UNDERGROUND SPACE USE

ANALYSIS OF THE PAST AND LESSONS FOR THE FUTURE

Copyright © 2005 Taylor & Francis Group plc, London, UK

PROCEEDINGS OF THE 31ST ITA-AITES WORLD TUNNEL CONGRESS, 7–12 MAY 2005, ISTANBUL, TURKEY

Underground Space Use

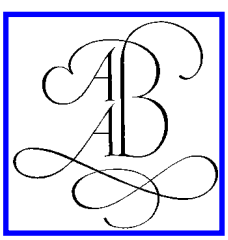
Analysis of the Past and Lessons for the Future

Edited by

Yücel Erdem
Turkish Road Association, Turkey

Tülin Solak
General Directorate of Highways, Turkey

Volume 1 & 2



A.A. BALKEMA PUBLISHERS LEIDEN / LONDON / NEW YORK / PHILADELPHIA / SINGAPORE

Copyright © 2005 Taylor & Francis Group plc, London, UK

Copyright © 2005 Taylor & Francis Group plc, London, UK

All rights reserved. No part of this publication or the information contained herein may be reproduced, stored in a retrieval system,or transmitted in any form or by any means, electronic, mechanical, by photocopying, recording or otherwise, without written prior permission from the publisher.

Although all care is taken to ensure the integrity and quality of this publication and the information herein, no responsibility is assumed by the publishers nor the author for any damage to property or persons as a result of operation or use of this publication and/or the information contained herein.

Published by: A.A. Balkema Publishers, a member of Taylor & Francis Group plc
www.balkema.nl and www.tandf.co.uk

ISBN Set (consisting of 2 volumes and CD-ROM): 04 1537 452 9
ISBN Volume 1: 04 1537 453 7
ISBN Volume 2: 04 1537 458 8
ISBN CD-ROM: 04 1537 459 6

Printed in Great Britain

Copyright © 2005 Taylor & Francis Group plc, London, UK

Preface xvii
Sponsors xix

53

Copyright © 2005 Taylor & Francis Group plc, London, UK

Observational method for tunnel construction in difficult conditions considering environmental impact to groundwater 93
H. Ohtsu, Y. Ohnishi, T. Nishioka, K. Takahashi & T. Yasuda

Research plan and construction outline of the Mizunami Underground Research Laboratory (MIU) in large depth for geoscience and geological disposal fundamental research 101
M. Sakamaki, T. Sato, S.-I. Mikake, T. Kanata, K. Nakamura, M. Kubo, K. Akiyoshi, M. Noda, Y. Nishikawa & J. Nobutoh

Water-tightening design and construction of tailbay tunnels at Kannagawa Power Plant 109
F. Kawashima, M. Yamasaki, H. Ozawa, S. Ishizaki, T. Otani & N. Igarashi

Study on state and pattern analysis of Tunnel Portal Slope in Korea 117
Y. Baek, O.I. Kwon, H.B. Koo & G.J. Bae

Desilting chambers of Nathpa Jhakri hydroelectric project – case study of problems during construction and remedial measures 123
S.P.S. Chauhan & R. Jeyaseelan

Oporto light train. Bolhão station design 129
R.S. Pistone & M.C. Costa

A design case study of the very wide 3-arch tunnel under the railroad station building 135
S.B. Chang, S. Kwon, S.J. Moon & S.D. Lee

Rock mass characterization and primary support design for the Boztepe Tunnel, Turkey 141
E. Sopaci, H. Akgün & M. Akinci

Tunnel and portal stability assessment in weak rock 149
M.K. Koçkar & H. Akgün

Three-dimensional regions in tunnels 157
H. Gercek

Surface settlement prediction for Istanbul Metro tunnels via 3D FE and empirical methods 163
S.G. Ercelebi, H. Copur, N. Bilgin & C. Feridunoglu

Transportation demands in Istanbul and New York 171
A. Gursoy

Experimental study for shear behavior of pseudo rock joint under constant normal stiffness condition 175
H.-R. Rim, H.-J. Choi, B.-K. Son, C.-I. Lee & J.-J. Song

The effect of spatial distribution in geotechnical design parameters on tunnel deformation 183
K.I. Song, G.C. Cho, I.M. Lee & S.W. Lee

Behaviour of a large cross-section tunnel in a large-scale model test 191
C.J. Lee, J.S. Kim, N.Y. Ryu, S.D. Lee, K.H. Jeong & J.W. Yang

GIS-based application and intelligent management of geotechnical information and construction data in tunnelling 197
C.Y. Kim, S.W. Hong, K.Y. Kim, S.H. Baek, G.J. Bae, B.H. Han & K.S. Jue

A new approach to estimate plastic region near tunnel considering excavation induced damage and in situ rock mass condition 205
M. Sagong & J.S. Lee

The influence of the round length on the stability of tunnel face and unsupported span 211
Y. Zoo, Lee, W. Schubert & C.-Y. Kim

Copyright © 2005 Taylor & Francis Group plc, London, UK

Effect of tunnelling and groundwater interaction on ground and lining responses 217
C. Yoo, S.B. Kim, H.C. Shin & S.C. Baek

Application of the multiple-layer supporting method to a tunnel in squeezing argillaceous rocks 225
S. Kemmochi, E. Taketsu, A. Ogawa, T. Aoki, M. Koike, R. Morita, H. Shirahata, N. Koya & M. Matsubara

On design analyses of NATM-tunnels 233
S.C. Möller & P.A. Vermeer

Case study of 3D fracture aperture density distribution technique on the assessment of tunnel safety at new constructing road 239
B.-J. Lee, J.-Y. Kim & Y.-S. Kim

A study on the reinforcement effect of Umbrella Arch Method and prediction of tunnel crown and surface settlement 245
S.-H. Kim, S.-H. Baek & H.-K. Moon

Numerical analysis of geotechnical parameters on subsidence due to underground mining 253
D.S. Cheon, S.O. Choi, Y.S. Jeon & C. Ryu

Model testing of perpendicularly spaced tunnels 259
S.-H. Kim

Design and construction of NATM underground station tunnel by using the forepoling method in difficult conditions for Athens Metro 265
P. Kontothanassis, N. Koronakis, A. Karinas & S. Massinas

Design of water isolation grouting for reducing high water inflows in urban shallow tunnels 271
N. Koronakis, P. Kontothanassis, D. Katsaris & J. Bournazos

Gotthard Base Tunnel – *Sedrun section* 277
Mastering squeezing rock zones
H. Ehrbar

Engineering geology and design of primary support of road tunnels. Cases from the Egnatia roadway 283
N. Kazilis & G. Aggistalis

Rock reinforcement design for unstable tunnels originally excavated in very poor rock mass 291
R. Osgoui & E. Ünal

Estimation of subsidence due to mining using artificial neural network – preliminary study 297
Y.B. Jung, D.S. Cheon & S.O. Choi

Model tests on shotcrete to analyze early age behavior of tunnel support 303
T.B. Celestino & D.A. Ferreira

Design aspects of the Bangkok Blue Line Extension 309
C. Photayanuvat, N. Phien-wej & S. Suwansawat

Teaching tunnels: knowledge management and on-line databases 315
R.-M. Faure, J.-F. Thimus, G. Hemond, N. Faure & B. Lecomte

The 9 km long Kallidromo Tunnel of the New Highspeed Railway Line Athens-Thessaloniki, Greece, Tunnel sections in squeezing ground 321
W. Wittke, B. Wittke-Schmitt & D. Schmitt

New high-speed railway lines Stuttgart 21 and Wendlingen-Ulm – approximately 100 km of tunnels 327
W. Wittke & C. Erichsen

Copyright © 2005 Taylor & Francis Group plc, London, UK

Status of Japanese underground research laboratory design and construction of 1000 m-deep shafts and research tunnels 335
T. Sato, M. Imazu, S. Mikake, T. Tamai, M. Yamamoto & M. Sakamaki

Tunnel portal problems in landslide areas – Black Sea Highway Project, Turkey 343
M. Vardar, B. Koçak & H. Karaoğlan

Jet-Grout application at Sarayköy Tunnel interval portals 347
M. Vardar, H. Karaoglan, K. Kaya & R. Mucukgil

Case study – deformations and remedial measures for Nefise Akçelik and Asarkayasi tunnels on Black Sea Costal Road Project 353
M. Vardar, H. Karaoglan, Z. Etkesen & E. Akis

Metsovitikos river north alignment of Egnatia Motorway. The concept and the tunnel designs 357
N. Kazilis, Ch. Georganopoulos & G. Aggistalis

New developments in excavation and construction technology for rock and soft ground tunnelling

New tunnel construction technique of pipe-roof method in saturated soft soil 365
J.k. Ge

Tunnelling in difficult ground and groundwater conditions 371
H. Quick & S. Meissner

Visualizing excavated soil flow in the cutter chamber of a large earth pressure balanced shield 377
H. Dobashi, Y. Sakurai, Y. Konishi, S. Ouchi, K. Matsubara, A. Kitayama & H. Takahashi

Planning and construction of Keelung River Yuanshantzu Flood-Diversion Tunnel Project 385
H. Shimizu, H. Hamada, T. Yasunaga, K. Taira & M. Kuniya

Application of the tunnel face reinforcement and fore-piling 391
T. Yamamoto, K. Murakami, S. Shirasagi, K. Negishi, K. Nishioka & T. Kobayashi

Tunnel excavation penetrating active landslide area – second-TOMEI Expressway Inasa No. 2 Tunnel 397
S. Tayama, K. Kanzawa, H. Hirano & S. Isoda

A deep open-cut excavation with three types of continuous retaining walls 405
H. Tsunoda, Y. Endo, I. Kamegaya, H. Kawakami, K. Fukumoto & A. Ueda

Application of the multiple-layer supporting method to a tunnel in squeezing argillaceous rocks 413
S. Kemmochi, E. Taketsu, A. Ogawa, T. Aoki, M. Koike, R. Morita, H. Shirahata, N. Koya & M. Matsubara

Support structure for tunneling in squeezing ground and secondary lining design 421
J. Yorita, M. Hanita, H. Takahara, K. Kawahara, H. Takahashi & M. Mitarashi

Ground reinforcement by the Pre-Supporting System Arch (PSS-Arch) method 427
K. Miyashita, H. Takahashi, M. Teranishi, S. Iwanaga, M. Inada, T. Matsuo & A. Nakakita

From research to practice "Development of Rapid Excavation Technologies" 435
S. Eskikaya, N. Bilgin, C. Balci & H. Tuncdemir

Jacked box tunnelling, a non-intrusive technique for constructing underbridges 443
J.W.T. Ropkins & D. Allenby

Ground borne vibration on the East Side Access Project Manhattan segment: issues and impacts 449
A. Benslimane, D.A. Anderson, N. Munfakh & S. Zlatanic

Copyright © 2005 Taylor & Francis Group plc, London, UK

An experimental study on the development of high performance shotcrete for permanent tunnel support 455
S.P. Lee, D.H. Kim, J.H. Ryu, J.Y. Yu, S.D. Lee, S.H. Han, M.S. Choi & C. Park

Successful application of the observational design method to difficult tunnel conditions – Driskos tunnel 463
P. Grasso, G. Scotti, G. Blasini, M. Pescara, V. Floria & N. Kazilis

Ground freezing improvement for TBM maintenance in Singapore 471
J. Itoh, Y.-S. Lee, S.-W. Yoo & S.-D. Lee

High pressure jet grouting in tunnels – a case study 477
A. Da Già, M. Marotta & G. Peach

Gotthard Base Tunnel: special aspects and state of the works 485
M. Rehbock-Sander & Y. Boissonnas

Dobrovskeho Tunnels in Brno, CZ 491
V. Horak, J. Pechman & J. Rozek

New method of underground structures using multi elements which are jointed with the specific junctions 497
M. Shimizu, A. Watanabe, K. Nishijima, M. Kurisu, K. Kuwabara, T. Genjun & E. Arakawa

Contract management, financing and risk analysis

The control of heavy squeezing phenomena in an Austrian road tunnel 505
N. Ayaydin & G. Huber

A study on the development of MI (Multiple Index) System for risk assessment of tunnelling in urban subway 509
Y.G. Wye, J.K. Park, D.U. You, C.R. Choi, Y.G. Kim & D.H. Lee

Determination of construction method for Young Dong Tunnel by risk assessment 515
Y.-II. Kim, Y.-H. Yoon, S.-K. Cho, J.-S. Kim & N.-Y. Lee

Managing the construction contract for the tunnels of the Bilbao Metro 521
J. Madinaveitia

Construction of highway tunnel financed by B.O.T. model management of risks in financing 527
Ünal İlker

Cost estimating and risk – management for underground projects 533
J.J. Reilly

A Tunneling Game Model for good tunneling practice 539
L. Rosas-Sanchez

Operation, maintenance, drainage, water proofing, rehabilitation, renovation and repair of underground structures

New waterproof structure for New Austrian Tunneling Method 549
T. Komatsu, T. Nakamura, H. Kanda & M. Takada

Behavior of support structure of existing tunnels during enlargement of cross section 555
H. Mashimo, T. Ishimura, N. Isago & S. Morimoto

The underground drainage system using New Tubular Roof Method 563
P. Inn-Joon, K. Jeong-Yoon, Y. Kwang-Ho, K. Chang-Won & K. Kyong-Gon

Copyright © 2005 Taylor & Francis Group plc, London, UK

Waterproofing of an emergency escape tunnel by employing an innovative sprayable membrane: the Giswil highway tunnel project, Switzerland 571
W. Meier, K.G. Holter & S. Haeusermann

BioSealing: how micro-organisms become our little allies in repairing leaks in underground constructions 575
V. Veenbergen, J.W.M. Lambert, E.E. van der Hoek, A.F. van Tol & S.I. Weersma

Tunnel automation systems 581
M. Barut

Quantitative assessment of structural fire endurance of concrete and shotcrete tunnel liners 585
A. Caner, S. Zlatanic & N. Munfah

Consolidation and excavation works for the upgrading of Frejus tunnel 591
M. Pescara, G. Russo, F. Valdemarin & P. Grasso

Rehabilitation of Malatya-Narlı No: 7 Railroad Tunnel 599
B. Divleli & E. Unal

Safety aspects of railway tunnel: Example of the Lötschberg railway tunnel 605
B. Crausaz, A. Weatherill & P. Gerber

Tunnel refurbishment under railway operations 613
A. W. Ackermann & F. Modetta

Renewal of the Alpine San Bernardino tunnel with traffic flowing 619
P. Wenger & L. Schönenberger

Energy-saving lighting system for road tunnel 625
S. Nagai, S. Ishida, M. Shinji & K. Nakagawa

Earthquake hazards and seismic design of underground structures

Seismic design method of immersed tunnel and effects of flexible joints 635
O. Kiyomiya

Seismic microzonation of Küçükçekmece-Halkalı region in Istanbul 641
H. Kılıç, P. T. Özener, M. Yıldırım, S. Adatepe & H. Demir

Seismic behaviour of tunnels in soft soil: parametric numerical study and investigation on the causes of failure of the Bolu tunnel (Düzce, Turkey, 1999) 649
A. Giannakou, P. Nomikos, I. Anastasopoulos, A. Sofianos, G. Gazetas & P. Yiouta-Mitra

Seismic assessment results and actual application in the complex ground conditions of Bolu tunnels after the 1999 Duzce earthquake 657
M. Ozben, F. Tokgozoglu & S. Isik

Volume 2

Geological and geotechnical investigations

Geotechnical & tunnelling conditions below buried valleys in Sydney, Australia. 669
Robert J. Whiteley

Geological risk assessment at the design stage in tunnel construction using GIS technique: the case of the A1 Highway Base Tunnel in the Apennines (Italy) 675
D. Furesi, M. Coli & G. Pini

Copyright © 2005 Taylor & Francis Group plc, London, UK

The study on the geotechnical factors effecting the excavation performance in Istanbul Metro Tunnels 681
Ö. Selimoglu

Geotechnical investigation program for the No. 7 subway line extension project, New York 687
E.C. Wang, R.B. Roberts, L.M. Hsia, C.M. Osborne, R. Jeremic & C.C. Chang

Some aspects for geotechnical investigations for TBM and NATM tunneling in rock 694
W. Wittke, J.H. Gattermann & P. Wittke-Gattermann

Rock mass classification and support design of the Kuskunkiran Tunnel in Van 701
E. Karahan, S. Cosar, S. Sözer & K. Kaya

Tunnel machines and mechanical excavations

The development and application of shield posture automatic measuring system 709
X. Yue

Research on shield tunneling technology in urgent curve metro tunnels 715
Y. Chen. J. Yang & J. Zhu

Geotechnical and mechanical interactions using the earth-pressure balanced shield technology in difficult mixed face and hard rock conditions 723
U. Maidl

Soil conditioning for EPB machines: balance of functional and ecological properties 729
L. Langmaack & Q. Feng

Clogging of TBM drives in clay – identification and mitigation of risks 737
M. Thewes & W. Burger

Tunnel support by fully grouted rock bolts for fast TBM advance 743
M. Alber & S. Rühl

Geodetic instrumentation for use on machine bored tunnels 749
N. Clarke-Hackston, M. Messing & E. Ullrich

Development of divergence construction technology for deep road tunnels 759
H. Shikata & T. Aso

Application of 'casting support tunneling system using TBM' to unconsolidated soil with high groundwater level 765
H. Iida, T. Kitagawa, K. Chishiro, T. Ono, Yu. Koyama & A. Koizumi

Shield tunneling technologies in Japan 773
T. Goto, T. Masaka, K. Miki & S. Takaku

Compact shield tunneling method 779
M. Matsuura, S. Takaku, Y. Nagashima & Y. Moriya

Continuous tight curved belt conveyor of R30m did a TBM drift excavation a lot of good-Shimizu No.4 tunnel on 2nd Tomei Expressway 785
M. Noda, Y. Inoue, T. Fujita & K. Akiyoshi

Study on the deformation and load bearing capacity of TBM shield tunnel lining in fire 793
H. Tajima, M. Kishida, T. Kanda & T. Morita

The design and construction of a shield tunnel which have a non-excavating extension part in the middle by the Japan longest distance class 801
M. Takahashi, T. Tsunekawa, T. Kamei, T. Tsuji & K. Takimoto

Copyright © 2005 Taylor & Francis Group plc, London, UK

Pressure gradients at the tunnel face of an earth pressure balance shield 809
A. Bezuijen, J.F.W. Joustra, A.M. Talmon & B. Grote

The performance of a roadheader in high strength rock formations in Küçüksu tunnel 815
N. Bilgin, D. Tumac, C. Feridunoglu, A.R. Karakas & M. Akgul

The performance of a full face tunnel boring machine (TBM) in Tarabya (Istanbul) 821
N. Bilgin, C. Feridunoglu, D. Tumac, M. Cinar, Y. Palakci, O. Gunduz & L. Ozyol

Slurry shield driven microtunnel applications in Istanbul 827
A.B. Akkaya, H. Copur, N. Omac & H.M. Yucel

Earth Pressure Balance tunnelling for two short drives for the New Mississippi Outfall, Denver, Colarado 833
J.Y. Kaneshiro, A.F. Stirbys & G.R. Fischer

Ground movements induced by Earth-Pressure Balanced, Slurry Shield and Compressed-Air tunneling techniques on the Toulouse subway line B 841
F. Emeriault, T. Bonnet-Eymard, R. Kastner, E. Vanoudheusden, G. Petit, J. Robert, J. Y. De Lamballerie & B. Reynaud

Large cross-section shield tunnel passing right under the Jyoban and Hibiya railway lines: Minowa tunnel of the Tsukuba Express Line 849
K. Sasaki, K. Sakamaki & S. Abe

Geotechnical problems encountered by tunnel boring machines mining in sedimentary rocks 857
C. Laughton

Uetliberg tunnel: comparison of drill and blast and mechanical heading 863
S. Maurhofer & M. Glättli

Microtunnelling in rock and soft ground strata – Asia Pacific experiences 871
Bala K. Balasubramaniam

Tunnel construction with Earth Pressure Balance shields and measures to minimize settlements under urban infrastructure in London 877
T. Schubert, K. Rieker, D. Court & C. Fice

FEM analysis of EPB tunneling bored underneath through underground obstruction 883
W. Teparaksa

Surface and subsurface ground deformation due to EPB tunneling in Bangkok subsoils 889
D. Luangpitakchumpol, W. Teparaksa, W. Pitaksaithong, C. Boonsong & J. Boonard

Ground improvement and settlement control

Tunneling and measurements in unconsolidated ground 897
T. Kitagawa, H. Iida, T. Sudo, T. Matsunaga, S. Akutagawa & S. Konishi

Construction method of shallow railway tunnel in loose sandy ground 903
T. Kitagawa, H. Iida, Y. Tadenuma, S. Konishi, T. Ono & K. Okutsu

Behavior of center diaphragm tunnel with large cross section in earth ground 911
N. Tomisawa & M. Tamotsu

Longitudinal arching characteristics around face of a soil-tunnel with crown and face-reinforcement – laboratory investigation 917
Y.-K. Choi, J.-H. Park, O.-Y. Kwon & S.-B. Woo

State-of-the-art microcement pre-injection for the Jong–Asker Rail Tunnel, Norway 925
H.O. Hognestad & E. Frogner

Copyright © 2005 Taylor & Francis Group plc, London, UK

Significance of grouting for controlling leakage in water tunnels – a case from Nepal 931
K.K. Panthi & B. Nilsen

Deformed ground massif state during tunnel construction 939
G.G. Balandyuk

Laboratory testing of grout properties and their influence on back fill grouting 941
A. Bezuijen, W.H. van der Zon & A.M. Talmon

Modified New Austrian tunneling method in clay soils 949
Y. Eyigun, K. Moroy & A. Saglamer

Advanced grouting techniques for tunnel constructions under sensitive buildings 955
U. Arslan, W. Krajewski & P. Ripper

Improvement of Wet-mix shotcrete performance by addition of High Reactivity Metakaolin 959
G.-J. Bae, S.-H. Chang, H.-S. Shin, H.-G. Park, M.-S. Lee, J.-K. Kim & J.-P. Won

The use of horizontal inclinometers for the optimization of the rock mass – support interaction 967
G. Volkmann & W. Schubert

Tunnel excavation works in Taksim-Kabataş funicular system project 973
E. Aykar, B. Arıoglu, N. Erdirik, A. Yüksel, T. Özbayır, E. Arıoğlu & R. Yoldaş

Resin-injection soil stabilization techniques used in underground construction carried on in big cities in Russia 981
A.B. Kondratov

Calculation of the stress intensity index of a sprayed concrete lining 985
R.B. Rokahr, R. Zachow & D. Zander-Schiebenhöfer

Prediction of ground deformation response for double tunnel Bangkok MRT subway 991
W. Teparaksa

Safety

New guidance on safety standards for road and railway tunnels 999
A. Focaracci

Study on anti-fire panel for vehicle fire in immersed tunnel 1005
Y. Matsuo, A. Mizobe & O. Kiyomiya

Proposed safety facilities for highway tunnels in Turkey 1013
I. Ünal & A. Nitta

Advanced studies on the propagation of fire in a motorway tunnel – case history by the test center 1019
S.J. Seirer & V. Wetzig

Dynamic fire spreading and water mist tests for the A86 east tunnel – description of the test set up and overview of the water mist tests 1025
X. Guigas, A. Weatherill, C. Bouteloup & V. Wetzig

Use of advanced fire fighting technologies of finely atomized water for fire protection of metro objects and tunnels 1031
A.S. Chirko, A.V. Karpyshev & M.D. Segal

Physical modeling of blasts and fires in tunnels 1035
V.P. Efremov, V.E. Fortov, V.V. Golub, M.E. Povarnitsyn, S.B. Viktorov & A.S. Chirko

Standardisation and research about fire safety in European traffic tunnels 1039
A. Haack

Copyright © 2005 Taylor & Francis Group plc, London, UK

Safety management – Checking Engineer in Conventional Tunnelling 1047
A. Beil & F. Aïssaoui

Prevention of accidents during the tunnel construction phase 1051
M. Bandmann, W. Chromy & A. Haack

Analytical methods and numerical modelling

From documentation to prediction – a computer-based method for discontinuity analysis and block stability assessment in Tunnelling 1059
M. Pötsch, W. Schubert & A. Gaich

Gallery connection between the annexed structure and the TBM tunnel in soft ground 1065
Ashraf A. Abu-Krisha

Development and application of a long face reinforcing method with GFRP tubes in mountain tunneling 1071
Y. Mitarashi, T. Matsuo, H. Tezuka, T. Tsuji, T. Haba & T. Okabe

Probabilistic analysis of blasting-induced rock damages in tunneling 1079
I.M. Lee, B.K. Park, K.H. Cho & C.W. Park

Re-analysis of Şanlıurfa tunnels by finite element method 1085
H. Tosun

Tunnel convergence analyses in heterogeneous/anisotropic rock masses 1091
C.Y. Kim, K.Y. Kim, S.H. Baek, S.W. Hong, G.J. Bae, S.H. Lee, W. Schubert, K. Grossauer & Y.Z. Lee

Determination of the mechanical properties of discontinuous rock masses by using PFC2D 1099
E.-S. Park, C.-H. Ryu & S.-H. Bae

Numerical simulations of SFRC precast tunnel segments 1105
G.A. Plizzari & L. Cominoli

Observed behavior of three-arch tunnel constructed in weathered soil 1113
K.H. Shin, J.K. Kim, S.R. Lee, Y.K. Kim & J.H. Noh

Evaluation of the stability and support design for the underground caverns in an abandoned gold mine 1121
S.K. Chung, Y.S. Jeon, C. Sunwoo & Y.B. Jung

Stability analyses of the dump site culvert in Tınaz Surface Mine 1127
Ö.C. Özcan & E. Ünal

Automated finite element model generation for tunnel forms 1135
A. Türer, Ökkeş Sultanoğlu & A. Şuyun

Three-dimensional numerical simulation of tunnel advancement on adjacent pile foundation 1141
C.H. Pang, K.Y. Yong & Y.K. Chow

Some considerations in finite element analysis of tunnelling 1149
C.H. Pang, K.Y. Yong & G.R. Dasari

3-D FEM analysis of closely spaced vertical twin tunnel 1155
Y. Zheng & W. Qiu

3D FEM analysis on mechanics behaviour of a new style railway tunnel portal 1161
J. Zhang, W. Qiu & F. Wang

Study on calculation method of frost force of tunnel in frozen earth 1167
W. Qiu & J. Wu

Copyright © 2005 Taylor & Francis Group plc, London, UK

Design, construction and supervision of tunnels in swelling rock 1173
W. Wittke & M. Wittke

Building response to tunnelling in Brazil Salvador Metro 1179
S.B. Foá, I. Chissolucombe & A.P. Assis

Prediction of ground-condition ahead of tunnel face using electric resistivity – analytical study 1187
G.C. Cho, J.S. Choi, G.H. Lee & J.K. Lee

3D numerical simulation of the future Pinheiros Station – Line 4-Yellow of the São Paulo Subway 1195
F.M. Kuwajima & H.C. Rocha

Field measurements and monitoring

Deformation monitoring of large tunnel wall under construction by digital photogrammetry measurement at Ritto Tunnel 1203
T. Nakai, M. Ryu, H. Miyauchi, S. Miura, Y. Ohnishi & S. Nishiyama

Channel Tunnel – monitoring strategy for the tunnel lining 1211
C. Choquet, A. Schwenzfeier & D.R. Lamont

Measurements of lining loads on a 3-arch tunnel in Daejeon subway, Korea 1215
H.J. Kim, S.H. Kim, G.J. Bae, J.K. Kim & D.S. Park

Impact on the environment of a shallow gallery excavated in Toulouse's molasses by a conventional method 1219
E. Vanoudheusden, G. Petit, J. Robert, F. Emeriault, R. Kastner, J.Y. de Lamballerie & B. Reynaud

Geotechnical online support for tunnels in difficult ground 1227
W. Schubert, K. Grossauer & B.A. Moritz

Evaluation of the influence of the rock mass structure on the deformation behavior of tunnels 1233
T. Solak & W. Schubert

The importance of displacement prediction 1239
K. Grossauer, W. Schubert & P. Sellner

The development of an in-situ AE monitoring system and its application to rock engineering with particular emphasis on tunneling 1245
H. Tano, T. Abe & Ö. Aydan

A real-time multi-parameter monitoring system for assessing the stability of tunnels during excavation 1253
Ö. Aydan, M. Daido, H. Tano, T. Tokashiki & K. Ohkubo

Immersed tunnels

Hydrodynamic forces on immersed tunnel elements during transportation and foundation 1263
B.P. Rigter & D. Schwanenberg

Marmaray project: requirements for the design and construction of the Bosphorus tunnel 1269
L.C.F. Ingerslev, H. Sakaeda, M. Takahashi & R. Castelli

Marmaray project: designing an immersed tunnel for the Bosphorus 1277
L.C.F. Ingerslev, H. Sakaeda & M. Takahashi

Dredged material management in immersed tube tunnel construction 1283
V. Tanal, F.S. Pehlivan, J.-N. Wang, Z. Ozerkan & I. Guler

Copyright © 2005 Taylor & Francis Group plc, London, UK

Sustainable design and construction aspects of immersed tube tunnels 1289
V. Tanal & F.S. Pehlivan

Seismic hazard assessment and earthquake resistant design considerations for the Bosphorus tunnel project 1295
J.-N. (Joe) Wang, M. Erdik & S. Otake

Marmaray project: safety and ventilation strategy, Bosphorus crossing tunnels 1305
S. Lykke, W.D. Kennedy, M.M. Babur & F. Asci

Marmaray project: geological and geotechnical investigations 1309
O. Şimşek, S. Mitani & O. Altun

Marmaray project: tunnels and stations in BC contract 1315
S. Mitani, H. Sakaeda, H. Şahin & Ümit Çelik

Marmaray project: marine operations, the Bosphorus crossing 1321
S. Lykke, H. Sakaeda, V. Tanal, F. Koyama & I. Guler

Marmaray Project: Project Management, the Marmaray Project 1325
S. Lykke, H. Belkaya, H. Sakaeda & H. Özmen

Marmaray Project: contract strategy and minor tactics 1331
R. Harrison, S. Lykke, H. Sakaeda & M. Çilingir

Copyright © 2005 Taylor & Francis Group plc, London, UK

Preface

The ITA annual congresses and meetings have become premier events in the international tunnelling and underground construction calendar.

We are very proud and honoured to host the ITA-AITES 2005 WORLD TUNNEL CONGRESS & 31st GENERAL ASSEMBLY with the theme "Analysis of the Past and Lessons for the Future" in Istanbul, the eternal city, where for more than 2,500 years East and West have met to form a melting pot for a variety of races, cultures, religions and political systems.

The 2005 congress is organized by the Turkish Road Association and General Directorate of Highways, with support from the International Tunnelling Association (ITA).

Hundreds of potential delegates and interested parties from all over the world had been invited to submit their papers and contribute to the development of our field. The response to free paper submission was very impressive and many of the accepted papers contained new information and demonstrated significant developments that had taken place within our field. We would like to reaffirm our appreciation to all of our colleagues for their guidance, their willingness to share knowledge and for their continued support.

The abstract books and the CD-ROM present the full length papers accepted by the Scientific and Technical Committee of World Tunnel Congress 2005 – Istanbul. A total of 277 Abstracts were received and reviewed. The Scientific and Technical Committee and the editors selected 200 of these for publication. The published papers are divided into 13 groups.

ITA-AITES 2005 Scientific and Technical Committee:

Prof. Dr. Emine AĞAR	TURKEY
to the beloved memory of Nefise *AKÇELİ*K	TURKEY
Associate Prof.Dr. Sadık BAKIR	TURKEY
Dr. Yücel ERDEM	TURKEY
Associate Prof.Dr. Nevzat ERSELCAN	TURKEY
Çetin FIRAT	TURKEY
Prof. Dr. Erol GÜLER	TURKEY
Prof. Dr. Alfred HAACK	GERMANY
Akın OYAT	TURKEY
Prof. Dr. Ahmet SAĞLAMER	TURKEY
Prof. Dr. Wulf SCHUBERT	AUSTRIA
Tülin SOLAK	TURKEY
Bülent ULUKAN	TURKEY
Prof. Dr. Remzi A. ÜLKER	TURKEY
Prof. Dr. Erdal ÜNAL	TURKEY
Prof. Dr. Mahir VARDAR	TURKEY
Dr. Harald WAGNER	AUSTRIA

We appreciate our publishing team at 'Taylor & Francis Group – A. A. Balkema' who have provided valuable advice in the preparation of the books and the CD-ROM.

The following groups have been closely involved in the Organisation of the Congress.

ITA-AITES 2005 Organising Committee:

Emine AĞAR	TURKEY
Ebru AKIŞ	TURKEY
Gönül BALKIR	TURKEY
Claude BERENGUIER	ITALY
Esin BÖGE	TURKEY
A. Tahir DENGİZ	TURKEY

Copyright © 2005 Taylor & Francis Group plc, London, UK

Sabri Özkan ERBAKAN	TURKEY
Yücel ERDEM	TURKEY (Chairman)
Çetin FIRAT	TURKEY
Vacip MERT	TURKEY
Susan NELSON	U.S.A
Akın OYAT	TURKEY
Erdem POYRAZOĞLU	TURKEY
Tülin SOLAK	TURKEY
Tamer ŞAHİN	TURKEY
İsmail TÜMAY	TURKEY
Bülent ULUKAN	TURKEY

ITA-AITES 2005 Advisory Committee:

Emine AĞAR	TURKEY
Andre ASSIS	BRAZIL
Claude BERENGUIER	ITALY
Alfred HAACK	GERMANY
Sung-Wan HONG	KOREA
Koichi ONO	JAPAN
Henk OUD	NETHERLANDS
Harvey PARKER	USA
Tae-Sung YOO	KOREA
Jian ZHAO	SINGAPORE

ITA-AITES 2005 Official Congress Organizer:

SETUR SERVICE TOURISTIC INC. ISTANBUL

O. Banu Sayman

The editors would like to acknowledge the great effort made by all these individuals in the organisation of the ITA-AITES 2005 Congress.

Tülin SOLAK – Yücel ERDEM

Copyright © 2005 Taylor & Francis Group plc, London, UK

Primary sponsors









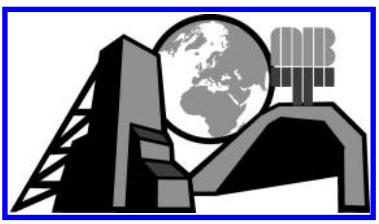




Supporters







Copyright © 2005 Taylor & Francis Group plc, London, UK

Tunnels, environment and public

Copyright © 2005 Taylor & Francis Group plc, London, UK

Positive impact of El Azhar road tunnels on environment, safety and tourism in Fatimid Cairo

A. Abd El Moamen Khalil
Lecturer of Civil Engineering, National Authority for Tunnels, Cairo, Egypt

ABSTRACT: A two level steel bridge along El Azhar street was constructed to solve the problems of transport and traffic congestion in seventies of the last century. The bridge and also the very crowded street caused a bad appearance of the historic buildings in addition to air and noise pollutions which affect badly on the residents and the visitors. To avoid these negative impacts, the ministry of transport and National Authority for Tunnels constructed two road tunnels passing under El Azhar street and connecting Salah Salem road with the city center. It is concluded in this paper that these tunnels contribute in reducing the negative impacts of the traffic flow and resulted in positive impact on environment and tourism in Fatimid Cairo.

1 INTRODUCTION

The Fatimid Cairo was built one thousand years ago by El Moez Li-Dinellah to be the capital of Islamic Egypt. It has many historic islamic buildings and monuments and it is a very attractive area for tourists and traders as they can find the most famous antique markets in Khan El Khalily and many other places.The main route in the area is El Azhar street which passing through it.

The ministry of transport built a two level steel bridge along the street to solve the problems of transport and traffic congestion in seventies of the last century. The bridge and also the very crowded street caused a bad appearance of the historic buildings in addition to air and noise pollutions which affect badly on the residents and the visitors.

To avoid these negative impacts, the ministry of transport and National Authority for Tunnels constructed two road tunnels passing under El Azhar street and connecting Salah Salem road with the city center. It is concluded that these tunnels contribute in reducing the negative impacts of the traffic flow and resulted in positive impact on environment and tourism in Fatimid Cairo.

2 FATIMID CAIRO DESCRIPTION

2.1 *Natural environment*

2.1.1 *Climate*

It is 35.5°C of the average high temperature and 21.0°C of the average low temperature in summer at Cairo where locates at the south part of Nile delta. And it is 18.5°C and 7.1°C in winter respectively. Moreover, the precipitation in Egypt is little and also the rainfall is about 24.3 mm through the year of the Cairo City. Table 1 shows the weather in Cairo.

Table 1. Weather in Cairo.

Season	Temperature Max	Temperature Min	Humidity (%)	Rainfall (mm)
Winter	18.5	7.1	59	24.3
Summer	35.5	21.0	56	0.0

2.1.2 *Population*

The growth rate of population in last 13 years was 13% which shows average rate of 1.3% per year. Greater Cairo has a population of 17 millions, with area of 7000 ha.

2.2 *Establishment of Fatimid Cairo*

When the Fatimid region (969–1171) settled in Cairo under the leadership of El Moez Li-Dinellah it was called “Cairo of El Moez” because they decorated its four suburbs with luxurious buildings, delightful spots and gardens. This increased its delightfulness and beauty. It was the settlement of rulers and princes, where they had built about 360 historic islamic buildings.

The Al-Azhar Mosque (the most blooming), established in 972 (361 H) in a porticoed style shortly after

Copyright © 2005 Taylor & Francis Group plc, London, UK



Figure 1. Photo of Fatimid Cairo.

the founding of Cairo itself, was originally designed by the Fatimid general Jawhar El-Sequili (Gawhara Qunqubay, Gawhar al-Sakkaly) and built on the orders of Caliph Muezz Li-Din Allah. Located in the center of an area teaming with the most beautiful Islamic monuments from the 10th century, it was called "Al-Azhar" after Fatama al-Zahraa, daughter of the Prophet Mohamed (Peace and Prayers Be Upon Him). Figure 1 shows a photo of Fatimid Cairo.

It imitated both the Amr Ibn El-As and Ibn Tulun Mosques. The first Fatimid monument in Egypt, the Azhar was both a meeting place for Shi'a students and through the centuries, it has remained a focal point of the famous university which has grown up around it. It was under Yaqoub Ibn Cals that the mosque became a teaching institute. This is the oldest university in the world, where the first lecture was delivered in 975 AD.

Today the university built around the Mosque is the most prestigious of Muslim schools, and its students are highly esteemed for their traditional training. While ten thousand students once studied here, today the university classes are conducted in adjacent buildings and the Mosque is reserved for prayer. In addition to the religious studies, modern schools of medicine, science and foreign languages have also been added.

Architecturally, the mosque is a palimpsest of all styles and influences that have passed through Egypt, with a large part of it having been renovated by Abdarrahman Khesheda. There are five very fine minarets with small balconies and intricately carved columns. It has six entrances, with the main entrance being the 18th Century Bab El Muzayini (barber's gate), where students were once shaved. This gate leads into a small courtyard and then into the Aqbaughawiya Medrasa to the left, which was built in 1340 and serves as a library. On the right is the Taybarsiya Medersa built in 1310 which has a very fine mihrab.

The Qaitbay Entrance was built in 1469 and has a minaret built atop. Inside is a large courtyard that is 275 by 112 feet which is surrounded with porticos supported by over three hundred marble columns of ancient origin. To the east is the prayer hall which is larger than the courtyard and has several rows of columns. The Kufic inscription on the interior of the mihrab is original, though the mihrab has been modified several times, and behind is a hall added in 1753 by Abd el-Rahman Katkhuda. At the northern end is the tomb medersa of Jawhar El-Sequili. Nowadays, the ministry of culture renewals all these ancient buildings which are lying in the area from north of Gamaleya to Bab El Wazir in the south and from Salah Salem road at the east to port said at the west.

As shown in Table 2, the number of tourist visited Egypt has high increase of 60% between 1993 and 1997.

Table 2. Number of tourist visited Egypt (Unit: thousand people, %).

	Year					
Nationality	1992	1993	1994	1995	1996	1997
All nationalities						
Number	3207	2508	2582	3133	3896	3961
Percent	100	100	100	100	100	100
Arabs						
Number	1103	922	932	823	897	967
Percent	34.4	36.8	36.1	26.3	23.0	24.4
Europeans						
Number	1555	1082	1030	1515	2021	2120
Percent	48.5	43.1	40.0	48.3	51.9	53.1
Americans						
Number	224	188	182	229	259	256
Percent	7.0	7.5	7.0	7.3	6.6	6.5
Others						
Number	325	316	438	566	719	636
Percent	10.1	12.6	16.9	18.1	18.5	16.0

3 URBAN TRANSPORT IN CAIRO

Cairo City is the capital of Egyptional country, and the biggest city in the African Continent which has 17 millions people. As a public transport system of Cairo city, it is composed of metros, buses mini buses, micro-buses, water buses, tram-metros, etc.

Due to economic development in Cairo, population has concentrated into the city, motor cars have rapidly increased and a choronic traffic jam has often occurred at major junctions in recent years. Such increase of traffic cars has not only brought the air and noise pollution, but also obstruction of economic activities and expansions.

On the other hand, the government agencies concerned started the construction of the underground metros as a drastical urban transport countermeasures in Cairo.

3.1 *Negative impact of transport modes*

In-movement licensed vehicles in Cairo in the end of year 1999 are shown in Table 3.

Copyright © 2005 Taylor & Francis Group plc, London, UK

Table 3. Licensed vehicles.

Type of vehicle	No. of vehicles
Private cars	515402
Taxi	63445
Buses	
Public	5116
Private	5080
Tourism	4717
School	1387
Lorry & truck	104098
Motor-cycles	98327
Others	66163
Total	863735



Figure 2. A photo of El Azhar bridge.

Based on several studies of the transport and facilities, transport problems were identified in Fatimid Cairo and are summarized as follows:

1) Congestion Roads caused by large numbers of vehicles due to high demand for the transport service in peak hours.
2) Crowded modes of transport especially on public sector modes for some routes passing through crowded districts due to insufficient supply against high demand.
3) Low degree of efficiency and comfort on some public modes.
4) Unnecessary fuel consumption caused by low speed traveling.
5) Long duration of trip time especially on peak hours.
6) Air and noise pollutions.

The studies which had been carried out in seventies of the last century agreed that the main solution to meet the requirements of urban transport inside Fatimid Cairo is to build a steel bridge of two levels in order to connect El Darrassa in the East of El Azhar street with the city center of Cairo, in addition to keeping the on ground surface traffic. The bridge was built in the beginning of eighties passing through El Azhar street, and it transfers the traffic flow which is coming from Salah Salem road to El Opera Square and also in the opposite direction. Figure 2 shows a photo of El Azhar bridge.

The bridge causes many negative impacts on the historic Fatimid area which can be summarized in the following items:

- Air pollution with carbon monoxide and ozone.
- Noise pollution.
- Bad appearance and prohibiting sight seeing.

3.1.1 *Air pollution*

Carbon monoxide results from incomplete combustion of fuel and is emitted directly from vehicle tailpipes. Incomplete combustion is most likely to occur at low air-to-fuel ratios in the engine. These conditions are common during vehicle starting when air supply is restricted (“choked”), when cars are not tuned properly, and at altitude, where “thin” air effectively reduces the amount of oxygen available for combustion (except in cars that are designed or adjusted to compensate for altitude).

Nationwide, two-thirds of the carbon monoxide emissions come from transportation sources, with the largest contribution coming from highway motor vehicles. In urban areas, the motor vehicle contribution to carbon monoxide pollution can exceed 90.

Ozone is a form of molecular oxygen that consists of three oxygen atoms linked together. Ozone in the upper atmosphere (the “ozone layer”) occurs naturally and protects life on earth by filtering out ultraviolet radiation from the sun. But ozone at ground level is a noxious pollutant.

Ozone is a severe irritant. It is responsible for the choking, coughing, and stinging eyes associated with smog. Ozone damages lung tissue, aggravates respiratory disease, and makes people more susceptible to respiratory infections. Children are especially vulnerable to ozone’s harmful effects, as are adults with existing disease. But even otherwise healthy individuals may experience impaired health from breathing ozone-polluted air.

Ozone is not emitted directly but is formed in the atmosphere through a complex set of chemical reactions involving hydrocarbons, oxides of nitrogen, and sunlight. The rate at which the reactions proceed is related to both temperature and intensity of the sunlight. Because of this, problematic ozone levels occur most frequently on hot summer afternoons.

Hydrocarbons and nitrogen oxides come from a great variety of industrial and combustion processes. In typical urban areas, at least half of those pollutants come from cars, buses and trucks.

Copyright © 2005 Taylor & Francis Group plc, London, UK

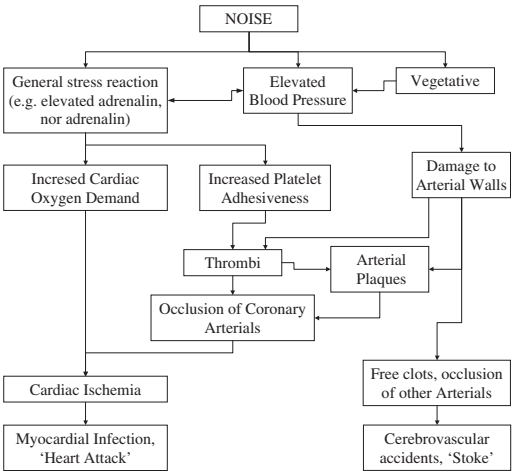


Figure 3. Effect of noise on human body.

3.1.2 *Noise pollution*

People who are exposed to high noise levels for short discontinuous periods may lose part of their hearing for some period, but those who are exposed to high noise levels for long continuous periods may lose part or all hearing abilities. Headache, stress and nervous instability may happen to the human body during the period of hearing loss.

The physiological effects are classified to short and long terms such as fatigue, headache, startle response, muscle tension response, respiratory reflexes, heart, circulation responses, and damage in the heart and brain as shown in Figure 3.

As El Azhar bridge is formed from steel sections, structure borne noise generated due to traffic flow is higher than standard regulations. It was found that air borne and structure borne noise levels are ranging 60 to 80 dB.

3.2 *Necessity of El Azhar road tunnels construction*

Within the framework of an overall revival and development plan for the glorious touristic area. The project of El Azhar road Tunnels has been proposed. The main objectives of this project are:

1) Providing a safe and efficient underground transport mean.
2) Creating a vehicular free surface for tourism and pedestrian purposes.
3) Reduction of air and noise pollution on the ground surface of El Azhar street.

To achieve the above mensioned objectives the ministry of transport and The National Authority for tunnels decided to construct two tunnels under

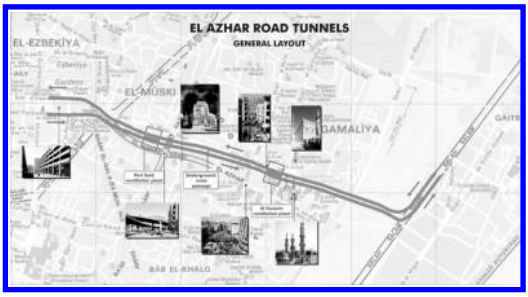


Figure 4. Outline of El Azhar tunnels.

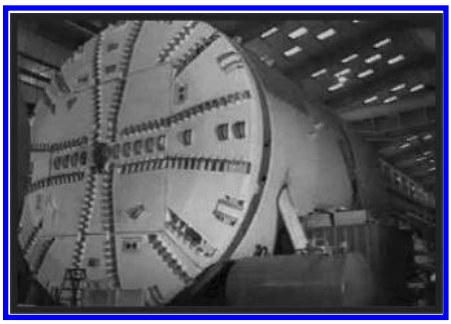


Figure 5. Tunneling boring machine.

El Azhar street. The north tunnel transferes the traffic flow from Salah Salem road to El Opera square and the south tunnel for the other direction as shown in Figure 4. The length of each tunnel is about 2.65 km.

- *Alignment constraints and difficulties*

1) Passing underneath the existing main sewer tunnel, at a depth of 17 m below ground level in Port Said Street.
2) Avoiding any damage to the existing old buildings and interference with the piled foundations of an existing bridge in El Azhar Street.
3) Avoiding and/or diverting existing utilities.

- *Tunnel cross section*

The bored tunnel section was constructed using two bentonite slurry shield tunnel boring machines which shown in Figure 5. Each of these was 9.44 m in diameter and 66 m long, and articulated in order to enable them to follow the designed alignment of the tunnels where each tunnel should have 2 traffic lanes per one direction.

- *Ventilation system*

In addition to the tunnels, the project contains 4 ventilation stations, where they are working for the two tunnels. Every station contains fans for drawing and

Copyright © 2005 Taylor & Francis Group plc, London, UK

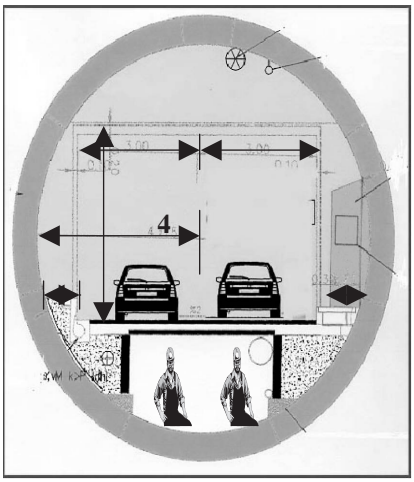


Figure 6. Tunnel cross section.



Figure 7. El Hossin ventilation station.

entering pure air and other fans for exhausting air. Figures 7 & 8 show El Hossin and Portsaid ventilation stations respectively.

- *Safety measures*

The choice of tunnel concept for traffic flow has been much attention. Two alternative tunnel concepts can be discussed in a safety perspective:

1) Single bored tunnel for two opposite traffic directions.
2) Two bored tunnels where every tunnel has a separate direction.

From a fire safety point of view it has been argued that twin bored tunnels are safer than single bored tunnels and it is preferable to distribute the emmisions of vehicles on large area. Also, construction of two tunnels reduced the rate of accedents in comparison with a single tunnel, especially that the tunnels are connected with 3 escape routes for cars and 5



Figure 8. Portsaid ventilation station.

escapes for transferring people in-between the tunnels and to the street level. The followings safety measures have been taken into consideration and implemented:

1) CCTV coverage, by remotely controlled color cameras, along the whole length of the tunnels and their approaches.
2) Controlled lighting to ensure that driver's sight is not affected by the varying levels of light from the surface to the interior of the tunnels.
3) Fire Detection instruments, along the tunnels, to detect smoke and excessive heat.
4) Fire Extinguishing Systems including pressurized fire mains, fire hydrants, hose reels and unit fire extinguishers containing powder and CO_2.
5) Air quality monitoring instruments, to check the degree of noxious fumes and alarms which will alert the operators to any problems with the ventilation equipment.
6) Emergency telephones.
7) Four dewatering pump stations, to prevent flooding of the tunnels.
8) Standby generators in case of loss of the main power supply.
9) Continuously manned Operations Control Rooms.
10) Emergency escapes every 100 m along the tunnels to transfer people from road level to the underpass where they can escape to the street level.

4 CONCLUSION

The urban traffic in Fatimid Cairo, which boasts its history of more than one thousand year, has always been congested on the ground of its ancient history. The streets in the city have changed to be in a torrent of automobiles owing to an overflow of vehicles by a runaway motorization in recent years. There is no doubt that building of El Azhar tunnels is contributing in solving many transport and traffic bad effects,

Copyright © 2005 Taylor & Francis Group plc, London, UK

thus it helps in protecting and keeping the historic monuments and buildings in the Fatimid Cairo. The positive impacts of building the tunnels can be concluded as follows:

1) It was necessary to build El Azhar road tunnels to reduce the trip time from half an hour to 4 minutes, and to avoid traffic jams.
2) The tunnels contribute in reducing air and noise pollutions by about 60% in case of removing the steel bridge.
3) The tunnels are the alternative of El Azhar bridge which should be removed to avoid the bad appearance in the historic Fatimid Cairo.
4) The tunnels have been constructed and equipped with very modern safety Aspects.

Copyright © 2005 Taylor & Francis Group plc, London, UK

Why did the hydropower industry go underground?

Einar Broch
Norwegian University of Science & Technology, Trondheim, Norway

ABSTRACT: In Norway more than 99% of a total annual production of 125 TWh of electric energy is generated from hydropower. 4000 km of tunnels has been excavated for this purpose, and the country has 200 underground powerhouses. Special design concepts have over the years been developed related to this massive use of the underground. One such speciality is the unlined, high-pressure tunnels and shafts. Another is the so-called air cushion surge chamber which replaces the conventional vented surge chamber. This paper will give a brief introduction to these and other solutions, and explain the advantages of utilizing the underground to its fullest possible extent for hydropower projects.

1 INTRODUCTION

Topographical and geological conditions in Norway are favourable for the development of hydroelectric energy. The rocks are of Precambrian and Paleozoic age, and although there is a wide variety of rock types, highly metamorphic rocks predominate. From an engineering point of view they may in general be classified as typical hard rocks.

More than 99% of a total annual production of 125 TWh of electric energy is generated from hydropower. Figure 1 shows the installed production capacity of Norwegian hydroelectric power stations. It is interesting to note that, since 1950, underground powerhouses are predominant. In fact, of the world's 500 underground powerhouses almost one-half, i.e. 200, are located in Norway. Another proof that the Norwegian electricity industry is an "underground industry" is that it today has more than 4000 km of tunnels. During the period 1960–90 an average of 100 km of tunnels was excavated every year.

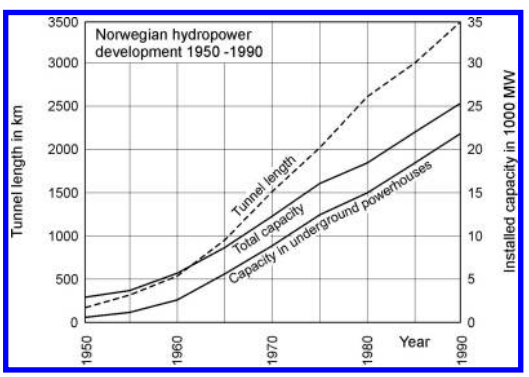


Figure 1. The development of Norwegian hydroelectric power capacity and accumulated length of tunnels excavated for the period 1950–90.

Through the design, construction, and operation of all these tunnels and underground powerhouses, valuable experience has been gained. This experience has been of great importance for the general development of tunnelling technology, and not least for the use of the underground. The many underground powerhouses excavated in rock masses of varying quality are to a large extent the forerunners for the varied use of rock caverns which we find all around the world today.

Also, special techniques and design concepts have over the years been developed by the hydropower industry. One such Norwegian speciality is the unlined, high-pressure tunnels and shafts. Another is the so-called air cushion surge chamber which replaces the conventional vented surge chamber. These specialities are described in further detail in Broch (2002).

Most of the Norwegian hydropower tunnels have only 2–4% concrete or shotcrete lining. Only in a few cases has it been necessary to increase this to 40–60%. The low percentage of lining is due not only to favourable tunnelling conditions. It is first and foremost the consequence of a support philosophy which accepts some falling rocks during the operation period of a water tunnel. A reasonable number of rock fragments spread out along the headrace or tailrace tunnel will not disturb the operation of the hydro power station as long as a rock trap is located at the downstream end of the headrace tunnel. Serious collapses

Copyright © 2005 Taylor & Francis Group plc, London, UK

or local blockages of the tunnels must, of course, be prevented by local use of heavy support or concrete lining when needed.

2 EARLY REASONS FOR GOING UNDERGROUND

During and shortly after the First World War there was a shortage of steel leading to uncertain delivery and very high prices. At that time the traditional design was to bring the water down from the intake reservoir or the downstream end of the headrace tunnel to the powerhouse through a steel penstock. Both the penstock and the powerhouse were above ground structures as shown in Figure 2.

With the lack of steel for a penstock, the obvious alternative was to try to bring the water as close to the powerhouse as possible through a tunnel or a shaft. As a result, four Norwegian hydropower stations with unlined pressure shafts were put into operation during the years 1919–21. The water heads varied from 72 to 152 m. One (Skar) was a complete failure due to too low overburden of rock, only 22 m rock cover where the water head was 116 m. One (Toklev) has operated without any problems ever since it was first commissioned.

The Svelgen hydropower station, with a water head of 152 m, had some minor leakage during the first filling. A short section of the shaft was lined with concrete and grouted with cement. Since then the shaft has operated without problems. The fourth station, Herlandsfoss, had a 175 m long, horizontal high-pressure tunnel with water head of 136 m. Leakage occurred in an area of low overburden, 35–40 m, and the short penstock had to be extended through the whole tunnel to the foot of the inclined pressure shaft. The shaft itself had no leakage. Further details in Broch (1982).

Although three out of four pressure shafts constructed around 1920 were operating successfully after some initial problems had been solved, it took almost 40 years for the record of 152 m of water head in unlined rock at Svelgen to be beaten. Through 1958, nine more unlined pressure shafts were constructed, but all had water heads below 100 m. Until around 1950 the above-ground powerhouse with penstock was the conventional layout for hydropower plants as demonstrated in Figure 2.

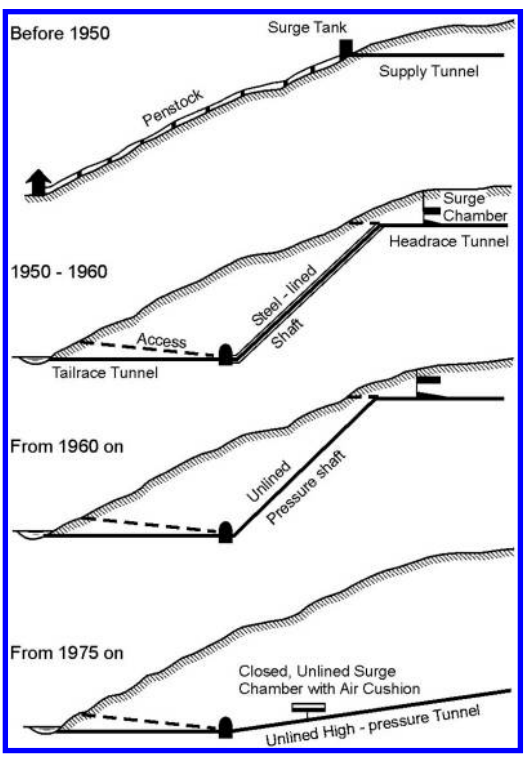


Figure 2. The development of the general lay-out of hydroelectric plants in Norway.

3 DEVELOPMENT AFTER 1945

3.1 *Underground powerhouses*

In a few early cases, underground location of a powerhouse was chosen as the only possible option (Bjørkåsen, 1921). During and after the Second World War, the underground was given preference out of considerations to wartime security. But with the rapid advances in rock excavation methods and equipment after the war, and consequent lowering of the costs, underground location came to be the most economic solution. This also tied in with the development of concrete lined, and later unlined pressure shafts and tunnels, to give the designer a freedom of layout quite independent of the surface topography.

Except for small and mini-hydropower stations, underground location of the powerhouse is now chosen whenever sufficient rock cover is available. Frequently the overall project layout requires the powerhouse to be placed under very deep rock cover where rock stresses may be substantial. This requires an investigation of the stress condition in advance for finding the most favourable orientation of the cavern and the optimum location, orientation and shape of ancillary tunnels and caverns.

In the early powerhouse caverns the rock support of the ceiling was limited to rock bolts. To safeguard against rockfalls, a 25–30 cm thick arch of in-situ concrete was placed some distance below the ceiling, see Figure 3.

Copyright © 2005 Taylor & Francis Group plc, London, UK

In poor rock masses, the ceiling was often reinforced by an arch of concrete in contact with the rock. In the latter case a light arch ceiling would be suspended below the roof arch to improve appearance and to intercept any water leakage.

The present-day solution prescribes systematic bolting of the rock ceiling immediately after excavation of the top heading, followed by fibre-reinforced shotcrete from 70 to 150 mm in thickness, according to rock quality. It is also common practice to install deeply bolted girders for the powerhouse crane right after the excavation of the top heading, see Figure 4.

In this way the crane can be installed and be available early for concrete work and installation of spiral cases etc. without having to wait for concrete structures to be built up from the floor level. If needed, the crane girders may be provided additional support later on by columns, cast in place before handling the heaviest installation loads.

In the most common layout the transformer hall is located parallel to the main hall, at a sufficient distance for rock support, and a transport tunnel is utilised as tailwater surge chamber, but other solutions have also been used, see Figure 5.

3.2 *Unlined high pressure tunnels and shafts*

When the hydropower industry for safety reasons went underground in the early 1950s, they brought the steel pipes with them. Thus, for a decade or so most pressure shafts were steel-lined. During the period 1950–65, a total of 36 steel-lined shafts with heads varying from 50 to 967 m (with an average of 310 m) were constructed.

The new record shaft of 286 m at Tafjord K3, which was put into operation successfully in 1958, gave the industry new confidence in unlined shafts. As Figure 6 shows, new unlined shafts were constructed in the early 1960s and since 1965 unlined pressure shafts have been the conventional solution. Today more than 80 unlined high-pressure shafts or tunnels with water heads above 150 m are successfully operating in Norway, the highest head being almost 1000 m. Figure 6 clearly demonstrates that increasing water heads reflect an increasing confidence in unlined pressure shafts.

The confidence in the tightness of unlined rock masses increased in 1973 when the first closed, unlined surge chamber with an air cushion was successfully put into service at the Driva hydroelectric power plant. This innovation in surge chamber design is described in detail by Rathe (1975). The bottom sketch in Figure 2 shows how the new design influences the general layout of a hydropower plant. The steeply inclined pressure shaft, normally at 45°, is replaced by a slightly inclined tunnel, 1:10–1:15.

Instead of the conventional vented surge chamber near the top of the pressure shaft, a closed chamber is excavated somewhere along the high-pressure tunnel,

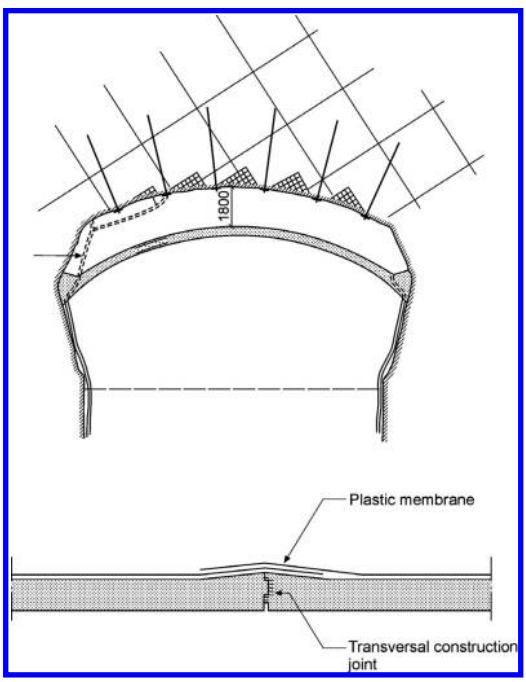


Figure 3. Typical design for a free span concrete arch.

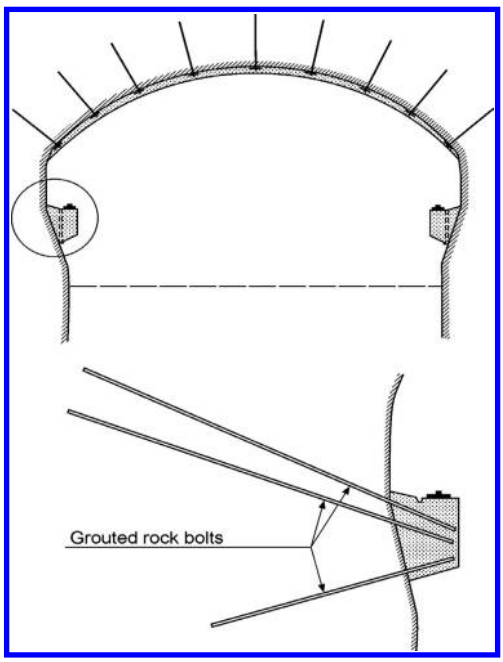


Figure 4. Steelfibre reinforced shotcrete arch and rock bolt supported crane beam.

Copyright © 2005 Taylor & Francis Group plc, London, UK

preferably not too far from the powerhouse. After the tunnel system is filled with water, compressed air is pumped into the surge chamber. This compressed air acts as a cushion to reduce the water hammer effect on the hydraulic machinery and the waterways, and also ensures the stability of the hydraulic system.

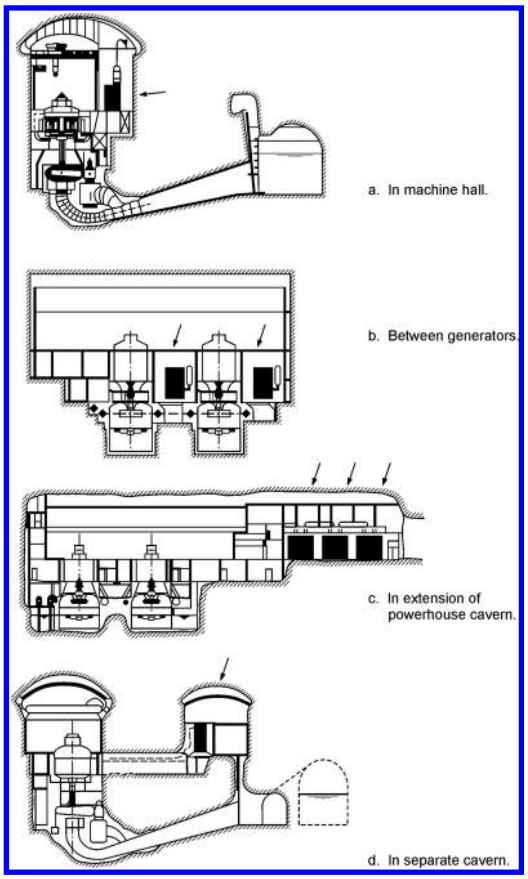


Figure 5. Common transformer locations.

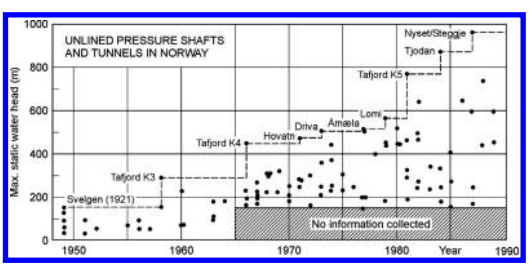


Figure 6. The development of unlined pressure shafts and tunnels in Norway.

In the years before 1970 different "rule of thumbs" were used for the planning and design of unlined pressure shafts in Norway. With new and stronger computers a new design tool was taken into use in 1971–72. This, as well as the "rule of thumbs", are described in detail in Broch (1982). It is based on the use of computerised Finite Element Models (FEM) and the concept that nowhere along an unlined pressure shaft or tunnel should the internal water pressure exceed the minor principal stress in the surrounding rock mass.

Very briefly, the FEM models are based on plain strain analysis. Horizontal stresses (tectonic plus gravitational) increasing linearly with depth, are applied. Bending forces in the model are avoided by making the valley small in relation to the whole model. If required, clay gouges (crushed zones containing clay) may be introduced.

Whichever method is chosen, a careful evaluation of the topography in the vicinity of the pressure tunnel or shaft is necessary. This is particularly important in non-glaciated, mountainous areas, where streams and creeks have eroded deep and irregular gullies and ravines in the valley sides. The remaining ridges, or so-called noses, between such deep ravines will, to a large extent, be stress relieved. They should therefore be neglected when the necessary overburden for unlined pressure shafts or tunnels is measured. This does not mean that pressure tunnels should not be running under ridges or noses – only that the extra overburden this may give should not be accounted for in the design, unless the stress field is verified through in-situ measurements, see Broch (1984) for further details.

As the permeability of the rock itself normally is negligible, it is the jointing and the faulting of the rock mass, and in particular the type and amount of joint infilling material, that is of importance when an area is being evaluated. Calcite is easily dissolved by cold, acid water, and gouge material like silt and swelling clay are easily eroded. Crossing crushed zones or faults containing these materials should preferably be avoided. If this is not possible, a careful sealing and grouting should be carried out. The grouting is the more important the closer leaking joints are to the powerhouse and access tunnels and the more their directions point towards these. The same is also valid for zones or layers of porous rock or rock that is heavily jointed or broken. A careful mapping of all types of discontinuities in the rock mass is therefore an important part of the planning and design of unlined pressure shafts and tunnels.

Hydraulic jacking tests are routinely carried out for unlined high-pressure shafts and tunnels. Such tests are particularly important in rock masses where the general knowledge of the stress situation is not well known or difficult to interpret based on the topographical conditions alone. The tests are normally

Copyright © 2005 Taylor & Francis Group plc, London, UK

carried out during the construction of the access tunnel to the powerhouse at the point just before the tunnel is planned to branch off to other parts of the plant, like for instance to the tailwater tunnel or to the tunnel to the bottom part of the pressure shaft.

To make sure that all possible joint sets are tested, holes are normally drilled in three different directions. By the use of Finite Element Models the rock stress situation in the testing area as well as at the bottom of the unlined shaft are estimated. At this stage the relative values of the stresses at the two points are more important than the actual values. During the testing the water pressure in the holes is raised to a level which is 20 to 30% higher than the water head just upstream of the steel-lining, accounting for the reduced stress level at the testing point. There is no need to carry out a complete hydraulic fracturing test. The crucial question is whether or not the water pressure in the unlined part of the shaft or tunnel is able to open or jack the already existing joints. Hence the importance for making sure that all possible joint sets are tested.

4 UNDERGROUND HYDROPOWER PLANTS WITH UNLINED WATERWAYS

To demonstrate the design approach an example of an underground hydropower plant will be shown and briefly described. Figure 7 shows the simplified plan and cross section of a small hydropower plant with only one turbine. No dimensions are given, as the intention is to show a system rather than give details. Similar layouts can be found for Norwegian plants with water heads in the range of 200–600 m.

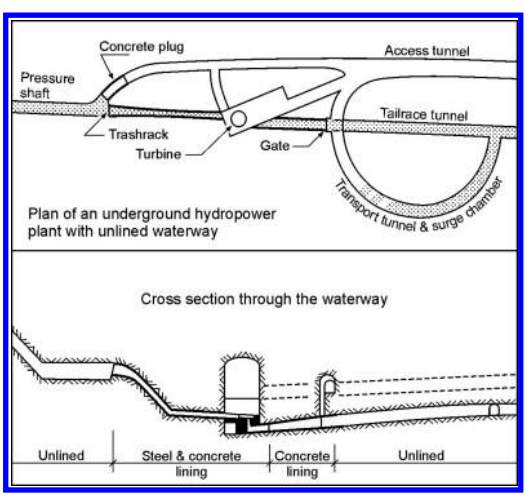


Figure 7. Plan and cross section of an underground hydropower plant with unlined waterways.

The figure is to some extent self-explanatory. A critical point for the location of the powerhouse will normally be where the unlined pressure shaft ends and the steel lining starts. The elevation of this point and the length of the steel-lined section will vary with the water head, the size and orientation of the powerhouse, and the geological conditions, in particular the character and orientation of joints and fissures. Steel lengths in the range of 30–80 m are fairly common.

The access tunnel to the foot of the unlined pressure shaft is finally plugged with concrete and a steel tube with a hatch cover. The length of this plug is normally 10–40 m, depending on the water head and geological conditions. As a rough rule of thumb the length of the concrete plug is made 4% of the water head on the plug, which theoretically gives a maximum hydraulic gradient of 25. Around the concrete plug and the upper part of the steel-lined shaft a thorough high-pressure grouting is carried out. This avoids leakage into the powerhouse and the access tunnel. Further details about the design of high-pressure concrete plugs can be found in Dahlø et al. (1992) or Broch (1999).

5 OPERATIONAL EXPERIENCE FROM UNLINED PRESSURE SHAFTS AND TUNNELS

The oldest unlined pressure shafts have now been in operation for 80 years. None of the pressure shafts and tunnels, with water heads varying between 150 and 1000 m which have been constructed in Norway since 1970, has shown unacceptable leakage. It is thus fair to conclude that the design and construction of unlined high-pressure tunnels and shafts is a well proven technology.

It is normal procedure to fill a shaft in steps or intervals of 10–30 hours. During the intervals the water level in the shaft is continuously and accurately monitored by an extra-sensitive manometer. By deducting for the inflow of natural groundwater and the measured leakage through the concrete plug, it is possible to calculate the net leakage out from the unlined pressure tunnel or shaft to the surrounding rock masses. The loss of water from a tunnel is large during the first hours, but decreases rapidly and tend to reach a steady state after 12 to 24 hours, depending on the joint volume that has to be filled.

6 CONCLUDING REMARKS

Experience from a considerable number of pressure tunnels and shafts have been gathered over a long period of time. These show that, providing certain design rules are followed and certain geological and topographical conditions are avoided, unlined rock

Copyright © 2005 Taylor & Francis Group plc, London, UK

masses are able to contain water pressures up to at least 100 bars, equaling 1000 m water head. Air cushions have proven to be an economic alternative to the traditional open surge shaft for a number of hydropower plants. The geotechnical design of the air cushion cavern should follow the same basic rules as for other rock caverns.

REFERENCES

Broch, E. 1982. The development of unlined pressure shafts and tunnels in Norway. *Rock mechanics: Caverns and pressure shafts* (Wittke, ed.). 545–554. A.A. Balkema, Rotterdam, Also in *Underground Space* No. 3, 1984.

Broch, E. 1982 B. Designing and excavating underground powerplants. *Water Power and Dam Construction* 34:4, 19–25.

Broch, E. 1984. Design of unlined or concrete lined high pressure tunnels in topographical complicated areas. *Water Power and Dam Construction* 36:11.

Broch, E. 1999. Sharing Experience with Concrete Plugs in High-Pressure Tunnels. *Hydro Review Worldwide*, Vol. 7, No. 4, 30–33.

Broch, E. 2002. Unlined high pressure tunnels and caverns. *Norwegian Tunnelling Society*, Publ. No. 12, 7–11.

Dahlø, T.S., Bergh-Christensen, J. & Broch, E. 1992. A review of Norwegian high-pressure concrete plugs. *Hydropower -92*. (Broch and Lysne, ed.). 61–68. Balkema, Rotterdam,.

Goodall, D.C., Kjørholt, H., Tekle, T. & Broch, E. 1988. Air cushion surge chambers for underground power plants. *Water Power & Dam Constr*., Nov. 29–34.

Rathe, L. 1975. An innovation in surge chamber design. *Water Power & Dam Constr*., No. 27, 244–248.

Copyright © 2005 Taylor & Francis Group plc, London, UK

Workforce competence in the United Kingdom tunnelling industry

R. Ibell
London Bridge Associates, Surbiton, UK

P.J. Jewell
Kellogg Brown & Root (KBR), Leatherhead, UK

D. Allenby
Edmund Nuttall Limited, Camberley, UK

ABSTRACT: For a number of reasons, there is an ongoing and increasing need for the UK tunnelling industry to ensure competence amongst its workforce at all levels. This paper reviews the background and describes a number of initiatives being taken by the industry to address this need for the workforce at all levels (operatives, engineers and management).

1 INTRODUCTION

There is an ongoing and increasing requirement for the United Kingdom (UK) tunnelling industry to ensure that its workforce at all levels (operatives, engineers and management) are competent to undertake their respective duties. This requirement for competence is being driven by high expectations of government, clients, insurers, as well as tunnelling contractors and consultants themselves, in terms of the quality, safety and environmental management of the work, and the confidence of delivery to time and budget.

This paper reviews the background to these high expectations. It then describes a number of initiatives which the industry is taking to address these expectations, and the roles of organisations such as the British Tunnelling Industry (BTS), the Pipe Jacking Association (PJA) and the United Kingdom Society for Trenchless Technology (UKSTT) in supporting such initiatives.

2 THE NEED TO DEMONSTRATE COMPETENCE

By its very nature, tunnel construction is inherently much more risky than most other forms of civil engineering. In the past there has been a reluctant acceptance of accidents and collapses in the mining and tunnelling industries being inevitable from time to time, but such events have now become totally unacceptable.

The UK tunnelling industry has had its fair share of challenges to respond to in recent years. In 1994 the industry's mood of confidence was dented by the collapse of tunnels being mined by New Austrian Tunnelling Method (NATM) techniques at Heathrow Airport's Central Terminal Area. There has since been a small number of ground subsidences associated with closed face tunnel boring machine (TBM) advances, which were unpredicted and difficult to explain. Inevitably, events like these do not help to give clients the confidence that the industry is competent.

At the same time, there is increasing recognition that the construction industry as a whole should and indeed can offer better value for money than it has been doing. Promoted by Sir John Egan and others, a number of high level initiatives, such as process driven approaches and partnering, have begun to instil into the construction better means of delivery, driving down overall project costs by up to 30%. Two of these initiatives, self-certification and design/construct contracting, have been adopted on a number of tunnelling projects. Self-certification is a good example of an initiative which brings with it a need for greater self responsibility and competence at all levels of the workforce. How can clients be confident that the whole tunnelling workforce is fit to deliver projects in these new ways?

Historically there has been a "grandfather rights" tradition in the workforce. Neither has it been obligatory for engineers and managers to have to demonstrate competence throughout their careers. This has

Copyright © 2005 Taylor & Francis Group plc, London, UK

now changed, brought about by a number of considerations, including:

- The changing legislative background, particularly in relation to workplace, designer and construction safety obligations.
- The expectations of the insurance industry. Insurers have been regarding tunnelling projects as high risk verging on being unacceptable. The Association of British Insurers (ABI) and the BTS have responded to this situation with the publication of a Joint Code of Practice (Ref. 1).
- Increased requirements from Clients for companies to demonstrate the competence of staff, to the occasional extreme of requiring tunnelling personnel to be formally certified as competent.
- The tunnelling industry itself, in responding to these increased expectations.

3 THE NATURE OF COMPETENCE

The authors have chosen to discuss the nature of competence because it is an ill defined term, although much used. Competence is widely accepted to mean that a person has any or all of the following – manual skills; an inherent ability; received training; a qualification; a practical and capable outlook; a sound mind.

However, the authors consider that competence is better defined as a combination of knowledge; experience; and inherent behavioural characteristics. They also believe that competence is specific to and should always be assessed against a particular set of circumstances or situation. This is because safe and productive tunnelling, more than almost any other form of construction, is a team operation with all team members needed to be confident through competence.

The process by which competence is achieved is broadly summarised in Figure 1.

The requirement to assess competence has come from a number of directions. ISO 9001 (Ref. 2) requires "*that we assess the competence of our staff*". The Joint Code of Practice (Ref. 1) requires for tunnel projects, training plans and a policy for the employment of skilled operatives. Requirements for a competent team (Managers, Engineers and Operatives) will also come from contract requirements, particularly for schemes involving self certification.

4 VERIFICATION OF TUNNELLING OPERATIVES

For many years Electricians, Mechanics (fitters), Carpenters and other building trades have had processes to train and approve their skills. Only in recent years has the UK tunnelling industry come to consider the need



Figure 1. Route to competence.

to train and verify the skills of many of its employees, for example Plant Operators, Crane Drivers, Concrete Constructors and, most notably, Tunnel Miners.

The UK Government introduced National Vocational Qualifications (NVQs) in 1986, including the declared object to recognise "*skills that were not otherwise recognised by existing available qualifications*".

An Occupational Working Group (OWG) has been established for each sector of the construction industry that wishes to have NVQs. The Tunnelling OWG was formed in 1993. The OWG is formed of representatives from the industry and the Construction Industry Training Board (CITB), and its function is to propose the content of the NVQs and submit them for accreditation.

NVQs are vocational qualifications and involve assessment by trained assessors who are themselves experienced in the particular discipline. They are not training based as such, and certainly are not training certificates, but are based on assessments of the candidates' performance and knowledge. There are five levels of NVQs:

- **Level One** is unskilled.
- **Level Two** is skilled.
- **Level Three** is for skilled supervisors.
- **Level Four** is for Senior Technicians and Engineers
- **Level Five** is for Managers.

The UK tunnelling industry's focus to date has been at the skilled tunnellers (Level 2) and is the only current fully accredited NVQ Level, although accreditation for Level 1 is currently being set up. First piloted in 1994, the initial tunnelling NVQ scheme suffered from over complexity and take up by the industry was low. More recently NVQs have been simplified, without reducing the requirements, and take up has much improved as a result.

The qualification is structured around units, as shown in Figure 2.

Units relate to operations, and defined in each unit are performance criteria together with the knowledge and understanding which underpin the performance. The assessment of a candidate can be carried out by a

Copyright © 2005 Taylor & Francis Group plc, London, UK

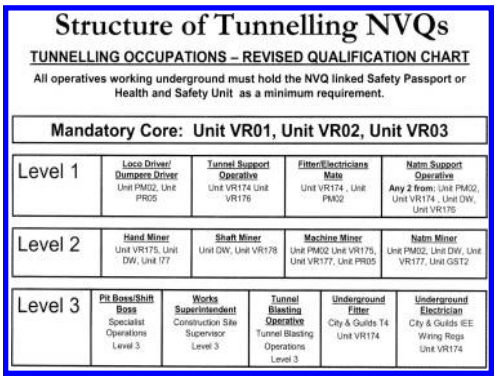


Figure 2. Structure of tunnelling NVQs.

combination of ways and if necessary over a considerable period, and is usually carried out on a site, where skills can be evidenced and signed off for their qualification. The assessors must work under an internally and externally verified accreditation centre, normally an employer who has to convince the Awarding Body that the proper checks and procedures are in place to ensure that the assessment is properly carried out.

A major challenge for the tunnelling industry is to resolve its short term, project to project outlook, which constrains long term career opportunities for skilled operatives; and instead create a real incentive to achieve qualifications.

Given the cyclical nature of the UK's tunnelling business activity, it is important too that the whole construction industry is encouraged to understand that the core competencies demonstrated by these NVQs permit the NVQ holders to be able to transfer readily into other forms of construction.

Recently, the substantial CTRL project with its large workforce provided the opportunity, with the help of the CITB, to establish a project based accreditation centre which registered some 300 operatives for NVQs, and achieved 40 full NVQs at Level 2. By August 2004 a total of 349 tunnelling NVQs had been registered and 76 NVQs awarded. The response from the tunnellers has been very positive. They have taken pride in achieving their qualifications. The authors also consider that recognising the skills of the tunnellers has encouraged a sense of responsibility which has spin offs in other areas, particularly in relation to health and safety.

5 UNIVERSITY STUDENT TRAINING INITIATIVES

It has long been recognised that many young tunnel engineers have had little or no exposure as undergraduate and postgraduate students to actual project related problem solving situations. Unless fortunate enough to have obtained some vacation work with tunnelling companies, they will continue to enter the industry with a lack of any practical experience.

An excellent example of an initiative taken to address this problem is provided by an arrangement between the University of Newcastle and Edmund Nuttall Limited. Together they have developed an integrated initiative to train students in the principles of underground construction using actual tender and construction information. This approach responds directly to the desire of the UK Institution of Civil Engineers (ICE) to see engineering taught in a holistic and multi-disciplinary way. Students are shown how their knowledge of geology, hydraulics, soil and rock mechanics, structures, etc. is put into practice to solve the technically demanding problems faced daily in the industry.

This unique course commenced in September 2001, and is delivered through a series of supporting lectures on shaft sinking and tunnelling using carefully chosen examples to highlight the importance of a comprehensive ground investigation, its interpretation in three dimensions, and the correct choice of construction method(s) to suit the ground conditions. One such project was a 7.8 km long, 2.85 m internal diameter wastewater tunnel constructed along the west side of Langstone Harbour, Portsmouth, UK, in two concurrent sections of 4.0 km and 3.8 km from an intermediate shaft, 7.5 m internal diameter by 28 m deep (Figure 3).

This project was chosen because it was technically challenging and demanded control of both ground water and ground during shaft and tunnel construction. In order to add realism to the design project students were not informed of the actual construction methods uses, or shown site documentation such as reports, temporary works drawings, photographs, etc., until the relevant project section detailed below had been satisfactorily completed. They were however presented with selected Tender Documentation and guided through a logical sequence from project conception to completion, typically producing:

- an interpretative geological report
- a conceptual design which they refined into the final design
- a number of design elements
- and the most advantageous construction method(s).

In achieving the project requirements students learned the importance of:

- a comprehensive well considered site investigation
- the accurate assessment of ground conditions and behaviour prediction
- the determination of the most appropriate construction methods, and

Copyright © 2005 Taylor & Francis Group plc, London, UK



Figure 3. Portsmouth tunnel, UK.

- producing concise, well written and illustrated reports with logical thinking and clearly presented conclusions.

This course introduced students to the "real world" and showed them how to apply their underpinning knowledge to solve a technically challenging problem in a logical manner within an agreed timeframe. Clearly students who graduate from this course are better equipped and prepared for industry than their counterparts and will, in the future, fulfill a valuable role in geotechnical engineering.

6 CONTINUING PROFESSIONAL DEVELOPMENT ROLE

The increasing obligations on the whole UK tunnelling industry to deliver projects better, require the highest standards of effective leadership and management. It will no longer be enough for senior professional tunnellers to rely and trade upon their work experiences alone; they will be obliged to demonstrate Continuing Professional Development (CPD) throughout their careers.

In some professional institutions, for example the Institution of Structural Engineers (IStructE), CPD is already mandatory for members. ICE presently treats CPD as obligatory but not mandatory, and provides a CPD record form, which its members and fellows are encouraged to maintain up to date.

The authors consider that CPD records provide a valuable tool for professional tunnellers to help demonstrate their continuing competence. If really necessary, and other evidence is not readily available, CPD records could be used to prove to Clients that senior staff are appropriately trained in areas of critical knowledge, for example familiarisation with the latest CDM Regulations. Directors of tunnelling companies should be encouraged to ensure that their more senior staff maintain CPD, not just for the immediate benefit of the companies themselves but also to underpin confidence in the whole UK tunnelling industry.

7 THE ROLE OF PROFESSIONAL SOCIETIES AND INDUSTRY ASSOCIATIONS

Organisations with a primary interest in the wellbeing of the UK's tunnelling industry, such as the BTS, PJA and UKSTT, have recognised that the pursuit of demonstrable competence is of increasing importance for both individual and corporate members.

For its part the BTS has concluded that it has a duty to monitor competency levels and support all individual and corporate members in their quest to demonstrate competence. In recent years it has made major contributions to advancing the state of knowledge amongst members and the wider construction industry about tunnelling requirements. For example, it was proactive in establishing a dialogue with insurers and preparing the joint Code of Practice (Ref. 2) with insurers. It has led a Closed Face Tunnelling Working Group which has published guidance (Ref. 3), and has also produced a model Specification for Tunnelling (Ref. 4) and a Tunnel Lining Design Guide (Ref. 5). The BTS's active representation on the Tunnelling OWG and support of NVQs is testament to its commitment to operatives.

During 2003 the BTS considered the necessity and desirability to introduce a Registration scheme for tunnelling professionals. The Society concluded that to take no action in this regard carried with it a real risk that the BTS would fail to move forward with the changing times, but also recognised that it would be almost certainly impractical, probably unnecessary, and in any case premature, for the BTS to invoke a full scale Registration scheme. An interim measure being considered is to set up of a tier of key Tunnelling Professionals, who could fulfil a number of functions, including having an accrediting role if Registration is eventually introduced.

8 CONCLUSIONS

In responding to increasing demands from clients and others, ongoing training is required at all levels of the UK's tunnelling workforce. Competence, however, is about much more than obtaining qualifications on paper, being a combination of knowledge, experience and behaviour.

The UK tunnelling industry has taken note of these increasing expectations, and is doing much to provide a workforce which is competent, effective and well managed at all levels. Organisations including the BTS, PJA and UKSTT are playing an active role in supporting the industry's endeavours in this regard.

Copyright © 2005 Taylor & Francis Group plc, London, UK

REFERENCES

1. Association of British Insurers (ABS) and British Tunnelling Society (BTS), 2003, *Joint Code of Practice for Risk Management of Tunnel Works in the UK.*
2. British Tunnelling Society (BTS), 2004, *Closed Face Tunnelling Machines and Ground Stability*, In Publication.
3. British Tunnelling Society (BTS), 2000, *Specification for Tunnelling*, Thomas Telford, London.
4. British Tunnelling Society and The Institution of Civil Engineers, 2004, *Tunnel Lining Design Guide*, Thomas Telford, London.
5. ISO 9000: 2000 Quality Management Systems – *Fundamentals and Vocabulary, British Standards.*

Copyright © 2005 Taylor & Francis Group plc, London, UK

Microtunnelling or trench excavation: a comparison of the two alternatives

Daniele Peila
DIGET, Georesources and Land Department, Turin Technical University, Italy
CNR – IGAG, National Research Council of Italy

Marta Bottero
DIGET, Georesources and Land Department, Turin Technical University, Italy

ABSTRACT: The technical and economic feasibility of an underground construction should involve not only geological, geotechnical and technological aspects, but also the evaluation of the factors that are related to the interferences of the construction procedures and techniques with the population and with the environmental components of the site.

The paper compares two different excavation alternatives, microtunnelling and trench excavation, for an urban sewer construction project using the Analytic Hierarchy Process.

1 INTRODUCTION

The need for new transport systems, new spaces for shops, offices, car parks, social and recreational activities and innovative service networks such as telephone cables, sewers and gas pipes is one of the reasons for the increase in underground works in urban areas. When a new service pipe has to be installed at a shallow depth below the surface it is normal practice either to excavate from the surface, to install pipes in trenches or to bore a small underground tunnel.

Open space works can cause problems for the surrounding environment and these aspects have to be considered for a correct technical-economic analysis of such a project; the microtunnelling technique, in fact, allows the surface area directly involved by construction to be reduced (Stein et al, 1989; Thomson, 1995).

Therefore, for a correct comparison of these two operational procedures, it is necessary to take into account the different environmental and social aspects.

The comparison can be performed with the Analytic Hierarchy Process (AHP) which is a multicriteria technique that provides useful support when a choice between several alternatives with different objectives and criteria has to be made (Fusco & Nijkamp, 1997; Nijkamp et al. 1990; Voogd, 1983).

2 THE ANALYTIC HIERARCHY PROCESS

The Analytic Hierarchy Process (AHP) is a procedure and computation approach that is suitable for dealing with complex systems related to making a choice from among several alternatives and which provides a comparison of the considered options.

The AHP helps organize the rational analysis of the problem by dividing it into its single parts, in a hierarchical form. The analysis then supplies an aid to the decision makers who, making several pairwise comparisons, can appreciate the influence of the considered elements in the hierarchical structure and give a preference list of the considered alternative solutions (Saaty, 1980; Saaty & Vargas, 1990; Mondini & Nati Poltri, 1996).

The AHP has been used to analyse different kinds of social, political-economic and technological problems. It uses both qualitative and quantitative variables. The fundamental principle of the analysis is the possibility of connecting information, based on knowledge, to make decisions or previsions; this knowledge can be taken from experience or derived from the application of other tools. Among the different contexts in which the AHP can be applied, mention can be made of the creation of a list of priorities, the choice of the best policy, the optimal allocation of resources, the prevision of results and temporal dependencies and the assessment of risks and planning (Saaty & Vargas, 1990).

The analysis is based on three fundamental principles:

1. breaking down the problem;
2. pairwise comparison of the various alternatives;
3. synthesis of the preferences.

The "*breaking down principle*" consists in subdividing the problem into simple clusters that are

Copyright © 2005 Taylor & Francis Group plc, London, UK

Table 1. Saaty's fundamental scale.

Value	Definition	Explanation
1	Same importance	Two decision elements equally influence the parent decision element
3	Moderately more important	One decision element is moderately more influential than the other
5	Much more important	One decision element has a greater influence than the other
7	Very much more important	One decision element has significantly more influence over the other
9	Extremely more important	The difference between the influences of the two decision elements is extremely significant
2, 4, 6, 8	Intermediate judgment values	

represented by different levels in a hierarchal structure. The decomposition is carried out from the top to the bottom, starting from the objective going on to the criteria and sub-criteria and then to the final alternatives.

The "*pairwise comparison principle*" consists in giving a rate to each cluster to measure the importance of each level in the hierarchy. Each single element is evaluated using pairwise comparison. The comparisons are made on a 9-point scale, the so-called "*Saaty's fundamental scale*", which is represented in Table 1.

The numerical judgments established at each level of the hierarchy are made up using pair matrixes.

Let n be the number of criteria in a certain level of the hierarchy and m the number of the alternatives, there are therefore n matrixes with m lines and m columns in that level. An example of a pairwise comparison matrix is given in Figure 1.

All the pairwise comparison matrices have two fundamental properties:

- The principal diagonal is always composed of values that are equal to one (because each criterion *i* is compared to itself);
- The matrices are reciprocal (in assigning a value from 1 to 9 to the comparison between the element *i* and the element *j*, the reciprocal value corresponds to the comparison between *j* and *i*).

The last step of the procedure consists of a comparison of the various alternatives, referring to the given judgments and extracting the related principal autovector from each comparison matrix.

n	1	2	3	…	m
1	1				
2		1		Reciprocal values	
3			1		
…				1	
m	Judgements values				1

Figure 1. Pairwise comparison matrix.

The principal vector measures how the components, at each hierarchy level, contribute to reach the objective with reference to which comparison has been performed. Each autovector must be weighted with regards to the priority of the considered criteria. The final list, obtained by summing all the autovectors, is a vector that provides the part played by each alternative in reaching the initial goal.

3 TRENCH EXCAVATION AND MICROTUNNELLING COMPARISON USING AHP

The AHP methodology, as described in chapter 2, has been used to compare traditional trench excavation with microtunnelling for the installation of a pipe in an urban area based on the data of a real case in Turin (Italy) of a sewer installation using trench excavation under a local urban road.

The fundamental goal of the analysis was to define which excavation technique was most compatible, from the point of view of the public and private actors who are involved in the construction process, taking into account the environmental and social aspects.

The first step of the analysis is the definition of the hierarchical structure to represent the problem (Bottero & Peila, 2004). The general criteria considered for the comparison are:

– direct construction costs;
– indirect construction costs;
– social costs;
– environmental costs.

All these costs together give the "global cost" of the construction.

In this research the analyses were carried out taking into account the results of a questionnaire that had been distributed to the population in the surrounding area with the goal of focusing the most relevant social impact on the people who live around the work area and on the economic activities such as shops.

Copyright © 2005 Taylor & Francis Group plc, London, UK

Table 2. Priority list of the subcriteria related to the "indirect construction costs" criteria.

Damage to private property	0.038
Damage to other infrastructures	0.066
Reduction in the life cycle of the road surface	0.242
Increase in road maintenance	0.242
Relocation of services that interfere with the works	0.412

Table 3. Priority list of the "traffic costs" subcriteria.

Measures for the diversion of traffic circulation	0.041
Time loss due to traffic increase and traffic jams	0.170
Choice of new routes for public transport	0.044
Installation of new road signs	0.040
Higher number of road accidents	0.115
Driving efficiency	0.299
Cost increase for public and private transport	0.291

3.1 *Analysis of the general criteria*

3.1.1 *Direct construction costs*

The direct construction costs involve the installation of pipes and consist of the total economic resources involved in the "physical" work and in the recovering of the site at the end of the works.

These costs, with reference to the considered example, are higher for microtunnelling than for trench excavation. Obviously different economic conditions are present when crossing under rivers, buildings or very sensitive infrastructures or when groundwater is present. These specific conditions are not considered and discussed in this work.

3.1.2 *Indirect construction costs*

The indirect costs are the expenses for materials, machinery and works not directly related to the construction phase.

The following costs are taken into account in the analysis:

1. costs due to damage to private property;
2. costs due to damage to other infrastructures;
3. costs due to the reduction in the life cycle of the road surface;
4. costs due to the increase in road maintenance;
5. costs due to the relocation of already existing infrastructures that interfere with the works.

In the considered example the highest cost value is given to the relocation of infrastructure (point 5).

The priority list that is obtained from the compilation of the pairwise comparison matrix and from the subsequent normalization is reported in Table 2.

If the two alternatives are compared with reference to the indirect construction costs, the surface excavation is the most critical.

Microtunnelling, in fact, involves the occupation of a limited area for the construction site and reduces damage to road surfaces, to private property and to the existing infrastructures. The use of microtunnelling also minimizes the relocation of the already existing underground infrastructures, which is limited to the shaft area instead of to the whole pipe length.

3.1.3 *Social costs*

The social costs are the costs borne by society during the operations. They are related to the externalities caused by the interferences between the construction site and the economic activities of the area.

The following costs are therefore taken into account:

1. problems of traffic circulation;
2. safety aspects of the work sites;
3. disturbance to commercial and recreational activities in the area;
4. landscape factors;
5. human factors.

Considering the complexity of the topics involved in these five aspects, it is necessary to further subdivide them.

The criterion related to traffic costs is therefore subdivided into the following main elements:

1(a) measures for the diversion of traffic circulation;
1(b) time loss due to traffic increase and traffic jams;
1(c) choice of new routes for public transport;
1(d) installation of new road signs;
1(e) higher number of road accidents;
1(f) driving efficiency;
1(g) cost increase in public and private transport.

When making the judgements, the increase in the costs for public and private transport, the driving efficiency and the increased number of road accidents are considered to be the most important. The priority list is reported in Table 3.

If these criteria are taken into account, trench excavation is worse than microtunnelling.

The criterion related to work safety (point 2) is linked to the costs borne by the contractors and by society for the safety of the workers in the construction site area.

In the analysis, these costs are considered, for this preliminary analysis, as being directly proportional to the surface of the construction site. The greater the area, the greater the exposure of the workers to risks (in fact, smaller shafts site areas are usually properly retained and safety measures are better enforced).

Therefore, as the construction site is larger for trench excavation than for microtunnelling the costs for safety are considered higher for the former solution.

The criterion related to the disturbance to commercial and recreational surface activities (point 3) is directly connected to the physical hindrances created by the construction site on the spaces for shops and

Copyright © 2005 Taylor & Francis Group plc, London, UK

facilities. In order to make a correct evaluation, it is necessary to have detailed information on the difficulties that are actually borne by the shopkeepers or on the temporary closing of shops or facility areas. This is obtained using the results of the questionnaire. It is, however, evident that the disturbance is higher for traditional excavation, especially when the roads are closed to both vehicular and pedestrian circulation.

The criterion related to landscape factors (point 4) has to be evaluated considering the negative impact generated by the construction site on the "urban and territorial values" of the area. In the analysis, this criterion was sub-divided into the following categories:

4(a) perceptive-visual aspects;
4(b) fundamental elements of the landscape.

In generic terms, the transformation of the urban landscape due to the construction site is reversible and when the works are over it is possible to restore the previous conditions or even improve them and the two options are therefore considered as equal.

The criterion related to human factors (point 5) is associated to the negative impact, caused by the construction site, as felt by the inhabitants of the area surrounding the job site. In the analysis, this criterion is sub-divided into:

5(a) aspects related to public safety;
5(b) aspects related to public health;
5(c) aspects related to the quality of houses.*

Even though the impact of a construction site for the installation of a sewer pipe system is transitory and stops when the works are over, it leads to the highest number of complaints from the population, as was clearly shown by the questionnaire.

In the analysis, public safety and health are considered to prevail over the quality of the houses, which, generally speaking, is not affected very much by this kind of excavation. The priority list is reported in Table 4.

It is intuitive, with reference to these factors, that trench excavation is more critical than microtunnelling because the former tends to create a higher impact in terms of dust emissions, noise and vibrations.

3.1.4 *Environmental costs*

Environmental costs are used to quantify the permanent negative effects on the environmental components of the area. In the analysis, this factor is divided into five criteria and the same weight is given to each of them: air, soil, water, physical agents and natural agents.

* These elements involve the possible disturbance for the inhabitants of the area due to the construction site, with reference to the impact on the building quality (noise, dust, vibrations, …).

Table 4. Priority list of the "human factors" subcriteria.

Public safety	0.455
Public health	0.455
Quality of houses	0.090

With reference to air, trench excavation has been considered to have more serious effects than microtunnelling because of the greater consumption of fuel for the excavation and transport machines and consequently the greater gas emissions in the atmosphere.

With reference to soil, trench excavation has a greater environmental impact than microtunnelling, but the latter requires more geological and geotechnical investigations for a better knowledge of the underground conditions.

With reference to water, the potential interferences between the operations and the quality of the surface and underground waters were taken into account: trench excavations can in fact interact with groundwater, generate pollution and affect surface water circulation (at least for the period of construction) while microtunnelling has a lower impact.

The physical agents are related to the impact of the construction site on the life of the inhabitants in the area due to noise and vibrations while natural agents refer to the impact of the operations on the vegetation conditions of in the area. In both cases, microtunnelling is considered preferable to trench excavation.

3.2 *Comparison of the two alternatives*

In order to develop a comparison between the alternatives, it is necessary to give specific weights to each cost.

These weights can be obtained starting from the pairwise comparison matrix for the general criteria. The results are summarized in Table 5.

If Table 5 is analysed, it is possible to observe that in this study some of the aspects that are usually underestimated by decision makers such as indirect construction costs and social costs are considered and high weights are given to them. This choice is arbitrary in the analysis and is closely linked to the decision making process. Different choices can obviously be made.

In the studied example, the evaluation was made while trying to highlight the point of view of the society and therefore the social and environmental costs take on a great importance.

The priority list obtained following the procedure described in paragraph 2 is reported in Table 6.

If the two alternatives are compared, on the basis of the chosen priorities (Table 5), it can be seen that trench excavation has a score of 0.23 while microtunnelling has a score of 0.77.

Copyright © 2005 Taylor & Francis Group plc, London, UK

Table 5. Pairwise comparison matrix for the general criteria.

	Direct construction costs	Indirect construction costs	Social costs	Environmental costs
Direct construction costs	1	1/3	1/3	2
Indirect construction costs	3	1	1	5
Social costs	3	1	1	5
Environmental costs	1/2	1/5	1/5	1

Table 6. Priority list of the general criteria.

Direct construction costs	0.137
Indirect construction costs	0.394
Social costs	0.394
Environmental costs	0.075

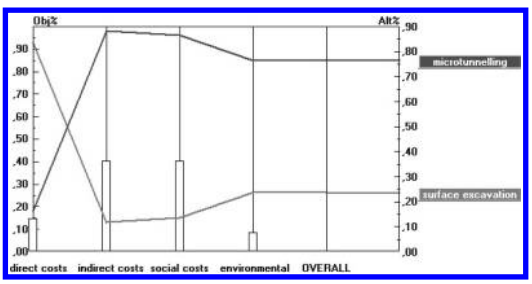


Figure 2. Performance graph.

Therefore, if the indirect construction costs, the social costs and the environmental costs are taken into account, microtunnelling appears to be preferable to trench excavation. Only if the analysis is performed maximizing the direct costs, does the trench excavation become preferable to microtunneling as it is possible to see in the graphs of Figures 2 and 3.

The Performance graph of Figure 2 highlights the priorities of the final alternatives, as regards the general criteria; the graph shows the course of the two alternatives (represented by two lines) with reference to each criterion (represented by a vertical bar proportional to the respective weight) and to the total priority list.

The graphs in Figure 3 show the relationships that exist between the two alternatives in function of the chosen weights of the general criterion (represented by the vertical line).

Figure 3(a) shows that if the weight of the direct construction costs is increased (moving the vertical bar to the right side of the graph from the chosen value of 14% to the value of 100%) and consequently the weights of the other criteria are decreased (in a proportional way to their initial weight) the trench method is preferable when a weight of 53% is given to the direct

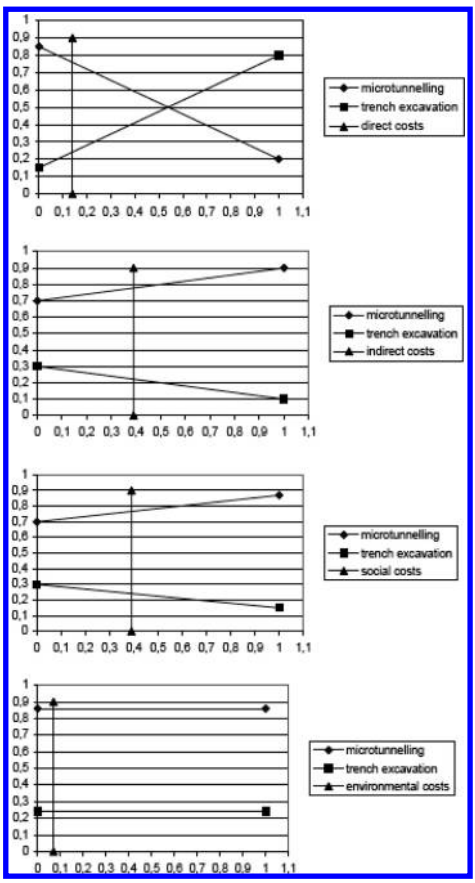


Figure 3. Gradient graphs with reference to the considered criteria.

construction costs. In all the other cases, microtunnelling is always a better solution than trench excavation and these differences increase with a rise in the weight of the indirect, social and environmental costs.

With specific reference to direct construction costs, some analyses carried out in Germany highlighted the influence of depth of the excavation and of the presence of groundwater (Stein et al. 1989) on the comparison

Copyright © 2005 Taylor & Francis Group plc, London, UK

between microtunnelling and trench excavation: if there is groundwater or the pipe is deep, the microtunnelling alternative is the best solution ever when the direct costs are considered.

Furthermore, in some cases, microtunnelling is the only possible technique, for example when crossing under infrastructures that cannot be interrupted such as canals, railways or very important roads or when there are buildings or delicate surface structures close by.

4 CONCLUSIONS

The comparison of trench excavation and microtunnelling that was carried out in this analysis shows that if indirect construction costs, social and environmental costs are considered with appropriate weights, microtunnelling excavation for the installation of a sewer in urban area is a better solution than conventional trench excavation.

Analytical tools that are able to help decision makers to correctly evaluate all the factors which are involved are nowadays available. Tools such as the one used in this paper are suitable and should be used to make the correct decision when comparing these two possible underground construction alternatives.

REFERENCES

Albers, L. & Nijkamp, P. 1989. Multidimensional analysis for plan or project evaluation. How to fit the right method to the right problem, in Barbanente A. (ed), *Metodi di valutazione nella pianificazione urbana e territoriale. Teoria e casi studio*, Bari: IRIS-CNR n. 6.

Bentivegna, V., Mondini, G., Nati Poltri, F. & Pii, R. 1994. Complex evaluation methods. An operative synthesis on Multicriteria techniques; *Proceedings of the IV International Conference on Engineering Management,* Melbourne, Australia.

Bottero, M. & Mondini, G. 2003. Towards the sustainability in mining wastes management: an application of the Analytic Herarchy Process; *International Symposium on Industrial Minerals and Building Stones, 15–18 settembre 2003*, Istanbul, Turkey.

Bottero, M. & Peila, D. 2003. Microtunneling o scavo a cielo aperto: l'applicazione dell'analisi di gerarchia per il confronto tra le due tecnologie, *Geoingeneria Ambientale e Mineraria,* XL, GEAM, 63–74.

Bottero, M. & Peila, D. 2004. Microtunnelling or trench excavation: comparison of the two alternatives, presented for pubblication of Tunnelling and Underground Space Technology.

Fusco Girard, L. & Njkamp, P. 1997. *Le valutazioni per lo sviluppo sostenibile della città e del territorio*. Milano: Franco Angeli.

Pelizza, S., Peila, D., Pigorini B., Artigiani, E. 1997. Analysis of microtunnel performances in granular soil; *No Dig*, Genova: 41–48.

Roy, B. & Bouyssou, D. 1995. *Aide Multicritére à la Décision: Méthodes et Cas.* Paris: Economica.

Saaty, T.L. 1980. *The Analytic Hierarchy Process.* New York: MacGraw Hill.

Saaty, T.L. & Vargas, L.G. 1990. *The Analytic Hierarchy Process Series*. University of Pittsburg.

Staheli, K. 1995. *Microtunnelling in California*. 1995 RETC: 393–405.

Stein, D. et al. 1989. *Microtunnelling. Installation and Renewal*. Berlino: Ernst and Sohn.

Sterling, R. 1997. Underground Technologies for Livable Cities. *Tunnelling and Underground Space Technology*. Volume 12, number 4: 479–490.

Thomson, J. 1995. Pipejacking and Microtunnelling. London: Blackie Academic & Professional.

Copyright © 2005 Taylor & Francis Group plc, London, UK

Tunnels related to Metro, Highway and Sewerage schemes in Istanbul

Dr. M. Cetin Gumusoglu
Regional Director (Eurasia), Parsons Brinckerhoff Ltd, Istanbul, Turkey

ABSTRACT: Tunnels related to Light Rail Transit System (LRTS), Metro, Highway and Sewerage schemes which have been implemented in the last decade in Istanbul, have led to valuable data regarding tunneling methods to be implemented in Istanbul. This is particularly important for this major metropolitan city as minimum of 200 km of metro tunnels are planned to be implemented in the next decade with the capital expenditure of 10 Billion US Dollars. In this paper construction methods, theoretical analyses and geotechnical monitoring pertaining to Incirli tunnel on LRTS, Tantavi and Kisikli Tunnels on Umraniye connection of E5 and E6 Motorways, Taksim-4. Levent metro and Istanbul sewerage tunnels have been discussed. Good correlation was achieved between measured and calculated values and predictions have been made on probable advance rates and costs to occur in the future tunnels to be constructed in and around Istanbul with a possibility of results setting general global trends in similar rock masses.

1 INTRODUCTION

In this paper construction of Incirli Tunnel located on LRTS 2nd Phase, Kisikli and Tantavi tunnels located on Umraniye connection of E5 and E6 Highways, Taksim-4. Levent section of Istanbul Metro and Bebek-Baltalimani sewerage tunnel, which is part of major Istanbul Sewerage Project, have been discussed and based on the data obtained from geotechnical monitoring of these tunnels, valuable data regarding possible advance rates and costs of the tunnels to be constructed in Istanbul have been developed.

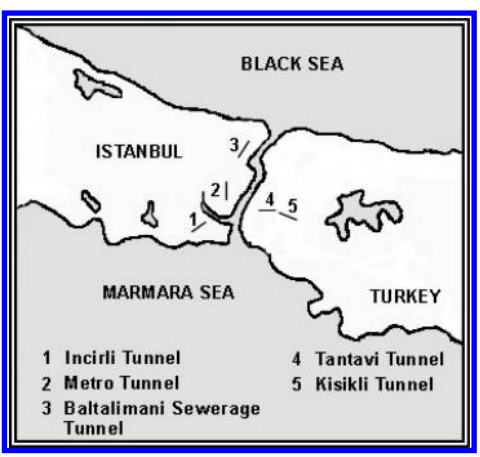


Figure 1. Location of infrastructure tunnels in Istanbul.

2 TUNNELS HISTORICALLY CONSTRUCTED IN ISTANBUL

History of infrastructure tunnels constructed in Istanbul extend beyond the century.

First transport tunnel in Istanbul is the 574 m long tunnel constructed between Beyoglu and Karakoy in 1874 (5). This was in fact commencement of 1st metro construction on BO Basis, 2nd in the world after London Metro. Since then not much has been achieved due to World Wars, economical difficulties etc. until 1980s.

Within the scope of infrastructure developments undertaken in Istanbul during the last 20 years, interceptor tunnels have been constructed since 1985 within the scope of Istanbul Sewerage Project. Within the project of Southern Golden Horn interceptors, approximately 7 km tunnel construction has been undertaken with internal diameters varying between 2.2–2.8 m. Within Northern Golden Horn interceptors project, approximate length of 5 km tunnel has been driven with internal diameters varying between 2.6–3.2 m and within the scope of Besiktas-Baltalimani interceptors, 8 km tunnel was constructed with internal diameters varying between 3.2–3.6 m (4).

Parallel to population growth mass transit systems gained priority at the city center in parallel to high density of passenger movement. In order to provide a solution to Istanbul's decaying urban transport problem, initially LRTS system construction had started in 1986 and Phase I incorporating Aksaray–Esenler–Zeytinburnu has been put into operation by 1993.

Copyright © 2005 Taylor & Francis Group plc, London, UK

Later 2nd stage construction, between bus terminal and airport, had started in 1991 and was completed in 1997. This 9.6 km long section of LRTS includes 1545 m long Incirli Tunnel, between Bakirkoy and Atakoy.

Istanbul Metro Phase I construction, connecting the city's commercial and cultural centre Taksim and 4. Levent, had started in 1992 and completed in 2000. Phase II construction is currently ongoing.

Highway tunnels were built on peripheral motorways around Istanbul in order to assist problems of traffic congestion and to connect both E5 and E6 motorways where necessary. Among these highway tunnels Kisikli and Tantavi tunnels were driven on the Anatolian side for the connection of E5 and E6 Highways at Umraniye between 1995 and 1997.

Accordingly when infrastructure works gained acceleration throughout the last 20 years, approximately 30 km tunnels were driven in Istanbul at separate locations due to transport and environmental goals and valuable data gathering was achieved regarding construction and cost aspects of these infrastructure tunnels.

3 INFRASTRUCTURE TUNNELS IN ISTANBUL

3.1 *Construction method*

Properties of tunnels driven in compliance with the New Austrian Tunneling Method (NATM) (7) are given in Table 1. Only Baltalimani tunnel in the table is constructed with shielded roadheader tunnel mechanism and without implementing the NATM.

Main principle of NATM is to convert the rock mass surrounding the tunnel to a load carrying rock mass. Achievement of this main principle requires utilization of supporting elements such as shotcrete, wire mesh, rock bolt, steel supports and fore poling when necessary. Support and excavation details showing the typical sections implemented in stages for Incirli Tunnel, for Kisikli – Tantavi tunnels and for Istanbul Metro tunnels are presented in the author's previous publication (5).

For Incirli, Kisikli, Tantavi and Metro Tunnels, following geotechnical investigations prior to design, three types of excavation and support systems have been determined and certain alterations have been implemented in these excavation systems as required following in-situ geotechnical monitoring carried out during tunnel excavation (1, 6).

Main reasons for selection of NATM method were as follows:

1. Rapid adaptation to varying geotechnical conditions.
2. Easy adaptation to varying sections.
3. A proven track record in weak and fractured rock masses.
4. Avoiding disturbance of soil and rock with deformation measurements and minimizing settlements on the surface.

3.2 *Geological–geotechnical conditions*

3.2.1 *Incirli tunnel*

Incirli Tunnel has been constructed in formations constituting of Upper Miocene old clay-marn and limestone (1). In the region these formations exist occasionally as carboniferous or as discordance on Eocene and on the tunnel alignment soil mainly consists of Gungoren Formation, Bakirkoy Formation and clays.

Table 1. Characteristics of Istanbul infrastructure tunnels.

Tunnel properties	Incirli Tunnel	Kisikli Tunnel	Tantavi Tunnel	Metro Tunnel	Baltalimani Tunnel
Location	Bakirkoy-Atakoy	Camlica	Umraniye	Taksim-4. Levent	Bebek-Baltalimani
Type	Single tube-double track	Twin Tunnel	Twin Tunnel	Twin Tunnel	Single Tube
Length (m)	1,337	634	210	4,987	2,342
Cut & cover (m)	68	68	60	700	–
Station (m)	140	–	–	1,080	–
Total (m)	1,545	720	270	6,677	2,342
Excavation section (m^2)	75	145	145	36	16
Concrete cover thickness (cm)	40	20	20	40	45
Concrete type	BS30	BS30	BS30	BS25	BS30
Tunnel excavation (m^2)	100,000	105,000	39,500	250,000	40,000
Shotcrete (m^2)	17,000	5,500	2,000	50,000	7,000
Internal lining concrete (m^2)	19,000	6,150	2,300	57,000	15,000

Copyright © 2005 Taylor & Francis Group plc, London, UK

Gungoren Formation consists of sand, silt-clay, clay and marn. Any sand layer has not been encountered at the tunnel level. Green-grey colored silty-clay is quite hard with claystone lithology at certain levels and limestone consists of marn and sand intrusions.

Geotechnical parameters of Gungoren Formation are listed below:

Soil Grade	: CH
Liquid Limit (LL)	: 67%
Plastic Limit (PL)	: 27%
Plasticity Index (PI)	: 40%
Natural Water Content (Wn)	: 38%
Unit Weight (yn)	: 1.81 t/m^3
Density (Gs)	: 2.73
Saturation Level (S)	: 97%
Swelling	: 0.78%
Compression Coefficient (Cc)	: 0.24
Consolidation Coefficient (Cv)	: 0.031 cm^2/min
Cohesion (c)	: $>$1.5 kg/cm^2
SPT N/30	: 63
Elasticity Modulus (Em)	: 579 kg/cm^2

Bakirkoy Formation: Dominant lithology is limestone in Bakirkoy Formation. Cream-white colored limestone include occasional thin clay bands and display transversal and vertical transactions with marn layers. Limestone comprising thin-thick layers, which are occasionally massive, include mactra fossils in abundance at certain levels. Along the tunnel alignment approximate thickness of limestone varies between 10–20 m.

Average physical and mechanical parameters of Bakirkoy Formation are as follows:

Unit Weight (yn)	: 2.29 t/m^3
Natural Water Content (Wn)	: 0.92%
Uniaxial Compressive Strength (σ_c)	: 222 kg/cm^2
Cohesion (c)	: 40 kg/cm^2
Internal Friction Angle (Ø)	: 48
Elasticity Modulus (Em)	: 25.000 kg/cm^2
Poisson Ratio (v)	: 0.25
Total Core Ratio (TCR)	: 60%
Rock Quality Designation (RQD)	: 16%

3.2.2 *Kisikli tunnel*

Kisikli Tunnel located between B.Camlica and K. Camlica is constructed in an excessively sophisticated geological structure and major rock formations are quartzite, arcose, clay stone-siltstone intrusions and intersecting volcanic dykes.

Geotechnical parameters of claystone-siltstone intrusions and volcanic formations encountered on the alignment of the tunnel are given in Table 2 enclosed.

3.2.3 *Tantavi tunnel*

Tantavi Tunnel is constructed in over weathered clay-siltstone, silt-clay stone and volcanic dykes intersecting along joints and fault zones.

Geotechnical parameters of volcanic formations are listed below:

Unit Weight (yn)	: 2.53 t/m^3
Natural Water Content (Wn)	: 0.71%
Uniaxial Compressive Strength (σ_c)	: 545 kg/cm^2
Cohesion (c)	: 13 kg/cm^2
Internal Friction Angle (Ø)	: 30
Elasticity Modulus (Em)	: 59.000 kg/cm^2
Poisson Ratio (v)	: 0.30
Total Core Ratio (TCR)	: 50%
Rock Quality Designation (RQD)	: 10%

3.2.4 *Metro tunnels (Taksim-4.Levent)*

Metro tunnels are generally constructed in Paleozoic aged Thracian Formation.

Table 2. Typical geotechnical parameters of formations encountered along Kisikli Tunnel.

Parameters	Sandstone	Claystone-siltstone	Diabase-Andesite
Unit Weight (yn)-t/m^3	2.29	2.57	2.31
Natural water content (Wn)-%	8.95	1.0	15.8
Uniaxial compressive strength σ_c-kg/cm^2	360	1,080	620
Cohesion (c) kg/cm^2	18	46	14
Internal friction angle (Ø)	34	38	31
Elasticity modulus (Em)-kg/cm^2	80,000	79,000	40,000
Poisson Rate (v)	0.27	0.35	0.28
Total core ratio (TCR)-%	35	65	30
Rock quality (RQD)-%	15	34	20

Copyright © 2005 Taylor & Francis Group plc, London, UK

Table 3. Typical geotechnical parameters of formations encountered along Metro Tunnel (Taksim–Sisli).

Parameters	Claystone-siltstone	Quartzite	Volcanics
Unit Weight (yn)-t/m^3	2.60	2.30	23.2
Natural water content (Wn)-%	1.5	7.5	14.0
Uniaxial compressive strength σ_c-kg/cm^2	540	250	720
Cohesion (c) kg/cm^2	30	30	35
Internal friction angle (Ø)	35	30	50
Elasticity modulus (Em)-kg/cm^2	20,000	60,000	58,000
Poisson Rate (v)	0.35	0.29	0.30
Total core ratio (TCR)-%	70	60	50
Rock quality (RQD)-%	25–50	50–75	50–75

Table 4. Typical geotechnical parameters of formations encountered along Baltalimani Tunnel (Bebek–Baltalimani).

Parameters	Sandstone	Claystone-siltstone	Limestone	Shale
Unit Weight (yn)-t/m^3	2.32	2.30	2.29	2.38
Natural water content (Wn)-%	0.85	9.0	0.95	1.0
Uniaxial compressive strength σ_c-kg/cm^2	555	300	874	520
Cohesion (c) kg/cm^2	35	25	50	18
Internal friction angle (Ø)	37	32	41	33
Elasticity modulus (Em)-kg/cm^2	27,000	71,000	70,000	43,000
Poisson Rate (v)	0.23	0.26	0.25	0.30
Total core ratio (TCR)-%	70	55	60	50
Rock quality (RQD)-%	25–50	25–50	0–25	0–25

Thracian Formation consists of grey-brown-green colored, weak-medium strength sandstone-siltstone and clay stone, with fine-mid size grained thin-thick layers, weathered and occasionally over weathered, altered, curly, with faults and very frequent fractures, and volcanic Andesite and Diabase dykes intersecting these along faults and weak zones. Related geotechnical parameters are enclosed in Table 3.

3.2.5 *Baltalimani tunnel (Bebek-Baltalimani)*

Paleozoic rock formations representing a continuous sedimentation from lower Devonian to Middle Carboniferous are found on the tunnel alignment. These are locally covered by 5 to 15 m thick Neogen Deposits of clay, silt, sand and boulders of 2–30 m. Devoninan and Carboniferous Buyukada and Thracian Formations, which form the bedrock, are cut by andesite and diabase dykes of 1–30 m thickness.

Buyukada Formation of Upper Devonian Age consists of micritic and nodular limestone and carbonate rich shale. It is strongly folded, little jointed and has massive appearance. The joints are generally vertical to bedding and have vertical to subvertical dip.

Thracian Formation as indicated above consists of mudstone, shale-greywacke and conglomerate units. It is closely jointed and strongly folded. RQD in Thracian Formation is comparatively low. The geotechnical parameters for the rock masses on the alignment of Bebek-Baltalimani tunnel have been provided in Table 4 enclosed.

3.3 *Geotechnical measurements*

All the tunnels constructed in Istanbul are naturally located under highly populated areas.

Hence, geotechnical measurements have been carried out at critical sections along the tunnel alignments during construction, in order to minimize expected settlements following the excavation and to be able to implement possible alterations in the support system without losing time. During the monitoring of these measurements below equipment/systems have been used as necessary:

1. Approach bolts installed within the tunnel
2. Settlement bolts installed outside the tunnel
3. Rod/Tape Extensometers
4. Inclinometers
5. Pressure Cells

Most critical sections subject to geotechnical measurements are shown in Figure 2 for Incirli Tunnel and in Figure 3 for Kisikli Tunnel. Metro tunnels extend totally under Cumhuriyet and Buyukdere avenues, and Baltalimani Tunnel follows Bebek-Baltalimani coastal

Copyright © 2005 Taylor & Francis Group plc, London, UK

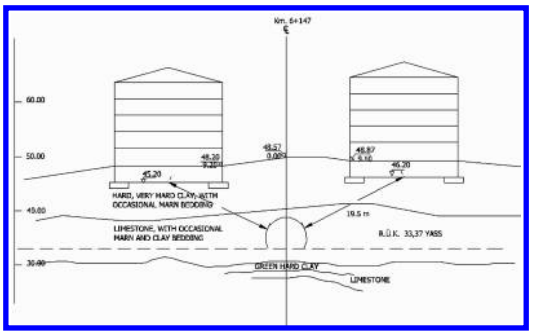


Figure 2. Typical crossing under buildings along Incirli Tunnel.

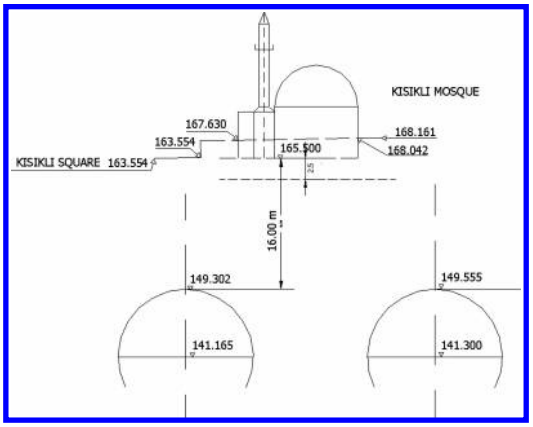


Figure 3. Kisikli Tunnel crossing under historical Kisikli Mosque.

road alignment and therefore these tunnels are less critical from subsidence point of view.

Maximum deformation values measured within the tunnel for Incirli Tunnel, Kisikli Tunnel, Tantavi Tunnel, Metro and Baltalimani Tunnels are presented in Figure 4 in a comparative manner.

For all tunnels finite element analysis was performed and in these analysis geotechnical parameters given in Section 3.2 obtained from laboratory results were used. In the finite element analysis NATM excavation steps and shotcrete was simulated and elasto-plastic material model was attributed to the rock and lining concrete (3). In the calculations permissible maximum deformation for Incirli, Kisikli, Tantavi, Metro and Baltalimani tunnels were assumed to be 100 mm. In finite element analyses, as rock masses remained within the elastic zone it was possible to compare the calculated values with some empirical methods developed based on the elastic theory. Finally, it was observed that good correlation has

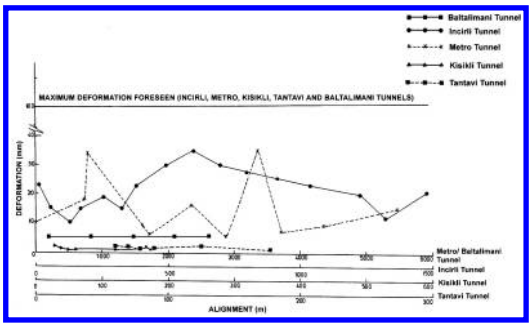


Figure 4. Comparison of convergence (deformation within the tunnel) values obtained with measurements at Incirli, Kisikli, Tantavi, Metro and Baltalimani tunnels.

been achieved between calculated, numerically checked and measured convergence values (5).

4 SITE OBSERVATIONS

1. For tunnels constructed under urban settlement zones, precise geotechnical measurements have been undertaken to avoid damage to existing buildings and to secure safety of excavation. Consequently with the utilized methods of geotechnical monitoring any serious damage to important historic and commercial buildings have been avoided.
2. Apart from Incirli Tunnel other transport tunnels constructed in Istanbul have been generally driven in Paleozoic Formations. Geotechnical monitoring of these tunnels usually display similar behaviour in spite of major local variations. On the other hand Incirli Tunnel is constructed in comparatively younger Upper Miocene formations. Whilst geotechnical parameters of these formations are still suitable for tunnel construction, they are more problematic compared to Paleozoic formations.
3. During Incirli Tunnel construction which was driven in weak to very weak rock conditions and under settlement areas with shallow cover, subsidences prospected in design and actual monitoring of excavation have been found in conformity to a great extent.

   In Incirli Tunnel, parallel to the lithology and structural situation, at the tunnel crest centerline with thin cover and thick fill, maximum 83 mm subsidence and 35 mm convergence values were observed. During Incirli Tunnel excavation shotcrete was applied continuously at the forepoling and face, apart from limestone dominant sections.
4. In Kisikli and Tantavi Tunnels excavation, different excavation techniques were implemented due to highly variable rock and soil conditions and this had negative effect on tunnel advance rate.

Copyright © 2005 Taylor & Francis Group plc, London, UK

During the excavations of Kisikli and Tantavi tunnels most critical factor was highly variable rock mass conditions. At Kisikli Tunnel very hard quartzite and softer but excessively weathered and altered volcanic dykes have been encountered. Excavation in clay stone and siltstone encountered apart from quartzite and volcanic dykes was relatively easier and it has been possible to work with shovel. Stand-up period of these formations was sufficient enough for shotcrete implementation. However, collapses have been encountered at jointed and faulted sections.

During the excavation of Kisikli and Tantavi tunnels geotechnical measurements were made with "tape extensometer" within the tunnels and tacheometer was used outside the tunnel along the axis. These monitoring studies have revealed very small values. (Maximum 6–7 mm deformation). However, it was observed that sudden settlements occurring until installation of measurement bolts for extensometers could not be accounted for successfully at site.

5. Significant surface settlements were not encountered at the surface along the alignment of Istanbul Metro Tunnel. However, within the tunnel, deformation up to maximum 35 mm was measured (6). In general maximum deformation values were obtained from horizontal readings close to the tunnel invert.
6. A choice of full-face type tunnel boring machine for Baltalimani tunnel was proven to be wrong under severe ground conditions and pulled back after a drivage of 1230 m and replaced by a shielded roadheader. This was due to insufficient geological investigations during the bidding stage and the subject is still on the legal dispute involving claims both from the contractor and the client. After utilization of shielded road headers no significant settlements have taken place on the surface and only negligible convergence displacements up to 5 mm have been encountered on the tunnel periphery. No serious collapses have also taken place. Subsequently, the tunnel has been successfully driven to completion with advance rates of 5 m/day on average.

5 CONCLUSIONS

Since 1985, parallel to the development of infrastructure schemes in Istanbul, approximately 30 km tunnels with varying diameters between 2.2 –13.6 m were constructed in Istanbul at separate locations for transport and environmental purposes and a major data has been accumulated regarding construction problems, advance rates and cost aspects of these tunnels. This data base could provide valuable insight in particular for the metro construction prospects, which

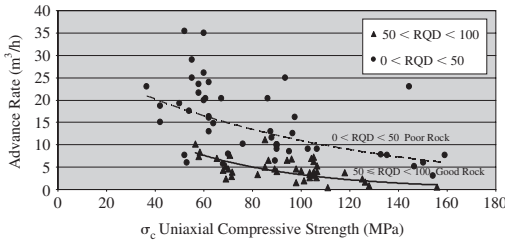


Figure 5. Advance rate of Tunnels with respect to RQD and uniaxial strength of rock masses.

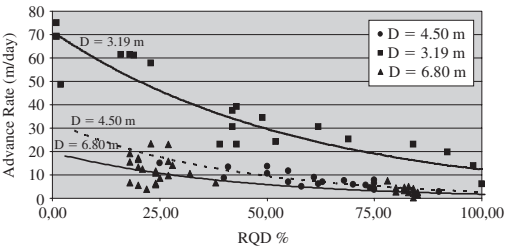


Figure 6. Advance rate of Tunnels with respect to RQD and diameter.

will be expanded all over Istanbul with minimum 200 km length during this decade. The accumulated data also presents valuable insight to underground constructions to be constructed at various parts of the world under similar conditions.

Relevant construction data could be summarized below related to infrastructure tunnels constructed in Istanbul:

1. The most appropriate and economic solution for small/medium diameter sewerage and metro tunnels in Istanbul is to utilize mechanized methods and by using "shielded roadheader". In highway/railway tunnels incorporating variable and big excavation diameters and in cases of variable soil conditions, implementation of the New Austrian Tunnelling Method has revealed good results.
2. Advance rates and costs of metro and sewerage tunnels are given in Figures 5, 6 and 7 with respect to rock strength and quality and diameter of tunnels. As can be seen in Figures 5 and 6, tunnel advance rate in general is affected by the rock mass quality (2). For good rocks with RQD $\geq$ 50, the advance rate is observed to be around 3–5 m/day and in medium to low quality rock with 0 $<$ RQD $<$ 50 the advance rate is found to be 13–15 m/day in the rock masses frequently encountered in Istanbul.
3. Problematic sections in tunnel excavations are generally very hard diabase dykes or highly fractured sections incorporating large blocks. Water

Copyright © 2005 Taylor & Francis Group plc, London, UK

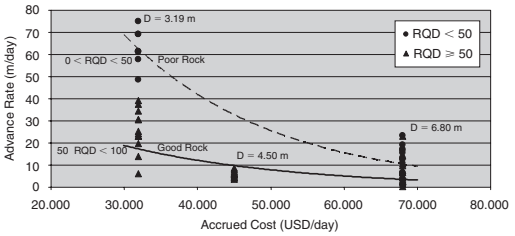


Figure 7. Accrued costs of tunnels with respect to advance rates.

ingress is generally at very low or controllable level.

4. Cost data summarized in Figure 7 have been derived from general construction statistics obtained from the various tunnel excavations discussed above including the support systems implemented. Based on the data in Figure 7 and taking into account length and advance rate of excavation the tunneling costs can be calculated as a rule of thumb (Diameter $\times 1000$ \$/m), as an average and empirical approach. Considering that rock masses encountered in Istanbul tunnels are in general of medium strength and quality, above general and empirical approach may even be adopted in calculating the approximate costs for other tunnels elsewhere in similar ground conditions, as well as being very beneficial in forecasting approximate budget for future infrastructure tunnels in Istanbul.

REFERENCES

(1) Ayaydin, N.,1992, Estimated Settlements Regarding Incirli Deep Tunnel, Yapi Merkezi, Istanbul.
(2) Bilgin, N., Seyrek, T. & Shahriar, K., 1990, Road-headers Glean Valuable Tips for Istanbul Metro, Tunnels & Tunneling, pp. 29–32.
(3) Gumusoglu, M.C.-Bray, JW & Watson, J.O., 1987, Analysis of Underground Excavations Incorporating the Strain Softening of Rock Masses, Proc. of 6th ISRM Congress for Rock Mechanics, Montreal.
(4) Gumusoglu, M.C. & Adiguzel, E., 1991, Modern Technologies used in Istanbul Sewerage Tunnels, Proc. Of XIth Tech. Cong. of Chamber of Civil Eng., pp. 693–703, Istanbul.
(5) Gumusoglu, M.C., Aslan, E., Ozbayir, T., 1995, "Metro and highway tunnels in Istanbul", Proc. of XIIIth Tech. Cong. of Chamber of Civil Engineers, pp. 433–447, Ankara.
(6) Lbay, N., Kuckertem, D. & Senturk, C., 1994, Geotechnical Monitoring Report for Istanbul Metro, I. Phase 2nd Section (Taksim-Sisli), Istanbul Greater Municipality, Istanbul.
(7) Rabcewicz, L.V., 1964, The New Austrian Tunnelling Method, Water Power, Vol. 16, pp. 153–157 (part 1).

Copyright © 2005 Taylor & Francis Group plc, London, UK

Underground space use in Ancient Anatolia: the Cappadocia example

A. Erdem
Istanbul Technical University, School of Architecture

Y. Erdem
ERER Engineering, Contracting and Consulting Company

ABSTRACT: Globalization enabled people to learn about the world in which they live in than ever before in the past. Today's global culture is determined by a rapidly growing communication network and advancing technologies. As a consequence, sustainability of local natural environments and cultural heritages becomes a global issue, while local sites become learning grounds for global communities. As one of the best example of man's symbiotic relationship with nature Cappadocia, located in Central Anatolia, offers many possibilities and lessons for underground habitation. This paper aims to discuss the ancient settlement of Cappadocia unique for its creative subterranean space use. The focal points of discussion are the physical geography and dominating forms of underground space use.

1 INTRODUCTION

Globalization enabled people to learn about the world in which they live in than ever before in the past. Today's global culture is determined by a rapidly growing communication network, expanding extend of knowledge and information and advancing technologies. As a consequence, sustainability of local natural environments and cultural heritages becomes a global issue, while local sites become learning grounds for global communities.

Due to the recent debates on energy consumption, cost efficiency and sustainability, new architectural strategies and trends emerged in the last decades. A greater awareness of energy efficient techniques in building design has developed and have been applied. Many alternative strategies have been adopted that reflect an evolution towards a set of redefined values in construction, maintenance and utilization. This new architecture is usually determined by prefixes such as sustainable, ecological, environmentally conscious or symbiotic in the related discourse. Among these is a design approach most commonly referred to as earth sheltered or subterranean architecture.

Although underground space use has historical roots in many cultures, the reemergence of the phenomena in the western world has occurred for many diverse and interrelated reasons. Usually the reasons for going underground is more than one: to conserve energy, to overcome tight zoning regulations, to minimize the entity's impact on historic buildings in the vicinity, to enlarge open space capacity,… Rafael Moneo's recent expansion to the Prado Museum, Sverre Fehn's Ivar Aasen Center in Orstad, Renzo Piano's underground extension to the Morgan Library in New York, Herzog and de Meuron's media art facility in California could be listed as prominent examples of this approach. Other examples may include a number of works by David J. Bennett, Philip Johnson's underground art gallery in Connecticut, Kevin Roche's Winthrop Rockefeller Archaelogy Museum and I.M. Pei's underground extension to Louvre.

1.1 *Historical perspective*

Through the course of time, one may find many examples of the situation where underground spaces provided potentials to meet shelter needs of man. Protection from predators and climatic conditions, lack of building materials were among the reasons for going underground. In 4000 B.C. inhabitants of the Banpo site in China lived in semiunderground pit dwellings with A-frame roof supporting a thin layer of soil. The thermal advantages of the earth's temperature moderation in a harsh climate, together with an ability to create shelter with minimum materials, energy and mechanization consequented in the mass construction of these caves to our day (Carmody & Sterling, 1985).

Between second and fifth centuries, Romans adopted a similar approach in Tunisia to overcome the disadvantages of the extremely hot and arid climatic

Copyright © 2005 Taylor & Francis Group plc, London, UK

conditions. The outcome was the below-ground atrium dwellings constructed at Bulla Regia. Other examples of the earth-integrated vernacular architecture in the Mediterranean region exist in the Gaudix region of Spain, in Sicily, and on the Isle of Santorini, Greece. Indian cliff dwellings of Mesa Verde, Colorado, subterranean houses of the central Australian desert and mined houses of South Australia set other examples. Among these examples the Cappadocia region in Anatolia is a valley dominated by cave buildings (Carmody & Sterling, 1985).

2 SUBTERRANEAN ARCHITECTURE OF CAPPADOCIA

As one of the best example of man's symbiotic relationship with nature Cappadocia, located in Central Anatolia, offers many possibilities and lessons for underground habitation. It is very interesting to observe a variety of answers to the question "why go underground?" dating back to the days of Byzantine Cappadocia, 400 A.D. The terrain was transformed within the hands of its inhabitants who hollowed out the soft rock into churches, houses and monasteries, evolving an entire architectural tradition from its unique material. The outcome is fascinating to the eye; it is as if nature and man competed to create a special terrain, as Charles Texier stated in 1882, "… *before descending from the plateau, which dominates this territory, I paused for a while, amazed at the spectacle before me. I know of no other corner of the world where there exists so striking and remarkable a phenomenon*." (Rifat, 2000).

2.1 *Geographical conditions and topography of the region*

Cappadocia, characterized by the natural features and subterranean architecture has been proclaimed a world heritage site by UNESCO in 1985. The story of this unique region covering almost 10000 hectares goes back far in time to Neocene, around 25 million years ago (Tuncel, 1998). The forces inside the earth started to form the cracks in the crust, through which molten magma came out, thus creating the volcanic mountains in the vicinity. They continued to erupt, producing the layer of volcanic tuff which gradually erupted into the unique landscape of our time. Volcanic emissions of lava and solid material buried the entire region under horizontal layers of widely diverse hardness, color and depth. Wind and rain then set to work to sculpt the rock, creating the strange pinnacles with their caps of more durable rock. This is how "fairy chimneys" were formed (Tuncel, 1998).

There exists a variety of shapes and sizes, but it is not only the diverse shapes of these formations that

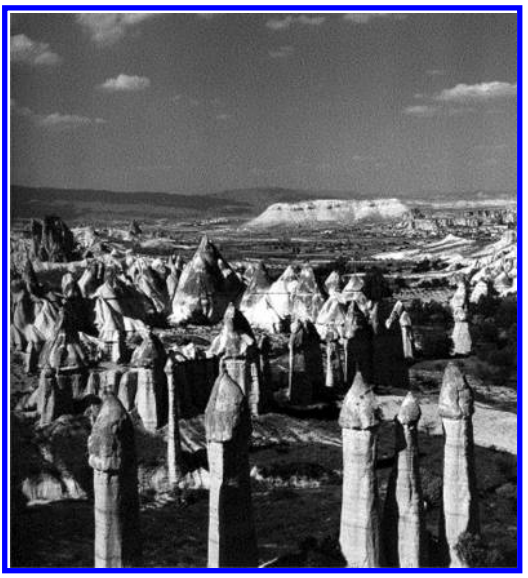


Figure 1. Pinnacles of Cappadocia.

are unique to the region. The diversity of color is no less remarkable, ranging from white, yellow and pink to grey and black, depending on the varieties of rock in each area. Where white rhytolitic tuff is abundant, and in the absence of a surface covering hard rock, the result is badlands topography, determined by sharp or rounded ridges forming white waves over large areas. Yellowish white columns occur in areas of rhytolitic tuff where red and pink columns in areas of red rhytolitic tuff. When man started to settle in the area, they took their cue from the wind and water and began sculpting the soft tuff to create shelter. The rock cones formed practical and versatile houses when the inside was carved.

2.2 *The Byzantine times*

The Byzantine period of Cappadocia starts in 395 A.D. when the region was inherited by the Eastern Roman Empire. The fame of Cappadocia today rests to a large extend on its Byzantine period rock churches and chapels. The volcanic terrain enabled a unique subterranean architecture carved from the soft tuff cliffs and pinnacles of the region. But although the carver masters adopted a different method of construction, they created spaces simulating the interiors of buildings constructed with stone and mortar. They modeled columns, vaults, arches and other architectural elements of their time. These elements did not have any structural function but were mere symbolic elements.

Instead of the classical definition of architecture as the creation of spaces for determined functions by

Copyright © 2005 Taylor & Francis Group plc, London, UK

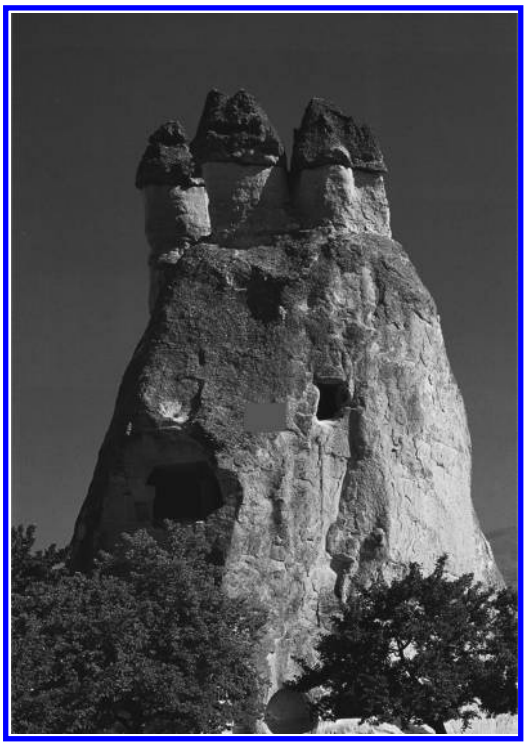


Figure 2. Monk Symeon's cell, Zelve (Akyürek, 1998).



Figure 3. Monk Symeon's Cell, Zelve. The small cell connects to an upper room. There is also a chapel on the lowest level (Akyürek, 1998).

enclosure with structural elements, here the interior space is created within solid matter by hollowing it out (Akyürek, 1998).

A large space could be completed in a couple of months, while the carver masters or architects did not require the complex knowledge required by their counterparts. The only limitation for the carver architect was the size of the rock mass that he was carving to form the spaces (Kostof, 1972).

2.3 *Dominating typologies*

In Cappadocia, one may find a variety of typological entities that differ in size and complexity: hermits' cells, dwellings, churches, monasteries and connected underground settlements. Inner rooms and spaces also vary in shape. The main idea is to carve out spaces within the limits of the pinnacles and stones, thus modifying the plans to fit the shape of the stones to be carved were a common practice among the carver masters. Consequently, each of the rock building was unique and none conformed to strict formal standards of Byzantine architecture.

The carving methods enabled Cappadocian masters to imitate the decorative elements of structural architecture by carving them along with the interior space. Although most of the buildings display no architectural features from the exterior, the interior spaces are decorated by frescoes or sculptured ornaments.

2.3.1 *Hermits' cells*

The simplest architectural form in the region is that of cells where hermits lived a reclusive existence. These carved cells or chambers contained niches to serve a variety of functions. They are usually devoid of decorations. The rocks which formed the landscape became dwellings for the monks when hollowed out.

2.3.2 *Churches*

Although there is a number of surviving subterranean architecture examples in the region, the highest percentage consists of religious buildings. In Cappadocia it is possible to find examples of religious buildings from early Christian to late mediaeval periods. However the architectural tradition flourished through the course of time and most of the existing churches highly decorated with frescoes date from the late tenth and early eleventh century. There are five main types of church in Cappadocia, single nave churches, double nave churches, basilicas, cruciform churches, and cross-in-square plan churches (Akyürek, 1998).

Copyright © 2005 Taylor & Francis Group plc, London, UK

Single nave churches consist of a nave and a large apse. The main space is rectangular in plan and roofed by a barrel vault. Access to the churches is through a single door in the shorter west wall. The apses are usually higher than the nave, and delineated by a screen carved from the rock. There exists a rectangular rock altar in the apse.

Double nave church plan was widely implemented during the Byzantine Empire. The plan type is common for both rock and structural churches of the era. The naves are separated by a series of small openings or arcades of pillars and arches.

Basilicas have rectangular plans that are divided into three or more aisles by a series of columns. The middle aisle is usually the widest and highest, ending with a semicircular apse. The basilica plan was used in early rock architecture in Cappadocia for cathedrals and important monastery churches. Carving the particular plan scheme was relatively difficult and so was reserved for religious entities of higher importance.

Cross-in-square plan type is typical of medieval Byzantine architecture. Following the tradition of the Great Palace in Constantinople, this plan spread all over the empire. The dome over the square central area is supported by four columns, and vaults on four sides of the dome form a cross plan roof.

There are also churches with irregular or amorphous plans which were probably dictated by the rock structure of the site.

2.3.3 *Monasteries*

From seventh century on, vast number of monasteries and chapels were formed in the Cappadocia terrain. Monasteries of Cappadocia are complex structures including refectory, dormitory and church all carved into the stone. The monasteries were comparatively small edifices, largest having a capacity for fifteen to twenty monks at a time. The monasteries were unique in their organizations as well: they combined the concept of a collective life under the lavra system unique to the East, and the more orthodox idea of individuality and isolation from others. This principle was reflected in the plan schemes as well. There are allocations both for private cells and spaces for communal functions.

2.3.4 *Tombs*

The sacral buildings of Cappadocia were frequently used for burials, a custom that has its roots in medieval Byzantine times. The dead were buried in either church floor or the wall niches in the narthex.

2.3.5 *Houses*

The housing tradition of Cappadocia goes beyond the Byzantine era. It is not easy to estimate the start of the subterranean architecture. The inhabitants of the terrain discovered the means of dealing with the rock before the Christian era. For them, carving out houses was preferable to ordinary construction methods. The houses created provided better inner climatic conditions and easy to maintain. They were also easy to defend in times of war or civil unrest.

2.3.6 *Multistory settlements*

Besides churches and monasteries constructed in the vicinity, there are also multistory settlements created by the Byzantine carver masters. These settlements are entirely underground and formed by uniting or linking a series of underground rooms or chambers. The plan schemes resemble complex labyrinths. Although there are a number of such settlements, the most impressive ones are at Derinkuyu and Kaymakli (Ousterhout, 1995). Like their above ground counterparts these settlements also contain a series of functional spaces allocated for residential, religious, administrative and public functions.

3 CONCLUSIONS

Many societies exist with their codes and customs, just as are transitory sorts of places. Architecture does not only build to shelter communities, it also builds powerful means of expression and communication. In Cappadocia, one does not only experience a powerful architectonic existence but also the cultural message conveyed through the transformation of a natural setting to a sound habitat. Remarkable identity of the setting is the consequence of a very strong symbiotic relation. Not only the formation of architectonic enclosures by working with the physical and material potentials of the terrain but also the realization of a dichotomy between private and public/religious life possess lessons for future developments.

Cappadocia sets a unique example of subterranean settlement with its dominating architecture and spectacular landscape. The carver architects or masters of the region adopted Byzantine forms and features but redefined them while creating the unique spaces of the dominant architecture. One may find architectural spaces in a variety of scales ranging from single rooms to totally integrated subterranean cities. The spaces that could survive till our day have attributes that provide lessons to contemporary practitioners as well: the spaces provide sound insulation against excessive weather conditions, the inner climatic conditions of the caves and their low levels of humidity provide perfect storage potentials for agricultural products and wine, the caves are also possess higher potentials to withstand earthquakes. Moreover, the underground architecture of Cappadocia sets a unique example for man's symbiotic relation with nature, while constituting a prominent example of highlighting local values and creating environmentally conscious

Copyright © 2005 Taylor & Francis Group plc, London, UK

settlements and spaces. In a way, analysis of the precedent provides many lessons for the future.

REFERENCES

Carmody, A. & Sterling, R. 1985. *Earth Sheltered Housing Design*. New York: Van Nostrand Rheinhold Company

Rifat, S. 1998. Cappadocia through the eyes of the travelers. In M. Sözen (ed), *Cappadocia*: 486–496, Istanbul: Ayhan Sahenk Foundation Publications.

Tuncel, M. 1998. A landscape in the making. In M. Sözen (ed), *Cappadocia*: 16–43, Istanbul: Ayhan Sahenk Foundation Publications.

Akyürek, E. 1998. Fourth to eleventh centuries: Byzantine Cappadocia. In M. Sözen (ed), *Cappadocia*: 194–225, Istanbul: Ayhan Sahenk Foundation Publications.

Kostof, S. 1972. *Caves of God: The Monastic Environment of Byzantine Cappadocia.* Massachusetts: The MIT Press.

Ousterhout, R. 1995. Historical design in the environment: examination of a Byzantine settlement in Cappadocia. In *Proceedings* at 1995 ASCA West Central region Conference: 13–19, University of Illinois at Urbana-Champaign.

Agacinski, S. 1995. Architectonic enclosure. In C.C. Davidson (ed), *Anyplace*: 24–31, New York: The MIT Press.

http://www.subsurfacebuildings.com

Copyright © 2005 Taylor & Francis Group plc, London, UK

Explosion tests in drainage pipes of long tunnels

V. Wetzig
Hagerbach Test Gallery Ltd. Sargans, Switzerland

ABSTRACT: Accidents due to petrol leaks have caused serious accidents in the drainage pipes of urban sewer systems in the past. Ten years ago, a petrol train ran off the rails and petrol escaped into the Zurich sewer system. Several hundred metres of the urban sewer system were destroyed due to an explosion of the petrol gases.

To avoid similar accidents in the new Swiss AlpTransit base tunnels, which are 35 km and 57 km long, a protection system has been developed and tested using real explosions.

In the base tunnels through the Swiss Alps, all fluids and water leaking out of the trains will be collected in waste water drainage systems. These drainage systems include maintenance openings measuring 100 m, which will be a weak point in case of an explosion in the drainage system.

The probability of an explosion of this sort in the drainage system is quite low, but should such an accident occur, subsequent trains could be affected and fire fighters could be trapped.

A constant water flow and the use of siphons should prevent propagation throughout the entire drainage system. The efficiency of methods of this kind has been proven in real-scale explosion tests over a length equivalent to one section of the drainage system. The aim of these tests was to prove that an explosion could not cross a maintenance shaft so as to affect a subsequent drainage section.

The tests used methane gases which were ignited in a simulated shaft. Different concentrations of methane were used to simulate different levels of explosion and detonation. The pressure of detonation and the propagation velocity of the flames were measured (frequency: 5000 Hz).

With a water flow of 5 l/sec in the drainage system, the explosion was cooled down and suppressed after about 50 m. Rapid increases in pressure and flame velocity were documented in each test. After reaching a certain value, the explosion was suppressed and the flames were extinguished. It emerged that serious explosions would be suppressed earlier than those of lower intensity.

Siphons are not necessary in order to halt the development of an explosion.

1 INTRODUCTION

The release of liquid and combustible hazardous substances such as petrol inside a tunnel can also result in explosive atmospheres in the tunnel drainage pipes. Accidents involving escaping petrol that reaches large-volume inner-city sewage systems indicate that an explosive event in the pipes can have catastrophic consequences.

In long rail tunnels, an event of this sort may cause an explosive incident to spread below the subsequent train or among the rescue teams arriving at the site.

To prove that the drainage system equipment selected for the AlpTransit rail tunnels is adequate for the safety requirements, explosion tests for this purpose were carried out on pipe sections which correspond to the dimensions of the AlpTransit installations.

The aim of the tests was to furnish experimental proof that an explosion, which is triggered in a pipe section between two maintenance shafts, is unable to spread beyond the shafts and the immersion tubes located in them across longer sections of the drainage system in the tunnel installation.

A closely related aspect is proof that the shaft structures, including the immersion tubes, do not suffer any damage, which would reduce the required outflow capacities for the system at the dimensioned pressures of 10 bar (radial) and 20 bar (axial).

2 EXPLOSION MECHANISM

If petrol flows into the drainage pipes after an accident, the shafts and pipes of the drainage system will fill with petrol as a consequence. The petrol will flow out of the pipes into the shafts, where residues that vaporize are left behind.

If, due to any mechanism whatsoever, an ignition event reaches the pipe system that is filled with combustible/explosive gases, an explosive event will occur.

The term ‘explosion’ is used to group together all the processes involved in a sudden conversion of

Copyright © 2005 Taylor & Francis Group plc, London, UK

substances, regardless of whether a deflagration or a detonation is involved.

The explosive event itself consists of a pressure wave and a flame front. The explosion is only deemed to have been extinguished or interrupted if both the elements of such an event are halted.

The explosion process depends on various factors in this case:

- the composition of the explosive mixture
- the type of ignition
- the pipe length
- the pipe geometry
- the closure at the end of the pipe
- the design of the shaft (open, closed)

The potential effects of an explosion depend, in particular, on the concentration of combustible substances and the geometry of the system under consideration.

In long and extended systems, such as the drainage channels in this case, the combustion gases spread along the longitudinal axis and push the as yet uncombusted mixture in front of them. This causes an increase in the turbulence in the uncombusted mixture, and hence an acceleration of the progression of the reaction with an increasing combustion reaction. The pressure effects increase in direct proportion to the velocity of propagation of the explosion and in extensive systems; they may attain values of 20 bar to 30 bar.

The larger the diameter of the system, the longer will be the initial distance for an accelerated explosion and hence the transition to a detonation. This distance is also extended in the case of concentrations which deviate from the stoichiometric petrol vapour/air mixture.

3 TEST SET-UP

3.1 *General test concept*

The explosive event was triggered in a run of pipes leading into the shaft. In the first phase, the run of pipes carrying the explosion was selected with a length of approx. 30 m, and this figure was extended to approx. 72 m as the tests proceeded further. A real-scale simulation of the shaft is connected to this pipe. A short run of pipes is positioned on the side of the shaft facing away from the explosion. The explosion was deemed to have been interrupted if no flame was detected in this pipe run.

The explosive event was recorded along the pipe carrying the explosion, in the shaft and in the pipe leading away from the shaft, by means of pressure sensors in the radial and axial directions, and by flame detectors.

The tests were carried out in three phases:

- pre-tests
- tests on 30 m-long pipe sections, with and without constant flow
- tests on 70 m-long pipe sections, with constant flow

The pre-tests were used to determine the gas mixture concentrations which led to the application of the required pressures at the open end of the pipe, taking account of the gas mixture, the pipe length and the pipe geometry. In this way, the dimensioning event was reproduced on the unprotected pipe system.

Following this, tests were carried out on 30 m-long pipe sections and the corresponding shaft structures. Tests were initially carried out on dry pipes, and then in a further testing phase; a constant flow of 51 of water per second was simulated in the pipes.

On the basis of the results obtained, it was decided to add a further testing phase in which a longer pipe section (approx. 72 m) was examined in front of the shaft.

4 RESULTS

On the basis of experience, above-stoichiometric methane–air mixtures produce more stable results, so the pre-tests were carried out with methane proportions of 10 and 10.5%. In this case, a methane content of 10% leads to pressure values which are significantly higher than the target values stated. Methane contents of 10.5 lead to pressure values which are at the lower limit of the target range of 10 bar (radial) and 20 bar (axial). For these reasons, a methane concentration of 10.3% was selected as the initial situation for the tests.

The first tests were carried out on dry pipes and water-filled shafts. As expected, the pressure in the pipe rose as the length increased. However, the expected pressures, which had also been proven in the pre-tests, were not attained. In the shaft itself, the massive extension of the cross-section combined with the shaft cover leads to a significant reduction of pressure. Only minimal overpressure is measured in the secondary pipe.

Various measures were implemented in attempts to attain the required pressures in the area where the drainage pipe opens into the shaft. Firstly, the methane concentration was gradually shifted towards the stoichiometric optimum. Even with 10% methane, axial pressures of only 7 bar were attained as compared to the pre-tests, where axial pressures of up to 40 bar had been achieved.

When the constant flow was introduced into the test set-ups, the attainable explosion pressures fell even further, to maximum values of approx. 1 bar.

However, a flame breakthrough occurred in the area of the shaft in all of the tests, meaning that the desired interruption of the explosive event was not achieved.

Since the pressure loss in the 30 m-long pipe section was significant, further tests were carried out with a longer pipe section (approx. 72 m).

Copyright © 2005 Taylor & Francis Group plc, London, UK

In these tests on a long pipe section, conditions were ascertained in the initial stage of the explosion that were analogous to those in the preceding tests. However, in the further course of the pipe, there is complete extinguishing of the flame front. This effect is apparent with different gas concentrations, down to the stoichiometric optimum of 9% methane. In the shaft itself, no flames and hence no potential ignition events for the continuation of the explosion are detected. The tests suggest that as the ideal stoichiometric value is approached, and hence in the case of more violent explosions, there is faster extinguishing of the flame front.

The effect whereby the progression of the explosion can be braked and even halted by the constant flow in the pipes can only be explained as follows: the incipient explosion whirls up the water in the constant flow and disperses it over the cross-section of the pipe, thus cooling the explosion and preventing its development; in addition, it may be assumed that the water vapour may exert an inerting influence in certain circumstances. This principles has been successfully used by the mining industry for a long time in order to prevent the propagation of explosions in coal pits. Accordingly, decisive importance attaches to constant flow for the purpose of limiting explosive events in the drainage systems of the AlpTransit.

5 CONCLUSION

The tests that were carried out showed that explosive pressures of the order of significantly more than 20 bar may occur in dry pipes, even in short pipe sections of approx. 30 m. When a constant flow is introduced into the experimental set-up, the explosive pressures fall below 1 bar. However, a breakthrough of the flames through the immersion tubes is registered in the shafts. The low pressure level is not exceeded, even with gas compositions which are optimal in terms of explosion technology. In a second phase of testing, the explosion behaviour in longer pipe sections (approx. 72 m) was examined. In all the tests carried out, it emerged that the explosion flame – which is critical for the continuation of the explosion – is extinguished within a pipe length of 60–70 m. Accordingly, critical importance is attached to constant flow for the control of explosive events in the drainage pipes of the AlpTransit.

The tests carried out were performed under the most optimal conditions for an explosion process. In an actual incident, such conditions will only be present for short periods of time, which are probably in the range of seconds. Likewise, no consideration is given to the consumption of oxygen due to the burn-off of hydrocarbons in the pipes, which will make it even less probable that optimal conditions for an explosion would be present.

Copyright © 2005 Taylor & Francis Group plc, London, UK

A multi-level tunnel for Amsterdam Zuidas

L.I. Vákár
Holland Railconsult, Utrecht, the Netherlands

Th.S. de Wilde
Holland Railconsult, Utrecht & Delft University of Technology, the Netherlands

E.L. Megens
Holland Railconsult, Utrecht, the Netherlands

ABSTRACT: The Zuidas (South-Axis) will develop into the second city centre of Amsterdam. The station will become the fifth station of the Netherlands. Several alternatives for the development of both infrastructure and urban habitat have been studied. Till recently, only two alternatives remained: the 'Dike' model, developed from the point of view of the infrastructure, but frustrating urban development, and the 'Dock' model, developed from the point of view of city planning, but neglecting the infrastructural and also the real estate requirements and therefore leading to a long building time. This paper will discuss a new design principle for the 'Dock' alternative: Stapeldok (Multistorey Dock) [1]. It is based on an underground longitudinal stacking of heavy-rail and light-rail, forming a multi-level tunnel. Real estate can be built on top of it, up to the desired height of one hundred meters. This design principle is being worked out presently as a third alternative. It has several benefits for both the infrastructure and the urban habitat that will be developed around and above it, including improved public quality [2], [3], more efficient phasing and lower overall costs.

1 INTRODUCTION

The Amsterdam Zuidas (South-Axis) lies between two southern districts of Amsterdam. It consists of a bundle of infrastructure for trains, metros and cars (Figure 1). There is a small station at present: Amsterdam Zuid/WTC. The present railway tracks will be augmented with new ones for the high-speed lines to both France and Germany. The station will become the fifth station of the Netherlands [3].

Planning for the development of the Zuidas began in 1994 and two alternative designs have remained for tracing out this bundle of infrastructure through the city. In the most ambitious alternative, the 'Dock' model, the infrastructure is built over with one million square meters of real estate (Figure 2). This paper



Figure 1. Zuidas at present.



Figure 2. The Zuidas in future with infrastructure built over.

Copyright © 2005 Taylor & Francis Group plc, London, UK

will present a new design principle based on a multi-level tunnel. This multi-level tunnel model optimises the phasing, overcomes important technical difficulties of existing alternatives and has positive financial consequences. Beside these advantages, the public quality and the flexibility are improved.

2 EXISTING ALTERNATIVES

At present there are two alternatives. The first alternative is the 'Dike' model that plans to extend the infrastructure on the existing embankment and to develop building sites only on both sides of the infrastructure. The second alternative is the 'Dock' model that plans to bring the entire infrastructure for heavy-rail (six tracks), light-rail (four tracks) and the motorway (four lanes on both sides) underground at level minus one to enable overhead construction of one million square meters of real estate extra. The latter alternative of building over railway tracks is the largest in its sort in Europe.

2.1 *'Dike' model*

In the 'Dike' model (Figure 3), the extension of the infrastructure takes place on the existing embankment. From the point of view of the infrastructure this is obviously the simplest model, but the infrastructural bundle is a wide, lasting obstacle in the city, frustrating the development of a new city centre. New real estate can only be developed on both sides of the infrastructure and the development of housing is limited by regulations for noise and air quality. This will lead to a mono-functional office development that lacks urban quality.

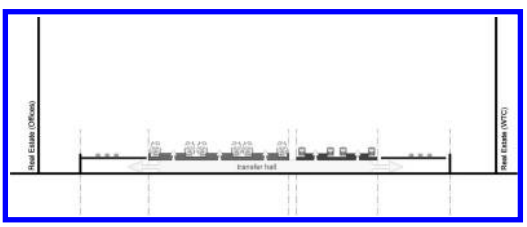


Figure 3. Infrastructure extended at plus-one level, the railways on the left and the metro on the right.

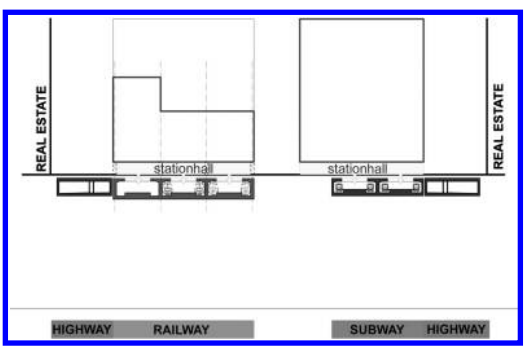


Figure 4. Infrastructure located at minus-one level, the railways on the left side and the metro on the right side.

2.2 *'Dock' model*

The 'Dock' model (Figure 4), with the infrastructure underground, at minus-one level, has obvious urban advantages over the 'Dike' model [4]. Up to one million square meter of real estate can be built over the infrastructure, thus connecting the city districts on both sides of the infrastructure bundle on existing street level and forming a new city centre. Compared with the 'Dike' model, this model is much more expensive. The extra costs must be earned back by real estate developments over the tunnels. Apart from the elevated price, this model has some important disadvantages.

First of all, this model contains two stations, one for the heavy-rail, one for the light-rail, approximately a hundred meters apart, with an urban axis in between. This leads to streams of passengers, pulling their trolleys through the future city centre. Besides, two stations take up a lot of commercial space at ground level. Another serious problem is the lack of possibilities to realise car parks for the real estate developments, as the underground space is already occupied by the infrastructure.

A major problem is the phasing of the building activities. The difficulty is that the present infrastructure should stay in use during construction of the underground docks, leaving little space for the construction of new tunnels. The entire surface of the bundle is part of the building site. This leads to a building time of not less than eighteen years and several temporary infrastructural measures, including temporary stations for trains and metros, separated from each other by a building site. This is not only expensive, it also leads to inconvenience to the public. In addition, the building of the real estate above the infrastructure only starts after eighteen years in the centre, leaving a gap in the city heart and in the financing of the project, during that time.

3 'MULTI-LEVEL TUNNEL' MODEL

On the IABSE Conference '*Structural Engineering for Meeting Urban Transportation Challenges*' in Lucerne in 2000 an alternative was suggested for the Zuidas project, that is to build the metro tracks underground and the railway tracks at plus-one level, thus

Copyright © 2005 Taylor & Francis Group plc, London, UK

leaving a large area available where, without any restrictions, building of real estate could take place [2]. In order to bring the entire infrastructure underground and to overcome the disadvantages of the existing 'Dock' model, this alternative has recently been improved and worked out as a multi-level tunnel, the so-called 'Stapeldok' (Multistorey Dock) [1]. It leads to several benefits for both the infrastructure and the urban habitat that will be developed around and above. It is compared to the 'Dock' model in Figures 4 and 5.

3.1 *Infrastructure*

In the multi-level tunnel alternative, the motorway and heavy-rail are positioned at minus-one level, while light-rail is placed at minus-three level under the heavy-rail. This is possible, because light-rail can cope with much steeper slopes than heavy-rail and has shorter platforms. At minus-two level a transfer hall between heavy-rail and light-rail finds its place, the station hall being situated at ground level.

The infrastructure of the metro has to be weaved in and weaved out underground under the railway infrastructure on the sides. Above it all, real estate developments are constructed. The weaving of the infrastructure under the real estate developments is represented in Figure 6.

3.1.1 *Construction*

The excavation for the multi-level tunnel will be built with slurry walls and an underwater concrete slab with tension poles. The tunnel being approximately 26 meters deep, it will rest on the stable sand soil layers, which start at the same depth at that location. The slurry walls bear at the same depth of 40 meters to act as an excavation wall, as well. The tension poles will be brought in under water up to minus 60 meters, after the ground between the slurry walls will be removed and the slurry walls will be propped.

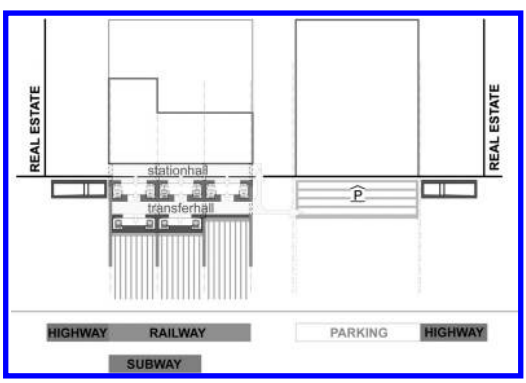


Figure 5. 'Stapeldok': a multi-level tunnel alternative.

3.1.2 *Phasing*

An important advantage of the multi-level tunnel is the phasing of the building activities (Figure 7). It is possible to build the tunnel, while leaving the rail infrastructure intact during construction. This prevents the use of expensive temporary infrastructural structures. The rail infrastructure can be migrated to the new positions without an intermediate stage. Also, there will be no building site between the different means of transport during most of the construction process, so changing of transport modality will be convenient even during the building stage. The building time of the infrastructure can be reduced from eighteen years of the 'Dock' model to thirteen years only. The roads will be brought underground both sides of the area to make space for the construction of the rail infrastructure.

Because the phasing is much faster, the development of real estate can set off sooner, starting from the new city centre, which will be available much earlier. This has important positive effects on the finance of this project because benefits can be realised much earlier.

3.1.3 *Flexibility*

Future infrastructural needs can be met in an easy way. This applies both in longitudinal direction, where a third light-rail platform can be added, apart from infrastructure possibilities under the urban axis, as for the transverse direction, where it will be possible to add a crossing light-rail line in the future at minus-two level, next to the transfer hall at that level.

3.2 *Urban surroundings*

The multi-level tunnel has important positive effects on the urban surroundings. Real estate, up to a height of one hundred meters, can be built at any desired place on top of the slurry walls of the longitudinally stacked tunnels, as these walls are present over the entire length of the tunnels.

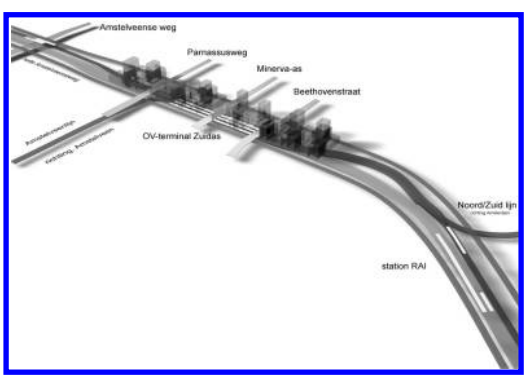


Figure 6. Impression of the longitudinal stacking in the 'Multi-level tunnel'.

Copyright © 2005 Taylor & Francis Group plc, London, UK

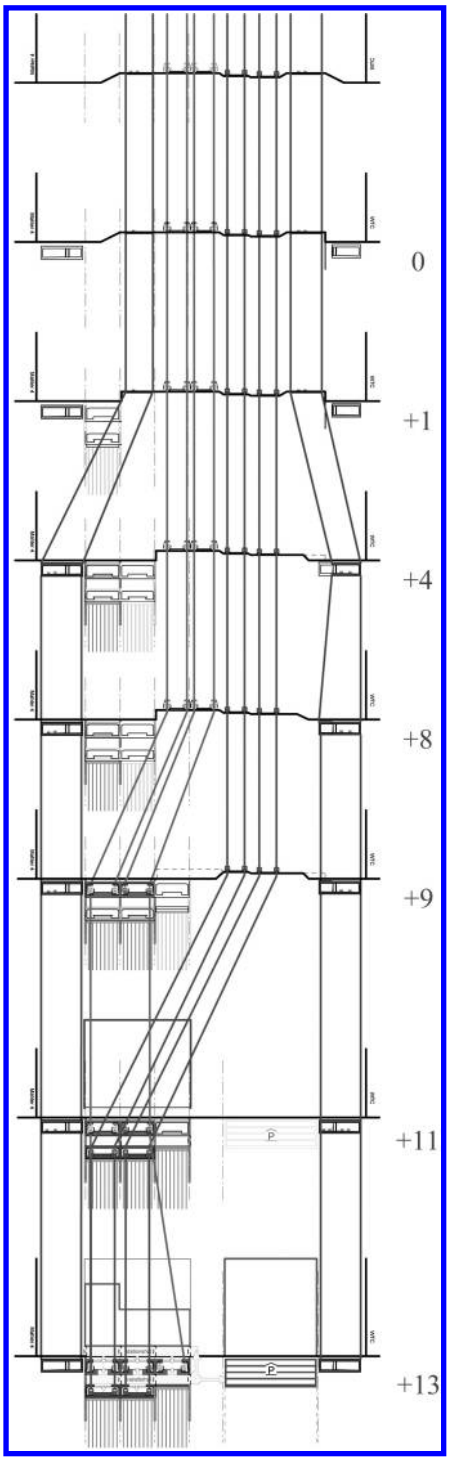


Figure 7. Phasing of the multi-level tunnel.

On the parcels beside the tunnels, building of real estate is not restricted anymore and car parks can be freely built under the real estate.

3.2.1 *Construction*

The longitudinal walls between the tunnel partitions at 21.60 meters centre to centre will spread the weight of the real estate on top of it, so it is possible to build on top of these walls without additional foundation. Of course a 'transfer' structure will be needed between the office grid of 3.60, 5.40 or 7.20 meter, commonly applied in the Netherlands and the 21.60 meter grid of the infrastructure [2],[5].

Next to the multi-level tunnel, no 'transfer' structure is required, but a standard foundation has to be made instead.

3.2.2 *Quality*

The quality of the real estate increases, as underground car parks will be available. There will also be more shopping space at ground level in the center of the project next to the station, as the two stations are integrated. The construction of the new district can start from the centre and gradually grow, thus creating high urban quality from the start on.

A secondary effect is created for existing real estate beside this building site. A lot of buildings have already been developed and some are under development. These all profit from a shorter building time of the infrastructure.

3.2.3 *Flexibility*

Half of the real estate can be freely developed. As the centre can quickly be built, it is possible to delay the rest of the real estate building activities till the moment when it suits best, without leaving an open city heart. Building on top of the multi-level tunnel hardly requires pre-investments, so there is no need to accomplish all the real estate within a short period of time.

3.3 *Integral public transport terminal*

The quality of the station will improve enormously compared to the existing 'Dock' alternative, combining all modalities within one station and thus making the interchange between transport modalities possible without leaving the station. The transfer hall that is integrated at minus-two level enables an efficient interchange in which transferring passengers don't have to gain ground level.

Creating an efficient integral public transport terminal means short transfer connections for a passenger between heavy rail, light rail and other modalities likes buses and taxis. By placing the infrastructure of heavy rail and light rail on top of each other, we are able to create a convenient arrangement. These modalities

Copyright © 2005 Taylor & Francis Group plc, London, UK

are linked with each other within the compact terminal. Passengers no longer need to cross the central axis road with their trolleys when transferring from one modality to the other, like in the 'dock' model. Transfer becomes quicker and more comfortable.

By introducing a transfer level on minus-two level, between the heavy rail tunnels and the metro tunnels, the passengers can overview the station within moments. They can see all levels and vertical transport equipment, like stairs, escalators and elevators and find their way to another level or exit easily. The tunnel walls between the tracks can be perforated to create more view and visual relation between the different platforms. The station will be visually larger; it will have a better atmosphere and will provide more social safety for the passengers.

The new integral terminal will be the first building on the Zuidas-site and will be the future city centre of this new area. The terminal will be a 'connector' between all future developments and between the two existing urban areas on the north and south side. Therefore it is important that all temporary stages in phasing this project will have a high urban quality. Because of the efficient phasing, the temporary situations during the construction of the tunnels and the use of the existing infrastructure will be of higher quality for the passengers, as the current situation will not change until the migration to the final position of the platforms.

3.4 *Financial aspects*

The 'Multi-level Tunnel' model has some lower investments compared to the 'Dock' alternative and some higher returns.

3.4.1 *Lower investments*

Although the tunnel infrastructure itself will require higher investments due to the depth of the excavation and the longer slopes to gain the depth of the light-rail station, overall investments will be lower. This is because on the one hand the building cost of the real estate on top of the multi-level tunnel will be lower, as no additional foundation will be required. On the other hand, the building cost of the real estate next to the multi-level tunnel will be lower, as no 'transfer' structure will be required between the grid of the real estate and the one of the infrastructure. The reduction of construction time reduces the interest expenses and financial risks substantially, as the time gap between profits and expenses diminishes.

3.4.2 *Higher returns*

As the building time and inconvenience will be reduced, the surrounding real estate will have higher rents. New real estate will also have higher rents, thanks to the increased quality of the station and its surroundings, the extra shopping space at ground level next to the station, the car park possibilities and the fact that the development will start at the station in the centre of the new city. Also, the benefits from the issue of the land will become available earlier. In addition, the return on investments of the real estate begins substantially earlier at the multi-level tunnel side, as no foundation has to be built there.

4 SAFETY

The fore mentioned 'Multi-level Tunnel' model has some points of attention, when compared with the 'Dock' model: Safety will be more an issue, because of the stacking of functions and as the depth of the station will increase. This applies mainly for the internal safety for the rail infrastructure. This is the safety of the passengers due to for instance fire in a train or metro, due to derailment or explosions. Escape routes play an important role, here, as well as the possibilities for the fire brigade and the first aid team to access the place of the accident. A quick study on these challenges indicates, that they can be easily overcome.

For external safety, that is the safety of the real estate due to accidents within the infrastructure underneath or vice versa, the situation is better than with the 'Dock' model, because only half of the real estate will be built over the rail infrastructure, when compared with that model.

In co-operation with the central government, the Rail Management Company, the city of Amsterdam and private investors, the possibilities of this 'Multi-level Tunnel' will be worked out in the next phase.

5 CONCLUSION

In the South of Amsterdam a second city centre is planned: Amsterdam Zuidas. In this project railway infrastructure is extended, also for the high-speed train, and up to 2.2 million square meters of real estate is planned, making it the largest project in its sort in Western-Europe. For this development, two models are under consideration, the 'Dike' model and the 'Dock' model. The first frustrates real estate developments and the latter not only neglects the infrastructural requirements, but frustrates real estate developments as well. For this reason a multi-level tunnel has been developed. This multi-level tunnel offers a substantial increase of quality and flexibility for both infrastructure and real estate. It also enables an extreme reduction of building time from eighteen to only thirteen years. This reduction of building time is possible due to improved phasing. It also reduces the interest costs and financial risks.

Copyright © 2005 Taylor & Francis Group plc, London, UK

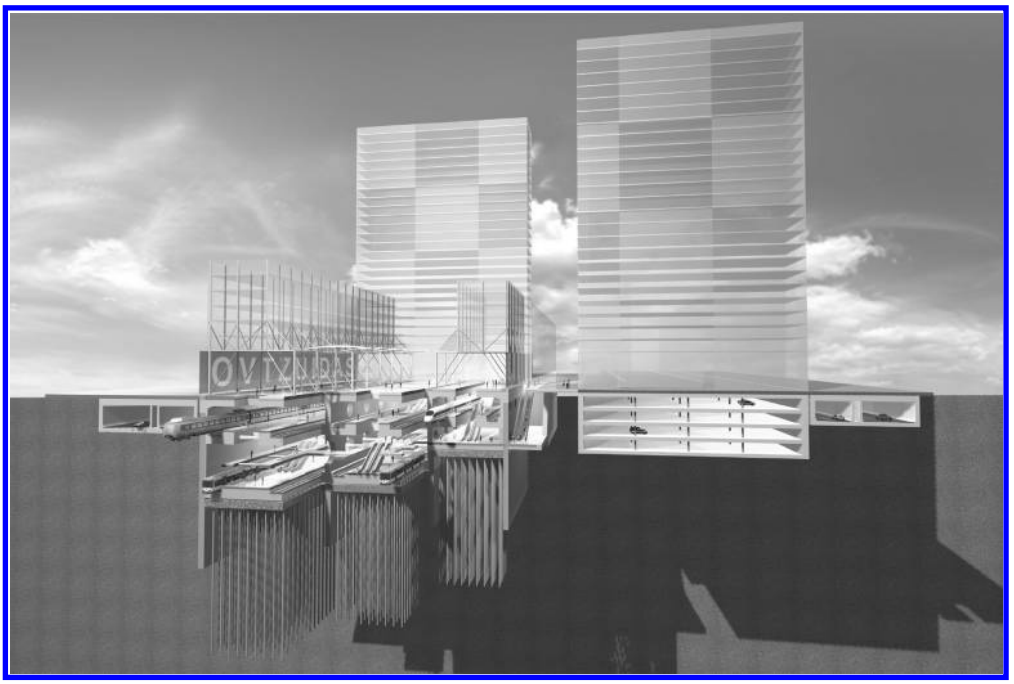


Figure 8. Impression of the 'Multi-level tunnel'.

The 'Multi-level Tunnel' (Figure 8) is a design principle in which knowledge of both infrastructure and real estate are combined enabling faster construction at lower overall costs and higher overall returns. Governmental parties, railway related parties, and private investors reacted positively to this alternative. That is why this new design principle is presently being worked out for the Amsterdam Zuidas.

REFERENCES

[1] Vákár, L.I., Wilde, Th.S. de, & Megens, E.L., September 2004, 'Multistorey Dock for Amsterdam Zuidas?' in: IABSE Report Volume 88, '*Metropolitan Habitats and Infrastructure*', Digital proceedings for IABSE Symposium 2004 '*Metropolitan Habitats and Infrastructure*', Shanghai, China.

[2] Vákár, L.I., & Snijder, H.H., 2001, 'Railway Station Structures Designed for Densely Populated Urban Areas', *Structural Engineering International*, Vol. 11, No. 2, 2001, pp. 128–138.

[3] Wilde, Th.S. de, & Vákár, L.I., August 2003, 'Flexibility and quality of HST railway stations and surrounding areas', in: IABSE Report Volume 87, '*Structures for High-speed Railway Transportation*', Digital proceedings for IABSE Symposium 2003, Antwerp, Belgium.

[4] DRO (Physical Planning Department of Amsterdam), 2001, '*Visie op de Zuidas*' *('View on the Zuidas')*, Amsterdam, the Netherlands.

[5] Wilde, Th.S. de, 2003, 'Structures for covering railways with real estate', '*System-based Vision for Strategic and Creative Design*' (Bontempi, F., ed.), A.A. Balkema Publishers, Lisse, the Netherlands, pp. 1009–1015.

Copyright © 2005 Taylor & Francis Group plc, London, UK

Planning research, development and design aspects on underground structures

Copyright © 2005 Taylor & Francis Group plc, London, UK

Design of pressure tunnels of Ermenek hydro power plant

M. Marence & A. Oberladstätter
Verbundplan GmbH, Salzburg, Austria

ABSTRACT: The Ermenek hydro power plant, currently under construction, with numerous underground facilities represents a big challenge the rock mechanics and tunneling works, especially for the pressure tunnel situated in the very heterogeneous rock mass with exchanging of weak and hard rock units. The tunnel is excavated by TBM, lined with concrete lining and loaded with internal pressure of up to 13 bar (130 m of water). Design requirements and design considerations with selected solutions are presented.

1 INTRODUCTION

The Ermenek hydro power plant is located in southern Turkey and collects the water of the Ermenek river and its tributary, the Erik river. The double-curved arch dam is located in a narrow gorge and has a height of 210 m with a crest length of only 123 m. Most of the hydro power plant facilities, except the dam and the main powerhouse, are placed below ground. Grouting galleries with a total length of approximately 10 km, covering a grouting area of 1.5 km^2, are designed in 4 levels in a vertical distance of approximately 70 m in order to make a grout curtain in karstified limestone (Figure 1).

The waterway comprises a 8.1 km long headrace tunnel with 5.60 m internal diameter and 1.1 km inclined shaft. With a gross head of 327 metres, two vertical shaft Francis turbines with a capacity of $2 \cdot 150 = 300$ MW are situated in a surface powerhouse. The project also includes the power plant scheme Erik with the 4.2 km long headrace tunnel, vertical pressure shaft with 170 m height, cavern powerhouse with $2 \cdot 3.4$ MW horizontal Francis turbines and tailrace tunnel in the Ermenek headrace tunnel. Both power plants with an annual production of 1 014 GWh are foreseen to be completed in 2007.

Together with the grouting galleries, spillway tunnels, gate, surge and elevator shafts and access tunnels, the project forms a tunnel net of more than 30 km. The excavation of most facilities, except headrace tunnels is carried out by drilling and blasting according to the NATM. The open TBMs: The Ermenek machine with a diameter of 6.70 m and the Erik machine with a diameter of 3.93 m excavate both headrace tunnels.

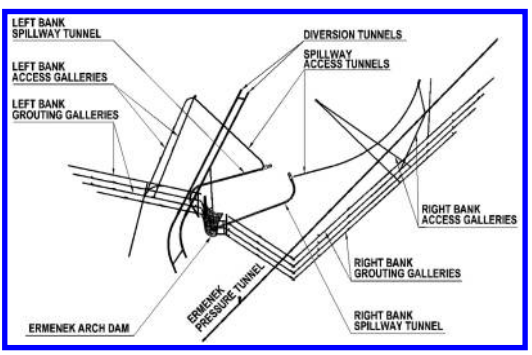


Figure 1. Underground structures in the vicinity of the Ermenek dam.

2 ERMENEK PRESSURE TUNNEL

2.1 *General*

The Ermenek pressure tunnel has length of 8.1 km with an excavation diameter of 6.70 m, is excavated by open hard rock TBM. The tunnel starts with an open surface intake structure, passing the gate shaft the surge shaft and ending in the valve chamber. TMB excavation starts from the valve chamber situated approximately one kilometre from the entrance portal. The gate shaft with excavation diameter of 8.0 m and height of 55 m will be excavated by NATM. Because of the tight time schedule the excavation of the surge tank with its 11 m excavation diameter and a height of 150 m is done independently of the tunnel excavation from the level above tunnel. After completing the

Copyright © 2005 Taylor & Francis Group plc, London, UK

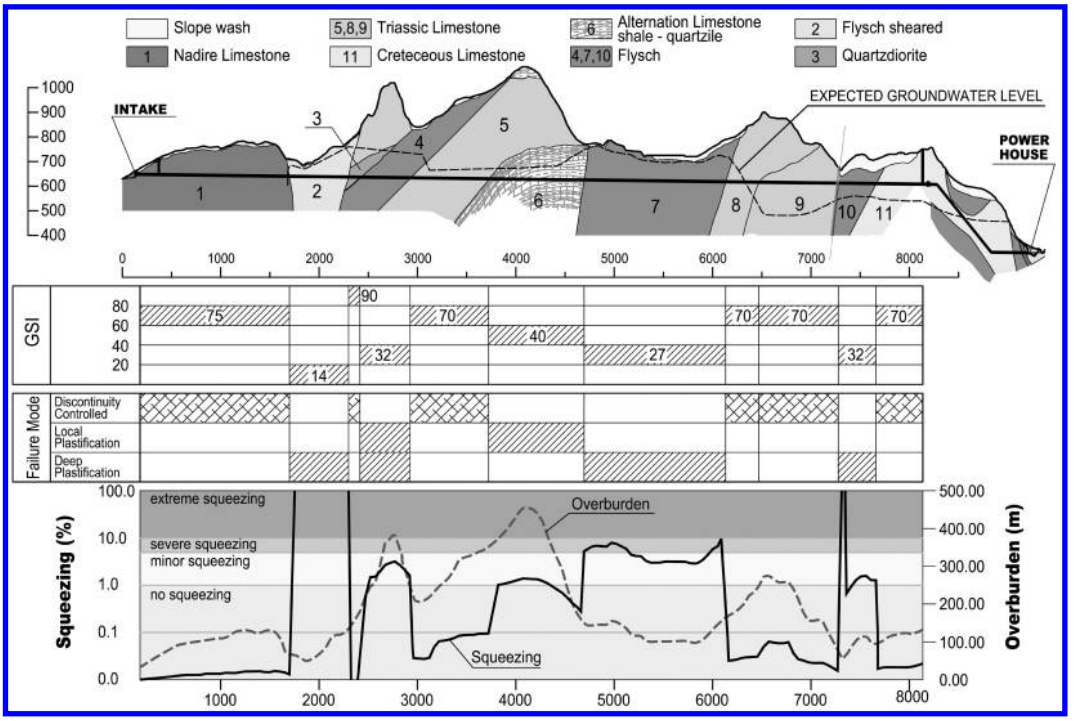


Figure 2. Longitudinal section of the pressure tunnel with rock behavior and squeezing potential.

TBM excavation connection shaft between the tunnel and surge shaft will be excavated.

Difficult geological conditions, especially several changings between the relatively hard and strong limestone with weak layers of flysch rock is a big challenge for the machine, but also for design of the primary and final lining.

2.2 *Geotechnical design of excavation and primary support*

The underground excavation and application of the support system is an interaction between ground properties and the selected excavation method in a defined period of time. Definition of the ground properties with its scatter represents a difficult task for the design of each structure in the ground. During the design period – independent of the design stage – type, characteristics and behavior of the ground are only known in points, along a line and/or only on the surface and together with other unknown factors, such as primary state of stress and groundwater, and can only be estimated by a characteristic value or by a range of values. Frequently, during the project phases with additional exploration works, the estimated values have to be changed or adopted. The design method is used that is flexible enough to allow these changes (Marence, 2003).

The design process started with definition of the regions with similar geological characteristics, so-called homogeneous regions. For these regions the geomechanical significant parameters (key parameters) and their characteristics are defined. The definition of these parameters is mostly done by geologists, however in cooperation with geotechnical engineers and is based on all obtainable information collected from the geology "in situ" and laboratory tests. Such information defines the ground type of the ground unit. For the Ermenek pressure tunnel geological conditions along the tunnel route have been separated in eleven rock mass types ("units") as shown in Figure 2. This un-oriented geology is put into relation with the orientation and geometry of the excavation and the information about groundwater, primary state of stress and other specific parameters are included. Also, qualitative geological and geotechnical information is transformed into quantitative parameters defined as fixed values or with their scatter. Then the key parameter and the RMR (Bieniawski, 1989) and GSI (Hoek, 2002) value for each rock mass type have been defined, All this information leads to the definition of the ground behavior type, which defines ground behavior including all important factors and excavation methods without considering the primary support and excavation phases. The categories of the

Copyright © 2005 Taylor & Francis Group plc, London, UK

Table 1. Input data and rock mass parameters for representative rock mass types (flysch and limestone).

Rock mass type	Flysch: claystone, siltstone and sandstone	Limestone
Comp. strength* [MN/m^2]	18/1–130	80/80–140
GSI [–]	32	70
m_i [–]	7	10
Rock mass friction angle [°]	31	52
Rock mass cohesion [MN/m^2]	250	2200
Rock mass E-modulus [MN/m^2]	1400	27 000
Rock mass comp. strength [MN/m^2]	0.3	14

* Intact rock mass.

ground behavior types are defined based on recommendations of the Austrian society for geomechanics (ÖGG, 2001).

The next design step was the calculation of the strength-, frictional- and elastic parameters of the rock mass as demonstrated for the units 10 – flysch and 11 – limestone which are representative for the project (Table 1).

In order to do the calculation for heterogeneous rocks like flysch rocks, which are built up of alternating layers of sandstones, siltstones and claystones the uniaxial compressive strength and the constant m_i of the intact rock has to be defined at first. For the heterogeneous rock mass with strength values of components from 1–130 MN/m^2 it was done based upon the relative percentages of their occurrence. The "weighted average" rock strength (18 MPa) and m_i (7) have been calculated according to Hoek and Marinos (2000). In case of the limestone units (like unit 11) the laboratory values of the compressive strength ranged from 80 to 140 MN/m^2 and for safety reasons the lower value was selected as input parameter for the calculations.

The failure mechanism strongly depends upon the stress conditions. A rough estimation of the failure mechanism is based upon the ratio between rock mass strength and in situ stress Hoek (1999) or by defining a squeezing potential (Hoek & Marinos, 2000 and Barla 2001). The squeezing potential is defined as a ratio between radial deformation of unsupported tunnel and tunnel radius defined as a percentage. The simple closed form solution for circular tunnel in a hydrostatic stress field is seldom met in the field, but the method gives useful indication about the tunnel support requirements and possible problems (Marence, 2003). The squeezing potential is used as a first estimation of the failure mechanism, defining regions where discontinuity conditional failures or plastification and squeezing rock conditions can be expected (Figure 2).

Considering all of these data the possible failure mechanisms (ground behaviour types) can be defined. The Austrian society for geomechanics (ÖGG, 2001) distinguishes eleven different ground behaviour types. A unique calculation method covering all ground behaviour types does not exist. The calculation method, analytical and numerical, must be appropriate for the assumed behaviour type. Three frequently encountered failure mechanisms are: block failure, local plastification and squeezing rock conditions. A suitable model gives answer on suitability of selected excavation process and support measures and gives possibility for risk assessment (Marence, 1998). In case of structurally controlled instabilities kinematic models are used for surface and underground excavations. The condition of joints and their orientation in relation to the designed structure are decisive for stability and several software products are available for such calculations. In case of homogenous and isotropic rock mass conditions continuous models like finite element or finite difference models are used.

Based on the calculations the primary support system is defined. Support is defined taking into consideration requests of the TBM:

- installation of the support in the region L1 immediately after the head and in L2 behind the machine
- application of shotcrete in the L1 region is restricted to the support classes where immediate support and rock sealing is necessary
- support with steel rings as an immediate support in weaker rock mass

The support systems are grouped in 6 support classes giving smooth transition from class to class. The first three classes, M1–M3, define the support in the blocky rock mass such as limestone and the last three, M4–M6, for the much weaker flysch rock. The support class M5 (weak rock) is shown on Figure 3. The support consists of steel arches TH 36 on the stroke distance of 1.70 m, systematic bolting in L1 and additionally in L2 region with 3.60 m long grouted bolts and 5 cm shotcrete in L1 and additional 10 cm shotcrete in L2 region reinforced with two layers of wire mesh.

On site, after each excavation cycle, the geological conditions on face are compared with design values, the suitability of the designed system is checked and a decision about support class application is done. In case of over- or under-estimation of the designed support system, the system can be easily adopted to the actual circumstances.

Geotechnical design gives possibility for understandable and comprehensive design with the option of intervention and adaptation in each project stage, based on the new knowledge, and during the construction works according to the as found conditions.

Copyright © 2005 Taylor & Francis Group plc, London, UK

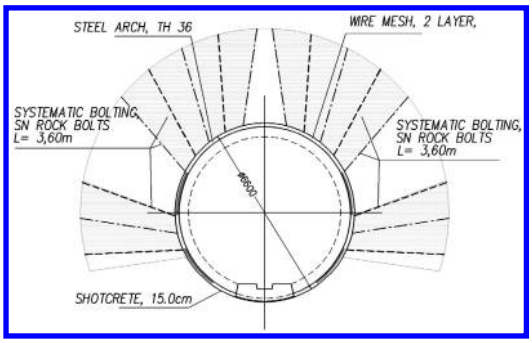


Figure 3. Primary support classes M5 for weak rock (flysch).

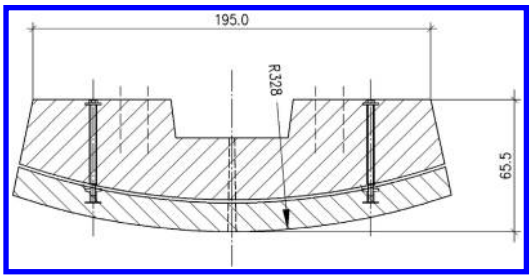


Figure 4. Two-part pre-cast concrete segment.

2.3 *Pre-cast invert segment*

The pre-cast concrete segment is used as a TBM sleeper. The segment is designed as a reinforced concrete element. Based on the selected final lining technology the segment is made of two parts – bottom and top part that are screwed together. The reinforcement design is made for separate parts (transport) and for the connected system (operation).

Five different segment types have been designed, distinguishing the technology and additional geometric conditions from the support requirements – gaps for the still rings in bottom part. A simple sketch of one invert segment type is shown in Figure 4.

2.4 *Final lining design*

2.4.1 *Reinforced or un-reinforced lining*

Main loading for the pressure tunnels is internal water pressure – static and dynamic pressure caused by maintenance of turbines and valves. The internal water pressure causes tensile forces in the lining. This, because of low concrete tensile strength, is an unfavourable loading and needs special treatment. Different methods to decrease, eliminate or overtake tensile forces are developed. In the Ermenek pressure tunnel two systems are selected: un-reinforced and reinforced concrete lining.

The plane, un-reinforced, concrete lining, as the most economic final lining, is adapted only for tunnels where only small tensile stresses in lining occurs during operation. In pressure tunnels subject to high internal pressures the plane concrete lining has to be pre-stressed in order to keep it free from fissures. The pre-stressing is made in form of grout injection in the gap between the final lining and the surrounding rock mass. In case that prestressing is not possible, tightening of the tunnel can be done by thin foils (plastic or thin steel lining), reinforced concrete and by high internal water pressure by classical thick steel penstock. By the Ermenek project sections where full prestressing was not possible the final lining is reinforced. A tight reinforced lining is achieved by special design requirements on lining and consolidation injections around the tunnel.

2.4.2 *Design based on Seeber theory*

Seeber (1984) defines the design method for unreinforced final linings of the pressure tunnels. The grout is pumped under high pressure into the contact joint between primary and final lining, a circumferential gap is opened and filled with cement grout. With the grout pressure exerted in the circumferential gap, the concrete ring is pre-stressed against the rock and the deformations of both sides are fixed by the hardened cement grout. To reduce adhesion between shotcrete and concrete and to achieve the circumferential gap opening the shotcrete separation layer is applied on the contact surface. In other to maintain the pre-stressing effect permanently, the rock mass has to be sufficiently firm and the rock stresses around the tunnel must be high enough to take the pre-stressing pressure. The final lining and the surrounding rock mass take the internal water pressure dependent on their stiffness. In the case that the pre-stressing by the injection is high enough, the lining will remain in compression during the operation and can be left unreinforced.

The selection of the injection pressure and optimal lining thickness is based on the simple graphic load-line method (Figure 5). The method is based on the assumption of the circular tunnel in homogeneous rock mass with full around radial pre-stressing. The injection pressure is limited to the concrete compressive strength and a minimal primary stress in the rock mass during the injection phases and by leaving the lining in compression during operation. An additional design condition is the groundwater pressure in case of an empty tunnel.

The same design philosophy as for the unreinforced concrete lining is used for the design of the reinforced lining. The reinforced lining is used where full grouting is not possible, because of too low overburden or too weak rock mass. The grouting with maximal allowed pressure – minimal initial stress – is applied. Grouting with pressure of 10 bars guarantee

Copyright © 2005 Taylor & Francis Group plc, London, UK

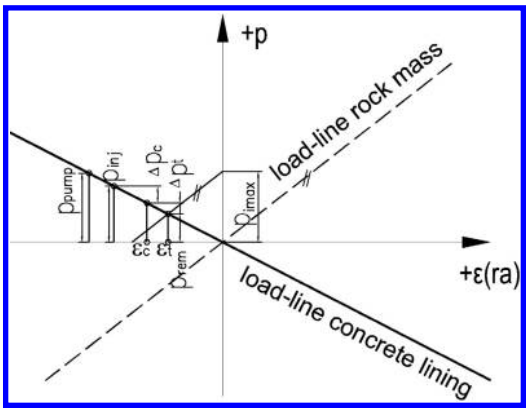


Figure 5. Load-line design method.

a contact between final lining and the rock mass after cooling the lining. The contact is necessary to achieve smooth and continuous force distribution between lining and rock and also to include the surrounding rock in the bearing of the internal pressure. Higher grouting pressures, applied if possible, additionally reduce the reinforcement amount in the lining.

To achieve the continuous reinforcement in the lining, the pre-cast segment must be removed and replaced by reinforced concrete. The two-part pre-cast segment allows removing the upper part without demolishing the primary tunnel lining and endangering the tunnel stability.

The preliminary calculations by spreadsheet program are suitable for parameter sensitivity analyses in pre-design. The calculations are performed for each geological unit with necessary division; dependent on overburden, groundwater and other important parameters. The comparison of results shows good agreement between this spreadsheet program and finite element calculations (Marence, 1996).

2.4.3 *Numerical model*

The spreadsheet calculations are based on the analytical solution with idealized assumptions that are not fully satisfying in practice. The most influenced parameters rock mass anisotropy and primary state of stress can be easily included in the finite element calculations. The calculations follow on the numerical modeling of the excavation and primary support (Swoboda, et al. 1993) including the stresses around the tunnel after excavation: The model includes all important influences such as self weight, shrinkage and creep of lining, contact and consolidation grouting, cooling of the lining by filling and internal water pressure.

The numerical model cannot portray all nature phenomenas, but should include the most important parameters of influence. Detailed description of the finite element modeling the pressure tunnels is described in Marence (1996). The most important model part is modeling of the gap between the linings and its behavior before and after grouting. The calculations are performed by the finite element program FINAL (Swoboda, 2004) simulating possible loading cases and modelling phenomena that occurs.

In case of unreinforced final lining, the lining must stay in compression and the stresses in lining are checked. For reinforced lining the reinforcement design is performed on the results of the finite element calculations. The reinforcement amount must satisfy following criteria:

- higher than minimal reinforcement in compression and tension
- designed for actual loadings with full safety
- crack width less than 0.30 mm

The crack with width of 0.30 mm means not absolutely tight lining, but technically tight system. In case of crack width less than 0.30 mm no erosion by wash out of fine particles in the rock joints is expected and self-cure process by filling with sediments will occur (Schleiss, 1997). In case of water sensitive regions – tunnel situated near the surface or in a vicinity of potentially unstable slope the crack width criterion is tightened up.

2.4.4 *Grouting philosophy*

The grouting is performed in two steps: contact grouting and consolidation grouting.

The contact grouting achieves the contact between the final lining and surrounding rock in the tunnel crown. A gap in the crown is a result of self weight deformations and shrinkage of the concrete. Also, in the crown during concreting void (highest point) can occur. Because of all this effects for all tunnels, independent of function (traffic or conducts), contact grouting is performed. The contact grouting is performed in the tunnel crown with low pressure 2–3 bar in the crown.

The consolidation grouting has a function to achieve continuous contact between the final lining and surrounding rock mass after shrinkage of lining by drying of concrete (draught in tunnel) and cooling of the lining by water (occurs by first filling of the system). The consolidation grouting by radial hole method is selected.

By the radial hole method the grouting is performed through mostly radially arranged boreholes. During the grouting procedure the grout penetrates into the surrounding rock and the gap between the final lining and the rock mass. A separation layer – lime paint or thin plastic foil – installed in the gap will easily activate the gap. The grouting injected in the gap between lining and the rock mass results in the so-called pre-stressing effect on the final lining. To achieve the nearly constant pressure in the gap and nearly continuous loading on the lining the distance

Copyright © 2005 Taylor & Francis Group plc, London, UK

between grouting holes, in radial and longitudinal direction, should not be larger than 2–3 metres measured on the final lining extrados. In the rock mass around the tunnel open joints or plastified zones occur and must be filled with the consolidation grouting to achieve a continuous support for the final lining.

In addition, the consolidation grouting decreases the rock mass permeability and increases the rock mass stiffness and strength. Reduction of the permeability up to 20 times can be achieved. The strength and stiffness of the rock mass will not be changed with such effort, but in case of anisotropic rock the minimal values of strength and stiffness will be increased, which will cause a more uniform system around the tunnel. The reduction of the permeability is important to decrease the water loses by both solutions where technically tight lining is necessary. Technically tight means that the lining is not impermeable, but the water losses can be neglected. Additionally, the leaked water in tight surrounding will increase the water pressure outside resulting in less loading on the lining.

The length of the gap grouting holes is defined based on the following criteria:

- Achieving the continuous support around the tunnel and continuous pre-stressing pressure on lining, the length should be in order of the tunnel radius
- In case of weak rock mass the plastified zone should be fully grouted
- In highly karstified regions with two and three dimensional karst phenomena (open joints and caves) the pattern of longer boreholes (up to tunnel diameter) for exploration is foreseen
- The open joints, especially semi-parallel to the tunnel axis, and caves that are encountered during the excavation must be filled with concrete before installation of the final lining.

Generally, the system of relatively short boreholes set with tight pattern is more efficient as long boreholes set in wide pattern.

3 CONCLUSION

The design of pressure tunnel with the geotechnical design, developed as a design of excavation and primary support of underground works, is extended on the design of the final tunnel lining. The geotechnical design represents a flexible procedure that can be adopted to any project stage. During the excavation the geotechnical design of the excavation and primary support is adopted to the encountered conditions, not only to achieve a stable, safe and economical solution, but also to collect additional data necessary for the final lining design. In the pressure tunnels the final concrete lining and surrounding rock mass make an integrated bearing system. The better the rock mass behavior is known, more the final lining and the consolidation grouting can be optimized.

In the project, generally, two types of final lining are selected; unreinforced and reinforced concrete lining. The unreinforced concrete lining is used in rock mass that can be grouted by sufficient pressure. The main criterion is no tensile stress during the operation in the lining. In case of reinforced lining the consolidation grouting is used to achieve continuous contact with the surrounding rock mass and reducing the reinforcement amount.

REFERENCES

Austrian society for geomechanics (ÖGG) 2001, Richtlinie für die Geomechanische Planung von Untertagebauarbeiten (Recommendations for geomechanical design of underground works). Österreichische Gesellschaft für Geomechanik.

Barla, G. 2001: Tunnelling under squeezing conditions. In Tunnelling Mechanics, *Eurosummerschool*, Innsbruck, pp 169–268.

Bieniawski, Z.T. 1989: *Engineering rock mass classification*. Wiley, New York.

Hoek, E. 1999: Support for very weak rock associated with faults and shear zones. Proc. *Int. symposium on rock support and reinforcement Practice in Mining.*, Kalgoorie, Australia.

Hoek, E. & Marinos, P. 2000. Predicting tunnel squeezing problems in weak heterogenous rock masses. *Tunnels and Tunnelling*. *Nov. & Dec. 2000.*

Hoek, E., Carranza-Torres, C.T. & Corkum, B. 2002. Hoek-Brown failure criterion – 2002 edition. *Proc. North American Rock Mechanics Society*, Toronto, Canada.

Jung, G. & Marence, M. 2004. Comparison of international and Austrian rock mechanical design procedures. *EUROCK 2004 & 53rd Geomechanics colloquium. Schubert (ed.), in press.*

Marence, M. 1996. Finite element modelling of pressure tunnel. In. J.-A. Dèsidèri et al. (ed) *Numerical Methods in Engineering '96*. Proc. of 2nd ECCOMASS Conf. Paris September 1996, Willey.

Marence, M. 2003. Geotechnical design of underground structures. In. *Underground Construction*, 563–572, London, Hemming Group.

Schleiss, A. 1997. Design of reinforced concrete linings of pressure tunnels and shafts. *Hydropower and Dams*, Vol.3, pp 88–94.

Seeber, G. 1984. Recent developments in the design and construction of power conducts for storage power stations. *Idraulica del territorio montano*, Bressanone, Italy.

Swoboda, G., Marence, M. & Mader, I. 1993. Finite element modelling of tunnel excavation. *Engineering Modelling* Vol. 6, No. 1–4, pp 51–63

Swoboda, G. 2004. Program FINAL – Finite element analyses of linear and non-linear structures under static and dynamic loadings – Version 7.2. University of Innsbruck.

Copyright © 2005 Taylor & Francis Group plc, London, UK

Three-dimensional rock mass documentation in conventional tunnelling using JointMetriX3D

A. Gaich
3G Software & Measurement GmbH, Austria

W. Schubert & M. Pötsch
Institute for Rock Mechanics and Tunnelling, Graz University of Technology, Austria

ABSTRACT: JointMetriX3D is a novel system that generates reproducible records of tunnel faces based on metric 3D images. The photogrammetric approach allows measurements from the 3D images, such as positions, lengths, or areas, as well as orientations either by discontinuity surfaces or traces. From those data discontinuity spacing and frequency as well as stereograms are generated. The 3D images itself represent a reproducible record of the tunnel face preserving the information on the actual rock mass conditions allowing analyses also at a later time. Measurements can be taken at any required number and extent, even in regions that are not accessible. The improved data serve as proof of the actual conditions but also as substantial information for the decision making on site.

1 INTRODUCTION

Conventional tunnelling requires continuous adaptation of the excavation and support method to the actual ground conditions in order to get an economical and safe construction (Schubert et al., 2003). This observational approach requires among others the continuous collection of information on rock mass type, structure, and quality, as well as the system behaviour. Very important in this context are geometric properties of the rock mass and especially the discontinuity network as observed at every tunnel face and subsequently descriptive parameters which altogether supports to establish a plausible rock mass model.

Traditional methods of geological data acquisition are prone to errors (Fasching, 2001). First of all, there are sampling difficulties, human bias, and instrument errors. Secondly time restrictions lead to incomplete data and finally getting access to relevant locations is often difficult or hazardous. The resulting mapping usually do not allow to objectively reproduce the actual rock mass conditions. Data not recorded immediately are lost as excavation proceeds or support is applied.

The presented JointMetriX3D system overcomes those problems and opens new possibilities for optimisations on the tunnel site. JointMetriX3D bases on the generation of a high resolution metric 3D image of every tunnel face which is then analysed and assessed on a computer. This way the visible rock mass structures are completely recorded and geometric data on the rock surface and the discontinuity network are easily measured at an arbitrary number. There are no access restrictions and results are instantly available for further processing. The 3D image is an objective documentation of the rock mass conditions which makes analyses possible even if a specific rock face is does no longer exist.

2 WORKFLOW

Figure 1 outlines the required steps when applying the system.

Firstly, images using the high resolution panoramic image scanner are taken from two different angles (stereoscopic images). In order to enable measurements later, the imaging system should be calibrated, i.e. known deviations of the optical system from the ideal behaviour are determined and thus correctable.

Secondly the images are processed in order to get a 3D image using photogrammetric principles complemented by computer vision strategies. This step is done by a purpose-built software that can deal with panoramic images.

Then the 3D image is ready for taking measurements using another purpose-built software component that allows the quantification and management of geometric entities such as positions, lengths, areas, or spatial orientations given by dip and dip direction.

Copyright © 2005 Taylor & Francis Group plc, London, UK

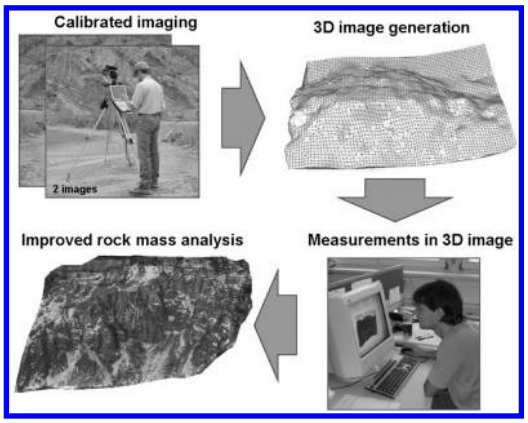


Figure 1. Data flow using the JointMetriX3D system.

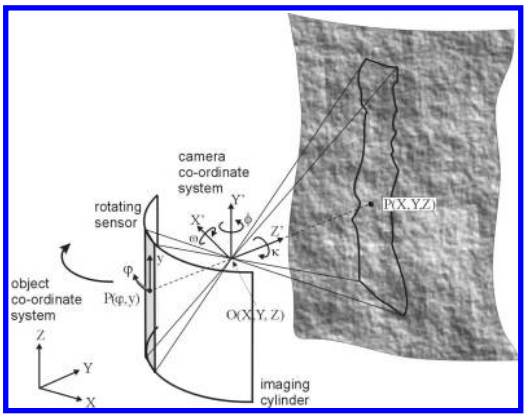


Figure 2. Geometry of panoramic line-scanning.

The results are structural maps, stereonets, descriptive and statistical rock mass parameters normally not determinable with reasonable efforts using traditional mapping.

3 IMAGING AT THE TUNNEL SITE

When taking images at a tunnel site one has to deal with several circumstances. Besides good visibility and *high resolution*, a sort of *referencing* mechanism is required in order to get a relationship between the data acquisition system and the surrounding which subsequently relates the derived measurements to the tunnel. A practical way to perform this relationship is to use reference points which means points of known positions in a superior co-ordinate system.

High resolution denotes that fine details are visible within the images which is crucial for documentation and analysis purposes. When doing conventional data acquisition the human observer also relies on the power of his/her visual capabilities. So it is obvious that any recording system must try to get as detailed information as possible when stating to be a documentation system. This is by the way a counting argument to use images instead of other sensors, such as lasers for example. If there are just intensities representing a rock face lacking of colour, lithological units and their borders as well as discontinuity traces might be misinterpreted or even not identifiable.

3.1 *The panoramic scanner*

A panoramic image is one that shows a full 360° field of view at least in one direction of the image. One approach to get a panoramic image is to move a camera along an rotation axis. When posing the rotation axis nearly vertically one gets an image that geometrically resides on a vertical cylinder, if an ideal rotation is assumed.



Figure 3. Imaging at the tunnel site. Note that only one person is required to operate the scanner.

The actually used imaging system is a rotating line-scanner. It has three CCD arrays one for each of the colour channels red, green, and blue. Each of the arrays has more than 5300 sensor elements which is a determinant magnitude for the resulting resolution that is composed by the vertical field of view in meters divided by the number of sensor elements.

The scanner is mounted on a tripod and controlled by a field notebook computer that instantly stores the acquired image data. During imaging the scanner rotates along a defined axis taking the panoramic image column by column. This principle decouples the vertical field of view (then depending only on the used lens) from the horizontal one (depending on the rotational motion). Figure 2 shows the imaging principle when using a panoramic line-scanner.

Since it is an imaging system there is of course a need for illumination. Usually one big flood light posed vaguely at the tunnel axis is sufficient to light the tunnel face up (see Figure 3).

Copyright © 2005 Taylor & Francis Group plc, London, UK

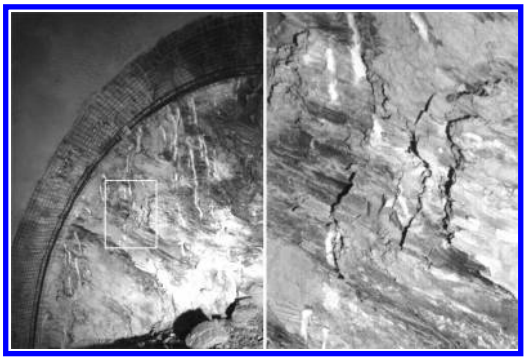


Figure 4. Parts of a tunnel panorama; the left side shows the tunnel face of a top heading excavation, the right side a detail taken from the same image. The geometric resolution is about 2 mm/pixel.

The panoramas taken at tunnel sites show typically a resolution in the mm-range. The resulting panoramas have a size of about 100 million picture elements (megapixels) which is clearly beyond conventional digital cameras. A section of a panorama is given in Figure 4. It shows a part of a tunnel face and a detail zoomed out from it. The image was taken at a two-track railway tunnel site in Austria (top heading).

3.2 *Referencing*

In order to get a relationship between the images and the tunnel, points with known co-ordinates in the tunnel system are required to be visible within the images. These points, denoted as reference points, are often available at conventional tunnel sites anyway where they are used to monitor displacements (Schubert & Steindorfer, 1996). For that reason the points are gauged regularly, often on a daily base.

An arising question is how to use those points optimally? If a conventional camera is assumed and one takes an image farther away from the tunnel face in order to capture also the reference points, the tunnel face covers only a small area of the whole image, thus giving required resolution away. Getting a closer view of the tunnel face entails that reference points disappear from the field of view of the camera.

This problem can be solved if panoramic images are used which allow the combination of high resolution at the tunnel face and a large field of view, thus making also the reference points visible. Figure 5 shows the geometric arrangement for imaging at a tunnel face. Reference points, in photogrammetry also denoted as ground control points, are indicated as well as possible camera standpoints. Note that there is no need for setting up the imaging system specially. The actual scanner poses are determined right from the observation of the reference points. In order to get proper echoes from the reflective reference points visible in the back, small light sources are mounted directly on the panoramic scanner.

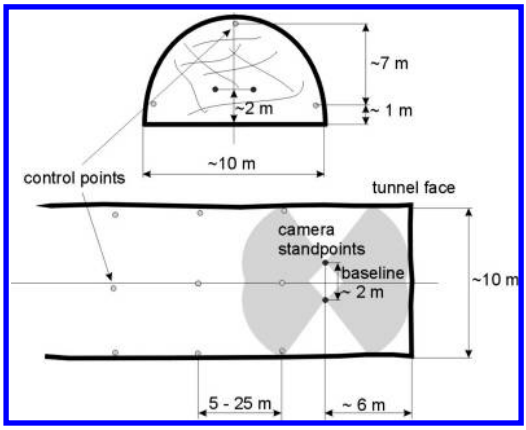


Figure 5. Schematic arrangement for imaging a tunnel face. The grey wedges indicate the useful parts from the 360° panoramas.

Once the relationship between the reference points and the acquired images is established, the results are referenced as well which means that derived measurements are related to the co-ordinate system of the reference points.

3.3 *Geometric arrangement*

As mentioned in section 2 there is a need for taking two images for getting measurements later. The two images can be taken simultaneously or subsequently. Each of the two panoramas contain the tunnel face and a view of the already excavated area as indicated with the grey wedges in Figure 5.

The time need in front of the tunnel face is some minutes typically. Within this time slot that is used usually before shotcreting all geometric data of rock surface and the discontinuity networks, as well as the referencing information is recorded.

4 3D IMAGE GENERATION

The generation of a 3D image uses principles of classical photogrammetry (Slama, 1980) complemented by more recent insights from computer vision where among others the calibration of off-the-shelf cameras was addressed (Faugeras, 1993). Having two images of the same region taken from different angles the so-called Shape from Stereo principle is applicable (Figure 6). Several tasks are required before a 3D image is ready (cf. Gaich, 2001):

– Calibration of the imaging system
– Determination of reference points

Copyright © 2005 Taylor & Francis Group plc, London, UK

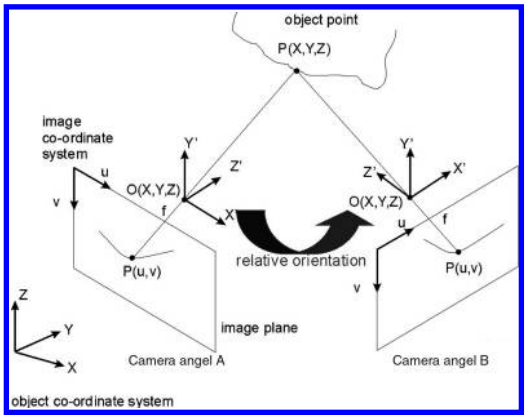


Figure 6. Shape from stereo principle.

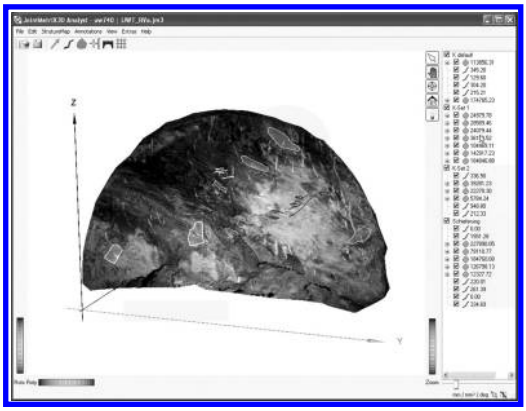


Figure 7. Snapshot showing the 3D image of a tunnel face and some measured structure data.

– Identification of corresponding image points
– Computation of 3D point cloud
– Connection of the 3D points to a surface mesh
– Geometric alignment of image and mesh

5 ASSESSMENT OF 3D IMAGES

5.1 *3D viewing*

Once a 3D image is ready, measurements can be taken from it. A purpose-built software is ready that allows to inspect a 3D image from any designated side. A turn and zoom mechanism brings any portion of the 3D image into any wanted pose. As additionally the 3D image is highly resolving, the human assessor gets this way a real impression on the rock mass conditions. Figure 7 shows a snapshot of the software with the 3D image of a tunnel face.

5.2 *Direct measurements*

From the 3D image geometric measurements are taken. At any of the possible poses of the 3D image, graphical markers can be placed "onto" it using the computer mouse. These marks denote points or regions of interest, e.g. visible discontinuity traces or discontinuity surfaces. The graphical marks themselves consists of 3D sample points and each of the sample points is given in the used object co-ordinate system, thus all measurements taken from the 3D image are inherently three-dimensional and digital.

5.2.1 *3D measuring point*

Any visible location can be marked by a measuring point getting it in the 3D Cartesian co-ordinates of the superior co-ordinate system, thus the position of any wanted location can be measured.

5.2.2 *Linear elements*

Discontinuity traces as well as lithological borders or geological strata are marked by linear elements providing instantly the true lengths in meters. Linear elements are represented as polygonal lines that follow the surface in 3D.

5.2.3 *Area elements*

Any region within a 3D image can be annotated by an arbitrarily defined closed polygonal. The sample points of the polygonal are determined directly from the 3D surface which brings the marked region also into 3D. The area of the marked patch is instantly provided in square meters.

5.2.4 *Orientations by discontinuity surfaces*

If a discontinuity surface is identified during the 3D analysis, it can be marked by an area element. The area element usually covers a number of smaller surface elements from which the 3D image is composed of. The software takes all affected surface elements and calculates a mean normal vector which represents a robust way to get an orientation measurement. Output is provided instantly by dip and dip direction and a graphical marker.

5.2.5 *Orientations by traces*

There is a second way to determine a discontinuity orientation mostly not possible during conventional field work. If a discontinuity trace is present that has a significant change in depth, i.e. the trace is not observed to be on a planar surface, the software calculates dip and dip direction from the trace alone by fitting a plane to the 3D polygonal. The plane is visualised as a spatial triangle that intersects the 3D surface as indicated in Figure 8.

Copyright © 2005 Taylor & Francis Group plc, London, UK

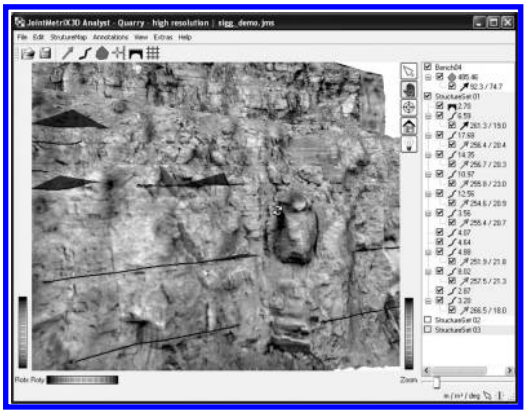


Figure 8. Discontinuity traces and computed orientation measurements indicated by spatial triangles.

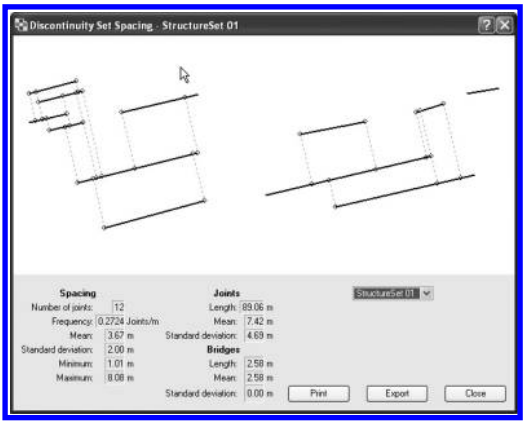


Figure 9. Computer generated sketch of the discontinuity network marked in Figure 8. The dashed lines indicate the scanline direction for determining the spacing.

5.3 *Derived measurements*

As the system allows 3D measurements that lead to geometric magnitudes in a given co-ordinate system, all descriptive rock mass parameters that base on geometric information of a rock face and the discontinuity network can be derived from those measurements.

5.3.1 *Spacing*

Spacing in this context is referred to as normal spacing, according to definitions given in the textbook by Priest (1993). For each discontinuity set, a plane of projection perpendicular to the mean orientation value is determined automatically. The plane of projection ensures that not the apparent spacing that is dependent from the actual shape of the surface is determined as it would be if just a single two-dimensional image is used.

All discontinuity traces of a set are then intersected with the plane of projection. Now the distance between adjacent discontinuities is measured along scanlines. The direction of the scanlines is also determined automatically which happens to be perpendicular to the mean orientation. Using a plane-sweep algorithm it is determined which discontinuities are adjacent.

Figure 9 shows the automatically generated sketch from the measurements shown in Figure 8. Continuous lines indicate the intersections of discontinuities and the plane of projection and dashed lines represent scanlines. This plot serves for visual inspection to verify a plausible spacing determination.

5.3.2 *Stereograms*

The measurements taken from the 3D image are grouped to sets by the user. Each set can be instantly visualized in polar nets in order to get an impression of the spatial distribution fastly where it is possible to choose between equal area or equal angle projections.

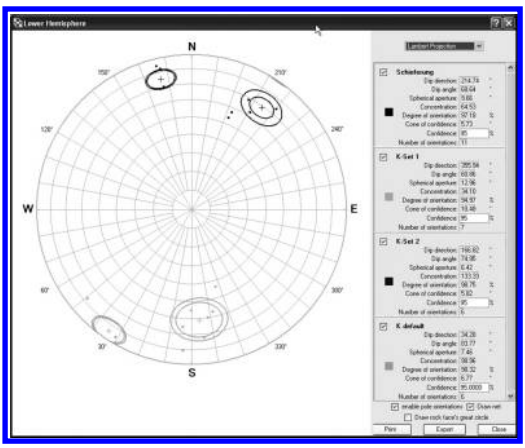


Figure 10. Lower hemisphere equal-area projection polar net of the identified discontinuity sets which is instantly available together with statistics on their distribution.

The stereograms deliver also some statistical figures, such as the spherical aperture or the cone of confidence for each discontinuity set. Figure 10 and Figure 11 outline such plots. The output is instantly updated when new orientation measurements are applied.

5.3.3 *Histograms*

Structural information that is annotated on the 3D image is stored as 3D information. Therefore true lengths of discontinuity traces are available. An export functionality allows to generate data files from which histograms as shown in Figure 12 are derived using external standard software.

Copyright © 2005 Taylor & Francis Group plc, London, UK

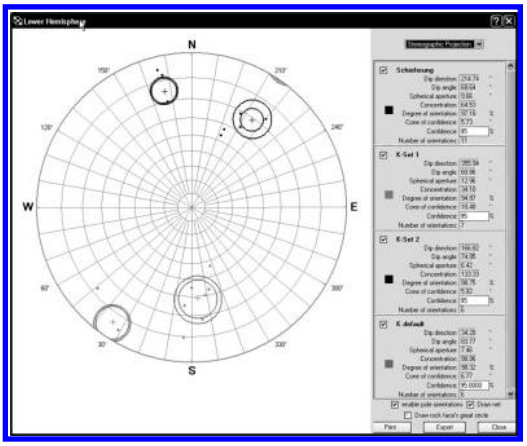


Figure 11. Stereographic projection of the same data set as shown in Figure 10.

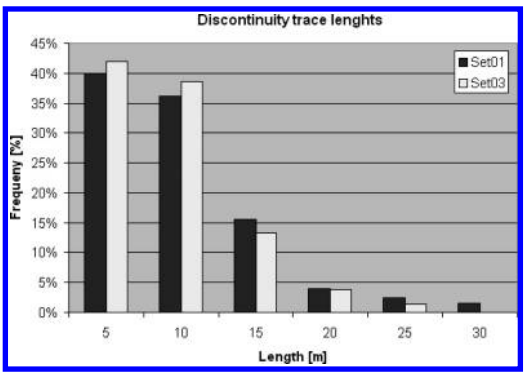


Figure 12. Discontinuity trace length distribution of two sets from a quarry assessment.

6 CONCLUDING REMARKS

The described system allows to record a tunnel face in a reproducible, objective way. Without needing knowledge on photogrammetry or computer vision one acquires relevant parameters of a rock wall quickly and preserves this way complete (visual) information of the actual rock mass conditions. Using this approach the data acquisition task is decoupled from the analysis task – the analysis can be performed even when the actual tunnel face does no longer exist.

Getting measurements from 3D images implies that this is an indirect measurement principle, therefore it is obvious that not all rock mass parameters can be determined by the system, for example discontinuity filling or strength parameters. However, indirect measurements increase safety as measurements can also be taken at inaccessible and possibly hazardous locations.

A 3D image resulting from the system represents an objective record of a tunnel face due to its high resolution, true colour, visual information and its three-dimensionality. It is no problem to do assessments at any later point in time or even support rock mass analyses from a distant location, as the data give a realistic impression to the observer.

Taking 3D images of a tunnel face in a regular manner, leads to an improved rock mass model that supports the understanding of the observed behaviour and serves as input for decisions on excavation and support on site. This specially bears the potential for saving construction cost since decisions on site are better if better information on the ground conditions is present.

An unbiased and reproduciberecord of the rock mass conditions can also a valuable asset in calim support and defence.

The JointMetriX3D system can also be applied on larger scale rock faces such as pit walls or quarries. Images of rock walls up to 300 m high can be taken from a distance of several hundreds of meters which allows an assessment of even hardly accessible slopes.

REFERENCES

Fasching, A. 2001. *Improvement of Acquisition Methods for Geotechnical Data.* PhD thesis. In Riedmüller, G., Schubert, W., Semprich, S. (eds) Schriftenreihe Gruppe Geotechnik Graz Heft 12b, Graz University of Technology.

Faugeras, O. 1993. *Three-Dimensional Computer Vision*. MIT Press, Boston, MA.

Gaich, A. 2001. *Panoramic Vision for Geotechnical Analyses in Tunnelling*. PhD thesis. In Riedmüller, G., Schubert, W., Semprich, S. (eds) Schriftenreihe Gruppe Geotechnik Graz Heft 12a, Graz University of Technology.

Gaich, A., Fasching, A. & Schubert, W. 2003. Improved site investigation. Acquisition of geotechnical rock mass parameters based on 3D computer vision. In Beer, G. (ed.) *Numerical Simulation in Tunnelling*: 13–46, Springer, Wien.

Schubert, W. & Steindorfer, A. 1996. Auswertung und Interpretation von Verschiebungsmeßdaten im Tunnelbau. *Ingenieurvermessung.* Bonn, Dümmler.

Schubert, W., Goricki, A. & Riedmueller, G. 2003. The Guideline for the Geomechanical Design of Underground Structures with Conventional Excavation. *Felsbau-Rock and Soil Engineering 21*, *Nr. 4*, Glueckauf Press, Essen.

Priest, S.D. 1993. *Discontinuity Analysis for Rock Engineering*. Chapman and Hall, London.

Slama, Ch. C. (ed.) 1980. Ma*nual of Photogrammetry.* 4th edition. American Society of Photogrammetry, Falls Church, VA.

Copyright © 2005 Taylor & Francis Group plc, London, UK

Highway D5 Pilsen highway by-pass – the Valik Tunnel

Ing. Jiří Svoboda
Main Tunnel Expert, Pragoprojekt Prague, Czech Republic

Ing. Miloslav Salač
Expert for Underground Construction, Metrostav Prague, Czech Republic

ABSTRACT: The Valik Tunnel is the last construction to finish the D5 highway, which connects Prague as the capital of the Czech Republic with the German border. Construction of this tunnel will enable to finish the Pilsen highway by-pass. Work preparation of the construction is characterized by a social and ecological antipathy. Design preparation and the choice of a technical solution has a longtime process. The final tunnel design, its statical assessment, the technical solution proposal and complex geological conditions have predicted the execution of a unique tunnel construction in the Czech Republic. The tunnel is designed as a twin-tube connected by a central cast-in-situ pillar in the primary lining. The tunnel is 380 metres long with the 330 metres mined section, width of the whole structure is 33 metres. The tunnel will be bored by NATM with double shell. Geological conditions are very complex, rock class 5a is the result of the final classification proposal. It has resulted from the investigation regarding the tunnel cross section and a low overburden. The design of the tunnel technological equipment for the operation fully corresponds with all safety requirements and meets the demands of European standards.

1 INTRODUCTION

Car transport in the towns is a phenomen whose negative impact on population and environment is increasing together with increasing number of cars. In the last few years very unfavourable situation has developed in most Czech towns, especially in Prague, Brno, Ostrava and Pilsen (the centre of the Western Czech District). This situation needs radical and prospective solution.

Current route net of Pilsen is no longer able to satisfy demands of its users. Therefore it is needed to quickly finish the construction of capacity road outside city aglomeration. In Pilsen, by-pass, which is the part of the higway D5 (Prague-Rozvadov-Germany), is being built. Originally, open cut was designed in the alignment of the tunnel. However, on the basis of people's and ecologists' claims it was replaced by driven tunnel.

The project of the whole by-pass road itself was being prepared for more than 9 years and was being accompanied by legal disputes. The legal disputes finally ended by decision of the Supreme Court of the Czech Republic in February 2000.

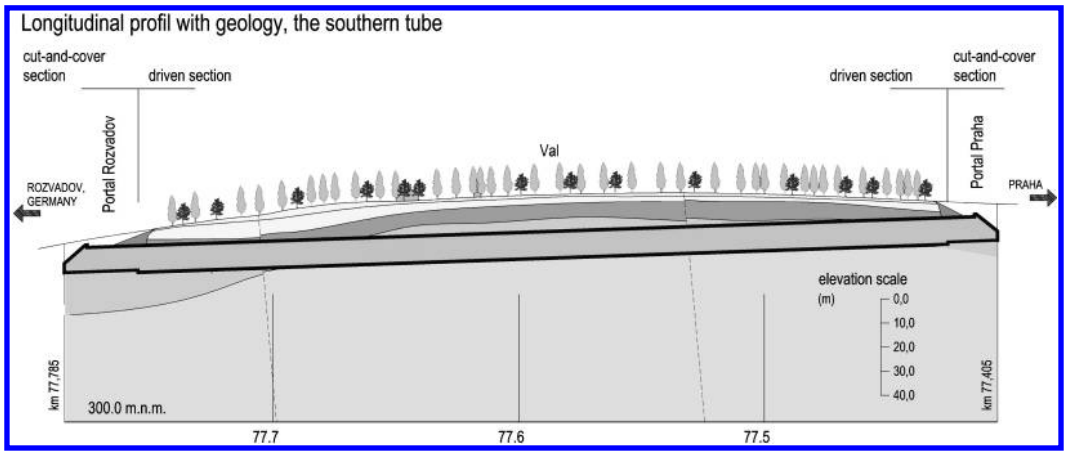
The motorway by-pass around of the town Pilsen is in the centre of attention of professional and non-professional public in the course of the last years of the old and new century. The technical experts, environmental specialists and environmentalists have got into argument during the preparation of the project. The future tunnel with a double tunnel profile will be 380 m long, 8,2 m high (in the vault head) and width of 11,5 m between kerbs. Tunnel tubes are proposed to be close without central rock pillar.

The maximal longitudinal gradient is 4%. Tunnel tubes are situated closely to each other without a central rock pillar which is replaced by a reinforced concrete pillar. This solution brings crucial saving in total range of permanent land occupation, especially in the area of pre-portal open cuts.

By this the demand for minimal intervention to the nature from ecologists and residents was fulfilled. Technical solution of tunnel construction is further more difficult than of common motorway tunnel. Therefore it needs solid knowledge of rock environment. The client "Czech Highway Directorate" decided to realize detailed exploration by a geological exploratory gallery situated in the axis of the motorway in the middle of the future-tunnel profile.

The future tunnel Valík is the part of completion of motorway D5, construction 0510/IB Černice – Útušice. This contruction comprise motorway route between km 76,510 and 79,980, from which 380 m is in the

Copyright © 2005 Taylor & Francis Group plc, London, UK



driven tunnel under the hill Valik. The tunnel is the dominant and crucial part of this construction.

2 GEOLOGICAL AND HYDROGEOLOGICAL CONDITIONS

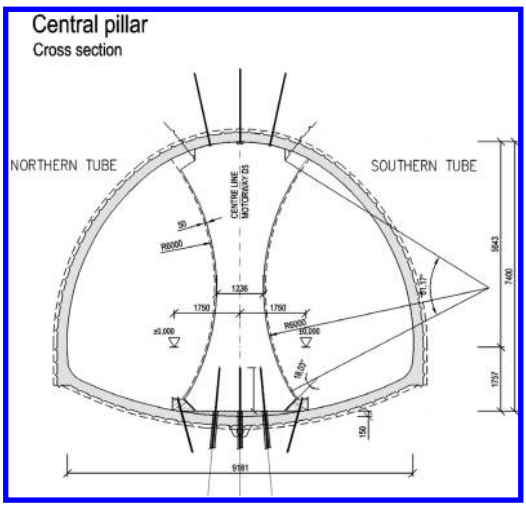
The hill Valik that is situated approx. 2 km north-east from village Štěnovice and 2 km south-west from Černice is from geological point of view created by slightly metamorphed proterozoic slate (moslty filets), strongly and intensively rough, weathered with clay-filled cracks of mostly up to 2 mm width. Encountered crack system in the explorary gallery signalises a high danger of overbreaks and falls of rock in the roof and sides. We can say that structural rock features (crack-to-space-volume ratio, size of rock pieces, solidity characteristics of cracks) determine excavation and stable ratios mostly in the fourth and fifth technological class of the New Austrian Tunneling Method (rock class NATM).

Hydrogeological conditions are rather convenient. We can assume that the boring of motorway tunnels will run in dry rock environment. Thin groundwater seepages in invert can be assumed only in the middle part of the tunnel in the chainage approx. 150–190 m.

Already during preparatory exploratory works and the processing of documentation for construction assignment, the board of geotechnical monitoring was working. The board coordinated exploratory and design works and nowadays it continues in its work during the whole tunnel boring.

3 TECHNOLOGY OF CONSTRUCTION

The construction technology of Valík tunnel is based on the principle of New Austrian Tunneling Method (NATM). Because of the aggravated geology and on



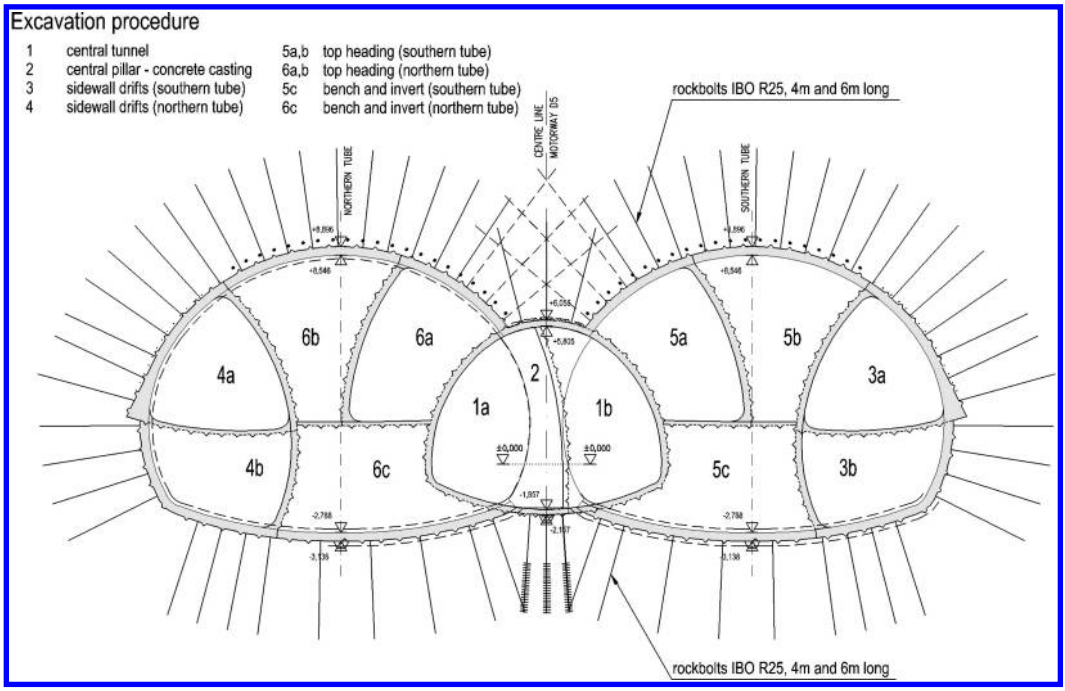
the basis of exploratory gallery results a new vertical excavation sequencing is designed. The primary lining is made from sprayed concrete that is strengthened by lattice girders and by the system of anchors and forepoling.

Under and above the central pillar the part of rock environment is strenghtened by anchors, micropiles and control cement grouting. The inner tunnel lining is reinforced concrete, cast in-situ, with intermediate waterproofing umbrella isolation. Moreover, "vivid" model of geotechnical monitoring is also a part of construction management, that is run by a company independent of the contactor. Constistenly an observation method is used.

4 CONSTRUCTION MANAGEMENT

The construction is pursued on the principle of an observation method, in which original (basic) proposal

Copyright © 2005 Taylor & Francis Group plc, London, UK



of the construction is continuously judged and can be changed even during the construction. The basic construction solutions are designed, including the range of reconstruction. Moreover, the limits of behaviour, e.g. deformation settlements of overburden, convergence etc., are determinated. The upfront solution (project and material as well) has been prepared earlier to replace the original solution in case of necessity. The detailed design of geotechnical measuring, including limits and trends, has been elaborated. In the construction, the responsible relationship of all participants is elaborated and approved. These participants have got competences and also communication means. They are able to react quickly as a team in case of exceeding of fixed limits of behaviour, which signalize an insufficiency of basic solution and call for its replenishment or replacement by upfront solutions. In the construction, the "Board of geotechnical monitoring" works under leadership of construction designer. The Board has clearly fixed competences and rights.

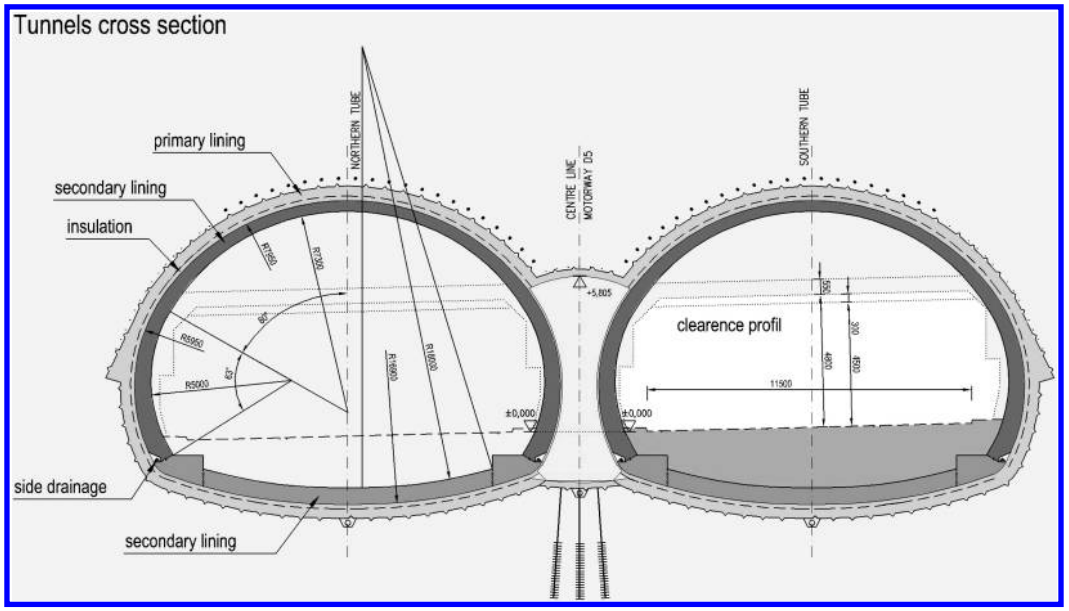
5 THE STATIC SOLUTION

The geological conditions are much worse than the building permit's design expected. Therefore, two independent static calculations were elaborated for the documentation of the construction assignment. These calculations were judged by an expert of Czech Highway Directorate. On the basis of expert opinion of Czech Highway Directorate, the third control static calculation was elaborated.

Static and stabilizing solution revealed all general features, especially from a view of process of the construction and support of individual rock classes. Moreover, it confirmed the reliability of designed size of central, highly loaded pillar. The area of failure is concentrated in the area between the tunnels above the central pillar, in the area in bedrock of the pillar in the right tunnel and the contact place of the pillar and invert, in the area of the left connection of invert and the side of the left tunnel. These areas will be needed to strengthen by grouting and anchors. During the construction it will be necessary to consistently use the system of safety umbrellas.

The first static and stability solution was carried out with the help of programme system PHASES 2.2 by the finite element method with the use of propability approach with the settlement of preliminary and output quantities of the solution. The second static calculation was realized in the programme PLAXIS for different combinations of preliminary parametres in the way that it is possible to optimize the proposal of preliminary tunnel lining with the regard of high variability of rock environment. The static calculations were realized in two professional workplaces in Prague and Ostrava.

Copyright © 2005 Taylor & Francis Group plc, London, UK



6 TECHNOLOGICAL FACILITY

The construction of the tunnel is equipped by extensive technological facilities in the terms of Czech technical norms for technology of tunnel facilities together with incorporation of other requirements, especially from Police of the Czech republic and Fire Brigade. The requirements concern especially air piping, tunnel lighting, radio connection, managing system of transport and technology, electric fire signalization, electronic safety signalization, fire tunnel duct with water source, etc.

7 PREPARATORY WORKS

For security of sensitive intervention to surrounding environment, passportization of wood and buildings in the zone of danger (especially cottages in cottage settlement V Americe) will be secured already before the opening of the tunnel construction. Furthermore, the monitoring of water level in wells will continue. In case of its serious fall the contractor will guarantee the well deepening or spare bores – if this method is effective. In case of total water loss the other compensation method of water source will be proposed – in accord with the water law.

For objective public informedness there will be the information system for public contact in the facilities of the contractor. A conference room together with pemanent exhibion for public is the part of information center. The exhibition includes promotional informative material for interested persons. For announced public (excursion, groups) the information center provides professional commentary with movie projection of tunnel boring and other technically interesting construction details.

8 THE TUNNEL SECURITY

Tunnel Valík fulfill "wefewfe". This directive newly regulates preventive measures and measures providing minimal security rate in case of accidents in the tunnel. Each tunnel, whose design has not been approved yet by an administrative body during 18 months after legal efficiancy of the directive, has to fulfill this directive.

The tunnel is only 380 m long, however, it has planned high intensity of transport, total 13250 vehicles a day in one direction. This number includes 3200 heavy goods vehicles (data for year 2020). Tunnel has two tubes, oneway and sorted in the class I. The construction measures, technological facility including independent fire driveways and emergency exits fulfill all safety criteria.

In the sense of this directive the administrative body will have to appoint a tunnel manager (public or private body) who will be responsible for tunnel operation. This body will elaborate explanatory reports for each important event or accident that will happen in the tunnel. For each tunnel a tunnel manager will appoint

Copyright © 2005 Taylor & Francis Group plc, London, UK

a security worker who will look after all preventive and security measures for ensuring security of users and operational personnel.

A security worker can be a member of tunnel personnel of emergency units (firemen, police), however he has to be independent in all questions regarding tunnel security. Moreover, a security workers must not be subjected to any orders from the employer in the security questions. A security worker can be responsible even for several tunnels in the region.

A security worker will pursue the following functions:

- he plans the organization of an intervention of emergency units, including operational schemas,
- he plans, realizes and evaluates safety operations,
- he takes part in the planning of safety schemas,
- he trains operational nad safety personnel, organizes regular practise,
- he looks after the maintanence, repairs of tunnel equipment and facility.

For tunnel Valík the detailed work order will be elaborated as a part of documentation of construction realization. The working system will intimately provide solutions for security operation of tunnel Valík.

9 OPERATION ORDER PRINCIPLES

Operation order priciples were elaborated for the tunnel Valík as a companion documentation of assigned construction documentation.

This documentation only deals with operation of local unmanned dispatching near Rozvadov portal, which is a regional dispatching for management of tunnel in Svojkovice. The tunnel Valík will be fully run by employees of Police of the Czech republic. Technical employees of Czech Highway Directorate will maintan the facility.

Tunnel is equipped by technological facility that serves for increasing of security in tunnel operation and for decreasing transport risk. Selected important functions are collectively processed in tunnel subcentral office placed near a portal Rozvadov and moreover they are centrally archived and run by the operating service situated in the Maintenance Highway Service Centre in Svojkovice in the building of Police of the Czech Republic. There is only one operation service workplace that consists of several rooms equipped by appropriate technics, technological and social background for the operation.

The proposal of transport and operation order of the tunnel is also a part of the "Principles". The transport order is based on different transport situations. Basic operation alternatives are following:

- regular regime,
- special regime without the police participation,





- special regime with the police participation,
- exceptional operation,
- emergency operation.

The characteristic of critical situations of transport is intimately described in the documentation. It is mostly transport and technological excesses in the tunnel. The tunnel is equipped by transport and technological facilities that enables to run transport and technology for all alternatives of transport operation in the tunnel and in its foreground. The set of "transport situations" has been settled. The set is the basis for processing of detailed proposal of tunnel signalling.

In case the tunnel is closed, the transport will be directed to local roads in close fly-over crossings; in the direction from Prague to the fly-over crossing Černice D5 – X – 1/20, from Rozvadov to the fly-over crossing Útušice – Jih D5 – X – 1/27. By-pass routes on local roads have been discussed with the Police of the Czech Republic.

The "Plan of fire-fighting" in different parts of the tunnel has been intimately processed and discussed already in the preliminary phase. On the basis "Fire design" was necessary to finish the design of individual arrival fire roads to individual portals including fire ascending areas.

10 CONCLUSION, CURRENT STATE OF REALIZATION

Metrostav Inc. is the contractor. All design works including work design are guaranteed by Pragoprojekt

Copyright © 2005 Taylor & Francis Group plc, London, UK

Inc. Stavební geologie Praha Inc. provides geotechnical monitoring. The construction itself started by preparatory works in the fourth quarter in the year 2003. The tunnel is expected to be finished by 30. 10. 2006. Nowadays (September 2004) the central auxiliary tunnel has been bored and casting of the temporary central pillar is being made. The excavation of transport tunnels will start in the last quarter of 20.

Copyright © 2005 Taylor & Francis Group plc, London, UK

A risk based methodology for optimum tunnel configuration

Donald P. Richards
Parsons Brinckerhoff, USA

Malcolm A. Hudson
Parsons Brinckerhoff, UK

Michael Whitaker
Parsons Brinckerhoff, Dubai

ABSTRACT: In planning new underground metros, a primary concern is to optimize the tunnel configuration in terms of operational safety, construction cost and schedule and environmental impact, within the prevailing regulatory framework. With improvements in Tunnel Boring Machine technology over the last 25 years, it is now feasible to construct large diameter bored tunnels with two parallel tracks running in the same tunnel, within crowded urban areas in poor ground and high ground water conditions. However, satisfactorily undertaking this form of construction should not be considered the only governing parameter. As the completed tunnels will be used for long-term of passenger transportation, operational safety as well as maintainability should be of equal, if not of more importance than construction capability alone. This paper outlines many of the risks that should be considered, their probability of occurrence and the magnitude of their consequences should a risk event ever materialize and the impact of local regulatory requirements.

1 INTRODUCTION

1.1 *Metro planning*

In planning new underground metros, a primary concern is to optimize the tunnel configuration in terms of operational safety, initial and life cycle cost, construction schedule, and environmental impact, all within the prevailing regulatory framework. With improvements in Tunnel Boring Machine technology over the last 25 years, it is now both technically and commercially feasible to construct large diameter bored tunnels with two parallel tracks running in the same tunnel, within crowded urban areas with poor ground and high ground water conditions. However, the ability to satisfactorily undertake this form of construction, should not be considered the only governing parameter. Since the completed tunnels will be used for long-term transportation of passengers in a safe and efficient manner, operational safety as well as maintainability should be of equal, if not of more importance than construction capability alone.

Operational safety of an underground Metro system is subject to different standards and guidelines, depending on the country in which it is built. In undertaking the evaluation of whether to adopt twin-tube single track parallel tunnels or a mono-tube double track tunnel, the design, construction and operations risks should all be considered from both a civil and systems engineering and a regulatory perspective. This regulatory framework has led to various tunnel configurations in a number of countries as shown in Table 1.

This paper outlines many of the types of operational risks that should be considered as well as a method of rating the risks for their potential impact on the project, considering their probability of occurrence and the magnitude of their consequences should a risk event ever materialize. It considers the one form of regulatory framework as well as a discussion of perceived differences between this, EU Countries and the U.S.

1.2 *Use of risk assessments: qualitative versus quantitative*

For planning purposes, it is considered adequate to perform preliminary risk assessments using a more qualitative rather than quantitative approach, since many project details are not sufficiently defined to justify quantitative methodologies requiring input of detailed project information. Once a project advances

Copyright © 2005 Taylor & Francis Group plc, London, UK

Table 1. Tunneling configuration adopted on recent Metro systems in Europe.

Method	Location	Configuration
Twin tube	London	Jubilee Line Extension opened in 1999. Bored single-track tunnels.
	Munich	5.74 m diameter bored single track tunnel with cut-and-cover.
	Nuremberg	Cut and cover, some bored single track.
	Vienna	Partly single track bored, partly double track cut-and-cover.
	Copenhagen	Bored single track tunnels.
Mono tube	Paris	Meteor line opened in 1998. First section of line in twin track tunnel
	Toulouse	Fully automated unmanned rubber tyred metro, twin track tunnel
	Athens	Lines 2 and 3 were opened in January 2000. Twin track tunnel.
	Barcelona	Line 9 total length 42.5 km of which 34 k. are underground. Twin track with partial vertical separation.
	Lyon	"Magally" system runs in twin track tunnels.
	Madrid	Metrosur and Line 10 extension with 27 km generally mono tube tunnels.

into the preliminary engineering phase of development, more sophisticated statistical approaches are justified.

2 OVERVIEW

2.1 *Regulatory requirements in UK and elsewhere*

Specific directives for railways in Europe apply basically to regional railway systems while urban underground systems are subject to local regulations. In European countries, safety certification is either subject to self-certification by the transit agency or compliance with country laws such as the UK requiring the submission of safety cases which require risk assessment and cost benefit analyses which show that all risks are either ALARP (As Low As Reasonably Practicable) or mitigated to this level at reasonable cost. See Table 2 for an overview of these requirements.

Table 2. Regional railway legislation.

System	Configuration	Reasons
European Heavy Rail	Up to 1 km can be mono/twin. Beyond 1 km subject to specific requirements	European Codex 779-9 relates only to regional railways. See Codex Item I 20
European Urban Transit	Should Comply with Local Policy	No European Directive
UK Railways Systems	Must Satisfy UK Health & Safety Requirements	UK Law
Irish Railway Systems	Must Satisfy Irish Health & Safety Requirements	Irish Law: must comply with Railway Order requirements.
USA Urban Transit	Self Certification Subject to State Safety Oversight	See FTA "Handbook for Transit Safety" & Security Certification

3 RISK ASSESSMENT FOR TUNNEL CONFIGURATION

The bored tunnel risk assessment considered three tunnel configuration arrangements:

1. Twin tube tunnels with single track;
2. Monotube tunnel with two tracks; and
3. Monotube with two tracks and central dividing wall.

Figure 1 shows a single-track twin tube 5.6 m diameter tunnel cross-section. The tunnel centreline is the same as the track centreline. The tunnel structure would typically be constructed of a pre-cast concrete segmental lining. A passenger walkway is provided along the inner wall of each tunnel in accordance with the Irish Draft Guidelines for the Design and Construction of Railway Infrastructure and Rolling Stock. Access to a place of safety is provided by cross passages between the two tunnels, spaced according to regulatory requirements.

Figure 2 shows a typical cross section of a monotube double track 8.5 m diameter tunnel with tracks positioned side by side. The tunnel structure would typically be constructed of pre-cast concrete segmental lining without a central wall. The centreline of the tunnel lies between the two tracks with passenger walkways located along the sidewalls. Access to a place of safety is provided by vertical shafts to the surface, again spaced according to regulatory requirements.

Figure 3 shows the monotube tunnel with the provision of a vertical central dividing wall. Construction is similar to the Figure 2 scenario, but the diameter

Copyright © 2005 Taylor & Francis Group plc, London, UK

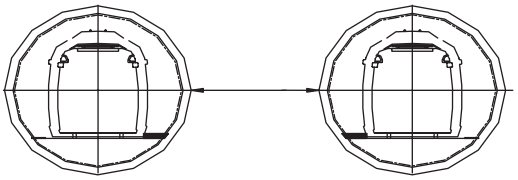


Figure 1. Twin tube tunnel configuration – nominal 5.6 m twin tube tunnels.

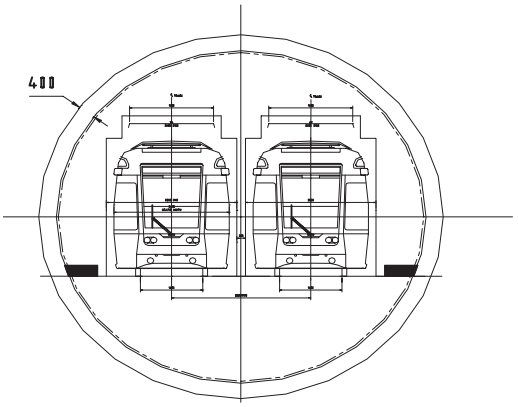


Figure 2. Mono tube tunnel configuration – nominal 8.5 m twin track tunnel – no central wall.

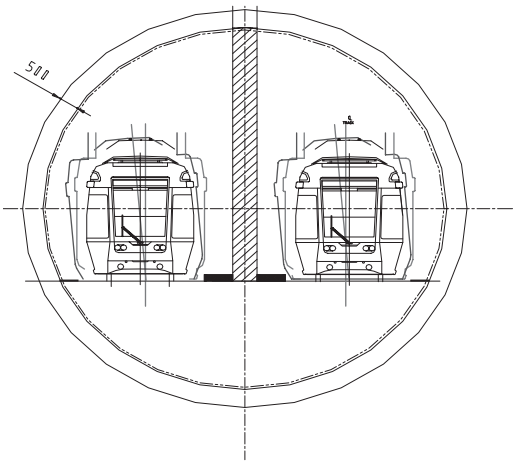


Figure 3. Mono tube tunnel configuration – nominal 10 m mono tube tunnel with central wall.

of the tunnel increases to 10 m to accommodate the central wall. Walkways are positioned in the centre of the tunnel along each side of the dividing wall leading to access points through the wall, thus providing a place of safety on each side of the wall.

4 DESCRIPTION OF RISK CONCEPTS

The acceptance of risk (i.e., a tolerable rate of dangerous failures) is based on defined principles and standards. ALARP (As Low As Reasonably Practicable) is the method used when collective risks are considered. This means that all risks affecting all persons using the system and the environment are taken into account.

The ALARP principle classifies risks according to frequency and severity. For example, for each different class of possible accidents, a maximum allowable upper limit of risk is defined which must not be exceeded. Above this limit risks are “Intolerable” and risk reducing mitigation measures must be implemented. Below this limit, and extending to a lower limit beyond which risks are “Tolerable” is the region of ALARP risk. In the ALARP range, mitigation measures should also be undertaken, but normally only if they are economically justified.

For an underground Metro system risk assessment, a multi-disciplinary team of experienced, independent professionals should be convened, each representing worldwide twin tube and monotube tunneling experience in design, construction and operation.

For purposes of a Risk Assessment Workshop, the participants should be divided into at least three teams to correspond with different phases of the project – design, construction, and system operation. As a first step, each group should identify and agree upon on the risks to be considered, ratings to be assigned and the appropriate mitigation measures required.

Following the risk assessment workshop, mitigation costs for all risks determined to be in the Intolerable and ALARP categories should be developed. In order to make informed decisions regarding implementation of mitigation measures, cost benefit assessment in the planning phase is usually limited, and restricted to (a) ALARP risks, since mitigation of all intolerable risks is mandatory; and (b) systems operations risks, because of the high priority usually given to systems performance and passenger safety.

During this process the risk assessment report evolved based on review comments from RPA and the workshop participants.

5 METHODOLOGY FOR RISK ASSESSMENT FOR TUNNEL CONFIGURATION

For the preliminary planning phase of a project, the risk assessment can be based on the tunnel section only without consideration of the risk inherent in other structures. All risks deemed pertinent to the operational safety case for the tunnel should be considered. Environmental, regulatory, contractual, legal, commercial, financial and property availability issues, which

Copyright © 2005 Taylor & Francis Group plc, London, UK

were deemed not to be relevant to the safety case, need not be considered in the planning phase.

While these limitations are important they are not expected to affect the choice of tunnel configuration based on safety, but should be considered in deciding on the overall acceptability of the three tunneling scenarios. The risk register for the assessment of bored tunnel methods should include all pertinent risks such as:

1. Systems risks – covering the rolling stock and electrical and mechanical systems
2. Civil risks – covering the physical infrastructure.

For the purposes of this presentation, civil risks are excluded since operational safety is the key issue in selecting a final tunnel configuration. These systems risks were then further subdivided into the three project phases:

1. Design
2. Construction
3. Operations.

The risk workshop participants should then rate each risk in terms of probability of occurrence and severity for each of the three tunnel scenarios: twin tube (T), monotube (M) and monotube with divider wall (M/D). The rating designations were: Intolerable (I); ALARP High A (H); ALARP Low A (L); and Tolerable. The risk model can be represented by:

$$R = F \times C$$

R = Risk Rating
F = Frequency of Occurrence
C = Magnitude of Consequences

The probability of occurrence for systems risks should be considered as:

1 = Improbable, extremely unlikely; Improbable: 1 in 100 years
2 = Remote chance of occurrence; 1 in 1000 projects; Probability: 1 in 50 years
3 = Occasional, or likely to occur; 1 in 100 projects; Probability: 1 in 10 years
4 = Probable, multiple occurrences; 1 in 10 projects; Probability: 1 in 5 years
5 = Frequent occurrences likely; Occurs every project; Probability: Once per year.

The severity of the consequences should be considered as:

1. Insignificant
   - No operational delays expected
   - No extra costs
   - No lost time injuries
2. Minor
   - Operational delays of hours expected
   - Extra costs easily accommodated
   - Potential for serious injury
3. Significant
   - Operational delay <1 day expected
   - Costs may be significant
   - Potential for a fatality
4. Major
   - Operational delay <1 week expected
   - Substantial cost impact likely
   - Single fatality likely
5. Catastrophic
   - Operational delay of weeks or months
   - Cost impact excessive
   - Multiple fatalities likely

For evaluation of mitigation measure requirements, the risk ratings were categorized as:

- Tolerable; R = 1–6
- ALARP; R = 8–12
- Intolerable; R = 15–25

6 MAJOR RISKS

As a reference case history, a study conducted for planning of the Dublin Metro will be considered. In that risk evaluation, the systems risks identified, as they relate to operational safety, included 17 design risks, 9 construction term risks and 40 operational risks. The major risks ($R > 15$) were:

Design
- Unauthorized access control
- Excessive electromagnetic interference
- Inadequate stray current protection

Construction
- None were considered critical

Operations
- Tunnel/Train Fire
- Inadequate emergency response plan
- Tunnel/station flooding
- Security – vandalism/urban violence
- Inadequate maintenance

7 RISK MITIGATION

For Dublin Metro systems, mitigation measures were considered for Intolerable risks, and the higher ALARP risks. For the risks considered for mitigation, several mitigation measures were recurrent for a solution to reducing a number of different risks.

The provision of platform screen doors occurs repeatedly as a mitigation measure for many of the key risks (e.g., vandalism, unauthorized access, passenger train interface). In the cost-benefit analysis this measure was considered to significantly reduce the risk of platform train interface hazards by a factor of 10.

Copyright © 2005 Taylor & Francis Group plc, London, UK

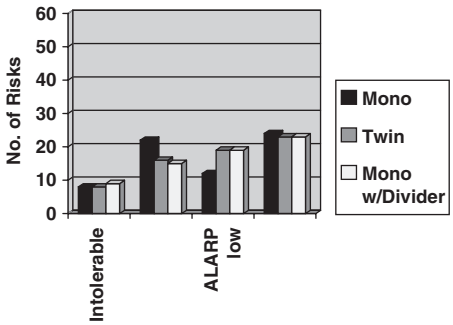


Figure 4. System risk summary – pre-mitigation.

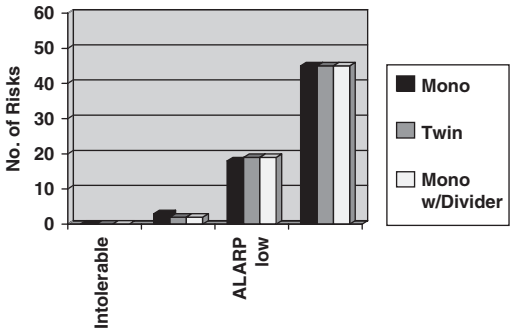


Figure 5. System risk summary – post-mitigation.

Platform screen doors could be a significant mitigation measure, but are not mandatory. The use of platform screen doors would have to be interfaced with the potential use of automatic Train Operation (ATO). It may be possible to replace ATO with an automatic train docking system at a significantly lower cost.

Tunnel fires either within the train or tunnel are one of the key risks, which can have major consequences. Mitigation measures should be designed into the system such as the provision of an escape walkway (benches), tunnel ventilation, material and equipment selection, minimizing train fire load and fire detection and suppression facilities.

Figure 4 shows the systems assessment results prior to mitigation of risk.

Figure 5 shows that after mitigation, the systems assessment results in all options being relatively risk equal and constructible with acceptable risks.

8 COST BENEFIT ANALYSES

Cost benefit evaluations were conducted only for systems related risk mitigation measures for the long-term performance stage of the project. In addition, they were limited to the ALARP risks, as mitigation measures for Intolerable risks are considered mandatory, not optional.

Metro accident statistics were collected and analysed to determine the potential safety benefits of the identified mitigation measures. The risk to the Dublin Metro tunnel section was estimated from both London Underground risk data and US transit accident statistics by scaling the operational services level (train miles).

For the major systems mitigation measures considered, the cost/benefit results are included in Table 3.

At this stage of the project, the "apparent" findings should be considered somewhat preliminary in nature for the following reasons:

1. There is an inherent uncertainty in carrying out quantitative cost/benefit analyses at this early stage of a project due to lack of detailed back-up information.
2. The analysis results presented do not reflect costs associated with damage to the infrastructure or loss of operation as a result of an incident.
3. They do not reflect the additional cost of enlarging the mono-tube tunnel sufficient to accommodate the central dividing wall.

9 CONCLUSIONS AND THEIR RELEVANCE TO OTHER REGULATORY SYSTEMS

1. All tunnel configuration options, based upon the Dublin case, are considered approximately risk equal after risk mitigation measures are applied.
2. A monotube tunnel with a centre wall could not be justified from a cost/benefit perspective due to the short length of tunnel. Because of the increased tunnel diameter, the station width and depth also must increase and the overall capital cost is likely to exceed the cost of a twin tube system.
3. Mitigation measures, both mandatory and optional (but desirable from cost/benefit perspective) in the ALARP category, should be included in the project design scope, and adjustments made to the construction cost and risk contingency cost estimates.
4. The decision on tunnel configuration must ultimately be acceptable to the local and regional regulatory agencies regarding railway safety. In the case of Dublin Metro, the over riding concern was emergency services access distance from a place of safety, tunnel ventilation efficiency in a fire scenario and reduction of collision risk in tunnel. Thus, the twin tube configuration was considered to best perform against these parameters.
5. The over-riding underground Metro operational concerns related to fire in the tunnel and train collision and these two issues predominated in the final decision on Dublin Metro tunnel configuration. Resolution of these concerns under other regulatory philosophy, could be considered, to be also offered

Copyright © 2005 Taylor & Francis Group plc, London, UK

Table 3. Cost benefit results – systems performance ALARP mitigations.

Mitigation measures safety benefits	CPF €m	1. year	CPF €m/ year	2. per year	VPF € per year	PF
Platform screen doors						
Reduces train/platform accidents				5.3E−2		
Collisions with people				4.3E−2		
	10.0	25	0.3	9.7E−2	1.6E+5	2.5
Central Kerb – derailment containment						
Reduces derailment consequences				1.9E−2		
Reduces collision potential				3.0E−3		
	4.0	100	0.04	2.3E−2	3.8E+4	1.1
Central Divider wall						
Reduces derailment impact				2.0E−2		
Reduces derailment collision potential				3.0E−3		
Reduces tunnel fire consequence				9.2E−4		
	15	100	0.15	2.4E−2	3.9E+4	3.9
Tunnel Portal fencing						
Reduces accident potential	0.05	25	1.8E+3	3.2E−3	5.2E+3	0.4

CPF: Cost of preventing fatality.
VPF: Value of preventing a fatality.
PF: Proportion factor.
1.: Operational life.
2.: Reduction in average fatalities assessed by mitigation.

by the monotube. It is therefore considered that the basis for a decision on tunnel configuration is dependent on experience of local operating systems and consideration of emergency scenarios which sets the weighting of safety risks.

ACKNOWLEDGEMENTS

The authors would like to thank and acknowledge the contributions of all of their professional colleagues from Parsons Brinckerhoff in the US, UK, and Ireland, and from Franklin & Andrews in Ireland. In addition, they would like to thank Mr. Henri Frey for contributing his "continental" European perspective. Last but not least they would like to thank their professional colleagues at both the Railway Procurement Agency in Dublin, and the Irish Department of Transport – Interim Railway Safety Commission in Blackrock, for their continued support and constructive criticism during the execution of the study on which this paper is based.

REFERENCES

Ad hoc Meeting of the Multidisciplinary Group of Experts on Safety in Tunnels (rail) (Second Session, 25–26 November 2002, agenda item 3) High Speed Line South: Safety Concept – Green Heart Tunnel, Informal Document No 10.

Andersen, T. and Paaske, B.J., Safety in railway tunnels and selection of tunnel concept.

British Standards Institution, 2001, Project Risk Management – Application Guidelines, BS IEC 62198, London.

Draft Guidelines for the Design and Construction of Railway Infrastructure and Rolling Stock, (Guidance to Railway Safety Act, 2002). Department of Transport, Ireland.

FTA Handbook for Transit Safety & Security Certification.

Harris, Miller, Miller & Hanson Inc., 1995, Transit Noise and Vibration Impact Assessment – Final Report, U.S. Dept. of Transportation Report DOT-T-95-16.

HSE "HID's Approach To 'As Low As Reasonably Practicable' (ALARP) Decisions" (SPC/PERMISSIONING/09).

HSE Guidance On 'As Low As Reasonably Practicable' (ALARP) Decisions In Control Of Major Accident Hazards (COMAH)-(SPC/PERMISSIONING/12).

HSC 2001 The joint Inquiry into Train Protection System

HSE 2002 Nuclear Safety Directorate Demonstration Of ALARP – Executive Summary T/AST/005.

HSE (2001) Reducing risk and protecting people.

International Association of Public Transport, 2003, Fire Prevention and Fire Fighting in Metros.

UIC Leaflet, UIC 779-9 R Safety in Railway Tunnels.

United Nations Economic and Social Council, Economic Commission for Europe, Inland Transport Committee, Ad Hoc Multidisciplinary Group of Experts on Safety in Tunnels (Rail), 2003, Third Draft of the Recommendations of the Multidisciplinary Group of Experts on Safety in Tunnels (Rail), July.

United Nations Economic and Social Council, Economic Commission for Europe, Inland Transport Committee, European Codex, 779-9 Safety in Tunnels.

Vlasov, S.N., Makovsky, L.V. and Merkin, V.E. 2001, Accidents in Transportation and Subway Tunnels – Construction to Operation, ELEX-KM Publishers, Moscow.

Copyright © 2005 Taylor & Francis Group plc, London, UK

Effect of ground water on tunnel face stability in the soft ground

S. Konishi & T. Ono
Railway Technical Research Institute, Japan

T. Kitagawa, H. Iida & A. Isogai
Japan Railway Construction, Transport and Technology Agency, Japan

T. Matsunaga
Pacific Consultants Co., Ltd, Japan

ABSTRACT: The Sambongihara tunnel, a double-track Shinkansen tunnel, is now construction to a small overburden in the soft ground by the shotcrete tunneling method or the so-called New Austrian Tunneling Method (NATM). At the construction site, the ground water level is high throughout the whole section, and the ground near the tunnel face is a sandy soil with a clay layer, whose position at the face varies as the tunnel construction work advances. The ground water flows both in the lower and upper sandy layers separated by the clay layer. Therefore, deep well method is adopted to lower the ground water level, since the ground water level normally has significant influence on the stability of the tunnel face. However, it is difficult to lower the ground water level in the upper sandy layer. This paper describes an outline of this tunnel, measurements of the groundwater level, results of face observation, results of the simulation analysis based on the plastic theory, or the so-called rigid plastic finite element analysis (RPFEA), and discusses the influence of groundwater level and conditions of ground layer on the tunnel face stability.

1 INTRODUCTION

To ensure the tunnel face stability, which is normally subjected to the influence of ground water, it is effective to lower the ground water level for tunnels constructed below the ground water level.

This paper describes a method to evaluate the tunnel face stability by rigid plastic finite element analysis (RPFEA) giving consideration to the effects obtained by the above-mentioned method. In the analysis, the effect of ground water on the tunnel face is expressed by applying a water pressure as a force on the ground.

2 CONSTRUCTING PROGRESS OF SAMBONGIHARA TUNNEL

2.1 *Outline of tunnel construction*

Tohoku-Shinkansen is planed along the 675 km-route from Tokyo to Shin-Aomori, of which the section between Tokyo and Hachinohe has already been put in service. Construction work is now in full swing to extend Tohoku-Shinkansen from Hachinohe to Shin-Aomori (82 km-route).

Twelve shallow tunnels have been planed or constructed in the soft ground between Hachinohe and Hakkoda Tunnel. Some of double- track Shinkansen tunnels are now under construction in the soft ground by the shotcrete tunneling method or the so-called New Austrian Tunneling Method (NATM). Among these tunnels, the 4,280 m-long Sambongihara Tunnel has an excavation width of 10.5 m and faces as high as 5.25 m at the upper half section. The overburden of the tunnel is about 23 m on an average, and 45 m at the maximum (Figure 1).

The geology near this tunnel is mainly composed of sandy soil, and alternation of strata is formed of

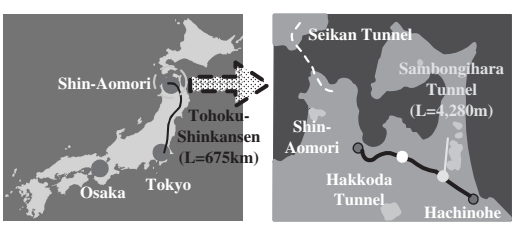


Figure 1. Location of Sambongihara tunnel.

Copyright © 2005 Taylor & Francis Group plc, London, UK

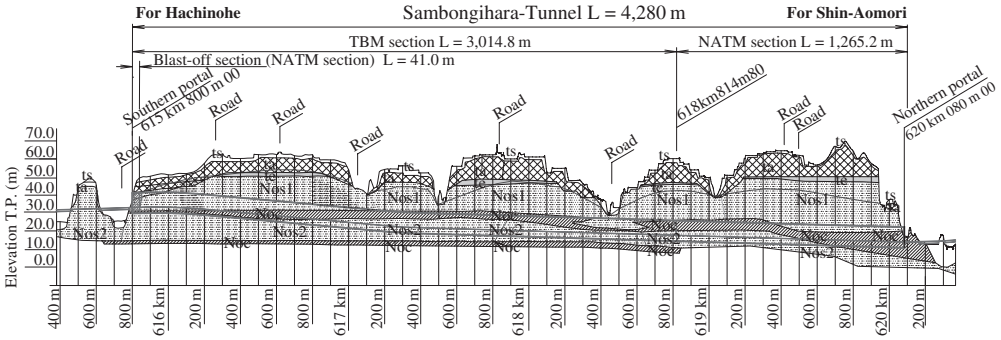
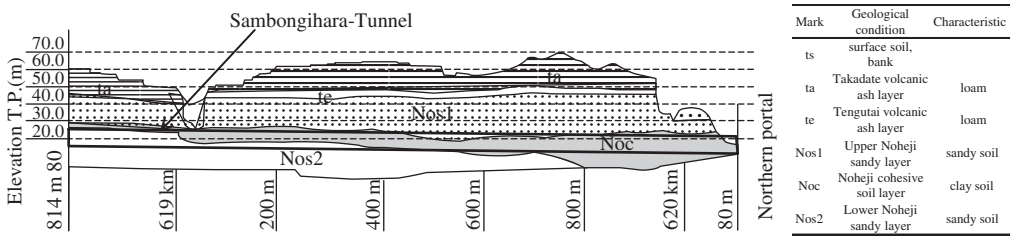


Figure 2. Geological profile of the Sambongihara-tunnel.



Mark	Geological condition	Characteristic
ts	surface soil, bank	
ta	Takadate volcanic ash layer	loam
te	Tengutai volcanic ash layer	loam
Nos1	Upper Noheji sandy layer	sandy soil
Noc	Noheji cohesive soil layer	clay soil
Nos2	Lower Noheji sandy layer	sandy soil

Figure 3. Geological profile of the Sambongihara tunnel (NATM section).

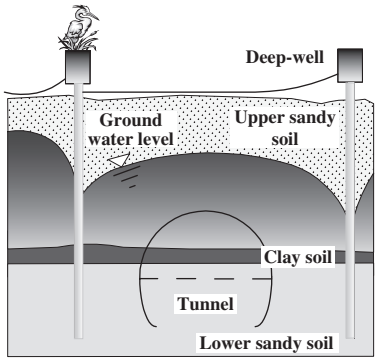


Figure 4. Situation of the actual tunnel.

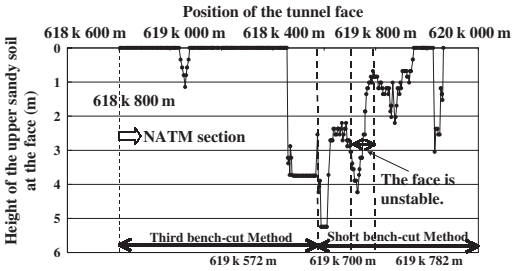


Figure 5. Relationship between the height of the upper sandy soil at face and the excavating pattern.

sandy soil and clay soil at the tunnel face (Figure 2 and Figure 3). The problems involved in the construction work are the flow of sandy soil; the ground water level of about 15 m above the tunnel crown; the fine fraction contents of 3 to 30%; and the uniformity coefficient of 1 to 9. In order to lower the ground water level near the face, therefore, this tunnel is excavated with the deep well method simultaneously applied.

2.2 *Tunnel face*

The ground near the tunnel face is sandy with a clay layer, whose position at the face varies as the tunnel

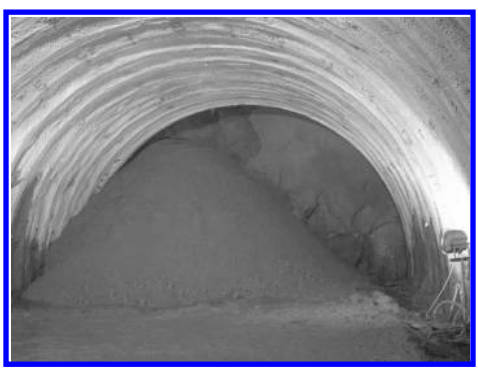


Figure 6. View of the face collapse.

Copyright © 2005 Taylor & Francis Group plc, London, UK

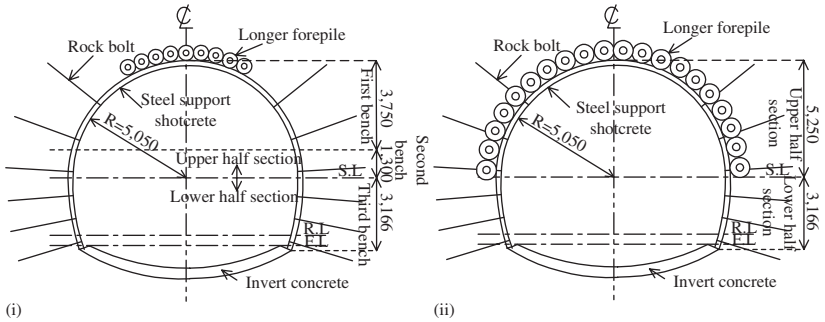


Figure 7. Excavating patterns. (i) Third bench-cut method, (ii) Short bench-cut method.



Figure 8. Excavation. (i) Longer forepile, (ii) Third bench-cut method.



Figure 9. Pumping well.

construction work advances (Figure 4). Moreover, the upper sandy soil was heterogeneous whereas the lower soil was homogeneous. Under these conditions, the ground water level in the lower sandy layer was fully lowered by the deep well method. However, it was difficult to lower the ground water level in the upper sandy layer. The face was unstable, in particular, where the upper sandy soil was high at the face (Figure 5). Small degrees of face collapse occurred twice in the tunnel, since the ground water level normally has significant influence on the stability of the tunnel face (Figure 6). Fortunately, however, nobody was injured, since the face conditions were sufficiently monitored and evaluated.

Longer forepiles were used instead of short forepiles to ensure the stability of the crown. Additionally, the tunnel was excavated by the third bench-cut method instead of the short bench cut method to lower the height of the face to maintain stability of the face (Figure 7 and Figure 8).

2.3 *Ground water lowering method*

For the shotcrete tunneling method, it is important to lower the ground water level near the tunnel face before excavation because the face is open.

In the tunnel, pumping wells bored by the deep well method are located at intervals of 20 m toward the tunnel axis in zigzags, at the distance of 10 m from each tunnel side. Additionally, observation wells are located on their fringe for monitoring fluctuation of the ground water level (Figure 9 and Figure 10).

The ground water level was lowered almost linearly before the face approach the pumping well. However, the ground water level was lowered only at the crown of tunnel (Figure 11).

2.4 *Study of the face stability*

The characteristics of the upper sandy layer are as follows.

- The position at the face varies as the tunnel construction work advances.
- The ground is heterogeneous.
- The ground is easy to collapse due to the ground water.
- It is difficult to lower the ground water level in the layer.

The upper sandy soil exists over the entire face where the clay layer is positioned at the foot of the upper half section. Therefore, the water pressure by the ground water in the soil works on the face, to make the face significantly unstable.

Consequently, the stability of the face is studied based on the relationship between the height of the sandy soil on the face and the ground water level

Copyright © 2005 Taylor & Francis Group plc, London, UK

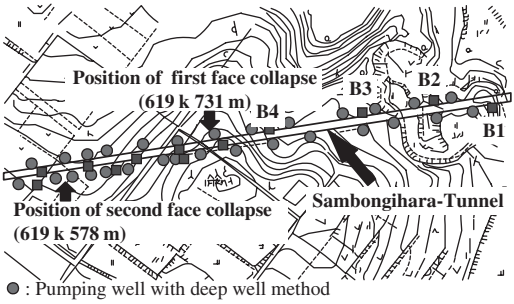


Figure 10. Location of the pumping wells and observation wells.

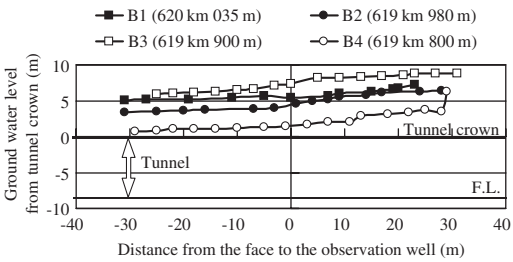


Figure 11. Relationship between ground water level and tunnel advances.

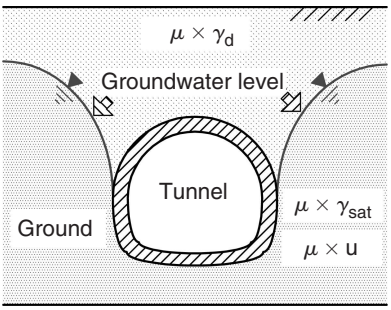
which is calculated by RPFEA giving consideration to the effect of the ground water.

3 SIMULATION ANALYSIS

3.1 *Rigid plastic finite element analysis*

Rigid plastic finite element analysis (RPFEA) pays attention only to the plastic state on the ground, and uses the upper bound theorem. Limited analysis is formulated by applying the FEA based on the plastic theory with this analysis. The method has attracted attention in the field of metal processing for the express purpose of calculating the magnitude of the force to process the metal (Hayes and Marcal, 1967; Kobayashi et al. 1973; Mori et al. 1979). In the geotechnical engineering, it can also be used as the analysis method in order to evaluate slope stability, stability of tunnel face and bearing capacity.

The method expresses only the state of the moment when plastic strain of the ground increases rapidly, or the state of the moment when the ground begins to break, and has some merits as shown below (Tamura et al. 1999; Konishi et al. 2000, 2002).



Here

γ_d : Unit weight of soil above the ground water level

$\gamma_d = \rho_d g$

γ_{sat} : Unit weight of soil under the ground water level

$$\gamma_{sat} = \frac{\rho_s - \rho_w}{1+e} g$$

ρ_d : Dry density of soil

ρ_s : Density of saturated soil

e : Void ratio

Figure 12. Change with unit weight of soil due to the change in the ground water.

– The elastic coefficient, which is useless under the critical state, is unnecessary.
– The method can well express the elastic flow near the critical state, of which errors become large with an elasto-plastic model.
– The initial stress is not required.

RPFEA is applied with the Drucker-Prager criterion by assuming the associated flow rule. The unit weight of soil and water-pressure are treated as body forces.

In the analyses, the following three factors are taken into account (Konishi et al. 2002).

– Change in the unit weight of soil due to the change in the ground water level (Figure 12).
– Change in the effective stress due to the change in the unit weight of soil and pore water pressure.
– Strength of the ground due to the change in the effective stress.

The stability of tunnel face is evaluated by acceleration μg as a face collapse occurs. The value of μg, in which g is the acceleration of gravity and μ is the load factor, is calculated by RPFEA. The method has the same test concept of tunnel face stability as that of the centrifuge test machine (Schofield, 1980). Not only the unit weight of soil γ but also the pore water pressure u are multiplied by the load factor μ as a face collapse occurs. The load factor μ is a measure barometer of stability. We considered that a face collapse actually occurs, when the load factor becomes $\mu \leqslant 1$. Then, we investigated the relationship between the height of

Copyright © 2005 Taylor & Francis Group plc, London, UK

face and the ground water level at a face collapse by this method.

Basic equations for the analyses are as follows (Tamura et al. 1984, 1987)

Equation of equilibrium:

$$\sigma_{ij,j} + f_i = 0 \tag{1}$$

Compatibility equation:

$$\dot{\varepsilon}_{ij} = \frac{1}{2}\left(\dot{u}_{i,j} + \dot{u}_{j,i}\right) \tag{2}$$

Stress-strain rate relation:

$$\sigma'_{ij} = \frac{\sqrt{2}k}{\sqrt{6\alpha^2 + 1}}\frac{\dot{\varepsilon}_{ij}}{\dot{\bar{e}}} + \lambda\left(\delta_{ij} + \frac{3\sqrt{2}\alpha}{\sqrt{6\alpha^2 + 1}}\frac{\dot{\varepsilon}_{ij}}{\dot{\bar{e}}}\right) \tag{3}$$

Kinematical constant:

$$\dot{\varepsilon}_{kk} + \frac{3\sqrt{2}\alpha\dot{\bar{e}}}{\sqrt{6\alpha^2 + 1}} = 0 \tag{4}$$

Constraint on the velocity on the basis of the upper boundary theorem:

$$\int_V f_i \dot{u}_i dV + \int_{S\alpha} \bar{T}_i \dot{u}_i dS = 1 \tag{5}$$

Relation between stresses and pore water pressure

$$\sigma_m{}' = \sigma_m - \mu u \tag{6}$$

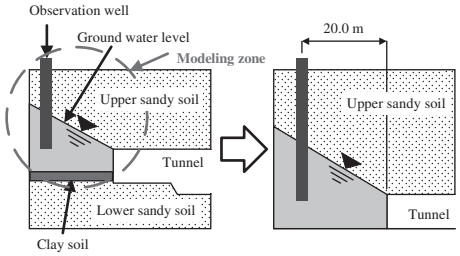
$$\sigma_{ij}{}' = s_{ij} + (\sigma_m - \mu u)\delta_{ij} \tag{7}$$

For the purpose of simplicity, we introduce the following notation:

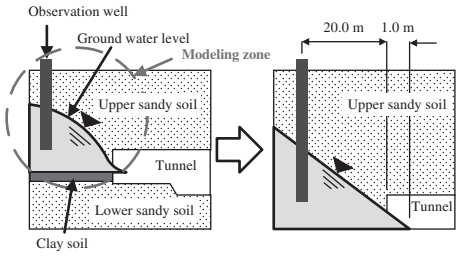
$\sigma_{ij,j}$: Total stress tensor
f_i : Nodal force
$\dot{\varepsilon}_{ij}$: Strain rate tensor
$\dot{u}_i$: Nodal velocity vector
$\sigma'_{ij,j}$: Effective stress tensor
k,α : Material constant of the Drucker-Prager criterion

$$k = \frac{\sqrt{3}c\cos\phi}{3 + \sin^2\phi},\quad \alpha = \frac{\sin\phi}{\sqrt{3\left(3 + \sin^2\phi\right)}}$$

ϕ : Internal friction angle
c : Cohesion of soil
$\bar{\dot{e}}_{ij}$: Equivalent strain rate, $\bar{\dot{e}} = \sqrt{\dot{\varepsilon}_{ij}\dot{\varepsilon}_{ij}}$
λ : Magnitude of the indeterminate component



(i)



(ii)

Figure 13. Model for analysis. (i) Ground water level is in the tunnel crown at the face (Model No. 1), (ii) Ground water level is at the lowermost level of the upper sandy soil at the 1 m point behind the face (Model No. 2).

δ_{ij} : Kronecker's delta symbol
$\dot{\varepsilon}_{kk}$: Volumetric component
$\bar{T}_i$: Surface traction
$\sigma_{m'}$: Mean principal stress
σ_m : Effective mean principal stress
s_{ij} : Principal stress difference

The critical values of $\dot{u}_i$, λ and μ are found out by these equations.

3.2 *Model for analysis*

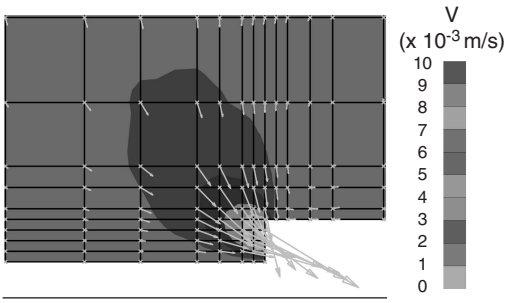
Sandy soil, in which exists above clay soil at the observation point is modeled in the RPFEA (Figure 13). Parameters for analysis are the height of upper sandy soil at tunnel face, apparent cohesion and the ground water level at the observation well. The ground water level input at the 20 m point ahead of the face, because the pumping well is located at intervals of 20 m toward the tunnel axis.

The ground water level is assumed by two types of models in this analysis.

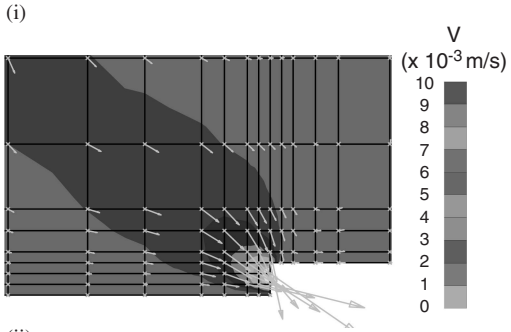
These models are as follows.

– The ground water level is assumed to be a straight line that connects the ground water level of the observation well, which is located at the 20 m point

Copyright © 2005 Taylor & Francis Group plc, London, UK



(i)



(ii)

Hw: Difference between the ground water level at the 20m point ahead of the face and level of the tunnel crown
Hf: Height of a face that can stand by itself

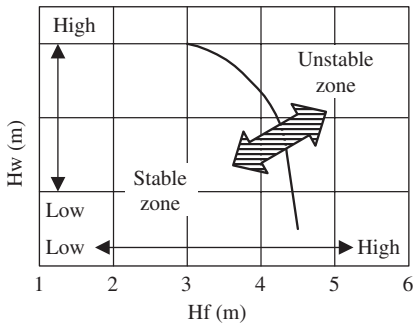
Figure 14. Velocity field at the face collapse. (i) Hf = 4 m, Hw = 0 m, (ii) Hf = 3 m, Hw = +20 m.

ahead of the face, and the tunnel crown at the face (hereinafter referred to as Model No. 1, Figure 13-i).
– The ground water level is assumed to be a straight line that connects the ground water level of the observation well, which is located at the 20 m point ahead of the face, and the lowermost level of the upper sandy soil at the 1 m point behind the face (hereinafter referred to as Model No. 2, Figure 13-ii).

Here, according to the observational results, the ground water level at the observation well is lowered almost linearly before the face approaches the observation well (Figure 10). Therefore, the ground water level is assumed to be a straight line in both models of this analysis.

3.3 *Analysis result*

Figure 14 shows some results of the analyses, and relative distributions of velocity vectors of displacement at the moment when plastic strain increases abruptly. As the ground water level becomes higher, the ground movement toward the face changes into the lateral direction.



Hw: Difference between the ground water level at the 20 m point ahead of the face and the level of the tunnel crown
Hf: Height of the face that can stand by itself

Figure 15. Concept of nomogram.

4 PROPOSAL OF A SIMPLE METHOD TO EVALUATE THE FACE STABILITY

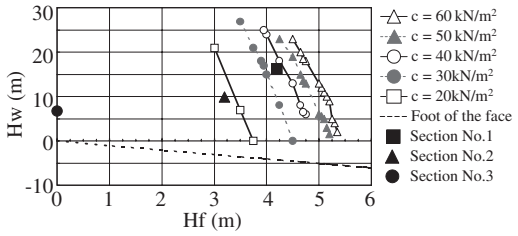
Nomograms made up based on the results of RPFEA are proposed to simply evaluate the tunnel face stability. In the nomograms, lines are indices to evaluate the face stability. The left zone shows that the face is stable, whereas the right zone shows the condition of unstability (Figure 15). Since analysis is performed by using two types of models, two nomograms is proposed (Figure 16). These nomograms are as follows.

– Nomogram No. 1 is made up based on analysis results by using Model No. 1 (hereinafter referred to as Nomogram No. 1, Figure 16-i).
– Nomogram No. 2 is made up based on analysis results by using Model No. 2 (hereinafter referred to as Nomogram No. 2, Figure 16-ii).

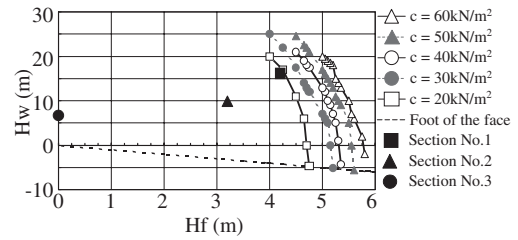
Because the values of cohesion of sandy soil obtained by soil tests varied widely depending on the position and other conditions, several values of cohesion are input. The results indicate that cohesion influences face stability to a large extent. It is thought that the slant of the line expresses the effect of lowering ground water level on face stability. In other words, it is effective to lower the under ground water to the crown level, in order to ensure face stability. The results also show that the height of the face is effective for stability. Therefore, attention must be paid to the stability of the face, when the level of the clay layer goes down.

Next, construction results are input in these nomograms to evaluate the adequacy of analysis. Table 1 shows construction results. When clay soil exists over the entire face (section number No. 3), it shows that the face is stable according to the construction results in the nomograms. On other hand, when an alternation of strata with sandy soil and clay soil is formed at the

Copyright © 2005 Taylor & Francis Group plc, London, UK



(i)



(ii)

Figure 16. Proposed nomogram. (i) Nomogram No. 1, (ii) Nomogram No. 2.

Table 1. Construction results.

Section number	Geological condition	Hf (m)	Face stability	Hw (m)
No. 1	Alternation of strata	4.2	Unstable	16.2
No. 2	Alternation of strata	3.2	A little unstable	9.9
No. 3	Clay soil	0	Stable	6.7

face (section number No. 1), the face is unstable. Since the nomogram based on the analysis coincides with the construction results, it is effective to evaluate the face stability by using there nomograms.

A comparison of the nomograms shows that lowering the ground water level to the foot of the face is effective for face stability.

5 CONCLUSION

– It becomes clear that it is possible to evaluate the face stability, which is affected by the ground water, by applying RPFEA while giving consideration to the effects obtained by the ground water.

– It is confirmed that three factors concerning the lowered ground water level is effective to evaluate the face stability. These factors are the fluctuation of the unit weight of soil due to the fluctuation of the ground water level, fluctuation of the effective stress caused by the fluctuation of the unit weight of soil and pore water pressure, and fluctuation in strength of the ground induced by the fluctuation of the effective stress.

We will compare analysis results and construction data, and study the methods to evaluate cohesion, set an appropriate ground water level and create an optimum model in the future.

REFERENCES

Hayes, D.J. & Marcal, P.V. 1967. Determination of upper bounds for problems in plane stress using finite element techniques, Int. J. Mech. Sci., Vol. 9, pp. 245–251.

Kobayashi, S., Lee, C.H. & Shah, S.N. 1973. Analysis of rigid-plastic deformation by the matrix method, Plasticity and Forming, Vol. 14, No. 153, pp. 770–778 (In Japanese).

Mori, K., Shima, S. & Osakada, K. 1979. Analysis of free forging by rigid-plastic finite element method based on the plastic equation of porous metals, Trans. JSME, Vol. 45, No. 396, pp. 965–974 (In Japanese).

Tamura, T., Adachi, N., Konishi, S. & Tsuji, T. 1999. Rigid-plastic finite element method for frictional materials, Journal of geotechnical engineering, JSCE, No. 638/3-49, pp. 301–310 (In Japanese).

Konishi, S., Asakura, T., Tamura, T. & Tsuji, T. 2000. Evaluation of tunnel face stability for sand strata with clay layers, Journal of geotechnical engineering, JSCE, No. 659/3-52, pp. 51–62 (In Japanese).

Konishi, S. & Tamura, T. 2002. Evaluation of tunnel face stability in sandy ground with clay layers, Journal of Geotechnical Aspects of underground construction in soft ground, 3rd international symposium Is-Toulouse, ISSM and TC28, 6th session, pp. 53–58 (In English).

Konishi, S. & Tamura, T. 2002. Effect of draw down on tunnel stability during excavation, Journal of applied dynamics, JSCE, Vol. 5, pp. 307–316 (In Japanese).

Schofield, A.N. 1980. Cambridge Geotechnical Centrifuge operations, 20th Rankine Lecture. Geotechnique 30, No. 3, pp. 227–268.

Tamura, T., Kobayashi, S. & Sumi, T. 1984. Limit analysis of soil structure by rigid plastic finite element method, Soils

Tamura, T., Kobayashi, S. & Sumi, T. 1987. Rigid-plastic finite element meth od for frictional materials, Soils and Foundations, JSSMFE, Vol. 27, No. 3, pp. 1–12 (In English).

Copyright © 2005 Taylor & Francis Group plc, London, UK

Development of anchor sheet segment and push resin joint

S. Okamoto & Y. Yamamoto
Obayashi Corporation, Tokyo, Japan

T. Kunifuji
Ishikawajima Construction Materials Co. Ltd., Tokyo, Japan

ABSTRACT: Two technologies have been developed for sewerage tunnels, which are subjected to highly corrosive environments, to improve durability and reduce life-cycle costs. The first technology is the anchor sheet segment method, a technique of tunnel lining, and the second one is push resin (PR) joints, which are corrosion resistant joints for reinforced concrete ring segments. The anchor sheet segment method, in which primary lining is coated with a high-density polyethylene resin sheet, improves tunnel durability and reduces lining thickness and the area of excavation. The metal-free, resin-based PR joints do not require anticorrosive measures and allow speedy construction because segments can be joined by sliding them in the tunnel axis direction.

1 INTRODUCTION

When constructing sewerage shield tunnels, a general approach for the sake of cost effectiveness and construction performance is to use steel segments for primary lining and cast-in-place concrete for secondary lining. In this case, the secondary lining has functions of corrosion prevention, waterproofing, and smoothing of the inner surface, which are not sufficiently achieved by the conventional primary lining.

Measures such as prevention of segment corrosion by secondary lining, rustproofing of metal joints, and filling of bolt boxes are necessary in particular in sewerage tunnels because of possible erosion of the inner surface by sandy particles, degradation of concrete by hydrogen sulfide generated from sewage, and metal corrosion. Moreover, the secondary lining concrete would lose its anticorrosive capability if it was degraded during the service period.

Considering that some resins are durable even in highly corrosive environments, we have conducted research and development on lining technologies that eliminate the need for corrosion proofing or rustproofing even in such environments and that reduce the life-cycle costs of sewerage tunnels.

In this paper, we describe considerations made for the development of the anchor sheet segment method and push resin (PR) joints and report experimental results and the features of these technologies.

2 ANCHOR SHEET SEGMENT

2.1 *Purpose of development*

The conventional approach of secondary lining by cast-in-place concrete has been adopted in sewerage tunnels for preventing corrosion of primary lining, which is a structural component, removing tunnel meandering, ensuring inner surface smoothness, and improving cut-off of water. Recent advancement in construction technologies now allows us to ensure excavation precision, cut-off of water, and inner surface smoothness only by primary lining, but there still is no fundamental solution for the early degradation of concrete. Thus, there is a need to develop a method of durable inner lining.

Anticorrosion lining methods developed for shield tunnels include pasting, spraying, and bolting resin material on the inner surface after tunnel construction. Two processes, tunneling and lining, are required in either method, and there has been a problem of segregation of coating from segments.

The anchor sheet segment method, which uses a resin of high durability and abrasion resistance, was

Copyright © 2005 Taylor & Francis Group plc, London, UK

developed as a lining method for sewerage shield tunnels. In this method, inner surface coating is completed by performing only primary lining.

2.2 *Outline of the method*

The outline of the anchor sheet segment method is described below. When manufacturing reinforced concrete segments for the primary lining of the shield tunnel, a high-density polyethylene resin sheet of 2 to 3 mm in thickness is placed in a concrete form. The sheet has stubs on the back side for complete bonding with concrete (Figure 1).

Accordingly, anchor sheet segments with high-density polyethylene resin on their inner surface are manufactured. By using the segments to construct a shield tunnel, inner surface coating is provided simultaneously with primary lining.

2.3 *Mechanical properties of anchor sheet*

The inner coating of a sewerage tunnel needs to be resistant to abrasion and damage caused by flow of solid matter and adaptable to deformation and cracking in the reinforced concrete segments, so that hazardous matter in the sewage will not get in contact with the segments.

To test the performance of the anchor sheet as a sewerage tunnel lining, the basic mechanical properties of the sheet were tested as shown in Table 1.

The test results indicate that the anchor sheet has the following properties:

- large tensile strain, ensuring adaptability to deformation and cracking of concrete
- high abrasion resistance, with the thickness of abrasion being less than one hundredth of that of concrete
- high imperviousness, with a low coefficient of water absorption
- high impact resistance
- low roughness coefficient, compared to concrete

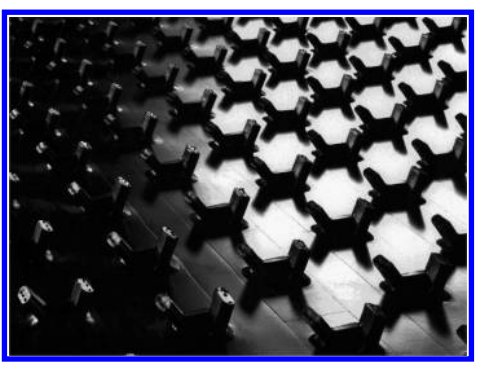


Figure 1. Back side of anchor sheet.

2.4 *Chemical resistance of anchor sheet*

In place of the conventional secondary lining made of cast-in-place concrete, the inner surface coating of a sewerage shield tunnel should protect primary lining from corrosion. The coating should therefore be resistant to various chemicals arising from the sewage.

To confirm the chemical resistance of the anchor sheet, the rate of mass change was measured by an immersion test (Table 2). The anchor sheet is found to be sufficiently resistant to various chemicals and can thus be used as an inner coating for sewerage tunnels.

2.5 *Features of the anchor sheet segment method*

The anchor sheet segment method has the following features:

- Because roughness coefficient is reduced to n = 0.010, compared to n = 0.013 to 0.014 on the inner surface of conventional concrete pipes, inner tunnel diameter can be reduced while retaining the same flow rate capacity.
- The thickness of abrasion is 0.8 mm, compared to 100 mm in concrete. The anchor sheet is highly resistant to abrasion caused by flow of sandy particles.

Table 1. Mechanical properties of anchor sheet.

Item	Unit	Value	Test method
Tensile strength	MPa	15.7	JIS K7113
Tensile strain	%	300	JIS K7113
Rockwell hardness	HRR	18	JIS K7202
Roughness coefficient	–	0.010 (0.014[*1])	–
Abrasion coefficient	mm	0.8 (100[*2])	JIS A5209 7.8
Coefficient of water absorption	%	0.07	JIS K7209
Charpy impact strength	KJ/m	61.0	JIS K7111

[*1] Test value on mortar
[*2] Test value on concrete (f_{ck} = 21 N/mm^2)

Table 2. Results of anchor sheet immersion test.

Item		Measured value (mg/cm^2)	Reference value* (mg/cm^2)
NaCl	(10%)	0.00	0.05
H_2SO_4	(30%)	−0.01	0.05
HNO_3	(40%)	+0.01	0.10
NaOH	(40%)	−0.02	0.05
C_2H_5OH	(95%)	+0.09	0.40

* JIS (Japan Industrial Standard) K 6761

Copyright © 2005 Taylor & Francis Group plc, London, UK

– The anchor sheet is highly resistant to chemicals and highly impervious. Secondary lining with cast-in-place concrete, which has been done conventionally to prevent corrosion by hydrogen sulfide and other substances, can therefore be eliminated.
– The low roughness coefficient and the elimination of secondary lining allow reductions in shield diameter and construction cost.
– Stubs on the anchor sheet ensure complete bonding of the resin coating with the concrete.
– The quality of the anchor sheet, which is produced at the factory, does not depend on the construction conditions. Quality control is easier compared with methods that involve lining by spraying, painting, and sheet attachment after segment assembly.

2.6 *Practical application*

The anchor sheet segment method has been used in two construction projects in Japan (Figure 2), which involved installation of pipes having inner diameters of about 2000 mm. Up to now, the method has been applied to tunnels of about 1000 m in total length.

Favorable results have been obtained, with the ability to reduce cost and period of construction confirmed. Some more time is required to demonstrate the high chemical and abrasion resistance of this method.

2.7 *Cost effectiveness*

Cost effectiveness was compared between two cases: secondary lining is applied to a shield tunnel using steel segments in the first case, and the anchor sheet segment method is used in the second case. The results indicate that the total construction cost can be reduced by 5% by adopting the anchor sheet segment method. Because maintenance is not required during the service period in the second case, further reduction in life-cycle cost can be expected.



Figure 2. Shield tunnel completed by the anchor sheet segment method.

Furthermore, construction period can be reduced by 20% because secondary lining is not conducted.

2.8 *Prospects*

The anchor sheet segment method has been put into practical use and its performance has been confirmed successfully.

As a next step, application of anchor sheets to sharply curved sections and sections where reinforced concrete segments are not used is being considered.

Steel segments are being used in sharply curved sections of shield tunnels to increase segment stiffness. In sewerage tunnels, steel segments need to be lined for corrosion prevention and inner surface smoothing.

If there is enough space for thick lining on steel segments, secondary lining by cast-in-place concrete is applied. If there is not enough space for thick lining, anchor sheets are used for secondary lining so that the steel segments can be protected from corrosion by the thin lining.

Anchor sheets are planned to be applied to sharply curved steel segments in a sewerage tunnel being constructed in Japan, and the performance of this work is to be tested.

By applying anchor sheets to steel segment sections, the entire sewerage shield tunnel including sharply curved sections benefits from the high durability, chemical resistance, and abrasion resistance of the sheets. Furthermore, design and construction of sewerage tunnels are expected to be more economic.

3 PR JOINTS (PUSH RESIN JOINTS)

3.1 *Purpose of development*

Steel joints are generally used for shield segments. In sewerage tunnels, however, anticorrosive measures such as rustproofing and mortar finishing on the joints are required because corrosion of steel by hydrogen sulfide and other substances is expected. Steel joints that allow segments to be joined through one-touch operation have recently been developed for practical use, but the cost of these joints in the entire segment construction would be large. Therefore, development of low-cost, compact joints has been required in particular for small-diameter tunnels. Under these circumstances, we developed PR joints, which are corrosion-resistant, cost-effective resin joints for connecting ring segments.

3.2 *Development principals*

About 70% of the sewerage shield tunnels subjected to highly corrosive environments have small excavation diameters of 3 m or less. With the aim of developing

Copyright © 2005 Taylor & Francis Group plc, London, UK

joints for small-diameter sewerage tunnels, the following principles were identified:

– Use a material that does not require anticorrosive measures even in highly corrosive environments.
– Achieve cost reduction in comparison with conventional steel joints plus anticorrosive measures.
– Reduce the joint size for adaptation to segments having outer diameters of 3 m or less, which are in greatest demand.
– Design the joints to allow one-touch operation so as to support speedy construction.

3.3 *Material selection*

Among resins that are resistant to acid, alkali, and weathering, polyamide was selected as a joint material because of its high tensile strength and general versatility (Table 3). This resin is thermoplastic and its productivity can be improved by injection molding. Glass fiber is added to the resin for reinforcement, so that the resin retains strength in a compact form.

3.4 *PR joint structure*

As shown in Figure 3, the PR joint consists of male and female parts that mate with each other. The male part has a head <1> and an anchor <2>, whereas the female part consists of threaded fillers <3> and a holder <4>. The threaded fillers on both sides of the holder are held within the holder, and the male and female parts are engaged by the fillers to prevent separation.

3.5 *PR joint performance test*

To confirm the basic performance of the PR joint and make it ready for practical use, the following performance tests were conducted.

3.5.1 *Single joint tensile test*

The tensile strength of a single PR joint was tested (Figure 4).

The test results are shown in Table 4. The average tensile strength of a joint pair is found to be 43.1 kN Assuming a water seal that can cope with a water pressure of 0.25 MPa, the maximum tensile force that acts on any part of the joint is about 13 kN. A safety factor of 3 is therefore achieved.

3.5.2 *Joint insertion and tensile tests*

A joint insertion test was performed to investigate the level of insertion load during segment assembly and whether there is any effect on the concrete around the joint. A tensile test was performed by using the same joint specimen to confirm the tensile strength of the joint embedded in segments and to calculate the tensile spring constant of the joint (Figure 5).

Table 3. Properties of reinforced polyamide.

Item	Unit	Value
Specific gravity	–	1.5
Tensile strength	MPa	205
Flexural strength	MPa	290
Compressive yield strength	MPa	190
Shear strength	MPa	95

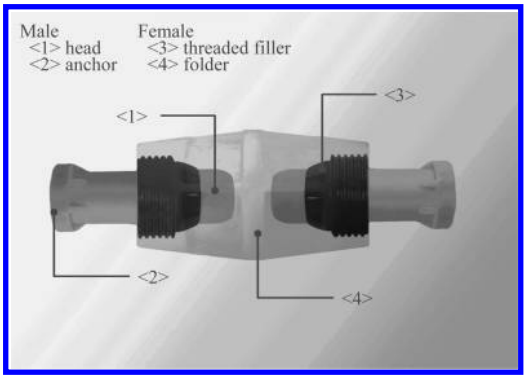


Figure 3. PR joint structure.

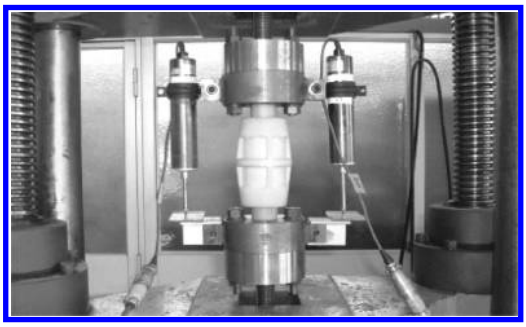


Figure 4. Single joint tensile test.

Table 4. Result of single joint tensile test.

Case	Max. load (kN)	Displacement (mm)
1	42.0	8.1
2	43.7	9.3
3	43.5	9.1
Average	43.1	8.8

The results of the joint insertion test indicate that a joint pair can be put into an engaged state by an inserting force of about 0.2 kN. This means joint insertion can be done by using a usual erector. No

Copyright © 2005 Taylor & Francis Group plc, London, UK

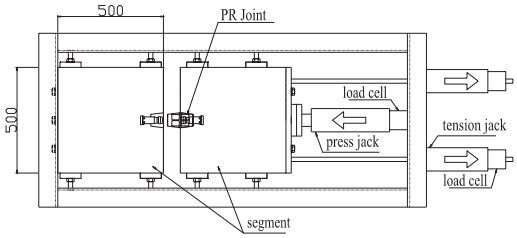


Figure 5. Schematic diagram of insertion and tensile test.

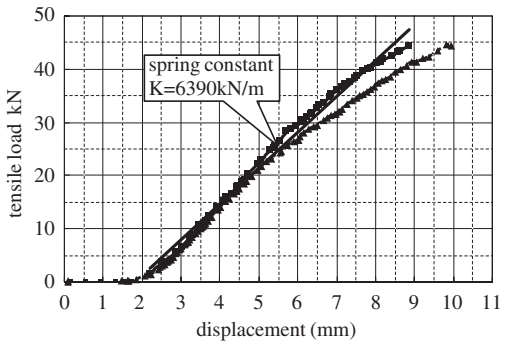


Figure 6. Results of joint tensile test.

irregularities such as cracks were found on the concrete around the joint.

The results of the joint tensile test are shown in Figure 6, where the vertical axis represents tensile load and the horizontal axis represents joint displacement. Excluding the effect of looseness in joint assembly, a tensile spring constant of 6390 kN/m was obtained. A tensile strength of 44.5 kN, which is comparable to the value of 43.1 kN obtained by the single joint tensile test, was also obtained. This indicates that the tensile strength of the PR joint is not changed even when it is embedded in concrete. We have thus confirmed that the joint functions properly without a decrease in strength even in water-added environments, such as those during concrete curing.

3.5.3 *Joint shear test*

A shear test was done by using a platy specimen to confirm the shear strength of the joint and to calculate its shear spring constant. As shown in Figure 7, a platy specimen simulating a main segment and a splice segment was connected by using four joints. A vertical load was applied to the main segment so that the joints were subjected to shear force. Two cases were tested: presence and absence of a gap between the main and splice segments.

The test results are shown in Figure 8, where the vertical axis represents vertical load and the horizontal

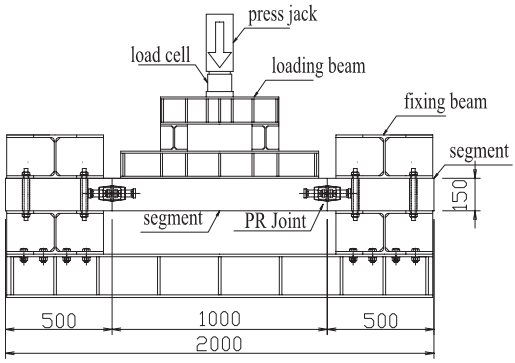


Figure 7. Schematic diagram of joint shear test.

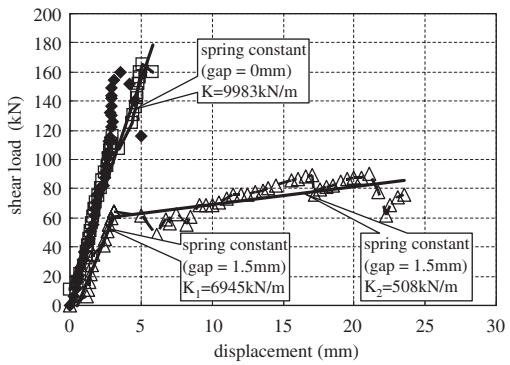


Figure 8. Results of shear test (specimen containing four joints).

axis represents vertical displacement. Maximum load was smaller when there was a gap between the segments, and different shear spring constants were obtained for the two cases. A joint shear strength of 22.6 kN/joint and initial shear spring constants of 7000 to 10,000 kN/m were obtained from the test results.

3.5.4 *Shear creep test*

Because resin materials are generally susceptible to creep deformation, we had to investigate the creep behavior of the joint under long-term shear force to bring the joint into practical use. To investigate the creep behavior, shear force was applied to a joint specimen by using a test device that is similar to the one used in the joint shear test. Creep loads of 3.2 and 4.8 kN were assumed in consideration of the maximum shear force (4.04 kN) that was expected to act on the joint from segment design on a trial basis described in the next section.

The results of the creep test are shown in Figure 9.

Copyright © 2005 Taylor & Francis Group plc, London, UK

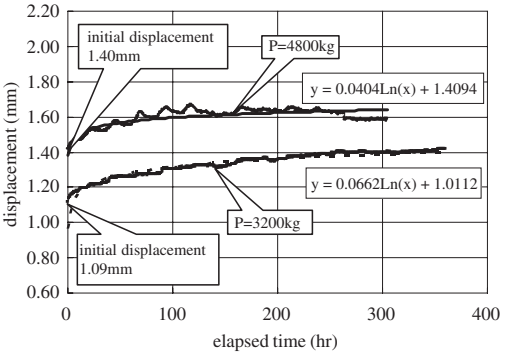


Figure 9. Results of shear creep test.

Based on an approximate expression deduced from the test results, creep deformation after the elapse of 50 years is estimated to be 1.9 mm. This is within the range where water can be cut off by usual seal.

3.6 *PR joint applicability*

Based on the results of the above-mentioned tests, we specified parameter values for the design of the PR joint as shown in Table 5.

By using the specified values of design parameters, we designed segments on a trial basis. While assuming an effective overburden of 10 m and a finished inner diameter of 2800 mm, soil conditions were varied as parameters.

The results of the trial design (Table 6) indicate that shear force τ on the joint has a maximum value of 4.04 kN when N-value is less than 2 and the soil type is alluvial cohesive soil. Because the shear strength of the PR joint obtained by the shear test is 22.6 kN even when there is a gap between the segments, safety factor Fs for the shear force that acts on the joint is 5.6. This indicates that the PR joint can also be applied to soft ground.

3.7 *Features of PR joints*

The key features of segments using PR joints are as follows:

– The joint, made of polyamide-based resin, is resistant to corrosive substances such as hydrogen sulfide and salt.
– Segments can be joined by one-touch operation without bolting, so that speedy construction is supported.
– Because joints are embedded within segments, tunnels with smooth inner surfaces can be constructed.
– Manufacturing and transport of segments are facilitated because joints do not protrude from segment sides.

Table 5. Design parameters of PR joint.

	Spring constant (kN/m)	Strength (kN)
tensile	6390	44.5
shear	6945～9983	22.6

Table 6. Results of trial design.

Case	1	2	3
Soil type	sand	clay	clay
SPN value	30<N	4<N<8	N<2
Loading Condition	loosened earth pressure	full overburden	
Displacement(mm)	−1.21	−2.35	−2.61
Shear stress (kN/joint)	1.32	2.79	4.04
Judgment	OK	OK	OK

– There is greater freedom in taper segment assembly because segments can be used regardless of their entrance and face sides.

3.8 *Cost effectiveness*

The cost effectiveness of PR joints was compared with that of steel bolt joints, which are lowest in price. A cost cut of 10% is expected by using PR joints, in comparison with the use of steel bolt joints combined with anticorrosive measures. This is because the resin used for the PR joint is low priced compared to metal in general and does not require anticorrosive measures. In the future, the cost of the PR joint may be further reduced by mass production and streamlining of manufacturing.

Because maintenance is not required during the service period, the PR joint is obviously advantageous in terms of life-cycle cost.

3.9 *Prospect*

The basic performance of the PR joint, including its structural behavior and applicability, was confirmed by various performance tests. By designing segments on a trial basis, we confirmed that the PR joint can well be applied to practical use.

The PR joint also surpasses conventional joints in economy.

In the future, trial construction will be conducted for further confirmation, and resin-based joints for

Copyright © 2005 Taylor & Francis Group plc, London, UK

combining pieces are to be put into practical use with the aim of developing segments that use no metal joints.

4 CONCLUSION

With the aim of improving the durability and life-cycle cost of shield tunnels, the anchor sheet segment method and the PR joint were developed while focusing on the high durability of resin material. The development enables reductions in the total cost of sewerage tunnels.

Adopting the anchor sheet segment method allows omission of secondary lining, reductions in roughness coefficient, excavation area, and construction cost as well as maintenance cost because of the high durability of the resin. Adopting the PR joint allows joint cost reduction, maintenance cost reduction because of improved corrosion resistance, and extension of the service lives of structures.

In the future construction of sewerage and other tunnels in highly corrosive environments, the high durability of resin can be used effectively in providing a rational anticorrosive measure to allow life-cycle cost reduction.

REFERENCES

Yamamoto, Y. et al. 2004. Development of PR Joint, Proceedings of the 59th Annual Conference of Japan Society of Civil Engineers.

Copyright © 2005 Taylor & Francis Group plc, London, UK

Observational method for tunnel construction in difficult conditions considering environmental impact to groundwater

H. Ohtsu & Y. Ohnishi
Kyoto University, Kyoto, Japan

T. Nishioka
Hanshin Expressway Public Corporation, Kyoto, Japan

K. Takahashi & T. Yasuda
Pacific Consultants Co. Ltd., Osaka, Japan

ABSTRACT: This study reports on the application of observational method to groundwater work in mountain tunnel construction, which was performed for the purpose of making the work economical and rational while dealing with tunnel related groundwater issues, and describes the development of suitable analytical and evaluation techniques. The tunnel to which this method was applied is a mountain tunnel excavated in alternating sand stone and slate from between the Mesozoic and Paleozoic Eras. Some sections on the route were going straight below surface waters or near important lakes, imposing environmental and groundwater requirements. In the application example presented, the observational method based groundwater work made it possible to effectively evaluate groundwater and thereby make the work economically efficient and environmentally friendly by incorporating the proposed evaluation technique in the excavation process.

1 INTRODUCTION

In Japan, tunnel work has conventionally been based on engineering knowledge such as the discipline of rock mechanics. Due to the recent trend of revitalizing urban functions through improvement of traffic networks, there is often no choice but to construct tunnels near built-up areas. In such a case, not only the construction work itself but also the surrounding natural and social environments raise crucial issues, and as a result, it is often essential to take relevant conservation measures to deal with environmental factors[1),2)]. The authors have so far examined groundwater prediction methods to help establish groundwater environment conservation measures [3)].

2 OVERVIEW OF OBSERVATIONAL-METHOD-BASED GROUNDWATER WORK

The groundwater issues involved in tunneling have two aspects: the work itself and the surrounding environment. With regard to the work itself, it is concerned with the need for groundwater measures for safety purposes, such as through prevention of cutting face failure that could be incurred by a large amount of leakage. With regard to the surrounding environment, it is concerned with such issues as the impacts of groundwater drainage on the surrounding groundwater environment and the impacts of groundwater level reduction on existing water resources. This study reports on the application of observational method to groundwater work in the construction of Inariyama Tunnel, which was performed for the purpose of making the work economical and rational while dealing with tunnel-related groundwater issues, and describes the development of suitable analytical and evaluation techniques. The observational method based groundwater work developed in this study is a system of tracking and evaluating the excavation process by rapidly repeating the processes of validation and prediction analysis based on the immediately preceding excavation data and consists of the following analytical stages:

(i) Groundwater model development: Based on the topographical, geological and groundwater information obtained prior to tunnel excavation, a large three-dimensional prediction model representing the hydro-geological conditions, aquifer structure and surface waters is developed.

Copyright © 2005 Taylor & Francis Group plc, London, UK

(ii) Validation analysis immediately preceding excavation data: Using the three-dimensional model, complex groundwater behavior during excavation is predicted through three-dimensional saturated-unsaturated seepage analysis[4]. The immediately preceding excavation data are feed backed to the prediction model to verify the model.

(iii) Prediction analysis: The groundwater behavior of as-yet-excavated area is predicted while attempts are made to improve the precision of prediction model. In the construction of the Inariyama Tunnel, the incorporation of proposed observational method for three sections, namely Sections A, B and C shown in Figure 1 (running close to a aqueduct tunnel, surface water or precious lake) allowed for the successful implementation of relevant conservation measures.

3 CLOSE POSITIONAL RELATIONSHIP WITH EXISTING AQUEDUCT TUNNEL (SECTION A)

3.1 *Tunneling conditions and surrounding environment*

Topographically, Section A was composed of gently inclined, highly weathered and eroded mountainous slopes having hilly areas and alluvial fans at their base. The surrounding geology consisted of the Tamba layer group (clayslate, shale, sandstone and chert) between the Carboniferous Period of the Paleozoic Era and the Jurassic Period of the Mesozoic Era. The strike of the strata ran from northwest to southeast; whose dip was generally south facing; and there were several fault-crushing belts running from northeast to southwest.

The Inariyama Tunnel had double cutting faces, namely eastern tunnel and western tunnel main tunnel, whose sectional area was both 80 m^2, as shown by the standard section in Figure 2. The existing aqueduct

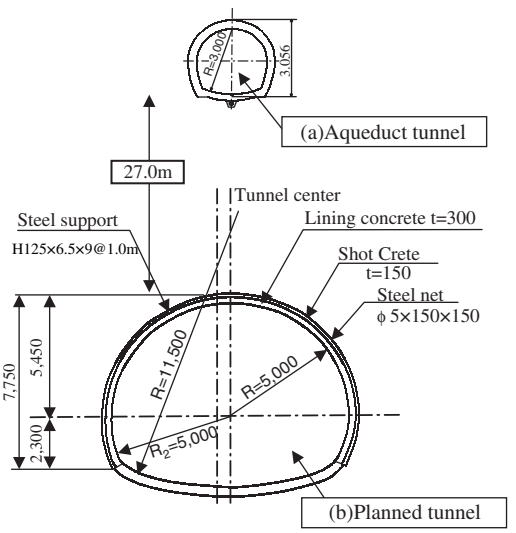


Figure 2. Tunnel cross section.

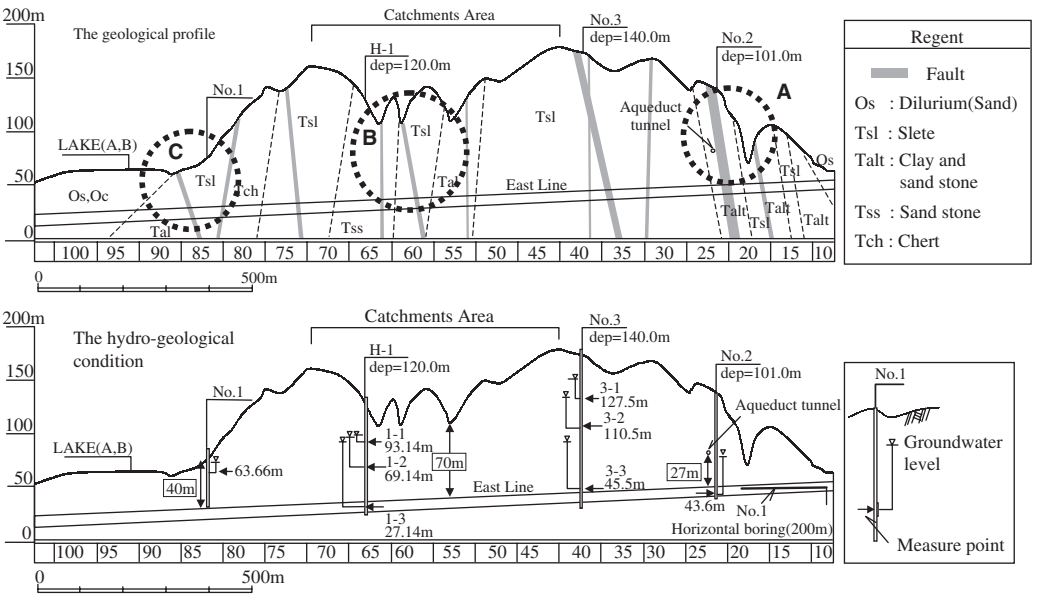


Figure 1. The geological profile of tunnel longitudinal section.

Copyright © 2005 Taylor & Francis Group plc, London, UK

tunnel, which presented a serious issue by running closely to the planned tunnel, had a flow volume of 12,000 to 13,000 m^3/hour and was one of the crucial water supply lifelines.

The aqueduct tunnel and planned route were running closely to each other, with a clearance of approximately 27 m and a crossing angle of 57°. According to the results of Lugeon test on No. 2 borehole, the crossing point had the following hydro-geological characteristics: the permeability coefficient of rock with fewer cracks was $k = 3.0 \times 10^{-5}$ to 1.0×10^{-4} cm/s, while that of the fault-crushing belts showed a large value of $k = 1.0 \times 10^{-2}$ cm/s. Viewed from the well core, the fault-crushing belts were found in every 2 to 5 m, and as a result, the whole ground was forming a huge fault-crushing belt. The groundwater level inside the well core was approximately GL-60 m, which was close to the water surface level inside the aqueduct tunnel. As a result of the No. 1 horizontal boring performed before the commencement of work, a great amount of leakage water was found inside the borehole and the fault-crushing belts were suffering intensive leakage, showing the actual leakage water of 500 to 700 L/min, while other regions showed 100 L/min or less. The permeability coefficient of fault-crushing belts obtained in the Lugeon test was $k = 1.3 \times 10^{-2}$ cm/s.

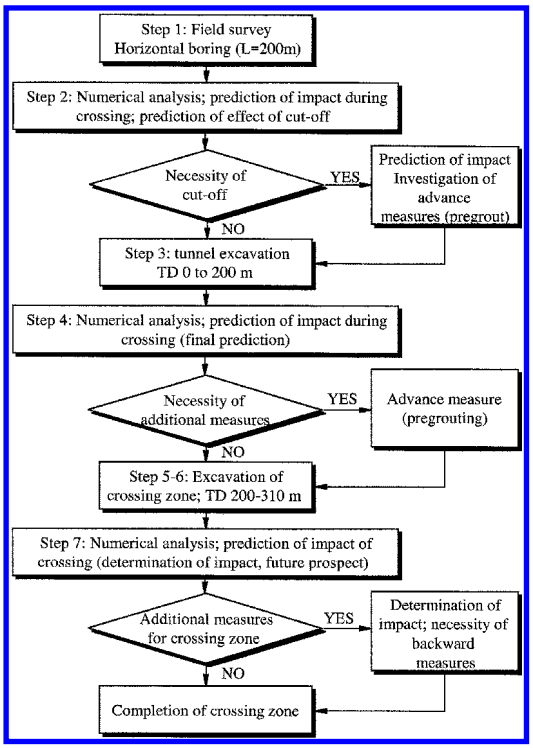


Figure 3. Flowchart of observational method.

3.2 *Observational-method-based groundwater work in Section A*

The procedure for observational-method-based groundwater work in Section A is shown in Figure 3. It is a procedure of repeatedly modifying the prediction model based on horizontal boring and preceding excavation data to predict the impacts on yet-excavated areas, thereby evaluating the necessity of measures or the size of predicted impacts. Figure 4 shows the prediction model for Section A.

In Section A, tunnel excavation was found to give the following impacts: either drawing a large amount of water from the drinking water lifeline, i.e. the aqueduct tunnel, through highly permeable fault-crushing belts, or loosening the ground around the aqueduct tunnel by lowering the groundwater level. However, since the aqueduct tunnel did not allow the direct observation of impacts, it was considered effective to evaluate the impacts using the impact values obtained

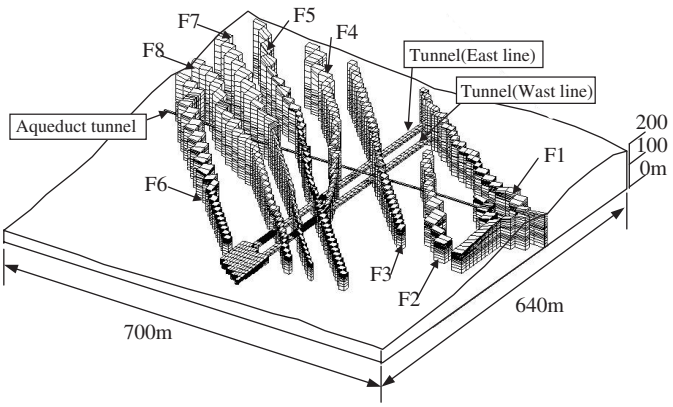


Figure 4. The prediction model for Section A.

Copyright © 2005 Taylor & Francis Group plc, London, UK

in numerical analysis. Based on the water volume ratio to the current flow volume, the allowable impact was determined to be the seasonal fluctuation of up to 4.0 to 7.6 m^3/min.

3.3 *Validation analysis during excavation of Section A*

3.3.1 *Evaluation of hydraulic characteristics of fault-crushing belts (Step 2)*

In Step 2, the properties of fault-crushing belts (existence and width) were added or modified using the actual horizontal boring data, and the horizontal boring was reproduced on the analytical model, faithfully representing the measured drilling process. At this stage, verification was conducted based on the actual amount of leakage during boring, and the hydraulic characteristics such as the permeability coefficient were obtained. Then, the groundwater behavior around the crossing point during main tunnel excavation was predicted and the impacts on the aqueduct tunnel evaluated. Furthermore, the need for measures was examined based on the results of preliminary prediction. According to the results of Step 2, the amount of drawing water was predicted to be 1.15 m^3/min, which suggested there was no need to take any cutoff measure such as large-scale chemical injection, and that it would be adequate to pay attention to the fault-crushing belts and adopt cutoff measures when it was considered necessary.

3.3.2 *Verification of prediction results and measured data (Step 4)*

Up to the crossing point, the actual leakage showed a peak amount of 1 to 2 m^3/min, which rapidly declined in accordance with the progress of tunneling.

Figure 5 is the comparison between the prediction results and measured data of the groundwater level of No. 2 borehole and main tunnel leakage. According to the results of impact prediction in Step 4, it was predicted that the tunnel leakage would increase near the crossing point to approximately 2.0 m^3/min, and the groundwater level of No. 2 borehole would rapidly decrease accordingly. The measured data mostly corresponded to the prediction results both in terms of groundwater level and tunnel leakage. Figure 6 shows changes in pressure head distributions at the crossing point. It helps understand that the aqueduct tunnel was affected by way of the fault-crushing belts crossing with the tunnel route, and the impacts of total head reductions during excavation were extended to the vicinity of ground surface along the fault.

3.4 *Reflection of impact evaluation results on actual work*

The repeated modifications of analytical model and execution of numerical analysis in accordance with

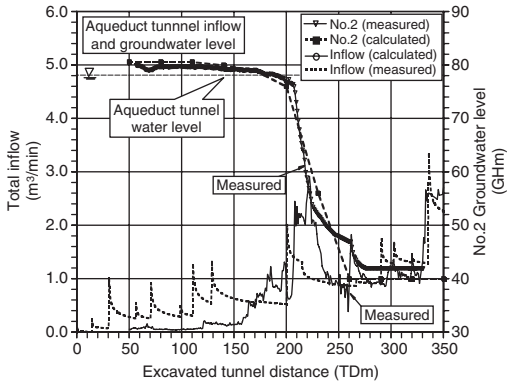


Figure 5. The comparison between the prediction results and measured data.

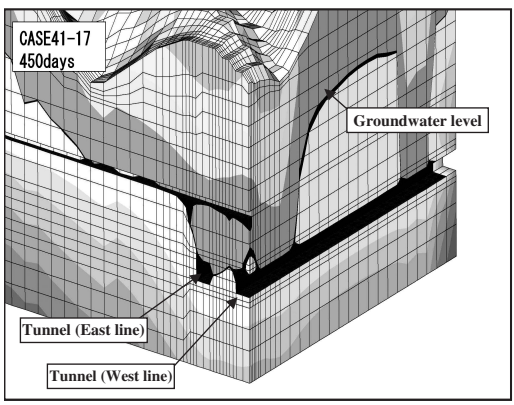


Figure 6. Result of groundwater level change(Step4).

excavation progress made it possible to precisely identify the groundwater behavior and impact development mechanism. Making them consistent with the monitoring data allowed the highly reliable impact prediction. In the actual work, since the amount of tunnel leakage and the impacts on aqueduct tunnel were below the allowable impact values, it was determined unnecessary to take any cutoff measures, such as grouting, which had been considered before the commencement of excavation. Thus, no specific measures against any groundwater impacts were taken.

4 EVALUATION OF IMPACTS ON SURFACE WATER SYSTEM (SECTION B)

4.1 *Observational method based groundwater work in Section B*

The prediction model used for Section B is shown in Figure 7. The allowable impact values were determined

Copyright © 2005 Taylor & Francis Group plc, London, UK

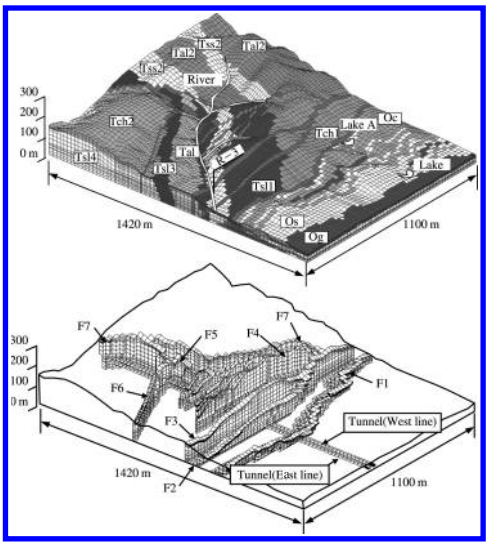


Figure 7. Distribution of fault zone in the 3-D geological profile for Section B, C.

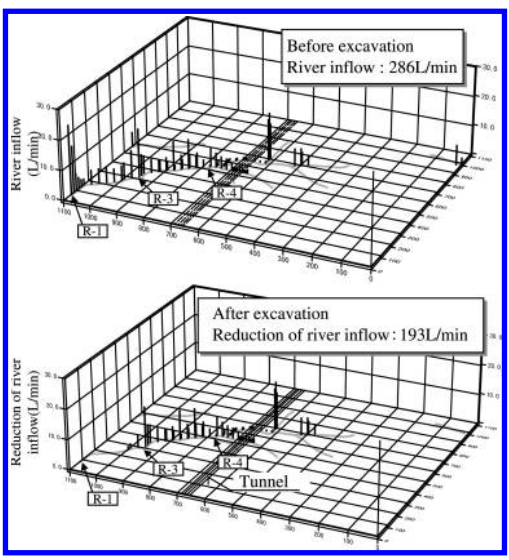


Figure 8. Results of river inflow.

using the base flow of surface waters as the reference value. As an emergency measure during work, it was determined to restore the surface water by providing publicly supplied water, the volume of which was proposed based on the results of validation analysis.

4.2 *Validation analysis during work on Section B*

Figure 8 shows the results of impact analysis for the flow of surface waters in Step 0. The upper diagram shows the condition where the excavation was not giving any impacts. The lower diagram shows the distributions of impact reduction while excavating through Section B. From the Figure, it was predicted that the base flow was 286 L/min before passing through the tunnel and then reduced by 193 L/min after passing, which would be a reduction of approximately 70%. The reduction of surface waters was particularly significant near the tunnel.

4.3 *Reflection of impact evaluation results on actual work*

As compared with the base flow of 150 to 200 L/min obtained from past hydrological survey records, it was predicted that the excavation work would almost dry up the surface waters. As an emergency measure in the actual work, the pumping-up procedure was taken, utilizing publicly supplied water.

5 EVALUATION OF IMPACTS ON NEARBY LAKES (SECTION C)

5.1 *Observational-method-based groundwater work in Section C*

Figure 9 shows the procedures for observational-method-based groundwater work to deal with lakes in Section C. The evaluation of the impacts on lakes meant the determination of end point location for mountain tunneling by NATM. In other words, it was to do with the determination of the mountain tunnel section to be excavated by the drainage type NATM, which would be able to minimize the impacts on nearby lakes. There was F1 Fault near the shield machine rotation shaft, which suggested that the section could be prone to problematic groundwater behavior in the fault-affected area and impacts on the groundwater recharge mechanism of the lakes. In other words, the observational-method-based groundwater work in Section C focused on the evaluation of impacts in accordance with the progress of main tunnel excavation, as well as the hydraulic characteristics of F1 Fault.

5.2 *Validation analysis during work on Section C*

Prior to the excavation of Section C, horizontal boring was performed for the purpose of confirming groundwater and the geology of the area near the shield machine rotation shaft. For Section C, the results of horizontal boring were treated as the evaluation target. Two cases, namely the maximum and minimum impacts were assumed (in Step 3), and the boring work itself was covered in the validation analysis.

Copyright © 2005 Taylor & Francis Group plc, London, UK

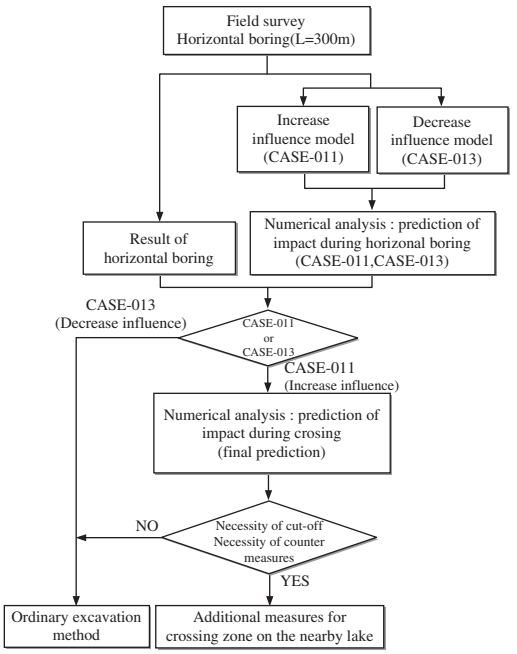


Figure 9. Flowchart of observational method.

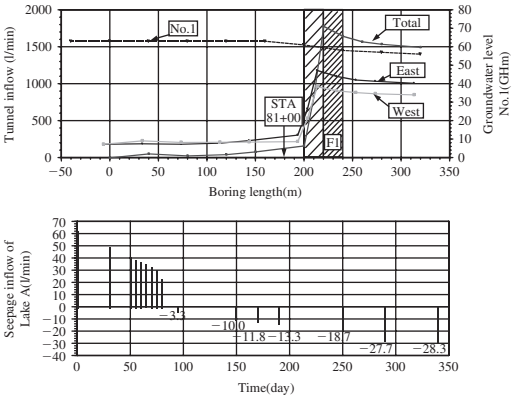


Figure 10. Seepage inflow and tunnel inflow(CASE-011).

5.2.1 *Validation of drained water during horizontal boring*

Through comparison between the prediction results for the two analytical conditions, namely the maximum and minimum impacts, and the measured horizontal boring data, it was confirmed that there would be a relatively large amount of drained water during horizontal boring, showing a relatively good correlation to the maximum impact condition (CASE-011) as far as shown by the measured data. For this reason, the CASE-011 model was used for the impact analysis of main tunnel excavation.

5.3 *Prediction results and impact evaluation in Section C*

Given the results of validation analysis described above, the prediction analysis for the impacts on lakes during main tunnel excavation was performed, assuming the maximum impact condition (CASE-011), where F1 and the disturbed sand-mud alternating layer before it both had a high permeability of $k = 10^{-3}$ cm/sec.

5.3.1 *When excavating F1 fault by NATM*

Figure 10 shows the prediction of tunnel leakage in relation to the boring length during main tunnel excavation after drainage boring, the water level of No. 1 borehole and the amount of seepage from the lakes. The main tunnel leakage was almost none at F2 before F1 due to the drainage effect of horizontal boring, but then increased to approximately 650 to 850 L/min in the sand-mud alternating layers near and through F1 in both westbound and eastbound main tunnels. Then, as in the case of horizontal boring, the increase stopped in the Osaka group at the far end. While the amount of drained water showed such a tendency, the reduction in the water level of No. 1 borehole was the sum of the reduction caused by horizontal boring and the reduction caused by the progress of main tunnel excavation. The final water level reduction caused by main tunnel excavation was 4 to 6 m. Together with the reduction caused by horizontal boring, the total water level reduction was predicted to be approximately 10 to 12 m. The amount of seepage from the lakes was decreased in accordance with the lowering of water level. The initial amount of seepage before excavation was 64 L/min, and the progress of main tunnel excavation was predicted to result in the final seepage of approximately 28 L/min.

5.3.2 *When the excavation is stopped at No. 81+00 before F1 fault*

The prediction results for the case where the main tunnel excavation was stopped before F1. The main tunnel leakage was almost none at F2 before F1 due to the drainage effect of horizontal boring, but then increased to approximately 100 to 120 L/min in the sand-mud alternating layers just before F1 in both westbound and eastbound main tunnels. While the amount of drained water showed such a tendency, the water level of No. 1 borehole showed almost no reduction. The final water level reduction was predicted to be approximately 8 m, which was caused solely by horizontal boring. The initial amount of seepage before excavation was 64 L/min, and the progress of main tunnel excavation was predicted to result in the final seepage of 0.4 L/min. Therefore, it

Copyright © 2005 Taylor & Francis Group plc, London, UK

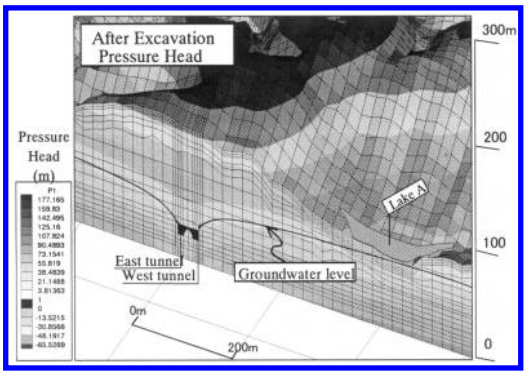


Figure 11. Results of ground water level change around the lake (Lake A).

was evaluated that the impacts on the lakes could be well controlled if the main tunnel excavation was stopped before F1. Figure 11 shows the reduction of groundwater level between the tunnel and lakes and pressure head distributions inside the ground.

5.4 *Reflection of impact evaluation results on actual work*

In controlling the impacts on lakes during tunneling work, it was considered necessary to take measures to control the amount of water drainage during main tunnel excavation. Because the impacts on lakes and surface waters are the reflection of complex groundwater behavior and aquifer structure, it is highly necessary to develop an appropriate drought prevention plan with the consideration for drought impacts and thereby control leakage and monitor surface water reduction. Based on the results of impact analysis, preparations have now been made to take necessary measures to restore the water shortage during and after the work.

6 CONCLUSIONS

The proposed observational method for groundwater work makes it possible to perform highly reliable tunneling work by accurately feed backing the data obtained for each tunneling step to the actual work. As compared with the conventional impact evaluation method using monitoring data, the use of analytical models derived from past construction records has the advantage of identifying the impact development mechanism in advance, allowing the quantitative prediction and evaluation of impacts. This would be impossible when only limited monitoring data are available.

Since the conservation of groundwater environment is difficult to evaluate in advance, it often takes the form of follow-up measures after the ex-post impacts have been confirmed in the conventional practice. However, the increasing call for environmental conservation has resulted in the pressing need for prior preparations before incurring any problems. With this regard, the importance of prior evaluation based on the groundwater behavior mechanism is supposed to be emphasized. In addition, since the proposed method can help reduce the risk of cost over-run by enhancing reliability through reevaluation during work, it is supposed to advance the efforts to implement prior preparations for environmental conservation purposes.

REFERENCES

1) Ohnishi, Y, & Tanaka, M. 1996. *Evaluation of the Effect of Tunnel Excavation for Surrounding Groundwater. (In Japanese) Proc . IGCS . Japan . 31*: 2137–2138.
2) Ohnishi, Y., Tanaka, M., Yasuda, T. & Takahashi, K. 1997. *Evaluation of the Effect of Tunnel Excavation for Surrounding Groundwater. (In Japanese) Proc . IGCS. Japan. 32*: 1997–1998.
3) Ohnishi, Y., Ohtsu, H., Yasuda, T., & Takahashi, K., 1998. *Assessment of Influence in Ground Water Surroundings at Urban Tunnels. Proc. ITA. World Tunnel Congress, 98*: 489–494.
4) Ohnishi, Y., Shibata, H. & Nishigaki, M. 1985. *Finite Element Analysis of Seepage Flow in Regularly Jointed Rock Mass. 5th Int. Cont. on Numerical Methods in Geomechanics. Nagoya.* 673–680.

Copyright © 2005 Taylor & Francis Group plc, London, UK

Research plan and construction outline of the Mizunami Underground Research Laboratory (MIU) in large depth for geoscience and geological disposal fundamental research

Masanori Sakamaki, Toshinori Sato & Shin-ichiro Mikake
Mizunami Underground Research Laboratory, Japan Nuclear Cycle Development Institute, Mizunami, Gifu, Japan

Tsutomu Kanata, Keigo Nakamura, Makoto Kubo, Kenji Akiyoshi & Masaru Noda
Obayashi Corporation, Mizunami, Gifu, and Tokyo, Japan

Yoji Nishikawa & Jun Nobutoh
Shimizu Corporation, Tokyo, Japan

ABSTRACT: One thousand meter-deep shafts and several level drifts will be excavated in the Mizunami Underground Research Laboratory (MIU) Project. Design and layout of the shafts and drifts are determined considering the geological and project condition, schedule, and investigation plan for characterization of the geological environment and engineering technology for the fundamentals of geological disposal.

This paper describes the design and construction condition, layout and design of the shafts and drifts of the MIU, and mechanical stability, ventilation and environmental concerning. Details of the design of shafts and drifts are determined, and safety of the design and construction of the MIU are discussed. Countermeasures and safety are also described in this paper.

1 INTRODUCTION

Mizunami Underground Laboratory (MIU) is one of the facilities to be constructed deep in the ground under a long-range plan for nuclear energy development in Japan. The principal target of research is crystalline rock (granite).

The MIU Project involves research on the fundamentals of geological disposal technology for high-level radioactive wastes. The project is being implemented by Japan Nuclear Cycle Development Institute (JNC) as part of fundamental geoscience research for the research and development of geological disposal technology.

The research shafts and galleries excavated under the project are expected to serve as places for establishing the technology for comprehensive investigation of the deep geological environment and developing the foundations of engineering technology for deep underground applications. The research shafts and galleries are also expected to help further the public's understanding of the deep geological environment as indicated in the Long-term Program for Development and Utilization of Nuclear Energy.

The program calls for the excavation of shafts and galleries at depths of up to 1,000 m from four viewpoints:

1. Use as places for the demonstration of the reliability of geological disposal technology at an estimated depth of 1,000 m in hard rock formations and, at the stage (i.e., the current stage) where a disposal site has not yet been selected, for fundamental research and development to be performed after constructing shafts and galleries down to a promising depth
2. Significance from the standpoint of engineering technology of shaft and gallery excavation at great depths where higher levels of technology is needed for groundwater and rock burst control
3. Significance as geoscience research concerning deep formations required by the plan drawn up by the national government
4. Economy of shaft excavation

The MIU Project was launched in 1996. In January, 2001, it was decided to excavate research shafts and galleries at a site in a tract of land owned by Mizunami City. Then, the research shafts and galleries and facilities

Copyright © 2005 Taylor & Francis Group plc, London, UK

and equipment necessary for shaft and gallery excavation were designed. In March, 2003, the first phase of research shaft and gallery excavation (excavation to a shaft depth of 300 m to be completed by March, 2005) began.

Research on the technologies for the design of research shafts and galleries in deep formations, construction planning, the excavation and maintenance of research shafts and galleries, and quality control may be thought of as research on the foundations of engineering technology for deep underground applications.

The purpose of the present study is to design research shafts and galleries that can be used in heterogeneous geological environments and that make it possible to conduct research at depths of up to 1,000 m; show examples of construction plans and develop a systematic approach to construction planning; and demonstrate the feasibility of constructing research facilities and disposal facilities in deep formations.

This paper reports on the construction plan for the MIU Project, focusing on the design and excavation methods for research shafts and galleries and safety measures such as the research shaft and gallery layout and cavern stability.

2 CONSTRUCTION PLANNING

2.1 *Basic requirements for planning*

(1) *Site conditions*

The underground research shafts and galleries for the MIU Project will be constructed in a tract of land owned by the Mizunami Municipal Government located in the town of Akiyo in Mizunami City, Gifu Prefecture. JNC leases about 7.8 ha of land from Mizunami City and install equipment for excavating research shafts and galleries in a one-hectare area of prepared land. The construction site is close to many public facilities including a park and hands-on learning facilities. In locating the equipment, therefore, it is necessary to take into consideration the fact that many citizens including school children visit those facilities.

(2) *Topography and geology*

The municipally-owned tract of land mentioned above is a hilly area with an elevation of about 200 m. In this area, granite (Toki granite) masses from the Cretaceous Period of the Mesozoic Era are distributed widely, and the granite masses are covered by Neogene sedimentary rock formations (Mizunami group). It is estimated that the sedimentary rock/granite interface at the excavation site is at a depth of 170 m.

(3) *Investigation and research plan*

The investigations and research for the MIU Project are conducted in three major phases.

The investigations and research conducted in the phase (Phase 2) in which research shafts and galleries are excavated can be classified into two groups: (1) water pressure and water quality monitoring using boreholes drilled from the ground surface, and (2) investigations and tests concerning the geology, groundwater hydraulics, groundwater geochemistry and rock mechanics measured through investigations and tests conducted in shafts and galleries.

The investigations and research in the latter group need to be coordinated with construction activities such as shaft and gallery excavation. In cases where the effect of shaft excavation on the surrounding rock or groundwater is investigated, it is necessary to start the investigations before shaft excavation.

The research conducted in the phase (Phase 3) in which the research shafts and galleries are used is mostly carried out in shafts or galleries. The galleries need to be laid out so that investigations and research in different fields such as those listed below can be carried out in appropriate zones. When conducting investigations and research, it is necessary to have the ability to flexibly allow changes in research shaft and gallery design or construction plan on an as-needed basis.

- Geological structure investigations: geological investigation through shaft/gallery wall observation, shaft/gallery investigation of 3D geology, water quality mechanism investigation, etc.
- Hydraulic investigations of groundwater: borehole permeability test, full-scale permeability test, permeability-under-thermal-stress test, crack-by-crack or fault-by-fault permeability test, etc.
- Geochemical investigations of groundwater: geochemical monitoring, oxidation–reduction study, water quality mechanism study, etc.
- Mass transfer investigations: large-scale mass transfer test, crack-by-crack or fracture zone-by-fracture zone mass transfer test, etc.
- Rock mechanics investigations: shaft/gallery excavation disturbance test, long-term behavior test, in-situ rock mass test, stress measurement, etc.
- Engineering technology: test of influence of artificial materials on rock masses, excavation disturbance reduction/rehabilitation test, coupled behavior test, etc.

(4) *Materials and equipment to be brought in*

The dimensional requirements for shafts and galleries need to be determined taking into account such factors as the efficiency and economy of excavation work, materials and equipment to be brought in and the research space requirements. Large equipment and boring machines necessary for the excavation of galleries and for research are to be brought in through the shafts. When designing shafts and planning their construction, therefore, it is important to ensure that

Copyright © 2005 Taylor & Francis Group plc, London, UK

those machines and equipment can be disassembled and brought into the shafts. Similar considerations apply to galleries as well. JNC's experience in past research projects indicates that the gallery diameter should be at least about 3 m.

(5) *Entrants*

Persons who enter shafts during shaft excavation may include not only excavation workers but also JNC employees, university or other researchers, and visitors.

(6) *Construction schedule*

The MIU Project aims to yield research results that can be reflected in disposal projects implemented by Nuclear Waste Management Organization of Japan (NUMO) and the safety standards and guidelines formulated by the national government. It is assumed that the shaft excavation results will be used as the technological foundation NUMO needs to select detailed investigation areas by around 2010. Major milestones of the MIU Project, therefore, are to reach a shaft depth of 1,000 m by around 2009 and complete the elevator by around 2010. In order to achieve these milestones, the excavation of the shaft entrance will be started in mid-2003, and shaft excavation using a drilling rig will be started by the end of 2004.

2.2 *Facility design*

(1) *Layout and functions of research shafts and galleries*

Investigation and research items for the MIU Project have been identified, and the layout of research galleries has been determined by referring to data obtained from existing boreholes and four adjacent deep boreholes. The basic layout is as follows:

- Shafts: two shafts (main shaft and ventilation shaft)
- Galleries: horizontal drifts excavated at two depths (mid-depth level, bottom level) of the two shafts

The geology of the MIU Project site is similar to that of the adjacent areas mentioned above. The sedimentary rock formation at the MIU Project site is slightly thicker, but the bedrock is identical (Toki granite). The layout in the municipally owned tract of land in Mizunami City, therefore, was modeled after the proposed basic layouts in the adjacent areas, and the standard layout was developed, taking into consideration such conditions as the site boundary and the construction schedule.

Figure 1 shows the layout of the research shafts and galleries. The layout will be reviewed from time to time on the basis of newly acquired geological environment information and details will be added accordingly.

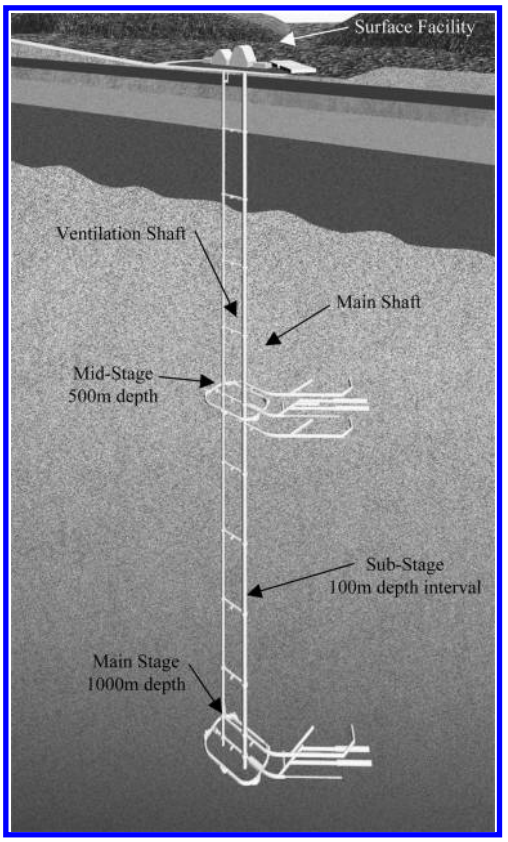


Figure 1. Layout of the research shafts and galleries of MIU.

The functions of each shaft and gallery are as follows:

- Main shaft: serving as the route through which excavated material generated by gallery excavation is removed and heavy equipment necessary for excavation is brought in and out.
- Ventilation shaft: space in which the elevator is installed after the completion of excavation to the depth of 1,000 m and a ventilation shaft for the entire shaft and gallery system.
- Mid-depth stage and main (bottom) stage: the principal places of research in Phase 3 (research using shafts and galleries).
- Test galleries: places where tests involving gallery excavation are conducted.
- Sub-stages: passageways between the two shafts and spaces where pump stations for removing groundwater flowing into the research shafts and galleries.

Copyright © 2005 Taylor & Francis Group plc, London, UK

(2) *Specifications for research shafts and galleries*
The inside diameter requirements for the shafts and galleries have been determined, taking into account the functionality and constructability requirements for the shafts and galleries. The inside diameter requirements for the galleries have been determined so that investigations and tests can be conducted and construction work can be carried out easily. The dimensions of the shafts and galleries are as follows:

- Main shaft: inside diameter: 6.5 m, depth: 1,025 m
- Ventilation shaft: inside diameter: 4.5 m, depth: 1,010 m
- Mid-depth and bottom stages: inside diameter: 3–8 m, length: 785 m
- Substages: inside diameter: 3 m, length: 35 m.

(3) *Analysis of mechanical stability of caverns*
For the analysis of the stability of the shaft and gallery caverns and the determination of support requirements (e.g., lining concrete, shotcrete, rock bolts, H-beams), methods used in the field of civil engineering such as tunnel engineering in which details are determined according to the rock mass conditions. Since, however, the depths involved are great and there are special sections such as connections between shafts and galleries, the numerical analysis method was used for those sections.

The rock mass conditions and the input conditions for numerical analysis were determined on the basis of the results obtained from existing boreholes (depth: 500 m) adjacent to the municipally owned tract of land in Mizunami City. Analyses were conducted, parameterizing the stress acting on the rock mass and the rock mass condition.

First, as a simple analysis, an elastic analysis was performed for allowable stress evaluation. In cases where the allowable stress was exceeded, the tunnel supports were strengthened and, by conducting a detailed two-dimensional FEM (finite element method)-based elastoplastic analysis, support conditions were modified.

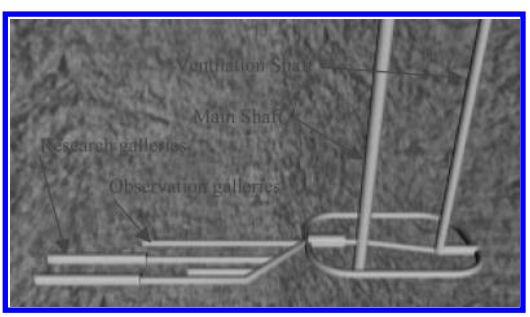


Figure 2. Detailed layout of the research galleries of main stage of MIU.

For the connections between the shafts and galleries, three-dimensional FEM analyses were conducted to evaluate their three-dimensional effects. From analysis results, strains are concentrated in the connection zone and near the corners, but their distributions are limited.

On the basis of the three-dimensional FEM analysis results, the degree of influence of the mechanical stability of the connection zone on a typical shaft cross section was analyzed, and it was ascertained that the allowable stress for the support of the typical cross section was not exceeded.

(4) *Equipment design based on ventilation analysis and fire response measures*
Fire is one of the hazards that are most likely to occur in the research shafts or galleries, so the most important thing is to ensure that there will be evaluation routes and enough time for evacuation in the event of a fire. It was thought that it would be difficult to secure a safe space, other than the two shafts, that makes it possible to escape to the ground surface in the event of a fire (i.e., a third shaft) or to secure safe fire compartments within the two shafts. It was also thought that there might not be enough evacuation time. As the basic concept of safety measures, therefore, it was decided that in the event of a fire, people in the shafts or galleries should evacuate to shelters, and requirements such as safe locations (safe compartments), evacuation time, and the size, shape and other attributes of shelters were identified. To identify shelter requirements, a ventilation network analysis, which is often conducted in the field of mining, was performed, assuming cases of fire emergency.

The construction process was divided into a number of stages, and consequences of a fire were analyzed for different fire sources. The shelter locations and specifications were determined on the basis of the analysis results thus obtained, and it was decided to locate shelters in all galleries. Ventilation equipment and fire fighting equipment were also designed.

2.3 *Construction plan*

(1) *Excavation method*
(1) Shaft excavation method
Excavation methods used for shaft construction include blasting methods such as the short step method, the long step method, NATM (New Austrian Tunneling Method) and mechanical excavation methods such as the methods using tunnel boring machines (TBM) or raise boring machines. Among the blasting methods, the short step method, in which blasting and lining are repeated at short intervals, has been used in many projects including projects that required excavation in poor rock mass conditions.

Copyright © 2005 Taylor & Francis Group plc, London, UK

The short step method enables excavation at high advance rates. Mechanical excavation methods require the pre-existence of a shaft or tunnel at the target depth. This means that TBM excavation must be preceded by drainage boring and that raise boring requires a shaft or tunnel so that equipment can be brought in advance. For this reason, these methods are not suitable for use in the MIU Project. For the MIU Project, it was decided, in view of the advantages of the short step method, to sink the two shafts (main shaft and ventilation shaft) concurrently by the short step method. In shaft excavation, the percentage of mucking time in total excavation time increases as depth increases. For efficient mucking, therefore, the kibble change method [method in which two kibbles (iron containers) are used] was used. The relationship between the excavation cycle and the advance per shot in blasting operations was studied, and it was decided to use the a modified shot step method, in which a 1.3-meter shot is repeated twice and a 2.6-meter-thick concrete lining is placed, as a safe and most efficient method of excavation.

(2) Gallery excavation method

Excavation methods used for galleries (drifts) can be broadly classified into two types: the blasting method, which is often used for excavation in hard rock, and the mechanical excavation method, which uses roadheaders or tunnel boring machines. Since the galleries at the MIU are relatively short, it was decided to use the efficient and economical NATM (blasting-based excavation method in which shotcrete and rock bolts are used for support) except in cases where the mechanical excavation method is used for research purposes such as excavation disturbance testing.

(2) *Surface plant for shaft excavation*

Excavation equipment and auxiliary equipment at the ground surface include derricks, hoists, scaffolding, ventilation equipment, water supply and drainage equipment, concrete plant, power receiving equipment and emergency power generation systems. The equipment that cannot be reinstalled or replaced, such as derricks and hoists, was designed specifically for the depth of 1,000 m, and the equipment that can be added or extended at later stages, such as wastewater treatment plant, was added or extended as shaft and gallery excavation progressed.

(3) *Safety measures*

(1) Measures against unexpected groundwater inflows

One of the phenomena that are likely to be encountered during shaft or gallery excavation is unexpected groundwater inflow. Related geological features that are likely to be encountered during excavation include unconsolidated strata, fault fracture zones and permeable fractures. These geological features could cause an unexpected inflow of a large quantity of groundwater ("unexpected groundwater inflow"). Unexpected groundwater inflow may have a serious impact on the progress of shaft and gallery excavation through such problems as the suspension of excavation or excavation equipment troubles.

In order to devise effective measures against unexpected groundwater inflows, therefore, investigations and studies were conducted with respect to the following items:

- Studying reported cases of unexpected groundwater inflows
- Devising measures against unexpected groundwater inflows in the research shafts and galleries
- Study of methods for evaluating the influence of groundwater control measures on the geological environment.

In sedimentary rock formations, groundwater inflows often occur from unconsolidated strata. Groundwater inflows might be accompanied by sediment flows. Grouting is not likely to be very effective in controlling groundwater inflows.

Groundwater, in some cases under great pressure, may gush out of fracture zones in granite formations. Large-scale fracture zones may be detectable by exploratory boring or other means of pre-excavation investigation. Representative methods for preventing unexpected groundwater inflows are drainage boring (drainage method) and the injection of cement slurry or other grouting materials (grouting method). Although both methods can be used as control measures against unexpected groundwater inflows, the grouting method, which does not cause substantial lowering of groundwater levels, was chosen in order to conserve the geological environment of the research shaft and gallery site. So, problems that need to be addressed in order to use this method during the research shaft and gallery excavation were identified, and concrete measures to be taken were determined.

One major problem is that there is no grouting pump or other grouting tool that can be used under very high pressure (since the groundwater level is close to the ground surface, the hydrostatic pressure at the depth of 1,000 m is 10 MPa). One way to solve this problem is to drill a number of drainage holes in a radial pattern from the bottom of the shaft so that, by reducing groundwater pressure in a limited area, grouting can be used effectively as a means of groundwater control. The grouting plan thus adopted calls for grouting over a horizontal distance of three times the radius of the shaft from the center of the shaft. The grouting depth is the length of the "unexpected groundwater inflow" zone plus the excavation diameter above and below the unexpected groundwater inflow zone. Grout is to be composed of normal Portland cement and a cement-setting accelerator.

Copyright © 2005 Taylor & Francis Group plc, London, UK

(2) Rock burst control measures
Because it is possible that rock burst (bursting with a sharp sound of rock fragments from the surface of a shaft or gallery being excavated) occurs during shaft or gallery excavation, information on past rock burst events, both in Japan and abroad, was collected by literature research to review possible factors contributing to the occurrence of rock burst, such as geological conditions and shaft/gallery layouts. An analysis was also conducted to predict the occurrence of rock burst during the excavation of the shafts and galleries of the MIU. The results of the analysis indicated possibilities of rock burst in the cases where weak rock regions such as fault zones are excavated at a depth of 1,000 m or in the cases where a large-diameter shaft or gallery is bored or a new shaft or gallery is drilled near an existing shaft or galley. If, therefore, excavation is carried out under such a geological environment or in the case of such a shaft or gallery layout, acoustic emission (AE) monitoring, which has a proven track record as a means of rock burst detection, is conducted and measures such as reducing the advance per shot in blasting operations are taken.

(4) *Environmental conservation measures*
As shown in Figure 1, the construction site is close to an urbanized area and to many public facilities. In order to minimize adverse environmental effects, it is necessary to take into consideration the control of the effects of noise and vibration on adjacent facilities during construction, the influence on well water, and the water quality of water released into the river.

With respect to noise and vibration control, studies were conducted to conform to the relevant laws and regulations and find ways to reduce adverse effects in the most cost-effective manner. To be more specific, the locations and noise levels of noise sources were identified, and noise levels at nearby locations were calculated. Then, for specified types of construction tasks related to rock drills, concrete plants and other equipment, specifications for the panels for soundproof buildings on the ground surface were determined so that the standards under the relevant laws and regulations were satisfied.

In the construction phase, noise and vibration measurements in and adjacent to the construction site are conducted periodically to check on the effectiveness of noise control measures.

The influence on river water and well water is evaluated by measuring flow rates and water level. Water released into the river is treated appropriately in a wastewater treatment plant so that the requirements under the relevant laws and regulations are satisfied.

3 CONCLUSION

Foundation work at the shaft entrance locations at the MIU site began in July, 2003. The ground surface bird view of the main shaft construction site is shown in Figure 3 and the excavation work at the bottom of the main shaft is shown in Figure 4. The long term monitoring will be done using adjacent deep boreholes (a borehole length of 1,300 m).

On the basis of the information newly acquired from these investigation and research, the design and the construction plan will be reviewed and modified if necessary. Various data will also be acquired as excavation progresses so as to verify the validity of



Figure 3. Ground surface bird view of the main shaft construction site of MIU.



Figure 4. Excavation work at the bottom of the main shaft at MIU.

Copyright © 2005 Taylor & Francis Group plc, London, UK

the design and the construction plan and reflect new findings in the subsequent excavation plans for the research shafts and galleries.

REFERENCES

JNC (2000): H12 Project to Establish the Scientific and Technical Basis for HLW Disposal in Japan, Project Overview Report, 2nd Progress Report on Research and Development for the Geological Disposal of HLW in Japan, JNC Technical Report TN1410 2000-001, Japan Nuclear Cycle Development Institute, Tokai-mura Japan.

Toshinori SATO, Shin-ichiro MIKAKE, Takeshi TAMAI, Masanori IMAZU, Masanori SAKAMAKI (2003): Toward a Depth of 1,000 m from the Ground Surface - Construction Scheme of Mizunami Underground Research Laboratory,-JNC Technical Report, Japan Nuclear Cycle Development Institute, Mizunami Underground Research Laboratory, Tono Geoscience Center, Japan. (in Japanese)

Copyright © 2005 Taylor & Francis Group plc, London, UK

Water-tightening design and construction of tailbay tunnels at Kannagawa Power Plant

Fumiharu Kawashima
Tokyo Electric Power Co., Ltd., Japan

Masanao Yamasaki
Tokyo Electric Power Co., Ltd., Japan

Hiroaki Ozawa
Tokyo Electric Power Co., Ltd., Japan

Seigoh Ishizaki
Nishimatsu Construction Co., Ltd., Japan

Tatsuhiko Otani
Nishimatsu Construction Co., Ltd., Japan

Noboru Igarashi
Mitsubishi Heavy Industries, Ltd., Japan

ABSTRACT: The Kannagawa Power Plant, owned by Tokyo Electric Power Company, is presently under construction and is scheduled to start operation in July 2005. The effective water head is 653 m and the maximum output is 2,820 MW. The tailbay tunnel is just downstream of the power plant; thus there might be a significant influence of high water pressure on the cavern due to water leakage from the water tunnels. Therefore, the water-tightening design of tailbay tunnels near a large cavern requires special precautions. In this paper, the authors report on the concept of water-tightness design and the results of grouting of the tailbay tunnel.

1 INTRODUCTION

The Kannagawa Power Plant, owned by Tokyo Electric Power Company, is presently under construction and is scheduled to start operation in July 2005. As shown in Figure 1, the upper dam is located in Minami-Aiki Village in Nagano Prefecture and the lower dam is located in Ueno Village in Gunma Prefecture. The effective water head is 653 m and the maximum output is 2,820 MW.

The tailbay tunnel just downstream of the power plant consists of four water tunnels with inner diameters of 4,100 mm and two water tunnels with inner diameters of 5,800 mm. The former composes the section from the large cavern (power plant) to the first junction and the latter composes the section from the first junction to the second junction. The length of the tailbay tunnel is 190 m and the maximum design internal water pressure is 2.2 MPa.

The overburden is about 500 m and the geology is basically Mesozoic hard rock masses whose matrices are sandstone and mudstone, having a modulus of deformation of 2,500 to 5,500 MPa. The permeability of these rock masses is very low, and the mean and maximum permeability are under 1 Lu and 2 Lu, respectively. And no dominant fault zones were identified.

The large cavern of the power plant has a width of 33 m, a height of 52 m and a length of 216 m. The power generation equipment in this cavern will be installed gradually, according to the power demand in the future. Therefore, the cavern will be left in a partially unequipped state just after excavation.

The design concept for the stability of the cavern is to keep the underground water confined to the bottom of the cavern by the drainage tunnels around it. Consequently, there might be a significant influence of high water pressure on the cavern due to water leakage

Copyright © 2005 Taylor & Francis Group plc, London, UK

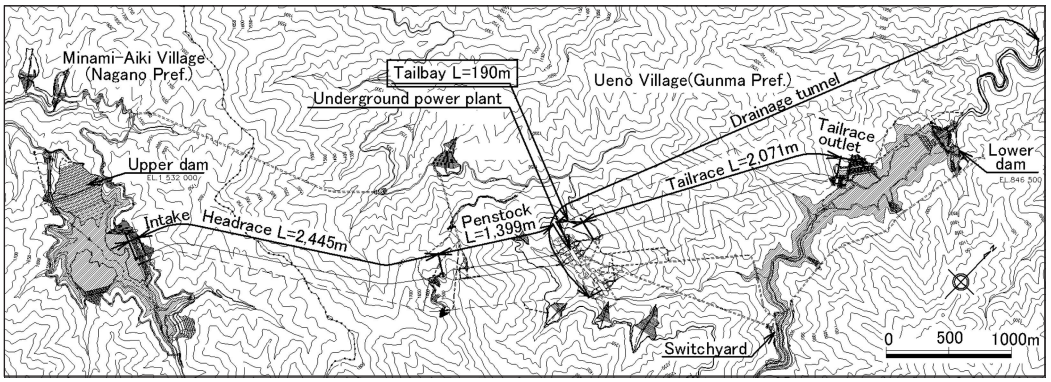


Figure 1. Location map of Kannagawa Power Plant.

from the water tunnels through the loosened rock masses, which may be damaged by blasting. From the permeability tests, the loosened rock masses may have a width of 1 to 2 m around the water tunnels and the maximum permeability is about 100 Lu or more. Therefore, the water-tightening design of the tailbay tunnel near a large cavern requires special precautions.

This paper reports on the water-tightening design and construction of the tailbay tunnel just downstream of the power plant.

2 THE CONCEPT OF WATER-TIGHTENING DESIGN OF TAILBAY TUNNELS

The tailbay tunnels near the large cavern are about 60 m in length and the junction sections are made of steel linings. But for cost savings, the tunnels in other sections are made of reinforced concrete.

In view of several other power plant projects, water leakage from the connections of 4100-mm-diameter steel linings and concrete linings where the seepage paths are particularly short, was regarded as a principal risk, and so the water-tightening design of the tailbay tunnel was carried out accordingly. Figures 2 and 3 show a longitudinal profile and a plan view of the tailbay tunnel, respectively.

2.1 *Design of steel lining*

The 60-meter-long section from the draft tube was designed as a steel lining section to ensure water-tightness as shown below:

- Steel lining stress under the internal water pressure (max. 2.2 MPa) while water flow is stopped must be 216 MPa or less.
- Critical buckling pressure under the external water pressure while the steel lining is empty must be 1.5 times the external water pressure (max. 0.8 MPa).

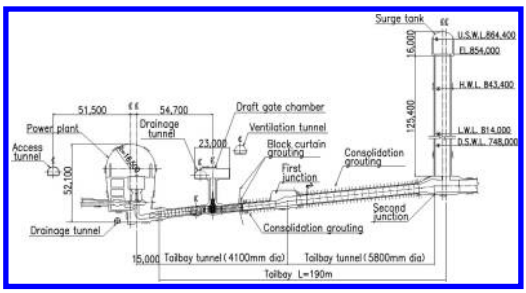


Figure 2. Longitudinal profile of the tailbay tunnels.

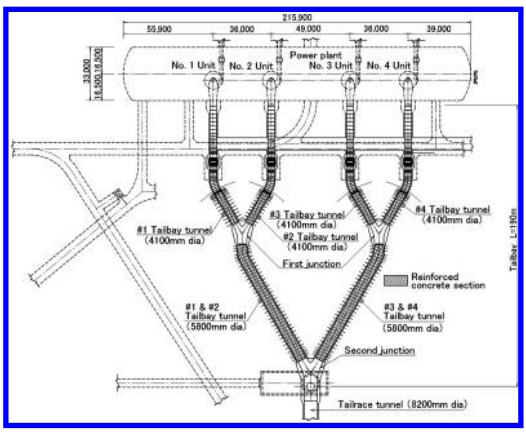


Figure 3. Plan view of the tailbay tunnels.

The steel lining is designed in order to maintain stability against either internal water pressure or external water pressure. The internal water pressure is estimated based on a situation in which the four power generation machines are stopped at the same time. The external water pressure is underground water pressure,

Copyright © 2005 Taylor & Francis Group plc, London, UK

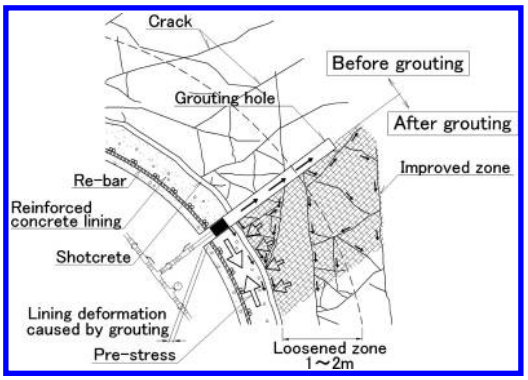


Figure 4. Pre-stressing by grouting.

which is estimated based on the investigation of the water pressure and the infiltration analysis.

2.2 *Design of reinforced concrete lining*

The 4100-mm-diameter tailbay tunnel section between the steel lining and the first junction was designed as a reinforced concrete structure.

In the sections of reinforced concrete, there is a risk that permeability will be higher than that of the steel lining. Therefore, the design concept of the RC tunnels should be a non-cracking concrete lining against the maximum internal water pressure (2.0 MPa), and pre-stressing of the lining by the consolidation grouting is expected.

In the lining design, it was decided to use a large amount of reinforcement (105 cm^2/m) that can be placed at the construction site for the lining thickness of 55 cm, and to use high-strength concrete (design strength: 40 MPa).

2.3 *Design of consolidation grouting*

2.3.1 *Mechanism of pre-stressing*

Figure 4 illustrates pre-stressing accomplished by consolidation grouting. By showing the states of the rock masses and lining concrete before and after consolidation grouting, it is assumed that the mechanism of pre-stressing is as follows:

- In loosened regions, water-tightness is improved by cement milk injected into open joints in the rock masses and bedding planes. When the cement milk infiltrates, the concrete lining is moved toward the inside of the tunnel and becomes pre-stressed.
- In low permeability regions outside the loosened regions, however, penetration of cement milk required for pre-stressing cannot be expected. So, mainly concrete-rock or concrete-lining interfaces were considered as areas to be grouted.

2.3.2 *Pre-stress to prevent cracking*

The amount of tensile stress that occurs in the lining under the maximum internal water pressure (2.0 MPa) is calculated by means of the method of Otto Frey-Baer. As a result, the tensile stress of concrete is calculated at 7.0 MPa, which is larger than the tensile strength of the concrete (3.0 MPa). It means that cracks occur when the lining is subjected to the maximum internal water pressure. Therefore, the concrete has to be pre-stressed up to 4.0 MPa (=7.0 MPa − 3.0 MPa).

In this case, if the pre-stress introduction ratio is assumed to be 30%, in order to introduce the target pre-stress, the required grouting pressure is 2.5 MPa (determined by the thick-cylindrical shell theory). In order to ensure successful grouting, however, a maximum grouting pressure of 2.8 MPa has been adopted.

2.3.3 *Improvement of water-tightness*

The loosened region around tailbay tunnel #1 extends over a distance of 2 m into the surrounding rock masses. In the loosened region, there are areas where permeability exceeds 10 Lu, and there are even extremely permeable areas where more than 100 Lu was recorded. The thickness of the loosened regions in the rock masses around tailbay tunnels #2, #3 and #4 are about 1 m. The permeability of the surrounding rock masses exceeds 10 Lu locally, but never exceeds 100 Lu.

In view of the distribution of permeability values and cracks around the tunnels, it was decided that the length of the grouting hole should be 3 m into the rock masses for tunnel #1, where the loosened region was about 2 m deep; and 2 m into the rock masses for tunnels #2, #3 and #4, where the loosened region was about 1 m deep.

Anticipating a failure to achieve the required pre-stress, it was decided that a mean permeability of 1 Lu should be adopted as the target level so that piping would not occur under the maximum internal water pressure.

3 CONSOLIDATION GROUTING

3.1 *Consolidation grouting of tailbay tunnel*

The results of the consolidation grouting of the head-race tunnel in Kannagawa Power Plant confirmed that the primary grouting sufficiently lowers the permeability of the rock masses. Considering this fact, the basic policy of the consolidation grouting is set up as follows:

- The permeability of rock masses around the tunnel is sufficiently lowered only by the primary grouting.
- After secondary grouting, priority is given to pre-stressing the concrete lining; the main point is to introduce pre-stresses appropriately.

Copyright © 2005 Taylor & Francis Group plc, London, UK

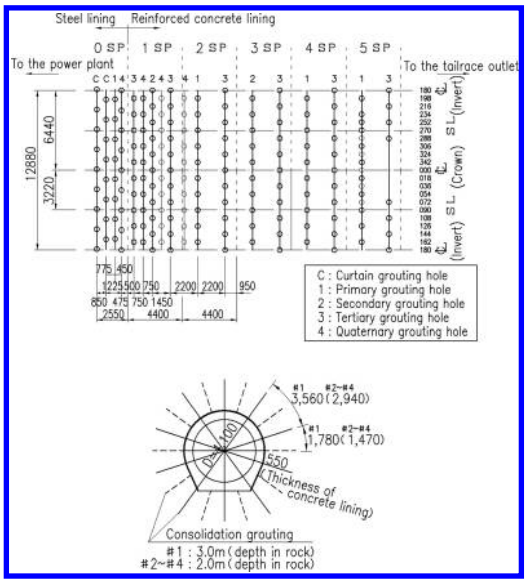
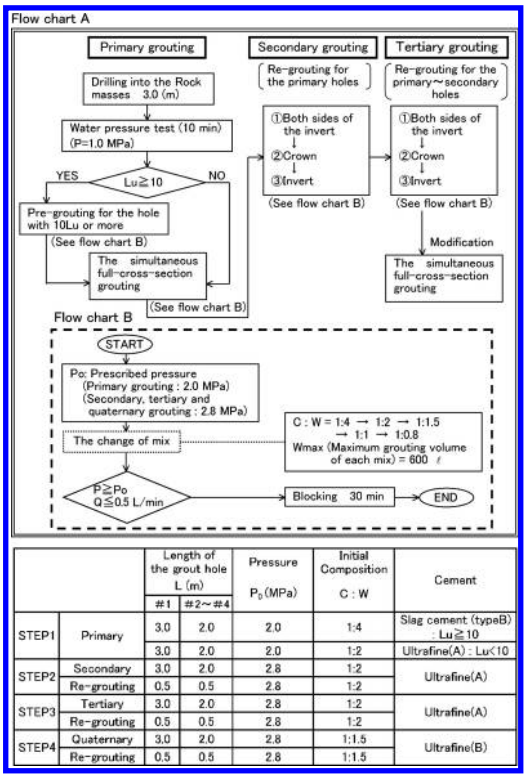


Figure 5. Consolidation grouting.



		Length of the grout hole L (m)		Pressure P_0 (MPa)	Initial Composition C : W	Cement
		#1	#2~#4			
STEP1	Primary	3.0	2.0	2.0	1:4	Slag cement (typeB) : Lu≧10
		3.0	2.0	2.0	1:2	Ultrafine(A) : Lu<10
STEP2	Secondary	3.0	2.0	2.8	1:2	Ultrafine(A)
	Re-grouting	0.5	0.5	2.8	1:2	
STEP3	Tertiary	3.0	2.0	2.8	1:2	Ultrafine(A)
	Re-grouting	0.5	0.5	2.8	1:2	
STEP4	Quaternary	3.0	2.0	2.8	1:1.5	Ultrafine(B)
	Re-grouting	0.5	0.5	2.8	1:1.5	

Figure 6. Grouting flow chart.

Based on this basic policy, the consolidation grouting of the 4100-mm-diameter tailbay tunnel was planned.

Figures 5 and 6 show the grouting design and grouting specifications for the 4100-mm-diameter tailbay tunnel. The grouting specifications are reviewed and modified from time to time according to the degree of improvement and the amount of pre-stress being introduced.

(1) Grouting pressure

In the primary grouting, the improvement of the water tightness was the main purpose. Thus, in order to be easily pre-stressed by secondary and subsequent grouting, it was decided that the grouting pressure should be 2.0 MPa, which is equivalent to the maximum design internal water pressure.

On the other hand, the main purposes of the secondary and subsequent grouting are to introduce pre-stresses appropriately. Thus, in order to ensure successful grouting, however, a maximum pressure of 2.8 MPa has been adopted (see 2.3.2).

(2) Grouting method

All primary holes were grouted simultaneously by the full-cross-section grouting method in order to minimize pressure decreases during the cement milk infiltration process.

The grouting sequences for the secondary and subsequent grouting holes were determined according to the pre-stresses introduced by the primary hole grouting. If the pre-stress level achieved was not enough, priority was given to the pre-stressing of the invert, which had been considered to be the most difficult to pre-stress, considering the excavated shape of the tunnel.

In order to minimize flexural tensile stress in the invert lining concrete, grouting was carried out in this order: (a) the walls on both sides of the invert, (b) the crown, and (c) the invert.

In the actual grouting process, it was confirmed that the pre-stress introduced was lost, especially, in places away from the grouting holes when, for example, the flow rate decreased during pre-blocking grouting (while the specified level of pressure was maintained).

We can assume that the loss of pre-stress was caused by the decrease of pressure in the region near the front end of the penetrating cement milk, and partly because the cement milk was diluted by the progress of cement milk penetration.

In view of these results, the simultaneous full-cross-section grouting method was reviewed and modified. Furthermore, the grouted holes were also drilled again (0.5 m into the rock masses) and additional grouting was carried out.

(3) Grouting material and initial composition

The grouting material used for the primary grouting holes with a permeability of 10 Lu or more was slag cement (type B), and the initial composition was C:W = 1:4.

Copyright © 2005 Taylor & Francis Group plc, London, UK

For the primary grouting holes with a permeability of lower than 10 Lu and for the secondary and subsequent grouting holes, ultrafine cement was used to minimize the dilution of the grouting during penetration. Ultrafine cement made by A corporation (Blaine fineness: 9,300 cm^2/g; 50% grain size: 3.5 μm), which had also been used at several other power plant projects, was used. For the quaternary holes, ultrafine cement made by B Corporation (Blaine fineness: 13,000 cm^2/g; 50% grain size: 2.5 μm) was used, because a higher Blaine fineness value was desired. The latter cement cost is almost the same as that of the former one.

In consideration of viscosity and bleeding, an initial composition of C:W = 1:2 was adopted as shown in Figure 6. However, in the actual grouting process, it was difficult to pre-stress at this initial composition. Thus, in order to reduce the dilution, the initial composition was changed to C:W = 1:1.5.

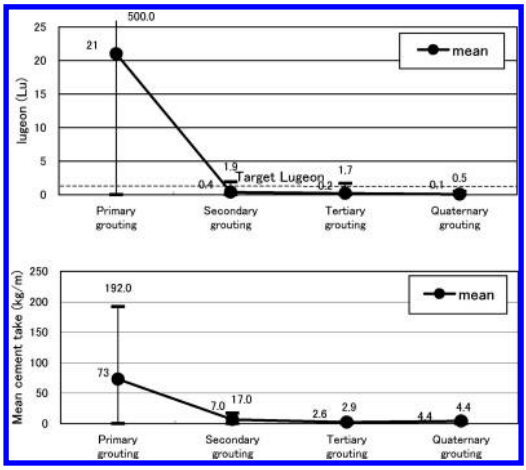


Figure 7. Lugeon and cement take vs. grouting stages.

3.2 *Improvement of water-tightness*

Figure 7 shows the quantities of cement used in grouting holes of different stages. As shown, the pre-grouting mean permeability and maximum perme-ability during primary grouting were 21 Lu and 500 Lu, respectively, while the pre-grouting mean permeability and maximum permeability at the secondary holes were 0.4 Lu and 1.9 Lu. These results clearly indicate the effects of the simultaneous full-cross-section grouting and the use of ultrafine cement for the primary grouting.

The fact that the pre-grouting permeability of the quaternary holes never reached 1 Lu (max. 0.5 Lu) indicates that a sufficient level of water-tightness was achieved by the grouting of tertiary or earlier holes.

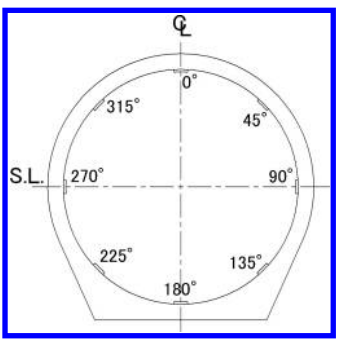


Figure 8. Locations of strain gauges.

3.3 *Pre-stresses*

In order to check the amounts of pre-stress actually introduced, pre-stress measurements were conducted by using strain gauges on the inside surface of the lining concrete, as shown in Figure 8.

Figure 9 is an example of the measurement results, and shows the surface strain time history and the distribution of strains in the cross sections. The target pre-stresses have been largely achieved mainly on both sides of the invert, but the target levels have not been attained at other locations.

Figure 10 also shows that the pre-stresses introduced were achieved mostly by primary grouting.

3.4 *Comparison with the grouting in the weak rock masses at the headrace tunnel of Kannagawa Power Plant*

Grouting was also performed in the weak rock masses at the headrace tunnel of Kannagawa Power Plant for the purpose of pre-stressing. As a result, the required level of pre-stress was achieved.

The geology of the headrace tunnel is composed mainly of serpentinite and mudstone. These rock masses are heavily weathered, and their modulus of deformation is 38 to 780 MPa, which is extremely low compared with the values of the tailbay tunnels (2500 to 5500 MPa). And permeability exceeds 10 Lu locally.

As shown in Figure 11, relatively large quantities of cement milk were injected into the weak rock masses at every grouting stage and the effects of grouting are obvious. Therefore, the quantity of cement used seems to greatly affect the amount of pre-stress introduced.

Differences in the quantity of cement injected are likely due to the composition of rock masses. Since there are partially argillized regions along cracks in the weak rock masses, relatively large quantities of cement milk can be injected. Hence, the weak rock masses are located within a relatively small area, and

Copyright © 2005 Taylor & Francis Group plc, London, UK

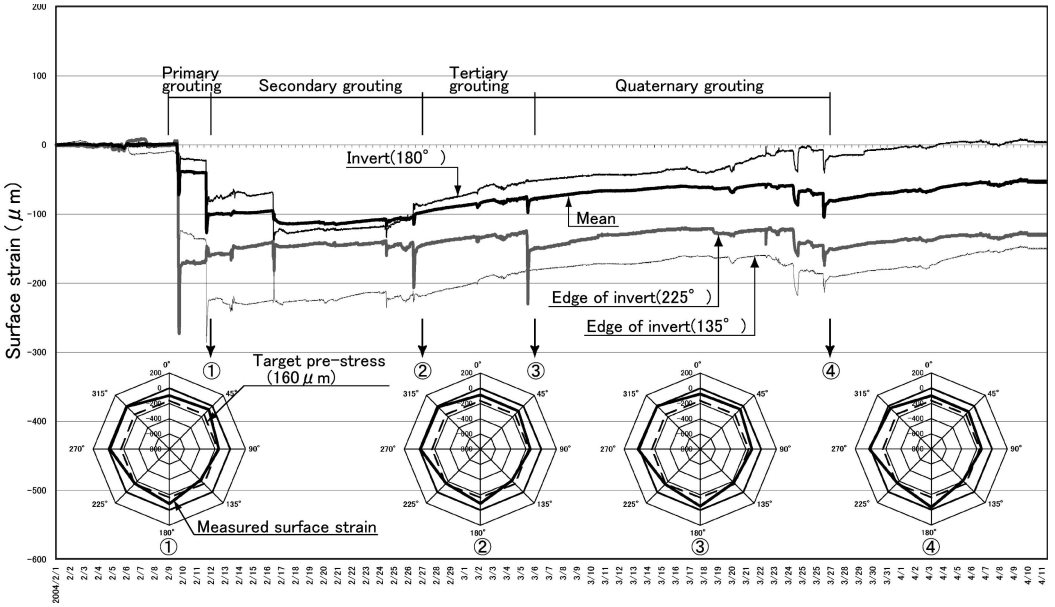


Figure 9. Strains vs. time.

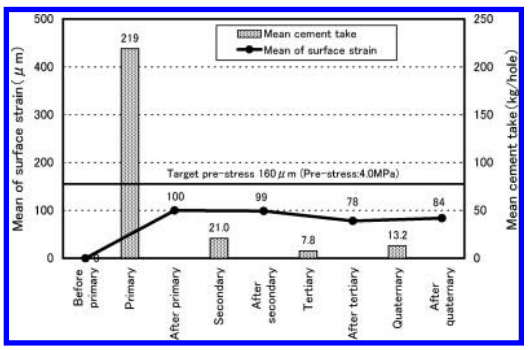


Figure 10. Strains and cement take vs. grouting stages (Tailbay tunnel).

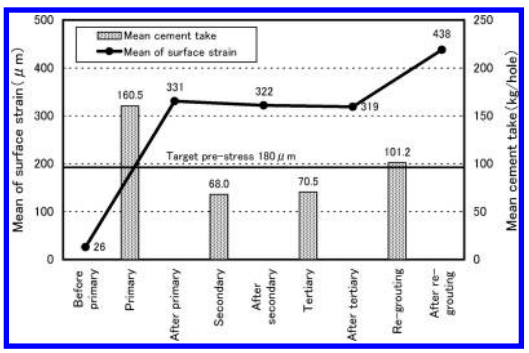


Figure 11. Strains and cement take vs. grouting stages (Headrace tunnel).

it is assumed that the surrounding hard rock masses provided enough reaction for pre-stressing.

On the other hand, at the tailbay tunnel in extremely hard rock masses, only local open cracks were grouted and, therefore, no other region could be grouted.

Considering that in cases where extremely hard rock masses are to be grouted (as in the case of the grouting carried out at the tailbay tunnel), it may be necessary, for example, to provide voids behind the concrete lining prior to grouting.

4 CONCLUSION

In the 4100-mm-diameter reinforced concrete tailbay tunnel, it was expected that pre-stressing of the lining (i.e. non-cracking concrete lining) could be achieved by consolidation grouting. But, in general, the target pre-stress was not attained.

Meanwhile, it has been confirmed that the permeability of the rock masses around the tunnel was sufficiently lowered. Therefore, there was no significant influence of water leakage from the water tunnels on the cavern of the power plant.

The grouting in the tailbay tunnel section has already been completed, and the filling of the water tunnels began at the end of July 2004. The present water pressure is 1.2 MPa, so the design internal water pressure (2.0 MPa) has not yet been reached. In addition, water leakage into the adjacent drainage tunnels has

Copyright © 2005 Taylor & Francis Group plc, London, UK

not been observed. Monitoring of tailbay tunnel behavior will be continued.

REFERENCES

Ito, K., Takatsu, H. & Nozawa, K. 1992. Design and construction of headrace tunnel at Sabigawa Pumped-storage Power Plant. *Electric Power Civil Engineering*, 241: 12–21. (in Japanese)

Japan Electric Power Civil Engineering Association, 1986. Design and construction of underground structures for electric power facilities. (in Japanese)

Copyright © 2005 Taylor & Francis Group plc, London, UK

Study on state and pattern analysis of tunnel portal slope in Korea

Y. Baek, O.I. Kwon, H.B. Koo & G.J. Bae
Korea Institute of Construction Technology, Goyang, Korea

ABSTRACT: The number of tunnels are in fact increasing as a part of linear improvement project of general national highway and road enlargement and pavement project. Recently, collapses of portal slope are also occurring considerably, due to local raining from severe rain storm and abnormal weather. Accordingly, it was risen a necessity to efficiently respond to tunnel portal slope damage and maintenance in Korea and oversea nations. This paper is a basic proposal to execute a survey on the current status and state of the tunnel portal slopes that were already installed and are now being operated along general national highways, and also to execute state evaluation for the purpose of managing those effectively. As a research method, domestic tunnels were analyzed in accordance with geometrical shape such as access type, portal form, and tunnel type, etc. via field survey to analyze the types of tunnel portal slopes along national highways. State evaluation classification sheet is presented to divide classes for the danger state of the surveyed portal slopes, and then the related grades are divided. It is mainly aimed at classifying the tunnel portal slopes along national highways with using this state evaluation, to use it as basic data so that continuous maintenance can be executed in the future in accordance with danger classes.

1 INTRODUCTION

In Korea, it is inevitable for tunnel to be generated following the construction of roads because more than 70% of land is mountainous area in view of topography features. It is actually tremendous national loss, i.e. cut-off of traffic and loss of lives due to collapses of Tunnel portal slope and entrance/exit slopes every year. The total number of tunnels, which are managed by nationwide 18 national highway maintenance & construction offices, are 105 tunnels, and the dispersion status of 5 regional construction management offices is as shown in Table 1. It was surveyed that there were many number of tunnels in Seoul Regional Office, Busan Regional Office, and Daejon Regional Office, and the average extension was resolutely the longest in case of Daejon Regional Office.

This research is aimed at: analyzing the overall status based on the data collected from direct surveying and observation on national highway's tunnel portal slope; evaluating the construction and stability of portal slope; and then using it as basic data for the arrangement of future maintenance measures and the related researches.

Table 1. Tunnel dispersion status along the national highways in Korea.

Regional Offices	Total	Seoul	Wonju	Daejon	Igsan	Busan
No. of tunnel	105	28	20	23	20	24
Average length	608	458	653	729	607	568

2 ANALYSIS ON THE CURRENT STATUS OF TUNNEL PORTAL SLOPE

The data acquired from field survey was used for the analysis on the current status of tunnel portal slope along national highways and its state evaluation. The fields that were utilized for this data analysis are as shown in Table 2. As shown in Table 2, the current status was analyzed dividing it into tunnel name, the number of tunnel portals, and the number of portal slopes. Those differences are due to such tunnels of national highway as being divided into up-stream and down-stream, coming and going lane tunnels, and tunnels without portal slope. The number of portal slopes refer to the numbers in the field surveys, which were used in field survey of portal slope, and it were divided into as followings when we watch the portal in front of it; "front slope" that is located upper part of entrance of tunnel; "left slope" that is located at the left side connected to entrance of tunnel; and "right slope" that is located at the right side. For the respect tunnel entrance of tunnels, there are cases that all three of left, front, right slopes exist, while cases that are different,

Copyright © 2005 Taylor & Francis Group plc, London, UK

Table 2. The numbers of tunnels and portal slopes per management offices.

Regional construction management offices	Highway maintenance & construction offices	Number of tunnel name	Number of portals	Number of tunnel sites
Seoul	Suwon	2	6	4
	Uijeongbu	7	17	14
Wonju	Hongcheon	12	26	16
	Gangneung	–	–	–
	Jeongseon	4	8	4
Daejon	Nonsan	5	10	7
	Chungju	7	17	14
	Boeun	–	–	–
	Yesan	1	1	2
Igsan	Gwangju	6	15	9
	Jeonju	1	2	1
	Namwon	4	8	5
	Suncheon	3	8	5
Busan	Daegu	–	–	–
	Jinju	2	4	4
	Pohang	4	8	6
	Yeongju	7	14	10
	Jinyeong	3	6	4
Total		68	151	105

Table 3. Number of tunnel type and tunnel length.

Tunnel type	No. of tunnel	No. of portal	Division	Length (m)	Remarks
Single lane parallel tunnel	37	89	Minimum	150	Gwangju office (Chuwolsan tunnel)
Double lane tunnel	30	60	Maximum	1,960	Chungju office (Bakdaljae tunnel)
Single lane tunnel	1	2	Average	608	

due to the topographical causes such as access type, etc. mentioned earlier. To see it by regional office, the number of portals of Seoul Regional Office are 23, which shows the least dispersion, and the numbers of portals of Wonju Regional Office, Iksan Regional Office, and Busan Regional Office are similar each other.

For the analysis on tunnel portal slope, the respect tunnel field was divided into entrance and exit. Also, to analyze the portal in detail, it was divided into the location of portal, single tunnel, and double lane tunnel. The reason why is that can be used in maintenance system in the future, which will be applied in view of maintenance. Table 3 shows the result of analysis on the number of tunnels per tunnel type and tunnel extension. From Table 3, "single lane parallel tunnel" refers to a couple of tunnels of which portal's locations are the same and up/down streams are divided into two tunnels, while "double lane tunnel" refers to a tunnel of which up/down streams are the same. Also, "single lane tunnel" refers to a tunnel that just one lane among up and down streams is made by tunnel. As a result of analysis, it shows that single lane parallel tunnels occupy most of tunnels in Korea. In case of single lane tunnel, there is Maamsan tunnel in the jurisdiction of Jinyeong office, of which down stream lane is made by tunnel, hence it is only one tunnel of the case. For tunnel length, it was surveyed that Chuwolsan tunnel in the jurisdiction of Gwangju office is the shortest while the longest one is Bakdaljae tunnel within the jurisdiction of Chungju office.

The location and types of tunnel portals were analyzed in view of maintenance such as future maintenance and introduction of real-time monitoring system. Table 4 is the results of analysis on access types and portal form. First, analysis on access types will be presented and then the analysis on portal form will be described.

Generally, the access type of entrance of tunnel is influenced the most from topography or weather, which may be divided into total of 5 types depending on the relation between topography and tunnel central axis: "slope orthogonal type", the best idealistic location

Copyright © 2005 Taylor & Francis Group plc, London, UK

Table 4. Access types and portal forms of tunnel entrance.

Access type	No. of portal slope	Portal form		No. of portal slope
Slope orthogonal type	10	Gravitational type	Gravitational-subgravitational	3
Slope slant intersection type	46	Facing wall type	Wing	99
Slope parallel type	11		Arch wing	7
Base root parallel type	40	Projecting type	Cylinder open-cut	39
Valley ccess type	44		Parapet	2
			Projection	1
			Bell-mouth type	0

relation of tunnel building line and slope; "slope slant intersection type" where tunnel building line accesses slightly against slope; "slope parallel type" that slant intersection is most extreme; "base root parallel type" that accesses along the ridgeline of topography and the excavations of entrance of tunnel is the least along the line; and "valley access type" that accesses along the valley of topography. As a result of analysis, the most common access types are in the order of slope slant intersection type, valley access type, base root parallel type, slope parallel type, and slope orthogonal type. This is regarded as a result of the Korean condition of which topography is mountainous, and of the current basic plant that road linearization is proceeded. Also, it shows that there are many tunnels of valley access type to minimize the length of tunnels, and that the tunnels parallel with slope are relatively less in consideration of the eccentric earth pressure that is influential on tunnel stability.

Then, portal forms were analyzed. The form of portal, which makes tunnel entrance, is selected in consideration of topography, geography, drain, etc., in order to protect portal from rockfall, snowslide, Water leakage, etc. The forms of portals are largely divided into gravitational type, facing wall type, and projecting type. As a result of analysis on data, it shows that most of the tunnel portal forms in Korea are wing type of facing wall type and cylinder open-cut type of projecting type shows the next frequency. It seems that the portal form of tunnel is selected and constructed to minimize the damage to original ground due to road establishment using the land and terrain of a variety of mountainous topography in Korea.

3 TUNNEL PORTAL SLOPE STATE EVALUATION

3.1 *State evaluation decision method*

A necessity is derived to evaluate the state of the surveyed tunnel portal slope for the purpose of the efficient maintenance. It is regarded that the state of tunnel portal slope can be evaluated according to the criteria of the proposed state evaluation and then targets of concentrated management can be selected, which also can be used as data to arrange medium and long term measurements. For the systematic management of tunnel portal slope, first, integrated decision should be made in consideration of basic data of tunnel portal slope, portal slope state evaluation, and damage probability. In this paper, basic value is given for the items that state evaluation of portal slope can be executed, and then quantified value is given for the respect parameter, to give a grade finally. State evaluation grades are divided into total of 5 grades as like as in the result of safety diagnosis of structures.

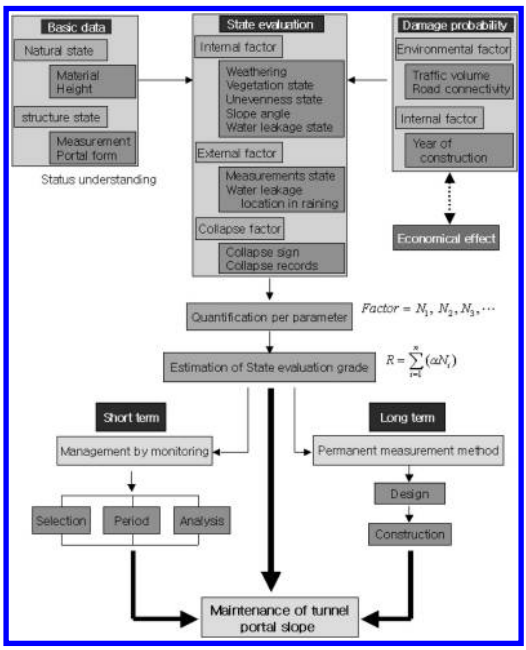


Figure 1. Flow chart of tunnel portal slope state evaluation.

Figure 1 roughly shows a flow chart that the state evaluation of tunnel portal slope is performed and then continuous maintenance is executed in the future. In general, for the management of portal slope, it is

Copyright © 2005 Taylor & Francis Group plc, London, UK

Table 5. State evaluation classification sheet for tunnel portal slopes.

Item			Grade I	II	III	IV	V	VI
Basic data	Material		Soil slope, rock slope, mixed slope					
	Height		Vertical height at the highest point of portal slope					
	Measurements method		Writes measurement method for the previously constructed					
	Portal form		Gravitational type, facing wall type, projecting type, and classified into 7 in detail					
Portal slope state	Weathering	Division	Fresh	S.W	M.W	H.W	C.W	R.S
		Rating	0	3	5	7	9	11
	Vegetation state	Division	Good	Fair	Poor	–	–	–
		Rating	0	3	5	–	–	–
	Unevenness state	Division	flat	Regular	Unevenness	–	–	–
		Rating	0	3	5	–	–	–
	Slope angle	Division	<30°	<50°	<60°	60°<	–	–
		Rating	1	4	7	10	–	–
	Water leakage state	Division	Dry	Damp	Wet	Flowing	–	–
		Rating	0	2	5	8	–	–
	Measurements state	Division	Good	Fair	Poor	–	–	–
		Rating	0	4	8	–	–	–
	Water leakage location in raining	Division	N/A	Lower part	Middle part	Upper part	–	–
		Rating	0	2	5	8	–	–
	Collapse sign	Division	N/A	Low	Regular	High	–	–
		Rating	0	4	8	12	–	–
	Collapse records	Division	N/A	Rockfall	Surface Failure	Collapse	–	–
		Rating	0	4	8	12	–	–
Collapse damage probability	Year of construction	Division	5 years	<10 years	<20 years	20 years <	–	–
		Rating	1	3	5	7	–	–
	Traffic volume	Division	<5,000 cars	<10,000 cars	<20,000 cars	>20,000 cars	–	–
		Rating	1	3	5	7	–	–
	Road connectivity	Division	Expressway	Highway	Local road	Village road	N/A	–
		Rating	0	1	3	5	7	–

arranged to decide whether to execute state evaluation and then to manage it using monitoring system in view of short term base, or if permanent measurements is necessary or not in respect to whether to arrange urgent measures because stability is not secure.

The value allotment of state evaluation grade of tunnel portal slope is comprised of 16 evaluation items at large. It was largely divided into 3 units, and 12 evaluation items were given with values, which were the basic scores for the state evaluation classification of portal slopes. Among those things, material, height, measurements method and portal form, which are corresponding to basic data, were not given with the values, instead, they were used as basic data only.

Table 5 is a classification sheet that is proposed to execute state evaluation. For each value allotment, the value distributions are different using the order of the higher possibility to have influence on stability in consideration of the collapse and stability of portal slope. Total state evaluation grade can be calculated as

$$R = \sum_{i=1}^{n} (\alpha N_i) \tag{1}$$

Where, R is the score of state evaluation total sum, and N is the value of each parameter.

The state evaluations of tunnel portal slope were divided into 5 grades using that is a calculation of total sum per detailed evaluation item. Table 6 shows criteria representing state evaluation classification of tunnel portal slope. This state evaluation criteria will utilized as a reference for whether to apply monitoring and permanent measurements method in view of the maintenance of portal slopes.

State evaluation of tunnel portal slope was executed using the data after completing field survey.

Copyright © 2005 Taylor & Francis Group plc, London, UK

Table 6. State evaluation criteria and measurement method.

Grade	Division	Details of tunnel portal slope
A	$0 < R < 30$	Considerably favorable status of both of construction and management Tunnel portal slope that has low priority of measurement preparation within short period including maintenance
B	$31 < R < 40$	When finding of slight damage state When urgent preparation of measurement is not required because it is already constructed according to measurements method, but it is necessary to arrange medium and long term measurement, which is divided and managed as a maintenance target. Portal Slope for which it is necessary to arrange measurement for some of sections where the stability is low
C	$41 < R < 50$	State that partial collapse is possible and so partial measurement is required. Portal Slope under the state of requiring medium and long term measurement while it has rare possibility of large scale collapse of portal slope
D	$51 < R < 70$	State that possibility of collapse is a little and so it is necessary to arrange a measurement as soon as possible Portal Slope that requires you of being somewhat cautious when you use road
E	$71 < R < 100$	State that stability is not secured and so it is necessary to arrange and execute a measurement as soon as possible Portal Slope that it should be performed to review the stability by experts for the entire sections

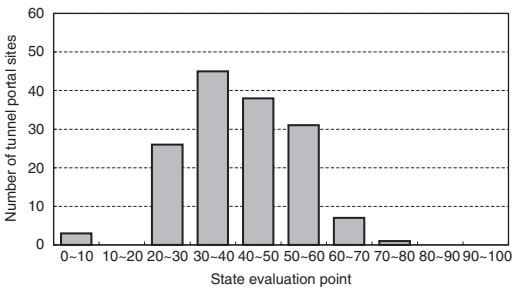


Figure 2. Graph of state evaluation analysis result.

To see the distribution ratio, it shows normal distribution form. Figure 2 shows the state evaluation distribution form by graph.

4 CONCLUSION

Pattern of portal slopes were analyzed through status investigation targeting at the tunnel portal slopes on the national highways in Korea. Total of 151 tunnel portals were analyzed, and a state evaluation classification sheet was proposed. The followings are summarizations of research results that were performed in this paper.

(1) The total number of tunnels, which are managed by 18 national highway maintenance & construction offices, are 105 tunnels. To see the current status of dispersion per regional office, it was surveyed that the number of tunnels was the most in case of Seoul Regional Office and Busan Regional Office while Daejon Regional Office was the longest in view of average extension.

(2) As a result of analysis for the current status and state evaluation of tunnel portal slope, it shows that most of tunnel types are single parallel tunnels in case of Korea. To see it in view of extension, it was surveyed that the extension of Chuwolsan tunnel was the shortest, while Bakdaljae tunnel of Chungju office was the longest. Calculating the average extension of the surveyed data is 608 m.

(3) It shows that most of access types are in the order of slope slant intersection type, valley access type, base root parallel type, slope parallel type, and slope orthogonal type. Most of portal forms are mainly wing type of facing wall type, and cylinder open-cut type of projecting type is the next frequent one.

(4) For the state evaluation, basic value was given and quantified value was also given for each parameters, which were finally divided into 5 grades. State evaluation distribution shows somewhat modified normal distribution.

(5) In case of Tunnel portal slope, it is very difficult to survey the potential structural collapses as it is very difficult to make an observation on discontinuity due to very good development state of vegetation. Accordingly, it is required to perform researches in regard to the establishment of maintenance method using monitoring technology as well as development of stability evaluation technique or surveying technique to complement that in the future.

Copyright © 2005 Taylor & Francis Group plc, London, UK

ACKNOWLEDGMENT

This study is part of a research program funded by Ministry of Construction and Transportation under grant No. C103A1000013-03A0200-01310.

REFERENCES

Korean National Railroad (2003), pp.1～42. Volume 5, Tunnel, Railroad design handbook (road bed)

Pung-hui Lee, Jae-sang Shin, Il-hwan Kim, U-seong Kim, Yeong-geun Kim (2003), "Design criteria of environmental friendly tunnel portal considering road safety", pp.18～33, No.4, Volume 5, Tunnel Technology, Korean Tunnelling Association

Korea Infrastructure Safety & Technology Corporation (2003), "Detailed guides for safety check and precision safety diagnosis (cutting slopes)", p.118, Volume 1, Ministry of Construction and Transportation

Korea Institute of Construction Technology (1999), "Road design handbook(I)", pp.600-1～623-5, Volume 1, Ministry of Construction and Transportation

Copyright © 2005 Taylor & Francis Group plc, London, UK

Desilting chambers of Nathpa Jhakri Hydroelectric Project – case study of problems during construction and remedial measures

S.P.S. Chauhan & R. Jeyaseelan
Central Water Commission, New Delhi, India

ABSTRACT: The 1500 MW Nathpa Jhakri hydroelectric Project located in Kinnaur & Shimla district of Himachal Pradesh (India) envisages harnessing of Hydro-power potential of river Satluj in the form of run-of-the-river development. It is a mega project with many major features and first of its kind in the Himalayan region. The technical support to the project was available from various fora. The panel of experts (POE) which comprised of many experts of national and international repute were regularly visiting the project. Central Water Commission, the apex body in the field of water resources development, was principal consultant. A consortium of Electrowatt Engineering Services ltd. (Switzerland), Nippon Koei co. ltd. (Japan) and Water and Power Consultancy Service ltd. (India) was associated with the project as Retainer Consultant. Besides this, advice and services of other expert individuals and institutions were availed from time to time.

A discharge of 486 cumecs (including 81 cumecs for flushing) is drawn from river Satluj by a 60.5 m high concrete gravity dam through four intakes. The diverted water passes through four underground Desilting Chambers, and 10.15 m diameter 27.4 km long Head Race Tunnel leading to a 301 m deep Surge Shaft of 21.5 m diameter. From here the water is conveyed through three pressure shafts to feed six generating units of 250 MW each housed in an underground power house. Water leaving the six units flows through draft tube tunnels in to a collection gallery. It finally returns to river Satluj through a 980 m long 10.15 m dia. Tail Race Tunnel and an outfall system.

1 DESILTING CHAMBERS

The water drawn through four independent intakes is conveyed by means of 6.0 m diameter, horse shoe shaped four inlet tunnels and 50 m long transitions to the four underground desilting chambers located on the left bank of the river Satluj. Each of the chambers is 525 m long, 16.31 m wide at the center and 27.5 m high inclusive of 5 m hopper portion. The chambers are egg-shaped, having circular arch roof, curved walls and hopper shaped bottom. They are spaced 45.6 m center to center leaving a rock pillar of about 29 m between adjacent chambers. At the top of the hoppers, inspection platforms are provided on both sides. At the bottom of the hoppers are the setting trenches and flushing conduits. Desilted water goes out through four outlet tunnels which connect the Head Race Tunnel. The silt is flushed out through Silt Flushing Tunnel back into river Satluj. The desilting complex is one of the largest such complexes in the world. Simplified plan and section of the chamber is given in Fig. 1(a) & (b).

2 TOPOGRAPHY, GEOLOGY AND ORIENTATION OF THE DESILTING CHAMBERS

The desilting arrangement is provided underground in the left bank hills with steep cliffs and escarpments. The hill mass rises continuously for about 1500 m from the Satluj river at El.1450 with 40° to 70° slopes. The desilting chamber complex area has a lateral cover of about 250 m to 750 m and a vertical cover of about 300 m to 600 m.

During preconstruction investigations geological explorations were conducted in the desilting chambers area through a drift across the chambers and along the full length of one of the chambers. The rocks in the area are predominantly compact and massive augen gneiss and gneiss with minor bands of biotite schist, sericite schist and are intruded by amphibolite, granite, pegmatite and quartz veins. In this rock mass shear seams 1–5 cm and 5–50 cm width are common. The general foliation direction (strike N 70 W – S 70) is 30° askew to the direction of river flow. The rock mass has four sets of major joints in addition to the foliation joints. The interfilling consists of clay gouge and rock flour Geo-technically chambers are largely in class II and III rock with about 5% in class IV and

Copyright © 2005 Taylor & Francis Group plc, London, UK

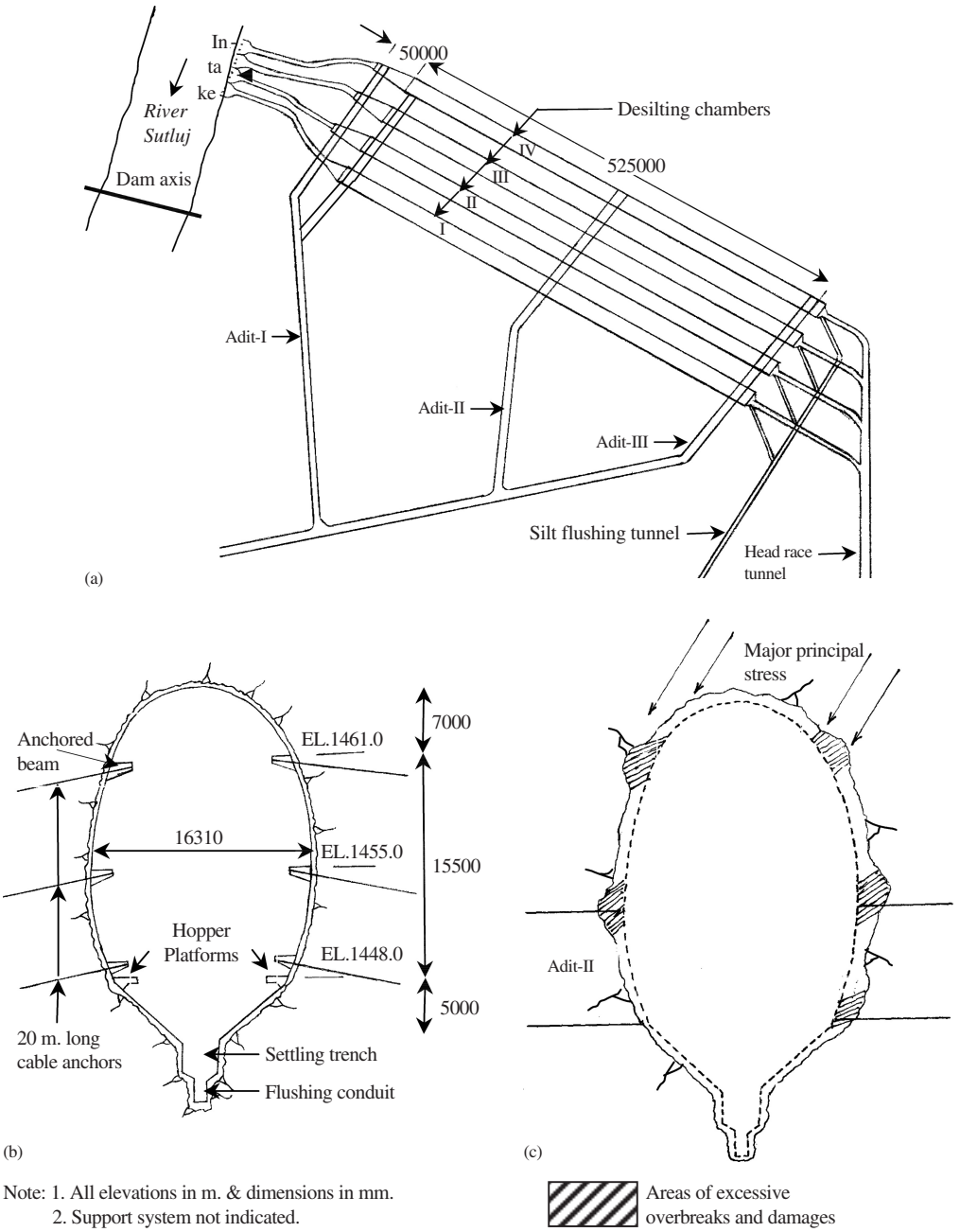


Figure 1. (a) Schematic plan of desilting chambers; (b) Cross section showing gantry beams; (c) Typical excavated section.

V rock. During construction exhaustive geological mapping of the excavated surfaces was carried out. No appreciable difference in the predicted geology and the actually encountered geology was observed.

The alignment of desilting chambers has been kept in the direction N 28 E-S 28° W which is about 42° askew to the foliation direction and 72° askew to the direction of flow of river.

Copyright © 2005 Taylor & Francis Group plc, London, UK

3 EXCAVATION METHOD AND SUPPORT SYSTEM

Excavation was done using conventional drill and blast method in different sequences. The central gullet was excavated first followed by side slashing to achieve the full width of the chambers. Excavation proceeded from top to bottom with a bench depth of 5.0 m. Smooth blasting technique were to be employed. During excavation considerable over-breaks occured almost at all locations. It was particularly excessive near the haunches reaching up to 2.0 m at some places. Due to this the surface of the desilting chamber became quite uneven and localized pockets of high stress concentration were formed. The issue of controlling the overbreaks was addressed after two major rock falls in May 2000 and pre-reinforcement of rock before careful and controlled blasting was resorted to.

Later on when shotcrete detachment and rock falls became substantial and it was noticed through instrumentation data that blasting in one chamber had some effect on other chambers also, further precautions about sequence of blasting and muck removal were adopted to minimize the effect.

To begin with support system was designed as rock bolts and shotcrete with wire mesh as initial support followed by a final lining of 300 mm thick concrete. The support system was changed to rock bolts and steel fiber reinforced shotcrete (SFRS) instead of shotcrete with wire mesh as initial support. The final lining also was decided to be of SFRS with minimum 150 mm thickness in walls and 200 mm in the roof. The SFRS was considered to be a better and faster alternative. However the hopper and conduit portion were to be concrete lined only. In general the support system was initial layer of 50 mm thick shotcrete with 32dia, 6 to 7.5 m long pattern rock bolting. The additional thickness of SFRS which was to be done subsequently as final lining was not to be considered as part of support system. The support system for weak zones was to be decided as per specific geological conditions and mainly comprised of additional thickness of shotcrete and closer and/or longer rock bolts.

The empirically designed support system was reconfirmed by numerical modeling to ensure the adequacy of the support system and modifications if so required. Numerical modeling was done for different stages of construction, loading conditions and locations involving change of geometry as intersection with the adits etc. Location specific geological parameters were used for the modeling.

The desilting chambers are to be operated under varying hydrostatic pressure due to diurnal variation in the reservoir level as well as the possibility of any of the adjacent chambers being empty. Therefore, efficient drainage of the rock mass was absolutely necessary. Initially it was proposed to provide 75 mm dia 6.0 m deep drainage holes in a pattern of 1.5×1.5 m in the roof and 2.5×2 m in the walls. Subsequently keeping in view the possibility of draining out of fine material from the rock joints and enhancement of permeability of the rock mass due to drainage holes, it was decided to provide only 0.6 m deep drainage holes in good rock. Weak and highly jointed portions were avoided while providing the drainage holes. Consolidation grouting was done only in areas where excessive seepage was indicated due to geological features.

4 OCCURRENCE OF INSTABILITIES AND REMEDIAL MEASURES

Construction of the desilting chambers started from Oct. 1995. No problems were faced during excavation of the roof portion and first benching of 5 m depth, except that excavated surface was quite uneven and considerable overbreaks took place particularly in the haunch portion. However while benching down from EL 1456 to 1451 a shotcrete fall (about 2×3 m) was observed on 26/8/1999 in chamber IV. A rock fall of about 100 m^3 took place in chamber II near the junction of construction adit II. Some cracks in the shotcrete specially the sub-horizontal cracks in the haunch area were also noticed. These incidences were considered to be localized due to geological features and destressing of rock and shotcrete. Localized enhanced support in the form of additional or longer rock bolts was suggested and carried out. The need for effective instrumentation and approach arrangements was re-emphasized for monitoring of the behavior of rock mass and application of the remedial measures.

In April and May, 2000 larger shotcrete falls were observed in chambers III and IV. Large rock falls also took place in chamber IV near the junction of Adit II. Fig. 1(c) indicates the locations when excessive overbreaks and damage to the shotcrete was noticed during excavations. These incidences raised concern about the safety of the chambers. Requirement for suitable approach to all parts of the desilting chambers was felt badly. There was difference of opinion among various experts involved with the project about the kind and quantum of enhancement of support system as well as method of approach and accessibility to all parts of the chambers. Finally three rows of concrete beams anchored to the rock with the help of 20 m long blind cable anchors of 60 ton capacity were proposed to be provided at haunch level (EL 1461.0), at middle EL 1455.0 and above the hopper portion (EL 1448.0 m). Spacing of cable anchors was 7.5 m. Cables were pretensioned for 30 ton only leaving balance capacity to accommodate the rock movement. In between the anchors dummy holes through the beams

Copyright © 2005 Taylor & Francis Group plc, London, UK

left for installation of additional cable anchors if required in future. Three mobile gantries operating from these beams were also proposed to be provided in each chamber for providing access to all areas of the chambers for inspection and taking up any repair and maintenance measures.

Meanwhile the project was hit by an unprecedented flood on 1st August, 2000. The approach roads were washed off and flood waters entered the desilting chamber also. Contractor also suffered loss of men and machinery due to this flood. Work could be restarted in May/June, 2001 only. The excavation work in chamber IV could be resumed in Nov., 2001. The delay put pressure on the project authorities to complete the desilting chambers as their completion had become critical for commissioning of the project. Focus was put on completion of chamber IV and III at the earliest. Provision of three beams with cable anchors and mobile gantries took considerable time and the first set of mobile gantry in chamber IV could be available by November, 1992 only.

In July–August, 2002 excavation for hopper portion i.e. EL 1446.60–1440.30 of chamber IV was completed. During this period eight shotcrete falls took place from the crown portion of the chambers. By this time the top gantry beam had been cast which could be used for a closer inspection of the haunch and roof portion. A team of geologists was entrusted with the task of thorough inspection of the roof/walls of the desilting chamber. The scope of work of the team included:

- To identify, delineate and map all instabilities.
- Identify areas where enhancement of support is required.
- Identify the cause of cracks vis-à-vis geological features.
- Suggest suitable repair and additional support system.

The team inspected the desilting chamber IV using the top gantry beam as a platform since the mobile gantry was yet not available. Findings of the team of geologists are summarized below:

- SFRS had cracked extensively and crack width showed a tendency of increasing with time. Cracking was more pronounced in the haunch portion.
- Most of the rock/shotcrete falls and damage to the shotcrete had taken place near the right hand haunch portion of the crown.
- The support system failed to serve its purpose to a large extent as the interaction between rock, shotcrete and rock bolts was not to the desired extent. It was apprehended that the initial movement in rock had taken place before the installation of the support system.
- Shotcrete had debonded and bulged at many places.
- Some rock bolts had also failed and bearing plates had deformed to a saucer shape.

As remedial measures the team recommended:

- Positive support for the roof portion, similar to the gantry beams provided in the walls.
- Scaling of damaged shotcrete and fresh coats of shotcrete.
- Enhancement of the support system with suitably designed rock bolts.

In August 2002 excavation for the conduit portion of chamber IV was taken up. During this period again few shotcrete falls were observed. This led to stopping of work by the contractor on the pretext of unsatisfactory safety environment. This along with the geologists report created alarming situation. Opinions of experts were once again differing with regard to the repair and rehabilitation measures. Doubts were also raised about efficacy of the SFRS as final lining. Provision of RCC lining and positive support to the roof were considered. The extent to which damaged/detached shotcrete could be delineated and scaled without damaging the surrounding rock was also a big question. All the alternatives had their own limitations and practical problems besides the time and costs involved in applicaton of such measures.

The opinion of Norwegian Geotechnical Institute (NGI) was also sought and their expert made a thorough inspection and review of the support system in the chambers. The report of the expert covered various issues like topographical effects on the stress conditions in the rock, application of the support system and the remedial measures etc. The causes of various instabilities in the desilting chambers can be summarized as:

- Predominance of valley side effect due to topographical conditions which affected the direction of major principle stresses leading to high subhorizontal stresses in the rock. This caused shearing and spalling of rock specially near the right hand haunch level of the chambers and debonding of the shotcrete.
- Removal of considerable mass of rock for excavation of chambers also caused high intensity stresses in the remaining rock mass causing dialation and shearing of the rock pillars between the chambers.
- Debonding of shotcrete and rock was also due to lack of interaction between rock bolts and shotcete as the rock bolts were provided before shotcreting with bearing plates flush with the rock.
- Lack of bond between rock and shotcrete caused shearing of rock through shotcrete.

Exhaustive remedial measures were suggested in the report which are summarized as below:

- Identifying the areas of debonded shotcrete through hammering.

Copyright © 2005 Taylor & Francis Group plc, London, UK

– Compensating the missing bond between rock and shotcrete by installing additional rock bolts with their bearing plates outside the shotcrete. Use of larger sized bearing plates with butterfly wings to further enhance the grip between rock bolt and shotcrete.
– Stitching of surrounding sheared rock with rock bolts of 6–7 m length with the rock bolt plates out side the shotcrete.
– Stitching of weaker areas, where dilation of rock pillars was apprehended, with 12 m rock anchors/ cable anchors.
– Weaker seams (like pegmatite) to be stitched with rock bolts on the sides with steel straps across the weak seams.
– To provide additional cable anchors through dummy holes in the gantry beams at identified locations (through use of bore hole camera) to prevent shearing of the rock pillars. These cable anchors were to grouted at end only leaving rest of the length of cable anchors to accommodate the rock movement.
– Continuous monitoring of rock behaviour throughout the construction and unilateral filling of the chambers.

With the availability of mobile gantries in Nov, 2002 onwards the rehabilitation measures suggested by the NGI expert were started and the construction of desilting chambers continued with great caution. Exhaustive location specific rehabilitation measures were adopted based upon geological details mapped earlier by the geologists as well as the information gathered through inspection of the chambers. Extent of the rehabilitation measures can be gauged by the fact that in chamber IV alone 1257 additional rock bolts of lengths 6 m, 7.5 m and 12 m were installed besides hundreds of rock anchors of 2–3 m length. Proper monitoring was done through instrumentation. Simultaneous numerical modeling for specific reaches was done with back analysis of monitored data and additional support requirement was modified based on the numerical analysis results. Blasting sequences in adjacent and other chambers were carefully planned. Commissioning schedules were also readjusted so that entire excavation in adjacent chamber should be completed before commissioning of any chamber. The chambers have since been commissioned in 2003 and 2004 and no problems have been reported so far during operations.

5 NUMERICAL MODELLING

Numerical modeling technique was extensively used for evaluating the performance of not only the desilting chambers but other underground cavities of the project also. Initially 2D modeling was done with the available geotechnical parameters to assess the adequacy of the empirically designed support system. At later stages 3D models were generated and the geotechnical/geological parameters were revised as per the actual site conditions to have a more realistic idea of the rock mass behaviour. Parameters were further revised through back analysis on the basis of observed instrumentation data to arrive at suitable support requirements during the last phases of the construction and rehabilitation. The technique was found particularly suitable for deciding the appropriate rock reinforcement measures around adit II, which was a major opening intersecting the desilting chambers. The weaker geological zones were also effectively analyzed by this technique. The unilateral filling of the chambers was of great concern to the designers, specially with the suspected shearing and opening of the joints deep inside the rock pillars. This condition was also analysed and it was seen that there was no appreciable effect of unilateral filling on the stress conditions in the rock pillars. Overall it has been a very useful tool for the designers in deciding the suitable support measures at crucial stages.

6 INSTRUMENTATION

It was envisaged right from the beginning that behaviour of the surrounding rock mass shall be monitored throughout the construction phase. Multiple point bore hole extensometers and piezometers were installed at selected locations. As chambers remained largely dry during the excavation, collection of pore pressure data was discontinued. The deformation data could not be collected consistently due to repeated damage to the instruments. Due to inaccessibility of the upper reaches, repair or replacement of these instrument was also difficult. It was only in the later stages when the problem of instabilities assumed serious proportion that concerted efforts were made to collect reliable instrumentation data about deformation and convergence. This was made possible by the access and approach provided by the mobile gantries. Borehole cameras were used to identify the depth and the locations where the joints had opened or the shearing had taken place in side the rock pillars. The instrumentation data was useful in monitoring the behaviour of the chambers and numerical modeling at later stages of the construction and rehabilitation of the desilting chambers.

7 CONCLUSIONS

Given the magnitude of the project and the Himalayan geology some problems were anticipated. However there are always some lessons to be learnt from

Copyright © 2005 Taylor & Francis Group plc, London, UK

any experience. In the present case these may be concluded as:

- A holistic approach of stresses and their direction around openings, geological features and interaction between rock and support elements should be adopted to arrive at suitable support measures for underground excavations.
- A more controlled and careful excavation of the chambers would have mitigated the problems to large extent.
- Arrangement of access to all the portions of the chambers at all stages of construction would have been very useful in collecting consistent instrumentation data, inspection and early repairs and rehabilitation of deficiencies and instabilities. This would have also enabled considerable saving of time and cost.
- The numerical modeling technique can be effectively used for understanding the rock mass behaviour but it is essential that the parameters used in the analysis are realistic and representative of the actual rock mass.

ACKNOWLEDGEMENT

Authors are grateful to the various experts and organisation whose works and reports have been referred to in writing of this paper. Authors are also thankful to the project authorities for their close and continuous interaction with Central Water Commission, the principal consultant, providing all the necessary data and documents throughout the conception and construction of the project.

REFERENCES

Geological reports of Geological Survey of India in the year 1995.

Design Memorandums put up to the Panel of Experts and Central Water Commission from 1996 to 2003.

Reports of various Panel of Experts meetings held from 1996 to 2003.

National Institute of Rock Mechanics reports on numerical modeling of desilting chambers submitted during the year 1996 to 1997, and 2000 to 2003.

Report of the team of Geologists September, 2002.

Reports of Dr. E. Grimstad of Norwegian Geotechnical Institute in the year 2003.

Copyright © 2005 Taylor & Francis Group plc, London, UK

Oporto light train. Bolhão station design

Sarra Pistone, R. & Costa, M.C.
COBA, Consultores de Engenharia e Ambiente, Lisboa, Portugal

ABSTRACT: The Bolhão underground station is located in the common stretch of lines A, B and C of the "Metro do Porto" (Oporto Light Train system) at a depth of 12 m, is situated downtown in one of the main commercial area of the city, under important buildings dating from the beginning of the twentieth century and the declared town patrimonial heritage chapel "Capela das Almas". Basically the station layout consists of two perpendicular caverns with diameters ranging up to 20 m. An escalator gallery connects the lower mezzanine with the upper mezzanine level and with the operational rooms placed in a lateral shafts, open pit excavated in granite saprolites, alluvial soils and old landfills. In this paper the main aspects of the excavation design of the caverns are discussed as well as the after construction main features.

1 INTRODUCTION

The Bolhão underground station, located within the common stretch of the lines A, B and C of the Oporto Light Train System, is situated in a densely built zone of the city, under the Bolhão Market, multi-storey buildings dating from the beginning of the past century and the declared town patrimonial heritage chapel "Capela das Almas".

The underground station comprises essentially a main cavern for the 70 m long platform, and a transversal gallery that intersects the platform perpendicularly, through which is granted access to the lower mezzanine at the platform level. At the crossing of the two galleries (Intersection), the cavern height is raised, throughout a 21 m long section, in order to enable the insertion of the access to the upper mezzanine, access which is done by means of a third smaller gallery (Figure 1).

The set of underground works is completed with open pit access shafts excavated from the Alexandre Braga street and beneath the Fernandes Tomás street, comprising the technical installations associated to the station, and additionally by the access shaft and the Camélias emergency exit.

The access shafts are delimited by a retaining structure comprising a secant pile cut off that confines the area to be excavated. The Fernandes Tomás shaft, has an approximate total length of 44 m, an inner width of about 11 m and a depth of some 26 m. The Alexandre Braga shaft has an identical total length and an inner width of about 9 m.

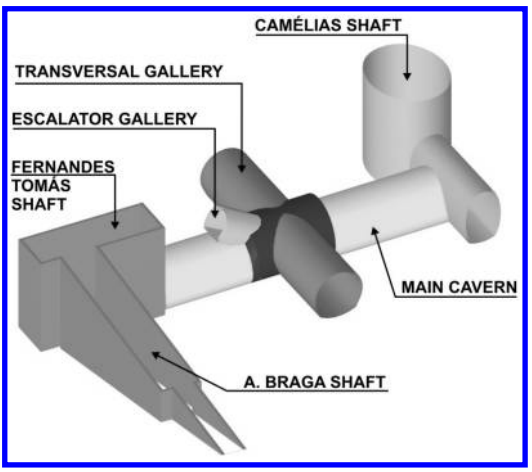


Figure 1. Tridimensional diagram of the Bolhão station.

2 GEOLOGICAL AND GEOTECHNICAL MODEL

Boreholes with core recovery accompanied by "in situ" testing were performed, namely standard penetration tests, dilatometric and pressuremetre tests, Lugeon type water injection test and Lefranc permeability test. Special reference is also made to the seismic tomography procedures carried out, as well as the placing of piezometers for monitoring the evolution of water levels.

Copyright © 2005 Taylor & Francis Group plc, London, UK

In geological terms, the Bolhão station is located within the "Oporto Granite", subjacent to fill materials, alluvial soils and granite saprolites, which can reach a total thickness of about 13 m. The "Oporto Granite", generally comprising a medium to coarsely grained two-mica granite, presents several degrees of weathering and fracturing, which results in strong variations of its mechanical characteristics.

Sarra Pistone and Rebelo (2003) presented the geological and geotechnical model upon which the final design of the station was based.

The geomechanical complexes encountered, duly characterized according to their degree of fracturing and weathering, and associated design parameters are presented in Table 1.

The rock and soil masses found during the excavation correspond entirely to those foreseen in the geological and geotechnical study.

The western end of the Cavern essentially encountered rock mass classified as G3 geomechanical complex. The intersection of both galleries came across G3 and G4 materials in the western half. Only in the eastern half occur G5 soils that were not properly detected in that position during the design stage. The G5 soil consists of a N-S oriented strip (Figure 2), wedge-shaped in the vertical section (see Figure 10), delimitated by soils of the G4 geomechanical complex.

The actual position of the most weathered soils not only interfered with the foundation of the historical buildings, but also compromised the stability of the cavern intersection zone.

Due to the fact that both caverns have similar roof levels, the intersection top presents an almost plain configuration, requiring the primary support to be reinforced with a special arch-shaped structure with adequate bearing and stiffness characteristics to face up to the adverse conditions encountered during the excavation.

3 PRIMARY SUPPORT DESIGN

The numeric analysis of the Bolhão station underground excavations was undertaken with the aid of Plaxis v 7.2 and Phases^2 v 5.027 software.

A perfectly plastic linear-elastic law was used to describe the behavior of materials. In the case of Plaxis, the Mohr-Coulomb failure criterion was used, whilst in the Phases^2 program, it was possible to use the Mohr-Coulomb criterion for (G5 and G7 soils) and the Hoek-Brown criterion for rock masses (G3 and G4). The geomechanical parameters used are summarized in Table 1, having been based on information gathered during the early stages of the design phase, as well as data collected from the complementary geotechnical survey.

As only 2-D modeling was performed, the simulation of the lap between the excavation of the cavern and the installation of the primary support was materialized with recourse to a load split routine. The load split considered was 0.5. Furthermore, an analysis of the system global stability and deformability was undertaken, using a 60% load split figure. On the other hand, the verification of the primary support strength was carried out by splitting merely 30% of the mass load.

In the design of the primary support it was considered, for shotcrete, a 5 MPa compressive strength after 24 h and 25 MPa after 28 days, a deformability modulus of 5 GPa after 24 h and 15 GPa after long term and a steel area corresponding to the one used in each section. The excavation was assumed to be totally drained.

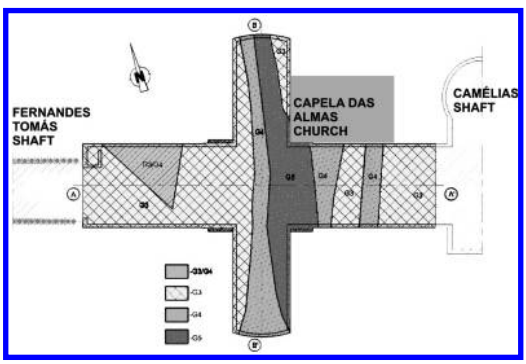


Figure 2. Actual geological model of the station. Plant view.

Table 1. Design parameters.

G.C.	Weath. and fract. degrees	γ kN/m^3	E MPa	σc MPa	Mohr-Coulomb ϕ′ (º)	Mohr-Coulomb c′ MPa	Hoek-Brown m	Hoek-Brown s
G7	–	19	40	–	28	0	–	–
G5	W_5 F_5	20	150	–	35	40	–	–
G4	W_4 $F_{4–5}$	23	600	10	35	75	0.67	0
G3	W_3 F_4 a F_3	24	1500	25	40	150	0.98	7.5 e^{-4}

Copyright © 2005 Taylor & Francis Group plc, London, UK

4 FINAL STRUCTURE DESIGN

The main cavern structure is constituted by a vault comprising a three-center arch and has an excavation section of about 186 m^2 (Figure 3). At the Intersection, the section diameters are increased, reaching a height of 15,05 m and a maximum width of about 17,4 m. The excavated section is approximately 244 m^2 (Figure 4).

The transversal gallery extends throughout 62 m, comprises a circular roof and has an excavated section of about 160 m^2. In order to accommodate the escalators, the elevators and remaining infrastructures expected to be installed beneath the platform, it was decided to lower the level of the tunnel invert and increase its curvature by means of a set of three arches (Figure 5).

The escalator gallery between mezzanines has an inner width of 6,3 m and a maximum height of about 5,5 m. In order to improve its performance, during excavation, its shape is approximately circular, comprising a central circular arch and two side arches at the connection to the tunnel invert (Figure 6).

Inside the station, the escalator gallery is suspended from the intersection vault by means of two 0,5 m thick vertical walls, blocked at the bottom with two 1,3 m high beams. The beam adjacent to the transversal gallery also comprises a support for the escalators and for the lower mezzanine slab.

The final lining was provided with a waterproofing system, comprising a PVC membrane and a mechanical protection geotextile, connected to longitudinal drains placed in the connections of the sidewalls to the tunnel inverts.

Due to the importance of the interaction between the structure and the surrounding mass, stresses upon the gallery final lining were evaluated resorting to the Plaxis software. The structure was simulated with bar elements and soils were modeled through 6-knot triangular finite elements, based upon the elasto-plastic behavior laws defined by the Mohr-Coulomb failure criteria.

The geotechnical scenarios considered for each one of the galleries were defined according to the real geological and geotechnical conditions observed during the excavation of the upper mezzanine of the cavern

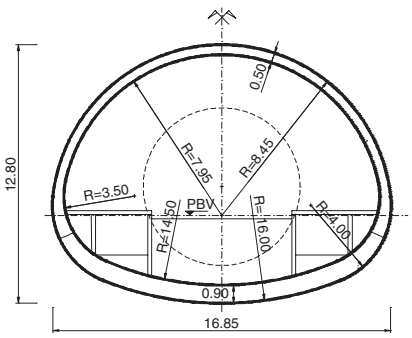


Figure 3. Typical section of the main cavern.

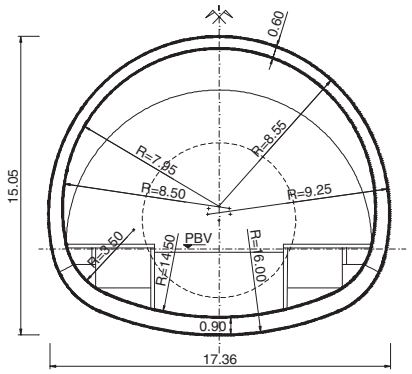


Figure 4. Section of the intersection.

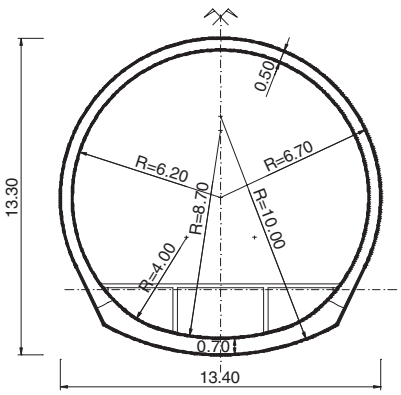


Figure 5. Section of the transversal gallery.

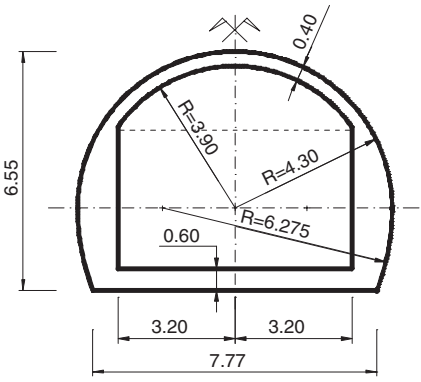


Figure 6. Section of the escalator gallery.

Copyright © 2005 Taylor & Francis Group plc, London, UK

and of the transversal gallery, having been decided to consider its insertion in a zone assimilated to the G4 geomechanical complex.

All excavations and primary support installation stages were simulated, and at the end all stresses were transferred on to the final lining. Creep effects of the mass and of the reinforced concrete structure were considered in the calculations, in a simplified way, through the introduction of a last phase in which the strenght parameters of materials were reduced. In order to assess the behavior of the gallery intersection the entire structure of the underground station was modeled tridimensionally with quadrangular finite shell elements (Figure 7), being the interaction with the mass simulated through radial springs.

The loads considered in the design were, besides the structure self weight, the hydrostatic pressure and the load transferred from surrounding ground.

5 EXCAVATION METHOD – PRIMARY SUPPORT

The excavation design took into consideration two basic conditions, namely the full drainage of the mass, resorting to long drains drilled from the railway tunnel already excavated and the application of the Observational Method (NATM). That method enables the adjustment of the constructive and primary support phasing according to the actual geological and geotechnical conditions found on site and to the soil response to the excavation, evaluated through the installation of a monitoring system.

The adopted constructive method considered two principal excavation phases, both for the cavern (including the intersection) and for the transversal gallery, undertaken in 1,5 m or 1,0 m steps, according to the geotechnical conditions. The first phase corresponds to excavation of the upper mezzanine and the second phase to the lower mezzanine.

In general the primary support consist in 0,30 m, thick reinforced shotcrete, (with steel fibres or weld mesh), Lattice girders type PS 115 20/30 and Swellex type dowels. In poorer geotechical conditions, selfboring anchorage with an inclination of 45°, were used (Figure 8).

The rock overburden at the intersection zone ranges down to a minimum of 4 m, being the remaining overburden (8 m) composed of saprolites, alluvial soils and land fills.

The almost plain configuration of the roof at the intersection zone and the reduced rock overburden require the execution of a reinforcement structure on the primary support in this zone, built in two stages, in order to enable the simultaneous progress of the excavation works in the transversal gallery and in the lower mezzanine of the cavern.

This reinforcement structure was achieved through a piece of reinforced shotcrete, increasing the thickness of the primary support and inserting a reinforcement mesh in the inner surface.

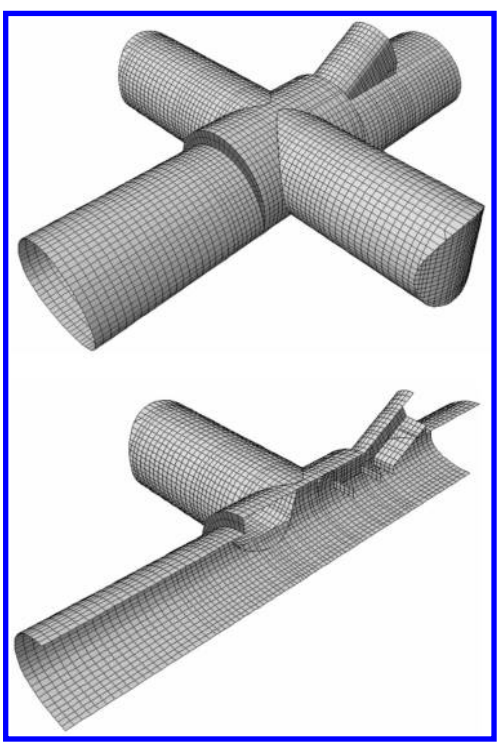


Figure 7. 3-D Model of the underground station structure.

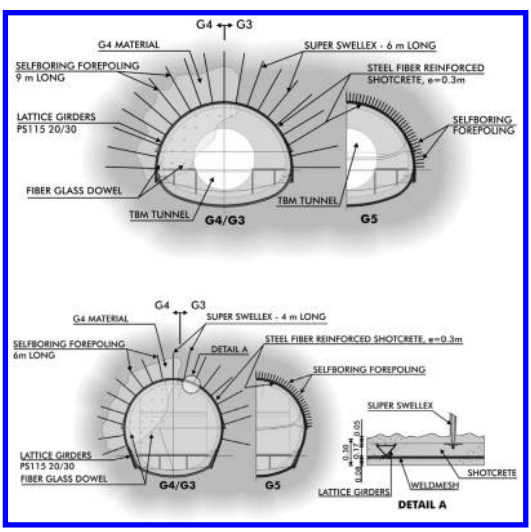


Figure 8. Primary support.

Copyright © 2005 Taylor & Francis Group plc, London, UK

Two reinforced concrete beams were placed on the base of the upper mezzanine in order to distribute the mass loads during opening of the first phase of the transversal gallery and during the excavation of the second stage of the cavern (Figure 9).

6 MONITORING WORKS DURING CONSTRUCTION

Sarra Pistone and Rebelo (2003) presented the monitoring plan upon which the excavation process follow-up was based. This plan included instruments currently used in this type of works, namely: Inclinometers, multipoint extensometers, precision leveling bench marks, piezometers and convergence marks inside the galleries monitored through optical methods.

The instruments were distributed amongst 8 monitoring profiles throughout the Fernandes Tomás Street, whilst monitoring log PM4 extended throughout Stª Catarina Street. The monitoring plan was adjusted to the real conditions verified during the excavation of the galleries and respective phasing.

6.1 *Alert and alarm system*

The excavation alert and alarm system was based upon the maximum estimated displacements. The following elements were of paramount importance for the assessment of the overall stability:

- Detailed and systematic geological and geotechnical survey in all excavation faces;
- Study of the displacement-time curves, namely first and second order increments that correspond to the speed and to the acceleration of displacements, respectively;
- Comparison between systematically obtained results in different monitoring sections;
- Comparisons with the numeric models out puts;
- Interpretation of deformations of the rock mass according to the position of the principal geological discontinuities.



Figure 9. Overall aspect of the intersection zone upon conclusion of the excavation works.

The alert and alarm limits in terms of settlements during excavation of the main cavern and transversal gallery were defined in the design using the criteria of independent excavations, i.e., considering that the excavation of the transversal gallery would only be initiated once the main cavern excavation works, primary support and final lining were completed, as was originally anticipated in the design.

In order to meet the requirements of the construction chronogram, the final edition of the excavation and primary support design was prepared under premise that the first phase excavation works of the cavern and of the transversal gallery be concluded before benching of both galleries, which implied a different primary support behavior and a reduced stiffness of the entire works.

Conceptually, it was assumed that should the excavation be undertaken in two phases, vault and bench, (as was eventually the fact), the reference settlements at the Intersection would be roughly equivalent to the sum of the displacements calculated for each gallery.

Another important updating of the displacements limit was due to the adjustment to the geological conditions verified "in situ", namely the presence of a material G5 on the western half of the station and transversal gallery intersection.

The surface settlements alarm and alert limits, timely reviewed and used for excavation monitoring, are the ones that figure in Table 2.

Table 2. Alert and alarm levels.

	Cavern						Transv. gallery						Intersection			
	G3		G3/4		G5		G3		G3/4		G5		G3/4		G5	
Phases	1	2	1	2	1	2	1	2	1	2	1	2	1	2	1	2
Alert (mm)	11	12	11	12	12	13	4	5	5	5	6	7	16	17	18	20
Alarm (mm)	18	19	18	19	19	21	6	8	8	8	10	11	26	27	29	32

Copyright © 2005 Taylor & Francis Group plc, London, UK

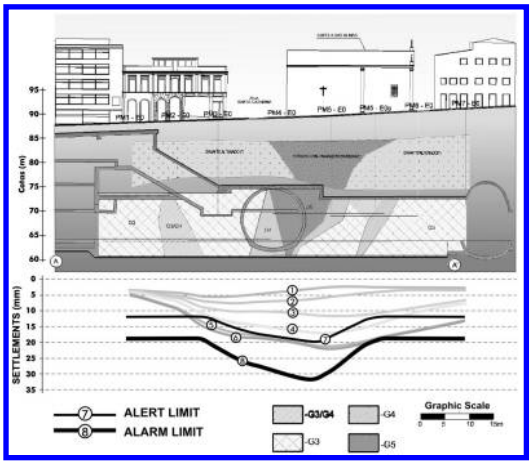


Figure 10. Fernandes Tomás street. Geological and monitoring profile.

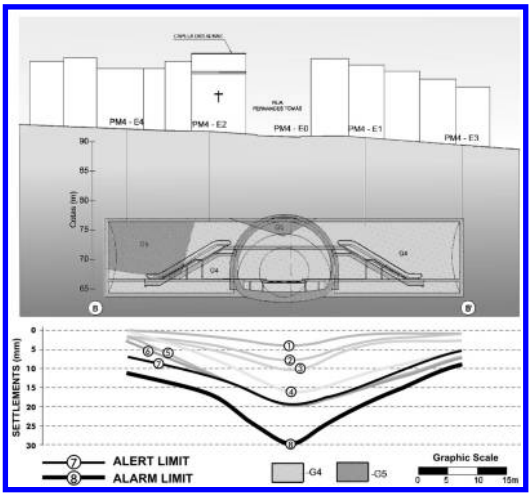


Figure 11. Santa Catarina street. Geological and monitoring profile.

7 MONITORING RESULTS – CONCLUSIONS

Once concluded the station excavation and stabilized the readings from the monitoring instruments, it was verified that the measured settlements match rather well those foreseen in the alert and alarm criteria presented in Table 2.

Regarding the building monitoring, and particularly in the case of the "Capela das Almas" the distortion levels reached a maximum 1/6000 throughout St[a] Catarina Street and 1/2200 throughout Fernandes Tomás Street, values that can be considered as very inferior to the limits imposed by the building risk evaluation study (BRA) that pointed to maximum acceptable distortion levels for the "Capela das Almas" of 1/850.

In Figures 10 and 11 the station longitudinal profiles are shown, viewed from the Fernandes Tomás and Santa Catarina Streets, respectively. In the same profiles were included the data from the available geological model and, at an adequate scale, the settlement curves corresponding to the most representative episodes of the station's construction works.

A reasonable agreement can be observed between the predicted and registered settlements, with a certain curve asymmetry corresponding to the occurrence of G5 soils in the Intersection zone.

The approach adopted, in what concerns design methodology, revealed to be adequate for overcoming the difficulties created by the different constraints inherent to the construction of shallow underground works in a sensitive urban environment.

ACKNOWLEDGEMENTS

The authors wish to thank the company Metro do Porto, S.A. and Transmetro ACE for authorizing publishing of this paper. This acknowledgement is extensive to all persons that participated in the design and construction teams, thus contributing for the success of the project.

REFERENCES

NORMETRO. Technical Report – General Geotechnical-Geomechanical Report for underground sections (lines C, S and connection branch C-S). Final Design 0/06/0/DE/00.00/220/TM/RT/012001/A/03(2000). Not published.

Sarra Pistone, R.; Rebelo, V. (2003) – "*Oporto Light Train – Bolhão Station. Geological Model and Excavation Design"*. Spanish-Portuguese Meeting on Subterranean Works – Importance of Geotechnical Survey and Monitoring. Madrid (487,498).

TRANSMETRO, ACE – "*Durability requirements for reinforced concrete structures in underground stations"*. Technical Report, 2003.

COBA – "*Bolhão Station. Underground Station. Final design for excavation and primary support*". Design undertaken for TRANSMETRO, ACE, 2003.

COBA – "Bolhão Station. Underground Station. Final Design for the Final Lining". Design undertaken for TRANSMETRO, ACE, 2003.

Copyright © 2005 Taylor & Francis Group plc, London, UK

A design case study of the very wide 3-arch tunnel under the railroad station building

S.B. Chang, S. Kwon & S.J. Moon
Yooshin Engineering Corporation, Seoul, Korea

S.D. Lee
Ajou University, Suwon, Korea

ABSTRACT: This paper presents the design case of the 3-arch tunnel under the railroad station building. The former construction method was the underpinning method supported by pipe-roof. However, it was changed to a 3-arch tunnel to improve the construction condition and the safety. The 3-arch tunnel is 28 m wide and 10 m high, which is the widest tunnel in Korea. Overburden is 23 m and the ground consists of a weathered rock and a weathered soil. The allowable settlements for the railroad station building and rail tracks are limited very strictly. Accordingly, the plan of tunnel excavation, the support for the tunnel stability, and the settlement minimization were executed conservatively and reviewed by numerical analysis.

1 INTRODUCTION

Recently, tunnelling method is preferred rather than cut-and-cover method in order to reduce the damage of existing structures and the obstruction to traffic. The subways planned in Korea require shallow depth and large-sectioned tunnels for passenger's convenience.

This paper introduces the design case of 3-arch tunnel under existing rail tracks and Daejeon station building(Chang et al. 2002). The former construction plan was the underpinning method supported by pipe-roof. However, it was changed to 3-arch tunnel due to its poor construction conditions and probable risk of ground settlement. Important requirements in this tunnel design are to secure the stability of large-sectioned 3-arch tunnel and to minimize the damage occurred from the construction of station building and existing rail tracks (Fig. 1).

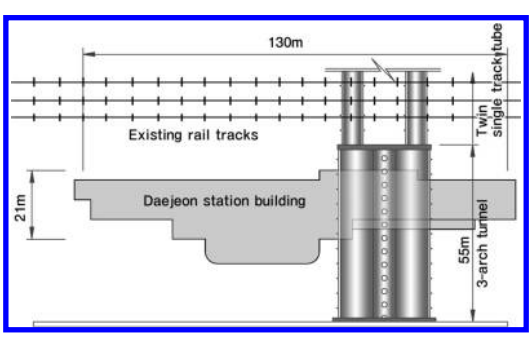


Figure 1. Plan view of 3-arch tunnel and station building.

2 SITE CONDITIONS

Daejeon station building was constructed 45 years ago. It was built on timber and concrete piles. The 3-arch tunnel runs under the station building and rail tracks at 23 m depth. According to the safety diagnoses of station building, allowable differential settlement is less than 12 mm and angular distortion ranges from 1/600 to 1/500. Allowable settlement referred to the standards of rail tracks maintenance is only 7 mm.

The soil profile begins with an upper layer consisting of fill, alluvial and weathered soil followed by a layer of weathered rock and bedrock (Fig. 2).

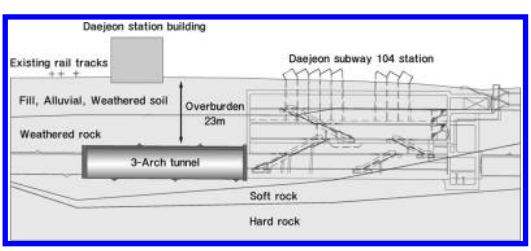


Figure 2. Profile and site conditions.

Copyright © 2005 Taylor & Francis Group plc, London, UK

The ground water level has been drawn down by the trench excavation for Daejeon subway 104 station. Before the tunnelling, ground water is 21 m below the ground surface. The ground at tunnelling depth consists of weathered rock. The coefficient of permeability of weathered rock varies from 7.17×10^{-5} to 1.17×10^{-4} cm/sec.

3 CROSS-SECTION DESIGN

This tunnel has to provide sufficient space for platform, columns and ventilation facilities. Each design requirements are listed in Table 1.

This 3-arch tunnel is 28 meters wide and 10 meters high, which is the widest tunnel in Korea. The cross-sectional area to be excavated is 284 m^2. Figure 3 shows the normal cross-section of 3-arch tunnel.

There are two important requirements considering the design of 3-arch tunnel cross-section.

- Ground settlement must be controlled so that the station building and rail tracks may remain usable during the construction.
- The 3-arch tunnel with a large section must be stable.

The cross section is designed in order that ground settlement is small and occurs gradually during the construction. But the cross-section has to divided in many parts for staged excavation, which can make the construction period long. After all, the ground settlement and safety are prior to other problems in this project.

Table 1. Design requirements for 3-arch tunnel.

Items	Requirements
Columns	Circular shape (diam. 1.9 m) Longitudinal spacing: 5.0 m Lateral spacing: 9.5 m
Ventilation ducts	Cross sectional Area: 11.34 m^2
Platform clearance	Height: 3.0 m
Structure gauge	According to the design standards of Daejeon subway

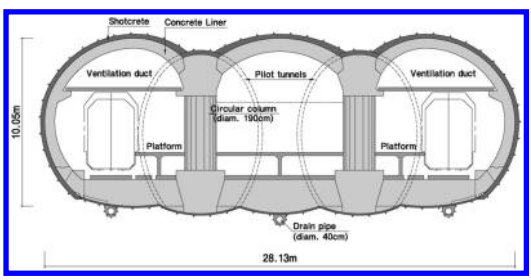


Figure 3. Standard cross-section of 3-arch tunnel.

4 EXCAVATION AND SUPPORT

To lessen noise and vibration problem and to protect the station building from blasting, mechanical excavation is adopted. Pilot tunnelling with ring-cut and invert is carried out to minimize the settlement and to enhance the stability of the tunnel. Tunnel advance length is 0.8 m and early floor closure is obtained by short-bench-cut method.

This 3-arch tunnel is supported by shotcrete with wire mesh and steel ribs installed every 0.8 m interval. The crown of tunnel is excavated with a temporary invert to reduce heaving of the bottom and stress concentration at the corner of the bottom. Figure 4 shows typical supports and reinforcements of 3-arch tunnel. Because of poor ground conditions, additional reinforcing measures are required as well as basic tunnel supports. Additional reinforcements are listed in Table 2.

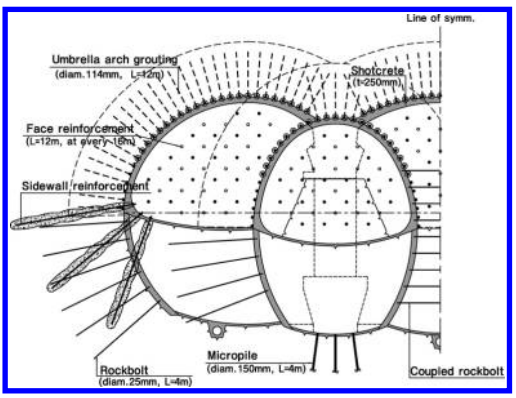


Figure 4. Supports and reinforcements.

Table 2. Additional reinforcements for soft ground conditions.

Items	Reinforcements measures
Umbrella arch grouting	– Steel pipe (diam. 114 mm) – Longitudinal spacing: 4 m
Face reinforcement	– Length: 12 m – Longitudinal spacing: 8 m
Micropile	– Column foundation reinforcement – Pile length: 4 m
Coupled rockbolt	– Central pillar reinforcement
Sidewall reinforcement	– Length 5 m – Longitudinal spacing: 0.8 m
Connection reinforcement between 3-arch tunnel and single track tube	– Umbrella arch grouting – Shotcrete at end face – Face reinforcement

Copyright © 2005 Taylor & Francis Group plc, London, UK

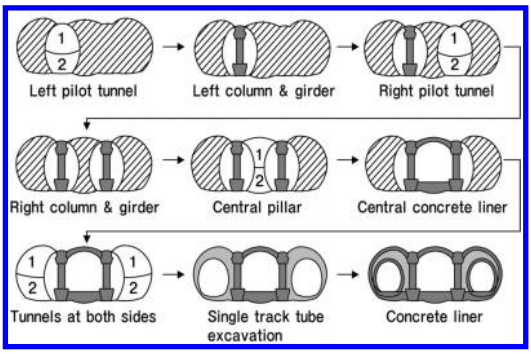


Figure 5. Construction sequence of 3-arch tunnel.

Table 3. Settlement criteria of Daejeon station building.

	Differential settlement	Angular distortion
Lateral	8.3 mm – 10 mm	1/500–1/600
Longitudinal	10 mm – 12 mm	1/500–1/600

As it was mentioned previously, cross-section is divided into ten sub cross-sections to minimize ground settlement and enhance tunnel stability. Figure 5 shows the construction sequence of sub cross-sections.

5 GROUND SETTLEMENT

5.1 *Settlement criterion*

In general, the maximum settlement and differential settlement are used to estimate the building stability. In this project, differential settlement criterion is applied for building because the maximum settlement criterion is not strict and appropriate to Daejeon station building which is wide rather than high. Settlement criteria of the station building are listed in Table 3. According to the standards of rail tracks maintenance, maximum allowable settlement is 7 mm.

5.2 *Settlement estimation with numerical analysis*

Settlement estimation is performed by three-dimensional numerical analysis. Calculated settlements are measured with respect to longitudinal and lateral directions considering column and wall spacing of the station building. Figure 6 shows the three-dimensional numerical model.

As for Daejeon station building, calculated settlement satisfy the criterion of differential settlement both in longitudinal and lateral directions. However, the existing rail tracks require maintenance because calculated settlements exceed the maximum allowable settlement. The estimated settlements are plotted in Figures 7 and 8.

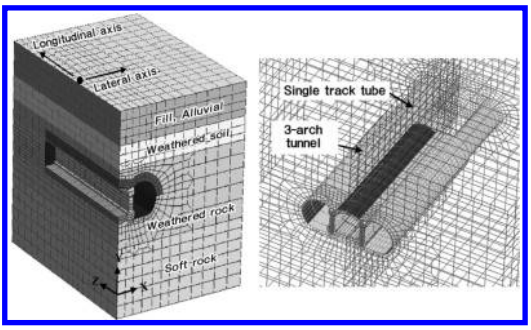


Figure 6. Three dimensional numerical model.

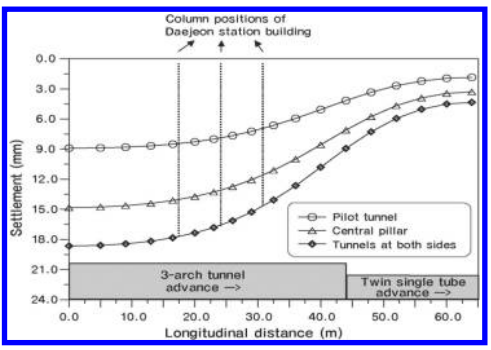


Figure 7. Estimated ground settlement (longitudinal direction).

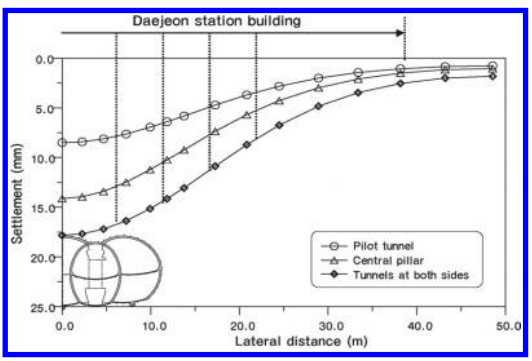


Figure 8. Estimated ground settlement (lateral direction).

6 MONITORING PLAN

Detailed monitoring plan is required to check stability of the existing structures and 3-arch tunnel.

Copyright © 2005 Taylor & Francis Group plc, London, UK

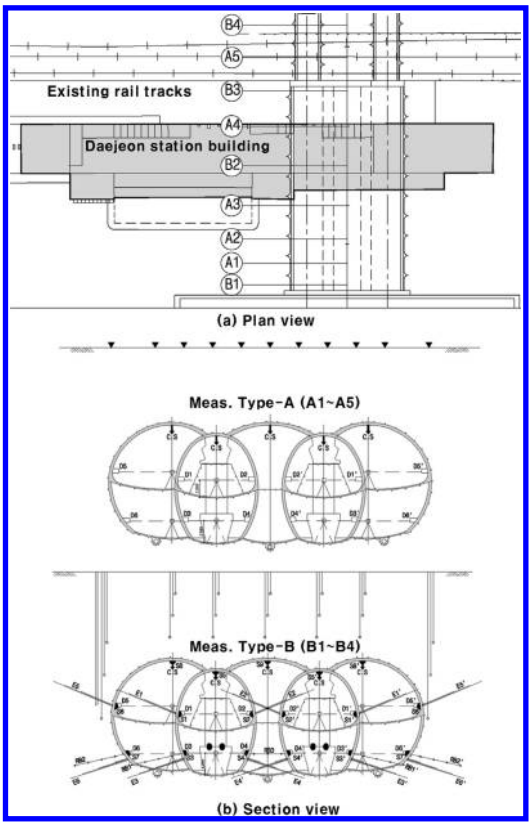


Figure 9. Arrangement of measurement lines and instrumentations.

Instrumentation items are selected with regard to the behavior which is uncertain during the design stage. Measurement lines are placed at every 5–10 m (Fig. 9). Daejeon station building is monitored by inclinometer and crack gauge. In order to monitor the 3-arch tunnel in service stage, load cells and strain gauges are placed into columns and concrete liner.

7 WATERPROOFING SYSTEM

Usually, 3-arch tunnel is vulnerable to water leakage at construction joint between column and concrete liner. To prevent this problem, detailed and multiple waterproofing measures are planned.

Waterproofing membrane and fleece are placed in arch and sidewalls. Hydrophilic waterstop is used at construction connecting parts. If leakage occurs, the leaking water will be drained through longitudinal split drain pipe. Figure 10 shows the detailed waterproofing measures.

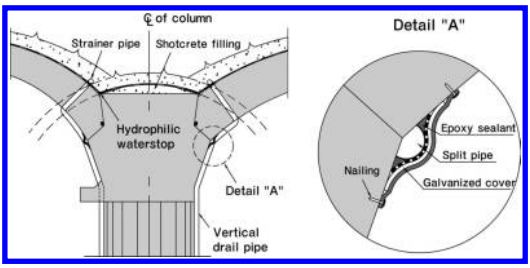


Figure 10. Waterproofing system.

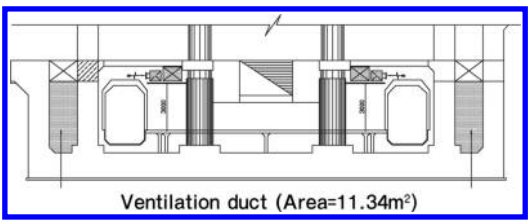


Figure 11. Ventilation duct arrangement (former design).

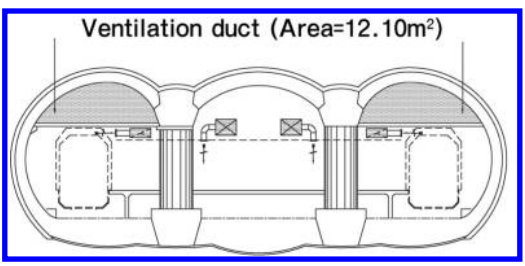


Figure 12. Ventilation duct arrangement (changed design).

8 VENTILATION DUCT ARRANGEMENT

Owing to the engineering change of construction method, ventilation duct arrangement has to be changed. In former design, ventilation duct was connected via sidewall of rail tracks. Because this 3-arch tunnel has insufficient sidewall space, the ventilation duct is planned passing above the rail tracks. This alteration causes the position of stairs to be changed. Figures 11 and 12 show the alteration of ventilation duct arrangement.

There are two alternatives in choosing the material of ventilation duct. One is prefabricated steel duct and the other is concrete slab type. The concrete slab type is chosen because it has more advantages in fire resistance and maintenance.

Copyright © 2005 Taylor & Francis Group plc, London, UK

9 CONCLUSIONS

Recently, the soft ground tunnelling with a large-section has a growing tendency because it provides sufficient solution in urban subway construction. For this reason, more effective measures are required to prevent large deformation and enhance the stability. The authors hope this design case will be helpful to design of urban large-sectioned tunnel.

REFERENCES

Chang, S.B., Moon, S.J., Kwon, S., Huh, D.H. & Bae, G.J. 2002. A design case study of 3-arch tunnel under the Daejeon station building (I). *Tunnelling technology. Korean tunnelling association* 3(4): 247–259.

Copyright © 2005 Taylor & Francis Group plc, London, UK

Rock mass characterization and primary support design for the Boztepe Tunnel, Turkey

E. Sopaci & H. Akgün
Department of Geological Engineering, Middle East Technical University, Ankara, Turkey

M. Akinci
TEMELSU International Engineering Services Inc., Ankara, Turkey

ABSTRACT: The Ordu province in local scale and northeastern Turkey in regional scale comprise of volcanic arc related rock masses. These modes of origin accommodate both volcanic and flysch type rock masses that have transitions so often with each other. The Boztepe tunnel will mostly be driven through this type of lithology. In order to assess the rock masses surrounding the tunnel from a geotechnical point of view; surface, subsurface and laboratory investigations have been implemented. Internationally accepted rock mass classification systems (RMR, NGI-Q-system and GSI) have been utilized via information gathered mostly from surface geotechnical investigations. In an attempt to check the validity of the empirical tunnel supports, stress analyses around the tunnel openings have been executed through employing finite element analyses by the Phase^2 package program. Kinematical and limit equilibrium analyses of the tunnel portals have been employed for portal slope stability considerations.

1 INTRODUCTION

The purpose of this study is to design the tunnel and portal support of the Boztepe Tunnel (T-1) of the proposed Ordu Peripheral Highway via rock mass classification systems. Accordingly, the stability investigation of portals and the tunnel support determination through rock mass classifications constitute the primary purpose of this study. For the purpose of the stability assessment of the tunnel consisting of two tubes, the following steps have been carried out:

(1) Elaborating literature survey for theoretical background about tunnel and portal design, (2) Assembling, correlating and interpreting of previous studies for the project area to comprehend geological conditions, (3) Characterizing rock masses along the proposed tunnel route by international rock mass classification systems such as Geomechanics Classification System, RMR; Norwegian Geotechnical Institution Q-System, NGI-Q and Geological Strength Index, GSI. In this particular article, supports determined from the NGI-Q system have been assessed as a case study. The proposed Ordu Peripheral Highway is planned to deviate at KM: 21 + 000 from the Bolaman – Ordu Highway, which is under construction, and join the existing Ordu – Giresun highway at KM: 40 + 114 (Figures 1–2).

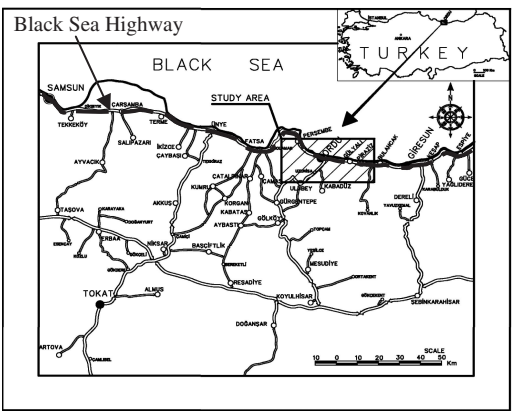


Figure 1. Location map of the study area, Ordu, Eastern Black Sea Region of Turkey.

2 GENERAL GEOLOGY

The project area regarding its geological characteristics is included in the central part of the Black Sea Region. While the eastern portion of the Black Sea Belt is mostly represented by volcanic rocks, the western part is dominated by sedimentary rocks. In this frame,

Copyright © 2005 Taylor & Francis Group plc, London, UK

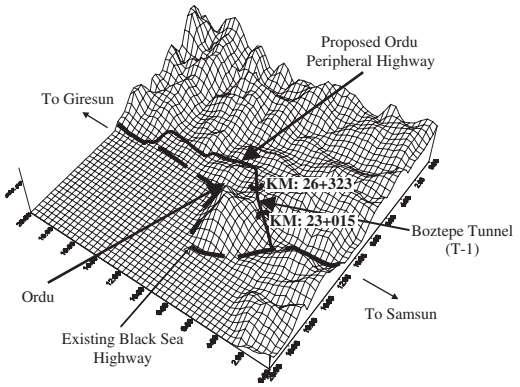


Figure 2. The proposed route for the Ordu Peripheral Highway.

the project area accommodates volcanic rocks together with contemporaneous sedimentary rocks (Terlemez and Yilmaz, 1980). The geological units in the area are firmly connected with the regional tectonic movements.

The presence of volcanic rocks juxtaposed to sedimentary rocks in the project area can be explained by submarine volcanism. More precisely, the geological units derived from island arc volcanism of regional scaled tectonic movements characterize the Ordu region and its province.

Upper Cretaceous aged Mesudiye formation is the oldest lithostratigraphic unit near the project area and its lower bound can not be observed. The inferred thickness of this formation is about 1000 m. The alignment of the Boztepe Tunnel will be mostly cut by the Mesudiye formation. It is comprised of agglomerate, basic lava flow, limestone, tuffite, mudstone, siltstone and sandstone. The description of this formation was first made by Terlemez and Yilmaz (1980). Agglomerates of the Mesudiye formation are dark gray, brownish colored, massive and sometimes very thick to thick bedded. The size of the andesitic and basaltic clasts varies from gravel to block. These clasts are angular and poorly sorted. The andesitic and tuffic cement of this agglomerate is either weak or tight. The clast contact is absent in case of weak cementation. Within the formation, pyroclastics are more dominant than interlayers of fine sandstone, claystone, tuffite and lenses of pelagic red limestone (Keskin et al., 1998). Mesudiye formation is the product of an arc volcanism related with the subduction of the northern branch of Neo-tethys. The sedimentary component of this formation, nevertheless, has occurred under the circumstances where submarine volcanism ceased. The most striking feature of the Mesudiye formation is its Kapanbogazi member consisting of red, pink and claret red colored, thin to medium bedded limestone, marl, mudstone, claystone, sandstone and tuff either in the form of lenses or interlayers. This member can also be traced as a key bed (Keskin et al., 1998). Another formation to be driven by the initial portion of the Boztepe tunnel is Akveren formation which may be correlated to the Fatsa formation of Terlemez and Yilmaz (1980). Akveren formation is formed by sedimentary rocks such as limestone, sandy limestone, marl, siltstone and sandstone alternations. Some tuffite interlayers have also been reported around Kumru, Korgan and Fatsa where the formation outcrops extensively (Keskin et al., 1998). The cumulative thickness of the formation reaches up to 750 m.

3 GEOTECHNICAL ASSESSMENT OF THE ROCK MASSES

The geotechnical assessment of the study area has been implemented in three stages as surface, subsurface and laboratory investigations. During the surface investigations, the properties of the discontinuities of the rock masses, which control the rock mass behavior, were investigated. Their spacing, aperture, persistency, roughness along with the weathering and groundwater conditions were examined for the assessment of the rock mass strength. About ten boreholes with a total length of more than 1000 m have been drilled for the Boztepe Tunnel (T-1) in order to observe the rock mass geotechnical condition at the tunneling depths. The laboratory tests, as a last stage, were performed on samples recovered from the drillings. The intact rock parameters were determined through these laboratory tests (Table 1).

The geotechnical description of the rock masses has been presented through integration of rock mass properties and intact rock properties. In this regard, the field findings representing rock mass properties and the drilling results coupled with laboratory tests reflecting intact rock properties were interpreted to complete the geotechnical description of the rock masses. Volcanic rocks of Mesudiye formation showing similar mass strength parameters along both tunnel alignments are the andesitic and basaltic agglomerate. The differentiation between basaltic and andesitic agglomerates by the unaided eye is only possible through their colors. The rock mass characteristics of them do not vary so much, hence the engineering parameters of these are given in the subtitle entitled "agglomerates". Light-dark gray, greenish and blackish agglomerate is formed by lapilli (4.0–64.0 mm) and volcanic bomb (>64.0 mm) sized fragments within the matrix of andesitic and basaltic tuff and volcanic ash. The 1.5–2.0 m thick uppermost part of this unit comprises of block sized rock fragments owing to mechanical and organical weathering. In spite of this particular zone, agglomerates are slightly weathered and fresh in general. According to the hammer rebound,

Copyright © 2005 Taylor & Francis Group plc, London, UK

Table 1. The laboratory test results of the intact rock samples.

Km	Lithology encountered at boreholes	Average uniaxial compressive strength (MPa)	Average Young's modulus (GPa)	Average Poisson's ratio
23 + 100 23 + 250	Flysch (Marl + Clst + Lst)	50	16.3	0.193
23 + 250 23 + 625	Flysch (Clst + Marl + Sst) Volcanics (Agg. + Tuff)	33	11.1	0.215
23 + 625 23 + 915	Volcanics (Agglomerate)	37	12.3	0.150
23 + 915 26 + 200	Flysch (Clst + Lst + Sst) Volcanics (Agg. + Tuff)	47.3	28.2	0.308
26 + 200 26 + 300	Volcanics (Agg. + Bslt)	97	–	–

Clst: Claystone; Sst: Sandstone; Lst: Limestone; Bslt: Basalt; Agg.: Agglomerate

agglomerates are usually moderately strong (UCS, uniaxial compressive strength, is between 12.5–50.0 MPa) and sometimes strong (UCS is between 50.0–100.0 MPa). The most striking property of the agglomerates is their massive structure. Scarce bedding planes were observed. The joints and bedding planes having a general orientation of 115/15° are discontinuous, undulating and irregularly rough. The spacing of the discontinuities is between 200–600 mm revealing RQD (Rock Quality Designation) = 50–75%. The 1–5 mm opened (aperture) discontinuities are slightly altered and filled with non-softening, non-cohesive rock mineral or crushed rock filling. Some layers of andesitic and basaltic tuff compared to the agglomerates serve poorer conditions regarding grain size, weathering and strength parameters. In this frame, the moderately weathered sections of the tuff are moderately strong (UCS is between 12.5–50.0 MPa) to weak (UCS is between 1.25–5.0 MPa), and the slightly weathered and fresh sections are moderately strong (UCS is between 12.5–50.0 MPa). These sections are highly fractured where the RQD value ranges between 25–50% and the average joint spacing is 60–200 mm. Basaltic lavas can easily be distinguished by their dark gray and blackish colored outcrops. Being mostly fresh and slightly altered, they exhibit moderately strong (UCS is between 12.5–50.0 MPa) character. The aperture of the discontinuity is between 1–5 mm. The discontinuity walls are coated with iron-oxides at the surface. Having a spacing of 60–200 cm, basaltic lavas have the RQD value between 75–90%.

Brown, greenish and dirty white colored alternation of claystone, sandstone, marl and limestone of Akveren formation displays its typical characteristics in the vicinity of the Boztepe Tunnel (T-1) entrance portal. The percentages of the lithologies are similar to those of the Upper Cretaceous sedimentary rocks mentioned earlier. This flysch type formation has gone through extensive tectonic processes through which some levels of this mass have been highly weakened. The greenish marl and brown claystone, which are the weakest components, are highly weathered and their strengths are very weak to weak (UCS is between 1.25–5.0 MPa). The bedding planes are moderately persistent (3–10 m) together with undulating and irregularly rough surfaces whose aperture size is between 1–5 mm. These surfaces are slightly altered and sometimes coated with calcite fillings. Having a spacing between 60–200 mm, claystone and marl have an RQD value between 25–50%. The limestone, however, alternating with them is slightly weathered to fresh and moderately strong (UCS is between 12.5–50.0 MPa). It has bedding planes with a general orientation of 120/20° and 3–10 m persistency with undulating and irregularly rough surfaces possessing an aperture size between 1–5 mm. These surfaces are slightly altered and sometimes coated with calcite and quartz fillings. Having a spacing between 200–600 mm, limestone has an RQD value between 50–75%. The dirty white sandstone is slightly to moderately weathered and moderately strong (UCS is between 12.5–50.0 MPa). The coarse and angular grains are mostly derived from volcanic rocks and limestone. Bedding planes with a general orientation of 120/20° are moderately persistent (3–10 m). Their surfaces are undulating and irregularly rough with an aperture size between 1–5 mm. These surfaces are slightly altered. Having a spacing between 200–600 mm, sandstone has an RQD value between 50–75%.

4 ROCK MASS CLASSIFICATION

Inside the tunnel, the rock masses of the similar lithologies and the shear strength parameters have been

Copyright © 2005 Taylor & Francis Group plc, London, UK

Table 2. Domain characterizations of the Boztepe (T-1) tunnel.

Boztepe (T-1) tunnel							
Domain name	T1-Pn (Entrance)	T1-1	T1-2	T1-3	T1-4	T1-5	T1-Px (Exit)
Km chainage	23 + 015 23 + 050	23 + 050 23 + 375	23 + 375 24 + 000	24 + 000 25 + 000	25 + 000 25 + 775	25 + 775 26 + 290	26 + 290 26 + 323
Lithology in tunnel	Tuff, Agg., Clst.	Clst, Sst., Marl	Agg.	Clst., Agg., Tuff	Clst., Tuff	Bslt., Clst., Agg.	Agg.

Table 3. NGI-Q and RMR classifications for Boztepe (T-1) tunnel.

Section	Domain name	NGI-Q	RMR
Tunnel	T1-Pn	0.64	38.65
	T1-1	2.00	50.75
	T1-2	18.80	69.51
	T1-3	3.60	53.20
	T1-4	1.00	50.77
	T1-5	4.90	59.01
	T1-Px	0.77	39.46

grouped into the same structural domains or geological mass units (Table 2). Thereupon, these domains have been treated as homogenous rock mass sections in order to assign unique support system for each domain. At open-cut excavations of the portals, the lithological units or formations can generally be grouped into two categories as volcanics and flysch type deposits in sense of their engineering behaviors. Rock mass classification systems, namely, RMR, NGI-Q system and GSI have been employed to obtain the rock mass shear strength parameters and the empirical underground support design.

The results of the NGI-Q system and RMR are presented in Table 3–4 (Barton et al., 1974; Bieniawski, 1973).

In determining the rock mass shear strength parameters, RMR values have been processed and the rock mass classes have been determined.

In the Q system of Barton et al. (1974), when a portal is of concern, joint number (J_n) is assigned a value twice the value that would be assigned to a region if there were no intersection and portal. At the portal locations, therefore, the tunneling quality index Q of a region is reduced to by half of its original value. Accordingly, someone may consider the use of reduced values of RMR for portals. Actually, if one considers $Q_{portal} = Q/2$ in the empirical expression $RMR = 9LnQ + 44$, the rock mass rating for the portals becomes $RMR_{portal} = RMR\text{-}6.24$. Therefore, RMR_{portal} values have been considered at the portal faces while determining the rock mass shear strength parameters for the portal slope stability analyses (Table 5).

5 ROCK MASS STRENGTH

The geotectonical conditions juxtapose volcanics and flysch type deposits so often in the project area. Therefore, the in-situ strength of the whole rock mass, which is hard to estimate, may show some differences than the estimated rates. Most of the time, this in-situ condition serves better ground conditions than the estimated ones for engineering applications. The evaluation of the rock mass strength has been executed by the software RocLab Version 1.004 (Rocscience Inc., 2002) based on the generalized Hoek-Brown failure criterion (Hoek et al., 2002). The brief information of the rock mass strength parameters is given in Table 6.

6 IN SITU AND INDUCED STRESS ANALYSIS

The determination of the in situ and induced stresses and deformations developed around the Boztepe tunnel and the interaction of the proposed support categories with the tunnel ground have been investigated by Phase^2 (Rocscience, 2003). In the analyses, four support categories determined by empirical relations for four different ground conditions categorized by NGI Q system in Table 4 have been examined to observe the efficiency and accuracy of the support systems. Boztepe tunnel has been modeled as double tube with 12.0 m of span and 9.0 m height horseshoe shaped tunnel. The field stresses at portals have been modeled by gravity loading. Along the Boztepe tunnel, four different ground conditions each of which supported by separate support categories have been determined as stated before. During the in situ and induced stress analysis, the critical section (Category III in Table 4) has been examined. Hence, the geotechnical parameters of this domain have been determined via GSI and utilized in the analyses (Table 7) whose mesh model is given in Figure 3.

The maximum stress concentration develops at the corner of the excavations whereas the maximum displacements occur at the base of the tunnel excavation.

Copyright © 2005 Taylor & Francis Group plc, London, UK

Table 4. Support recommendations by NGI-Q system for Boztepe (T-1) tunnel.

Intervals		(I) $10 \leqslant Q < 40$	(II) $4 \leqslant Q < 10$	(III) $1 \leqslant Q < 4$	(IV) $0.4 \leqslant Q < 1$
Domains		T1-2	T1-5	T1-1, T1-3, T1-4	T1-Pn, T1-Px
Q		18.80	4.90	1.00-2.00-3.60	0.64-0.77
RMR		69.51	59.01	50.75, 69.51, 50.77	38.65, 39.46
NATM		A2	B1	B2, B2, B2	B3, B3
Suggested Support Categories by Q-system	Roof	Untensioned grouted dowels (Ø26 mm, spacing 1.5–2 m, L = 3.80 m + Chainlink mesh anchored to bolts and intermediate points + when needed tenisoned rockbolts (Ø26 mm, spacing 1 m, L = 3.80 m)	Tensioned rockbolts (Ø26 mm, spacing 1–1.5 m, L = 3.80 m) + Chainlink mesh anchored to bolts and intermediate points + when needed tenisoned rockbolts (Ø26 mm, spacing 0.8–1 m, L = 3.80 m)	5–10 cm shotcrete + Tensioned rockbolts (Ø26 mm, spacing 1–1.5 m, L = 3.80 m) + Chainlink mesh + when needed tenisoned rockbolts (Ø26 mm, spacing 0.8–1 m, L = 3.80 m)	5–12.5 cm shotcrete + Tensioned rockbolts (Ø26 mm, spacing 1 m, L = 3.80 m) + Chainlink mesh + when needed tenisoned rockbolts (Ø26 mm, spacing 0.8–1 m, L = 3.80 m)
	Wall	No support required	2–3 cm shotcrete + Spot reinforcement with untensioned grouted dowels (Ø26 mm, spacing 1.5–2 m, L = 3.35 m) + when needed tenisoned rockbolts (Ø26 mm, spacing 0.8–1 m, L = 3.80 m)	2.5–5 cm shotcrete + Tensioned rockbolts (Ø26 mm, spacing 1 m, L = 3.80 m) + when needed tenisoned rockbolts (Ø26 mm, spacing 0.8–1 m, L = 3.80 m)	5–7.5 cm shotcrete + Tensioned rockbolts (Ø26 mm, spacing 1 m, L = 3.35 m) + when needed tenisoned rockbolts (Ø26 mm, spacing 0.8–1 m, L = 3.80 m)

Table 5. RMR classification for Boztepe tunnel portals.

Portal			
		Side slopes	Portal face
Position	Lithology	RMR	RMRp
Entrance	Volcanics	48.55	42.31
	Flysch	45.92	39.68
Exit	Volcanics	53.20	46.96
	Flysch	45.92	39.68

During the analyses, the maximum displacement has been measured as 8.56 mm at the base of right tube.

The results indicate that the deformations and the loads on support elements are acceptable, and that the empirically determined support members have been proved to be satisfactory (Sopaci, 2003)l.

7 PORTAL SLOPE STABILITY ANALYSES

The stability of the cut slopes of the Boztepe Tunnel portals is controlled by the Upper Cretaceous volcanics and the concurrent flysch. The sandstone and limestone member of Akveren formation (flysch) intertonguing with the volcanics has continuous and distinct bedding planes with 120/20 and 11/15 dip direction and dip amount, respectively. According to the contractor's specifications, the maximum excavation height of the cut slopes was designed to be about 15.0 m above which 5.0 m wide benches were planned. While the cut slopes on the left and right have 1h:3v inclination, the portal face was designed to be 1h:5v for lower slope and 1h:2v for upper slope. In general, the rock mass dominating the portal areas was classified as FAIR ROCK according to RMR classification. This rock mass, in fact, is formed by volcanics and concurrent flysch deposits. The shear strength parameters used in the analyses of this two different lithology groups were determined by RMR classification. Consequently, the shear strength parameters of the volcanics have been determined to be the average of "FAIR ROCK" limits whereas the lower limits of "FAIR ROCK" interval have been chosen for the concurrent flysch.

This is due to the non-homogeneous lithology and strength behavior of the flysch. In addition to this, the first 5–6 m from the ground surface displays highly weathered character as a "VERY POOR ROCK", which can be treated as residual soil. In this particular article the analyses executed for the entrance portal have been given as a case study. According to the kinematical analyses' results of the most critical entrance portal, there is no risk for either plane or toppling

Copyright © 2005 Taylor & Francis Group plc, London, UK

Table 6. The comparison of lab results and the field estimations on rock mass shear strength parameters.

		Hoek-Brown				Mohr-Coloumb		Field estimates			
Domain	Lithology	m_i	σ_{ci} (MPa)	c (MPa)	ϕ (°)	c (MPa)	ϕ (°)	m_i	σ_{ci} (MPa)	c (MPa)	ϕ (°)
T1-2	Volcanics (Agglomerate)	36	11	0.80	41.7	11.6	32				
	Volcanics (Agglomerate)	48	3.6	0.28	44.1	6.8	27	19	30	0.3–0.4	35–45
	Volcanics (Agglomerate)	7	42	1.87	27.4	15.7	27				
T1-3	Flysch (Limestone)	150	1.4			6.7	29	16	35	0.2–0.3	25–35
T1-5	Volcanics (Agglomerate)	16	26	1.46	34.4	13.5	31	17	40	0.2–0.3	25–35
T1-Px	Volcanics (Agglomerate)	87	2.3			13.5	33	19	25	0.2–0.3	25–35

Table 7. Shear strength parameters utilized in the finite element analysis.

Domain	m_i	s_i	m	s	γ (kN/m^3)	c (MPa)	ϕ (°)	E (MPa)	ν
T1-Px	19	1	1.86	0.0007	23	0.192	53	2108	0.2–0.3

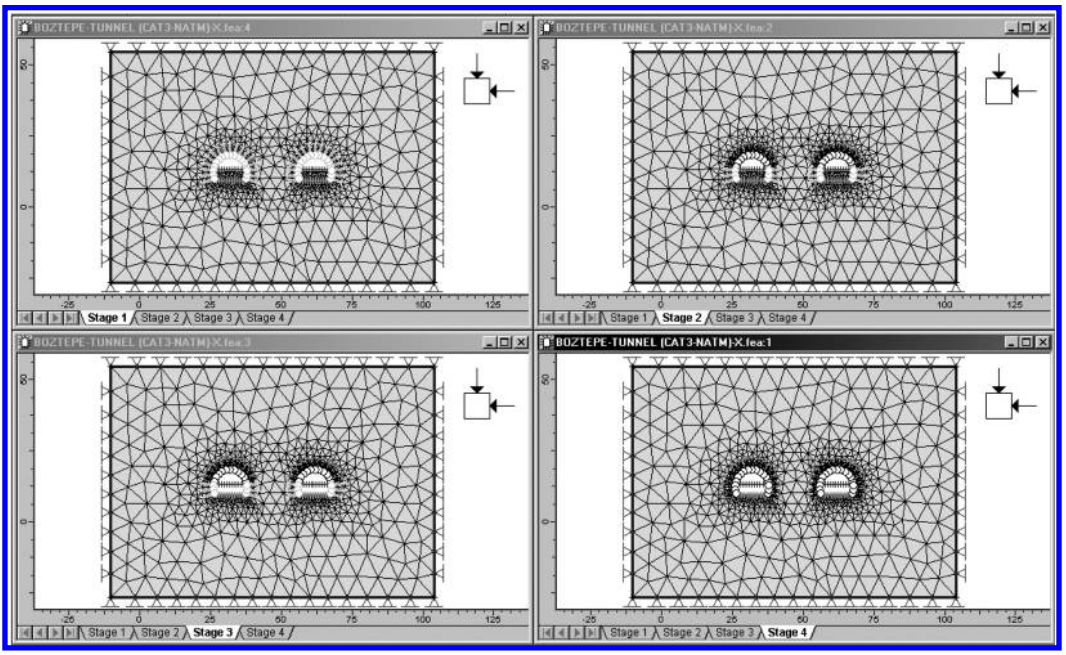


Figure 3. Finite element mesh for the analysis of the Boztepe (T-1) tunnel.

failure. Therefore, the limit equilibrium analyses will not be performed. However, due to the existence of the formerly mentioned weathered zone (residual soil) at the portal areas, the portal slopes have been studied by circular failure analysis by SLIDE (Rocscience, 2003). Table 8 displays the analysis results of the most critical portal excavation (Sopaci, 2003).

Copyright © 2005 Taylor & Francis Group plc, London, UK

Table 8. Boztepe (T-1) Tunnel/Circular Failure Analyses.

Entrance portal					
Left tube			Right tube		
Slope gradient	c (kPa)	ϕ (°)	Slope gradient	c (kPa)	ϕ (°)
1:2	50	15	1:2	50	15
	200	25		200	25
1:5	250	30	1:5	250	30
F.S.: 2.048 ($a_h/g = 0.1$)			F.S.: 1.758 ($a_h/g = 0.1$)		
F.S.: 2.291			F.S.: 1.969		

8 CONCLUSIONS

According to the constructed geotectonical model, surface and subsurface investigations; the rock masses surrounding the Boztepe Tunnel have been classified by NGI-Q system into four main rock classes each of which is supported by different support systems. After the implementation of NGI-Q system, four tunnel support categories have been determined. The related geotechnical rock mass parameters forming the tunnel have been determined in order to model the field conditions into a finite element analysis program. These parameters, which are gathered from empirical classifications (e.g. GSI) and from the lab tests, have been correlated. According to this comparison, "ϕ" values can be said to be successful when they are compared with the results from lab tests. In case of "c" values, on the other hand, the results display wide range of numbers. The Mohr-Coulomb criterion can only calculate the cohesion of intact rock samples without integrated with GSI or RMR ratings. However, Hoek-Brown criterion calculates the rock mass c and ϕ values via GSI which is taken as 50 (average rock quality) by RocLab. This is the reason why c values of Hoek-Brown criterion are much smaller than that of Mohr-Coulomb. On the other hand, the values approximated via RMR, which are more conservative values rather than that of the Hoek-Brown criterion, have been utilized in the slope stability analyses.

The results of the finite element analyses verify that the empirical support design and portal excavation design for the Boztepe tunnel are satisfactory.

REFERENCES

Barton, N., Lien, R., and Lunde, J., 1974, Engineering Classification of Rock Masses for the design of Tunnel Support, Rock Mechanics, Vol.6 No.4, pp. 189–236.

Bieniawski, Z.T., 1973, Engineering Classification of Jointed Rock Masses, Trans S. Afr. Inst. Civ. Engrs. 15, pp. 335–344.

Hoek, E., Carranza-Torres, C., and Corkum, B., 2002, Hoek-Brown Failure Criterion – 2002 edn.

Keskin, İ.,Yergök, A. F., Kara, H., Dönmez, M., and Arslan, M., 1998, Geology of Ünye-Fatsa-Kumru-Korgan (Ordu), Geological Investigation Department of the General Directorate of Mineral Search and Exploration (MTA), Ankara.

Rocscience, Inc., Phase^2 V.5.00, 2D finite element program for calculating stresses and estimating support around underground excavations, Rocscience Inc. 31 Balsam Ave., Toronto, Ontario M4E 1B2, Canada, 2003.

Rocscience, Inc., RocLab Version 1.004, Rock Mass Strength Analysis Program Using the Hoek-Brown Failure Criterion, Rocscience Inc. 31 Balsam Ave., Toronto, Ontario M4E 1B2, Canada, 2002.

Rocscience, Inc., SLIDE V.5.00, 2D limit equilibrium slope stability for soil and rock slopes, Rocscience Inc. 31 Balsam Ave., Toronto, Ontario M4E 1B2, Canada, 2002.

Sopaci, E., 2003. Stability investigations along the Ordu peripheral highway (KM: 21 + 000–KM: 40 + 114). Ms. Thesis, Middle East Technical University, Turkey.

Terlemez, İ., and Yilmaz, A., 1980, Stratigraphy of the Area between Ünye-Ordu-Koyulhisar-Resadiye, Bulletin of the Geological Society of Turkey, Vol. 23, pp. 179–191.

Copyright © 2005 Taylor & Francis Group plc, London, UK

Tunnel and portal stability assessment in weak rock

M.K. Koçkar & H. Akgün
Department of Geological Engineering, Middle East Technical University, Ankara, Turkey

ABSTRACT: The purpose of this study is to present an algorithm for tunnel and portal support design in weak rock conditions. Basic principles of engineering design are introduced and the main stages of the design process are delineated through assessing a highway tunnel case study in Turkey. This case study involved the investigation of the engineering geological and geotechnical characteristics of the rock material and rock mass of the tunnel grounds; evaluation of the field stresses, the applied loads and the deformations around the underground excavations; assessment of the validity of decision making (i.e., alternative selection); and finally, suggesting appropriate support and stabilization techniques for optimum tunnel design.

1 INTRODUCTION

The main objective of this study is to present an algorithm for tunnel and support design in weak rock conditions through a highway tunnel case study in southern Turkey which involved investigating the engineering geological and geotechnical characteristics of the rock material and rock mass of the tunnel grounds, and suggesting appropriate support and stabilization techniques. Figure 1 gives a detailed flow chart of the design algorithm.

The algorithm started with the statement (or definition) of the design and performing literature review regarding the geology and geotechnical characteristics of the project site, a preliminary site reconnaissance visit to identify major lithologies, structural features and to collect data and decide on possible in-situ test locations. Then, information was gathered from geological, geotechnical, geophysical field investigations along with seismic studies in the project area. Preparation of engineering geological maps and geological cross-sections from site exploration, assessment of the seismicity of the study area, determination of RQD from boring data, selection of representative rock core samples for geomechanics laboratory testing and determination of discontinuity characteristics through scan-line survey was performed for rock material and rock mass characterization. Laboratory tests were performed to determine the geomechanical parameters of rock masses. For poor quality (weak or squeezing) rock masses, the Geological Strength Index (GSI) was utilized to obtain the relevant geomechanical parameters since it was almost impossible to recover representative core samples for laboratory testing.

In the model formulation and analysis of solution components of the design steps (empirical, analytical and numerical methods), the tunnel grounds were classified according to internationally accepted rock mass classification systems, namely, the Q-system, the Rock Mass Rating (RMR) method as well as NATM (New Austrian Tunneling Method). Empirical tunnel support types and categories were selected for each of the three classification systems. Back analysis was performed during the initial stages of portal excavation on failed rock slopes to provide the constants of the selected constitutive model and to perform a check on the reliability of the shear strength parameters. By using the appropriate rock mass strength parameters (i.e., shear strength, deformation modulus, Poisson's ratio, dilation angle, etc.), deformations and stress concentrations around the underground excavations were investigated and the interactions of the empirical support systems with the rock masses were analyzed by using numerical modeling (i.e., FEM, FDM) methods under static and dynamic conditions to interpret and specify the alternative solutions for the reliability of decision making. Consequently, appropriate support recommendations and stabilization techniques were introduced for optimum design. Regarding the stability of the portals and cut slope sections, slope stability analyses were performed along the tunnels. Kinematic and limit equilibrium methods were performed for the failed rock slopes. Slope stability analyses of weak rock and soil-like lithologies were analyzed by finite element and slope stability softwares under static and dynamic conditions to check the reliability of the results and to specify the best alternative for portal design. Finally, recommendations were made regarding the required

Copyright © 2005 Taylor & Francis Group plc, London, UK

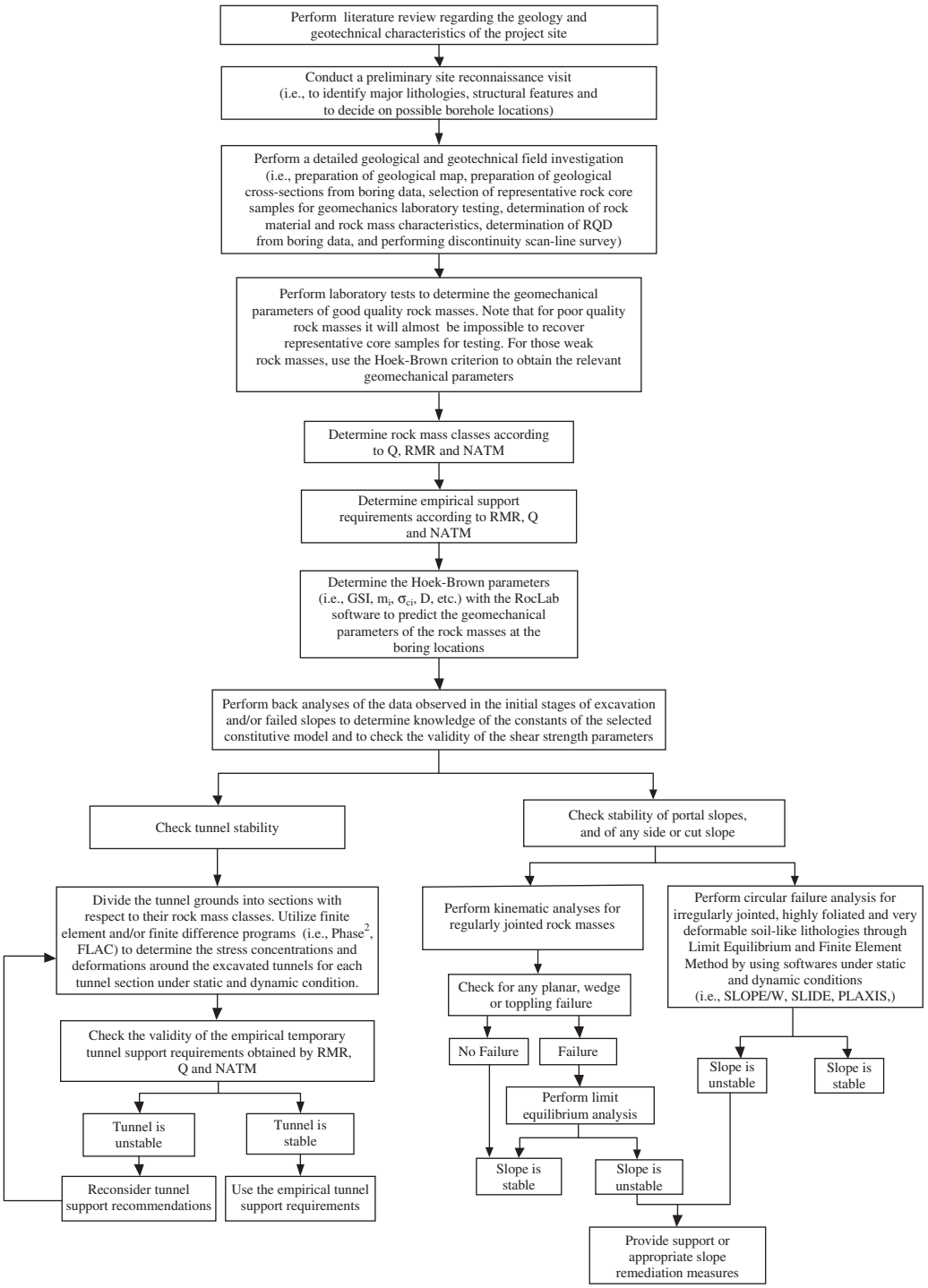


Figure 1. Flow chart of the design algorithm for assessing support requirements in weak rock conditions (Modified from Koçkar & Akgün, 2003).

Copyright © 2005 Taylor & Francis Group plc, London, UK

support design or appropriate slope remediation measures.

2 ASSESSING TUNNEL CASE STUDIES

Engineering design was assessed through a highway tunnel case study in southern Turkey along the coast of the Mediterranean Sea (Figure 2). The tunnels, known as Ilıksu 1 and 2, are located along the 4th division route of the Antalya-Alanya D-400 highway. A cut slope section lies in between these two tunnels (Koçkar, 2001; Koçkar & Akgün, 2003).

The study area is overlain by the Alanya Massif which is the name given to a large area of metamorphic rocks situated towards the east of Antalya Bay in the Eastern Mediterranean region (Özgül, 1984). Geologic units that belong to the Yumrudağ Nappe that is the structurally highest unit of the Alanya Massif were observed in the project area. Yumrudağ Nappe consists of a thick carbonate sequence (regularly bedded, recystallized limestone) underlain by a schist unit metamorphosed under low-grade greenschist facies. Due to tectonic activity, the rock mass can be highly heterogeneous in some of the lithologies of the schist unit. Pelitic schists, calc schists, graphitic phyllites and alternations of these lithologies are the major lithologies of the schist unit that are highly problematic (Koçkar, 2001).

Detailed geological and geotechnical field investigations along with seismic studies were carried out in the project area in order to constitute the geological model and to determine the engineering geological properties of the tunnel grounds. Pelitic schist, which is partly intercalated with calc schists, will be cut along the tunnel route (Figure 3). This lithology is green to greenish gray, moderately to highly weathered, and possesses weak to moderately weak strength. It is easily separated along the foliation planes, which are highly persistent. The uniaxial compressive strength (UCS) is classified as very low, with a measured range of 3 to 29 MPa. The Rock Quality Designation (RQD) of the pelitic schist ranges between zero to 81%.

Phyllite, which is mostly intercalated with calcchists and limestone bands is the most problematic unit of the study area. This lithology is blackish to dark gray, possesses weak to moderately weak strength, and is moderately to highly weathered. In phyllite, the joint systems are not well developed and rock masses are highly heterogeneous (Figure 4). It is highly sheared, deformed and has very poor quality rock mass properties. UCS of the rock is classified as low, with a measured range of 16 to 50 MPa. The RQD of phyllite ranges between zero to 62%.

Calc schist is observed to be intercalated with limestone bands and phyllite. Calc schist is light to dark gray and almost always includes calcite veins. The

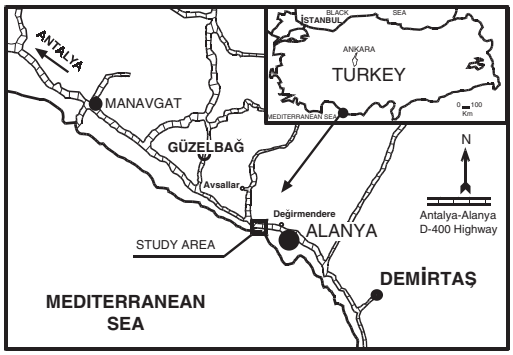


Figure 2. Location map of the project area.



Figure 3. Tectonically deformed, folded, laminated and foliated pelitic schist unit.

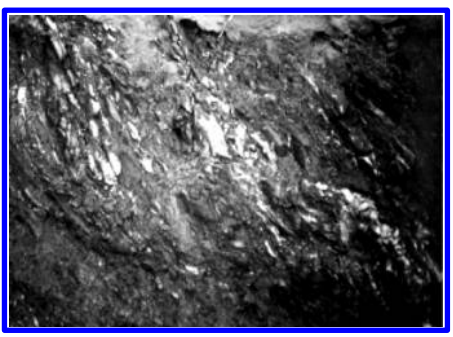


Figure 4. Graphitic phyllite. A heterogeneous rock mass comprising of highly foliated sheared and very deformable soil-like lithologies.

foliation planes and rare joint systems control the discontinuous nature of the rock mass. It is slightly to moderately weathered and has moderate to high strength. It possesses poor rock quality due to intercalation with pelitic schists and phyllites. The UCS is measured to range between 62 to 92 MPa. The RQD of the calc schist ranges between zero to 20%.

Copyright © 2005 Taylor & Francis Group plc, London, UK

Table 1. Summary of the rock mass classification results for different rock masses in the project area.

Tunnel location	Tunnel section (km)	Lithology	Q-system	RMR	NATM	Support requirements
Iliksu 1	127 + 545–127 + 685	R.Lst.	2.107–7.305	53–59	B1–B2	Fair Quality
	127 + 685–127 + 800	Phyllite	0.234	31	B3	Poor Quality
	127 + 800–127 + 870	R.Lst./Pelitic schist	5.693	58	B1–B2	Fair Quality
	127 + 870–128 + 074	R.Lst./Pelitic schist	0.571–0.971	31–46	B3	Poor Quality
Cut slope section	128 + 074–128 + 155	Pelitic schist	0.571	46	B3	Poor Quality
Iliksu 2	128 + 155–128 + 195	Phyllite/Calc/ Pelitic schist/R.Lst.	0.900	31	B3	Poor Quality
	128 + 195–128 + 317	Phyllite/Calc/ Pelitic schist	0.125–0.804	31	B3	Poor Quality

Recrystallized limestone is exposed in most parts of the project area and generally overlies all of the units. Karstic features are locally observed in limestone. In the recrystallized limestone unit, rock masses are often very blocky. It is gray to light gray, strong, and slightly weathered. The UCS of recrystallized limestone is high, with a range of 30 to 117 MPa. The RQD values range between 61 to 73%.

The geotechnical properties of the units comprising the area were assessed using three empirical rock mass classification systems, namely the Q-system (Barton et al., 1977), RMR (Bieniawski, 1989) as well as NATM (New Austrian Tunneling Method) by using correlations with the RMR and Q (Turkish General Directorate of Highways, 1997). The results of the rock mass classifications for different rock masses observed in the project area is presented by Table 1.

A summary of the empirical temporary support systems and related support requirements were selected for each three classification systems (Koçkar and Akgün, 2003).

The shear strength parameters and geomechanical properties of the rock masses were determined by the Hoek-Brown criterion for weak rock masses (Hoek et al., 1992 & Hoek, 1994). Determination of the strength of closely jointed, foliated and heterogeneous weak rock masses is hardly possible because it is not always possible to recover representative core samples. In order to overcome these difficulties, the extended GSI has been used for very poor quality of rock masses (Hoek & Brown, 1997), namely for the extremely poor quality schistose rock masses and phyllites (Hoek et al., 1998) as well as for heterogeneous rock masses (Marinos & Hoek, 2001) in the study area.

In the project area, the major lithologies of the very poor quality schist units are weak, laminated, foliated, tectonically deformed, highly heterogenous and differentially sheared (Figure 3 & 4). The recrystallized limestone rock masses are generally very blocky. At some locations, the rock mass blocky/ disturbed/ seamy due to intense folding or karstic nature or the presence of schistosity bands.

The Hoek-Brown input parameters (Hoek et al., 2002) and the ranges of GSI values of the lithologies corresponding to the rock mass quality at each tunnel section were obtained. The ranges (upper and lower bounds) of the Hoek-Brown input parameters and the ranges of GSI values, an estimate of the geomechanical properties and post-failure behavior of the rock masses are summarized in Table 2 (Modified from Koçkar & Akgün, 2003).

To determine the stability of the portal, side or cut slope sections, slope stability analyses were performed. In order to check the stability of the proposed cut slopes consisting of regularly jointed rock masses, kinematic analyses were initially performed to determine the type and possibility of the occurrence of any kinematic failure. Next, limit equilibrium analyses were performed on the regularly jointed rock slopes for wedge and plane types of failures (Hoek & Bray, 1981).

The results of the kinematic analyses on regularly jointed, recrystallized limestone showed that only wedge failure was possible on the north cut slope of the Ilıksu 1 tunnel entrance portal. After performing a wedge limit equilibrium analyses for saturated conditions, it was determined that wedge failure was not expected for the north cut entrance portal slope of the Ilıksu 1 tunnel. Planar failure was kinematically possible for both the north cut and south cut slopes along the Ilıksu 1 tunnel entrance portal. After performing a plane failure limit equilibrium analyses for saturated

Copyright © 2005 Taylor & Francis Group plc, London, UK

Table 2. Geomechanical properties of fair quality, poor quality and very poor quality rock mass at the project area as determined by RocLab (2002).

Geomechanical properties	Fair quality	Poor quality	Poor to very poor quality
Intact rock strength (σ_{ci}) (MPa)	58–75	45	5–35
Hoek-Brown constant (m_i)	10–9	8	6–8
Geological Strength Index (GSI)	55 ± 5–50 ± 5	30 ± 5	18 ± 5–22 ± 5
Disturbance factor, D	0.5	0.5	0.5
Hoek-Brown constant (m_b)	0.832–1.173	0.285	0.121–0.171
Hoek-Brown constant (s)	0.0013–0.0025	0.0001	1.79e-5–3.04e-5
Constant (a)	0.504–0.506	0.5220	0.538–0.550
Friction angle (ϕ')	51–57°	42°	20°–28°
Cohesive strength (c'), MPa	0.357–0.487	0.121	0.023–0.085
Global strength (σ_{cm}), MPa	7.019–9.553	2.832	0.167–1.520
Rock mass tensile strength (σ_{tm}), MPa	0.089–0.133	0.014	0.001–0.006
Uniaxial compressive strength (σ_c), MPa	1.991–3.061	0.344	0.012–0.130
Deformation modulus (E_m), MPa	5712–7938	1591	266–885
Poisson's ratio (ν)	0.25	0.27	0.30
Dilation angle (φ°)*	6.3°–7°	2.6°	0°–1°

*The post-peak or post failure characteristics of the rock masses are determined by using experience in numerical analysis on a variety of practical problems (Hoek & Brown, 1997).

Table 3. Summary of the stability results for the portal faces of the Iliksu tunnels consisting of weak rock masses.

Section	Lithology	Soil properties	F.S. with SLOPE /W (Simplified Bishop Method)	F.S. with PLAXIS 7.2 (Phi-c reduction by using Standard Coulomb Condition)		Stability condition ($F > 1.5$)
				Static	dynamic (pga = 0.2 g)	
Iliksu 1 exit portal	Pelitic schist	$\gamma = 26.65\,kN/m^3$, $\phi = 23°$, $c = 78\,kPa$	1.34	1.31	1.21	unstable
Iliksu 2 entrance portal	Phyllite, calc and pelitic schist	$\gamma = 25.0\,kN/m^3$, $\phi = 18°$, $c = 42\,kPa$	0.94	0.93	0.85	unstable
Iliksu 2 exit portal	Calc schist and phyllite	$\gamma = 25.0\,kN/m^3$, $\phi = 22°$, $c = 70\,kPa$	1.28	1.23	1.16	unstable

conditions, no plane failure was expected along the north and south cut portal slopes of the Ilıksu 1 tunnel.

Slope stability analyses of irregularly jointed, highly foliated and very deformable soil-like lithologies were analyzed by the slope stability software Slope/W (Geo Slope, 1999) using Bishop's simplified method under static conditions, and by the c-ϕ reduction option of the finite element analysis software PLAXIS 7.2 (2001) under static and dynamic conditions (considering that the project area lies between IIIrd to IVth degree seismic zone according to the earthquake zonation map of Turkey). The results of the analysis shows that slope stability problems are expected on the exit portal face of the Ilıksu 1 tunnel and the entrance and exit portal faces of the Ilıksu 2 tunnel. The results are summarized in Table 3 for static and dynamic conditions. Stability of the cut slope section that is planned to be constructed between the two tunnels was analyzed by Slope/W and PLAXIS 7.2 as well. It needs to be mentioned that the studies presented herein have been cited by Rocscience Inc. (2004) in "Phase^2 Project Gallery Website". According to these analyses, stable and unstable zones exist along the cut slope section. Recommendations regarding support types for the slope faces along with the north and south side cut slopes of the portals and cut slope sections were made.

A back analysis was performed within calc schist on a failed slope that has developed most probably due to insufficient support and stress relief during portal excavation. Calc schist was regularly bedded and did not show intense intercalation with highly foliated, laminated, sheared and very deformable soil-like lithologies. The back analysis was applied to two wedge types of failures that occurred within each other in order to determine the shear strength parameters. The results of the back analysis led to $\phi' = 25°$

Copyright © 2005 Taylor & Francis Group plc, London, UK

and c′ = 58 kPa. The shear strength parameters were also determined with the generalized Hoek-Brown failure criterion with the slope application option. According to the GSI results (from Table 3), the range of the shear strength parameters of calc schist are as follows: c = 36–67 kPa; ϕ = 20–25° which indicates a very good agreement between the shear strength parameters obtained through the GSI method and those obtained through back analyses for very poor quality rock masses.

The finite element software package Phase^2 (2001) was used to determine the induced stresses and deformations developed around the Ilıksu tunnels and to investigate the interaction of the proposed support systems with the tunnel ground. The objective of Phase^2 was to check the validity of the empirical temporary tunnel support requirements. Modeling with Phase^2 consisted of four stages. In the first stage, in situ stress distributions were examined. In the following two stages, the principal stress distributions (σ_1, σ_3), the safety factor, yield points (shear, tension) and the induced displacements that developed around the tunnels were analyzed using top heading followed by excavating the entire tunnel. In the final stage, the effectiveness of the temporary support systems was investigated.

Tunneling through weak condition is a very problematic situation because the rock mass around the opening looses its inherent strength under the influence of in-situ stresses. Therefore, the most unsuitable conditions (poor to very poor quality rock mass) that could be faced during tunneling were taken into consideration in modeling this tunnel section. The results of the numerical stress analysis of the tunnel section (Km: 128 + 155–128 + 317) which encompasses the total displacements in the rock mass as a result of the four stages with and without support are shown in Figure 5 (Stage 3 & 4). Compared to the unsupported excavation, displacements have been drastically reduced. After installation of the support system, the total displacement has nearly been reduced by three-folds with respect to the induced displacement without support. Therefore, it may be concluded that the support recommendations given for the Ilıksu 2 tunnel are satisfactory (Koçkar & Akgün, 2003).

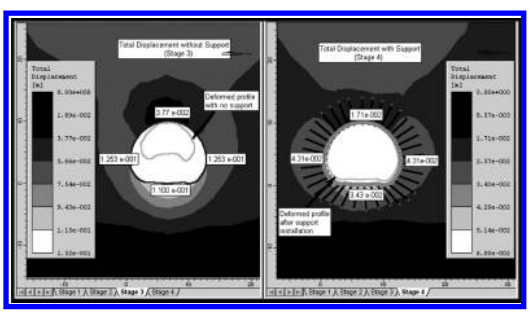


Figure 5. Total induced displacement contours and their deformed mesh at the Ilıksu 2 tunnel portal locations.

3 CONCLUSION

The purpose of this study is to introduce the principles of engineering design and to present an algorithm for the main stages of the design process for tunnel and portal support in weak rock conditions through investigating a tunnel case study in southern Turkey.

ACKNOWLEDGEMENTS

The authors would like to thank Mr. H. Özaslan of Yüksel Proje International A.Ş. for his kind assistance throughout the project.

REFERENCES

Barton, N., Lien, R. & Lunde, J. 1977. Estimation of support requirements for underground excavations. *Proceedings 16th Symposium on Rock Mechanics, Minneapolis, USA.*

Bieniawski, Z.T. 1989. Engineering rock mass classification. A.A. 251. Cape Town: Balkema.

Geoslope. 1999. Slope/W-Slope stability Software. Geo Slope International Ltd, Calgary, Alberta, Canada.

Hoek, E. 1994. Strength of rock and rock masses, *ISRM News Journal*, 2(2): 4–16.

Hoek, E. & Bray, J.W. 1981. Rock Slope Engineering. Institution of Mining and Metallurgy. 358. London.

Hoek, E. & Brown E.T. 1997. Practical estimates of rock mass strength. *Int. J. of Rock Mech. Min. Sci. & Geomech. Abstr.*, 37 (8): 1165–1186.

Hoek, E., Wood, D. & Shah, S. 1992. A modified Hoek- Brown criterion for jointed rock mass. *Proc. Rock Characterization, Symp. Int. Soc. Rock Mech.: Eurorock '92*, (Edited by Hudson, J.A.). London, Brit. Geotech. Soc., 209–214.

Hoek, E., Marinos, P. & Benissi, M. 1998. Applicability of the geological strength index classification for very weak and sheared rock masses. The case of the Athens Schist Formation. *Bulletin Engineering Geology Environment.*, 57: 151–160.

Hoek, E., Caranza-Torres, C.T. & Corkum, B. 2002. Hoek-Brown failure criterion-2002 Edition. *Proc. North American Rock Mechanics Society*, Toronto, Canada.

Marinos, P. & Hoek, E. 2001. Estimating the geotechnical properties of heterogeneous rock masses such as flysch. *Bulletin Engineering Geology Environment.*, 60: 85–92.

Koçkar, M.K. 2001. Engineering geological investigations along the Ilıksu Tunnels, Alanya, *M. Sci. Thesis*, Middle East Technical University. 333. Ankara, Turkey.

Koçkar, M.K. & Akgün, H. 2003. "Methodology for tunnel and portal support design in mixed limestone, schist and phyllite conditions: A case study in Turkey", *International*

Copyright © 2005 Taylor & Francis Group plc, London, UK

Journal of Rock Mechanics & Mining Sciences, Vol 40/2: 173–196.
Özgül, N. 1984. Alanya tectonic window and geology of its western part. *The Geological Society of Turkey, Ketin Symp.*, The Geological Society of Turkey, Ankara, 97–120.
PLAXIS Version 7.2. Finite Element Code Soil and Rock Analyses. 2001. PLAXIS BV, P.O. Box 1675, 3000 BR Rotterdam, Netherlands.
Rocscience Inc. 2001. Phase^2. 2D finite element program for calculating stresses and estimating support around underground excavations. Rocscience Inc., Toronto, Canada.
Rocscience Inc. 2004. RocLab. Rock mass strength analysis using the Hoek-Brown failure criterion. Rocscience Inc., Toronto, Canada.
Rocscience Inc. 2004. Application of finite element method to slope stability. Rocscience Inc., Toronto, Canada. (http://www.rocscience.com/library/Phase2ProjectGallery.asp)
Turkish General Directorate of Highways. 1997. List of specifications of the underground tunnel excavations with NATM practice. 105 (in Turkish).

Copyright © 2005 Taylor & Francis Group plc, London, UK

Three-dimensional regions in tunnels

H. Gercek
Dept. of Mining Engineering, Zonguldak Karaelmas University, Zonguldak, Turkey

ABSTRACT: In the stress and stability analysis of underground openings, cross-sectional plane-strain analyses are common; yet, in tunnels, there are some regions that must be analyzed three dimensionally. The typical examples of such regions are: the excavation face, portals, intersections with other underground openings, and regions with sudden geometrical changes. The paper involves some considerations regarding the stability and analysis of these three-dimensional regions. Significance of these regions and the problems encountered in such regions are discussed. Then, major considerations that should be taken into account during the stress and stability analysis of the three-dimensional regions in tunnels are presented.

1 INTRODUCTION

Theoretically, the state of stresses and displacements around an underground opening is three dimensional. Ideally, therefore, three-dimensional (3-D) methods should be used for the proper analysis of stresses and displacements occurring around openings. Even with today's powerful numerical methods and friendly computer programs, 3-D stress analysis is complex and requires experience for implementation and interpretation. In tunneling, nevertheless, this complicated analysis can be, and usually is, replaced by a much simpler, cross-sectional plane-strain analysis when one of the principal components of in situ stresses is acting (or assumed to be acting) parallel to the longitudinal axis of the opening. However, the result of this kind of analysis corresponds to the deformed (i.e. final) state of the tunnel. Also, it does not tell us how the stresses and displacements develop along the tunnel length.

The underground openings, around which the distribution of stresses can be studied by two-dimensional analyses, are called "two-dimensional (2-D) openings." Yet, even in a tunnel, which is the most typical example of 2-D openings, there are some regions which must be analyzed three dimensionally. These are as follows (Fig. 1):

(a) the excavation face,
(b) portals,
(c) intersections with other underground openings, and
(d) regions with sudden geometrical changes, i.e. cross-sectional (shape, size) or directional changes.

In this paper, important considerations regarding these 3-D regions are presented. Firstly, from tunneling point of view, the significance of each region is explained. Secondly, special problems encountered in the excavation of these regions and factors affecting their stability are discussed. Finally, major

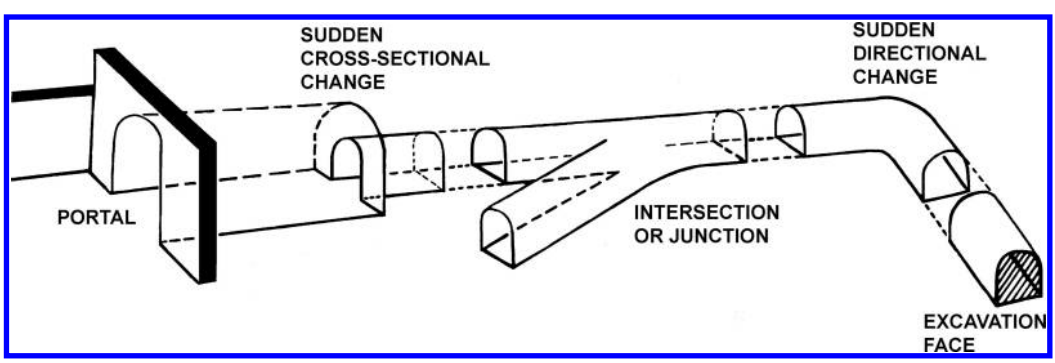


Figure 1. An imaginary view of the three-dimensional regions in tunnels.

Copyright © 2005 Taylor & Francis Group plc, London, UK

considerations to be taken into account for the stress and stability analysis of such regions are presented.

2 THREE-DIMENSIONAL REGIONS

It should be emphasized that the 3-D nature of the regions discussed here arises from purely geometrical considerations. In other words, it is assumed that the existing in situ stress field justifies a plane-strain analysis of a regular or normal section of the tunnel, and the state of induced stresses around the special region becomes three dimensional due to the change(s) in the cross-sectional geometry and/or direction along the longitudinal axis of the opening.

2.1 *The excavation face*

The excavation face of a tunnel is a dynamic region that moves along the route during the construction and ceases to exist at some stage. In many cases, multiple excavation faces are employed. Frequently and due to the stability considerations, excavation is carried out in multi stages instead of full face. No matter how the face is excavated, the ground conditions encountered at the face is an indication of the behavior of surrounding medium far behind the face.

Because of the so-called "half-dome action" of Terzaghi (1946), the stability situation of the face is somewhat better than that of the region behind the face. In fact, according to Italian ecolé, "everything revolves at the face: a tunnel with an unstable face will collapse, even though its walls may be supported (Duffaut & Piraud 2002)."

Researchers in tunneling have always been fascinated by the stresses and displacements occurring around the advancing face of a tunnel. The major reason behind this fascination is that the distribution of stresses and displacements around the face gives valuable information on the stability and support requirements of the tunnel, which is the most important aspect of tunnel design in terms of safety and economics. Yet, the complicated geometry and boundary conditions of the problem have excluded the possibility of finding a closed-form solution to this problem that must be analyzed three dimensionally.

Unavailability of a closed-form solution for this interesting problem has directed the researchers to the utilization of numerical analyses mainly; in addition, to a lesser extent, in situ measurements and physical models (e.g. 3-D photoelasticity) have been employed to study the problem. Numerous analyses employing numerical methods started during the mid 70s (Descoudres 1974, Ranken & Ghaboussi 1975, Hocking 1976, etc.), and they have continued into the 21st century (Eberhardt 2001, Tonon & Amadei 2002, Unlu & Gercek 2003). The numerical studies have involved elastic (isotropic or transversely isotropic), elasto-plastic, viscoelastic, etc. material behavior. They have been performed for studying tunnel convergence, analyzing of rock-support interaction, determining excavation disturbance zone, evaluating tunnel face stability, etc. Some of these studies were reviewed and summarized by Pelli et al. (1991).

Also in recent years, significant research has been devoted to the stability and deformation behavior of tunnel face reinforced by longitudinal pipes or bolts (Yoo 2002, Ng & Lee 2002, Kamata & Mashimo 2003, Yoo & Shin 2003).

2.2 *Portals*

Geometrically, portal of a tunnel may be defined as the intersection of the tunnel with surface. Yet, the portal, due to its inherent conditions, should be considered as a special region where an underground opening intensely interacts with the surface that usually includes natural or man-made slopes. More properly, "the portal is defined as a unique structural region of which primary purpose is to provide safe access for men, materials, and equipment from the surface to a subsurface excavation over a definable project life (Rogers & Haycocks 1988)."

Portals and structures built in these areas vary depending on the function of the tunnel, topography of the area, and conditions of the site. Especially, architectural features of portal structures emphasize the importance of the tunnel. In a sense, "the portal of a tunnel may be considered the business card of its builder (Müller 1978)." Today, modern approach in the design of portals and related structures involves both technical and environmental criteria (Peila & Pelizza 2002).

Portals are known to be difficult regions for tunnel engineers due to the special problems listed below (Pacher 1974, US Army Corps of Engineers 1978, Gercek 1990).

(a) Compared to the other parts of the tunnel, rock masses at portal sites are highly discontinuous and usually of low quality due to weathering. The development of a self supporting-arch over the tunnel requires adequate (two diameters or more) rock cover.

(b) Creation of an excavation face and its advance at the portal sites may affect the stability of natural and/or man-made slopes seriously and in several ways. For example; the toe of the slope is unloaded, loosening behavior is triggered, and dynamic loads are imposed by blasting.

(c) At portal regions, in situ stresses influenced by the topography and geology of the site may be highly nonuniform, and their effect on stability may not be easily predictable.

(d) In the case of drill-and-blast excavation, overbreak is high due to poor quality rock mass and

Copyright © 2005 Taylor & Francis Group plc, London, UK

Table 1. Failure classification for tunnel portals (Rogers & Haycocks 1988).

External failure types	Internal failure types
Overall mass slide *	Crown face overbreak **
Upper slope slide	Internal crown/rib failure
Outer rib slide	Invert failure
Upper slope subsidence/ collapse	Seal rupture ***

* Least common, most disastrous.
** Most common, least reported.
*** In inactive or abandoned portals.

interaction with the free slope surface during the initial rounds.

(e) Historically, in terms of seismic performance, damage at and in the vicinity of portals may be significant (Hashash et al. 2002).

(f) At the time of portal excavation, it is generally too early for the construction crew to act as a team and develop an understanding of the rock mass.

Because of one or a combination of these problems, failures are experienced frequently at or around the portals of tunnels. Rogers & Haycocks (1988), based on over 300 case studies, developed a location-based classification system for the failures encountered at portals (Table 1).

For the design and stability of tunnel portals, the following studies, though not exhaustive, are worth mentioning. US Army Corps of Engineers (1978) gave a detailed account of portal design approaches and guidelines (including types of portals, portal treatments, portal excavation procedures, etc). Barisone et al. (1983) reviewed Italian practices (e.g. umbrella arch method, diaphragm of piles, etc.) employed for excavation of tunnel portals in difficult ground. Rogers & Haycocks (1989) developed excavation/support guidelines for portals of tunnels (diameter $\leqslant 9$ m) for the Geomechanics Classification System of Bieniawski (1989). Incidentally, Barton et al. (1974) considered portals in a separate excavation category and allowed provisions for them in their Q-System classification. Peila & Pelizza (2002) presented criteria for technical and environmental design of tunnel portals. Del Greco & Oggeri (2004) summarized the stability and reinforcement techniques of rock slopes above portals in northern Italy.

2.3 *Intersections or junctions*

An intersection involving tunnels is a region where the common points of two or more individual tunnels are located. This is a purely geometrical definition. Actually, it is a region where the tunnels that form the intersection or junction interact closely with each other.

Underground intersections are frequently developed in many subsurface construction projects, e.g. subway systems, power station complexes, sewer or water-supply networks, military and defense installations, etc. Also, conceptual designs of underground repositories for high-level nuclear wastes generally involve a labyrinth of underground passageways with numerous junctions. Similarly, in underground mining operations, intersections involving galleries and shafts are common. As a matter of fact, in some mining practices (e.g. block caving and room-and-pillar methods), intersections are an inherent feature of the production method.

Intersections provide continuity of functions of tunnels along different routes crossing one other; therefore, the stability of intersections is crucial. Yet, the potential for instability is more pronounced in these regions due to the following reasons (Gercek 1986, 1996).

(a) At an intersection, the roof span is greater than those of the openings involved, and, obviously, a larger span corresponds to a shorter stand-up time and greater rock-load height.

(b) Geological discontinuities pose difficulties for the design of intersections. For example, a favorable orientation of a dominant joint set for one opening may be undesirable for the other(s). An extreme example of such a possibility is shown in Figure 2a.

(c) At the intersection, the support provided by the sidewalls of an opening is removed. In a jointed and blocky rock mass, the removal of confinement and creation of additional free surfaces may expose some blocks or wedges that can move in more than one direction (Fig. 2b).

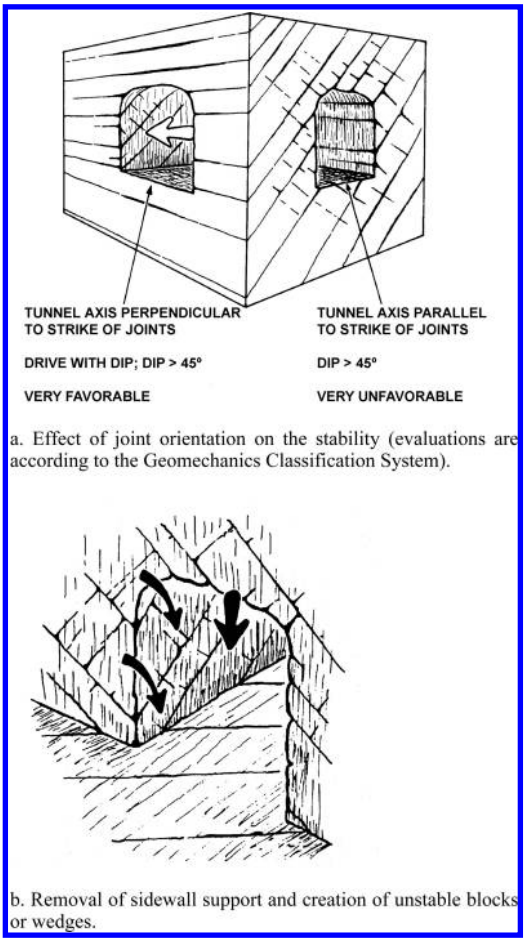
(d) At intersections or junctions, induced stresses occurring around individual openings are, in a sense, superimposed. Particularly, sharp intersection corners are regions of high stress concentration and, if possible, they should be avoided.

In fact, the intersection region includes not only the conditions and characteristics of the individual openings but also additional problems created by the new geometry. Therefore, the design of tunnel intersections requires special consideration. The possibility of encountering adverse conditions (i.e. significantly different from those existing around the individual openings) should be taken into account.

For the intersection problem, too, there is no closed-form solution for the distribution of stresses. Earlier studies were carried out by using 3-D photoelasticity (Kaneshige et al. 1964, Riley 1964).

Also, many studies involving numerical analyses have been done on the subject; however, most of those studies included results dependent on a particular case. In this respect, a comprehensive study carried out by Hocking (1978) on the stresses around two- and three-way tunnel intersections or junctions was remarkable.

Copyright © 2005 Taylor & Francis Group plc, London, UK



a. Effect of joint orientation on the stability (evaluations are according to the Geomechanics Classification System).

b. Removal of sidewall support and creation of unstable blocks or wedges.

Figure 2. Some of the stability problems at intersections (Gercek 1986).

Gercek (1986, 1996) presented recommendations for the design and support of tunnel intersections. Furthermore, some of the rock mass classification systems offer provisions for the intersections. For example, in the Q-System of Barton et al. (1974), the Q value of a region is reduced to one-third of its original value at the intersections. In the application of Geomechanics Classification System, Bieniawski (1978) recommends the use of next lower quality rock mass class when an intersection is involved.

As a matter of fact, the rock mass rating (RMR) for the intersection may be estimated by (Gercek 1996):

$$RMR_{intersection} \approx RMR - 10 \quad (1)$$

Here, it should be noted that the intersections involving underground openings with significantly different sizes may be considered as special cases. For example, during the construction of Dinorwic underground power station at North Wales, there were 35 intersections within the tunnel system, and more than 50 intersections of tunnels with the caverns were treated as portals, apart from 15 actual portals (Peterson & Arthur 1979, Ellis et al. 1979).

2.4 *Regions with sudden geometrical changes*

These regions, actually, can be considered as special types of intersections. The reason for their inclusion in a separate category is that the region with sudden geometrical change belongs to a single tunnel, i.e. no other opening is involved.

In tunnels, sudden geometrical changes may involve cross-sectional or directional changes or both. Sudden cross-sectional changes occur either by enlarging or decreasing the cross-sectional area of the opening. This kind of geometrical changes may be accompanied by changes in the shape of the tunnel. In any case, it has long been established that, if stability problems of some degree exist in a project, decreasing the cross-sectional area of the excavation generally improves the stability; inversely, enlarging the area of the excavation somehow worsens the stability picture. If possible, therefore, cross-sectional enlargements should be made gradually.

In the case of sudden directional changes, the outcome may not be readily predictable. Of course, effect of anisotropic in situ stresses or the orientation of discontinuities will be the major concern regarding the stability. For tunnels driven in an anisotropic in situ stress field, sometimes the directional change dramatically affects the stability (Gercek & Genis 1999). Also, concerning the orientation of tunnel with respect to the dominant joint sets, sudden directional changes may significantly affect the stability picture (Fig. 2a). Actually, in most tunneling projects, directional changes are gradual, or the overall change in direction may not warrant more than a single cross-sectional analysis.

In summary, the 3-D regions in tunnels are important but they pose some problems to designers.

3 CONSIDERATIONS FOR ANALYSIS

For proper stress and stability analysis of 3-D regions in tunnels, there are a number of considerations that should be taken into account, and these are as follows.

Firstly, the domain to be analyzed should include the zone of influence of the 3-D region. It is the zone outside of which the effect of the 3-D region practically diminishes. For the excavation face, the zone of influence starts about two tunnel diameters ahead of the face and extends to some distance behind the face. This distance is about two to four diameters for a linear

Copyright © 2005 Taylor & Francis Group plc, London, UK

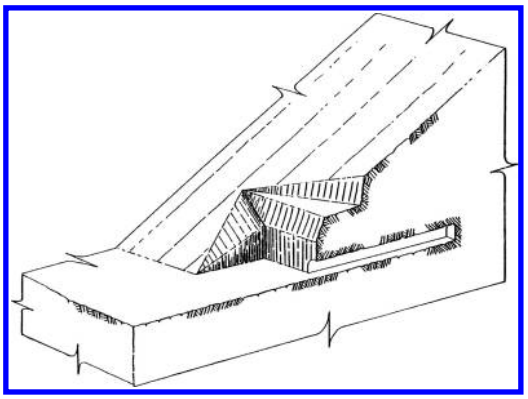


Figure 3. An hypothetical domain for modeling the portal and excavation face of a tunnel (Gercek 1990).

elastic rock while it can be several diameters for elasto-plastic material behavior (Unlu & Gercek 2003).

The size of the zone of influence of a portal depends on topographical and geometrical features of the site. In this context, the size is influenced by the extent to which the slopes of the portal cut are affected by the tunnel excavation. In addition, the geomechanical characteristics (e.g. quality and behavior of the rock mass) are among the significant factors to be considered. Figure 3 shows a possible domain that can be considered in the stress analysis of a tunnel portal and excavation face.

The extent of the zone of influence of an intersection, under a certain state of in situ stresses, primarily depends on the intersection configuration. It is influenced by the geometry (i.e. size and shape) of individual openings and by their orientation with respect to each other (Gercek 1986). Particularly, the angle of intersection affects the 3-D zone within the pillar between the branch tunnels. For sharp angled bifurcations in Y- or X-junctions, this extent may reach several tunnel diameters; alternatively, for T- or +-junctions formed in an elastic medium, the influence of intersection is practically zero at about two tunnel diameters from the center of intersection (Kaneshige et al. 1964, Hocking 1978).

For the regions of sudden geometrical changes, the extent of the zone of influence depends on the degree/severity of the change. Unfortunately, this matter is yet to be investigated, and, for this purpose, a series of parametric studies may be helpful.

Secondly, realistic modeling of the in situ stresses and boundary conditions may be a problem. Except for the portals, the in situ stress tensor can be taken as constant throughout the problem domain for all the 3-D regions if they are located at a considerable depth. For portals, this tensor is expected to be highly variable within the domain. Without sacrificing the accuracy, every effort should be made to simplify the geometry, boundary conditions, in situ stresses, etc. For example, in many of the numerical studies involving the excavation face, a circular tunnel located in a hydrostatic in situ stress field is considered to simplify the problem, increase the tractability of results, and facilitate the use of axisymmetric solutions.

Thirdly, in the stress analysis of underground openings, it used to be a formidable task to model complex 3-D configurations accurately. Today, thanks to the very capable and friendly computer codes, it is much easier to model, discretize, modify, visualize, and analyze such situations. For example, FLAC^{3D} finite difference computer program (Itasca 1997) includes special library functions to assist the user to model the excavation face and tunnel intersections easily. Also, the application of 3-D visualization technology (Nonomura et al. 2004) has been very informative.

Finally, simulation of sequential excavation and support installation gives valuable insight into the identification and causes of potential instabilities; then, it can be possible to take actions to improve the stability or remedy the problems. Again, even with the high level of sophistication reached by the current stress analysis programs, such simulations are difficult and, to some degree, simplifications are necessary.

4 CONCLUSION

Stress and stability analysis of the 3-D regions in tunnels is discussed. It is emphasized that the 3-D nature of these regions should be appreciated since the interaction of factors affecting the stability complicates the problem. Although the tunnel engineers understand that each case must be treated on its own merits, the issues discussed in this paper should be given due consideration for the proper modeling and analysis of the 3-D regions.

REFERENCES

Barisone, G., Pelizza, S. & Pigorini, B. 1983. Italian experiences with tunnel portals in difficult ground. In *Proc. Eurotunnel'83*: 157–163. Bucks, UK: Access Conf. Ltd.

Barton, N.R., Lien, R. & Lunde, J. 1974. Engineering classification of rock masses for the design of tunnel support. *Rock Mechanics* 6(4): 189–206.

Bieniawski, Z.T. 1978. Personal communication. Dept. of Mineral Engineering, Penn State University, University Park, PA.

Bieniawski, Z.T. 1989. *Engineering Rock Mass Classifications*. New York: Wiley.

Del Greco, O. & Oggeri, C. 2004. Reinforcement design and control of rock slopes above tunnel portals in northern Italy. *Int. J. Rock Mech. & Min. Sci.* 41(3). *Proceedings of thé ISRM SINOROCK 2004 Symposium*, Paper 3B02.

Copyright © 2005 Taylor & Francis Group plc, London, UK

Descoudres, F. 1974. Analyse tridimensionelle de la stabilité d'un tunnel au voisinage du front de taille dans une roche élasto-plastique. In *Advances in Rock Mechanics; Proc. of the 3rd Int. Congress on Rock Mechanics* 2: 1130–1135. ISRM.

Duffaut, P. & Piraud, J. 2002. Ideas on tunnel stability. *Tribune* (22), http://www.ita-aites.org

Eberhardt, E. 2001. Numerical modelling of three-dimensional stress rotation ahead of an advancing tunnel face. *Int. J. Rock Mech. & Min. Sci.* 38: 499–518.

Ellis, I.T., Douglas, T.H. & Copeland, B.G.T. 1979. Dinorwic power station, North Wales: design and construction of tunnels and shafts. In M.J. Jones (ed.) *Tunnelling'79*: 15–29. London: Institution of Mining and Metallurgy.

Gercek, H. 1986. Stability considerations for underground excavation intersections. *Mining Science & Technology* 4(1): 49–57.

Gercek, H. 1990. Stability of and design of portals for tunnels and galleries (in Turkish). *Kaya Mekanigi Bulteni* (4): 3–8.

Gercek, H. 1996. Stability of excavation intersections in underground mining. In *Milestones in Rock Engineering – The Bieniawski Jubilee Collection*: 265–274. Rotterdam: Balkema.

Gercek, H. & Genis, M. 1999. Effect of anisotropic in situ stress field on the stability of underground openings. In G. Vouille and P. Berest (eds), *Proc. of the 9th Int. Congress on Rock Mechanics* 1: 367–370. Rotterdam: Balkema.

Hashash, Y.M.A., Hook, J.J., Schmidt, B. & Yao, J.I. 2001. Seismic design and analysis of underground structures. *Tunnelling & Underground Space Technology* 16: 247–293.

Hocking, G. 1976. Three-dimensional elastic stress distribution around the flat end of a cylindrical cavity. *Int. J. Rock. Mech. Min. Sci. & Geomech. Abstr.* 13: 331–337.

Hocking, G. 1978. Stresses around tunnel intersections. In A. Burt (ed.), *Computer Methods in Tunnel Design*: 41–60. London: Institution of Civil Engineers.

Itasca 1997. *FLAC^{3D}* Fast Lagrangian *Analysis of Continua in 3 Dimensions V. 2.0*, Users Manual, 5 vols., Minneapolis, MN: Itasca Consulting Group, Inc.

Kamata, H. & Mashimo, H. 2003. Centrifugal tests of tunnel face reinforcement by bolting. *Tunelling & Underground Space Technology* 18(2–3): 205–212.

Kaneshige, O., Kawamoto, T. & Okamura, H. 1964. On the state of stress distribution around the crossing gallery (in Japanese). *J. Min. & Metall. Inst. Japan* 80: 659–664.

Müller, L. 1978. *DerFelsbau, Dritter Band: Tunnelbau*. Stuttgart: Ferdinant Enke Verlag.

Ng, C.W.W. & Lee, G.T.K. 2002. A three-dimensional parametric study of the use of soil nails for stabilising tunnel faces. *Computers & Geotechnics* 29(8): 673–697.

Nonomura, S., Kimura, H., Nakamura, J. & Tamura, S. 2004. Design and construction of tunnel intersection area with special structure. *Tunnelling & Underground Space Technology* 19: 490.

Pacher, F. 1974. Zur Sicherung grosser Tunnelvoreinschnitte. *Rock Mechanics,* Suppl. 3: 79–88.

Paterson, T. & Arthur, L.J. 1979. Tunnel portals at Dinorwic. In M.J. Jones (ed.), *Tunnelling '79*: 3–14. London: IMM.

Peila, D. & Pelizza, S. 2002. Criteria for technical and environmental design of tunnel portals. *Tunnelling & Underground Space Technology* 17: 335–340.

Pelli, F., Kaiser, P.K. & Morgenstern, N.R. 1991. The influence of near face behaviour on monitoring of deep tunnels. *Canadian Geotechnical Journal* 28: 226–238.

Ranken, R.E. & Ghaboussi, J. 1975. *Tunnel Design Considerations: Analysis of Stresses and Deformations Around Advancing Tunnels*. Final Report to Federal Railroad Administration, Report No. FRA OR&D 75–84, Washington, DC: Department of Transportation.

Riley, W.F. 1964. Stresses at tunnel intersections. *J. Eng. Mech. Div. Proc. ASCE* 90: 167–179.

Rogers, G.K. & Haycocks, C. 1988. Portal stability in rock. In *Proc. 7th Int. Conf. on Ground Control in Mining*: 76–83. Morgantown, WV: West Virginia University.

Rogers, G.K. & Haycocks, C. 1989. Rock classification for portal design. In A.W. Khair (ed.), *Rock Mechanics as a Guide for Efficient Utilization of Natural Resources; Proc. 29th US Symp. on Rock Mechanics:* 23–30. Rotterdam: Balkema.

Terzaghi, K. 1946. Introduction to tunnel geology. In P.V. Proctor & T.L. White, *Rock Tunneling with Steel Supports*, Youngstown, OH: Commercial Shearing and Stamping Co.

Tonon, F. & Amadei, B. 2002. Effect of elastic anisotropy on tunnel wall displacements behind a tunnel face. *Rock Mech. & Rock Engineering* 35(3): 141–160.

Unlu, T. & Gercek, H. 2003. Effect of Poisson's ratio on the normalized radial displacements occurring around the face of a circular tunnel. *Tunnelling & Underground Space Technology* 18: 547–553.

US Army Corps of Engineers 1978. *Tunnels and Shafts in Rock*. Engineer Manual EM 1110-2-2901, Washington, DC: Department of the Army.

Yoo, C. 2002. Finite element analysis of tunnel face reinforced by longitudinal pipes. *Computers & Geotechnics* 29(1): 73–94.

Yoo, C. & Shin, H.K. 2003. Deformation behaviour of tunnel face reinforced with longitudinal pipes – laboratory and numerical investigation. *Tunnelling & Underground Space Technology* 18(4): 309–319.

Copyright © 2005 Taylor & Francis Group plc, London, UK

Surface settlement prediction for Istanbul metro tunnels via 3D FE and empirical methods

S.G. Ercelebi, H. Copur, N. Bilgin & C. Feridunoglu
Istanbul Technical University, Faculty of Mines, Mining Eng. Dept., Maslak, Istanbul, Turkey

ABSTRACT: In this study, surface settlement is predicted for tunnels which are to be excavated in the section of 5 + 635–5 + 735 meters between Sehzadebasi and Yenikapi stations of Istanbul Metro line. Precautions in order to minimize the ground settlement are also suggested. Geology in this section is composed of clay, claystone, sand and marl. Tunnels, 36 m^2 in cross-section, are excavated employing NATM method. Umbrella method of pre-excavation and shotcrete for temporary support are employed. Between crown and bench excavation, a 2.40 meter distance is kept constant. Settlement prediction is made with 2 different methods, empirical and 3D finite element method. Empirical method is based on Gaussian curve suggested by O'Reilley. For 3D finite element, 3D Tunnel program is used. For 3D analysis, excavation and ground reinforcement steps are simulated exactly as applied in the field. The results of 2 methods are found to be in good agreement.

1 INTRODUCTION

Istanbul Metro line has been constructed in 2 phases. The first construction phase was started in 1992 and opened to public in 2000. The second phase between Taksim and Yenikapi is under construction by Anadolu Metro joint venture. The route of metro line phases 1 and 2 are shown in Figure 1.

1.1 *The geology*

Trakya formation of the Carboniferous age is found in the study area consisting of fine-grained, laminated, fractured and interbedded siltstone, sandstone and mudstone. A formation locally named Suleymaniye overlays Trakya Formation. Suleymaniye Formation includes competent or deformed claystone and marl with interbedded clay and sand horizons. Some diabase or andesite dykes are also encountered. Many faults and geologic discontinuities exist in the area due to Hercinian and Alpine Orogenies. The overburden thickness above the tunnels varies between 17 to 25 meters, averaging 21.5 meters.

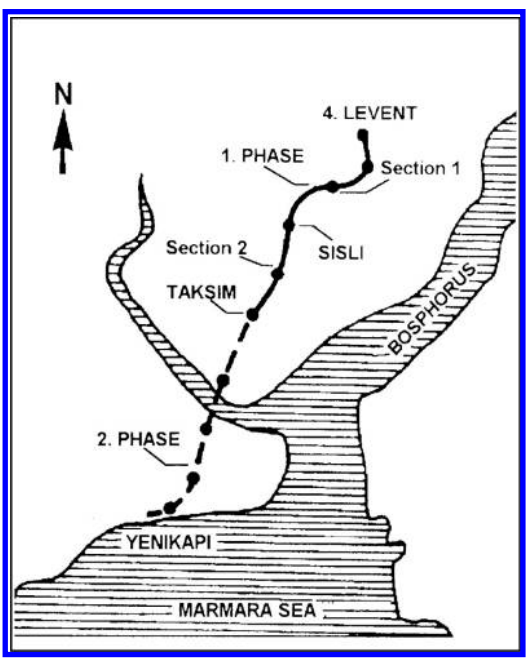


Figure 1. Main route of Istanbul metro line.

1.2 *Method of construction*

New Austrian Tunneling Method (NATM) is used in the study area of Type A tunnel. Currently used temporary tunnel support includes 4 to 6 m long rock bolts, wire mesh and shotcrete. Prior to excavation, an umbrella of steel pipes are installed with a 5^0 dip in a truncated conic shape made on the crown of the tunnel. Umbrella length is 9 m of which excavation is carried on under 6 m. Truncated cone shape allows the 3 m overlapping of two adjacent umbrellas.

Copyright © 2005 Taylor & Francis Group plc, London, UK

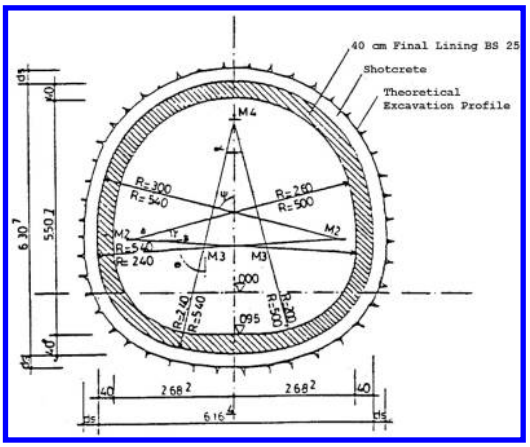


Figure 2. Typical cross section of single track tunnel, Type A.

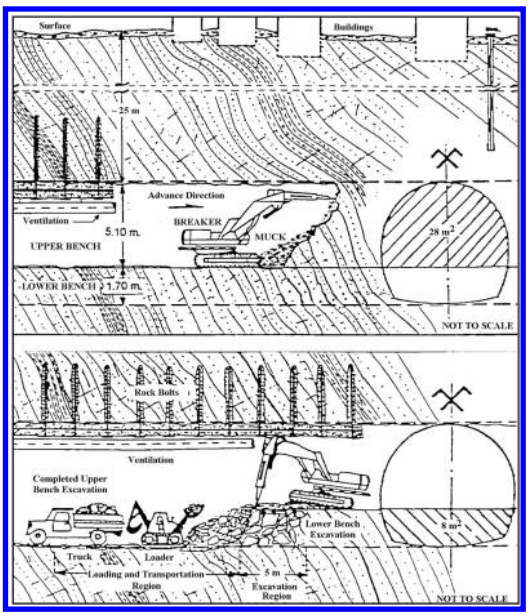


Figure 3. Method of construction in Istanbul Metro tunnels (Bilgin, 2002).

Depending on tunnel diameters, the final lining is undertaken with 35 to 45 cm thick in-situ cast concrete. Type A tunnel (Figure 2) has a cross-section of 36 m^2 and the upper half of 28 m^2 is excavated first and the lower part is excavated later which is 2.40 m behind the upper part (Figure 3).

There are mainly two settlement prediction approaches: (i) empirical, based on empirical formulas derived from past observations, (ii) numerical

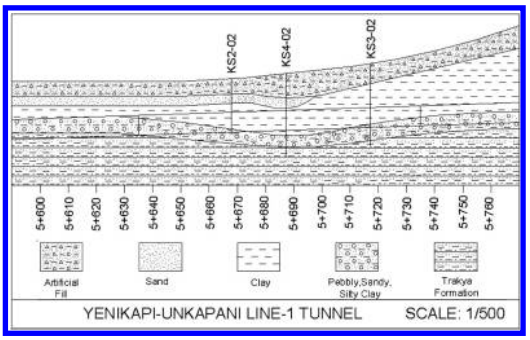


Figure 4. Geological cross-section.

analysis such as finite element approach, which is the most popular method. In this study, both methods are employed to predict the surface settlement above the tunnels of the chainage between 5 + 635 m and 5 + 735 m of phase 2 of line 2. A new excavation sequence and support system are recommended in order to prevent the damage to the nearby buildings. This section has the most difficult ground conditions. Geological cross-section of the study area is presented in Figure 4. Laboratory and in-situ tests are applied to define the geotechnical features of the formations tunnels passed through. Summary of the geotechnical properties are presented in Table 1.

2 EMPIRICAL PREDICTIONS

Settlement parameters used in empirical estimations and notations are presented in Figure 5. Assumptions used in the estimations are as follows:

- Cross-section of the tunnel is circular.
- Tunnel is shallow.
- Tunnel passes through clay formation.
- Tunnelling method is NATM.
- Estimations are valid for completed primary support (wire mesh + shotcrete + bolts + lattice).
- Since the excavation of other tunnel next to 35 m is completed, the settlement interaction between the tunnels is ignored.
- Long term consolidation settlement is ignored.

Equations used in estimations are as follows:

$$S = S_{max} \cdot e^{\left(\frac{-x^2}{2 \cdot i^2}\right)} \qquad \text{(O'Reilley, 1982)} \tag{1}$$

$$i = \frac{i_1 + i_2 + i_3}{3} \tag{2}$$

$$i_1 = 0.386 \cdot Z_0 + 2.84 \qquad \text{(Arioglu, 1992)} \tag{2a}$$

Copyright © 2005 Taylor & Francis Group plc, London, UK

Table 1. Geotechnical properties of formations.

Strata	Unit weight (kN/m^3)	Elastisity Modulus (kN/m^2)	Cohesion (kN/m^2)	Poisson Ratio	Angle of Friction
Fill	18.0	5,000	1.0	0.40	10
Sand	17.0	15,000	1.0	0.35	25
Süleymaniye formation	18.9	38,000	20.0	0.33	14
Tarkya formation	25.0	60,000	80.0	0.20	25

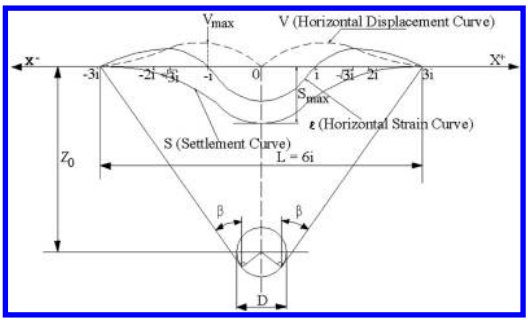


Figure 5. Settlement parameters and notation.

$$i_2 = 0.5 \cdot Z_0 \quad \text{(Glossop, 1978)} \tag{2b}$$

$$i_3 = 1.392 \cdot \left(\frac{D}{2}\right) \cdot \left(\frac{Z_0}{D}\right)^{0.704} \quad \text{(Arioglu, 1992)} \tag{2c}$$

$$S_{\max} = 0.785 \cdot \left(\gamma \cdot Z_0 + P_s\right) \cdot \left(\frac{D^2}{i \cdot E}\right) \text{(Herzog,1985)} \tag{3}$$

$$ds/dx = 0.606 \cdot \left(S_{\max}/i\right) \quad \text{(O'Reilley, 1982)} \tag{4}$$

$$d^2s/dx^2 = 0.445 \cdot \left(S_{\max}/i\right) \quad \text{(O'Reilley, 1982)} \tag{5}$$

$$\varepsilon_t = 0.445 \cdot \left(\frac{S_{\max}}{Z_0}\right) \quad \text{(O'Reilley, 1982)} \tag{6}$$

$$\varepsilon_c = 0.445 \cdot \left(\frac{S_{\max}}{i^2}\right) \quad \text{(O'Reilley, 1982)} \tag{7}$$

$$H_{mx} = i \cdot \sqrt{3} \quad \text{(O'Reilley, 1982)} \tag{8}$$

where,

S = theoretical settlement (gauss error function, normal probability curve)

Table 2. Building damage classification.

ds/dx	$S_{\max}$ (mm)	Damage
<0.002	<10	Ignored
0.002–0.005	10–50	Slight
0.005–0.02	50–75	Medium
>0.02	>75	High

$S_{\max}$ = maximum settlement (m)
x = transverse horizontal distance from the tunnel center line (m)
i = point of inflexion (m)
Z_0 = tunnel axis depth (m)
D = equivalent tunnel excavation diameter (m)
γ = natural unit weight of formation (ton/m^3)
E = elasticity modulus of formation (ton/m^2)
P_s = total surcharge load (ton/m^2)
ds/dx = maximum slope
d^{2}s/dx^2 = maximum sagging curvature
ε_t = maximum horizontal strain (tensile) (m)
ε_c = maximum horizontal strain (compressive) (m)
H_{mx} = point of maximum curvature (m).

Equations (2) and (3) were derived from both shield excavated and NATM tunnel data (Arioglu, 1992). Other equations (4, 5, 6, 7, 8) were derived theoretically from the theoretical settlement function given in Equation (1), (O'Reilley, 1982).

Damage to the buildings due to settlement can be classified as in Table 2, (Attewell et al., 1986).

Input parameters and results of the empirical settlement predictions for Yenikapi-Unkapani Line-2 tunnel previously excavated in Trakya Formation are presented in Table 3. As it is seen, the maximum settlement and maximum slope values are 37 mm and 0.002, respectively, and possible level of damage to the nearby buildings is slight.

In-situ settlement and building displacement measurements are performed on ground surface and

Copyright © 2005 Taylor & Francis Group plc, London, UK

Table 3. Settlement prediction for Yenikapi-Unkapani Line-2 Tunnel in Trakya formation.

Input	Estimations (m)
$D = 6.77$ m	$i = 10.2$
$Z_0 = 20.0$ m	$S_{max} = 0.0370$
$\gamma = 2.50$ tonne/m^3	$ds/dx = 0.0022$
$E = 6000$ tonne/m^2	$d^2s/dx^2 = 0.0016$
$P_s = 13.0$ tonne/m^2	$\varepsilon_t = 0.0008$
Building Damage: Slight	$\varepsilon_c = 0.0004$
	$H_{mx} = 17.7$

Table 4. Results of surface settlement measurements for Yenikapi-Unkapani Line-2 tunnel in Trakya formation.

Street	Behnameci				Azimkar
Point	Y-5093	Y-5095	Y-5105	Y-5103	Y-5119
S (m)	0.012	0.024	0.016	0.010	0.044
x (m)	18	9	6	11	6
i (m)	10.2	10.2	10.2	10.2	10.2
S_{mak} (m)	0.057	0.035	0.019	0.018	0.052
% diff.*	+54	−5	−49	−51	+41

* Percent difference from predicted value of 0.037 m.

different buildings in Yenikapi-Unkapani Line-2 tunnel to validate the empirical method. The results of settlement measurements are summarized in Table 4 and Figure 6. As seen, the empirical predictions are lower than the measured settlements in some cases and higher in others. However, overall the empirical predictions can be assumed to be approaching to actually occurred settlements. Displacement measurements performed on surface and different buildings validate the empirical model. Therefore, it is also possible to use the empirical method for settlement predictions to be occurred in Yenikapi-Unkapani Line-1 tunnel to be excavated later in Suleymaniye Formation.

Input parameters and results of the empirical settlement predictions for Yenikapi-Unkapani Line-1 Tunnel (between chainage 5 + 635 and 5 + 735) to be excavated in Suleymaniye Formation are presented in Table 5 for the worst case ($E = 2000$ tonne/m^2) and Table 6 for the best case ($E = 3000$ tonne/m^2). As seen, the predicted maximum settlements are around 88 mm (with maximum slope of 0.0052) for the worst case and 59 mm (with maximum slope of 0.0035) for the best case. Possible levels of damage to the near buildings are medium for the worst case and slight for the best case. Variation of maximum settlement versus elasticity modulus is presented in Figure 7.

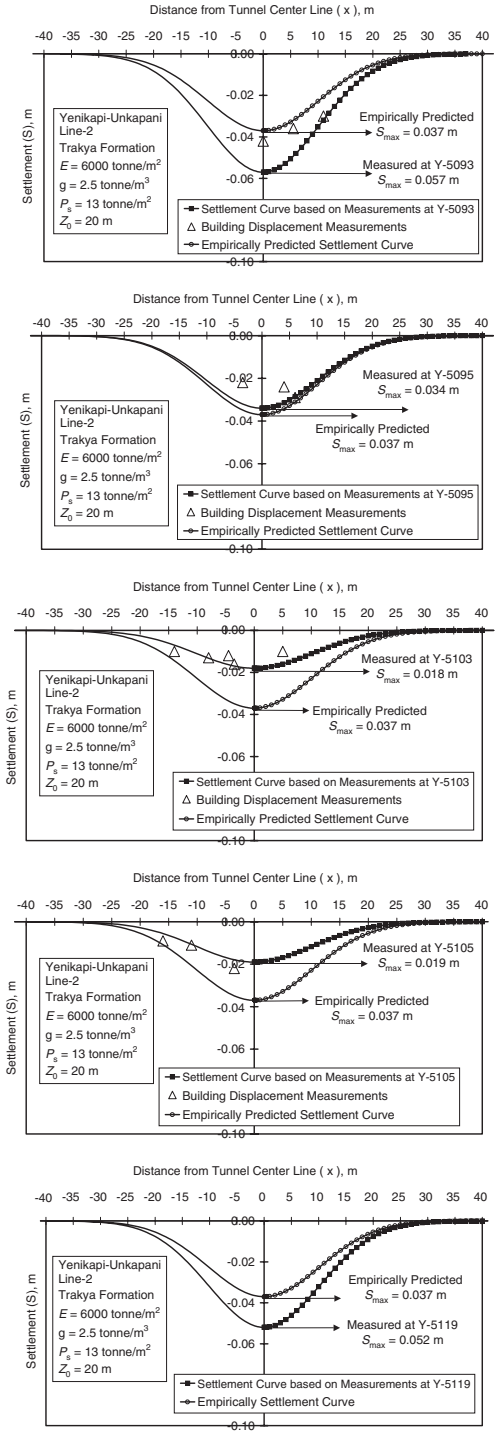


Figure 6. In-situ surface settlement and building displacement measurements in Yenikapi-Unkapani Line-2 tunnel.

Copyright © 2005 Taylor & Francis Group plc, London, UK

Table 5. Settlement prediction for Yenikapi-Unkapani Line-1 tunnel in Suleymaniye formation (the worst case).

Input	Estimations
D = 6.77 m	i = 10.2 m
Z_0 = 20.0 m	S_{max} = 0.0884 m
γ = 1.86 tonne/m^3	ds/dx = 0.0052
E = 2000 tonne/m^2	d^2s/dx^2 = 0.0038
P_s = 13.0 tonne/m^2	ε_t = 0.0020 m
Building Damage: Medium	ε_c = 0.0008 m
	H_{mx} = 17.7 m

Table 6. Settlement prediction for Yenikapi-Unkapani Line-1 tunnel in Suleymaniye formation (the best case).

Input	Estimations
D = 6.77 m	i = 10.2 m
Z_0 = 20.0 m	S_{max} = 0.0589 m
γ = 1.86 tonne/m^3	ds/dx = 0.0035
E = 3000 tonne/m^2	d^2s/dx^2 = 0.0026
P_s = 13.0 tonne/m^2	ε_t = 0.0013 m
Building Damage: Slight	ε_c = 0.0006 m
	H_{mx} = 17.7 m

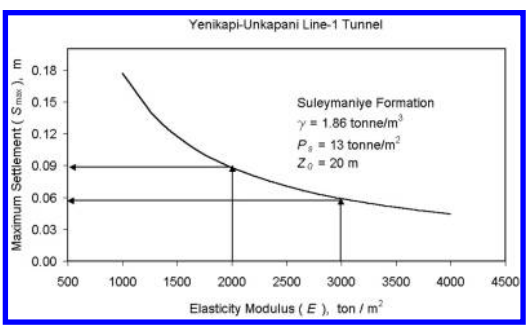


Figure 7. Variation of settlement according to elasticity modulus for Yenikapi-Unkapani Line-1 tunnel in Suleymaniye formation.

3 3D FINITE ELEMENT MODELLING

An important concern of tunnelling is the development of surface settlements. As for the tunnel heading stability, a 3D analysis is needed for a proper prediction of surface settlement. To investigate its development, 3D Finite Element model analysis is performed. For this analysis, Plaxis 3D Tunnel program is used. 3D Tunnel program is capable of simulating staged excavation sequences as in NATM tunnelling. Using this program, the NATM tunnel with a cross-section of 36 m^2 and a cover of around 20 m is modelled with an unsupported excavation length of 0.60 m. Each phase consists of 0.60 m of excavation. Within the same phase, a shotcrete lining and rock bolts are applied to support the previous excavation. Umbrella system is activated previous to excavation. The shotcrete lining has a thickness of 30 cm and rock bolts are 4 to 6 m in length.

Table 7. Properties of support system

Item	Elastisity modulus (kN/m^2)	Poisson ratio	Normal stiffness (kN/m)	Flexural rigidity (kNm^2/m)
Young shotcrete	1.0×10^7	0.2		
Hard shotcrete	2.85×10^7	0.2		
Rock bolt			2×10^5	
Umbrella		0.2	5.7×10^6	19,950

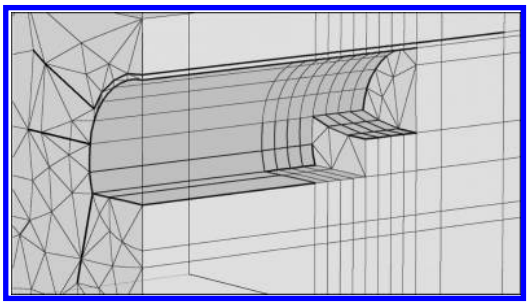


Figure 8. Partial FE model.

3D model is chosen because for 2D FE models, it is not so easy to estimate pre-relaxation factors (sometimes called stress reduction factors), which is fraction of load effecting on tunnels, and purely based on practical experience. With the 3D model, estimation of pre-relaxation factor is no longer required when excavation stages can be modelled not only in cross-section but also in the longitudinal section, e.g. excavation of the bench and invert can be modelled in the actual distance behind the excavation of the top heading. A typical sequential tunnel excavation in accordance with the principles of the New Austrian Tunnelling Method is modelled more realistically by the 3D FE. The model involved modelling of the ground, shotcrete, bolting and umbrella. Shotcrete time dependent behaviour is modelled in such a way that two sets of parameters for the shotcrete, young and hard, has been included. When placing the lining for the first time, the young is assigned to the lining and for the next excavation step this is changed to hard.

The physical properties of supporting system, including umbrella, bolting and shotcrete, used in the calculations are shown in Table 7.

The FE model consists of 11,936 elements and 34,140 nodes. Figure 8 shows the partial finite element

Copyright © 2005 Taylor & Francis Group plc, London, UK

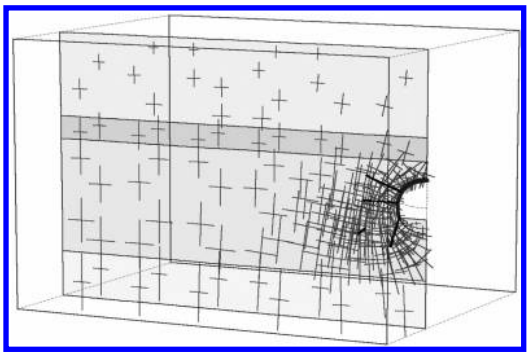


Figure 9. Stress arc after bench excavation.

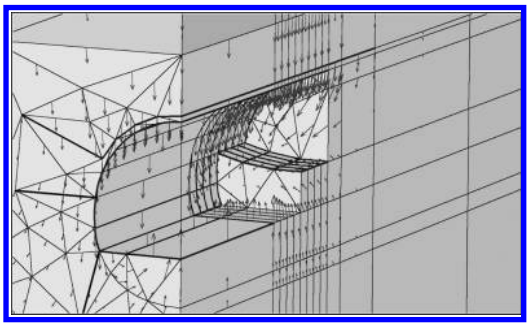


Figure 10. Total displacement vectors around tunnel.

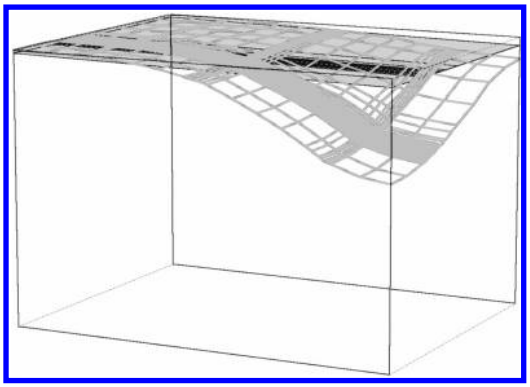


Figure 11. Settlement profile in the shape of Gaussian curve.

model at a later excavation stage with the top heading advancing.

The thickness of slices in 3D model are chosen according to the distance between the excavation steps, 0.60 m, and the actual distance between the excavation faces of top heading and bench, 2.40 m. Invert excavation and final lining are not modelled in the numerical model.

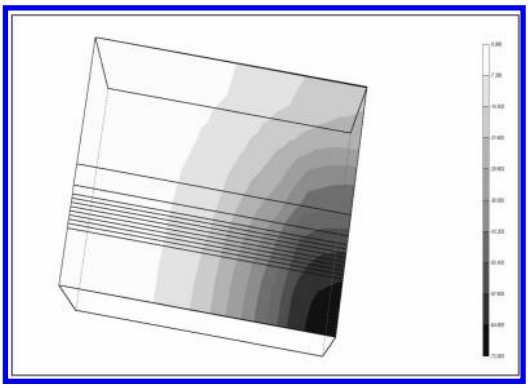


Figure 12. Settlement contours on the surface.

As the result of analysis, stress arc acting around the tunnel after bench excavation is shown in Figure 9, and total displacement vectors are shown in Figure 10.

The maximum ground settlement is estimated as 54.4 mm after 2.40 m of top heading and 72.7 mm after the bench excavation. Corresponding total tunnel closure is calculated as 130 mm. Vertical displacement profiles on the surface, when bench advances, are shown in Figures 11 and 12. In Figure 11 settlement profile in the shape of Gaussian curve is clearly evident. Maximum settlement is directly above the tunnel axis.

4 CONCLUSIONS AND SUGGESTIONS

Surface settlement is predicted for tunnels which are to be excavated in the section of 5 + 635 to 5 + 735 meters between Sehzadebasi and Yenikapi stations of Istanbul Metro line using two settlement prediction approaches. This section has very difficult ground conditions. Empirical method resulted as the maximum settlement will be between 59 and 88 mm. Numerical method predicted the maximum ground settlement about 72.7 mm. As seen the results of two methods are to be in close agreement.

Although possible levels of damage to the nearby buildings are in medium level, this can not be acceptable. Therefore, precautions to reduce the surface settlement are suggested. First suggestion is the ground improvement before excavation. Among the ground improvement techniques, jet grouting is found to the most applicable technique in this particular tunnelling section. Since grouting from surface is very difficult because of the buildings, it is suggested that it should be applied from the existing shaft where possible or from the inside of the tunnel prior to the excavation. It is also suggested that underpinning should be applied to the buildings where the foundation is weak.

Copyright © 2005 Taylor & Francis Group plc, London, UK

ACKNOWLEDGEMENTS

Istanbul Great Municipality is appreciated due to their valuable support during the studies as a part of this project performed by the authors.

REFERENCES

Arioğlu, E. 1992. Surface movements due to tunnelling activities in urban areas and minimization of building demages. *Short Course*, Istanbul Technical University, Mining Eng. Dept.

Attewell, P.B., Yeates, J. & Selby, A.R. 1986. *Soil movement induced by tunnelling and their effects on pipelines and structures*. New York: Chapman and Hall.

Bilgin, N., Dincer, T. & Copur, H. 2002. The performance prediction of impact hammers from Schmidt hammer rebound values in Istanbul metro tunnel drivages. *Tunnelling and Underground Space Technology* 17: 237–247.

Heath, G.R. 1997. Structures how ground settlement affects them. *Tunnels and Tunnelling International*, pp. 38–40.

Herzog, M. 1985. *Die Setzungsmulde über seicht liegenden Tunneln*. Berlin, pp. 375–377.

Glossop, N.H. 1978. *Soil deformation caused by soft ground tunnelling.* Ph.D. Thesis, University of Durham.

O'Reilley, M.P. & New, B.M. 1982. Settlement above tunnels in the United Kingdom, their magnitude and prediction. *Proc. Tunneling 82*, Brighton, pp. 173–181.

Plaxis 3D Tunnel manual. *Finite element code for soil and rock analyses.*

Copyright © 2005 Taylor & Francis Group plc, London, UK

Transportation demands in Istanbul and New York

Ahmet Gursoy
Parsons Brinckerhoff

ABSTRACT: This paper presents a summary comparison of the transportation demands in Istanbul and New York, particularly in reference to mass transit. Originally a much detailed version was prepared for my book titled "A New Yorker by Choice" published in 2003 and now is available on the Internet. The study was prepared primarily to bring out similarities between two cities, in terms of Underwater Crossings for mass transit needs, and to compare the location selection of Tube tunnel crossing in Istanbul, versus the tunnel connections provided at 13 different locations in New York City, to provide almost similar passenger demand and volume.

1 INTRODUCTION

In developed countries scale of economic progress and the growth in national wealth are measured by the efficiency indicators of private sector and government, and the national transportation index.

The loss in national wealth due to inefficiencies in transportation systems have been a great concern in European parliaments and for the lawmakers of the United States Congress. In the United States, recognizing the $370 billion annual loss in national wealth caused by the inefficiencies in transportation, the U.S. Congress passed two laws in the last thirteen years:

- Intermodal Surface Transportation Efficiency Act (ISTEA) in 1991
- Transportation Equity Act for the 21st Century (TEA-21) in 1998.

Both laws are designed to shift the public ridership from private cars to higher occupancy modes of travel to achieve greater efficiencies in national transportation. Unfortunately in Turkey or in Istanbul, the loss in national wealth due to inefficiencies in transportation are not available for comparison.

Historically in Istanbul, transportation studies conducted from 1959 to 1977 were basically bridge location studies that led to the construction of two bridge crossings over Bosporus. Although these studies collected useful data, they failed to systematically examine alternative transportation corridors as well as a complete range of alternative transportation modes. Consequently, they did not provide the level of engineering and data needed to convince local decision makers and international lending agencies to advance any mass transit project into the implementation stage. For this reason, in May 1984, the Ministry of Public Works and Settlement, General Directorate of Railways, Harbors and Airports of the Government of Turkey, and the U.S. Trade and Development Agency issued a request for technical proposals for engineering services to conduct a comprehensive transportation planning study, as well as feasibility studies and preliminary design for an integrated rail system comprising a proposed Bosporus railroad tube tunnel and the Istanbul Metro System. The project was awarded in 1985 to Istanbul Rail/Tunnel Consultants (IRTC), a consortium of American and Turkish firms with Parsons Brinckerhoff International, Inc. as the lead consultant.

The transportation planning study, feasibility study and preliminary design of the Bosporus tube tunnel and the Istanbul Metro were completed in 1988. This comprehensive planning effort not only identified Istanbul's transportation needs, but also provided the needed database to support future growth in transportation and the provision of goods and services in the region – and thereby the economic well-being of Turkey. (Istanbul and the Marmara region provides 25% of the total gross domestic product – GDP – of Turkey). The recommended rail line that includes 1.6 km long tube tunnel, is a 12.5 kilometers long rail corridor and connects with the existing rail lines at Kocamustafapasa Station on the European side and to Sogutlucesme Station on the Asian side. The Istanbul Metro is a predominantly underground double-track heavy rail facility extending from Topkapi in the southwest to 4th Levent in the north, with yard and shop facilities at Topkapi.

The study identified current and projected transportation deficiencies; performed systematic testing and evaluation of a range of alternative transport systems; and examined a variety of different technologies

Copyright © 2005 Taylor & Francis Group plc, London, UK

using a multi-criteria evaluation process with an explicit value judgment trade-off analysis. This led to the development of a set of recommendations for transportation improvements in the Istanbul metropolitan area. The summary report, supported by 60 individual task reports, examined alternatives and recommended preliminary engineering of facilities and systems. It included environmental studies; evaluation of impacts to historic and archaeological resources; land use studies; estimation of capital and operating costs and operating revenues; and economic and financial evaluations.

It is interesting to note that when the 1985 study was initiated there was no Ministry of Transportation in the Turkish government. The Ministry of Transportation was established during the execution of this study.

2 MASS TRANSIT COMPARISON OF ISTANBUL AND NEW YORK

The population of Istanbul had climbed from 4.5 million in 1987 to 9.5 million in 1998. Today it is unofficially reported to be 13 million.

A comparison in transportation demands between Istanbul and New York is necessary for the following reasons:

1. Similar population density (9.5 million versus 7.2 million) in both cities.
2. Separation of land by three bodies of water in each city.
3. Similarity in demand for "commuter rail" traffic (250,000 passengers daily in Istanbul versus 464,000 passengers per day in New York City).
4. Each is a major contributor in the GDP of their respective national economies.
5. Each serves as a role model in their own country.
6. Istanbul is in the process of completing a new metro system, and New York City has been operating a 96 years old system with 90% efficiency.

Success of a mass transit system is measured by its efficiency. For example, New York City Transit carries 6.5 million passengers daily (4.5 million by metro, 2 million by public bus) of the city's 7.2 million population, creating 90% efficiency. To generate this efficiency, the metro system offers 24 different routes reaching into the four boroughs of the City (Manhattan, Queens, Bronx, and Brooklyn) over a double-track rail system totaling 368 km and serving 483 stations. The central business district (CBD) of New York City, the borough of Manhattan, is surrounded by four bodies of water: the Hudson River and Atlantic Ocean on the west and south and the East River and Harlem River on the east and north. The boroughs of the Bronx, Queens, and Brooklyn are located along the eastern shores of the East and Harlem Rivers. Therefore, the separation of New York's CBD created by the East and Harlem Rivers is very similar to the separation of Istanbul's CBD created by the Bosporus and the Golden Horn.

Unlike the Bosporus, the East and Harlem Rivers are crossed every day to employment centers in Manhattan not only by automobiles but by 13 different metro tunnels that carry 2.3 million passengers a day. In addition, 232,000 passengers travel to Manhattan by commuter rail every day from the suburbs of Westchester and Long Island, and 200,000 passenger trips a day from the adjacent states of New Jersey and Connecticut (464,000 passenger trips per day). To provide the proper distribution of 24 different metro routes, in addition to the 13 rail tunnels, and 4 rail bridges within the city limits, the system makes use of 2 rail tunnels under the Harlem and Hudson Rivers. Interestingly, with the exception of the 63rd Street Tunnel (completed in 1972), there has been no new infrastructure added to the New York City transit system in the last 50 years. This demonstrates how well the original planning was prepared to be able to maintain 90% efficiency for the last 90 years. The man with the vision to start the metro planning in 1883 was William Barclay Parsons, who became the chief engineer of the New York City Metro and later the founding father of Parsons Brinckerhoff in 1885.

3 IS USKUDAR-SIRKECI CONNECTION NECESSARY

Commuter lines of Gebze and Halkali carried 300,000 passengers daily in 1994 and 250,000 passengers in 1997. Combined with the light rail and tramway, a total of 470,000 daily passengers used the existing rail system in 1994 and 515,000 in 1997, a 9.6% increase (see Tables 1 and 2).

Tables 1 and 2 also indicate that total daily vehicular traffic demand (travel trips) was 6.467 million in 1994 and 7.588 million in 1997. A comparison of the two tables indicates that in the last 3 years while road-based daily trips increased by 17%, daily rail-based trips increased by only 5%, and light rail users increased 300%. The reason for this is that the east and west commuter lines are not interconnected and they are in desperate need of rehabilitation. Despite the decrease in commuter rail users, the light rail users increased by 300%.

According to a 1997 joint study performed by the Istanbul Technical University (ITU) and the Greater Municipality of Istanbul, the projected commuter rail traffic for the year 2015 at the proposed Sirkeci-Uskudar crossing will be on the order of 60,000 to 65,000 passengers per peak hour, per peak direction

Copyright © 2005 Taylor & Francis Group plc, London, UK

Table 1. Daily vehicle trips by mode in Istanbul (1994).

Mode	Vehicles	Daily passengers (000)	Private	Public	Total
ROAD BASED					
Automobile	850,000	1,200	16.4%	–	–
Taxis	17,000	600	8.2	–	
Dolmus	600	50	0.7	–	
Minibus	6,664	1,000	13.6	–	
Private Bus	806	500	6.8	–	
IETT Bus	2,314	1,700	–	23.2%	
School/Empl. Bus	24,810	1,417	19.3	–	
Subtotal	–	**6,467**	**65.5%**	**23.2%**	**88.2%**
RAIL BASED					
Commuter	101	300	–	4.1	
Nostalgic Train	5	6	–	0.1	
LRT	79	40	–	0.5	
Tramway	26	130	–	1.7	
Funicular Tunnel	2	20	–	0.3	
Subtotal	–	**496**	**–**	**6.7%**	**6.7%**
WATER BASED					
Passenger Ferry	59	300	–	4.1	
Sea Bus	10	20	–	0.3	
Dolmus Boat	200	50	0.7	–	
Subtotal	**–**	**370**	**0.7%**	**4.4%**	**5.1%**
TOTAL	**–**	**7,333**	**65.7%**	**34.3%**	**100%**

Table 2. Daily vehicle trips by mode in Istanbul (1997).

Mode	Vehicles	Daily passengers (000)	Private	Public	Total
ROAD BASED					
Automobile	1,141,344	1,200	14.14%	–	–
Taxis	17,416	348.3	4.1	–	
Dolmus	590	47	0.55	–	
Minibus	5,055	1,100	12.96	–	
Private Bus	307	93	1.1	–	
Private Bus (Halk)	837	600	–	7.07%	
IETT Bus	2,377	2,000	–	23.56	
School/Empl. Bus	25,700	1,700	20.3	–	
Gypsy Vehicle	1,552	500	5.89		
Subtotal	**–**	**7,588.3**	**58.76%**	**30.63%**	**89.39%**
RAIL BASED					
Commuter	101	250	–	2.94%	
Nostalgic Train	3	6	–	0.07	
LRT	26	120	–	1.41	
Tramway	34	130	–	1.53	
IETT Tunnel	2	15	–	0.18	
Subtotal	**–**	**521**	**–**	**6.14**	**6.14%**
WATER BASED					
Passenger Ferry	59	300	–	3.53	
Sea Bus	17	30	–	0.35	
Dolmus Boat	236	50	0.59%	–	
Subtotal	–	**380**	**0.59**	**3.89**	**4.48%**
TOTAL	–	**8,489.3**	**59.35%**	**40.65%**	**100%**

resulting in 533 million passengers per year. For the year 2010, estimated yearly commuter rail traffic at the Sirkeci-Uskudar crossing is estimated to be 484 million or 1.33 million passengers per day.

Comparison of traffic demands of the two cities (1.3 million passenger per day at a single crossing of Sirkeci-Uskudar connection in Istanbul versus 2.3 million passenger per day carried by the New York

Copyright © 2005 Taylor & Francis Group plc, London, UK

City's Subway System with the help of 13 connecting tunnels) shows the great efficiencies inherent with the Sirkeci-Uskudar tube tunnel connection carrying 58% of the total demand with one single tunnel.

It can be clearly seen that these projections represent a significant volume of traffic that cannot be ignored. On the contrary, they underline the need for mass transit service at Sirkeci-Uskudar, serving primarily the low income, blue-collar workers who cannot afford to use automobiles. I am sure in time a midpoint crossing at Bosporus will be built to meet the growing demands of its time but not now.

While the Istanbul Metro is slowly progressing by completing the first (7 km) segment in 8 years, Turkish Authorities must pay great attention on significance of the recent rail accidents took place within the existing rail system, particularly within the Ankara-Istanbul segment. In order to accomplish a meaningful breakthrough in rehabilitation of the national rail system, a comprehensive national rail policy must be developed and debated openly in public.

4 NEW TRENDS IN MASS TRANSIT PLANNING AND THE PUBLIC PRIVATE PARTNERSHIP

As newly developed nations enter into the business of mass transit and metro construction, the passenger comfort factor in station allocation is being replaced by the concept of denser people transfer with less attention to station allocations. This is primarily due to the insufficient capital funding available during transportation planning for overly crowded cities in these developing nations. For example, in Mexico City the metro system carries 5 million passengers per day and services five different routes (lines) very effectively within the CBD. However, the system's overall efficiency drops to 23 percent when scaled to the city's total population of 22 million. Similar conditions exist in Sao Paulo, Brazil and Seoul, South Korea.

In contrast, the New York City metro was planned from the beginning with the consideration of passenger comfort, which resulted in construction of 483 stations for the 368-km metro line throughout the four boroughs. On the other hand, in Hong Kong, the short 50-km metro line carries 3 million passengers a day from the city's highly dense population of 6 million, achieving 50% efficiency by metro system alone (63% in New York City) without surface transportation.

As a civil engineer promoting infrastructure design and rehabilitation globally for the last fifty years, I learned early on that financial success of a major transportation infrastructure project will be greatly enhanced if the "urban development" component is included within the planning and in the application phase of the project. Inclusion of "urban development" by the use of public-private partnership would help to finance the project at an early stage, and would also shorten the time of loan payments by increasing the rate of return. Having seen the successful examples in San Francisco and Singapore during 1960's, in 1980's I am confident that it can be repeated in Istanbul with great success.

Copyright © 2005 Taylor & Francis Group plc, London, UK

Experimental study for shear behavior of pseudo rock joint under constant normal stiffness condition

Hong-rae Rim, Hae-jun Choi
CHUNG SUK Engineering Co., Ltd., Seoul, Korea

Bong-Ki Son, Chung-In Lee & Jae-Joon Song
Seoul National University, Seoul, Korea

ABSTRACT: The CNS (Constant Normal Stiffness) shear test was carried out for the artificial saw-tooth joints and the replica samples of three natural rock joints by using a servo-controlled direct shear test machine. The inclination angle of the saw-tooth joint ranged from 0° to 30° in 8 steps, and the average inclination angles of the replica samples were 9.4°, 10.0° and 13.9°, respectively. The CNS tests were conducted for 9 cases with 3 kinds of initial normal stress (0.15 MPa, 0.35 MPa, and 1.0 MPa) and 3 kinds of constant normal stiffness (0.2 MPa/mm, 0.5 MPa/mm, and 1.0 MPa/mm). Characteristics of acoustic emissions from the artificial saw-tooth joints and replicas of the natural rock joints during the CNS shear test were also investigated.

1 INTRODUCTION

Understanding the shear behavior of rock discontinuities is critical for understanding mechanical behavior of rock mass, because the shear movement of rock mass occurs mainly along the discontinuities such as faults, joints and fissures. Direct shear tests on the rock discontinuities can be divided into two types: Constant normal load (CNL) direct shear test, where the normal load on the discontinuity remains constant during the shear test, and constant normal stiffness (CNS) direct shear test, where the normal load varies according to the normal dilation.

The CNL direct shear test can be applied to predict the shear behavior of a rock slope, where the normal load on the discontinuities is relatively small and constant. The CNL direct shear test, however, has been used also for many underground rock joint shear tests, just because of neglect of the difference between rock slope and underground, or because CNL test equipment is simpler and easier to set up than CNS test equipment.

For the underground rock joints as shown in Figure 1, the normal stress on the rock joint is determined by normal stiffness and normal displacement of the joint. In CNS direct shear test, the constant normal stiffness can be obtained by inserting a spring between a load frame and a joint sample or by adopting a servo-controlled shear machine. Of course, the servo-controlled machine is more versatile and provides more precise results.

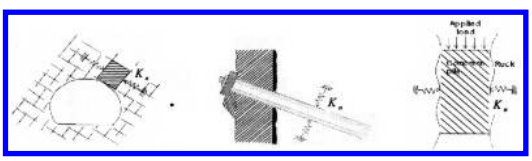


Figure 1. Examples of the constant normal stiffness condition (after Mouchaorab et al., 1994).

Johnston et al. (1987) carried out the CNS direct shear test and numerical analysis for saw-tooth rock-concrete joints. They classified the joint shear mechanism obtained from the CNS test into four steps: In the first step, the shear stress increases from zero with no dilation; in the second step, dilation destroys the cohesive bonding; in the third step, there is asperity sliding of joint plane; and in the fourth, there is asperity shearing.

By the CNS direct shear test for regular triangular and rectangular joint samples made of cement mortar, Mouchaorab and Benmokrane (1994) explained the relation between inclination angle of joint asperity and shear parameters such as peak shear stress, peak normal stress, and peak normal displacement. The values of these shear parameters increased until the inclination angle became 15°∼25°, but decreased past this range of inclination angle. The peak shear displacement decreased until the inclination angle

Copyright © 2005 Taylor & Francis Group plc, London, UK

reached 40°, and it remained nearly constant over the inclination angle range of 40° to 90°.

Indraratna et al. (1999) investigated CNL and CNS direct shear tests for regular saw-tooth rock joints made of casting plaster. In their tests, the shear strength from the CNS test was higher than that from the CNL test, while the friction angle and dilation from the CNS test were lower than those from the CNL test. They observed that the friction angle remained almost constant when the constant normal stiffness was applied, regardless of the initial normal stress.

In this study, we made a servo-controlled hydraulic direct shear machine that could carry out the CNS and the CNL direct shear test. Then, we prepared pseudo rock joints made of cement mortar which were regular saw-tooth joints and a replica of natural rock joints. This paper introduces the shear machine and the result of the CNS direct shear test in which three kinds of initial normal stress and three kinds of constant normal stiffness were applied for both types of joint samples.

2 PREPARATION OF SAMPLES

Cement mortar was used to make the pseudo rock joint. Uniaxial compressive strength of the cement mortar increased from 40 MPa to 47 MPa as the curing time increased from 50 hours to 74 hours. Elastic modulus showed the same tendency according to the length of the curing time: it increased from 12.4 GPa to 14.0 GPa, while the indirect tensile strength and Poisson's ratio remained nearly constant at 4 MPa and 0.21, respectively, as the curing time increased from 50 hours to 74 hours.

The regular saw-tooth joint sample was made by using the mold frame as shown in Figure 2. The size of mold frame was 155 mm in width, 150 mm in length and 110 mm in height. The mold frame was divided into two parts: 65 mm and 90 mm in width. Each part was used for the upper or lower joint block. A thin plate shown in Figure 3 was inserted between two frames.

The inclination angle of the saw-tooth joint ranged from 0° to 30° in 8 steps: 0°, 5°, 10°, 12.5°, 15°, 17.5°, 22.5° and 30°. The saw-tooth joint sample was named following the format of 'AJ-inclination angle-initial normal stress-constant normal stiffness'. For example, a sample named 'AJ-12.5-0.35-0.5' means that regular saw-tooth joint sample with an inclination angle of 12.5° was tested under initial normal stress of 0.35 MPa and constant normal stiffness of 0.5 MPa/mm.

Replica samples were obtained from the natural rock mass joint at the tunnel construction site of 25 m depth in Korea. Three kinds of replica samples were

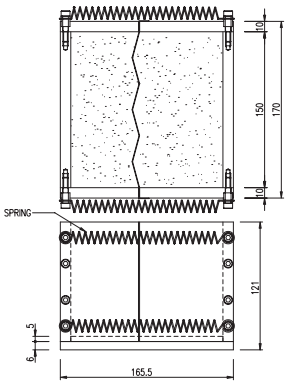


Figure 2. Schematic diagram of mold frame.

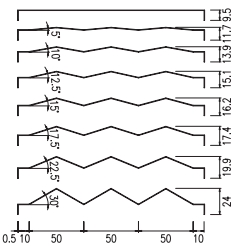


Figure 3. Schematic diagram of inserted frame for different inclination angles.

duplicated from three kinds of natural rock mass joint-with JRC (Joint Roughness Coefficient) of 6～8, 10～12, and 16～18, respectively.

Conjugate joints of a natural rock joint were made by replication of prepared natural rock joint using plaster. Then aluminium casting was applied to make a pair of replica surfaces for the upper and the lower joint surface. The image of the aluminum replica is shown in Figure 4. A complete replica mold frame is shown in Figure 5. The frame is 110 mm in width, 150 mm in length, and 80 mm in height. Test joint blocks made of cement mortar using the replica mold frame.

The replicated samples were named according to the following rules: notation of class is 'NJ', JRC of 16～18 is 'H', JRC of 8～10 is 'M', and JRC of 6～8 is 'L'. The format of replica sample name was 'NJ-roughness profile-initial normal stress-constant normal stiffness'. For example, 'NJ-H-0.15-0.2' means that the replica sample with JRC of 16～18 was tested under an initial normal stress of 0.15 MPa, and constant normal stiffness of 0.2 MPa /mm.

The saw-tooth sample and replica sample were measured for the roughness before the direct shear test. Among the many parameters of profile roughness, this study adopted 4 kinds of parameters such as

Copyright © 2005 Taylor & Francis Group plc, London, UK

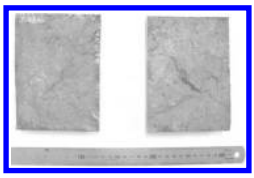


Figure 4. A view of surface of aluminum replica of natural joint.

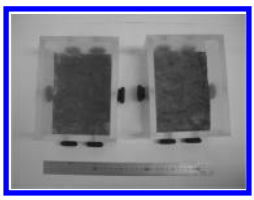


Figure 5. A view of mold frame for natural joint replica.

Table 1. Summary of roughness parameter for saw-tooth joint sample.

Sample number	Z_2	i_{ave}	D	R_s
AJ-0	0.0396	1.1426	1.000241	1.003695
AJ-5	0.1194	6.4779	1.000586	1.015516
AJ-10	0.1895	9.9309	1.001820	1.039185
AJ-12.5	0.2232	12.3093	1.001985	1.051105
AJ-15	0.2647	14.4829	1.002691	1.072423
AJ-17.5	0.3153	16.6679	1.005088	1.101715
AJ-22.5	0.4037	21.5497	1.007381	1.166115
AJ-30	0.5674	29.1401	1.009989	1.327031
NJ-H	0.3194	13.8969	1.010615	1.187143
NJ-M	0.2590	10.0032	1.007791	1.152468
NJ-L	0.2548	9.4137	1.006812	1.141555

root mean square of joint slope Z_2, average inclination angle of joint i_{ave}, fractal dimension D, and surface roughness coefficient R_s (Belem et al., 2000). The average inclination angle of a joint i_{ave} was used for comparing the results between the saw-tooth sample and replica sample. The roughness parameters obtained is shown in Table 1.

3 DIRECT SHEAR MACHINE

Direct shear tests were performed by the servo-controlled hydraulic direct shear machine of Rock Engineering Laboratory in Seoul National University, Korea. A shear load actuator and a normal load actuator can be independently controlled. Schematic diagram of the direct shear machine is shown in Figure 6.

The normal load actuator (1) contains an internal LVDT (Linear variable displacement transducer), and

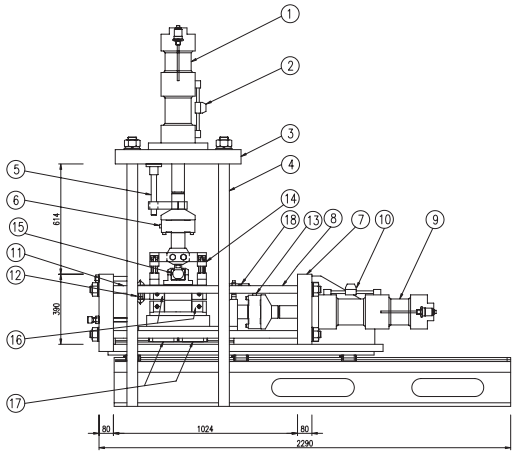


Figure 6. Schematic diagram of the direct shear machine.

the actuator is controlled by a normal load servo-valve (2). The shear load actuator (9) is similar to the normal load actuator (1) with respect to feature and function. Another servo-valves (10) is attached to shear load actuator.

The normal stiff plate (3) supports the normal load actuator (1), each normal stiff rod (4), and guide rod of the normal linear motion (5). The shear stiff plate (7) performs the same role as the normal stiff plate. The capacity of each load cell (6) and (13) is 20 tonf.

The roller bearing (12) transmitted shear load to the reaction plate (11), and it reduced the friction in the normal load direction caused by dilation. The bearings of linear rail (17) guides the lower shear box (16) so that the box moves linear with low friction.

4 CONSTANT NORMAL STIFFNESS (CNS) DIRECT SHEAR TEST

The CNS tests were conducted for 9 cases with 3 kinds of initial normal stress (0.15 MPa, 0.35 MPa and 1.0 MPa) and 3 kinds of constant normal stiffness (0.2 MPa/mm, 0.5 MPa/mm and 1.0 MPa/mm) for the saw-tooth joint sample and replica sample. The shear displacement rate was maintained at 2 mm/min for all tests and the signals from measuring instruments were recorded at regular intervals of 1 second.

The shear parameters were defined as follows. The first peak shear stress τ_{p1} was defined as the shear stress that changes suddenly at the shear displacement that does not exceed 3 mm. The second peak shear stress τ_{p2} was defined as the largest point of the shear stress. And linear dilation angle d_n was defined by the slope of the linear interval from 30% to 80% of the normal displacement.

Copyright © 2005 Taylor & Francis Group plc, London, UK

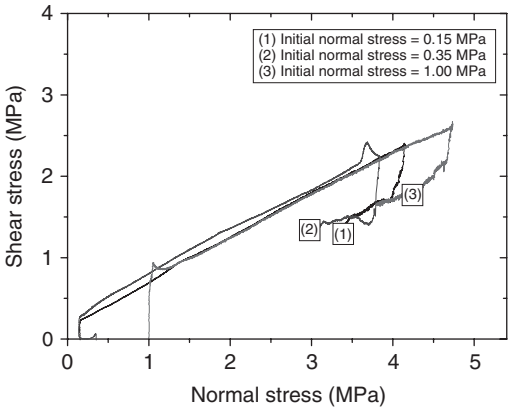


Figure 7. Normal stress verse shear stress curve (AJ-22.5, stiffness = 0.5 MPa/mm).

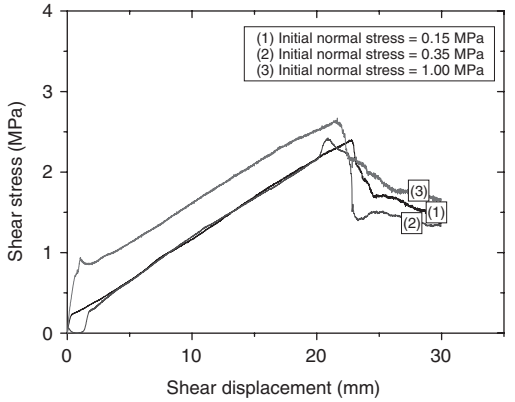


Figure 8. Shear displacement versus shear stress curve (AJ-22.5, stiffness = 0.5 MPa/mm).

4.1 *Constant normal stiffness direct shear test for saw-tooth sample*

The typical CNS test for saw-tooth samples are presented in Figure 7 and Figure 8. These graphs show CNS test results of AJ-22.5-0.15-0.5', 'AJ-22.5-0.35-0.5', and 'AJ-22.5-1.0-0.5'.

According to the analysis of the CNS direct shear tests, shear parameters could be classified into two groups. One highly correlated with the initial normal stress, and the other with the constant normal stiffness. Specifically, the first peak shear stress τ_{p1} strongly correlated with the initial normal stress. The second peak shear stress τ_{p2}, peak normal stress σ_u, shear displacement at peak normal stress, ultimate dilation, and linear dilation angle d_n strongly correlated with the constant normal stiffness.

In this study, we verified the linear correlation between shear parameters and inclination angle. Shear parameters such as the first peak shear stress, the second peak shear stress, peak normal stress, and linear dilation angle depended on the increase of the inclination angle.

From the (a) of Figure 9, the first peak shear stress and the inclination angle positively correlated. When the initial normal stress increased from 0.15 MPa to 1.00 MPa, the slope of regression line of the inclination angle versus the first peak shear stress increased from 0.009 to 0.055, and the Y axis-intercepts at this state increased from 0.08 to 0.34. For the increase in the inclination angle from 5° to 30° and the increase in the initial normal stress from 0.15 MPa to 1.00 MPa, the first peak shear stress can be expressed by the experimental equation below.

$$\tau_{p1} = (0.06 + 0.28\sigma_{n0}) + (-0.003 + 0.057\sigma_{n0})\, i \quad (4.1)$$

where, τ_{p1} is the first peak shear stress (MPa); σ_{n0} is initial normal stress (MPa); and i is the inclination angle.

The second peak shear stress was highly affected by the constant normal stiffness. Figure 9 (b) indicated that the second peak shear stress and inclination angle positively correlated, and also that the second peak shear stress started to decrease from 22° of inclination angle under 1.0 MPa/mm of constant normal stiffness. This situation gave results which were in agreement with the results of Mouchaorab and Benmokrane (1994).

For the linearly regressed 3 lines, correlation coefficient of the slope was 0.9960, and correlation of the Y axis-intercept was −0.9974. Thus, for increase in inclination angle from 5° to 22° and the increase in constant normal stiffness from 0.2 MPa/mm to 1.0 MPa/mm, the second peak shear stress can be expressed by the experimental equation below.

$$\tau_{p2} = (0.48 - 0.90K_n) + (-0.006 + 0.241K_n)\, i \quad (4.2)$$

where, τ_{p2} is the second peak shear stress (MPa); K_n is constant normal stiffness (MPa/mm).

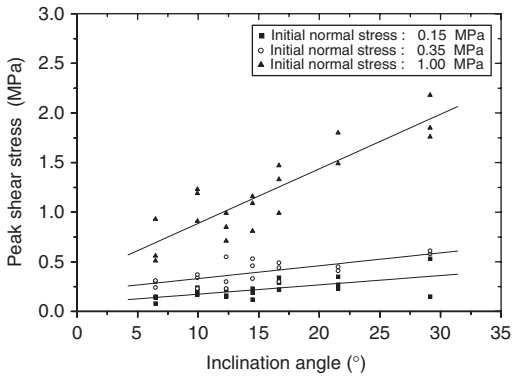
Similarly, peak normal stress and dilation angle were expressed by the experimental equations below from Figs 9 (c) and (d).

$$\sigma_u = (0.75 - 0.57K_n) + (0.027 + 0.269K_n)\, i \quad (4.3)$$

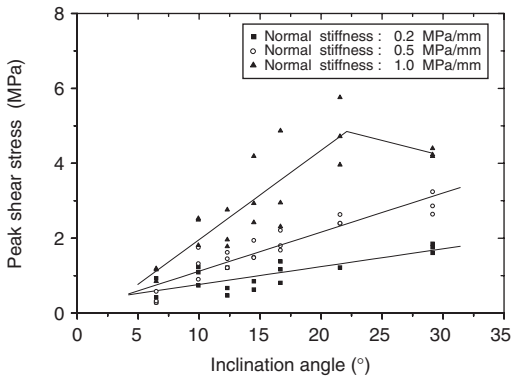
$$d_n = (3.04 - 1.87K_n) + (0.902 - 0.151K_n)\, i \quad (4.4)$$

where, σ_u is the peak normal stress, d_n is the linear dilation angle.

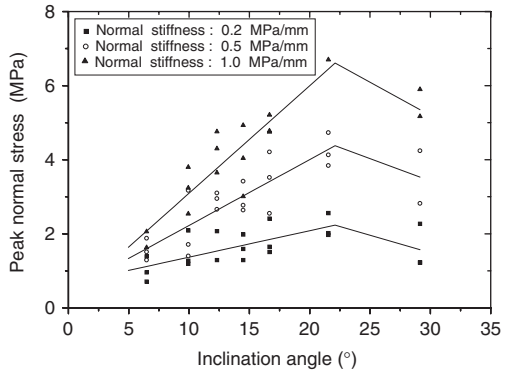
Copyright © 2005 Taylor & Francis Group plc, London, UK



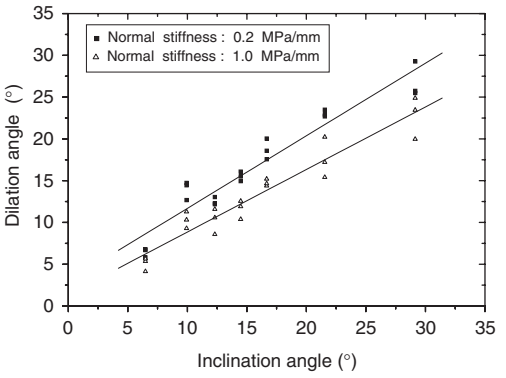
(a) The first peak shear stress



(b) The second peak shear stress



(c) Peak normal stress



(d) Dilation angle

Figure 9. Scatter plot of saw-tooth sample under CNS condition.

4.2 *Constant normal stiffness direct shear test about replica*

Figures 10 and Figure 11 show the typical results of a CNS test for the replica samples. The test conditions were 'NJ-L-0.15-0.5', 'NJ-L-0.35-0.5', and 'NJ-L-1.0-0.5'.

The behavior of the replica joint samples was similar with that of saw-tooth joint sample. However, their overall behavior was quite different, such as non-linear curves in the shear behavior of the replica joint samples. These phenomena could be explained by acoustic emission.

From the shear stress versus normal stress curves of the NJ-L-0.15-0.5 sample, a friction angle was calculated in the normal stress range of 0.2 MPa∼0.8 MPa, and the friction angle was about 40.5°. A friction angle of the NJ-L-0.35-0.5 sample was about 40.9° in the normal stress range of 0.35 MPa∼0.7 MPa, and a friction angle of the NJ-L-1.0-0.5 sample was about 38.3° in normal stress range of 1.25 MPa∼1.5 MPa. A friction angle of a replica joint could be calculated from one replica joint shear test under the CNS condition.

4.3 *Characteristics of acoustic emissions during shearing*

Figure 12 shows the shear stress and AE rate versus shear displacement for the saw-tooth joint sample and replica sample under the initial normal stress of 0.1 MPa and constant normal stiffness of 0.2 MPa/mm. The shear behavior could be divided into three periods according to the characteristics of the AE count.

In Figure 12a, AE counts starts around the first peak shear stress in period I. AE counts were very low in period II. This result means that the whole regular saw-tooth asperities were just climbing between the interfaces of the saw-tooth asperities. Because a local asperity tip failed, however, AE counts were high only around 9 mm of the shear displacement. In period III, as

Copyright © 2005 Taylor & Francis Group plc, London, UK

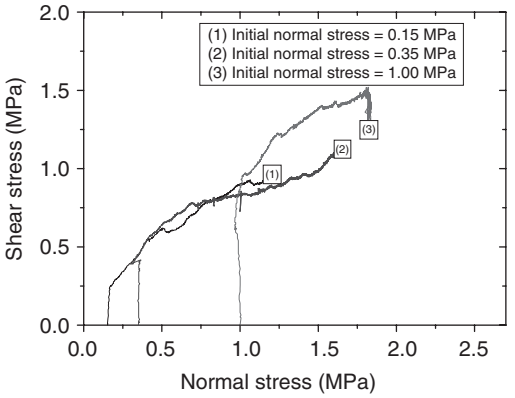


Figure 10. Normal stress verses shear stress curve (NJ-L, stiffness = 0.5 MPa/mm).

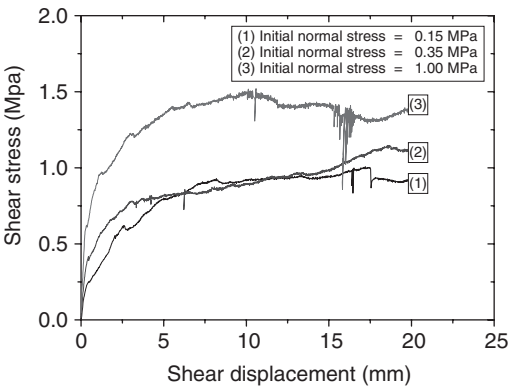


Figure 11. Shear displacement verses shear stress curve (NJ-L, stiffness = 0.5 MPa/mm).

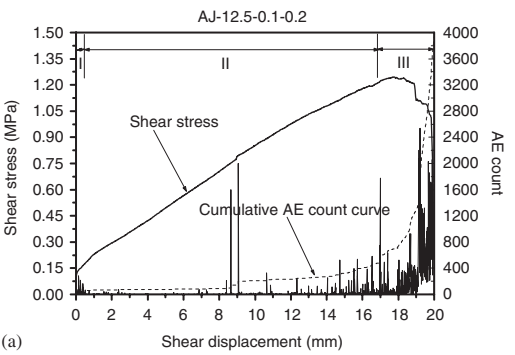


Figure 12a. Shear stress & AE count versus shear displacement curve for saw-tooth joint sample.

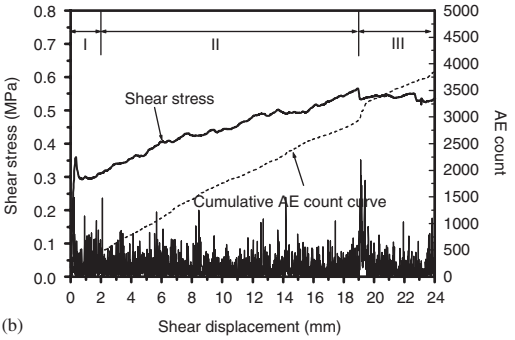


Figure 12b. Shear stress & AE count versus shear displacement curve for replica joint sample.

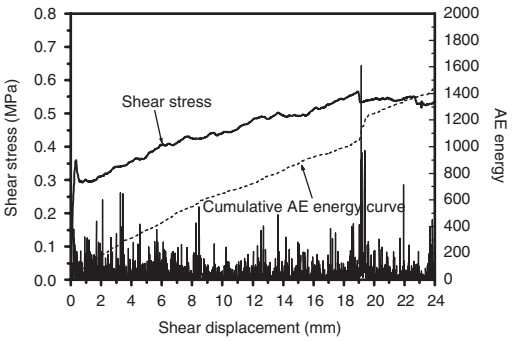


Figure 13. Shear stress & AE energy versus shear displacement curve for replica joint sample.

whole saw-tooth asperities were sheared off, AE counts increased dramatically. In Figure 12b for the replica sample, AE counts occurred until the normal stress started to increase during period I, and AE counts increased linearly during period II. In period III, AE counts increased similarly to AE counts of period II. However, on the boundary between period II and period III, the first order asperity failed and the shear stress was constant even when the normal stress increased.

The AE records showed that the cumulated AE counts for the saw-tooth joint sample were much lower than AE counts for the replica sample during period II. These phenomena may be due to the fact that as the normal stress increased, the asperities of the replica sample sheared off continuously.

In Figure 13, which showed the shear stress and AE energy versus the shear displacement for the replica sample, AE energy phenomena were similar to AE counts phenomena. This result agreed with the results of C. Li & E. Nordlund (1990).

Copyright © 2005 Taylor & Francis Group plc, London, UK

5 CONCLUSIONS

The CNS direct shear tests were performed to more fully understand the shear behavior of underground rock joint. Pseudo rock joints, such as regular saw-tooth joint sample and replica sample of natural rock joint, made of cement mortar were used for the CNS direct shear tests. The following conclusions were drawn.

1. Under CNS direct shear test for the saw-tooth joint, shear parameters can be classified into two groups. The first peak stress strongly correlated with the initial normal stress, but the second peak shear stress, peak normal stress and dilation angle strongly correlated with the constant normal stiffness.
2. The shear curves of replica joint were similar to those of saw-tooth joint sample.
3. A friction angle of a replica joint can be calculated from the data obtained from one replica joint shear test under CNS condition.
4. The shear behavior can be divided into three periods according to the characteristics of AE count and AE energy.

REFERENCE

Bae, Ki-Yoon, Lee, Sang-Geun & Lee, Chung-In, 2002, Development of a 3D rock joint roughness measurement system using a laser type displacement meter, in *Rock Engineering Problems and Approaches in Underground Construction*, Seoul, Korea: 825–832.

Belem, T., Homand-Etienne, F. & Souley, M., 2000, Quantitative Parameters for Rock Joint Surface Roughness, *Rock Mechanics and Rock Engineering*, **33**(4): 217–242.

Benmokrane, B., Mouchaorab, K.S. & Ballivy, G., 1994, Laboratory investigation of shaft resistance of rock-socketed piers using the constant normal stiffness direct shear test, *Canadian Geotechnical Journal*, **31**(3): 407–419.

Hencher, S.R. & Richard, L.R., 1989, Laboratory direct shear testing of rock discontinuities, *Ground Engineering*, **22**, p. 24–31.

Indraratna, B., Haque, A. & Aziz, N., 1999, Shear behavior of idealized in filled joints under constant normal stiffness, *Geotechnique*, **49**(3): 331–355.

Jiang, Y., Tanabashi, Y., Xiao, J. & Sakuma, N., 2003, Mechanical and hydraulic behavior of rock joints under constant normal stiffness conditions, in *Proceedings of the First Kyoto International Symposium on Underground Environment*, Kyoto, Japan: 103–110.

Johnston, I.W., Lam, T.S.K. & Williams, A.F., 1987, Constant normal stiffness direct shear testing for socketed pile design in weak rock, *Geotechnique*, **37**(1): 83–89.

Li, C. & Nordlund, E., 1990, Characteristics of acoustic emissions during shearing of rock joints, *Rock joints, Barton & Stephansson (eds)*: 251–258.

Mouchaorab, K.S. & Benmokrane, B., 1994, A New Combined Servo-Controlled Loading Frame/Direct-shear Apparatus for the Study of Concrete of Rock Joint Behavior Under Different Boundary and Loading Conditions, *Geotechnical Testing Journal*, **17**(2): 3–12.

Seidel, J.P. & Haberfield, C.M., 2002, Laboratory Testing of Concrete-Rock Joint in Constant Normal Stiffness Direct Shear, *Geotechnical Testing Journal*, **25**(4): 391–404.

Copyright © 2005 Taylor & Francis Group plc, London, UK

The effect of spatial distribution in geotechnical design parameters on tunnel deformation

K.I. Song & G.C. Cho
Korea Advanced Institute of Science and Technology, Daejeon, Korea

I.M. Lee
Korea University, Seoul, Korea

S.W. Lee
KonKuk University, Seoul, Korea

ABSTRACT: It is very important to assess accurately geotechnical design parameters along the periphery of tunnel excavation. The geotechnical parameters most commonly used in numerical modeling for tunnel design are usually obtained by subsurface exploration and in-situ characterization before tunnel construction. These parameters generally indicate representative properties or the average values of the circumferential ground of tunnel in global scale. However, tunnel behavior during and after construction may be greatly affected by the spatial distribution of geotechnical parameters even in case that their average values are constant. The spatial variation of geotechnical parameters also may affect the long-term temporal response (e.g., creep) of tunnel behavior. Deformation characteristics of tunnel are apparently governed by anisotropic and spatially distributed geotechnical parameters rather than by isotropic and uniform geotechnical parameters. Thus, in this paper, a statistical approach on numerical modeling is suggested to explore the effect of spatial distribution in design parameters on tunnel deformation. A commercial program, FLAC2D, is used as a numerical analysis tool. As an input, normally distributed data sets were randomly generated based on statistical properties. The generated geotechnical design parameters were assigned to elements or/and zones. This process makes it possible to assess the spatial distribution effects on the deformation of tunnel. The site considered herein is a subway tunnel of Pusan, Republic of Korea, consisting of residual soil and soft rock. Various geotechnical parameters are investigated in view of tunnel deformation and their effects are quantitatively estimated in terms of an influencing distance from the outline of the tunnel. According to numerical analysis results, critical zones where the spatial distribution of design parameters affects the deformation behavior are clearly present, and the influencing distance from the tunnel is various with each geotechnical parameter. Finally, this paper presents what is the most sensitive geotechnical property, which should be investigated precisely, and the practical investigation distance from a tunnel.

1 INTRODUCTION

Geotechnical design parameters are usually obtained through in-situ and/or laboratory tests. The mean value of measurements is often used for a design parameter even though its variation exists noticeably. Parametric variation concept has been rarely considered in most of geotechnical designs. There are two kinds of sources for variation of design parameters: One is spatial distribution and the other is uncertainty.

Uncertainty of geotechnical parameters should be distinguished from their spatial distribution. Uncertainty means that the material property of soil/rock has characteristic unreliability. In reliability-based design, the uncertainty of geomaterial is significant for a specific site characterization. Therefore, the geotechnical properties can be taken in a reasonable range at a particular site during simulation processing. There are three major geotechnical uncertainties, governing the variability of geoproperties, such as inherent soil characteristics, measurement errors, and transformation fallacies (Phoon 1999).

Spatial distribution of soil has been considered for ecological and environmental modelling (Jury 1985). Likewise, the spatial distribution of geoproperties is important for mechanical behavior in case of

Copyright © 2005 Taylor & Francis Group plc, London, UK

Table 1. Material properties used for numerical modeling.

Material property	Weathered soil	Weathered rock
Unit Weight (kg/m^3)	1800	2200
Cohesion (Pa)	1E4	5E4
Friction Angle (Degree)	30	35
K_o	0.5	0.7
Young's Modulus (Pa)	1.7E7	1E8
Poisson's Ratio	0.35	0.3
Shear Modulus (Pa)	6.3E6	3.8E7
Bulk Modulus (Pa)	1.89E7	8.3E7
Young's Modulus for lining (Pa): 5E9		

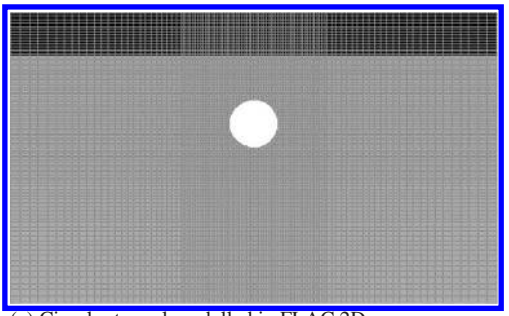
underground structures surrounded by the variable soil/rock. Rock/soil itself is not an isotropic material but an anisotropic and non-homogenous material. These characteristics are induced by the formation process and the state of stress of ground. Spatial distribution takes the macro scale in the range of interest.

The effect of variation of geotechnical parameters on tunnel safety or deformation based on the statistical concept is rarely studied (Schweiger 2001). Selection of geotechnical parameter is also an important subject for analysis. Taylor series finite difference method (Benjamin 1970) is a reasonable way to select sensitive parameters which affect the deformation on tunnel. In this paper, the effect of the spatial distribution in geotechnical parameters on tunnel deformation is studied through numerical analyses based on the statistical concept. From this study, it is possible to answer two questions: "Which geoparameter causes the large deformation on tunnel?" and "What is the practical range of investigation around tunnel?"

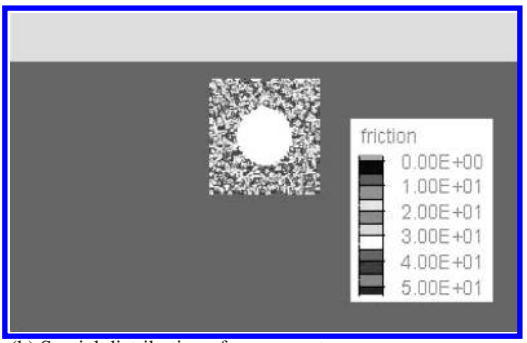
2 SPECIFICATION OF TUNNEL MODELLING

The site considered herein is a subway tunnel of Pusan in Korea, consisting of residual soil and weathered rock. The shape of the tunnel is assumed as circular to facilitate comparison. The radius of the circular tunnel is 5 m. The tunnel is located in the depth of 18 m from the ground surface. Material properties used for numerical modeling are summarized in Table 1. These values represent the mean value of each property. The tunnel model was simulated using a commercial FDM program FLAC (Itasca 1996).

Figure 1(a) shows the generated mesh for numerical analysis of tunnel and Fig. 1(b) shows spatially distributed friction angle with the range of 100% (i.e., 2D, two times of tunnel diameter) from the tunnel excavation periphery. The area of the one element of the model grid is 0.25 m^2, so that the spatial distribution



(a) Circular tunnel modelled in FLAC 2D



(b) Spatial distribution of geoproperty

Figure 1. Numerical model for spatial distribution analysis.

effect of each geotechnical parameter can be precisely evaluated at a realistic scale.

3 STATISTICAL THEORY ADOPTED

3.1 *Normal distribution of geotechnical parameter*

The general coefficient of variation (COV) has been commonly used to quantify the variability of soil and rock properties for a long period (Harr 1987). The COV is defined as standard deviation (σ) divided by mean (μ).

$$COV = \frac{\sigma}{\mu} \times 100\% \quad (1)$$

Each material property of soil and rock can be regarded as a normal random variable that has a certain probability error. Especially, friction angle and unit weight have been shown that their spatial distribution follow normal distribution parameterized with mean and COV (Lumb 1966, Hoeg and Murarka 1974, Lacasse and Nadim 1996, Low and Tang 1997, Phoon and Kulhawy 1999, Tanit et al. 2004). It is assumed herein that all geotechnical parameters have normal distribution characteristics.

Copyright © 2005 Taylor & Francis Group plc, London, UK

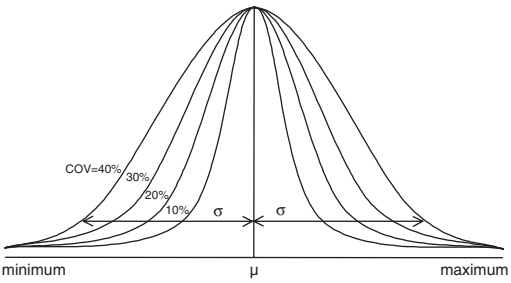


Figure 2. Normal distribution curve of standard deviation.

3.2 *Application on numerical modeling*

Normal distribution of properties can be generated by mathcad (Mathsoft 2001) with specific mean and standard deviation. The generated data is randomly assigned to each grid point over the area of interest. When COV is zero, the mean value of parameter is assigned to the whole range of soil and rock layers. This case is considered as a reference model. The magnitude of variation for each parameter increases as the COV increases. Figure 2 shows the normal distribution curve of various COV values (i.e., COV = 5%, 10%, 20%, 30%, and 40%). Numerical analysis is performed for each case of COV.

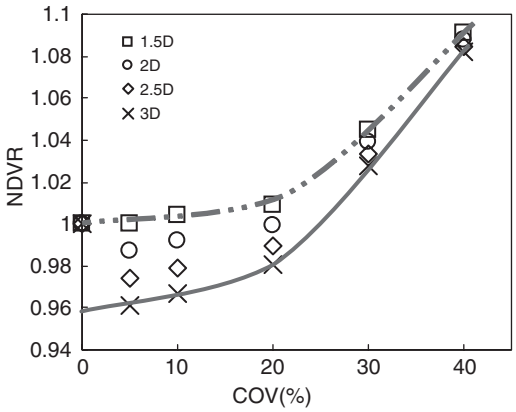
4 NUMERICAL ANALYSIS RESULT – SPATIAL DISTRIBUTION EFFECT

Normalized deformation variation ratio (NDVR) is defined as the deformation (δ_{COV}) at a certain COV with respect to the reference deformation (δ_{ref}) as follows:

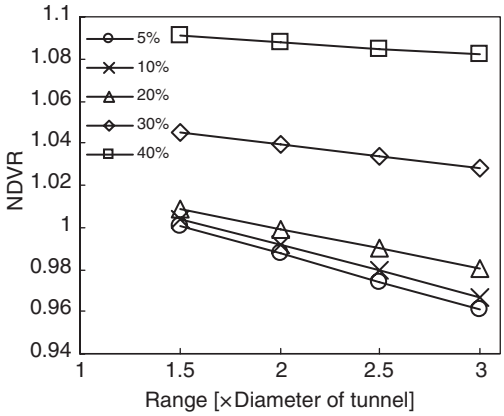
$$NDVR = \frac{\delta_{COV}}{\delta_{ref}} \tag{2}$$

δ_{ref} is the deformation obtained by the mean value (i.e., when COV = 0% for all geotechnical parameters). The reference deformation obtained is 22.21 mm at the crown of tunnel and 38.70 mm at the bottom of tunnel. The NDVR varies with distance from the tunnel opening periphery and COV. For instance, the range of 100% (i.e., 2D) covers the regular quadrilateral area of 400 m^2 as shown in Fig. 1(b).

Three points are monitored and averaged at each analysis to get reasonable deformation characteristics at the crown and bottom of tunnel. Since specific weak elements may lead to large deformation on tunnel surface, three to five analyses are performed and averaged for all cases to avoid any bias effect.



(a) COV-NDVR



(b) Range-NDVR

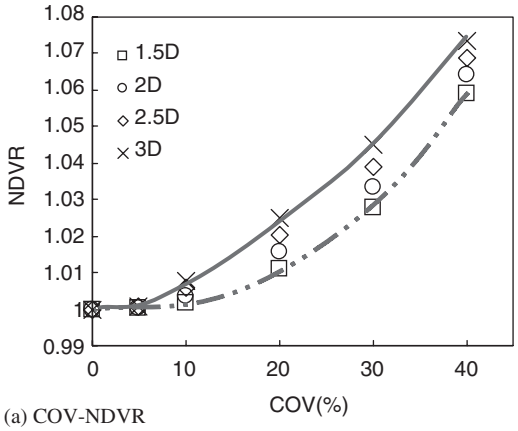
Figure 3. The effect of spatial distribution in modulus on deformation at crown.

4.1 *Bulk modulus and shear modulus*

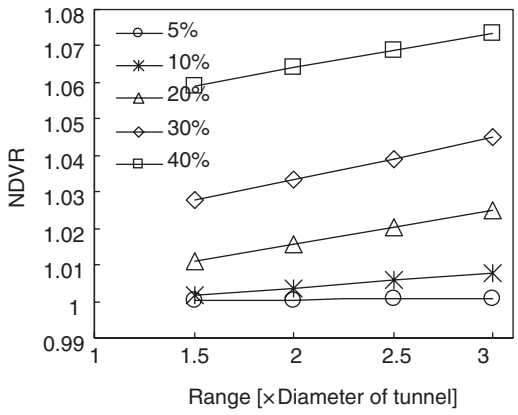
Bulk modulus (B) and shear modulus (G) are important material parameters in geotechnical engineering problem. These two parameters (B, G) can be alternatively changed by Young's modulus (E) and poisson's ratio (ν). In this study, bulk modulus and shear modulus controlled to simulate the spatial distribution effect of modulus on tunnel deformation.

Numerical analysis results are shown in Fig. 3 and Fig. 4. The NDVR is biggest when COV = 40% and Range = 1.5D. However, as the distance increases, deformation gets smaller for all COV cases. The NDVR at crown is larger than that of bottom. In case of crown, the area near to the tunnel governs the deformation because the NDVR at the crown of 1.5D is larger than that of 3D. However, in case of bottom, the result is opposite. And, the NDVR slope becomes steeper as the COV increases along the range. From Fig. 3 and Fig. 4, the COV of 20% is susceptible variation of

Copyright © 2005 Taylor & Francis Group plc, London, UK

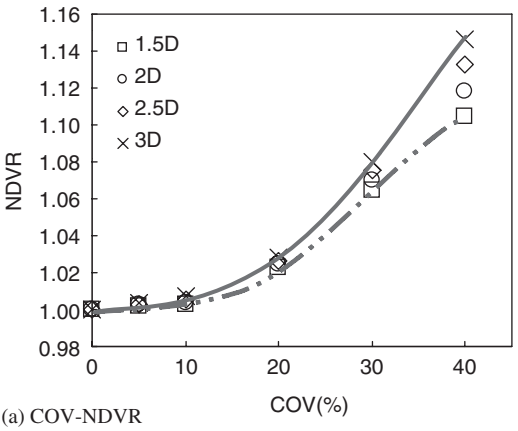


(a) COV-NDVR

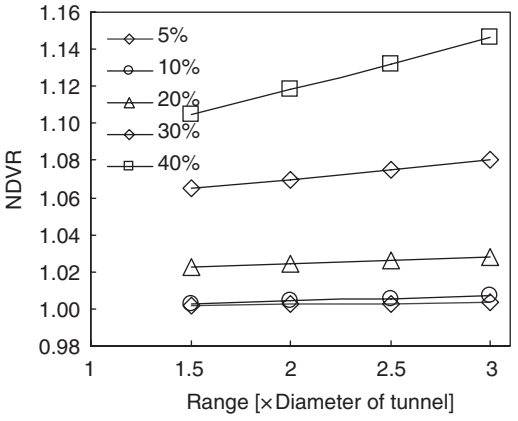


(b) Range-NDVR

Figure 4. The effect of spatial distribution in modulus on deformation at bottom.



(a) COV-NDVR



(b) Range-NDVR

Figure 5. The effect of spatial distribution in friction angle on deformation at crown.

modulus effect on tunnel deformation. The range of 1.5D is enough for crown and bottom.

4.2 *Friction angle*

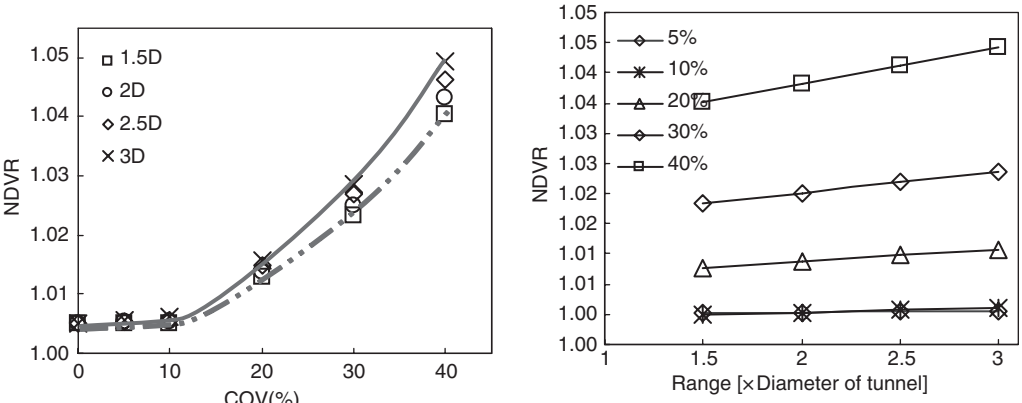
The governing equation of tunnel deformation adopted in FLAC2D is suggested by Salencon (1969). Friction angle is strongly related to the governing equation. From the literature review, the COV of friction angle is small of 12% (Schultze 1972).

Numerical analysis result for the effect of spatial distribution in friction angle on deformation is shown in Fig. 5 and Fig. 6. The NDVR at crown reaches 1.14 when the COV of friction angle is 40% and the variation range covers the 3D area. The slope of range-NDVR relation becomes steeper as the range increases. The deformation of bottom is not significant. However, the NDVR of bottom due to friction angle variation is not small at all compared to other design parameters. From this numerical analysis result, it is concluded that the friction angle variability is the most important factor for deformation on tunnel compared to other geotechnical parameters. However, 10%~20% variation of friction angle is not critical for large tunnel deformation.

4.3 *Cohesion*

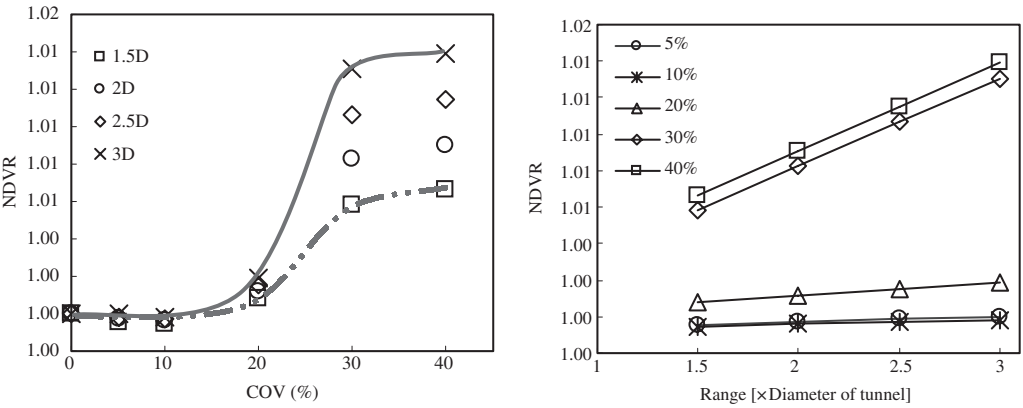
The COV of cohesion is around 40% (Fredlund and Dahlman 1972). As shown in Fig. 7 and Fig. 8, the 20% variation of cohesion little affects deformation on tunnel. As the COV increases, the NDVR of crown converges in all cases of the range. This means that cohesion variation plays more important roll on bottom deformation than crown deformation. However, the NDVR induced by the cohesion variation is very

Copyright © 2005 Taylor & Francis Group plc, London, UK



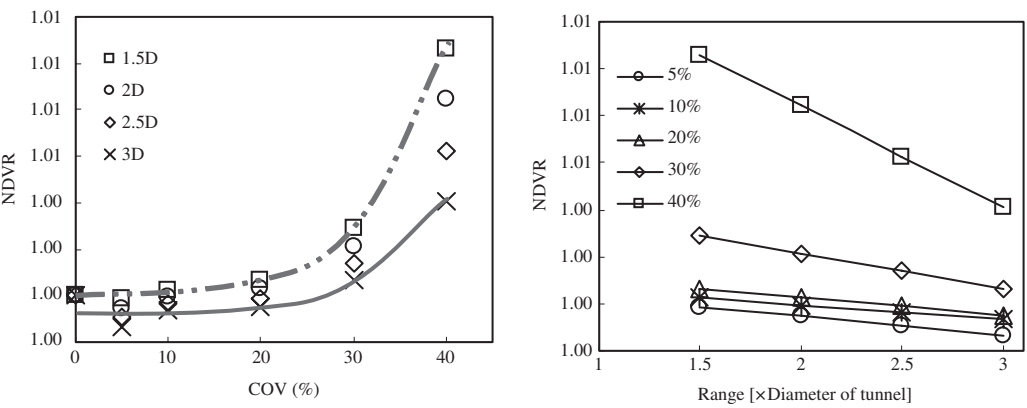
(a) COV-NDVR (b) Range-NDVR

Figure 6. The effect of spatial distribution in friction angle on deformation at bottom.



(a) COV-NDVR (b) Range-NDVR

Figure 7. The effect of spatial distribution in cohesion on deformation at crown.



(a) COV-NDVR (b) Range-NDVR

Figure 8. The effect of spatial distribution in cohesion on deformation at bottom.

Copyright © 2005 Taylor & Francis Group plc, London, UK

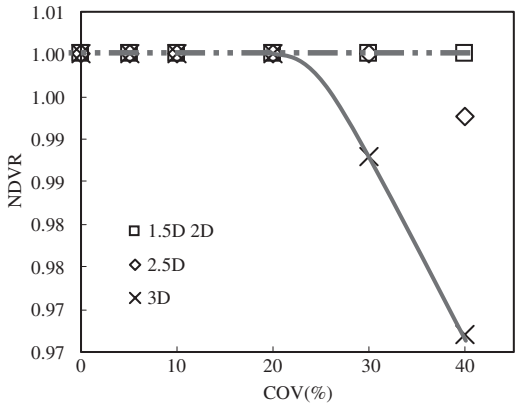


Figure 9. The effect of spatial distribution in tensile strength on deformation at crown.

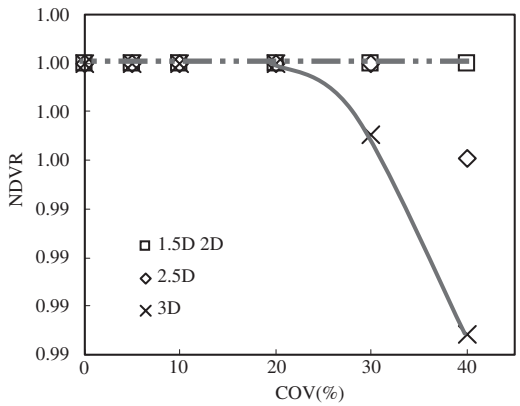


Figure 10. The effect of spatial distribution in tensile strength on deformation at bottom.

small about 1%. From the analysis result, the cohesion effect on deformation is smaller than that of elastic moduli and friction angle. Therefore, cohesion variation is not a critical parameter for deformation characterization.

4.4 *Tensile strength*

The numerical results of tensile strength are shown in Fig. 9 and Fig. 10. The variation of tensile strength does not cause a big deformation at a small COV and in the range close to tunnel. However, as the range becomes larger, the NDVR gets smaller, suggesting that the deformation caused by the tensile strength variation is smaller than the reference case. Almost similar deformation characteristics are observed at the crown and bottom of tunnel. Very small NDVR of about 0.97~0.99 reflects the little effect of tensile strength on bottom and crown deformation of tunnel. This is attributed to the fact that the governing deformation equation adopted in FLAC2D has no tensile strength term.

5 FINAL REMARKS

In this paper, a statistical approach on numerical analyses is suggested to explore the effect of spatial distribution in design parameters on the tunnel deformation. The NDVR with respect to the COV and the range from the tunnel surface was investigated for each geotechnical parameter. The effect of spatial distribution of each parameter was evaluated in terms of deformation at the crown and the bottom of tunnel. The friction angle is the most significant geoproperty which should be investigated precisely. The range from 50% to 100% (1.5D~2D) around the tunnel is a proper ground investigation scope.

Various rock types can be replaced for this numerical modelling to verify and generalize the observed tendencies. For practical purposes, an equivalent parameter reduction factor may be introduced to numerical analysis according to rock type and design parameters. The spatial distribution effect of seepage force acting on the undrained tunnel and permeability in rock mass also can be included in the analysis of tunnel behavior using the method suggested herein.

ACKNOWLEDGEMENT

This paper was supported by the Underground Space Construction Technology Center under the Ministry of Construction and Transportation in Korea (grant C04-01).

REFERENCES

Cho, G.C., Lee, J.S., Santamarina, J.C. 2004. Spatial Variability in Soils: High Resolution Assessment with Electrical Needle Probe. Journal of geotechnical and geoenvironmental engineering, Vol. 130, No. 8, pp. 843–849.

Chung, Y.S. & Choi, K.S. 1996. Development of Stochastic Finite Element Model for Underground Structure with Uncertainties in the Physical Properties in Discontinuous Rock Mass, Korea Civil Engineering Society, Vol. 16, No.1–6, pp. 669–681.

U.S. Army Corps of Engineers. 1997. Engineering and Design tunnels and shafts in rock.

Harr, M.E. 1987. Reliability Based Design in Civil Engineering. Dover Publications, INC., pp. 1–74.

Hayter, A.J. 2002. Probability and Statistics for Engineers and Scientists. Duxbury. pp. 232–285.

Hoek, E. & Brown, E.T. 1980. Underground excavations in Rock, The Institution of Mining and Metallurgy, London.

Copyright © 2005 Taylor & Francis Group plc, London, UK

Itasca Consulting Group. 1996. FLAC – Fast Lagrangian Analysis of Continua, Version 4.0, Minneapolis, MN:ITASCA Consulting Group, Inc.

Jury, W.A. 1985. Spatial variability of soil properties. In: Hern, S.C., Melancon, S.M. (Eds.), Vadose Zone Modeling of Organic Pollutants. Lewis, Chelsea, MI, pp. 245–269.

Phoon, K.K. & Kulhawy, F.H. 1999. Characterization of Geotechnical Variability. Canadian Geotechnical Journal, 36(4), pp. 612–624.

Phoon, K.K. 1995. Reliability-based design of foundations for transmission line structures. Ph.D. Thesis. Cornell University.

Salencon, J. 1969. Contraction Quasi-Statique D'une Cavites Sysmetrie Spherique Ou Cylindrique Dans Un Milieu Elastoplastique. Annales Des Ponts Et Chauss, Vol. 4, pp. 231–236.

Schweiger, H.F., Thurner, R., Pottler, R. 2001. Reliability Analysis in Geotechnics with Deterministic Finite Elements. The International Journal of Geomechanics, Vol. 1, No. 4, pp. 389–413.

Tanit, C. 2004. Reliability-Based Design for International Stability of Mechanically Stabilized Earth Walls. Journal of geotechnical and geoenvironmental Engineering, Vol. 130, No. 2, pp. 163–173.

Copyright © 2005 Taylor & Francis Group plc, London, UK

Behaviour of a large cross-section tunnel in a large-scale model test

C.J. Lee, J.S. Kim & N.Y. Ryu
Construction Division, Samsung Heavy Industries Co., Ltd, Korea

S.D. Lee
Department of Civil Engineering, A Jou University, Korea

K.H. Jeong & J.W. Yang
Dodam Engineering and Construction Co., Korea

ABSTRACT: Behaviour of a large cross-section prototype tunnel has been investigated by carrying out a large-scale model test. In order to simulate the prototype tunnel to be constructed in sandstone and mudstone, the model ground has been formed by using layers of rectangular concrete bricks, having apparent rock mass rating (RMR) index of about 67. The model test consists of simulation of excavating the model ground in several stages including pilot tunnel excavation. In addition, tunnel behaviour under the service condition after completion of the tunnel excavation has been studied. It has been found that most of the ground displacements develop during the pilot tunnel excavation, after which insignificant ground displacements occur. Based on the measurements, an empirical equation for rock load that can be used in the preliminary tunnel design has been proposed. The insight into the tunnel behaviour observed from the model test will be reported and discussed.

1 INTRODUCTION

The use of 2-arch tunnels in Korea has been rapidly increased in recent years since they are more environmentally friendly compared to conventional two parallel tunnels (Yun 2002). In practice, the 2-arch tunnel can be regarded as a special case of two parallel tunnels with very short centre-to-centre distance. However, since central part of the 2-arch tunnel may be subjected to the large ground displacement due to insignificant arching effect near the centre of the tunnel, central part of the tunnel (pilot tunnel) is often supported by centre pillar constructed after completion of the pilot tunnel excavation. There have been a series of researches on the behaviour of 2-arch tunnels in soils and weathered rocks (Matsuda 1998, Yun 2002, Celestino et al. 2004). On the contrary, to date, the behaviour of 2-arch tunnels in mountainous areas composed of hard rock is not well understood among engineers.

The purpose of the current research is to study the behaviour of a large cross-section (187.6 m^2) prototype tunnel to be constructed in sandstone and mudstone in southern part of Korea by carrying out a large-scale model test. The prototype tunnel is about 23.9 m in width and 8.2 m in height as shown in Figure 1. The prototype tunnel has been designed based on the New Austrian Tunnelling Method (NATM), widely used in Korea. In addition, the diameter of the pilot tunnel to be built before construction of the main tunnel is 10 m. Since the behaviour of tunnels constructed in hard rock heavily depends on geological characteristic, the current model test used a number of concrete bricks to represent the prototype ground condition. The model test consisted of the pilot tunnel excavation, left and right tunnel excavation and application of a surface loading upon the completion of the tunnel excavation. In the model test behaviour of the tunnel has been monitored by measuring ground displacement, rock load and lining displacement. The findings from the model test have been successfully included in the design of the prototype tunnel and the tunnel design has been finalised.

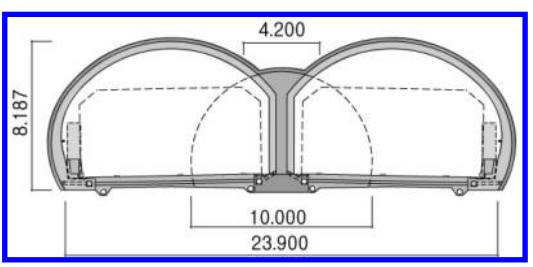


Figure 1. Sectional view of the prototype tunnel (unit: m).

Copyright © 2005 Taylor & Francis Group plc, London, UK

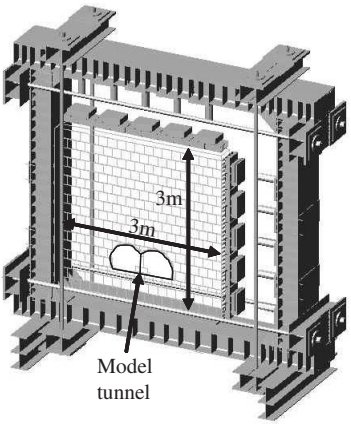


Figure 2. Sectional view of the model tunnel.

2 THE MODEL TEST

2.1 *The model package*

The size of the model ground was 3 m × 3 m in area and 0.27 m in thickness as shown in Figure 2. The model tunnel consisted of left, centre and right tunnel and centre pillar as noted in Figure 2. The inside of the model container was coated with grease to reduce side friction so that shear transfer at the ground and the container interface could be minimised. In the model test, scale factor of 20 was used. Hence the dimension of the model test was reduced by 20. The pilot tunnel was 0.54 m in width and 0.36 m in height. The main characteristic of the model test is application of both the vertical and lateral loading by using a loading system to duplicate similar stress conditions near the prototype tunnel prior to the tunnel excavation. The maximum magnitude of the vertical and lateral loading that can be applied was 250 tonf/m^2. However, since the current research was based on a commercial project only important features of the prototype tunnel has been modelled.

2.2 *The model ground*

It has been well known that rock mass is not uniform and there exist discontinuities in a rock mass (Hoek & Brown 1980). The behaviour of tunnels and surrounding ground is therefore heavily dependent on the engineering characteristic of the rock mass (GEO 1992). In this study to model characteristic of sedimentary rock, the model ground was made of a number of concrete bricks (see Figure 2). The brick had friction angle of 32° and cohesion of zero based on the direct shear tests. The dry density of the block was 2,020 kgf/m^3 and average compressive strength was 254 kgf/cm^2. The model ground was arranged to have similar RMR rating, widely used in tunnel design in Korea, of the prototype ground (Bieniawski 1984). The model ground used in the model tests had slightly rough surface with aperture thickness less than 1 mm. Overall the model ground had total RMR rating of 67 and hence the model ground was classified into class number II, i.e., Good rock.

2.3 *The center pillar*

In order to measure the rock load acting on the centre pillar, load cell was installed prior to the formation of the model ground. In the real tunnel excavation, the centre pillar is to be installed after completion of the pilot tunnel. However, to measure loosening load during the pilot tunnel excavation the centre pillar was installed prior to the assembly of the model ground. Thereafter the pillar load has been arranged to zero to measure rock load, exclusively associated with the main tunnel excavation.

2.4 *The tunnel lining*

The model tunnel lining has been installed after completion of the tunnel excavation. The model lining was made of steel plate and represented prototype concrete lining of 400 mm in thickness. The thickness of the steel model lining was decided to be 6 mm based on the following scaling law in equation (1).

$$E_m I_m = E_p I_p / n^4 \quad (1)$$

Where E = elastic modulus; I = 2nd moment of inertia; m = model; p = prototype; n = scale factor (20).

2.5 *Instrumentation*

In the model test the behaviour of the tunnel and the ground due to excavation was monitored using LVDT (Linear Variable Displacement Transducer, ground displacements and lining displacement) and load cell (pillar load). The location of LVDTs is shown in Figure 3. In the current research the behaviour of tunnel at six different stages have been monitored as follows:

Stage a: Formation of the model ground
Stage b: Excavation of upper part of the pilot tunnel
Stage c: Excavation of lower part of the pilot tunnel
Stage d: Arrangement of load cell reading to zero
Stage e: Excavation of the left tunnel
Stage f: Excavation of the right tunnel

In addition, the internal displacement of the tunnel lining under the service condition has been monitored and the location of LVDTs is shown in Figure 4.

2.6 *The test procedures*

The model test was conducted under a uniform surface loading of 100 tonf/m^2 with the lateral earth pressure

Copyright © 2005 Taylor & Francis Group plc, London, UK

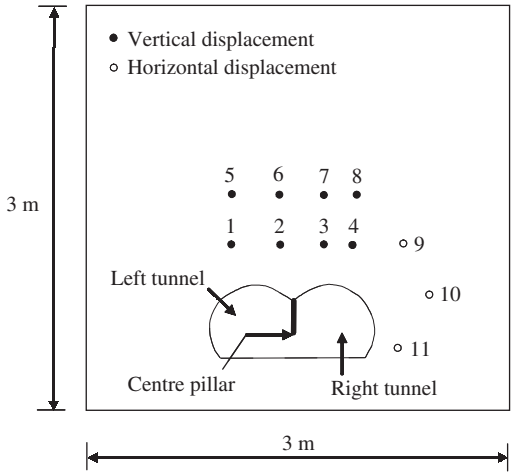


Figure 3. Location of LVDTs in the model test.

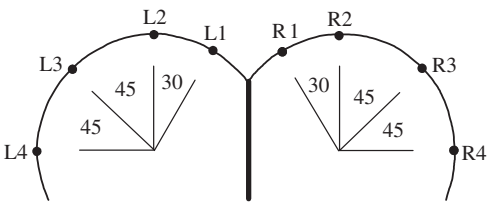


Figure 4. Location of LVDTs in the lining (unit: degree).

of 150 tonf/m^2 and hence the earth pressure coefficient was 1.5, which was closed to the measured value from field tests (1.54). The stress condition of the model ground represented vertical stress of the prototype roughly 50–100 m in depth, depending on geological condition of the prototype ground near the tunnel. The model test was carried out in the following sequence (refer to Figure 5):

1. Installation of the centre pillar and formation of the initial ground (Figure 5a)
2. Excavation of the pilot tunnel (Figure 5b)
3. Excavation of upper part of the main tunnel (Figure 5c)
4. Completion of the tunnel excavation (Figure 5d)
5. Installation of tunnel lining
6. Application of surface loading

3 THE MEASURED RESULTS FROM THE MODEL TEST

3.1 *Changes of vertical ground displacements*

In order to measure vertical ground displacements during the tunnel excavation at different stages, ground

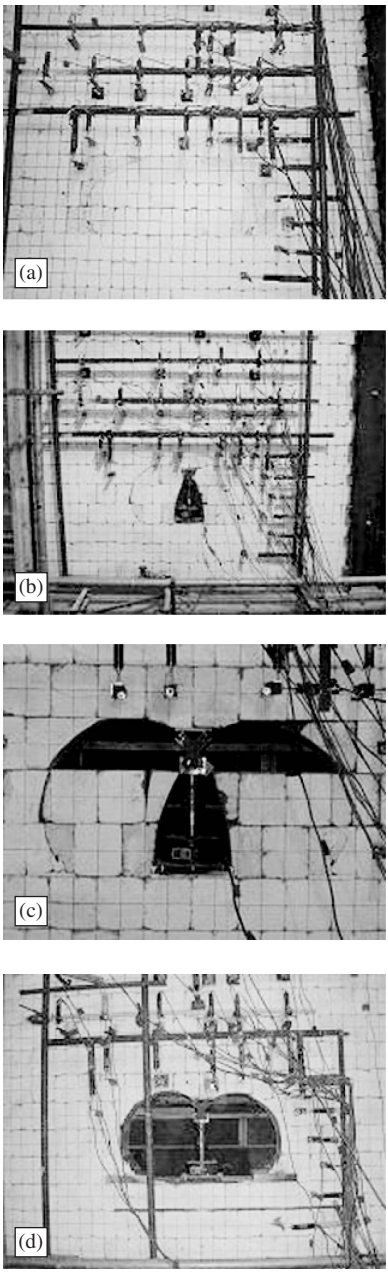


Figure 5. Modelling of tunnel excavation.

displacements at 0.25 W and 0.5 W above the tunnel crown have been monitored (0.25 W: points 1–4; 0.5 W: points 5–8), where W is the width of the tunnel. The locations of the measuring points are shown in Figure 3. Figure 6 shows changes of the vertical ground displacement during the excavation stages. It is noted

Copyright © 2005 Taylor & Francis Group plc, London, UK

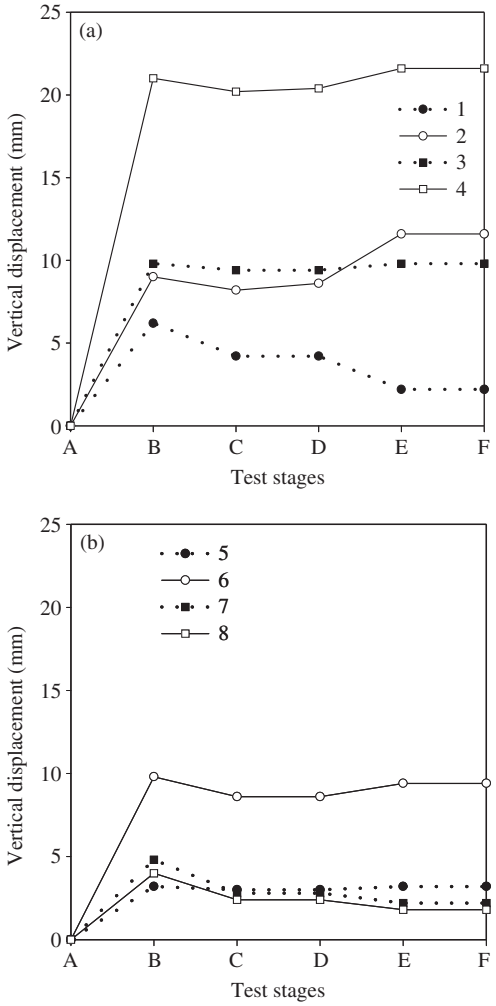


Figure 6. Changes of vertical displacement.

that the measured displacements referred in the current paper are prototype displacements by multiplying the measured displacements with the scale factor (20). It is shown that there is a sudden increase in the vertical ground displacements during stage b after which insignificant ground displacements were developed. The ground displacements measured at 0.5 W are generally smaller than those measured at 0.25 W. In addition, considering the measured vertical ground displacements from all LVDTs used in the model test most of the ground displacements occurred within 0.25 W. This implies that the length of rock bolts should be longer than 0.25 W to reinforce disturbed area effectively. It is interesting to note that excavation of the right tunnel resulted in insignificant vertical displacements at points 1–2 and 5–6. Overall the

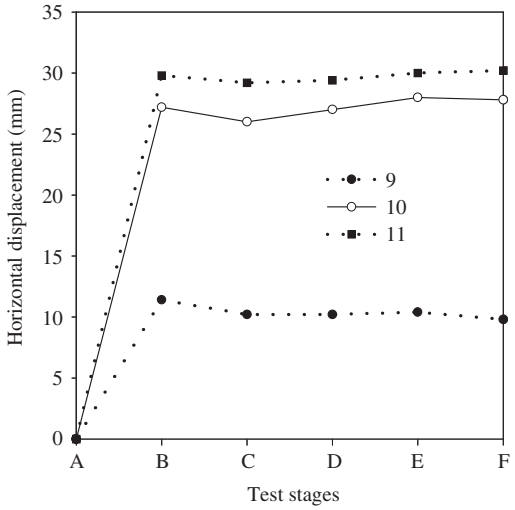


Figure 7. Changes of horizontal displacement.

measured ground displacements imply that the centre pillar was rigid enough to restrain ground displacement. In addition, this high rigidity could probably reduce the interaction between the left and the right tunnel.

3.2 *Changes of horizontal displacements*

In order to evaluate stability of the side wall, the lateral ground displacements at the right part of the tunnel have been monitored using LVDTs. The locations of LVDTs are shown in Figure 4 (points 9–11). As shown in Figure 7 the majority of the displacements occurred at stage b after which insignificant changes of the ground displacements developed. This is consistent with the development of the vertical ground displacements. In general the stress condition of the ground after tunnel excavation may be different from the in-situ condition. In particular, direction and magnitude of the principle stresses will be changed due to stress re-distribution through the arching effect, hence the measured results indicate that majority of the stress change occurred during stage b after which the stress condition may not be changed much. Overall the measurements suggest that the stability of the 2-arch tunnel depends mainly on the excavation of the pilot tunnel. Therefore, the pilot tunnel should be stabilised prior to excavation of the other part of the tunnel. In addition, the measured results show that the longer the distance from the tunnel base the smaller the lateral ground displacement.

3.3 *Centre pillar*

A 2-Arch tunnel can be regarded as a special type of two parallel tunnels. However, arching effect may be

Copyright © 2005 Taylor & Francis Group plc, London, UK

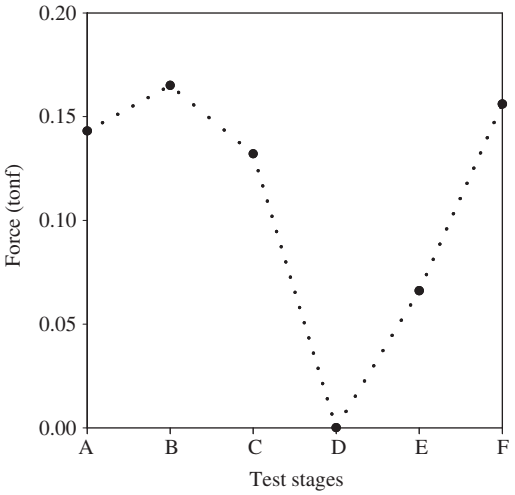


Figure 8. Changes of force on the pillar.

insignificant near the centre of the tunnel and hence the stability of the central part of the tunnel may be reduced, thereby leading to an increase in the rock load acting on the centre pillar. In practice, design of the centre pillar requires the information of the magnitude of the rock load.

Figure 8 shows changes of the measured load at the centre pillar. The changes of the measured load prior to the main tunnel excavation, i.e., left and right tunnels, are not significant. Upon the completion of the pilot tunnel excavation, the reading of the load cell has been re-set to zero to measure the changes of the rock load during the main tunnel excavation. The measurement shows a gradual increase in the load as the excavation steps preceded. The measured load before stage d means the load to be supported by shotcrete, rock bolt and steel rib, while the final load of about 0.16 tonf is the actual rock load to be supported by the centre pillar. This increase implies that the centre pillar stabilise the tunnel during left and right tunnel excavation, thereby leading to insignificant increase in the ground displacement during the main tunnel excavation as discussed previously.

Matsuda (1998) proposed an empirical equation of rock load for a tunnel in soils and weathered rocks by considering soil depth (H) and tunnel centre-to-centre distance (B). However, to date studies of rock load that can be used in preliminary tunnel design for 2-arch tunnels in rock is rather limited. In the current study, an empirical relation for rock load based on the measurement is proposed for the rock when RMR is greater than 60. The empirical equation proposed from the current research is $H = 0.15B$, where B is the centre-to-centre distance between left and right tunnels. Although more study is obviously required, this

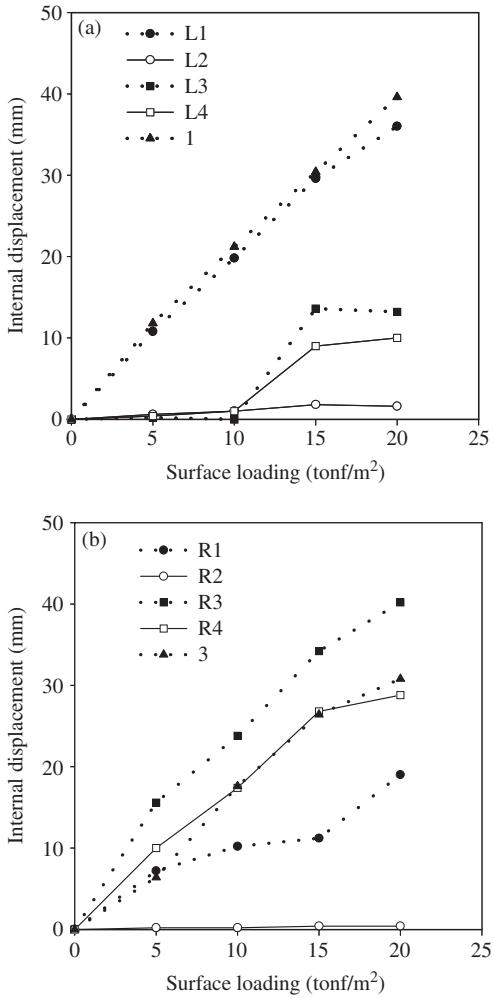


Figure 9. Changes of internal displacement.

relation may be used for the preliminary design of the centre pillar for 2-arch tunnels.

3.4 *The tunnel behaviour under service loading*

In general, concrete tunnel lining constructed in NATM may not take any structural load since shotcrete, rock bolt and steel rib may take all external loads. However, creep effects resulted from weathering of the ground may apply some load on the lining. In the model test to simulate tunnel behaviour under a service condition, a surface loading has been applied with K_0 of 1.5 (vertical stress: 5, 10, 15, 20 tonf/m^2).

Figure 9 shows an increase in the internal displacement of the tunnel lining with an increase in the surface loading. Figure 4 shows locations of the LVDTs

Copyright © 2005 Taylor & Francis Group plc, London, UK

used to measure internal displacement of the lining. In addition, net increase in the vertical ground movement during the surface loading is included in the figure for comparison (points 1 and 3, see Figure 3). In the graph the positive displacement implies the displacement toward the centre of the tunnel, implying reductions in the tunnel size. Generally speaking, the internal lining displacements are increased with an increase in the surface loading. Overall the displacement is not symmetric with the centre of the tunnel. This is probably related to the disturbance caused by tunnel excavation. The points L2 and R2 show the minimum lining displacement. The measured ground settlement is similar to the maximum lining displacements. The measured ground settlements due to the surface loading were larger than those measured during the tunnel excavation. This implies that substantial ground settlement can be developed in the long-term process of tunnel use.

4 CONCLUSIONS

A large-scale model test has been performed to study the behaviour of the large cross-section prototype tunnel. Following conclusions can be drawn from the model test:

1. Ground displacements mainly occurred within 0.25 W, where W is the tunnel width. This suggests that rock bolt length should be longer than 0.25 W to prevent loosening of the rock. In addition, most ground displacements occurred during the pilot tunnel excavation. Hence, it may be important to install rigid centre pillar prior to main tunnel excavation.
2. Based on the limited information obtained from the measurement, the rock load acting on the centre pillar may be $H = 0.15B$, where B is the centre-to-centre distance between left and right tunnels when RMR is more than 60. However, obviously more research is required to generalise the proposed relation.
3. The behaviour of the tunnel under the service condition has been simulated by applying surface loading. The displacement of lining increased nearly inearly with an increase in the surface loading. The ground displacements due to the surface loading were larger than that measured displacements developed during tunnel excavation.
4. Based on the model test, it has been decide to increase rigidity of the centre pillar and the design of the prototype tunnel has been finalised. The construction of the tunnel is expected to be commended on early 2005.

ACKNOWLEDGEMENTS

The current paper is based on the joint research between Samsung Heavy Industries and A Jou University. The authors would like to thank researchers at geotechnical research laboratory of A Jou University for their assistant in the model test described in this paper.

REFERENCES

Bieniawskti, Z.T. 1984. Rock mechanics design in mining and tunnelling, Balkema: Rotterdam.

Celestino, T.B., Re, G., Leite, R., Rocha, H.C. & Vasconcellos, C.A. 2004. The design and construction of the Vila Madalena station for the Sâo Paulo Subway. Underground space for sustainable urban development. Proc. of. 30th ITA-AITES World Tunnel Congress. (Edited by Shirlaw, Zhao & Krishnan). (1) 350–357.

Geotechnical Engineering Office (GEO). 1992, Guide to cavern engineering. Geoguide 4. Civil Engineering Department, Hong Kong.

Hoek, E. & Brown, E.T. 1980. Underground excavation in Rock. Instn. of Mining & Metallurgy.

Matsuda, T. 1998. Discussion: behavior and settlement control of twin tunnel in soil ground. Tunnels and Metropolises.

Yun, S.Y. 2002. A study on design method of large scale twin tunnel by analyzing of construction practice. MEng thesis. Graduate school of industry. Han Yang University. Korea (*in Korean*).

Copyright © 2005 Taylor & Francis Group plc, London, UK

GIS-based application and intelligent management of geotechnical information and construction data in tunnelling

C.Y. Kim, S.W. Hong, K.Y. Kim, S.H. Baek & G.J. Bae
Geotechnical Engineering Research Dept., Korea Institute of Construction Technology, Korea

B.H. Han
Civil Eng. & Tech. Team, Civil Division, Samsung Corporation, Ltd., Korea

K.S. Jue
Division of Civil Works, Hyundai Engineering & Construction Co., Ltd., Seoul, Korea

ABSTRACT: Ground and rock mass considered in tunnelling have characteristics such as uncertainty, heterogeneity and structural complexity because they have been formed undergoing various geological events for a long period. So, it is difficult for engineers to predict and judge the behaviors of rock mass in tunnelling. In this paper, the authors suggest a GIS-based intelligent management system, which is named ITIS (Intelligent Tunnel Information System), for site investigation, design and construction in tunnelling and introduce the application of this system for several urban and mountainous tunnel sites under construction in Korea.

1 GENERAL INSTRUCTIONS

In general, experiences play an important role in construction of underground structures such as a tunnel. The reason for this is due to the difficulty of gathering sufficient information on the geology and evaluating the true mechanical behavior of the ground at the design stage. Also geological information is difficult to quantify because of imprecise and incomplete data observation, and the tunnel design is carried out with insufficient information on the geology and the mechanical behavior of the ground.

The concept of 3-D visualization system certainly gives a new aspect in the field of geotechnical engineering. The analysis and interpretation with attention to geotechnical or geological data using 3-D visualization techniques are valid to understand geotechnical site characteristics. Furthermore, the adequate analysis prevents construction delay and additional cost, and leads to minimize geological and geotechnical uncertainties. As 3-D visualization system has become popular in recent years, the authors have started to investigate how to systemize the experiences and decision making procedures of experts in tunnel design and construction by using GIS, virtual reality, artificial intelligence and database system since 1999. A national research laboratory (NRL) in Korea was established to develop the Intelligent Tunnelling Information System (ITIS).

2 ITIS SYSTEM DESIGN & DEVELOPMENT

2.1 *System architecture (software & hardware)*

Arriving at the correct design for the information system before embarking on its development is very important. Site investigation, tunnel design and construction data are generally existed in forms of manually completed documents, project reports, regional geotechnical maps and geotechnical relational database, etc. And the analysis of these data that located against some form of map or plan is generally two dimensions. ITIS is an integrated D/B management, analysis and visualization system for geotechnical projects especially in tunnelling. It is a true client-web server database system. The client-web server model for distributed computing allows multiple client PCs to request data from a single server PC on which resides a database and the software for servicing client requests. The structure of ITIS is shown in Figure 1.

All geological information can be stored in file database in the machine of main system. The client part (tunnel construction sites) can input its construction

Copyright © 2005 Taylor & Francis Group plc, London, UK

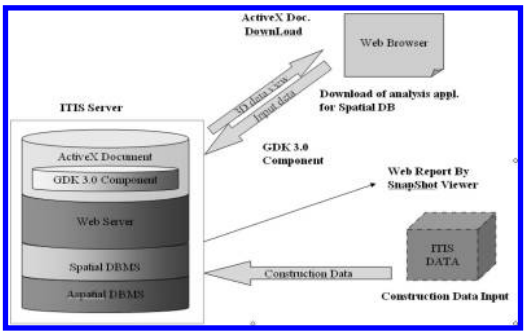


Figure 1. The structure of ITIS.

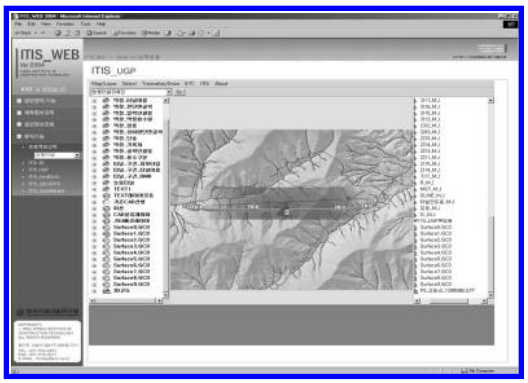


Figure 2. ITIS graphical user interface.

data into the SQL server and geographical and spatial data into the GMS (Geomania Server, GIS Server). It provides the environment that makes much easier to create 3-D subsurface model and analysis results and creates presentation-quality. In developing ITIS the important considerations are easy-operating environment and PC-Windows-based for civil engineers who have antiquated computing capabilities. ITIS was developed using C++, Open GL and Delphi for language, and GEOMania, GDK (GEOMania Development Kit) and GEOMania/3D for program and runs on Pentium PC operating under Windows 9X/NT compatible operating system.

Using the graphical user interface, the user can operate the system with the mouse and the keyboard. The system consists of input, output, and analysis/interpretation modules. There are a lot of input data available such as basic geological information acquired from borehole, field investigation and geophysical exploration, in situ test, laboratory test, pre-investigated reports and tunnel initialization information, including start and endpoints. These data are managed and analyzed in a lump to make a 3-D model and

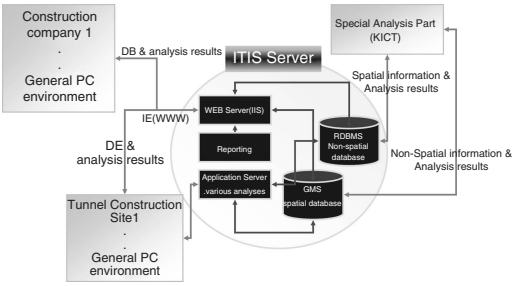


Figure 3. Structural concept of data transmission.

several types of analysis with adapting mathematical and scientific algorithms. Within the system it is possible to zoom, move, rotate, cut, select a gradient and custom coloring, and copy/paste directly to other Windows compatible software. The user can take cross sections in all directions and create subsurface profiles in the cross sections. All of cross sections created are easily compared with each other.

Using the report functionality, the user can get most of the requested information. The extensive pre-prepared report formats are available. Furthermore, the query options can be used to generate lists of data that exist within the database. These can be exported a pre-prepared files. Figure 2 shows the ITIS graphical user interface with 3-D windows.

2.2 *Database structure*

The core part of Database of ITIS is the SQL DB Server and GMS spatial DB Server. Both database are the repository for all data managed by the system. The cornerstones of this data structure are five primary entities: construction contract, site investigation, design, construction and analysis.

3 MODULES OF ITIS

3.1 *Visualization module for site investigation data and structure*

The module allows engineers and scientists to input, edit and manage data, and create 3-D models easily. Once logged on to the system, the user meets the Graphical User Interface (GUI). The GUI comprises two units. One enables the user to use all the functions such as file management, digital map editing, data input and analysis, drawing, setting of options, and help. The other is used for creating 2-D and 3-D models with selecting projects. It is possible to zoom, measure scaled distances, drag, select layers, and copy/paste directly to other compatible programs.

Copyright © 2005 Taylor & Francis Group plc, London, UK



Figure 4. Input and output windows for borehole information.

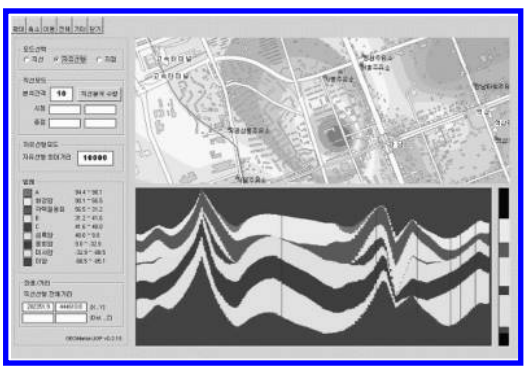


Figure 5. Creation of cross-section using geostatistics.

This module treats most of the data observed and measured in site investigation.

- Three-dimensional geomorphologic data (x, y coordinates and elevation)
- Borehole location and depths of samples and stratigraphic samples taken in borings
- Physical property and other attribute data measured at outcrops
- In situ and laboratory test results
- Tunnel initialization information, including start and endpoints

The user manages systematically all the data that the user wants to include in the project by using Object-Oriented Database System (OODB). Figure 4 shows the input and output windows for borehole information. Details of boreholes collected and observed are entered into a borehole database. It consists of project, company and borehole classes. With using the boring log function, borehole log is created from data and is automatically updated when the data is modified. A standard heading and contents of columns could be selected to form a suitable log format.

Figure 5 shows the windows of cross-section by krigging method. This module allows the user to visualize two-dimensional surfaces, fence diagrams and three-dimensional solid models. In 2-D surface the user creates surface models and contours for geology, rock mass classification, mechanical properties of several stratigraphic 2-D surface models.

They also support the same features as 2-D surface models. All of the created cross sections are easily compared with each other. This function is useful to discuss or verify complex geologic site conditions and to solve a problem of disagreement between staffs concerned with construction projects. For creating 3-D model borehole and 2-D surface information are used and analyzed with adapting mathematical and scientific algorithms in a lump. The process of generating 3-D model from the relative data is quick and simple. Hong et al. (2001b) introduced the procedure of making 3-D model in detail.

3.2 *Prediction module for ground surface settlement and damage assessment*

Some tunnel and underground excavation inevitably disturbs the ground and the original stress field, which in turn causes ground movement leading to surface settlement. The ground movements can be large enough to disrupt the function of nearby structures and utilities. Particularly, in urban areas, the freedom of choice of alignment and tunnel depth is rather limited. The module is for the prediction of ground surface settlements incorporating artificial neural networks (ANN). In this module, ANN is incorporated with '113' of monitored field results to predict surface settlement for a tunnel site. This module uses a concept of relative strength of effects (RSE) in sensitivity analysis for various major factors affecting the surface settlement in tunnelling. The module is connected to the ITIS visualization system and shows the predicted area as contours with trough according to a stage of excavation. Figure 6 is a window that shows 2-D settlement prediction with trough according to a stage of excavation in Seoul subway. The module also gives a prediction result of 3-D settlement with adjacent building continuously during excavation.

3.3 *Selection module for tunnel auxiliary reinforcement*

In tunnel construction it is important to predict or define the cause of the abnormal phenomenon and then to carry out the countermeasure against the major cause. For building up this module a lot of types of tunnel failure were surveyed and the detail

Copyright © 2005 Taylor & Francis Group plc, London, UK

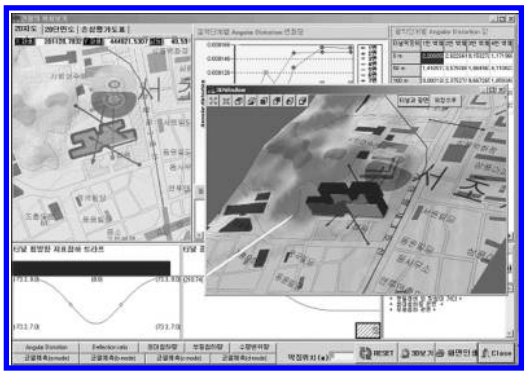


Figure 6. Surface settlement prediction with predicted damage class of adjacent building.

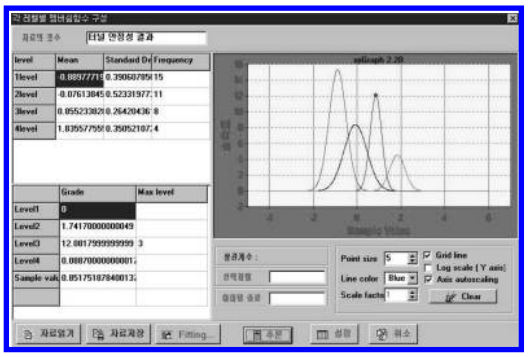


Figure 7. Safety evaluation of tunnel face.

causes were studied after many cases of tunnel failure were collected. The module was developed to predict the safety of tunnel and choose proper tunnel reinforcement system using fuzzy quantification theory and fuzzy inference rule based on tunnel information database. The system has two main parts. In first part, tunnel information input items are decided based on the tunnel face mapping information that can be easily obtained in-situ site. Tunnel information database consists of major face mapping items and tunnel safety effect factors such as adjacent building and overburden above tunnel, but in this system, only face mapping data expressed 4 levels was used. Main input data was made of uni-axial compressive strength, RQD, joint space, joint condition, joint direction and water inflow that are almost RMR classification factors. In second one, using fuzzy quantification theory II, fuzzy membership function is composed and tunnel safety level is inferred through this membership function. The comparison result between the predicted reinforcement system level and measured ones was very similar. In-situ data were obtained in three



Figure 8. The inference result of tunnel collapse type.

tunnel sites including subway tunnel under Han River. This system will be very helpful to make the most of in-situ data and suggest proper applicability of tunnel reinforcement system escaping from the dependence of some experienced experts for the absent of guide. The module is used with information of ground surface settlement together. And the D/B part is concluded in ITIS system. Figure 7 shows an example of the safety evaluation of tunnel face.

3.4 *Prediction module for potential tunnel face failure*

This module was built to predict the pattern and magnitude of tunnel collapses using Neural Network system. The module uses tunnel face mapping and other geological information that are stored in the D/B of ITIS. The inference-learning module uses the back-propagation algorithm that is based on the generalized delta rule by Rumelhart et al. (1986). It is the most popular learning procedure for multi-layer neural networks among more than 50 neural network models. Neural Network for the module is consisted of two main modules; inference module for tunnel collapse pattern and inference-learning module for tunnel collapse using the data obtained from 20 sites in Korea. Input data for predicting tunnel collapse pattern are 16 factors such as condition of shear zone, discontinuity conditions near by shear zone, geometry of joint with tunnel, water inflow, face condition, excavation method, the effect of configuration in earth, rock mass structure, rock mass classification, rock type, overburden, tunnel depth, tunnel geometry, RQD, joint condition and joint spacing. The system is proven to be capable of the estimation of tunnel collapse types and magnitudes effectively. However the effluent data of tunnel collapse should be accumulated in the system to infer the results with a reasonable accuracy. Figure 8 shows the inference result of tunnel collapse type and magnitude.

Copyright © 2005 Taylor & Francis Group plc, London, UK

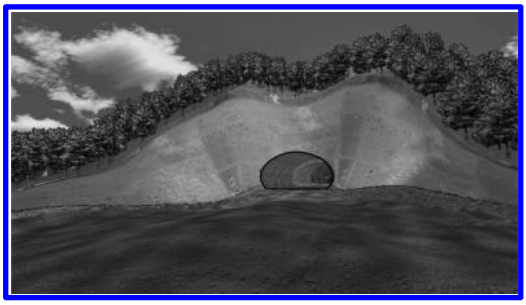


Figure 9. VR screen shots of the portal in tunnel.

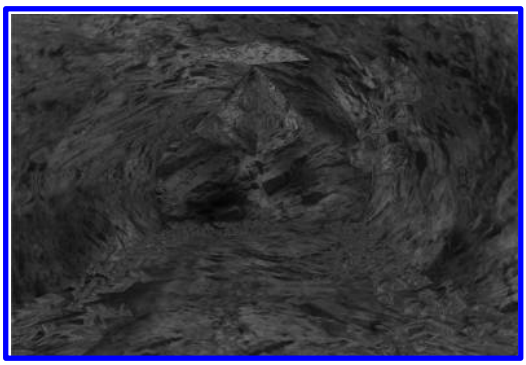


Figure 10. VR screen shots of wedge failure.

3.5 *VR for visualization of tunnel construction sequences*

VR technology is providing engineers and geologist with new and interactive ways to model the design and construction of tunnel. Virtual environment, in which the visualization of the design and construction progress is effected, shows to be ideal for simulating geological features, the predicted results for ground surface settlement and face failure. The system prototype has been tested on two tunnel construction sites. Figure 9 and Figure 10 shows examples of the prototype system's outputs. The system will be extended to the main tool for visualization and also linked up with the D/B and other modules in ITIS.

4 APPLICATION IN URBAN AND MOUNTAINOUS TUNNELS

4.1 *Urban tunnels in design stage*

In case of tunnel excavation in urban area it is most important to keep the stability of buildings near the construction site from ground settlement and blasting. Stability analysis can be carried out both in design and construction stage of tunnel excavation. Building damage assessment in design stage was conducted in

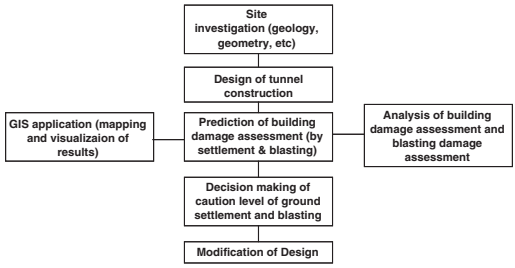


Figure 11. Analysis flow of building damage assessment of urban tunnel.

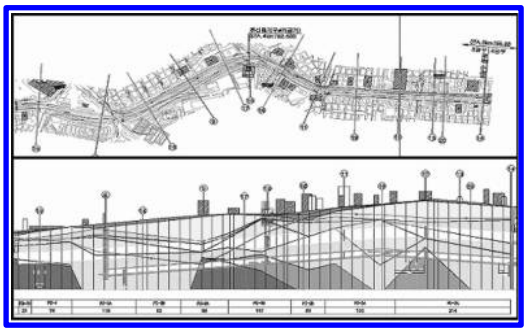


Figure 12. Design map and geological condition of Busan subway tunnel.

urban subway tunnel in Busan. Figure 11 shows the procedure of building damage assessment. There are 20 section to be examined and 36 buildings to be assessed in this tunnel. Figure 12 shows the design map and geological conditions of this area.

Overburden layers of the tunnels in most cases are composed of weathered rocks, residual soils and alluvial soils. Using predicted settlement traph, building damage assessment parameters such as angular distortion, deflection ratio, building maximum settlement were decided. Such parameters put into conventional building damage assessment criteria predicted the probability of building damage. Figure 13 shows the damage assessment result.

Blasting damage to the buildings were assessed from the peak particle velocity of blasting wave. In design stage, we don't have much information about the charateristics of blasting wave propagation because test blasting in urban area is not apt to be performed. Thus blasting vibration parametes (K, n) were obtained by prediction of artificial neural network(ANN) from various results of test blasting in other sites. The extent of blasting damage to buildings depends on the distance from the blasting source and the amount of expolsives with same delay time. ITIS automatically predicted the damage of buildings we wanted to know

Copyright © 2005 Taylor & Francis Group plc, London, UK

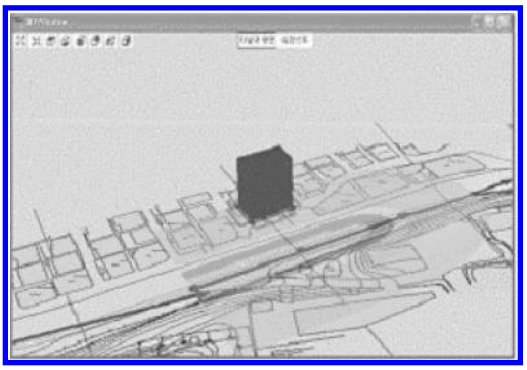


Figure 13. Building damage assessment result by the ground settlement.



Figure 14. Building damage assessment result by the blasting.

and the effective zone of blasting damage was contoured in the 2D and 3D GIS map (Figure 14).

4.2 *Mountainous tunnel under construction*

Neung-Dong tunnel and Moo-Geo express way tunnel are now under construction and with this system they have 3D visualized map of the geology and tunnel geometry and accumulate database of construction information such as tunnel face mapping results, special notes and pictures of construction and 3D monitoring data, all matters on the stability of rock bolts and shotcrete, and so on. Considering complex process of tunnel construction and engineers' unwillingness about adding burden to their current work, web-based application is devised and applied.

Tunnel face mapping can tell us a lot of inevitable clues about tunnel behaviour and stability. The ITIS system can accumulate the database on information of tunnel face mapping during tunnel construction and visualize it on GIS map. Figure 15 shows the sample data of tunnel face mapping database in Neung-Dong tunnel.



Figure 15. Tunnel face mapping sample of Neung-Dong tunnel.

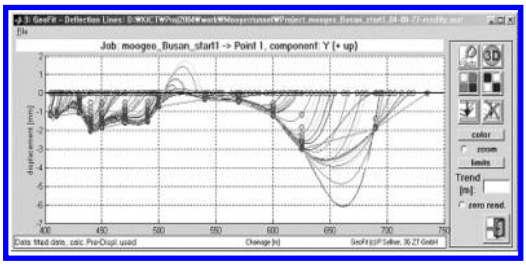


Figure 16. Displacement fitting result of Moo-Geo tunnel.

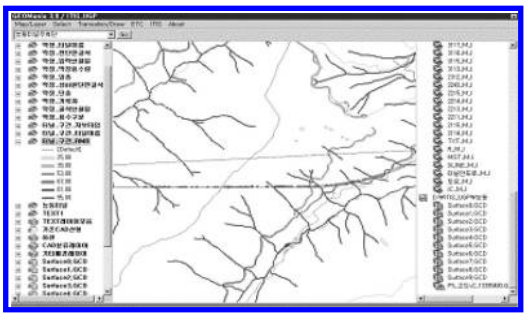


Figure 17. GIS visualization of various monitoring data.

During tunnel excavation a systematic monitoring is important for the determination of support type and quantity, as well as for controlling the tunnel stability. Geodetic methods of absolute displacement monitoring allow determining the spatial displacement vector of each measured point. And after the construction is finished, monitoring for maintenance and management of tunnel is planned to be performed. Special monitoring items are axial force of rock bolt, shotcrete stress, ground displacement and 3D absolute monitoring. Each item has its own database table and all items are connected with one another through the key field, excavation chainage.

Copyright © 2005 Taylor & Francis Group plc, London, UK

All the information from face mapping and monitoring can be visualized on GIS map. And some can be charted by real time analysis in the system.

5 CONCLUSIONS

The authors have developed Intelligent Tunnelling Information System (called ITIS) that is an integrated expert system including visualization, evaluation and prediction technology of tunnel survey, design, construction and reinforcement system based on D/B, Artificial Intelligence, 3-D visualization and Virtual Reality technologies. And the system has been applying to tunnels in design stage and under construction. ITIS is powerful management system for tunnelling and its use in Korea is steadily increasing. ITIS will be modified and developed to have the functions to establish international on-line database system which makes tunnel engineers share their construction information in real time.

ACKNOWLEDGEMENT

This research has been performed as a part of National Research Laboratory project provided by KMOST (Korea Ministry of Science & Technology). The authors greatly appreciate their financial support.

REFERENCES

Hong, S.W., Bae, G.J., Seo, Y.S., Kim, C.Y., Lee, S.W. & Lee, K.H. 2001a. The development of geotechnical interpretation system for tunnelling. *AITES-ITA 2001*. 715–721.

Hong, S.W., Bae, G.J., Seo, Y.S., Kim, C.Y., Lee, S.W. & Lee, K.H. 2001b. 3-D simulation analysis for visualizing geotechnical site investigation. *Proc. 15th Int. Conf. Soil Mech. and Geotech. Engng*. Istanbul. 27–31. Aug. 2001.

Kim, C.Y., Bae, G.J., Hong, S.W., Park, C.H., Moon, H.K. & Shin, H.S. 2001a. Neural network based prediction of ground surface settlements due to tunneling. *Computers and Geotechnics*. 28. 517–547.

Kim, C.Y., Park, C.H., Bae, G.J., Hong, S.W. & Oh, M.Y. 2001b. Countermeasure Expert System for Tunnelling Failure. *AITES-ITA 2001*. 409–416.

Copyright © 2005 Taylor & Francis Group plc, London, UK

A new approach to estimate plastic region near tunnel considering excavation induced damage and in situ rock mass condition

Myung Sagong, Jun S. Lee
Korea Railroad Research Institute, Kyunggi, Korea

ABSTRACT: An approach for the estimation of the radius of plastic region and the stress distribution in elastic and plastic regions near tunnel is proposed. Together with elasticity of cylindrical opening and Hoek-Brown 2002 criterion, the radius of plastic zone and stress distribution around a tunnel can be estimated. In addition, the use of Hoek-Brown 2002 criterion provides the application of the damage induced during construction and the characteristics of in situ rock mass condition. The results from the proposition show increase of the radius of plastic zone and decrease of the peak tangential stress as rock quality becomes poor.

1 INTRODUCTION

Tunnelling in the underground produces open space larger than the final shape of a tunnel. Construction of the open space turns continuous condition of in situ rock masses into discontinuous state with respect to stress and flow. Due to the constructed open space, in situ stress will rotate along the perimeter of the tunnel and the rotated stress will concentrate near the crown or springline of the tunnel depending on the anisotropy of the in situ. This concentration of the stress will damage in situ rock mass in the form of the initiation and propagation of cracks, thus increased density and length of cracks near tunnel can be found (Cai et al. (2001)). In this paper, we will define this type of damage as structural damage.

Not only the structural damage but also the constructional damage produced during mechanical excavation and blasting on the rock masses can be developed during tunnelling. Pusch and Stanfors (1992) carried out three different types of blasting, normal careful and very careful, on the Äspö tunnel located at a depth of 50 m from the ground and subjected to 10, 7, and 1.5 MPa of major, intermediate and minor principal stresses to investigate blasting induced damage near the tunnel. The degree of damage (disturbance) is evaluated by geological fracture characterization, logging, acoustic emission, vibration measurements and hydraulic testing in boreholes. The observed ranges of the generation of new fractures are 1.5–2.1 m for normal blasting, 1.0–1.7 m for careful blasting and 0.6–1.4 m for very careful blasting. The test results support that the blasting induced damage on the rock mass is not negligible. In consequence, the estimation of the plastic region near rock tunnel must consider not only the structural damage induced by arching and stress concentration but also the constructional damage during excavation. In this study, we like to present an approach to calculate the stress state in plastic and elastic regions and the radius of plastic zone near tunnel by considering structural and constructional damages.

Estimation of plastic region near rock tunnel requires the use of proper yield criterion applicable to the material. In this paper, we adopt the Hoek and Brown criterion for the yield criterion and assume that the rock mass in the plastic zone exhibits a perfectly plastic behavior. Hoek and Brown criterion have been popularly adopted for the yield criterion (Brown et al. (1993), Wang (1996), Pan and Brown (1996), and Carranza-Torres and Fairhurst (1999)). With the refinement of the Hoek and Brown criterion new approaches to estimate the plastic zone near tunnel were proposed. For example, the proposition of Brown et al. (1983) is based upon 1980 version of Hoek-Brown criterion and Carranza-Torres and Fairhurst (1999), 1997 version of Hoek-Brown criterion which increases its applicability by introducing the Geological Strength Index (GSI). In this study we will introduce 2002 edition of Hoek-Brown criterion which incorporates damage factor "D" representing the degree of damage induced during construction.

Copyright © 2005 Taylor & Francis Group plc, London, UK

2 ANALYTICAL SOLUTION FOR THE ELASTIC AND PLASTIC REGIONS NEAR A TUNNEL IN ROCK MASS

2.1 *Hoek-Brown criterion 2002*

The suggested 2002 edition of Hoek-Brown criterion (Hoek et al. 2002) is as follows:

$$\sigma_1 = \sigma_3 + \sigma_{ci}(m_b \frac{\sigma_3}{\sigma_{ci}} + s)^a \quad (1)$$

where, σ_1 and σ_3 are major and minor principal stresses at the failure of rock masses containing discontinuities; σ_{ci}, the uniaxial compressive strength of the intact rock core; m_b, Hoek-Brown constant in consideration of rock type (m_i) and Geological Strength Index (GSI) $m_b = m_i \exp((GSI - 100)/(28 - 14D))$; D, a factor considering damage produced by blasting and stress relaxation in rock masses, which varies from 0 to 1 (see Table 1 for details); s and a, Hoek-Brown constants which are functions of GIS and D.

$$s = \exp(\frac{(GSI-100)}{(9-3D)}),$$
$$a = \frac{1}{2} + \frac{1}{6}(e^{(-GSI/15)} - e^{(-20/3)})$$

Introduction of D factor and calculation of Hoek-Brown constants s and a are the major difference between Hoek-Brown$_{1997}$ (lower case represents the edition of the criterion) and Hoek-Brown$_{2002}$. Hoek-Brown$_{2002}$ adopts smooth continuous transitions of s and a for the entire GSI range which, in contrast, are discontinuous functions when GSI is 25 in Hoek-Brown$_{1997}$.

Table 1. Details on the damage factor D (Hoek et al. 2002).

Description on the rock mass	Suggested value of D
Excellent quality blasting or excavation results in minimal disturbance to surround rock mass	0
Mechanical or hand excavation results in minimal disturbance to the surrounding rock	
Squeezing results in significant floor heave	0.5
Very poor quality blasting in a hard rock results in severe local damage	0.8
Small scale blasting in civil engineering slope results in modest rock mass damage	0.7 (Good blasting) 1.0 (Poor blasting)
Very large open pit mine slopes suffering significant disturbance	1.0 (Production blasting)
Soft rock damaged during ripping and dozing	0.7 (mechanical excavation)

For the calculation of the radius of elastic and plastic regions near tunnel the following conditions are assumed in this study:

1) Tunnel shape is circular and the applied load is axi-symmetric
2) Hydrostatic and plane strain conditions are assumed
3) The assumed shape of plastic boundary is in circular
4) Rock masses near tunnel show elastic-perfectly plastic behavior

Based upon the above assumptions the derivation of the analytical solutions is shown in the next section.

2.2 *Calculation of the stress in the plastic region (0 < r < b)*

The equilibrium of polar coordinate system shown in Figure 1 can be represented as follows:

$$\frac{d\sigma_r^p}{dr} + \frac{\sigma_r^p - \sigma_\theta^p}{r} = 0 \quad (2)$$

where, σ_r^p and σ_θ^p are radial and tangential stresses in the plastic zone. Since the shear stress at the hydrostatic condition equals to zero, the radial and tangential stresses are major and minor principal stresses; $\sigma_r^p = \sigma_1$, $\sigma_\theta^p = \sigma_3$. Substitution of these into equation (1) changes the equation with radial and tangential stress terms which are applicable to equation (2).

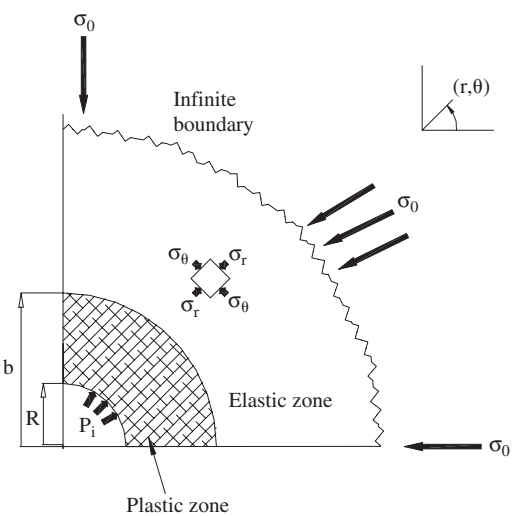


Figure 1. Elastic and plastic zones near a tunnel.

Copyright © 2005 Taylor & Francis Group plc, London, UK

Substitution of the radial stress term into equation (2) turns into as follows:

$$\frac{d\sigma_r^p}{dr} = -\frac{\sigma_{ci}\left(m_b\frac{\sigma_r^p}{\sigma_{ci}}+s\right)^a}{r} \tag{3}$$

The solution of equation (3) is

$$\frac{1}{1-a}\left(m_b\frac{\sigma_r}{\sigma_{ci}}+s\right)^{1-a} = m_b \ln r + C \tag{4}$$

Application of the boundary condition that the internal pressure at the perimeter of the tunnel (r = R) is P_i produces the following equations:

$$\sigma_r^p = \frac{\sigma_{ci}}{m_b}\left\{\left[\left(m_b\frac{P_i}{\sigma_{ci}}+s\right)^{1-a} + m_b(1-a)\ln\left(\frac{r}{R}\right)\right]^{\frac{1}{1-a}} - s\right\} \tag{5}$$

$$\sigma_\theta^p = \sigma_{ci}\left[\left(m_b\frac{P_i}{\sigma_{ci}}+s\right)^{1-a} + m_b(1-a)\ln\left(\frac{r}{R}\right)\right]^{\frac{1}{1-a}} \times \left\{\frac{1}{m_b} + \left[\left(m_b\frac{P_i}{\sigma_{ci}}+s\right)^{1-a} + m_b(1-a)\ln\left(\frac{r}{R}\right)\right]^{-1}\right\} - \frac{s\sigma_{ci}}{m_b} \tag{6}$$

Finally equations (5) and (6) represent the radial and tangential stresses in the plastic region.

2.3 *Calculation of the stress in the elastic region ($b < r < \infty$)*

When an opening exists at an infinite media, the solutions representing stress distribution in a hollow cylindrical opening subjected to uniform internal and external stresses are

$$\sigma_r^e = X + \frac{Y}{r^2} \tag{7}$$

$$\sigma_\theta^e = X - \frac{Y}{r^2} \tag{8}$$

where, X and Y are variables. Application of the boundary condition that the radial stress at the infinite boundary is equal to the far field stress ($r = \infty$, $\sigma_r^e = \sigma_0$) produces that $X = \sigma_0$. In addition, application of the boundary condition that the equality of radial and tangential stresses at the interface of elastic and plastic regions to equations (7) and (8) (at r = b, $\sigma_r^e = \sigma_r^p$, $\sigma_\theta^e = \sigma_\theta^p$) produces the following equations:

$$\sigma_0 + \frac{Y}{b^2} = \frac{\sigma_{ci}}{m_b}\left\{\left[\left(m_b\frac{P_i}{\sigma_{ci}}+s\right)^{1-a} + m_b(1-a)\ln\left(\frac{b}{R}\right)\right]^{\frac{1}{1-a}} - s\right\} \tag{9}$$

$$\sigma_0 - \frac{Y}{b^2} = \sigma_{ci}\left[\left(m_b\frac{P_i}{\sigma_{ci}}+s\right)^{1-a} + m_b(1-a)\ln\left(\frac{b}{R}\right)\right]^{\frac{1}{1-a}} \times \left\{\frac{1}{m_b} + \left[\left(m_b\frac{P_i}{\sigma_{ci}}+s\right)^{1-a} + m_b(1-a)\ln\left(\frac{b}{R}\right)\right]^{-1}\right\} - \frac{s\sigma_{ci}}{m_b} \tag{10}$$

When the variables X and Y are solved from equations (9) and (10), the following equations describing stress distribution in the elastic region are obtained:

$$\sigma_r^e = \sigma_0 - \frac{\sigma_{ci}}{2}\left[\left(m_b\frac{P_i}{\sigma_{ci}}+s\right)^{1-a} + m_b(1-a)\ln\left(\frac{b}{R}\right)\right]^{\frac{a}{1-a}}\left(\frac{b}{r}\right)^2 \tag{11}$$

$$\sigma_\theta^e = \sigma_0 + \frac{\sigma_{ci}}{2}\left[\left(m_b\frac{P_i}{\sigma_{ci}}+s\right)^{1-a} + m_b(1-a)\ln\left(\frac{b}{R}\right)\right]^{\frac{a}{1-a}}\left(\frac{b}{r}\right)^2 \tag{12}$$

In consequence, stress distribution in elastic and plastic regions near a tunnel can be obtained from equations (5), (6), (11), and (12). However, for the determination of elastic stress, the radius of plastic region must be calculated in advance. Since the radius of plastic region, b, can not be calculated in a closed form equation, the radius can be obtained from the iterative calculation of equations (5) and (11). The radius of plastic zone is determined when the difference between elastic and plastic radial stresses at the interface of elastic and plastic regions is within 0.01%.

3 VERIFICATION OF THE METHOD

3.1 *Stress distribution near tunnel*

Stress distribution in the elastic and plastic regions can be determined by using equations (5), (6), (11) and (12). Figure 2 shows stress distribution around the tunnel with radius of 5 m, subjected to 2 MPa of

Copyright © 2005 Taylor & Francis Group plc, London, UK

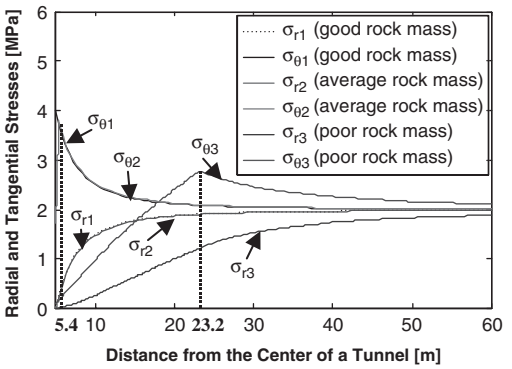


Figure 2. Stress distribution around a tunnel constructed in good, average, and poor qualities rock mass.

Table 2. Engineering properties of the rock mass (Hoek, 1998).

Rock mass quality	GSI	σ_{ci} (MPa)	m_i	D	R (m)	σ_0 (MPa)	b (m)
Good	75	150	25				0
Average	50	80	12	0.8	5	2	0.4
Poor	30	20	8				18.2

confining stress and constructed by poorly controlled blasting (D = 0.8). Furthermore, Figure 2 displays the stress distribution near tunnel for three different rock quality conditions: good, average, and poor. The engineering properties of three different rock mass qualities are shown in Table 2.

In Figure 2 when the rock masses are good and average, no apparent difference between the two cases on the stress distribution is observed. The observed plastic zone radii are 0 and 0.4 m for both conditions. Thus, in Figure 2 tangential stress for average rock mass is discontinuous at 5.4 m from the center of the tunnel. Since no plastic region is observed for good rock mass condition, stress developed near the tunnel is in elastic state. However, with poor rock mass quality, the observed plastic range is extended up to 23.2 m from the center of the tunnel. The characteristics of the stress curves are as follows: the peak tangential stress decreases with rock quality and the convergence of radial stress to the far field stress requires longer distance as rock quality becomes worse.

3.2 *Comparison with previous results*

Verification of the proposed method is carried out in comparison with previously proposed approach by Carranza-Torres and Fairhurst (1999). They provided

Table 3. Engineering properties used for the comparison between Carranza-Torres and Fairhurst (1999) and current study.

	σ_{ci} (MPa)	P_i (MPa)	GSI	m_i	R (m)	σ_0 (MPa)	b (m)
C&F	30	5	50	10	5	30	8.2
S&L							8.18

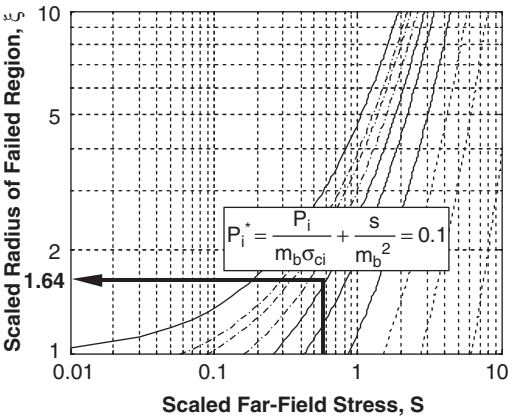


Figure 3. Graphical procedure to obtain the dimensionless parameter ξ (Reproduced from Carranza-Torres and Fairhurst (1990)).

closed-form equations for the radius of plastic zone and related stress and displacement by using Hoek-Brown$_{1997}$. They also used Londe (1988)'s rescaled Hoek-Brown criterion to provide a general applicability to the solution. In their approach the radius of plastic region is multiplication of the dimensionless parameter and the radius of tunnel.

The same rock mass and loading conditions are applied to the procedures of Carranza-Torres and Fairhurst (1999) and this study. The used input values are summarized in Table 3.

The applied uniaxial compressive strength of rock mass is 30 MPa; internal pressure 5 MPa; GSI 50; m_i 10; radius of the tunnel 5 m; and far field stress σ_0 30 MPa. In Table 3 C&F represents the results from Carranza-Torres and Fairhurst (1999) and S&L from current study. Table 3 shows that the radius (b) of plastic region calculated from Carranza-Torres and Fairhurst (1999) and this study are quite similar. The calculated dimensionless parameter ξ is 1.64 from Carranza-Torres and Fairhurst (1999) (see Figure 3). Therefore, the radius of plastic region, which is the multiplication of the dimensionless parameter and the radius of tunnel, is 8.2 m.

Copyright © 2005 Taylor & Francis Group plc, London, UK

4 PARAMETRIC STUDY

The use of equations (5), (6), (11), and (12) requires input parameters such as uniaxial compressive strength of intact rock, GSI, damage factor. In this section, relative importance of the uncertainty associated with these parameters is evaluated. From the parametric study sensitivity of each parameter is investigated.

Figure 4 shows the influence of damage factor on the radius of plastic zone near a tunnel.

As can be seen from the figure, increase of damage factor extends the radius of plastic region. In this case solely by structural damage the radius of plastic zone extends to 8.2 m. Therefore, the damaged zone of the tunnel reaches 3.2 m from the perimeter of the tunnel. Increase of damage factor "D" enlarges the plastic zone. When the damage factor is about 1, the size of plastic zone does significantly increases compared to that of structurally damaged case; when damage factor is zero.

Figure 5 shows the variation of the size of the plastic zone with damage factor and uniaxial compressive strength of intact rock. For average rock quality, GSI = 50, m_i = 10, the assumed range of uniaxial compressive strength of intact rock is from 50 MPa to 120 MPa. In this range the maximum size of plastic zone, 1.8 m, occurs when the damage factor is 1. However, with increase of uniaxial compressive strength the plastic zone decreases to 0.3 m. Increase of compressive strength decreases the radius of plastic region to 1.5 m. This represents that for average rock mass condition, the adopted constructional method is more influential than the strength of the in situ rock mass on the generation of plastic zone.

Figure 6 represents the influence of geological strength on the size of plastic zone when the damage factor is 0.8. Poor quality rock mass shows the largest size of plastic region, as expected. A comparison between Figures 5 and 6 shows that GSI is more influential on the generation of plastic zone than the damage factor. In consequence, GSI is the most sensitive parameter than the compressive strength of rock mass and construction method on the generation of plastic zone.

Figure 7 shows linear correlation between the radius of tunnel and radius of plastic zone. Similar linear correlation on the size effect between the radius of tunnel and plastic zone can be found from Carranza-Torres and Fairhurst (1999), because the radius of plastic zone is a linear function of the dimensionless parameter and tunnel radius. As indicated by Hoek and Brown (1980), the stability of a tunnel relates with the stability of rock blocks near tunnel. Therefore, even though the Kirsh's elastic solution does not include the size term of a tunnel, the stability of tunnel is affected by the size of tunnel. Since

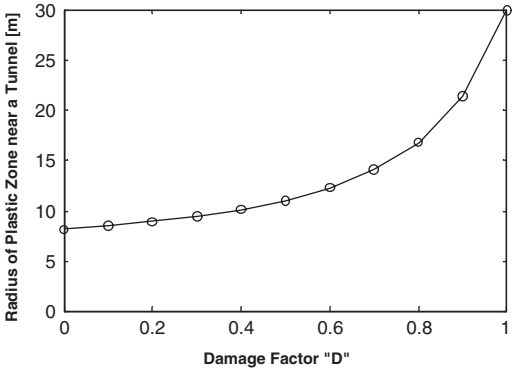


Figure 4. Influence of damage factor on the radius of plastic zone under following condition: R = 5 m, m_i = 10, σ_{ci} = 30 MPa, P_i = 5 MPa, σ_0 = 30 MPa, GSI = 50.

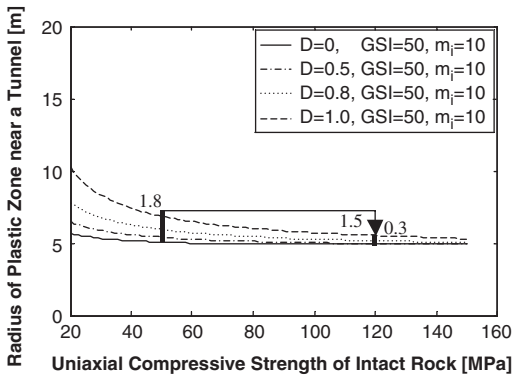


Figure 5. Radius of plastic zone with variation of uniaxial compressive of intact rock and damage factor.

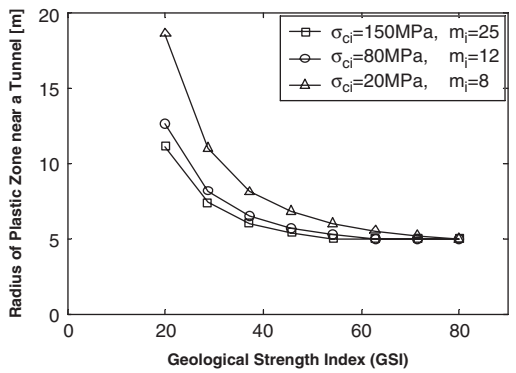


Figure 6. Radius of plastic zone with variation of Geological Strength Index (GSI).

Copyright © 2005 Taylor & Francis Group plc, London, UK

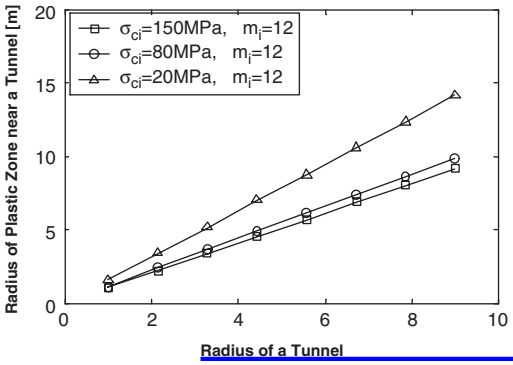


Figure 7. The size of plastic zone with different radius of a tunnel.

Figure 7 shows that the radius plastic zone increases with radius of tunnel, increased amount of reinforcement such as rock bolts and shotcrete will be required.

5 CONCLUSIONS

In this study an approach to calculate the radius of plastic region and the stress distribution in elastic and plastic zones near a circular tunnel is proposed. The proposed approach adopts Hoek-Brown$_{2002}$ criterion for yield criterion thus it can consider geological features of rock masses, rock types, compressive strength of rock mass as well as the degree of damage induced during construction. For the derivation of the equations circular tunnel subjected to the hydrostatic stress condition in a homogeneous and isotropic ground is assumed.

The proposed method is verified from the comparison with the result from Carranza-Torres and Fairhurst (1999). With the proposed equations, the calculated radius of plastic zone increases as rock mass quality becomes worse. In addition, the peaks of tangential stress decrease with rock quality.

The parametric study shows that Geological Strength Index is more influential than the uniaxial compressive strength of intact rock and damage factor on the determination of the size of plastic region. In addition, the size of the plastic region is in proportional with the tunnel radius.

REFERENCES

Brown, E.T., Bray, J.W. & Landanyi, B. 1983. Ground Response Curves for Rock Tunnels, *Journal of Geotechnical Engineering*, 109(1): 15–39.

Cai, M., Kaiser, P.K. & Martin, C.D. 2001. Quantification of rock mass damage in underground excavations from microseismic event monitoring *International Journal of Rock Mechanics and Mining Science* 38: 1135–1145.

Carranza-Torres, C. & Fairhurst, C. 1999. The elasto-plastic response of underground excavations in rock masses that satisfy the Hoek-Brown failure criterion, *International Journal of Rock Mechanics and Mining Sciences*, 36: 777–809.

Hoek, E. 1998. Rock engineering course note by Evert Hoek, *http://www.rocscience.com/hoek/PracticalRockEngineering.asp*, retrieved on Oct. 5, 2004.

Hoek, E., Carranza-Torres, C. & Corkum B. 2002. Hoek-Brown failure criterion-2002 edition. *5th North American Rock Mechanics Symposium and 17th Tunneling Association of Canada Conference: NARMS-TAC*: 267–271.

Londe, P. 1988. Discussion on the Determination of the Shear Stress Failure in Rock Masses, *Journal of Geotechnical Engineering*, 114(3): 374–376.

Pan, X.–D. & Brown, E.T. 1996. Influence of Axial Stress and Dilatancy on Rock Tunnel Stability, *Journal Geotechnical Engineering*, 122(2): 139–148.

Pusch, R. & Stanfors, R. 1992. The zone of disturbed around blasted tunnels at depth, *International Journal of Rock Mechanics and Mining Science & Geomechanics Abstract*, 29(5): 447–456.

Wang, Y. 1996. Ground Response of Circular Tunnel in Poorly Consolidated Rock, *Journal of Geotechnical Engineering*, 122(9): 703–708.

Copyright © 2005 Taylor & Francis Group plc, London, UK

The influence of the round length on the stability of tunnel face and unsupported span

Young-Zoo, Lee & Wulf Schubert
Institute for Rock Mechanics and Tunneling, Graz University of Technology, Graz, Austria

Chang-Yong, Kim
Korean Institute of Construction Technology, Koyang, Kyunggi-do, Korea

ABSTRACT: A number of research projects on the face stability of tunnels have been carried out in the past. However, the influence of the round length has not been thoroughly investigated, although it is an essential factor for the stability and excavation costs. This paper presents typical failure mechanisms of the face including the unsupported span in relation to the round length in weak rock tunnels, whose behavior is not governed by discontinuities. A series of small-scale model tests and numerical analyses by PFC-2D (Particle Flow Code, Itasca) were carried out to define failure modes at the face and unsupported span. Five failure modes according to its shape and extent are suggested for excavation planning. The influence of the lining stiffness and overburden on the overbreak and round length has been investigated in the model tests. Failure mechanisms, their initiation and propagation have been also investigated by PFC analyses and compared to the results of the model tests. Overbreak in the unsupported span does not affect the face stability as long as the face is initially stable and the round length is small enough not to cause excessive overbreak or daylight collapse. Therefore, the decision on the round length should be made in consideration of the interaction of overbreak and support rather than the face stability itself.

1 INTRODUCTION

Conventional excavation for tunnels requires the determination of each round length in consideration of the ground condition, support capacity, construction cost and time, etc. (Baudendistel 1997). Presently most of the decisions in the design and construction stage are based on personal experience. Although the round length has a considerable influence on the stability of excavation and construction cost, most of research has focused on the stability of face itself and the influence of round length has not been thoroughly investigated.

In this paper, failure mechanisms at the face and unsupported span are investigated by small-scale model tests and numerical analyses using Particle Flow Code (PFC 2D, Itasca, USA). Weak rock or rock-like soil, whose behavior is not governed by discontinuities such as joint, bedding or foliation are considered in this study. Therefore, overbreak mainly results from stress-related failure, not from the geometry of discontinuities or blasting damage. Regarding the depth of tunnel, overbreak is more dominant in low or medium stress environments than associated with squeezing or rock burst. Therefore, this paper focuses on shallow and medium depth tunnels.

1.1 *Terminology*

To avoid confusion of, 'Round length' is defined as the length of unsupported span which is excavated at once before support is installed. 'Unsupported span' is composed of crown, shoulder and sidewalls, and 'face' is a vertical plane perpendicular to the tunnel axis. 'Overbreak' has a limited volume in underground and 'collapse' means overbreak reaching the ground surface (so-called 'Daylight collapse').

2 SMALL-SCALE MODEL TESTS

2.1 *Modeling in small scale*

Small-scale model tests were carried out to simulate the overbreak and collapse as round length is increased. The overbreak shape and its propagation were observed

Copyright © 2005 Taylor & Francis Group plc, London, UK

and recorded by digital video camera at each round. The influence of overburden and lining stiffness on the failure mechanism was also investigated in model tests. The scale for these models is 1:40 and various cases were simulated. Sand material used for tests is classified in SW (well-graded sand) according to Unified Soil Classification System (ASTM D2487-83).

– $D_{max} = 2.0\,mm$, $D_{10} = 0.2\,mm$
– $Cu = D_{60}/D_{10} = 7.5$
– $Cc = D_{30}^2/(D_{60}–D_{10}) = 1.63$

Water content is 1.6~2.0% and apparent cohesion can be calculated as below (Terzaghi 1954).

$$C_{apparent} = \frac{H \cdot \gamma}{4\sqrt{K_p}} = 1.5\ \text{kPa} \quad (1)$$

where $H = 0.2\,m$ = height; γ = unit weight; K_p = passive earth pressure coefficient using friction angle $\varphi = 32°$.

The primary lining is made of vinyl sheet and small steel wires for the flexible lining, while for stiff linings a 2 mm thick plastic plate is used. Tunnel diameter is 10 m and rock bolts are not modeled. After the excavation of each '1 m' round, the behavior was observed for at least 15 minutes before continuing with excavation. Once first overbreaks occurred, the round length was reduced to '0.5 m'.

2.2 *Results of model tests*

The results of model tests are summarized in Table 1. 'Stable round length' is a round length without overbreak and 'collapse round length' is round length causing daylight collapse. 'Maximum round length' is the maximum length with overbreak before daylight collapse.

Most of overbreaks are cone-shape and extended to the ground surface at the collapse round length, forming a so-called 'chimney-shape collapse', forming a crater at the surface. In all cases, the face was stable before daylight collapse occurred. It showed that excessive overbreak or collapse can affect the face stability, but the round length is not key factor for the face stability (Figs 1–4).

2.2.1 *Influence of overburden*

The model test showed that with increasing overburden also the stable round length increases. In addition, the collapse at low overburden occurs more abruptly, due to the low confining pressure.

2.2.2 *Influence of lining stiffness*

Larger round lengths are possible with stiff linings than with flexible linings. Considering stable round length, both cases do not show significant difference, however maximum and collapse round length are different. It means that the first overbreak mainly depends on the ground strength but its propagation and collapse can be affected by the lining stiffness.

The test results suggest that the initial strength and stiffness of shotcrete linings are very important factors controlling the overbreak and thus should influence the decision of round length.

Table 1. Results of small-scale model tests.

Cases	Stiff lining		Flexible lining	
overburden	1D	2D	1D	2D
Stable R/L	1.0	2.0	1.0	2.0
Max. R/L	3.5	4.5	3.0	3.5
Collapse R/L	4.0	5.0	3.5	4.0

*R/L = round length in meter; D = tunnel diameter; 1D and 2D are overburden.

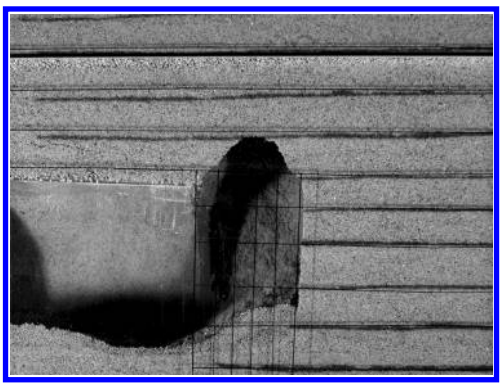


Figure 1. Typical overbreak at unsupported span in model test.

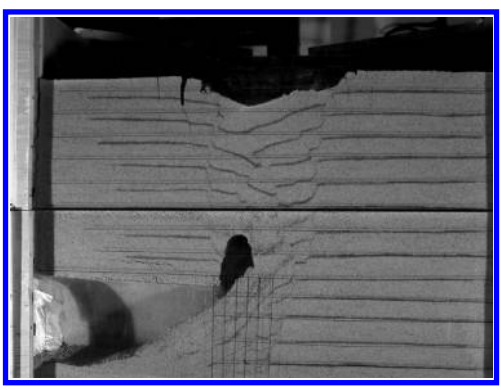


Figure 2. Daylight collapse in stiff lining case with 2D overburden in model test.

Copyright © 2005 Taylor & Francis Group plc, London, UK

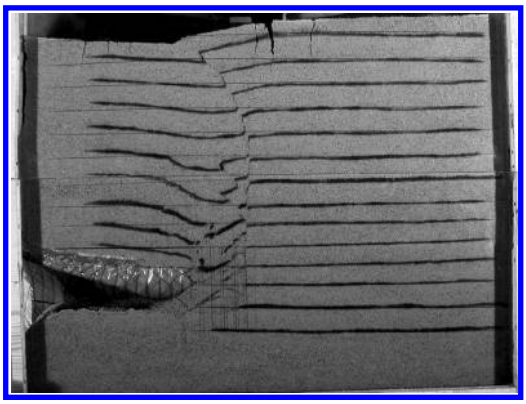


Figure 3. Daylight collapse in flexible lining case with 2D overburden in model test.

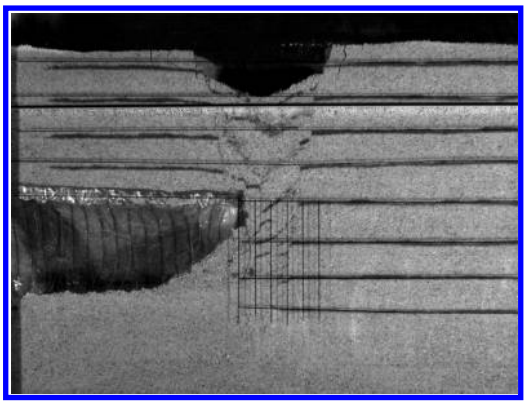


Figure 4. Daylight collapse in flexible lining case with 1D overburden in model test.

2.2.3 *Relationship of overburden and lining stiffness*

While with an overburden of 1D and a flexible lining a distinct chimney develops and the lining damage is minor, in the case with an overburden of 2D the lining suffers heavy damage, causing also a longer crater at the surface (Figs 2–4).

This means that in case of collapse with an overburden of 2D the load on the lining is considerably higher. For the safety of laborers, high stiffness and strength of lining is necessary to minimize the consequences of a chimney type failure in the unsupported span.

3 NUMERICAL ANALYSES USING PARTICLE FLOW CODE (PFC)

To investigate the failure mechanism and the propagation of failure, as well as the stress distribution during overbreak and collapse a particle flow code (PFC, Itasca, USA) was used. Although the problem is clearly 3-dimensional, characteristic phenomena can be shown also in the 2-dimensional model.

The contact force plots show clearly the stress flow and the formation of arching stress. Analyses were performed as well longitudinally, as also in cross sections. The bond strengths between the particles were varied, while the friction angle was kept constant. The reason for this procedure is that cohesion is more important for the stability of face and unsupported span in shallow or medium depth tunnel than the friction angle.

3.1 *Longitudinal section analysis*

This analysis can show the development and changes of arching stress around the face during the occurrence of overbreak and collapse. The lining is modeled by a 'wall' element, therefore the lining is assumed to be a rigid boundary, similar to the 'stiff lining' in the model tests.

The first step is to simulate the failure mechanism without excavation as bond strength is gradually increased from zero. The properties and analysis conditions are as below;

- Tunnel diameter(D) = 10 m
- Overburden (H) = 20 m (2D)
- Ball size = 25.4∼38.1 cm
- Normal stiffness (Kn) = 1e8 N/m
- Shear stiffness (Ks) = 1e8 N/m
- Friction angle (f) = 30°
- Normal bond (Sn) = 0, 84000, 85000 N
- Shear bond (Sb) = 0, 84000, 85000 N

If ground is cohesionless (zero bond strength), the face starts to ravel, resulting in a daylight collapse. However, a limited volume of overbreak occurs at the face, if ground is a little cohesive as shown in Figure 5 and other small-scale model tests (Vavrovsky 1987). With sufficient cohesion the face is stable and the excavation can be commenced (85000 N bond strength).

In a next step the failure mechanism is investigated as round length is increased, beginning with the stable face without unsupported span (85000 N bond strength). Excavation is carried out at '1 m' steps until the collapse occurs.

At '4 m' round length, the first overbreak occurs in the unsupported span, while the face is still stable (Figs 6–7). Although the ground at the face is loosened, it does not ravel and overbreak always occurs at the unsupported span. The same behavior was observed in the model tests.

At 5 m round length, the overbreak extends to the surface and a daylight collapse develops. In the beginning an overbreak occurs in the unsupported span, followed by the development of a natural ground arch.

Copyright © 2005 Taylor & Francis Group plc, London, UK

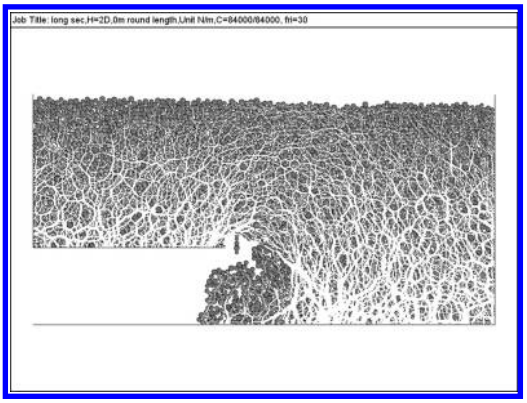


Figure 5. Longitudinal section of PFC analysis showing overbreak at the face before excavation with contact force chains (bond strength is 84000 N).

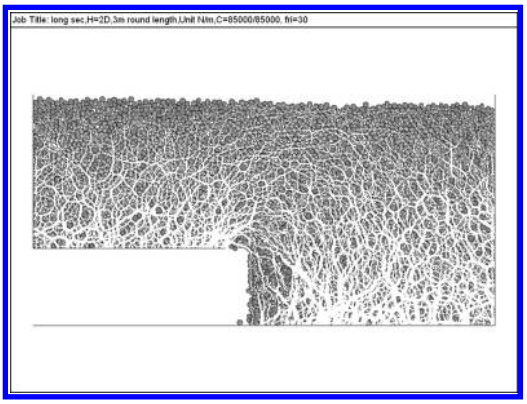


Figure 6. Longitudinal section of PFC analysis showing no overbreak with stable face after 3 m excavation.

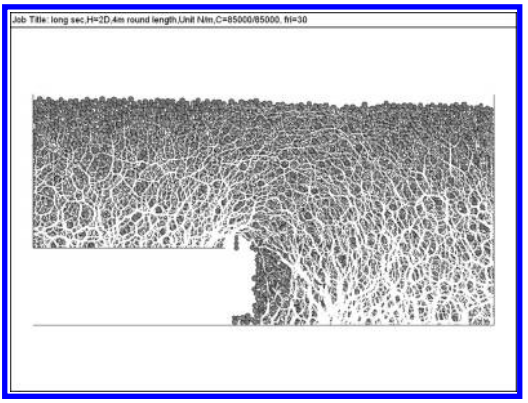


Figure 7. Longitudinal section of PFC analysis showing overbreak in the unsupported span after 4 m excavation.

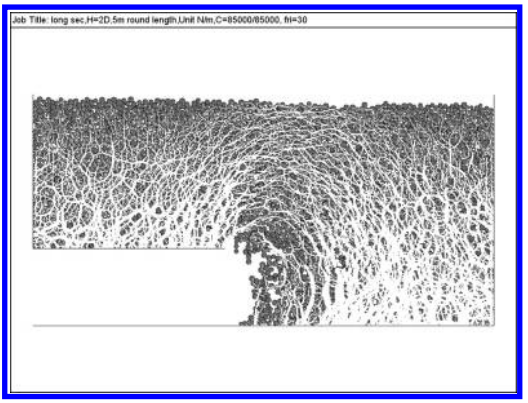


Figure 8. Longitudinal section of PFC analysis showing overbreak propagation after 5 m excavation.

Eventually also the arch fails and partially the face. As overbreak progresses, the arching stress decreases (Figs 8–9).

Concerning the stress on the lining, it has been reported by many researchers that the larger the round length, the higher the lining stresses are (Chang 1994). However, it was found in model tests and PFC analysis that lower stresses act on the lining near to the face at the moment of overbreak because of the arching effect above the overbreak (Fig. 7). Afterwards, higher stress acts on the lining at the moment of collapse, as shown in the model tests and PFC analyses, because arching stress is disturbed and ground load acts as a dead load (Fig. 8).

3.2 *Cross section analysis*

It is reported that most of overbreak is triggered at the shoulder of the unsupported span and extends to the crown (Shin & Lee 2001). This phenomenon could also be observed in the small-scale model tests. Very rarely the overbreak begins at the sidewalls. Basically, it is the same reason why overbreak always occurs at the unsupported span rather than at the face, even if stress concentration is higher at the face.

Overstressing induces the loosening of the ground at the sidewall, before overbreak occurs at the shoulder. However, the material at the sidewalls keeps in place because of kinematical conditions and this loosening triggers a change of the arching stresses (Fig. 10). This change results in stress relief at the shoulder, which triggers the overbreak. Afterwards, the overbreak changes the arching stress again and it triggers stress relief again at the crown (Fig. 11). In this way, overbreak occurs at the shoulder and propagates to the crown. If ground is weak enough or confining pressure is low, overbreak extends to the surface and results in a daylight collapse (Fig. 12).

Copyright © 2005 Taylor & Francis Group plc, London, UK

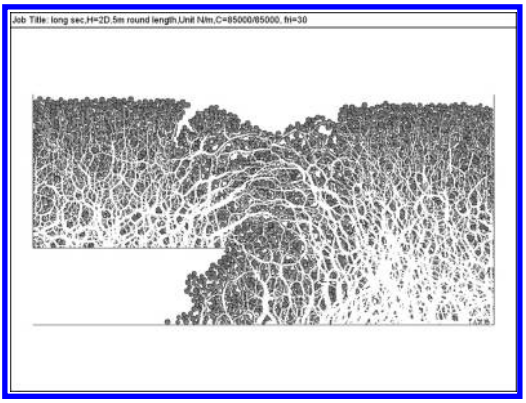


Figure 9. Longitudinal section of PFC analysis showing daylight collapse after 5 m excavation.

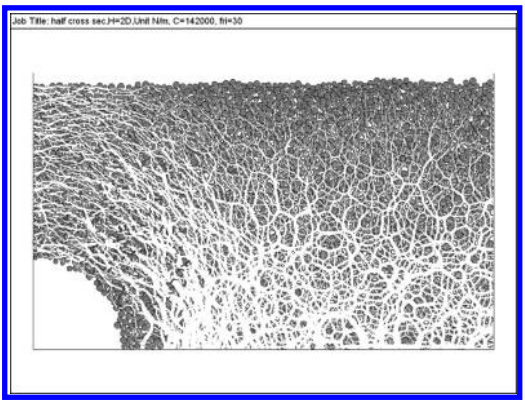


Figure 10. Cross section of PFC analysis showing stress relief at the sidewall with contact force chains.

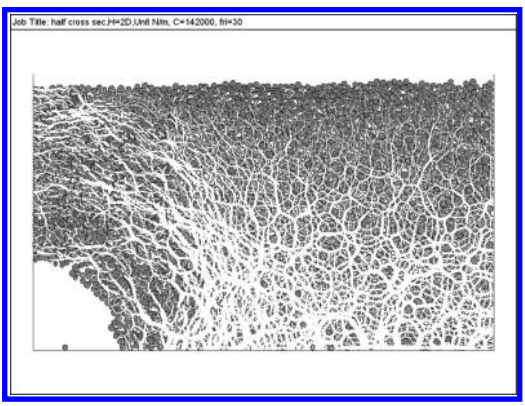


Figure 11. Cross section of PFC analysis showing the initiation of overbreak at shoulder with contact force chains.

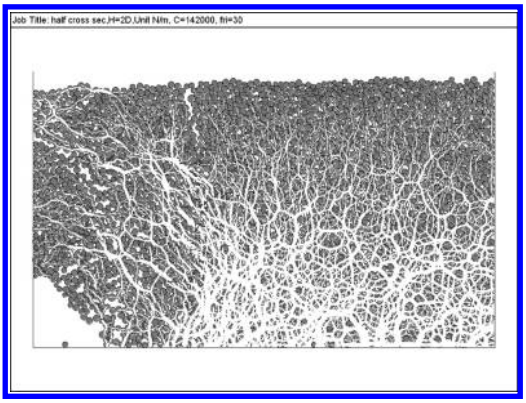


Figure 12. Cross section of PFC analysis showing the propagation of crack to crown from shoulder with contact force chains.

Researchers using FEM models obtained similar results but these do not cover the detailed procedure from the initiation of overbreak to the collapse because of the restriction of the method (Shin & Lee 2001, Vermeer et al 2002).

4 SUGGESTED FAILURE MODES

According to model tests and PFC analyses, 5 types of failure modes can be suggested for the decision of round length and support method. With decreasing cohesion the failure modes change. Those modes are described in chapters 4.1 to 4.5 for the same overburden and lining condition.

4.1 *No overbreak with stable face*

In this case, an increase of the round length can be considered. However, the decision should be made carefully to avoid overstressing of the lining, excessive volume of overbreak and daylight collapse.

4.2 *Overbreak with stable face*

In this case, the optimization of the round length is essential for the excavation plan and safety. Overbreak starts at the shoulder of the tunnel and it propagates to the crown. However, it does not result in a daylight collapse and the face and sidewall are still stable during this failure. The increase of the round length leads to increase an of overbreak volume and construction costs, but also to a reduction of construction time. Therefore, the round length should optimized to achieve a minimum in the construction costs with an acceptable safety level. A safety margin should be maintained to avoid a daylight collapse.

Copyright © 2005 Taylor & Francis Group plc, London, UK

4.3 *Daylight collapse with stable face*

In this case, excessive round length results in a daylight collapse. During the propagation of overbreak to the ground surface, the face could also partially collapse, depending on the support and ground conditions. The round length should be kept well below the critical value to avoid excessive stresses in the shotcrete lining.

4.4 *Overbreak with unstable face*

In this case, the unsupported face is not stable and collapses even without excavation, leading to a small scale overbreak. However, the overbreak does not propagate to the ground surface because of the ground strength. Practically, excavation can be continued without significant interruption in this case and face supports such as face bolts can be applied to guarantee a stable face.

4.5 *Daylight collapse with unstable face*

In this case, the face is unstable and collapses before excavation is commenced and it leads to a daylight collapse. Cohesionless ground typically shows this failure mode and excavation is practically impossible without pre-support and face support such as pipe roof and face bolts.

5 CONCLUSIONS

According to the results of small-scale model tests and PFC analyses, it is clearly found that the overbreak in the unsupported span does not affect the stability of the face, as long as the face is initially stable and the chosen round length does not cause excessive overbreak or daylight collapse.

The initiation of overbreak occurs at the shoulder of the unsupported span and extends to the crown. This initiation is governed by the ground condition, round length and initial stress, rather than the lining stiffness. However, the lining stiffness plays an important role when the failure propagates, eventually leading to a daylight collapse.

Stress acting on the lining is increased as the round length is increased. However, stress is relieved at the lining near to the face, if overbreak occurs in small scale so that arching stress is not significantly disturbed. During the development of daylight collapse, excessive ground loads act on the lining like a dead load because the ground arch fails. Therefore the stiffness of the lining is important for the safety of workers in case of a daylight collapse.

A large round length leads to failure when the overburden depth is not enough for the development of a natural arch above the overbreak. However, daylight collapse does not necessarily lead to the distortion of the lining in shallow tunnels because of low ground loads.

Regarding the determination of round length and support method, five failure modes are suggested, which should be considered for optimization of the construction. The round length should be decided to avoid overstressing of the lining and daylight collapse, and limit overbreak to acceptable limits. As the stiffness and strength of the lining plays a certain role in the propagation and extent of failure, also the advance rate should be optimized in case of shotcrete linings.

Various parametric studies and evaluations of case histories are planned to arrive at a kind of "rule" for the determination of the optimum round length for design and construction purposes.

REFERENCES

Baudendistel, M. 1997. Significance of the unsupported span in tunnelling. *Tunnelling 85*: 103–108.

Chang, Yanting. 1994. *Tunnel support with shotcrete in weak rock-a-rock mechanics study*. Stockholm: Royal Institute of Technology.

Itasca. 1999. *PFC2D User's guide.* Minneapolis: Itasca consulting group.

Shin, J. H. & Lee, I. K. 2001. A study on the failure mechanisms of the mixed-face tunnels in decomposed granite. *J. of Korean Geotechnical Society 17 (4)*: 317–329 (In Korean).

Terzaghi, K. 1954. *Theoretische Bodenmechanik*. Berlin-Goettingen-Heidelberg: Springer.

Vavrovsky, G. M. 1987. *Entspanung, Belastungsentwicklung und Versagensmechanismen Bei Tunnelvortrieben Mit Geringer Ueberlagerung*. Leoben: Leoben University.

Vermeer, P. A., Ruse, N. & Marcher, T. 2002. Tunnel heading stability in drained ground. *Felsbau 20 (6)*: 8–18.

Vermeer, P. A., Marcher, T. & Ruse, N. 2002. On the ground response curve. *Felsbau 20 (6)*: 19–24.

Copyright © 2005 Taylor & Francis Group plc, London, UK

Effect of tunnelling and groundwater interaction on ground and lining responses

C. Yoo & S.B. Kim
Sungkyunkwan University, Korea

H.C. Shin
Seoul Metropolitan Government, Korea

S.C. Baek
Hyundai Engineering and Construction, Korea

ABSTRACT: On account of increased public concern regarding the impact of tunnelling on surrounding environments, the control of groundwater has become an essential part of the planning, design, and construction of a tunnelling project. This paper presents the results of an investigation on interaction mechanism between tunnelling and groundwater using a 3D stress-pore pressure coupled finite-element model. It is shown that the ground and lining responses are significantly influenced by the relative permeability of the lining, and that the circumferential pre-grouting is an effective means for minimizing the tunnelling and groundwater interaction. Practical implementations of the findings from this study are discussed in great detail.

1 INTRODUCTION

In response to rapid growth in urban development there has been a pressing need for construction of new tunnels for transportation systems and underground utilities. Construction environments for urban tunnelling situations, however, are becoming increasingly unfavorable. For example, a new subway line, Line 9, is being constructed in Seoul, Korea. The entire construction project runs across west and east parts of Seoul, along Han river, and consists of cut and cover sections as well as drill and blast tunnel sections. An example of difficult tunnelling conditions being encountered is illustrated Figure 1. As seen, a 10-m diameter tunnel is planned to be excavated partly through a water bearing alluvial layer consisting of predominantly fine sands directly under an existing expressway, requiring cutting parts of existing piles. Apart from the interaction between the expressway and tunnelling, concerns are raised on the effects of groundwater and tunnelling interaction on the tunnelling performance. In such situations, it is essential to understand principles of the effect of tunnelling and groundwater interaction on the tunnelling performance in order to provide optimum mitigation measures, if necessary.

Tunnelling beneath the groundwater table causes changes in the state of stress and the pore water pressure distribution. In such tunnelling problems, there are three important issues that have to be addressed during design and construction including construction, stability, and environmental issues. First, water inflows during tunnelling significantly hamper the tunnelling works, thus resulting in an increase in the construction costs. Second, as the stress-strain-strength

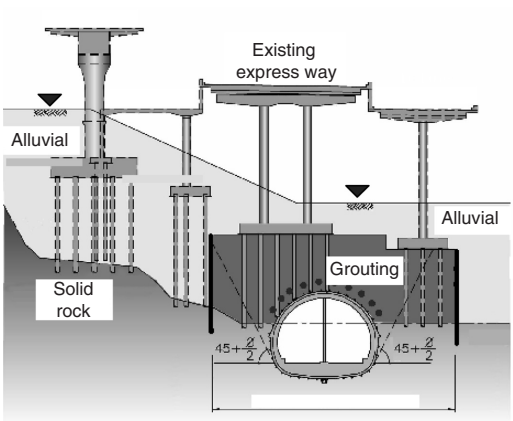


Figure 1. An example of difficult tunnelling condition in Seoul Metro Subway Line 9 construction project.

Copyright © 2005 Taylor & Francis Group plc, London, UK

characteristics of the surrounding ground are governed by the effective stress, the change in the pore water pressure distribution during the tunnelling process can affect the short- and long-term tunnel stability. Third, the direct environmental consequence of water inflows during tunnelling is the draw down of groundwater level in the surrounding aquifer. The related ground subsidence occurring as a result of the reduction in water pressures in the soil layers can damage nearby structures/utilities.

Despite the importance of understanding the stress-pore water coupled effect on tunnelling performance, studies concerning this subject are limited. Some of the available studies related to this subject focused more or less on the hydrodynamic nature of the problem dealing with the influence of the seepage flow towards the tunnel (Schweiger et al. 1991; Katzenbach 1995), and of the lowering of the water table (Adachi et al. 1988) on the stability of the opening and on the loads carried by its liner. Other studies of similar nature are specifically related to the effects of tunnelling on the groundwater regime in the surrounding medium (Daito and Ueshita 1988; Ueshita and Daito 1985). Gunn and Talyor (1984), Atwa and Leca (1994), Pottler et al. (1994) and Schweiger et al. (1999) have performed numerical analyses on the problem similar to that addressed in this study, but with the steady-state seepage analysis or sequential seepage analysis and stress analysis, which can not accurately model the fully coupled interaction behavior between the tunnelling and the groundwater. More recent studies include those by Shin et al. (2002a,b) in which the effect of ground water on the long-term tunnel behavior was studied using a plane strain and an axisymmetric finite-element models.

As part of a pre-investigation on the tunnelling conditions of the Seoul Metro Subway construction project aiming at reviewing initial designs and establishing construction guidelines, a parametric study was performed on various factors affecting the tunnelling performance using a fully coupled 3D finite-element model. This paper presents the 3D finite-element model, simulation strategy, and finally, practical implications of the findings.

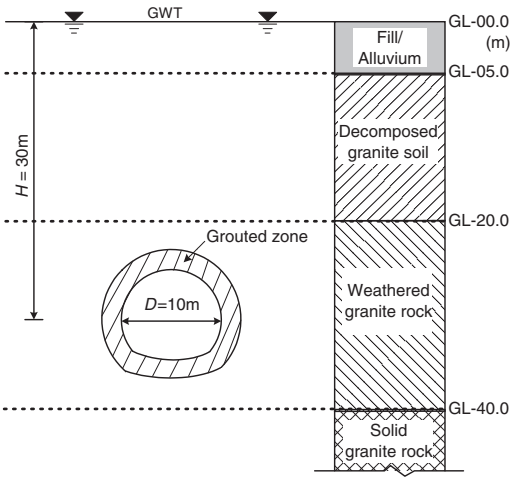


Figure 2. Ground profile for tunnelling condition analyzed.

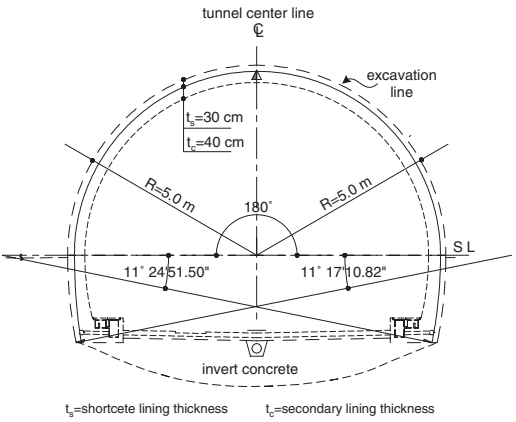


Figure 3. Tunnel cross section.

2 PARAMETRIC STUDY

2.1 *Cases studied*

A parametric study using a 3D finite-element model was performed on a typical 10-m-diameter horseshoe shaped tunnel constructed 25 m below the ground surface in the ground condition frequently encountered in Seoul, Korea. Figure 2 shows the ground profile considered in this study. The tunnel is excavated through a moderately weathered granite rock layer of Grade III, according to the engineering classification of weathered rock (Waltham 1994). For simplicity, the groundwater table was assumed to be located at the ground surface level. In regard to the post-tunnelling groundwater flow regime, a draw down condition with no recharge at the ground surface during the tunnelling process was assumed. Such a post-tunnelling groundwater flow condition was purposely selected to look into rather extreme cases in terms of the groundwater drawdown, although one can argue that in reality such a condition is only valid during a very dry season as there usually exists near-surface recharge from leaking water pipes in urban conditions.

Cross section of the 10-m-diameter tunnel is shown in Figure 3. The tunnel is assumed to be constructed using the conventional drill and blast technique with a

Copyright © 2005 Taylor & Francis Group plc, London, UK

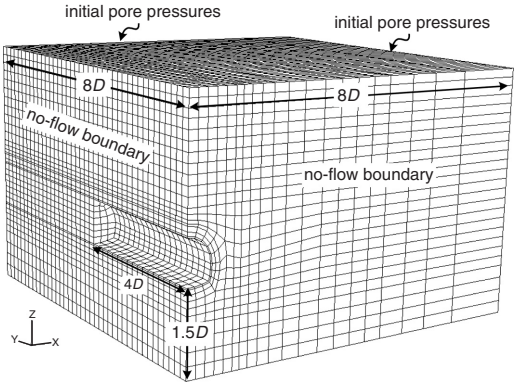


Figure 4. Finite-element model.

30-cm-thick shotcrete lining. Although rock bolts are usually installed as part of the primary support in this type of tunnelling condition, no rock bolts were considered for the sake of modeling simplicity.

2.2 *3D finite-element model*

In order to realistically capture the interaction mechanism between the tunnelling and the groundwater, a fully coupled 3D finite-element model capable of simulating the sequential tunnelling process was adopted for analyses. The tunnel was assumed to be excavated full face, and therefore, only one half of the domain was considered in the finite-element model by making use of the symmetry about the tunnel centerline. The finite-element mesh extends to a depth of two times the tunnel diameter (D) below the tunnel springline and laterally to a distance of $8.0D$ from the tunnel centerline. Appropriate hydraulic boundary conditions are also prescribed in the model. The details of the hydraulic boundary conditions are shown in Figure 4.

The ground was discretized using 8-node trilinear displacement and pore pressure elements with reduced integration (C3D8RP), while the shotcrete lining was modeled using 4-node doubly curved general-purpose shell elements with reduced integration with hourglass control and finite membrane strains (S4R). The finite permeability of the shotcrete lining was simulated based on the approach by Shin et al. (2002a), in which shell elements are combined with continuum elements having a prescribed permeability. For those cases with pre-grouting, the grouting effect is modeled by changing the material properties to those of the grouted zone at designated steps. In the analysis, the soil and rock layers were assumed to be an elasto-plastic material conforming to the Extended Drucker-Prager failure criterion together with the non-associated flow rule, while the shotcrete was assumed to behave in a linear elastic manner. Table 1 shows the material properties for the ground.

Table 1. Material properties used.

Material	c' (kPa)	ϕ' (°)	ψ (°)	k (m/sec)	E (MPa)	K_o
Fill	5	30	20	2×10^{-6}	30	0.4
Decomposed granite soil	50	38	15	1×10^{-6}	70	0.5
Weathered granite rock	100	40	15	6×10^{-7}	100	0.5
Solid granite rock	200	45	15	1×10^{-9}	100	0.7
Grouted zone	200	50	10	6×10^{-9}	500	0.5
Shotcrete	–	–	–	1×10^{-8}	2000	–

In order to form a database that can help identify the interaction mechanism between the tunnelling and the groundwater, a number of cases were constructed by varying the permeability k_L/k_S of the lining relative to the ground through which the tunnel is excavated. In addition to k_L/k_S a number of cases with different pre-grouting schemes with varying overlap length (L_G) between each grouting round were analyzed. For comparison, a total stress analysis with no consideration of the stress-pore pressure coupled effect was additionally conducted on the same tunnelling condition.

3 RESULTS AND DISCUSSION

3.1 *Shotcrete lining responses*

The axial force distributions in the shotcrete lining are shown in Figure 5 for a section $2.0D$ behind the tunnel face. Normalized forces $T/\gamma' HD$ are presented in this figure, where T is the calculated shotcrete axial force per unit length of the tunnel drive and γ' is the average effective unit weight of the ground above the tunnel axis. Four important trends can be observed in this figure. First, it is evident that the total stress analysis yields significantly smaller lining forces than the coupled analyses in some cases, especially at the invert, demonstrating that the lining forces can be significantly underestimated when performing a total stress analysis with no consideration of the stress-pore pressure coupled effect. Second, the variation in the lining forces with k_L/k_S tends to be more pronounced below the springline, thus suggesting that a special consideration be given to the invert stability when designing the lining for cases with smaller k_L/k_S. Third, no significant variation can be observed among the cases having a same k_L/k_S despite the differences in the level of the drawdown H_D. Fourth, for the finite lining permeability cases of $k_L = 1 \times 10^{-8} m/s$, in

Copyright © 2005 Taylor & Francis Group plc, London, UK

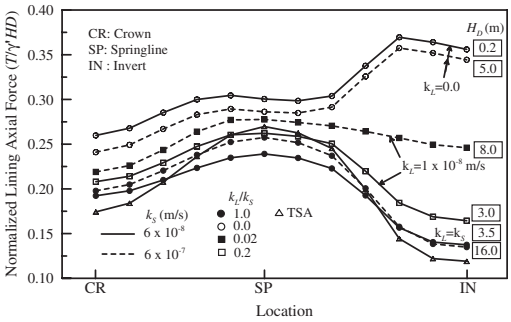


Figure 5. Variation of lining axial force with k_L/k_S.

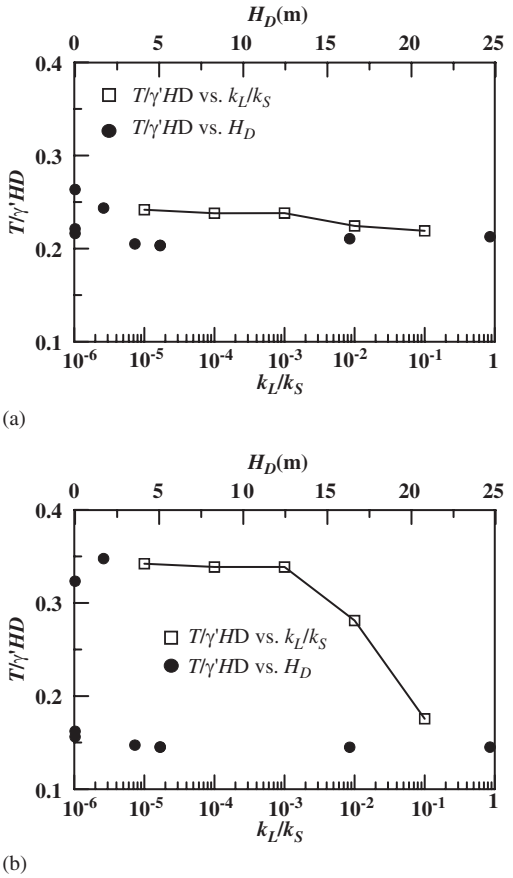


Figure 6. Variation of lining axial force with k_L/k_S and H_D: (a) crown; (b) invert.

which two different relative lining permeability ratios are considered, i.e., $k_L/k_S = 0.2$ and 0.02, the lining forces for $k_L/k_S = 0.02$ are significantly greater than for $k_L/k_S = 0.2$, especially at the invert, although H_D for $k_L/k_S = 0.02$ is approximately three times larger than for $k_L/k_S = 0.2$. The results imply that the relative lining permeability k_L/k_S is a more important controlling factor in the development of lining forces than the post-tunnelling groundwater level, and that correct evaluation of the lining permeability is thus an important task in the context of lining design as it governs the actual pore water pressures acting on the lining.

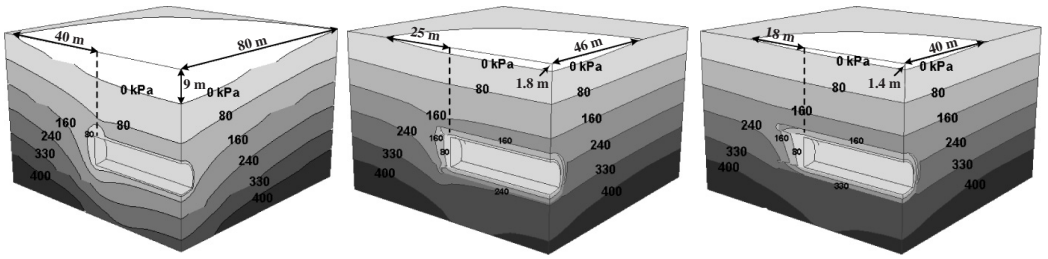
The effects of relative lining permeability ratio (k_L/k_S) and drawdown level (H_D) on the lining response are illustrated in different forms in Figure 6. Salient features shown in this figure are two fold. First, the axial lining force at the crown does not appear to be significantly influenced by k_L/k_S whereas there is a tendency for the lining force to decrease with increasing k_L/k_S at the invert. Second, no significant tie can be established between $T/\gamma' HD$ and H_D. Such results are in contrast to the current design practice in which design water pressures are selected based on the hydraulic head above the tunnel crown. Further study is required to establish the relationship between the drawdown level and the lining forces.

3.2 *Effect of pre-grouting*

The effect of pre-grouting on the groundwater regime and the tunnelling performance is examined for the case of $k_L/k_S = 0.02$. Four different overlap lengths L_G are considered, i.e., $L_G = 0.4D$, $0.6D$, $0.8D$, and $1.0D$. It should be noted that no solutions were obtained for cases $L_G < 0.4D$ due to numerical difficulties arising from the face instability, suggesting that $L_G = 0.4D$ is a critical overlap length below which the tunnel stability cannot be assured for the tunnelling condition considered in this study.

Illustrated in Figure 7 are the pore water pressure distributions after the face advances to a distance $4.0D$ from the front boundary. Also shown in this figure is a table summarizing the magnitudes and extent of the drawdown for the cases analyzed. As seen in Figure 7, the pre-grouting tends to significantly reduce the magnitude and the extent of the drawdown. In fact, the drawdown is kept below 1.8 m when employing the pre-grouting with $L_G \geq 0.4D$ as opposed to 9 m for the case without the pre-grouting. The lateral (X_D) and longitudinal (Y_D) extents of the drawdown zone are also reduced almost by half when adopting the pre-grouting. With regard to the effect of L_G, it appears that the overlap length L_G does not appear to significantly influence the magnitude of the drawdown, exhibiting $H_D = 1.4 \sim 1.8$ m for all cases. The longitudinal extent of the drawdown ahead of face (Y_D) is more influenced by L_G, showing a 30% reduction when increasing L_G from $0.4D$ to $1.0D$. The water pressures ahead of the face also decrease with increasing L_G, as illustrated in this figure.

Copyright © 2005 Taylor & Francis Group plc, London, UK



(a) w/o pre-grouting (b) L_G=0.4D (c) L_G=1.0D

L_G	H_D (m)	X_D (m)	Y_D (m)
0.0D	9 m	80 m	40m
0.4D	1.8 m	46 m	25m
0.8D	1.6 m	44 m	20m
1.0D	1.4 m	40 m	18m

Note
L_G = longitudinal extent of grouuting ahaed of face
H_D = drawdown
X_D = lateral extent of drawdown
Y_D = longitudinal extent of drawdown ahaed of face
L_G = 0.0D inidicates no pre-grouting.

Figure 7. Pore water distributions for with and w/o pre-grouting: (a) w/o pre-grouting; (b) $L_G = 0.4D$; (c) $L_G = 1.0D$.

The positive effect of the pre-grouting on the ground settlements and the face displacements is well illustrated in Figure 8. As seen in Figure 8(a), the settlement troughs for the pre-grouting cases are considerably narrower and shallower, showing a maximum settlement of 13 mm as opposed to 70 mm for the case without the pre-grouting. As for the drawdown, the overlap length L_G appears to have insignificant effect on the surface settlements, showing the maximum values in the range of 8∼13 mm for $L_G = 0.4\sim1.0D$. The reduced settlements are mainly attributed to the decreased level of groundwater drawdown, although the umbrella effect by the grouted zone ahead of the face also provides a positive effect. It should be noted that pre-grouting provides an umbrella effect that reduces the earth load ahead of the face, thus promoting the face stability. The pre-grouting is also effective in reducing the face axial displacements as seen in Figure 8(b). One important observation is that when $L_G = 0.4D$, the face displacements are even larger than without the pre-grouting. The increased pore water pressures ahead of the face and insufficient umbrella effect are mainly responsible for such a trend. Care should b e exercised when selecting the overlap length L_G to avoid the face instability problem. In addition, no further benefit in terms of reducing the face displacement is apparent when $L_G > 0.6D$. Considering the repetitive nature of the grouting work, the threshold value of $L_G = 0.6D$ can be regarded as an optimum overlap length $L_{G,opt}$ required between two successive cycles, since any shorter length would yield rather large face and ground deformations.

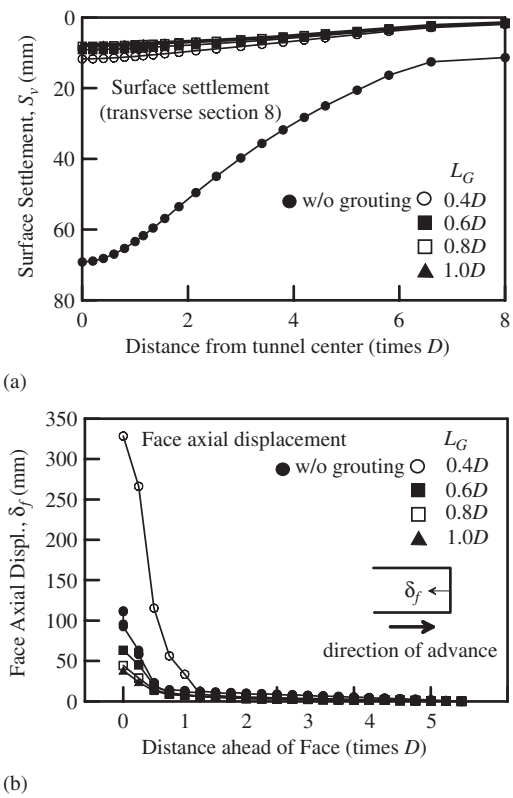


Figure 8. Effect of overlap length of pre-grouting on ground deformation: (a) Surface settlement; (b) Face displacement.

3.3 *Effect of face-grouting*

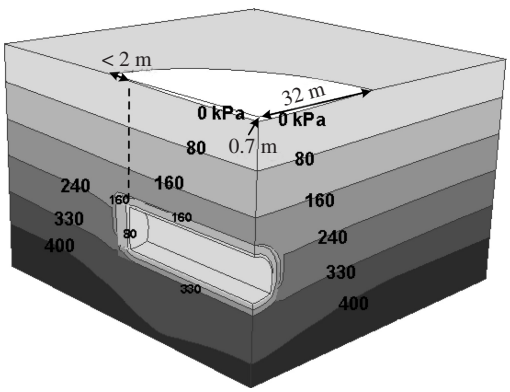
As demonstrated, the circumferential pre-grouting cannot completely prevent the lowering of the groundwater

Copyright © 2005 Taylor & Francis Group plc, London, UK

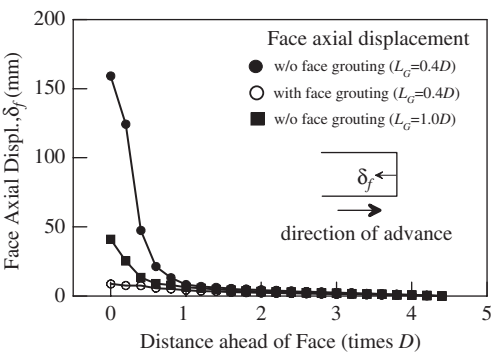
table. Moreover, when the overlap length is not sufficient, i.e., $L_G < 0.6D$, maintaining the face stability becomes a critical issue due to high water pressures built up ahead of the face. A possible measure to cope with such problems is to employ face grouting in combination with the circumferential pre-grouting.

Illustrated in Figure 9 are the results for face grouting extending 0.4D ahead of face, i.e., $L_{FG} = 0.4$D, in addition to the circumferential grouting of $L_G = 0.4D$. As can be seen in Figure 9(a), the face grouting significantly reduces not only the magnitude of the drawdown but also the lateral and longitudinal extents of the drawdown when compared to the case employing the circumferential grouting of $L_G = 0.4D$ only. Also shown is that the drawdown level ahead of the face is almost reduced to zero, and the lateral drawdown extent cut by half.

The face grouting in fact can significantly reduce the face and ground deformations not only by preventing the water inflow from the face but by the enhanced stress-strain-strength characteristics. This is well illustrated in the plots of the face movements in Figure 9(b). The maximum face displacement for the face grouting case is only 10% of that for the case without face grouting. One important observation is that the overall performance of the case $L_G = 0.4D$ with face grouting is much better than the case $L_G = 1.0D$ without face grouting. This suggests that a shorter overlap length for the circumferential grouting can be adopted when employing the face grouting. Such results have a significant practical implication since a shorter overlap during the grouting work would significantly reduce the work cycle time. A similar trend is seen in the settlement troughs, although not presented here.



(a)



(b)

Figure 9. Effect of face grouting: (a) Pore pressure distribution; (b) Face displacement.

4 CONCLUSIONS

This paper examined the interaction mechanism between tunnelling and groundwater using the results from a series of 3D stress-pore water coupled analyses on a hypothetical tunnelling condition frequently encountered in urban areas in Korea. Attention was paid to analyzing the results so that the effect of relative lining permeability on the pore water pressure regime as well as the ground and lining responses could be identified. The effect of a pre-grouting scheme was also analyzed. On the basis of the results of the present study, the following conclusions can be drawn.

1. For a range of the relative lining permeability with respect to the ground permeability, the maximum shotcrete lining force varies by more than 200% depending upon the relative lining permeability. The relative lining permeability is a more important factor than the post-tunnelling groundwater level in view of the shotcrete lining response to tunnelling construction.
2. When adopting a circumferential pre-grouting in the tunnelling conditions considered in this study, an optimum overlap length ($L_{G,opt}$) below which the tunnelling performance is markedly declined is found to be $L_{G,opt} = 0.6D$.
3. A face grouting when used in combination with a circumferential pre-grouting can significantly reduce the required overlap length for the circumferential grouting.

ACKNOWLEDGEMENTS

This research is supported by Korea Ministry of Construction and Transportation under the contract No. 03-A01-06. as well as by Hyundai Engineering and Construction. The financial support is greatly acknowledged.

Copyright © 2005 Taylor & Francis Group plc, London, UK

REFERENCES

Adachi, T., Kikuchi, T., and Kimura, H. 1988. Behaviour and simulation of soil tunnel with thin cover. *Prof. 6th Int. Conf. on Numerical Methods in Geomechanics*, Innsbruck, 1585–1590.

Atwa, M. and Leca, E. 1994. Analysis of groundwater seepage into tunnels. *Proc. Int. congress on tunnelling and ground conditions*, Cairo, Egypt, 303–310.

Daito, K. and Ueshita, K. 1988. Prediction of tunnelling effects on groundwater condition by the water balance method. *Prof. 6th Int. Conf. on Numerical Methods in Geomechanics*, Innsbruck, 1585–1590.

Gunn, M. J. and Taylor, R. N. 1984. Discussion on Atkinson and Mair (1983). *Géotechnique* 35(1), 73–75.

Hibbitt, Karlsson, and Sorensen, Inc. 2002. *ABAQUS users manual, Version 6.3*, Providence, R.I.

Katzenbach, R. 1985. The influence of soil strength and water load to the safety of tunnel driving. *Prof. 5th Int. Conf. on Numerical Methods in Geomechanics*, Nagoya, 1207–1213.

Pottler, R., Hagemeister, A., Schweiger, H. F., and Faust, P. 1994. Influence of tunnel drive on groundwater level. *Proc. 8th Conf. of the Int. Association for Computer Methods and Advances in Geomechanics*, Morgantown, 1249–1258.

Schweiger, H. F., Pottler, R. K., and Steiner, H. 1991. Effects of seepage force on shotcrete lining of a large undersea cavern. *Proc. 7th Conf. of the Int. Association for Computer Methods and Advances in Geomechanics*, Cairns, 1503–1508.

Shin, J. H., Addenbrooke, T. I., and Potts, D. M. 2002a. A numerical study of the effect of groundwater movement on long-term tunnel behavior. *Géotechnique*, 52(6), 391–403.

Shin, J. H., Potts, D. M., and Addenbrooke, T. I. 2002b. Three-dimensional modeling of NATM tunnelling in decomposed granite soil. *Géotechnique*, 52(3), 187–200.

Schweiger, H. F., Schuller, H., and Pottler, R. 1999. Some remarks on 2D models for numerical simulation of underground construction with complex cross-sections. *Proc. 9th Conf. of the. Association for Computer Methods and Advances in Geomechanics*, China, 1303–1308.

Ueshita, K., Sato, T., and Daito, K. 1985. Prediction of tunnelling effect on groundwater condition. *Prof. 5th Int. Conf. on Numerical Methods in Geomechanics*, Nagoya, 1215–1219.

Waltham, A. C. 1994. *Foundations of Engineering Geology*, Blackie Academic & Professional, London. Glasgow.

Copyright © 2005 Taylor & Francis Group plc, London, UK

Application of the multiple-layer supporting method to a tunnel in squeezing argillaceous rocks

S. Kemmochi, E. Taketsu & A. Ogawa
Japan Railway Construction, Transport and Technology Agency, Yokohama, Japan

T. Aoki, M. Koike & R. Morita
Taisei Corporation, Tokyo, Japan

H. Shirahata, N. Koya & M. Matsubara
Obayashi Corporation, Tokyo, Japan

ABSTRACT: Squeezing phenomena accompanied by the support failures have occurred at Konari work section of Iiyama Tunnel for Hokuriku Shinkansen (a bullet train line) in a Neogene mudstone formation where the overburden exceeded 180 m. To cope with this large squeezing earth pressure, the multiple-layer supporting method has been applied for this tunnel as reported in our previous paper mainly on the failing behavior of the first-layer supports and its numerical analyses. Further severe squeezing phenomena occurred in the shear-disturbed zone located at around the boundary between Konari and Itakura work sections. In this paper, the improvement of the multiple-layer supporting method in this zone is described including the predictive numerical analyses and the application results.

1 INTRODUCTION

Iiyama Tunnel for Hokuriku Shinkansen (a bullet train line) runs through the boundary of Nagano and Niigata Prefectures and has a great length of 22.2 km. It is divided into six work sections for construction. In Itakura and Konari work sections, 3,660 m and 3,800 m in length respectively, that locate first and second from the Niigata-side portal, we encountered the squeezing phenomena in mudstones of Miocene, Neogene formations. The maximum convergence tended to exceed 200 mm especially in sections whose overburden went beyond 180 m. In our previous paper (Kemmochi et al., 2004a & 2004b), the application of the multiple-layer supporting method in squeezing rocks in Konari work section was reported. The characteristic behaviors of the first-layer support members especially on the stress variation were investigated with the in-situ measurements and three-dimensional numerical anal yses. Consequently, it was found that the behaviors of the convergences and support stresses were able to be expressed by the numerical analyses in which the work execution procedures were fully sequentially incorporated.

Further severe squeezing phenomena occurred in the shear-disturbed zone located at around the boundary between Konari and Itakura work sections. To deal with such large earth pressures, strengthening of the first-layer support members and the early-time application of the second-layer support were investigated with the predictive numerical analyses. Whereas large convergences more than 500 mm occurred actually in the shear-disturbed zone, the tunnel was safely excavated with the execution procedures and the support specifications that had been designed based on the findings of the predictive analyses. The performances of the first- and second-layer supports were confirmed with the various in-situ measurements.

In this paper, the application of the multiple-layer supporting method in the shear-disturbed zone is described.

2 PREDISTIVE NUMERICAL ANALYSES ON TUNNELING IN THE SHEAR-DISTURBED ZONE

In our previous paper (Kemmochi et al., 2004a & 2004b), we have shown that the three-dimensional numerical analyses with elasto-perfectly plastic rock model together with yieldable support models can explain the measured displacement and support-stress behaviors. We have also studied the cases of high-strength first-layer support members (Kemmochi et al.,

Copyright © 2005 Taylor & Francis Group plc, London, UK

2004c). In these investigations, the second-layer support was supposed to apply at the location distant from the top-heading face by 3.5D where D is the tunnel width and is 10 m here. Whereas the first-layer support somewhat failed before the application of the second-layer support, cases in which the second-layer support became broken as severe as it lost its support function had not been targeted.

In this chapter, a poorer rock condition is assumed so as to correspond to rocks in the shear-disturbed zone. Cases of high-strength first-layer support and the early-time application of the second-layer support are studied with the numerical analyses for the prediction.

2.1 *Analysis conditions*

The rock and support properties used in the numerical analyses are given in Table 1. The stiffness (i.e. Young's Modulus) of each first-layer support member is set one-fifth of the material property based on the findings in our previous study (Kemmochi et al., 2004a & 2004b) so as to reasonably express the measured response of the support stress change with the rock displacements. This behavior is considered to result from the loosened boundary between the support and rocks at the tunnel interior. Such technical treatment is often adopted in numerical analyses. The stiffness reduction is not applied for the second-layer support since its close contact with the first-layer support can be assured in practice.

Regarding the excavation sequence, the first-layer support is closed by applying the invert at the location distant from 10 to 14 m from the top heading face and subsequently, the second-layer support is applied at the section of 10 to 22 m away from the face. Two support patterns are tested: high-strength and normal support members viz.:

– Case 1: First-layer support (high strength) + Second-layer support (normal)
– Case 2: First-layer support (normal) + Second-layer support (normal)

2.2 *Analysis results*

2.2.1 *Displacement*

The horizontal convergences at a cross section of the top heading are shown in Figure 1 and Table 2. As given in Table 1, Case 1 with high-strength first-layer support has the convergence of 79% of that of Case 2 with normal-strength supports before the application of the second-layer support. It has the convergence of 10% of that of Case 2 after the application of the second-layer support. The difference in displacement before the application of the second-layer support would result from the different stiffness of the first-layer support. In contrast, the displacement ratio after the application of the second-layer support is much

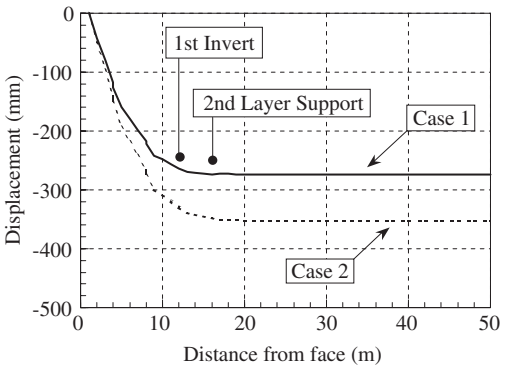


Figure 1. Convergence.

Table 2. Convergences.

Displacement (mm)	Case 1	Case 2	Case 1 / Case 2
Total	−274.2	−353.7	0.78
Before 2nd layer support	−273.6	−347.8	0.79
After 2nd layer support	−0.6	−5.9	0.10

Table 1. Parameters used for predictive numerical analysis.

	Specification	E [GPa]	ν	C [MPa]	ϕ [°]	Yield stress [N/mm^2]
Ground		0.2	0.3	0.26	16.5	–
1st Layer support [high strength]						
Shotcrete (1/5 stiffness)	t = 250 mm	1.36	0.2	18.0	0	(36.0)
Steel support (1/5 stiffness)	HH200	40	–	–	–	390
1st Layer support [normal]						
Shotcrete (1/5 stiffness)	t = 250 mm	0.68	0.2	9.0	0	(18.0)
Steel support (1/5 stiffness)	H200	40	–	–	–	235
2nd Layer support [normal]						
shotcrete	t = 150 mm	3.4	0.2	9.0	0	(18.0)
steel Support	H125	200	–	–	–	235

Copyright © 2005 Taylor & Francis Group plc, London, UK

less whereas the same specification is applied for their second-layer supports. This would mainly result from the difference in the yield strength of their first-layer supports. Namely, since Case 1 has significant extents of yielded parts in the shotcrete and steel supports in comparison with those of Case 2 (see Figure 2 with reference to the following Section 2.2.2), the first-layer support of Case 1 has greater virtual stiffness than that of Case 2 before the application of the second-layer support.

2.2.2 *Stress in first-layer support*

Figure 2 shows the yielded parts of the first-layer support before the application of the second-layer support. Regarding the yielded zones of the shotcrete (black-colored parts), the shotcrete of Case 1 remains in elastic state (so does it even after the application of the second-layer support in this case) whereas that of Case 2 contains yielded zones widely spread from the crown to the shoulder. Concerning the yielded parts of the steel supports (grey-colored thick-lined parts), the yielded parts of the steel supports of Case 1 are limited in the crown region whereas the steel supports of Case 2 yielded in almost all the parts.

Thus, the use of normal-strength support members in Case 2 would result in severe failure e.g. crush of shotcrete or rupture of steel supports since both the shotcrete and steel supports are yielded especially in the regions of the crown and shoulder of the top heading.

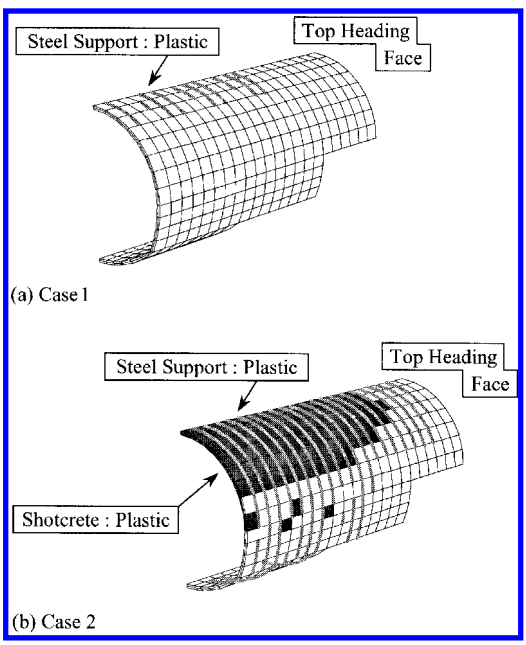


Figure 2. Yielded zones of first-layer support.

2.2.3 *Stress in second-layer support*

Figure 3 shows the yielded parts of the second-layer support after the excavation completed. The yielded zones in the second-layer shotcrete distributed from the invert to the sidewall at after the sections close to the construction joint. The yielded zones of Case 1 are wider than those of Case 2. In case of use of high-strength support members (Case 1), the second-layer support is partly yielded mainly at the invert region. Nevertheless, the shotcrete support would be considered to retain the total stability since the first-layer shotcrete is not yielded at all. Moreover, since the position of the yielded zones of the second-layer shotcrete in both Cases 1 and 2 is limited at the invert and sidewall near the construction joint and all the arch region of the second-layer support remain in the elastic state, it can be insisted that the working safety be secured.

3 CONSTRUCTION RESULTS

The support patterns used in the shear-disturbed zone are shown in Table 3. Based on the recent work experiences, tunneling was at first conformed to Pattern A with which the second-layer support was basically applied at the position of 3.5D away from the top-heading face; D is the tunnel width and is 10 m here. However, the convergence exceeded

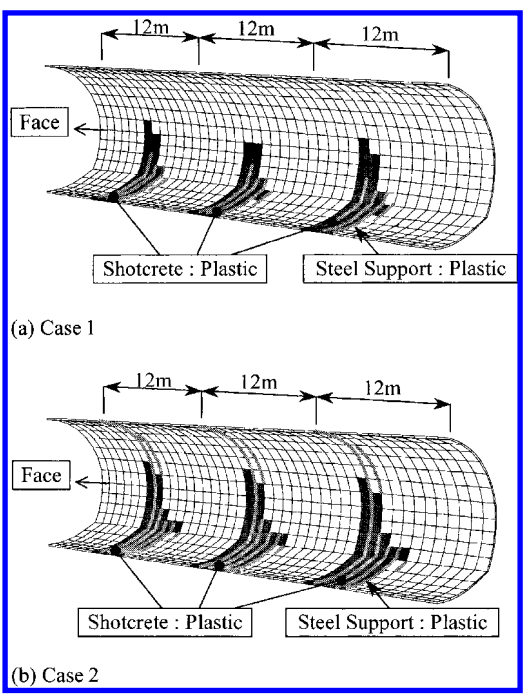


Figure 3. Yielded zones of second-layer support.

Copyright © 2005 Taylor & Francis Group plc, London, UK

Table 3. Specifications of supports.

			Support pattern A	Support pattern B
First layer	Arch	Steel support	200H (SS400)	200H (SS540)
		Shotcrete	25 cm thick fiber reinforced 18 N/mm^2	25 cm thick Fiber reinforced 36 N/mm^2
		Rock bolt	4.0 m × 10 4.5 m × 16	4.0 m × 10 4.5 m × 16
	Invert	Steel strut	200H (SS400)	200H (SS540)
		Shotcrete	25 cm thick 18 N/mm^2	25 cm thick 36 N/mm^2
Second layer	Arch	Steel support	125H (SS400)	150H (SS400)
		Shotcrete	12.5 cm thick 18 N/mm^2	15 cm thick 18 N/mm^2
	Invert	Steel strut	–	150H (SS400)
		Shotcrete	–	15 cm thick 18 N/mm^2



Photograph 1. Failure of first-layer invert.

300 mm at the position of 1.5D from the top-heading face and it did not tend to converge. The shotcrete cracked resulting in spalling at the tunnel crown and shoulder. Especially at the crown, the steel supports were yielded and some of them were ruptured. The second-layer support was applied here over the first-layer support but the displacement did not tend to converge. It was observed that the shotcrete was crushed and that the invert steel struts were consecutively ruptured when the backfill over the first-layer invert was removed, as shown in Photograph 1. It was considered that these circumstances resulted from the insufficient bearing capacity of the first-layer support against such unexpectedly large earth pressure.

The predictive analyses described in the previous chapter indicated that strengthening of the first-layer support would be effective in a poor rock condition of the shear-disturbed zone. Hence, the supports of Pattern B with high-strength shotcrete and high-standard steel supports were used for tunneling (see Table 3 and Figures 4 and 5). Since the supports of Pattern B were used, the convergences had been stabilized at around 200 mm as shown in Figure 6. Moreover, the second-layer supports became scarcely damaged and the stability of the tunnel structure was secured.

4 VERIFICATION WITH MEASUREMENTS

Measurements of the stresses of the support members in addition to those of the convergences were performed to confirm the effects of strengthening the first-layer support members and of the early-time application of the second-layer support with the supports of Pattern B.

4.1 *First-layer support*

The stress change of the first-layer shotcrete with time is given in Figure 7. The stresses at all of the measured points rapidly increased at the early phase. The sudden stress decrease indicated the shotcrete failure at the nearby location. It was found that subsequently, the stresses turned into re-increase after the application of the second-layer support.

Figure 8 shows change of the axial rim strains of the first-layer steel support with time. Both the strains at crown and invert increased rapidly just after the installation and soon exceeded the yield strain of 0.21%. However, the application of the second-layer support restrained the strains from further increase.

4.2 *Second-layer support*

The stress change of the second-layer shotcrete with time is given in Figure 9. The stresses at the crown,

Copyright © 2005 Taylor & Francis Group plc, London, UK

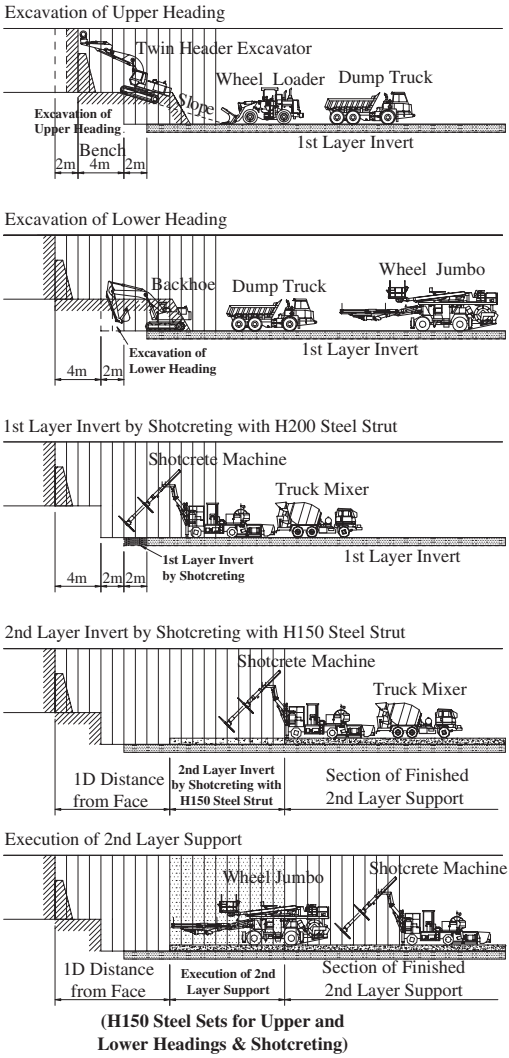


Figure 4. Work execution procedure.

shoulder and sidewall were within relatively low level below 6 N/mm^2. On the contrary, the stress measured at the invert reached the design strength of 18 N/mm^2.

Figure 10 shows change of the axial rim strains of the first-layer steel support with time. While the axial strains were within the relatively small level below 0.1%, that of the invert was greater than the others and exceeded 0.1%.

Consequently, one could conclude that the second-layer supports remained stable in the arch and sidewall position judging from the stress state measured. On the contrary, the support members at the invert including the shotcrete and steel strut were in high stress state.

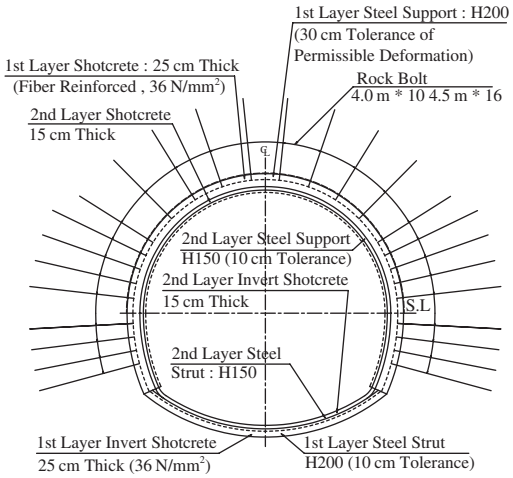


Figure 5. Support pattern B.

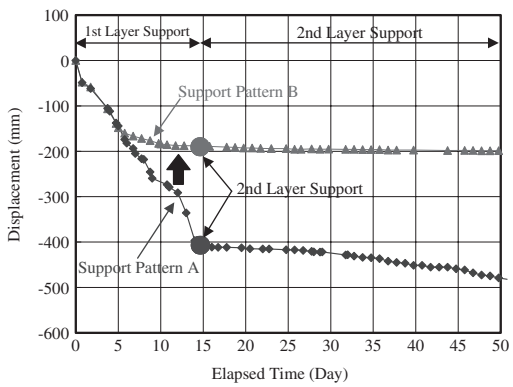


Figure 6. Convergence.

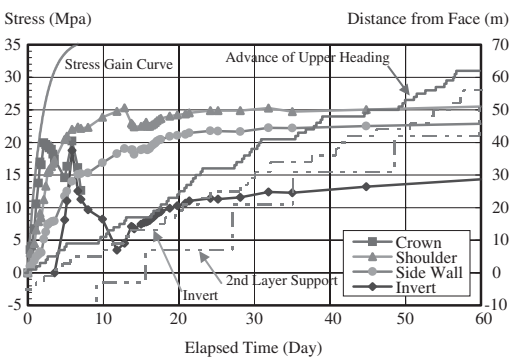


Figure 7. Axial stresses of first-layer shotcrete.

Copyright © 2005 Taylor & Francis Group plc, London, UK

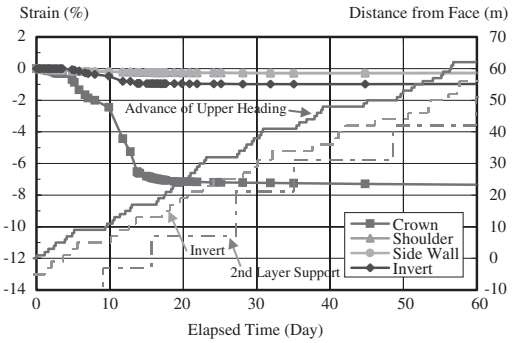


Figure 8. Axial strains of first-layer steel supports.

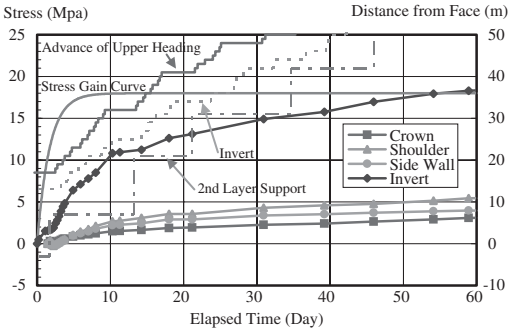


Figure 9. Axial stresses of second-layer shotcrete.

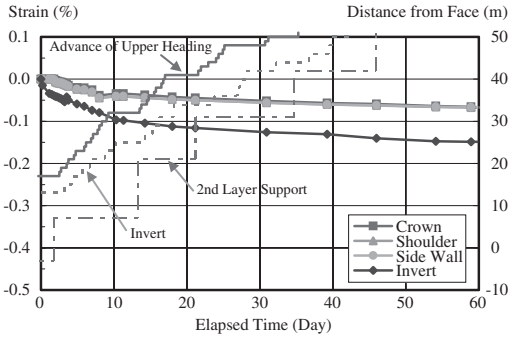


Figure 10. Axial strains of first-layer steel supports.

4.1 *Summary*

While the first-layer support was partly in the yielded state, its displacements became converged after the application of the second-layer support. Thereat, restoration of the support function of the first-layer support was observed.

The second-layer support was able to keep its soundness in the support function although the limited part at the invert was in the yielded state.

5 COMPARISON OF RESULTS OF MEASUREMENT AND PREDICTIVE ANALYSES

5.1 *First-layer support*

It was obtained from the predictive analyses that the use of high-strength shotcrete and high-standard steel supports for the first-layer support would avoid yielding the shotcrete and would restrain the yielded extent of the steel supports, as indicated in Figure 2. Correspondingly, the measurement results indicated that both the shotcrete and steel supports resulted in significant yielding and failure at the crown and invert. However, the shoulder and sidewall were fairly sound, as shown in Figures 7 and 8. It was considered that the actually worked earth pressure (or in-situ stress) was greater than that used in the predictive analyses. Hence, damage of the first-layer support was severer in the actual construction than it was in the predictive analyses. However, the overall trends of the support behaviors were well demonstrated by the predictive numerical analyses.

5.2 *Second-layer support*

In the results of the predictive analyses, the yielded zones of the second-layer shotcrete were limitedly distributed at the invert and sidewall, as shown in Figure 3. Correspondingly, the stress of shotcrete reached the design strength only at the invert in the actual measurement and the stresses in the second-layer support at the arch region remained below the design strength level, as given in Figures 9 and 10. Thus, the predictive analysis results were in relatively good accordance with the measured behaviors.

6 CONCLUSIONS

The application of the multiple-layer supporting method in the shear-disturbed zone was investigated where significant squeezing phenomena occurred. The main findings are listed below:

1. In the shear-disturbed zone where the deformation was significantly large, the multiple-layer supporting method was successfully applied by strengthening the first-layer support members so as to restrain the yielding and failing and by applying the second-layer support at as close to the top-heading face as 1D (or 10 m). This combination of the high-capacity first-layer support with the early-time application

Copyright © 2005 Taylor & Francis Group plc, London, UK

of the second-layer support effectively secured the tunnel stability in such a difficult ground condition.
2. The three-dimensional analyses in which the work execution procedures were fully sequentially incorporated were found to be capable of investigating the appropriate combination of the first- and second-layer supports and the suitable timing of the application of the second-layer support.
3. The multiple-layer supporting method is a highly flexible and rational tunneling method in squeezing rocks in that the specifications and the application timings of the first- and second-layer supports can be effectively adjusted.

REFERENCES

Kemmochi, S., Taketsu, E., Morita, R. & Aoki, T. 2004a. Investigation into loosened zones and deformation behaviors of a tunnel in a squeezing ground by means of the multiple-layer supporting method. Proceedings of the World Tunnel Congress, Singapore, E03, p. 6 (CD-ROM).

Kemmochi, S., Taketsu, E., Morita, R. & Aoki, T. 2004b. Investigation into loosened zones and deformation behaviors of a tunnel in a squeezing ground by means of the multiple-layer supporting method. Tunnelling and Underground Space Technology, Vol. 19, No. 4–5, pp. 408–409.

Kemmochi, S., Taketsu, E., Aoki, T., Kamemura, K. & Morita, R. 2004c. Three-dimensional analysis on the deformation behavior of a tunnel in squeezing rocks. Proceedings of the 11th Japan Symposium on Rock Mechanics, pp. 9–16.

Copyright © 2005 Taylor & Francis Group plc, London, UK

On design analyses of NATM-tunnels

S.C. Möller & P.A. Vermeer
Institute of Geotechnical Engineering, University of Stuttgart, Germany

ABSTRACT: The design of tunnels requires a proper estimate of surface settlements and structural forces in linings. Here it is not feasible to use three-dimensional finite element calculations, as they are engineering time consuming. Instead relatively simple two-dimensional analyses are required. Here effects of three-dimensional arching are accounted for by the so-called Load Reduction Factor. Unfortunately there is very little data on the appropriate value of this factor. In order to improve this situation comparison is made between simple 2D and fully 3D analysis. In this paper results for circular NATM- (New Austrian Tunnelling Method) tunnels are shown. Influences of coefficient of lateral earth pressure at rest, stiffness ratio of ground and tunnel lining, strength parameters as well as geometric influences of tunnel diameter and cutting length are quantified. Moreover field data from a tunnel are considered in order to arrive at guidelines for the selection of the Load Reduction Factor.

1 INTRODUCTION

A frequently discussed topic is the question, whether structural forces in tunnel linings as well as settlements should be computed by a fully three-dimensional analysis or whether more simple two-dimensional models are sufficient.

No doubt, a tunnel constitutes predominantly a three-dimensional stress-strain-situation and three-dimensional Finite-Element (FE) analyses have been adopted in engineering tunnelling practice. But such analyses are still very time consuming. For large tunnel projects with several kilometres of excavation and various cross sections three-dimensional analysis cannot be used as a design tool. In this case two-dimensional analyses are required.

Two-dimensional FE-analyses have been applied already for a long time. For the calibration of such analyses an assumption about the three-dimensional arching effect has to be made in order to compensate the missing third dimension. This is done by means of the so-called load reduction factor, but assumptions have to be made about its magnitude.

The present paper systematically compares three-dimensional to two-dimensional FE-analyses in order to arrive with more information on proper load reduction factors. Analyses are both carried out for the design of tunnel linings, i.e. bending moments and normal forces, as well as for settlements due to tunnelling.

Finally results of structural forces in tunnel linings and surface settlements are shown for the underground railroad Steinhaldenfeld-Tunnel in Stuttgart, Germany.

2 TWO-DIMENSIONAL FE-ANALYSES

In order to simulate sequential tunnel excavation in a two-dimensional FE-analyses, an assumption about the third dimension has to be made. As two-dimensional analyses can not account for the three-dimensional arching effect at the tunnel heading an artificial support pressure $\beta \cdot \sigma_0$ is applied, as indicated in Figure 1. Here σ_0 is the initial stress before construction of the tunnel and β is the load reduction factor. In this paper we will simply refer to β as the unloading factor.

In practice there are a number of different approaches, but for the present study the so-called load reduction method (Schikora & Fink 1982), also known as the β- or λ-method, has been adopted.

Figure 1 shows the two calculation phases of the load reduction method, being related to the so-called ground-response or Fenner-Pacher curve (Pacher 1964). Starting from the initial geostatic stresses σ_0, with $\sigma_h = \mathrm{K}_0 \cdot \sigma_\mathrm{v}$, where K_0 is the coefficient of lateral earth pressure at rest, ground elements inside the tunnel are switched off in the first phase. Inside the tunnel a support pressure of the amount $\beta \cdot \sigma_0$ (with $0 < \beta < 1$) is left to account for the missing three-dimensional arching at the tunnel heading. To this point only the ground is loaded and settlements of the amount S_1 occur. In the second phase the support pressure is removed and the lining is activated. Final settlements of the amount S_{tot} occur in this phase due to the combined loading of ground and lining. Structural forces in the lining occur only during the second phase.

Copyright © 2005 Taylor & Francis Group plc, London, UK

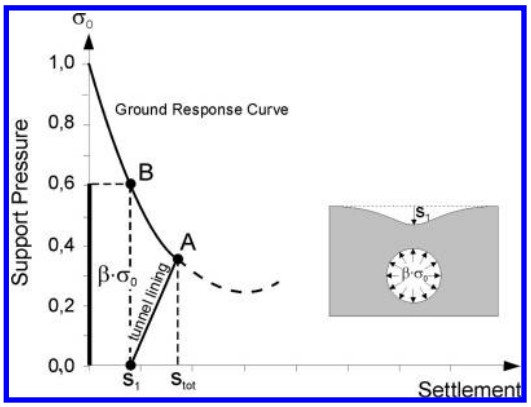


Figure 1. Display of load reduction method adopting ground response curve.

The amount of support pressure β, which is determining the moment of placement of tunnel lining installation, is directly influencing the magnitude of both settlements and structural forces. A larger factor β corresponds to an early installation of lining with larger structural forces and less settlements, a smaller factor leads to lower structural forces in the lining and larger settlements correspondingly.

3 THREE-DIMENSIONAL FE-ANALYSES

Figure 2 shows a three-dimensional FE-mesh in a half-symmetric condition. NATM-tunnels with a circular cross section have been analyzed. The mesh of Figure 2 compriseses a tunnel diameter of $D = 7\,m$ and a cutting length of $d = 1.5\,m$. It yields a total height of $57\,m$, a length of $120\,m$ and a width of $60\,m$.

Different meshes with diameters of $9\,m$ as well as $11\,m$ and cutting lengths of $d = 0.5\,m$ as well as $1\,m$ have also been analysed. All meshes had a cover of $H = 21\,m$ and a width of $60\,m$. The minimum mesh length was taken eighty times the cutting length d. All measures were large enough to ensure for no influences of the mesh boundaries.

To simulated the excavation process of NATM-tunnels the so-called 'step-by-step'-method (Wittke 1984) has been used. Again starting from initial geostatic stresses, the excavation sequence as indicated in Figure 2 has been repeated. In step $i - 1$ ground elements inside the tunnel are removed to simulate an excavation of cutting length d. Once this excavation step is numerically simulated in step i the excavation is repeated for the next cutting length and at the same time the tunnel lining for the previous excavation is activated to support the ground. These calculation phases are repeated in steps $i + 1$ to $i + n$ until a representative steady-state solution has been obtained.

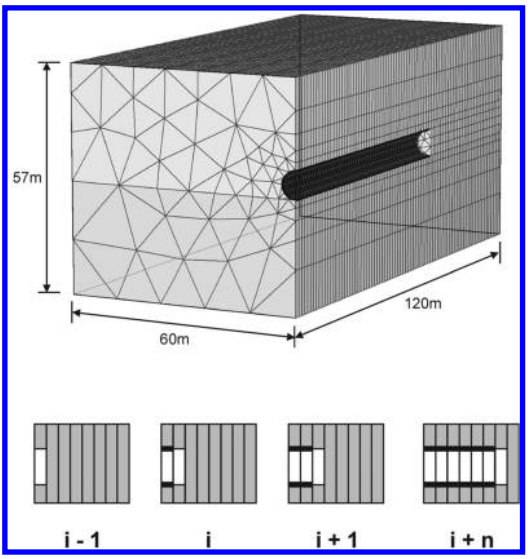


Figure 2. Three-dimensional FE-model, with $D = 7\,m$ and $d = 1.5\,m$.

For more details on the required excavation length the reader is referred to Vermeer et al. (2002) and Bonnier et al. (2002).

4 COMPARISON OF TWO- AND THREE-DIMENSIONAL FE-ANALYSES

For a particular tunnel geometry and a particular set of material properties, the finding of the corresponding β-value sometimes requires an iterative procedure. This is best explained by considering settlements as shown in Figure 1. Here a complete ground response curve is obtained from a two-dimensional FE-analysis and the settlement S_{tot} is obtained from a three-dimensional FE-analysis. For tunnels in truly elastic ground and $K_0 = 1$, the line from point A to point S_1 in Figure 1 is linear. In such a linear case it is straightforward to compute the inclination of line $A-S_1$ and to find point B with the corresponding β-value. This simple procedure even holds true for non-linear ground. Indeed for deep tunnels with $K_0 = 1$ there is a more or less axis symmetric state of stress around the tunnel giving a cylindrical compression of the lining. As long as this lining behaves elastically line $A-S_1$ in Figure 1 will be linear.

For shallow tunnels in non-linear ground, however, circular tunnel linings deform into ellipses with complex stress distributions and line $A-S_1$ is not longer linear. In such cases point B with its corresponding β-value has to be computed iteratively.

The above β-finding procedure applies to settlements. Instead of considering settlements, one may

Copyright © 2005 Taylor & Francis Group plc, London, UK

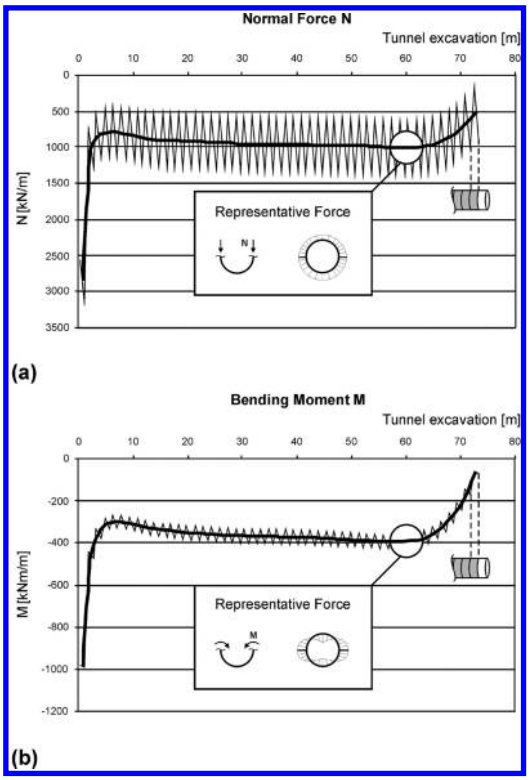


Figure 3. Evaluation of three-dimensional structural forces, (a) normal forces and (b) bending moments.

also compute ground response curves for bending moments and/or normal forces in linings. The settlement in Figure 1 might for instance be replaced by the maximum bending moment or the maximum normal force, as both of them increase when reducing the support pressure $\beta \cdot \sigma_0$. No doubt, all three curves will be somewhat different and one will find three different factors:

β-settlement,
β-bending moment,
β-normal force.

In the following results of β-values of bending moments and normal forces will not be plotted as discrete curves but are shown in a band width for structural forces in general.

5 EVALUATION OF STRUCTURAL FORCES AND SETTLEMENTS

Figure 3 shows a representative situation of three-dimensional distributions of bending moments and normal forces after an excavation of $50 \cdot d$. Both distributions show a significant increase at the left mesh boundary. These forces are non-physical but are effects related to the roller boundaries of the FE-mesh (Bonnier et al. 2002). Due to the stepwise excavation of NATM-tunnels results show a zigzagging pattern, which approaches a steady-state solution (Vermeer et al. 2002, Bonnier et al. 2002) after a total excavation length of about $10 \cdot d$. In order to compute β-values for the two-dimensional analyses the average value of these zigzag distributions (thick line in Figure 3) has been considered. The representative structural forces from the three-dimensional analyses were taken in the middle of the tunnel lining as indicated in the insert of Figure 3.

6 ON GROUND AND LINING STIFFNESSES

In tunnelling large amounts of soil and/or rock are excavated so that the ground underneath the tunnel is unloaded. Moreover, stress changes decrease with depth so that the soil or rock underneath the tunnel experiences on average only very small stress decrements. In such cases soil or rock will behave extremely stiff. Rather than using complex material models which account for stress and strain-level depending stiffnesses and which distinguish between loading and unloading, computations will be carried out for relatively simple material models with a constant stiffness modulus E both for loading and unloading. In order to account to some extend for the unloading and the small strain in the deep ground below the tunnel, a two-layer mesh is used for all analyses and the deep ground layer is taken much stiffer than the upper layers.

The lining plate elements were simulated by using a linear elastic model. The increase of the shotcrete lining stiffness E_l with time has been accounted for by using a stepwise increase with excavation phases. Starting from an initial stiffness of $E_l = 7500\,\mathrm{MN/m^2}$ in step i an increase to $E_l = 15000\,\mathrm{MN/m^2}$ in step $i + 1$ has been adopted.

On considering β-values, it should be emphasized that they depend on the lining thickness, the ground stiffness and the tunnel diameter, which can be combined into two relative stiffness factors

$$\alpha_1 = \frac{E \cdot R^3}{E_l \cdot I_l} \quad \text{and} \quad \alpha_2 = \frac{E \cdot R}{E_l \cdot t_l} \tag{1}$$

where R is the tunnel radius, E_lI_l the bending stiffness of the lining an t_l the thickness of the lining. In all cases that will be considered both relative stiffness factors are small and β-values are dominated by the stiffness and the strength of the ground.

Copyright © 2005 Taylor & Francis Group plc, London, UK

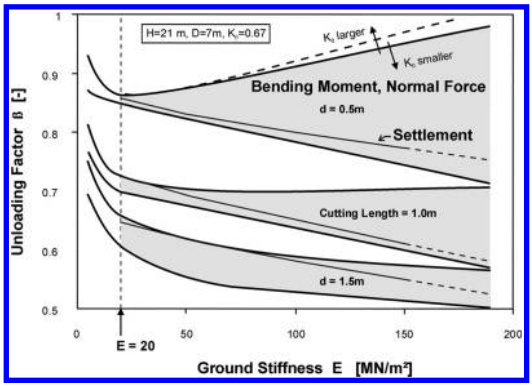


Figure 4. Influence of ground stiffness and cutting length for linear elastic ground. The results shown here were obtained from a tunnel with $D = 7\,m$, but are also valid for $D = 9\,m$ and $D = 11\,m$.

7 LINEAR ELASTIC ANALYSES

First of all a linear elastic constitutive model for the ground behaviour has been used to simulate the influences of ground stiffness E, horizontal stress factor K_0, tunnel diameter D and cutting length d. All analyses were carried out for a ground without ground water. The unit weight of the ground is taken to be $\gamma = 20\,kN/m^3$ and the Poisson's ratio $\nu = 0{,}3$. These values were kept constant throughout all analyses. All following results have been observed for a tunnel with a cover of $H = 21\,m$.

No interfaces between tunnel and ground have been applied as full bonding of the lining is considered.

Figure 4 shows the influence of ground stiffness E and cutting length d on the unloading factor β. Both for structural forces and settlements the unloading factor β is decreasing with increasing cutting length d. This seams logical, as a tunnel without a lining, i.e. $d = \infty$, has to have an unloading factor of $\beta = 0$ (no forces in the lining). Because of different unloading factors for bending moments and normal forces a band width for structural forces is plotted. The band width of structural forces is influenced by K_0. For smaller values of K_0 the upper lines of the scatter ranges drop down, for larger values of K_0 much wider scatter ranges are observed. For a smaller ground stiffness however, the influence of K_0 tends to disappear. With increasing ground stiffness a decrease of unloading factors is observed. The β-values for settlements always remain within the bandwidth for structural forces.

8 ELASTO-PLASTIC ANALYSES

Following the linear elastic evaluations the elasto-plastic Mohr-Coulomb model has been used to determine the influences of the strength parameters φ' and c'. The friction angle has been varied by considering $\varphi' = 20°$, $30°$, and $40°$. A wide range of the cohesion has been accounted for by $c' = 20$, 40, 60, 80, 100, 120, 160, 200, and $400\,kN/m^2$. In these studies dilation was neglected by using a dilatancy angle equal to zero.

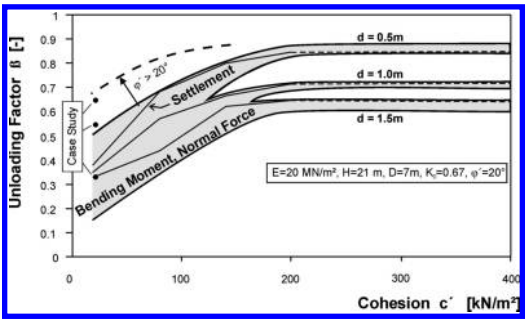


Figure 5. Influence of friction angle, cohesion and cutting length for elasto-plastic ground.

As the elastic analyses the elasto-plastic analyses are carried out with full bonding, i.e. without interfaces between tunnel and ground.

Figure 5 shows results of unloading factors for different cutting lengths, constant ground stiffness of $E = 20\,MN/m^2$ and a constant friction angle of $\varphi' = 20°$. With increasing cohesion the observed β-ranges approach a horizontal plateau which corresponds to the linear elastic solution (left side of curves in Figure 4). The elasto-plastic solution begins to deviate from the linear elastic one at a cohesion of $c' = 200\,kN/m^2$. For larger friction angles the linear elastic part of the scatter range is extending to smaller values of cohesion.

Unloading factors for settlements again remain within the observed bandwidth of structural forces. It is important to note, that the findings from Figure 5 correspond to the particular ground stiffness of $E = 20\,MN/m^2$. For a higher stiffness results will render smaller values of unloading factors as can be seen from Figure 4.

9 INFLUENCE OF TUNNEL COVER

The influence of the tunnel cover has yet not been observed in full detail. But for an elasto-plastic ground with $\varphi' = 40°$ and $c' = 40\,kN/m^2$ a tendency for structural forces of this influence can be given. Figure 6 shows a linear relationship between the unloading factor β and the tunnel cover H. With increasing tunnel cover unloading factors tend to drop down.

More detailed research will be carried out to investigate, whether β and H correspond in a linear relationship and if the steepness of the observed curve is influenced by the strength parameters φ' and c' or the

Copyright © 2005 Taylor & Francis Group plc, London, UK

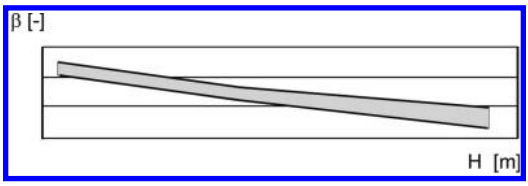


Figure 6. Qualitative influence of tunnel cover H on unloading factor.

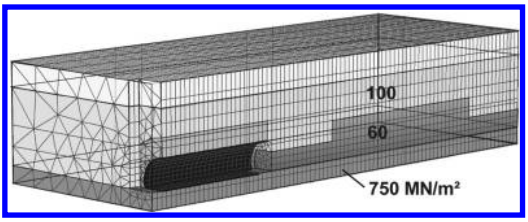


Figure 7. Three-dimensional FE-model of Steinhaldenfeld-tunnel.

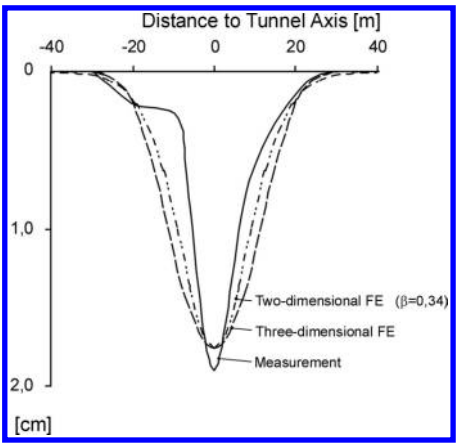


Figure 8. Calculated and measured transverse settlement trough.

Table 1. Ground properties of Steinhaldenfeld-tunnel.

	Cover layer	Upper Keuper Marl	Lower Keuper Marl	Limestone
Unit weight γ [Kn/m^3]	20	24	23	23
E-Module E [Mn/m^2]	15	100	60	750
Poisson's ratio ν[−]	0,375	0,2	0,35	0,2
Friction angle φ′[°]	25	25	25	25
Cohesion c′[Kn/m^2]	10	25	25	200

ground stiffness. Moreover, the influence of tunnel cover on the unloading factor for settlements has not been evaluated yet.

10 CASESTUDY STEINHALDENFELD-TUNNEL

Figure 7 shows a three-dimensional FE-model with excavation of top heading of Steinhaldenfeld-tunnel in Stuttgart, Germany. In addition to a full three-dimensional FE-analyses two-dimensional analyses have been carried out in order to arrive at unloading factors for this more complex tunnel from site. In the following results of unloading factors for structural forces and surface settlements of Steinhaldenfeld-tunnel will be shown.

10.1 *Ground properties*

The ground of Steinhaldenfeld-tunnel shown in Table 1 consists mainly of overconsolidated marl, which may be considered to be a hard ground as well as a soft rock. As ground water was of minor influence for this project the analysis was carried out without considering any water pressures. Moreover, it was assumed, that no pore pressures would develop by performing a drained analysis. The ground behavior was described by the Mohr-Coulomb model with parameters given in Table 1.

For the simulations of anchors additional ground properties have been used. Anchor forces have been modeled by an increased cohesion.

Figure 7 shows a relative thin ground layer underneath the tunnel excavation. This is due to the fact, that the ground stiffness of deeper layers is a factor ten times higher than the stiffness of the layers above the tunnel.

10.2 *FE-analysis of steinhaldenfeld-tunnel*

For the three-dimensional analysis of the top heading hoarse shoe profile with a diameter of *9.6 m* an excavation of *57* cutting lengths with $d = 1.2\,m$ has been simulated. For further details the reader is referred to Möller et al. (2004).

Figure 8 shows the results of computed and measured transverse settlement troughs. It is observed that the Mohr-Coulomb model predicts a relatively wide and shallow trough, which deviates from the measured one. At least for the steepness of the settlement

Copyright © 2005 Taylor & Francis Group plc, London, UK

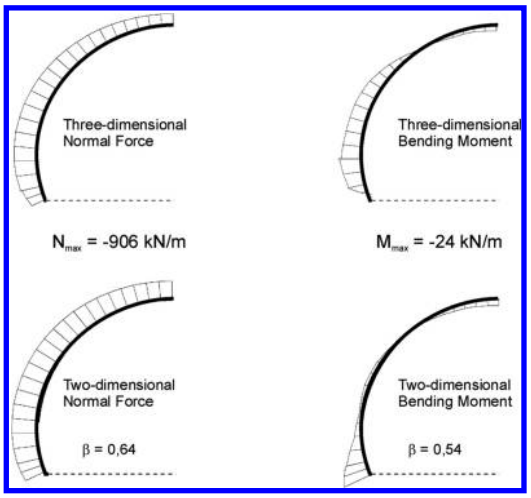


Figure 9. Comparison of three- and two-dimensional structural forces.

trough it is well known, that the elasto-plastic model in most cases is not able to predict reality (Herle 2003). Further details on the longitudinal settlement trough of Steinhaldenfeld-tunnel can be found in Möller et al. (2004) and Vermeer et al. (2003).

The best fit for a two-dimensional settlement analysis was found for an unloading factor of $\beta = 0.34$. Figure 9 shows unloading factors for structural forces. For the bending moment $\beta = 0.54$ and for the normal force $\beta = 0.64$ was observed. Again it becomes obvious, that different unloading factors for settlements as well as for bending moments and normal forces have to be used, to match exact three-dimensional solutions.

By comparing the β-values of Steinhaldenfeld-tunnel to the present study the unloading factor for settlements matches the solution of Figure 5 quite well, where as for structural forces one obtains slightly higher values. By considering the influence of Figure 6 solutions for more shallow tunnels yield higher unloading factors. Taking into account the smaller cover of *16 m* of Steinhaldenfeld-tunnel the unloading factors for structural forces still seam to match present findings satisfactory.

11 CONCLUSIONS

The present study shows results of unloading factors for two-dimensional FE-analyses. Both structural forces in linings and settlements for circular NATM-tunnels have been evaluated for a linear elastic and an elasto-plastic ground. Linear elastic as well as elasto-plastic analyses show, that the cutting length has the most significant impact on unloading factors. The coefficient of lateral earth pressure at rest and ground stiffness have a minor influence, but should not be neglected.

Elasto-plastic results show, that friction angle and cohesion have a considerable influence on unloading factors. The smaller the shear strength of the ground the smaller the unloading factors. For design analyses in elasto-plastic ground with $H = 21\,m$, $E = 20\,MN/m^2$ and $d = 1\,m$ it is advised to take $\beta = 0.7$ for structural forces and $\beta = 0.3$ for settlements, remaining on the save side of obtained results.

First analyses on the influence of tunnel cover have shown, that unloading factors tend to increase with tunnel depth. In particular regarding friction angle and cohesion further research on the tunnel cover needs to be carried out.

A case study on Steinhaldenfeld-tunnel in Stuttgart, Germany has given first evidence, that present findings are representative for practical applications. But never the less these results have to be treated with caution as many questions, such as influences of geometry of tunnel cross section, securing means like anchors etc. or complex ground layering still remain open. In these cases it is more appropriate to use a three-dimensional FE-analysis.

REFERENCES

Bonnier, P.G., Möller, S.C., Vermeer, P.A. 2002. *Bending Moments and Normal Forces in Tunnel linings*. 5th European Conference Numerical Methods in Geotechnical Engineering (NUMGE). Paris: Presses de l'ENPC/LCP: 515–522.

Herle, I. 2003. *Constitutive models for numerical simulations*. In: Rational Tunnelling. Summerschool, Innsbruck: Ed. D.Kolymbas: Logos Verlag Berlin: 27–60.

Möller, S., Lehmann, T., Rogowski, E. 2004. *Dreidimensionale Finite-Element-Berechnung der Setzungsmulde am Beispiel des Steinhaldenfeldtunnels in Stuttgart*. Kolloquium Bauen in Boden und Fels. Tagungsband 4. Ostfildern: TAE: 275–282.

Pacher, F. 1964. *Deformationsmessungen im Versuchsstollen als Mittel zur Erforschung des Gebirgsverhaltens und zur Bemessung des Ausbaues*. In: Felsmechanik & Ing. Geologie, Suppl. I: S.149–161.

Schikora, K., Fink, T. 1982. *Berechnungsmethoden moderner bergmännischer Bauweisen beim U-Bahn-Bau*. In: Bauingenieur: 193–198.

Vermeer, P.A., Bonnier, P.G., Möller, S.C. 2002. *On A Smart Use of 3D-FEM in Tunneling*. Proceedings 8th International Symposium on Numerical Models in Geomechanics (NUMOG VIII), Rome: A.A. Balkema Publishers, Lisse: 361–366.

Vermeer, P.A., Möller, S.C., Ruse, N. 2003. *On the Application of Numerical Analysis in Tunnelling*. Post proceedings 12th Asian Regional Conference on Soil Mechanics and Geotechnical Engineering (12 ARC). Singapore, 4–8 August 2003, 2: 1539–1549.

Wittke, W. 1984. *Felsmechanik*. Berlin/Heidelberg/New York/Tokyo: Springer Verlag.

Copyright © 2005 Taylor & Francis Group plc, London, UK

Case study of 3D fracture aperture density distribution technique on the assessment of tunnel safety at new constructing road

Byung-Joo Lee
Korea Institute of Geoscience & Mineral Resources (KIGAM), Daejeon, S. Korea

Jung-Yul Kim & Yoo-Sung Kim
Soam Consultant Co., Ltd., Daejeon, S. Korea

ABSTRACT: Although surface mapping would provide lots of geological and structural data, there has been a tendency that in reality the attitude of dominant fracture groups from discontinuities around the tunnel route have been properly used as a design parameter. Even the intersecting planes of faults with the planned tunnel, that plays an important role in tunnel design, tend to be estimated only in a geometrically intuitive way. Due to such uncertainties, the information won't be readily used for tunnel design. Thus, this paper introduces an evaluation method enable to project all the available structural data from surface mapping into an arbitrary 3D-block encompassing the tunnel, where each fracture aperture is, if possible, considered. With this, the interpretation of fracture system around the tunnel route has been fundamentally eased and hence other valuable design parameters can be additionally estimated.

1 INSTRUCTION

Geological mapping data which are rock distribution, geological age, the relationship between the each rock and geological structure, give a lot of information for tunnel design. Most important data of them are the discontinuities of geologic structure. By surface geological mapping, we can draw the geological cross section to the tunnel level. But for confirming the section bore hole drilling must be carried out. The purpose of this paper that through the data of the surface fractures the discontinuities are estimated and analyzed to the tunnel route by three dimensional fracture aperture density distribution techniques. For example, pre-Cambrian gneiss and schist area, which are new constructing the road, are selected (Fig. 1) and for analyzing them, at each point dip angle, dip direction and aperture was measured (Figs 1 & 2).

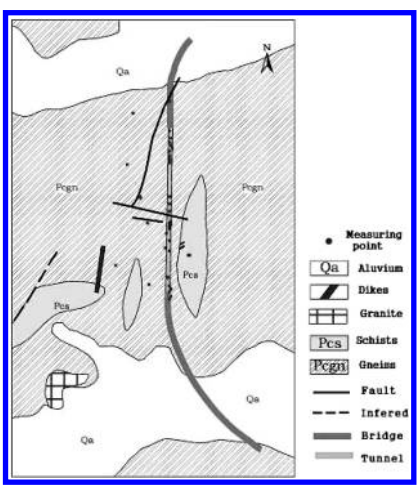


Figure 1. Geological map around new constructing road.

2 FRACTURE FACE MAPPING

Fracture face mapping means an evaluation method used to form an image of fracture lines determined by intersecting of each fracture plane with an arbitrary plane section (normally vertical section) crossing the borehole where structural data are available. As illustrated in Figure 3, if fracture data are obtained in borehole A and the arbitrary section corresponds to the plane containing borehole A and B, the intersected fracture line D_AD_B can be derived from the depth *DepDif*, that is,

$$\theta = \theta_A - \theta_{AB}$$
$$DepDif = r \cdot \tan\beta = r \cdot \tan\alpha \cdot \cos\theta$$

α, θ_A : true dip and dip direction of fracture plane

θ_{AB} : azimuth of a selected vertical plane section

Copyright © 2005 Taylor & Francis Group plc, London, UK

assuming that all fractures be planar with fixed aperture, although many fractures are geometrically complex and others are altered chemically, according to the abundant experiments in recent years, it would seem that the mapping technique could be applied to benefit the design of numerous engineering works such as tunnel excavation, slope stability, dam foundation and diverse environmental works (Kim et al., 2002 a,b &c).

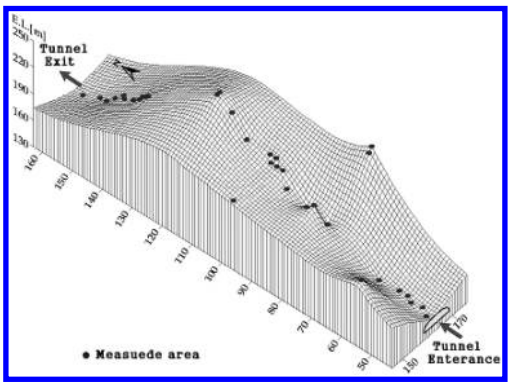


Figure 2. Measuring point of the joint and fault on three-dimensional geographical surface.

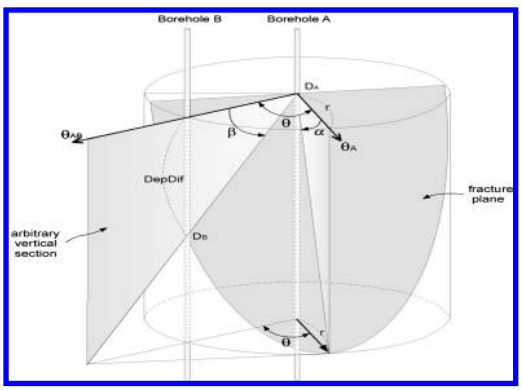


Figure 3. Fracture plane-arbitrary vertical section geometry, where two boreholes lie on the vertical section.

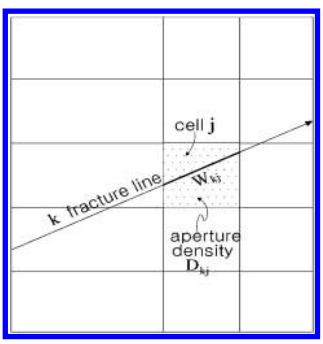


Figure 4. Net describing parameters for a fracture line for the cells.

3 FRCTURE APERTURE DENSITY DISTRIBUTION

A main feature of this strategy consists in incorporating information of fracture aperture size in the result of fracture face mapping, because the aperture provides a potential for estimating fracture permeability. As indicated in Figure 4, a selected plane section of medium around a borehole or the cross section between two boreholes is discredited into a two dimensional grid of cells (rectangular elements). As each elongated (straight) fracture (k fracture line) passes through the cells, the corresponding aperture size value is successively summed up in each cell, depending on the fracture length segment W_{kj}. As mentioned above, the fracture lines are estimated from fracture face mapping algorithm. If the fracture line does not pass through a particular grid element, the segment length W_{kj} is set to zero. The final value (aperture size value of each cell) D_j derived from all the detected fractures constitutes the fracture aperture density distribution of the selected plane section. (Kim et al., 2002d). That is, the aperture value D_{kj} in each cell j for k fracture line can be expressed as :

$$D_{kj} = W_{kj} \cdot A_k ,$$
$$j = 1, 2, \ldots, I \qquad I = M \times N \text{ (2-D grid)}$$

I : total number of grid elements
A_k : aperture size value of K fracture line
The final fracture density D_j is then given simply by

$$D_j = \sum_k D_{kj}$$

4 THREE-DIMENSIONAL PRESENTATION OF FRACTURE MAPPING AND FRACTURE APERTURE DENSITY DISTRIBUTION

As the permeability of hard rock is mainly influenced by fractures, a three-dimensional view of fractures around the test borehole is very helpful to examine some prevailing water flow routes, to envisage a future grouting or excavation plan. This far, the estimated fractures lines are imaged only on the plane section crossing the test hole (see Fig. 3). However, for a three-dimensional presentation, the fracture lines should be determined by intersecting of each fracture plane with an

Copyright © 2005 Taylor & Francis Group plc, London, UK

arbitrary plane section apart from the test hole, as indicated in Figure 5. Figure 6 illustrates the corresponding geometry of fracture plane, arbitrary plane section S and fracture line, with the previous geometry description in Figure 5 in mind. The goal of this algorithm is to find the positions D_{S1}, D_{S2} which allow determining the fracture line on section S. To this end, the depth ranges $DepDif_1(D_{s1} - D_A)$ and $DepDif_2$ are beforehand calculated. In geometry condition, they are:

$$\beta_1 = \tan^{-1}(\tan\alpha \cdot \cos\theta_1)$$
$$DepDif_1 = H_1 \cdot \tan\beta_1 = H_1 \cdot \tan\alpha \cdot \cos\theta_1$$

$$\beta_2 = \tan^{-1}(\tan\alpha \cdot \cos\theta_2)$$
$$DepDif_2 = H_2 \cdot \tan\beta_2 = H_2 \cdot \tan\alpha \cdot \cos\theta_2$$

Thus, the depths z_1, z_2 of cross points D_{s1}, D_{s2} are given:

$$z_1 = D_A - DepDif_1 \quad , \quad z_2 = D_A - DepDif_1 - DepDif_2$$

Finally, regarding the geometry relation shown in Figure 7, the horizontal coordinates of $D_{s1}(x_1, y_1)$ and $D_{s2}(x_2, y_2)$ can be easily computed:

$$x_1 = x_0 - H_1 \cos\gamma$$
$$y_1 = y_0 - H_1 \sin\gamma$$
$$x_2 = x_1 + H_2 \cos(90° - \gamma)$$
$$y_2 = y_1 - H_2 \sin(90° - \gamma)$$

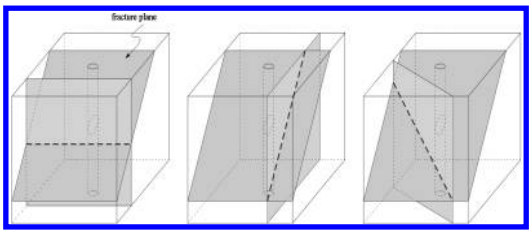


Figure 5. Fracture lines are constructed by intersecting of arbitrary vertical sections with the same fracture plane.

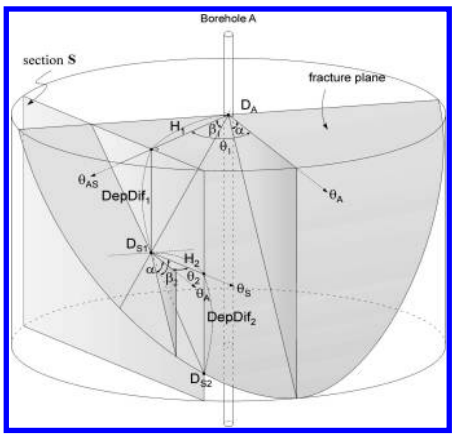


Figure 6. Fracture plane-arbitrary vertical section geometry for three-dimensional fracture face mapping.

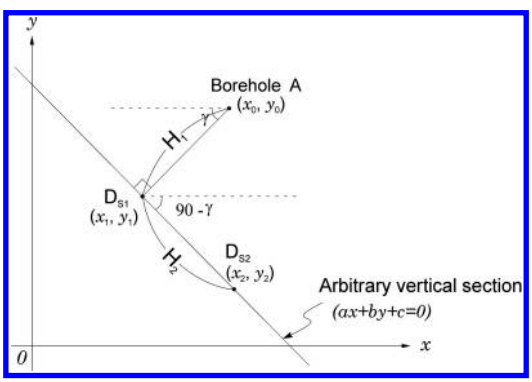


Figure 7. Geometry for calculating the coordinates of D_{S1} and D_{S2}.

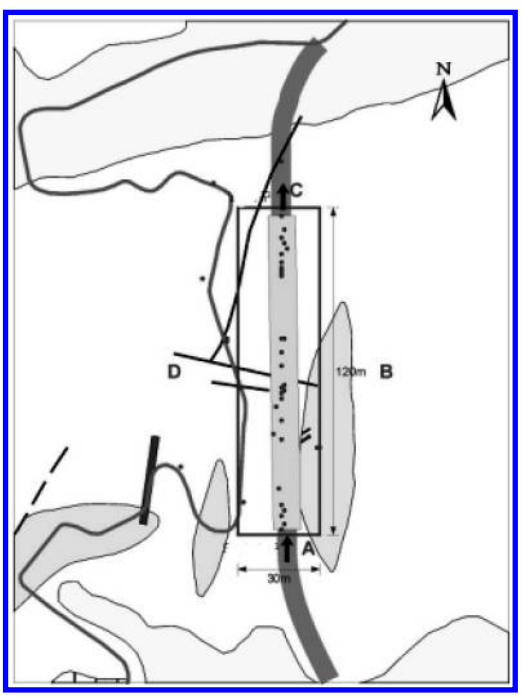


Figure 8. Tunnel site (rectangular area) for 3-d fracture aperture density. A, B, C, D represent the cross section lines.

Copyright © 2005 Taylor & Francis Group plc, London, UK

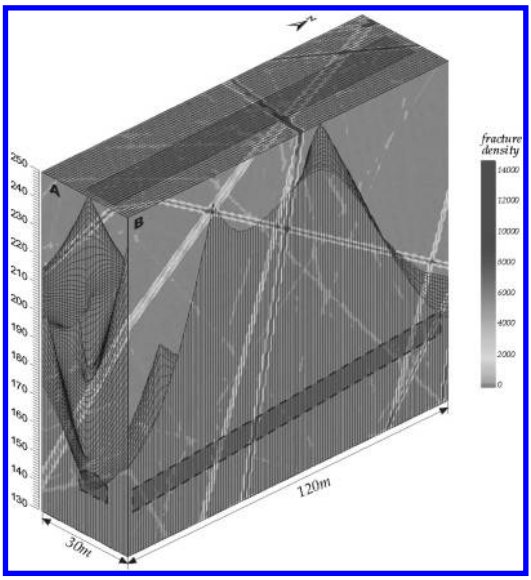


Figure 9. Block diagram from surface to bottom of tunnel, 30 m × 120 m × 120 m, by 3-d fracture aperture density.

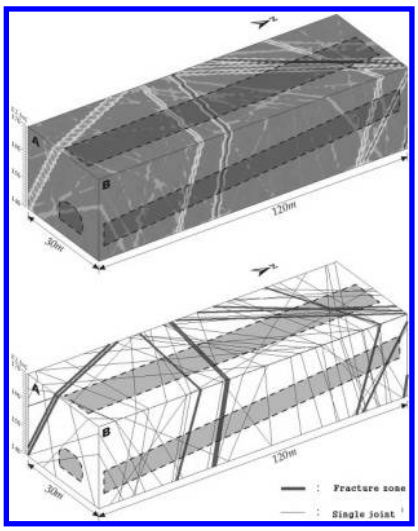


Figure 10. Through the tunnel route, three-dimensional fracture zone and joint distribution.

where $H_1 = \dfrac{|ax_0 + by_0 + c|}{\sqrt{a^2 + b^2}}$

The intersected line, that is, the fracture line from fracture plane and arbitrary plane section apart from the test hole is then determined by two point, $D_{s1}(x_1, y_1, z_1)$, $D_{s2}(x_2, y_2, z_2)$ in space. The corresponding fracture

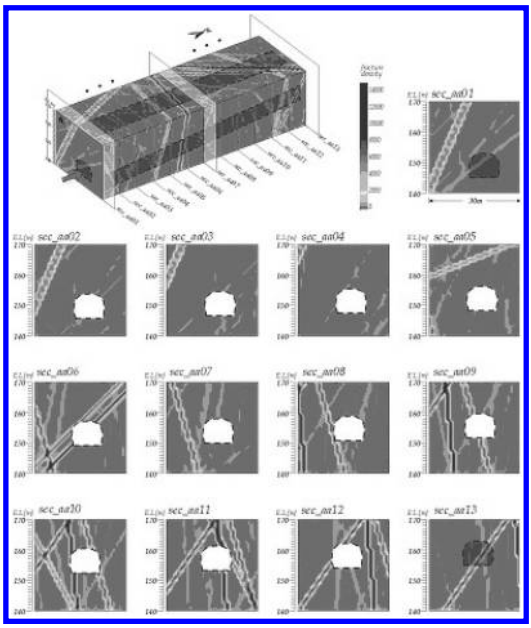


Figure 11. Vertical cross section across the tunnel per every 10 m at the tunnel route.

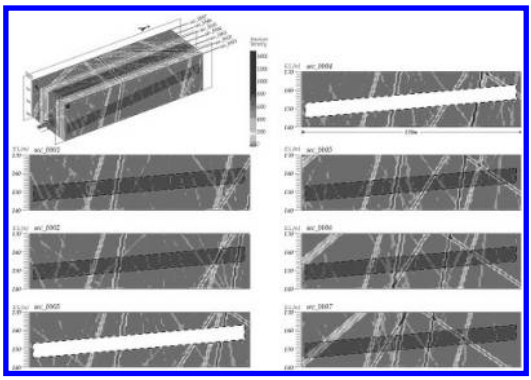


Figure 12. Vertical cross section along the tunnel per every 10 m at the tunnel route.

aperture density value in each cell can be also evaluated in the same manner shown in Figure 4.

5 APPLING AT NEW CONSTRUCTING TUNNEL SITE

Figure 8 is selected area (rectangular area) for the 3-d fracture aperture density and A,B,C,D represent the cross section lines. Figure 9 shows the block diagram having three dimensional fracture zones and joint

Copyright © 2005 Taylor & Francis Group plc, London, UK

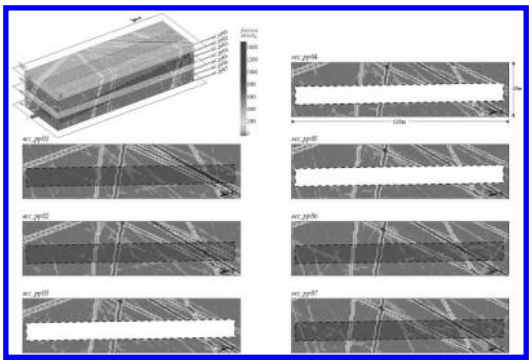


Figure 13. Horizontal cross section along the tunnel per every 10 m at the tunnel route.

patterns by the surface fracture mapping data. By these two figures, the surface fracture pattern is well reflected to underground tunnel level (Figure 10). At vertical cross section across the tunnel and along the tunnel and horizontal cross section along the tunnel per every 10 m show Figure 11, 12 and 13.

6 CONCLUSION

Even though geological mapping data give a lot of information for tunnel design, there has been a tendency that in reality the dips and directions of dominant fracture groups from discontinuities around the tunnel route have been properly used as a design parameter. Even the intersecting planes of faults with the planned tunnel, that plays an important role in tunnel design, tend to be estimated only in a geometrically intuitive way. Due to such uncertainties, the information won't be readily used for tunnel design. Through the data of the surface fractures, the discontinuities are estimated and analyzed to the tunnel route by three dimensional fracture aperture density distribution techniques. At new constructing tunnel site, through the tunnel route vertical and horizontal cross section per 10 m are estimated by three-dimensional fracture aperture density distribution technique.

REFERENCES

Kim, J. Y., Kim, Y. S. and Hyun, H. J. (2002a) Televiewer rock strength as an approach to estimate the strength of in situ Rocks, *Proc. the KGS Spring Conference 2002*, Seoul, Korea, 237–244.

Kim, J. Y., Kim, Y. S., Kim, H. S., Back, K. H. and Kim, K. S. (2002b) Accurate quantitative assessment of grouting efficiency in fractured rocks by evaluating the aperture sizes of fractures, *Proc. the KGS Spring Conference 2002*, Seoul, Korea, 695–702.

Kim, J. Y., Kim, Y. S. and Kim, K. S. (2002c) Development of fracture face mapping algorithm and its applications to the design of various engineering and environmental works, *Proc. the KGS Spring Conference 2002*, Seoul, Korea, 119–126.

Kim, J. Y. and Kim, Y. S. (2002d) Evaluation of fracture density distribution for the design of grouting works in fractured rocks, *Proc. the KGS Spring Conference 2002*, Seoul, Korea, 627–634.

Copyright © 2005 Taylor & Francis Group plc, London, UK

A study on the reinforcement effect of Umbrella Arch Method and prediction of tunnel crown and surface settlement

Seon-Hong Kim
Yooshin Engineering Corporation, Seoul, Korea

Seung-Han Baek
Korea Institute of Construction Technology, Korea

Hyun-Koo Moon
Hanyang University, Seoul, Korea

ABSTRACT: Umbrella Arch Method (UAM) is commonly used for tunnel design in order to reinforce the ground around tunnel and stabilize the tunnel face. However, since the design and construction work with UAM have been done on the basis of only the practical experience of engineers, it needs to analyze quantitatively the reinforcement effect of UAM. In this study, Finite Element Method was applied for analysis of the quantitative reinforcement effect with deformation modulus of ground and overburden. As a result, the settlement increases as overburden increases and decreases with the increase of the deformation modulus of ground. Also, the prediction equations for crown settlement and surface settlement, which are represented as exponential function, have been suggested through the regression analysis.

1 INTRODUCTION

When a tunnel is constructed on poor and soft ground, some kinds of auxiliary method for stability of tunnel are applied in order to secure the stability of tunnel. Among various auxiliary methods, Umbrella Arch Method (UAM) is commonly being applied in Korea, but UAM is used only based on the empirical knowledge without any organized theory and quantitative analysis on the effect of UAM.

Recently, plenty of case studies for UAM on various site conditions as well as parametric studies by numerical analysis are being performed. Harazaki et al. (1998) presented the result that UAM is effective method for the stability of tunnel face and for the improvement of ground in front of tunnel face by measuring surface settlement and stress of steel pipe at road tunnel. Bae et al. (1997) analyzed loosened area and displacement in front of tunnel face in case whether UAM was applied to or not. As a result, UAM is more effective method for stability of tunnel than other auxiliary methods. Kim et al. (1998) also analyzed ground behavior around tunnel and clarified the role of the steel pipe and grouting material as support material by assuming the ground applied steel pipe and grouting material as a complex material. They estimated the characteristics of design factor as well in case of applying UAM. Ryu et al. (1995) suggested that transversal reinforcement range is the important design factor to minimize the ground settlement by using numerical analysis.

In this study, by taking mechanical properties of ground and overburden parameters, the reinforcement effect of UAM is analyzed by 3-dimensional finite element method and the prediction equations for tunnel crown and surface settlement are suggested by regression analysis.

2 REINFORCEMENT EFFECT OF UAM

2.1 *Model and modeling condition*

In this study, by using the Pentagon3D™ which is one of 3-dimensional FEM programs, an numerical analysis has been performed on the construction sequence of mini-bench method and the procedure of reinforcement during a tunnel excavation. The tunnel section of the model was set to have 10.5 m of width, 9 m of height and about 10 m of equivalent diameter. Also, 6 models that have the overburden thickness of 5, 10, 15, 20, 25, 30 m (0.5∼3.0D) from the tunnel crown were prepared (Kim, 2003).

Copyright © 2005 Taylor & Francis Group plc, London, UK

Figure 1 shows the model of the finite element mesh when overburden thickness is 30 m, and the model was set by considering the shape of the tunnel section, strata, construction sequence, steel pipe and dividing strata into boundary of upper and lower half. In order to consider the influence of boundary condition due to the excavation, the modeling was performed to make the side part of boundary extend more than five times of tunnel diameter and the lower part of boundary extend more than four times of tunnel diameter. To analyze the reinforcement effect of UAM, a series of arrangement has been made as the steel pipe (diameter: 60.8 mm, thickness: 3 mm, length: 12 m) to the 0.4 m of distance in transverse direction and 6 m of distance in a longitudinal direction as a range of angle of 120° from a center of tunnel. As for the 5 rows from the opening section of tunnel, the steel pipe was designed upward as angle of 15°. For the analysis of relative reinforcement effect according to the ground condition such as deformation modulus and overburden thickness, the same range of reinforcement was applied. The analysis procedure of excavation and reinforcement has been set to total 35 stages as application of UAM and excavation, soft shotcrete, and hard shotcrete. The advance was 1 m and the bench length of the upper and lower half were 4 m, half times of tunnel height.

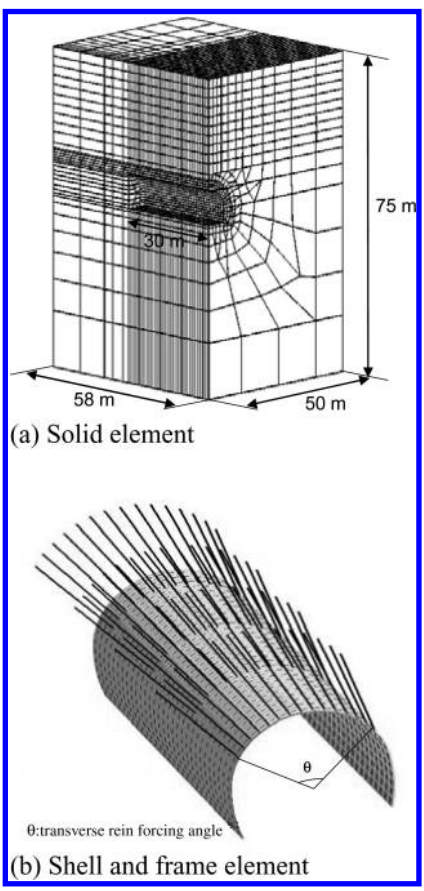


Figure 1. The 3-dimentional finite element model.

In this study, to analyze the characteristics of ground motion and the reinforcement effect, 7 kinds of mechanical property of ground were used as shown Table 1. Also, 3-dimensional numerical analysis has been performed on total 84 cases from the combination of the seven mechanical properties, six different overburden thicknesses, and appliance of UAM.

The ground where the steel pipe and the grouting material have been inserted was assumed as a complex material, and the transverse deformation modulus deduced from the 'strain energy theory' was applied to the equivalent material property of complex material. When the volume fraction of grout is between 0.4 and 0.5, grouted grounds indicate two times of deformation modulus to the original ground. Referring to the mean grouting rate (20∼0%), two times of deformation modulus of the original ground was applied to the deformation modulus of grouted ground (Kim and Moon, 2001).

2.2 *Results for surface settlement*

An analysis was performed on the surface settlement of transversal direction at the top of tunnel, referring to the variation of the deformation modulus of ground and overburden thickness. Figure 2 shows that in Ground A, the surface settlement ratio for maximum varies with normalized transverse distance, the surface settlement ratio was about 61∼70% at the inflection point and about 8∼12% at the point of 2.5i when UAM was not applied. And also, when UAM was applied, the surface settlement ratio decreased little by little. Ground B-G was similar tendency with

Table 1. Mechanical properties of ground and shotcrete.

Ground type	E (MPa)	ν	coh (MPa)	ø (°)	γ (t/m^3)
Weathered soil					
A	20	0.30	0.015	30	1.9
B	50	0.30	0.03	30	2.0
Weathered rock					
C	100	0.28	0.05	32	2.1
D	300	0.27	0.07	33	2.2
E	500	0.27	0.1	33	2.2
Soft rock					
F	1,000	0.26	0.2	34	2.4
G	3,000	0.25	0.3	35	2.5
Shotcrete	10,000	0.20	–	–	2.5

Copyright © 2005 Taylor & Francis Group plc, London, UK

Ground A, generally, as the overburden thickness become thinner, the slope of surface settlement curve tend to increase at the inflection point. Also, as shown the Table 2, as the deformation modulus of ground increased, the settlement ratio decreased. This is proved that as deformation modulus of ground increased, the reinforcement effect of UAM decreased.

2.3 *Results for crown settlement*

In this chapter, the crown settlement on variation of deformation modulus and overburden thickness is analyzed. Figure 3 shows the variation of crown settlement ratio with normalized axial distance in Ground A. In Ground A the crown settlement ratio at the tunnel face increased little by little as the overburden thickness increase and decreased in case that UAM was applied. Also, as the overburden thickness increased, the slope of crown settlement ratio curve increased and the distance from the starting point of crown settlement relatively increased. Ground B-G were similar tendency with Ground A. Generally the more the deformation modulus increased, the more the crown settlement at the tunnel face decreased. As shown the Table 3, as the deformation modulus of ground increased, the settlement ratio decreased. This indicates that as deformation modulus of ground increased, the reinforcement effect of UAM decreased.

3 PREDICTION EQUATION OF SURFACE SETTLEMENT

3.1 *Single regression analysis*

In order to predict surface settlement, it was performed single regression analysis from the result of numerical analysis with the following exponential function, and it is determined coefficient i and k.

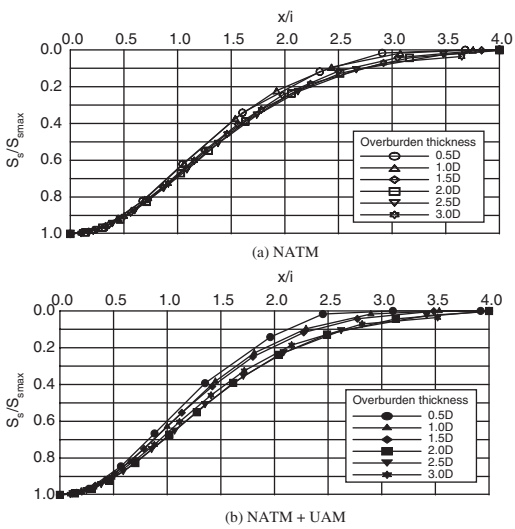


Figure 2. Variation of surface settlement ratio with normalized transverse distance in ground A.

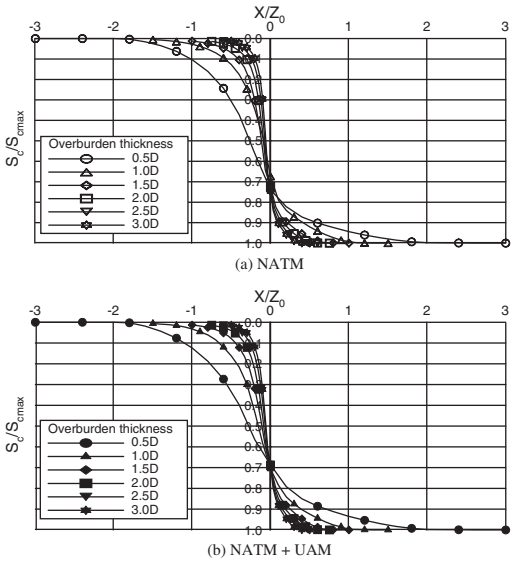


Figure 3. Variation of crown settlement ratio with normalized axial distance in ground A.

Table 2. Maximum surface settlement. Unit: mm

Ground type	NATM						NATM + UAM					
	0.5D	1.0D	1.5D	2.0D	2.5D	3.0D	0.5D	1.0D	1.5D	2.0D	2.5D	3.0D
A	22.6	27.3	32.7	33.1	33.1	32.6	16.3	25.6	28.4	29.7	30.0	29.4
B	9.4	14.0	14.6	15.1	16.1	15.9	7.1	11.9	13.0	14.5	14.6	14.6
C	6.72	8.02	8.62	8.78	8.90	8.31	4.88	6.91	7.66	7.92	8.06	7.99
D	2.83	3.40	3.57	3.63	3.64	3.63	2.13	2.91	3.18	3.29	3.33	3.35
E	1.85	2.18	2.26	2.30	2.31	2.31	1.42	1.90	2.04	2.11	2.13	2.14
F	1.23	1.34	1.35	1.34	1.33	1.31	1.07	1.24	1.28	1.28	1.26	1.25
G	0.46	0.49	0.50	0.50	0.50	0.49	0.38	0.47	0.47	0.47	0.47	0.47

Copyright © 2005 Taylor & Francis Group plc, London, UK

Table 3. Crown settlement with varying ground type and overburden.

Ground type		NATM						NATM + UAM					
		0.5D	1.0D	1.5D	2.0D	2.5D	3.0D	0.5D	1.0D	1.5D	2.0D	2.5D	3.0D
A	S_0(mm)	21.0	30.1	50.1	65.4	84.0	103.3	13.3	27.5	38.6	50.0	61.5	74.4
	S_{cmax}(mm)	28.4	44.6	69.3	90.3	113.9	138.5	19.3	39.0	55.3	72.5	89.9	107.8
	S_0/S_{cmax}(%)	74.0	67.4	72.3	72.4	73.7	74.6	68.7	70.6	69.9	69.0	68.4	69.0
B	S_0(mm)	4.7	14.8	16.9	23.8	34.6	42.2	3.5	10.7	13.1	21.3	26.7	32.6
	S_{cmax}(mm)	10.7	23.4	30.5	40.9	54.0	64.8	8.2	18.2	24.9	35.4	44.0	52.7
	S_0/S_{cmax}(%)	44.0	63.1	55.4	58.3	64.1	65.2	43.2	58.7	52.7	60.4	60.7	61.8
C	S_0(mm)	2.7	5.9	9.4	15.3	20.3	17.2	2.3	4.9	7.7	11.5	15.3	16.9
	S_{cmax}(mm)	7.07	12.6	18.1	24.9	31.7	33.7	5.6	10.3	14.8	19.8	25.1	29.6
	S_0/S_{cmax}(%)	38.5	47.0	52.2	61.5	64.0	50.9	40.6	47.3	52.0	58.2	61.0	57.3
D	S_0(mm)	1.0	1.9	3.2	4.5	6.4	8.1	0.7	1.6	2.6	3.6	5.0	6.3
	S_{cmax}(mm)	3.3	5.5	7.6	10.0	12.5	15.1	2.5	4.4	6.2	8.1	10.1	12.2
	S_0/S_{cmax}(%)	28.8	35.5	41.6	45.3	50.8	53.4	29.6	36.6	42.0	44.9	49.1	51.7
E	S_0(mm)	0.5	1.1	1.7	2.4	3.1	4.1	0.4	1.0	1.5	2.1	2.7	3.3
	S_{cmax}(mm)	2.2	3.5	4.9	6.3	7.8	9.4	1.7	2.9	4.0	5.2	6.4	7.6
	S_0/S_{cmax}(%)	24.0	31.2	34.3	38.0	40.0	43.6	26.3	34.0	36.8	40.0	42.0	43.9
F	S_0(mm)	0.36	0.66	0.94	1.21	1.49	1.81	0.3	0.6	0.9	1.1	1.4	1.7
	S_{cmax}(mm)	1.5	2.2	2.9	3.7	4.5	5.3	1.2	1.9	2.6	3.3	4.0	4.7
	S_0/S_{cmax}(%)	24.7	30.8	32.4	32.9	33.1	33.9	26.5	32.4	34.0	34.5	34.7	35.3
G	S_0(mm)	0.1	0.2	0.3	0.4	0.5	0.6	0.1	0.2	0.3	0.4	0.5	0.6
	S_{cmax}(mm)	0.5	0.8	1.1	1.4	1.7	2.0	0.4	0.7	1.0	1.2	1.5	1.7
	S_0/S_{cmax}(%)	16.1	25.6	28.4	29.3	29.7	29.8	17.5	27.8	30.6	31.6	32.0	32.2

$$S_s = S_{s\,\max} e^{\left(-x^2/ki^2\right)} \quad (1)$$

where x is the lateral distance from tunnel center, k is coefficient determined by the characteristics of ground and overburden thickness, and i is the inflection point determined by the characteristics of ground and overburden thickness.

According to the regression result, inflection point i and coefficient k were increased as ground thickness was increased, and were not correlated with the deformation modulus of ground. Figure 4 shows the variations of i, k with increasing the deformation modulus of ground.

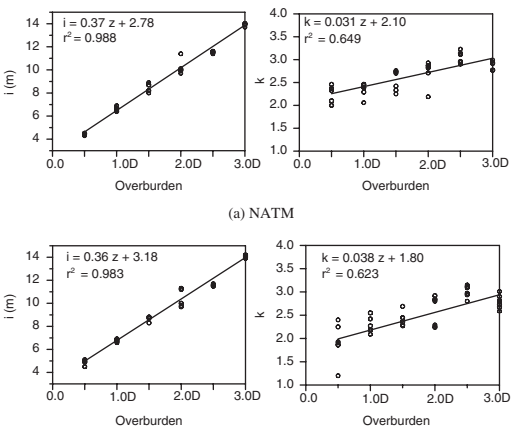


Figure 4. Regression results of inflection point i and coefficient k with increasing overburden.

3.2 *Multiple regression analysis*

A multiple regression analysis assumed the form of Equation (2) which is based on results of numerical analysis for maximum surface settlement after converging in the center of tunnel, and the multiple regression analysis was performed with overburden thickness, deformation modulus of ground and surface settlement.

$$S_{s\max}\left(\frac{1}{E}, z\right) = a_s \frac{1}{E} + b_s z + c_s \frac{z}{E} + d_s \quad (2)$$

Where E is the deformation modulus of ground z is overburden thickness from the surface to tunnel crown, and a_s, b_s, c_s and d_s are constants obtained from regression results.

From the result of a multiple regression analysis, in case that UAM was not applied, the maximum surface settlement represents Equation (3) and its coefficient

Copyright © 2005 Taylor & Francis Group plc, London, UK

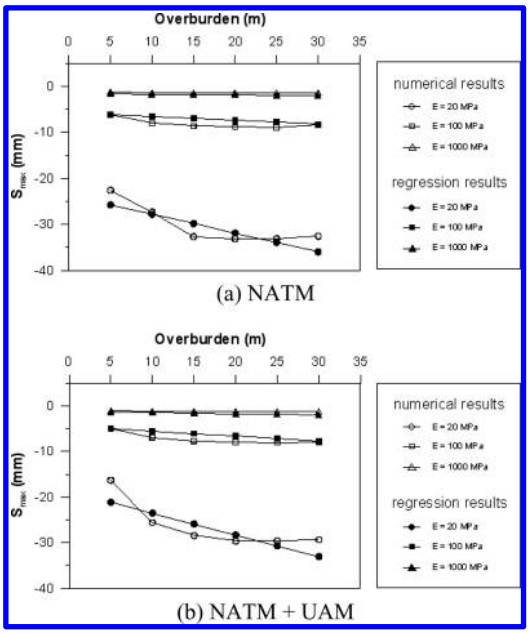


Figure 5. Comparison of maximum surface settlement between numerical analysis and regression analysis.

of determination was more than 0.98. In case that UAM was applied, the maximum surface settlement represents Equation (4) and its coefficient of determination was more than 0.97. This is shown in Figure 5.

$$S_{s\max} = -\frac{4.51\times10^{2}}{E} - 5.31\times10^{-3}z - 8.06\frac{z}{E} - 1.15 \quad (3)$$

$$S_{s\max} = -\frac{3.57\times10^{2}}{E} - 1.49\times10^{-3}z - 9.22\frac{z}{E} + 0.89 \quad (4)$$

Where S_{smax} is the maximum surface settlement (mm), z is overburden thickness (m) and E is the deformation of soils.

4 PREDICTION EQUATION OF CROWN SETTLEMENT

4.1 *Single regression analysis*

To predict the crown settlement curve, using numerical analysis result, single regression analysis was performed to the following equations which are formed a exponential function.

$$\begin{aligned} S_c &= S_o e^{a_1 x} && x \le 0 \\ S_c &= S_{c\max} - (S_{c\max} - S_o)e^{a_2 x} && x \ge 0 \end{aligned} \quad (5)$$

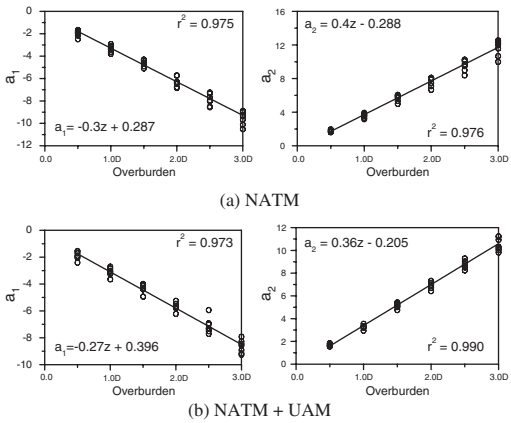


Figure 6. Regression results of unknown coefficients a_1 and a_2.

In above Equation (5), x = X/z, X is the longitudinal distance from the tunnel face, z is the overburden thickness from tunnel crown to the ground surface, a_1 and a_2 are the coefficient determined by the characteristic of ground and overburden thickness.

According to regression result, a_1 and a_2 were increased as ground thickness was increased, and were not correlated with the deformation modulus of ground. Figure 6 shows the variations of a_1 and a_2 with increasing the deformation modulus of ground.

4.2 *Multiple regression analysis*

Based on the result of numerical analysis, the crown settlement and the maximum crown settlement after converging at the tunnel face, assumed the form of Equation (6). Then it is performed the multiple regression analysis with overburden thickness, deformation modulus of ground and crown settlement.

$$S_0, S_{s\max}\left(\frac{1}{E}, z\right) = a_c\frac{1}{E} + b_c z + c_c\frac{z}{E} + d_c \quad (6)$$

In above equation, a_c, b_c, c_c and d_c, are the constants through regression analysis.

As a result of multiple regression analysis, the crown settlement at the tunnel face can be presented Equation (7) when UAM was not applied and presented Equation (8) in case that UAM was applied. The maximum crown settlement can be presented Equation (9) when UAM was not applied and presented Equation (10) in case that UAM was applied. The plots of these results are shown Figure 7 and Figure 8. At the prediction equation of crown settlement from the tunnel face, the coefficient of determination, in case that UAM was not applied, presents 0.998, and presents

Copyright © 2005 Taylor & Francis Group plc, London, UK

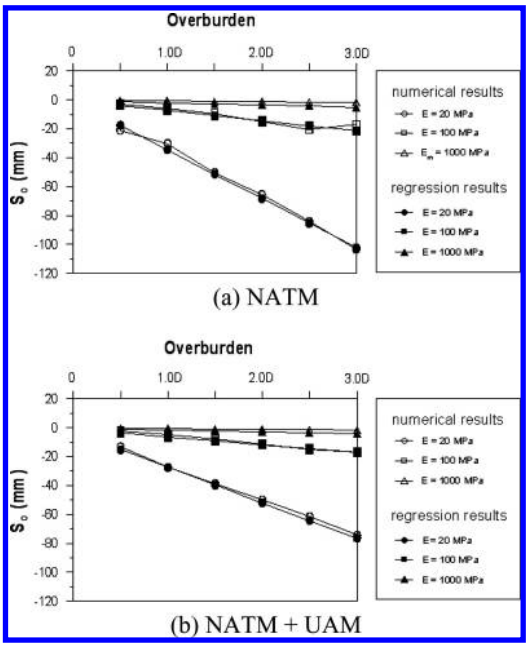


Figure 7. Comparison of crown settlement between the numerical analysis and regression analysis.

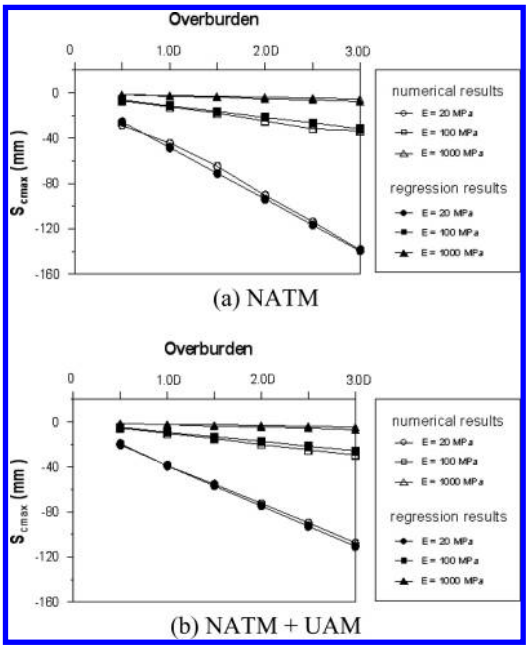


Figure 8. Comparison of maximum crown settlement between numerical analysis and regression analysis.

0.993 in case that UAM was applied. From these equations, it presents that S_0 is the crown settlement (mm) at the tunnel face, z_0 is overburden thickness (m), and E is the deformation modulus of ground.

$$S_0 = -\frac{1.97}{E} - 2.28\times10^{-2} z - 6.73\frac{z}{E} - 0.482 \quad (7)$$

$$S_0 = -\frac{46.2}{E} - 5.77\times10^{-2} z - 4.78\frac{z}{E} - 0.708 \quad (8)$$

$$S_{c\max} = -\frac{47.5}{E} - 0.148z - 88.0\frac{z}{E} - 0.468 \quad (9)$$

$$S_{c\max} = -\frac{47.0}{E} - 0.149z - 69.1\frac{z}{E} - 0.158 \quad (10)$$

5 CONCLUSIONS

In this study, the prediction equation for crown and surface settlement was deduced through parametric study on the deformation modulus and thickness and regression analysis. The results of this study are summarized as follows.

From the results of numerical analysis for settlement, the reinforcement effect of UAM was good in a soft and shallow ground.

The range of settlement ratio was 0.61 to 0.73 at an inflection point, and it was higher than the previous other studies. So, considering the measurement error in the fields, the limit of settlement range is not 2.5i but 3.0i.

From the regression results for surface settlement, unknown coefficient i and k was correlated with ground thickness and not with deformation modulus of ground. Coefficient i and k could be expressed linear function. From the multiple regression analysis, the coefficient of determination is more than 0.97. In case of crown settlement, coefficient of a_1 and a_2 are correlated with a ground thickness and the coefficient of determination is more than 0.99 from multiple regression result.

The prediction equations for surface and crown settlement could be expressed with the deformation modulus of ground and ground thickness. From these equations the crown and surface settlement can be estimated, therefore it is expected to be able to evaluate reinforcement effect of UAM and the stability of tunnel and structures adjacent to tunnel.

REFERENCES

Bae, G. J., Kim, C. Y., Moon, H. D., Hong, S. Y. 1997. A Study on the Ground Movement around Tunnel Reinforced

Copyright © 2005 Taylor & Francis Group plc, London, UK

by Umbrella Arch Method, *TUNNEL & UNDERGROUND, J. of Korean Society for Rock Mech.* 7(4) pp. 299–309.

Harazaki, I., Aono, H., Matsuda, A., Aoki, T., Hakoishi, Y. 1998. Field observation of large tunnel supported by umbrella method: Case of Maiko Tunnel in Kobe, Japan. *Proc. of the World Tunnel Cong. 98 on Tunnels and Metropolises*. Vol. 2. pp. 1009–1014.

Kim, C. Y., Bae, G. J., Moon, H. K., Choi, Y. K. 1998. A Study on the 3-dimensional Finite Element Analysis for the Tunnel Reinforced by Umbrella Arch Method. *TUNNEL & UNDERGROUND, J. of Korean Society for Rock Mech.* 8(3). pp. 209–225.

Kim, G. J. & Moon, H. K. 2001. A Theoretical and Numerical Study on the Effects of Prereinforced of Tunnel Face *(in Korean). TUNNEL & UNDERGROUND, J. of Korean Society for Rock Mech.* 11(4). pp. 328–338.

Kim, S. H. 2003. *A Study on the Reinforcement Effect of Umbrella Arch Method and Prediction of Tunnel Crown and Surface Settlement (in Korean)*. Ph D. thesis, Hanyang University. p. 136.

Ryu, C. S., Shin, S. W., Kim, Y. J., Kim, Y. J. 1995. Three-Dimensional Finite Element Analysis on Tunnel Behavior Reinforced by Umbrella Arch Method. KGS Fall '95 National Conference. 28. Oct. 1995. Seoul. Korea. pp. II_11-II_16.

Copyright © 2005 Taylor & Francis Group plc, London, UK

Numerical analysis of geotechnical parameters on subsidence due to underground mining

D.S. Cheon, S.O. Choi, Y.S. Jeon & C. Ryu
Korea Institute of Geoscience & Mineral Resources, Daejeon, Korea

ABSTRACT: Subsidence is a major problem associated with underground coal mining, causing damage to subsurface and surface structures. To avoid adverse impacts of subsidence, a reliable prediction is essential. But subsidence due to underground mining is a very complicated phenomenon which depends upon numerous factors. Due to a large number of parameters influencing the behavior of the rock mass and surface above the excavated space, it is difficult to determine all the parameters and it is even more difficult to determine their relative impact. However the relative impact of parameters and its effect on subsidence is very important to predict the subsidence. Hence in this paper parametric analysis on subsidence were carried out using FLAC^{2D} for horizontal underground mining. From numerical experiments result the major important geotechnical parameters related to the ground subsidence were selected and their weighted values were determined.

1 INTRODUCTION

Underground mining causes the formation of ground subsidence trough. Ground subsidence is acting a serious problem on the surface and surface structure, and is threatening the public safety in a residential area. Thus subsidence estimation is the important to avoid adverse impacts of subsidence, a reliable prediction is essential. The knowledge about the surface activity caused by mining and the prediction of subsidence enable efficient repairs of the mining damage, and has a positive impact on the economic results of mining. Thus understanding accurate subsidence mechanism is very important to predict the ground subsidence.

There are various prediction methods proposed by researchers and they can be classified into three methods (Alejano,1999). The first methods for the prediction of ground subsidence are empirical methods – including graphical methods, profile functions and influence functions. These methods are based on the correlation of the measuring data and the related measuring results. These types of methods are a good to predict subsidence in the region where initial data were taken, but the results are valid only for the investigated area. So their geographic extension is usually restricted.

Second methods are physical models which entail the construction of a scale model of the strata involved by a material such as plaster. This expensive technique helped to understand subsidence mechanism but it was not a good tool to predict displacement.

The last ones are numerical methods, which are based on numerical approximations of the governing equations such as the differential equation, the strain-displacement relation, the stress-strain equation. They finally produce the induced displacements and stress in the analyzed area. They can be considered as the most rigorous and sophisticated subsidence prediction techniques. However, Due to a large number of parameters influencing the behavior of the rock above the excavated space, these methods need a painstaking characterization of the materials involved in the subsidence phenomenon. Also It is difficult to determine all the parameters, and it is even more difficult to determine their relative impact.

Thus this study focused on the parametric analysis related to the shape of opening, rock mass properties, in-situ stress and etc. And also focused on selection of the major important geotechnical parameters and determination relative weighted value on them using FLAC^{2D}.

2 NUMERICAL MODEL FOR SUBSIDENCE

2.1 *Analysis condition*

The subsidence phenomena taking place when a flat coal seam is mined are analyzed in this section stating with the numerical modeling. FLAC^{2D} code has been selected to perform simulations.

Figure 1 shows the geometry and boundary conditions. Horizontal displacement has been restrained in

Copyright © 2005 Taylor & Francis Group plc, London, UK

the central vertical axis; as well as in the left boarder, which is located far enough from the mined seam so as not to influence the general displacement pattern. Vertical displacement has been restrained along the bottom axis of the model. Mesh average dimension decreases from the boundaries to eh surroundings of the excavation, where significant stress and displacement gradient take place.

In order to describe the geometry of the extracted coal seam the following basic terminology has been adopted.

- h is the average depth below surface of the flat coal seam or overburden thickness
- W is the panel width, or width of extraction of the longwall
- M is the extraction height or thickness of extraction taken on the longwall.

2.2 *Geotechnical parameters related to subsidence*

Subsidence due to underground mining is a very complicated phenomenon which depends on upon numerous factors. Some important parameters for the prediction of subsidence are shown in Table 1.

Other parameters are RMR, strength of the rock, creep properties of rock mass and etc.

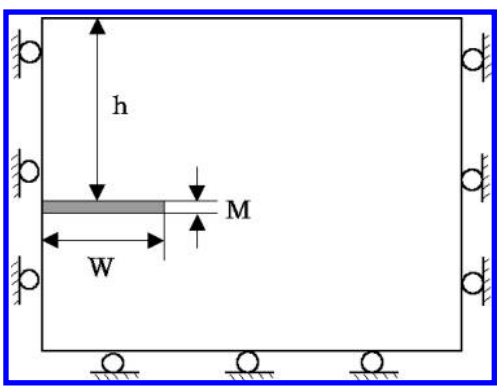


Figure 1 Horizontal opening model and its boundary conditions.

3 ANALYSIS OF GEOTECHNICAL PARAMETERS

To make a first approach to the problem, a simple geometry is selected (W = 40 m, h = 200 and M = 2.5 m). And In-situ stresses is used from the measured value in the several coal mines in KOREA. In this condition, numerical results are shown in Figure 2 which shows the maximum and minimum principal stress distribution around horizontal mine opening obtained from FLAC^{2D} analysis.

3.1 *Effect of the shape of opening and the ratio of horizontal to vertical stress on subsidence*

In order to investigate the effect of shape of opening on subsidence, numerical analysis were performed with the change of overburden thickness(h), width(W), thickness(M) of horizontal opening. Measuring point of subsidence is the surface line above the center of horizontal opening. Table 2 shows the input parameter used in this numerical modeling.

3.1.1 *Subsidence trough*

Figure 3 shows typical subsidence trough with the change of opening width at h = 150 m, 300 m, respectively. As shown Fig. 3, maximum subsidence (S_{max}) increased with W increasing. And S_{max} and Influence distance of subsidence in case at h = 300 are more enlargement than in case at h = 150 m.

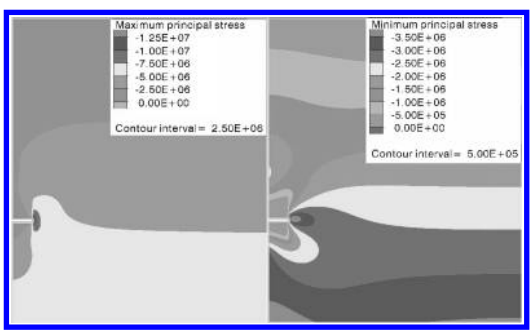


Figure 2 Maximum and minimum principal stress distribution around horizontal opening model obtained from FLAC^{2D} analysis.

Table 1. Important parameters affecting the ground subsidence.

	Shape of opening	In-situ stress	Geotechnical properties	Discontinuity	Groundwater
Parameter	Thickness (M) Overburden thickness (h) Width (W) Inclination	Magnitude s_h/s_v (K)	Rock mass modulus (E_m) Poisson's Ratio (n_m) Cohesion (c_m) Friction (ϕ_m) Density (ρ)	Normal stiffness (k_n) Shear stiffness (k_s) Cohesion (c_j) Friction (ϕ_j)	Level

Copyright © 2005 Taylor & Francis Group plc, London, UK

3.1.2 *Effect of width (W), overburden thickness(h) and thickness(M) of opening*

Maximum subsidence is the main concerning factors in subsidence problem. So in this section, this factor was evaluated with h, W, M at fixing K and rock mass properties.

Figures 4–6 show S_{max} against width, overburden thickness and thickness respectively. The results show that S_{max} increased with increasing W and was rarely affected by overburden thickness. It was found from the results that W is most important parameter among shape parameters.

Table 2. Input parameters for numerical analysis.

Factors	h (m)	W (m)	K	E_m (MPa)
Input value	150	40	0.5	6,758
	200	60	1	
	300	80	1.5	
		100		
Factors	c_m (MPa)	ϕm(°)	n	M (m)
Input value	0.625	30	0.22	2.5

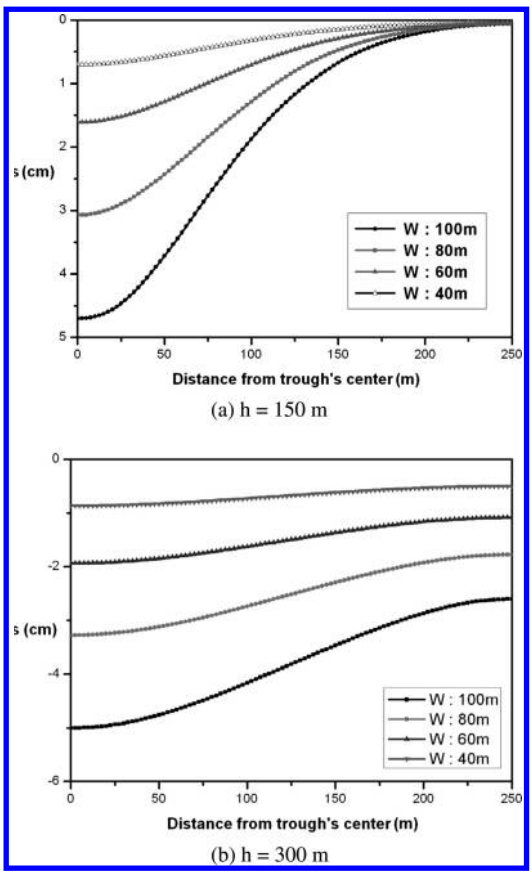


Figure 3 Ground subsidence graph with the change of opening width.

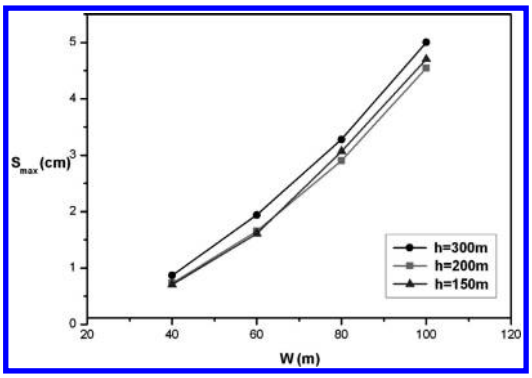


Figure 4 Maximum subsidence with the change of width (W).

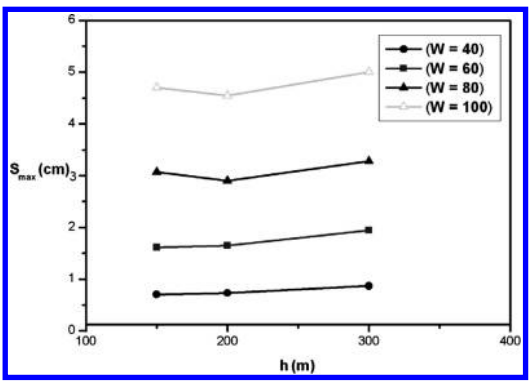


Figure 5 Maximum subsidence with the change of overburden thickness (h).

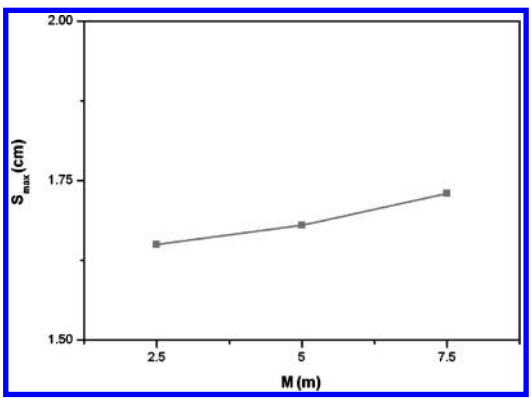


Figure 6 Maximum subsidence with the change of thickness (M).

Copyright © 2005 Taylor & Francis Group plc, London, UK

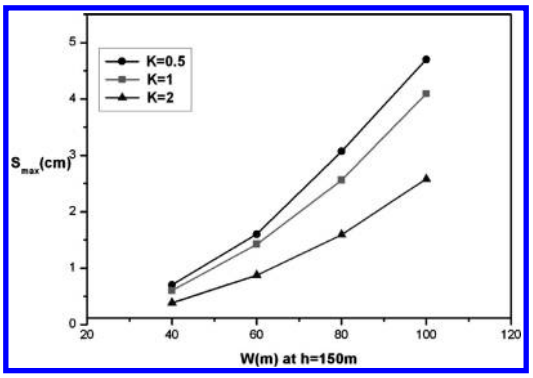


Figure 7 Maximum subsidence with the change of the K.

3.1.3 *Effect of the ratio of horizontal to vertical stress (K)*

With shape of the opening and rock mass properties fixed, subsidence is analyzed with the change of the K. As above mentioned, W is the main parameter. Thus in this section numerical analysis for effect of K on subsidence is performed with varying Width at fixed overburden thickness. Figure 7 presents the S_{max} with the change of K and width. Results indicated that S_{max} increased with increasing K.

3.1.4 *Sequence of the shape parameter and K*

The following sequence of the major factor to affect the subsidence is obtained from the above results.

$$[W] > [K] > [h] > [M]$$

But, this sequence is obtained from the simple horizontal opening model with the change of the shape factors (W, h, M) and K, so more detail and complicated analysis is required to order the sequence.

3.2 *Effect of rock mass properties*

To investigate effect of rock mass parameters on subsidence, parametric analyses were performed with standard horizontal opening geometry.

Usually parameters of rock mass properties related to maximum subsidence and influence distance in subsidence simulation are as follows.

a. Rock mass modulus (E_m)
b. Poisson's ratio (E_m)
c. Cohesion (c_m)
d. Friction angle (ϕ_m)
e. Groundwater
f. Cohesion of discontinuities (c_j)
g. Friction angle of discontinuities (ϕ_j)
h. Normal stiffness of discontinuities (k_n)
i. Shear stiffness of discontinuities (k_s)
j. Angle of coal seam (α) etc.

Table 3. Input parameters for geotechnical parametric studies.

Factors	E_m (GPa)	n	c_m (MPa)	ϕ_m (°)	Groundwater level (m)
Standard model	20	0.22	1	30	None
Input value	80	0.2	22.6	50	0
	60	0.23	13.7	40	−50
	40	0.26	8.3	45	−100
	20	0.29	5.1	35	−150
	2.8	0.32	3.1	30	−200
	2.2	0.35	1.9	25	−250
	1.7		1.2		
	1.3		0.7		

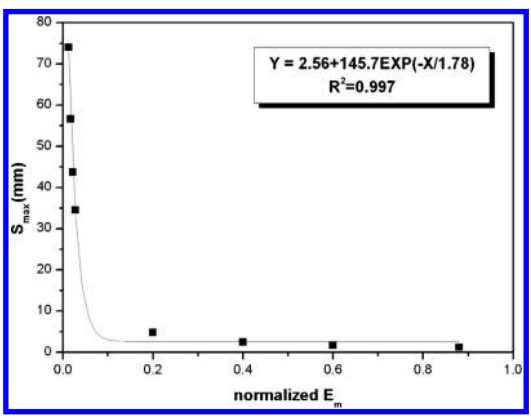


Figure 8 Maximum subsidence against normalize E_m.

Rock mass density among these parameters was fixed at 2,400 kg/cm^3 considering the small variance between different rocks. And (a)–(e) parameters are used for parametric studies considering continuum analysis code, FLAC^{2D}.

Analysis model has the mesh with 250 m wide, 300 m height large enough to allow full trough development without interferences from the boundary conditions. And opening thickness is 2.5 m, overburden thickness is 200 m, ratio of horizontal to vertical stress is 1.0. Table 3 shows the input parameters for rock mass properties. Used input parameters were obtained from RMR which range is from 20 to 90 at 10 intervals. Rock mass modulus (E_m) is calculated from the empirical equation proposed by Bieniawski (1989), Serafim & Pereira (1983). Rock mass strength properties (c_m, ϕ_m) are calculated from the empirical equations proposed by Trueman (1988). And Poisson's ratio is typical range of rock mass. Figures 8–12 show the maximum subsidence developed with the change of normalized parameters.

Copyright © 2005 Taylor & Francis Group plc, London, UK

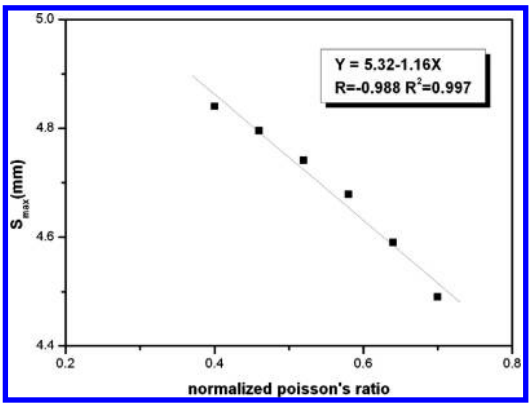


Fig. 9 Maximum subsidence against normalized Poisson's ratio.

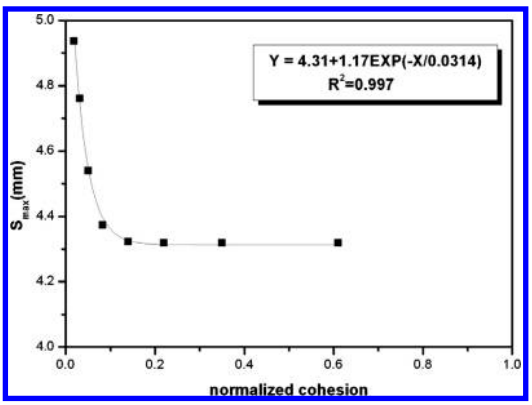


Fig. 10 Maximum subsidence against normalized cohesion.

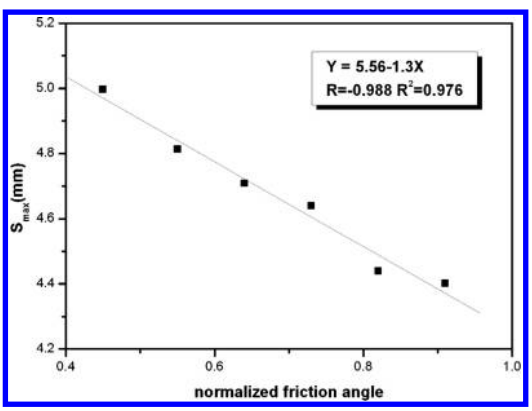


Fig. 11 Maximum subsidence against normalized friction angle.

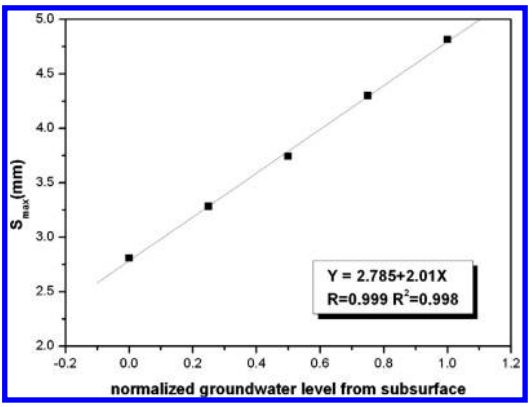


Fig. 12 Maximum subsidence against normalized groundwater level.

Table 4. Sequence of major input parameters on subsidence and its relative weighted value.

Sequence	[E_m] > [Groundwater level] > [Cohesion] = [Friction angle] > [Poisson's ratio]
Parameter	Weighted value (%)
E_m	93.38
Groundwater	4.12
Cohesion	0.75
Friction angle	0.75
Poisson's ratio	0.38

3.3 *Determination of weighted value for rock mass parameters*

From above continuum analysis, sequence of the rock mass parameters on subsidence was known. And using the normalized relations for various parameters, relative weighted values of parameters were determined as shown in Table 4.

Cohesion and Friction angle is the variable of the Mohr-Coulomb criteria and these are deeply related the plastic failure zone which is direct effect to the surface vertical displacement. This is supported by the numerical analysis in this study. These two parameters change give the similar S_{max} and subsidence profiles. Weighted values for parameters were determined based on these two parameters.

4 CONCLUSION

To investigate the major parameters on subsidence, various numerical tests were conducted. From what has been discussed above, numerical results can be summarized as follows.

Copyright © 2005 Taylor & Francis Group plc, London, UK

1) Sequence of shape parameters was ordered by [Width], [Ratio of the horizontal to vertical stress], [overburden thickness], [opening Thickness].
2) Sequence of rock mass parameters was ordered by [E_m], [Groundwater], [Cohesion] = [Friction angle], [Poisson's ratio].
3) Weighted values of rock mass parameters are determined and E_m is very important parameters compared to the cohesion, friction angle and Poisson's ratio.
4) Thus for analysis of the subsidence the evaluation of the K and E_m, which are only obtained from the site investigation, should be careful.

But these results were obtained from the only simple numerical simulations. Thus it is necessary to perform further study for understanding clearly the effect of parameters with more detail and complicated models, also the results should be verified with the real subsidence sites.

REFERENCE

Alejano, L.R., Oyanguren, P.R. & Taboada., J. 1999. FDM predictive methodology for subsidence due to flat and inclined coal seam mining, *Int. J. Rock Mech. & Min. Sci*. 36: 475–491

Ambrozic, T. & Turk, G. 2003. Prediction of subsidence due to underground mining by artificial neural networks. *Computers & Geoscience* 29: 627–637

Bieniawski, Z.T. 1989. *Engineering rock mass classifications*. John Wiely&Son

Hiramatsu, Y., Okamura, H. & Sugawara, K. 1989. Surface subsidence and horizontal displacement caused by mining induced coal seams, *Proc. 4th Int. Cong. On Rock Mech.* 2 : 665–670

NCB 1975. *Subsidence engineer's handbook.* London: National Coal Board

Ren, G. Whittaker, B.N. & Rddish, D.J. 1989. Mining subsidence and displacements prediction using influence functions methods for steep seam. *Mining Sci. & Tech.* 8: 235–252

Serafim, J.L. & Pereira, J.P. 1983. Considerations on geomechanics classification of Bieniawski. *Proc. Int. Symp. On Eng. Geol. And Underg. Constr.* 1: 31–42

Singh, R.P. & Yadav, R.N. 1995. Prediction of subsidence due to coal mining in Raniganj coalfield, West Bengal, India. *Engineering Geology* 39: 103–111

Trueman, R. 1988. *An evaluation of strata support techniques in dual life gateroad*, Ph.D. Wales

Whittaker, B.N. & Reddish, D.J. 1989. *Subsidence : occurerence, prediction and control*. Amsterdam: Elsvier

Yao, X.L., Reddish, D.J. & Whittaker, B.N. 1989. Non-linear finite element analysis of surface subsidence arising from inclined seam extraction. *Int. J. Rock Mech. & Min. Sci*. 30:

Copyright © 2005 Taylor & Francis Group plc, London, UK

Model testing of perpendicularly spaced tunnels

Sang-Hwan Kim
Department of Civil Engineering, Hoseo University, Asan, Korea

ABSTRACT: This paper describes a study of the effect of shield tunnel construction on the liners of existing nearby perpendicular tunnels. The research programme investigated the influence of tunnel proximity and alignment, liner stiffness on the nature of the interactions between closely spaced tunnels in clay. A total of two sets of carefully controlled 1 g physical model tests, including same test for repeatability, were performed. A cylindrical test tank was developed and used to produce clay samples of Speswhite kaolin. In each of the tests, three model tunnels were installed in order to conduct two interaction experiments in one clay sample. The tunnel liners were installed using a model tunnelling machine that was designed and developed to simulate the construction of a full scale shield tunnel. The first tunnel liner was instrumented to investigate its behaviour due to the installation of each of the new tunnels. The interaction mechanisms observed from the physical model tests are discussed and interpreted.

1 INTRODUCTION

In recent years many new tunnels have been planned and designed or constructed near to existing tunnels in order to develop and extend underground transportation systems. In the design of new tunnels, it is important to ensure that any existing underground transportation systems in close proximity to the proposed tunnelling activities can continue to operate safely both during and after construction. Therefore, it is necessary to understand the interaction mechanisms between new and existing tunnels, to ensure that no damage occurs to the existing tunnel. In general, this interaction may be strongly dependent on the spacing between the tunnels. If the new tunnel is constructed at a large distance from the existing tunnel, the individual tunnels can be considered separately as single tunnels and analysed as such. However, if the influence zones of the two tunnels overlap, some degree of interaction between tunnels will take place. This interaction will affect the state of stress and the displacements in the ground around the tunnels, the ground surface displacements and the support loads.

The structural interactions that occur between closely spaced tunnels are associated with a variety of mechanisms. For tunnels that are located one above the other, additional mechanisms may come into play. For example, if a new tunnel is constructed beneath an existing tunnel, then this may lead to settlements in the upper tunnel. Further mechanisms have also been proposed; for example Hansmire *et al*. (1981) suggest that, for shield tunnelling, the stresses developed between the shield and the ground may lead to significant structural effects in any nearby tunnels. It is clear that the problem of interaction between adjacent tunnels is highly complex, and any structural interaction will depend on the geometry of the tunnels, the properties of the liner and the soil and the method of tunnel installation.

Interaction between closely spaced tunnels has been studied in the past using a variety of approaches. Much of the published work is based on measurements made during the construction of full scale tunnels. Some work is also reported in which finite element analysis was used to study the problem. Very little research, however, seems to have been carried out based on the use of reduced scale laboratory testing.

Hansmire *et al.* (1981) reported a set of measurements that were made during the construction of a new sewer in close proximity to a pair of subway tunnels. In this case, the sewer was perpendicular to, and above, the two existing tunnels. Excavation for the sewer led to an increase in the vertical diameter of the two existing tunnels in the zone immediately beneath it. This increase in diameter is, presumably, associated with a reduction in vertical stress acting on the tunnels. When the shield was advanced, however, the vertical diameter of the existing tunnels tended to decrease. Hansmire *et al*. suggested that this latter observation was associated with shear stresses developed between the shield and the soil.

Typical numerical analyses of the interaction between tunnels are described by Ghaboussi and Ranken (1977) and Leca (1989). In these studies, a

Copyright © 2005 Taylor & Francis Group plc, London, UK

variety of tunnel spacings and procedures to model tunnel construction were adopted. In both cases a two-dimensional approach was used in which the soil model was elastic. For the configurations investigated, the interactions between two parallel tunnels were small when the centre-line spacing was greater than about two tunnel diameters. Addenbrooke and Potts (1996) reported numerical analyses of the interaction between two tunnels constructed within a month of each other, using a small strain non linear soil model. They concluded that the interaction between two tunnels passing at depth depends on relative tunnel position (to the side or vertically above) and on the spacing. Driving a new tunnel above an existing tunnel has significantly less influence on the existing tunnel lining than driving a new tunnel to the side.

Little work has been carried out to investigate the interactions between tunnels using laboratory scale model tests. In recent years, however, much research on single tunnel behaviour has been carried out using centrifugal modelling, for example, particularly in the Cambridge Soil Mechanics Group by Cairncross (1973), Atkinson *et al.* (1974), Atkinson and Orr (1976), Potts (1976), Seneviratne (1979), Mair (1979) and Taylor (1984). It is difficult to simulate tunnel construction in a centrifuge. However, Nomoto *et al.* (1994, 1996) and Imamura *et al*. (1996) describe the design and development of a miniature shield tunnelling machine for a centrifuge.

In the performance of a tunnel liner, the relative flexibility of the liner and the surrounding soil is of fundamental importance. Peck *et al*. (1972) suggested that the relative stiffness of an embedded tunnel liner may be characterised by two dimensionless numbers termed the 'flexibility ratio' and the 'compressibility ratio'. The analytical basis for these parameters was derived by Burns and Richards (1964) and Höeg (1968) taking account of soil-structure interaction. The flexibility ratio (F) determines the relative bending stiffness of the lining and the compressibility ratio (C) defines the relative stiffness of the lining in hoop compression. These ratios are expressed by:-

$$C = \frac{E\,R\,(1-\nu_L^2)}{E_L\,A\,(1+\nu)(1-2\nu)} \quad (1)$$

$$F = \frac{E\,R^3\,(1-\nu_L^2)}{E_L\,I\,(1+\nu)} \quad (2)$$

where E_L, ν_L, R, A and I are respectively the Young's modulus, Poisson's ratio, radius, cross-sectional area and second moment of area of the liner, and E and ν are the Young's modulus and Poisson's ratio of the soil. Note that $E = 2(1 + \nu)G$, where G is the shear modulus. The term $(1 - \nu_L^2)$ assumes that the liner is continuous longitudinally and may be omitted for segmental liners with compressible joints between successive rings.

Peck *et al*. (1972) suggested that tunnel liners may be considered flexible if F is greater than about 10. Then the stresses acting on the interface between the liner and the soil may lead to significant liner displacements, and the nature of the stress distribution will be determined, in part, by the liner stiffness. In general, tunnels in soil have a value of C less than 1, while for rock tunnels C is greater than 1 (Sinha, 1989). However for short-term undrained behaviour of clay, with ν equal to 0.5, C becomes infinite and the liner hoop stiffness of no consequence. Typical values of F for real tunnels lie in the range of about 5 to 300; however tunnels with a substantial concrete secondary lining may be stiffer than this, while segmental linings with articulated joints between segments may be extremely flexible.

The project described in this paper sought to study the highly complex soil/structure interaction problem of closely spaced perpendicular tunnels in soft ground by high quality 1 g laboratory scale model tests, with direct measurement of the additional bending moments and deformations induced in an existing tunnel by the installation of new tunnels nearby.

The project was confined to the study of tunnels in normally consolidated clay. At the start of the project, the need to develop accurate and repeatable methods of tunnel installation was identified and so a model earth pressure balance tunnelling machine was developed. Radial movements of the tunnel liner were identified as representing important interaction data; new instruments for making these measurements were therefore also developed. The tunnel linings used in the study consisted of thin steel tubes that were instrumented with strain gauges, pressure cells and pore pressure transducers.

2 DEVELOPMENT OF TESTING EQUIPMENT AND PROCEDURES

2.1 *Introduction*

Two sets of model tests were carried out. The behaviour of perpendicular tunnels was studied in a cylindrical tank (Figure 1).

The test tank was designed such that each clay sample could be used to conduct two independent interaction tests. In order to achieve this, three positions were made available for tunnel installation.

2.2 *Perpendicular tunnel tests*

Two perpendicular tunnel tests were carried out, including a repeated test to check the consistency of

Copyright © 2005 Taylor & Francis Group plc, London, UK

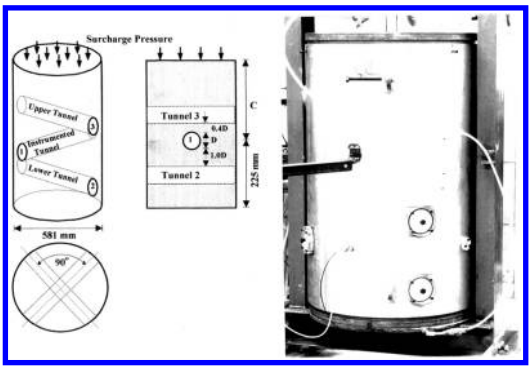


Figure 1. Cylindrical test tank.

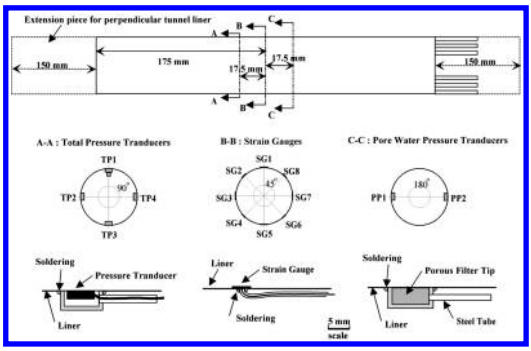


Figure 2. Tunnel liner instrumentation.

Table 1. Specification of tests.

Test no.	CY1	CY2
OCR	1	1
P_{sur} (kPa)	89.04	88.2
t (mm)	0.254	0.356
F	214	75
s_u (kPa)	23.6	22.7
G (kPa)	4712	4530

the testing procedures. The tests were carried out with a surcharge of value P_{sur} applied to a stress controlled boundary on the top surface of the clay in order to provide the required value of OCR. The tests are specified in Table 1.

The values of OCR listed in Table 1 were calculated using the actual values of overburden stress acting at the level of the tunnels in the model tests. The thickness (t) of the tubular steel liners was chosen to ensure reasonable values of the flexibility ratio F, of about 70 and 200. Although, based on Peck's criterion, both of these tunnels would be classified as flexible, in the discussion of the results given below the liner for which $t = 0.254$ mm is termed 'flexible' and the liner for which $t = 0.356$ mm is termed 'stiff'.

The values of soil shear modulus given in Table 1 were estimated from the measured values of undrained shear strength and the appropriate value of OCR, on the basis of charts presented by Duncan and Buchignani (1976) and further information from Wroth *et al.* (1979), assuming a plasticity index of 31%. The clay shear strength was measured while the surcharge loading was applied, by means of a shear vane inserted into the sample through ports installed in the front panel of the test rig. Shear vane measurements were also made after removal of the surcharge and after swelling had taken place; these latter results, of course, do not correspond directly to the soil strengths that were relevant to the tests although the two sets of data could be correlated.

2.3 *Instrumentation*

A variety of instrumentation systems were adopted as summarised below. A study on the accuracy of the measurements is given by Kim (1996).

(1) Monitoring of Sample Preparation
Two transducers were installed in the side of each test tank in order to measure total stresses and pore pressures during consolidation. Sample settlement and consolidation pressure were also recorded.

(2) Instrumented Tunnel
Instrumentation of the first tunnel to be installed is illustrated in Figure 2 and included:
- Eight strain gauges spaced equally around the circumference to measure hoop strains on the liner exterior. Strains recorded using these gauges were used to estimate liner bending moments on the assumption that hoop forces were small.
- Four miniature total pressure cells.
- Two pore pressure transducers.

(3) Measurement of Radial Movements
Two different types of radial displacement measuring devices, RDMD1 and RDMD2, were developed and used to monitor the radial displacements of the liner.

The RDMD1 consisted of four strain gauged cantilevers made from stainless steel, mounted on a specially machined aluminium block, to measure radial displacements of the crown, invert and both springlines of the tunnel liner. The maximum range of each cantilever was 20 mm corresponding to the maximum elastic deflection. Each cantilever was 70 mm long, 5 mm wide, 0.25 mm thick and inclined to the horizontal at 40°. A dome-shaped tip was attached to the free end of each cantilever to ensure good contact with the measuring points.

This device was found to be sensitive to temperature variations, and the RDMD2 was developed to overcome this problem. It measured the liner deformations by converting the displacement

Copyright © 2005 Taylor & Francis Group plc, London, UK

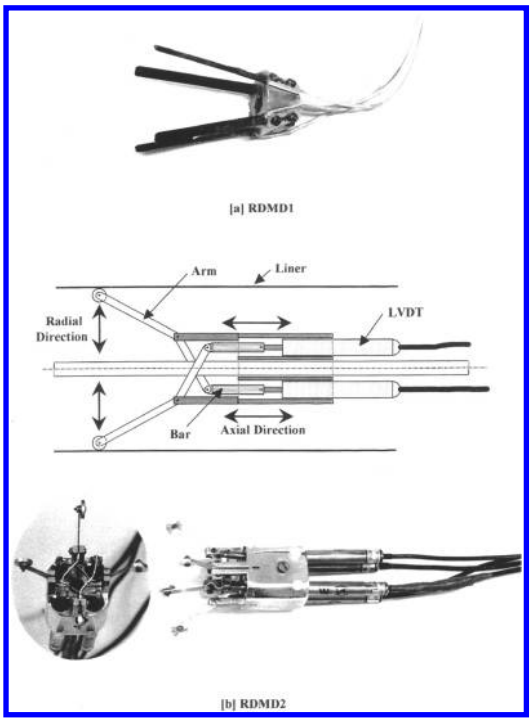


Figure 3. Radial displacement measuring devices (RDMD1 and 2).

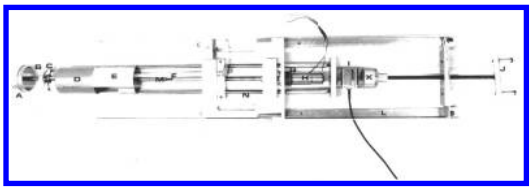


Figure 4. Model tunnelling machine.

direction from radial to axial through four arms rotating about pin supports on a mounting block and connected by pin-jointed bars to corresponding LVDTs. A small roller was mounted at the end of each arm to move smoothly on the liner. The LVDTs had a maximum working range of 10 mm.

2.4 *Model tunnelling machine*

A model tunnelling machine, based on an earth pressure balance shield, was therefore developed as shown in Figure 4. The rotary cutting head consisted of a flat plate with two cutting blades. The head was connected to a shaft which was rotated by an electric motor in order to excavated the soil. Soil removed by the cutting head was washed back through the tunnel using a

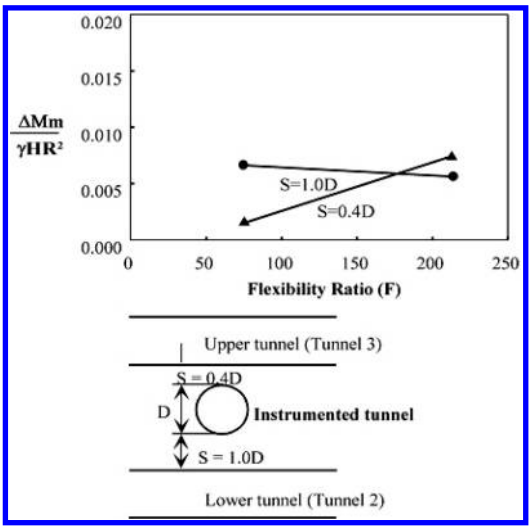


Figure 5. Variation of incremental bending moments.

water jet system. The lining was jacked into the soil immediately behind the cutting head which was oversized slightly in order to produce a ground loss of about 6%.

To operate the machine, a small guide shaft was first placed in the sample along the tunnel axis. This shaft was installed to a high accuracy using a reference frame bolted to the side of the tank, and was then used to locate the cutting head during tunnel installation.

3 MODEL TEST RESULTS

The normal stress interaction effects were strongly dependent on the new tunnel positions. As would be expected, the largest stress interaction effects occurred at the crown for the upper tunnel case and at the invert for the lower tunnel case.

Figure 5 shows the variation of the normalized incremental bending moments ($\Delta M/\gamma HR^2$) plotted against flexibility ratio (F) for installation of the new perpendicular tunnels. Here ΔM is the maximum incremental bending moment developed in tunnel 1 after installation of each of tunnels 2 and 3, at the crown for the upper tunnel (close spacing, $S = 0.4D$), at the invert for the lower tunnel (distant spacing, $S = 1.0D$). The moment interaction effects are strongly dependent on new tunnel position and liner stiffness rather than tunnel spacing. It is clear that in the upper tunnel case ($S = 0.4D$), the interaction effects were much greater for the flexible liner than the stiff liner, whereas in the lower tunnel case ($S = 1.0D$), the influence of liner stiffness seems to be small. For the lower tunnel case, the moment interaction effects are relatively similar in magnitude to those measured in

Copyright © 2005 Taylor & Francis Group plc, London, UK

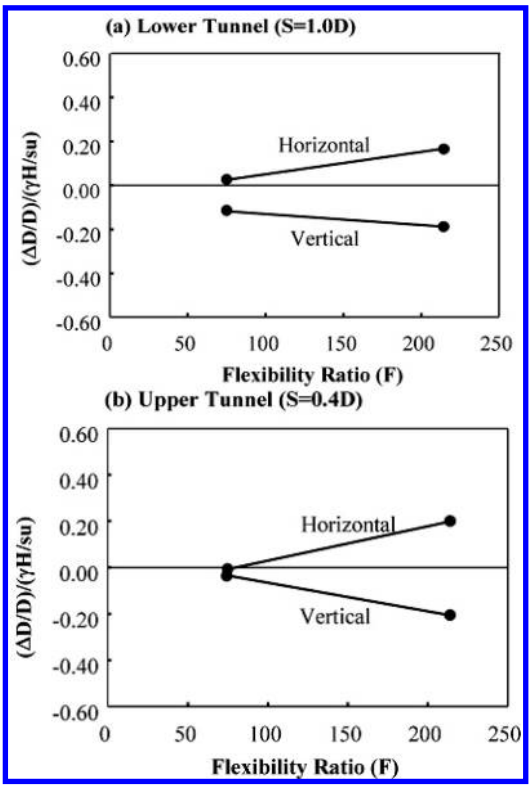


Figure 6. Variation of incremental diameter change with W/D.

the corresponding parallel tunnel tests, while for the upper tunnel case the interaction effects are much smaller than for the corresponding parallel tunnel tests, in spite of the fact that the upper tunnel was closer than the lower tunnel. The differences between perpendicular and parallel tunnels tend to increase with increasing stiffness of the liner.

Figure 6 shows the diameter changes (ΔD) of the existing tunnel after construction of the new tunnels plotted against flexibility ratio (F). The distortion interaction effects for perpendicular tunnels are strongly dependent on the liner stiffness. The variations in diameter changes are much larger for the flexible liner than for the stiff liner. It is worth noting that the diameter changes seem to be very similar in both upper and lower tunnel cases. However following construction of the lower tunnel, the instrumented tunnel also displaced downwards by a significant amount, presumably as a result of settlement generated by the lower tunnel. The deformation interaction effects in perpendicular tunnels are relatively smaller than those observed in the corresponding parallel tunnel tests, the differences being much greater in the upper tunnel case than in the lower tunnel case.

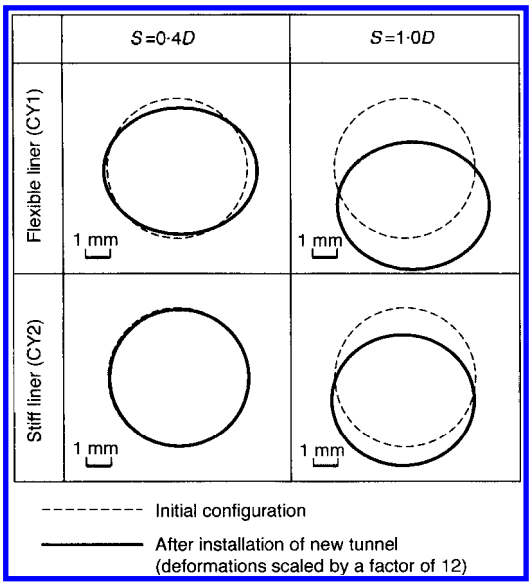


Figure 7. Deformed cross-sections for perpendicular tunnels.

Figure 7 shows the deformed cross sections of instrumented tunnel after adjacent perpendicular tunnel construction. These data indicate that, in all cases, installation of a new perpendicular tunnel caused increases in the horizontal diameter, and corresponding decreases in the vertical diameter, of the adjacent tunnels. It is thought that this tendency is associated with additional ground deformations caused by the jacking forces used to advance the shield and the tunnel liner. These additional deformations are thought to be sufficiently large to counteract the expected tendency of the vertical diameter of the adjacent tunnels to increase as a result of stress relief. A similar trend is apparent in the field data reported by Hansmire *et al.* (1981) relating to the construction of perpendicular staked tunnels in New York. These field data show that the interaction effects developed in adjacent tunnels are strongly influenced by the magnitude of the jacking force used to advance the shield. Large jacking forces tended to cause the horizontal diameter of adjacent tunnels to increase; when smaller jacking forces were adopted then the horizontal diameter of adjacent tunnels trended to decrease.

The observed interaction behaviour of the perpendicular tunnels appears to be dominated by liner installation effects.

4 CONCLUSIONS

(a) High quality tests were carried out at laboratory scale for closely-spaced perpendicular tunnels.

Copyright © 2005 Taylor & Francis Group plc, London, UK

(b) A model tunnelling machine was developed to allow accurate and repeatable tunnel installation procedures to be adopted.
(c) For the cases studied, tunnel installation was shown to modify the stresses acting on the liner of an existing adjacent tunnel. These stress increments led, in turn, to liner deformations and induced bending moments. In extreme cases, the induced bending moments were found to be a factor of two or three greater than the maximum liner moment before adjacent tunnelling took place.
(d) The results of the perpendicular tunnel tests suggest that, in these cases, interaction effects are predominately caused by jacking forces applied to the liner and the tunnelling machine during tunnel installation.
(e) The perpendicular tunnel tests indicated interaction effects that were generally more severe than those expected in the field. It was observed that a perpendicular tunnel constructed beneath the instrumented tunnel tank led to relatively large movements.
(f) The experience gained from these tests indicates that the interaction mechanisms that operate between adjacent tunnels are highly complex.

REFERENCES

– Addenbrooke and Potts (1996). Proceedings of Int. Conf. on Tunnelling in Soft Ground, April, in press.
– Atkinson, J.H., Cairncross, A.M. and James, R.G. (1974). *Model tests on shallow tunnels in sands and clay*. Tunnels and Tunnelling, 6(3), pp 28–32.
– Atkinson, J.H. and Orr, T.L.L. (1976). *Experiments on model tunnels in stiff clay*. Proc. 6th European Conf. Soil Mech. Found. Eng., Vienna, 1.1, pp 227–280.
– Cairncross, A.M. (1973). *Deformations around model tunnels in stiff clay*. Ph.D. Thesis, University of Cambridge.
– Duncan, J.M. and Buchignani (1976). *An engineering manual for settlement studies.* Geotech. Eng. Report, Dept of Civil Eng. Univ. of California at Berkeley, p 94
– Ghaboussi, J. and Ranken, R.E. (1977) *Interaction between two parallel tunnels*. Int. J. Num. and Analyt. Meth. in Geomech. 1, p 75–103
– Hansmire, W.H., Parker, H.W., Ghaboussi, J., Casey, E.F. and Lentell, R.L. (1981). *Effects of shield tunnelling over subways*. Proc. 3rd Rapid Exca. and Tunnelling Conf., pp 254–276.
– Kim, S.H., Burd, H.J. and Milligan, G.W.E. (1996). *Interaction between closely spaced tunnels in clay*. Proceedings of Int. Conf. on Tunnelling in Soft Ground, April.
– Leca, E. (1989). *Analysis of NATM and shield tunnelling in soft ground*. D.Phil. Thesis, Virginia Polytechnic Institute and State University.
– Mair, R.J. (1979). *Centrifugal modelling of tunnel construction in soft clay*. Ph.D. Thesis, University of Cambridge.
– Peck, R.B. (1969). *Deep excavations and tunnelling in soft ground*. Proc. of the 7th ICSMFE, Mexico, State-of-the-Art Report Volume, pp 225–290.
– Peck, R.B., Hendron, A.J. and Mohraz, B. (1972). *State of the art of soft-ground tunnelling*. Proc. 1st Rapid Excavation and Tunnelling Conference AIME, 1, p 259–286
– Seneviratne, H.N. (1979). *Deformation and pore pressure dissipation around shallow tunnels in soft clay*. Ph.D. Thesis, University of Cambridge.
– Wroth, C.P., Randolph, M.F., Houlsby, G.T. and Fahey, M. (1979). *A review of the engineering properties of soils with particular reference to the shear modulus.*Cambridge University Engineering Department Report CUED/D – Soils TR75.

Copyright © 2005 Taylor & Francis Group plc, London, UK

Design and construction of NATM underground station tunnel by using the forepoling method in difficult conditions for Athens Metro

P. Kontothanassis, N. Koronakis, A. Karinas & S. Massinas
Omikron Kappa Consulting Ltd, Athens, Greece

ABSTRACT: This paper describes the detailed engineering design process in terms of the relative geotechnical interpretation stage, the subsequent multistaged numerical simulation steps by using SOFISTIK software, the critical decision making points and the actual results achieved during the construction of Ag. Savas underground station tunnel for Athens Metro.

1 GENERAL DESCRIPTION OF AGIOS SAVAS UNDERGROUND COMPLEX

1.1 *Project layout*

Agios Savas underground complex is a part of the new extension LINE 3 of Athens' metro. The project is considered to be very complicated (Figs 1, 2), since it contains an underground station of 110 m in length (1), the main building (2) close to the station tunnel and a cut&cover dome (3) which will be connected with the main building via an underground cross gallery (4). Furthermore, four underground inclined galleries (5) with stairs are foreseen for the transportation between the dome, the station and the main building.

For the excavation and temporary support of the station tunnel, a forepoling method was applied in order to overcome the time schedule delays, which are generally produced by a typical side drifting method.

The piling work in the area of Agios Savas Station building pit began at January 2003 and the contractor J/V AKTOR SA-IMPREGILO SpA will fulfill the civil works until the beginning of 2008.

According to the construction sequence, the following stages are foreseen:

- Installation of the retaining system of the building pit and south dome (concrete piles and prestressed anchors) and partial excavation of the building pit.
- Excavation of the station tunnel with forepoling method and top heading and bench.
- Implementation of the final lining of the station tunnel and excavation of the deep part of the building pit with top-down method.
- Concreting works of the building (up to a certain level) and the dome.

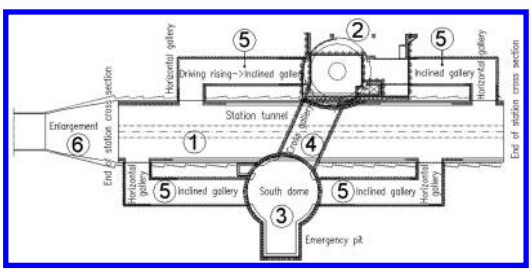


Figure 1. Plan view of Agios Savas underground complex at the final construction stage.

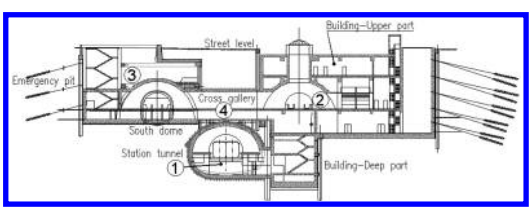


Figure 2. Section of Agios Savas underground complex. Station tunnel will be constructed in advance.

- Construction of the remaining underground parts (inclined galleries and cross gallery).
- Concreting works of the remaining part of the building.

2 FOREPOLING METHOD OF THE STATION TUNNEL

2.1 *Presentation of the temporary support system*

The overburden thickness of the station's tunnel is approximately 18 m. The geological formation at the

Copyright © 2005 Taylor & Francis Group plc, London, UK

depth of the station tunnel consists of conglomerates and marl with small layers of sand and clay. The hydrogeological conditions are favourable for the project, in this specific area, since the inflow water quantities are rather neglectable.

Excavation is performed by the use of a hydraulic hammer. Old shafts have been discovered during the excavation of the station, since the area was continuously inhabited during the last 3000 years (considered to be a part of the old ancient Athens).

The excavated cross section of the station's tunnel ranges' between 195 m^2 (at the minimum excavation) to 215 m^2 (at the maximum excavation enlargement). The width of the top heading and bench is 20.2 m, the total height of the tunnel is 14.25 m (in the maximum enlargement), while the excavated height of the top heading exceeds 8 m (Fig. 3).

In order to implement the first series of forepoles, it was necessary to enlarge the running tunnel's cross section, thus creating the required space for installing the forepole tubes at the station's cross section (Part 6 in Figure 1). The enlargement must be gradually increasing from the running tunnel's cross-section to the station's cross-section, creating a stable and statically acceptable excavation. A transition part of the running tunnel has already been constructed from the running tunnel to the station. The length of the transition part was determined at 20 m (Fig. 4). The excavated cross section of the transition part of the running tunnel ranges between 91 m^2 (minimum excavation) to 213 m^2 (maximum excavation enlargement).

The excavation and temporary support system is based on the following:

– Top heading round length 1.00 m.
– Forepoling tubes St37, Φ193.7/179.5 mm, 12 m length, placed at average axial distances of 0.60 m per 6 round lengths of top heading.
– Shotcrete shell of 40 cm minimum structural thickness, C25/30. However, in the junction areas of temporary invert and elephant feet the structural thickness requirement increases for providing a better structural system with smooth geometrical corners and for avoiding stress concentrations.
– Steel sets placed at each round length, HEB 180, St37.
– Rock bolts of 6 m length, S500, 25 mm in diameter, installed at a grid 1.00 m × (each top heading round length) (cross × axial spacing) at the sidewalls of bench (except from the final and temporary invert) and pairs of rock bolts for steel sets secure.
– Reinforcement layers T188 mesh type, (external, intermediate and internal) are installed.
– Temporary invert with prefabricated steel reinforcement cages for faster installation and two layers of steel mesh T188 and shotcrete 35 cm thickness, C25/30.
– Reinforced final invert (with two steel meshes T188), shotcrete 40 cm minimum thickness C25/30.

Two (2) different support classes have been provisioned. The principal considerations for the design and determination of the main/composite/transitional excavation and temporary support classes pointed to:

– The homogenisation and compatibility between the excavation and temporary support classes relevant to their basic structural components (shotcrete shell, rockbolts grid, temporary and final inverts thickness). The excavation and temporary support classes determined according to this consideration are more flexible, so the application of the composite and transitional excavation and temporary support classes is facilitated.

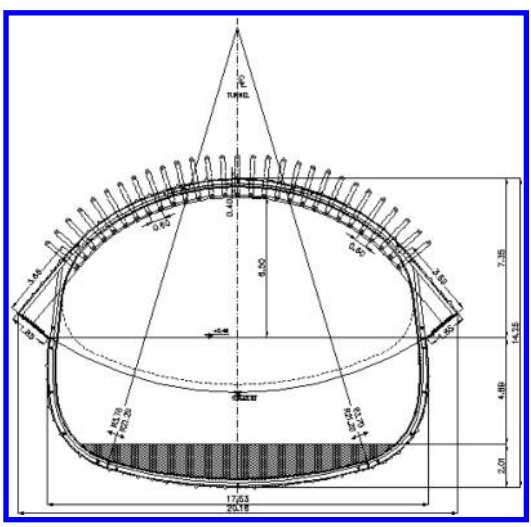


Figure 3. Excavation geometry of the typical cross section (maximum enlargement).



Figure 4. Top heading construction of the transition section of the running tunnel.

Copyright © 2005 Taylor & Francis Group plc, London, UK

– Adjustment according to the ground conditions anticipated during the excavation, even if each excavation and temporary support class has a specific application range.

2.2 *Special conditions and different support system implemented*

Due to the particularities of each different part of the project, a possible alteration of the excavation and temporary support classes proposed was anticipated. Due to this fact, by evaluating the ground profiles, the hydrological regime and the probable difficulties expected to be faced during the excavation, additional ground improvement techniques were recommended (drainage holes, probable application of consolidation grouting) in order to provide the as secure as possible design in case of unfavorable conditions in the excavation face area.



Figure 5. Installation of the forepoling tubes at the top heading of the station tunnel.



Figure 6. Top heading excavation of the station tunnel. Installation of the HEB 180 steel arches.

The excavation of the station tunnel is influenced in specific areas by the presence of piles (South Dome and Building Pit) as well as by the presence of the prestressed anchors (Fig. 7). As for the station tunnel's excavation in the area the Deep building Pit piles, there are a lot of construction difficulties to be confronted, which concern mainly the demolition of some of the piles and the connection of some of the remaining ones with the temporary support shell of the station tunnel.

Furthermore, the presence of the deep Building Pit's piles at the north side of the station tunnel, prevents the construction of the typical elephant foot. Due to this reason, station tunnel's north side temporary support shell is connected to Deep Building Pits piles via a special structural connection system with the use of steel dowels, anchored on the existing piles by injection of special adhesives (Fig. 8).

The prestressed anchors of Building Pit's south side and the cross and the E/M Service openings (connected to the South Dome and Building Pit) are also presented.

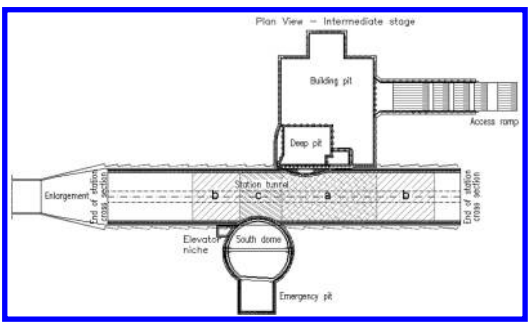


Figure 7. Plan view of the different parts of the station tunnel that are influenced by the neighbouring constructions of (a) piles of the building pit, (b) anchors of the building pit and (c) piles of the south dome.

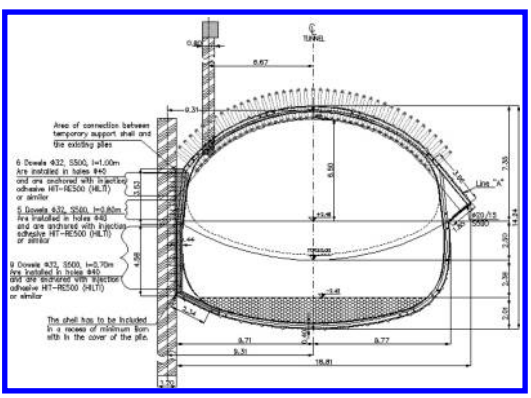


Figure 8. Connection details between temporary support shell and existing piles of the building pit.

Copyright © 2005 Taylor & Francis Group plc, London, UK

According to the above-mentioned reasons and especially due to the presence of the Building Pit's and South Dome's piles at the face and at the crown of the station tunnel's excavation, there is a number of forepole tubes which cannot be normally installed. Instead of those forepole tubes, spiles have been installed, in order to avoid any interruption of the applied presupporting system in the station tunnel's crown.

3 CALCULATION PROCEDURE ACCORDING TO 3D MODELS

One of the most important parameters to be taken into consideration, during tunneling in urban environment, is the stability of the face of the station tunnel. By providing sufficient stability on station tunnel's face with the application of efficient temporary support measures, the construction of the project is secured and the surface settlements will be limited to their minimum values; thus the surface constructions (buildings) and relevant installations will be secured by irrecoverable damages.

In the present project detailed analyses have been performed by the use of a powerful computational code SOFiSTiK3D, in order to approach in general the effectiveness of the application of the support measures, the settlements along the station tunnel, the face stability and the rockmass relaxation at the excavation face area in relation to the distance of the face. By taking into account the results of the 3D model, the (stiffness core relaxation E/in situ ground stiffness Eo) coefficient was determined, for each distinguished load case and excavation and temporary support class in the 2D analyses. The convergence of the rockmass as determined according to the 3D analysis was presented in special diagrams. The analytical dimensioning and structural adequacy check of each support class is performed according to the 2D analyses.

The 3D analyses in combination with the specific 2D analyses have been performed in order to ensure the requirements relevant to:

- Maximum surface settlements.
- Safety factor in the station tunnel's face.
- Safe construction sequence.

4 SETTLEMENT CALCULATION vs ACTUAL SETTLEMENT MEASUREMENTS

The surface settlements as well as the convergence and the adequacy of the temporary shell of the station tunnel were calculated according to detailed 3D analysis with sophisticated models (Fig. 9).

Figure 10 presents the surface settlements calculations, after 30 m of top heading and bench excavation.

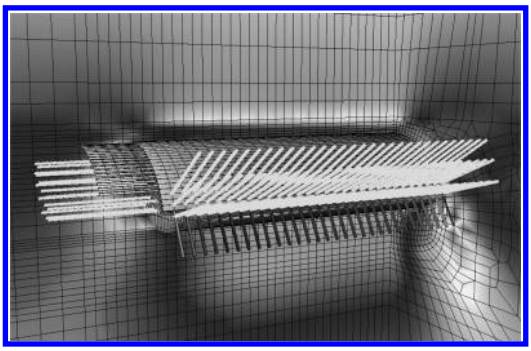


Figure 9. Analytical 3D model of the station tunnel by taking into account the forepoles, the fiberglass bolts in the tunnel face, the shotcrete lining, the micropiles, the anchors, etc.

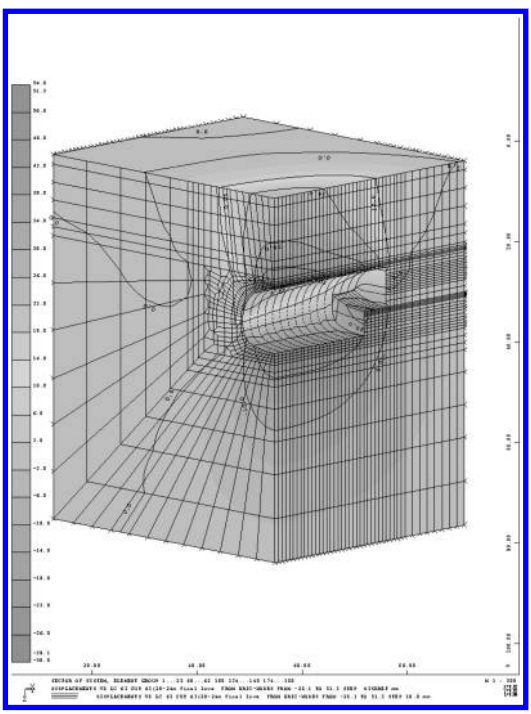


Figure 10. Surface settlement calculations after 30 m of excavation and temporary support of the station tunnel.

During the construction of the Station tunnel and according to the measured values acquired for the top heading excavation, the predicted settlement values were significantly confirmed in a substantial part of the underground station.

The adequacy of the shotcrete lining, as well as, the settlements and the behavior of the surrounding buildings were intensively monitored by a dense

Copyright © 2005 Taylor & Francis Group plc, London, UK

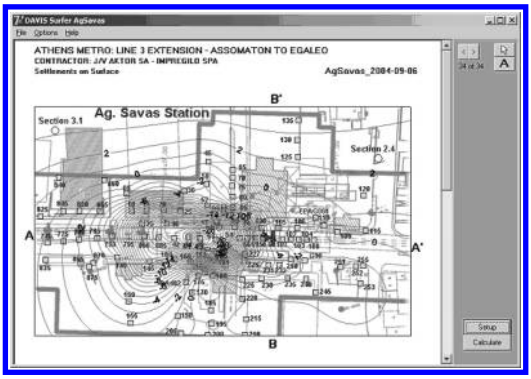


Figure 11. Contour plots of the surface settlements measurements after 50 m of excavation and temporary support of the station tunnel.

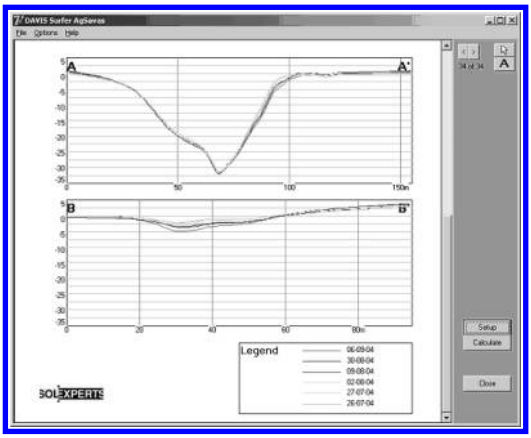


Figure 12. Plot curves of the surface settlements measurements after 50 m of excavation and temporary support, in the longitudinal section AA and the transverse section BB of the Station tunnel.

geotechnical system. Figures 11 & 12 present partial plots of the daily-evaluated data.

According to the results of the 3D analysis concerning the excavation and temporary support classes, important conclusions have been arised regarding the station tunnel's face stability and the surface settlements calculations.

The most important temporary support measures for the stability of the station tunnel's face and the restriction of the surface settlements are the fiberglass bolts and the forepoles (steel tubes). It's a fact that the fiberglass bolts combined with the forepoles reduce not only the extent of the plasticity zone, in front of the station tunnel's face, but also the magnitude of the surface settlements.

The proper cooperation of the fiberglass bolts and the forepoling umbrella vanishes the displacements of the face, the magnitude of the surface settlements and decreases the probability for chimney development. From the above mentioned, the most important aid is the determination of the appropriate number of the fiberglass bolts applied in the station tunnel's face and the appropriate number of forepoles applied in the station tunnel's crown.

5 CONCLUSIONS

The station tunnel design and construction is based on the application of NATM tunnelling, in two discrete stages (top heading and bench) and on the systematic use of grouted forepoling umbrellas. Special problems encountered during the design refer to the close proximity of the station tunnel to the adjacent building pit and the auxiliary galleries and shafts of the station complex, as well as the structural and geometrical efficient transition from the smaller running tunnel section to the required profile of station tunnel.

The tunnel alignment underpasses a significant Athens avenue with heavy traffic and the influence zone of the tunnel includes several commercial buildings and manufacturing sites. There are very few station tunnels in urban areas under such low cover (approx. 18 m) worldwide to be designed and constructed by this method (without any type of side drifting) under such strict construction sequence, time, traffic, settlement and geotechnical constraints.

The choice of the forepoling method has proven to be successful for the project, since the time needed for the construction of the top heading was 5.5 months and the total estimated time for the full cross section of the station will be less than 10 months, despite the specific modifications of the forepoling method that was necessary in different parts of the project.

The safe construction of the station tunnel via forepoling method and the limitation of the surface settlements could be provided by the control of the station tunnel's face stability in combination with an adequate shotcrete shell and an immediate construction of the temporary invert (in the present design this construction sequence was applied). Guidelines relevant to the better use and cooperation of the applied support measures in the station tunnel's face are also provided and concern the following:

– The maximum forces on the forepoles/spiles applied in the station tunnel's crown, depend on the round length, their foundation conditions and mainly on the deformability and strength of the station tunnel's face.
– By supporting the station tunnel's face with fiberglass bolts, its strength is improved, so the opening,

Copyright © 2005 Taylor & Francis Group plc, London, UK

the deflection (sagging) and the bending moment of the forepoles/spiles is decreased.
- The stresses of the forepoles/spiles can be restricted by increasing their quantity or by applying additional support to the station tunnel's face.
- The fiberglass bolts grid may in each case become denser according to the support requirements met during the excavation, but the immediate increase of the forepoles/spiles is not always possible.
- The in situ recognition of the geomechanical behavior of the weak formation is of great importance and also critical for the normal construction process and the restriction of the surface settlements.

REFERENCES

Omikron Kappa Consulting Ltd and Ingenieurburo EDR GmbH, March 2003, Agios Savas Emergency exit and South Dome Pit, Temporary Retaining Structures.

Omikron Kappa Consulting Ltd and Ingenieurburo EDR GmbH, October 2003, Agios Savas Building Pit, Temporary Retaining Structures.

Omikron Kappa Consulting Ltd, February 2004, Excavation and temporary support of the transition part of the running tunnel, KP 2 + 180.32 to KP 2 + 200.32.

Omikron Kappa Consulting Ltd, March 2004, Excavation and temporary support of the Station tunnel, KP 2 + 200.32 to KP 2 + 312.19

Copyright © 2005 Taylor & Francis Group plc, London, UK

Design of water isolation grouting for reducing high water inflows in urban shallow tunnels

N. Koronakis, P. Kontothanassis & D. Katsaris
Omikron Kappa Consulting Ltd, Athens, Greece

J. Bournazos
Technical Manager AKTOR S.A., Athens, Greece

ABSTRACT: The paper presents a decision making process for the determination of the numerous grouting parameters during design and the necessary corrective and evaluation actions during field trials or systematic grouting. Special application of design and execution of grouting for shallow tunnels in urban areas is given. The evaluation of field trials is also discussed, thus fine-tuning the design and optimizing the water sealing efficiency.

1 GENERAL PLANNING – DECISION MAKING PROCESS

1.1 *Design considerations*

Successful treatment of a soil or rock-grouting problem depends on the basic understanding of the general engineering fundamentals, soil or rock mechanics, hydrogeology and environmental geochemistry. A grouting engineer must make a proper use of the geotechnical engineer's "toolkit" in order to determine the soil's or rock's flow properties, nature and structure – these factors are the cornerstones of any grouting program design.

1.2 *Decision making process – parameters*

The grouting concept must always be based on the idea to start performing the work by using the easiest and simplest available technique.

The decision making process in a grouting programme consists of several parameters, some of which are mentioned below.

1.2.1 *Injection & drilling sequencing*

The simplest injection hole layout is the parallel pipe array, in which all the injection pipes are placed parallel to each other. Construction constraints may require a fan array, in which the pipes diverge.

Injection staging involves primary, secondary, tertiary, and quaternary grouting stages, the last two being optional depending on the project requirements. Primary grouting refers to initial grout penetration in ungrouted zones where adjacent grout bulb boundaries are either in partial contact or not. Secondary grouting refers to grouting the gaps between primary grout boundaries. Tertiary and quaternary grouting targets spots that the first two stages missed. The result is a grouted soil or rock mass with overlapping grout bulbs.

Ultimate injection hole spacing for most grouting projects range from 0.8 to 2 m. Typically, the greater the distance between injection holes, the less definitive the grout front becomes. When grout holes are spaced too close, the result is excessive drilling costs.

All holes of an intermediate set in any section of the grout curtain are grouted before the next set of intermediates is drilled. If grout frequently spreads from one primary hole to another, an increase in the primary spacing is necessary. As the split spacing technique reduces the intervals between grout holes, the average grout consumption per linear meter of hole should also become smaller.

1.2.2 *Permeability*

In-situ field permeability tests give more accurate results than lab permeability tests performed on representative field samples. Laboratory test results often have systematic errors. Furthermore, undisturbed cohensionless soil samples are difficult to obtain since they fall apart easily. Permeability is measured in cm/sec expressed by the variable k:

- $k = 10^{-6}$ or less: ungroutable
- $k = 10^{-5}$ to 10^{-6}: groutable with difficulty by grouts under 5cP viscosity and ungroutable for higher viscosities

Copyright © 2005 Taylor & Francis Group plc, London, UK

– k = 10^{-3} to 10^{-5}: groutable by low-viscosity grouts but with difficulty when k is more than 10 cP
– k = 10^{-1} to 10^{-3}: groutable with all commonly used chemical grouts
– k = 10^{-1} or more: use suspended solids grout or chemical grout with a solids filler.

Field permeability test methods are the double packer test and the well pumping test.

1.2.3 *Injectability*

At present, there are no truly reliable small scale or laboratory methods which will accurately determine the injectability limits of soils or rocks. Tests are typically conducted with cylinders, which are filled with soil and grouted from the top down. These methods do not take into account the impact of boundary conditions on the ultimate injectability.

Thinner soil layers require higher injection pressures at a given injection rate and by decreasing the injection rate the effect of the layer thickness can be somewhat compensated.

A very general rule of thumb used in conjunction with the permeability coefficient of soil has been that:

– $k > 1 \times 10^{-1}$ cm/s are injectable with regular cement based (suspension grouts)
– $k > 5 \times 10^{-3}$ cm/s are injectable with microfine cement based (suspension grouts)
– $k > 1 \times 10^{-4}$ cm/s are injectable with solution grouts
– Reducing the cohesion of the grout mix, while maintaining a stable grout mix, can enhance its penetration.

It is important to establish the upper limit of silt content in a given soil that will still enable acceptable penetration. A soil with a "suitable" d_{10} d_{50} or d_{85} which would lead one to believe that it is perfectly injectable may be found in the field to not be injectable with microfine or suspension grouts due to the silt content.

1.2.4 *Grout mix design*

The choice of grout type is a function primarily of the aperture of the rock joints and cost for grouting projects that involve filling fissures. The use of stable grouts formulated with locally available ordinary Portland cement is recommended. Based on experience, the aperture of joints that can be grouted with ordinary Portland cement is:

(a) 500 microns without special care.
(b) 400 microns with extra care using high quality grout.

The groutability of fine cracks is related to the width of the crack and the grain size of the grout material, expressed as a groutability ratio for rock in the following formula:

$$Groutability\ Ratio = \frac{Width\ of\ Fissure}{D_{95}\ of\ Grout} \quad (1)$$

For groutability ratios greater than 5, grouting is considered consistently possible. For groutability ratios less than 2, grouting is not considered possible.

The D95 and practical grouting range for various grouts are provided in Table 1.

For each application of grout, it is necessary to select a starter mix, and then as grouting of the hole proceeds, decide whether to thicken the mix during grouting. Choosing a good starter mix will come from experience at a particular site after several holes have been grouted. At most sites a good starting point is a 2:1 (water ÷ cement by weight) mix.

1.2.5 *Injection pressure*

A long standing rule of thumb for calculating the maximum allowable grout injection pressure has been 1 lb/in^2 per foot of packer depth in rock (22.59 kN/m^2 per meter of packer depth in rock) plus half the depth of overburden. This rule is based on the weight of rock and overburden directly above the grout hole. While this approach to determining maximum injection pressures may be applicable when grouting in poor or unknown geological conditions at shallow depth, 10 m or less, it is felt to be too conservative for

Table 1. Joint aperture range for various cement grouts.

Cement grout	D95 of grout	Practical joint aperture
Ordinary Portland	80–100 microns	>400 microns
High early Strength	40–60 microns	>200 microns
Microfine cement	10–20 microns	>50 microns

Table 2. Suitable grout vs. permeability.

Lugeon value	Permeability	Grouting material
4	5.2×10^{-7} m/s	Microfine cement grout
8	1.0×10^{-6} m/s	Microfine cement grout
15	2.0×10^{-6} m/s	Microfine cement grout
30	3.9×10^{-6} m/s	Cement rout with stabilizing additives
60	7.8×10^{-6} m/s	Cement grout with stabilizing additives
120	1.6×10^{-5} m/s	Cement grout with thixotropic additives

Copyright © 2005 Taylor & Francis Group plc, London, UK

most other rock grouting. To reinforce the philosophy of using higher injection pressures, the European rule of thumb for safe grouting pressures is 1 kg/cm^2 per meter of packer depth. This is about four times the US rule of thumb.

1.2.6 *Completion & refusal criteria*

Grouting may be continued to absolute refusal at the maximum grouting pressure, although this is not usually done. There are two methods that are most frequently used to determine when grouting is complete. One specifies that grouting shall continue until the hole takes no grout at three fourths of the maximum grouting pressure. The other requires that grouting continues until the hole takes grout at the rate of 30–40 lt or less in 10 min measured over at least a 5-min period. This is often modified according to the mix and/or pressure applied.

If there is doubt about the completeness of treatment in any zone or area, a check hole or holes should be drilled. However, a quicker and less expensive check can be made by drilling and pressure testing of another grout hole. If tight when pressure- tested with water, the rock is satisfactorily grouted; if the hole takes water, additional grouting is indicated.

1.3 *Corrections & evaluation actions during field trials or systematic grouting*

It is well known, that there is not any grouting program worldwide established in the form of certain preliminary investigations and technical guidelines that was not finally subjected to significant modifications during the actual evaluation process and the exploitation of the results of the learning curves achieved on site. There are always significant control or even reset actions that are required for optimizing the grouting process efficiency and productivity as a whole, mainly taken by the on site engineers responsible in close cooperation with the designer, by taking into account the changeable prevailing conditions and the heterogeneity of the ground as well as the equipment and mix design possibilities. The contractor must establish a reliable monitoring and evaluation engineering team officially responsible for the decision making required at a daily basis on an immediate response on site, in conjunction with the systematic on site involvement of the designer in all the critical steps or cases actually anticipated.

Each grouting program has unique characteristics because of its immediate connection and interaction with the geological and geotechnical profile of the region in interest.

For instance, an ascending (up-stage) grouting method should change if an unstable to drilling ground layer causes significant problems to the drilling crew and the productivity. Possible actions are to reduce the borehole's diameter if possible or to apply a descending (down-stage) grouting method.

Cataclastic rocks, breccia or conglomerates usually reduce the lifetime span of packers. So, it's common for packers to be destroyed because some sharp rock cuts its protective rubber cover. Reducing the borehole's diameter usually helps because there is not much movement and friction of the packer's surface on the borehole wall during its swelling.

The most significant part of the grouting design is the determination of the completion and refusal criteria that the grouting engineer would apply on site. A successful choice of these parameters can judge the success of the grouting program as a whole. Usually, the completion and refusal criteria consist from a volume and pressure-time control guideline. If the completion criterion is achieved then grouting has to stop or the grout mix to change. So, a volume control guideline has to take into consideration the agitator's capacity. This is critical because in this case the wastes are eliminated and this is of major importance especially in an urban environment. A pressure-time control guideline has to be calibrated according to the response of the rockmass in grouting as well as to the productivity targets of the project. So, if the time to reach the refusal pressure is significant and the pressure rises asymptotically in relation to time then the criteria should be calibrated accordingly.

1.4 *Usual problems during the application and evaluation of a grouting program on site*

Besides to the equipment capacities, the expertise of the crew and the grouting engineer is the most significant factor for the success of the grouting project. The readiness, the ability to judge and evaluate the design on site as well as the ability to translate and sense the grouting process are necessary characteristics that a grouting crew should have developed. A new learning curve is needed and for this reason the designer and the grouting engineer on site must be in close contact. The designer knows the marginal values and acceptance limits of each critical parameter. The grouting engineer on site is usually stressed by the need for organizing the optimum production system in relation with quality control aspects.

Usually, parameters such as, the completion and refusal criteria, the extent and sequence of drilling and grouting as well as the management of grout mixes (quantities, additives, time of preparation) and applied pressures are major subjects for discussion and calibration during the advance of the grouting project. However, the above-mentioned parameters are also the tricky subjects where misunderstandings occur and are not always applied strictly according to the initial design provisions.

Copyright © 2005 Taylor & Francis Group plc, London, UK

2 SPECIAL APPLICATION OF GROUTING DESIGN IN ATHENS METRO

2.1 *General description*

The present paragraph refers to the execution of grouting works for water control purposes of a ventilation shaft, the access gallery and the chamber in the area of a running shallow track tunnel, for the construction of the western extension of Athens Metro Line 3, with conventional (NATM) method (Fig. 1). The basic demand of the design is to use construction methods to achieve all the demands of settlement requirements and to reduce or eliminate water inflows to acceptable limits, which will permit the safe and feasible construction of the access gallery and chamber. The overburden thickness is approximately 22 m.

The main geological formations encountered in the area of interest, consist of (from ground surface to depth) alluvial deposits (mainly clayey gravels and sandy clay gravels), conglomerates and breccias ranging from loose to cemented and cohesive, sandy and clayey marls with sandstone intercalations and Athens schist as the main underlying bedrock.

The whole geological background is characterized by considerably high heterogeneity due to the frequent alterations and erratic lithological, petrographical and stratigraphical structures and characteristics of the main horizons by taking into account almost all the existing types of water permeability origin, ranging from the alluvial nature of the soil and soil like formations, which is mainly governed by the grain size distribution and the cohesion, up to the fissured rock properties of the highly cemented conglomerates, which are mainly determined by the joint properties and the composition of the matrix material. It is obvious that several modifications and differential arrangements have to be applied, especially in the "grey" (boundary) areas between soil like and weak rock nature of the conglomerate formation, which actually governs the response of the underground excavation and temporary support of the underground opening, with regard to the underground water inflows, seepage and piping phenomena.

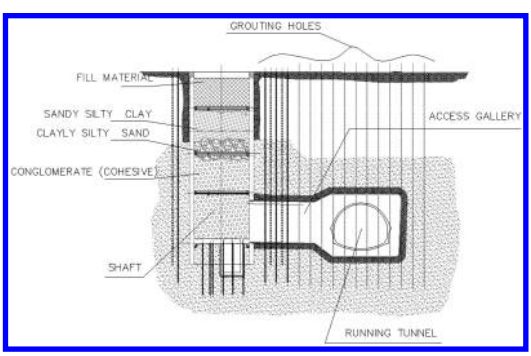


Figure 1. Longitudinal section of the shaft, access gallery and chamber with the running tunnel.

Unexpectedly high ground water inflows were observed during the construction (January–February 2003) of the shaft (approx. 220 m^3/h, with very little water table drawdown).

The conglomerate is usually relatively well cemented and its permeability is high, mainly due to the existence of open cracks, fissures and other discontinuities providing selective flow paths. The large thickness of the conglomerates results in a high "average" permeability of the aquifer.

The hydraulic parameters assessed for this region gave the following values:

Permeability $k = 1 \times 10^{-3}$ m/sec, Transmissivity $T = 8 \times 0^{-3}\,m^2$/sec to $3.5 \times 10^{-2}\,m^2$/sec, Storativity $S = 0.04$.

The above values show that the water inflow in the area of the tunnel face is too high and well beyond the inflows (Figs 4–5), which can be reliably controlled by drilling drainage boreholes ahead of the tunnel's face. In addition to that, the pumping tests have shown that the drawdown cone is very sharp, which indicates that only few metres (3–5 metres) away from the tunnel face the water pressures will be practically hydrostatic, thus creating a large hydraulic head which can cause face blow-outs and collapse. Such events can occur in areas where the conglomerate is locally less cemented resulting in lower shear strength. A typical case can be a block of less cemented conglomerate having a width of 2–5 metres ahead of the tunnel face, with better-cemented material beyond that distance. The high water pressures in the more competent material can cause blowout of the less competent conglomerate at the tunnel face resulting in an extended face collapse.

2.2 *Grouting programme*

Since the shaft has already been driven up to its final bottom level, all the grouting work was performed from surface. Several preparatory works took place i.e. reestablishment of a surface collar plug in the ground surrounding the top shaft level by placement of 20 cm of lean concrete (B10), use of thrown bulk sand in the shaft, for acting due to its own weight as a natural plug on all the existing discontinuities, cracks of the shotcrete and the existing open holes. A certain hole pattern was designed, consisting of three main (I, II, III) and two auxiliary [(I-II), (II-III)] rows of holes divided in primary (A), secondary (B) and tertiary (C) holes (Fig. 2).

The final spacing of the main rows of holes was 2 m × 2 m and by taking into account the installation of the auxiliary holes (if needed), it was 2 m × 1 m.

Copyright © 2005 Taylor & Francis Group plc, London, UK

The borehole sequencing was based on circumferential advance of the drilling and grouting works (inside each row) as the initial priority and after the completion of each row the work was expanded to the next row etc. For avoiding undesired leakages of pressured air and grout due to existing interconnections between adjacent boreholes, these were placed in distances ranging from 6 up to 12 m (in general 8 m).

The final depth of all the main rows of holes exceeds the depth of the shaft for 6 up to 7 m. Certain bottom shaft holes were executed in order to provide the necessary water isolation in this critical area of the shaft. The whole grouting concept was based on the stage up method in stages of 3 m of grouting in conjunction with the use of conventional single pneumatic packers for each stage.

The "roof" (upper) grouting stage does not exceed approx. 13 m of depth. A variety of grout mixes (w/c) was available (per weight): 2:1, 1.5:1, 1:1, 0.8:1, 0.6:1, with 0, 1 and 2% (per weight of cement) bentonite. For special purposes, a mix of 0.5:1 (per weight) with special additives for antishrinkage effects and easier pumping, was also available, been distinguished by almost similar thixotropic characteristics like the 1:1 mix.

The achieved verticality of the holes was of major importance due to the close arrangement of the holes and any effort was made for avoiding more than 0.5 m deviation in the bottom of the holes. Casing of the holes was necessary.

The borehole design has been based on the assumption that the minimum crack sizes of the conglomerate exceed 0.5 mm (500 μm). Due to the petrographic features of the conglomerate formation, the majority of the existing discontinuities to be grouted was distinguished by horizontal or subhorizontal dips (since most of the existing fissures are erosional, oxidization or of weathering nature), thus making in-shaft grouting a non preferable alternative, in regard to its efficiency. Different mixes were used in different rows of holes or even in different stages in one hole, due to the existing heterogeneity of the fissured conglomerate structure based on the fast and reliable evaluation of the existing grouting results, by taking into account the resultant combinations of grout intake, pressure, time and composition of mix.

Due to the fact that the basic direction of water inflow in the area of the shaft comes mainly from North to South, an asymmetrical hole arrangement was applied in order to balance the applied hydrostatic pressures in the area of the shaft and to contribute to the most efficient water isolation of the structure through grouting. The applied pressures in any case did not exceed 15 bars being necessarily differentiated according to the depth level of each stage and to the mechanical properties of the formations for avoiding uplift phenomena and hydrofracturing.

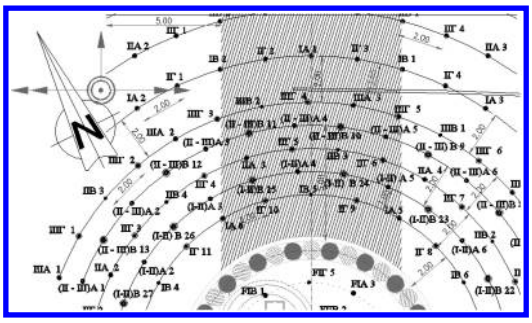


Figure 2. Plan view of a typical borehole grouting pattern around the shaft and the access gallery.

2.3 *Evaluation of field trial tests and conclusions*

Grouting in this ground profile was successive and therefore necessary for the decrease of the expected water inflows of the underground openings. Moreover, it is emphasized that grouting was applied with the simplest possible method. No special grout mixes were used as well as any sophisticated procedures or equipment. The method applied was an ascending one, with one pneumatic packer and simple grout mixes.

The actual consumption of grout is the only reliable tool for the evaluation of the grout process (Fig. 3). There was a significant consumption of grout while the Lugeon tests indicated a coefficient of permeability of 10^{-6} m/sec and even less. The initial pump-out tests indicated a coefficient of permeability of 10^{-4} to 10^{-3} m/sec, which correlates well with the actual grout consumption.

In order to correlate the grout consumption (which depends from flow Q and time T) with permeability, the following Table 3 is presented.

Table 3 shows that in order to achieve a mean value of flow 35 lt/min and pressure 8.5 bars (the mean values used for grouting in situ), then the permeability

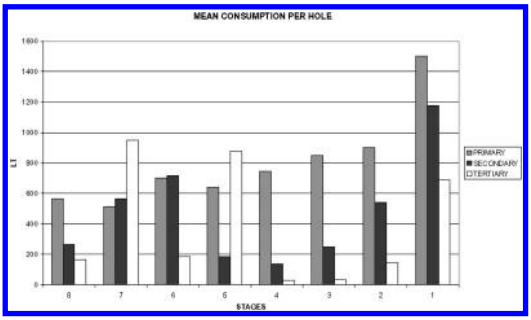


Figure 3. Mean consumption of grout per hole for each stage for all the executed primary, secondary and 8 tertiary boreholes. Average values, Primary = 802 lt, Secondary = 479 lt, Tertiary = 384 lt.

Copyright © 2005 Taylor & Francis Group plc, London, UK

Table 3. Injectability formula $Peff = \frac{Q \cdot Vi \cdot \delta i}{2 \cdot k \cdot v \cdot e} \ln\left(\frac{R}{r_o}\right)$

Injectability formula				
Grout injection rate	Q (lt/sec)	35	35	35
Kinematic Viscosity of grout	Vi (sec)	47.25	47.25	47.25
Viscosity of water	v (sec)	35	35	35
Specific gravity of grout	δi (kN/m^3)	14.02	14.02	14.02
Hydraulic conductivity of soil with water	k (m/sec)	10^{-5}	10^{-4}	10^{-6}
Thickness of soil horizon	e (m)	3	3	3
Constant depending on soil type (1–10)	R	5	5	5
Radius of borehole	r_o (m)	0.05	0.05	0.05
Grout pressure	Peff (kN/m^2/m)	848	85	8477
	Peff (bar/m)	8.48	0.85	84.77



Figure 4. Shaft during pump-out test.

coefficient should be 10^{-5} m/sec and higher. The above value of effective grout pressure is directly proportional to the grout spread in the soil and therefore the effective groutable radius. The effective pressure



Figure 5. Water inflow from drainage holes in the shaft.

presented to Table 3 corresponds to 1 m radius which is the spacing interaction between primary, secondary and tertiary boreholes.

Furthermore the specific grout consumption (volume of grout/volume of grouted region) taking into consideration only the primary and secondary holes reached the value of 3.7%. The specific grout consumption for the primary holes, was 2.5% and for the secondary holes 1.2%. The significant decrease of the grout consumption between the primary and secondary holes reaching the 50% reduction is a robust factor for the success of the grouting programme.

REFERENCES

Omikron Kapa Consulting Ltd, July 2003, Technical Report No 3AW3CW395R905A, Prof. Daniel – New detailed final design of grouting works for shaft, access gallery and associated works.

Omikron Kapa Consulting Ltd, March 2004, Technical Report No 3HW3CW401R901A, Evaluation report of investigation grouting results and testings in Prof Daniel shaft.

Copyright © 2005 Taylor & Francis Group plc, London, UK

Gotthard Base Tunnel Sedrun section mastering squeezing rock zones

Heinz Ehrbar
AlpTransit Gotthard Ltd., Lucerne, Switzerland

ABSTRACT: Since more than three years the main tunnel of the Gotthard Base Tunnel is under construction. In the central section of Sedrun large zones with squeezing rock are predicted. The project takes the high forces and the necessary deformations into account. For the rock support steel ribs are the main elements. Special on site tests were carried out to check the effectiveness of the chosen rock support.

1 FUNDAMENTAL CONSIDERATIONS REGARDING PLANNING AND IMPLEMENTATION

Since the route of the Gotthard Base Tunnel (GBT) was decided, it has been known that in the Sedrun section two constructional difficult zones – the Tavetsch Intermediate Massif (TIM) (North) and the Urseren Garvera Zone (UGZ) – must be cut through. In both zones, squeezing rock conditions are expected to be encountered.
The main questions during design and construction are:

1. With what type of ground conditions are we confronted?
2. What phenomena could hinder the successful construction of a tunnel?
3. What are the constructional measures to overcome these phenomena, so that a tunnel can be constructed safely at an acceptable cost?

In each phase of the project, answers to these questions have been, and are, found by application of the procedure shown simplified in Fig. 2.
The main project steps are:

- Geological exploration
- Description of the rock mass based on the geological exploration
- Assessment of the rock mass with regard to excavation of the underground cavity
- Determination of the cross section
- Determination of the rock support
- Determination of the method of excavation
- Determination of the requirement for constructional aids
- Definition of the radial and longitudinal procedures (construction sequence)

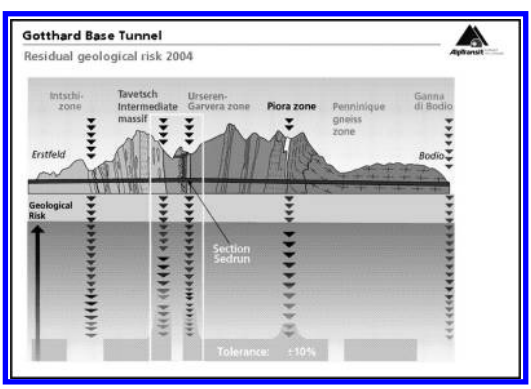


Figure 1. Gotthard Base Tunnel, geological risk zones.

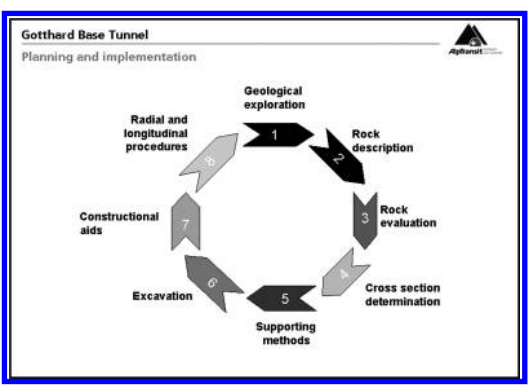


Figure 2. General planning procedure.

Copyright © 2005 Taylor & Francis Group plc, London, UK

2 CONSTRUCTIONAL FOUNDATION

2.1 *Geological exploration*

The owner AlpTransit Gotthard Ltd. (ATG) already decided at an early stage to explore the geologically difficult zones with extensive test-bore campaigns and other investigations. The following test-bore campaigns were conducted:

1991:	Diagonal bore SB 1	L = 838 m
1991:	Diagonal bore SB 2	L = 543 m
1993:	Diagonal bore SB 3.1	L = 780 m
1997:	Diagonal bore SB 4.1	L = 1750 m
1997/98:	Diagonal bore SB 3.2	L = 1716 m

The Urseren Garvera zone was not explored with test bores. However, since this tectonic unit had been traversed during construction of the headrace tunnel for the Vorderrhein hydropower scheme, and when building the Gotthard road tunnel, sufficient knowledge and experience was available.

During the construction phase, horizontal test bores are made in both of the single-track tunnels, to the north as well as to the south. Depending on the rock conditions, the test bores are either percussion or core bores. The length of the bores varies between 36 m for the percussion bores and from 150 m up to 400 m (in the region of the Nalps dam) fore the core bores. Depending on the evaluation of the potential hazard of water ingress, the test bores are protected with preventers.

2.2 *Description of the rock situation*

The test bores to the north have indicated that the 1.1 km long Tavetsch Intermediate Massif North consists to approximately 70% of soft, kakiritic rocks displaying ductile fracture behaviour. Approximately 30% of the rock is hard and displays brittle facture behavior. Hard and soft rocks alternate in narrow vertical layers. Where the material resembles loose rock, it is saturated with water.

2.3 *Assessment of the rock mass*

The assessment of the rock serves to forecast the composition and behavior of the rock which will be encountered when constructing the underground cavity. This evaluation, as well as an evaluation of the rock in relation to water and gas, was made project-specifically based on known hazard scenarios.

In the Tavetsch Intermediate Massif (North) as well as in the Urseren Garvera zone, the predominant hazard is the phenomenon of squeezing rock.

In view of the high overburden of 900 m and more, as well as the fact that the rock is saturated with water, the squeezing conditions are classified as extreme.

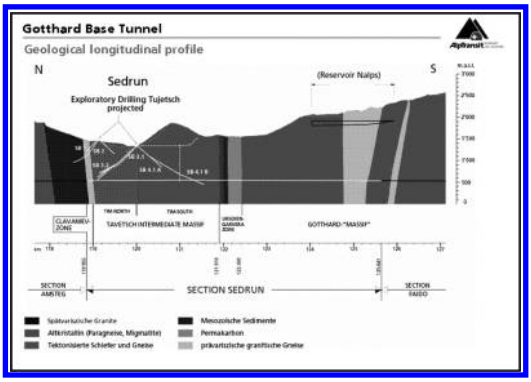


Figure 3. Sedrun section, longitudinal geological profile.

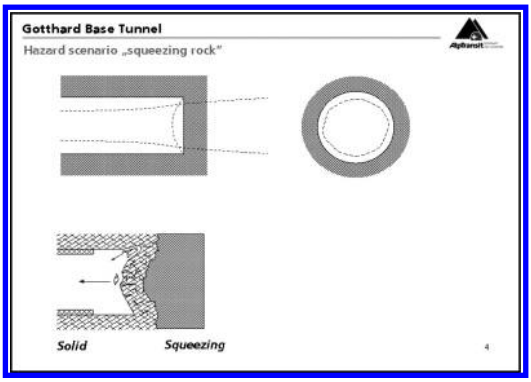


Figure 4. Hazard scenario "squeezing rock".

The phenomenon of squeezing rock will manifest itself both radially as well as at the work-face as a tendency of the excavated cavity to converge. In the longitudinal direction, given the expected alternation of different vertical layers of rock, the phenomenon will be accentuated as potential instabilities at the workface.

3 CONSTRUCTIONAL MEASURES

Experience of tunnel construction indicates that rock pressure decreases as the amount of rock deformation increases. The amount of constructional resistance needing to be applied can therefore be substantially reduced if a certain amount of deformation is permitted. However, in the case of strongly squeezing rock such as occurs in the Sedrun section, permitting greater deformation alone is insufficient to achieve a stable situation.

Despite permitting deformations of the order of several decimeters, extremely massive supporting forces must be applied to keep the excavated cavity

Copyright © 2005 Taylor & Francis Group plc, London, UK

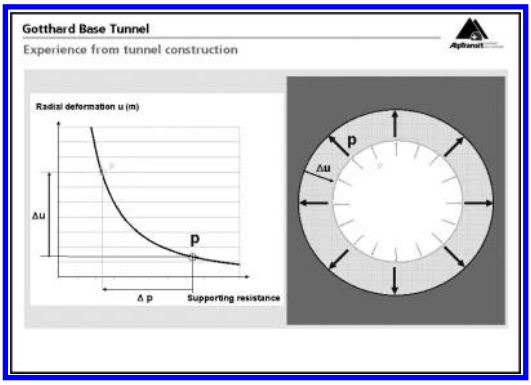


Figure 5. Experience of tunnelling in squeezing rock.

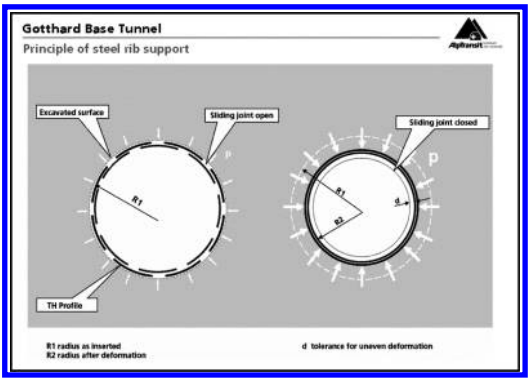


Figure 7. Principle of steel rib support.

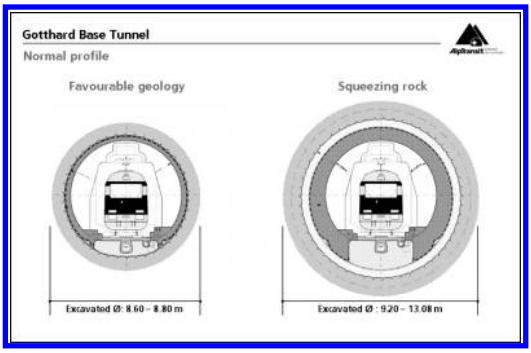


Figure 6. Normal profiles.

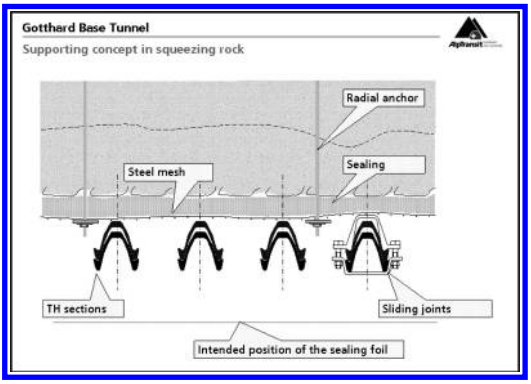


Figure 8. Supporting concept in squeezing rock.

open. Without permitting deformations, it would be technically practically impossible to create the forces needed to keep the excavated cross section open.

3.1 *Design of the cross section*

The specifications for the high-speed railway line in the GBT stipulate a minimum free air cross section Fair of 41.0 m^2. The high forces on the construction expected from the true rock pressure demand a structurally optimal form. For this reason, through-out the entire Sedrun section, the only cross section which can be used for the single-track tunnel is a circle, whereas in sections with favorable geological conditions the base of the tunnel is made flat to assist construction operations.

3.2 *Mining engineering methods of support*

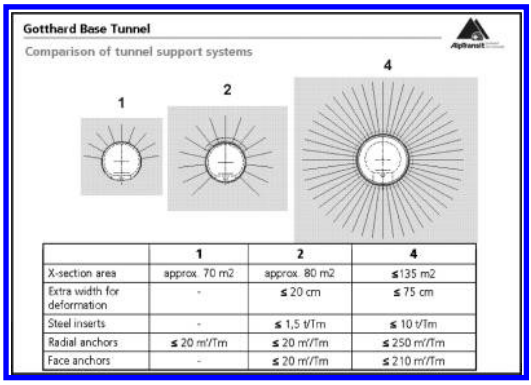
Considerations based on the principles of rock mechanics resulted in a concept being sought which would fulfill the conditions specific to the Sedrun situation, i.e. a concept which would allow a high degree of deformation but also provide a high level of outward resistance when completed.

In their search, both owner and project engineers endeavored to find a solution based on proven technology. The technique applied in German coal mines of using deformable steel inserts with Toussaint-Heintzmann (TH) sections fulfilled the specified requirements.

After excavation of the cavity, two steel ring inserts each consisting of eight segments are assembled to form two concentric rings. The joins can slide over each other to a predefined limited extent, which allows the overall system to deform radially. When fully compressed, the system attains a maximum load-bearing pressure of approx. 1.8 MPa.

The insertion process is shown idealized and symmetrical in Fig. 5. However, this idealized situation will rarely be achieved in practice. The GBT project allows a degree of tolerance for uneven deformation, which in the mining industry leads to the term ‘swimming inserts’.

Copyright © 2005 Taylor & Francis Group plc, London, UK



	1	2	4
X-section area	approx. 70 m2	approx. 80 m2	≤135 m2
Extra width for deformation	-	≤ 20 cm	≤ 75 cm
Steel inserts	-	≤ 1,5 t/Tm	≤ 10 t/Tm
Radial anchors	≤ 20 m/Tm	≤ 20 m/Tm	≤ 250 m/Tm
Face anchors	-	≤ 20 m/Tm	≤ 210 m/Tm

Figure 9. Comparison of tunnel support system.

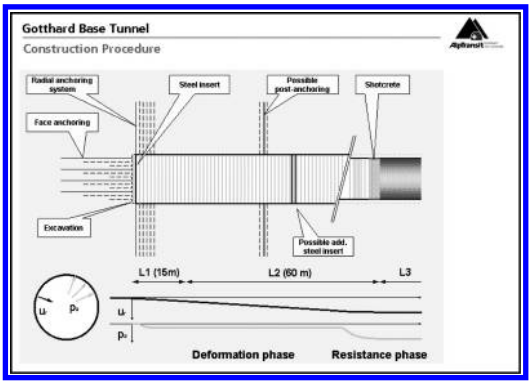


Figure 10. Construction procedure.

In the most extreme case, the steel rings are inserted practically 'shoulder to shoulder'. In addition to the steel inserts, the system is also reinforced with a systematic radial anchoring using up to 25 m of anchor per tunnel meter. The tunnel face is also anchored to a similar extent.

After the steel rings have been inserted, they are permanently concreted into place with shotcrete.

The overall supporting concept in the Sedrun section is modular, so as to allow optimal deployment of the associated machinery.

3.3 *Constructional aids*

Constructional aids are measures which enable driving under exceptional conditions by improving the rock (increased strength, rigidity, reduced permeability, etc.) and assuring the stability of the tunnel face.

In the main contract for the construction of the Sedrun Section, the following measures are foreseen:

- long advance drainage;
- grouting (individual grouting, grouting shields, grouting bodies);
- reinforcement of tunnel-face anchors and lances;
- re-profiling if necessary.

3.4 *Construction procedure*

The procedures for creating the profile are based on the following considerations:

The exploratory bores which have been made in the TIM (North), and the associated laboratory tests, indicate that in the TIM (North) an extreme amount of squeezing must be expected. Quick closure of the ring is therefore essential to keep the cross section open. For this reason, in the Sedrun section full-face excavation will always be used followed by immediate ring closure. The procedure for closing the ring will be as follows:

- After each advance, the steel rings are inserted (2 × TH 44, minimum distance 33 cm).
- 12 m long radial anchors are inserted to form an anchoring system.
- 18 m long tunnel-face anchors are inserted after every 6 m of advance.
- When the full length of the sliding join has been taken up, the circular force in the steel insert and with it the risk of buckling, increases. For perfect embedment, and to ensure the full load-bearing capacity, the steel rings are then completely shotcreted in. In the project, it is assumed that the insertion phase is completed 75 m behind the tunnel face.
- Within this distance of 75 m it is stipulated that over the entire cross section additional supporting measures must be possible, namely
  - insertion of additional steel rings
  - re-anchoring during the deformation process
  - application of a shotcrete lining after the deformation process is complete.

For this construction procedure to be possible, some major logistical challenges have to be mastered. The driving equipment must be capable of coping with enormously different dimensions (e.g. tunnel faces from 65 m^2 to 135 m^2). Also, the limited amount of space in the temporary base of the tunnel restricts the extent to which machines can pass each other. Because of this, large parts of the installations are placed on a following hanging plat-form.

For installation of the steel rings, as well as for various tasks at the tunnel face, so-called tunnellining machines are being used for the first time in railway tunnel construction. These machines allow insertion of steel inserts using two working platforms and a manipulator arm; application of the tunnel-face sealing

Copyright © 2005 Taylor & Francis Group plc, London, UK

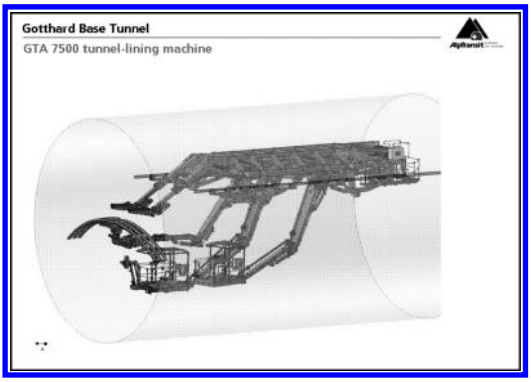


Figure 11. GTA 7500 Tunnel lining machine.



Figure 12. Steel rib tests, small test.

from the work platform by means of spray nozzles; cutting the tunnel-face anchors to length with hydraulic pincers.

Such installations for insertion of steel supports are used in mining, but not with the dimensions required on the Sedrun section where a weight of 50 tones has to be suspended from overhead rails.

The tunnel-lining machine is augmented with a backup suspension platform from the ROWA Company.

4 INNOVATIVE IN SITU TESTS FOR STEEL RIB SUPPORT

The concept described above is, as stated, based on already known technology. However, in the Sedrun section, tunnel cross sections of up to 13 m diameter must be excavated. Since experience with such large dimensions is lacking, critical questioning of important assumptions such as, for example, the insertion procedure and the assumed load-bearing capacity of the steel ring inserts was necessary before implementation.

The owner, AlpTransit Gotthard Ltd., therefore decided to contractually re-quire the contractor to perform a suitability evaluation of the proposed system. In consequence, tests ordered by ATG were performed on the construction site at a scale of 1:1.

The principle used in the tests is for the rock pressure to be simulated by means of inflatable rubber cushions. Such cushions are known in lifting technology for lifting heavy weights.

To gain greater familiarity with the system, a large number of small tests were performed on a single ring segment. This allowed the participants to test the necessary adaptations to the system with low outlay.

The tests began in the autumn of 2003 and were completed in spring 2004.

The results of the tests confirmed the theoretical calculations with the predicted accuracy. The selected

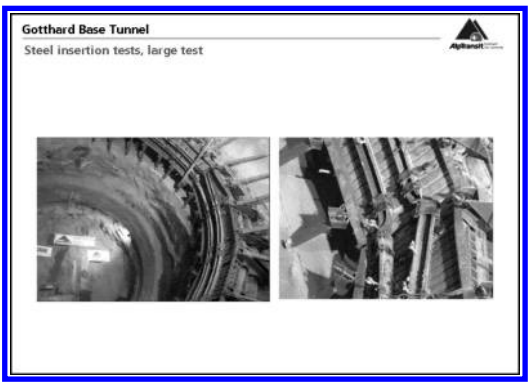


Figure 13. Steel rib tests, large test.

concept can therefore be judged to be suitable. However, the tests also showed potential limitations of the system.

In a subsequent large test, two complete steel rings with a diameter of 13 m were loaded to failure. With a closing distance of 60 cm, the knowledge regarding compression behavior and load-bearing capacity which was gained in the small test was confirmed.

At the same time, a certain margin for unexpected conditions, and potential for possible optimization, was also identified. It became evident that the direction of insertion of the shape of the steel-profile is of only minimal significance. In practice, the focus will be mainly on optimizing the system of single rings with smaller distances between the rings, since the additional load-bearing capacity of a double ring is not significantly greater than that of a single ring. Everyone involved in the project is aware that, despite the utmost care in preparation, further optimization will have to be achieved. For this purpose, a permanent working group with representation of the construction contractors, the project engineers, the local construction

Copyright © 2005 Taylor & Francis Group plc, London, UK

management, and the owner has been set up so as to be able to respond swiftly when required.

It was certainly right to perform the tests on the construction site rather than in the laboratory. This gave the driving team the opportunity to experience for the first time the techniques which will have to be used and the immense forces which will be encountered. This aspect must not under any circumstances be underestimated, since compression of the steel inserts is accompanied by loud noises which are not usual in tunnel construction.

5 CONSTRUCTION STATUS AND OUTLOOK

Since the contract was signed in April 2002, an enormous amount of work has been completed by the Transco Sedrun consortium. First, extensive installation works had to be done both above and below ground to make systematic construction work at all possible. At the same time, Shaft 2 was sunk, and lined with fireproof shotcrete, thereby becoming the first underground structure to be completed in the Sedrun section.

Since November 2003, driving at up to nine workplaces at tunnel level has proceeded practically unhindered by installation activities. Between 400 m and 700 m of tunnel system were constructed each month at a depth of more than 1.5 km under the mountain of Tgom.

In mid-May 2004, the transition zone to the area of squeezing rock was reached in the northward drive. Until autumn 2004 even in zones of bad rock quality no phenomena of squeezing rock occurred at Sedrun. In December 2004 rock masses with a high potential of squeezing were detected in the exploratory drillings. From the beginning of the year 2005 the construction procedure will follow the before mentioned method in the northern drive.

It is self-evident that under conditions with highly squeezing rock only greatly reduced rates of advance are possible. Whereas in favorable geology advance rates of more than 7 m of excavated tunnel per working day are possible, in squeezing-rock zones the advance rates fall to less than 1.0 m per working day.

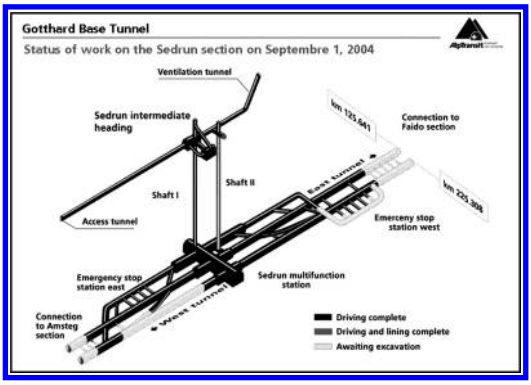


Figure 14. Status of work, September 2004.

The facts as described lead to the following key dates for the construction schedule of Lot 360:

- Start of construction — April 2002
- Shaft II sunk — End-May 2003
- Start driving north — July 1, 2003
- Start driving south — August 1, 2003
- Start driving in squeezing-rock zones — Summer 2004
- Breakthrough at north — July 2008
- Breakthrough at south — October 2008

REFERENCES

Ehrbar H., Schällibaum I., Kälin J., "Gotthard Base Tunnel, Construction Lot Sedrun, A Challenge for Tunnel Construction", ITA World Tunnel Congress, Milano 2001

Kovári K., Amberg F., Ehrbar H., "Mastering of Squeezing Rock in the Gotthard Base Tunnel", World Tunnelling, June 2000

Lombardi G., 1971, "Zur Bemessung der Tunnelauskleidung mit Berücksichtigung des Bauvorganges, Schweizerische Bauzeitung, 89. Jhg., Heft Nr. 32

Copyright © 2005 Taylor & Francis Group plc, London, UK

Engineering geology and design of primary support of road tunnels. Cases from the Egnatia roadway

N. Kazilis & G. Aggistalis
Tunnels Discipline Head, Egnatia Odos A.E. Thessaloniki, Greece
Tunnelling Engineer, Egnatia Odos A.E. Thessaloniki, Greece

ABSTRACT: On the basis of our experience in tunnel design and construction, the most important issue is the careful recognition and evaluation of the engineering geological units along the tunnel route, and the proper estimation of those engineering geological characteristics of the rock mass that will control the underground excavation of the tunnel. In such cases, the selection of the appropriate temporary support measures can only be done, after the recognition of the significance of these characteristics on the behavior of the tunnel excavation. The experiences gained from the design and construction of selected tunnel cases from the Egnatia roadway project in Northern Greece (Macedonia) are presented in this paper. Specifically, in four tunnels (under construction or under design), the key engineering geological characteristics that proved to control the tunnel excavation are explained, and the support measures designed and implemented against those rock mass features are given. A short description of the Egnatia roadway construction project is also given.

1 EGNATIA ODOS PROJECT

The 680 km Egnatia Motorway is a modern motorway and the only road link spanning Northern Greece from its western to its eastern border. The Egnatia Motorway is the modern revival of the great Roman highway known as the Via Egnatia which was also one of the roads walked by Saint Paul (figure 1).

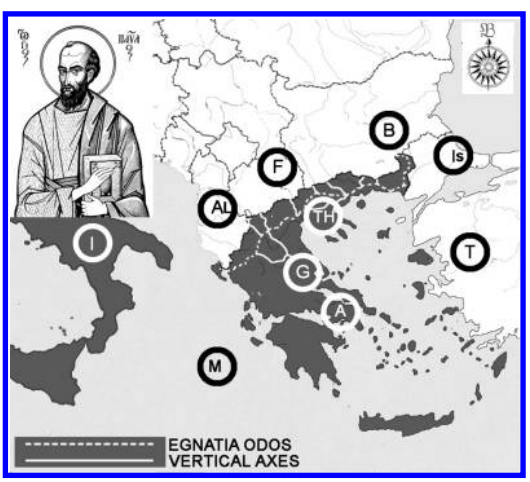


Figure 1. Map of Egnatia Motorway in the context of the Trans-European network, Saint Paul. **G**: Greece, **TH**: Thessaloniki, **A**: Athens, **AL**: Albania, **F**:Fyrom, **B**: Bulgary, **T**: Turkey, **IS**: Istanbul, **I**: Italy, **M**: Mediterranean Sea.

Nine major vertical road axes provide links to Albania, Fyrom, Bulgaria and Turkey, and the whole system is served by 720 km of service roads. The Egnatia Motorway was designed to the specifications of the Trans-European road network. It is a closed dual carriageway motorway with a central reserve, two traffic lanes plus an emergency lane per carriageway, for a total width of 24.5 metres. The project works include 75 twin tunnels of a total combined length of a 100 km.

In September 1995, the Greek Government set up the firm Egnatia Odos A.E. (EOAE), the object of which is to design, build, and operate this motorway (Georganopoulos & Kazilis 2001). Following an international tender toward the end of 1995, it appointed Kellogg, Brown and Root as a provider of project management services. EOAE has about 300 staff in the head office in Thessaloniki and various regional offices (Rawlings et al, 2001).

2 TUNNEL CASES

2.1 *General*

Egnatia Odos AE has compiled Design Guidelines for all engineering disciplines involved in the construction

Copyright © 2005 Taylor & Francis Group plc, London, UK

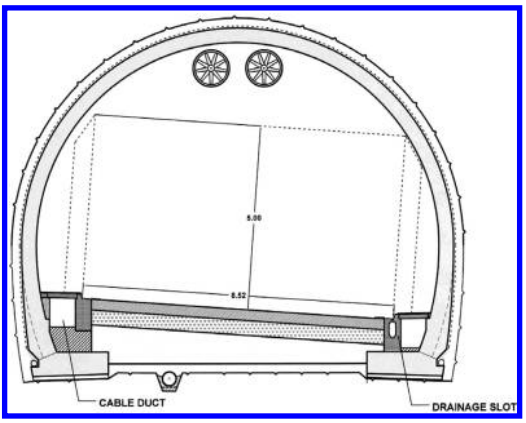


Figure 2. Egnatia Odos tunnel typical cross section.

of the highway (Kazilis, 1999). A part of this document concerns the tunnel design guidelines and covers both bored tunnels and Cut and Cover tunnels. All Egnatia tunnels are designed as twin tunnels. Cross passages are provided every 300–400 metres. Emergency vehicle turn-overs are provided every 1000 metres along parking areas. Figure 2 shows the Egnatia Odos tunnel typical cross section.

2.2 *General geological information*

Egnatia motorway passes through almost all of the geological history of Greece by crossing nine major geotectonic units. Figure 3 shows, in simplified terms, the major geotectonic units along the route of Egnatia Odos.

All of the units described above are overthrusted one over the other. The general direction of this overthrusting is from east to west. Although this is a very simplified approach, the actual tectonics and interrelationships of these units is quite complex.

Most of the tunnels are being built in the west and central sections. This is due to the mountainous terrain resulting from the formation of the Ionian, Pindos and Eastern Greece geotectonic units. Tunnelling works have been executed in a variety of rock mass conditions that range from very good quality rock masses such as massive limestones, granites, sandstones, gabbro, to very poor quality rock masses such as clay schists or sheared claystones that mainly belong to the flysch formations of the Pindos geotectonic unit (No.3 in figure 5). This geotectonic units is the most disturbed in the geological setting of Greece .

2.3 *Excavation and temporary support design. Engineering geological considerations*

Egnatia Odos A.E. has developed tunnel design guidelines that cover all the aspects of a tunnel design. Particularly, for the design of the excavation and

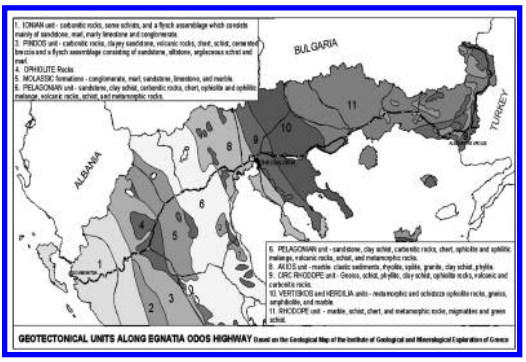


Figure 3. Geotectonical units along Egnatia motorway.

Table 1. Design stages for the excavation and temporary support measures.

Stages
1. Assessment of the strength and deformability of the geomaterial along the tunnel. Use of acceptable systems (e.g. GSI).
2. Calculation of deformations and plastification zones along the tunnel **without considering support measures.** Use of analytical equations taking into consideration the stress field and the rockmass strength.
3. Preliminary selection of support classes based on experience and empirical methods.
4. Calculation of deformations and plasticization zones along the tunnel **considering support measures.** Use of analytical equations taking into consideration the stress field, the rockmass strength, and the support pressure provided per support class.
5. Identification of problems. High deformations, front instabilities for each support class, etc.
6. Use of numerical analyses to confirm and finalize the support classes based on the anticipated failure mode. Use of numerical software e.g. UDEC, SOFISTIC, FLAC, PHASES.

temporary support, are proposed the design steps described in table 1.

Table 1 covers only the part of the tunnel support design methodology that deals with the dimensioning of the support measures. Before this stage, the preparation of a very detailed geological/ geotechnical interpretative report which is based on the factual data of the ground investigation program is required. Part of this report is the identification of the engineering geological units along the tunnel, their detailed description, the description of their arrangement and their contacts. Of outmost importance is the identification of those geological characteristics along the tunnel,

Copyright © 2005 Taylor & Francis Group plc, London, UK

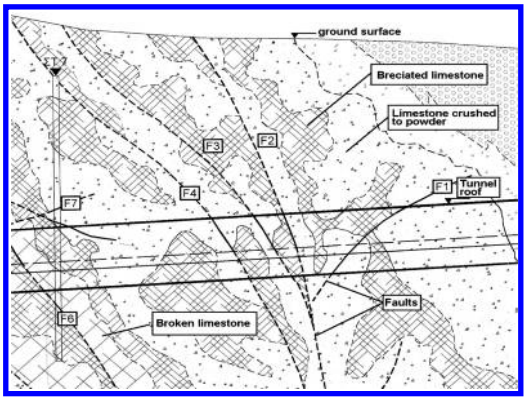


Figure 4. Part of the geological longitudinal section of the tunnel which was prepared during the excavation of the tunnel (Raptis G, 2002).

that will play an important role on the excavation of the tunnel.

Many times the description these particular geological characteristics of the geological formations are beyond the scope of the well known rock mass classification systems, but they play the most important role both on the tunnel design philosophy and on the tunnel construction. It is crucial for the tunnel designer, to identify them, and adjust/propose the support measures in the support classes to the potential dangers which are associated with these geological features.

In the paragraphs that follow, design and construction aspects from selected tunnel cases from the Egnatia Odos project are presented. In these cases the influence (in the spirit described above) on the design and construction of selected geological characteristics are presented.

2.4 *Agia Mavra tunnel (S2)*

Agia Mavra tunnel is a 700-metre twin road tunnel in northern Greece. The tunnel was excavated in a heavily fractured and brecciated (kataclasitic) limestone resulting from over-thrusting or from tectonic displacements and falls (Marinos, 2001). This geomaterial is characterized by the presence of numerous brittle cohesionless shear zones (Laws et al, 2003) of significant thickness, which are oriented parallel to the general direction of the faulting in the area. The values of permeability measured (Megalomastora, 2000) in this material is medium to high ($k \geq 10^{-5}$ m/sec). Figure 4 shows a part of the geological map prepared during the excavation of the tunnel.

This limestone was classified in four (4) rock mass classes based on the block size of the intact rock. The block size of the intact rock was ranging from >10 cm down to a powder like limestone material or fault gauge. In the better rock mass qualities the block size



Figure 5. Brecciated limestone (Hoek & Marinos unpublished EOAE report). Drill hole 100 mm in diameter, in limestone breccia (Hoek & Marinos unpublished EOAE report).



Figure 6. Ground flow in the powder like limestone material at the tunnel excavation front of Agia Mavra tunnel.

of the limestone pieces increases. However in any case the rock mass pieces are not cemented each other and it is only the interlocking of the these pieces (or the friction) that holds them connected. Figure 5 shows an outcrop of the brecciated limestone, and a close up view of a 100 mm diameter drill hole in this material.

This material was met to a significant proportion of the tunnel length during excavation and its presence was associated with significant tunneling problems such as cave-ins, face instabilities and in some cases ground flows of the powder like limestone material. Figure 6 shows a ground flow in the powder like limestone material at the tunnel excavation front.

Copyright © 2005 Taylor & Francis Group plc, London, UK

Table 2. Summary of the support measures used in Agia Mavra tunnel.

Structural thickness of shotctete shell	From 15 cm to 25 cm fiber reinforced
Temporary invert	20 cm thick fiber reinforced shotcrete in the worst support classes
Final invert	25 cm thick reinforced with wire mesh
Rock bolts	Self-drilling 200 KN to 300 KN, 5 m to 6 m long, 1,5 m × 2m to 1,5 m × 1 m pattern
Steel sets	HEB120 to HEB 160 every 1,5 m to 1,0 m
Face support	5 cm to 10 cm shotcrete in combination with fiberglass face anchors
Prereinforcement rock bolts & forepoles	Self drilling rock bolts 6 meters long Ø30 to Ø51/11, Ø114 forepoles 12 meters long

In this case, the engineering geological characteristic that practically controls the rock mass behavior during the excavation of the tunnel is its brecciation and the lack of cohesion and cementation in between the rock pieces.

The selection of the appropriate support measures and excavation methodology, is based on the aforementioned engineering geological characteristics of the geomaterial, and is based on a combination of actions for: (a) creating cohesion or cementing the rock mass, it, (b) excavating through a stable rock mass with altered properties (after its cementation).

This was achieved with the introduction of techniques of grout injection ahead of the tunnel face.

Prereinforcement elements were used for the support of the tunnel roof at the excavation front.The implementation of these elements served two purposes: (a) to inject the grout in order to introduce cohesion in the rock mass and (b) to secure safe working conditions at the tunnel face. Several adjustments in the application of the aforementioned support methods and techniques took place during tunnel excavation. These adjustments were about improving and adapting the grout mixtures to the rock mass conditions and modifying the support measures to safely tackle the differentiations of the geological conditions at the tunnel excavation front. A summary of the temporary support measures used to tackle the different rock mass classes along the tunnel, ranging from a good quality limestone down to the powder like limestone material is given in the table 2 (Lefas I et al, 2001).

2.5 *Dodoni tunnel*

Dodoni tunnel was excavated through limestones mainly of good to fair quality. The main difficulty

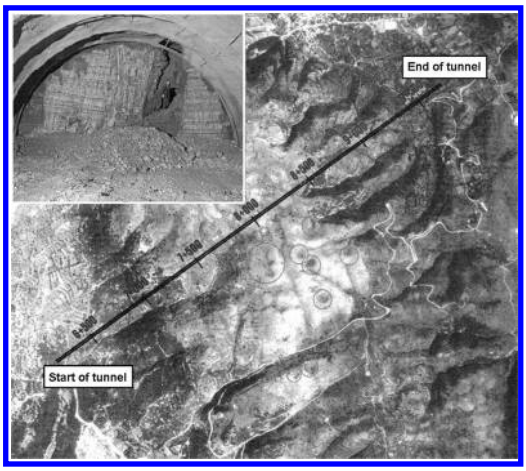


Figure 7. Traces of the carstic voids (in the circles) seen from the air (Malios & Katsivelis, 2001). Cave-in occurred during tunnel excavation.

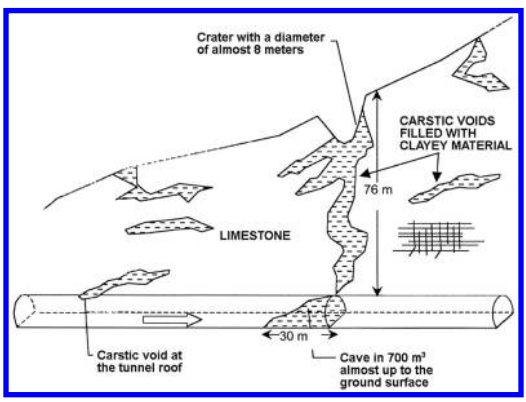


Figure 8. Cave-in occurred during tunneling under a carstic void. After the collapse a crater was formed at the ground level 76 meters above the tunnel roof (Malios & Katsivelis, 2001).

during the excavation of the tunnel was the presence of carstic voids in the limestone that in most cases was filled with soft clayey material. Figure 7 shows from the air the presence of the traces of carstic voids. In some cases significant face instabilities occurred. Figure 8 shows a sketch of the development of a carstic void met at the tunnel excavation front. The excavation methodology and the support measures which were selected to tackle these engineering geological features were developed considering mainly the geometrical development of the carstic voids and the potential volume of the in-filling clayey material. The support measures selected in order to safely pass through these features were able to undertake the "dead" loads of the material which was filling the

Copyright © 2005 Taylor & Francis Group plc, London, UK

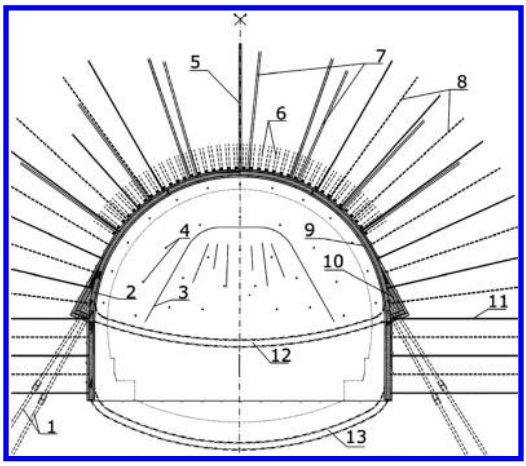


Figure 9. One of the temporary support cross section applied in carstic voids locations (Malios & Katsivelis, 2001). 1. Mikropiles, 2. IPB160, 3. Face buttress with 10 cm shotcrete, 4. Fiberglass anchors, 5. Grout injection holes, 6. Forepoles Ø114, 12 m long, 7. Drainage holes, 8. Self-drilling rock bolts, 9. 30 cm shotcrete layer, 10. Foundation of top heading, 11. Pair of rock bolts.

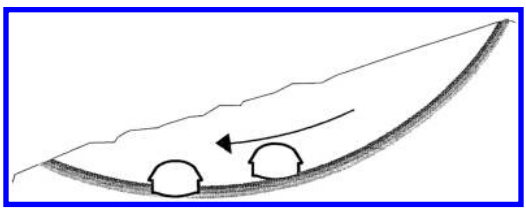


Figure 10. The twin tunnel S3 in section 5.2 of Egnatia Odos in the context of the potential slip surface of the cut slope (Hoek & Marinos).

voids. This material is obvious that has a zero self supporting capacity and when the tunnel excavation reach it, it will empty driven by the gravity and seepage pressure, in the tunnel opening, unless the appropriate measures are taken.

The support measures selected and adjusted on the basis of the aforementioned anticipated "key" geological engineering conditions. In other words they were able to undertake the 'dead' ground loads induced from the filling the voids materials without any allowance for deformations. Therefore, stiff support systems were developed with the use of steel sets and pre-reinforcement elements. These elements were able to bridge the carstic voids ahead of the tunnel face and to transfer the load of the in-filling the void material, on the sound ground at either side of the void, or at the foundation area of the top heading.

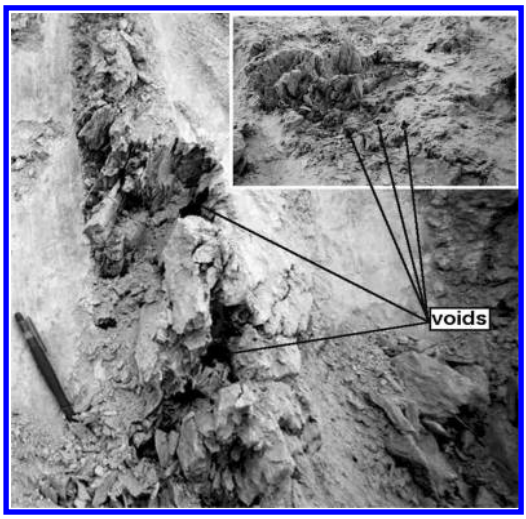


Figure 11. Disturbed phyllitic limestone in S3 tunnel. Visible are the numerous open joints denoting the loosening of the rock mass of the ancient landslide.

A probe-drilling (Hoek & Marinos) program was developed in order to investigate the presence of the carstic voids ahead of the tunnel face and to be able to implement the pre-reinforcement elements before the excavation reach the void. Figure 9 shows details of one of the temporary support cross section applied in carstic voids locations.

2.6 *S3 tunnel*

Tunnel S3 was excavated in a phyllitic limestone at the hillside of an ancient stable big landslide (figure 10). The convergence occurred during tunnelling, produced a crack propagation in the rock mass that reached the ground surface. A number of cracks then appeared on the ground surface above the tunnels and the excavation works stopped. At that time only the excavation of the top heading of the tunnel had been completed. The movements in the tunnel were showing some development.

The support measures initially selected was a heavy stiff tunnel supporting system comprised of steel sets, heavy forepoles and shotcrete. The support section also included temporary and permanent inverts. For the continuation of the tunnel excavation works a series of monitoring data was evaluated. However, the most important issue that re-evaluated was the engineering geological characteristics of the rock mass. Here the key geological engineering parameter of the rock mass that was proved to have a significant bearing on the tunnel behavior was the "open" and loose structure of the rock mass (figure 11). It must be noted that very high permeability values was measured

Copyright © 2005 Taylor & Francis Group plc, London, UK

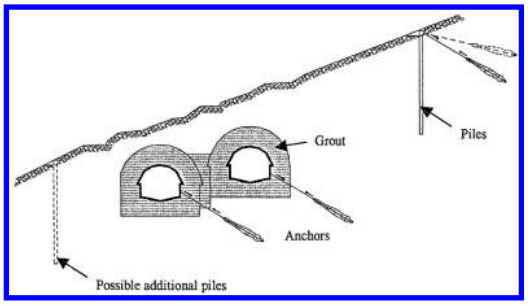


Figure 12. Support measures implemented to secure tunnel stability (Hoek & Marinos).



Figure 13. Appearance of the contact of conglomerates and alternations of siltstones with sandstones.



Figure 14. Appearance of good quality of alternations of siltstones with sandstones.

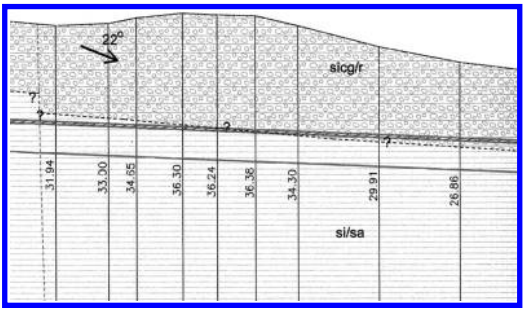


Figure 15. Part of the geological longitudinal section of Velanidia tunnel. The tunnel roof passes along the contact of the conglomerates on the top with the siltstone/sandstone intercalations.

(Koronakis, 2002) in this material ($k \geqslant 10^{-3}$ m/sec). In particular, the rock mass was characterized by the presence of numerous open joints. According to our opinion, the opening of these joints was the result of the ancient landslide movement that disturbed the geomaterial and resulted in a massive loosening of the rock mass at the hillside.

After the careful evaluation of all the available data one of the main measures (Koronakis, 2002, Hoek & Marinos) proposed to secure the tunnel was the implementation of a grouting program around the perimeter of the tunnel (figure 12). The task of the grout injection program around the tunnel was to introduce cohesion in the rock mass by filling up the voids around the tunnel and therefore to strengthen it in a length of almost six meters around the tunnel excavation perimeter.

The whole system, excavation opening, supporting shell and grouted rock mass around the tunnel was anchored with long prestressed anchors behind the potential slip surface of the ancient landslide. Other measures proposed to secure the tunnel are beyond the scope of this paper.

2.7 *Velanidia tunnel*

Velanidia tunnel is to be excavated in molassic formations (under low overburden) that consists of intercalations of siltstones, sandstones, and conglomerates of various qualities. These formations are wedging one in the other and their contacts are sometimes irregular. The formations are slightly tectonized and faulted in big anticlines and synclines. The geological formations in their contacts are sometimes of very poor quality especially for the formation of the conglomerates (figures 13 and 14).

The water movement along the contact of the conglomerate and the siltstone has often loosened the structure of the conglomerate as it has dilute the matrix of the conglomerate and moved it away. The poor quality of the conglomerates at these contacts has been found in the ground investigation program.

The excavation in some part of the tunnel is expected to progress parallel to such type of contacts (figure 15).

This geological setting is one of the key geological engineering parameters that has a significant bearing on the selection of the support elements. In the tunnel design (Malios, 2004) and in order to secure the tunnel excavation front when such ground conditions are expected the support measures that have been proposed include pre-reinforcement elements installed ahead of the tunnel excavation front. These conditions will be investigated through a probe drilling program and a methodology for the selection of these pre-reinforcement elements based on the evaluation of the probe drilling results.

Copyright © 2005 Taylor & Francis Group plc, London, UK

3 REMARKS

In the tunnel cases presented above, the importance of the good understanding and interpretation of the geological features on the selection of the tunnels stabilization measures have been shown. Many times the description these particular geological characteristics of the geological formations are beyond the scope of the well known rock mass classification systems, but they play the most important role both on the tunnel design philosophy and on the tunnel construction. In such cases, the selection of the appropriate temporary support measures can only be done after the recognition and understanding of these characteristics. The initial selection of these temporary support measures is independent of the numerical calculations that will follow in order to verify the structural integrity and adjust, refine the support measures selected. The use of shotcrete and rock bolts only as a tunnel temporary support, the use of yielding support systems, the use of pre-reinforcement elements, the use of fully grouted rock bolts instead of immediately activated rock bolts, or the use of ground improvement techniques, can be justified on the basis of a good understanding of the geological engineering characteristics of the rock masses, and the estimation of their impact on the tunnel stabilization.

REFERENCES

Georganopoulos, C. & Kazilis, N.: Innovations in Tunnel design management in Egnatia Odos A.E., Scientific meeting, Ioannina, Greece, 7 & 8 December 2001.

Hoek, E. & Marinos, P.: Unpublished experts reports for Egnatia Odos A.E.

Kazilis, N. The tunnels of Egnatia Motorway: In *"THE TUNNELS OF EGNATIA ODOS"*, Scientific meeting, Ioannina, Greece, 15 & 16 October 1999.

Koronakis, N.: Egnatia Odos AE, Section 5.2–5.3, S3 tunnel, definitive design of stabilization measures. Omikron Kappa Ltd, Athens, Greece, 2002. Unpublished.

Lefas, I., Dalas, A & Koronakis, N.: Tunnels in brecciated materials, section 1.1.6, tunnel S2, conceptual design and implementation. Proceedings of the Conference: The Egnatia Odos tunnels, Ioannina, Greece 7&8 December 2001.

Laws, S., Eberhardt, E., Loew, S. & Descoeudres, F.: Geomechanical properties of shear zones in the Eastern Aar massif, Switzerland and their implication on tunneling. Rock Mechanics and Rock Engineering, Vol. 36, No4, September 2003.

Malios, I. & Katsivelis, I.: Dodoni tunnel in limestone formations with carstic voids, experiences – design: Proceedings of the Conference: The Egnatia Odos tunnels, Ioannina, Greece 7&8 December 2001.

Malios, Y.: Egnatia Odos AE. Section 4.1.2s. Definitive design of excavation and temporary support of Prionia and Velanidia tunnels. Malios & Associates S.A. 2004. Unpublished.

Marinos, P.: The appropriate use of geological information in the design and construction of motorway tunnels, Scientific meeting, Ioannina, Greece, 7 & 8 December 2001.

Megalomastotra, P.: Definitive geological – geotechnical design of S2 tunnel. EDAFOMECHANIKI Ltd, Athens Greece, December 2000. Unpublished.

Raptis, G.:I. SARANTOPOULOS A.E. – ASTALDI S.p.A. Longitudinal geological section of the right branch of S2 tunnel from ch. 30 + 269,00 to ch. 31 + 135,00. Unpublished report 20.03.02.

Rawlings, C., Silva, R., Kazilis, N., Aggistalis, G., Rachaniotis, N. & Mantziaras, P.: The tunnels of Egnatia Motorway Project, Northern Greece, London conference, Tunnelling 2001.

Copyright © 2005 Taylor & Francis Group plc, London, UK

Rock reinforcement design for unstable tunnels originally excavated in very poor rock mass

R. Osgoui & E. Ünal
Mining Engineering Department, Middle East Technical University, 06531 Ankara, Turkey

ABSTRACT: Number 7 Malatya railroad tunnel was excavated through the toe of a paleo-landslide material in 1930. Ever since that date, this horseshoe shape tunnel, having width and height of 5 m and 6 m, respectively, struggled with stability problems. A large amount of deformation (170 cm) developing through the years and leading to miss alignment of the tunnel was observed. In this paper, firstly a new approach developed for classifying very poor quality rock mass was presented. Secondly, evaluations were made on the stability of the tunnel. Thirdly, information is provided on rock reinforcement design. Finally, the results of finite element analysis (FEA) conducted for evaluating the stability of unreinforced tunnel and the tunnel reinforced by self drilling anchors (MAI-bolt) designed based on empirical method were given.

1 INTRODUCTION

Today, rock bolting is used in almost all types of underground constructions. Knowledge of the rock mass behavior and support effects of rock bolts are vital for the design and construction of underground structures in rock.

Malatya- Narli No: 7 railroad tunnel, situated at the central part of turkey, is a rail-road one that was initially excavated inside a valley of very poor quality rock mass. Due to the effect of the *in-situ* stress in the course of time, the deformations of the tunnel were exceeding the limit in which a huge collapse occurred and the tunnel was closed to the traffic.

In this study, the site investigation, the rock mass classification, and the experimental design of the rock bolt system were carried out in order to open the tunnel and to make it safe. At the same time, the numerical method was investigated to verify the empirical design approach.

During conducting this study, a new approach for classifying very poor quality rock mass was extracted.

2 ROCK MASS CLASSIFICATION

Rock mass classifications, which serve as powerful design aids in underground construction when used in conjunction with observational, analytical and numerical methods, provide a basis for characterizing the rock mass. For the qualification of the rock mass, RMR (Bieniawski, 1974, 1989), Q (Barton, 1974, 2002), and GSI (Hoek, 1994, 1997, 2000, 2002) systems are widely being used. These systems have been evolving due to the requirement of modifications for the different case studies; however, there are still doubts and confusions on the applications.

The rock mass surrounding the Malatya tunnel is composed of very poor rocks such as metasiltestone, clayey and silty sandstone, shale and phyllite.

Usually, the overall very poor quality rock mass is highly heterogeneous and anisotropoic owing to the combined effect of advanced weathering and severe tectonic stressing that gave rise to intense shearing which resulted in highly weathered rock masses. However, in view of the fact that the whole rock mass around the Malatya tunnel was completely decomposed and disintegrated as a result of the effect of highly historical horizontal stress (similar to great landslide), the rock mass was regarded as the homogenous material. Therefore, in order to investigate the tunnel section using the rock mass classification system, the tunnel length is considered as a unit along its axis.

The test results of core specimens taken from 67 boreholes were used as the input parameters for the assessment of rock mass classification systems. During rock mass classifying, it was difficult to obtain representative samples of the worst quality materials, especially when there are alternating weak materials. Then, Due to difficulty in retrieving the intact rock pieces, the uniaxial compressive strength σ_{ci}, and the material constant m_i, for example, are determined from tables published elsewhere.

Copyright © 2005 Taylor & Francis Group plc, London, UK

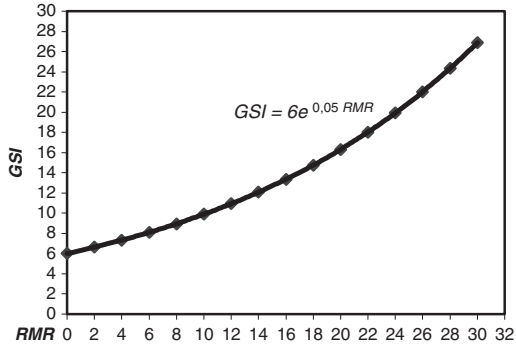


Figure 1. GSI vs RMR for very poor quality rock mass where RMR <30.

A good approach for classification of very poor rock mass as a case study for Athens schist formation was developed by Hoek, Marinos and Benissi (1998). As demonstrated, the new category named disintegrated rock, which defined as poorly interlocked, heavily broken rock mass with a mixture of angular and rounded rock pieces, was appropriate to Malatya tunnel ground.

For very poor quality rock mass where the value of RMR <30, a new exponential correlation between Rock Mass Rating (RMR) and Geological Strength Index (GSI) was developed by authors as shown in the Figure 1.

$$GSI = 6e^{0.05\ RMR}$$

This correlation is compatible with the relation obtained from case studies data of the Alpine region carried out by Morales *et al.* (2004). Moreover, the above relation satisfies the definition of the GSI introduced by Hoek (1994) in such a manner that when RMR = 0, the minimum value of GSI is 6.

More recently, Coşar (2004) showed a relation between GSI and RMR for weak rock mass (RMR <40) has been given by distributive graph as demonstrated in Figure 2.

In Malatya tunnel, on the basis of core logging, the value of RQD for almost all cores were estimated to be zero; further, the RMR or M-RMR has not been calculated soundly. For this reason, the two approaches could have been taken into consideration to be more sensible. The first one was to evaluate the cores based on observational judgment. In this respect, the rock mass was classified in five categories (R1, R2, R3, R4, R5) on the basis of its geological characteristics. In order to make this classification in terms of engineering parameters, a new supplementary classification was integrated as given in the Table 1. This classification system is capable of characterizing the very poor quality rock mass with respect to engineering parameters of rock mass like rock mass strength and rock

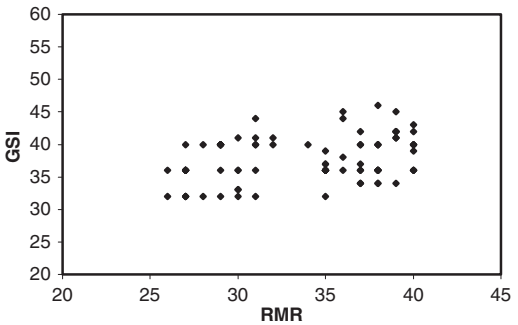


Figure 2. Distributive abundance of GSI vs RMR for weak rock mass in which RMR <40 (after Co şar, 2004).

Table 1. New quantitative classification system for very poor quality rock mass and its correlation with GSI system.

GSI	Very poor quality rock mass strength (kPa)	Definition	Very poor quality rock mass deformation modulus (MPa)	Definition
6 to 7	250–290	R1	344–424	E1
7 to 8	290–370	R1	424–584	E2
8 to 10	370–450	R2	584–744	E3
10 to 13	450–550	R3	744–944	E4
13 to 16	550–650	R4	944–1144	E5
16 to 21	650–750	R5	1144–1344	E6
21 to 27	750–850	R6	1344–1544	E7

mass deformation modulus using defined indices. For example, the rock mass defined by R_3E_2 indicates the rock that its strength and modulus falls into the range of 450–550 kPa and 424–584 MPa, respectively.

The next approach was to use the GSI system due to very poor quality rock mass. The Geological Strength Index (GSI), introduced by Hoek (1994), Hoek *et al.* (1995, 1997, 1998, 2000, and 2002) provides a system for estimating the reduction in rock mass strength for different geological conditions. For very poor quality rock masses the value of RMR is very difficult to estimate and the balance between the ratings no longer gives a reliable basis for estimating rock mass engineering parameters. Consequently, Bieniawski's RMR classification should not be used for estimating the GSI values for poor quality rock masses. Furthermore, for poor quality rock masses GSI <30, relatively few intact core pieces longer than 100 mm are recovered and it becomes difficult to determine a reliable value for RMR. In this circumstance, the physical appearance of material recovered in the core should be used as a basis for estimating GSI. Therefore, the GSI guideline chart introduced by, Hoek, Marinos, and

Copyright © 2005 Taylor & Francis Group plc, London, UK

Table 2. The value of various rock mass classification systems of the Malatya tunnel.

Rock unit	RMR	GSI	New classification
Very poor quality rock mass	0	5–6	R1–E1

Benissi (1998), Marinos and Hoek (2000, 2001) was considered as a sole means of evaluating the GSI for Malatya ground. The interesting specification of this chart was to take into account two various types of poor rock masses in terms of their structure, namely; disintegrated and foliated/ laminated/ sheared rock masses.

A latest rock mass classification system based on GSI system developed by Morales *et al.* (2004) falls the Malatya poor quality rock mass into class 8. This class defines the poor rock mass as a result of intense joining or very low strength near to soils. In other words, the rock masses included in this class are those with a high fracture rating in which the joints are very close, without predominant weak surfaces. This group also includes rock masses where the material itself, or because of weathering, is low strength. This class also includes very weathered rock masses. Circular failure and rotating landslides are the most characteristic forms of instability. The GSI is under 27 and the σ_{ci} is no more than 15 MPa in this class. The value of RMR, GSI, and new classification systems for Malatya tunnel are presented in the Table 2.

3 STABILITY EVALUATION

Based on results gained from the closed-form solutions of the development of rock mass failure surrounding an unsupported circular tunnel subjected to equal stresses in all directions carried out by Duncan-Fama (1993) and Hoek, Kaiser and Bowden (1995), a rock mass is considered to be weak when its *in-situ* uniaxial compressive strength is less than about one third of the *in-situ* stress acting on the rock mass through which the tunnel is being excavated (Hoek, 1999). In this case, a sudden increase in convergence of tunnel occurs. As a first approximation, the *in-situ* stress can be assumed to equal the product of the depth below surface and the unit weight of the rock mass. Considering that the vertical *in-situ* stress due to gravity loading was 1.54 MPa with the assumption that the unit weight of very poor rock mass was 0.022 MN/m^3 as well as the rock mass strength was 0.156 MPa, the rock mass strength to *in-situ* stress ratio would be 0.101. Hence, even from this point of view, a huge amount of convergence would have been anticipated as the maximum wall deformation of tunnel had been recorded about 60 cm. Sakurai (1983) has suggested that the stability of tunnels can be assessed on the basis of the strain in the rock mass surrounding the tunnel. The strain is defined by the ratio of tunnel convergence to tunnel diameter. A critical strain of approximately 2% represents the boundary between stable tunnels that required minimal support and unstable tunnels that require special consideration in terms of support design. Monitoring of the Malatya tunnel implied that this critical value of strain was also exceeded.

4 ROCK REINFORCEMENT DESIGN

The support requirements for the Malatya tunnel were estimated from the data of engineering classification of rock mass (empirical design approach). Further, the rock bolt support appropriate to the Malatya tunnel was empirically designed and installed. The MAI-bolts, which is a self driving full column cement-grouted bolts, were chosen to be more suitable for very poor quality rock mass because drill holes are usually closed before installing the bolt and the injection operation associated with rock-bolting make the ground improved in terms of engineering parameters like strength, modulus of deformation, and Hoek-Brown constants. In other words, since the extent of yielding or broken zone is directly related to the material properties, any improvement of the strength and frictional parameters must reduce the extent of overstressed rock. The MAI-bolts develop load as the rock mass deforms. Relatively small displacements are normally sufficient to mobilize axial bolt tension by shear stress transmission from the rock to the bolt surface (Indraratna and Kaiser, 1990).

In order to increase the stability, 110 m long section of the tunnel was supported systematically by MAI-bolts having a diameter of 32 mm, length of 6 m or 9 m and spacing of 1 m (Divleli and Ünal, 2004). A total of 15 rock bolts were installed around the tunnel and the invert of the tunnel. Floor was supported by installing 5 grouted bolts with the length of 5 m. The rock reinforcement details of number 7 tunnel are shown in Figure 3.

For the rock reinforcement design, the section of the tunnel to be supported was divided into three parts namely; A1, A2, and B. A systematic rock bolting was performed at that section. The MAI-bolts having 32 mm diameter, 6 m and 9 m length were installed in the parts A and B, respectively. A total of 20 rock bolts were installed at a cross-section of tunnel whereby the roof of the tunnel could be reinforced by 5 MAI-bolts while the two sides of walls were supported by 10 MAI-bolts, and the invert of the tunnel floor could be formed by installing 5 grouted bolts with the length of 5 m.

Copyright © 2005 Taylor & Francis Group plc, London, UK

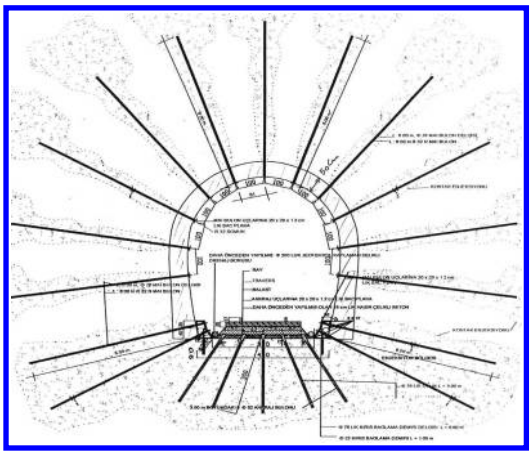


Figure 3. The sketch of rock reinforcement layout.

The bolt density parameter β, which reflects the relative density of bolts with respect to the tunnel parameter and the convergence reduction of the tunnel walls, can be expressed as follows:

$$\beta = \frac{\pi d \lambda a}{S_L S_T}$$

where d is the bolt diameter, λ friction factor for bolt/ground interaction, a is tunnel radius, and S_T, S_L are circumferential and longitudinal bolt spacing, relatively. For the Malatya tunnel, with the event that $d = 32$ mm, $\lambda = 1$, $a = 2.7$, S_T, $S_L = 1 \times 1$ m, the value of β is calculated as 0.271. It means that a design with high bolt density was carried out at Malatya tunnel to control and reduce the convergence (closure) of the tunnel. For very high bolt densities ($\beta = 0.3$), convergence reductions of about 60% can be obtained (Indraratna and Kaiser 1990). The ratio of the bolt length to tunnel radius (L/a) is between 2.22 and 3.33 in Malatya tunnel. Since the reduction in total convergence attained is more pronounced for long bolts, it is expected that the convergence control of tunnel would be appropriately performed. For example, at $\beta = 0.3$ and *in-situ* stress of 14 MPa, a convergence reduction of approximate 60% can be achieved by long bolts.

5 NUMERICAL ANALYSIS OF TUNNEL STABILITY

The main concern of numerical analysis of an underground opening like tunnel is that of exactly modeling that depicts the real situation in which tunnel analysis is to be solved. The program PHASE^2 (A 2nd Plastic Hybrid Finite Element- Boundary Element Analysis for Calculating Stresses and Estimating Support Around Underground Excavations) (Rocscience, 1999) is used for modeling the ground and tunnel and calculating stresses and displacements to evaluate the extension of the broken zone surrounding tunnel in terms of strength factor.

In the constitutive model of very poor rock masses, it is assumed that the surrounding rock mass behaves as an elasto-perfectly plastic material in which failure involving slip along intersecting discontinuities is assumed to occur with zero plastic volume change i.e. zero dilatancy angle and non-associated flow rule of plasticity (Osgoui, 2004). In the post failure behavior of rock mass, a nonlinear Hoek-Brown yield criterion and a linear Mohr-Coulomb plastic potential with the constant dilatancy angle are used to model the stress-strain regime for very poor rock mass.

As mentioned previously, the Malatya tunnel was originally driven through a tectonized paleo-landslide material, which regards as a very poor rock mass. The primary support system of the tunnel is comprised of concrete lining combined with steel arch. Since its construction, the Malatya tunnel has been influenced with in-situ geomechanical problems like the effect of high horizontal stress and pore water pressure that ultimately led to serious collapse.

In order to correctly model the tunnel, four stages are considered as follows:

1. modeling the ground before excavation.
2. modeling the tunnel regarding previous situation (primary support system included).
3. modeling the tunnel concerning installation of the new reinforcement system.
4. modeling the tunnel pertinent to ground consolidation.

The input parameters of the rock mass for performing the numerical methods are given in Table 3.

5.1 *Results of numerical analysis*

Main focused issue of the results was the yield zone in the rock mass surrounding the tunnel and induced displacements around the excavation. The strength factor, which is the ratio of available rock mass strength to induced stress in accordance with the chosen failure criterion, reveals the yield zone. The maximum induced displacements around the tunnel show the progression of displacement on excavation boundary at various stages of tunneling. Maximum principal stresses, total induced displacements, and minimum strength factors for three stages are presented in the Table 4 while Figure 4 demonstrates the extent of the failure in terms of strength factor for stage 2 (primary support system i.e. before rock-bolting), stage 3 (after rock-bolting), and stage 4 (after ground consolidation).

Copyright © 2005 Taylor & Francis Group plc, London, UK

As can be deduced from Table 4, the maximum induced displacement was recorded on left wall as 0.015 m at stage 2. It should be noted that this value is corresponding to induced displacement at the time of stable tunnel in which the strength factor is around unit i.e. the collapse was more likely to occur, on the other hand, this value of displacement was irrespective of large deformation at the time of land-sliding or active loading. After systematic rock bolting the displacement increment (tunnel convergence) would have been under control to follow a consistent value of 0.013 m. In the case of ground consolidation, the displacement increment followed again a consistent rate.

Table 3. Input parameters for performing numerical analysis.

Property	Value
Failure criterion	Hoek & Brown (2002 version)
Geological strength Index (GSI)	5 or 6
Material type	Isotropic
Young's modulus (MPa)	167.68
Poisson's ratio	0.2
Compressive strength (MPa)	0.156
*m parameter (peak)	0.235
*s parameter (peak)	2.6e-5
Material type	Elastic analysis performed Plastic analysis performed
Dilation angle	Zero (non-associated)
*m parameter (residual)	0.235 (Elasto-perfectly plastic analysis)
*s parameter (residual)	2.6e-5 (Elasto-perfectly plastic analysis)

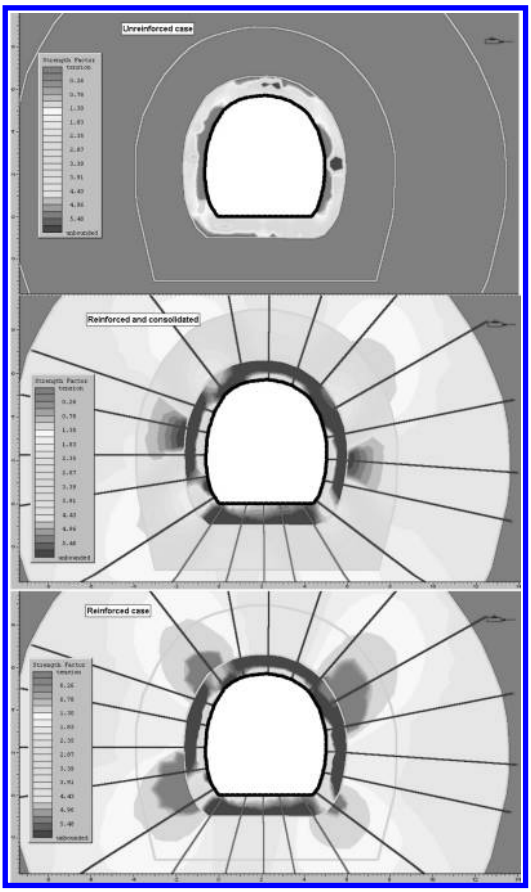


Figure 4. Extension of the failure zone around the tunnel and its decrease using rock bolting and consolidation.

Table 4. Results from finite element analysis for 3 stages of tunneling.

Location	Parameter	Stage 2 (primary support system)	Stage 3 (reinforced tunnel by rock-bolts)	Stage 4 (reinforced tunnel + ground consolidation)
Roof	Total displacement (u_t) m	1.5E-2	1.2E-2	1.2E-2
Right wall		1.3E-2	1.3E-2	1.3E-2
Left wall		1.6E-2	1.3E-2	1.3E-2
Floor		1.4E-2	1.3E-2	1.3E-2
Roof	Maximum principal stress (σ_1) MPa	11.33	4.19	3.68
Right wall		2.95	1.51	1.22
Left wall		5.46	2.38	1.95
Floor		10.75	4.26	3.68
Roof	Minimum strength factor	1.22	3.29	3.68
Right wall		Tension*	1.58	2.01
Left wall		Tension	1.45	1.85
Floor		1.57	3.30	3.70

* The strength factor is less than one and the collapse is certain to occur.

Copyright © 2005 Taylor & Francis Group plc, London, UK

As far as the strength factor is concerned, the tunnel was bound to collapse at stage 2 due to tension extension around tunnel as substantiated by numerical analysis. However, a great improvement in strength factor of tunnel boundary and rock mass around tunnel would have been made in the stage 2, where a systematic rock-bolting operation was carried out. The tension forms of failure mode could have been exchanged into strength factor of 1.48 and 1.58. Having been consolidated, the quality of rock mass surrounding the tunnel was improved in terms of engineering parameters; hence, the strength factor of tunnel boundary was remarkably increased. The main objective of rock mass consolidation was to increase the span of the tunnel for the railroad traffic requirements.

6 CONCLUSIONS

This study was carried out with a view to firstly classify very poor quality rock mass based on engineering parameters such as strength and modulus and to identify the effect of rock bolting on tunnel reinforced by MAI-bolts.

A new relationship, furthermore, correlating the GSI-system and RMR for very poor quality rock mass (RQD and RMR are equal to zero) was extracted.

A very poor rock mass entails a high-density rock bolting having the length more than span of the tunnel. For this purpose, a systematically rock bolt system with relatively high density ($\beta = 0.271$) and the ratio of bolt length to tunnel radius ($L/a = 2.22$ and 3.33) was designed.

Numerical analysis of tunnel proved that with the help of the rock bolting, a considerable increase in strength factor (decrease in extension of tension zone) around tunnel could be obtained. On the other side, displacements could be controlled.

REFERENCES

1. Bieniawski, Z.T., 1974. Geomechanics classification of rock masses and its application in tunneling. Advances in Rock Mechanics 2, part A, pp. 27–32. National Academy of Sciences, Washington, D.C.
2. Bieniawski, Z.T., 1989. *Engineering Rock Mass Classifications*. Wiely, New York.
3. Barton, N., Lien, R. and Lunde, J., 1974. Classification of rock masses for design of tunnel support. *Rock Mech*. 6 (4), pp. 189–236.
4. Barton, N., 2002. Some new Q-value correlation to assist in site characterization and tunnel design. *Int. J. Rock Mech. Min. Sci*. 39(1), 185–216.
5. Hoek, E., 1994. Strength of rock and rock masses. *ISRM News Journal* 2(2): 4–16.
6. Hoek, E., Kaiser, P.K. and Bawden, W.F. 1995. *Support of underground excavation in hard rock*, A. A. Balkema.
7. Hoek, E and Brown, E.T., 1997. Practical estimates of rock mass strength. *Int. J. Rock Mech. Min. Sci. Geonech. Abstr* 34(8), 1165–1186.
8. Hoek, E., Carranza-Torres, C. and Corkum, B. 2002. Hoek-Brown failure criterion – 2002 edition. In R. Hammah,W. Bawden, J. Curran, & M. Telesnicki (Eds.), *Proceedings of NARMS-TAC 2002, Mining Innovation and Technology. Toronto – 10 July 2002*, pp. 267–273. University of Toronto.
9. Hoek, E., Marinos, P. and Benissi, M. 1998. Applicability of the Geological Strength Index (GSI) classification for very weak and sheared rock masses. The case of the Athens Schist Formation. *Bull. Eng. Geol. Env. 57*(2), 151–160.
10. Marinos, P. and Hoek, E. 2000. GSI- A geologically friendly toll for rock mass strength estimation. *Proc. Geo Eng 2000 Conference*, Melbourne.
11. Morales, T., Etxebarria, G., Uriarte, J. and Valderrama, I., 2004. Geomechanical characterization of rock masses in Alpine region: the Basque Arc (Basque-Cantabrian basin, Northen Spain). *Eng. Geol* 71, 343–362
12. Coşar, S., 2004. Application of rock mass classification systems for future support design of DIM tunnel near Alanya. *MSc Thesis*. Middle East Technical University, Ankara.
13. Duncan, Fama, M.E., 1993. Numerical modelings of yield zones in weak rocks. In: Hudson, J.A. (Ed.). *Comprehensive Rock Engineering*, vol. 2. Pergamon, Oxford, pp. 49–75.
14. Sakurai, S., 1983. Displacement measurements associated with the design of underground openings. Proc. Int. Symp. *Field measurements in geomechanics*, Zurich 2, 1163–1178.
15. Divleli, B and Ünal, E., 2005. Rehabilitation of Malatya- Narli No: 7 railroad tunnel. *World Tunnel Congress '2005 and 31st ITA General Assembly*. In press.
16. Indraratna, B and Kaiser, P. K., 1990. Design for Grouted Rock Bolts Based on the Convergence Control Method. *Int. J. Rock Mech. Min. Sci. Geonech. Abstr 27* (4), pp 269–281.
17. Rocscience, 1999. A 2-D finite element program for calculating stresses and estimating support around the underground excavations. Geomechanics Software and Research, Rocscience Inc., Toronto, Ontario, Canada.
18. Osgoui, R. 2004. Stress-strain regime used for solution of a circular tunnel excavated in very poor quality rock mass. *A partial work on PhD study*. Unpublished. Middle East. Tech. Univ. Turkey.

Copyright © 2005 Taylor & Francis Group plc, London, UK

Estimation of subsidence due to mining using artificial neural network – preliminary study

Y.B. Jung, D.S. Cheon & S.O. Choi
Korea Institute of Geoscience & Mineral Resources, Daejeon, Korea

ABSTRACT: Artificial neural network (ANN) model can be used for the subsidence estimation instead of empirical methods, methods based on influential functions and on mechanical model. Also, using relative strength of effect (RSE) and global relative strength of effect (GRSE), the relative impacts of input variables on output variables can be identified quantitatively. In this study, we use back-propagation neural network (BPN) and developed ANN program using visual basic. Firstly, the developed program was tested for verification data set generated from simple nonlinear equation and the results were satisfactory. The training data for subsidence estimation were obtained from 50 numerical analyses for preliminary study. And another 10 data not included in training data were used for checking the validity of ANN model. The developed ANN model shows a good estimation results. Also it was found that the width and the depth of excavation are most influential input variables on magnitude of maximum subsidence from RSE and GRSE analysis.

1 INTRODUCTION

Usually underground excavation causes surface subsidence. The estimation of subsidence due to excavation is an important task for the stability of surface structure and excavation process itself.

Because of a large number of parameters influencing the behavior of rock above the excavated area, the prediction of excavation consequences is a demanding task. But it is difficult to determine all the parameters and it is more difficult to determine their relative impact.

Displacement causes damage in surface building. Therefore, the goal of most researches is to estimate the impact of underground excavation on building, surface transport system and so on. From the direct measurement of displacement in mines or tunnel and on the surface, methods for the prediction of surface subsidence were developed (Kratzsch, 1983).

The first methods for the prediction of subsidence were empirical prediction methods. These methods are based on the correlation of the measured data and the related measured results with the geometric parameters of the excavation. As these methods are derived from the measurements in a specific area, the results are valid only for the investigated area.

The second group of prediction methods is prediction methods based on influential functions. The influential function is used to describe the value of the effect of elementary part of the excavation on the formation of subsidence. This group of prediction methods is based on some assumptions which simplify the calculus and make the methods generally applicable. The methods are simple and efficient, but it is difficult to calculate the coefficients in the equations of influential functions.

The model prediction methods are originated from mathematical-physical models. The elastic and plastic models of subsidence belong to this group of prediction methods. In this case, the subsidence problems are usually solved by numerical methods such as the finite element method, the finite difference method or boundary element method.

Another prediction method is the prediction of subsidence with artificial neural network (ANN). ANN model can be constructed using the results of case studies and the influential parameters on surface subsidence can be identified using the concept of relative strength effect (Yang & Zhang, 1998).

In this article, the results of elasto-plastic analyses are used as training and validation data sets for subsidence estimation as a preliminary study.

2 ARTIFICIAL NEURAL NETWORK

2.1 *ANN*

The artificial neural network (ANN) is a computational method inspired by studies of the brain and

Copyright © 2005 Taylor & Francis Group plc, London, UK

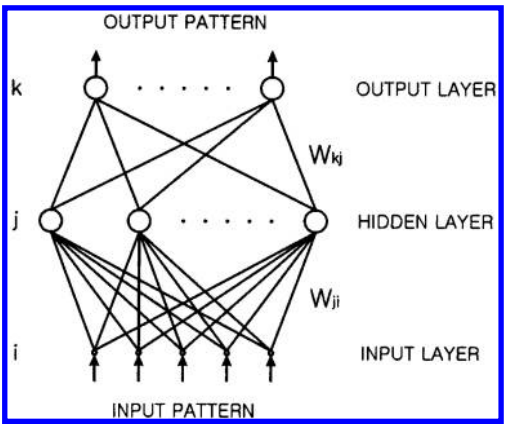


Figure 1. The concepts of multi-layer perceptron (Pao, 1989).

nervous systems in biological organisms. An ANN is constructed of highly interconnected network of many basic neurons. Two of the characteristics of ANNs are their capability of self-organization and autonomous-learning. ANNs are well suited to problems involving matching input pattern to a set of output patterns where deep reasoning is not required.

In this paper, back-propagation neural networks (BPN) were used to estimate the ground subsidence and find key factors on subsidence. The back propagation algorithm is a gradient descent method in which weights of the connections are updated using parallel derivatives of error with respect to weights. It has been shown that BPNs are ANNs that are the most popularly used and they are well suited for problems of classification, prediction, adaptation control, system identification, and so on (Pao, 1989).

The development processes of BPNs consist of three steps: defining the network architecture, training the network, and testing the network. The basic task of defining the network architecture is to decide the number of layers, number of nodes in each layer, and types of interconnection between nodes. BPN architecture generally contains three layers: input layer, hidden layer, and output layer (see Fig. 1).

Most BPNs use one or two hidden layers. Next, raw data are generally divided into two groups: a training data set and a test or validation data set. Within the BPN training process, several experiments with different BPN architectures, transfer functions, learning rules, learning and momentum rates need to be done to decide the appropriate combinations. In a supervised BPN training, the connection weights are adjusted continuously until termination conditions are met. The adjustment of connection weights is referred to learning or training. Furthermore, the test data set is used to verify the appropriateness of the trained network.

2.2 *RSE & GRSE*

The effect of inputs on outputs can be determined using RSE (relative strength of effect) and GRSE (global relative strength of effect) concepts (Yang & Zhang, 1998).

RSE_{ki} (i-input variable, k-output variable) has the following properties.

1. RSE_{ki} expresses the influence of different input values on one of the output values. The larger the value of RSE_{ki} becomes, the greater is the effect on the output.
2. The sign of every RSE_{ki} indicates how the input affect the output, a positive action applies on the output when $RSE_{ki} > 0$, and a negative action when $RSE_{ki} < 0$, and the output has no relation with the input when their $RSE_{ki} = 0$.
3. RSE_{ki} is a relative value which is different from the differentiation of a function approximated by the neural network, so the RSE_{ki} does exist even if the differentiation of this function does not exist.
4. RSE_{ki} varies with the variance of the position of the input point in input space, so the effect of the input value taking on the output value varies with the changing of the position of the input point in input space.

According to these RSE properties, we can establish and pay attention to the factors which dominate the state of the output, and ignore those factors which have RSE_{ki} near to zero. Thus, we obtain the necessary knowledge to enable the control of subsidence with the key factors, optimizing the likelihood that the rock mass as perturbed by engineering will behave in the way we expect.

GRSE is a simple form of RSE where the transfer function is assumed to linear function. Therefore, only the weights are used for calculation of GRSE. Albarez (2000) also suggested WWF (weighted weight factor) term similar with GSRE. Detailed information and calculation procedures of RSE and GRSE are described by Yang et al. (1998).

3 VERIFICATION

An ANN program for subsidence estimation was developed using visual basic and named SEPA (subsidence estimation & prediction using ANN).

Simple data set generated from following equation is used to check the prediction performance of developed program.

$$z = 0.5x^2 + 0.1xy - 0.9y^2 \quad (1)$$

Copyright © 2005 Taylor & Francis Group plc, London, UK

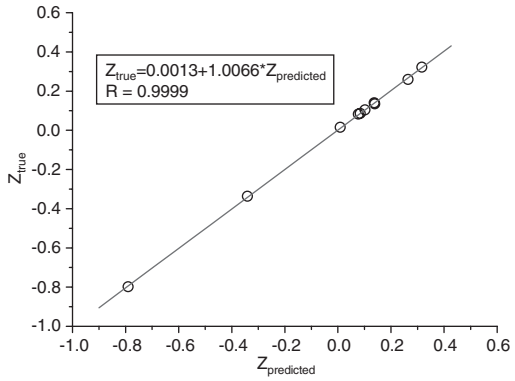


Figure 2. The relationship between true values and predicted values from ANN model.

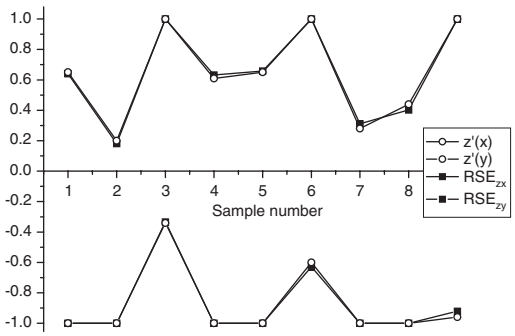


Figure 3. RSE distribution for the verification data set.

Training data set has 30 input(x,y)-output(z) pairs and another 10 data are used for validation of SEPA. We set ANN architecture as 2-4-4-1, learning rate as 0.95, momentum as 0.8 and maximum iteration number as 100,000.

After training, the RMSE of training data set was 2.735e-3 and that of validation data set was 4.85e-3. The RSEs of ANN are similar with the scaled derivative of eqn. (1) (see Figs 2 & 3). From these results, the applicability of developed program for nonlinear problems was proved.

4 APPLICATION

4.1 *Training*

As a preliminary study on subsidence, total 60 numerical analyses were carried out for different geometrical and mechanical conditions. From those numerical results, 9 input variables and 2 output variables were selected. Table 1 shows the input and output variables and their units. The training data set has 50 data randomly selected from the total data set and remaining 10 data were used as a validation data set.

The prediction performance of ANN is dependent on the learning rate, momentum, number of layer, number of layers and so on. Therefore, we tested for 8 different ANN model using test data and chose M2-1-4 model because it shows the smallest RMSE (Table 2). Fig. 4 shows the training process using training data set for M2-1-4 model and fig. 5 shows the training results for maximum subsidence and subsidence range. The predicted values are consistent with the target values.

Table 1. The input and output variables for SEPA.

Parameter		Description	Range	Unit
Input	X1	Overburden height, z	0∼1000	m
	X2	Width of cavern, W	0∼1000	m
	X3	Height of cavern, h	0∼100	m
	X4	K-ratio, k	0∼5	–
	X5	RMR	0∼100	–
	X6	Shear modulus(G)	0∼10000	MPa
	X7	Bulk modulus(K)	0∼10000	MPa
	X8	Cohesion, c	0∼10	MPa
	X9	Friction angle, f	0∼90	degree
Output	Y1	Maximum subsidence, Smax	0∼1	m
	Y2	Subsidence width, Srange	0∼5000	m

Table 2. The tested ANN architectures and their RMSEs.

Model no	Structure	Learning rate	Momentum	RMSE
M2-1-1	9-10-10-2	0.7	0.7	5.5889E-03
M2-1-2	9-10-10-2	0.7	0.8	3.9856E-03
M2-1-3	9-10-10-2	0.9	0.7	3.2064E-03
M2-1-4	9-10-10-2	0.9	0.8	2.7363E-03
M2-2-1	9-5-5-2	0.7	0.7	8.2132E-03
M2-2-2	9-5-5-2	0.7	0.8	8.3530E-03
M2-2-3	9-5-5-2	0.9	0.7	1.4021E-02
M2-2-4	9-5-5-2	0.9	0.8	6.7837E-03

4.2 *Validation*

Data set which are not used at training stages were applied to M2-1-4 model for validation. Table 3 and Fig. 6 show the prediction results.

Copyright © 2005 Taylor & Francis Group plc, London, UK

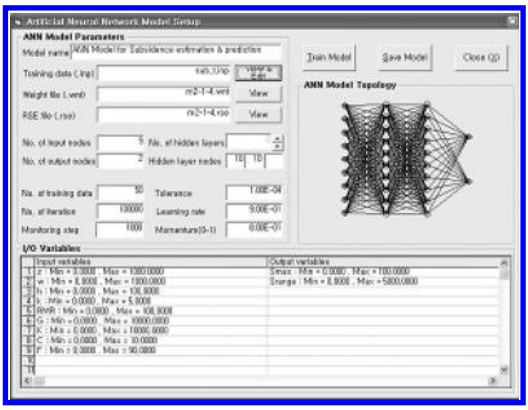


Figure 4. The outlook of developed program and training procedure.

Table 3. Target values and ANN outputs.

	Target		ANN output	
No	S_{max} (m)	S_{range} (m)	S_{max} (m)	S_{range} (m)
1	0.019	250.0	0.02010	246.2
2	0.007	0.0	0.00672	0.0068
3	0.028	250.0	0.02611	249.3
4	0.016	250.0	0.01724	254.8
5	0.009	0.0	0.00763	0.021
6	0.013	117.5	0.01372	191.6
7	0.040	250.0	0.03994	250.6
8	0.011	67.5	0.01556	89.19
9	0.019	117.5	0.01889	108.3
10	0.019	87.5	0.01821	78.24
		RMSE =	0.00179	24.84

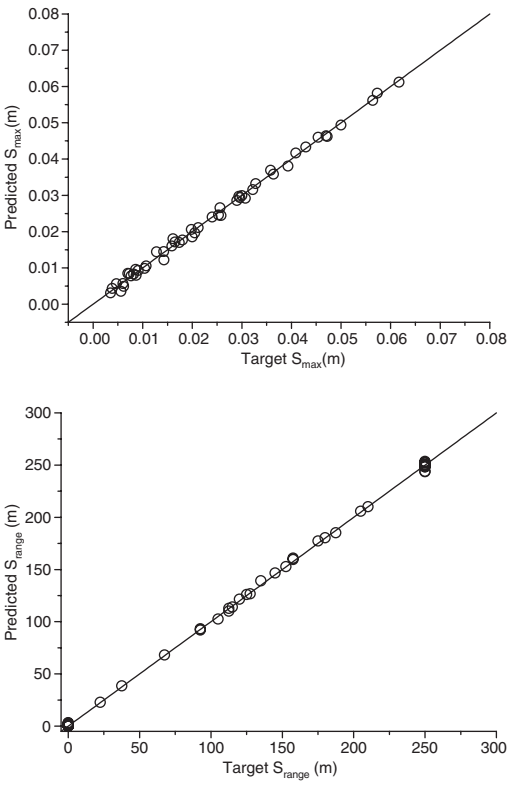


Figure 5. The results of ANN training stage (upper: Smax, lower: Srange).

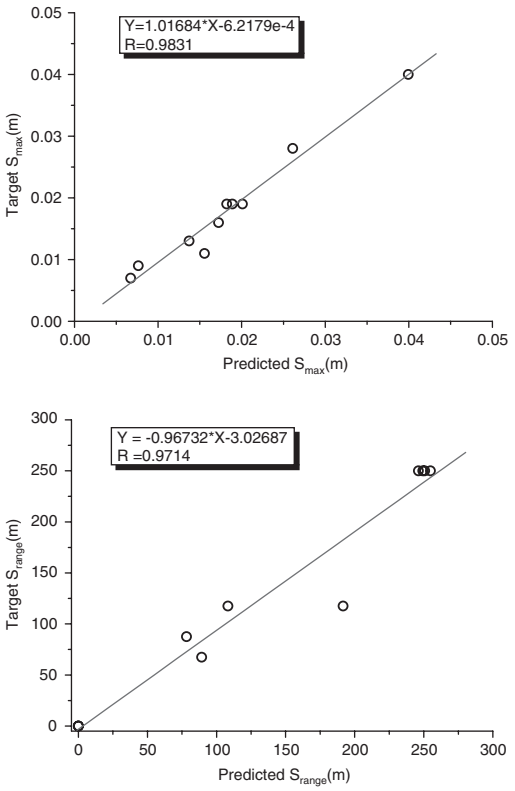


Figure 6. Prediction results for validation data set (upper: maximum subsidence, lower: subsidence range).

The RMSE for Smax is 0.00179 and that of Srange is 24.84. In case of Srange, relatively large RMSE was obtained because we truncate Srange data as 250 m when the real Srange exceeds 250 m. The correlation coefficients for two outputs are bigger than 0.97 and shows good prediction results.

From these results, the applicability of ANN model was verified but it needs field applications of real field

Copyright © 2005 Taylor & Francis Group plc, London, UK

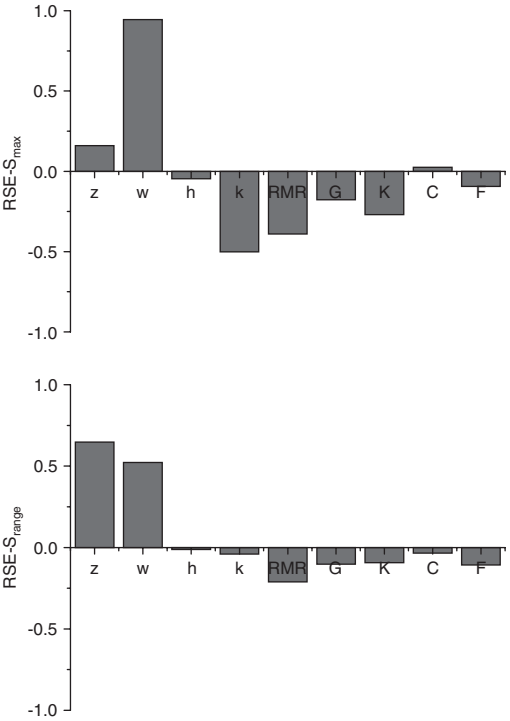


Figure 7. The RSE distribution for training data set (upper: Smax, lower: Srange).

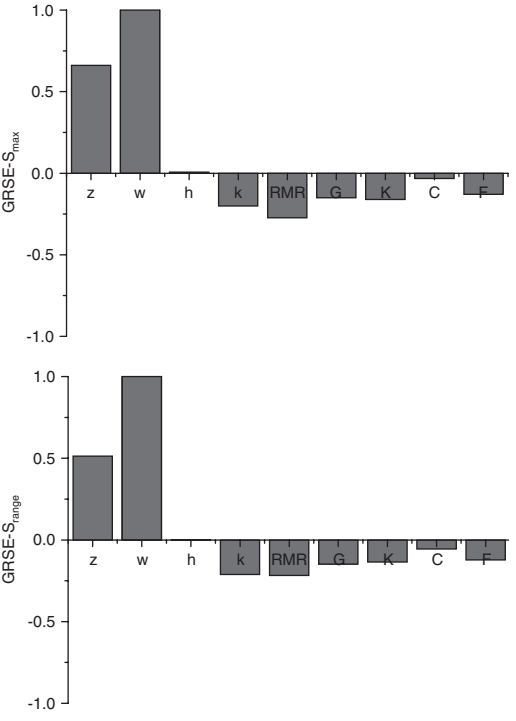


Figure 8. The GRSE distribution for training data set (upper: Smax, lower: Srange).

data for various geological and mechanical conditions for ANN model to become a generalized prediction model.

4.3 *Parameter identification*

To find key factors of subsidence, RSE and GRSE analyses were carried out on the M2-1-4 model.

The average of RSEs between maximum subsidence and subsidence range and input variables are shown in Fig. 7. The depth and width of excavation have positive effects on subsidence and subsidence range. The ratio of horizontal and vertical stress, RMR, bulk modulus, shear modulus and friction angle have negative effects on subsidence as we expected. In case of cohesion and height of excavation, RSEs are positive contrary to our expectation but the magnitudes of RSEs are small and could be ignored.

In case of GRSE, the results were similar with RSE and accordance with our expectation (Fig. 8).

The depth has positive effect on subsidence considering the mean RSE value but the RSE is a dynamic term varies with the position in input space. Considering the standard deviation of this RSE, the RSE between depth and subsidence can have negative values. Therefore, more case studies on this parameter must be carried out.

5 CONCLUSIONS

ANN model was constructed from the results of numerical analyses on various geometrical and mechanical conditions simulating ground subsidence. Also, the key factors were identified using RSE and GRSE. From above mentioned studies, the following results are obtained.

1. ANN program for subsidence estimation was developed and applied to verification data generated from simple equation. It was shown that ANN model was suitable for the prediction of nonlinear problems from the results.
2. The developed program was applied for the results of numerical analyses. After training, the developed ANN model can be used for prediction of maximum subsidence and subsidence range with an error range respectively 2 mm and 25 m.
3. From the analyses of RSE and GRSE, the key factors on subsidence were identified. The geometrical

Copyright © 2005 Taylor & Francis Group plc, London, UK

factors, depth to excavation and width of excavation have dominant effect on subsidence.

This study is a preliminary one for ground subsidence estimation and prediction. Quantitative field survey will be done and new prediction model will be set up using those data.

ACKNOWLEDGEMENT

This paper is based on the research funded by Korean ministry of science & technology.

REFERENCES

Albarez, G., 2000, Neuro-Fuzzy Modeling in Engineering Geology, A.A.Balkema, Rotterdam, 244p.

Ambrozic, T. and G. Turk, 2003, Prediction of subsidence due to underground mining by artificial neural networks, Computers & Geosciences 29(5): 627–637.

Kratzsch, H., 1983, Mining Subsidence Engineering, Springer, Berlin, 543p.

Pao, Y. H., 1989, Adaptive pattern recognition and neural networks, Addition-Wesley.

Yang, Y. and Q. Zhang, 1998, The Application of Neural Networks to Rock Engineering Systems (RES), International Journal of Rock Mechanics and Mining Sciences 35(6): 727–745.

Copyright © 2005 Taylor & Francis Group plc, London, UK

Model tests on shotcrete to analyze early age behavior of tunnel support

T.B. Celestino
University of São Paulo, São Carlos – SP, Themag Engenharia Ltda, São Paulo – SP, Brazil

D.A. Ferreira
BVP Engenharia, Belo Horizonte – MG, Brazil

ABSTRACT: The early age behavior of shotcrete is analyzed in field model test in terms of temperature, strain and strength evolution for two different curing conditions: regular and under the action of electric gradient. Shotcrete was sprayed on a vertical slope and the electric gradient was kept constant during the first 6 hours of age. Increasing loads were applied and then kept constant for 12 days. The load applied on 100 × 100 cm panels simulated the increase of internal forces typical of tunnel shotcrete support. The use of electric gradient increased the strength at 6-h age by about 40%. The electric gradient increases the range of stress-independent strains. Elastic and viscous strain components due to load are decreased with electric gradient. Important influence of water loss due the contact with dry soil was found in the inner fiber, affecting both short and long term deformability parameters.

1 INTRODUCTION

Shotcrete tunnel support requires significant strength at early age. A method to improve the hardening rate of shotcrete has been developed, without the use of chemical substances. The method consists of applying electric gradients to fresh concrete and has presented good results.

For cast concrete, laboratory experiments have shown strength increase of the order of 100% at 12-hour age, as compared to concrete produced under the same condition without the action of electric gradient (Ferreira, 1997, Ferreira & Celestino, 1999). No strength loss was observed at 28-day age, as usual with some chemical additives of thermal curing. The method efficiency was checked with different types of cement and concrete mixes, as reported by Ferreira & Celestino (2001).

The first application of the method on shotcrete was presented by Ferreira et al. (2002), who showed results from specimens sprayed on wooden panels. Strength increase in the range of 40–50% at 6-hour age and up to 40% at 28-day age was obtained. Overall, the results were better for shotcrete than for cast concrete, due to differences in microstructure of the two materials.

For application of the method in underground works, a broader study about the effects of the electric gradient on shotcrete mechanical properties other than strength is necessary, as well as better understanding about the electrical and hydraulic interactions of shotcrete with the surrounding ground mass. Previous studies concentrated on evaluating strength increase only.

Ferreira (2003) presented for the first time results of field applications of the method. Shotcrete was sprayed directly on soil with different moisture conditions to analyze the electrical interaction and current leakages. The effect of loading at early age was analyzed by studying structural models subjected to loading histories similar to those occurring in shotcrete support of shallow soft ground tunnels.

This paper presents the results of the response of one of the structural models analyzed. Panels with dimensions 100 × 100 cm were shotcreted directly on vertical slopes of Cenozoic fine clayey sand with porous structure, and basaltic saprolite. These panels were subjected to increasing load since 6–7 hour age simulating the external actions on shotcrete tunnel support.

Strain response was recorded by means of vibrating wire strain gages. Strength increase was indirectly evaluated by means of a penetrometer. Measurements were taken both from specimens subjected to electric gradient and reference specimens (regular curing conditions). The information is therefore relevant to

Copyright © 2005 Taylor & Francis Group plc, London, UK

understand the behavior of shotcrete cured under regular conditions as well as subjected to electric gradient when loaded at early age.

Analysis of the phenomena responsible for strength increase under the action of electric gradient will be presented elsewhere.

2 EXPERIMENTAL PROGRAM

The experimental program was carried out in two stages:

Stage 1 – Observation of the behavior during the application of the electric gradient, recording the electric current, temperature and strains (shrinkage and thermal strains).

Stage 2 – Application of increasing loads to the shotcrete panels starting at 7 to 9-hour through 12-day age, recording the resulting strains.

Details of the experimental programs are presented next.

2.1 *Materials*

Dry mix shotcrete was produced by a CP 3 machine manufactured by Este Engenharia. The cement used was CP II E 32 (a slug modified cement). Aggregate consisted of 10 mm maximum size granitic crushed rock from the São Paulo Metropolitan region, and medium sand. No additives were used for set accelerating. Water-cement ratio was approximately 0.40.

Table 1 presents the mix used.

2.2 *Electric gradient application*

The application of electric gradient in the field followed the same procedures as in the laboratory (Ferreira & Celestino, 1999, 2001).

The electric gradient was applied to shotcrete panels with dimensions 100 × 100 × 20 cm sprayed directly on a vertical slope.

The electrodes consisted of 12.5 mm diameter rebars, spaced at 80 cm. The material used for the electrodes and their spacing were defined resembling the design of lattice girders for soft ground tunnel support. For an application in a real tunnel construction, lattice girders are the ideal electrodes.

A sketch of the application of the electric gradient is presented in Figure 1.

The electric gradient started to be applied about 30 minutes after the completion of the shotcreting operation. It was kept constant for 5½ hours. During this period, the total electric current, the temperature and strains measured at internal points of the specimens were recorded.

Three panels were simultaneously shotcreted: the first one, to be subjected to electric gradient and mechanical loading; the second (reference sample) subjected to mechanical loading only; and the third, aimed at obtaining stress independent strains, not subjected to electric gradient or mechanical loading.

Table 1. Shotcrete mix.

Material	kg/m^3
Cement	352
Sand	1198
Crushed rock	705

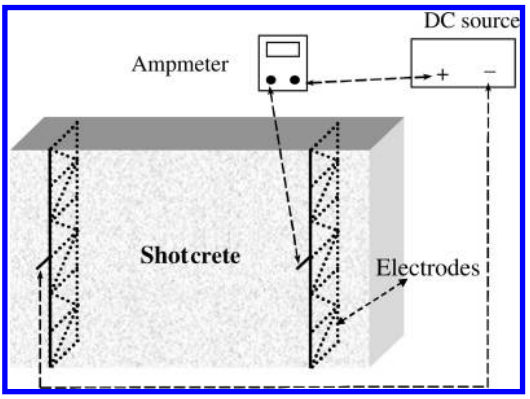


Figure 1. Sketch of the application of electric gradient.

2.3 *Loading system*

The loading system was designed to duplicate the loading history to which shotcrete supports of shallow soft ground tunnels are subjected. Similar studies for final loads on shotcrete were presented by Fernandez-Delgado et al. (1976), Holmgren (1976) and Chang (1974). Those authors studied the actions imposed by rock masses, different from those resulting of the soil-shotcrete interaction to be analyzed here.

Figure 2 shows a scheme of the loading frame. The frame was positioned parallel to the slope surface prior to the shotcreting operation. The load was applied by a hydraulic jack and distributed to the panel by means of a beam, positioned immediately after the application of the electric gradient.

2.4 *Instrumentation*

The shotcrete panels were instrumented with 153-mm long vibrating wire strain gages with 1 $\mu\varepsilon$ sensitivity, specific for shotcrete applications. Similar devices were used by Kuwajima (1991) for the SLRT tunnel in Canada.

Strain gages were placed at both the internal and external fibers, about 2.5 cm from the soil surface and 3.0 cm from the free surface respectilvely, at 3 different

Copyright © 2005 Taylor & Francis Group plc, London, UK

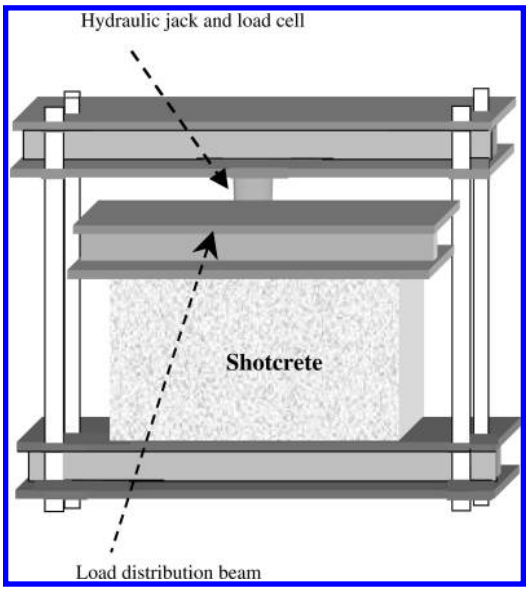


Figure 2. Loading system schematic view.

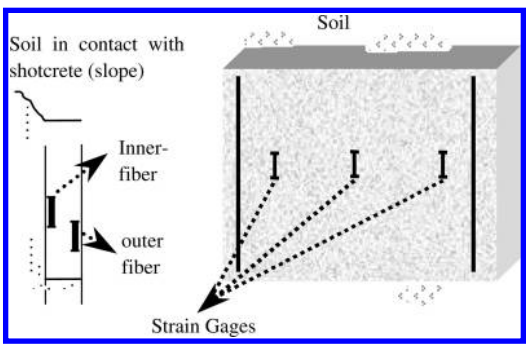


Figure 3. Panel instrumentation.

locations between the electrodes, spaced at 20 cm. Reference panels were instrumented with a single pair of strain gages.

Figure 3 shows schematically the instrumentation of the panels.

Strain gage readings started to be taken just after shotcreting had been completed. This allowed to obtain stress independent strains both at the contact with the soil surface and at the shotcrete free surface. Strains were also read during the loading stage. The data acquisition system was programmed to take continuous readings throughout 12 days at 5-minute intervals for the first 6 hours, progressively increasing to 12-hour intervals after the 7th day. Readings taken at 5-minute intervals for the first 5 hours allowed to observe the strain behavior at ages before final cement setting.

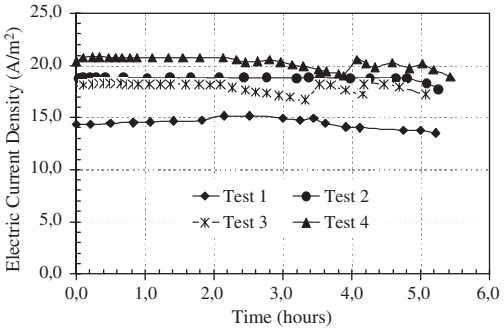


Figure 4. Evolution of electric current density in the first hours.

3 SHOTCRETE BEHAVIOR DURING ELECTRIC GRADIENT APPLICATION

The electric gradient was kept constant for 5½ hours. During this period, electric current density, temperature, strains and the evolution of compressive strength were recorded.

Shotcrete compressive strength at early age was indirectly determined by using a Meynadier penetrometer, employing a correlation proposed by Prudencio (1993). Details about this correlation are presented by Ferreira & Celestino (2001).

Strain and temperature readings taken during this period had the purpose of checking the effects of the electric gradient on shrinkage and temperature increase.

3.1 *Electric current and mechanical strength*

The intensity of the electric gradient adopted was 0.58 V/cm. This value was lower than that previously adopted in a laboratory test program on shotcrete panels, reported by Ferreira et al. (2002).

In order to check the possible effect of current leakage through soil, an isolating PVC membrane was placed on the slope surface before spraying shotcrete. Figure 4 presents the results of electric current. Tests 2 and 3 correspond to specimens with the isolating membrane. Specimens 1 and 2 were sprayed on porous non-saturated soil; specimen 4 was sprayed on basalt saprolitic clayey soil and specimen 3 on an intermediate soil.

Electric current recorded was of the order of 3A, regardless of the presence of the isolating membrane. The total electric current measured passes through the soil-shotcrete system, but the current density was calculated considering only the area of the shotcrete panel cross section.

The electric current was independent of the presence of the isolating membrane, probably because of damages caused during the shotcreting operation. More significant influence of the soil type was found.

Copyright © 2005 Taylor & Francis Group plc, London, UK

Probable leakages through the saprolitic, saturated clayey soil were responsible for higher current values.

The evolution of shotcrete electric resistivity was known previously from laboratory tests on panels reported by Ferreira (2002). Using those values, it was possible to evaluate the leakage current through the soil mass, which was found to be of the order of 1A, or approximately 35% of the total current.

Compression strength evolution was similarly independent of the membrane.

Shotcrete subject to electric gradient had strength increase of about 100% at 4-hour age and about 50% at 6-hour age. Figure 5 presents the results obtained with the Meynadier penetrometer through the first seven hours.

3.2 *Temperature and stress-independent strains*

Stress-independent strains were measured during the first hours while the electric gradient was applied. Figure 6 shows the results of strains on the panel subjected to electric gradient as well as the reference panel of test number 3. Those strains depict the behavior of shotcrete at ages before final setting.

Stress independent strains are affected by the electric gradient. The reference panel presents shrinkage at the internal fiber caused by loss of water to the dry soil. This was not the case for saprolitic soil.

At the external fiber, the behavior is determined by the temperature and air relative humidity. In this test, expansion dominated through the first 5 hours.

In the neighborhood of the electrode positive pole, the tendency for expansion is more pronounced. The highest trend for shrinkage at the internal fiber was found close to the negative pole and the lowest at the positive pole. This is due to electro-osmosis. The electric current initially carries water to the negative pole, increasing the water-cement ratio and the shrinkage susceptibility there. Opposite phenomenon occurs at the positive pole. Intermediate behavior occurs at the central region.

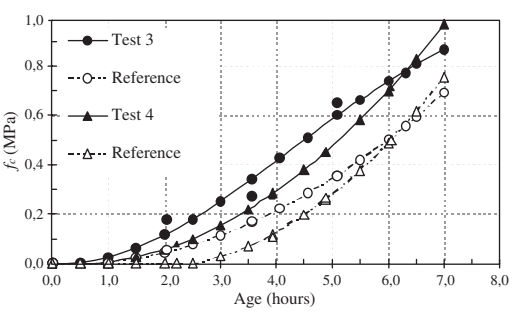
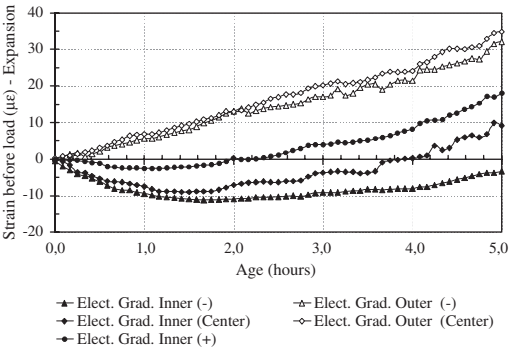


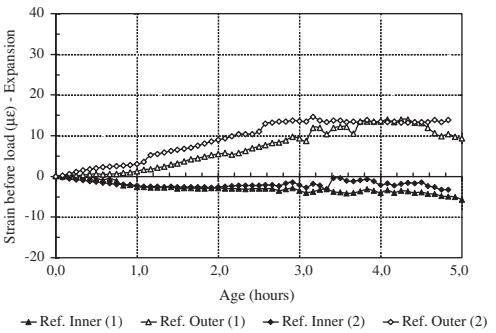
Figure 5. Strength evolution measured with the Meynadier penetrometer at early age.

Temperature was also recorded and the results are presented in Figure 7.

The effect of the electric gradient on the temperature evolution is similar to the influence on strains: there is no change in the general trend, but the differences of readings taken at the internal and external



(a) Electric gradient panel



(b) Reference panel

Figure 6. Stress-independent strains in concrete specimens up to 5-hour age: panels subjected to electric gradient and reference panels.

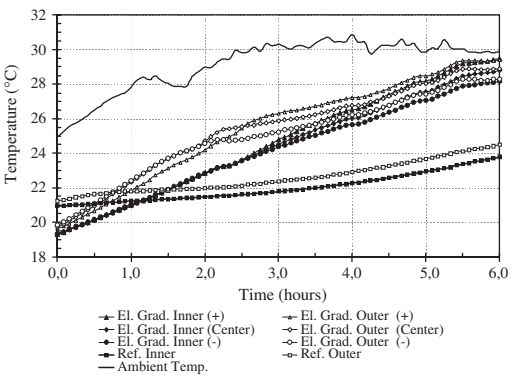


Figure 7. Evolution of temperature during the first hours.

Copyright © 2005 Taylor & Francis Group plc, London, UK

fibers are amplified. Temperature at the internal fiber tends to be lower due to the higher capacity of heat transfer to the soil. In the case of dry soils, convection plays an important role and enhances the heat transfer rate. Shotcrete subjected to electric gradient suffers temperature increase of about 10°C at 5-hour age above the increase observed in reference specimens.

4 LOAD DEPENDENT STRAINS

Shotcrete panels were subjected to loading at ages between 7 and 9 hours, after application of the electric gradient. Loads were applied in stages with duration between 18 and 36 hours, progressively increasing throughout 12 days. Figure 8 presents the as planned and the effectively applied loading histories, according to measurements of a load cell and a pressure cell installed below the load distribution beam. Loads were simultaneously applied to the specimen subjected to electric gradient, and to the reference specimen.

Figure 9 presents the strain evolution after loads started to be applied. The difference in behavior of the internal and external fibers can be clearly observed in both specimens, subjected to electric gradient and reference. Golser et al. (1988) and Kuwajima (1991) also observed such difference in behavior in tunnels, but the phenomenon was attributed to bending moments, definitely not present here, and shrinkage due to air drying at the external fiber.

In this case, the difference in behavior is due to the differences of possibilities of water and heat exchange not only with the air, but also with the soil mass. Water migration from shotcrete to non-saturated soils may give rise to much more severe shrinkage than that occurring at the air contact surface, changing properties for the whole life of the material.

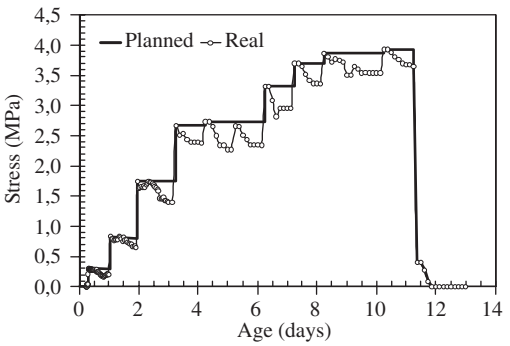


Figure 8. Loading history on shotcrete during the first 12 days.

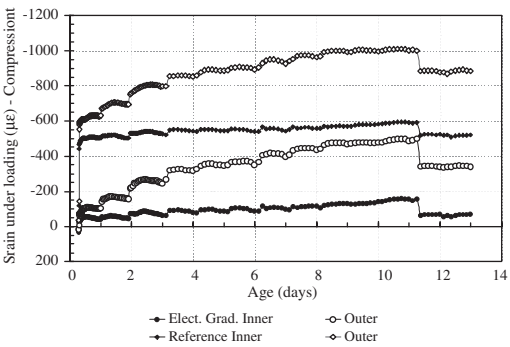


Figure 9. Strains in shotcrete under loading.

4.1 *Shotcrete with electric gradient versus reference shotcrete*

Figure 9 shows that load dependent strains in the shotcrete panel subjected to electric gradient are lower than those in the reference panel. This type of behavior is consistent since the early stages of loading throughout the whole period of observation. For the final loading stage corresponding to 11-day age, the application of electric gradient resulted in decreasing strains from 500 $\mu\varepsilon$ at the internal fiber and 1000 $\mu\varepsilon$ at the external fiber to 200 and 450 $\mu\varepsilon$ respectively.

Readings taken at 10-minute intervals at the initial stages of loading allowed to identify instantaneous and delayed strain components analyzed by Schubert (1988), Golser et al. (1989) and Aldrian (1991). Creep rates obtained by using the rheological model proposed by those authors were also lower for specimens subjected to electric gradient. Rehological behavior results will be presented elsewhere.

After unloading, strains were recorded for about two days. The low level of elastic behavior is observed, as evidenced by the large permanent strains. They reached 83% of the maximum strain under load for the reference specimen and 56% for the specimen subjected to electric gradient.

5 CONCLUSIONS

Results of an experimental program were presented with information about the mechanical behavior of shotcrete at early age, including both stress dependent and independent strains for specimens cured under regular conditions and under electric gradient.

The application of the electric gradient method in field conditions presented good results for the increase of strength and the decrease of deformability.

Structural models were developed to study early age shotcrete response to loads similar to those observed in shallow soft ground tunnels. The results were obtained by loading shotcrete panels sprayed on soil slopes loaded at ages as early as 7 hours.

Copyright © 2005 Taylor & Francis Group plc, London, UK

The electric gradient applied was of the order of 0.58 V/cm, lower than the value adopted in a previous laboratory test program on shotcrete specimens sprayed on wooden panels. Electric current leakages to the soil mass were of the order of 35%, and they depended on the type of soil, being lower for non-saturated soil.

In spite of the low values of electric gradient, strength increase of about 40% was achieved at 6-hour age. The deformability was substantially decreased with the application of electric gradient.

With respect to stress independent strains, their trend is not affected by the electric gradient, but only the amplitude of their values.

Unloading at 12-day age showed more pronounced elastic behavior for shotcrete subjected to electric gradient, with larger recoverable strains.

ACKNOWLEDGMENTS

This research was sponsored by FAPESP, the research funding agency for the State of São Paulo, Brazil, under contracts number 98/02595-0 and 00/01421-0.

The authors are indebted to Este Engenharia, for the loan of the shotcreting equipment and to the companies Holcim Brasil and Pedreira Riúma, for the donation of cement and aggregate for the experiments.

REFERENCES

Aldrian, W. 1991. *Beitrag zum materialverhalten von früh belastetem spritzbeton*, Dissertation, Mountanuniversität, Leoben, Austria.

Chang, Y. 1994. *Tunnel support with shotcrete in weak rock – A rock mechanic study*. PhD. Thesis, Royal Swedish Institute, Stockholm, Sweden.

Fernandez-Delgado, G.F.; Mahar, J.W.; Parker, H.W. 1976. Structural behavior of thin shotcrete liners obtained from large scale test. *Proc. Shotcrete for Ground Support,* ACI Publ. SP-54: 399–442.

Ferreira, D.A. 2003. *Interaction of ground mass and shotcrete structural models subjected to electric gradient for tunnel support*. (in Portuguese) PhD. Thesis. Escola de Engenharia de São Carlos, University of São Paulo.

Ferreira, D.A. 1997. *Study about a physical method for strength increase of young shotcrete by applying electric gradient aiming at tunnel support* (in Portuguese). M.Sc. Dissertation, Escola de Engenharia de S. Carlos, University of São Paulo.

Ferreira, D.A.; Celestino, T.B. 1999. Physical method to increase shotcrete early-age strength. *Proc. Shotcrete for Underground Support VIII.* United Engineering Foundation, São Paulo, Brazil: 94–107.

Ferreira, D.A.; Celestino, T.B. 2001. Use of electric gradient to increase shotcrete early age strength. *Proc. Int. Conf. Modern Tunnelling Science and Technology*, Kyoto, Balkema, 1: 463–468.

Ferreira, D.A.; Celestino, T.B.; Bortolucci, A.A. 2002. Shotcrete response to the electric gradient method. *Proc. of Shotcrete for Underground Support IX.* Japan Tunnelling Assoc., Kyoto: 138–151.

Golser, J.; Schubert, P.; Rabensteiner, K. 1989. A new concept for evaluation of loading in shotcrete linings. *Proc. of International Congress on Progress and Innovation in Tunnelling,* Montreal: 79–85.

Holmgren, J. 1976. Thin shotcrete layers subjected to punch load. *Proc. Shotcrete for Ground Support,* ACI Publ. SP-54: 443–460.

Kuwajima, F. M. 1991. *Behavior of shotcrete in shallow tunnels*. Ph.D Thesis, Alberta University, Edmonton, Canada.

Prudêncio Jr, L.R. 1993. Contribuições à dosagem do concreto projetado. PhD Thesis, University of São Paulo, Brazil.

Schubert, P. 1988. Beitrag zum rheologischen verhalten von spritzbeton. *Felsbau,* 6(3): 150 – 153.

Copyright © 2005 Taylor & Francis Group plc, London, UK

Design aspects of the Bangkok Blue Line Extension

C. Photayanuvat
Mass Rapid Transit Authority of Thailand

N. Phien-wej
School of Civil Engineering, Asian Institute of Technology, Pathumthani, Thailand

S. Suwansawat
Department of Civil Engineering, Faculty of Engineering King Mongkut's Institute of Technology, Ladkrabang, Bangkok, Thailand

ABSTRACT: The Bangkok Blue Line Extension is the second phase of the subway system in Bangkok implemented to mitigate traffic problem in the Metropolitan area. The tunnel will be excavated underneath the old Chinatown, a densely populated urban district, historical areas, and cross underneath the major river in Bangkok. Since, there are very limited working spaces on the ground level, design and construction methods will be optimized to reduce effects of the construction on ground surface and existing structures. A large dual-track tunnel with 11 meter in outer-diameter and twin tunnels with 6.3 meter in outer-diameter are considered. Selecting a suitable type of tunnel boring machines is also crucial since the machine must be capable of excavating a tunnel throughout various geological conditions including soft to stiff clay layer, dense sand layer, and sand layer with high water pressure without inducing large ground movements.

1 PROJECT BACKGROUND

Bangkok crams around 10 million people into a rapidly growing area. Anyone travels through the city braces for an ordeal of wasting hours in impenetrable traffic. Concern about Bangkok's increasing heavy traffic led to the implementation of the first phase of the Bangkok Blue Line Subway project which was completed and opened in 2004. The initial phase was only 20 km long and mainly concentrated in the heart of the city. This only mitigates the traffic problem to some degree. To address the problem, the mass transportation system must be expanded to other parts of the city to serve commuters who live in outskirts of the metropolitan area. Thus, the Bangkok MRT plans to construct the Bangkok Blue Line Extension as the second phase of the subway system in Bangkok. The extension line is composed of two contracts which are the North Contract and the South Contract. The North Contact will be an elevated system of 13 km extended from the northern end of the initial Blue Line. The South Contact is 14 km long that 6.5 km of the route will run underground expanded from the southern end of the initial phase (Fig. 1). The underground work will consist of tunneling work and 4 stations, which has to be constructed in very limited areas. The construction is expected to start in the year 2005 and will take 3 years to complete the project. In this article, only underground work will be discussed.

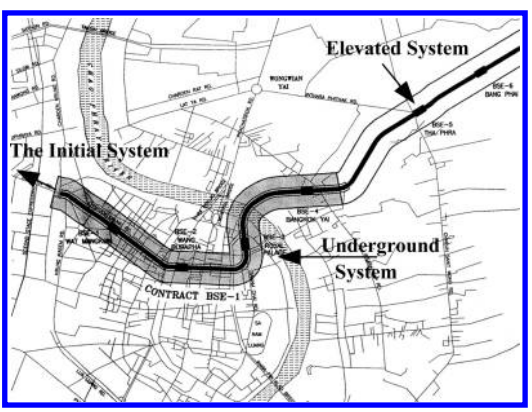


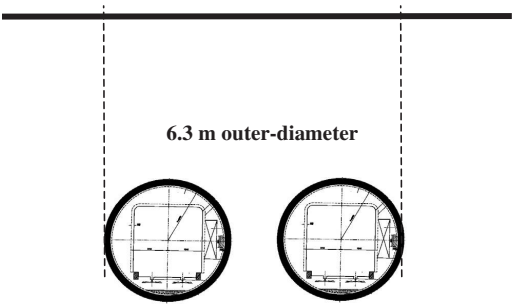
Figure 1. Bangkok Blue Line Extension (South Underground Contract).

Copyright © 2005 Taylor & Francis Group plc, London, UK

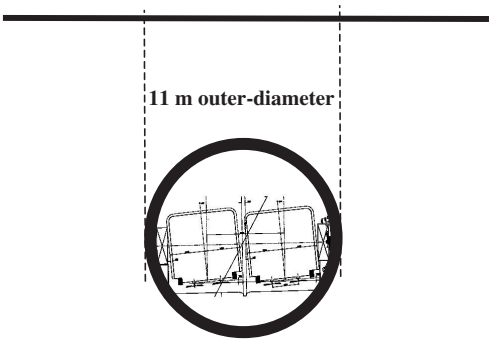
2 TUNNEL DIMENSION

The tunnel will be excavated underneath main streets inside the old China Town district, where population is very dense and traffic is always busy. Furthermore, buildings lined up along the tunnel route are very old and a number of buildings have become national heritage. Since the roads are narrow and buildings are very sensitive to ground movement induced by tunneling, tunnel dimension and method of construction have become major concerns in the design. The completed subway system or the initial phase of the Blue Line already employed the single-track twin-tunnel. Hence, using the same size of tunnel was the first choice for the extension project since designers and site engineers have already experienced what should be done and what should be avoided to implement the tunnel. Besides, it will be less difficult if supporting systems of the new tunnel correspond to the former system.

However, the twin-tunnel of 6.3 meter in outer-diameter (Fig. 2a) requires safe clearances between tunnels during construction. In some cases, the tunnel will be excavated underneath narrow streets so that the twin tunnels if used have to be excavated very close to each other causing induction of high stress to the tunnel lining. This may lead to damages or deflections of the lining. Another alternative therefore come across that a dual-track tunnel with 11 m in outer-diameter should be used in this case (Fig. 2b). Nevertheless, a large-diameter tunnel may require less horizontal space but its excavation volume will be larger than that of the twin-tunnel. Besides, excavation speed of a large-diameter TBM is slow and induces more ground loss volume than that induced by small-diameter tunnels although they may yield the same percentage of ground loss magnitude (i.e. 0.5–2% would be expected) since their excavation volumes are different.



(a) Two single-track tunnels



(b) A dual-track tunnel

Figure 2. Two alternatives of the tunnel used in the project.

3 METHOD OF CONSTRUCTION

In recent years, most soft ground tunneling projects have adopted the Earth Pressure Balance shield and slurry shield techniques. The EPB shield is usually considered particularly suitable for cohesive or silty ground that does not contain cobble or boulder obstructions and in which the water head at the face is not high. In other words, the more homogeneous and consistent the soil, the more successful the technique is. Although the EPB shield is capable of working in sandy conditions using foam or injected polymer technique, this might be problematic. On the other hand, the slurry shield method is quite well suited for tunneling in non-cohesive ground. However, it requires a circulation or slurry separation plant that can be a problem in the crowed city with limited working areas like Bangkok.

Due to experiences in the initial Blue Line project, eight EPB shields (Fig. 3) have been successfully excavated the tunnel by inducing minor ground loss. However, excavating within a sand layer can lead to large surface settlements and in the case of high water

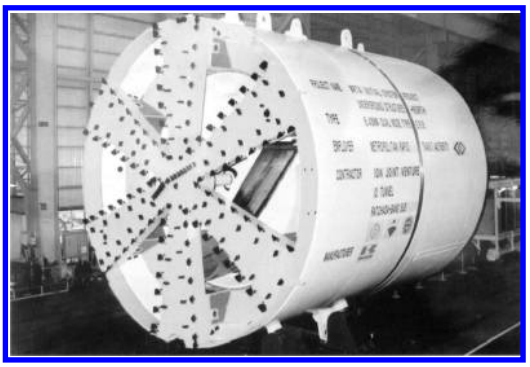


Figure 3. An EPB shield used for the construction of the initial Bangkok Blue Line.

Copyright © 2005 Taylor & Francis Group plc, London, UK

table level, it was very difficult to manage EPB shields and to control water intrution problem even though many technigues such as foam injection and jet grouting had been used. In the Extention Line, selected shields will have to cut through a dense sand layer and even underneath a river bed where sand deposits will be expected. Therefore, if EPB shield is selected to be used for the new project, there will be some challenging problems waiting for tunnel engineers.

The tunnel alignment also pass close to a heritage and sacred area of Bangkok where a royal palace, a holy temple, and a royal park are located. Using cut-and-cover technique for excavating a tunnel station within this region is prohibited. Only a ventilation and an access shaft may be allowed. Building a large subway station from underground without open-cut is not simple and very risk. Hence, other excavation alternatives have been discussed. NATM (New Austrian Tunneling Method) has been studied for this purpose. In this alternative, workers have to excavate a large open area connecting between tunnels to build a subway station. Another alternative is to employ a triple-head shield or detachable three-section sheild as illustrated in Fig. 4. This type of shield consists of three sections as shown in the diagram below. The central section is used to excavate the space between the twin tunnels to build a passenger platform.

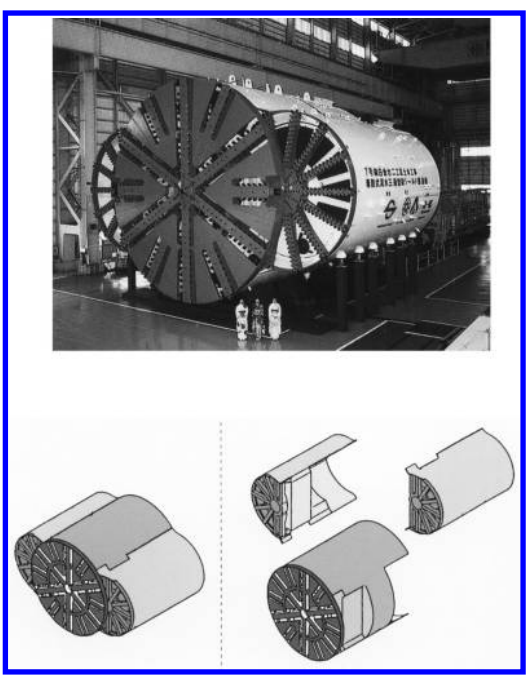


Figure 4. Detachable three-section shield considered to be used in the Bangkok Blue Line Extension project.

4 GEOLOGICAL CONDITION

Bangkok is lying in the Chao Praya delta plain. Its topography is low and flat being approximately 0.5 to 1 meter above sea level. The subsurface conditions along the Bangkok Blue Line Extension is that soft clay underlain by stiff clay and dense sand as shown in Fig. 5. Most of the tunnel alignment is located at 20–30 m deep from the ground surface or within a stiff clay and a sand layer. However, in some parts of the route, tunnels will be entirely excavated deep into the dense sand layer particularly when the tunnel is cross under the Chao Praya river.

As mention earlier, the subsurface condition highly affects the design of the tunnel construction. Since the tunnel alignment will be located within different soil types, the shield therefore will have to be capable of excavating a tunnel throughout various geological conditions including soft to stiff clay layer, dense sand layer, and sand layer with high water pressure without inducing large ground movements.

5 HYDROLOGICAL CONDITION

Hydrological condition is always an important factor involved in designing of any underground construction in Bangkok since pumping of ground water from the aquifers for both domestic and industrial purposes has reduced the piezometric head beneath the city. The depression in ground water level was initially centered on Bangkok, but as industry moved out of the city and pumping increased in the industrial areas to the south and east of the city, the piezometric levels in these areas became depressed at the same time as those in Bangkok recovered.

There are two main effects of the depression in the water tables. First, the localized depression of the water table has caused migration of ground water from the surrounding areas, which has allowed saline water from the Gulf of Thailand to infiltrate the aquifers. Secondly, the reduction in pore pressure

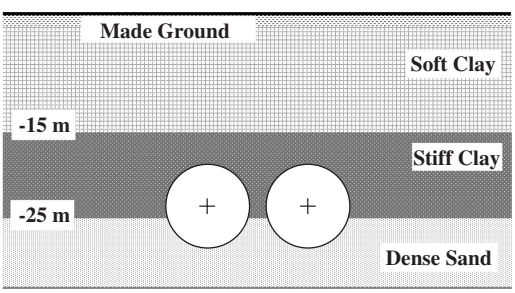


Figure 5. Typical subsurface condition along the alignment of the Bangkok Blue Line Extension project.

Copyright © 2005 Taylor & Francis Group plc, London, UK

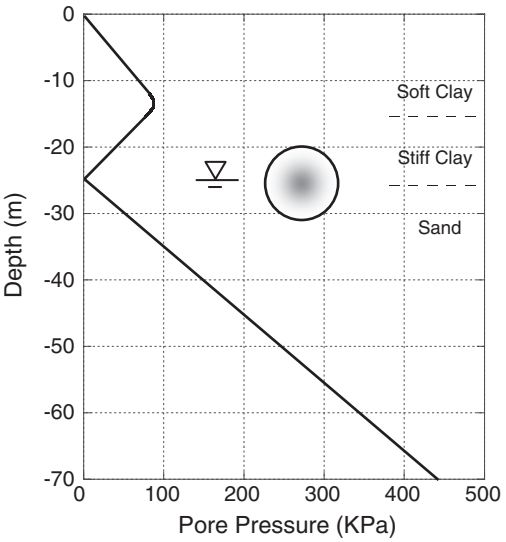


Figure 6. Typical pore water pressure profile in Bangkok.

has caused consolidation of the substrata leading to significant long-term ground settlement across the region.

The effect on the Bangkok Aquifer of this pumping has been to lower the piezometric levels within the aquifer by underdrainage through connection with the aquifers below. Beneath the site of the Extension Line, the piezometric levels were reduced from what would have originally been a hydrostatic profile from near the ground level (i.e. before any pumping occurred), to a level of about 23 m below ground level by 1979. The piezometric level in the Bangkok Aquifer does not appear to have changed from this level between 1979 and the present day. The First Stiff Clay and Bangkok Soft Clay above are underdrained near their base, however, because of replenishment from the surface and its relatively low permeability, the Bangkok Soft Clay has a hydrostatic profile from near ground level to approximately 10–12 m below ground level (Fig. 6).

Even though the ground water has no significant impact on most of the tunnel alignment during construction, it will have more and more effects on the tunnel lining due to the rising ground water level in the future. Hence, the lining has to be designed to withstand the increase of water pressure.

6 CONSOLIDATION SETTLEMENT

The extraction of ground water has lead to significant consolidation settlement within the substrata. 1.6 m of surface subsidence has occurred in the Bangkok area between 1933 and 1987 with approximately 800 mm to 1000 mm occurring at the Blue Line Extension site. Today, the rate of settlement reduces from the past. This reduction in rate is probably due to the restriction of groundwater extraction as discussed earlier, and the subsequent rise in piezometric pressures in the aquifers below the Bangkok Aquifer.

Data from the four settlement monitoring stations with settlement pins installed at depth in the vicinity of the initial route indicate that compression of the Bangkok Soft Clay may have been between about 2 mm and 15 mm/year in 1996. It is not possible from the data available to determine the rates of settlement in the strata beneath this. However, as stated above it seems likely that there is very little movement at a depth of 200 m and below.

The piezometric pressures in the Bangkok Aquifer have been relatively stable at 22–24 m below the ground surface over the period 1979 to 1997. The ground settlement monitored over this period is likely to be principally due to consolidation of the clay overlying the Bangkok Aquifer. The rate of settlement monitored in l996 at 20 m below ground level appears to be only some l0% of that monitored in l981 and, given no further decrease in piezometric level within the Bangkok Aquifer, it can be expected that this reduction in settlement rate may continue in the future. However, consolidation settlement is considered during design and construction stages. Construction techniques and procedures for excavation, tail void grouting, and ground improvement are specified not to induce high excess pore water pressure leading to long-term settlements over the tunnel alignment.

7 CONCLUSIONS

From the design point of view, the Bangkok Blue Line Extension is a challenging tunneling project in an urban environment. Limitations of spaces, traffic, existing structures and various geological conditions along the tunnel alignment are considered as key factors in the design and construction. Two types of tunnels are studied to determine which alternative is more suitable in this project. Subsurface and hydrological conditions also affect tunnel lining design. The lining must be able to withstand increased water pressure due to the high water table. Moreover, appropriate tunneling techniques will be used to minimize ground settlement but not significantly induce excess pore water pressure causing consolidation settlement over the tunnel alignment. Additionally, selected TBM must be able to excavate the tunnel through different soil types without causing any major problem.

Copyright © 2005 Taylor & Francis Group plc, London, UK

REFERENCES

Maconochie, D. J., Suwansawat, S., and Chang C. C. 2001. Tunneling for the Chaloem Ratchamongkon Line in Bangkok. *Proc. 2001 of Rapid Excavation and Tunneling Conference (RETC)*. Colorado.

Phienwej, N. 1998. Tunnelling for Infrastructure Development in Thailand. *Tunnelling and Underground Space Technology* 13(3): 317–330.

Photayanuvat, C. and Schulz C. 2003. New Realization of Driving Shield Tunnel Boring Machines in Thailand. *Proc. the ITA World Tunneling Congress 2003*. Rotterdam: Balkema.

Suwansawat, S. 2003. The M.R.T. Chaloem Ratchamongkhon Line: A Road to Success of the First Subway Project in Bangkok. *Proc. the 21st Conference of Asean Federation of Engineering Organizations (CAFEO)*. Indonesia.

Suwansawat, S. 2003. The Challenging Subway Project in Bangkok: New Hope of Thais in Solving Traffic Problem. *Proc. the 8th Conference of the Association for Computer Aided Architectural Design Research in Asia.* Thailand.

Copyright © 2005 Taylor & Francis Group plc, London, UK

Teaching tunnels: knowledge management and on-line databases

Prof. René-Michel Faure
CETU, France

Prof. Jean-François Thimus
Université Catholique de Louvain, Belgique

Ing., Gérard Hémond
Solem Expertises SA, Carouge, Suisse

PhD student, Nicolas Faure
Solem France SA, Archamps, France

Ir. Bertrand Lecomte
Université Catholique de Louvain, Belgique

ABSTRACT: We present the structure and the use of a knowledge database of tunnel for teaching purposes. This database, called KBT, is complementary to the e-learning tool DIDACTU. The development of KBT will give an important help to teaching providing text an images to illustrate courses.

1 INTRODUCTION

During its last meeting, in Singapore at ITA/AITES symposium, the Working Group n°18, that works for providing new materials for teaching undergrounds works, decided to improve its action for teaching tunnels giving to teachers and students new tools by the way of the WEB. This paper describes one aspect of these efforts about a database named KBT.

Teaching is a way for the transmission of the knowledge from elder to younger. In a prospective approach of knowledge about tunnels we can define knowledge under three forms that are:

- Concepts, for which we can use glossaries and ontology's.
- Conceptual relations that we find in text (granite IS A rock) and that we find in algorithms (calculation codes),
- Selected cases for case based reasoning (in fact a combination of the two previous item).

An e-learning tool, the educational software DIDACTU that was presented at the Singapore conference (Faure et al, 2004), is a tool for the transmission of knowledge. We can find in it a glossary, some on line codes, texts in which rules are expressed in usual language, not with the usual formalism of logic, and the description of some cases of tunnels.

This tool appears as an important step in knowledge management, but not the last one, because there is not a strong formalism for these three kinds of knowledge and systematic and automatic acquisition of knowledge is not possible. It is a little more than a course in which the professor selects and presents documents, and as it is done with usual navigation tools, the use of this knowledge depends mainly of the user. (Faure, Thimus, 2004)

In a brief first part, this paper presents the bases of a classification of concepts used in tunnel works, with a clear definition of each one. Some possibilities of this formalism are mentioned.

In a second part, as it was decided in WG 18, we describe the KBT database of tunnel cases that we have developed and implemented thought the net. The selected cases of tunnels must have an interest for teaching and even they are not numerous, the singularities of the cases must be described with accuracy. So, for a better use of the database, KBT is closely linked with the e-learning tool DIDACTU.

A third part describes the use of KBT.

2 CLASSIFICATION OF CONCEPTS USED FOR TUNNEL WORKS

Knowledge is expressed with words, so knowledge representation begins with words, said Sowa, (Sowa,

Copyright © 2005 Taylor & Francis Group plc, London, UK

2000). Words are ambiguous, so we must express them with definitions in order to resolve their ambiguity. A word and its definition is what we call a "concept", which refers to every and each item which matches the definition and – hence – the name. So, that we call concept is each thing and tool clearly identified in tunnel works. A jumbo, a beam, a computer code, a theory are concepts. The identification of these concepts is done by automatic language treatment running on chosen texts. An expert of the world of tunnel give definition for any concept and set it in a tree that checks subsumed relations (IS A) between all concepts.

The same process applies to various relations between concepts, mainly aggregation (IS A PART OF); the sum of these various trees, featuring the same concepts, offers a kind of common reference for concepts organisation in the field of tunnels. This helps to define some conceptual neighbourhoods, which, we hope, will allow some reasoning in a next future or for the educational software DIDACTU a new kind of navigation and for the knowledge base KBT a new query mode.

This part is still under development, and shall be presented next symposium.

3 MAIN CONCEPTS LEADING TO THE KBT DATABASE

3.1 *What is an "interesting" tunnel and for what use?*

When teaching, examples are used for showing some feature or some problem that may occur during the construction of a tunnel. Interesting tunnel are these where something unexpected occurs and where an original solution must be founded. For a teacher, but also for a young engineer, the discussion that can develop when showing the case is usually fruitful, and the student will remember the causes of the incident and its remedial. Several cases, well chosen, would be an appreciated help when teaching, or for new engineers, who wish to upgrade their own knowledge.

3.2 *What were the previous works about databases?*

The previous works about on-line databases are numerous, and the authors contributed to these progresses (Faure et al, 1992). A recurrent subject of discussion about that kind of database is the property of the data. In the WASSS project (Faure, 1999), (Faure et al, 2001) we have decided to share the data into two parts, the first one that we call meta-data, which are information on the data, and the data itself. The meta-data are access free, but the detailed data remains under the acknowledgement of its owner. It is quite heavy and we worried about the management of the rights (Faure et al, 2002). For the actual release of KBT we skip that approach and we think that all data must be free for a gentle use of the database.

One other aspect of that kind of database is the feeding of it. Preparation of a case must be very light, if we want obtain numerous cases. We observed that for a men knowing correctly the case he want to display, the capture of the structured data all must no be longer than few minutes, and we conceive KBT as to agree with this constraint. The building of the web

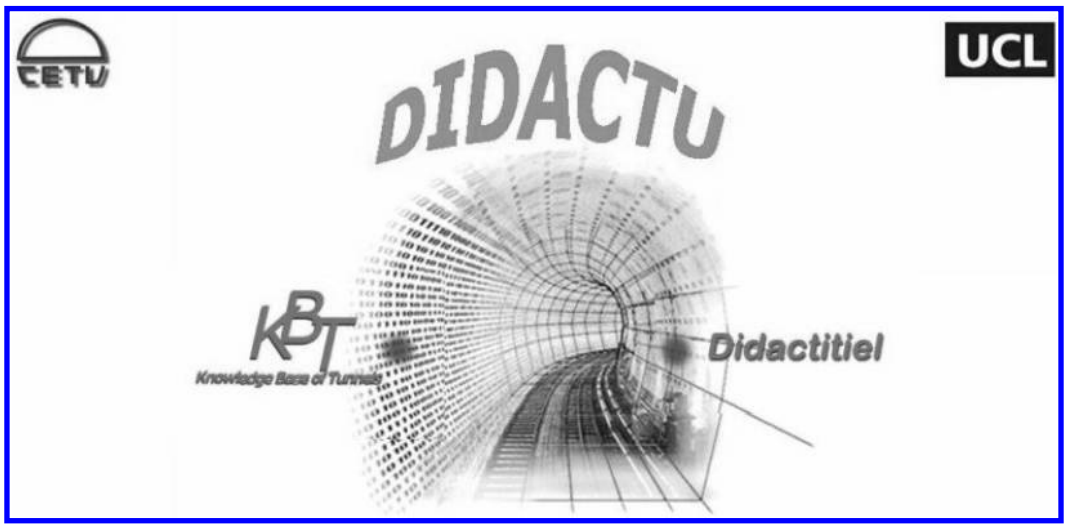


Figure 1. First page when entering DIDACTU with the link to KBT.

Copyright © 2005 Taylor & Francis Group plc, London, UK

pages presenting the case may be longer, but as the form is completely free, it is easy for the writer to describe his case generally already existing on an other format, and he can use images, maps, sketches and also web links. The WEB page(s) is written in his own language, as KBT allows the use of several languages.

4 THE ON-LINE KBT DATABASE

KBT means: "Knowledge data Base for Tunnels". The word knowledge is used in its full signification, that is to say, that we want collect not only information about tunnel, but also reasoning about it when an incident occurs. For this, when filling the database four kinds of data are asked in a chosen language among French, Italian, Spanish, German and English.

4.1 *What data for KBT?*

4.1.1 *General data about the tunnel*

These data are asked in a form, the user must fill:

Name of the tunnel
Country
GPS coordinates of the two entrances
Owner of the tunnel
Builder (name of the company)
Number of tubes
Mean declivity

Shape of section (circular, horse shoe shape, elliptic, rectangular.…) (a combo list)

Length of the tunnel
Excavated volume
Name of the road (railways) that uses the tunnel
Date of the opening
Date of writing the form
Name of the writer
Used language for web pages.
References: other documents in which information about the tunnel can be found.
Internet address: where the tunnel is presented, if any.

4.1.2 *Meta knowledge*

It is a list of questions with answer: "yes or no". If the feature is present or developed in the web pages the writer clicks on the yes button. The first questions are about:

General map,
Profile,
Geotechnical report,
Calculus references,
Photos,
Experimentation or particular study,
Other: if any other kind of information, one line for answer.

The other questions concern the following themes, if they are developed or not in the web pages. Those themes are:

Do you meet difficulties with a weak soil?
Do you have problems with water?
Do you have problem during building?
Do you have problem of subsidence?
Do you have problem with the driving of TBM?
What other problem do you have for this tunnel?

(One line for answer)

4.1.3 *Some information about the works and the design*

All these information are predefined and the writer has only to click on combo list. This information will be used for querying the database, and is stored in an access like database. As a tunnel is a linear structure this information is required three times, for each portal and for the most difficult section.

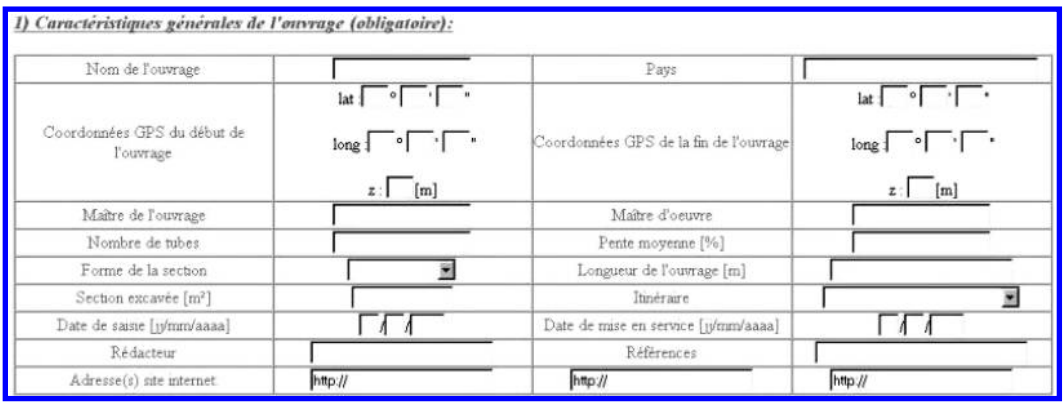


Figure 2. Part of the form for entering general data.

Copyright © 2005 Taylor & Francis Group plc, London, UK

KBT presents combo lists for:

Geological stage for soil:
(mainly rock as soil is "quaternary")
Cambrian (Cambrien),
Carboniferous (Carbonifère),
Cretaceous (Crétacé),
Devonian (Dévonien),
Eocene (Eocène),
Jurassic (Jurassique),
Lias (Lias),
Miocene (Miocène),
Ordovician (Ordovicien),
Pliocene (Pliocène),
Precambrian (Précambrien),
Quaternary (Quaternaire),
Silurian (Silurien),
Trias (Trias).

Lithology:
a short list chosen by some tunnel experts.
Amphibolite, (Amphibolite),
Andesite, (Andésite),
Anhydrite, (Anhydrite),
Slate, (Ardoise),
Clay (Argile),
Clayshale (Argile schisteuse),
Claystone (Argilite),
Arkose, (Arkose),
Basalt, (Basalte),
Limestone, (Calcaire),
Calcareous shale, (Calcschiste),
Coal, (Charbon),
Cellular dolomite, (Cargneule),
Cinérite,
Conglomerate, (Conglomérat),
Cornéenne, (Cinérite),
Chalk (Craie),
Diorite, (Diorite),
Dolerite, (Dolérite),
Dolomite, (Dolomie),
Gabbro, (Gabbro),
Gneiss, (Gneiss),
Granit, (Granite),
Granodiorite, (Granodiorite)
Sandstone, (Grès),
Gypsum, (Gypse),
Halite, (Halite (sel gemme)),
Felsite, (Leptynite),
Brown coal, (Lignite),
Marble, (Marbre),
Marl, (Marne),
Calcareous Marl, (Marno-calcaire),
Siliceous limestone, (Meulière),
Micaschist, (Micaschiste),
Microgranite, (Microgranite),
Pelite, (Pélite),
Peridotite, (Péridotite),
Pumice, (Ponce),
Quartzite, (Quartzite),
Rhyolite, (Rhyolite),
Sand (Sable),
Schist, (Schiste),
Serpentinite, (Serpentinite)
Syenite, (Syènite),
Sylvinite, (Sylvinite),
Tephra, (Téphra),
Volcano tuff, (Tuf volcanique),
Trabertine, (Travertin).

Digging system:
Drill and blast, (Abattage à l explosif),
TBM, (Tunnelier),
Roadheader, (machine à attaque ponctuelle),
Digger, (pelle mécanique),
Rock breaker, (brise roche).

Soil treatment:
Freezing, (Congélation),
Jet-grouting, (Jet grouting),
Injection, (Injection),
Water lowering, (Rabattement de nappe).

Mucking system:
Rails, (système à rails),
Lorries, (Camions ou charge et roule),
Conveyor, (Bande transporteuse),
Pipe line, (Pipe line).

Reinforcement during digging:
Bolts on front face, (Boulonnage du front),
Pre-mill shell, (Voûte prédécoupée),
Fore polling, (Poussage de tubes),
Umbrella arch (Voûte parapluie),
Umbrella arch et pre-cutting, (Voûte parapluie et prédécoupage).

Support:
Formed concrete, (Béton coffré),
Extruded concrete, (Béton extrudé),
Sprayed concrete, (Béton projeté),
Bolt, (boulon),
Bolt + Sprayed concrete, (Boulon + Béton projeté),
Rib, (Cintre),
Rib + sheeting, (Cintres + Blindage),
Rib + Sprayed concrete, (Cintres + Béton projeté),
Rib + bolt + Sprayed concrete, (Cintres + Boulons + Béton projeté),
Concrete segment, (Voussoir béton),
Metal segment, (Voussoir métal).

Structure:
Vault, (Voûte),
Cut and cover, (Tranchée couverte),

Copyright © 2005 Taylor & Francis Group plc, London, UK

Slurry wall, (Paroi moulée).
Portal:
Embankment, (Remblai),
Without embankment, (à l'air libre),
Retaining wall, (Soutènement de paroi),
Safety net, (Filet de protection).

Lining:
Reinforced concrete, (Béton coulé armé),
Formed concrete, (Béton coulé non armé),
Sprayed concrete, (Béton projeté),
Massonery, (Maçonnerie),
Concrete segment, (Voussoir béton),
Metal segment, (Voussoir métal).

Waterproofing:
Global watertightness system, (Dispositif d'étanchéité global (DEG))
Liner on the back of the vault, (Géomembrane en extrados),
Drain + Cavity membrane, Drain + géoespaceur),
Waterproof coating on the vault, (Enduit hydrofuge en intrados),
Bituminous sheet on the back of the vault, (Membrane bitumineuse en extrados),

Water outlet, (Exhaure)(a number with unity),

Max depth of the tunnel (overburden), (Profondeur maximale du tunnel).

4.1.4 *Web pages*
The web page(s) that we can add is really the transcription of the knowledge, the writer want to deliver about this tunnel. A photo, a sketch or a few lines may express this knowledge very simply, but it can also be developed, if necessary, on several web pages. All these pages are linked to the previous data.

4.1.5 *Commentaries*
The writer can express there his opinion, or the reason why he find this case worthy to be stored and shown to all people, and why it can be useful for teaching.

4.2 *The use of the database KBT*

4.2.1 *How to fill the database?*
Who wants to present a case inside KBT, must first build freely the web page(s) presenting the case.

After that, he goes on the web site of KBT, and fills the form we describe upper. After that he send by e-mail the web page to the web master of KBT. The page is read and the web master put all the information in KBT. For any problem detected by the web master an exchange of mails will solve it, the data are and remain under the responsibility of the writer and the web master will never modify anything without the acknowledgement of the writer.

4.2.2 *How to query the database KBT?*
Directly from a list of cases or from a map where all cases are displayed with icons, the reader can reach any case.

By a serial query language (SQL like), the reader makes a choice of all tunnels corresponding to his criteria's.

5 CONCLUSION

KBT appears as an easiness to manage database, a powerful complement to DIDACTU, and as it is in all main language, we hope that it will grow quickly.

Contact: rene-michel.faure@equipement.gouv.fr or thymus@gce.ucl.ac.be

BIBLIOGRAPHY

Faure R.M., Mascarelli D., Vaunat J., Leroueil S., Tavenas F., 1992, Present state of development of XPENT, expert system for slopes stability problems.; 6th Int. Congress on Landslides Bell editor Christchurch. p1671–1678.

Faure R-M., 1999, Data-bases and the management of landslides. Int. Symp. on Landslides. Shikoku (Japan). IS Shikoku '99, p 1317–1330.

Faure R.M., Locat J., Thimus J.F., Picarelli L., 2001, Base de données internationale sur les glissements de terrain, Revue Française de Géotechnique. Numéro 95 et 96: Mouvements de terrain, pp 183–187.

Faure R.M., Thimus J.F., Hémond G., 2004, DIDACTU, an e-learning tool for underground works. Proc. ITA Congress, Singapore.

Sowa J.F., 2000, Knowledge representation, Brooks/Cole editor.

Faure R.M., Thimus J.F., 2004, Contribution of on line tools on Internet for the teaching of slopes and tunnel stability, Proc of Engineering geology for infrastructure planning in Europe. A European perspective, Liège, Springer ed. pp 59–68.

Faure R.M., Thimus J.F., Robert A., Schubert W., Bourgeois E., Bois A.P., 2002, Base de connaissance internationale sur les tunnels, Tunnels et Ouvrages Souterrains, n°170, pp 94–98.

Copyright © 2005 Taylor & Francis Group plc, London, UK

The 9 km long Kallidromo tunnel of the new highspeed railway line Athens-Thessaloniki, Greece, tunnel sections in squeezing ground

W. Wittke, B. Wittke-Schmitt & D. Schmitt
WBI – Prof. Dr.-Ing. W. Wittke Consulting Engineers for Tunneling and Geotechnical Engineering Ltd., Aachen/Stuttgart, Germany

ABSTRACT: In course of the new highspeed railway line from Athens to Thessaloniki, the approx. 9 km long Kallidromo tunnel is to be constructed with two single-track tubes. After completion of approx. 2 × 1.5 km on either side, the works had to be interrupted in 2002. Difficult heading and failures of the support had to be dealt with in squeezing ground. Design for the remaining tunnel sections was re-done. For the tunnel sections in squeezing ground, a yielding support with a slotted shotcrete membrane and a special type of yielding anchors is foreseen in the new design.

1 PROJECT

In course of the new highspeed railway line from Athens to Thessaloniki, the approx. 9 km long Kallidromo tunnel is to be constructed (fig. 1). The tunnel consists of two single-track tubes with a distance of the tunnel axes of approx. 35 m, which is planned to be increased to 65 m in the center section of the tunnel. Cross-cuts are planned every 500 m. The tunnel tubes are drained. The height of overburden amounts to up to approx. 530 m.

The first sections of Kallidromo tunnel were constructed according to the shotcrete method. After completion of approx. 2 × 1.5 km on either side, the works had to be interrupted in 2002, since the envisaged construction time and budget were strongly exceeded. This was mainly due to difficult heading and failures of the support in squeezing ground conditions.

Design of the remaining 2 × 6 km was re-tendered. Re-start of construction is planned for the beginning of 2005.

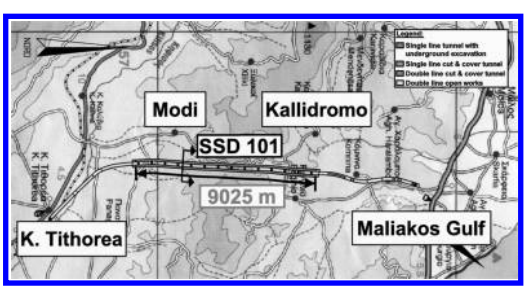


Figure 1. Kallidromo tunnel, plan view.

2 GEOLOGY

The tunnel sections remaining to be excavated are located in silty clay, layers of the ophiolitic sequence and limestone (fig. 2, ALEXIADOU & MIGIROS 2003).

A structural and mechanical model for the clay was derived from back-analysis of the monitored displacements measured in the already excavated Southern tunnel sections. Homogeneity and isotropic behavior were assumed. Back-analysis lead to a very high deformability (E ∼ 60 MN/m^2) and a low strength (σ_u ∼ 0 to 1 MN/m^2). In view of the overburden height, which amounts to up to approx. 220 m in the corresponding tunnel section, and the low strength of the clay, squeezing behavior is to be expected also for the upcoming phase of construction.

In the area of the layers of the ophiolitic sequence, the tunnel has a height of overburden between approx. 300 and 530 m. The layers to be expected are schistous serpentinite (se.s), serpentinite (se) and to a minor extent schists, cherts and basic lavas. The schistous serpentinite has a distinct schistosity with limited shear strength, which forms the dominant discontinuity, resulting in anisotropic strength and deformability of the se.s. Material properties of the se.s vary. Sections with lower and higher strength are observed. The se reveals basically the same characteristics as the se.s, however, it has no distinct schistosity, and the properties are slightly more favorable. In both layers, shear zones with properties of a cohesive soil have to be expected on 15 to 20% of the length. As a rule, the thickness of the shear zones varies between 1 to 3 m, with a maximum thickness of 15 to 20 m. In the area of

Copyright © 2005 Taylor & Francis Group plc, London, UK

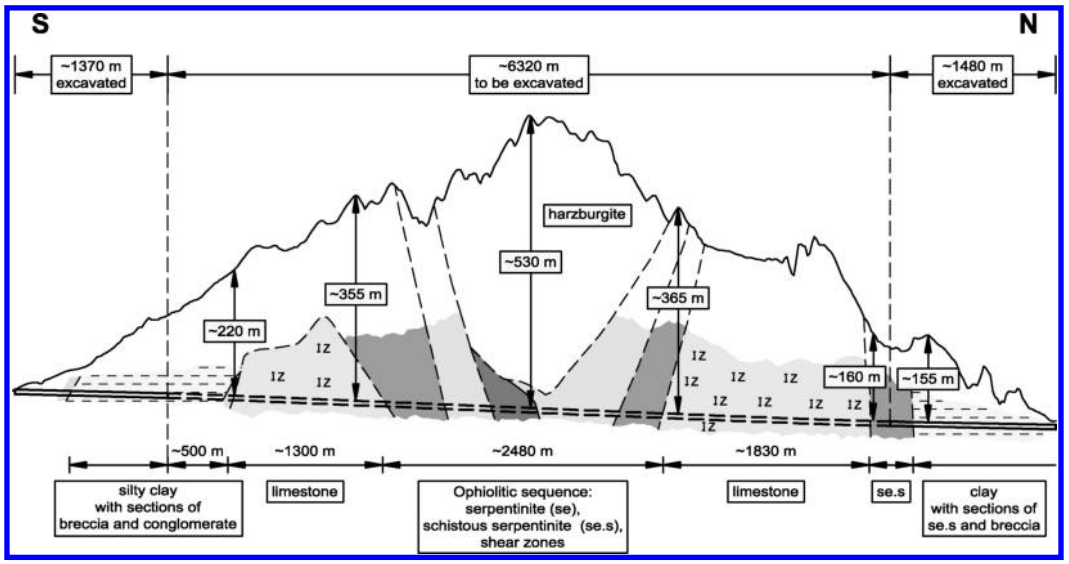


Figure 2. Kallidromo tunnel, longitudinal section.

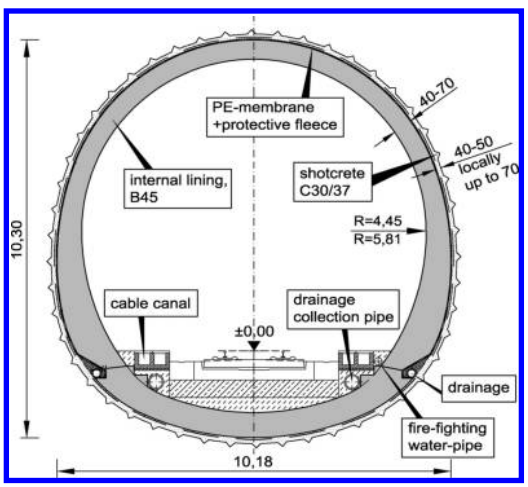


Figure 3. Typical cross-section, closed invert (WBI/NAMA 2003).

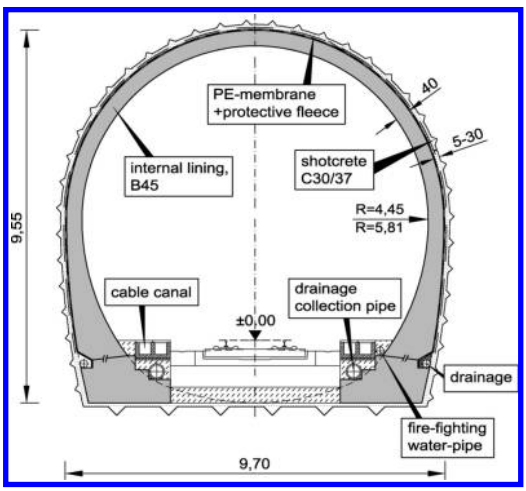


Figure 4. Typical cross-section, open invert (WBI/NAMA 2003).

the shear zones as well as in se and se.s with medium to poor properties, squeezing behavior is to be expected.

The limestone has a comparatively high strength and a low deformability. It is partly thickly bedded and partly thinly bedded. Locally highly fractured zones are observed.

3 CROSS-SECTIONS

The tunnel sections in clay and in the layers of the ophiolitic sequence are planned with a closed invert (fig. 3).

The tunnel sections in limestone are planned with an open invert (fig. 4). In both cases, a clear diameter of approx. 9 m is foreseen.

4 TUNNEL SECTIONS IN CLAY

4.1 *Tunnel sections already excavated*

At the Southern side, the tunnel has been excavated on a length of approx. 1.370 m. The height of overburden in the section excavated in clay results to approx. 150 m.

Copyright © 2005 Taylor & Francis Group plc, London, UK

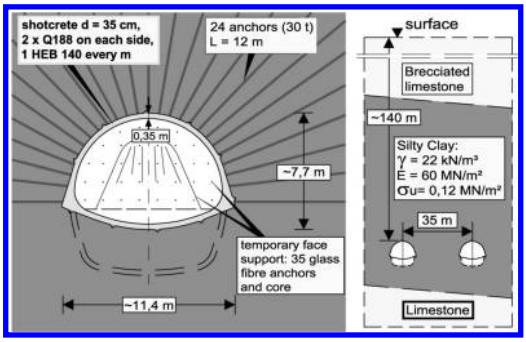


Figure 5. Kallidromo tunnel, cross-section and ground conditions, southern section in silty clay (ERGA OSE S. A & WBI/NAMA 2003).

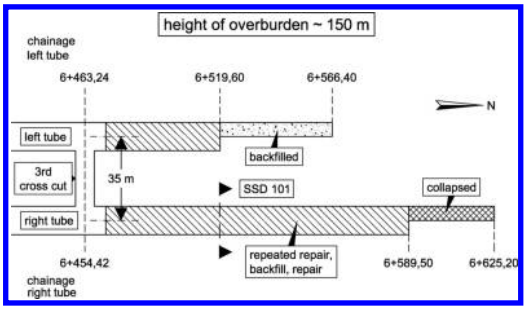


Figure 6. South heading, silty clay, plan with status of excavation (ERGA OSE S. A.).

A vault excavation with a shotcrete membrane of up to 35 cm thickness and extensive anchoring was carried out (fig. 5). The temporary face was supported with glass fibre anchors (ERGA OSE S.A.).

The temporary vault invert of the advancing right tunnel tube had to be repaired after a roof settlement of approx. 25 cm had occurred within approx. 1 month (figs. 6, 7).

Due to this measure, displacements converged. However, as excavation of the second, left tube proceeded, displacements in the right tube increased again remarkably. Thus, the invert was repaired a second time. Again, stabilization of the tunnel was achieved. However, after approx. one month, displacements again increased (fig. 7). One tunnel section collapsed, the remaining sections of the area in question could be filled with sandy gravel in time and thus were stabilized (figs. 6, 8).

Also the sections marked by "repeated repair…" in fig. 6 were backfilled to avoid collapse. Prior to the interruption of the works these sections were excavated and a stiff support was installed (fig. 6). This was feasible, because large radial displacements already had occurred, before the tunnel was backfilled.

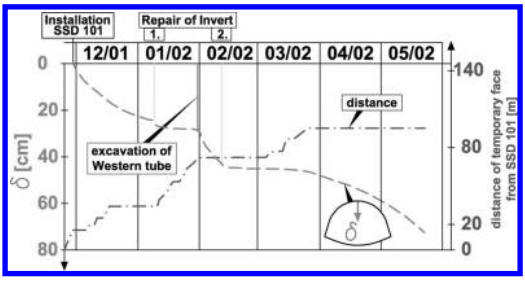


Figure 7. Kallidromo tunnel, measurement cross-section SSD 101, eastern tube.

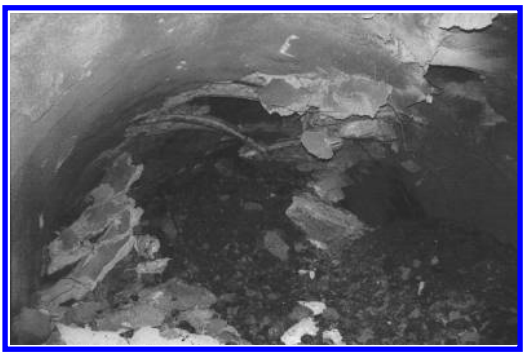


Figure 8. Kallidromo tunnel, failure of support.

4.2 *New design*

With the existing design for stiff support, the new excavation and support in the squeezing clay was however not possible. Therefore, the design was re-done. In the new design for the tunnel sections in clay (WBI/NAMA 2003), it is accounted for the squeezing behavior by a yielding support and a full face excavation. A slotted shotcrete membrane and yielding anchors are foreseen (figs. 9, 10), both allowing for radial displacements. After the displacements, which are necessary to allow for the formation of an arch in the rock mass next to the tunnel, occurred, the slots in the membrane are closed and the anchors are tied in. The remaining loads can be taken over by the support without failure.

Based on the results of the back-analysis of monitored displacements mentioned in section 2, three-dimensional and pseudo-three-dimensional stability analyses were carried out. An elastic viscoplastic constitutive law was used (WITTKE 2000). The finite element mesh (figs. 11, 12) is finely discretized in the area of the tunnel. The shotcrete segments as well as the slots are simulated. Five calculative steps were used for the analyses (fig. 13). After simulation of the in situ state of stresses and the preceeding stress relief in the area of the tunnel, excavation and installation of the slotted shotcrete membrane and the yielding anchors were

Copyright © 2005 Taylor & Francis Group plc, London, UK

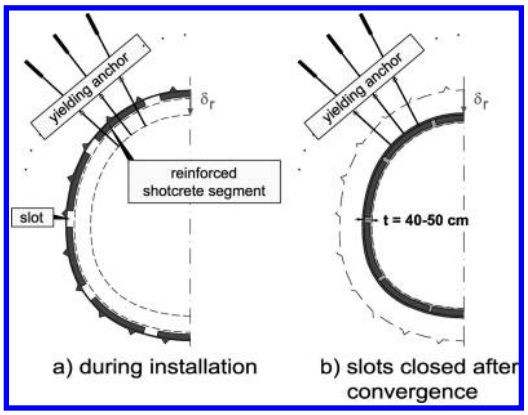


Figure 9. Yielding support, principle (WBI/NAMA 2003).



Figure 10. Shaft Konrad, yielding support in squeezing rock in a depth of 1000 m.

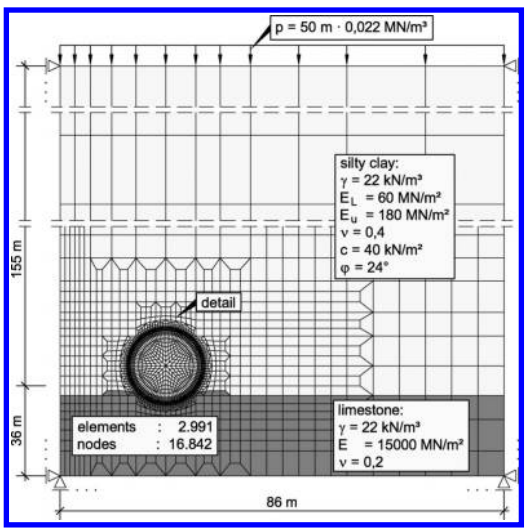


Figure 11. South heading in clay, yielding support, calculative section, FE-Mesh (WBI/NAMA 2003).

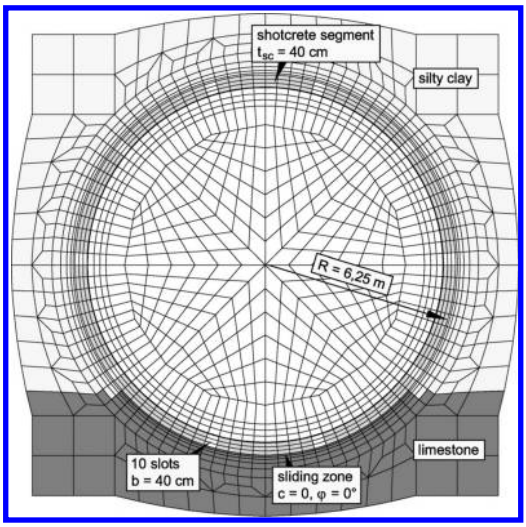


Figure 12. South heading in clay, yielding support, FE-Mesh, detail (WBI/NAMA 2003).

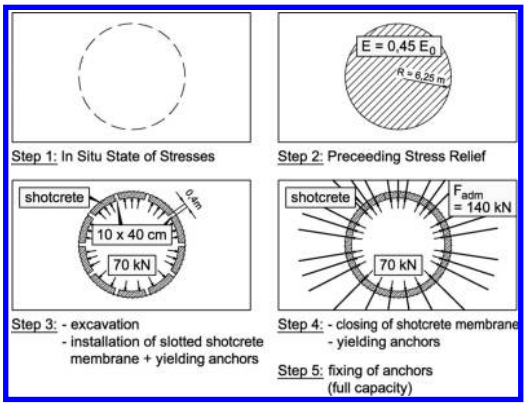


Figure 13. Yielding support, calculation steps 1 to 5 (WBI/NAMA 2003).

simulated in the third step of analysis, followed by an iteration to simulate the radial displacements. The factor to simulate stress relief was derived from the above mentioned back-analysis of the monitored displacements. In the fourth and fifth calculative step, the closing of the shotcrete membrane and the tying-in of the anchors are simulated. In the "yielding state", the yielding anchors are simulated with single loads equivalent to the yielding load. After tying-in, the anchors are simulated with rod elements and their admissible anchor load.

In this way, a realistic simulation of the sequence of excavation and support, of the radial displacements, the stresses in the rock mass and support and the stress

Copyright © 2005 Taylor & Francis Group plc, London, UK

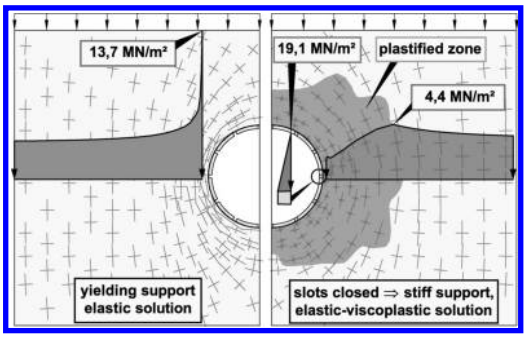


Figure 14. Kallidromo tunnel, "arching-effect" (WBI/NAMA 2003).

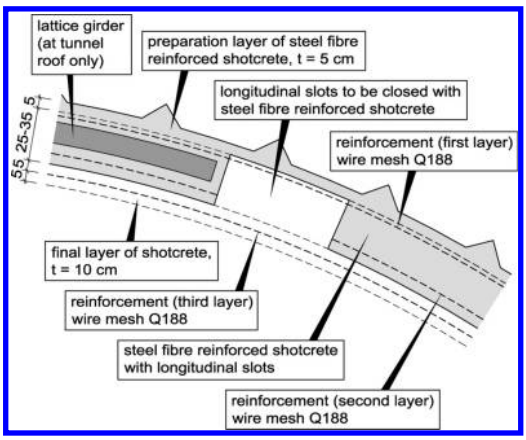


Figure 15. Slotted shotcrete membrane, detail tunnel roof (WBI/NAMA 2003).

re-distribution due to the "arching effect" is possible (fig. 14).

The analyses show that due to the low strength of the clay and the comparatively high overburden, radial displacements of 80 to 100 cm, for unfavorable conditions even up to approx. 120 cm, will be necessary in order to avoid failure of the support. In order to allow for such large displacements, a high number of comparatively long slots in the shotcrete membrane is necessary. Therefore, existing solutions e. g. with sliding steel arches (cp. Schubert 1996 & Sánchez Fernándes & Terán Benítez 1994), which allow only for smaller displacements, cannot be applied. Furthermore, special types of yielding anchors are necessary, since the calculated radial displacements extend far into the rock mass such that the steel rod in the anchor's bond length also experiences large strains. The solution chosen for the slotted shotcrete membrane is shown in principle on fig. 15.

The yielding anchor (fig. 16a) reaches 12 m into the ground. It is a wedge yoke anchor with 4 m bond

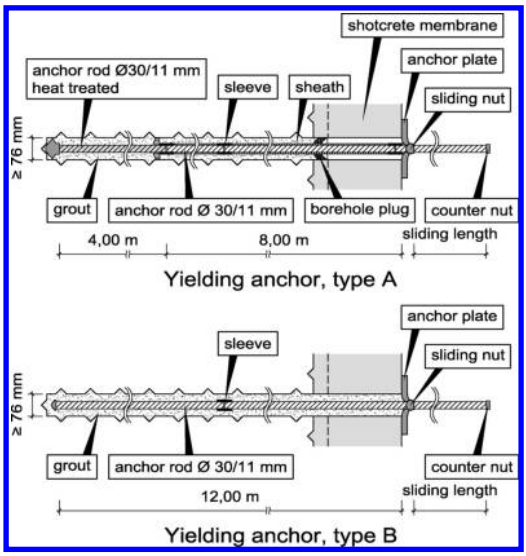


Figure 16. Yielding anchor (WBI/NAMA 2003).

length. The bond length consists of a special, heat-treated steel which allows for comparatively large plastic strains before failure. For compensation of the radial displacements of the shotcrete membrane, a sliding nut is foreseen, which slides along the anchor rod as soon as the load of 70 kN, considered in the FE-analyses, is reached. The outstand of the anchor rod is chosen depending on the expected radial displacements. After closing the slots in the shotcrete membrane, the anchors are tied-in so that they reach their full capacity. During construction, the bearing behavior of the anchors is to be monitored. Possibly, fully grouted anchors with a yielding head can alternatively be installed (fig. 16b).

The chosen solution also provides the flexibility needed to adapt the design to changing ground conditions and overburden heights as well as unexpected conditions. This is necessary since limited exploration was carried out and thus uncertainties regarding the ground conditions remain. For the same reason, quite a high number of excavation and support classes with varying size of excess excavation, slot width and shotcrete membrane thickness was foreseen in the design.

5 TUNNEL SECTIONS IN SERPENTINITE AND SCHISTOUS SERPENTINITE

As already mentioned, varying ground conditions and a high overburden are to be expected in these tunnel sections. The stability analyses as well as back-analysis of displacements monitored in an already excavated

Copyright © 2005 Taylor & Francis Group plc, London, UK

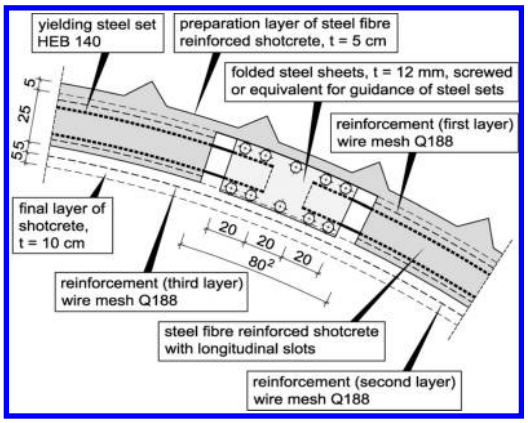


Figure 17. Yielding support, slots for small displacements, detail (WBI/NAMA 2003).

tunnel section in se.s (Northern heading) show that a stiff support with shotcrete and anchors will be sufficient in the areas of se and se.s with good material properties. In these sections, an advancing vault excavation with open invert is foreseen. The temporary face is supported with glass fibre anchors and shotcrete. Locally, an advancing support with mortar spiles is foreseen. However, in the sections with medium to poor properties as well as in the shear zones, a yielding support will be necessary. The required radial displacements amount to up to approx. 60 cm and are thus smaller than in the clay. However, the uncertainty regarding the ground conditions – the approx. 2.500 m long, complex section was explored with 5 drillholes only – as well as the range of change in ground conditions are far higher than in clay so that flexibility and adaptability of the support are even more important.

In principle, the same design is foreseen as for the yielding support in clay. In addition, a modified solution with sliding steel arches is foreseen for sections where smaller radial displacements are sufficient (fig. 17).

6 TUNNEL SECTIONS IN LIMESTONE

Since the limestone is competent, an unsupported open invert is foreseen in the corresponding tunnel sections (fig. 4). Full face blasting excavation with minimum support by shotcrete and anchors is foreseen where possible. In the more fractured sections, vault excavation with shotcrete membrane and anchors and potentially advancing support with spiles is foreseen.

REFERENCES

Alexiadou, H.; Migiros, G. 2003: Geological longitudinal section, geological report. Athens, July 2003. Not published.

Erga Ose S.A.: original design and documents on heading carried out up to now. Not published.

Sánchez Fernándes, J. L.; Terán Benítez, C.E. 1994: Túnel de Trasvase Yacambú-Quibor. Avance actual de los trabajos de excavación mediante la utilización de soportes flexibles aplicados a rocas con grandes deformaciones. Integral approach to applied rock mechanics, M. van Sint Jan, ed. Editec, Santiago, 1, 489–497.

Schubert, W. 1996: Dealing with squeezing conditions in Alpine tunnels. Rock Mech. Rock Engrg. 29(3), 145–153.

WBI/NAMA 2003: Design for tunnel sections of Kallidromo tunnel, which remain to be excavated. Aachen/Athens. Not published.

Wittke, W. 2000: Stability Analyses for Tunnels, Fundamentals. Geotechnical Engineering in Research and Practice, WBI Print 4. Verlag Glückauf GmbH, Essen, Germany.

Copyright © 2005 Taylor & Francis Group plc, London, UK

New high-speed railway lines Stuttgart 21 and Wendlingen–Ulm – approximately 100 km of tunnels

W. Wittke & C. Erichsen
WBI – Prof. Dr.-Ing. W. Wittke Consulting Engineers for Tunneling and Geotechnical Engineering Ltd., Aachen/Stuttgart, Germany

ABSTRACT: For the large scale projects new high-speed railway line (NBS) Wendlingen-Ulm and Stuttgart 21, a total of approx. 100 km long single- and to a small extent also double-track tunnel tubes are foreseen.

In the course of the NBS Wendlingen-Ulm, among other structures, the 8.7 km long Boßlertunnel and the 4.7 km long Steinbühltunnel are planned. The Boßlertunnel is located in Brown Jurassic. Locally, squeezing rock is to be expected. The Steinbühltunnel is located in White Jurassic, which is locally strongly karstified. For both tunnels, it was investigated whether an advancing test section and through-going exploratory adits respectively would lead to a safer design with regard to construction costs and time.

A total of approx. 52 km single- and double-track tunnel tubes is foreseen for the project Stuttgart 21. The paper exemplary illustrates the Fildertunnel. With regard to tunneling, the tunnel sections in swelling unleached Gypsum Keuper are of major importance. The principle of resisting support is planned to be carried out.

1 INTRODUCTION

Approximately 100 km of tunnels are foreseen for the construction of the new high-speed railway lines Wendlingen-Ulm and Stuttgart 21. Tunneling in squeezing rock as well as in karstified rock is decisive with regard to construction time and costs of the tunnels for the new high-speed railway line from Wendlingen to Ulm (Wittke W. 2004b). The design and construction of tunnels in swelling rock is a major challenge in connection with the project Stuttgart 21.

2 NEW HIGH-SPEED RAILWAY LINE WENDLINGEN–ULM

2.1 *Tunnels*

The new high-speed railway line Wendlingen–Ulm is planned to go from Wendlingen, passing Aichelberg and Merklingen, to Ulm (Fig. 1). Four comparatively large tunnels are foreseen. The Albvorlandtunnel near Wendlingen is planned with a length of 7.9 km. The ascent to the Swabian Alb from Aichelberg to Merklingen with a length of approx. 13.5 km is also planned to go below ground. In this section, the line is crossing the Filstal. This valley needs to be spanned by a bridge. Therefore two separated tunnels, the Boßlertunnel with a length of 8.7 km and the Steinbühltunnel with a length of 4.7 km, are required.

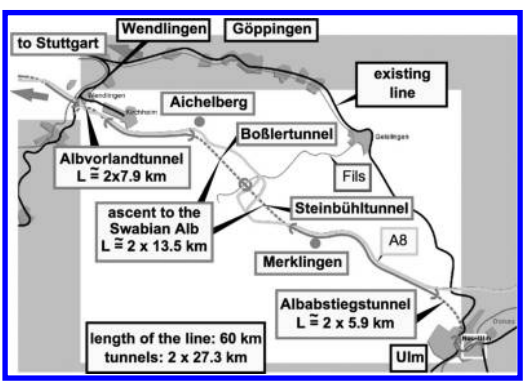


Figure 1. New high-speed railway line from Wendlingen to Ulm.

The fourth tunnel is the 5.9 km long Albabstiegstunnel near the city of Ulm (Fig. 1).

All tunnels are to be constructed as single-track tubes with cross-cuts at distances of ⩽1000 m. The total length of all single-track tunnel tubes results to approx. 55 km.

2.2 *Boßlertunnel – tunneling in squeezing rock*

For the ascent to the Swabian Alb to the west of the Filstal, the Boßlertunnel is planned with a length of 8.7 km (Fig. 2).

Copyright © 2005 Taylor & Francis Group plc, London, UK

Over a length of approx. 6 km, the tunnel tubes are crossing the layers of the Brown Jurassic (Figs. 2 and 3). The Brown Jurassic α, which is also known as Opalinuston, consists of a sequence of mudstones and marlstones. The thickness of the Brown Jurassic β amounts to approx. 75 m. In the lower and upper part two sandstone layers, the Lower and Upper "Donzdorfer Sandstone", are located. The middle part is formed by an alternating sequence of mudstones and sandstones, the so-called "Personatensandsteinzone". Above the Brown Jurassic β, mudstones and marlstones, in which layers of limestone are embedded, are located. The permeability of the mudstones and marlstones is very low. The sandstone and the limestone are aquifers.

Above the Brown Jurassic the layers of the White Jurassic α to γ are located (Fig. 2). The White Jurassic α consists of an approx. 90 m thick sequence of marlstones. In the lower part of it mudstones are embedded and in the upper part limestones. The White Jurassic β and γ, which consists of limestones with deposits of marlstone and are partly karstified, are located above the White Jurassic α.

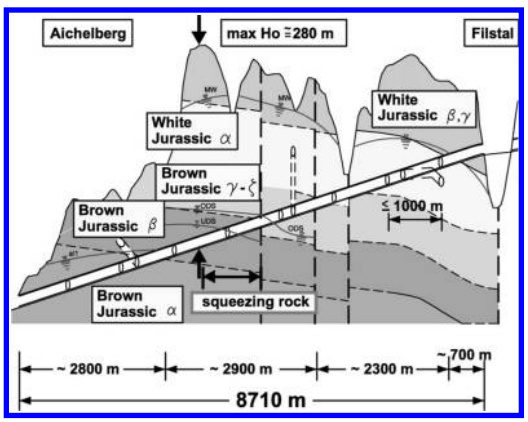


Figure 2. Geological longitudinal section, Boßlertunnel.

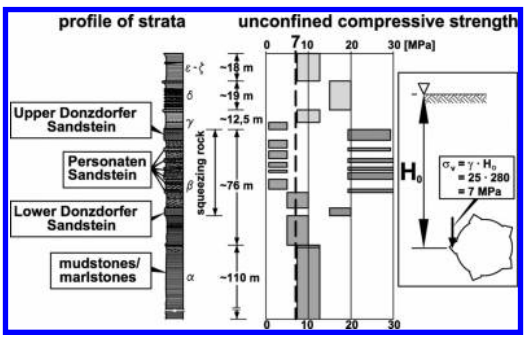


Figure 3. Layers of the Brown Jurassic.

According to the results of explorations carried out up to now, several ground-water reservoirs exist in the Brown and White Jurassic, which are separated by mudstone and marlstone deposits with very low permeability. At the moment, the water pressures at the level of the tunnel tubes are estimated to be ≤9 bar for the White Jurassic.

The unconfined compressive strength of the mudstones of the Brown Jurassic β, δ and ε to δ is comparatively low (Fig. 3). For the Brown Jurassic β, values of 0.5 and 5.0 MPa were evaluated. In the section in which the tunnel is located in the Brown Jurassic, the overburden amounts to 280 m. It cannot be excluded that in these layers the low strength of the mudstones will be exceeded during excavation of the tunnel tubes and squeezing rock conditions occur.

The effect of squeezing rock is illustrated in Figure 4. The Yacambu tunnel in Venezuela could not be completed for a long time, because the shotcrete support could not withstand the high rock pressure.

The excavation of the Boßlertunnel in the Brown Jurassic β with an overburden of some 280 m, therefore, is one of the challenges of the new high-speed railway line Wendlingen–Ulm. Using the shotcrete method, a yielding support could be taken into consideration (Rückel & Wittke 1991, Zimmer & Wittke 1996, Fig. 5). With regard to a possible TBM heading, it is presently planned to excavate an advancing test section in the Brown Jurassic β for additional exploration. If this full scale exploration leads to the conclusion that a TBM heading in the layers of the Brown Jurassic β, which are difficult with respect to tunneling, is associated with a too high risk, the tunnel section in the Brown Jurassic β would have to be excavated using the shotcrete method. In the remaining tunnel section of approx. 10 km, however, TBM headings could be carried out.



Figure 4. Tunnel Yacambu (Venezuela), squeezing rock.

Copyright © 2005 Taylor & Francis Group plc, London, UK

2.3 *Steinbühltunnel – tunneling in karstified rock*

Figure 6 shows a geological longitudinal section of the Steinbühltunnel, which is located to the south of the Filsbachtal. The length of this tunnel amounts to approx. 4.8 km.

The tunnel tubes are located in the layers of the White Jurassic β to δ_4 above the average water level. The alignment and the gradient were chosen correspondingly. The water level of the karst aquifer varies. During rainfalls, it is rising by several 10 m. Thus, also for this tunnel the water pressure is expected to be within 3 to 5 bars and the tunnel tubes need to be sealed along the whole circumference by a watertight lining which is dimensioned against water pressure.

The layers of the White Jurassic are karstified. In the Swabian Alb, many karst phenomena and cavities are known. Examples are the "Mordloch" (Fig. 7) and the "Falkensteiner Höhle", a 5 km long cave in the White Jurassic δ. Furthermore, karstified master joints occur in the layers of the White Jurassic β to δ (Fig. 8).



Figure 5. Shotcrete method in squeezing rock, deformable lining.

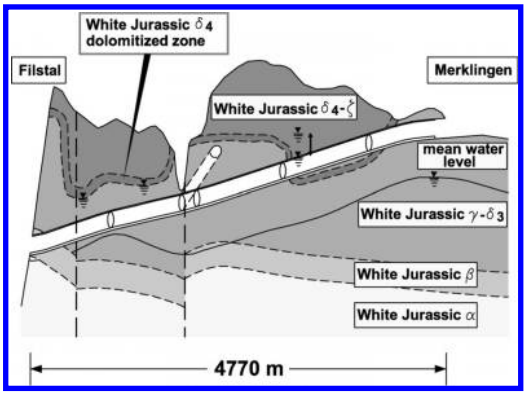


Figure 6. Geological longitudinal section, Steinbühltunnel.

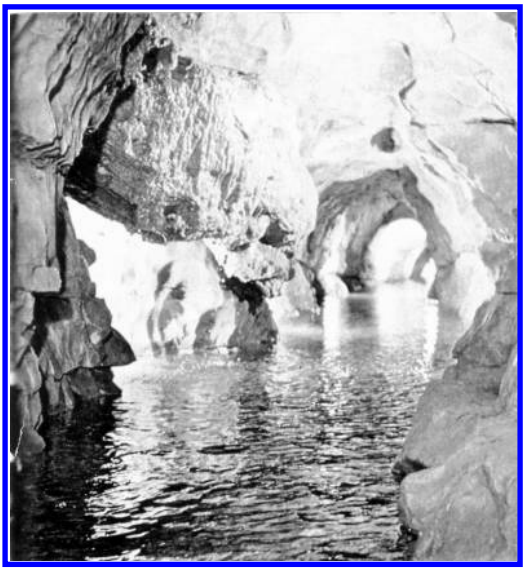


Figure 7. Mordloch, karst channel in the White Jurassic β (Binder 1989).



Figure 8. Karstified master joints in the White Jurassic γ.

Copyright © 2005 Taylor & Francis Group plc, London, UK

In Figure 9, the main types of karstification in the layers of the White Jurassic are illustrated.

Figure 10 shows a vertical section through the cave "Laichinger Tiefenhöhle", in which the contour of one tunnel tube of the new high-speed railway line is plotted.

Since it cannot be excluded that karst phenomena of importance for tunneling are encountered during the excavation of the Steinbühltunnel, corresponding support measures are foreseen in the tunnel design. Figure 11 exemplary shows the support of a tunnel tube in case of a karst cavity located above the tunnel's roof. For stability reasons a concrete body is to be constructed between the tunnel and the karst cavity. Thus, the karst cavity as the main flow path will be maintained so that groundwater conditions remain unchanged during tunneling. Figure 12 exemplary shows the support in case of a karst cavity located underneath the invert of the tunnel.

Also for the Steinbühltunnel it was investigated whether the excavation of advancing exploratory adits in karstified rock is of use. This investigation led to the recommendation to drive two advancing exploratory adits located within the cross-sections of the tunnel tubes over the full length of the Steinbühltunnel

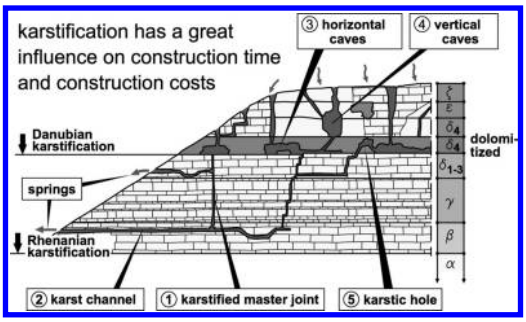


Figure 9. Main types of karstification in the White Jurassic.

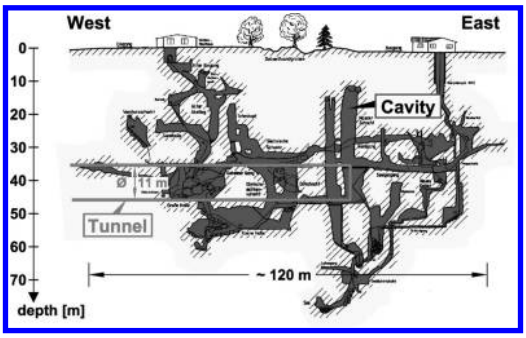


Figure 10. Possible cavities in the cross – section of the tunnel.

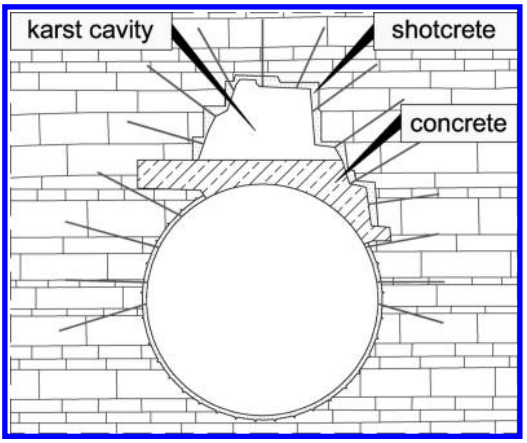


Figure 11. Support of tunnel in karstified White Jurassic, karst cavity above the roof.

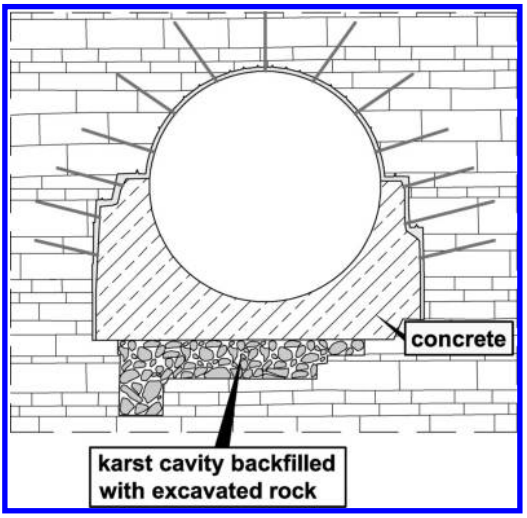


Figure 12. Support of tunnel in karstified White Jurassic, karst cavity underneath the invert.

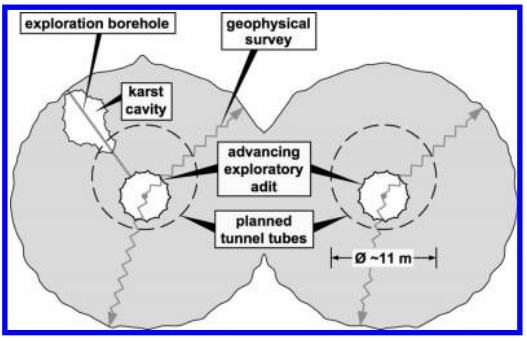


Figure 13. Exploratory adit in karstified rock, Steinbühltunnel.

Copyright © 2005 Taylor & Francis Group plc, London, UK

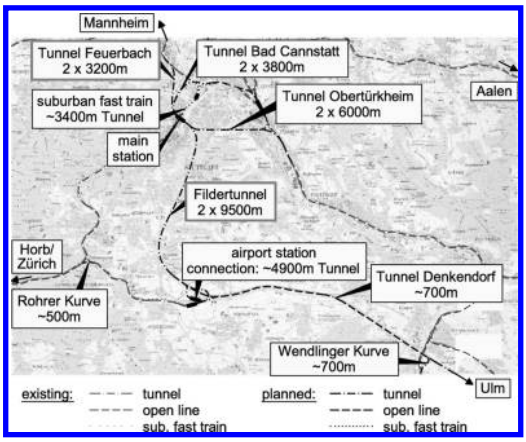


Figure 14. Stuttgart 21, overview.

(Fig. 13). From these adits, karst cavities adjacent to both tunnel tubes can be explored by seismic methods and supplementary drillings and also stabilized if required. If these measures are carried out prior to the excavation of the tunnel tunnel tubes, the risk for TBM-tunneling is considerably reduced.

3 STUTTGART 21

3.1 *Tunnels*

In the city of Stuttgart, five tunnels are planned (Fig. 14). The tunnel Feuerbach with a length of approx. 3.2 km is connecting the high-speed railway line Mannheim-Stuttgart with the new main station. The Fildertunnel with a length of approx. 9.5 km shall provide the main connection from the new main station to the Stuttgart airport and further to the new high-speed railway line Wendlingen–Ulm. As further essential tunnel structures, the tunnel Bad Cannstatt with a length of approx. 3.8 km and the tunnels to Ober- and Untertürkheim are to be constructed. The tunnel Obertürkheim undercrosses the Neckar river in a comparatively low depth. The total length of this tunnel is approx. 6 km.

To remove traffic from the ground surface and to improve the suburban fast train connections, additional tunnels with a length of approx. 3.4 km are planned. For the connection to the airport, further tunnels with a length of approx. 4.9 km are foreseen. In addition several comparatively short tunnels like the Rohrer Kurve, the Wendlinger Kurve and the tunnel Denkendorf are planned.

The total length of all single-track and double-track tunnel tubes for the project Stuttgart 21 is approx. 52 km. In the following, the Fildertunnel with its special features with respect to tunneling will exemplary be presented.

3.2 *Fildertunnel – tunneling in swelling rock*

The Fildertunnel, which leads from the new Stuttgart main station to the Filder Plain, has a length of approx. 9.5 km (Fig. 15).

The tunnel crosses all layers forming the valley of Stuttgart, which are located above the "Lettenkeuper". At the beginning of the tunnel, the cross-section is located in the leached Gypsum Keuper over a length of 200 to 300 m. In the following, it passes sulfate rock containing gypsum and anhydrite over a length of approx. 4.3 km. Here, the leaching front is located 30 to 45 m above the roof of the tunnel. Underneath the anhydrite level, which is located 20 to 30 m above the tunnel's roof, the sulfate rock consists mainly of anhydrite. The tunnel is located in the "Schilfsandstein", the "Kieselsandstein" as well as the "Unteren Bunten Mergel" and "Oberen Bunten Mergel" over a length of approx. 750 m. The sandstones and siltstones of the "Stubensandstein" are crossed by the tunnel over a length of some 2.5 km. The remaining tunnel sections are located in the "Knollenmergel" and the silty mudstones and sandy limestones of the Black Jurassic (Lias α).

The unleached Gypsum Keuper is a major challenge for design and construction of the Fildertunnel. It consists of a horizontal alternating sequence of sulfate-containing clay- and siltstones and pure sulfate rock. The sulfate is found in two different modifications, as gypsum and as anhydrite. Both modifications can be found at the same time, if the rock is dry. If water gains access to the rock, however, anhydrite transforms into gypsum. This chemical process results in an increase of the solid volume by approx. 60%. This volume increase is denoted as swelling.

The swelling behavior of the unleached Gypsum Keuper is also influenced by the water uptake of clay minerals.

The volume increase due to swelling causes major swelling deformations. If these are confined, great swelling pressures occur, which have led to severe damages of tunnel linings in many cases in the past.

The maximum overburden of the Fildertunnel amounts to 225 m. The design concept for the Fildertunnel is based on the principle of resisting support (Fig. 16). Thus, the lining is designed to resist the developing swelling pressure.

In a greater distance to the leaching front the unleached Gypsum Keuper has a very low permeability according to experience. Because of the comparatively great distance of the tunnel gradient to the leaching front, it is to be expected that the rock mass remains dry and thus no swelling occurs, if no water gains access to the rock during the stages of construction. This was an important criterion for determination of the gradient. Another criterion was to have the tunnel passing the leaching front in an area in which the

Copyright © 2005 Taylor & Francis Group plc, London, UK

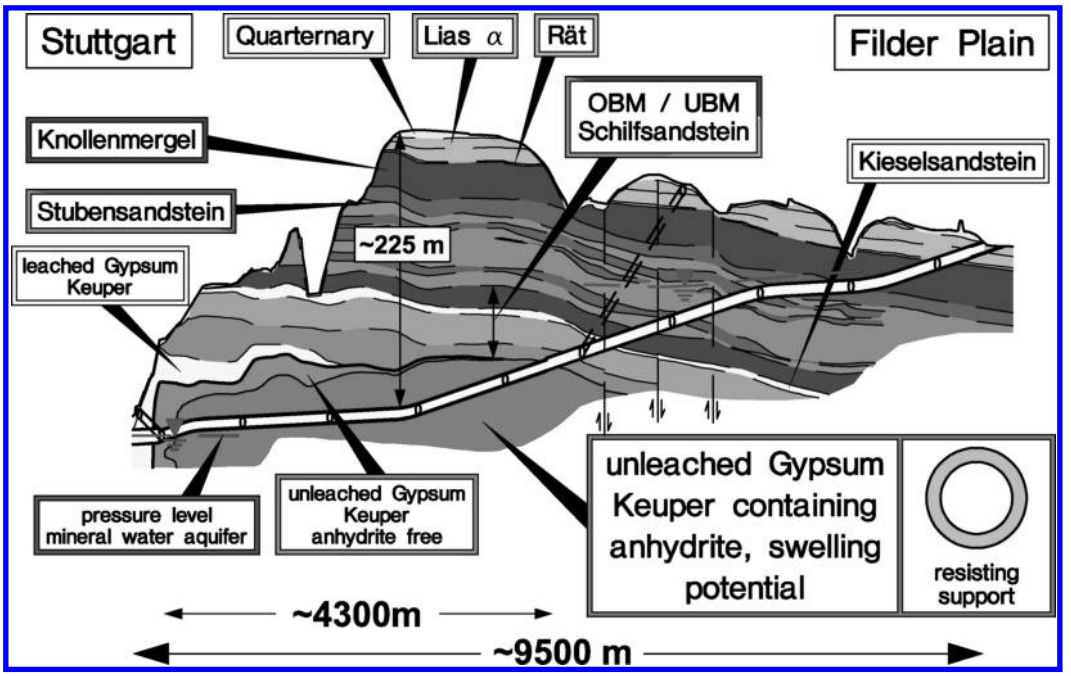


Figure 15. Geological longitudinal section, Fildertunnel.

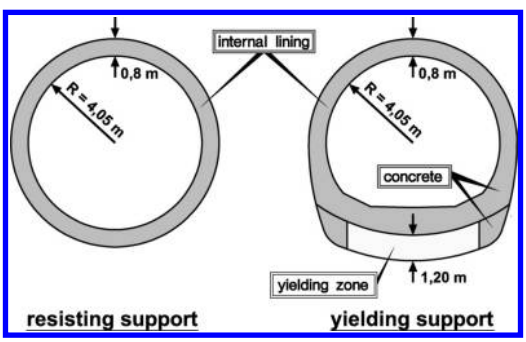


Figure 16. Design principles for tunnels in swelling rock.

overlaying rocks are almost dry. Furthermore, due to the chosen deep location of the gradient, a tunnel lining subjected to swelling pressure underneath the invert can be supported by a sufficiently thick rock layer consisting of hard rock. Thus, significant heavings of the tunnel tubes due to swelling are not to be expected.

The principles of resisting support and yielding support respectively are presently used for the design of tunnels in anhydritic, swelling rock (Fig. 16). In both cases, it is assumed that water to initiate the maximum swelling load and full swelling respectively is available in sufficient quantities. Consequently, the designed measures have to be carried out over the full length of the tunnel in swelling rock.

Based on observations, the hypothesis was made that, in the area of the transition from water bearing to anhydritic rock, self-sealing due to swelling occurs around the tunnel, if the resisting principle is applied. As a consequence of this self-sealing effect, seepage through the rock along the tunnel, and thus also swelling, is interrupted at a certain distance from the water bearing formation (Wittke M. 2003, 2004).

In a research project carried out by WBI, a rock mechanical and hydraulical model and a corresponding 3D-FEM-code have been developed, which describe the corresponding phenomena. It is expected that the results of this work will lead to remarkable cost savings along with the design of tunnels in swelling rock.

REFERENCES

Baur, R. 2002. *Tunnelbau im Projekt Stuttgart 21. Geotechnik* 25 (3): 153–156.

Baur, R. & Erichsen, C. 2000. *Challenges in tunneling according to 40 km tunnels for the DB Projekt Stuttgart 21. Proc. of the EUROCK 2000 symp., Aachen 2000*. Essen: Verlag Glückauf.

Beiche, H. 1991. *Bemessung und Bau eines Tunnels in anhydrithaltigem Gebirge. Proc. 9. Nat. Felsmechanik Symposium, Aachen 1990*. Essen: Verlag Glückauf.

Bernhardt, K. & Rock, D. 1995. *Der Engelbergbasistunnel: Bau und Finanzierungskonzept eines Autobahntunnels mit*

Copyright © 2005 Taylor & Francis Group plc, London, UK

außergewöhnlichen Querschnittsabmessungen in schwierigen Gebirgsverhältnissen. Forschung + Praxis 36, Proc. World Tunnel Congress, Köln 1995.

Binder, H. 1989. *Höhlenführer Schwäbische Alb.* Konrad Theis Verlag.

Grob, H. 1972. *Schwelldruck am Beispiel des Belchentunnels. Proc. Int. Symposium für Untertagbau.* Luzern: 99–119.

Grüter, R. & Liening, B. 1976. *S-Bahn Stuttgart, Planung und Bau der Haltestelle Schwabstraße (Baulos 11) und der unterirdischen Wendeanlage (Baulos 12), Teil I. Proc. Baugrundtagung, Nürnberg 1976.*

Jäckle, P. 2002. *Die Tunnel der Neubaustrecke Wendlingen – Ulm. Geotechnik* 25 (3): 157–161.

Kiehl, J. R. 1990. *Ein dreidimensionales Quellgesetz und seine Anwendung auf den Felshohlraumbau. Proc. 9. Nat. Felsmechanik Symposium, Aachen 1990*. Essen: Verlag Glückauf.

Kirschke, D., Kuhnhenn, K. & Prommersberger, G. 1991. *Der Freudensteintunnel: Eine Herausforderung für den planenden Ingenieur.* Ibw 7: 5–39.

Klonsdorf, G. & Schaser, F. 1991. *Baudurchführung des Freudensteintunnels, Bergmännische und offene Bauweise.* Ibw 7: 118–172.

Marquart, P. 2004. *Die Geologie weist ihren Weg – Tunnelbau in den Gebirgsformationen rund um Stuttgart und auf der Schwäbischen Alb. Geotechnik* 27 (2): 99–103.

Paul, A. & Wichter, L. 1992. *Das Langzeitverhalten von Tunnelbauwerken im quellenden Gebirge – Neuere Meßergebnisse vom Stuttgarter Wagenburgtunnel. Proc. 10. Nat. Felsmechanik Symposium, Aachen 1992.* Essen: Verlag Glückauf.

Rückel, M. & Wittke, W. 1991. *Abschluß von Einlagerungskammern in druckhaftem Gebirge, Konzept und in situ Nachweis. Proc. 9. Nat. Felsmechanik Symposium, Aachen 1990.* Essen: Verlag Glückauf.

Wittke, M. 2003. *Begrenzung der Quelldrücke durch Selbstabdichtung beim Tunnelbau im anhydritführenden Gebirge. Geotechnik in Forschung und Praxis, WBI-PRINT 13.* Essen: Verlag Glückauf.

Wittke, M. 2004. *Bemessung von Tunnels im quellfähigen Gebirge unter Berücksichtigung der Selbstabdichtung. Geotechnik* 27 (2): 136–141.

Wittke, W. 2004a. *Planung, Bau und Überwachung von Tunneln in quellfähigem Gipskeuper. Geotechnik* 27 (2): 104–111.

Wittke, W. 2004b. *Ursachen und Vermeidung von Termin- und Kostenüberschreitungen bei Tunnelbauten der Infrastruktur,* unpubl.

Wittke, W. & Rißler, P. 1976. *S-Bahn Stuttgart, Planung und Bau der Haltestelle Schwabstraße (Baulos 11) und der unterirdischen Wendeanlage (Baulos 12), Teil II. Proc. Baugrundtagung, Nürnberg 1976.*

Wittke, W., Wittke, M. & Wahlen, R. 2004. *Zum Quellgesetz für anhydritführenden, unausgelaugten Gipskeuper. Geotechnik* 27 (2): 136–141.

Wittke-Gattermann, P. 1998. *Verfahren zur Berechnung von Tunnels in quellfähigem Gebirge und Kalibrierung an einem Versuchsbauwerk. Geotechnik in Forschung und Praxis, WBI-PRINT 1*. Essen: Verlag Glückauf.

Zimmer, M. & Wittke, W. 1996. *Entwurf und Ausführung eines verformbaren Ausbaus in stark durckhaftem Gebirge. Proc. 11. Nat. Felsmechanik Symposium, Aachen 1994*. Essen: Verlag Glückauf.

Copyright © 2005 Taylor & Francis Group plc, London, UK

Status of Japanese Underground Research Laboratory – Design and construction of 1000 m-deep shafts and research tunnels

T. Sato, M. Imazu, S. Mikake, T. Tamai, M. Yamamoto & M. Sakamaki
Japan Nuclear Cycle Development Institute (JNC), Tono Goescience Center (TGC), Mizunami Underground Research Laboratory, Mizunami, Gifu, Japan

ABSTRACT: Two one-thousand meter deep shafts and research galleries at several levels will be excavated in the Mizunami Underground Research Laboratory (MIU) Project. Design and layout of the shafts and galleries were determined considering design and construction constraints, schedule, and the investigation plan for characterization of the geological environment and engineering technologies. This paper describes the limiting conditions, layout and design of the shafts and galleries of the MIU, and the results of mechanical stability, ventilation and earthquake-resistance and seismic stability analysis. Details of the design of shafts and galleries and safety of the design and construction of the MIU were confirmed based on the results of these analyses. The excavation plan and current status of facility construction are also described in this paper.

1 INTRODUCTION

One of the features of the geological disposal policy in Japan is the establishment of Underground Research Laboratories (URLs). The URLs must be distinct from an actual disposal facility, as outlined in the Atomic Energy Commission (AEC) report (AEC, 2000). Research on the deep geological environment will provide the basis for R&D on geological disposal of high-level radioactive waste. The AEC stipulated that research at the underground laboratories should also contribute to Japan's scientific research on the geological environment.

JNC's URL projects are directed towards improving the reliability of geological disposal technologies and developing advanced safety assessment methodologies. It will ensure that the implementation of geological disposal is based on a thorough scientific and technological basis. The URLs in these projects are classified into purpose-built generic URLs as described in the OECD/NEA report (OECD/NEA, 2001), and are distinct from on-site (site-specific) URLs to be constructed at potential waste disposal sites. In order to cover the general geological environment in Japan, two URLs, one for crystalline rock and another for sedimentary rock have been planned, one is the Mizunami Underground Research Laboratory (MIU), the other is the Horonobe Underground Research Laboratory (Hnb-URL) (JNC, 2002; 2001). One of purpose of this plan is to confirm the technical reliability of the geological disposal methods, as indicated by the Second Progress Report (JNC, 2000).

The site of the URL project for crystalline rock is located in Mizunami, Gifu. The regional geology consists of Tertiary and Quaternary sedimentary rocks overlying Cretaceous granitic basement. Conceptual design for the MIU at present is as follows.

- Two 1000 m shafts, the Main Shaft (6.5 m ϕ) and the Ventilation shaft (4.5 m ϕ);
- Two experimental levels, the Main Stage at 1000 m and the Middle Stage, at 500 m depths.

The site of the URL project for sedimentary rock is located at Horonobe, Hokkaido, north of the main island of Japan. The geology consists of Tertiary sedimentary rocks. Conceptual design for the Hnb-URL at present is as follows.

- Two 500-m shafts and one Ventilation shaft;
- One experimental level, the Main Stage at around 400 m depth.

As of July 2003, shaft portals were being constructed at Mizunami, and land development work had started at Horonobe.

This paper describes design constraints, layout and design of the shafts and galleries of the MIU, and results of the mechanical stability studies, ventilation and earthquake resistance and seismic stability analysis. Details of the design of shafts and galleries were determined, and safety of the design and construction

Copyright © 2005 Taylor & Francis Group plc, London, UK

plans of the MIU were assessed and confirmed based on the results of these analyses. The excavation plan and current status of facility construction are also described in this paper.

2 BASIC DESIGN CONDITIONS

2.1 *Location*

The URL project for crystalline rock is located in Mizunami, Gifu, in the central part of Honshu, the main island of Japan (Figure 1). The MIU facility and related surface plant will be constructed on land in Akeyo-cho leased from Mizunami City. The site is about 7.8 hectares and located in the Intergarden of Tono Frontier Science Research City. This area has many public facilities, which draw many people to the area. This situation may affect or constrain traffic flow to the site during execution of the programme, depending on circumstances.

2.2 *Geology and mechanical properties*

The shafts and galleries of the MIU project will be excavated in the late Cretaceous Toki Granite. The Toki Granite has been faulted, and subjected to several episodes of uplift and subsidence in the Miocene to Pliocene, indicated by the lacustrine and marine sedimentary formations unconformably overlying the granite. The thickness of the sedimentary formations in this area is about 170 m.

The average P-wave velocity, unconfined compressive strength and Young's modulus of intact granite are 5.5 km/sec, 150 MPa and 50 GPa, respectively.

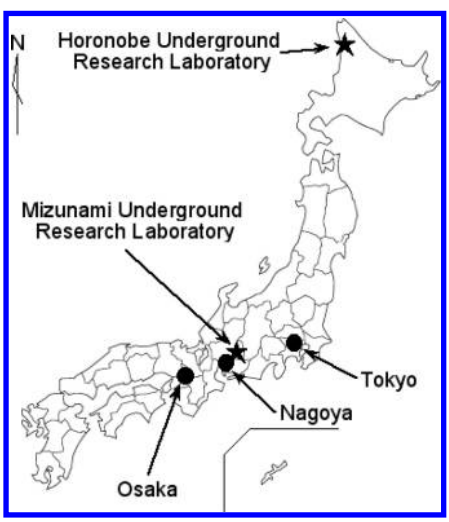


Figure 1. Location of Underground Research Laboratories.

2.3 *Function of shafts and design constraints*

The size and shape of shafts and galleries were determined based on considerations of efficiency and economics of excavation, the machinery and materials to be transported in the shafts and in the galleries and needed at the investigation sites. Figure 2 shows the layout of MIU facility. The function of shafts and design constraints are as follows.

2.3.1 *Access method*

Access methods can be basically grouped into vertical shaft and inclined-tunnel type (inclined ramp). The vertical shaft type was selected as the access method for the MIU, because of the shape and size of the site, schedule, and excavation economics.

2.3.2 *Number of shafts*

In general, an ideal number of shafts is three or more, one for ventilation and others for movement of personnel and materials, air supply, and egress in the event of fire or accidents. With three or more shafts, personnel in the shafts and galleries could get to surface through the one of the air supply shafts. Because of the limited construction area at the MIU, there is no option to excavate a third shaft. So, the basic concept for the MIU is that personnel can take refuge in the shafts and in the refuge stations excavated in each gallery, and return to surface after the fire is extinguished. Therefore, the number of shafts in the MIU layout is two, the Main shaft and the Ventilation shaft.

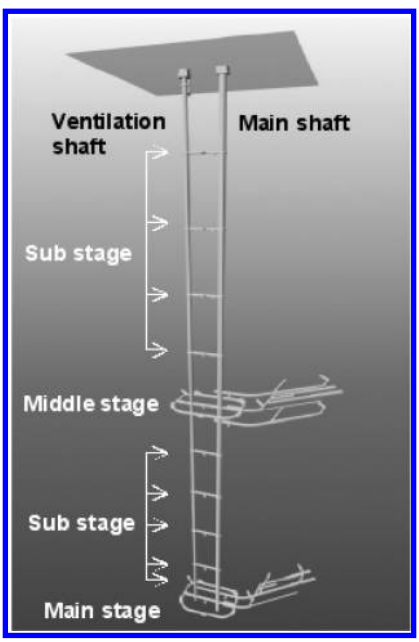


Figure 2. Conceptual design of Mizunami URL.

Copyright © 2005 Taylor & Francis Group plc, London, UK

2.3.3 *Shape and size of shafts*

The cross-section geometry of the shafts is circular selected after consideration of mechanical stability, workability, safety and economics of construction and maintenance.

The inner diameter of the Main and Ventilation shafts were determined to be 6.5 m and 4.5 m, respectively, for the following reasons.

- Schedule: One of the MIU project milestones established is to reach 1000 m depth by FY 2009.
- Space requirements: Ease of transport of materials and equipment needed for excavation of galleries and investigations, installation space for equipment, and plumbing.
- Workability (minimum space for excavations): Applicable short-step shaft excavation method.

Actual shaft excavation sizes in Japan are shown in Figure 3 and include the Main and Ventilation shafts of the MIU for comparison.

2.3.4 *Depth of shafts*

One of the purpose of the MIU project is to confirm the technical reliability of the basis for geological disposal methods, indicated by the Second Progress Report (JNC, 2000) discussed above. In this report, the maximum depth of a disposal facility is to be 1000 m in the case of hard rock. Therefore the target depth of geoscience research at the MIU is also 1000 m for this reason. So, the MIU shafts will extend to 1000 m depth and research galleries will be constructed as deep as 1000 m as specified in the Master Plan of the MIU project (JNC, 2002).

2.3.5 *Function of shafts and galleries*

The functions of shafts and galleries at the MIU are as follows.

- Main shaft: Transport route for construction and research materials necessary for excavation of galleries and for investigations, and for transport of muck (waste rock) to the surface.
- Ventilation shaft: Ventilation (including space for fans) and space for hoist installed after excavation to 1000 m.

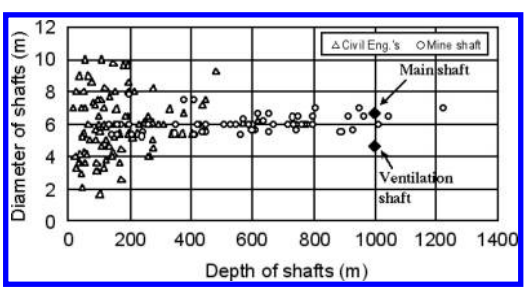


Figure 3. Actual shaft excavation sizes in Japan.

- Sub stages: Galleries that will connect the Main and Ventilation shafts and provide space for pumps, water supply, air conditioner, electrical equipment, and, space for investigations intended for understanding depth-dependency and excavation disturbance.
- Main and Middle stages: Space for Phase III (Operation Phase) investigations including Research galleries, TBM tunnel, Loop Galleries, refuge shelters and drilling stations.
- Measurement galleries: Galleries for investigations intended to understand excavation disturbance due to extension of the Main and Middle stages.

2.4 *Schedule*

The results of the geoscience research carried out in the MIU project will be applied as the technological basis for safety regulations of the government and for the HLW disposal program to be carried out by the Nuclear Waste Management Organization of Japan (NUMO). In consideration of NUMO's program, one of the milestones for the MIU project is to reach 1000 m around FY 2009.

3 DESIGN OF THE MIU FACILITY

3.1 *Surface facilities*

Figure 4 shows the plan for surface facilities constructed for shaft excavation. Soundproof panels and materials will be used to enclose equipment at surface, especially the headframes and thus to control excessive noise from the construction and operational activities.

3.1.1 *Equipment at surface around the shafts entrance*

Equipments at the entrance to the shaft are as follows:

- Headframe (Figure 5)
- Equipment for muck shoot

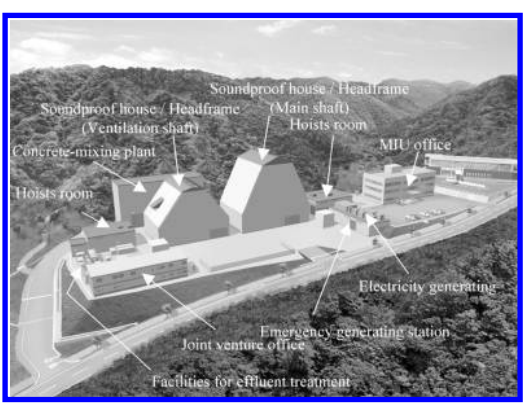


Figure 4. Conceptual layout of surface facilities.

Copyright © 2005 Taylor & Francis Group plc, London, UK

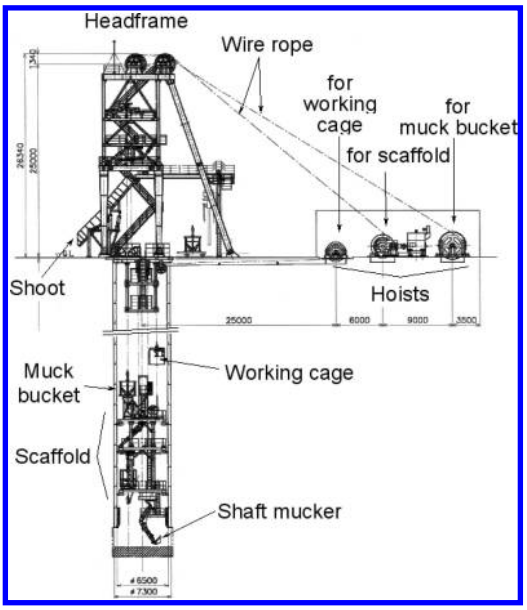


Figure 5. Headframe and hoists for shaft excavation.

- Hoisting equipment (Several hoists, the scaffold, muck buckets and working cage) (Figure 5)
- Storage space for muck
- Drill jumbo transport equipment
- Standby space for muck and concrete buckets
- Motorized muck cars and rails
- Dust collectors.

3.1.2 *Shaft-sinking equipment*

Triple-deck scaffold will be used in shaft-sinking. There are platforms for the working cage and concrete hopper in the upper deck, concrete shoot and electric control board on the middle deck. The lower deck is used for changing muck buckets. The shaft mucker is installed below the lower deck.

3.1.3 *Auxiliary equipment*

These includes the concrete-mixing plant, water supply, drainage, ventilation and air supply systems, air conditioner and electrical equipment needed for shaft excavation and operation.

3.2 *Shaft design*

3.2.1 *Support system*

Initially, support system designs were based on the rock classification determined from core observation and determination of the physical and mechanical properties of core samples obtained from boreholes near the construction site. This method is the same as the one used for design of highway and railway tunnels in Japan (JH, 1998; JR, 1996). Calculations using theoretical analysis were performed to check support stress intensity and normal strain of the rock. But this analysis is based on many assumptions. Significant factors such as gallery cross-section geometry, excavation procedure, the effect of supports, etc. must be considered in the theoretical analysis.

Therefore, 2-D FEM analysis was performed to understand mechanical stability of the rock and support. Support stress intensity, local safety factors and maximum shear strain of rock are judgment indicators used in this analysis. Support was determined based on this numerical analysis (Sato, et al., 2003).

Based on the results of the numerical analysis, normal strain of the rock around the shafts and galleries and support stress intensity were determined. For the deep part of sedimentary rock, the shafts and galleries are predicted to be stable using a high strength (40 MPa) concrete liner and H-section steel. Table 1 shows the standard support patterns of the shaft.

Table 1. Support patterns of Main part of shaft.

Rock classification	B	CH	CM	CL	D	E
Rock bolts						
Length (m)	–	–	–	–	–	–
Circular line (m)	–	–	–	–	–	–
Spacing (m)	–	–	–	–	–	–
H-section tunnel support						
H-125	–	–	–	Need	Need	Need
Concrete liner (m)	0.4	0.4	0.4	0.4	0.4	0.4
Liner plate	–	–	–	–	–	Need

3.2.2 *Main part of shaft*

Standard cross section of the main parts of the Main and is shown in Figure 6. The inner diameter of the Main shaft and the Ventilation shaft are 6.5 m and 4.5 m, respectively. The thickness of concrete liner is 40 cm for each shaft. In the case of CL and D classification rock, H-section steel supports (125H) will be installed in the concrete liner. Steel liner plate will also be added in the case of E type rock.

3.3 *Earthquake-resistant design of shaft*

To ensure safety and efficiency during construction of the MIU facility, it is essential that the shafts and galleries are not only stable during excavation but also remain stable and resistant to damage with respect to earthquakes. Numerical analyses using static techniques were performed to understand stress on the

Copyright © 2005 Taylor & Francis Group plc, London, UK

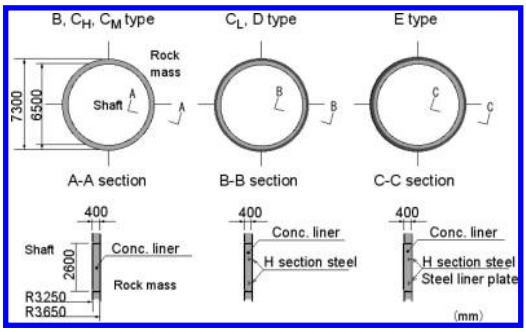


Figure 6. Standard cross section of Main shaft.

concrete liner and the surrounding rock mass under static loads, and for comparison to intensity of a dynamic load, assuming a significant earthquake generated by movement on the nearest active fault, having a maximum ground acceleration equal to 478.6 gal. Calculations of the principal stresses, the major shear strains and the local safety factors in the excavated shafts and arising from an earthquake after shaft excavation showed that the changes in these parameters are very small. The stresses induced in the design supports induced by an earthquake are lower than the allowable value.

3.4 *Ventilation analysis*

The MIU consists of a complex underground layout and deep, long excavations. Hence, they require rather sophisticated ventilation programs because of huge pressure losses and air volumes. In order to design the ventilation system applied to construction, and to understand the direction and velocity of airflow, a ventilation network analysis has been performed (Sato, et al., 2003).

To derive the results of the airflow rate analysis, one part of the ventilation analysis, required calculation of air volume versus air velocity limitations, the gas inflow and dust generated by shotcreting. The capacity and optimum location of the ventilation equipment were determined based on these results. The ventilation system, which during construction will consist of auxiliary fans with an air ducting system, will be changed to a tunnel ventilation system when the shafts reach 500 m depth.

4 CONSTRUCTION PLAN

4.1 *Construction of the upper and lower part of the shaft entrances*

The foundations of the headframes were fixed to base rock, the upper part of the Mizunami group. The depths of the base rock corresponding to the upper part of the entrance to the Main shaft and Ventilation shaft are at GL-9.0 m and GL-10.5 m, respectively. H-section steel was installed for guide-walls, and excavation of the top of the shaft was done using a drag shovel. Photo 1 shows the overall view of the top, the entrance to the Main shaft.

The shafts will be excavated to approximately 50 m depth and shaft-sinking equipment set-up, including the mobile scaffold for excavating deeper than 50 m depth. The short-step method, which is performed over a single step (1.0 m length), with drilling, blasting, mucking, and installation of shaft lining carried out for every cycle, was selected. Photo 2 shows the construction of the lower part of the entrance to the Ventilation shaft.

4.2 *Activities in the main part of shaft*

Although there are several shaft excavation methods, basically they are grouped into blasting methods (long-step method, short-step method, NATM (New Austrian Tunneling Method), etc.), and mechanical excavation methods (Raise boring, free cross section excavation machines, etc.). The short-step method, which is performed over a single step, with length ranging approximately from 1.0 to 2.5 m, and drilling, blasting, mucking, and shaft-lining carried out every cycle, was selected, for the reasons of rapid excavation and actual, proven applications in many excavations with poor rock conditions in Japan.

The ratio of mucking time to excavation cycle time will increase with depth. So we adopted a 2 muck bucket system, and 2 consecutive drill, blast and mucking steps (1.3 m + 1.3 m) and 1 shaft-lining step (2.6 m) per cycle to optimize cycle time for shaft excavations. In the case of poor rock conditions, the excavation method will change from 2 drill and blasting steps and 1 shaft-lining step per cycle to the normal short-step method (a single 1.3 m drill and blast cycle and a 1.3 m shaft-lining step) for safety against rock fall.

There are three hours allotted for geoscience investigations such as geological mapping, t photography of shaft walls, etc., in the excavation cycle time. Figure 7 shows the excavation cycle time of the Main shaft at 500 m depth.

4.3 *Concrete liner and shotcrete*

SEC (Sand Enveloped with Cement) system, patent pending by Livecon Engineering Co. Ltd., has been selected for supplying the concrete liner and shotcrete. A concrete-mixing plant has been constructed at the MIU site for support of the shaft and gallery excavations. Two-stage mixing of concrete is proposed for improving the quality of concrete in this system. Strength, bleeding, permeability and durability are improved with this method. On the other hand,

Copyright © 2005 Taylor & Francis Group plc, London, UK

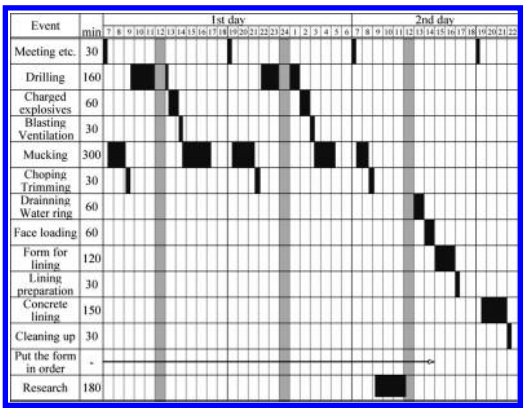


Figure 7. Cycle time of shaft excavation (ex. Main shaft; CH).

Table 2. Details of concrete liner and shotcrete.

Location	Strength in advance N/mm^2	Slump of cement mm	Max. dimension of coarse aggregate mm
Entrance to shaft			
Upper part	24	120	25
Lower part	24	120	25
Concrete liner			
Connection part	40	120	25
Main part of shaft	24	120	25
Shotcrete			
Connection part	36	180	15
Main part of shaft	18	80	15

ready-mixed concrete is sufficient for use in the upper and lower parts of the shaft entrances. Table 2 shows the details of concrete liner and shotcrete used in the construction of MIU.

4.4 *Measurement items*

Convergence measurements and geological mapping of the excavation face, the A-measurements are considered to be requirements for daily safety management. These will be performed during excavation of all galleries and intersections of shaft and galleries.

The following measurement items, the B-measurements, will be applied to typical geologic formations about every 50 m in the shafts. B-measurements will also be performed in two sections in each gallery.

- Convergence measurements, rock mass displacement measurement
- Measurement of rock bolt axial stress
- Stress measurement of supports

The following measurements will be performed in each excavation cycle in the shafts and galleries and in the connections between the shafts and galleries.

- Photography of shaft walls by digital camera
- Geological mapping (geological features, rock mass classification, RMR, weathering, alteration, structure (type, geometry, strike and dip, filling materials in fractures and faults), seepage, etc.)
- Infrared thermograph of shaft walls using a digital camera
- Measurement of groundwater inflow rate and geochemical analysis of sampled water
- Groundwater sampling and measurement of physicochemical parameters (Temp, pH, Eh, EC, DO), of seepage from shaft walls using water collection rings.

Measures to limit inflow of groundwater and mitigate rock bursts will be applied in the excavation of shafts and galleries, especially in the deeper parts of the MIU. Analytical approach and in-situ measurements have been performed to provide information of these phenomena.

5 SUMMARY

This paper describes the outline of the design constraints, the layout and design of the shafts and galleries of the MIU, and the results of mechanical stability, ventilation and seismic stability analysis to assess resistance to earthquakes. Details of the design of shafts and galleries were determined, and safety of the design and execution method for construction was confirmed based on the results of these analyses. The excavation plan and current status of the facility construction are also described.

By July 2003, entrances to the shafts were constructed, and excavation of lower part of shaft entrance was started in March 2004. Current status (September 2004) of construction is excavation of the shafts to a depth of 40 m has been done and construction of the concrete mixing plant was completed. Additional information will be obtained from future surface-based investigations. In the site, the MIZ-1 borehole is being drilled to a depth of 1300 m along borehole axis from surface. Based on any new information, design and construction of MIU will be optimized.

REFERENCES

Atomic Energy Commission, Japan (2000): Long-Term Program for Research, Development and Utilization of Nuclear Energy (Unofficial Translation).

Nuclear Energy Agency/Organization for Economic Co-operation and Development (2001): The Role of

Copyright © 2005 Taylor & Francis Group plc, London, UK

Underground Laboratories in Nuclear Waste Disposal Programmes.
JNC (2002): Master Plan of the Mizunami Underground Research Laboratory Project, *JNC Technical Report*, JNC TN7410 2003-001.
JNC (2001): Horonobe Underground Research Laboratory Project, Plan of surface-based Investigation, *JNC Technical Report*, JNC TN1410 2001-001.
JNC (2000): Second Progress Report on Research and Development for the Geological Disposal of HLW in Japan, H12 : Project to Establish the Scientific and Technical Basis for HLW Disposal in Japan, *JNC Technical Report*, JNC TN1410 2000-001～-004.
Japan Highway Public Corporation (1998): Third-Volume Tunnel Construction Major Designing Points, 1998.10, in Japanese.
Japan Railway Construction Public Corporation (1996): Design and Construction Guideline for NATM, *Japan Railway Construction Public Corporation*, 1996.3, in Japanese.
T. Sato, S. Mikake, M. Sakamaki, K. Aoki, S. Yamasaki, N. Shigeta and S. Takeda (2003): Underground Research Laboratories in JAPAN – What are the Important Factors for Facilities Design, *Proceedings of ICEM'03 : The 9th International Conference on Environmental Remediation and Radioactive Waste Management, September 21–25, 2003*, Examination Schools, Oxford, England, ICEM03-4736.

Copyright © 2005 Taylor & Francis Group plc, London, UK

Tunnel portal problems in landslide areas – Black Sea Highway Project, Turkey

M. Vardar
Istanbul Technical University -Faculty of Mines, Turkey

B. Koçak & H. Karaoğlan
Emay Int. Eng. Cons. & Trade Co. Ltd., Turkey

ABSTRACT: Since the last few years the amount of Express Road – Highway works in Turkey are increasing. In this article two different important tunnel projects in Turkey are represented, which are Sarayköy and Cayeli tunnels located between Trabzon and Hopa. The tunnels are constructed under a thin rock cover between the tunnel roof or sidewalls and ground surface and have slope-portal stability problems due to huge landslides. In this paper, information of the projects is given and stability problems with their field applied solutions are discussed.

1 INTRODUCTION

Since the last few years the amount of Express Road-Highway works in Turkey are increasing. In this article two different important tunnel projects in Turkey are represented, which are Sarayköy and Cayeli tunnels located between Trabzon and Hopa (Figure 1).

Eastern Black Sea Coastal Express Road is constructed for Republic of Turkey, General Directorate of Highways, 10th District Directorate by LİMAK and CMM. The final application projects are designed by EMAY under consulting of ITU and UBM. This route is one of the important projects, because it connects northeast neighbors (Georgia, Armenia and Azerbaijan) to Turkey and Europe. This road is constructed from Samsun to Hopa separated into two groups. Group I is from Samsun to Trabzon and Group II from Trabzon to Hopa. Here part Group II is explained. This Express road part Group II is constructed in four regions, which are; Çarşıbaşı-Araklı, Araklı-Iyidere, İyidere-Cayeli, Cayeli-Hopa. Tunnel studies are the most important subjects of the engineering activities in this project. There is a big need for reliable information and interpretation about state of tunnel alignment, behavior of the rocks on the vicinity of tunnel, expected problems and their solutions during the design works.



Figure 1. Location Map of Sarayköy and Cayeli Tunnels.

As mentioned above due to geomorphologic conditions several bridges, viaducts and tunnels must be constructed. According to the project specifications all these tunnels are double tube tunnels with a length changing from 2025 m to 3636 m, a clear width of 10.25 m and a clear height of 6.85 m, each at the full section of approximately 82.5 m^2. The clear distance of the two tunnel tubes is 11 m. On the slope sides especially, on portals the pillar thickness decreases to a thickness of 4 m and lesser. They are named as Sarayköy, Cayeli, Konakönü, Pazar and Arhavi Tunnels.

One of the problems on these projects is tunneling under a thin rock cover between the tunnel roof or sidewalls and ground surface and the other is slope-portal stability problems due to huge landslides. In these circumstances, the stability of the tunnel may be so short that there is no time to install conventional temporary support just before the excavation face and wall's collapse. In situations like these, tunnel admit at a steep mountain slope, the weathered and crushed rock makes it necessary to pre-treat and reinforce the roof – side walls of the tunnel with fore-poling and

Copyright © 2005 Taylor & Francis Group plc, London, UK

concrete wall supported by rock bolts, steel arches with shotcrete.

The engineering geological profile of the Eastern Black Sea Coast, can be characterized and summarized by a heterogeneous alternating sequence of following rock materials; Young formations; Clayey siltstone with sand and gravel, Basaltic tuff-agglomerate; and Eocene formations; Volcanic dyke- monsogabro and basalt.

The tunnels have been driven in difficult conditions due to geology, high morphology, surface-ground-water flow and slope instabilities in portal areas. Occasionally, however, the projects run into serious problems where the rock is very brittle, weathered or crushed.

2 CASE STUDY

2.1 *Sarayköy tunnel*

In the first stage of the project, the route was designed without tunnels. In this case the road was going to be constructed with high-steep slopes. Because of the geological conditions, landslides and creep problems in the area, the projects have been changed from slope excavations to tunnels.

Black Sea region with high rainy climate and steep morphology increases landslide-creep risks and weathering processes in gravelly, silty clayey media, altered tuffs-basaltic tuffs and agglomerates. These unfavorable geological conditions necessitate the use of special supporting-excavation methods or pre-treatment and precautions such as jet-grout columns, wire mesh, shotcrete, soil nails-anchors and drainage networks to ensure stability.

At sites, where landslides are expected, as well as at unfavorable geological settings, such as altered and weak formations, roof jet grouting provides a very effective support. It prevents loosening at the tunnel crown and also reduces stresses affecting the tunnel. Additionally, deformations on the tunnel can be highly reduced, allowing the usage of less lining materials. Jet grout application has provided many advantages such as improvement of the soil quality without any environmental disturbance, reduction of loosening and deformations, providing construction safety.

This method also helped to improve the excavation rates. The design of jet-grout application depends on three major criteria that can be classified as: the quality of soil – cement mixture; the length of the jet-grout pile and its compaction; and the diameter of the piles. The permeability, strength, and the supporting limit of the pile are also factors of quality. These factors were taken into consideration during the construction of the Sarayköy tunnels. Monitoring applications showed that adequate quality has been obtained for a safe construction.

Field observations revealed that the tunnel portals were affected by creeping and landslides developed at valley sides and mechanical drillings were performed to characterize their mechanical behavior. These drillings show that the tunnel ground consists of a 40–80 cm-thick humus-soil covering a variable thickness layer of gravel and clay overlaying highly altered basaltic tuffs and agglomerates. The first layer, gravel-silt-clay, has a unit weight of 19–21 kN/m^3, $\phi = 18°$, and cohesion c = 60 kPa. The second layer, the weak – very weak, strongly altered basaltic tuffs and agglomerates have a unit weight of 23 kN/m^3, $\phi = 24°$, and cohesion c = 220 kPa.

In order to overcome the instabilities during excavation-construction stages jet-grout and soil nails have been applied to prevent risky slope movements. For Sarayköy tunnel, Rize and mid route portals are given as example. Jet-grout reaches from the topsoil layer, down to rock formation, i.e. basaltic tuffs and agglomerates. For strength improvement, jet-grouts are supported by 6 m-long, φ 26 steel soil nails extending 2.5 m in the vertical direction and 2.4 m in the horizontal direction with an angle of 11–14°.

The tunnel is constructed in three different construction systems, which can be explained as; build and cover; cut and cover; underground NATM tunnel (Figure 2, 3). In order to ensure stability of slopes, after completing build and cover section, cut and cover part is constructed with steps of 5 m while covering completed part with artificial fill.

At mid portals, similar construction processes with the East portals are applied. In addition to the retaining walls and pretreatment works, a different jet grout system is applied with a pattern of inclined columns

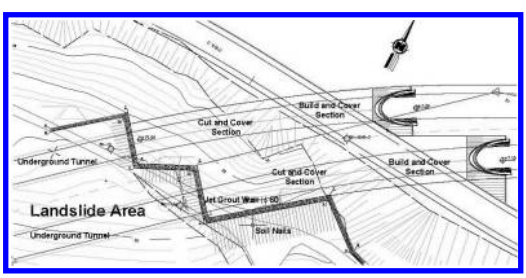


Figure 2. Planar view of Portals, unstable slope, jet grout wall and soil nails, Rize (East) Portal.

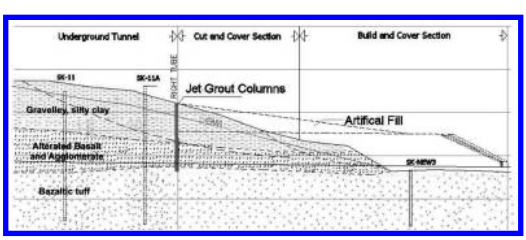


Figure 3. Geological cross section of Rize (East) Portal.

Copyright © 2005 Taylor & Francis Group plc, London, UK

in reverse angles are performed at shallow locations to constitute a preserving roof over the tunnel. With help of this roof, fore poling is applied between the columns and the tunnel tubes are constructed by NATM principles. Figure 6 shows the cross section of this critical area.

2.2 *Cayeli tunnel*

As a part of an express road project of General Directorate of Highways in Eastern Black Sea Region of Turkey 1.34 and 1.06 km long two tubes Cayeli tunnel have been driven in difficult conditions due to high morphology, surface and ground water flow and slope instabilities in portal areas. Occasionally, however, Cayeli tunnel project run into serious problems where the rock is very brittle, weathered or crushed, another challenge is tunneling under just a thin rock cover between the tunnel roof or side walls and ground surface. In such conditions, tunnel at a steep mountain slope, the weathered and crushed rock makes it necessary to reinforce the roof and side walls of the tunnel with fore poling and concrete wall supported by rock bolts, steel arches and shotcrete.

Slope tunnels have always created problems during construction; therefore they are preferred neither by the designers nor the contractors. On the other hand, this kind of tunnel may be required under certain topographical or other constraining conditions and can be considered as the exciting side of the engineering design art. Due to the difficulty of modeling the native field with many unknowns, tunneling needs to be carried out on unexpected conditions. Successful tunneling depends on the quality of the field studies and the laboratory. Since the working material is nature, the physical and mechanical properties of the soil or the rock have to be studied in detail. These findings should then be analyzed to determine the behavior of the ground during construction. This is the only way to predict failure points and set up the suitable supporting elements in optimum time.

According to the detailed researches, the features in the design of slope tunnels can be grouped as:

Surface strengthening applications: Peeling till reaching rock surface, applying shotcrete and wire mesh to stop loosening. Rock bolts should be applied to prevent shear stresses while taking into consideration the fractures and squeezing zones of rock. The application should provide as much monolith and isotropic conditions as possible.

Retaining Walls: If the pillar thickness between the slope surface and the tunnel, is less than 2 m fillings should be applied to increase the thickness to 4 m. Retaining walls should be applied to support the filling.

Supporting Mould Arc: Considering the of the tunnel excavation, I160 steel lining should be applied, from the retaining wall foundation up to tunnel crown. Steel supports are connected to each other by φ 26 steel. A plate with a thickness of 3 mm should be

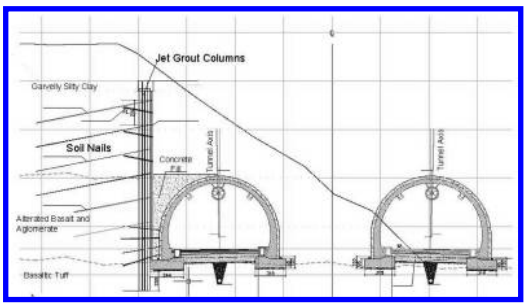


Figure 4. Cross section of east portal with both tunnel construction systems and pretreatment elements.



Figure 5. Jet grout application at Sarayköy portal area representing the excavation stage of cut and cover tunnel.

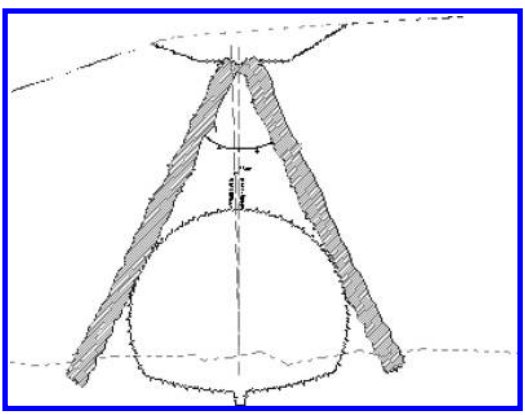


Figure 6. Jet-Grout Application at shallow parts of the mid portals.

Copyright © 2005 Taylor & Francis Group plc, London, UK

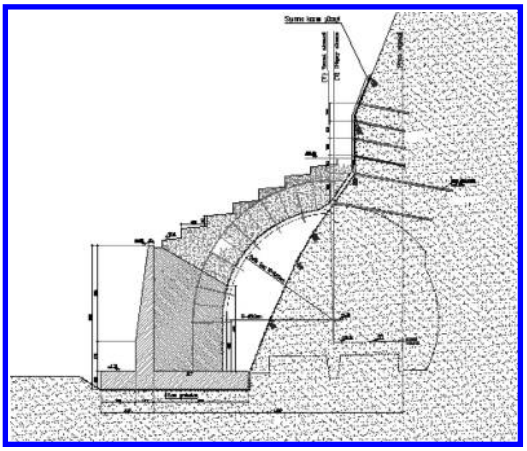


Figure 7. Supporting elements of the Çayeli Slope Tunnel right(s).

assembled under the steel support. Shot Crete and wire mesh should be applied on the steel support.

Ray Reinforcement: Ray Reinforcement consisting of φ 26 steel should be applied around the tunnel, systematically as rock bolts, with the same distance.

Lower part filling: The backside of the retaining wall should be filled with B20 concrete to make an artificial pillar.

Upper part filling: Ray reinforcement should be covered with B14 concrete, which needs to be applied up to the upper part of the tunnel.

Tunnel excavation and construction: The slope side of the double tunnels should be excavated first by the drill and blast excavation.

All of the above-mentioned steps are critical in the design of tunnels and their application to more difficult conditions, such as slope tunnels, showed that excavation-construction of the tunnel could be performed without facing any unexpected and unwanted problems.

To avoid any unwanted movements, reinforcement wall is set in front of these critical zones. This supports



Figure 8. Picture of the Çayeli Slope Tunnel right(s).

the slope, and the stability of the tunnel. Figure 7 shows the supporting elements. Figure 8 shows the slope tunnel in field.

REFERENCES

Vardar, M., 1977, Zeiteinfluss auf das Bruchverhalten des Gebirges in der Umgebung von Tunneln, Veröff. des Institutes für Bodenmech. und Felsmech. der Univ. Karlsruhe

Vardar, M., 1989, Die Wirkung der ingenieurgeologisch-felsmechanischen Verhaeltnisse auf die Planung und Verwirklichung der Istanbuler Abwasserstollen, Geologie Felsmechanik Felsbau Festkolloquium L. Müller-Salzburg, Trans Tech Publications

Vardar, M., H. Karaoğlan, C. Koçak, 2002, A Contribution to the Importance of the Bearing Capacity and the Unite Rock Element Displacement of the Rock Masses at the Design and Dimension of the Slope Tunnels, 1st International Symposium of Istanbul Technical University Faculty of Mines on Earth Sciences and Engineering, p. 194

Copyright © 2005 Taylor & Francis Group plc, London, UK

Jet-grout application at Sarayköy tunnel interval portals

Mahir Vardar
Prof. Dr., İstanbul Technical University, Mining Faculty, İstanbul, Turkey

Halil Karaoğlan
Civil Engineer (M.Sc), Emay International Eng. Consulting&Trd Co. Ltd., İstanbul, Turkey

Kenan Kaya
Geological Engineer (M.Sc.), KGM Technical Research Department, Ankara, Turkey

Rıza Mucukgil
Geological Engineer (M.Sc.), KGM Technical Research Department, Ankara, Turkey

1 SUMMARY

The Double Tube Sarayköy tunnels are constructed in the scope of the Black Sea coastal road projects by the Republic of Turkey, General Directorate of Highways, 10th District Directorate and are located on İyidere-Çayeli section. On the 1818 meters-long tunnel route, main entrances are on the Trabzon and Rize sides, and two additional portals are required (where) due the valley on the mid-route.

Every portal in the project is expected to present difficult geological ground conditions such as crossed gravel, silted clay satiated on water, decomposed tuffs-basaltic tuffs and agglomerates. Experiments show that past landslides and creeping have already developed at those sites. These unfavorable geological conditions necessitate the use of jet-grout and soil nails at these portals to ensure stability. We propose that the weak and unstable zones on the tubes need to be supported by intersecting jet-grout pillars, creating a supporting roof. In this study, we describe and discuss in detail this support system, which will be applied in Turkey for the first time.

Sarayköy tunnels, located on Iyidere – Çayeli section, constructed between km 111+780 and 113+420 have a total length of 1818 meters. As mentioned in the summary, the geological and geotechnical problems associated with these tunnels mandated a wide range of field observations and extensive use of instrumentation. Topographical observations revealed that the tunnel portals were affected by increased creeping and landslides developed at valley sides and mechanical drillings were performed to characterize their mechanical behavior.

These drillings show that the tunnel ground consists of a 40–80 cm-thick soil covering a layer of gravel and clay. Highly alliterated basaltic tuffs and agglomerates that are much weaker are located beneath these layers. Sarayköy tunnels' interval portals are going to be constructed into the gravel-silt-clay, and the tunnel foundation will be extended from alliterated basaltic tuffs and agglomerates to stronger basaltic tuffs and agglom-erates.

The first layer, gravel-silt-clay, has a unit weight of 21 kN/m^3, $\varphi = 18°$, and cohesion (c) = 60 kPa. The second layer, the weak – very weak, strongly alliterated basaltic tuffs and agglomerates have a unit weight of 23 kN/m^3, $\varphi = 24°$, and cohesion (c) = 220 kPa.

During the excavation of the interval portals, supporting systems containing jet-grouting and soil nails have been adjusted to prevent risky slope movements. On the interval portals, from km 112+580 to km 112+635, φ 60 jet-grout piles are going to be constructed.

Figures 1 and 2 show the details of the frontal and the planar view of the intermediary portals, respectively.

As mentioned above, the supporting types that will be used in the Sarayköy tunnels are structurally important since they will be implemented for the first time in Turkey, on the interval portals are performed. In the figure below, φ 60 jet grout pile applications on the interval portals from km 112+580 to km 112+635 are shown.

Jet-grout reaches from the topsoil layer, down to rock formation, i.e. basaltic tuffs and agglomerates. For strength enhancement, jet-grouts are supported by 6 m-long, φ 26 steel soil nails extending 2.5 m in the vertical direction and 2.4 m in the horizontal direction with an angle of 11–14°.

To obtain more stable conditions above the tunnels, jet-grouts, intersecting at an angle harmonious with the topography, are applied from km 112+605

Copyright © 2005 Taylor & Francis Group plc, London, UK

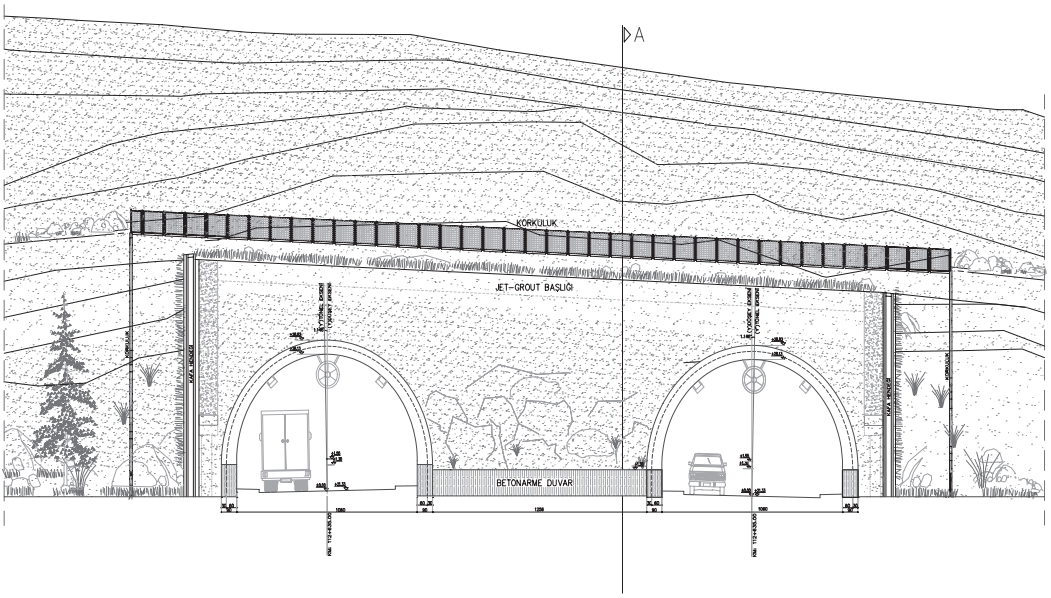


Figure 1. Frontal view of intermediary portals, Sarayköy tunnel.

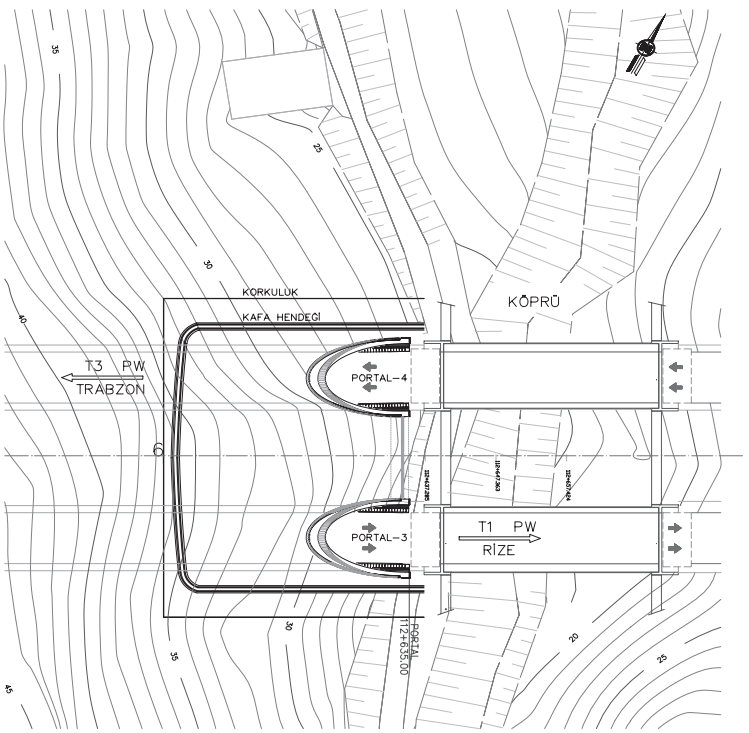


Figure 2. Planar view of the portals.

Copyright © 2005 Taylor & Francis Group plc, London, UK

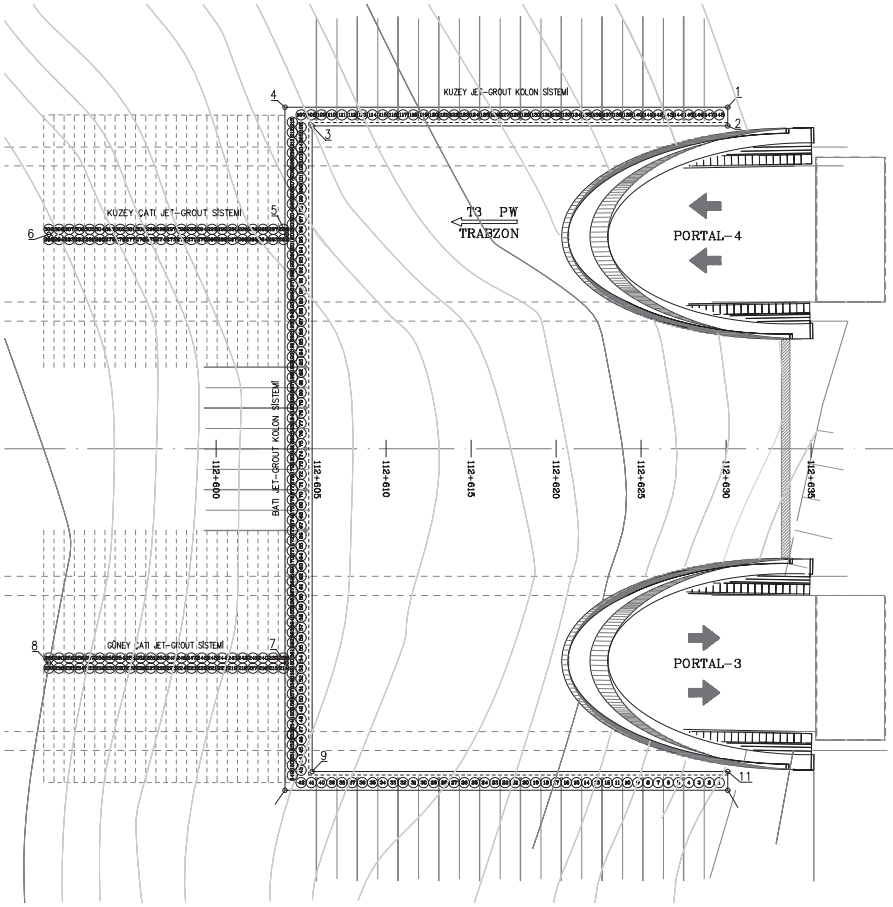


Figure 3. Jet-grout application, the planar view of the portals.

to km 112+590. Figure 4 shows the intersecting jet-grouts cross sectional view.

At sites, where landslides are expected, as well as at unfavorable geological settings, such as alliterated and weak formations, roof jet grouting provides a very effective support. It prevents any loosening on the tunnel crown and also reduces stresses affecting the tunnel [1,2]. Additionally, deformations on the tunnel can be highly reduced, allowing the usage of less lining materials. Jet grout application has provided many advantages such as improvement of the soil quality without any environmental disturbance, reduction of loosening and deformations, providing construction safety. This method also helped to improve the excavation rates.

The design of jet-grout application depends on three major criteria that can be classified as: the quality of soil – cement mixture; the length of the jet-grout pile and its compaction; and the diameter of the piles. The permeability, strength, and the supporting limit of the pile are also factors of quality. These factors were taken into consideration during the construction of the Sarayköy tunnels. Monitoring applications showed that adequate quality has been obtained for a safe construction. Figure 5 shows the cross-sectional view of the jet-grout application.

Jet-grout methods can be classified into three groups. These are:

– Single fluidity
– Double fluidity
– Triple fluidity.

Single fluidity method is the simplest method of the three [3,4]. In this method, rapidly injected mortar cuts the soil, changes its location and connects with the soil. Mortal pressure differs between 20–40 MPa,

Copyright © 2005 Taylor & Francis Group plc, London, UK

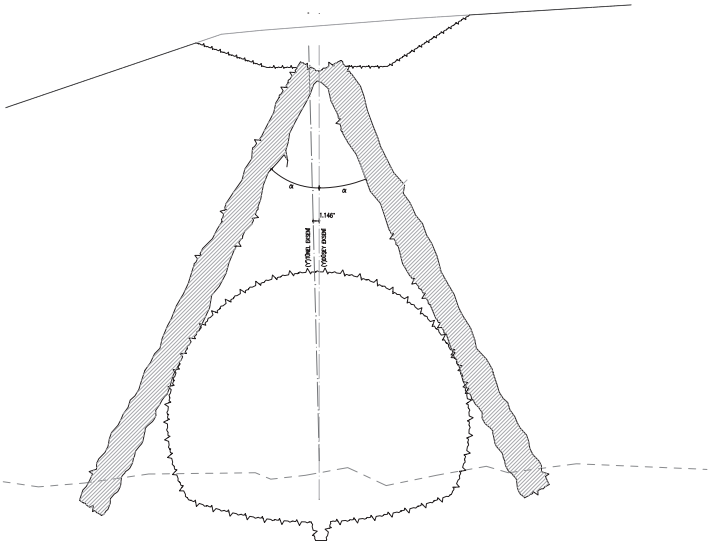


Figure 4. Jet-grout application.

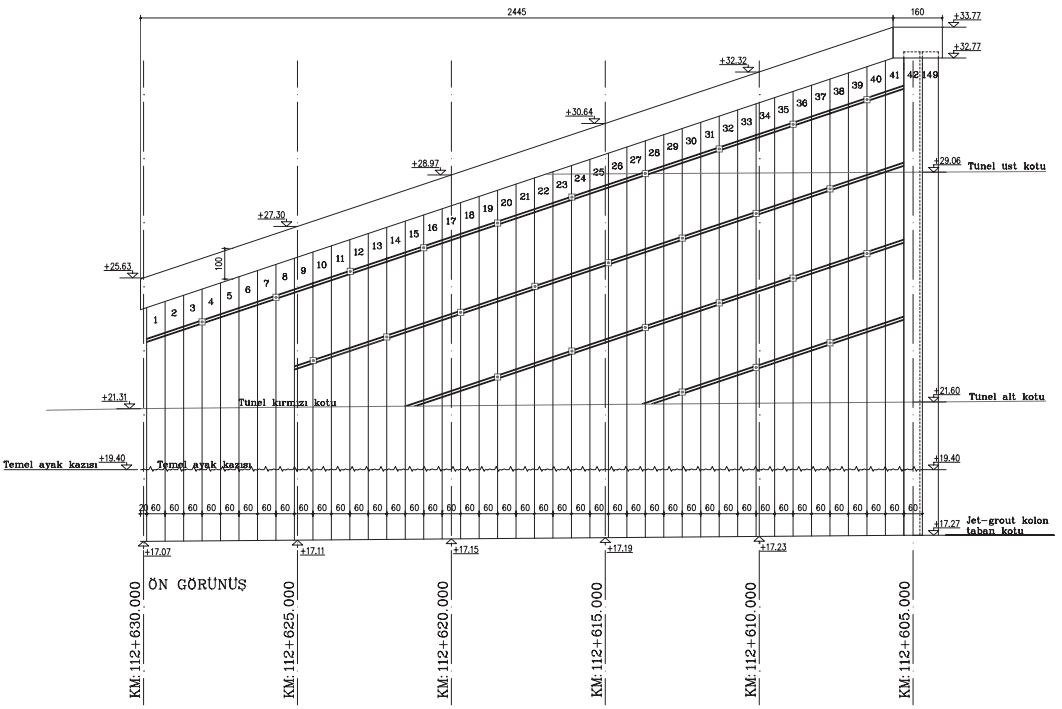


Figure 5. The cross-section of the Jet-grout application.

Copyright © 2005 Taylor & Francis Group plc, London, UK

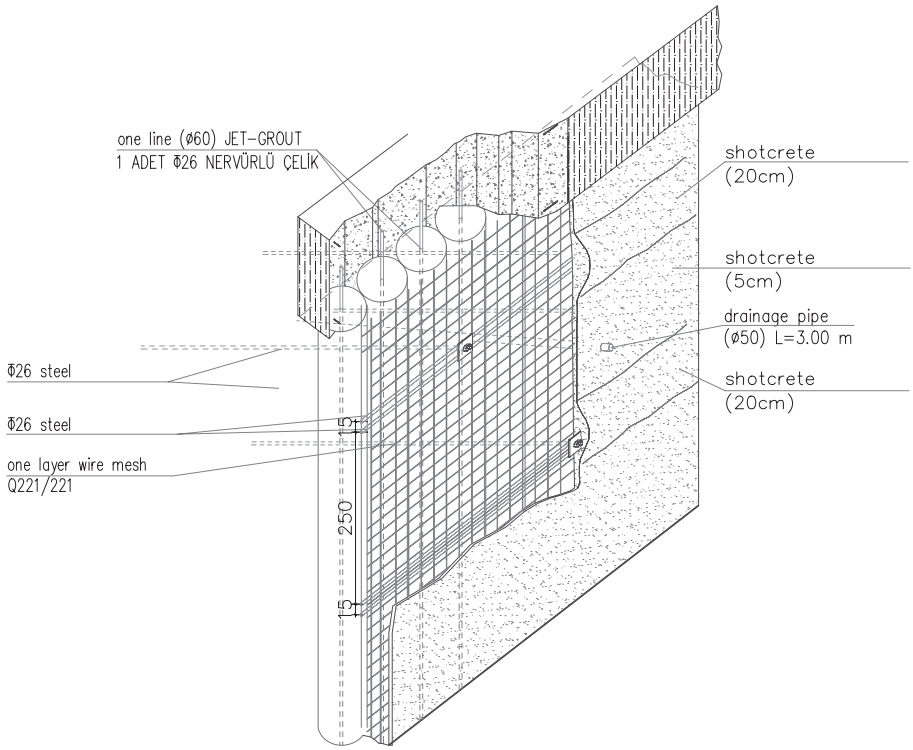


Figure 6. The Jet-grout application.

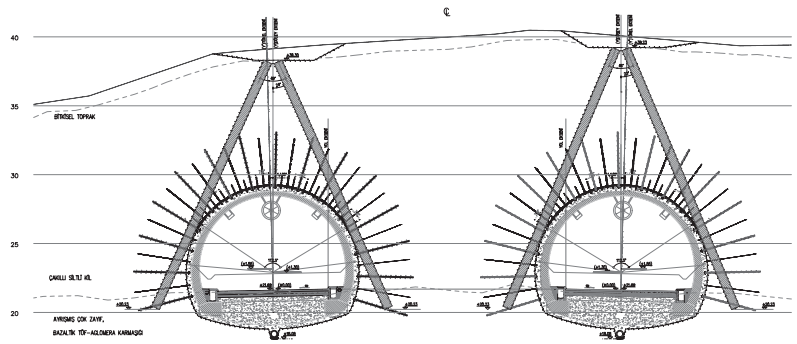


Figure 7. The cross-section of Jet-grout application on Sarayköy tunnels.

injection velocity is about 50 m/sec, and Debby 3 lt/sec. Rotating pipe is pulled up at 100–150 mm/sec. In the other techniques, the effectiveness of the jet-grouts decreases, as the column becomes horizontal. Experience shows that the jet-grout column compresses the soil as far as half the column diameter. The diameter of the single fluidity columns is smaller than the others. For soil containing clay, the diameter is chosen to be 40–80 cm, and for soil with separated particles, as 50–120 cm. The equipment limits the usage of the single fluidity system. The power of the cement pump and the delivered velocity determines the diameter of the column. During the application of the jet-grout columns, pumps, which can pump cement mortal at a velocity of 150–450 lt/min with a pressure of 60 MPa and work up to 8 hours, are preferred. Figure 6 shows the jet-grout application at the tunnel.

Copyright © 2005 Taylor & Francis Group plc, London, UK

Figure 7 shows the cross-sectional view of the application on the double tube Sarayköy Tunnels detailing the intersecting jet-grout columns.

REFERENCES

Mitchell, J.K., 1981. *Soil Improvement Methods and Their Aplications in Civil Engineering.* Sixteenth Henry M.Shaw Lecture in Civil Engineering, North Caroline State University.

Morino, A., Grasso, P.G. & Pelizzi, A., 1989. *Bolletino della Associazione Mineraria Subalpina*.Torino.

Petros, P.X., Lee, W.A. & Donald, A.B. *Ground Control and Improvement*.

Balasubramaniam, A.S., Chandar, S. & Bergado, (eds), 1982. *Recent Developments in Ground Techniques*.

Copyright © 2005 Taylor & Francis Group plc, London, UK

Case study – deformations and remedial measures for Nefise Akçelik and Asarkayası tunnels on Black Sea Costal Road Project

M. Vardar
Istanbul Technical University-Faculty of Mines, Turkey

H. Karaoğlan
Emay Int. Eng. Cons. & Trd. Co. Ltd, Turkey

Z. Etkesen & E. Akiş
General Directorate of Highways, Turkey

ABSTRACT: Nefise Akçelik Tunnel and Asarkayası tunnel are constructed in the scope of Black Sea Coastal Road Project in Turkey. Basalt agglomerates and tuffs formed as submarine volcanism along the twin tunnels alignment. For Nefise Akçelik and Asarkayasi tunnels the lengths are 3776 meters and 306 meters, along the problematic sections overburden heights are 375 meters and 110 meters respectively. After completion of excavation and installation of primary supports, high displacement occurred. The morphology is controlled by young tectonic activity and erosion. Along the fault zone there are water incomes into the tunnels. In this paper engineering geological and geomechanical reasons for deformations are described and rehabilitation design approaches are given as case studies.

1 INTRODUCTION

Both of the tunnels are constructed in the scope of Black Sea Coastal Road Project in Turkey. This coastal route project is one of the important projects as it connects northeast neighbors (Georgia, Armenia and Azerbaijan) to Turkey and Europe.

Nefise Akçelik tunnel is the longest double tube tunnel with a length of 3776 m in Turkey. Depth of the tunnel is 33 meters in portals and ranges between 75–375 meters throughout the route. The diameter of the tunnel is 12.6 meters and the cross section area after excavation is 80.96 m^2. The problematic sections, where high deformations occurred are approximately 117 meters for the left tube and 49 meters long for the right tube.

Asarkayasi tunnel has a length of 306 and 310 meters for the left and right tubes respectively. Depth of the tunnel is 20–30 meters in portals and reaches 110 meters throughout the route. The diameter of the tunnel is 12.6 meters and the cross section area after excavation is 90.99 m^2. The problematic sections are approximately 35 meters + 28 meters = 63 meters long for the left tube and 37 meters long for the right tube.

Tunnels are driven under difficult conditions due to morphology and geology. In addition to these conditions, there is water income into Nefise Akçelik Tunnel. In Asarkayasi Tunnel, there is no excessive ground water flow. The morphology on the tunnels route is controlled by young tectonic activity and erosion.

Deformations were occurred after completion of excavation and installation of primary support system of Nefise Akçelik and Asarkayasi Tunnels. Surface geology, fault systems, tunnel geological mapping, deformation records were evaluated to estimate the stress distribution and rock parameters in problematic sections.

This paper presents example of deformations occurred in tunnels through weak geological sections and summarizes the rehabilitation design approaches for problematic sections.

2 NEFİSE AKCELİK TUNNEL

Along the problematic section, according to New Australian Tunnelling Method (NATM), B2 rock support (rock bolts and shotcrete) and B3 rock support (rock bolts, shotcrete, steel ribs, without invert) had been installed in the problematic sections of left tube and right tube respectively.

Copyright © 2005 Taylor & Francis Group plc, London, UK

Convergence measurements were recorded and geological mapping were done during construction. In May 2002, excavation and primary support of the right tube was completed. In August 2002, excavation of the left tube was done by blasting. After blasting, the shotcrete at the roof and shoulders in the right tube cracked heaved and fell Maximum deformation measured was 14 cm. As an immediate measure for this situation, after re-excavating, extra bolts (6–8 m) were installed.

The tunnel construction was stopped due to financial problems up to May 2003. During this period, deformations continued. Since the deformation rate was beyond acceptable limits, inner lining could not be constructed.

After June 2003, following investigation studies were done; surface geology and fault systems were restudied, radial deformations (24 points on one cross-section) were recorded with 2 meters intervals. Deformations are evaluated due to last 1.5 months records. According to the tunnel geological mapping (Fig. 1) (considering the fault systems, water effect, weak zones) and deformation records, the parameters of the surrounding rock types were determined by back analyses. Then, rehabilitation project was designed.

According to the studies, it was seen that the morphology on the tunnel route is controlled by tectonic activity and erosion. Because of this, the region is surrounded by steep valleys and rivers still continue to erode the valley beds. At the section, where high deformations occurred, the tunnel is driven parallel to east-west directional fault controlled valley, where the fault and tunnel crosses each other. As it can be seen on Figure 2, the tunnel is compressed by tectonic forces at this section.

2.1 *Results of investigation studies*

The tunnel route is settling along the Upper Cretaceous basaltic, andesitic lavas and pyroclasts, and overlapped by Upper Cretaceous – Eocene sediments and carbonate rocks, Brinkmann (1974). Nefise Akçelik tunnel is driven throughout volcano-clastic series. These series include basaltic lavas (basalts, diabase), basaltic pyroclasts (andesitic, basaltic tuff-agglomerate) and sedimentary rocks (claystone, mudstone, shale) as lithological units. Tunnel base map was prepared to observe the lithologies and fault direction beneath the surface.

Volcanic units are usually jointed and filling materials are calcite and clay. Fillings have a thickness ranges between 1 mm to 15 cm. Also opened cracks are common. This structure yields to the circulation of the groundwater throughout the joint systems. In the tunnel driven zone, groundwater is collected and the tunnel becomes a collector gallery. That drain system affects the clay and tuff units at the invert, and the units become softer. So that tuffs altered and clay zones become softer.

2.2 *Engineering geology and deformations of the left tube*

Clay zones are the product of basalt lavas and calcite filled basalts, altered by groundwater. Clay zones cause to excessive deformation problems at the invert. There are no displacements in clastic units (agglomerates), but also water income is excessively high in these units. Left tube is crossed by NW-SE and NE-SW directional faults. As tunnel driven, the fault systems caused to cracking and loosening strength of the volcanic units.

The last 1.5 month displacements were ~5 cm at the roof, 13 cm at side walls and 20 cm at the bottom.

2.3 *Engineering geology and deformations of the right tube*

NW-SE and NE-SW directional faults cross each other along the right tube. This structure yields to produce clay zones. The tunnel base includes clayey

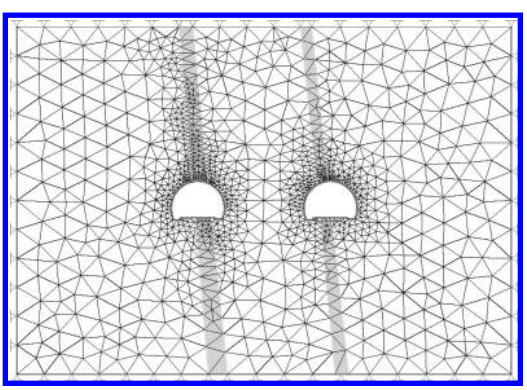


Figure 1. Geological model used for numerical analysis.

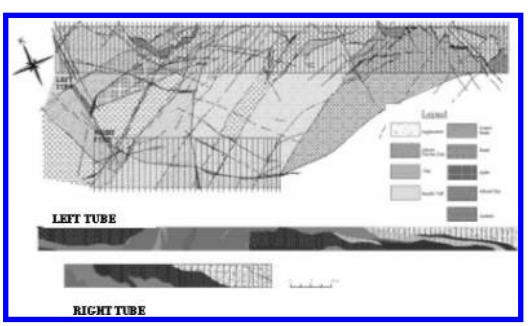


Figure 2. Tunnel level geology map and cross-section chainage 10+683.00–10+800.60 km for the left tube and 10+693.10–10+742.10 km for the right tube.

Copyright © 2005 Taylor & Francis Group plc, London, UK

silty lithologies. Andesitic and basaltic clay layers overlap these lithologies. Andesitic and basaltic tuffs are weak between chainage in problemitic section, and separated with clayey units by NW-SE directional faults.

The last 1.5 month displacements were 5 cm at the roof, shoulders and left side wall, 9.5 cm right side wall.

2.4 *Rehabilitation project*

The rehabilitation project was consists of following steps; drainage measures, forming the ring with invert.

For right tube (from B2 to B3 rock support) excavation and construction stages: (Fig. 3a)

Top heading:
Excavation between existing steel ribs
Installation extra ribs, shotcrete and wire mesh.
Installation extra bolts (Ø28, L = 6 m)
Invert:
Invert excavation and installation of drainage system.

If required, forming the ring with installation extra bolts at toes (L = 12 m) and at the bottom (L = 6 m) of the invert.

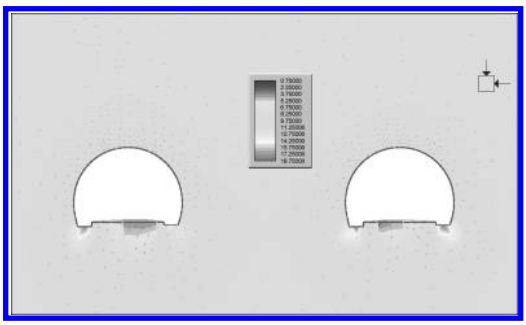


Figure 3a. Excavation and construction stages for B2 to B3 support.

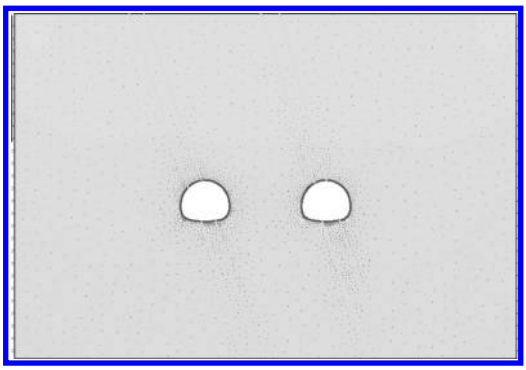


Figure 3b. Excavation and construction stages for B3 rock support.

Construction of foundations beams between foundations and inner lining.

For right tube (B3 rock support) (Fig. 3b)

Excavation of invert and installation of drainage system.

Forming the ring with installation wire mesh, shotcrete and steel ribs.

Installation of bolts at the toes (L = 8–12 m)

If required, installation of bolts (L = 6 m) at the bottom of the invert.

Construction of foundation beams between foundations and inner lining.

3 ASARKAYASI TUNNEL

NATM C2 rock support had been applied during construction since the deformations were lower than expected, the invert was not constructed.

Convergence measurements were recorded and geological mapping were done during construction. In the problematic sections over breaks on shoulders and roof stability problems at face occurred.

After completing the excavation and primary support, the inner lining and drainage system could not be constructed due to financial problems.

After two years records showed heaving and settlements at the bottom on shoulders and side walls. The deformations were acceptable but continued so the inner lining could not be constructed.

Following investigation studies were done; surface geology and fault systems were restudied, radial deformations, tunnel geological mapping (Fig. 4) (considering the fault systems, weak zones) were evaluated. Parameters of surrounding rock type were determined by back analysis. Then rehabilitation project was done.

3.1 *Result of investigation*

The morphology is similar with the Nefise AKÇELİK tunnel. During construction no excessive water income was exposed. Water was formed as dropping, seepage and small springs.

The tunnel is crossed perpendicularly by N-S directional fault. Fault zone material consists of

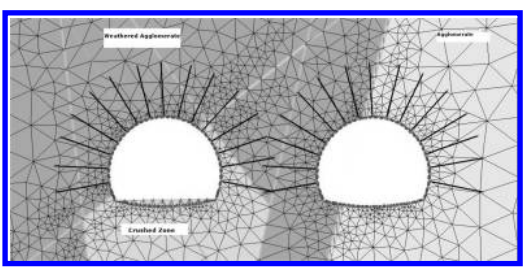


Figure 4. Geological model used for numerical analysis.

Copyright © 2005 Taylor & Francis Group plc, London, UK

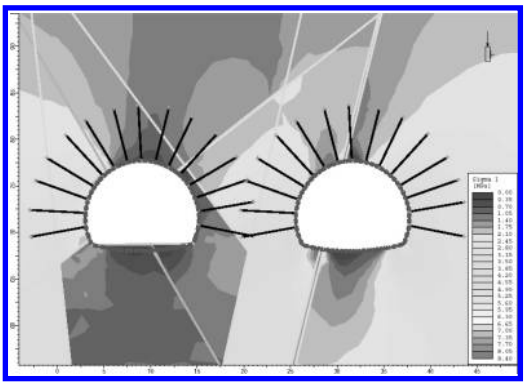


Figure 5. Analysis Results for Rehabilitation Project – Stress Distribution Around Tunnels

agglomerates volcano bres, mudstone, claystone, basaltic tuff, with very weak strength, highly weathering fractured and cracked.

3.1.1 *Left tube*

In first problematic section 35 m in length the tunnel was excavated in andesite, riyolit, riyadesit. The formation is moderately high weathered, has moderately strong-very weak strength. Because of extremely high alliterations, prophilites occured. Units have random and uncontinued discontinuities. Joint filling material is Mn0 and clay.

In second problematic section 28 m in length the formation similar with the first section. Fault zone dip direction is through the tunnel.

Fault zone materials consist of swelling clay at the bottom of the tunnel. 10 cm heaving occurred at the bottom depending on swelling clay, 3 cm convergence occurred in the tunnel.

3.2 *Rehabilitation project*

Considering geological mapping, deformations, the geological model was prepared and the parameters were determined by back analysis. Then the rehabilitation project was designed.

Since the deformations are smaller than Nefise Akçelik tunnel deformations, the lighter measurements were sufficient.

The rehabilitation project includes following stages: (Fig. 5)

- Excavation of the bottom for invert (~2 m).
- Installation drainage system at the bottom of invert.
- Forming the ring with shotcrete, wire mesh and steel ribs.
- Filling the invert with concrete.

4 CONCLUSION

Nefise Akçelik and Asarkayasi tunnels route has a morphology controlled young tectonic activity and erosion. The area crossed fault systems and geological weak zones. As a result of stopping the tunnels construction and insufficient drainage system caused the deformations in the tunnels. Deformation records related with the construction may lead the project without living that kind of problems.

According to engineering geological and geomechanical evaluations, new design projects including invert, extra supports drainage systems were applied. Deformations decreases under the limit values and inner linings were constructed.

REFERENCES

Nefise Akçelik Tüneli Hesap Raporu Nisan 2004 (Emay)

Karadeniz Sahil Yolu Bolaman-Perşembe Arası Asarkayası Tüneli Kesin Proje Jeoteknik Raporu ve Tünel Hesap Raporu Temmuz 2004 (Emay)

Bolaman-Perşembe Devlet Yolu Hapan Tünelindeki Problemleri Inceleme ve Değerlendirme Raporu Temmuz 2003 KGM-TADB.

Bolaman-Perşembe Yolu ve Hapan Tüneli İnceleme Raporu Ağustos 2003 KGM TADB

Copyright © 2005 Taylor & Francis Group plc, London, UK

Metsovitikos river north alignment of Egnatia motorway. The concept and the tunnel designs

N. Kazilis[1], Ch. Georganopoulos[2] and G. Aggistalis[3]
[1] *Tunnels Discipline Head, MBA, MSc, BSc, DIC, Egnatia Odos A.E. Thessaloniki, Greece*
[2] *Civil Engineer, Consultant, Former Design Manager of Egnatia Odos A.E. Thessaloniki, Greece*
[3] *Tunnelling Engineer, MSc, CEng MIMMM, Egnatia Odos A.E. Thessaloniki, Greece*

ABSTRACT: This paper describes the concept and the tunnel designs of a part of a highway alignment of the Egnatia roadway across Northern Greece. The selection of the alignment of the road was done basically on the early thorough geological evaluation of the terrain at either side of the Metsovitikos river. An old single carriageway alignment south of the river was abandoned as the road was passing through unstable slopes. The old alignment was placed on a terrain that was, mild morphologically and friendly, since no major structures such as tunnels or major bridges were required. After a detailed value engineering, that was carried out in house, by the Egnatia Odos A.E. personnel, it was proved that the placement of the alignment north to Metsovitikos river was a no risk and a cost effective solution. North to the Metsovitikos river the alignment had to pass through a steep terrain where tunnels and major bridges were required. However, the road could be constructed with no risk as the geological conditions were very good and were characterized by the presence of good quality thick bedded sandstones and siltstones, and the construction of big structures such as tunnels and bridges could be completed with no major problems. Most important, the road could be constructed as a double carriageway instead of single carriageway originally thought about south of the Metsovitikos river. The major structures of this alignment are 6 twin tunnels 4,1 klm cumulative length, and an access road of a major interchange linking Egnatia roadway to the Metsovon city and the old national road and three major bridges. The construction started 1999 and the road is scheduled to open to traffic, mid 2005.

1 EGNATIA ODOS PROJECT

The 680 km Egnatia Motorway is a modern motorway and the only road link spanning Northern Greece from its western to its eastern border. The Egnatia Motorway is the modern revival of the great Roman highway known as the Via Egnatia which was also one of the roads walked by Saint Paul.

Nine major vertical to Egnatia road axes provide links to Albania, Fyrom, Bulgaria and Turkey, and the whole system is served by 720 km of service roads. The Egnatia Motorway was designed to the specifications of the Trans-European road network. It is a closed dual carriageway motorway with a central reserve, two traffic lanes plus an emergency lane per carriageway, for a total width of 24.5 metres. The project works include 75 twin tunnels of a total combined length of a 100 km.

In September 1995, the Greek Government set up the firm Egnatia Odos A.E. (EOAE), the object of which is to design, build, and operate this motorway (Georganopoulos & Kazilis, 2001). Following an international tender toward the end of 1995, it appointed Kellogg, Brown and Root as a provider of project management services. EOAE has about 300 staff in the head office in Thessaloniki and various regional offices (Rawlings et al, 2001).

2 TUNNEL INFORMATION

2.1 *General*

Egnatia Odos AE has compiled Design Guidelines for all engineering disciplines involved in the construction of the highway (Kazilis, 1999). A part of this document concerns the tunnel design guidelines and covers both bored tunnels and Cut and Cover tunnels. All Egnatia tunnels are designed as twin tunnels. Cross passages are provided every 350–400 metres. Emergency vehicle turn-overs are provided every 1000 metres along parking areas.

Copyright © 2005 Taylor & Francis Group plc, London, UK

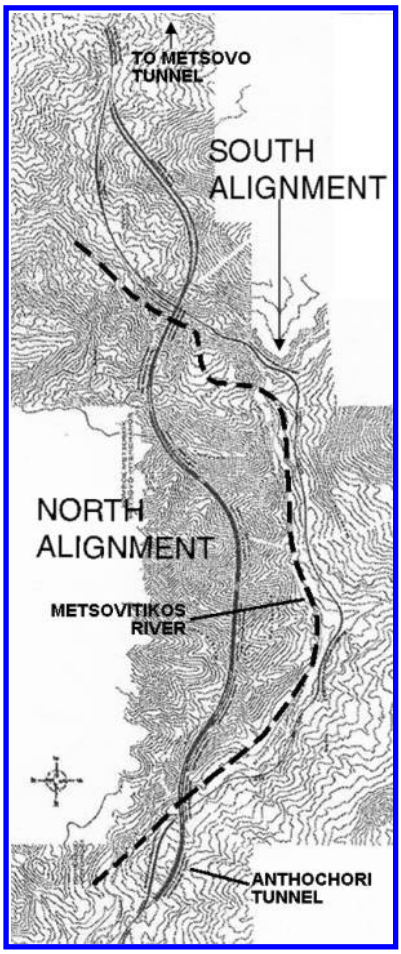


Figure 1. North and south alignments of the Egnatia highway that run almost parallel to the Metsovitikos river.

3 THE CONCEPT OF THE METSOVITIKOS RIVER NORTH ALIGNMENT

3.1 *History*

During '80s a 3.6 klm long tunnel named Metsovon tunnel was constructed in the middle a mountainous alpine terrain named Pindos. For a long period of time the eastern and western accesses to this tunnel was a serious problem. In 1992 an alignment was designed for the western access of the Metsovon tunnel. This alignment run parallel to the south side of the Metsovitikos river (see Figure 1) following a mild slope terrain and generally provided for small cuts and embankments in a single carriageway model.

In 1996 the responsibility for the design and construction of the this part of the road transferred to Egnatia Odos A.E. For the continuation of the design of the alignment, an extensive geological and geotechnical investigation and design took place, associated with the design of the potential stabilization works. The investigation / design proved that along this alignment existed active landslides that required extensive stabilization measures. These measures included a long drainage tunnel running parallel to the alignment for most of its length and a big number of horizontal and vertical drainage measures, aimed to "embrace" the body of the road. The total estimated cost for this part of the road running from Anthochori tunnel (the start point of the alignment) up to the western portal of Metsovon tunnel was estimated to be about 260 million €. This alignment (called the south alignment) was a single carriageway highway and had the disadvantages of a continuing maintenance of the drainage measures, a hidden remaining geotechnical risk as most of the road was crossing landslip areas, the lack of connection of Egnatia Odos to the Metsovo city and most seriously, the constraint to leave Egnatia Odos highway as a single carriageway in this part.

This situation caused serious considerations in the Design Department of Egnatia Odos A.E., and a decision was made for a serious reconsideration of the highway solution. The thinking of the design department engineers was focused on the north side of the Metsovitikos river. The steep terrain of this side of the river, which was a sign of good geological conditions, forced the design department leadership to examine a highway alignment through the steep slopes of the northern side of Metsovitikos river. A preliminary alignment set up, and a thorough value engineering study took place. This study was based on a thorough evaluation of the geometrical data of the alignment, the geology, the geotechnical, the environmental and maintenance issues. The new alignment called now the "north alignment" was able to solve all the disadvantages mentioned above associated with the south alignment and proved to be (as a dual roadway)a cost effective solution. A short comparison of the two alignments is given in the table 1.

After approval of this proposal from the Egnatia Odos Board of Directors, design contracts were assigned for the completion of the definitive designs associated with the alignment.

3.2 *Tunnels of the Metsovitikos river north alignment. General technical information*

The Metsovitikos river northern alignment of Egnatia motorway contains six tunnels. These are listed below in table 2. A summary of their technical data is also given.

In tunnels Kalamion and Agios Nikolaos EOAE adopted enlarged tunnel cross sections in order to accommodate the acceleration lanes of a complete interchange located in between these tunnels

Copyright © 2005 Taylor & Francis Group plc, London, UK

Table 1. Engineering and cost comparison of the Egnatia roadway alignments, south and north to the Metsovitikos River.

North alignment up to the entrance of Metsovo tunnel	South alignment up to the entrance of Metsovo tunnel
Length: ~9,3 Km	Length: ~9,0 Km
Six (6) twin tunnels of length ~4.1 Km and one single in the Metsovon interchange	One (1) tunnel of length almost 0.7 Km
Three major bridges of total length ~1500 m	Mainly cuts and embankments, and bridges almost 4 Km in length
One major interchange	Long drainage tunnels and extensive river training works
Double carriageway	Single carriageway
Bidding cost:	Estimated cost:
270 million €	260 million €

Table 2. Tunnels along the north alignment.

Tunnel	Technical information
Anthochori	Length: ~700 m, Geology: sandstone boulders in sheared claystone
Votonosi	Length: ~500 m, Geology: alternations of massive siltones and sandstones
Dio Korifes	Length: ~730 m, Geology: alternations of massive siltones and sandstones
Krimnos	Length: ~1080 m, Geology: alternations of massive siltones and sandstones
Kalamion	Length: ~800 m, Geology: alternations of massive siltones and sandstones
Agios Nikolaos	Length: ~360 m, Geology: alternations of massive siltones and sandstones

(Ekonomopoulos, 1999). Figure 2 shows a layout plan of the Metsovon interchange. The typical cross section of Egnatia Odos and the enlarged cross sections adopted in these two tunnels are given in the figures 3,4 & 5.

3.3 *Tunnel designs*

The scope of works of the tunnel designs was claimed from the designers to prepare definitive / application tunnel designs and to submit their designs in stages. The stages of the different design submissions were included:

a) submission of the project appraisal report, a document that describes all the data related to the design of the tunnel, it gives the design methodology and proposes the necessary extra geological / geotechnical investigation works that are needed, b) submission of the geological / geotechnical evaluation report, a submission that includes the evaluation of all geological/ geotechnical investigation results along with the

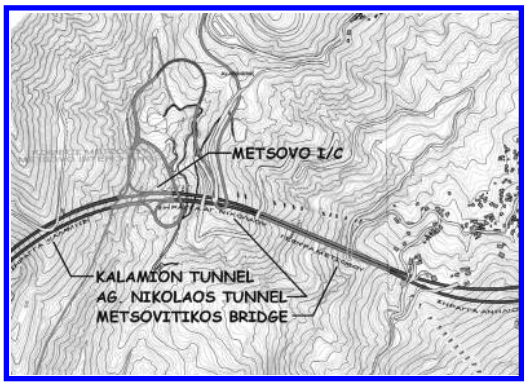


Figure 2. Metsovon interchange including the Kalamion and Agios Nikolaos tunnels.

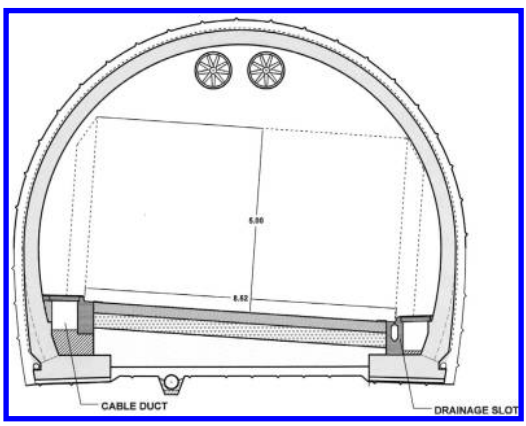


Figure 3. Typical 2 (two) – lane tunnel cross section.

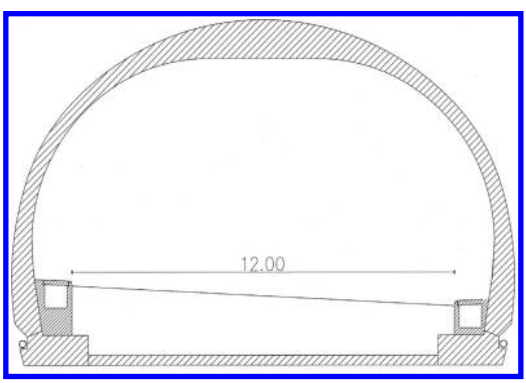


Figure 4. Three – lane cross section used in Agios Nikolaos and Kalamion tunnel.

Copyright © 2005 Taylor & Francis Group plc, London, UK

necessary geological / geotechnical drawings (layout plans, longitudinal sections and cross sections), c) submission of the excavation and portal support designs, d) submission of the underground excavation and support design of the tunnel, e) submission of the design of the final lining of the tunnel.

3.4 *Geological / geotechnical evaluation reports*

For the design of the tunnels a detailed geological / geotechnical investigation campaign started early 1997. This campaign generally included geological mapping along the tunnels in 1:500 scale at the main body of the tunnel and 1:200 scale at the tunnel portal areas. Boreholes were executed every ~200 apart while in some cases of difficult geology like anthochori tunnel, boreholes were executed every 100 m to 50 m apart (Pantzartzis, 1999). From the geological / geotechnical investigation it was confirmed that the geology along the tunnels was friendly for the construction of the tunnels. Specifically, most of the tunnels were to be build in massive to medium bedded alternations of hard sandstones and siltstones. Only in Anthochori tunnel soft ground conditions were predicted. In this case the tunnel had to be excavated through a huge overthrust zone in between two major geotectonic units Greece. The material of this overthrust zone is in the form of a tectonic mélange which contains hard sandstone boulders "swimming" in soft sheared claystone with soil behavior.

3.5 *Excavation and support designs of the tunnel portals*

The task of the excavation and support designs of the tunnel portals was to keep the open excavation to the minimum possible. This was achieved relatively easily due to the favorable geology (hard rock excavation). In most cases the excavation and support designs were included open excavations at the portals reinforced with rock bolts, shotcrete and drainage. The main danger was to keep potentially unstable rock wedges in place. A typical excavation of such a portal is given in the figure 6.

Despite the good geological conditions the design of the Votonosi eastern portal (figure 7) was forced to adopt big excavation in hard rock in order to accommodate the necessary equipment for construction of the Megalorema Bridge using the incremental launching method. The cut slopes was reinforced with long prestressed anchors and protected with a wire mesh.

In the case of Krimnos eastern portal (figure 8), and due to the very steep morphology and the thick weathering mantle at part of the tunnel portal area the designer adopted the construction of a vertical "berliner" type wall tied back with prestressed anchors.



Figure 6. Excavation arrangement of the Krimnos tunnel entrance portal excavation.

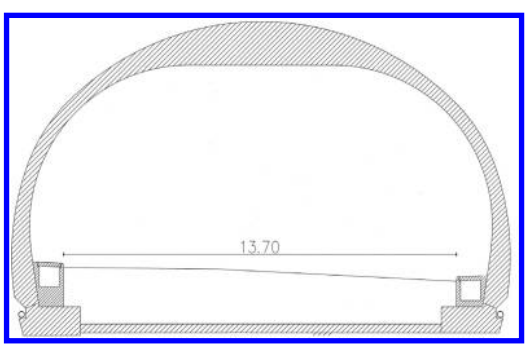


Figure 5. Enlarged three – lane cross section used in Kalamion tunnel.



Figure 7. Construction of the Votonosi tunnel eastern portal and the Megalorema Bridge.

Copyright © 2005 Taylor & Francis Group plc, London, UK

3.6 *Underground excavation and support designs of the tunnels*

For the excavation and support of the tunnel mainly five (5) typical excavation and support sections were designed following the principles of conventional tunneling, that are excavation by drill and blast or mechanical excavation, in two phases: top heading and bench. Special excavation and support cross sections were designed for the portal areas. The basic support material elements for the underground excavation support are the shotcrete, fully grouted rock bolts, lattice girders and steel sets, forepoles of different diameters, mainly Ø25 S500s rebars, Ø51 perforated hollow tubes with grout and Ø114 perforated hollow tubes with grout in the most adverse geological conditions, and mainly in cases were dead loads were anticipated ahead of the tunnel phase. A summary of the temporary excavation and support sections used is given in the table 3.

The adverse geological / geotechnical conditions in Anthochori tunnel were tackled using heavy support including 30 cm to 40 cm thick shotcrete shells, long self drilling rock bolts (9 m to 12 m), heavy steel sets or lattice girders, and face stabilization measures in the form of fiberglass anchors and forepoles.



Figure 8. Construction of the "Berliner" type vertical wall at Krimnos tunnel eastern portal.

3.7 *Final lining designs*

The placement of the excavation and temporary support is followed by the construction of a steel reinforced cast concrete final lining. The final lining is concreted in 12 m to 12.5 m segments after the placement of a geotextile and the waterproofing geomembrane on the surface of the temporary support. The final lining is dimensioned mainly using the DINs 1054, 1055, 4017, 4018, 1045-1, 1055-100, the Egnatia Odos tunnel design guidelines named OSMEO and the special Greek design, seismic regulation codes as Greece is placed in a highly seismically active environment.

3.8 *Tunnel construction*

The construction of the project started October 1999 and most of the civil works design of the tunnels was completed late 2000. The tunnel designs were prepared and approved from Egnatia Odos A.E. and issued to the contractors in stages: first the design of the temporary excavation and support measures for the portals and the underground part and at a later stage the design of the final cast in place concrete final lining. The type of contract is a "construct only" contract. The project is scheduled to open to traffic mid 2005. Figures 9 & 10 shows part of the project almost finished.

4 CONCLUSIONS

1. The friendly, mild topography of a terrain should not be the only criterion for the initial selection of a highway alignment. The geological conditions must be equally taken severe consideration.
2. The detailed combined geological – geotechnical investigations are absolutely necessary mostly in

Table 3. Summary of the support measures used for the construction of the tunnels.

	Excavation and support cross sections				
Support elements	A	B	C	D	E
Excavation phases	2	2	2	3	3
Excavation step per phase (m)	3–6	2.5–5	2–4	1–2–4	1–2–4
Shotcrete (cm)	5	10+ fibres	15+ fibres	20+ fibres	25+ fibres
Wire mesh	1T131				
Steel sets/lattice girders	–	–	LG70/26/D26	HEB120	HEB140
Rock bolts	Ø25, 4 m, 8/9 pieces	Ø25, 4 m, 11/12 pieces	Ø25, 4 m, 14/15 pieces	Ø25, 4 m, 7 pieces & 6 m	Ø25, 4 m, 7 pieces & 6 m
Face reinforcement				18 pieces 20 Ø76, 12 m	20 pieces26 Ø114, 12 m

Copyright © 2005 Taylor & Francis Group plc, London, UK



Figure 9. West portal of Votonosi tunnel and Votonosi bridge.



Figure 10. Votonosi bridge in between Anthochori and Votonosi tunnels.

the initial stages of a highway design. Spending money in such investigations, in the initial stages of a highway design is a good investment that in most of cases saves a lot of money.

3. The initial scenarios about the geological, geotechnical conditions and the costs, of the Metsovitikos river northern alignment, have been fully confirmed, as construction is almost finished.

REFERENCES

Ekonomopoulos, I., Kontothanasis, P.: Agios Nikolaos tunnel. Design and Construction Methods. Proceedings, Scientific meeting, Egnatia Odos S.A., Ioannina, Greece, 16 & 18 December 1999.

Georganopoulos, C., Kazilis, Pardalis, K.: The northern alignment of Metsovon. Results of a coordinated effort – lessons learned. Proceedings, Scientific meeting, Ioannina, Egnatia Odos S.A., Greece, 7 & 8 December 2001.

Georganopoulos, C. & Kazilis, N.: Innovations in Tunnel design management in Egnatia Odos A.E., Proceedings, Scientific meeting, Egnatia Odos S.A. Ioannina, Greece, 7 & 8 December 2001.

Kazilis, N.: The tunnels of Egnatia Motorway: In *"THE TUNNELS OF EGNATIA ODOS"*, Proceedings, Scientific meeting, Egnatia Odos S.A, Ioannina, Greece, 15 & 16 October 1999.

Pantzartzis, P., Botsialas, Ch.: Anthochori tunnel, Geological, geotechnical Investigations. Proceedings, Scientific meeting, Ioannina, Egnatia Odos S.A., Greece, 16 & 18 December 1999.

Rawlings, C & Silva, R., Kazilis, N., Aggistalis, G., Rachaniotis, N., Mantziaras, P.: London conference, Tunnelling 2001.

Tunnels and Tunnelling: Egnatia's tunnels feel the squeeze. Tunnels and Tunnelling International, November 2004.

Copyright © 2005 Taylor & Francis Group plc, London, UK

New developments in excavation and construction technology for rock and soft ground tunnelling

Copyright © 2005 Taylor & Francis Group plc, London, UK

New tunnel construction technique of pipe-roof method in saturated soft soil

J.k. Ge
Shanghai No. 2 Municipal Engineering Co., Ltd, China

ABSTRACT: The tunnel of Shanghai center ring located in the intersection of Hongxu-Beihong road is the first case to adopt pipe roof construction method in China, and also the largest tunnel section engineering of pipe roof in soft saturated layer in the world. Based on this case, a creative method of jacking cultivate box in pipe roof is presented. The scheme of this engineering is discussed in details in order to provide experience for other similar projects.

1 INTRODUCTION

As a trenchless technique, pipe roof method used to pass roads, railways and airport runways has gained good effects in underground construction engineering such as in Japan, America, Taiwan China etc. The steel pipes are connected by means of interlocks and then form a closed roof. In the gap of interlock, some water-stop material or cement pasted is injected to form a waterproof pipe curtain. After soil reinforced, excavation and brace set are carried out simultaneously, then the structure system is installed until all soil excavated. Alternative is also feasible, like the method of Japanese ESA (endless self-advancing method), which cultivate box is cast beforehand in shaft then pulled each other as soil excavated. Because of the effect of pipe roof, ground settlement decreases dramatically.

The tunnel, whose axis is North-South direction, located in the intersection of Hongxu-Beihong road is the important part of Shanghai center ring. This large section and long distance shallow tunnel passes through Hongqiao road and Xijiao Hotel along Hongxu road, and then connects with Beihong road (Figure. 1). Because of heavy traffic on Hongqiao road and many pipeline under it, as well as protection the environment of Xijiao Hotel zone, the creative method of cultivate box jacking in pipe roof (RBJ) is coming to generate after many times' proof and optimization (Shanghai No.2 Municipal Engineering Co., Ltd, 2003).

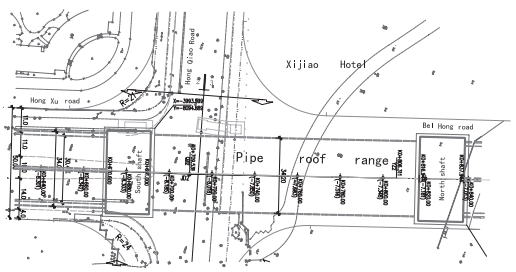


Figure 1. Plane view of the pipe roof engineering.

2 BRIEF INTRODUCTIONS TO PROJECTS

2.1 *Structure parameters*

1) The sizes of two shafts (North shaft and South shaft): 24.6 m long, 41 m broad and 17 m deep. The shafts are constructed by continuous concrete wall, which is 0.8 broad and 31 deep.
2) The range of soil reinforcement near the hole at both shafts is 8 m long, 38 m broad and 18 m high. The soil strength q_u after reinforced is up to 0.8 Mpa.
3) Steel pipe roof : 80Φ970 × 10 pipes with interlock forms a '$$' type of pipe curtain, which is 126 m long. Steel angle L100 × 80 × 10 is weld to form interlock.
4) Cultivate box: rectangular 2-hole RC structure, two directions and 8 driveways. Its outline size is

Copyright © 2005 Taylor & Francis Group plc, London, UK

34.7 m broad and 7.85 m high. The upper floor is 1.3 m thick, the bottom 1.4 m and middle wall 0.8 m. The box is divided into 8 segments and each one is 15.5 long. 4 segments are cast and jacked in each shaft (Figure. 2).

5) Depth of soil above pipe is 4.5 m∼5.0 m

2.2 *Engineering geology*

Box and pipe roof are located in ③ grey mock silty clay and ④ grey mock clay, which are both saturated soft soil with high water content, low permeability and poor bearing capacity. Mechanical and physical properties of soil are list in Table 1.

2.3 *Engineering environment*

Hongqiao road is primary road with heavy traffic, and the pipeline under the road is crisscross. Moreover many high quality hotels are located in this district of Xijiao Hotel. Because of these reasons, the ground settlement has a restrict requirement. Ground uplift value should be less than 30 mm and settlement less than 50 mm.

3 GENERAL CONSTRUCTION PROCESS

See Figure 3

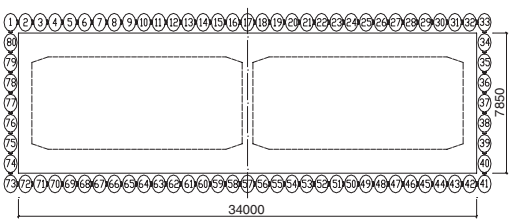


Figure 2. Schematic plan of pipe roof and cultivate box.

4 CHARACTERS OF RBJ METHOD

1) It is suitable for large section and long distance trechless tunnel in saturated soft soil.
2) Excavation face stability can be obtained by grid shield, as a result the soil inside pipe roof don't need reinforced.
3) The structure of covered tunnel constructed previously can provide counterforce for advancing box, no need reinforcing the soil around shafts.
4) Jacking method that replaces the reciprocal pulling one makes the force transformation system concision.
5) Integrated and reliable bracing and lubricating muddy between the box and pipe can decreases not only the ground settlement but also the drag force during the procedure of box advancing.

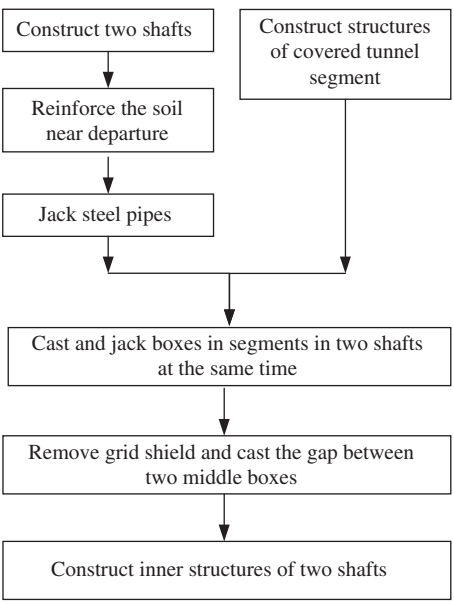


Figure 3. General construction process.

Table 1. Physical and mechanical properties of soil.

Layer sequence	Soil name	Depth of the layer bottom m	Water contend W %	Wet gravity ρ KN/m^3	Compression coefficient $a_{v0.1-0.2}$ MPa^{-1}	Modulus of Compression $E_{s0.1-0.2}$ MPa	Peak strength of R-test C kPa	Peak strength of R-test ϕ (°)	Unconfined compressive strength Intact soil q_u kPa
③	Grey mock silty clay	6.00∼8.40	45.6	17.3	0.96	2.36	14.4	13.0	30.7
④	Grey mock clay	14.50∼16.50	48.1	16.9	1.15	1.97	14.0	10.5	40.2

Copyright © 2005 Taylor & Francis Group plc, London, UK

6) Bottom steel pipes can be regarded as reference plane guiding the boxes advancing.
7) It can reduces engineering cost, shortens construction time and be safe and reliable.

5 JACKING TECHNIQUE OF STEEL PIPES

In order to save construction time, six pipe-jacking driving machines (slurry balance) operate concurrently in South shaft. Each machine drives 30 m per day. As for steel pipe driving with interlock, the crucial technique is high-accuracy attitude control, including axis deviation and rotation control (Dilpl.-Ing.Max Scherle, 1999). Over limits deviations can induce interlock deformable or crack, result in closure obstacle of interlocks between pipes, and then impact the boxes regular advancing. The control accuracy of this engineering is 30 mm up-down deviation, 50 mm left-right deviation and 2° rotations. The following measures are taken to ensure the high accuracy of attitude control.

1) Accuracy control system of pipe driving machine. Trail control system of computer software is adopted to guide construction, and slurry balance shield ensure the excavation face stability. In addition, reflection laser rectification system, inclinometer sensors, jack stroke adjustment sensors and rotation sensors are installed in machine to improve the jacking accuracy.
2) Special tectonic measures to improve maneuverability of rectification.
   In order to ensure the head section of driving machine to be able to rectify the direction of back stiff steel pipe, one way is to improve the ratio of distance to diameter and the other is to follow three transitional steel pipes. The pipes are connected with hinges, which can rotate slightly, and then formed a kind of multi-segments hinge system. Thus, the rectified jacks can drive the following steel pipes to change directions so as to achieve the aims of rectification and guideline. The rotation is prevented by use of stop mass set in transitional pipes, cutter head reverse motion and one-side kentledge.
3) Reasonable construction procedure and jacking sequence.
   Reasonable pipe jacking sequence can control the cumulative deviation of steel pipes within the permissible range. In this project, pipes are jacked in sequence at first. Reference pipe is installed only when the deviation can't satisfy the accuracy requirement; correspondently abnormity interlock was installed to enclose pipes according to the survey results. In addition, it is also important to establish accuracy management and monitor procedure, such as operation and deviation alarm system by use of attitude curve of head section.

6 CONSTRUCTION TECHNIQUE OF CULTIVATE BOX JACKING

6.1 *Seal structure design and assemble in hole*

Because of 20 cm gap existing between box and pipes and the gap filling with high viscous slurry to sustain the load, it is important to design and install reliable seal structure around the hole. Seal structure is installed in GML beam, connected firmly with the steel bar in beam by preembedded steel plate in seal structure. The structures are made of steel spring plate, seal rubber band and press plate. Two layers of structures are set in order to gain good effect (Figure. 4). Some preformed injected holes are set between the GML beam and double seal structures. Sealing slurry can be inserted in the gap between the first and second hinge if the seal structure cannot gain expected effect.

6.2 *Grid shield design and resemble*

Steel grid shield can cut clay, as well as sustains face stability in the case of the unreinforced soil inside pipe roof. In order to control the settlement within permissible range, the soil pressure on grid shield should be controlled to fluctuate round rest earth pressure during box advancing. Gate is fixed on each grid that can open and close as required. Earth pressure can be adjusted to rest earth pressure by means of advancing rate, grids size, and numbers and distribution of opening gates. Adopted value of soil strength is 0.3 MPa while designing grid shield. Whole grid shield is divided into 20 big grids in horizontal direction and 3 in vertical direction, and the big grid subdivided into small grids. The net horizontal distance of middle two big grids is 1500 mm, others 1300 mm. Vertical net distance from bottom grids to upper grids is 1715 mm, 1400 mm and 1435 mm respectively. The length of grid shield (embedded into soil) is 1300 mm. Every big grid is subdivided into some small grids, and the length of small grid is

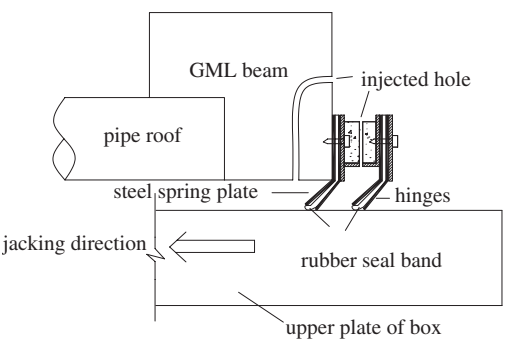


Figure 4. Schematic of seal structure.

Copyright © 2005 Taylor & Francis Group plc, London, UK

500 mm. Big grids are made of structural section and steel plate by bolt or wedding and formed a spatial criss-cross bearing system to bear earth pressure and sustain pipe roof. Small grids are welded to big grids and also form a spatial criss-cross structure system. All big grids are divided into 12 components, which are fabricated in plant, and then assembled into whole grid shield in site.

6.3 *Process of box departing hole*

1) Stability of reinforced soil near the departure hole.
   Continuous concrete wall at the place of hole will be removed when the large section box leaves the hole. In order to sustain the stability of soil at departure hole, 8 m long soils are reinforced, 3 m of these are cement mixing pile and the others are grouting method (Xia, 1999).
   – Parameters of reinforced soil (Liu, 1998)
     Parameters of soil reinforced by cement mixing pile: $q_u = 0.8$ MPa, $c = 65.4$ kPa, $\varphi = 15.0°$ $\gamma = 16.9$ kN/m^3
     Parameters of soil reinforced by grouting method: $p_s = 1.2$ MPa, $c = 45.0$ kPa, $\varphi = 12.7°$, $\gamma = 16.9$ kN/m^3
   – Calculation results
     Safety factor is 1.2 calculated by simplified Bishop Slice Method on the assumption that the pipes can't bear overburden soil. It is obvious that the soil excavation face is safe.
2) Continuous concrete wall removable at departure hole.
   When the grid shield and first segment box jacked into the seal structure along the advancing platform and only 0.8 m distance existed to the wall, then the concrete wall can be removed quickly by blast. Blast hole and blast loading are prepared beforehand.
3) Excavation of reinforced soil.
   When the grid shield is jacked through reinforced zone, the following measures are taken to excavate reinforced soil.
   At beginning, small grids are not welded in big grids.
   – Excavation in layers and blocks from up to down in orders.
   – Combination with small-size fluid power picks, hydraulic shovels and air picks to excavate.
   – Translation from big grids to small one is key to sustain stability of excavation face during box departure. This should be done at appropriate time in advance.

6.4 *Jacking force control of box advancing*

1) Estimation of resistance force of box advancing:
   – Head resistance force: $F_1 = \gamma HA_1 = 18 \times 10 \times 34.2 \times 7.85 = 48325$ KN

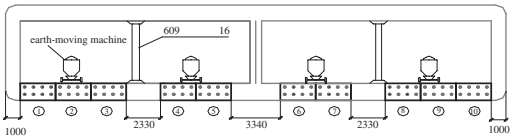


Figure 5. Arrangements of jacks (10 groups).

   – Frictional resistance force of upper box: $F_2 = \gamma hA_2\ \mu = 18 \times 6 \times 34.2 \times 63 \times 0.15 = 34905$ KN
   – Frictional resistance force of bottom box: $F_3 = (\gamma hA_2 + G)\ \mu = (18 \times 6 \times 34.2 \times 107 \times 63 \times 25)0.15 = 60184$ KN
   – Frictional resistance force of double sides of box: $F_4 = 2A_3 \times f_1 = 2 \times 7.85 \times 63 \times 12 = 11869$ KN.
2) Local bearing capacity of back bearing structure: $б = 2500 \times 8/2.4 \times 1.4 = 5952$ KN/m^2 $<$ 30000 KN/m^2.
3) Frictional estimation of 200 m long covered tunnel segments:
   $F5 = A_4 f_2 = 84 \times 200 \times 20 = 336400$ KN.
4) controlling jacking force: $F_0 = 200000$ KN.
5) Jacks arrangement.

According to total jacking force, 80 jacks are needed. They are divided into 10 groups, 8 per group (Fig. 5)

6.5 *Attitude control of box jacking*

Box is jacked along the bottom pipes. Because of gaps existing between pipes and boxes, together with stiff connection between them, the advancing boxes must be on line. Only when they are on line, the turning point cannot be formed at box joints to avoid retarding construction.

1) Altitude deviation control.
   Box is expected to jack at bottom pipe during boxes advancing. It can be seen in Fig. 6 that moments of A axis generated by forces can be divided into two rotation directions. F, Q, q generate low-head moments (clockwise), and the Pv, P_H, τ, P_1 generate up-head moment (counter clockwise). Above values of forces and distance to A axis affect the balance of moment during box advancing directly. Known from calculation that no matter one or four segments of boxes is considered, the low-head moments are much higher than up-head moments. So, in general, box cannot generate up-head phenomenon. If the boxes are tending to be up head in case, excavation way can be adjusted to decrease earth pressure of front face.

Copyright © 2005 Taylor & Francis Group plc, London, UK

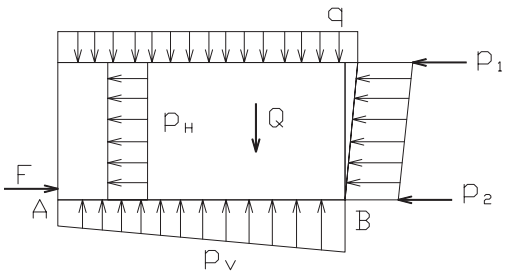


Figure 6. Force sketch of box.

2) Center deviation control of box.
   Center deviation control of box is critical as well as difficult during advancing. Main ways are as following:
   – Real-time and continuous surveying the boxes attitude by means of automatic measurement system to instruct box rectification.
   – Adopting computer synchronous control system of fluid power jacking, it can not only satisfy the 80 jacks in-step, but also realize manual rectification by groups.
   – Setting guide pier at double sides of box in shaft to restrict center deviation while box departure.
   – Adjusting excavation quantity of soil at left or right side to rectify center deviation.

6.6 *Ground settlement control as box jacking*

1) Stability control of excavation face.
   When boxes are jacked through improved soil into unreinforced soil, which is saturated soft clay with horizontal multi-layer sands, earth pressure and free water pressure may be able to induce the excavation face of grids unstable, as well as soil and water collapse. In order to avoid these hazards, the following measures can be used. Small grids are installed in big one to control soft soil extrusion; soil near excavation face can be reinforced or drained to improve strength through grids directly in case of local unstable soil occurred; all gates are closed after one box finished advancing until the next segment is ready.
2) Injection process of bentonite slurry.
   Special slurry with water-stop is injected into the gap between boxes and pipes in time while jacking (North China petroleum university, 1974). So this type of slurry not only satisfied the seal requirement, but also maintains stationary pressure to sustain and lubricate.
3) Slurry substitution.
   The bentonite slurry should be substituted after all box jacked. Substitution slurry is composed of cements mixed with fly ash, and the latter proportion is up to 30%.

7 CONCLUSIONS

It is feasible to adopt pipe roof method combined with box jacking (RBJ) to construct large section in saturated soft soil.

(1) Deviation of pipe jacking can be controlled within permissible range by means of high accuracy direction control system.
(2) 8 m long soils reinforced at the front of departure hole can maintain the stability of excavation face while box departure.
(3) It is feasible to use big grids combined with small grids to sustain stability of excavation face.
(4) It is safe and reliable to use covered tunnel as back bearing structure.
(5) Injected special slurry can not only restrain ground settlement but also reduce resistance forces.

REFERENCES

A3.5 bidding documents of center ring of Shanghai (Beihong road pipe roof tunnel)[R], Shanghai No.2 Municipal Engineering Co., Ltd, 2003 (in Chinese)

Dilpl.-Ing.Max Scherle, Qi pingsheng translation, 1983, pipe jacking engineering, Chinese construction press Beijing, (in Chinese)

M.Y. Xia, J.L. zeng, 1999, construction manual of underground engineering, Chinese construction press, (in Chinese)

North China petroleum university, 1974, drilling mud, Beijing fuel and chemistry press, (in Chinese)

Z.F. Liu, 1998, new technology of soil and foundation, Haicao Press, (in Chinese)

Copyright © 2005 Taylor & Francis Group plc, London, UK

Tunnelling in difficult ground and groundwater conditions

Dipl.-Ing. H. Quick & Dipl.-Ing. S. Meissner
Dipl.-Ing. H. Quick, Ingenieure und Geologen GmbH, Darmstadt, Germany

ABSTRACT: In the course of the a new highspeed railway line the Tunnel Offenbau is built in difficult ground and groundwater conditions. Due to these conditions and the bordering village Offenbau the Tunnel is constructed in top cover technique combined with compressed air in order to guarantee the serviceability of the housing at all times. The construction of the tunnel was accompanied by an extensive monitoring programme, which included the monitoring of tunnel and the neighbouring constructions. Moreover, the monitoring is required for the conservation of evidence of the housings and all structural objects.

1 GENERAL INSTRUCTIONS

The Tunnel Offenbau undercrosses a small mountain hill and is located between the existing highway A9 and the village Offenbau. The Tunnel was planned to built in open cut technique (Phase 1). Due to the difficult soft ground and groundwater conditions and the nearby village the tunnel had to be re-planned and was constructed by means of the top cover technique combined with compressed air as well as additional groundwater lowering in order to reduce the required air pressure (Phase 2).

2 GROUND AND GROUNDWATER CONDITIONS (PHASE 1)

In the first phase of the construction a ground investigation was conducted. The explored ground consisted of quaternary fills (sands and clay/silt) and soft weathered claystone respectively claystone.

The groundwater condition were characterized by one unconfined groundwater level in the quaternary fills.

3 TUNNELLING METHOD (PHASE 1)

In the phase 1 the Tunnel was planned in open cut technique with slopes. The unconfined groundwater level was lowered with wells. During the first stages slope stability problems, large settlements of the tunnel segments and settlements of the surface due to the groundwater lowering occurred. To explore the ground more in detail an additional ground investigation (phase 2) was initiated.

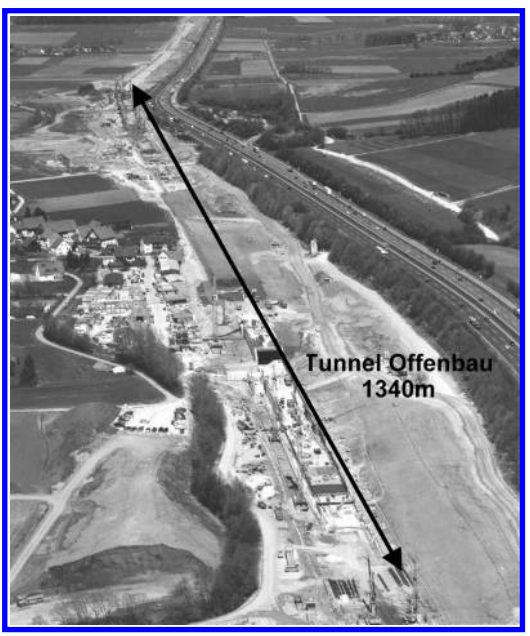


Figure 1. Overall situation of the Tunnel Offenbau.

4 GROUND AND GROUNDWATER CONDITIONS (PHASE 2)

Due to the additional ground exploration (Phase 2) it was possible to forecast the ground and groundwater condition lateral to the line more in detail. All obtained data was interpreted and so the following prognosis of the ground and groundwater conditions was made.

Copyright © 2005 Taylor & Francis Group plc, London, UK

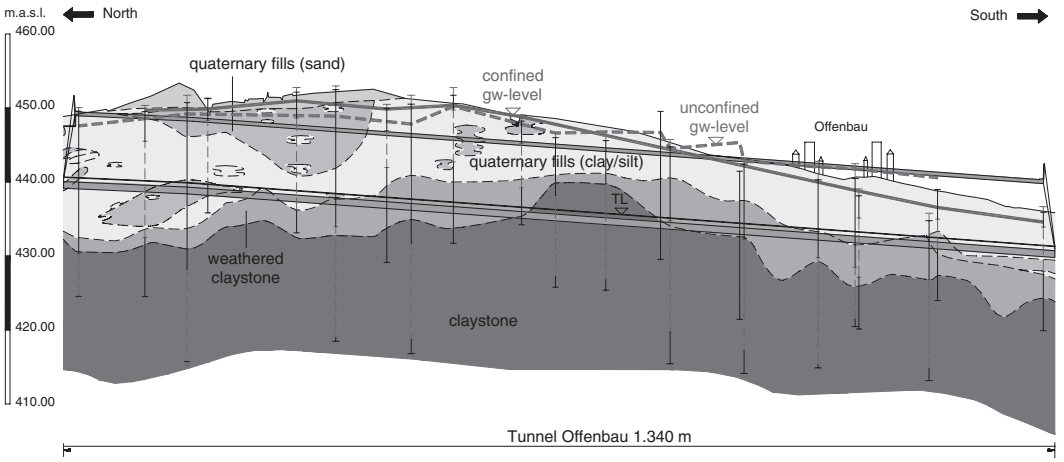


Figure 2. Geotechnical longitudinal section (Phase 2).

The ground conditions are characterized by quaternary fills (sands and clay/silt) and soft weathered claystone with only little stiffness respectively claystone. Within the quaternary fills surfaces with reduced shear parameter were found. The weathered claystone and the claystone tends to swell.

In the area of the tunnel two groundwater levels were found: An unconfined groundwater level in the quaternary fills and a confined (subartesian and artesian) aquifer in the claystone underneath the weathered soft clay. (Fig. 2).

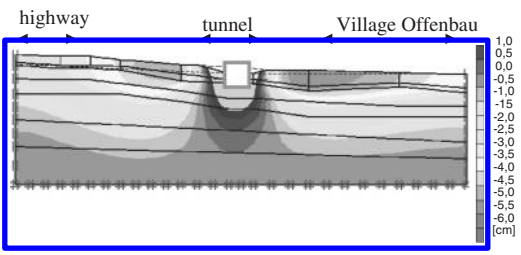


Figure 3. Analysis of the settlements.

5 TUNNELLING TECHNIQUE (PHASE 2)

The re-planned tunnelling technique had to take into account the new conclusion from the geotechnical investigation (phase 2), such as the lower stiffness of the ground, the surfaces with little shear resistance, the confined groundwater level in the claystone and the swelling processes in the claystone. A further boundary condition for the construction of the tunnel was the limitation by authorities of groundwater withdrawal. The serviceability of neighbouring construction such as the village and the highway had to be guaranteed at all times. The proof of the serviceability was carried out with numerical analysis. Figure 3 shows settlements due to a groundwater lowering of the unconfined und the confined groundwater level for the tunnelling in open cut technique (phase 1).

Therefore, a groundwater lowering (up to 16 m) of the two groundwater levels could not be taken into account.

The tunnel was consequently re-planned in top cover technique combined with compressed air pressure and if necessary additional groundwater lowering to reduce the maximum air pressure. The tunnel was constructed in 7 stages:

1. Construction of the watertight bored pile walls along both sides of the tunnel. During construction these piles have the function of a retaining wall, later on these piles conduct the all loads into deeper ground layers with higher bearing capacity (claystone). To verify the verticality of the piles and to reduce any imperfection (later on air loss problems), each pile was measured and documented with a inclination system. Furthermore each pile excavation was geologically documented to draw a comparison with the prognosticated geological situation (Fig. 4).
2. Excavation between the walls and construction of the reinforced tunnel roof (top cover). The reinforcement tunnel roof is attached to the pile wall.
3. Earthwork: filling up the ground to the former surface.
4. Driving (excavation) of the upper half under compressed air (driving from south to north).
5. Driving (excavation) of the lower half under compressed air (north to south) with additional

Copyright © 2005 Taylor & Francis Group plc, London, UK



Figure 4. Construction of the watertight bored pile walls.



Figure 5. Construction of the tunnel roof (top cover).



Figure 6. Compressed air driving – air lock.

groundwater lowering to limit a maximum air pressure value of <1,0 bar.
6. Construction of the invert (temporary).
7. Construction of the inner lining under atmospheric pressure (Fig. 8).

In the construction phases 4 to 5 the loads from the air pressure and the uplift (groundwater) are transferred via the tunnel roof into the bored piles into the ground. The piles receive tension load. In the construction phases 6 and 7 as well as in the finale state



Figure 7. Construction of the invert (temporary).



Figure 8. Construction of the inner lining.

the loads from groundwater and swelling processes as well as the dead and live loads are conducted via the invert/lining into the piles. According to the groundwater level the piles receive tension respectively compression load.

The quaternary groundwater seepage at right angle to the tunnel is guaranteed by 5 inverted siphons. The seepage of the groundwater in the claystone is possible due to the bored piles with different length. For the proof of the seepage extensive numerical groundwater calculation were done.

6 PILE LOADING TEST

For the first design of the pile foundation of the tunnel (Phase 2) the pile capacity parameter derived from the recommendation of the German technical rule. To determine these parameters more accurate or even to optimise the design pile loading tests were carried out.

Two static and dynamic loading tests with pile length of 22 m and 27 m regarding the actual load were planned. For this an extensive monitoring programme with pressure cells and strain gages in the piles was installed (Fig. 9). Two piles (PN) end in the layer

Copyright © 2005 Taylor & Francis Group plc, London, UK



Figure 9. Measuring systems for the pile loading test.

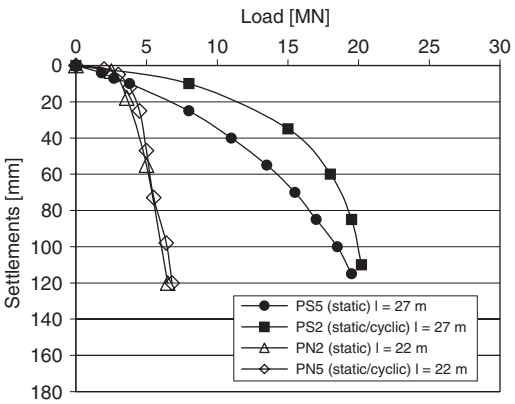


Figure 10. Results from the pile loading test.

of the weathered claystone, the other two piles (PS) end in the claystone with higher bearing capacities.

After execution of the four pile loading tests the pile capacity parameter, such as the ultimate skin resistance and ultimate end bearing were evaluated. According to the results of the pile loading tests the pile bearing capacity could be increased in comparison to the first assumption of phase 2. Furthermore, nearly no impact was observed due to the cyclic loading on the result of the pile capacity parameter (Fig. 10).

With the determination of these parameter approx. 10000 m of piles have been reduced compared to the first design of the phase 2.

7 TUNNEL DATA

In the following the leading data of the tunnel is presented:

- Length of tunnel: 1340 m
- Tunnel width (clearance): 12.30 m

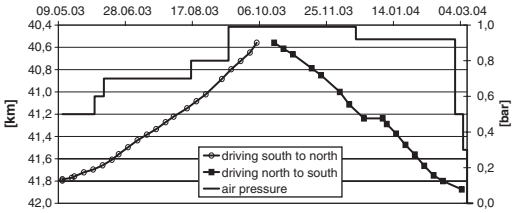


Figure 11. Timetable of the construction.

- Clear section: 92 m^2
- max. overburden: 7.5 m
- Secondary piles: 17 m beneath invert
- Primary piles: 2 m beneath invert
- Piles: 70000 m
- concrete for piles: 56000 m^3
- Armour: 8700 to

The Tunnel was constructed in the years 2003 and 2004. In May 2003 the driving (excavation) of the upper half under compressed air (driving from south to north) began. The air pressure was increased depending on the confined groundwater level in the tertiary claystone (Fig. 11). In October 2003 the driving was reversed and the lower half of the tunnel was excavated under compressed air and additional groundwater lowering regarding the maximum air pressure of 1,0 bar. In March 2004 the driving was finished and the invert (temporary) was installed and the compressed air shut down.

8 MONITORING PROGRAMME

The monitoring programme of the Tunnel Offenbau consisted of geodetical cross sections, geodetical bolts within the tunnel, inclinometer, extensometer and groundwater piezometer. According to the strict regulation of max. settlements of the neighbouring constructions, the emphasis of the programme was to observe the impact of the air pressure driving in addition with the groundwater lowering in the claystone. The measuring systems of the geodesy and the piezometer were observed and interpreted weekly.

9 RESULTS OF THE MONITORING PROGRAMME

The largest impact due to the construction of the tunnel was expected for the construction stages 5/6 (driving under compressed air supported by a groundwater lowering in the tertiary clay). Figure 12 shows the lowering of the confined tertiary groundwater level orthogonal to the tunnel meanwhile construction stages 5/6. The tertiary groundwater was lowered

Copyright © 2005 Taylor & Francis Group plc, London, UK

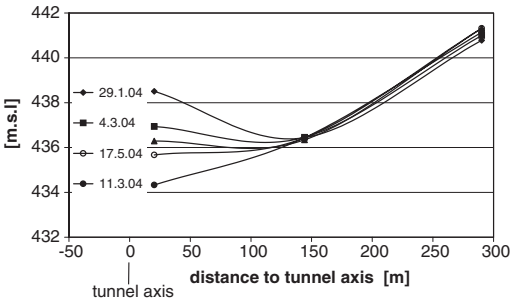


Figure 12. Tertiary groundwater lowering – cross section.

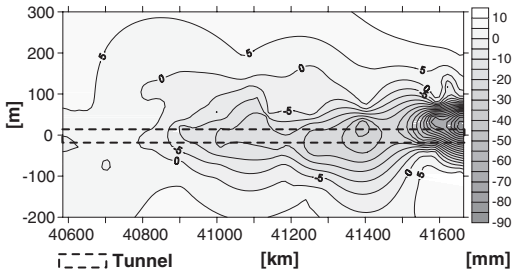


Figure 13. Surface settlements (17.03.04) – plan view.

directly next to the tunnel approx. 4 m (29.01.04 – 11.03.04). In March 2004 the lowering was shut off and the groundwater level raised. In a distance to the tunnel axis of 150 m no impact could be observed.

The surface settlements due to the construction of the tunnel with additional groundwater lowering are shown in Figure 13. The settlements reached a maximum of 2 cm. Only in the southern part, where the surface had to be artificially filled up to the tunnel roof, the settlements added up to approx. 9 cm.

10 CONCLUSION

The Tunnel Offenbau had been planned in open cut technique. Due to the new conclusions concerning the ground and groundwater conditions the tunnel had to be re-planned. After all the tunnel was constructed successfully in top cover technique with compressed air driving and additional groundwater lowering of the confined groundwater level. The groundwater lowering was used to limit the air pressure during construction to a maximum of 1,0 bar. The construction of the tunnel was accompanied by a extensive monitoring programme to observe all impact on all neighbouring constructions. By means of this programme the serviceability of the neighbouring constructions as well as of the tunnel itself was evaluated. Moreover, with the monitoring the conservation of evidence of the housings and all structural objects was possible.

In order to optimise the tunnel construction pile loading tests in consideration of all boundary conditions were carried out.

Copyright © 2005 Taylor & Francis Group plc, London, UK

Visualizing excavated soil flow in the cutter chamber of a large earth pressure balanced shield

H. Dobashi, Y. Sakurai, Y. Konishi & S. Ouchi
Metropolitan Expressway Public Corporation

K. Matsubara, A. Kitayama & H. Takahashi
Obayashi Corporation

ABSTRACT: Of the Metropolitan Expressway Central Circular Shinjuku Route, which is being constructed by the Metropolitan Expressway Public Corporation, tunnels of the SJ51 to SJ53 Sections were decided to be excavated using a world-largest earth pressure balanced shield, which has an outer diameter of 12.02 m. In the conventional earth pressure balanced shield method, plastic flow of excavated soil within the cutter chamber, which is indispensable for stable excavation, has never been analyzed, and the method has been little used to excavate tunnels of over 10 m in diameters. In this project, a system for visualizing the flow of soil inside the chamber was decided to be developed and introduced. This paper describes an overview of the system and results of its application.

1 INTRODUCTION

The Metropolitan Expressway Central Circular Route (hereinafter referred to as the "Central Circular Route"), which is being constructed by the Metropolitan Expressway Public Corporation, is a circular expressway to be located outside the Circular Route 1, and will be about 47 km long. Approximately 26 km, or almost 60% of the total length, has been completed and is in service. The remaining 20 km is the Central Circular Shinjuku Route (hereinafter referred to as the "Shinjuku Route"), which constitutes the western arc of the circular route and is actively being constructed, and the Central Circular Shinagawa Route, which will be the southern arc and is under a procedure for project execution. The Central Circular Route aims to alleviate traffic congestion in Tokyo Metropolis by providing a detour route for vehicles passing through the city and decentralizing the vehicles and to create a radial and well-balanced traffic network. The Route is also expected to improve the environments in the metropolis by reducing exhaust gas as a result of congestion alleviation, and its completion is awaited.

The Shinjuku Route is 11 km long and connects Aobadai, Meguro Ward, Tokyo, and Kumano-cho, Itabashi Ward. The section is constructed mainly by the shield tunneling method to smoothen construction in crowded areas and minimize impacts to residents. The shield section is divided into eight sections, each of which involves shield tunneling of over 10 m diameter. Figure 1 shows an overview of the project, and Figure 2 shows an overview of the Metropolitan Expressway Central Circular Shinjuku Route.

Tunnels of over 10 m in diameter are usually excavated using the slurry shield method, which is easy to control the face stability. However, the earth pressure balanced (EPB) shield method and a shield machine that has an outer diameter of 12.02 m, the largest in the world, were decided to be used in this project due to the following reasons:

(1) The site to construct the starter shaft was too small to accommodate the necessary equipment for slurry shield, and



Figure 1. Overview of the project.

Copyright © 2005 Taylor & Francis Group plc, London, UK

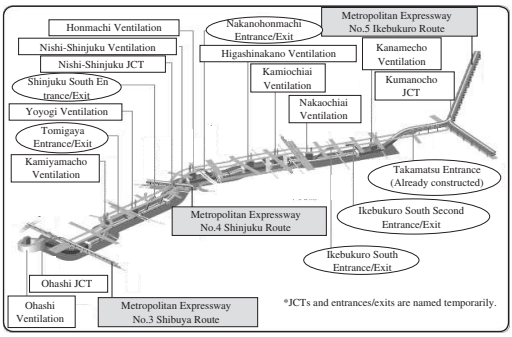


Figure 2. Central circular Shinjuku route.

(2) The overburden depth could be as shallow as 7.3 m (0.6D), and slurry may erupt to the surface affecting peripheral buildings.

Earth pressure balanced shields have been little used for large diameter tunnels since the plastic flow of excavated soil within the chamber, which is indispensable for stabilizing the face, has been little understood and no monitoring methods have been established.

In this project, a system for analyzing excavated soil flow in the cutter chamber was developed and introduced to evaluate and understand the conditions of excavated soil in the chamber aiming to execute appropriate face control and contribute to the planning and design of future earth pressure balanced shields.

This paper describes an overview of the new visualization system and results of its application to an actual project.

2 OVERVIEW OF THE PROJECT

An overview of the project is shown in Table 1.

The soil of the ground to excavate consists of alternate layers of dense Musashino gravels (N value: 12 to over 50, hereinafter referred to as the "Mg layer"), very dense Tokyo gravels (N value: over 50, hereinafter referred to as the "Tog layer"), and Tokyo clayey soil, which mainly consists of silt with strips of fine sand (hereinafter referred to as the "Toc layer") up to about 350 m from the starting shaft. The Mg and Tog layers contain gravels of about 100 mm diameter (assumed maximum diameter: 300 mm), have high water content, and showed moderate permeability coefficients whose order is 10^{-3}. The section up to about 1,000 m consists mainly of the Tog layer. Solidified layers of Edogawa clayey soil (N value: 11 to over 50, hereinafter referred to as the "Edc layer") lies under the tunnel. The remaining section up to the arrival shaft consists of alternate layers of Edc and moderate to very dense Edogawa sandy soil (N value: 12 to over 50, hereinafter referred to as the "Eds layer"). A soil profile is shown in Figure 4.

Table 1. Overview of the project.

Project name	Tunnel excavation project of SJ51 to SJ53 (Clockwise Route)		
Owner	Metropolitan Expressway Public Corporation		
Period of the project	March 14, 2002 to February 15, 2005		
Excavation method	Earth pressure balance shield method (air bubble)		
Contents			
Diameter of the shield	12.020 mm (world largest)		
Tunnel length	2,018.1 m	Outer diameter of segment	11,800 mm
Segment type	Reinforced concrete, ductile, steel		
Amount of soil to excavate	229,766 m^3	Over-burden depth	7.3～23.4 m

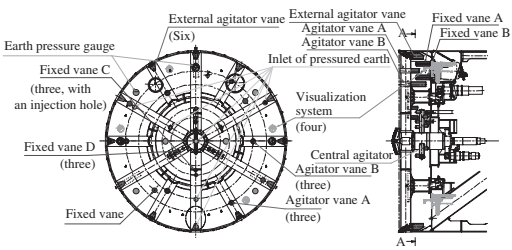


Figure 3. Overview of the shield.

3 DEVELOPMENT AND INTRODUCTION OF VISUALIZATION SYSTEM

3.1 *Problems of large earth pressure balanced shield*

In earth pressure balanced shield, (1) the flow of excavated soil, (2) earth pressure on the face, and (3) the amount of excavated soil should be appropriately controlled to stabilize the face. Especially, the plastic flow of excavated soil must be maintained otherwise soil may erupt from the screw conveyer, destabilizing the face and affecting the ground surface. Large-diameter earth pressure balanced shield has been difficult to understand whether the excavated soil and additives are appropriately mixed and stirred and the plastic flow of the soil is maintained or not in its cutter chamber.

Copyright © 2005 Taylor & Francis Group plc, London, UK

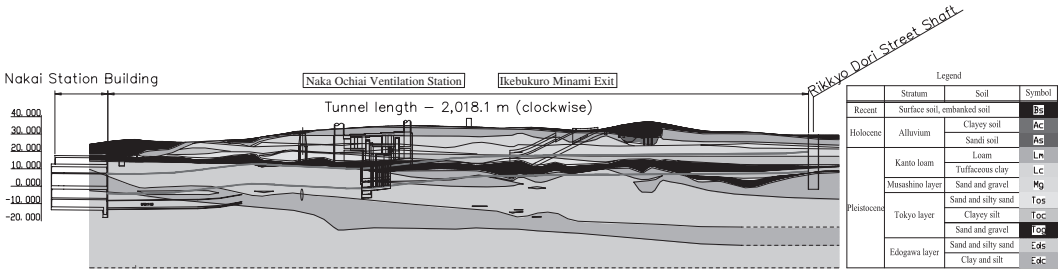


Figure 4. Soil profile.

Table 2. Problems concerning the stability of the face of a large-diameter earth pressure balanced shield and counter-measures.

Stability of face	Problem	Countermeasure
Plastic flow of excavated soil	Selection and injection methods of additives	Additives were tested using the natural ground to excavate and then selected Three kinds of air bubbles were prepared, from which the one appropriate for the ground was selected: Type A (for clayey soil and silt) Type B (for sand) Gelled foam (for sand and gravel) Injection holes were arranged as shown in Figure 3 so that the additives were injected into the natural ground uniformly
	Improvement of agitation of excavated soil in the chamber	Central agitators were arranged along the inner periphery of the machine, where the soil is difficult to agitate: Fixed vanes and agitator vanes were arranged as shown in Figure 3
	Monitoring and evaluation of plastic flow of excavated soil in the chamber	A system for visualizing the inside of the chamber was developed and implemented
Earth pressure control	Understanding the earth pressure distribution in the chamber	Earth pressure gauges were arranged in the chamber as shown in Figure 3
	Setting of appropriate control earth pressure	Control earth pressure was established by considering the actual earth pressure distribution. The validity of the control pressure was verified using a differential settlement gauge
Water pressure control	Prevention of soil eruption into the shield machine	Primary and secondary screw conveyors were installed apart to reduce earth and water pressures, and plug zone was formed to cut off water. Two or more earth pressure gauges were installed in the screw conveyors to detect sings of eruption in advance

Measures were taken in this project as shown in Table 2 to ensure the plastic flow of excavated soil in the chamber of a large earth pressure balanced shield, which involved selection of effective additives, improvement of stirring performance, and development and introduction of a system for visualizing the flow in the chamber.

3.2 *Overview of the visualization system*

Plastic flow of soil, which is indispensable for the stabilization of the cutting face of an earth pressure balanced shield, occurs when the shear stress of the soil, which is caused by certain external force, exceeds a certain value ($\tau 0$) and produces shear rate (Figure 5).

Copyright © 2005 Taylor & Francis Group plc, London, UK

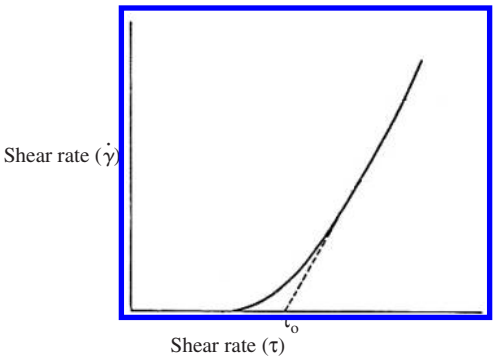


Figure 5. Plastic flow state of soil.

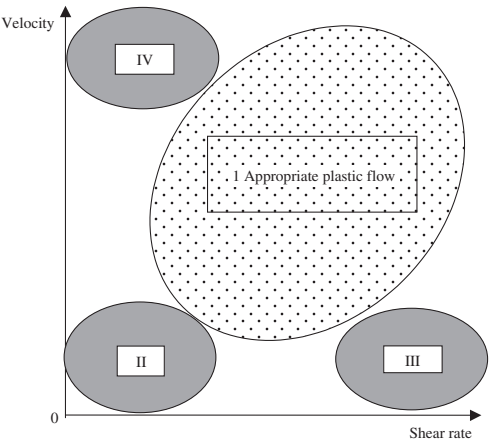


Figure 6. Relationship between the velocity of soil and shear rate.

Shear stress signifies force per unit area that causes flow of excavated soil, and shear rate means changes in shear strain per unit time.

Velocity is given to excavated soil in a cutter chamber by the rotation of the cutter, and shear stress is produced be fixed mixing bars and agitators. When the excavated soil in the chamber is in plastic flow, shear rate should have been generated along with the production of shear stress. Conditions of excavated soil in cutter chambers classified based on velocity and shear rate are shown in Figure 6. In Range I, the velocity and shear rate are appropriate, suggesting plastic flow of soil. In Range II, where both the velocity and shear rate are small, the soil is not likely to be in plastic flow but should be retained and in a state difficult to agitate. In Range III, where the velocity is small and the shear rate is large, the soil is likely to be very flowable. In Range IV, where the velocity is large and shear rate is small, soil is not in plastic flow, and agitation is little effective.

The system developed to visualize the flow of soil in the cutter chamber estimates the plastic flow state using the concepts of velocity and shear rate of soil within the chamber, analyzing the soil flow by modeling the inside of the chamber (Figure 7), and simulating the velocity and shear rate. To verify the precision of the simulation, electric rotating flappers were developed and installed to the periphery of the bulkhead to measure changes in torque (Photograph 1). The flappers are rotated by electric motors and measure changes in torque of rotation. Changes in torque monitored by the flappers and changes in torque estimated by the simulation are compared to examine the validity of the simulation. Back analysis is conducted based on the changes in torque monitored by the flappers to evaluate the states of soil in the chamber.

This system aims for appropriate excavation control in which the plastic flow state of excavated soil is reflected by inspecting simulation result. The simulation is also expected to contribute to optimum designs

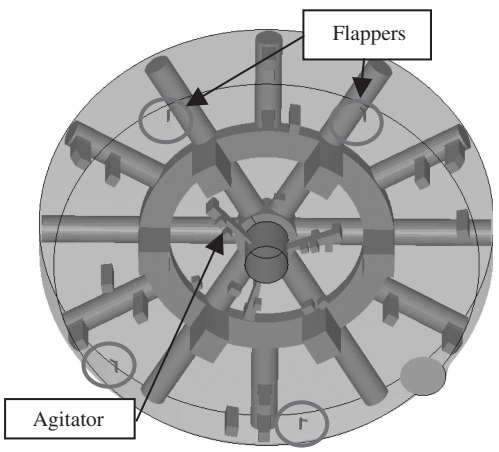


Figure 7. Model.



Photograph 1. Measurement instrument (flapper).

Copyright © 2005 Taylor & Francis Group plc, London, UK

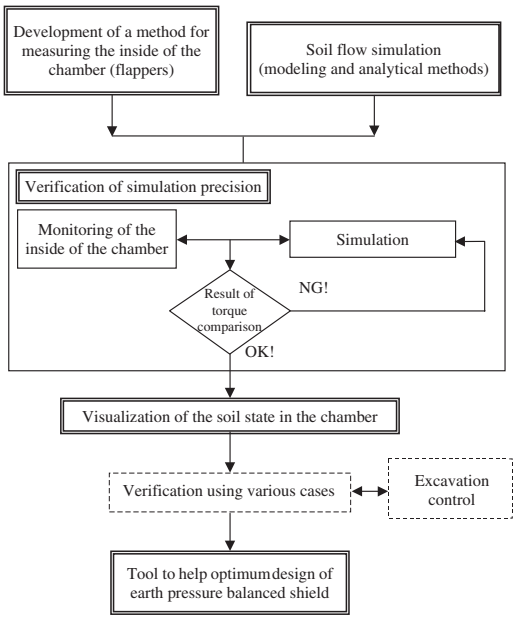


Figure 8. Flow of development and introduction.

and plans of earth pressure balanced shields of small to medium diameters as well as large diameters and those that have profiles other than circular.

A flow of development and implementation of the system is shown in Figure 8.

The system was developed and implemented by first verifying the precision of simulation using the shield machine of this project, checking the precision, and then evaluating the plastic flow state of the soil in the chamber.

3.3 *Implementation of the system in the project*

(1) Verification of simulation precision

The precision of simulation was verified by comparing the changes in torque monitored using the flappers under the ground conditions shown in Figure 9 and excavation conditions shown in Table 3, and the changes in torque calculated by the simulation to which the conditions in Figure 9 and Table 3 were inputted.

The results are shown in Figure 10. The changes and values were similar, showing that the simulation was precise.

(2) Visualization of soil states in the chamber

When the shield excavated the tunnel under the conditions shown in Figure 9 and Table 3, the face was stable and no soil erupted from the screw conveyor. The excavation states suggested that the soil in the chamber was in plastic flow. The results of simulation of the soil states in the chamber are described.

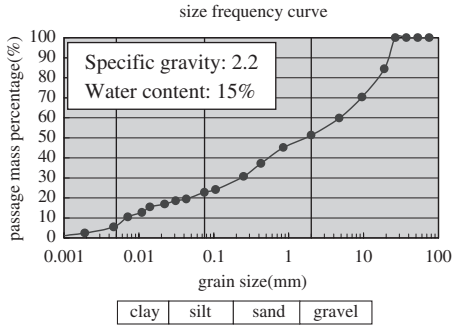


Figure 9. Ground conditions.

Table 3. Excavation conditions.

Excavation conditions	
Agitator revolution speed	1.365 rpm
Cutter revolution speed	0.46 rpm
Flapper revolution speed	1.88 rpm
Excavation speed	20 mm/min
Ground conditions	See Figure 9

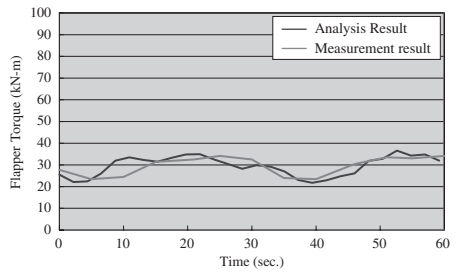


Figure 10. Result of flapper torque comparison.

Figures 11 to 13 show the velocity distribution (left) and shear rate distribution (right) at three cross sections of 1) near the face (z = 1.7 m, z: distance from the bulkhead), 2) at the center of the chamber (z = 0.9 m), and 3) near the bulkhead (z = 0.45 m), respectively. Velocity is expressed in vector quantity, and arrows show the direction and the quantity of flow. Shear rate is expressed in scalar quantity, and the quantity is expressed in color brightness. According to the simulation, the distribution of both the velocity and shear rate was not uniform transversely, and was different between the periphery, near the cutter support, and near agitators. Their longitudinal distributions were also different between the face and the bulkhead.

Figure 14 plots velocity (m/sec) at arbitrary points on the Y axis against the shear rate (1/sec) at the

Copyright © 2005 Taylor & Francis Group plc, London, UK

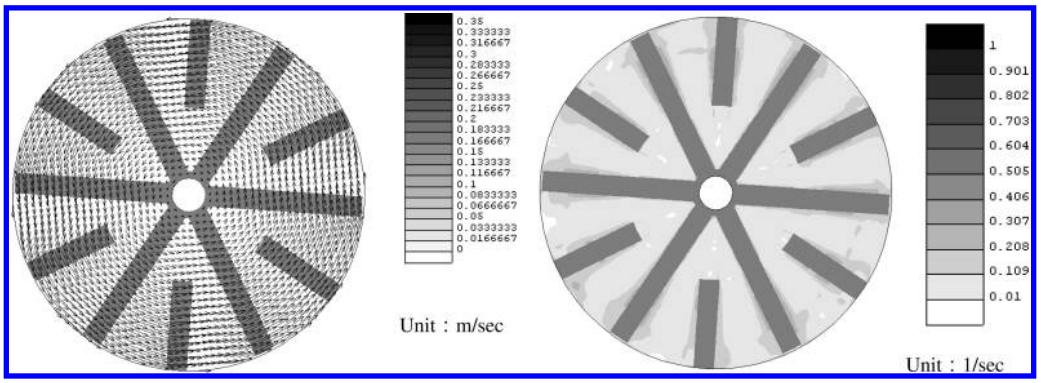


Figure 11. Velocity distribution and shear rate distribution at z = 1.7 m (near the cutter face).

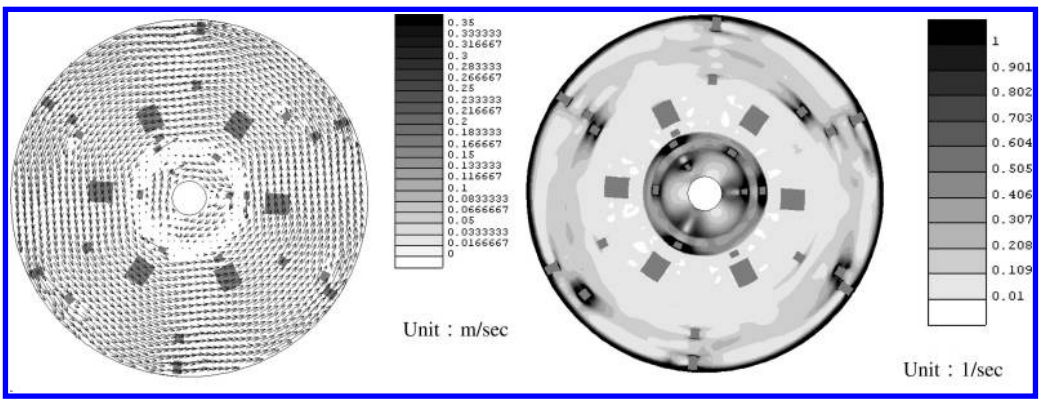


Figure 12. Velocity distribution and shear rate distribution at z = 0.9 m (at the center of the chamber).

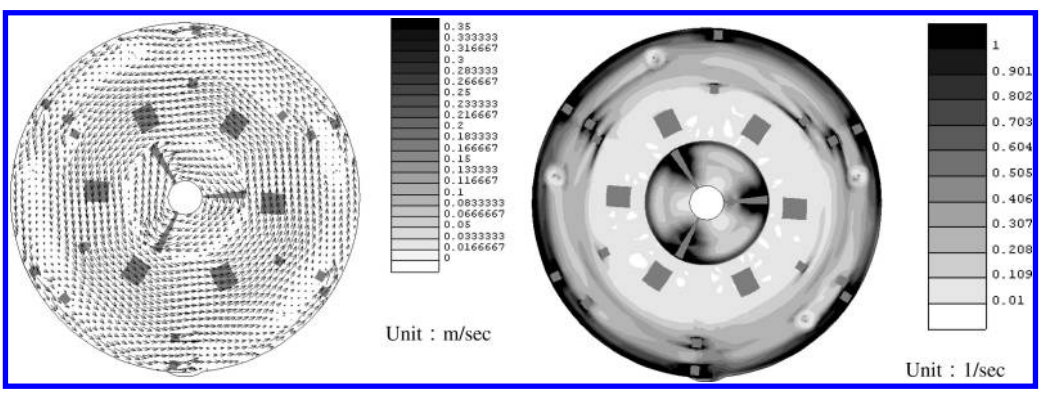


Figure 13. Velocity distribution and shear rate distribution at z = 0.45 m (near the bulkhead).

points in log on the X axis. The figure shows, from left to right, the distribution at profiles z = 1.7 m, 0.9 m and 0.45 m. The transverse zone was broadly divided into the 1) agitator area (0 to 1/3 R, R: radius of the shield), 2) cutter support area (1/3R to 2/3R), and 3) peripheral area (2/3R to 1R), which are shown by different marks in the plot.

A tendency is shown that the relationships near the cutter face (z = 1.7 m) are far from the center of the graph but the points for nearer the bulkhead

Copyright © 2005 Taylor & Francis Group plc, London, UK

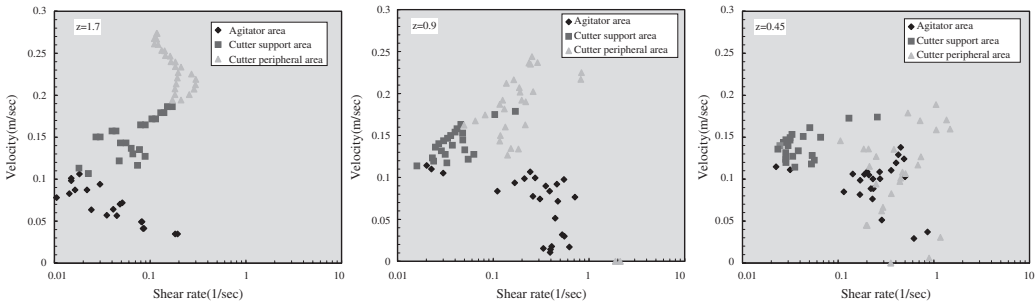


Figure 14. Relationship between velocity and shear rate for each profile.

(z = 0.45 m) are nearer to the center. Especially, increases in shear rate are apparent in the agitator area and peripheral area.

On the other hand, in the cutter support area, velocity and shear rate were both uniform from the cutter face to the bulkhead.

Based on the classification used for Figure 5, the monitored data in the agitator and peripheral areas approached the center of the graphs as the soil approached the bulkhead likely because the soil was increasingly converted into plastic flow as it approached the bulkhead by the effects of the fixed vanes and agitators. On the other hand, in the cutter support area, the data are located more to the left of the graphs than the other data, and shear rates were low even when the velocity of the soil was as fast as the speed of the cutter rotation (about 0.15 m/sec), suggesting that the soil moved together with the cutter as solid masses and was difficult to be in plastic flow. The simulation showed that there were areas within the chamber where the soil was difficult to be in plastic flow, but the simulation was regarded to simulate a state in which the soil in the chamber was in plastic flow since the cutter was stable and the soil was steadily discharged during the actual excavation that was subjected to the simulation analysis. The results of simulation also suggested that the cutter support area may need to be further investigated for designing and planning new shield machines.

4 CONCLUSIONS

The system for visualizing the state of excavated soil in cutter chamber was developed and introduced. The precision of the simulation was verified in an actual tunneling project, and the system was effective to evaluate the state of soil in the chamber. The soil to excavate is anticipated to change in this project, and simulation precision will be verified under various soil and excavation conditions to evaluate the states of soil in the chamber.

During this project, the precision of simulation will be improved, appropriate excavation control will be conducted by reflecting the plastic flow of excavated soil, and establishment of a system that contribute to optimum designs and plans of earth pressure balanced shields of small to medium diameters as well as large diameters and those that have profiles other than circular is aimed for.

Copyright © 2005 Taylor & Francis Group plc, London, UK

Planning and construction of Keelung River Yuanshantzu Flood-Diversion Tunnel Project

H. Shimizu, H. Hamada & T. Yasunaga
KAJIMA Corporation Keelung River Project Office, Taipei County, ROC

K. Taira & M. Kuniya
KAJIMA Corporation, Tokyo, Japan

ABSTRACT: Keelung River Yuanshantzu Flood-Diversion Tunnel project is located in about 30-km eastside of Taipei City, the Republic of China (Taiwan). Its purpose is to divert flood-water in Keelung River to the East Sea. This Project comprises water intake facilities on the Keelung River, a drainage NATM tunnel, and facilities that discharge flood-water into the sea. This project adopts "Design-and-Build" contract, and contractor was selected through "International Open Tender with Technical Proposal" method. Therefore, the contractor is required to make its detailed design with consideration of actual site conditions, and to satisfy construction period by adopting accelerated construction method. This paper briefly introduces our planning and construction records.

1 INTRODUCTION

The Keelung River Yuanshantzu Flood-Diversion Tunnel project (hereafter referred as "the project") is planned as a main part of "Keelung River Flood Mitigation Scheme". It is to divert 1,310 cms (cubic-meter per second) flood water into the tunnel out of 1,620 cms based on 200-year return-period calculation.

The project's practice was accelerated by Xiang-Shen Typhoon (2000) and Nali Typhoon (2001) that caused a huge damage by flooding in Taipei Metropolitan Area, and the Water Resources Agency (hereafter referred as "the Owner") as well as local residents requested quick completion of the project.

The Owner adopted "Design and Build" contract, and we were selected through "International Open Tender with Technical Proposal" method that considers not only cost by also contractors' ability to satisfy construction period and required quality. Therefore, it is necessary for us to make our detailed design that includes wide range of construction items with consideration of productivity, and satisfy construction period by adopting accelerated construction methods.

In this paper, we briefly introduce our construction planning and records as;

- Accelerated construction methods to satisfy period.
- Auxiliary methods to excavate difficult parts under safety condition.

2 OUTLINE OF THE PROJECT

2.1 *Tunnel outline*

Main quantity of the project is summarized as follows:

- Period: June 5, 2002 to December 27, 2004
- Length: 2,484 m (#1:1,152 m, #2:1,332 m)
- Three-Adits (#1,2 in Jiu-Feng, #3 in Intake), 641 m in total
- Standard Excavation Cross Section: about 171 square-meter
- Excavation Diameter: 14-m, Finish Bore: 12-m, Inclination: 1%
- Lining Concrete: thickness between 0.7 m (Arch) and 1.8-m (Invert), concrete strength: 45 N/sq-mm
- Excavation Volume: about 425,000 cubic-meter
- Concrete Volume: 116,000 cubic-meter
- Excavation Method: Top Heading with Bench Cut Method, Drill and Blasting Method, NATM

2.2 *Geological condition*

Figure 2 shows geological condition shown in the Basic Design. It is mainly mixed layer of Sand-Stone and Shale, and boundaries inclines from Intake side to Outlet one. Difficult conditions concentrate in #2 Tunnel upper-side where exist coal layers, disused coal mines, methane gas area, and "Fan-Zi" fault.

Copyright © 2005 Taylor & Francis Group plc, London, UK

Because the Basic Design shared the Owner's geological investigation results in detail, we could prepare in an early stage for additional geological investigations and arrange some special equipment, such as a big ventilation fan for the methane gas area. Details are summarized in Section 4.2.

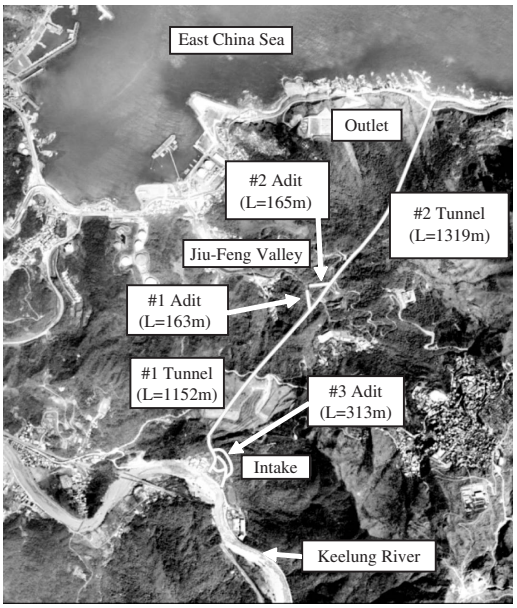


Figure 1. Aerial-view of the project.

3 CHARACTERISTICS AND PROBLEMS OF THE PROJECT

3.1 *General characteristics of the project*

General characteristics of the project are as follows;

- Its total construction period is 28 months that is shorter than other same scale projects. Except for preparation works, actual construction period is less than two years including Adits' works.
- Standard excavation cross section is 14-m in height and 170 sq-m. It requires multi-bench excavation method and careful consideration of muck transportation.
- Related to support pattern in the Basic Design, it is stiffer than our standard in Japan, such as thickness of shotcreting. It affects "cycle-time" of excavation works.
- To deal with local people's requests, there were many restrictions related to noise and vibrations.

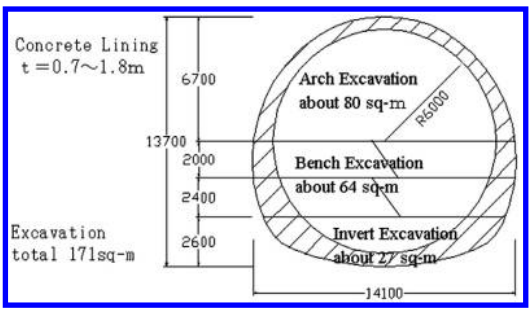


Figure 3. Standard cross section of the tunnel.

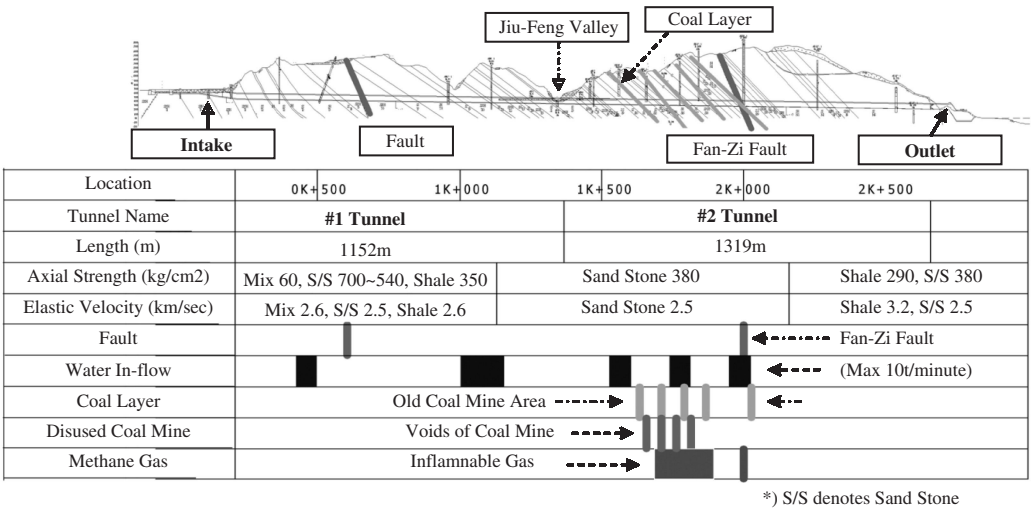


Figure 2. Geological conditions shown in the basic design.

Copyright © 2005 Taylor & Francis Group plc, London, UK

Because it was prohibited to make blasting at night (9pm to 7am), we had to adjust cycle schedule.

Difficulties of the project are summarized as, "Within short construction period with restrictions of working hours, we have to complete huge quantity of works." To solve these difficult conditions, we adopt some accelerated methods to satisfy period. It is summarized in Section 4.1.

3.2 *Difficult Parts for Excavation in the Project*

There are some difficult parts for excavation in the project as;

- In the middle of tunnel, there exists a stream where rock cover is minimum 4-m. In the Basic Design, it was planned to adopt "Open-cut Method". In our detailed design, we change it to continue tunnel excavation without "Open-cut" after water-stop grouting from surface ground.
- At the #1 Tunnel portal, tunnel cross section changes drastically from height 20-m, width 19-m egg-shaped profile (328 sq-m) to standard circle within 31.5 m section. It is necessary to plan carefully how to execute such a big cross section excavation.
- As mentioned in "Geological Condition", there are several bad rock zones in the #2 Tunnel upper side. We have to pay attention to coal layers, disused coal mines, a methane gas area, and the Fan-Zi fault where the Basic Design predicts huge water in-flow.

Construction methods in each item are summarized in Section 4.2.

4 PLANNING AND CONSTRUCTION RECORD OF THE PROJECT

4.1 *Accelerated construction methods to satisfy period*

To deal with many difficult conditions, we made some "Change-Design" in our detailed design to increase rate of construction. It was flexible as compared with normal projects thanks to the "Design and Build" contract.

4.1.1 *Increase #3 Adit to multiply number of cutting faces*

The Basic Design includes only two Adits in Jiu-Feng Valley. We increased #3 Adit (L = 313 m) near #1 Tunnel's portal based on following reasons;

- #1 Tunnel's portal excavation is about 100,000 cubic-meters, and needs time before starting tunnel excavation. #3 Adit saves several months of tunnel period.
- #3 Adit enables the project to increase number of cutting faces. Actually, we made maximum six cutting faces at the same time for arch excavation, and four ones for bench and invert excavation.
- There exists a cross section transition area at #1 portal, and it needs a lot of time for excavation and lining works (Refer to Section 4.2.2). It takes about four months for lining works, and it is required to close transportation at the #1 Tunnel portal during this period. #3 Adit facilitates traffic for other #1 tunnel works.

4.1.2 *Support pattern in the detailed design and ideas to accelerate excavation*

To minimize the cycle-time of excavation works under safety condition, we made our detailed design and a construction plan based on following ideas;

- In our detailed design, we set an interval of support in each type within a certain range. During construction, we try to adopt the maximum interval in each type (Refer to Figure 4).
- We try to select a light support pattern under consultation with our geologist as well as monitoring results. As summarized in Table 1, actual length of Type II (1304 m) is much bigger than that in the detailed design (500 m).
- Except for the bad rock zones, we adopt lattice girder support instead of H-beam one. It is lighter in weight and we expect quick installation.

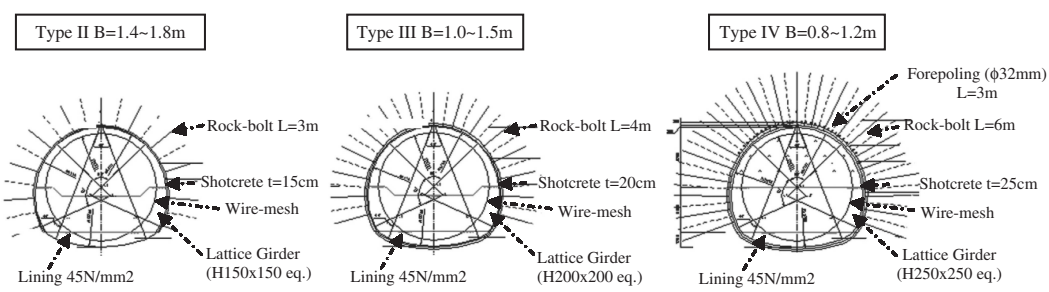


Figure 4. Support pattern in the detailed design.

Copyright © 2005 Taylor & Francis Group plc, London, UK

Table 1. Compare each support type length in detailed design and actual construction.

Support type	II	III	IV	V
Detailed design (m)	500	1197	392	395
Actual construction (m)	1304	883	220	77
Actual (%)	52	36	9	3

– As shown in Figure 3, we divide the bench excavation, 4.4 m in height, into two steps. Its main reason is to facilitate safety arrangement of traffic. Additionally, it enables us to arrange slope for the temporary road quickly which may contribute to shorten the cycle-time of excavation works.

4.1.3 *Ideas to accelerate concrete lining*

As shown in Figure 3, thickness of the concrete lining is between 0.7-m and 1.8-m with double-arrangement of rebar. To minimize period for lining works, we adopt following methods;

– To prevent thermal cracks owing to high concrete design strength of 45 N/sq-mm, we replaced 45% of cement with "blast-furnace slag" cement. Additionally, we adopt "wire-mesh" near surface to prevent cracks.
– Cross section of the concrete lining is about 46 sq. m. Judging from workability and cycle-time analysis, we divided concrete lining works into two forms (Invert, Arch), and set its span as 9-m. In this case, concrete volumes in Invert and Arch are 180 cu.-m and 280, respectively.
– Our cycle-time analysis shows that concrete lining works need at least two days for one-cycle works. To satisfy construction period, we arrange each three sets of invert forms as well as arch ones. In the project, three to six forms worked at the same time for about 10-month period.

4.2 *Auxiliary methods to excavate difficult parts under safety condition*

4.2.1 *Thin rock cover zone in Jiu-Feng Valley*

In Jiu-Feng Valley that locates in the middle of the tunnel, there exists thin rock cover zone minimum 4 m above tunnel crown. For safety excavation of the tunnel, we made following procedures;

1 At first, we made three core-drilling tests inside this zone and confirmed that bed-rock 2 m below ground level was relatively fresh and solid.
2 Based on the test result, we came to the conclusion that a cutting face in this zone could be stable with water-stop grouting and ground improvement from above ground level.



Photograph 1. Water-stop grouting in Jiu-Feng Valley.

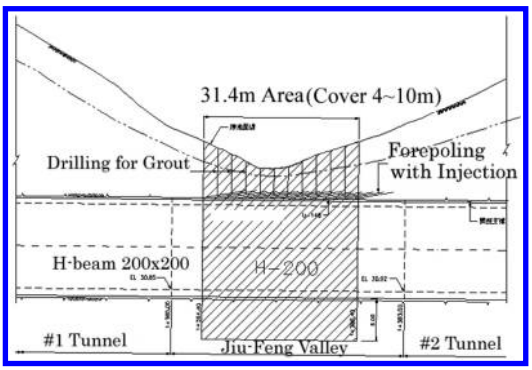


Figure 5. Auxiliary methods in Jiu-Feng Valley.

3 To select a method for water-stop grouting, we made "Lugeon-test", six points in total. Results showed that Lugeon number were between 0.2 and 20. We divided grouting methods into two as;
   – Where the Lugeon number is less than 10, we immediately make "water-glass" grouting.
   – If the number is more than 10, at first we make "cement-milk" grouting to fill cracks. Afterwards, we drill again and make the water-glass grouting.
4 For tunnel excavation, we made forepoling with injection of silica resin for the most critical area of 31.4-m in length where rock covers were between 4 m and 10. In this area, we set H-beam (200 × 200) for support every 1.0 to 1.2 m that was stiffer in initial shear strength than the lattice girder. (Ref. Figure 5)

Thanks to above procedure, seepage water during excavation was less than 1-ton per minute, and crown settlement was within 2 cm.

4.2.2 *Cross section transition at #1 Tunnel portal*

In the #1 Tunnel portal area, cross section changes from 20 m height, 19 m width egg-shaped profile to

Copyright © 2005 Taylor & Francis Group plc, London, UK

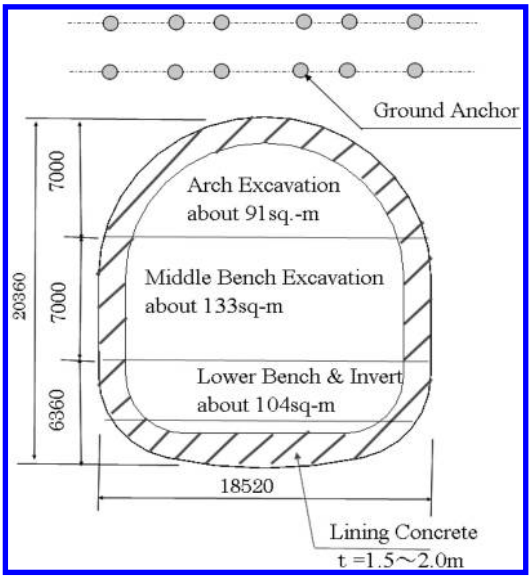
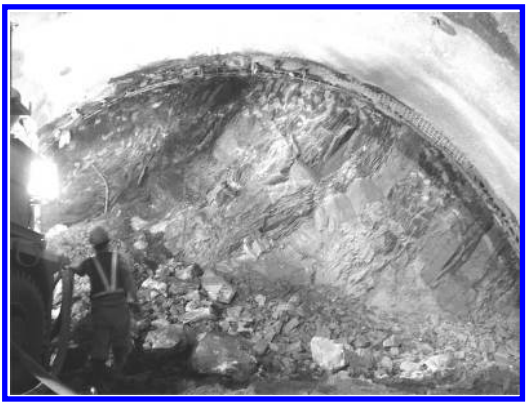


Figure 6. Cross section at #1 Tunnel portal.



Photograph 2. Part of a disused coal mine, upper-left includes fragments of wood.

standard one within 31.5 m section. Its maximum area is 328 sq-m, and we select 4-bench excavation method as shown in Figure 6. One bench height was maximum 7 m, but we judged it feasible based on following reasons;

– Based on results of core drilling tests, geological condition in this area looks well.
– Top arch have been fastened by twelve ground anchors.
– #3 Adit enables us to excavate the area in both sides, i.e., from outside as well as inside the tunnel. Therefore, muck transportation arrangement is relatively easy.

We select the stiffest support pattern as 30 cm shotcreting with lattice girders equivalent to H-250 × 250 mm in this area. Monitoring results of crown displacement during excavation was less than 10 mm.

4.2.3 *Auxiliary methods for coal layer, disused coal mine, and methane gas*

During excavation of #2 Tunnel upper-side, there actually existed some coal layers with thickness around 50 cm. We also hit some areas that might be parts of a disused coal mine. It had already been squashed completely and there was no void, but ground condition there was fragile and accumulated water came out together with fragments of woods.

Whenever we met above-mentioned special ground conditions, we immediately made shotcreting for first-support, and then executed grouting of silica-resin if necessary, in accordance with results of site observation and monitoring. During excavation, its maximum displacement was within 30 mm.

Related to methane gas, we set gas monitoring equipment near the cutting face and continued measurement 24-hour to prevent an accident. Actually, we found some parts by alarming of the equipment where the methane gas concentrations were beyond first caution level of 5% LEL.

Because it was expected in advance since planning stage, we arranged a big volume ventilation fan with 3,000 cubic meters per minute capacity. It could thin down the concentration to safety level.

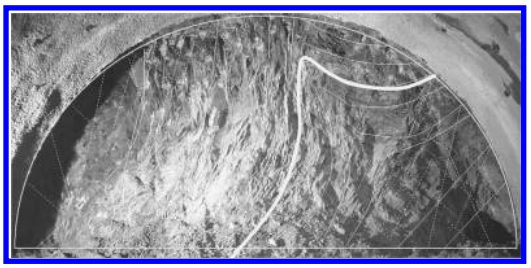
4.2.4 *Auxiliary method for "Fan-Zi" fault zone*

As mentioned in "Geological Condition", the Fan-Zi fault was one of our biggest concerns, because the Basic Design predicted huge water inflow of 10-ton per minute. To detect the location of the Fan-Zi fault, we made long-distance horizontal core-drilling tests (maximum 300 m at once, total 972 m) before excavation as well as non-core drilling test by a jumbo-driller every 30 m. Both tests could not identity clear location of the Fan-Zi fault that might include clay, crushed stone, and high-pressure water.

During excavation in the area (1 k + 980 m to 2 k + 050 m, 70 m in total, rock cover about 120 m) where the Basic Design predicted existence of the Fan-Zi Fault, cutting face kept stable with no crushed stone. However, afterwards it occurred many cracks in shotcrete after excavation, and monitoring results showed big and continuous displacements (Figure 7). Additionally, cutting face showed wavy layer arrangement, and then we realized that we were in a fold zone. (Ref. Picture 3)

To hold the displacement, we used many auxiliary methods as additional shotcreting, long rock-bolts (6 m, 9 m), and silica-resin injections. Thanks to these

Copyright © 2005 Taylor & Francis Group plc, London, UK



Photograph 3. Wavy layer arrangement of cutting face inside the fold zone.

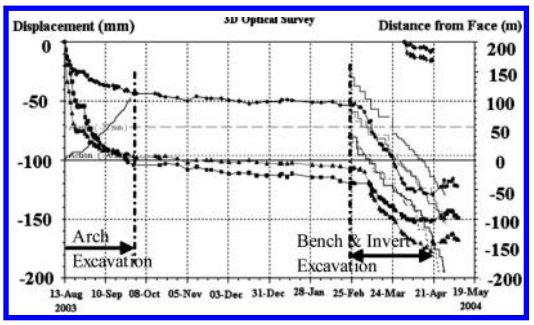


Figure 7. Monitoring results of displacement in the fold zone.

measures, crown displacement was stabilized after two months of arch excavation.

For arch excavation, its record showed that actual injection volume of the silica-resin was 3 to 4 kg/m that was smaller than our plan of 10 to 20 kg/m. It showed that there were few cracks and voids in rock, and grouting could not stabilize the displacement efficiently. For bench and invert excavation, we revised our plan of auxiliary methods to hold the displacement as mainly using long rock-bolts and invert shotcreting.

For bench and invert excavation, we tried to hold the displacement within 200 mm in total that was equal to margin for displacement in our detailed design. Since there was about four-month period before the bench excavation starts, we tried all kinds of measures before starting excavation, such as additional rock-bolts together with silica-resin injection. During bench and invert excavation stage, we also tried to cast invert lining concrete as quick as possible. Actually, these auxiliary methods decreased rate of the bench and invert excavation (average 130 m/month decreased to 80 m/month), and invert lining as well as arch one (average 140 m/month) soon caught up just behind the excavation area. It was favorable to hold displacement.

After casting the invert lining, the displacement was stabilized significantly as shown in the Figure 7.



Photograph 4. Additional rock-bolt together with silica-resin injection in the fold zone.

We made monitoring at 7-point within this area, and total displacements in each point were between 12 cm and 18 cm.

5 CONCLUSION

As mentioned in Section 4.1, one of the most difficult points in the project was how to complete large quantity of works within a limited period. We solved this problem mainly by increasing number of cutting-face and concrete forms.

Originally, we tried to shorten period by reduction of support and lining related quantities through "Change-Design". But it was required to solve many difficult problems to complete the detailed design, such as impact and wear of concrete surface by flowing stones during flood diversion. It could not be solved within a short period, and consequently we had to select a relatively conservative design.

Related to auxiliary methods for difficult parts, we were very successful in the small rock cover zone, and in advance preparation for the coal zone, methane gas and water in-flow. However, we had a lot of difficulties in holding displacements in the fold zone that we did not forecast in advance. In this point, we fully realized difficulties to excavate tunnel in a foreign country where we did not have enough data and experience.

Another impressive event was an emergency flood-diversion on September 11, 2004 that diverted flooding water into the tunnel that was still under construction by the Owner's instruction. It was just before completion of the tunnel, and we got damages in concrete forms and other construction equipment. However, our completed products got almost no damage at all.

We hope this paper would be a good reference for future projects.

Copyright © 2005 Taylor & Francis Group plc, London, UK

Application of the tunnel face reinforcement and fore-piling

T. Yamamoto, K. Murakami & S. Shirasagi
Kajima Technical Research Institute, Chofu, Tokyo, Japan

K. Negishi & K. Nishioka
Fujikawa Tunnel Project, Kajima Corporation, Shizuoka, Japan

T. Kobayashi
Fuji Project Office, Japan Highway, Japan

ABSTRACT: In Fujikawa Tunnels, the TBM pilot and enlargement tunnel excavation method was applied on this project. The pilot tunnel was firstly driven by a hard rock TBM with providing vital information for subsequent tunnel enlargement work.

Firstly, the three-dimensional numerical analysis was conducted with taking the displacement of the tunnel face into consideration to evaluate various auxiliary methods for ground improvement such as long, meddle and short span fore-pilings using steel, and face reinforcing bolts using glass fiber. As a result, most effective auxiliary method was chosen corresponding to the size and depth of loosened zones at the tunnel crown. Consequently, long and middle span fore-pilings technique was chosen as most effective auxiliary methods.

Secondly, the test section was excavated and ground behavior was monitored to confirm the analysis results. Actual ground behavior at the test section was very similar to the estimated one by the analysis.

1 INTRODUCTION

The 4500-m-long three-lane Fujikawa tunnel between Fujikawa-cho and Shibakawa-cho, Shizuoka prefecture on the Daini-Tomei Expressway has a large excavated cross section of approximately 200 m^2. A pilot tunnel excavated above the main tunnel using a 5-m-diameter TBM is enlarged by drill-and-blast methods. The geology consists of the Iwabuchi volcanic rock formation composed of Quaternary andesite and tuff breccia. In the poor soil section, the crown of the pilot tunnel collapsed frequently during the excavation by TBM. The expansion of loose areas over a wide area and large crown collapse were therefore expected to occur during the enlargement of the pilot tunnel.

Auxiliary methods were therefore required in the poor soil section. Three-dimensional numerical analysis was made to select optimal auxiliary methods according to the loosening of the ground. As a result, the behavior of the ground and supports during tunnel excavation could be evaluated in advance. Three-dimensional time-series effects of auxiliary methods could be grasped. Three auxiliary methods were implemented on a trial basis in a section of nearly uniform geological property. They are medium (6.5 m) and long (12.5 m) forepoling methods using steel pipes of a medium diameter of 76.3 mm, and face reinforcing bolt method using glass fiber reinforced pipes. Comparing the analysis results with measurements enabled the verification of the effects of the auxiliary methods and helped prepare data for rational design of auxiliary methods according to the loosening of the ground.

2 EVALUATION OF AREA LOOSENED BY PILOT TUNNELING

2.1 *Loosening of ground*

Face and crown collapses occurred frequently in the Iwabuchi volcanic rock formation during TBM excavation of the pilot tunnel. Figure 1 shows the elevations of loose areas above the crown of the pilot tunnel at different points. The red dotted line indicates the elevation right after excavation and the blue solid line represents the elevation at the end of displacement after sufficient time passed since the TBM passed the point. The value along the red line is more than double that along the blue line at STA. 1045 + 70. The expansion of the loose area and more crown collapses were of concern during the enlargement of the pilot tunnel. Applying auxiliary methods according to the

Copyright © 2005 Taylor & Francis Group plc, London, UK

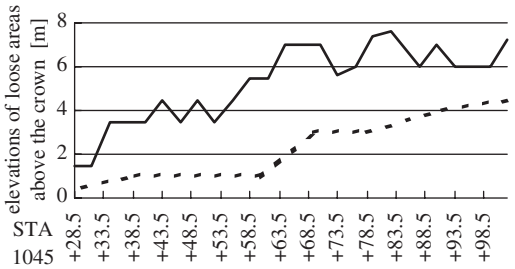


Figure 1. The elevations of loose areas above the crown of the pilot tunnel at different points.

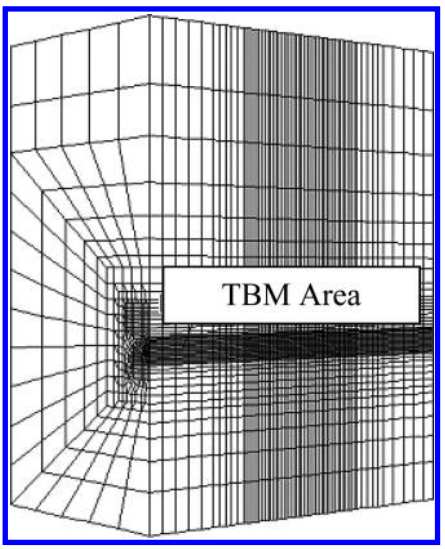


Figure 2. Basic mesh.

loosening of the ground was therefore considered necessary. Then, back analysis was made using the physical property values of the ground as parameters to reproduce the loosening condition shown in Figure 1.

2.2 *Analysis method*

The finite difference analysis method was used. Unlike in the finite element analysis that produces solutions using static equilibrium equations, the governing equation is formulated using a kinetic equation in finite difference analysis methods. The finite difference analysis is therefore suitable to problems of large deformations such as collapse behavior and the expansion of plastic areas during tunnel excavation. The analysis method has recently been adopted for examining forepoling works, face bolts and cable bolts on an increasing number of occasions. In this study, FLAC3D, three-dimensional numerical analysis software, an expansion of finite difference code FLAC, was used. A Mohr-Coulomb constitutive relation was employed.

Table 1. Material parameters.

Density	24 kN/m^3
Young's Modulus	500 MN/m^2
Poisson's Ratio	0.3
Cohesion	20 MN/m^2
Friction Angle	34 degrees

The analysis space is shown in Figure 2. The earth cover is 80 m. Space of a length of 3D is reserved between the tunnel walls to the side boundary. Space of a length of 2D or more is reserved longitudinally between the face and the boundary. The initial earth pressure was determined based on the analysis of the self-weight of the ground and given as an external force during the excavation of the pilot and main tunnels.

2.3 *Results of analysis*

The elevation of loose area when the displacement of the crown of the TBM pilot tunnel settled was classified into "less than 1.5 m", "1.5 m to 3.5 m", "3.5 m to 5.5 m" or "more than 5.5 m". The physical property value of the ground reproducing each elevation was identified. In this study, analysis was made at a loose area elevation of "1.5 m to 3.5 m" to which pilot implementation of auxiliary methods was most applicable. The physical property values of the ground and the distributions of loose area identified are shown in Table 1, respectively. The loose areas were assumed to be plastic in analysis.

3 ANALYTICAL STUDY OF AUXILIARY METHODS

3.1 *Auxiliary methods and study methods*

In order to select auxiliary methods before excavating the main tunnel, the displacement was estimated to verify the effectiveness of auxiliary methods. A case where no measures were taken and four other cases where auxiliary methods were implemented were assumed. In the latter four cases, steel pipe length and the range of pipe driving in degrees of a circle were used as parameters. The five cases are outlined in Table 2 and Figure 3. The mesh shown in Chapter 2 was used in analysis. Auxiliary methods were modeled using beam elements. The behavior of the ground and supports was evaluated during the excavation of the top heading. Excavation was modeled so

Copyright © 2005 Taylor & Francis Group plc, London, UK

Table 2. Analysis cases.

Case	Material	Diameter [m]	Length [m]	Pitch [mm]	Range [degree]
I	no	–	–	–	–
II	Steel	30.5	4	600	120
III	Steel	76.3	6.5	900	120
IV	Steel	76.3	13.5	600	120
V	Steel	76.3	13.5	600	90

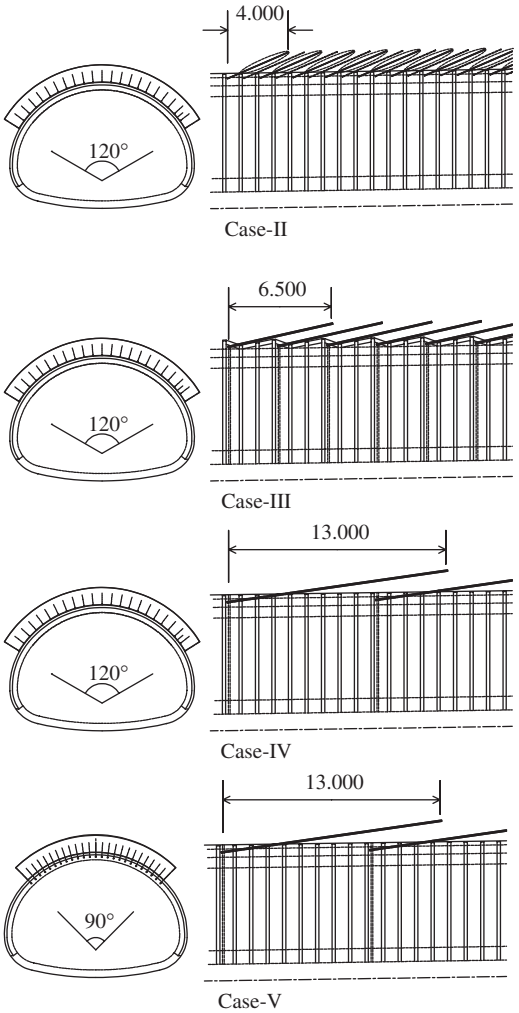


Figure 3. Auxiliary methods of analysis.

that the first 30-m section was excavated at a time and the next 40-m section was excavated consecutively one meter at a time. The cohesion of the soil was increased by 50% in view of soil improvement by grouting.

Table 3. Parameters of auxiliary methods

	Medium forepoling	Long forepoling	Face bolt
Length	9.0 m	9.0 m	7.0 m
Material	Steel pipe		GERP
Diameter	76.3 mm	76.3 m	76.0 mm
Length	6.5 m	12.5 m	7.5 m
Range	90 degree		–
Pitch	900 mm	600 mm	1,500 mm
Number	17 or 18	27	6

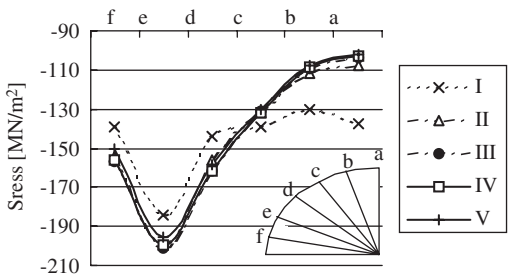


Figure 4. The stress acting on the steel support.

3.2 *Results of estimation*

Table 3 shows the displacement, the area where the maximum shear strain g exceeded 0.2% and the plastic zone while the pilot tunnel was excavated by TBM. The displacement at each point was reduced as the auxiliary system became more substantial from grouted forepoling to medium to long forepoling. The steel pipe length (in cases III and IV) or the range of pipe driving in degrees of a circle (in cases IV and V) made little difference in reduction of displacement. All the medium and long steel piles had an internal diameter of 76.3 mm. They were nearly as effective as steel piles of a large diameter of 114.3 mm. The stress acting on the steel support is shown in Figure 4. The figure shows that auxiliary methods reduced compressive stress near the crown but caused the compressive stress at the foot to increase slightly. The phenomenon occurred probably because loads on the forepoling were transmitted to the ground at the foot of the tunnel via supports behind the face causing the axial force and bending moment near the crown to decrease and the bending moment at the foot to increase. Similar tendency was found for all the auxiliary methods selected, under the soil conditions in this study.

The yield stress of steel support was 440 MN/m^2 and was below the strength of steel support in all the cases. Applying grouted forepoling was considered to pose no problems in analysis under the conditions in this study. The method was, however, later found more

Copyright © 2005 Taylor & Francis Group plc, London, UK

costly than the other auxiliary methods. Then, medium to long forepoling methods using steel pipes of medium diameter were implemented on a trial basis in Case V where pipes were driven in a range of 90 degrees of a circle based on a series of analysis results. The objective was to verify the effectiveness of these methods.

4 PILOT IMPLEMENTATION OF AUXILIARY METHODS

Analytical studies were made of the effectiveness of auxiliary methods selected according to the loosening condition. Then, medium to long forepoling methods using steel pipes of medium diameter were implemented on a trial basis at STA.1042 + 59.8 to + 34.3 to verify their effectiveness. Face reinforcement, which was found effective for varying heights of loose area, was also implemented on a trial basis. The three auxiliary methods are outlined in Table 3.

4.1 *Tunnel deformation*

The settlement of crown, convergence and settlement at the foot in the cross section under study until the excavation of the top heading are given in Figure 4. Neither analysis nor measurement showed no significant variance among the three auxiliary methods. A review of respective methods, however, revealed that crown settlement was relatively large in analysis while the measurement was nearly none although convergence was nearly the same either in analysis or in measurement.

This may be because no considerations were given in analysis to either the simple liners installed at intervals of one meter as TBM supports or the long steel pipe forepoling installed for protection since face collapse occurred successively during pilot tunnel excavation. The settlement at the foot was larger in medium and long forepoling that in face reinforcement because the load of loosened ground on the steel pipe was transmitted to the foot via steel supports.

4.2 *Stress of steel supports*

The stress of the steel supports for respective auxiliary methods is shown in Figure 5. The analysis value is almost in agreement with the measurement near the shoulder (point d through e in Figure 6) in medium and long forepoling methods. The measurement is higher than the analysis value by approximately 200 MN/m^2 at the crown. In face reinforcement, measurements are higher than the analysis values by 100 MN/m^2 on the shoulder and by approximately 300 MN/m^2 at the crown. Face reinforcement is effective for controlling displacement but is detrimental to the sharing of the load of loosened ground acting on

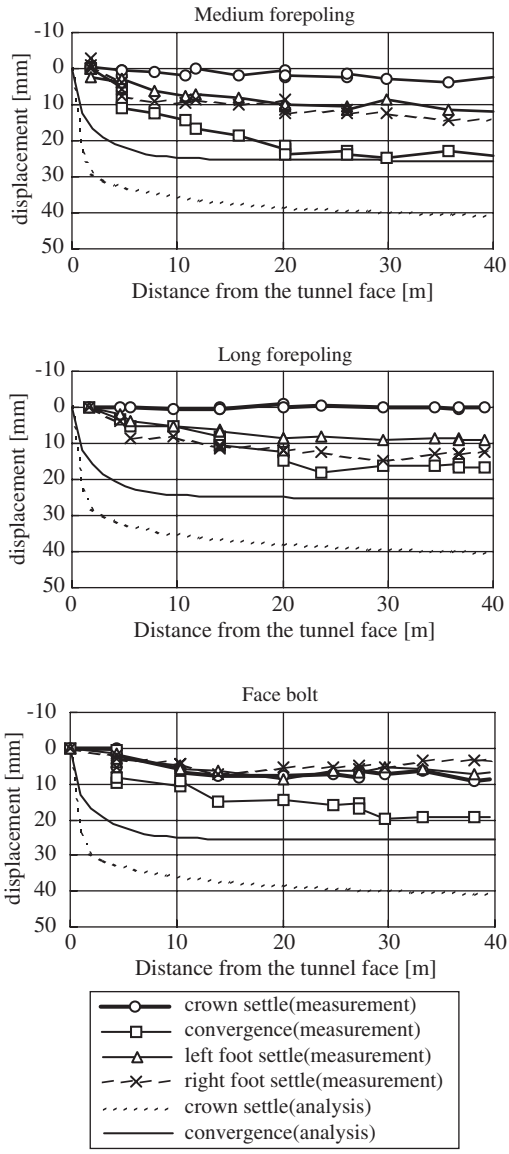


Figure 5. Settlement of crown, convergence and settlement at the foot in the cross section.

the steel support because face bolts are removed consecutively as excavation progresses. Then, compressive stress higher than a yield stress of 440 MN/m^2 acts on steel supports, and additional shotcrete or bolts may be required. In medium and long forepoling, the compressive stress of steel supports is relatively low probably because an integrated arch shell area is formed in the ground and transmits the load of loosened ground in front of the face to behind the face and enables load sharing.

Copyright © 2005 Taylor & Francis Group plc, London, UK

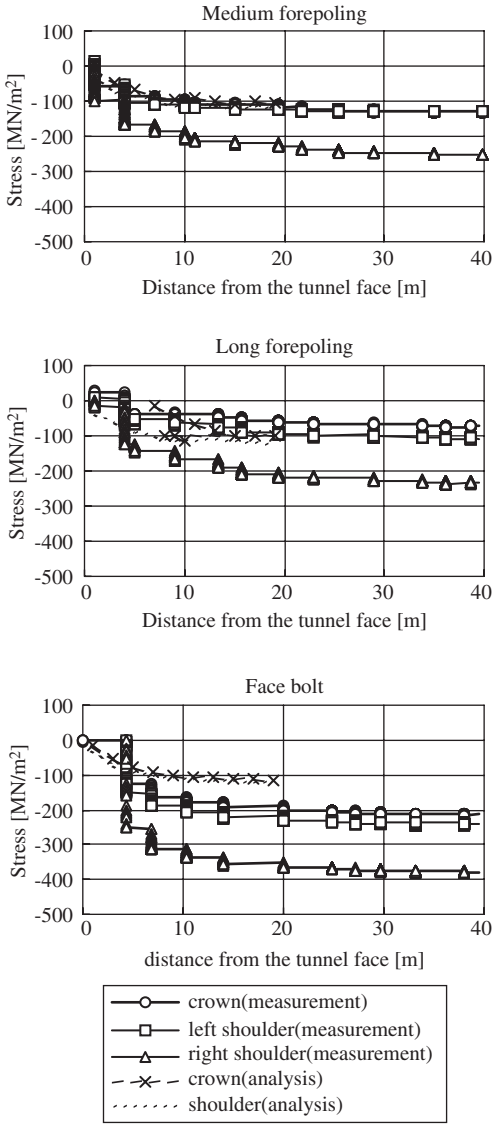


Figure 6. The stress acting on the steel support.

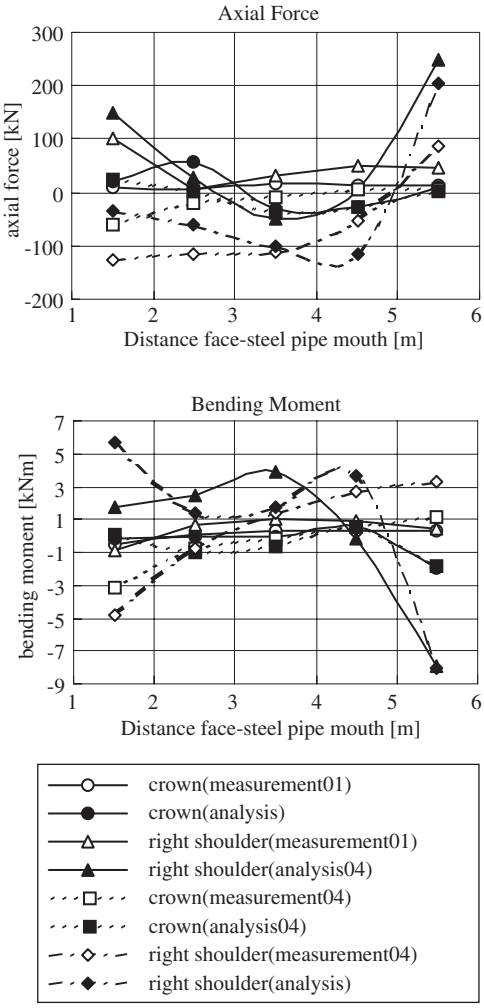


Figure 7. The stress acting on the steel pipes installed at the crown and on the right shoulder in medium-length forepoling.

4.3 *Stress resultants at the cross section of steel pipe forepoling*

The stress resultants (axial force and bending moment) acting on the steel pipes installed at the crown and on the right shoulder in medium-length forepoling are shown in Figure 7. 01 and 04 in the legend indicate that the distance from the steel pipe mouth to the face is 1 and 4 m (along the dash-dot line), respectively. The steel pipe mouth was connected and fixed to the steel support using shotcrete. As excavation progressed, the ground moved toward the tunnel opening, so compressive axial force occurred at the base of the steel pipe driven diagonally upward. The tip of the steel pipe was fixed to the ground by the grout, so downward movement of the ground to the tunnel opening caused tensile stress. The measurement of bending moment indicates deflection behavior toward the tunnel opening at a point 5.5 m from the mouth. It suggests that the load of loosened ground was carried around the point. When the face advanced 1 m, little bending moment occurred at the crown because a steel support existed at a point 1.5 m from the mouth of the steel pipe. When the face advanced 4 m, little

Copyright © 2005 Taylor & Francis Group plc, London, UK

bending moment occurred because steel supports had been installed. In the case of long forepoling, soil behavior was nearly the same as in medium-length forepoling although of slightly complex nature. The agreement between measurements and analysis results was thus verified.

5 CLOSING REMARK

When a tunnel of large cross section was excavated following the TBM excavation of a pilot tunnel, physical properties were identified corresponding to the loosening of ground and the effectiveness of auxiliary methods was evaluated using three-dimensional finite difference methods. The objective was to select auxiliary methods according to the loosening of the ground. Auxiliary methods were implemented on a trial basis under nearly identical soil conditions, and measurements were compared with analysis results. As a result, data were obtained for selecting optimal auxiliary methods. This study provided two findings. (1) Driving medium-diameter steel pipes in a range of 90 degrees of a circle results in effective forepoling regardless of pipe length where the loose area is at an elevation of 1.5 to 3.0 m. (2) Applying face bolts for reinforcement is highly effective for controlling displacement but is likely to increase the stress of steel supports. In the future, construction will be carried out according to the varying soil conditions based on a series of analysis results obtained in this study, while paying attention to cost effectiveness.

REFERENCES

Yamamoto, Takuji et al. 1999. Results of application of forepoling using medium-length steel pipes, *Proceedings of Tunnel Engineering 9*: 167–172. Tokyo: Japan Society of Civil Engineers.

Yukiyoshi, Kitamoto et al. 2003. A study on the reinforcement effects of grouted steel pipe forepoling, *Proceedings of the Japan Society of Civil Engineers 736/III-63*: 167–177. Tokyo: Japan Society of Civil Engineers.

Copyright © 2005 Taylor & Francis Group plc, London, UK

Tunnel excavation penetrating active landslide area – Second-TOMEI Expressway Inasa No. 2 Tunnel

Satoshi Tayama
Japan Highway Public Corporation, Shizuoka, Japan

Koji Kanzawa & Hiroyuki Hirano
Shimizu Corporation, Inasa No.2 Tunnel Construction Site, Shizuoka, Japan

Susumu Isoda
Shimizu Corporation, Civil Engineering Division, Technology Department No.2, Tokyo, Japan

ABSTRACT: During the construction of Inasa No.2 tunnel, both portals, northern starting point and southern ending point, have been subject to large-scale landslides. Based on the obtained knowledge through the construction at the north portal with intensive measurements and observations, this paper describes the landslide mechanism caused by tunnel excavation nearby, and the effect of countermeasure to control landslide actually implemented in the construction of tunnel.

1 INTRODUCTION

In case of constructing a tunnel in a mountainous region, especially where the overburden is shallow such as portal zones, tunnel excavation could induce a landslide and have actually been reported. Although much is yet to be known about the causal relationship between landslides and tunnel excavation, many studies have enabled the formulation of technical guideline.

The portals of Inasa No. 2 Tunnel are located in large-scale landslide areas. In the north portal area, as the tunnel was to be constructed through the landslide zone over a distance of about 220 m, there was great concern about the possibility of a landslide induced by the tunnel excavation.

This paper reports the results of landslide, ground surface observations and tunnel measurements conducted during the construction of Inasa No. 2 Tunnel in the north portal landslide zone. The paper also describes the obtained knowledge about the design and construction of a tunnel considering the influence of tunnel construction on landslide behavior, and about the slip-reducing effect of countermeasures.

2 PROJECT SUMMARY

2.1 *Outline of tunnel*

Inasa No. 2 tunnel is located between Nagoya and Shizuoka cities as shown in Figure 1, in Chubu area of Japan. It is a two-lane tunnel, about 1,500 m in length, planned as part of newly Second-TOMEI expressway currently under construction. The cross-sectional area of excavation is about 110 m^2, and tunnels of both lanes are excavated from the north portal end.

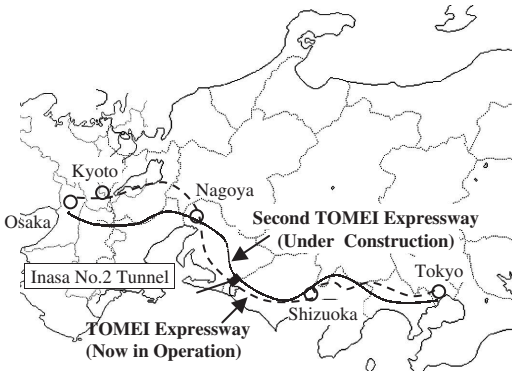


Figure 1. Location of Inasa No.2 tunnel.

2.2 *Geology*

The tunnel was to pass through gently rolling 200 to 400 meter mountains. The geology of the site consists of Mikabu greenstone categorized as Mesozoic and Paleozoic Sanbagawa metamorphic rock. The geology of the tunnel zone is composed of diabase

Copyright © 2005 Taylor & Francis Group plc, London, UK

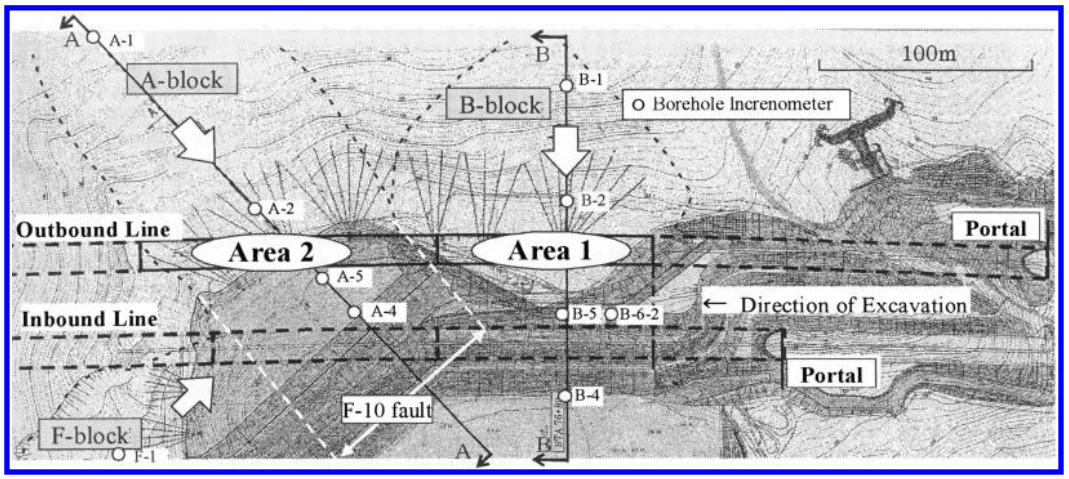


Figure 2. Plain view of northern portal area.

Table 1. Outline of landslide block in northern portal area.

Block	Scale of landslip			Geology (main)
	Width	Length	Depth (ave)	
A-block	100 m	240 m	14.4 m	Hyaloclastite
B-block	130 m	100 m	13.7 m	Diabase
F-block	60 m	120 m	10 m	Hyaloclastite

interbedded with schalstein, serpentinite and hyaloclastite. Especially the bedrock in the north portal area is composed of these kinds of rock, all of which are covered with talus deposits.

Survey results indicate that multiple fault fracture zones and many landslide blocks exist near the hyaloclastite zones. As shown in Figure 2, there are three large landslide blocks (A,B and F-block) along the slope over the tunnel, and landforms such as terraces and trench-like depressions are found at the ground surface. Table 1 briefly describes the scale and geology of these slide blocks. Moreover, it has been known from the geological survey that there is a large-scale fault fracture zone called "F-10 Fault" just under the landslide face of A-block.

The results of borehole inclinometer measurement, electro-optical distance measurement and landslide observation indicated that B-Block was not moving, and A-block and F-Block were already moving at the rates of about 10 mm/month and 20 mm/month, respectively, before the construction work began. Because of these adverse geological conditions, landslide control measures and slope stabilization measures were quite important during the tunnel construction at the north portal. Therefore, counterweight fill was carried out as a means of landslide control, and appropriate slip control measures were implemented according to the relative locations of the tunnel and landslide blocks.

3 RELATIVE LOCATIONS OF LANDSLIDE BLOCKS AND TUNNEL

3.1 *Position of landslide and tunnels*

Figures 2 to 4 show the relative locations of the tunnel and the slide blocks. As shown, the outbound line tunnel is located directly below A- and B-block. And the inbound line tunnel is to cut off the slip surface itself at the compression zone of B-block. In addition, F-10 Fault is situated right under A-block, so the inbound line tunnel was expected to encounter highly argilliferous and extremely bad-conditioned ground. However, these tunnels are not located so as to influence the behavior of F-block.

The relative locations of the slide blocks and the outbound line tunnels are shown in Table 2, which also describes the geology and other information of two areas handled in this paper.

3.2 *Factors to induce landslide*

There are three possible causes of a landslide under the influence of tunnel construction; loosening caused by tunnel excavation, cutting off of slip surface, and the removal of loads from the slide block.

These causes are deeply related to the location of the tunnel relative to the landslide block.

The following paragraphs describe the behavior of landslide blocks observed in the north portal area, and the locations of landslide blocks relative to the tunnel.

As mentioned before, there are three large landslide blocks near the north portal. Prior to tunnel

Copyright © 2005 Taylor & Francis Group plc, London, UK

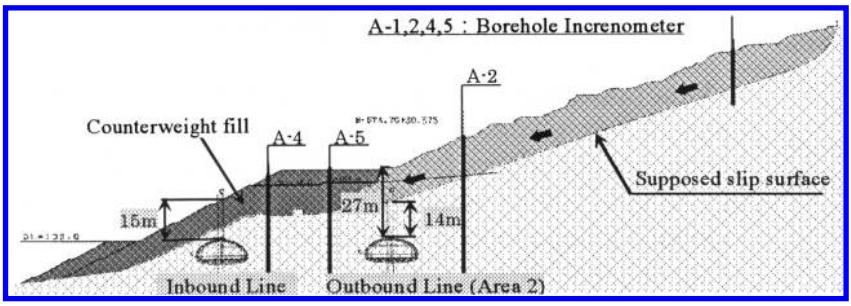


Figure 3. Cross-section view of landslide A-Block.

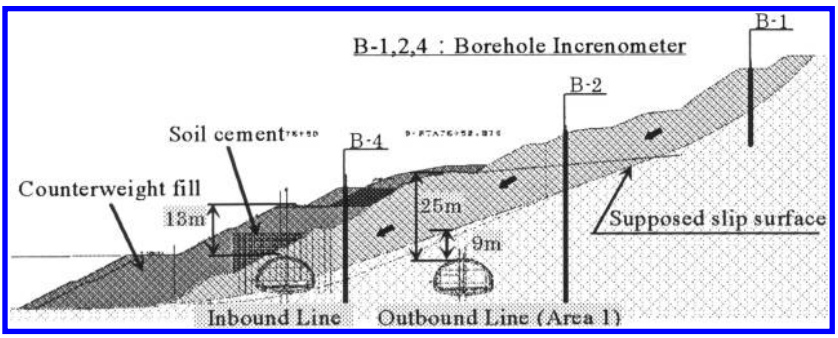


Figure 4. Cross-section view of landslide B-Block.

Table 2. Area classification of outbound line tunnel in northern portal area.

Landslide block	Area 1 B-block	Area 2 A-block
Spatial relationship with landslide block	Right under the **central** part of landslide block	Right under the **terminal** part of landslide block
Vertical distance to landslide face	9 m	14 m
Overburden height	25 m	27 m
Geology of excavated area	Highly fractured diabase (main)	Highly argillized fault fracture zone
Implemented support	H-150 steel t = 200 shotcrete 6 m × 24 rock bolts	H-200 steel t = 250 shotcrete 6 m × 24 rock bolts AGF fore poling
Excavation method	Full face excavation with 4-meter bench	

construction, some countermeasure works to control landslide were implemented for these slide blocks. On the assumption that tunnel construction would reduce the cohesion of the slip surface or the internal friction angle, or that it reduce the weight of the slide block due to the cutting off of the slip surface and tunnel excavation, a landslide stabilization study was conducted to find ways to satisfy the design safety factor by means of counterweight fills (approx. 280,000 m^3) and thereby ensure overall landslide block stability. The provided counterweight fill began to stabilize the behavior of A- and F-block, which were moving before the counterweight fill was carried out and tunnel excavation was started.

4 LANDSLIDE BEHAVIOR AND COUNTERMEASURES DURING THE EXCAVATION OF OUTBOUND TUNNEL

4.1 *Outbound tunnel B-block section (Area 1)*

For this landslide problem, the counterweight fill in which the influence of the tunnel excavation was taken into consideration in its design, was conducted prior to the excavation as a means of satisfying the design safety factor. On top of that, since B-block landslide behavior was no longer observed until then, it was considered that the landslide block would not be affected by the tunnel excavation.

In the excavation of outbound line tunnel which started earlier of two, since rather rigid and hardly

Copyright © 2005 Taylor & Francis Group plc, London, UK

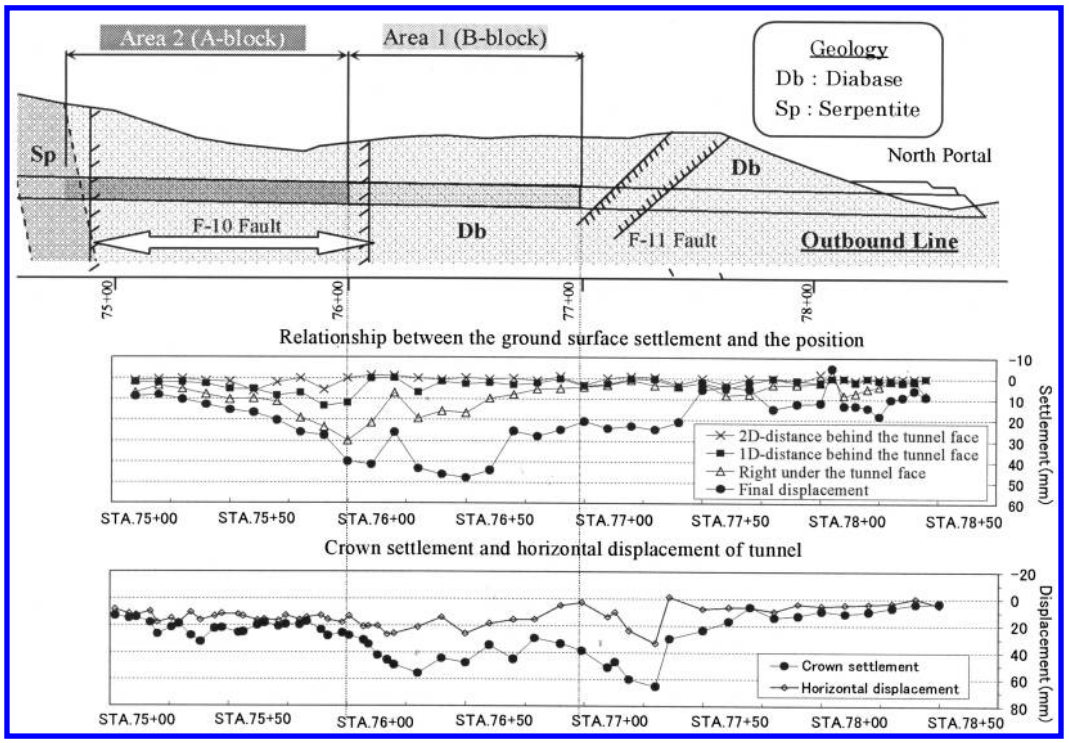


Figure 5. Behavior of tunnel and ground surface during the excavation of outbound tunnel.

fractured rock classified as CL-Class had appeared in tunnel face at the time of exploratory boring, normal support pattern using steel arch support: H-150, shotcrete: $t = 200$, and 6 m × 24 rock bolts, was applied when excavation was actually conducted.

The result of measurement on ground surface and tunnel during the excavation are shown in Figure 5. It indicates that crown settlement and convergence were not particularly large, 30–50 mm and 10–30 mm respectively. However, ground surface settlement was relatively large up to 30–50 mm. Furthermore, when the tunnel face passed a point about 2D – distance (D: diameter of excavated tunnel) behind the primary slide-survey line of the B-block, landslide began to occur at almost the same slip surface as anticipated, despite its absolute stop of landslip behavior before the beginning of excavation work.

Figure 6 shows the landslide displacements of B-block indicated by the borehole inclinometers, whose locations are shown in Figures 2, 4. As shown, borehole inclinometer B-2 indicated a maximum displacement rate of 0.69 mm/day and a cumulative displacement of about 20 mm. It is ascertained that landslide began to occur almost as soon as the tunnel displacement occurred after excavation. Thus was showed quite a close relationship between the tunnel displacement and landslide.

Though some time has passed after the tunnel face passed under the primary slide-survey line of slide block, tunnel displacement continued to increase and did not converge. Then it was decided to construct the invert concrete earlier than usual. As the invert was finished, then tunnel displacement finally converged and landslide movement stopped.

4.2 *Outbound tunnel A-block section (Area 2)*

Landslide of A-block had been already active before the tunnel construction began. In view of this fact and the behavior of B-block, it was thought that the influence of tunnel excavation on landslide occurrence would be a large-scale one even though some countermeasure works, considering sufficiently the influence of tunnel excavation, have conducted to control landslide.

It was thought that during the excavation of the A-block section (Area 2), behavior similar to the one observed in the B-block section (Area 1) would occur. Since the A-block section was located in the F-10 fault and a highly argillized fracture zone had been found, several measures including the support system were discussed and considered to control the loosening of the surrounding ground when the tunnel is excavated. As a result, it was decided to apply more rigid support pattern than the originally designed one. This

Copyright © 2005 Taylor & Francis Group plc, London, UK

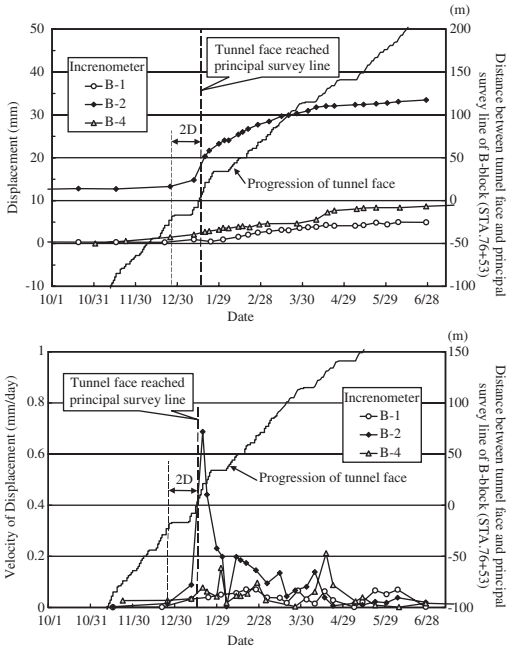


Figure 6. Behavior of landslide B-Block.

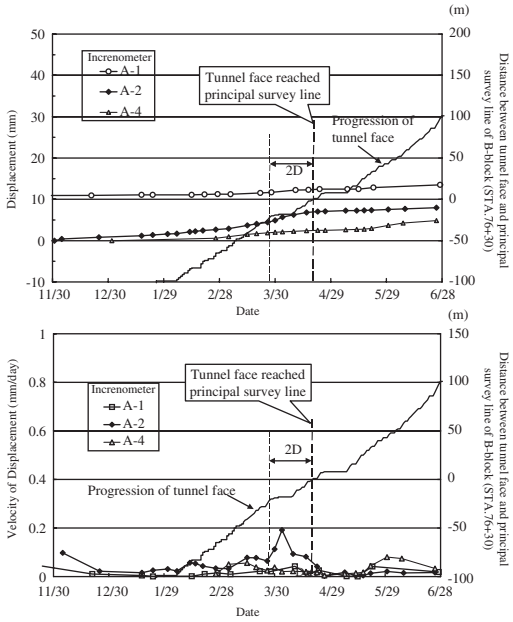


Figure 7. Behavior of landslide A-Block.

pattern consists of steel arch support: H-200, shotcrete: $t = 250$, rock bolts: 6 m × 24 bolts and 12-meter long steel fore poling system called AGF, to reduce the loosening of the ground at crown, especially ahead of face.

It was also decided to construct the invert concrete earlier than usual in order to make a ring by invert and H-steel support as soon as possible if displacement did not converge after excavation, as making the support ring-shaped will make the support itself and surrounding ground physically stable and thus the displacement would be considerably reduced.

In the actual construction of outbound line tunnel in A-block, by applying the rigid support pattern mentioned above, surface settlement was reduced to about 20 mm, as shown in Figure 5. And also the measured landslide displacements of A-block are shown in Figure 7. This figure shows that the maximum displacement rate and cumulative displacement of A-block were reduced to 0.20 mm/day and about 6 mm, respectively. Thus, the displacement of A-block was reduced to about one-third of that of B-block. After the tunnel face passed, the displacement of A-block showed a tendency to converge earlier than the case of B-block.

4.3 *Effectiveness of long fore poling (AGF)*

Long fore poling AGF method has been used in many projects as a way to reduce surface settlement or prevent crown collapse. In the A-block section (Area 2) of the outbound tunnel, the effectiveness of the AGF was confirmed in reducing surface settlement. As a result, landslide occurrence was minimized.

Let us take a look at the loosening-reducing effect of the AGF method. In the B-block section (Area 1) and the A-block section (Area 2) of the outbound tunnel, ground settlement measurement was conducted to determine the loosening zone around the tunnel. And the results are shown in terms of strain distributions. As shown in Figure 8, in the A-block section there are clearly discernible active and passive areas, and the preliminary support effect of AGF is indicated. In the B-block section, however, there is no clearly discernible active or passive area.

There is no standardized concept of "loosening" due to tunnel excavation so far. In this report, therefore, "loosened zone" was defined as a region in which the mechanical properties of ground are altered under the influence of tunnel excavation, and an inflection point of strain distribution curve was regarded as the end of a loosened zone. Accordingly, as shown in Figure 8, in the A-block section about 3.5 m (0.25D) above from the tunnel was regarded as the end of the loosened zone. In the B-block section, though there is not as evident inflection point observed as that in the A-block section, the ground displacement began increasing steeply at the point of about 7 m (0.5D) above from the tunnel. So this point was regarded as the boundary of the loosened and non-loosened zone. Thus it is thought

Copyright © 2005 Taylor & Francis Group plc, London, UK

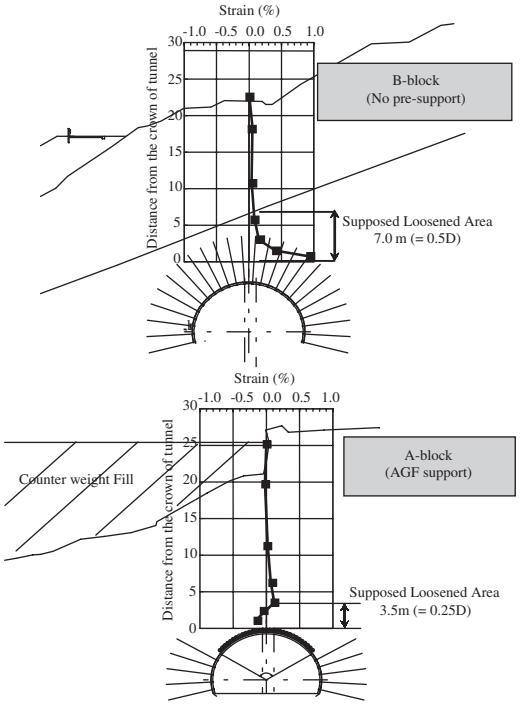


Figure 8. Results of ground displacement measurement.

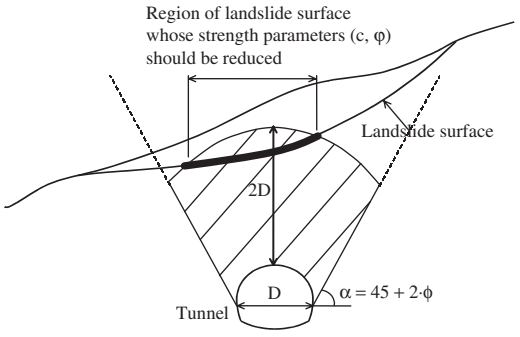


Figure 9. Influence of tunnel excavation on landslide.

that the extent of the loosened zone was reduced to about 50 percent by applying the AGF method.

4.4 *Mechanism for inducing a landslide*

Prior to the excavation of outbound tunnel at B-block (Area 1), counterweight fills were designed through stability analysis that takes into account the influence of loosening of ground around the tunnel, and implemented. However, considerable landslide occurred while the tunnel was excavated. In the conventional

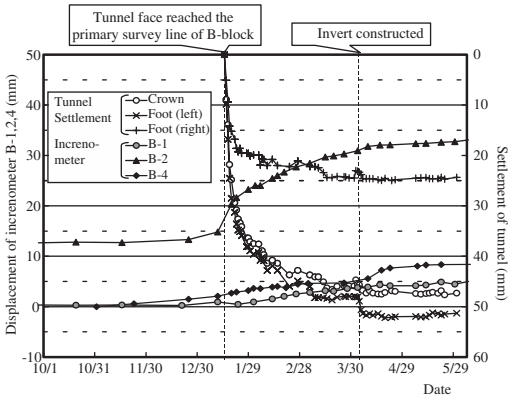


Figure 10. Relationship between the landslide behavior and tunnel displacement in B-block section.

approach, the influence of the tunnel upon landslide occurrence outside a landslide area is evaluated by assuming the loosened zone within the distance of 2*D* above the tunnel, as shown in Figure 9, and reducing the strength parameters such as *c*; the cohesion, and ϕ; the angle of internal friction, of the ground of slip surface within this distance.

This method of evaluating the influence of the tunnel in terms of decreases of the strength parameters works on the assumption that once a landslide has occurred, landslide behavior would continue if no countermeasures to control landslide are taken. On the contrary, as shown in Figure 10, the landslide behavior of B-block correlates closely with tunnel displacement after excavation, and landslide behavior stops as tunnel settlement converged after the construction of the invert.

In the conventional method with shotcrete and rock bolt, unlike in the old sheet pile method, loosening of the surrounding ground does not reach the distance of 2*D* unless it is intended to excavate highly squeezing ground. This is clearly indicated by the results of ground displacement measurement conducted in many tunnels. The loosened zone around the tunnel in the B-block section was within about 0.50D, as is shown in Figure 8, and it did not reach the slip surface, but it did induce landslide movement.

As mentioned before, this kind of landslide movement, previously, has been explained by means of assuming that plasticization occurs, and of reducing the strength parameters (c, ϕ), i.e., for the slip surface as a result of "loosening" induced by tunnel excavation. However, it can be explained more appropriately by thinking that landslide movement is caused by temporary decrease of vertical stress at the slip surface, which was resulted from the displacement of surrounding ground. When a tunnel is excavated, a grand arch is formed right outside the loosened zone, and consequently the stress state of the ground is altered.

Copyright © 2005 Taylor & Francis Group plc, London, UK

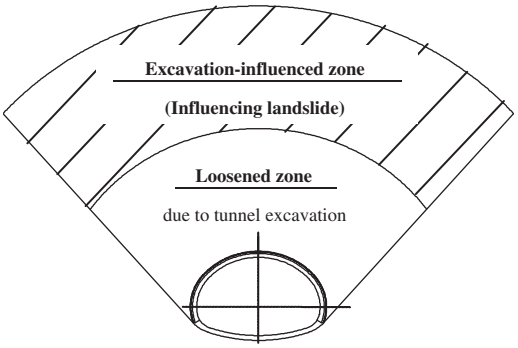


Figure 11. A zone for influencing landslide.

This is the redistribution of stresses in the ground due to tunnel excavation. If there is a slip surface in this stress-redistributed region, vertical stress at the slip surface is temporarily removed and then a landslide is induced. Then, when tunnel displacement begins to decrease, stress redistribution of surrounding ground would be completed, and the temporarily removed vertical stress is restored so that landslide movement gradually comes to a halt.

Let us summarize the concept of loosening. According to the results of measurements conducted during the construction and to other several reports, a "Loosened zone" due to tunnel excavation can be determined as a region where the mechanical properties of ground are altered under the influence of tunnel excavation. And outside this region, additionally, a "Excavation-influenced zone" can be assumed, defined as a region where the ground may behave under the influence of tunnel displacement, and may also induce the landslide inside this region. These regions are shown in Figure 11.

5 CONCLUSION

This paper has reported the behavior of landslide, ground surface and tunnel, which were monitored and measured during the construction of the north portal section of Inasa No.2 Tunnel. The findings of this study concerning three things; landslide behavior under the influence of the tunnel, design and construction of tunnels considering the influence on landslide movement, and the effectiveness of landslide control measures, are summarized as follows:

- If the tunnel is located outside a landslide area, tunnel excavation may induce a landslide even if landslide control measures allowing for the influence of the tunnel excavation are taken. It is thought to be due to the redistribution of stresses in the surrounding ground caused by tunnel excavation. Controlling tunnel displacement can fairly reduced the landslide behavior.
- If a loosened zone due to tunnel excavation is defined as a region where the mechanical properties of ground are altered under the influence of tunnel excavation, a zone of influence on landslide movement may be regarded as a region under the influence of tunnel displacement, which spreads more widely than a loosened zone.
- In the ground where the tunnel face requires no support, and loosening of ground ahead of tunnel face does not extend beyond the length of long fore poling (AGF), the AGF method is effective in reducing loosening around the tunnel and the settlement of ground surface.

As mentioned above, tunnel construction in a landslide area is an extremely difficult task. It is therefore important to make well-informed predictions, conduct monitoring during construction, and feed back the monitored results for the subsequent stages of construction. Because landslide behavior due to tunnel construction and the effectiveness of landslide-control countermeasure works have been investigated in this study, we would like to make effective use of the findings of this study for tunnel construction in the south portal landslide area.

REFERENCES

Osamu, Sakagaki. 1983. Landslide countermeasure works around the tunnel portal. *Tunnels and Underground*., vol.12, No.10: 37–43

Shunsuke, Sakurai. 1983. Study on Loosening Zone in Connection with Tunnel Excavation. *Tunnels and Underground.,* vol.14, No.1:35–41

Copyright © 2005 Taylor & Francis Group plc, London, UK

A deep open-cut excavation with three types of continuous retaining walls

Hiroshi Tsunoda, Yasuhiro Endo, Isao Kamegaya & Hisanobu Kawakami
Metropolitan Expressway Corporation

Katsuji Fukumoto & Akio Ueda
Obayashi Corporation

ABSTRACT: Construction of a Metropolitan Expressway ventilation structure in downtown Tokyo requires a 35 m-wide, 230 m-long and 22 m-deep underground excavation using a cut-and-cover method under a congested trunk road. In addition, a 36 m-deep excavation is required for connecting the ventilation structure and the expressway tunnels. Consequently, 48 m-deep continuous retaining walls are designed to cut off the underground water, and no dewatering is planned.

In Japan, the most popular method for building a continuous retaining wall of this depth is the Soil Mixing Wall method. However, due to the surface conditions, three different types of continuous retaining wall methods are utilized at one excavation site. This paper introduces the details of these three methods, as well as special features, advantages and disadvantages. In addition, differences in quality between these three methods are discussed, including straightness and verticalness, unconfined compressive strength and permeability of the walls.

1 INTRODUCTION

As more and more people move into larger cities, the pressure on cities to develop efficient inhabitable space is increasing. Elevated structures are being incorporated into transportation systems, such as roads and railways, but due to the constraints of urban space in big cities, the use of underground structures has become more popular in recent years.

Underground construction methods are classified as either open-cut excavation method or non-open-cut excavation method. Though a shield tunneling method is currently being rapidly developed, the most common method is still the open-cut excavation method.

When the open-cut excavation method is adopted in an urban area, there is a need to minimize the adverse effects on the surrounding environment, because residents in the neighboring communities continue their daily activities. Using this method in big cities is especially difficult, as the extremely efficient use city space makes it difficult to find space to work, and noise, vibration and air pollution problems caused by construction need to be addressed. Also, conservation of underground water has become a more important issue of concern in recent years, so selecting a construction method that minimizes the adverse effects on surrounding community is the key to success in urban construction projects.

2 OUTLINE OF THE METROPOLITAN EXPRESSWAY CENTRAL CIRCULAR SHINJUKU ROUTE

The construction of the expressway system in Tokyo Metropolis began in the 1960s, but the construction of circular expressways lags far behind the construction of radial expressways, as shown in Figure 1.

The Central Circular Shinjuku Route is an 11 km-long western section of the Central Circular Route.

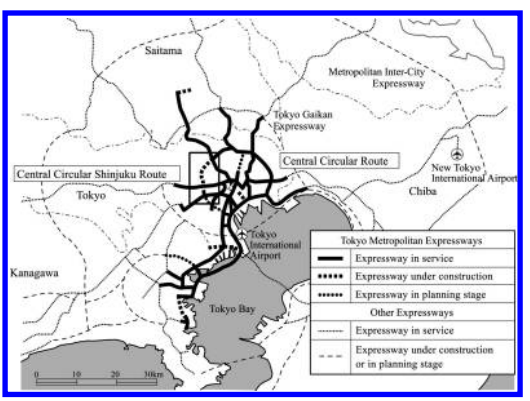


Figure 1. Greater Tokyo motorway network.

Copyright © 2005 Taylor & Francis Group plc, London, UK

It is designed with two lanes in each direction and has a design speed of 60 km/h. To accommodate the land use patterns along the route, and in order to preserve a sound environment and make efficient use of limited public urban space, the Shinjuku Route is designed as a tunnel structure under the circular road Route No.6, which will be widened to 40 m in the same period. Therefore, the alignment of the tunnel, the types of underground structures, and the construction methods must take into account constraints such as the crossing of rivers, subways, trunk roads and railways, as well as the accommodation of major existing public utilities. As is typical with urban expressways, it has a short average distance between access ramps, with six access ramps to the ground-level street and three junctions with radial routes of other Metropolitan Expressways, as shown in Figure 2.

3 OUTLINE OF THE NAKAOCHIAI VENTILATION STATION CONSTRUCTION

Nakaochiai ventilation station is 230 m long, 35 m wide, 22 m deep and constructed under the circular road Route No.6. The expressway road is built under the ventilation station using the shield method, so the excavation for connecting the ventilation station and the expressway roads reaches a depth of 36 m.

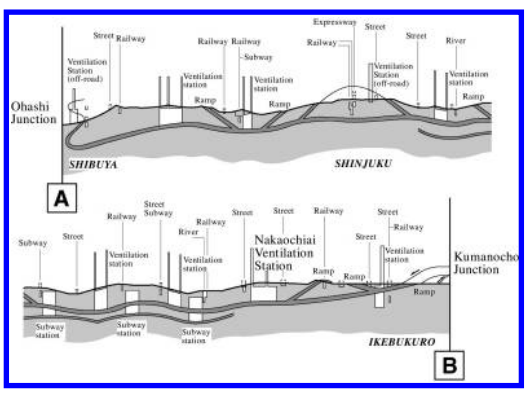


Figure 2. Overview of the central circular Shinjuku route.

The ventilation station is built in stable diluvial strata. There is a layer of Kanto loam and clay from the surface to a depth of 10 m, followed by a layer of Musashino gravel and Tokyo gravel to a depth of 22 m. The ground underneath the Tokyo gravel layer is the 1st Edogawa sand layer, which is stable diluvial sand, and its N value is more than 100. The 1st Edogawa clay layer lies under the 1st Edogawa sand layer.

The underground water level is about 10 m from the surface, which is approximately at the top of the Musashino gravel layer. The Tokyo gravel layer and the 1st Edogawa sand layer both have artesian ground water. When an earth retaining system was designed for the Nakaochiai ventilation station, a continuous retaining wall was adopted to prevent adverse effects on the surrounding area by dewatering. Therefore, the retaining wall extends to the 1st Edogawa clay layer, which is about 46 m below the surface.

The wall in the standard section consists of H-488 × 300 steel piles at 600 mm spacing. For the section where excavation is 36 m deep for connection to the tunnels, H-900 × 300 steel piles are used at 450 mm spacing, because no ground resistance is expected where the section between the two tunnels is excavated. The plan view and layout of the continuous retaining wall are shown in Figure 3. The cross-sections are shown in Figure 4 and Figure 5.

4 ADOPTED CONSTRUCTION METHODS OF CONTINUOUS RETAINING WALLS

In Japan, the most common method for building a continuous retaining wall is the Soil Mixing Wall (SMW) method. In the SMW method, a hole is drilled with an earth auger, and when the auger is extracted, it is rotated backward so that the excavated soil mixes

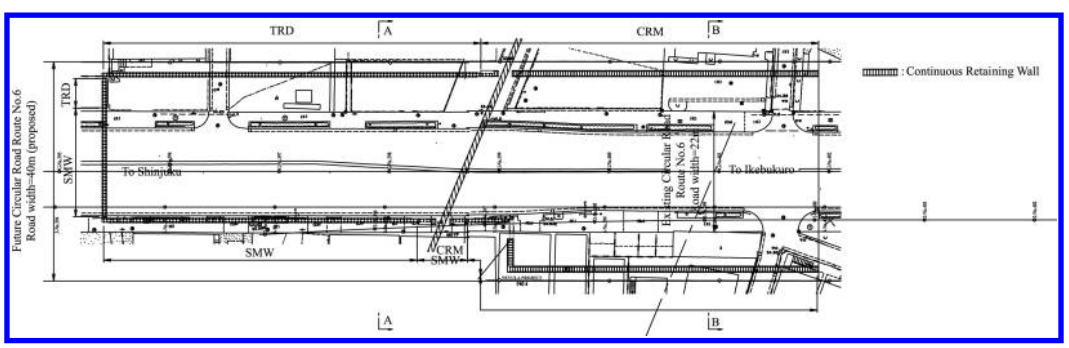


Figure 3. Plan view and layout of continuous retaining wall.

Copyright © 2005 Taylor & Francis Group plc, London, UK

with cement slurry injected from the tip of the auger to produce soil cement. Then, a soldier pile is inserted into the hole. This method produces less noise and less vibration compared to driving sheet piles, and it

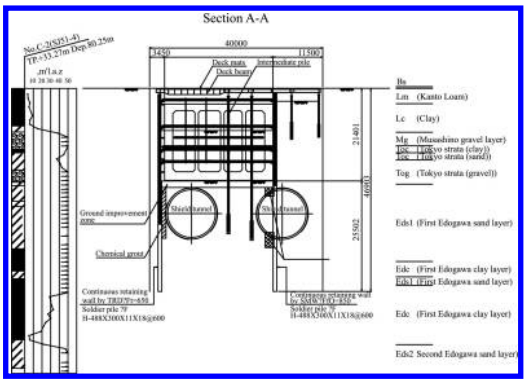


Figure 4. Sectional view (Standard section).

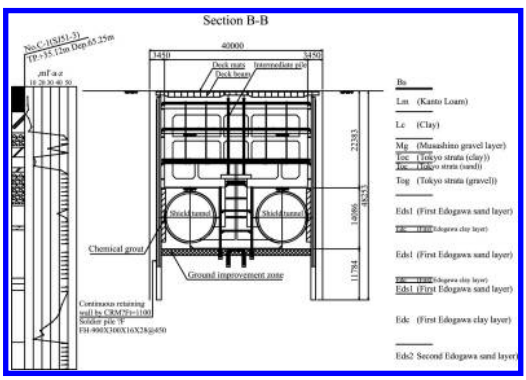


Figure 5. Sectional view (Connecting section to tunnel).

can be applied in various ground conditions. However, due to limitations of the base machine, the maximum diameter of a hole is 900 mm and the maximum size of a soldier pile is H-700 × 300. Also, since holes are drilled with triple augers, the spacing of holes is set as 600 mm.

In the Nakaochiai project, an H-900 × 300 soldier pile was designed for the section that connects to the tunnels, so the SMW method cannot be applied. As a result, the Continuous Walls Using Recycled Mud (CRM) method was adopted. The CRM method is a kind of slurry wall method in which a horizontal multi-axis cutting wheel excavator is used. Two differences from the conventional slurry wall method are that soldier piles are used rather than reinforcing bars, and soil cement is used rather than concrete. The original plan was to make soil cement from reclaimed excavated material and cement in the CRM method, but since a soil cement plant cannot be set up due to noise and vibration problems, the soil cement for this project is purchased from a commercial concrete plant. The size of the element, which is 1100 mm wide and 3200 mm long, is the same as for a conventional slurry wall.

In addition, in a 70 m outbound section where the street could not be shifted due to surface conditions, the working area is not large enough to accommodate an SMW machine. Therefore, the Trench Cutting Remixing Deep Wall (TRD) method was adopted. In the TRD method, a large cutting blade is inserted into the ground, and the ground is excavated and mixed with cement slurry by rotating the cutting chain installed around the outside perimeter of a cutting blade. Then, soldier piles are installed into the trench as the machine advances.

Table 1 is a selection table of continuous retaining wall methods, and Figure 6, Figure 7 and Figure 8 show the general view and a procedures for each method.

Table 1. Selection table of continuous earth retaining methods.

Items	SMW	TRD	CRM
Wall depth approximately 50 m	○	○	○
Geology:			
Diluvial clay	○	○	○
Diluvial sand	○	○	○
Diluvial gravel	○	○	○
Size of soldier piles			
H-488 × 300	○	○	○
H-900 × 300	×	×	○
Width of work area			
10.0 m	○	○	○
7.64 m	×	○	○
Construction cost (SMW = 100)	100	107	139
Remarks	Used in standard section	Used where work area is narrow	Adopted where the section between two shield is excavated

Copyright © 2005 Taylor & Francis Group plc, London, UK

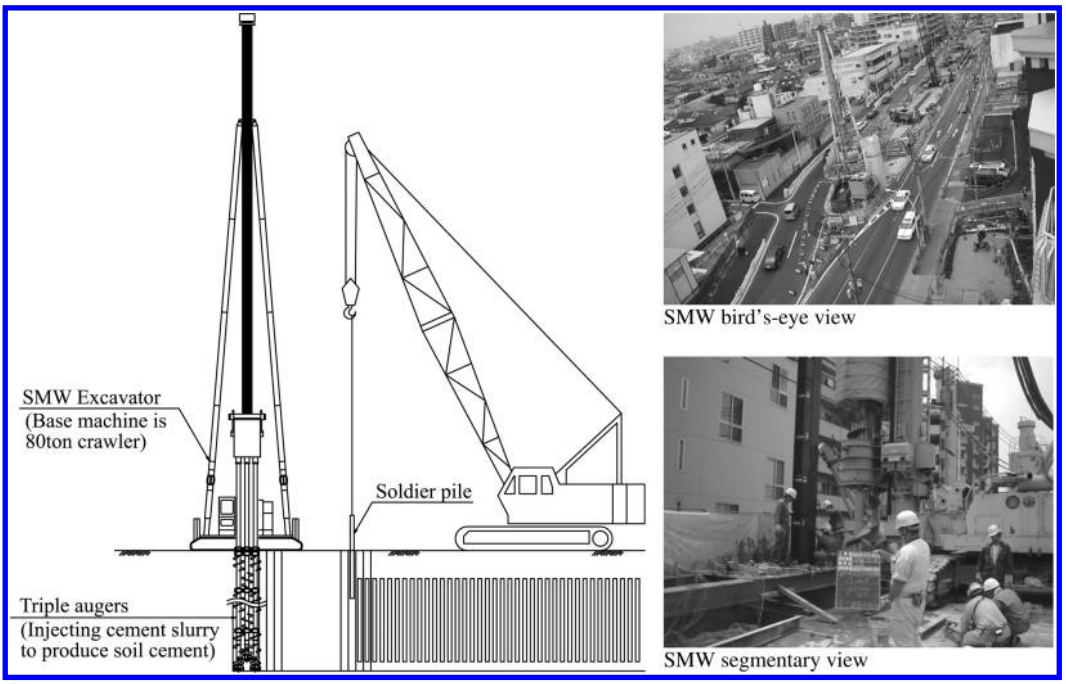


Figure 6. General view of SMW operation.

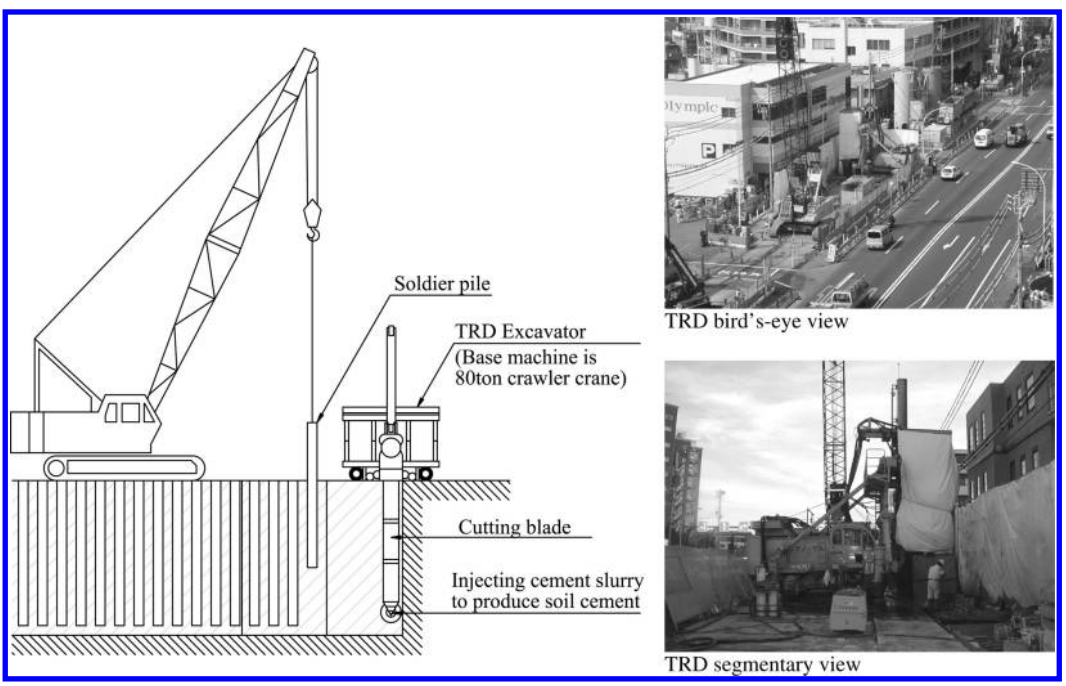


Figure 7. General view of TRD operation.

Copyright © 2005 Taylor & Francis Group plc, London, UK

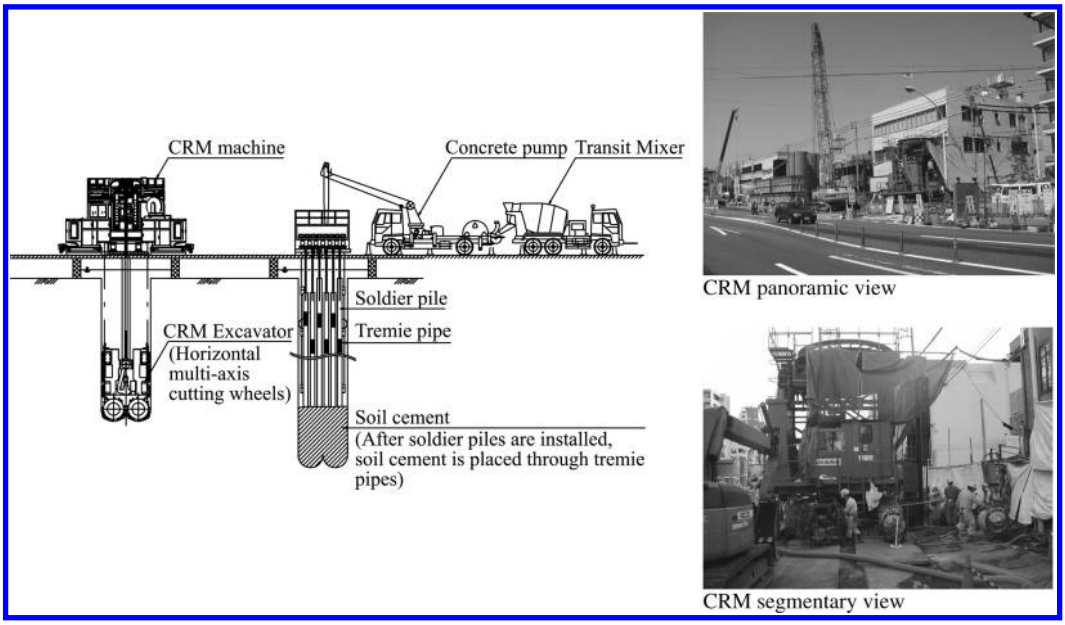


Figure 8. General view of CRM operation.

5 CONSTRUCTION RESULTS OF EACH METHOD

5.1 *Production rate*

The daily production rate of each method is shown in Table 2.

Since the CRM method requires multiple stages of operation, the average daily production rate is lower than the other methods. In addition, the CRM method requires relatively large equipment, such as a soil cement plant, so the mobilization and demobilization time is longer than for the other methods. No significant difference in production rate is observed between the SMW method and TRD method. Since there are no underground utilities crossing the wall line in this project, the production rate of the TRD method is comparable to that of the SMW method. But in general, it takes about a week to excavate and to lower the cutting blade in position when using the TRD method, so it is not considered suitable for projects in which there are underground utilities crossing the wall line.

Table 2. Daily production rate.

Items	SMW	TRD	CRM
Total wall area (m^2)	4,090	3,484	5,860
Working days (days)	71	60	216
Average daily production rate (m^2/day)	57.6	58.1	27.1

5.2 *Accuracy of wall*

The excavation accuracy of each method is shown in Table 3. Accuracy perpendicular to the wall line is best in the CRM method, followed by the TRD method and the SMW method. Since the TRD method is a continuous operation along the wall line and construction joints are created only at the end of the day, the water-tightness of the wall is considered better than the in the SMW method. In the CRM method, if joints are cleaned up well and the placement of soil cement is controlled, the water-tightness of the wall is also secured.

To the contrary, holes drilled using the SMW method may be curved and may not overlap each other if the wall is more than 40 m deep. Therefore, the SMW method should be applied carefully when performing deep excavation in highly permeable ground, and particular attention should be paid to water leaking from the wall while excavating.

5.3 *Quality of soil cement*

The quality of soil cement in each method is shown in Table 4. The design strength and permeability of the soil cement of the wall is 500 KN/m^2 and 1×10^{-6} cm/sec accordingly. All methods satisfy the design requirements. In the SMW method, soil and cement slurry are mixed with an auger rotating horizontally, so the

Copyright © 2005 Taylor & Francis Group plc, London, UK

Table 3. Accuracy of excavation.

Items	SMW	TRD	CRM
Deviation along the wall line (mm)	−168 to 200	Continuous operation along the wall line	−3 to 50
(Verticalness = deviation/depth)	(−1/280 to 1/235)		(−1/1550 to 1/934)
Deviation perpendicular to the wall line (mm)	−157 to 186	−5 to 90	−5 to 45
(Verticalness)	(−1/300 to 1/253)	(−1/930 to 1/517)	(−1/950 to 1/1036)
Combined deviation (mm)	1 to 216	NA	NA
(Verticalness)	(1/2769 to 1/218)		

Table 4. Quality of soil cement.

Items	SMW	TRD	CRM
Axial compression strength (KN/m^2)			
Upper area (Clay) (GL-2 to 3)	2,624	2,680	2,895
Middle area (Gravel) (GL-20 to 21)	5,475	2,700	2,247
Lower area (Sand) (GL-40 to 41)	4,862	4,700	1,506
Permeability (cm/sec)			
Upper area (GL-2 to 3)	2.72×10^{-8}	2.76×10^{-8}	4.20×10^{-7}
Middle area (GL-20 to 21)	3.23×10^{-8}	4.57×10^{-8}	5.51×10^{-8}
Lower area (GL-40 to 41)	1.92×10^{-8}	3.69×10^{-8}	2.79×10^{-8}

strength of the soil cement fluctuates depending on the properties of the in-situ soil. In this project, the top 10 m is Kanto loam and clay, so the strength of the top 10 m of soil cement is relatively weaker than other sections. On the other hand, in the TRD method, a chain cutter along the edge of the blade rotates to mix soil and cement slurry, so the quality of soil cement is considered fairly uniform, regardless of depth. However, remarkable uniformity of soil cement is not observed in this project. In the SMW method and TRD method, the compressive strength of the soil cement varies depending on the in-situ soil, but the permeability of the soil cement is fairly uniform.

In the CRM method, cutting slurry is replaced with soil cement produced in a commercial plant, so the quality of soil cement is relatively uniform. Since the specific gravity of soil cement is as low as approximately 1.5, it is considered that soil cement may be mixed with cutting slurry when it is placed. The ground at the bottom 10 m of the excavation is highly permeable and contains abundant water, so the specific gravity of the soil cement is set as 1.6 and a viscous agent is added to prevent soil cement from mixing with cutting slurry. Judging from the results of quality assurance boring, the permeability of the area where the viscous agent is added is 1/10 that of the upper section, so the higher specific gravity and viscous agent work as expected.

5.4 *Encountered problems*

As indicated above, all three different continuous retaining wall methods satisfy the design requirements in this project. However, a large deviation is observed in the installation of soldier piles. Since the excavation depth is only 22 m, the length of a soldier pile is approximately 31 m, even though the length of the wall is 48 m. Therefore, the bottom of a pile is not supported by the ground and may move when the next section is excavated in the TRD method. In the SMW method, the diameter of an auger is determined by excavation depth, so an 850 mm auger is required for a 48 m-deep wall. The size of a hole is 850 mm, which is much larger than the size of the H-488 × 300 soldier pile, so the pile may move when the next hole is excavated. In either case, piles are lined up fairly well along the wall line, but pile spacing may vary because piles may move along the wall line. Reinforcing steel plates are installed where spacing of piles is too wide.

6 CONCLUSION

Since a continuous earth retaining wall is relatively impermeable, dewatering is unnecessary and adverse effects on the surrounding environment are minimized. Therefore, continuous earth retaining wall methods

Copyright © 2005 Taylor & Francis Group plc, London, UK

are currently in widespread use in open-cut excavation. Many different continuous earth retaining wall methods have been proposed, so it is very important to select the most suitable methods for the project, depending on geological conditions, wall depth, size of working area, size of soldier piles, existing underground utilities, and so on.

These three different retaining wall methods are adopted for this project, so additional observations and explorations are conducted to identify the properties of these methods, which may help engineers in future projects. Though all three of these methods satisfy the required performance and quality, there is still some room for future improvement, such as with the installation of soldier piles in the trench, construction around underground utilities, and size reduction of construction equipment.

Underground construction in urban areas will continue to increase in the future, so more innovative construction methods are anticipated.

Copyright © 2005 Taylor & Francis Group plc, London, UK

Application of the multiple-layer supporting method to a tunnel in squeezing argillaceous rocks

S. Kemmochi, E. Taketsu & A. Ogawa
Japan Railway Construction, Transport and Technology Agency, Yokohama, Japan

T. Aoki, M. Koike & R. Morita
Taisei Corporation, Tokyo, Japan

H. Shirahata, N. Koya & M. Matsubara
Obayashi Corporation, Tokyo, Japan

ABSTRACT: Squeezing phenomena accompanied by the support failures have occurred at Konari work section of Iiyama Tunnel for Hokuriku Shinkansen (a bullet train line) in a Neogene mudstone formation where the overburden exceeded 180 m. To cope with this large squeezing earth pressure, the multiple-layer supporting method has been applied for this tunnel as reported in our previous paper mainly on the failing behavior of the first-layer supports and its numerical analyses. Further severe squeezing phenomena occurred in the shear-disturbed zone located at around the boundary between Konari and Itakura work sections. In this paper, the improvement of the multiple-layer supporting method in this zone is described including the predictive numerical analyses and the application results.

1 INTRODUCTION

Iiyama Tunnel for Hokuriku Shinkansen (a bullet train line) runs through the boundary of Nagano and Niigata Prefectures and has a great length of 22.2 km. It is divided into six work sections for construction. In Itakura and Konari work sections, 3,660 m and 3,800 m in length respectively, that locate first and second from the Niigata-side portal, we encountered the squeezing phenomena in mudstones of Miocene, Neogene formations. The maximum convergence tended to exceed 200 mm especially in sections whose overburden went beyond 180 m. In our previous paper (Kemmochi, et al., 2004a & 2004b), the application of the multiple-layer supporting method in squeezing rocks in Konari work section was reported. The characteristic behaviors of the first-layer support members especially on the stress variation were investigated with the in-situ measurements and three-dimensional numerical analyses. Consequently, it was found that the behaviors of the convergences and support stresses were able to be expressed by the numerical analyses in which the work execution procedures were fully sequentially incorporated.

Further severe squeezing phenomena occurred in the shear-disturbed zone located at around the boundary between Konari and Itakura work sections. To deal with such large earth pressures, strengthening of the first-layer support members and the early-time application of the second-layer support were investigated with the predictive numerical analyses. Whereas large convergences more than 500 mm occurred actually in the shear-disturbed zone, the tunnel was safely excavated with the execution procedures and the support specifications that had been designed based on the findings of the predictive analyses. The performances of the first- and second-layer supports were confirmed with the various in-situ measurements.

In this paper, the application of the multiple-layer supporting method in the shear-disturbed zone is described.

2 PREDISTIVE NUMERICAL ANALYSES ON TUNNELING IN THE SHEAR-DISTURBED ZONE

In our previous paper (Kemmochi, et al., 2004a & 2004b), we have shown that the three-dimensional numerical analyses with elasto-perfectly plastic rock model together with yieldable support models can explain the measured displacement and support-stress behaviors. We have also studied the cases of

Copyright © 2005 Taylor & Francis Group plc, London, UK

high-strength first-layer support members (Kemmochi, et al., 2004c). In these investigations, the second-layer support was supposed to apply at the location distant from the top-heading face by 3.5D where D is the tunnel width and is 10 m here. Whereas the first-layer support somewhat failed before the application of the second-layer support, cases in which the second-layer support became broken as severe as it lost its support function had not been targeted.

In this chapter, a poorer rock condition is assumed so as to correspond to rocks in the shear-disturbed zone. Cases of high-strength first-layer support and the early-time application of the second-layer support are studied with the numerical analyses for the prediction.

2.1 *Analysis conditions*

The rock and support properties used in the numerical analyses are given in Table 1. The stiffness (i.e. Young's Modulus) of each first-layer support member is set one-fifth of the material property based on the findings in our previous study (Kemmochi, et al., 2004a & 2004b) so as to reasonably express the measured response of the support stress change with the rock displacements. This behavior is considered to result from the loosened boundary between the support and rocks at the tunnel interior. Such technical treatment is often adopted in numerical analyses. The stiffness reduction is not applied for the second-layer support since its close contact with the first-layer support can be assured in practice.

Regarding the excavation sequence, the first-layer support is closed by applying the invert at the location distant from 10 to 14 m from the top heading face and subsequently, the second-layer support is applied at the section of 10 to 22 m away from the face. Two support patterns are tested: high-strength and normal support members viz.:

– Case 1: First-layer support (high strength)
  + Second-layer support (normal)
– Case 2: First-layer support (normal)
  + Second-layer support (normal)

2.2 *Analysis results*

2.2.1 *Displacement*

The horizontal convergences at a cross section of the top heading are shown in Figure 1 and Table 2. As given in Table 1, Case 1 with high-strength first-layer support has the convergence of 79% of that of Case 2 with normal-strength supports before the application of the second-layer support. It has the convergence of 10% of that of Case 2 after the application of the second-layer support. The difference in displacement before the application of the second-layer support would result from the different stiffness of the first-layer support. In contrast, the displacement ratio after the application of the second-layer support is much less whereas the same specification is applied for

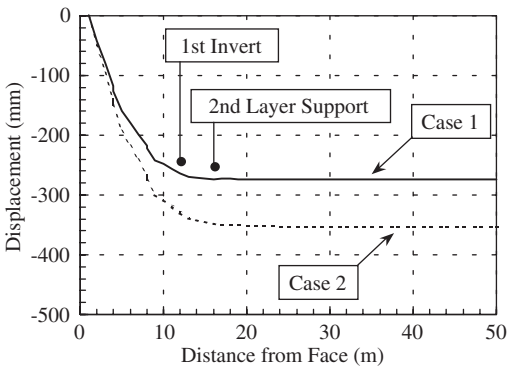


Figure 1. Convergence.

Table 2. Convergences.

Displacement (mm)	Case 1	Case 2	Case 1/ Case 2
Total	−274.2	−353.7	0.78
Before 2nd Layer Support	−273.6	−347.8	0.79
After 2nd Layer Support	−0.6	−5.9	0.10

Table 1. Parameters used for predictive numerical analysis.

	Specification	E [GPa]	ν	C [MPa]	ϕ [°]	Yield Stress [N/mm^2]
Ground		0.2	0.3	0.26	16.5	–
1st Layer Support [High Strength]						
Shotcrete (1/5 Stiffness)	t = 250 mm	1.36	0.2	18.0	0	(36.0)
Steel Support (1/5 Stiffness)	HH200	40	–	–	–	390
1st Layer Support [Normal]						
Shotcrete (1/5 Stiffness)	t = 250 mm	0.68	0.2	9.0	0	(18.0)
Steel Support (1/5 Stiffness)	H200	40	–	–	–	235
2nd Layer Support [Normal]						
Shotcrete	t = 150 mm	3.4	0.2	9.0	0	(18.0)
Steel Support	H125	200	–	–	–	235

Copyright © 2005 Taylor & Francis Group plc, London, UK

their second-layer supports. This would mainly result from the difference in the yield strength of their first-layer supports. Namely, since Case 1 has significant extents of yielded parts in the shotcrete and steel supports in comparison with those of Case 2 (see Figure 2 with reference to the following Section 2.2.2), the first-layer support of Case 1 has greater virtual stiffness than that of Case 2 before the application of the second-layer support.

2.2.2 *Stress in first-layer support*

Figure 2 shows the yielded parts of the first-layer support before the application of the second-layer support. Regarding the yielded zones of the shotcrete (black-colored parts), the shotcrete of Case 1 remains in elastic state (so does it even after the application of the second-layer support in this case) whereas that of Case 2 contains yielded zones widely spread from the crown to the shoulder. Concerning the yielded parts of the steel supports (grey-colored thick-lined parts), the yielded parts of the steel supports of Case 1 are limited in the crown region whereas the steel supports of Case 2 yielded in almost all the parts.

Thus, the use of normal-strength support members in Case 2 would result in severe failure e.g. crush of shotcrete or rupture of steel supports since both the shotcrete and steel supports are yielded especially in the regions of the crown and shoulder of the top heading.

2.2.3 *Stress in second-layer support*

Figure 3 shows the yielded parts of the second-layer support after the excavation completed. The yielded zones in the second-layer shotcrete distributed from the invert to the sidewall at after the sections close to the construction joint. The yielded zones of Case 1 are wider than those of Case 2. In case of use of high-strength support members (Case 1), the second-layer support is partly yielded mainly at the invert region. Nevertheless, the shotcrete support would be considered to retain the total stability since the first-layer shotcrete is not yielded at all. Moreover, since the position of the yielded zones of the second-layer shotcrete in both Cases 1 and 2 is limited at the invert and sidewall near the construction joint and all the arch region of the second-layer support remain in the elastic state, it can be insisted that the working safety be secured.

3 CONSTRUCTION RESULTS

The support patterns used in the shear-disturbed zone are shown in Table 3. Based on the recent work

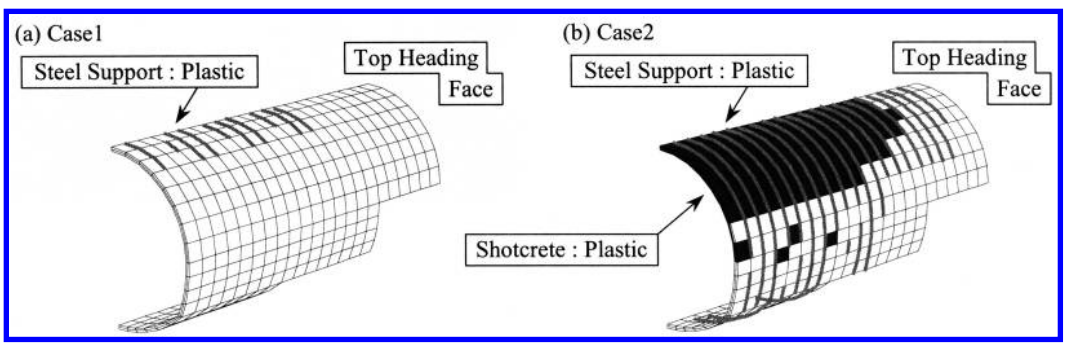


Figure 2. Yielded zones of first-layer support.

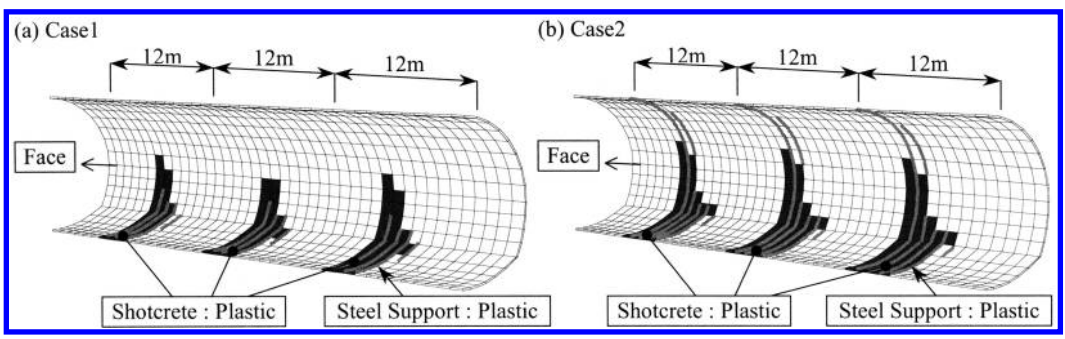


Figure 3. Yielded zones of second-layer support.

Copyright © 2005 Taylor & Francis Group plc, London, UK

Table 3. Specifications of supports

			Support Pattern A	Support Pattern B
First Layer	Arch	Steel Support	200H (SS400)	200H (SS540)
		Shotcrete	25 cm Thick	25 cm Thick
			Fiber Reinforced	Fiber Reinforced
			18 N/mm^2	36 N/mm^2
		Rock Bolt	4.0 m × 10	4.0 × 10
			4.5 m × 16	4.5 m × 16
	Invert	Steel Strut	200H (SS400)	200H (SS540)
		Shotcrete	25 cm Thick	25 cm Thick
			18 N/mm^2	36 N/mm^2
Second Layer	Arch	Steel Support	125H (SS400)	150H (SS400)
		Shotcrete	12.5 cm Thick	15 cm Thick
			18 N/mm^2	18 N/mm^2
	Invert	Steel Strut	–	150H (SS400)
		Shotcrete	–	15 cm Thick
				18 N/mm^2



Photograph 1. Failure of first-layer invert.

experiences, tunneling was at first conformed to Pattern A with which the second-layer support was basically applied at the position of 3.5D away from the top-heading face; D is the tunnel width and is 10 m here. However, the convergence exceeded 300 mm at the position of 1.5D from the top-heading face and it did not tend to converge. The shotcrete cracked resulting in spalling at the tunnel crown and shoulder. Especially at the crown, the steel supports were yielded and some of them were ruptured. The second-layer support was applied here over the first-layer support but the displacement did not tend to converge. It was observed that the shotcrete was crushed and that the invert steel struts were consecutively ruptured when the backfill over the first-layer invert was removed, as shown in Photograph 1. It was considered that these circumstances resulted from the insufficient bearing capacity of the first-layer support against such unexpectedly large earth pressure.

The predictive analyses described in the previous chapter indicated that strengthening of the first-layer support would be effective in a poor rock condition of the shear-disturbed zone. Hence, the supports of Pattern B with high-strength shotcrete and high-standard steel supports were used for tunneling (see Table 3 and Figures 4 and 5). Since the supports of Pattern B were used, the convergences had been stabilized at around 200 mm as shown in Figure 6. Moreover, the second-layer supports became scarcely damaged and the stability of the tunnel structure was secured.

4 VERIFICATION WITH MEASUREMENTS

Measurements of the stresses of the support members in addition to those of the convergences were performed to confirm the effects of strengthening the first-layer support members and of the early-time application of the second-layer support with the supports of Pattern B.

(1) First-layer support.
The stress change of the first-layer shotcrete with time is given in Figure 7. The stresses at all of the measured points rapidly increased at the early phase. The sudden stress decrease indicated the shotcrete failure at the nearby location. It was found that subsequently, the stresses turned into re-increase after the application of the second-layer support.
Figure 8 shows change of the axial rim strains of the first-layer steel support with time. Both the strains at crown and invert increased rapidly just after the installation and soon exceeded the yield strain of 0.21%. However, the application of the second-layer support restrained the strains from further increase.

Copyright © 2005 Taylor & Francis Group plc, London, UK

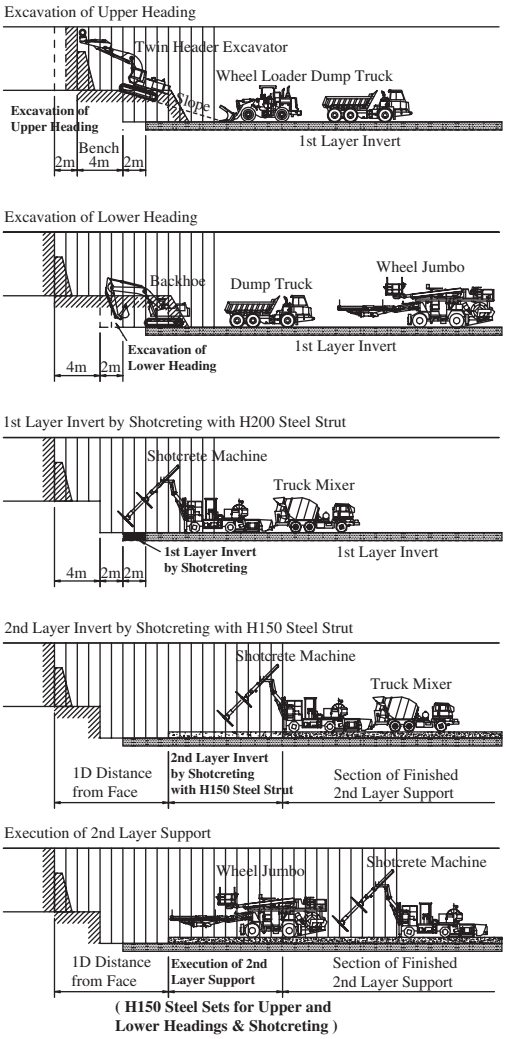


Figure 4. Work execution procedure.

(2) Second-layer support

The stress change of the second-layer shotcrete with time is given in Figure 9. The stresses at the crown, shoulder and sidewall were within relatively low level below 6 N/mm^2. On the contrary, the stress measured at the invert reached the design strength of 18 N/mm^2.

Figure 10 shows change of the axial rim strains of the first-layer steel support with time. While the axial strains were within the relatively small level below 0.1%, that of the invert was greater than the others and exceeded 0.1%.

Consequently, one could conclude that the second-layer supports remained stable in the arch and sidewall position judging from the stress state measured. On the contrary, the support members at the invert including the shotcrete and steel strut were in high stress state.

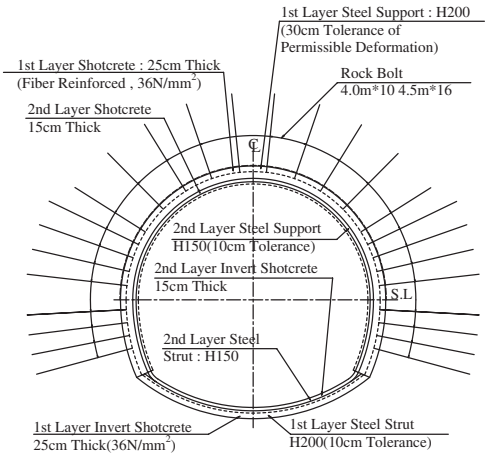


Figure 5. Support pattern B.

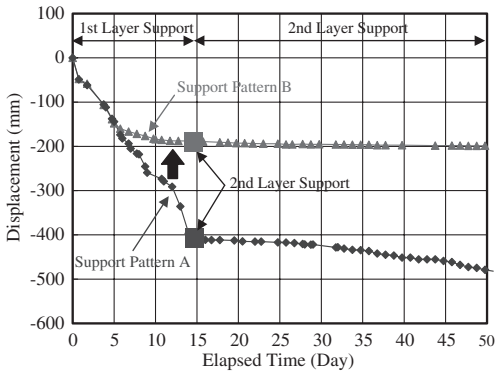


Figure 6. Convergence.

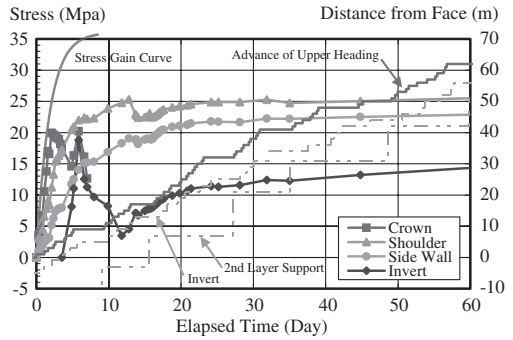


Figure 7. Axial stresses of first-layer shotcrete.

Copyright © 2005 Taylor & Francis Group plc, London, UK

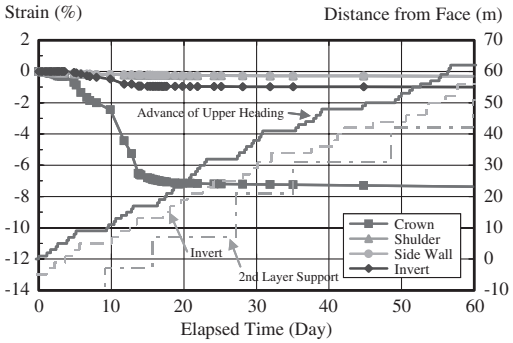


Figure 8. Axial strains of first-layer steel supports.

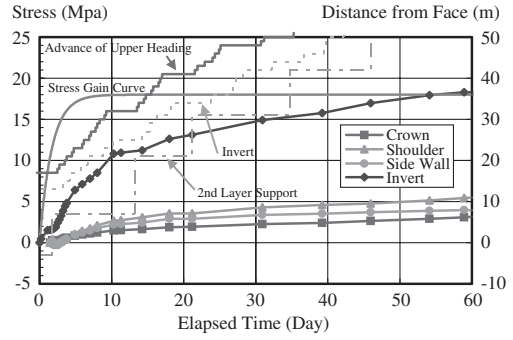


Figure 9. Axial stresses of second-layer shotcrete.

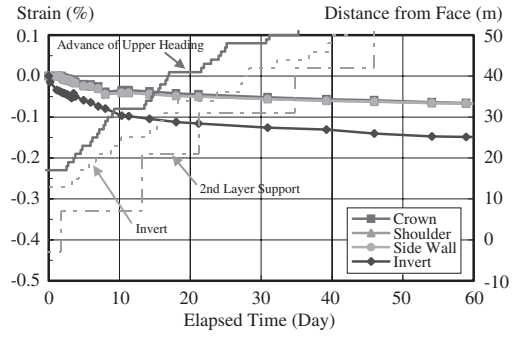


Figure 10. Axial strains of first-layer steel supports.

(3) Summary

While the first-layer support was partly in the yielded state, its displacements became converged after the application of the second-layer support. Thereat, restoration of the support function of the first-layer support was observed.

The second-layer support was able to keep its soundness in the support function although the limited part at the invert was in the yielded state.

5 COMPARISON OF RESULTS OF MEASUREMENT AND PREDICTIVE ANALYSES

(1) First-layer support

It was obtained from the predictive analyses that the use of high-strength shotcrete and high-standard steel supports for the first-layer support would avoid yielding the shotcrete and would restrain the yielded extent of the steel supports, as indicated in Figure 2. Correspondingly, the measurement results indicated that both the shotcrete and steel supports resulted in significant yielding and failure at the crown and invert. However, the shoulder and sidewall were fairly sound, as shown in Figures 7 and 8. It was considered that the actually worked earth pressure (or in-situ stress) was greater than that used in the predictive analyses. Hence, damage of the first-layer support was severer in the actual construction than it was in the predictive analyses. However, the overall trends of the support behaviors were well demonstrated by the predictive numerical analyses.

(2) Second-layer support

In the results of the predictive analyses, the yielded zones of the second-layer shotcrete were limitedly distributed at the invert and sidewall, as shown in Figure 3. Correspondingly, the stress of shotcrete reached the design strength only at the invert in the actual measurement and the stresses in the second-layer support at the arch region remained below the design strength level, as given in Figures 9 and 10. Thus, the predictive analysis results were in relatively good accordance with the measured behaviors.

6 CONCLUSIONS

The application of the multiple-layer supporting method in the shear-disturbed zone was investigated where significant squeezing phenomena occurred. The main findings are listed below:

1. In the shear-disturbed zone where the deformation was significantly large, the multiple-layer supporting method was successfully applied by strengthening the first-layer support members so as to restrain the yielding and failing and by applying the second-layer support at as close to the top-heading face as 1D (or 10 m). This combination of the high-capacity first-layer support with the early-time application of the second-layer support effectively secured the tunnel stability in such a difficult ground condition.
2. The three-dimensional analyses in which the work execution procedures were fully sequentially incorporated were found to be capable of investigating

Copyright © 2005 Taylor & Francis Group plc, London, UK

the appropriate combination of the first- and second-layer supports and the suitable timing of the application of the second-layer support.

3. The multiple-layer supporting method is a highly flexible and rational tunneling method in squeezing rocks in that the specifications and the application timings of the first- and second-layer supports can be effectively adjusted.

REFERENCES

Kemmochi, S., Taketsu, E., Morita, R. & Aoki, T. 2004a. Investigation into loosened zones and deformation behaviors of a tunnel in a squeezing ground by means of the multiple-layer supporting method. Proceedings of the World Tunnel Congress, Singapore, E03, p. 6 (CD-ROM).

Kemmochi, S., Taketsu, E., Morita, R. & Aoki, T. 2004b. Investigation into loosened zones and deformation behaviors of a tunnel in a squeezing ground by means of the multiple-layer supporting method. Tunnelling and Underground Space Technology, Vol. 19, No. 4–5, pp. 408–409

Kemmochi, S., Taketsu, E., Aoki, T., Kamemura, K. & Morita, R. 2004c. Three-dimensional analysis on the deformation behavior of a tunnel in squeezing rocks. Proceedings of the 11th Japan Symposium on Rock Mechanics, pp. 9–16.

Copyright © 2005 Taylor & Francis Group plc, London, UK

Support structure for tunneling in squeezing ground and secondary lining design

J. Yorita, M. Hanita & H. Takahara
Iiyama Railway Construction Office, Japan Railway Construction, Transport and Technology Agency, Nagano, Japan

K. Kawahara & H. Takahashi
Nagoya Branch, Kumagai Gumi, Co. Ltd., Aichi, Japan

M. Mitarashi
Kumagai Gumi, Co. Ltd. Tokyo, Japan

ABSTRACT: The Iiyama tunnel is a large-scale tunnel about 22 km long on the Hokuriku Shinkansen Line at the boundary between Nagano and Niigata prefectures. Since the Nabetate-yama tunnel on the Hokuhoku Line, where large squeezing earth pressures were induced, is located near this project, similar geological conditions were expected to exist at the Iiyama tunneling site. Squeezing ground was encountered as predicted from the initial stage of excavation. We dealt with this difficulty by increasing the support rigidity and closing the section earlier. It was impossible however to completely control tunnel deformation, making it impossible to ensure the specified section in some places. As a result, multiple support was adopted to continue excavation in the squeezing ground. This paper discusses the support design for replacement of supports and the concept of secondary lining.

1 INTRODUCTION

The Iiyama tunnel is a large-scale tunnel about 22 km long planned at the boundary between Nagano and Niigata prefectures on the Hokuriku Shinkansen Line (between Nagano and Joetsu). The Nabetate-yama tunnel, where pressure generated during excavation from squeezing soil caused serious difficulties in construction, is located thirty kilometers north-east of this project site. The geological conditions in the Iiyama tunneling site were expected to be similar to those in the Nabetate-yama tunneling site.

At the Tomikura sector, as expected, squeezing ground was encountered from the every early stage of excavation. We dealt with this situation by increasing the rigidity of supports and closing the section earlier. It was impossible however to completely control tunnel deformation, and we could not ensure the specified section in some places. As a result, we adopted a multiple support system with a support (hereinafter referred to as secondary support) inside the primary support, to maintain structural integrity of the supports. Using this strategy, we have continued excavating the squeezing ground with some success.

This paper discusses the support structure for excavation in the squeezing ground, in-situ measurement results, support design at the time of replacement of supports with re-excavation, and the concept of the secondary support.

2 OVERVIEW OF THE PROJECT

Project name:

Tomikura sector of the Iiyama Tunnel project on the Hokuriku Shinkansen Line

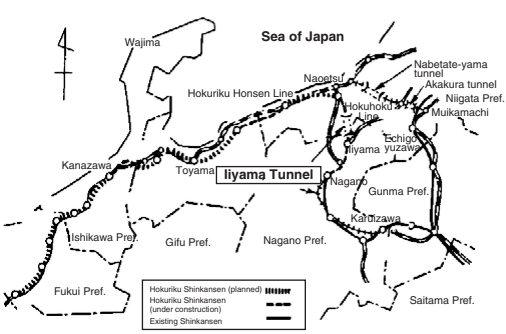


Figure 1. Location of the Iiyama tunnel.

Copyright © 2005 Taylor & Francis Group plc, London, UK

Planned Work period:
from June 30, 1998 to December 31, 2005
Tunneling features:
Excavation length 4,504 m (total length 22,225 m)
Excavation section about 72 to 102 m^2
Longitudinal gradient 30/1,000
Excavation method:
full face cutting with auxiliary bench
Excavation equipment:
full face cutter (boom header)

3 GEOLOGY

The tunneling site is located in a zone called Northern Fossa Magna, with well-developed folds, characterized by significant geological deformation. The geology of the Tomikura sector consists of, from the lower position, Tertiary Teradomari formation, Shiiya formation (Miocene formations), Nishi-yama formation, and Haizume formation (Pliocene formations). The lithofacies are composed of semi-abysssal and abyssal sediments generated by submarine volcanic activities (mudstone and tuff), and neritic and continental sediments containing a large volume of coarse grain particles.

It is known that the sedimentary rocks of Miocene, Neogene and Pliocene in the Niigata coast and Higa-shikubi hills contain petroleum and natural gas in some places. Petroleum and natural gas gushed out from the tunneling face also in the Tomikura sector.

The mudstone and tuff of this geological age generally contains much squeezing clay-like mineral (montmorillonite).

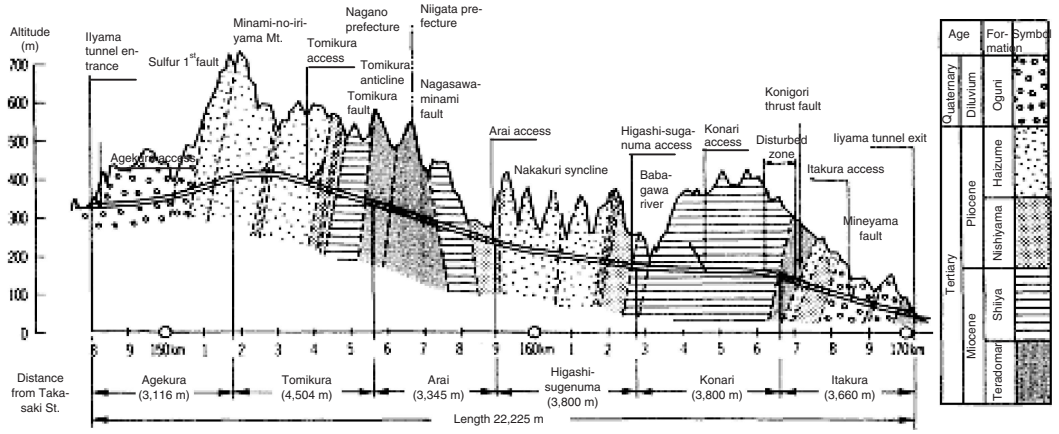


Figure 2. Geological diagram of the Iiyama tunneling site.

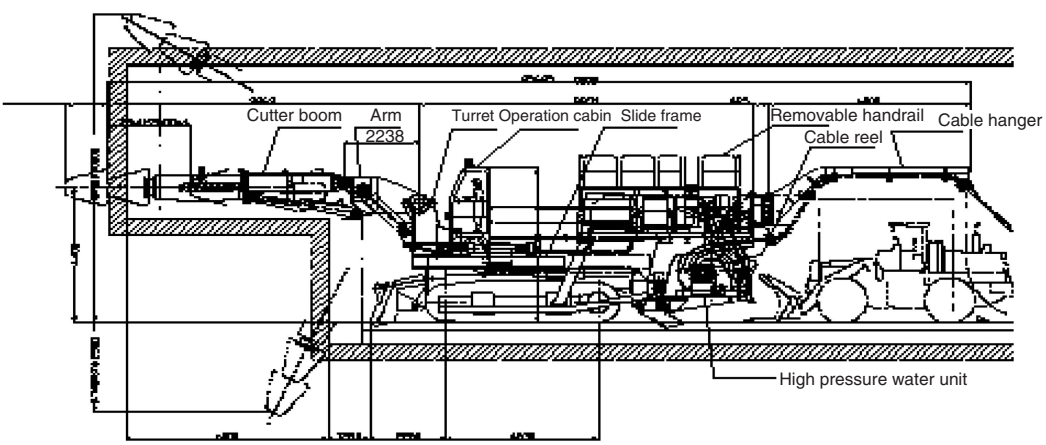


Figure 3. Full-face cutter (boom header).

Copyright © 2005 Taylor & Francis Group plc, London, UK

4 TUNNELING OPERATIONS

Mechanical excavation with a boom header was selected. As shown in Figure 3, the equipment enables full face cutting, and is provided with a sliding mechanism that can achieve a bench length of about 6 m and a boom capable of cutting also the invert, for stabilizing the face. With this equipment design, it is possible to close sections early, as the primary invert can be placed just near the face. In addition, by survey boring prior to face cutting, we have been attempting to find in advance inflammable gas, water inflow and adverse ground conditions. This survey boring is implemented with an explosion-proof rotary boring machine, in the direction of 20 degrees to the tunnel excavation axis, with an upward gradient of about 2 degrees, at intervals of 100 m advance. This is because the strike of the stratum crosses the tunnel alignment with a degree of about 45 degrees, and in order to ensure water drainage gradient.

5 DAMAGE OF THE SUPPORTS

From the initial stage of excavation, squeezing ground was encountered, with horizontal displacements around 150 mm. But, just after tunneling entered the Shiiya formation, from the location 154.840 km (distance from Takasaki Station), the horizontal displacement abruptly increased, causing significant buckling of steel supports and spalling of sprayed concrete (Figure 4). Consequently, it became necessary to increase support strength.

Figure 5 shows the changes in horizontal displacement and crown settlement in the Tomikura sector. At the location 155.173 km, a horizontal displacement of 900 mm and a crown settlement of 300 mm were recorded.



Figure 4. Damaged primary support.

6 MEASURES AGAINST DEFORMATION

6.1 *Early closure of sections*

In tunneling in squeezing ground or in very weak ground, early section closure is effective since the surrounding ground is plasticized because of loosening during excavation. By using the machine shown in Figure 3, the primary invert was placed near the face, enabling the section to be closed early.

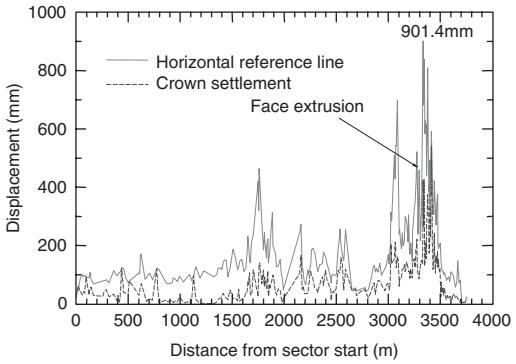


Figure 5. Horizontal reference line and change.

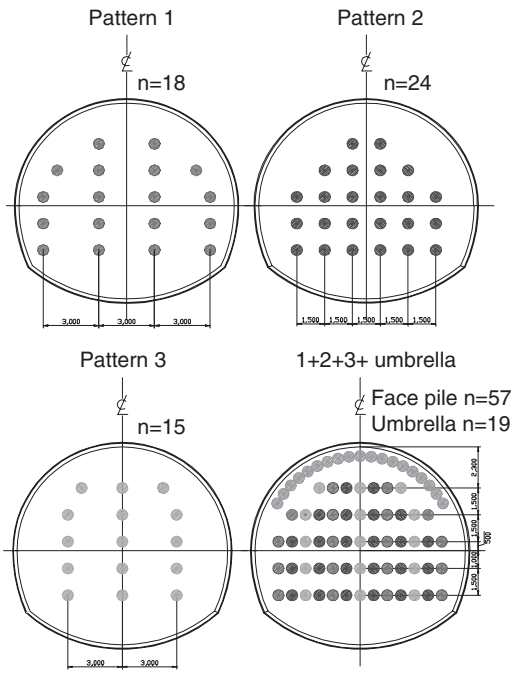


Figure 6. Long face piling pattern.

Copyright © 2005 Taylor & Francis Group plc, London, UK

6.2 *Long face piling*

Although the section was closed temporarily as early as possible, at the location 155.212 km, the face extrusion exceeded 3 m and the convergence was more than 900 mm. Consequently, long face bolts were driven to stabilize the face.

Glass-fiber-reinforced plastic tubes (76 mm in outer diameter) were used to stabilize the face, which could be driven by double-tube boring. Bolts 15.5 m long were placed at 4 m intervals in the three patterns shown in Figure 6 to ensure the tube joints were well distributed.

The face piling reduced initial displacement by 50% as shown in Figure 7.

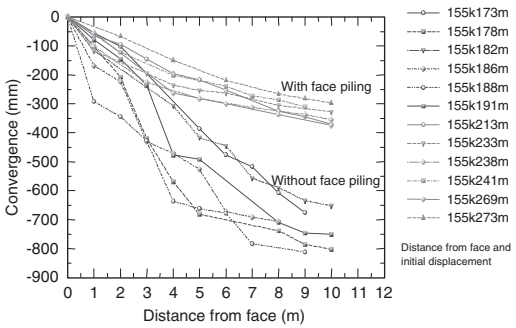


Figure 7. Reduction of initial displacement by long face piling.

6.3 *Multiple support*

The support pattern was changed in response to the predicted final displacement. However, as shown in Figure 4, it was impossible to completely control deformation, causing buckling of steel supports, spalling of sprayed concrete, failure of rock bolts and heaving of the primary invert. At locations where it was difficult to ensure the specified section, we judged that it was not efficient to place more rigid primary supports.

The multiple support concept was therefore adopted. This technique tolerates a certain displacement of the primary support resulting in some degradation of its structural performance. By placing the secondary support inside the primary support, the structural integrity of the supports as a whole is maintained (Figure 8).

The multiple support offers the following merits in comparison with the replacement of supports.

(1) Since re-excavation for replacing supports is not needed, no further release of in-situ stress is induced, reducing pressures acting on the support.
(2) Supports installed at the time of initial excavation are not removed. The multiple support restrains the tunnel wall tri-axially, and resists ground pressure well.
(3) Replacement of supports needs re-excavation, which may cause difficulty in tunneling management. In contrast, the multiple support is installed as planned, facilitating the management of tunneling operation.

Figure 9 illustrates the results of convergence measurement in the zone with multiple support. Without the multiple support, the tunnel wall deformation tends to increase gradually for a long time (3 mm per month) even when the face distance exceeds 1,000 m. However, with the multiple support, the deformation rate tends to converge, though the initial deformation rate is almost the same.

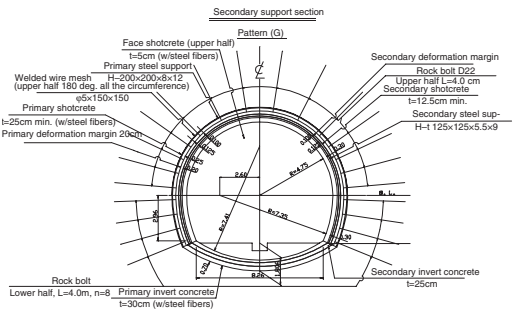


Figure 8. Secondary support pattern.

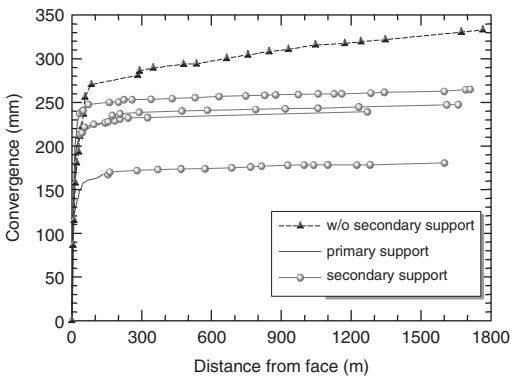


Figure 9. Convergence measurement results of the zone with the multiple support.

7 DESIGN OF THE SECONDARY LINING

7.1 *Concept of the secondary lining in the zone where deformation does not converge*

The concrete lining of tunneling in ordinary ground is considered to be a member for improving the primary support, and no load is assumed to apply on the lining.

Copyright © 2005 Taylor & Francis Group plc, London, UK

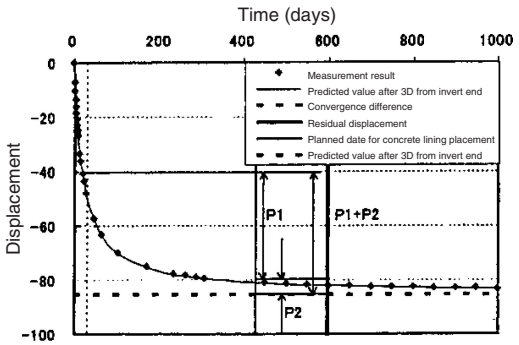


Figure 10. Concept of load acting on the concrete lining.

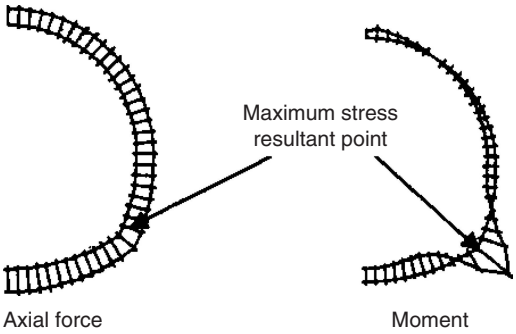


Figure 11. Stress resultant in lining 40 cm thick.

However, if concrete lining is placed in a zone where displacement has not converged yet, displacement is restrained by the lining, thereby inducing loads on the concrete lining. In design, it is therefore necessary to consider loads acting on the concrete lining, predicting the behavior of ground for a long period.

7.2 *Prediction of loads acting on the concrete lining*

Displacement before replacement of supports does not converge, but maintains a very small displacement rate, generally keeping good balance with the ground. Hence, stresses redistributed by replacement of supports correspond to the reaction of supports installed. In the sector in question, the secondary support is constructed. The reaction (P1 load) of this support is estimated from its displacement (Figure 10). Since, displacement in squeezing ground such as this sector continues for a long time, the restraining force due to the displacement must be considered as load (P2 load). The final displacement is given by the formula:

$$u(t) = t/(a + bt)$$

Where u(t) represents measured displacement, t elapsed time, 1/a initial displacement rate, 1/b final displacement.

Conservatively, the total of P1 and P2 is taken as load acting on the concrete lining.

7.3 *Design of the support and primary lining*

Based on the ground properties calculated from the convergence and crown settlement and the loads mentioned above, the stress resultant in the concrete lining (steel-fiber reinforced concrete) was obtained, and design was made by the limit state design method. The design procedures are described below.

(1) Calculation of ground properties

With the measurement results for the location where the largest displacement occurred in the sector discussed here, FEM back-analysis was made to calculate the ground properties.

(2) Prediction of loads acting on the concrete lining

By making the loads discussed in 7.2 act on the lining, the ratio of load acting on the lining to the stress released due to excavation was calculated at the different measuring points. As a result, the load on the lining was assumed to be 5% of the total in-stress release.

(3) Calculation of stress resultant in the concrete lining

The stress resultant was determined for seven different lining thicknesses ranging from 30 to 60 cm by the frame structure analysis. An example of the results is shown in Figure 11.

4) Verification of section

Verification was made with the design stress resultant obtained in step (3). The results are summarized in Table 1.

(5) Verification of cracking width

The criterion for crack width obtained is 0.25 mm or less. Because the amount of reinforcing steel fibers is limited to 60 kg/m3, the three contents shadowed in Table 2 are feasible. The results of the verification demonstrated that the most suitable design is achieved with design strength of concrete lining 30 N/mm2, lining thickness 55 cm and content of steel fibers 47.4 kg per cubic meter of concrete.

Table 1. Tensile strength required of SFRC (kgf/cm^2).

		Strength (kgf/cm^2)			
		180	240	300	400
Lining thickness (cm)	30	–	–	–	–
	35	–	–	25	20
	40	–	25	15	15
	45	–	15	15	10
	50	15	10	10	10
	55	10	10	5	5
	60	5	5	5	5

Copyright © 2005 Taylor & Francis Group plc, London, UK

Table 2. Steel fiber content for design strength of 30 N/mm^2.

Lining thickness (cm)		40	45	50	55	60
Tensile strength of SFRC (kgf/cm^2)	10					**19.5**
	15				**47.4**	**50.0**
	20			73.4	77.1	80.6
	25		97.2	102.2	106.8	111.2
	30	11.7	125.0	130.9	136.5	141.7

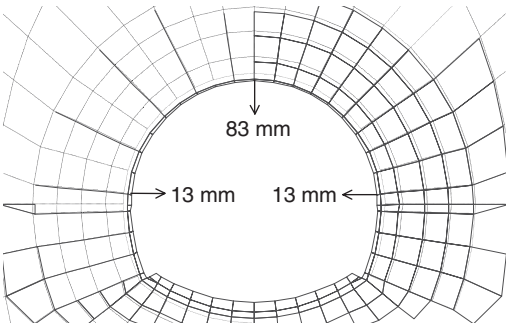


Figure 12. Predicted displacement after timber replacement.

(6) Study of the supports replacement pattern

Assuming support patterns, two-dimensional FEM analysis was performed with a load equal to 5% of the total in-situ stress release due to excavation. This analysis verified that the stress induced in each support pattern is within the tolerance. Based on the analytical results, the support structure is composed of steel support of H150, sprayed concrete 20 cm thick, 16 rock bolts each 4.0 m long and deformation margin 10 cm.

The predicted displacements after supports replacement were 26 mm (convergence) and 83 mm (crown settlement) as shown in Figure 12.

8 CONCLUSIONS

For dealing with difficulties in tunneling in squeezing ground of the Tomikura sector of the Iiyama Tunnel, early section closure, long face piling and multiple support were implemented with successful results. This paper also discussed the concept and placement of concrete lining for the zone where displacement did not converge completely, though the convergence rate was very small. In continuing the tunneling, it will be essential to fully consider the measurement results of ground behavior in the design, and, even after placing concrete lining, to measure stresses generated in the concrete, and feedback the results to the design.

Copyright © 2005 Taylor & Francis Group plc, London, UK

Ground reinforcement by the Pre-Supporting System Arch (PSS-Arch) method

K. Miyashita, H. Takahashi & M. Teranishi
Ishikawa prefecture government, Japan

S. Iwanaga, M. Inada, T. Matsuo & A. Nakakita
Kumagai Gumi Co., Ltd., Tokyo, Japan

ABSTRACT: The Wakunami Tunnel on the Kanazawa Loop Expressway in Ishikawa prefecture is composed of a binocular tunnel for through lanes, and an approach-lane tunnel that runs just above the binocular tunnel. This type of structure is very rare in Japan.

The geology of the site is unconsolidated alteration of diluvial saturated sand and mud. Residential buildings stand on the surface, and the overburden is small. For this project a new method, named PSS-Arch (Pre-supporting System Arch), was developed. This technique inserts curved steel pipes from the center drift, into the ground along the excavation circumference of the main tunnels. Since main tunnels are excavated inside the supports installed in advance, higher safety is ensured and ground settlement is well controlled. This paper discusses the development and application of this new method.

1 INTRODUCTION

The NATM has become the standard technique in mountain tunneling projects, and mechanized construction has made remarkable advances. Under the circumstances, further labor saving and improved work safety are required. There is greater risk when workers are present near the tunneling face, which is prone to falling rocks or collapse. People involved in tunneling projects have been insisting "no goal is more critical than safety at the face."

In recent mountain tunneling sites in weak ground, where it is difficult to ensure face stability, long forepiling using relatively rigid piles with chemical injection is the most common method used to effectively prevent face collapse and falling rocks. Since these auxiliary stabilizing techniques are implemented alternately with tunnel driving, the reinforcing range ahead of the face is limited, and therefore sufficient safety is not ensured at the face.

An increased number of binocular tunnels by the urban NATM have been recently constructed, Various auxiliary stabilizing techniques are used for avoiding surface settlement in sites with small overburdens and protecting underground facilities, thereby causing increased construction costs.

In this context, the "PSS-Arch" method has been developed. This technique, using the Pre-Supporting System arch, is designed to improve safety in binocular tunneling sites by preventing falling rocks and collapse at the face, reduce construction cost by eliminating a significant amount of auxiliary stabilizing work, improve construction quality by minimizing surface settlement, and shorten the time required by stabilizing simultaneous with face cutting. This technique was applied to the Wakunami Tunneling site on the Kanazawa Loop Expressway. This paper reports the overview and construction record of the PSS-Arch method.

2 OVERVIEW OF THE PSS-ARCH METHOD

(1) *Overview of the method*

Curved steel pipes are inserted into the ground, by means of curved boring. Before driving the main tunnels in the binocular tunneling project, supports are installed in advance from the center drift. In addition, chemical is injected through the steel pipes to improve the ground with an efficiency equivalent or superior to that of forepiling with chemical injection.

Copyright © 2005 Taylor & Francis Group plc, London, UK

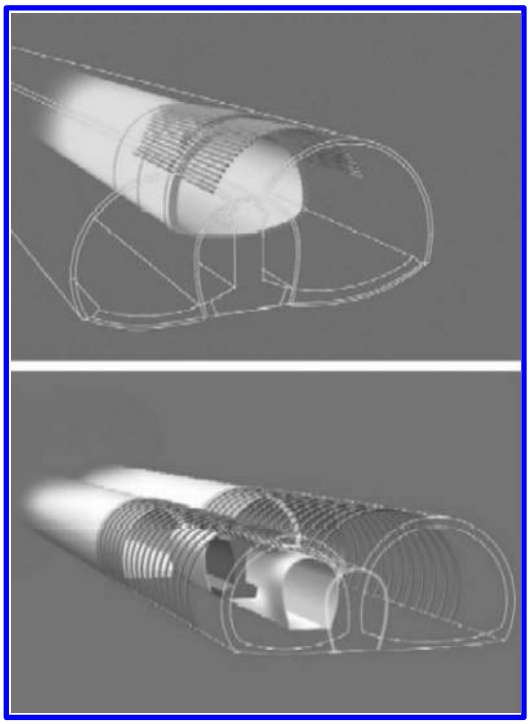


Figure 1. Schematic diagram of the auxiliary stabilizing methods. (upper: long forepiling, lower: PSS-Arch)

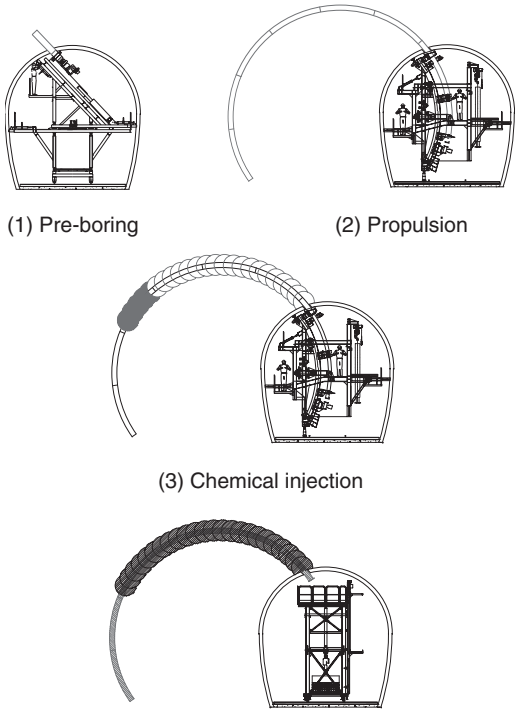


Figure 2. Operation sequence.

Furthermore, the steel pipes filled with mortar form continuous highly rigid supports far ahead of the main tunneling face.

(2) *Merits of the method*

Since main tunnels accommodating through lanes (lead tunnel and subsequent tunnels) are driven inside the supports installed in advance, this method limits the displacement ahead of the face more effectively. Moreover, with supports penetrating from the tunnel cutting base, settlement is limited more effectively. On the other hand, this method has no effect upon the excavation procedures, significantly shortening the time required for construction. Furthermore, this method offers a very high level of safety, because it effectively limits the displacement ahead of the face, reducing surface settlement and face collapse, and decreasing work needed at the face for installing supports.

Figure 1 shows the schematic diagram of the conventional forepiling and PSS-Arch method.

(3) *Procedure*

Figure 2 shows the work sequence of the PSS-Arch method.

(1) Pre-boring
Using a large-diameter boring machine, holes are drilled into the sprayed concrete of the center drift support.

(2) Propulsion
Curved steel pipes, each 3 m long, are driven and welded to each other until the specified length for the support is reached. The slurry is directly sucked by the vacuum pump placed outside the tunnel, to be discharged.

(3) Chemical injection
After primary injection between ground and steel pipes, secondary injection is performed, using a water-glass-solvent-based inorganic setting agent to improve the ground.

(4) Filling the steel pipes
The steel pipes serving as pre-supports are filled with mortar to improve their rigidity.

(4) *Verification of the effect of the PSS-Arch method by numerical analysis*

In a site using this method, supports are installed in the ground before the face arrives. Therefore, this technique is expected to have a significant effect in limiting displacement ahead of the face and settlement.

Copyright © 2005 Taylor & Francis Group plc, London, UK

The effect is evaluated by two-dimensional and three-dimensional finite element analyses. In the three-dimensional FEM analysis shown in Figure 3, two cases are studied to compare the effects of different construction procedures for limiting displacement ratio and settlement: ordinary excavation with supports (H-200) installed immediately after face arrival and PSS-Arch steel pipes (267.4 mm in diameter) driven in advance. The analytical results, as shown in Figure 4, demonstrate that there is no significant difference in ratio of displacement ahead of the face: 38% with the ordinary case and 34% with the PSS-Arch, but the crown settlement with the PSS-Arch is 48% of that with the ordinary method.

The two-dimensional analysis in Figure 5 shows that the surface settlement in tunneling by the PSS-Arch is 74% of that with ordinary auxiliary support (AGF). Both two-dimensional and three-dimensional analyses verified that the PSS-Arch is more effective than the AGF for limiting displacement ahead of the face and settlement.

3 PSS-ARCH TECHNIQUE

(1) *Excavation mechanism*

The excavation mechanism of the PSS-Arch for curved steel pipe propulsion is, unlike the conventional rotating system, a non-rotating type newly developed. Excavation is performed by pushing the cutter mounted at the pipe end, with water-jet and compressed air. The sludge is discharged through the central sludge pipe (internal pipe) under negative pressure generated by a vacuum pump. This is a truly innovative technique without precedent. (Figures 6 and 7).

(2) *Propulsion system*

The chain feed type propulsion system with a propulsion force of 80 kN is adopted. The inner pipe is pushed from the rear end, while the leading end of the outer pipe is pulled. To cope with insufficient propulsion force due to confining pressure of the surrounding ground, the system is provided with two sub-propulsion jacks (350 kN each) that can be used with the chain feed (Figure 8). A special flange that can follow deformation of the outer pipe was developed and mounted on the joints of the inner pipes (Figure 9). This design avoids the risk that the inner drilling machine cannot be retrieved because of deformation of the outer steel pipe during propulsion.

(3) *Steel pipe connection system*

Before connecting steel pipes, their angle and direction are modified. They are temporally welded,

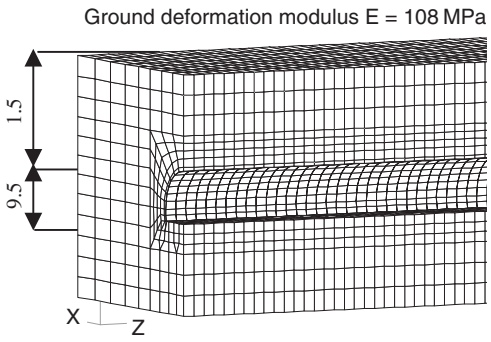


Figure 3. 3D analysis model.

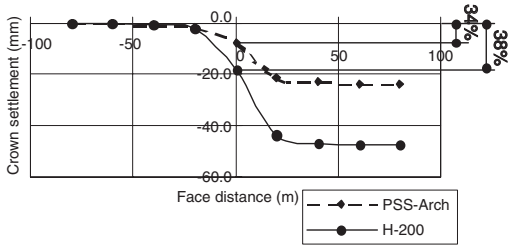


Figure 4. Change in crown settlement with face distance.

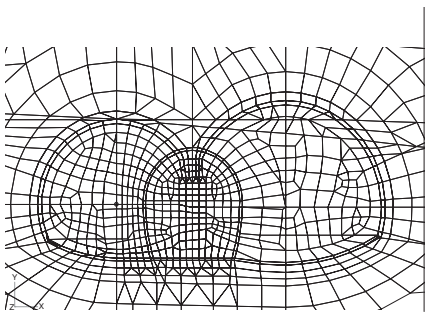


Figure 5. 2D analysis model.

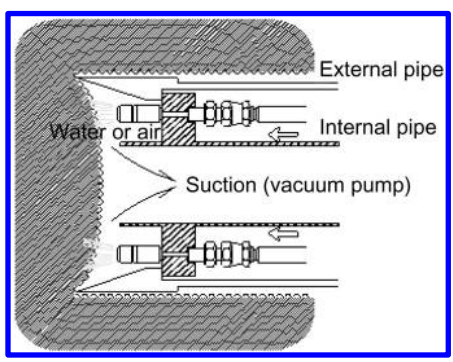


Figure 6. Boring system.

Copyright © 2005 Taylor & Francis Group plc, London, UK

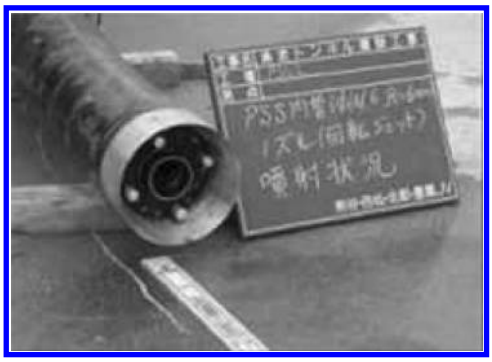


Figure 7. Cutter and nozzle.

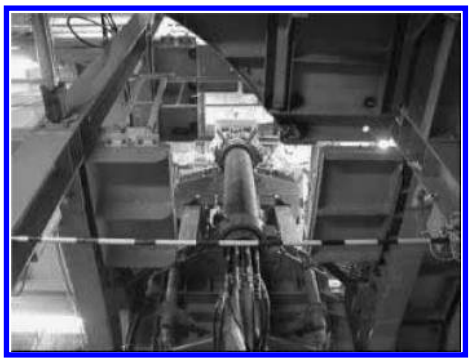


Figure 8. Propulsion system.

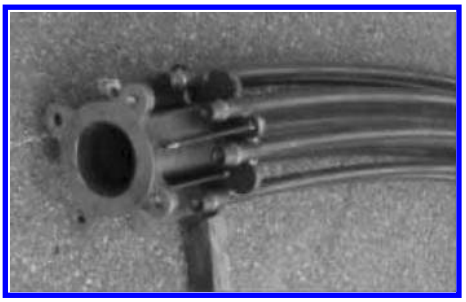


Figure 9. Internal pipe with special flange.

then permanently welded by an automatic welder (Figure 10).

(4) *Chemical injection system*

A chemical agent is injected into the ground by two newly-developed double packers, in which each unit works independently. Use of this packer significantly reduced the injection time (Figure 11).



Figure 10. Automatic welding of steel pipes.

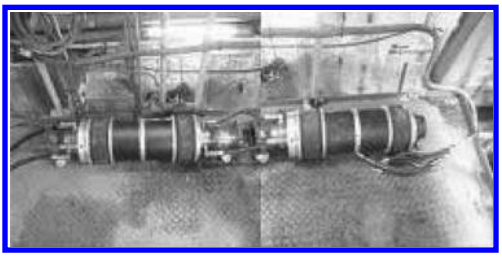


Figure 11. Double packer.

4 RECORD OF THE APPLICATION TO THE WAKUNAMI TUNNEL PROJECT

(1) *Summary of the project*

Project name:	Kanazawa Loop Expressway (mountain side), Suzumi Shinjo Line Road renovation (Wakunami Tunnel)
Site:	Between Nishiki-machi and Okuwa-machi, in Kanazawa City, Ishikawa Prefecture
Work period:	September 30, 2000 to August 31, 2005
Project tunnel:	
Center drift:	excavation/lining length 636 m excavation section 50.2 m^2
Main tunnel (mountain side):	excavation/lining length 636 m excavation section 71.5 m^2
Main tunnel (sea side):	excavation/lining length 636 m excavation section 111.2 m^2
Approach-lane tunnel:	excavation/lining length 154 m excavation section 120.6 m^2

The Wakunami Tunnel, part of the Suzumi-Shinjo Line of the urban road project, connects Nishiki-machi with Okuwa-machi in Kanazawa City. Two

Copyright © 2005 Taylor & Francis Group plc, London, UK

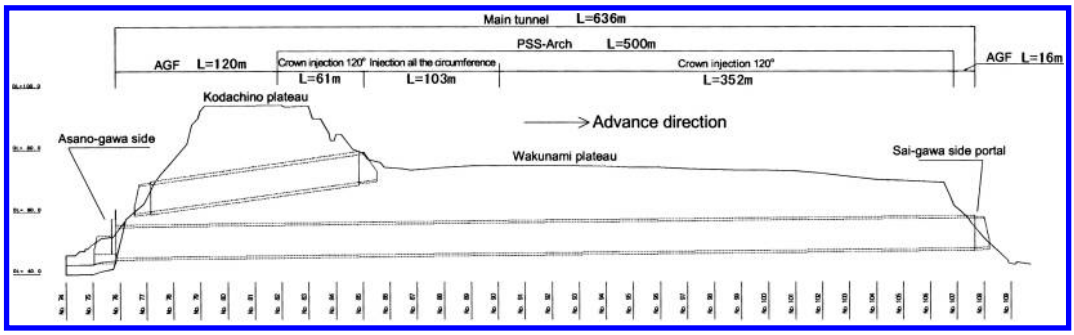


Figure 12. Tunneling site using the PSS-Arch method.



Figure 13. Image of completed tunnels.



Figure 14. Pre-boring machine.

rivers, the Asano-gawa and Sai-gawa Rivers, flow near the entrances to the tunnel. An approach-lane tunnel runs just above the binocular tunnels accommodating the main lanes. This structure is unprecedented in Japan.

There is a residential zone on the surface. The overburden is small, with a minimum depth of about 12 m. The distance between main tunnels and approach-lane tunnel is no more than 3 to 12 m.

The geology traversed by the tunnel alignment consists of unconsolidated fine-grain sandstone and silt generally in Okuwa stratum of early Quaternary Pleistocene epoch. The groundwater level is generally high. Since the uniformity coefficient is less than 4 and the fine grain content is less than 10%, the groundwater significantly affects the ground stability by causing sand to flow-out and the crown to collapse.

The PSS-Arch technique was developed and selected by the value engineering approach to control the surface settlement, ensure work safety at the face, and reduce the cost. Of the total length of 636 m in the main tunnels, a section of 500 m long uses the PSS-Arch option. Figure 12 shows the section by the PSS-Arch, and Figure 13 the image of the completed tunnels.

(2) *Status of tunneling using the PSS-Arch method*

Figures 14 to 19 are views of the tunnel construction using the PSS-Arch method.

At the initial stage, workers were not familiar with the procedure of this new technique, causing delays and troubles in construction. In addition, because of the geology with intercalated silt layers, progress was slow, with one work cycle taking 17 hours. However, by improving the machines and work procedures, one cycle is currently about 9 hours.

The positioning precision of steel pipe propulsion depends upon the geological conditions. In some places, because the pipe hit gravel or an adjacent pipe, propulsion was impossible. In such places, supports are erected as in the conventional practice during excavation.

(3) *Effect of the PSS-Arch method*

By the use of the PSS-Arch method, the ground around the tunnel is relatively well consolidated in the excavation of the main tunnels, and steel pipe supports are installed in advance, which remarkably reduces the risk of face collapse and falling rocks.

Copyright © 2005 Taylor & Francis Group plc, London, UK



Figure 15. Steel pipe propelling machine.



Figure 16. Chemical injection platform.



Figure 17. Pre-boring.

The graphs in Figure 20 represent the measurement results (crown settlement in the drift, settlement at the foot of the upper half, settlement just above the tunnel and surface settlement).

These measurements were made when the subsequent tunnel excavation reached the point TD80



Figure 18. Steel pipe propelling.



Figure 19. Chemical injection.

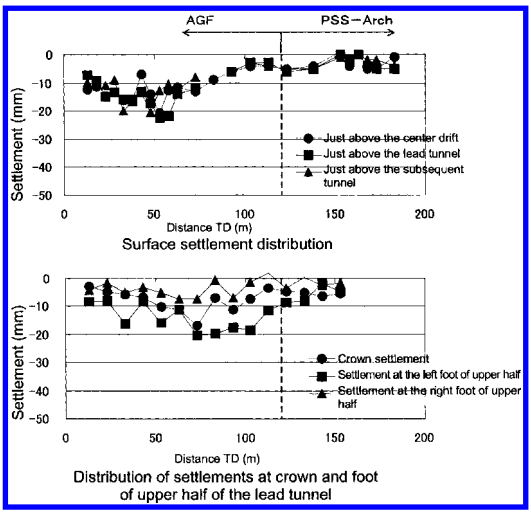


Figure 20. Measurement results.

Copyright © 2005 Taylor & Francis Group plc, London, UK

(tunnel diameter × 80) (as of June 2004). It is not possible to definitively evaluate the effect of the PSS-Arch. At the completion of the lead tunnel excavation, the settlements at all portions (crown, foot of the upper half, just above the tunnel and surface) in the PSS-Arch section of the lead tunnel are smaller than those in the AGF section. Although the geological conditions are different between the two tunnels, we can consider that the data verify the displacement control effect of the PSS-Arch. It is necessary, however, to re-evaluate the effect of the PSS-Arch method after the tunnel construction has progressed further and more extensive measurement data have been obtained.

5 CONCLUSIONS

The PSS-Arch discussed above was developed to be well suited to the geology of the Wakunami Tunnel. To satisfy this goal, the cutter blade system with water jet was used for propelling steel pipes. This excavation mechanism is suitable only for unconsolidated sandy grounds such as the Wakunami tunneling site. This technique may be utilized for tunneling in soft ground with a small overburden in urban districts. However, if the ground contains gravel over 10 cm in diameter, trouble would occur in propulsion with the steel pipe diameter used in the Wakunami project (267.4 mm). We will improve the excavation system, aimed at wider application to projects such as new construction of binocular tunnels, ultra-large-section tunnel with entry and exit ramps in urban areas and widening and repair of existing tunnels.

ACKNOWLEDGEMENT

The authors wish to extend our sincerest thanks to professor Ota at Tokyo Institute of Technology, and members of the mountain side trunk road construction committee, for helpful advice in applying the PSS-Arch method, and officials of Ishikawa Prefecture who selected this method by using the value engineering approach after conclusion of the contract.

Copyright © 2005 Taylor & Francis Group plc, London, UK

From research to practice "Development of Rapid Excavation Technologies"

S. Eskikaya, N. Bilgin, C. Balci & H. Tuncdemir
Istanbul Technical University, Mining Engineering Department, Istanbul, Turkey

ABSTRACT: This paper is a summary of a research sponsored by NATO Sfs programme, on "Development of Rapid Excavation Technologies" for the Turkish mining and Tunneling Industries.

Full-scale cutting tests were carried out on rock samples collected from different tunneling sides and machine performance was predicted for each case due to a model developed using specific energy values. Tunnel boring machines application in Tuzla-Dragos Tunnel gave a unique opportunity to compare predicted and actual machine performance data.

An empirical model for the prediction of roadheaders and jackhammers performances was also created using a database collected from several tunnel excavation activities. This model makes possible to predict net cutting rate of a machine using power of the machine, rock compressive strength and RQD (Rock Quality Designation) of the rock formation.

A detailed research programme was carried out using numerical modeling software (Franc 2D/L) and a small scale rock cutting rig to investigate the effect of rock stresses on machine performance. Previously described cutting performance models for roadheaders were reevaluated using the results of numerical modeling and data cutting test results under stressed conditions.

Underground environmental measurements were taken in Istanbul Metro Tunnels and Middle Anatolian Lignite Mine to compare dust and noise levels accountered in tunnel drivages both with roadheaders and impact hammers.

1 INTRODUCTION

Turkey has a large potential for tunneling projects in both civil and mining industries. Nearly a total of 140 km/year of various tunnels are being constructed, including mine developments, drifts, raises and shafts, hydroelectric projects, underground storage, highway, metro, sewer and irrigation tunnels (Bilgin et al, 2000). However the advance rates, in many cases, are too small which necessitates new excavation technologies for more efficient tunneling. The primary goal of the research program described in this paper was significantly advance the current level of excavation technology utilized in the Turkish Mining and Civil Underground Construction Sectors to speed up project completion schedules, to reduce costs and improve worker health and safety. This goal was planned to be accomplished by conducting research in new excavation techniques and introducing them into the industry by field implementation of the research findings (Bilgin et al, 2000)

2 LABORATORY FACILITIES

Laboratory facilities were created under the specific purpose of providing the tunneling and mining industries with solid solutions to practical problems. The laboratories contain a selection of equipment that allows physical testing of every type of commercially available rock cutting or drilling tools at full scale and also, rock mechanics equipment, ventilation-health and safety equipment.

2.1 *Full scale linear cutting machine*

The linear cutting machine used includes a stiff reaction frame on which cutter and dynamometer (load cell) are mounted. The triaxial pillar-type dynamometer with 50 tons of thrust capacity monitors orthogonal forces acting on the cutter. The rock sample is cast in concrete within a heavy steel box to provide the necessary confinement during testing. A schematic drawing of the linear cutting machine used is presented in Figure 1.

Copyright © 2005 Taylor & Francis Group plc, London, UK

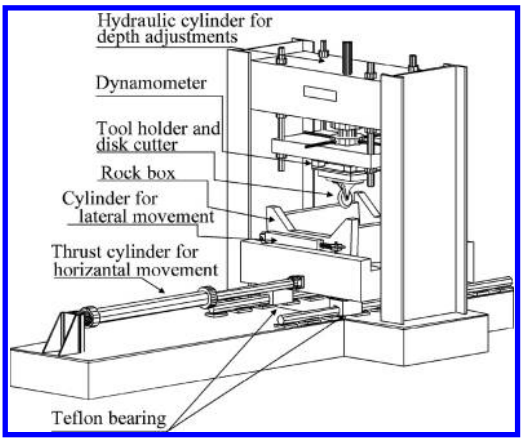


Figure 1. Schematic drawing of linear cutting machine.

A servo controlled hydraulic actuator forces the sample through the cutter at a preset depth of cut, width of spacing and constant velocity. The dynamometer measures the normal, drag, and sideways forces acting on the cutter during the cut. The rock box is moved sideways after each cut by a preset spacing to duplicate the action of the multiple cutters on a mechanical excavator.

The data acquisition system includes dynamometer, amplificator and personnel computer. The data acquisition card includes eight independent channels and monitors and collects data from the dynamometer. Data sampling/recording rate is adjustable up to 50,000 Hz. The recorded data is evaluated by a custom macro program.

2.2 *Horizontal drill rig*

The horizontal drilling rig is equipped with an electric motor of 132 kW and it is full hydraulic controlled. It is designed to have a maximum torque of 3500 kgm, a penetration rate of 0–60 m/h, maximum bit weight of 50 t and a maximum lateral thrust of 20 t. The experimental table may be easily accommodate the rock specimen in size of 1.5 × 1.0 × 1.0 m. The rotational speed may be adjusted between 0–40 rpm or 0–80 rpm by connecting two hydraulic motors in series or parallel (Ergin et al, 2000, Kuzu et al, 1999).

2.3 *Small scale rock cutting rig*

This cutting test on small rock samples is discussed in details by McFeat and Fowell. The test results, which may be classified as index values, are evaluated according to previously accumulated field performance data (McFeat-Smith, Fowell, 1977–1979, Balci, 2004).

3 LABORATORY AND FIELD STUDIES TO IMPROVE THE PERFORMANCE OF TBM'S AND PERFORMANCE PREDICTION MODEL

One of the main factors governing the cutting efficiency of a tunnel boring machine is the optimum chip failure occurred between the cutting grooves during the cutting process and the laboratory full scale cutting tests give the unique opportunity to observe the chip failure under controlled conditions. As a basic rule of rock cutting mechanics, specific energy, defined as the energy consumed per unit volume of the excavated rock, is optimum for a given s/d (cutter spacing/cutting depth) ratio. Cutter spacing is a constant value of a TBM cutting head, which dictates that for a given rock formation the laboratory predetermined cutting depth will determine the optimum thrust force values of the excavating machine. In the light of these main rules, an intensive laboratory full scale cutting test program was planned to obtain the relationship between cutting depth and cutter force values, specific energy and s/d ratio for different type of cutters for Tuzla tunnel.

The compressive strength of the rock sample tested was 579 ± 56 kg/cm^2, and tensile strength was 36 ± 3 kg/cm^2

The relationship between rolling force, cutting force, thrust force and depth of cut, for unrelieved cutting for CCS disc cutter are shown in Figure 2.

Thrust force (FT mean thrust force, F'T mean peak force) may be defined as vertical cutter force; rolling force (FR mean rolling force, F′R mean peak rolling force) and cutting force may be defined as horizontal cutter forces.

The relationships between specific energy values and s/d (cutter spacing/cutting depth) ratios are given in Figure 3.

3.1 *Steps followed for machine performance prediction*

Steps followed for machine performance prediction are as follows; determine the basic characteristics of the TBM to be considered for the specific job (number of cutters, cutter spacing, thrust and torque available etc.), use full scale cutting test results to obtain specific energy values for optimum s/d (cutter spacing/cutting depth) ratio, obtain optimum thrust value of the machine using cutting depth – thrust force graph from number of cutters and mean rolling force, calculate the torque of the machine for a predetermined cutting depth, calculate the possible power consumption of the machine, calculate the possible excavation rate using optimum specific energy values and the estimated power consumption (Bilgin et al, 1999).

Copyright © 2005 Taylor & Francis Group plc, London, UK

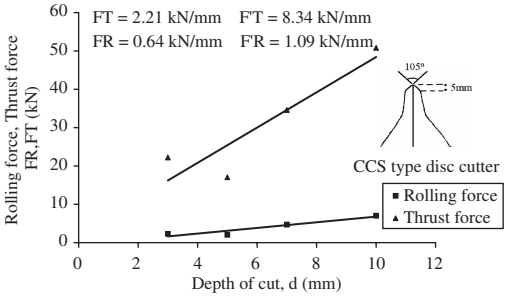


Figure 2. The relationship between rolling thrust forces and depth of cut.

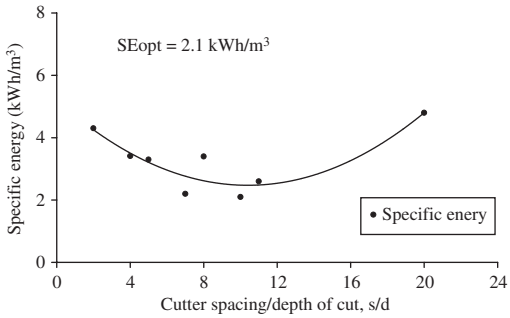


Figure 3. The relationship between specific energy and s/d ratios.

The TBM, which was in consideration for possible use in Tuzla–Dragos Tunnel was a double shielded Robbins 165-162/E 1080 machine, having diameter of 5 m, number of cutters 36, rotational speed 6 rpm, maximum thrust force 785 t, cutting head power 600 HP.

3.2 *Machine performance prediction*

- Optimum specific energy value from Figure 3 is SE = 2.1 kWh/m^3
- Optimum s/d value from Figure 2 is found to be between 8 and 10
- From machine specification cutter spacing is s = 7.5 cm
- For s/d = 8; d = 7.5/8 = 1 cm
- For s/d = 10; d = 7.5/10 = 0.8 cm
- From Figure 2 for CCS cutter type F′T = 8.34 kN/mm
- For d = 8 mm, total machine thrust is 36 × 8 × 8.34 = 2400 kN
- For d = 10 mm, total machine thrust is 36 × 10 × 8.34 = 3000 kN
- Total machine thrust must change between 2400 kN and 3000 kN
- Torque of the machine calculated from Table 1 using Equation 1:

$$\sum_{i=1}^{i=n} r_i XFR \tag{1}$$

where n = number of cutters; $r_{i=}$distance from the cutter to the center of the cutting head; FR is mean rolling force obtained from Table 1; for cutting depth of 8 and 10 mm.

- Torque for the cutting head for d = 8 mm, 36 × 1.375 × 8 × 0.64 = 253 kNm
  Torque for the cutting head for d = 10 mm; 36 × 1.375 × 10 × 0.64 = 317 kNm
- Expected power of the machine

$$P = 2\pi NT \tag{2}$$

In this Equation 2; P is in kW, N rpsec, T torque in kNm.

- Expected power of the machine for cutting depth of 0.8 mm.

$$P = 2\pi \frac{6}{60} x317\,kW; P = 200\,kW$$

- Expected power of the machine for cutting depth of 10 mm.

$$P = 2\pi \frac{6}{60} x253\,kW; P = 160\,kW$$

$$Net\,excavation\,rate\,(m^3/h) = k\frac{P\,(kW)}{SE\,(kWh/m^3)} \tag{3}$$

where k is energy transfer ratio, which is estimated to be around 0.7∼0.8, for the below calculations k = 0.8 is taken.

- Net excavation rate = 60∼70 m^3/h

In competent rock an average machine utilization factor of 30% and 16 hours working time per day will result a daily advance rate of

$$\frac{16hx60m^3x0.3}{hx\pi\frac{25}{4}m^2} \cong 15m/day$$

The predicted excavation rate is for competent rock, it is obvious that the geological discontinuities will increase the net excavation rate to a certain level and high amount of RQD or water income in rock

Copyright © 2005 Taylor & Francis Group plc, London, UK

formation with high amount of clay will decrease the daily advance rate due to regional collapses, face instability and chocking the cutters etc. These factors effected tremendously the advance rate of the TBM during Tuzla-Dragos tunnel drivages.

During field studies it is observed that the actual values were very close to predicted values (Bilgin, 1999).

4 FIELD STUDIES TO CREATE PERFORMANCE PREDICTION MODELS FOR ROADHEADERS AND IMPACT HAMMERS

Roadheaders and impact hammers have been widely used both in civil and mining industries since 1970. A contractor is always interested in predicting the machine performance prior to starting a tunnel project that will definitely define the tunnel drivage economy. The past few research works were focused on the prediction of the performance of roadheaders or TBM's from laboratory rock cutting tests. The work originated in Newcastle Upon Tyne University dealt with the correlation of in-situ data with the results of core cutting tests (McFeat-Smith, Fowell, 1977–1979). In that study the specific energy obtained from small scale rock cutting test was the key factor in the machine performance prediction. A more realistic model was developed by using full scale rock cutting test results in Earth Mechanics Institute of Colorado School of Mines by Ozdemir (Rostami, Ozdemir, Neil, 1994, Cigla, Ozdemir, 2000, Cigla, Yagiz, Ozdemir, 2001). However, the work described in this paper differs from the two previously mentioned in the fact that it is based on the statistical interpretation of the field data that has been collected since 1988 from different sewerage tunnels in Istanbul.

The model described in this paper only deals with the one aspect of performance prediction, i.e. instantaneous cutting rate defined as net cutting rate obtained when the machine is in cutting mode (Bilgin et al, 1988, Bilgin et al, 1990, Bilgin et al, 1997). The improved equations are stated below:

For roadheaders

$$ICR = 0.28P(0.974)^{RCMI} \quad (4)$$

For Impact hammers

$$ICR = 4.24P(RCMI)^{-0.567} \quad (5)$$

$$RCMI = \sigma_c \left(\frac{RQD}{100} \right)^{2/3} \quad (6)$$

Table 1. Actual and predicted cutting performance of roadheaders and impact hammers in selected zones in Istanbul Metro.

Zone	Excavator	Compressive strength MPa	RQD	Actual ICR m^3/h	Predicted ICR m^3/h
A	Roadheader	80	40	28	24
B	ATM 75	76	25	35	34
C		88	70	14	12
D	Roadheader	102	40	16	22
E	ET 250	94	30	25	31
F		110	60	11	12
G	Impact	118	70	10	11
H	Hammer	120	80	8	10
I	BRH 250	85	30	14	18

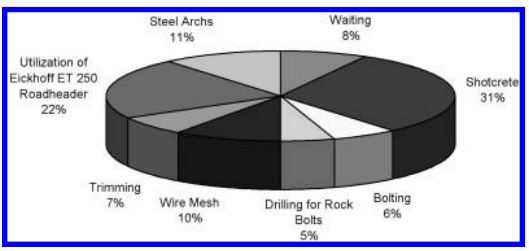


Figure 4. Overall performance of tunnel drivage in Taksim platform tunnel 2.

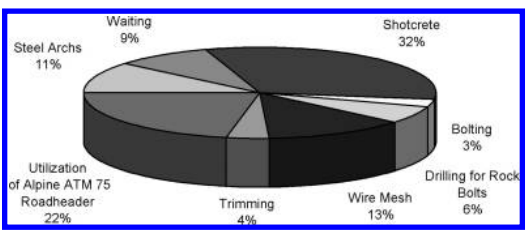


Figure 5. Overall performance of tunnel drivage in Taksim platform tunnel 1.

However it should be emphasized that equation 3 is improved using Schmidt hammer values (Bilgin et al, 2002).

In these equations; ICR = Instantaneous or net cutting rate in m^3/h; P = Cutting power of the machine in HP; $RCMI$ = Rock mass cuttability index; σ_c = Uniaxial compressive strength in MPa, RQD = Rock quality designation.

Different zones in Istanbul Metro were used to compare actual values and predicted values of net cutting rate as using Equations 4, 5 and 6. It is clearly seen from the relevant table 1 that the predicted values are

Copyright © 2005 Taylor & Francis Group plc, London, UK

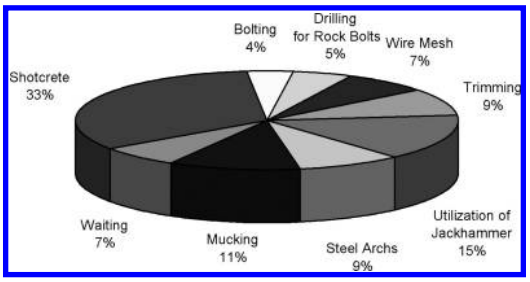


Figure 6. Overall performance of tunnel drivage in Levent line 2 tunnel.

very close to the actual values of net cutting rates suggesting that the model described by (Bilgin et al, 1996) is valid for both spiral and drum head roadheaders.

Overall performance of roadheaders and impact hammers are given in Figures 4–6.

5 STUDIES ON CREATING A MODEL TO PREDICT THE PERFORMANCE OF TUNNELING MACHINES UNDER STRESSED CONDITIONS

In the past, different models on performance prediction of different excavation machines were developed based on site observations, laboratory small- and full-scale cutting tests. However, it is important to note that none of these models takes into account the rock stresses for machine performance prediction.

First cutting experiment carried out by Pomeroy in different coal samples showed that a modest level of stress can close up the cleats in coal, making it more difficult to cut (Pomeroy, 1958). However it is reported by Roxborough and Phillips that experiments undertaken on a rock which was largely free of discontinuities, confining stress up to 200 kg/cm^2 was found no measurable effect on cutting force, normal force and specific energy (Roxborough et al, 1981). These studies are pioneering in their field and limited in number and only to unrelieved cutting conditions. During realization of the research programme described in this paper, it is decided that some laboratory rock cutting experiments under stressed conditions should be carried out in order to make clearer this phenomenon. A numerical model should also be run to support the findings of rock cutting experiments under stress conditions.

Several samples were needed for relieved and unrelieved cutting experiments. Two artificial materials, plaster and concrete were used during experiments to keep constant the homogeneity characteristic of the test material.

The stress analyses were performed using software 'Franc2D/L' (Swenson et al, 1997). It is a crack propagation simulator for two-dimensional layered structures. The finite element method is used in Franc2D/L to compute the stresses and displacements in an arbitrary structure subjected to arbitrary boundary conditions. The material is assumed to be linear elastic. Franc2D/L needs a pre-generated (initial) mesh. The initial meshes were developed using software 'Casca' (Swenson et al, 1997), which is distributed together with Franc2D/L.

A shaping machine equipped with a chisel pick having a rake angle of −5° and width of 12.5 mm is used as a cutting rig. Tool cutting, normal and side force are measured using a triaxial piezoelectric. Lateral stresses are given to cutting samples with the aid of hydraulic pistons.

Numerical modeling showed that for unrelieved cutting lateral stresses dramatically decrease tensile stresses around the cutting groove up to a certain level of lateral stresses, in this case, a lateral stress of 1/5 or 1/4 of sample compressive strength in magnitude, causing an increase of around 60 percent in cutter force. However, for relieved cutting the effect of lateral stresses are less apparent, causing an increase in cutter force around 20 or 30 percent more than unstressed conditions. Experimental cutting tests justify the findings of numerical modeling used in this study. These results emphasize that specific energy values found in full-scale relieved cutting tests should be multiplied at least with a factor of 1.3 in performance prediction models, if tunnels under stresses are considered (Bilgin et al, 2000).

6 STUDIES ON THE ENVIRONMENTAL PROBLEMS OF TUNNEL EXCAVATION

The noise measurements in Istanbul Metro Tunneling works Phase 1, were carried out in 4. Levent shaft and associated tunnels of Sisli –4. Levent Line.

It is observed that the main source of the noise at the top of the shaft is ventilator given fresh air to the tunnels. The noise measured 1 m away from the ventilator was L_{eq} = 88.6 dBA. At different places of shaft plant the values of L_{eq} > 80 dBA were observed.

It is concluded that within a circle having a diameter of 10 m from the center of the ventilator, the daily working time for the workers should be limited to 3–4 hours if it is necessary. Otherwise the ventilator should be in operation under a noise proved environment and earring protectors should be given to the workers.

It is understood that the noise levels of L_{eq} = 91 dBA where the excavators are working and the noise levels of L_{eq} = 93.5 dBA where the shotcrete equipment is working, reach to a dangerous level to effect negatively the hearing health of the workers (Okten et al, 1998).

Underground workers usually suffer greatly from the unfavorable environmental conditions of tunnel

Copyright © 2005 Taylor & Francis Group plc, London, UK

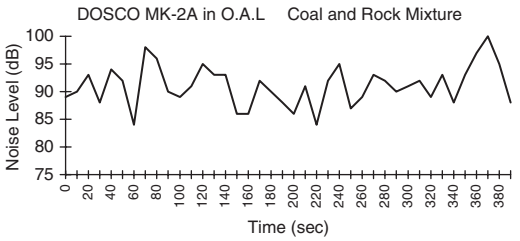


Figure 7. The variation of noise level with time in Middle Anatolian Lignite Mine.

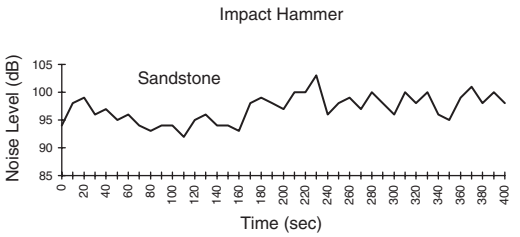


Figure 8. The variation of noice level with time in Istanbul Metro Tunnel.

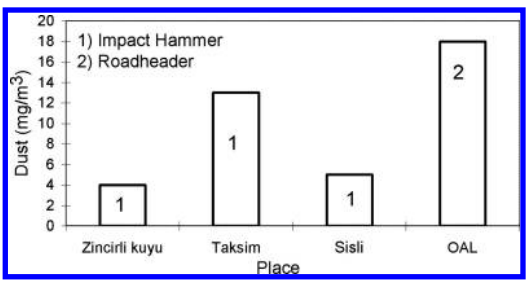


Figure 9. The variation of dust content in air in different tunnels.

projects, i.e., dust, noise, humidity etc. Underground measurements were taken during the past six months in Istanbul Metro Tunnels and Middle Annotation Lignite Mine. This gave an opportunity to compare dust and noise levels encountered in tunnel drivages both with roadheaders and impact hammers. Casella 113, a gravimetric dust collector and RS-103 sound level meter were used for in-situ measurements. The following Figures 7, 8 and 9 are the typical examples emerged from this investigation.

7 CONCLUSIONS

A detailed research programme carried out showed that, optimum specific energy obtained from full scale cutting tests using real life cutter may be used with confidence in predicting net cutting rate of TBM's or any mechanical excavators. However specific energy should be multiplied at least with a factor of 1.3 in performance prediction models, if tunnels under stresses are considered.

It is also demonstrated that rock mass cuttability index defined as a product of rock compressive strength and RQD may be used as a guide in predicting cutting and breaking rates of roadheaders and impact hammers.

Noise and dust are also main factors in an efficient working environment. Noise levels in impact hammers are as high as roadheaders. However dust generation in impact hammer is proved less than in roadheader application.

ACKNOWLEDGMENT

The research study described in this paper is sponsored by NATO SfS programme. The generous help and advice of Prof. Dr. Levent Ozdemir from CSM, and research staff from ITU are acknowledged.

REFERENCES

Balci, C. 2004. Comparison of small scale and full scale rock cutting tests to select mechanized excavation machines. *Ph.D. Thesis in Turkish,* Istanbul Technical University:269.

Bilgin N., et al, 2000. Development of Rapid Excavation Technologies for the Turkish Mining and Tunneling Industries. *NATO TU-Excavation Project Report.* Istanbul Technical University, Mining Eng. Dept.:172

Bilgin, N. Dincer, T. & Copur, H. 2002. The performance prediction of impact hammers from Schmidt hammer rebound values in Istanbul metro tunnel drivages, *Tunnelling and Underground Space Technology*, 17(3): 237–247

Bilgin, N. Balci, C. Acaroglu, O. Tuncdemir, H. & Eskikaya, Ş. 1999. The Performance Prediction of a TBM in Tuzla-Dragos Sewerage Tunnel, *World Tunnel Congress*: 817–822. Rotterdam: Balkema.

Bilgin, N. Balci, C. Tuncdemir, H. Eskikaya, Ş. et al, 1999. The Performance Prediction of a TBM in difficult ground condition, *AFTES-Journeesd'Etudes Internationales de Paris*: 115–121.

Bilgin, N. Kuzu, C. & Eskikaya, Ş. 1997. Cutting performance of jack hammers and roadheaders in Istanbul Metro drivages. *Proceedings, World Tunnel Congress, Vienna.* 455–460. Rotterdam: Balkema.

Bilgin, N. Seyrek, T. & Sahriar, K. 1988. Roadheader performance in Istanbul Golden Horn clean up contributes valuable data. *Tunnels and Tunnelling* 20(6): 41–44.

Bilgin, N. Seyrek, T. Erdinç, E. & Sahriar, K. 1990. Roadheader glean valuable tips for Istanbul Metro. *Tunnels and Tunnelling.* 22(10): 29–32.

Bilgin, N. Yazıcı, S. & Eskikaya, Ş. 1996. A model to predict the performance of roadheaders and impact hammers in

Copyright © 2005 Taylor & Francis Group plc, London, UK

tunnel drivages. *Proceedings, Eurock 96*, *Torino*: 715–720. Rotterdam: Balkema.

Bilgin, N. Tuncdemir, H. Balci, C. Copur, H. & Eskikaya, S. 2000. A Model to Predict the Performance of Tunneling Machines Under Stressed Conditions, *World Tunnel Congress SA*.

Cigla, M. & Ozdemir, L. 2000. Computer Modeling For Improved Production of Mechanical Excavators, *Society for Mining, Metallurgy and Exploration (SME) Annual Meeting*, Salt Lake City, UT.

Cigla, M. Yagiz. S. & Ozdemir, L. 2001. Application of Tunnel Boring Machines in Underground Mine Development, *International Mining Congress*, Ankara, Turkey.

Ergin, H. Kuzu, C. Balci, C. Tuncdemir, H. & Bilgin, N. 2000. Optimum bit selection and operation for the rotary blast hole drilling through HDR- a case study at KBI Murgul mine. *International Journal of Surface Mining Reclamation and Environment*, 14: 296–204.

Eskikaya, S. Bilgin, N. Dincer, T. & Ozdemir, L. 1998. A model to predict the cutting performance of rapid excavation systems. *Proceedings of the Seventh International Symposium on Mine Planning and Equipment Selection, Calgary*: 575–579. Rotterdam: Balkema.

Kuzu, C. Ergin, H. Balci, C. & Bilgin, N. 1999. Bohrkopfauswahl mit HDR-Einsatz für die Sprengbohrlöcher im Kupfertagebau Murgul, *Glückaufforschungshefte*, 60(2): 57–59.

McFeat-Smith, I. & Fowell, R.J. 1977. Correlation of rock properties and the cutting performance of tunnelling machines. *Proceedings of a Conference on Rock Engineering.* The University of Newcastle Upon Tyne: 581–602.

McFeat-Smith, I. & Fowell, R.J. 1979. The Selection and application of roadheaders for rock tunnelling. *Rapid Excavation and Tunnelling Conference, Atlanta*: 261–280.

Okten, G. Tuncel, Z. & Kuzu, C. 1998. An Investigation of Noise Pollution in Istanbul Metro Tunnel Drivages, Enviromental Issues and Waste Management in Energy and Mineral Production: 189–193. Rotterdam: Balkema.

Pomeroy, C.D. 1958. The effect of lateral pressure on the cutting of coal by wedge – shaped tools. *Proceedings of a Conference on Mechanical Properties of Non-Metallic Brittle Materials.* Conference organised by National Coal Board. Published by Butterworths Scientific Publications, London: 469–478.

Rostami, J. Ozdemir, L. & Neil, N.M. 1994. Performance prediction. A key issue in mechanical hard rock mining. *Mining Engineering.* November: 1263–1267.

Roxborough, F.F. & Phillips, H.R. 1981. Applied rock and coal cutting mechanics. *Workshop Course. 156/81*. Australian Mineral Foundation. Adelaide: 1.1–20.6.

Swenson, D. & James, M. 1997. Franc2D/L, Version 1.3 User's Guide, *Kansas State University*: 87.

Swenson, D. James. M. & Hardeman, B. 1997. Casca, Version 1.4 User's Guide. *Kansas University*: 26.

Copyright © 2005 Taylor & Francis Group plc, London, UK

Jacked box tunnelling, a non-intrusive technique for constructing underbridges

J.W.T. Ropkins
John Ropkins Limited, London, UK

D. Allenby
Edmund Nuttall Limited, Camberley, UK

ABSTRACT: Jacked box tunnelling is a non-intrusive technique for constructing underbridges beneath existing surface infrastructure such as railways and highways. The technique avoids the inconvenience and costs of disruption to traffic associated with traditional cut-and-cover methods. The paper describes the technique in outline and the measures used to control ground disturbance during tunnelling. Typical applications of the technique on two projects in the UK are described, one under a busy main highway and one under an urban railway station.

1 THE TECHNIQUE

1.1 *Outline of technique*

The technique is outlined in Figure 1 which shows the stages of construction for a new vehicular underbridge beneath a four track railway.

A reinforced concrete box is cast on a jacking base adjacent to the railway embankment, see Figure 1(a). A purpose designed tunnel shield is provided at its leading end, and thrust jacks are provided at its rear end reacting against the jacking base. Anti-drag systems (ADS) are installed and the box is jacked forward to the embankment. The box is then tunnelled through the ground by carefully excavating 150 mm off the face and jacking the box forward by a corresponding increment, this sequence being repeated many times, see Figure 1(b). When the box has reached its final position, see Figure 1(c), the shield, jacking equipment, etc are dismantled and the portal wing walls and roadway are constructed, see Figure 1(d).

The technique enables surface infrastructure to remain in place and traffic usage to continue uninterrupted throughout the construction process. Ground disturbance during tunnelling is carefully controlled so as to keep surface displacements within acceptable limits.

The technique is suitable for use in many types of ground, both natural and made ground, where face stability can be controlled using open faced shield tunnelling methods. On some projects ground conditions have been improved by geotechnical processes such as dewatering, grouting or freezing in order to render them suitable for tunnelling.

In all cases a comprehensive site investigation and archive survey is necessary to identify the ground types, their strength and stability characteristics, and the ground water regime. Obstructions must be identified and their impact on both excavation and face stability assessed. Surveys of the overlying infrastructure are also necessary to establish their type, form, structural integrity and ability to withstand displacements.

Risk assessments must be performed to identify any mitigation measures required during design, construction and installation.

1.2 *Control of ground disturbance*

Surface settlement is an unavoidable consequence of conventional tunnel excavation. It results in a shallow trough formation developing over the tunnel alignment whose magnitude and extent are dependent upon the physical and time dependent properties of the ground, the effectiveness of face support, the speed of erection of the tunnel lining and the effectiveness of its primary grouting, and the rate of tunnel advance.

In jacked box tunnelling the same consequences apply with the added complications of a tunnel lining that is advanced through the ground and a tunnel lining/ground interface that cannot be grouted until tunnelling has been completed.

The principal sources of ground disturbance and the measures used to control them are as follows.

Copyright © 2005 Taylor & Francis Group plc, London, UK

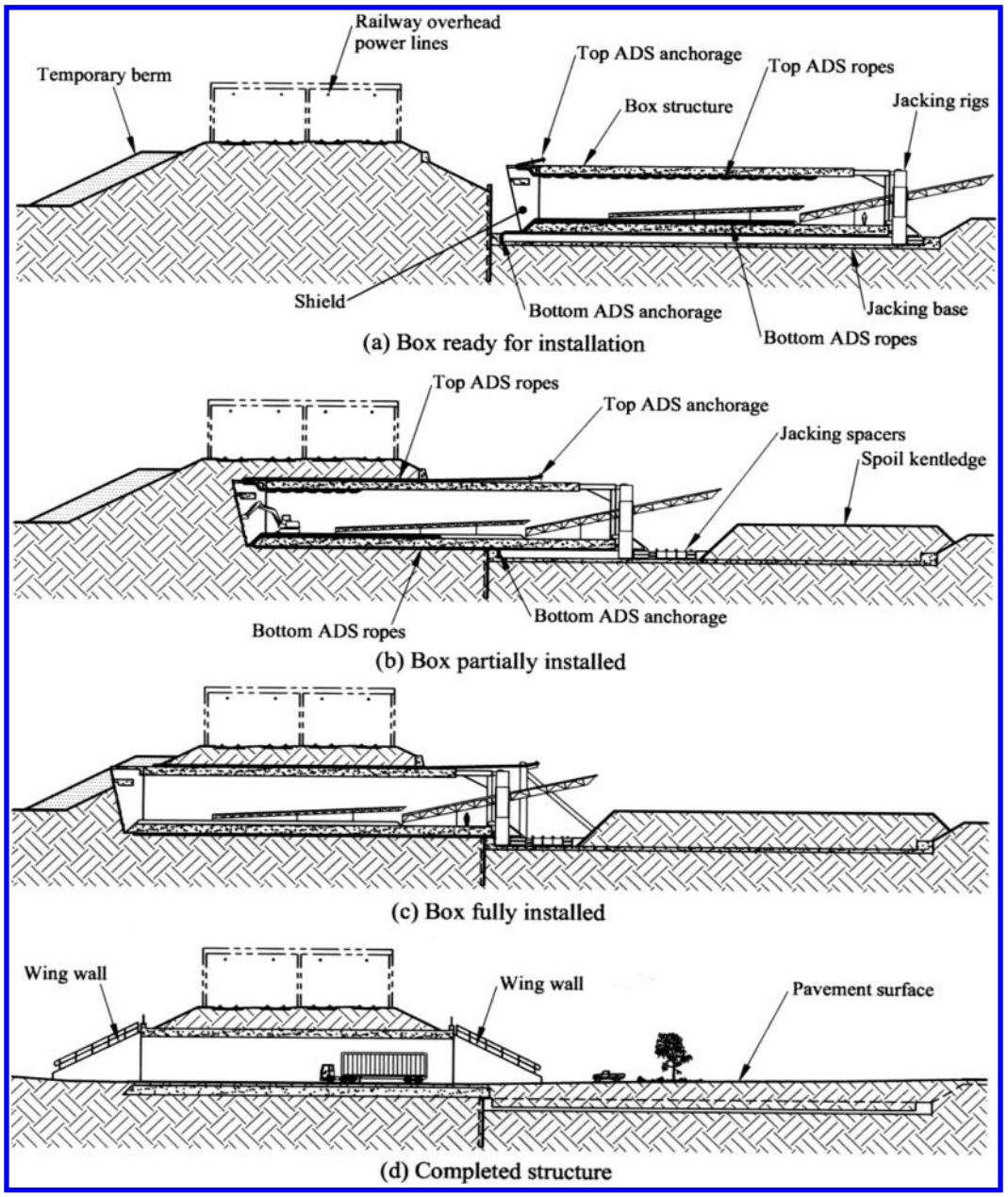


Figure 1. Jacked box tunnel construction stages.

1.2.1 *Control of ground drag*

Referring to Figures 1(b) and 1(c), it will be seen that as the box is jacked forward there will be a tendency to drag the ground. In the case of a wide box with shallow cover the ground on top of the box could be dragged forward, causing major disturbance and possible disruption to the overlying infrastructure. Similarly, the underside of the box will tend to drag and shear the ground, resulting in remoulding accompanied by a loss in volume causing the box to dive.

These effects are controlled using proprietary top and bottom anti-drag systems (ADS) as illustrated in Figures 1(a) to 1(c) which effectively separate the external surface of the box floor and roof from the adjacent

Copyright © 2005 Taylor & Francis Group plc, London, UK

ground during tunnelling (Ropkins 1998). They comprise arrays of closely spaced greased wire ropes anchored to the jacking base with their free ends passed through guide holes in the shield and stored with their free ends inside the box. As the box advances the ropes are progressively drawn out through the guide holes in the shield and form a stationary layer between the moving box and the adjacent ground. In this manner the ground is isolated from the drag forces and remains largely undisturbed.

Ground drag on the sides of the box is normally prevented by lubricating with bentonite slurry.

1.2.2 *Control of face loss*

In soft ground a cellular shield configuration is normally adopted with the internal walls and decks buttressing the tunnel face. A cutting edge around the perimeter of the shield accurately cuts the hole through which the shield body and box structure pass. The shield provides safe access to the tunnel face for miners and machine operators and egress for the anti-drag systems.

The ground must have sufficient strength to arch safely across the open cells and must accept the incremental advance of the shield into it without distress. Sometimes it is necessary to improve the ground in advance of tunnelling. This is normally achieved using geotechnical processes such as dewatering (Allenby & Ropkins 2003), grount injection (Ropkins 1998) or in particularly difficult situations the ground may be stabilized by freezing, (Allenby & Ropkins 2003).

1.2.3 *Constructional tolerances*

The shield perimeter cutting edge is designed to cut a hole slightly oversize of the box sides and roof in order to relieve ground pressure on the shield and box and to accommodate construction tolerances. It is important to keep the designed over-cut to a minimum to control settlement caused by ground movement towards the box sides and roof. This is done by ensuring that all external box and shield surfaces are straight, smooth, free from steps and defects, and that opposite faces are parallel and free from twist and distortion. These requirements are achieved by rigorous control of setting out, the use of high quality shuttering materials, checking finished surfaces and rectification of defects.

1.3 *Tunnelling system design*

The main components of the tunnelling system are the shield, anti-drag systems, jacking system, jacking pit, jacking base and jacking pit headwall entry procedure. These interact with one another and the system designer must determine their optimum configuration to achieve simplicity of design and installation.

Some engineers propose the use of a pre-installed canopy of steel tubes above the box to safeguard the tunnel face. The authors do not favour this concept as such an installation would cause more ground disturbance over a longer period of time than would result from the jacked box tunnelling technique described in this paper. It would also undermine the integrity and effectiveness of the technique.

In the two projects discussed an assessment of the jacking load using appropriate site geotechnical parameters, with top and bottom anti-drag systems, showed that sufficient jacking capacity could be mobilised through shear interaction between the jacking base and jacking pit ground interfaces to permit a monolithic underbridge structure to be installed. This simplified underbridge design, construction and installation, and provided each client with a high quality joint and maintenance free structure.

2 VEHICULAR UNDERBRIDGE AT JUNCTION 15A, M1 MOTORWAY, NORTHAMPTON, UK

A vehicular underbridge 14 m wide, 8.5 m high by 45 m long was installed under the M1 motorway at Junction 15A to upgrade the existing A43 intersection. Figure 2 illustrates the underbridge installation with 1.6 m minimum cover to the motorway hard-shoulders (Allenby & Ropkins 2004).

The motorway embankment comprises an engineered clay fill overlying boulder clay with a 3.5 m depth of compacted pulverised fuel ash under each carriageway. An open face reinforced concrete cellular shield divided into three working levels, each with seven compartments, was designed to support the face. The top level compartments were designed for hand mining and the lower two levels for machine mining using 360° Mecalec excavators. Figure 3 shows a rear view of the shield.

A top anti-drag system covering the full roof width was necessary to isolate the roof from, and support, the pulverised fuel ash. The bottom anti-drag system comprised two 3.5 m wide tracks of rope forming slide paths for the underbridge to travel on and of sufficient width to prevent the allowable bearing pressure on the underlying boulder clay from being exceeded. In Figure 3 the top anti-drag ropes can be seen stored on scaffolding suspended inside the underbridge, the bottom anti-drag ropes are stored under the false floor on which the excavation is taking place.

Four jacking rigs were used giving a total installed jacking capacity of 7,200 tonnes.

The contract documents specified settlement criteria for the carriageway surfaces based on trigger levels referenced to settlement/heave at any point, and/or a variation in longitudinal grade and/or a change of cross-fall across any traffic lane or hard shoulder.

Copyright © 2005 Taylor & Francis Group plc, London, UK

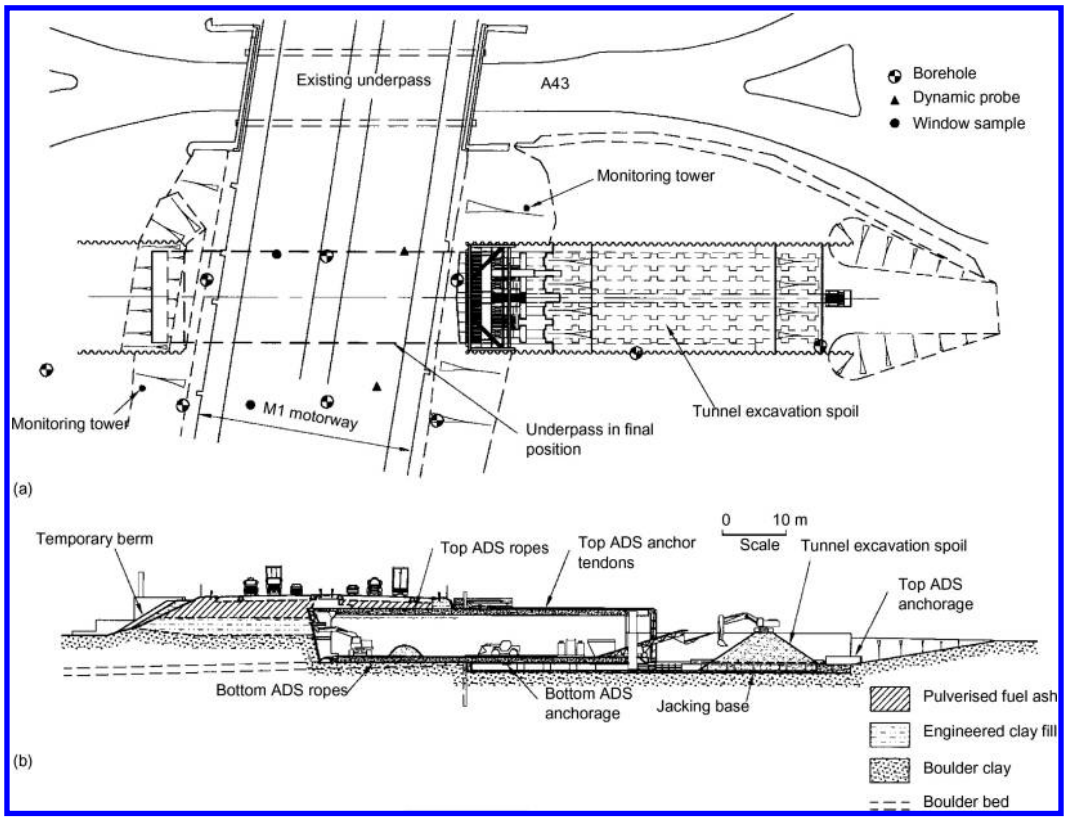


Figure 2. Vehicular underbridge, Junction 15A, M1 motorway.



Figure 3. Rear view of tunnelling shield, Junction 15A, M1 motorway.



Figure 4. Completed underbridge, Junction 15A, M1 motorway.

During underbridge installation two direct reading reflex theodolites, mounted on 9 m high towers one each side of the motorway, monitored settlement points on a grid across the motorway.

Careful control of the jacking and excavation operations during underbridge installation maintained all three running lanes in each carriageway well within specified tolerances without the need for resurfacing, the maximum recorded settlement being 28 mm. The tunnelling operation took 3 weeks to complete following shield entry and required a maximum jacking thrust of 4,500 tonnes. The completed underbridge is shown in Figure 4.

Copyright © 2005 Taylor & Francis Group plc, London, UK

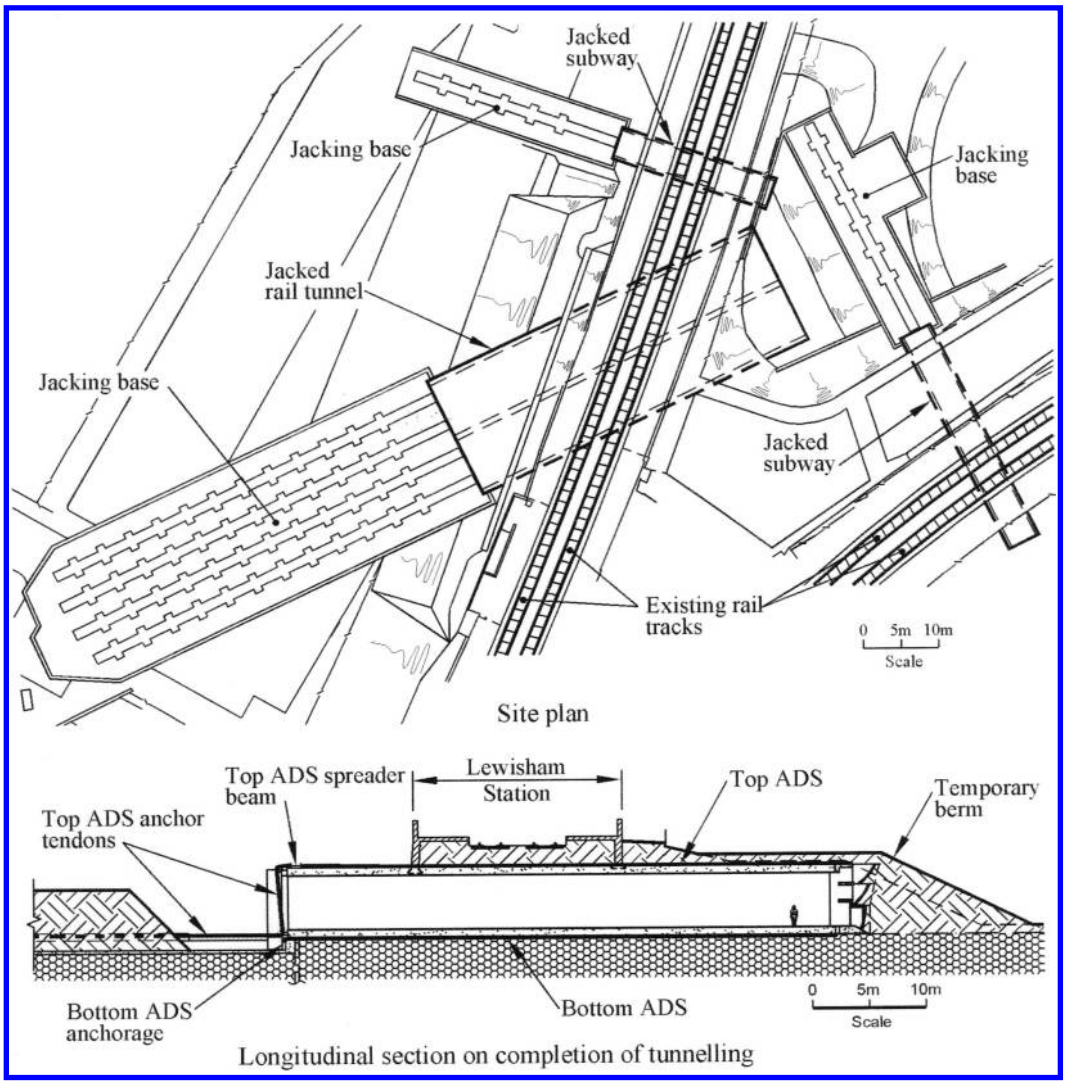


Figure 5. Rail underbridge, Lewisham railway station, London.

3 RAIL UNDERBRIDGE AT LEWISHAM RAILWAY STATION, LONDON, UK

At Lewisham railway station a twin cell rail underbridge measuring 17 m wide, 6.2 m high by 48 m long was installed at a severe skew to the railway with 1.7 m of cover to the rail sleepers, see Figure 5. The underbridge passed under the inner platform foundations and through the outer platform wall foundations.

A composite steel and reinforced concrete shield, illustrated in Figure 6, was designed to control a mixed face comprising very loose, weak silt and sand in the top half overlying a soft squeezing clay. The steel section was designed to penetrate the loose material inducing face stability through applied pressure and friction developed between the ground and embedded cutting edges, dividing walls and horizontal decks. The reinforced concrete section was designed to buttress the clay with its dividing walls and to accurately trim the invert to the required profile.

Top and bottom anti-drag systems were used, the top anti-drag system being anchored via wire rope tendons and compensation jacks to the rear of the jacking base. In this way the stability of the monolithic underbridge was used to transfer the top anti-drag system load of 800 tonnes from a high level down to the

Copyright © 2005 Taylor & Francis Group plc, London, UK



Figure 6. Tunnelling shield, Lewisham railway station.



Figure 7. Completed underbridge, Lewisham railway station.

jacking base level. Four jacking rigs were used giving a total installed jacking capacity of 7,200 tonnes.

The severe skew gave rise to differential horizontal loads along the underbridge sides and differential embedment loads across the width of the shield. These were accommodated in the system design by means of side guides and by the planned application of eccentric jacking thrust as required.

During the three week installation period ground movements were controlled to within specified tolerances. This enabled the railway and railway station to remain fully operational throughout and avoided potential damage to an adjacent passenger waiting shelter. The underbridge was installed to within 25 mm of true line and level and required a maximum jacking thrust of 4,500 tonnes. Figure 7 shows the completed underbridge in service.

4 CONCLUSIONS

The exceptional degree of control on ground and surface movements afforded by the technique enables surface infrastructure to remain intact and traffic systems to be maintained fully operational throughout the underbridge construction process.

The costs of traffic disruption associated with conventional cut-and-cover construction are avoided and the final product is a high quality maintenance free structure.

The authors believe that this relatively new technique will be used widely in the future as highway and railway authorities and their consultants around the World come to recognize its safety and reliability and appreciate its benefits.

ACKNOWLEDGEMENTS

The authors wish to acknowledge the assistance and encouragement afforded by Edmund Nuttall Ltd and John Ropkins Ltd in the preparation of this paper.

REFERENCES

Allenby, D. & Ropkins, J.W.T. 2003. Geotechnical aspects of large section jacked box tunnels. In M.W. Frost, J. Jefferson, E. Faragher, T.E.J. Roff & P.R. Fleming (eds), Transportation Geotechniques: 39–66. London: Thomas Telford.

Allenby, D. & Ropkins, J.W.T. 2004. The use of jacked box tunnelling under a live motorway to form a vehicular underpass. Geotechnical Engineering 152, Issue GEI, October 2004: 1–10.

Ropkins, J.W.T. 1998. Jacked box tunnel design and construction. In ASCE (ed), Proceedings of the Sessions of Geo-Congress 98, Special Publication No 87, Boston, 1998, Boston: ASCE.

Copyright © 2005 Taylor & Francis Group plc, London, UK

Ground borne vibration on the East Side Access Project Manhattan segment: issues and impacts

A. Benslimane, D.A. Anderson, N. Munfakh & S. Zlatanic
Parsons Brinckerhoff Quade and Douglas, New York, USA

ABSTRACT: The East Side Access Project will connect the Long Island Railroad to New York's Grand Central Terminal on the east side of Manhattan. It is one of the largest tunneling projects ever undertaken in New York. A series of tunnels and caverns will be excavated in rock to connect the existing 63rd Street tunnels to twin three-level caverns beneath existing Grand Central Terminal (GCT). Construction activities for the East Side Access (ESA) Project will include blasting activities beneath several structures along Park Avenue in Manhattan, including Metro North Railroad (MNR) structures and overlying buildings. This paper presents the methodology and results of a study conducted by the authors to investigate any impact the vibrations generated by blasting may have on these structures. The attenuation of blast-generated vibration can be predicted based upon a combination of the attenuation of the measured vibrations through rock and though the structures. Isoseismic plots were generated showing expected controlled drill-and-blast activities induced vibrations for various round lengths as a function of distance at various levels of the existing structures surrounding the newly excavated GCT shafts. A strain criterion was also developed to account for the effect of close proximity blasting on the columns and foundations of the adjacent structures. Based on the findings of the vibration study, provisions were specified for test blasts to be performed by the contractor prior to production blasting. Predictions were also made for the expected vibration levels induced by Tunnel Boring Machine (TBM) and Roadheader and areas of zone of influence were identified.

1 INTRODUCTION

The East Side Access Project (ESA) is a major capital construction project that is carried out by the Metropolitan Transit Authority (MTA) in conjunction with the Long Island Rail Road (LIRR). The project, upon its completion, will provide Long Island commuters with direct access to Manhattan's Grand Central Terminal (GCT), which will help relieve congestion at Penn Station and provide direct access to the East Side of Manhattan. The connection is to be accomplished by providing a new rail line between the Sunnyside Yard in Queens and the GCT in Manhattan using the lower level of the existing 63rd Street Tunnel under the East River and new tunnels in Queens and Manhattan (Figure 1).

The Manhattan segment of the East Side Access project is situated under mid-town Manhattan's densely populated residential and business hub from East 63rd Street and Second Avenue to the intersection of Park Avenue and East 38th Street. The Manhattan segment consists of three major underground construction elements (Figure 2): (i) Manhattan Tunnels

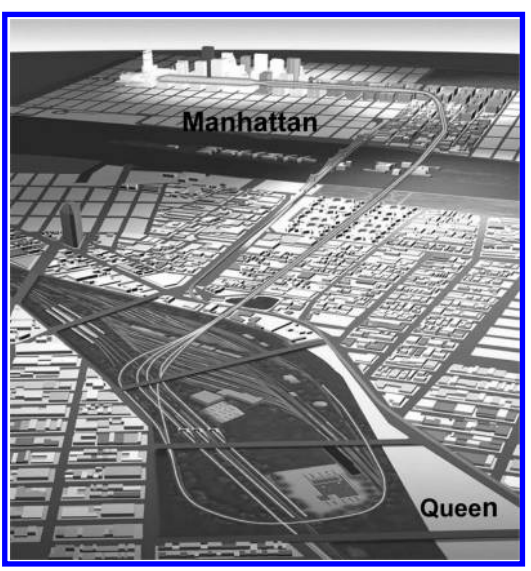


Figure 1. Location plan.

Copyright © 2005 Taylor & Francis Group plc, London, UK

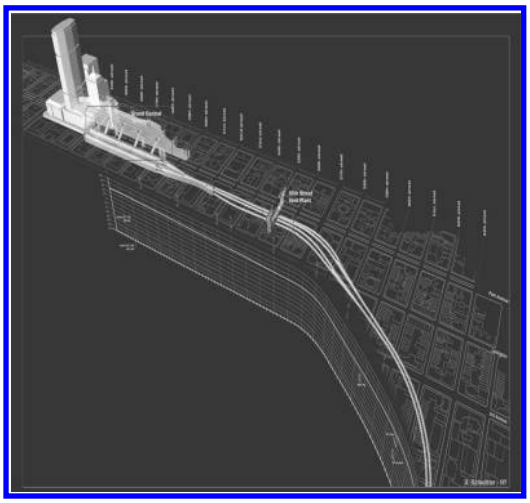


Figure 2. Manhattan Tunnels.

including the 55th and 50th Street ventilation structures, (ii) GCT Caverns, tunnels and shafts connecting new the LIRR terminal to the existing GCT Madison Concourse and the 44th Street ventilation structure, and (iii) Tail track tunnels and caverns and 38th Street ventilation structure.

The Manhattan Segment tunnels and caverns will be built under various existing operating New York City Transit (NYCT) subway lines, and Metro North Railroad (MNR) commuter tracks originally constructed to accommodate numerous foundations of high-rise buildings.

2 CONTROLLED DRILL-AND-BLAST ACTIVITIES INDUCED GROUND BORNE VIBRATION

Construction activities for the East Side Access (ESA) Project will include controlled drill-and-blast activities beneath several structures along Park Avenue in Manhattan, including Metro North Railroad (MNR) structures and overlying buildings. It will also involve controlled drill-and-blast activities beneath several structures in two areas: 63rd Street and Second Avenue, and 58th Street and Lexington Avenue. These structures include NYCT tunnels (IRT Lexington Avenue Line at 59th Street and 63rd Street Tunnel) and overlying buildings.

It is worth noting that for drill and blast areas other than GCT, in addition to the vibrations propagated through the rock from the controlled drill-and-blasting site, vibration can travel through the soil, to the foundations of the overlying structures, and up through the structures. In some cases, vibration does not strictly attenuate with distance, where resonances in an overlying soil layer can locally amplify vibration in certain frequency ranges. Knowledge of such conditions is important in blast delay design to avoid constructive interference at such frequencies.

A study was conducted to investigate the impact the vibrations generated by controlled drill-and-blast activities may have on these structures. Determination of the likely levels of vibration is necessary to provide contractors with guidelines for the explosive charge and delay configuration during blasting, as well as to establish estimates of expected blast vibration for interested parties. Ground borne vibration due to drilling and TBM/Roadheader operations were also addressed.

A method was developed to determine the attenuation, or decay with distance from the source, of such vibration from its origin at the base of the lower level of the MNR tracks, through columns in Grand Central Terminal (GCT) and building columns to the structures themselves. The train passage at the lower level of GCT was used as the main source of vibrations in the absence of a design-phase test blast program. The Contractor will perform test blasts before production controlled drill-and-blast activities starts for each construction contract. This test blast program will confirm the applicability of the vibration regression equations resulting from this report, recognizing that significant extrapolation is required in this approach. Furthermore, the test blast program will aid in determining necessary adjustments to the controlled drill-and-blast activities procedure.

The purpose of the study was to facilitate suggested drill and blast procedures for construction of GCT shafts and the drill and blast segments of the Manhattan tunnel excavation contract. Construction of vertical ventilation, stair and elevator shafts, escalator wellways, and inclined escalator shafts will take place from the lower level of GCT and will involve controlled drill-and-blast activities directly below and adjacent to the operating MNR tracks and adjoining MNR and building structures. The Manhattan cavern excavation contract will include construction of starter pits for raise bores at the escalator shafts adjacent to columns at GCT lower level, raise bores for some vertical shafts as well as construction of access adits that would reach to the bottom of the raise bores from a bored tunnel constructed using Tunnel Boring Machine (TBM) methodology.

In addition, construction of approach tunnel, TBM assembly chambers, starter tunnels, and Wye structures will involve controlled drill-and-blast activities directly below and adjacent to NYCT tunnels and adjoining building structures. During construction of Manhattan tunnels, in addition to the vibrations propagated through the rock from the controlled drill-and-blast activities site, vibration can travel through the

Copyright © 2005 Taylor & Francis Group plc, London, UK

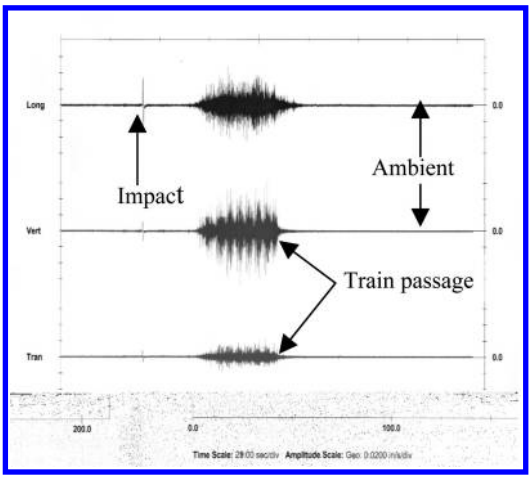


Figure 3. Typical train passage vibration event.

foundations and columns of the overlying structures up through the structures.

For this study, measurements were taken in the major structures. Ambient vibration from both the normal cultural activities in the neighborhood of these buildings, as well as that generated by train passage within the MNR tunnels, was measured. These vibrations have characteristic signatures that allow them to be distinguished from local and random vibration sources (Figure 3).

The attenuation of the train-generated vibration was used to estimate the attenuation of blast-generated vibration. Regression equations were generated relating the train-induced vibrations in GCT to vibrations measured in the buildings.

It is well established that blast vibration is a function of both the horizontal distance of the blasting source from the affected structures as well as the explosive charge weight. The appropriate relationship is termed "Scaled Distance" (SD) and is defined as:

$$SD = \frac{D}{\sqrt{W}} \tag{1}$$

where D is the distance from the blast in feet, and W is the explosive charge (in pounds) per 8 millisecond delay interval. The vibration is, in turn, a function of the Scaled Distance through a site-specific equation as follows:

$$PPV = A \times SD^{-B} \tag{2}$$

where PPV is a measure of vibration (Peak Particle Velocity in inches per second), and A and B are site-specific constants. To accurately determine A and B for relevant portions of the ESA Project area prior to production controlled drill-and-blast activities, the Contractor will be required to detonate test blasts, while monitoring at various distances from each blast. Since no design-phase test blasts were possible, other means of estimating the vibration propagation conditions are needed and were developed.

As mentioned earlier, peak particle velocity is the standard criterion for associating vibration generated by controlled drill-and-blast activities with the potential for structural damage. However, for this study, peak particle velocities varied significantly during train passages, due to wheel flats and other irregularities in the vibration generation as the trains pass. Therefore, a root-mean-square (RMS) analysis of the vibration of the train passages was used, which is typical of normal transit vibration studies. VdB values were calculated from the RMS values to determine the level of vibration relative to the expected vibration values from train passage.

To determine the attenuation of vibration with distance in the structures, it was necessary to determine appropriate distances. The study by Oriard, et al. (1985) was used as a basis for distance determination. The authors noted that a reasonable correlation was found for the vibration based upon the sum of the propagation distance through the ground and the vertical distance through the structure. Therefore, the closest approach for the train to the measurement location was established as the horizontal distance, and the distance from the track bed was established as the vertical distance.

Measurements at various distances were used to establish several regression equations. These equations determined the attenuation of the vibration with distance for several areas. The data were divided into several groups, based upon location.

The relationship known as the "crest factor," which is the ratio of the PPV to the maximum RMS values, was used to derive an expected PPV level from the measured RMS. The FTA Guidelines (p. 7–3) indicate that for ground-borne vibration from trains, the crest factor is usually 4 to 5. A mean value of 5.8 was computed from the collected data, however, to be conservative, the FTA estimate of 5 was used. The attenuation relations were modified to determine the variation of PPV with distance, as shown in Figure 4. This information was combined with vibration data obtained from controlled drill-and-blast activities at Hunter College in 1974, which is located close to the ESA project site, and in similar rock type (Figure 5). Attenuation ("B") was determined to have a slope of −1.69. The 95% value is calculated at

$$PPV = 59 \times D^{-1.69} \tag{3}$$

The horizontal and vertical distance measurements were combined to determine the expected levels of

Copyright © 2005 Taylor & Francis Group plc, London, UK

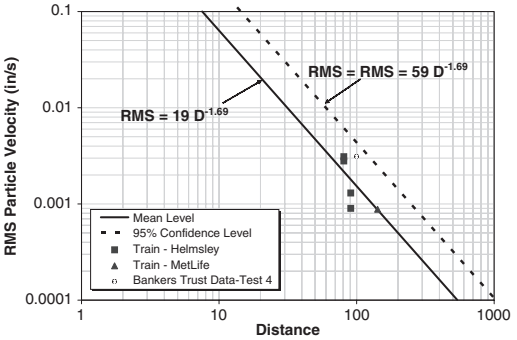


Figure 4. Typical variation of Peak Particle Velocity (PPV) with distance for typical buildings along the Manhattan ESA alignment.

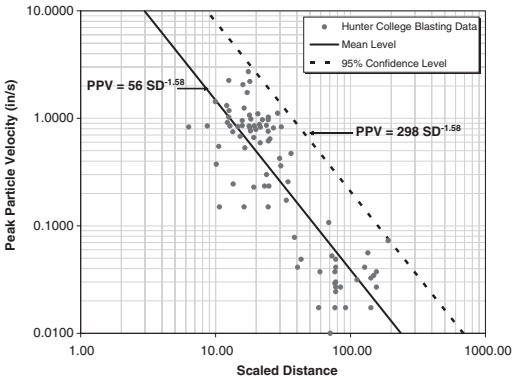


Figure 5. Hunter college blast vibration data.

vibration at various levels in buildings, due to four-foot round length explosive charges of 3.92 pounds per 8 millisecond delay interval.

This charge weight is determined from the explosive type available and approved for use in New York City by FDNY, as well as the minimum practical round length.

Isoseismic diagrams (contour plots of expected vibration levels of constant amplitude) for the two vibrations limits of 0.5 inch/sec and 1.92 inch/sec and for the GCT lower level, upper level, ground surface level and the first floor of the previously mentioned buildings were derived.

Frequency spectra were determined for ambient and train-generated vibration in the buildings, and next to and on steam pipes in the study area. The spectra were calculated using Fast Fourier Transforms, and further separated into 1/3-octave bands. Both the frequencies excited by train passage, as well as resonant frequencies of building elements and utility pipes, were determined.

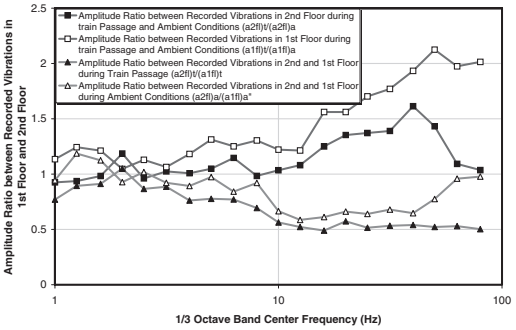


Figure 6. Amplitude ratio between recorded vibrations between 1st floor and 2nd of typical buildings along the Manhattan ESA alignment.

As result of this study, the frequencies to be avoided in order to not cause resonance that would amplify blast vibrations were determined for both buildings and utility pipes.

Figure 6 show these ratios for typical building along the Manhattan ESA alignment.

Although there are minor differences, similar characteristics are observed for all of the buildings. The square symbols (filled and open) show the ratios between train passage and ambient vibration. The ratio is greater than 1 for most frequencies, which would be expected, with the vibration concentrated at frequencies above 40 Hz. This indicates that the train passage generates vibration that is primarily related to the source; i.e., the trains themselves generate 40 to 80 Hz vibration. There is another peak at around 4 Hz, of smaller amplitude, discussed below.

The triangle symbols (filled and open) show the ratios between the upper and lower floors measured in each building for the train passage and ambient respectively. The ambient vibration shows a fairly consistent amplitude ratio of less than one for most frequencies. This means that the vibration decays with amplitude upward through the structure. This is true even at the high frequencies (40 to 80 Hz) propagated by the train passage, which are measured as being amplified relative to ambient.

There is an exception at low frequency. The train passage generates vibration at 4 Hz that is amplified relative to the ambient and for the upper floor relative to the lower. This is likely due to floor resonance in the buildings.

The significance of this is related to recommended blast design for the Contractor. Design that incorporates relatively long delays of explosives, i.e. 250 millisecond delay, might generate vibrations that would propagate and resonate in these structures, and therefore be more noticeable. Such design should be avoided.

Copyright © 2005 Taylor & Francis Group plc, London, UK

It is also worth noting that the within the ESA project, a study was conducted to assess the projected impact of ground borne noise and vibration levels inside buildings along ESA alignment in Queens and Manhattan due to operations of LIRR commuter rail train into and out of Grand Central Terminal in Manhattan.

To characterize the effect of vibration propagating from trains running in the LIRR tunnels to the ground surface, or in bedrock to the foundation level in the rock (where taller buildings are founded), the transfer mobility measurement were performed using a standard drill rig during the geotechnical investigation. Three street surface borings were used for the vibration propagation measurement in Manhattan (VM-2, MA-103, and MA-104). All three boreholes were located in the curve section of the Manhattan alignment, between 62nd and 63rd street, Lexington and 3rd Avenues. It was concluded that substantial amplification of the vibration could occur in the upper soil layer at the soil /rock interface. Impact of such amplification will be determined during the test blast program.

3 CONTROLLED DRILL-AND-BLAST ACTIVITIES-INDUCED STRAIN

For close proximity controlled drill-and-blast activities, the effect of blasting is measured by blast-induced dynamic strain in the columns and foundations of the adjacent structures. Peak particle velocity is used as a criterion for whole structure response; a strain criterion is used where the response of a particular structural element is desired. Instead of using detailed structural modeling (which is impractical for complex and aged GCT structures and the numerous overlying buildings), the strain in the columns of the buildings can be related to the input vibration based upon a plane-strain relationship, of the form:

$$\varepsilon = \frac{PPV}{c} = \frac{1}{c} PPV = \alpha . PPV \qquad (4)$$

where ε is the (dimensionless) strain, PPV (in/sec) is the vibration, and c (in/sec) is the wave propagation velocity in the building column.

A conservative estimate can be calculated assuming a typical wave propagation velocity in concrete of 10,000 ft/sec ($\alpha \approx 8.3$). This will give a lower bound on the wave propagation velocity, and therefore an upper bound on the strain. This conservative assumption is further confirmed by Figure 7 where correlations of strain gauges measurements vs. PPV from 2 major tunneling projects are presented: (i) the Weehawken Tunnel where strain gauges were mounted on duct banks, controlled drill-and-blast activities conducted at tunnel crown level and rock type was diabase

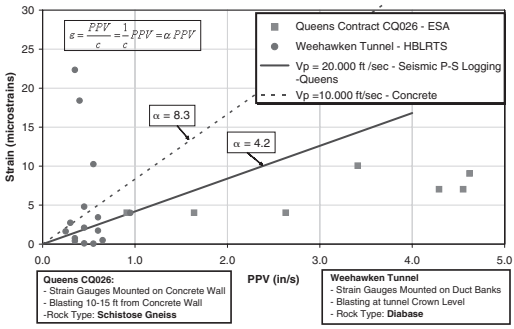


Figure 7. Correlation of stain gauge measurements vs. PPV.

(Ott et al., 2004). (ii) East side Access Queens Contract where strain gauges mounted on concrete wall, blasting conducted at 10–15 ft from concrete wall and rock type was Schistose Gneiss.

Based upon these calculations, the maximum expected strain level at close locations is 209 microstrains, for blasting one foot away from building column footings. This level is well below the level of approximately 700 microstrains that Tart et al. (1980) showed could cause concrete spall. Based on successful application of this method on other projects, strain level threshold criteria were set at 150 microstrains (Alert Level), and 500 microstrains (Upset Level). During the construction, considering the age and condition of existing MNR structures, if strain measurements between 150 microstrains and 500 microstrains are obtained, provision in the contract documents will be made requesting the Contractor to inspect the affected columns and footings in close proximity to the controlled drill-and-blast activities and make sure that no visible concrete spalling has occurred before proceeding with subsequent controlled drill-and-blast activities. In isolated cases where measurements of 500 microstrains may be reached, the Contractor will be requested to halt blasting activities and adjust the blasting procedure.

4 TBM/ROADHEADER INDUCED GROUND BORNE VIBRATION

Vibration from operating TBM machines is influenced by distance, structural rock conditions, physical rock properties, ground water and depth of overburden. At the Chattahoochee Tunnel Project near Atlanta, Georgia, measured PPV intensities created by an 18.4-ft Robbins machine in granodiorite ranged from 0.02 to 0.08 in/s. The average depth of this tunnel is about 200 feet from ground surface. When monitoring data was compared to depths of overburden, engineers discovered that PPV readings were inversely proportional

Copyright © 2005 Taylor & Francis Group plc, London, UK

to the depth of overburden. This stands to reason, because it is well known that high-frequency vibration attenuates more rapidly in loose material and some energy is lost due to reflection at the overburden-rock interface. Since most buildings in Manhattan are founded directly in the bedrock and the depth of the TBM tunnels is less than 200 feet, it would be wise to assume that predicted PPV values will occur in the high-range of curves based on historical data.

The rotation and design of mechanical cutting heads on hard-rock TBM machines typically generates ground vibration with frequencies ranging from 20 to 80 Hz. However, several cases are known where TBMs caused very low frequency motion (<5 Hz). In these instances, such as at the Metrowest Tunnel in Massachusetts and the DC Metro Project, it is believed that "machine-shaking" while mining through blocky or faulted ground caused the low-frequency ground motion. The intensity of low-frequency motion does not attenuate as rapidly as the components of motion occurring in higher frequencies so measured PPV values would be accordingly higher at the ground surface.

The TBM ground vibration levels were estimated using historical data from three tunnel projects in hard rock: Buffalo Light Rail Rapid Transit Tunnel data summarized by Flanagan (1993), Metro West Water Supply Tunnel reported by Hager Geoscience (1999), Chattahoochee Tunnel and TBM data provided by Fornaro et al. (1994). The analysis of the measured data was used for these projects. As illustrated on Figure 8, the following 95% statistical confidence level equation was derived to facilitate estimates of vibration intensities that will be felt by residents above the Manhattan work.

$$PPV = 93.5 \times (D)^{-1.4} \quad (5)$$

where PPV = Tunnel Boring Machine-Induced Peak Particle Velocity (in/s), and D = Distance (ft).

Isoseismic diagrams (contour plots of expected vibration levels of constant amplitude) for the two

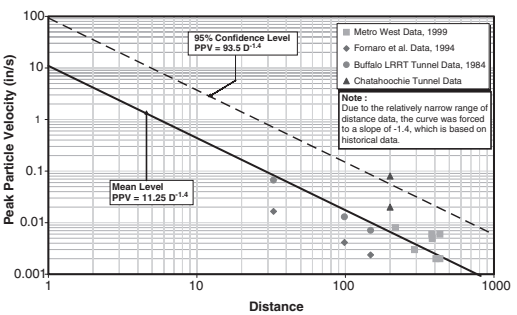


Figure 8. PPV prediction data and regression curve for TBM in hard rock.

vibrations limits of 0.5 inch/sec and 1.92 inch/sec, for the NYCT structures, ground surface and the 2nd floor of typical buildings along the Manhattan ESA alignment were derived.

5 CONCLUSION

Findings of the vibration study are critical to completing the instrumentation and monitoring program, determining the extent of the structure and utility protection during construction (limits of a protective construction mesh), setting the limits of required structural/utility condition assessment at the onset of the construction that would involve controlled drill-and-blast activities, and validating the criteria for construction activity-induced vibrations for use in contract documents. The findings will be modified to facilitate prediction of vibrations through the existing overlying structures due to construction activities from other ESA contracts. The findings will be confirmed through a construction-phase test blast program where minor adjustments to the controlled drill-and-blast procedures will take place. Recommendations for protective measures for the overlying structures, utilities at GCT, and NYCT Tunnels as well as blast design are drawn from the conclusions of this study and included in the contract documents.

REFERENCES

Flanagan, R.F. (1993) "*Ground vibrations From TBM's and Shields,*" Tunnels and Tunneling, October, pp. 30–33.

Fornaro, M., Patrucco, M. and Smabuelli, L., (1994) "*Vibrations from Explosives, High Energy Hydraulic Hammers and TBM's; Experience from Italian Tunnels,*" Gallerie E Grandi Opere Sotterranee, December, pp. 30–37.

Metro West Water Supply Tunnel Project. (1999) "*TBM Vibration Monitoring Reports*" prepared by Hager Geoscience, Inc, for Stone and Webster Civil and Transportation Services, Inc., April 1999.

MTA/Long Island Rail Road East Side Access. (2003) "*Ground Borne Vibration Study*", dated July.

MTA/Long Island Rail Road East Side Access – Preliminary Engineering: *Ground-borne Noise and Vibration Impact Report*", dated January 2001.

Oriard, L.L., Richardson, T.L. and Akins, K.P. (1985), "*Observed High-Rise Building Response to Construction Blast Vibrations,*" Proceedings of Symposium on Vibration Problems in Geotechnical Engineering, ASCE National Convention, Detroit, Michigan, October.

Ott, K.R., Haq, S. and Anderson, D.A. (2004), "*Blasting Adjacent to High Voltage Duct Banks*," Proceedings of North American Tunneling Conference, 2004.

Tart, R.J., Oriard, L.L. and Plump, J.H. (1980), "*Blast Damage Criteria for a Massive Concrete Structure in Minimizing Detrimental Construction Vibrations*", ASCE, NY, pp. 125–140.

Copyright © 2005 Taylor & Francis Group plc, London, UK

An experimental study on the development of high performance shotcrete for permanent tunnel support

S.P. Lee, D.H. Kim, J.H. Ryu & J.Y. Yu
LG Engineering & Construction Corp., Seoul, Korea

S.D. Lee & S.H. Han
Korea Highway Corp., Seoul, Korea

M.S. Choi
Silkroad C&T, Seoul, Korea

C. Park
Korea Institute of Geoscience & Mineral Resources, Daejeon, Korea

ABSTRACT: Recently, the study of high performance shotcrete as a permanent tunnel support has gained an increasing amount of attention in Korea. However, several attempts to adapt permanent shotcrete lining tunnel with PCL(Precast Concrete Lining) instead of conventional in-situ concrete lining, have been abolished due to the lack of trust on the performance of rock bolt and shotcrete as a permanent tunnel support. Therefore, in this study, target performance levels of shotcrete (compressive strength over 40 MPa, flexural strength over 4.5 MPa) were set up to achieve long-term durability for the life-time of tunnel. The maximum size of aggregate was 10 mm and hooked-ends type steel fiber were used for mix design. The alkali free accelerator was mainly utilized for the test, and the aluminate and the silicate accelerators were used for comparison. The silica fume of 4, 7, 10% was added substituting the same amount of cement. 987 test samples consisting of cylinder, beam, round panel(by RTA, Australia) and square panel(by EFNARC) were prepared using a shotcrete machine, Meyco Suprema. Several tests on the samples were carried out by the elapsed time of 3, 7, 28 days and 3 months and will be continued to the elapsed time of 6, 12 and 24 months. The compressive strength, the flexural strength and the flexural toughness were measured to monitor the performance of shotcrete according to each elapsed time. Finally, the optimum mix composition was proposed to meet the target performance level of the shotcrete as a tunnel support.

1 BACKGROUND

1.1 *Shotcrete specification of each country*

According to the list of the permanent shotcrete lining (2003 ITA working group 12, shotcrete use), permanent shotcrete lining was used at 168 tunnels (total length of 610 km approx.) in 14 different countries (Table 1). The types of tunnels where permanent shotcrete lining has been applied include road, rail, subway tunnel and oil cavern. However, the way to apply the permanent shotcrete lining to those types of tunnels differs each country. For example, in Czech, the thickness of shotcrete was increased to 45 cm rather than increase of the strength, while the high strength shotcrete whose compressive strength is up to 45 MPa, was applied in Austria.

In northern Europe, the compressive strength over 40 MPa is widely used for the permanent shotcrete lining. Especially, in Japan, the compressive strength of high strength shotcrete is defined to be over 36 MPa. In Korea, many researches and experiments considering various admixture and mixture design of shotcrete have been performed. Nevertheless, there is still hesitance adopting high performance shotcrete as a permanent support without concrete lining for tunnel.

1.2 *Target specification of high performance shotcrete*

The quality of high performance shotcrete as a permanent tunnel support should be higher than that of conventional shotcrete, where compressive strength of

Copyright © 2005 Taylor & Francis Group plc, London, UK

Table 1. List of permanent shotcrete lining tunnel (ITA, 2003).

Name	Country	Type	Length (m)	Shotcrete thickness (cm)	Compressive strength of shotcrete (MPa)
Subway Line B	Argentina	Subway	500	60	17
WMC Leinster Nickel	Australia	Mining tunnel	60,000	7.5	45
Hall Stadt	Austria	Road	1,063–1,203	15	29–69
BC rail	Canada	Rail	640	10	40
Lo Prado II	Chile	Road	2,800	15–30	>30
Praha	Czech	Subway	140	45	>20
Taino	Japan	Rail	351	7	37
Y-2	Korea	Cavern road	1,594	5–14	20
Freifjord	Norway	(undersea)	5,086	6.5–14	36(C45)
Laedal	Norway	Road	24,500	6–5	32(C40)
Disentiser	Switzerland	Rail	346	30–45	34.4
Sodra	Sweden	Road	16,600	6–9	>40

Table 2. Northern Europe strength standard (EFNARC, 1996).

	Compressive strength (MPa)			
Strength class	Cylinder	Core (cylinder)	Cube	Flexural strength (MPa)
C30	24	20.5	30	3.4
C35	28	24	35	–
C40	32	27	40	–
C45	36	30.5	45	4.2
C50	40	34	50	–
C55	44	37.5	55	4.6
C60	48	41	60	–

21 MPa is normally applied in Korea. However, the anticipated level of high performance shotcrete can be different according to the conditions and usage of the tunnels each country. In this study, the target specification of high strength shotcrete (compressive strength over 40 MPa, flexural strength over 4.5 MPa) was set to satisfy that of C50 in Northern Europe with long-term durability (Table 2).

2 MIX DESIGN

Project-specific tests and experiments should be conducted to determine the proper mix design of shotcrete and to assess the performance when particularly proposed materials and application procedures are applied. Since it was almost impossible to take account of all components that consist of shotcrete mix, experiments were conducted varying the amount of the two ingredients, accelerator and silica fume which are believed to be the most critical component to determine the mechanical characteristics of the shotcrete based on previous studies. Selected contents and types of components are follows.

2.1 *Aggregate*

The maximum size of aggregate used in these experiments was specified to 10 mm.

2.2 *Steel fiber*

Steel fiber improves the tensile strength, the resistance against crack, and the toughness of shotcrete. Among various types of steel fiber, hooked ends type, which has the diameter of 0.5 mm and the length of 30 mm, was selected with the amount of 40 kgf/m^3 considering constructibility.

2.3 *Accelerator*

It is important to select the appropriate type and exact amount of accelerator for rapid strength development and long lasting strength. It is reported that Alkali free accelerator is not harmful to human and less reduces the strength when compared with the Aluminate and Silicate type. In this study, the Alkali free (8%) was used as a standard accelerator. However, for the comparison, performance of the shotcrete when different accelerator such as Aluminate (5%) and Silicate (10%) was applied was also investigated.

Copyright © 2005 Taylor & Francis Group plc, London, UK

Table 3. Mix composition of each session.

No.	Slump (cm)	W/C ratio (%)	Fine-aggregate ratio (%)	Content (kgf/m^3)								Parameter
				W	C	Coarse Agg.	Fine Agg.	Steel fiber	Silica fume	Plasticizer	Accelerator	
1	12 ± 3	43.1	65	207	480	566	1008	40	0 (0%)	4.8 (1%)	AF (8%)	Silica fume accelerator
2	12 ± 3	43.1	65	207	480	566	1008	40	0 (0%)	4.8 (1%)	AL (5%)	Accelerator
3	12 ± 3	43.1	65	207	480	566	1008	40	0 (0%)	4.8 (1%)	SL (10%)	Accelerator
4	12 ± 3	43.1	65	207	461	564	1004	40	19 (4%)	5.76 (1.2%)	AF (8%)	Silica fume
5	12 ± 3	43.1	65	207	446	562	1000	40	34 (7%)	6.72 (1.4%)	AF (8%)	Silica fume
6	12 ± 3	43.1	65	207	432	560	997	40	48 (10%)	7.68 (1.6%)	AF (8%)	Silica fume

* AF: Alkali free, SL: Silicate, AL: Aluminate.

2.4 *Cement and Water/Cement (W/C) ratio*

The type of cement used was portland cement and the amount was 480 kgf/m^3. W/C ratio was designed to be 43% in favor of mixing works at field.

2.5 *Silica fume*

Silica fume is he highly pozzolanic mineral admixture, which has been mainly used to improve the durability and strength of the concrete. In this study, the performance of shotcrete was investigated when the amount of silica fume was changed to 0, 4, 7, and 10% substituting the same amount of cement.

2.6 *Plasticizer*

Plasticizer plays a role in distributing shotcrete to the target surface. This component reduces the water content without hardening time delay, excessive air induction, and decrease of shotcrete strength. In this study, polycarbon AE superplasticizer was selected for the plasticizer.

3 SPECIMEN MANUFACTURING

The testing shotcrete machine 'Meyco Suprema' which has a computer controller was used for the precise control of accelerator component. Total of 987 specimens with different shapes such as cylinder, beam, round panel (by RTA, Australia) and square panel (by EFNARC) were manufactured for 5 separate sessions (Table 3, Table 4 and Table 5).

To manufacture the spray type shotcrete specimens, steel structures for fixing molds were made at construction site of Hyunpoong-Kimchon highway (Figure 1). The task of spraying shotcrete was performed by hand (Figure 2). Test specimens were cured in the field being covered by curing blankets to prevent evaporation of moisture and to minimize the effect of temperature and humidity change. After 1 day when specified strength was acquired, test specimens were demolded and marked with numbers to identify the session and type of the specimens. Thereafter, test specimens had been cured for another 2 weeks at the site before it was finally move to the laboratory to prevent the decrease of strength when being transferred.

4 EXPERIMENT RESULTS

4.1 *Accelerator*

Compressive strengths were measured at 3, 7, 28 days, and 3 months. The compressive strength increases with the time (Figure 3). It was also found that the among test specimens, only Alkali free accelerator satisfied target compressive strength of 40 MPa at 28 days. At 3 months, the compressive strength of Aluminate was highly increased to satisfy the target strength.

It can be seen that with Alkali free and Aluminate accelerators, the flexural strength was satisfactory being over 4.5 MPa (Figure 4), while, the flexural strength was below 4.5 MPa with Silicate accelerator at 7 days and 28 days. The flexural strength of specimens with Aluminate increased 14% from elapsed time of 7 days to 28 days, but the flexural strength of samples with Alkali free decreased 11% during the same period.

4.2 *Silica fume*

With the fixed amount of Alkali free accelerator at 8%, the compressive strength of all samples satisfied 40 MPa for the elapsed time of 28 days when the amount of Silica fume ranged between 0 and 10% (Figure 5). Especially, when the content of Silica fume was 4%, the compressive strength was over 50 MPa. The result observed at 28 days showed that the strength improved with the increase of Silica fume up until certain point and decreases afterward. The effect by the

Copyright © 2005 Taylor & Francis Group plc, London, UK

Table 4. Manufacturing program of specimens.

Silica fume (%)	Accelerator	Steel fiber	Box (core) cylinder elapsed time	Pouring cylinder elapsed time	Spraying beam		Pouring beam		Box (cut) beam elapsed time	Spraying square 28d	Pouring square 28d	Spraying round 28d	Pouring round 28d
					Elapsed time	Pin	Elapsed time	Pin					
0	PL	40	18(3)	21	–	–	18	2	–	–	3	–	3
	AF		42(7)	–	12	2	–	–	30(15)	6	–	6	–
	Sum		60(10)	21	14	–	20	–	30(15)	6	3	6	3
	PL	40	–	21	–	–	18	2	–	–	–	–	–
	AL		42(7)	–	12	2	–	–	6(3)	–	–	–	–
	Sum		42(7)	21	14	–	20	–	6(3)	–	–	–	–
	PL	40		21	–	–	6	2	–	–	–	–	–
	SL		42(7)	–	12	2	–	–	6(3)	–	–	–	–
	Sum		42(7)	21	14	–	8	–	6(3)	–	–	–	–
4	PL	40	42(7)	42	–	–	36	2	–	–	3	–	3
	AF		42(7)	–	12	2	–	–	30(15)	–	–	6	–
	Sum		84(14)	42	14	–	38	–	30(15)	6	3	6	3
7	PL	40	18(3)	42	–	–	36	2	–	–	3	–	3
	AF		42(7)	–	12	2	–	–	30(15)	6	–	6	–
	Sum		60(10)	42	14	–	38	–	30(15)	6	3	6	3
10	PL	40	18(3)	42	–	–	36	2	–	–	3	–	3
	AF		42(7)	–	12	2	–	–	30(15)	6	–	6	–
	Sum		60(10)	42	14	–	38	–	30(15)	6	3	6	3
Total sum			348(58) 987	189	72	12	150	12	132(66)	24	12	24	12

* PL: Plain sample for reference, number in ( ) means number of Box.

Copyright © 2005 Taylor & Francis Group plc, London, UK

Table 5. Type of test samples and specification.

Type	Specification	Remarks
Cylinder Mold	D 100 × 200 mm	–
Cylinder Core	400 × 650 × 200 mm (Box sample)	Coring (D 100 mm)
Beam Mold	150 × 150 × 550 mm	–
Beam Cutting	400 × 650 × 200 mm (Box sample)	Cutting (150 × 150 × 550 mm)
Panel Round	D 800 × 75 mm	–
Panel Square	600 × 600 × 100 mm	–



Figure 1. Steel device for fixing molds.



Figure 2. Manual spraying of shotcrete.

amount of the Silica fume is not critical. So, further observation should be made for this.

All flexural strengths were over 4.5 MPa at 28 days and the highest flexural strength was observed with 4% of Silica fume (Figure 6). Without Silica fume, the flexural strength decreased about 11% from the elapsed time of 7 days to 28 days. On the contrary, if the Silica fume was added, the flexural strength increased about 10% regardless of the its quantity.

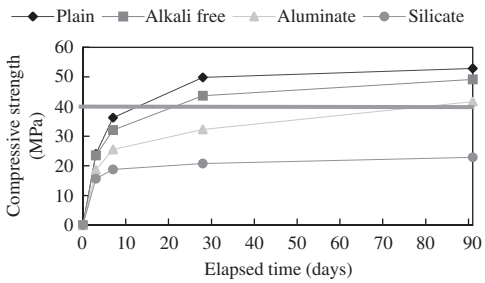


Figure 3. Compressive strength for each accelerator.

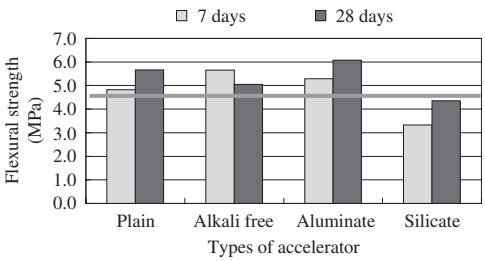


Figure 4. Flexural strength for each accelerator.

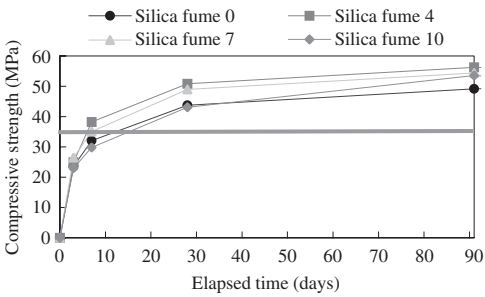


Figure 5. Compressive strength for the amount of Silica fume.

4.3 *Panel tests*

Panels were manufactured in specific size to simulate the behavior of shotcrete sprayed and cured in the real

Copyright © 2005 Taylor & Francis Group plc, London, UK

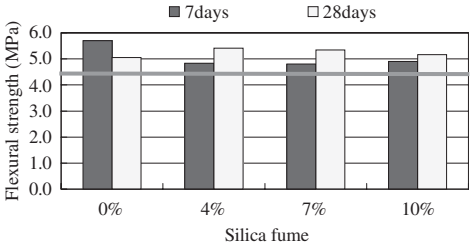


Figure 6. Flexural strength for the amount of Silica fume.

Table 6. Comparison of panel tests.

Classification	Round panel (RTA)	Square panel (EFNARC)
Specimen size	R 800 × 75 mm	600 × 600 × 100 mm
Loading velocity	10 mm/min	1.5 mm/min
Max. settlement	40 mm	25 mm
Support condition	3 Point Support	4 edge Support
Shape of loading	Half sphere	Square

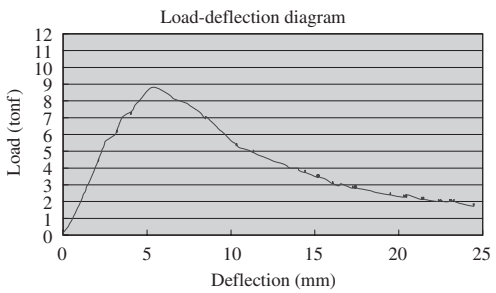


Figure 7. Load-deflection graph of Square panel.

tunnel. Flexural toughness can be evaluated measuring the energy absorption by Square Panel tests and Round Panel tests (Table 6).

The load-deflection diagram of the test methods for square panel and round panel was compared (Figures 7 and Figure 8). In square panel test, maximum strength was reached following gently developing curve. While, in the round panel test, the load fell rapidly after peak value was reached in the early stage. It is thought this phenomenon was due to the change of the support point as the tests progressed.

The absorption energy of EFNARC panel ranges between 780 J and 1250 J, and for the RTA panel it was between 280 J to 450 J (Figure 9). It can be seen that the degree of dispersion is fair. The line on the Figure 10 signifies linear relationship between the absorption energy of EFNARC panel and that of RTA panel suggested by Bernard. According to the relationship

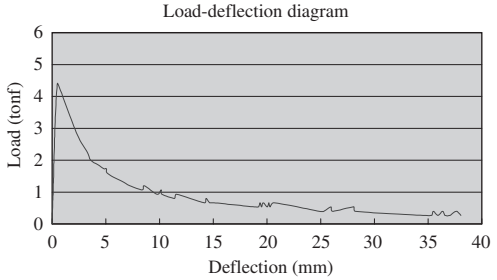


Figure 8. Load-deflection graph of round panel.

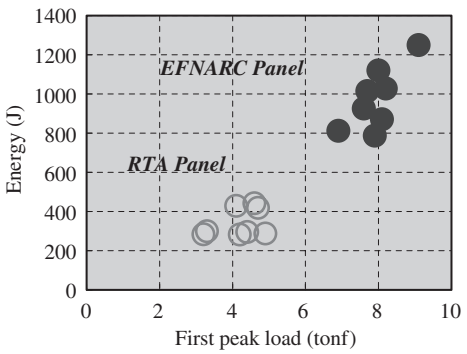


Figure 9. Relation between early cracking load and absorption energy.

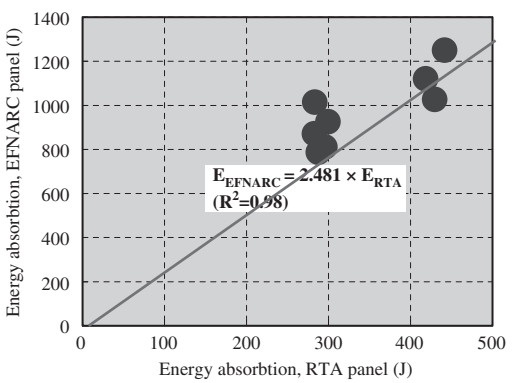


Figure 10. Correlation of RTA and EFNARC panel.

absorption energy of 1000 J by EFNARC panel corresponds to 400 J of RTA panel. In this experiment, the correlation coefficient (R^2) was investigated as 0.68, which is considerably low compared with the 0.98 from Bernard's experiment (1998). This was believed to be due to the wind and so on which effected properties of shotcrete when it was manufactured outside.

Copyright © 2005 Taylor & Francis Group plc, London, UK

5 CONCLUSION

1. Among 3 accelerators applied to experiment, only Alkali free accelerator achieved target strengths (compressive strength over 40 MPa and flexural strength over 4.5 MPa at 28 days).
2. When Alkali free was added 8%, the objective strength was acquired regardless of the amount of Silica fume.
3. Without Silica fume, the flexural strength decreased with the elapsed time. The highest compressive strength was observed to be 4% of Silica fume among 0%, 4%, 7% and 10%. According to the previous researches by others, the amount of Silica fume when the max strength was acquired was 15%. This was believed to be due to the influence of conditions in manufacturing site such as wind and this should be eliminated to secure the validity of the data for the further research.
4. Comparing strength of shotcretes with respective accelerators in the same condition, the strength dropped significantly with addition of Silicate and considerably with Aluminate. With Alkali free accelerator the decrease of the strength was not noticeably observed when compared with the data of the specimens with no accelerator.
5. The correlation between EFNARC panel and RTA panel was investigated. However, it was found that the correlation value of this experiment was lower than that of Bernard's experiment.
6. Strength tests of specimens have been carried out by the elapsed time of 3 months and the further tests are scheduled to be in 6, 12, and 24 months.

More experiments and studies will be followed to find various ranges of mix composition satisfying target specifications of shotcrete. Also studies are required to define the test standards and the specifications of high performance shotcrete in Korea.

REFERENCES

Jong-Hyun Ryu, Seung-Hwan Han, Jin-Cheol Kim, Tae-song Ahn, Sang-Don Lee (2002), "An Experimental Study on Flexural Toughness of SFRS", Journal of Korea Concrete Institute, Vol. 14, No. 1, pp.581–586.

Bernard, E. S. (1998), "Correlations in the Performance of Fiber Reinforced Shotcrete Beams and Panels", University of Western Sydney.

EFNARC (1996), European specification for sprayed concrete.

EFNARC (1999), European specification for sprayed concrete Guidelines for specifiers and contractors.

Highway Research Center (2001), "Enhancement and Quality Control of Steel Fiber Reinforced Shotcrete", Korea Highway Corp.

ITA Working Group on Shotcrete Use (1993), Shotcrete for rock support: a summary report on the state of the art in 15 countries. Tunnelling and Underground Space Technology, Vol. 8, No. 4, pp.441–470.

Knut, F. & Tom, A., "Advantages of Permanent Wet-mix Sprayed Concrete Tunnel Linings – Project Experiences".

Marc Jolin and Denis Beaupre (2003), "Understanding Wet-mix Shotcrete: Mix Design, Specifications, and Placement", Shotcrete. Summer 2003, American Shotcrete Association.

RTA, Test method T373 (1999), "Determination of the toughness of a fibre reinforced shotcrete mix – round determinate panel test".

Copyright © 2005 Taylor & Francis Group plc, London, UK

Successful application of the observational design method to difficult tunnel conditions – Driskos tunnel

P. Grasso, G. Scotti, G. Blasini, M. Pescara & V. Floria
Geodata S.p.A., Turin, Italy

Kazilis N.
Egnatia Odos A.E., Athens, Greece

ABSTRACT: Difficult geotechnical conditions were encountered during the construction of the twin bore Driskos tunnel (Egnatia Odos Motorway, Greece). Excessive tunnel deformations and primary support failures were experienced in different tunnel sections. To resume the tunnel excavation, a new design for the bench phase was adopted which was essentially based on the concept of a flexible observational approach. Back analysis of tunnel behaviour in the heading phase (A-Phase) allowed to define a reference model for subsequent excavation (B-Phase). Real time monitoring data analysis and direct tunnel inspections helped to control and, when necessary, to modify the provisions of the new design. Safe and fast tunnel completion was successfully achieved.

1 INTRODUCTION

Driskos Tunnel is a twin bore tunnel (Fig. 1.1), with 11.00 m internal diameter for each bore, crosses the North-East Greek Pindos mountain chain under 220 m maximum overburden, comprised in the Egnatia Odos Motorway, Section 2.3. Pillar width between the bores is approximately 13 m.



Figure 1.1. Driskos tunnel, Left Bore. Additional reinforcement (18 m long prestressed anchors) is visible around Ch. 8 + 800. Also visible are the concreted sidewalks and the platform in the neighbor completed section (view towards the Exit Portal side).

2 OVERVIEW OF PREVIOUS TUNNEL CONSTRUCTION PHASES

The detailed design required to excavate the cross section of both bores in two steps: the top heading (A-Phase) and the bench (B-Phase). During the A-Phase excavation, excessive deformations (up to 210 mm tunnel closure) and primary support failures (Fig. 2.1) were recorded along a stretch (Ch. 8 + 500 to 8 + 800) of the Left Bore (LB), with an overall length of 300 m.



Figure 2.1. Steel ribs yield in the overstressed LB stretch.

Copyright © 2005 Taylor & Francis Group plc, London, UK

Displacements increased after the top heading excavation of the second parallel tube (Right Bore, RB), reaching a maximum value of 310 mm.

Additional support works were carried out to strengthen the original (HEB160 1.0 m distance, 25 cm thick shotcrete shell, ϕ32 mm 6.0 m long fully grouted rockbolts, 25 cm thick temporary shotcrete invert arch) support section. In particular no. 10 prestressed cable anchors (18 m long) between steel ribs, grouted rockbolts (9 m long) in some portions of the tunnel and 6.0 m long micropiles at the base of the supporting shell were installed; the latter were also incorporated into a steel reinforced continuous concreted beam element that was laid at the base of the steel ribs along both sidewalls.

Nevertheless, the records of the convergence measurements (Fig. 2.2) showed that stable conditions were only reached 7 months after the commencement of the A-Phase excavation, with a resulting excess convergence that, in several points, exceeded by more that 15 cm the expected values.

The Client (Egnatia Odos Company), forced both by the occurrence of such difficult geological/technical conditions and by the necessity of catching up with the Project's construction schedule that required to proceed with the B-Phase excavation, decided to entrust the design for the bench excavation phase to an independent designer, able to react fast to the events and to follow "on site" construction works. To this purpose the JV of GEODATA SpA (Italy) and ODOTECHNIKI Ltd (Greece) JV was appointed and asked to proceed with the design of strengthening of the temporal support of the top heading and B-Phase (benching) excavation of both bores.

Re-design activities were also extended to another problematic tunnel section in the Right Bore, between Ch. 8 + 128 and Ch. 8 + 195, where excessive and unexpected stability problems were encountered during the A-Phase excavation of a lay-by section.

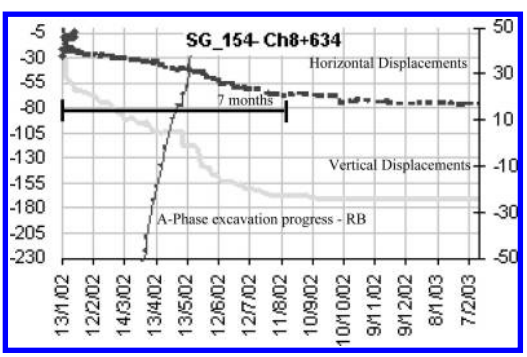


Figure 2.2. Typical deformation pattern of Driskos tunnel (LB at Ch. 8 + 634. Right Y axis = displacement [mm]; left Y axis = excavation face distance [m].

3 FLEXIBLE DESIGN APPROACH

Underground construction works normally pose significant challenges and require special efforts in order to accomplish them in a safely and timely manner. One of the main difficulties is to be capable of providing a sufficiently reliable predictive ground model. It has been recognized for a long time that the most effective way to face ground conditions uncertainty consists in adopting a flexible approach, otherwise referred to as observational approach.

Such an approach was adopted and implemented for the design and construction phases relevant to the critical Driskos tunnel sections.

The approach requires a very coordinated and integrated design and construction follow-up team to be set up, capable of fast reacting against the occurrence of anomalous or unpredicted conditions.

Three principal logical steps of the observational approach can be recognized:

- Setup of a predictive geomechanical model.
- Implementation of control measures during the construction phase, to empirically proof the adequacy of the model and of the construction scheme (support system and excavation technique; Bock, 2000).
- Structured though flexible decision making process to react against the occurrence of anomalous conditions and continuous analysis of recorded data to feedback into the predictive model (model update). Counter measures have to be defined *prior* to the excavation works and with reference to a significantly wide range of possible events scenarios.

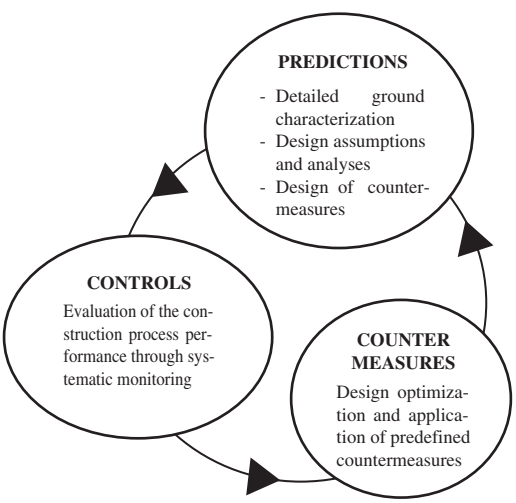


Figure 3.1. Logical steps of an observational design & construction flexible approach.

Copyright © 2005 Taylor & Francis Group plc, London, UK

The process in itself is typically recursive with successive feedback across the phases chain, as represented in Fig. 3.1.

3.1 *The predictive model*

Main design steps to define the reference prediction model were:

a. Focus on existing constraints and requirements.
b. Thorough study of available information and definition of a geomechanical model.
c. Definition of the key parameters that the back analysis process has to focus on.
d. Sensitivity study of tunnel's behaviour using the *ground reaction curves* method.
e. Definition of the actual tunnel conditions based on back-analysis FEM models and setup of different scenarios.
f. Modelling of the bench excavation over the possible scenarios.

3.1.1 *Constraints and requirements*

The locations of the critical tunnel sections were quite inside the tunnel route; in order to limit the impact over the whole Project's schedule, the critical tunnel sections were secured and left behind for subsequent actions. The rest of the tunnel's LB was excavated and the final concrete lining put in place.

This resulted in a very limited, if any, allowance of fitting the deformed tunnel section to the surrounding zones. In practice, no allowance was indeed available for additional settlement to occur beyond very limited values, otherwise the proposed remedial measures for the completion of the tunnel would have been thwarted and an extensive tunnel remining would have to be carried out.

Tunnel re-profiling, through partial demolition and reconstruction of the support system, was recognized as technically uncertain, potentially unsafe and time consuming and, therefore, it was discarded.

Both the Client and its technical advisors recommended to envisage a solution that should not have required any intervention or modification of the existing support system. A reduction of the tunnel's internal radius from 5.50 m to 5.25 m was hypothetically envisaged, provided that the support capacity of the final lining would have been guaranteed, thus entailing the necessity of maintaining external loads within acceptable limits.

3.1.2 *Definition of the reference model*

The main available reference data were:

– Tunnel's A-Phase construction records including face mappings compiled during the excavation.
– Reports of the Contractor's Designer including the suggested measures to proceed with tunnel excavation, after the onset of anomalous deformations.
– Technical and design reports issued by an appointed Experts Panel.
– Geotechnical and topographic monitoring data.

The excavated rocks, belonging to the Pindos Flysch unit, are represented by siltstone-sandstone sequences, locally very tectonized and sheared, which are referred to in the literature as complex formations.

According to both the system proposed by the A.G.I. (Italian Geotechnical Association; 1979 ISRM Congress and following updates) and the one based on the GSI concept (Marinos and Hoek, 2002), the encountered flyschoid rock masses can be classified as shown in Table 3.1.

With reference to the A.G.I. classification, it is important to observe that tunneling experiences in similar geomechanical and overburden conditions (e.g. in the Italian Appennines) have shown high squeezing behavior with B2–B3 elementary geotechnical complexity.

The issue about potential problems in tunnelling trough heterogeneous rock masses, as well as pitfalls and uncertainties for their geotechnical characterization, was addressed in a dedicated section of the Design Guidelines issued by the Client (O.S.M.E.O. 2003).

Based on available documentation and past experience in similar ground conditions, the following input parameter values and related probabilistic distributions of these parameters were defined (Table 3.2), to perform a back-analysis of the tunnel's behaviour.

An elastic-brittle-plastic constitutive law was adopted to describe the geomechanical behavior of rock mass. In this respect, a significant shear strength

Table 3.1. Geotechnical complexity and flysch classification.

Geotechnical complexity (A.G.I.)	B1/B2(→B3)
Flysch type (M&H)	D/F

Note: the slash symbol indicates staggered sequences among different technical units.

Table 3.2. Characteristic values and associated distributions of main geomechanical parameters.

Distribution	TRUNC. TRIANG. (5–15–30) σ_c [MPa]	TRUNC. TRIANG. (3–7–11) m_i [–]	TRUNC. TRIANG. (10–25–35) GSI [–]	UNIF. (0.025–0.027) γ (MN/m^3)
Min	10	5	15	0.025
Max	25	9	30	0.027

Notes: σ_c = Intact rock strength; m_i = constant of intact rock (Hoek e Brown, 1980); γ = unit weight of rock mass; TRUNC. TRIANG. = truncated triangular distribution.

Copyright © 2005 Taylor & Francis Group plc, London, UK

reduction in the post-failure field was indeed hypothesized; residual GSI values were defined according to Russo et al. 1998.

With reference to in situ stress field conditions, it was considered reasonable to take into account a k0 horizontal to vertical stress ratio interval ranging between 0.8 to 1.2.

3.1.3 *Back analysis*

In order to correctly understand the occurred deformation phenomena a thorough examination of the possible associated causes was carried out.

Several possible mechanisms/causes were investigated and broadly grouped into two categories: "geomechanical causes" and "construction causes". Based on the available knowledge, an occurrence likelihood was assigned to each category, as shown in Table 3.3.

Monitored tunnel deformations were integrated by adding an amount of displacement related to the initial (or so called "lost") convergence, i.e. the tunnel closure that normally occurs before the installation and zero reading of convergence monitoring sections. The initial deformations were analytically evaluated using the ground reaction curves, which were generated by adopting the geomechanical parameters listed in Table 3.2.

The total displacements (initial + measured) were then compared with the existing tunnel clearances as measured by a systematic topographic survey. Such comparisons, in some cases, clearly put in evidence inconsistencies (up to 31 cm of vertical displacements in excess to those referred to the convergence), thus suggesting that construction causes could also have played an important role in producing the final tunnel configuration.

This evidence was kept in due consideration when the construction study of the bench phase was undertaken.

A two-dimensional FEM model was set up that included the information gathered through the construction phase monitoring in order to model the tunnel's behaviour and carry out a parametric study to verify the suitability of the adopted geomechanical parameters. The Phase 2 code (developed by Rocscience) was used.

The model also took into account the observed asymmetric tunnel deformation condition that resulted after the completion of the A-Phase excavation.

Table 3.3. Checklist of possible causes for the observed excessive tunnel deformations.

Possible mechanisms/causes
Geomechanical causes
Inadequate geomechanical classification
Anomalous in situ stresses
Creep phenomenon
Swelling
High water pressure
Construction causes
Effects of water during drilling
Weaknesses in the connection between temporary invert and steel ribs
Inappropriate length and type of rock reinforcement elements
Misalignment of the steel ribs
Over excavation /cave-in and subsequent insufficient confinement of the surrounding ground, causing loosening and unforeseen gravitational loading
Disturbed/softened foundation zone of the primary support shell
Delay in installing the primary support

3.1.4 *FEM numerical analyses*

The numerical analyses put in evidence the following aspects:

- A plastic zone extension of 7–9 m around the excavation perimeter developed after the top-heading phase, thus leading to an almost complete plasticization of the 13 m width pillar between the twin bores (Fig. 3.2)
- A k_0 (horizontal/vertical stress ratio) value of 1.2 resulted to be the most appropriate for fitting monitoring data
- The top heading primary support resulted overstressed at the end of the A-Phase excavation as actually occurred during the construction phase; the next B-Phase excavation would have increased the phenomenon up to a critical state.

3.1.5 *Design and construction provisions*

To account for the observation made in A-Phase, to increase the reliability of the support system and to ensure a sufficient intrinsic safety margin, the B-Phase bench excavation primary support was designed for achieving the following objectives:

a. Optimize and strengthen the support system. The geometry of the steel ribs sets was optimised to

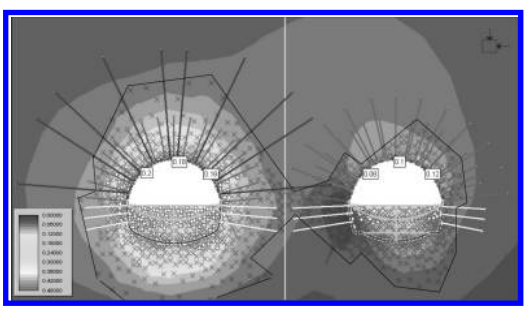


Figure 3.2. Two dimensional FEM back-analysis model of A-Phase excavation stage. The plasticized volume around the twin bores is contoured.

Copyright © 2005 Taylor & Francis Group plc, London, UK

better accommodate loading actions; ribs legs were modified from a straight to a rounded configuration; a steel arch was introduced to have a full reacting closed support section; an extended "elephant ear" support foot was introduced at the base of ribs legs to limit the onset of concentrated loads and possible additional settlements. Bench sidewalls reinforcement consisted of an array of fully bounded fast reacting, 240 kN capacity, 6–9 m long rock bolts (to this purpose Swellex Mn24 rock bolts were employed); the primary support section is shown in Fig. 3.3.

b. A complete and immediate closure of the primary support shell. A connection of the sidewalls ribs legs was provided through a steel arch along the curved invert section. A joint articulated steel rib was designed so as to allow the excavation and support of bench and invert sections to be accomplished in a unique solution, thus considerably reducing the duration of the excavation cycle. A construction sequence was studied to guarantee the permanent availability of the bench/invert section to support and lining operations; excavation should proceed directed away from the face, keeping main machinery working from the upper A-Phase level; in Fig. 3.4 steel ribs positioning from the upper A-Phase level is shown.

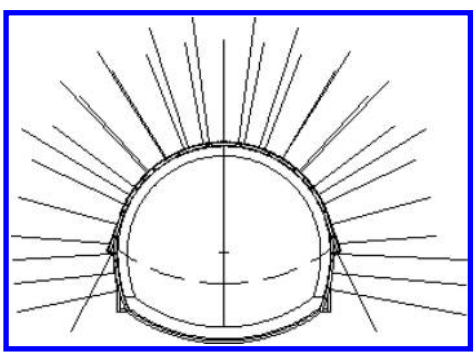


Figure 3.3. B-Phase excavation primary support section type (Left Bore).

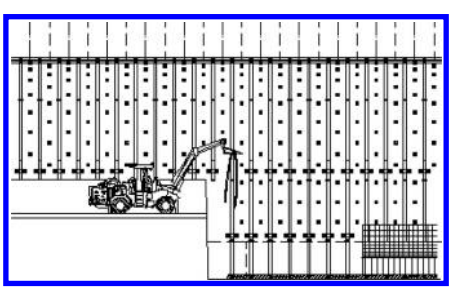


Figure 3.4. B-Phase excavation: articulated B-Phase steel ribs positioning from the upper A-Phase level.

3.1.6 *Monitoring scheme*

A monitoring scheme was required to verify the adequacy of the adopted geomechanical model and the proposed support system in order to eventually introduce a design and construction optimisations. A monitoring scheme was defined to monitor the relevant parameters such as:

- Tunnel walls displacements (3D optical survey; Fig. 3.5).
- Rock mass deformation (sliding deformometers and inclinometers columns).
- Groundwater pressure variations (piezometric cells).

In Fig. 3.6 a special monitoring section (two of such sections were foreseen) is represented.

4 THE CONSTRUCTION PROCESS

As a consequence of site organisational requirements, the contractor's and site supervision's management proposed to resume the B-Phase excavation from the parallel RB. It was then decided to exploit this opportunity in order to monitor the behaviour of the opposite more critical tunnel branch and collect additional information for possible model refinements. In this

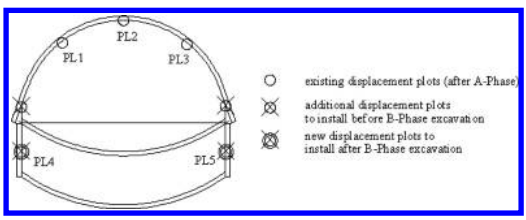


Figure 3.5. 3D displacements optical survey layout.

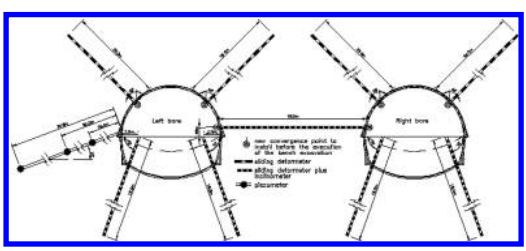


Figure 3.6. Special monitoring section layout.

Copyright © 2005 Taylor & Francis Group plc, London, UK

respect, the first 35 m of B-Phase excavation in the RB were considered as a trial zone.

Here bench excavation rounds were eventually maintained within a maximum unsupported span of 2.0 m, after the initial 1.0 m length could be modified according to the encouraging results that were being coming from the trial zone construction.

Table 4.1 summarizes the main production results (advancement rates) achieved in both bores through the adoption of the new design.

The monitoring data unexpectedly indicated that the outer sidewall of the RB (i.e. opposite to the central pillar) experienced the largest deformation values, particularly in the invert zone.

The adopted countermeasure consisted in reversing the rockbolts pattern: longer (9.0 m) elements were then moved from the pillar to the sidewall, while shorter (6.0 m) elements were installed inside the pillar; with such adaptation more homogeneous and stable conditions were achieved along the remaining of the RB.

Monitoring data analysis over the trial zone confirmed one of the most stringent and constraining provision introduced by the new design: in fact, the stabilizing effect of the immediate installation of the primary support was clearly demonstrated. The maximum unsupported span along the bench excavation was then limited to 2.0 m; the complete support system was installed within that distance.

4.1 *Construction performance controls*

Figure 4.1 shows the tunnel inner perimeter displacements after completion of the B-Phase excavation along the LB. As indicated by the figure, the redesigned temporary support reacted more quickly in comparison to the one put in place during the A-Phase excavation; stable deformation trends were achieved shortly after the passage of the bench face.

Tunnel's deformation patterns in the RB showed that deformations begin to manifest at a distance of approximately 1 diameter ahead the face and tended to stabilize (gradient <1 mm/day) at a distance of 3 diameters behind the face.

Deformations were on average more significant on the outer sidewall (asymmetric behaviour), which was not predicted by the numerical model. A more symmetric condition was achieved after the modification of the sidewalls rockbolts pattern had been introduced.

By processing the monitoring data registered during excavation of the trial zone, it was pointed out that the deformations at the tunnel's LB, reach a top gradient at a distance of circa 10 m (<1 diameter) backwards from the benching RB face, after which they quickly got to stabilization. On the contrary, the gradients on the RB kept on increasing till a distance of approximately until 30 m (<3 diameters) from the benching face, where they finally dropped to stabilized values.

4.2 *Comparison between predicted (FEM model) and observed deformations*

In Tables 4.2a and 4.2b a comparison between predicted and observed tunnel deformation for both bores is reported. The figures are referred to the additional displacements caused by the B-Phase excavation (i.e. A-Phase contribution is not considered).

Relevant comments to the below comparative tables are as follows:

a. Displacements predicted by the numerical model with few exceptions were generally fairly in accordance with the recorded values
b. As anticipated by the model analysis, the influence of the LB excavation activity over the RB was confirmed to be irrelevant

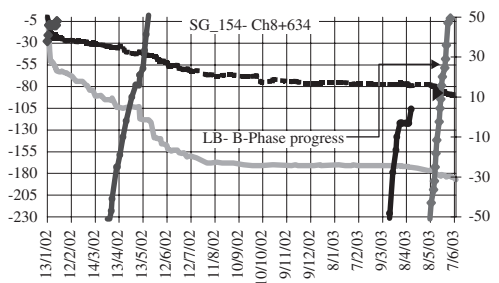


Figure 4.1. Typical deformation pattern of Driskos tunnel (LB at Ch. 8 + 634. Right Y axis = displacement [mm]; left Y axis = excavation face distance [m].

Table 4.1. Production rates obtained with the implementation of the new design approach.

Tunnel stretch	Starting date	Achieved	Length (m)	Excavated area (m^2)	Working days	Production rate (m/day/face)
RB	17-Feb-03	14-Apr-03	300	107.4	43	4.0
LB	16-Apr-03	6-Jun-03	300	110.9	37	6.0
RB-PA	18-Jun-03	4-Jul-03	67	140.2	14	4.8

Copyright © 2005 Taylor & Francis Group plc, London, UK

c. The relatively high k_0 value (1.2) introduced as input variable to the numerical model didn't find a direct confirmation from the observed tunnel behaviour; in particular along the RB the extent of horizontal displacements has been much less than predicted.

4.3 *Construction modifications after the completion of the B-Phase excavation*

Tunnel deformation in the LB during the A-Phase excavation caused an excessive settlement of the tunnel profile and raised the issue about how to accommodate the final lining section inside the available clearance (45 cm thick, 5.50 m internal radius).

Having discarded a partial tunnel reshaping and rebuilding since before the B-Phase excavation, the only viable solutions consisted in reducing the tunnel lining inner radius and/or lowering the tunnel alignment.

The reduction of the internal tunnel radius (5.50 m to 5.25 m, which could have been viable because of the availability on site of a quickly adaptable formwork), although suitable for a considerable tunnel stretch wouldn't be adoptable for the more critical sections (insufficient lining thickness).

The modification of the tunnel alignment to a maximum value of 30 cm was accepted and actually implemented. As a consequence, this entailed some modifications of the final lining sidewalls geometry to be introduced in order to properly accommodate the lateral drainage system.

The proposed design solution consisted of a geometrical and structural reshaping of the connection between the invert arch and sidewalls, that eventually was modified from linear to curved.

A similar modification had to be introduced for the formwork; this was carried out with little effort because the formwork itself allowed such adaptation.

Table 4.2a. RIGHT BORE – End of RB bench excavation (displacements in mm).

	PL4	PL1	PL2	PL3	PL5
Monitoring[(1)]					
Horizontal	11	10	5	24	18
Vertical	11	23	16	29	14
FEM Analysis					
Horizontal	105	15	0	23	90
Vertical	20	30	20	30	20

Table 4.2b. LEFT BORE – End of LB bench excavation, final step (displacements in mm).

	PL4	PL1	PL2	PL3	PL5
Monitoring[(1)]					
Horizontal	4	8	0	7	5
Vertical	5	17	16	21	5
FEM Analysis					
Horizontal	15	0	0	8	30
Vertical	0	0	20	10	0

[(1)]Cfr. Fig. 3.5 for plots location.

5 CONCLUDING REMARKS

Difficult tunneling conditions were encountered during the construction of the Driskos tunnel (Egnatia Odos Motorway); to overcome them an experienced design team made up of Geodata SpA and Odotechniki Ltd. was appointed which successfully adopted a flexible design approach.

The systematic application of the observational method once more can be considered as the most effective and reliable approach when dealing with challenging underground environments.

The continuous feedback among the main conceptual components of the method (i.e. Predictions-Controls-Countermeasures), where contractually allowed, provides an effective problem-solving and decision-making process, which is of paramount importance when a Project is subject to relevant risks of cost overruns and/or disruptive schedule delays.

This is of great help to the Client side because it effectively contributes to maintain the potential for (additional) claims within acceptable limits; on the other hand also the Contractor side is benefited because construction optimization solutions can be evaluated quickly and, more importantly, on the base of factual evidences that come from direct observations.

ACKNOWLEDGEMENTS

Authors acknowledge the Egnatia Odos A.E. General Management for the permission to publish the paper, the Egnatia Odos A.E. technical staff, the Construction Management and Contractors personnel for the collaborative and open-minded environment experienced during the authors' on-site stay period.

C. Seferoglou and colleagues (Odotechniki Ltd., Athens) are also gratefully acknowledged for the fruitful and stimulating collaboration.

REFERENCES

A.G.I. (Italian Geotechnical Association, 1979) "*Some Italian experiences on the characterization of structural complex formations*" – Proc. of Intern. Congress on Rock Mechanics, Montreaux, vol. I, pp 827–846.

Copyright © 2005 Taylor & Francis Group plc, London, UK

Bock H. (2000) "*European Practice in Performance Monitoring for Tunnel Design Verification*" – Tunnel & Tunnelling International, July (part 1) and September (part 2) issues.

Egnatia Odos AE – O.S.M.E.O. – Tunnel Design (Internal Document) (2003) "*Potential Tunnelling Problems in Heterogeneous Rock Masses*".

Marinos P. and Hoek E. (2002) "*GSI: A Geologically Friendly Tool for Rock Mass Strength Estimation*" –

Hoek E., Kaiser P.K. and Bawden W.F. (1995) "*Support of Underground Excavation in Hard Rock*" – A.A. Balkema, Rotterdam.

Hoek E. and Brown E.T., (1980) "*Underground Excavations in Rock*" – The Institution of Mining and Metallurgy, London, p. 527.

Russo G., Kalamaras G.S. and Grasso P. (1998) "*A discussion on the concepts of geomechanical classes, behavior categories and technical classes for an underground project*" – Gallerie e grandi opere sotterranee, No. 54, pp. 40–51.

Copyright © 2005 Taylor & Francis Group plc, London, UK

Ground freezing improvement for TBM maintenance in Singapore

Jhun Itoh, Yang-Soo Lee, Su-Wan Yoo & Seung-Do Lee
Samsung Engineering & Construction, Korea

ABSTRACT: Authors have constructed sewerage project DTSS (Deep Tunnel Sewerage System) in Singapore. For the maintenance of face and bulkhead of TBM, the space in the front of the machine needed to be established. The object ground is composed of marine clay, silty sand, sandy silt with N values from 0 to 10 indicating very weak ground. The soil improvement was indispensable in order for safe working conditions underground. It was decided that the ground improvement by chemical and jet grouting was not feasible from the results of laboratory tests. Although authors noticed that the freezing method adopted in the joint of Tokyo Trans Bay Tunnel, the average annual temperature in Singapore is higher than that of Tokyo at above 25°C, giving rise to thermal problems, such as frost temperature and pitch of lance. This paper describes the design and application of the freezing method under the high temperature condition.

1 INTRODUCTION

In general, ground freezing methods are practicable if the natural moisture content of the ground exceeds 10%. Both fault and marine clay material in Singapore satisfy this requirement. Frost heave may occur in some soils due to freezing, depending on the permeability and in-situ stress. The conversion of pore water to ice and migration of the pore water to the freezing front may cause such heaves. However, if the soil drains at the same rate as the progress of the freezing front, expansion does not occur.

Clean, uniform sand and gravel are not susceptible to frost expansion. Significant expansion is possible in silts and clays (applying intermittent refrigeration during maintenance stage can minimize that expansion). Further causes of movements are a consequence of stress relaxation upon excavation and finally of thaw consolidation. In the climate conditions of Singapore, however, the measure is not recommended due to high temperature (the ground has an average temperature of above 25°C) and also the lack of local experience.

The reason of adopting ground freezing method at the site in the underground condition of the current location is that the TBM is not stable and not safe enough to carry out the regular maintenance of TBM and minor repair works without ground stabilization based on the additional soil investigation and analysis of boring data. The ground surrounding TBM is high permeability clay which is difficult for grouting. Also jet grouting is difficult to be used considering the swelling of ground.

It was decided to adopt a ground freezing method among the various options of ground improvement methods for stabilizing the tunnel face. The purpose of the ground freezing is to stabilize water earing/mixed face ground by freezing the underground water in front of TBM cutter head for the regular maintenance of the machine, such as replacement of cutter bits and minor repair works.

2 OUTLINE OF GEOLOGY

The formation is named after its extensive occurrence in the Kallang river basin. The Kallang formation covers a large portion of the total surface of Singapore, especially eastern part of the island. Five members are recognized within the formation, and these are referred to informally the marine member, alluvial member, littoral member, transitional member and reef member. The young sediments of marine alluvial, littoral and estuarine origin are generally loose or very soft in consistency and have often given rise to difficulties in foundation and excavation. The marine member is most critical due to its extensive occurrence in thick layers (Fig. 1).

Weathering results in softening of the upper section showing its color from bluish-greenish grey (when fresh) to yellowish, reddish, grayish brown (when weathered). The formation is described as being poorly lithified and very dense. Local zones of cementation were observed, but it usually disintegrated after few days of exposure. In order to delineate the various

Copyright © 2005 Taylor & Francis Group plc, London, UK

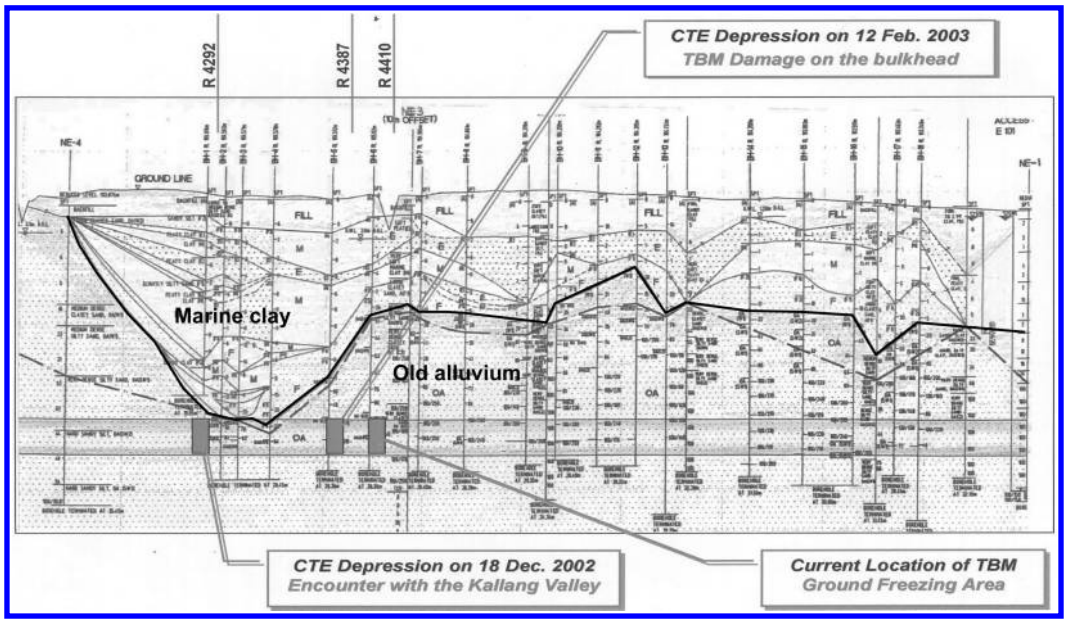


Figure 1. Cross-section view of the geological features.

weathering zones, they were categorized into three groups based on the SPT value as follows.

- HWOA: $N < 30$; Highly weathered, uncemented old alluvium
- WOA: $30 \leqslant N < 80$; Completely to slightly weathered, uncemented old alluvium
- OA: $80 \leqslant N$; Not weathered, light cemented old alluvium

Particle size distribution from large number of samples has been taken from the old alluvium along the existing MRT (Mass Rapid Transit) line from Kallang River to bedrock. The data show that the soil, in general, consists of both clayey and sandy textured soil and 62% of the sample is predominantly cohesionless soil of clayey sand texture. The remainder 38% is cohesive soil of clayey silt or silty clay of typically medium plasticity. A cross-section profile shows typical morphological features identified in the old alluvium. It was also reported that there is strong evidence of overconsolidation in the old alluvium, with the overconsolidation ratios from four to five.

3 OUTLINE OF PROJECT (DTSS)

3.1 *Tunneling system*

In Deep Tunnel Sewerage System (DTSS) contract, the distance of T04 Ang Mo Kio tunnel is 7.3 km and its diameter is 5.3 m excavated by shield TBM which crosses Singapore from north to south. The purpose of the tunnel projects is construction of the sewerage which is one of the sanitary facilities in Singapore. The total length of DTSS is 48.1 km and construction section is divided into six, T01 to T06 (Fig. 2).

The outer diameter of the tunnel is 5.2 m, and the inner diameter is 4.3 m. Initial ground support is pre-cast segment (t = 225 mm), and final support is concrete lining (t = 225 mm) with membrane (t = 2.5 mm). The tunnel has been excavated by earth pressure balance (EPB) shield TBM, and the tunnel system is shown in Figures 3–5.

3.2 *TBM tunneling status*

Manufacturing of TBM started in Kobe, Japan on May 2000, and arrived in Singapore on January 29th 2001. Excavation of tunnel was 6,615 m (4,410 segment rings) as of July 2003.

The repair such as exchange of cutter bits was needed at the point of 667 m of the remaining excavation. The damage on TBM occurred for the first time at the depression by the CTE (CenTral Express) side. The damage on TBM at this time was worn-out of bulkhead. The temporary restoration of TBM was made to move ahead 30 m in old alluvium section, because the geology of this point existed marine clay in the tunnel upper part and was unstable ground condition. TBM tunnel status is summarized in Table 1, and the performance of TBM by July 2003 is listed as follows.

Copyright © 2005 Taylor & Francis Group plc, London, UK

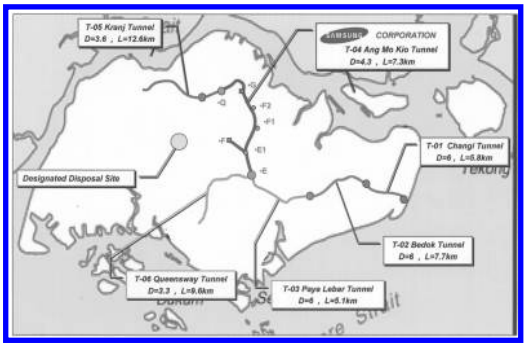


Figure 2. Location of the project.

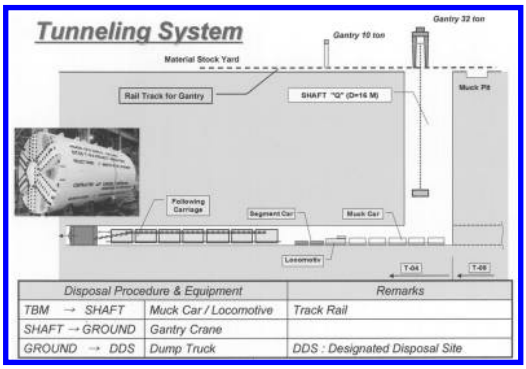


Figure 3. Tunneling system.

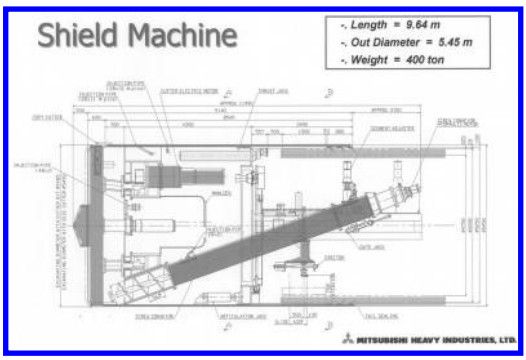


Figure 4. Shield Machine.

- Distance of excavation : 6,615 m
- Period taken : 29 months
- Monthly average : 228 m
- Best monthly record : 478 m
- Monthly average of 2001 : 252 m
- Monthly average of 2002 : 305 m
- Monthly average of 2003 : 25 m

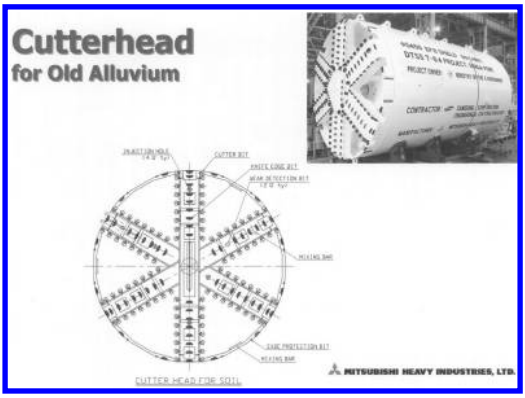


Figure 5. Cutter head for Old Alluvium.

Table 1. Summary of TBM tunneling status.

Description	Date	Remarks
TBM manufacturing	May∼Nov 2000	6 months
TBM delivery	1 month	from Japan (Kobe)
Launching	29 Jan. 2001	
Tunnel excavation	as of July 2003	6,615 m (4,410 rings)
Remained length of Tunnel	as of July 2003	657 m (438 rings)
TBM damage on bulkhead	12 Feb. 2003	Depression on CTE
TBM rescue & repair	Mar.∼Apr. 2003	Tunnel restoration
Ground freezing	May∼June 2003	Hoek loss + Linde gas
Expected completion	39 Sep. 2003	

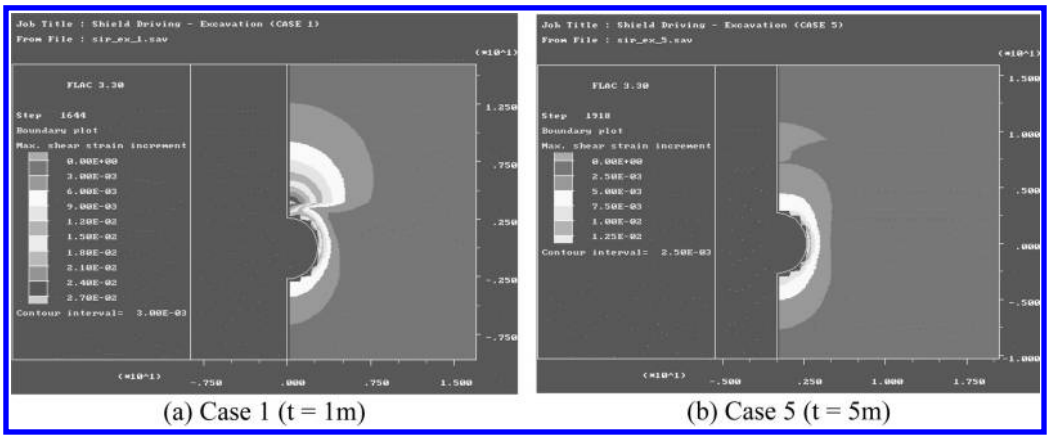
4 DESIGN OF THE FREEZING METHOD

4.1 *Selection of freezing method*

TBM moved up to the point where old alluvium (comparatively strong ground) exists, furthermore small cavern for repair needed to be built in front of TBM face. About the position by which ground is stabilized, TBM passed through the valley of marine clay; old alluvium layer of the securable position is over 5 m. Based on numerical analyses for the maximum shear strain (Fig. 6), the thickness of old alluvium was determined for TBM stabilization. The numerical modeling had done for five cases based on the thickness of old alluvium as follows.

- Case 1: 1 m of old alluvium
- Case 2: 2 m of old alluvium
- Case 3: 3 m of old alluvium

Copyright © 2005 Taylor & Francis Group plc, London, UK



(a) Case 1 (t = 1m) (b) Case 5 (t = 5m)

Figure 6. Maximum shear strain for thickness of old alluvium.

Table 2. Methods of ground improvement.

Description	Deep well	Permeation grouting	Jet grouting	Ground freezing
Strong points	Most economic Easy & fast Success in Singapore (DTSS T05) Least drilling holes	Familiar & well-known Immediately mobilized Experienced sub-contractor in Singapore	Familiar & well-known Immediately mobilized Stronger support than permeation grouting Experienced sub-cont in Singapore	Easy to get approval Success cases in Singapore (DTSS T05) High percentage of success in the 1st trial Less drilling holes (<grout).
Weak points	High risk of settlement Difficult to get approval High risk of failure Grout may not be stable after dewatering No experience Not to mobilize at once Field test required	Not able to estimate exact quality of grout Difficult to select optimum material & method Grout may affect TBM restart Failed cases in Singapore Low percentage of success in the 1st trial Not easy to get approval	Not able to estimate exact quality of grout Less drilling holes (<permeation grouting) Low percentage of success in the 1st trial Accuracy of drilling is essential Not easy to get approval	Impossible to remove freezing pipes after completion Complicated system of freezing & pipe installation Expensive copper pipes No experience Proper access for liquid nitrogen tank & tank lorry Accuracy of drilling is essential
Drilling	# of hole: 10~20 Required period: 2~3 weeks	# of hole: 120 (approx.) Required period: 6~8 weeks	# of hole: 100 (approx.) Required period: 6~8 weeks	# of holes: 30~40 Required period: 2~3 weeks
Estimated period	6~8 weeks	12 weeks	12 weeks	6~8 weeks
Estimated amount	SGD 300,000~ SGD 400,000	SGD 550,000~ SGD 1,000,000	SGD 550,000~ SGD 600,000	SGD 550,000~ SGD 600,000

– Case 4: 4 m of old alluvium
– Case 5: 5 m of old alluvium

Also, the ground improvement needed to be carried out so that work could be safe in the cavern. Four methods of ground improvement (deep well, permeation grouting, jet grouting, ground freezing) were given to the candidate, and their brief descriptions of four methods are summarized in Table 2.

Copyright © 2005 Taylor & Francis Group plc, London, UK

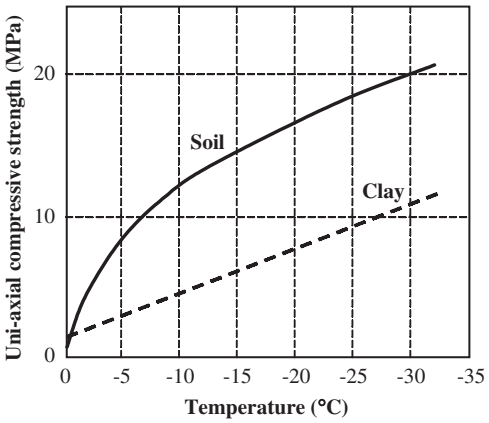


Figure 7. The relationship between uniaxial compressive strength and temperature of frozen soils (Takashi et al. 1981).

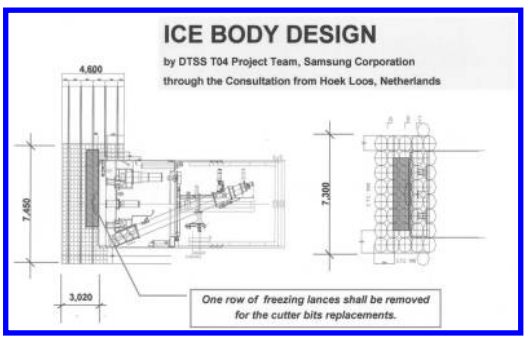


Figure 8. Design of the ice body.

4.2 *Design*

The pitch of the freezing lance (pipe) was calculated by adopting an analytic method (Carslaw & Jaeger 1959). Frost temperature and freezing period were designed by an experimental graph. Making the necessary foundation strength to be 1.5~2.0 MPa, the freezing temperature was decided to be − 20°C from the relation between uniaxial compressive strength and temperature of frozen soils. (Fig. 7).

Hence, the design of freezing method has been decided as follows (Figs 8 & 9).

- Uniaxial strength of ice body : 1.5~2.0 MPa
- Liquid Nitrogen : −196°C
- Frost temperature : −20°C
- Pitch of lance : 0.9 m × 0.9 m

4.3 *Numerical analyses*

In order to examine the temperature distribution caused by ground freezing and its effect on ground

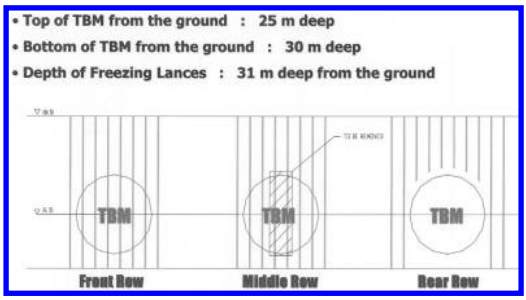


Figure 9. Front view of freezing lances.

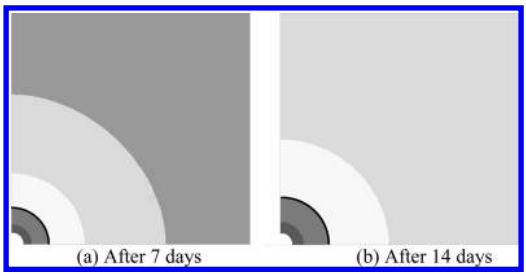


Figure 10. Temperature distribution for single lance.

improvement, numerical analyses have been performed by using a finite difference method (Cundall 1995).

4.3.1 *Thermal analyses*

The basic law defining the relation between the heat-flux vector and the temperature gradient is Fourier's law. This constitutive law for a stationary, homogeneous, isotropic solid is expressed as follows:

$$q_i = -k_{ij} T_{,j} . \tag{1}$$

where T is the temperature, k is the thermal conductivity tensor, and the comma indicates derivative.

For thermal analyses, thermal conductivity and convection heat transfer become important parameters. Here, thermal properties of DTSS site have been determined from a back analysis. Also, the initial and freezing temperatures were set to 25°C and − 25°C, respectively.

For single lance layout, temperature distribution shows that hear transfers in a radial fashion, in which a thick line indicates freezing boundary, a line of 0°C (Fig. 10). For double lance layout where lance spacing is 90 cm, it important to notice that the freezing boundary becomes much wider, and freezing bulk is generated after two weeks (Fig. 11).

4.3.2 *Mechanical analyses*

In order for examining the effect of ground freezing on tunnel stability, numerical analyses for tunnel

Copyright © 2005 Taylor & Francis Group plc, London, UK

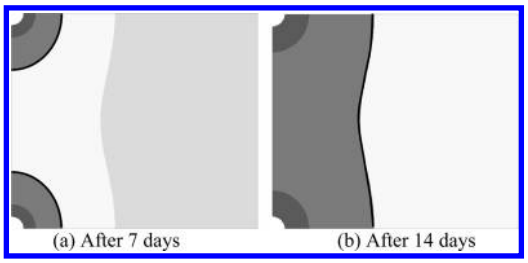


Figure 11. Temperature distribution for double lances.

Table 3. Mechanical properties of the ground freezing region.

	Marine clay	Old alluvium
E (MPa)	5.6 (500*)	20.2
ν	0.5	0.5
γ (ton/m^3)	1.65	1.85
ϕ (°)	20	35
c (MPa)	0.00	0.21

* Enhanced values after ground freezing.

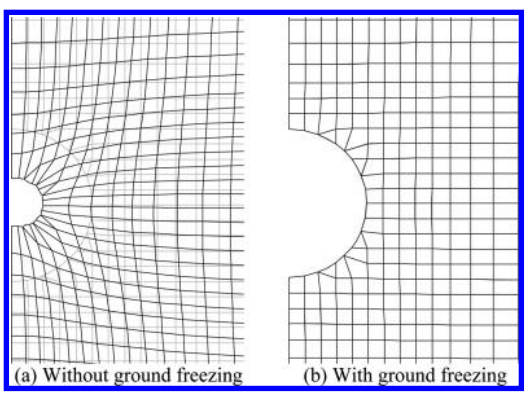


Figure 12. Deformation of the tunnel.

excavation have been performed without and with considering ground freezing. Mechanical properties are shown in Table 3, in which Young's modulus after ground freezing has been determined from the relation between uniaxial compressive strength and frozen soil temperature (Fig. 7), and the relation between Young's modulus and uniaxial compressive strength.

Figure 12 shows the result of numerical analyses for tunnel excavation. As can be seen, tunnel deformation with ground freezing (0.2 mm) is much lower than that without ground freezing (71.9 mm).

Based on the design procedure mentioned so far, the following construction steps have been performed.

– Installing the freeze lances
– Installing all pipe work
– Installing all measurement equipment and controlling equipment
– System test
– Freezing
– Maintaining the freeze
– Stop freezing
– Rigging down

5 CONCLUSION

The freezing method was successfully applied in Singapore of annual temperature of above 25°C so that the repair works for face and bulkhead of TBM were safely performed. During and after the construction, the following items were taken into account and the construction was completed.

1. Pitch of lances
   – The effective diameter of ice body was measured with 0.7 m∼1.0 m.
   – The uniaxial compressive strength of frozen ground without groundwater was over 2.0 MP.
2. The effect of difference between permeable and impermeable layers.
   – The ground was perfectly frozen without groundwater, but it was not frozen by the groundwater on the tunnel face where two ways of groundwater were observed.
   – The groundwater, which seemed to flow along the boundary between permeable and impermeable layers, was kept while it was not frozen.
3. The freezing situation between soil and the attachment part of skin plate of TBM
   – The situation of skin plate and frozen state of attachment part in the ground without the way of groundwater were good.
   – The soil was stiff when the part of cutter head was frozen, which must be melted by the water applying in the long term.

REFERENCES

Carslaw, H.S. & Jaeger, J.C. 1959. *Conduction of heat in solids*. Oxford.

Cudall, P.A. 1995. *FLAC User's Manual*. Itasca Consulting Group.

Takashi, T. Ohrai, T. Yamamoto, H. & Okamoto, J. 1981. Experimental study of uniaxial compressive strength of homogeneously frozen clay. *Japanese Society of Civil Engineering* 315: 83–93. (Japanese)

Copyright © 2005 Taylor & Francis Group plc, London, UK

High pressure jet grouting in tunnels – a case study

A. Da Vià[1], M. Marotta[1] & G. Peach[2]
[1]*ITAI Engineering & Construction Co.*
[2]*Independent Tunnelling Consultant*

ABSTRACT: Using the authors experience gained on design and construction management on one particularly difficult NATM tunnel located in Taiwan this paper reviews by way of two collapses how high pressure jet grouting (400 bars) was successful and efficient implemented, with benefits for both client and contractor. The paper will discuss two collapses case studies. These collapses occurred in the Top Heading of a 120 m^2 tunnel being excavated by NATM. The first collapse was 90 m and the second collapse was 290 m in length. In both cases the tunnel were completely blocked, and the collapse extended up to the surface. This paper will detail how high pressure jet grouting was decided upon as the preferred recovery methodology and the management process that was adopted in order to fast tract the jet grouting design. The details of the surface trials will be covered and the configuration of the vertical and horizontal jet grouted columns will be explained in detail. The plant requirements will be covered including the additional plant required and the modifications that were carried out to the existing site plant. This was all carried out within an extremely tight construction programme. This paper will explain the programme arrangements planned and then in detail discuss the as built performance giving the details of times for design, mobilization, cycle time per canopy, along with all the time performance data for the individual jet grouting elements employed with the jet grouting option. The instrumentation requirements will be explained and the field data recovered with be discussed and lesson learnt covered.

1 INTRODUCTION

1.1 *Hukou tunnel north*

The Hukou tunnel is part of the 345 km Taiwan High Speed Railway, a US$ 15 billion project, under BOT model, running from Taiwan's capital, Taipei, to the second major city, Kaoshiung located in the south of Taiwan. Operational services are scheduled for October 2005.

Civil works have been constructed by 12 major Joint Ventures, for a total of 39 km of mined tunnels, 8 km of Cut & Cover tunnels, 251 km of viaduct and bridges, and 31 km of Cut & Fill embankments.

For tunnels, the necessity of double track required the excavation section of approximately 110∼120 m^2, in order to guaranty a finished tunnel cross section of minima of 90 m^2 in accordance to aerodynamic requirements associated with the high-speed train velocity of 300 km/h.

NATM has been the main excavation methodology.

The Hukou tunnel, with a total length of 4.3 km, is the third longest tunnel, after the Paghuashan tunnel (7.4 km) and the Linkou tunnel (6.4 km), and is considered as one of the most difficult tunnels on the project. It includes 2 Emergency exits (Adit A and B). This paper will review the collapse that occurred in the Northern section of Hukou tunnel.

1.2 *Geology of Hukou tunnel north*

The Hukou Tunnel alignment cuts through the Hukou terrace in unconsolidated, un-lithified sedimentary materials, dated as Pleistocene.

The Tientzuhu Formation, mostly encountered at North portal section, consists of a poorly graded gravel bed and with sandy and silty lenses, ranging from a few meters to 30 m in thickness.

The Yangmei formation is mainly composed of alternating silty clay and silty sand, with an estimated thickness of 900 m and underlies the whole area traversed by Hukou tunnel.

Three major fault structures were encountered during the excavation of the northern Tunnel section and three collapses have occurred within the vicinities of these three geological structures. The three faults arranged according to the sequence encountered during the excavation are (1) Adit-A, (2) Yanghsiwo, and (3) S-1032 faults.

Copyright © 2005 Taylor & Francis Group plc, London, UK

Table 1. Homogeneous hydro geological zones.

Zones	Zone limits From	To	Remarks
Zone I	64 + 200	64 + 402	Low water table
Zone II	64 + 402	66 + 000	High water table
Zone III	66 + 000	66 + 200	Low water table

1.3 *Hydro geological conditions*

Hydro geological conditions along the Hukou Tunnel North alignment generally were determined by geological structures. The Yanghsiwo Fault in the north and S-0132 fault in the south play the role of impermeable barriers for inclined water-bearing sandy layers and divide the area in to three main zones:

First and third zone initially had low water level providing dry conditions to the excavation while in the central portion the original groundwater level was close to the ground surface and several aquifers with different hydraulic heads were crossed by tunnel excavation.

A total of 224 deep wells from the surface, with diameters of 300–350 mm, drilled to a depth 20–25 m below the tunnel invert with a 3–5 hp pump, were constructed from both sides of tunnel alignment at an offset of 10–15 m from centerline.

Total pumped water quantity reached the volume of 4,718,743 m^3 by June 2004.

Distance between wells varies from 25 m to 15 m for these areas, with high critically permeability and water accumulation due to fault barrier, located at the borders of the Zone II.

1.4 *Possible effects of dewatering on collapses*

The Zone II mainly consists of alternate sandy layers (aquifer) and less permeable beds, but permeable enough to transmit water, similar to silty-clay layers (aquitard). Prior to any dewatering, an internal equilibrium between the "wet" and "dry" side of each fault was in place. Dewatering causes a compression of the aquifer system, where the support previously provided by the pore fluid is transferred to the granular structure.

When the load of the granular structure remains less then any previous maximum load (pre-consolidation stress), dewatering creates only a small elastic deformation of the aquifer system with a small displacement at the surface.

Long term pumping raises the stress on the aquitard's beyond the maximum pre-consolidation stress, the aquitard compact in an irreversible mode.

The dewatering was carried out only on the "wet" side of each fault for a period long enough to cause a migration of the internal stress on the aquitard's. As more fluid is squeezed from the interior of the aquitard, larger internal stress propagates into the aquitard, until a point where the internal stress exceeds the pre-consolidation stress and the compressibility dramatically increases.

This could have caused an interruption of the internal stress equilibrium between the wet and dry side of each faults.

For the South Collapse area, deformation monitoring carried out during construction did not show any significant alarm values until a few hours before the collapse occurred. This could be because of the nature of the clayey soil surrounding the tunnel being able to suddenly release the stress.

2 COLLAPSES

2.1 *Introduction*

During the construction of the Hukou tunnel, three collapses occurred.

A first minor collapse happened during the excavation of the Adit A (emergency exit tunnel), while approaching the main tunnel alignment.

The major two collapses (named North and South in relation to their position from the Adit) both occurred nearby the two previously described faults.

2.1.1 *North collapse*

North collapses occurred at chainage 64 + 520 on 2nd Aug. 2002 (nearby the southern "wet" side of the Yanghsiwo fault) when top heading had already holed through, and during bench excavation with permanent invert concrete just 10 m behind and with temporary ring closure of the heading in front assured by a structural temporary invert shotcrete. During collapse the ground surfaces (overburden 60 m) sank and a crater, with diameter of 16 m by 9 m depth, was clearly visible.

The collapsed area covered a total length of approximately 90 m with a total volume of collapsed soil estimated as 7000 m^3. Visible cracks occurred in inner lining, showing a total collapse-affected area of approximately 180 m.

2.1.2 *South collapse*

South collapse started on 31st October 2002 whilst top heading excavation was ongoing, with cracking and stripping of shotcrete, nearly 50 m behind the face. Collapse itself started at chainage 66 + 012, approximately where the S-1032 fault intersect the tunnel at the East side around 80 m behind the face, and developed by a domino effect until the 3rd November 2002, with a total of 14.000 m^3 of material entering the

Copyright © 2005 Taylor & Francis Group plc, London, UK

tunnel. Emergency measures including reinforcing rings, timber props and an air mortar backfilled bulkhead stopped the advance of the collapse some 271 m from the original tunnel face.

Affected area was however judged as far as 350 m beyond the collapsed area, as settlements of 40 mm were measured in the area between the already executed invert concrete and the top heading. Installation of additional rings and timber supports was performed immediately, stopping the ongoing deformations.

2.2 *Loss mitigation work*

For both collapses a similar approach was taken in order to stop further failures, consisting in the backfilling of surface craters, in the installation of additional support rings and in the strengthening by means of cement grout through self-drilling bolts, in the affected areas.

2.3 *Preliminary void filling*

Initially for the north collapse, pressure grouting from surface was planned in order to fill voids and for improve soil characteristics in the surrounding of the area to be re-excavated.

However, the result of the site investigation showed a limited efficiency of this methodology for the actual site conditions, caused by leaking from inside the tunnel and by the impossibility to recover consolidate sand samples. Therefore initial plan was reduced and grouting from surface considered for void filling only; same principle was applied to second south collapse.

2.4 *Redesign of supports*

2.4.1 *North collapse*

Redesign finalized two support classes, for re-profiling (RD-2) and for re-excavation in full collapsed area (RD-1 ref. Figure 1)

New designed support classes, differs from the originals by the use of H beam instead of lattice girders, the increased thickness of inner lining, the use of high strength shotcrete, the removal of rock bolting and the introduction of jet grouting technology as main consolidation/support element.

2.4.2 *South collapse*

New designed supports for south collapse applied the same principles already adopted for the north collapse redesign, but dimensioned bigger due to, more critical collapse distance and higher overburden. Six to nine meters rock bolts were included on the tunnel shoulders.

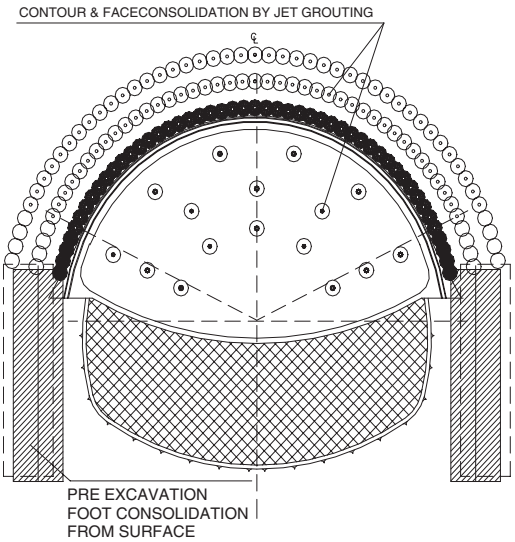


Figure 1. RD1 jet grouting consolidation scheme.

For both collapses the reinstatement of dewatering system by wells was mandatory prior to re-excavation commencement.

2.5 *Introduction to jet grouting methodology*

Considering the nature of a collapsed area, and the result of the site investigation, it was necessary to choose and design a consolidation system able to:

- Guaranty a certain geometrical accuracy of the treatment area.
- Fit different ground conditions
- Avoid impact on the dewatering system
- Be easily estimated in term of execution time, material consumption and costs.
- Use existing plant wherever possible.
- Be verified in field trials before implementation.
- Be robust and flexible.

High pressure jet grouting was judged as the most feasible technology able to fit the listed requirements.

In the jet grouting methodology, first a borehole, drilled up to the desired depth, is carried out with a rotary drilling machine with the end element of the drilling rod provided of both cutting tools and nozzle for injection.

At the completion of the drilling the treatment is then executed by gradual withdrawal of the rod with controlled step time, and at same time, by the rotation of the rod and the attached head with nozzle that radialy jets the cement slurry in to the soil with high energy and impact (400 bar), mixing it with injected

Copyright © 2005 Taylor & Francis Group plc, London, UK

material and creating a solid cement column. The volume of treated soil can vary in accordance to the speed of rotation, the number and diameter of the nozzles, and the pressure of injection. Those parameters are defined at first by site trials.

Jet grouting effectiveness changes in accordance with the soil characteristics. Its efficiency increases from cohesive to un-cohesive soils (typically the circumstances occurring in a collapsed area).

Therefore the jet-grouting technique is more efficient exactly where is more necessary to execute soil improvement.

It should be noted that execution of jet grouting did not affect the dewatering system during the two collapses reconstruction work.

2.5.1 *Details of arch canopy and face consolidation*

The redesign proposed a ground treatment by means a reinforced jet-grouting canopy, able to create an artificial arch to contain the area to be excavated.

The columns reinforcement by grouted steel pipes gives continuity to the structure in materials where jet grouting is less efficient. The flexibility of this methodology is mostly in creating a double structure: an arch structure guaranteed by the longitudinal co-penetration of the columns, and a longitudinal beam structure given by the steel pipes.

Face consolidation by mean of horizontal jet grouting columns reinforced with fiberglass rods was designed in order to limit a possible face extrusion and with the purpose to reduce the pre-convergences ahead of the face and avoid further failures.

Fiberglass rod, as column reinforcement, provides the same continuity as the steel pipe in the arch canopy; however the nature of fiberglass material (high tensile strength and low shear strength) allows an easy cutting by mining equipment while excavation proceeds.

Design parameters are showed in Table 2 & 3.

2.5.2 *Details of foot consolidation*

Jet grouting arch canopy itself could act as a load if poor bearing capacity of the soil occurs at the top

Table 2. Jet Grouting parameters for canopy and face consolidation.

Parameters	Value	Unit measure
Expected column diameter	600	mm
Pressure of injection	400	ba
Flow of injection	3–10	m^3/h
Speed of raising rod	24–48	cm/min
Speed of rotation	8–15	RPM
Nozzle numbers	1	set
Nozzle diameter	2.2–3.8	mm

Table 3. Crown/face consolidation – North & South Collapses.

Class	North	South
Crown protection canopy	Jet grouting	Jet grouting
Type	Sub-horiz.	Sub-horiz.
Execution from	Tunnel	Tunnel
Module length (m)	5–7*	7
Number of columns per module	48	48
Expected column dia. (mm)	600	600
Columns length (m)	15	15
Overlap (m)	8–10*	8
Overlap (numbers of)	2–3*	2
Face consolidation	Jet grouting	Jet grouting
Execution from	Tunnel	Tunnel
Excavation module length (m)	10	7
Number of columns per module	16–20	20–35
Expected column dia. (mm)	600	600
Columns length (m)	15	15
Overlap (m)	5	8

* First and second values are related to Re-excavation (RD-1) and Re-profiling (RD-2) classes.

Table 4. Jet grouting parameters for vertical columns from surface.

Parameters	Value	Unit Measure
Expected column diameter	2000	mm
Pressure of injection (air)	20–25	bar
Pressure of injection (cement)	450	bar
Flow of injection (air) (×1000)	10–15	l/min
Flow of injection (cement)	150–190	l/min
Speed of raising rod	6–12	cm/min
Speed of rotation	10–15	RPM
Nozzle numbers	1	set
Nozzle diameter	2.2–3.8	mm

Table 5. Foot consolidation for North & South Collapses.

Class	North	South
Foot consolidation	Jet grouting	Jet grouting
Type	Vertical	Vertical
Execution from	Surface	Surface
Execution prior to	Heading	Heading
Expected column dia (mm)	2000	2000
Column length (m)	8.00	10.00
Columns spacing (m)	1.50	1.50

Copyright © 2005 Taylor & Francis Group plc, London, UK

heading foundation. For this reason it was necessary for pre-excavation foot consolidation methodology to be adopted this enables transfer of the load into depth. The full collapse area disturbed soil is below the top heading foot, sub-horizontal columns, executed from tunnel below the heading, were not judged as sufficient and excluded because of the difficulty of drilling at the optimum angle. The time taken to drill these sub-horizontal columns would greatly impact upon the cycle/programme time.

Bi fluid technology was then applied in order to install large diameter vertical columns from the surface with sufficient bearing capacity. In each of the collapses world record depths were achieved.

In the bi-fluid system, the shearing action is accomplished by the high-pressure injection of cement slurry controlled by a ring of compressed air at approximately 20 to 25 bars. It reduces the dispersion of the cement slurry, and thus increases the penetration action, permitting the execution of larger diameter columns (up to 2 m in diameter)

For the previously described jet grouting process it was decided to execute the pre-drilling, the jetting rod installation, and the jet grouting operation with separate plant in order to speed up the cycle time.

The temporary filling of the pre-drilled holes, by bentonite-cement slurry, solved the problem of keeping their medium term integrity.

In additional the execution of a pre-drilling provided a chance to check, by inclinometer instrumentation, the actual deflection from theoretical vertical axis of each drilling. Actual average deviation on North collapse has been 0.29% corresponding to 17 cm at 58 m depths, with a maximum deviation of 0.74%, within the required specifications (less then 1%).

The section applied for south collapse re-excavation consisted in a double canopy jet grouting, 15 m in length for 7 m excavation. The layout, including vertical column from surface, differs from the one applied for north collapse mainly for the elevation of the vertical columns, extended at an elevation of 2 m higher then top heading foot and executed with a 90 m average overburden, this protected the sides of heading during excavation. A higher number of face jet grouting was necessary in order to stabilize the face. An average number of 36 (with a maximum of 43) fiber glass reinforced columns, 15 m in length, were performed each 7 m-excavation module, with columns pattern studied time by time in accordance to the actual face observation.

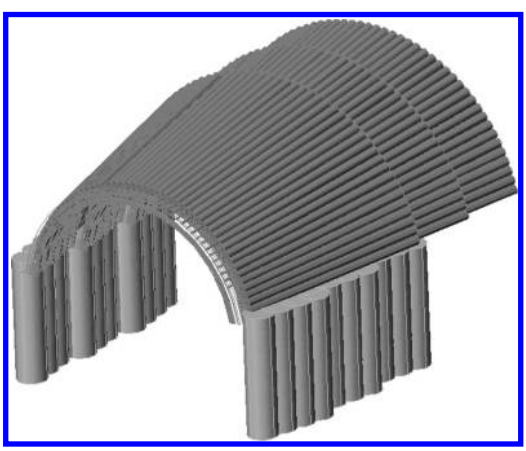


Figure 2. 3D model – RD1 Jet grouting 5 m modules.

3 DEFORMATION MONITORING

Monitoring was executed with extreme attention during the entire project.

Settlement and convergence were measured by high accuracy optical survey, with at least twice daily near the areas affected by construction activities (excavation, grouting, etc.), including surface settlement.

In additional, geotechnical instrumentation from inside the tunnel (pressure cells, Steel ribs and shotcrete strain gauges, rock bolt axial force meter), and from surface (extensometers, inclinometers), was locally utilized in accordance to special conditions, as during collapses re-excavation.

A comparison between maximum-recorded deformations is shown in Table 6.

The tunnel deformations behavior, and as a consequence allowable limits before failures, was variable in similar overburdens in accordance with the geological conditions. Settlement increased for top heading, bench, or invert in accordance to the bearing capacity of their foundation, causing rotation in case of non-homogeneous material in the tunnel sides. The allowable deformation before failure is not only depending on those factors, since the south collapse occurred in an area with low value deformations and with good geological conditions able to support an excavation rate that was for the previous 4 months over 5 m/day, including arch protection by pipe roofing.

Table 6. Maximum settlement and convergence.

Area	Stage	Max Settl. (mm)	Max Conv. (mm)
North collapse	before collapse	350	330
North collapse	re-excavation	60	40
South collapse	before collapse*	<50	40
South collapse	re-excavation	80	80

* Related to top heading only where collapse started.

Copyright © 2005 Taylor & Francis Group plc, London, UK

Table 7. Equipment and plant.

Category	Characteristics	Set	Location
Pre-drilling		1	Surface
Rod installation		1	Surface
Crane		1	Surface
Drilling/ jet grouting	2 booms	1	Tunnel
Drilling/ jet grouting	1 boom	1	Tunnel
High-pressure pump	max 400 bars	3	Surface
High-pressure pump	max 700 bars	4	Surface
Silos		2	Surface
Mixer plant		2	Surface
Agitator		2	Surface

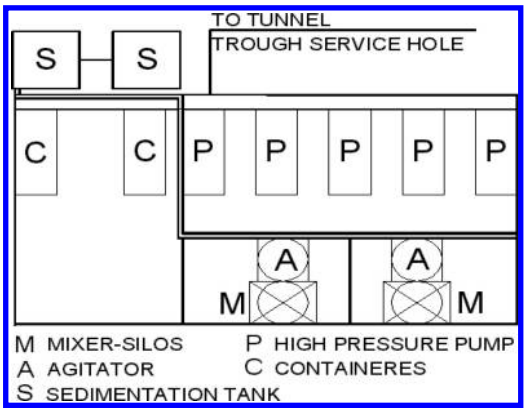


Figure 3. Collapse #2 surface plant arrangements.

Table 8. Chronology of North Collapse area (180 m).

Date	Status	Progress days
2nd Aug 2002	Collapse	0
31st Aug 2003	End of emergency measures	29
1st Oct. 2002	Start of site investigation	60
October 2002	Start re-design	
14th Jan 2003	Start excavation from S to N	165
1st Mar. 2003	Start pre-drilling from surface	211
25th Mar. 2003	Start re-profiling from N to S	235
26th July 2003	Break trough of heading	358
July 2003	End of re-design	
27th Sep. 2003	Break trough of bench	421
10th Nov. 2003	Invert concrete completion	465
11th Jan. 2004	Arch concrete completion	527

4 PLANT AND EQUIPMENT FOR JET GROUTING EXECUTION

In order to optimize the arrangement, for both collapses a single plant was installed on the surface, for the execution of jet grouting from either surface and inside tunnel. This was possible by the drilling of services holes from surface to the tunnel roof, from where high-pressure pipes, service pipes and cables were installed.

The surface arrangement frees the required space in tunnel, therefore it could be applied also to small tunnels, or where top heading is shortly followed by other excavation and/or concreting phases.

5 OVERALL PROGRAM

South collapse was the most critical in term of overall schedule.

When the collapse happened the completion of excavation was scheduled within 3 months.

At start of re-excavation the gained delay was already of over 5 months.

At completion of lining work the delay was reduced to 1fi month, and it was fully recovered by the track work execution.

Break trough of headings occurred after 358 days (north collapse) and 461 days (south collapse) respectively.

It's therefore clear how the South collapse reconstruction, extending for a length 50% higher then the north one, was positively beneficed by the first collapse experience, in term of management, design (22 months for North Collapse VS 11 months for South collapse), workmanship and plant.

Major technical improvements consisted in the use of a two booms drilling machine for the execution of the jet grouting from tunnel, in the use of an additional guide lattice girder with pre-installed steel pipe through which jet grouting drilling could be executed without penetrating the shotcrete layer, and in a systematic void filling from surface through the jet

Copyright © 2005 Taylor & Francis Group plc, London, UK

Table 9. Chronology of South Collapse area (271 m).

Date	Status	Progress days
31st Oct 2002	Collapse	0
6th Nov 2002	End of emergency measures	6
December 2002	Start of re-design	
22nd Jan 2003	O.S.C.* heading completion	83
31st Jan 2003	End of loss mitigation works	92
15th Apr 2003	Start pre-drilling from surface	166
31st May 2003	Start Jet Grouting from surface	212
25th June 2003	Start heading excavation N to S	237
19th July 2003	End of surface jet grouting	261
9th Oct 2004	Start heading excavation S to N	343
October 2004	End of re-design	
26th Dec 2003	Start bench excavation N to S	421
2nd Feb 2004	O.S.C.* for invert concrete	459
4th Feb 2004	Break trough of heading	461
8th Mar 2004	O.S.C.* for arch lining	494
9th Mar 2004	Break trough of bench	495
10th Mar 2004	Break trough of invert	496
31st Mar 2004	End of Invert Concreting	517
27th Apr 2004	End of Arch lining concrete	544

* O.S.C. as Original Schedule date of Completion.

grouting pre-drilling holes, in order to create better conditions for jet grouting execution.

6 CONCLUSIONS

6.1 *General consideration*

The great engineering and management experience gained during the Hukou tunnel construction is a good example of fully recovery of very unfavorable and unexpected conditions.

With the occurrence of two major collapses and a tight construction schedule in front, finally no delay was caused to the further line development.

The use of the Jet grouting methodology was successfully implemented from management side to construction side using the experience of all the qualified personnel involved in the project.

Effectiveness of this consolidation methodology has been confirmed, proving it as applicable even to worst soil conditions.

The possibilities of utilize existing plant, with some minor improvement, provides a fast mobilization time with benefit on the construction schedule.

A remarkable issue is that jet grouting didn't affect the dewatering pumping system, considering the small difference (∼7 m) between the alignment of the pumping wells and the one of the vertical jet grouted columns.

For future projects, a special consideration should be taken on effect of dewatering in particular geological conditions.

Effect of speed of excavation in relation to the designed type of supports should also be further analyzed.

With an optimum arrangement, the consolidation and excavation time for a 7 m module can be around 8 days, permitting an excavation progress rate greater the 26 m/month.

Use of jet grouting technology permits the development of standardized procedures, resulting in a quite constant excavation ratio, providing benefits on scheduling and cost estimations.

Copyright © 2005 Taylor & Francis Group plc, London, UK

Gotthard Base Tunnel: special aspects and state of the works

M. Rehbock-Sander & Y. Boissonnas
Amberg Engineering Ltd., Regensdorf-Watt, Switzerland

ABSTRACT: The Gotthard Base Tunnel will be the world's longest traffic tunnel, with a length of 57 km. The tunnel is part of the New Alpine Transverse in Switzerland. The dual purpose of this project is to provide a high speed link for rail passengers between Germany in northern Europe and Italy in southern Europe and to transfer freight traffic from road to rail. It represents an essential step toward actively protecting the Alps and making an important contribution to preserving the environment in general. At the present time the construction work is proceeding at both portals and at the three intermediate access points. Over 33% of the total length of the tunnels and galleries have been excavated. Some difficult parts of the of tunnel have been completed successfully, but others with over 2,000 m of overburden and poor rock mass properties remain to be excavated.

1 INTRODUCTION

The transalpine rail routes through Switzerland are more than one hundred years old. Because they no longer meet the requirements of ever-increasing rail traffic between north and south, they are now being rebuilt. The present Gotthard rail route is in fact a mountain railway: the northern and southern access ramps – with a maximum speed of 80 km/h and a maximum gradient of up to 2.2% – climbs up to about 1,100 m a.s.l. where the old Gotthard rail tunnel is located (approximately 900 m higher than the city of Milan).

The Swiss government has approved construction of two new railway axes – the Gotthard and Lötschberg axes – through the Alps.

The Gotthard Base Tunnel (GBT), the longest NEAT tunnel, is divided in five sections, the lots Erstfeld, Amsteg, Sedrun, Faido and Bodio. In order to shorten construction time and for ventilation purposes the tunnel is driven from several sites concurrently (see Fig. 1).

2004 is an important year for building the GBT: presently the construction works are proceeding at both portals (Erstfeld in the north, Bodio in the south) and at the three intermediate access points (access tunnels in Amsteg and Faido, shaft in Sedrun).

The GBT consists of two parallel single tubes that are connected by cross cuts about every 310–325 m. With a minimum radius in curves of 5000 m and a maximum gradient of 0.7%, the GBT will be the first flat railway through the Alps. The high speed passenger trains will travel at speeds of 200 km/h to 250 km/h and freight trains at speeds of 140 km/h.

The Sedrun and Faido sections each include a multifunctional station (MFS). In emergencies, the MFS's provide safe rooms for passsengers. Furthermore they include special emergency train stops (sheltered areas) that are linked by a gallery system to enable passengers to transfer from one tube to the other. They also allow trains to switch from one tube to the other by using a tunnel interchange.

Up to August 2004, about 50 km of tunnels and galleries or 33% of the entire project (153.3 km) has been excavated. Based on the progress made in the different sections, the current overall time schedule indicates that the excavation work will be finished in March 2010 and the first train will run through the GBT in April 2015.

2 GEOLOGY AND GEOLOGICAL CONDITIONS

More than 90% of the total length of the GBT passes through the three major gneiss zones Aar Massif, Gotthard Massif and the Penninic Gneiss Zone. These zones are considered essentially favourable for tunnelling, especially in view of the fact that zones with significantly high overburden consist of practically vertical layers that will be driven through perpendicularly.

Copyright © 2005 Taylor & Francis Group plc, London, UK

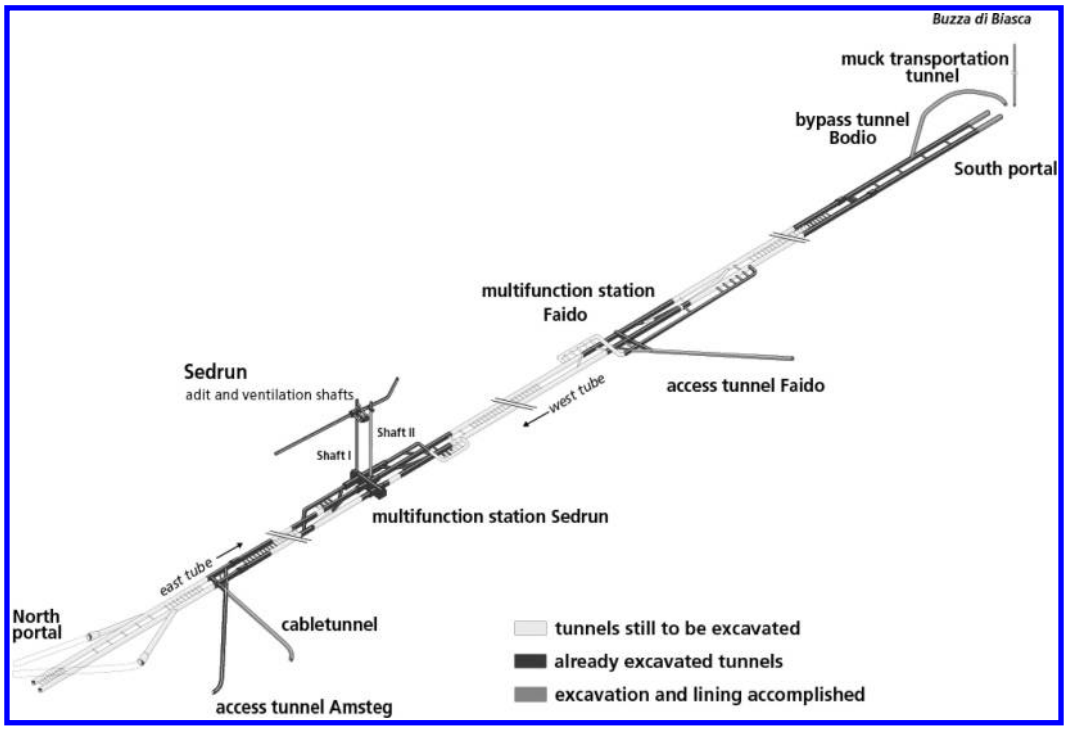


Figure 1. Gotthard Base Tunnel, status of construction, July 2004.

Most of the GBT will have an extremely high overburden: more than 1000 m for roughly 30 km, more than 1500 m over 20 km, and it can even be more than 2000 m for approximately 5 km. The maximum overburden is about 2300 m.

Technically difficult sections will be encountered beneath the fault zones in the aforementioned Massifs, in the Tavetsch Intermediate Massif (TZM), in the Urseren Gavera Zone and in the Piora Basin. Geological investigations were conducted in the Piora Basin from 1993 to 1997 and in the TZM from 1991 to 1998.

The Piora Basin is a zone of sedimentary rock. The investigation scheme consists mainly of an investigation tunnel located 350 m above the base tunnel level. At this level, the structure and the thickness of the basin were examined by means of exploratory drillings. These revealed very poor rock quality with differing proportions of sugar-grain dolomite and water pressure as high as 130 bar. Inclined preventer-protected exploratory bores of over 1000 m length fortunately showed that at base tunnel level the Piora basin consists of stable dolomite marble or dolomite anhydrite. No water was found in any of the bores.

The TZM was also explored. All drill-cores attested the very poor quality of the rock in the TZM, consisting of highly fractured phyllites, shales and metamorphic gneisses. The geological prediction indicates that extreme squeezing behaviour can be expected. Hence the TZM North in the Sedrun section is the geotechnically most difficult part of the GBT.

3 STATUS AND RECENT CHALLENGES OF THE MAIN LOTS

3.1 *Erstfeld Section*

On July 19, 2004, the construction works at the northern Ertsfeld portal, the starting point of the last section, began and in the next month preparations will proceed for the main work in the tunnel. Tenders for the Erstfeld tunnel section have been invited and a decision will be taken in mid-2005. The contract will be awarded in autumn 2005. The section consists of two 7.2 km long single-track tunnels. Driving will begin at the end of 2006.

3.2 *Amsteg Section*

The base tunnel in the Amsteg section is connected to the surface by a 1.8 km long access gallery. The heading of this access gallery began in December 1999 and is being used now for the transport of personnel and materials. The contract comprises two single tubes

Copyright © 2005 Taylor & Francis Group plc, London, UK

of 11.4 km length leading to the southern part, which will be excavated with TBM's.

The installation of the TBM's with a diameter of 9.58 m each started in autumn 2003 and has been carried out in a staggered pattern. In the initial phase the 141 m long rump machine forms the TBM running unit. After the excavation of about 415 m in each tube, the machines were fitted with their back-ups to complete the in situ floor, the logistics station and the extension installations. The TBM's have now grown to their final length of 441 m, which makes them the world's longest tunnelling machines.

The regular operation of the TBM in the eastern tube started on October 1, 2003, and the TBM has driven about 3,500 m. The western tube unit was completed at the end of 2003 and the TBM has been in regular operation since January 2004. It has already excavated 3,000 m (16%).

At the beginning of February 2004, performance has declined because the predicted Intschi Zone was encountered, in which poorer geological conditions prevail and partially squeezing conditions were expected. The two tunnel tubes pass through the Intschi Zone over a length of about 950 m.

In the eastern tube, roughly 470 m of the Intschi Zone was driven by mid-April. Then in two fault zones, comprising sheared and folded serizit phyllites with a length of roughly 15 m, the machine deviated from its intended position over a distance of about 100 m. Horizontal deviations from the intended axis of up to 45 cm were measured. By means of the installation of reinforced support especially in the wall zone, the machine's gripping effectiveness was improved so that it could again be driven along its intended axis. The section that deviated from the intended position was reworked prior to placement of the in situ concrete floor. The vault area has to be redeveloped before the inner vault is installed.

The third forecast fault zone was driven at the beginning of May 2004. The western tube machine entered the Intschi Zone at the end of April.

The TBM's are supplied by a two track tunnel railway from the portal of the access tunnel to the floor concrete site.The mucking of the TBM-driven tubes is achieved with belt conveyors.

The machine back-ups in the vicinity of the floor concrete site are designed as suspended platforms. This makes it possible to pour the concrete floor below the TBM independent of the driving operation.

The 37 cross-passages of the Amsteg section will be excavated by conventional drill-and-blast (emulsion explosives). A self-travelling suspended platform was introduced to ensure that the supply trains for the TBM are not obstructed by the installation of the cross passages. This platform contains feeders with conveyor belts to load the mucking trains.

3.3 *Sedrun Section*

For logistical and geological reasons, the Sedrun section is the most complicated section of the base tunnel. The adit (1000 m), the inclined ventilation shaft (450 m), the cavern at the top of the first shaft and the 835-m-deep vertical access shaft were completed in several preparatory construction lots. The entire logistical supply for the heading of a total tunnel length of 2×6.8 km (4 simultaneous tunnel drives, together with other minor drives) has to be done through the access tunnel and the double shaft system. Up to 6,000 tonnes of excavated material have to be handled every day.

Excavation work at tunnel level began according to schedule in the third quarter of 2003. The construction of shaft II was also completed parallel to the start of driving. All construction site installations for excavating the MFS and the single-track tunnel were successfully completed. At the end of July 2004, 1927 m of the western tube and 1242 m of the western tunnel had been excavated. Typical cross sections are shown in Figure 2.

In autumn 2004, the Tavetsch Intermediate Massif (TZM) will be reached. The TZM is the biggest challenge of the entire GBT with respect to the geotechnical predictions. The geotechnical prognosis is based on five exploratory drillings from the surface of the terrain. One of these exploratory drillings penetrated the entire extent of the TZM. It shows a complete picture of the TZM, which consists of intensively crumbled, kakiritic mica gneisses, mica slates and mica phyllites. The results of the geological forecast predict extreme squeezing behaviour of the rock. Squeezing behaviour implies that the ground has the capacity to close the cavity again after excavation. Because deformations occur very slowly, the absolute order of magnitude is hardly predictable.

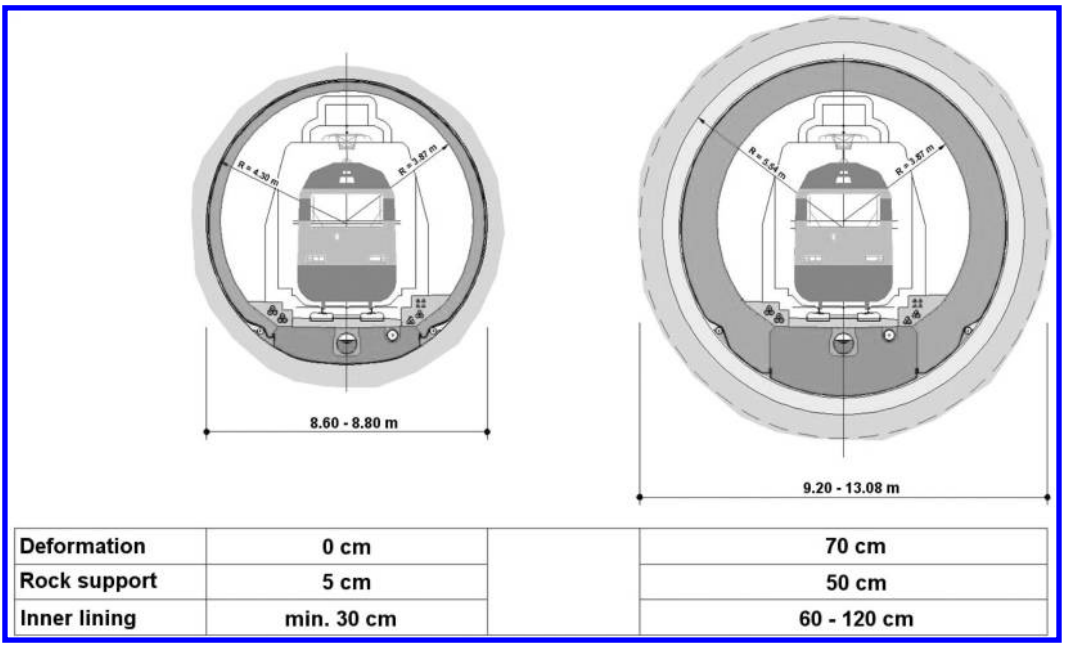
In the TZM with an overburden of up to 2000 m, radial deformations of up to 70 cm and a daily heading rate of about 80 cm are expected. The cavity support must ensure high resistance and allow large radial deformations of up to 70 cm. The designed support consists of yielding steel arches and pattern bolting with radial bolts of up to 12 m in length. The steel arches (TH 44 mine profile) are set up in form of a double ring. The arches are installed every 1.66 m, and every 0.33 m in extreme cases.

The cross-section of the single tubes increases from about 80 m^2 to more than 130 m^2 (see Fig. 2).

3.4 *Faido Section*

In Faido the Base Tunnel is opened up via an inclined 2.7 km long access adit. The construction of this gallery began in December 1999 by means of conventional drilling and blasting. Close to the adit portal,

Copyright © 2005 Taylor & Francis Group plc, London, UK



Deformation	0 cm		70 cm
Rock support	5 cm		50 cm
Inner lining	min. 30 cm		60 - 120 cm

Figure 2. Tunnel Sedrun, typical cross sections.

extensive processing plants – for recycling of a part of the muck and for the production of concrete aggregates – and conveyor belt systems for the transportation of debris have been constructed.

The MFS Faido was planned according to the geological prediction in favourable rock conditions. In summer 2002, however, an intensive fault zone was encountered totally unexpectedly. It passes through the large caverns of the multifunctional station at a very acute angle. An intensive investigation program was carried out to define the best place for the huge cross-over caverns with cross sections up to 260 square meters and with an overburden of nearly 1,500 m. As a result of these investigations it was possible to adapt the layout of the multifunctional station with the aim of placing the large caverns in favourable rock conditions in the southern part of the MFS. To date, about 6.7 km of tunnels and galleries and two cross-over caverns have been successfully excavated. The northern headings in the single track tubes are still within the fault zone and still need very intensive rock support. The yielding steel support has proven to be an effective system in the rock conditions with up to 40 cm of radial deformations (see Fig. 3).

Since 2003 rock bursts were noticed in the MFS Faido. These rock bursts are a sudden reduction of pressure in the rock with the release of enormous amounts of energy. Rock bursts are seismic events that cause injury to persons or damage to underground workings. The general and essential feature of



Figure 3. Tunnel Faido, yielding lining.

rockbursts is their sudden, violent nature. Rock bursts occur when the stresses around an excavation exceed the rock mass strength. The higher the overburden and the more compact the rock, the greater the probability of rock bursts occurring. As a rule, rock bursts can neither be predicted nor prevented.

The rock bursts at the MFS Faido occur mainly at the face. Not all of the drives are affected. In January 2004 material broke out of the face unexpectedly in the single-track tube east-north. As a result, the drive was switched from full-face to partial excavation (crown heading).

Copyright © 2005 Taylor & Francis Group plc, London, UK

Table 1. Definition of terms and measures in case of rock bursts.

	Term (event)	Perceived phenomena	Measures
E1	Release	– cracking sound – rumbling	– document observations in shift and daily report of contractor – intensify observations – partial excavation (crown heading) – Overhead protective nets over entire crown – shotcrete on face – vaulted face – face anchor bolts
BS1	Light rock bursts	– concussions – dust raised – heavy face spalling during loosening in the form of plates up to about 5 m^3 and about 1 m deep	Additional to E1: – strengthen face bolting – leave wedge of material in front of face – intensify and strengthen system bolts – strengthen overheading netting
BS2	Medium rock bursts	– extreme concussions – concussions even 3–6 h after excavation – dust clouds from crown – face spalling less than 5 m^3 already prior to loosening – bend anchor plates into L2	Additional to BS1: – denser, yielding rock burst anchoring
BS3	Extreme rock bursts	– extreme concussion – several successive concussions – concussions after more than 3 h – shotcrete spalling L2 – cracking of shotcrete on face – face spalling greater than 5 m^3 even before loosening – overbreak formation – anchor heads torn off near abutment	Additional to BS2: – denser bolt pattern if damage pattern requires it – pattern bolting/strengthening – face bolting, reduction – bolt spacing, reduction – pressure relief blasting – submit event report (short report)

Starting in March a great increase in the number of rock bursts was suffered in the single – track tube east-north. Measures had to be taken to minimize the effects of rock bursts and similar phenomena. The "Rock burst working party" was set up.

While normal rock pressure is countered with relatively yielding supports, rock bursts call for support measures capable of withstanding dynamic loads. The difficulty faced during a drive is to determine the prevalent kind of danger one will encounter. Frequently a combination of danger sources is faced, so that complicated support measures are required.

To ensure safe working when faced with possible rock bursts, the following basic measures are considered:

- Sealing of the face with steel-fibre shotcrete (against loosening of small stones in the face)
- Face anchors with large anchor plates
- Wedge of excavated rock left in front of the face (to keep people from getting too close to the face)
- Switch to crown heading
- Vaulted face form (to anticipate the excavation shape normally occurring as a result of stresses)

Additional measures may be required if the rock bursts are especially violent. A "Rock Burst Information Sheet" spells out the measures to be taken when rock bursts occur and also defines the terms involved. Table 1 is also part of this information sheet.

3.5 *Bodio Section*

Extensive construction work was taking place at the southern Portal in Bodio before autumn of 2002 in preparation for the heading of the main tunnel lot. It included a bypass adit (to bypass the loose rock zone at the portal), the mucking tunnel (3.2 km) that will serve as a conveyer belt tunnel, the opencast tunnel (380 m long) including the portal, the processing plants that recycle the debris into concrete, and finally the tunnel section in loose rock material (410 m) that follows the open cast construction.

Copyright © 2005 Taylor & Francis Group plc, London, UK

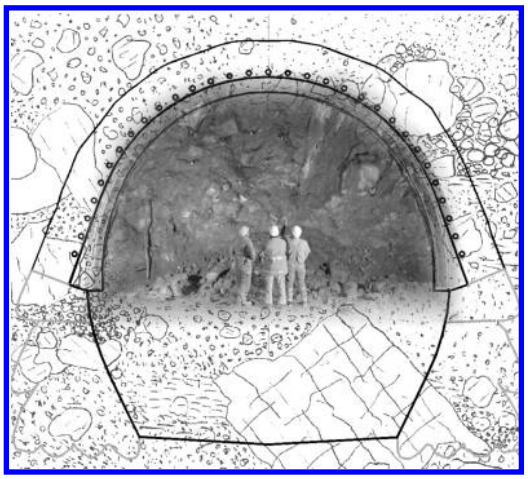


Figure 4. Tunnel Bodio, cross section in loose rock material.

This tunnel was excavated through rock fall and loose rock material. To drive the heading through this zone auxiliary measures were taken, such as putting a pipe umbrella in place and undertaking a large amount of grouting (see Fig. 4). The heading of this section was completed successfully in June 2003, on time and within budget.

The two 15 km base tunnel tubes in Bodio, leading north in the direction of Faido, started in the cavern at the end of the bypass. In January and February of 2003, the two TBM's in the Bodio section – each with a diameter of 8.80 m and installed in underground installation chambers – began their work.

The TBM in the eastern single tube has now cut 4,500 m, the one in the western tube 5,500 m.

In 2003 the roughly 600 m installation for the rear "inner vault" construction site – the so-called "worm" – was assembled at the Bodio yard in front of the tunnel. The concreting of the lining support and of the lining itself was started in the west tube in April 2004. About 500 m of final lining have been executed using the specially designed vault formwork, which possesses a certain adaptability. It is used to optimize the support taking into account any TBM deviations and the actually installed supporting elements.

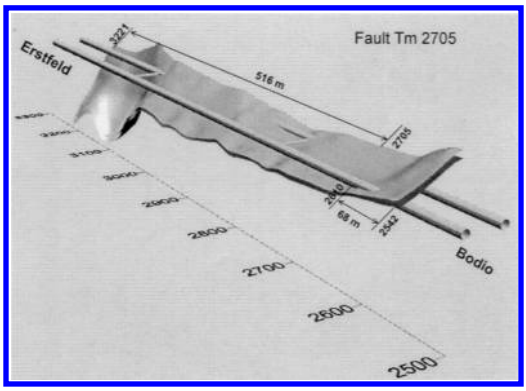


Figure 5. Tunnel Bodio, unexpected fault zone.

Shortly after the TBM's started in Bodio, they encountered an unpredicted fault zone. The tunnel tubes followed the flat zone about 500 m in the eastern tube and nearly 60 m in the western tube. The average heading rate was approximately 2.45 m per day. In autumn 2003 the fault zone was successfully passed through and the average heading rate increased to 13.13 m (TBM west) and 12.21 m (TBM east) per day (see Fig. 5).

4 OUTLOOK

2004 is a decisive year for the construction of the Gotthard Base Tunnel, as it marked conclusion of the starting-up phase for construction work in all five contract sections. Now it is imperative to ensure that the high expectations are confirmed in constructional, logistical and scheduling terms and to master the challenge of driving through extremely sophisticated geology. In Amsteg the TBM in the western tube reached the Intschi Zone at the end of April 2004. In Sedrun the drive towards the north will reach the squeezing TZM in autumn 2004 and the drive towards the south will reach the squeezing Useren Gavera Zone in late-summer 2004. The drill-and-blast operation in the Faido MFS as well as the TBM drives in Bodio will work towards the target of "arrival of both TBM's in the Faido MFS at the end of 2005".

Copyright © 2005 Taylor & Francis Group plc, London, UK

Dobrovskeho Tunnels in Brno, CZ

V. Horak, J. Pechman & J. Rozek
Civil Engineers (MSc), Amberg Engineering Brno, a.s., Brno, the Czech Republic

ABSTRACT: The paper deals with the design of two parallel road tunnels passing under a densely built-up area on a ring road in the city of Brno. Critical parameters for this unique tunnel construction will be adverse ground conditions in neogenous clay, large excavation area, very low overburden and a residential area situated above. The twin-tube tunnel of 1.25 km in length will be constructed by driving. At present, construction work is finished on three exploration adits. Special attention is paid to evaluation of estimated subsidence and to minimization of possible damage to existing structures.

1 PROJECT OVERVIEW AND GEOLOGY

1.1 *Project overview*

The Dobrovskeho Tunnels are the core component of the newly built northwestern section of the city ring road in Brno, Czech Republic. The Dobrovskeho I Tunnel is located beneath Dobrovskeho street, the second tube is situated in parallel about 60 m to the south. Both tubes pass under a densely buit-up area, which means that the excavation will have to traverse under or near buldings up to seven storeys high. The tunnel is connected at both portals to large intersections with grade separation.

The estimated construction time of the whole project is 5.5 years and the opening is planned for 2010.

1.2 *Geology*

The geological conditions in the area are monotonous. The cover (3–10 m thick) is made up by fills and loess loams. Basis of the Quaternary cover is represented by gravel sediments (groundwater collector), which are not continuous. Its underlay is formed by limey, silty clays of Tertiary (Neogene) origin (more than 60 m thick).

The clays are heavily tectonically faulted, locally in zones up to several tens of metres thick. They have a blocky to irregularly fragmenting disintegration, commonly with radial structures at the fracture surface, which is uneven, bowl-curved.

The clays are of very high plasticity (MV or CV according to USC system) and in semi-solid to solid consistency state, depending on the depth. When in contact with ground water, they display squeezing properties.

2 TUNNEL DESCRIPTION

2.1 *General*

The project consists of two parallel tubes designed for unidirectional traffic, each 1.25 km long. The dominant part of the entire length will be driven using conventional excavation methods and sprayed-concrete lining, while short section at the portals (150 m and 50 m, respectively) will be constructed by cut-and-cover method.

The vertical alignment of tunnel axes is governed by the minimum necessary overburden thickness in clays and by the links to the existing roads. The resulting overburden height varies between 6 m and 22 m.

Both tubes are connected by four transverse walkways. In each bore, there is an emergency lay-by. Maximum distance between SOS niches is 175 m.

Approximately in the middle of the tunnel is situated an underground ventilation and machinery facility, where the control room and back-up energy centre is located.

2.2 *Driven sections*

The standard driven cross-section is horseshoe-shaped with an arched invert (see Fig.1). The excavation area is 125 m^2. The cross-section is divided by an intermediate ceiling into the traffic area and ventilation area. The traffic clearance envelope is 8.50 $\times$ 4.5 m.

Primary excavation support is formed by steel arches and shotcrete reinforced with wire meshes. Total thickness of primary support is 350 mm. The tunnel is sealed with a closed waterproofing membrane. The final RC concrete lining has minimum thickness of 450 mm.

Copyright © 2005 Taylor & Francis Group plc, London, UK



Figure 1. Digital rendering of eastern portal area.

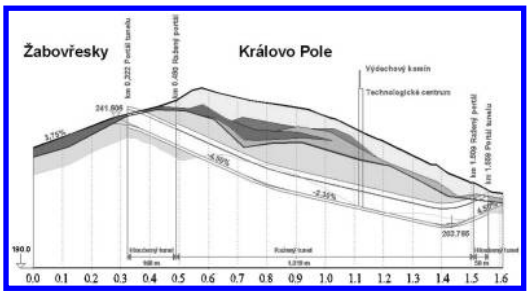


Figure 2. Geologic longitudinal profile of Dobrovskeho Tunnel.

2.3 *Cut and cover sections*

At the approach to the driven tunnels, the cut-and-cover sections are proposed for structural and technological reasons. The design of cut-and-cover sections is a part of the solution of alignment of roads and engineering structures at the three-level grade separation at the western portal in Žabovřesky. Closed tunnel tubes are situated in the bottom level, the intermediate level is formed by covered galleries and surface roads, and bridges and retaining walls are in the top level. This complex engineering task is complicated further by the fact that the construction must be carried out while maintaining the traffic and operation of all buried utilities concentrated in the area.

The construction pit is secured by braced or anchored pile walls. Load-bearing structure of the tunnel tubes is cast in-situ concrete frame.

2.4 *Underground ventilation and machinery facility*

One of the transverse walkways is linked to the underground facility for ventilation and machinery, whose seven underground floors and one ground floor house all necessary technological equipment, subsidiary

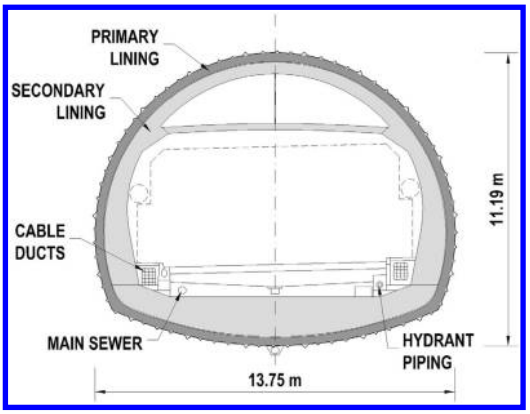


Figure 3. Standard cross-section of driven tunnel.

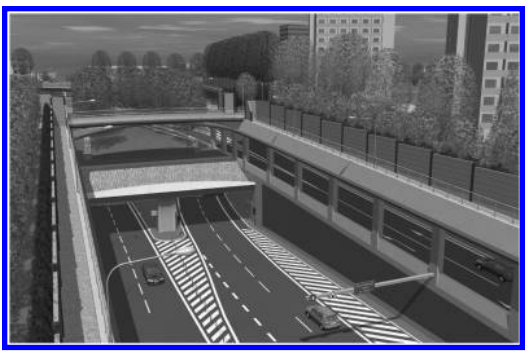


Figure 4. Digital rendering of western portal area.

control room and service rooms, as well as an escape staircase and personal evacuation lift.

3 CONSTRUCTION PROCEDURE

Mined sections of the tunnel will be driven using the core construction method with vertical and horizontal division of excavation (Paramentstollen). Primary rock support will consist of steel girders and mesh-reinforced shotcrete. Design of final lining incorporates cast in-situ reinforced concrete with precast RC members in the invert for faster advances in installation.

4 EXPLORATION ADITS

4.1 *Objective and configuration*

The tunnel design has to cope with three main adverse consequences of the tunnel location: relatively difficult ground (Neogene clay), comparatively low overburden (6 to 22 m) and a number of existing buildings that could be affected on the surface.

Copyright © 2005 Taylor & Francis Group plc, London, UK

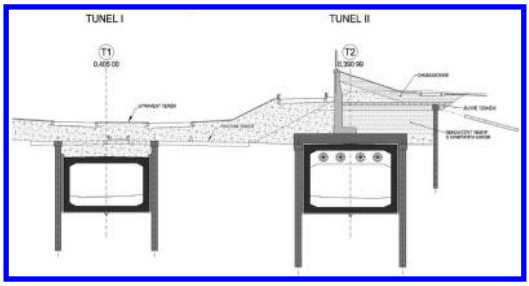


Figure 5. Cross-section of western cut-and-cover section.

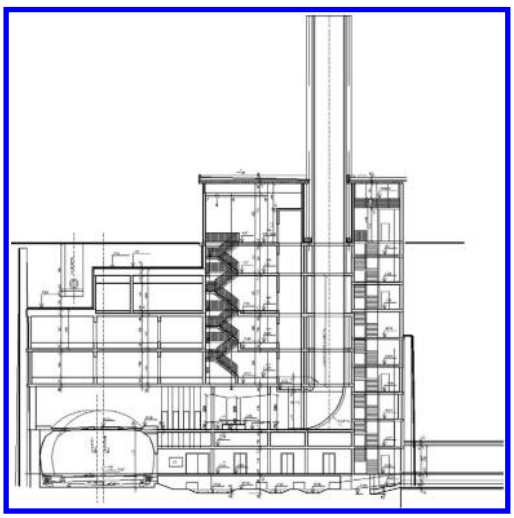


Figure 6. Cross-section of the underground technology centre.

That is why a detailed geotechnical investigation programme including excavation of exploration galleries was carried out before the start of the tunneling project proper. The objective of these exploration works was:

- to obtain detailed data for design and construction of the future tunnels.
- to try out excavation and construction techniques.
- testing of structural properties of the primary lining
- description of the interactive relationship between the excavation and its environment, with respect to the ground settlement and effect on buildings.

Three exploration adits were excavated. The total length is $2 \times 831\,\text{m} + 365\,\text{m} = 2027\,\text{m}$. They are located inside the future tunnel cross-section and respect the proposed construction procedure (see Fig.5). Cross-sectional area of one adit is approximately $15\,\text{m}^2$.

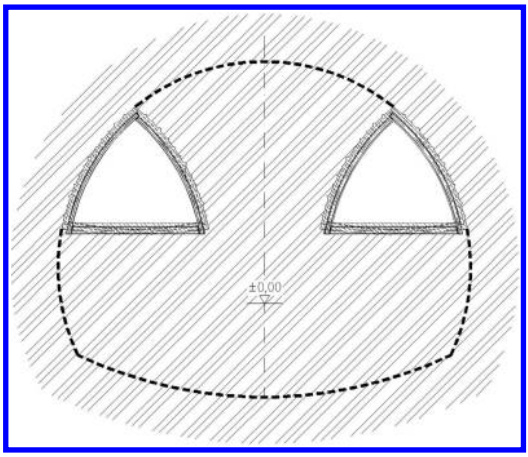


Figure 7. Location of exploration adits in the cross-section.



Figure 8. Portal of exploration adits.

4.2 *Lessons learned*

The investigation revealed several important facts for design in these specific conditions:

- Displacement development is long-term, final displacement is reached only after about 280 days. Clay behaves like a 'viscous liquid'.
- Deformations in the invert influence substantially the overall displacements.
- Stiffness of the primary support has to be increased proportionally with the excavation area.
- Partial excavation steps have to be carried out and support has to be installed in the shortest time possible. Interruptions in excavation cycle result in increments in displacements and in settlement trough area.
- The settlement trough is relatively narrow. Points of inflexion lie approximately 20 m from the tunnel axis.
- Excavation in very shallow sections and under sensitive structures on surface requires additional measures, such as ground improvement, grout screens

Copyright © 2005 Taylor & Francis Group plc, London, UK

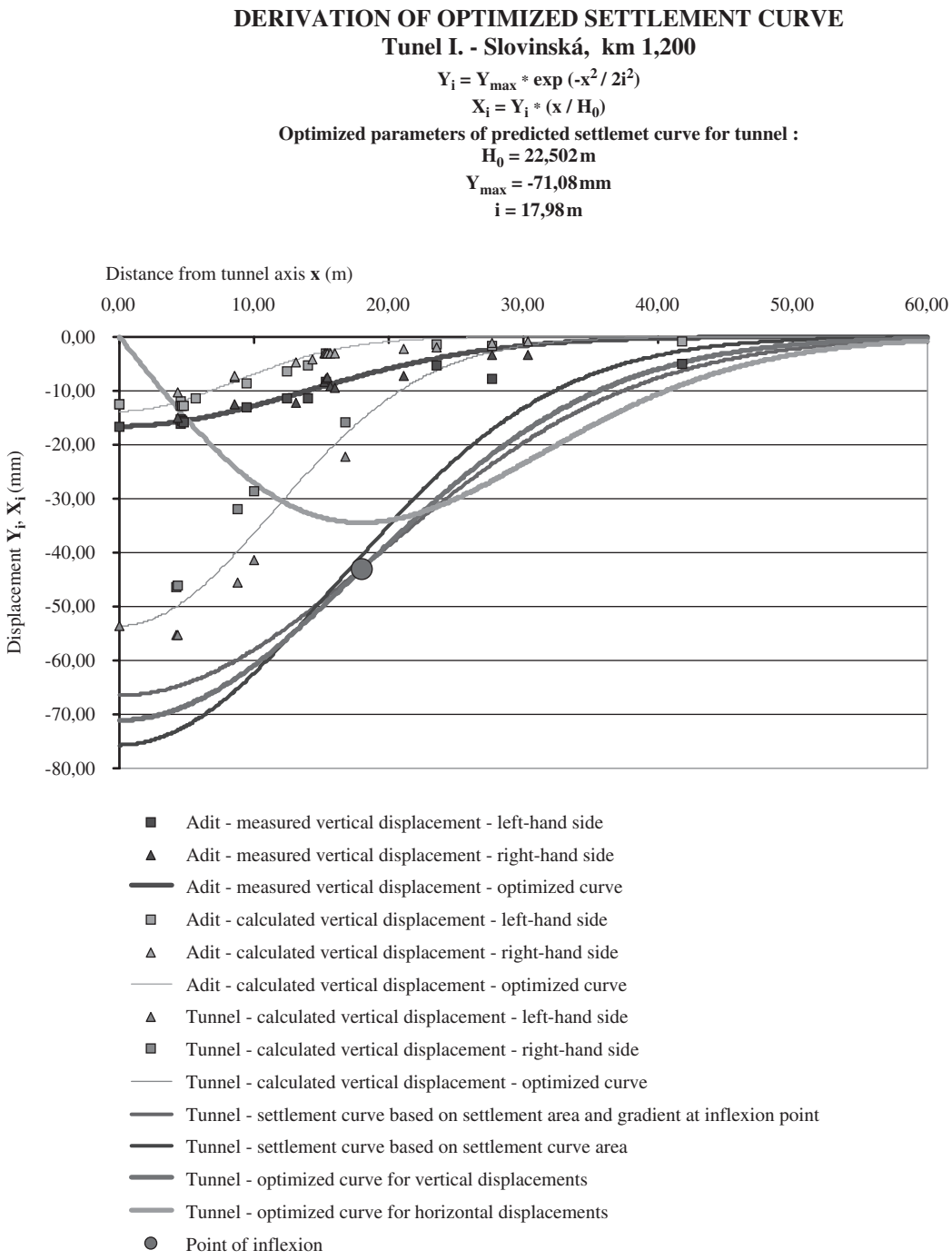


Figure 9. Sample representation of settlement curve derivation.

Copyright © 2005 Taylor & Francis Group plc, London, UK

and pipe umbrellas, as well as the use of up-to-date boring techniques and grouting materials.

5 SUBSIDENCE PREDICTION

The probable impact on existing ground structures was evaluated by means of settlement trough analysis. The used methodology of prediction incorporates mutual interactive extrapolation of ground investigation data, real settlements measured during construction of exploration galleries and data obtained by mathematical modelling.

5.1 *Input data*

The source data were obtained from

- Monitoring of exploration adits (convergence measurement, extensometers, precise levelling)
- FLAC mathematical model – modelling of complete excavation and construction process ('zero' state, partial excavation and installation of temporary support, stabilization of displacements, installation of final lining, traffic load, degradation of temporary lining during lifetime of the tunnel). The model also included 3D effects near tunnel face, the effect of pipe umbrellas and development of deformations over time.

5.2 *Initial settlement curves*

Based on the statistical analysis of corresponding data arrays, three initial settlement curves were defined:

- Settlement curve based on measured final settlements after completion of exploration adits.
- Settlement curve based on mathematical modelling of construction stage after completion of exploration adits.
- Settlement curve based upon mathematical model of final construction stage after completion of the tunnel and reaching final displacement values.

Then, 'calculated' and 'measured' curves were compared as to the shape and magnitude. The decisive factors taken into account for comparison were

- Calculated area of settlement curve (volume loss).
- Calculated maximum gradient of deflection curve (gradient at the poi nt of inflexion).

Due to larger deviation of several individual points the area of settlement curve taken into further considerations was increased by 50% of standard deviation.

5.3 *Predicted settlement curve*

Two partial curves were derived from the 'calculated' settlement curve for completed tunnel.

- Curve based on settlement curve area ratio only (this curve is affine to the calculated one).
- Curve based on both settlement area ratio and gradient ratio.

To derive optimum parameters of final settlement curve, their significance with respect to the risk of damage to surface structures was evaluated as follows:

1 A curve with lower gradient is affine to real surface deformation curve after excavation of exploration adits and has smaller negative impact on existing buildings, therefore brings about higher risk in possible damage and costs of remedial measures needed.
2 A curve with larger gradient is affine to calculated deformation curve, the settlement trough is narrower and deeper. The negative impact is bigger on a narrow strip of buildings, where the risk of unexpected damage is relatively low due to support measures prior to tunnelling. On the other hand, the scope of affected buildings in greater distance from tunnel axis could be underestimated in this way.

Experience gained from analysis of exploration adits shows that real settlement trough is flatter and wider compared to the calculated curve. In conclusion, the parameters of the resulting settlement curve, which serves for prediction of the shape and magnitude of surface deformations, are derived as mean parameters from the two above mentioned curves.

In total 28 cross-sectional profiles were evaluated. A sample representation of optimized curve derivation can be seen on Figure 9. A vertical displacement contour plan of the affected area was drawn based on the optimized data, which served as a basis for important decisions preceding the tunnel construction:

- the design of supporting measures on existing buildings,
- planning of relocation and repairs of existing utilities (sewers, gas and water pipelines etc.)
- planning of temporary traffic routes during construction.

6 CONCLUSION

Difficult local geological conditions combined with challenges posed by urban environment make the Dobrovskeho Tunnels project an outstanding engineering task, a first of its kind not only in the Czech Republic.

Copyright © 2005 Taylor & Francis Group plc, London, UK

New method of underground structures using multi elements which are jointed with the specific junctions

M. Shimizu, A. Watanabe, K. Nishijima, M. Kurisu, K. Kuwabara, T. Genjun & E. Arakawa
East Japan Railway Company, Tokyo, Japan

ABSTRACT: There are several construction methods for non-open cut underground structures under traffic roads, however, there are some problems about the ground deformation due to constructions etc. This paper presents that the development of new type of construction method using multi elements made of steel and concrete, aiming to overcome some problems in matured methods, and shows the strength character of the elements and application of the method to real civil engineering construction projects.

1 INTRODUCTION

The construction methods for non-open cut underground structures crossing traffic roads had been developed in recent decades (JNR 1986, EJR 2001, JRCEA2001, JREC 2001). Table 1 shows the typical non-open cut methods for constructing a crossing structure under the traffic roads, and each method had different histories of development and modification based on construction experiences and related studies. Method 1 is an excavation method supported by steel pipes that were installed in ground. Concrete box culvert was constructed under the supported steel pipes. There are two types methods with/without evaluation of junction rigidity of pipes. The influence to traffic roads should be mitigated by accurate design about pipe deformation. Method 2 is pushed/pulled concrete box culverts which were already constructed in a shaft. Pipes for mitigation of ground deformation were usually installed in the ground in advance for pushing/pulling box culverts. There are two chances of influences to traffic roads in the construction sequences, and the box pushed/pulled stages could damage traffic roads even damage mitigation pipes were constructed. Method 3 is pushed/pulled constructed concrete box culverts which are already made in a shaft, box shape roof elements for mitigation of traffic roads deformation were simultaneously pushed in the ground. There were two influence chances of ground deformation on pushing elements and pushing/pulling box culverts. Method 4 is pushing steel/pre-stressed concrete elements and building beam shape structures. A framed structure could be made using pre-stressed cables installed through elements. In many cases, by using this method, the rigidity of junction of elements were not commonly calculated/designed since the rigidity for the framed structures with junctions were not evident. The elements were pushed from a start shaft, thus in a case that a length of crossing traffic roads were long, the pushing facilities should be large enough for pushing. This method was commonly used in a lower-beam type structures same as the lower-beam type bridge composed of crossing horizontal beams and longitudinal beams and abuts, thus the shoes under the beams were constructer although their maintenance were difficult in a ground. Due to this, construction methods to build framed structures without shoes below beams were rather preferable. And, the design procedure, e.g., anti-earthquake design, is rather complicated compared to framed box culvert.

Table 1. General description of non-open cut construction methods.

Method	General description
Method 1	Steel pipes are used for support the ground and culverts are made inside the pipes.
Method 2	Box culverts are pushed/pulled, usually with pipes for mitigation of ground deformation.
Method 3	Box culverts are pushed/pulled with box-shape roof elements.
Method 4	Steel/pre-stressed concrete elements are pushed and framed structure, usually lower beam type is implemented.
Method 5	Steel elements with junctions is pushed/pulled and frame jointed elements structure is made.

The considering some issues for stable construction under traffic roads in some existing construction

Copyright © 2005 Taylor & Francis Group plc, London, UK

methods, a new type of underground structure using multi elements, Method 5, was developed. The main characters of the development were as follows; 1) speed and accuracy on location of elements for crossing traffic roads were higher in the case of pulling the elements rather than pushing elements, 2) composite elements of metal and concrete with specific junctions would be used for a framed structure.

This paper describes the development of the new construction method on following issues; 1) strength characteristics of new type elements including junctions, 2) application of the method to under railway structures and its ground behavior.

2 CHARACTERISTICS OF NEW CONSTRUCTION METHOD

Figure 1 shows the schematic diagram of formed structure constructed by new construction method. Frame

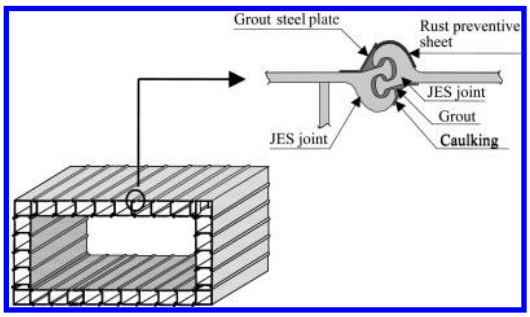


Figure 1. Schematic diagram of structure made by JES method.

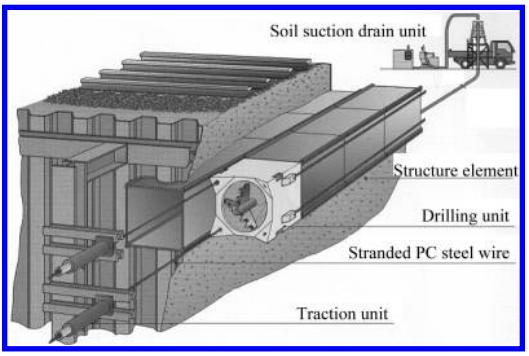


Figure 2. Schematic diagram showing pulling elements.

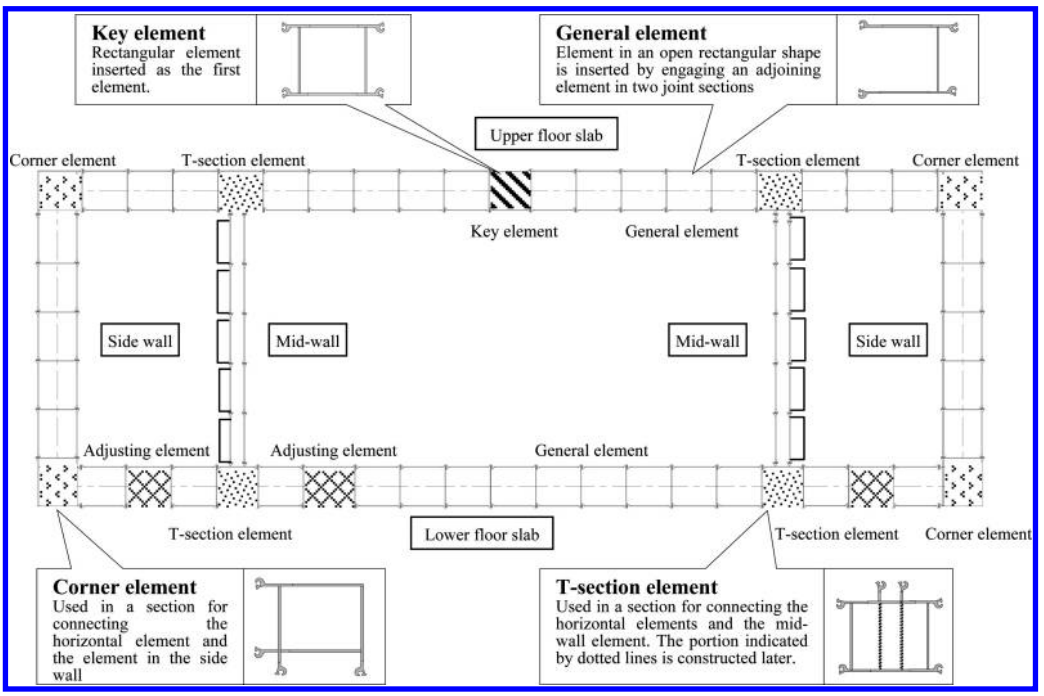


Figure 3. Example of element layout in JES method.

Copyright © 2005 Taylor & Francis Group plc, London, UK

box culvert is constructed by multi-elements made of steel elements with junctions. The method was called a JES method which stands for Jointed Element Structure. The inside of an element is filled up with concrete to get strength and rigidity as the framed structure. Figure 2 shows the typical framed structures with elements. Each element was set in a start shaft and was pulled by stranded PC steel wires from an end shaft. Figure 3 shows the schematic diagram pulling the elements by stranded PC steel wires from an end shaft.

3 STRENGTH AND RIGIDITY CHARACTERISTICS OF THE ELEMENTS AND BEAM MADE OF THE ELEMENTS

The bending strength and shear strength of a beam which were confirmed by the laboratory test and which were made from the element were described below.

3.1 *Strength of junctions*

Static tension tests were performed as shown in Figure 4. The tests were done with grouting in the space of junctions. The tests results are shown in Figure 5. The load-displacement relationship was indicated that the static tension strength of junction is above the yield strength (233 kN) of 13 mm steel plate (SM400 type)of which thickness was used as the standard element shapes. The test results show that the strength of junction is above the steel plate flange with designed thickness. Thus, it is confirmed that the strength of junction is not weaker than flange plate.

Fatigue strength of junction was tested as same junction element pieces in Figure 4. Several stress amplitude (stress was converted to equivalent stress to 13 mm steel plate thickness) was loaded, changing the number of cycles. The test results were plotted as S-N (stress amplitude-number of cycles) curve as shown in Figure 6. The design S-N curve was set

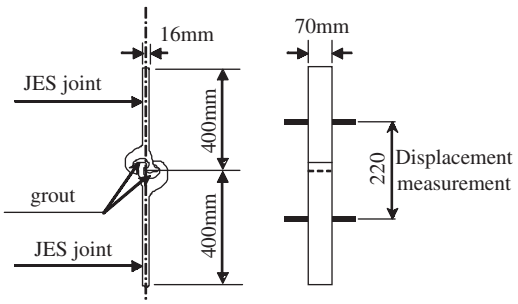


Figure 4. Schematic diagram of tension test of junction.

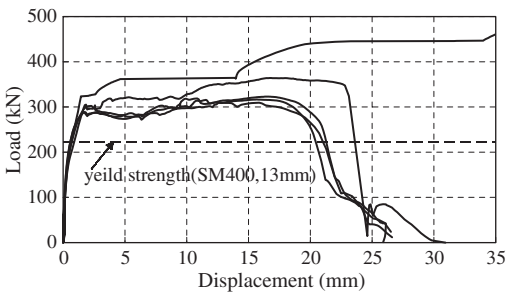


Figure 5. Relationship between load and displacement.

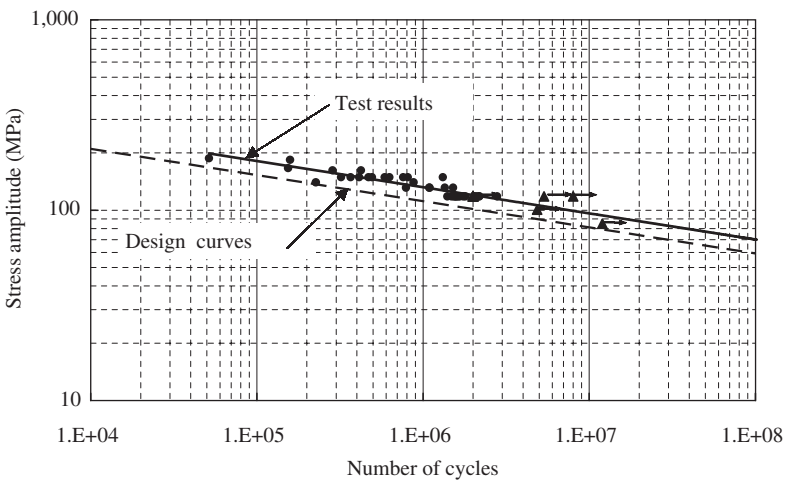


Figure 6. Relation between stress-amplitude and number of cycles in fatigue tests of element junction.

Copyright © 2005 Taylor & Francis Group plc, London, UK

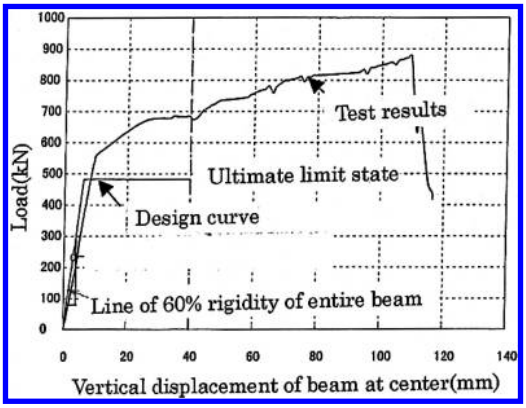


Figure 7. Comparison between test results and design curve of bending strength.

below the test results curve keeping the certain margin. Thus, the fatigue failure of junctions can be avoided by keeping the design curve.

3.2 *Strength characteristics of beam composed of elements*

Bending and shear strength of beam made of JES elements were tested to propose the design equations. The bending and shear strength of the steel element with filled concrete might be rather complex. Due to its complexity of structure, the design equations might be rather practical if the strength behavior was assumed to be similar as that of reinforced concrete, just simplifying the element steel plates as reinforced steel in the beam and concrete inside elements was assumed as the concrete in reinforced concrete. Thus, strength tests of beams were performed to confirm that the above simplicity was reasonable and safe for the above simplicity was reasonable and safe for the design.

The bending test was performed as shown in Figure 7. The load-displacement relationship was shown in Figure 7. The experiment curve and the curve calculated by design theory of simple reinforced concrete were compared in Figure 7. The followings were confirmed; 1) the ultimate strength of the beam with elements could be simplified with safety margin as reinforced concrete theory; 2) rigidity before the yield point could be assumed as 60% of entire section.

The shear tests with certain variety of shear span were performed as following; shear span ratio a/d = 1,1.5,2 (a: shear span; d: effective height of beam), using d = 400 mm beams made of elements. The comparison with test results and calculated shear strength based on reinforced concrete was shown in

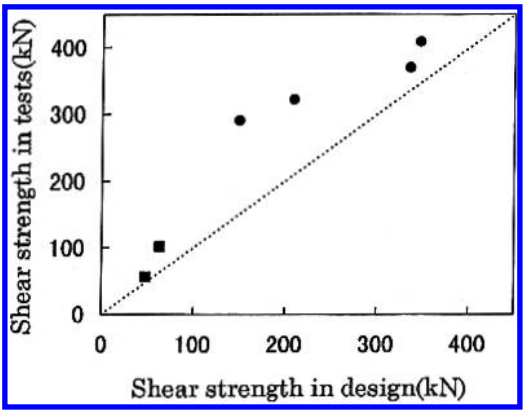


Figure 8. Comparison between test results and design curve in shear strength.

Figure 8. The calculated shear strength in the Figure 8 was based on the either calculated shear strength of the shear strength of the concrete inside the steel plate and the shear steel plate, and the smaller one was the calculated/designed shear strength, i.e., weaker strength between the concrete shear strength and steel plate shear strength in the element was the one of the element. From the comparison, the beams which were composed of elements can be simply assumed as the one from the above reinforced concrete theory.

Based on the above, the bending and shear strength were designed assuming as the simple reinforced concrete beams and their simplicity had safe margin.

4 CONSTRUCTION OF TUNNNEL BY THE NEW METHOD

Although this method of construction has a construction actual result exceeding 40 until now, it introduces the structure which was the largest as for the scale here. The construction was what builds a railroad tunnel with a diameter of 10.8 m, and a length of 107 m in parallel directly under an established railroad. The sectional view of a structure is shown in Figure 9. The tunnel is located in cohesive soil. Photo 1 shows the tunnel feature.

The steel elements have the shape of trapezoid, 800 mm in height with bases of 700 mm and 800 mm length, and were manufactured using 16 mm tick steel plate (SM400). The elements were manufactured in 6 m and 8 m lengths, the maximum length that could pass through the shaft opening. These were successively welded together into elements of full tunnel length while being pulled through the ground.

The method is often adopted in the construction of grade separations with railways and highways, and there were examples of construction of crossings

Copyright © 2005 Taylor & Francis Group plc, London, UK

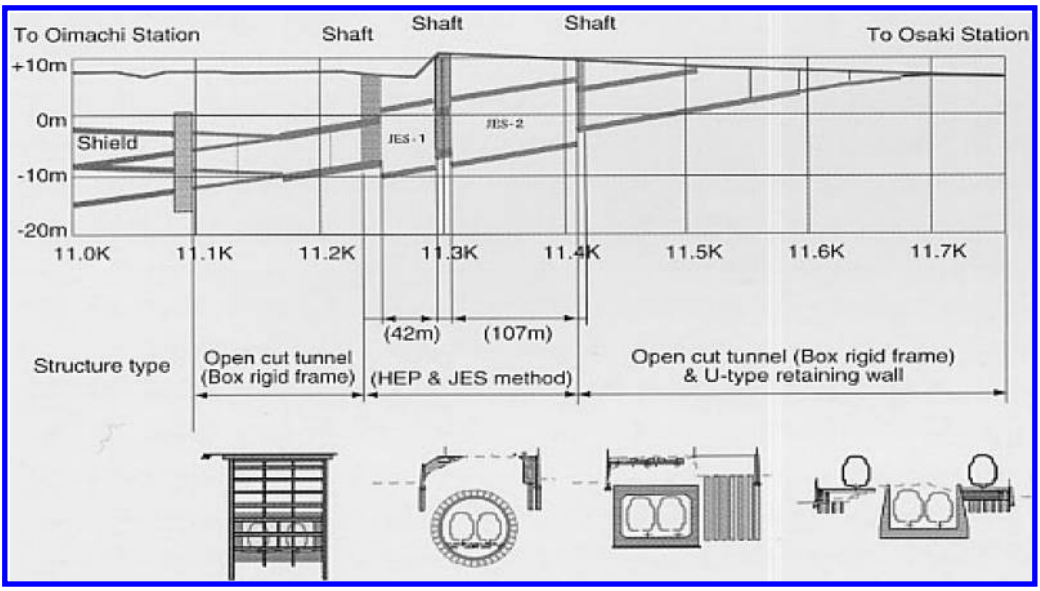


Figure 9. Tokyo Waterfront Area Rapid Transit Line.

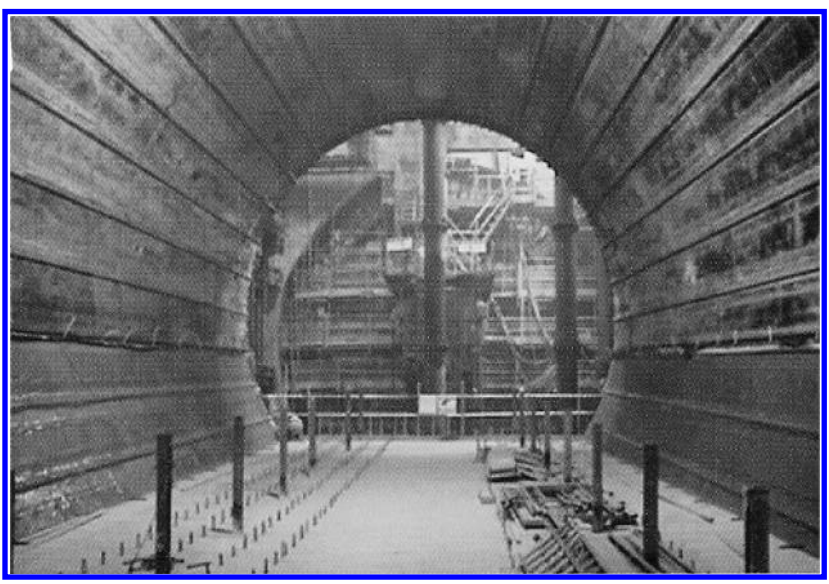


Photo 1. Osaki tunnel.

under double track railway lines (pulling distance on the order of 20 m), but this was first time for a pulling distance of 107 m. Therefore, test construction was performed prior to the actual construction, and various definite improvements were made, including change of element configuration, improvement of the pulling equipment, and determination of the pulling force. In actual construction, pulling of the first element was begun in March 2001 and the pulling operation at the tunnel was completed in October.

Through the completion of this construction within the prescribed time, it is considered that superiority of this method, its safety and ease of performance, in the construction of grade separations with railways and

Copyright © 2005 Taylor & Francis Group plc, London, UK

highways has been proven, and that the method can be included in a broad comparison of construction method.

5 CONCLUSIONS

This paper presents new type of underground structure using multi elements, describing the characteristics of the method, strength of junction, strength and rigidity characteristics of the beam composed of elements, and the case study of the constructions. The new construction method was evaluated from the element test of the joints to real construction implementation. Authors could assume that this method would be rather efficient for construction of tunnel under traffic roads compared with alternatives. Authors would be acknowledge Dr. Ishibashi, director of Structure Engineering Center of East Japan Railway, and Mr. Saito of Tekken Corporation for their guide for the developments of the construction method. Further developments on speed up of construction sequences would be expected, and related works were under study, and their outcome would be presented near future.

REFERENCES

Japanese National Railway. 1986. Planning manual of under railway structure.

East Japan Railway. 2001. Design and construction manual of JES method.

Japan Railway Civil Engineering Association. 2001. Planning manual of under railway structure.

JR East Consultants. 2001. Technical paper on High Speed Element Pull (HEP) & Jointed Element Structure (JES).

Copyright © 2005 Taylor & Francis Group plc, London, UK

Contract management, financing and risk analysis

Copyright © 2005 Taylor & Francis Group plc, London, UK

The control of heavy squeezing phenomena in an Austrian road tunnel

N. Ayaydin & G. Huber
IGT-Geotechnik und Tunnelbau, Salzburg, Austria

ABSTRACT: In the western part of Austria for an Expressway a road tunnel with two tubes each 5,8 km are under construction. The "Strenger-Tunnel" named tunnel crosses east-west striking and south dipping quartzphyllonites and quartzitic schists with an overburden up to 800 m. The geological condition shows a number of fault zones, parallel to the axis. On a length of appr. 2.500 m heavily squeezing rock mass behaviour were encountered. Due to the high overburden investigation bore holes were not possible on the whole length of the tunnel during design and tendering process. An adaptable contract and experienced tunneling personal on owners side (designer, supervision and geologist), and also experienced personal on contractors side were chosen to manage the expected geotechnical difficulties. Large deformations up to 80 cm were to be mastered with continuous adjustment of rock bolt lengths and numbers, as well as with the installation of yielding steel elements in slots of shotcrete lining.

The optimization of the support measures were based on the interpretation of the geotechnical measurements and on geological documentation of the tunnel face.

The adaptability and economic application of the New Austrian Tunnelling Method (NATM) has been proven once more at this project.

1 GEOLOGY

The Strengen Tunnel is situated in the alpine region of western Austria. The tunnel has two tubes, each 5,8 km long, and was excavated in so-called "Landecker Quarzphyllit", which consists mainly of east-west striking and south dipping quartzphyllonites and quartzitic schists with low water-inflow. The tunnel's geological conditions were dominated by a number of fault zones, nearly parallel to the tunnel axis, which followed the tunnel excavation over long distances. In fault zones, mylonitic and totally disturbed strips of two and more meters in thickness appeared in the immediate vicinity of the tunnel. As a result, heavy squeezing rock conditions occurred especially in the central part of the tunnel.

Due to the high overburden of up to 800 m, only few exploratory drillings were possible prior to the construction phase.

2 GEOMECHANICAL BEHAVIOUR

The geotechnically extremely problematic spatial distribution of the main discontinuities was marked by steep, mainly south-dipping, faulting. Furthermore, the faulting was acutely tangential to parallel to the main tunnel axis.

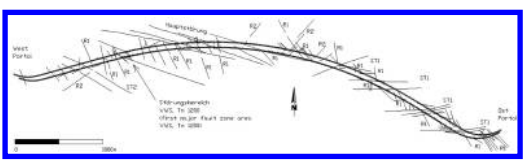


Figure 1. Tectonic analysis of the fault zones (ST1,2 orientation of the major fault zones; R1,2 Riedel shears).

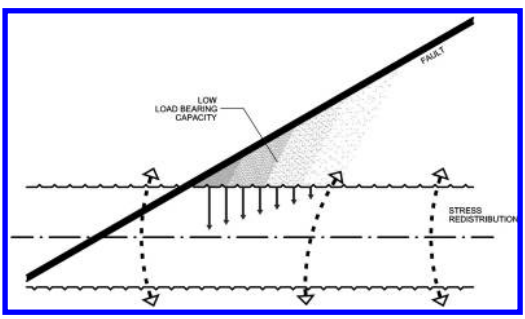


Figure 2. Schematic layout of faults and their influence on stress redistribution.

In the middle section of the tunnel, the parallel faulting accompanied the excavation for long distances, whereby the fault bundles, which were located close outside the tunnel cross-section, induced strong

Copyright © 2005 Taylor & Francis Group plc, London, UK

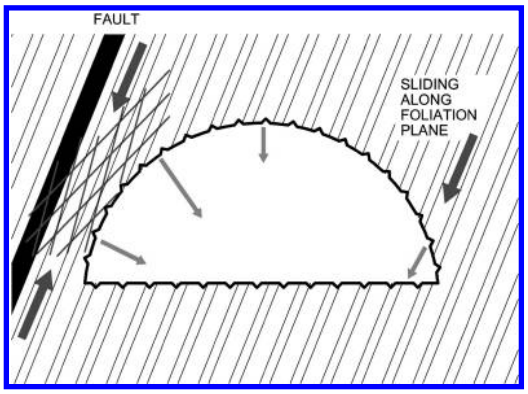


Figure 3. Dominant geomechanical model in zones with overburden >500 m.



Figure 4. Fault in tunnel-face.

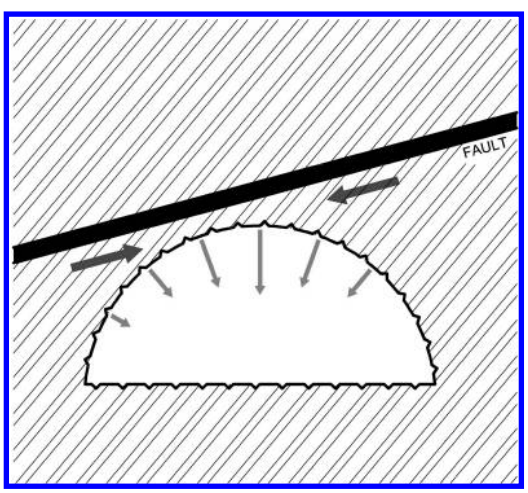


Figure 5. Geomechanical model in zones with moderately dipping faults.



Figure 6. Fault dipping moderately to the south.

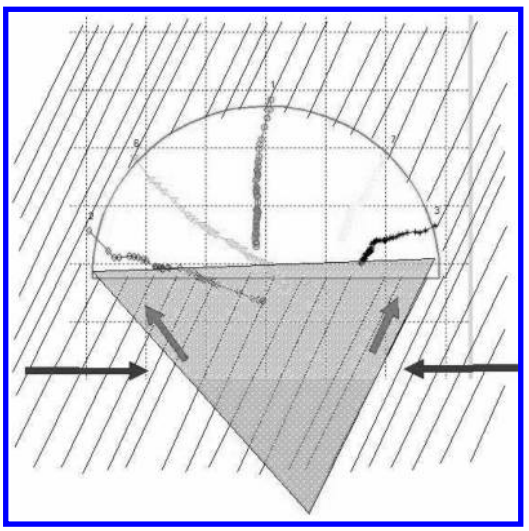


Figure 7. Geomechanical model of bottom-lift (after Prof.W. Schubert).

deformations over long periods of time. These were, depending on the relocation of the faulting, mostly asymmetrical.

Steeply dipping discontinuities, acutely tangential or parallel to the tunnel axis, predominated along long stretches of the excavation. This geometry meant that the faults influenced the tunnel drive over distances of several hundred meters. As a result of the high degree of faulting, rock mass strength parallel to the faulting had to be graded as moderately poor to poor. The geodetic displacement measurements displayed, especially in the eastern drives at of an overburden of about 500 m, strata-induced asymmetrical deformation and long-continuing displacements. The typical compression of "rhomboedric chips" in phylite was evident, which lead to strong dilation (displacement at right-angles

Copyright © 2005 Taylor & Francis Group plc, London, UK



Figure 8. Bottom-lift of 1,2 m.

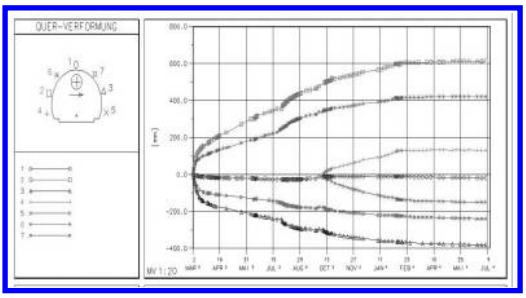


Figure 9. Typical results of geotechnical measurements.



Figure 10. High deformations exceeding provided deformation tolerances.

to the load), whereas on the right side of the tunnel, sliding occured along the plane of discontinuity.

Medium-steep to shallowly south and south-east dipping faults and sheers resulted in pronounced settling in the side walls and roof areas.

In the central area of the tunnel, with the predominately parallel striking planes of discontinuities and the accompanying longitudinal faulting, marked uplift of the bottom were evident some time after excavation.

3 DEFORMATIONS

The strata-induced long term deformations (asymmetric), due to exceeding the ground deformation tolerance over distances of several kilometers, despite "moderate" initial displacement, reached as much as 60 mm. The maximum displacements within the measured cross-section were, in accordance with the plane of discontinuity, in the southern tunnel area. The results some months after initial monitoring showed a decreasing deformation of about 4 mm per month; however, this was only after a combination of refurbishing the existing support and installing additional bolts and completing succeeding construction phases, such as bench and bottom.

In contrast, the connecting tunnels, where discontinuities was at right-angles to the excavation, only slight deformation were detected. This illustrates the influence of the orientation of the discontinuities and fault planes with respect to the tunnel axis.

4 SUPPORT MEASURES

Adaptable tunnelling methods provide a number of possibilities for adapting tunnel advance and support measures to a wide field of ground behaviour. The necessary support to counteract squeezing phenomena in the central tunnel area was based mainly on massive bolting. This meant as many as 30 or more SN bolts with a load capacity of 350 KN had to be installed per tunnel meter.

The bolt length of sometimes 8 m, sometimes 6 m, and also sometimes 12 m, was determined by the surrounding rock and the degree to which rock mass strength was exceeded, as well as the distance from the excavation cavern to the faulted zones. In accordance with the geomechnical model, bolting was asymmetrically installed. Bolt frequency and length was determined by the degree of measured displacement.

Because of the strong radial deformation, the shotcrete lining could not be monolithically implemented, and was therefore subdivided by two to four longitudinal deformation slots. In order to maintain the load

Copyright © 2005 Taylor & Francis Group plc, London, UK



Figure 11. Top heading with extensive bolting and deformation slots and with lining-stress controllers.



Figure 12. Detail of deformation slots with lining-stress controllers.



Figure 13. Lining- stress controllers after deformation.

capacity of the lining, the slots were fitted with steel lining-stress controller (yielding steel) elements. Ideally, the rigidity of these elements is slightly less than that of the shotcrete lining. This largely prevented uncontrolled destruction of the lining. Lattice girder arches were implemented at distances of 1,0 m to 1,2 m.

5 CONTRACTUAL ISSUES

In order to effectively control such difficult phenomena, which can hardly be reliably predicted at high overburden, both the owners and the contractors need experienced decision-making staff (supervisors, geologists, geotechnical experts, and staff for geotechnical measurements) on site.

However, over and above the technical problems, contractual processes are decisive. Flexible tunnelling methods also require flexibility in tendering documents, calculation of costs, and payment regulations. To meet these demands, the Austrian standard, ÖN B2203 (1994 and 2001), was chosen. This standard represents an entirely new approach to classification of excavation costs; namely, a numerical evaluation of the influence of excavation costs by support and round lengths for top heading and bench, and non-numerical invert excavation classification according to open length and construction type.

Achievable performance, and with it also the costs of conventional tunnel driving, depend above all on round-lengths and the intensity of support measures that have to be implemented. Performance is, furthermore, influenced by the subdivision of the cross-section and of the rock mass strength.

The excavation classes of top heading and bench are defined by two characteristic values. The first of these is round-length, the other is the support factor, which reflects the cost of support measures. Support measures include various types of support, each of which influence the excavation progress to different degrees. An evaluation of individual support measures is therefore necessary. The rating factor, a dimensionless quantity per support unit, indirectly reflects the difficulty of implementation.

The new standard has been applied in 20 rail and road tunnels during the past ten years. Today we can say that the goal of the code, namely to create an objective and accountable basis for calculation and cost accounting, has been successfully achieved.

REFERENCES

Felsbau 1/2004 spec. issue Strenger Tunnel

H.Westermayr Außergewöhnliche Deformationen.… DACH Treffen Tagung Luzern

Univ.-Graz; Prof.W.Schubert Numerical simulations and reports by Dept. of Rock Mechanics and Tunnelling.

Copyright © 2005 Taylor & Francis Group plc, London, UK

A study on the development of MI (Multiple Index) System for risk assessment of tunnelling in urban subway

Y.G. Wye, J.K. Park, D.U. You, C.R. Choi, Y.G. Kim & D.H. Lee
Sambo Engineering Co. LTD., Seoul, Korea

ABSTRACT: A quantitative method for estimating the risk factors in tunneling, called by the MI(Multiple Index) System is suggested in consideration of the complex effect in subway construction. It is verified that various risk factors can be expressed by stability and environment index using numerical and multi-variate statistical analysis. Stability index, MI-S includes the factors of safety of ground condition, the amount of ground settlement, condition of inflow and earthquake as a variable, and environment index, MI-E includes vibration and noise by blasting and metro train under construction and operation as a one. Finally, the applicability of quantitative assessment method using stability and environment index are evaluated and utilization method in designing tunnel in Seoul subway is reviewed.

1 INTRODUCTION

Urban subway have many problems and risks such as safety, stability and environmental influence in excavation and operation, because that is generally constructed in the vicinity of the existing structures and excavated at weathered soil and rock in shallow depth. Therefore, it is important that support system and reinforcement method should be determined reasonably and quantitatively in consideration of stability of tunnel, the settlement of adjacent structures and environmental influences such as vibration and noise by blasting.

However, tunnel design mainly depends on empirical method due to the absence of quantitative assessment criteria for the risk factors. It is necessary for the new assessment method to consider the risk factors including stability and environmental effect in designing the tunnel at urban region.

In Korea, many subways are planned and constructed in Metro city, such as Seoul, Daegu, Daejeon and Kwangju, but the popular complaints are occurred, according to unstability of buildings, noise and vibration by blasting and train operation. Thus, the various risk factors in tunneling must be studied at the planning stage for the reasonable construction of subway.

In this study, MI(Multiple Index) for considering the risk factors in tunneling is developed and MI system is suggested to assess quantitatively the risk in urban subway tunnel such as ground condition, ground water, adjacent buildings, noise and vibration. Firstly, considering the stability and environmental influence in urban subway tunnel, the risk factors are selected and can be expressed by stability and environmental index using numerical and multi-variate statistical analysis. Stability index, MI-S includes the factors of safety of ground condition, the amount of ground settlement, and condition of inflow, and environment index MI-E includes vibration and noise by blasting metro-train under construction and operation.

Also, MI system is applied to verify the validity in tunnel design at urban subway and planned the excavation, reinforcement and measurement. It is reviewed that MI system can be used as a quantitative index in tunnel design through the application case of tunnel in Seoul subway.

2 DEVELOPMENT OF MI SYSTEM

2.1 *Constitution of MI System*

It is necessary for consideration for various factors in tunnel design at urban subway because of safety and stability tunnel and buildings. Especially, importance of environmental factors such as noise and vibration under tunneling and operating are increasing. In this study, influence factors are selected considering stability and environment effect in tunneling. As shown in Table 1, total 8 factors are selected and evaluated for MI(Multiple Index) system.

2.1.1 *Risk factors for stability in tunnelling*

(1) Ground Condition: Tunnel stability is analyzed by using shear strength reduction method(SSR),

Copyright © 2005 Taylor & Francis Group plc, London, UK

which is repeatedly calculated the safety factor of tunnel for quantitative evaluation in according to reduction of shear strength (c, ϕ) of soil and rock.

(2) Ground Settlement: Influence of adjacent buildings in tunnel excavation is evaluated by numerical analysis. In this study, maximum strain and settlement of buildings are analyzed for stability of adjacent buildings.

(3) Inflow of Groundwater: Ground water is inflow in tunnel according to ground excavation and effected the stability of tunnel. In this study, seepage and flow analysis are conducted for evaluation of inflow of groundwater in tunnel.

(4) Earthquake: It is important of influence of earthquake in urban subway. Thus, tunnel stability for earthquake is evaluated by dynamic analysis using amplification of earthquake vibration.

2.1.2 *Risk factors for environment in tunnelling*

(1) Vibration and Noise by Blasting under Tunnel Construction: Vibration and noise by blasting under tunnelling are evaluated the equation of vibration and noise from experimental blasting in borehole.

(2) Vibration and Noise by Metro Train under Operation: Subway are planned near buildings and the buildings are effected by vibration and noise by train operation. Noise and vibration by metro train is calculated by equation (1) and (2).

Table 1. Risk factors and constitution of MI-System.

Risk factors in tunnelling			MI-System
Stability and Safety for tunnel structure	Ground condition	M_F	Stability index MI-S
	Ground settlement	M_S	
	Groundwater	M_W	
	Earthquake	M_E	
Environmental influence for adjacent buildings	Vibration and noise by blasting under construction	M_{V1} M_{N1}	Environment index MI-E
	Vibration and noise by metro train under operation	M_{V2} M_{N2}	

$$L_a = 59 - 20 \log d \ [dB(a)] \quad (1)$$

$$L_v = L_o - [A_1 \log (r/r_o) + A_2 r] \quad (2)$$

2.2 *Evaluation of multiple index*

2.2.1 *Grouping of multiple index*

The various factors that effected in tunnel stability are expressed quantitatively by using statistical analysis. Thus, the correlations of these factors are analyzed through multi-variate statistical technique for the grouping the factors.

In this study, the factors are divided two groups, one is stability index, MI-S including M_F, M_S, M_W, and M_E, the other is environment index, MI-E including M_{V1}, M_{N1}, M_{V2} and M_{N2}. The results are shown in Table 2 and Figure 1.

2.2.2 *Classification of multiple index*

The value of these risk factors are calculated by the various analyses and classified by some ranges, as shown in Table 3. But, the criterion of these classifications for Multiple Index is necessary for the more verification.

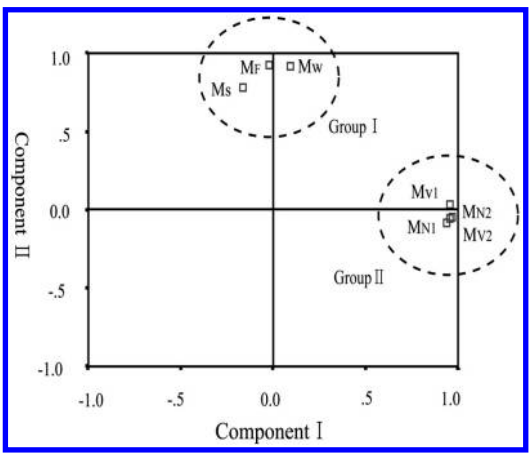


Figure 1. The result of multi-variate analysis.

Table 2. Correlation analysis for risk factors.

	M_F	M_S	M_W	M_{V1}	M_{N1}	M_{V2}	M_{N2}
M_F	1.0000						
M_S	0.821	1.0000					
M_W	0.567	0.550	1.0000				
M_{V1}	0.025	0.102	−0.149	1.0000			
M_{N1}	−0.096	0.019	−0.141	0.857	1.0000		
M_{V2}	−0.081	0.023	−0.161	0.915	0.928	1.0000	
M_{N2}	−0.093	0.029	−0.223	0.863	0.875	0.856	1.0000

Copyright © 2005 Taylor & Francis Group plc, London, UK

2.2.3 *Grading of Multiple Index*

The value and class for each factor for stability and environment are summed and graded 5 classes. The class means the stable and risky grade, that is, MI-S are graded from S1 to S5, and MI-E are graded from E1 to E5, as shown in Table 4.

3 APPLICATION OF MI SYSTEM

3.1 *The outline of subway tunnel*

This project is one of the extensions of Line 3 at Seoul subway, from Garak-dong to Ogum-dong. Total length is 1577 m including two stations. The tunnels consist of 2-Arch tunnel at Station 302 and 303, main tunnels with double and three tracks. The geological longitudinal profile of this subway is shown in Figure 2, the deep layer of alluvial soil is investigated at beginning and the fault zone at terminal region.

3.2 *Evaluation of MI in subway tunnel*

The risk factors of Multiple Index are selected for influence of stability and environment for tunnel. Also, the value for the factors were calculated from numerical analysis at 20 m intervals and showed the distributions of value of Multiple Index for all tunnel sections in Figure 3 and Figure 4.

As shown in Figure 3, M_F is showed the low values at the section with weathered soil and rock and faulted zone. M_S, that is, stability for adjacent buildings is the low grade at main tunnel sections because of shallow depth to buildings. Also, inflow of ground water at 302 tunnel sections is greatly increased and M_F is showed the low values. The influence of earthquake for tunnel, M_E is showed the low values at faulted zone in terminal section.

The results of vibration and noise by blasting and metro train under construction and operation are shown in Figure 4. The effects of noises by blasting and metro train are greatly increased at cut and cover section in shaft and station. Also, the effects of vibration by blasting are greatly increased at Station 302 section that many buildings are located at near distance.

Finally, the distribution of Multiple Index, MI-S and MI-E are obtained from these analyses for the stability and environmental effect, as shown in Figure 5. The classes of MI-S are high ranked at Station 302 section and faulted zone in terminal because of

Table 4. Grading of Multiple Index (MI-S and MI-E).

	MI-S		MI-E	
Remarks	Class	Range	Class	Range
Very Stable	S1	20<	E1	20<
Stable	S2	21–40	E2	21–40
Medium	S3	41–60	E3	41–60
Risky	S4	61–80	E4	61–80
Very Risky	S5	81>	E5	81>

Table 3. Evaluation of Multiple Index.

		Class				
Multiple Index		I	II	III	IV	V
M_F	Factor of safety	1.5<	1.5–2.0	2.0–2.5	2.5–3.0	3.0>
	Marks	10	8	6	4	2
M_S	Max.tension strain	0.1>	0.1–0.05	0.05–0.01	0.01–0.005	0.005<
	Marks	10	8	6	4	2
M_W	Inflow rate (m^3/min/km)	3.0>	3.0–2.5	2.5–2.0	2.0–1.5	1.5<
	Marks	10	8	6	4	2
M_E	Acceleration (g)	0.3>	0.3–0.25	0.25–0.2	0.2–0.15	0.15<
	Marks	10	8	6	4	2
M_{V1}	Velocity (cm/.sec)	0.4>	0.4–0.3	0.3–0.2	0.2–0.1	0.1<
	Marks	10	8	6	4	2
M_{N1}	dB	70>	70–60	60–50	50–40	40<
	Marks	10	8	6	4	2
M_{V2}	dB	70>	70–60	60–50	50–40	40<
	Marks	10	8	6	4	2
M_{N2}	dB	40>	40–35	35–30	30–25	25<
	Marks	10	8	6	4	2

Copyright © 2005 Taylor & Francis Group plc, London, UK

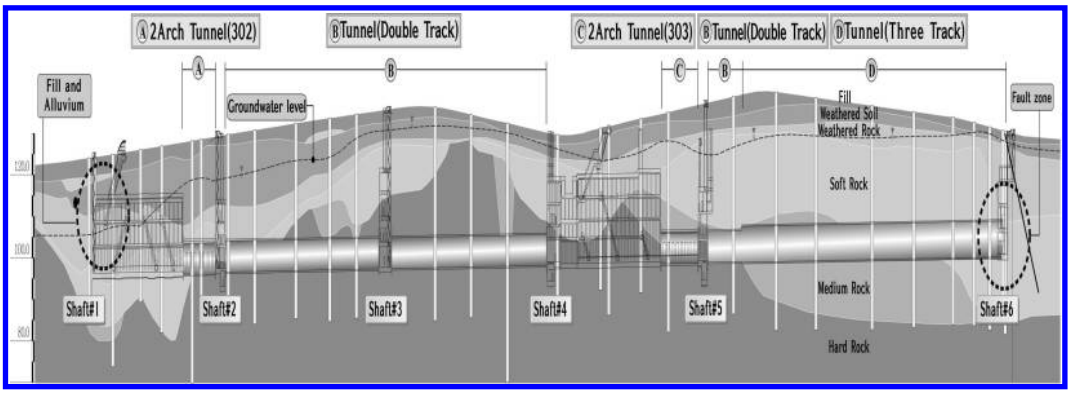
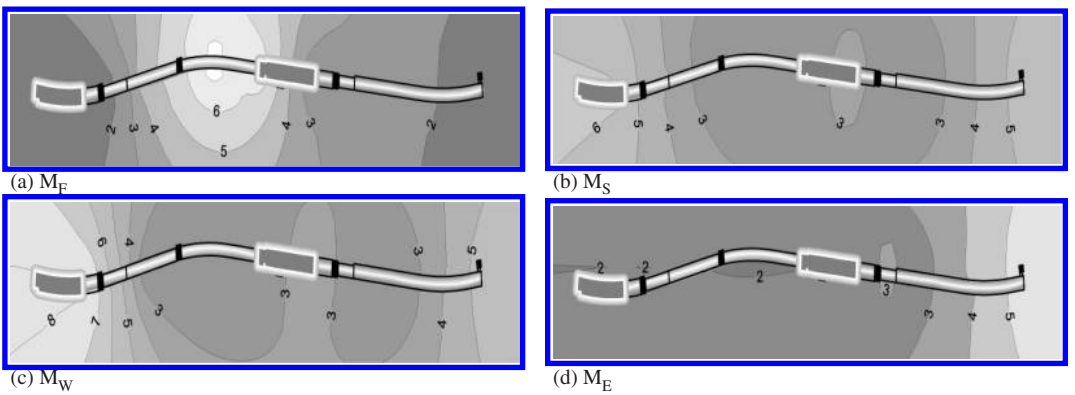


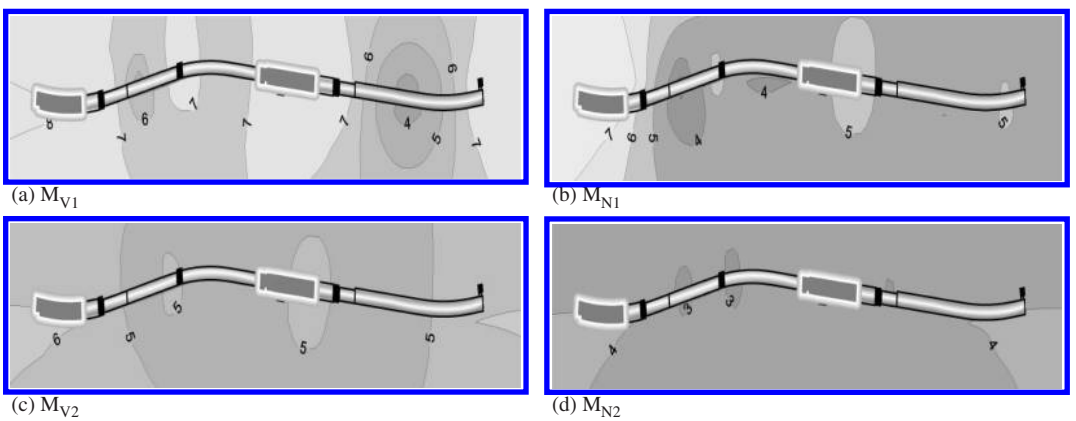
Figure 2. Geological longitudinal profile of extension of Line 3 in Seoul subway.



(a) M_F (b) M_S

(c) M_W (d) M_E

Figure 3. Distribution of the risk factors of MI-E in subway tunnel.

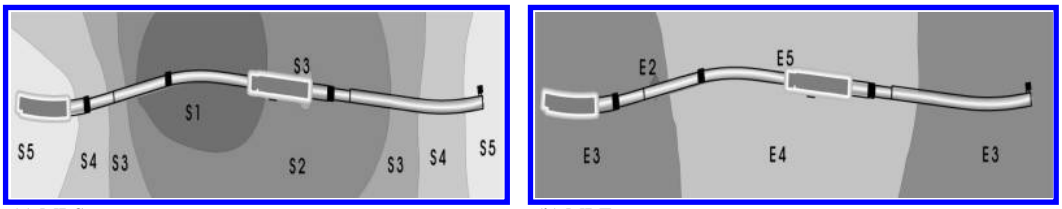


(a) M_{V1} (b) M_{N1}

(c) M_{V2} (d) M_{N2}

Figure 4. Distribution of the risk factors of MI-E in subway tunnel.

Copyright © 2005 Taylor & Francis Group plc, London, UK



(a) MI-S (b) MI-E

Figure 5. Distribution of Multiple Index in subway tunnel.

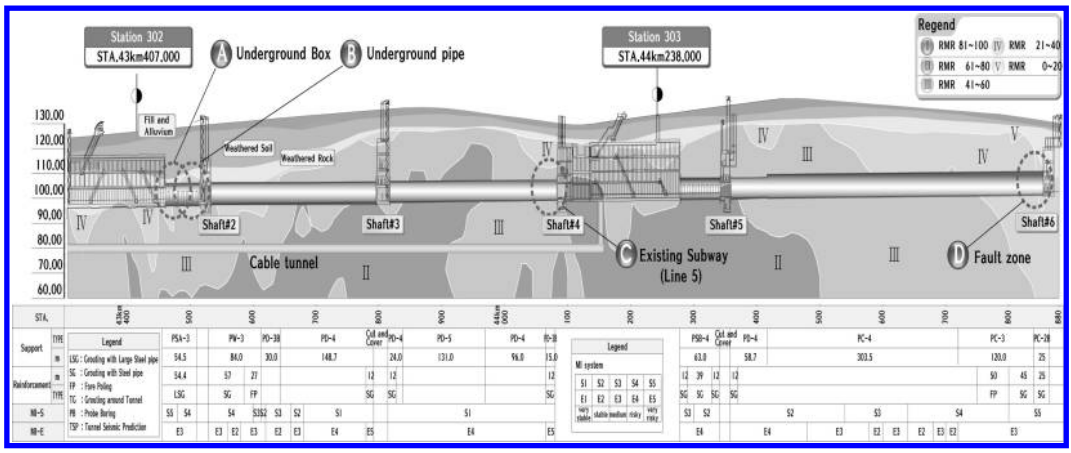


Figure 6. Application of MI System for tunnel design in Seoul subway.

ground condition and large cross section. The class of MI-E are high ranked at main tunnel section with double track cross section due to near excavation.

3.3 *Application for MI System in subway tunnel*

MI(Multiple Index) system is applied to the optimum design of subway tunnel, such as the selection of excavation, reinforcement, grouting and measurement. For total section of tunnel, the value and class of MI-S and MI-E are evaluated and compared to the class of rock mass, such as RMR and Q-system. The case of application for MI system for subway tunnel is shown in Figure 6.

In this case, mechanical excavation is designed at the section of the class of MI-S, S5 and the class of MI-E, E5. Blasting excavations are applied at the others. Ground grouting for preventing inflow of groundwater is applied at the section of the class of MI-S, S5. Also, measurements of vibration and noise are planned at the tunnel section of the class of MI-E, E4-E5 for minimizing the environmental influence in tunnelling at urban region.

4 CONCLUSIONS

There are many risk factors in tunnelling in urban region. In this study, MI system is suggested to assess quantitatively the risk factors in urban subway tunnel, such as ground condition, groundwater, adjacent buildings, noise and vibration. The factors are selected considering the stability and environment and graded through numerical analyses and empirical equation, thus two groups are classified using multi-variate statistical analysis, that is, the index for the tunnel stability, MI-S and the index for environmental influence, MI-E. The Index is divided by the 5 classes and evaluated the stable and risky grades.

MI system is applied to verify the validity in tunnel design at urban subway in Seoul and planned reasonably the excavation method, reinforcement type and measurement. It is showed that MI system can be used as a quantitative index in tunnel design through the case of subway tunnel. But the criteria and the evaluation method for the risk factors must be reviewed through the verification and application in tunnel design and construction.

Copyright © 2005 Taylor & Francis Group plc, London, UK

REFERENCES

Y.G. Wye, J.K. Park, S.K. Jwun and Y.G. Kim (2002), "Development and Application Multiple Index for Reasonable Tunnel Design" The Proceedings of Korean Society for Rock Mechanics and Engineering, pp. 31–42.

C.R. Choi, J.K. Park, D.U. You, Y.G. Kim and D.H. Lee (2003), "Development and Application MI System for Tunnel Design", The Proceedings of Korean Tunnelling Association, pp. 260–261.

The Report for Tunnel Design for 3-line Extension 302 Division at SEOUL Subway(2003), Seoul Metropolitan Government.

P.B. Attewell and J.P. Woodman (1982), "Predicting the Dynamics of Ground Settlement and Its Derivatives caused by Tunneling in Soil", Ground Engineering, Vol. 15, No. 8, pp. 13–22.

P.B. Attewell and R.K. Taylor (1984), "Ground Movements and Their Effects on Structures", Survey University Press, USA.

E.M. Dawson et al. (1999), "Slope Stability Analysis by Strength Reduction", Geotechnique Vol. 49, No. 6, pp. 835–840.

Copyright © 2005 Taylor & Francis Group plc, London, UK

Determination of construction method for Young Dong Tunnel by risk assessment

Yong-Il Kim
Daewoo E&C CO., Ltd, Deputy General Manager, Ph.D.

Young-Hoon Yoon
Daewoo E&C CO., Ltd, Project Manager

Sang-Kook Cho
Daewoo E&C CO., Ltd, Executive Managing Director

Jang-Su Kim
Korean National Railroad, Construction Manager

Nai-Yong Lee
Daewoo E&C CO., Ltd, Manager

ABSTRACT: The construction method for the Young Dong Tunnel has been chosen following detailed risk assessment. In this paper, the specific risks to the project programme, associated with adopting either mechanical excavation in the form of a shielded TBM, or drill and blast excavation methods, are assessed. From the risk assessment results, and taking other important factors into account, such as project sensitivity and local experience, the recommendation is made that the relatively low risk drill-and-blast method is the most appropriate for construction of the Young Dong Tunnel.

1 INTRODUCTION

The major part of the Young Dong Railroad Relocation Project proposed by Korean National Railways (KNR) consists of the construction of a tunnel in rock approximately 16.3 km long with a span of approximately 8 m, it will be the longest tunnel in Korea (Fig. 1). The tunnel is designed to carry a single-track railway in a large radius loop below mountainous terrain in eastern Korea. The maximum depth of the tunnel is approximately 400 m with most of the alignment being at depths in excess of 100 m.

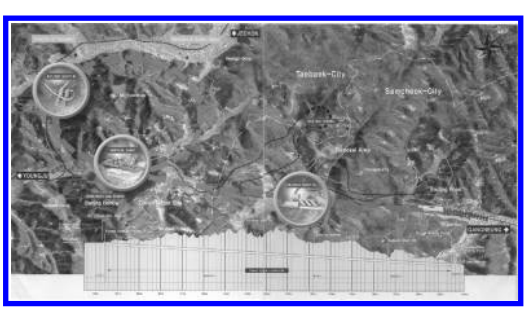


Figure 1. Route map.

2 GEOLOGY OF THE SITE

The proposed tunnel alignment passes through geological formations ranging from Cambrian to Triassic in age. Expected lithologies intercepted by the alignment include conglomerates, quartzite, sandstones, shales, limestone and coal measures. Cretaceous volcanics also outcrop in the area but these are expected to be well above the proposed invert level. (Fig. 2)

The key geological factors recognized for assessing appropriate construction methods for the tunnel are as follows:

- potentially high water pressures, up to 40 bars (40 kgf/cm^2) pressure
- fault zones, possibly associated with significant groundwater inflows

Copyright © 2005 Taylor & Francis Group plc, London, UK

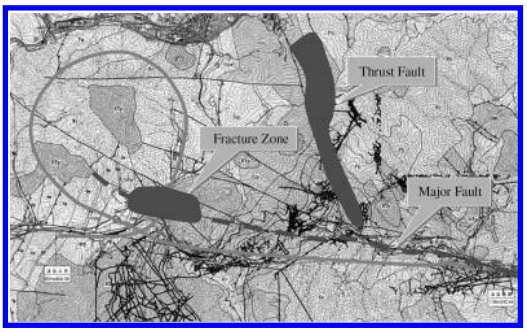


Figure 2. Geology of the site.

- highly sheared and closely jointed rocks
- some rocks with high strength and abrasively
- possible karstified (cavernous) limestone with groundwater
- coal measures rocks and old mine workings.

3 RISK ASSESSMENT METHOD

A risk assessment method has been developed to make a quantitative and objective assessment of the construction methods of Young Dong Tunnel. The risks associated with tunnel excavation are dependent on the hazards encountered and are defined with respect to programme (rather than other issues such as safety or cost).

The likelihood of a hazard occurring is assumed to be at one of three levels, thus: 1. Probable, 2. Occasional, 3. Remote.

In turn, the degree of consequence of each hazard is assumed to be at one of five levels, namely: 1. Catastrophic, 2. Critical, 3. Serious, 4. Marginal, 5. Negligible.

The description and scale of the above levels of likelihood and consequence are given in Table 1 below.

The level of risk for each hazard can be determined by finding its likelihood of occurrence and considering its consequence. The level of risk associated with the hazard is then established conventionally as follows:

$$\text{Level of Risk} = \text{Likelihood} \times \text{Consequence}$$

Once the level of risk has been ascertained, it can be compared with Table 2 below to identify the action that should be taken to mitigate the risk.

Having made an assessment of the risk associated with each hazard, appropriate mitigation measures are considered. The residual risk remaining after mitigation is then assessed in the same way to determine acceptability or otherwise.

Table 1. Definition of risk to programme.

Title	Description	Scale
Likelihood		
Probable	Likely to occur during the construction of the tunnel, possibly on more than one occasion	3
Occasional	Likely to occur at least once during construction of the tunnel	2
Remote	Unlikely to occur during construction of the tunnel	1
Consequence		
Catastrophic	Total loss of a section of tunnel	5
Critical	Major damage or delay to tunnel or major environmental impact affecting programme	4
Serious	Some damage or delay to tunnel or some environmental impact affecting programme	3
Marginal	A routine maintenance repair to tunnel or minor hindrance	2
Negligible	Of little consequence to programme	1

4 RISK ASSESSMENT

The assessment of risks associated with the use of a shielded TBM to excavate a hard rock tunnel is presented in Table 3, and that for drill and blast excavation is presented in Table 4.

5 RESULTS AND DISCUSSION

It can be seen from an initial inspection of Tables 3 and 4 that the number of hazards associated with a shielded TBM at Young Dong would be much greater than for the drill and blast method. The principal reasons for this include the:

- The sophistication of modern TBMs which require a high level of technological input for their successful operation and maintenance
- The relative inflexibility of mechanized excavation and lining systems to deal with conditions for which they may not have been specifically designed
- The dependence of the tunnel progress entirely on the performance and reliability of a single item of mechanical plant.

Copyright © 2005 Taylor & Francis Group plc, London, UK

Table 2. Risk classification.

Likelihood	Consequence				
	Catastrophic	Critical	Serious	Marginal	Negligible
Probable	15	12	9	6	3
Occasional	10	8	6	4	2
Remote	5	4	3	2	1
Score					
10–15	Very high risk – not acceptable for tunnel construction – need to apply mitigation measures to eliminate or reduce risk				
6–9	High risk – apply mitigation measures to eliminate or reduce risk. Residual risk at this level indicates need for active management control and response plans to be well developed with well trained personnel, materials and plant readily available				
1–5	Low risk – may be accepted if mitigating measures are in place under active management control				

Table 3. Programme risk assessment for excavation by shielded TBM with segmental lining.

			Risk level				Residual risk level		
	Hazard	Risk	L	C	R	Mitigation measures	L	C	R
1	Highly jointed rock mass	Ravelling ground, roof falls	3	4	12	1. Shielded TBM 2. Probing and pre-injection grouting	2	2	4
2	Fault zones	Soft ground with potential roof falls	3	4	12	1. Drag bits on cutter head 2. Shielded TBM	3	3	9
3	Squeezing ground	Ground “comes on” to the TBM	3	4	12	1. Provision of “enlarging” cutters 2. Provision of adequate trust	3	3	9
4	Cavities in the rock mass	Instability of tunnel face, roof falls	3	4	12	1. Provision of TSP 2. Provision for probe drilling	2	3	6
5	High strength rock	High UCS for rock mass	3	3	9	1. Shallow cutting head 2. Double shield TBM with grippers	3	2	6
6	Abrasive rocks	Increased rate of disk cutter wear	3	3	9	1. Shallow cutting head 2. Back-loaded disk cutters	3	2	6
7	Variable quality rock mass	Mixed face conditions causing mucking difficulties	3	4	12	1. Provision of drag bits to excavate “soft” ground 2. Shielded TBM with gripper	3	3	9
8	Mechanical failure	Failure of mechanical component	3	4	12	1. Shallow cutting head 2. Provision of variable speed drive 3. Reversible cutting head	2	3	6
9	Water ingress, possibly	Water in cavities, entering face during excavation	3	4	12	1. Bolted segmental lining provided with compression gaskets 2. Probing and pre-injection grouting	2	3	6
10	Fire in TBM	Fire in TBM	1	5	5	1. Fire suppression system 2. Non-flammable oils and lubricant	1	4	4
11	Segmental lining erection	Risks of segments drop	3	5	15	1. Fail-safe segment erector 2. Safe segment handling system	1	5	5
12	Tunnel ventilation	Possible occurrence of explosive gases	3	5	15	1. Fresh air to the TBM and face 2. Atmospheric monitoring system	1	4	4
13	Broken drill	Cutter-head damage	2	4	8	1. Provide retrieval equipment	1	4	4

Copyright © 2005 Taylor & Francis Group plc, London, UK

Table 4. Programme risk assessment for excavation by drill and blast.

	Hazard	Risk	Risk level L	C	R	Mitigation measures	Residual risk level L	C	R
1	Highly jointed rock mass	Ravelling ground, roof falls and sidewall and/or face instability	3	4	12	1. Reduce length of excavation advance 2. Reduce powder factor to lessen blast damage	2	2	4
2	Fault zones	Soft ground or mixed face conditions	3	4	12	1. Increase rock support 2. Probe drilling ahead of the excavation face	3	2	6
3	Water ingress	Water in cavities entering excavation	3	4	12	1. Pre-injection grouting 2. Provision of pumps to cope with high flows	2	2	4
4	Cavities in the rock mass	Instability of tunnel face, roof fall and side wall instability	3	4	12	1. Provision of TSP to identify cavities in advance of excavation 2. Provision of probe drilling	2	3	6
5	Tunnel ventilation	Explosion risk	3	5	15	1. Provision of adequate fresh air 2. Atmospheric monitoring system	1	4	4
6	Mechanical breakdown	Failure of key item of plant	3	3	9	1. Planned maintenance strategy 2. Maintain spare plant items	3	1	3
7	Use of explosives	Premature detonation	2	5	10	1. Use non-electric detonators 2. Comply with safety regulation	1	5	5

Table 3 identifies a total of 13 significant hazards connected with the TBM method. The risk classifications can be summarized as follows:

	Number of hazards before mitigation	After mitigation
Very high risk	9	0
High risk	3	8 (Average score 6.9)
Low risk	1	5

Thus, although it can be seen that the areas of very high risk can be successfully eliminated, the majority of the residual risks are classified as "high", with an average score of 6.9 (in a "high risk" range of 6–9, see Table 2).

Table 4 identifies a total of 7 significant hazards connected with the drill and blast method. The risk classifications in this case can be summarized as follows:

	Number of hazards before mitigation	After mitigation
Very high risk	7	0
High risk	0	2 (Average score 6.0)
Low risk	0	5

Again it can be seen that all areas of very high risk can be successfully eliminated, but in this case slightly more than 70% of the residual risks are classified as "low". The residual risks in the "high risk" category have an average score of 6.0 (in a "high risk" range of 6–9, see Table 2).

The *average* level of risk of *all* hazards after mitigation in each case can be summarized thus:

- TBM method
  - 13 No. hazards in total
  - Average risk classification after mitigation 6.00 (marginally "high")
- Drill and blast method
  - 7 No. hazards in total
  - Average risk classification after mitigation 4.60 ("low")

It is recognized that the above assessment of programme risk is largely qualitative and to a certain extent subjective. Also, the differences in the numerical scores are not large, although this is partly due to the simple scoring system adopted. However, a general trend is apparent which indicates that

- There are likely to be for more significant risks which may impact on programme associates with the use of a TBM than with the drill and blast method – a total of 13 No. for TBM compared with 7 No. for drill and blast
- The level of residual risk after mitigation is likely to be generally higher with a TBM than with drill and blast.

Copyright © 2005 Taylor & Francis Group plc, London, UK

6 CONCLUSION

A risk assessment method has been developed and applied to make a quantitative and objective assessment of the construction methods of Young Dong Tunnel.

The risk assessment results show that the drill – and – blast method would be a relatively low risk approach, whereas a shielded TBM would provide a generally higher risk approach in Young Dong area with the hazards of coal measures rock, old mine workings, and fault zones.

REFERENCES

Halcrow (1999), *Tunnel Construction Methods, Young Dong Railroad Relocation Project Report to Daewoo E & C Co., Ltd.*

Halcrow (1999), *Geology Review and Recommendations for Ground Investigations, Young Dong Railroad Relocation Project Report to Daewoo E & C Co., Ltd.*

Halcrow (1999), *Tunneling Through Coal Measures Methods and Case Histories, Young Dong Railroad Relocation Project Report to Daewoo E & C., Ltd.*

Copyright © 2005 Taylor & Francis Group plc, London, UK

Managing the construction contract for the tunnels of the Bilbao Metro

J. Madinaveitia
IMEBISA, Bilbao, Spain

ABSTRACT: A number of special factors arising from the local political and administrative system influence the management of the entire Bilbao Metro construction project.

After a brief summary of this particular political framework, the paper provides a detailed description of the way underground work on the Bilbao Metro is monitored and controlled.

1 BILBAO AND ITS METRO

Bilbao is the financial capital of the Basque Country. Located in northeast Spain overlooking the Bay of Biscay, some one hundred kilometres from the French border, the city's port is one of the most important in the area, with quays and wharves with natural clearance of more than thirty metres.

Founded as a city in 1300 on a bend in the river, fourteen kilometres from the sea, Bilbao started life as a fishing port, later flourishing as a centre of trade and commerce.

With the advent of the industrial revolution, the city's iron mines became increasingly valuable, helping to create a shipbuilding industry that produced the vessels needed to take the iron to England. The vessels returned loaded with English coal for the city's own budding iron and steel industry.

To accompany the industrial development, residential areas gradually grew up on both banks of the river down to the sea, bringing the overall population in the city and environs to more than one million.

The river valley is very narrow and communications are basically linear, running along each bank so as not to interfere with port and industrial facilities, as far as the city's financial and commercial district, which is where most of the city's road bridges are located. With such priority being given to navigation along the river, road traffic congestion was inevitable, and the 1980s saw major problems on the roads into the city centre. Circulation levels threatened to bring many streets to a complete halt.

To solve this problem, in part at least, the Metro was designed as a mass passenger service. Line 1 of the Metro began to operate in 1995.

Adapting to the shape of the valley and servicing the demand for return journeys in and out of Bilbao, the Bilbao Metro is designed as a kind of Y. The left and right upper branches provide a service along either bank of the river, while the shared lower stem runs under the city centre and the old mediaeval quarter before continuing upriver to the larger districts to the east of the city.

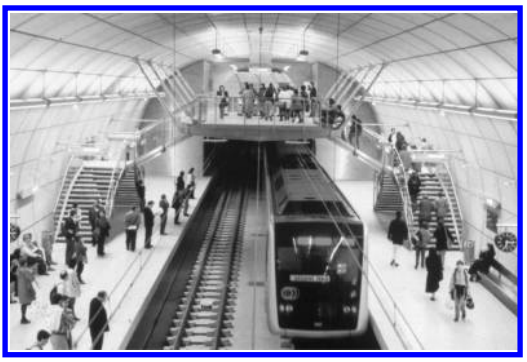


Photo 1. Station with passengers.

The branch running along the right bank of the river uses an old rail track that was upgraded, while the rest of the Metro, both the line on the opposite bank and the shared section and its prolongation to the east, is newly built and runs underground. (Photo 1)

With two lines eventually covering forty kilometres in all, 32 kilometres are now in service and work is well advanced on a further four, which are scheduled to be inaugurated in two phases, the first in January 2005.

2 POLITICAL AND ADMINISTRATIVE BACKGROUND

The Kingdom of Spain is a constitutional regime that acknowledges the autonomous nature of the regions within the kingdom. The regime, which logically involves a far-reaching process of decentralization,

Copyright © 2005 Taylor & Francis Group plc, London, UK

has a number of unusual features when it comes to finding solutions in different areas of the administration.

The Basque Country in particular has a somewhat peculiar political administrative system, which needs to be gone into in some detail if we are to understand the way the Bilbao Metro project is managed.

The Statute of Autonomy of the Basque Country recognizes the region has a Parliament, elected by universal suffrage by the region's voting population. The parliament elects the President of the Government, who puts together an autonomous government to wield the powers that the central Spanish government has totally or partially transferred to it.

To execute its programme, every year the autonomous government presents to its own Parliament a Budget that includes the regulatory capacity to collect general taxes. However, the Basque Government does not collect these taxes directly, as they are collected by an intermediate body in each of the three Basque provinces known as the *Diputación*, or Provincial Council, also part of the autonomous system.

The Basque Country comprises three provinces, Alava, Vizcaya and Guipúzcoa, each of which has a certain subsidiary level of autonomy, with their own provincial parliaments known as *Juntas Generales*, or General Assemblies, also elected by universal suffrage.

The *Juntas Generales* elect a *Diputado General*, or Chief Executive, who then forms his own government for the province in question, with a view to applying its programme of government. The government of the *Diputación* in each province has the power to collect taxes.

By an agreement between the three *Diputaciones*, or Provincial Councils, and the Basque autonomous government, the latter's budget receives funds collected through these taxes.

Through this complex mechanism, the autonomous community takes responsibility for these taxes, transferring part of them to the central government to cover the costs of non-transferred general services such as defence.

3 LEGAL AND FINANCIAL FRAMEWORK

A law of the Kingdom of Spain created the "Bilbao Metro". This law defined the main parameters of the legal and financial framework for the project, its subsequent execution and the way the new transport system should be run.

The Spanish Government's Ministry of Transport & Public Works took responsibility for preliminary reports and studies, the decisions regarding which districts and areas should be provided with a service, general service planning and development and the drafting of projects for infrastructure, construction management and bringing the service into operation.



Photo 2. Finished tunnel.

Under the law a local body, the *Consorcio de Transportes de Bizkaia*, or Vizcaya Transport Consortium, was also set up to complete the projects by providing the superstructure. Among other things, the Consortium was charged with the responsibility of operating the system directly or of creating an operator. The latter option was chosen and the company called Metro Bilbao, S.A. came into being.

The *Consorcio de Transportes de Bizkaia* was originally created by the Spanish Government's Ministry of Transport & Public Works, the Vizcaya *Diputación*, or Provincial Council, and the town councils involved in the consortium, these being in principle the ones through which the new rail line was to be routed. (Photo 2)

From the financial viewpoint, the law states that the Spanish Government's Ministry of Transport & Public Works should finance 50% of the total investment, with the other 50% being distributed between the Vizcaya Provincial Council (*Diputación*), which would take responsibility for 25%, and the town councils in the consortium, which would share the remaining 25%, basically in accordance with population size. As a result of the transfer of powers to the autonomous community, the financial burden accepted by the Spanish Government's Ministry of Transport & Public Works was taken over by the Basque autonomous government.

The Vizcaya Provincial Council (*Diputación*) agreed to take responsibility for the 25% originally accepted by the town councils.

In short, financing for the Bilbao Metro project is currently shared 50% each by the Basque Government and the Vizcaya Provincial Council, the latter acting through the Vizcaya Transport Consortium (*Consorcio de Transportes de Bizkaia*).

4 PROJECT MANAGEMENT

The Basque government is responsible for managing the project through its Transport & Public Works Department.

Copyright © 2005 Taylor & Francis Group plc, London, UK

To carry out this project the Transport Department created a small company to manage project engineering and the works themselves. The company is called IMEBISA (**I**ngeniería para el **ME**tro de **BI**lbao, **S.A**.).

Using the preliminary studies produced by the Spanish Ministry of Transport & Public Works, the Basque Government came to its own conclusions about population distribution and demand, producing its "Bilbao Metro Construction Plan".

Besides consolidating certain routes, the Plan also had to go through public information procedures. Amendments and suggestions received from private individuals and, in particular, the municipal districts affected, were discussed and included to the extent that they upheld the initially established service criteria.

Alongside the public information procedures, which involved nearly a year of meetings and juggling with alternative routings, the Basque Government commissioned a Functional Project for the Metro and a financing report.

Likewise, for the execution of construction projects, IMEBISA drafted the basic conditions, which, together with the specifications included in the Functional Project, were to be used in the call for tenders leading to the selection of the engineering firm or firms to draft the actual projects. In this case, IMEBISA appointed one of its engineers as Project Director, to ensure the winning engineering firm would act under his orders while the work was under way.

For financial reasons, and the investment capability of the Basque Government and the Vizcaya Provincial Council, the Bilbao Metro Construction Plan was divided into construction sections, so that in each section, once work had been completed, the service could be extended to new districts, thus increasing the service itself and adjusting this to demand as far as possible.

Construction work on each section is subject to an open international call for tenders, and is published in the official EU gazette in Brussels.

The Basque Government entrusted IMEBISA with the task of successfully completing this contract. To this end, it is organized as the body responsible and director of a multidisciplinary monitoring and control team.

The members of this team are chosen by IMEBISA through an open, public call for tenders, largely for technical and financial proposals presented by engineering firms in the works zone.

In practice the management, monitoring and control team affects different areas of work, the most important of these being:

- *General management and acceptance of the monthly financial advance certificates for the works*

The IMEBISA engineer acting as works director is responsible for the general management of the works, in sole command and the acceptance of monthly financial advance certificates for the works. His functions include coordinating the other people working in the monitoring and control teams, defining the responsibilities of each group and identifying potential areas of conflict, acting as arbitrator in such cases. He does this work directly or delegates it to his technical assistants who occupy themselves with specific work areas.

- *Monitoring and controlling project specifications and plans*

The Works Management established by the contract between the Basque Government and different constructors includes notary-style attributions to enable it to certify that work executed has been done in accordance with project specifications, scrupulously following detailed plans.

- *Controlling quality of materials*

All materials arriving at work sites must have the corresponding quality certificates issued by specialist companies unconnected with the suppliers. All intermediate transport, loading, unloading and storage systems must also be controlled and accepted.

- *Acceptance of procedures governing execution and on-site arrival of the main project units*

Constructors must submit to the approval of the Works Director all material fabrication and on-site arrival processes. For tunnel boring, they are required to present the work sequence, active and passive safety measures to be applied during work runs or phases, and the possibility in real time of having all the necessary extraordinary resources and measures available should incidents arise. In all cases the Constructor, as the party with the human and material means to execute the work, takes responsibility for the methods used and measures to take; even so, these must have been previously agreed on with the Works Director, who may propose (not impose) modifications or changes if he considers that they would improve quality or safety levels.

- *Monitoring and controlling tunnel supports*

Roadheaders are used to bore the Bilbao Metro tunnels. Roadheaders are highly versatile machines greatly suited to the type of rock found in the area. They also permit changes of section and routing with ease. **(**Photo 3**)**

The base rock is marly limestone with rock mass strengths of between 30 and 50 Mpa, crossed at random by basic rock of volcanic origin with strengths of 100 to 120 Mpa. Massiveness is the main characteristic of rock in Bilbao, with faults in the mass being rare. This, together with its high tenacity (relatively high traction strength values) makes breaking it up with hammers a slow, often low yield operation.

However the rock cooperates substantially in its own stability, thus enabling support monitoring and control to facilitate progress at low cost within some

Copyright © 2005 Taylor & Francis Group plc, London, UK



Photo 3. Roadheader at rest at heading with head and heading rock in view.

very strict parameters. It is important to protect the rock as soon as possible with a layer of shotcrete to ensure the heading is not affected by weather-related factors or damp.

Support generally varies from a simple layer of shotcrete to systematic bolting in zones likely to break into blocks. In some degraded zones metal ribs are also used.

The project offers a range of solutions depending on the expected characteristics of the rock; the support to be used is decided at each heading. Three independent geologists identify and evaluate the rock, which enables the quality of the appraisals to be checked in each case.

- *Real time monitoring of tunnel and boring auscultation, including potential influence on overlying buildings*

The Bilbao Metro tunnels and some station caverns (more than 20,000 cubic metres hollowed out) run underneath buildings, some of them very old (particularly in the mediaeval district), where building and quality standards and conditions may vary tremendously. During construction and, to a lesser extent, during service operations rock response to the aggressive nature of tunnel boring is controlled.

Auscultation equipment most used inside the tunnel involves convergence measurements and movements in the rock mass, measured by rod extensometers. Rod extensometers, inclinometers and levels are also applied on the outside. All data goes onto a computer system that shows the evolution curves of the measurements at all times. The evolution facilitates action on support, which is reinforced when auscultation suggests it is needed.

- *Monitoring inspection points*

This apparently routine action is actually very important to the quality of the work, as it monitors and controls, in many cases visually only, hundreds of different aspects.

- *Health and safety at the works in general*

Bilbao Metro projects include a detailed study of safety and health conditions at the works, particularly with regard to tunnel and station cavern boring.

Specific references by the Constructor to work methods and the machinery to be used on-site complete the study, once again because only the Constructor is in a position to execute the work.

- *Acceptance of safety procedures for each major unit of works*

Before beginning the execution of each unit of works, the Constructor presents his definition of the work method, the material and human equipment and teams to be used and a study of the potential risks in each zone, establishing the individual and group protective measures to be taken into consideration for each work position and activity.

These partial reports are submitted to the general works safety coordinator, who analyzes them and has the power to increase safety measures if he considers it necessary.

- *Watching and guarding the installations*

This works health and safety team function basically involves controlling worker and team access to the works site, establishing control measures for visits and ensuring that all points where people might be able to get into the works are properly watched.

- *Environmental watch and consolidation of corrective measures*

The environmental watch team concentrates on controlling three areas. First, works on the surface that are most likely to affect traffic, pedestrians and the local people require an effort to keep people informed and areas with fences in perfect conditions, with publicity and graffiti being removed at once. Inside tunnels, in cooperation with safety officials, the environmental watch should know about lighting levels, air quality (percentages of oxygen and noxious gases) and noise at work headings, in access ways and galleries and completed tunnels. Finally during tunnel boring work, large amounts of rubble need to be removed, usually by lorries with dirty wheels, which means the most comprehensive cleaning system possible in the circumstances is required. Water pumped out from the tunnels usually carries a large percentage of slime, which has to be eliminated before the water can be added to the city's general drainage system. In the works for the Bilbao Metro it is obligatory to install a decantation system fitted with a dust and slime briquette maker that ensures total recovery of decanted water. All these systems are controlled by the environmental watch team, which at any given time implements the measures needed to find out how far the work is in compliance with the contract specifications.

Copyright © 2005 Taylor & Francis Group plc, London, UK

- *Geometric control of works (topography and detailed tachymetry)*

The Constructor has to plot works and execute them correctly in geometric terms. However Works Management has a geometric monitoring and control team covering the most important points of linear works, alignments, clearances, etc.

- *Controlling measurement and units of works*

Works contracts generated by the Basque Government are usually of the kind involving the payment of unit prices, which requires proper control of the measurement of works executed.

- *Relations with public officials and political authorities from the municipal districts 'hosting' the works*

Although works on the Metro are public and the Basque Government is totally responsible, it should not be forgotten that physically speaking the work is executed in different municipalities.

- *Relations with the Vizcaya Transport Consortium (Consorcio de Transportes de Bizkaia)*

Pursuant to the law that founded this organization, the superstructure of the line must be directly managed by Transport Consortium. Consequently, the infrastructure Works Management transfers its watch and maintenance responsibility to the Consortium as soon as sections are freed up.

- *Relations with local people in the works area*

Last but by no means least, the local people, who are most affected by the works, must be kept properly and regularly informed.

5 ECONOMIC CONTROL: RISK ANALYSIS

The Basque Government contract offered under calls for tender involve payment per unit prices.

The project produces a detailed, thorough-going report on the measurements of the units of works to be paid for only if they have been executed in compliance with the conditions established in the specifications sheets. The specifications sheet, which is an integral part of the contract, establishes the origin and quality of the materials and the way units of works should be measured and paid.

Once the work is under way, the amount of work done is measured every month by means of measurements agreed by both parties. These measurements are provisional, i.e. they may be corrected in the following months if it is shown that errors may have been made.

In underground works, this month-by-month numerical and economic control is particularly important because units of works can often only be checked as they are executed, being subsequently hidden and not susceptible of verification.

Generally, all prices have a margin of risk accepted by the Constructor in his tender, although some factors creating uncertainty in the price of boring in tunnels in particular need emphasising.

Pursuant to the contract for payment by unitary prices for tunnel boring, payment would be made for:

- Cubic metres of tunnel boring, including waste material clearance and transport to tip
- Cubic metres of concrete projected as primary support, in accordance with the thicknesses defined for each type of heading in the project
- Metres of support bolting, when the project establishes the need for bolting to reinforce support in zones where there is risk of block falls
- Kg of support ribs, to be placed in position in zones where the rock has deteriorated badly and the support needs reinforcing.

Understandably, if the rock is good quality and only shotcrete support is required, the boring process has greater continuity than when rock quality is poor and other kinds of support items are needed, which requires time. For the boring process this is time lost and is not paid for. This risk, which depends on the kind of terrain that may appear at a heading cannot be assumed a priori by the Constructor, so the Specifications Sheet includes devices for reducing the occurrence of such risk.

Basically these devices involve different formulas that take account of two or three rock characteristics at each heading and which, in accordance with these characteristics, establish a percentage supplement or reduction to be applied to the payable boring price. Other prices, such as shotcrete, bolts and ribs, remain unvaried. A limit of 20% on the basic figure tendered by the Constructor is placed on the risk accepted by the Owner.

The rock characteristics included in the formula are established in the following way. During the weekend stoppage for machinery maintenance, a probe is made at the heading. The sample taker, which must be at least twenty metres in length, is completely removed.

Before the probe is performed, the Works Management support monitoring and control official and the Constructor's Works Manager agree on two or three zones for sampling. The samples are then sent to the laboratory. The results of tests on these samples affect the payment formula.

Our experience in the works on the Bilbao Metro is that although this method of sharing risk in the more complicated unit of works is not perfect, it does help to offset, at least in part, time lost when problems arise due to poor quality rock.

6 CONCLUSION

The construction of tunnels and station caverns for the Bilbao Metro follows a fairly complex administrative

Copyright © 2005 Taylor & Francis Group plc, London, UK

process that is reflected in the way the construction phase is subsequently managed.

As the body responsible for defining and developing all rail transport systems in the autonomous community, the Basque Government approves in its budgets the financial participation required to cover 50% of the investment, proposes the works plan for each section, and negotiates with the Vizcaya Provincial Council (*Diputación*), which finances the other 50%. Once the two institutions have reached an agreement and the amount to be invested is fully available, the call for tenders for each section is announced.

From this point, IMEBISA takes over the operation, being responsible for results up to the time the works are completed and judged ready for operational service and use by the public as a new system of transport.

Copyright © 2005 Taylor & Francis Group plc, London, UK

Construction of highway tunnel financed by B.O.T. model management of risks in financing

Dr. Ünal İlker
Managing Partner
Yapi Teknik Engineering and Consulting Co. Ltd.

ABSTRACT: The Built-operate-transfer (B.O.T.) model is used in the financing of infrastructure projects. The actors of B.O.T. operations are the owner, the sponsor (borrower) and the lender. The risks of the investment must be thoroughly studied, shared among the actors and transferred to others if needed. The investment in a highway tunnel by B.O.T. model carries most of the risks common to B.O.T. projects and additional risks due to the unknowns specific to highway and tunnel projects. An analyses of the risks is presented with some suggestions specific to GÖÇEK Project.

1 INTRODUCTION

Among the financing models of infrastructure projects, B.O.T model has been utilized in many fields, such as power production, water management, transportation projects, motorways...

The three main actors in B.O.T. financed projects are: the owner, the lender and the sponsor.

The owner authorizes the sponsor to built (B) the project and collect the revenues during a given period of time called operation (O) period. At the end of the operation period, the sponsor transfers (T) the project and his rights to the owner.

The sponsor provides equity capital, sometimes with the participation of the owner. The sponsor sets the financing from the lenders, borrower being the sponsor or the project (a specially established project company). The sponsor contracts the realization of the project to the contractors and the operation of the project to an operator.

The revenues of the project operation are used to service debt, pay operating and maintenance costs and provide a return to both lenders and sponsor.

All three actors of a B.O.T. project are facing the risks but sponsors assume most of them. These are risks due to the studies, to the constructions and to the operation.

The management of the risks by identification, classification and evaluation are required by all actors and must be thoroughly prepared.

2 DESCRIPTION OF THE PROJECT

The Göcek region is in the south-west Anatolia and the small Göcek town is well known as a touristic port and famous with it's marina.

Dalaman airport is the nearest airport in the region and the road between the Dalaman airport and Göcek is the turkish national highway D400 connecting Marmaris and Muğla to Fethiye both very touristic regions.

This highway crosses a mountainuous region between Göcek and Dalaman. A tunnel of 830 meters long has been proposed to shorten the distance Göcek-Dalaman by three kilometers but the driving time, especially in high season will be shortened by 30 to 45 minutes.

A private turkish group has applied to built the tunnel by B.O.T model and has signed the contract with the Turkish Highway Authorities as a private company in the form of a joint venture, on November 14, 2003. The contract states that the partners of the joint venture will form a new company, named here as "Project Company" and the only activity of this company will be the activities related to the accomplishment of the contract. This company will:

- Construct the tunnel according to the design given by the owner and commission it
- Operate and maintain the tunnel and the connection roads

Copyright © 2005 Taylor & Francis Group plc, London, UK

– Collect the tolls fixed by the contract with the owner, from vehicles using the tunnel and repay the debts and loans
– Keep the national road section by passed by the tunnel in operation

According to the contract, the investment period (construction period) is two years from the date of site delivery to the Project Company and the operation period is twentysix years from the date of the acceptance of the construction by the Turkish Highway authorities and the start of the effective operation.

The total investment cost is estimated to 9.676.000 US dollars and out of this sum, 8.864.000 is the cost of the construction of connection roads and the tunnel.

The highway transportation is a public service which is offered by the state to the citizens and it is free of charge. Any highway which is subject to a toll collection must be proposed to offer better conditions than another highway which gives the same services with lower conditions but toll free.

A B.O.T. project is a private investment devoted to revenues and benefit. The examples of such projects are numerous in "dam + hydroelectric power plant" constructions and airport constructions but these examples do not have the same constraints than a highway project. The energy produced will be sold under specified conditions and the quality of the product is not discussed. In the case of an airport, alternatives are very much restraint. In the case of an highway "Quality and benefits of the service – toll asked" is a relation which must be very carefully studied to receive the expected number of passage. Your project has always an alternative...

3 DESCRIPTION OF THE RISKS

The risks in any B.O.T. project can be classified under three titles:

– Statuory risks
– Financial risks
– Project risks

These risks cover a period of time running from the signing of the B.O.T. agreement to the end of the operation period. The parties of the B.O.T. agreement have also to consider that the studies done before the signature of the agreement and on which the conditions of the agreement are based may be erroneous and may introduce some risks. These risks are mainly due to the feasibility study done before the signature of the B.O.T. agreement. As explained hereunder, in some cases these risks are subject to transfer to the owner. We will include them in the project risks.

Statuory risks

The statuory risks are mainly due to the legislations and administrations. In some cases, it can also be related to the international conjucture.

Among the Statuory risks, we can name:

For most of the B.O.T. projects,

– Changes in the legislation
– Breach of statuory legislation

For a transportation project,

– Changes in national transportation policy
– Changes due to international conjucture for touristic areas
– Environmental objections

As can be seen, the statuory risks cover the whole project period but are mostly related to the operation phase.

Among the Financial Risks, we can name,

– Increase in foreign exchange rates, decrease of national income
– Increase in taxations
– Increase of transportation costs which will affect the number of passages in the case of the tunnel project
– Failure to raise required equity
– Failure of required financing

As can be seen, some risks, such as financing and equity are only related to the construction phase, while the others are related to the whole project period or operation period.

Among the Project Risks, we name,

– Mis- evaluation in the financial part of the feasibility study
– Geological and geotechnical risks
– Inadequacy of design, poor estimates
– Construction contract risks, not completion in time and within the budget
– Threat by terrorist or political organisations
– Major accidents, interruption of operation.

4 MANAGEMENT OF RISKS

As Management of risks, we understand, once the risks are identified, the classification, the evaluation, the control, the transfer or the sharing of these risks.

The major risk factors who will threaten the good financial operation of the project have been listed above. In a "Risk Management" study these risks will be studied in detail for the project, will be classified by period and by actors of the project and will be evaluated. Once the risks are evaluated, the management study will propose to the actors of the project, solutions for control of the risks and their transfer to others or sharing among the actors.

Copyright © 2005 Taylor & Francis Group plc, London, UK

The typical steps of the risk management are:

- Prepare detailed study of the risks and their classification
- Identify the preventive measures to avoid the risk or to reduce it's effects
- Search for the possibility of reducing the risk by further investigations
- Establish contingency plans to deal with the risks if they occur
- Evaluate the financial effects of the risk, considering factors such as cost and probability
- Consider the transfer of the risk to others and it's cost
- Consider the sharing of the risks among the actors.

The risk management is usually done once the B.O.T. project agreement is under discussion but we believe that the risk management study must start during the preparation of the feasibility study, when some technical preventive measures can be included in the design and the financial evaluations can be more risk oriented.

It is a fact that, today some sensitivity analyses are included in the feasibility studies and evaluate the risks on some assumptions but these are far from being a risk management analysis. They are limited to the most critical variables of the project and their outcome is the evaluation of the effect of changes in the variable on the final cost or the internal rate of return.

A risk analysis can be quantitative or qualitative. The qualitative risk analysis is limited to the identification of the risks and an estimate of their effects on cost and time. This is done by check lists established according to previous experiences, interviews with key actors and brainstorming of the project team. The risks of geological source to happen during the construction of a tunnel, the remedial measures (additional supporting is an example) and their effect on the cost and time is a qualitative analysis.

The quantitative risk analysis can be deterministic or probabilistic. The deterministic analyses is a simple method which do not consider the probability of occurrence and analysis each risk independently while the probabilistic analysis considers the risks as variables and each risk has a probability distribution giving the frequency of occurrence or probability of exceedence.

Many models and computer programs are available for the probabilistic analysis of the risks.

In the case of a tunnel project with B.O.T. model, a critical variable is the number of passages per year. The traffic studies will give a number of passages and the feasibility study will be based on this value. The deterministic analysis will consider a variation in the number of passages and will calculate it's financial effect while a probabilistic analysis will consider the reasons of the variation, their probability of occurrence, the combination of the reasons and will give a range of values of decrease in the number of passages, their financial effect and their probability.

In a project, there are always possible contingencies for the occurrence of the risks. The contingency plans show the measures to be taken to minimize the effects of the risk with additional costs if any. As an example we can give the case of an accident in the tunnel during the construction. If the works are stopped for a while from one front, they can continue from the other front and the effect on the cost of the project will not be a big amount but if the contingency plan asks for the change of the alignment, with increase in the length of tunnel, it's effect on the cost and time will be important.

The risk analysis and the study of contingencies makes the risk and it's financial effects well defined in case of occurrence and the question is who will bear the financial consequences of the risk or to whom this risk can be transferred.

There are some steps to follow:

- Share the risk among the actors, by appropriate clauses in the agreements among actors

And then at the level of actors:

- Provide funds or reserve money to compensate the risks
- Provide external borrowings to answer to the financial effects of the risk if it occurs
- Transfer the risk to the insurance companies and pay the primiums of insurance

5 RISK MANAGEMENT IN THE CASE OF GÖÇEK TUNNEL

The main risks for the project have been estimated as being:

- Construction risks due to geological conditions
- Revenue risks due to the numbers of vehicles using the tunnel

A risk matrix for the project is given in table 1.

We will develop here these two main risks named above, one related to the construction period and the other to the operation period.

Geological and Geotechnical Investigations

The geological conditions are of prime importance for the construction of a tunnel. Unexpected geological condition will increase the cost of tunnel construction and the duration of the construction.

These unexpected geological conditions such as existing land slides, undetected faults, weak rock conditions, soft soils and excessive underground water can be the origin of a cost overrun upto 40% in the civil construction works which are 80% of the investment in Göçek Tunnel.

Copyright © 2005 Taylor & Francis Group plc, London, UK

Table 1. Example of risk matrix for Göçek project.

Risk Event	Risk Period	Risk Bearing Actor	Risk Probability	Potential Consequences	Contingency	Cost to Project	Possible Transfer to
Statuory							
– Change in legislation	Project	All actors	Low	Project stopped	None	Unknown	Owner
– Breach of statuory legislation	Project	All actors	Low	Delay	None	Low	Sponsor
– Changes in national transportation policy	Operation	Sponsor	Low	Operation loss	None	Low	Owner
– Changes in international conjucture	Operation	Sponsor	Moderate	Operation loss	None	Low	Owner
– Environmental	Project	Sponsor	Moderate	Delay	None	Unknown	–
Financial							
Foreign exchange rates	Construct	Sponsor	Moderate	Budget exceeded	Use local equipment	Low	Owner
Increase in taxation	Operation	Sponsor	Moderate	Revenue loss	None	Low	Owner
Decrease in number of passages	Operation	Sponsor	Moderate	Revenue loss	None	Moderate	Owner
Failure to raise equity	Construction	Owner + lender	High	Project stopped	Change sponsor	Low	New sponsor
Failure to raise financing	Construction	Owner + Sponsor	Moderate	Project stopped	Change lender	Moderate	Insurance
Project							
Mis evaluation in feasibility	Project	Sponsor	Moderate	Revenue loss	May exist	High	–
Geological + geotechnical	Construction	Sponsor	High	Delay	May exist	High	–
In adequacy of design + poor estimates	Construction	Sponsor	Moderate	Budget exceded	May exist	Moderate	Insurance
Raise of construction cost	Construction	Sponsor	Moderate	Revenue loss	May exist	Moderate	Insurance
Delay in construction	Construction	Sponsor	Moderate	Revenue loss	May exist	Moderate	Insurance
Threat terrorism	Project	Sponsor	Low	Delay	None	Low	–
Major accidents interruption of operations	Operation	Sponsor	Low	Delay	None	Low	Insurance

* Project period: construction period + operation period.

In many cases the cost of site investigations is less than 0.5% of the engineers estimate of works. In a publication of U.S. National Committee for Tunnelling Technology in 1984, this ratio was suggested as 3% to be able to control the tunnelling cost within 10%. We must add that the investment put into site investigation should be commensurate with the complexity of the geological conditions and the size of the project.

The owner of Göçek tunnel, Turkish State Highways General Directorate is not participating to the risks due to geological conditions. In some hydropower projects in Turkey the owners accept to reflect to the energy price the extra cost which may come from the risks due to underground conditions but in the case of Göçek tunnel, the majority of the costs are the tunnel construction costs and the owner cannot bear this risk. A proposed solution could be the transfer of the risk to the contractor by setting a turn key contract for the construction of the tunnel but in the case of Göçek tunnel the sponsors are also construction companies and they are willing to built the tunnel by their own. The sponsors are called to bear extensive geological and geotechnical investigations to minimize the geological risk they are bearing.

Additionally, an experienced construction team for tunnelling, a proper choice of excavation methods and equipment, a continuous geological survey during construction works are the factors to minimize the geological risks.

Copyright © 2005 Taylor & Francis Group plc, London, UK

Traffic studies

The revenues of the project are based on traffic studies.

The number of vehicles using the tunnel are found by extrapolation of the traffic counts made between years 1990 and 2000. The traffic counts have been made as passage of cars, busses and trucks. The total number of passages in 1990 was 2013 vehicles per day and with an average increase of 4.7%, this number reached 3179 in 2000.

The traffic density depends on the tourism and economic activity in the region and it is very difficult to make accurate estimations for the coming twentyeight years. The risk due to the revenues related to the number of passages is identified by sensitivity analysis but still the probabilities are undefined. The number of passage will depend very much from international conjucture and tourism activities in the region as most of the tourist in the region are foreigners. The development of the region will also influence the traffic estimation and the number of passages. It is noted that the region, due to it's touristic potential calls the turkish investors to invest in the region and these investments increase the economical activity which is a positive factor for the traffic estimations.

The proposals to manage the risk in revenues are various.

As examples we propose:

- The owner may guaranty a minimum number of passages and if this number is not achieved, the toll price or operation period can be revised.
- The owner can leave to the sponsor to determine the tolls and the sponsor has to operate the tunnel in free market conditions, even varying the toll according to seasons and vehicle classes.

6 CONCLUSIONS

Any B.O.T. project has risks which can be managed but a B.O.T. project for a highway tunnel presents conditions more severe than other projects as in Göçek Tunnel case where most of the risks are carried by the sponsors and where the owner gives the design of the project as part of the agreement and fix the toll in the same agreement made with the sponsors.

The sponsors must rely on a realistic "Risk Management Study" for their investment.

The main risk is issued from very often under estimated geological and geotechnical investigations and on which the design and planning of tunnel works are based. The sponsors have to invest in the investigations before accepting the design proposed by the owner.

In the case of GÖÇEK tunnel, the sponsors are "Road and Tunnel Constructors". The goal of the sponsors is to built the project which is their speciality but the financial operations behind are quite new for them. In such a B.O.T. project a finance specialist must be between the sponsors or hired by the sponsors for financing matters. The owner may have good reasons to ask for such a specialist group.

The revenues in the form of "toll collection" must not be fixed by the agreement between the owner and the sponsor. In Göçek project, the maintenance of the existing road is in the charge of the owner and the owner may be very strict on this item but leave the sponsor to operate his tunnel under the free market conditions, his competitor being the existing road that will be maintained by the owner.

Copyright © 2005 Taylor & Francis Group plc, London, UK

Cost estimating and risk – management for underground projects

J.J. Reilly
President, John Reilly Associates International, Framingham, Massachusetts, USA

ABSTRACT: This paper gives examples of cost estimation problems for large, complex infrastructure and underground projects, compares differing cost estimating approaches for two such projects and describes a cost validation and risk elicitation/identification process recently developed by the Washington Department of Transportation (WSDOT) with the author and colleagues. The paper builds on previous papers (e.g. Reilly & Brown, 2004) which described the cost estimation problems and proposed a suggested solution which was subsequently implemented by WSDOT in its Cost Estimate Validation Process (CEVP®). Recommendations are given for those owners of complex projects who wish to know a "more realistic probable cost" for their projects.

1 THE COST-ESTIMATION PROBLEM

The public is skeptical of our ability, as a profession, to accurately estimate (i.e. predict) the final costs of large, complex public projects and also of our ability to manage these projects to established budgets. The public asks us:

- "Why do costs seem to always go up?"
- "Why can't the public be told exactly what a project will cost?" and,
- "Why can't projects be delivered at the cost you told us in the beginning?"

Our inability to answer these questions consistently is a consequence of many factors – principally an inadequate analysis and correction of poor cost estimating practices (Flyvbjerg et al. 2002, 2003). Additionally, poor project management and poor communication with the public further adds to the problem.

The number of high-visibility projects where it appears to the public and the media that costs are "running away" or "out of control" seems to be increasing – and the cost increases involved are large.

Examples include the Jubilee Line Transit Project in London – 2 years late and £1.4 billion (67%) over budget (the budget which was communicated at time of decision to proceed); the Channel Tunnel – £3.7 billion (80%) over budget; Denmark's Great Belt Link – 54% over budget; the 2003 Woodrow Wilson bridge tender in Virginia – 72% over estimate and, Boston's Central Artery Project – billions over the initial budget and years late (Salvucci, 2003).

As will be discussed later, early identification and management of risk is a key to meeting cost and schedule for large, complex underground projects (Arup, 2000).

One study (Reilly & Thompson, 2000) found that specific, relevant project cost information was usually unobtainable. Little objective history could be found, including findings that would support recommendations for improvement. Because of the difficulty in obtaining hard data, firm conclusions could not be reliably drawn, but the following findings were reported by owners:

1. There are significant cost and schedule overruns suggestive of poor management in at least 30%, and possibly more than 50%, of the projects.
2. It appears that the factors that most directly influence success or failure are a) expertise and policies of the owner and b) procurement procedures.
3. The professional teams engaged in projects were judged to be competent, by the owners, leading to the conclusion that problems in poorly performing projects may lie primarily with the ability of the owner to lead and manage the project process.
4. Risk mitigation was not well-understood or applied, even in elemental ways. This was considered to be a promising area for development, in particular as it related to cost overruns and unforeseen events.
5. Reported cost and performance data – especially for "good" results – should be treated very cautiously. Consistent, complete and relevant data are very hard to get and almost impossible to validate after project completion.
6. Conclusions based on reported cost data, unless the conclusions are grossly evident (e.g. meta-findings), should also be treated with caution.

Copyright © 2005 Taylor & Francis Group plc, London, UK

Other studies confirm the problem. One study (Flyvbjerg et al. 2002) surveyed 258 projects spanning 70 years and found that the problem of accurate cost forecasts has been chronic for that time period.

Moreover, as an industry, planning, design and construction professionals, and owners, have not corrected the chronic underestimation of the real cost of infrastructure projects. If they had done so, there would have been a uniform number of results over budget as under budget. They concluded that the problem is both an inability to estimate accurately, and also a bias to estimate on the optimistic side.

Fundamental issues underlie the cost estimation problem. The ultimate consequence is a rejection of public funding for projects – such as rejection of new taxes for highway projects in Washington State and Virginia, both in 2002.

1.1 *Cost estimating – two Boston examples*

Two projects from the Boston area illustrate different aspects of cost estimating – and also that not all projects fail in this respect. From the public's point of view, the Central Artery and Tunnel Project (CA/T) and the Massachusetts Waster Resources Authority (MWRA)'s Boston Harbor Cleanup Program (BHP), were at the extremes of project performance – with respect to the cost estimates:

1. The CA/T Project was initially presented in 1986 as costing under $3 billion. But this number did not correspond to the actual project, as constructed, with respect to scope, complexity and time. In 1990, as construction was about to begin, the "official" estimate was $6 billion (Salvucci, 2003). Three years later it was "$7 billion, not more than $9 billion" (Leidon, 1993). The project will ultimately be delivered in 2005 at more than $15 billion.
2. The Boston Harbor Cleanup Project initially presented a cost range of $4 to $4.9 billion. In 1992, at a very early stages of construction, a thorough review of the project cost was performed and the estimate was changed to $3.65 billion. The project was delivered a decade later for $3.8 billion. This is considered a cost estimating and project management success.

Among the many differences in these two projects are the way that the original estimates were prepared and presented – which dramatically affected the initial cost estimate – and, the "number" that the public remembers to this day.

1. The CA/T costs were in 1986 dollars with no escalation or contingency (consistent with FHWA requirements at the time) and the costs did not include provision for additional scope elements or all of the necessary "soft" costs.
2. The BHP estimate was built from estimated costs for the projected final program. It included contingencies and escalation to the projected mid-point of construction and it included all anticipated scope and "soft" costs envisioned.

Each project cost estimate was different – in scope, context and timeframe – and was being used, and understood, differently for each agency. However, the public – and the media – never understood these major differences. The majority of the "public" had, and still has in the case of the CA/T, no knowledge that the numbers represented two completely different scopes, contexts and timeframes. For the CA/T the media has (unreasonably) continued to use the incomplete 1986 number as the basis of comparison in every discussion of cost on the program. Therefore, public opinion has been shaped, and mis-informed, by these poorly understood cost numbers.

1.2 *Cost-validation – MWRA's MetroWest Tunnel*

Another example from Boston illustrates how cost estimating procedures can be changed to improve cost estimating practice. MWRA became concerned that the estimated project costs for the MetroWest Water Supply Tunnel were significantly underestimated and so a critical review of the cost estimate, and the cost estimating procedures, was initiated.

A intensive review of the design team's estimate was done by a group of independent professionals with project management, design and construction experience. The group included persons with specialized experience in estimating and constructing this type of project, viewed from a contractor's perspective.

The result was a revised cost estimate that included all costs including planning, design, permitting, compliance, land costs, mitigation costs, construction management, contingency and construction costs – all escalated as appropriate.

This new cost estimate was used in all subsequent public discussions. MWRA delivered the MetroWest Tunnel Project on schedule and under the approved budget and, in doing so, demonstrated a cost-validation process that was reasonable and which corrected an early, inadequate cost estimate.

The MWRA's experience in critical cost review and its revised cost estimating approach became one of the three critical foundations of WSDOT's Cost Estimate Validation Process – CEVP®.

1.3 *WSDOT evaluates cost estimating problems*

In 2001, WSDOT was looking at a large highway construction program, of the order of US $30 billion. The cost estimating and communication problems, cited above, led the Secretary of Transportation to ask for (1) a critical evaluation of the problem and

Copyright © 2005 Taylor & Francis Group plc, London, UK

(2) development of a better cost estimating methodology. Findings included the following:

1. There is a general failure to adequately recognize that an estimate of a future cost or schedule involves substantial uncertainty (risk).
2. The uncertainty must be included in the cost estimating process.
3. Costs, especially construction costs, must be validated by qualified professionals, including experienced construction personnel who understand "real-world" bidding and construction.
4. Large projects often experience large scope and schedule "changes" which affect the final cost. Provision for this must be made in the cost estimates and management must deal competently with these changes.

WSDOT decided to address these findings by:

1. Using an improved cost estimating methodology,
2. Incorporating cost validation and uncertainty,
3. Communicating "ranges of probable cost" to the public, media and key political decision makers.

Essential elements of the new process included an external review by independent, professionals, including "validation" of base cost and schedule estimates and assumptions, replacing "contingencies" (which are allowances for unknowns) with explicit cost and schedule uncertainty (risks and opportunities). A key objective was to move from "single value" cost estimates to cost estimates which are communicated as "ranges of probable cost".

2 THE WSDOT COST ESTIMATE VALIDATION PROCESS (CEVP®)

Accordingly, in January 2002, the WSDOT Secretary of Transportation tasked small group of consultants and WSDOT managers to develop a new cost estimating procedure. The result WSDOT's Cost Estimate Validation Process – CEVP®.

2.1 *CEVP®*

CEVP® develops a probabilistic cost and schedule model to comprehensively and consistently define the probable ranges of cost and schedule required to complete each project. The basic approach requires a peer-level review, or "due diligence" analysis, of the scope, schedule and cost estimate for a project and then to incorporate uncertainty (uncertainty includes both risk and opportunity) to produce a range of probable cost and schedule.

Specific objectives of the method are to evaluate the quality and completeness of "base costs" together with the inherent uncertainty in the estimate.

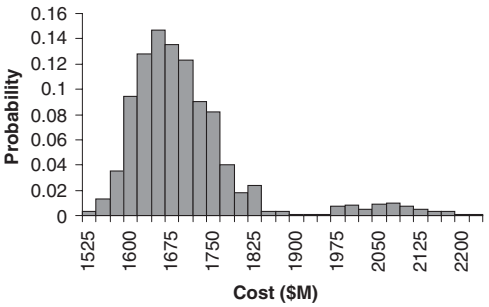


Figure 1. Future costs are a "range of probable costs".

The results of the assessment are expressed as a probable distribution of cost and schedule values for the project (Figures 1 and 2). In summary (Reilly et al. 2004), the CEVP® process:

1. Critically examines the Project estimate to validate all cost and quantity components using independent external professionals.
2. Removes all "contingency" and allowances for unknowns.
3. Replaces contingency and other approximating allowances with individually identified and explicitly quantified uncertainty events (risks plus opportunities).
4. Builds a model of the project – normally in an Excel spreadsheet – from a flow-chart of key planning, design, permitting and construction activities. Included are quantification of cost and critical path schedules. The model assigns the quantified uncertainty events to activities with the associated probabilities and impacts.
5. Runs a simulation to produce the projected "range of probable cost and schedule".
6. Report the results (Figure 1).

3 CEVP® WORKSHOP

Two key elements of the CEVP® process are cost validation and risk elicitation (the third required element is the subsequent communication of results to the public and political decision-makers).

Because the CEVP® process has been described previously in several papers (Reilly & Brown 2004) this paper will detail two core processes – cost validation and risk identification.

3.1 *CEVP® – Cost validation*

The CEVP® Team consists of the project team and the CEVP® specialists working closely together since it is critical that the results of the CEVP® process are understood and "owned" by the project team.

Copyright © 2005 Taylor & Francis Group plc, London, UK

The CEVP® cost workshops are led by a manager with program delivery experience, supplemented by CEVP® team members with both design and real-world construction experience. The use of personnel with experience in contractor's methods is necessary to bring that perspective into the cost review for a well-shaped determination of "base cost" – the cost if "all goes as planned and assumed". The process consists of the following:

1. The project team first briefs the CEVP® specialists on the detailed scope of the project and identifies cost and schedule risks that have been included in the project estimate.
2. The CEVP® cost specialists discuss the cost estimate with the project team, reviewing what the estimate represents and the basis of its development. They discuss what metric has been used to calibrate the estimate and what contingencies have been included in the estimate.
3. A review of the scope of the project is completed with the project team on an element by element basis to assure that all elements and phases of the project have been accounted for.
4. The estimate is reviewed to assure that items such as: right of way, mobilization, permitting, mitigation, temporary facilities and utilities, construction phasing requirements, seasonal constraints, cuts/fills, hazardous material issues, archaeological issues, storage and disposal of material, haul distances, compaction and testing, protection of work, testing of mechanical and electrical systems, occupancy permits, de-mobilization, etc. have been recognized and addressed – from a cost standpoint.
5. The schedule for the project is also reviewed – is it realistic?, does it consider adequate time for mobilization?, set-up of temporary facilities and utilities?, construction permitting?, construction phasing?, dealing with differing site conditions?, traffic or operational issues?, seasonal constraints?, site access limitations?, testing of piping?, electrical and signals?, SCADA systems? etc.
6. Unit prices and production rates that have been assumed for the major items of work are reviewed, asking if the production numbers (the basis of the units costs) are reasonable and if there are any risks that those unit prices may not have taken into account – such as high ground water or the presence of organic material.
7. The contingency that is included in each unit price – or the entire estimate – is identified and removed from the cost estimate. This is done in order to develop the "base cost" of the project (the contingency is subsequently replaced by the probable cost of risk and opportunity events).
8. During the discussions, and upon completion of the above review, items of work that may be missing, over- or under-estimated are identified and recorded. Estimates for missing items are developed and recommendations for adjustments are made. Finally, an agreed "base cost" is determined. This becomes the base to which the cost of potential risk and opportunity events are added by the cost/schedule uncertainty model.

3.2 *CEVP® – Risk identification and elicitation*

The risk part of the CEVP® workshops are led by an experienced risk elicitator (risk analyst) who is familiar with uncertainty theory, de-biasing techniques and the structure of a subsequent cost and risk model.

Other workshop participants include representatives from the project team who have familiarity with the plans, strategies, assumptions and constraints on the project, plus subject matter experts (SME's) who bring an independent perspective on important areas of project uncertainty.

The identification and quantification of uncertainties requires a balance of project knowledge, risk analysis expertise, cost estimating expertise, and objectivity. Project knowledge and the independent expertise of SME's are essential to identify the uncertainties. Risk analysis expertise is required to capture balanced information on risk and model uncertainties. The risk workshop preparation includes the following activities:

1. Appropriate (but limited) training of participants in the principles and procedures of uncertainty (risk and opportunity) assessment,
2. Preliminary work to capture the plan and strategy of the project in a draft "flowchart",
3. A preliminary list of risks and opportunities,
4. Identification and validation of base costs (as described previously).

The goal of the risk workshop is to identify, quantify and model the uncertainty in project cost and schedule. The principal activities are:

1. Identification of potential risks and opportunities. This is done in an open brainstorming process that typically begins with a prior list of potential uncertainties from the project team, lists from similar projects and other sources. In the workshop, it is necessary to provide a critical environment that allows for this initial information to be combined with other suggested risks. As a practical matter, the team should identify a screening criteria to help produce a prioritized list of significant cost and schedule risks.
2. Characterization of potential risks and opportunities. This process combines subjective and objective information to identify the consequences to the project if each of the risks were to occur. Typically there are varying opinions on the range of consequences,

Copyright © 2005 Taylor & Francis Group plc, London, UK

such as increased cost or schedule delay. The risk elicitator is responsible for guiding the group to an appropriate agreement regarding the consequences of the risks – i.e. probability of occurrence and impact. Independence and correlation among risks is also defined, positively or negatively.
3. Analyzing the risk information and base costs.

The risk and opportunity events that are the output of the workshop should be defined to be independent as far as possible. When this is not possible, the dependencies among events must be defined and accounted for. In addition, each risk or opportunity event must be allocated to the project activities that are affected by it or, if a given event affects multiple project activities, significant correlations among occurrences need to be addressed. Significant uncertainties and correlations among event impacts also need to be defined. This information is incorporated in the cost and schedule to produce the model results.

Risk elicitation within CEVP® is an iterative process that must combine subjective and objective information. Uncertainty characterizations and probabilities are defined simultaneously to provide reasonable, practical descriptions of uncertainty.

3.3 *Completion of the CEVP® process*

The project's "range of probable cost and schedule" is determined by combining the base costs determined from cost validation and the risks plus uncertainties identified from the risk workshop in a model which:

1. Integrates base costs with risks and opportunities (uncertainties) in a probalistic model
2. Reports the CEVP® results as a "range of probable cost and schedule"

Results of the model analysis are presented as cost and schedule probability distributions, usually in a graphical form (Figure 2) with supporting tabulations of characteristic statistics. First order descriptions and models are sufficiently accurate and are used for most projects. These distributions can describe a variety of situations of interest including:

1. Current dollar (time of assessment) cost and year of expenditure cost ($YOE)
2. Fully funded or partially funded scenarios
3. Comparative design options
4. Probable date of completion for the project
5. Probable schedule to meet project milestones

The specific form of the reported results can vary depending upon need and the results can be used for a number of applications, including:

1. Project assessment / management re-direction
2. Risk management plans

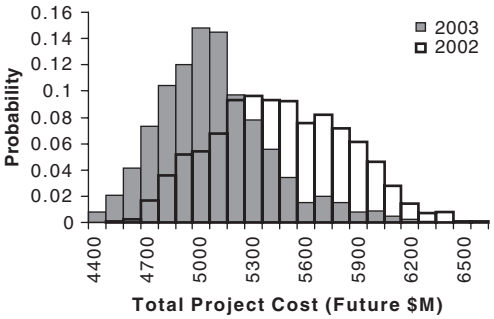


Figure 2. Improvement in probable cost (mean and distribution), successive CEVP® workshops, Alaskan Way Project.

3. Data input to value engineering workshops
4. Integrated management of multiple projects
5. Better internal and external communications
6. Financial management options and alternatives

CEVP® is iterative in nature. For many project applications it is appropriate to conduct a reassessment of the project from time to time to update project changes, cost and schedule estimates. The following example of 2003 results compared to 2002 results for a complex highway project in Seattle, shows a reduction in both probable cost and uncertainty (range).

3.4 *Current developments*

CEVP® is proving to be a useful process for estimating and communicating ranges of probable costs and schedules, as well as explicitly identifying and quantifying risks, for large, complex projects early in the planning and design phases. There is better information that the public, and elected officials, can use to make sound decisions and that engineers can use to better manage their projects.

WSDOT has internalized the process and uses it, and a simpler "Cost Risk Assessment" process, for many of its projects.

The U.S. Federal Transit Administration and the Federal Highway Administration have each investigated the CEVP® results. They have concluded that CEVP®, or a similar process, should be used for large, complex projects. As of this writing further demonstration projects and educational seminars are underway and WSDOT has been designated "Lead Agency" status in this work.

4 FINDINGS

1. WSDOT found that CEVP® focuses early attention on the significant cost and schedule risks for a

Copyright © 2005 Taylor & Francis Group plc, London, UK

project and increases the project team's awareness of risk.
2. Use of experienced external subject matter experts, who have constructed similar projects, is good value and gives an independent check on key assumptions.
3. Because risks are explicitly defined, a risk management plan (Grasso et al. 2002) can be quantified earlier. This allows significant management and control of cost and schedule earlier in a project (Arup 2000) and allows a more explicit communication of cost and schedule (and changes thereto) with the public and key political decision makers.
4. WSDOT found that CEVP® permitted a more intuitive communication with the public which better related to "… what people already know".
5. WSDOT recognized the value that cost validation and risk assessment provides.
6. WSDOT recognized that CEVP® is not a "magic bullet" or a "quick fix". WSDOT therefore committed to improve its cost estimating process by implementing the CEVP® program on a state-wide, long-term basis and training staff in the technique.

5 RECOMMENDATIONS

1. Owners of complex infrastructure and underground projects should consider using a WSDOT CEVP® type process for early cost validation and risk identification.
2. Such a process leads to an explicit, quantified definition of potential risk events – this becomes a basis for a quantified risk management plan for each project.
3. Periodic updates to the model can be used to assist with, and explain rationally, project changes. They can, additionally, evaluate and compare alternatives.
4. Such a process has promise to assist owners in determining a more realistic "range of probable cost" which can enable better communication about, and management of, these projects.

   This is only possible if the owner truly wants to know the realistic "range of probable costs" and is prepared to communicate this to the public and decision makers.
5. It is recognized that significant concerns have been raised that, if we tell the public the more realistic probable costs, which tend to be greater than other estimates, projects will never be funded and authorized. Such concerns imply that we cannot trust the public with the real cost information. If true, such a position has moral implications that the profession needs to address.

ACKNOWLEDGEMENTS

The WSDOT project teams and CEVP® consultants rose admirably to the challenge of implementing a new process which questioned established ways of cost estimating. It required a high-level of dedication and persistence to develop and implement the new process and then report the CEVP® results, for 10 mega-projects, in only 4 months.

The CEVP® process, and its successful application, would not have been possible without the commitment and expertise of the following personnel: WSDOT – Secretary MacDonald, John Conrad, David Dye, Cliff Mansfield, Jennifer and Adam Brown, Monica Bielenberg; MWRA – Michael McBride; Consultants – John Reilly, Bill Roberds, Dwight Sangrey, Travis McGrath, Keith Sabol, Art Jones, Richard Rast, plus Paul Silvestri and his National Constructors Group; University of Colorado – Keith Molenaar & Jim Diekmann; plus, many others who have been, and are now working on, these projects and this process.

REFERENCES

1. Arup 2000, London Jubilee Line, Secretary of State's Agent (Arup), "End-of Commission Report", July
2. Flyvbjerg, B., Holm, M., Buhl, S. 2002 'Underestimating Costs in Public Works, Error or Lie? American Planning Association Journal, Vol. 68, No. 3
3. Flyvbjerg, B., Bruzelius, N. & Rothengatter, W. 2003 'Megaprojects and Risk: An Anatomy of Ambition' Cambridge University Press, March, 208 pages. ISBN: 0815701284
4. Grasso, P., Mahtab, M., Kalamaras, G. & Einstein, H. 2002, 'On the Development of a Risk Management Plan for Tunnelling', Proc. AITES-ITA Downunder 2002, World Tunnel Congress, Sydney, March
5. Leidon, C. 1993 "The Connection – Central Artery Project" National Public Radio Broadcast, Boston
6. Reilly, J. & Thompson, R. 2001 "International survey, 1400 projects", internal report
7. Reilly, J. 2003, "Towards Reliable Cost Estimates", Tunnels & Tunneling, North American Edition, September, Viewpoint Article, p4
8. Reilly, J. & Brown, J. 2004 "Management and Control of Cost and Risk for Tunneling and Infrastructure Projects" Proceedings, World Tunneling Conference, International Tunneling Association, Singapore, May
9. Reilly, J., McBride, M., Sangrey, D., MacDonald, D. & Brown, J. 2004, "The development of CEVP® – WSDOT's Cost-Risk Estimating Process" Proceedings, Boston Society of Civil Engineers, Fall/Winter
10. Salvucci, F. 2003 "The 'Big Dig' of Boston, Massachusetts: Lessons to Learn", T&T North America, May
11. WSDOT CEVP® Website www.wsdot.wa.gov/projects/cevp/default.htm

Copyright © 2005 Taylor & Francis Group plc, London, UK

A tunneling Game Model for good tunneling practice

Leonardo Rosas-Sanchez
University of Colorado at Boulder

ABSTRACT: In this paper, a game theory approach is presented for maximizing the performance of the tunneling industry. The Tunneling Game Model (TGM) is a two-person cooperative game which is formulated as a bargaining situation. The two players are the "owner" and the "contractor" who have the opportunity to collaborate for mutual benefit. Two utility functions are proposed to determine the psychological characteristics of the players. The construction of each utility function is based on sustainability, professional-technical agreements, and risk allocation in the contract documents.

1 INTRODUCTION

Tunneling is a crucial component in the development of infrastructure. Tunnels can help making our cities healthier, safer and sustainable. Unfortunately, the great potential of tunneling is minimized in practice due to adversarial behavior and relationships of those involved in tunneling projects.

The risk for both owners and contractors is inherent in a tunneling project. This risk, realistically, cannot be entirely avoided or eliminated. But, it can be managed and controlled. However, in practice, allocation and assumption of intolerable risk increases the probability of disputes, claims, and eventual litigation or arbitration.

The risk aversion and non-cooperative attitude in the tunneling industry have caused lack of investment in underground facilities. In this paper, the Tunneling Game Model (TGM) is presented as a two-person cooperative game where the contractor's and owner's interests are not strictly competitive.

2 TUNNELING AS A RISKY GAME

The physical conditions encountered underground (nature, quality, and quantity) and the impact of these conditions during construction process cannot be precisely anticipated prior to excavation or related construction activities. The behavior of underground conditions may be dependent on construction means and methods selected by the contractor, which typically will no be known until sometime after the design is completed and the construction contract is awarded.

Despite efforts to prepare and disclose to the contractor available information, underground conditions encountered during construction may differ (to a greater or lesser degree) from those indicated. Moreover, the construction means and methods selected by the contractor may differ from those assumed in the design, and any variation may significantly impact the anticipated behavior of ground conditions during the construction process. Therefore, the risk for both the owner and the contractor is inherent in tunneling projects. And the success of the tunneling project may vary if the risk can be effectively managed and fairly allocated between both parties.

The risk in tunneling practice is normally allocated and assumed. For instances: (1) the owner does not authorize adequate preconstruction site investigation; (2) the owner does not disclose to the contractor the anticipated site conditions information; (3) the owner decides not to carry any contingency for different site conditions that might be encountered during construction; (4) the contractor bids a project without conducting any site inspection; (5) the contractor acts in conscious disregard of disclosed or available information; or (6) the contractor enters into a contract without contingency for the risk of different site conditions.

Realistically, the risk inherent in tunneling projects cannot be entirely avoided or eliminated. However, it can be managed and controlled, providing that it is identified in a timely fashion during the planning phase by means of adequate investigation, and then appropriately addressed in the design, and providing that the pertinent results of the investigation are disclosed to the bidders.

Copyright © 2005 Taylor & Francis Group plc, London, UK

If tunneling would be visualized as a game, two players have the position to control the decision making concerning risk identification, allocation, and management. They have the opportunity, if not the obligation, to achieve a successful tunneling project.

The project success can be measured by the schedule, the budget, or the positive project participant relationships. Achieving this goal requires a continuous, disciplined, and diligent effort by all the project players, to deal and interact with each other in good faith and in an equitable way, throughout the entire planning, design, and construction processes.

Tunneling and sustainability

Tunneling plays (and will play more) a crucial component in infrastructure development, especially in urban areas. The Global Plan of Action emphasizes the importance of innovative urban planning and design solutions to guide future development of urban areas in harmony with the natural environment.

The major constrain in infrastructure development is the availability of land. Thus, promoting sustainable urban land use will involve innovative utilization of the underground space for the rapid growth of urban mobility, the management of growing volumes of urban waste, and the supply of water to the cities and the removal of waste water.

Unfortunately, the sustainable potential of tunneling is minimized in practice due to the behavior of the participants. Tunneling is now perceived as synonymous to claims, disputes, and overrunning.

3 GAME THEORY

Social phenomena can take several forms: (i) people are acting sometimes against each other, or sometimes cooperatively with each other; (ii) people have different degrees of information about each other; and (iii) people's aspirations lead them to conflict or cooperation.

Game theory is a theory of decision making. It considers how one should make decisions and, how one does make them. Each person's decisions are linked to each person's goals. Game theory is a discipline whose mathematical properties can be applied to social, economic, and political problems. Social events can best be described by models taken from suitable games of strategy. These games in turn are amenable to through mathematical analysis. The theory of games enables us to examine the complexity of society in an entirely new light, hoping to lift the discussion from a purely verbal state.

In a game, each player (at least two) must assess the extent to which his/her goals match or clash with his/her the goals of others and decide whether to cooperate or compete. Each player will pick a strategy (make a decision). As a result of this choice, and possible chance, the result will be a reward or punishment for each player: the payoff. A player needs not be a single person. If each member of a group has exactly the same position about how the game should turn out, members of a group may be considered as a single player.

A strategy in game theory is a complete plan of action that describes what a player will do under all possible circumstances. It is assumed that players always do their best.

The nature of the game is determined by rules. Whether players can communicate and make binding agreements, the information they have, and the ability to share payoffs are all of interest; but more important are the number of players involved and the extent to which their interests coincide or conflict.

In every game, game theory looks for a 'solution', a description of what each player should do and what the outcome should be. By viewing a complex situation as a game, each player can translate the intuitive insights of an experienced observer into a quantitative model.

Utility theory is the mechanism that allows us to express a person's preferences in a consistent pattern so he/she can make rational decisions. The he/she choices are often made on the basis of the way the alternatives are expressed.

Two-Person, Zero-sum games

The term 'zero-sum' means the players have diametrically opposed interests. The term comes from parlor games like poker where there is a fixed outcome of money around the table.

Two strategies are in equilibrium (they come in pairs, one for each player) if neither player gains by changing strategy unilaterally. The outcome (sometimes called the payoff) corresponding to this pair of strategies is defined as an equilibrium point.

Assume that player B knows player A's strategy in advance. Since B would choose the minimum value of any A chooses, A should choose a strategy that yields the maximum of these minimum values; this value is called the '*maximin*', and it is very least that A can be sure of getting. Now imagine the rules are changed so that A knows B's strategy in advance. A would be expected to choose the maximum, so B should choose the value that minimizes the maxima. That outcome is called '*minimax*'.

If the minimax equals maximin, the payoff is an equilibrium point and the corresponding strategies are an equilibrium strategy pair. Since the game is represented by a matrix, the payoff associated with an equilibrium point is the smallest in its row and the largest in its column. If a game has an equilibrium point, it is easy to choose appropriate strategies and predict the outcome.

Copyright © 2005 Taylor & Francis Group plc, London, UK

In game theory, the most important and fundamental theorem is the Von Neumann's & Morgenstern **minimax theorem**. It states that one can assign to every finite, zero-sum two-person game a value υ. The theorem considerably simplifies the study and analysis of games. The outcome is intimately related to both players' behavior and each is at the mercy of the other's caprice.

The virtue of the minimax his/her strategy is security. With it, each player can obtain your full value, and have the assurance that he/she could not do better. As a consequence of the minimax theorem, the general, zero-sum, two-person game has a good theoretical foundation. But, like a game of perfect information, it rarely exists in practice. The difficulty is the requirement that the game has to be zero-sum, with the essential assumption that players have diametrically opposed interests.

Utility theory

Game theory is a tool for making decisions, but before one decides how to get what he/she wants, he/she must first decide what he/she wants. There are many situations in which people do not act so as to maximize their expected winnings. This has not anything to do with the formal theory; it is an observation about life. Many games having a negative average nevertheless attract a large number of players; lottery players have a small chance to win a fortune, and insurance policyholders avoid the small chance of having a catastrophe befall them.

A utility function is simply a "quantification" of a person's preferences with respect to certain objects. The player's preferences are said to be intransitive. If the preferences of a player are sufficiently consistent, that is, if they satisfy certain requirements, the preferences can be expressed concisely in the form of a utility function. There is no hope of completely describing subjective feelings quantitatively, of course, but using utility theory, it is possible to convey enough of these feelings under certain conditions.

It is supposed that the preferences of each player are expressed by a utility function and that the payoffs are given in 'utilities' in which utility functions are expressed. Referring again to the zero-sum game, it is a game in which the sum of all the payoffs (in utilities) is always zero. When two players are involved in a zero-sum game in this new sense, their interest must necessarily be opposed.

Player's preferences are observed first and then the utility function is established. Players may act as 'though' they were maximizing their utility functions. 'To act rationally' according to this criterion means to choose from among the available courses of action the one which promises to maximize expected value (or minimize expected cost). 'Irrational behavior' can be avoided by identifying and controlling the significant variables.

Two-person cooperative games

In this game, it is assumed that: (1) all pre-play messages formulated by one player are transmitted without distortion to the other player; (2) all agreements are binding, and they are enforceable by the rules of the game; and (3) a player's evaluations of the outcomes of the game are not disturbed by these pre-play negotiations. The negotiations are in integral aspect of the strategic possibilities. In this way, the outcomes can be made to depend upon the negotiations.

The players can act cooperatively through pre-play communication. Imagine a point (u, v) in a surface R' is said to be jointly dominated by a different point (u', v') of R' if both u' $\geqslant$ u and v' $\geqslant$ v. Clearly, the players need not consider any point which is jointly dominated by another one of R'. Thus, after a little preliminary negotiation, they can be expected if they are rational, to confine their attention to the jointly un-dominated outcomes.

Treating the game in a non-cooperative manner, player 1 can guarantee himself an amount υ_1 and player 2 an amount υ_2; and it is unreasonable to suppose either player will accept less than his maximin value in the negotiations. This point is called the negotiation set of the game.

Solutions of an outcome from the multiplicity of points in the negotiation set depend upon certain psychological aspects of the players which are relevant to the bargaining context. At this point, the bargaining personalities of both players will begin to enter; each can hurt the other in different degrees.

Arbitration schemes

In some situations, 'rational' people fail to reach an agreement. For this reason, players may often be willing to submit their conflict to an arbiter, an impartial outsider who will resolve the conflict by suggesting a solution.

Since there is not a defined criterion of 'fairness', a set of precise desiderata that any acceptable arbitration scheme must fulfill has to be formulated. Once these desiderata are formalized as axioms, then the problem is reduced to a mathematical investigation of the existence of and characterization of arbitration schemes which satisfy the axioms. The ideal is that the desiderata can be considered a full characterization of the arbitration scheme.

Bargaining models

A 2-person bargaining situation involves two individuals who have the opportunity to collaborate for mutual

Copyright © 2005 Taylor & Francis Group plc, London, UK

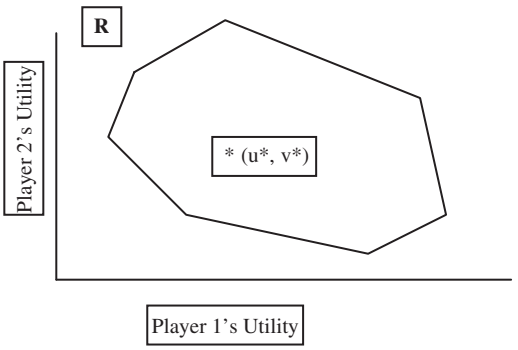


Figure 1. Nash's Bargaining Problem.

benefit in more than one way. The simplest case is the cooperative two-person game. In general terms, the bargaining problem is idealized by supposing that the two individuals are highly rational and: (1) payoffs are in utility terms; and (2) no interpersonal comparisons of utility are assumed. Moreover, it is supposed that each player has full knowledge of the personal utility of the other.

Nash's bargaining model

In Figure 1, a bargaining problem is characterized by a region R of the plane and a special point (u*, v*) of R. The following interpretation holds: if no trade occurs, the payoff is (u*, v*), and a trade takes place if and only if both players agree upon a unique point of R which then constitutes the payoff. A bargaining game is denoted by [R, (u*, v*)].

Without formalizing the negotiation procedure precisely, the existence of a status quo point (u*, v*) is assumed. Geometrically, a *status quo* point is within the boundary of the feasible region R. It represents the payoff to each player if they do not agree, or if negotiations break down. The *status quo* point corresponds to each player's security level. The security level of a player is the maximum payoff which that player can obtain regardless of what the other player does.

The choice of the *status quo* point (u*, v*) may vary with different assumptions about the attitudes behavior and bargaining strengths of the players. But whatever *status quo* point is adopted, it will not itself generate a solution although it will obviously play a part in finding it.

Nash [7] proposed the following solution to the bargaining game: (1) change the origin of measurement of utility for each player so that the point (u*, v*) is transformed into (0, 0) and the resulting transformation of R is R'. In other words, the *status quo* gives zero payoff; and (2) in the region R' find the unique point (u_0', v_0') such u_0'*v_0' is the maximum of all products u*v, where (u, v) is in R. The point (u_0', v_0') is the Nash's solution to the bargaining game [R, (u*, v*)] obtained by utility transformations.

The *status quo* trade is at the origin, or, in other words, the zeros of the individual utility functions are arbitrarily chosen to be the case of no trade. This is the anticipation of no cooperation between the bargainers. The Nash's "solution" concept does not predict of what happens in bargains. Here, the asymmetry in the roles of the players enters into the solution. The model does not equate the *status quo* positions of the players.

Ethically, this may be unfortunate, since asymmetry works to the detriment of the 'poor man' and to benefit for the 'rich man'. Nash's approach may not be ethically fair, but this solution proposes to give a 'fair' arbitrated value of the bargain when the strategic aspects are taken into account.

4 SUSTAINABILITY

Today's process industry decisions face new economic realities that come closer to the principle of sustainability. However, traditional economic evaluation methods are not able to account for sustainability and do not measure ecological aspects within the enlarged task of ecological process engineering.

The concept of sustainability can be considered to be the base of strategic planning in two ways: (1) it is an inherent long-term concept. Thus it allows long-term planning in the face of radically changing boundary conditions; and (2) the reference systems are natural flows or states and their variations. Hence, planning on this basis is independent of social conventions like threshold values which may vary with time.

In [9], an operational working hypothesis of sustainability consistent with the needs of ecological process engineering is introduced. Base on this definition, sustainability requires three criteria: (1) *anthropogenic material flows must not exceed the local assimilation capacity and should be smaller than natural fluctuations in geogenic flows*. This requirement maintains the quality of the material base for ecosystems (soil, aquifers, atmosphere, etc.); (2) *anthropogenic material flows must not alter the quality and the quantity of global material cycles*; most of the dominant global material cycles (like carbon, nitrogen, and water cycle) have natural buffer stocks. This requirement defines the input streams for industrial systems; and (3) *the natural variety of species and landscapes must be sustained or improved*. It calls for maintaining the important interaction between man and nature at a physical as well as psychological level and for the use of nature's resources under the boundary conditions of aesthetics. Degrading land and species irreversible will impede our own chance to improve our quality of

Copyright © 2005 Taylor & Francis Group plc, London, UK

life and it will deprive future generations of an important basis for living.

Process industry needs a strategic measure that takes environmental and social considerations into account as a base for decisions on future projects. A number of interesting approaches to this problem already exist to create strategic measures which can evaluate the viability of processes under new constrains of competition.

Sustainability indexes

The Sustainable Process Index (SPI) is based on an operationalized form of the principle of sustainability. The core of the SPI evaluation is the calculation of the area needed to embed a process completely into the biosphere. SPI helps to define a whole process more widely by including raw material generation, energy production, by-product treatment and recycling into the process. Thus, ecological process engineering can deal with process design and optimization much more consistently with respect to ecological problems.

SPI evaluates technical processes according to their competitiveness under completely sustainable conditions. It is based on data which are known at an early stage of planning. Therefore, it can be used for screening different process alternatives as well as different technological possibilities of supplying a necessary service.

The factor "Area" as the basic unit for the computation of the SPI was chosen. The reason behind this choice is that in a sustainable economy the only real input that can be utilized in the long term is solar energy. Moreover, area is a limited resource in a sustainable economy (flow to soil, water or air requires a certain area) since the surface of the planet is finite.

By taking into account the dual function of area as a recipient of solar energy and as a production factor, the SPI can measure and relate the ecological impact of a process with respect to the quantity and quality of the energy and mass flows it reduces. The specific area is a comparative measure of sustainability if certain services paths to deliver a service are related.

5 TUNNELING GAME MODEL (TGM)

Definition

The Tunneling Game Model (TGM) is a cooperative game where the players are permitted to communicate prior to playing the game, to make binding agreements, and to use randomized strategies. It is formulated as a bargaining situation which involves two players "owner" and "contractor" with different utility functions. Both players have the opportunity to collaborate for mutual benefit.

The TGM assumes the existence of a *status quo* point (u*, v*) which represents the payoff to each player if they do not agree. The choice of the *status quo* point may vary with different assumptions about the attitudes behavior and bargaining strengths of the players.

The negotiation set consists of all un-dominated payoffs for which each player gets at least his maximin value. In the bargaining context, the selection of an outcome from the multiplicity of points in the negotiation set depends of the psychological characteristics of the players.

Utility Functions

The construction of the utility functions with the form $U = X^aY^bZ^c$ is proposed, where X represents "sustainability", Y represents professional-technical agreements (geotechnical investigation, schedule, budget, and engineering services during construction), and Z represents risk allocation and contract documents. The power allocation may facilitate the contribution of each component towards U.

Component X

Here, the concept of sustainability can be considered to be the base of strategic planning. SPI evaluates technical process (technological possibilities of supplying a service) according to their competitiveness under completely sustainable conditions.

Component Y

The professional-technical component can be divided into different phases: (1) define the level of confidence of the subsurface conditions; (2) define the level of confidence of the engineering and chemical properties, and groundwater conditions; (3) assess how the potential ground conditions will behave when subjected to a range of anticipated construction means and methods; (4) design the tunneling support to accommodate not only the final loads, but also the construction methodologies that are compatible with the ground conditions and be sufficiently robust to accommodate reasonable variations in both the ground conditions and normal variations in construction; and (5) define the designer's participation through construction, since the design is not complete until construction is completed.

The site investigation provides the design parameters, information for selecting and judging construction means, methods, and performance. Cutting corners in the ground characterization phase can lead to increased cost resulting from a conservative design and can increase the risk of a significant differing site conditions claim, or adverse performance of the

Copyright © 2005 Taylor & Francis Group plc, London, UK

structure. Design phase costs can also be reduced by restricting the scope of the engineering service. Similarly, eliminating the designer's role during construction will also reduce costs. However, the costs "saved" by such scope reductions are more than offset by the costs of the added construction risk and claims, and other costs associated with the resultant risk of diminished quality of the design and construction of the project.

The schedule defines the time line, and it is a condition precedent used in most contracts. It is important that the schedule be both reasonable and integrated with the entire effort and within the control of the designer; not depending on the contractor's performance, since the contractor's performance is not within the control of the engineer.

Component Z

The contract must be flexible enough because underground engineering involves significant construction phase elements, including design modifications required to address variables such as differing site conditions or unanticipated behavior of site conditions arising out of the construction means and methods selected by the contractor.

As a general rule, more risk assumed by the owner, a lower initial bid construction is expected. Conversely, a higher initial bid construction is expected as a result of defensive designs, contractor contingency costs, etc. The optimal position varies significantly from project to another depending on the risk tolerance and attitude of the owner. For private sectors, where reasonable risks can be accepted and funded, a more aggressive position may be appropriate. In contrast, the public owners, where changes are not easily accommodated, a more conservative approach may be appropriate.

The contract, ideally, provides a clear, written understanding of the obligations and responsibilities of each party. The contract should also include provisions that address the procedures for changing the terms of the contract and its requirements, resolving disputes, indemnification, insurance requirements, and termination and default.

Solution

The solution of the TGM is the Nash's solution to the bargaining game obtained by utility transformations. This 'solution' concept does not predict of what happens in bargains. But, it proposes to give a 'fair' arbitrated value of the bargain when the strategic aspects are taken into account. This solution can only be said to exist if the players are committed to Nash' solution.

The Nash's solution defined as a single point is not an ethical statement. However, it can be complemented axiomatizing the solution of a general cooperative game. A set of precise desiderata that any acceptable arbitration scheme must fulfill can be formulated as axioms. In the TGM, the players may agree to submit to an arbiter who is committed to find the solution with a pre-specified method.

6 SUMMARY

The TGM tries to show how risk aversion and adversarial relationships cause owner authorities and contractors to not reach their potential satisfaction.

In the TGM, the owners have the power to define the rules of the game. Then, the players make agreements, but would eventually cheat in order to maximize their own revenues.

7 CONCLUSIONS

The TGM offers a chance to include the concept of sustainability into the tunneling strategic planning process. It may allow a rational discussion of different technological alternatives in infrastructure development.

The TGM encourages: (1) the preparation of appropriate geotechnical reports and data, and adequate contract documents for the execution of design; (2) the importance of the professional's observational services during the construction; and (3) the inclusion in the contract documents of fair and impartial procedures for the timely submission and resolution of disputes and claims involving different site conditions.

The TGM provides an education tool for owners and contractors in the tunneling industry. An uneducated owner, for instance, may prefer the competitive fee biding approach, the low-bid process to the procurement of professional services. In this way, the benefits of the new technological development, engineering design evolution, and new experience are never utilized in this tunneling project.

The TGM proposes delivery of services in accordance with clearly defined standards and expectations, and preserves the professional right's and defines, allocates, and mitigates risk exposure. The players are obligated to understand the fundamental tunneling issues.

The TGM recognizes the value of continuity from design into construction. Unanticipated conditions are inevitable and require modifications or adaptations of the design. The failure by the owner in recognizing this issue is one of the primary causes of claims, cost escalation, and poor quality in tunneling projects.

The TGM offers the opportunity to lay the foundation for educating the tunneling participants about the principles of fair and realistic risk allocation on tunneling projects, and how these principles encourage

Copyright © 2005 Taylor & Francis Group plc, London, UK

successful (technically and management) tunneling projects.

Adversarial positions should have no place in civil engineering projects. Hopefully, the Tunneling Game Model (TGM) may help in the solution of the adversarial relationships; a current big challenge for the tunneling industry.

REFERENCES

[1] Aliprantis C., Chakrabarti. *Games and Decision Making*

[2] Chambers N., Simmons C., Wackernagel M. *Ecological Footprints as an Indicator of Sustainability*

[3] Colman A. *Game Theory & Its Applications in the Social and Biological Sciences*

[4] Edited by David J. Hatem, Esq. *Subsurface Conditions; Risk Management for Design and Construction Management Professionals*

[5] Edited by Jian Zhao, J. Nicholas Shirlaw & Rajan Krishnan. *Tunnels and Underground Structures*

[6] Goel R., Dube A. *Status of Underground Space Utilization and Its Potential in Delhi*. Tunneling and Underground Space Technology, Vol. 14, Number 3, 1999

[7] Luce D. & Raiffa H. *Games and Decisions*

[8] Mesterton-Gibbons M. *An Introduction to Game-Theoretic Modelling (Second Edition)*

[9] Narodoslawsky M. & Krotscheck C. *The Sustainable Process Index (SPI): evaluating process according to environmental compatibility*, Journal of Hazardous Materials 41 (1995) 383–397

[10] Narodoslawsky M., Krotscheck C. *Integrated Ecological Optimization of Process with the Sustainable Process Index*; Waste Management 20 (2000) 599–603

[11] Roberts D. *Sustainable Development and the Use of Underground Space*; Tunneling and Underground Space Technology, Vol. 11, Number 4, 1996

[12] Underground Construction Research Council of ASCE in cooperation with AIME. *Report of: A Program for Improving the Effectiveness of Underground Construction*. The Use of Underground Space to Achieve National Goals

Copyright © 2005 Taylor & Francis Group plc, London, UK

Operation, maintenance, drainage, water proofing, rehabilitation, renovation and repair of underground structures

Copyright © 2005 Taylor & Francis Group plc, London, UK

New waterproof structure for New Austrian Tunneling Method

Toshihiko Komatsu & Toshio Nakamura
Maeda Corporation, Tokyo, Japan

Hiroshi Kanda & Masaji Takada
Kanto Regional Bureau, Railway Construction Headquarters of the Japan Railway Construction, Transport and Technology Agency, Tokyo, Japan

ABSTRACT: Along with increases of tunnels and other social overhead capital, reduction of total costs is an urgent necessity. New Austrian Tunneling Method (NATM) is increasingly used to construct tunnels in urban districts as well as in mountainous areas because the method is rational and economical. Cracks on lining concrete and water leakage are a serious problem, and measures are needed to minimize maintenance and repair works since tunnels are difficult to repair while in service.

The authors developed a system that enables smooth application of lining sheets for NATM, free from the effects of unevenness on sprayed concrete surface. This system can reduce cracks on lining concrete and produce highly watertight tunnel structure, and thus can prolong the service life of the tunnel and reduce the maintenance and repair costs. This paper describes the concepts and execution methods of this system.

1 INSTRUCTION

Tunnels in mountainous areas are waterproofed to reduce the restrain from the back of the lining and control cracks usually by nailing waterproofing sheets on sprayed concrete surface. However, this method is prone to excessive and insufficient allowance of waterproofing sheets, which causes entrainment of the sheets in lining concrete, blockage of grouting, insufficiency of lining thickness, and voids behind the sheets. A practical method should be developed to apply sheets tightly to sprayed concrete so that the sheets do not block injection of grout.

Watertight tunnels are increasingly designed to minimize environmental impacts by discharge of underground water from tunnels, and watertight construction is highly demanded. In Europe, where a large number of watertight tunnels are constructed, the thickness of waterproofing sheets is 2.0 mm to 3.0 mm, and is 4.0 mm for high water pressures. To apply such thick sheets, various measures are taken, such as spraying a finish layer on sprayed concrete surface and using temporary lining, which are expensive.

The authors developed a system that enables smooth application of waterproofing sheets, free from the effects of unevenness on sprayed concrete surface. The method involves spreading of waterproofing sheets on formwork, injection of grout in the space between the sheets and sprayed concrete surface, and ensuring adhesive force between the geotextile sheets and the grout. This system enables lining of waterproofing sheets to be performed simultaneously with grout injection, and solves problems that have caused cracks, such as restraining of sheets and voids behind the lining. In-situ joining works can also be reduced by using wide sheets, and breakage of sheets can be prevented by smoothing unevenness. Thus, the resultant linings are highly watertight and are little prone to cracks. The high quality of the linings will minimize necessary maintenance and repair works and prolong the service life of the tunnel. This paper describes the concepts and execution methods of this system based on the construction of Minimi Nagareyama Tunnel of Tsukuba Express Railway.

2 PROBLEMS OF CONVENTIONAL METHODS

Conventional methods usually control cracks on lining, which are caused by external restrain, and leak of water from the cracks by applying waterproofing sheets on the sprayed concrete surface. Waterproofing sheets must be applied with an allowance appropriate to the unevenness of the sprayed concrete surface and rock bolts. When the amount of allowance is not appropriate

Copyright © 2005 Taylor & Francis Group plc, London, UK

but is insufficient or excessive, the following problems may arise:

1) The waterproofing sheet is pulled or deflects while placing the lining concrete, disturbing the filling of concrete,
2) Variation arises in the effect of the sheet to mitigate restrain of the sprayed concrete and at the back of the lining concrete, increasing the risk of cracks on the lining concrete,
3) The risk of damaging the waterproofing sheet with edges of reinforcement increases while assembling the reinforcement,
4) When the waterproofing sheet is damaged behind deflection, the chance of overlooking the damage is large, and
5) When water pressure acts from the back of a breakage, a water channel may be formed along the waterproofing sheet, causing leak of water over a wide area.

Therefore, the sprayed concrete surface behind the waterproofing sheet needs be finished smooth. However, preparing smooth surfaces require extra spraying, time, and cost, and is usually not performed.

3 NEW METHOD PROPOSED

Practical waterproof structures that adhere well to sprayed concrete surface but do not disturb concrete filling should be developed for the lining of tunnels. Since waterproofing sheets also serve to mitigate the restrain at the back of lining concrete, the quality is also important. Points that must be revised to improve the quality of the waterproof and lining structures were investigated. The investigation showed that waterproofing sheets need to be finished so as to adhere tightly to the surface of sprayed concrete and to result in smooth tunnel shape.

To satisfy these requirements, a new method was developed based on the concept of preparing bases appropriate for applying waterproofing sheets rather than the conventional idea of adjusting waterproofing sheets to the unevenness of sprayed concrete surfaces.

Schematic cross sections of tunnel structure for the conventional and new methods are shown in Figure 1.

4 NEW METHOD PROPOSED

Three issues must be solved to materialize the tunnel structure shown in Figure 1, which are the 1) performance for construction (construction methods), 2) economy, and 3) quality. Measures for these issues are described in the rest of this section.

4.1 *Performance for construction (construction methods)*

As shown in Figure 1, the base for waterproofing sheet can be prepared smooth by setting formwork (such as arch centers) and grouting filler between the sprayed concrete surface and the form. Although waterproofing sheets can be pasted after regularizing the sprayed concrete surface, sheets were decided to be spread on the formwork in advance to reduce the labor of pasting the sheets, minimize voids behind the sheets, and thus maximize the performance and quality of construction.

The new method involves setting and fixing waterproofing sheets on the specified parts of the external wall of formwork and filling the space between the sheet and concrete with foamed mortar or other kind of filler. The method unites the waterproofing sheet, filler, and sprayed concrete, and results in a smooth and even surface covered by the waterproofing sheet. To implement the method, materials of waterproofing sheet, backfill materials, and sheet installation equipment (form wagon) needed to be improved.

Based on the investigations, waterproofing sheets were decided to have the same structure as those used for the conventional method (waterproofing sheet plus 3 mm-thick geotextile pasted together at factory). The

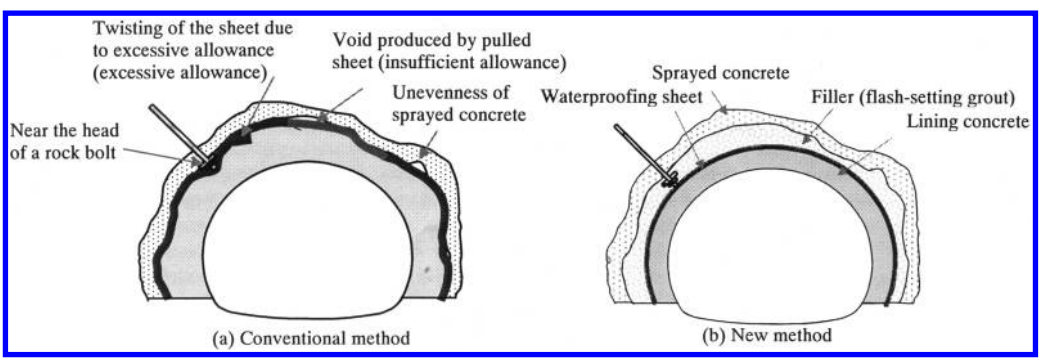


Figure 1. Schematic diagram of tunnel structure.

Copyright © 2005 Taylor & Francis Group plc, London, UK

entire sheet is to be adhered on the wall using the adhesive force between the filling material and geotextile. A sheet spreader was decided to be installed on the sheet installation equipment. The manufacture of the equipment and actual sheet application work were likely possible using conventional tunnel construction technologies. A form wagon is illustrated in Figure 2.

Backfill materials needed to be checked for the adhesive force between sprayed concrete and geotextile (adhesion), the performance for filling the space between the sprayed concrete and geotextile (flowability), and the consolidation time (flash setting) so that the materials do not leak from the bulkhead and bottom of the formwork. Methods used for selecting backfill materials are described below.

(1) Selecting backfill materials

As backfill materials, air milk and two-part flash-setting grout used for the shield tunneling method were investigated.

Of the two kinds of filler, air milk was found in test application that a large volume of milk was needed since foam burst by the pressure during grouting and the heat of hardening was much larger than expectation. Since it takes long to consolidate, a large amount of milk leaked from the uneven sections of the sprayed concrete surface and the bulkhead (air tubes), and the formwork deformed due to working loads. On the other hand, the two-part flash-setting grout used for the shield tunneling method showed no such a leakage problem and was efficient to work with. Based on these results, the two-part flash-setting grout was decided to be used as the backfill materials.

(2) Consolidation time and adhesive force

Backfill materials should not cause leaks (but consolidate fast) as well as they need to be flowable. An indoor experiment was conducted to examine the relationship between flowability and consolidation time by changing the gelling time from 10 to 30 seconds. The optimum gelling time was found to be 30 seconds.

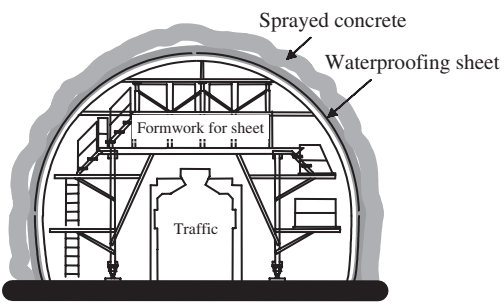


Figure 2. Tunnel formwork wagon for installing waterproofing sheets.

The mix proportion of the backfill materials were determined based on the target gelling time. Basic experiments were conducted to examine the adhesive force between sprayed concrete and the backfill materials and between the backfill materials and the waterproofing geotextile sheet. The experiments showed that at 2 hours the backfill materials had adhesive forces much larger than target adhesive forces, which were calculated to be 20-fold larger than the necessary values determined from the dead weights of the materials, for both between the sprayed concrete and the backfilling materials (necessary force: $1.4 \times 10{-}3\ N/mm^2$) and between the backfilling materials and geotextile (necessary force: $1.8 \times 10{-}5\ N/mm^2$). Since curing time of over 10 hours is planned for practical implementation, the two-part flash-setting grout was shown to have sufficient adhesive force and performances required for backfilling materials.

(3) Working method

The backfilling materials were grouted according to the following procedure:

1) Waterproofing sheets were spread and set on the formwork. The height and center of the formwork were adjusted.
2) Air tubes were arranged along the external wall of the formwork for the section to be filled with grout. Bulkhead was constructed. Three inlets were established. Grout was first injected from one of the side inlets (SL + 4 m), then from the other side inlet, and finally from the center inlet at the top.
3) Filling is completed after checking that the fill materials have returned from the air relief at the top.

A schematic diagram of a bulkhead form and its photograph during construction are shown in Figure 3.

4.2 *Economy*

The new method needs almost double costs of those in the conventional methods for equipment (form wagon for sheet installation, inner forms and sheet installation equipment). On the other hand, construction costs (wages, costs of materials and costs for running the plant) were almost the same with those of the conventional method with a slight increase of 3.5%. The difference was thus attributable to the costs of equipment.

Since the cost of equipment per unit area is determined by the length of the tunnel to be constructed, the costs can be reduced in relatively short tunnels, such as the tunnel tested (361 m), by using a lining center as the formwork for sheets. Six meters of sheets were assumed to be installed per day, but the length can be increased to 10 m to reduce labor costs. The

Copyright © 2005 Taylor & Francis Group plc, London, UK

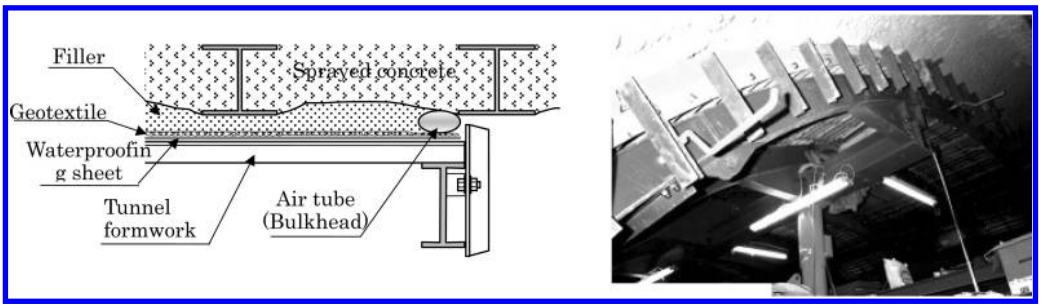


Figure 3. Waterproofing sheet installed on formwork.

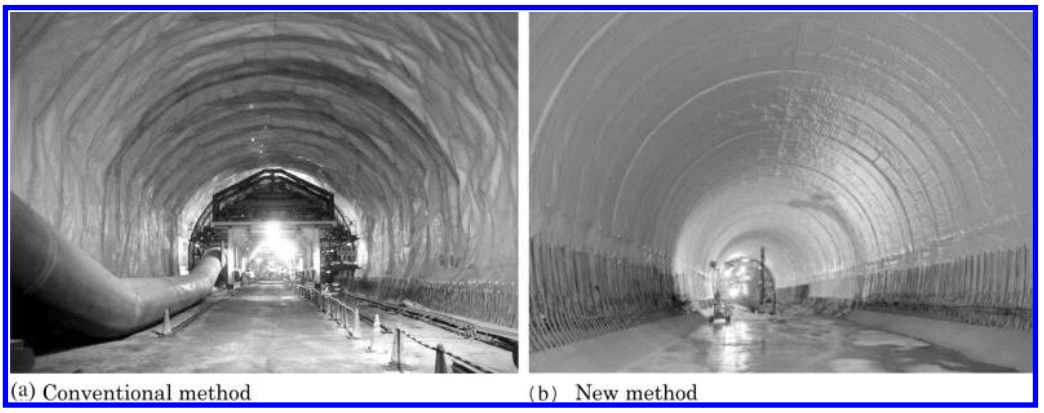


Figure 4. Tunnel surface with waterproofing sheets applied.

adhesion strength of the backfill materials was larger than the standard strength, and the mix proportion can be modified to reduce costs.

4.3 *Quality*

Figure 4 shows a tunnel finished with the conventional method and a tunnel lined with waterproofing sheets using the new method.

The tunnel of the conventional method was concerned for excessive and insufficient allowance of the sheets. On the other hand, the surface of the lining in the new method was smooth except at welded sections, satisfying the required quality.

5 EFFECTS OF THE NEW METHOD

The new method should be effective to:

(1) Ensure the quality of the resultant lining concrete.
  1) The thickness of the lining concrete will be uniform because the surface of waterproofing sheet is smooth. Voids will be reduced.
  2) The isolation function of waterproofing sheet will be improved and become uniform.
  3) Concrete can be filled smoothly between the surface of tunnel and waterproofing sheet, enabling the sheet to be tightly adhered.

(2) Improve the waterproof performance
  1) Wide sheets that are as wide as the formwork length can be applied, reducing the welding work at the site, and the quality of the lining as a whole becomes more reliable than linings applied using the conventional method.
  2) Sheets become less prone to breakage by the heads of rock bolts and projections than in the conventional method.
  3) Sheets become less prone to damage by edges of reinforcement while assembling the reinforcement.
  4) Since waterproofing sheets will be smooth and tightly adhered to sprayed concrete, firm water barrier can be formed and can stop leak of water over a wide area (enabling points to be repaired to be identified).

(3) Reduce costs (possibility of VE)
  1) Economical and highly strong materials, such as HDPE (high density polyethylene), can be

Copyright © 2005 Taylor & Francis Group plc, London, UK



Figure 5. Process of the new method.

used for waterproofing sheets since the sheets need not to be as flexible as to bend along unevenness of sprayed concrete surface.

2) The process of treating the heads of rock bolts and smoothing the surface of sprayed concrete is reduced, enabling the period of tunnel excavation project and the mount of concrete materials to be reduced.
3) Structures that conforms with required water proof performance can be constructed by using the method for necessary sections and selecting appropriate sheet materials (For example, only at joints, only for the top heading, and for the entire surface).
4) Costs for stopping and treating leak water can be reduced.

(4) Improve working environment

1) Sheets will be applied by machines instead of manpower, reducing labor.
2) Sagging of sheets will be reduced, improving the working environment and efficiency of assembling reinforcement.
3) The lining construction using the new method is shown in Figure 5 in a time historical order.

6 FUTURE TOPICS AND CONCLUSIONS

This paper described the effectiveness of the new method.

There are still topics that must be solved, such as methods for discharging water leaking from sprayed concrete surface if there is any, and ensuring the injection of the grout to the crown. Simple formwork and improved backfill materials should be developed to improve efficiency and reduce costs. The significance of the new method should also be investigated in terms of watertightness and quality of linings.

The proposed new method solves the structural defects of the conventional methods from the root and prolongs the service life of mountain tunnels. The system can produce very strong, reliable and highly watertight linings using wide waterproofing sheets, smooth sheet surfaces with no voids behind the lining, and highly strong materials such as HDPE (high density poly ethylene), and can be applied to construct perfectly watertight tunnels in urban areas. The method will be used for a large number of tunnels and will be developed into a standard construction method.

Copyright © 2005 Taylor & Francis Group plc, London, UK

Behavior of support structure of existing tunnels during enlargement of cross section

Hideto Mashimo, Toshiaki Ishimura, Nobuharu Isago & Satoshi Morimoto
Public Works Research Institute, Tsukuba, Ibaraki, Japan

ABSTRACT: In Japan, with upsizing of vehicle or increase of traffic volume, the number of tunnels in which passage of two vehicles and passage of pedestrians are difficult due to the narrow cross sections has been increased. To reconstruct existing tunnels rationally and economically, to arrange the right-sizing support structure by taking account of the existing tunnel characteristics is important. Field measurements at four existing road tunnels for enlargement were carried out to clarify the behavior of support structure during enlargement of existing tunnel's cross section. From these results, the influence of enlarging existing tunnels was clarified and the effectiveness of rock bolting which was installed prior to enlargement of existing tunnels in restraining the ground movement was confirmed.

1 INTRODUCTION

The number of the tunnel with small cross section, which does not allow smooth traffic flow or passage of pedestrians, is increasing due to upsizing of vehicle or increase of traffic volume. Also enlargement of section or reconstruction for existing tunnels is needed because the deformation in permanent lining by aging of tunnel or change of ground conditions occurs. However the support structure for enlargement of tunnel section or reconstruction is referred to one for new tunnels by no clear design method established in current stage. More economical and mechanically rational design method for enlargement or reconstruction, such as considering the effect of a pilot tunnel or the existence of loosened area around an existing tunnel, should be established.

Several field measurements in four tunnels which enlarged their cross sections were achieved to collect basic data, such as the deformation or the strain in lining of an existing tunnel and the stress in the support at enlarged tunnels, for the purpose of establishing the design method. The outline of measurements and the results will be shown in the following.

2 MEASUREMENT OUTLINE

Field measurements were achieved in four tunnels shown in Table 1. All cases were the enlargement of cross section for an existing tunnel. Tunnel A, B and C were enlarged under the active road condition, that is, without disruption of current traffic flow. Crown settlement, convergence and strain at the surface of lining to grasp the influence for existing lining, and stresses of steel rib and shotcrete and axial force in rock bolt to grasp the behavior of the enlarged tunnel were measured in tunnel A and B. The additional rock bolts were diagonally cast at the wall of tunnel B and its behavior was monitored to examine their effect. In addition, the rock bolts were placed as the pre-reinforcement of ground before the enlargement of tunnel and their axial forces were measured in tunnel C and D.

3 MEASUREMENT RESULT OF TUNNEL A

3.1 *Measurement method*

Field measurements for the existing tunnel were carried out in section 4 and 5 shown in Figure 1(a). Strain of lining, using the space above the protector by attaching strain gauge shown in Figure 1(b), and convergence and crown settlement of four measurement lines were measured. Stresses of steel arched rib and shotcrete and axial force of rock bolts were measured in enlarged tunnel shown in Figure 1(c).

3.2 *Result*

3.2.1 *Measurement result of existing tunnel*

Figures 2 and 3 shows the strain of lining in circumferential direction, the convergence in section 4 and 5 with tunnel face advance.

Copyright © 2005 Taylor & Francis Group plc, London, UK

Table 1. Items of measurement in each tunnel.

Tunnel	A	B	C	D
Existing tunnel (old)				
Construction:	Conventional method			
Open (year)	1973	1950	1962	1938
Length (m)	975	116	146	82
Width (m)	9.8	6.0	6.0	6.0
Height (m)	6.3	4.9	5.0	5.1
Lining thickness (m)	50–70	30	35	30
Enlarged tunnel (new)				
Construction:	NATM			
Excavation type	Mech.	Mech.	Blast	Mech.
Length (m)	170*	120	146	102
Width (m)	15.6	12.5	9.75	12.5
Height (m)	8.0	7.0	7.1	7.0
Lining thickness (m)	40–45	30–35	30	30–35
Max. overburden (m)	38	38	42	30
Geological specification				
Geology	Sandstone Schist Tuff	Mudstone	Andesite	Silty mud-stone
UCS (MPa)	16~30	1~9	13 (weak) 150 (mean)	4~10
Measurement items**				
Old	(a) (b)	(a)		
New	(c)	(c)	(d)	(d)

*: Only around portal area
**(a): Crown settlement, convergence
(b): Strain of lining
(c): Stresses of steel rib/shotcrete, axial force of rock bolt
(d): Axial force of rock bolt in previous stage

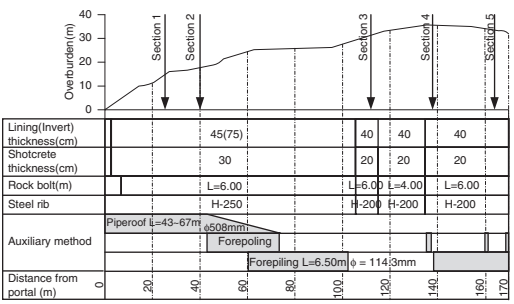


Figure 1(a). Outline of tunnel A.

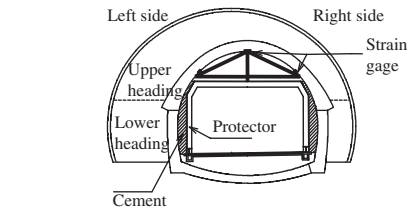


Figure 1(b). Strain measurement of lining at tunnel A.

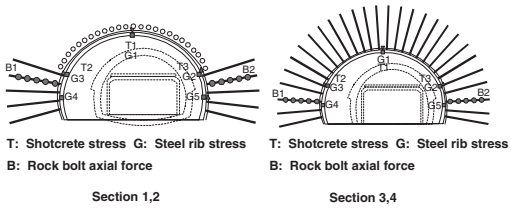


Figure 1(c). Measurement point of stresses and axial force at enlarged tunnel A.

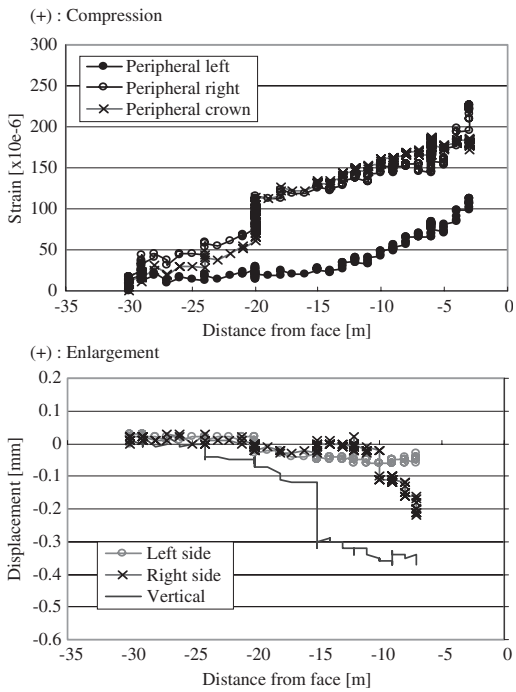


Figure 2. Measurement result of lining at section 4 of existing tunnel A.

The strain of lining increased when the face approached at a point of 30 m, which was equivalent to 2D (D: tunnel diameter), from the measurement point in section 4. The value was almost constant up to a point of 15 m (1D) and increased again from the place. The convergence, which was measured at three lines shown in Figure 2, started changing when the face approached at a point of 25 m (1.5D) from section 4. These tendencies may correspond with the

Copyright © 2005 Taylor & Francis Group plc, London, UK

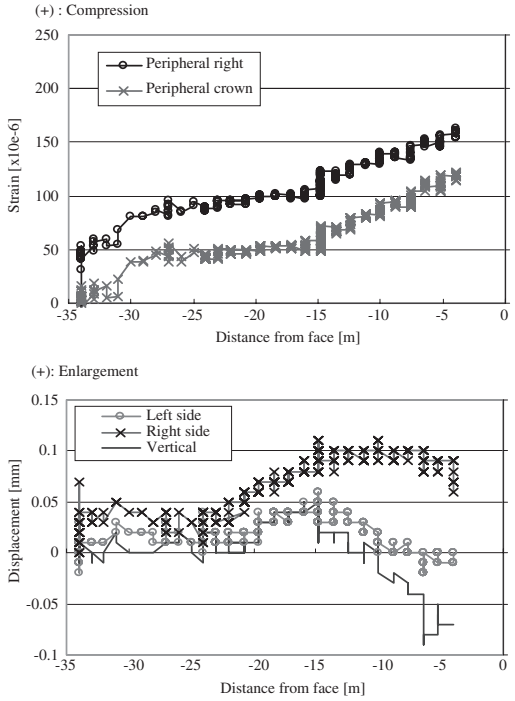


Figure 3. Measurement result of lining at section 5 of existing tunnel A.

strain one. This value drastically changed at 15 m (1D) from section 4 because the convergence changed from the expansion to the contraction of cavern while the crown settlement did not almost change.

The strain of lining clearly increased when the face approached at a point of 25 m (1.5D) from the measurement point in section 5 and drastically increased at a point of 3 m from there. The convergence started changing for contraction when the face approached at a point of 25 m from section 5.

3.2.2 *Measurement result of the support in enlarged tunnel*

Figure 4 shows the final values of crown settlement and convergence in enlarged tunnel. The overburden at the measurement sections 1 and 2, which was near tunnel portal, was under 20 m and it was thought thin. Crown settlement was large while convergence was not so. The geology around this area was bad and the loosened area was confirmed above the crown. Pipe-roof method was planned from the design stage. Section 3 and 4, which were over 100 m away from the portal, adopted the injected forepoling and the displacements were within 10mm. This value was relatively smaller than the one with the same degree of ground condition.

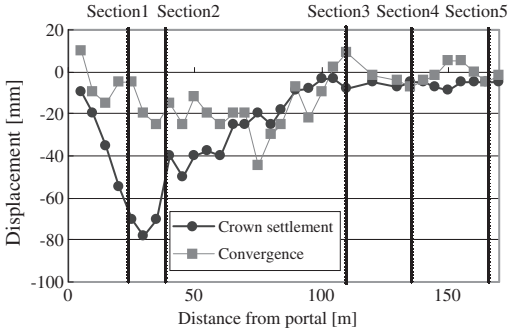


Figure 4. Displacement of tunnel A.

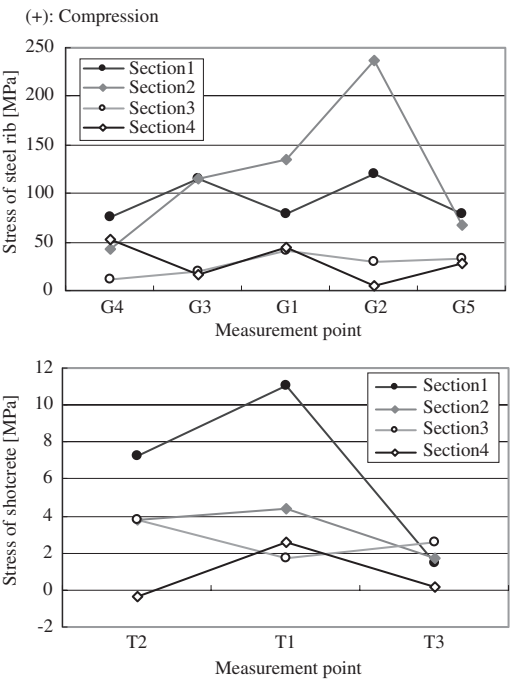


Figure 5. Final values of stresses at every measurement point from all of sections.

Figure 5 shows the final values of each stress. Stress on steel rib was relatively high in section 1 and 2 where the overburden was under 20 m while the stress was low in section 3 and 4. This tendencies was true of the result of shotcrete measurement.

Figure 6 shows the measurement result of rock bolts. Axial force was high in section 2 where the stress on steel rib and shotcrete was high, to the contrary, not so in section 4.

From the results above, stresses and axial force were not so high when the overburden was over a certain

Copyright © 2005 Taylor & Francis Group plc, London, UK

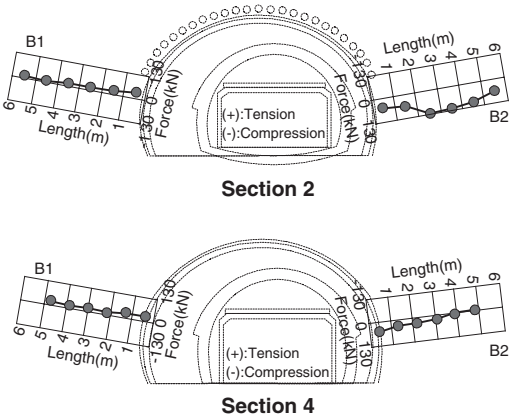


Figure 6. Axial force distribution of rock bolts in enlarged tunnel A.

value with exception, and it means the capacity of support system in this tunnel could be validated.

4 MEASUREMENT RESULT OF TUNNEL B

4.1 *Measurement method*

Field measurements were carried out in three sections shown in Figure 7(a). Convergence and crown settlement of existing tunnel lining using the space above the protector. Stresses of steel arched rib and shotcrete and axial force of rock bolts were measured in enlarged tunnel shown in Figure 7(b). Around section 2 along a tunnel length of 10m, five rock bolts, whose material and length were same as ones in other area, were placed diagonally to the advance direction in both walls and the results were compared with ones from section 3, which did not cast them. The order of excavation section was upper, lower left-sided, lower right-sided, footing left-sided and footing right-sided.

4.2 *Result*

4.2.1 *Measurement result in existing tunnel*

Figure 8 shows the crown settlement of the lining of existing tunnel. Crown settlement was within 0.5 mm and relatively small in all areas and convergence was also small. No drastic change was admitted with the advancement of the enlarged tunnel.

4.2.2 *Measurement result in enlarged tunnel*

Crown settlement and convergence in the enlarged tunnel were also shown in Figure 8. Crown settlement was within 20 mm and small. No clear relation was admitted between the support pattern and overburden. Convergence was also small but tendency of change was a little different. The value was almost zero in

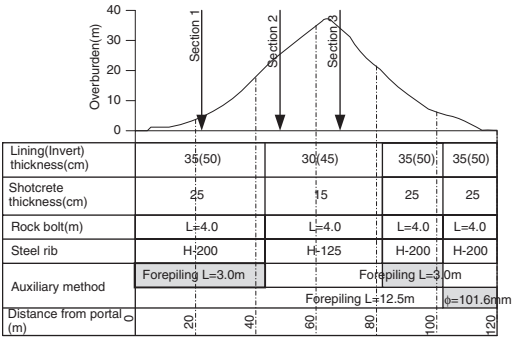


Figure 7(a). Outline of tunnel B.

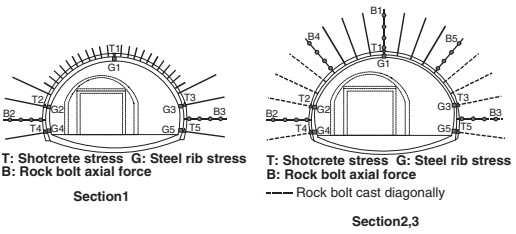


Figure 7(b). Measurement point of stresses and axial force at enlarged tunnel B.

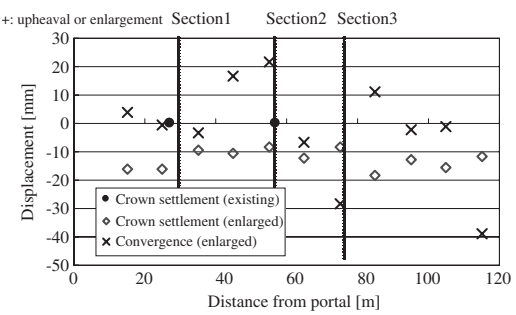


Figure 8. Displacement of tunnel B.

section 1, and moving to mountain side in section 2 and to tunnel side in section 3 was found.

Figure 9 show the final values of each stress. When the results from section 1 and 3 were compared, section 1 which was smaller overburden had the larger stress. The result from section 2 where the additional rock bolts were placed showed a little larger stress comparing with one from section 3, however, the value may be with in the capacity of support. Stress on shotcrete was under 4 MPa and small, and no large load from ground may not be acted on each support.

Figure 10 shows the measurement result of rock bolt in three sections. The maximum tensile value was

Copyright © 2005 Taylor & Francis Group plc, London, UK

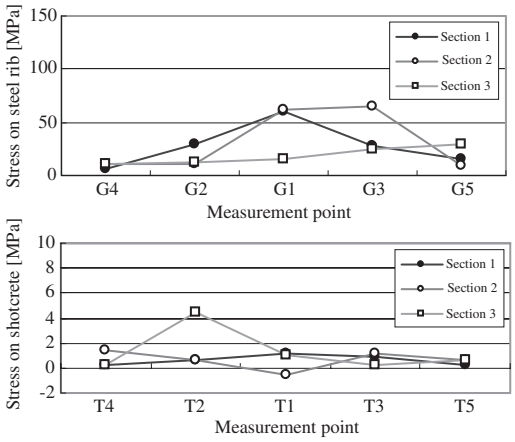


Figure 9. Final values of stresses at every measurement point from all of sections.

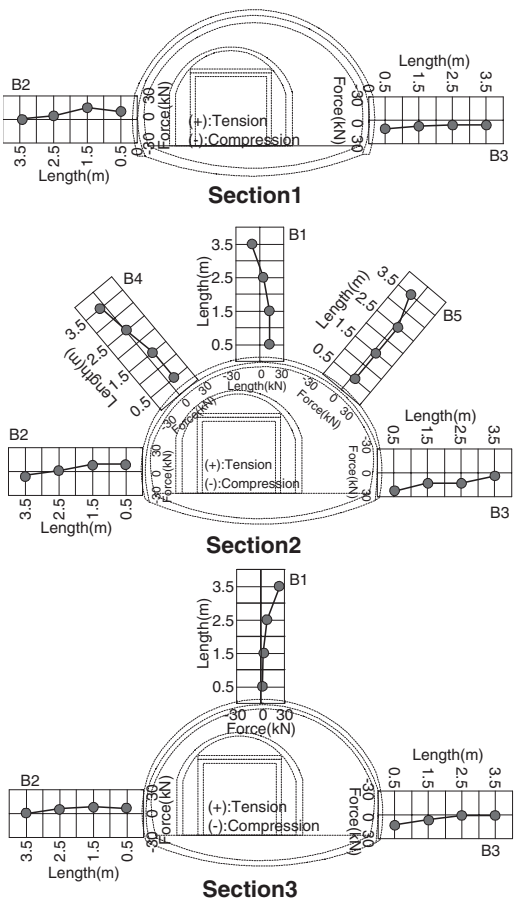


Figure 10. Axial force distribution of rock bolts in tunnel B.

20 kN in all sections and no clear difference was admitted about the angle of bolt placement to tunnel walls.

From the results above, stresses and axial force were not so high in every section and the capacity of support would be confirmed in this tunnel. No clear difference was admitted about the direction of rock bolts placement under this condition.

5 MEASUREMENT RESULT OF TUNNEL C

5.1 *Measurement method*

Field measurement was carried out in one section shown in Figure 11. FRP rock bolts with a length of 3 m were placed around the crown all over the existing tunnel to reinforce it. The axial force of three rock bolts was measured. Only the bolt for measurement was adopted with a length of 6 m. Enlargement construction was performed after the removal of pavement and roadbed in existing tunnel.

5.2 *Result*

Figure 12 shows the axial force of rock bolt at crown (B2) until the bolt was cut off by excavation for enlargement. All of the bolts measured indicated tensile with the start of roadbed excavation and the lining deformed downwards. The force was changed to compression with the enlargement. Tensile force of 60 to

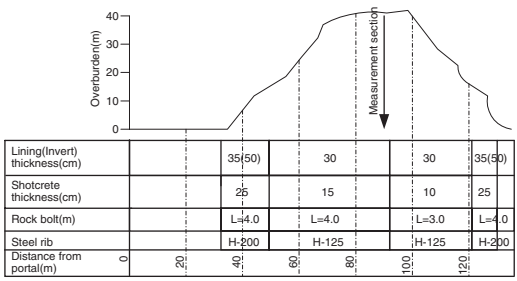


Figure 11(a). Outline of tunnel C.

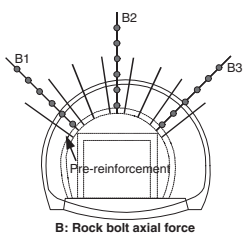


Figure 11(b). Measurement point of axial force at existing tunnel C.

Copyright © 2005 Taylor & Francis Group plc, London, UK

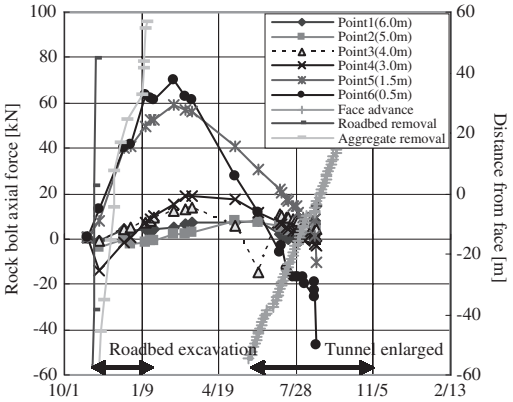


Figure 12. Axial force of rock bolt during enlargement stage at tunnel C.

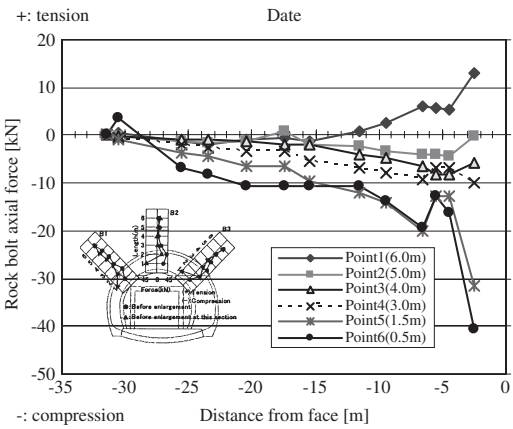


Figure 13. Axial force of rock bolt at every measurement point at tunnel C.

70 kN occurred to the tunnel perimeter of 2 to 3 m shown in Figure 12.

Figure 13 shows the axial force distribution at the measurement section. One is the tendency of axial force changes with the advance of tunnel face. The value was initialized as start of tunnel enlargement. The other is the distribution of axial force to back of the ground just before the enlargement excavation. When the face approached at 10 m before the measurement section, axial force prominently changed to compression. In addition, the change drastically occurred at 2.5 m. It means the influential area of existing tunnel by enlargement would be approximately 10 m (1D). From the distribution of force, compressive force occurred to a tunnel perimeter of 3m and the vicinity of wall was maximum.

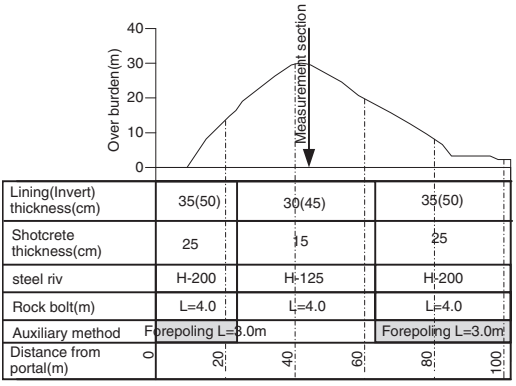


Figure 14(a). Outline of tunnel D.

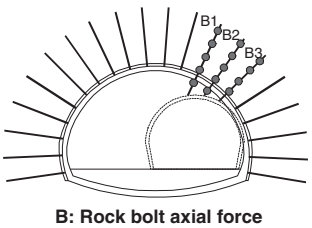


Figure 14(b). Measurement point of force at tunnel C.

6 MEASUREMENT RESULT OF TUNNEL D

6.1 *Measurement method*

Field measurement was carried out in one section shown in Figure 14. Three rock bolts with diameter of 50 mm, fully grouted and self-drilling type were placed for 10 m long around the center of tunnel. The axial force of bolts was measured within this zone. These bolts were placed before the excavation of enlarged tunnel and it would be composed of support member after the excavation. Measurement was continued by cutting off a part of bolt when tunnel face approached the section.

6.2 *Result*

Figure 15 shows the axial force distribution with time of rock bolt at shoulder (B2) and the convergent value just before the face passed. No large change of axial force with the advance of face was admitted, however, tensile force increased just after the face passed the measurement section and the force converged after some interval. Constrain of ground deformation around the area from crown to shoulder of tunnel will be expected when the rock bolt cast in advance from this result. Convergence in enlargement was approximately

Copyright © 2005 Taylor & Francis Group plc, London, UK

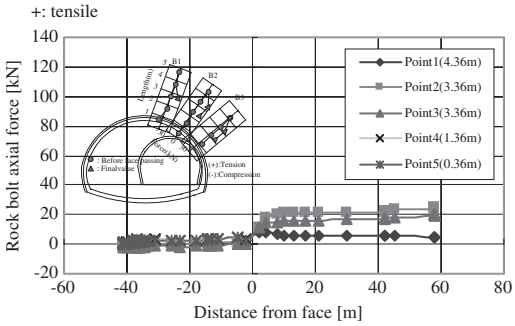


Figure 15. Axial force of rock bolt at every measurement point at tunnel D.

5 mm and it was thought to be very small. Axial force of rock bolt indicated maximum value at a point of 3.36 m from tunnel wall, where was equivalent to 1.5 m from the wall after cutting off the bolts. Other results showed the same tendency and final value of force was almost 20 kN and relatively small.

7 CONCLUSIONS

Field measurement at four tunnels whose sections were enlarged was achieved and the following results were acquired:

1) Influential area to pre-constructed tunnel by enlarging tunnel section was at most 1.5～2D (D: enlarged tunnel diameter) to the advance direction of tunnel face
2) Stress at steel rib or shotcrete in enlarged tunnel was relatively small when certain overburden was confirmed.
3) Axial force of rock bolt in enlarged tunnel was small and no clear difference was admitted as for the direction of rock bolt casting such as vertically or diagonally to tunnel wall.
4) Constrain of ground deformation around crown and shoulder of tunnel could be expected when the rock bolt cast in advance to reinforce the excavation area.

Copyright © 2005 Taylor & Francis Group plc, London, UK

The underground drainage system using New Tubular Roof method

P. Inn-Joon
Dept. of Civil Eng, Hanseo University, Seosan, Korea

K. Jeong-Yoon
KNTS Co., Ltd., Seoul, Korea

Y. Kwang-Ho
Dept. of Civil Eng., The Univ. of Suwon, Kyungki-Do, Korea

K. Chang-Won
Dept. of Geotech. Eng, Chung-Suk Engineering. Co. Ltd

K. Kyong-Gon
KNTS Co., Ltd., Seoul, Korea

ABSTRACT: Recently, the development of the underground structures is going to be inevitably necessary due to the increase in population and traffic volume that has been caused to the ground congested and the heavy traffic jams. For this reason, underground structures such as subway, underground shopping centers, lifeline facility and so on, have been increasing. On the other hand, Several economical, social and environmental problems have being concurred such as the heavy traffic caused by delaying construction, various kinds of accident induced by weak ground conditions, the damaged circumstance, and the civil appeal for noise and vibration. Therefore, the safer and more beneficial methods of underground construction are on the rise. In this research, the N. T. R (New Tubular Roof) method was modified and utilized for solving those problems. This method was modified suitable for Korean geotechnical conditions, and was made up for the weak points-the lack of stability due to the water leakage from walls and tops, maintenance, and construction procedures-in the prior methods. This paper dealt with the features and the procedure of N.T.R Method. It is also mentioned the applicable capacity to the method for underground development in Korea using the data measured from a construction site for underground drainage system and the results from numerical analysis for the stability of that system.

1 INTRODUCTION

The increase of population and traffic in urban areas has urged civil engineers to develop underground structures, which also cause various problems related to the construction process, maintenance and water leakage. Therefore, the safer and more suitable for Korean geotechnical conditions methods of underground construction have been required. In connection with the above problems and requirement, N.T.R (New Tubular Roof) method was proposed . In this research, the overall features, construction procedures were overviewed and applicable capacity of N.T.R method were inspected, furthermore, practical measurement data of a tunnel using N.T.R method were obtained and compared to the result of numerical analysis.

2 MAIN FEATURES OF N.T.R

2.1 *Main features*

Large-caliber steel pipes are injected to the target place and excavated inside with position measurement in every 1 meter. Direction controlling valve is attached to the guide pipe for curved or straight alignment. The sides of pipes are cut and linked by steel plate welding transversely to avoiding water leakage and collapsing of adjacent soils. Through the connected areas, H-Beam or reinforcing bar as a stiffness enhancer is set up for building concrete frame structure. Recently, N.T.R method is widely applied to underground space, subway, lifeline facilities, tunnel and so on in S. Korea. Especially, direct construction

Copyright © 2005 Taylor & Francis Group plc, London, UK

of underground structures makes various problems such as traffic, passage restriction, existing underground structures, surface settlement nullified. The main features of N.T.R are as follows;

1. The costs of maintenance due to erosion can be reduced.
2. Waterproof effect is remarkable due to welding connection of transverse plate.
3. Construction in shallow depths (Minimum of 1D) is possible, so the optimum longitudinal gradient is obtained. In this case, total costs can also be cut down.
4. The internal surface of N.T.R structure is flat because slab or lining are formed in consecutive pipes.
5. There are no problems related to the surface such as traffic, passage restriction, surface settlement, etc.
6. Suitable for urban underground structures (tunnel, underground shopping centre, etc) due to no vibration and noise.
7. Homogeneous section can be assembled in connection with other types such as NATM.
8. No potential hazard due to soil collapse. All operations are performed in large-caliber steel pipes.
9. Easy set of curved alignment by direction device on guide pipe.
10. There is no limitation of longitudinal length of pipe (Practically, 400 meters of N.T.R).
11. Advantages in internal excavation, removal of excavation volume, transportation of materials due to large-caliber steel pipes.
12. Direct disposal of gravel by manpower during excavation
13. Independence of climatic conditions, i.e. the period of construction can be reduced.
14. Excavation in soft or hard rock is possible by control blasting method such as smooth blasting.
15. Initial excavation area is much less than normal tunneling, therefore, N.T.R method is acceptable in soft ground, collapsing soils and water inflow problem.

2.2 *Comparing to other methods*

There are a few methods using in underground construction such as Detouring, Front Jacking method, Pipe Roof method and T.R.M.

Detouring method is to make a detour around construction site temporarily and open-cut the ground. This is a low-cost method and experienced, however, extra space for transportation is required.

Front Jacking method is usually applied to undercrossing pass beneath the existing roads or structures. Steel pipes are drawn by PC wire and hydraulic cylinder jack, then, precast-concrete structure is located to the excavated place. It does not cause any traffic disturbance, however, direction or gradient change is not possible.

Pipe Roof method is mainly applied to understructure, tunnel opening. Steel pipes are injected to the ground in arch shape and resist overburden pressures. The area under the steel pipes arch is excavated and lining is installed. It also does not cause traffic disturbance and many application sites are exist in Korea, however, boring holes for steel pipe are left relatively long time, so this method has weakness in settlement problem.

T.R.M (Tubular Roof Method) is quite similar to N.T.R method. Large-caliber steel pipes are utilized as main pipes in longitudinal direction. Additionally, small-caliber pipes are linked among main pipes and building up roof, then, external areas of linking pipe are grouted. It has similar advantages to N.T.R, however, uncertainties for water leakage from connecting section means high costs of maintenance. Overall, N.T.R method is superior in some respects for excavation problems in urban area. It modified the weak points-the lack of stability due to the water leakage from walls and tops, surface settlement, maintenance, and construction procedures-in the prior methods (K. Jeong-Yoon et al., 2000).

3 PROCEDUERS

The construction types are classified into two categories according to reinforcing structure inside steel pipes; the one is reinforced concrete girder type and the other is H-Beam type. Arch shape and box shape are possible both in each type. Field conditions, size of section, and period are considered to determine construction type. Generally, reinforced concrete girder type is more common due to some advantage of costs and manipulation. The procedures of this type are illustrated below (K. Jeong-Yoon, 2003).

3.1 *Setting of the operation site (including disposal exit and reacting wall)*

It is recommended that the dimension of operation site should be minimized owing to traffic congestion and the effect of adjacent buildings. The depth of operation site has to be extended as far as design depth of the whole structure and establish waterproof system in case of water leakage or ground settlement due to drainage. Hydraulic jack and propulsion rail are installed in the aftermath of setting the reaction wall.

3.2 *Position measurement and installing guide pipe*

It is required to measure the position of injection and control the direction of guide pipe for precise advance

Copyright © 2005 Taylor & Francis Group plc, London, UK



Figure 1. Operation site construction.

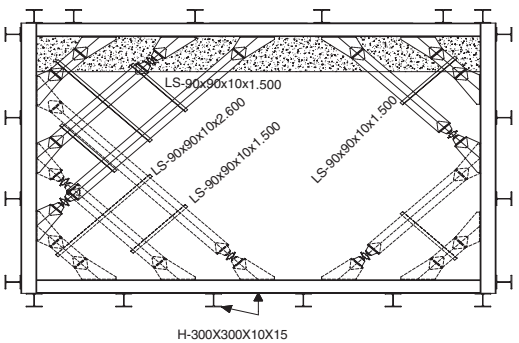


Figure 2. Example of resisting system for operation site.



Figure 3. Installing guide pipe.

in every 1 meter. Total length of pipe is almost 1 m to 6 m according to site condition and connection ring is assembled between pipes for homogeneous section and convenience of linking process.

3.3 *Injection of pipes and excavation*

Hydraulic jack inject steel pipes and soil or soft rock inside pipes excavated by manpower. The advancing

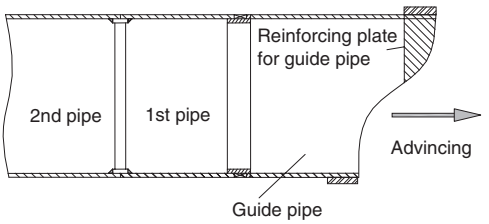


Figure 4. Guide pipe details.

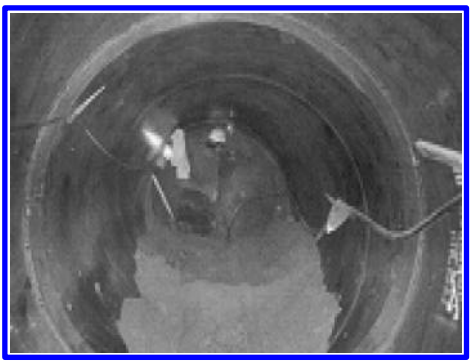


Figure 5. Excavation in pipe.

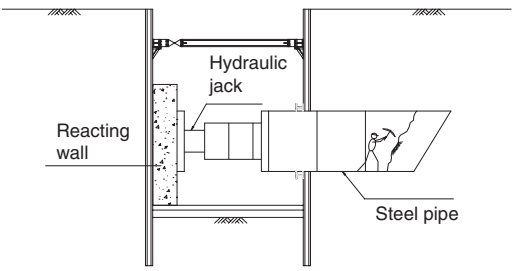


Figure 6. Injection and excavation.

length per each step is 1 m approximately. In principle, injection is followed by excavation inside and the position of pipes should be checked in every 1 or 2 meters. In case of error in positioning, modify the alignment using direction controlling device attached on the guide pipe.

The minimum error range is ±50 mm and bentonite mixture is also injected around pipes to reduce frictional resistance in the ground.

3.4 *External grouting*

External grouting is required to reinforce relaxed ground near pipes because the injection of pipes disturbs the ground around pipe perimeter. Soil and

Copyright © 2005 Taylor & Francis Group plc, London, UK

groundwater inflow, water leakage at the connection and ground relaxation will be prevented.

3.5 *Installing reinforcement ring and waterproofing*

Reinforcement ring is installed interior pipes when the side of pipe is cut for linking transversely using steel plate to resist earth pressure and water leakage. At this stage, connecting steel plate is welded on the installed pipes and ventilation process also be on work.

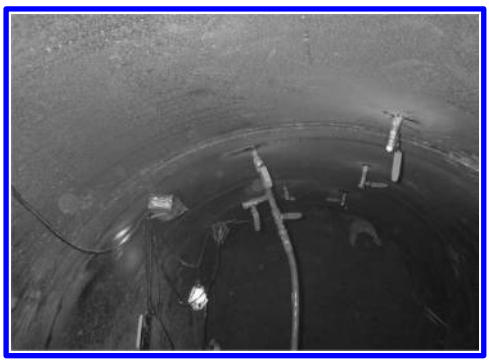


Figure 7. External grouting from inside.

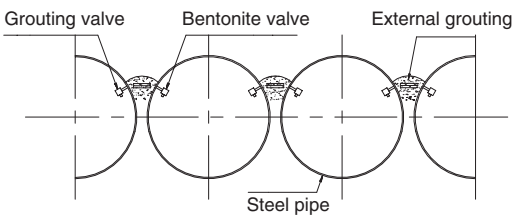


Figure 8. External grouting plan.



Figure 9. Installing reinforcement ring and welding.

3.6 *Building girder and mold*

After linking steel plate transversely, the side of pipes is cut in longitudinal direction, reinforcing structure (steel bar or H-Beam) is inserted in connected pipes. Under the reinforcing structure, mold for concrete construction is set.

3.7 *Concrete fill in pipes*

Pipes along wall are filled with concrete, then upper pipes forming roof are filled. In the roof pipes, PVC

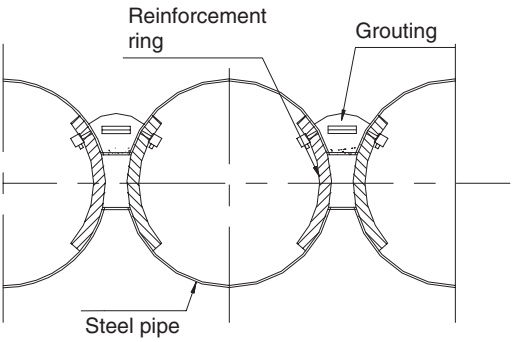


Figure 10. Installing reinforcement ring plan.

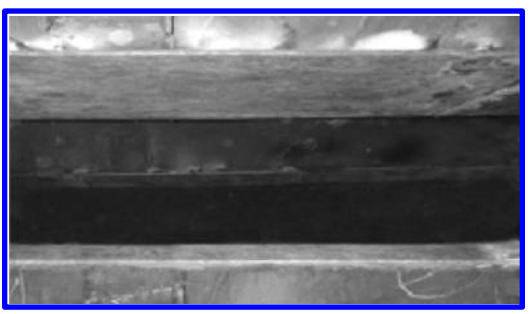


Figure 11. Building girder and mold.

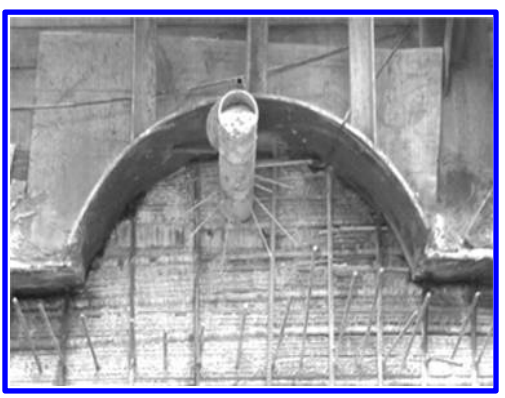


Figure 12. Concrete inside pipe.

Copyright © 2005 Taylor & Francis Group plc, London, UK

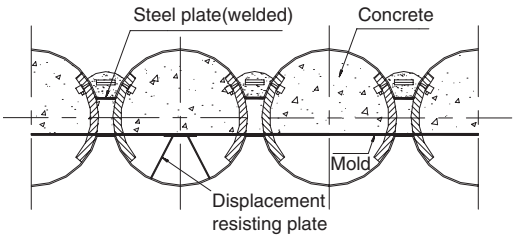


Figure 13. Concrete filling plan.



Figure 14. Inside excavation.



Figure 15. Invert construction.

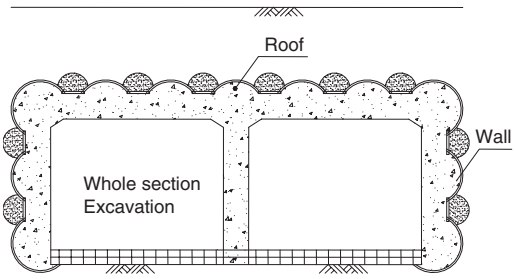


Figure 16. Inside trimming and invert construction plan.

pipe (D = 100 mm) and grouting injection tube have to be installed. Secondary concrete is followed by primary slab concrete. Finally, other gap in pipes is filled with cement mile grouting.

3.8 *Inside excavation and trimming*

After curing of concrete, the whole section under pipes is excavated and trimmed along the mold line. Some part of pipes cut in the previous procedure should be removed at this stage.

3.9 *Invert construction*

As the last stage, invert structure is established after roof and wall are completed.

4 APPLICATION CASE STUDY

4.1 *Site overview*

Practical case study that evaluated the benefits of N.T.R method is performed in this research. N.T.R method is applied to drainage tunnel through 60 m of 360 m in total. Soil layers are composed of gravel, sand (STP N value = 7 to 10, saturated), weathered soil and base rock from surface. Target place for applying N.T.R method is located at 6.8 m depth of surface. Shallow depth may cause the settlement of adjacent National Highway; therefore N.T.R method is determined as the best for avoiding settlement and other surface problems (see Fig.17).

4.2 *Stability study by numerical analysis*

Numerical analysis to verify the stability of N.T.R. tunnel using finite difference method (FDM) is performed. FLAC2D and FLAC3D are utilized to evaluate ground displacement and stress of pipes, respectively and each result is compared to field measurement data. Firstly, in 2-D plane strain analysis, construction procedures are divided into 4 stages. Figure 18 shows each stage. Figure 19 shows the deformed mesh at

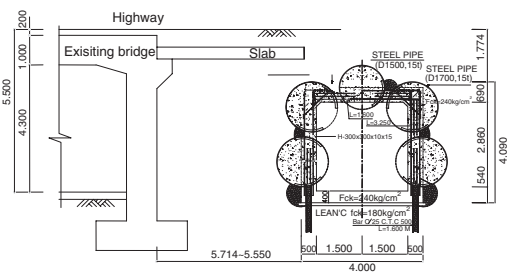


Figure 17. N.T.R section of the site.

Copyright © 2005 Taylor & Francis Group plc, London, UK

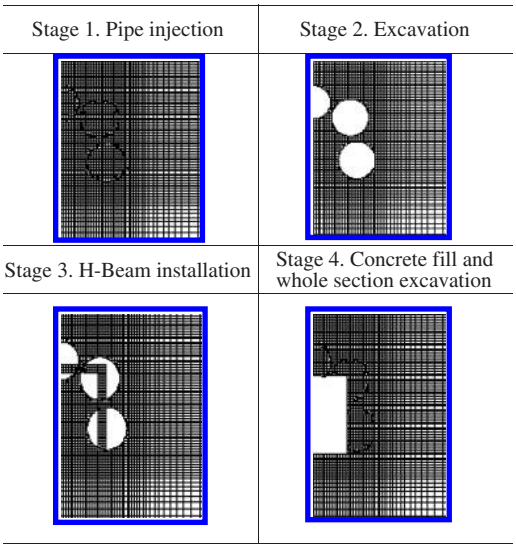


Figure 18. Mesh generation and analysis stages.

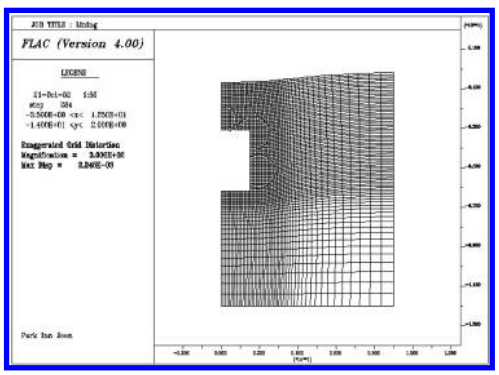


Figure 19. Deformed mesh at the last stage.

last stage. Total settlement of crown was 2.248 mm and lateral displacement was 2.246 mm. This result is compared to field measurement data in following Section 4.3.

Secondly, in 3-dimensional analysis for steel pipes, stress distribution and concentration trend was reviewed. Two kind of steel pipe; (1) 2500 mm of exterior diameter, 24 mm of thickness, (2) 2000 mm of exterior diameter, 20 mm of thickness. Reinforcement ring(I-Beam) dimension is $150 \times 150 \times 7 \times 10$ and allowable stress is set to 2375 kgf/cm^2. Figure 20 shows 3-D grid at the stage of excavation.

Maximum stress, which occurs at the stage of cutting pipe side to connect them transversely, is estimated 433.1 kgf/cm^2 of axial and 0.169 kgf/cm^2 of

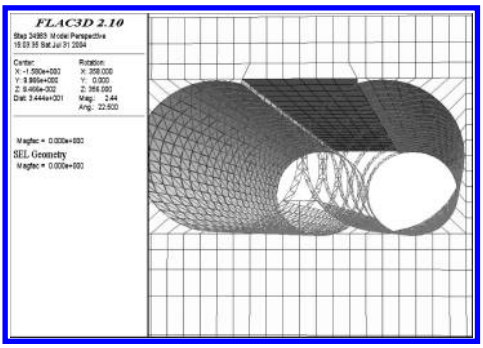


Figure 20. 3D grid.

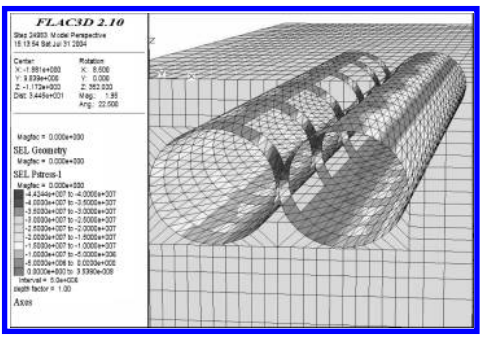


Figure 21. Stress contours.

Table 1. Station of field measurement site (N.T.R area).

Station	17+5	17+15	18+5	18+15	19+5	19+15	Total
Crown	1	1	1	1	1	1	6
S.L.	2	2	2	2	2	2	12

shear. Figure 21 displays stress contours and concentration at the edge cut.

4.3. *Field measurement (Kim, Jeong-Yoon et al., 2003)*

The displacement gauges are installed in crown station and in Spring Line station, respectively attached and monitored from March to June in 2002 in N.T.R tunnel. The measurement data shows in tables 1 and 2.

4.4. *Review of each results*

The results from numerical analysis and field measurement both show the stable state of N.T.R tunnel. From table 3, computed displacements using FLAC are quite similar to practical field data from the site, therefore, numerical analysis can be useful and

Copyright © 2005 Taylor & Francis Group plc, London, UK

Table 2. Field measurement result (in mm).

Location	Station	Max. disp.	Limitation	Stability
Crown	17+5	0.33	30	O.K
	17+15	1.92	30	O.K
	18+5	0.26	30	O.K
	18+15	−1.83	30	O.K
	19+5	1.71	30	O.K
	19+15	0.72	30	O.K
S.L.	17+5	−2.00	30	O.K
	17+15	−2.00	30	O.K
	18+5	−1.00	30	O.K
	18+15	2.00	30	O.K
	19+5	−2.00	30	O.K
	19+15	1.00	30	O.K

* + means extrusion in S.L, uplift in Crown.

Table 3. Comparison of each results.

	Max. disp. (field data)	Max. disp. (FLAC)
Crown	1.92 mm (STA.17+5)	2.248 mm
S.L.	2.00 mm (STA.18+15)	2.246 mm

worthwhile means to estimate displacement or stress distribution.

5 CONCLUSION

The applicable capacity of N.T.R (New Tubular Roof) method for underground development in Korea have been verified using the data measured from a construction site for underground drainage system and the results from numerical analysis for the stability of that system. Applying N.T.R method to practical site in Korea, it restrained crown settlement, especially shallow tunneling, and numerical analysis shows concurrence of displacement result approximately. Practically, the application case was highly successful in Korea and that means N.T.R has many advantages in urban excavation and tunneling as it mentioned in previous chapters.

REFERENCES

Kim, Jeong-Yoon. 2003. The method of building underground structure using the space in the steel pipes injected to the ground, Application of new technology authorization. *Ministry of Construction and Transportation.* S. Korea.

Kim, Jeong-Yoon, Park, Inn-Joon & Kim, Kyong-Gon. 2003. The development of underground structure using new tubular roof method. *Journal of the Korean Tunneling Association*, Vol. 5, No. 4.

Copyright © 2005 Taylor & Francis Group plc, London, UK

Waterproofing of an emergency escape tunnel by employing an innovative sprayable membrane: The Giswil highway tunnel project, Switzerland

W. Meier
Murer AG, Erstfeld, Switzerland

K.G. Holter & S. Haeusermann
Degussa Construction Chemicals (Switzerland) Ltd, Zuerich, Switzerland

ABSTRACT: An innovative method for the waterproofing of tunnels was employed for the 4 m diameter bored tunnel, an emergency escape facility for the recently completed Giswil highway tunnel in central Switzerland.

Successful waterproofing was achieved by a sprayable membrane system, consisting of a minimum 3 mm thick spray applied membrane which is located between two layers of sprayed concrete. The membrane provided bonding to the rock support sprayed concrete substrate, as well as to the inner layer of sprayed concrete which was applied onto the membrane after the initial curing.

The membrane was applied to the full tunnel profile including the invert, to provide a single shell undrained solution. The double sided bonding which the system provides, ensured no migration of water along the membrane-concrete interfaces. Hence, a continuous waterproof single-shell sprayed concrete structure was achieved.

1 INTRODUCTION

The 1960 m long Giswil road tunnel in Canton Obwalden in central Switzerland will provide a bypass for the town of Giswil. The project consists of a two-lane road tunnel and an emergency escape tunnel running parallel to the main tunnel. The main road tunnel is located in mica schists and excavated by drill-and-blast. The final structure consists of a double shell concrete lining with drained waterproofing by means of a PVC sheet membrane and a geotextile fleece for drainage.

The emergency escape tunnel was excavated by a 4 m diameter hard-rock TBM and supported by pattern rock bolting and sprayed concrete. A length of approximately 10 m in each end of the tunnel was excavated by drill-and-blast. In the portal areas cut-and-cover concrete tunnels were constructed.

The engineer wished to achieve a waterproofing solution in the outermost parts of the escape tunnel in both ends which provided:

- No water ingress in the bored part of the tunnel
- A successful solution for waterproofing continuously from the bored tunnel, through the blasted part of the tunnel to the cut-and-cover concrete tunnel at the portal
- Compatibility between the waterproofing of the cut-and-cover concrete tunnel and the waterproofing of the rock tunnel

2 DESIGN

The emergency tunnel was designed with an undrained lining with sprayed concrete and sprayable waterproofing membrane. The adjacent parallel road tunnel was designed as a drained structure with cast-in-place concrete lining and conventional PVC sheet membrane with drainage geotextile. Figure 1 below shows a cross section with the layout of the two tunnels.

The final lining of the emergency tunnel consists of a sandwich structure with two layers of sprayed concrete with an impermeable sprayable membrane between the two concrete layers. The membrane bonds to both the substrate steelfibre reinforced sprayed concrete (primary rock support) as well as the sprayed concrete layer (unreinforced) which covers

Copyright © 2005 Taylor & Francis Group plc, London, UK

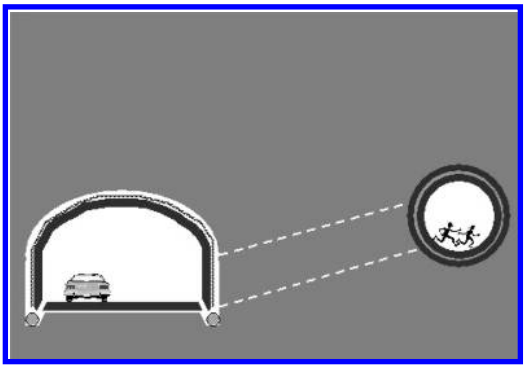


Figure 1. The main road tunnel and the emergency escape tunnel, principal sketch, cross section. Ventilation and drainage details are not complete and not to scale.

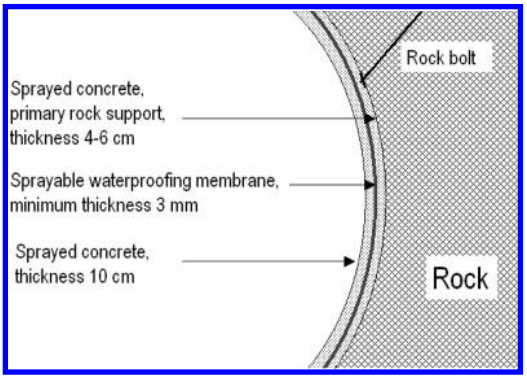


Figure 2. Sprayed concrete lining in the TBM excavated tunnel with sprayable membrane in a continuous structure between two layers of sprayed concrete. Cross section, not to scale.

the membrane. Figure 2 below shows the details of this structure.

3 THE WATERPROOFING MEMBRANE

The sprayable waterproofing membrane employed on this project represents an innovative technical solution for waterproofing. The membrane itself is a polymerbased cementitious product delivered as a powder. The application involves the adding of water by means of a dry spraying process, similar to that of spraying of dry-mix sprayed concrete. The only processes which take place during the curing of the membrane is the drying of the polymer component and the hydration of the cementitious component.

The membrane will bond to the substrate surface as well as the sprayed concrete which is applied on top of the membrane surface. Figure 3 shows how the



Figure 3. Sprayable waterproofing membrane system. The photo shows a core sample of sprayable waterproofing membrane with a thickness of 3 mm, between two layers of sprayed concrete.

membrane appears between the two sprayed concrete layers.

Since the membrane bonds to both its interphaces with concrete, water cannot migrate along the membrane. This also means that the membrane itself is an undrained waterproofing.

4 APPLICATION, WORKING SEQUENCE

The undrained waterproofing solution in the entire tunnel profile imposed a careful planning of the sequence of the different parts of the application.

The establishment of the lining with sprayable membrane and sprayed concrete consisted of the following steps:

- Removal of the water seepages in the tunnel contour
- Application of the substrate concrete unless sprayed concrete had been applied as primary rock support
- Application of the waterproofing membrane in the walls and the crown
- Spraying of the layer of inner concrete
- Application of the waterproofing membrane in the invert
- Spraying of concrete in the invert

The water seepages in the contour had to be removed temporarily in order to avoid problems with the bonding of the membrane to the substrate. This was done by means of one-component polyurethane injections and two-component acrylic injections, Figure 4. This operation was more extensive in this particular case than ususal, due to the request from the engineer of an undrained waterproof structure, and hence, no drainage

Copyright © 2005 Taylor & Francis Group plc, London, UK



Figure 4. Removing of water ingress points by injections with one-component polyurethane.



Figure 5. Manual application of sprayable waterproofing membrane with a small dry shotcreting machine.

channels or stripes could be established behind the membrane.

Application of the membrane was done manually with a normal dry shotcreting machine of the smallest available type. In order to produce a controllable spray of membrane, a small and even output of material was desirable. The equipment set-up and application is shown in Figure 5.

Thickness control of the applied membrane was done by spot checks with a needle. The minimum thickness required to achieve an impermeable membrane is 2 mm. Because it's virtually impossible to achieve an even membrane thickness of 2 mm, the target thickness for the application was set to 3 mm. By thorough control after application, no areas with membrane thicknesses below 2 mm were found.



Figure 6. Application of wet-mix sprayed concrete after the application of the sprayable waterproofing membrane.



Figure 7. Complete system in place in the walls and the crown. Stripes of waterproofing membrane are left uncovered in the lower walls in order to provide for a continuous membrane when applying the membrane in the invert.

After the application of the membrane, the inner layer of sprayed concrete was applied. This operation followed approximately 24 hours after the application of the sprayable membrane. For this purpose wet mix sprayed concrete with a designed thickness of 10 cm was applied. Mechanized application with a spraying robot mounted on a small tracked vehicle proved to be highly efficient. The application of the inner lining of sprayed concrete is shown in Figure 6.

The establishment of the waterproofing in the invert required a special effort in ensuring that a continuous membrane was achieved. A 15 cm wide longitudinal stripe of membrane in the lower part of each of the walls was protected and hence, left uncovered of concrete when the application of sprayed concrete took place. This can be seen in Figure 6 above.

After the application of concrete in the walls and the crown, the invert was thoroughly cleaned. Sprayed

Copyright © 2005 Taylor & Francis Group plc, London, UK



Figure 8. Applying the sprayable waterproofing membrane in the invert.

waterproofing membrane was then applied. Hence, in order to achieve a continuous membrane from the walls through the invert, an overlapping of the waterproofing membrane was sprayed on the stripes in the lower parts of the wall.

Several small seeping points in the invert remained after the final application of sprayed concrete in the invert. This was due to wet spots and small ponds in the invert which caused difficulty of achieving a sufficiently rapid curing of the membrane. The remaining seepages were left "open" under the floor in the invert, and hence drained by gravity to the portal.

5 CONCLUSIONS

The single-shell sprayed concrete lining concept with an integrated waterproofing membrane proved successful for the Giswil emergency escape tunnel. The flexibility and simplicity in application of the system, as well as the compatibility to the waterproofing system of the portal structure made it a cost-effective solution.

REFERENCES

Garshol, K. (2000). Permanent waterproofing with sprayable membrane in combination with sprayed concrete – experiences (Norwegian), *Norwegian Rock Mechanics Conference,* Oslo, Norwegian Society of Chartered Engineers

Copyright © 2005 Taylor & Francis Group plc, London, UK

BioSealing: how micro-organisms become our little allies in repairing leaks in underground constructions

V. Veenbergen, J.W.M. Lambert & E.E. van der Hoek
GeoDelft, Delft, Netherlands

A.F. van Tol
Delft University of Technology, Delft, Netherlands

S.I. Weersma
Visser & Smit Bouw BV, Papendrecht, Netherlands

ABSTRACT: This paper presents a new method for leak repair in underground constructions like sheet piles, clay layers and contamination retaining barriers, being developed at GeoDelft in close cooperation with Delft University of Technology and Visser & Smit Bouw BV. The method is called BioSealing and has been patented. The method makes use of "micro-organisms present in the soil by nature" and groundwaterflow to a leak. BioSealing can be used to decrease the flow through geotechnical constructions as well as to prevent migration of contaminants out of contaminant retaining constructions. Several tests have been carried out to study the influence of different nutrition, materials, concentrations, catalysts, temperature and scale. In this paper the method of BioSealing is described and illustrated by results from laboratory experiments and the results of a field experiment.

1 INTRODUCTION

1.1 *General*

In civil engineering as well as and in environmental geotechnics underground water retaining barriers are frequently applied. Especially in densily populated areas the need for underground structures is strongly rising. This results in more application of underground water retaining barriers. During civil engineering projects water barriers such as sheet piles are necessary to be able to work under dry conditions and to prevent large quantities of extracted groundwater. For environmental purposes water retaining barriers are designed to prevent migration of (toxic) contaminants. Examples are underground barriers underneath waste disposal sites, chemical industry plants and gasoline stations.

Underground water retaining constructions are designed to be impermeable. Although a general agreement exists that prevention of leaks has a high priority this appears not always to be possible. Unfortunately, in practice a lot of these (temporary) water barriers in underground constructions appear to be more permeable than they are designed for. Failure is caused by, for example, broken sheet pile joints, cracks in sheets, imperfect connection between vertical walls or heterogeneous clay layers. Especially in dense populated environments this may cause damage: occasional leaks lead to the need for excessive groundwater extraction (involving higher costs and potential problems with drainage permissions), damage in the surroundings by settlements and large delay in the construction time. Contaminant migration may lead to environmental risks and/or additional amount of groundwater to be extracted with cleaning and disposal costs.

After it is decided the leak needs to be repaired a number of methods are available to do so. Repairing a leak in a traditional way however is expensive and sometimes even impossible because the locations of leaks are hardly accessible for big and heavy equipment. The available methods to repair the leak in situ so far (for example injection of grouts and gels) have numerous disadvantages. They are often expensive and unfriendly for health and environment [see Council Regulation (EEC, 793/93)]. In some countries it is even not allowed to use gels. The excessive amount of injection fluids is another disadvantage of the traditional methods, because the location of the leak is not exactly known. State-of-the-art methods can detect a leak within a distance of several meters. This accuracy

Copyright © 2005 Taylor & Francis Group plc, London, UK

is realistic with electrical leak detection techniques such as ECR and EFT, developed in Germany and in the Netherlands and Germany recently tested on several sites. Therefore, a need exists for easier, more effective and less expensive methods for leak repair.

1.2 *BioSealing: a new promising solution*

Under certain circumstances the natural chemical, physical and biological properties of the soil and groundwater can lead to spontaneous precipitation and so blockage of the pores parallel with drinking water production where clogging is a problem. Near groundwater extraction wells clogging takes place which puts limits on the possible amounts of extraction and causes many problems and costs. These clogging processes are caused by natural processes in the underground. The idea of BioSealing was to stimulate conditions such that these natural clogging processes can take place easily.

The flow through leaks need not to be stopped for 100%. In the case of BioSealing repair of leaks is interpreted as "to reduce the permeability at the location of the leak". One of the purposes set when this method was designed was to reduce the permeability with at least a factor 5. This factor is a bit arbitrary, but realistic. For example a clay layer of 100 m^2 has a vertical hydraulic conductivity of $k_v = 10^{-7}$ m/s and local (1 m^2) $k_{v;local} = 10^{-5}$ m/s. The predicted flow is x m^3/d through the clay layer, however due to a local leak of 1 m^2 the flow is 2x m^3/d. As it is seen in figure 1, reducing $k_{v;local}$ with a factor 5 will reduce the flow to x + 0,2*x = 1,2x m^3/d. Consequently, such a deviation from the predicted extraction rate might be acceptable.

A property of a leak is the flow directed to a leak due to the difference in head over a leak. The presence of the already mentioned micro-organisms and chemicals nearby the leak is therefore guaranteed. The micro-organism stay relative for a long time in front of and after the leak in comparison with the short period when they pass through the leak. The method of BioSealing makes optimum use of these circumstances.

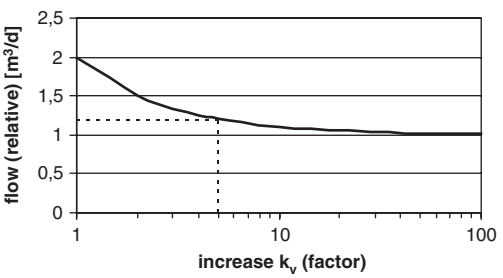


Figure 1. Flow through a horizontal clay layer as a function of the permeability of a leak.

2 LABORATORY TESTING

In a first stage the BioSealing process was tested in a laboratory setting. The objective of the laboratory test was to discover which nutrition presents the best chance of success and after that whether or not it was possible to control the clogging process in a defined environment. In a later stadium the location of the clogging process and the durability of the clog were studied.

2.1 *Setup and operation of the flow column*

The apparatus is shown in the scheme of figure 2. This apparatus has been used in all laboratory tests presented here. In large PVC columns filled with natural Dutch Pleistocene sand an iron or PVC separation plate with a hole ∅0,04 m was placed, representing a leak. The experiments were performed under "anaerobic" conditions using water as transport medium for nutrition. The water flow, as in real circumstances, was directed towards and through the leak. The flow was in upward direction to prevent specific flow channels to occur due to gravity. To initiate the flow a separate storage tank was used with a higher water level than the test column (the so called "law of the communicating vessels"). This results in a flow under constant pressure. The nutrition was added to a separate inlet.

6 Manometers (divided over the height of a column) showed the difference in hydraulic head over a part of the column. The head gradient, often denoted by i [–], could be calculated with the in-between distance. By doing so the exact location of the clog could be determined by increasing i over a part of the column.

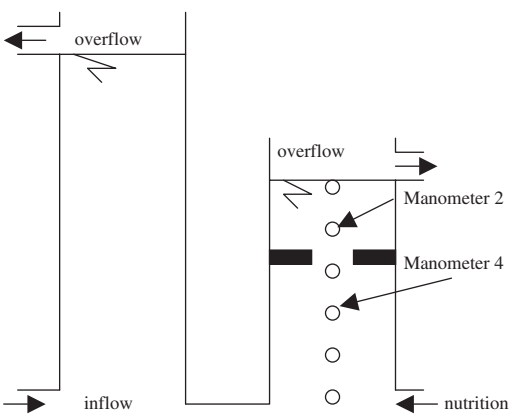


Figure 2. Experimental setup.

Copyright © 2005 Taylor & Francis Group plc, London, UK

Groundwater velocities in the test were based on travel time between injection and hole in real conditions. This travel time was estimated for building pits using customary groundwater conditions, knowledge of leaking conditions and the knowledge that new leak detection techniques can find the leak within 5 meters accuracy.

2.2 *Execution and results of the first series experiments*

After a small series of survey experiments, the next step was to find out the most promising mechanism. From the first session of these experiments it was concluded that biological clogging could be identified to be a promising mechanism in comparing with precipitation of iron oxide or deposition of lime.

The purpose of the next series of experiments was to find out which nutrition was the most promising to activate bacteria. Three kinds of nutrition were investigated: syrup (treacle), Nutrolase (simple decomposable protein) and Solvicol (hard decomposable starch).

The best results were achieved by adding Nutrolase. Nutrolase is a residue of the production of potato starch by Avebe. It was found that clogging starts with biomass and later this clogging is being reinforced by a (biologically induced) chemical precipitation of iron sulphide.

2.3 *Influence of different boundary conditions*

The purpose of the last series of laboratory experiments was to optimize the mechanism by studying the influence of different boundary conditions like: the material of the plate with the leak (PVC or iron, because of the precipitation of iron sulphide), the effect of catalysts such as nitrate, the variance in the concentration of Nutrolase and the choice of the (number of) injection(s).

To compensate the fluctuating water level, the result is presented by the factor of clogging C:

$$C_i = \frac{\left(\frac{\Delta Q}{\Delta h_i}\right)_{t=0}}{\left(\frac{\Delta Q}{\Delta h_i}\right)_{t=t}} \qquad (1)$$

where ΔQ = decline in flow; and Δh = difference in head between 2 manometers.

At the start of the monitoring C = 1 and by decreasing permeability or difference in groundwater level C will increase. It appears that the material of the plate had no influence at the clogging, as it is seen in figure 3 (p1–p2, for example, in figure 3 means between manometer 1 and 2). Manometer 2 and 3 are

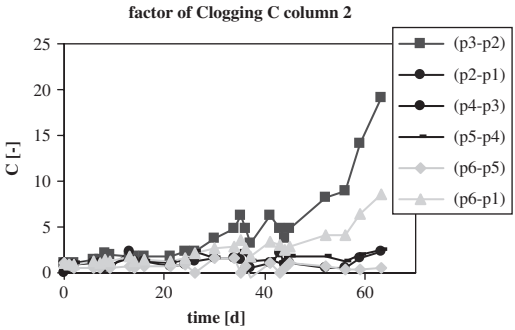


Figure 3. Result of column 2 with PVC plate.

situated above and under the plate, as it is shown in figure 2. Figure 3 shows that the clogging appeared only around the leak (P2–P3). In the other parts of the column the factor of clogging does not increase. It follows that the factor of clogging of the whole column (P1–P6) also increases. High concentration or adding catalysts lead to the formation of gas that causes temporary clogging. After the gas has disappeared the flow is reinstalled. The gas formation may also be caused by high temperature in laboratory circumstances.

The most important result was a decrease of permeability with a factor 5–20 and even totally blockage of columns by adding Nutrolase. After stopping the nutrition supply the micro-organisms stayed near the leak for the duration of the test, which was 4 months in this case. This leads to the conclusion that BioSealing is a durable solution. The clogging process takes place in an anaerobic environment, because otherwise the iron sulphide will oxidize and dissolve.

In the laboratory experiments the clogging always appeared around the leak, independently of the flow speed, the size of the leak and the kind of nutrition. One could expect clogging before the leak, but after excavating it seems that iron sulphide is precipitated after passing the leak.

It was found that biomass does not flow as fast as groundwater, because it biomass gives preference to attach the soil grains. From the laboratory experiments this retardation factor was calculated to be a factor 10–15.

3 FIELD EXPERIMENT

3.1 *Location*

To check the results of the laboratory tests under natural circumstances (like temperature, heterogeneity, size of the leak or natural flow) in the beginning of 2004 a field experiment was designed. The objective of the field experiment is to reach a reduction of the

Copyright © 2005 Taylor & Francis Group plc, London, UK



Figure 4. A 20 ft sea-container is buried at the Maasvlakte.

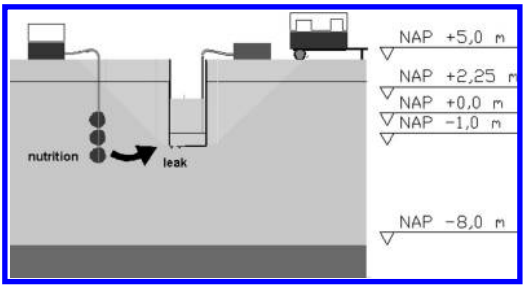


Figure 5. Schematic representation of the experimental setup.

flow rate at the location of the leak with at least a factor 5, which is required to make the method accepted as a real option for trouble-shooting. The experiment was carried out at the factory site of Lyondell Chemicals Nederland B.V. at the Maasvlakte (port of Rotterdam). This location has been selected because of the presence of sandy subsoil, the presence of groundwater at reachable depth and the relationship with Lyondell due to geotechnical soil investigations in the past.

3.2 *Design of the experiment*

Representation, prevention and inspection of unwanted leak, costs and possibilities to monitor were factors that played an important role in the design of the experiment. Finally three 20 ft sea-containers were buried on vertical position with known leaks of different measure and shape, as shown in figure 4. These leaks are located in the bottom of the containers.

The difference in hydraulic head (3 to 4 meters is realistic in a building pit) was maintained by a horizontal drain in the containers in combination with a pump. This resulted in a flow rate of 3,5–8,5 m^3/day. The drain has been constructed in a gravel filter to avoid blocking. The circumstances nearby the drain are similar to those nearby the leak: streamlines come together and the flow rate increases. It is therefore not unrealistic that clogging occurs nearby the drain, which is an unwanted effect. The large porosity of the gravel filter has to avoid this potential problem of clogging.

To avoid the influence of oxygen in the anaerobic process of reducing the permeability in the vicinity of the leak, it is necessary to have at least one meter groundwater above the bottom in the container, which results in a groundwater level in a container at maximum 5 m below surface level. Figure 5 shows a schematic drawing of the experimental setting.

To stimulate the micro-organism activity, Nutrolase is injected at various places and various depths upstream the containers by using an injection method similar to grouting. It is generally known that clogging may occur near the injection point by injection of nutrition. During the experiment, after injecting nutrition, water is injected to clean out the immediate vicinity in order to prevent clogging.

It is also possible to inject the nutrition under high pressure to be able to squeeze the nutrition through the clogs near the injection point. During the experiments nutrition is injected under at least 1 bar up to 6 bar to reach maximum micro-organism activity. However, injection by high pressure can also result in vertical or horizontal fracturing, so prudence is called for. Per container about 500 l Nutrolase is injected.

To collect more information about the behavior of the nutrition and micro-organisms in field conditions a monitoring plan was designed. The process is monitored by standpipes, a water meter and several pieces of apparatus to measure chemical properties of ground water (pH, EC, oxygen, redox potential). A decreasing redox potential indicates for example an increasing micro-organism activity and a decreasing flow indicates a decreasing permeability nearby the leak. Also the monitoring plan provided a possibility to be able to make adjustments in the parameters that can be influenced in case of unforeseen developments.

3.3. *Results*

It took about 6 weeks before the waterdemand of container 2 has decreased a factor 5 (which was the aim) in the first session of the experiment. The graph where the factor of clogging C as a function of time is presented in figure 6.

3 weeks after the start the redox potential drops away to a more or less constant value of −100/−200 mV Ag/AgCl which indicates formation of iron sulphide as it is seen in figure 6. From this moment on, the factor C starts also increasing continuously. The last injection took place on 22 April 2004.

For the formation of iron sulphide an electron is needed, so the electric conductivity EC of the

Copyright © 2005 Taylor & Francis Group plc, London, UK

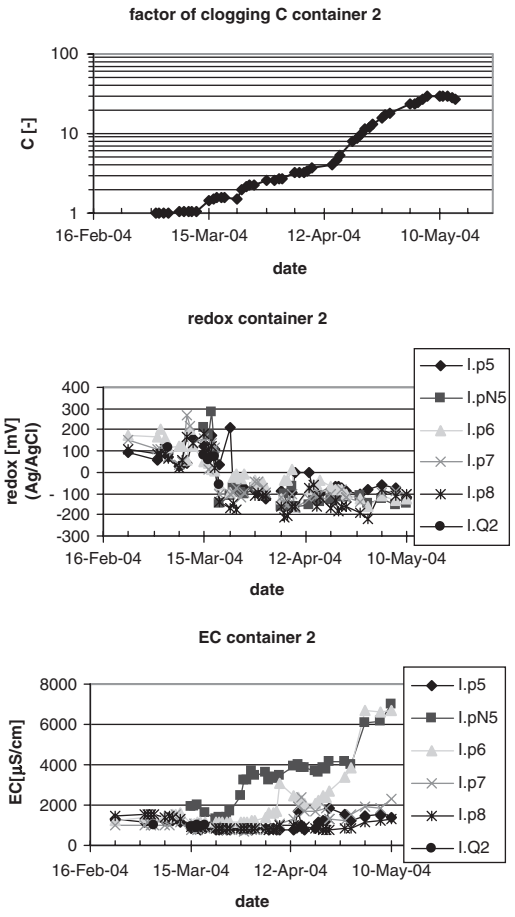


Figure 6. Downwards: factor of clogging, redox potential and electric conductivity EC vs. time (numbers at the right side of the graphs are the number of the standpipes).

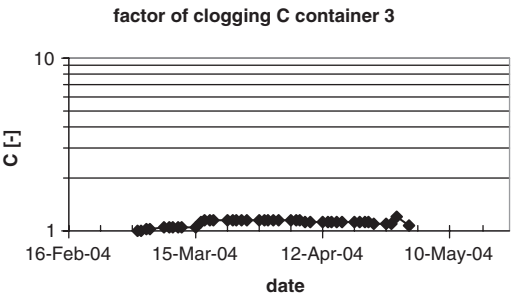


Figure 7. Results of the "blank container"; the first period without adding nutrition and from 14 may 2004 with nutrition.

groundwater has to increase. The last graph in figure 6 confirms this theory: at the same time that the redox potential decreases, the EC increases. However, the increase is also partly caused by the nutrition. Nutrolase is a saline liquid (EC ≈ 30000 mS/cm thinned down with water 1:5).

Simultaneously container 3 was drained off, but no nutrition was injected. It was found that the flow rate didn't vary. So the decrease of the flow rate in container 2 in 6 weeks is due to the mechanism activated by injecting Nutrolase. Also in container 3 after 14 May 2004 Nutrolase was injected, what resulted in an increasing factor of clogging of this container.

To reduce time needed for decreasing the permeability with a factor 5, it was decided to inject daily nutrition in the second session. Nevertheless, it took also about 6 weeks to reduce the flow rate with a factor 5. The results of a third container are in the same order of the 2 containers discussed in this paper.

In July 2004 the containers were digged up and several interesting observations are done. For example the whole volume of soil between the injection points and leak is colored black. This means that not only clogging occurs near the leak, but also between container and injection point. However, the soil is colored most intense black near the leak, as shown in figure 8. The lower side of the figure is in the hole of a container and the upper side is 1 m above the bottom of the container.

The clog was still in existence by container 2 3 months after the last injection. It looks like that the retardation factor is the same as was estimated from the laboratory experiments. After studying the results of different analysis of groundwater samples, it seems that the biomass absorbs to the soil skeleton. This might be the reason that it takes several weeks before clogging in the leak occurs. Biomass does not flow as fast as groundwater.

4 DISCUSSION

The field experiments have been finished successfully. BioSealing will provide both the field of civil engineering and environmental geotechnics with a method for decreasing permeability of the soil, which will not only be useful for the repair of leaks. The solution is environment-friendly because use is made of natural micro-organisms and natural occurring physical, chemical and biological processes that are stimulated by adding natural nutrition like Nutrolase.

As already mentioned, the purpose of the field experiment was to prove the mechanism of BioSealing. To optimize the clogging process it is necessary to do more research to biological processes.

The clogging process has proved to be durable for at least 3 months because it does not reverse after stopping the supply of nutrition. To consider other

Copyright © 2005 Taylor & Francis Group plc, London, UK

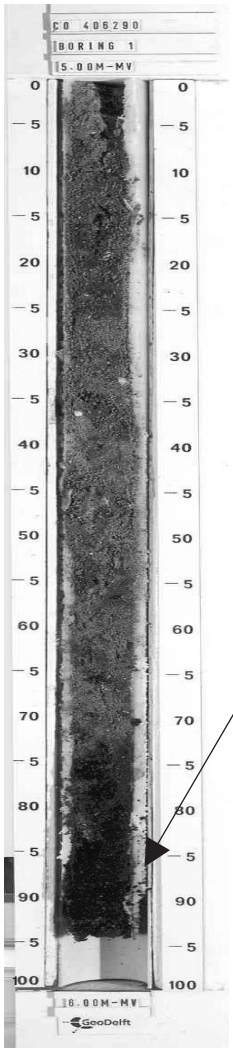


Figure 8. Photograph of a soil sample from just above a leak.

applications than building pits, like wells or dikes, it is necessary to perform durability tests for at least a year, for example. It also prevents waste of clean drinking water which occurs when additional drainage is necessary to keep the water out of the construction site or to prevent migration of contaminants.

But also decreasing the permeability of a whole volume of soil is one of the aims for the future. A matching application is for example decreasing the permeability of the sandy core of dikes, so less clay is needed.

5 CONCLUSIONS

BioSealing turns out to be a promising technique for leak reparation. Under representative circumstances a decrease in permeability with a factor 5–30 is measured within 6 weeks. Accelerating the clogging mechanism is one of the future aims. The method is environmental friendly ("only adding sugar") and durable, although more studies have to be carried out to know the real durability.

Additional to the fact that BioSealing was intended to be developed for building pits or repairing geosynthetics, after the experiments it seems to be promising that other applications of this method can be considered. At this moment the most actual issue that can be studied is the prevention of local salt water seepage through clay layers (wells) in polders. For this purpose there is already contact with the relevant district water board.

One of the problems to be solved is if no soil skeleton is present behind the leak. If this study to prevent seepage through wells turns out to be successful, a new world of possibilities is expected to open up. Leaking underground car parkings, tunnels, caves etc. could be a interesting applications in that case.

The research on BioSealing is incorporated in a larger research program called SmartSoils®. Within this program, research is conducted on how micro-organisms can be used to improve the properties of the soil, for example the strength. In contrary to BioSealing, these micro-organisms have to be brought into the soil.

ACKNOWLEDGEMENTS

The authors would like to thank Visser and Smit Bouw B.V. and the Delft University for their cooperation in this project, Lyondell Chemicals Nederland B.V. for their help in providing a testing location and AVEBE for providing Nutrolase. The research has been funded by the Ministry of Economic Affairs, for which the authors are grateful.

Copyright © 2005 Taylor & Francis Group plc, London, UK

Tunnel automation systems

M. Barut
General Directorate of Highways, Ankara, Turkey

ABSTRACT: The length of the road network of the General Directorate of Highways exceeds 62.000 km. This network covers 114 tunnels at present, but most of them are small scale tunnels. In line with motorways and divided roads initiatives the Highways Authority will be operating considerable amount of medium and large sized tunnels in 2010s. Safety is the most important phenomena for underground structures. Tunnels need some systems and facilities in addition to institutional measures to provide safety. In this paper the tunnel automation systems in the content of technical measures will be summarized and some examples will be given, and an evaluation will be made for the future of tunnel operation in Turkey.

1 SAFETY IN TUNNELS

1.1 *General safety properties*

Technology is the key element in order to increase safety in transport facilities. The ITS (Intelligent Transport Systems) concept advises application of high level technologies to roads, such as communication, control and information technologies in particular. The final aim of which is saving of human life, time, budget, environment and energy. Interaction between infrastructure, user and vehicle will be strengthened by means of using technology. Even if ITS utilizes the highest technologies it is an institutional issue. Same idea is valid for tunnel systems. In fact, tunnel systems are the extensions of ITS in tunnels. Tunnels have additional safety features. Contaminated air, poor visibility, accessibility difficulty and fire possibility in the event of an accident are the most significant factors must be taken into account. Safety systems are the primary way of improvement safety level of an underground structure. The systems to be installed in tunnels can be itemized. However there is no unique reply to the question of "What are the parameters and criteria for the type and size of systems shall be installed in a tunnel?". Parameters can be generalized, but there is no homogeneous application for systems in practice. Various design criteria are being used for safety systems in the world at present. The type and size of systems to be installed in tunnels depend on assessment parameters. Each tunnel has its own conditions. So each tunnel is a unique structure in terms of systems.
The main tunnel parameters shall be taken into consideration:

- Tunnel length,
- Traffic volume,
- Tubes number,
- Lanes number,
- Availability of dangerous goods vehicle traffic,
- Percentage of heavy good vehicle traffic,
- Gradient,
- Proposed vehicle speed,
- Geographical conditions,
- Availability of peak hour traffic,
- Wind velocity and direction,
- Uni-directional or bi-directional traffic,
- Landscape,
- Curve,
- Etc.

1.2 *Automation systems*

The tunnel parameters mentioned above shall define the type and size of systems. These are particularly electrical, electronic and electromechanical equipments. All the systems are connected to single main control unit. Sub-control units can be established for a group equipments. But, finally sub-control units are also subject to main control centre in a tunnel. The systems can be grouped as:

- Power,
- Illumination,
- Traffic control,
- Control centre,
- Telecontrol,
- CCTV,
- Incident detection,
- Fire detection,
- Hydrants and fire extinguishers,
- Air quality control and ventilation,
- Radio broadcasting,

Copyright © 2005 Taylor & Francis Group plc, London, UK

– Wireless communication,
– Service telephone,
– Emergency call,
– Announcement,
– Emergency power.

In practice a slight difference may be seen in categorizing the systems. Extra detail can be given to each element of this list and sub-units can be defined. Such as illumination systems comprise normal lighting, emergency lighting and evacuation lighting. Traffic control systems can be grouped into traffic control inside tunnel and traffic control outside tunnel. Other technical measures shall be integrated part of systems. These are;

– Operation,
– Vehicles,
– Road users.

An operation model consistent with logic of systems shall be set up. Extra counter-measures for dangerous goods vehicles and heavy goods vehicles and dissemination of necessary information to users are other necessities.

2 EUROPEAN UNION APPROACH ON TUNNEL SAFETY

2.1 *The contents of the Directive*

The European Union put "Directive 2004/54/EC of the European Parliament and of the Council of 29 April 2004 on minimum safety requirements for tunnels in the trans-European road network" into effect on 30 April 2004. The Directive proposes organizational and technical requirements for tunnels longer than 500 m. The Organizational requirements are appointing of;

– Administrative authority,
– Inspection body,
– Tunnel manager,
– Safety officer.

The technical requirements focus on;

– Infrastructure,
– Vehicles,
– Information to users.

The Directive also proposes refurbishment of existing tunnels by the minimum requirements.

2.2 *Summary of minimum requirements*

The Directive takes into account daily traffic volume per lane and length of tunnel as major classification criteria. The threshold value for traffic volume is given as 2000 vehicles. The proposed systems and other measures to be taken into consideration are summarized below.

– Tubes number,
– Gradient,
– Emergency walkways,
– Emergency exits,
– Cross-connection for emergency services,
– Crossing of the central reserve outside each portal,
– Lay-bys,
– Drainage for flammable and toxic liquids,
– Fire resistance of structure,
– Lightning,
– Ventilation,
– Emergency station,
– Water supply,
– Road sign,
– Control centre,
– Monitoring systems,
– Equipment to close the tunnel,
– Communication systems,
– Emergency power supply,
– Fire resistance of equipment.

Table 1. Existing tunnels in operation.

	500 m–1000 m	>1000 m	Total
Motorways	3	4	7
State roads	6	4	10
Total	9	8	17

Table 2. AADT of tunnels.

	Korutepe	TAG	75th Year
AADT	30.000	8.000	12.000

3 TUNNEL OPERATION IN TURKEY

3.1 *Existing tunnels*

Entire road network covers 114 tunnels. Motorway tunnels longer than 500 m are equipped with various systems in addition to lightning. State road tunnels with considerable length have only lightning equipment and no other systems. Existing tunnel numbers for primary motorway tunnels are given in Table 1.

The longest ones in three separate closed motorways are equipped with extra systems. Table 2 indicates AADT (Annually Average Daily Traffics) of tunnels.

The installed systems is given in Table 3.

3.2 *Summary of systems*

The systems mentioned in Table 3 will roughly be explained.

Copyright © 2005 Taylor & Francis Group plc, London, UK

Table 3. Systems in tunnels.

System	Korutepe	TAG	75th Year
Power	√	√	√
Illumination	√	√	√
CCTV	√	√	√
Traffic control	√	√	√
Control centre	√	√	√
Telecontrol	√	√	√
Incident detection			
Fire detection	√	√	√
Hydrant and Extinguisher	√	√	√
Ventilation and air quality	√	√	√
Radio broadcasting		√	√
Wireless communication	√	√	√
Service telephone	√	√	√
Emergency call	√	√	√
Public announcement			√
Emergency power	√	√	√

3.2.1 *Power*
Power system supplies electricity demand of all equipment and it comprises power control unit, transformer, switchgear.

3.2.2 *Illumination*
CIE (Commite' International d' Eclairage) rules are applied for lightning. High pressure sodium type luminaries are adopted. The level of illumination is set automatically by SCADA (Supervisory Control and Data Acquisition System).

3.2.3 *CCTV*
CCTV (Closed Circuit Television System) aims at continuous monitoring traffic inside tunnels and at portals for 24 hours. In case of push button activation or fire extinguisher removal scene of incident area is automatically captured and displayed on monitor in control centre.

3.2.4 *Traffic control*
Traffic control systems comprises sub-systems such as VMS (Variable Message Signs), three colored traffic sign, variable type lane matrix sign, vehicle classification and counting, vehicle height checking equipment, signs for emergency exits, illuminated or unilluminated all kinds of vertical signings and horizontal markings. The tunnel approaches are integral part of tunnel in terms of traffic control.

3.2.5 *Control centre*
Control centre is located in control room. All the systems are subject to control centre. It is a kind of SCADA centre. It gathers information, processes it and control systems connected to it. It is also monitoring and management centre of tunnel. Several tunnels can be centralized into single control centre. Tunnel operation strictly needs to contact with emergency services; fire brigade, police, ambulance.

3.2.6 *Telecontrol*
The purpose of telecontrol system is to transmit and control signals to and from installed all equipments. The information flow is carried out under supervision of redundant computer through metallic, co-axial or fiber optic cable. The whole system forms a LAN (Local Area Network). PLC (Programmable Logic Control) units are elements of control of devices in tunnel.

3.2.7 *Incident detection*
Incident detection system automatically senses abnormalities in traffic such as stopping vehicle, reverse moving or pedestrian in tunnel.

3.2.8 *Fire detection*
Smoke and linear fire detectors aim at detecting of a fire. Additionally emergency call niches and emergency exits are equipped with emergency bush buttons.

3.2.9 *Hydrants and extinguisher*
Portable fire extinguisher at every emergency stations and hydrants are the elements of fire extinguishing in tunnel.

3.2.10 *Ventilation and air quality control*
Dust particle concentration, air velocity, air flow direction, and CO concentration are of importance for ventilation. Longitudinal type ventilation is adopted. Evacuation of contaminated air is carried out by jet fans.

3.2.11 *Radio broadcasting*
Radio broadcasting system help users to give emergency messages broadcast in FM channels. Leaky feeder emits radio signal inside tunnel.

3.2.12 *Wireless communication*
Wireless communication equipment provides comprehensive communication for maintenance staff, ambulance services, police and fire brigades.

3.2.13 *Service telephone*
In order to provide communication between maintenance staff service telephone system are installed. Service telephone boxes communicate with control centre and other service telephones.

3.2.14 *Emergence call*
Emergency call boxes are mounded at every specified interval such as at every two hundred meters. In the event an alarm signal from call boxes an alarm sign will be prompted on the screen at control centre.

Copyright © 2005 Taylor & Francis Group plc, London, UK

Table 4. Tunnels under construction.

	500 m–1000 m	>1000 m	Total
Motorways	7	2	9
State roads	13	9	22
Total	20	11	31

3.2.15 *Public announcement*
In order to give voice messages to users public announcement systems are installed only in 75th Year Tunnel. Loudspeakers are mounted along the tunnel.

3.2.16 *Emergency power*
In the case of failure of main power emergency generator is automatically started to feed the systems. If emergency generator fails to start battery based uninterrupted power supply continues to supply essential loads.

3.3 *Future prospect*

When the ongoing construction activities on motorways are completed tunnel numbers longer than 500 m will be given as in Table 4.

The number of tunnels in operation will account for 48 in near future. Providing that completion of 16 tunnels at design stage the Highways Authority will be operating 64 tunnels over 500 m in 2010s.

4 AN EVALUATION ON TUNNEL OPERATION IN TURKEY

4.1 *New organizational charts for tunnels*

Not only technical requirements but also organizational formation is necessary for tunnel safety. Present organizational charts appoint only a few posts directly related to operation of tunnels in motorways and do not cover operation units of tunnels. Constructing of new tunnels has been continuing at a growing rate. New organizational units should be set up to meet the requirements of tunnel operation and maintenance.

4.2 *Comparison with EU countries*

If tunnel number of Turkey is compared with European Union Countries' Turkey will rank the fourth in 2010. Table 5 indicates tunnel figures of some countries at the top.

Table 5. Tunnel numbers, longer than 500 m in some European Union Countries and Turkey by years.

	Country	2002	2010
1	Italy	227	246
2	Austria	52	64
3	Germany	37	55
4	Turkey	17	48
5	Greece	7	45
6	France	31	35
7	Spain	20	25

4.3 *New operational properties with regard to state road tunnels*

- The first time a different financing method adopted for state roads. Built Operate Transfer method will be used to build and operate a tunnel.
- Together with longer state road tunnels, tolling of tunnel will be inaugurated. This will be an open type toll collection.
- The number of state road tunnels larger than 500 m in state roads will exceed that of motorways'. Operation activities will begin for state road tunnels and become significant issue.

4.4 *Setting up criteria for tunnel systems*

For application of systems to tunnels a design guideline is needed to provide homogeneous application.

4.5 *Tunnel operation regulation is to be renewed*

The maintenance, operation and protection of tunnel systems are carried out by the Tunnel Operation Regulation put into force in 2000. Existing regulation should be revised in consideration of new developments in technically and operationally.

4.6 *Relation with EU*

Turkey is a candidate country to the European Union. Transport is a common policy in the European Union. When the membership is realized transport acquis will be an obligation for member states and will have been transposed into internal legislation by the time membership occurs. That's why the progress concerning tunnel operation in the European Union should be pursued.

REFERENCES

Tunnel Operation Regulation, General Directorate of Highways.
Tunnels, Structures Forming Height, Underpasses on Highways, General Directorate of Highways.
Directive 2004/54/EC of the European Parliament and of the Council of 29 April 2004 on minimum safety requirements for tunnels in the trans-European road network.

Copyright © 2005 Taylor & Francis Group plc, London, UK

Quantitative assessment of structural fire endurance of concrete and shotcrete tunnel liners

A. Caner, S. Zlatanic & N. Munfah
Parsons Brinckerhoff, New York, USA

ABSTRACT: Tunnel fires can result in human casualties, structural damage, service disruptions and financial loss. Tunnel liners made of concrete or shotcrete can explosively spall at fires with high heat release rates and temperatures, and heat release rates are typically more severe in tunnel fires than in building fires. In the past, structural fire performance studies for concrete members focused mainly on buildings; not much work has been done regarding tunnels. This paper discusses an analytical method to quantify the structural fire safety of the concrete or shotcrete tunnel liners for a defined fire event. The proposed analysis for quantifying demand and capacity of the tunnel liners during a fire combines a heat transfer analysis and a non-linear structural analysis that includes type of fire, concrete mix design, temperature-induced material degradation and ground-tunnel liner interaction. It concludes by recommending methods to minimize fire damage.

1 INTRODUCTION

1.1 *Tunnel fires*

Most tunnels exposed to prolonged fires have been heavily damaged or have collapsed, resulting in service disruptions, significant structural damage and, most important, loss of lives (Both & Breunese 2003, Khoury 2002, and Tatnall 2002). In the aftermath of a fire, returning the tunnel to service is very costly. Fires in the Channel Tunnel in the U.K., Mont Blanc Tunnel in France, Howard Street Tunnel in the U.S. and St. Gotthards Tunnel in Switzerland are some examples of such disasters. It took years to reinstate service in these structures.

In the 1990s, ventilation systems were extensively tested by the Massachusetts Highway Department at Memorial Tunnel in West Virginia. Test data on released smoke and heat influenced the design of the tunnel ventilation program on Boston's massive Central Artery/Tunnel project (Massachusetts Highway Department 1995, Robena 1995). The focus of these tests, however, was on human safety, not structural safety or stability. Moreover, the tunnel structural members were heavily insulated so as to incur no damage during the 98 short duration tests (from 15 minutes to 30 minutes). The Memorial Tunnel in West Virginia was also utilized to simulate the Howard Street Tunnel Fire of Baltimore (McGrattan & Hamins 2003)

1.2 *Tunnel fire rating curves*

Tunnel fires are rare events and cannot be classified as service loads in structural design. For structural analysis or design check, different fire rating curves are developed for tunnels representing extreme fire events. These curves are mainly used for structural fire rating (PIARC 1999), and are not a function of the size of the tunnel or ventilation system, or represent the burning of a single vehicle. Furthermore, it was observed by Takekuni et al. (2003) that the small-size tunnels have higher temperature readings on tunnel liners than the large-size tunnels when subjected to the same type of fire.

Figure 1 shows a number of fire rating curves. Curve 1, called the cellulosic curve, is based on the

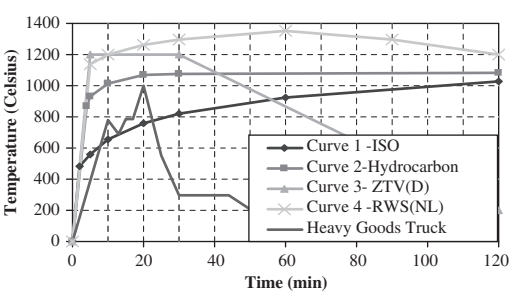


Figure 1. Tunnel fire rating curves.

Copyright © 2005 Taylor & Francis Group plc, London, UK

burning rate of materials found in general building contents. Curve 2, the hydrocarbon curve, is applicable where small petroleum fires might occur. Curve 3, the ZTV curve (developed in Germany), represents a case in which temperatures rapidly rise to 1200°C in 5 minutes. Curve 4, the RWS curve (developed in the Netherlands), simulates the burning of a fuel tanker with a fire load of 300 MW. Information on fire rating curves can also be found in the work of Khoury (2002).

For buildings, a standard fire curve is used for fire rating analysis and is an envelope of different individual fires. In ACI216R-89 (Reapproved 2001) fire load combination is treated as an extreme event like a seismic load combination. Fire rating is typically measured in hours.

1.3 *Damage to concrete and shotcrete liners*

Damage to concrete and shotcrete liners is a function of the heat release rate and peak temperature of the fire as well as concrete mix design. During the first half an hour of a fire event, a major concern is to prevent explosive spalling of the concrete. At the later stages, of the fire a major issue is the material degradation, because an increase in structural demand and simultaneous decrease of structural capacity during a lasting fire event can result in serious structural damage.

It was observed that high-strength concrete having silica fume subjected to a fire with a 5°C/min heating rate can explosively spall at a temperature as low as 240°C (Flynn 1999). Explosive spalling is a function of the concrete moisture content, concrete mix design, heat release rate of the fire and applied compressive stresses. When the temperature in the concrete rises rapidly, the moisture in the concrete cannot find a path to escape and turns into steam. The steam's building pressure may cause the explosion of the concrete. When a concrete with high moisture content by weight (say more than 3% to 4% by weight) and with low permeability is subjected to a fire with high heat release rates, explosive spalling can be expected (Khoury 2002, Tatnall 2002, Phan & Carino 2000, Kutznig 1999).

At the later stages of a fire, concrete, shotcrete and steel start to degrade and lose functionality (ACI216R-89 Reapproved 2001). Therefore, the load-carrying capacity of the concrete liner decreases. For thermally restrained structures such as tunnels the structural demand increases. When the demand exceeds the load-carrying capacity of the liner, the collapse of the tunnel can be expected.

1.4 *Current fire endurance evaluation methods*

The design or analysis aids for fire endurance of columns, beams, walls and slabs can be found in several publications such as American Concrete Institute, ACI 216R (2003), American Society of Civil Engineers, ASCE (2003), Milke (1999), Dotreppe et al. (1999), Lie & Irwin (1993), Huang et. al (1999) and Rignerth (2000). These design aids are typically focused on building fires.

Khoury et al. (1985) investigated the thermal stresses in axially loaded concrete cylinders for different types of concrete used at nuclear reactor pressure vessels. The thermal strains in the concrete could not be determined using elastic analysis. Transient creep at early stages of fire reduced the thermal stresses. At cooling, transient creep did not have any benefit on concrete elements. The maximum radial temperature difference in the central region of a cylinder specimen was linearly related to the rate of heating and inversely related to the thermal diffusivity.

A specific design guideline was developed by Parsons Brinckerhoff for the part of Hudson Bergen Light Rail System project related to Weehawken Tunnel in New Jersey. In this guideline, an analytical method was established to evaluate the condition of the concrete- or shotcrete-lined tunnels when exposed to high temperatures at different stages of the fire. The guideline was structured to allow some minor repairable damage to the liner for the selected extreme fire event.

1.5 *Need for research*

It is important to quantify the structural fire safety of concrete or shotcrete tunnel liners. Such assessments will enable engineers to implement design measures that will avoid catastrophic disasters, yet still allow tunnels to accept some minor damage after major fires with long durations. Corrective repair and maintenance activities can then be applied easily with little or no disruption to tunnel operations.

2 GUIDELINE

The purpose of this guideline is to quantify increase in demand and decrease in capacity of tunnel sections under fire. The fire rating of the tunnel liner can be defined in terms of time required to equal the structural demand to the liner structural capacity.

2.1 *Design philosophy*

In U.S., the final liners of tunnels are typically designed for daily loads such as dead load, rock load and hydrostatic load. In the last decade, load combinations and resistance factors listed in the American Concrete Institute's *Building Code Requirements for Structural Concrete* (ACI318 1999) and prior versions of the code have been used in the U.S. A common

Copyright © 2005 Taylor & Francis Group plc, London, UK

load-factored combination based on this code for daily loads is:

$$1.4DL + 1.7(HL + RL) \quad (1)$$

where DL = dead load, HL = hydrostatic load and RL = rock load (all the force and moment terms are in units of N or N-mm respectively).

The forces obtained from the above equation must be less than the ultimate capacity of the section as follows:

$$\phi R_n > R_u \quad (2)$$

where ϕ = resistance factor, R_n = nominal resistance capacity, which can be a force or moment, and R_u = factored loads.

The factored loads can be determined from structural analysis of the tunnel sections and the nominal resistance can be determined through a standard moment-curvature analysis or through an axial force-moment interaction curve.

Fires are not service loads, so the load combination including an extreme fire event can be taken without the load factors, as suggested by ACI216R-89 (Reapproved 2001). Other extreme events, such as seismic design check of structure were done using a similar philosophy, shown as:

$$DL+(HL+RL)+FL(t)=R_u(t) < \phi_r R_{nr}(t) \quad (3)$$

where $FL(t)$ = fire induced structural load (sum of the primary and secondary forces at the investigated time of fire), ϕ_r = the resistance factor (= 1.0 for extreme events per ACI216R-89 (Reapproved 2001)), and $R_{nr}(t)$ = reduced capacity due to material degradation at the investigated time of the fire.

2.2 *Computing demand*

The analysis of thermal gradient for bridge concrete members was explained in great detail in the work of Shushkewich (1998). A similar approach with some modifications can be used for tunnels to determine the primary and secondary forces due to fire.

Primary forces have two components: thermal forces and equilibrating forces. Thermal forces are a function of the temperature profile inside the liner. The temperature profile inside the concrete or shotcrete liner can be:

- Taken or interpolated from applicable experimental data. Some of the temperature data for different fires and for different type of concrete and shotcrete can be found in ACI216R-89 (Reapproved 2001), Tatnall (2000), Mangs & Rahkonen (1990).
- Predicted using transient heat transfer analysis. More information on heat transfer analysis can be found in the work of Reddy (1985). Temperature-dependent thermal properties of concrete shall be used to predict the temperature profile in the concrete (Kodur & Sultan 2003, ACI216R-89 Reapproved 2001, Flynn 1999).
- Computed using a software package such as RADTherm (2003). This particular software requires manual update of thermal properties of the concrete at different temperatures and requires an iterative solution.

To derive thermal forces from thermal strains, the concrete section can be divided into layers at its depth. Stress in each layer can be determined from stress-strain curves of the concrete. The force in each layer is simply the area of the layer times the stress in the concrete layer. The total thermal force at the section is simply the summation of the forces in each layer. Such analysis techniques have been used in many applications of concrete analysis (Zia et al. 1995). The only difference in fire analysis is that the stress-strain curve of the concrete is not constant at the depth of the concrete due to high temperatures. A sample for temperature dependent stress-strain curves for a concrete with a 28 day compressive strength of 28 MPa is shown in Figure 2. Similar stress-strain curves can also be found in ACI216R-89 (Reapproved 2001).

The temperature profile due to fire will generate compressive thermal forces close to the hot surface. These thermal forces will be equilibrated by a tensile axial force and a bending moment at the neutral axis of the tunnel liner cross-section. These forces are called equilibrating forces.

The equilibrating forces will be input into the structural model of the liner to determine the secondary forces due to fire. In this step, loads due to dead, hydrostatic and rock or soil pressure shall also be included. A general structures analysis software with non-linear analysis capabilities such as LARSA (2004) can be used to determined the secondary forces. Ground-tunnel liner interaction shall be included in such

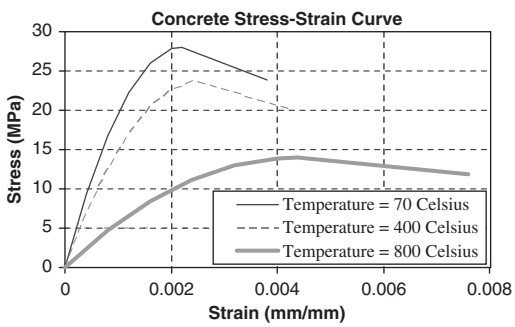


Figure 2. A sample set of concrete stress-strain curves.

Copyright © 2005 Taylor & Francis Group plc, London, UK

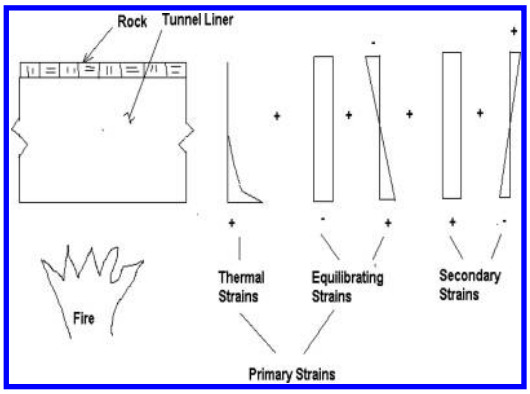


Figure 3. Primary and secondary strains induced by fire.

analysis in addition to material degradation and geometric non-linearity. In ground-tunnel liner interaction, the compression stiffness of the waterproofing system can also be included. Material degradation properties can be manually updated based on the temperature inside the concrete or shotcrete liner by iteration.

At each step mentioned above, the strains shall be computed since the forces are not addable due to non-linear material behavior. The primary and secondary strains are shown in Figure 3. The creep strains can be added to to the primary and secondary strains and estimated based on ACI 216R-89 (Reapproved 2001). The total fire load can again be determined using temperature modified stress-strain curves and the transformed area of the section.

2.3 *Computing capacity*

The reduced capacity of the liner cross-section can be determined through a temperature-modified moment-axial interaction analysis. Again, in such analysis the liner cross-section will be divided into layers, and the material properties of each layer will be a function of the temperature. An in-house software package called "FIRECAP" was developed to quantify the demand and the capacity of the tunnel section.

3 MITIGATION OF FIRE DAMAGE AND REPAIR METHODS

3.1 *Concrete or shotcrete liners*

After a fire, concrete sections exposed to temperatures in excess of 300°C should be removed. The reason for selecting such temperatures is that tests of the compressive strength characteristics of concrete specimens heated to 300°C, then cooled to room temperature and stored in air at 75 percent relative humidity for six days, revealed that those specimens lost 40 percent of their compressive strength (ACI216R-89, Reapproved 2001).

The depth of fire-damaged concrete can be determined by using heat transfer analysis or by chemical analysis of concrete Voids should be patched with patching materials with similar characteristics to the concrete mix design used for the original tunnel to maintain structural integrity.

3.2 *Reinforcement*

If the reinforcement in the concrete was exposed in the fire as a result of the spalling, it should be removed. The new reinforcement should be spliced to the existing reinforcement.

3.3 *Waterproofing*

Waterproofing membranes are typically used in combination with geotextile drainage fabrics to prevent water leakage and relieve hydrostatic pressure at the new tunnel liners. Such waterproofing systems will also help controlling the moisture content in the concrete liner by preventing infiltration of ground water from the external surface of the liner, and may serve as a valuable means of mitigating the total effects of the fire. If the waterproofing membrane was damaged or melted as a result of the fire, the waterproofing should be properly replaced and spliced to the existing one.

3.4 *Micro-polypropylene fibers*

Micro-polypropylene fibers in concrete will start melting over 130°C and will increase the permeability of the concrete layers close to the hot surface at the early stages of the fire. Increased permeability of the concrete will allow the steam to escape from the concrete without exploding it. After fire, an evaluation of the need for major repair should be determined on a case-by-case basis. Furthermore, with the more permeable concrete the chance of explosive spalling may be minimal in the event of another fire at the same location. (The fibers, however, do decrease the workability of the concrete and add to the overall cost of the concrete mix.)

3.5 *Insulation*

If the tunnel liner is insulated through the application of fire-rated coatings, and if these insulation materials are damaged during a fire, they should be replaced by the same type of material based on the fire performance history of the material. The insulation materials could be a spray-on type or a board type. In a thermally restrained tunnel, if the thermal barriers such as spray-on materials or fire boards are made integral to the tunnel liner, they should also be able to

Copyright © 2005 Taylor & Francis Group plc, London, UK

resist the structural stresses induced by fire. Thermal barriers are typically considered a costly measure (Both & Breunese 2003).

3.6 *Sprinklers*

Sprinkler systems may be used as way to extinguish the fires, but they, too, are considered costly because of costs associated with their installation, maintenance and drainage. Implementation of sprinkler systems in tunnels is not practical and is not typically done.

3.7 *Ventilation*

Ventilation systems are typically provided for human safety. In the early stages of a fire, the ventilation system can help in cooling down the temperatures at the exposed surface of the liner, and can improve overall structural safety in the tunnel.

4 CONCLUSION

The following conclusions are based on evaluation of the effects of a fire on concrete and shotcrete tunnel liners:

- The structural concrete or shotcrete liner can be designed to withstand the tunnel fire up to a certain period of time while accepting some minor repairable damage to the liner.
- The fire endurance of the tunnel liners can be estimated using the proposed analysis method.
- Tunnel liners should be analyzed to determine the fire rating of the design.
- Using micro-polypropylene fibers in the concrete or shotcrete mix design can minimize explosive spalling of the tunnel liner.
- Use of thermal barriers can help reducing the fire temperatures on concrete or shotcrete lining and can improve structural safety.
- Ventilation systems will improve structural fire safety in the early stages of the fire.
- More experimental data on tunnel fires are needed on material level for different types of concrete, shotcrete and fibers.

REFERENCES

ACI216R-89 Reapproved 2001. Fire endurance of concrete elements. *ACI 2003 Manual of Concrete Practice*, Farmington Hills, Michigan.

ACI318 1999. *Building code requirements for structural concrete*, Farmington Hills, Michigan.

ASCE/SEI/SFPE 29–99 2003. *Standard calculation methods for structural fire protection*, Reston, Virginia.

Both C., Wolinsk G.M. & Breunese A.J 2003. Spalling of concrete tunnel linings in fire., *(Re)Claiming the Underground Space*, Sauver, Swets & Zeitlinger, Lisse, 227–231.

Dotreppe, J-M., Franssen, J.-M. & Vanderzeypen, Y. 1999 Calculation methods for design of reinforced concrete columns under fire conditions., *American Concrete Institute, Structural Journal*, (96)1, January–February, 9–18.

Flynn, D.R. 1999. Response of high performance concrete to fire conditions: review of thermal property data and measurement techniques*, NIST GCR 99–767*, U.S. Department of Commerce Building and Fire Research Laboratory National Institute of Standards and Technology, Gaithersburg, Maryland.

Huang, Z., Burgress, I.W. & Plank, R.J. 1999. Nonlinear analysis of reinforced concrete slabs subjected to fire. *American Concrete Institute, Structural Journal*, (96)1, January–February, 127–135.

Massachusetts Highway Department 1995, *Memorial tunnel fire ventilation test program*, Test Report, Massachussets.

Khoury, G.A., Grainger, B.N. & Sullivan, P.J.E. 1985 Transient thermal strain of concrete: literature review, conditions within specimen and behavior of individual constituents. *Magazine of Concrete Research*, 132, September, 131–144.

Khoury, G.A. 2002. Passive protection against fire. *Tunnels and Tunneling International*, November , 40–42.

Kodur, V.K.R. & Sultan, M. A. 2003. Effect of temperature on thermal properties of strength concrete., *Journal of Material in Civil Engineering*, 15(2), 101–107.

Kutznig, L. 1999 Fire resistance of high performance concrete with fiber cocktails., *LACER*, No. 4**,** 185–192.

LARSA (2004), *Quickstart guide for version 6.08.r46*., Melville, New York.

Lie & Irwin 1993. Fire resistance of reinforced columns. *American Concrete Institute, Structural Journal*, (90)1, January–February, 52–60.

Mangs, J. & Rahkonen, O.K. 1990. Fire testing of shotcrete samples in a small furnace. *Shotcrete for Underground Support V*, ASCE 297–313.

Milke, J. 1999. Analytical methods to evaluate fire resistance of structural members. *Journal of Structural Engineering* 125(10), 1179–1187.

McGrattan, K.B. & Hamins, A. 2003. Numerical simulation of the howard street tunnel fire., *NUREG/CR-6793, NISTIR 6902*, Baltimore, Maryland.

PIARC Committee on Road Tunnels (C5) 1999. Fire and smoke control in road tunnels., *World Road Association*, Athens, Greece.

Phan, L.T. & Carino, N.J. 2000. "Fire Performance of High Strength Concrete: Research Needs.", *NIST, ASCE/SEI Structures Congress*, Philadelphia, PA.

RADTherm 2003. *Manual-version 7.0*. Calumet, Michigan.

Reddy, J.N. 1985. An introduction to the finite element method*, McGraw Hill, International Edition*, Singapore.

Rignerth, J. 2000 Simplified design of fire exposed concrete beams and columns – An evaluation of eurocode and swedish building code against advanced computer models., *Department of Fire Safety Engineering*, Lund University, Sweden.

Robena, J.N. 1995 Tunnel fire testing to evaluate ventilation systems, *Public Roads*, Winter 1995, 58(3).

Copyright © 2005 Taylor & Francis Group plc, London, UK

Shushkewich, K.W. 1998 Design of Segmental Bridges for Thermal Gradient, *PCI J*. 43(4), 120–137.

Takekuni, K., Akifumi S. & Yokota, Masahiro 2003. The Characteristics of Fires in Large-Scale Tunnels on Fire Experiments inside the Shimizu No.3 Tunnel on the New Tomei Expressway, *(Re)Claiming the Underground Space, Sauver, Swets & Zeitlinger*, Lisse, 179–184.

Tatnall, P.C. 2002. Shotcrete in Fires: Effects of Fibers on Explosive Spalling, *Shotcrete*, American Shotcrete Association, Farmington Hills, Michigan, 10–12.

Zia, P., Caner A. & El-Safty, A.K. 1995. Jointless bridge decks. *Research Report No. FHWA/NC/95-006*, Center for Transportation Engineering Studies, North Carolina State University, Raleigh, NC.

Copyright © 2005 Taylor & Francis Group plc, London, UK

Consolidation and excavation works for the upgrading of Frejus Tunnel

M. Pescara, G. Russo, F. Valdemarin, P. Grasso
Geodata S.p.A., Torino, Italy

ABSTRACT: Within of the works for upgrading the historical railway line from Turin to Modane, the most important is the famous tunnel of the "Traforo del Frejus": being a piece of pioneering work for its geometry and excavation method, completed in 1871, still today it constitutes an efficient communication way through the Alps both for commodity and for passengers. The works currently in course on the Italian side consist in lowering the actual rail level by approximately 60 cm and upgrading the technological apparatuses. The benching, that will be realized after the consolidation works, will be executed with an AHM105 road-header that will excavate even under the foundation level of the existing lining structures. Due to the constraints to assure the non-stop exploitation of the tunnel at least on one track, the benching will be executed in two phases, alternately along the two railroads; great importance has been given therefore in this paper to the practical construction aspects.

1 INTRODUCTION

The upgrading activities are part of the overall works to empower the historical Turin-Modane line managed by the railway administrations of Italy (RFI) and France (RFF), in order to allow the transportation of particular trains and to improve the safety endowments of the whole system.

In particular, the undergoing works includes:

- adjustment to shape B1 from the Italian portal till the Italy-France border;
- implementation of a more advanced system for managing the train circulation (BAB C.c). (3/3);
- upgrade of the safety system based on new RFI guidelines for existing tunnels.

With respect to the new shape, it will be obtained by lowering the current rail plane by 60 cm and re-adjusting the two tracks in plan. As regards the system's adjustment, the new necessary apparatuses will be placed inside new or adapted niches.

The demolition and excavation works would follow a systematic consolidation of the tunnel lining and rock. The civil works have been anticipated by the site organization, and thus the tunnel, with proper facilities (ventilation, illumination and electricity). All the activities have been carried out entering the tunnel on one single track to assure no interruption of the international traffic; the shipyard aspects have been organized considering the possible intersection with the commercial traffic at Bardonecchia station.



Figure 1. The Italian historical portal of the Frejus.

2 PROJECT INFORMATION

2.1 *Characteristic of the work*

The Frejus Tunnel, bored between 1857 and 1871, connects Bardonecchia (I) to Modane (F), over the length of approximately 13636 m (6791 m in Italy).

The tunnel is double track, with a maximum overburden of 1600 m, and an inclination varying from 1‰ to 30‰; the maximum height a.s.l. is 1296 m at the Border Line. In plan view the tunnel alignment is

Copyright © 2005 Taylor & Francis Group plc, London, UK

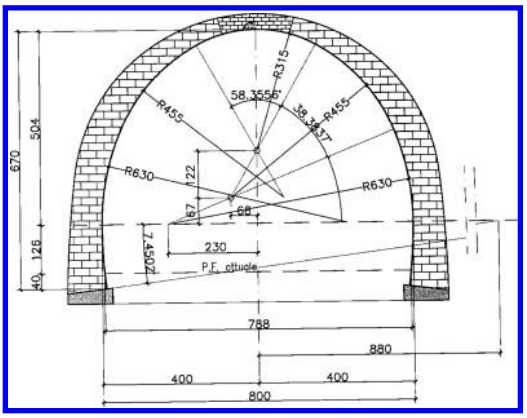


Figure 2. Geometry of the cross-section (measures in cm).

mainly straight (central part), with only some curves near the two portals; the straight part prosecutes outside through the directional tunnels, used for topographic controls.

The tunnel can be divided in at least three stretches on the Italian side:

- the first, starting from the portal (Pk 84 + 225), of approximately 600 m, is in curve (radius 704 m), and it is constituted from an artificial horseshoe shape tunnel leaned to the mountain wall; on the opposite side (river side), at regular distances (30 m) 9 windows of approximately 4 m height are present;
- the second is a natural tunnel, again located in curve (400 m radius approximately), which ends with the intersection of the directional tunnel, where the section is 12 m wide;
- the third is the straight part; the shape is horseshoe with raised crown; the maximum width is approximately 7.9 m, while the height from the rail level is varies from 6.0 m to 6.3 m.

The lining is in masonry, mainly made of stone blocks at the sidewalls and bricks at the crown; locally, however, the lining can be all made of stone blocks apart from the top portion of the crown which is always in bricks. The lining thickness varies from 80 cm at the sidewalls to 45 cm at the crown.

The lining construction has been executed positioning the bearing structure with the help of wood moulds and filling up with blocks, concrete and detritus the voids to obtain a good contact with the rock mass; such a system, as demonstrated by "georadar" investigations lead to possible presence of important voids in the crown.

Starting some decades ago many instability phenomena in the crown (cracking and splitting of the masonry has appeared) over long stretches of the Frejus tunnel have been recorded with increasing intensity.

Chart 1. Classification parameters.

GSI	σ_c (MPa)	m_i
35–65	20–80	5.15

GSI = Geological Strength Index;
σ_c = compression strength of the rock mass;
m_i = constant of Hoek & Brown for the intact rock.

Chart 2. Representative geomechanical parameters for a section and used for the numerical analysis.

E_d	$\sigma_c \approx \sigma_{cm}$	m_b (=m_i)	s (=s_i)	m_r	s_r
[GPa]	[MPa]	[–]	[–]	[–]	[–]
10	30	10	1	1.017	$8.1 \cdot 10^{-4}$

E_d = deformability modulus;
$\sigma_c \approx \sigma_{cm}$ = compressive strength of the rock mass;
m_b, s, m_r, s_r = const. of the rock mass for the Hoek & Brown's failure criterion.

Along the tunnel, a lot of different niches are distributed in order to allow the personnel recovery and the lodging of technological systems. At the center of the tunnel floor, under the ballast, a conduit, approximately 80 cm width and 80 cm depth, covered with stone slabs is located for drainage purpose.

2.2 *The geomechanical characterization*

The Frejus tunnel is excavated in the formation of the calceschists of the "Serie Piemontese" (Schistes lustrés), which have been assembled in wide plicative structures. From the geologic-geomechanical point of view the calceschists shown a remarkable variability (structure from almost massive to foliated) essentially due to their state of tectonization.

The geomechanical characterization has been developed on the basis of various in situ and laboratory tests. Chart 1 shows the main parameters used as a reference for the design analysis.

In order to calibrate the numerical model, some back-analysis have been performed, starting from the stress-deformation lining conditions, and using different sets of geomechanical values. Chart 2 shows the values of the main parameters which allowed to obtain the best fit: the rock mass is simulated as an "intact" rock with σ_c = 30 MPa and an elasto-plastic ideally brittle behaviour.

With reference to the in situ stress, it has been verified a deficit of the vertical stress (σ_v) compared with the geostatic value (σ_o) since σ_v/σ_o = 0.8–0.9; this phenomenon is coupled with values of the k_0 (ratio horiz./vert. in situ stresses) quite variable and generally

Copyright © 2005 Taylor & Francis Group plc, London, UK

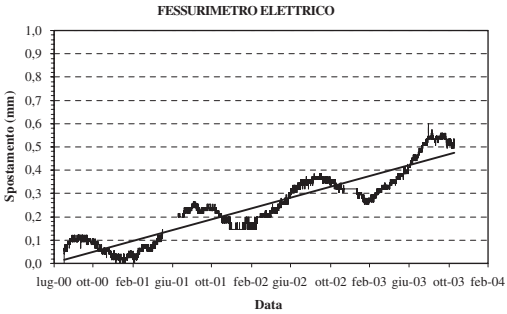


Figure 3. Movement of one crack monitored over years in the crown of the tunnel.

comprised between 0.7 and 1.3 but sometimes also near to 1.6–1.7 (see also Berest et al. 1980 and more recently Carpegna et al. 1999).

Moreover, it is important to point out that 1 of the 5 samples of calcescists, on which creep tests have been performed, showed a significant deformation trend along time (constant load for 20–30 days).

2.3 *Measures of the actual strain–stress conditions and back-analysis calculations*

In addition to the geologic-geomechanical investigations, in situ and laboratory tests have been carried out for definitioning the stress conditions of the lining and the strength of its constituent materials. Among the others, hereafter the results of the tests carried out on the materials and the flat jack tests are shown. Also the readings of a crackmeter located on the cited cracks are reported.

The flat jack tests highlighted values of high and asymmetric stresses in the structure, especially if compared with the mean compression strength values of the materials.

Comparing, with the needed degree of approximation, the values of stress in the lining reported by Bernede et al. (1996) and the ones in Chart 4, it is possible to define an increase in 35years of the normalized tangential stress in the lining ranging from about 0.04–0.07 to 0.10–0.26.

Moreover, the inspections of the lining's foundations revealed, thus poor bearing conditions.

The back-analysis calculations, performed with the FLAC, have attempted to reproduce the actual condition of stress and strain inside the structure, synthetically characterized by:

- asymmetry of loads;
- high stress values;
- tendency of the structure to converge at the sidewalls with consequent high compression stresses at the intrados of the crown.

Chart 3. Strength and deformability of samples of lining (2000).

Material	Parameter	Minimum	Media	Maximum
Briks and mortar	σ_c (MPa)	2.3	5.7	12.0
	E_t (GPa)	0.4	1.4	2.7
Bloks and mortar	σ_c (MPa)	7.7	20.6	38.4
	E_t (GPa)	10.7	28.1	52.65

Chart 4. Results of the flat jack tests (pressure of restoration expressed in MPa).

Station	Right sidewall	Right spring-line	Left spring-line	Left sidewall
85 + 800	3.5	3.0	3.5	1.0
86 + 700	5.0	2.5	2.5	9.0
87 + 500	3.5	4.5	5.0	3.5
88 + 600	2.5	2.5	6.0	6.0
89 + 200	4.4	6.6	4.0	7.3
89 + 268	4.9	5.9	6.6	5.9
89 + 600	6.5	3.0	8.5	3.5
89 + 765	3.1	4.9	2.9	8.7
89 + 800	–	3.2	2.6	3.5
90 + 600	5.0	7.0	5.0	4.0

Such conditions have been reproduced by either assuming the presence of a void in the crown, or imagining a perfect between rock mass and lining. In particular, the presence of voids in the crown (lack of confinement to oppose the deformation on the upper part of the arch), increases the tendency to the transversal closure, causing high stress in the crown.

3 DESIGN INTERVENTION DEFINITION

3.1 *The targets of the intervention*

Starting from the results of the above mentioned studies, numerical analyses have been performed to evaluate the effects of the excavation on the structure. Such calculation allow to define the target to be reached through the consolidation works which shall permit the excavation in safety conditions:

- to contrast the lining converge trend aggravating the compression state at the crown, and thus limiting further weakening of the structure;
- to prevent a settlement of the structure due to the sliding of the loose material beneth the foundation during the excavation phase, in case this material has low mechanical characteristics;
- to completely support the arch in the zones where it will be partially demolished to create the new niches or in particularly delicate sections;
- to support punctually the masonry arch in correspondence of the portal of any niche.

Copyright © 2005 Taylor & Francis Group plc, London, UK

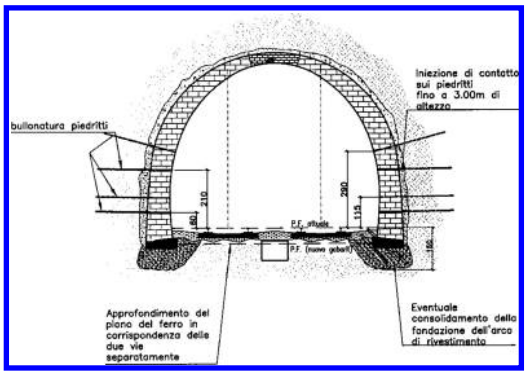


Figure 4. Section type for the consolidation of the tunnel (cm).

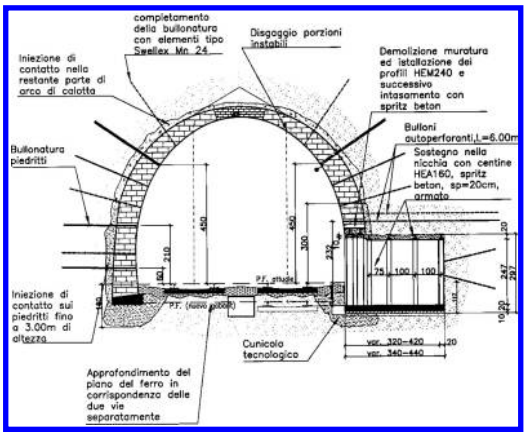


Figure 5. Section-type for consolidation in correspondence of the niches (cm).

Each of the above targets is reached by designing specific intervention.

Contrast the convergence

The potential convergence of the sidewalls was contrasted by installing systematic radial rockbolts on the lower part of the structure, rigidly tying the lining to the surrounding rock mass.

Such intervention was anticipated by a mortar injection to fill the voids between the linign and the rocks mass. The use of CT-bolts rockbolts, has moreover concurred to increase the stability because of the pretensioning given to the elements themselves. The length of the bolts was limited in order to allow the placement without interfering with the installation in rail line under exploitation.

Control of the settlements of the foundation

A systematic consolidation of the lining foundation was performed by mortar injections through PVC tubes with "manchette".

Complete support of the arc

This target was reached throughcompleting the mortar injections and radial rockbolting for the entire arch.

In particular it has been used:

- rockbolts type Swellex Mn24 equipped with a short case located near the plate to avoid the detrimental expansion of the bolt inside the masonry;
- the mortar injection for contact purpose was transformed at the crown in an injection to fill voids, especially when cracks were present.

Support of the niches' portal

Before the start-up of lining demolition, a heavy steel gateway inserted in the lining that is capable of taking the actual stresses in the masonry.

The installation of the gateway is anticipated by systematic bolting of the lining (with self-drilling bolts) along the niche's contour with the double function:

- to facilitate the arching over the gateway, preventing the collapse of the masonry;
- to act as an umbrella protection during the excavation of the niche.

3.2 *The executive phases*

About the execution phases, the design prescribes that:

- the benching can begin on one track way only (whichever of the two), provided that the consolidation is completed on both sides and at the crown, where required;
- the bolting of any portion of the arch will follow the injection of the same portion before the injection of an adjacent portion, in order to reduce the rising of any asymmetric loads;
- the volumes and the pressures of injection should be continuously monitored and recorded for further back-analysis.

4 THE EXCAVATION PROCESS

4.1 *The excavation of bench by the road-header*

The bench excavation will be performed using a Voest-Alpine AHM105 road-header with a specific procedure, an unusual one for such an equipment. Indeed, the machine will work digging in advance a bench 3.90 m wide (half width of the tunnel) and 60 cm thick for the whole length of the tunnel, advancing of very few centimetres for each passage.

Copyright © 2005 Taylor & Francis Group plc, London, UK

The working cycle will be:

- "*forward step*" – constitutes the sinking of the head in the front for a depth of 5 ÷ 6 cm with the road-header's arm laterally extended to reach and cut the maximum width of the section to be excavated;
- "*cutting step*" it is the phase of the real excavation, carried out by lateral movement of the head;
- continuing of the excavation by repeating the above two steps, starting from the opposite side of the bench.

The decision to work with a reduced sinking of the head, (equal to 1/10 of the attainable value during of standard excavation), is the need to avoid full stabilisation of the machine at every new excavation cycle, obtaining therefore an increased overall advance rate.

4.2 *The excavation of the niches by pre-cutting with a circular saw*

The need to maintain the railway traffic on one track during the excavation of the niches implies:

- to avoid compulsorily the use of explosive (forbidden in tunnel);
- to limit as much as possible the negative effects on the portion of lining not to be demolished;
- to use operating machine that does not interfere with the rail line under exploitation.

For these reasons a set of machines for the controlled demolition has been selected for excavating the niches, using diamond mono/pluridisk saws in association to electrical demolishing robots.

The entire cycle of excavation for each niche implies the employment of two independent teams, operating both from a railway wagon:

- the team A, equipped with monodisk saws and robot demolisher, cuts the lining, excavates it and installs the gateway of all the niches;
- the team B (working in front of the road-header, equipped with pluridisk saws and shotcreting equipment, cuts the rock mass, excavates it, installs the temporary supports and the final shotcrete lining for the niches.

5 MONITORING OF THE STRUCTURE

In accordance with the targets of the design interventions, a monitoring system has been installed to assure the safe progression going on of the works.

In particular it serves to:

a. record lining convergences;
b. verify the foundations settlements;
c. verify the effects induced from the lining demolition works mainly near the new niches;
d. check the deformation of the lining in correspondence of the niches.

The monitoring system is based upon a hierarchical system divided in three levels and includes:

- the sensors and the topographic pins;
- the acquisition data units;
- the centralization, management and distribution data collocated (GIS-based).

In practice, independent from the typology of the sensors, all the monitoring data (digital or manually collected) converge in an unique management & distribution system, based on a GIS-Web platform.

The system allows real time monitoring data management and the automatic execution of alarm procedures when the readings exceed predefined thresholds. The contextualisation in the GIS system of the monitoring measurements with design data and tunnel survey data, allows to identify and to understand the instrumentally recorded phenomena and to bring them back to their correct physical meaning.

Thanks to the GIS-Web platform all the monitoring measurements are distributed in real time (with a protected Internet login) to the Contractor, the Owner, the Engineer and the Designer.

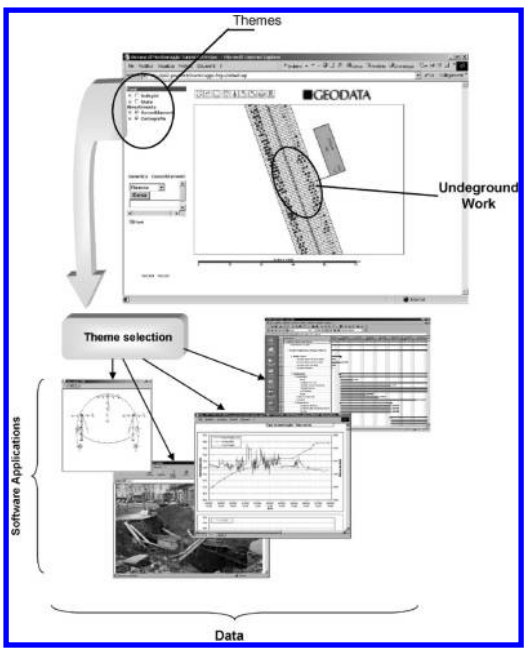


Figure 6. The monitoring with the GIS-Web platform.

Copyright © 2005 Taylor & Francis Group plc, London, UK

5.1 *Monitoring the bench excavation*

The monitoring scheme for the bench excavation, performed by the road-header, is based on the implementation of two section-types:

- *Current Section* (SC) spaced every 50 m of tunnel, consists of optical reflectors for the determination of the 3D convergence;
- *Special Section* (SP), located in problematic zones (n.10 in total), consists of flat-jacks, dynamometric cells on the bolts and optical reflectors, for the determination of the lining stress-deformation conditions.

This monitoring scheme is supplemented by a vibrometrical monitoring system made of three moving sections (SV based on the use of 3D geophones), which follows the road-header excavator in order to control the potential production of any dangerous effects on the masonry lining.

5.2 *The monitoring for the excavation of the niches*

One of the most critical works is the demolishing of the lining to create the entrance for the new niches, because of the summed effects of the excavations. In all those zones it is activated a real-time monitoring of the convergence and settlement of the lining immediately above the niche excavation profile. The section is made with two disto-lasers located near the niche to be excavated, and an electrical crackmeter (if relevant). The registered data from these instruments are centralized in a readout-unit for local data storage, able to transfer via SMS the readings to an external datalogger. To increase the safety direct readings at the site are also possible due to the presence of a graded support where the distometer will collimate; this will allow a visual estimation of the deformation induced from the excavations activities.

6 THE JOBSITE AND THE TUNNEL EXPLOITATION

One of the main problems for organizing the site to implement any possible design solution was the constraints to have the tunnel under exploitation at least on one track: the commerce and the long-distance trains (Eurostar and TGV) have to be maintained, deviating on highway just the local transit. The most part of the activities are undergoing in such a condition since only for few hours divided in 2 "windows" a complete interruption has been foresaw. This means that the cited constraints does not allow to delimit the work site area and to carry out any activity by normal people, which must be protected.

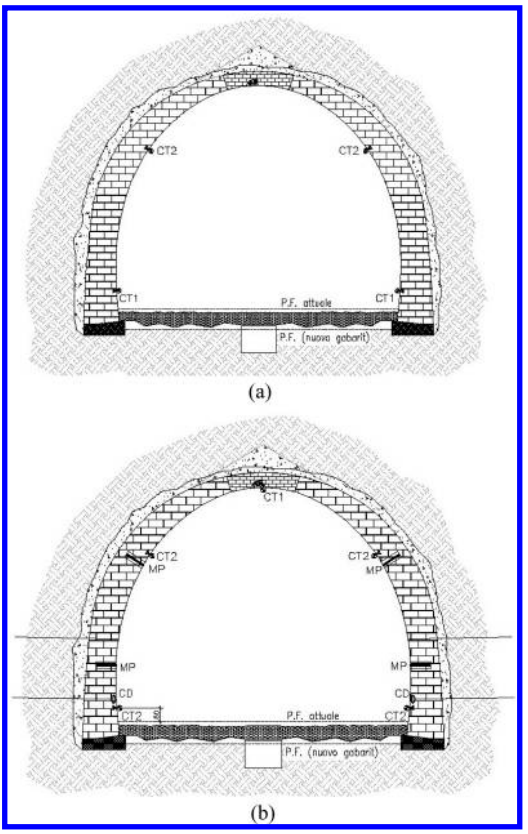


Figure 7. Scheme of current (a) and special section (b).

6.1 *The control of the workings "in shape"*

The need to have a well defined "respect zone" for the transit of trains on the adjacent rail track influences all the construction activities and also the design of the consolidation and excavation techniques. In particular, from the design point of view, the following choices have been made:

- limiting the length and the typology of bolts;
- pre-supporting the roof of the niches with self-drilling bolts jointed in parts of 1.5 m in length;
- studying the dimensions of road-header and its technological wagon;
- studying the dimensions of all operating machines.

In addition, also the following recommendations are to be observed during all the works:

- the wagons used to transport the shifts and the equipment have been all equipped with gates in the direction of the rail track under exploitation;
- protection personnel, specifically trained for, is always present with every operating crew.

Copyright © 2005 Taylor & Francis Group plc, London, UK

6.2 *The accurate composition of the convoys*

A careful planning of the site activities has been constantly conducted prior to every operation in tunnel. In particular, the sequence of the operations has been rigidly maintained, at the price of sacrificing the productivity. The composition of the crew for every shift is planned by a specialized personnel having the responsibility to know the position of every operating wagon and the forecast production for every team, to avoid interferences between the single squads.

7 CONCLUSIONS

This paper has synthetically introduced the primary aspects of the design and the construction of the civil works for the adaptation of the gauge of the historical Frejus Tunnel to the traffic demand.

The works had to constantly face with the actual static conditions of the tunnel and with the constraints to assure the exploitation of at least one single track; the latter strongly conditioned all the design choices.

A strategic part of the design is the control made by the designer directly during the construction, in order to optimise the interventions and thus the smooth operation of the railway traffic. Particular attention has been also dedicated to write the excavation procedures for the works undergoing, especially those one related to the road-header excavation control of the lining behaviour.

ACKNOWLEDGMENTS

The authors would like to thanks the managements of Frejus Scarl, composed of CLF SpA – as mandatory, AR.FER Srl, GEFER SpA, SALCEF SpA, PASOLINI VCB Srl, RTS S.A:, VALDITERRA SpA, as mandans, for the availability of the data and for their support as well as encouragement during preparation of this article.

Copyright © 2005 Taylor & Francis Group plc, London, UK

Rehabilitation of Malatya-Narlı No: 7 Railroad Tunnel

B. Divleli & E. Unal
Department of Mining Engineering, Middle East Technical University, Ankara, Turkey

ABSTRACT: In this paper, a case study associated with the rehabilitation of Malatya-Narlı No: 7 Railroad Tunnel is presented. The rehabilitation work included cleaning of two collapses and stopping of deformations occurring in the tunnel as well as characterizing the rock-mass by evaluating the cores obtained 67 drill holes. Due to two collapses occurred in the tunnel a large sinkhole developed at the surface. And the tunnel closed to the train traffic for about 10 months (September, 2002–July, 2003). Originally, the tunnel was excavated by Germans in the paleo-landslide material in 1930. The very poor rock-mass surrounding the tunnel consists of limestones, metavolcanics and schists. The problems related to the stability of the tunnel can be categorized into four main groups apart from the collapses and the sinkhole, namely; excessive displacements occurred in the tunnel, reduced tunnel span, poor rock-mass and underground water. Ground water circulating in the rock-mass has always given rise to stability problems. During field studies, 15 deformation monitoring stations were installed aimed at determining the deviation from tunnel alignment. In order to provide stability of the tunnel Self Drilling Anchors (MAI bolts) were recommended.

1 INTRODUCTION

The No: 7 Railroad Tunnel, having a length of 357 meters, was constructed inside the toe of a landslide material in 1930 using drilling and blasting method. Originally, the tunnel was excavated in horse-shoe-shape having a width of 5.5 meters and height of 5.25 meters. No: 7 Tunnel has experienced stability problems ever since the opening of the tunnel. The main problems are associated with the existence of a very poor rock mass around the tunnel, underground water and excessive deformations causing misalignment and time dependent deformation (creep).

2 LOCATION OF THE TUNNEL

No: 7 Tunnel is located on the route connecting Malatya, Adiyaman, Gaziantep and Kahramanmaras to each other. The tunnel takes place at the back of Alisliseki which is the part of Kapidere creek. Kapidere creek flows from North to South direction and passes through bottleneck at the location of No: 7 Tunnel.

3 ROCK MASS CONDITIONS

The rock-mass around the tunnel is melange type having a complex geology. The rock-mass around the tunnel consists of metavolcanics, schist, fractured limestone blocks, antigorite and radyolite in patches. The matrix material consists of clay and schist having low swelling potential. Limestone blocks are generally closely jointed and highly fractured. There are also voids inside the rock mass. RQD value around the tunnel is generally equal to zero (Ergun et al., 2002).

4 UNDERGROUND WATER CONDITIONS

The lithological units surrounding the tunnel consists of disintegrated schist and metavolcanics taking part as blocks in the matrix material. The complex structure indicates a medium permeability. However, the permeability level increases due to existence of dense cracks and fractures in limestone. The water-table is about 8–14 meters below the tunnel floor and it is located at the top of an alluvial strata. It is probable that this water table located on the alluvial strata triggers the tunnel to be displaced from the mountain side towards the creek side. On the other hand, the water precipitation leaking into the rock-mass around the tunnel has always given rise to instability (Ergun et al., 2002).

5 PROBLEMS AND CORRECTIVE MEASURES

The stability problems observed in and around No: 7 Railroad Tunnel can be categorized into six main groups.

Copyright © 2005 Taylor & Francis Group plc, London, UK

5.1 *Excessive displacements occurred in the tunnel*

An obvious misalignment was observed within 105 meters of the tunnel between km 155 + 550 and 155 + 655 and 35 meter section of it (between km 155 + 569 and km 155 + 604) was displaced about 1.70 meters over the years.

5.2 *Collapses occurred during rehabilitation work*

The first collapse in the tunnel occurred on July 30, 2002 due to breakage of the existing concrete-lining during enlargement of the tunnel span. The unsupported span was about 3 meters just before the collapse. This collapsed material flowed from the roof filled a 21-m long section of the tunnel between km 155 + 666 and 687. The volume of the collapse material flowed into the tunnel was estimated to be 500 m^3. Because of this collapse the tunnel stayed close to traffic for about 10 months. While cleaning up of the collapse material in the tunnel, a new collapse occurred at a 3 meter long section, on February 7, 2003 in such a manner that the loose material at the roof poured into the tunnel. The collapse occurred in No: 7 Tunnel is shown in Figure 1.

5.3 *Sinkhole developed at the surface due to collapse and rock mass flow into the tunnel*

As a result of two collapses occurred in the tunnel a sinkhole was developed at the ground surface as a result of 500 m^3 material flowed into the tunnel from the tunnel roof. The dimensions of the sinkhole were about 15 × 10 × 20 meters. The sinkhole developed in No: 7 Tunnel is shown in Figure 2.

5.4 *Reduced tunnel span and height preventing trains to pass freely*

The tunnel between km 155 + 550 and 155 + 655 have displaced through the creek side resulting an undulating shape of the tunnel, a reduced roof-span, deformed steel-arches, and cracked concrete-lining. Consequently, there were two serious problems namely, a reduced span and unstable tunnel. It was realized that there were number of sections through which trains could not pass.

5.5 *Poor rock mass causing instability*

As part of the project work carried out by METU Mining Engineering Department for TCDD (Unal, 2003), 67 coreholes drilled from inside the tunnel at various locations. It was determined that the rock mass around the tunnel is very weak and contains voids in the "displaced section" of the tunnel, in general, the RQD index value of the rock is equal to zero: Total Core Recovery (TCR), on the other hand, changes between 17 and 48%. TB-2 borehole drilling



(a)



(b)

Figure 1. (a) Apperance of the collapse. (b) Last stage of clearance of the collapse.



Figure 2. Sinkhole developed at the surface as a result of the collapse.

Copyright © 2005 Taylor & Francis Group plc, London, UK

made at the 122.5 meters from the Narli entrance progressed in alluvial sand at depth between 11.5 m and 21 m from the tunnel floor and terminated within ophiolite. Figure 3 shows a typical core box obtained from the drillings.

5.6 *Surface and underground water reducing tunnel stability*

The water always weakens the disintegrated rock mass and exerts pressure on concrete-lining thus reduce the stability. During the earlier studies, it was comprehended that the tunnel had been driven in paleo-landslide of melange type. Consequently, it is always expected to have underground water inflow at different sections of the tunnel, especially from the mountain side. During investigations it was also seen that a water drainage gallery at a distance of 40 m to the tunnel on the mountain side had been opened parallel to No:7 Tunnel aimed at relieving the effect of water. Nonetheless, this precaution worked partially, and the tunnel continued to deform together with the drainage gallery through the years. Along the both sides of the tunnel, drainage ditches were constructed inside the invert at the floor. The drainage pipes having a diameter of 200 mm and surrounded by geotextile were inserted along the tunnel bottom. In addition, along the mountain side of the tunnel, galvanized and perforated drainage pipes having a diameter of 75 mm and length of 10 m and spacing of 5.0 meters were inserted into the tunnel wall with a staggered pattern. The location of the upper holes of the drainage pipes were 2.0 meters and the lower holes were 0.5 m from tunnel bottom. At the creek side of the tunnel, in Sections 2, 3, 3/4 border, 4 and 8, drainage pipes having a length of 3.0 meters were inserted. On the earth surface above the tunnel, a total of 11 drainage wells, spaced 15 meters to the each other and having a diameter of 300 mm were sank vertically from the surface to the drainage gallery, in order to collect the surface and underground water inside the drainage gallery. During rehabilitation work, the earlier collapse in the drainage gallery was cleaned up. Drainage pipes having spacing of 1.0 meter, a diameter of 100 mm and a length of 0.50 meter were inserted into the walls of the drainage gallery. Figure 4 shows applied surface drainage system and details related to the surroundings of the tunnel.

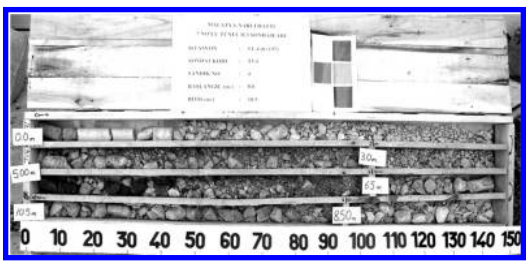


Figure 3. A typical core box obtained from the drillings.

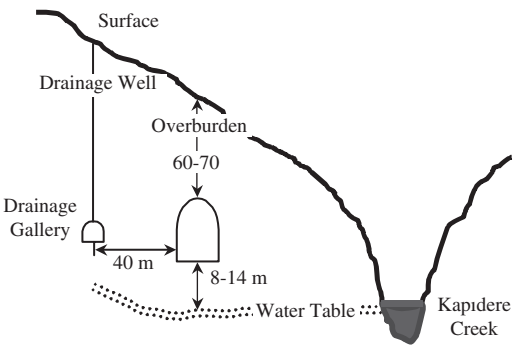


Figure 4. Surface drainage system and details related to the surroundings of the tunnel.

6 ROCK REINFORCEMENT IN NO: 7 RAILROAD TUNNEL

Based on existing rock mass conditions and the numerical studies carried out by using Phase 2D software, the lowest safety factor in the roof was found as 1.2. Consequently, Self Drilling Anchors (SDA) and ground injection were decided to be carried out. Figure 5 shows installation of Mai Bolts around the tunnel walls and floor of the tunnel.

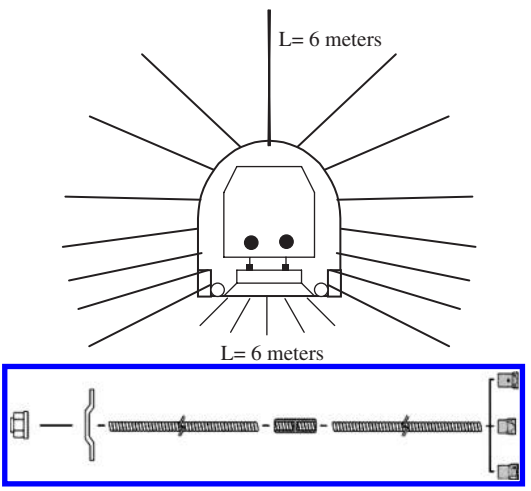


Figure 5. Installation of Mai bolts around the tunnel and floor of the tunnel.

Copyright © 2005 Taylor & Francis Group plc, London, UK

6.1 *Reinforced sections (at the walls of the tunnel)*

Before application of the bolting system, the tunnel has been divided into different support sections according to the bolting pattern used as A1, B and A2. The bolt lengths used in the tunnel was 6 meters. Section B was the most problematic section of the tunnel affected by excessive deformations and displaced towards the creek side as much as 1.70 meters. Figure 6 demonstrates application pattern and SDA applied sections of the tunnel.

6.2 *Stability of the floor*

After examining the cores drilled in different sections of the tunnel, it was realized that improvement of the tunnel floor was essential especially at Sections 2, 3, 4 and 9 owing to the voids under the bottom of the tunnel. There were neither concrete and invert nor support in the tunnel bottom at locations between km 155 + 545 and 631 and km 155 + 631 and 661. There were just ballast, concrete invert having a thickness of 0.15 m and other fittings under the rail.

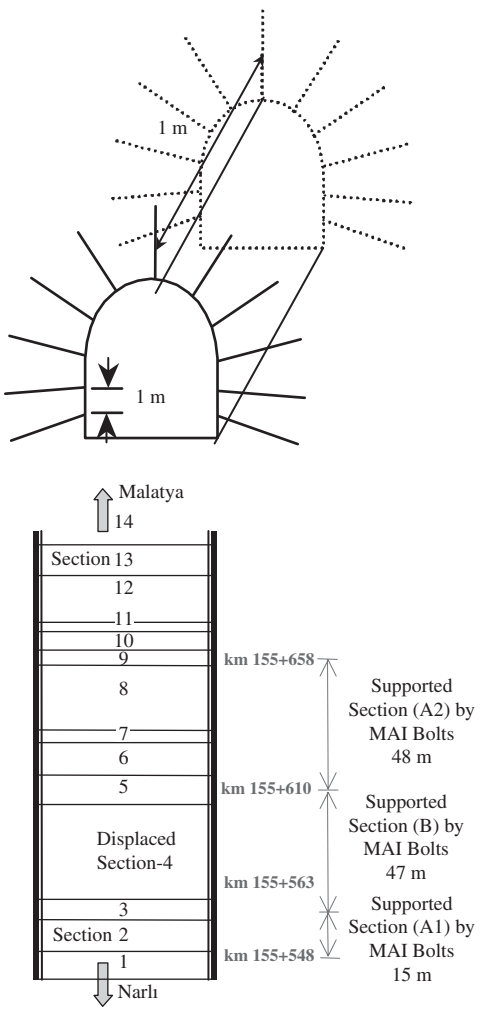


Figure 6. Mai bolt application pattern and SDA application sections A1 and A2.

7 FIELD MEASUREMENTS IN NO: 7 MALATYA-NARLI RAILROAD TUNNEL

In order to determine the short-term behaviour of the tunnel and to evaluate its stability, before rock reinforcement applications, a series of measurements were carried out by means of Distometer having a sensitivity of 0.01 mm (Divleli, 2004). During field studies a total of 15 deformation stations were installed in the tunnel. 11 of these stations were located in the deformed part and 5 of them in the non-deformed part of the tunnel. Each station consisted of 4 rebars. The two of them were fixed in roof and floor and other two in walls of the tunnel. The rebars fixed in the wall at the mountain side, between Stations 2 and 8 were 8.0 meters in length. Whereas the remaining rebars were 0.50 m. The reason why 8.0 meters long rebars were fixed at the mountain side was because of providing a relatively stationary (not moving) anchorage inside the rock mass and thus measuring the displacement towards the creek side. Figure 7 shows convergence measurement at a station.

Convergence measurements were taken as three times between the dates January, 22 and April, 30 in 2004. Consequently, the movement occurring due to displacement of the tunnel from the mountain side towards the creek side was tried to be determined. The measuring period was about 100 days. The measurement could not be taken after this period because rock reinforcement application was started in the tunnel. Table 1 shows measured convergence values.

The convergence values measured at Stations 9, 10, 11, 12 and 13, installed in tunnel Sections 8, 9, 10 and 12, were less than 1.0 mm. Although more data is needed to be able to interpret the results, it can be concluded at this stage that 167 meters of the tunnel is stable (including Section 14). The maximum horizontal movement was 8.78 mm at Station 4 probably due to compressive stresses acting from the mountain side. Consequently, it was concluded that there were still movement in Section 4. Sections 2 and 3 were the most problematic sections in the tunnel in terms of water effect, especially in rainy seasons. At Station 1, installed in Section 2 both horizontal closure and vertical dilation were observed. The rock mass in Sections 3 and 4, approximately 40 m in length, have a tendency of shifting from mountain side towards creek side. Based on the measurements carried out in

Copyright © 2005 Taylor & Francis Group plc, London, UK



(a)



(b)

Figure 7. Convergence measurement at a station.

the tunnel, it can be concluded that i. In tunnel Sections 2, 3, 4 and 7 (Stations 1, 2, 4, 5 and 8) there were both horizontal and vertical movements. ii. In tunnel Sections 6 (Station 7) there was horizontal movement only. Consequently, the rock mass in Sections 2 to 9 are still instable and requires rock reinforcement.

8 CONCLUSIONS

No: 7 Tunnel located between Malatya-Narlı railroad route was excavated within the heel material of a paleo-landslide. This was a big mistake in selecting a tunnel location on the first place. The No: 7 tunnel continuously faced with serious stability problems ever since it has been constructed.

During rehabilitation work, the two collapses occurred in different sections of the tunnel have been cleared up. In addition, a serious problem, namely the reduced tunnel span was extended to its normal width thus allowing normal train traffic-run again. In order to reduce the effect of water, drainage measures were taken on the surface and inside the tunnel.

To comprehend the short-term behaviour of the tunnel a total of 15 convergence stations were installed at different sections of the tunnel. The results of measurements indicated the possibility of tunnel shifting in particular locations. Hence, additional rock reinforcement was recommended.

REFERENCES

Ergun, U., Doyuran, V., Unal, E., and Ozgenoglu, A., 2002, "Malatya-Narlı Hattı km 155+465-822 Arasında Yer

Table 1. Measured convergence values.

Station No	Section No	Distance from Narlı side, m	Deformation (Vertical), mm		Deformation (Horizontal), mm	
			18.03.2004	30.04.2004	18.03.2004	30.04.2004
1	2	92	−1.98	−3.67	1.22	2.4
2	3	102	1.29	4.78	−1.87	1.22
3	4	115	0.84	0.31	−1.03	0.19
4	4	125	1.54	−0.21	7.91	−8.78
5	4	135	2.88	0.94	1.68	−0.48
6	5	146	0.49	1.15	−0.23	1.38
7	6	156	−0.19	0.30	1.48	−0.72
8	7	164	−1.26	−1.06	6.66	3.55
9	8	175	−0.74	−2.19	1.84	0.34
10	8	186	−0.78	−1.80	0.45	−0.08
11	9	195	−0.47	−0.82	0.07	0.19
12	10	200	−0.62	−0.06	0.27	1.25
13	12	210	0.53	−1.04	0.26	−0.1
14	12	221	0.43	−0.21	0.21	−0.56
15	13	231	0.27	−0.14	0.14	0.13

Copyright © 2005 Taylor & Francis Group plc, London, UK

Alan Tünel Islah Çalismalari Ön Raporu", METU, 31 pages.
Ergun, U., Unal, E., Doyuran, V., and Ozgenoglu, A., 2003, "Malatya-Narlı Hattı km 155+465-822 Arasında Yer Alan Tünel Islah Çalısmaları ve Dıger Seçenekler Hakkında Sonuç Raporu", METU, 64 pages.
Unal, E., 2003, Consultation Reports on Rehabilitation of No: 7 Tunnel, September 2003, November 2003 and December, 2003 (in Turkish).
Divleli, B., 2004, "Rehabilitation of Malatya-Narlı No: 7 Railroad Tunnel Master Thesis, 145 pages".

Copyright © 2005 Taylor & Francis Group plc, London, UK

Safety aspects of railway tunnel: Example of the Lötschberg railway tunnel

B. Crausaz, A. Weatherill & P. Gerber
FDK (BG & Emch + Berger AG), Switzerland

ABSTRACT: After the serious accidents, which happened in tunnels in the last years, most of the countries have established 'Task Forces' in order to evaluate the safety of existing tunnels and to establish new safety measures. Taking as example the Lötschberg railway tunnel, new safety measures particularly regarding ventilation system are presented in this paper. In view of the recent events of the year 2001 (terrorism act of the 11 of September and Gotthard fire on the 24th of October) particular attention should be turned on related safety aspects.

1 INTRODUCTION

The serious accidents, which happened in the Mont-Blanc and Tauern tunnels in 1999 and more recently in the Gotthard Tunnel, have highlighted the intrinsic difficulties of road and goods traffic in tunnels. Most of the countries with tunnels as part of their national infrastructures have established special 'Task Forces' which have decreed directives and instructions concerning traffic in road and rail tunnels. The safety aspects, particularly related to ventilation, of the Lötschberg rail tunnel project are analysed (35 km long) construction of which began in 1998 and will be completed in 2007.

The catastrophic fire of October 2001 in the Gotthard Tunnel has highlighted the performance of ventilation systems, the dangerous potentiality of goods transportation and the human factor.

North–South traffic and goods transport in Europe have to pass through the Alps where the relief and climate concentrate the links to few options, particularly to tunnels for convenience. Due to increasing traffic throughout the years, particularly goods transportation, these bottlenecks are overloaded. Therefore, even if fewer accidents happen intrinsically in tunnels compared to the remaining network, their configuration increases the consequences. As the probability of accidents raises in parallel to the traffic increase, safety aspects have to be improved.

2 THE LÖTSCHBERG RAIL BASE TUNNEL

2.1 *Presentation and characteristics of the tunnel*

2.1.1 *Switzerland: a country of transit*

Switzerland has always been an important transportation junction and transit country in the middle of Europe despite the obstacle imposed on it by the Alps. In these last thirty years, the transportation of goods between the North and the South of Europe has increased by a factor of six.

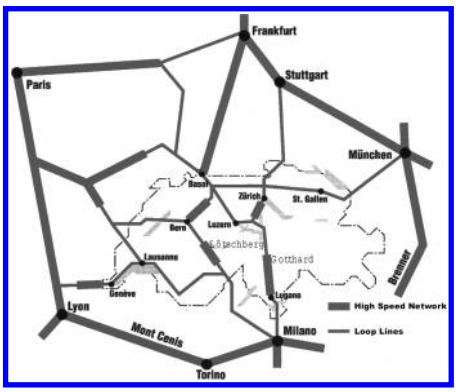


Figure 1. Rail & road links through the Alps.

2.1.2 *The consequences in Switzerland*

With the overloaded transportation network (rail and road), the environment is badly affected by noise and pollution. The quality of life and road safety are decreasing along the major highways. The saturation limits have long been exceeded.

2.1.3 *The AlpTransit*

Switzerland has been able to convince the European Community of the need to pursue a coherent transportation policy. With the Transit Agreements, the combined rail and road traffic also includes Europe.

Copyright © 2005 Taylor & Francis Group plc, London, UK

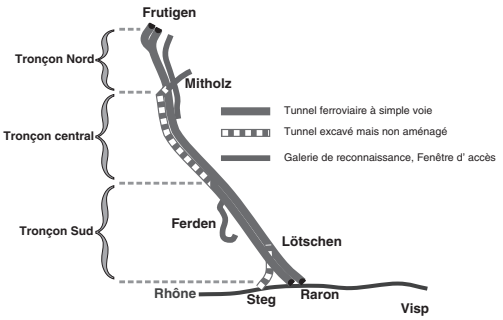


Figure 2. The Lötschberg base tunnel.

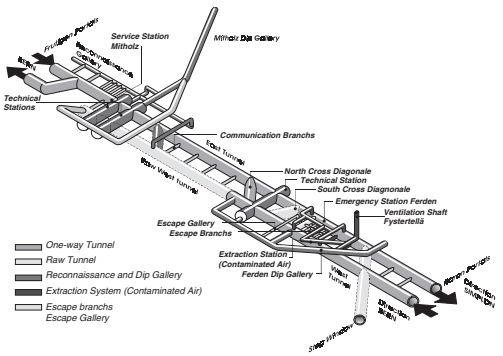


Figure 3. Overview of the Lötschberg base tunnel.

The role of the Alps is preserved for tourism and for the protection of the environment, because trains do not emit so many noxious substances. AlpTransit, the new railway link, will permit to cross easily the Alps. This project is based on four constituent elements:

– The key element will be the new and additional railway route Arth-Goldau – Lugano with the Gotthard (57 km) and Monte-Ceneri (13 km) base tunnels
– The base railway route from Frutigen to the Rhône valley (Lötschberg Tunnel, 34.6 km) will complete the picture in order to avoid a concentration of traffic on the Gotthard
– The Simplon route connected to the French TGV (Macon–Geneva) will connect the French part of Switzerland to the northern part of Italy and France
– The traffic routes East of Switzerland will be improved (Zurich–St-Gall).

2.1.4 *The Lötschberg base tunnel*

The Lötschberg base tunnel will be built to accept different classes of train, from goods transportation to passenger trains. The tunnel will also accommodate high-speed trains and therefore will be designed for a maximal speed of 250 km/h.

Basically the tunnel is a two-tube tunnel comprising a rail tunnel East and West. But in the first phase the two-way tunnel will be open from Raron (South Portal) to the North of the emergency station in Ferden. The remaining part of the tunnel northwards will be a one-way tunnel as far as train operation is concerned (except at the North Portal in Frutigen).

3 SAFETY CONCEPT OF THE TUNNEL

Despite railways being a statistically safe form of transportation (due to guidance per rails, professional drivers, etc.) rail accidents may still happen. Even if accidents occur less often in tunnels (e.g. no level crossings, which cause most of the train-related accidents) the severity of the accidents increase seriously due to the tunnel configuration, not to mention the psychological impact attributed to such events. In Switzerland, the last accidents with fatalities occurred in 1971 and in 1932. The safety concept of the Lötschberg tunnel should bring a substantial improvement compared to the existing lines of the rail network. With a partial two-tube tunnel, access via two galleries, as well as a window gallery and reconnaissance gallery, an essential improvement in rail tunnel safety should be achieved.

3.1 *Safety philosophy*

Safety is considered basically as the characteristic of quality, which has to be guaranteed throughout its life period. It is based on the following four elements:

– Protection objectives (‘protection of the endangered person’ i.e. passengers, personal, etc. and ‘protection of the natural environment, the constructions and technical installations and their use’ by order of importance)
– Danger analysis and evaluation of risk
– Safety measures
– Implementation.

These objectives are considered to be obtained when:

– Principle 1: all necessary measures have been met in relation to the potential danger
– Principle 2: all necessary measures have been met in relation to the technical and scientific standards which are applicable and the relevant circumstances.

The railway operator is responsible for its installations and the safety measures. In relation to the opening of the railway network for ‘free access’, international jurisdiction takes on new importance. Protection objectives and safety measures play a very important role for the operator.

Copyright © 2005 Taylor & Francis Group plc, London, UK

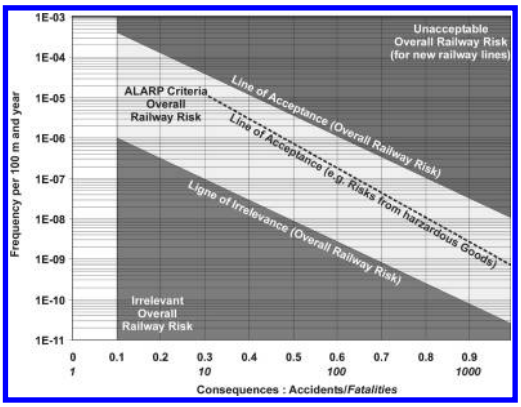


Figure 4. F-C diagram.

3.2 *Methodology of the risk assessment*

As part of the complex process of constructing a long railway tunnel, a safety analysis and concept serve the future operator to guaranty a high level of safety. The procedure consists of two steps:

1. A Qualitative Safety Analysis in order to limit the range of accident scenarios and related concepts, and to identify appropriate safety measures for all the tunnel sections. It should also define the appropriate laws and applicable national and international norms and regulations.
2. A Quantitative Risk Analysis is used on the relevant hazard scenarios derived from step 1 only where this previous step was not able to define appropriate measures. Using international and domestic statistical data (available in Switzerland from the CFF and the BLS) and considering the effects of the safety measures, each event is quantified with the frequency of its occurrence and the extent of its consequences.

In order to better define the remaining risks after having taken all essential preventive and curative measures, (so-called 'residual risk'), the representation used is the frequency-consequences diagram, which allows for optimisation of the safety measures by means of applying specific assessment criteria and evaluating the acceptability of the risk in order to adjust said assessment criteria.

The diagram is subdivided into three ranges:

– unacceptable overall railway risk for new railway lines.
– ALARP (As Low As Reasonably Practicable) Criteria for overall railway risk.
– Irrelevant overall railway risk.

In the area limited by the unacceptable risk and the irrelevant risk, the risk is to be reduced as far as it is technically and operationally possible and should be contained within reasonable limits.

The risk assessment has been carried out taking the following critical events into consideration:

– Industrial accidents
– Accidents involving injury (passengers, others)
– Fire (all type of trains)
– Derailments
– Collisions
– Losses of hazardous goods
– Operation failures
– Terrorism/violence.

3.3 *Objectives*

From the results of the risk analysis, several objectives have been identified. A new tunnel cannot be designed without adopting the following measures:

– Measures to prevents incidents (appropriate conveys, railway well-maintained)
– Measures to reduce fatalities and damages
– Measures to improve self-rescue opportunities
– Measures to improve the possibilities of external rescue.

The measures will also affect the rolling materials, but here, as the tunnel will be open to free access, requirements of materials on trains cannot be guaranteed. Due to the length of the tunnel and the difficulties involved for rescuers to get to the scene of the accident, self-rescue measures are essential during the initial phase. The safety measures should also ensure that rescuers are able to accomplish their duties.

3.4 *Self-rescue*

The event sequences, which have occurred in the past in tunnels, show that a great priority has to be attributed to self-rescue measures, particularly during fire. Given the great velocity at which a fire spreads and due to the high temperature, reduction of oxygen concentration, loss of visibility and propagation of toxic fumes, those persons who are able to escape rapidly have a fair chance of getting themselves to safety on their own.

Therefore, the following aspects have to be considered:

– Length of escape paths and indicators
– Equipment along the escape gallery (lighting, ventilation)
– Communication infrastructure (telephone, radio, etc.)
– Education for tunnel users.

Copyright © 2005 Taylor & Francis Group plc, London, UK

3.5 *Rescue by third parties*

In order to facilitate the job of external rescuers, some measures have to be considered such as:

- Accessibility of tunnel portal
- Accessibility to the scene of the accident (extraction of and fresh air supply)
- Rapidity of intervention (training, planning, etc.).

4 ITERATIVE PROCESS USING RISK ANALYSIS

The safety planning is an iterative process that is constantly updated on the last tends in various domains.

The iterative process encompasses domains such as operation scenarios, alarm and rescue concept, quantitative risk analysis and Aerodynamics calculations.

4.1 *Designing escape ways by simulation of crowd movement*

As example of the iterative process to check the safety concepts, the escape ways in the emergency station have been designed in number, size and the interval between them based on simulation of crowd movement.

The methodology of designing escape ways by simulation of crowd movement is based on the simulation of movement of crowd in order to be able to predict the position of persons at any time. To know the location of persons is very important in order to delimit the risks encountered by these persons as regard to their exposure to high temperature and toxic fumes. The characteristics of crowd movement is based on Predtechenskii & Milinskii. The movement speed of persons depends largely of the crowd density, which is calculated with the floor surface of definite classes of people.

After the stop of a train in the emergency station, the simulation enables to calculate at any time the number of persons remaining in the train, on the station platform, blocked in front of doors and in the safe area.

With this methodology the platform width, the number of escape doors and their width can be determined in order to design a safe evacuation of the train passengers in the emergency station.

4.2 *Interval between cross passages*

With similar methodology, the interval between cross passages (communication branches) has been conducted. In the case of emergency stop in the tunnel, passengers have to evacuate through cross passages.

The limitation of the number of cross passages is of economical interest. An iterative safety planning based on risk management assessment, simulation of crowd movement and simulation of smoke propagation has been conducted by varying the distance between cross passages.

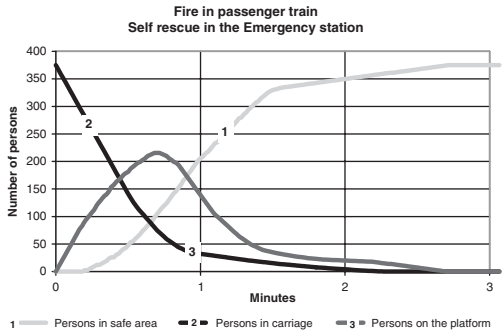


Figure 5. Example of passengers repartition during evacuation in the emergency station.

The results are shown with the F-C diagram for different interval between cross passages. The interval has been fixed to 333 m.

The distance between these cross-passages influences the self-rescue proceedings and the exposition time during which passengers are exposed to smoke.

The effects on the individual risk, varying the distance between the cross-passages e.g. to 500 metres, are examined by the simulation of crowd movement.

The simulations showed that depending on the position of the train referring to the position of the cross-passages and depending on the position of fire within the train, the evacuation time for passengers may vary distinctively, considering:

- longer escape routes
- longer stay in smoke-laden air
- mutual obstruction of escaping passengers with partial back-ups.

The risk profiles (Fig. 6) show the significant increase of consequences for the event 'fire in a passenger train and stop elsewhere in the tunnel'. Considering all scenarios, the distance between the cross-passages is in a certain range a less decisive parameter for the summarised overall risk profile (Fig. 7). This fact can be explained by the other preventive measures taken (e.g. emergency stop stations with ventilation which can be reached in most of the cases of a fire in a passenger train) in the safety concept, having much larger effects on the risk profile. Nevertheless it was decided to keep the 333 m distance warranting self-rescue conditions as safe as practicable in the Lötschberg base tunnel.

4.3 *Simulation of lethal zones*

The calculation of smoke movement and lethal zone is used as part of the iterative process of safety planning,

Copyright © 2005 Taylor & Francis Group plc, London, UK

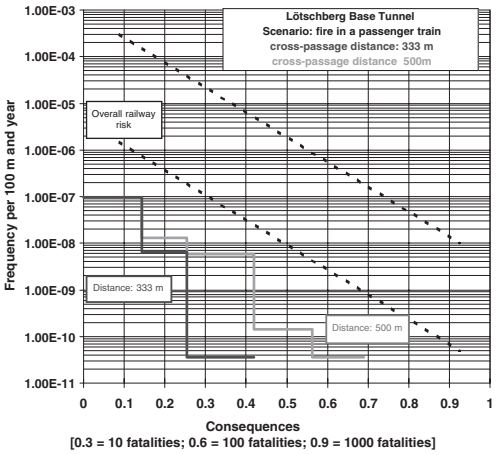


Figure 6. F-C diagram for different interval between cross passages – scenario 'fire in a passenger train'.

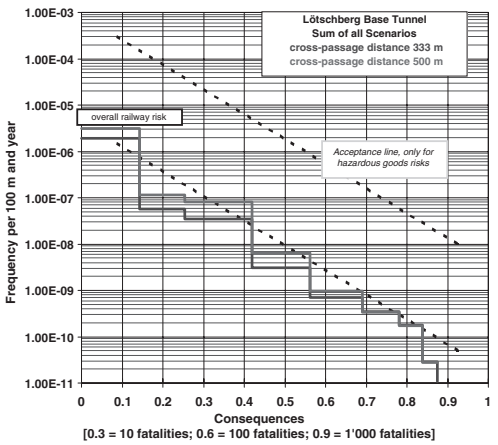


Figure 7. F-C diagram for different interval between cross passages – sum of all scenarios.

for determining among others the number of fatalities due to exposure to high temperature and toxic fumes generated by the fire. The limit of dangerous exposure to smoke is difficult to evaluate. It depends largely of the time of the exposure and of the concentration of toxic fumes. To determine a limit after which a person is no more able to self-rescue is defined with the help of a so called FED (Fractional Effective Dose) variable. The FED is the quotient of the quantity of CO_2, CO and O_2 to the quantity of this gas, which causes an incapacity of self-rescue. The FED is integrated on the gas concentration, which the person is exposed to.

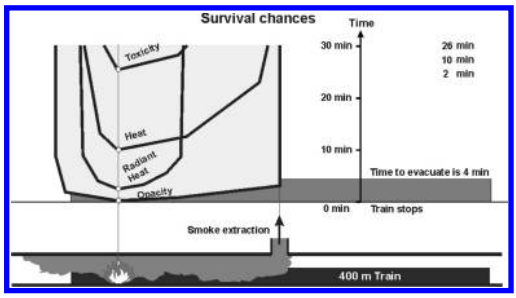


Figure 8. Results simulation of the survival chances in the tunnel (Emergency station) with the program TUFISI.

The same approach on toxic gases can be used for the heat duress. Heat causes thermal shock (hypothermia), skin and breathe burn.

One of the calculation tools used was the program TUFISI (TUnnel FIre SImulation), which used a mathematical model based on 2 layers separated in a number of parallelepipedal segments. Each segment is divided in 2 layers, with homogeneous properties, the upper one represents the hot gas while the under one the cold gas.

This program was validated by the Memorial Tunnel Fire Test Program in West Virginia and in Ofenegg Tunnel in Switzerland.

The tool enables to calculate the dimension, temperature and density of the upper and under layers, the speed flows, heat production as well as different gas concentrations and distance of visibility.

The fire is entered as a fuel source burned variably along the time depending of the rate of oxygen (reference fire of a passenger train with max. 20 MW).

The following lethal conditions can be determined:

– Distance of visibility
– Toxic gas production (CO_2, CO, lack of O_2)
– Heat.

The ventilation in the emergency station should improve the protection of passengers during self-rescue. The ventilation will extract smoke and provide with fresh air the station in order to enable an evacuation free of smoke.

Two scenarios were studied: the first one ventilation of the safe zone without extraction, the second one with extraction.

The output of the first scenario shows that the smokes spread South and North along the train. Toxic gases and visibility hamper self-rescue. On the other hand the heat duress is confined around the fire. The output of the second scenario, i.e. with smoke extraction, shows that the local extraction impedes self-rescue from fire to the extraction point. Therefore the opening of an appropriate damper based on fire location leads to the reduction of this zone.

Copyright © 2005 Taylor & Francis Group plc, London, UK

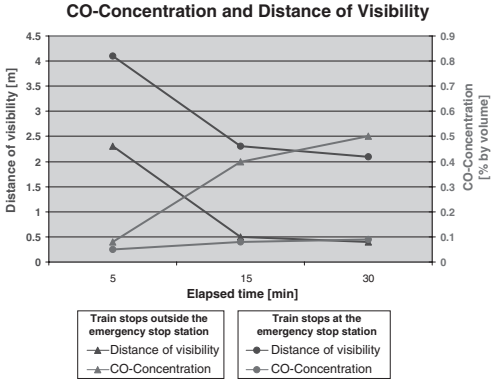


Figure 9. Co-concentration and distance of visibility for two scenarios (downwind).

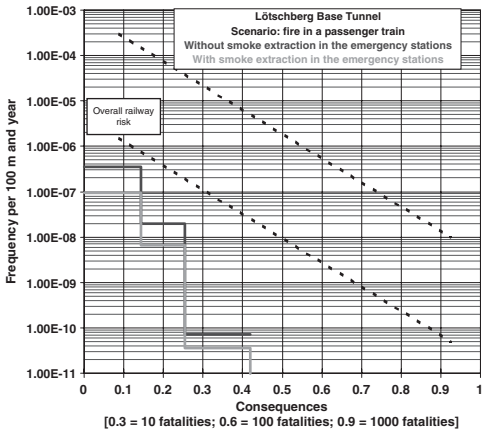


Figure 10. F-C diagram with and without smoke extraction in the emergency station – scenario 'fire in a passenger train'.

The outcomes of the calculations are then used as inputs in the safety planning.

As example the following F-C diagram shows the improvements due to extraction in the emergency station compared to without extraction.

5 VENTILATION CONCEPT FOR FIRE

5.1 *Service and emergency stations*

The safety measures will prevent a train already on fire from entering into the tunnel. Should this occur or in the event that a train should catch fire in tunnel, experience has revealed that the train will continue to roll a considerable distance (about 20 km). Two stations, the service station Mitholz (which can later be transformed into to an emergency station) and the emergency station Ferden situated at approximately 20 km from the opposite portal, will greatly facilitate self-rescue, evacuation and intervention of the rescuers. Of course, it stands to reason that there can be no certainty that trains will be able to stop at these stations. It is therefore necessary that any safety concept include scenarios for a train stopping along the entire length of the tunnel.

The service station Mitholz will serve as a rescue station in the event that a train on fire stops in the station. A platform of the length of the station (approx. 440 m.) will cater for the victims of an emergency, who will then move to the reconnaissance gallery Kandertal. From there, they will pass through airlocks and be evacuated by buses.

Ventilation will be raised to its maximum capacity in order to ensure a safe environment for the self-rescue of the passengers from the service station to the reconnaissance gallery.

The emergency station Ferden is made up of two rail stations, one per tunnel (East and West) with a length of 450 m. A platform will enable the victims of an accident to use one of the six escape galleries spaced at intervals of 85 m and which lead to a protected and ventilated zone between the two tunnels. Any injured travellers can be picked up by ambulance, which can enter the tunnel from the Ferden dip gallery and reach this zone via the lock under the ventilation station of Ferden. The evacuation of any victims will follow by train via the safe tunnel.

In an emergency mode, the fresh air ventilation system in Ferden will provide air to the escape zone and the safe tunnel as well as to the tunnel, where the train is on fire by passing through the escape galleries. Any victims fleeing the scene will thus have a safe escape route free of smoke.

Smoke is extracted via seven dampers, one of which will be opened nearest to the position of the fire, so as to ensure optimal extraction of smoke as well as maximum visibility in the tunnel. The smoke is extracted by the ventilation station Fystertellä through a ventilation shaft.

5.2 *Safety concept in case of fire outside (South) of the emergency station*

In case that a burning train has come to a stop South of the emergency station (i.e. in the twin tunnel), the evacuation of passengers shall occur through communication branches spaced every 333 m nearest the location where the train has stopped. Another train will take the victims to the exterior of the tunnel. The ventilation system will go into emergency mode; the fresh air system (station Ferden) will blow its maximum air capacity at the same time that the exhaust system (station Fystertellä) will begin extracting at its

Copyright © 2005 Taylor & Francis Group plc, London, UK

maximum air capacity. This will create a pressure difference between the safety zone and the tunnel with the train under fire in order to prevent the smoke from hampering any escape efforts through the communication branches.

Coherent planning is needed in order to provide for the safe passage of trains, to allow the rescue train access to the tunnel and to prevent any other trains from entering the tunnel during an emergency. Planning is also required in order to organise rescue operations.

6 CONCLUSION

The objective of this paper was to show the benefit of an iterative process of safety planning in the design of a modern railway long tunnels.

Safety concepts have to take into account the following consequences of an accident or fire in a tunnel:

- The consequences of what might at first appear to be an incident of a relatively harmless nature can rapidly take on dramatic proportions
- In the case of fire, the most dreaded incident, the smoke and heat can rapidly cause the scene and the surrounding area to become a potentially fatal place
- The problems encountered when evacuating tunnel users and getting rescuers to the scene of the accident.

In this last case scenario, the time it takes rescuers to get to the scene is often longer than life expectancy in an emergency situation. Victims of an accident or emergency must be able, in an initial phase, to take charge of their own rescue (self-rescue).

The route along where evacuation takes place or rescuers progress to the fire place must not be located in the affected tunnel. An escape gallery or tunnel or other access route must provide access to the scene of the accident as well as allowing victims to be evacuated.

Tunnel operators and fire-fighters must be subject to regular drills, which must be as realistic as possible.

Past experience and experiences currently being acquired in the area of tunnel security aim at constructing or improving tunnel infrastructure in order to:

- Detect abnormal situations and rapidly inform tunnel workers and users of any danger
- Provide protection and facilitate evacuation of tunnel users and access of rescue workers
- Optimise preparations in view of the possibility of fire.

The safety planning is a tool to find measures for the highest security objectives. Nevertheless the risk factor will never be reduced to zero even though we must do everything in our power to reduce the risks to the greatest extent possible.

Copyright © 2005 Taylor & Francis Group plc, London, UK

Tunnel refurbishment under railway operations

A.W. Ackermann
Civil Engineer FH (B.Sc.), Amberg Engineering Ltd., Regensdorf, Switzerland

F. Modetta
Civil Engineer ETH (M.Sc.), Amberg Engineering Ltd., Regensdorf, Switzerland

ABSTRACT: Because numerous railway tunnels have reached an advanced age, many being well over 100 years old, railway companies are faced with the task of insuring safety and serviceability of their structures through refurbishment measures. In the interest of the railways, construction methods are employed which enable operations to be disturbed as little as possible. The refurbishment of rail tunnels during operations places tough demands which must be dealt with during project planning and realization. Cramped spatial conditions, short net intervals for works and often dangerous working conditions require suitable and innovative solutions.

1 REASONS FOR REFURBISHMENT

1.1 *Maintenance and renewal of structural materials*

The insufficient condition of structural materials often necessitates construction measures in order maintain the safety of the structure.

Another common goal of construction measures may be to guarantee operational safety and to reduce the required amount of maintenance. Typical construction measures for these purposes include the localized waterproofing and drainage of water so that damage to railway installations can be prevented and/or to prevent the protrusion of ice into the clearance envelope. Furthermore, refurbishment measures also have a preventative character against advancing damage to structural materials.

1.2 *New operational requirements*

Occasionally increased clearance demands necessitate construction measures. More powerful and larger engines, panorama vehicles and wagon-loading transport require a larger clearance envelope. Higher speeds require a correction of the track position or an optimization of the geometrical alignment. Additional utilities may also require more space for installations.

1.3 *Increasing safety*

Fires in various road tunnels in recent years (Mont-Blanc, Tauern, Gotthard-roadtunnel) have led operators and authorities to increase the amount of self-rescue equipment in railway tunnels. Installations such as escape paths, fire resistant lighting and handrails all require specific construction measures.

2 STATE ASSESSMENT

The condition of a tunnel must be known in order to develop an effective refurbishment concept. As the knowledge of the current condition increases in detail and accuracy, the more precisely an evaluation of construction measures can be carried out.

The purpose of investigations is to assess the structural elements of a tunnel as well as the installations (track, signals, etc.). But other external factors such as geology and hydrology, the clearance requirements of rolling stock and compliance with the current regulations must also be integrated into the state assessment.

3 ECONOMIC FACTORS

3.1 *Construction costs*

Refurbishment measures in tunnels during railway operations are generally quite expensive. The rates of construction performance lie significantly lower than that which is achieved under normal conditions.

The construction contractor generally has only short work intervals available (i.e. night shifts). Often the length of night shift is between four to six hours. The available length of a shift is dependent upon the traffic frequency of the affected railwayline.

Main lines of railways, especially, have undergone a heavy increase in traffic density in recent years. A good example is Swiss Federal Railways, which intends to

Copyright © 2005 Taylor & Francis Group plc, London, UK

offer 30% more capacity on their network over the next ten years. With these circumstances in mind, it can be assumed that the time available for tunnel refurbishment works will decrease in the near future.

The construction process is hindered by cramped space or by interruptions due to railway traffic.

Due to the crowded conditions in a rail tunnel, only smaller construction machines and equipment can be used. Even today, numerous construction procedures must still be carried out by hand.

3.2 *Costs for the owner*

Reductions in operations and temporary measures such as the replacement of rail service with buses result in reduced profits for the railway operator. Additionally, public rail transportation can suffer from profit reductions caused by hindrances in operations due to construction works. Works which cause hindrances over longer periods of time increase the risk that the customers who are forced to use individual transportation during construction will not return to public transportation once service is restored. In addition, the public, i.e. the potential rail market, tends to perceive restrictions to rail traffic negatively. The damage to reputation resulting from suspensions in services which are perceived as too frequent or too long is not directly calculable in terms of money, but is surely disadvantageous to the railway.

Other costs to the client during tunnel refurbishment works include those associated with safety personnel, use of special rail wagons for the construction trains, project management, and various railway specialists which may be needed for to provide services such as provisional power supply, etc.

3.3 *Study of variations*

Due to the high costs and the extremely difficult operational constraints, the following questions must be answered before the start of a refurbishment project:

– is a new tunnel more economical?
– does the tunnel have to be refurbished during operations or can the traffic be diverted for a defined period of time?

These questions must be answered within the scope of the earliest design phase, the preliminary design.

A comparison shows that the meter price of a comprehensive refurbishment under difficult conditions can reach an order of magnitude equivalent to that of new construction.

The example of the Disentiser Tunnel of the Matterhorn Gotthard Bahn shows that a study of alternatives does not necessarily have to favor refurbishment.

Table 1. Comparison of average refurbishment and renewal costs carried out during operations with new construction costs.

Construction costs	Costs per meter Euro/ meter tunnel
Lining refurbishment (waterproofing and drainage, lining repairs, local profile enlargement, local strengthening of lining)	1,500–3,500
Renewal/Replacement of tunnel lining	6,000–15,000
Renewal/Replacement of tunnel invert	6,000–15,000
New construction 1 track-Tunnel	10,000–20,000
New construction 2 track-Tunnel	10,000–30,000



Figure 1. Construction of the new Disentiser Tunnel (right) during operation of the old tunnel (left), which was permanently filled after the new tunnel was put into service.

3.4 *Ensuring operational safety*

For tunnel refurbishments during operations, reduced or even normal rail operations must be maintained over the entire construction period. For the contractor, this means:

– The safety of the structure must be permanently guaranteed.
– The clearance envelope may not be violated during periods of operation.
– The construction site must be prepared and cleared in short intervals of time so that the line can be put back into service on time.
– In cases in which rail service and construction occur simultaneously (e.g. in double-track tunnels), the construction works may not hinder railway traffic, and at the same time, the safety of the workers must be ensured.

It is easy to see that tunnel refurbishments during operations place significant technical and logistical demands upon the affected parties.

Copyright © 2005 Taylor & Francis Group plc, London, UK

Two case studies and the solutions applied to them will be presented in the following chapters of this report.

4 CASE STUDY: MAGNACUN AND TASNA TUNNELS (CONSTRUCTION 2000 TO 2002)

4.1 *Condition before refurbishment*

The line between Bever and Scuol-Tarasp of the Rhatian Railway in Lower Engadine passes through several tunnels which were built at the beginning of the 20th century. The two longest tunnels are the Magnacun Tunnel with 1,909 meters and the Tasna Tunnel with 2,351 meters.

Both structures are constructed entirely of broken and cut natural stone masonry. Their condition had become increasingly worse over the last few years.

The tunnel lining of both tunnels was heavily saturated in some sections. The joint mortar was heavily deteriorated and locally destroyed due to frost effects.

Masonry bonds at the abutments of the side walls were locally loosened. Horizontal and vertical cracks were discovered at several locations in masonry joints or completely through stones.

Further damage included missing stones which had fallen from the tunnel vault as well as various spalls in shotcrete which had been applied to strengthen the lining.

Aggressive groundwater was the cause of local deterioration of existing shotcrete and corrosion to the rails.

The clearance conditions in both tunnels were extremely tight throughout and insufficient in some areas.

4.2 *Geology*

The Magnacun-Tunnel is driven through a sliding mass of a gorge in the "Unterengadiner Fenster" formation which consists mainly of slate with gypsum layers, gneiss and amphibole. Surface slope movements can be observed in the entire region. It had to be concluded that the slope movements influence the area of the tunnel.

The Tasna Tunnel lies geologically in an extremely difficult terrain of slates containing gypsum and a thrust fault.

4.3 *Refurbishment concept*

The concept of the works was selected to minimize immediate costs. For this reason, only selected sections of both tunnels were chosen for refurbishment. Careful monitoring had to be carried out in these sections to ensure clearance requirements were met. The tendering of works included the classification of the tunnel into various priority classes.

4.4 *Installations and logistics*

Construction had to be carried out during rail operations. Work in the tunnels could therefore only be carried out in night shifts, whereby the last scheduled train was replaced by bus service. During the day, trains were able to provide scheduled services.

Travel to the tunnel portals was only possible by rail. For this reason, all supply and waste disposal had to be handled by construction trains. All works also had to be carried out from these trains. Driving on the tracks with road vehicles was not possible as the risk of track damage was too high and could have resulted in interruption in rail traffic.

In 2000, two different construction trains were in use, one for sealing and shotcrete works and the other for demolition and support works (shotcrete, rock bolts, and reinforcement). Both consisted of several flat cars upon which mixing equipment, aggregates silo, supply installations, vault saw and high pressure water equipment were installed. Parking and material loading stations for both of these construction trains were provided near the Ardez rail station.

In 2001 and 2002, a third construction train was deployed from the Scuol-Tarasp station. A specialty of this construction train was the Dubrava shotcrete system which enabled fully automatic dosing of water, cement and additives.

Stationary equipment was placed at the portals of both tunnels in the form of large doors with integrated ventilation systems for use during construction. The doors were closed and put into operation during the night shifts. Mobile equipment included a small backhoe as well as a mobile drilling rig.

Near the railway stations Ardez and Scuol-Tarasp, installation areas were set up for material deliveries and preparations for works at the tunnel sites. The



Figure 2. Construction train at the installation site in Ardez.

Copyright © 2005 Taylor & Francis Group plc, London, UK

delivery of construction materials up to the reloading points was carried out by rail. At both locations the construction trains were loaded in the daytime for the approaching night shift. Mortar and cement were put on pallets and reloaded over a temporary ramp. The installation area in Ardez had the necessary containers for construction management, workers and incidentals.

4.5 *Safety*

Because the works were carried out during the nightly break in operations, a clear division between construction and railway operations existed. Before the start of each nightshift, the affected section of the line was closed to railway service. Each morning the stretch was officially reopened. During the nightly closure, the catenary system was turned off and earthed.

Each morning before reopening, the construction site and the track was checked to ensure the clearance envelope was not infringed upon.

4.6 *Work intervals*

The partial renewal was realized during the construction season of 2000–2002. It must be taken into consideration that the works were carried out in eight to nine hour shifts at night and that normal operations were conducted during the day.

The work interval provided by the client includes the entire break in normal railway operations. The amount of time for travel to and from the construction site as well as the preparation time at the start (including the grounding of the catenary system) and the clearing of the site at the end of the night shift must be subtracted. These tasks took about 30 minutes each night.

Because of the location of both tunnels at about 1400 m above sea level, works could only be carried out seasonally from spring until fall. Concrete work was not possible at winter temperatures.

The works each year were carried out from mid-April until mid-November. This results in a 7 month construction period.

4.7 *Construction costs*

Thanks to the chosen installations concept, it was possible to carry out the works without disturbing normal rail service.

The partial refurbishment was carried out within budget.

The costs can be summarized as follows:

Construction:	ca. 6,750,000 Euro of which approx. 20% was for installations
Costs of the owner:	ca. 1,120,000 Euro
Meter costs:	ca. 1,850 Euro/Tm

The costs of the client made up about 15% of the total costs.

4.8 *Summary*

The logistical concept developed for the partial refurbishment of the tunnels Magnacun and Tasna which consisted of deploying of one or more construction trains proved successful. It enabled the contractor to quickly prepare for works and to clear the site each day. If works in the future must be carried out in the invert of the tunnel, other solutions will have to be found.

5 CASE STUDY: EMMERSBERG TUNNEL (CONSTRUCTION 2004)

5.1 *Condition before refurbishment*

The 761 meter Emmersberg Tunnel which was opened in 1895 is located on the railway line Etzwilen-Schaffhausen, between the stations Feuerthalen and Schaffhausen. The tunnel has an elliptical profile and was lined with natural stone masonry made of cut limestone (upper Jurassic). The owner and operator of the tunnel is the Swiss Federal Railways who was also the client for this project.

Exploratory bores and maintenance works in the tunnel invert (1998) showed that no substructure had been built in Emmersberg Tunnel. The ballast was separated from the moraine rock surface (hardened glacial deposits) only by an approx. 5 cm thick sand layer.

The ballast layer of 20 to 25 cm thickness measured from the top of the sleepers was generally too shallow. This resulted in a poor stability of the track system, which suffered local twisting and settling of the rails.

Groundwater could not be effectively drained as a result of sand deposits in the drainage system, longitudinal drainage pipes which were located too high and the lack of drainage perpendicular to the tunnel axis. Water backed up in the tunnel invert which caused a saturation of the underground, resulting in mud deposits and ultimately the instability of the track system.

The instability resulted in a rocking movement of the rolling stock, through which dangerous scraping collisions with the tunnel walls were possible.

During various inspections of the tunnel, points of water infiltration with the presence of sand deposits were observed in the side walls and in the tunnel crown.

These wet areas reduced the durability as a result of heavy corrosive effects upon the track supports and the rails.

5.2 *Geology*

The tunnel passes through a solid moraine as well as very fine and somewhat dry partially saturated

Copyright © 2005 Taylor & Francis Group plc, London, UK

sand. The geological conditions in the direction of Feuerthalen was predicted to be a fine water-bearing sand, while the geology in the last 300 m of the tunnel in direction Schaffhausen was expected to be predominantly moraine, and in the worst case dry sand. During construction it was discovered that this area contained predominantly fine grained water-bearing sand which led to some difficulties during project realization.

5.3 *Refurbishment concept*

The clearance problematic as well as that of the track system and substructure were solved through renewal of the tunnel invert including a lowering of the track level. At locations where clearance violations were expected even after the lowering of the invert, local profile enlargements were conducted.

The concept called for a phased construction approach. In a first phase, preparations and some of the works in the vault were carried out during night shifts. This preliminary phase lasted nine weeks. During the subsequent main phase, an eight week interruption in rail operations was planned for works in the tunnel invert. After putting the tunnel back into service, the rest of the works in the tunnel vault was planned to be completed in a final phase during night shifts. Renewal of the invert during operations with use of a temporary construction bridge was not applied due to cost considerations.

As a substitute for the temporarily suspended rail operations during the main phase, bus replacements for commuters were arranged. Cargo transport was temporarily rerouted.

5.4 *Installations and logistics*

In the preliminary phase, all works took place during the night. A construction train was used in which the wagons were used for the purpose of material transport and as working platforms. Various construction materials and equipment were transported into the tunnel, unloaded and utilized. Cutting works were carried out with a special saw mounted onto rail wagon.

Rail-compatible equipment was used at times such as a backhoe mounted with wheel flanges and equipped with drilling equipment.

Shotcrete supply to the site was realized with silos which were located at the installation site. The material was transported to the construction site using a transport pipe. The shotcrete was delivered during the day by truck and loaded into the silos.

As suggested by the contractor, a provisional access ramp to the tunnel was built leading from a vehicle accessible lot up to the elevated level of the railway. The ramp enabled access to the railway during phases in which the line remained in operation as well as direct access to the tunnel during the main phase of refurbishment.



Figure 3. Preparation of access ramp.

Driving over the track with road vehicles was also prohibited during this project. Otherwise rail operations during the day could not be guaranteed.

Rail-compatible vehicles, on the other hand, were allowed and could access the tunnel directly over the ramp during all phases of the project.

During the main phase, the construction materials and equipment were stored directly next to the tracks.

The installation concept allowed a large degree of flexibility, because the construction site was not 100% dependent on rail access. In addition, the transition from the preliminary phase to the main phase could be realized smoothly.

5.5 *Project changes*

On July 7, 2004, a water-bearing sand pocket located approx. 300 m from the portal Schaffhausen was encountered during excavation work in the invert. Due to the fact that several buildings are located above the tunnel, ground settlements had to be avoided. The working procedures were therefore adapted to the new circumstances. The length of invert excavation and concreting stages were reduced to 2.5 m. To provide extra support during construction, two steel braces were applied in each excavation stage.

The bearing capacity of the invert was increased. Over 300 m, a reinforced slab invert constructed of cast-in-place concrete was built in order to resist any horizontal forces from the masonry lining.

5.6 *Work intervals*

During the preliminary phase, night shifts were limited to six hour intervals. 20 minutes were needed for both preparations at the start of each shift and for

Copyright © 2005 Taylor & Francis Group plc, London, UK

clearing the line at the end of each shift. Advantageous for the contractor was the short access distance of approx. 300 m from where construction train was parked to the tunnel.

Because of the change in construction procedures, the main phase of works was increased from eight to eighteen weeks. During the main phase, works were carried out seven days a week and in three shifts.

The final project phase which was carried out during night shifts was reduced to seven weeks by realizing some of the vault refurbishment during the longer main phase.

5.7 Construction costs

Construction works are scheduled for completion on December 11, 2004 with additional costs of approx. 1 million euros. The total construction costs at that time are estimated at 3.5 million euros. In the area with the strengthened invert slab, construction costs will be approx. 7,500 euro/tunnel meter.

6 FINAL COMMENTS

Complete closure of a tunnel during refurbishment works is today only possible on railway lines of secondary importance.

The higher the traffic frequency, the more likely the option of building a new tunnel will be realized, in some cases combined with a subsequent refurbishment of the existing tunnel. Additionally, as the number high-speed rail lines come into operation, new challenges for the refurbishment of tunnels during railway operations arise due to the fact that works on and next to an operating high-speed line are nearly impossible.

On the other hand, planners and contractors continue to work on new innovations. New methods of construction as well as innovative installation and logistics concepts are constantly under development in order to meet the new demands of modern rail traffic, and to ensure the continued necessity of maintenance and refurbishment works can be carried out in the future.

SOURCES

Ackermann A.W, Modetta F. 2003. Final Report, "Tasna- und Magnacuntunnel, Teilerneuerung"

Modetta F, 2003. Project Design Report, "Linie 820 Feuerthalen – Schaffhausen, Sanierung Emmersbergtunnel".

Copyright © 2005 Taylor & Francis Group plc, London, UK

Renewal of the Alpine San Bernardino tunnel with traffic flowing

Peter Wenger
Amberg Engineering Ltd., Sargans, Switzerland

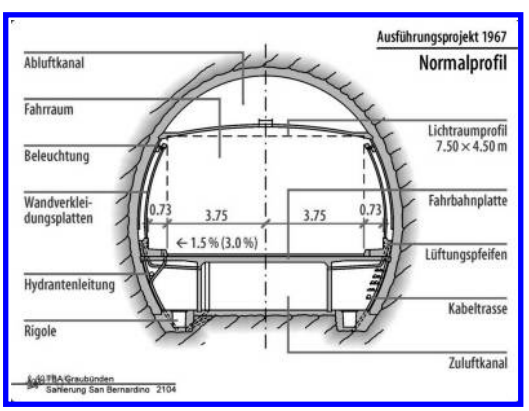
Louis Schönenberger
Amberg Engineering Ltd., Chur, Switzerland

ABSTRACT: The tunnel was opened 38 years ago and is therefore renewed thoroughly by:

– Adjusting the safety concept (new ventilation for fire and operation, emergency exit gallery)
– Replacement of the carriageway under traffic, with one open lane from Monday to Friday and two open lanes on weekends.
– New carriageway as reinforced concrete slab without joints under a number of special conditions as for examples operational within 24 hours after curing, concrete treatment with add on layers and curing during low temperatures.

1 TUNNEL PRIOR TO RENEWAL

The San Bernardino road tunnel lies at an altitude of 1600 m. above sea level and is 6.6 km long. On the south side it drops off with a gradient of 0.4%, on the north side with a gradient of nearly 1%. The tunnel was officially opened for traffic on December 1, 1967.



Two-way traffic prevails in the tunnel. A single-shell concrete arch supports the rock, and thin-walled concrete lining elements keep seepage water off the roadway. An enterable fresh air duct flanked by utility ducts are arranged under the roadway. The exhaust air duct is located above the traffic space.

In addition to the two ventilation facilities at the north and south portals, the tunnel is ventilated by two underground facilities, Aria and Sasso, which are connected with the surface by inclined shafts. The cross ventilation system is dimensioned for peak traffic of 1500 vehicles per hour. Secondary ducts spaced 5 m apart blow fresh air into the traffic space, and identically spaced openings in the intermediate ceiling extract the exhaust air.

The average daily traffic of nearly 2300 vehicles in 1968 grew to over 6200 vehicles (more than 10% of them trucks) in 2003.

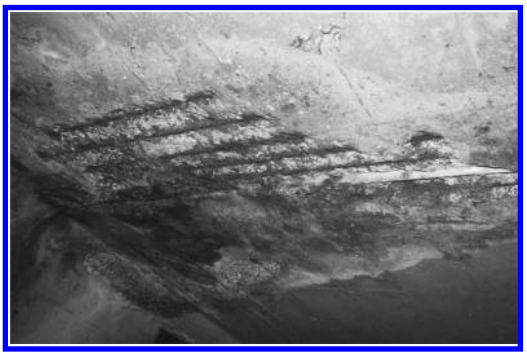
Over 35 years of operation have left their marks on the tunnel. A systematic visual inspection and various investigations have shown that, while the tunnel is still serviceable, progressive damage over the years has jeopardized its operational safety. Consequently, various parts of the basic structure and the electro-mechanical equipment are badly in need of refurbishment and modernization.

The existing roadway slab has suffered corrosion damage, some of it very severe. Around the joints – every 2.5 m – the bottom layer of reinforcement is in very poor condition. The conditions here are highly conducive to corrosion. Wherever the concrete coverage is insufficient, heavy rust damage is found. The damage is caused mainly by the practice of spreading de-icing salt in the winter combined with a lack of effective sealing.

The intermediate ceiling is generally in good condition, which indicates that it can be expected to

Copyright © 2005 Taylor & Francis Group plc, London, UK

remain sufficiently durable in the future. Only the first 250 meters of intermediate ceiling at the north and south portals have to be renewed to eliminate the damage caused by salt spreading. Except for these portal areas, the mainly unreinforced tunnel crown has suffered only local damage from aggressive ground water.



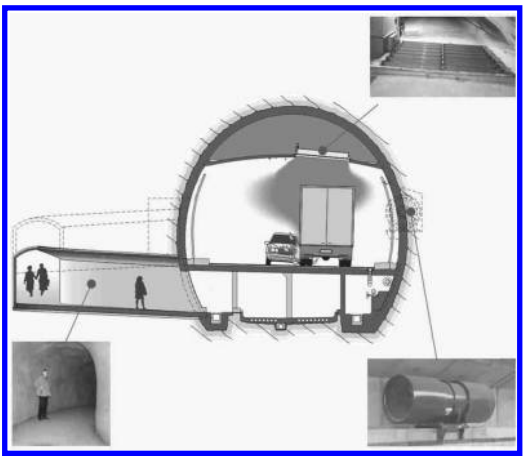
The following objectives were established for the San Bernardino Tunnel renewal project:

- Safe operation to be ensured at all times.
- Durability and quality of the structural substance to be maintained and secured (service life of at least 50 years without further renovation).
- Electromechanical systems to continue serving operation of the tunnel for 25 years without renovation.
- Closure of the tunnel during the construction work is out of the question for political reasons. So the flow of traffic has to be maintained while the work is done. Other cantons or regions may not be subjected to additional traffic as a result of the project.
- Any traffic obstruction should be restricted to a short period of time. The work in the tunnel's traffic space is to be limited to just a few years, and no traffic obstruction will be tolerated during the heavy traffic period of summer.

The renewal project should result in easier operation and servicing of the tunnel equipment, and also in reduced maintenance expenses.

The catastrophic tunnel fires that occurred in France and Austria in the spring of 1999 necessitated a review of the safety concept in the event of a fire. This review produced the following project amendments and modifications:

- Installation of an escape route that employs the two central channels under the roadway as escape and life-saving galleries, and construction of escape exits spaced 350–375 m apart on the west side of the tunnel to provide access to the escape gallery.
- Adaptation of the ventilation system, especially the fire ventilation, to the present state of the art in this field.



2 RENEWAL PROJECT

During the structural renewal of the San Bernardino Tunnel, various parts of the structure are being renovated or replaced:

2.1 *Lowering of the invert*

The tunnel invert around the central channel was lowered by 50 cm. The need to demolish most of the existing concrete base solved the problem of the concrete damage that had occurred over the years. Lowering the invert provided the additional overhead clearance required for future use of the channel as an escape and life-saving gallery.



The cramped conditions necessitated the use of special, extra-compact machines for this work.

Mechanical excavation equipment was used to demolish the concrete and excavate the invert rock. Special tractors and cars were used to cart the debris out of the tunnel.

When the new concrete base was poured, it also included a cable conduit installation that includes all of the cable connections required for operation of the

Copyright © 2005 Taylor & Francis Group plc, London, UK

tunnel during the construction phase. Formerly, these cables were carried on open racks in the west channel.

2.2 *Escape exits*

A total of 17 escape exits were built on the west side of the tunnel to connect the traffic space with the escape gallery.



Because the blasting work had to be carried out in the immediate vicinity of the existing structure without interrupting the flow of traffic, some rather drastic restrictions had to be imposed. For one thing the work had to be done during the low-traffic nighttime hours, and for another the charge quantity was limited to 200 g per blast. The excavation work was monitored by means of continuous vibration detection.

2.3 *New ventilation system*

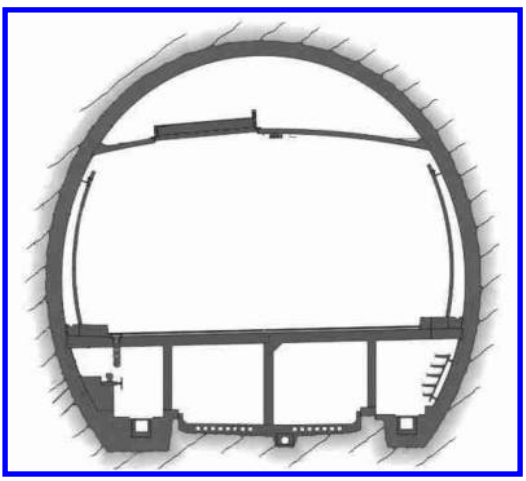
The ventilation system was converted from transverse air flow to longitudinal air flow with extraction at regularly spaced intervals. If needed, fresh air can be blown into the traffic space at both underground ventilation facilities. Two groups of 6 jet-fans each are needed to regulate the longitudinal air flow.

For the point-by-point air extraction system, openings roughly 5 m^2 in size were broken out of the intermediate ceiling every 96 m and articulated fire dampers were installed in them. The old extraction openings were closed off with plates. The jet-fans are placed in niches along the side of the traffic space. The mechanical excavation work and concrete placement were carried out during the night without interrupting the traffic flow. The jet-fans installed in the niches are about 1.40 m in diameter and have a power rating of 37 kW.

2.4 *Renewal of the roadway*

The central element of the refurbishment project is renewal of the roadway. This includes the preliminary work, the actual renewal of the slab, and the roadway finishing work.

The various preparatory jobs included removal of the wall panels and the lighting system installed above the panels on both sides, milling away of the old pavement over the entire roadway width, and demolition of the catwalk on the east side to provide the necessary clearance for traffic during the roadway renewal.



The new roadway consists of a jointless, reinforced slab that is supported across its width by three walls and bears on the vault in both side-walls. Two of the support walls are located at the same points as the existing walls, while the third divides the central channel into the new escape and life-saving galleries.

The finishing operations that complete the roadway renewal comprise:

- Sealing: The entire surface of the slab is sealed to protect it against harmful effects from the traffic space. Sealing is achieved by applying a fully bonded web of polymer/bitumen.
- Catwalk: The catwalks installed on both sides of the roadway consist essentially of prefabricated concrete elements.
- Pavement: Conventional two-layer bridge pavement with 6 cm of HMT B16S topped off by a 3 cm layer of AB 8S.
- Roadway drainage: Every 25 m the roadway water exits through drains and flows down into the cast-iron sewer under the roadway slab. Settling/flushing traps are installed every 100 m (or every 50 m near the portals).

The individual worksteps of these finishing operations are carried out in rapid succession, because this work is also done with the traffic flowing and is subject to the same restrictions as the slab renewal work.

Copyright © 2005 Taylor & Francis Group plc, London, UK

2.5 *Renewal of the traffic space*

The traffic space renewal includes refurbishment of the intermediate ceiling and the crown, plus prefabrication and installation of the wall panels.

Investigations of the condition of the intermediate ceiling and the crown led to the conclusion that the intermediate ceiling is generally in good condition and, assuming unchanged or better humidity levels in future, does not require total refurbishment. It was therefore decided merely to repair local damage and observe the future ambient conditions with a monitoring system.

At both ends of the tunnel, however, the condition of the reinforced intermediate ceiling (over the first 300 m or so inside each portal) is poor and requires thoroughgoing refurbishment. This means jetting off the concrete down to the reinforcement, replacing the reinforcement where necessary, and then reprofiling with high-grade sprayed mortar.

3 SPECIAL ASPECTS OF THE RENEWAL PROJECT

3.1 *Restrictions on working hours*

During the construction work, the following restrictions and rules have to be observed.

- Work starts on Sunday at 22.00 hours and stops on Friday at 14.00 hours. Single-lane traffic wherever and whenever work is in progress.
- During weekends, holidays and the 4-week period of heavy traffic in summer, two-lane traffic must be maintained at all times.
- Maximum length of the work site is 800 m, and only one work site is permitted in the tunnel at any given time.
- Maximum 20 minutes of tunnel closure for setting up and clearing the work site. Separation of normal traffic from works traffic.

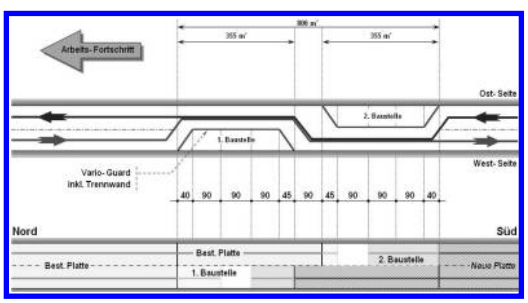
3.2 *Slab renewal in stages*

In order to observe these restrictions without impairing work progress, a concept was developed involving step-by-step operations at two mutually independent subsites.

These two subsites, set up in tandem with a traffic crossover in between, cover a total length of 800 m. The first subsite is used for renewing the west side and erecting the new central partition. The east side is then renewed at the second subsite. Work progresses at the same rate at both subsites.

A fixed weekly cycle was defined for renewing the roadway slab at the west and east work sites. Within one week, the following work has to be completed to replace 90 meters of slab:

- Cordoning off of the existing roadway for demolition of one lane with a row of posts in the middle of the existing roadway.
- Cutting of the existing slab into transportable sections of concrete.
- Removal and carting off of the concrete sections
- Installation of formwork elements, placement of reinforcement, and pouring of concrete for the new slab.
- And finally topping off of the concrete surface with an epoxy layer.



3.3 *Traffic control*

It was necessary to develop a safe and efficient traffic control system for the specific purpose of handling the single-lane traffic within the 800 m long work site. The system had to take these factors into consideration:

- In view of the rear-end collision that had occurred in the Tauern Tunnel (Austria), a solution with a red light ahead of the work site with resultant backups in the tunnel was out of the question.
- At both portals, the entry of jobsite vehicles via a separate access had to be possible as frequently as necessary.
- These works vehicles had to be able to enter and (more importantly) leave the work site in the tunnel safely and as frequently as possible.
- The truck traffic on the San Bernardino route, which was held back and allowed to pass alternately in one direction only, did not have to be accorded any special treatment by the work site traffic control system.

In spite of these supplementary conditions, the traffic capacity had to be maximized and the the cycle time kept as short as possible.

The traffic control installation VRA02 was developed to meet the above requirements.

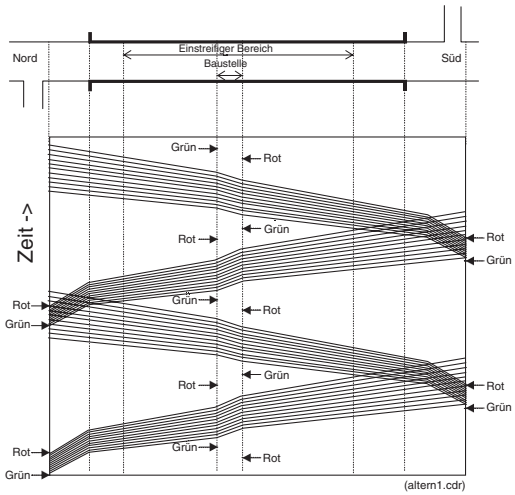
Briefly, the traffic control system works this way:

- The traffic lights at the portals are set to operate so that the batch of vehicles released by the green

Copyright © 2005 Taylor & Francis Group plc, London, UK

light reaches the single-lane zone at the work site in time to pass through it smoothly.

Traffic lights are also placed ahead of and following the work site to prevent vehicles arriving too early or too late from entering the single-lane zone.



Besides fullfilling all of the above requirements, this optimized control system keeps the cycle time to about 15 minutes under normal traffic conditions, which is considered tolerable for the drivers.

3.4 *Concrete roadway slab*

Early strength. The need to make the tunnel available for 2-lane traffic on weekends means that the new section of roadway must be able to withstand traffic quite early. The concrete formulation and the formwork design were established with this in mind:

– Early strength of the concrete
  The concrete can be driven on only after 24 hours. At this point its compressive strength must be at least 10 N/mm^2.

Because this requirement is mandatory for releasing the roadway for traffic, the slab's changing strength must be monitored. The concrete's weighted maturity according to de Vree was prescribed for this measurement. The temperature change of the concrete as a function of time is measured at 6 different points and integrated over time with the help of the so-called maturity computer. As soon as the sum arrived at in preliminary tests has been reached, the concrete has achieved the necessary early strength. Along with this indirect measuring method, the strengths of test cubes are measured regularly after 24 hours.

– Load-bearing formwork design
  Because the concrete's bearing capacity after 24 hours is not sufficient to withstand the lateral forces around the wall supports with the necessary safety margin, the formwork must be able to absorb the traffic loads and also be exceptionally stiff. The deformations that do occur must be so small that the concrete can absorb them without suffering damage.

Concrete curing. Special curing measures are required to suit the young concrete for traffic. The surface is sealed with epoxy resins to prevent drying out and provide additional protection against chloride penetration. Sealing with epoxy has the added advantage that it affords relatively long-term protection of the concrete surface despite the traffic-caused erosion. Because the epoxy coating also serves as substrate for the main seal, it must be compatible with this seal.



800 grams of epoxy and 2.1 kilograms of silica sand per m^2 are applied to the freshly poured, semi-rigid concrete. The heat produced by the setting concrete helps cure the epoxy, so that it is sufficiently strong by the time the road is released for traffic.

Frostproofing measures. Because of the altitude (more than 1600 meters above sea level), the work is carried out in climatic conditions that are sometimes extreme. This necessitates the use of frostproofing measures during the mixing, transport, placement and curing of the concrete.

The following requirements must be met:

– Production of the concrete
  The mixing plant must be capable of producing concrete with outside temperatures as low as −20°C. The admixtures must be stored in encased boxes or silos. The fresh concrete temperature must reach 20°C at all times, which means that the mixing water and admixtures must be heated.

– Transport of the concrete
  The concrete must have a temperature of at least 15°C when it is poured. Temperature losses during transportation of the concrete should be kept as

Copyright © 2005 Taylor & Francis Group plc, London, UK

low as possible (short transit time, preheating of transport vessel, insulation of transport vessel).

– Shelter
  A shelter must be built for protection of the concrete pouring location in the traffic space. It protects against drafts and reduces the energy consumed for heating.
– Heating
  The concrete work locations have to be kept at a temperature of no less than 15°C. This ensures that the concrete will reach its required early strength. In addition, the channels under the roadway slab and the shelter in the traffic space are heated. Oil burners are used for heating.

3.5 *Safety aspects of tunnel operation*

The tunnel, which is more than 30 years old, no longer satisfies today's safety requirements. So the entire tunnel had to be adapted to the currently applicable safety specifications. The new requirements were drawn up on the basis of ASTRA.

The most important changes made to meet today's safety standards are:

– New fire ventilation system with extraction points every 96 meters and a linear fire detection installation.
– Creation of an escape route with 17 exit connections from the traffic space into the escape gallery.
– Creation of a life-saving gallery for the emergency squad.
– Installation of fire emergency lighting every 50 meters on the tunnel side with the escape exits.
– Simple and clear signs marking all safety equipment and escape routes.
– New hydrant system with pillar hydrants roughly every 125 meters.
– New SOS niches with emergency phones and fire extinguishers roughly every 250 meters.
– Visual guidance installation on both catwalks.
– New wall cladding panels in light colors to improve lighting conditions.

Various studies were carried out to investigate the effects of fires on the intermediate ceiling (such as simulated calculations, static double-checks, fire tests in the Hagerbach Test Galleries VSH). The studies and tests showed that, assuming the newly installed fire ventilation system functions properly, the intermediate ceiling will not be damaged by passenger car fires (from 1 MW to 5 MW fire) and will suffer only local damage in the event of bus or truck fires (from 20 MW to 30 MW fire).

3.6 *Safety aspects during construction*

During the construction phase, the safety needs of vehicle occupants, contractor personnel, electrical contractors, supervisory staff and tunnel operation must be observed. Various measures are taken to ensure this:

– Renewal in stages
  The ventilation system was renewed before the main work started. So more efficient extraction of fumes would help limit the effects if a fire should ever occur during the construction phase.
– Jobsite
  Various measures have been instituted to protect the tunnel traffic from immissions from the work sites and vice versa. These include:
– The use of Vario-Guard barriers and a partition reaching to the intermediate ceiling separates the traffic space clearly from the work site.
– Increased light intensity in the work zone.
– Integration of the tunnel ventilation system into the construction ventilation.
– Life-saving and alarm scheme

Establishment of organizational measures and provision of various equipment for improving safety (such as communication devices, life-saving apparatus, fire extinguishers, etc.).

4 CONSTRUCTION PROGRAM AND COSTS

4.1 *Costs*

– Electromechanical systems (hardware and software).
  Costs totaling CHF 41 million or about 19%.
– Construction work.
  Costs totalling CHF 142 million or about 64%.
– General expenses (planning and design, work related to tunnel operation, etc.).
  Costs totalling CHF 37 million or about 17%.

4.2 *Construction program*

The renewal work started in 1998 and is expected to be complete at the middle of 2007.

Lowering of the invert Construction (Lot 1) had to be carried out first in order to provide the necessary space for the subsequent activities. This work started in mid-1998 and was completed at the end of 2001.

Construction (Lot 3) with the safety installations started in mid-2001 and was completed at the beginning of 2003, when the roadway renewal work was starting.

The main construction phase (Lot 2), including renewal of the roadway, started at the end of 2002 and is scheduled to be completed by the end of 2006.

Construction (Lot 4), which includes installation of the wall cladding and the electromechanical systems in the traffic space, will be completed by mid-2007.

This means that the totally renewed San Bernardino Tunnel is expected to commence normal operation after a construction period of 9 years.

Copyright © 2005 Taylor & Francis Group plc, London, UK

Energy-saving lighting system for road tunnel

S. Nagai
Eight Consultants Co., Ltd, Japan

S. Ishida
Chuden Engineering Consultants, Japan

M. Shinji & K. Nakagawa
Yamaguchi University, Japan

ABSTRACT: Road tunnel lighting system requires brightness for safe recognition visually, in order to avoid other vehicles and passengers, and as a result, standard values to be maintained level are determined. In general, road tunnels in JAPAN, brightness is adjusted from time to time depending on the brightness outdoors and by employing peak and off-peak periods in compliance with standard values. However, lighting is continuously kept on regardless of the existence of users during a 24-hour period. The ESTL (Energy-Saving Tunnel Lighting) system the authors proposed in this paper is a system targeting mountain tunnels for which traffic volume is remarkably low, and contributes to the prevention of the greenhouse effect through a drastic reduction in CO_2 levels. At the same time, ESTL reduces energy waste, secures safety and provides a comfortable visual environment. In this paper, authors introduce the ESTL system, and discuss economical effects of this system. And numerical simulation will be done to estimate actual traffic conditions and electric power consumption amounts.

1 BACKGROUND OF THE SYSTEM CONSTRUCTION

It is required to challenge for the environmental issues around world. And each country's response toward reduction of greenhouse gases in the atmosphere has significantly changed since the Kyoto Protocol in 1997. Most of the causative agents of global warming are from carbon dioxide (CO_2) generated by combustion of fossil fuels, and reduction of this CO_2 is a critical problem-solving key. In households and offices, activities are performed, as measures for CO_2 reduction, such as diligently turning off the lights in rooms not in use, adjusting the set temperature of air conditioning, introducing energy-saving type high-efficiency equipment, and shifting over to hybrid cars, where use of natural energy, such as solar power generation and wind power generation, is also becoming steadily popular.

In the road lighting field, development of appliances high in lighting efficiency and introduction of new light sources are also proceeding rapidly, but with road lighting installed at a minimum to ensure safety, substantial CO_2 reduction is difficult under present circumstances. This time, focusing on road tunnels that particularly consume power in road lighting, we have proposed and constructed a new system to significantly reduce the amount of electric energy used. Road tunnel lighting should have sufficient brightness for drivers to safely view and avoid other vehicles, obstacles, road alignments, etc., and standard values to be maintained are also specified. In general road tunnels, the in-tunnel brightness is adjusted as needed to meet a standard according to outdoor luminance and the period of time, where lighting is kept on regardless of the presence or absence of users on a 24-hour basis.

The ESTL (Energy-Saving Tunnel Lighting) construction method we proposed here contributes to the prevention of global warming through significant CO_2 reduction, targeting extremely low traffic mountain tunnels, by adjusting the in-tunnel brightness in conjunction with sensing technology while ensuring safety and a comfortable visual environment, so that the required brightness is secured only for the utilization time.

2 SYSTEM CONFIGURATION

This system, employing high-efficiency Hf fluorescent lamps (High frequency fluorescent lamp) excelling in

Copyright © 2005 Taylor & Francis Group plc, London, UK

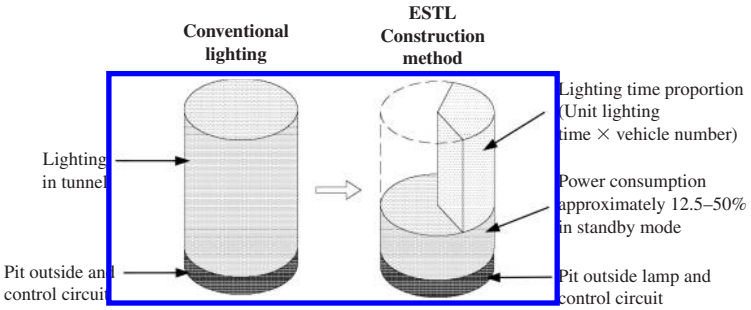


Figure 1. Power-saving model.

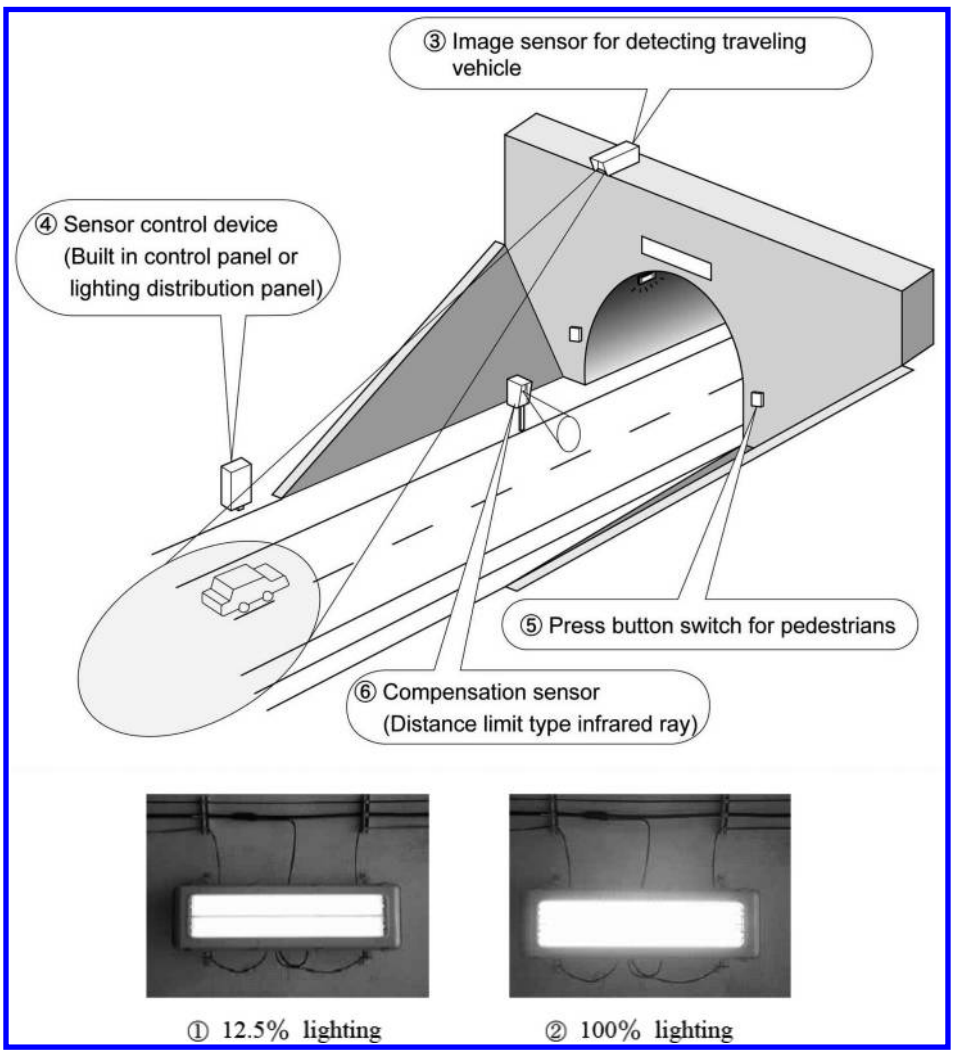


Figure 2. System configuration.

Copyright © 2005 Taylor & Francis Group plc, London, UK

color reproducibility as light sources, provides a user-friendly visual environment, in which the lighting is maintained at 12.5%–50% optical output when no vehicle passes, and when the approach of a vehicle is detected by the image sensor provided at the entrance of the pit, the in-tunnel lighting is turned on to a 100% lighting condition to meet a standard until the vehicle passes through the tunnel. The system configuration in actual operation is shown in Figure 2.

3 SYSTEM OPERATION FLOW

The system operation of ESTL are as follows;

1. When no vehicle passes, the tunnel lighting is in standby mode consuming as low as 12.5% power (1).
2. The image sensor for detecting a traveling vehicle (3) detects a vehicle outside the tunnel pit.
3. The sensor control device (4) judges the approach of a vehicle to turn on the in-tunnel lighting in a 100% lighting condition according to outdoor luminance and the period of time (2).
4. For pedestrians, base lighting is assured with a push-button switch (5) provided at the entrance of the pit.
5. In the event of detection by mistake or abnormal traveling that could not be judged appropriately, it can be handled by back up with a compensation sensor (6).
6. After passage of a vehicle or pedestrians, the low power consumption state is restored by a timer.

The image sensor for detecting a traveling vehicle measures the changes of brightness in the image processing detection area by using the luminance signal video signals, which judges the presence or absence of a vehicle from the difference in luminance between the road surface and a vehicle.

Since it can respond to vehicle speeds of approximately 10 to 80 km/h, and is able to determine the direction, and also offers high accuracy and a wide range of detection, vehicles entering a tunnel across the center line and two-wheeled vehicles can also be



Figure 3. Image sensor for detecting traveling vehicle (3).



Figure 4. Detected image.



Figure 5. Sensor control device (4).



Figure 6. Press button switch for pedestrians (5).

Copyright © 2005 Taylor & Francis Group plc, London, UK



Figure 7. Compensation sensor (6).

detected. In this system, a control device performs processing from capturing of images to judgment of the presence or absence of a vehicle and determination of the direction of entry, and then control signals are output to lighting circuits.

4 LIGHTING CONTROL FLOW

Figure 8 shows the control flow of the ESTL construction method, in which outdoor luminance, such as clear weather, cloudy, or nighttime, is judged by an automatic dimmer, and each circuit of A to C is turned on/off to obtain an in-tunnel brightness suitable to the condition. In clear weather, circuits from A to C are turned on, and in cloudy weather, circuits B and C are turned on, and during nighttime, circuit C is turned on. Since this system is adopted for extremely low traffic tunnels, a 12.5% upper stage lighting standby condition results in most periods of time. On the contrary, all circuits are always operated in a 100% lighting condition as shown in a middle stage in typical tunnels, where power is wasted in most periods of time with no passage.

5 EFFECT OF INTRODUCTION

A data logger was attached to the control section of a tunnel in which this system had been introduced to collect data of traffic condition, lighting time of each circuit, power consumption, etc., for one month. Table 1 shows a summary of the data.

6 EFFECT OF INTRODUCTION

As a result of introduction of this system in this tunnel, the average daily traffic of which is 175 vehicles, we could confirm that the tunnel lighting had operated at 28.1% power consumption of the conventional system.

This corresponds to 698.9 kg CO_2 in terms of CO_2 emissions that are reduced by one-month operation, which means that approximately 8.4 t CO_2 is reduced yearly. (Calculations are based on 0.36 kg CO_2/kWh from data by the Ministry of the Environment.)

The reduction effect of the system increases with decreasing passage of vehicles and during days with longer-time lighting of the clear weather circuit. While the reduction rate tends to drop in rainy weather in which the tunnel entrance does not need to be so bright during the daytime because the power required for one day is itself small. Figure 10 shows one day's movement in power consumption. From this, it can be seen that this system operates at 25–30% power of a conventional system during the nighttime, when a nearly constant reduction effect can be obtained, and although the standby power requirement during the daytime is slightly high, the reduction in the amount of power used is considerably wide since the power of entrance lighting, which is remarkably large in a conventional system, is minimized by the ESTL construction method.

7 CONSIDERATION AND FUTURE PROSPECTS

As in the above, a considerable amount of energy could be saved by the ESTL construction method.

However, continued efforts must be made to further upgrade the effect and ease restrictions on system construction through redoubled improvements. This system needs to be in a standby mode in a low output condition due to the necessity of raising safety and optical output to specified values instantaneously upon sensor detection, wherein normally the standby lighting is carried out at 12.5% output.

However, since the air temperature affects the lighting rise time and luminous flux (amplitude of the optical output), such a contrivance would be necessary to compensate for it as slightly raising the output during standby when the temperature is low. Also, the unit lighting time per user is set from the passing time that is determined by tunnel extension and traveling speed, and in the tunnel we have introduced, one minute is the timer-controlled unit lighting time per vehicle.

For this reason, the lighting time is extended in relatively heavily-trafficked tunnels because following users are always detected, resulting in continuous

Copyright © 2005 Taylor & Francis Group plc, London, UK

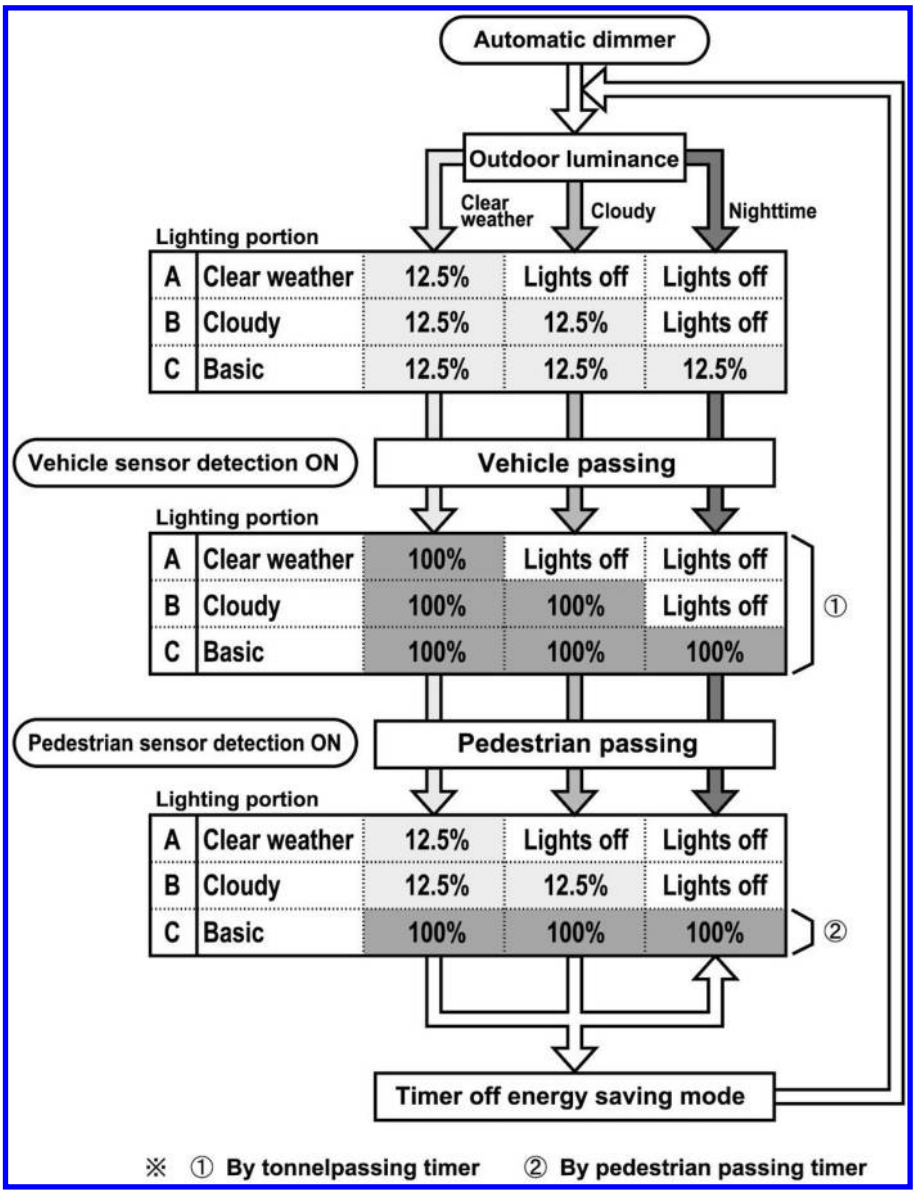


Figure 8. Lighting control flow.

lighting at 100% output, where the effect of introduction becomes small.

Consequently, the non-use time should continue for a certain period in target tunnels, and this system is of great use in a case where use is slack during the daytime when is power consumption is high. We have determined from several studies that introduction of this system is effective in tunnels when daily traffic is 500 vehicles or less.

As stated above, effective use of this system is limited to low traffic tunnels, but many applicable tunnels exist in countries with a great number of mountainous areas like Japan. Under today's considerable mission of safeguarding the global environment, contributions to the greatest possible extent are necessary in the road traffic field, and we would like to contribute to this by realizing as many systems as possible.

Copyright © 2005 Taylor & Francis Group plc, London, UK

Table 1. Collected data (May 2004, Measurement data of "O" tunnel in Shimane prefecture).

May Day	Air temperature (°C)	Lighting time by circuit (h)				Passage (times)		Measured electric energy (kWh)	Assume electric energy of a conventional system (kWh)	Effect (measured value/ assumed value)	CO_2 reduction (kg-CO_2)
		Entrance lighting		Basic	Outside the pit (nighttime)	Vehicle detection	Pedestrian push button				
		Cloudy	Clear								
1	17.1	11.2	6.6	24.0	10.8	116	0	25.89	98.35	26.3%	26.1
2	19.0	10.7	8.5	24.0	10.8	113	0	26.68	102.19	26.1%	27.2
3	17.3	9.4	1.1	24.0	11.1	103	0	22.30	80.29	27.8%	20.9
4	15.4	7.5	0.0	24.0	11.3	75	2	20.46	73.40	27.9%	19.1
5	14.6	11.9	7.7	24.0	10.5	119	0	27.97	102.62	27.3%	26.9
6	15.4	11.5	4.4	24.0	10.4	223	0	28.98	93.17	31.1%	23.1
7	17.1	11.7	4.3	24.0	10.5	302	0	28.35	93.38	30.4%	23.4
8	18.2	11.5	4.8	24.0	10.5	102	0	26.16	94.24	27.8%	24.5
9	18.4	7.7	2.0	24.0	11.2	67	0	20.43	78.98	25.9%	21.1
10	19.0	9.0	3.9	24.0	10.8	82	0	22.61	86.60	26.1%	23.0
11	16.7	8.5	2.9	24.0	11.2	72	2	20.87	83.04	25.1%	22.4
12	20.6	10.8	4.5	24.0	10.5	288	0	26.44	91.95	28.8%	23.6
13	17.5	4.2	0.5	24.0	12.0	60	0	19.07	67.78	28.1%	17.5
14	17.9	11.0	6.8	24.0	10.4	324	0	29.39	98.31	29.9%	24.8
15	15.3	10.9	0.0	24.0	10.7	70	0	21.35	80.56	26.5%	21.3
16	17.2	10.2	0.2	24.0	11.0	65	1	20.96	79.66	26.3%	21.1
17	17.8	10.6	2.7	24.0	10.7	286	0	24.98	86.91	28.7%	22.3
18	17.9	11.9	3.7	24.0	10.3	320	0	26.91	92.19	29.2%	23.5
19	13.8	6.9	0.0	24.0	11.2	297	0	21.45	72.07	29.8%	18.2
20	13.9	8.3	0.0	24.0	11.1	177	0	21.79	75.07	29.0%	19.2
21	19.3	10.6	4.9	24.0	10.2	205	0	25.57	92.46	27.7%	24.1
22	17.8	12.0	4.2	24.0	10.2	60	1	23.98	93.67	25.6%	25.1
23	15.4	11.3	5.5	24.0	10.1	84	2	25.17	95.50	26.4%	25.3
24	15.9	11.4	3.9	24.0	10.0	357	0	27.53	91.54	30.1%	23.0
25	16.9	11.4	3.1	24.0	10.1	386	0	27.57	89.50	30.8%	22.3
26	19.5	11.6	5.2	24.0	10.3	340	0	27.76	95.43	29.1%	24.4
27	19.9	11.7	2.9	24.0	10.0	126	0	23.34	89.60	26.0%	23.9
28	21.6	12.0	3.6	24.0	10.1	403	0	28.70	92.09	31.2%	22.8
29	19.5	7.7	0.2	24.0	10.6	69	1	20.30	74.14	27.4%	19.4
30	22.3	8.3	3.2	24.0	11.1	56	2	22.39	83.36	26.9%	21.9
31	17.4	6.1	0.0	24.0	11.6	86	1	21.83	70.46	31.0%	17.5
Total (※ Avg.)	17.6 ※	10.0 ※	3.3 ※	24.0 ※	10.7 ※	175.3 ※	0.4 ※	757.18	2698.51	28.1% ※	698.9

Copyright © 2005 Taylor & Francis Group plc, London, UK

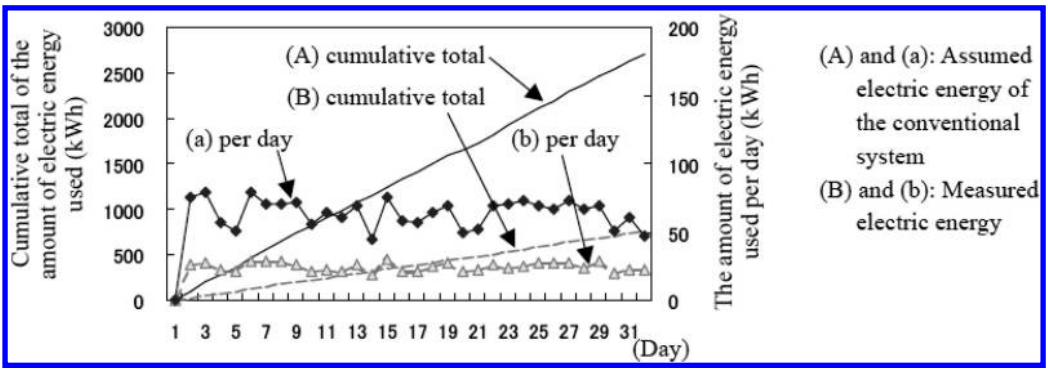


Figure 9. Cumulative total of power consumption.

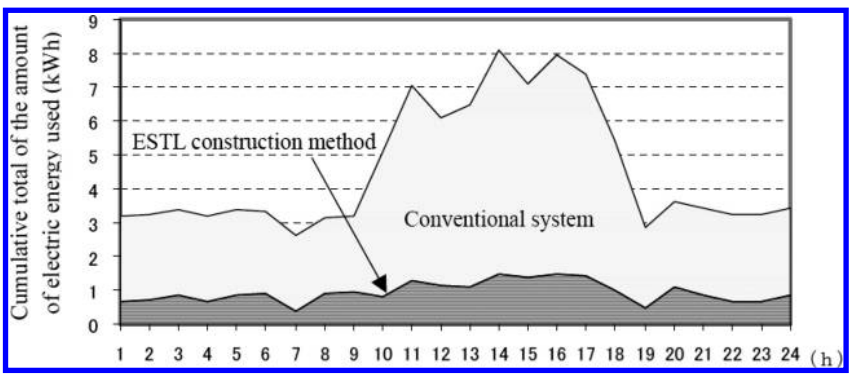


Figure 10. One-day power consumption status (May 10, 2004).

REFERENCES

Nagai, S., Unno, T., Miki and Shobusaki, M., 2003. A case study on ecological lighting system on road tunnels. Proc. Of JSCE Annual meeting Tokushima, Japan (in Japanese)

Nagai, S. and Takiguchi, K., 2004 Introduction of examples of mountain tunnel energy-saving lighting system (ESTL). Proc. of 11th World Congress on ITS., Nagoya. Japan.

Copyright © 2005 Taylor & Francis Group plc, London, UK

Earthquake hazards and seismic design of underground structures

Copyright © 2005 Taylor & Francis Group plc, London, UK

Seismic design method of immersed tunnel and effects of flexible joints

O. Kiyomiya
Waseda University, Tokyo, Japan

ABSTRACT: The immersed tunnels in Japan are constructed in vigorous earthquake activity areas and in soft ground. Since rigid joints are often disadvantageous, flexible joints should be used for absorption of large deformation due to earthquake force. For this reason, various studies and analyses have been conducted to develop higher deformation performance flexible joints. Dynamic response analysis has been introduced to estimate sectional force and displacement at the immersed tunnel. Seismic design method and effect of flexible joints for the earthquakes are presented in this paper. Newly developed flexible joint that is called Crown Seal Joint is mainly discussed.

1 INTRODUCTION

Many immersed tunnels have been constructed in areas where seismic effects are large in Japan. Performance-based design method using dynamic response analysis has been proposed by author and other researchers. The immersed tunnel is required to be stable and to receive no damage against middle-scale earthquake motion. The other hand, it is required not to collapse and water seepage against very large earthquake motion. Dynamic response analysis is adopted for the seismic design to ensure required performances. To increase seismic resistance of the immersed tunnel, flexible joints or soil improvement methods are widely adopted in design. This paper presents seismic design concept in Japan for the immersed tunnel, dynamic response model and calculation results. Immersed tunnel with rigid joints at soft ground area is impossible to design as to large sectional forces of the tunnel elements and large ground movement in vigorous earthquake area. To cope with this problem, flexible joints with large movement capacity as to axial direction and rotation at joint parts. A couple of new type flexible joints are developed and response of the immersed tunnel is studied by dynamic response analysis when these flexible joints are adopted between tunnel elements.

2 SEISMIC DESIGN METHOD

2.1 *Outline*

It is newly specified that the structures of highest importance such as the immersed tunnels shall be designed by seismic performance-based design. Contents of this design method is described in "Design Manual of Immersed Tunnel" published by Coastal Engineering Research Center in Japan. In performance-based design, some important requirements are evaluated as follows.

(1) Rout of the immersed tunnel should be avoided at changing part of ground property and at active fault zone. (2) When the immersed tunnel crosses the very soft sand where has potentially liquefaction, loose sand should be improved. (3) Water-tightness of joints and element should be secured during earthquakes. (4) Structural members should be not collapsed or heavy damage. (5) Rapid restoration and rescue system should be secured after earthquakes. Estimation of safety of the immersed tunnel during earthquakes should be estimated by proper methods.

Therefore the design earthquake must be properly defined and acceptable level of structural performance must be clearly identified. Two levels of design earthquake motion are specified as:

Level 1: Earthquake motions, which are likely to occur once or twice during the lifetime of the structure (a return period of about 75 years).

Level 2: Maximum credible earthquake motions, which are infrequent rare events, but when they occur, they are excessively intense (a return period of more than several hundred years).

The extent of the damage for the structures of highest importance must remain fully serviceable after temporary restoration measures for Level 1 earthquake motion. For level 2 earthquake motion, serious damage of the tunnel should be avoided. Damage levels are classified into three degrees. In degree 1, stresses

Copyright © 2005 Taylor & Francis Group plc, London, UK

Table 1. Performance based design.

	Level 1	Level 2
Return period of earthquake	50–75 year	500–1000 year
Damage level	Small damage No repair	Before collapse Repair
Stress of members	Within allowable stress	Over yield stress but within ultimate stress or strain
Analysis method	Dynamic analysis	Dynamic analysis
Material property	Elastic	Non-linear

in the members should be within allowable stresses. In degree 2, the stress should be within yield stress of each material. In degree 3, strain should be with allowable strain of each material and members are required to be not collapsed. Damage degree 1 responds to level 1 earthquake motion. Degree 2 & degree 3 responds to level 2 earthquake motion.

2.2 *Calculation model*

Calculations are carried out for both axial direction and cross section of the immersed tunnel. In general, effect of the flexible joint is for the axial direction of the tunnel. Cross section force is not related to the flexible joint. It is recommended to use the analysis based on soil-structure interaction analysis, generally using mass-spring system as shown in Fig. 1 or the finite element model. The sectional force and displacement along the immersed tunnels shall be also estimated by the dynamic analysis for the total structural system with ambient ground including effects of topography and geology at planned tunnel sites. The response of the ground and the tunnels can be calculated in time series by numerical integration. With the model, response of the surface layer can be calculated as below equation.

$$[M]\{\ddot{y}\}+[C]\{\dot{y}\}+[K]\{y\}=-[M]\{\ddot{e}\} \quad (1)$$

where [M]: mass matrix, [C]: damping matrix, [K]: rigid matrix by K_1 and K_2 springs,{ë}: input acceleration, {ÿ}: acceleration vector of mass, {″}: velocity, {y}: displacement.

The immersed tunnel is assumed as a beam supported by springs representing soil rigidity. One end of each spring is considered to displace same as the displacement of the ground calculated by the total model of surface layer.

When non-linear properties of the structure and ground are taken into consideration in the model as

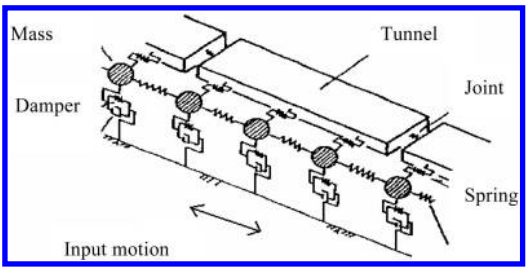


Figure 1. Mass-spring system.

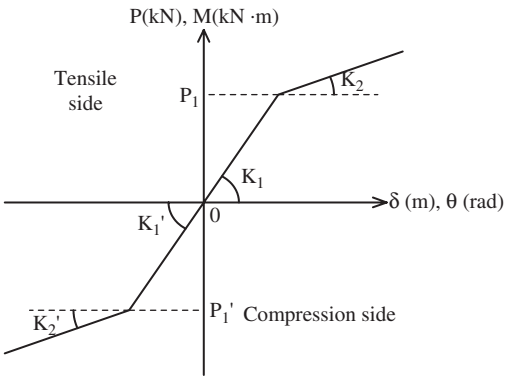


Figure 2. Material non-linear (bi-linear model).

shown in Fig. 2. Compressive rigidity of the axial direction of the tunnel is determined by concrete part of the element. First point in compressive side in below figure presents crack rigidity and horizontal line presents concrete crushing part. Tensile rigidity of the axial direction is determined by steel part of the element. First point in tensile side presents yield of the steel.

The spring constants have also non-linear properties. In the conventional way, the spring constants are assumed to be equivalent rigidities.

2.3 *Input wave*

For input data record to the dynamic response analysis, a couple of acceleration records are adopted. Two kinds of the earthquake record are considered in the design: one record is assumed to be the earthquake that the epicenter is narrow and the magnitude is not so large. This wave record has properties of short dominant periods and short duration time like as shock waves. Another record is assumed to be the earthquake that the epicenter is far and the magnitude is large. This wave record has long dominant periods and long duration time. When the earthquake records are obtained near the construction site, these records are adopted. When there is no record, Tokachi-oki Earthquake

Copyright © 2005 Taylor & Francis Group plc, London, UK

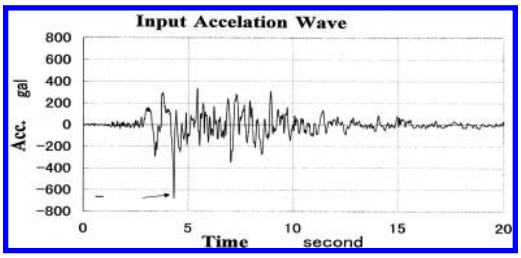


Figure 3. Input acceleration record (Kobe 1995).

record (1968) and Kobe Earthquake record (1995) as shown in Fig. 3 are usually used. Recently artificially acceleration waves are calculated considering epicenter length, magnitude, scale of the active fault, etc.

3 FLEXIBLE JOINT

3.1 *PC-rubber gasket type flexible joint*

First case of the flexible joints was adopted at Tokyo Port Immersed Tunnel that was completed in 1976. Rubber gasket and Omega type steel plate were used for the flexible joints between elements. For Tokyo Second Channel Tunnel, the flexible joints with rubber gasket and PC cables as shown in Fig. 4 were installed between the immersed tunnel elements. This type of flexible joints is very effective for absorption of large relative deformation at the joints parts. They have been widely installed since then and several immersed tunnels have these type joints.

In general, maximum absorption displacement of this type of the flexible joint is about 50 mm for total external forces such as temperature, ground settlement, earthquake and so on.

PC cables resist tensile force and rubber gasket resists axial force at the joint parts. PC cables in the bulkhead are connected each other by a coupler at the joint part. The coupler absorbs dislocation of the PC cables. The couplers are seal by rubber tapes to cope with corrosion of the coupler and PC cables. Shear keys are arranged at floor slab and participation walls to resist shear forces due to earthquake forces, ground settlement and so on.

Figure 5 shows force and moment components at the joint. Namely, this type of joint is available for horizontal direction in view of both axial force and bending moment. The spring constant for tensile side is governed by PC cable mechanical property and that for compression side is by rubber gasket property that has strong non-linear property.

Spring constants (Kp and Kc) for tensile side and compression side are obtained by next equations.

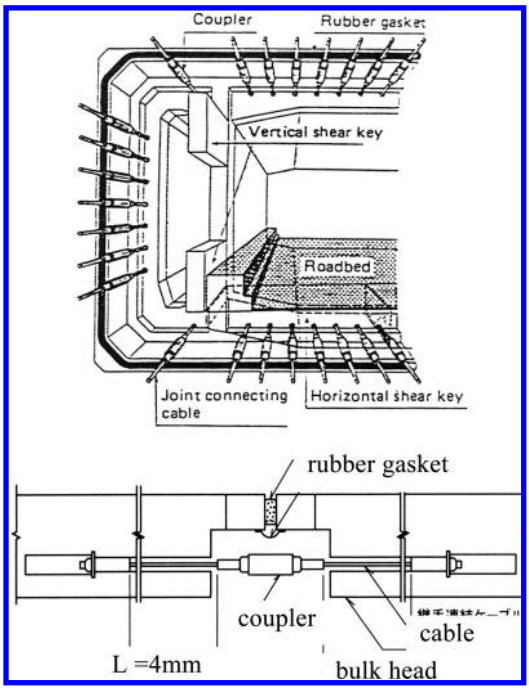


Figure 4. PC-rubber gasket type flexible joint.

$$Kp = Ep\ N\ Ap/L \quad (2)$$

where Ep: Young's modulus of PC cable, N: No. of PC cables, Ap: Cross section area of PC cable, L: Length of PC cable

$$Kc = (Pmax\text{-}P_0)/(\delta max\text{-}\delta_0) \quad (3)$$

where Pmax: Maximum compression load of rubber gasket, P_0: Initial compression load for joint work, δmax: Maximum compression displacement, δ_0: Initial compression displacement in Fig. 6 shows load–displacement relationship of the rubber gasket.

3.2 *Crown Seal joint*

Ohsaka Bay in Japan is located on the alluvium layer and large ground settlement is now observed. While the man-made island is reclaimed, new Umeshima Immersed Tunnel at Ohsaka Bay is now under construction. About 1 m un-uniform ground settlement is calculated by one dimensional consolidation analysis and by two dimensional finite element method to predict consolidation settlement along the tunnel axis for 100 years. PC-rubber gasket type joint is not available for the new immersed tunnel. New type flexible joint called Crown Seal joint to cope with the large ground

Copyright © 2005 Taylor & Francis Group plc, London, UK

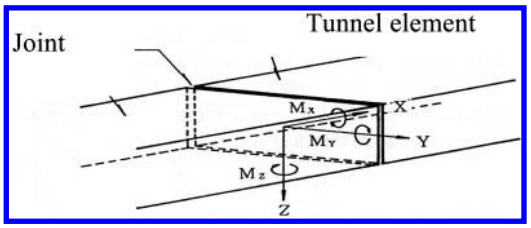


Figure 5. Resist components at the joint.

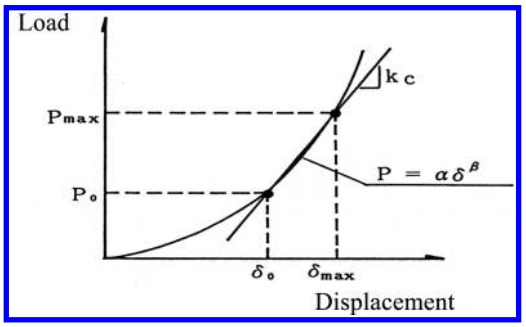


Figure 6. Mechanical property of the rubber gasket.

settlement is required to exploit. Figure 7 shows outline of the Crown Seal joint.

Rigid joint is installed beside the crown seal joint for joining work. Required performance of crown seal joint is presented as below.

(a) Crown Seal Rubber Block

Self-seal for water-tightness is secured by noses at the block for ordinary load condition 1 and level 1 earthquake. Self-seal is also secured by attachment plate at flange part for load level 2 earthquake. This water-tightness capacity is designed to be within 25–30 cm of horizontal displacement at the joint part.

(b) Stopper Cable: PC Cable

PC cable is not structural member at ordinary state but stopper for unpredictable displacement. No tension force is introduced for ordinary load condition. Axial stress of PC cable is within yield stress for level 1 and level 2 earthquake.

(c) Secondary Omega Type Rubber Seal

Secondary seal is installed for leakage from the rubber gasket and this is a kind of double failure safe system. The water-tightness capacity is designed to be within 60–80 cm of horizontal displacement at the joint part.

(d) Cushion Rubber Block

Cushion rubber block does not contact to other side bulkhead for ordinary load condition. Cushion rubber block and bulkhead beam is not broken for to absorb impact force during level 1 and level 2 earthquake.

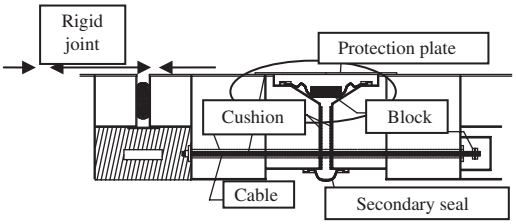


Figure 7. Outline of the Crown Seal Joint.

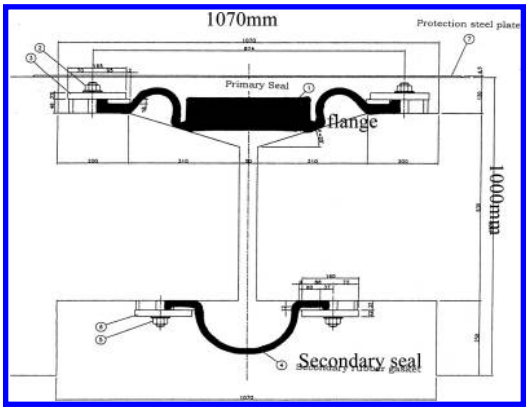


Figure 8. Detail of the rubber gasket part.

Table 2. Comparison of joints.

	PC cable-rubber gasket	Crown Seal joint
Tensile force	PC cable	No
Axial force	Rubber gasket	No
Shear force	Shear key	Shear key
Moment	Transmission	No
Watertightness	Rubber gasket	Nose of block and flanges
Secondary watertightness	Omega type	Omega type
Displacement capacity (mm)	50–80	250–300

No force is transmitted at the joint part for axial direction and bending direction for this flexible joint.

Configuration and material property of the rubber block and the flange material as shown in Fig. 8 is determined by finite element analysis. The flange part of the rubber block is reinforced by the textile. Tensile side of the rubber block is also reinforced by same textile. Effectiveness of the crown seal joint is confirmed by indoor model test. In the model test, water

Copyright © 2005 Taylor & Francis Group plc, London, UK

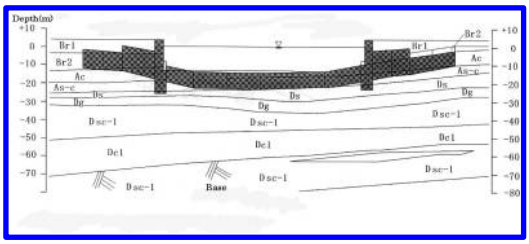


Figure 9. Soil condition of surface layer.

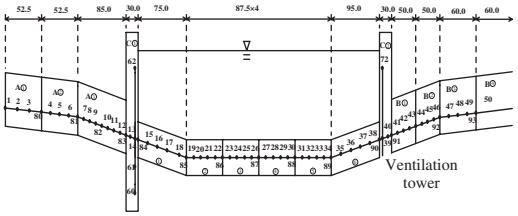


Figure 10. Calculation model.

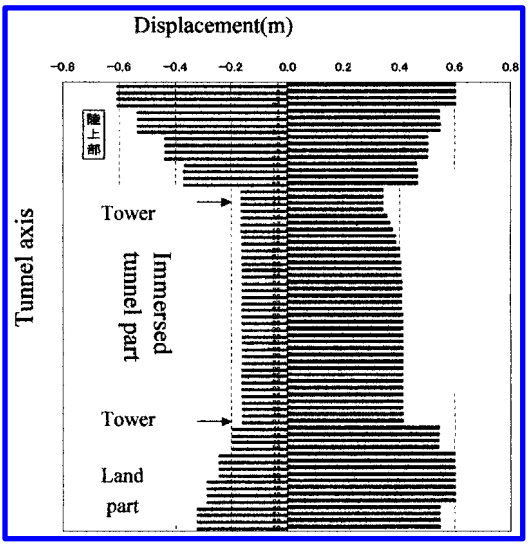


Figure 11. Displacement distribution along tunnel.

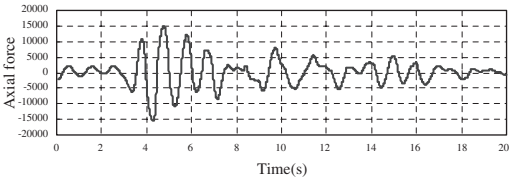


Figure 12. Axial force time series at tunnel.

tightness is checked for various positions according to movement at the joint part. Table 2 shows comparison of both flexible joints.

4 A CALCULATION EXAMPLE

4.1 *Calculation model*

In this paper, a calculation results by the dynamic response analysis to compare the effect of the flexible joint is described. This calculation is carried out for Kobe Minatojima Tunnel near Ohsaka Bay. The total length of the Kobe Minatojima Tunnel is 990 m and the length of the immersed tunnel is 520 m. The immersed tunnel part consists of 6 elements and two ventilation towers are located at both ends of the immersed tunnel part. The length of each element fabricated by steel-concrete composite members is 87.5 m. Its height is 9.1 m and its width is 34.6 m respectively. Surface layer as shown in Fig. 9 consists of soft clay and its engineering base rock locates at depth of 53–70 m. Dominate period of left land part in the figure is 1.1~1.9 s, that of the channel part is 0.9 s and right land part is 1.2 s according to S wave survey.

The outline of the model is shown in Fig. 10. The tunnel part including the land parts is replaced by 50 beam elements. The immersed tunnel part has seven joint parts. The ventilation tower at the land part is connected with the tunnel element by the flexible joint. Flexible joint by PC rods are installed at the land tunnel part at interval of 25–30 m. Earthquake acceleration record is input at the engineering base rock.

4.2 *Calculation result*

Sectional forces of the tunnel do not depend on the ground acceleration but the ground deformation. Fig. 11 shows maximum displacement distribution at each location along the tunnel axis.

Max displacement of 60 cm is calculated at the land part and displacement at immersed tunnel part is smaller than that of the land part. Therefore large relative displacement is calculated at the revetment where the ventilation tower is located. These ground displacement are used as input data for a beam model supported springs.

Figure 12 shows time series of axial force waves during the earthquake. This result is obtained for the PC cable-rubber gasket type flexible joint at the tunnel element. Relatively long period of 0.5 Hz is dominant for Kobe Earthquake acceleration records as shown in Fig. 3. This input acceleration record was obtained at − 81 m location in Kobe Earthquake in 1994.

Table 3 represents maximum values obtained by the calculation. Large values of the axial forces are calculated for the rigid joint. When the PC cable-rubber gasket type joint is adopted, the axial force

Copyright © 2005 Taylor & Francis Group plc, London, UK

Table 3. Comparison of maximum values.

Joint type	Rigid joint	PC & gasket	Crown Seal
Tensile force at tunnel kN	183000	147800	20400
Com. force at tunnel kN	319200	155300	20280
Bending moment at joint kNm	4503000	263800	215
Joint relative displacement mm	0	35	125

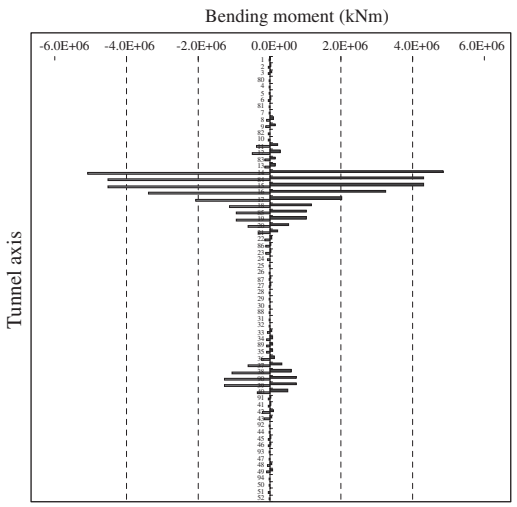


Figure 13. Bending moment distribution for rigid joint.

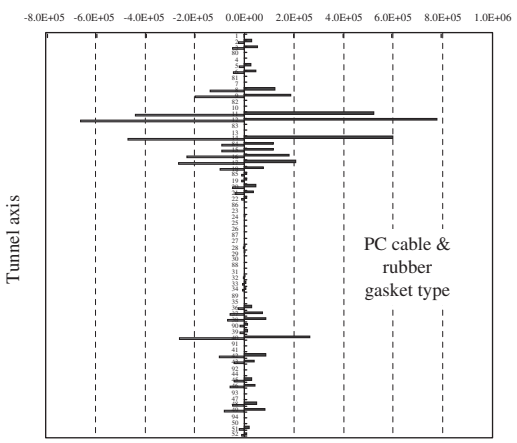


Figure 14. Bending moment distribution.

decreases rather than that of the rigid joint. Relative displacements of the flexible joints are large value. Displacement of 35 mm for the PC cable and rubber gasket type flexible joint and that of 125 mm for the Crown Seal joint are calculated. These values are within required allowable displacement for each joint in the design as shown in Table 2.

Figures 13 and 14 show bending moment distribution along the tunnel axis for the rigid joint and PC cable & rubber gasket type flexible joint. Large value of the bending moment is calculated at the revetment location. For Umeshima Tunnel, Crown Seal joints are used for the tunnel at the revetment parts and PC cable-rubber gasket type flexible joint are used for the tunnel part at the navigation channel part.

7 CONCLUSIONS

(1) Flexible joints have been developed to cope with ground settlement and earthquake movement. PC cable and rubber gasket type joint is widely adopted for several immersed tunnels in Japan. No trouble about joint part has been observed since this type of flexible joints was installed.
(2) Recently, large deformation capacity for the flexible joint is required. Crown Seal joint is exploited. This joint is adopted for Umeshima Tunnel that is under construction at Ohsaka Bay where consists of very soft surface layer.
(3) Effects of the flexible joints for earthquakes are verified by dynamic response analysis. Maximum axial forces and bending moments of tunnel elements with the Crown Seal joint decrease to very small values in comparison to the rigid joints.

REFERENCE

1) Coastal Engineering Research Center: 2002. Design Manual of Immersed Tunnel
2) Osamu KIYOMIYA: 1995, Earthquake-resistant Design Features of Immersed Tunnels in Japan, *Tunneling and Underground Space Technology* 465, Vol. 10, No. 4, pp. 463–475
3) ChristianIngreslev and Osamu KIYOMIYA: 1997, Earthquake Analysis, *Immersed and floating tunnels working group report*, ITA, Vol. 2, No. 2, pp. 76–80
4) Osamu KIYOMIYA: 2004, Flexible joints between elements for large deformation, *ITA World Conference (Singapore)*

Copyright © 2005 Taylor & Francis Group plc, London, UK

Seismic microzonation of Küçükçekmece-Halkalı region in Istanbul

H. Kılıç, P. Tohumcu Özener, M. Yıldırım
Yıldız Technical University, Faculty of Civil Eng., Geotechnical Department, 34340 İstanbul, Turkey

Ş. Adatepe
Kasktaş, Piling and Drilling Contracting Co. Inc., Istanbul, Turkey

H. Demir
Geogrup Engineering Comp., Istanbul, Turkey

ABSTRACT: In this study, the local soil conditions at Küçükçekmece-Halkalı in Istanbul are investigated and a microzonation study is carried out with respect to soil amplification in accordance with the new Microzonation Manual **(MERM, 2003)**. Within the framework of a project implemented for investigation of the region with respect to suitability for settlement, the geological and tectonic characteristics of the region were investigated with the aid of soil exploration borings. Additionally, the results of the geophysical surveys and microtremor measurements were also utilized. In order to be able to investigate the effects of local soil conditions on the dynamic behavior, site response analysis are performed with EERA by utilizing the findings of field and laboratory investigations. The outcomes of the numerical analysis and emprical equations are processed by GIS techniques in order to produce microzonation maps in terms of soil amplification.

1 INTRODUCTION

Seismic microzonation can be defined as the estimation of response of soil layers under earthquake excitations and variation of earthquake forces that will act on structures taking into account the earthquake characteristics that may occur in the investigated region. In the last decade, both the increase in the availability of experimental and instrumental data and the developments in the evaluation of ground conditions and ground amplification analyses (Hartzall et al., 1997) have led to significant developments in microzonation studies. Following the Kocaeli earthquake on August 17, 1999, the effects of earthquakes on public safety and economy have initiated the "Microzonation For Earthquake Risk Management" project was started by the General Directorate of Disaster Affairs and basic principles were defined for seismic microzonation on the municipality basis. The seismic microzonation in the municipality basis together with earthquake resistant design code provide safe urban development in terms of land use and structural design.

Küçükçekmece-Halkalı districts of Küçükçekmece province are located at about 10 km north of the active right-lateral fault segment of North Anatolian Fault and are in the 1st (most active) seismic zone. Since, Istanbul in general, and Küçükçekmece in particular, are at high risk of being hit by a major earthquake, earthquake risk analysis is needed to be performed by dividing Istanbul and its districts into subregions. Within the framework of a project prompted by Küçükçekmece Municipality, the suitability for settlement of a total area of 25.95 km^2 involving Küçükçekmece-Sefaköy regions and Halkalı-İkitelli regions were investigated through geological, geophysical and geotechnical studies.

In this study, by taking into consideration the local site conditions, a seismic microzonation study was carried out in terms of soil amplification in accordance with the Seismic Microzonation Manual prepared by World Institute for Disaster Risk Management (DRM) in order to evaluate and assess the probable effects of an expected Marmara earthquake in the Küçükçekmece-Halkalı region.

The microzonation method used is based on the recommendations of the Microzonation Manual and comprises of 5 stages. These stages are summarized as following:

1. The geological and tectonic characteristics of the region were determined and the geotechnical features of the local soil conditions were investigated through soil exploration borings. The results of the geophysical measurements were also evaluated from

Copyright © 2005 Taylor & Francis Group plc, London, UK

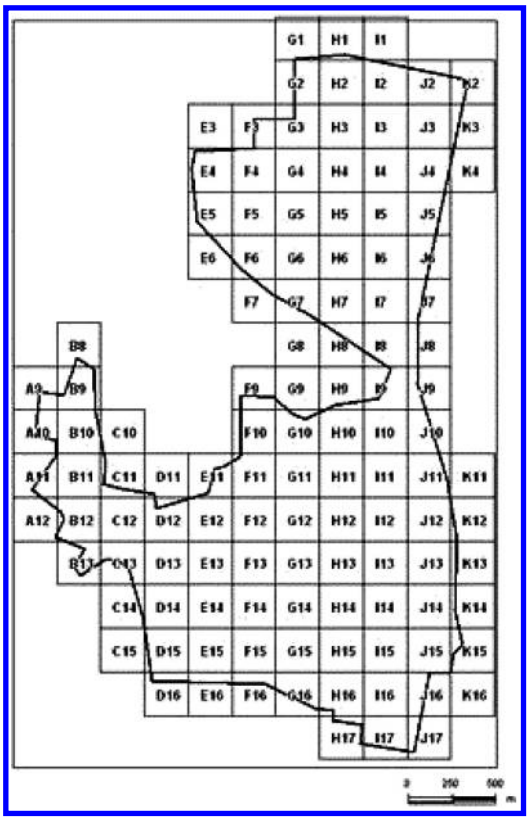


Figure 1. The grid map of the region.

the point of view of local site effects **(Özaydın vd. 2002)**.

2. The earthquake hazard of the region was determined and regional earthquake hazard parameters were determined by KOERI (Kandilli Observatory and Earthquake Research Institute). The regional earthquake hazard and required earthquake parameters were determined for a return period of 475 years. For simulation of time domain ground motions, a program code **TARSCTHS (2000)** was used.
3. The research area was divided into 250 m × 250 m grids as shown in Figure 1 and for each grid representative soil profiles were determined and classified according to Turkish Earthquake Code, NEHRP **(BSSC, 2001)** and equivalent shear wave velocities.
4. For each grid dynamic site response analysis were performed with EERA (2000) by using simulated earthquake time-histories. As a result of the site response analyses, peak ground acceleration, spectral accelerations and soil amplification at the ground surface were determined.
5. Since the site characterizations and the analyses performed involve various approximations as well as some assumptions, it was preferred not to assign any numerical values for the parameters. In order to produce microzonation maps in terms of soil amplification, the area was divided into three zones as A, B and C as described in the Microzonation Manual (MERM, 2003) by using GIS. Here, the Zone A shows the most unsuitable 33 percentile, Zone B the medium 34 percentile and Zone C shows the most favourable 33 percentile. The percentile values are determined based on the frequency distributions of the calculated parameters obtained from the results of the site response analysis.

2 THE GEOLOGY OF THE REGION

The formations outcropping in the area start with the lithologies belonging to Middle Eocene Kırklareli formation. This formation rests unconformably on the "graywacke" sequences of Trakya formation (Carboniferous) and is composed of limestone and argillaceous limestone. At its base, it starts with a cream–white, locally loosely cemented, sometimes carbonaceous basal conglomerate, and continues upward with thinly to medium bedded, occasionally thickly bedded, karstic, compact limestone. Kırklareli formation is overlain by younger deposits of Upper Oligocene–Upper Miocene, which are quite widespread in the area. These start with sand and gravel, gray–cream in color, and continue upward uninterruptedly with green, thinly to medium bedded, horizontal to slightly dipping, overconsolidated clay, and interbedded clay and sand layers **(Yıldırım ve Savaşkan, 2002–2003)**. In the upper levels (Upper Miocene) of the sequence, granular lenses, and organic, soft to medium stiff clay lenses respectively named Çukurçeşme and Güngören formations are encountered. The uppermost level of the deposition, called Bakırköy formation, is characterized by mactra-bearing, argillaceous limestone interbedded with clay and fine sand.

As can be seen from the geological map of the investigated area given in Figure 2, younger deposits of Miocene, which are quite widespread on the south part of the area and are up to 70 m thick on the hill plateu, decrease in thickness on the north towards TEM highway and are replaced by limestones of Kırklareli formation. The limestones may either outcrop or are encountered at shallow depths of 5 –15 m on the north parts of the site. The cross-section A-A′ through the area and the typical sequence of geological formations are shown in Figure 3.

The Ayamama streambed forming the eastern boundary of the investigated area is mostly composed of young alluvial deposits, varying in thickness from 3–10 m. The area is poor in groundwater resources, but the aluvial deposits contain some groundwater seeping from Ayamama river.

Copyright © 2005 Taylor & Francis Group plc, London, UK

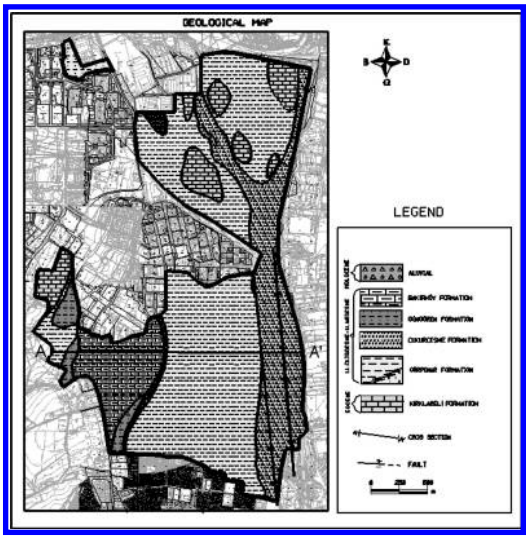


Figure 2. The geology map of the region.

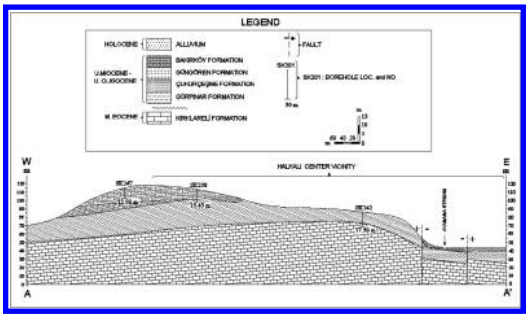


Figure 3. The cross section A-A′ of the region.

2.1 *Geotechnical investigations*

The geotechnical information gathered from a total of 30 boreholes of 10–25 m depth and a total of 38 exploration pits are summarized as below. Standart Penetration Tests were executed at several intervals during the soil exploration borings at the site and disturbed and undisturbed soil samples were recovered. The variation of SPT-N values with depth for different formations are given in Table 1 and the natural water content (w_n), consistency limits (w_L, w_P) of the cohesive formations and natural unit weight (γ_n) of the formations encountered in the study area are given in Table 2. The grain size distribution of the soil formations is summarized in Table 3. The observations at exploration pits of 1.10–4.90 m depth were utilized to define the geologic formation boundaries, formation types and to determine the level of ground water table.

Table 1. SPT-N Blow counts for the formations in the study area.

	SPT-N blow counts	
Soil description	Range	Average
Fill	6–16	10
Alluvial soil	9–26	18
Bakırköy formation (clay levels)	4–57	20
Güngören formation	9–48	16
Çukurçeşme formation	41-Refusal	50
Gürpınar formation (4.0–7.50 m)	7-Refusal	20
Gürpınar formation (7.50–10.50 m)	10-Refusal	20
Gürpınar formation (>10.50 m)	10-Refusal	30
Kırklareli formation (clay levels)	14-Refusal	60

Table 2. Natural water content, consistency limits and natural unit weight of the formations in the study area.

Soil description	w_n (%)	w_L (%)	w_P (%)	γ_n (kN/m^3)
Fill	28–32	60–64	28–30	18
Alluvial soil	17–34	32–57	18–28	18
Bakırköy formation*	22–32	20–56	21–37	19
Güngören formation	21–59	40–109	24–48	19
Gürpınar formation (1)	15–45	43–98	19–38	20
Gürpınar formation (2)	16–39	51–103	22–38	20
Gürpınar formation (3)	15–54	40–108	20–45	20
Kırklareli formation*	29–35	50–77	23–34	19

*Clay levels; (1) (4.0–7.50 m arası); (2) (7.50–10.50 m arası); (3) (>10.50 m)

Table 3. Grain size distribution of the formations in the study area.

Soil description	Gravel (%)	Sand (%)	Silt-clay (%)
Fill	0–65	0–28	0–70
Alluvial soil	0–14	47–83	17–53
Çukurçeşme formation	0–41	48–85	11–23
Gürpınar formation	0–34	28–78	7–53

The undrained shear strength values determined from the unconfined compression tests and UU triaxial compression tests conducted on undisturbed samples recovered from Güngören formation, and uniaxial compression tests and point load tests executed on samples recovered from Kırklareli and Bakırköy rock formations are given Table 4.

Copyright © 2005 Taylor & Francis Group plc, London, UK

Table 4. The shear strength parameters for formations.

Soil description	cu (kPa)	q_u (kPa)	q_c (kPa)
Gürpınar formation (♦)	30	25–111	–
Bakırköy formation*		–	1646–116872
Kırklareli formation*	–	–	874–142810

*Limestone; (♦)Clay

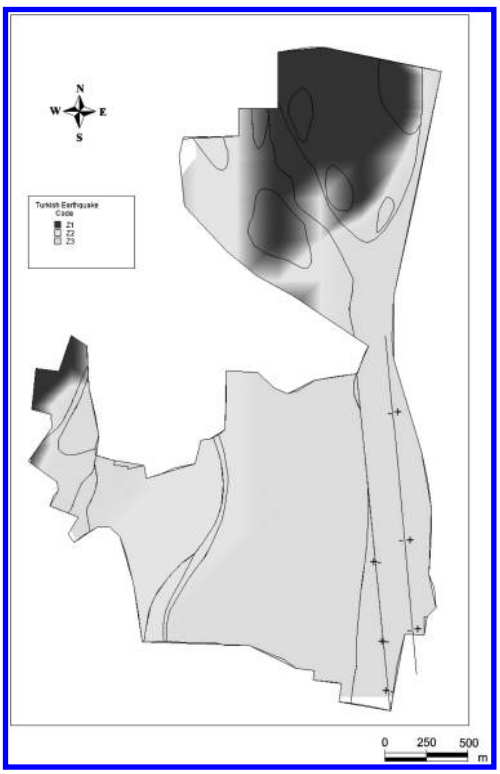


Figure 4. The site soil classification according to Turkish Earthquake Code.

2.2 *Site classification and shear wave velocity distribution in the study area*

The site classification at each grid was carried out according to both Turkish Earthquake Code (TEC, 1998) and NEHRP (BSSC, 2001). The region is determined to include Z1, Z2, and Z3 site classes according to Turkish Earthquake Code and C, D and F site classes according to NEHRP. The site classification maps with respect to Turkish Earthquake Code and NEHRP are shown in Figure 4 and Figure 5 respectively. Site soil classification maps showed that the Kırklareli limestone and Gürpınar formation

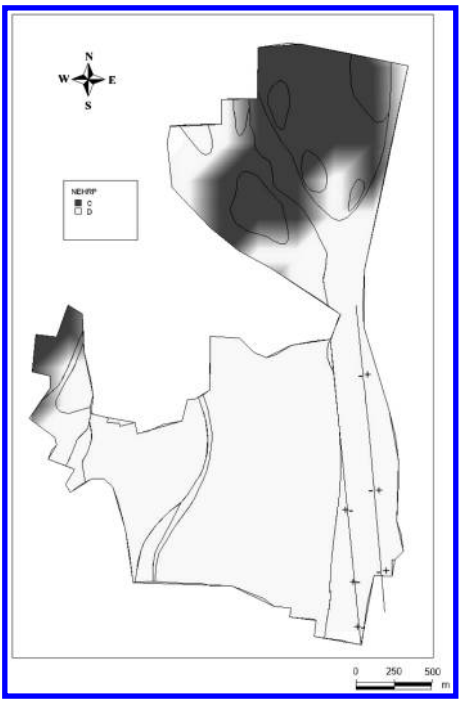


Figure 5. The site soil classification according to NEHRP (BSSC, 2001).

litologies are classified as Z1/C. The zones of Z2/D are seen to be found in the clay interbedded limestones of Bakırköy formation and in certain portions of Gürpınar and Çukurçeşme formations. The site class Z3/D appear in Güngören, Gürpınar and in major portion of alluvial site.

Based on the available site investigation results, typical soil profiles are identified for each grid and using the variation of SPT-N values with depth, the shear wave velocity profiles were computed based on the empirical relationship proposed by İyisan (1996). As a consequence, the shear wave velocities are determined to vary between 105 m/s and 554 m/s and the equivalent shear wave velocities for the topmost 30 m were determined to vary between 182 m/s and 527 m/s.

3 SITE RESPONSE ANALYSES

In this study, dynamic site response analyses were conducted using EERA which provides a procedure to define inputs and outputs in Excel routines based on equivalent linear analysis program SHAKE 91 (Idriss and Sun, 1992). The regional earthquake hazard of the site was determined based on probabilistic approach and the computer code TARSCTHS (2000)

Copyright © 2005 Taylor & Francis Group plc, London, UK

was used for simulation of earthquake motion. The representative and hypothetical soil profiles defined in the middle of each 250 m × 250 m grid were used in **EERA (2000)**. For each soil layer in the soil profiles, total unit weight, thickness, shear wave velocity, G/G_{max} and damping relationships are provided as inputs.

3.1 *Seismic microzonation with respect to ground motion*

Site response analyses were conducted for Halkalı region using the selected soil profiles and the input time histories obtained for each grid from the regional probabilistic earthquake hazard study. The basic intention of the site response analysis is to estimate the effect of local site conditions in assessing the site amplification with respect to ground shaking. The peak spectral amplifications based on equivalent shear wave velocity were calculated using the emprical relationship given by **Midorikawa (1987)**,

$$A_k = 68V_s^{-0.6} \quad (1)$$

where A_k is the spectral amplification and V_s is the equivalent shear wave velocity. The peak spectral amplifications are calculated based on Eq. (1).

As a result of the one-dimensional (1-D) dynamic site response analysis with respect to the earthquake characteristics for probability of exceedance of 10%, peak ground acceleration (PGA), maximum spectral acceleration (SA) and soil amplification were determined. In the evaluation of maximum spectral accelerations, the average spectral acceleration between 0.1 s and 1.0 s periods is defined and mapping procedure was performed according to the average spectral acceleration $Sa_{(ave)}$. The peak spectral accelerations are also computed based on Eq. (1). In the evaluation of the cumulative frequency distribution of these calculated values, since $S_{(\%67)} > 1.3S_{(\%33)}$ was not justified, the study area was divided into two zones as A and C, where Zone A shows the upper 50% percentile and Zone C shows the lower 50% percentile (MERM, 2003). The variation of average spectral acceleration values calculated by site response analysis for probability of exceedance of 10% is shown in Figure 6. In Figure 6, average spectral accelerations for probability of exceedance of 10% are observed to vary between 0.438 g and 1.414 g and the areas which possess spectral accelerations greater than 0.785 g were defined as Zone A_s and the areas with less than 0.785 g were defined as Zone C_s with respect to cumulative frequency distribution criteria.

The variation of spectral amplifications computed from equivalent shear wave velocity based on Midorikawa are shown in Figure 7. Here, the spectral amplifications are seen to vary between 0.96 and 1.98. The areas with greater than 1.33 amplification are shown as Zone A_v and the areas which show less than 1.33 amplification are as C_v with respect to cumulative frequency distribution.



Figure 6. Variation of average spectral accelerations for probability of exceedance of 10%.

The seismic zonation with respect to ground shaking is accomplished based on the evaluation of average spectral accelerations obtained by site response analysis (Fig. 6) and by peak spectral amplifications calculated using equivalent shear wave velocity (Fig. 7). The resulting microzonation map obtained from this approach is shown in Figure 8 with respect to the probability of exceedance of 10%. Here the zone A_{GS}, representing relatively highest shaking level, corresponds to overlapping zones of A_s and A_v, the zone B_{GS}, relatively medium shaking level, corresponds to overlapping zones of A_s and C_v or C_s and A_v and the zone C_{GS}, relatively low shaking level, corresponds to overlapping zones of C_s and C_v. There seems to be some inconsistencies at some points between site classification and computed site amplifications. This is probably due to the fact that the site response analysis would sometimes give unrealistically high spectral amplification or very low peak ground acceleration values depending on the thickness of the deposit, estimated initial shear moduli, and also on the characteristics of the input acceleration time histories.

Copyright © 2005 Taylor & Francis Group plc, London, UK



Figure 7. The variation of spectral amplification computed from equivalent shear wave velocity based on Midorikawa (1987) equation.

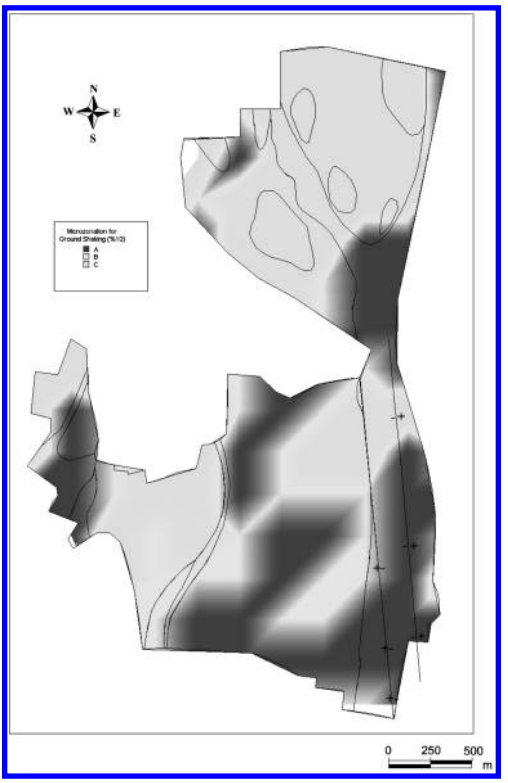


Figure 8. Ground shaking zonation map with repect to probability of exceedance of 10%.

3.2 *Evaluation of the seismic zonation maps*

The comparison of microzonation map for the ground shaking shown in Figure 8 and the geology map shows that the plateu at the southern part of the investigated region where marl and argillaceous limestone of Bakırköy formation outcrops, the northern parts where limestone of Kırklareli formation is outcropping and the high sand content clay levels of Gürpınar formation constitute the more favorable zones B and C. The southern parts of the region where clays of Gürpınar formation in thickness of 70 m and the alluvial deposits of Ayamama stream and western slopes where high organic content clays of Güngören formation is outcropping form the more risky zone A.

4 RESULTS

In this study**,** a seismic microzonation study with respect to soil amplification was carried out in accordance with the seismic microzonation manual prepared by World Institute for Disaster Risk Management (DRM) in order to evaluate and assess the probable effects of an expected Istanbul earthquake in the Küçükçekmece-Halkalı region in western Istanbul.

The dynamic site response taking into local soil conditions of Küçükçekmece-Halkalı region was determined based on the earthquake hazard parameters derived for probability of exceedance 10% in 50 years. The microzonation map for ground shaking seems to be compatible with geological map and local site classification maps with respect to NEHRP and Turkish Earthquake Code. The seismic microzonation study performed with respect to new microzonation manual showed that the Bakırköy formation which is quite widespread in the plateu of southern side of the region and limestone of Kırklareli formation which outcrops on the north of the area and high sand content levels of Gürpınar formation constitute the more favorable zones of B and C. On the other hand, the clays of Gürpınar formation, alluvial deposits of Ayamama river and the western slopes where Güngören formation outcrops constitute the unfavorable zone A.

Copyright © 2005 Taylor & Francis Group plc, London, UK

ACKNOWLEDGEMENTS

The authors are grateful to Professor Mustafa Erdik, Research Asst. Karin Şeşetyan and Research Asst. Mine Demircioğlu for valuable contributions on the probabilistic evaluation of earthquake susceptibility of Küçükçekmece-Halkalı region. The authors would also like to thank Professor Atilla Ansal for his support and helpful discussions during the application of microzonation manual.

REFERENCES

MERM (2003), Microzonation Manual, World Institute for Disaster Risk Managament.

Özaydın, K., Yıldırım, S. and Yıldırım, M. (2002), "İstanbul İli Küçükçekmece İlçesi Halkalı ve İkitelli Yerleşim Bölgeleri İmar Düzenlemesi 1-2-3-4 ve 5. Uygulama Sahalarının Jeolojik ve Jeoteknik Etüd Raporu ve Yerleşime Uygunluk Açısından Değerlendirilmesi" Yıldız Teknik Üniversitesi Geoteknik Anabilim Dalı, İstanbul, (in Turkish).

Yıldırım, M., Savaşkan, E., (2002), "İstanbul Tersiyer Çökellerinin Stratigrafisi ve Mühendislik Özellikleri", Uluslararası Mühendislik Jeolojisi Türk Milli Komitesi (MJTMK) Bülteni, 25. Yıl, sayı 18, sayfa 48–62 (in Turkish).

Yıldırım, M., Savaşkan, E., (2003), "İstanbul Bölgesi Tersiyer Çökellerinin Stratigrafisine Yeni Bir Yaklaşım ve Çökellerin Mühendislik Özellikleri", İstanbul'un Jeolojisi Sempozyumu, Sayfa: 87–102, TMMOB Jeoloji Mühendisleri Odası – İstanbul.

İyisan, R., (1996), "Geoteknik özelliklerin belirlenmesinde sismik ve penetrasyon deneylerinin karşılaştırılması", Doktora Tezi, İTÜ Fen Bilimleri Enstitüsü, İstanbul, (in Turkish).

Bayındırlık ve İskan Bakanlığı Afet İşleri Genel Müdürlügü, AIGM (1998) "Afet Bölgelerinde Yapılacak Yapılar Hakkında Yönetmelik, Türkiye Deprem Yönetmeliği (TDY)".

BSSC-Building Seismic Safety Council (2001), "NEHRP (National Earthquake Hazards Reduction Program) Recommended Provisions for Seismic Regulations for New Buildings and Other Structures", 2000 Edition, Part I: Provisions FEMA 302.

NEHRP (1997), Recommended Provisions for Seismic Regulations for New Buildings and Other Structures, FEMA-303, Prepared by the Building Seismic Safety Council for the Federal Emergency Management Agency, Washington, DC.

Midorikawa, S., (1987), " Prediction of isoseismal map in the Kanto plain due to hypothetical earthquake. (In Japanese with English Abstract) Journal of Structural Engineering. Vol. 33b, pp. 43–48.

Bardet, J.P., Ichii, K., and Lin, C.H., (2000), "EERA: A Computer Program for Equivalent-linear Earthquake site Response Analyses of Layered Soil Deposits", University of Southern California, Los Angeles.

Papageorgiou, A., Halldorsson, B. and Dong, G. (2000), TARSCHTS: "Target Acceleration Spectra Compatible Time Histories" University of Buffalo, Dept. Of Civil, Structural and Environmental Engg., NY.

Idriss, I.M. and Sun, J.I. (1992), "User's Manual for SHAKE91" Center for Geotechnical Modelling, Department of Civil Engineering, University of California, Davis.

Copyright © 2005 Taylor & Francis Group plc, London, UK

Seismic behaviour of tunnels in soft soil: parametric numerical study and investigation on the causes of failure of the Bolu tunnel (Düzce, Turkey, 1999)

A. Giannakou, P. Nomikos, I. Anastasopoulos, A. Sofianos, G. Gazetas & P. Yiouta-Mitra
National Technical University, Athens, Greece

ABSTRACT: This paper presents a parametric investigation of the seismic response of circular tunnels. The dynamic response due to seismic shaking is analyzed numerically making use of the finite difference method. The analyses are conducted in plane strain, parametrically varying the diameter of the tunnel and the thickness of the lining. Idealized Ricker wavelets are utilized as dynamic excitation, being representative of real seismic events. The results, including maximum differential displacements between the crown and the invert, as well as the maximum bending moments and axial forces in the lining, are found to compare well with existing elastic solutions. As a real case study, the paper investigates the causes of failure of the Bolu tunnel during the 1999 Düzce (Turkey) earthquake. It is concluded that the intensity of the seismic motion due to the proximity to the seismic source must have played a major role. The 1 m convergence observed before the earthquake, that was due to squeezing ground conditions, not only contributed to the reduction of the soil strength surrounding the tunnel, but also drove the lining very close to failure even before the earthquake struck. Had the tunnel not been in such a limiting state, it would possibly have survived the earthquake.

1 INTRODUCTION

1.1 *General*

Underground structures are generally considered to be "immune" to earthquakes, proven by their successful seismic performance in the past. However, most tunnels are designed and constructed without any seismic consideration. During the last few years, and after the collapse of the Daikai subway metro station in Kobe, Japan, the need for this consideration of earthquake loads in the design of underground structures has become clear. The collapse of the 400-m-long section of the twin bored tunnel of Bolu, Turkey, confirmed in a tragic manner the need for earthquake resistant tunnel design.

Underground structures have features that make their seismic performance different from the usual surface structures, such as their complete enclosure in rock or soil, and their significant length in comparison to the dimensions of their cross-section. The main causes of seismically induced failures in tunnels are liquefaction, fault rupture and strong seismic shaking. Regarding the recorded seismic performance of underground structures, the following general observations, among others, can be made:

- As the thickness of the overburden increases, the seismic competence of the tunnel generally improves.
- Tunnels in soft soil are more vulnerable than tunnels in rock.

1.2 *Past performance of underground structures*

Two cases of collapse of an underground structure due to severe earthquake shaking have been reported so far. The Hyogoken-Nambu earthquake in Kobe in 1995 caused the collapse of the underground subway station in Daikai, which had been constructed with the cut & cover method. The design of the station, made in 1962, did not take into account seismic actions. It is the first underground construction to fail during a seismic incident. During the earthquake the station's central columns collapsed leading to the collapse of the ceiling slab and the 2.5 m sinking of the soil cover.

The November 12, 1999 Düzce earthquake caused the collapse of the Bolu tunnels, 300 m from their east

Copyright © 2005 Taylor & Francis Group plc, London, UK

portal. The tunnels had a total length of 3360 m and a cross-section 15 m in height and 16 m in width. Their construction constituted a challenge since the project had to cross a number of fault zones in parallel to the Anatolia fault. At the moment of the earthquake an 800 m section had been excavated, while the permanent lining had been completed at a length of 300 m. The collapse took place in clay gauge material in the unfinished section of the tunnel. The lining of the collapsed section included shotcrete and anchors. Various mechanisms have been proposed to explain the collapse of the tunnels. They include: strong seismic shaking, displacement along the direction of the fault gauge material, and landslide mechanisms.

Finally, it should be noted that underground structures in the United States survived the Loma Prieta and the Northridge earthquakes with only minor damage. However, the level of seismic shaking was much lower than the maximum anticipated events, in which case a significantly increased level of damage should be expected (Hashash et al., 2001).

2 THEORETICAL BACKGROUND

2.1 *Dynamic response of tunnels*

Usually, the dynamic response of a tunnel is approached through the use of an elastic circular beam subjected to deformations imposed by the surrounding soil. Underground structures are subject to two types of seismically induced deformations: a) along the longitudinal axis of the tunnel: axial compression and extension, in combination with longitudinal bending, and b) in the transverse direction (i.e. perpendicular to the tunnel axis): ovaling of circular cross-sections, which will be the subject of this paper, and racking of rectangular cross-sections (see Fig. 1). The axial distress is caused by seismic waves traveling parallel to the tunnel axis, causing alternating compression and tension. Ovaling or racking deformations, on the other hand, are caused by those components of the seismic waves which produce motions perpendicular to the tunnel axis.

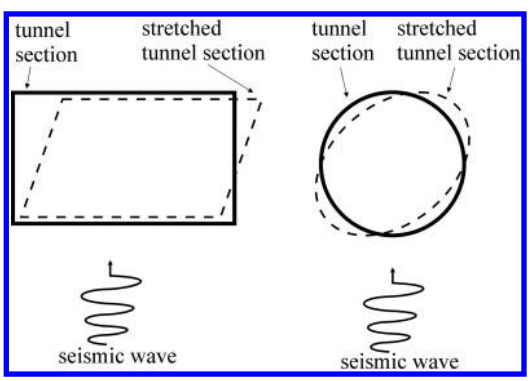


Figure 1. Deformation of tunnel cross section due to shear wave propagation.

2.2 *Free-field ovaling deformation*

The shear distortion of the ground caused by vertically propagating shear waves is probably the most critical for underground structures. To estimate the shear distortion imposed to the tunnel, not taking into account Soil–Structure Interaction (SSI), usually termed as the free-field shear strain, there are two possibilities: i) evaluation of the shear strain profile induced by a seismic excitation, making use of the equivalent linear one-dimensional wave propagation method (SHAKE, 1972), ii) for deep tunnels located in relatively homogenous soil or rock, use of the simplified procedure proposed by Newmark to estimate the maximum free-field shear strain γ_{max} from the equation:

$$\gamma_{\max} = \frac{V_s}{C_s} \tag{1}$$

where V_s is the peak particle velocity; and C_s the shear wave velocity.

2.3 *Ovaling deformation taking Soil–Structure Interaction into account*

When the tunnel is relatively rigid compared to the surrounding soil, it tends to resist and modify the imposed deformations instead of complying with them. Taking into account Soil–Tunnel Interaction, plays a decisive role in the realistic determination of the tunnel response. The strains developed on the lining depend on the compressibility ratio and the flexibility ratio of the structure, the overburden pressure (γh), and the lateral earth pressure coefficient (K_0). In order to simulate the seismic loads generated by shear waves, the free-filed shear stress replaces the overburden pressure and the coefficient of lateral earth pressure is assumed to be equal to 1 to approximate simple shear.

The tunnel rigidity in relation to the surrounding soil is quantified through the compressibility and flexibility ratios (C and F), which are measures of the resistance against tension and bending (resistance to ovaling) (Hashash et al., 2001, which refers to Merritt et al., 1985).

$$C = \frac{E_m(1-\nu_l^2)r}{E_l t(1+\nu_m)(1-2\nu_m)} \tag{2}$$

Copyright © 2005 Taylor & Francis Group plc, London, UK

$$F = \frac{E_m(1-\nu_l^2)r^3}{6E_l I(1+\nu_m)} \quad (3)$$

where E_m = the Young's modulus of the medium; ν_m = the Poisson's ratio of the medium; E_l = the Young's modulus of the lining; ν_l = Poisson's ratio of the lining; t = thickness of the lining; I = Moment of inertia of the lining; and r = Tunnel radius.

If we assume full slip conditions, without tangential shear force, the diametric strain $\Delta d/d$, maximum thrust T_{max} and maximum bending moment M_{max} are given by (Wang, 1993):

$$\frac{\Delta d}{d} = \pm\frac{1}{3}K_1 F\gamma_{max} \quad (4)$$

$$T_{max} = \pm\frac{1}{6}K_1\frac{E_m}{(1+\nu_m)}r\gamma_{max} \quad (5)$$

$$M_{max} = \pm\frac{1}{6}K_1\frac{E_m}{(1+\nu_m)}r^2\gamma_{max} \quad (6)$$

where

$$K_1 = \frac{12(1-\nu_m)}{2F+5-6\nu_m} \quad (7)$$

According to the literature, full slip on the tunnel-soil interface is possible only for tunnels in soft soil or in cases of very intense seismic loading. For most tunnels, the condition on the tunnel-soil interface is between full slip and no-slip, therefore the two cases must be studied for critical forces on the lining and critical deformations of the soil. Despite the above, assuming full slip under simple shear conditions, we may be led to substantial underestimation of the maximum thrust, therefore the assumption of the no-slip condition is recommended when calculating the thrust on the lining, as conservative:

$$T_{max} = \pm\frac{1}{6}K_2\frac{E_m}{(1+\nu_m)}r\gamma_{max} \quad (8)$$

where

$$K_2 = 1 + \frac{F[(1-2\nu_m)-(1-2\nu_m)C] - \frac{1}{2}(1-2\nu_m)^2 + 2}{F(3-2\nu_m)+(1-2\nu_m)C + C\left[5/2 - 8\nu_m + 6\nu_m^2\right] + 6 - 8\nu_m} \quad (9)$$

On the other hand, the full slip condition gives more conservative results in terms of bending moment and lining deflection. Penzien and Wu (1998) developed similar elastic solutions for the thrust, shear force, and bending moment on the tunnel lining due to distortion. These solutions yield results for the thrust and moment that are similar to those by Wang for sliding conditions. However, the value of the thrust from Wang's solutions is much higher than the one calculated by Penzien for no-slip conditions.

3 NUMERICAL SIMULATION

3.1 *The finite difference model*

The dynamic response of the tunnel is analyzed numerically making use of the finite difference code FLAC (Itasca, 1998). The numerical model, depicted in Figure 2, consists of a 70 m thick soil deposit overlying rigid bedrock. Three different tunnel diameters are parametrically investigated with the overburden height kept constant at 32 m. The lateral boundaries of the model extend 50 m from the tunnel center. A linear elastic constitutive model is used for the soil, assuming unit weight ρg = 1.8 t/m^3, Young's modulus E_m = 350 MPa and Poissoin's ration ν_m = 0.45. The concrete tunnel lining is simulated through the use of two-dimesional beam elements. Young's modulus for the lining is taken as E_l = 24 GPa and Poisson's ratio ν_l = 0.2. Three tunnel radii are taken for the numerical analysis: r = 4, 6 and 9 m with lining thicknesses t = 0.3, 0.45 and 0.675 m respectively, thus keeping the flexibility ratio of the lining constant.

Idealized Ricker wavelets, with dominant frequencies of 1 Hz and 2 Hz, and PGA = 0.4 g are utilized as dynamic excitation, applied at the base of the model. Since the shear wave velocity of the soil layer is about C_s = 260 m/s, the 1.0 m by 1.0 m zones used in the numerical analysis should not interfere with the propagation of shear waves having frequencies up to approximately 25 Hz.

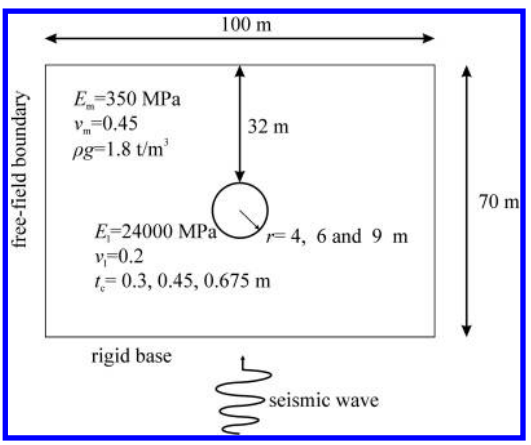


Figure 2. FLAC model used in the numerical simulations.

Copyright © 2005 Taylor & Francis Group plc, London, UK

Rayleigh damping was used with constant damping ratio equal to 10%, corresponding to a central Rayleigh frequency lying between the predominant frequencies of the dynamic excitation and the fundamental frequency of the soil layer. Free field boundary conditions were assigned at the lateral edges of the model.

The analysis is conducted in three consecutive steps:

1. Establishment of the initial state of stress of the soil deposit under gravitational loading with lateral earth coefficient $K_0 = 0.8$.
2. Establishment of the state of stress after the excavation of the tunnel and placement of the lining.
3. Dynamic excitation.

3.2 *Discussion of results*

Results include the measurement of maximum differential displacements between the crown and the invert of the tunnel caused by the excitation, as well as the maximum bending moments and axial forces developed in the lining. The results of the analyses are summarized in Table 1.

Furthermore in Figure 3a the time history of the bending moment exerted on the lining is shown for the case of tunnel radius 4 m and 1 Hz Ricker pulse. The maximum bending moment occurs at time t = 1.32 sec. The corresponding horizontal differential displacement time history is shown in Figure 3b.

As it is observed from Figure 3 the maximum bending moment on the lining occurs when the differential displacement of the crown and the invert of the tunnel is maximized. Similar conclusions arise for the rest of the numerical models.

Table 1 clearly indicates the effect of the dynamic excitation on the stability of the tunnels studied. This effect is primarily observed on the bending moment magnitudes. The dynamic analyses yield bending moments an order of magnitude higher than the ones due to static loading. This effect may be also observed for the axial thrust of the tunnel lining, but in this case it is less pronounced.

The increase of the lining moments and axial forces is much more pronounced for lower excitation frequencies (Ricker of 1 Hz). In this case, the excitation dominant period becomes comparable to the fundamental period of the soil layer:

$$T = \frac{4H}{C_s} = \frac{4 \cdot 70\ m}{260\ m/s} = 1.08\ \text{sec}$$

The effect of the wavelet frequency on the soil deposit response may be observed in Table 2, where the maximum acceleration at the ground surface is presented.

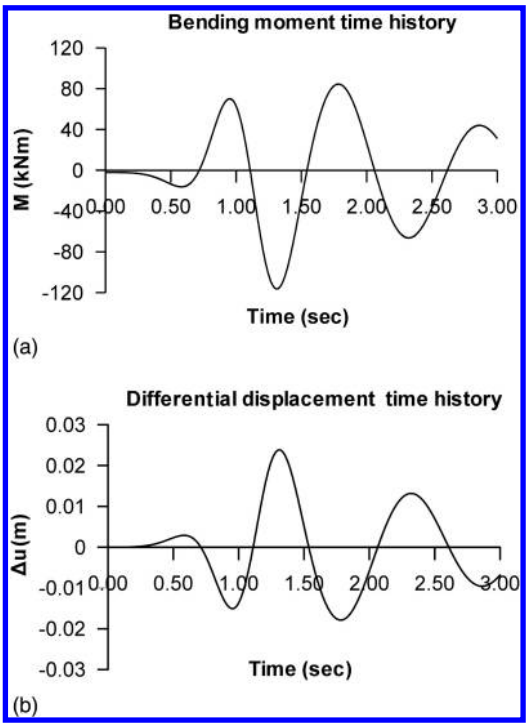


Figure 3. (a) Time histories of bending moment and (b) differential displacement of the crown and the invert of the tunnel for tunnel radius 4 m and Ricker wavelet frequency 1 Hz.

Table 1. Summary of results of the numerical analysis.

Tunnel radius (m)	Excitation frequency (Hz)	Static analysis		Dynamic analysis		
		M (kNm)	T (MN)	M_{max} (kNm)	T_{max} (MN)	Δu_{max} (cm)
4	1.0	12	2.2	116	3.6	2.38
4	2.0	12	2.2	34	2.5	0.63
6	1.0	27	3.5	244	5.3	3.67
6	2.0	27	3.5	73	3.8	0.90
9	1.0	52	5.6	587	7.8	5.58
9	2.0	52	5.6	162	5.8	1.29

Table 2. Peak ground acceleration at the surface calculated from the numerical models.

Tunnel radius (m)	Excitation frequency (Hz)	Peak Ground accelaration (g)	Peak particle velocity (tunnel level) (m/s)
4	1.0	0.67	0.65
4	2.0	0.47	0.23
6	1.0	0.67	0.65
6	2.0	0.46	0.23
9	1.0	0.66	0.65
9	2.0	0.46	0.23

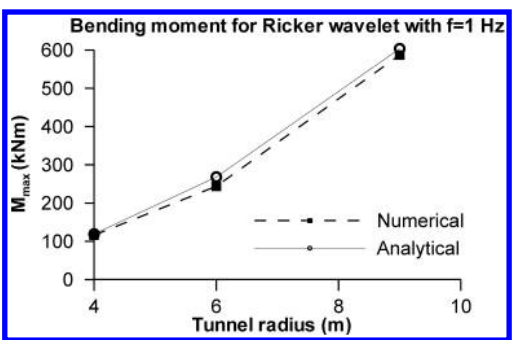
Copyright © 2005 Taylor & Francis Group plc, London, UK

3.3 *Comparison with analytical procedures*

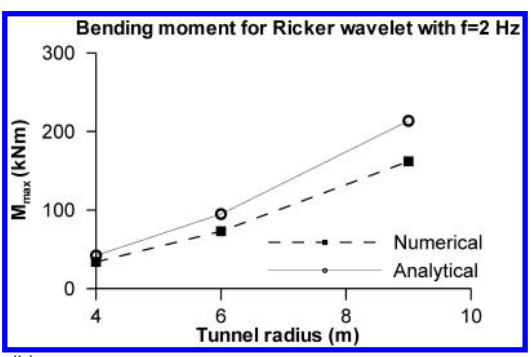
As mentioned earlier, the seismic response of tunnels can be analyzed by the use of closed form solutions (Hashash et al., 2001). According to this procedure, the dynamic motion at the tunnel depth must first be estimated, based on the peak ground acceleration. Table 2 presents the maximum acceleration at the ground surface as well as the values of the peak particle velocity at the depth of the tunnel.

Table 3. Bending moments and axial forces on the lining evaluated with analytical procedure from eqs (1) through (9).

Tunnel radius (m)	Excitation frequency (Hz)	γ_{max}	Full slip		No slip
			M (kNm)	T (MN)	T_{max} (MN)
4	1.0	0.00250	119	0.03	1.2
4	2.0	0.00088	42	0.01	0.4
6	1.0	0.00250	268	0.05	1.8
6	2.0	0.00088	95	0.02	0.6
9	1.0	0.00250	604	0.07	2.7
9	2.0	0.00088	214	0.02	1.0



(a)



(b)

Figure 4. Comparison of numerical and analytical results for the dynamically induced bending moments on the tunnel lining.

Thus the maximum shear strain at the depth of tunnel may be calculated from eq.(1) with C_s = 260 m/s for the soil parameters selected for the analyses. Maximum bending moments and thrusts on the lining of the tunnel may be evaluated from eqs (2) through (9). The results of this procedure are presented in Table 3.

In Figure 4 the maximum bending moments on the lining derived from the FLAC models with respect to tunnel diameter are compared to those calculated using the aforementioned analytical procedure, showing quite an agreement between the analytical and numerical results.

4 THE BOLU TUNNEL

4.1 *Analysis of the seismic performance of the Bolu tunnel*

In order to investigate the Bolu tunnel failure during the 1999 Düzce earthquake, a fully non-linear analysis was conducted, using the finite difference code FLAC. The geometry of the tunnel and the soil properties used in the analyses were obtained from the literature and a first approach to the causes of the tunnel failure is attempted herein.

The dimensions and the shape of a typical cross section of the part of the tunnel that collapsed are shown below, according to Dalgic (1999). The lining of this cross-section consisted of 70 cm of shotcrete and was simulated in the analyses with beam elements.

The Düzce earthquake record, scaled at 0.6 g to take account of the proximity of the tunnel to the fault, was reasonably selected as the excitation (Figure 6).

The soil profile used in our analyses is the one proposed by Amberg & Rousso (2001) while the shear wave velocities and the shear moduli were taken from O' Rourke et al. (2001). Therefore, starting from the

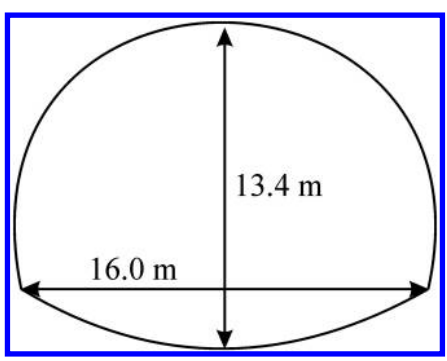


Figure 5. Geometry of the cross section that was used for the analysis.

Copyright © 2005 Taylor & Francis Group plc, London, UK

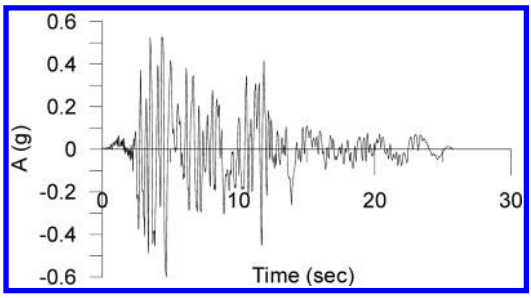


Figure 6. Düzce record.

base of the model and moving upwards the soil properties are:

- Bedrock: $V_s = 2500$ m/sec, and $\rho = 2.7$ ton/m^3,
- High plasticity flyschoid: $V_s = 650$ m/sec, and $G = 850$ MPa,
- Sandstone: $V_s = 695$ m/sec, and $G = 1000$ MPa,
- High plasticity flyschoid: $V_s = 610$ m/sec, and $G = 750$ MPa,
- Sandstone: $V_s = 695$ m/sec, and $G = 1000$ MPa

Two different models were developed to simulate the particularly significant convergence phenomena that took place before the earthquake and played a significant role in the reduction of the strength characteristics of the soil surrounding the tunnel. In both models the nonlinear soil behavior is simulated using the Mohr-Coulomb failure criterion.

In the first case the modulus of elasticity of the soil zone surrounding the tunnel, which is 16 m thick (i.e. one tunnel diameter), is reduced to 65% of the flyschoid's initial modulus of elasticity. In this way, we attempted to simulate the plastic zone surrounding the tunnel after the excavation. This approach is shown schematically in Figure 7. In the second model the lateral earth pressure coefficient k_0 was increased to 1 attempting to simulate the squeezing ground stress conditions that led to the enormous tunnel convergences of the order of 1 m.

4.2 *Discussion of results*

The results of the analyses of both models show a significant increase of the axial force and bending moment that act on the lining. This increase is more intense at the invert and at the elephant foot.

For the axial load, we observe that its value during the static equilibrium ($N_o \approx 12$ MN) drives the lining concrete to a limiting condition. Specifically, if we consider concrete C 20/25, the maximum compressive force the lining is capable of undertaking is 20 MPa $\times$ 0,7 m^2 $\approx$ 14 MN. Since the analysis aims at investigating the failure, no safety factors are taken into account. Additionaly, the nominal strength value

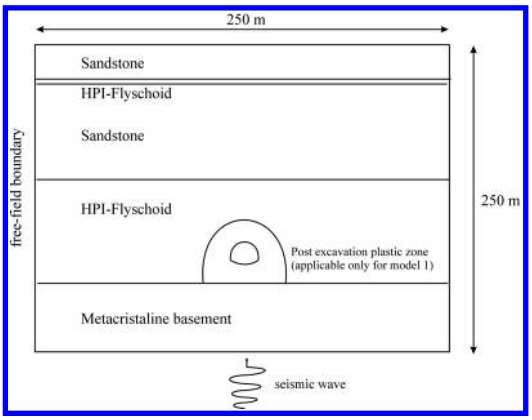


Figure 7. Soil profile of the models adapted for the numerical simulations.

of 20 MPa may be considered as a minimum limit, since the real value of the concrete strength often exceeds this value by far.

5 CONCLUSIONS

Our parametric study showed that the soil layer properties in combination with the seismic excitation characteristics can play a decisive role in the distress of the tunnel section, i.e. the bending moments and axial forces that develop within the tunnel lining. Moreover, the stiffness of the tunnel is found to be a very important parameter with respect to the magnitude of the bending moments and forces that act on the lining. Therefore, for a proper seismic design both the strength and flexibility of the tunnel should be considered. Finally, our numerical analysis results are found to compare well with analytical solutions, which in some cases constitute an upper bound estimate of the internal forces in the lining.

As far as the study of the Bolu tunnel is concerned, it is concluded that the increased intensity of the seismic motion as well as the proximity to the seismic source must have played a major role towards the collapse of the tunnel. Furthermore, the soil conditions have contributed to the aggravation of the situation. Indicative of the latter is the fact that the part of the tunnel that collapsed laid inside fault gauge material. Finally, the significant convergence of the tunnel ($\approx$1 m) observed before the earthquake due to squeezing ground conditions, not only contributed to the reduction of the soil strength surrounding the tunnel, but also drove the lining very close to failure before the earthquake struck. Had the tunnel not been in such a limiting state, it would possibly have survived the earthquake with only minor damage.

Copyright © 2005 Taylor & Francis Group plc, London, UK

REFERENCES

Amberg, W., Russo, M. 2001. Seismic Design of Underground Structures – The Bolu Tunnel. *Proceedings of the AITES-ITA 2001 World Tunnel Congress*. Milano, (I), Vol.1, 137–147.

Dalgic, S. 2002. Tunneling in squeezing rock, the Bolu tunnel, Anatolian Motorway, Turkey, *Engineering Geology* Is.67, 73–96.

Hashash, Y.M.A., Hook, J.J., Schmidt, B., Yao J.I-C. 2001. Seismic design of underground structures. *Tunnelling and Underground Space Technology* 16 (4), 247–293.

Itasca Consulting Group Inc. 1998., *FLAC2D, Version 3.40: Fast Legrangian Analysis of Continua – User's Manual.*

Merritt, J.L., Monsees, J.E., Hendron, A.J., Jr., 1985. Seismic design of underground structures. *Proceedings of the 1985 Rapid Excavation Tunneling Conference*, Vol. 1, 104–131.

O'Rourke, T.D., Goh, S.H., Menkiti, C.O., Mair, R.J. 2001. Highway tunnel performance during the 1999 Düzce earthquake *Proceedings of the Fifteenth International Conference on Soil Mechanics and Geotechnical Engineering*, Istanbul, Turkey.

Penzien, J., Wu, C. 1998. Stresses in linings of bored tunnels. *Int. J. Earthquake Eng. Struct. Dyn*. 27, 283–300.

St. John, C.M., Zahrah, T.F. 1987. Aseismic design of underground structures. *Tunneling Underground Space Technology* 2 (2), 165–197.

Wang, J.-N. 1993. Seismic Design of Tunnels: A State-of-the-Art Approach. Monograph 7. Parsons, Brinckerhoff, Quade and Douglas Inc.

Copyright © 2005 Taylor & Francis Group plc, London, UK

Seismic assessment results and actual application in the complex ground conditions of Bolu tunnels after the 1999 Duzce earthquake

M. Ozben
Technical Research Department, K.G.M., Ankara, Turkey

F. Tokgozoglu & S. Isik
Yuksel Proje Uluslararasi A.S., Bolu, Turkey

ABSTRACT: The Anatolian Motorway Gümüsova-Gerede Section, a portion of the Trans-European Motorway (TEM) network, will link Ankara to Istanbul and Turkey to Europe. Stretch-2 of the Gumusova-Gerede motorway, a portion of which is under construction comprises twin tunnels of 2790 m and 2963 m. The tunnels are being excavated in a faulted and heavily tectonised sequence. Being in the first degree seismic environment in of the North Anatolian Fault Zone, the tunnels were significantly affected by Duzce Earthquake of 12th Nov. 1999. This paper describes the detailed studies undertaken as part of the re-assessment of the effects of the 1999 Düzce earthquake having the magnitude of Mw = 7.2 on the 18 m diameter highway tunnels. Following the earthquake, detailed seismic design studies have been carried out. The aim of the seismic design is to allow for serviceability of tunnels for emergency usage and easy repair within a short period after a new seismic event. The new design strike a balance between too stiff a lining and too soft a lining (which might attract excessive grounds loads). To verify the new design, a comprehensive instrumentation program was implemented to monitor the actual tunnel performance. Some instrumentation results are presented here which provide an insight into tunnel behaviour in such poor ground conditions.

1 INTRODUCTION

The construction of the Gumusova-Gerede section of the Trans-European Motorway (TEM) commenced in 1988 with various stretches completed and opened to the public traffic at intervals between December 1992 and August 1996.

Bolu mountain crossing twin highway tunnels, are 18 m in excavated diameter and lengths of 2963 m and 2790 m according to the new alignment. The ground pillar between two tunnels is approximately 50 m. Overburden above the tunnels is up to maximum 250 m, with the majority of the tunnels under a cover of 80–150 m. Ground water levels were 45%–95% of the overburden cover above the tunnel crown along the new alignment. The face excavation area of twin tunnels varies between 133 m^2–260 m^2, depending on ground conditions, lining thickness and deformations. Each tube comprises 13.00–8.2 m excavation diameter for an equivalent circle.

The twin tunnels are being excavated in a faulted and heavily tectonised sequence. Tunnel design was prepared based on standard Austrian Rock Classification system (1992–1994). The original tunnel design was performed according to NATM principles, with shotcrete, rock bolts and light steel sets. The highway tunnels are located in a first degree seismic environment in to the North Anatolian Fault Zone, and were significantly affected by the Duzce earthquake of 12th November 1999. The epicenter of the Duzce earthquake was approximately 20 km from the northern Asarsu portals of the tunnels. The peak ground acceleration (PGA) at the project site was measured as 0.81 g. The performance of Tunnels have been assessed at different stress levels arising from excessive loading in different seismic hazards caused by the earthquake using the intrinsic characteristic structure of soil. The findings have been used in developing the basic method and philosophy in determination of main lines for re-designing the tunnel. This also plays a significant role in ground water pressure. Following Turkey earthquakes of 17 August and 12 November 1999 detailed site investigation and seismic design studies have been carried out. Two seismic hazards affecting the tunnels have been considered.

Copyright © 2005 Taylor & Francis Group plc, London, UK

Table 1. Measured strength and stiffness parameters

	Peak		Residual		
Unit	ϕ[6]	c[6](kPa)	ϕ[6]	c[6](kPa)	G_o/σ'_v[7]
High PI[5] flysch clay (clayey matrix 80% to 100%)	15°–17°	100	9°–12°	50	500[1]
Blocky flysch clay (clayey matrix 60% to 65%)	20°–25°	100	13°–17°	50	650[1]
Area 3 FG[3] clay	13°–16°	100	9°–12°	50	700[1]
AS/EL FG[3] clay	18°–24°	100	6°–12°	50	NA[4]
Metasediments	25°–30°	50	20°–25°	25	825[1]
Crushed MCB	20°–25°	50	15°–20°	25	950[1]
Sound MCB[2]	55°	1500	NA[4]	NA[4]	High

[1]From high quality pressure meter tests; [2]Metacrystalline basement rock; [3]Fault gouge; [4]Not available; [5]Plasticity index [6]ϕ', c′ = effective stress friction angle and cohesion, respectively; [7]G_o/σ'_v = ratio of max shear modulus to initial vertical effective stress.

2 GROUND CONDITIONS

The tunnels are excavated through highly tectonised and faulted sequences of rocks, and intermixed series including flyschoid of mudstones, siltstones-limestones and amphibolite, with stiff heavily slickensided, highly plastic fault gouge clay. The proportion of the clayey matrix by volume varies from about 30% to 100%. In some zones, the ground consisted of uniform fault gouge with no hard inclusions forming the least favorable conditions. To date such zones have been encountered in thickness of up to 50 m along the tunnel alignment, which also extend sub-vertically up to ground level (i.e. overburden cover 80 m to 120 m of poor material). The mixed ground conditions have made tunneling difficult. Along some sections of tunnel the dip of the slickensided surface has been toward the face with the potential for large blocks to slide into the work area. Face bolting was used to reduce this risk. In 1998/99, a detailed characterization of the ground ahead of the tunnel faces was implemented via a pilot tunnel test program (Geo Consult 1998). The mechanical properties are given in Table 1.

The geology at and near the fault zone consists of highly tectonised and intermixed series of mudstones, siltstones and limestones with stiff heavily slickensided highly plastic pure foult gouge clay. This fault gouge clay layer is between metasedimentary rocks (and quartzic rocks and amphibolite of the Metacrystalline basement strata (MCB). The meta sedimentary rocks comprise metasiltstone, metalimestone, quartzic limestone, crystallized limestone, blocks with bedded and slickensided low to medium plastic firm to stiff sandy silty to clay fault gouge matrix). This fault gouge material is at the interface between Asarsuyu – Elmalik geological formation. The proportion of the clayey matrix varies substantially between the different geotechnical units, such that the worst ground comprises wide zones of uniform pure fault gouge clay (Ozben 2003). Figure 1 shows the location of some of the more extensive fault gouge zones.

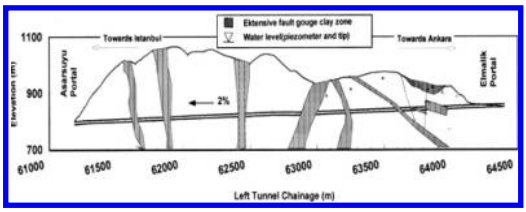


Figure 1. Tunnel geology-fault zones and ground water tables.

3 EARTHQUAKE PERFORMANCE OF TUNNELS

Site inspection of the tunnels was carried out after the Duzce earthquake. The damage patterns discovered are summarized below.

3.1 *Relevant site observations*

The epicentre of the Mw 7.2 earthquake was approximately 20 km (Erdik 2001) from Asarsu portals of the tunnels. The surface rupture of the fault was within 3 km of these portals. Peak acceleration and velocity recorded at the nearest strong motion station at Bolu were 0.81 g and 66 cm/s, respectively. It was initially concluded that this damage was due to ground shaking alone since no surface ruptures had been observed to cross the tunnel alignment and no fault offset displacements were evident within the accessible parts of the tunnels. In the main Asarsu tunnels within the metasediments, slight-moderate damage was observed as slabbing and spalling of shotcrete, and also longitudinal cracking and deformation of the potentially weak Top Heading-Bench joint.

In the Asarsu Left Tunnel Bench Pilot Tunnels (BPT) in fault gouge clay, moderate – severe damage was observed. Invert heave of 0.5 to 1.0 m occurred, together with damage to the shotcrete arch lining comprising shotcrete concrete (S/C) slabbing, spalling,

Copyright © 2005 Taylor & Francis Group plc, London, UK

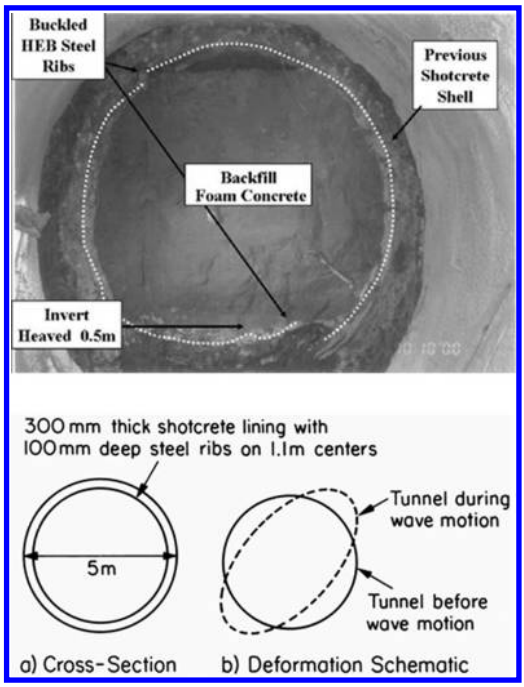


Figure 2. Picture during re-mining of Bench Pilot Tunnels (BPT) showing typical floor heave and buckled steel rib + shotcrete shell. (a-b) BPT Cross-Section and Seismic Distortion.

S/C compression crushing and associated steel rib buckling at crown, shoulder and knee areas (Figure 2) (O'Rourke, Goh, Menkiti, Mair 2001)

In both Asarsu main tunnels, cracking of the monolithic concrete invert was observed as longitudinal tensile-type cracks. Running close to the centerline and occasional shear-type cracks deviating away from the centerline towards the sides. Crack widths were 0.5 cm–5 cm, depending on ground conditions, invert thickness and reinforcement levels. In the Asarsu Right (ASR) tube in fault gouge clay, various levels of reinforcement bar had been installed in the invert – allowing a quantitative assessments to be made. It was found that 51 cm^2/m shear steel cages installed at the sides of inverts in clayey metasediments successfully prevented shear-type cracks. However, 25 cm^2/m tensile reinforcement mats placed near the top of the invert similar to the ground could distribute and limit (but not prevent) tensile cracking.

Inspection pits in this area showed a steel-concrete bond failure mechanism, rather than tensile failure/necking of the 36 mm diameter ribbed bars. Most critically, it was noted that the reinforcement for the Option 3 support system lead tunnel successfully prevented the development of any tensile or shear cracks in inverts within the low strength Asarsu/Elmalik (AS/EL) main fault gouge clay.

In general, the site observations confirmed that the observed damage pattern is consistent with loading induced by vertically propagating earthquake shear waves. This supports the basic assumptions of the dynamic analyses that are being conducted.

Severe damage in the form of complete collapse of two parallel 16.5 m diameter main tunnels occurred during the earthquake near the southern Elmalik portals. The tunnels were excavated in main fault gouge clay, at a center-to-center separation of 54 m and supported by 45 cm–75 cm of shotcrete (f_{cu} = 20/30 MPa). Large deformations necessitating re-profiling works had occurred in this area before the earthquake. During the earthquake itself, the right tube lining was breached with inrush of clayey material and complete blockage of the tunnel so that miners had to escape through a cross-adit and via the left tube. At this time the left tube was collapsing with falling blocks of shotcrete and clay. Within 1–2 hours of the main shock, the left tube too had become blocked by clay debris. The collapse in the right tube propagated upwards through 50 m of cover to cause a 5 m diameter sinkhole and concentric ground cracks at the surface during the earthquake. Progressive failure occurred, confirmed by the generation of another 8 m diameter sink hole over the left tube, through 122 m of cover, some 4.5 months after the earthquake (Menkiti, 2000).

3.2 *Instrumentation results*

Following the earthquake; concrete crushing, shear cracking and offset displacement of the lower footing were observed in Bernold No.2, near the face excavations in the surviving Asarsuyu drives. Pre and post earthquake deformation readings are available which allow an assessment of the induced deformations in Bernold blocks 1&2. Figure 3 shows the 3-D optical deformation reading for Bernold 1. It is acknowledged that the accuracy of this system is limited to several millimetres. It can be seen that a settlement of about 10 mm and a convergence of about 14 mm is indicated as having being induced by the earthquake. Rigid body offset displacement of 150 mm is also indicated by the 3-D data. Pre and post-earthquake measurements were available at 5 different sections in the inner lining within clayey metasediments. Figure 4 shows the typical configuration with pressure cells and embedded strain gauges at various points around the inner lining. The lining hoop stress changes at the crown of Block 54 are also shown, as typical results. Figure 4 shows also the earthquake induced radial stresses on inner lining from pressure cells and embedded strain gauges. Peak values of up to 10 MPa (equivalent to about 17% of the overburden) are induced at the crown and feet of the arch lining, representing a significant proportion of the

Copyright © 2005 Taylor & Francis Group plc, London, UK

strength reserve (O'Rourke, Goh, Menkiti and Mair 2001). The results of geotechnical instrumentation show that permanent increases in bending moment and compressive hoop stress equivalent to about 17% of the overburden were induced by ground shaking.

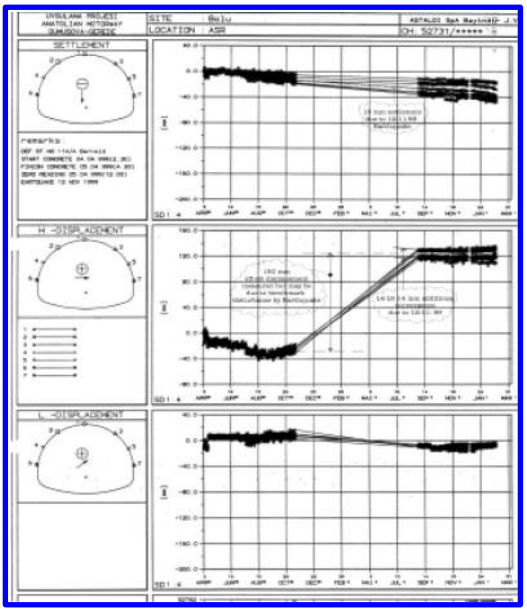


Figure 3. (3D) optical deformation reading for Intermediary Lining (B40 MPa, ds = 60 cm) from station 114/A in ASR tunnel on before and after earthquake.

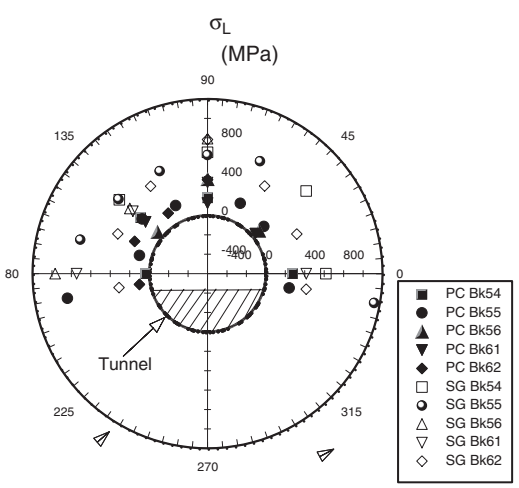


Figure 4. Earthquake induced radial stresses (kPa) on inner lining from pressure cells and embedded strain gauges.

4 SEISMIC CONSIDERATION AFTER 17 AUGUST GOLCUK AND 12 NOVEMBER DUZCE EARTHQUAKES

Following the 17 August and 12 November Duzce earthquakes of 1999, the Client (KGM) instructed an upgraded seismic criteria. Before the 12.11.99 earth quake the Contractor was asked to review the seismic design of the Bolu tunnels utilising detailed dynamic analyses to quantify earthquake effects. Following the 1999 earthquakes, the Client instructed a higher design earthquake design together with stringent performance requirements for the motorway immediately after the design event.

As a consequence, detailed dynamic analyses have been conducted to estimate the tunnel seismic loading and to provide a basis for determining the lining reinforcement. As input into this assessment a site specific seismic hazard assessment study had been carried out. The study was divided into two parts:

- A probabilistic site specific assessment of earthquake ground shaking (Erdik and Yilmaz 2000).
- An assessment of the fault rupture hazard in the site vicinity (Barka and Lettis 2000)

The project's philosophy is that the primary support may become over stressed during the design earthquake, but the inner lining remains undamaged. The new design earthquake was defined as a 2000 year return period event. Based on a probabilistic site specific seismic hazard update study conducted by Erdik, M. and Yilmaz, C. (2000), this design event was calculated to correspond to a peak ground acceleration of 0.81 g (Figure 5).

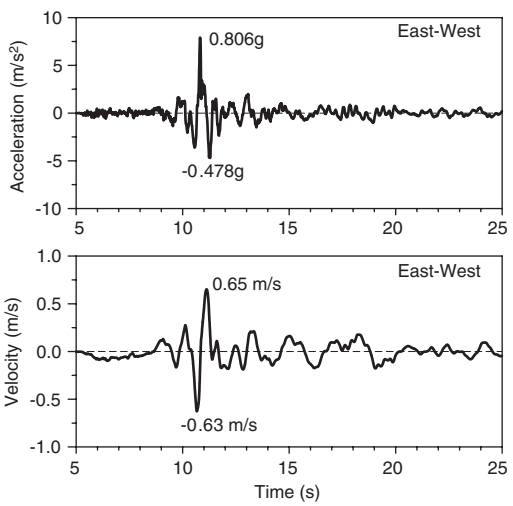


Figure 5. Strong Motion Time Records. Bolu Station Records for 12/11/99 Mw = 7.2 Earthquake E-W Records.

Copyright © 2005 Taylor & Francis Group plc, London, UK

The motorway tunnel is located in within the Anatolian through region. The review assessed the potential of faults in the vicinity of the project site to rupture within the design life of the motorway. Two potential active faults that may cross the tunnel alignment were identified. The Bakacak Fault is one of these active faults. In the event of rupture along these faults the associated earthquake was determined to be of (Mw = 6¼ to 6½) moderate level. The associated fault system is called the North Anatolian Fault Zone (NAFZ). The NAF is a right-lateral transformation fault, representing the boundary between the Black Sea and the Anatolian Plates. It extends a total length of about 1500 km running east-west. The Bakacak fault is identified as a short secondary fault in the step-over region between the two major NAF branches in the Bolu region (i.e. the northern Düzce branch and the southern Mudurnu branch). The location of the Bakacak fault is stated by the authors to cross left tunnel between Ch.62 + 800 and 63 + 000. This layer of fault gouge is at the interface between the Asarsuyu and Elmalik geologic domains identified in tunnel face logs (included 4 associated Bench pilot tunnels BPTs) and through vertical boreholes. According to the results of tunnel seismic design studies performed two potential earthquake hazards affecting the tunnels have been considered (Menkiti, Mair, O'Rourke and Russo, 2000). The hazards are:

- Strong Ground Shaking
- Fault Rupture Displacement

Seismic lining design loads have been derived for static loading and ground shaking, consistent with the Client's seismic performance specifications. The most severe loads from a pool of 11 earthquake records reflecting site conditions and including near field effects, were adopted for design (Menkiti, Kurzweil, Golser, 2000). It was found that the continuous zones of poor fault gouge clays required Option 3&4 support were the most critical. The Bakacak fault of this size may generate an Mw = 6¼ to 6½ earthquake with up to 30 to 50 cm of fault rupture. Conservatively a design value of 0.5 m has been adopted. Therefore high ground loads would be applied to the lining due to fault displacement.

A solution incorporatinf seismic displacement joints has been adopted (Lombardi, May 2001). A fault crossing design and retrofit strategy that addresses the above points has been developed. It consists of wide closely spaced seismic joints (every 4.4 m) to accommodate the fault rupture by slip and/or rotation. Seismic Joints would be created in the complete lining (BPTs, Bernold lining, Inner lining and Invert) at 4.4 m intervals in order to allow articulation. Figures 6 & 7 shows the typical inner lining and invert with seismic joints.

Inner lining block length of 4.4 m was chosen to suit the existing construction round length of invert and Bernold lining. This design strategy is ideally suited to accommodate the low probability event of distributed slip without significant damage to the tunnel. Concentrated slip and large relative movements may be concentrated at 1 or 2 seismic joints, necessitating local speed reductions prior to repairs. The rupture of the Mw = 7.2 12th November 1999 Düzce earthquake was about 5 km from Bolu Mountain crossing. In the Bakacak fault crossing the design has considered the following load cases.

a) Static loading plus severe ground shaking (design 2000 year return period of earthquake)
b) Static loading plus moderate ground shaking (M_w = 6–6.5) plus permanent fault offset.



Figure 6. Seismic joints of 4.40 m spacing and 0.50 m spanning are currently being constructed at the Bakacak Fault crossing.

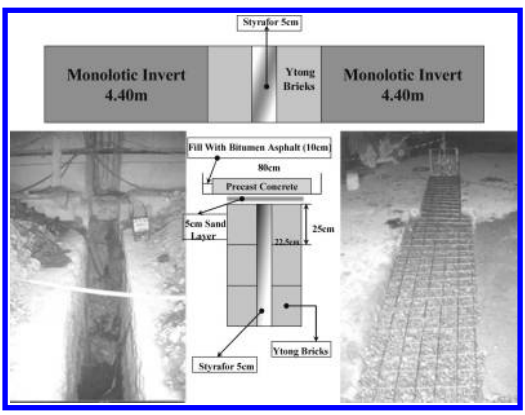


Figure 7. Detailed seismic joints in the monolithic invert.

Copyright © 2005 Taylor & Francis Group plc, London, UK

It is intended to cross the Bakacak fault zone using Option 4 design. Some modifications of the Option 3 and Option 4 design have been necessary to account for the new earthquake design criteria, imposed after the 1999 Golcuk and Düzce earthquakes. From the suite of 11 records the 3 most adverse have been selected as input into detailed Flac analyses to generate design lining loads. The momentary peak load, therefore considers the maximum peak load from the worst of the 11 accelerograms a severe loading condition. For the locked-in load, present after the earthquake the average lining loading derived from the 3 most severe earthquakes is used. As a result of dynamic analyses and following detailed dynamic analyses of the load case of severe ground shaking (Mw = 7.2) for Option 3 and Option 4 it was noted that Bakacak fault rupture was more critical than a medium size earthquake event. Weak ground conditions mean that the static loads would be high and a robust basic design would be required. The high dynamic strains are dissipated and attract the high dynamic loads on the existing tunnel support system under the seismic ground shaking. Therefore, negative dynamic loading is exerted on the already existing static load. For that reason, extra amount of steel reinforcement was required for the Bakacak fault crossing section of the tunnels. The dynamic analyses indicate that large quantities of steel are necessary for Option 3. Lower reinforcement is predicted for Option 4, which is inherently more resistant to earthquake loading. In both cases upgrade of the inner lining and Bernold lining concrete from B30 to B40 is required. Steel fibre has also been used in Bernold lining. These represent significant support upgrades relative to that required for static loading alone.

This design strategy is ideally suited to accommodate the low probability event of distributed slip without significant damage to the tunnel. This is done by concentrating concentrated slip, large relative movements may at 1 or 2 seismic joints, necessitating local speed reductions prior to repairs.

5 CONCLUSIONS

With 1999 earthquakes, very good earthquake performance experience was gained from completed tunnel section. Despite very high level seismic loading and fault displacement, very good earthquake performance of the tunnels was observed.

Following the earthquake, The Client asked for a higher design earthquake resistance (2000 year return period) together with stringent performance requirements for the motorway immediately after the design event. As a consequence detailed dynamic analyses have been conducted to estimate the tunnel seismic loading and to provide a basis for determining the lining reinforcement. Also, for the active faults crossing, articulations have been provided to accommodate the main part of the lateral displacement in the fault.

In conclusion, Bolu tunnels are very important with regard to the validity and practicality of the models developed for the seismic performance of tunnels.

Comparison of the damage observed and geological conditions and also design followed has indicated that these could be the basis for assessing the performance of tunnels and identifying the potentially hazardous zones.

REFERENCES

Geo Consult, (May 28,1998), *Experimental Investigations During Construction of Pilot Tunnel, Gümüsova-Gerede Motorway* project report No.45110/R/2148.

William Lettis & Asssociates Inc. & A.Barka, (September 30, 2000), *Geologic Characterisation of Fault Rupture Hazard*, Gümüsova-Gerede Motorway project report.

Tokgozoglu, F. & Isik, S. (October 6, 2002), *Seismic Consideration Of Bolu Tunnels After Duzce Earthquake and Possibile oluation Proposal*, International Conference/ Workshope & Exhibition on Tunnelling & Underground Space Use.

Geo Consult, (July 15, 1998), *Design Methodology Unexcavated Sections Gümüsova- Gerede Motorway*, project report, No.45110/R/2149.

Ozben, M. (2003), *Engineering Geology of Bolu Mountain Tunnel and Encountered Geological and Geotechnical Problems During Excavation and Their Effect on Tunnel Excavation and Support System,* Ph.D. Thesis.

Menkiti, C.O. & Mair, R.J. & Miles, R. (April 2001), "*Tunnelling in Complex Ground Conditions in Bolu, Turkey*" for Publication in the Proceedings of Underground Construction 2001.

Menkiti, C.O. & Işık, S. (April 7, 2001), *Investigation of Toughness, Energy Absorption Capacity and Modulus of Elasticity Observations of Tunnel Steel Fibre Reinforced Shotcrete and Intermediate (Bernold) Lining Concrete in Bolu Tunnels* of The Gümüsova-Gerede Motorway by Yüksel & Rendel JV.

Menkiti, C.O. & Işık, S. (June 8, 2000) *Stiffness-Strain Relationships From Pressuremeter Tests, Interface Fault Clay in Bolu Tunnels of* The Gumusova-Gerede Motorway by Yuksel & Rendel JV

Menkiti, C.O. (December 5, 2000), *Review of Deformations of Bernold Lining Blocks in Asarsuyu Right Tube, Originally Damaged By the 12/11/99 Earthquake and Then Further Deformed By Recent Construction Works.*

Lombardi, (May 2001), Gümüsova-Gerede Motorway *Asarsuyu Tunnels, Detailed Seismic Analysis-Op.3 + Op.4 and Active Fault Crossing-Design Philosophy and Joint Requirements*.

O'Rourke, T.D., Goh, S.H., Menkiti, C.O. & Mair, R.J. (2001), *Highway Tunnel performance during the 1999 Duzce earthquake.*

Menkiti, C.O., Mair, R.J., O'Rourke, T. & Russo, M. (October 9, 2000), *Minutes of Meeting on The Seismic Design Review of Bolu Tunnels.*

Menkiti, C.O. & Kurzweil, H.C. & Golser, W. (November 14, 2000), *Minutes of Meeting on The Seismic Design Review of Bolu Tunnels (Fault Crosing).*

Copyright © 2005 Taylor & Francis Group plc, London, UK

Geological and geotechnical investigations

Copyright © 2005 Taylor & Francis Group plc, London, UK

Geotechnical & tunnelling conditions below buried valleys in Sydney, Australia

Robert J. Whiteley
Coffey Geosciences Pty. Ltd., Sydney, Australia

ABSTRACT: Sydney's coastline reflects a drowned river system, 10 to 30 m deep, overlying deeper buried valleys 60 to 70 m deep. These buried valleys incise Sydney's main tunnelling medium, Hawkesbury Sandstone, and are infilled with sands and silts. While this Sandstone is an excellent tunnelling medium, conditions beneath the buried valleys are more variable due to valley heave and pose a major tunnelling risk in the Sydney region. Most tunnellers appreciate the potential difficulties with such features but not the value of geophysics, in particular borehole seismic tomography, in detailing these conditions prior to encountering them. Borehole seismic tomography accurately delineated complex features below the floor of buried valleys along two major tunnels in Sydney, the Epping Rail Link and the Northside Storage Tunnel. The ability of seismic imaging to extend borehole information in difficult and environmentally sensitive areas with detail on poor ground, geological structures, likely areas of local stress concentrations within the rocks and areas of potential water inflow allowed tunnellers to prepare in advance for these challenging conditions.

1 INTRODUCTION

Sydney is Australia's largest city with a population of 4 million. Major transport and wastewater tunnelling projects were begun in the Sydney region during the last decade of the 20th century and are continuing today with total value of tunnelling of about 4 billion Euros.

Over this period, rapid technological development of TBM's has contributed to successful tunnelling in Sydney, however, a major factor is the local geology. Sydney is underlain by essentially, flat-lying sedimentary rocks of the Sydney Basin (Branagan, 1985) with most rock tunnelling in the upper geological units of this Basin. These comprise the Triassic Ashfield Shale, Hawkesbury Sandstone and the underlying Narrabeen Formation. The main tunnelling unit is the Hawkesbury Sandstone. This is a high strength (25–70 MPa, typically 35 MPa) quartzose sandstone, some 280 m thick, that is an excellent tunnelling medium with few geotechnical constraints (Parker et al., 1999).

Like many cities, Sydney was developed near the coast around a magnificent harbour. The coastline is rugged and reflects an older river system drowned by the current, globally elevated sea levels. These drowned rivers are typically from 10 to 30 m deep and frequently overly even deeper buried valleys. These buried valleys are incised into the Hawkesbury Sandstone to depths of about 60 to 70 m below the present sea level and are infilled with sands and silts, mainly of Tertiary and Quaternary age. They are often highly irregular in section and profile and the rock beneath them is more deeply weathered and fractured due to the relatively rapid erosion that formed them and the valley heave processes that followed. These buried valleys present a major geotechnical risk and significantly add to tunnelling costs in the Sydney region. While most tunnellers appreciate the challenges of tunnelling where these features occur (e.g. Herrenknecht et al., 2004) they do not appreciate the value of geophysical methods in detailing these conditions prior to encountering them.

In the Sydney region geophysical methods including gravity, seismic refraction and marine seismic reflection have successfully located buried valleys along various tunnelling routes (Whiteley and Parker, 2001).

This paper, presents case studies using borehole seismic tomography to provide detailed information on the more complicated geotechnical conditions below buried valleys that had to be traversed during in rock tunnelling for two major tunnels in Sydney.

2 BOREHOLE SEISMIC IMAGING

Seismic imaging from boreholes with surface-to-borehole and crosshole transmission tomography has been available to the tunnelling industry for some time (Whiteley, 1998). However, these methods are still only applied where difficult subsurface conditions are

Copyright © 2005 Taylor & Francis Group plc, London, UK

expected or where surface conditions such as river crossings are expensive to investigate by alternative methods such as overwater drilling. The most frequently used imaging parameter is P-wave velocity. This can be related to engineering parameters such as rock strength (Table 1) and Q (Barton, 1998). What is less well understood is the relationship between seismic velocity and local stress fields that are present in rocks prior to tunnelling or are created during and following tunnelling.

Stress is known to affect the elastic properties of rocks and seismic wave propagation through them. In granular materials, such as sandstones, P-wave velocity increases with increasing external stress with the greatest effects at low stress levels, decreasing as stress levels increase (Radcliffe et al. 1986). These effects are closely related to the behaviour of microcracks in the rock and to its prior stress history that governs crack distribution and orientation. Increasing stress rapidly increases seismic velocity in a non-linear manner in response to crack closure and to actions at grain contacts. Once pressures exceed about 200 MPa velocity increases more slowly and in a manner that is related to the mineral constituents and the intrinsic elastic properties of the rock.

The situation is more complex during non-uniform stress relief within already stressed rocks, this tends to open existing microcracks and to promote microcrack growth, lowering seismic velocity. However, lower strength rocks may release stress completely, fail and essentially transmit P-waves at or near the fluid velocity whereas the higher strength rocks tend to concentrate residual stresses and to exhibit higher seismic velocity than would be expected at their burial depth.

In the Sydney region extensive stress measurements (Enever, 1999) has estimated that, for the depth interval 0 to 200 m in which all of the tunnelling to date has occurred the major horizontal principal stress due to tectonic forces about 6.5 MPa above the overburden stress but can be much greater in areas of high surface or buried topographic relief. As a result the seismic velocity distribution can be quite complex beneath buried valleys as the earlier non-uniform stress relief produced by differential removal of material has imposed a complex local stress regime. These features are evident on the seismic images provided in the following case studies.

Table 1. Correlation of seismic velocity with engineering parameters.

UCS (MPa)	Geotechnical classification	Seismic velocity (km/s)
<10	Low strength rock	<2.0
10–20	Medium strength rock	2.0–2.5
20–60	High strength rock, stratified, jointed	2.5–3.5
>60	Very high strength rock, stressed	3.7–7.0

3 EPPING RAIL LINK

The Epping rail link (Fig. 1) is a new 13 km long addition to Sydney's commuter rail network and consist of twin bore rail tunnels and three new stations (Rozek, 2004). The underground tunnels are 7.2 m in diameter at depths between 15 and 60 m with a single river crossing in the Lane Cove National Park. Tunnel construction commenced in September 2003 using two refurbished Robbins TBMs that are programmed to achieve 120 to 180 meters per week, in Hawkesbury Sandstone, with dive structures predominantly in Ashfield shale. The route is programmed to open in mid-2008. The Lane Cove River crossing is environmentally sensitive and is currently being excavated using cut and cover construction within temporary cofer dams to maintain river flow and minimise environmental impacts. Considerable effort was expended in geotechnical investigations for this crossing while the various construction options were being considered.

Figure 2 shows the seismic image obtained along the alignment at the Lane Cove River crossing (Fig. 1). This was obtained between three boreholes (TD13, 14 and 16) that provided direct calibration with the subsurface conditions. The seismic image was achieved

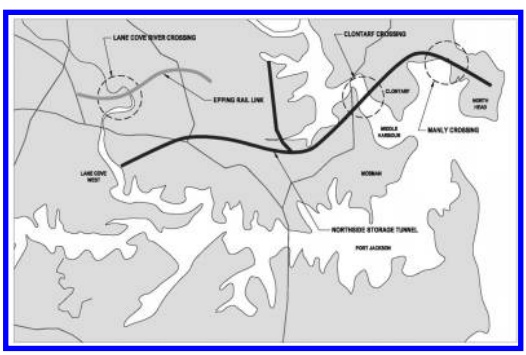


Figure 1. Location of tunnelling projects in the Sydney region.

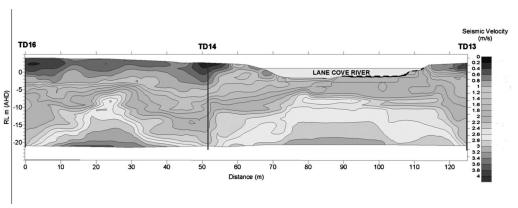


Figure 2. Seismic image across the Lane Cove river.

Copyright © 2005 Taylor & Francis Group plc, London, UK

using a combination of land and marine seismic refraction, surface-to borehole and crosshole seismic methods as described by Whiteley (2000). Typical seismic source and receiver spacings were 1 to 3 m. The cost of obtaining this image was equivalent to the cost of one of the cored boreholes and much less than the cost of an overwater borehole, that, incidently, would have missed the buried valley.

The seismic image in Fig. 2 is relatively simple and shows that the current river channel is underlain by moderately weathered sandstones (1.9 to 2.8 km/s) with little or no sediment cover. This cover (0.3 to 1.8 km/s) thickens to the sides of the channel and an older buried river channel near TD14 and extending to about 11 m below the present river level has been located beneath fill and sediments to the side of the river. An increased thickness of moderately weathered sandstone is also present in the base of the channel with similar increased thickness near the ends of the seismic line. These are believed to reflect major regional jointing and faulting patterns. Higher velocity material at depth represents the fresh sandstone with velocities of from 2.9 to 3.8 km/s. These are typical of Class 1 Hawkesbury Sandstone (Pells, 1985). The relative lack of complexity on this image indicates that significant local stress fields have been dissipated or are relatively uniform. The tunnel is being constructed beneath the river with 1 to 2 m of cover.

4 NORTHSIDE STORAGE TUNNEL

The Northside Storage Tunnel (NST) acts as a temporary underground storage volume for heavily contaminated wastewater overflows from Sydney's northern suburbs of about 18,000 megalitres per year that were the main polluter of Sydney Harbour (Henderson and Cuttler, 1999). This tunnel is 3.8 to 6.5 m diameter, beneath a rock cover about 25 to 150 m thick, extending for 16 km in an east-west direction to a treatment plant on the coast with further 3.7 km north-south connection to the existing wastewater network (Fig. 1). Prior to construction, variable bedrock depths were anticipated with deep buried valleys at Manly and Clontarf (Fig. 1). These buried valleys exerted the major geotechnical constraints to this project.

At Manly, two vertical boreholes (NS1 and NS26) were drilled 55 m apart on either side of the buried valley axis to a depth of 120 m or about 65 m into the sandstone bedrock to assess whether the valley floor contained any major structural features such as stress relief zones, dykes or faults. Cross-hole seismic tomography was completed between these holes to about 25 m below the proposed tunnel level. The seismic image (Fig. 3) shows the valley floor interface and a complex distribution of seismic velocities within the rocks in the range 2.8 to 4.2 km/s. This distribution reflects strength variations in the rock mass with higher velocities due to stress concentrations and dipping or folded strata. Increased fracturing due to stress relief was interpreted as the cause of lower velocities in the rock below the central region of the image extending to about 15 m below the valley floor. Following this seismic interpretation, a further an inclined borehole NS34 (Fig. 4) was drilled between the vertical boreholes. Significantly more fracturing was present in the inclined borehole than in the two earlier boreholes with clear evidence of the faulting and shearing that was predicted from the seismic image. Six low-angled, shear zones were encountered in the inclined hole within the seismic low-velocity zone on the seismic image. This zone occurs within the high velocity zone (4.0 km/s, Fig. 3) and corresponds to very high strength rock units. High horizontal stresses of 4 to 6 times the overburden stress were measured in this zone and a fault was also present. However, the high seismic velocities demonstrate that it was a discrete feature within very strong and stressed rock units. Using this information the tunnel was designed for 23 m of rock cover and poor ground conditions consistent with valley

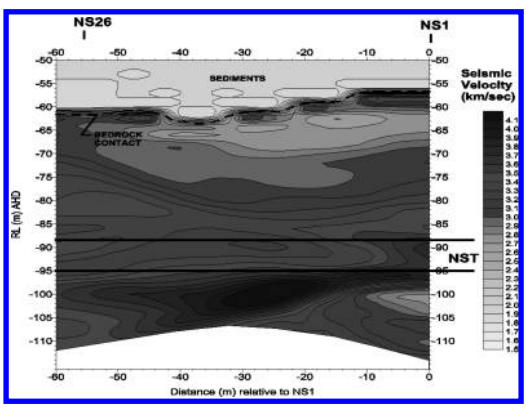


Figure 3. Seismic image below the Manly buried valley.

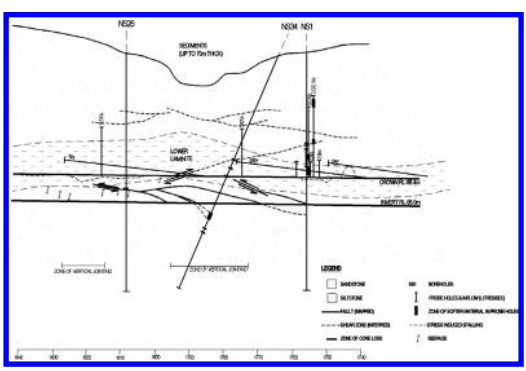


Figure 4. Geological section below the Manly buried valley.

Copyright © 2005 Taylor & Francis Group plc, London, UK

heave, with fault and bedding plane shears in a 30 to 50 m wide zone beneath the valley floor. In this region probing-ahead was also recommended with localised heavy support and pre-tunnel grouting ahead of the TBM to control any potential groundwater inflow from discrete faults or shear structures.

The geological section obtained from detailed geological mapping in the actual tunnel during and from the probe holes is shown in Fig. 4. Rocks in the exposed tunnel contained a series of widely spaced, low-angled thrust faults and bedding plane shears 10 mm to 200 mm thick and about 5 to 10 m apart. These could be traced to the boreholes and extended through high strength, un-fractured sandstone or siltstone with only minor seepage evident. These features, in high strength rock, are consistent with the high seismic velocities on the seismic image at the tunnel horizon. These ground conditions were no major constraint to the TBM even though some roof spalling due to stress relief did occur requiring additional support. The siltstone (the "Lower Laminite" bed in Fig. 3) provided evidence for the fold structure evident on the seismic image. This laminite bed occurred at the tunnel crown seems to have acted as a low permeability barrier between the tunnel horizon and the upper, more-fractured, seismic low-velocity zone that is present immediately below the valley floor.

The NST also had to negotiate a water crossing at Middle Harbour (Fig. 1) but it was not possible to drill overwater due to heavy boat traffic and high environmental sensitivity. However, inclined boreholes from the shore and marine geophysics located a deep buried valley below and to the side of the Harbour. High permeability zones and fractured rock were encountered in some of these boreholes and there were concerns regarding the potential for substantial water inflows and poor ground conditions. Seismic imaging with a combination of crosshole and surface-to borehole methods with hydrophone arrays laid on the Harbour floor was used to extend the information beneath the Harbour and between the inclined boreholes. The seismic image obtained is shown in Fig. 5. This clearly defines the base of the sediments and substantial low velocity zones beneath the Harbour indicative of poor ground conditions. A potential fault or shear zone identified beyond the inclined boreholes was of particular concern. Generally lower velocity rock was indicated at the tunnel level. Local zones of higher velocity above section of the tunnel roof indicated possible local stress concentrations. The tunnelling contractor was advised of these features prior to initiating the crossing.

Figure 6 shows the actual conditions that were encountered in the tunnel that was to the north of the seismic image section. The TBM was progressing from the east at the rate of 250 m/week but as it entered the rock below the buried valley (palaeochannel, Fig. 6) probing ahead was commenced and

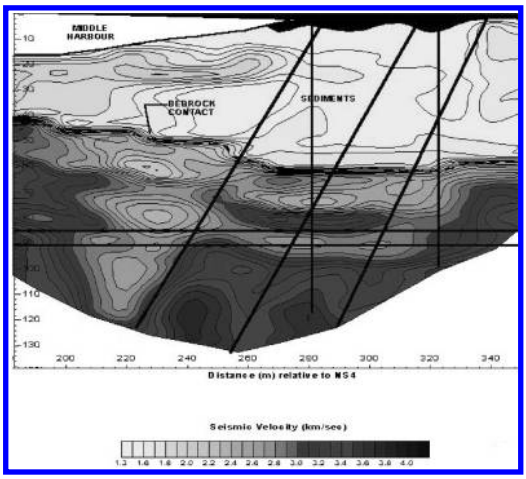


Figure 5. Seismic image below the Clontarf buried valley.

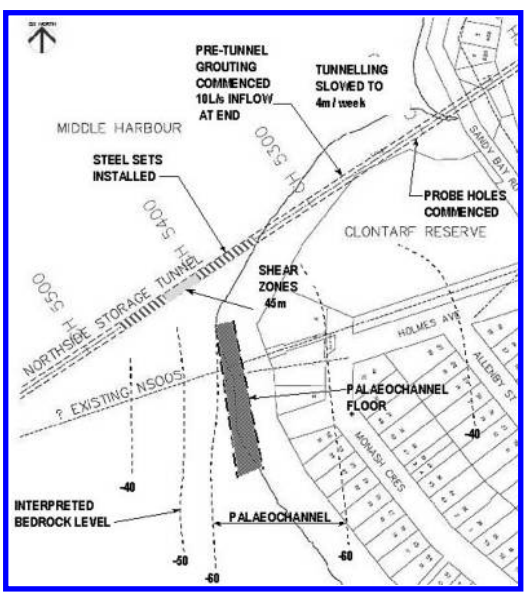


Figure 6. Tunnelling conditions below the Clontarf buried valley.

progress slowed to 4 m/week because grouting was needed to stem water inflows of up to 10 litres/sec. As the tunnel progressed beneath buried valley floor the poor ground predicted from the seismic image was encountered and required installation of steel sets to support the roof. A 45 m wide shear zone was encountered beyond the valley floor. These conditions were again consistent with the features that were predicted from the seismic image.

Copyright © 2005 Taylor & Francis Group plc, London, UK

5 CONCLUSIONS

Rock tunnelling conditions in the sandstone and shale rocks of the Sydney region are generally excellent, however, poor ground conditions beneath deep buried valleys beneath or near water crossings present major geotechnical risks and significantly increase tunnelling costs. The value of borehole seismic imaging in defining these conditions and contributing to a detailed understanding of these geotechnical issues has been clearly demonstrated using case studies from two major tunnelling projects in Sydney.

The ability of the seismic images to extend the information from boreholes in difficult and environmentally sensitive areas and to provide detailed information on the extent of the poor ground, geological structures, likely areas of local stress concentrations within the rocks and potential water inflow allows tunnelling contractors to be prepared in advance for these difficult conditions.

REFERENCES

Barton, N. 1998. Keynote lecture. L. DaSilva et al. (ed.), *Rock mass characterization from seismic measurements. Proc. SAROCKS'98, 2nd Brazilian Symposium, 5th South American Rock Mechanics Congress, Nov. 22–25 1998.* Brazil: Santos.

Branagan, D.F. 1985. Overview of the geology of the Sydney region. In Pells, P.N.J. (ed.) *Engineering Geology of Sydney, 1985*, 3–48. Rotterdam: Balkema.

Enever, J.R. 1999. Near surface in-situ stress and its counterpart at depth in the Sydney metropolitan area. *Aust. Geomechanics, June 1999*, 65–76.

Henderson, A.D. & Cuttler, R.J. 1999. *Northside Storage Tunnel Project. Proc. 10th Aust. Tunnelling Conference, 21–24 March 1999*, 47–53. Australia: Melbourne.

Herrenknecht, M. Rehm, U. & Liebler, B. 2004. *Tunnelling in Changing Geology. Proc. World Tunnelling Congress, 22–27 May, 2004*, paper D07, 1–11. Singapore.

Parker, C., Whiteley, R. & Gee, B. 1999. *Innovative investigation techniques used for geotechnical modelling of the Northside Storage Tunnel Project. Proc. 10th Aust. Tunnelling Conference, 21–24 March*, 193–205. Australia: Melbourne.

Pells, P.N.J. 1985. Engineering properties of Hawkesbury Sandstone, In Pells, P.N.J. ed. *Engineering Geology of Sydney, 1985*, 179–198. Rotterdam: Balkema.

Radcliffe, K.S., Thill, R.E. & Jessop, J.A. 1986. Use of acoustic velocity in predicting stress under uniaxial compression. In *115th Ann. AIME Mtg.* Repr. 86–147, 1–11.

Rozek, J. 2004. *Parramatta Rail Link-Design and Construction. Proc. 30th ITA-AITES World Tunnel Congress, 22–27 May, 2004*, paper C03,1–8.

Whiteley, R.J. 2000. *Seismic imaging of ground conditions from buried conduits and boreholes. Proc. Paris 2000, Petrophysics meets Geophysics, 6–8 Nov. 2000*, paper B-15. France: Paris.

Whiteley, R.J. & Parker, C. 2001. *Application of geophysical and geotechnical technologies to major tunnels in Sydney, Australia. 2001 Proc. Rapid Excavation and Tunneling Conference, SMME*, Ch. 24, 285–298. USA: San Diego.

Copyright © 2005 Taylor & Francis Group plc, London, UK

Geological risk assessment at the design stage in tunnel construction using GIS technique: the case of the A1 Highway Base Tunnel in the Apennines (Italy)

D. Furesi, M. Coli & G. Pini
Department of Earth Sciences, University of Florence

ABSTRACT: In this paper we try to predict silica risk on workers for the Base Tunnel of the A1 Highway in the Tuscan Appennines (VAV), (8600 m double tube). Risk is calculated by quantifying single parameters of the equation (R = I*H*E*V). The silica level which is breathed by workers during tunnel excavation is strictly connected to local geology and to the duty of the worker and with tunneling method too. Silica risk has been analyzed for the more exposed duties (wheel loader man, excavator driver and foreman). The parameters were evaluated by available data coming from the High Speed Railway project (TAV) (70 km of tunnels, 80 km of railway), excavated in similar geological conditions and techniques. By creating a database containing the risk equation parameters a GIS software has been used and divided the tunnel profile in various segments representing different risk levels.

1 INTRODUCTION

The Autostrada del Sole (A1 Highway) was build in the "60"s and projected for 20,000 vehicles per day, but nowadays up to 50,000 vehicles run everyday between Firenze and Bologna. In the beginning of the 80's a project to potentiate the traffic capacity was carried out (VAV project). The Base Tunnel will allow a faster crossing of the Apennine mountains. It will be about 8.6 km long, double tube, with 160 m^2 section and it will be excavated with drill and blast and mechanic machineries.

One of the principal safety concerns in excavation is the breathing of crystalline SiO_2 for miners that work most of their time near the front. During the excavation of the tunnels for the High Speed/High Capacity railway (TAV project), the ASL (the regional Authority on prevention at work) of Florence and Bologna developed a monitoring system for worker's health.

Based on monitoring and analogies of excavation methods and geology of both the VAV and TAV projects, and on mineralogical analysis of the rock masses drilled, a prediction on silica risk for workers in the excavation of the Base Tunnel can be attempted.

2 SILICA RISK

2.1 *The Silicosis*

Silicosis most commonly occurs as a diffuse nodular pulmonary fibrosis. It is caused by the inhalation and deposition of respirable crystalline silica particles (less than 10 μm in diameter) (Ziskind *et al*., 1976; IARC, 1987).

The most important factor in the development of silicosis is the concentration of dust containing respirable silica in workplace air and the percentage of respirable silica in the total dust.

Crystalline silica is considered carcinogenic to man (IARC). In 2000 the ACGIH modified the TLV (Tolerable Limit Value) of breathable quartz from 0.1 mg/m^3 to 0.05 mg/m^3.

In Tuscany, after ten years of monitoring death from silicosis before the age of 65 the predicted death rate is 0.6% of the exposed population (Merler *et al*., 1998).

2.2 *The TAV monitoring*

The monitoring of the exposition to dust is categorized into the different roles of the workers. The weighted mean of exposition level to respirable silica, is calculated and put in histograms. Data collected from 2001–2003, stressed that workers close to the front of the excavation are subjected to a particularly high concentration of microcrystalline silica.

The "wheel loader man" is exposed the most to silica risk (79% of the time he works with a microcrystalline silica level which is more than the recommended TLV), then there is the "excavator driver" (77%) and then the "foreman" (67%) (Figure 1).

Copyright © 2005 Taylor & Francis Group plc, London, UK

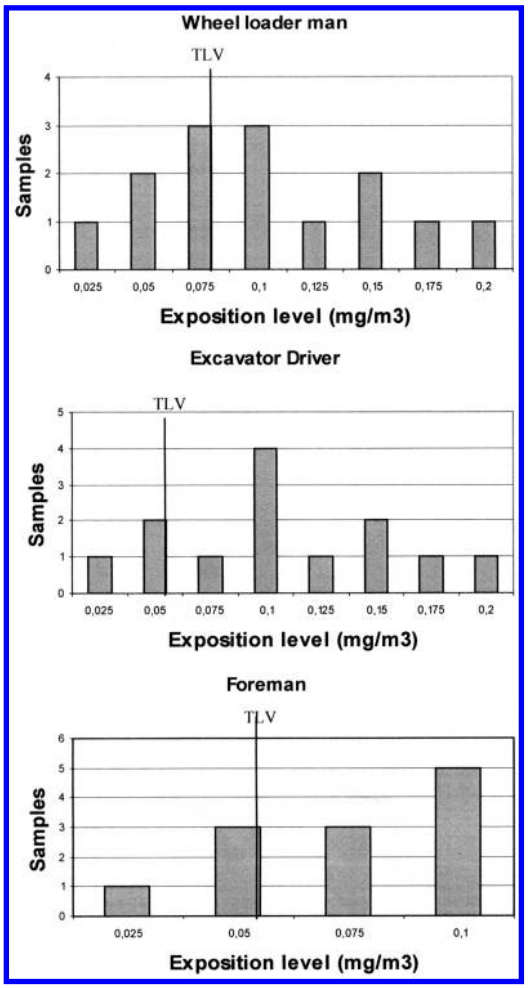


Figure 1. Histograms of frequencies of the monitoring samples. Most of the samples are over the recommended TLV in all the jobs analysed.

3 THE BASE TUNNEL AND THE TAV PROJECT

In the 80's the manager of the Italian highway network devised a new project, called VAV, in order to potentiate the traffic capacity of the main Italian Highway, the A1.

The Base Tunnel crosses the Apennine chain and it is 8.6 km long and double tubed; it has a 160 m^2 section and it will be completed in five years. Four pilot tunnels were excavated (about 5 km in total length), in order to investigate the underground geological setting.

The other important project which crosses the Apennines and which is almost completed is the TAV project. The TAV project consists in the construction of single track double tube tunnels, connecting Firenze and Bologna with a high velocity/high capacity railway.

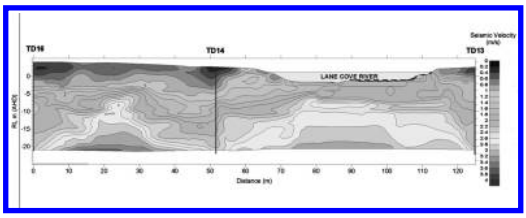


Figure 2. Geological cross section of the Base Tunnel North side. Legend: CDP1, CDP2 and TCG1 are silico – clastic turbidites; SIL, MVV, AVC are mainly siltstones and shales (Courtesy by SPEA – Soc. Autostrade).

The TAV tunnels are nearby the VAV and excavated in very similar rock masses, mainly flysch and siltstones (Figure 2). Excavation methods used for the VAV will be the same methods that were used by the TAV, i.e. machineries and explosives. This similarity allows us to make predictions on geological risks connected to the excavation.

Silica risk is quantified using monitoring data on TAV workers from 2001 to 2003 and mineralogical analysis of the excavated rocks which were conducted by the University of Firenze Department of Earth Sciences.

4 RISK ANALYSIS

For the risk assessment the equation

$$R = I * H * E * V \quad (1)$$

has been adopted, where:

I, Intensity: is expressed as a number that refers to a unique predetermined scale of intensity. This scale must be comparable with other phenomena. It correlates the intensity of the phenomena with its consequences (Table I).

H, Hazard: is the potential that the intensity (as defined above) of a phenomena occurs in a particular site, during a certain time interval. This depends on the regional and local geological setting. In general, hazard is expressed in terms of annual probability of occurrence or in terms of return period (Table II).

E, Elements at risk: human elements (people, things, economic activity, social structure, public services, infrastructures and goods, socio-economic value of cultural heritage) that are present in a particular area exposed to hazard.

In calculating silica risk only human elements must be considered (Table III).

$$E = (E1a + E\ 1b + E1c) \quad (2)$$

Copyright © 2005 Taylor & Francis Group plc, London, UK

Table I. Scale of Intensity, from DRM modified, 1990.

Intensity	Grade	Consequence
Negligible	1	IMPROBABLE ACCIDENTS No important damage
Low	3	ISOLATED ACCIDENTS With long exposition time potential diseases are possible
Medium	6	SOME FATALITIES Possible diseases for most exposed workers
High	10	VARIOUS FATALITIES Probability of diseases is high for most exposed workers
Very high	15	MANY FATALITIES Health diseases possible for all workers, even with short exposure time

Table II. Scale of Hazard (modified by Fell, 1994).

Hazard	Grade	Return period (yrs)	Annual probability
Extreme	28	1	100%
High	21	5	20%
Elevated	15	20	5%
Medium	10	100	1%
Low	6	1.000	1‰
Very low	3	10.000	0.1‰
Improbable	1	100.000	0.01‰

Table III. Value of the elements at risk with regards to human life (E1), (source from DRM, 1990).

Deaths (E1a)	Chronic disease (E1b)	Not chronic disease (Elc)
1	2–3	0.2–1

V, Vulnerability: is the degree of loss in human activity (economic, social, cultural, installation, infrastructure) resulting from a potentially damaging phenomenon. In general, it is expressed with a variable from 0 (no elements at risk) to 1 (all elements at risk) and it depends on the elements at risk and on intensity. It is expressed as:

$$V = V_S * V_T * (V_{D1} + V_{D2}) \quad (3)$$

These four factors vary between 0 and 1 and are:

V_S: spatial probability expressed in % between 0 (0%) and 1 (100%), with regards to area and/or building

V_T: temporal probability expressed in % between 0 and 1, with regards to area and/or building

V_{D1}: foreseeable material damage with regards to area and/or building

V_{D2}: foreseeable human loss expressed in % between 0 and 1.

4.1 *Determining Intensity (I)*

Referring to the consequences listed in table I, Intensity refers to the silica content of the excavated rock mass.

Mineralogical analysis on sandstones/pelites (S/P) excavated rock masses for the TAV project resulted in 33% for sandstones and 15.5% for pelites. By measuring the S/P ratio at the tunnel level, the weighted average of silica content along the tunnel profile is 21.4%. The TAV's monitoring of workers resulted in 5.6% as respirable silica. Therefore the respirable silica during the excavation is the 26% of the silica content of the rock mass.

Considering the similarities of the geology and mineralogy of the rock masses in TAV and VAV, the 26% can also be considered valid for the S/P excavated rock masses of the VAV.

Mineralogical and petrographical analysis on sandstones and pelites was also carried out for the New Italian Geological Map project, scale 1:50.000. The silica content of the various geological formations that will be crossed by the VAV resulted between 23.3% and 36.5%. Therefore, according to (4), the respirable silica contents will be between 6% and 9.6% during the excavation.

The 26% should not be considered in siltstone formations. The silica content of the siltstone formation measured in the TAV is of 11.8%. Respirable silica in that tunnel is about 2.6%, so the percentage is 22%.

Assuming that percentage is also valid for siltstone formations along the VAV, the respirable silica will range between 2% and 3%.

Referring to Table I, in the excavation of siltstone formations we considered low consequences (Grade 3) for workers, whereas medium consequences (Grade 6), are foreseeable for the excavation in flysch formations.

4.2 *Determining Hazard (H)*

Hazard (H) is the annual probability for a worker to be exposed to breathing of microcrystalline silica. Assuming 8 hours of duty for 270 days working per year it can be calculated a 24% of annual exposition. Referring to Table II we assigned a value of 21.2 for all three duties.

4.3 *Determining Elements at risk (E)*

In the original formulation of (1), the element E was subdivided into five sub-elements, E_{1a}, E_{1b}, E_{1c}, E_2,

Copyright © 2005 Taylor & Francis Group plc, London, UK

E_3. E_2 and E_3 refer to the elements at risk with regard to land use and their socio-economic value, such as schools, hospital, primary roads, etc. In this paper we considered only the (2), because only human life is connected with silica risk, so E_2 and E_3 are zero.

Because microcrystalline silica is considered a suspected carcinogenic for humans and it can lead to death, the value 1 can be assumed for E_{1a}.

E_{1b} and E_{1c} was assumed 2 and 0.2 (the minimum possible values) respectively, so the (2) is 3.2.

4.4 *Determining Vulnerability (V)*

Various terms of the (3) were evaluated. V_s in underground excavation is assumed to be 1, (i.e. 100%), because the phenomenon "respirable silica during excavation" always occurs.

V_t depends on the different duties; the monitoring of TAV workers shows that the wheel loader man has the most exposed duty. For 79% of his working time he is exposed to a higher respirable silica level than the recommended TLV (cfr. figure1), so V_t assumes the value of 0.79.

The excavator driver spends 77% of his time over the recommended TLV, so the V_t rating is 0.77.

The foreman is the least exposed duty, even if he is 67% of the time over the TLV. His V_t rating is 0.67.

In considering silica risk it can be assumed that material damages with regards to area and/or building are not foreseeable, so $V_{D1} = 0$.

Statistical analysis on active workers, between 1987 and 1996, demonstrate that the mortality rate from silicosis is about the 0.6% (Merler *et al.*, 1998). The foreseeble human loss V_{D2} is 0.006.

5 RISK ASSESSMENT

5.1 *Classification of (R)*

Once single parameters of (1) has been determined the calculation of R is possible. Referring to the geological profile of the VAV (Figure 1), R depends on lithology and job role (Table V).

It is now important to define a referring scale of the Risk (R). By combining all possible rates of the elements of (1), 1,473 values were obtained, which ranges from a minimum of R = 0 to a maximum of R = 4,760. These are distributed as a log-normal (figure 3). In a cumulative ascending form, sample values have been divided in five risk classes, according to the increasing order of magnitude (Figure 4).

It results in siltstones silica risk is Low, whereas it is Medium in S/P rock masses.

5.2 *A further classification*

The (1) was calibrated for natural hazards, so the levels of silica risk result quite low if compared to the entire range of risk values. Nevertheless, working for a long time in high concentrations of silica dust can cause serious damage such as pulmonary tumors. In order to stress the importance of reducing silica dust concentrations and to better the conditions of the workers, a more specific classification is proposed.

Since silica risk is only connected with human life, ratings regarding other aspects (land use, socio-economic value of goods at risk, damages to buildings or cultural heritage,...) will never be used, i.e. they will always be considered as zero. By combining only the ratings of the elements of (1) in analyzing silica risk, the range of possible values of R goes from 0 to 9. Values are distributed as a Beta which displayed in a

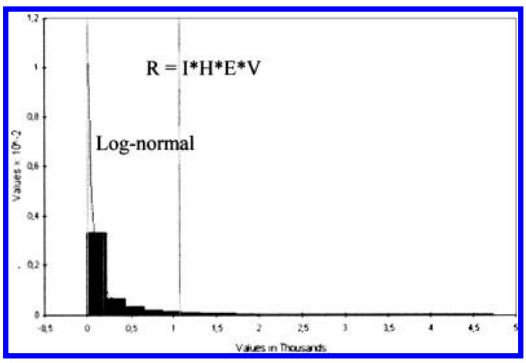


Figure 3. Distribution of the values of (1). The log-normal distribution best fit input data.

Table V. Calculation of R depends on lithology and job role.

Job role	Lithology	I	H	E	V	R
Wheel loader man	S/P	6	21.2	3.2	$4.74*10^{-3}$	1.93
Wheel loader man	Siltstones	3	21.2	3.2	$4.74*10^{-3}$	0.97
Excavator driver	S/P	6	21.2	3.2	$4.62*10^{-3}$	1.88
Excavator driver	Siltstones	3	21.2	3.2	$4.62*10^{-3}$	0.94
foreman	S/P	6	21.2	3.2	$4.02*10^{-3}$	1.64
foreman	Siltstones	3	21.2	3.2	$4.02*10^{-3}$	0.82

Copyright © 2005 Taylor & Francis Group plc, London, UK

cumulative form allows us to define five classes by a 20% interval (Figure 5).

This can be seen as a "zoom" on silica risk and it points out that R is Elevated in S/P rock masses and High in siltstones.

6 RISK PROFILE FOR THE BASE TUNNEL OF THE A1 HIGHWAY

One of the limits of this procedure of risk analysis is the reliability of input data. In fact, the silica content in the excavated rock masses comes from the petrologic analysis performed for the New Italian Geological Map project, scale 1: 50.000 and they are referred to samples spread on a wide area; no further analysis were performed specifically on the VAV area. A simple visualization of the results of R along the tunnel may not be very useful in the future as more accurate data could eventually be available and therefore, some of the elements of (1) could change. This will obviously affect the final result of R.

A database of the single elements of (1) has been created, directly linked to a GIS software. The database can be updated once more accurate input data becomes available and that, in turn, will update the GIS layout in real time.

Figure 6 shows an example of the inferred safety risk profile for the wheel loader man. It is also shown in the main tables of the Access database.

This method allows a quantitative definition of risk, so that the designer can plan prevention and mitigation measures which reduce the ratings of the elements of (1). First, a definition of acceptable risk must be stated, then the analysis must be newly performed with reduced values. If R is acceptable the considered prevention and mitigation measures must become part of the entire project.

The (1) can be used for analyzing different kinds of geological risks, for example hydrogeological, grisou, asbestos, etc.. The main problem is the definition of

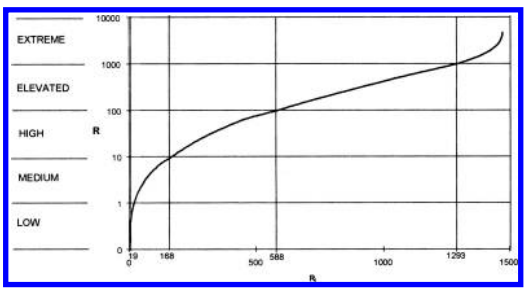


Figure 4. Cumulative ascending distribution of R values. The limits of the five classes of risk correspond with the flex points of the curve.

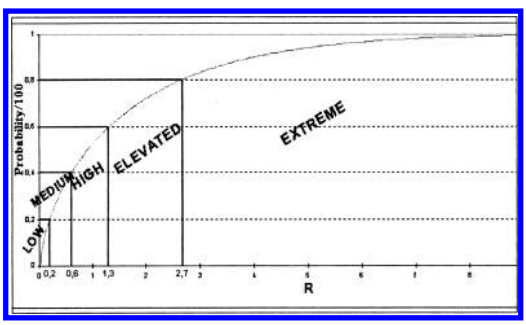


Figure 5. Cumulative distribution of R. Only the element of (1) connected with silica risk has been considered. Silica risk can range only between 0 and 9. The five classes have a 20% of amplitude.

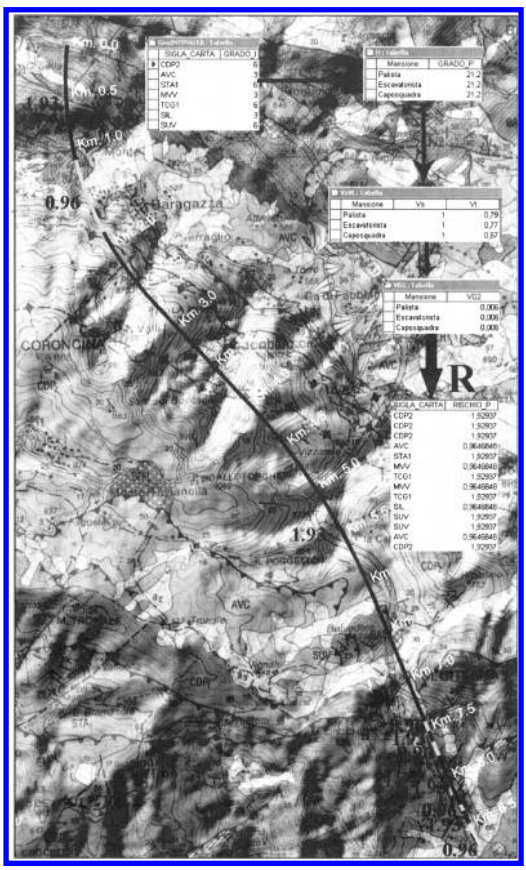


Figure 6. Inferred safety risk profile for the wheel loader man. Numbers close to the trace of the Base Tunnel are the R values for silica risk. It is shown in the Access database which manages the GIS layout. The database is easily updatable. Geological sketch from Nuova Carta Geologica d'Italia scala 1:50.000, Foglio 252 Barberino di Mugello.

Copyright © 2005 Taylor & Francis Group plc, London, UK

the term V (vulnerability), because statistic data are needed. In particular, the likelihood definition of some extreme events (grisou explosion or big water inflows) is the most difficult part in risk analysis and a very developed geological knowledge is required.

7 CONCLUSIONS AND LIMITS

In this paper a method to evaluate risk for workers in tunnelling at the design stage is proposed. This method allows us to make predictions of risks regarding safety and health of workers, according to the types of the input data.

The limit of this method is in the reliability of input data. Regarding this example of silica risk, the TAV monitoring only reports global exposition data during excavation, whereas the excavated lithology should also be specified. This would permit a better correlation between exposition values and excavated rock mass. Moreover, further mineralogical analysis should be done on excavated lithologies, in order to better quantify silica content. This type of organized monitoring would allow a more careful evaluation of the intensity (I) and a better definition of risk (R).

The implementation of this method with GIS software allows to update immediately the elements of risk equation and to manage results during the design and execution stages, in real time.

As it can be seen from the GIS simulation, silica risk is elevated for long tracts of the VAV. Appropriate preventative measures must therefore be taken into account (efficient ventilation system, water spreading on the excavated rock, Personal Protective Equipment, …), especially during excavation in S/P rock masses.

REFERENCES

Bertacchini M., Gelmini R. & Ponzana L. 1987. Le arenarie di monte Cervarola: caratteri sedimentologici e petrografici di alcune sezioni dell'Appennino Modenese. Mem. Soc. Geol. It. 39, pp. 35–47.

DRM – Délégation aux Risques Majeurs. 1990. Les études préliminaires à la cartographie réglamentaire des risques naturels majeurs. Secrétariat d'Etat auprés du Premier Ministre chargé de l'Environnement et de la Prévention des risques technologiques et naturels majeurs. La Documentation Française. pp. 143.

FELL R. 1994. Landslide risk assessment and acceptable risk. Canad. Geotech. J., 31/2, 261–272.

IARC. 1987. IARC monographs on the evaluation of the carcinogenic risk of chemicals to humans: Silica and some silicates. Vol. 42. Lyon, France: World Health Organization, International Agency for Research on Cancer.

Merler E., Barchielli A., Sorso B., Giovannetti L. & Cardini, C.E. 1998. La mortalità per silicosi polmonare in regione Toscana nell'ultimo decennio dimostra che gli effetti sulla salute dovuti all'esposizione lavorativa a silice.

Morgan G.C., Rawlings G.E. & Sobkowicz J.C. 1992. Evaluating total risk to communities from large debris flows. In: Geotecnique and natural hazard. BiTech. Publishers, Vancouver B.C., pp. 225–236.

Nuova Carta Geologica d'Italia scala 1 : 50.000, Foglio 252 Barberino di Mugello.

Ziskind M., Jones R.N. & Weill H. 1976. Silicosis. Am Rev Respir Dis *113*:643–665.

Copyright © 2005 Taylor & Francis Group plc, London, UK

The study on the geotechnical factors effecting the excavation performance in Istanbul Metro Tunnels

Ö. Selimoğlu
Department of Mining Engineering, Istanbul Technical University, Istanbul, Turkey

ABSTRACT: The purpose of this study is to present a study on the geotechnical factors effecting the excavation performance through investigating two lines metro case studies that are located along the Istanbul Metro in southwest Turkey. Detailed site investigations and performance analysis were carried out in the tunnel face of the line Galatasaray – Taksim Metro. First, geological discontinuities and face conditions were recorded for each time. Rock samples were collected and later, they were subjected to rock mechanics tests in the laboratory. During the performance studies, advance rates, net breaking rates of hydraulic impact hammers, the percentage of the each working item (time spent to drill bolt holes, wire meshing, shotcrete, muck removal, etc.) were recorded carefully. All the shift data were statistically analysed, and net breaking rate was correlated with rock mass properties. The results were promising for prediction of excavation performance for future applications in order to increase the excavation efficiency and to decrease tunneling cost.

1 INTRODUCTION AND OBJECTIVES OF THE RESEARCH

The population of Istanbul has increased in the last two decades to more than 10 millions. The Municipality Authorities planned to solve the transportation problem in the city by starting construction of 16 km two lines metro at the end of 1992. Although, in the past, few research works were carried out on the "Geotechnical factors effecting the excavation performance in Istanbul Metro Tunnels", it is believed that the accumulation of data base and more detailed studies are necessary for more efficient and economical applications in the future.

One of the most important factors in determining the excavation economy and the job duration time of a tunnel project is the performance of mechanical excavator used, and the performance prediction plays an important role in decision making of a contractor.

In the past, some investigations were focused on the prediction of the performance impact hammers from rock mass properties and machine parameters. It is believed that further research works are necessary to make more realistic performance prediction approach. The main objectives of this research work may be cited as to collect data from tunneling site, to determine the geological discontinuities in the tunnel face, to carry out rock mechanics tests on the samples collected from tunnel, to correlate rock mass properties with the net breaking rates of hydraulic impact hammers, to test the validity of previously mentioned prediction models and to contribute to the science of rock breakage.

2 THE GEOLOGY

Paleozoic sedimentary formations from Lower Devonian to Middle Carboniferous are dominant in the area. Many geological discontinuities were developed due to Alpine and Hercinian Orogenies making RQD (Rock Quality Designation) values changing between 0 to 90% and uniaxial compressive strength between 30 to 150 MPa. The rock formation, locally named Trakya Formation is formed of fine grained, laminated, fractured and interbedded siltstone and mudstone. Some diabase and andesite dykes have also been encountered while driving the tunnels and these effected progress rates as they were significantly harder than rock excavated along the major part of the tunnel routes (Bilgin, N, 1997). During the excavation in the Galatasaray-Taksim Metro Line, tunnel face always had a mixed geological condition which also effected the instantaneous breaking rate directly.

3 METHOD OF CONSTRUCTION

The NATM (Australian Tunneling Method) was chosen as the tunnel construction method. L.V. Rapcewics published first the principles of NATM in his book

Copyright © 2005 Taylor & Francis Group plc, London, UK



Figure 1. Applications of hydraulic impact hammer in Istanbul metro tunnels.

"Gebirgsdruck and Tunnelbau" in 1994. From 1956 to 1958 the first large size tunnels were designed and built by him in Venezuela (Johann, G., 1995). The philosophy of NATM was summarized by Prof. Dr. T. Brown as the inherent strength of the rock strata around the tunnel should be conserved, deformation of the ground should be controlled and excessive deformation should be avoided. These conditions may be achieved by systematic rock bolting, wire meshing and shotcreting. The primary support will partly or completely represent the total support required. The length of tunnel left unsupported at any time during construction should be as short as possible. If possible, the tunnel should be driven with minimum disturbance of the strata by blasting (Brown, E.T., 1990).

The main tunnel type A has an area of 36 m^2, but also in different lines depending on requirement, area of tunnel is changing 36 m^2 to 100 m^2. Tunnel excavation is realized by hydraulic impact hammers mounted in excavators as seen in Figure 1. Roof bolting, wire meshing and spray concrete are realized immediately after the excavation to avoid the initial deformations, Figure 2. The upper bench of 28 m^2 of tunnel cross section is excavated at first then the lower bench of 8 m^2 is excavated later. The lower bench is excavated 30 m behind the first bench. 3 to 3.6 m long rock bolts, type of Q221/221 wire meshes, steel archs and thickness of 10 to 20 cm shotcrete were used as temporary tunnel support. For permanent tunnel support, depending on type of profile, the final lining is undertaken with 35 to 45 cm thick with a type of Q221/443 wire mesh added.

4 ROCK MASS PROPERTIES AND THE PERFORMANCE OF IMPACT HAMMERS

Different zones were chosen for detailed site investigations. In each zone, data about tunnel geology, rock mass structure, intact rock properties and instantaneous

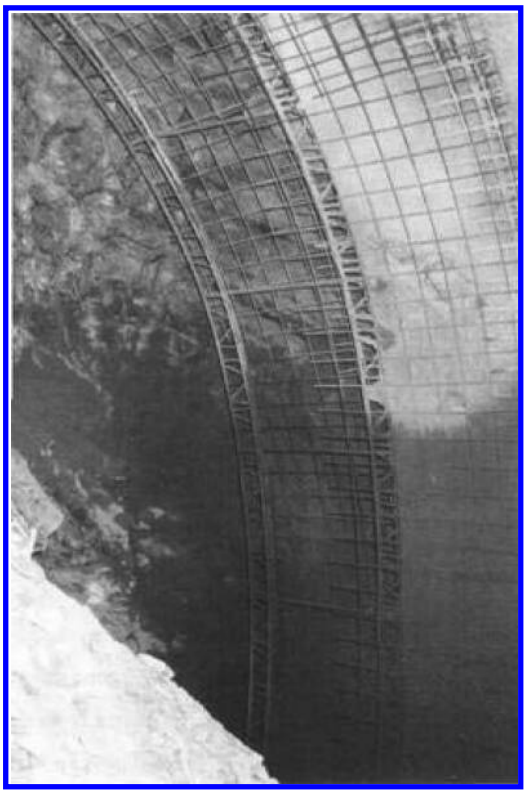


Figure 2. Applications of temporary tunnel support.

Table 1. Breaking rate of impact hammer and rock properties in Galatasaray-Taksim Metro Line 1.

Tunnel chainage (m)	Rock description	Compressive strength (kg/cm^2)	RQD	Impact hammer breaking rate (m^3/h)
9394	Sandstone	732	60	25
9406	Shale	1103	75	12.3
9407	Mudstone	905	60	16.6
9409	Mudstone	905	45	17.8
9427	Weathered diabase	803	60	19.4

or net breaking rate of impact hammers were carefully collected. RQD was determined by the tunnel geologist using volumetric joint count (J_v) as described by Brown (Brown, E.T., 1981).

Sample rock's descriptions, compressive strengths, RQD values and impact hammer breaking rate are given in Table 1 and 2 for each line.

Rock samples were taken from the tunnel face for laboratory tests. Thin sections were prepared for

Copyright © 2005 Taylor & Francis Group plc, London, UK

Table 2. Breaking rate of impact hammer and rock properties in Galatasaray-Taksim Metro Line 2.

Tunnel chainage (m)	Rock description	Compressive strength (kg/cm^2)	RQD	Impact hammer breaking rate (m^3/h)
9364	Diabase	784	60	22.3
9367	Interbedded shale sandstone	763	60	23.3
9380	Sandstone	833	35	43.6
9384	Weathered sandstone	834	35	19.4
9387	Diabase	1063	75	14.6
9400	Diabase	1253	75	9.7
9401	Weathered diabase	1067	60	15.9

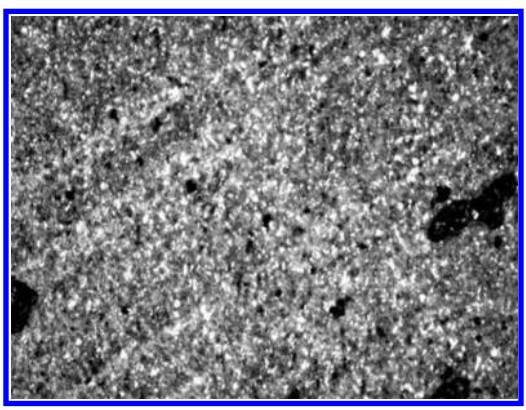


Figure 3. Thin section of mudstone sample taken from tunnel chainage 9407 m.

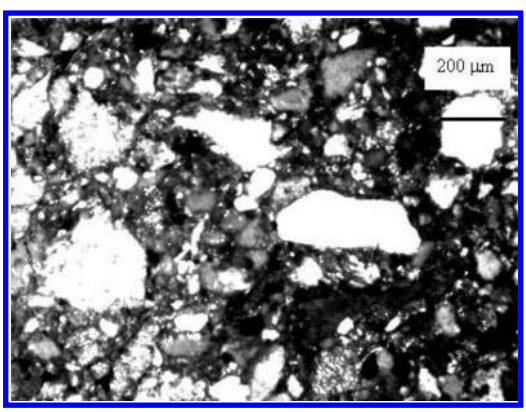


Figure 4. Thin section of sandstone sample taken from tunnel chainage 9380 m.

petrographic identification under microscope. Figures 3 and 4 show typical view of mudstone under microscope from tunnel chainage 9407 m (Galatasaray-Taksim Metro Line 1) and sandstone from tunnel chainage 9380 m (Galatasaray-Taksim Metro Line 2).

5 THE COMPARISON OF PREDICTED AND MEASURED PERFORMANCE DATA

Factors effecting the breaking performance of mechanical excavators can be summarized as below.

- Rock intact and rock mass properties
- The skill of machine operator
- Impact hammer design characteristics, blow frequency, below energy etc.

In Galatasaray-Taksim Metro Line 1 and 2, Caterpillar Model 90 hydraulic hammer is used for excavation operations.

The empirical approach which predicts the instantaneous breaking rates of impact hammers is defined below by equation 1 and 2 (Bilgin 1988, 1990).

$$IBR = 4.24 \times HP(RMCI)^{-0.567} \quad (1)$$

$$RMCI = \sigma_C \times (RQD/100)^{2/3} \quad (2)$$

where IBR = instantaneous breaking rate, m^3/h; HP = power of the impact hammer, HP; RMCI = rock mass cuttability index, MPa; σ_c = uniaxial compressive strength, MPa.

However it is important to note that this equation is only valid where the ground water income does not exist and the face is not mixed face. Sometimes the face is not uniform and two or more different formations are in contact with each other. Those contact zones make easy to break the rock form the face which increases the excavation rate. Figure 5 shows the relationship between actual breaking rate values of hydraulic impact hammer and rock mass cuttability index in Galatasaray-Taksim Metro Line 1 and Line 2. As expected breaking rate decreases with increasing rock mass cuttability index. Instantaneous breaking rates of impact hammers in different zones were calculated using equations 1 and 2 and compared with actual values in Table 3. As it can be seen from this table, there is a significant difference in predicted and actual values. This demonstrates clearly that the model described by Bilgin is only valid in non mixed geological conditions.

6 PERFORMANCE STUDIES

Daily advance rates obtained in August 2000, in Galatasaray-Taksim Metro Line 1 and 2 are given in

Copyright © 2005 Taylor & Francis Group plc, London, UK

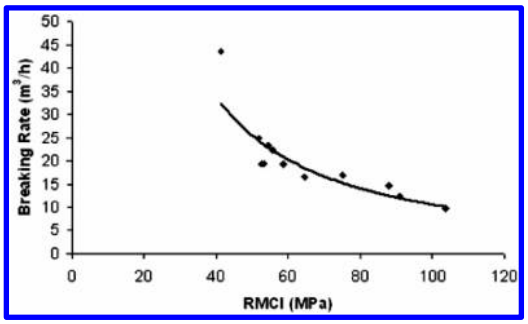


Figure 5. The relations between breaking rate of impact hammer and rock mass cuttability index.

Table 3. Actual and predicted values of breaking rate of hydraulic impact hammers.

Tunnel face	Tunnel chainage (m)	Actual values (m^3/h)	Predicted values (m^3/h)
Diabase, mudstone	9394	25	9.5
Sandstone, mudstone, diabase	9406	12.5	6.9
Sandstone, mudstone	9407	16.6	8.4
Mudstone, sandstone	9409	17.8	9.4
Shist, diabase	9427	19.4	8.9
Mudstone, diabase	9364	22.3	9.1
Diabase, sandstone	9367	23.3	9.2
Diabase, sandstone	9380	43.6	10.8
Mudstone, diabase	9384	19.4	9.4
Mudstone, diabase	9387	14.6	7.0
Diabase, mudstone	9400	9.7	6.4
Diabase, mudstone	9401	15.9	7.6

Figure 6 and 7. As it may be observed from these figures, daily advances in mainly change from 2 to 3 m and with few exceptions to 4 m. These figures can be accepted too low if compared to other mechanized excavation systems, i.e. excavation with TBM (full face tunnel boring machines). The advance rates of a TBM is high since more cutting power is transmitted to the tunnel face and mainly all the tunneling operations are done in the same time, for example, muck removal or tunnel support with precast segment may be realized while the rock is being excavated by the TBM. However, the tunneling operations in Istanbul Metro Tunnels are independent from each other. Excavation by impact hammer is first realized and later muck removal, rock bolting, wire meshing and shotcreting operations are carried out consequentially. This is clearly shown in Table 4 which gives the time spent in one day for each operation. It is important to note that only 20% of tunneling time is spent to excavation and 26 to 31% of the time spent for muck

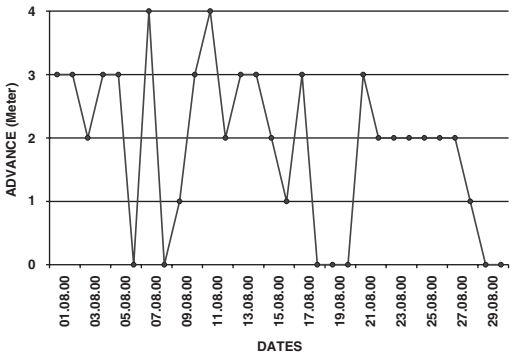


Figure 6. Tunneling advance (m) in August 2000 in Galatasaray-Taksim Metro Line 1.

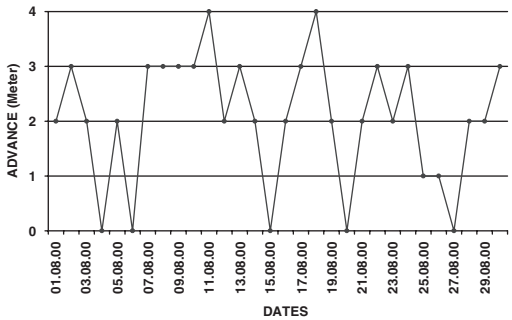


Figure 7. Tunneling advance (m) in August 2000 in Galatasaray-Taksim Metro Line 2.

Table 4. The percentage of time spent for each tunneling operation in a cycle of one day in Galatasaray-Taksim Metro Line 1 and 2.

	Daily advance rate		
Tunnel Operation (%)	2 meter	3 meter	4 meter
Excavation by impact hammer	20	20	23
Muck removal and rock bolting	31	31	26
Drilling for temporary tunnel support	8	10	8
Mounting steel arches	14	15	22
Wire meshing and shotcreting	21	21	19
Waiting and break down	6	3	2

removal and rock bolting, 8 to 10% to drilling for temporary support of the tunnel face, 14 to 22% to mounting of steel arches, 19 to 21% to wire meshing and shotcreting and 2 to 6% to waiting and breakdown. As it is mentioned before for rock mechanics tests, rock samples were collected from the tunnel face. In Figure 8 and 9, net breaking rate graphic of

Copyright © 2005 Taylor & Francis Group plc, London, UK

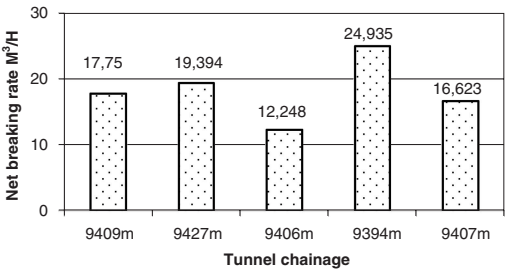


Figure 8. Net breaking rate graphic of rock samples that are collected from Galatasaray-Taksim Metro Line 1.

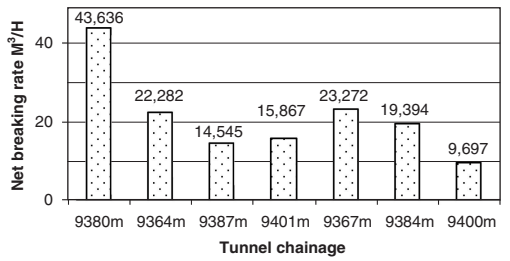


Figure 9. Net breaking rate graphic of rock samples that are collected from Galatasaray-Taksim Metro Line 2.

rock samples that are collected from Galatasaray-Taksim Metro Line 1 and 2.

7 CONCLUSION

In situ investigations carried out in Metro Tunnel of Galatasaray – Taksim Line proved that the instantaneous breaking rates of hydraulic hammers are significantly related to rock mass cuttability index described as the product of rock compressive strength and RQD. New Australian tunneling method is used in Istanbul Metro Tunnels. Detailed performance analysis showed that daily advanced rates are too low changing mostly from 1 m to 3 m. Tunnel boring machines are recommended for future rapid and efficient tunnel excavations. However high initial capital investment for tunnel boring machine applications, should be considered if compared with current applications.

ACKNOWLEDGEMENT

This research study was carried out in Istanbul Metro Tunnels under the construction of "Anadolu Metro Ortaklığı". The author would like to express his appreciation to the following people: Mr. D. Küçükertem, Mr. M. Hizel, Mr. B. Çakiroğlu, Mr. F. Sezer for the helps in the construction site. Thanks are due to Prof. Dr. N. Bilgin and Assoc.Prof. Dr. S.G. Erçelebi Assist. Prof. Dr. H. Çopur for their guidance of the research and helps to write this paper.

REFERENCES

Bilgin, N., Seyrek, T. & Shahriar, K. 1988. Roadheader performance in Istanbul, Golden Horn clean up contributes valuable data. *Tunnels and Tunneling* 20 (6): 41–44.

Bilgin. N., Seyrek, T., Erdinç, E. & Shahriar, K. 1990. Roadheaders glean valuable tips for Istanbul Metro. *Tunnels and Tunneling* 22 (10): 29–32.

Bilgin, N., Kuzu, C., Eskikaya, Ş. & Özdemir, L. 1997. Cutting performance of jack hammers and roadheaders in Istanbul Metro Drivages. *World Tunnel Congress 97*: 445–460.

Brown, T. 1981. *Rock characterization, testing and monitoring.* New York: Pergamon Press.

Brown, T. 1990. Putting NATM into perspective (Nov' 81). *Tunnels and Tunneling* Summer (Special issue): 9–13.

Johann, G. 1995. NATM, history, definition, principles. *Summer course*: 4/1–4/11. IACES bureau of Vienna.

Selimoglu, O. 2001. Detailed analysis of excavations in Istanbul Metro in Taksim-Yenikapi Line between Galatasaray and Taksim. *Diploma thesis* (in Turkish): Istanbul Technical University.

Copyright © 2005 Taylor & Francis Group plc, London, UK

Geotechnical investigation program for the No. 7 subway line extension project, New York

E.C. Wang, R.B. Roberts, L.M. Hsia & C.M. Osborne
Parsons Brinckerhoff Quade & Douglas, Inc., New York, U.S.A.

R. Jeremic
Yu & Associates, Inc., Elmwood Park, New Jersey, U.S.A.

C.C. Chang
Parsons Brickerhoff Quade & Douglas, Inc., New York, U.S.A.

ABSTRACT: The existing MTA-New York City Transit's (MTA-NYCT) No. 7 Subway was built in the early 1900's and currently terminates at Times Square near 41st Street and Eighth Avenue. As part of the City's redevelopment of the west side of Manhattan, the MTA-NYCT's No. 7 Subway extension project will add approximately 1.5-miles of twin tunnel alignment to the current line. The proposed alignment will extend from the existing Times Square Station west beneath 41st Street then turn south under Eleventh Avenue and terminate between 24th and 25th Streets. The project will include two new stations, a two-track line station near 41st Street and Tenth Avenue and a three-track terminal station at 34th Street and Eleventh Avenue. The alignment lies in close proximity to a number of major underground structures. The tunnels and station caverns will be constructed in the Manhattan Schist, which has been extensively intruded by pegmatitic and aplitic veins along and across the foliations. The lithology of the bedrock as well as the orientation and condition of the rock mass discontinuities are critical to the design of the tunnel boring machines.

1 INTRODUCTION

The proposed No. 7 Subway Line Extension project in New York City is configured as a two-track subway, extending approximately 1.5 miles of twin tunnel primarily in hard bedrock. Continuing the subway westward from the existing Times Square terminal station at Eighth Avenue in 41st Street, the extension follows 41st Street to Tenth Avenue and then negotiates a 650-foot (200-m) radius turn south into Eleventh Avenue. The alignment continues south along Eleventh Avenue to the end of the extension between 24th and 25th Streets. The subway extension will incorporate a new line station at Tenth Avenue in 41st Street and a new terminal station at 34th Street in Eleventh Avenue (see Figure 1).

Subsurface geotechnical investigations are on-going to support the design and the EIS efforts.



Figure 1. Site location plan.

2 GEOLOGIC SETTING

The following represents the current working knowledge of local geology, combined with field

Copyright © 2005 Taylor & Francis Group plc, London, UK

observations from investigation borings and subsequent review of recorded rock core samples.

The project alignment mainly occupies the portion of western Manhattan along 41st Street from 8th Avenue to Eleventh Avenue and from 41st Street to 26th Street along Eleventh Avenue. The area forms part of the Manhattan Prong of New England Upland Province.

The hard crystalline metamorphic bedrocks form the ridges and valleys within this province.

3 EXISTING STRUCTURES AND INFRASTRUCTURE

Existing structures and infrastructure in the vicinity of the project alignment include NYCT structures, Port Authority Bus Terminal, Lincoln Tunnel East Approach (South, Central and North tubes), Amtrak Empire Line and Hudson River Tunnels, the Eleventh Avenue Viaduct, the 8th Avenue Subway (Lines A, C, and E), as well as privately owned properties above or adjacent to the proposed alignment. The vertical separation from the underground structures was one of the important considerations in selecting the final tunnel alignment. Operational constraints, including maximum 0.5 per cent grade within stations and 3.0 per cent maximum grade for the running tunnels also influenced the vertical alignment of the proposed subway extension. Construction of the existing structures date from the early turn of the 20th century to the 1950s, with expansions completed during the 1970s.

4 INVESTIGATION PROGRAM

A comprehensive study of archive data from accessible sources including geological maps, memoirs, monographs and geotechnical reports were performed prior to field investigations being undertaken. The subsurface geotechnical investigation program has subsequently been undertaken in stages to satisfy the requirements of design development.

The actual methods used for the subsurface geotechnical investigation included the following:

- Conventional soil boring;
- Conventional and oriented rock core drilling;
- Borehole testing – Packer permeability testing, borehole acoustic televiewer survey, in-situ stress measurement using hydraulic fracturing method (ASTM D4623), suspension P & S velocities measurement, and determination of rock mass modulus by borehole dilatometer method;
- Digital core scanning – photographic scanning to preserve a visual record of the rockcore;
- Rock outcrop stereophotogrammetry survey to map discontinuities planes in outcrops;
- QA/QC procedure for rockcore logging;
- Soil and rock laboratory;
- Asbestiform minerals determination.

5 SITE CONDITIONS

The thickness of the overburden deposits varies substantially along the alignment. The project borings indicate that the soil cover is relatively thin along 41st Street and generally increases in thickness westward toward Eleventh Avenue and southward towards 25th Street. The overburden typically consists of glacial and post-glacial soils, overlain by recent manmade fill. Generally, the naturally derived soils include glacial till, modified glacial drift, sand and gravels, and some glacio-lacustrine silts and clays.

In Figure 2, the project alignment is superimposed on a topographic map of Manhattan published by Egbert L. Viele in 1874. The map indicates an ancient creek once flowed in a westerly direction, crossing Ninth through Eleventh Avenues between 39th Street and 42nd Streets. Another ancient creek is indicated crossing the project alignment in Eleventh Avenue between 29th and 32nd Streets. Such drainage features are often indicative of zones of weakness in the underlying rock mass (i.e. fault zones, joints, and fractures) and can potentially be associated with high water inflows if encountered in excavations.

The project area comprises the youngest group of Manhattan Formation i.e., the Manhattan Schists. Although commonly referred to as schists, these crystalline schists vary in mineralogical composition from quartzose schists, quartz-felspar schists, quartz-garnet mica schists, biotite schists, hornblende schists to muscovite schists. Numerous pre-, post- to late-kinematic (during Cameron thrust activity) pegmatitic intrusions of varying sizes (80 feet wide to a fraction of an inch)



Figure 2. Project alignment superimposed on the E.L. Viele Topographic map of 1874.

Copyright © 2005 Taylor & Francis Group plc, London, UK

have been emplaced within these schists along and across the foliations and along fractures and joints in the area. These intrusions have locally elevated the metamorphic grade and modified the texture of these schists, which almost resemble aplitic, gneissic to granitic rocks.

Serpentinite, together with talc and chlorite schists, have been encountered in the borings between 27th and 28th Street on Eleventh Avenue. These rocks seem to have been intruded along the fractures and fault planes during Late Taconic to Early Acadian Orogeny. They are highly sheared and are seen as talcose schists, which display a distinct pulverized nature.

6 ESTABLISHMENT OF ROCK PROFILE

Probe drilling and seismic refraction surveys have been used to supplement the core drilling in areas where the rock profile approaches the alignment of the proposed tunnels. The seismic refraction surveys largely proved unsuccessful due to some or all of the following:

- Excessive soft compressible organic stratum within the overburden;
- Interference of sounding waves due to existing street traffic vibrations and utility obstructions near surface;
- Where two materials do not exhibit contrasting velocities, or where velocities gradually increase with depth, a clear refracted signal is not generated;
- The depth relations of the water table and bedrock may constitute a significant problem for the seismic refraction. This problem is that of a "blind layer" where the thickness of the saturated overburden is less than about half the depth of bedrock. In such cases, seismic energy from it will be received as a first arrival of seismic energy, and all methods used to reduce the seismic data to determine the depth of bedrock use only first arrivals. Thus, the saturated layer will not be detected where it is close to bedrock;
- A "hidden layer" occurs where a lower velocity material underlies a higher velocity material, a common situation in stratified sediments.

7 ROCK TYPES

Based on the cores recovered by the borings, the rocks along the alignment have been simplified into the following principal rock types:

- Pegmatitic Rocks: Includes igneous rocks including but not limited to pegmatite, granite, granitic schist/gneiss, quartz and granofels;
- Serpentine Rocks: Includes serpentinite, talc schist and chlorite schist;
- Schistose Rocks: Includes schist, schistose gneiss, and amphibole schist.

8 STRUCTURAL GEOLOGY

Structurally, the rocks of Manhattan Formation have undergone multi deformational events. The imprints of these events can be seen from various discontinuities observed in the rock cores. The most prominent fold episode during the deformational event D3 has developed the main regional macroscopic antiformal (F2) structure in Manhattan Island, which has modified the cleavage/foliation (S1) generated by isoclinal recumbent folding (F1) during the second phase of deformation (D2). The orientations of cleavage/foliation (S2) during the deformational event D3 trend NNW to NE and dips at low to high angles to either W/NW to SW or E/NE to SE, according to the orientation of respective attitude of bed rocks due to the F2 folding. The orientations of cleavage/foliation and associated fractures and joints are classified according to deformational events which are described below: (Refer to Shah, et al., 1998)

- D1 – the first foliation/bedding formed-(So): Orientation is obliterated;
- D2 – the foliation/cleavage trends E/W to ENE/WSW, highly obliterated, can only be seen near the fold cores (F1);
- D3 – represents the main foliation/cleavage in the area trending NNW/SSE to NE/SW due to large scale antiformal folding (F2), dipping either to the East or West;
- D4 – developed large scale shearing and fracturing due to the Cameron thrust faulting. Though this fault is not encountered in the area, the effect is seen in the rocks by shearing and chloritization;
- D5 – the rocks show moderate to steep plunging folds (F3). Foliations trend WNW/ESE with the development of S3 cleavages. These cleavages due to the extreme stresses resulted into slickensides, joints, fractures and faults on all scales. This event marks the most important fault/fracture system in the area and is associated with the Manhattanville (125th Street) fault, which had been developed in this deformational phase (Middle Devonian – Acadian Orogeny).

9 ZONES

For design and construction purposes, the geology along the tunnel alignment has been divided into 8 zones determined from the subsurface conditions

Copyright © 2005 Taylor & Francis Group plc, London, UK

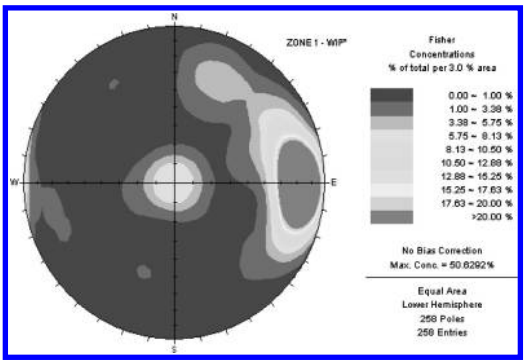


Figure 3. Stereoplot of discontinuities.

(e.g., ground type, lithology, rock strengths, rock mass Q-values and groundwater conditions) obtained from the boreholes, field tests and rock laboratory tests. Presently, further investigation is ongoing. This new data will confirm the zone boundaries. For illustration purpose, a stereographic pole plot of dip angles and dip directions of foliation and foliation joints obtained from the oriented rock core discontinuity data is shown in Figures 3. This plot is derived from oriented core, acoustic borehole televiewer and outcrop mapping using Rocscience software.

The resulting orientation and condition of these joint sets have been evaluated with respect to the opening orientation and geometry using the Unwedge software program for stability analyses of potential wedge formations within the rock mass. These data will also be used in the final tunnel liner design.

10 HYDROGEOLOGY – GROUNDWATER CONDITIONS

Manhattan schist is generally not saturated, as groundwater is held in the open joints within a generally tight rock mass. Groundwater flow is controlled by the random interconnection of these more open joints as observed in deep excavation in and around the New York City. Groundwater levels measured in the soil tend to follow the bedrock elevation, suggesting that they are probably perched on top of the bedrock, where rock forms a ridge and within the soil above the rock in bedrock valleys. The sources of groundwater recharge in Manhattan include infiltration in parklands, leaking sewers, drains and water lines, and the adjacent East River and Hudson River. Though the recharge in the bedrock mass is unlikely to be from precipitation filtration due to the relatively impermeable nature of the city streets and buildings, there is evidence that the natural groundwater flow may be lateral following the old buried stream beds.

11 HYDROTHERMAL MINERALIZATION

A 3-inch metallic sample was recovered from one of the borings (PE-23) at a depth of 145 feet (44 m) below existing ground level (El. −51 feet [15.5 m] NYCT Datum). The report on the laboratory testing conducted on the sample from indicates that the sample could not be cut by diamond saw. Characteristics of the metallic sample are similar to vein-type hydrothermal mineralization. Such mineralization is associated with intrusive igneous activity similar to the origin of the Pegmatite rocks. The mineralization is transported by super-heated hydrothermal fluids and deposited as veins within cracks and fractures in the host rocks. The mineralization will potentially exist in vein form within the Schist and Pegmatitic rocks. Vein thicknesses can vary considerably.

12 ENVIRONMENTAL INVESTIGATIONS

Environmental investigations have been undertaken along the project alignment to establish the presence, or otherwise, of potential contaminants associated with former land uses. The results of these investigations are beyond the scope of this paper.

13 CONCLUSIONS

The site geotechnical subsurface investigation program has been performed in four phases in support of the design from conceptual design to final design. The final design phase of subsurface exploration is currently on going. The investigations have included archive searches, stereophotogrammetry surveys of rock outcrop, test borings in soil and bedrock, oriented rock cores, borehole testing, and extensive laboratory testing. The results from these comprehensive site investigations have been interpreted to provide a geological model for the No. 7 Subway Line Extension. The geologic structure has been found to be complex, with regions of significant faulting, shearing, alteration and folding, particularly in the southern end of the project and at two stations on Eleventh Avenue and Tenth Avenue, respectively. The investigations have provided an updated and comprehensive record of the discontinuity system in the area. The expected excavation conditions with due regard to construction methodology have been developed for the running tunnels. The data obtained from the subsurface investigations has been interpreted and used to derive geotechnical parameters for design and to facilitate selection of construction methodologies. The data will also be used to baseline the ground conditions for contract purposes.

Copyright © 2005 Taylor & Francis Group plc, London, UK

ACKNOWLEDGEMENT

The authors gratefully acknowledge P. W. McGrade, Program Manager of MTA-NYCT for his permission and D. A. Donatelli of PB Team for his cooperation and support to publish this paper.

BIBLIOGRAPHY

1. Baskerville, C. A. Bedrock And Engineering Geologic Maps Of New York County and Parts of Kings and Queens Counties, New York, and Parts of Bergen and Hudson Counties, New Jersey, *U. S. Geological Survey*, 1994.
2. Shah, A. N., J. Wang, and N. C. Samtani, Geological Hazards in the Consideration of Design and Construction Activities of the New York City Area, Environmental & Engineering Geoscience, Vol. IV, No. 4, Winter 1998, pp. 524–533.
3. Stumm, F., A. Chu, A. D. Lange, F. L. Paillet, J. H. Williams, and J. W. Lane, Jr. Use of Advanced Borehole Geophysical Techniques to Delineate Fractured-Rock Ground-Water Flow and Fractures Along Water-Tunnel Facilities in Nortern Queens County, New York, U. S. Geological survey, WRIR 00-4276, December 2001.

Copyright © 2005 Taylor & Francis Group plc, London, UK

Some aspects for geotechnical investigations for TBM and NATM tunneling in rock

W. Wittke, J.H. Gattermann & P. Wittke-Gattermann
WBI – Prof. Dr.-Ing. W. Wittke Consulting Engineers for Tunneling and Geotechnical Engineering Ltd., Aachen/Stuttgart, Germany

ABSTRACT: Driving of tunnels in rock can be carried out by means of the New Austrian Tunneling Method (NATM) and by Tunnel Boring Machines. When applying the NATM it is possible to adapt the amount and thickness of the temporary support as well as the thickness of the internal lining to the different rock conditions to be expected along the tunnel alignment. Furthermore in case rock conditions encountered during construction differ from the predictions it is easy to modify support and lining accordingly. Also support of the temporary face can be carried out as required. The tunnel driving according to the NATM is however time-consuming in certain cases.

Thus, the application of a TBM is often an economic alternative. Using this method, the excavation diameter, the thickness of the lining and the type of the machine have to be selected in an early phase of the project. This includes an assessment of the stability of the working face. Thus, a TBM heading is far more sensitive to a change of the predicted ground conditions. This will be illustrated by means of two practical examples (chapter 2 and 3). For the second example the problems with machine tunneling could have been avoided by selecting a different type of machine.

Also with regards to the stability of the temporary face, the selection of an adequate machine is decisive (chapter 4). It results that the knowledge of the rock conditions must be far more reliable if it is planned to select a TBM-heading.

1 INTRODUCTION

A profound exploration of the ground conditions within the design phase is decisive for the technical and economical success of a tunnel construction. Since below certain depths the overburden stresses can not be carried by the support and lining respectively, parts of the load must be carried by the arch which develops in the rock around the tunnel. For a reliable assessment of this arch action and the load resulting for the support, the mechanical properties of the rock mass and adequate stability analyses are decisive. Also for the selection of the equipment for excavation the mechanical properties, especially the intact rock strength and it's mineral composition, are important.

Thus, the rock conditions combined with stability analyses are of central importance for selecting a suitable and economic support and construction method.

Common construction methods are the New Austrian Tunneling Method (NATM) and the construction with a tunnel boring machine (TBM).

Applying the NATM one can choose between a full face or sequential excavation. The latter can e. g. consist of an advancing vault heading with or without a temporary shotcrete supported invert, which is followed by the excavation of bench and invert of the total cross section. Besides the mode of heading the tender documents for a NATM driven tunnel should also describe the amount of support, such as the thickness of the shotcrete as well as the amount of anchoring and steel arches and its variation along the alignment of a tunnel. Variation of the thickness of the shotcrete support and the internal lining for the predicted ground conditions is easily feasible, because it is possible to change the excavation diameter along the alignment. It is also possible to increase and decrease the thickness of the shotcrete and the internal lining as well as the amount of anchoring along the alignment of a tunnel in case of unforeseen ground conditions occur.

Especially for long tunnels a TBM-heading can be more economic than the NATM. Figure 1 gives an overview on tunnelling machines. The type of machine must be defined in an early phase of the project, well before the start of construction. Also the required excavation diameter and thus the required thickness of a segmental or a cast in place lining including a potential support, have to be determined

Copyright © 2005 Taylor & Francis Group plc, London, UK

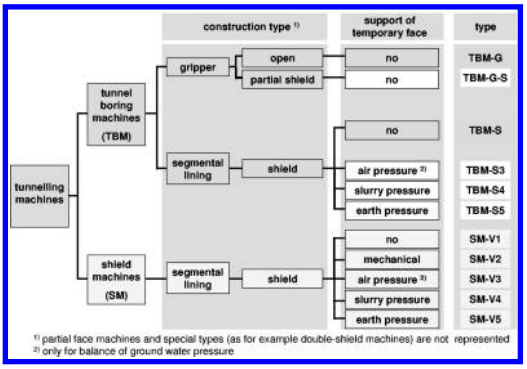


Figure 1. Overview of tunneling machines (cp. Daub 1996).



Figure 2. Water transmission tunnel in squeezing rock, Yacambu, Venezuela.

well in advance. This includes the required overcut, to compensate for radial displacements of the tunnel circumference, resulting from excavation. Furthermore, the method of a potential support of the temporary face as used for a slurry or earth pressure balanced shield, must be determined at an early point in time.

Having the above explanations in mind it becomes clear that a TBM heading is far more sensitive to a change of the predicted ground conditions. This will be illustrated by means of two practical examples (chapter 2 and 3). For the second example the problems with machine tunneling could have been avoided by selecting a different type of machine.

Also with regards to the stability of the temporary face, the selection of an adequate machine is decisive (chapter 4).



Figure 3. Shaft Konrad, yielding support in squeezing rock.

2 TUNNELS IN SQUEEZING ROCK

The water transmission tunnel of the Yacambu project in Venezuela is located in so-called squeezing rock (fig. 2). This tunnel was excavated by a tunnel boring machine (TBM-G) and supported by steel arches, shotcrete and anchors. This support failed because the rock mass strength was small in comparison to the stresses resulting from the weight of the overburden. Thus, the stiff support was overloaded because the rock adjacent to the tunnel became plastic. Displacements in the order of magnitude of decimeters had to be allowed for to enable the formation of an arch with large span in the rock mass around the tunnel.

An adequate design would have consisted of a shotcrete membrane with horizontal slots, fixed by yielding rock anchors (figs. 3 and 4). Such a support would have allowed for radial displacements to enable the above cited arching action within the rock mass. After certain displacements combined with the partial closing of the slots would have occured, the remaining gaps would have had to be closed by shotcrete and

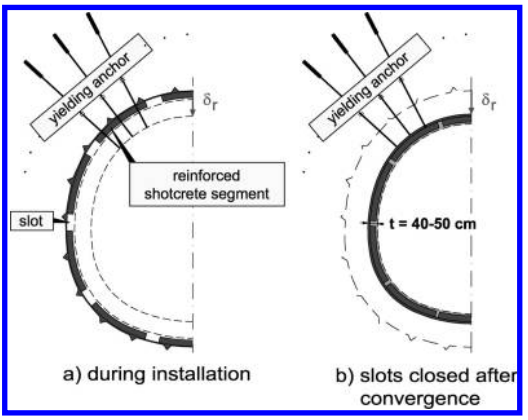


Figure 4. Yielding support, principle (Wittke 2005).

the anchors would have had to be fixed thus creating a stiff support. This process is strongly time-dependent because of the time-dependent plastic behavior of the rock mass.

Copyright © 2005 Taylor & Francis Group plc, London, UK

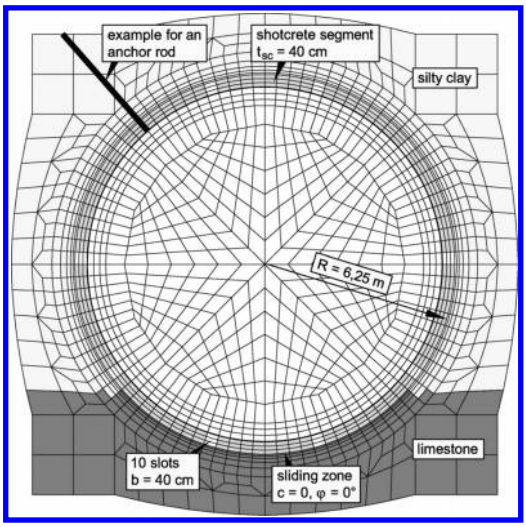


Figure 5. Yielding support, detail of FE-mesh (Wittke 2005).

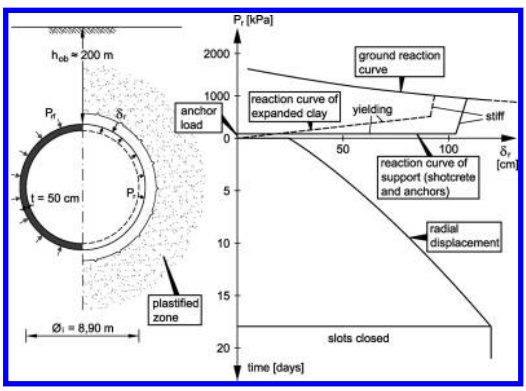


Figure 6. Example for analyses for a yielding support in squeezing rock (WBI/NAMA 2003).

Such a rock mass behavior can be simulated by an elastic-viscoplastic stress-strain law (Wittke, 2000). The stresses and displacements around the tunnel and within the support can be modeled by a corresponding finite-element program (Wittke, 2000). An example for an adequate finite-element mesh is represented in fig. 5.

As a result of corresponding analyses the radial displacements of the excavated surface are plotted versus the required radial support pressure (fig. 6). The reaction curve of a yielding support is a horizontal line with a radial pressure p_r, resulting from the anchoring. Once the slots are closed this line becomes steep (stiff support). Equilibrium is reached when the ground reaction curve is intersected.

The corresponding time displacement curve is also represented in fig. 6.

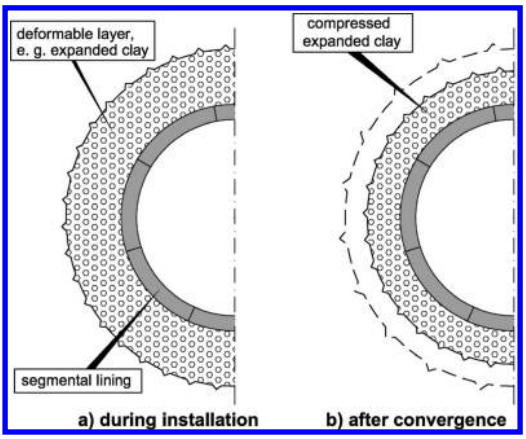


Figure 7. Support for TBM-heading in squeezing rock, principle.

A design for a tunnel in squeezing rock, constructed by a shielded tunnel boring machine with a segmental lining (SM) can foresee a deformable layer of expanded clay to be installed behind the segmental lining at the tail skin (fig. 7). The corresponding reaction curve of support is shown in fig. 6. This yielding support gains it stiffness by grouting of the zone of expanded clay at the required point in time. It is clear that for the latter solution a precise prediction of the ground reaction curve is required, already during the planning phase. If this prediction is on the unsafe side the risk of overloading of the segmental lining is high. If it is too much on the safe side the solution is not economic anymore. If the ground conditions vary the design has to account for the most unfavorable conditions and thus can not be optimized. Also if the required displacements result to a couple of decimeters the positioning and fixing of the segments will be difficult.

However, the same difficulties of prediction exist when the NATM solution is applied. The support in this case, however, can be better adapted to the existing conditions and also easily be modified along the alignment of the tunnel. Also a local repair is possible, if the first prediction did not meet reality.

However, if the conditions are uniform and predictable throughout the tunnel, a machine can be the better alternative.

3 TUNNEL BORING MACHINE IN SEDIMENTARY ROCK

The 21 km long water transmission tunnel for the project Misicuni is located near the city of Cochabamba, Bolivia (Wittke 2004) (figs. 8 and 9). The tunnel with a diameter of 3.5 m is located in faulted sedimentary

Copyright © 2005 Taylor & Francis Group plc, London, UK

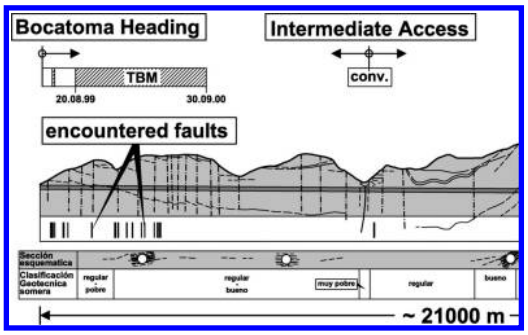


Figure 8. Proyecto múltiple Misicuni Bolivia, longitudinal section (part 1 of 2).

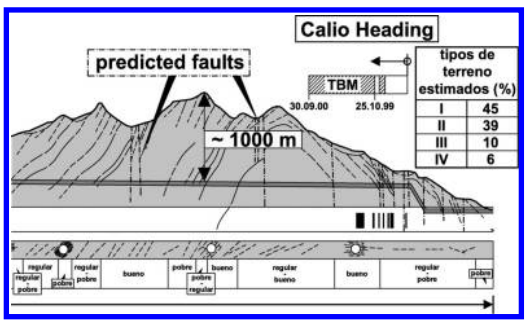


Figure 9. Proyecto múltiple Misicuni Bolivia, longitudinal section (part 2 of 2).

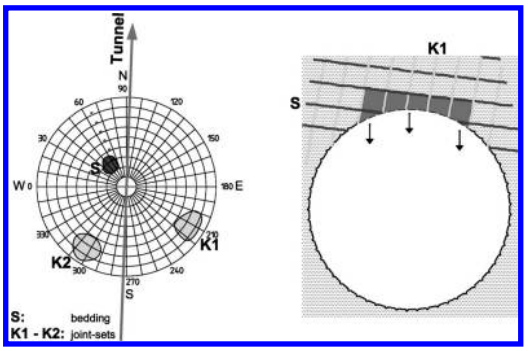


Figure 10. Proyecto múltiple Misicuni, bedding and joints, instabilities at tunnel roof.

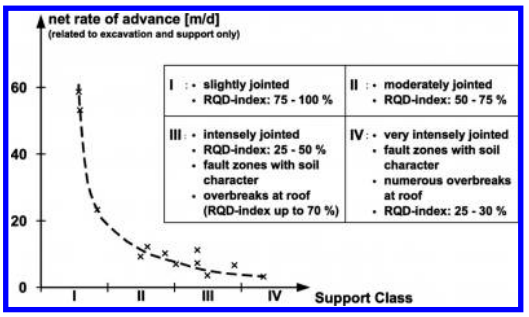


Figure 11. Proyecto múltiple Misicuni, net rates of advance per day and support classes.

rock. The bedding and the bedding parallel discontinuities reveal a shallow dip over long sections of the alignment (fig. 10). In combination with the distinct jointing following two vertical sets (K1 and K2), rock blocks were created above the tunnel roof, which have led to instabilities (fig. 10). The tunnel is being excavated from both sides with a hard rock tunnel boring machine (TBM-G, fig. 1). These two headings are named Bocatoma and Calio heading respectively (fig. 8 and 9). Because of the high overburden of up to 1000 m, only one intermediate access for conventional excavation through a shaft was feasible.

It is obvious that because of its length the conventional excavation of the whole tunnel by NATM would have led to an extremely long construction time. Thus, the decision to install 2 TBMs on each side was correct in principle.

Nevertheless, the achieved rates of progress were not satisfactory. In the tender documents the rock was subdivided into four classes (I to IV) with different intensity of jointing (fig. 11). For class number I no support was expected to be required.

For rock classes II–IV anchor and shotcrete support of different intensity was planned and also necessary. Due to lack of space in the area of the tunnel boring machine it was however very difficult and time consuming to install these support measures. Furthermore the anchors and the shotcrete could only be installed behind the cutter head, eventhough rock blocks already fell down ahead and above the cutter head and of course also behind the cutter head.

As long as the support class I could be used, the net rates of advance were very high (fig. 11). However, when the support classes III or IV were needed, which unfortunately very often was the case, the rates of advance were extremely low and unsatisfactory. It revealed that the selected tunneling machine was not suitable for the given task. The consequence was an extreme delay of construction time and a considerable cost increase. A tunnel boring machine with a shield and a segmental lining would have been a far better choice for the encountered ground conditions.

To realize this would however have required a much better description and assessment of the orientation and intensity of bedding and jointing already in the planning phase. A simple rock mass classification could not serve the purpose.

Copyright © 2005 Taylor & Francis Group plc, London, UK

4 STABILITY OF THE WORKING FACE IN SOFT ROCKS OR IN MIXED FACE CONDITIONS

In certain rock formations, especially in soft rocks, a support or stabilization of the working face is required.

If the tunnel is driven using the NATM the stabilization of the working face can be reached by means of a layer of shotcrete, anchoring, an inclined working face and a supporting core. If the instability is caused by ground water flow, advanced drillings for dewatering represent a feasible measure.

Furthermore, stability can be increased by reducing the area of the working face which can be achieved by sequential excavation.

In figure 1 possible measures for stabilization of the working face in case of a TBM-heading are presented. As long as the temporary face and the adjacent roof are stable along most of the tunnel length a tunnel boring machine with a shield is often the most economic solution. To avoid risks and to cope with local instabilities the option to install preceding anchors and spiles at the roof respectively, is advisable. The rates of advance of such machines are normally quite high. However, if supporting measures at the working face are required over long sections of the tunnel alignment, tunnel boring machines with slurry and/or earth pressure balanced shields respectively might be a better alternative. Furthermore fluid and earth pressure balanced shields respectively can be economic within heterogeneous ground conditions, such as rock and soil at the working face within the same cross section (mixed face conditions).

Figure 12 shows the range of application of Hydroshields in soils as a function of the grain size distribution (Maidl et al., 1995). A high content of fines can require a very costly separation of the returned soil from the slurry. Also adhesion to the cutting tools can lead to problems. If the content of coarse-grained material is very high a stabilization of the working face can not be achieved by means of a hydroshield, because the slurry penetrates into the ground.

A corresponding diagram for the applicability of an EPB-shield in soil is represented in figure 13. Depending on the type of the soil and the water pressure, water or other additives are required for feasibility.

TBM tunneling in rock using EPB shields requires that the excavated rock can be transformed into a mud with an adequate soft to very soft consistency, a high "water-binding" capacity and low permeability. During excavation the in-situ rock is mechanically crushed to chips by the cutting tools. These chips are to be converted into a mud in the course of mingling with ground water. It may also be necessary to add water, clay suspensions or other conditioning additives.

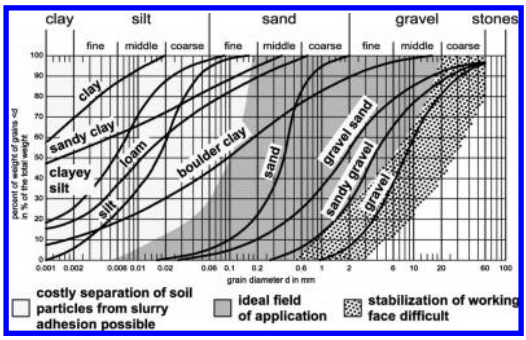
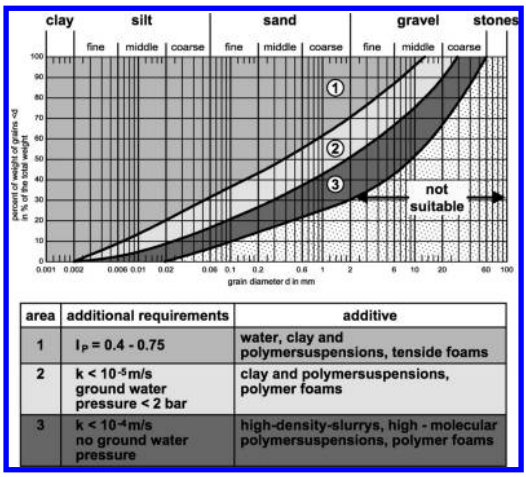


Figure 12. Field of application of a hydroshield (Maidl 1995).



area	additional requirements	additive
1	I_P = 0.4 - 0.75	water, clay and polymersuspensions, tenside foams
2	k < 10^{-5} m/s ground water pressure < 2 bar	clay and polymersuspensions, polymer foams
3	k < 10^{-4} m/s no ground water pressure	high-density-slurrys, high - molecular polymersuspensions, polymer foams

Figure 13. Possibility of conditioning of ground for feasibility of an EPB-shield (Maidl 1994).

In order to gain more informations about the applicability of earth pressure balanced shields in rock WBI has carried out some preliminary laboratory tests (Gattermann & Kiehl, 2003). Samples from a project near Stuttgart were taken and crushed into pieces of 1–3 cm size (fig. 14). By means of a rather simple test setup it was tested, whether this granular material and water as additive can be transformed into a mud. This equipment consists of a column drilling machine, an agitator and a container of synthetic material. The speed of rotation of the drilling machine was 150 revolutions per minute. The duration of the test was 10 minutes each.

Before and after the test the grain size distribution of each sample was determined in WBI's soil mechanics laboratory. The resulting grain size distribution were compared with the required grain size distribution according to figure 13. Exemplary, figure 14 shows

Copyright © 2005 Taylor & Francis Group plc, London, UK

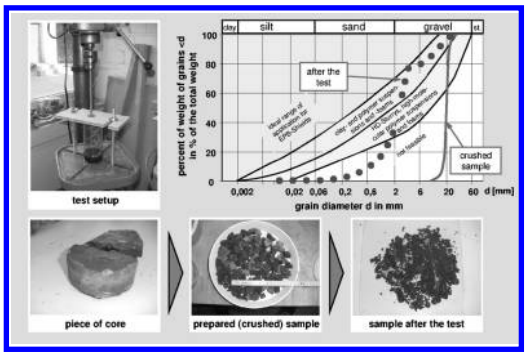


Figure 14. Preliminary tests on feasibility of conditioning of rock with water (Marl, "Obere Bunte Mergel") (Gattermann 2004).

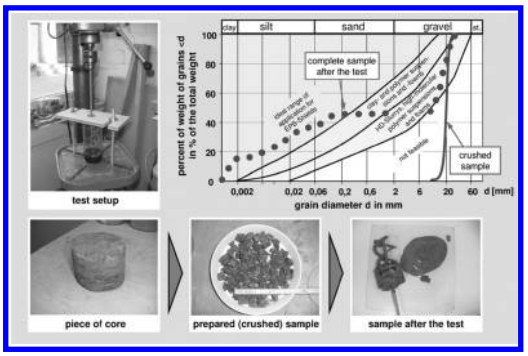


Figure 15. Preliminary tests on feasibility of conditioning of rock with water (mudstone of the "Lias α").

the test results for a sample of marl of the so called "Obere Bunte Mergel". The grain size distribution lies partly in the area which is according to Maidl (1994) not suitable for EPB-shields. Obviously the conditioning with water was not completely successful in this special case.

The results of two other tests are represented in figures 15 and 16. One can see that liquefaction of the mudstone of the Lias α is feasible whereas the tests on samples of Unleached Gypsum Keuper were not successful.

For rotation of the cutter head, the driving torque must be greater than the resisting torque. The resisting torque results from rotation of the tools on the temporary face and from rotation of the earth mud.

To avoid a rotation of the shield of the TBM, the resulting driving torque must be transferred to the rock mass and/or the segmental lining. This is mainly achieved by friction between the shield and the rock and by tangential deviation of the jacks. It has to be taken into account that – unlike the situation during TBM-heading in soil – the gap between the rock and the shield is not closed. Thus, the shield is not loaded by rock pressure along the complete circumference and the torque can only be transferred to the rock in the area of the invert. The remaining torque must be transferred to the segmental lining by tangential deviation of the jacks.

It has to be ensured that the properties of the earth mud are in a range, which allows to transfer the required driving torque to the rock and/or the segmental lining. For a special project it was found that the properties of the earth mud are to be $\varphi < 15°$ and $\tau_0 < 25\,kN/m^2$ respectively (Gattermann, 2004).

Furthermore EPB shields in rock include the risk of a tearing of the working face which can lead to an instability of the working face. A great amount of stones or coarse gravel within the earth mud can lead to a mechanical blockade of the cutting roles.

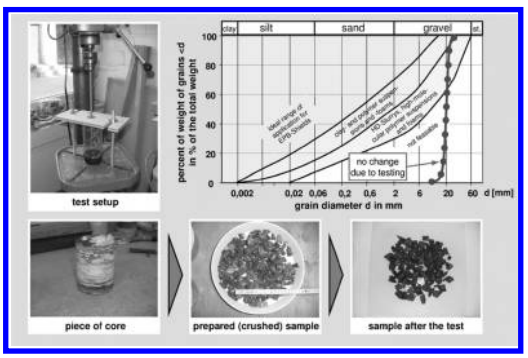


Figure 16. Preliminary tests on feasibility of conditioning of rock with water (Unleached Gypsum Keuper).

The relative movement between the soil and the cutting wheel goes along with a high wear of the tool kits and the cutting wheel.

It is obvious, that a sound prediction of the stability of the working face is necessary in an early phase of the project. Also the type and feasibility of a face support must be decided upon rather early. In case an EPB shield is selected, it should be checked in advance whether it is possible to convert the in situ rock into a suitable earth mud. Thus, the risk of EPB shields could be considerably lowered, the most favorable conditioning material could be specified and suitable cutting tools could be chosen.

REFERENCES

Deutscher Ausschuß für Unterirdisches Bauen (DAUB) 1996: Empfehlungen zur Auswahl und Bewertung von Tunnelvortriebsmaschinen.

Gattermann, J. H.; Kiehl, J. R. 2004: EPB-Vortriebe im Fels – Verbreiung des Gesteins, erforderliches

Copyright © 2005 Taylor & Francis Group plc, London, UK

Drehmoment und Verrollung. Geotechnik 27 (2004) Nr. 2, P. 208–213.
Maidl, U. 1994: Erweiterung der Einsatzbereiche der Erddruckschilde durch Bodenkonditionierung mit Schaum. Dissertation.
Maidl, B.; Herrenknecht, M.; Anheuser, L. 1995: Maschineller Tunnelbau im Schildvortrieb. Berlin. Ernst & Sohn, Verlag für Architektur und technische Wissenschaften.
WBI/NAMA 2003: Kallidromo Tunnel, Final Design, TBM design. Aachen/Athens. Not published.
Wittke, W. 2000: Stability Analyses for Tunnels, Fundamentals – Geotechnical Engineering in Research and Practice. WBI-PRINT 4. Verlag Glückauf GmbH, Essen, Germany.
Wittke, W. 2004: Ursachen und Vermeidung von Termin- und Kostenüberschreitungen bei Tunnelbauten der Infrastruktur. Oral presentation. Baugrundtagung, Leipzig, Germany.
Wittke, W.; Wittke-Schmitt, B.; Schmitt, D. 2005: The 9 km long Kallidromo Tunnel of the New Highspeed Railway Line Athens – Thessaloniki, Greece. Tunnel Sections in Squeezing Ground. ITA 2005, submitted for publication.

Copyright © 2005 Taylor & Francis Group plc, London, UK

Rock mass classification and support design of the Kuskunkiran Tunnel in Van

Ercüment Karahan
Mining Engineer, SEMAT Eng. Ltd., Ankara, Turkey

Songül Coşar
Geological Engineer (M.Sc. Mining Eng.), PETRA Eng. and Cons. Ltd., Ankara, Turkey

Şenol Sözer
Geological Engineer, PETRA Eng. and Cons. Ltd., Ankara, Turkey

Kenan Kaya
Geological Engineer (M.Sc.), KGM Technical Research Department, Ankara, Turkey

ABSTRACT: The purpose of this study is to investigate the geological and geotechnical characteristics of the rock mass and to suggest appropriate excavation and support recommendations, and rock mass strength parameters along the Kuskunkiran Tunnel in Van. The study area consists of calc schist, graphitic schist, meta-sandstone, meta-conglomerate and recrystallized limestone. The rock mass was classified according to the RMR, Q, and NATM classification systems and the tunnel ground was divided into sections according to the rock mass classes. Then, the geomechanical parameters and the support recommendations were selected based on these classification systems. Appropriate geomechanical parameters (i.e., Hoek-Brown material constants m and s, cohesion, internal friction angle, modulus elasticity etc.) were used, deformations and stress concentrations around the tunnel were investigated and finally the interaction of the support systems with the excavated rock masses were analyzed by using finite element method.

1 INTRODUCTION

1.1 *Purpose and scope*

The purpose of this study to investigate the geological and geotechnical characteristics of the rock mass and to suggest excavation and support recommendations, and rock mass strength parameters along the Kuskunkiran Tunnel located at the Van-Tatvan Road between Km 0+910 and Km 3+147.50 in Van (Figure 1).

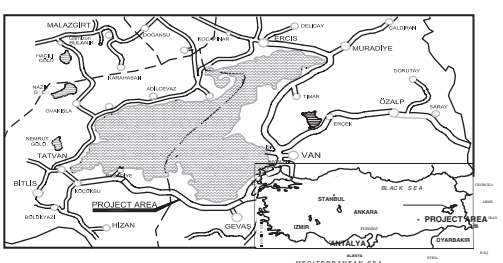


Figure 1. Location map of the project area.

1.2 *Project area*

The project area is located 25 km west of Gevaş on the Van-Tatvan Road between Km 0+910 and 3+147.50 in eastern Turkey. 2237.50 m long Kuskunkiran Tunnel has a flute shape, with a span of 12 m and a height of 10 m.

2 GEOLOGY

In the project area and its close vicinity, Permo-Carboniferrous aged Muş-Bitlis Massive and Quaternary deposits are distinguished. Muş-Bitlis Massive consists of calc schist, graphitic schist, meta-sandstone, meta-conglomerate, recrystallized limestone and marble.

3 ENGINEERING GEOLOGY

A detailed geological and geotechnical study was carried out in the project area. In order to determine the

Copyright © 2005 Taylor & Francis Group plc, London, UK

geotechnical properties of the rocks exposed and cut along the tunnel route, field measurements (i.e. identification of lithological units, determination of discontinuity characteristics, etc.), core-box survey (determination of lithological units, total core recovery (TCR), rock quality designation (RQD), joint conditions such as weathering, roughness, persistency, aperture, etc.) and laboratory testing on samples taken from the core borings were performed. The rock descriptions include both rock mass and rock material characteristics that based on ISRM (1981). Along the 2237.50 m long Kuskunkiran Tunnel, a total of 1851 m of drilling was performed with 18 boreholes. A strip geological map and cross-section showing borehole locations along the tunnel route were prepared based on field geology and core-box survey.

The main rock types observed in the project area include calc schist, graphitic schist, meta-sandstone, meta-conglomerate.

Schist, which is rarely intercalated with meta-conglomerate, meta-sandstone, recrystallized limestone and marble, will be cut along the all tunnel route (Figure 2). Schists are dark gray, fine grained, slightly to moderately hard, slightly to moderately weathered and weak to moderately weak. It is easily separated along the foliation planes, which is highly persistent. Field and core-box observations show that thin foliation planes (5–15 cm) are tight (<1 mm). The joint walls are planar, rough to smooth. Apertures are <0.5 mm wide and sometimes filled with quartz infilling. Average spacing of joints in the schist ranges between 5 and 50 cm. The uniaxial compressive strength and point load strength index of the schists range between 3 and 116 MPa, and 1.14 and 6.12 MPa, respectively. The Rock Quality Designation (RQD) ranges from 5% to 75%.

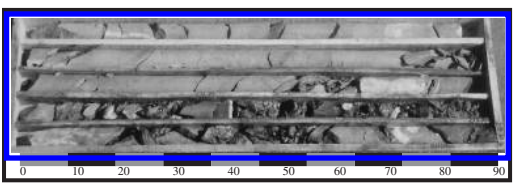


Figure 2. A view of core samples taken from calc schist-graphitic schist alternation at borehole YSK-3 along the Kuskunkiran Tunnel route.

Conclusions should state concisely the most important propositions of the paper as well as the author's views of the practical implications of the results.

4 ROCK MASS CLASSIFICATION, STRENGTH PARAMETERS AND EMPIRICAL SUPPORT DESIGN FOR THE KUSKUNKIRAN TUNNEL

For the design of the Kuskunkiran Tunnel, RMR, Q, and NATM classification systems were used and the support systems were selected according to these classification systems. The rock mass classifications results, geomechanical properties of rock mass and the empirical temporary support recommendations, including rock bolt, shotcrete, wiremesh and steel ribs, are summarized in Tables 1, 2, and 3, respectively.

5 NUMERICAL ANALYSIS FOR KUSKUNKIRAN TUNNEL

The objective of the numerical analysis is to check the validity of empirical temporary tunnel support requirements given in Table 3. For this aim, the finite element software package Phase^2 has been used to determine induced stresses and deformations developed around tunnel excavation and to investigate the interaction of proposed support systems with the tunnel ground.

Table 1. Summary of the rock mass classification results in the project area.

			Rock mass classification ratings			
Tunnel section/km	Borehole no	Lithology	Q	RMR	RMR (=9lnQ+44)	NATM
Tunnel entrance	SK-8, SK-9	Schist	0.917	42	43	B3
0+900–2+000	SK-1, SK-2, YSK-2	Schist	4.00	53	56	B2
2+000–3+147.50	SK-3, SK-4, SK-5, YSK-3, YSK-4	Schist	0.666	40	40	B3
2+000–3+147.50 (Weak and highly weathered)	SK-4, SK-5	Graphitic schist	0.1666	30	28	C2
Exit portal	SK-5, YSK-5, SK-10, SK-11, ÇSK-1, ÇSK-2, ÇSK-3, ÇSK-4	Schist	0.417	37	36	B3

Copyright © 2005 Taylor & Francis Group plc, London, UK

The excavation section of Kuskunkiran Tunnel will be twin tube flute shaped with 12 m span and 10 m height. The tunnel ground has been divided into sections with respect to rock mass geomechanical properties that have been evaluated at the borehole locations along the tunnel route. Dominating rock class of the Kuskunkiran Tunnel according to ONORM 23 is B2 between entrance-middle part and B3 between middle part-exit of the tunnel. Also in weak and highly disintegrated zones of graphitic shists, rock class of C2 may be encountered. Furthermore, tunnel excavation at portals should be evaluated carefully because of low overburden thickness and weathering conditions around excavation.

So, four different Phase2 excavation and support model (B2, B3, C2 and Portal) has been constituted to evaluate the interaction between proposed support systems with surrounding ground. The model prepared for B3 Excavation and Support System, one of the most severe conditions that would be faced during tunneling, is shown in Figure 3, at its last stage when all excavation and supporting activities has been finished.

The B3 excavation and support model has been constituted by nine stages to simulate the real excavation and support phases. The Hoek-Brown Failure Criterion is used for finite element analysis. In the first stage, insitu stress distribution (gravity loading due to thickness of overburden) is examined. The overburden height is approx. 300 m, which is the biggest height along the tunnel. In the following two stages, left tube top heading excavation and supporting activities are completed. In the forth and fifth stages,

Table 2. Geomechanical properties of rock mass for each section at the project area.

	Undisturbed rock					Disturbed rock					
Tunnel section/ km	Modulus of elastisity	Cohesion c (kPa)	Friction angle ϕ°	m	s	Modulus of elastisity E_m	Cohesion c (kPa)	Friction angle ϕ°	m	s	Unit weight γ (kN/m^3)
Tunnel entrance	0.615	250	46	1.638	0.00159	1.833	170	37	0.537	0.000224	27
0+900–2+000	7.511	825	47	2.426	0.0054	4.882	570	39	0.983	0.0011	27
2+000–3+147.50	3.082	560	41	1.525	0.00127	2.003	360	31	0.481	0.000167	27
2+000–3+147.50 (Weak and highly weathered)	1.000	300	29	1.067	0.000419	0.650	180	19	0.278	0.0000393	27
Exit portal	1.831	200	43	1.371	0.000912	1.190	130	33	0.408	0.000108	27

Table 3. Summary of the tunnel support requirements for the Kuskunkiran tunnel.

Support system	B2	B3	C2
Excavation	Top heading and bench	Top heading and bench	Top heading and bench
Advance length			
Top heading	2–2.50 m	1–1.50 m	<1.00 m
Bench	<3.50 m	<3.00 m	<3.00 m
Invert	–	<3.00 m	<3.00 m
Support Type			
Rock Bolt			
Diameter	Æ 28	Æ 28	Æ 28
Spacing	2.00 × 2.00	1.00–1.50 × 1.50	1.00–1.50 × 1.50
Length	4 m	4–6 m	4–6 m
Shotcrete class and thickness	B20 15 cm	B25 20 cm	B25 25 cm
Wiremesh type	Q221/221	Q221/221	Q221/221
	1 layer	2 layer	2 layer
Steel rib type and spacing	–	I160,1–1.50 m	I160,1.00 m
Forepoling spacing and length	–	0.3–0.4 m, 4–6 m	0.3–0.4 m, 4–6 m

Copyright © 2005 Taylor & Francis Group plc, London, UK

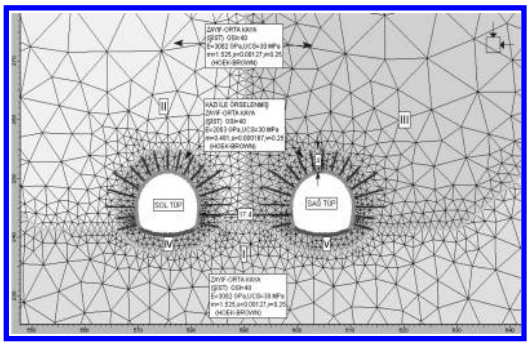


Figure 3. B3 excavation and support model.

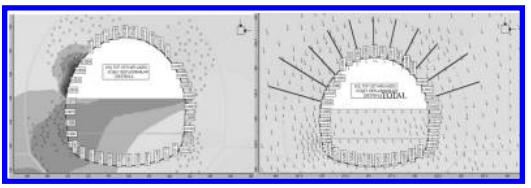


Figure 4. Total displacements in second and third stages.

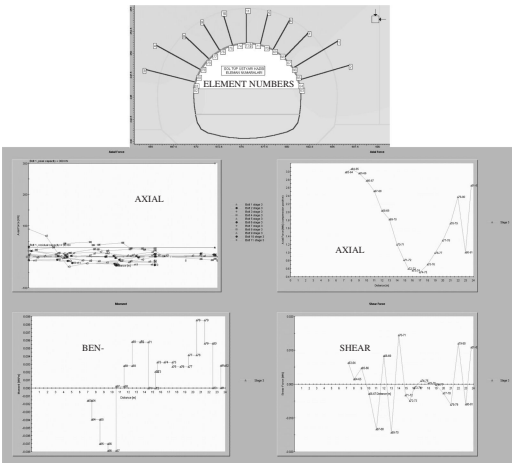


Figure 5. Total loads and moments carried by support elements at third stage.

bench excavation and supporting of left tube is finished and in the last four stages excavation and supporting of right tube is finished in the same manner of left tube.

The distance between excavation perimeters of left and right tubes are 17 m. A disturbed zone of 4 m thickness around tunnel excavation is supposed to be formed after blasting and bolt installation.

For the optimum simulation of excavation and support stages, Phase2 provides Load Split possibility to split the loads between stages. This means that, the loads carried by an unsupported excavation is not the total load, but only a part of it. The rest of the load is carried by the unexcavated section of tunnel. It is assumed that (and should be), total load is carried by fully supported section of the tunnel which is also at a sufficient distance of tunnel face.

According to this, as shown in Figure 3, Load Split has been utilized for undisturbed rock masses II and III and disturbed Rock Masses IV and V. At the second stage where the top heading excavation of left tube is finished, II and IV masses are loaded with a percentage of r1. In the third stage where the support of top heading (20 cm thick shell of shotcrete, fully bonded 4–6 m long and 28 mm diameter untensioned grouted rock bolt, wire mesh and steel rib) is completed, the rest of load (1-r1) is added and these masses will be fully activated. In the same manner, III and V Rock Masses are loaded with a percentage of r2 at the sixth stage for Right Tube, and the rest (1-r2) is loaded in the seventh stage for full activation.

The determination of r1 and r2 percentages is quite difficult, because it depends on various parameters such as rock mass quality, time deviations during excavation and supporting phases, application quality of supports etc. But it is clear that, r1 and r2 percentages of rock masses will be decreased with increasing quality of rock mass because of increasing time and dimension of unsupported span. For B3 excavation and support system, the advance length of top heading is 1.00–1.50 m and, full supporting should be completed before a new advance. So an unsupported section will be at max. 1.50 m distance from tunnel face and r1 percentage is estimated as 60% with the consideration of safety conditions. The construction period of right tube will be started after the completion of left tube, so r2 percentage is also estimated as 60% since the induced stress conditions created by left tube excavation will be completed before right tube excavation.

Total displacements are shown in Figure 4 where top heading excavation (second stage) and top heading support systems (third stage) is completed. Maximum displacement reaches to 36 mm in the third stage from 25 mm in the second stage. This verifies that the r1 percentage (60%) is correctly estimated and some displacement of unsupported rock mass is provided before installation of support as expected between excavation and supporting stages and as suitable for the NATM philosophy.

Total loads and moments carried by support elements at top heading of left tube (third stage) are shown in Figure 5. Maximum axial force on bolts is 9 tons which is originated in third bolt element at side wall of the excavation. Maximum axial force, bending moment and shear forces developed on shotcrete elements are 310 tons, 0.8 ton * m and 1.5 tons respectively at roofs

Copyright © 2005 Taylor & Francis Group plc, London, UK

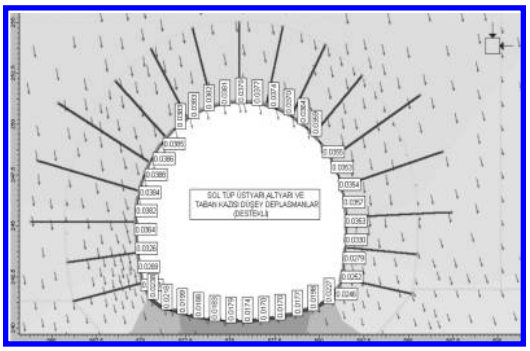


Figure 6. Total displacements at fifth stage.

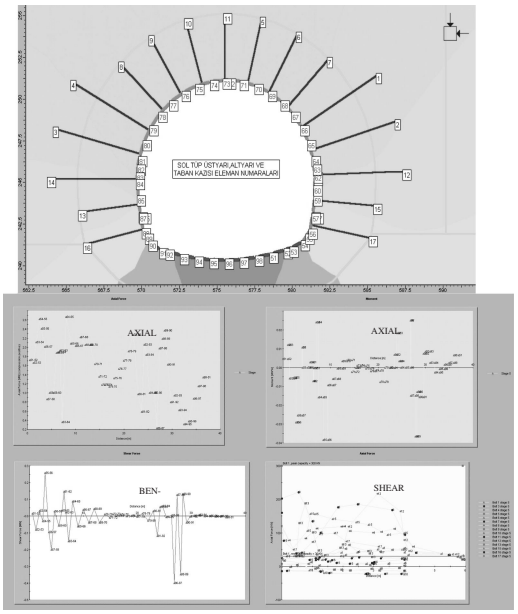


Figure 7. Total loads and moments at fifth stage.

and side walls of the tunnel. It is clear that, the loads carried by shotcrete elements are quite below their capacities.

Total displacements (Figure 6), originated after completion of full section excavation and support (top heading, bench and invert) at left tube (fifth stage), is increased to 38 mm at the roof of the tunnel compared to 36 mm, after top heading excavation and support, there has been a small increase as expected in homogeneous rock conditions without big scale discontinuities.

At this fifth stage, axial forces originated on bolt elements are increased to 22 tons on elements 6 and 12 at roof and side wall. Maximum bending moments, shear forces and axial forces developed on shotcrete elements are 3.8 ton * m, 35 ton and 270 ton respectively at side

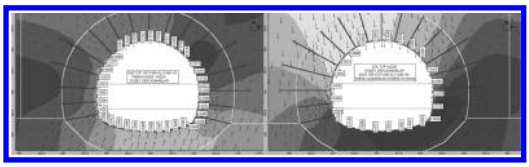


Figure 8. Total displacements at ninth stage.

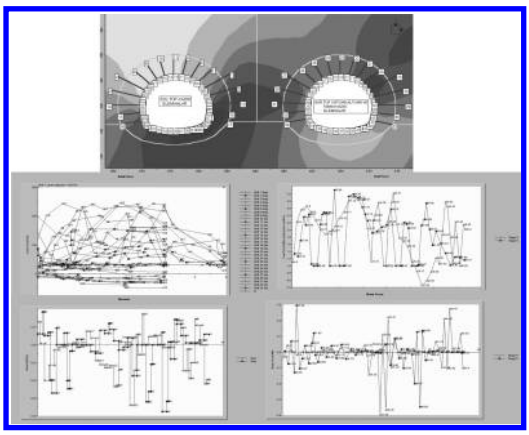


Figure 9. Total loads and moments at ninth stage.

walls of excavation. Compared to third stage, axial forces are slightly decreased which may be expected on condition that drastic increase in bending moments and shear forces.

After completion of full section excavation and support of right tube (stage nine), total displacements of both tubes are shown in Figure 8. Compared to fifth stage (without excavation of right tube), maximum displacements are increased to 56 mm from 38 mm at the roof of left tube. For the right tube, maximum displacements are developed on the left side of excavation as 42 mm.

Figure 9 shows loads and bending moments developed on bolt and shotcrete elements both for left and right tubes at ninth stage. Maximum axial force originated on bolt elements are 25 tons on element number 17 of right tube side wall and on element number 18 of left tube side wall. There is a slight increase from 22 tons to 25 tons before and after right tube excavation. Maximum loads carried by shotcrete elements are 310 tons as axial force on left tube, 3.8 ton*m as bending moment on left tube and 40 tons as shear force on right tube. Compared to fifth stage, there are slight increases on maximum axial and shear forces and there is no change on bending moments.

As seen from the previous figures, the difference in loads developed on support elements between fifth stage where full section excavation and support of left tube has been completed and ninth stage where full

Copyright © 2005 Taylor & Francis Group plc, London, UK

section excavation and support of right tube has been completed is only 2 tons of increase of maximum axial force on bolt elements and 5 tons of increase of maximum shear force. Also total displacements on left tube have been increased approx. 20 mm. There is no yield on any support element. This actually means that the distance between two tubes is properly selected and creates no any instability even in weak rock conditions. In the last stage of model, maximum axial and shear forces and bending moments that shotcrete elements have been exposed are;

On 65–66 Element;

M = 0.0025 MN * m = 0.25 ton * m = 25 000 kg * cm

N= 3.1 MN = 310 tons = 310 000 kg (Max. Value)

On 87–88 Element;

M = 0.038 MN * m = 3.8 ton * m = 380 000 kg * cm (Max. Value)

N = 2.1 MN = 210 ton = 210 000 kg

T = 0.4 MN = 40 ton = 40 000 kg (Max. Value)

Minimum and maximum stress concentrations constituted by the Axial Force-Bending Moment on the shotcrete shell of 20 cm in thickness will be:

On 65–66 Element;

Sxx,max = $310000/(100 \times 20) + 6 \times 25000/(100 \times 20^2) = 155 + 3.75 = 158.75$ kg/cm^2

Sxx,min = $155 - 3.75 = 151.25$ kg/cm^2

On 87–88 Element;

Sxx,max = $210000/(100 \times 20) + 6 \times 380000/(100 \times 20^2) = 105 + 57 = 162$ kg/cm^2

Sxx,min = $105 - 57 = 48$ kg/cm^2

Under these maximum stress concentrations, it will not occur any instability with B25 shotcrete of 200 kg/ cm^2 bearing capacity. Also, the average shear stress constituted by shear force on shotcrete will be $t = 40000/(20 \times 100) = 20$ kg/cm^2 which can be easily carried by shotcrete, steel rib and wire mesh combination.

Therefore it is concluded that the excavation and support systems recommended for B3 Rock Class of Kuskunkiran Tunnel in Table 3 is satisfactory.

6 CONCLUSION

In this study, the engineering geological characteristics of rock mass are assessed and appropriate support systems and stabilization techniques along Kuskunkiran Tunnel are suggested. A detailed engineering geological study is carried out in project area. Rock mass classification systems, namely, the RMR system and the Q system have been applied. The tunnel ground is classified according to NATM by using a correlation with RMR and Q system. The Hoek-Brown material constants m and s and elastic modulus of rock masses are obtained by using RMR (Rock Mass Rating) and GSI (Geological Strength Index). The Rock masses of Kuskunkiran Tunnel ranges from poor quality to fair quality rock mass.

The finite element package Phase^2 is used to determine the loads, deformations and induced stresses developed around Kuskunkıran Tunnel excavation and to investigate the interaction of proposed support system with the tunnel ground. One of the most severe conditions that would be faced during tunneling is taken into consideration to model the tunnel ground. It is concluded that the suggested empirical support systems are satisfactory.

REFERENCES

Barton, N., Lien, R. & Lunde, J., 1974. Engineering Classification of Masses for the Design of Tunnel Support, *Rock Mechanics* Vol.6, No.4, pp.189–236.

Bieniawski, Z.T. 1989. *Engineering Rock Mass Classifications*, Newyork: Wiley.

Hoek, E. 2000. *Rock Engineering Course Notes,* http://www.rocscience/Hoek's Corner, last date accessed April 2004.

Hoek, E. 2004a. A Brief History the Development of the Hoek-Brown Failure Criterion, Discussion Paper # 7, http://www.rocscience.com/Hoek's Corner, 9 p, last date accessed June 2004.

Hoek, E., Carranza-Torres, C., Corkum, B., 2002. Hoek-Brown Failure Criterion – 2002 Edition, http://www.rocscience/Hoek's Corner, last date accessed April 2004.

ISRM (International Society for Rock Mechanics), 1981. *Rock Characterization, Testing and Monitoring – ISRM Suggested methods*, Oxford: Pergamon Press.

Petra Müh. Müş. İnş. Ltd. Şti., 2004. *Van-Tatvan Yolu Kuskunkiran Tüneli Kesin Proje Raporu.*

Petra Müh. Müş. ve İnş. Ltd. Şti., 2004. *Van-Tatvan Yolu Kuskunkiran Tüneli Kesin Proje Jeolojijk-Jeoteknik Raporu.*

Singh, B., Goel, R.K., 1999. Rock Mass Classification, *A Practical Approach in Civil Engineering*: 267 pages.

Copyright © 2005 Taylor & Francis Group plc, London, UK

Tunnel machines and mechanical excavations

Copyright © 2005 Taylor & Francis Group plc, London, UK

The development and application of shield posture automatic measuring system

Xiuping Yue
Shanghai No. 2 Municipal Engineering Co. Ltd., Shanghai, China

ABSTRACT: Correctly measuring real-time shield postures and promptly working out the deviation during shield driving is a prerequisite to successful tunneling proceeding and good quality. This paper gives a general introduction of the theory of the automatic shield three-dimensional posture tracing and measuring system which emerges from the Leica TCA as well as its distinctive characteristics known as simple in operation, real-time and accurate in giving the actual position of the shield. The analysis of the construction data also indicates its super performance in promptness, accuracy, flexibility and stability.

1 INTRODUCTION

During the tunneling with shield method, the automaticity of the shield is becoming higher, the driving velocity is faster, and these two factors make a lot of pressure on measurement and induction. For giving the deviation of directivity duly and precisely and rectifying the deviation during the construction of tunneling, there are only several precise guidance systems which are used in the tunneling with shield method in the international. So far, the precise guidance systems are used a little in the engineering, the reasons are: 1 the equipment charge or the tenancy charge is high; 2 the users are required a lot and it is not easy for the technologists to master; 3 the operation and the maintenance of some systems is complicated, and it needs some other assistant methods to make sure the precision reliability.

We analyze the reasons for using the guidance system such a little, take other thoughts in allusion to these adverse factors to establish the new frame, and form the new system combining the current newest technological equipments. This paper gives an introduction of this new system's theory, technique, development and application.

2 THE RIGID THEORY OF THE SHIELD POSTURE

Considering the shield as the rigid is easily understood according to the space geometry theory, which is three points of the rigid which are not collinear uniquely determine the spatial position and the posture of the rigid (Fig. 1). That is, once such three points of the rigid are determined, then the position in space (coordinate) of each point of the rigid is determined uniquely. From that, the necessary and sufficient theorem of the rigid spatial location is derived as follows: the premise of the determination of the rigid position and posture is that three points of the rigid which are not collinear are determined.

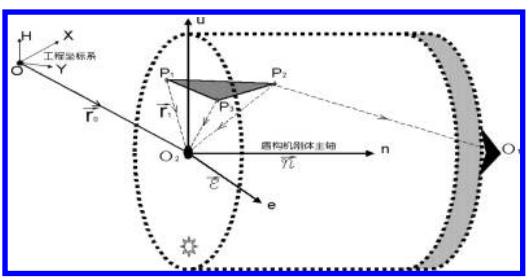


Figure 1. Three points spatial location.

The set of the three points' positions is important, and the selection of the positions is arbitrary in theory – but not collinear. To determine the temporal posture of the shield (rigid), the selection of the three practical points is according to the following principle: the closer the lengths of sides of the triangle formed by the three points are and the bigger the area of the triangle is, the more accurate it is to locate the posture of the shield. In practical application, whether the result of the location agrees to the demand of the normative precision is taken as the evaluation criterion.

The coordinates of feature point and exact value of the posture angle of the shield can be calculated from

Copyright © 2005 Taylor & Francis Group plc, London, UK

the real time coordinates of the three measuring points with vector reduction method. That is, to get the current three-dimensional coordinates (X_{01}, Y_{01}, Z_{01} and X_{02}, Y_{02}, Z_{02}) of the center points O_1 and O_2 of the feature part in the notch and the shield end with three-dimensional vector reduction. And then, according to the theoretical value corresponding to the design, we get the amount of deviation comparing the two values.

3 AUTOMATIC MEASURING METHOD OF THE POINT LOCATION

The automatic measuring equipment is with the new techniques, this always brings us the change in methods. Leica automatic measuring technique is the main supporting technique to realize the automatic measuring of the shield posture.

To realize the theory, the accurate measurement of the three-dimensional coordinates of the three target points is the key, and using the automatic function of the total station to achieve the accurate measurement of the three-dimensional coordinates is the key for the system to realize the automatic guidance. The former is the problem of theory and arithmetic, the latter is the capability of performance, and both of them are the frame factors to structure the automatic operating system.

3.1 *Automatic measuring technique*

Automatic measuring technique is incarnated concentratedly in the main performance of the automatic total station:

- Automatic operating. The total station has waiting motor inside, which can drive all the operation while the measuring by using 12V DC. Such as turning the alidade of the instrument, reversing normal and reverse telescope of the telescope to measure, turning the telescope to search the target prism and so on.
- Automatic collimating. Due to the different design of the instrument manufacturers, there are two different automatic collimating methods:
  - One method is with active prism, namely equipping the luminaire in the scutcheon of the prism. Such as Trimble 5600 automatic total station, the scutcheon send the ray by itself, the total station can capture this kind of ray and collimate the prism automatically. The virtue is it can not be interfered by other reflecting objects, the defect is that structure of the prism is complex, the installation and the maintenance is inconvenient, 12V DC is supplied necessarily.
  - Another method is to install coaxial ATR device in the telescope of the total station. It sends laser beam to the prism, the laser beam reflected by the prism is captured by CCD camera in the device and the central position of the prism is computed, so the motor can be driven to turn the telescope for collimating the target accurately. The virtue is that it uses usual measuring prism, the structure is simple, the installation is handy, no maintenance is needed basically, power supply is not necessary. The defect is that it can be interfered by other reflecting objects. Considering the construction situation and the spot condition, here we select Leica TCA1800 automatic total station which is using the second automatic collimating method.



Figure 2. Leica TCA1800.

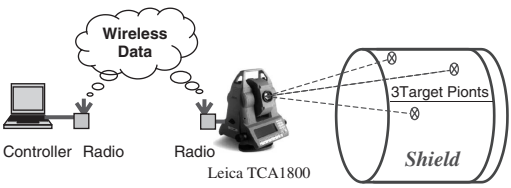


Figure 3. Supporting wireless data traffic mode.

- Automatic measurement. The automatic total station is kind of total station with computer. The inner microcomputer can process both-way communication with outer controlling computer. So it can not only output the measured data to the outer computer, but also receive the software order from the outer computer to measure the distance, horizontal angle and vertical angle automatically, accordingly, the automatic measuring with nobody watching over the whole process is realized.
- Wireless data traffic. Wireless method can be adopted to control the operation of the instrument in the tunnel, which is shown in Fig. 3. The selection for the radio is RFM96W, the waterproof data transfer radio of PCC (Pacific Crest Corporation) in USA. Its virtue is smaller volume, light weight and low power waste.

The automatic measuring technique is made up of two parts: one part is to equip the automatic total station, another part is to equip computers and related software according to the needs of the measuring item.

Copyright © 2005 Taylor & Francis Group plc, London, UK

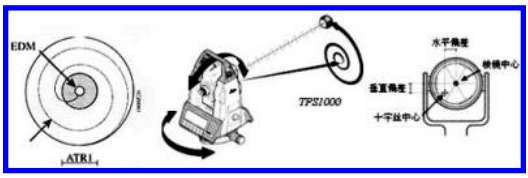


Figure 4. ATR Scan.

3.2 *Automatic target recognising (ATR) technique*

This is a target searching and recognising technique with active way. Leica TCA1800 automatic total station can send infrared ray, and use autocollimation theory and CCD picture processing function to realize the automatic target recognising and collimating whether in day or night.

Automatic target recognising (ATR) and collimating can be separate into three processes: target searching process, target collimating process and measuring process. When starting ATR to measure, if there is no prism in the viewing field of the CCD camera of the total station, the target searching process goes first; once the prism appears in the viewing field, it will turn into target collimating process immediately; and after reaching the collimating allowable precision, the measuring process for distance and angle starts.

Using both ATR way and manual way to check and determine the collimating deviation is very necessary in angle measuring. Because it is only in this case that the two methods can achieve the optimal match.

3.3 *Precise align*

The three processes carried out in above order forms the trait of precise location: searching process, target collimating process and measuring process.

When using the ATR measuring technique, the motor turns the telescope spirally to collimate the center of the prism and let it in the deviation set in advance. Usually the cross lines is nearby the center of the prism. The reason that the cross lines is not in the center of the prism is for optimizing the measuring speed. For determining the deviation, ATR is used to measure the horizontal offset and vertical offset between the cross lines and the center of the prism. These offsets are used to correct the horizontal angle and the vertical angle shown in the instrument. So the final results are given by the center of the prism, they are precisely located.

Recently, Leica issues more advanced product, the new generation TPS1200 super station (X-Function), it has better extraocular antireflection capability (advanced image processing) and can reduce the viewing field of target recognising to one third of primary one (Fig. 5).

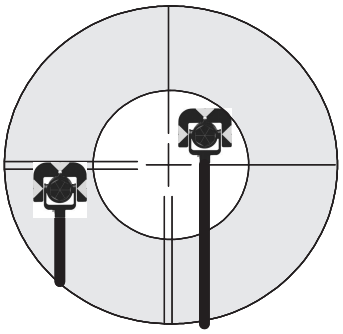


Figure 5.

4 SYSTEM FRAME AND FUNCTIONAL CHARACTERISTICS

According to the analysis of the relative merits of the similar systems, we redesign the whole frame, and there are some differences in theoretical principle and method relative to the traditional method: 1 system operating does not adopt the guidance way that laser beam points to the receiving target, but calculate the shield precisely according to the coordinates of the three measuring points, abandon the usual integral calculating method for shield posture factors, so the error cumulation is avoided; 2 the high precision fully automatic measuring robot which has the secondary developing function – Leica TCA total station is adopted to make the whole measuring process fully automatic and computer intelligent control; 3 the measuring set mode and calculating process are simplified to increase the accuracy according to the spatial vector reduction instead of the traditional concept that plane plus altitude in theory.

As shown above, we adopt the TCA1800 and accessorial fittings of Leica corp. in Switzerland to structure the basic frame for hardware running and obtain the measuring factors as the base of the system work.

4.1 *Hardware constitution and performance*

(1) Fully automatic total station: The TCA1800 automatic measuring total station of Leica corp. in Switzerland is adopted as the major measuring instrument, its angle measuring precision is $\pm 1''$, distance measuring precision is 1 mm + 2 ppm; this instrument can fix two prisms in the same viewing field and realize precise measuring.
(2) Measuring accessorial equipments: They include prism, reflecting plate and so on.
(3) Automatic striking up foundation: Germany GEO Laser, large horizontal correction extension ($10°48'$), quick and sensitive reaction ($\pm 32''$).

Copyright © 2005 Taylor & Francis Group plc, London, UK

(4) Industrial computer: The system adopt industrial controlling computer, it runs well in jogging 5°～50°C and 80% relative humidity condition, and it is dustproof, shockproof, dampproof under working condition.
(5) Both-way communication (total station ⇆ computer) equipment: System long-distance Both-way communication equipment equips the special components, wire communication distance is allowed 1000 meters long (usually operating requirement of the system is satisfied in 200 meters). According to single machine model, two waterproof PPC radios are used for data traffic.

Considering the equipment constitution, we know that the system do not use gyroscope, and the laser sending and receiving device is not necessary to be assembled. The transducer device or dip meter which is relied on before is also abandoned. Consequently the system constitution is furthest simplified and the robustness is increased. Finally the minimization and optimization are achieved. As shown in Fig. 1, the spatial vector three-dimensional location frame directly gives the coordinates (X, Y, Z) and angle deflection (α, β, γ) of the arbitrary (feature) point in the shield.

In fact, the best feature of this system is that the measuring objects – all the six factors of the rigid spatial posture are directly computed according to the coordinates of the measuring points.

4.2 *Three running modes*

The system has the ability to adjust to the likely running mode for different tunnels and working environment, which makes the management convenient and satisfies the purpose needed by the project construction.

- Automatic running of a single total station is the simplest form (Fig. 6). As the manner in common use, it is often to adopt PCC radio in remote communication.
- Automatic measuring of two total stations is the most suitable running mode adapting to all kinds of tunnel variety (Fig. 7). It can solve continuous propulsion problem of small-radius or big-curvature very well. The two measuring stations form two angels of broken line, whose function of turning in pointing direction could not be obtained by other systems. This method makes the system more perfect because of dynamic station's automatic tracking.
- Measuring mode is a three-target point method by observing front shield. This method is very flexible in using. We can set the position of the apparatus arbitrarily, and adopt any method that can confirm three-target point coordinates exactly. By inputting three-target point coordinates into the computer, we can gain the same result as the automatic running. Thus, this way can examine the accuracy of the automatic running, or backdate the past dates, or use as a convenient method to calculate the value of human measuring.

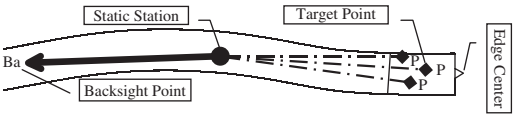


Figure 6. Single machine running mode.

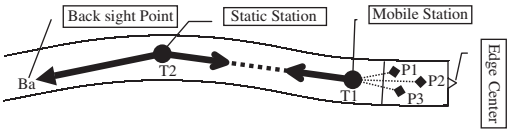


Figure 7. Double machine running mode.

4.3 *Functional traits*

The premises of supervising shield to drive accurately according to design are to measure in time and gain the exact special position and posture direction, and control the propulsion of the shield by these, and correct betimes. This system's functional traits are mainly expressed:

(1) Special synchronous following-ahead method: the system adopt following-ahead measuring method (Fig. 7), which overcome the observing difficulty and inconveniency well that is produced by digging-plan going ahead and the testing points going farer and farer.
(2) three-dimensional vector lead calculating: the system makes full use of the functions that have been possessed by measuring robot (Leica TCA total station), and it measures the three-dimensional coordinates of the points directly. It uses a new way of calculation – "spatial vector" to solve the problem strictly in attitude factors, and these six factors are gave once (six degrees of freedom).
(3) Without auxiliary transducer equipment.

The system continuously measures the position in three-dimension space and the posture by tracking. The main information showed in computer screen includes these: displaying horizontal deviation and vertical deviation of double shield ends (the center of the notch and the center of shield end) and intersection three posture angle of rigid shield in graph,

Copyright © 2005 Taylor & Francis Group plc, London, UK

Example 1. The analysis of on-the-spot survey data precision estimate for shield at the no driving state.

Number of sampling	Error: Horizontal notch error of deviation unit (mm)	Error: Vertical notch error of deviation unit (mm)	Error: Horizontal shield end error of deviation unit (mm)	Error: Vertical shield end error of deviation unit (mm)	Remarks
15	1.1	2.2	1.1	2.5	• Sampling at random • On-the-spot survey data of no driving state, as the gist of instructing driving
5	4.3	3.3	6.9	7.0	
15	1.7	2.0	3.6	2.7	
40	1.1	1.55	1.3	1.8	
RMSE	±1.6	±1.9	±2.6	±2.8	±2.3 (mm)

giving the time of measuring and the distance of the shield notch.

5 EXAMPLES OF ENGINEERING APPLICATION

Example 1: first we adopt double machine running mode. In December 2001, the system applied successfully in the shield driving of North Zhongshan road station to Yanchang road station in north-extending project of Shanghai No. 1 subway. It achieved accurate leading and joint-up checking. This project contains two tunnels, the up line and the down line, and the single line is totally 1267 meters long. Each tunnel includes 15 horizontal curves (straight line, transition curve, circular curve) and 17 vertical curves (grade line, circular curve), the linear form is very complex.

First on down line (mileage SK15 + 804∼ SK16 + 103) the system was installed and debugged successfully. Because down line encountered obstacle of filling pile in front when it went ahead, it transferred to be installed on up line until the up line was joint up exactly on March 7, 2002, and it gained satisfactory result. Precision is showed in the table.

Example 2: single-machine running mode. From August 20, 2003 to October 22, 2003, in Shanghai East Fuxing Road it was applied to project of south line shield driving across the river, and it leaded to run-through accurately. This application made wireless data traffic realized remote control and telemetry (Fig. 3). The monitoring and manual measuring data gained by us was identical in reflecting the state of shield driving, so this proved that the interior and exterior of the system accorded with stability. The error in continuous measuring results was in ±1 mm, which excelled the result showed in the table.

From the statistic data in the table, we can find that the data precision is very high when the shield at the state of no driving. This illuminate that the conformance is very good when system runs.

Conclusion 1: when the automatic measuring system runs continuously, the precision of the result is very high.

Conclusion 2: the result between the automatic measuring system and manual measuring system is identical in statistic.

6 CONCLUSION

By the practically running in project and adaptable inspection in a great variety of difficult condition, the system manifests nicer capability.

1) Real time – automatic measuring reflect the current spatial state of the shield.
2) Dynamic characteristics – double machine mode automatic follow ahead, which solves the problem of changing direction in curve bend well.
3) Simplicity – the structure of the system is simple and suitable. The operation and the maintenance are convenient.
4) Accuracy – the result is accurate and the precision is high, which satisfy the requirement of criterion.
5) Stability – the system can adapt to shaky and moist environment, and run continuously in a long time.

The application indicate that shield posture automatic monitoring system with simple structure, stable operation, high precision and convenient maintenance has the ability to supply a reliable leading for construction of shield driving.

REFERENCES

[1] Jianhang, Liu. July, 1999. *Construction of tunnel*. Shanghai: Technology and Science Publishing House.

Copyright © 2005 Taylor & Francis Group plc, London, UK

[2] *TPS1000 theodolite locating system manual*. Leica instrument Ltd.
[3] The total report of the research and development of the shield posture automatic observation system. Shanghai No. 2 Municipal Engineering Co. Ltd. May, 2004.
[4] Xiuping, Yue. January, 2004. The development and the application of the shield posture automatic observation system. *China Municipal Engineering*.
[5] *GeoCOM Reference Manual Version 2.20*, Leica AG, CH-9435 Heerbrugg (Switzerland).
[6] SLS-RV Guidance System For Pipe Jacking Technical Description, VMT GmbH.
[7] www.vmt-gmbh.de, The Guidance Professina.

Copyright © 2005 Taylor & Francis Group plc, London, UK

Research on shield tunneling technology in urgent curve metro tunnels

Yong Chen, Junlong Yang & Jiwen Zhu
Shanghai No.2 Municipal Engineering Co., Ltd Rail Transit Construction No.1 Branch Company, China

ABSTRACT: This paper analyzed the usual problems that frequently happen on the shield tunneling by special urgent curve. Based on the construction of the special urgent curve tunnel project between Yishan road and Tingche chang road, the author put forward the driving technology on the shield tunneling by urgent curve.

1 INTRODUCTION

Urgent curve tunnel line type will be applied more and more in developing rail transit due to the confinement of the planning and structures. Studying on the shield tunneling construction technology of urgent curve tunnel line type will benefit similar later project.

2 ANALYSIS AND COUNTERMEASURE FOR URGENT CURVE SHIELD TUNNELING CONSTRUCTION

Generally speaking, if a radius of curvature adopts the minimum value or approximate minimum value of code in design, then we consider the curve as urgent curve. We call it "urgent curve" in the following for convenience.

2.1 *Controlling technology for urgent curve tunneling axis*

In the urgent curve part, the shield machine can't fit the urgent curve completely because of the straight-line type rigid body. The smaller the radius is and the longer the machine body is, the harder to fit the curve completely.

In order to control the construction axis of urgent curve tunnel, one of the most effective measures is to shorten the length of machine head, add articulated device in the middle of shield machine, over break by using copying device on cutting head.

1) use of shield machine articulated device

Using articulated device of shield machine could match the curve of front canister, back canister of shield machine, and make a curve state providing a good consolidation space for duct piece.

Figure 1 provides there modes of shield machine tunneling state. Mode (a) stands for mode in which inner side need full over break during construction. In this mode, the articulated angle isn't sufficient and the over break is too much, there is gap between outer point D on the back of shield machine and liability of unstability of shield machine position.

The articulated angle in Mode (b) are called limiting articulated angle θ_{cr}. It can be calculated given the radius of curve and dimension of shield machine. As the conformation of shield machine, it is ideal to adopt θ_{cr} as the articulated angle. In this case, the outside of shield machine will contact ground fully, the construction will be the steadiest and the value of over break δ will be the smallest.

Mode(c) stands for the over articulated state, the tail of shield machine and the front of cut head exceed the tunneling arc, and the outside of it knock the surrounding ground. The soil resistance will be very large because the machine compact the ground.

2) use of copying tool

The applying result will impact the function of articulated device of shield machine. Over break too much will impact the earth seriously while over break insufficiently will affect the function of articulated device so that the design radius can't be achieved.

So, during the urgent curve tunneling construction, mode (b) in fig. 1 should be adopted in setting up the journey of copying tool and tunneling articulated angle. The calculation of over break quantity of copying tools in this mode is shown as follows:

The calculation of over break amount (fig. 2): (analysis based on the vertical condition of duct piece cross-section in side of cut head and back canister of shield). The coordinate of point P:

$$X_p = L_2 + D/2 \tan\theta/2$$

$$Y_p = R_o$$

Copyright © 2005 Taylor & Francis Group plc, London, UK

the coordinate of point Q:

$$X_Q = X_p + (D/2\tan\theta/2 + L_1)\cos\theta$$
$$Y_Q = Y_p - (D/2\tan\theta/2 + L_1)\sin\theta$$

the coordinate of point V:

$$X_v = X_p + (D/2\tan\theta/2 + L_1 - l)\cos\theta - D/2\sin\theta$$

$$Y_v = Y_p - (D/2\tan\theta/2 + L_1 - l)\sin\theta - D/2\cos\theta$$

Angle α_v of point V and axis Y:

$$\alpha_v = \tan^{-1}(X_v / Y_v)$$

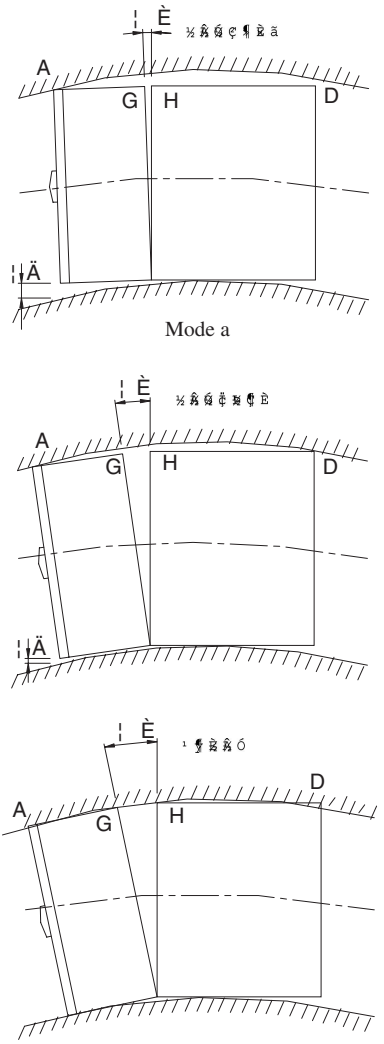


Figure 1.

Least inscribed radius R_{min}

$$R_{min} = \sqrt{\left(\frac{L_2\tan^2\theta + (R_y - D/2)\tan\theta}{1+\tan^2\theta}\right)^2 + \left(\frac{L_2\tan\theta + R_y - D/2)}{1+\tan^2\theta}\right)^2}$$

over break quantity δ

$$\delta = \frac{R_v - R_{min}}{\cos(\alpha_v - \theta)} = \frac{\sqrt{X_v^2 + Y_v^2} - R_{min}}{\cos(\alpha_v - \theta)} \quad (1)$$

where D: external diameter of shield; θ: the middle turn angle; R_0: internal diameter of curve).

2.2 *Analysis on deviation the whole tunnel to arc outside due to lateral component force*

As the shield tunneling one ring, the end surface and the normal of this position will form a angle, and produce a component force under the action of jack. (see in fig. 3).

Calculation of Lateral component force: (see in fig. 3: sketch map for lateral component force)

$$\theta = \tan^{-1}\frac{l}{R_0} = \tan^{-1}\frac{l}{R_c + D/2}$$

$$F_{\text{ô}} = F_{\times} Sin\theta \quad (2)$$

where $F_{\text{总}}$ = acting force of shield jack; $F_{\text{纵}}$ = counterforce normal to duct piece surface; $F_{\text{侧}}$ =

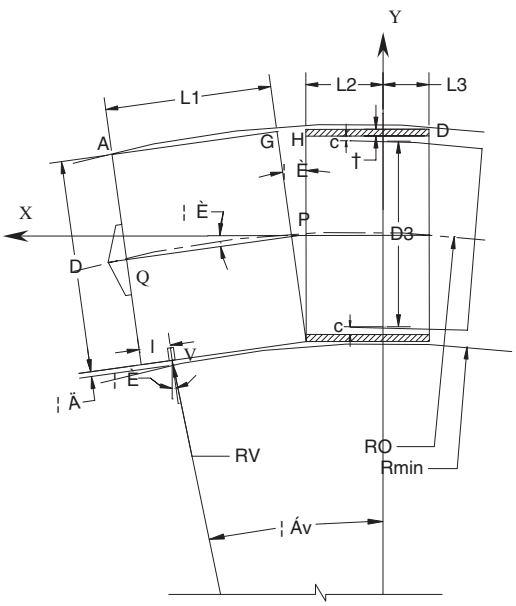


Figure 2.

Copyright © 2005 Taylor & Francis Group plc, London, UK

counterforce parallel to duct piece surface; RC = radius of arc line; D = external diameter of duct piece; L = width of duct piece.

Conclusions can be drawn that, the value of lateral pressure $F_{侧}$ are depend on $F_{总}$ and θ, while the value of θ is depend on L and R_c, D. While D is invariable, the smaller L is, the larger R_c will be. So, during designing the dimension of duct piece, duct piece with smaller width should be adopted. During the construction, $F_{侧}$ are invariable value after entering the curve part, the value of lateral component force $F_{侧}$ is decided by the acting force of shield jack $F_{总}$. In order to reduce the elastic deformation of the earth, acting force of shield jack $F_{侧}$ should be considered to be reduced.

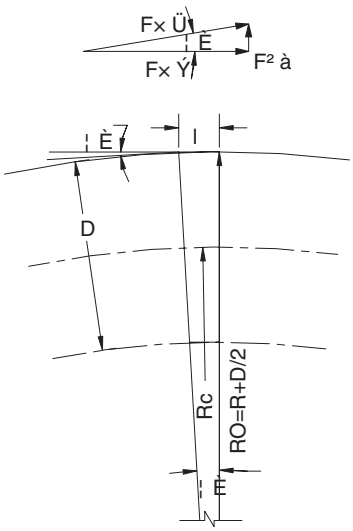


Figure 3.

Furthermore, due to the construction gap between shield crust and ectotheca of duct piece, during the construction, tunneling gap and grout filling quantity of timing grout cannot be done in completely synchronism and completely consistence. If the early stage strength of grout filled in tunneling gap cannot meet the demand, the duct piece will deviate to external side of arc under the action of lateral pressure. The maximum value of tunnel deviation will be (D1–D2)/2 (D1 is external diameter of shield, D2 is internal diameter of shield).

In this point of view, the author deem, it is reasonable to adopt two-shot grout in synchronism grout, because two-shot grout is quick-freezing grout with high early age strength, good liquidity and filling uniformity. So it can fill the construction gap and achieve certain strength in a shorter time, cooperating with original soil to reduce deviation of duct piece to outside arc due to the lateral pressure. (see fig. 4)

2.3 *Addictive factor resulting in earth disturbance due to larger rectifying quantity during tunneling*

Compared with the construction of straight line, the construction of urgent curve will be influenced by the following there factors except the ground deformation factor in the construction of straight line tunneling:

1) Due to tunneling along urgent curve, the shield machine is in a rectifying deviation condition and copying tool are turned on, the actual tunneling face is ellipse, so the actual over break quantity is larger than that in theory.
2) On the normal condition of adopting appropriate technology and correct operation, urgent curve tunneling will add ground losing by 0.5～1%

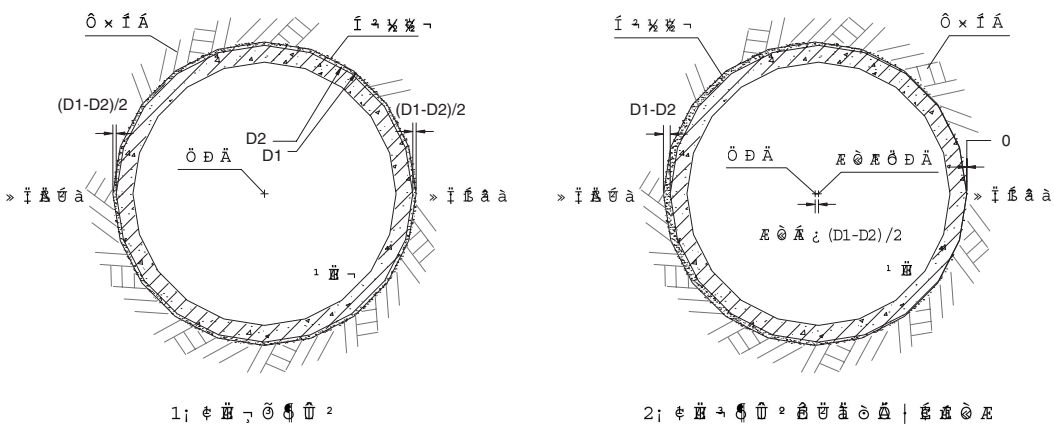


Figure 4. Sketch map for deviation of duct piece due to thelateral pressure.

Copyright © 2005 Taylor & Francis Group plc, London, UK

$8L^2\pi R/(R+R_c)$ (l is the length of shield machine; R is the external radius of shield machine; R_c is the tunneling curve radius).

3) Larger rectifying will result in larger disturbance of ground and long time's after settlement.

The corresponding countermeasure is dynamic management and information construction, controlling the grouting time and grouting quantity. According to specific situation, grout for another time if necessary.

3 PROJECT EXAMPLES

3.1 *General situation of the project*

Yishan road parking tunnel of Shanghai rail transit Mingzhu line project (second phase), with a total length of the tunnel is 462.64, is a in and out line to Puhui tang parking. The tunnel line are designed to cross among pipe group and bridge pier of two flyover crossing.

The tunnel in this zone is "U" type in horizontal with a minimum radius of curvature of 250 m and curve part take a part of 87.02% in the total length. This tunnel joints with a open excavation tunnel of R150 m at its end, transition curve point is arranged in working well, so, the leaving cavern tunnel is located in transition curve part connecting R150 m tunnel, the equivalent radius of curvature in this position is only 178.3 m.

The tunnel in this zone is "V" type vertical, up grade and then down grade, with a minimum radius of curve of 2000 m. Plane curve with of radius of 250 m and vertical curve with a radius of 2000 m cross together, forming a long distance urgent curve metro tunnel in space. (see in fig. 5)

So, the difficulty of this project become the " two first" in the shield tunneling construction in Shanghai:

The first is that this project is the first time to adopt φ 6340 shield for long distance urgent curve tunnel, with a radius of curvature merely 250 m, and curve part take a part of total length of 87.02% in the total length.

The second is that this project is the first time to cross platform on piles of Mingzhu line first period project in such a near distance, the nearest distance from shield to platform is merely 1.35 m.

Tunnels in this zone adopt prefabricated reinforced concrete lining structure. The width of duct piece is 1012 mm, the external diameter is 6200 mm,and the internal diameter is 5500 mm, the design strength of concrete is C55. The line are consolidated with stack bond method.

3.2 *Engineering geology condition*

According to the engineering geology prospecting report, the shield tunneling in ④$_1$ layer muddy clay, which belong to high sensitivity, high plastic, high compressive, low strength, low permeability saturated soft soil, containing mica, organic, shallow salty sand, the soil is rather uniform. In this soil layer, the shield can construct easily, but creeping in this soil layer is rather large, the soil is easily to bong to shield. The physical mechanics character indexes of this layer are shown in attached table 1.

3.3 *Main construction technology*

3.3.1 *Technology for controlling axis*

3.3.1.1 Adopt shield machine with articulated device and copying tool

ϕ6340 articulated style earth pressure balance shield machine produced by Japan San-ling company are adopted in this project, the head of shield machine is about 8625 mm, the distance from articulated point to cutting head is 4990 mm, horizontal turn angle is ±1.5°, vertical turn angle is ±0.5°. The minimum design radius of this tunnel is 200 m, but the

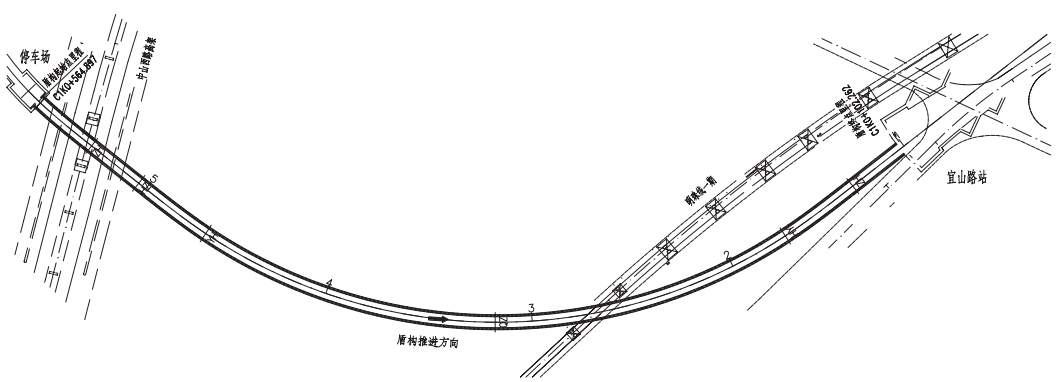


Figure 5.

Copyright © 2005 Taylor & Francis Group plc, London, UK

construction of a tunnel with a minimum equivalent radius of 178 m can be finished with the use of articulated device of shield machine and copying tool. It is proved that this kind of shield machine is a construction machine with advance technology, good performance, proved by the construction of tunnel between Yishan parking of Mingzhu line second period project.

The shortcomings of this shield machine are that in-step grouting system can't adopt two-shot grouting.

3.3.1.2 Turn on the shield articulated device, tunneling the curve posture beforehand

Calculate the articulated angle according to design radius of the curve. Turn on articulated device of shield machine to make angle of front canister and back canister and curve anatomies, tunneling the curve posture beforehand, to provide good consolidation space for duct piece.

During the construction of tunnel between Yishan road parking project, shield machine is in the range of small radius transition curve with a radius of 178 m when it leave the cavern. So, during the tunneling construction in 4～5 m of reinforced area, turn on the shield articulated device with a articulated horizontal turn angle of 1.5° cooperate with turning on copying tool to over break. From the entrance into transition part, reduce the horizontal turn angle step by step until arriving straight-line part. In this time, the angle becomes zero, then tunneling in straight line.

When tunneling R = 250 m curve part during the construction of tunnels between Yishan road parking, the actual middle turn angle θ is 0.8° (see in attached table 2), coming accordance with theory calculated value 0.703°.

3.3.1.3 Adopt copying tool to carry out over break in the inside of curve to favor rectify deviation

Factors of two aspect should be considered during using copying tools, the first one is the over break range of the copying tools. Over break can be carried out in random position around through setting up copying tools. Copying tools are adopted to over break in the inside of curve to facilitate rectifying deviation. The second one is over breakage. Calculate according to formula (1): R = 250 m, theory over breakage δ is 21 mm; in the transition curve part, it is an invariable function value.

During the construction of tunnels between Yishan road parking, R = 250 m, the actual over breakage δ is about 8 mm (see in attached table 3), less than theory over breakage.

The author analysis, because the foundation in Shanghai is rather soft, the shield machine can tunneling along the axis though it compress the inside earth after turning on the articulated device. So, during the construction, the actual over breakage will be less than theoretic over breakage.

Table 2. Articulated angle.

Code number	Construction parameter	Unit	Ring number			
			294	295	296	297
1	Articulated angle (up and down)	deg	0	0	0	0
2	Articulated angle (left and right)	deg	0.8	0.8	0.8	0.8

Remark: ring 294～297 is on the R250 m curve.

Table 3. Distance covered by copying tool.

Construction parameter	Unit	Ring number			
		294	295	296	297
Distance covered by copying tool	mm	−7	−8	−8	−8

Remark: ring 294～297 is in R250 m curve.

Table 1. Physical mechanics character index for ④$_1$ layer muddy clay.

Code number of soil layers	Name of soil layer	Gravity r KN/m^3	Water content W_O %	Porosity ratio e_o	Liquid limit W_L %	Plastic limit W_P %	Quick consolidation shear (peak value)		Unconfined compressive strength			Static lateral pressure factor K_0
							Cohesive strength C kPa	Inner friction angle Φ (°)	Undisturbed soil q_u kPa	Manipulated soil q'_u kPa	Sensitivity S_t	
④$_1$	Muddy clay	16.7	50.4	1.43	43.4	23.0	14	12	39	6	7.7	0.58

Copyright © 2005 Taylor & Francis Group plc, London, UK

3.3.2 *Technical measures controlling the deviation of tunnels to outside of curve induced by lateral component force*

The radius of curve of tunnels between Yishan parking is 250 m, the thrust of jack produced lateral component force $F_{à} = 151.8$ KN (see in formula 2). The in-step grout adopted in this project is initial grout with a low early strength. It will flow due to lateral compression and duct piece will deviate to the outside of curve, so, this kind of grout can meet the demand of resisting.

According to the actual measurement during the early stage of the construction of tunnels between Yishan road parking, the deviation after duct piece leave the shield machine is between 40～80 mm in round curve part, coming accordance with elastic deformation hypothesis and deviation analysis of duct piece in construction gap (theoretical deviation is $(6340 - 6200)/2 = 70$ mm). See in attached table 4.

During the construction of this project, the following main measures are adopted for controlling the construction:

3.3.2.1 The reserved deviation of the direction of shield tunneling

In order to control the final deviation of tunnel axis in the range of the demand of code, reserved deviation should be considered for tunnels during the construction of tunnels.

Driving the shield machine along the secant of the curve, the axis is in the inside of curve during consolidating the duct piece; reserve certain space for the deviation of duct piece due to lateral component force. The determination of reserved deviation is decided by the compound analysis of theoretical calculations and experience of construction practice, while the ground condition of tunneling area should also be considered. The reserved deviation is 40～60 mm during the construction of tunnels between Yishan road and parking.

3.3.2.2 Control the tunneling speed and thrust of the jack

During the normal tunneling, in order to ensure the schedule, the tunneling speed of shield machine often reaches about 50 mm/min and the matching thrust is rather big. During the tunneling of urgent curve tunnels, according the matured construction experience, it is necessary to reduce the tunneling speed, that is to reduce the total thrust of jack and lateral component force in the same time, which is benefit for reduce the deviation to the outside of curve.

So during the tunneling of urgent curve tunnels, a reasonable thrust and tunneling speed must be determined properly. The reasonable tunneling speed must not increase the additional thrust in order to reduce the lateral component force and disturbance to soil. It is necessary to note that the tunneling speed is not an invariable value, and it can change with the change of construction condition, geology condition, and curve type. It should be adjusted to obtain a best construct result.

To be noticed, when the shield machine start to work, the tunneling speed should be increased by a small acceleration to avoid oversize of the thrust of jack.

During the construction of tunnels between Yishan Parking, the total tunneling thrust is controlled at about 10000 KN. See in table 5.

3.3.2.3 Select pertinence measures of applying in-phase grouting and secondary grouting together

Because the shield machine used in the construction of tunnels between Yishan road and parking can not adopt two-shot grout as the in-phase grouting, two factors are considered when selecting the in-phase grouting grout, the first one is to fill the round gap in the outside of duct piece to avoid subsidence of the ground; the second one is to raise the early stage strength of

Table 4. Deviation due to lateral component force after duct piece leaves shield tail.

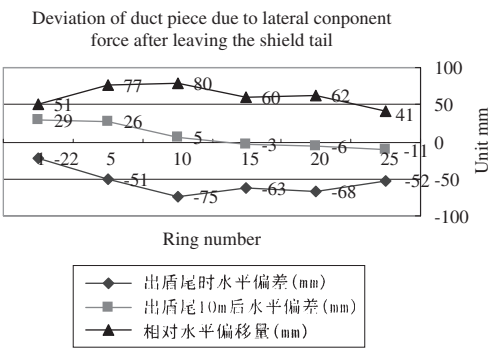


Table 5. Tunnels between Yishan road and parking road shield driving Journal sheet (Shanghai 14 shield).

Code number	Construction parameter	Unit	Ring number 294	295	296	297
1	No.1 jacking speed	mm/min	19	19	21	19
2	No.6 jacking speed	mm/min	19	19	20	19
3	No.10 jacking speed	mm/min	19	19	22	19
4	No.18 jacking speed	mm/min	19	19	20	19
5	Sj total thrust	× 10 kN	1005	1025	1011	989
6	Moment of cutter head	kNm	970	995	957	957

Copyright © 2005 Taylor & Francis Group plc, London, UK

grout to resist the influence of lateral component force. During the actual construction, measures of applying in-phase grouting and secondary grouting together are adopted in this project.

1) In-phase grout

During the construction, with the tunneling of shield machine, "construction gap" appeared between duct piece in shield tail and the ground, and then carry out the in-phase grouting with grouting pipe in the shield tail.

Consider the grouting quantity and grouting pressure together according to the construction condition, geology condition during in-phase grouting. Generally speaking, the grouting quantity should be controlled at about 130–180% of "construction gap" (notice that the grouting quantity in urgent curve tunnels is bigger than that of straight-line tunnels), and the grouting pressure is about 0.3～0.5 Mpa. The grouting speed should be kept accordance with tunneling, that is, grouting when is shield machine is working and stop grouting when tunneling is paused. During the construction, enhance the monitoring to the subsidence of ground. Adjust in-phase grouting through information construction to avoid subsidence and oversize upheaval of ground.

We select the following mixture ratio for inertia grout:

2) Secondary grouting

In order to avoid the problem of low early stage strength of grout and large influence of lateral component force, carry out secondary grouting around duct piece through grouting hole to resist the component force after duct piece leave shield tail for 5～6 ring. The grout is quick coagulate two-shot grout with a higher early stage strength.

The mixture ratio of two-shot grout: see in table 7.

Gist for construction technology:

Install the special ball valve as splash-proofing equipment completely, opening up the reserved hole with churn drill or chisel, then close special ball valve (to avoid the leakage of ground water or grout), joint the grouting pipe with special ball valve to prepare grouting. Adjust grouting quantity and pressure according to monitoring result during secondary grouting. Remove the grouting pipe and close the hole after grouting.

Control the secondary grouting pressure under 0.3 Mpa; control grouting flow at about 10～15 L/min.

In this project, the axis of the tunnel is stable in general and there is no distinct deviation after secondary grouting.

At the same time, the problem of large over breakage of ground, large disturbance, large subsidence's of ground in the construction of urgent curve tunnels are solved.

Table 6.

Yellow sand (kilogram)	Fay ash (kilogram)	Pottery clay (kilogram)	Water (kilogram)
32%	30%	11%	27%

Remarks: the consistency of this recipe 7～9 cm.

Table 7.

Grout	First grout				Second grout
Material	Water	Cement (Portland-cement 42.5)	Fly ash	Bentonite	Water-glass (35°)
Mixture ratio (kg)	100	100	66	5	30～50

Add proper accelerator, the mixture ratio of the first and the second grout is determined by field test and initial setting time should be 10–20 minute.

4 CONSTRUCTION RESULT

After taken the measures stated in the article, the whole tunnel axis is controlled in the range of −50～50 mm and the subsidence of ground are controlled in the range of −20～5 mm after the completion of tunnels between Yishan road and parking. All the indexes of this project achieved the standard of high quality project. At present, this project has been appraised as the first high quality structure project in Shanghai.

5 CONCLUSIONS

1) During the constructions of urgent curve tunnels with shielding method, there are both common aspects with ordinary tunnels and its particularity. We should pay more attention to studying and controlling the difference aspect.
2) During the constructions of urgent curve tunnels with shielding method, select suitable shield machine, seizing the characters of the big curvature, small radius, difficulties to control the shield machine, apply copying tool and articulated device, optimize all kinds of parameter in a smaller and stricter range.
3) During the constructions of urgent curve tunnels with shielding method, aiming at the character of duct pieces which are easily to deviate to the outside of curve, it is better to apply two-shot grout as in-phase grouting. When adopting inertia grout, carry out deviation prediction and secondary grouting, enhancing monitoring and dynamic management.

Copyright © 2005 Taylor & Francis Group plc, London, UK

REFERENCES

Jianhang, Liu & Xueyuan Hou(Ed). 1990. *Handbook of construction technology for underground structures of municipal projects of soft soil (in Chinese).*

Jianhang, Liu & Xueyuan, Hou(Ed). 1991. *Shield tunneling method (in Chinese).* The railway publishing house in china.

Tinghui, Bai. 2001. *Research on the shield tunneling across the close underground structures*. A dissertation presented to the academic committee of Tongji University. (in Chinese)

Yun Bai. 2000.*The soil disturbion and deformation analysis caused by the shield construction.* Corpus for the technology of the soft tunneling and underground projects (in Chinese).

Copyright © 2005 Taylor & Francis Group plc, London, UK

Geotechnical and mechanical interactions using the earth-pressure balanced shield technology in difficult mixed face and hard rock conditions

U. Maidl
Maidl + Maidl Consulting Engineers, Bochum, Germany

ABSTRACT: The use of EPB shields in the so-called mixed face conditions has set new demands to man and machine in EPB shield tunneling. EPB shields were initially conceived to drive in the pressurized closed mode in soft ground, whereas hard rock TBMs were designed to work in the unpressurized open mode. The present use of EPB shields in hard rock and mixed face conditions requires the combination of both technologies by finding best compromise solutions. This paper deals firstly with the geotechnical and mechanical interactions between machine and ground. Further on the critical points such as tool wear and tool replacement are exposed, together with a proposal of best solutions.

1 INTRODUCTION

In the last years, the application range for Earth Pressure Balanced (EPB) shields has been significantly extended to coarser grained grounds. This has mainly been possible due to the contribution of the newly developed processes employing foam ground conditioning. As a result, EPB shields can also increasingly be used in mixed face and hard rock conditions.

The particular advantage provided by this wider application range is the fact that the surface installations necessary to handle with the muck are hardly different to those used when excavating with a TBM.

There are a number of projects which have been driven and are being planned in such conditions.

2 EPB SHIELD PRINCIPLE

EPB shields assure the stability of the tunnel face by means of a supporting pressure produced with the excavated ground. The ground which is loosened by the cutting tools placed on the cutter-head, is pressed into the mining chamber through the openings on the cutter-head. In the mining chamber it is mixed with the plastic earth mixture. Equilibrium is reached when the earth mixture in the chamber is not compressed any more by the ground and by the water pressure on the tunnel face. Extensive details on EPB shield tunneling are provided in (Maidl B. et al. 1996).

2.1 *Application ranges*

The traditional application range for EPB shields in soft ground is described in (Maidl, U. 1995). The optimal application range lies in soft clayey soils and clays with liquid to plastic consistency. Experience with EPB technology in coarser grained soils has been made in some European projects, such as at the Botlek tunnel in the Netherlands, reported in (Gurkan & Frietzsche 2001; Maidl & Jonker 2001; Rehm 2002), where it has been demonstrated that the EPB technique works well in combination with foam conditioning in water saturated sand.

The extension of the application range for EPB shields to coarse grained soils is thoroughly treated in (Maidl, U. 1995). Furthermore, in (Maidl, U. 1997) it is shown how the foam conditioning allows the active control of the supporting pressure, enhancing the spoil flow on its way through the cutter-head and the mining chamber.

2.2 *Mixed face conditions*

Nowadays it is possible to work with EPB shields in the mixed face conditions, however in many cases these conditions still result in a hindrance of the boring process. At first sight talking about mixed face conditions assumes basically encountering both soil and rock on the tunnel face. However, this definition does not comprise other situations where the mere presence of only rock or soil on the tunnel face with different geotechnical properties yields the same difficulties as those due to the definition given above.

Copyright © 2005 Taylor & Francis Group plc, London, UK

This subject is extensively treated in (Steingrímsson et al. 2002), where projects in hard rock conditions are reported which had to overcome typical problems related to mixed face conditions. The characteristics of the tunnel face in the different projects presented vary. Such conditions are sometimes characterized by rocky conditions with stronger dykes crossing the tunnel face, or other times by simply encountering the contact between two rock layers with different strengths (see sections 2.3 and 2.4).

2.3 *Operation modes*

When working with an EPB shield there are three modes in which the shield can be operated, open mode, transition mode and closed mode.

2.3.1 *Open mode*

Shield tunneling in the open mode is possible when the tunnel face is self-supporting and water inflow causes no hydrogeological as well as no operational problems. When abrasive rock is present on the tunnel face it is essential to operate the shield in the open mode (when possible) in order to avoid the cutter tools wear and overloads. These are problems that characterize the drives in mixed face conditions and which will be discussed further on.

2.3.2 *Transition mode*

The main feature of the transition mode is operating with a closed but not earth pressurized working chamber. The tunnel face is supposed to be self-supporting. This feature makes it different from the closed mode. The intention is to deal with controllable water inflow and to handle intermediate conditions from the open into the closed mode. The working chamber is partly or completely filled with excavated ground and/or water, and a very low confinement pressure between 0.1 and 0.2 bar is required to control the water inflow.

In the transition mode it is possible to perform stops by attaining equilibrium with the groundwater pressure.

2.3.3 *Closed mode*

The main aim of the closed mode is to assure stable excavation conditions when crossing through water bearing soils and to minimize settlements at the ground surface. This is achieved by pressurising the excavated ground inside the mining chamber and balancing the pressure of the spoil in the chamber with the earth and groundwater pressures present on the tunnel face.

2.4 *Hard rock TBMs vs. EPB shields*

The problems which arise in EPB shield tunneling in mixed face conditions are partly due to the incompatibility between the mixed geological/geotechnical conditions and the machine design.

It is clear that the design and process technology of a hard rock TBM and of an EPB shield must be different, since the encountered ground features are substantially distinct.

In EPB shields the cutter-head is provided with openings through which the loosened ground is pressed into the mining chamber.

TBM cutter-heads are mainly characterised by having buckets distributed around the perimeter and also on the front of the cutter-head. The buckets pick up the loosened ground and, through the turning of the cutter-head, deposit the spoil into the mining chamber.

Concerning the mucking procedure, EPB shields extract the muck from the bottom of the pressurized mining chamber across to the unpressurized tail shield by means of a pressurized screw conveyor. TBMs generally transfer the muck onto a conveyor belt located already inside the unpressurized mining chamber by means of muck chutes built up on the rear side of the cutter-head. The chutes collect the loosened ground in the mining chamber and with the help of the turning of the cutter-head deposit the material onto the conveyor belt. Aiming to improve the extraction of the muck from the mining chamber, the cutter-head and the mining chamber are designed as a drum which allows the whole system to turn round together.

3 GEOTECHNICAL AND MECHANICAL INTERACTIONS

3.1 *Cutter tool wear*

One of the main problems which characterises the drives in mixed face conditions is the rapid tool wear.

Figure 1 illustrates the parameters which play a role in the cutter tool wear, which is controlled by the type of ground which is being bored, the machine parameters and the operational parameters.

The relationship between the ground-machine parameters and the wear of the cutters has been scientifically analysed by means of laboratory tests and is dealt with in (Gehring 1995; Gehring 1997; Rostami et al. 1994). In reference to the operational parameters, scientific models developed aiming to establish their relationship with the encountered ground conditions are very complex.

3.2 *Interaction of forces*

The pressurized conditions in EPB shields yield a complex interaction of the existent forces. Figure 2 illustrates the distribution of forces in an EPB shield in mixed face conditions. The total thrust force applied

Copyright © 2005 Taylor & Francis Group plc, London, UK

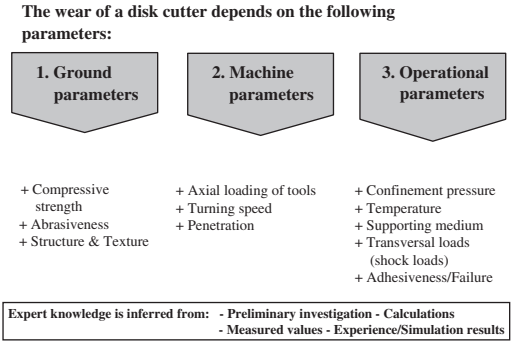


Figure 1. Main control parameters for the disk cutter wear.

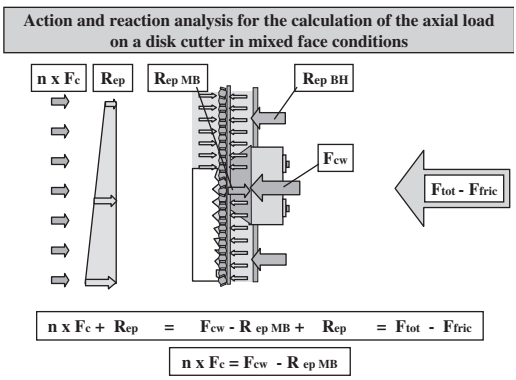


Figure 2. Action and reaction analysis of the forces present in an EPB shield drive.

by the jacks onto the last installed ring is distributed into the following forces:

- F_{tot}: total thrust force
- R_{ep}: reaction force of the total earth pressure
- R_{ep} BH: reaction force of the earth pressure transmitted to the bulkhead
- R_{ep} MB: reaction force of the earth pressure transmitted to the main bearing
- F_{cw}: force transmitted to the cutter-head
- F_c: force on each one of the disk cutters which are in contact with the face
- F_{fric}: frictional force of the shield against the excavated ground profile
- n: number of disk cutters in contact with the hard tunnel face

Most of the total thrust is distributed between the earth pressure reaction (Rep) and the cutter forces (nxFc).

In Figure 3 the particular total thrust applied by the jacks, the earth pressure reaction (Rep) and the force which is transferred to the disk cutters (Fcw-Rep

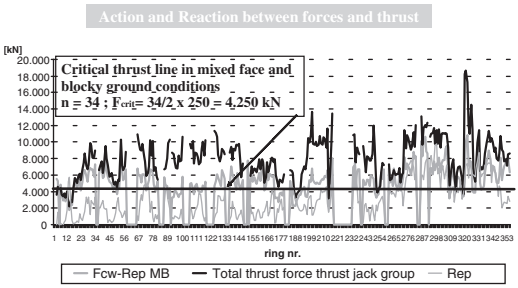


Figure 3. Representation of the cutter-head thrust, the total thrust and the reaction of the earth pressure for a specific project.

MB), from a specific project carried out in mixed face conditions have been represented.

Assuming that the maximal admissible load on 17″ disk cutters ranges between 230 kN and 250 kN, and also that only 50% of the cutters are in contact with the tunnel face, it can be clearly appreciated in Figure 3 how the peak loads exceeded the admissible thrust for the cutters. It has to be taken into account that in such conditions quite more than 50% of the cutters might not be in contact with the tunnel face.

The overload of the disk cutters due to mixed face and blocky ground conditions in the peak loads can actually well exceed the maximal admissible force by a factor of 4.

The difficulties encountered in the control of the shield forces are patent in Figure 3, since in EPB shield tunneling the total thrust, the earth pressure reaction and the cutter-head thrust usually describe quite parallel curves without specially distinctive peak loads.

3.3 *Open mode mixed face*

In this case the interaction between the tunnel face and the cutter-head is highly influenced by the existence of hard or harder rock only in part of the face. This effect can be negatively accompanied by the so-called blocky ground conditions. These consist in a tunnel face characterized by an irregular zig-zag pattern with rocky blocks sticking out of the tunnel face surface as illustrated in Figure 4.

The existence of hard or harder rock only in part of the face (mixed face conditions) and the non-uniform contact between the cutter-head tools and the tunnel face (blocky ground), results in only a few cutting tools being effectively in contact with the rocky tunnel face. Based on the applied thrust force, the disk cutters may thus be overloaded.

3.4 *Transition mode*

Contrary to a hard rock TBM operating in open mode, the rock chips loosened by the disk cutters cannot not

Copyright © 2005 Taylor & Francis Group plc, London, UK

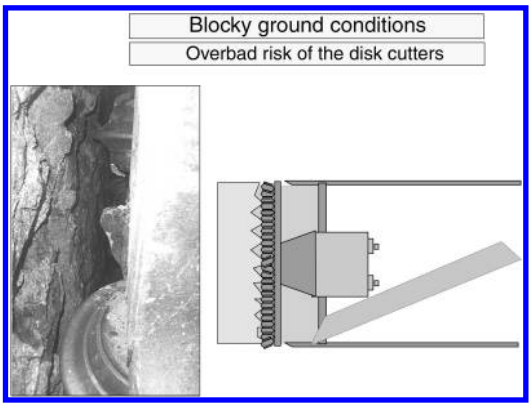


Figure 4. Blocky ground conditions.

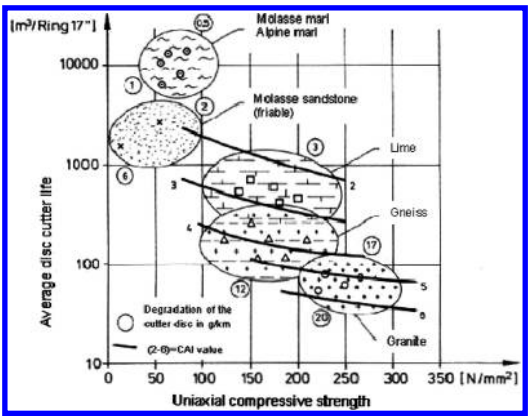


Figure 5. Average disk cutter life for different uniaxial compressive strenghts and CAI values (Maidl B. et al. 2001).

be collected by the buckets to be transferred into the empty mining chamber. In this mode the loosened ground usually remains stopped between the cutter-head and the tunnel face. Additionally, the loosened material and the groundwater form a paste that remains between the tunnel face and the cutter-head, which keeps on turning and grinding unnecessarily the already loosened material (secondary wear).

The contact zones which separate the two ground types can be related to high permeability and water flow. In this case it is mostly not possible to drive in the transition mode.

3.5 *Closed mode*

The total thrust applied by the shield is mainly distributed between the thrust transmitted to the cutter tools and the earth pressure reaction.

Using the closed mode requires a particularly plastic and compressible spoil in the mining chamber in order to achieve a better control on the earth pressure in the chamber. Additionally liquid to soft consistency, low internal friction and abrasiveness and a low permeability of the spoil are required to assure the best performance of an EPB shield.

It is difficult to attain such ground properties in mixed face conditions and the deformability of the spoil is usually too low.

4 PROBLEMS

4.1 *Tool wear*

Normally in mixed face conditions, the normal methods used for the determination of the cutter tool wear, mainly based on the abrasivity of the ground and the length run by the disk cutters as shown in (Gehring 1995), are not adequate to achieve a realistic estimation of the cutter's life. Figure 5 presented in (Maidl B. et al. 2001) illustrates the life of a disk cutter for different uni-axial compression strengths and different values of the CAI (Cerchar Abrasiveness Index). Experience in mixed face conditions has shown that the average cutter life can lie well under 100 m3 of excavated ground per disk cutter.

The main causes for the high tool wear are listed below.

- Overload of the disk cutters.
- Poor material inflow which results in secondary wear and clogging of the disks.

Transversal shocks of the cutters against the blocky ground when the cutter-head turns, which can eventually result in blocking of the cutters.

Furthermore, blocky face conditions do not allow the disks to work in the suitable conditions to attain their expected penetrations. Hence, advance rates are further reduced.

4.2 *Tunnel face stability*

It is clearly reported in (Steingrímsson et al. 2002) that experience yields a decrease of the applied thrust in mixed face conditions, in order to reduce the massive vibrations caused by the cutters bouncing on and off strong and weak layers. Additionally, as mentioned above, the total thrust must also sometimes be reduced in order not to overload the disk cutters.

Therefore, due to the deficient deformability of the earth supporting medium in mixed face conditions, such a decrease of the total thrust results in an unwanted decrease of the confinement pressure.

Hence, not only the control on the load transmitted to the cutter tools is partially lost, but also the confinement pressure control is hindered, and thus the risk of ground failure increases.

Copyright © 2005 Taylor & Francis Group plc, London, UK

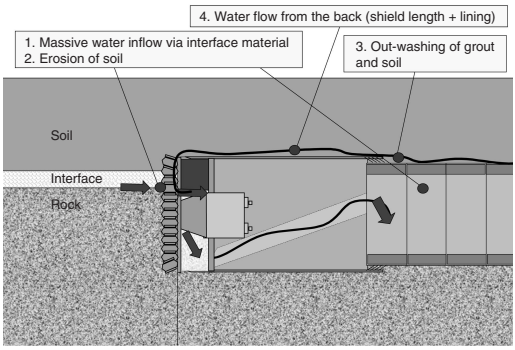


Figure 6. Representation of the erosion and water inflow process in mixed face conditions.

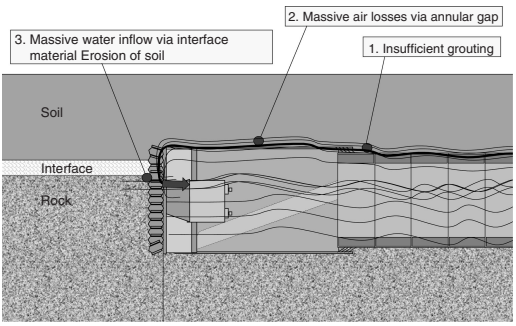


Figure 7. Representation of the erosion and water inflow process during compressed air interventions.

Furthermore, the contact zones between soft soil and a hard rock are often related to an increase of the permeability. The higher permeability of the contact zone can yield water inflows into the mining chamber. A water pressure gradient is then created between the tunnel face and the annular gap at the tail shield. This process can eventually lead to an erosion of the soft ground and of the grout injected in the annular gap in the way described next and illustrated in Figure 6.

0. Disturbance of the water pressure which creates a loss of equilibrium and a pressure gradient.
1. Water inflow into the mining chamber through the interface layers and into the annular gap.
2. Consequently, the erosion of the soft ground begins and its shear parameters become poorer. The area affected by the water flow and the erosion extends. This results at the same time in a dramatic increase of the water inflow.
3. Erosion of the grout in the annular gap occurs.

Since the control over the pressure applied from the mining chamber is partially lost, water starts to flow forward from the rear part of the shield and from the lining towards the tunnel face.

Eventually it comes to a point where it is impossible to stop the water inflow into the mining chamber with the existing technology and additional measures become necessary.

4.3 *Air interventions*

Due to the high wear of the cutters frequent compressed air interventions are required in order to check and replace the cutters. According to experience and to the state-of-the-art in soft soil conditions, closed mode is required in order to assure a good grouting quality and to seal the annular gap.

The operation in open mode and transition mode in combination with a high water inflow in mixed face conditions results eventually in the formation of air channels through which the applied air pressure dissipates. The process can be described in the following steps illustrated in Figure 7.

0. In open and transition modes (unpressurized chamber) with high water inflows a water pressure gradient is formed between the pressure in the annular gap and the working pressure at the tunnel face. Erosion of the soft soil and of the grout occurs in both the annular gap and the tunnel face.
1. The annular gap grouting has an insufficient quality (see step 0).
2. Therefore, massive air losses may occur in the annular gap during interventions, since no additional supporting medium, such as the bentonite cake in slurry shields, is available.

Due to the high air losses and the insufficient air pressure, water flow and erosion of soft ground formation takes place. This leads to an additional increase of the permeability and water inflow. In the final state the quality and behaviour of the soft ground decreases and hence neither the stability of the tunnel face nor of the ground above the shield can be guaranteed.

5 SOLUTIONS

In order to more effectively cope with the mixed face conditions the following solutions can be foreseen:

– The cutter-head design ought to be specially adapted: spacing between cutters, opening ratio, size of the disk cutters, double disk cutters, conical shaped openings on the cutterhead.
– Wear protection of all the steel construction.
– A complete and continuous monitoring of the shield drive (machine parameters, surface movements).
– In order to guarantee the best standards to the spoil as supporting medium, the use of foam to condition the ground gives very good results.

Copyright © 2005 Taylor & Francis Group plc, London, UK

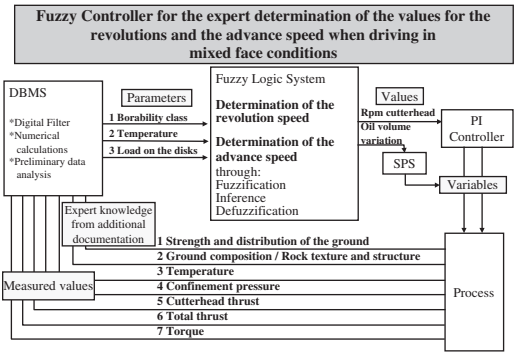


Figure 8. Process overview for an expert system based on fuzzy logic.

– Control of the interaction between the forces aiming to avoid overloads and shock loads. An experienced shield driver is required.
– Best compromise solutions have to be attained between the advance rate and the revolutions.
– Development of expert systems based on fuzzy logic. An overview of the process is illustrated in Figure 8. From a data base management system (DBMS), the following parameters: borability class, temperature in the mining chamber and force on the cutters are submitted to the fuzzy logic system which, based on expert knowledge, determines the values for the cutter-head revolutions and the speed of the oil to be injected in the jacks.

6 FINAL REMARK

The intention of this paper has been to clarify which geotechnical and mechanical interactions account for the new challenges arisen from EPB shield tunnelling in mixed face conditions, aiming to set the best basis to decide and perform the necessary enhancements to the shield design and to the process technology which can help to overcome the encountered difficulties.

REFERENCES

Gehring K. 1995. Leistungs- und Verschleißprognosen im maschinellen Tunnelbau. *Felsbau* 13 Nr. 6. 439–448.

Gehring K. 1997. Classification of Drillability, Cuttability, Borability and Abrasivity in Tunnelling. *Felsbau* 15 Nr. 3. 183–191.

Gürkan E., Frietzsche. 2001. Verkehrstunnel in den Niederlanden in Schildbauweise. *Tunnel* 8/2001.

Maidl, B., L. Schmid, W. Ritz, M. Herrenknecht. 2001. *Tunnelbohrmaschinen im Hartgestein*. Berlin: Ernst & Sohn.

Maidl, B., M. Herrenknecht, L. Anheuser. 1996. *Mechanised shield tunnelling*. Berlin: Ernst & Sohn.

Maidl, U. 1995. Erweiterung der Einsatzbereiche der Erdruckschilde durch Bodenkonditionierung mit Schaum. *Technical reports of the Institute of structural engineering* No. 95–4. Ruhr University Bochum.

Maidl U., J.H. Jonker. 2001. Bauausführung Betuweroute: Erfahrungen beim Schildvortrieb. *Tunnel* 8/2001.

Rehm U. 2001. Botlektunnel – ein Meilenstein in der Erddrucktechnologie. *Tunnel* 8/2001.

Rostami, J., L. Ozdemir, D.M. Neil. 1994. Performance prediction: A key issue in mechanical hard rock mining. *Mining engineering*, Vol. 11, 1263–1267.

Steingrímsson J.H., E. Grøv, B. Nilsen. 2002. The significance of mixed-face conditions for TBM performance. *World tunnelling, annual Technical Review*. 435–441.

Copyright © 2005 Taylor & Francis Group plc, London, UK

Soil conditioning for EPB machines: balance of functional and ecological properties

Lars Langmaack
Degussa Construction Chemicals (Europe), Darmstadt, Germany

Qiu Feng
Degussa Construction Chemicals, Zuerich, Switzerland

ABSTRACT: Earth Pressure Balancing (EPB) tunnel boring machines using soil conditioning additives have become more and more frequent in the world of tunnelling. Their ability to produce & secure the earth pressure equilibrium together with consideration on their ecological and toxicological aspects belongs to the most important factors of a successful TBM drive.

1 GENERAL

The correct and effective use of soil conditioning additives is not always obvious.

The success of EPB machines – especially in non-homogeneous, highly porous or adhesive ground conditions – depends on good mechanical engineering combined with highly effective soil conditioning additives. Examples of these successful combinations are Madrid MetroSur, Toulouse Metro and Rome Railway tunnel projects.

An additional important point for the choice of soil conditioning additives is also their possible impact on the surrounding environment. Risk assessments concerning the emission into ground water during application, the working place concentrations and emissions from the land filling of the treated soil are necessary.

2 TBM DESIGN VS GEOLOGY

EPB tunneling is used in homogeneous as well as heterogeneous ground conditions. Famous examples for EPB drives in very heterogeneous geological formation are BPNL Lyon with a 10.98 m diameter NFM machine (Bentz et al 1997) and Barcelona Metro L9 with a 12,06 m diameter Herrenknecht machine (Gabarró et al 2003). The soil distribution of these two projects is indicated in Figure 1.

As a consequence of the soil heterogeneity, the TBMs cannot be designed for the optimum of a specific geology, but for the overall optimum (Rehm 2004). This implicates a compromise from the machine technology point of view which has to be optimized by using different soil conditioning agents.

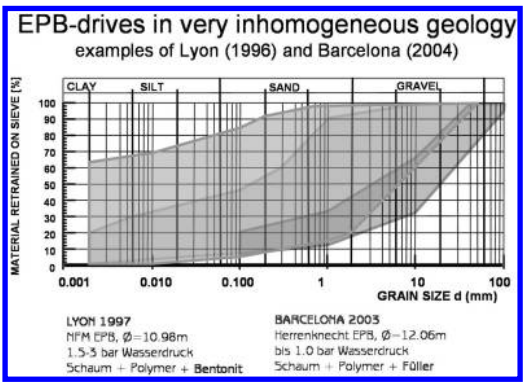


Figure 1. Soil distribution of Lyon and Barcelona (Langmaack 2004).

The 3 most important factors for soft ground tunneling – apart from the hard rock geology – are the

- Soil permeability
- Ground water pressure
- Risk of clogging and adhesion

2.1 *Soil permeability*

The soil permeability for EPB drives can reach values of up to $k = 10^{-3}$ for the most porous soils (BPNL Lyon, Turin) and comes down to practically impermeable clay (Heathrow T5).

The TBM drives in clay soil, either full face or mixed face, often suffer from face clogging and adhesion problems as described in 2.3.

Copyright © 2005 Taylor & Francis Group plc, London, UK

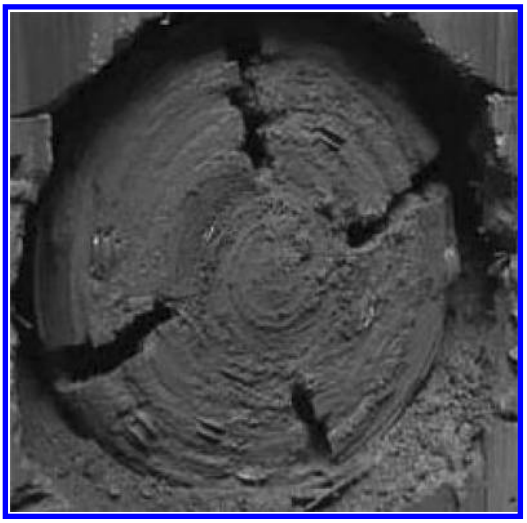


Figure 2. Clay clogging on the TBM cutterhead.

In porous soils, the typical problems are a very instable tunnel face, uncontrolled soil and water ingress as well as loss of face pressure through the soil. These problems were lately described for the Milan Metro project (Grandori et al 2003). Of importance to a successful TBM drive is the mechanical adaptation of the TBM itself including shield opening factor, number and choice of tools and finally the right soil conditioning with foams and polymers combined with a complete filled working chamber. The use of pure foams will not be successful, details see in chapter 3.2.

2.2 *Ground water*

An important influence for EPB drives in soft ground is the ground water level and therefore the ground water pressure. The higher the water pressure, the more difficult uncontrolled water ingress and settlement risks can be avoided. From the machine technique point of view only few things can be done like long screw conveyors to decrease the pressure gradient, installation of piston pumps after the screw conveyor, … The most important factor to successfully control the water is to fill the TBM working chamber completely with a homogeneous and impermeable soil paste by help of foams and polymers. Successful site examples have been demonstrated at the Botlek Tunnel and Aviles Sewage Tunnel drives as described in the literature and in chapter 6.1.

2.3 *Clogging and adhesion*

EPB drives in clay formations, either full face or mixed face, often run into clogging and adhesion problems.

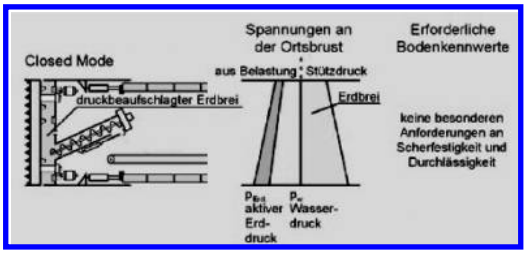


Figure 3. EPB mode (Babendererde 2003).

Figure 2 shows how easily the cutterhead openings can be closed and cutterhead tools can become ineffective by clogging clay. The problem of clay clogging and adhesion will always lead to difficult TBM steering, slow advance rates and extensive cleaning. From the machine technique point of view only few things can be done like the design of an open cutterhead, especially in the central position, and well placed mixing devices in the working chamber. Again one of the most important factors to successfully reduce the clay clogging and adhesion is the use of foams and/or special anti-clay polymers (details see chapter 3.3). Site examples where successful implementation of these technologies has been observed are on the Madrid MetroSur (MBT Online) and Roma 4 Venti (MBT Online) tunnel projects as described in chapter 6.2 or Toulouse Metro in chapter 6.3.

3 NECESSISITY OF SOIL CONDITIONING

Only the use of soil conditioning additives makes it possible to fill the TBM working chamber, to reduce the TBM torque and to reduce the abrasion. No other modes of advance are suitable, and especially not in case of instable ground and sensitive surface areas (Babendererde 2003, figure 3).

The earth pressure equilibrium can only be achieved if the TBM working chamber is filled completely with soil (Herrenknecht et al 2003, Steiner et al 1994). Therefore the soil must be treated during excavation with soil conditioning agents:

- Foams
- Polymers for porous soil
- Polymers for clay soil

either separately or in combination.

3.1 *Foam*

The main demand of foam as conditioning additive is to obtain a suitable soil rheology to build up and maintain the necessary support pressure in the working chamber and prevent high pressure variations. Foam incorporated in the earth paste has the same effect as

Copyright © 2005 Taylor & Francis Group plc, London, UK

the big air bubble in Slurry machines. The reduction of torque and abrasion are very important additional effects, too. Foam is produced by turbulent mixing of a surfactant solution with air (Langmaack 2000).

The main surfactant properties are:

- fluidising effect on soils because of the decrease of surface tension. Soil particles are no longer bound to each other by linked water
- electrostatic repulsion effect which can separate two particles attracting each other by electrostatic forces.

Laboratory tests as well as the site experience show, that often each soil type, from stiff clay to sandy gravel, requires more or less its own type of foam to reach the best effectiveness. Figure 4 demonstrates the effects of a foaming solution on clay and clayey sand. Due to test limitations, it was impossible to use foam. The tests are used to distinguish effective from ineffective agents; the quantity indications as given in figure 4 must not be transformed to site use and will be drastically reduced when using the same surfactant as foam due to the additional effect of air bubbles.

Of importance is the reduction of the angle of internal friction as well as the cohesion. In clay soil, the reduction of cohesion is one of the main tasks of foam. The type of surfactant which shall be used for a specific site has to be determined by preliminary laboratory tests with the original in-situ type of soil.

3.2 *Polymer for clay soils*

As indicated already in the foam chapter 3.1, soil conditioning additives shall decrease the clogging and adhesion characteristics of clay soil. Therefore anti-clay polymers have to adsorb on the clay particle surface. They have to carry a high charge density to separate the soil particles and they should furthermore be able to create a steric barrier in order to avoid re-agglomeration effects.

These demands can be fulfilled by surfactants and anti-clay polymers, but anti-clay polymers are much more efficient.

Anti-clay agents are mainly used to support the destructuring properties of the foam, but they might be introduced without foam, too. Figure 6 illustrates the effect of those polymers in clay soil.

Using only foam and water, the clay particles agglomerate immediately and show extensive adhesion to metal surfaces (figure 6 left part). Using a TBM in this mode, the cutterhead as well as the working chamber will get plugged. Only the additional use of anti-clay polymer results in separated clay lumps and decreases to a minimum their adhesion (figure 6 right part). A correct EPB mode with a reasonable TBM advance rate and minimal maintenance and stoppages is only possible to achieve under these conditions.

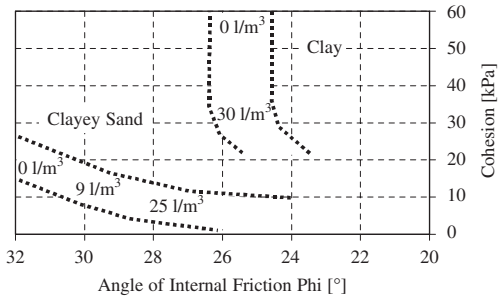


Figure 4. Surfactant solution effects on soil (Jancsecz et al 1999).

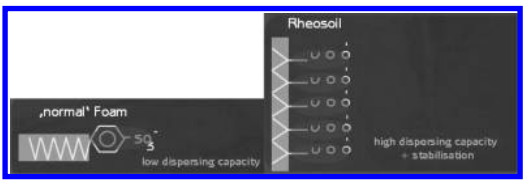


Figure 5. Difference between foam and polymer.



Figure 6. Clay behavior without and with anti-clay polymer.

3.3 *Polymer for porous soils*

In contrast to the anti-clay polymers, the polymers for porous soil have to create cohesion in order to obtain a pasty soil rheology.

A couple of polymers can be used in porous soils:

- water binding polymers to dry out (liquid) soils
- soil structuring polymers which are useful in loose, coarse soils to change the soil rheology and which prevent sedimentation
- foam stabilising polymers.

Some polymer developments are based on hydrocarbon chains and are produced by bacterial fermentation. These polymers are water soluble, biodegradable and compatible to the foam surfactants. Both of them are safe for foam generators and consequently they can be mixed with the foaming solution. Polymers also induce a more stable support pressure in the working chamber during boring and when stopping the machine.

Copyright © 2005 Taylor & Francis Group plc, London, UK

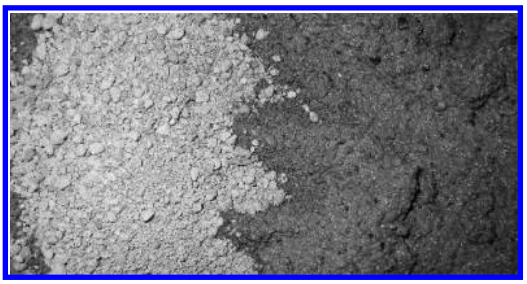


Figure 7. Comparison of original pure dry porous soil and as homogeneous paste after mixing with foam and polymer.

All polymers should be preferably in liquid form to avoid dosing problems and additional installation to get a solution or suspension out of the powder.

4 ECOLOGICAL AND TOXICOLOGICAL PROPERTIES OF SOIL CONDITIONING AGENTS

As substantiated in chapter 2 and 3, the use of soil conditioning products is unavoidable when using a EPB machine. They have not only to fulfill performance criteria but also toxicological and ecotoxicological criteria. In consequence the possible impact on the surrounding environment plays an important role for the choice of soil conditioning additives and is one of the exclusion criteria.

In order to determine the possible risk of a product, a risk assessment study should be carried out. The most important factor in this study is the risk evaluation to human beings and the environment. It is mainly determined by the following four points:

- The amount of substance entering the environment
- The chemical and physical properties of a substance which determine the distribution in the environment. In most cases this is the leachability into ground water. In addition, bioaccumulation has also to be taken into consideration
- The toxicity of a substance for the environment, respectively the toxicity towards aquatic organisms and for humans
- The elimination process (degradation and/or immobilization) also determines the distribution in the environment. Organic substances can be degraded in three separate ways:
  - Biodegradation: by organisms which already exist in the soil or added separately
  - Hydrolysis: degradation in presence of water
  - Photolysis: degradation under influence of light.

For a complete risk assessment, the emission into ground water during application, the working place concentrations and emissions from the land filling of the treated soil have to be taken into consideration.

4.1 *Definition of toxicity*

Toxicity is the intrinsic capacity of substances to cause negative effects to organisms. Toxic effects depend on the amount of a substance which is available to the organism. Toxicity tests carried out in the laboratory are used to predict the so called 'safe concentrations' at which no negative impact on the organisms is expected. The acute toxicity differentiates toxicity to mammal organisms and toxicity to aquatic organisms. For mammals the lethal oral dose for 50% of the population (LD_{50}) is listed in mg substance per kg of organism weight, for aquatic organisms the lethal concentration for 50% of the population (LC_{50} or EC_{50}) is listed in mg per liter of water.

4.2 *Definition of bioaccumulation*

Bioaccumulation is a process by which organisms concentrate chemicals within themselves. This can result either from their food or directly from the surrounding environment.

4.3 *Definition of biodegradation*

Biodegradation is the breakdown of an organic substance by the action of micro-organisms. Before degrading completely to water and CO_2, substances may degrade to smaller intermediates.

Persistence is the ability of substances to resist degradation.

5 SUITABLE SOIL CONDITIONING PRODUCTS

Suitable soil conditioning products should only be those, which show the desired functional properties and in the same time are as safe as possible for the workers and the environment. This implicates a judgment of the acute aquatic toxicity, potential for bioaccumulation, biodegradation and chronic aquatic toxicity by risk assessments.

5.1 *Toxicological recommendations*

The most sensitive area is the acute aquatic toxicity. Tests should be done according OECD Guidelines 201 to 203.

Generally, the LD_{50} and $L(E)C_{50}$ product data shall be as high as possible. For all types of Polymers the $L(E)C_{50}$ data for Daphnids and Algues shall be preferably >100 mg/l water in order to be not classified for

Copyright © 2005 Taylor & Francis Group plc, London, UK

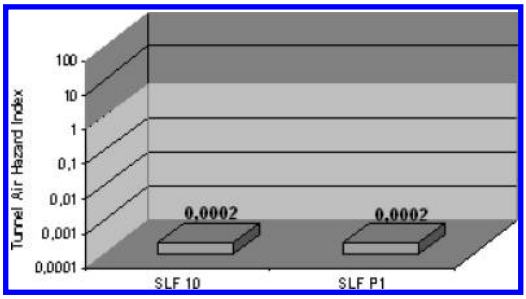


Figure 8. Example of human risk assessment, air hazard index.

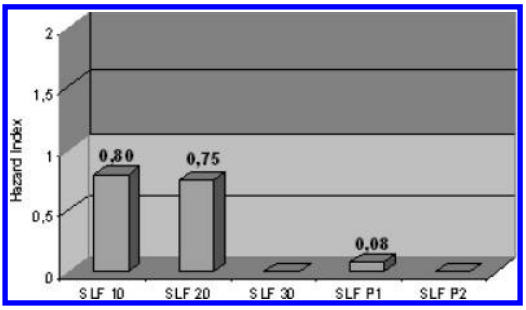


Figure 9. Example of worst case environmental assumptions for various soil conditioning polymers and foams, hazard index.

acute toxicity. Foams, due to their reduction of surface tension, should reach LC_{50} data of >10 mg/l concerning fish (class acute III).

5.2 *Ecological recommendations*

The ecological properties of a product are judged by biodegradation data, using OECD Guidelines with a defined amount of starting bacteria.

Generally, soil conditioning products shall be either

- readily biodegradable or
- not biodegradable (inert material) and non-toxic.

Both possibilities guarantee the lowest possible impact to the surrounding ecology.

5.3 *Preferable risk assessment results*

5.3.1 *Risk for workers*

The expected impact on the environment should generally be low if the substances are adequately handled and the recommendations of the Material Safety Data Sheets are implemented.

Ideally the concentrations in the tunnel air are even under worst case assumptions more than 1,000 times below the respective occupational exposure limits (air hazard index = 1) as shown in figure 1.

5.3.2 *Risk for the environment*

No risks to surface water from emission due to pumped tunnel water or run-off water should be expected, providing that the water is drained into the municipal sewage system for treatment.

The potential infiltration of ingredients into the ground water during the product application should not cause any relevant risk for the environment. Based on the available information of the ingredient concentration in the treated soil, it should be able to be disposed on an appropriate landfill site without any special pre-treatment.

6 SITE EXAMPLES

The following chapters introduce 3 TBM sites with difficult geologies, where the soil conditioning performance and Ecotoxicological properties lead to success.

6.1 *Aviles Sewer (Spain)*

The Aviles Site works with a Lovat EBP machine, diameter 3.40 m. After facing stiff clayey silt, the soil changed over a length of approximately 1.000 m to pure gravely beach sand with a seawater pressure of up to 3,0 bar. The grain size distribution is shown in figure 10.

Only the use of foam in this type of geology resulted in incorrect pressure in the working chamber, uncontrolled water inflow and very slow TBM advance rates.

There was no possibility on the machine to introduce additional filler suspension into the working chamber. An extra installation had been too costly and too time intensive. The alternative solution was to use additional Polymers – in order to make the soil as plastic as possible to be able to install a counter pressure against the seawater and to reduce the water content of the outcoming soil. The result is shown in figure 12 and visualises the tremendous change.

With the above mentioned soil conditioning by using a combination of foam and structurising polymer, the average daily progress achieved 27 meters with a maximum daily performance of 50.50 meters with fully filled and pressurized working chamber up to 3 bars and without any trouble with water income.

Details concerning this jobsite are given by Fernandez 2002 and Langmaack 2001.

6.2 *Roma 4 Venti (Italy)*

The Herrenknecht 7.90 m diameter EPB TBM S-184 operated by Astaldi / Impregilo JV was working on

Copyright © 2005 Taylor & Francis Group plc, London, UK

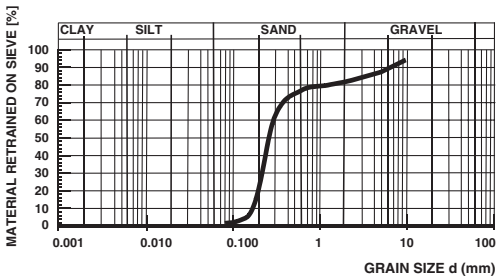


Figure 10. Grain size distribution curve of Aviles Sand.



Figure 11. Sand excavation only with foam.



Figure 12. Sand excavation with foam & polymer.

the Rail Link Tunnel project in Rome, Italy. After heading first through silty sand (tuff) formation, the ground later changed into very sticky and adhesive Vatican Clay. In order to overcome clay clogging at the cutterhead and stirring problems as well as very low advance rates, it was necessary to use Foam in combination with anti-clay additives.

Figure 13 shows the TBM breakthrough in the receipt shaft with a clean cutterhead, using foam and anti-clay additives. The clogging problems could be drastically reduced and the TBM speed increased.



Figure 13. Clean cutterhead after breakthrough.

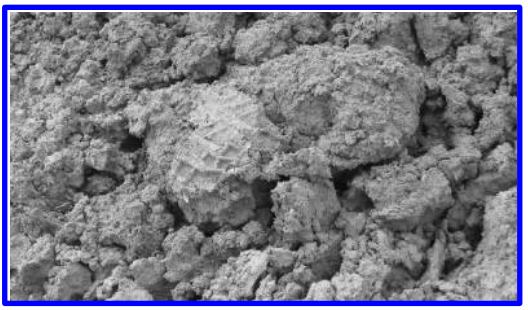


Figure 14. Soft but not adhesive soil after excavation.

Further project details are given by Marchionni et al 2002 and MBT Online Roma 4 Venti.

6.3 *Toulouse Metro (France)*

The Herrenknecht 7.72 m diameter EPB TBM S-208 operated by Vinci / Eiffage JV was working on the Toulouse metro extension project Lot 2 in France. The geologic formation is dry clayey silt with incorporated sand lenses under water pressure. In homogenious clay formation it was possible to excavate in dry mode under air pressure, but as soon as the sand lenses were hidden, the face support collapsed and water ingress was observed. This resulted in overall slow advance rates, extensive TBM cleaning, conveyor belt difficulties and last but not least in doubts on face stability and surface settlements.

Only by using foam and anti-clay polymer together with water it was possible to create a non adhesive, non-clogging soil paste to fill the working chamber completely and work in EPB mode. Figure 14 illustrates the quality of the excavated soil.

The TBM showed reasonable advance rates of 40–50 mm/min also in the EPB mode, no water ingress occurred any more and the face support could be secured. Figure 15 shows the clean cutterhead after the TBM breakthrough.

Copyright © 2005 Taylor & Francis Group plc, London, UK

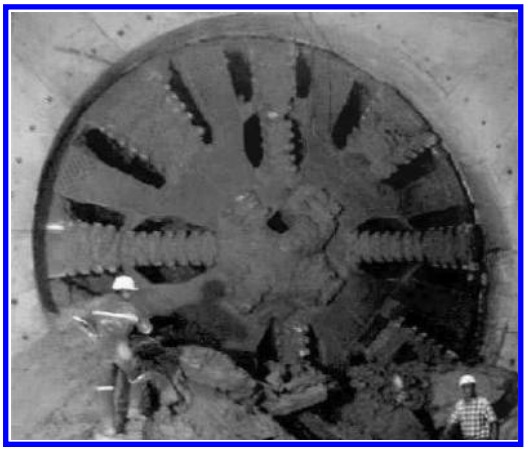


Figure 15. Clean cutterhead after breakthrough.

7 CONCLUSION

As demonstrated by the site examples, it is possible to drive a TBM successful and rapidly also through difficult geologies. In addition to the choice of a well adopted TBM machine, the use of the right soil conditioning additives is vital – for very permeable soil under ground water table as well as for clay soil with high clogging and adhesion potential.

Additionally, all additives used in the site examples passed strict risk assessment studies to ensure minimum impact on the workers and the environment. Neither during construction nor on the disposal sites a negative influence of the soil conditioning additives occur.

REFERENCES

Babendererde 2003 *TBM mit Slurry- oder Erddruckstützung – Einsatzbereiche und Zuverlässigkeitsanalyse* Felsbau 21 (2003), No.5, p. 155 ff

Bentz et al 1997 *Optimierung des schaumgestützten EPB-Vortriebs, Boulevard Périphérique Nord de Lyon* STUVA Tagung Berlin 1997, Alba Verlag Berlin, 1998, Volume 37, p. 88, ISBN 3 87094 636 9

Fernandez 2002 *Aviles Sewage Tunnel, a tunnel below sea water level* AFTES 2002 Toulouse, p. 131 ff, Specifique ISBN 951 04 16 2 4

Gabarró et al 2003 *Metro Barcelona Linea 9 – Europe's greatest metro project with tunnel boring machines of large diameter* ITA 2003 Amsterdam, p 637 ff, Balkema ISBN2: 90 5809 542 8

Grandori et al 2003 *Turin Metro Systems – Design and operation of EPB TBMs beyond the limits of this technology* Felsbau 21 (2003), No.6, p. 34 ff

Herrenknecht et al 2003 *Geotechnische und mechanische Interaktion beim Einsatz von Erddruckschilden im Fels* STUVA Tagung 2003, Dortmund, p. 175 ff, Bauverlag ISBN 3 7625 3602 3

Jancsecz et al 1999 *Advantages of soil Conditioning in shield tunneling: Experiences of LRTS Izmir* ITA 1999 Oslo, p. 865 ff., Balkema ISBN 90 5809 063 9

Langmaack 2000 *Advanced Technology of Soil Conditioning* North American Tunnelling Congress, Boston 2000, A.A. Balkema, Rotterdam, Brookfield, 2000, p. 525 ISBN 90 5809 162 7

Langmaack 2001 *Application of new TBM Additives* BAUMA 2001, 6th int. symposium for tunnel construction Verlag Glückauf GmbH, Essen, 2001, p. 27, ISBN 3 7739 5964 8

Langmaack 2004 *EPB-Vortrieb in inhomogenen Böden: Möglichkeiten neuer Konditionierungsmittel* Tunnel- und Tiefbautagung 2004, Györ, p. 121 ff

Marchionni et al 2002 *Galleria Quattro Venti in Rom* Tunnel No.8, 2002, p. 8 ff

MBT Online Madrid MetroSur www.degussa-ugc.com

MBT Online Roma 4 Venti www.degussa-ugc.com

Rehm 2004 *maschineller Tunnelvortrieb unter sehr schwierigen geologischen Verhältnissen* Tunnel- und Tiefbautagung 2004, Györ, p. 99 ff

Steiner et al 1994 *Face support for a large Mix - Shield in heterogeneous ground condition* Proc. of Tunnelling '94. London : Chapman & Hall

Copyright © 2005 Taylor & Francis Group plc, London, UK

Clogging of TBM drives in clay – identification and mitigation of risks

M. Thewes
STUVA e.V., Cologne, Germany

W. Burger
Herrenknecht AG, Schwanau, Germany

ABSTRACT: Tunnelling through clay soils with a shield machine can result in serious clogging of the TBM, which in turn can lead to delays in construction time and to conflicts regarding additional costs. In the paper new insights about clogging and corresponding problems in practice are discussed. An approach to prevent clogging problems is presented, covering the range from design to execution. The objectives are to provide those who are involved in a tunnel project with a tool to assess the danger of clogging and to list the available technical and operational measures to prevent it. Among the main aspects of the paper are the effect mechanisms of "sticky" clay soils, the identification and classification of soils with clogging potential, measures against clogging in design and operation, and recommendations for geotechnical investigations in clayey soils.

1 INTRODUCTION

1.1 *General problem*

During tunnel drives with shield machines in clay formations strong clogging may occur, especially when using a fluid-supported tunnel face and a slurry circuit mucking system. The consequences include difficulties for the excavation process. At first, the clogging hinders the transport of the spoil in the cutting wheel, excavation and suction inlet area and then leading to further obstructions which can result in a complete interruption of the material flow. If clogging cannot successfully be mitigated, they can lead to a drastic performance reduction due to a reduced advance rate and to the time required for additional cleaning efforts.



Figure 1. Clogging in the invert of a fluid-supported TBM.

1.2 *Development from first clogging to standstill*

In practice, two developments can be observed from the first appearance clogging to a complete blockage, stemming from the two areas mainly responsible for clogging – the cutting wheel and the suction inlet area. These mechanisms can also be overlapping.

Often the problem first occurs in the suction inlet area due to a build-up of material in front of the inlet grill. An accumulation of excavated clay fills up the bottom area (Fig. 1) and is then compressed by further spoil. In a short time, the suction inlet area and the excavation chamber can be filled with clay. The compaction of the material in the rear working chamber can even be increased by the cyclic movements of a jaw crusher, pushing the spoil which has settled in the bottom area up towards the side.

In the second case, clogging occurs in the cutting wheel area (Fig. 2) there is first a build-up on the cutting tools, particularly in the cutting wheel centre. As a consequence, clay discs typically occur in front of the cutting wheel. This applies, in particular, to the centre areas of cutting wheels not provided with an active centre cutter, as the excavated material cannot directly flow from the cutting tool towards the excavation chamber but has to flow parallel to the tunnel face over a certain

Copyright © 2005 Taylor & Francis Group plc, London, UK

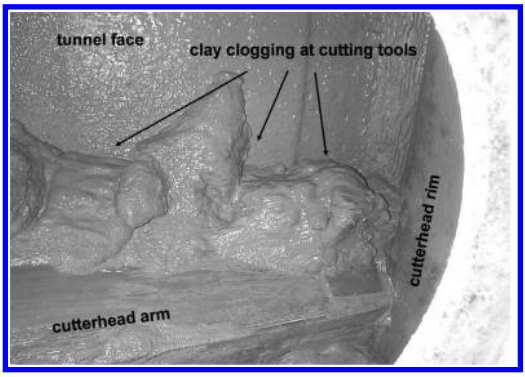


Figure 2. Clogging at the cutterhead of a fluid-supported TBM.

distance. The effect of the clogged centre area of spoke-type cutting wheels (and also for the entire surface area of closed-type cutting wheels) is that the soil is displaced instead of being cut. This can lead to high contact pressures of the cutting wheel resulting in an increase of the torque and stalling in the worst case.

A mixed tunnel face with clay and gravel or clay and sand can lead to additional stability problems of the tunnel face, as the required fluid support is no longer provided when the excavation chamber is clogged. Furthermore, the abrasive paste may lead to a high wear, in particular in the area of the gauge cutters around the periphery due to the great speed differential between the rotating cutting wheel and the stationary cutting edge of the shield.

2 GEOTECHNICAL ASPECTS OF CLOGGING

2.1 *Clogging potential as a sum of four single effect mechanisms*

In order to classify soils clay formations regarding their clogging potential, a research programme on the adhesion of clay on steel has been carried out (Thewes). The programme was based on practical research regarding the clogging potential as well as laboratory tests with clay samples. The clogging potential of a clay formation was defined as the interaction of four single effect mechanisms (Fig. 3):

- the adhesion of clay particles on a component surface,
- the bridging of a clay particles over openings in the path of the spoil transport,
- the cohesion of clay particles, sticking to each other,
- the low tendency of a clay towards dissolving in a water.

From these four mechanisms, adhesion is the most important single effect mechanism and characterises

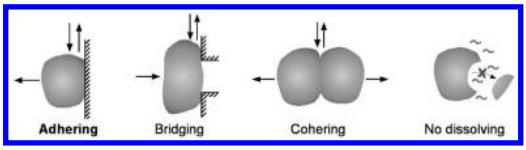


Figure 3. Clogging potential – interaction of single effect mechanisms.

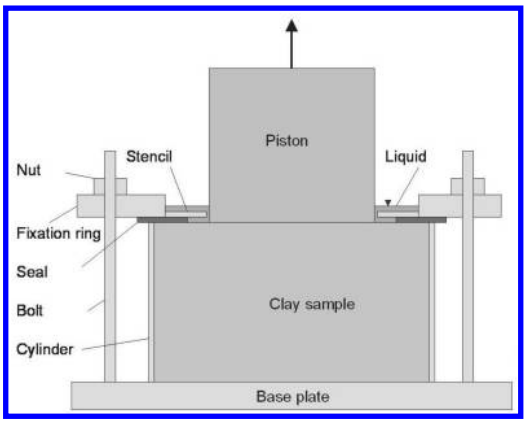


Figure 4. Schematic diagram of separation test for clay adhesion.

best the "sticky" character of clay. Depending on the relative movement between soil and steel it can be subdivided into normal and tangential adhesion.

2.2 *Laboratory test to define clay adhesion*

A laboratory test has been developed in order to evaluate the adhesion between the soil sample and a steel piston when it is pulled vertically from the sample (Fig. 4). Wetting (with a fluid similar to the support fluid of a fluid-supported shield) is vital prior to soil and steel contact.

The adhesion tests have been carried out with samples from six clay formations varying in their mineralogical composition. Besides the usual soilmechanical testing there was also a mineralogical analysis performed for each of the six sample soils.

In the various test series a number of influential test parameters were varied: The consistency of the soil, the wetting time before the contact of the piston with the soil, the contact time of the piston with the soil, and the type of the wetting fluid.

The normal adhesion of soil and steel proved to depend strongly on the content of swelling clay minerals and the consistency of the soil. Further factors of influence were the wetting time, the contact time, and the type of wetting fluid.

Copyright © 2005 Taylor & Francis Group plc, London, UK

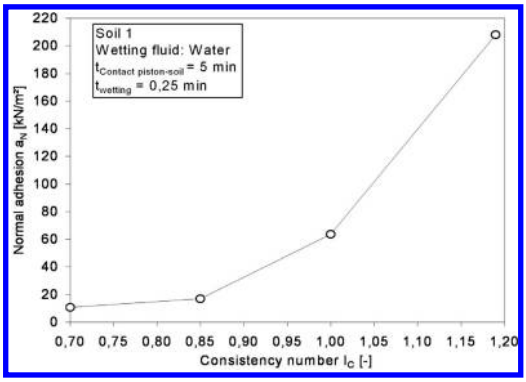


Figure 5. Results of adhesion tests with varying consistency.

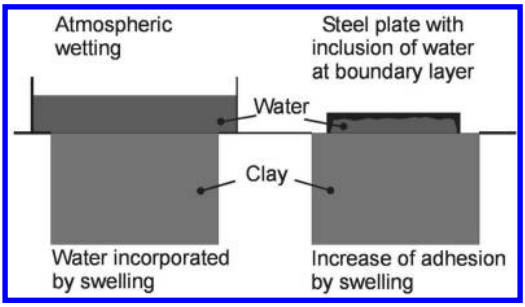


Figure 6. Schematic diagram on the model for adhesion of a swelling clay formation.

With increasing wetting time a decrease of the measured adhesion was observed. On the contrary, with increasing contact time an increase of adhesion was measured.

In a variation study a wide spectrum of the consistency of one of the soils was used. The results in Figure 5 show that the normal adhesion is increasing strongly with increasing consistency (stiffness). This increase has not been detected in older research about adhesion because the wetting with a fluid has not been used before.

The comparison of the various sample soils showed that only those soils with a significant content of swelling clay minerals, such as montmorillonite or illite, could develop adhesion. The adhesion measured in kaolinitic clays was comparatively low.

During the tests, adhesion values of up to 208 kN/m^2 have been measured. This compares a column of clay of approximately 11 m length, which is "suspended" to a steel interface by adhesion!

2.3 *New understanding of adhesion from the tests*

The test results allowed the development of a model for the principle mechanism during the adhesion of swelling clay as shown in the schematic sketches of Figure 6. On the left side, the sketch shows the wetting of a soil sample with water under atmospheric pressure. The pore pressure in the swelling clay is much lower than in the water. The resulting pressure difference causes the clay to absorb the water and the clay swells.

On the right side of the sketch, a steel plate is shown which has been wetted prior to soil contact. As even a polished steel plate is rough in microscopic terms, there is a small amount of water enclosed between the soil and the steel surface. The clay, like in the first example, tries to absorb the enclosed water. After a certain period of time, as no water can flow to be absorbed by the clay, a subpressure with a value similar to the pore water pressure of the clay develops in the water, which is encapsulated at the clay-steel interface. The result is a tensile stress at the interface (adhesion).

2.4 *Identifying and classifying soils with clogging potential*

During the research programme a broad practical study was carried out regarding soils with clogging potential. The geological information from many tunnel drives, where problems of different scales occurred due to clogging, was analysed. During these projects conventional fluid-supported shields were used which originally were not designed for cohesive clay soils. The evaluation of this data leads to a classification of the soils into three categories:

- Soils with *high clogging potential* lead to substantial problems during excavation and required daily cleaning works. The modifications, which were subsequently installed underground, only led to a reduction but not a solution of the problem.
- Soils with *medium clogging potential* could be mastered after a number of mechanical modifications of the shield machine and its slurry circuit along with changes in the operation of the machine (reduced advance rate, longer flushing periods).
- Soils with *low clogging potential* required a reduction in the advance rate and additional flushing periods, but could be overcome only by reducing the excavation speed of the TBM without making major alterations of the machinery.

In all three categories information on grain size distribution, consistency limits and the natural moisture contents of the excavated clay was available. Figure 7 shows the relationship between the consistency and plasticity indices and the categories for the clogging potential. This diagram provides an indication of clogging risks for fluid-supported shield drives.

Copyright © 2005 Taylor & Francis Group plc, London, UK

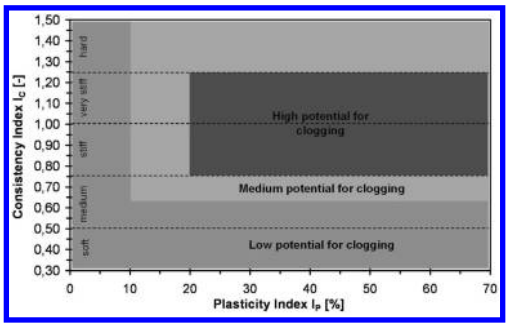


Figure 7. Clogging potential of clay formations regarding plasticity and consistency.

3 PREVENTION AND MITIGATION OF CLOGGING

3.1 *Preventive measures against clogging of fluid-supported shield machines*

For all fluid-supported shield tunnel projects where a significant amount of clay has to be excavated, it is recommended to consider preventive measures in terms of the design of the tunnelling system and the separation plant, even if the clay only shows a low potential for clogging. The principle measures in the design of the shield machine to prevent clogging generally are as follows:

- Generate large soil chips to reduce the adhesion-prone surface of the excavated clay in relation to its volume.
- Avoid narrow passages and other obstructions for the transport of a clay chip from the tunnel face to the slurry line.
- Avoid clay accumulation and minimise the time spent by the clay chips in the chamber by increasing the ratio of the suspension flow rate to the volume of excavated soil.
- Avoid clay agglomerations through increased agitation in areas which are prone to material settlement.

For clays with low to medium clogging potential the risk of adhesions generally is low, whereas a risk of clogged openings still remains during spoil transport, depending on the consistency of the material (bridging). In this regard, narrow passages should be avoided. Unfavourable elements in terms of design are the closed-type cutting wheels, the centre area of spoke-type cutting wheels and grills, used in front of the suction inlet.

A clay with medium to high clogging potential can adhere to all parts of the machine, to which is comes into contact with over a sufficient length of time. In order to use a fluid-supported shield in such a soil, a consequent and costly optimisation is required regarding the entire excavation and transport process:

- Narrow passages (on the cutting wheel) must be avoided,
- the soil flow should not lead to direct impacts on components (cutting tools, sieve, stone crusher),
- 90° degree angles in the corners of the excavation chamber must be broken or rounded,
- in areas where material may settle turbulence must be created (flushing nozzles, agitators) and,
- the flow rate of the suspension in the excavation chamber must be maximised (circuit and flushing concept).

3.2 *Operational measures against clogging for fluid-supported shields*

Once clogging occurs in fluid-supported shield drives, there remain but few operational measures in order to restrict the resulting problems:

- A drastic reduction of the advance rate.
- An optimisation of the cutting tool penetration in order to get a favourable size of the clay chips.
- A maximum suspension flow rate with a feeding system directly at the cutting wheel or in the excavation chamber.
- Flushing pauses or flushing of the excavation chamber during ring-building.
- Operation with a partial air support in the excavation chamber (only possible with a stable tunnel face).
- The use of chemicals as additives.

3.3 *Clogging during EPB-shield drives*

Even though fluid-supported shield machines are at the focus of this paper, at this point a reference to earth pressure balance shields (EPB) is necessary. When tunnelling with EPB-shields in stiff to hard clay, usually the excavated soil has to be conditioned in order to use it as a supporting medium at the tunnel face. Experience, i.e. in the London clay, has shown that conditioning with water or bentonite suspension only may not be sufficient in this case, because also an EPB-shield can suffer from clogging of the cutterhead and in the excavation chamber.

In opposition to the fluid-supported shields, however, the problem of clogging can be avoided very efficiently with the foam conditioning system, which now is generally installed in EPB-shields. The surfactants used in foam production are very effective in inhibiting the clay from swelling and thereby keep it from adhering to surfaces. Even clays with a high clogging potential have already been mastered with EPB-shields using a foam conditioning system.

Copyright © 2005 Taylor & Francis Group plc, London, UK

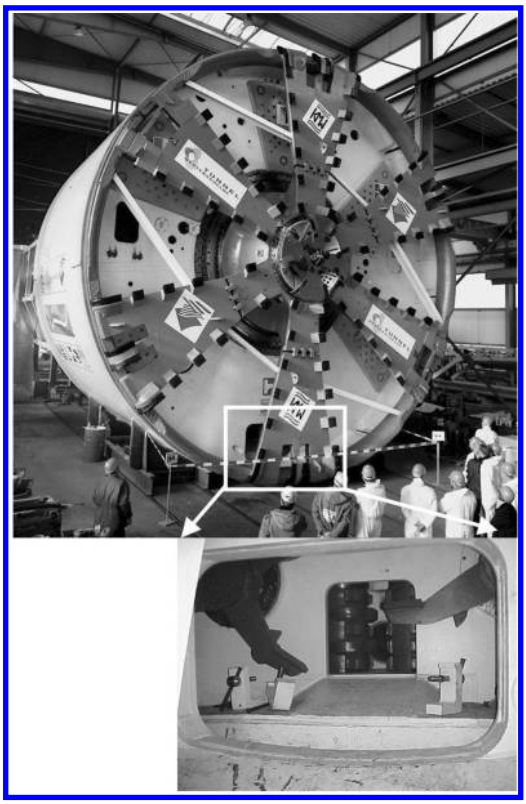


Figure 8. Herrenknecht shield machine with detail of the suction inlet area.

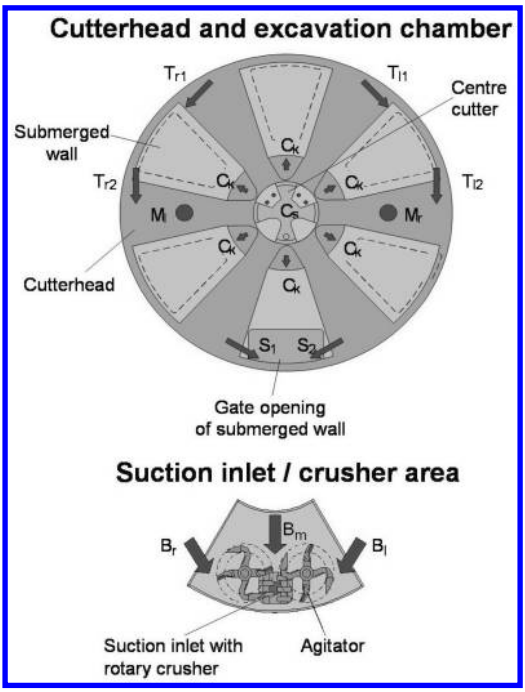


Figure 9. Scheme of the flushing circuit of the Herrenknecht TBM.

A comparatively larger problem with clogging and stickiness of clay can develop in the mucking system. While the transport of excavated clay with belt conveyors usually causes little problems, the transport of clay with muck-skips on trains often becomes difficult and inefficient. On various sites the capacity of muck-skips has been reduced by clogging by as much as 20%. This even has lead to a loss of production, when the installation of an additional car with an extra muck-skip was not possible due to geometrical reasons in the back-up system of a TBM.

3.4 *Experience from a successful fluid-supported tunnel drive in very adhesive clay*

The Westerschelde tunnel in the Netherlands was a pioneering project in terms of the geotechnical evaluation of the clogging potential of the soils to be encountered and the design of the shield machine for the prevention of clogging. The Boom Clay a tertiary, overconsolidated, highly plastic, illitic-montmorillonitic and thus strongly swelling clay was encountered over two thirds of the total length of the tunnel ($2 \times 6{,}600$ m). The success of the project was closely linked to the possibility of a trouble-free advance through the Boom Clay.

Identifying the high clogging potential of the Boom Clay led to a consequent optimisation of the cutting wheel, the excavation chamber, the suction inlet areas of both mixshields, manufactured by Herrenknecht AG (Herrenknecht). Furthermore, the clogging potential has been taken into account during implementation of a sophisticated flushing system in the excavation chamber and design of the data acquisition system (Sager, Maidl).

The cutting wheel (Fig. 8) was designed as open-spoke cutting wheel with rim and the form of the cutting arms was streamlined. Soft-ground cutting tools were used, allowing for the excavation of isolated clay chips. A centre cutter with a diameter of 2.5 m was installed on the axis of the machine, equipped with individual feed and slurry lines. The excavation chamber was lined with steel sheets to avoid clogging-prone angles.

In the crusher chamber rotary crushers with two agitators were installed (Figs 8, 9). These crushers were able to break larger lumps of the hard clay to an adequate size for pumping. The chosen combination of rotary crushers and agitators did not restrict the slurry flow in the same way as a combination jaw crusher and sieve would have.

Copyright © 2005 Taylor & Francis Group plc, London, UK

In the excavation chamber and the suction inlet area an innovative flushing system was implemented (Fig. 9). The feed flow of max 2,200 m^3/h could be distributed individually to various parts of the excavation chamber and the suction inlet area.

Both tunnel boring machines have successfully excavated the Westerscheldetunnel including the sections in the Boom Clay. Despite the very high clogging potential of the Boom Clay, the tunnelling works did not come to a stop due to clogging in any part of the tunnel drives. Using the flushing system an excavation chamber, which was clogged by about 70% could still be cleaned by the machine itself.

4 CONCLUSIONS

4.1 *Geotechnical Studies for future shield drives*

Problems in shield driving caused by clogging can be avoided most efficiently when an existing clogging potential is detected beforehand and the tunnel boring equipment as well as the estimated performance rate are adapted correspondingly. The geological expertises for future construction works with fluid-supported shields should take this aspect into account. The geotechnical evaluation of cohesive soils thus should consider the following requirements:

- Evaluation of the plasticity number and the consistency number of all relevant clays to indicate the clogging potential according to Figure 7.
- Clay mineral analyses to define the mass fraction of the most important minerals (caolin, illite, montmorillonite, smectite, quartz etc). Starting from a content of swelling clay minerals (illite, montmorillonite) above 10%, adhesion must increasingly be taken into account.
- More detailed information regarding clay formations to evaluate more accurately the length of the tunnel and amount the tunnel face affected.

4.2 *Adhesion tests in practice*

Unfortunately, little practical information on the relation between adhesion tests and practical tunnelling experience has been published at present. The results of various adhesion tests developed by different geotechnical laboratories cannot be compared to each other because of differences in the testing procedures. Therefore, bidding contractors cannot evaluate the results of adhesion tests in construction practice, yet. This will be the case as long as there will be no unified geotechnical test procedure allowing extensive testing of characteristic soils, which are known for their clogging potential in tunnelling. Until then, clients, engineers, and contractors will at least be able work with the qualitative indication of the clogging potential as described in this paper.

4.3 *Final remark*

The economic success of a tunnelling project can depend very much on the clogging potential of the encountered clay formations. The production progress in clay can be 2/3 (see above) or possibly as low as 1/10 of the regular progress in granular soil. The clogging potential thus represents a decisive characteristic with high influence on the performance of tunnelling works with fluid-supported shield machines. A careful evaluation of the clogging potential and the adhesion clays to be encountered as well as a good quantification of the affected length of a tunnel can be helpful in establishing more contractual transparency and in avoiding disputes in the construction stage.

REFERENCES

Herrenknecht, M. 2001. Praktische Hinweise zur Anpassung von Tunnelvortriebsmaschinen an die Erfordernisse beim Vortrieb. *In Forschung + Praxis 39, Proceedings of the STUVA-Symposium 2001 in Munich, 2001*. Gütersloh: BertelsmannSpringer Bauverlag.

Sager, H.-J. & Maidl, U. 1999. Innovative Methoden zur Begegnung der Verklebungsproblematik bei den Flüssigkeitsschilden der Tunnel unter der Westerschelde. *Forschung + Praxis 38, Proceedings of the STUVA-Symposium 1999 in Frankfurt a.M.* Düsseldorf: Alba Verlag.

Thewes, M. 1999. *Adhäsion von Tonböden beim Tunnelvortrieb mit Flüssigkeitsschilden, Berichte aus Bodenmechanik und Grundbau Vol. 21, Bergische Universität Wuppertal*. Aachen: Shaker Verlag.

Copyright © 2005 Taylor & Francis Group plc, London, UK

Tunnel support by fully grouted rock bolts for fast TBM advance

M. Alber & S. Rühl
Ruhr-University Bochum, Engineering Geology, Bochum, Germany

ABSTRACT: Hard rock TBM advance rates may be estimated from rock mass properties, in situ stresses and basic TBM characteristics. High TBM utilization rates may be achieved by designing support systems, e.g. rock bolts, that confine the tunnel convergence and that are speedily installed. For several rock types the bond strengths between resin and rock were evaluated by executing novel laboratory tests. Strength criteria for the contact between resin and host rock were formulated. The bond strength may be so high that the load transfer from a rock mass to steel rebar exceeds its yield strength. Implications of these findings for tunneling are shown and procedures for designing fully grouted bolt support for fast TBM advance are addressed.

1 INTRODUCTION

1.1 *Tasks in hard rock TBM tunneling*

The two basic tasks in TBM tunneling, as for any underground excavation, are (i) to excavate and remove the rock and (ii) to maintain tunnel stability until the final lining, if necessary, is installed. Application of rock engineering for TBM drives should be directed towards solving these tasks which define the TBM performance and finally the project delivery time and project economics (Alber, 2001).

Performance prediction of TBM drives requires the estimation of both TBM penetration and utilization. The rate of penetration (m/h), defined as the distance mined divided by TBM operating time, depends on the TBM design (thrust, torque, disc size and spacing) as well as the rock mass properties that withstand penetration. TBM utilization is defined as the percentage of shift time during which mining occurs and depends on equipment and non-equipment downtimes (McFeat-Smith & Tarkoy, 1979). Maintenance of equipment and tunnel are typically scheduled on a regular basis and are mainly fixed quantities. Two major factors in estimating utilization rates are (i) the stability of the rock mass and (ii) the proper support systems as incorporated in the TBM. Figure 1 shows schematically two pairs of interactions between TBM and rock mass that influence performance data. Rock mass strength and disc thrust may determine the TBM penetration while rock mass behavior often requires support installation and influences so TBM utilization.

Particularly TBM tunneling in weak rock requires great efforts for fast support installation to confine tunnel convergence to admissible levels for the TBM.

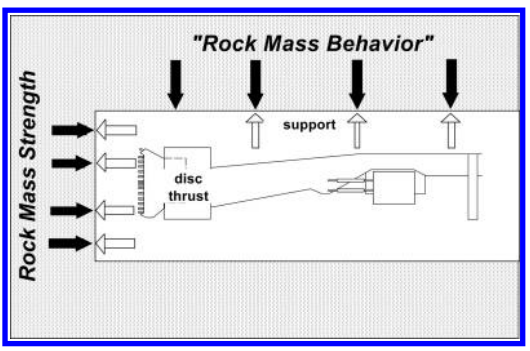


Figure 1. Interactions between rock mass and TBM.

This paper describes some recent results from tests on the load behavior of fully grouted rock bolts with respect to its application to support installation with TBM tunneling in weak rock.

1.2 *Estimation of TBM penetration rates*

The penetration rate of a TBM is typically estimated from some properties of intact rock (Tarkoy, 1995; Nelson, 1993; Bilgin et al., 1999), often the uniaxial compressive intact rock strength σ_C. However, the influence of discontinuity spacing and conditions on the penetration rates is well known (Wanner & Aberli, 1979; Büchi, 1984). The prediction method of the Norwegian Institute of Technology (NIT 1988 und 1990) was the first to take rigorously the influence of discontinuity spacing on the penetration rate via the fracturing factor k_s into account. Recently, rock mass classification systems Q and RMR were introduced to

Copyright © 2005 Taylor & Francis Group plc, London, UK

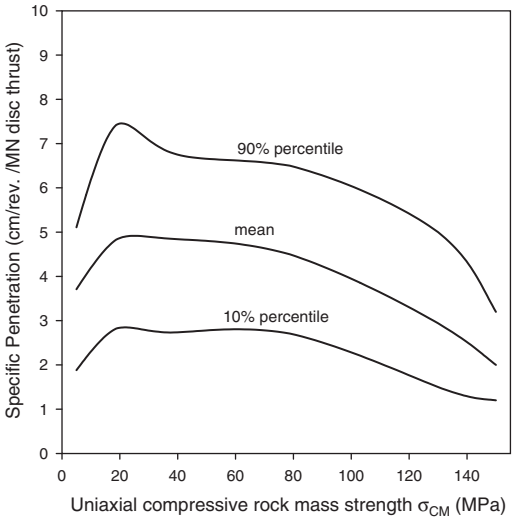


Figure 2. Specific penetration of a TBM as a function of the uniaxial compressive rock mass strength.

derive penetration rates as well as advance rates of hard rock TBMs (Barton, 2000; Alber 1996).

A prediction method based on the uniaxial compressive rock mass strength σ_{CM} was proposed by the author (Alber, 1996). This rock mass parameter includes both σ_C and discontinuity features and covers thus the main rock mass characteristics that influence the penetration rate of a TBM. The uniaxial rock mass strength σ_{CM} may be estimated by characterizing a rock mass with the RMR-System (Bieniawski, 1989) and the use of the Hoek-Brown failure criterion. The well known formula is

$$\sigma_{CM} = \sigma_C \sqrt{s} \tag{2}$$

where σ_C is the uniaxial compressive strength of the intact rock and s a constant computed with

$$s = \exp\,[(RMR-100)/9] \tag{3}$$

The RMR-value has the maximum rating for parameter groundwater and no rating adjustment for joint orientation.

From the analyses of more than 110 km of TBM-tunnels a relationship between uniaxial rock mass strength σ_{CM} and specific penetration SP was found as shown in Figure 2.

The curves are applicable to rock masses and TBM systems as described in the database (Table 1). It may be noted that no hard and abrasive metamorphic rock masses are included in the database and consequently, the application of Figure 2 for predicting penetration rates in those rock masses will not be successful (Ribacchi & Lembo Fazio, 2004).

Table 1. Database.

Recorded tunnel length:	110 km
Diameter :	2,9 m–6,5 m
RMR:	10–95
Intact rock strength:	20–320 MPa
Rock mass strength:	≈1–160 MPa
Overburden:	20–1240 m
TBM penetration:	0.5–8.3 m/h
Disc-size:	15.5–19 (in.)
Cutterhead rpm:	2,3–10 rpm
Thrust:	110–240 kN/disc
TBM utilization:	5%–80%
Recorded tunnel stations:	4650
Rock types: sandstone, mudstone, limestone, dolostone, dolomitic shale, shale, basalt, dolerit, mylonit (in faults)	

1.3 *Estimation of TBM utilization rates*

The prognosis of the utilization rate, defined as the actual boring time as percentage of the available shift time in a given rock mass is barely described in the rock engineering literature. Büchi (1984) showed for a Swiss project the decrease of the utilization rate with increasing discontinuity frequency, and McFeat-Smith (1987) and Ichikawa (1993) gave a tentative correlation between utilization and rock classes for rock masses in Hongkong. The estimation of the TBM utilization rate is difficult since it depends on many factors such as maintenance, cutter change, and rock support.

In the course of this research utilization rates were mainly seen as a function of support installations. The necessary ground support is a function of the rock mass behavior upon excavation. The respective behavior depends on the ratio of rock mass strength to induced stresses at the tunnel wall. This ratio may be expressed by the Factor of Safety FS at roof centerline, computed by dividing the uniaxial compressive rock mass strength σ_{CM} by the tangential stress at roof centerline σ_{Roof}.

$$FS = \sigma_{CM} / \sigma_{Roof} \tag{4}$$

The relationship between the Factor of Safety and the TBM utilization is shown in Figure 3. It may be seen that in stable rock mass behavior ($FS > 2$) the TBM-utilization ranges from 25 to 50% and averages at 40%. For FS between 1.25 and 2 the average utilization reduces to 35%. For $FS < 1.25$ the TBM's utilization is well below 35% and may even drop to zero in tunnel sections in which the ratio of strength to stress approaches zero. The rock mass to be tunneled by a TBM may be classified upon its behavior in three groups, namely stable, friable and squeezing rock masses. Friable and particularly squeezing rock masses slow down a TBM considerably and support measures should be installed as close to the face as possible and

Copyright © 2005 Taylor & Francis Group plc, London, UK

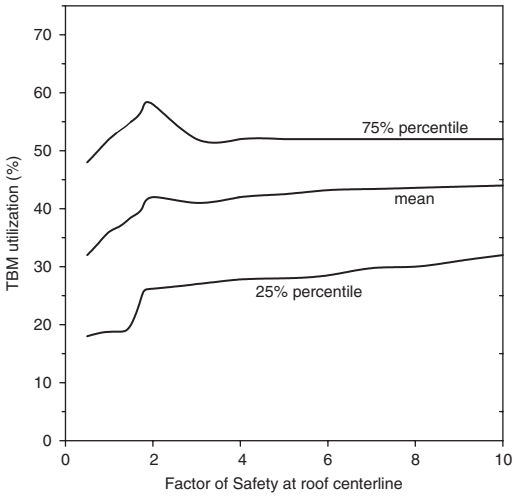


Figure 3. Relation between TBM-utilization and Factor of Safety at roof centerline.

fast as possible. The design engineer has in those rock mass behaviors the task to select support measures that provides sufficient support pressure to control the convergence and more importantly, to incorporate the installation process in such ways into the TBM production cycle that utilization remains as high as possible.

It has been shown (Alber, 1998) that the use of just one support measure, e.g. bolting, is preferable to combined measures such as bolting and shotcrete with respect to utilization rates of TBMs. However, bolting alone in weak rock masses must be carefully evaluated for providing sufficient pressure. Research has been carried out to investigate the load behavior of fully resin-grouted rock bolts in rock and rock masses towards quantifying its support capacity.

2 LOAD BEHAVIOR OF FULLY RESIN-GROUTED ROCK BOLTS

Laboratory and field tests have been conducted to quantify the load capacity of rock bolts. The rock bolts used in all tests are threaded steel bars with specifications given in Table 2. Young's modulus of the steel is about E = 215 GPa and Poisson's ratio $\nu = 0.3$, respectively. Specification of the resin is given in Table 3.

For testing the loading behavior of the system bolt-resin-rock under confining pressure special tests have been conducted. Cores of diameter 110 mm and of length approximately 400 mm from site investigations in two different shales, limestone and two types of concrete cores, representing sandy samples, have been used to represent rock masses to host resin grouted bolts. A hole of diameter 32 mm was dry drilled into

Table 2. Basic bolt data.

Bolt diameter:	25 mm
Bolt tensile strength:	700 MPa ≅ 320 kN load
Bolt yield strength:	450 MPa ≅ 220 kN load

Table 3. Basic resin data.

Resin type:	2 components in 1 capsule
Capsule diameter:	28 mm
Capsule length:	500 mm
Capsule volume:	308 ml
Setting time (@25°C):	4.5 min (maximum)
σ_C after 24 h @25°C:	>70 MPa

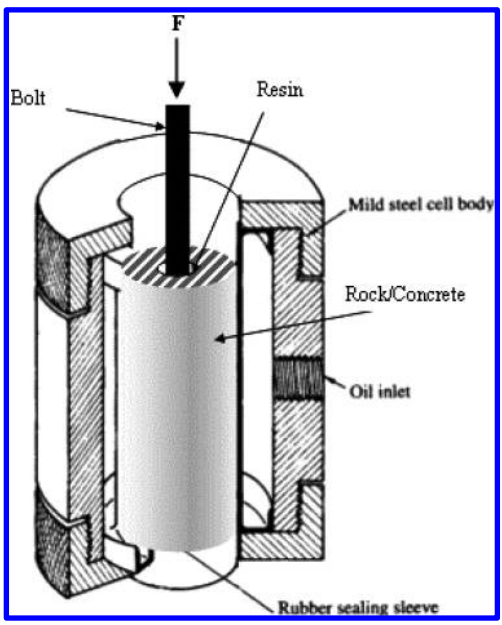


Figure. 4. Schematic view of the set-up for determining the load behavior of the system bolt-resin-rock in a triaxial cell after Hoek and Franklin.

the specimen and short resin grouted bolts have been placed into the samples. The samples have been inserted into a triaxial cell and then placed into the loading frame to evaluate the shear strength of the system by punching through the bolt under various confining pressures. The setup is schematically shown in Figure 4. Axial force (i.e. shear force) on the bolt was increased until nonlinear displacement of the bolt was recorded, then the confining pressure, i.e. the normal stress on the system bolt-resin-rock was increased and another axial loading cycle was started. Additionally some load–unload cycles were performed to evaluate plastic deformation of the system. The bolts were carefully removed from the host rock after the tests.

Copyright © 2005 Taylor & Francis Group plc, London, UK

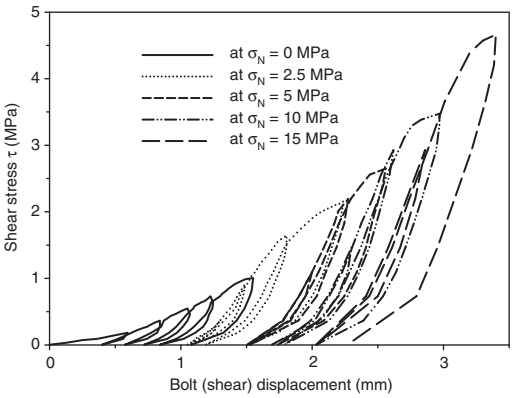


Figure 5. Shear stress vs. bolt (shear) displacement from laboratory testing of "sandy" rock under various confining pressures.

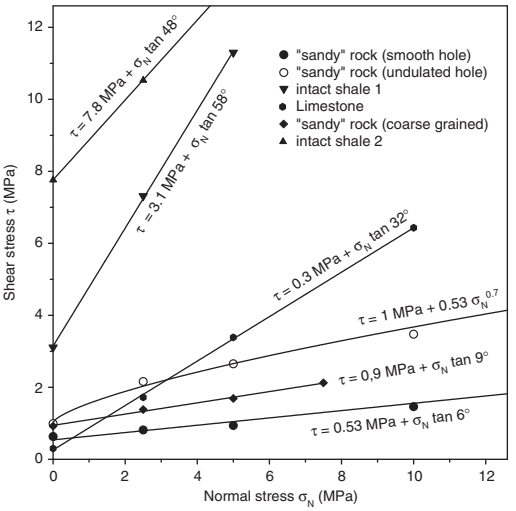


Figure. 6. Shear strength vs. normal stress for different systems bolt-resin-host rock.

The resin-grouted bolts in the four different host rock types were axially loaded to different levels and the displacement of the bolts were recorded at equilibrium, i.e. at constant displacement. In all tests at least three stages of confining pressures were applied, typically at 0 MPa, 2.5 MPa, 5 MPa, sometimes up to 10 MPa and more (Figure 5). The shear stresses were calculated from the bolt load (shear force) and the bond area between resin and rock. The confining pressure from the triaxial cell on the rock sample was taken as the normal stress on the interface between resin and rock. This assumption was verified by numerical modeling of an axial symmetric model using the Finite Element Analysis (Phase^2, 2004). Figure 5 shows the shear stress vs. bolt (shear) displacement obtained from the system bolt-resin-"concrete". In all tests the bond between resin and rock was the decisive factor of the loading capacity of fully resin-grouted bolts in rock.

All lab tests are summarized in Figure 6 showing peak shear stresses at boundary between grout and rock at different confining pressures. Those tests allow the formulation of failure criteria for the bond between resin and host rock in the form of Mohr-Coulomb equation

$$\tau = c + \sigma_N \cdot \tan\phi \tag{5}$$

where τ is the shear strength, c the cohesion, σ_N normal stress and ϕ the friction angle. The failure criteria are given in Figure 6.

It is evident that the strength of the system bolt-resin-host rock depends on the rock type. It has been shown elsewhere (Rühl & Alber, 2004) that the same applies to rock masses or, more specific, to the rock mass condition. Cohesion as well as friction angle are significantly lower in the "sandy concrete" host rock compared to values from the shale. From inspection of the grouted bolts after the tests it is suggested that loose sandy particles reduce the cohesion of resin with sandy rock and, moreover, the bolt and resin "slide" after the loss of cohesion through the hole and little frictional strength is obtained. Cohesion as well as frictional strength may be enhanced by undulating drill-holes. In contrast, a very strong bond between resin and shale is demonstrated by a high value for cohesion and friction angle. After the peak load a high residual capacity of >150 kN in the shale was recorded. Remarkably, the bond between bolt steel and resin was in all tests intact even under the high confining pressures and it appears that the bond strength between resin and host rock, as expressed by the Mohr-Coulomb failure criteria, describes the upper load limit in the system bolt-resin-rock mass.

2.1 *Implications for tunnel support*

It has been demonstrated in Figure 6 that for the sandy and calcite rock materials the cohesive strength of the interface resin rock is in the order of 0.3 and 1 MPa. For a fully grouted bolt of, say, 2 m length in a 32 mm borehole the contact area A between resin and rock is 201061 mm^2. The necessary forces to shear off the contact area is 60 kN (for $c = 0.3$ MPa) and 201 kN (for $c = 1$ MPa), respectively. The latter force 201 kN is close to yield strength of a standard 25 mm bolt, which is typically 220 kN.

A different situation exists with the bolts in shale. The cohesion is between 3.1 and 7.8 MPa, which corresponds to shear-off forces for a 2 m long bolt of 623 and 1568 kN, respectively. Those forces are way

Copyright © 2005 Taylor & Francis Group plc, London, UK

beyond the yield strength of the iron bar. Thus, in those rocks featuring high cohesive strength of the interface resin-rock the iron rebar will break upon rock deformation but the contact between resin and rock will remain intact. In those rocks it is necessary either to reduce the grouted length or to use high grade steel in order to fully utilize the bolt capacity.

3 TUNNEL SUPPORT BY FULLY GROUTED ROCK BOLTS FOR FAST TBM ADVANCE

The findings above may be employed for maintaining high TBM utilization rates e.g. in shale through tunnel support just by bolts. Consider a shale rock mass, characterized by a RMR-value of 65 (or GSI = 65) and an intact rock strength of 45 MPa, shall be excavated by a 5 m-dia TBM at a depth of some 300 m. Assuming a ratio of horizontal to (vertical stress $k = \sigma_h/\sigma_v = 1.5$ we have a virgin state of stress of $\sigma_v = 8$ MPa and a horizontal stress $\sigma_h = 12$ MPa. From elastic solution the maximum tangential stress at the roof is 28 MPa and at the sidewall 12 MPa. The uniaxial compressive rock mass strength is according to formulas (2 and 3) about 9 MPa and the Factor of Safety at roof centerline according to formula (4) is FS = 9 MPa/28 MPa = 0.32. The rock mass around the tunnel is overstressed and squeezing rock mass behavior may be expected. Elasto-plastic FE-analyzes suggests deep failure (3 m into the roof and 1 m into the sidewall) around the tunnel with convergence of 0.6%. Figure 4 suggests TBM-utilization rates as low as 15% due to time-consuming support installations. The task in TBM tunneling is now to design a support system that utilizes at best the machine, i.e., that keeps the machine penetrating the rock mass without interruptions by support installations.

3.1 *Support design for high TBM-utilization*

The first step in designing the support system is the knowledge about the penetration rates in the rock mass under consideration. Suppose the 5 m hard rock TBM features 40 discs of diameter 17″ (432 mm), the operational thrust per disc is 220 kN and the cutterhead rotates 10 times per minute. From Figure 2 the specific penetration SP in the shale rock mass of uniaxial compressive rock mass strength 9 MPa is SP = 3.5 ± 1.5 cm/rev/MN disc load. This translates to an average penetration rate 4.62 m per hour. The stroke length of the thrust cylinders is 1.5 m, so the excavation process will be interrupted roughly three times per hour and the net penetration rate might be some 4.3 m/h.

The task in support design for any underground excavation is to control the deformations. For TBM drives additional tasks are to confine the deformations so that the TBM does not get stuck as well as to maintain high utilization rates. The penetration would

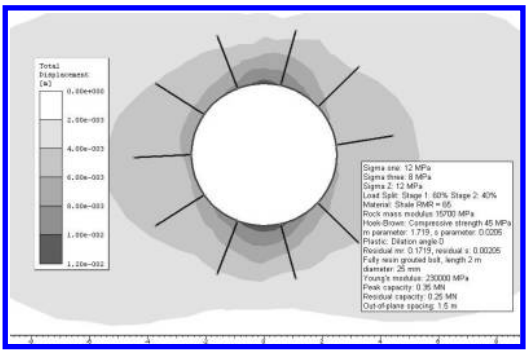


Figure 7. Total displacements after installation of fully grouted rock bolts.

be fully utilized if it is possible to support 4.3 lineal m of shale rock mass in one hour. It has been shown (Alber, 1998) that support by rock bolts or steel sets might be the least time-consuming procedure to for support installation within the main body of open hard rock TBMs. Steel sets provide very high support pressures, up to 0.8 MPa, but are somewhat difficult to handle and a steel set erector directly behind the cutterhead is necessary. Rock bolts on the other hand are rather easy to handle as well as easy to install. Fully grouted bolts provide furthermore immediate support and prevent corrosion of the steel bar.

Rock engineering calculations (ground reaction support analyses or some numerical modeling) yield for the situation under consideration the following specifications for rock bolt support: 10 bolts at centers 1.5 × 1.5 m, 25 mm diameter, 2 m long, borehole diameter 32 mm, fully grouted with resin as specified in Tables 2 and 3. However, due to the high cohesion of the interface resin-shale the bolts of yield strength 220 kN will break upon convergence of the rock. Consequently, a steel grade with yield strength of 350 kN will be necessary. With those specifications a support pressure of about 0.15 MPa is available. The result of numerical modeling (Phase^2, 2004) of the support measure is shown in Figure 7. The model takes into account that the rock mass significantly relaxes within the first 2 m behind the face, which is the distance from the face to the earliest bolt installation. Thus, the model features a load split between two stages (stage 1 = excavation, stage 2 = bolt installation 2 meters behind the face). A perspective view of the bolting pattern is given in Figure 8.

More important than rock mechanics considerations is for TBM tunneling however the speed of support installation. The following working procedure for the specified bolt installations is reasonable:

– Drill 2 m long hole: 2.5 min
– Insert resin capsules: 0.5 min

Copyright © 2005 Taylor & Francis Group plc, London, UK

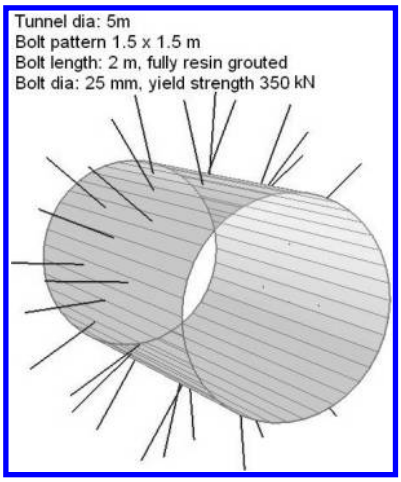


Figure 8. Perspective view of the bolting pattern.

– Insert steel rebar and spin it at 500 rpm: 1 min
– (Full load transfer after 4 min)
– Move to next drill hole: 1 min

Taking some delays into account the installation time for one bolt is some 5 min. With pattern bolting at 1.5 m centers there are on average 6.66 bolts per lineal m to install, which will take about 33 min. In other words, 1.8 lineal m of tunnel may be supported per hour. As the TBM is able to move 4.3 m/h ahead only 41% of the possible advance is achieved. Considering that a TBM is typically available only 60% of the shift time, the overall TBM-utilization with this kind of support system is 25%. Adding a second bolter as well as personal elevates the overall TBM-utilization to some 50%, which would be an outstanding achievement for a hard rock TBM in this rock mass.

4 CONCLUSIONS

It has been shown that hard rock TBM advance rates may benefit from careful considerations about support provided by fully grouted rock bolts. The first step is the estimation of penetration rates from rock mass characteristics and basic TBM data. The second step is to fully utilize the penetration achieved by designing a fast and efficient rock support system that integrates well into the TBM main body. In case of support by fully grouted rock bolts it appears necessary to consider the bond strength between resin and rock mass. With novel but simple laboratory test is has been demonstrated that

– the interface between steel and resin remains intact even at peak loads;
– the bond strength of between resin and rock is different for various rocks;
– the rock-specific bond strength has serious implications on the load capacity of the system steel-resin-rock, and
– that the bond strength may be so high that the load transfer from a rock mass to steel rebar exceeds its yield strength.

Implications of these findings were shown for a TBM in a squeezing rock mass and procedures for designing fully grouted rock bolt support for high utilization rates of the TBM were addressed. It has been shown that high TBM penetration rates are wasted if the proper support system has not been designed.

REFERENCES

Alber, M. 1996. Prediction of penetration and utilization for hard rock TBMs, *Proc. ISRM Int. Symp. Eurock'96*: 721–725. Balkema, Rotterdam.

Alber, M. 1998. Design of high speed TBM-drives, *Proc. 8th Int. IAEG Congr.*: 3537–3543. Balkema, Rotterdam.

Alber, M. 2001. Advance Rates of Hard Rock TBMs and Their Effects on Project Economics. *Tunnelling and Underground Space Technology*: 55–64. Elsevier.

Barton, N. 2000. *TBM tunnelling in jointed and faulted rock*, Balkema, Rotterdam.

Bieniawski, Z.T. 1989. *Engineering rock mass classifications.* Wiley, New York.

Bilgin, N., Balci; C., Acaroğlu, Ö., Tunçdemir, H., Eskikaya, Ş., Akgül, M. & M. Algan. 1999. The performance prediction of a TBM in Tuzla-Dragos sewerage tunnel, *Proc. World Tunnel Congress '99:* 817–822. Balkema, Rotterdam.

Büchi, E. 1984. *Influence of geological parameters on TBM advance rates* (in German), PhD thesis, University Bern.

McFeat-Smith, I. & P. J. Tarkoy. 1979. Assessment of tunnel boring machine performance, *Tunnels & Tunnelling* (12): 23–25.

Nelson, P.P. 1993. TBM Performance Analysis with Reference to Rock Properties, in *Comprehensive Rock Engineering* (J.A. Hudson, Ed.), Vol. 4: 261–292. Pergamon, Oxford.

NIT. 1988. *Hard Rock Tunnel Boring*. Norwegian Institute of Technology, Trondheim.

NIT. 1990. *Drillability*. Norwegian Institute of Technology, Trondheim.

Phase^2. 2004. *2D finite element program*, Vers. 5.0. Rocscience, Toronto.

Ribacchi, R. & A. Lembo Fazio. 2004. Influence of Rock Mass Parameters on the Performance of a TBM in Gneissic Formation (Farzo Tunnel). *Rock Mech. & Rock Eng.*: online publication www. springerlink.com. Springer, Vienna

Rühl, S. & Alber, M. 2004. Capacity of Resin Grouted Rock Bolts with Respect to Rock Mass Quality. *Proc. Aachen Int. Min. Symp. on Roofbolting in Mining*: 273–288. Verlag Glückauf, Essen.

Tarkoy, P.J. 1995. Comparing TBMs with drill+blast excavation, *Tunnels & Tunnelling*, October: 41–44.

Wanner, H. & U. Aeberli. 1979. Tunnelling Machine Performance in Jointed Rock, *Proc. 4th Symp. Rock Mech*. 573–580. ISRM, Montreux.

Copyright © 2005 Taylor & Francis Group plc, London, UK

Geodetic instrumentation for use on machine bored tunnels

N. Clarke-Hackston, M. Messing & E. Ullrich
VMT GmbH, Bruchsal Germany

ABSTRACT: As advance rates of TBM bored tunnels increase, it is essential that all aspects of the control of the machine and the tunnel support are able to operate at the desired rate. This paper describes the innovative ways that the basic guidance system has been adapted to cater for the TBMs that are currently in use used on the Gotthard tunnel where the traditional line of sight throughout the backup gear is continuously obstructed due to the use of a sprayed concrete support facility. The guidance system utilizes features from the well proven system for distance and curved pipejacking applications where the main reference is attached to the moving pipe (tunnel lining). Accurate steering of the tunnelling machine is essential if the segmental lining is to be efficiently installed. The use of ring sequencing software for the determination of the ring type and rotation, significantly aids the rapid placement of the most appropriate ring, which in turn can be monitored for any immediate convergence with the innovative chained inclinometer convergence measurement system. All of this information together with the surface mapping, geotechnical, and surface monitoring data bases can be fully integrated with the monitoring of the machines operating parameters in the Controlled Boring Process software integration package to give the machine operator a complete graphical display of all that is happening around him, to ensure optimum control and speed of safe advance.

1 INTRODUCTION

In the 10 years since its inception VMT GmbH has become the leading company for not only the supply of guidance systems for the full range of tunnel boring machines but also for the supply of a full service for the metrology needs of modern tunnelling projects.

For the navigation of tunnel boring machine projects with segmentally lined tunnels and unlined rock tunnels the SLS-T system has now been used on over 140 projects. Various derivatives have been developed to accommodate the ever changing demands of tunnelling machine design. From the dual system used on the Sophiaspoor tunnel in Holland on the continuously boring Herrenknecht machine to the tandem systems used on the Gotthard, Lötschberg and San Pedro machines. All systems are based on a laser or infra red beam reference that is projected from a motorized total station onto either and active target or retroreflective prism. The options available include ring management services where the sequence and orientation of tapered rings is determined and presented to the ring build crew in the erection area of the machine, automatic tailskin clearance measurement and the automatic steering option. Data transfer through a local network or via the internet is also available.

With the requirement for more information to be supplied to the machine operator with respect to geodetic, geo-technical and TBM operations, VMT GmbH has developed its CBP (Controlled Boring Process) feature that enables the integration of all this data into one common data-base to give near realtime evaluation of all incoming data for the continuous monitoring and visualization of surface structures and the display of deformations in front, above and behind the TBM. This will include the implementation of steering aid options for the shield driver and supply warning messages in case of dangerous drive conditions.

For pipejacked tunnels that are either curved or of extended distance the SLS-RV system has now been used on over 160 projects totalling over 100,000 m including many of the most complex curved alignments. The Seo Cho Project in Korea using a Herrenknecht AVN 2400 machine successfully completed a 789 m drive from a single shaft the drive included 5 curves 2×200 m radius one left, one right and 3×250 m radius, 2 right and 1 left. This complex alignment was necessary to keep the alignment under public rights of way.

The Convergence Measuring System based on the chained inclinometer principle for determining the deformation of the lining within the confines of the trailing gear of a TBM has now been supplied to several critical projects.

High precision measuring services for tunnel construction, automotive and aeronautical manufacturing

Copyright © 2005 Taylor & Francis Group plc, London, UK

industries using metrology systems based on Digital Photogrammetry, Lasertracker and Theodolite systems are routinely supplied for mould and segment measurements as part of a QA/QC procedure.

Additional Services include: Geodetic Network Measurement, Works Procedures and Method Statements, Conception and implementation of innovative solutions for metrology problems, Prediction of breakthrough tolerances, Calculation of Designed Tunnel Axis, Deformation Measurements, Consistency checks for new Ring Design, Ring Sequencing for entire Tunnel Drives, Surveying services for conventional tunnelling.



Figure 1. Theodolite on self-levelling tribrach & Shuttered prism – Lower Laser window.

2 DEVELOPMENT OF TANDEM SYSTEM

2.1 *Gotthard south*

The Gotthard tunnel posed numerous problems for the manufacturers of the Tunnelling machines and for the suppliers of the equipment that needed to be installed in it. The guidance system was one of the major items that had to be designed to accommodate the specific machine design.

Typically the guidance system utilizes a main reference that is mounted on the tunnel wall. These days this reference is a motorized total station incorporating a laser. This reference sights to an active target mounted on the body of the machine as close to the cutterhead as practical. A clear line of sight or "laser window" is maintained throughout the trailing gear to allow the reference to continuously activate the target. Movement of the machine relative to the reference can thus be determined and incorporated into a display for the machine operator. Unfortunately on the Gotthard South Machines tunnel support required the installation of wire mesh, rock bolts, steel ribs and shotcrete, in various combinations for initial ground support immediately behind the shield. Thus this area became a congested work area whilst the machine was advancing. In addition the secondary shotcrete line was installed in a purpose built shotcrete application chamber which unfortunately obscured the line of sight along the trailing gear. A system therefore had to de devised that made use of the available split laser window, comprising an upper portion from the wall mounted reference Total Station to prisms mounted on the forward part of the trailing gear, and a lower portion between a Laser Theodolite mounted on a self-levelling tribrach sighting to the Active target on the machine.

(Unfortunately excessive residual shotcrete in the air soon obstructed the front screen of the target so it was decided to replace it with 4 shuttered prisms. Sighting to these is sequenced and the shutter is only open for the duration of the measurement. This kept the prisms clean.) Transposition of the position from the upper laser window to the lower is carried out and the Laser Theodolite for the lower laser window is mounted on a self-levelling platform to enable the movement of the trailing gear to be accommodated in the measurement process. This and the principle of a moving reference is a key feature of the curved pipejacking system and the technology was easily transported into the tandem system.

3 RING SEQUENCING

3.1 *Basic requirements*

Steering the TBM along the correct tunnel alignment is the primary objective in any tunnelling project. However, when a pre-cast segmental lining has to be installed in the tunnel it becomes essential to, not only determine the position of the TBM, but also the space available for the optimum installation and orientation of the most appropriate ring type within the tailskin of the machine, taking into account any steering bias required by the TBM. This is particularly significant when tapered rings are used. Tapered rings are best suited for curved drives or straight tunnel alignments under difficult ground conditions, where the use of packers to accommodate ring positioning inaccuracies is not recommended.

3.2 *Optimum positioning*

Optimum positioning of the ring is a critical part of the tunnelling process and the manual determination of the parameters necessary to perform the calculations for ring placement can be a time consuming operation. Avoidance of ring damage and the machine becoming "iron bound" or the loss of the tail seal integrity is of paramount importance.

Among the tapered ring conceptions there are two distinct subsets: the UNIVERSAL ring and the mirrored pair of LEFT and RIGHT rings. The former is easier to produce and the latter ring conception permits easier ring erection.

Copyright © 2005 Taylor & Francis Group plc, London, UK

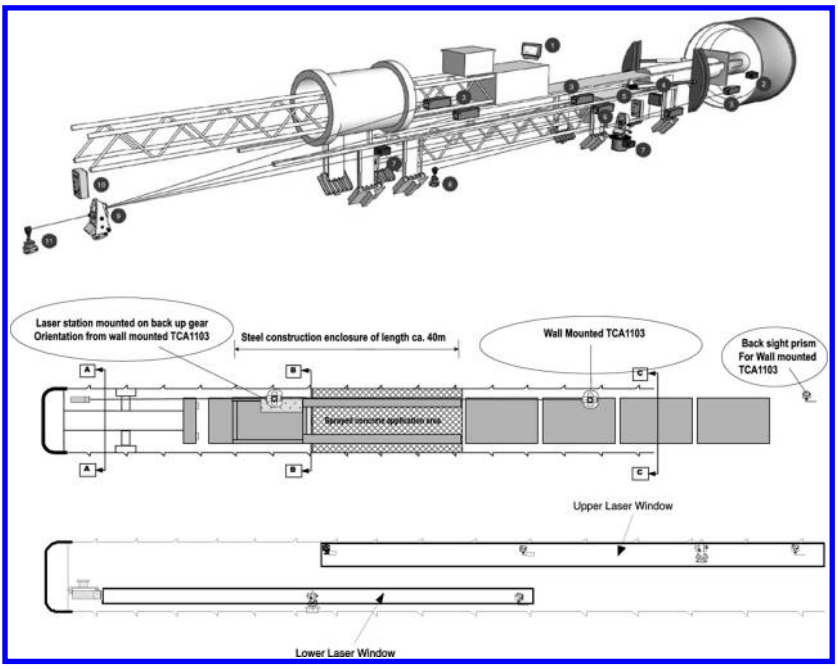


Figure 2. Tandem guidance system.

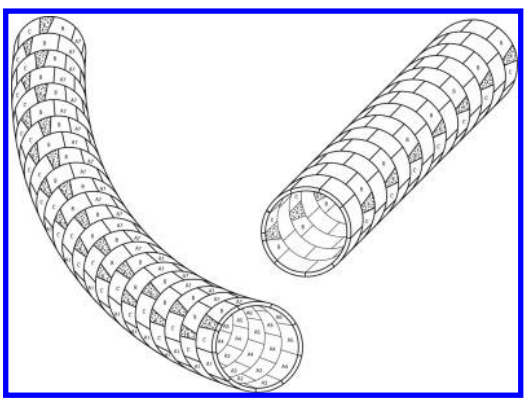


Figure 3. Tapered ring options.

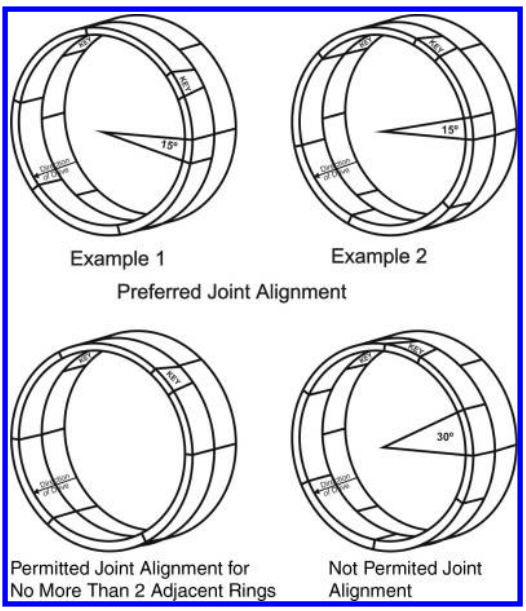


Figure 4. Typical ring alignment options.

To use a single Universal ring in a curve of the minimum radius for the ring's design, it is necessary to position the narrowest side of one ring next to the narrowest side of the preceding ring, allowing for joint overlap positioning.

Using the same Universal ring, a straight is achieved by positioning the narrowest part of one ring next to the widest part of the preceding ring.

During tunnel construction, the miners need to know what type of ring: UNIVERSAL, LEFT, RIGHT, or PARALLEL will be called next from the yard and in what rotational position the ring should be erected. Depending on the chosen rotational position, the ring will take, due to its taper, a certain tendency towards the centre of the shield tail or towards the iron. This has

Copyright © 2005 Taylor & Francis Group plc, London, UK

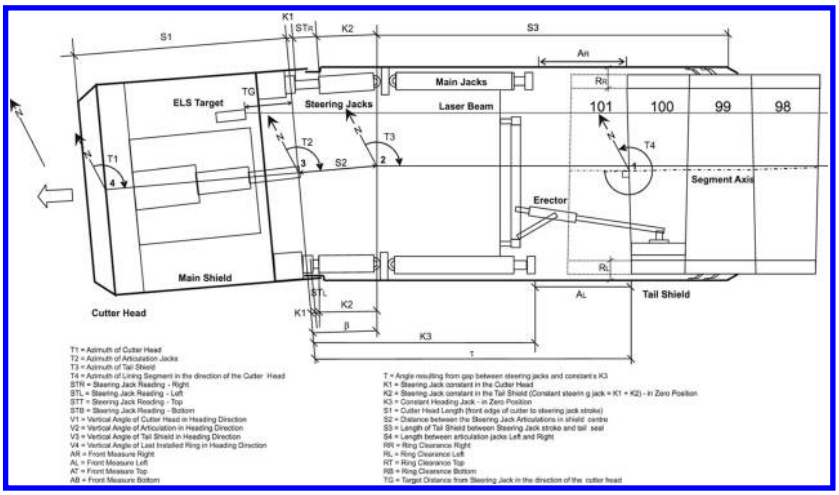


Figure 5. TBM geometric variables.

to be optimized to avoid causing problems to the outer side of the lining, if not to the tail sealing itself, with the risk of dangerous water inrush after having damaged the tail sealing. Therefore, attention must be paid to the best choice of the key position for each ring to be erected.

There may be cases where the selection of the appropriate key position for just the next ring could be judged by the miners themselves, without the assistance of a dedicated ring selection program. However, this would require quite a long standing experience in ring building. Most probably, even an experienced ring builder could not predict more than one ring at a time.

Often the engineering department asks for important characteristics of a corrective ring sequence which could not be evaluated manually: e.g. how large will the expected maximum offset be? At what station will the maximum offset take place? How many rings will be needed to regain the centre line with an offset of less than, say, ± 10 mm? etc.

3.3 *Machine variables*

Current tunnelling machines are becoming increasingly complex, see Figure 5. With more joints and articulations, the task of determining the precise position of the tail of the machine for ring building purposes is becoming increasingly complex. Such complexity can only be handled properly by a well-prepared ring selection program and correct instrumentation on the machine.

With more use of underground space the alignments for many projects have become increasingly complex. Taking the basic data from the clients' drawings for input to the guidance or ring sequencing system is subject to possible errors. The VMT ring sequencing software enables the primary geometrical alignment data to be input and converted to a DTA point coordinate table. This data is then used in the system software, or it can be easily exported into third party guidance systems.

When the machine has deviated from the theoretical alignment it is necessary to calculate the correction curve required to bring the machine back to the desired alignment. This correction curve must take into account the manoeuvrability of the tunnelling machine, the geometry of the ring and will be based on bringing the machine and the tunnel lining tangentially back onto the DTA.

Ideally the ring selection program forms part of the guidance system for the shield and is closely integrated to it. Alternatively, the VMT ring selection software and computer can be integrated with an existing guidance system (capable of suitable data output) or be supplied as a stand-alone package for use at the ring erection area.

The optimum choice for the next ring types and key-positions can be predicted by help of a ring selection program, which takes into account the actual conditions and proposes a ring sequence for the next few rings.

3.4 *Input parameters*

Whenever a ring sequence is calculated, the following input parameters must be taken into account:

- Current machine position, horizontally and vertically, by position, offsets and orientation to the current drive tendency.
- Type of the last erected ring and its key position, location within the shield tail, actual clearances and the orientation of the last erected ring by help of the push ram elongations.

Copyright © 2005 Taylor & Francis Group plc, London, UK

– Scheme of permitted and not-permitted ring sequences, with respect to non-aligned longitudinal joints and other local or temporary inclusions and exceptions.
– Available positioning options for the ring with respect to the steering of the machine.
– Characteristics for the preferred drive corrections.
– Length of the ring sequence selection required, e.g. 5…10, or up to the end of the project.

3.5 *Tailskin clearance measurement*

Measurement of the tailskin clearance can be carried out either manually, automatically with the SLuM system, utilizing 5 non-contacting laser distance measuring devices or other best estimate values can be entered.

3.6 *Plausibility checks*

To have a fully integrated system, as much data as possible should be gathered by electronic data collection from relevant sources and sensors, such as the guidance system itself, push rams, tail clearances, precedent computations, etc. However, manual collection and input of data is also available for systems without electronic data collection, or where one or more sensors fail to transmit their current data, or they are disqualified as implausible. The user has the option (even after qualified data transmission) to enter some or all data manually. This may be helpful occasionally, when given conditions are difficult and should be examined more closely by performing several tests runs with deliberately varied data.

The program then performs a comprehensive numerical computation, in order to:

– Examine if the manually input data is plausible,
– Determine if there is a solution to the given task, under the premises supplied to it,
– Select an optimum ring sequence and any related parameters for it,
– Warn the user where inconsistencies are detected and propose a remedy,
– Issue a Ring Sequence listing, for the shift engineer, the shield driver and for the yard,
– Produce a LOG-file of the last run with more details for the surveyor for inspection and revision, if needed.

After having print-out the last run, the person responsible should assess the results, validate them and supply the information to all relevant personnel.

4 MOULD & SEGMENT MEASUREMENT

Following on from their success in photogrammetric metrology for the precision measurement and evaluation of the moulds used for casting reinforced concrete segments and for the verification of the accuracy of the segments produced, VMT now offer its improved Laser Interferometer System for increased accuracy and speed in these measurements.



Figure 6. Leica Laser Interferometer LTD500.

The use of a Laser interferometer system now enables the accurate digitization of surfaces by direct polar coordinate measurement. Measurement to a single spherical corner cube prism enables the operator to comprehensively measure the full profile of the object to be measured.

Laser Interferometer Systems are usually employed where large numbers of spot points are to be surveyed with the highest accuracy and the shortest interruption to the production process.

Special attention has been drawn to the flexibility of the systems and the automated measurements and data evaluation process.

– Mobility of the system for measurements of the objects directly at the production location,
– Flexibility of the system can be configured to various control tasks,
– Short time requirements to survey the objects,
– Three-dimensional information about the objects,
– High accuracy,
– High degree of automation,

Copyright © 2005 Taylor & Francis Group plc, London, UK

– Interfaces to a wide variety of evaluation programs,
– Interfaces to most usual CAD systems,
– Interfaces to word processing and spread-sheet programs (like Word, Excel, etc.).

The object coordinates can either be confronted directly by a design to as-built comparison, be transferred to a CAD station, or be further processed by the system's geometric evaluation software (regular surfaces and free-form surfaces).

The precise control of the geometry of a mould by 3D survey before producing the first segment, as well as the control of the first produced segment itself is indispensable in order to check and verify any set of moulds. The direct comparison of the findings for related moulds and segments will permit the detection of deviations from the design values to sub-millimetre accuracy. The primary control is carried out ahead of, and independent to, the regular production. It comprises not only the geometric verification but the potential for verification of recesses for gaskets, bolts, identifiers, reference markers, etc.

Attention should be drawn to the requirement, that all moulds and segments shall be exposed to the same environmental conditions and are undergoing the same stock conditions.

As the most important result, the 3D-coordinates of the object points will be obtained in the format "point-name X, Y, Z, dx, dy, dz". These records are the object's coordinates in space along with an estimated accuracy of the internal quality criteria. The evaluation of the standard geometry and the comparison with design values and relevant tolerances will take place directly after the evaluation of spatial coordinates with help of the program "TUBGEO".

Secondary Control is the term to denote the cyclic verification of complete sets of segments (i.e. rings) and related sets of moulds. Typical cycle times might be for example "one ring and one set of moulds per week", or one may refer to the results of the Tertiary Control as the selection criteria. The object (segment or mould) to be checked will be taken off the production process (storage or carousel) and placed at a convenient location somewhere in the production hall. For a cyclic Secondary Control the verification of the 6 outer surfaces and from them derived distances and angles is essential.

The data processing runs semi-automatically by help of only a few simple menu functions. The main result of the data evaluation will be displayed in a summary report, this includes the measurements and clear statements about the tolerances, whether they have been kept or exceeded.

The process commences with the establishment of the frequency of measurement points to be taken. These may be at a time dependent interval, distance interval or by working to a grid matrix.



Figure 7. Stacked segments being measured at CTRL.

For the actual use of the Laser Interferometer System in the measurement of segments and moulds VMT have included dialogue aided scripting for the operator to clearly explain the processes of each measurement operation.

As the complete measurement of the mould or segment cannot be accomplished from a single standpoint it is necessary to relocate the Laser Tracker to a second standpoint.

To ensure that all the measurements taken can be reconciled within the same coordinate framework, index measurements are taken to the prism that is located in a "birds nest" cradle.

Between 4 and 6 of these indexing locations are established and the dialogue control informs the operator when to locate the prism in the appropriate cradle.

Upon commencement of a measurement cycle the operator places the retroreflective prism in the reference point receptacle on the Laser Tracker stand. The instrument is then able to carry out its own internal calibration and establishes its zero reference point. The operator then removes the retroreflective prism and making sure that the laser beam from the instrument is always in line of sight of the retroreflective prism he will commence the systematic tracing of the prism over the surface of the mould or segment that is to be measured; making sure to include all the significant surface points.

If the line of sight between the Laser Tracker instrument and the prism is broken then the prism must be replaced in the reference point receptacle on the Laser Tracker stand to re-zero the system. The measurement can then recommence at the point where line of sight was broken.

The typical time taken to conduct the measurements for all six surfaces including the relocation of the Laser Interferometer Instrument as well as the analysis of the results is approximately 30 minutes.

The Field proven TubGeo© software has already proven its functionality and enormous potential in

Copyright © 2005 Taylor & Francis Group plc, London, UK

numerous test measurements, and in several production plant operations, under tough industrial conditions. It has been developed employing modern software techniques in the programming language C++ with no restrictions in mind. With its help it is possible to calculate the external surfaces by "best-fit" and derive all relevant intersection measurements. The calculated output can be given numerically, graphically or in a combination of both. The resulting high-performance package including TubMes©, together with optional software such as (CAD Import/Export, Freeform surface calculation etc.) gives a tailor-made solution to suit individual needs.

5 RING CONVERGENCE MEASUREMENT

5.1 *Initial requirement*

Along many tunnel projects with segmental lining the Client has often defined specific locations, where different kinds of deformation measurements have to be performed by the Contractor. One important contribution is obtained by the observation of convergences of particularly interesting diameters, e.g. horizontal and vertical diameters.

Convergence measurements performed in previous years were based on either invar wires, or classical theodolite observations. The former are absolutely impossible along the back-up trailer, where the latter could be achieved at the very limit, but only with exceptional effort.

The most important considerations to the initial deformation of a ring – which has just been built- are the pressure of the jacks during next drive and subsequent load changes, e.g. the passing of the shield's tail, primary and secondary grouting, passing of the last back-up trailer and any potential long term effects.

5.2 *Chained inclinometer concept*

VMT has developed a system for convergence measurements, which avoid the disadvantages listed above and, hopefully, gain some new advantages.

It is based on the implementation of a series of inclinometers on the ring to be observed for deformation. One inclinometer is installed in each and every segment of the ring to be measured. The basic idea is the supposition, that any deformed ring could be considered as a chain of rigid elements, where each element (segment) remains rigid and does not in itself deform. Deformations can only take place along the longitudinal joints, which have to be treated as articulations. Any movements of the rigid segments have as primary components some changes of their vertical inclinations, which can be observed by appropriately installed inclinometers.

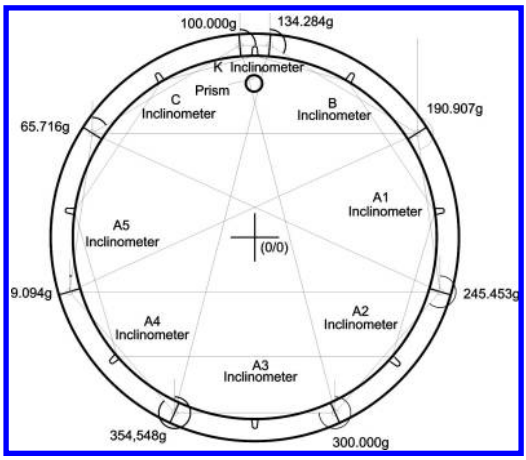


Figure 8. Chained inclinometer concept.

Having collected the tilt changes of the 6…7 inclinometers over time, the deformations of the entire ring can be derived.

Calculations of an open traverse in an arbitrary local coordinate system have to be performed for each data set (shortest cycle time approx. 5 secs). The coordinates obtained for the 6…7 articulations will permit the calculation of any interesting convergence line. Taking differences between any two arbitrarily chosen time instances (epochs) will supply the required convergence.

Fully automatic data collection on a freely selectable time interval over an arbitrarily long time period with only small requirements in terms of personnel and equipment can be achieved. A very detailed picture of potential deformations can be obtained – at fairly low cost. Confirmation of the absence of any movements can also be determined.

5.3 *Achievable accuracies*

The internal accuracy of the system is about ± 0.3 mm for periods of no load changes (determined over hundreds of data sets), e.g. during times of no tunnelling activities. Therefore, the typically occurring convergence during tunnel construction with segmental lining can be determined from 1 mm upwards.

Due to the recording of all data, calculations on convergence lines not initially considered important can be calculated at a later date. Also, one can freely chose any of the observed epochs as the current reference (zero epoch) and relate all further epochs to that one.

5.4 *Data analysis*

If access to the actual drive parameters over time (history) is available, e.g. stationing of the shield, jack

Copyright © 2005 Taylor & Francis Group plc, London, UK

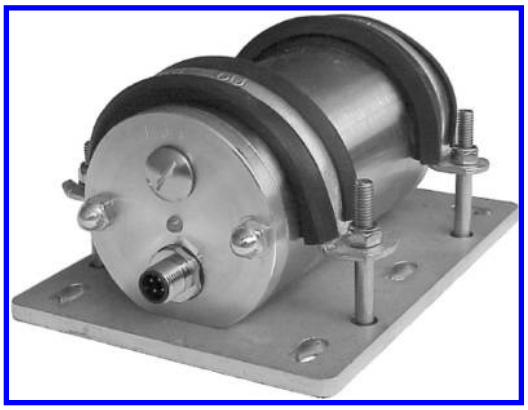


Figure 9. Chained Inclinometer unit.

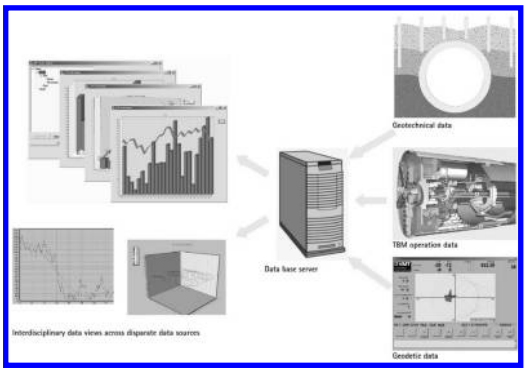


Figure 10. CBP data integration.

elongations of the push rams, pressure values, etc., such information could be related to the determined convergences by synchronizing both data bases over their time stamps. This way, inspection may be made for interrelations between the observed ring deformation and some drive data, which has not been assumed to date.

One reservation: in the case of significant movement at the longitudinal joints (radial and bird's mouthing) it would be necessary to measure them as well, even manually, in order to guarantee the accuracy as stated above. Should the requirements be less precise, e.g. only from 5 mm upwards, with an expected accuracy of only $\pm$ 2 mm, the somewhat laborious measurements and calculations could probably be omitted.

5.5 *Absolute results*

If absolute results (e.g. crown settlement or invert lifting) rather than relative vertical convergences are required, it is necessary to integrate the recorded values from the inclinometers with the measurement of a fixed reference point on the measurement ring, preferably in the crown area, and link these measurements to the main survey network. Installing a prism on one segment and monitoring any vertical movement can accomplish this. This data can then be integrated with the relative movement according to the time of the recordings to give absolute vertical dislocation data.

5.6 *Placement of inclinometers*

The precise location for fixing the inclinometers to the segments depends on the design of the segments. The user should look for niches within the segments, or any other protected spaces – these free spaces are almost always available for purposes of the segment erection or as bolt pockets. For fixing the inclinometers within such niches, it has been proven to use spray foam, which allows the installation of the inclinometer to the segment without causing any harm to the segment. Depending on the local circumstances metal frames have also been used, which can be connecting to the bolts between adjacent segments. Some help from the workshop is advised here.

5.7 *Technical data – Inclinometer*

– Sturdy aluminium casing (IP65), with additional paint protection (resistant against salt water)
– User-definable rotation of the angular position of each sensor
– Galvanic separation of the sensors from their casing
– Analogue/Digital conversion

6 CONTROLLED BORING PROCESS

It is clear from the operations that are mentioned above in relation to determining the position of the machine, ring placement and ring convergence that there is a requirement for the integration of these and other relevant parameters that are monitored into a central database for active processing. Other key parameters that are also typically monitored include the machine performance parameters and the geodetic monitoring of the surface and surface features.

The excavation of tunnels in the older cities of Europe where buildings that are of significant historical importance overlie the tunnel alignment presents a formidable challenge with regard to surface settlement associated with the machine boring process.

In response to these challenges a Controlled Boring Process system has been developed to integrate and analyse the monitored data to enable the Machine operator to receive advance warning of potentially hazardous situations. Such advance warning will enable the most appropriate actions to be taken to minimise the effects of the tunnelling process.

Copyright © 2005 Taylor & Francis Group plc, London, UK

Key areas of data integration are:

- Continuous monitoring of above ground deformations
- Integration of geodetic, geo-technical and TBM operation data into one common data-base
- Near real-time evaluation of all incoming data
- 2D and 3D visualisation
- Visualisation of surface structures and display of deformations in front, above and behind TBM
- Interdisciplinary data views across disparate data sources
- Implementation of steering aid options for the shield driver
- Warning messages in case of dangerous drive conditions

The program package provides the permanent project control, with optional network and internet connections specifically adapted to the security requirements of the project. One part of the CBP software offers a direct operation control for the shield driver. The installation of a CBP system is currently underway at the Randstad project in Rotterdam.

7 CONCLUSIONS

Rapid progress in the adaptation of Geodetic Instrumentation on machine bored tunnelling projects has been driven by the demand from an ever changing industry and supplied by dedicated teams of engineers from small companies that are flexible to reach to these demands.

REFERENCES

Broomfield, J. *Complex Pipejack Alignment in South Korea*. No-Dig International Nov/Dec 2003.

Clarke-Hackston, N. *Guidance for Extended Distance & Curved Pipe Jacking Applications*. Presented at the Microtunnelling Short-course. Feb 9–11 2000. Colorado School of Mines, Boulder, CO, USA.

Clarke-Hackston, N. *Guiding the way Forwards.* Tunnels & Tunnelling International, April 2003.

Großkopf, J. & Fischer, A. *Good cooperation leads to success*. Gute Zusammenarbeit führt zum Erfolg, April 2004.

Frenzel, C. & Rehm, U. *Controlled Boring Process (CBP) – a new approach to deformation-reduced tunneling in urban areas.* Oslo 2002.

Copyright © 2005 Taylor & Francis Group plc, London, UK

Development of divergence construction technology for deep road tunnels

H. Shikata & T. Aso
Shimizu Corporation, Tokyo, Japan

ABSTRACT: In recent years, the need for tunnel constructions at greater depths using shield tunneling is increasing for further tunnel projects in urban areas in Japan. In constructing divergence portions with main tunnels at greater depth, conventional methods such as cut and cover may not be appropriate due to the high cost of construction and the considerable influence on the surroundings.

The authors developed the new methods where the divergence portion and emergency parking zone from the pre-excavated main shield tunnel are constructed without any work from the ground surface.

The method to construct the divergence portion is called the Expandable and Shrinkable Tube Method for Junctions (ES-J method), and the method to locally expand the width in small lengths for emergency parking zones, etc., is called the Segment Expansion Method by Excavation (Seg-Jet method). This paper gives an outline of the ES-J method and Seg-Jet method, and their development technologies.

1 OUTLINE OF THE ES-J METHOD

The "ES-J method" is a technology to construct the divergence portion with a road tunnel without any work from the ground surface, where the main tunnel and the rampway tunnel are constructed by shield methods. To construct the overlapping portion, the rampway shield machine excavates a part of the main tunnel, and when the shield machine has completely excavated the required portion, the segments of both tunnels are joined.

The access road runs parallel with the main road for a certain length. This is to allow vehicles to adjust their speed before joining the main road. To construct the extra width for the parallel slip road, the shield machine excavating the main tunnel expands, and expanded tunnel segments are constructed within the expanded shield machine, making a length of the main tunnel wider. The rampway shield machine excavates up to the parallel slip lane, which is constructed by expanding the main tunnel shield machine.

1.1 *Features of the construction method*

1. As the shield machine can expand or shrink multiple times, divergence portions can be positioned at any points and any number of times.
2. The rampway tunnel and the main tunnel can be connected even after the main road tunnel is put into use as a road.

1.2 *Connection technology*

1.2.1 *Outline of the technology*

The rampway shield machine cuts into a part of the main tunnel. The portion of the main tunnel that is cut into is constructed of cuttable segments. The segments are made from concrete, using carbon fibers instead of iron reinforcing rods and are joined with plastic bolts. A temporary reinforced concrete wall is constructed in the main tunnel and the cutting side is filled with lean-mix mortar to stabilize the area around the shield machine at the time of cutting. The temporary wall carries the earth pressure exerted on the cut away portion of the main tunnel and the pressure caused at the time of cutting during the time from the cutting to the joining of the two tunnels.

Once the excavation of the rampway shield is complete, both tunnel segments are joined, the temporary wall is removed, and the divergence portion is constructed.

1.2.2 *Joining procedure*

The following shows the joining procedure, and Figure 1 shows the joint sequence.

1. During excavation of the main shield, cuttable segments are placed at the section where the rampway tunnel is to join the main tunnel.
2. After the excavation of the main tunnel is complete, the main lanes are put into use as a road tunnel until the rampway tunnel is constructed.

Copyright © 2005 Taylor & Francis Group plc, London, UK

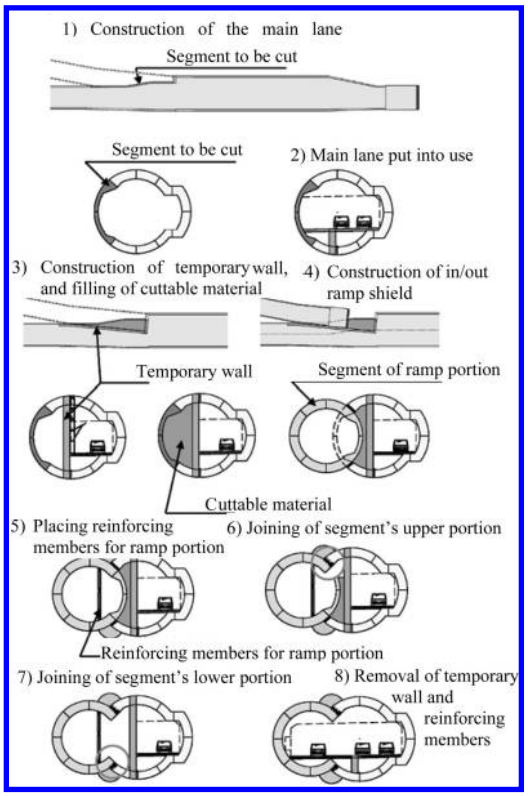


Figure 1. Joint sequence diagram.

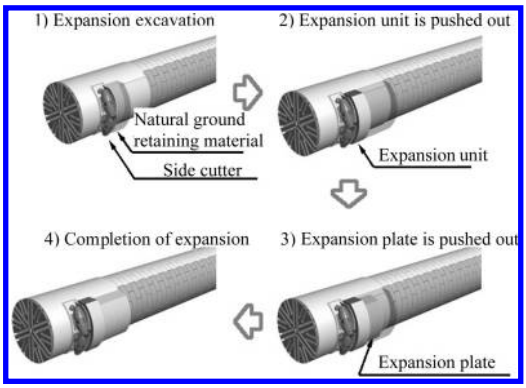


Figure 2. Expansion sequence diagram.

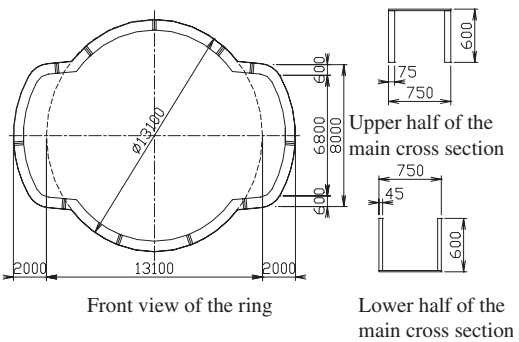


Figure 3. Expansion portion segment.

3. When constructing the rampway tunnel, a temporary wall is built on the main lane, and cuttable material, lean-mix mortar, is filled in the space between the temporary wall and the segments to be cut.
4. The rampway tunnel shield machine starts from the ground, and excavates its way down to and through the cuttable segments of the overlapping portion of the main tunnel.

5–8. The segments of the main tunnel and the rampway tunnel are joined.

1.3 *Shield expansion technology*

The joint between the expansion portion of a shield machine (expansion plate) and the main unit is a pin joint.

The following is an outline of the expansion procedure, and Figure 2 shows the expansion sequence.

1. The portion to be expanded is excavated by a side cutter.
2. The expansion unit is pushed out from the shield machine.
3. The expansion plate is pushed back gradually from the expansion unit.
4. When the expansion plate has been pushed all the way back to the rear end of the shield machine, a circular plate slides forward from the inside of the expansion plate and the shield machine's expansion process is complete.

1.4 *Analysis of construction*

The segments and the shield machine have been trial-designed. The segment has an outer diameter of 13.1 m, a width of 75 cm, and an expansion width of 2 m. For load conditions, an earth covering depth of 15.5 m is assumed, and the soil is assumed to be diluvial sandy soil.

1.4.1 *Segment*

1.4.1.1 Expansion portion of the segment

The depth of the beam for the segment is 600 mm, the same depth as for the general circular portion. Dimensions of the segment construction are shown in Figure 3.

Copyright © 2005 Taylor & Francis Group plc, London, UK

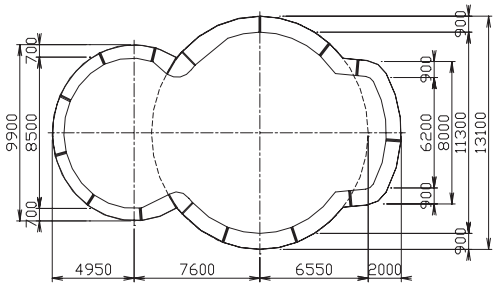


Figure 4. Front view of the segment ring of the joining section.

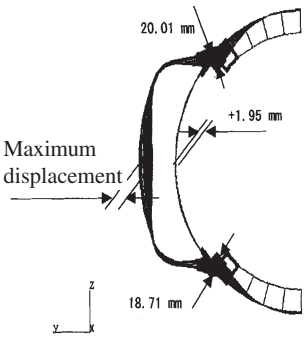


Figure 5. Displacements at the major positions of the member.

1.4.1.2 Joint portion of the segment

The depth of the beam is 900 mm in the main lane segment and 700 mm in the rampway tunnel segment. The main beam thickness is 30 to 60 mm. For the joint of the main tunnel with the rampway tunnel, direct welding plate construction is used. Dimensions of the construction are shown in Figure 4.

1.4.2 *Shield machine*

The skin plate thickness of the tail portion of the shield machine is 150 mm, and the expansion plate thickness is 160 mm. The displacements at the major positions of the member are shown in Figure 5.

2 OUTLINE OF THE SEG-JET METHOD

The "Seg-Jet method" is the method to construct expansion portions such as an emergency parking zones in shield tunnels without soil improvement. Figure 6 shows a schematic diagram of the Seg-Jet method.

Main shield tunnels are excavated by a normal shield machine, when excavating the shield tunnel's expansion length, an expandable circular segment is assembled in the shield machine. The expansion of the tunnel is

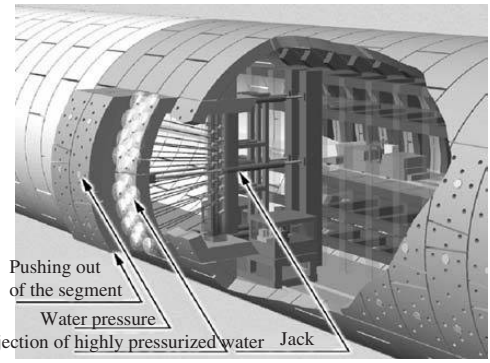


Figure 6. Schematic diagram of Seg-Jet method.

performed after the shield machine's excavating equipment (trailing equipment) passes the location to be expanded. Highly pressurized water is used to excavate the soil behind the pre-placed expansion segments and the rings of the segment are pushed out one by one. A jack system is used for pushing because it enables high-precision control of the pushing direction. Steel members are assembled to resist the reaction force of the jack when pushing the segment. The influence on the surrounding ground can be minimized during highly pressurized water excavation by controlling the excavation range and slurry amount. After completion of the specified pushing, the pushed segments are secured to the surrounding segments using bolts, and back filling to the outer surrounding completes the expansion.

2.1 *Development technology*

To establish the methods, the following main technologies have been developed.

2.1.1 *Simultaneous multiple injection excavation system*

In this system, many holes are provided in the segments to be pushed and excavating rods are protruded from the holes. The system enables excavation of the natural ground by the injection of highly pressurized water and high pressure air.

The diameter of the excavating rods is 40 mm, and injection of highly pressurized water (the pressure range is 20 to 40 MPa and injection volume range is 60 to 200 L/min.) and high pressure air (the pressure is 1 MPa and injection volume range is 0.5 to 2.5 m^3/min.) from the holes located in the side of the rod close to the tip allow a circular shape to be excavated by rotation of the tip of the rod.

2.1.2 *Jack system*

When the pushed segments are for the emergency parking zone size, the number of jacks to be used is

Copyright © 2005 Taylor & Francis Group plc, London, UK

eight, and each jack's stroke difference can be controlled to within ±1 mm regardless of the variation of the loads applied to the jacks. For this reason, the segments can always be pushed in a fixed direction and in an accurate manner.

2.2 *Segment trial-design*

2.2.1 *Construction of the segment*

After specifying load conditions, the segment was trial-designed with an outer diameter of 16 m and a width of 2000 mm. The pushing amount is 1900 mm. Soil property and loading conditions are assumed as follows: the earth covering is 50 m and the soil property is diluvial sandy soil. The depth of the beam of the circular portion segment is 700 mm, and 800 mm for the pushed segment. The dimensions of the segment are shown in Figure 7.

2.2.2 *Joint of the pushed segment*

After pushing the segment, the pushed segment is secured to the upper and lower segments using bolts. The joint requires 36 bolts of M36 (10.9). The stress applied to the bolts is shown in Table 1.

2.3 *Features and advantages*

1. Soil improvement is not required for expanding tunnels, and ground excavating equipment and pushing equipment to push the segments are simple.
2. The highly pressurized water injection enables restricted excavation of soil in the amount necessary to push the segment. Also, the control system for stabilizing the natural ground during excavation and when back filling is performed just after pushing segments can restrict ground changes during the tunnel's expansion.
3. When expanding the cross section of a tunnel, there is no need to have any contact with the natural ground, consequently all work can be carried out from within the tunnel, providing safe operation.

2.4 *Field experiments*

A series of field experiments was carried out to establish construction performance. The experiments concentrated on directly pushing segments. In the experiments, dummy ground was filled in the tank and tests were carried out in three stages.

2.4.1 *Excavating experiment using highly pressurized water and high pressure air*

The feasibility of whether or not highly pressurized water and high pressure air can excavate in a horizontal direction and discharge soil was examined. In the experiment, fluidized processed soil was filled in the 10 m^3 tank, when the stress reached 0.4 kN/mm^2, a

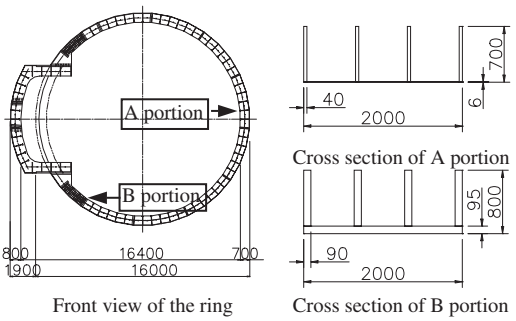


Figure 7. Dimensions of the segment.

Table 1. Stress applied to bolts.

	Applied stress N/mm^2	Allowable stress N/mm^2
Tension	355.7	380
Shear	226.3	270

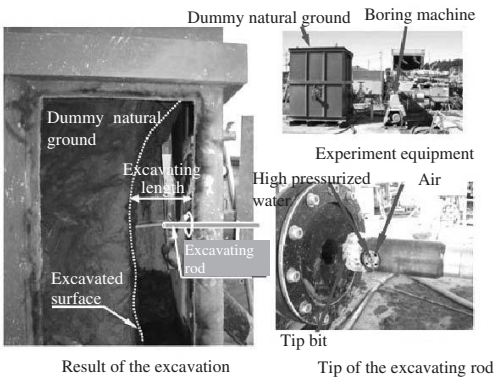


Photo 1. Excavating experiment.

40 mm-diameter excavating rod was inserted into the dummy ground and the ground was excavated. The soil excavated during the experiment was smoothly discharged through a three inch slurry pipe installed in the bottom of the tank. After the experiment, the diameter of the excavation was measured at 1200 mm. Photo 1 shows the set up of the experiment.

2.4.2 *Excavating experiment under high pressurized water*

The possibility of discharging soil when excavating under high pressurized water and maintaining groundwater pressure was examined assuming construction at great depth.

Water was applied at a pressure of 0.7 MPa to a high pressure tank in which fluidized processed soil

Copyright © 2005 Taylor & Francis Group plc, London, UK



Photo 2. Excavating experiment under high pressure.

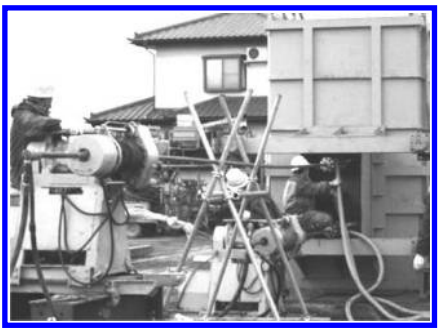


Photo 3. Excavating/Pushing experiments.

was filled, then a 40 mm-diameter excavating rod was inserted into the tank for excavation. Pressure was able to be maintained at 0.7 MPa and soil discharge was made possible by operating the valve installed on the 2 inch slurry discharge pipe during excavation. The stress of the fluidized processed soil was 0.2 kN/mm^2, and the excavated diameter was 1000 mm. Photo 2 shows the experiment equipment.

2.4.3 *Field experiment of pushing segment*

2.4.3.1 Outline of the experiment

The possibility of maintaining a highly accurate pushing direction for the segment by the jack system was examined while excavating.

In the experiment, dummy ground assuming a mudstone layer was filled in a steel box in which the segment to be pushed was installed, and 2 excavating rods and the jack system were used.

The size of the pushed segment was 800 mm in width × 1500 mm in height, the steel box was 2 m × 2 m × 3.5 m (height). Four 450 kN jacks were used in the jacking system. The dummy ground was made by mixing tuff loam, sand, and cement. On pushing the segment, while maintaining the pressure in the steel box at 0.03 MPa, the dummy ground was excavated by synchronizing the pushing amount of two excavating rods and the pushing distance of the segment. Photo 3 shows the experiment equipment.

2.4.3.2 Results of the experiment

The strength range of the dummy ground was 1.4 to 2.1 kN/mm^2. Comparing to the previous two experiments, the strength of the dummy ground was greater than that of the fluidized processed soil. This led to a smaller excavated diameter, and sometimes it was impossible to push the segment in the early stage of the experiment. Consequently the injection specification was changed, and the specified pushing length of 700 mm was obtained by reducing the inserting speed while maintaining the revolution speed of the excavating rod. The thrust force range of the pushing jack was 80 to 100 kN, and it resisted the friction force caused by the seal material. The stroke variation of the four jacks was within ±1 mm, and it was possible to smoothly extend them without causing galling. Table 2 shows the relationship between the injection specifications and possibility of the pushing.

Table 2. Injection specifications table.

Highly pressurized water	High pressure air	Excavating time	Possibility of the pushing
40 MPa × 100 L/min	1 MPa × 1 m^3/min	1 cm/20 sec	×
40 MPa × 100 L/min	1 MPa × 1 m^3/min	1 cm/40 sec	×
40 MPa × 200 L/min	1 MPa × 2 m^3/min	1 cm/60 sec	○

3 SUMMARY

The ES-J method, enabling divergence construction in a tunnel constructed by the shield method at any required position, and the Seg-Jet method, which enables expansion of the shield tunnel's cross section, have been developed. Both methods enable the expansion of a shield tunnel's cross section, but the ES-J method is more suitable for the divergence portion in two-lane cross section class tunnels as its expansion length is comparatively long and because of the expansion shield machine's manufacturing cost. The Seg-Jet method is suitable for emergency parking zones, etc., in two to three-lane cross section class tunnels, as they require a comparatively short expansion length. From here on, we will pursue cost efficiency and ease of construction, and also try to further improve the reliability and practicality of both methods.

Copyright © 2005 Taylor & Francis Group plc, London, UK

Application of 'casting support tunneling system using TBM' to unconsolidated soil with high groundwater level

Hiroomi Iida & Takashi Kitagawa
Japan Railway Construction, Transport and Technology Agency, Kanagawa, Japan

Keizo Chishiro
Sambongihara Tunnel Project Office, KUMAGAI GUMI CO., LTD., Aomori, Japan

Takatoshi Ono
Railway Technical Research Institute, Tokyo, Japan

Yukinori Koyama
Geo-Research Institute, Tokyo, Japan

Atsushi Koizumi
Waseda University, Tokyo, Japan

ABSTRACT: The Sambongihara Tunnel on the Tohoku Shinkansen Line, located between Hachinohe and Shin-Aomori stations, is a double-track tunnel 4,280 meters long. The geology of this tunneling site mainly consists of alternating layers of unconsolidated sandy soil under high hydraulic pressures and cohesive soil. Excavation of this tunnel began in August 2001 using the NATM from the Shin-Aomori side, but the tunnel face collapsed twice, preventing the tunnel construction from advancing as scheduled. We therefore conducted an in-depth study to develop a new tunneling technique, aimed at improving efficiency and safety of the work.

The new tunneling method uses a standard earth and mud pressure shield to maintain face stability and ensure good excavating capability. The technique developed will significantly improve the efficiency and safety of the work. This paper outlines the construction and design of the linings selected for this tunneling practice.

1 INTRODUCTION

The Sambongihara Tunnel, in the east district of Aomori, is a part of the extension project of the Tohoku Shinkansen Line between Hachinohe and Shin-Aomori (Fig. 1).

Initially the NATM was planned to be used for this project. The tunnel construction started in August 2001 from Shin-Aomori side, but two significant collapses occurred in March and September 2002. Development was therefore required of effective means to ensure safety in the work at the face and less impact on the structures on the surface, and countermeasures against delay in the work schedule.

To overcome these initial difficulties, a new technique named SENS was developed, which features improved safety, economy and work efficiency. As a result, the excavation by the NATM from Shin-Aomori side was stopped, and instead tunneling by the SENS from Hachinohe side started in July 2004, and is currently being used. This paper discusses the overview of the SENS method and reports the status of tunneling.

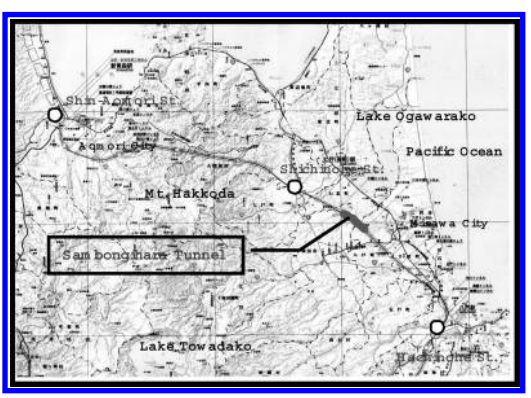


Figure 1. Location of the Sambongihara Tunnel.

Copyright © 2005 Taylor & Francis Group plc, London, UK

2 OUTLINE OF THE PROJECT

2.1 *Characteristics of the project*

The Sambongihara Tunnel is in a double-track section on the Shinkansen Line. Its excavation outer diameter is 11,440 mm, and finished diameter 10,180 mm, and the total length 4,280 m. After 1,265.2 m had been excavated, tunneling by the NATM was stopped, and plans were made to use the SENS for construction of the remaining 3,014.8 m. The section of this tunnel is shown in Figure 2, and the characteristics of the tunnel in Table 1.

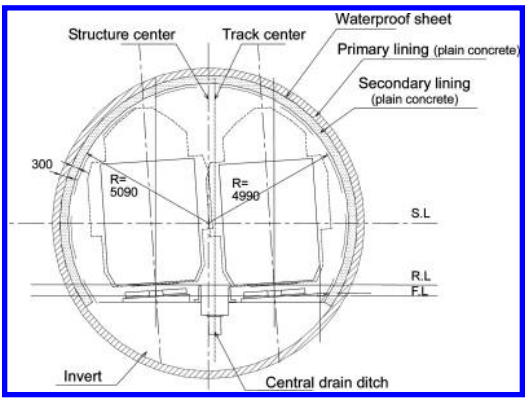


Figure 2. Tunnel section.

2.2 *Geological profile*

Figure 3 depicts the geological longitudinal section of the tunnel. The topography of the site consists of relatively flat diluvial upland of about 60 m in altitude and alluvial valley dissected by a river. The Noheji formation traversed by the tunnel alignment consists of alternating layers of unconsolidated sand and clay. The composition is upper sandy layer Nos1 with coefficient of uniformity about 5 and higher water permeability, cohesive soil layer Noc with complex distribution of volcanic ash cohesive soil, small gravel and coarse sand, and lower sandy layer Nos2 mainly with middle grain to coarse sand. The overburden in the SENS section ranges from 2 to 45 m, averaging 23 m. The groundwater level is above the tunnel crown in most places, and at the highest spot, about 17 m above the crown.

The ground to be excavated is in general relatively solid, allowing excavation by the NATM. However, as experienced when using the NATM, at the boundary between sand and cohesive soil layers, the fluidity of the upper Nos1 layer increased, due to water ingress to the face, causing the collapses.

Table 1. Characteristics of the tunnel.

Diameter of excavation	11,440 mm	Tunnel length	4,280 m
Inner diameter of primary lining	10,780 mm	NATM section length	1,265.2 m
Inner diameter of secondary lining	10,180 mm	SENS section length	3,014.8 m
Thickness of primary lining	330 mm	Maximum overburden	45 m
Thickness of secondary lining	300 mm	Minimum overburden	2 m
Width of a ring	1,200 mm	Average overburden	23 m

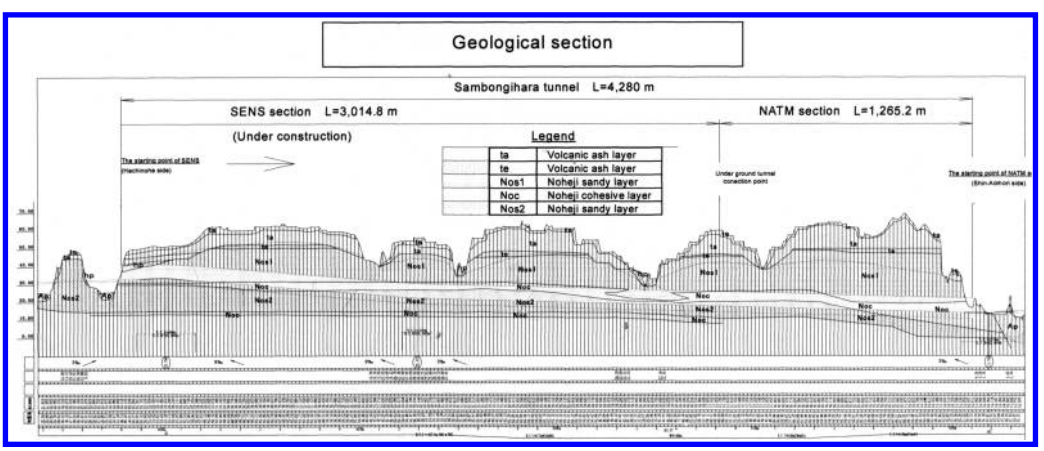


Figure 3. Geological longitudinal section.

Copyright © 2005 Taylor & Francis Group plc, London, UK

3 DEVELOPMENT OF THE SENS

3.1 *Definition of the SENS*

The tunneling methods are largely divided into shield tunneling and the NATM. The former technique uses a TBM to ensure 'face stability' and perform 'muck handling.' It is excellent in that tunneling in urban weak soil can be performed safely. However, since prefabricated segments are used for lining, it is as a general rule more costly than the NATM tunneling.

In contrast, the NATM is excellent from the economical viewpoint, but it is difficult to apply to weak or unstable soil.

In soil such as that at the Sambongihara Tunnel site, which is generally solid though a stratum of relatively high fluidity exists, the shield tunneling is suitable from the standpoint of 'face stability' and 'muck handling,' but lining with prefabricated segments is less economical. Figure 4 is a schematic diagram showing comparison of shield and the NATM techniques in terms of economy and ground properties.

For projects classified in the boundary range between the NATM and shield, an increasing demand is recognized for techniques that offer both a safe 'excavation mechanism' and a reasonable 'lining system.' The SENS is one of these techniques. It uses a TBM to maintain 'face stability' and ensure efficient 'excavation,' with concrete structural members cast in place at the tail.

The ECL is a technique similar to the SENS. The ECL is based on the same design practice for cast-in-place concrete as that for segments of shield tunneling. However, it is not economical for relatively solid ground, that of Sambongihara site for example. In addition, records of ECL projects reveal that much labor was needed in some cases for assuring quality because significant cracks and water leak occurred in the lining.

Considering the above, the authors applied the concept of ultimate state of the lining to simplify the lining structure, and to ensure satisfactory structural quality. The structure selected for achieving these goals is secondary lining inside the cast-in-place concrete.

This new method was named 'Casting Support Tunneling System Using TBM', and called SENS for short. SENS stands for Shield (S), ECL (E), the NATM (N) and System (S), since it is a method developed on the basis of these tunneling techniques.

3.2 *Lining*

As shown in Figure 2, the ground support is composed of a 330 mm thick primary lining and a 300 mm thick secondary lining.

The primary lining is expected to work as the shotcreting in the NATM. That is to say, it has a support

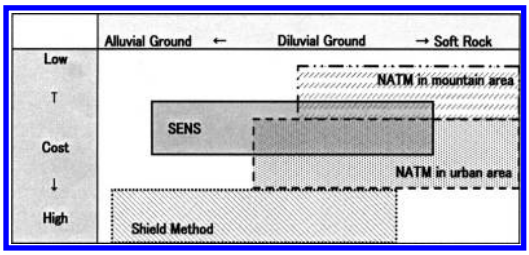


Figure 4. Difference of tunneling method.

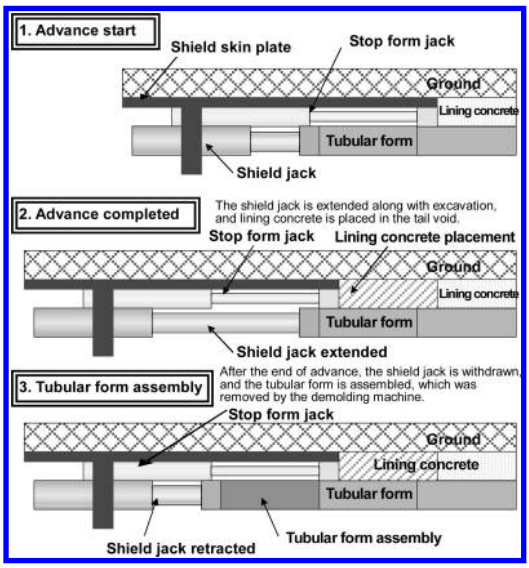


Figure 5. Operation process of the primary lining.

function for stabilizing the excavated cavity, but it tolerates some degree of groundwater infiltration and cracking. For designing the primary lining, the ultimate state was validated. As a result, plain concrete was selected, which is less thick than the segment of shield tunneling. The secondary lining that will not carry loads is placed after confirming that cast-in-place concrete deformation has well converged.

The primary lining concrete is, as illustrated in Figure 5, placed between ground and tubular form assembled at the tail. Concrete casting is simultaneous with tunnel advance. The ground is maintained by the liquid pressure of the concrete until the concrete hardens. However, while hardening, the ground continues to deform under the effect of excavation, so loads acting on the hardened concrete are expected to be smaller than those on the segment lining. The authors will measure stresses in the lining concrete to understand the mechanism of interaction between the ground and primary lining.

Copyright © 2005 Taylor & Francis Group plc, London, UK

4 TUNNELING OPERATIONS

4.1 *TBM*

Figure 6 shows the TBM and Figure 7 the entire view of the TBM and tubular form. As indicated in Figure 6, the TBM is 11,440 mm in outer diameter, 11,120 mm long. The earth and mud pressure shield was selected to prevent primary lining concrete from seeping into the face. The machine used in this project is equipped with a tubular form removal device (demolding machine), in addition to a tubular form erector as installed on the ordinary TBM.

As shown in Figure 5, concrete is injected simultaneously with tunnel advance, through the ports provided in the stop form, at the position surrounded by ground, stop form and tubular form erected at the tail. The stop form in the shape of a ring is located between skin plate and tubular form circumference. This form is supported against the TBM body by the stop form jacks. During advance, the accumulator in the hydraulic circuit moves the stop form forward and backward in the tunnel axis direction so that the concrete pressure is kept constant, even if there is a slight variation in advance speed or concrete supply rate. Each stop form jack cylinder is separated into four chambers, and the different jacks are synchronized so that the jack strokes are nearly the same as all the

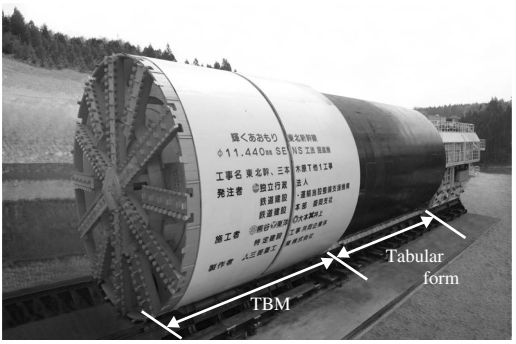


Figure 7. TBM and tubular form.

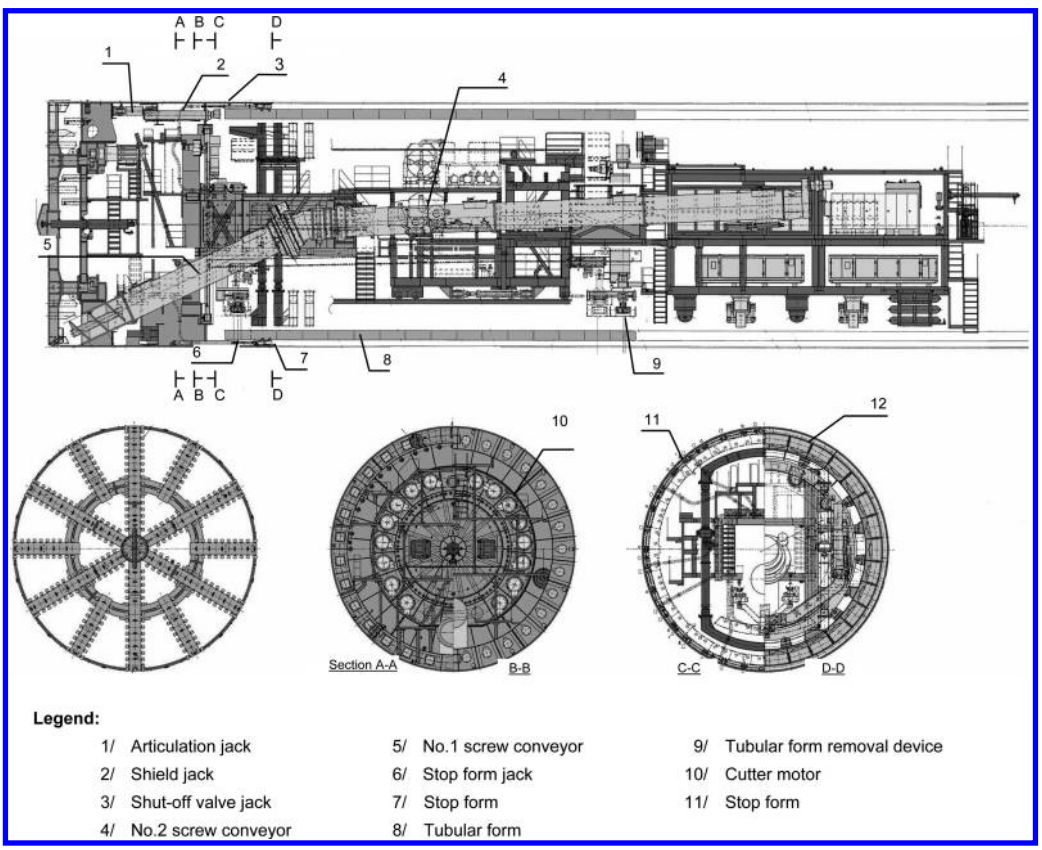


Figure 6. Entire view of the TBM.

Copyright © 2005 Taylor & Francis Group plc, London, UK

others. This regulation mechanism avoids significant inclination of the stop form.

In one work cycle, as shown in Figure 8, the tubular form at the end is removed simultaneously with advance, and at the end of advance, another tubular form is assembled. The advance and tubular form assembly take about 90 minutes respectively, so one cycle is about 3 hours. Advance is continuously performed while casting concrete. However, during advance, the concrete piping tends to clog and the stop form movement becomes irregular. To cope with this difficulty, advance is interrupted at intervals of ten rings, and the pumps and piping are cleaned, and the stop form is separated from the concrete surface after ten hours when concrete has set enough to sustain itself.

4.2 *Tubular form*

The section of the tubular form is illustrated in Figure 9. One ring of the form is 1.2 m wide. Sixteen rings are used in total. The tubular form assembled at the tail is removed and disassembled when it comes to the end along with tunnel advance, to be conveyed to the tail and used repeatedly.

The propulsion reaction of the shield is given by adhesion of concrete to the tubular form. With concrete of 24-hour unconfined compressive strength of 15 N/mm^2, an adhesion of 200 kN/m^2 of tubular form can be obtained. On this assumption, the adhesion area of 7rings of hardened concrete is necessary to ensure sufficient propulsion reaction. Therefore, the advance per day is limited to 8rings, so at least 8 concrete rings having 1day compressive strength remain.

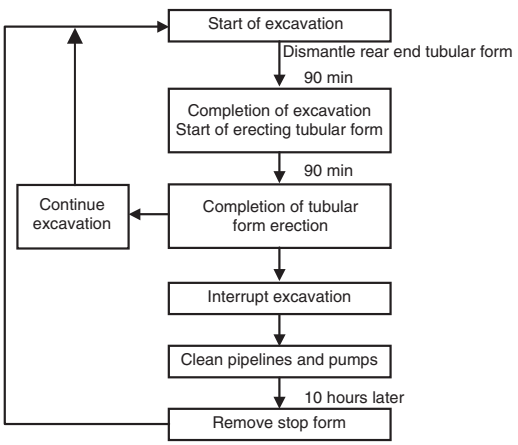


Figure 8. Operation cycle of primary lining.

4.3 *Concrete lining system*

Figure 10 is a schematic diagram of the concrete lining system. Concrete is manufactured at a plant installed in the site, and transported to the supply pump by agitator trucks. The concrete pump supplies concrete through the 6 inch piping to the remixer in the trailing carriage of the TBM. Concrete is conveyed from the remixer to six concrete lining pumps. Then the concrete is sent, via the two-way valve, through 3 inch piping and poured through 12 ports.

5 DEVELOPMENT OF CONCRETE

Concrete to be used in this project is subjected to the following restrictions:

– it takes a certain time to assemble a ring of the tubular form, following the advance for a distance of the preceding ring,

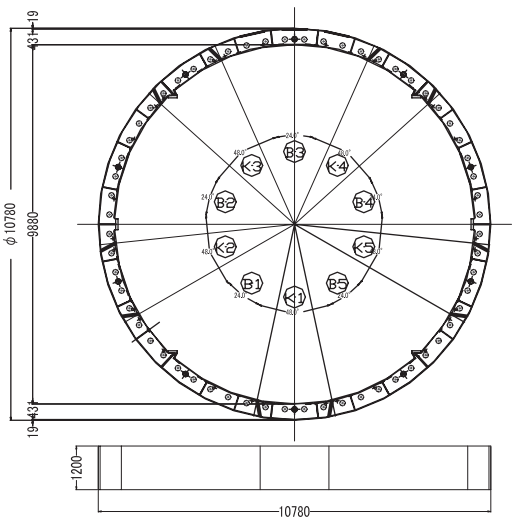


Figure 9. Section of tubular form.

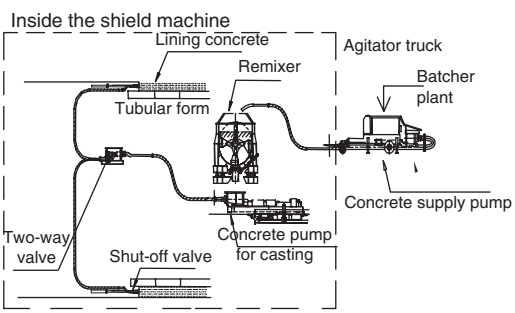


Figure 10. Concrete lining system.

Copyright © 2005 Taylor & Francis Group plc, London, UK

Table 2. Quality standard of concrete.

No.	Quality performance	Quality standard
1	Flowability	Flowability shall be maintained for hours that are the estimated time from mixing-up to casting.
2	Self-compactibility	Concrete shall entirely fill 330 mm thick space (lining thickness).
3	Segregation resistance	Concrete shall not segregate during pumping or filling.
4	Antiwashout	Loss of cement particles from concrete placed in water shall be limited.
5	Pumpability	The required amount of concrete can be conveyed under pressure, and conveyed concrete quality shall not degrade.
6	Early age compressive strength	The strength at one day shall be 15 N/mm^2 or more

– concrete is placed in water, and
– concrete shall exhibit the required strength by the time of form removal.

To satisfy these requirements, concrete having the properties given in Table 2 must be developed.

Among the properties shown in Table 2, the fluidity and exhibition of early age strength are incompatible with each other, as are antiwashout and pumpability. However, tests on fluidity and strength, and pumpability were conducted repeatedly to select the concrete mix specification with a non-segregating agent given in Table 3.

The management items shown in Table 4 have been set up, and the tunnel construction is now under way using the concrete satisfying these items. The antiwashout property test is based upon the Guidelines for Design and Work of Antiwashout Underwater Concrete (draft) published by the Japan Society of Civil Engineers. In this test, concrete is dropped into distilled water, and the amount of cement dissolved from the concrete into water is determined by the pH value, thereby evaluating the segregation in water. This test verifies that the concrete in question can be used satisfactorily without significant segregation in water.

6 CONSEQUENCE OF TUNNELING

6.1 *Displacement of lining*

The displacement of lining concrete is shown in Figure 11. The dotted lines represent settlement at the crown, right and left, whereas the solid line expresses the variation in distance between two points. Since the measurements were possible only after the trailing carriage passed away, the data cover points 50 meters or more from the face. The graphs demonstrate that the settlement at each point is less than 1 mm, and the variation in distance is no more than +/−1 mm. We can conclude therefore that the concrete moved very little after demolding.

Table 3. Mix proportion.

W/C %	S/a %	Unit weight (kg/m^3) W	C	S	G	Non-segregating agent W×%	Super plasticizer C×%
35	38	190	543	597	948	4.0	3.2

Table 4. Control values of concrete.

	Control value	Frequency
Specified slump flow	60 cm ± 5 cm	Once/day
Specified slump (After 4 hours)	80% of specified slump flow value	Once/day
Volume ratio of air	4.5 ± 1.5%	Once/day
Antiwashout test	pH ⩽ 12	Once/day
1-day compressive strength	More than 15 N/mm^2	Once/day
28-day compressive strength	More than 30 N/mm^2	Once/day
Unit water content	Specified water content + 20 kg	Once/50 m^3

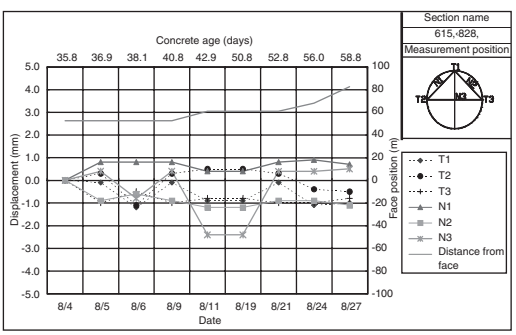


Figure 11. Variation of crown settlement and convergence with time.

6.2 *Cracks and water leakage*

As Figure 12 shows, the completed primary lining is almost free from cracking and water ingress. This

Copyright © 2005 Taylor & Francis Group plc, London, UK



Figure 12. Tunnel at completion of the primary lining.

ground support is better in quality than the primary lining of the NATM tunneling. Concrete filling is perfect, and no un-filled sections were observed from the surface. The ultrasonic test verified that the lining thickness conformed to the requirement.

7 CONCLUSIONS

As of August 2004, about 70 meters of the primary lining have been cast. To date, tunneling construction has made good progress and no abnormal displacements of concrete or surrounding ground have been found.

We will perform in-depth measurements of stresses induced in the lining concrete and displacement of the surrounding ground. Referring to data measurements, we will determine the loads acting on the cast-in-place primary concrete lining, in the hope of proposing a reasonable lining design technique that is well suited to the process of concrete casting in place.

Copyright © 2005 Taylor & Francis Group plc, London, UK

Shield tunneling technologies in Japan

T. Goto, T. Masaka, K. Miki & S. Takaku
Shield Tunneling Association of Japan, Tokyo, Japan

ABSTRACT: The Shield Tunneling Association of Japan, STA, was established in 1999, and its membership consists of 97 companies including leading general contractors, TBM and lining segment manufacturers. Fourteen proven and reliable shield tunneling methods have been registered with the association to date, and the association is helping to apply these shield tunneling methods to various projects and promoting widespread use of those methods. This paper introduces the history of shield tunneling methods in Japan and some of the latest shield tunneling technologies, focusing on the registered 14 shield tunneling methods.

1 OUTLINE OF THE ASSOCIATION

In recent years, use of underground spaces has been essential to the construction of urban infrastructure. Shield tunneling methods have been gaining increased importance as a means of creating underground spaces.

The Shield Tunneling Association of Japan was established in 1999, and its membership consists of 97 companies including leading general contractors, TBM and lining segment manufacturers. It has registered 14 reliable, time-tested and state-of-the-art shield tunneling technologies and methods. It has been collecting and organizing management, and thereby helping apply specific methods and enhancing and promoting shield tunneling technologies.

2 GENERAL

In 1939, shield tunneling was used successfully for the first time to construct a circular railway tunnel in Japan. In the 1960s, shield tunneling began to be used for various infrastructure projects in urban areas, and the open shield method had its heyday until the 1980s.

The period from 1980 to 1990 saw a transition from open TBM to closed TBM such as earth pressure balance shield machines developed in Japan. At present, 98 percent of TBM machines used in Japan are closed type. During the peak period in the 1980s, as many as 300 contracts were awarded each year for shield tunneling projects, and marked progress was made in infrastructure development.

Today, although the number of shield tunneling contracts awarded each year declined to around 150, the contract requirement is getting tougher such as deep tunnel under 1 MPa water pressure, highway tunnel of 16 m diameter, long distance drive (9 km) for trans Tokyo Bay tunnel, and increase of sections of rectangle and multi-circles. One of examples is shown in Figure 1.

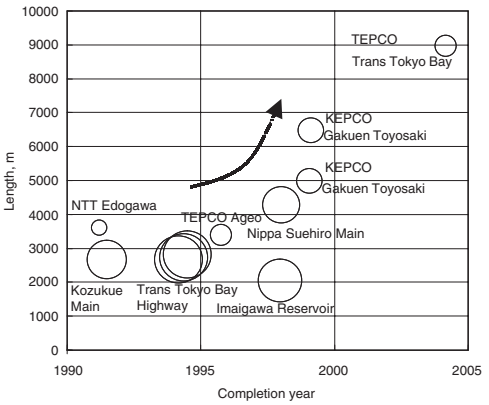


Figure 1. Example of long distance tunnel.

STA is providing technical support to the challenging projects with the registered 14 shield tunneling methods, and contributing to the development of Japan's shield tunneling technology.

3 FOURTEEN SHIELD TUNNELING METHODS

The 14 shield tunneling methods are registered to the Shield Tunneling Association of Japan and the details of each method are classified into "tunneling technology", "multiface", "non-circular", "special technique", and "lining technologies"; and described as follows with figures for each.

Copyright © 2005 Taylor & Francis Group plc, London, UK

3.1 *Tunneling technologies*

3.1.1 *DK shield method*

The DK Shield Method controls muddy soil pressure for tunnel excavation in three phases to minimize disturbance to the ground.

Mud making agent is injected into soil excavated by a cutter. The excavated soil is then kneaded forcefully with the agent using kneading blades and changed to muddy soil with plastic fluidity and impermeability.

Kneading chamber and screw conveyor are filled with muddy soil. Then, muddy soil is pressed by the thrust of a jack to resist groundwater pressure and earth pressure, providing face stability.

Muddy soil pressure is constantly monitored using pressure gauges attached to the bulkhead. Shield driving is controlled by changes in the rate of shield advance and the rotational speed of the screw conveyor so that muddy soil pressure becomes equivalent to the total of earth pressure at rest and water pressure.

It was experimented under water pressure of 0.7 MPa and concluded that it can be applied in underground as deep as 50 m.

3.1.2 *Rheological foam shield tunneling method*

The Rheological Foam Shield Tunneling Method is to excavate a tunnel while injecting foams into the face and the chamber. The foams are generated by special foaming agent. The tiny foams with properties similar to those of shaving cream improve the fluidity and the watertightness of excavated soil. Foams can also prevent the soil from sticking inside of the chamber. This enables smooth tunnel driving while maintaining face stability. In addition, the removed soil with foams can be defoamed and put back to the state as before foam injection. Then excavated soil can be easily transported and disposed of. Thus, the method also has economic merit.



Figure 2. DK Shield Method.

The Rheological Foam Shield Tunneling Method has been adopted on 404 projects, constructing a total length of 412 km as of April 2004.

3.1.3 *Chemical plug shield method*

An additive and the main chemical agent, CP-M, are mixed with the excavated soil in the chamber. Then, the assistant chemical agent, CP-S, is injected into the screw conveyor to create a cut-off plug from improved

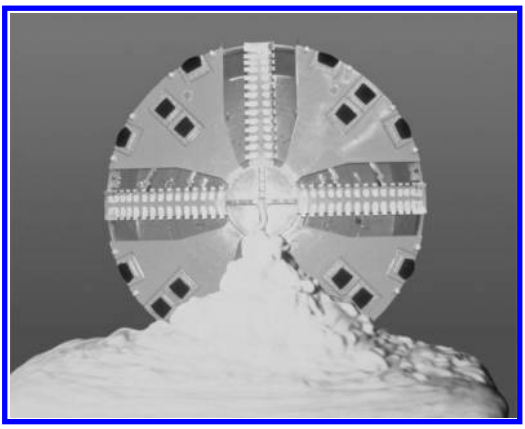


Figure 3. Rheological foam shield tunneling method.

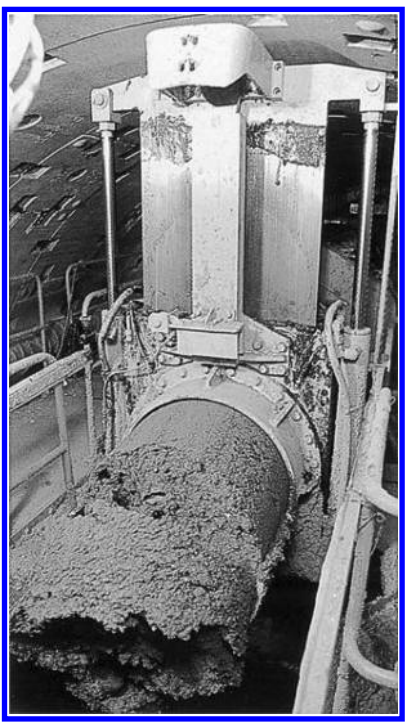


Figure 4. Chemical plug shield method.

Copyright © 2005 Taylor & Francis Group plc, London, UK

soil. This enables safe and accurate excavation in water-bearing gravelly soil under high water pressure, up to 1.0 MPa, while controlling face pressure and preventing face collapse due to blow and other soil disturbances.

The CP-M is added to conventional EPB's additive at the plant. The plant for the CP-S may be located in the tunnel. The excavated soil mixed with CP-M is mixed with CP-S and agitated in the screw conveyer, and rapidly changed into improved soil to form the cut-off plug.

3.2 *Multiface*

3.2.1 *Horizontal and vertical variation shield method*

Cross section can be changed continuously from horizontal to vertical multi-circular shape or vice versa. The cross articulation system enables free control of machine steering and orientation, and continuous change of multi-circular cross section from horizontal to vertical alignment or vice versa.

The cross articulation system articulates multiple front bodies of a shield machine in reciprocal directions and make respective bodies advance in different directions. The system enables shield machine to generate rotating forces and advance so that the tunnel spirals.

The machine can be divided. Therefore tunnel can be separated without intermediate shaft.

3.2.2 *Multi-circular face shield method*

The Multi-circular Face Shield Method places 2 or 3 cutter heads attached to shield machines in such a way that one locates ahead of others and overlaps each other. Connecting double or triple circular sections, or sections of different cross sections vertically or horizontally could offer tunnels of diverse cross section other than a circular section.

This enables simultaneous construction of upper and lower tunnels at a site with limited land under a narrow road by vertically connecting tunnel cross sections occupying a small area. Even in cases under restrictions on vertical space due to existing structures, a multi-circular-face shield method using horizontally connected cross sections can be adopted.

Tunnel cross sections fit for the construction condition or tunnel use can be provided efficiently.

3.2.3 *DOT tunneling method*

The DOT Tunneling Method is applied for an earth pressure balance shield machine with interlocking spoke-equipped multiple cutters that are positioned in the same plane to construct tunnels of double or triple cross sections.Adjacent cutters rotate in the opposite directions to avoid touching or smashing one another and are thus controlled synchronously.

Rolling of the shield machine is controlled by component force of thrusting jack by shifting along the circumference of the machine, and rolling control jacks placed on the longer sides of the machine.

The DOT shield machine is equipped with cantilever-arm type erector to erect joint and panel segments, so it provides wide working space.



Figure 5. Horizontal and vertical variation shield method.

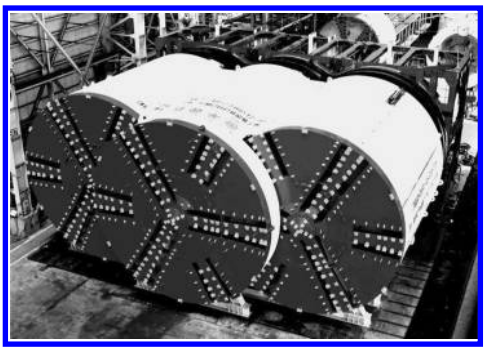


Figure 6. Multi-circular face shield method.

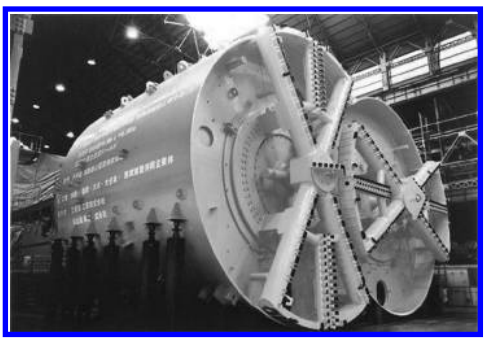


Figure 7. DOT tunneling method.

Copyright © 2005 Taylor & Francis Group plc, London, UK

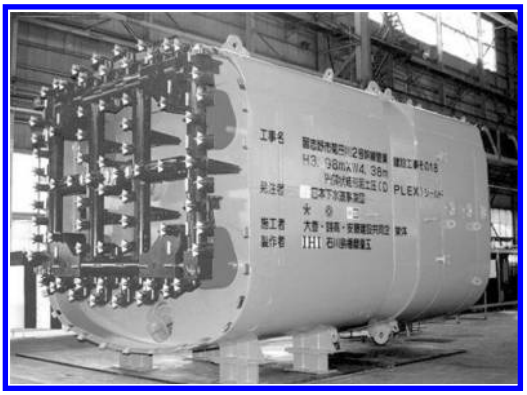


Figure 8. DPLEX shield method.

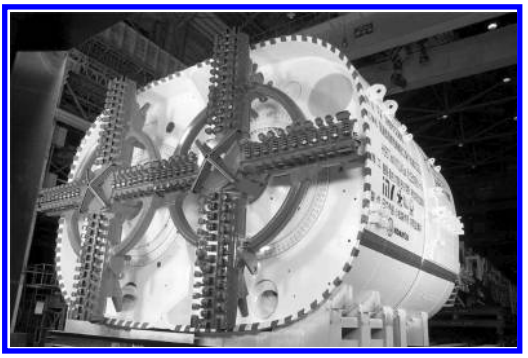


Figure 9. Wagging cutter shield method.

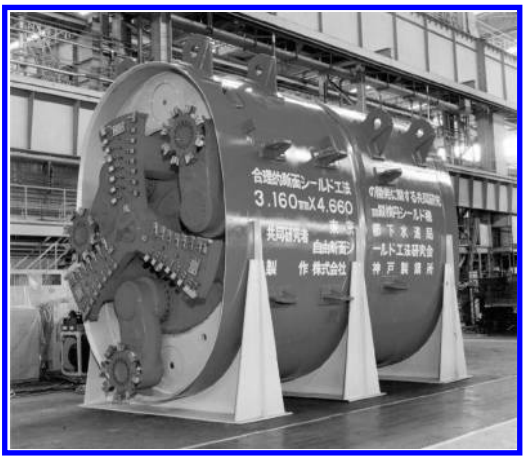


Figure 10. JIYU-DANMEN shield method.

The method provides a more reasonable shape with smaller unnecessary space in the cross section of railway and highway tunnels than circular shield tunneling methods.

3.3 *Non-circular*

3.3.1 *DPLEX shield method*

Supporting the cutter frame eccentrically at the ends of multiple crank shafts, and rotating the shafts in the same direction cause the cutter to move in a circle along the inside perimeter of tunnel cross section and create a cross section with a shape similar to the cutter. It means that this method creates tunnels of any cross section.

To stabilize the face, the EPB method, which has been adopted for circular shield machines and proofed highly reliable, is basically employed.

The cross-roof bit unique to this method enables cutting in all directions with the rake and relief angles being equal to each other.

A cutter with short turning radius requires low torque at the cutterhead. Multiple drive motors can be integrated into a compact unit. Thus, the shield tunneling machine can be assembled, dismantled and transported easily. The advantage is greater for larger shield machines.

A cutter with short turning radius means short bit sliding distance and reduces bit wear. Thus, tunnels can be excavated the length about three times that by conventional machines.

The cutterhead drive motor is small enough to enable full-face soil stabilization from within the shield machine. Soil in curved sections or in the vicinity of the tunnel can be stabilized from within the machine.

3.3.2 *Wagging Cutter Shield Method*

Wagging Cutter Shield Method enables to excavate various cross sections such as circular, multi-circular and rectangular sections by wagging cutter.

Cutters are wagged by reciprocating motion of hydraulic jacks. Thus, the driving mechanism is simple and the weight and length of the tunneling machine can be reduced.

The rotation of the cutters and the expansion and contraction of overcutters are automatically controlled to enable accurate excavation of corners of the cutting face in case of non-circular shape.

Long stroke overcutters, essential to the non-circular wagging cutter shield method, are required to have higher durability and reliability than ordinary cutters. The newly developed high-performance “spike” bit is capable of penetrating and cutting the earth when the overcutter is expanded or contracted, and before and after the cutterhead is wagged.

3.3.3 *JIYU-DANMEN shield method*

One of the major features of the JIYU-DAMMEN Shield Tunneling Method is its capability of excavating tunnels with various cross-sectional shapes such as oval, horseshoe and rectangle.

Adopting “planetary” cutters enables free selection of the tunnel cross sections. The main cutter excavates

Copyright © 2005 Taylor & Francis Group plc, London, UK

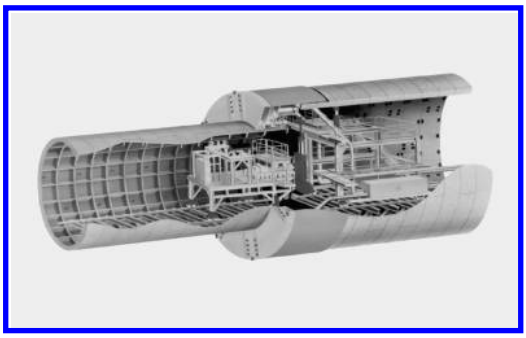


Figure 11. Enlargement shield tunneling method.



Figure 12. Rotating shield method.

the circular section at the center of the face, and the multiple planetary cutters excavate surrounding areas.

The planetary cutters, while rolling themselves, rotate along the perimeter of the rolling main cutter. The orbit of the planetary cutters can be changed freely by adjusting the angle of swing arms attached to them. Thus, various cross sections can be easily created.

Since a horseshoe-shape, oval or rectangular cross-sectioned tunnel can be designed, a large cross-sectioned tunnel may be excavated in the ground which is restricted in width and/or depth.

3.4 *Special technique*

3.4.1 *Enlargement shield tunneling method*

This method allows launching the Enlargement Shield from the launching base at an arbitrary location in an existing shield tunnel and excavates the tunnel longitudinally to enlarge the cross section of the tunnel.

First, base for launching circumferential shield is constructed and the circumferential shield excavates the earth around the existing tunnel. Enlargement shield machine is then assembled in the void created by the circumferential shield. Enlarged tunnel is constructed by the enlargement shield machine which runs outside the existing tunnel along the direction of the tunnel axis.

By the method, cross section can be enlarged for a desired length according to special need. The method offers even greater economy and shorter construction period in tunneling at greater depths.

3.4.2 *Rotating shield method*

The Rotating Shield Method enables to change the direction of the tunnel driving in such a way that spherical part with cutter rotates and launches out of it. It is called Horun. Using similar technique, for long distance driving, cutter bits are replaced inside the machine by rotating the spherical part so that the cutter faces inward. It is called Kurun.

In case of Horun method, excavation is carried out by a single shield machine continuously from the ground surface first driving in the vertical direction then in horizontal for the adit. Separate construction of shaft by d-wall or caissons, which is necessary for conventional shield tunnel, is not required, so it contributes to easier construction, shorter construction period and reduces cost.

Similarly, this mechanism enables a single shield machine to continuously excavates a tunnel, curving horizontally at a right angle. The machine is highly effective in underground spaces below congested intersections or occupied by buried structures where no vertical shaft can be driven for turning the shield machine.

In case of Kurun, the machine is effective in excavating long distances continuously. Cutter bits can be replaced simply by rotating the cutter head. The method has eliminated ground improvement and other measures required by conventional methods. It is especially beneficial for deep tunnel.

3.4.3 *Mechanical shield docking method*

2 machines from both sides are connected mechanically underground without ground improvement and inflow of earth and ground water. One machine equips insert ring and another its receiver.

Docking and dismantling of conventional shield machines has been done in narrow space where the ground was exposed. The Mechanical Shield Docking (MSD) Method enables steel rings to directly support earth and water pressures, and ensures safe and reliable work without exposing the ground.

Docking point can be selected freely without any restrictions of surface traffic or underground utilities. It is possible even under seabed.

The MSD Method causes neither ground settlement nor uplift and involves no surface work, so it has no impacts on surface traffic or the neighboring environment.

The MSD Method requires no auxiliary measures and enables easy mechanical shield docking, so it

Copyright © 2005 Taylor & Francis Group plc, London, UK



Figure 13. Mechanical shield docking method.

achieves a reduction of construction time, compared to conventional methods.

Costs can be reduced because no auxiliary measures for stabilizing the ground and shaft are required.

3.5 *Lining technologies*

3.5.1 *P&PC segment lining method*

The P&PC Segment Lining provides a lining ring of post-tensioned prestressed concrete structure by assembling a segmented concrete ring, giving it tension, and fastening it by inserting a prestressing single strand into the sheath that has already been embedded in the precast concrete segment.

Because an unbonded prestressing strand with low friction loss between the prestressing steel and sheath is used for the prestressing strand, sufficient prestress can be introduced by applying tension to only one position on the whole circumference. Furthermore, by using a combined anchoring device made of cast iron that has the tension side and fixing side integrated into one piece (X anchor) by embedding it in the segment, the reinforcement in the segment can be simplified and buildability of tensioning can be improved.

3.5.2 *Extruded concrete lining method*

Extruded Concrete Lining Method is to construct the lining by in-situ concrete at shield tail instead of precast segment. As the shield advances, fresh concrete is extruded and pressed considering groundwater pressure

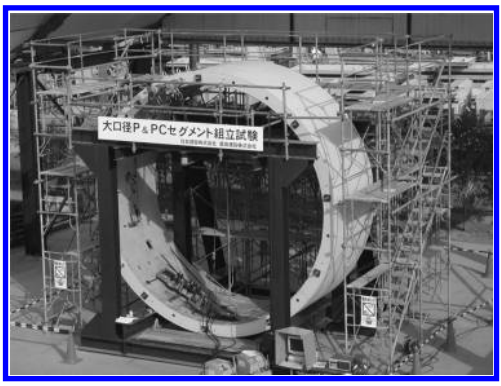


Figure 14. P&PC segment lining method.



Figure 15. Extruded concrete lining method.

and earth pressure in such a way that it prevents loosening of the surrounding earth, and the lining closely contacted to the earth is created.

This method allows flexible choice of lining based on the site conditions, out of reinforced concrete, non-reinforced concrete, fiber-reinforced concrete, steel-reinforced concrete and prestressed concrete.

4 CONCLUSIONS

14 shield tunneling methods registered to the STA were outlined.

Key words describing current Japanese shield tunneling are “deep”, “large diameter”, “long driving”, and “various sectional shape”. It is considered that this trend will continue. The STA intends to play a role for consultation to difficult projects using the 14 registered methods.

Meanwhile Japanese shield tunneling technologies have been mainly applied domestically. The STA considers the technology to be put on the world map and applied for the prime sponsor of ITA. The authors hope that we are contacted to provide the quality of the Japanese shield technologies.

Copyright © 2005 Taylor & Francis Group plc, London, UK

Compact shield tunneling method

Masayuki Matsuura & Setsuo Takaku
Bureau of Sewerage of the Tokyo Metropolitan Government, Tokyo, Japan

Yasushi Nagashima
Taisei Corporation Civil Engineering Technology Promotion Department, Tokyo, Japan

Yoichi Moriya
Obayashi Corporation Civil Engineering Technology Division, Tokyo, Japan

ABSTRACT: "Compact shield tunneling method" is a newly developed shield tunneling system, which is suitable for re-construction of aged sewer tunnels. This method was developed to achieve the targets such as, lower cost, shorter construction period, various construction environment, lower environmental impacts and lower maintenance cost. To achieve such targets, tunnel lining, shaft and mechanical equipment, are scaled down as much as possible.

1 INTRODUCTION

In Tokyo Metropolis, the rehabilitation and renewal of sewer systems is an urgent issue due to the aged sewers and increases in wastewater and stormwater runoff. Generally, shield tunneling confronts various problems, such as high construction costs, adverse effects on living environments, and densely used surface and underground spaces. Based on such backgrounds, the authors developed a new shield tunneling method, which is called the "Compact shield tunneling method" that is effective for constructing such main sewers. This paper describes the outline of this newly developed tunneling method and reports the actual execution on site.

2 OVERVIEW OF THE COMPACT SHIELD TUNNELING METHOD

The new shield system was developed based on the principal concept of minimizing both the sizes of linings to be set and the scales of the shafts and facilities during construction, and is called the "compact shield" system. This "Compact shield tunneling method" includes following technical elements.

(1) Integrated segment with grooved inner lining: Segmental lining consists of four segments. And these four segments will form three-hinged ring structure, which is structurally stable. Factory fabricated segments are united with secondary lining inside and have a ditch at the invert (Figure 1).
(2) Double articulate shield machine with integrated back-up facilities: Back-up facilities are located in the shield machine and not in the tunnel. Enough working space can be arranged in the tunnel. It contributes efficiency of the works and safety of the site. Also the shield machine is designed to be divided into three bodies and easily re-used at next projects (Figure 2).
(3) Tire-type transporting system with guide: There are no rail and sleeper inside tunnel. Instead of rail, new transportation system is used. With this

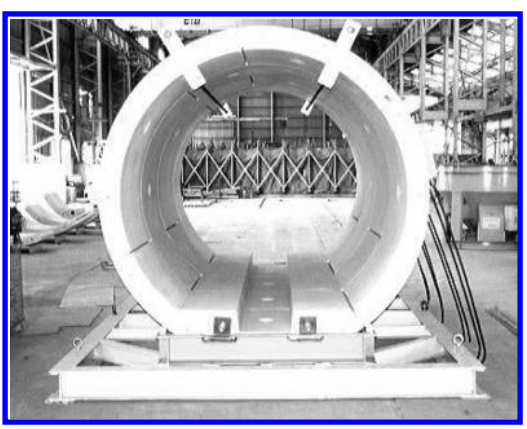


Figure 1. Integrated segment with grooved inner lining.

Copyright © 2005 Taylor & Francis Group plc, London, UK

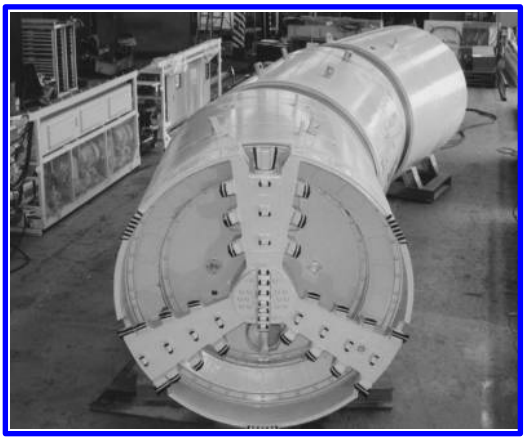


Figure 2. Double articulate shield machine with integrated rear facilities.



Figure 3. Tire-type transporting system with guide.

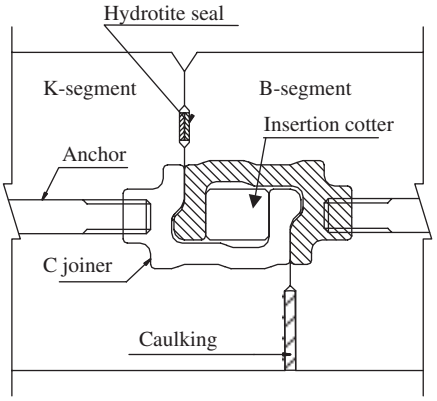


Figure 4. Firm joint.

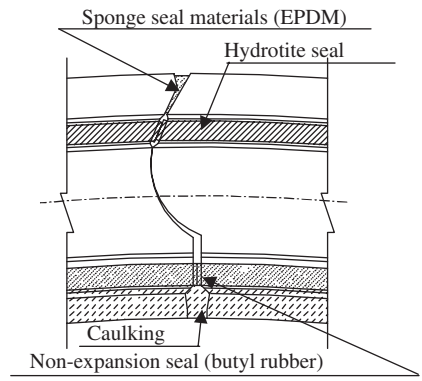


Figure 5. Structure of the knuckle joint.

new transportation system, trucks using for transportation of segments or excavated muck is guided with guide roller at the invert ditch, and steering is not necessary (Figure 3).

2.1 *Development of the segments*

2.1.1 *Smoothness of the inner surface*

The smoothness of the segment inner surface was ensured by adopting the joint structure that does not expose joint metals on the inner surface and applying caulking on the joints.

(1) Segment joint

To firmly connect Segment B and K, a horizontally inserting cotter-type structure was developed (Figure 4). The structure is assembled by inserting the C shape joint metal and then a wedge. The structure enables easy vertical adjustment and connection insertion of the K-segment inserted in longitudinal direction.

Knuckle joints, which give satisfactory results in precast materials, are used for the hinges (Figure 5). This structure cuts off water with its hydrotite seals around the knuckle joints and non-expansion seal and inner joint caulking applied along the inner edge of the inner lining even when the knuckle joints rotates. Hard sponge seal materials (EPDM) that were molded in the form of the gap are applied along the outer edge of the knuckle to prevent the back filling and soil from clogging into the gap along the outer edge.

(2) Circumferential joint

Circumferential joints are being developed, so as to have the standard form of rotary joints (Figure 6). As inserting the male fittings, the divided metal washers in female fittings are shifted by the flat springs and fit

Copyright © 2005 Taylor & Francis Group plc, London, UK

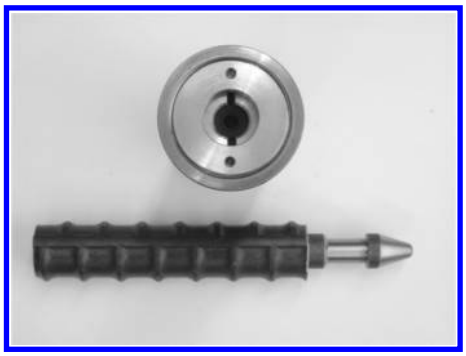


Figure 6. Rotary joints.

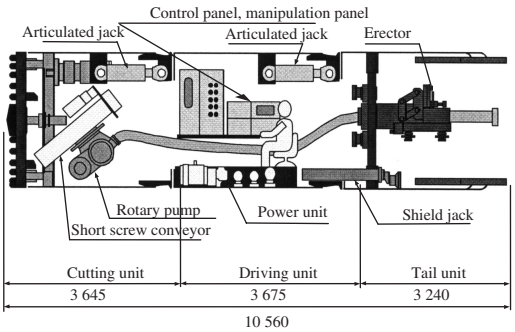


Figure 7. Outline of the shield machine and its integrated rear.

to the small diameter portion of the male fittings, and then the joints will resist the drawing force.

2.1.2 *Durability of the segment*

Installation of the sections (inner lining) that are not evaluated as lining structures inside the segments enables future repair works. The thickness of the inner lining was decided to be at least 50 mm by considering the carbonization depths derived from various carbonization equations (maximum value of 47 mm) and the working performances of replacing concrete for future repair works (approximately twice the size of the aggregate of the maximum diameter).

The flat invert section of the segment can be utilized as the pass for inspecting the sewer and provides a sewer shape that is likely appropriate for future mechanical and automated maintenance works. Addition of such a performance that enables efficient maintenance works to new sewers improves the durability of the sewer throughout its life cycle.

2.1.3 *Reducing the number of segment per ring*

To improve the economic performance by the use of the three-hinged structure and the reduction in the number of segment pieces, each segment should be divided into three pieces. However, the segments are thick since the inner lining was integrated, it may be very difficult to transport the segment pieces and to secure spaces for assembling the pieces. Therefore, a segment ring was decided to have three hinges and one rigid joint to both reduce the number of pieces and secure the statically determinate structure. Each segment ring is constituted by I-segment, which has an invert, and A-, B- and K-segments.

2.2 *Development of the shield machine*

The compact shield tunneling method installs large and thick segments, since a ring is divided into a small number of segments and the inner lining is integrated. The back-up facilities may impede the construction works. Various studies were conducted, and the problem was decided to be solved by extending the shield machine for one block to the rear side and integrating the back-up facilities within the machine.

The shield machine, which is long due to the extended block, was divided into three parts. Since each segment can separately start and be retrieved, it is possible to reduce the size of starting and arrival shafts.

2.2.1 *Double articulate shield machine with integrated back-up facilities*

An earth and mud pressure shield machine that can be separated into the cutting, driving, and tail units was developed (Figure 7). The cutting and driving units are equipped with articulated jacks and can negotiate sharp curves of R = 15 m.

(1) Cutting unit

The length of the cutting unit was reduced by adopting a short screw conveyer. The soil discharge system is connected to a rotary pump and pressure pumps the soil outside the shield machine. It is possible to precisely control the earth pressure at the cutting face by controlling the rotations of the screw conveyer and the rotary pump.

(2) Driving unit

The driving unit is equipped with facilities that are usually installed at the trailing cars, such as the power unit and control panels.

(3) Tail unit

The tail unit is equipped with the shield jacks and erectors.

2.2.2 *The mechanisms for assembling segments*

An erector and a segment feeding device were developed to enable the assemblage of large segment pieces.

The erector was modified by slightly moving the rotation center upward. A two-step lifting system that

Copyright © 2005 Taylor & Francis Group plc, London, UK

combines the link and slide mechanisms was developed to secure a lifting stroke of approximately 600 mm. These mechanisms enable large segment pieces to be lifted, rotated, and moved in tight spaces.

To feed large segment pieces from segment wagon to the position of erection, segment feeding rollers and segment feeding tables were developed.

2.3 *Development of the transportation systems*

A rational method was developed for transporting machines, tools, and materials, within tunnels by utilizing the characteristics of segments with invert.

2.3.1 *Entire composition*

The entire composition of the system consists of two segment wagons, one motor wagon, and five soil wagons, assuming to discharge soil on wagons. The system can transport the amount of soil that is excavated during the installation of one ring in one cycle.

2.3.2 *Tire-type non-steering transportation system with guide rollers*

A tire-type non-steering transportation system with guide rollers was developed, which moves along the invert groove at the bottom of the segments. The transportation wagons were installed with horizontal tire guide rollers so as to automatically drive along the invert groove.

3 EXPECTED EFFECTS

The implementation of the new compact shield machine is likely to produce the following effects. Here, the effects were calculated using the verification work that is described in Section 4 of this paper as a model, which was to construct a sewer of a finished inner diameter of 2,000 mm.

(1) Cross section

The outer diameter of the segment for constructing a finished inner diameter of 2,000 mm is reduced from 2,750 mm to 2,300 mm. This reduction decreases the excavation cross sectional area and the amount of soil to be excavated by 25% (Figure 8).

(2) Shaft space

The length of a starting shaft is reduced from 8.3 m to 5.6 m. The area of the shaft is reduced by 32%. The size of arrival shaft smaller than the starting shaft is sufficient for recovering the shield machine.

(3) Construction process

It is possible to eliminate the process of constructing the secondary lining. An estimation using the verification work model showed a reduction of approximately 47% in days necessary for constructing the shield tunnel section, from conventional 292 to 155 days.

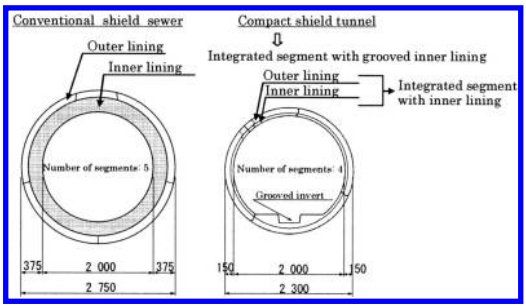


Figure 8. Cross sections of a conventional shield sewer tunnel and a compact shield tunnel.

(4) Economic performance

Reduced cross sectional area, reduced shaft spaces, and reduced construction periods are likely to result in reductions in cost.

(5) Environmental impacts

Reductions in both shaft space and construction periods minimize impacts on peripheral environments during construction. Reduction in excavation cross sectional area reduces the amount of discharged soil and the resultant environmental load for treating the soil. The amount of concrete is reduced since the lining is thin. Reuse of the shield machine reduces the amount of materials, such as steel, and wastes produced by disassemblage of the machine. The reduction in such materials reduced the amount of CO_2 emission otherwise produced.

4 RECENT CONSTRUCTION PROJECT

4.1 *Overview of the construction project*

The construction project aimed to enhance the capacity and renovate the deteriorated pipe section, at which main branches merge in Ojima 4 and 5-chome, Koto Ward, into a pipe of 2,000 mm in inner diameter using the compact shield method. This is the second project that uses the compact shield method following the reconstruction project in Misuji 3-chome and Torigoe 2-chome, Taito Ward. The same shield machine used for the previous project was used.

Project name: Reconstruction project near Ojima 4 and 5-chome, Koto Ward
Site of construction: Ojima 4 to 5-chome, Koto Ward, Tokyo
Owner: Bureau of Sewerage of the Tokyo Metropolitan Government
Constructor: Obayashi-Omoto Joint Venture
Period of construction: January 2003 to July 2005
Content: Compact shield tunneling method

Copyright © 2005 Taylor & Francis Group plc, London, UK

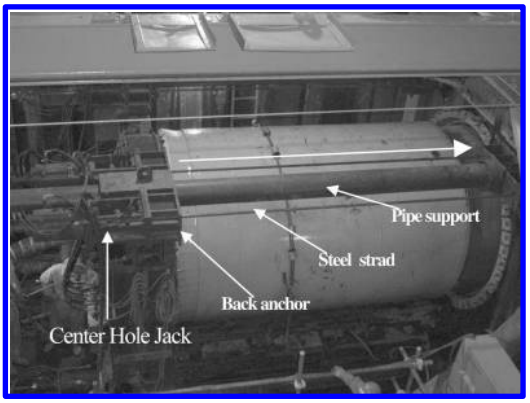


Figure 9. The Center Hole Jack Method.



Figure 10. Injection hole plugs with inserts.

Length of the tunnel to be constructed: L = 1,389.3 m
(1,203.9 m + 185.4 m)
Outer diameter of the shield: 2,430 mm
Outer diameter of the segments: 2,300 mm
Inner diameter of the finished pipe: 2,000 mm
Overburden: 8.0 to 8.9 m
Gradient: 0.2 to 0.29%
Minimum radius of curve: R = 30 m.

4.2 *Geology and locational conditions*

The site is located at the southeastern part of Tokyo, and is in the zero-meter area called Koto Delta. The soil to excavate using the shield machine consists of soft silt layers of about N = 0 to 3. There are a large-scale housing complex and commercial and quasi-industrial districts near the site; and the Ojima-chuo Ginza Street, where the starting shaft faces, is busy.

4.3 *Characteristics of the project*

This project uses the principal element technologies of the compact shield method described above and the following new technologies.

(1) Starting method
The compact shield machine was decided to be started separately in principle. "The Center Hole Jack Method" (Figure 9) is used to improve the excavation efficiency at initial excavation. With the method, measures for preventing the machine from moving back ward while jacks are resetted and installation and removal of struts became unnecessary.

(2) Segments
"Rotary joints", "injection hole plugs with inserts" (Figure 10), and "Sea-caulk" (Figure 11) were decided to be used for the first time throughout the entire section, as circumferential joint , injection hole plugs, and joint-filling compound of the setting type, respectively.

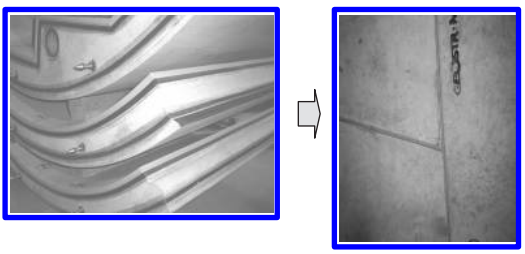


Figure 11. "Sea- caulk".

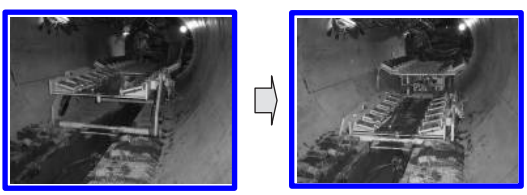


Figure 12. "Segment lifter".

(3) Segment supply method
Segments were decided to be supplied from a segment wagon to the segment feeding roller installed on an invert using an ordinary electric hoist and also a "segment lifter" (Figure 12) to lift and transport segments.

(4) Power supply method
The longest span in this project is 1,204 m, which is very long for a compact shield project. Power supply through low voltage cables, which were used in the previous project, was not applicable. Drops in voltage would be so large that it wakes construction difficult. Instead, a "high voltage transformer on a rear bogie" (Figure 13), which supplies power through high-voltage cables, was decided to be used after comparing the economy of candidate methods.

Copyright © 2005 Taylor & Francis Group plc, London, UK



Figure 13. "High voltage transformer on a rear bogie".



Figure 14. Completed tunnel.

4.4 *Progress of the project*

4.4.1 *Entire project*

The shield started in end October 2003 and completed excavating the 1,203.9 m section of the upstream side (western side) in mid June 2004. The shield machine was lifted from the arrival shaft, and is now being serviced to excavate the 185 m section of the downstream side (eastern side). The machine will start in February 2005.

4.4.2 *Separate starting using the Center Hole Jack*

The Center Hole Jack method was used for the first time to start a compact shield. The results of the use are described below.

(1) Operation principles of the Center Hole Jack

The operation principles of the Center Hole Jack involve releasing of the two chucks in front and behind the jack and closing the chucks to advance 200 mm each stroke. With this method, measures for preventing the machine from retrogressing while jacks are resetted replaced become unnecessary, and the working period is reduced.

(2) Results of construction

The data while the machine started show slight fluctuations, but the total driving force of the jack never exceeded 800 kN to drive the front body, 1,900 kN to drive the middle body, and 2,100 kN to drive the rear body. The earth pressure at the face was gradually raised to 0.11 MPa, which was the target pressure for the section where the ground had been improved to protect the cutting face, and the pressure was maintained even after the shield machine advanced through the natural ground.

The total driving force of the jack temporarily dropped at around 2,600 mm stroke length likely because the machine passed through the ground section that had been improved for cutting face protection. The driving force gradually increased thereafter because the propelling speed and the frictional resistance between the shield machine and the ground increased.

The results show that the method used to start the shield machine is as effective as ordinary earth and mud pressure shield machine in controlling earth pressure. The direction was also well controlled, and the shield drew the provided line. In respect to cycle time, it took 12 days from the setup of the cutting face to the completion of starting the rear body of the shield machine (including connecting the bodies). Since this method does not need to perform large-scale replacement works, such as charging rear wagons and demolishing temporary segments, this method is safe and is simpler than ordinary methods used for initiating shield excavation.

5 CONCLUSION

The third project of the compact shield tunneling method was ordered and is under preparation. The compact shield machine was designed to be used for three projects. Final evaluation of the method, including cost evaluation, will be performed using also the results of the next project. Up to present, the method reduced the costs by 8% as initially planned. In the next project, soil is planned to be transported using pressure pumps. The compact shield tunneling method will be further improved to establish a rational system that meets construction conditions.

REFERENCES

Maeda, M., Kushiyama, K. 2001, August. Development and practical use of compact shield tunneling system, Bureau of Sewerage, Tokyo Metropolitan Government, Sewerage rehabilitation project at Misuji-Torigoe Street. Tunnels and Underground, Vol. 32, pp. 55–63.

Copyright © 2005 Taylor & Francis Group plc, London, UK

Continuous tight curved belt conveyor of R30 m did a TBM drift excavation a lot of good-Shimizu No.4 Tunnel on 2nd Tomei Expressway

M. Noda & Y. Inoue
Obayashi Corporation, Shimizu No.4 Tunnel Construction Office, Shizuoka-shi, Shizuoka, Japan

T. Fujita
Japan Highway Public Corporation, Shizuoka Construction Bureau, Shizuoka-shi, Shizuoka, Japan

K. Akiyoshi
Obayashi Corporation, Civil Engineering Technology Division, Minato-ku, Tokyo, Japan

ABSTRACT: Authors of this paper report a 3,570 m-long TBM drift excavation with the continuous tight curved belt conveyor mucking system on twin 3-lanes tunnels for the first time in the world. This system was applied to 30 m radius with 180-degree U-turn section of in this site. TBM mucking from TBM body to temporary disposal area at portal was executed successfully with originally aided following outcomes. (1) Safety improvement due to single track utilization. (2) Working environmental improvement without muck car traffic. (3) Turbid water treatment plant downsizing due to easy separation of large fresh and turbid groundwater. (4) Construction period saving and cost reduction.

1 PROJECT OVERVIEW

Japan Highway Public Corporation is now constructing the Second Tomei Meishin Expressway with a total length of 502 km from Tokyo to Kobe, as an effort to develop a network of expressways covering the Pacific side of Japan. Shimizu No.4 Tunnel on 2nd Tomei Expressway is located at about 7 km northwest of the existing Tomei Expressway Shimizu Interchange. This tunnel consists of about 2,160 m up- and down-bound lines of 3-lanes, each having an inner cross section of about 180 m^2.

"TBM Drift Advancing and Enlargement Excavation Method" was used to excavate a total length of 3,560 m (see Figure 1). A top drift was first excavated from the eastern entrance (Tokyo side) of the down-bound line by using a 5.0 m-diameter TBM. At the point of 100 m before the western entrance (Nagoya side), TBM made a U-turn with a radius of curvature R30 m and changed its direction 180-degree to excavate the up-bound line. A curved belt conveyor was applied to remove muck continuously over a long distance from TBM body to tunnel exterior, although application of curved belt conveyors to tight curves has been considered to be difficult so far.

2 GEOLOGY

Shimizu No.4 Tunnel is geologically situated in the Shizuoka Group, consisting mainly of Neogene Miocene sedimentary rocks, on the eastern side of the Itoigawa-Shizuoka Tectonic Line. The uniaxial compressive strengths of the rocks are relatively high (50 to 170 N/mm^2) as Neogene sedimentary rocks. The bedrock consists of sandstone, gravel, and mudstone,

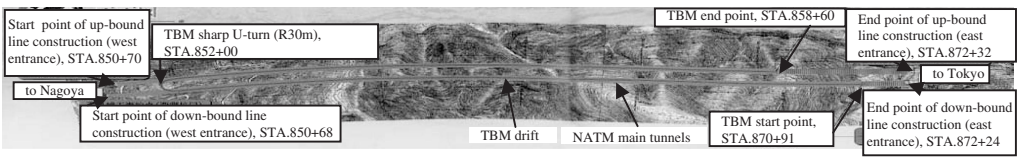


Figure 1. Shimizu No.4 Tunnel plan view.

Copyright © 2005 Taylor & Francis Group plc, London, UK

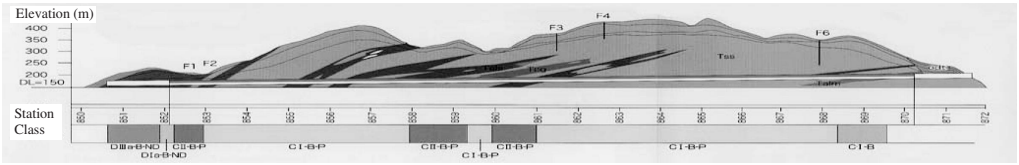


Figure 2. Up-bound line geological profile.

while sandstone is by far dominant in the tunnel section. The sandstone infrequently intercalates mudstone and gravel layers with thicknesses of 5 to 200 cm and thus consists of alternate layers in the entire tunnel section. Fresh sandstone is massive, hard and are resistant to weathering, whereas mudstone frequently contains fissures and is prone to weathering. Gravel layers are also massive and resistant to weathering like the sandstone layers. A geological profile of the up-bound line is shown in Figure 2.

3 MUCKING SYSTEM

3.1 *Initial plan and problems*

When a TBM tunnel makes a sharp U-turn of R30 m, as is the case with Shimizu No.4 Tunnel, muck cars on tracks are generally used. The most important challenge was treatment of groundwater inflow during TBM excavation because this tunnel is 2% down grade from the eastern to western entrance and groundwater inflow of 7 m^3/min was initially expected. In drainage planning, turbid water generated at the face had to be separated from fresh groundwater at already excavated areas, and drained outside. Also, equipment to cope with sudden groundwater inflow had to be installed in the tunnel. To achieve above purposes in consideration for safety, environment and workability in the tunnel, a continuous curved belt conveyor was applied instead of conventional steel muck cars originally planned.

3.2 *Continuous belt conveyor technology*

3.2.1 *Present status in Japan*

In Japan, continuous belt conveyors were first introduced into TBM tunneling and are now being used also for mountain tunneling. It is now found mostly on new Shinkansen lines and, in other cases, on waterways. This trend may be caused by difficulties in the use of dump trucks for mucking in tunnels with relatively small widths.

3.2.2 *Development of tight curved continuous belt conveyors*

Conventional continuous belt conveyors had a minimum radius of curvature R150 m roughly. Obayashi Corporation firstly started to develop the conveyor with a minimum radius of curvature R40 m and conducted a demonstration test in June 1999 at the company's Osaka Machine Shop to confirm the conveyor operation (see Photo 1). As a notable feature of this test machine, variable trough carrying idlers were developed and this allowed to vary the belt shape in optimum according to the curvature radius.



Photo 1. Demonstration test of a continuous curved belt conveyor for R40 m.

3.3 *Development of continuous belt conveyor for tight curvature*

3.3.1 *Comparison with conventional mucking method*

Although the application of continuous belt conveyors to TBM tunneling is not rare any more on 2nd Tomei Meishin Expressways, its application to radius of curvature R30 m, planned in this TBM drift, has been a challenge because conventional mucking method is used for previous Shimizu No.3 & No.1 Tunnels in similar condition. We considered adopting a continuous belt conveyor in view of its advantages of safety and environment while pursuing its technological development, and finally decided to apply it at this drift (see Table 1 and Figure 3).

Copyright © 2005 Taylor & Francis Group plc, London, UK

Table 1. Comparison of mucking methods.

Item	Steel muck car method		Continuous belt conveyor method	
Environment	– Although better than tire method, noise and vibration occur in the tunnel because of frequent muck cars traffic.	△	– Although rail cars are used for material delivery, more advantageous because traffic is much less frequent than muck car method.	○
Safety	– There are safety problems because a separate safety walkway is not affordable with 5 m-diameter tunnel.	△	– A safety walkway is affordable except those areas where drainage tanks are installed. – Mucking equipment, rail facilities and a safety walkway can be installed separately.	○
Economics	– In case of straight tunnel, continuous belt conveyor method is more economic than muck car method. When a curved section is included, continous belt conveyor method is still more economic in view of depletion expenses excluding development cost and equipment reuse.			
Period	10 months	○	10 months (including preparation)	○
Problems	– Separation of turbid and fresh groundwater, which is important for minimizing turbid water treatment capacity, is difficult because of reason below: If there is a certain amount of groundwater inflow, relay tanks to separate turbid water need to be installed at 250 m intervals. That the tunnel space allows only a single track near tanks poses serious restrictions on muck car operation and safety management.		– There has been no previous attempt of applying a continuous belt conveyor for a curve of R30 m in Japan or abroad. – Maintenance is very important because excavation may have to be stopped completely in case of failure in belt conveyor system.	
Evaluation	– Under this tunnel condition, there are problems regarding groundwater inflow and operation management.	△	– Excels in groundwater inflow measures, safety and working environment.	○

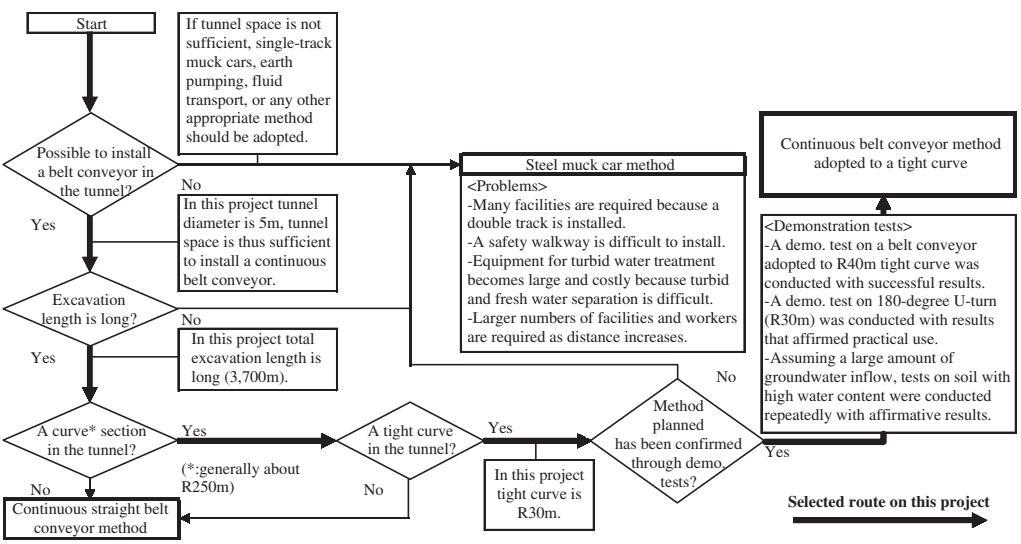


Figure 3. Flowchart of selecting mucking method.

Copyright © 2005 Taylor & Francis Group plc, London, UK

3.3.2 *Demonstration tests for 180-degree U-turn (R30 m)*

The continuous belt conveyor system for the demonstration testing of 180-degree U-turn (R30 m) was developed cooperatively by Obayashi Corp. and Taguchi Industrial Co., Ltd. The major challenge was to continuously connect the curved and straight conveyor sections. An actual system was assembled and its operational status was studied through demonstration tests (see Photo 2):

- First demonstration test in July 2001
- Second demonstration test in September 2001 (after improvement)

Test results indicated that this system was feasible, so it was introduced to this drift excavation.



Photo 2. Demonstration test of a continuous curved belt conveyor for R30 m.

Table 2. Features of R30 m continuous curved belt conveyor

Portion	Features
Belt	– Standard flat belt, strength 80 N/mm^2 (normally 60 N/mm^2)
Carrying side structure	– Belt is concaved in appropriate U-shape by using carrying idlers. – Carrying frame is tilted to reduce difference between inner and outer radii.
Return side structure	– Belt is kept upright so that inner and outer radii are the same.

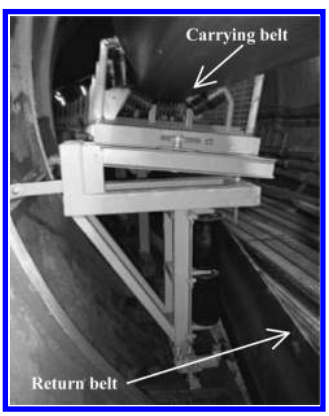


Photo 3. Curved belt conveyor in operation (frontal view).

3.3.3 *Features of developed system*

Main features of the continuous curved belt conveyor developed are shown in Table 2. As shown in Photo 3, the most conspicuous features of this system are trough shape of the carrying belt (upper side) and upright direction of the return belt (lower side).

4 TBM DRIFT ADVANCEMENT

4.1 *TBM specifications*

TBM applied in this drift is of 11.2 m-long closed shield type, reused as a third time, and can be articulated at its front, central, and rear portions by an angle of 6-degree each.

4.2 *Equipment in the drift*

Arrangement of temporary facilities in the drift is shown in Figure 4. These facilities do not differ significantly between the straight and U-turn sections. To operate the continuous belt conveyor smoothly, dedicated equipments were installed as follows.

4.2.1 *Turnover train*

When the tail of TBM back-up train is about to enter U-turn section (the face is 80 m ahead), a turnover train is added to the tail. This train, situated at the forefront of the belt, keeps the belt shape in stable by

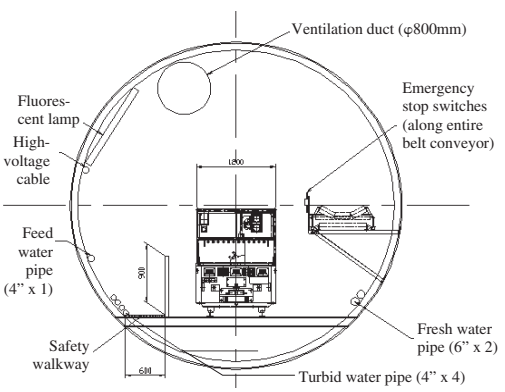


Figure 4. Temporary facilities installed in TBM drift.

Copyright © 2005 Taylor & Francis Group plc, London, UK

finely adjusting orientation, angle, height, and other aspects of the upper side carrying belt. This train changes the returned belt direction from upright to horizon and sends the back-up train back the belt.

When the tail of TBM back-up train is about to exit U-turn section (end point of the continuous curved belt conveyor), the turnover train is disconnected because it is no more needed.

4.2.2 *Return belt uprising and put-down devices of fixed type*

Return belt uprising device of fixed type is installed at the same time as the turnover train installation. This device changes the returned belt direction from horizon to upright only within U-turn section. During U-turn section advancing, returned belt is kept upright between this device of entrance side (see Photo 4) and another device on turnover train. When the train tail is about to exit U-turn section (when turnover train is removed), another return belt put-down device is installed at the end of U-turn section. Returned belt is kept upright between these devices on entrance and face sides of U-turn section until completion of the TBM advancing.



Photo 4. Return belt up-rising device (entrance side).

4.2.3 *Booster drive units*

When a continuous belt conveyor is extended by a certain length, power of main drive unit installed outside the tunnel becomes insufficient for operating the entire conveyor system. A booster drive unit is thus required to compensate for this insufficiency. This unit was installed when back-up train tail reached the critical length of 2,000 m from main drive.

5 CONSTRUCTION OF TBM DRIFT U-TURN SECTION

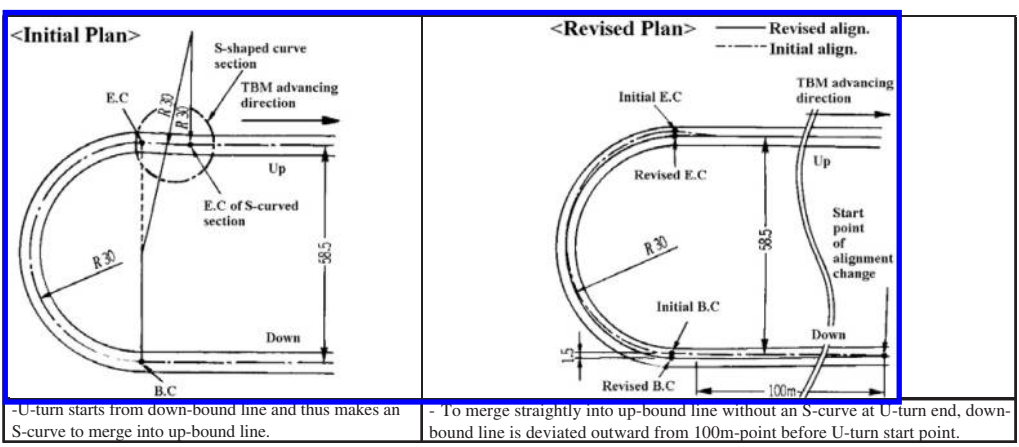
5.1 *Alignment control*

Alignment control is important when installing a continuous curved belt conveyor, because carrying frame installation may face difficulties if TBM does not advance along a line of nearly uniform curvature. Alignment control method adopted is described below.

5.1.1 *Horizontal alignment change*

Distance between centers of the up- and down-bound lines is 58.5 m, compared to 60 m diameter in U-turn section (R30 m); this means a compensation of 1.5 m length is needed. Initial plan was to make compensation by introducing an S-shaped curve section at the end of the curve (EC). When operating the continuous curved belt conveyor in this arrangement, however, the belt is very likely to deviate because belt tension in this section changes abruptly from originally inward to outward directions. Horizontal alignment was thus redesigned.

After discussions, a revised plan was made (see Figure 5). Original S-curved section is thus cancelled



-U-turn starts from down-bound line and thus makes an S-curve to merge into up-bound line.

- To merge straightly into up-bound line without an S-curve at U-turn end, down-bound line is deviated outward from 100m-point before U-turn start point.

Figure 5. Horizontal alignment plans.

Copyright © 2005 Taylor & Francis Group plc, London, UK

and U-turn section is shortened by 13 m. This contributes to reducing construction period by eliminating the preparatory work and excavation time for this S-curved section.

5.1.2 *Pilot survey boring*

To allow TBM to advance though the sharp U-turn section, drift needs to be enlarged to ensure sufficient clearances between TBM and drift wall. If U-turn section is situated in a rock mass prone to collapse, TBM advancing according to the planned alignment may become difficult because of the clogging of debris into TBM.

This problem is critical to this project because continuous curved belt conveyor system is applied. To make a precise U-turn in preferable conditions as much as possible, continuous core sampling by the percussion wire-line boring method was carried out before U-turn excavation.

Results of 130 m-long boring revealed the presence of a lot of weathering and conglomeratic fractured rock in the initially planned location. Start point of the U-turn section was thus shifted by 5 m short of initial plan toward entrance (eastern side).

During TBM advancing, 10 m-long collapse zone of about 70 to 100 cm in height has appeared in the middle of U-turn section.

5.1.3 *TBM alignment control method*

Surveying for TBM advancing is typically conducted repeatedly by using a gyroscope during day shift and night shift every day. The gyroscope can be used only for roughly guiding excavation; if TBM is laterally translated without changing its orientation, the machine's departure from the alignment cannot be detected until the next run of surveying. Surveying must be done frequently in particular in U-turn section for alignment control. In this project, a precise surveying system that requires less assistance was adopted for TBM alignment control. Three prisms (providing absolute positions from TBM center) are installed on TBM rear portion. This system indicates TBM position in real time by measuring the positions of two prisms with an electro-optical distance meter installed on drift roof behind TBM.

Measured data (planned horizontal alignment, TBM position relative to vertical alignment, and various machine data) are constantly displayed on the monitor installed in front of the TBM operator's seat.

5.2 *Problems in construction*

As TBM back-up train passes the BC point, the continuous curved belt conveyor is extended in parallel with TBM advancing. Carrying frames to support the belt mainly in the curved section are attached after advancing TBM by the length of the frame (3 m) plus

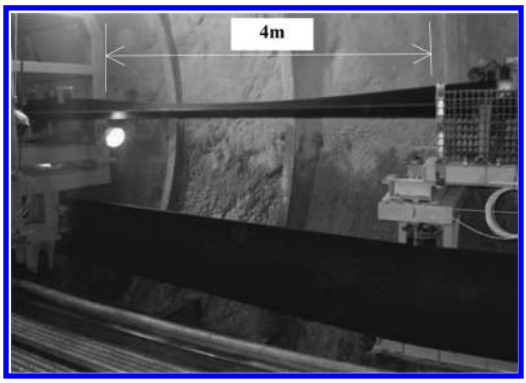


Photo 5. Unsupported belt section between back-up train tail and carrying frame.

1 m. Belt is unsupported between return belt up-rising device installed on the train tail and the already installed carrying frame (see Photo 5). Belt is subjected to significant inward tension in the curved section, and the possibility of belt deviation becomes very high when unsupported belt length becomes 4 m or more. Excavation was thus halted at this point to attach an additional frame, and belt is extended sequentially.

A belt conveyor frame in straight section can be attached easily by one worker. In contrast, about one hour was required to attach a frame in the curved section because of its heavy weight (95 kg/ea.). Maintenance activities such as checking, greasing and bolt tightening are very important because of the constant inward tension on the belt. During operation of the continuous curved belt conveyor, machinery members inside the belt are subjected to stress and its checking is required in view of safety. To maintain the belt conveyor performance, those members were checked while carrying frames are installed and belt conveyor was stopped in dayshift and night shift.

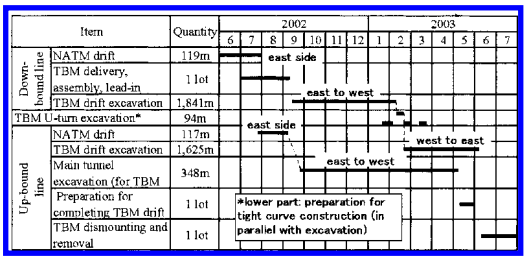
In the future, workability can be improved by reducing weight of members to shorten belt conveyor extension time and reducing number of members to shorten maintenance time.

5.3 *Excavation of U-turn section*

Excavation of the U-turn section was started on February 7, 2003. The BC point was set to the 1,960 m point of tunnel distance on the basis of the results of probe head boring. One stroke length was initially set to 500 mm, but TBM advanced straightly and derailed. The length was thus reduced to 400 mm, 300 mm, and finally 250 mm. As a result, U-turn section with a radius of curvature R30 m was completed, although the track shifted 1.5 m westward from initial plan.

Copyright © 2005 Taylor & Francis Group plc, London, UK

Table 3. Time schedule of TBM work.



6 EXCAVATION OF ENTIRE TBM DRIFT

TBM started to advance on September 9, 2002 and successfully completed its excavation on June 18, 2003 (see Table 3).

Front down-bound line was excavated while conducting advance drainage boring because the line had a down slope and a large amount of groundwater inflow was expected. As much as 400 L/min of inflow was observed in some drainage boreholes, but inflow from the face was about 100 L/min at the maximum.

If usual muck cars are used in latter up-bound line excavation, the numbers of muck cars and workers may need to be increased because of the extended length of transport and decreased speed of muck cars in the curved section. By introducing the continuous curved belt conveyor, the entire drift could be excavated at constant rate by the same number of workers, as if using a continuous belt conveyor for mucking in a straight section. Safety was improved and burdens on workers were lessened, because there was no complicated operation of mine cars exchange and no switch point installation or operations, and because construction was conducted solely on a single track.

As for the construction of the entire TBM drift, a maximum daily driving of 48 m and a maximum monthly driving of 576 m were achieved in spite of the increase of poor rock mass sections (DI class) than initial design and the involvement of belt conveyor extension. By applying this system developed, turbid water tanks could be installed easily (conventionally when excavation was stopped), and the time required to separate turbid water from fresh water was reduced. Also, workers could concentrate on the face in an improved environment because noise and vibration caused by muck cars were eliminated. As a result, excavation was completed about one month ahead of the schedule.

7 CONCLUSION

A continuous belt conveyor was applied to excavate TBM drift along a tight curve (R30 m, 180-degree U-turn) and expected goals were achieved. Safety improvement and efficient construction were enabled by adopting this new technology. In addition, physical and mental burdens on workers were reduced by improving the working environment both inside and outside the tunnel.

The scope of applying continuous belt conveyors has been widened by our success in the construction of a tight curve with a radius of curvature R30 m. Our approach can be applied to various construction works in future:

(1) Mucking equipment in urban deep underground construction.
(2) Application of above equipment to flexible alignment.
(3) Tight curved shield tunneling in urban areas.
(4) Disposal soil transport tunnels under road.

Copyright © 2005 Taylor & Francis Group plc, London, UK

Study on the deformation and load bearing capacity of TBM shield tunnel lining in fire

Hitoshi Tajima & Masahiko Kishida
Metropolitan Expressway Public Corporation, Japan

Toru Kanda
Nippon Civic Engineering Consultant Co., Ltd., Japan

Takeshi Morita
Shimizu Corporation, Japan

ABSTRACT: This paper describes the result of fire test with specimens of the same size as actual segment and the numerical analysis to reproduce the behavior of specimen during the test. The design load for the crown or spring line of actual tunnel is introduced into the specimen. The numerical analysis is executed many times to simulate the time history of deformation behavior and load bearing capacity of the specimens. This analytical technique consists of heat conduction analysis and nonlinear thermal stress analysis.

1 INTRODUCTION

In recent years there have been many cases where the secondary lining of shield tunnels has been omitted to reduce cost. However, with this type of structure the segments are directly heated in a fire, and there is concern that this will affect the structure of the tunnel. The authors have therefore carried out various investigations into the relative fire resistance of shield tunnel segments without a secondary lining. It is known that the fire resistance of RC segments is greatly affected by explosive spalling of the concrete, and that the characteristics of the spalling are affected by the stress conditions of the concrete. As shown in Figure 1, the stress conditions in a tunnel lining vary with position; near the crown there is sagging bending moment and near the spring line there is hogging bending moment. Here we report the results of tests in which the various parts of a tunnel cross-section were heated while being subjected to design cross-section loads. In particular, fire tests were carried out to determine the segment deformation behavior, and elasto-plastic thermal stress analysis was carried out to simulate the behavior of the test specimen during the test.

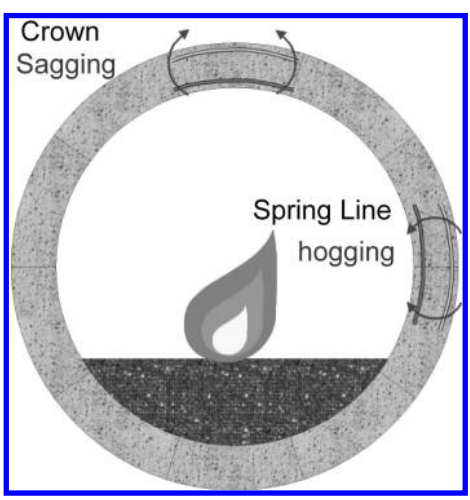


Figure 1. Cross sectional load in lining.

2 TESTING PROCEDURE

As shown in Figure 2, the RABT curve is adopted as the time-temperature curve. Figure 3 shows the dimensions and loading method of the test specimens, the thickness of which are the same as actual tunnel segments. The bending moment and axial force are induced with push-pull double acting jacks and tendon respectively. During the tests the bending moment is held constant by controlling the load in the jacks. However the axial force by the tendon is not controlled.

Copyright © 2005 Taylor & Francis Group plc, London, UK

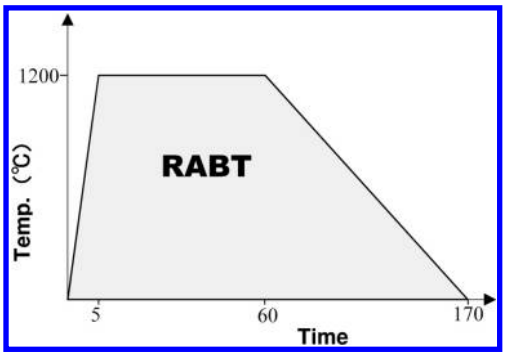


Figure 2. Time temperature curve.

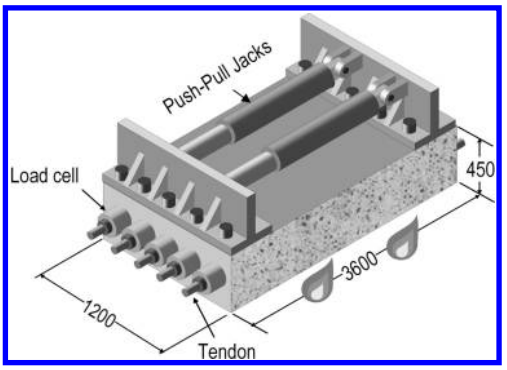


Figure 3. Dimensions of specimens.

Table 1. Mix proportion

	Water	Cement	Slag	Fine aggregate	Coarse aggregate	Super plastisizer	PP fiber
Ordinaly	136	200	200	814	1095	2.6	
PP	147	216	216	789	1046	2.81	1

Slump = 1.5 ± 1.5 cm.
Maximum size = 20 mm.

Table 2. Type of specimen.

Part	Crown		Spring line	
Bending moment	Sagging 324 mN · m		Hogging − 293 kN · m	
Axial force	Compression 1092 kN		Compression 1566 kN	
Fire protection	Insulation 15 mm	PP 1 kg	PP 1 kg	None
Specimen name	FP-P	FC-P	FC-N	OC-N

Because of this, the axial force increased slightly during heating as the test specimen expanded. During a fire, the thermal deformation of the tunnel lining is constrained and the axial force increases, so this test condition is a reflection of an actual phenomenon. The composition and types of test specimen are shown in Tables 1 and 2. Two specimens from ordinary concrete and two specimens from concrete containing 1 kg/m^3 of polypropylene fibers (hereafter referred to as PP fibers) were made. The addition of polypropylene fibers has been previously shown to reduce the amount of explosive spalling in ordinary concrete. Each used high strength concrete with a compressive strength of 72 N/mm^2. One of the test specimens made of ordinary concrete was treated with a 15-mm ceramic fiber insulation, and the other was left untreated.

High temperature strain gages were installed on the main rebar on the heated side of the specimen to measure the behavior of the rebar at high temperatures. The rebar layout and position of the strain gages is as shown below. The cover on the heated face 53 mm for the main rebar.

3 TEST RESULTS

3.1 *Deformation behavior*

To ascertain the residual deformation of the test specimens, measurements were continued beyond the time needed to prepare the RABT curve. Figures 5 to 8 show the concrete surface temperature and temperature of the main rebar on the heated side, strain in the main rebar, and vertical displacement of the uniformly heated test specimen. All measurements were taken in the middle of the 1650 mm span of the specimen and extended for 12 hours after the start of the test.

Copyright © 2005 Taylor & Francis Group plc, London, UK

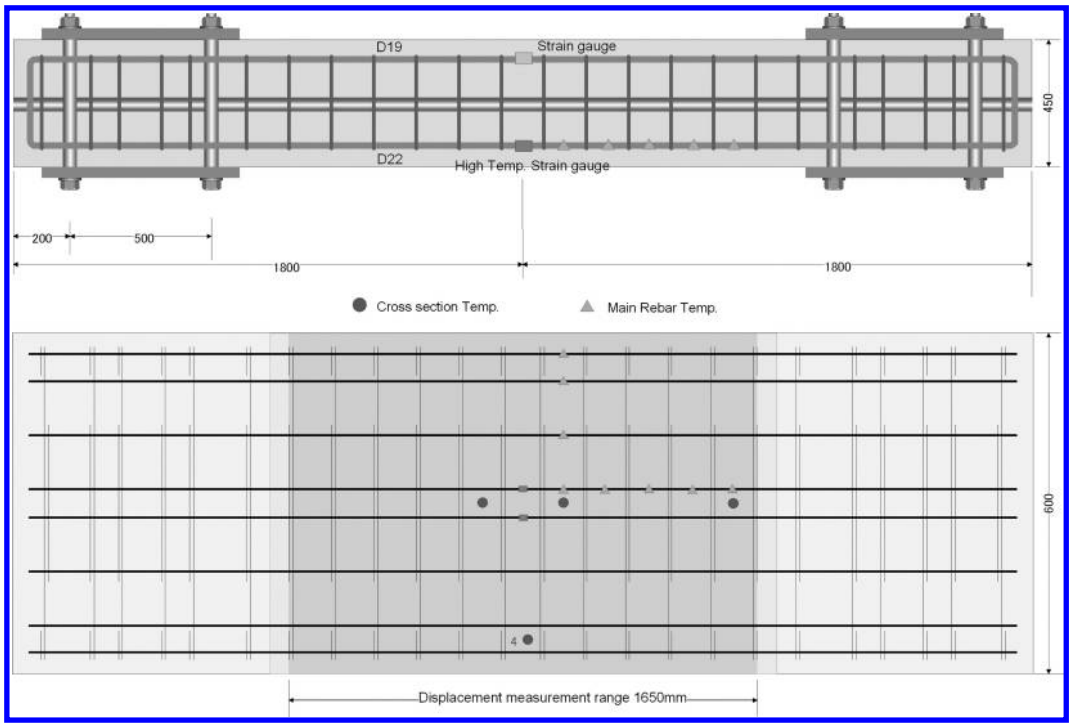


Figure 4. Rebar and sensor arrangement.

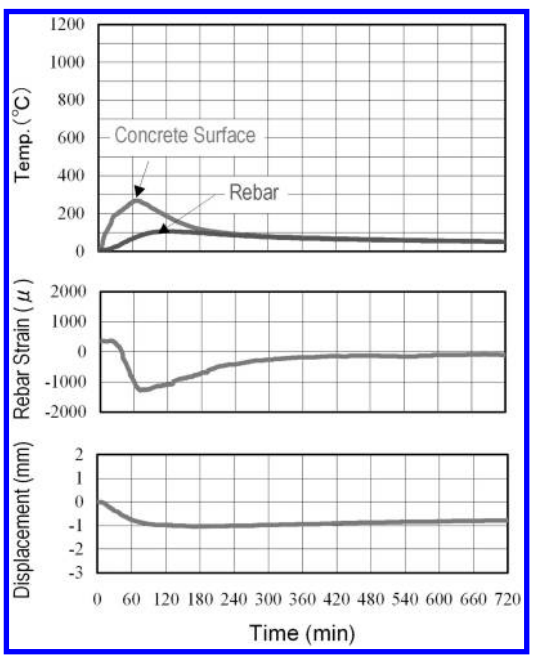


Figure 5. Insulation sagging (FP-P).

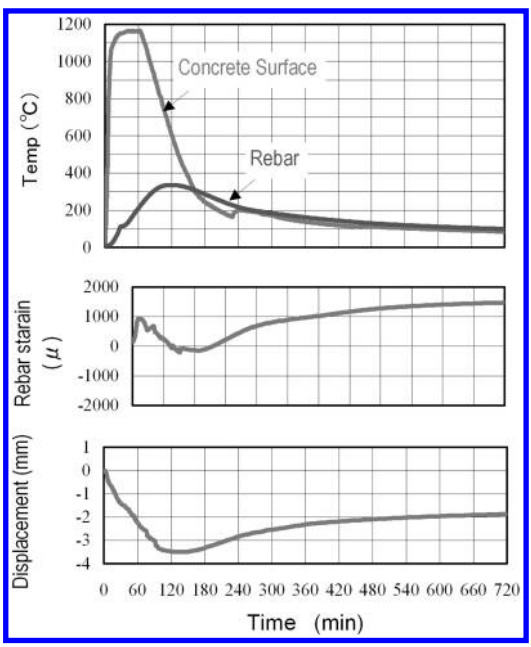


Figure 6. PP sagging (FC-P).

Copyright © 2005 Taylor & Francis Group plc, London, UK

In the tests for the specimens with insulation, the temperature of the concrete surface and main rebar remained low, and the displacements were very small. In the PP sagging test specimen there was virtually no spalling, and although the surface temperature of the concrete reached around 1200°C the temperature of the rebar was kept below 350°C due to the concrete cover. The displacement was relatively small at around 4 mm, but was several times larger than that of the specimen with the insulation. Also, the strain in the main rebar of the specimen with insulation returned to its initial state after completion of the heating, but in the PP specimen there was a residual strain of around 1500 μ.

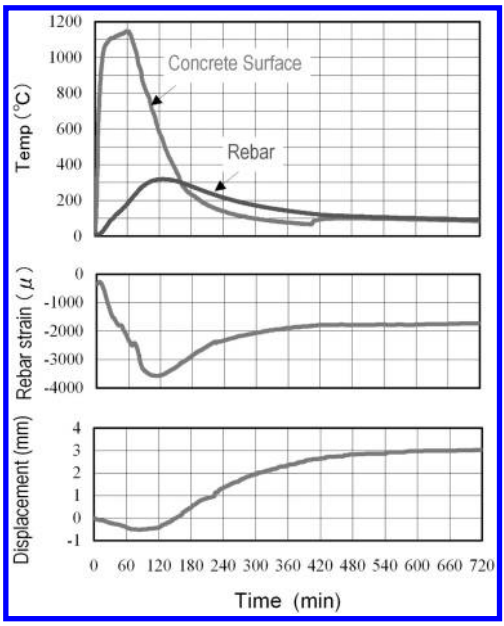


Figure 7. PP hogging (FC-N).

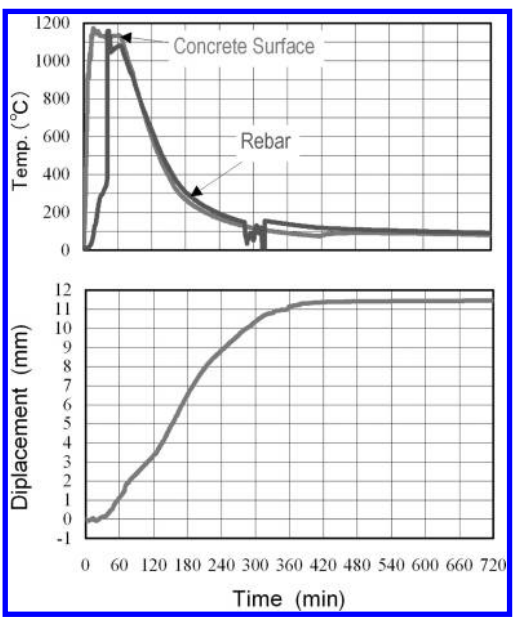


Figure 8. No insulation hogging (OC-N).

In the PP hogging specimen there was no spalling and the temperature of the rebar remained low, as in the sagging specimen. However, a compressive strain of over 3000 μ was temporarily induced in the rebar. Overall, although the PP specimens could not match the effect of those with fireproof linings, the residual displacement was around 3 mm, so this presents a promising and simple fireproofing method.

By comparison, the hogging specimen with no insulation displayed severe spalling and the temperature of the rebar rose to 1200°C, so it was not possible to measure the strain in the rebar. The residual displacement was also large, at 12 mm. However, even in this case the specimen was capable of maintaining the design cross-section load, and it would not have resulted in collapse of a tunnel.

3.2 *Damage to the concrete due to temperature*

It has been reported that the strength and elastic coefficient of concrete lining subjected to heat tends to decrease as the maximum temperature reached increases. Here we will discuss the phenomenon of carbonation due to heat. No spalling occurred in the concrete in which PP fibers were added; however the surface temperature reached 1200°C, so some degradation of the cover concrete could be expected. Figure 9 shows the detailed temperature history near the surface.

It can be seen that to maintain the temperature of the rebar below 350°C, a cover of around 60 mm was required. At a depth of around 50 mm from the surface, the maximum temperature reached 500°C.

Figure 10 shows the results of carbonation measurements made on a core taken from the heated surface of the same specimen. Previous research has shown that portlandite starts to decompose above 500°C, resulting in carbonation occurring in the concrete. However, in this case only the parts where the temperature exceeded 600°C were carbonated. This may be within the range of variation associated with varying concrete composition, or it could be the effect of the PP fibers. It is not possible to make a conclusion from these tests. In any case, after a fire it is necessary to repair the surface layer of concrete to which PP fibers have been added. The criterion for determining the depth to which concrete should be removed is whether there has been carbonation or not. In these tests the

Copyright © 2005 Taylor & Francis Group plc, London, UK

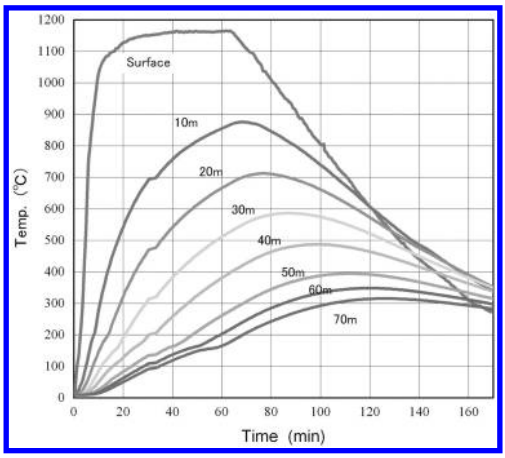


Figure 9. Temperature history of surface layer.

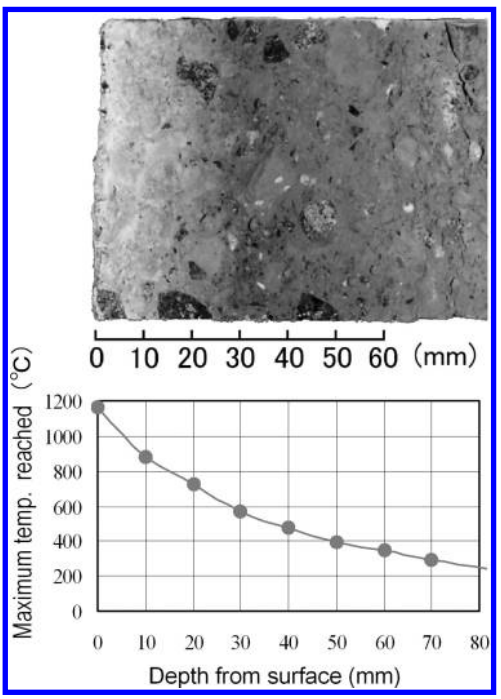


Figure 10. Carbonation due to heat.

thickness of the cover over the main rebar was 53 mm, and carbonation did not occur to that depth.

4 ELASTO-PLASTIC STRESS ANALYSIS

4.1 *Analytical technique*

The analysis consisted of thermal conduction analysis to determine the temperatures in the test specimens and elasto-plastic thermal stress analysis using the temperature results. The thermal conduction analysis used the finite difference method with temperature-dependant thermal properties determined by reference to the EUROCODE 4 model. The elasto-plastic thermal stress analysis used a fiber model with iterative calculations using the time integration. The concrete mechanical characteristics were modeled taking transient creep strains into account, and the mechanical characteristics of the rebar used the EUROCODE 4 model. For the analysis, the cross-section of the member was divided into fine elements, and the temperature of the member was assumed to vary stepwise with no variation in the temperature of each element within each time step.

4.2 *Analysis results*

Table 3 lists the analysis cases, while the analysis model is shown in Figure 11. For analyses of the crown (sagging), the segment with insulation (FP-P), and the segment using PP fiber reinforced concrete (FC-P) were used. For analyses of the spring line (hogging), the segment with PP fiber reinforced concrete (FC-N) and the segment using normal concrete (OC-N) were used. It was assumed that spalling did not occur in FP-P and FC-P. In the segment using normal concrete, it was assumed that spalling occurred between 4 and 12 minutes after the start of heating, and that the concrete cover was lost in stages to a total of 45 mm from the surface.

Figure 12–14 shows the internal temperature and displacement at the center of the member over time from the results of the analysis and tests. The maximum concrete temperature near the main rebar was about 100°C for FP-P, about 300°C for FC-P and FC-N, and about 550°C for OC-N. For sagging, the maximum displacement of the center occurred at between 120 and 180 minutes after the start of heating, and as they cooled they tended to return to their

Table 3. Analysis cases.

Analysis name	Fire protection	Position (Load Condition)	Spalling depth
FP-P	Insulation 15 mm	Crown (Sagging)	None
FC-P	PP Fiber	Crown (Sagging)	None
FC-N	PP Fiber	Spling line (Hogging)	None
OC-N	No protection	Spling line (Hogging)	45 mm

Copyright © 2005 Taylor & Francis Group plc, London, UK

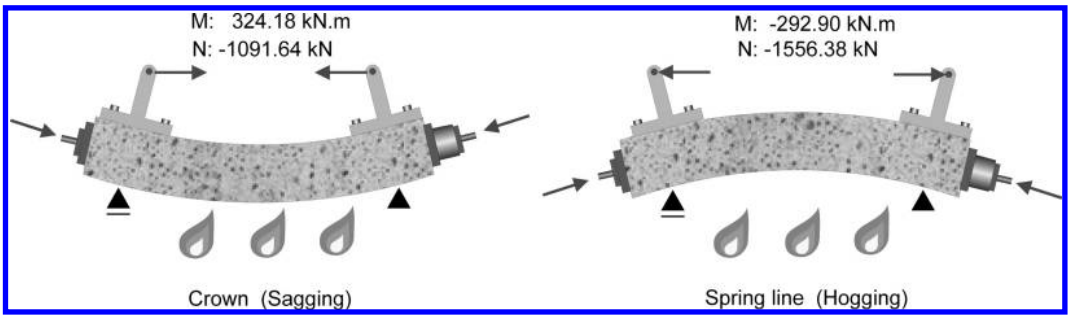


Figure 11. Analysis Model.

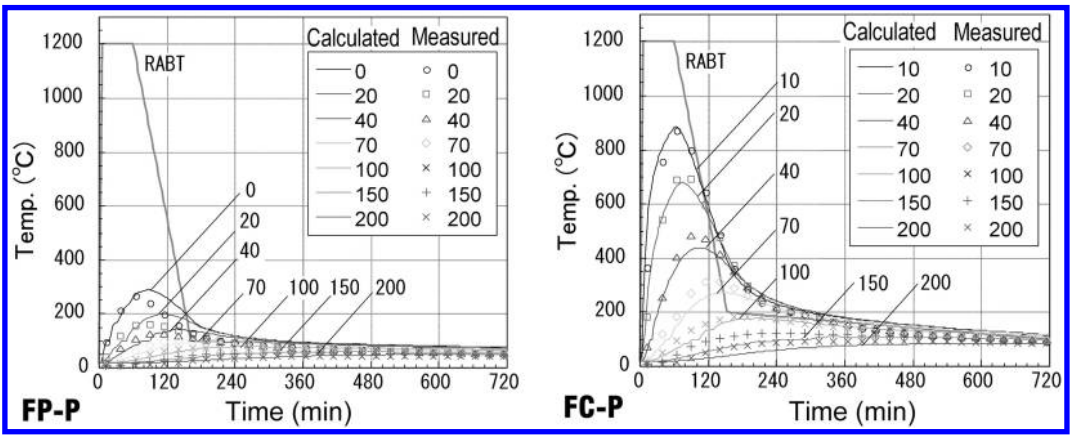


Figure 12. Comparison of analysis and test results (case FP-P, FC-P).

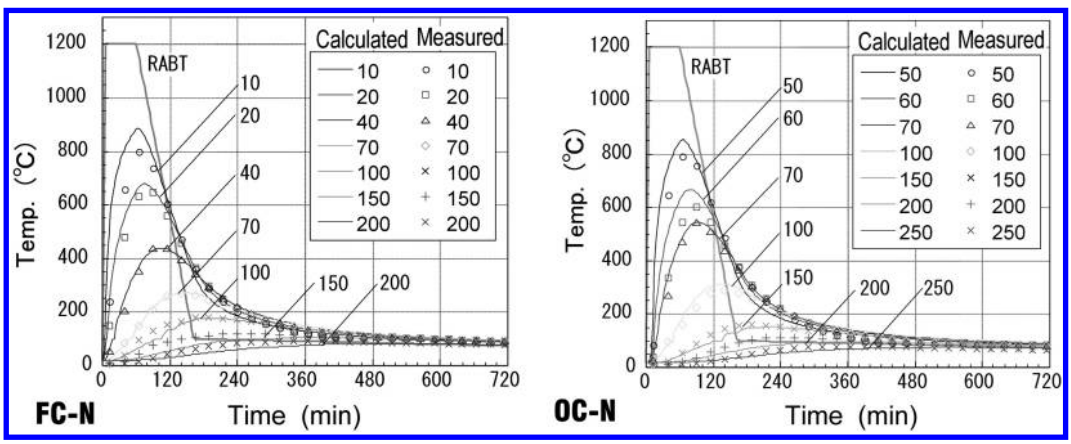


Figure 13. Comparison of analysis and test results (case FC-N, OC-N).

original state. On the other hand, for hogging the deformation increased as cooling proceeded. The magnitude of residual displacement after heating was FP-P < FC-P < FC-N < OC-N. In the case of sagging, the calculated values and measured values during heating approximately agreed. In the case of hogging, the calculated values and measured values approximately agreed after a point where the analysis

Copyright © 2005 Taylor & Francis Group plc, London, UK

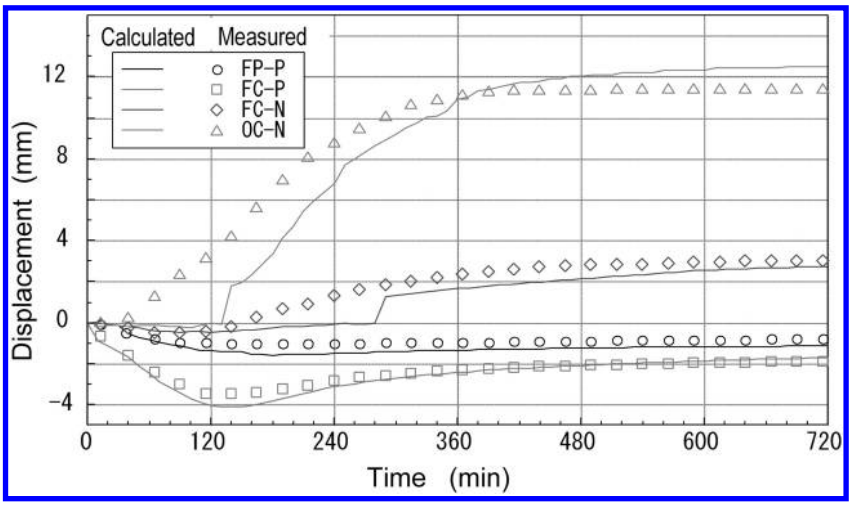


Figure 14. Comparison of analysis and test results (displacement).

indicated that cracking had occurred in the concrete in the rear face.

5 CONCLUSIONS

We conducted fire tests and elasto-plastic thermal stress analysis on specimens of tunnel segment members subject to the design cross-section force. The following are the conclusions.

(1) In specimens with insulation the deformations during a fire were small, and there was virtually no damage to the lining surface.
(2) There was no spalling in specimens containing PP fibers. The temperature rise in the rebar was suppressed by the concrete cover and deformations were small for both sagging and hogging, but the effect was not as pronounced as with the insulation.
(3) In both the containing PP fibers and the test specimens with no insulation, carbonation occurred on the heated face due to heating. The extent of this effect is thought to be those parts that reached 500°C or higher.
(4) Severe spalling occurred in the hogging test specimen with no insulation. The deformation was also large, but the specimen did not collapse and was capable of withstanding the design cross-sectional load throughout the test.
(5) Elasto-plastic thermal stress analysis was sufficiently accurate in simulating the deformation behavior of the specimens, although work remains to be done on modeling of cracking under hogging conditions.

In the future we intend to model the whole lining, taking the reactions of the foundations and other factors into account, and carry out thermal stress analysis to verify the overall safety of tunnels during fire.

REFERENCES

1) EUROCODE 4 Design of Composite Steel and Concrete Structures Part 1.2:Structural Fire Design, CEN/TC250/SC4, N39, prENV 1994-1-2, Second Draft, 1992
2) Morita,T., Schneider,U. and Franssen,J.-M.: Influence of Stress History Function in the Schneider-concrete-model under Fire Attack, FIRE SAFETY SCIENCE – PROCEEDINGS OF THE FIFTH INTERNATIONAL SYMPOSIUM, pp. 1057–1068, 1997

Copyright © 2005 Taylor & Francis Group plc, London, UK

The design and construction of a shield tunnel which have a non-excavating extension part in the middle by the Japan longest distance class

Makoto Takahashi
The Chubu Regional Bureau of Ministry of Land , Infrastructure and Transport, Nagoya, Japan

Teruyasu Tsunekawa, Tatsuji Kamei & Takashi Tsuji
JV of Kajima, Shimizu, and Okumura, Nagoya, Japan

Kunihiko Takimoto
Kajima Corporation, Tokyo, Japan

ABSTRACT: This shield tunnel, referred to as Kasugai Public Utility Conduit, was ordered by the Chubu Regional Bureau of the Ministry of Land, Infrastructure and Transport and, upon completion, will have an inner diameter of 4.2 m and total tunnel length of 6.82 km. Further, three underground sections will be cut and widened 2.5 m in diameter and 10～17 m in length from inside the path of the tunnel. The ground consists of hard, cobblestone-mixed, diluvial gravel layer. Boring is to be performed by use of one shield machine. With the aim of proper execution of construction, the following equipment and methods were utilized to carry out the highly difficult work successfully.

1. High-durability shield machine constructed by the relay bit construction method.
2. New quick block (QB) segments for high-speed automatic assembly and wedge block (WB) segments.
3. Construction method of underground widening in which a shield machine for widening the tunnel.

1 INTRODUCTION

The Kasugai Public Utility Conduit is the longest shield tunnel ever constructed in Japan, having a length of 6,800 m. It was constructed through application of the mud pressure technique using one shield machine to bore the cobblestone-mixed, diluvial gravel ground.

During the shield construction of recent years, extension of the boring distance has been discussed with the aim of reducing traffic congestion, improving conservation of the roadside environment, and reducing cost. The essential issue is to improve the durability of the shield machine, more specifically, the durability of the cutter bits subject to severe abrasion when boring the gravel ground. For this construction project, the latest technologies based on remarkable development results from private sectors were introduced and the VE system of design/construction proposal-type bidding was implemented for the bid contract with the aim of reducing construction cost.

The latest technologies proposed for this construction project are as follows:

(1) Shield machine:
Relay bit construction method (cylindrically reinforced shell bit) Automatic segment conveyance/assembly system
(2) Lining system:
five-divided, smooth, inner face segments
QB segments (W = 1,300 mm)
WB segments (W = 1,000 mm)
(3) Underground widening of junction sections:
Simultaneous boring-widening method

2 CONSTRUCTION PLAN

Figure 1 and 2 show the standard cross section and the top view of the proposed shield tunnel, respectively. The proposed shield tunnel includes 15 curved sections with R = 200 m (approx. 880 m) and the other sections are straight. At the end, a steep, curved section with R = 20 m exists.

Copyright © 2005 Taylor & Francis Group plc, London, UK

Figure 3 shows the estimated geological longitudinal cross section. The soil layer subject to shield boring consists of the diluvial deposit with compacted gravel bed (Dmg) and the hard cohesive soil layer (Pc), 80% or more of which is composed of the cobblestone-mixed gravel layer. The cobblestones are assumed to have the maximum grain size of 300 mm. The groundwater level (GL) is between −11.0 m and −5.0 m and the first section, which is about 800 m in length, is a waterless section.

As of the end of December 2004, boring work successfully reached the point of 4400 m (approx. 65%).

Also major features of the technological proposal for this construction project are explained in Figure 4 above:

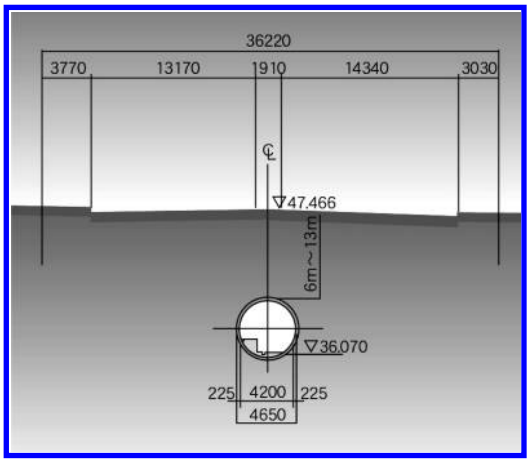


Figure 1. Standard cross section.

3 SELECTION OF SHIELD MACHINE

3.1 *Outline*

Major points to be considered in the selection of a shield machine and the relay bit construction method, which is one of the most characteristic features of the shield machine, are explained as follows:

(1) Load reduction of bits has been intended through use of an open spoke which facilitates boring of gravel.
(2) Through introduction of the center-support-type cutter head and hydraulic drive system, a space for relay bit changing work is secured. Further, proper attention was given to steep curve work

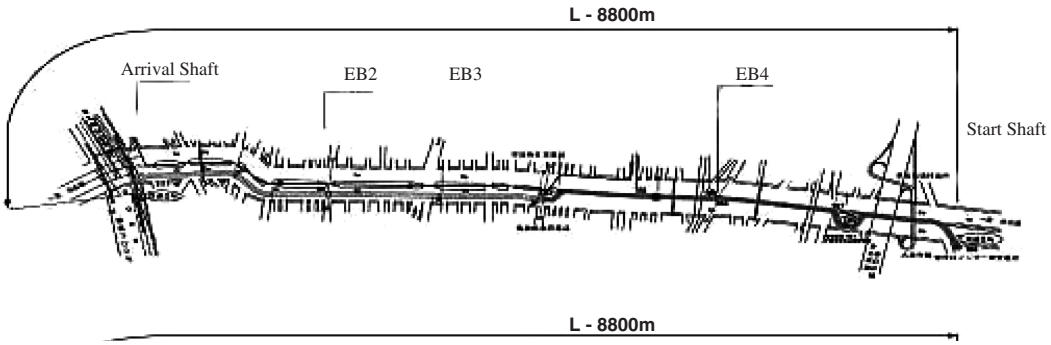


Figure 2. The top view of the proposed shield tunnel.

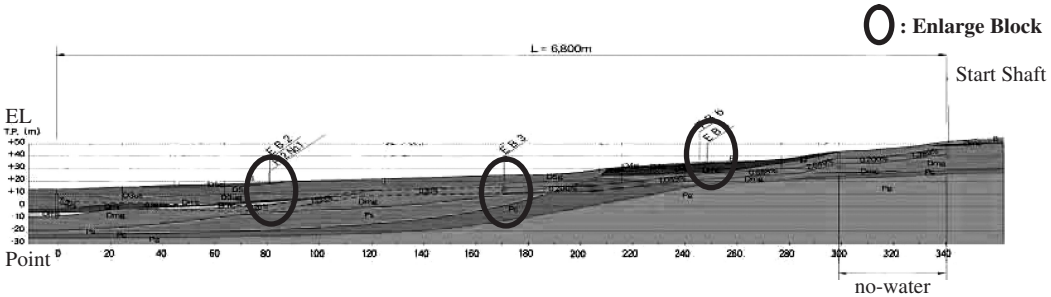


Figure 3. Geological longitudinal cross section.

Copyright © 2005 Taylor & Francis Group plc, London, UK

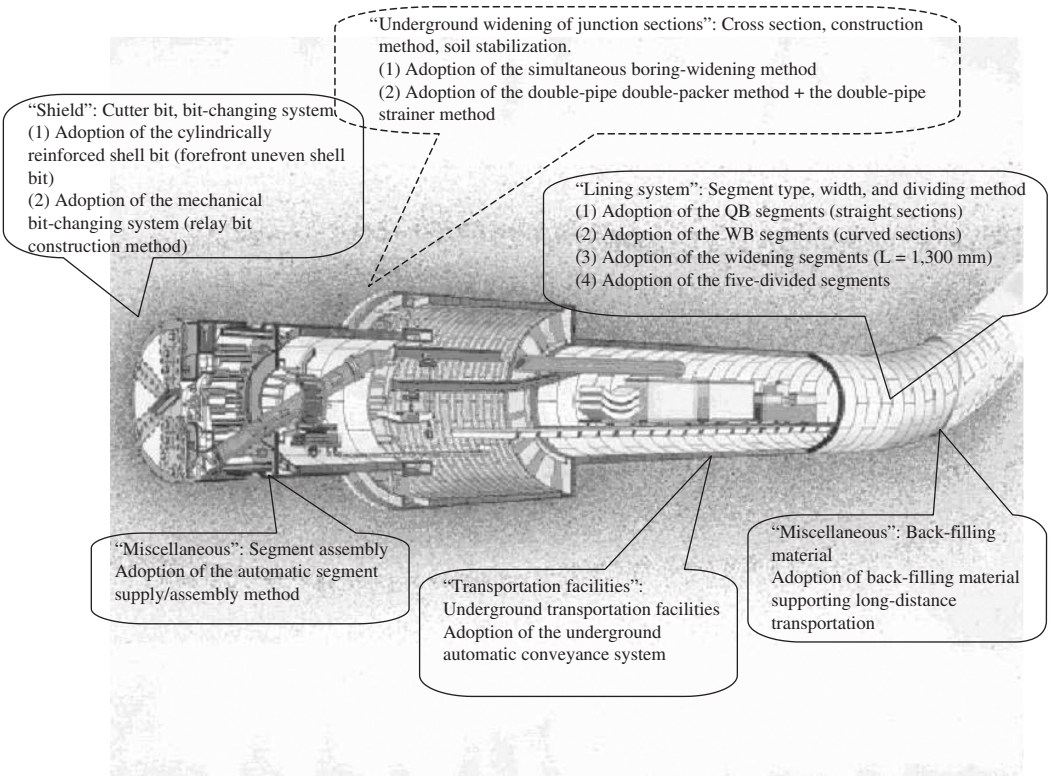


Figure 4. Overview of the VE proposal.

(R = 20 m) by adoption of the shortened front shell and articulation mechanism.

(3) Six cutter-head spokes have been adopted so that the number of bits on the same track is increased. Also, for increased durability, the large-sized bit, the cutting edge of which does not chip off easily, has been adopted.

Photo 1 shows the shield machine.

3.2 *Relay bit construction method*

In the relay bit construction method, a work space (approx. 80 cm × 80 cm) is provided inside the cutter spokes to allow a worker to enter from the rotation shaft of the cutter to replace necessary cutter bits.

The relay bit construction method is characterized by the following features:

(1) A work space provided inside the cutter spokes allows bit changing work without the need for stabilization of soil and pressurization by air in the working face.

(2) Bit changing may occur "at any time, at any place, and as many times as required" without regard for the soil conditions.



Photo 1. The shield machine.

(3) Bit abrasion can be visually inspected.

(4) When soil type changes during boring, the cutter bits can be replaced by those which are suitable for the new soil type.

(5) The method can be applied to both the slurry method and the mud pressure method.

Copyright © 2005 Taylor & Francis Group plc, London, UK

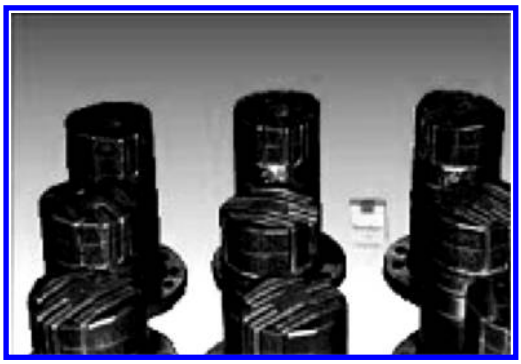


Photo 2. The relay bits.

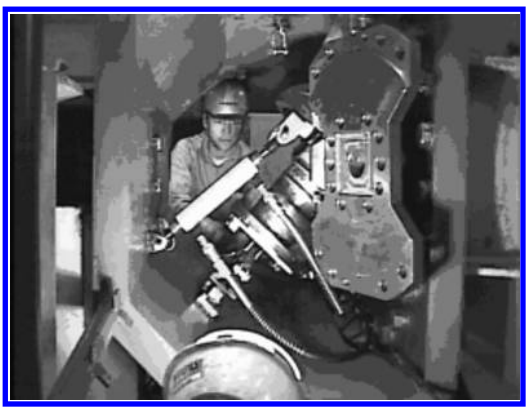


Photo 3. The bit-changing.

Photo 2 shows the relay bits. Photo 3 shows the bit-changing experiment which was performed before the start of construction.

As of the halfway point of the construction work, bit changing has been performed four times and boring has continued smoothly with the degree of abrasion being less than half of that originally expected.

Figure 5 shows the relationship between the soil volume bored per bit and the abrasion loss based on the data obtained during the first half of the construction work. These quantitative analyses will help serve as a guideline for future evaluation of durability.

4 ADOPTION OF NEW SEGMENT TYPES FOR HIGH-SPEED CONSTRUCTION

4.1 *Outline*

QB segments, characterized by their high economical efficiency, have a "pin + butt joint," thus eliminating the necessity for secondary lining. Due to elimination of bolt boxes and exposure of metal fittings on their

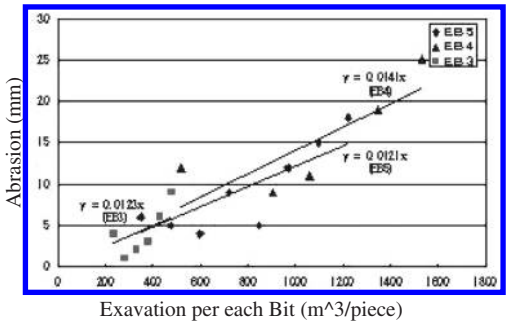


Figure 5. The relationship between the soil volume bored per bit and the abrasion loss.

surface, durability has been increased. Further, these segments are suitable for automatic assembly, enabling high-quality and high-speed construction work. QB segments serve as the basic segments for construction of the shield enabling high-quality and high-speed construction work. QB segments serve as the basic segments for construction of the shield tunnel and are used for a stretch of 5753 m (approx. equal to 85%).

WB segments, characterized by their high rigidity, which is even greater than that of QB segments, have joints composed of "pin + cotter." In construction of the shield tunnel, these segments are used in curved sections with R = 200 m where greater rigidity is required in comparison with straight sections.

4.2 *Demonstration of rigidity of QB segments*

Prior to finalizing the design of the QB segments, a demonstration was conducted by use of full-size specimens to more accurately confirm the rigidity of the QB segment ring.

The demonstration was conducted with concrete slab specimens complying with the QB segment specifications of 225-mm thickness, 1,300-mm width, and temporary fixing bolts/sealing material. Various demonstrations confirmed the rigidity of the QB segments, thus the design was finalized. The demonstration included the following:

(1) Bending test of the axial force introduced on the joint: Determination of the rotation spring constant of the segment joint and so forth
(2) Shear test of the segment joint: Determination of shearing resistance of the segment joint
(3) Ring joint (WLP joint) test: Determination of shear spring constant, required pushing force, and tension spring constant of the ring joint
(4) Segment-to-segment pressing test: Review of the specification of the erection guide

Copyright © 2005 Taylor & Francis Group plc, London, UK

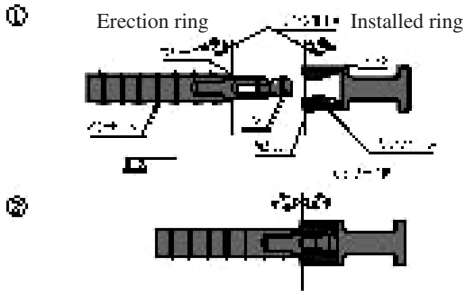


Figure 6. The outline of WLP [for Type I].

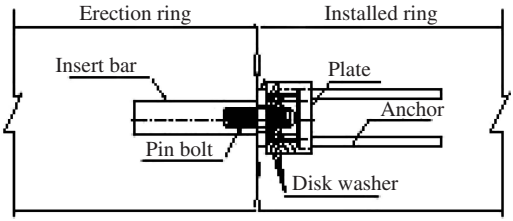


Figure 7. The outline of DS joint [for Type II].

4.3 *Improvement of QB segments*

It was decided that the QB segments [TYPE-I] used in the first half of this construction must be further improved; therefore, QB segments [TYPE-II] were developed.

The major changes from the QB segments [TYPE-I] are as follows:

(1) The WLP joint (ring joint TYPE-I) was changed to the DS joint (ring joint TYPE-II). This sharply reduced the joint fastening force so that the joints can be fastened with only an erector, without the use of a jack (Figures 6 and 7).
(2) Temporary assembly bolts were replaced with temporary single-pass metal fittings. As a result, fully automatic assembly using no manpower is realized. Further, because occurrence of irregularities is minimized, improvement in assembly accuracy is also expected.

Based on the changes mentioned above, the following advantages are expected to result from utilization of the QB segments [TYPE-II]:

(1) Cost reduction
(2) Improved safety in assembly of segments
(3) Reduction in the number of defects in segment cross sections
(4) Increase in accuracy of assembly of segment pieces.

Photo 4 shows the QB segments [TYPE-II]

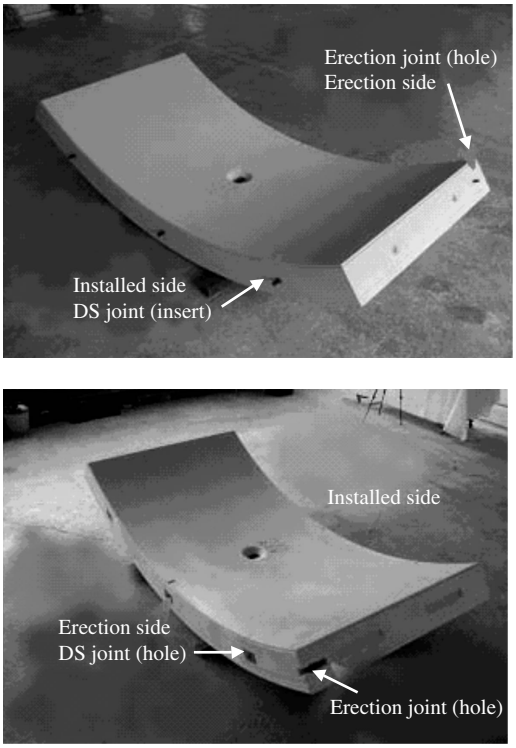


Photo 4. QB segments.

5 WIDENING OF SHIELD TUNNEL (SIMULTANEOUS BORING-WIDENING)

5.1 *Outline*

Construction sites requiring underground widening work are all located at the main traffic intersections on national roads. Power turnouts and communication turnouts are expected to be added to these widened sections in the future. According to the original design, the New Austrian Tunneling Method (NATM) method was first considered for underground widening. However, a new method was proposed and adopted, in which a widening boring shield machine is mounted outside a shield tunnel, without exavating the ground surface, after completion of the main line and boring is performed in the axial direction of the tunnel. An expected advantage of this method is minimization of the influence of loosened ground surface since the concentric cross sections are lined by segments.

In the widening construction method, the widening shield machine consisting of a shelter and a cutting edge is assembled underground after completion of soil improvement from the ground. When the natural ground in the section to be widened is dug by manpower, the widening shield machine is moved forward

Copyright © 2005 Taylor & Francis Group plc, London, UK

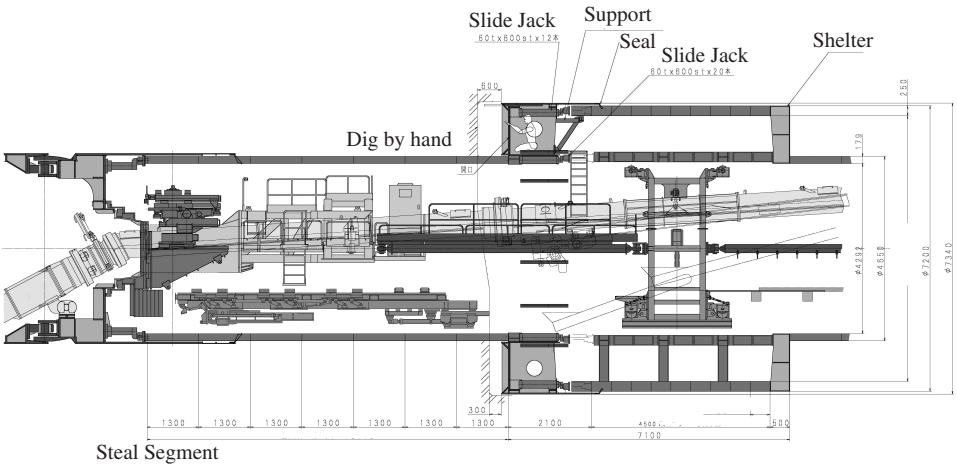


Figure 8. The outline of the boring-widening.

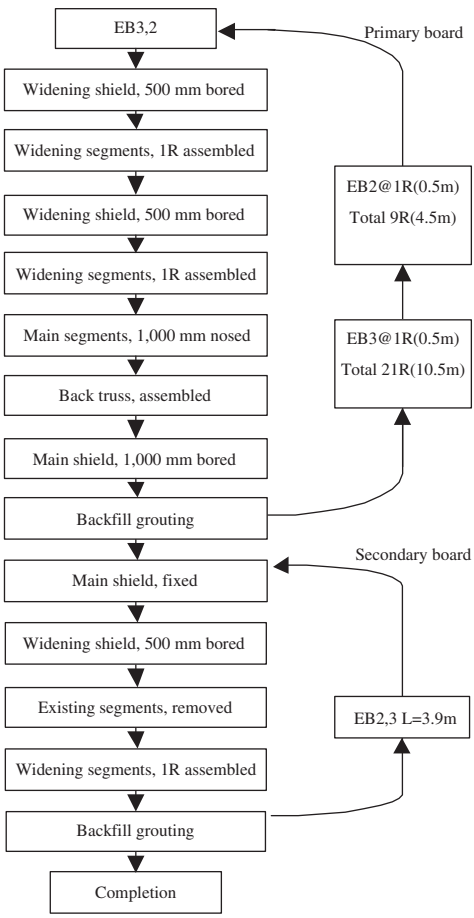


Figure 9. Flow of simultaneous boring-widening.



Photo 5. Full view of the EB.

at the same time as the shield machine with φ4,800 mm and the widening segments (made of steel) are assembled.

The widened section thus constructed is φ6,600 mm in inner diameter as against φ4,200 mm of the standard section, which is an increase of 2,400 mm in diameter.

In this construction work, a total of three, underground, widened sections are required to be built. Two of them have already been constructed. The actual work required for one of them, EB3, which was constructed by the simultaneous boring-widening method with the main line is briefly explained below:

5.2 *Actual result of section widened by simultaneous boring-widening method (EB3)*

In the construction of EB3, the face of the widening shield was located 3 D (D: outer diameter of the main

Copyright © 2005 Taylor & Francis Group plc, London, UK

shield tunnel) behind the main level face and boring was carried out alternately. The outline of EB3 construction is shown in Figure 8 and the construction cycle in Figure 9. Also, the outline of the completed construction is shown in Photo 5.

6 CONCLUSION

This construction work is highly difficult as a 6.8 km tunnel must be built by one shield machine under the ground, almost all of which consists of cobblestone-mixed diluvial gravel, and three sections along the path of the tunnel must be widened without breaking the ground surface. To successfully perform this construction work, a machine with high durability, segments for high-speed construction, and the underground widening method performed without breaking the ground surface have been utilized and have been producing good results. Various development results have been accomplished and we are determined to continue our efforts in this field.

Copyright © 2005 Taylor & Francis Group plc, London, UK

Pressure gradients at the tunnel face of an Earth Pressure Balance shield

A. Bezuijen
GeoDelft, Delft, Netherlands

J.F.W. Joustra
Tunnel Engineering Consultants (TEC)/Witteveen + Bos

A.M. Talmon
WL | Delft Hydraulics, Delft, Netherlands

B. Grote
T & E Consult

ABSTRACT: Measurements are presented that were performed in the pressure chamber of an EPB TBM. The TBM operated in saturated sand with a high water table. Foam was applied for soil conditioning. Different from a slurry shield there was no direct relation between vertical the pressure gradient and the density of the sand water foam mixture in the pressure chamber. The pressure measurements differ considerably for different rings. The density of the mixture was measured by taking samples from the pressure chamber during excavation. Densities found indicate a porosity higher than the maximum porosity of the sand. Horizontal pressure gradients were measured during drilling depending on the rotation direction of the cutter head. A possible explanation is presented in the paper.

1 INTRODUCTION

The Botlek Rail Tunnel was the second bored tunnel in The Netherlands and the first that was completed using an EPB shield. A considerable part of the tunnel was bored through Pleistocene sand under a high water table, see Figure 1. The water table was up to 23 m above the tunnel axis. Foam was used to stabilize the tunnel face.

The support pressure acting at the tunnel face can be seen as a combination of an absolute pressure and the vertical pressure gradient. In an EPB-shield, the average pressure is controlled by the screw conveyer and valves; the vertical pressure gradient is determined by a combination of the excavation process and material properties and cannot be controlled. Yet this gradient is of importance because it determines the pressure at the crown of the tunnel for a given pressure at the axis. The pressure gradient at the tunnel face of a slurry shield is determined by density of the slurry at the tunnel face. For an Earth Pressure Balance shield there appear to be more mechanisms that determine the gradient.

The paper deals with the pressure gradients measured, the densities of the mixture samples taken and possible mechanism that determine the gradients found.

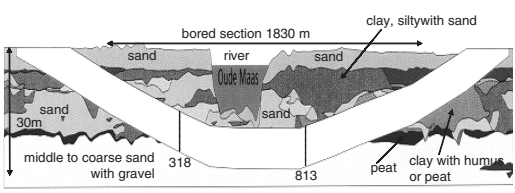


Figure 1. Geotechnical profile. The numbers indicate the approximate positions of rings, see further text.

2 MEASUREMENTS

2.1 *Measurements performed*

The following measurements where performed at the tunnel face: The density of the muck was measured by sampling the muck through a stopcock in the pressure bulkhead. The total pressure was measured at the bulkhead at 9 locations and the pore water pressure at 3, see Figure 2. The pore pressure gauges could be cleaned by a small water jet to avoid blocking of the filter. The status of the boring process was monitored as well as the amount of injected foam.

Copyright © 2005 Taylor & Francis Group plc, London, UK

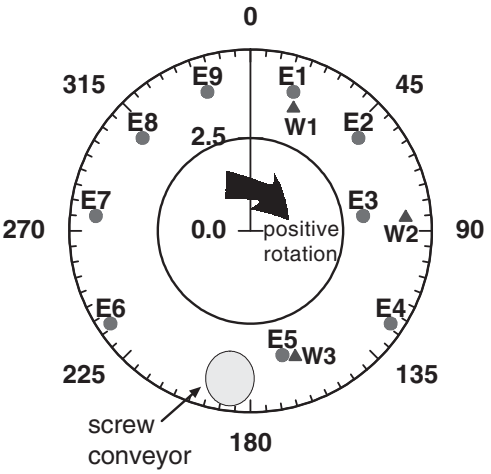


Figure 2. Position of instruments in the TBM looking from the tunnel to the TBM and definition of rotation.

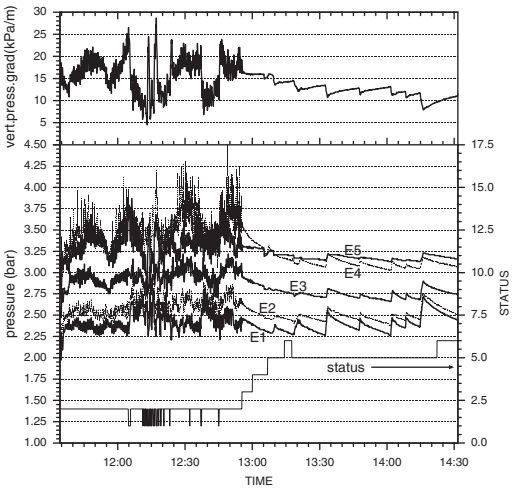


Figure 3. Ring 318 N. Pressures measured at the bulkhead, status of the TBM and the gradient determined from the pressures. Only a part of the pressure readings is shown, but all readings (E1 – E9) are used to calculate the gradient.

2.2 *Density measurements*

In order tot determine the exact composition of the muck inside the excavation chamber a sampling device was developed. This device simply consisted of a piece of pipe with some valves which was directly attached to the pressure bulkhead. By carefully opening the valves, some muck was allowed to flow out from the pressured excavation chamber through the sampling device. By subsequently closing the valves an exactly known volume of muck was extracted which would be analysed in a laboratory. In this way, the porosity and water content of the mixture could be determined, which could be converted tot the relative volumes of the different phases of the mixture (solid, liquid and gas).

A total of more than 20 samples of muck have been extracted from the centre of the excavation chamber at 6 different locations along the tunnel alignment. Although muck with a relatively high consistency proved problematic to collect because of its inability to flow easily, samples taken in a short time span were very comparable.

2.3 *Pressure measurements*

2.3.1 *Pressures and vertical gradients*

Pressures were measured during excavation of the Botlek Rail Tunnel at various locations at the pressure bulkhead; see for an example Figure 3. The vertical pressure gradients determined from these pressures are shown in the upper plot of Figure 3. (all figures with measurements present the ring number in the caption that was drilled during the measurement. S is the south tunnel, N the north). It shows that the gradient can be high during excavation but decreases when excavation stops (shown with the status, 2 means excavation, all other values mean stand still, see Table 1). The values measured for the vertical gradient can be put in perspective realizing that the gradient of the total vertical pressure in the not yet excavated soil is approximately 20 kPa/m, the density of the foam-water-soil mixture is approximately 13 kPa/m and the pore pressure has a gradient of 10 kPa/m. The measurements showed that the measured gradients can higher than 20 kPa/m, but also lower than 10 kPa/m. The vertical gradient decreases during ring building.

Table 1. Meaning of the status bit.

Status	Meaning
1	Temparary stop during excavation
2	Excavation
3	End of excavation phase
4	Start of ring building phase
5	Actual ring erection
6	Pause after ring erection

Another way to present the pressure measurements for the same ring is shown in Figure 4. It shows the pressures from gauges E1 until E5 for different time steps. It can be seen that there is a more or less linear increase with pressure apart form the lowest measurement position (E5) with various gradients. The pressure decreases at the position of E5, because this gauge is close to the screw conveyer, where the mixture is removed from the pressure chamber.

Copyright © 2005 Taylor & Francis Group plc, London, UK

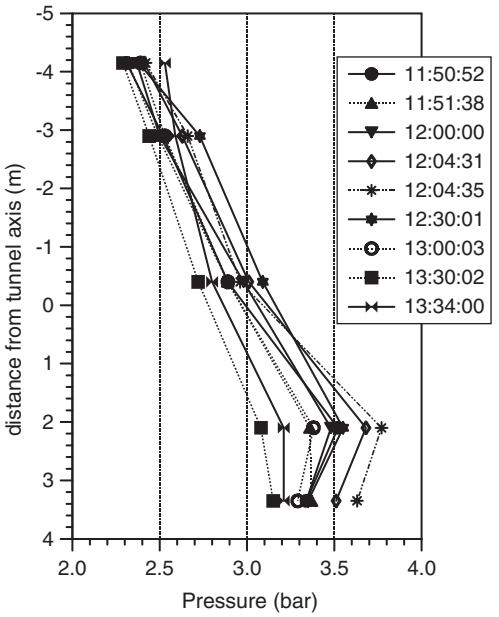


Figure 4. Ring 318 N. Pressure distribution along the gauges E1 until E5 for various time steps.

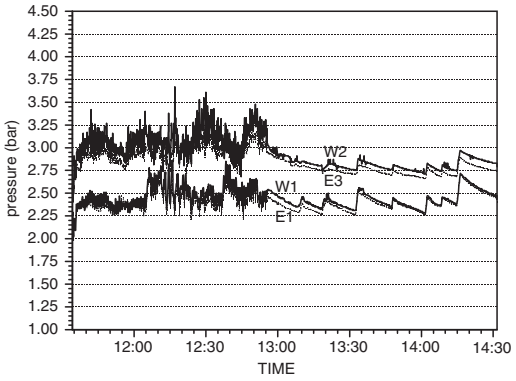


Figure 5. Ring 318 N. Total pressures and pore pressures compared.

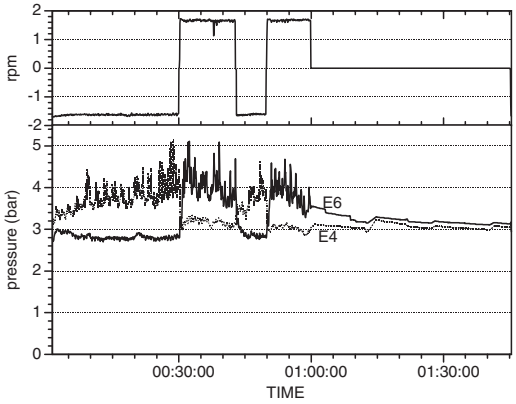


Figure 6. Ring 813 S. Pressures measured right (E4) and left (E6) of the TBM axis compared with the rotation of the cutter head, see also definition in Figure 2.

2.3.2 *Effective stress*

Pore pressure gauges were installed near some total pressure gauges, see Figure 2 to determine the effective stress in the soil water foam mixture. Results of both total pressure gauges and pore pressure gauges are shown in Figure 5. It is clear that both pressures are comparable, which means that the effective stress in the mixture is negligible. W3 did not function and therefore could not be compared with E5.

Figure 5 shows the pressures measured for only one ring. The conclusion that there is hardly any effective stress in the mixture is a more general one for this boring (Joustra, 2002). Although there are some indications that there is an effective stress near transducers E4 and E6 during the drilling of some rings, as will be dealt with later in this paper. The conclusion that there is hardly any effective stress is also confirmed by the density measurements performed. It was found that in most cases the porosity of the samples was above the maximum porosity. A porosity lower than the maximum porosity is necessary to have a grain skeleton and effective stresses.

2.3.3 *Horizontal pressure differences*

The measurements show for some rings remarkable horizontal pressure differences depending on the direction of rotation of the cutter head, see Figure 6 and Figure 7. Pressures varied 1 bar and more depending on the direction of rotation. The pressure variations are most significant for pressure gauges E4 and E6, less for the other gauges and more or less disappeared at the top of the tunnel, see Figure 7.

Pressure variations differ for different rings. Most rings have only small variations, see Figure 8. Also here pressures varied depending on the rotation direction, but the variation was so small that it could not be noticed in the original data, see Figure 3. By taking a moving average over 7 measurements to reduce the noise it is possible to see a variation of approximately 0.25 bar.

2.3.4 *Variations in pressure*

Comparing the results of Ring 318 N with those of Ring 813 S, it appeared that there is a considerable difference in the results of these rings. Compare Figure 6 with Figure 8 and Figure 4 with Figure 7. Measurements

Copyright © 2005 Taylor & Francis Group plc, London, UK

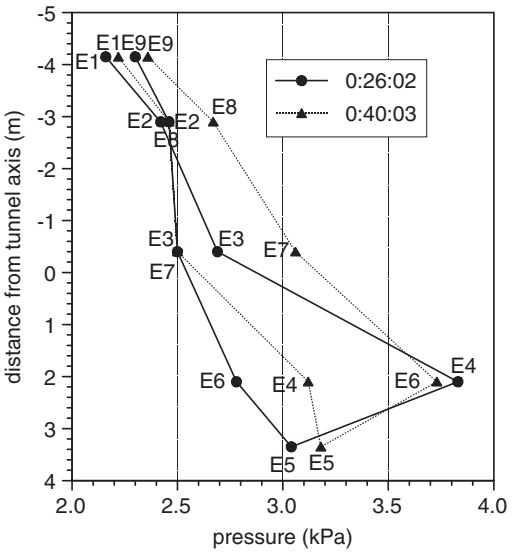


Figure 7. Ring 813 S. Distribution of pressures when the cutter head is rotating to the left (negative values) at 0:26:02 and to the right at 0:40:03.

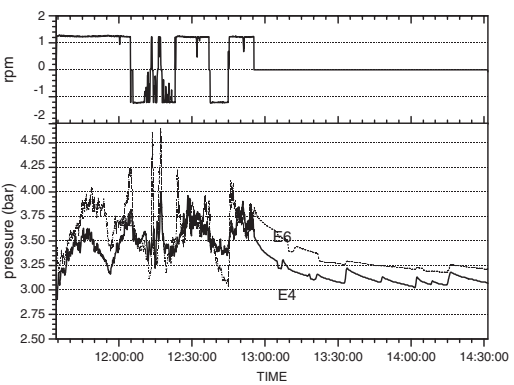


Figure 8. Ring 318 N. Pressures measured right (E4) and left (E6) of the TBM axis compared with the rotation of the cutter head, see also definition in Figure 2 (lines smoothed, see text).

from other rings showed also such differences (Joustra, 2002); although for quite a number of rings the soil conditions are comparable. The excavation process showed al lot of variability, which leads to the assumption that there is still a considerable margin of optimisation left with respect to the control of this process. The process is sensitive to pressure variations, because by the air involved these variations influence the volume in the mixture chamber and the performance of the screw conveyer. This was also found in laboratory experiments simulating the EPB process (Bezuijen & Schaminée, 2001). A more constant pressure may lead to a smoother drilling process with less stops. Now it can be seen from Figure 3, the status, that there are sometimes a lot of stops during drilling.

3 DISCUSSION

3.1 *Vertical gradient*

In a slurry shield TBM the vertical gradient found in the pressure chamber was equal to the gradient that corresponds with the density of the slurry (Bakker et al., 2003). In the predictions made for these measurements it was assumed that this was also the case for an EPB shield. However, this was not found for this tunnel. Pressure gradients varied during drilling and this variation is much larger than can be expected from variations in densities. Measured vertical gradients are sometimes larger than 20 kPa/m. Assuming that such a gradient is a good indication for the density would mean that there would be rather dense saturated sand in the pressure chamber, which is quite unlikely.

From the results it was concluded that also the yield stress of the soil has an influence on the pressure gradient. This can also be seen from the pressure drop that is present at E5 compared to the pressures E4 and E6, see Figure 4 and Figure 7. At the lower end of the tunnel, the screw conveyer removes the mixture from the pressure chamber and due to the yield strength of this mixture this leads to a pressure drop.

Assume a layer of sand-water-foam mixture between the cutter head and the pressure bulkhead of the pressure chamber at L metre apart. The adhesion between the cutter head or the pressure bulkhead and the mixture is τ_a and the density of the mixture is ρ_m. In case of vertical flow, equilibrium of forces leads to the following equation:

$$\frac{dP}{dx} = \rho_m g \pm 2\frac{\tau_a}{L} \qquad (1)$$

Depending on the flow direction the pressure gradient can be $2\tau_a$ /L higher or lower than the pressure gradient corresponding to the density of the mixture. In case of a flow with a horizontal component as can be expected in the pressure chamber between E6 and E5 as well as between E4 and E5, the influence of the adhesion becomes even bigger.

There is no direct field data from the shear strength of the mixture in the pressure chamber, but from measurements in the laboratory it was found that this shear strength is one to a few kPa. This means that with an average density of the mixture of approximately 1500 kg/m^3, the pressure gradient can vary as was measured depending on the direction of the flow. Lower values of the shear stress of 0.2 to 0.6 kPa were

Copyright © 2005 Taylor & Francis Group plc, London, UK

found from back calculation of the performance of the screw conveyer (Talmon & Bezuijen 2002). However these values are likely to be lower than in the pressure chamber due to the pressure relief in the screw conveyer that leads to a higher porosity.

From a physical point of view the concept of adhesion as described here is probalby too simple. Adhesion on flat iron surfaces can be less and the roughness, combined with the conhesion results in an apparent adhesion. However, also this apparent adhesion will result in the pressure gradient variations described here.

After the actual drilling, during ring building, the vertical pressure gradient decreases. Foam injections executed during ring building are necessary to keep a stable boring face, but also lead to a decrease in the average density of the mixture. The pressure loss is caused by ground water flow from the tunnel face to the ground water caused by the excess pore pressure in the chamber (see also Bezuijen et al., 2002 and Bezuijen, 2002). The water that flows out is compensated with foam that contains only about 10% water and 90% air.

Consequence of the relatively low measured vertical gradient during most of the drilling cycle, compared to the gradient that corresponds with the density of the soil, is that the pressure gradient is lower than the soil pressure gradient. It is sometimes mentioned as an advantage of the EPB shield that there is a better 'match' with the pressure gradient in the soil when compared with a slurry shield. For the ground conditions encountered here this is not the case. The relatively high permeability sand (k is 5.8 10^{-6} m/s when Ring 318 N was drilled 3.10^{-4} m/s during drilling of Ring 813 S) leads to expelling of water from the mixture. This reduces the density of the mixture. This with the influence of the yield stress that leads to a further reduction of the vertical gradient results in pressure gradients that are significantly lower than measured in a slurry shield (Bakker et al., 2003).

3.2 *Horizontal gradient*

Some horizontal gradient can also be explained by the yield stress of the air-sand-water mixture, assuming that the pressure chamber is not completely filled. The cutter head pushes the mixture in one direction and to get a stable situation it has to flow back. However, it can only flow back if there is a pressure difference large enough to overcome the yield stress. This pressure difference is created because there is more mixture on one side of the TBM than on the other side, see Figure 9.

The figure shows a possible pressure distribution on both sides of the axis (the centre part with a radius of 5 m) assuming that there is more mixture on the right side due to the rotation of the cutter head.

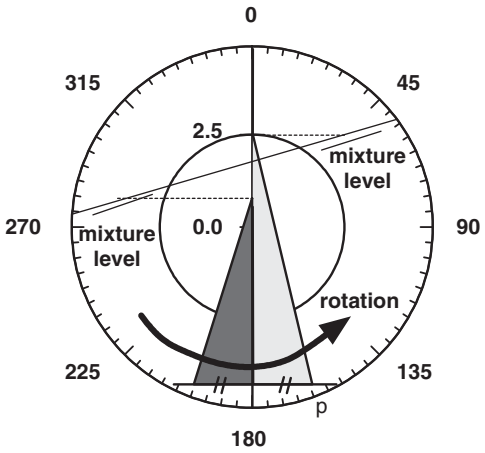


Figure 9. Sketch of possible pressure distribution due to rotation of cutter head without effective stress, see further text.

Assuming a stable situation, the pressure has to be the same on both sides at 180 degrees (the lowest point of the mixture, but is higher on the right hand side for other positions, because the mixture is higher on that side. The difference between both pressures is highest on the top level of the mixture on the left hand side.

A pressure distribution as shown in Figure 9 implicitly assumes that the pressure chamber is only partly filled with sand water foam mixture. This was measured for some rings (the pressure gauges on top of the TBM showed the same pressures) but not for all and not for Ring 813 s, see Figure 7.

The mechanism sketched above can explain some horizontal gradient, but not the approximately 100 kPa that was measured during the drilling of Ring 813 S. Assuming again a density of the mixture of 1500 kg/m^3, such a pressure difference corresponds to a different in height of at least 6.6 m, which is quite unlikely because that is more than halve of the height of the pressure chamber. Looking at the pressure gradient measurements, shown in Figure 7, there is no indication that there is an empty pressure chamber, over several metres from the top of the TBM. An empty pressure chamber would mean that the pressure remains constant, which is not the case.

A possible explanation for the high horizontal pressure gradient is the effective stress that can occur in the mixture chamber, see Figure 10. This Figure is the same as Figure 6, but the reading of pressure gauge E5 and pore pressure gauge W3 are added. From Figure 10 it is clear that the variation in the pore pressure, measured with W3, is much less than the variation in the total stress transducers E4 and E6 (the pressure fluctuations on the pore pressure gauge after drilling (rotation is zero), are caused by the cleaning

Copyright © 2005 Taylor & Francis Group plc, London, UK

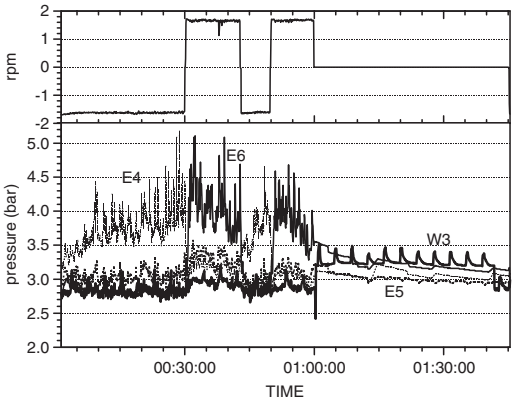


Figure 10. Ring 813 s. Pore pressure measured at W3 compared with the pressures measured at E4, E6 and E5 and the rotation of the cutter head. Variations in W3 after 1:00 are caused by the cleaning mechanism on the gauge.

system on the pore pressure transducer). E4 is more or less equal to the pore pressure transducer for negative rotation (turning to the left) and E6 is equal to the pore pressure transducer when the cutter head is turning in the opposite direction. In both cases the other pressure transducer is approximately 1 bar (100 kPa) above the pore water pressure.

When the cutter head is rotating in a way that the mixture is transported from screw conveyer, the mixture becomes more or less squeezed between the cutter head and the bulk head. This resulted locally in a high pressure. The pressures are lower at higher levels in the pressure chamber and close to the screw conveyer (see the reading of E5 in Figure 10). No effective stress was measured at these locations.

4 CONCLUSIONS

From the study described in this paper we came to the following conclusions:

- While boring in sand with an EPB shield an important function of the foam is to increase the porosity of the sand to such a value that deformation is possible with no or only limited grain stresses. This is different from boring in clay where the lubricating is more important (Mair et al., 2003).
- Significant differences between tunnel rings in comparable geology of the pressure measurements and other process parameters suggest that the regulation of the drilling process has some potential for optimisation. A better regulation can possibly improve the drilling process.
- The vertical pressure gradient is only to a certain extend influenced by the density of the mixture. Yield stress of the mixture also seems to have an influence.
- The vertical pressure gradient can be lower for a EPB using foam than for a slurry shield.
- Horizontal pressure gradients can be quite considerable over the tunnel face. These may be caused by compression of the sand grains in the mixture leading to effective stresses in some parts of the pressure chamber.

ACKNOWLEDGEMENTS

The laboratory tests were commissioned and supervised by BTL (Research foundation: Horizontal Drilling & Tunnelling) and COB (Centre for Underground Construction). The authors wish to thank these foundations for their permission to publish the results. The data on the Botlek Rail Tunnel presented here are derived from the COB-pilot project F300 in which the authors participate. The authors are very grateful to both COB and the builder of the tunnel BTC Botlek vof, with the granted opportunity to publish.

REFERENCES

Bakker K.J., Teunissen E.A.H., Berg P. van den, Smits M. Th. J.H., 2003, K100 research at the second Heinenoord tunnel. *Proc. ITA 2003, Amsterdam*,

Bezuijen A., Pruiksma J.P., Meerten H.H. van 2001. Pore pressures in front of tunnel, measurements, calculations and consequences for stability of tunnel face. *Proc. Int. Symp. on Modern Tunneling Science and Techn. Kyoto*.

Bezuijen, A., & P.E.L. Schaminée, 2001, Simulation of the EPB-shield TBM in model tests with foam as additive, *Proc. Int. Symp. on Modern Tunneling Science and Techn. Kyoto*.

Bezuijen A. Influence of soil permeability on the properties of a foam mixture in a TBM. *3rd Int. Symp. on Geotch. Aspects of Underground Construction in Soft Ground, IS-Toulouse*.

Joustra, J.F.W., 2002, Additional data analysis independent research project Botlek Rail Tunnel, the 'EPB-process' (in Dutch), *Delft University of Technology report. 2001.BT.5566*.

Mair, R.J., Merrit, A.S., Borghi, X., Yamazaki, H., and Minami T., 2003. Soil conditioning of Clay Soils. *Tunnels and Tunnelling International, April*.

Talmon A.M. & A. Bezuijen, 2002, Muck discharge by the screw conveyor of an EPB Tunnel Boring Machine, *3rd Int. Symp. on Geotch. Aspects of Underground Construction in Soft Ground, IS-Toulouse*.

Copyright © 2005 Taylor & Francis Group plc, London, UK

The performance of a roadheader in high strength rock formations in Küçüksu tunnel

N. Bilgin, D. Tumac & C. Feridunoglu
Istanbul Technical University, Mining Engineering Department, Istanbul, Turkey

A.R. Karakas & M. Akgul
STFA Co, Istanbul, Turkey

ABSTRACT: The main objective of this study was to investigate the performance of a roadheader used for the excavation of Küçüksu Sewage Tunnel having a length of 1037.52 m. The tunnel is located in Anatolian part of Istanbul and constructed by STFA for Istanbul Water and Sewerage Administration (ISKI).

Detailed statistical analysis showed that net advance rate of the roadheader is directly influenced by rock compressive strength, rock mass quality designation and water income.

In the second stage of the research study, a big rock block taken from the tunnel face was subjected to full-scale rock cutting tests in the laboratory using a linear cutting machine. Cutter force and specific energy values were recorded for different depths of cut and cutter spacings and likely net cutting rate of the roadheader excavating rock formation was predicted using specific energy and cutter head power.

In situ cutting rate and laboratory predicted values were compared in order to test the validity of the full scale rock cutting tests.

1 INTRODUCTION

The application of roadheaders in hard formations, has increased in recent years, considerably in both civil and mining engineering fields. The prediction of instantaneous (net) cutting rate and machine utilization time, determining daily advance rates, play on important role in time scheduling of the tunneling projects and in determining the economy of tunnel excavation. This paper is a summary of a research study in this respect.

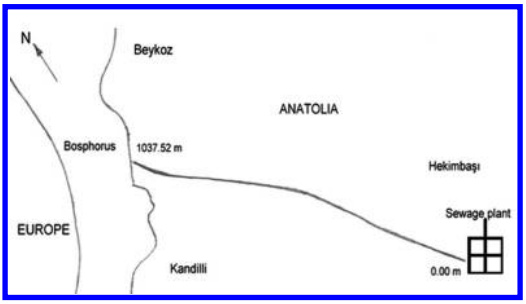


Figure 1. The route of Küçüksu tunnel.

2 DESCRIPTION OF THE TUNNEL PROJECT

Küçüksu tunnel is apart of sewage project which is situated between Küçüksu and Hekimbaşi in the Anatolian part of Istanbul. The route of the tunnel is shown in Figure 1. The project commissioned to STFA consists of a sewage plant having a capacity of 7 m^3/sn, three shafts and two tunnels having final diameters of 2.2 m and length of 95.8 and 1037.2 m. The tunnels were excavated using SM1 model shielded Herrenknecht roadheader which is shown in Figure 2, the machine had a cutting power of 90 kW and total power of 224 kW. The cutting head is axial type having 36 conical cutters of 75° tip radius. The excavation of tunnels started in 27th August 2002 and finished in 9th August 2003. The crew consisted of 5 civil engineers, three surveyors and 12 workers per shift. The excavated material was transported using Clayton locomotive of 21 hp and cars of 2.5 m^3 in volume. 2 × 7.5 kW ventilator and ventube of 500 mm in diameter realized the ventilation of tunnel.

Cross-section of the tunnel is shown in Figure 3. Precast segments prepared in tunnel side are used as initial tunnel support; each segment has a length of 0.75 m and thickness of 0.10 m. Each rig consists of 4 precast segments and an invent. In situ casted concrete

Copyright © 2005 Taylor & Francis Group plc, London, UK



Figure 2. SM1 model Herrenknecht roadheader.

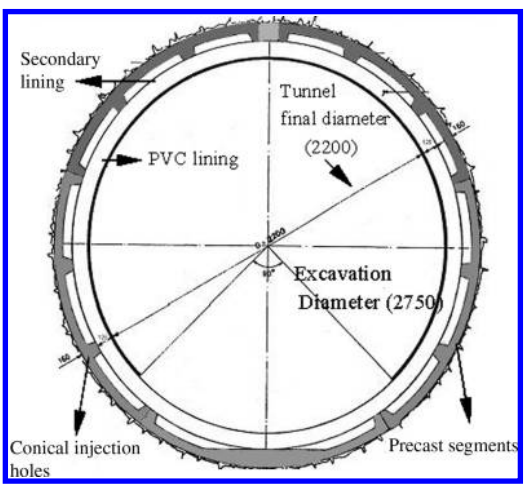


Figure 3. Cross section of the tunnel.

lining was used as secondary tunnel support and PVC lining to protect concrete from harmful effect of the sewage water.

3 TUNNEL GEOLOGY AND SOME ROCK PROPERTIES

Rock samples were collected systematically and geological observations were made during tunnel excavations.

The main rock formation is limestone (72%) having compressive strength values changing from 600 to 1452 kg/cm^2 and RQD values from 40% to 90%. 16% of the rock formations are andesite and diabase dykes with compressive strength from 741 to 1638 kg/cm^2 and RQD 80–90%.

Petrographic descriptions of the samples collected from different tunnel chainages are given in Table 1.

Table 1. Petrographic description of the rock formations.

Tunnel chainage	Petrographic description
251.25	Porphyritic andesite (fine and medium size hornblende and plagioclase matrix)
288.00	Limestone with %95 calcite content
288.75	Limestone with %95 calcite content
306.00	Carbonated sandstone
306.75	Carbonated sandstone
375.00	Siltstone with foliation, abundant with quartz and calcite
447.00	Medium size limestone with fossils
462.00	Limestone with large size calcite crystals
465.75	Limestone abundant with amphiboles and large plagioclase crystals
486.75	Limestone with fossils
506.25	Limestone with organic detritals
547.50	Altered andesite with albite, calcite and epidote crystals
560.25	Limestone with fossils
613.50	Large sized carbonated siltstone
630.00	Cretaceous aged andesite, hornblende ferro-crystals, altered plagioclase, fine graine amphiboles
645.00	Limestone with 90% calcite of 1 mm in size
660.00	Carbonated diabase, 50% of calcite crystals and feldspars
684.75	Carbonated siltstone, 35% calcite, 7–8% muscovite, fine grain quartz, crystals with 0,1 mm in size

A geological cross section of the tunnel with RQD and water income values in different rock strata is given in Figure 4.

4 PERFORMANCE PREDICTION OF THE ROADHEADER IN KÜÇÜKSU TUNNEL

In recent years the application of roadheaders in hard rock formations has increased considerably. However the prediction of the net cutting rate and machine utilization time determining daily advance rates still stays a key factor in determining the economy of tunnel excavation. Although in the past many roadheader performance prediction models were published (McFeat-Smith, Fowell 1977–79; Bilgin et al. 1990–1996–1997; Thuro, Plinninger 1998–1999; Çopur 1997–1998), one of the most realistic method to predict the cutting rate of any excavation machine in massive rock formations was reported to use cutting power, optimum specific energy and energy transfer ratio as given in Equation 1 (Rostami, Ozdemir 1994).

$$ICR = k\frac{P}{SE_{opt}} \quad (1)$$

Copyright © 2005 Taylor & Francis Group plc, London, UK

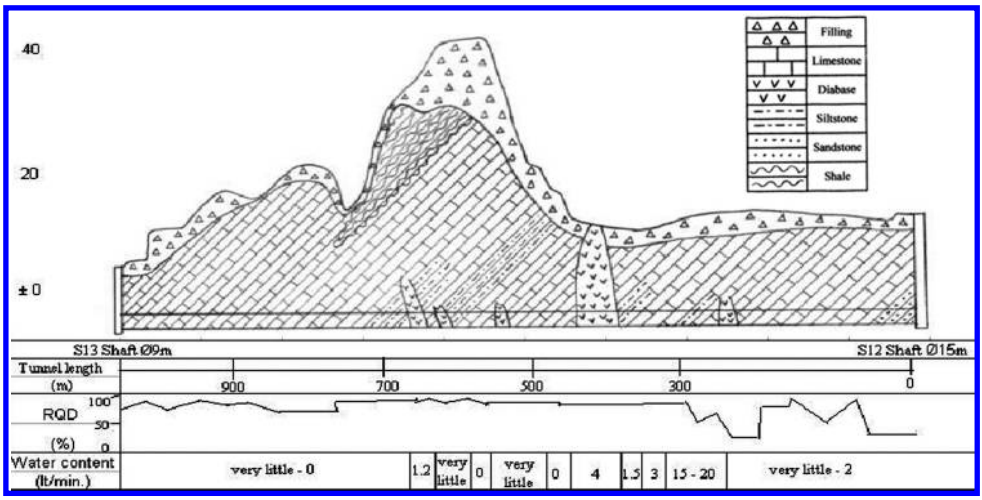


Figure 4. A geological cross section of the tunnel.

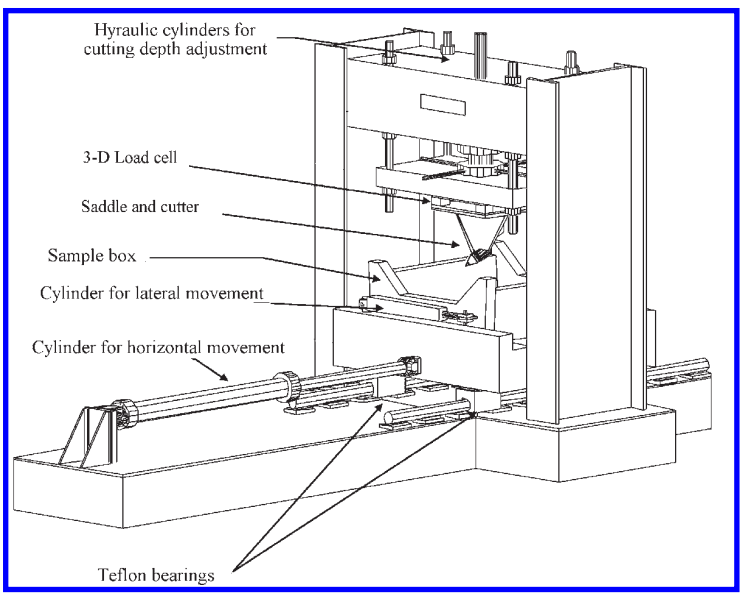


Figure 5. Schematic view of ITU LCM.

where, ICR is instantaneous cutting rate in m^3/h, k is energy transfer ratio from cutting head to the rock formation, P is cutting power of cutting head in kW and SE_{opt} is optimum specific energy in kWh/m^3.

It is strongly emphasized that the SE_{opt} should be obtained from full-scale linear cutting tests in optimum conditions using real life cutters. Rostami and Ozdemir pointed out that k changes between 0.40 for roadheaders to 0.90 for TBM's (Rostami, Ozdemir 1994).

A limestone block having a size of 30, 40, 50 cm was collected from one of the shafts in order to carry out full scale cutting tests in ITU laboratories

4.1 *Rock cutting test*

The linear cutting machine used in this study was built as an outcome of NATO supported project (Eskikaya 2000). The schematic view of the cutting rig is given in Figure 5. It includes a stiff reaction

Copyright © 2005 Taylor & Francis Group plc, London, UK

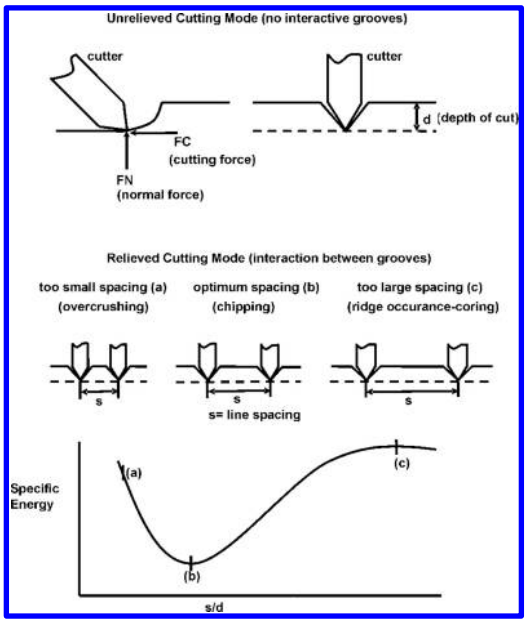


Figure 6. Unrelieved and relieved cutting modes and the effect of cutter spacing and depth of cut on specific energy.

frame on which the cutter and the force dynamometer of 50 t capacity are mounted.

A data acquisition system is used to record the cutter forces in three perpendicular directions. Data recording rate is adjustable up to 50,000 Hz. The hydraulic cylinders can move the sample box in which the rock sample is cast with concrete to eliminate pre-failure of the specimen.

The initial cutting tests are carried out in unrelieved mode to determine the variation of specific energy with depth of cut. This helps to find the optimum depth of cut value at which the relieved cutting tests will be carried out to determine the optimum specific energy and cutter spacing. Optimum specific energy will serve to predict the cutting rate of the machine intended to be used in the rock formation tested. Unrelieved cutting modes and the effect of cutter spacing and depth of cut are shown in Figure 6.

A limestone sample collected from tunnel face and having compressive strength value of 1100 ± 112 kg/cm^2 was subjected to rock cutting tests in the laboratory. The results are given in Figures 7, 8, 9. As seen in Figure 9 the optimum specific energy for d = 9 mm depth of cut is 7 kWh/m^3. As explained above the net cutting rate (ICR) of the roadheader used in Küçüksu tunnel may be calculated using equation (1). Bearing in mind that, energy transfer ratio k is reported to be 0.40 by Rostami and Özdemir (1997).

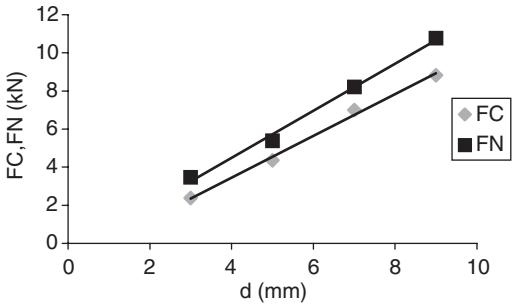


Figure 7. The variation of mean cutter forces with depth of cut.

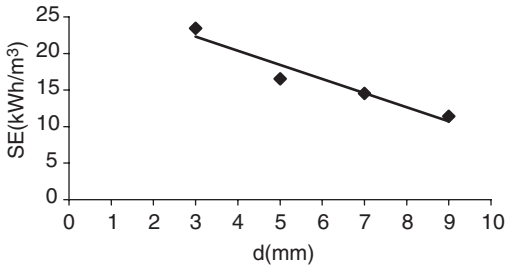


Figure 8. The variation of specific energy with depth of cut.

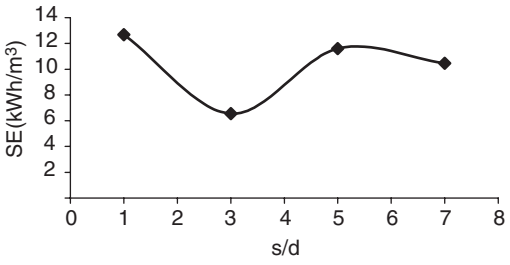


Figure 9. The variation of specific energy with s/d.

$$ICR = k\frac{P}{SE}$$

$$ICR = 0.4\frac{90kW}{7kWh/m^3}$$

$$ICR = 5.1m^3/h$$

5 RECORDING THE PERFORMANCE OF ROADHEADER AND COMPARISON OF PREDICTED AND ACTUAL VALUES

The performance of roadheader was recorded continuously during tunnel excavation. The summary of the roadheader performance is given Table 2 and Figure 10. Monthly advance rates of the roadheader are shown in

Copyright © 2005 Taylor & Francis Group plc, London, UK

Table 2. Summary of the roadheader performance.

The best daily advance (m/day)	9
The mean daily advance (m/day)	3.3
The best advance per shift (m/shift)	4.5
The mean advance per shift (m/shift)	2.1
The best weakly advance (m/week)	36.8
The mean weakly advance (m/week)	23.3
The best month advance (m/month)	106
The mean monthly advance (m/month)	81.7

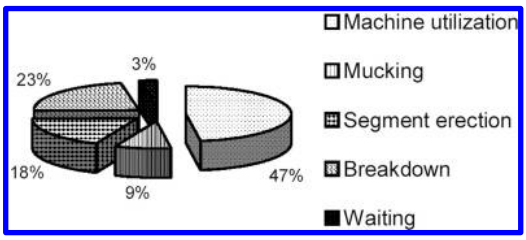


Figure 10. Overall performance of roadheader.

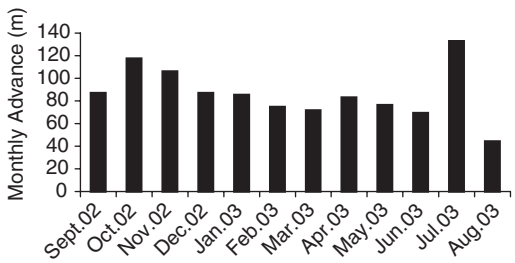


Figure 11. Monthly advance rate of roadheader.

Figure 11. However, to be more precise, rock samples were collected continuously from tunnel face for testing in the laboratory. Limestone, sandstone, siltstone, andesite and diabase zones were encountered in tunnel route as noticed in Figure 4. The mean compressive strength values of different rock formations are given in Table 3. The relationship between compressive strength and advanced rate for RQD values grater than 80% is given in Figure 12. This verifies findings of different research workers (Scheider 1988; Gehring 1977–1988; Vehigashi et al. 1987).

It is strongly emphasized that the predicted cutting rate of roadheader as calculated in section 4 is very close to the actual value for limestone as seen in Figure 12.

However during the field studies, it is observed that geological discontinuities specially RQD values less than 50% and water income effect tremendously the advance rates as observed recently in Nuh cement factory tunnel (Bilgin 2004). Excavation of Küçüksu tunnel is an experience in high strength rocks with RQD values greater than 80% leading a tremendous

Table 3. Mean compressive strength of the rock formation encountered during tunnel excavation.

Rock	Compressive strength (kg/cm^2 ± sd)
Limestone	1118 ± 240
Sandstone	557 ± 57
Siltstone	833 ± 71
Andesite	1200 ± 449
Diabase	770 ± 82

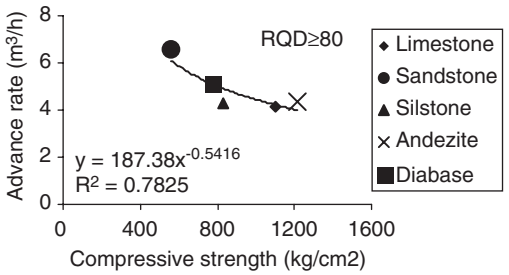


Figure 12. The variation of net cutting rate in different rock formations.

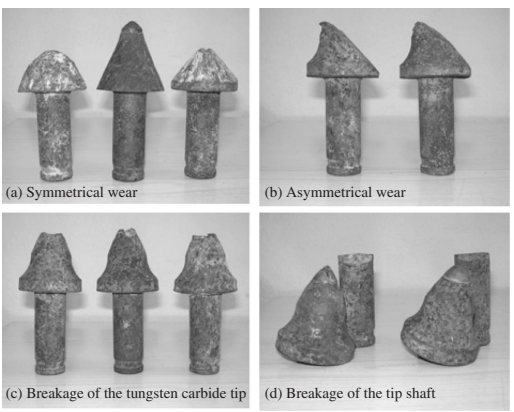


Figure 13. Classification of cutter wear in Küçüksu tunnel.

problem in cutter consumption. Four types of cutter wear were experienced in tunnel excavation, symmetrical wear 36%, asymmetrical wear 17%, breakage of tungsten carbide tips 7% and breakage of the cutter shaft 40%. The classification of the cutter wear is illustrated in Figure 13 and 14.

Breakage of the tungsten carbide tips are mainly due to the close contact of tips to the shield of roadheader. Peak normal forces up to 3000 kg were observed during laboratory rock cutting tests. The main raison of breakage of the cutter shaft may due to high forces encountered during the roadheader excavation. As seen from Table 4, the mean cutter consumption is

Copyright © 2005 Taylor & Francis Group plc, London, UK

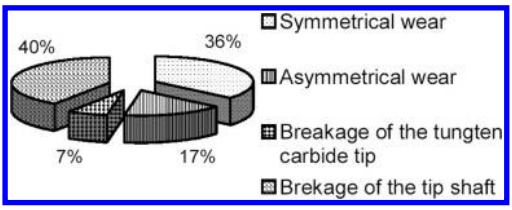


Figure 14. Classification of cutter wear in Küçüksu tunnel.

Table 4. The summary of cutter consumption.

Month	Formation	Cutter consumption (cutter/m^3)
September 02	Sandstone-Limestone	0.143
October 02	Limestone	0.264
November 02	Limestone-Diabase	0.305
December 02	Limestone-Siltstone	0.077
January 03	Limestone-Diabase	0.452
February 03	Limestone-Diabase	0.421
March 03	Limestone-Diabase	0.669
April 03	Limestone-Diabase	0.649
May 03	Limestone	0.390
June 03	Limestone	0.334
July 03	Limestone	0.180
August 03	Limestone	0.079
Total		0.330

0.33 cutter/m^3, varying from 0.077 cutter/m^3 in siltstone to 0.669 cutter/m^3 in limestone-diabase.

6 CONCLUSION

It is fact that the roadheaders are not recommended in high strength rock formations. However, the excavation of Küçüksu tunnel with a shielded roadheader of 90 kW of cutter power, showed that an instantaneous cutting rate of 5 m^3/h is possible to obtain in high strength rock formation having compressive strength values of more than 1000 kg/cm^2 with RQD values higher than 80%. The overall performance of the roadheader showed that machine utilization time of the roadheader was 47%. It is also important to note that the tool consumption is important disadvantage in excavating high strength rocks with peak values up to 0.7 cutter/m^3. Another important point emerging from this research study is that insitu cutting rate of roadheaders may be predicted from full scale cutting tests realized in the laboratory, using energy transfer ratio 0.40 from cutting head to rock formation.

7 ACKNOWLEDGMENT

The authors are grateful to STFA Tunnel Construction CO authorities for permitting to access to the tunnel side for collecting data. The tremendous help of Prof. Dr. Levent Ozdemir from **CSM EMI, USA** is also acknowledgement for helping to construct and design the laboratory cutting rig.

REFERENCES

Bilgin, N. et al. 1990. Roadheaders glean valuable tips for Istanbul Metro. *Tunnels and Tunnelling* (October), 29–32.

Bilgin, N. et al. 1996. A model to predict the performance of roadheaders and impact hammers in tunnel drivages. In G. Barla (ed), *Proceedings, Eurock'96*; 715–720, Rotterdam: Balkema.

Bilgin, N. et al. 1997. Cutting performance of rock hammers and roadheaders in Istanbul Metro drivages. In J. Golster et al. (ed), *Proceedings, World Tunnel Congress'97 Tunnels for People*: 455–460, Rotterdam: Balkema.

Bilgin, N. et al. 2004. Some geological and geotechnical factors affecting the performance of a roadheader in an inclined tunnel. *Tunnelling and Underground Space Technology*. November: 629–636.

Copur, H. et al. 1997. studies on performance prediction of roadheaders. In H. Gürgenci, M. Hood (ed). *International Symposium on Mine Mechanization and Automation*: A4-1 – A4-7, Brisbane, Old. Australia.

Copur, H., Ozdemir, L., Rostami, J. 1998. Roadheader applications in mining and tunnelling. *Mining Engineering* 50 (3), 38–42.

Eskikaya, S. et al. 2000. Development of rapid excavation technologies for the Turkish mining and tunnelling industries. *NATO TU-Excavation sfs Programme Project report:172*. Istanbul Technical University.

Gehring, K.H. 1988. A cutting comparison. *Tunnel and Tunnelling*, 21: 27–30.

Gehring, K.H. 1997. Classification of drillabilty, cuttability, boreability and abrasivity in tunnelling. *Felsbau*. 15: 183–191.

McFeat-Smith, I. & Fowell, R.J. 1977. Correlation of rock properties and the cutting performance of tunnelling machines. In E.L.J. Potts & P.B. Attawell (ed), *Conference on Rock Engineering:* 581–602, Geotechnical Society and Department of Mining Engineering; The University of Newcastle Upon Tyne.

McFeat-Smith, I. & Fowell, R.J. 1979. The selection and application of roadheaders for rock tunnelling. In A.C Maevis & W.A. Austrulid (ed), *Proceedings of the Papid Excavation and Tunnelling Conference*; 261–279, Atlanta.

Rostami, J. et al. 1994. Performance prediction: a key issue in mechanical hard rock mining. *Mining Engineering* (November), 1263–1267.

Schneider, H., 1988. Estimating cutting capability for boom-type roadheaders. *Engineering and Mining Journal*. Jan: 23–24.

Schneider, H. 1988. Criteria for selecting a boom type roadheader. *Mining Magazine*, Sep: 183–187.

Uehigashi, K., Tokairin, Y., Ishikawa, K., Kikuchi, T. 1987. Possibility of rock excavation by boom-type tunnelling machines. In: *Proc. of the 6th Australian Tunnelling Conference*. Melbourne. 253–259.

Copyright © 2005 Taylor & Francis Group plc, London, UK

The performance of a full face tunnel boring machine (TBM) in Tarabya (Istanbul)

N. Bilgin, C. Feridunoglu & D. Tumac
Istanbul Technical University, Mining Engineering Department, Istanbul, Turkey

M. Cınar, Y. Palakci, O. Gunduz & L. Ozyol
Tinsa Co., Istanbul, Turkey

ABSTRACT: The performance of a full face tunnel boring machine (Herrenknecht TBM) was evaluated within the research program of this study. TBM having a diameter of 2.9 m and cutting power of 560 kW was used to excavate the tunnel of 13270 m in length, which was situated between Sariyer and Baltalimanı. The main rock formations are Paleozoic aged sedimentary rocks, limestone, sandstone-siltstone, andesite dykes and sediment fillings. The project was commissioned to Tinsa – Öztaş – Hazinedaroğlu – Simelko consortium. The performance of TBM was recorded continuously for detailed shift analysis. A limestone block having dimensions of 0.4 × 0.5 × 0.4 m, representing majority of the rock formations was collected from one of the shafts. This rock block was subjected to full scale instrumented laboratory cutting tests using a disc cutter taken from the TBM. The relationship between thrust force and depth of cut was compared to the one obtained in the field. It is concluded that accumulated data and instrumented full scale rock cutting tests may serve as a valuable tool to predict the performance of full face tunnel boring machines in any type of rock formation.

1 INTRODUCTION

It is estimated that in the coming years the underground construction in Europe and in the other parts of the world will increase tremendously, typical examples are tunnels, microtunnels, storage caverns (oil, gas, waste etc.). Mechanical rock excavation offers many advantages over conventional drill and blast techniques. These include improved safety, minimal ground disturbances, elimination of blast vibration, reduced ventilation requirements etc. In addition, mechanical boring is capable of providing much higher rates of advance at lower cost than drill and blast excavation. A degree of uncertainty is always present on selecting equipment, predicting machine performance, estimating job duration, costs etc. However accumulated and published data from tunneling projects serve to improve predicting the machine performance and scheduling of job duration, this paper is prepared under this objective.

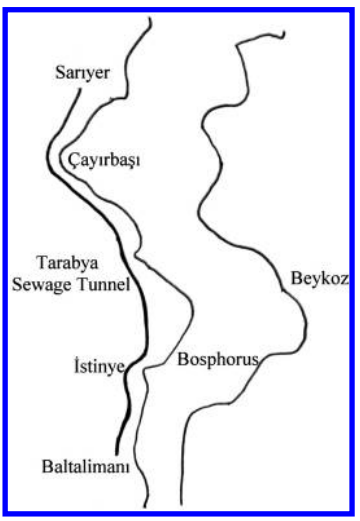


Figure 1. The general layout of the Tarabya Tunnel.

2 DESCRIPTION OF THE TUNNEL PROJECT AND TUNNEL GEOLOGY

Tarabya tunnel is a part of sewerage project, which is planned to clean the sea pollution in Istinye – Tarabya and Büyükdere bays around Istanbul Bosphorus. The tunnel having a length of 13,270 m and final diameter of 2 m is situated between Sarıyer and Baltalimanı as seen in Figure 1. 19 shafts are connected to the main

Copyright © 2005 Taylor & Francis Group plc, London, UK

tunnel with 15 tunnels being oval in shape with a size of 1200/1800 mm. Cross section of the main tunnel is given in Figure 2. The tunnel mainly passes through limestone and shale rock formations of Silurian-Devonian age and sandstone, siltstone rock formations of Carboniferous age. Some magmatic intrusions and sediment fillings are encountered in tunnel route.

Summary of the rock properties obtained from tender document is given in Table 1. The figures in Table 1 represent a tunnel length of 8847 m. The second part of the tunnel was also commissioned to the same contractors. However the second part of the tunnel was driven mainly in sediment fillings in majorities.

Some limestone samples were taken from the tunnel face in 18.09.2000 and 11.10.2000 for testing in the laboratories. It is noted that the compressive strength of the rock samples taken from the face could be different than given in general documents. The compressive strength values of the samples were 80 ± 7 MPa and 119 ± 16 MPa.

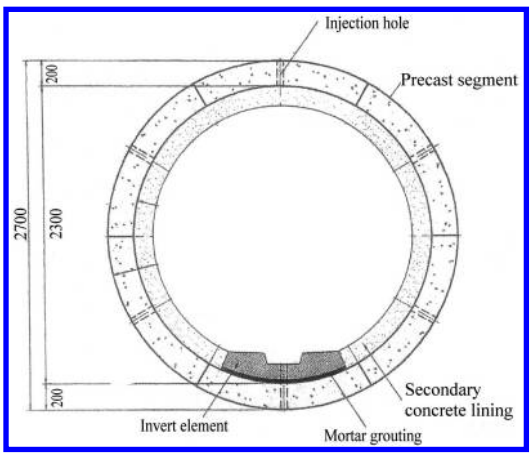


Figure 2. Cross section of the main tunnel.

Table 1. Summary of the rock properties encountered in tunnel route.

Rock formation % of the total	Compressive Strength (MPa)	Tensile strength (MPa)	Elastic modulus (MPa) × 10^3
Limestone 65%	44–81	4–5	9–15
Shale 17%	55–59	2.4	9–10
Sandstone-Siltstone 12%	59	–	–
Dykes 1%	32–40	3	6–7
Sediment Filling 5%	–	–	–

3 DESCRIPTION OF TBM AND WORK STUDY ON MACHINE ASSEMBLAGE

General characteristics of Herrenknecht TBM used in tunnel drivage are given in Table 2.

TBM came to the field in 31 May 2000 and machine assemblage time took 30 days. Table 3 summaries machine assemblage time for different jobs. A typical view of TBM is given in Figure 3.

Table 2. General characteristics of TBM used in Tarabya Tunnel.

TBM excavation diameter	2915 mm
TBM shield diameter	2870 mm
Disc number	20
Disc diameter	305 mm (edge width 10 mm)
Max. rotational speed	16 rpm
Max. torque applied	725 kNm
Number of thrust cylinders	6
Max. thrust force	3750 kN (250 bar)
Max power	620 kW

Table 3. Machine assemblage time for different jobs.

Preparation of the shaft bottom	6%
Descending the cutting head and shield	7%
Pushing cutting head and shield to face	7%
Preparation of the rails for back-up system	3%
Descending the back-up system	3%
Preparation of the steel arch supporting the first rig	3%
Assemblage of back-up and hydraulic system	25%
Preparation of the conveyor band	3%
Assemblage of the laser measuring system	7%
Assemblage of the cooling system	7%
Test running of TBM	11%
Electrical breakdown	15%
Cooling system breakdown	3%

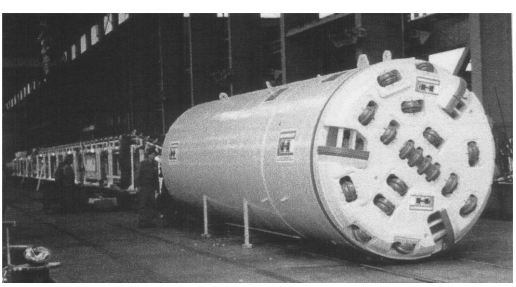


Figure 3. Typical view of TBM.

Copyright © 2005 Taylor & Francis Group plc, London, UK

4 RECORDING THE PERFORMANCE OF TBM

The tunnel excavation started in July 2000 and finished in November 2004. The performance of TBM was recorded continuously for detailed shift analysis. Table 4 is a summary of overall performance for 7700 m of tunnel drivage.

The performance of the TBM between chainage 981 and 7700 m are summarized in Figures 4–7. As seen from these figures the average machine utilization time is 35%, breakdowns are between 24 to 27% of shift time. However it is interesting to note that the share of disc changing within the breakdown time is between 36 to 41%, which is a quite high compared to other applications. The machine utilization time was found to change between 15% to 55% in general.

Machine utilization time is one of the most important factors in determining the machine advance rate. As seen from Figure 8, an increase in machine utilization time from 15% to 55%, increases the machine advance rate from 0.2 m/h to 0.8 m/h. Machine utilization time is defined as the ratio of the net cutting time of the machine to the total working time; i.e., shift time.

Table 4. Overall TBM performance for 7700 m of tunnel drivage.

The best shift advance	18 m
The mean shift advance	4.5 m
The worst shift advance	0.75 m
The best daily advance	24.75 m
The mean daily advance	11.50 m
The worst daily advance	0.75 m
The best monthly advance	531 m
The mean monthly advance	376.7 m
The worst shift advance	144.75 m

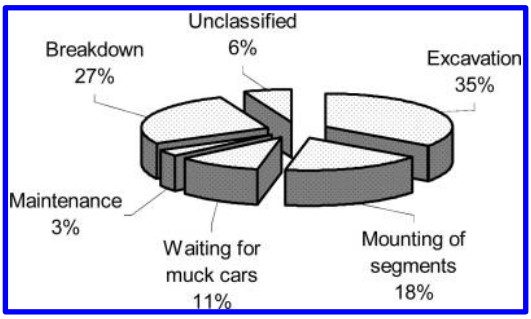


Figure 4. Machine performance between chainage 981–2260.

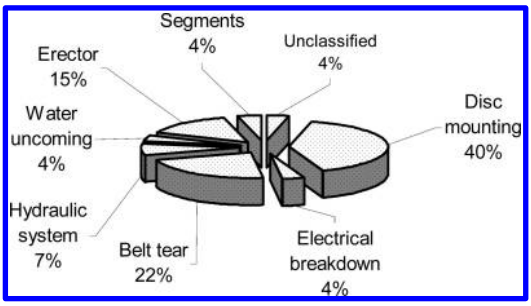


Figure 5. Classification of breakdowns between chainage 981–2260.

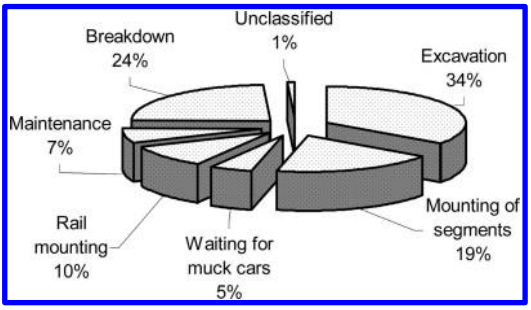


Figure 6. Machine performance between chainage 2500–7700.

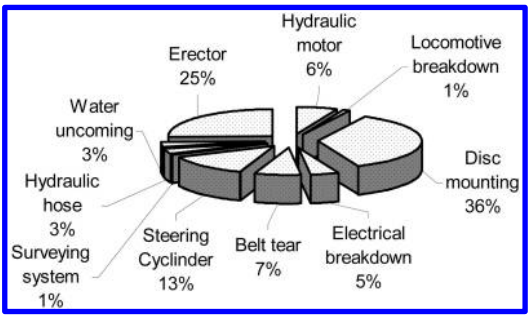


Figure 7. Classification of breakdowns between chainage 2500–7700.

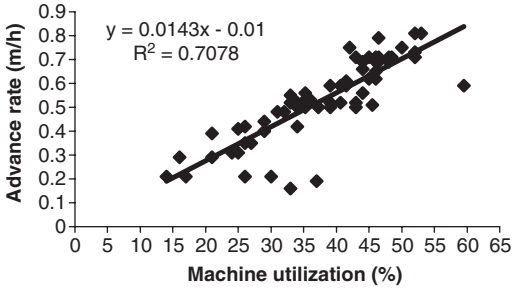


Figure 8. The relationship between machine advance rate and machine utilization time between chainage 981–2260.

Copyright © 2005 Taylor & Francis Group plc, London, UK

5 FULL SCALE ROCK CUTTING TESTS IN THE LABORATORY AND ESTIMATION OF THE MACHINE CUTTING RATE

The main objective of the laboratory rock cutting tests was to see how the in situ measured machine performance values were close to the predicted values from laboratory rock cutting tests, which will contribute to rock cutting mechanics for further industrial applications. For 4 mm depth of cut the measured net cutting rate was 9 m^3/h. Figure 9 represents the relationship between disc thrust force and depth of cut measured in the field for 1 rev/min when excavating limestone formation.

Full-scale rock cutting tests were carried out in the laboratory using the cutting rig as outlined in Figure 10. The rig was designed and manufactured within NATO-TU excavation project. A high quality aircraft aluminum block equipped with strain gauges is used as a dynamometer to record thrust forces up to 50 t. A data acquisition card included eight independent channels. Data recording rate is adjustable up to 50000 Hz.

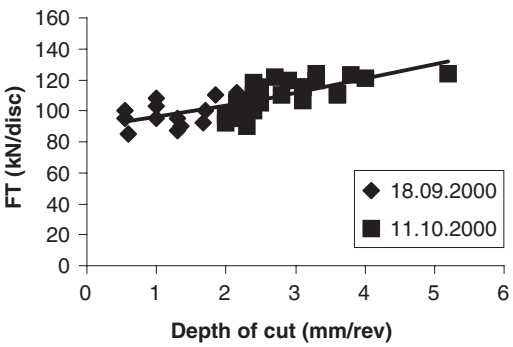


Figure 9. The relationship between disc thrust force and depth of cut measured in the field.

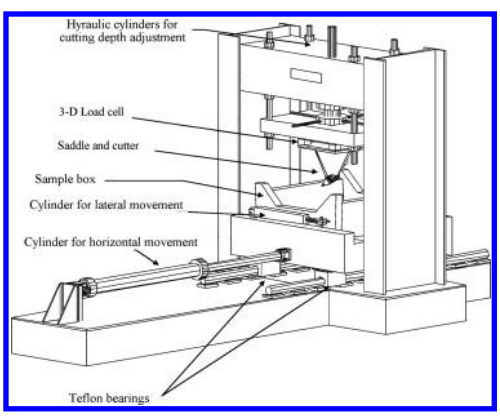


Figure 10. Schematic view of full scale cutting rig.

The hydraulic cylinders can move the sample box in which the rock sample is cast with concrete to eliminate pre-failure of the specimen. The cutter is fixed with a tool holder directly to the dynamometer. The specific energy obtained by dividing mean rolling force to yield (volume of rock removed per unit length) is a key factor in determining the efficiency of cutting process. It is advisable to work with operational parameters given minimum specific energy which is obtained for a given cutter spacing/depth of cut ratio.

The philosophy behind the laboratory rock cutting tests lies in the reality that as a basic rule of rock cutting mechanics, for a given cutting tool and rock formation, optimum specific energy is obtained for a defined s/d ratio. Specific energy is the energy to excavate a unit volume of rock (kWh/m^3) and s/d is cutter spacing/cutting depth ratio. This phenomenon is illustrated in Figure 11 (Ozdemir, 1992). The first and second cuts are inefficient, optimum chip is formed in the third pass given a minimum specific energy value which is preferred for an efficient excavation. Groove deeping should be always avoided for successful operations. Bearing in mind that the distance between disc cutters in a TBM cutting head is constant, the optimum s/d ratio will be directly dictate optimum cutting depth. The relationship between depth of cut, disc thrust force, disc rolling force, may be obtained directly from full scale rock cutting tests realized on big size rock blocks representing the rock formations which are likely to be found in tunnel line. Thrust force for a predetermined depth of cut will directly dictate total machine thrust which the machine operator must apply for an efficient cutting operation. Rolling force for a given disc cutting depth, may be directly used to calculate the power consumed during the cutting process. The torque and the power consumed in optimum cutting conditions may be calculated with the following Equations (Bilgin, 1999).

$$T = \sum_{i=1}^{i=n} r_i.FR \tag{1}$$

$$P = 2\pi NT \tag{2}$$

In these Equations FR is rolling force, n the total number of disc cutters in cutting head of the TBM, r_i is the distance from the cutter to the center of the machine, T is torque and N is revolution per minute of the cutting head and P is the power consumed during the cutting operation. Instantaneous cutting rate or net cutting rate may be calculated using the relation given in Equation 3.

Copyright © 2005 Taylor & Francis Group plc, London, UK

$$ICR = k \times \frac{P(kW)}{SE\ (kWh/m^3)} \quad (3)$$

In the Equation 3 (ICR) is instantaneous cutting rate in m^3/h, k is the energy transfer ratio changing between 0.7 and 0.8, (P) is power consumed during the cutting process and (SE) is optimum specific energy obtained in full scale laboratory cutting tests as explained in Figure 11.

The relationship between depth of cut and cutter forces obtained in the laboratory for a limestone having a compressive strength of 100 ± 8 MPa is given in Figure 12. A disc cutter taken from the TBM was used in rock cutting tests. Disc has a diameter of 305 mm and edge width of 10 mm. The actual cutter forces and measured values of thrust forces are given in Table 5. As seen from this table the field values are very close to laboratory results meaning that thrust force values obtained in the laboratory may lead to predict field depth of cut values for 1 rev./mm, hence net cutting rate of TBM.

In situ FT values for one disc are calculated by dividing total thrust force applied by thrust cylinders of TBM divided by total disc numbers. However actual thrust values delivered to rock surface is usually less then calculated values due to system efficiency and losses such as back-up system towage during mining or friction losses from contact between the shield and the rock. This is experienced to be around 20% during the excavation of Tarabya tunnel. It is reported by different investigators that net average cutter thrust force can be easily 40% less than average gross force calculated from hydraulic cylinder pressures (Nelson, 1993).

The optimum specific energy for the limestone rock formation excavated in Tarabya tunnel is calculated to be 5.7 kwh/^{3} for s/d ratio of 14. Cutter spacing of the face cutters in TBM is 86 mm, given an optimum

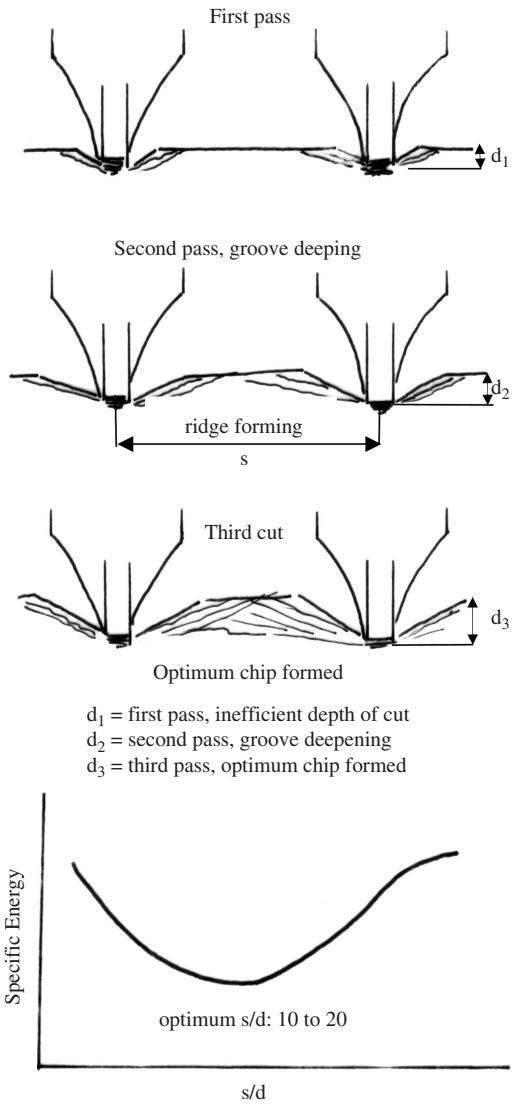


Figure 11. The relation between specific energy and optimum cutter spacing/depth of cut.

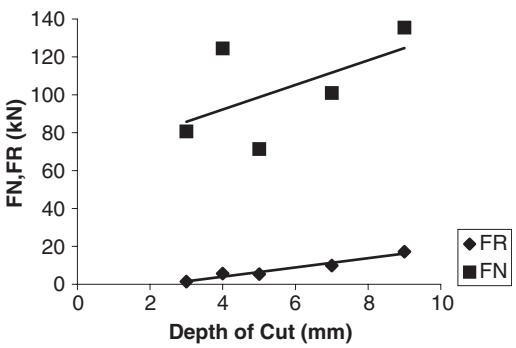


Figure 12. The relationship between depth of cut and cutter forces obtained in the laboratory.

Table 5. Field and measured thrust force values.

Depth of cut (mm)	Measured in situ FT (kN)	In situ FT with 20% less due to friction factors, (kN)	Measured laboratory values FT, (kN)
2	100	81	80
3	110	87	88
4	120	94	96
5	135	101	108

Copyright © 2005 Taylor & Francis Group plc, London, UK

depth of cut of 6 mm. Rolling force FR for one disc for 6 mm depth of cut is calculated to be 9.82 kN from Figure 12. The torque and the cutting power for optimum depth of cut are calculated using equation 1 and 2 as 142.4 kNm and 239 kW consecutively. In optimum cutting condition instantaneous cutting rate of the TBM may be calculated using equation 3 as given below.

$$ICR = 0.8x\frac{239}{5.7} m^3/h$$

$$ICR = 33.5\ m^3/h$$

Optimum thrust force for one disc cutter from Figure 12 is found to be 10.8 t Optimum thrust force that TBM operator should apply taking into account the 20% friction losses;

1.2 x 20 disc x 10.8 = 259 t

In field, during the excavation of Tarabya tunnel the instantaneous cutting rate of 33.5 m/h was obtained during some shifts.

6 CONCLUSION

Tunnel excavation in Tarabya started in July 2000 and finished in November 2004. The main rock formation excavated were Paleozoic aged sedimentary rocks, limestone, sandstone – siltstone and andasite dykes. The mean monthly advance rate of 377 m was obtained with a machine utilization time of 35%. It is shown that laboratory full-scale cutting tests may serve as a useful guide for an efficient excavation. It is shown that optimum cutting conditions were obtained using a total machine thrust force of 259 t given an optimum disc penetration of 6 mm/revolution.

7 ACKNOWLEDGEMENT

The authors are grateful to Tinsa – Öztaş – Hazinedaroğlu – Simelko consortium given access to field data and Prof.Dr. Levent Ozdemir from CSM, USA for helping to construct laboratory facilities.

REFERENCES

Bilgin N. et al. 1999. The Performance Prediction of a TBM in Tuzla-Dragos Sewerage Tunnel. In: T.Allen et al. (eds). *The World Tunnel Congress*, Oslo 31 May 3 June: 817–822, Rotterdam: Balkema.

Bilgin N. et al. 1999. The Performance Prediction of a TBM in Difficult Ground Condition. *AFTES-Journees d'Etudes Internationales de Paris,* 25–28 October, 115–121.

Nelson P. 1993. TBM Performance Analysis with Reference to Rock Properties, Mechanized Excavation. In: J.A. Hudson (ed). *Comprehensive Rock Engineering* 4: 27.

Ozdemir L. 1992. Short Course Notes. *Mechanical Excavation Techniques in Underground Construction,* 2 Volumes, ITU Faculty of Mines.

Copyright © 2005 Taylor & Francis Group plc, London, UK

Slurry shield driven microtunnel applications in Istanbul

A.B. Akkaya
Eregli Iron and Steel Plants A.S., Kdz Eregli-Zonguldak-Turkey

H. Copur
Istanbul Technical University, Mining Eng. Dept., Maslak-Istanbul-Turkey

N. Omac
CET Construction, Ltd. Sti., Levent-Istanbul-Turkey

H.M. Yucel
Istanbul Water and Sewage Authority, Aksaray-Istanbul-Turkey

ABSTRACT: Field performance of a shielded slurry microtunnel boring machine used for installing concrete pipelines in four different project sites in Istanbul is presented in this study. Herrenknecht AVN 1800C machine is used for installation of the wastewater pipelines. Brief descriptions of the projects are presented. Geological conditions and formations varying from rock to water-bearing sands and silts that the machine passes through the project sites are described briefly based on in-situ and laboratory site investigations. Field performance of the machine is summarized based on field observations and records, such as average system utilization and net advance rates, as well as downtime. The results demonstrate the success of microtunnelling to cope with varying ground conditions, which influence the boring performance to a great extent, without disruptions to the surface and underground utilities.

1 MICROTUNNELLING

Growing population and demand on prosperity increase the need for installation, replacement and rehabilitation of infrastructure systems (underground openings-mainly utility lines) in the urban areas. Urban areas are environmentally sensitive and include some obstacles in the surface such as highways, roads, railways, rivers, canals, buildings and airfields that are in the path of pipe lines. A special care should be taken in order to not disturb the surface structures due to surface settlement.

A set of pipes are placed (installed) underground in the most of the cases. Placement can be performed by either open cut (trenching, cut and cover construction methods) or using trenchless tunneling technologies (microtunnelling, pipe jacking, no-dig technologies). Advantages of trenchless construction method over cut and cover construction is presented in Table 1.

Trenchless tunneling includes the techniques for the installation, replacement, renovation and repair of pipes, ducts, cables and other underground apparatus with minimum excavation from the ground surface. It may also include associated techniques such as leak detection, inspection and location of existing infrastructure. Applicable diameters are up to 3.5 meters (maximum available pipe diameter). Microtunnelling can be defined as remotely controlled, steerable, continuous pipe jacking in all diameters whether man-accessible or not, which is used especially in the North America.

2 THE PROJECT

Istanbul Water and Sewage Authority (ISKI) started a project for wastewater collecting and refining system. CET Construction Co is awarded the contract to lay concrete pipes of 2,000 mm ID, including the sections of Kagithane Left Shore Collectors, North Halic Collectors and Tunnels, Kabatas to Baltalimani Tunnels, Kemerburgaz Tunnels, Baltalimani Wastewater Refining System, Baltalimani Discharge Line and Stream Improvement, North Halic Secondary Collectors and Tarabya Collectors and Tunnels.

Trenchless construction method is considered as the best solution for this project to not disturb the heavy traffic, many buildings, structures and utilities found in the project sites.

Copyright © 2005 Taylor & Francis Group plc, London, UK

Table 1. Advantages of trenchless construction over cut and cover construction.

- Minimizes risk of settlement, disruption to the surface structures, traffic, existing sewers, utilities and services during construction, reduces the social cost.
- Minimizes reconstruction work to road surfaces and restoration work to buildings.
- Working problems in contaminated ground would be eliminated as spoil is removed with the slurry or with no muck haulage systems (ground displacement methods).
- When working in contaminated ground, the only soil excavated is that of the pipe bore.
- Considerably reduces the amount of excavated material to be removed compared to an open cut excavation method, because only the pipe bore is excavated.
- Avoids the need to dewater the pipe trench, thereby significantly reducing the risk of collapse/settlement.
- Reduces need for man-entry and improves operator/worker safety, because of remote control capability.
- Accurate installation with line and grade tolerances of better than ±2.5 cm over even the longest drive lengths.
- Strength of pipe is typically greater than open cut pipe.
- Smooth internal finish giving good flow characteristics.
- No requirement for secondary lining.
- Prevention of ground water ingress by use of pipes with sealed flexible joints.
- Applicable to most soil types and conditions.
- Applicable to any depth.
- A virtually maintenance-free construction.
- Network design flexibility.
- Speedier construction (excavation, pipe installation and muck haulage continuously and simultaneously)
- Provides a cost effective modern solution.

3 THE MACHINE

Herrenknecht 1800C slurry microtunnelling machine fitted with an extension to skin up to 2,000 mm diameter and having a mix-shield cutting head is utilized by CET Construction Co in the project, passing through different ground conditions varying from water bearing sand to medium strength rock. A picture of the machine is presented in Figure 1. Some of the specifications of the microtunnelling machine and jacking frame are presented in Table 2.

Cutting wheel is of four-spoke design, fitted with replaceable slab cutters. Four arms (one behind every spoke) are used for the power transmission from the cutting wheel shaft. Those arms are also used as stone crusher. Slab cutters are carbide fitted. They are mounted into the prepared recesses on the front side of the cutting wheel and screwed with hex head screws from the rear. Center cutter is fitted with an especially hard facing and it forms a cone-shaped outline. Caliber cutters are mounted at two spokes of the cutting wheel.

Laser target and bypass are mounted in the machine can. The steering head is attached to the machine can by four hydraulic steering cylinders. These are used to direct the steering head and cutting wheel in the direction while pipe jacking. The machine can is also used as an abutment for steering movements. Also, switchgear cabinets for the power supply exist in the machine can.

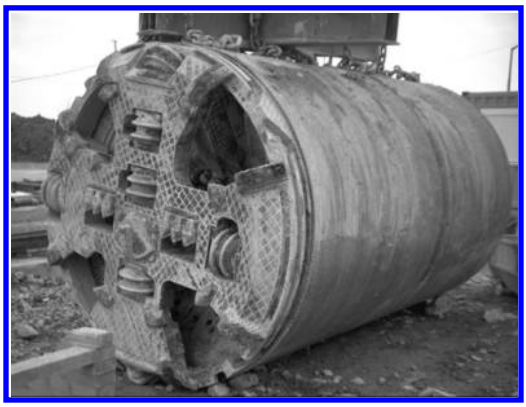


Figure 1. Herrenknecht AVN 1800C.

To prevent rotation between the machine can and the trailing tube, two torque reaction bars are provided between the two. In this way, the skin friction almost absorb the roll, which is a reaction of running the cutting head.

Laser target helps to control the machine. It records the position of the laser beam and sends the data via cable to the computer mounted in the control panel of the control container.

Push cylinders are used as propulsion group of jacking frame. They are designed with flat plates to move the push ring forward if the push cylinders are discharged. The push cylinders have a stroke of 1,830 mm.

The push cylinders are also used to move back the push ring to its start position. They are also controlled from the operators control panel in the control container or from the remote control panel located in the launching shaft.

The machine has a data logging system for recording machine operational parameters. These records are used for performance analysis in this study.

4 THE PIPES

Concrete pipes of 3 m length, 2 m ID, 2.4 m OD and around 10 tonnes weight, are produced at the site using self-compacting concrete. The pipes are designed to withstand jacking forces of up to 3000 tonnes, which is much more than required using the Herrenknecht machine. Due to the nature of the concrete, very smooth surfaces are obtained and jacking forces are substantially reduced when this smoothness is coupled with a bentonite lubrication system.

Copyright © 2005 Taylor & Francis Group plc, London, UK

Table 2. Machine and jacking frame specifications.

Company	Herrenknecht AG
Type	AVN 1800C
Production Year	2002
Cutting Wheel Length	2140 mm
Length after Cutting Wheel	3264 mm
Cutting (Excavation) Diameter	2496 mm
Shield Weight	7460 kg
Total Weight	19940 kg
Cutting Wheel Drive Motor	132 kW/400 V/50 H
Torque (Left and Right at 275 bar)	245545 Nm
Revolution (Left and Right)	0–3.4 rpm
Number of Drive Motors	1
Number of Steering Cylinders	4
Dia. of steering cylinders (piston/rod)	180/120 mm
Stroke of Steering Cylinders	100 mm
Steering Capacity per Cylinder at 500 bar (Extend/Retract)	1250/706 kN
Steering Angle (Up/Down)	4.7°
Steering Angle (Diagonal)	3.3°
Steering Angle (Left/Right)	4.7°
Diameter of Feed/Slurry Lines	125 mm
Diameter of Bypass	125 mm
Number of Bypass Cylinders	5 Stuck
Maximum Pressure of Bypass Cylinder	150 bar
Max. Pressure of Steering Cylinder	500 Bar
Jacking Frame Shaft Dimension	6 m × 5 m
Minimum Height (Shaft Bottom to Tunnel Axis)	1500 mm
Maximum Pipe Length	3000 mm
Maximum Outside Pipe Diameter	2450 mm
Clear Width	2500 mm
Number of Jacking Cylinders	2
Number of Lifting Points	4
Jacking Cylinder Size (Piston/Rod)	330/260 mm
Maximum Jacking Cylinder Stroke (First Stroke)	1690 mm
Second Cylinder Stroke	1830 mm
Total Cylinder Stroke	3520 mm
Maximum Pressure per Jacking Cylinder (Extend/Retract)	500/400 Bar
Jacking Cylinder Motor Power	30 kW/400 V
Total Jacking Force (Extend/Retract)	8548/2600 kN
Additional Hydraulic Pump Motor for Jacking Cylinders	22 kW
Feed Pump Drive Motor	55 kW/400 V

5 THE FORMATION AND PERFORMANCE

The first section is along the banks of the Kurbagalidere River and involves laying 700 m of 2,000 mm ID and 2,440 mm OD concrete pipes. This first section between the two existing pipelines is left untouched due to the extremely difficult geological conditions for man-entry pipe jacking methods, which requires a rather costly grouting all along the line. The geology comprised very fine sand and silty sand with a water table at about 2 to 3 m below the surface, which is a flowing ground. A total of 8 shafts are constructed at an average depth of 7 m using caisson shaft sinking methods. A general view of drive shaft and slurry separation system is presented in Figures 2 and 3, respectively. The back walls of all the launch shafts are jet grouted to provide stability during the pipe jacking operations. When works commence, the first 700 m are completed in about 3 months. The machine achieves speed up to 150 mm/minute and progress of up to 45 m is achieved in a 24 hour work. A typical daily advance rate achieved between two shafts in Kurbagalidere is presented in Figure 4.



Figure 2. A view of drive shaft.



Figure 3. A view of slurry separation system.

The second part of the project is in the Bostanci region of Istanbul close to the Marmara Sea. This section passes through quite different geology than that at Kurbagalidere. The geology comprises limestone with an average unconfined compression strength of 50 MPa, with ground changing to a clay formation in the middle and to a silty sand formation in the latter part of the section. A total of 9 shafts are constructed and the works are finished in 3 months with lower advance rates than at Kurbagalidere. However, much

Copyright © 2005 Taylor & Francis Group plc, London, UK

lower set up and pipe connection times are spent as the crew gains more experience. The positions of shafts (manholes) in Bostanci microtunnelling site is presented in Figure 5. A typical daily advance rate achieved between two shafts in Bostanci area is presented in Figure 6.

Kucukkoy microtunnel alignment with total length of 462 m includes sandstone, gravel, sand and silt, which create problems during construction. Totally 8 shafts/manholes are constructed in this section. Bentonite lubrication is also used to reduce the jacking forces. A typical daily advance rate achieved between two shafts in Kucukkoy is presented in Figure 7.

Kucukcekmece consists of clay, silt and gravel along the microtunnel alignment. An example of advance rate from Kucukcekmece is presented in Figure 8.

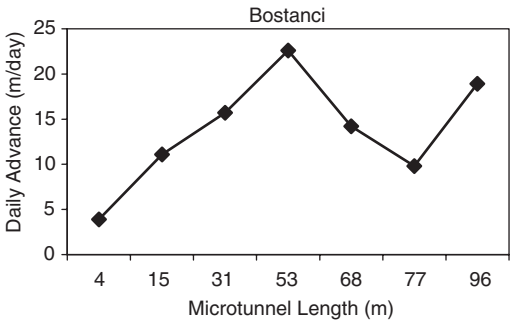


Figure 6. Microtunnel advance rate in Bostanci.

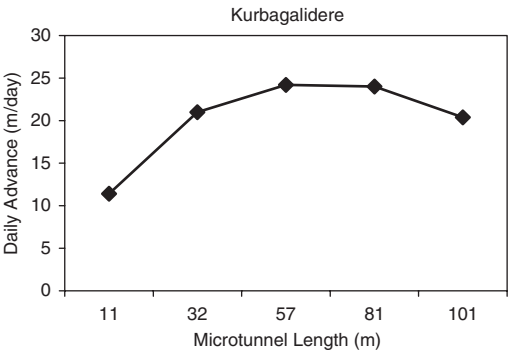


Figure 4. Microtunnel advance rate in Kurbagalidere.

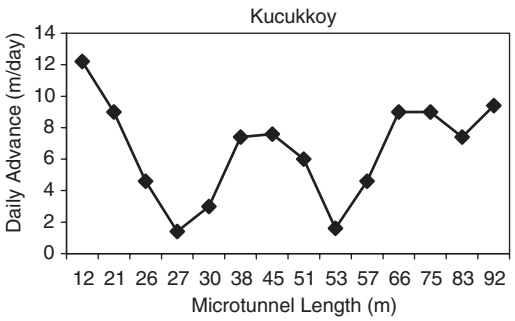


Figure 7. Microtunnel advance rate in Kucukkoy.

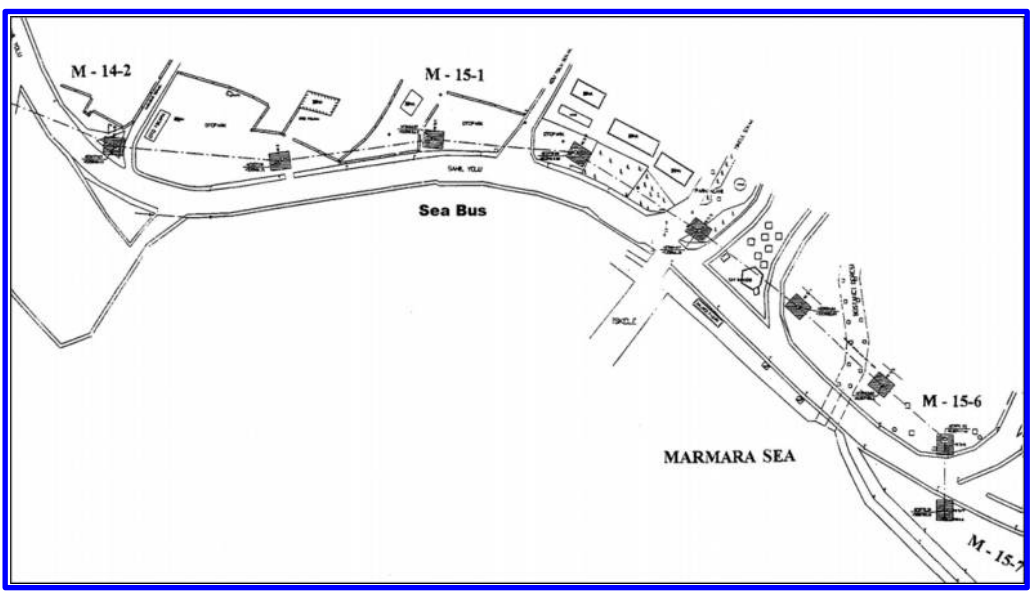


Figure 5. Positions of manholes in Bostanci.

Copyright © 2005 Taylor & Francis Group plc, London, UK

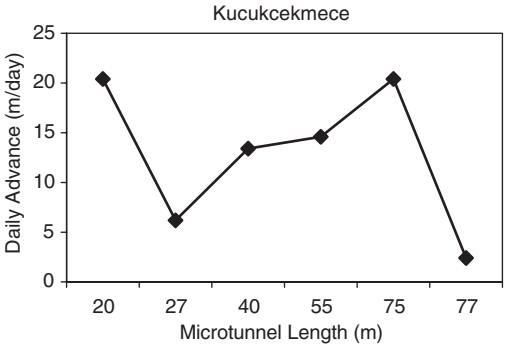


Figure 8. Microtunnel advance rate in Kucukcekmece.

Table 3. Overall performance of the machine.

Machine Utilization	32 to 35%
Machine Downtime	65 to 68%
Advance in Kurbagalidere	~6 pipes/day
Advance in Bostanci	~4 pipes/day
Advance in Kucukkoy	~3 pipes/day
Advance in Kucukcekmece	~5 pipes/day

The overall field performance of the machine are summarized in Table 3 based on the collected field data for all the sections mentioned above. Downtime, includes around 20% of slurry problems, 12% of power failure, 6% of cutter wear, 25 to 30% others and does not include lunch breaks.

6 CONCLUSIONS

Project owners and contractors in Turkey are getting aware of the merits of microtunnelling and other trenchless construction methods and the applications of these techniques increase rapidly in especially large urban areas such as Istanbul. The method reduces especially the social cost, minimizes the surface settlements and disruptions to heavy traffic of the largely urbanized cities and increases the quality of the finished utility lines.

This study summarizes the performance of Herrenknecht AVN 1800C, which is classified as a full-face excavation machine with slurry type muck removal system. The machine passes successfully through many different types of ground conditions including water bearing sand, silt and gravel and medium strength limestone and sandstone.

At the beginning of the works, the set up and pipe connection periods were rather longer than the expected as the crew had no previous experience for this kind of machine, and so the machine utilization time were quite low. But now, the crew is very experienced and machine utilization and daily advance rates are increasing eventually in every new microtunnel construction project.

7 ACKNOWLEDGEMENTS

This study is a part of Ahmet Baris Akkaya's PhD thesis. The authors are grateful to the Istanbul Municipality, Istanbul Water and Sewage Authority (ISKI), representatives of CET Construction Co and Istanbul Technical University Mining Engineering Department for their valuable help and support during the studies.

REFERENCES

Technical Documents about Herrenknecht AVN 1800
Construction Contracts of Istanbul Water and Sewage Authority (ISKI)
Geological Reports of the areas, ARI Mining Co
CET Construction Co, Data Reports from Microtunnel Machine Records

Copyright © 2005 Taylor & Francis Group plc, London, UK

Earth Pressure Balance tunnelling for two short drives for the New Mississippi Outfall, Denver, Colorado

J.Y. Kaneshiro & A.F. Stirbys
Parsons, Pasadena, California, USA

G.R. Fischer
Shannon & Wilson, Denver, Colorado, USA

ABSTRACT: Earth Pressure Balance (EPB) tunnelling technology has become economical at shorter and shorter lengths because of the combination of the availability of used EPB machines as well as increased urbanization and value of surface space. This paper presents an overview of design and construction of two EPB machine drives (554 m and 91 m) for the New Mississippi Tunnel Outfall for the Transportation Expansion Project (T-REX). The Contractor was Southeast Corridor Constructors, a Kiewit-Parsons, Joint Venture. The T-REX Project's New Mississippi Outfall is a US$ 30 million constructed value project, a small but important part of the US$ 1.2 billion highway widening and Light Rail Transit expansion project of Denver's Interstate Highway I-25.

1 INTRODUCTION

1.1 *Project description*

The Outfall conveys highway and other urban drainage to the South Platte River as well as provides long needed relief from flooding problems in the southeastern portion of the Interstate 25 highway corridor. The Outfall tunnel conveys storm water under I-25 then under Mississippi Avenue to the river. The Outfall consists of a number of distinct elements with water flowing and connecting from east to west as follows: an Energy Dissipation Structure, 91 m of 213 cm diameter jacked pipe EPB crossing under I-25, Junction Interceptor Structure, 554 m of 4 m ID tunnel excavated by EPB machine technology, a Transition Structure (connecting the circular section to a rectangular section and serving as the main tunnel driving shaft), 266 m of 5.5 m wide by 2.4 m high cut and cover box structure, and Outfall Structure at the South Platte River.

The Outfall crosses both the existing I-25 as well as the future improvements including under the Light Rail Transit, a new bridge abutment, widened lanes, and new retaining walls. The Outfall also crosses adjacent to several buildings and five bridges, under major traffic and utility intersections, and through difficult geology. The permitting, ROW easements, geotechnical investigation, design and construction was part of the design-build contract package. Close and continuous coordination with City, County, State, and Federal regulatory permitting agencies, railroads and other private businesses was required.

The geology consists of unconsolidated saturated alluvial river deposits and the Denver formation (sandstone, siltstone and claystone). The tunnelling conditions are difficult because tunnelling methods would have to be adapted to tunnelling efficiently and with little settlement in soil and weak rock, and in both soil and weak rock at the same tunnel cross section (mixed face conditions). Also, being down gradient of the Gates Rubber Plant, there was the possibility of encountering contaminated groundwater in the tunnel.

1.2 *Project planning and 30% design*

Colorado Department of Transportation and their representatives prepared Preliminary Engineering to 30% Documents for the New Mississippi Outfall for tendering as a design-build project. The design of the outfall consisted of two options: (1) a smaller diameter pipe jacked alignments versus (2) a primarily curved tunneled alignment (shown in plan on Figure 1). Both alignments are further to the north, crossing near the LRT station at Broadway and I-25, north of the Gates Rubber Plant.

The tender specification design standards provided for (a) pipe jacking and (b) tunnelling with conventional "hand mining" methods (also known as Sequential Excavation Method or New Austrian Tunnelling

Copyright © 2005 Taylor & Francis Group plc, London, UK

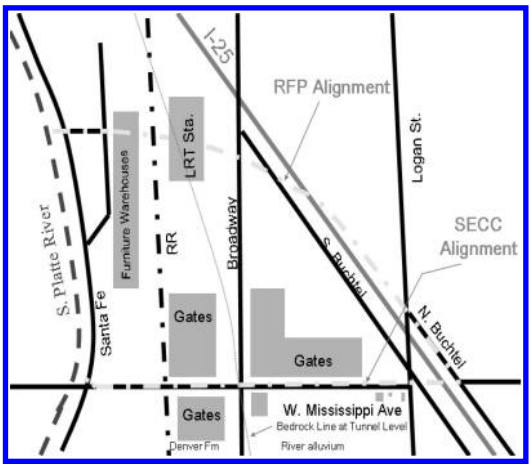


Figure 1. Site location map.

Method) or (c) tunnelling with a shielded tunnel boring machine. Provisions were made to supplement these tunnelling methods as required with dewatering and ground modification methods such as chemical grouting. The final liner specifications were geared for cast in place or a smooth finished shotcrete liner.

1.3 *Bid phase*

The Southeast Corridor Constructors (SECC) Team (Kiewit-Parsons with subcontractors: KCM, Earth Surface Systems, Shannon & Wilson, and Elmore Pipe Jacking) began evaluating the outfall option about 6 months prior to bid and selected the primarily tunnel alignment (as opposed to pipe jacking) to bid. The primarily tunnel alignment would require tunnelling under a furniture warehouse and underpinning several footings in weak rock or mixed face ground conditions, as well as tunnelling on a large gentle curve under I-25 in saturated sands. In order to cope with all ground conditions and the concern of contaminated groundwater, the team proposed using controlled tunnel face tunnelling methods; i.e., earth pressure balance (EPB) tunnelling. The weak rock tunnel section would be mined using a roadheader (excavator mounted on boom) and supported with shotcrete and steel ribs. Underpinning of the furniture warehouse foundation would be most effective from within the hand mined tunnel, where as the EPBM tunnel was more amenable to the soil or mixed face ground. The weak rock tunnel cross section would be larger than the EPB tunnel boring machine so that it could be advanced through the area that required underpinning to the mixed face and soil ground conditions. Also, the Team planned on using a precast concrete segmented liner as both the initial ground support as well as the final finished liner.

During the bidding period, the SECC Team also considered a new Mississippi Avenue outfall further to the south, but it was dismissed at the time due to clearance issues (Figure 1). The grade of West Mississippi Avenue was lowered to provide clearance for the LRT, so there was a sag in the road alignment. To avoid the clearance problems, the Team proposed a siphon taking advantage of keeping the entire tunnel alignment within the competent Denver formation, with the exception of the shafts themselves. The siphon concept was rejected by CDOT due to concerns of access and maintenance and due to concerns that the siphon would not be self cleaning.

2 DESIGN

2.1 *Alternative alignment selection*

After award of T-REX to SECC, the Team reconsidered the advantages of an alignment on Mississippi Avenue. The clearance issue at the LRT bridges was solved by changing the drainage structure section to a lower profile box culvert. From a hydrological standpoint, location of the outfall on Mississippi made better sense to fit in with the natural and urban drainage layout. The other main advantages of the Mississippi Alignment as compared to the alignment provided in the Tender Documents are as follows.

- CDOT would avoid the problem of obtaining the ROW from private interests, namely the Gates Rubber Plant.
- The Gates Rubber Plant was up gradient from potential hazardous waste plumes.
- The alignment is straight without curves, thus minimizing potential problems and slower advance on curves.
- Underpinning of the commercial businesses, mainly the furniture warehouse would be avoided.
- Crossing under the LRT Station at Broadway with potential mixed face ground would be avoided.
- Crossing under the highway obtusely and on a curve for a long distance in alluvial river deposits would be avoided.
- The alignment is a significantly shorter reducing the amount of tunnel and pipeline by about 550 m.

The New Mississippi Alignment Outfall (Figures 1 and 2) had its fair share of obstacles, which the design and construction had to overcome including:

- Similar difficult tunnelling and ground conditions as the original Tender Documents
- Similar concerns for rerouting utilities
- Economic concerns of a shorter tunnel
- Tunnelling under several important utilities under Broadway St.

Copyright © 2005 Taylor & Francis Group plc, London, UK

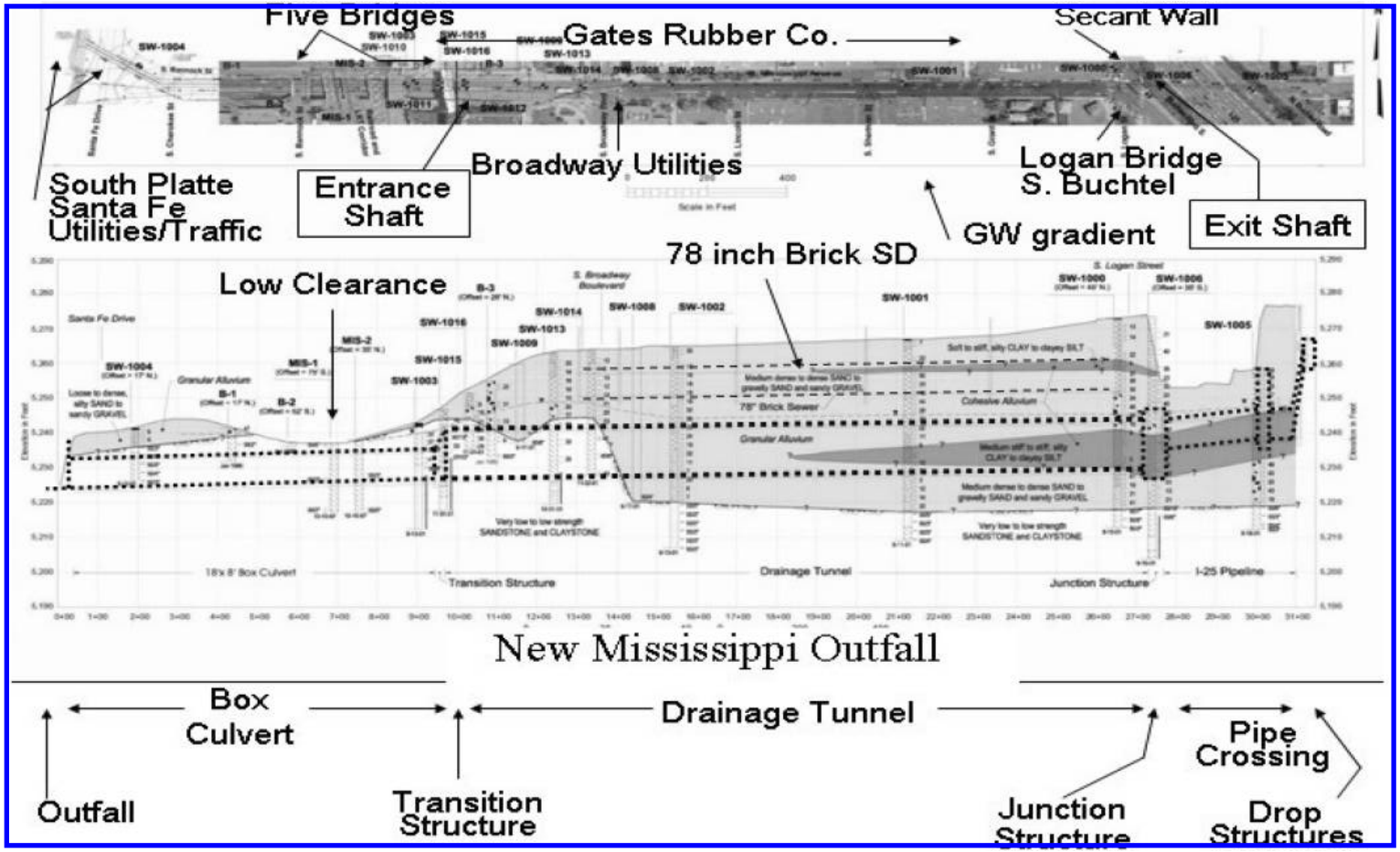


Figure 2. Plan and profile: Key elements and geotechnical conditions.

Copyright © 2005 Taylor & Francis Group plc, London, UK

- Clearance issues at the LRT and railroads and the sag on West Mississippi Ave.
- Underpinning of five bridge foundations and adjacent retaining walls and sidewalks
- Tunnelling adjacent to the Gates Rubber Plant Buildings
- Tunnelling under the existing brick storm drain outfall with less than half a diameter of cover

Meeting these challenges was accomplished as discussed in the following sections.

2.2 *Final design*

The geotechnical investigation and design began simultaneously in the early Fall of 2001. Previous borings in the area from the LRT bridges and other road and utility improvements combined with new borings led to the interpreted geologic and tunnelling conditions as illustrated in Figure 2. The New Mississippi Outfall alignment had essentially no geotechnical information as compared to the one provided in the Tender Documents. By selecting the new alignment and all its advantages, the Team also accepted all the disadvantages and risks of differing site conditions. Because the new project configuration consisted of significantly less tunnel, the Team considered constructing the alignment entirely by cut and cover, but in the final evaluation tunnelling was chosen. The tunnel is over 2 diameters depth at maximum cover, crosses under industrial and suburban neighborhoods, and crosses less than 3 m under a 50-year old three-course brick 198 cm ID storm drain from about Broadway Street to I-25. There would still be significant open cut and cover work, and the temporary shoring and underpinning bridges for the Burlington Northern and Santa Fe Railroad and the Union Pacific Railroad, access roads, and the LRT.

The geology is fill and saturated medium dense alluvium, predominantly fine to medium grain sands, overlying the Denver formation, which consists of claystone, siltstone, and sandstone. No contaminated materials were encountered during the investigation. The cut and cover rectangular culvert, outlet structure, and transition structure (see bottom of Figure 2 for location) were expected to be primarily in the Denver formation, whereas the tunnel began in the Denver formation at the transition structure on the west for about 150 m, changed to a combination of the Denver formation and alluvium (mixed face ground) under Broadway, for the remainder of the tunnel alignment, and through the junction structure, the pipeline under I-25, and the drop structure. The groundwater table appears to be fairly consistent year round at the crown of the tunnel; the hydrostatic pressure at the bottom of the face of the tunnel is only about 1/2 bar.

The outlet structure will serve as maintenance access so incorporated an access road, wing walls, apron, riprap, and plantings for aesthetic and environmental considerations. The apron and box were to be founded on piers as an extra measure of security for scour protection. The geotechnical conditions expected were alluvium, fill, and claystone near the surface since the South Platte River in the vicinity of the outlet was in bedrock.

In order to avoid clearance problems and provide a minimum of 0.9 m of cover at the sag of Mississippi Ave., the section was changed from a 4 m ID circular tunnel to an 5.5 m wide by 2.4 m high rectangular culvert. The disadvantage of a 5.5 m wide internal dimension section is that there is very little clearance, especially between the spread footing bridge foundations. Utility congestion was also of concern.

The culvert was situated in the Denver formation's swelling claystone and as such was designed for high swell pressures on the order of 240 to 480 kPa depending on the location. This required thicker 46 cm walls than would otherwise be required, exacerbating clearance concerns. To minimize and mitigate potential high swell pressures, the claystone was protected with shotcrete on the walls and a concrete slab within 48 hours after initial exposure. The underpinning design of the 5 bridge piers was performed by Brierley Associates (Denver) and incorporated mini or micro piles and soil nails. Underpinning incorporated two-35 mm rebar at 1.5 m centers, while soil nails were 25 mm rebar at 1.5 m centers with 10 cm of shotcrete.

Tunnel design consisted of a 23 cm thick, 5 piece and key. The segments were designed to be fastened together across both the radial/longitudinal and circle transverse joints with plastic dowels. The rings/keys were staggered to provide for cross sectional rigidity as well as to ensure gasket closure. The specifications required the rings be tapered for steering in case the operation should go of alignment, although the alignment was straight. There is very little tolerance for correcting the alignment over such a short length of tunnel given the design is a one-pass liner and gasket leakage considerations only allow a small amount of offset.

The tunnel was designed using two dimensional finite element frame models incorporating hinge elements at the joints and tangential and radial springs for soil-structure interaction. Various loading combinations were evaluated including full overburden and minimum overburden with live loads from the future light rail. Like the box culvert, the tunnel was also situated in claystone for a portion of the alignment and was designed for the potential high swell pressures.

The saturated alluvium carries very few fines and is uncemented, thus requiring special considerations with respect to controlling settlement. An extensive

Copyright © 2005 Taylor & Francis Group plc, London, UK

instrumentation and monitoring system was implemented including settlement points, multi-position and single position extensometers, and tiltmeters. Also, under Broadway where there are extensive utilities, provisions for compaction grouting were installed, which effectively helps to recover lost ground by jacking the ground back up by injecting bulbs of low slump concrete. Based on experience with controlled face tunnelling methods, a settlement trough due to tunnelling was anticipated, with the maximum settlement occurring above the tunnel crown, diminishing to zero at the edge of the trough. The shape of the trough is normally distributed over a width defined by about a 45-degree line measured from the springline of the tunnel. Maximum surface settlements were estimated to be 13 mm to 25 mm, depending on the experience of the earth pressure balance machine operator, representing a face loss of one percent. The Team recognized the sandy nature of the material was not ideal for earth pressure balance methods unless polymer additives were employed to condition the excavated soils (muck) to a "toothpaste" consistency to form a plug in the screw conveyor. The conditioned muck allows the spoils to be discharged into muck cars at atmospheric pressure without loss pressure (1/2 bar) at the tunnel excavation face.

The tunnel connects to the junction structure, which picked up flows at three sources. The junction structure, which also serves as the TBM receiving shaft, required construction of temporary shoring consisting of sheet piles with internal bracing. The temporary shoring and tunnel eye were designed by Atlantic Engineering (Seattle, WA). The sheet piles were designed to be driven to bedrock or a clayey member within the alluvium. Dewatering pump tests were performed to determine the feasibility of effective drawdown.

The crossing under I-25 was considered by open cut-and-cover and pipe jacking using a controlled-face tunnelling shield. Because of dewatering and traffic concerns, the crossing was select to be performed by pipe jacking. The junction structure also serves as the jacking pit for the 213 cm ID Class V reinforced concrete pipe.

The highway widening in the vicinity of the junction structure will accommodate the new LRT and a widened I-25. As such, a retaining wall will span across and over the tunnel. The tunnel is also in the vicinity of bridge piers for the new Logan Street Bridge. Special concern for design of the tunnel in this area was considered due to the passive loads, which would be generated in the piers due to the lateral loads spanning the tunnel. An inner liner was considered, isolated piers, and larger diameter stiffer piers, but eventually, the designer of the walls designed the piers to be tied back to minimize the passive pressures developed in the pier.

3 INSTRUMENTATION

Instrumentation was installed to monitor ground, utility, and existing structure deformations during excavation of the box culverts, west portal shaft, tunnel, east portal shaft, and I-25 crossing. Instrumentation monitoring systems included building settlement markers, utility settlement markers, tiltmeter plates, surface settlement markers, extensometers, and inclinometer casings.

A precondition survey was performed of the existing brick storm drain and old outfall. The survey revealed that the laterals connecting to the storm drain had already separated from the brick storm drains prior to tunnelling.

4 CONSTRUCTION

4.1 *Open cut section*

Construction and mobilization of the cut and cover portion of the project began in November 2001. Permanent underpinning of the bridges foundations and temporary shoring was performed by WLH Construction (Denver). The claystone behaved well, and no significant settlement occurred adjacent to the open excavations. Construction of the outlet structure, originally projected to be founded in the Denver formation. As it turned out depth to bedrock was from 7.5 to 11 m deep in this area and was due to an old paleo-channel or previous man made channels in the area. The original design incorporated piers as a second defense against scour. Since some of the piers would be impractically deep, and the outlet was already provided with grouted riprap, it was decided that certain piers were not required.

4.2 *EPB 554 meter drive*

Tunnel construction was performed by Elmore Pipe Jacking (Sylmar, CA), which was acquired by Affholder (Chesterfield, MO). Tunnel advance rates range from a low of 1.2 m to a high of 14.6 m. Average advance rate is about 6 to 7.2 m per day. The contractor typically worked 5 days per week, one 10 hour shift per day. Advance at the beginning was slow and messy, requiring large amounts of water to assist in excavating the claystone bedrock.

Precast concrete segment manufacturing began in December of 2001 by Economy Precast (Sylmar, CA). Mobilization of the Lovat Earth Pressure Balance TBM began in March of 2002, and began from the west end towards the east to the Junction structure at I-25. The segment forms and the TBM were previously used on the North Metro Interceptor II Sewer Tunnel near the San Diego Airport (ca. 1997). The

Copyright © 2005 Taylor & Francis Group plc, London, UK

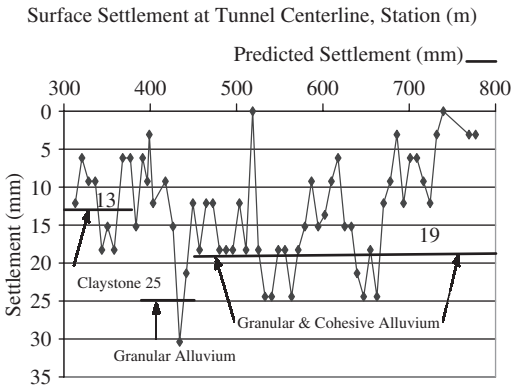


Figure 3. Actual surface settlement.

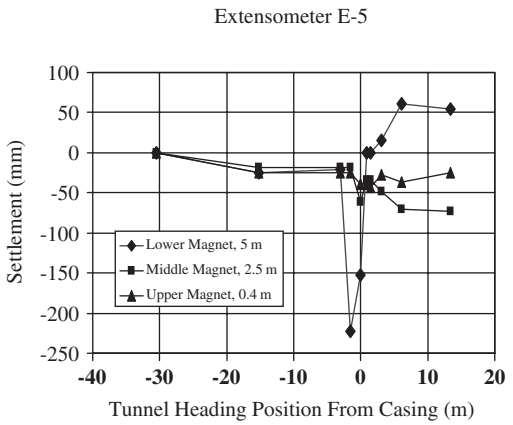


Figure 4. Settlement at Extensometer 5-E.

TBM had also been used on the Colombia Slough project in Portland, OR. The steel forms were originally made by EFCO and modified by Economy Precast into a one-pass system to accommodate gasket grooves and the dowelled and clipped connecting system. The TBM originally equipped with only a screw conveyor had been modified on the Colombia Slough project (ca. 1999) to also include a muck ring.

4.3 *Settlements for 554 meter drive*

Tunnelling under Broadway Street, under the utilities, and in particular under the brick storm drain went fairly smoothly. Settlement data indicates typically less than about 20 to 25 mm and occasionally less than about 5 mm heave. The actual settlement records from borehole extensometers along the alignment compared to the predicted settlement is shown in Figure 3.

After tunnelling 120 m, the lower magnet at 5 m depth or 2 m above the crown of the tunnel of Extensometer E-5, began showing rapid movement of over 200 mm as shown in Figure 4. The settlement was successfully arrested and never reached the surface by immediate compaction grouting by Denver Grouting (Hayward Baker) also as shown in Figure 4.

There were, however, several sinkholes along the alignment. On one occasion, the SECC Team shut down the tunnel subcontractor after three sinkholes occurred, which were promptly filled with concrete and the area was secured by compaction grouting. The largest sinkhole required ten 8 cubic meter trucks. Also, on another occasion, the City shut down the tunnel subcontractor after a sinkhole occurred a hundred meters behind the excavation face. In all sinkhole cases, there was no danger to the public or traffic concerns, as the road was in an industrial area.

The tunnel subcontractor performed ground penetrating radar surveys to ensure the City that no further sinkholes would occur. The tunnel contractor chose not to include polymer additives to condition the muck. Also flood doors in the cutterhead were not functioning properly, which led to the sinkholes during several shutdowns.

Construction of the junction structure shoring using sheet piles and internal bracing was completed successfully but the dewatering of the excavation had proven to be difficult. The Junction structure was not installed at the original design depth and some minor modifications were required to prevent flotation of the finished structure. Hole through of the tunnel was completed on August 16, 2002.

4.4 *EPB 91 meter drive*

Because of the difficulty experienced with dewatering at the Junction Structure, the I-25 crossing alignment was re-evaluated by Terracon and the elevation of the pipe was slightly modified so as to be constructed within a clay layer. Michels Pipeline Construction, Inc. of Brownsville, Wisconsin jacked a 213 cm Class V Reinforced Concrete Pipe using a 2.54 m OD Lovat boring machine with a muck ring. The 91 m crossing was accomplished in less than one week, working 24 hours per day. Dewatering was performed at both the jacking (Junction Structure) pit and the receiving pit by Griffin Dewatering Company of Omaha City, Nebraska. While tunnelling under I-25 no lanes were closed.

4.5 *Settlements for 91 meter drive*

Instrumentation indicated minimal settlement. A series of 6 surface settlement points were placed along the centerline of the alignment across the freeway. Measurements were taken at night. Maximum surface settlement of the Highway was less than 9 mm, and typically 0 to 3 mm. There was loss of ground, which

Copyright © 2005 Taylor & Francis Group plc, London, UK

occurred on the shoulder at the exit shaft adjacent to I-25 shutting down a lane temporarily. Otherwise, the crossing was completed successfully with no major incident.

5 CONCLUSIONS

The predicted geologic conditions at the outlet structure were different than expected. A boring at this location may have uncovered this problem, but since construction was in the open and the paleo-channel was small, there was little consequence on overall construction. For the remainder of the alignment, the anticipated geotechnical conditions and their behavior were as expected. No contaminated groundwater or earth materials were encountered, which could have been problematic with the RFP alignment.

Considering the tunnelling operations did not employ conditioners and malfunctioned during shutdowns, performance with respect to minimizing settlement, damage to adjacent structures and the brick storm drain was remarkable.

The Design-Build team optimized the alignment in terms of plan, profile and construction methods saving considerable dollars for all parties. The Contractor elected to propose the alternatives of (1) controlled face earth tunnelling using mechanized methods (EPB), (2) EPB tunnel/pipe jacking under I-25, (3) a one-pass precast concrete gasketed and dowelled segmented liner, and (4) an entirely different alignment. The first three proposed methods were made economical by the availability of previously used EPB machines and segment forms, which were specially modified for this project. These methods commonly economical for longer and larger tunnel projects were cost-effective despite the short length of tunnels given the urban environment and difficult ground conditions. Finally, the New Mississippi Outfall alignment proposed and constructed also fit naturally into the urban runoff setting and avoided costly right-of-way issues.

ACKNOWLEDGEMENTS

Special thanks to Maurcio Andrade of Kiewit and George Cotton of ESS who championed the cause for an alternative alignment, Roger Kilgore of KCM for assisting in difficult permitting issues, Andy Peterka of Economy Precast who led the effort to modify the forms for this project. Layout of text mail or by courier well packed and in time. Be sure that all pages are included in the parcel.

Copyright © 2005 Taylor & Francis Group plc, London, UK

Ground movements induced by Earth-Pressure Balanced, Slurry Shield and Compressed-Air tunneling techniques on the Toulouse subway line B

F. Emeriault, T. Bonnet-Eymard & R. Kastner
URGC Géotechnique, INSA, Lyon, France

E. Vanoudheusden*, G. Petit* & J. Robert
Arcadis ESG, Paris and Toulouse (*), France

J.Y. de Lamballerie
Maîtrise d'œuvre du Métro de l'Agglomération Toulousaine, Toulouse, France

B. Reynaud
Société du Métro de l'Agglomération Toulousaine (SMAT), Toulouse, France

ABSTRACT: A global comparison of the effects of different tunneling techniques (Earth-Pressure Balanced Shield, Slurry Shield and Compressed-Air) on ground movements and strain in the tunnel lining segments is performed through the analysis of the results of three monitoring sections installed during the excavation works of Toulouse subway line B. The comparison is justified by the homogeneous geology of the site and the almost constant depth of the tunnel. Tunneling parameters such as the confining pressure, the grouting pressure and volume of grout injected are considered in the analysis.

1 INTRODUCTION

The 12.6 km long subway line B of Toulouse (France) has been realized with three different tunnel boring machine (TBM) techniques: Contracts 2 and 5 are excavated with earth-pressure balanced TBM and Contract 4 with a slurry shield TBM (all three machines are approximately 7.7 m in diameter) while Contract 3 uses a compressed-air TBM of 5.3 m in diameter.

The encountered geology is homogeneous on the whole layout. The tunnels run through the Toulouse molasses (hard sandy clay with pockets and lenses of very dense sand). Geotechnical investigations have shown that in these formations, K_0 is greater than 1, generally close to 1.2 and that geotechnical characteristics are homogeneous ($\gamma = 22\,kN/m^3$, $S_u = 300\,kPa$, $c' = 30\,kPa$, $\phi' = 32°$). The average cover ranges between 10 and 20 m and the water table is mostly found 4 m below ground level.

Since the geology, stratigraphy and tunnel cover are almost identical, the differences in soil reaction can be explained by the tunnelling parameters such as the pressure used for the stabilization of the excavation face (earth, slurry or air pressure) and the grouting pressure used to fill the remaining annular void behind the tunnel lining.

2 MONITORING OF THE THREE SECTIONS

Particular attention has been paid to the movements induced by the excavation within the soil mass and on the existing buildings. Several monitoring sections have been defined on each of the four contracts consisting in inclinometers, multi-points borehole extensometers and precise levelling. Strains are also measured in the tunnel concrete lining segments (one pair of vibrating wire strain gauges per segment). A typical monitoring section is described in Figure 1.

Additional monitoring includes precise levelling of exiting buildings and, for some of the sections, tiltmeters (with automatic data acquisition), horizontal extension measurements and cracks opening measurements using Demec strain gauges. An example of a complete monitoring section can be found in Vanoudheusden et al. 2005.

For each type of TBM, one section has been selected and the measured vertical and horizontal ground movements are presented in addition to the average values

Copyright © 2005 Taylor & Francis Group plc, London, UK

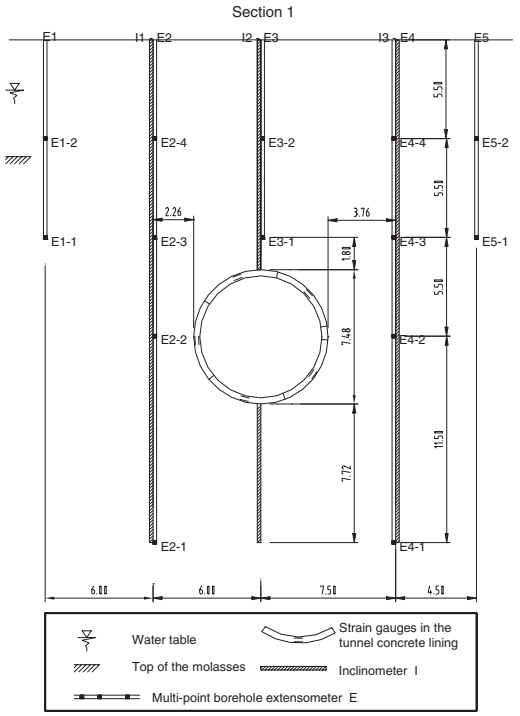


Figure 1. Typical monitoring section.

Table 1. Comparison of the 3 sections.

Section	1	2	3
TBM	EPBS	Air	Slurry
H (m)	12.8	16.0	18.5
D (m)	7.75	5.28	7.73
H/D	1.65	3.03	2.39
Annular void (m)	0.12	0.06	0.135
Water table level (m)	−2.8	−4.1	−4.7
Molasse cover (m)	6.3	10.0	10.3
Lenses of sand	yes	yes	no

of the main tunnelling parameters (the main characteristics of the sections are summarized in Table 1): Section 1 corresponds to an Earth Pressure Balanced TBM while Section 2 is related to an Compressed-Air TBM and Section 3 to the Slurry Shield technique.

3 TBM ADVANCEMENT AND PARAMETERS

Figure 2 shows that for the three sections the excavation rate is approximately constant. It is noteworthy that Sections 1 and 3 are reached when respectively a 2.9 km and 2.5 km long part of the tunnel has been

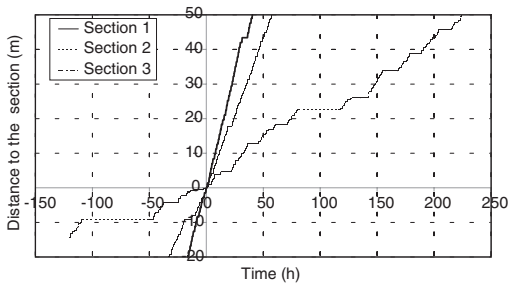


Figure 2. Distance to the monitoring section vs. time.

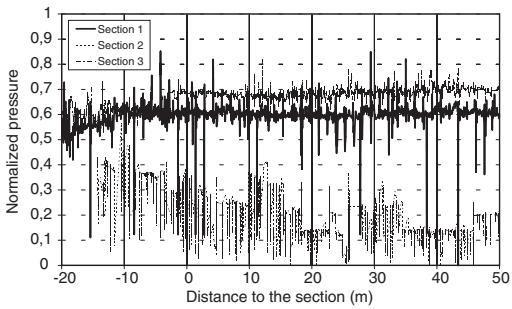


Figure 3. Normalized confining pressure P_{front}/σ_{v0} vs. distance to the monitoring section.

excavated whereas Section 2 is located only 50 m away from the entrance pit. Moreover, in this case, the excavation works are stopped during the night (between 9:00 pm and 6:00 am).

The tunneling parameters of interest for the analysis are the following:

– pressure at the front P_{front} (either earth, slurry or air pressure)
– grouting pressure P_{grout}
– volume of grout injected per ring V_{grout}

These parameters are measured by different devices every second.

3.1 *Stabilization of the front*

For each monitoring section, Figure 3 shows the variation of the pressure at the front (for Section 1 an average value is determined from the values recorded by the different pressure cells). In order to compare the results, this pressure is normalized by the total vertical stress at the tunnel crown σ_{v0}.

It can be observed that for Sections 1 and 3, the pressure at the front is almost constant with average values ranging from 0.6 σ_{v0} to 0.7 σ_{v0} (see Table 2). This confirms that the excavation rate is constant and that the geology is homogeneous within −20 m and +50 m of the monitoring section.

Copyright © 2005 Taylor & Francis Group plc, London, UK

Table 2. Comparison of mean tunnelling parameters.

Section	1	2	3
P_{front} (kPa)	155	44–118	243
U (kPa)	100	119	138
P_{front}/σ_{v0}	0.60	0.14–0.37	0.68
P_{grout} (kPa)	265	N/A	476
P_{grout}/σ_{v0}	1.00	N/A	1.24
V_{grout}/V_{theo}	1.20	1.90	1.18

The normalized pressure P_{front}/σ_{v0} recorded for Section 2 is relatively low (with values ranging from 0.14 to 0.37) whereas 55 m after the monitoring section this value rises suddenly to 0.6. The compressed-air tunneling technique enables the pilot to visually analyze the excavation front and its potential stability. Therefore in the [−20 m; +50 m] range, the clayey and overconsolidated characteristics of the molasses have laid the pilot to use a relatively low pressure at the front. After 55 m, the molasses becoming sandy and highly permeable, the pressure at the front had to be increased to avoid water inflow (due to the high hydraulic head) and instability of the excavation front. The average value of P_{front} then used (180 kPa) is close to the pore pressure at the level of the tunnel invert (177 kPa with H, D and water table level given in Table 1).

3.2 *Grouting pressure*

For Sections 1 and 3, the average grouting pressure can be determined for each installed tunnel ring. This pressure appears to remain constant in the [−20 m; +50 m] range and equal or slightly greater than the vertical stress at the tunnel crown (Table 2 summarizes the obtained values P_{grout} and the normalized value P_{grout}/σ_{v0}).

The grouting pressure is not available for Section 2 due to a technical problem.

3.3 *Volume of grout injected*

In addition to the average grouting pressure, the volume of grout injected per installed tunnel ring is an interesting parameter to analyze. The measured volumes remain almost constant in the [−20 m; +50 m] range for the three sections, their average value being given in Table 2 (normalized by the theoretical volume of void that has to be filled by the grout).

It appears that the volume of grout injected is slightly greater than the theoretical volume for Sections 1 and 3 (+20%). This difference can be explained by the over-cutting generally used by both TBM that is not accounted for in the theoretical volume and by an excess of injection (controlled by the pilot with an imposed level of grouting pressure greater than the initial vertical stress) that can explain the observed vertical movements of the ground surface (see 4.1).

For Section 2, the excavation technique itself leads to a major over-cutting: the measured volume of grout is almost twice the theoretical volume (determined with the 0.06 m difference between the TBM shield and the tunnel lining outer radii – see Table 1).

These conclusions should be carefully considered because it appears that the measure of volume is not easy to perform and therefore can be relatively inaccurate.

4 OBSERVED SOIL MOVEMENTS

4.1 *Surface settlements*

The vertical displacements of the ground surface have been measured by precise levelling of the 5 borehole extensometer heads and of levelling points installed either on the pavement and sidewalks or building facades. In the [−10 m; +12 m] range, one topographic survey is done for each installed tunnel ring (1.0 m or 1.4 m long).

Figure 4 shows that for Section 1 the TBM progression induces in a first stage upwards movements of the ground surface (with a maximum heave observed directly above the tunnel axis equal to 1.07 mm). After approximately 40 m, the different extensometer heads start to settle (see Figure 5). The final maximum settlement of 0.6 mm is reached 20 days after the passage of the TBM and is not observed directly above the tunnel axis but with a 12 m offset.

The same scenario is observed for Section 3 (see Table 3). The difference in maximal heave can be explained but the greater depth of the tunnel in Section 3, the other tunneling parameter being approximately identical (P_{front}/σ_{v0}, P_{grout}/σ_{v0}, V_{grout}/V_{theo}).

For Section 2, the observed ground surface movements are only settlements (with a final value of 1.8 mm above the tunnel axis). They are mainly due to the low pressure at the front, P_{front}/σ_{v0} ranging from 0.14 to 0.37. A second monitoring section located 70 m after Section 2 exhibits the same ground movements as Sections 1 and 3. As mentioned in 3.1, in this zone, the confining pressure is greater and P_{front}/σ_{v0} is close to 0.57.

4.2 *Horizontal displacements*

The horizontal movements have been measured for each section in three inclinometric casings located in the tunnel axis (I2) and on both sides of the tunnel approximately at a distance of D/2 away from the sidewalls (I1 and I3). The tip of the casing is one diameter

Copyright © 2005 Taylor & Francis Group plc, London, UK

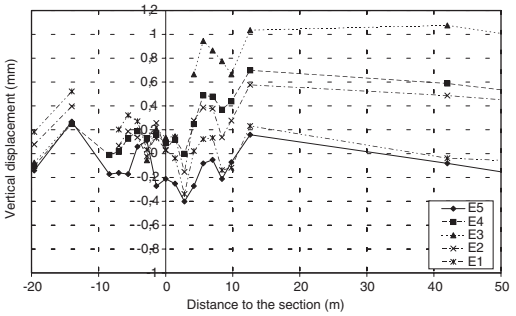


Figure 4. Vertical displacement of the extensometer heads vs. distance to the monitoring section (positive = heave – negative = settlement).

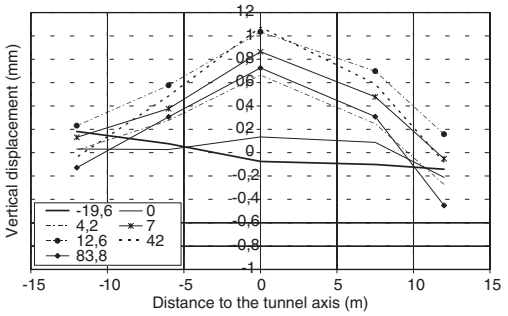


Figure 5. "Settlement" trough for different distances to the monitoring section (positive = heave – negative = settlement).

Table 3. Comparison of the settlement troughs.

Section	1	2	3
Settlement (mm)	0.6*	1.8	0.9*
Maximal heave (mm)	1.07	no heave	0.55

* The maximum value is not obtained for the leveling point placed directly above the tunnel axis.

below the tunnel invert. Unfortunately this total length generally does not prove to be sufficient to ensure bottom fixity of the casing.

The observed longitudinal horizontal movements (parallel to the tunnel axis) are generally small and close to the accuracy of the inclinometric measure (between 1 and 2 mm of maximum displacement on the total length). They correspond to displacements towards the TBM excavation chamber, the maximum being observed in the upper part of the tunnel, slightly above the center. Table 4 summarizes the results obtained for the three sections.

Table 4. Comparison of the horizontal displacements.

Section	1	2	3
Displacements parallel to the tunnel axis			
Maximum (mm)	N/S	−1.5	−1.7
Depth (m)	–	17	19–24
Depth/(H + D/2)	–	0.91	0.85–1.07
Displacements perpendicular to the tunnel axis			
Maximum (mm)	5.7	9	3.6
Depth (m)	18.5	17.5	22.5
Depth/(H + D/2)	1.10	0.94	1.00

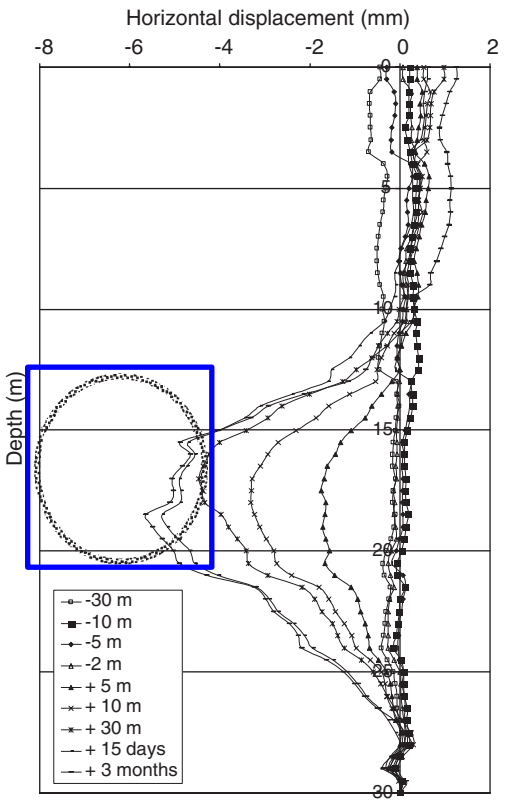


Figure 6: Horizontal displacements in the plane of the monitoring section.

The transversal displacements are more significant (Figure 6). They appear when the cutting wheel is 2 m before reaching the monitoring section and correspond to a convergence towards the tunnel. The maximum displacement is obtained in the lower part of the tunnel slightly below the axis. 15 days are necessary to obtain the final stabilized values.

From Table 4, it can be concluded that small convergence displacements are observed (for example

Copyright © 2005 Taylor & Francis Group plc, London, UK

3.6 mm for Section 3) when the normalized pressure at the front P_{front}/σ_{v0} and normalized grouting pressure P_{grout}/σ_{v0} present high values close to 1.0 or greater.

The simultaneous convergent horizontal displacements and ground surface heave can be explained by the high value of K_0 (greater than 1.0 and generally close to 1.2).

4.3 *Vertical displacements*

The vertical displacements at different locations within the soil are measured by five multi-points borehole extensometers. The typical monitoring section (see Figure 1) includes:

- two lateral 2-points extensometers at a distance of 2 D from the tunnel axis (E1 and E5),
- two 4-points extensometers at a distance of D/2 from the tunnel sidewalls (E2 and E4)
- a central 2-points extensometer (E3).

The differential vertical displacement between the anchor and the extensometer head are automatically recorded every 5 min.

Figure 7 presents the results obtained for the extensometer E2 of Section 1 and Figure 8 corresponds to E3 of the same section. These results are representative of what is measured on Sections 2 and 3. Positive values correspond to the shortening of the distance between the two points.

It can be concluded from Figure 8 that the two anchors of extensometer E3 present similar movements (even though the amplitude is small):

- when the cutting wheel reaches the monitoring section a sudden shortening of the distance between the anchor and the extensometer head appears indicating that the anchor moves upward (the displacement is then greater than the observed ground surface heave)
- the increase in the distance observed afterwards correspond to the progression of the shield with a reduction in diameter
- the third stage is caused by the grout injection that is sufficient to bring the distance between the anchor and the extensometer head to its initial value.

The determination of the total vertical displacements requires the addition of the vertical displacement of the extensometer head. Due to the limited number of topographic surveys, this operation has been performed in the case of extensometer E2 for three positions of the TBM (0, 7.0 and 84 m). The reference of displacement is chosen when the cutting wheel is 20 m before the monitoring section. The results are presented in Table 5.

For the deepest anchor E2-1, the vertical movements are very small (except for the measure corresponding to 0 m). It can be concluded that this point is not affected by the excavation operations because it is located at a distance D below the tunnel invert and that the total displacements for 0 m should be discarded (in italic in Table 5). The precision of the levelling of the extensometer head is probably responsible for this discrepancy.

E2-2 presents an increasing upwards movement. The final 0.17 mm displacement should be compared with the horizontal convergence observed in inclinometer I1 at the same depth: 4.7 mm (see Figure 6).

On the opposite, increasing settlements are observed for E2-3 with a maximum value of −0.35 mm which

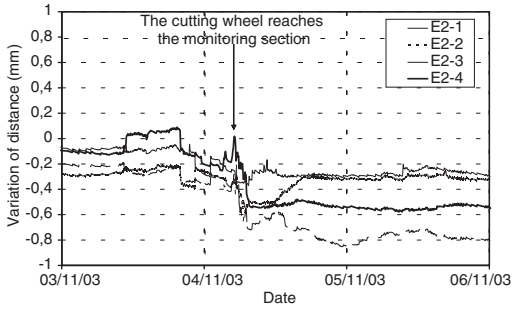


Figure 7. Differential vertical displacements of the 4 anchors of extensometer E2 and ground surface vs. time.

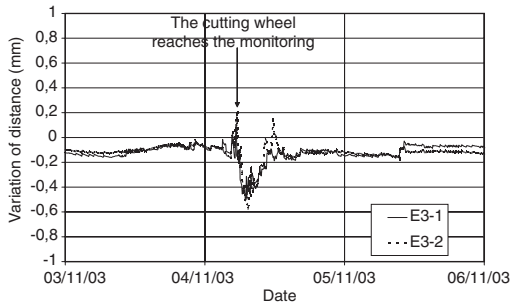


Figure 8. Differential vertical displacements of the 2 anchors of extensometer E3 and ground surface vs. time.

Table 5. Total vertical displacements (in mm) of the anchors of extensometer E2 for Section 1.

Distance to the section	−20 m	0 m		7 m	84 m
E2-1	0*	−0.12	–	+0.03	+0.03
E2-2	0*	−0.07	–	+0.13	+0.17
E2-3	0*	−0.19	–	−0.12	−0.35
E2-4	0*	−0.03	–	+0.20	−0.13

* Reference of the displacements is taken when the cutting wheel is 20 m before the monitoring section.

Copyright © 2005 Taylor & Francis Group plc, London, UK

should also be compared with the horizontal displacement measured at the same depth: 0.66 mm.

Finally for E2-4 (the closest anchor to the ground surface), the movements are very similar to those of the ground surface: heave is observed between −20 m and 7 m and afterwards settlement occurs.

5 STRAINS IN THE TUNNEL LINING

The variations of strains in the tunnel lining are measured in each monitoring section by 5 pairs of vibrating wire strain gauges installed in the lining segments at the intrados and extrados. Automatic data acquisition starts as soon as the ring is installed, one measurement is taken every 10 min.

Reference for the strains is taken before the lining segments are transported in the tunnel entrance shaft and thus before any load is applied. Negative μ-strains correspond to compression and positive values to extension. The average strain for each pair of gauges is presented in Figure 9 for Section 1. Table 6 draws the main conclusion of Sections 1 and 3.

The segment installation process generally induces an "initial" μ-strain affected by several factors that can not be clearly identified or assessed: temperature of the concrete, temperature of the strain gauges, load applied by the hydraulic jack ensuring the progression of the TBM, ….

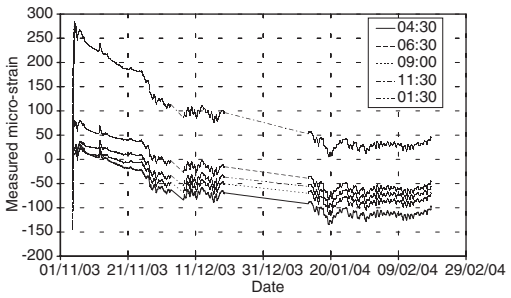


Figure 9. Strain gauges measurements vs. time.

Table 6. Comparison of the strains in the tunnel lining.

Section	1	2	3
Maximum μ-strain	[22;267]	N/S	[−41;185]
Position of maximum	Crown	–	Crown
μ-strain after 20 days	[−22;181]	N/S	[−52;155]
μ-strain after 3 months	[−115;30]	N/S	–

Generally, positive μ-strains are measured. This means that extension occurs but this extension can not be physically explained.

Nevertheless, approximately 24 hours after installation (which corresponds to a progression of the TBM of approximately 35–40 m), μ-strains start to decrease. This indicates that the lining segments are subjected to compression. Final values are obtained after approximately two months.

The difference observed in the range of maximum μ-strains for Sections 1 and 3 (see Table 6) can be partly explained by the greater grouting pressure P_{grout} and P_{grout}/σ_{v0} used in Section 3 leading to smaller initial extension μ-strains.

After approximately 3 months, the μ-strains measured in the 5 segments of the tunnel lining of Section 1 are stabilized. The induced increments of compressive stress that can be calculated from the decrease of μ-strains range from 2.75 MPa for the tunnel invert to 4.75 MPa for the tunnel crown. They can be related to an increase of the pressure applied by the soil and grout to the tunnel lining ranging from 247 kPa to 428 kPa. These stresses are close to the values of the vertical total stress σ_{v0} at the crown and invert of the tunnel (266 and 429 kPa). The greater final stress at the crown level could be explained by:

a) the fact that grout is injected essentially in the upper part of the annular void
b) the effect of buoyancy (the final "unit weight" of the tunnel is 10 times smaller than that of the molasses.

6 CONCLUSION

The effect of tunneling with different tunnel boring machines has been compared by the analysis of three monitoring sections installed on the Toulouse subway line B corresponding to similar depths and diameters of tunnel and to homogeneous ground conditions. The recorded vertical and horizontal movements can be related to the average values of tunneling parameters such as confining pressure or grouting pressure and injected volume.

It appears that, due to the particular ground conditions found in the Toulouse molasses, the vertical movements are much smaller than the horizontal ones. Depending on the confining pressure and grouting pressure, the convergent horizontal movements can be reduced and associated with either ground surface settlements or heave.

The use of multi-points extensometers installed vertically at a short distance of the tunnel sidewalls has shown that the vertical displacements of points located at different depth can be either increasing settlement, increasing heave or first heave and then settlement.

Copyright © 2005 Taylor & Francis Group plc, London, UK

Finally strain measurements in the tunnel lining, even though they are difficult to analyze in the first 24 hours after installation, show that progressive compression stresses appear in the lining segments. This compressive stresses can be related to the total stresses in the surrounding soil.

ACKNOWLEDGEMENT

The authors would like to thank for their financial support the French Ministry of Research and the Réseau Génie Civil & Urbain (RGC&U). They also would like to acknowledge the help of the different contractors in collecting data.

REFERENCES

Vanoudheusden E., Petit G., Robert J., Emeriault F., Kastner R., de Lamballerie J.-Y. & Reynaud B. 2005. Impact on the environment of a shallow gallery excavated in Toulouse's molasses by a conventionnal method. *Proceedings of ITA-AITES 2005, 7–12 May 2005, Istanbul, Turkey*.

Copyright © 2005 Taylor & Francis Group plc, London, UK

Large cross-section shield tunnel passing right under the Jyoban and Hibiya railway lines: Minowa Tunnel of the Tsukuba Express line

K. Sasaki, K. Sakamaki & S. Abe
Japan Railway Construction, Transport and Technology Agency

ABSTRACT: The Minowa Tunnel, constructed by the slurry shield method with an outer shield diameter of 10.2 mm, passed obliquely right under railway lines in service (Tokyo Metro Hibiya, JR freight, and JR Jyoban lines) for a length of about 300 m. The construction conditions were severe because the overburden of the tunnel in the intersection area is thin (1.2 to 0.4 times the tunnel diameter), an alluvial clay layer with N-values of 0 to 6 is prevalent in the area, and a sandy soil susceptible to collapse is present in the upper part of the tunnel. To ensure the integrity and safety of the railway facilities while operating the existing railway lines on usual schedule, the tunnel was constructed by preventing slurry eruption during shield advancement and suppressing abrupt settlement of the railway tracks.

1 INTRODUCTION

Tsukuba Express is a new railway line with a total length of 58.3 km between Akihabara in Tokyo and Tsukuba-shi in Ibaraki Prefecture (Figure 1). The Minowa Tunnel is situated on the line between Asakusa Station, under construction in Taito-ku, and Minami-Senju Station in Arakawa-ku. The double-track shield tunnel, with a length of 2219 m, a segmental outer diameter of 10.0 mm, and a finished inner diameter of 9.2 m, was constructed by the slurry shield method.

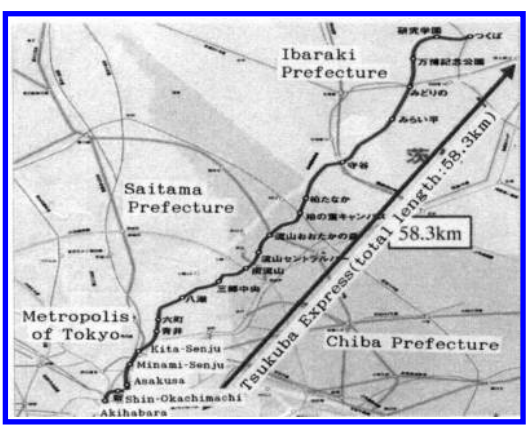


Figure 1. Schematic map showing the planned route of Tsukuba Express.

From Asakusa Station to Minami-Senju Station, as shown in Figure 2, the tunnel construction advanced below the Kokusai-dori street for about 1300 m through densely populated residential areas on an upward slope of 33 per mil, and the tunnel passed right under the Tokyo Rapid Transit Authority's (Tokyo Metro) Hibiya subway line, a JR freight line, and the JR Jyoban railway line. Advanced technologies and careful control on the construction were therefore required to prevent disturbances to key structures and to ensure the safety of the train traffic.

2 GEOLOGY OF THE AREA OF INTERSECTION WITH THE EXISTING LINES

The upper part of tunnel cross sections in the area of intersection with the railway lines in service (see Figure 3) has N-values of about 4 and grain-size composition of 70% sand, 16% silt, and 14% clay. Because the water-bearing sand layer consists of fine grains with high uniformity coefficients and low N-values,

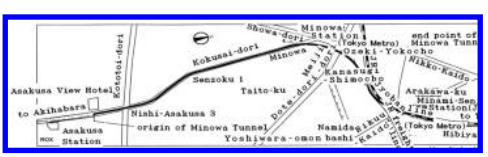


Figure 2. Plan view, sectional view, and profile of Minowa Tunnel.

Copyright © 2005 Taylor & Francis Group plc, London, UK

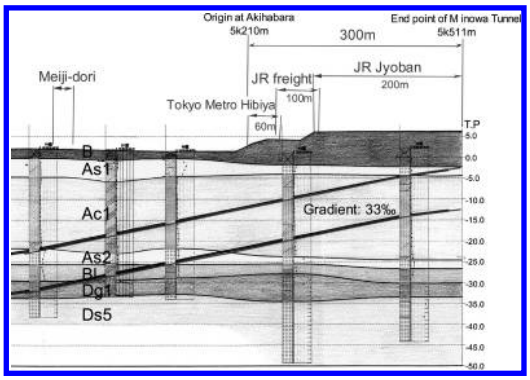


Figure 3. Geological profile of the soft cohesive soil section.

some problems were concerned: (1) susceptibility to fluidization, (2) susceptibility to failure, and (3) possible settlement and slurry eruption during shield advancement.

3 CHALLENGES REGARDING SHIELD ADVANCEMENT

The most important thing was to complete the tunnel within a set period under failure-prone geologic conditions with thin overburden, while ensuring the safety of the trains that frequently pass above the tunnel. To this end, three main challenges were identified: (1) improvement of the soil below the existing railway tracks, (2) development of methods and systems for simultaneous track measurement on the three existing lines, (3) setting and verification of shield advancement control values.

4 IMPACT PREDICTION AND CONTROL VALUE SETTING IN THE AREA OF INTERSECTION

Ground displacement in the area of intersection with the existing lines was predicted by finite element analysis before the tunneling. Because slurry eruption was expected from the thin overburden, slurry pressure in the analysis was set to the sum of natural water pressure + fluctuating pressure (20 kPa), which is lower than the lower limit (active earth pressure + water pressure + fluctuating pressure) usually adopted in the slurry shield method.

As a result, the maximum settlement, with soil improvement, on the ground level of the track was found to be 30 mm. The deformation modulus of the ground after chemical grouting was assumed to be twice that of the existing ground. For the unimproved

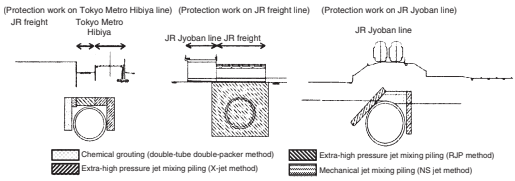


Figure 4. Protection work in the area of railway intersection.

ground, a settlement of 42 mm was predicted under the same conditions.

The final control value for track settlement was set to 24 m; this corresponds to 80% of the maximum settlement (30 mm) calculated by the finite element analysis. The first, second, and third control values on settlement were set at ±15 mm, ±20 mm, and ±24 mm, respectively.

Considering that ballast tracks intersect with the shield tunnel, a scheme was developed through discussions with the relevant railway companies to maintain the tracks promptly when a track displacement exceeding any of the control values occurs.

5 PROTECTION WORK IN THE AREA OF INTERSECTION WITH THE EXISTING LINES

With primary focus on ensuring the safety of the existing railway lines, soil improvement was carried out in the area of intersection to prevent slurry eruption and suppress settlement right above the shield tunnel.

The design and execution of the soil improvement were commissioned to the relevant railway companies. The soil improvement work is described here briefly based on the representative cross sections given in Figure 4. Soil improvement was applied to form roof-like structures covering the shield tunnel. The ends of the improvement areas were additionally improved with cement-base material. When closure was not allowed because of construction depth or other reason, chemical grouting (double-tube double-packer method) was carried out as a complementary measure.

Because the Jyoban line has an acute curvature of R = 300 at the intersection, the tracks on the line were reinforced by the work girder method and the electric poles on the line were reinforced by root wrapping, in addition to the soil improvement.

6 MEASUREMENT PLAN

Because the shield tunnel was to be excavated at any time of day or night, it was important to measure precisely and promptly within the operating hours of

Copyright © 2005 Taylor & Francis Group plc, London, UK

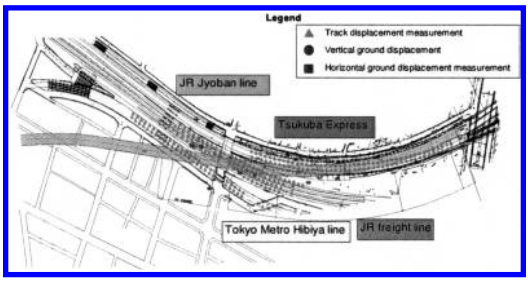


Figure 5. Plan view of instrument arrangement.

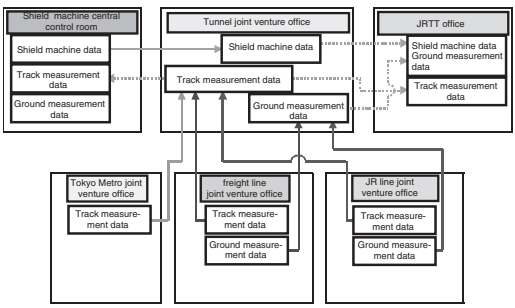


Figure 6. Schematic diagram of measurement scheme for the area of railway intersection.

each railway line to detect track displacement as early as possible and control the shield machine. Only shield advancement data are usually transmitted for control in shield tunneling. In the present case, however, relative track displacement measurement data on the existing lines and ground displacement measurement data (Figure 5) were also transmitted on a real-time basis through a dedicated telephone line to the shield machine central control room, the site office, the relevant railway companies, and an office of Japan Railway Construction, Transport and Technology Agency (JRTT). A measurement scheme was developed to this end (Figure 6), and shield advancement was controlled at the central control room by monitoring the measurement data.

To ensure the safety of trains in case of an emergency during shield advancement, track maintenance managers, who were authorized to operate an automatic train stop system, were stationed on a 24-hour basis.

7 SHIELD ADVANCEMENT CONTROL PLAN

If control values are inappropriately set, a serious accident can be caused during shield advancement right below the existing lines. To cope with this situation, slurry pressure, excavation volume, advance rate, and the pressure and amount of backfill grouting were controlled centrally. The control values of shield advancement are summarized in Table 1.

Table 1. Control values for excavation.

Item	Control value	Note
Face slurry pressure	Natural water pressure +20 kPa	Maximum is critical eruption pressure; minimum is natural water pressure
Excavation volume	−10% to +5% of theoretical excavation volume, within 2-sigma of the data of the past ten rings	
Advance rate	25 mm/min	Target value
Backfill grouting	Grouting rate: 110% Grouting pressure: Face slurry pressure +150 kPa	Relative to actual void

The control values were set based on past construction experiences in such tunnels as Ayasegawa and Kahei Tunnels constructed by JRTT on Tsukuba Express and the Mitejima Tunnel on the Tozai Line of West Japan Railway Company (JR West). The geological conditions of the Ayasegawa and Kahei Tunnels are similar to those of the Minowa Tunnel, whereas the Mitejima Tunnel represents a shield tunnel that successfully passed below railway lines in service.

7.1 *Setting of slurry pressure*

It is known from past experiences that preconsolidation upheaval and settlement may enhance subsequent consolidation settlement when excavating a tunnel through soft cohesive soil layers. Face slurry pressure was therefore basically set to the sum of natural water pressure (pore pressure) + fluctuating pressure (20 kPa), which is lower than the lower limit (active earth pressure + water pressure + fluctuating pressure) usually adopted in the slurry shield method. This setting was then tested in a trial section.

As shown in Figure 7, the lower limit of slurry pressure was set to the sum of natural water pressure + 20 kPa (fluctuating pressure). On the other hand, the upper limit was set to the sum of natural water pressure + earth pressure at rest + 20 kPa (fluctuating pressure) for the section between the left end of the graph and the 5.25 km point.

In the section beyond the 5.35 km point, the sum of natural water pressure + earth pressure at rest + 20 kPa (fluctuating pressure) exceeds the critical eruption pressure because the level of the road that runs beside the existing railway line is about 6 m lower than the railway embankment. The upper limit of slurry pressure

Copyright © 2005 Taylor & Francis Group plc, London, UK

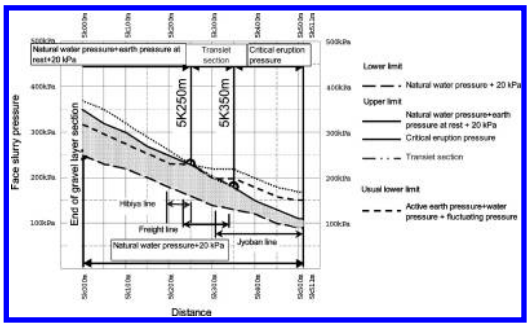


Figure 7. Slurry pressure setting.

in this section was thus given by the critical eruption pressure. The 100-m section between the 5.25- and 5.35-km points was considered as a transient section for the upper limit of slurry pressure, and face slurry pressure in this section was set within the range given by the upper limits of the adjacent sections.

It was judged from past experiences that the lower limit of slurry pressure (active earth pressure + water pressure + fluctuating pressure) usually adopted was too high to be applied to the excavation of the soft cohesive soil section.

7.2 *Normal*

Because the excavated soil was cohesive, excavation volume was controlled within −10% to +5% of the theoretical excavation volume.

To suppress settlement, excavation volume was controlled within 2-sigma (standard deviation) of the data of the past ten rings, instead of the usual approach of 3-sigma.

Advance rate had to be controlled to minimize the pressuring and deformation of the rock mass. Minimizing rock mass deformation leads to minimum effect on the tracks.

Settlement could be suppressed in test excavation performed repeatedly in a similar ground. The advance rate of 25 mm/min for the Kahei Tunnel was adopted in principle and was tested in the trial section.

7.3 *Control of backfill grouting*

An excessive pressure or an excessive amount of backfill grouting would lead to cracking and disturbance in the ground and thus secondary consolidation settlement. In full consideration of the results obtained in the Ayasegawa and Kahei Tunnels, the rate and pressure of backfill grouting were respectively set to 110% and the sum of face slurry pressure +150 kPa.

Other than the four main control items described above, the specific gravity of the slurry fed for excavation was controlled within the range of 1.10 to 1.30.

8 VERIFICATION OF CONTROL VALUES FOR SHIELD ADVANCEMENT

When the shield machine advanced to the soft cohesive soil section at around the 4.92 km point (near the Meiji-dori street), the shield advancement control plan described in Section 7 was gradually introduced and excavation on a trial basis was started.

At the 4.95 km point (Meiji-dori sidewalk), a ground surface settlement of 15 mm was observed during the passage of the shield machine. During the excavation through this point, slurry pressure was the sum of natural water pressure +20 kPa as initially planned, advance rate was 25 mm/min, and backfill grouting pressure was close to the sum of face slurry pressure +150 kPa. As shown in Figure 8, preconsolidation settlement occurred on the ground surface after it was subjected to the area of the influence of the shield machine (upper forward area within 45 degrees). Settlement was 5 mm at the time of face passage and increased by 2 mm to 7 mm at the time of tail passage. Ground surface upheaval associated with backfill grouting was not observed at the time of tail passage. It was considered that preconsolidation settlement occurred because of the low face slurry pressure and that subsequent settlement was enhanced as a result. In the first stage of adjustment, therefore, face slurry pressure was changed to the sum of natural water pressure +35 kPa, and the trial was continued without changing the other control values.

Settlement on the ground surface was measured again at around the 5.05 km point (Arakawa-ku highway). No preconsolidation settlement was observed, and settlement was 1 mm at the time of shield machine passage. With the set control values, verificational measurement was done in a cross section at the 5.07 km point (Figure 9), right before the area of intersection with the existing lines.

In the measurement cross section, ground surface settlement at the time of shield machine passage was 0 mm, and subsequent settlement was 7 mm at the maximum.

As shown in Figure 10, differential settlement gages right above the shield machine recorded a settlement of 5 mm at the time of machine passage and then an upheaval of 8 mm (to +3 mm) associated with backfill grouting. Consolidation settlement started after the machine passage, and convergence was achieved at a settlement of 14 mm.

Dipmeters were pushed toward the rock mass by 5 mm at the time of shield machine passage and remained there at the time of backfill grouting.

The dipmeters then slightly returned toward the tunnel and their displacement eventually stabilized at 3 mm.

As shown in Figure 11, the differential settlement gages indicated a settlement of 5 mm on the 11th day after the shield machine passage on April 9 and a

Copyright © 2005 Taylor & Francis Group plc, London, UK

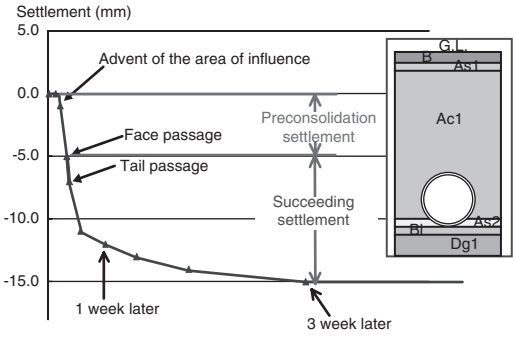


Figure 8. Ground surface settlement measured at the 4.95 km point.

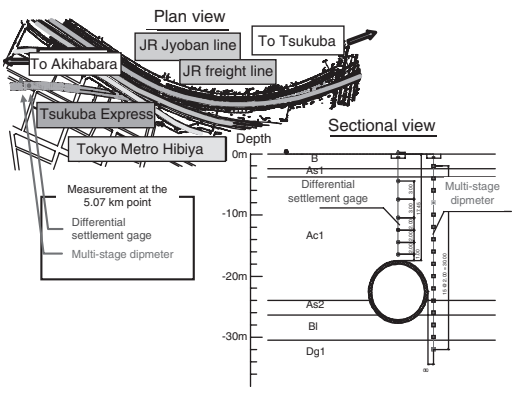


Figure 9. Outline of ground measurement arrangement at the 5.07 km point.

final settlement of 7 mm on the 28th day. The 5-mm settlement on the 11th day is 70% of the final settlement; the same trend is seen in the other six points.

On the basis of the trial results, slurry pressure was changed to the sum of natural water pressure +35 kPa, as one of the control values used for excavation below the existing lines.

9 SHIELD TUNNELING

To prevent any serious accident, excavation of the tunnel section below the existing lines was started at times other than the morning and evening rush hours.

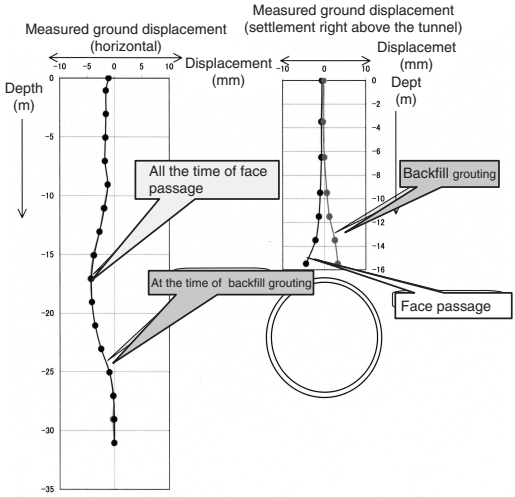


Figure 10. Ground measurement results at the 5.07 km point.

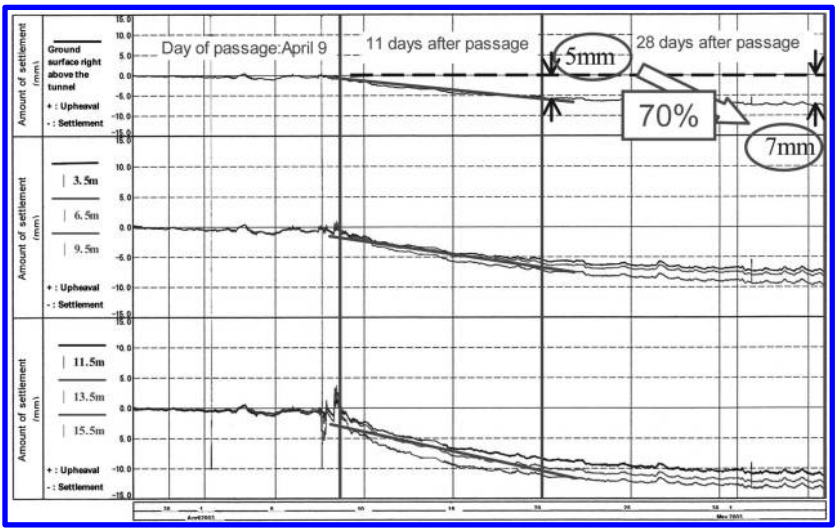


Figure 11. Ground measurement results over time at the 5.07 km point.

Copyright © 2005 Taylor & Francis Group plc, London, UK

As shown in Figure 12, face slurry pressure decreased by 5 kPa for each ten rings as calculated in consideration of the railway gradient, and excavation was completed within the set ranges of control values. Jack thrust increased temporarily around the Second Minami-Senju overbridge and in the full improvement section at the end of the tunnel but decreased as face slurry pressure decreased. Jack thrust is thus correlated with face slurry pressure.

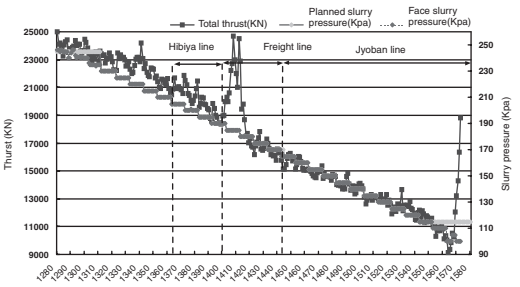


Figure 12. Jack thrust and slurry pressure.

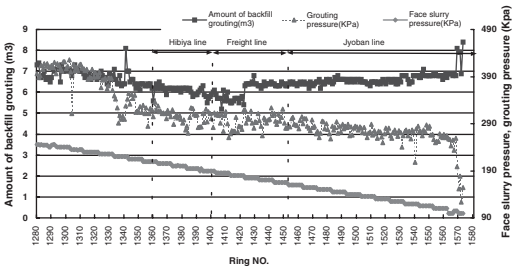


Figure 13. Amount of backfill grouting and grouting pressure.

Backfill grouting pressure was intensively controlled to the sum of face slurry pressure +150 kPa (see Figure 13), and grouting rates of 110% to 130% were achieved without upheaval or abrupt settlement.

As a result, the maximum ground settlement at the time of shield machine passage was 7 mm and the final settlement was 20.0 mm, which is smaller than the analytically predicted value of 30.0 mm.

10 CONTROL OF THE EXISTING LINES

Control of the railway lines in service was based on the relative displacement of the tracks (see Figure 14). Though the first control values were ±3.5, ±9.0, and ±6.0 mm for the Tokyo Metro Hibiya, JR freight, and JR Jyoban lines, respectively, JRTT adopted a value of ±5.0 mm for the Jyoban line (see Table 2) and monitored the measured data at the central control room.

The relative displacements measured during the passage of the shield machine, with a suppressed maximum of 3.6 mm, were below the first control value of each line. Because of the subsequent consolidation

Table 2. Control value.

	Tokyo Metro Hibiya line	JR freight line	JR Jyoban line
First control value	±3.5 mm	±9.0 mm	±5.0 mm
Second control value	±5.0 mm	±13.0 mm	±10.0 mm
Third control value	–	±24.0 mm	±15.0 mm

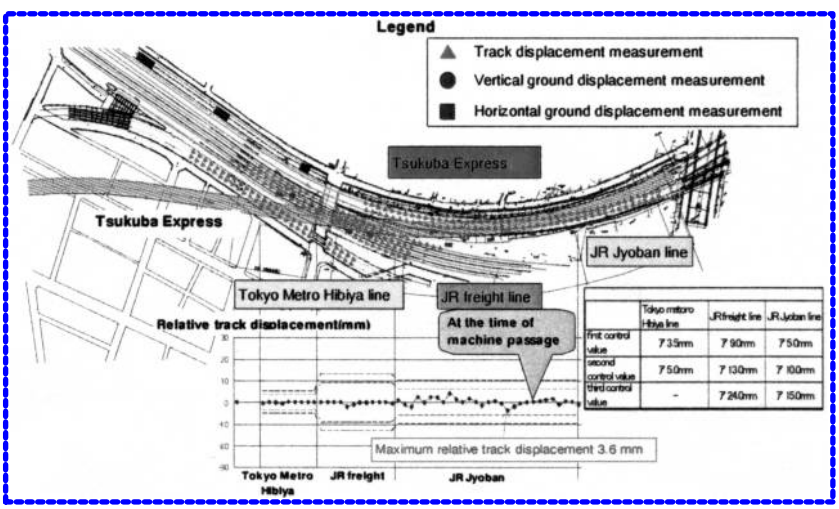


Figure 14. Measurement results of relative track displacement.

Copyright © 2005 Taylor & Francis Group plc, London, UK

settlement, the tracks were maintained as many as five times after the passage.

11 FINAL REMARKS

The shield tunnel was excavated successfully through the soft cohesive soil section with thin overburden below the existing railway lines without stopping the trains. This was achieved by addressing the three challenges identified preliminarily:

(1) The control values of shield advancement were tested in a trial section, and the optimum slurry pressure was found to be the sum of natural water pressure +35 kPa (fluctuating pressure). This setting was verified through measurements in a cross section at the 5.07 km point and used for the excavation below the existing lines.
(2) By taking such protective measures as soil improvement, work girders, and root wrapping of electric poles, the excavation was completed without slurry eruption or abrupt ground deformation.
(3) Track measurements on each railway line, ground measurements, and shield advancement data were centrally managed at the site office, so that excavation was completed successfully without substantially affecting the tracks. An emergency drill was carried out jointly with the relevant railway companies before the excavation to confirm the emergency contact scheme; this was also helpful in conducting the excavation smoothly.

In spite of the difficult conditions, such as excavation through the soft ground with thin overburden and excavation below tightly-scheduled railway lines in the metropolitan district, the shield machine finally reached Minami-Senju Station in June 2003 without any trouble while suppressing the impact on the existing railway lines to the allowable level. This was achieved through preliminary protection work, automatic measurement, track monitoring, extensive construction control, and excavation at times other than the morning and evening rush hours to avoid serious accidents. The excavation was done without affecting the railway lines in service through the planning of protection, measurement, and excavation, and a great deal of cooperation from the relevant railway companies during the construction work.

The cost and period of the construction were reduced by using wide segments with a width of 1.5 m.

Excavation of the tunnel has been completed, and equipment work is underway with the start of service expected in the fall of 2005.

Lastly, the authors hope that this study will be useful for future tunneling work involving intersections with railway lines in service.

Copyright © 2005 Taylor & Francis Group plc, London, UK

Geotechnical problems encountered by tunnel boring machines mining in sedimentary rocks

Christopher Laughton
Fermi National Accelerator Laboratory

ABSTRACT: Under favorable sedimentary rock mass conditions, the Tunnel Boring Machine (TBM) can excavate tunnel at rates unrivalled by other mining methods. However, the TBM's performance can be severely compromised by a wide range of adverse conditions encountered underground. In such conditions the TBM can become a liability.

This paper notes the excellent performance achieved by open TBMs in favorable rock mass conditions and describes how recurring geotechnical problems have negatively impacted TBM performance in other case histories. The impacts of these geotechnical problems and the various mitigation measures that have been taken to counter such impacts are reviewed and a recommendation made to encourage increased systematic reference to case history data sets during the planning and design of TBM tunnels in sedimentary rocks.

1 INTRODUCTION

Tunnel Boring Machine (TBM) performance in sedimentary rocks is negatively impacted by a variety of geotechnical problems. Even after extensive investigation, sedimentary rock masses can surprise the tunneling team with ground-related problems that had not been foreseen. The impacts of such problems might have been simply mitigated on the drawing board, but typically prove difficult to mitigate through methods and means change initiated during the course of construction.

Given that a site investigation may not bring to light all the ground-related problems that impact TBM performance, the planner is well advised to complement evidence from the investigative programme with reference to case histories. Reference to past experience will allow the team to better formulate and focus follow-on investigations and adapt the TBM and tunnel designs to the ground.

Past experience will enhance confidence that the systems selected are properly matched to the ground conditions.

2 FAVORABLE CONDITIONS

2.1 *Overview*

Sedimentary rock masses are commonly mined by TBMs. In a rock tunnel database of over 600 rock case histories (Nelson et al 1994), sixty percent of the tunnels were mined in sedimentary rocks. Argillaceous, arenaceous and calcareous rock types were all well represented in this data base.

Over the past forty years the tunneling industry has accumulated a wealth of data on TBM mining in sedimentary rocks. The planner of new tunnels has ready access to this data thanks to the efforts of those in the tunneling industry that have reported good and bad tunneling experiences in a highly comprehensive and professional manner.

The case history reports allow planners to calibrate their expectations directly with conditions experienced on "like-sites". In review, the database also allows the state-of-the-art TBM performances in various sedimentary rock types to be identified.

2.2 *Favorable conditions for open TBM mining*

A checklist of geologic factors ("geo-factors") impacting open TBM performance is shown in Figure 1. The "open TBM" referred to in this text is one configured with minimal shielding ("fingers") uses disc cutters and sidewall grippers. Favorable tunneling conditions for these "geo-factors" are described below, based on a discussion by Deere (1981).

Ideally, low to intermediate intact rock strengths are preferred for TBM tunneling. In this range, deep disc cutter indentation and high cutter penetration are achieved, and sufficient bearing capacity is available to support rock loads imposed by the machine on the invert and sidewalls of the excavation.

Copyright © 2005 Taylor & Francis Group plc, London, UK

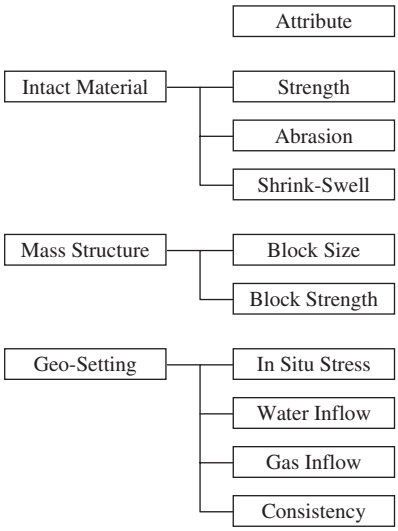


Figure 1. Geo-factors impacting TBM performance.

The absence of abrasive and slake-swell sensitive minerals are hallmarks of favorable tunneling conditions in sedimentary rocks.

The conditions of the rock structure will have a major influence on TBM performance. In particular, the wide spacing of rough-surfaced fractures and absence of alteration or weathering will auger well for excavation stability. An opening devoid of gravity-driven block or wedge fall-out will require the installation of little or no block support measures.

"Geo-setting" parameters, related to stress state, fluid pressure/flow and rock mass consistency can have a major impact on TBM performance.

A moderate in situ stress environment is desirable to provide for stable boundary conditions ensuring adequate normal stress across discontinuities without creating over-stress conditions.

The minimal presence, or ideally the absence, of water will also constitute a favorable tunnel conditions. Although the presence of water may not impact opening stability, it will generally be a "nuisance factor" and require an effort on the part of the tunneler to collect and remove from the tunnel.

A gas-free tunnel is favorable from both safety, and operational standpoints.

Lastly, rock mass consistency is also a highly desirable attribute of the geologic structure within which the tunnel is mined. Rock mass consistency will facilitate the early establishment of an optimized TBM operation (e.g. short learning curve) and eliminate the need for changes in key operating parameters en route.

Figure 2 shows the four basic critical activities that the open TBM-system needs to perform in order to advance the TBM one mining cycle: penetration, regrip, mucking and support installation. Over the past forty years, several case histories of open TBM performance under favorable mining conditions have been reported in the industry. Some of these case histories are described below by way of illustrating what can be achieved under favorable conditions.

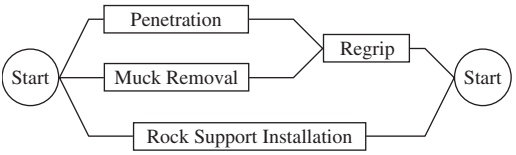


Figure 2. Open TBM mining cycle.

2.3 *Rapid tunneling in argillaceous rocks*

In 1966–7, a 3.2 m-diameter TBM mined the Oso Tunnel in a low strength shale (Sinha, 1986). The average advance rate achieved on this drive was over 60 m/day. A remarkable rate for its time, particularly given that the tunnel spoil was removed by rail cars.

Excellent average advance rates have also been achieved in inter-bedded sedimentary materials mined using open TBMs, notably in the Syar tunnel in Utah. Here, a 3.6 m-diameter tunnel mined through inter-bedded shale, siltstone, sandstone and limestone at an average daily rate in excess of 55 m (Busman & Rogers, 1991).

In reporting the high rates of mining above, it is notable that the averages quoted excluded zones of "bad ground". This is a clear reminder, should one be needed, that natural materials, such as rock or soil will present the miner with a range of conditions, some good, and some "not so good", and that often both are found within the same tunnel!

As can be surmised from the advance rates above, some clay-rich rocks can be driven to good effect using open TBM-systems. However, if the onset of slake-swell deterioration is anticipated during the construction period, the prudent designer/builder often opts to erect a full support liner (e.g. pre-cast segments) at the heading. The systematic placement of this liner will typically lead to slower, "support-bound" operations, e.g. the boring/mucking process in Figure 2 is routinely delayed to allow for liner installation to be completed.

2.4 *Rapid tunneling in arenaceous rocks*

High average advance rates have also been achieved in sandstones. A notable mining performance was reported on the Blue Mountain Project in Australia (Logan and Finnsson, 1995). On this drive, a 3.4 m-diameter, open TBM mined through intermediate

Copyright © 2005 Taylor & Francis Group plc, London, UK

strength sandstones at average rates in excess of one kilometer a month. This TBM performed in a "penetration bound" mode, as neither support nor mucking operations prolonged the mining cycle. Muck evacuation was by a continuous conveyor system and ground support was installed back from the heading, off the critical path of the mining cycle.

2.5 *Rapid tunneling in calcareous rocks*

Uniformly high rates of mining are perhaps most commonly reported in calcareous rocks. In moderate stress environments, "layer-cake" chalk strata can presents the tunnel team with near-ideal tunneling conditions. Chalk is both relatively weak and impermeable. On the Dallas Area Rapid Transit Project, a 6.5 m-diameter TBM achieved average rates of just under 60 m/day (Rogstad, 1995). On the Supercollider Project, Texas, a 4.9 m-diameter TBM mined at average daily rates approaching 100 m (Toohig, 1994). Many good and few bad TBM performances have been achieved in layer-cake chalk formations.

The somewhat stronger dolomitic limestone formations of Northern Illinois have also proven highly conducive to TBM mining. Over the last thirty years these rock units have been mined by a series of tunnels as part of the Tunnels and Reservoir Project (TARP) of the Metropolitan Water District of Greater Chicago. The recent use of high-power TBMs in these rocks has further pushed the "performance envelope" as predicted by recent research, sponsored by Fermi National Accelerator Laboratory (The Robbins Company, 1999 and Laughton, 2001).

2.6 *TBM-system limitations*

Although the TBM performances cited above are perhaps up to an order of magnitude faster than can be achieved using other systems, it must be noted that these state-of-the-art TBM advance rates represent only a fraction of the penetration capacity of the cutterhead. Even under favorable operating conditions, the cutterhead routinely operates for less than 50 percent of the available shift time. Factors unrelated to the ground reduce TBM performance way below its theoretical production levels. The TBM incurs delays for equipment repairs and replacements, unscheduled maintenance and an assortment of operational stoppages. The net result of these delays, even in favorable ground conditions, has been an average TBM-system delay of at least 18 minutes for every meter of tunnel mined (Laughton, 1998).

Studies of the causes and consequences of these delays is expected to prompt further incremental improvements in the system reliabilities, reduction in delay times and consequent improved utilization. However, planners of the system should be aware that the TBM is still far from being the manufacturing system that it is designed to be!

Even in the most favorable ground, a large gulf still remains between the maximum rate achieved on a stroke-by-stroke (mining cycle) and that achieved over the length of the drive.

3 TBM PROBLEMS IN SEDIMENTARY ROCKS

3.1 *Overview*

Although some TBM tunnels have been built under uniformly "favorable conditions" most have not. More generally, the tunnel, aligned to get from Point A to Point B, will need to be mined through a variable rock mass. The designer and miner should expect to meet a few problems en route. Commonly encountered problem types and their impacts on TBM performance are discussed below.

3.2 *Penetration and abrasion*

Although nowadays it is generally acknowledged that newer, larger disc cutters can efficiently cut even strong, and massive sedimentary rock there are still good reasons to fully evaluate the intact properties of the rock material.

Firstly, the higher penetration rates that can be achieved through the use of larger discs demand corresponding upgrades in mucking and support installation capacities. Appropriate reliability and capacity increments need to be built into all critical elements of the TBM-system design in order to take full advantage of the opportunities for faster mining that the larger discs can provide for.

Secondly, abrasive wear can be high in some sedimentary rocks, notably when abrasive minerals are present either as grains or as stringers, nodules or pockets within the rock matrix. Cutter replacement rates in such materials can be comparable to those reported in much stronger igneous and metamorphic rocks. Gehring (1994) reports on the high rates of cutter replacement experienced on the Clermont tunnel driven in sandstone. In this case, the "toughness" of the intact rock's "micro-structure" had not been noted during the site investigation campaign.

Thirdly, water and air coming into contact with shrink-swell rocks can have a detrimental impact on TBM performance. The onset of rock degradation under swell-slake action at any point during construction, can cause instability and necessitate stoppages to the TBM in order to perform remedial work. The presence of water at the face in slake sensitive rocks can also be problematic to the cutterhead and conveyor operations as the muck and water can form a slurry that

Copyright © 2005 Taylor & Francis Group plc, London, UK

can clog muck chutes and interrupt the evacuation process (Varley, 1990).

3.3 *Gravity-driven failure*

In stronger igneous and metamorphic rocks, field studies have consistently demonstrated that the presence of even a modicum of fracturing within a rock volume can markedly enhance the "penetrability" of the rock mass. Similar, albeit less pronounced, improvements in rock mass "penetratabilty" have also been observed in some stronger sedimentary rock masses (Laughton, 1998). However, in bedded rock units, increases in fracture density will also quickly lead to changes in heading support and extensions of the support time. This extension will typically result in "support-bound" TBM operation, which by definition, negates any positive influence that increased fracturing might have had on the penetration rate (Leonard, 1981).

As noted above, deteriorations in rock mass conditions and minor block or wedge fall-out observed at the support platform, will prompt increments in the amount of installed support and minor losses in TBM utilization. The occurrence of major instability at or in front of the support platform will lead to major reductions in utilization. In addition to requiring extensive hand mining and support installation, instability at the face can damage cutters, cause muck chute blockages and render cutter changes problematic.

As the stand-up time of the rock mass at the heading is reduced, the need for installing more support earlier and/or closer to the heading becomes critical in order for the TBM operation to remain viable (Martin, 1988). If stand-up time in a zone of tunnel becomes effectively zero, as may be the case in fault zones or karst or soil-like materials, the TBM may be stopped or even withdrawn to allow for changes in methods and means. These "showstopper events" have been encountered unexpectedly in all types of rock, their impact on production is so severe as to warrant inclusion in the planning of all TBM drives. In a TBM survey conducted by Nelson et al (1994), one such event was encountered, on average, every 3.3 km in karstic limestones and every 15.9 km in sandstones. Such showstopper events were, on average, much more widely spaced in non-karstic limestone (46.7 km) and claystone and shales (50 km).

3.4 *Stress-driven failure*

In some instances tunnel instability can be the result of overstress conditions occurring at the tunnel boundary.

In more brittle rock materials, high stress concentrations at the tunnel profile, that approach or exceed the uni-axial compressive strengths of the intact material, will cause "bed-buckling" or intact failure resulting in fall-out in close proximity to the advancing face.

In more ductile materials, overstress conditions will result in the onset of plastic deformations and potentially high rates of convergences that in some cases can squeeze and stall the TBM equipment in situ (Sinha, 1986).

3.5 *Fluid inflows*

TBMs can operate effectively even when subject to relatively large water inflows. However, the presence of water will take a toll on the electrical and mechanical systems and will lead to a decrease in the time between failures and potentially an increase in the time to repair of TBM components.

Water inflows and/or pressure can act to cause instability. The action of water can be sufficiently problematic for the TBM method itself to require modification or even outright abandonment. Where water inflow levels in excess of 100,000 liters per minute were encountered at the La Cloche tunnel the TBM system was withdrawn and drill and blast equipment used to complete the drive (AFTES, 1995).

A variety of hazardous atmospheres associated with asphyxiating, toxic, or explosive gases may be encountered during tunneling. Such gases include hydrogen sulphide, sulphur dioxide, methane and gasoline. These can occur naturally or may be the result of contamination. Sedimentary rocks are reservoirs for a number of such gases. Failure to properly mitigate and monitor these gases can have disastrous consequences. In some cases the mitigation measures required to counter gassy ground maybe so onerous as to make the project unviable.

4 MITIGATION THROUGH DESIGN

4.1 *Overview*

Any one or a combination of the ground conditions described above can cause major problems to a TBM operation. Most of these problems, can be, at least partly, mitigated through the adoption of appropriate design and construction measures. In general, measures are aimed at either "desensitizing" the TBM-system to the problem-causing condition(s) or modifying the ground prior to excavation.

As surmised from the discussions in section 3, the incorporation of extra "mitigating" equipment and/or activities can itself have a significant impact on the viability of the TBM option. The designer needs to develop a thorough understanding of what the ground conditions may be, how they will impact TBM operations and if such conditions can be effectively mitigated without unduly compromising productivity and/or raising project cost excessively.

Some steps that have been successfully adopted to improve a TBM-system's ability to negotiate adverse

Copyright © 2005 Taylor & Francis Group plc, London, UK

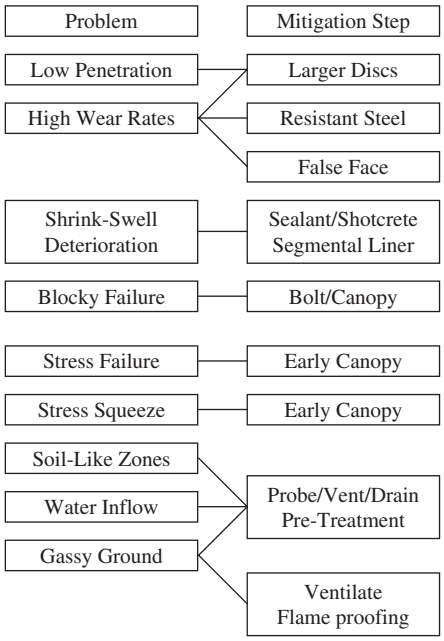


Figure 3. Mitigating ground problems.

rock mass conditions are outlined in Figure 3 and described above.

4.2 *Mitigation*

High cutter wear and low penetration are no longer the dominant factors that they used to be in determining the viability of the TBM option. In most rock units, the adoption of large disc technology allows for the quasi-totality of rock materials to be mined cost-effectively with adequate penetration per revolution and wear resistance.

False facing noted in Figure 3 provides for the mitigation of blocky fall-out conditions at the cut face that are noted in section 3.3. The presence of a false face reduces the space between the cutterhead and the cut face and minimizes the size of blocks that can fall. Back-mounted cutters are often adopted in conjunction with false facing as this measure all but eliminates the need for human intervention in front of the cutterhead to perform cutter inspections and replacements.

In recognized slake-swell conditions, as are commonplace in argillaceous materials, designers and contractors often choose to place shotcrete or pre-cast segments at the heading, as discussed in section 2.3. Protecting the rock within hours or days of excavation limits the exposure of the material to the deleterious impacts of water and humidity and preserves the long-term integrity of the rock matrix. In rocks that have only a moderate propensity for slake-swell behaviour, protection of the rock matrix may be limited to the placement of an invert segment. The placement of an invert segment can effectively seal the rock from water infiltration and provide a stable foundation for rail transport.

Fall-out occurring in front of the first point of mechanized support installation (platform) is generally problematic to a TBM operation. The presence of the TBM equipment itself makes access to the tunnel around and in front of the cutterhead impractical. It is difficult to arrest the onset and progression of rock mass failures in this volume of rock material. Two approaches have been used to handle failures at and in front of the tunnel heading.

The first approach uses extended TBM shielding (fixed or telescoping) to hold the failed mass "in-place" while a segmental lining is erected within the shielding. The rock load that develops on the shielding is transferred to the lining as the TBM shield moves forward. The second approach uses minimal shielding and a TBM configuration that provides for maximum access to the cutterhead. This configuration accommodates "miner-access" for the early recognition and arrest of fall-out conditions. Both approaches have some virtue with the latter approach perhaps best reserved for experienced mining crews who can recognize and react appropriately to the onset of failure at the heading. The former approach has experienced difficulties when high rock loads have built-up on the shielding. Not only can they trap the machine but the loads themselves can prove problematic to transfer to the installed ground support system, as discussed by Robbins (1988). Overbore systems have been devised to allow for "over-excavation" in order to accommodate ground squeezing and/or the placement of additional thickness of ground support. Continuous mining operations may be adopted in rapidly converging ground to avoid leaving the machine stationary for any period of time (long weekends).

In wet ground or in stretches of tunnel where the presence of soil-like zones might be expected, a variety of design and operational strategies have been used. Drainage, grouting and freezing have been adopted, either singly or in combination, to decrease water inflow and/or increase rock mass strength.

Practical measures to mitigate build-up in gas concentration at the heading can also be important. Mitigation measures include the removal of non-essential electrical equipment from underground, the use of fireproof-enclosures for electrical equipment and increased ventilation.

5 CONCLUSION

Sedimentary rock masses can present the tunnel team with highly favorable, if not ideal, mediums in which

Copyright © 2005 Taylor & Francis Group plc, London, UK

to build TBM tunnel. However, more generally, the rock mass will present the tunnel team with one or more problematic geotechnical conditions that can have significant negative impact(s) on TBM performance. It behooves the team (TBM manufacturers, tunnel designers and tunnel constructors) to work closely together to thoroughly study the site and relevant case histories, in combination in order to characterize the site and identify a shortlist of geotechnical problems that the site may present for the TBM-system.

The TBM can unquestionably yield the highest rates of advance and lowest cost tunnel under favorable mining conditions. However, even relatively short stretch of acute problems or extended reaches of chronic problem conditions can largely or completely negate the potential time and cost benefits projected for the TBM option. The manager of a TBM drive will need to develop an understanding and properly express the added risks that the TBM will bring to the project in order to plan the tunnel project, in general, and make good decisions about the design and construction aspects of the TBM operation, in particular.

Practitioners are well advised to prepare for the worst and hope for the best. As Stevens (1970) notes "the tunnel contractor's greatest dream is to bid a tunnel with a mechanical mole (TBM), estimating the excavated cost and time when the machine holes-through." This long-held "dream" remains largely unattained. TBM work rarely proceeds according to plan. During design, the team must take advantage of the site investigation and past experience to devise the best laid plan possible that fully balances the risks and rewards that adoption of a TBM can bring to a project and specifically prepared the builder for the worst that the ground may hold in store.

REFERENCES

AFTES. Working Group 4 (1995), "Fiche Signaletiques des Chantiers Mechanises." Tunnels et Ouvrages Souterrains, No 127 January-February.

Busman, P.R., Rogers, D.J. (1991), "Rapid Construction of the Syar Tunnel Central Utah Project." Rapid Excavation and Tunneling Conference, Washington, pp. 507–526.

Deere, D.U. (1981), "Adverse Geology and TBM Tunneling Problems." Proc. Rapid Excavation and Tunneling Conference, California, May, pp. 574–585.

Gehring, K. (1994), "Experience with TBM-Application under Extreme Rock Conditions in a South-African Project Leads to Development of High-Performance Disc Cutters." Proc. 7th International Congress of the Int. Engineering Geologists, September, Lisbon, Portugal, pp. 4243–4252.

Laughton, C. (2001), "Value Engineering the Construction of Long Tunnels in the Dolomites of Northern Illinois, USA." Proc. AITES-ITA World Tunnel Congress, Milan, Italy, June, pp. 287–294.

Laughton, C. (1998), "Evaluation and Prediction of Tunnel Boring Machines Performance in Variable Rock Masses." University of Texas at Austin, pages 313.

Nelson, P.P., Al-Jalil, Y.A. and Laughton, C. (1994), "Tunnel Boring Machine Project Data Bases and Construction Simulation." Geotechnical Engineering Center Report GR. 94-4 to the National Science Foundation, pages 323.

Leonard, J.W. (1985), "Designing Geotechnical Equipment." Tunnelling and Underground Transport, Future Developments in Technology, Economics, and Policy, Boston, US., April, pp. 117–120.

Logan, D., Finnsson, S. "The Blue Mountains Sewerage Scheme. A case history of the Hazelbrook to Katoomba Tunnels." Proc. Rapid Excavation & Tunneling Conference, California, 1995, pp. 269–275.

Martin, D. (1988), "TBM Tunnelling in Poor and Very Poor Rock Conditions." Tunnels and Tunnelling, Vol. 20, No. 3, pp. 22–27.

Robbins, R.J. "Tunnel Boring Machines for Use with NATM." Felsbau 6 Issue 2, pp. 57–63.

Rogstad, D. "Dallas Area Rapid Transit Subway Tunnel Project." Rapid Excavation and Tunneling Conference, San Francisco, 1995, pp. 425–443.

Sinha, R.S. (1986), "Tunnels: Machine Excavation – Rate of Progress – Machine Data." Bureau of Reclamation Report No. REC-ERC-86-8, July, pages 37.

The Robbins Company, "Tunnel Cost Reduction Study, Prepared for Fermi National Accelerator Laboratory". Batavia, Illinois, pages 40.

Toohig, T.E. "TBM Advance Rates." Personal Communication to C. Laughton, April, pages 27.

Varley, P.M. (1990), "Susceptibility of Coal Measures Mudstone to Slurrying During Tunnelling." Quarterly Journal of Engineering Geology, Vol. 23, pp. 147–160.

Copyright © 2005 Taylor & Francis Group plc, London, UK

Uetliberg tunnel: comparison of drill and blast and mechanical heading

S. Maurhofer
Overall Project Manager and Chief Construction Manager Uetliberg Tunnel, Amberg Engineering Ltd., Regensdorf-Watt, Switzerland

M. Glättli
Project Manager Uetliberg Tunnel, Amberg Engineering Ltd., Regensdorf-Watt, Switzerland

ABSTRACT: The official proposal in submission was to drive the molasse sections of the Uetliberg tunnel by drill and blast with a horseshoe cross-section. The Uetli Joint Venture submitted a variant with mechanical driving and circular cross-section, owing to the official proposal. Importance was attached to enlargement of the pilot heading in conjunction with undercutting technology. After a short project overview, this article illustrates the differences between the drill and blast and mechanical heading in the Uetliberg tunnel, focusing on the hazard scenarios and the rock support.

1 PROJECT OVERVIEW AND GEOLOGY

1.1 *Project overview*

The Uetliberg tunnel in Switzerland is the longest tunnel in Zurich's new Western Bypass Expressway.

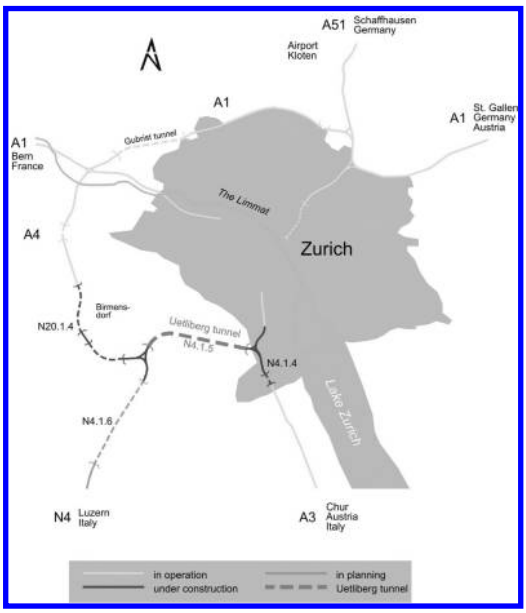


Figure 1. Project overview of the Uetliberg tunnel.

The project comprises two parallel tubes, each about 4.4 km long. The two tunnel tubes are connected every 300 m by a transverse walkway and every 900 m by a transverse roadway. The SOS niches are spaced 150 m apart.

1.2 *Geology*

From west to east, the Uetliberg tunnel passes under two parallel ranges of hills (Ettenberg and Uetliberg) with the Reppisch Valley in between. The core of both ranges consists of flat layers of the upper fresh water molasse and alternating deposits of sandstone and soft marl. Maximum overburden of the tunnel under the Uetliberg is about 320 m.

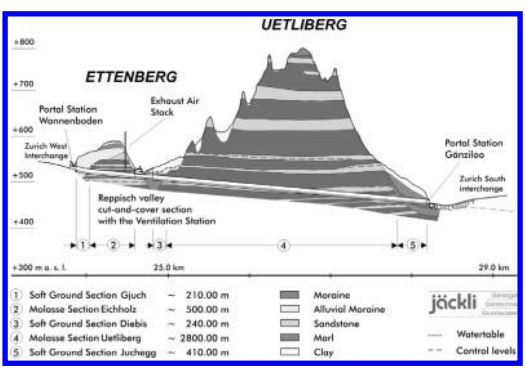


Figure 2. Geologic profile along the Uetliberg tunnel.

Copyright © 2005 Taylor & Francis Group plc, London, UK

Before the molasse sections of Eichholz (500 m) and Uetliberg (2800 m) were reached, three sections of soft ground (Gjuch, Diebis and Juchegg) had to be driven.

2 CONSTRUCTION PROGRAM AND PROCEDURES

From the Reppisch Valley construction site, the rock tunnel excavation is currently being driven downwards under the Uetliberg to the Zurich-South motorway interchange. This work was preceded by the excavation of soft ground sections using the core construction method in both tubes over distances of 250 m and 350 m from April 2001 to May 2002. At the end of the soft ground excavation at Diebis, starting caverns were excavated in the molasse under the Uetliberg for the tunnelling machine operations to follow in both tubes.

At the beginning of April 2002 an open pilot tunnel boring machine (TBM) Type Wirth TB III 500 E (diameter 5.00 m) was installed in the Basel tube. After starting in the middle of May 2002, the TBM drove the entire Ueltiberg molasse section. Since the beginning of May 2003, a tunnel bore extender (TBE) Type Wirth TBE 500/1440 using the undercutting technique has been traversing this entire molasse section under the Uetliberg to extend the centered pilot tunnel bore to the final profile of 14.00 to 14.40 m. Simultaneously with this bore extension, work has proceeded on driving the other pilot tunnel in the Chur tube untill the end of 2003. Afterwards the Chur pilot tunnel will enlarged to its final profile by the same bore extension procedure.

Starting from the Gänziloo pit, excavation has been proceeding since February 2002 in the two 450 m long rising tubes through the soft ground of the Juchegg section. In both tubes, the first 50 m were driven through Uetliberg loam with pipe screen protection, likewise using the core construction method.

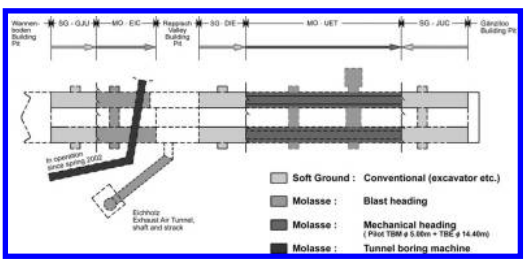


Figure 3. Heading methods of the Uetliberg Tunnel.

Since the beginning of April 2002, work has also proceeded on the downward tunnel starting at the west portal (Wannenboden) and leading under the Ettenberg towards the Reppisch Valley excavation site. The first hurdle here was the Gjuch soft ground section with a length of 220 m. It is followed by the 500 m long Eichholz molasse section, which was excavated by drill and blast and ripping.

3 TUNNEL CROSS-SECTIONS

3.1 *Soft ground sections and Eichholz molasse section*

The horseshoe cross-section used in all of the soft ground sections (SG) and for the drill and blast excavation in the Eichholz molasse section (MO-EIC) is about 14.70 m wide and about 12.70 m high. The face area is roughly 143 to 148 m^2.

3.2 *Uetliberg molasse section (TBE)*

The standard cross-section for the Uetliberg molasse section (MO-UET) is 14.40 m wide and 14.20 m high. The face area is about 160 m^2. Figure 4 shows in detail the elements of the tunnel cross-section.

Waterproofing, concrete invert, service duct (prefabricated elements), a cable conduit block and side backfilling are installed beneath the back-up equipment behind the TBE suspended from rock bolts in the ceiling. The concrete ring of the inner shell and the intermediate ceiling are installed successively later on in the rear areas.

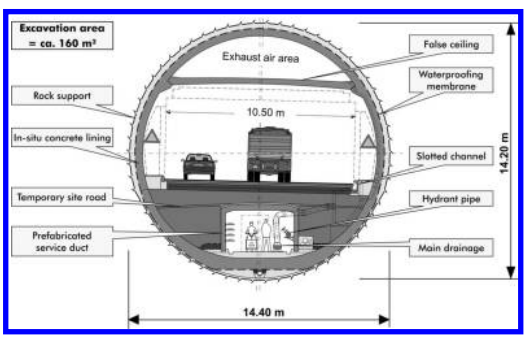


Figure 4. Standard cross-section of the TBE-section.

4 SOFT GROUND HEADING WITH THE CORE METHOD

All soft ground sections are driven with the core construction method, shown in Figure 5.

Normally, temporary support measures consist of steel arches (HEM 180 girders spaced 1 m apart) and a 25 cm thick layer of steel fiber reinforced shotcrete.

After about two years of construction and the installation of 10,000 tonnes of steel, it is now possible to issue a positive progress report for the first time. During this two year period, about 1800 meters

Copyright © 2005 Taylor & Francis Group plc, London, UK

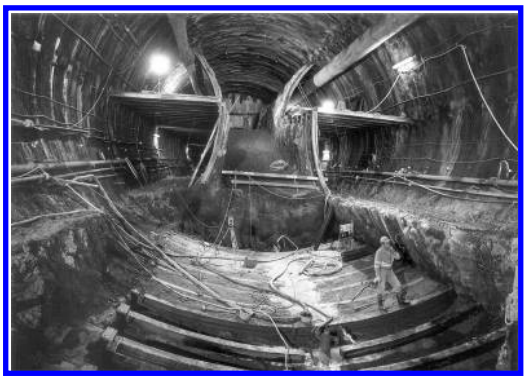


Figure 5. Core method for all soft ground heading.

of tunnel has been driven successfully through soft ground. The excavation rate specified in the contractor's bid, 1.2 m advance per day over the entire cross-section was achieved and even exceeded. The systematic installation of steel supports has made it possible to organize efficient and predictable tunnelling progress practically free of unpleasant surprises and complications despite these exceptionally heterogeneous geological formations. Overall support at the working face and support of the partial cross-sections was insured at all times with face anchors and cement injections.

5 DETAILED DESCRIPTION OF DRILL AND BLAST AND MECHANICAL HEADING IN THE UETLIBERG TUNNEL

5.1 *Drill and blast excavation of the Eichholz molasse section*

The 500 m long Eichholz molasse section is excavated by drill and blast with round lengths of 3 m, divided into crown, bench and base. Rock support generally consists of mesh reinforced shotcrete and rock bolts. Initially, the tunnel crown was driven over the entire length of the molasse stretch. As soon as breakthrough of the crown was achieved, work started on excavation of the core and the base.

5.2 *Pilot tunnel in the Uetliberg molasse section*

The TBM for the pilot tunnel has bored two 5.00 m diameter tunnels in both tubes.

Rock support used consisted of steel fiber reinforced shotcrete and glassfiber reinforced rock bolts 2.5 m long. The peak rate of advance was 42.6 m/workday in three shifts. The average rate over the entire section was 20 m/workday.



Figure 6. TBM-excavation of the pilot tunnel.

5.3 *Tunnel bore extender (TBE) in the Uetliberg molasse section*

Starting in November 2002, the TBE was assembled in the Diebis soft ground section and in the starting pit. The rock is excavated with the undercutting technique, known to be an effective cutting method ever since the early days of tunnel boring machines. With this technique, the cutting rollers work against the rock's tensile strength, which is much lower than its compressive strength.

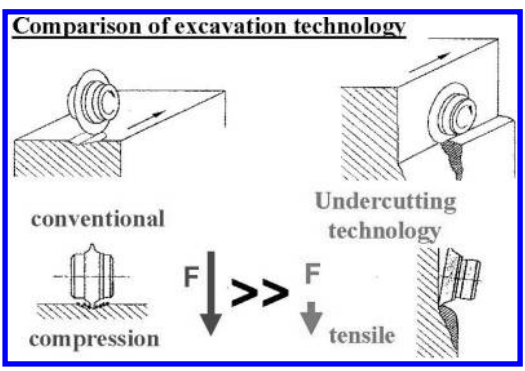


Figure 7. Principle of the undercutting technique.

The TBE enlarges the pilot tunnel of 5.00 m to a diameter of 14.20 to 14.40 m. The head of the TBE consists of a two piece cutterhead body with six cutter arms. It rotates on the inner kelly, which is braced and positioned in the pilot tunnel and in the extended tunnel cross-section. The cutters, which are offset both axially and radially from the tunnel axis, are mounted on radially movable slides on the cutter arms.

When the six arm boring head rotates, the rollers are shifted from an inner to an outer boring diameter. When the nominal boring diameter has been reached, the slides are retracted. Then the continuously rotating head is shifted by one 20 cm advance towards the face, and boring of the next round can begin.

Copyright © 2005 Taylor & Francis Group plc, London, UK

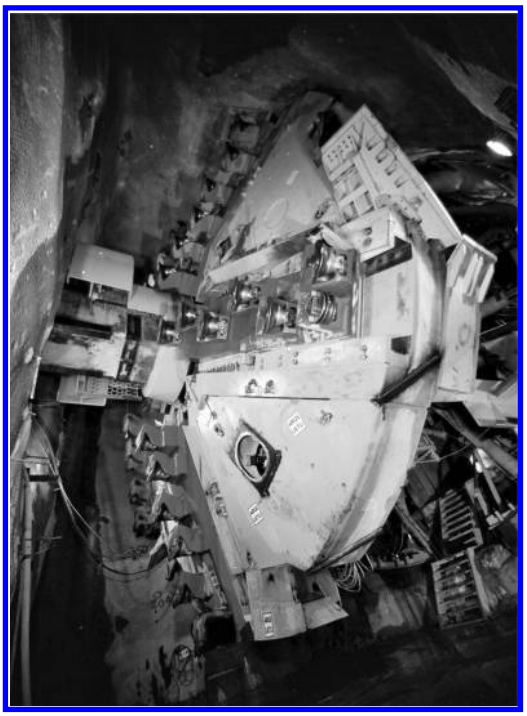


Figure 8. The TBE boring head.

Excavation support, comprising cable bolts, Swellex rock bolts, nets and shotcrete, is installed right behind the cutting head.

The erection of the TBE with its back-up equipment has a total length of about 180 m.

6 COMPARISON OF DRILL AND BLAST AND MECHANICAL HEADING

6.1 *Detailed geology of the molasse sections*

The upper fresh water molasse consists of interchanging strata comprising hard sandstone outcrops and soft marl layers plus a variation in the two strata. The marl layers split the sandstone outcrops. In addition, various marker beds can be encountered. These marker beds primarily consist of pale-reddish freshwater calcium, accompanied by black, carbonaceous, sandy marls and marly sandstone ranging in thickness between a few centimetres and a few decimetres. No actual bentonite horizon has been encountered. In addition, thin black horizons with carbonaceous substance were encountered.

Generally, the strata are flatly bedded. Separating planes which occur include stratification planes, bedding planes and cracks in the form of fissures. The marl layers feature strata thicknesses in the range of millimetres to centimetres and the sandstones feature strata thicknesses in the range of decimetres to metres. No cracks are observable in the marls. This contrasts with the sandstones where the fissures are closed or open only a few millimetres. There are also far larger fracture openings in the slope areas. Overall, plateform fissure structures can be anticipated. It is not possible to preclude the possibility of subsequent fractures in the crown area in the marls.

The permeability of the marls is low. They can be considered as more or less impervious. The sandstones have a low porosity but moderate fissure water may occur owing to the fissures. Overall however, it is possible to assume a moderate permeability.

6.2 *Official proposal for rock support in submission*

The original concept for driving the Uetliberg Tunnel foresaw conventional drill and blast for the molasse sections. What was envisaged was partial excavation with crown, bench – if applicable subdivided into core and wall heading – and an invert excavation – if applicable also in two stages.

The "circular cross-section/TBM driving" variant was also investigated again in addition to the "horseshoe section/conventional driving" variant during the course of the detailed project.

There were similar geotechnical hazard scenarios in the molasse section for both variants.

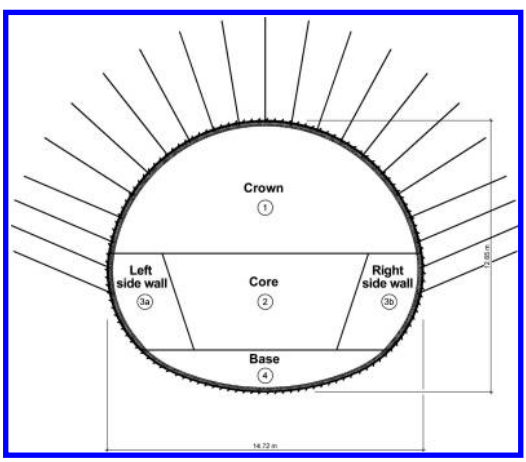


Figure 9. Standard cross-section according to submission, driving through molasse.

6.2.1 *Hazard scenarios*

The following hazard scenarios were defined in the molasse sections of the Uetliberg Tunnel:

– Springs in the marl
– Groundwater

Copyright © 2005 Taylor & Francis Group plc, London, UK

Table 1. Types of rock support in accordance with the submission documents for the regular cases in the molasse sections.

	Rock bolts			Shotcrete class B	Meshing
Type of rock support	L = …[m]	a_L = …[m]	a_Q = …[m]	d = …[cm]	Steel S500 [mm]
1	5.0	1.5	1.5	20	150/150/6/6
Capping: to 50 m					
2	5.0	1.2	1.2	25	150/150/6/6
Capping: 50–100 m					150/150/6/6
3	8.0	1.0	1.0	30	100/100/6/6
Capping: 100–200 m					100/100/6/6
4	8.0	1.0	1.0	35	100/100/6/6
Capping: > 200 m					150/150/8/8

– Strata loosening
– Capping height
– Fissuring
– Stratification
– Quartz content

Springs: The clay minerals contained in the marl strata tend to form springs if water collects in the crystal structure. Attention must be paid above all to adequate dimensioning of the cribbing, in particular in the invert vault, in order to cope with this hazard scenario. The geometry of an invert vault is of crucial significance in this case. Without invert vault, the stresses occurring from the spring process cannot be coped with. Ring closure of the overall vault as early as possible is important in this case.

Groundwater: The very low permeability and yield mean that driving operations are impaired only slightly. Open pre-drainage suffices for driving operations. However, a corresponding water pressure on the cribbing must be assumed for the operating state of the tunnel.

Strata loosening: It has been assumed that loosening up to approx. 6.0 m may occur in the crown. An appropriate design and adequate excavation dimensioning with corresponding rock bolt lengths are important in order to cope with this hazard.

Capping height: The capping height of the Uetliberg molasse section is max. about 320 m. The redistribution of stresses at such capping heights must be taken into consideration. Dimensioning of the rock support and of the interior vault designed for this is required. The criterion of the capping height was the crucial criterion for defining the type of rock support.

Fissuring: The fissuring occurs above all in the siltstones and sandstones. The fissures are predominantly closed fissures. The existing fissures must be stabilized by means of rock bolts.

Stratification: The rock structures involved all feature a predominant, subhorizontal stratification. The geological expertise explicitly pointed out the possibility of strata loosening in the tunnel crown.

Quartz: The only problems relate to work safety (dust) and wear. No further precautions are required from the design aspect.

6.2.2 *Means of support*

The capping height was defined as the crucial criterion for defining the types of rock support for the molasse sections.

Tenders were invited for driving through the Uetliberg molasse section by enlarging one of the pilot headings to be created beforehand in the crown and this would be followed by excavation with drill and blast (ripping of the bench or the invert) and simultaneous rock support with rock bolts, meshing and shotcrete.

When doing this, importance was attached to achieving a short distance between the invert closure and the driving point, two of the reasons being the very large cross-section and the spring phenomena anticipated in the marl in the invert.

6.3 *Bid – tunnel bore extender (TBE) variant*

The Uetli Joint Venture submitted for the Uetliberg molasse section a variant with mechanical driving owing to the official proposal, and importance was attached to enlargement of the pilot heading in conjunction with undercutting technology.

The most important arguments in favour of this mechanical driving were as follows:

– The geological report basically foresaw the possibility of mechanical driving.
– The official proposal foresaw opening of the crown over the entire width. No subdivision of the excavation cross-section in the crown was scheduled in the molasse section of Uetliberg.
– The official proposal already foresaw pilot headings for both tunnel tubes, even though these were in the form of roof headings.

Copyright © 2005 Taylor & Francis Group plc, London, UK

Table 2. Overview of the technical differences between the official proposal and the proposal covering tunnel bore extender with undercutting technology.

	Invitation to tender Official proposal	Tunnel bore extender (TBE)
Pilot heading		
Excavation	2 driving operations in parallel with 2 TBMs, Ø 4.50 m/4.70 m	2 driving operations consecutively with 1 TBM, Ø 5.00 m
Rock support	Rock bolts, meshing and shotcrete	Rock bolts, steel fibres and shotcrete
Enlargement		
Excavation	Enlargement of the pilot heading with drill and blast (crown)/ripping (bench/invert)	Enlargement of the pilot heading with TBE (undercutting technology)
Rock support	Rock bolts, meshing and shotcrete	Rock bolts, meshing and shotcrete
Standard cross-section	Horse-shoe cross-section	Circular cross-section
Invert vault	Flat, reinforced	Round, non-reinforced
Construction sequence	2 driving operations in parallel concrete vault and invert cribbing simultaneously	Driving operations one after the other Concrete vault in parallel

– An immediate ring closure is possible using a tunnel bore extender (TBE) which simultaneously excavates the entire cross-section. This met the requirements resulting from the geological and geotechnical considerations. A ring closure for this large diameter would only have been possible with a substantial distance from the face using a conventional excavation method such as drill and blast.
– Mechanical driving offers the option of already placing the interior works of the base in the follow-on area.
– From a structural engineering point of view, a virtually circular cross-section is better than a horse-shoe cross-section with invert vault.
– Contractors of the bidding Uetli Joint Venture already availed of experience with bore extender methods.

The Client, together with the Project Engineer, opted to award the contract to the Uetli Joint Venture with the "tunnel bore extender" variant.

6.4 *Design project – tunnel bore extender (TBE) variant*

6.4.1 *Hazard scenarios*

Since support of the drilled tunnel with the TBE is not performed by segments but classically with shotcrete and rock bolts, the hazard scenarios of TBE driving correspond to those of conventional driving as already illustrated in the submission for the official proposal.

The same geotechnical hazard scenarios result both for the pilot heading and for TBE driving as for the official proposal in the invitation to tender.

6.4.2 *Means of support*

The supports can be placed well in front behind the cutter-head in the case of TBE driving.

When driving the pilot heading, it was shown that the stipulated hazard scenarios from the official proposal were appropriate and assigned well to the rock situation encountered.

Table 3 compares the types of rock support of the official proposal from the invitation to tender with the versions with the TBE and undercutting technology.

The maximum thickness of the shotcrete was able to be reduced by 5 cm to 30 cm owing to the more structurally sound cross-sound with TBE driving. A general thickness of 10 cm for the shotcrete shell was selected in the invert. This is also related to the relatively fast placement of the final invert vault which is produced in the follow-on area.

The same can be said of the rock bolt spacing. A spacing of 1.2 m ×1.2 m was increased to 1.5 m ×1.5 m in type 2 of rock support and from 1.0 m ×1.0 m to 1.2 m ×1.2 m in types 3 and 4 of rock support. The use of pre-fabricated cable rock bolts was scheduled for TBE driving in order to allow flexible placement of the rock bolts.

The rock bolt lengths were also modified. While a rock bolt length of 8.0 m was foreseen in the official proposal even for the types 3 and 4 of rock support, a rock bolt length of 5.0 m, 6.0 m and 8.0 m is foreseen in the types of TBE rock support. Type 4 of rock support was split into a type 4a and a type 4b, whereby the difference relates to 6.0 m or 8.0 m long rock bolts.

Once third of the cable rock bolts are being replaced by Swellex rock bolts as a response to the adapted hazard scenario based on the experience of the first pilot heading driving operation in respect of strata loosening in the roof area. This measure was aimed at rapid attachment of the head protection which enhances work safety.

The reinforcement in the vault very largely corresponds to the official proposal with meshing from K 188 to K 235.

Compared to the official proposal, one further additional type of rock support, type 5, was constructed and foresees placement of steel vaults TH 29/58 at

Copyright © 2005 Taylor & Francis Group plc, London, UK

Table 3. Comparison of the types of rock support in the official proposal and in the TBE version (1 … 4 = types of rock support, official proposal; TBE 1 … TBE 5 = types of rock support, TBE).

	Rock bolts/steel vaults			Shotcrete		Meshing	
Type of rock support	L = …[m]	a_L = …[m]	a_Q = …[m]	Vault d = …[cm]	Invert d = …[cm]	Pitch/Ø [mm]	Meshing type [Steel S500]
1	5.0	1.5	1.5	20		150/150/6/6	K 188
TBE 1	5.0	1.5	1.5	20	10	150/150/6/6	K 188
2	5.0	1.2	1.2	25		150/150/6/6	K 188
						150/150/6/6	K 188
TBE 2	5.0	1.5	1.5	20	10	150/150/6/6	K 188
3	8.0	1.0	1.0	30		100/100/6/6	K 283
						100/100/6/6	K 283
						100/100/6/6	K 283
TBE 3	5.0	1.2	1.2	25	10	100/100/6/6	K 283
4	8.0	1.0	1.0	35		100/100/6/6	K 283
						150/150/8/8	K 335
TBE 4a	6.0	1.2	1.2	30	10	100/100/6/6	K 283
						100/100/6/6	K 283
TBE 4b	8.0	1.2	1.2	30	10	100/100/6/6	K 283
						100/100/6/6	K 283
TBE 5	Steel vaults TH 29/58			30	20	150/150/8/8	K 335

spacings of 1.3 m. For placement of the interior vault in the invert area, it was necessary to increase the shotcrete thickness from 10 cm to 20 cm with this type. K 335 meshing is fitted in this case.

7 CONCLUSION

After boring 2000 m with the TBE, we can say that the tunnel bore extender with the undercutting technique works well.

The mechanical heading with the TBE in the Uetliberg tunnel allows to reduce the excavation support, compared to drill and blast heading.

It is feasible to mechanically drive large cross-sections in the molasse without aid of concrete segments by constantly assessing the rock conditions. To be successful with this method, we need to have a selection of pre-defined types of rock support. The rock support has to be placed well forward, behind the cutter-head.

In fact there is more excavated material to remove because of the larger cross-section, but a part of this material can be used to backfill all service ducts in the tunnel sections.

All things considered the mechanical heading with the TBE proved to be an economic way to drive through the Uetliberg molasse section.

For further information, click on:
www.westumfahrung.ch (client) /
www.uetlibergtunnel.ch (project coordinator) /
www.arge-uetli.ch (contractors).

Copyright © 2005 Taylor & Francis Group plc, London, UK

Microtunnelling in rock and soft ground strata –Asia Pacific experiences

Bala K Balasubramaniam
Director, Amberg & TTI Engineering, Singapore

ABSTRACT: Singapore pioneered the use of advanced shield tunneling and microtunnelling technology in the eighties to install sewers in built-up urban areas. It used the technology extensively in the past two decades to install several hundred kilometers of sewers. Through the application of the advanced tunneling technology, it acquired a considerable know-how and experience in the use of various types of advanced shield tunneling systems, both larger (macro shield) and smaller (remote controlled non man entry size micro shields) diameter shield tunneling in a variety of ground conditions, ranging from very soft water charged clayey soil strata to high strength rocky strata.

Many Asia Pacific countries have benefited from the greater use of the advanced macro and micro tunnelling technology in Singapore. The lessons learned by the authorities, contractors and tunnelling equipment suppliers, thorough the use of the advanced shield tunnelling technology, microtunnelling in particular, in Singapore and Asia Pacific countries to install sewers, are indeed a very valuable resource.

This paper briefly discuss the use of advanced macro and micro shield tunnelling technology in Asia Pacific countries; Singapore, Australia and India in particular, in variety of ground conditions ranging from water charged soft soils to hard rock. The paper also contained some of the technical data collected during tunnel excavation in soft soils, soils with boulders and rock.

1 INTRODUCTION

Singapore enjoys a clean and healthy environment today. It is largely because of the comprehensive sewerage infrastructure construction programs implemented in the seventies and through eighties and nineties. Singapore used Earth Pressure Balance Shield tunnelling system for the first time in 1983 to install a 3000 mm diameter effluent outfall pipeline. Singapore also used advanced Slurry Shield tunnelling system in 1982 to install sewers in water charged sandy strata. Since then these shields and micro shields have been used very extensively to install sewers in Singapore.

In the past decade alone, more than 500 km of sewers were added. In addition Singapore will soon add 48 km of very deep sewers of diameters ranging from 3.3 m to 6 m and another 70 km of link sewers of diameters ranging from 0.75 m to 3 m to the sewer network. All these sewers are being also installed using advanced shield tunnelling technology.

Many Asia Pacific countries have also used the advanced tunnelling technology to install sewers in variety of ground strata ranging form soft soils with high water table to hard rock. Australia used the Slurry Shield micro tunnelling technology in Sydney and Melbourne in 1995/96 to install sewers in strata containing silty sand and cobble stones and also in full face siltstone. India used the technology in 1999/2002 to install sewers successfully in very complex ground strata comprising stiff silty sand with boulders and full face hard basaltic rock.

2 EARTH PRESSURE BALANCE SHIELD TO INSTALL SEWERS

Singapore was 2nd country outside of Japan, besides USA, to use Earth Pressure Balance Shield (EPBS) tunneling technology in 1983. The EPBS was used to construct a 3 km long and 3000 mm diameter effluent outfall pipeline in tunnel through water logged soft marine clay. Since then many EPBS and Slurry shields have been used in Singapore.

As the tunnel excavation was carried out in close proximity to very important structures and installations, the ground response to tunneling by EPBS was carefully monitored throughout the construction period using inclinometers, pizeometers, and tilt plate settlement plates for the entire 3 km long tunnel. The measured ground settlement along the entire 3 km long tunnel route is shown Figure 1. The average ground settlement was about 53 mm while the maximum was 169 mm.

Copyright © 2005 Taylor & Francis Group plc, London, UK

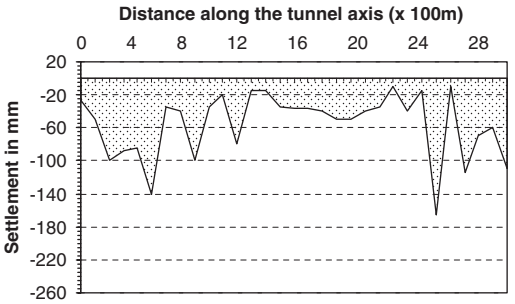


Figure 1. Soil response to EPBS tunnelling.

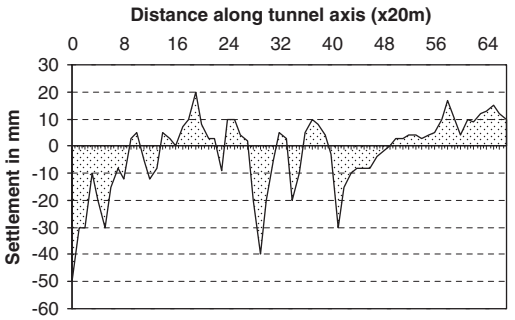


Figure 2. Soil responses to slurry shield tunnelling.

The performance of EPBS and the soil response to the tunneling by EPBS is discussed in details in the paper (Balasubramaniam, 1987). The measured vertical and lateral displacements of soil during tunnel excavation, as recorded by several inclinometers and settlement points along the tunnel route are also graphically presented in the paper.

3 SLURRY SHIELDS TO INSTALL SEWERS

Slurry shield was used in Singapore for the first time in 1982 to install medium size sewers in water charged silty sand strata. Since then several dozens of slurry shields have been used in Singapore.

Soil response to slurry shield tunneling was measured in a project where five slurry shields were used simultaneously in the early nineties to install 11 km of sewers of diameters ranging from 1200 mm to 2100 mm. A typical ground response to slurry shield excavation by a 1500 mm diameter shield through very soft marine clay strata is shown in Figure 2.

There was no significant ground settlement occurred along the sewer route and the average ground settlement was only 15 mm. The very low ground settlement was due to the fact that the slurry pressure at the tunnel was deliberately kept high to balance the soft marine clay. It is not easy to balance the tunnel face in marine clay due to its fluidity state. Its active pressure coefficient was estimated to be 0.9 and thus any slight reduction in slurry pressure will result in free flow of marine clay, causing ground above to settle, while any increase in slurry pressure will result in upheaval as shown in the Figure 2. The average upheaval of the ground was only 8 mm. (Balasubramaniam, 1993).

4 MICROTUNNELLING AND PIPEJACKING TECHNOLOGY TO INSTALL SEWERS

Hundreds of kilometres sewers of diameters ranging from 225 mm to 900 diameters were installed in Singapore since 1982 using microtunnelling and Pipejacking technology. Singapore's exposure to the technology and accumulated know-how and expertise in the trenchless application has enabled many neighbouring countries including Malaysia, Brunei, Thailand China, Korea, Taiwan and Hong Kong and lately India to adopt and use the technology.

Singapore has used several types of micro shields for trenchless sewer construction. It acquired world class knowledge and know-how in the use of various types of micro-tunnelling systems for sewer installations. Many micro-tunnelling technicians, operators and engineers from Singapore have provided expertise in micro-tunnelling operations to many countries in the Asia Pacific region.

Most commonly used microtunnelling system was slurry shield system. However Singapore has extensively used the following microtunnelling systems during the initial period in the early eighties for trenchless installation of sewers. Even today some of these machines are still being used.

Earth Arrow method
(two stage augur excavation process)
Iron mole method
(two stage slurry shield excavation process)
Horizonger method
(single stage augur excavation process)
Slurry shield method (Single stage excavation process).

4.1 *Microtunnelling in cobble stones in Sydney*

Sydney used the slurry shield microtunnelling system in 1995 to install a sewer in soil strata containing cobble stones. A microtunnelling system capable of boring through soft soil strata to rocky strata was used successfully to bore through cobble stones whose compressive strength was about 200 Mpa.

The geotechnical tests showed that the river cobbles to be hard quartzite/porphyry materials of strengths of 300–400 Mpa. The rock boring shield was equipped with roller bits capable of cutting rock formation of

Copyright © 2005 Taylor & Francis Group plc, London, UK

unconfined compressive strength up to 200 Mpa. The shield was capable of exerting large torque to break up rocks. The shield was also fitted with a more robust cone crusher capable of crushing hard rocks including cobble stones as hard as 300 Mpa.

The shield initially dipped into the ground and refused to respond to the steering jacks fitted to the shield head. It could not be brought back to the true alignment and continued to dip further. At one stage the alignment target in the shield could not be seen from the jacking pit.

The shield and the jacked in pipes were pulled back to the shaft and the bore was filled with sand. After modifying the configuration of the adapter and dummy pipe assembly, the tunneling was recommenced. This time, to restrain the shield from dipping, the flexible joints of the shield head and the dummy pipe and that of the adapter pipe which followed the dummy pipe were bolted to restrict the flexibility of the joints. The controlling of the shield becomes much easier after this modification.

4.2 *Microtunnelling in siltstone in Melbourne, Australia*

Microtunnelling was used in Melbourne, Australia in 1996 to install a 1500 mm diameter sewer through siltstone strata. The unconfined strength of the moderately weathered siltstone was about 1.7 Mpa. About 215 m long sewer was installed in this stretch using a 1500 mm diameter slurry shield. When the second leg of tunneling was commenced in the opposite direction, a much harder siltstone, in contrary to the low strength siltstone as originally envisaged, was encountered. The slurry shield tunnel machine could not bore through the harder siltstone whose unconfined compressive strength was about 13 Mpa.

After the modification of the cutter head by welding special cutter bits supplied by the manufacturer, the shield resumed excavation but at much slower speed. One of the main problems faced during the excavation was the rolling of the machine when high torque was applied to excavate the siltstone. Because of this constraint, the applied torque was limited to only about 50% to 60% of the full torque.

About 120 m of full face tunneling excavation was done in this harder siltstone. The next 40 m of the tunnel was excavated in siltstone and silty clay transition start. The remaining 55 m was excavated in water charged silty clay start. A plot of excavation rate in siltstone (and soft soils) is shown in Figure 3.

4.3 *Microtunnelling in basaltic rock in Mumbai, India*

Trenchless technology paved the way in Mumbai, India to install eleven missing sewer links across very busy railway corridors and along bottleneck stretches of streets in the city.

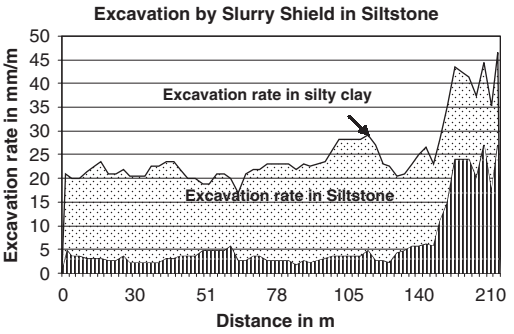


Figure 3. Graph showing the excavation rate in siltstone.

This World Bank funded first microtunnelling project in India made it possible for the Municipal Corporation of Mumbai to connect US$ 25 million worth sewer network that was discharging sewage for decades into storm water drains to the city's main sewage collection and disposal system. These missing sewer links could not have been installed by traditional open trench construction method.

It was apparent to the Municipal Corporation and World Bank that the only viable option to close these missing links was the use of trenchless technology but they were initially reluctant to adopt this option due to the lack of trenchless expertise available in India. The risks of failure and cost escalations that can be associated with the application of trenchless techniques on the difficult and complex sites and ground conditions were also factors that affected the use of the technology.

Mumbai's soil condition is complex and given the urbanised and built-up nature of the city, the project to install the sewer links by microtunnelling, especially across busy railway tracks and along congested and heavily used roads, turned out to be one of the most difficult and challenging microtunnelling projects.

Of major significance, beside very congested and difficult nature of the sites, was the soil conditions which varied from hard basaltic rock with compressive strengths in excess of 100 Mpa to water charged marine clay with boulder intrusions.

Three microtunnelling equipment, Herrenknecht AVN 1200, AVN1000 & AVN 800 were used in the project to install the 4.8 km of sewer conduits of diameters ranging from 350 mm to 1400 mm.

The contractor initially selected two microtunnelling machines, Herrenknecht AVN 800 and AVN 1000 that met the specified performance requirement in the contract for excavation of both soft and hard ground including rock expected to be encountered in the project. Another Herrenknecht AVN 1200 was mobilized by the contractor to install sewer through a much

Copyright © 2005 Taylor & Francis Group plc, London, UK

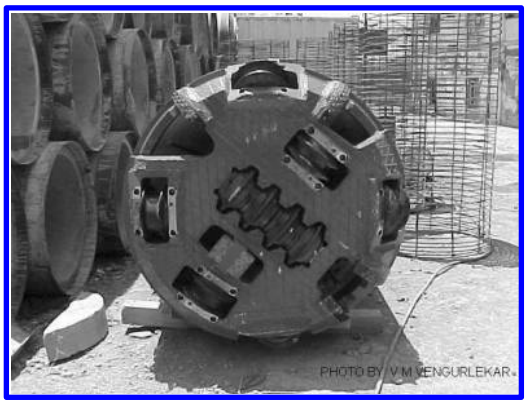


Figure 4a. AVN 1000 Slurry Shield.



Figure 4b. 1200 mm tunnel bore in basalt rock.

harder rock encountered in one of the four sites added subsequently.

After an initial teething and familiarization period, a record length of micro tunneling of 2.1 km was completed in a 10 month period representing an average monthly production rate of 210 m. This rate was achieved on a two nine hour shift basis and included set up and turn around time for the machines. The AVN 1000 machine achieved a maximum production of 15 m/day in hard rock at an average of 8 m/day while the AVN 800 achieved in hard rock a maximum of 30 m/day at an average of 10 m/day. Minimum production rate for both machines were 3 m/day.

Figure 4a shows a typical AVN 1000 slurry shield capable of excavating hard rock. Figure 4b shows a tunnel bore in rock after the microtunneling machine and the jacked-in pipes were pulled back.

The project has created a lot of enthusiasm and confidence in "Trenchless Technology" in India and many Indian cities are expected to use the technology in the future for sewerage installation works.

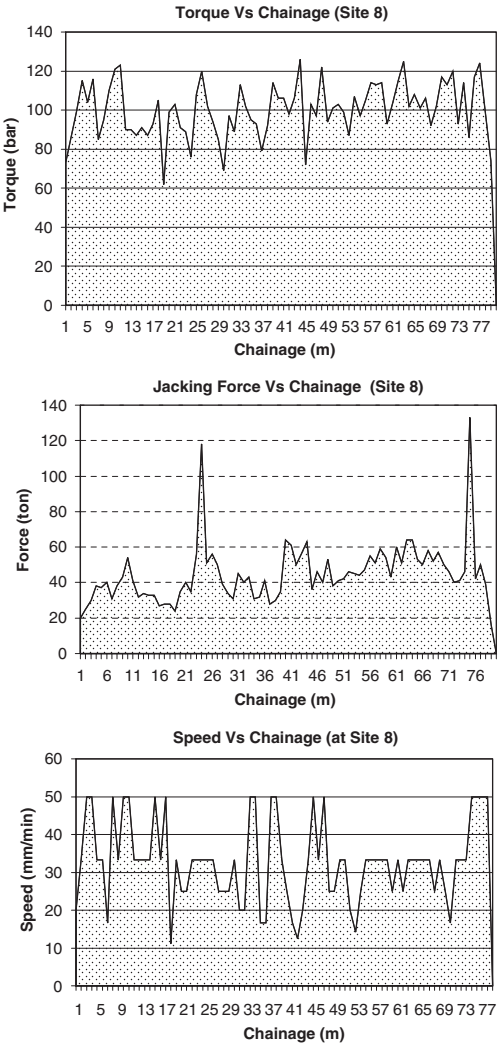


Figure 5. Measured excavation data in rock. Site 8: Andheri-Kurla (rock of ucs 50–100 Mpa).

4.3.1 *Excavation rate in basaltic rock*

Microtunnelling excavation was carried out in basaltic rock and granite stones of strengths from 50 Mpa to 300 Mpa. As a matter of fact the microtunnelling shields have gone through a very tough endurance test in this project as the rock encountered was not only hard but also very tough. The toughness of the rock made the excavation more difficult and slow. In one sewer stretch the rock strength reached as high as 340 Mpa.

The graphs in Figures 5 & 6 show typical jacking force applied in tone, excavation rate in mm per minute and the torque exerted by the cutter head to excavate

Copyright © 2005 Taylor & Francis Group plc, London, UK

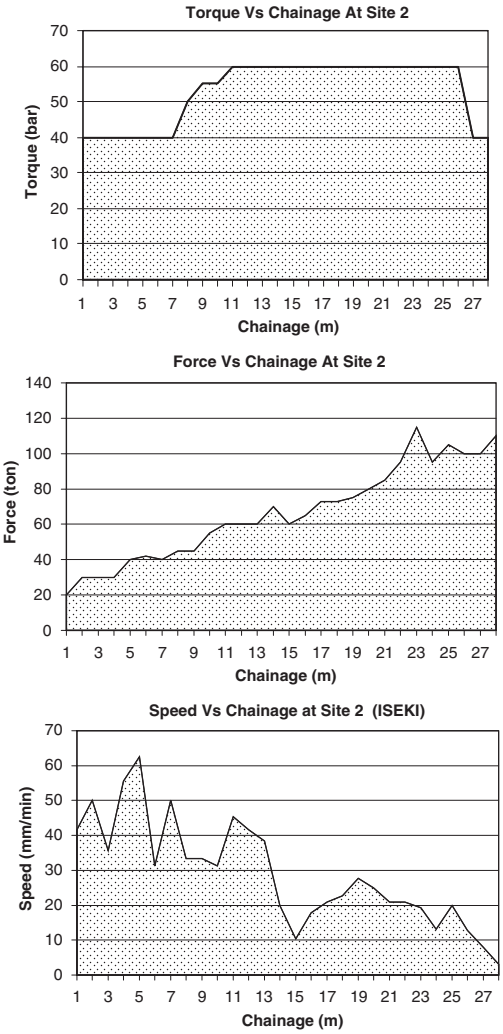


Figure 6. Measured excavation data in soft ground. Site 2: Mankurd Railway (Stiff and Soft soil with boulders).

the rock in bars. The rock strength in Mpa, the maximum and minimum excavation rate in mm per minute and the average torque in bars and the maximum jacking force applied in tons are also indicated in the graph.

The data plotted in Figure 5 corresponds to tunnel excavation in full face basaltic rock of strength up to 100 Mpa while the Figure 6 corresponds to the tunnel excavation in stiff clay with boulders.

CONCLUSION

The soil response to tunneling by Earth Pressure Balance Shield in soft clay was found to be good and the average ground settlement was found to be only 53 mm over a 3 km stretch of 3.75 mm diameter bore.

Moreover the lateral soil movement as revealed by inclinometer measurements was also found to be very encouraging. The performance of EPBS for tunnel excavation in soft ground was good as demonstrated by the measurements carried out in the project, on lateral and vertical soil displacements.

Similarly the soil response to Slurry Shield tunneling in soft clay was also found to be good. However the balancing of the tunnel face by the slurry pressure require good skills and experience of the operators to avoid upheaval and blow outs.

As demonstrated in the tunnel excavation in siltstone, accurate soil investigation is paramount to select the right kind of microtunnelling equipment. Trying to modify a machine meant for excavating soft ground to excavate harder ground as done in the Melbourne project will not only result in additional cost to the project but also delay the completion of the project.

The project in Mumbai is a good example to illustrate the above point. The geotechnical investigation done by the client has indeed helped drafting appropriate clauses in the contract document and to encourage the Contractor to select and invest on the right kind of microtunnelling equipment.

This was clearly demonstrated in the project where the Contractor was almost guided to use top of the range slurry shield capable of excavating hard rock.

The typical measurements such as torque, jacking force, speed of excavation for hard and soft ground excavation demonstrate that the torque required for the excavation varied considerably. The torque required for excavating hard rock was almost two times of that required for soft soils.

REFERENCES

Balasubramaniam, K, 2002. India's First Micro-tunneling Pro*ject – Planning, Procurement and Implementation – Consultant's Perspective. Fifth National Conference on Trenchless Technology, Australia.*

Balasubramaniam, K, Musa M.A, 1993. Mechanized Shields for Trenchless Sewer Construction in Singapore. Proceedings of the VIII Australian Tunneling Conference, Sydney, Australia.

Balasubramaniam, K, 1987. Construction of Effluent Outfall Pipeline in Tunnel Using Earth Pressure Balance Shield (EPBS). Proceedings of the Fifth International Geotechnical Conference, Singapore.

DiFrancesco, C, Balasubramaniam, K, 1996. Slurry Shield Tunnelling in Siltstones and Cobble Stones: Australian Experience. Proceedings of the International No-Dig 96 Conference in New Orleans, Louisiana, U.S.A.

Copyright © 2005 Taylor & Francis Group plc, London, UK

Tunnel construction with Earth Pressure Balance shields and measures to minimize settlements under urban infrastructure in London

Dipl.-Ing. T. Schubert & Dipl.-Ing. Dr. techn. K. Rieker
Wayss & Freytag Ingenieurbau AG, International Tunnelling and Engineering Division, Frankfurt am Main, Germany

David Court & C. Eng. FICE
Edmund Nuttall Ltd., London, UK

ABSTRACT: Tunnelling of Section C250 was performed with two EPB shields over a length of 5.3 km in the area of the city of London under London Underground and Network Rail facilities without interrupting operation. The construction ground conditions encountered – London Clay, Woolwich and Readings Beds, the Upnor Formation and Thanet Sands – placed vastly differing requirements on the supporting pressure of the EPB TBMs, conditioning, quantity surveying and volume control of the excavated soil as well as the dewatering measures.

1 GENERAL OUTLINE OF THE PROJECT

The Channel Tunnel Rail Link (CTRL) project comprises the construction of a 109 km long double-track railway section for the conveyance of passengers with an option for the conveyance of goods. This section extends from the Channel Tunnel Terminal at Folkestone to St. Pancras Station in the heart of London (see Figure 1).

The project will be realised in two steps. Section 1 comprises the 74 km long connection, which has already been put into operation, between the Channel Tunnel via Waterloo Connection to the already existing railway connection to London Waterloo International Station. Section 2 comprises the 39 km long connection between the North Kent Line Connection and St. Pancras Station in London with the Thames Tunnel, the three construction lots of the London Tunnel as well as Stratford Railway Station. Section 2 is scheduled to be put into operation in 2007.

2 SECTION 250 – RIPPLE LANE TO BARRINGTON ROAD

The Joint Venture Nuttall/Wayss & Freytag/Kier was awarded Contract 250 with an order volume of £115 million (approximately €175.8 million).

The site is situated in Dagenham, a quarter in East London. Here the transition from ground level to below ground level takes place. Contract 250 comprises a reinforced concrete ramp construction, 335 m in length, which leads into a 195 m long tunnel construction at Ripple Lane Portal constructed in the cut

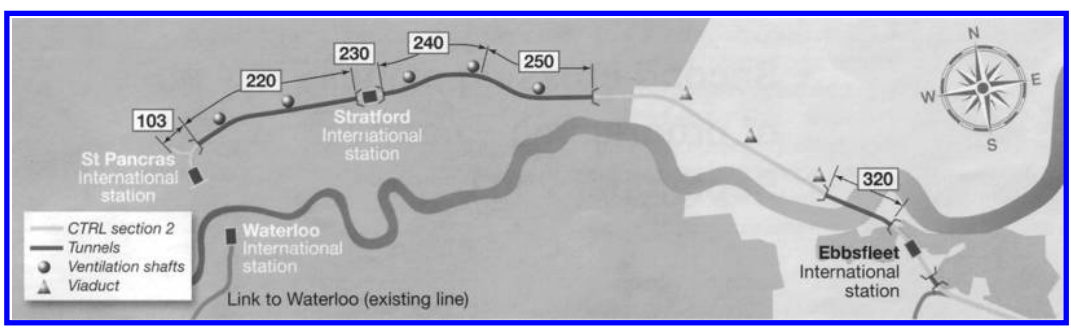


Figure 1. Overview of Channel Tunnel Rail Link contracts.

Copyright © 2005 Taylor & Francis Group plc, London, UK

and cover method, followed by two single-track tunnels with an inner diameter of 7.15 m, each 5300 m long. These tunnels were built using the shielded tunnelling method proceeding in a Westerly direction up to the destination shafts at Barrington Road.

In addition to the construction of the Wayside Ventilation Shaft, the contract also comprises the construction of seven cross passages between the two main tunnels with an inner diameter of 3.5 m. The first stage of the track bed for the two tunnels composed of unreinforced concrete completes the order.

3 GRADIENTS AND GEOLOGY

Since the railway line is designed for a speed of 300 km/h, the longitudinal inclination of the first 200 m is 4.6 per mill; that of the remaining part of the construction lot 3.6 per mill. The tunnels are driven with a minimum radius of approximately 2500 m. The minimum cover of 7 m is slightly smaller than the tunnel diameter. The first 500 m of the route pass through soft alluvial clay and a zone with terrace gravels and then into London clay over the full tunnel cross section for a length of approximately 2.5 km. Afterwards it passes through the Harwich, Woolwich and Reading Beds. Finally, directly in front of the destination shafts, the tunnel is driven through a zone consisting completely of Thanet Sands. Ground water under tension with pressures of up to 3.3 bar is encountered here, which penetrates the overlying layers of Woolwich and Reading Beds formations.

During the design phase, the client carried out field and simulation tests to investigate the ground water lowering possibilities. The aim was to simplify the construction of the tunnel and cross passages. As a result of these investigations it was decided to lower the ground water table in the Thanet Sands. (Woods 2003).

4 CLIENT'S DESIGN

London and Continental Railways (LCR), represented by the affiliated company Union Railways Limited, entrusted a joint venture consisting of the companies Arup, Bechtel, Halcrow & Systra under the name Rail Link Engineering (RLE) with the design, project management and realisation of the whole project.

As a result of the computer simulations of the aerodynamic influences on trains with speeds of 230 km/h as well as further detailed investigations, a consistent inner diameter of 7.15 m was chosen for the tunnel constructions.

In addition, the client carried out tests to compare precast concrete segments with reinforcing steel and those with steel fibres. The behaviour of the segments was examined under the influence of tensile stress resulting from transportation, storage, construction of the segments as well as under the pressure of the thrust of the TBM. As a result of the tests, the client decided to use segments reinforced by steel fibres. In the test, these segments had the following advantages:

- Higher permanent resistance to salty or aggressive ground water.
- Improved resistance against damage during transport.
- Cost saving compared with conventionally reinforced segments.

In addition to the steel fibres, polypropylene fibres at the ratio of 10 kg to 1 kg per cubic meter of the concrete mixture were also used. In case of fire, these fibres can reduce spalling of the concrete lining resulting from pressure in the pores produced by water vapour. (Craig 2003).

The required compressive strength is 60 N/mm^2. The 1.5 m wide rings consist of nine single segments and a key stone. The taper of the left and right segments was specified at 35 mm. Permanent screws were used for the connection of the annular joints in addition to three plastic string dowels for each single segment.

EPDM gaskets supplied by the company Heinke were used as seals. The gaskets were tested against 7.5 bar water pressure with a 5 mm joint displacement. (Craig 2003).

5 TUNNEL BORING MACHINES

Until the mid 90s, experiences with shield tunnelling in the United Kingdom tended to be unsatisfactory. This was due, among other things, to the delays experienced with the construction of the Jubilee Line Extension and the technical problems with the construction of the Heathrow Tunnel.

Shield tunnelling was perceived by investors and the public to be a very risky method of construction, the cause for these problems usually being "wrong machines" or "wrong construction ground".

As a result of this experience RLE called in an expert to define the type of machine and the minimum requirements of the TBMs for each contract section. It was the contractor's responsibility to choose two potential shield suppliers and to specify modifications and additional requests with regard to the TBM standards of performance.

As a result of these negotiations two EPB TBMs of the RMP 320SE type with an outer shield diameter of 8.15 m built by Lovat in Toronto/Canada were used for tunnelling on the construction lot (see Figure 2).

The total length of the tunnelling equipment consisting of an approximately 10 m long shield and ten trailers was 110 m. The TBMs were designed in such

Copyright © 2005 Taylor & Francis Group plc, London, UK



Figure 2. Lovat TBM in workshop after reception.

a way that they could be transformed from the "closed mode" with material removal via a screw conveyor to the "open mode" with direct material removal from the centre of the cutting wheel. The cutting wheel had an opening percentage of 35%.

Each of the five cutting arms was centrally equipped with scrapers and the material inlet slots had protective shields against wear. Two scrapers each at the working face and on the cutting wheel rim were equipped with hydraulic indicators for wear. The cutting wheel torque was 14,520 KNm at 1.4 rpm. If necessary, the cutting wheel could be completely closed by ten steel plates activated by hydraulic cylinders.

The whole front shield was flexibly connected to the central section of the shield so that steering movements of up to 250 mm were possible. The 29 thrust jacks produced a total thrust force of 73,950 kN. Their stroke was 2250 mm.

Eight foam injection ports allowed the addition of ground conditioners in front of the cutting wheel, either into the excavating chamber or into the screw conveyor alternatively.

Originally, the tail void grouting consisted of two double piston pumps that pressed cement mortar into the annular gap via four conduits in the shield tail sheeting. In the London Clay this system was replaced by rotary hose pumps. Instead of the conventional cement mortar, a two-component ETAC mortar was grouted via two injection points provided in the sidewall section. As soon as both components meet in the annular gap this mortar forms a stable gel stabilising the segment ring in its position after leaving the shield tail.

The material excavated from the tunnel face was removed by means of belt conveyor systems, which were designed for a capacity of 800 t/h per tunnel. The belt conveyor systems in the tunnel and at the surface were supplied by Continental Conveyor Ltd. The 800 mm wide conveyor belts had to be extended after every 300 m advance. To realise this, 600 m of belt were drawn into the belt store provided at the tunnel portal and connected with the tunnel belt by vulcanisation.

6 SETTLEMENT RISK ANALYSIS OF CONSTRUCTION GROUND

Keeping settlements resulting from tunnelling work and their effects on the urban London infrastructure to a minimum attracted our special attention from the very beginning.

All the more so as immediately after the start of the shield driving the tunnel alignment work passes under the railroad yards of London Tilbury & Southend Railway with only 7 m cover, followed shortly thereafter by the freight traffic centre of Freightliner, and then over the remaining distance by the operating railroad facilities of London Underground Ltd. and Network Rail. The alignment crosses below the complete length of Barking Station in a longitudinal direction and passes beneath numerous bridges and supply pipes. In addition, hundreds of homes exist directly above the tunnels.

Therefore, a three-stage risk analysis with regard to the effects of possible settlements of the construction ground on the existing infrastructure was carried out in the run-up to the execution of the constructions. In each case the most unfavourable construction ground conditions and settlement behaviour were assumed. At each stage, the low risk objects were excluded and objects with a higher risk were submitted to a further thorough investigation.

At the first stage of the examination, settlements of 2% volume loss were assumed along the alignment. At the second stage of the investigations, it was estimated that for section 2 a moderate or higher risk exists during the tunnelling work for nine bridge constructions, three stanchion walls, 200 buildings, one crane runway and three subway railway lines.

As there was only a limited ground cover over large distances of the C250 construction lot, the greatest number of these buildings existed along this section.

While stages 1 and 2 of the investigation were performed by RLE, it was the task of the contractor to carry out more detailed investigations at the third stage and to plan and realise suitable measures to minimise the effects of settlements on the structures. (Bowers 2003).

Therefore, 37 buildings in total were examined by the joint venture before the start of the shield tunnelling work. The following measures were taken:

– Portal crane runway in the Freightliner Depot: The construction ground consists of earth fills. The tunnel cover here is 11 m at maximum. A new runway was erected and founded on piles, which extended

Copyright © 2005 Taylor & Francis Group plc, London, UK

into the London Clay below the tunnel. During the tunnelling work no settlements occurred on the structure.

– Forward Control Building: The three-storey office building lies between the two tunnel tubes which were driven in succession with a cover of approximately 15 m. As a precaution, the buildings were evacuated during the shield driving work and a monitoring system was installed with the assistance of Cambridge University. Minor settlements occurred during the shield tunnelling without damage to the substance of the building.
– Box Lane Ramp and Renwick Road Bridge: These bridge constructions are the only access to the Freightliner Depot. The cover here is 16 m to 18 m. The road bridge showed considerable previous damage by fire. A system consisting of hydraulic presses was installed under the superstructures to hold them in the correct position if necessary. This area showed uniform settlements of 10 mm to 15 mm after the passage of both TBMs. It was not necessary to activate the hydraulic system.
– Alfred's Way Bridge, road crossing over railroad facilities: The pile foundation of the Eastern bridge abutment extended into the profile of the planned tunnel. The tunnel gradient was revised and lowered. The abutment was underpinned and newly founded on mini-piles. A jacking and monitoring system was installed, but did not need to be activated.
– Ripple Road Bridge: Length and position of the pile foundations in relation to the tunnels were examined by means of magnetometers. It was found that the minimum vertical distance was 600 mm. The gravel layers in the area of the upper piles and the anchoring points in the London clay were stabilized with cement mortar to minimise the settlements. The maximum settlement on the ground surface was 7 mm. Segments equipped with normal steel reinforcement in addition to the steel fibre concrete were installed below the bridge.

7 AUTOMATIC MONITORING

Besides the preparatory works of improving structures or reinforcing the foundation of structures, alternatively high frequency monitoring was conceived to detect settlement problems during the tunnel drives backed up by contingency plans to deal with the consequences of large movements.

High frequency monitoring means in this case a system of real time remote monitoring of surface railway structures in the Barking area. A list of affected structures is given in Table 1.

As the authorities (LUL and NR) stipulated monitoring data to be provided on a 24 h/7 day basis, which was the working rhythm of the tunnelling works, only an automated monitoring system (AMS) would meet this stipulation.

Table 1. Affected structures in the Barking area.

Affected structures	Construction
LUL underpass	Segmental Reinforced Concrete (RC) Box
Barking Station Overbridges (x3)	East Bridge: RC deck on RC "finger" columns Centre Bridge: brick abutments and piers supporting a "jack arch" deck West bridge: RC columns supporting RC deck
Barking Station Platforms	Brick construction
Northern Relief Road Overbridge (A123)	Steel box girder and RC slab supported by RC abutments and Pier
Queen's Road Bridge	Brick abutments supporting "jack arch" deck
Loxford Road Footbridge	Steel girder supported by RC Piers
Loxford Water Culvert	RC Culvert
LTE Flyover	RC railway flyover
LTS Flyover	RC railway flyover
River Roding Bridges (x3)	North Bridge: RC abutments and Piers supporting steel beams and RC slab Centre and South Bridges comprise wrought iron girders supported on ballast filled caissons and masonry bankseats
London-Tilbury-Southend mailine LUL District line Silverlink Gospel Oak line	
North Circular Road Viaduct (A406)	Multi-span composite deck viaduct

For the design of such a system the affected structures had to be fixed and their sensitiveness to be assessed, contours for 1% volume loss to be defined and positions of robotic total stations to be found. For this purpose, large-scale drawings, photographs and site visits were used.

Finally the following monitoring targets were installed:

– Ground monitoring targets at 10 m centres along the centre lines of the tunnels;
– Transverse monitoring arrays at approx. 50 m centres to control ground loss;
– Targets on the railway lines attached to rail shoes;
– Targets at the affected structures.

Copyright © 2005 Taylor & Francis Group plc, London, UK

As a result of the structural assessments three alert levels were defined:

– Green trigger: work may continue, review level twice daily.
– Amber trigger: further review of monitoring carried out; additional monitoring surveys implemented, visual inspections.
– Red trigger: all work stopped, third party notified immediately, detailed review of monitoring and TBM data.

Once the monitoring targets had been installed, a series of baseline readings was taken to provide a stable reference to compare changes as the TBMs passed.

After these preliminary works an initial set up of the robotic total stations instruments with auto target recognition was carried out. The instruments were mounted on pillars adjacent to the monitoring zones.

The initial baseline readings were observed by the surveyor and then transmitted back to the GeoMOS server using radio modems. This procedure was required to "train" the GeoMOS later to recognise the total station and its location in 3D space.

During the tunnelling activities the frequency of the monitoring corresponded approximately with a muck and ring build cycle of the TBM, i.e. one observation during each cycle was made.

In total 17 total stations operated simultaneously and observed up to 1000 targets.

The observed data was transmitted back to the GeoMOS server and stored.

From the stored data spreadsheets were developed to create simple user interfaces for the management of the AMS. Graphical spreadsheet outputs were part of the management strategy for the C250 TBM drives. (Preece et al., 2004)

8 TUNNELLING

Before starting shield tunnelling, the necessary support and grouting pressures were investigated with the aim of minimizing the construction ground settlements. For this examination, various cross-sections were chosen which from experience had to be evaluated quite critically due to their geology or the kind of the foundation of the construction. With the same aim different conditioners were tested on soil typical of the route in the construction material laboratory. Different grouts were designed and tested with raw materials available in situ. The results of these investigations formed the basis for the shield driving parameters established by project management.

Subsequently, the TBM was assembled and, after positioning in the tunnel eye steel structure, finally coupled to the back-up system, which had been completely equipped in the meantime.

A number of partition walls, stairways and intermediate ceilings for an escape and rescue structure had to be erected within the start shaft. The overall schedule had foreseen the handing over of the construction work to another contractor while the tunnel work was still in full operation.

In order to exclude the dangers emanating from these works and to save time, the joint venture developed a solution that dispensed with the use of a thrust frame and used permanent rings instead of blind rings.

A special steel ring was manufactured for this purpose and screwed to the first ring built under the protection of the shield tail. Hydraulic presses, which were lengthened with spacers and supported against the portal of the completed ramp structure, formed the support for the construction of the rings.

A lengthened shield cradle over the central axis of the tunnel tube prevented the lateral displacement of the segments. After completion of the ring construction, the spacers were removed and the tunnel tube was cautiously pushed to the rear. After a position was reached which allowed the construction of the next segment ring, the spacers were put back in and the bottom of the ring was lined with grout. With the aid of this method six complete rings per tunnel were built.

After the cutting wheel had passed the starting gasket, the radial cutting tools were installed and the excavation chamber filled with a sand-bentonite mixture from the surface via a borehole and the tunnelling work was started.

Our activities were accompanied by a comprehensive monitoring of settlements. Points previously fixed and measured at the surface, the railroad tracks and the buildings were checked at predetermined intervals. The controls included both manual and automatic measurement procedures as described in the paragraph above.

In addition, a so-called "Control Room Engineer" was installed on a 24-hour basis. He was in permanent contact with the engineers responsible for the tunnelling work and the monitoring.

All relevant tunnelling and measurement data converged at his desk. They were recorded during the advance work in a Log Book and compared with the nominal values. If there were differences, the Tunnel Agent present on site was informed. It was his responsibility to implement corrective measures.

The "Control Room Engineer" also ensured that RLE, LUL and Network Rail were informed. Should railway traffic be endangered by the tunnelling work, he was authorized to have the responsible Line Controller stop the railway traffic above the tunnel alignment.

Twice a day tunnel management met with the surveyors and a representative of RLE to evaluate the latest measuring and advance work data. As a result, the parameters for the shield drive were confirmed or adjusted.

Copyright © 2005 Taylor & Francis Group plc, London, UK

In order to keep settlements of the construction soil to a minimum, the quantities and volume of the excavated ground were continuously recorded during the advance work, shown digitally and graphically in the operating cabin and compared with the reference values. For this reason, the joint venture equipped both TBMs with volume scanners in addition to the conveyor type weighers already installed.

The data acquired on the TBM repeatedly showed differences. These were caused by the wear of the conveyor belts and changes in the belt tension. Since at that point of time the design of the belt conveyor system could no longer be changed, further conveyor type weighers were installed at the inclined conveyor belts of the supply shaft. By comparison of three data trends measurement errors could be excluded.

If the desired values were exceeded, first the volume of the injection grouting material was increased. Then, test bores and further grouting ensured that no cavities remained in the construction ground.

The injection of bentonite suspension into the tunnel crown via the shield casing proved to be another effective measure to reduce settlements during the advance work. In case of longer stoppages, bentonite was also injected into the crown and additionally via the grout injection lances. Thus, settlements could be minimised and it was easier to restart the shield.

From our point of view, the use of a TBM with an articulated forward shield and ground water lowering over the whole route did not contribute to minimize settlements.

As a result of the TBM manufacturer's philosophy almost the whole hydraulic system, including all oil tanks, heat exchangers as well as control and regulating equipment, was incorporated in the shield. This meant that the centre of gravity of the shield was quite near the front. In order to compensate for this, the shield was mainly controlled by Look-Up. This on the other hand, resulted in a permanent overcut.

Due to the ground water lowering all cross passages could be mined by hand under the protection of semi-mechanized tunnelling techniques. This is a traditional construction method in London and led to cost savings compared with the freezing measures that would otherwise have been necessary. However, in some route sections settlement of the construction soil was caused by dewatering. Here, too, the dewatering of the Thanet Sands had negative influences on the excavation of the soil with EPB shields. In some parts, water had to be added to condition the soil during advance work.

Finally, it should be pointed out that the settlement problems can above all be positively or negatively influenced by the miners during the tunnelling work. Of particular importance is the experience and sense of responsibility of the chief operator of the shift, foremen, and above all the shield drivers.

9 SUMMARY

Nearly throughout the whole shield drive values of between 0.3% and 0.4% of volume loss were achieved. Railway traffic above the tunnel route was able to proceed unhindered and without interruption. On the bridge structures beneath which the tunnel passes no damage or traffic hindrances occurred. All tunnel constructions were completed within the set time frame and budgets, thereby setting new standards for suburban tunnel construction in Great Britain.

REFERENCES

Bowers, K. 2003. Managing the CTRL ground movement risk. In Thomas, T. (ed.). *CTRL section 2 tunnelling*. London: Polygon Media Ltd.

Craig, R. 2003. Underground on section two. In Williams, L. (ed.). *World Tunnelling Channel Tunnel Rail Link supplement*. London: Mining Communications Ltd.

Preece, L., Mimnagh, F., Martin, J. & Harrison, S. 2004. Automatic monitoring on CTRL's C250 tunnels In Thomas, T. (ed). *Tunnels & Tunnelling International*. September 2004. Sidcup: Polygon Media Ltd.

Woods, E. 2003. Design decisions for CTRL 2's bored tunnels. In Thomas, T. (ed.). *CTRL section 2 tunnelling*. London: Polygon Media Ltd.

Copyright © 2005 Taylor & Francis Group plc, London, UK

FEM analysis of EPB tunneling bored underneath through underground obstruction

W. Teparaksa
Center of Soft Ground Engineering, Department of Civil Engineering, Chulalongkorn University, Thailand

ABSTRACT: The Premprachakorn flood diversion tunnel was the shortcut tunnel to divert the flood water in rainy season into the Choa Phraya river. The tunnel bored by means of EPB shield tunneling in very stiff silty clay layer at about 20–24 m depth. During flood diversion tunnel bored underneath the existing Bangkok main water supply tunnel and pile foundation of the bridge, instrumentation was monitored and compared with predicted FEM analysis. The prevention risk potential by means of predicting damage assessment is also presented and discuss.

1 INTRODUCTION

In rainy season, flooding in Bangkok city is one of the crisis to the city which is responsible by the Bangkok Metropolitan Administration (BMA). The first flood diversion tunnel so called Klong Premprachakorn flood diversion tunnel was constructed to divert the flood water in the area North of Bangkok and along the main highway from Bangkok International airport to Bangkok city to Choa Phraya river. This first shortcut tunnel was about 1.88 km long. The intake and pumping station was located at Premprachakorn cannel while the outlet shaft was on the Choa Phraya river bank as shown in Figure 1. Along the route, the tunnel was bored underneath through two underground obstructions as the existing Bangkok main water supply tunnel and the bridge crossing the cannel.

This paper presents the measuring surface and subsurface ground displacement caused by EPB shield tunneling. The FEM analysis to assess risk potential is also presented.

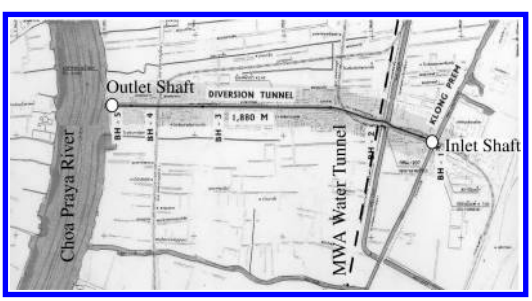


Figure 1. Layout of Premprachakorn flood diversion tunnel.

2 TUNNEL ALIGNMENT AND SOIL CONDITIONS

The Premprachakorn flood diversion tunnel was the first diversion tunnel shortcut the flooding water from Premprachakorn cannel to Choa Phraya river. The second and third diversion tunnels are now under design and construction period by divert the flood water from Sansab-Ladpro Cannel and Makkasan reservoir to Choa Phraya river, respectively (SECC, 2004). The tunnel has outside diameter of 4.05 m with reinforced concrete segmental lining of 180 mm thick and bored by means of EPB shield. The tunnel was seated in the very stiff silty clay layer alternated with dense silty sand layer at about 20–24 m below ground surface as shown in Figure 2. The tunneling work was started from outlet shaft at Choa Praya river. At station 1 + 534 from Choa Phaya river, the flood diversion tunnel was bored about 3 m underneath through the existing Bangkok main water supply tunnel as shown in Figure 3.

During diversion tunnel boring the main water tunnel is under service discharge water pressure of 50–80 kN/m^2. The structure of the existing main water tunnel is the concrete segmental lining of 0.2 m thick with secondary steel liner. Generally the TBM was bored based on the face pressure of about 100–120 kN/m^2 which is about 45–55% of the at rest earth pressure, however at portion where the tunnel have to pass underneath the existing main water supply tunnel, the face pressure was applied up to about

Copyright © 2005 Taylor & Francis Group plc, London, UK

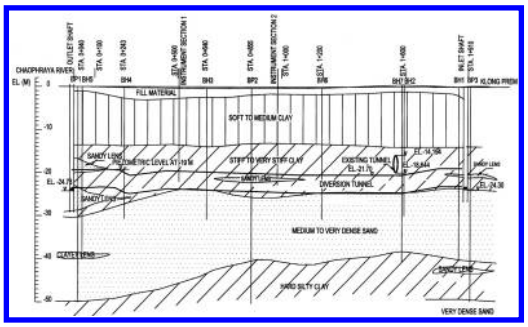


Figure 2. Cross section of flood diversion tunnel.

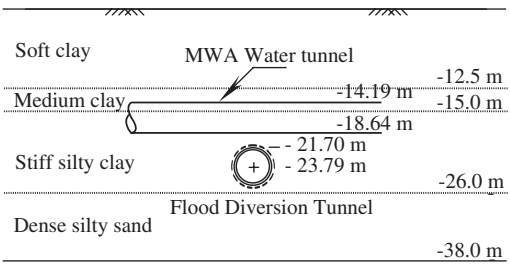


Figure 3. Diversion tunnel bored underneath water tunnel.

380 kN/m^2 in order to minimize the ground loss as well as soil displacement. This technique could be over come the obstruction, however, polymer lubricant had to add to solve the slip of stiff clay in the cutting process. This critical path was obviously controlled based on the fully instrumentation inspection (Deep ground settlement point). After just 18 m. through this water supply tunnel, at station 1 + 552 and 1 + 573 the diversion tunnel was also bored about 0.5–1.5 m below pile foundation of the main bridge across to the raw water cannel as shown in Figure 4. This bridge is quite old and its as-built drawing is not available. Therefore, the side echo integrity test were carried out under water to determine the pile length. Therefore, the exact pile length was not clear.

At the area of this tunnel bored through the sub-structure obstruction, the detail instrumentation were installed at 3 sections as station 1 + 502, 1 + 512 and 1 + 522 as shown in Figure 5 and monitored.

The general subsoil conditions of Bangkok sub-soils consists of 13–15 m thick soft marine clay underneath by stiff to very stiff silty clay layer to about 22–24 m depth. This soft clay is the sensitive clay having anisotropic behavior with water contents about 85–95% with undrained shear strength about 15.5–16 kN/m^2. The first dense silty sand layer is found beneath the very stiff silty clay layer to about 30–35 m depth and alternated by hard silty clay and second very dense silty sand layer. The piezometric

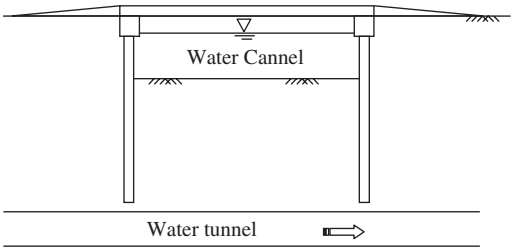


Figure 4a. Tunnel bored underneath bridge pile foundation.

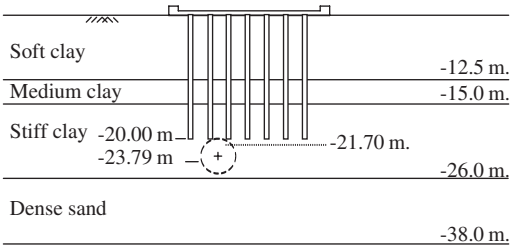


Figure 4b. Bridge crossing the raw water cannel.

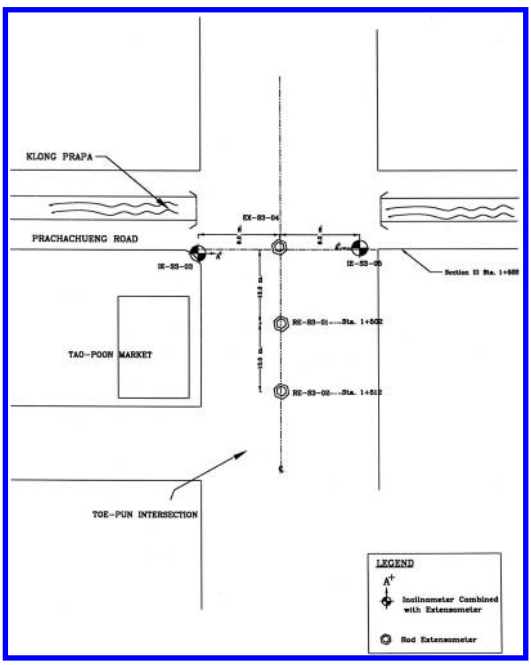


Figure 5. Layout of the instrumentation.

draw down water level was found at about 23 m depth below ground surface (Teparaksa, 1999 a, b, c and 2000 a) due to deep well pumping and lead to induced land subsidence in Bangkok city.

Copyright © 2005 Taylor & Francis Group plc, London, UK

3 DAMAGE ASSESSMENT BEFORE TUNNEL BORED THROUGH OBSTRUCTION

In order to prevent the risk potential on both Bangkok main water supply tunnel and pile foundation of the bridge across the raw water cannel, the damage assessment by means of FEM analysis was carried out. Two tested sections at station 0 + 506 and 0 + 980 were fixed with fully installation of instrumentation to verify the ground displacement response (Ground surface settlement point and extensometer).

The numerical approach to predict ground displacement response was performed based on FEM analysis. The two dimensional FEM namely PLAXIS (Teparaksa, 2002) is used for modeling of the interaction between soil and structure. With this approach, a complete modeling of the system including the stress–strain distribution and ground water condition, the deformation and section force in the lining was also possible.

3.1 *Ground modeling*

The constitutive model was based on an elasto-plastic (Mohr-Coulomb) failure criteria. As the recorded ground displacement response (Teparaksa, 2000 b and 2001), it was occurred in the short term conditions, therefore undrained soil parameters were assumed for the cohesive soil layers. The effect of ground water flow as well as consolidation was not considered in the model. The standard ground model used for the FEM analysis was based on the soil stiffness parameters. Generally the stiffness of the Bangkok subsoils has the non-linear behavior depended on the shear strain level. For practical point of view, the plain strain concept with the Mohr-Coulomb soil model was used in the FEM analysis. Menzies (1997) proposed the soil stiffness depending on the order of the shear strain as shown in Figure 6. The range of shear strain for bored tunnel was recommended in the range of 0.1–1.0%. Six number of self boring pressuremeter test were carried out along the MRT route. Teparaksa (1999 c) reported the results of the self-boring pressuremeter tests in Bangkok subsoil that the soil stiffness was depended on the degree of shear strain. Figure 7 (a) and (b) show the variation of shear modulus with shear strains for soft clay and stiff clay respectively. According to the shear modulus from pressuremeter test and the order of shear strain for tunneling works recommended by Menzies (1997) between 0.1–1%, the soil stiffness was assumed for FEM analysis as Eu/Su = 240 and 480 for soft clay and stiff clay, respectively. The strength and stiffness soil parameters were summarized in Table 1.

3.2 *Damage assessment*

The damage assessment was carried out by the author (Teparaksa, 2000 c) to predict the ground surface and subsurface response caused by EPB shield tunneling.

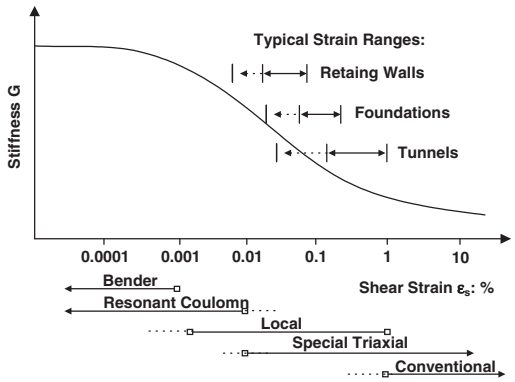


Figure 6. Typical shear modulus and shear strains for foundation works (after Mair 1993).

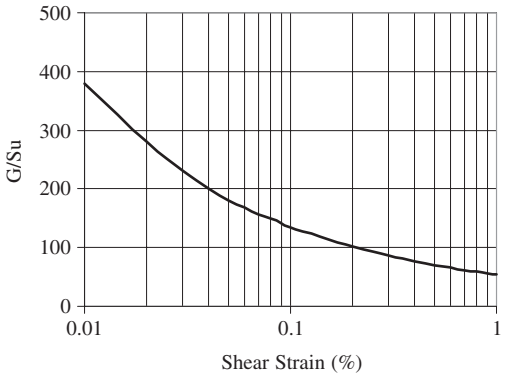


Figure 7a. Shear modulus of soft Bangkok clay.

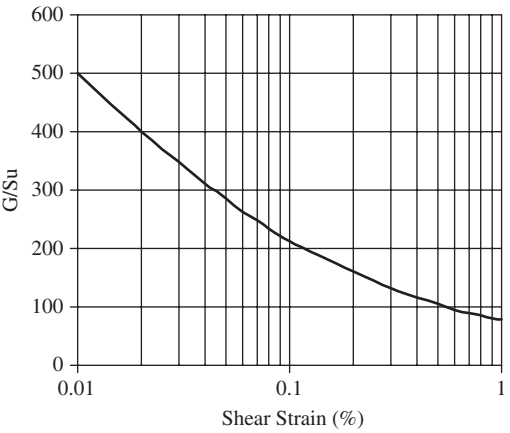


Figure 7b. Shear modulus of stiff Bangkok clay.

Copyright © 2005 Taylor & Francis Group plc, London, UK

Table 1. Soil parameter for FEM analysis.

Soil layer	Su (kN/m^2)	Eu/Su	E′ (kN/m^2)
Made ground	35	300	–
Soft clay	17–22	240	–
Stiff clay	100–150	480	–
Silty sand	–	–	$2000N_{60}$

Su : Undrained shear strength
Eu : Undrained modulus
E′: Drain Modulus

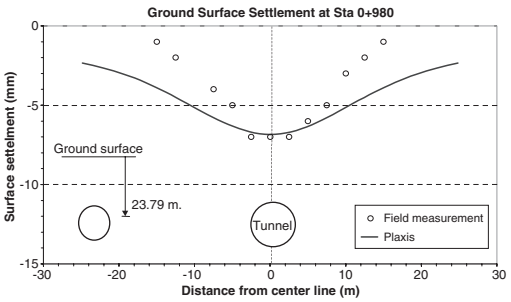


Figure 8a. FEM prediction of surface deformation compared with field measurement (station 0 + 980).

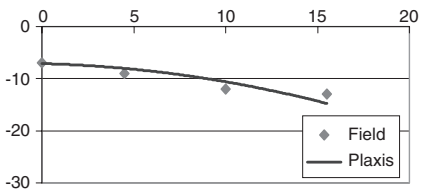


Figure 8b. FEM prediction of subsurface deformation compared with field measurement (station 0 + 980).

Figure 8 presents the predicted ground surface and subsurface response by means of FEM analysis compared to field measurements at station 0 + 980. The prediction agreed well with field performance.

4 GROUND DISPLACEMENT CAUSED BY TUNNEL BORED UNDERNEATH OBSTRUCTION

The damage assessment well predicted both ground surface and subsurface ground deformation. At station 1 + 522 where is about 10 m before crossing the MWA water tunnel. The predicted displacement of MWA water tunnel was about 19 mm at about 15 m below ground surface. Figure 9 presents the FEM predicted ground displacement compared with field measurement by surface settlement point and deep

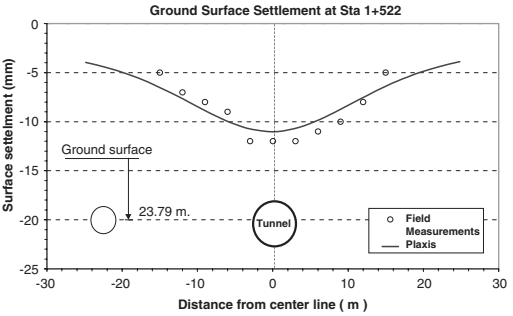


Figure 9a. FEM prediction of surface deformation compared with field measurement (station 1 + 522).

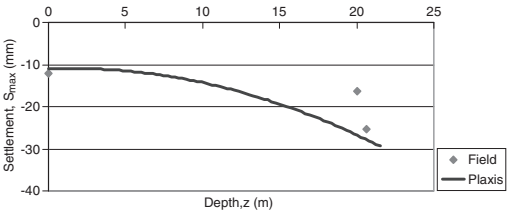


Figure 9b. FEM prediction of subsurface deformation compared with field measurement (station 1 + 522).

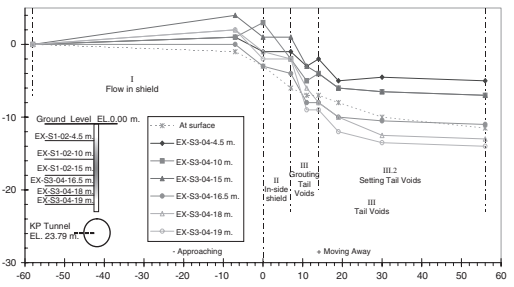


Figure 10. Ground surface and subsurface measured at various positions (station 1 + 522).

rod extensometer. The behavior of ground displacement both surface and subsurface at various position of TBM passing through the measured point (station 1 + 522) is presented in Figure 10. The deformation was divided into 3 stages as stage 1 soil flow into the shield, stage 2 deformation in the shield and stage 3 caused by tail void. The tail void induced the major displacement caused by EPB shield tunneling. At the station where the Premprachakorn flood diversion tunnel pass underneath the MWA water tunnel (station 1 + 534) and pile foundation of the bridge (station 1 + 522 and 1 + 573), only ground surface displacements was monitored. In the area of protection zone

Copyright © 2005 Taylor & Francis Group plc, London, UK

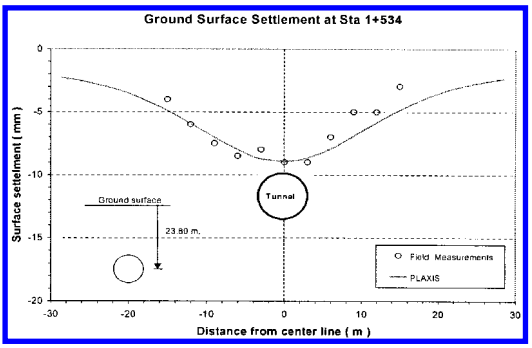


Figure 11. FEM prediction of surface settlement compared with field performance at station 1 + 534.

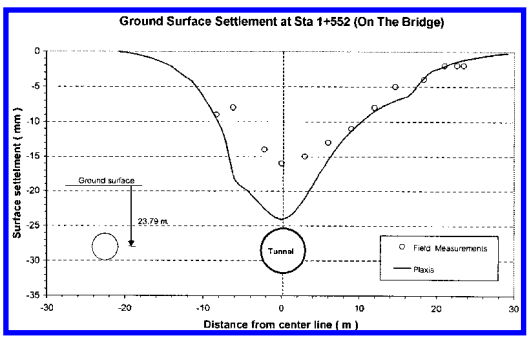


Figure 12. FEM prediction of surface settlement compared with field performance at station 1 + 552.

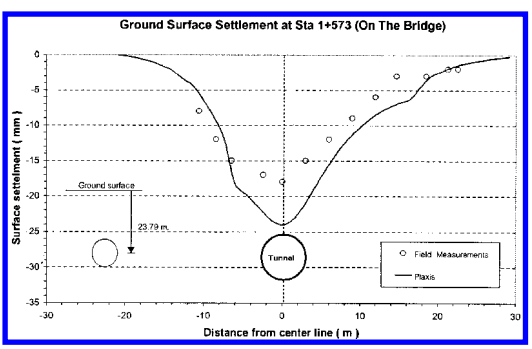


Figure 13. FEM prediction of surface settlement compared with field performance at station 1 + 573.

of MWA tunnel, there were not allow any drilling or boring even for deep instrumentation.

Figures 11–13 present the ground surface response predicted by means of FEM analysis compared with field measurement at station 1 + 534 (crossing the MWA tunnel), station 1 + 522 and 1 + 573 (crossing the bridge foundation), respectively. The Fem prediction agreed well with field performance.

5 CONCLUSIONS

The flood diversion tunnel was bored underneath two underground obstructions as existing main Bangkok water supply tunnel, and the bridge pile foundation crossing the raw water cannel. The damage assessment by means of FEM analysis to verify the risk potential was carried out and compared with measurements before reaching the obstruction. The behavior of ground surface and subsurface response during and after passing the obstruction was also present.

ACKNOWLEGEMMENT

The authors would like to express their gratitude to the Mass Rapid Transit Authority of Thailand (MRTA) for their permission of publishing this paper. Thanks also to all staff of the Strategia Engineering Consultants Co., Ltd. (SECC) for their supporting in the analysis as well as preparing the manuscript.

REFERENCES

Mair, R.J. 1993. Development in geotechnical engineering research, application to tunnels and deep excavations, *Proceedings of the Institution of Civil Engineers and Civil engineering.*

Menzies, B. 1997. Applying modern measures, *Ground Engineering,* pp. 22–23.

Teparaksa, W. 1999 a. Geotechnical aspects on the design and construction of the MRTA subway in Bangkok, *Journal of the Society of Professional Engineering Thailand,* Vol. 24, pp. 21–34.

Teparaksa, W. 1999 b. Performance of diaphragm wall and soil parameters for design and construction of sub structures in Bangkok subsoil, *Annual Conference on National Civil Engineering,* Engineering Institute of Thailand.

Teparaksa, W. 1999 c. Principle and application of instrumentation for the first MRTA subway project in Bangkok, 5th *International Symposium on Field Measurements in Geomechanics,* Singapore.

Teparaksa, W. 2000 a. Displacement behavior of soil for the first MRTA subway in Bangkok subsoil, 13th *KKNN Symposium on Civil Engineering,* Taipei, Taiwan, pp. 349–354.

Teparaksa, W. 2000 b. Design and construction of Klong Premprachakorn flood diversion tunnel, Special Lecture, *the Engineering Institute of Thailand*.

Teparaksa, W. 2000 c. Damage assessment on influence of MWA water tunnel due to bored tunnel of flood diversion tunnel, *Strategia Engineering Consultants Co.Ltd. (SECC)*, Bangkok, Thailand.

Teparaksa, W. and Pitaksaithong W. 2001. Behavior and Prediction of Soil Displacement During TBM Tunneling in Bangkok Subsoils, 7th *National Congress on Civil Engineering,* Bangkok, May.

Teparaksa, W. 2002. Training course on PLAXIS, *Two Plus Soft Co.Ltd.,* Bangkok, Thailand.

Copyright © 2005 Taylor & Francis Group plc, London, UK

Surface and subsurface ground deformation due to EPB tunneling in Bangkok subsoils

D. Luangpitakchumpol
Ph.D. Student, Chiang Mai University, Chiang Mai, Thailand

W. Teparaksa
Professor, Department of Civil Engineering, Chulalongkorn University, Thailand

W. Pitaksaithong, C. Boonsong & J. Boonard
Strategia Engineering Consultants Co.Ltd, Bangkok, Thailand

ABSTRACT: The Premprachakorn flood diversion tunnel (OD = 4.05 m.) first shortcut tunnel of the Bangkok Metropolitan Administration (BMA) to divert the flood water in the city to the Choa Phraya river. The MRT subway tunnel (OD = 6.3 m.) of Bangkok city just opened in 2004 consists of dual tunnel for 20 km. long. Both tunnels seated in the very stiff sillty clay layer with some alternated with dense sillty sand layer between 15–24 m. depths below ground surface. The empirical approaches for prediction ground surface settlement base on Peck (1969) and O'Reilly & New (1982) was presented. Based on subsurface ground response due to shield tunneling of two tunnel projects, newly developed correlation for prediction subsurface settlement is presented in terms of tunnel radius and tunnel depth.

1 INTRODUCTION

The infrastructure or civil works in Bangkok city, Thailand are recently designed as the underground utility constructed by means of tunnelling methods. Those are the high voltage underground cable tunnel, waste water treatment project, main water supply tunnel, flood diversion tunnel and Mass Rapid Transit (MRT) subway tunnel. All tunnels are bored by Earth Pressure Balance (EPB) shield. The experiences in construction planning, preventing the unforeseen damage as well as damage assessment were well performed (Teparaksa, 2003). The recent tunneling works such as the second and third phase of flood diversion tunnel or the next stage of MRT subway tunnel, the tunnels will be more complicated and must be crossed underneath the existing tunnel or substructures. The prediction or forecasting the performance of tunneling in terms of surface and subsurface ground movement is really required to verify the risk potential.

2 PROJECT DESCRIPTIONS AND SOIL CONDITIONS

Ground displacements measured by means of surface and subsurface settlement points of two tunnel constructed projects namely Klong Premprachakorn flood diversion tunnel belong to the Bangkok Metropolitan Administration (BMA), and MRT subway project were performed along the route. In Bangkok city, flooding problem is controlled by the BMA. The Klong Prempachakorn flood diversion tunnel is the first phase flood diversion tunnel to divert or shortcut the flood water in the rainy season from Premprachakorn cannel to Choa Phraya River with total length of 1888 m. as shown in Figure 1. The tunnel has outside diameter of 4.05 m. with reinforced concrete segmental lining of 180 mm thick and bored by means of EPB shield. The tunnel was seated in the very stiff silty clay layer

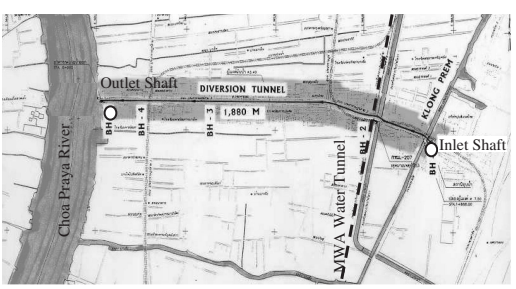


Figure 1. Layout of Premprachakorn flood diversion tunnel.

Copyright © 2005 Taylor & Francis Group plc, London, UK

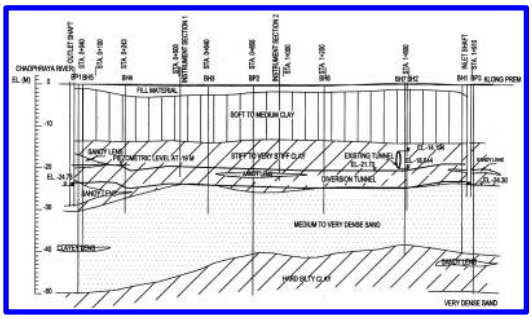


Figure 2. Cross section of flood diversion tunnel.

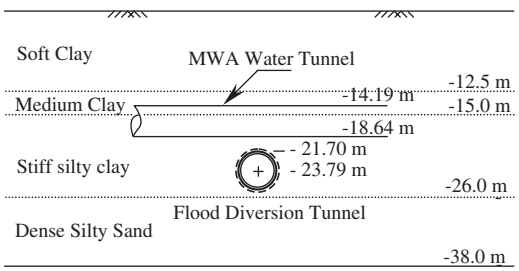


Figure 3. Diversion tunnel bored underneath water tunnel.

alternated with dense silty sand layer at about 22–24 m. below the ground surface as shown in Figure 2. The tunnelling work was started from outlet shaft at Choa Praya River.

At Station 1 + 534 from Choa Phraya River, the flood diversion tunnel was bored about 3 m. underneath through the existing Bangkok main water supply tunnel as shown in Figure 3.

During tunnel boring, the main water supply tunnel is under service discharge water pressure of 50 kN/m^2. The structure of the main water supply tunnel is the reinforce concrete segmental lining of 0.20 m. thick with secondary steel lining.

The MRT subway project, blue line is the first phase subway for 20 km. long in Bangkok city as shown in Figure 4. The MRT tunnel was dual parallel tunnel constructed by means of EPB shield with outside diameter of 6.3 m. with RC segmental lining of 0.30 m. thick. The dual tunnel was seated in the very stiff silty clay layer between 17–22 m. depths below ground surface. Generally, the dual parallel tunnel is arranged with spacing between tunnels of about 15 m. The surface and subsurface ground displacement was recorded between Sirikit (S6) and Bonkai (S5) station where MRT tunnel was bored about 4 m. underneath through the existing Bangkok main water supply tunnel.

The general subsoil conditions of Bangkok subsoils consists of 13–15 m. thick soft marine clay underneath by stiff to very stiff silty clay layer to about 22–24 m.

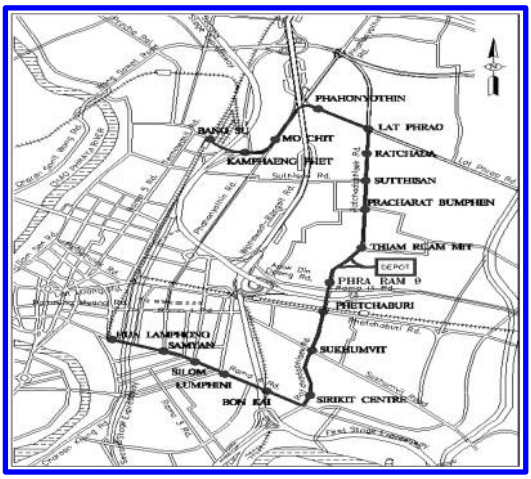


Figure 4. Layout of MRT subway.

depth. This soft clay is the sensitive clay having anisotropic behavior with water contents about 85–95% with undrained shear strength about 15.5–16 kN/m^2. The first dense silty sand layer is found beneath the very stiff silty clay layer to about 30–35 m. depth and alternated by hard silty clay and second very dense silty sand layer. The piezometric draw down water level was found at about 23 m. depth below ground surface (Teparaksa, 1999a, and b) due to deep well pumping and lead to induced land subsidence in Bangkok city.

3 GROUND SURFACE RESPONSE DUE TO SHIELD TUNNELLING

The ground surface settlement due to EPB tunnelling of the Klong Premprachakorn flood diversion tunnel was recorded by Teparaksa (2000). The tunneling work was started from outlet shaft on Choa Praya river bank (station 0+000). Three test sections were selected to represent the performance of EPB tunneling work as well as to improve and adjust influence parameters before driving underneath through the existing main water supply tunnel (MWA tunnel) at station 1+534. Three test sections were divided into 6 stations as section 1 at station 0+506, section 2 at section 0+980 and section 3 closed to MWA tunnel at station 1+522, 1+534, 1+552 and 1+573. The measured ground surface and subsurface deformation response due to EPB tunneling can be classified according to position of EPB shield passing through the measuring point into 3 stages as the deformation ahead the shield, deformation at the shield and deformation behind the shield (Figure 5). The first stage of ground deformation ahead the shield is due to the soil flow into the shield. The third stage of ground deformation is induced during

Copyright © 2005 Taylor & Francis Group plc, London, UK

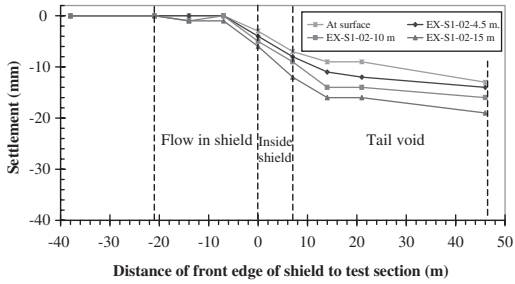


Figure 5. Behavior of ground response caused by bored tunnel.

grouting the tail voids as well as during setting period. It is clear that ground displacement response due to EPB shield tunneling mainly induced at the last portion so called "tail void" ground loss.

Peck (1969) and O'Reilly & New (1982), proposed the empirical method to estimate the ground surface settlement profile due to tunneling as:

$$S = S_{max} \exp\left(\frac{-x^2}{2i}\right) \quad (1)$$

$$i = KZ_0 \quad (2)$$

$$S_{max} = \frac{0.313 V_L D^2}{KZ_0} \quad (3)$$

where S = ground surface settlement at distance x from center line of tunnel (mm); S_{max} = maximum settlement at tunnel line (mm); x = distance (cross section) from center line of tunnel (m) ; i = transverse distance from center line of tunnel to the point of inflexion (m); Z_0 = depth of center line tunnel to ground surface (m); K = constant value depend on ground condition; V_L = volume loss ; D = diameter of tunnel.

Based on the recorded ground surface response at all tested sections of Klong Premprachakorn flood diversion tunnel, the ground loss was found in the order of 1–3%. The ground surface response and the estimated settlement profile proposed by Peck (1969) and O'Reilly & New (1982) at various test sections are presented in Figure 6 to 9. The measured ground surface deformation profile of the MRT subway project for the single and twin parallel tunnels at Sirikit (S6) and Bonkai station (S5) is presented in Figure 10. The estimated settlement profile proposed by Peck (1969) and O'Reilly and New (1982) is also presented in Figure 10.

The i-value for single tunnel and twin tunnel are in the order of 8–12 m. and 11–13 m., respectively. The K-value for single tunnel and twin tunnel are in the order of 0.45–0.55 and 0.7–0.8, respectively.

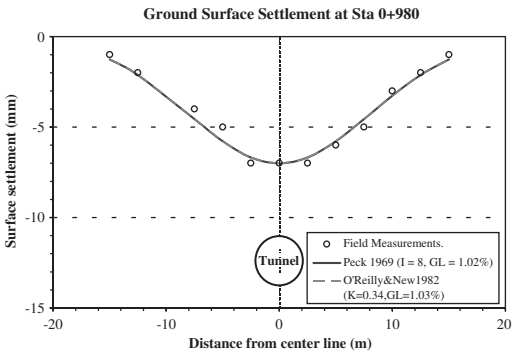


Figure 6. Estimated settlement profile at station 0+980 (Prempachakorn flood diversion tunnel).

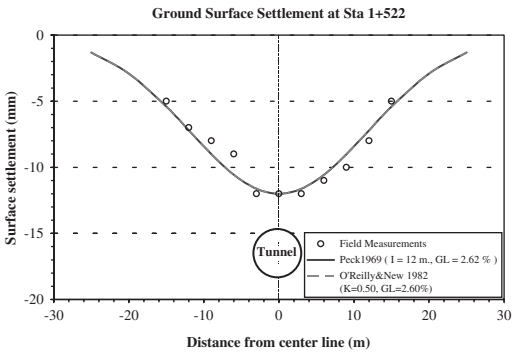


Figure 7. Estimated settlement profile at station 1+522 (Prempachakorn flood diversion tunnel).

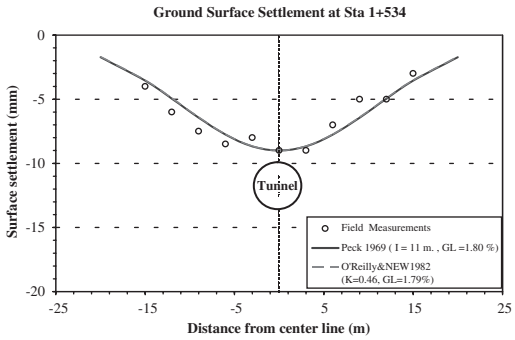


Figure 8. Estimated settlement profile at station 1+534 (Prempachakorn flood diversion tunnel).

4 SUBSURFACE GROUND RESPONSE

The subsurface ground response is measured by means of extensometer. Since the Klong Premprachakorn

Copyright © 2005 Taylor & Francis Group plc, London, UK

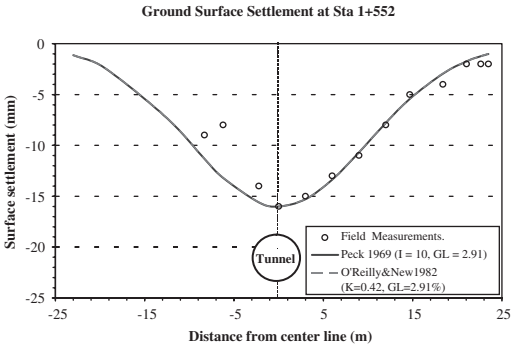


Figure 9. Estimated settlement profile at station 1+552 (Prempachakorn flood diversion tunnel).

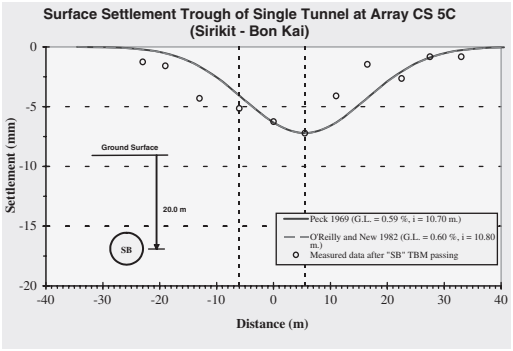


Figure 10a. Estimated settlement profile of MRT single tunnel.

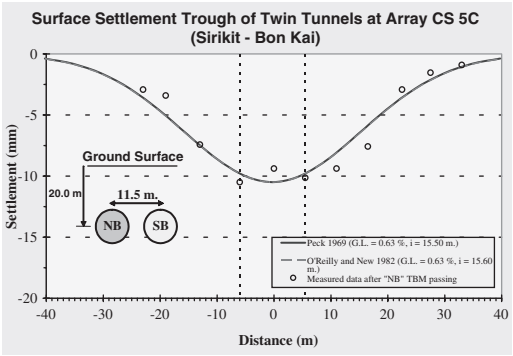


Figure 10b. Estimated settlement profile of MRT twin parallel tunnel.

flood diversion tunnel and MRT subway tunnel were bored underneath the existing MWA water supply tunnel, in order to verify the damage assessment, the subsurface ground settlement, especially at the depth



Figure 11a. Measuring of ground surface settlement.



Figure 11b. Measuring of ground subsurface settlement.

of main water supply tunnel was measured before EPB shield bored through the crossing point. Figure 11 presents the photograph of surface and subsurface ground measurement of flood diversion project. The maximum subsurface ground deformation generally is induced more than ground surface settlement. However, the influence zone is narrower as presented in Figure 12. Mair et al. (1993) proposed the method to estimate the subsurface ground deformation as presented in Figure 13.

The S_{max} at various depth could be determined as same as case of ground surface settlement from Equation 3. However, the K-value was varied against with depth of tunnel. The K and i value for determination of maximum subsurface settlement are:

$$K = \frac{0.175 + 0.325(1 - Z/Z_0)}{(1 - Z/Z_0)} \quad (4)$$

$$i = K(Z_0 - Z) \quad (5)$$

Based on the measured subsurface ground deformation due to shield tunnelling of the Premprachakorn

Copyright © 2005 Taylor & Francis Group plc, London, UK

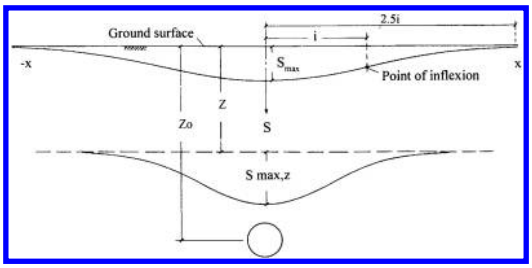


Figure 12. Subsurface settlement profile (Mair et al. 1993).

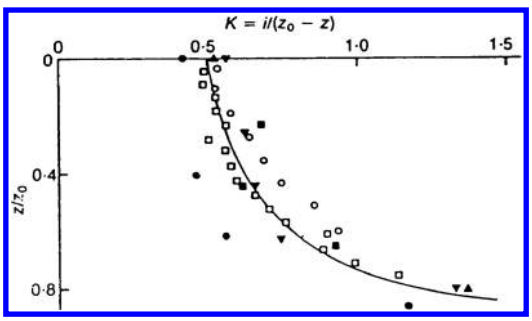


Figure 13. Variation of K-value proposed by Mair et al. 1993.

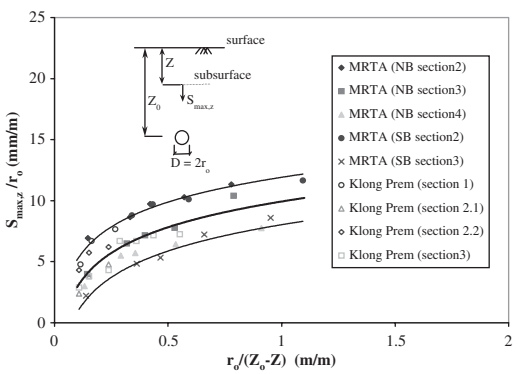


Figure 14. Proposed correlation of maximum subsurface settlement.

flood diversion tunnel and MRT tunnel, the estimated maximum subsurface ground settlement based on Mair et al. (1993) showed much different deformation with measurement. This is may be due to the Mair's approach concerned only depth of tunnel and not concern about the tunnel size. The new correlation to verify the maximum subsurface ground displacement is, therefore, proposed in terms of tunnel radius (r_o) as presented in Figure 14. This proposed correlation was only for shield tunnelling in the very stiff silty clay layer with outside diameter between 4–6.5 m. and ground loss about 1–3%.

5 CONCLUSIONS

The ground surface and subsurface response were measured during and after completion of the Klong Premprachakorn flood diversion tunnel and MRT subway tunnel of Bangkok city. The behavior of ground displacement at various tunnel boring stage is presented and discussed. The i-value proposed by Peck(1969) and K-value proposed by O'Reilly & New (1982) for predicting the ground surface settlement profile is in the order of 8-9 m., 11–13 m. and 0.45–0.55, 0.7–0.8 for single tunnel and twin parallel tunnel, respectively. The newly developed correlation for predicting maximum subsurface ground settlement is proposed in terms of tunnel radius and depth of tunnel.

ACKNOWLEDGEMENT

The authors would like to express their gratitude to the Bangkok Metropolitan Administration (BMA) and Mass Rapid Transit Authority of Thailand (MRTA) for their permission of publishing this paper. Thanks also to all staff of the Strategia Engineering Consultants Co., Ltd. (SECC) for their supporting in the analysis as well as preparing the manuscript.

REFERENCES

Mair, R.J., Taylor, R.N. and Bracegirdle, A. 1993. Subsurface settlement profiles above tunnels in clays. *Geotechnique 43*, No.2, pp.315–320.

O'Reilly, M.P. and New, B.M. 1982. Settlement above tunnels in United Kingdom-their magnitude and prediction, *Tunnelling'82*, Institute of Mining and Metallurgy, pp.173–181.

Peck, R.B. 1969. Deep excavations and tunnelling in soft ground, *Proc. of 7th Int. Conf. on SMFE*, State of the Art Report, pp.225–290.

Teparaksa, W. 1999a. Geotechnical aspects on the design and construction of the MRTA subway in Bangkok, *Journal of the Society of Professional Engineering* Thailand, Vol. 24, pp.21–34.

Teparaksa, W. 1999b. Principle and application of instrumentation for the first MRTA subway project in Bangkok, *5th International Symposium on Field Measurements in Geomechanics*, Singapore.

Teparaksa, W. 2000. Design and construction of Klong Premprachakorn flood diversion tunnel, *Special Lecture*, Engineering Institute of Thailand.

Teparaksa, W. 2003. Damage assessment for EPB shield tunnel bored and cut pile foundation of North park underpass, *Strategia Engineering Consultants Co., Ltd. (SECC).*

Copyright © 2005 Taylor & Francis Group plc, London, UK

Ground improvement and settlement control

Copyright © 2005 Taylor & Francis Group plc, London, UK

Tunneling and measurements in unconsolidated ground

T. Kitagawa & H. Iida
Japan Railway Construction, Transport and Technology Agency (JRTT)

T. Sudo
Taisei Corporation

T. Matsunaga
Pacific Consultants CO., LTD.

S. Akutagawa
Dept. of Architecture and Civil Eng, Kobe University

S. Konishi
Railway Technical Research Institute

ABSTRACT: This paper describes the results regarding the measurements and analysis to investigate the characteristics of ground surface settlement when a tunnel is advanced through unconsolidated ground. Rokunohe tunnel is a 3,810 m long railway tunnel in Hachinohe - Shin-Aomori section of Tohoku Shinkansen. It is located in almost flat diluvial tableland (Sambongihara plateau) at elevation of 60 m above sea level. The surface above the tunnel is mainly used for agricultural and housing land; therefore, the tunnel will pass beneath the public facilities such as roads, railways, water channels for agriculture. Hence, measurements of ground subsidence by using the auto tracking level were adopted to monitor the displacement of the ground resulting from the tunneling. These data were utilized for the verification of the adopted excavation method and auxiliary methods. The numerical simulation was also applied in order to interpret the measurement results. The prediction procedure of the deformation and overall direction of the investigation are described.

1 INTRODUCTION

As shown in figure 1, Rokunohe tunnel is a mountain tunnel in Hachinohe – Shin-Aomori section of Tohoku Shinkansen. Top heading and bench method with mechanical excavation is employed. Ahead of tunneling, deep wells are allocated along the tunnel route to lower the ground water level. In addition, well point drainages at the both sides of the upper bench are arranged to keep the floor dry.



Figure 1. Location of the Rokunohe tunnel.

Figure 2 shows the typical cross section of the tunnel. As an auxiliary method to stabilize the crown, the push-in-type forepoling with steel pipes of their diameters of 48.6 mm and of their lengths of 3 m were installed at the crown perimeter in the range of 150 degrees. The face bolts made by glass fiber reinforced plastic (GFRP) and face shotcrete were used to stabilize the face of the top heading.

The tunnel will cross under the public facilities such as roads, railways, water channels for agriculture. Hence, measurements of ground subsidence were carried out at the location of 510 m from the portal (at the vicinity of 614 km750 m) in order to monitor the stability of the ground and to grasp the influence of tunneling.

Copyright © 2005 Taylor & Francis Group plc, London, UK

2 GEOLOGY

Sambongihara plateau consists of Noheji sandy layer (Nos layer) as the basement and Neogene-Pliocene to Quaternary-Pleistocene pyroclastic materials of Mt.Hakkoda are the terrace layer. The tunnel section is located in Nos layer mainly. Figure 3 shows the geologic profile around the measurement area, and the soil properties of Nos layer are given in table 1. Nos layer consists of even grain sized sands including relatively few fine particles.

3 MEASUREMENT METHOD

In this area, it was difficult to survey the level points using the manually-operated equipment owing to heavy snow cover of up to 1 m thick. Settlement sensors made with a communicating vessels system can not be used due to possible freezing of the inner-liquid. Hence, the ground surface settlements were measured by means of auto tracking level together with leveling staves of a bar code type in order to monitor the displacement of the ground. The auto tracking level autonomously collimates the leveling staves according to the preset directions at an interval of 30 minutes, and reads the bar code to measure the difference of elevation. Although this system does not have the function of three-dimensional measurement, this measuring method is economical when the only vertical profiles are to be measured. The degree of accuracy is 1 mm at this range.

As shown in Figure 4, six scan lines were set on the ground at 10 m spacing and in total 78 leveling staves

Table 1. Soil properties of Nos layer.

Dry density	ρ_d (kN/m^3)	27～30
Void ratio	e	0.8～1.0
Fine fraction content	Fc (%)	5～18
Uniformity coefficient	Uc	2.9
Natural moisture content	Wn (%)	21～34
Relative density	Dr (%)	＞100%
Coefficient of permeability	k (m/sec)	8.0 × 10^{-5}
Cohesion	C (kN/m^2)	0
N-value		30～50

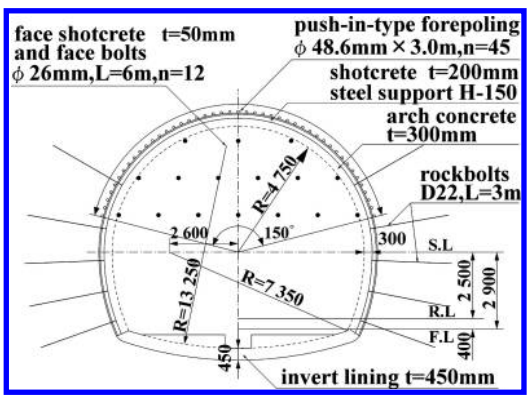


Figure 2. Typical cross section.

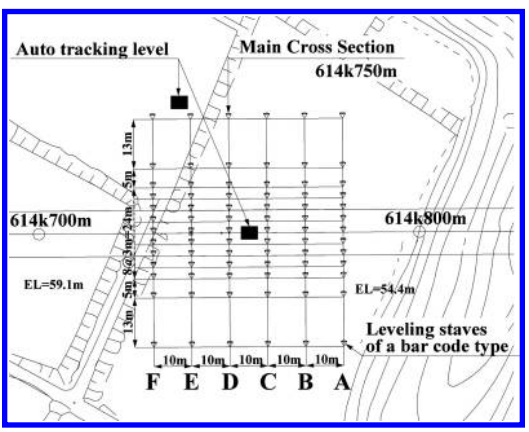


Figure 4. Plan of Ground Surface Measurement Area.

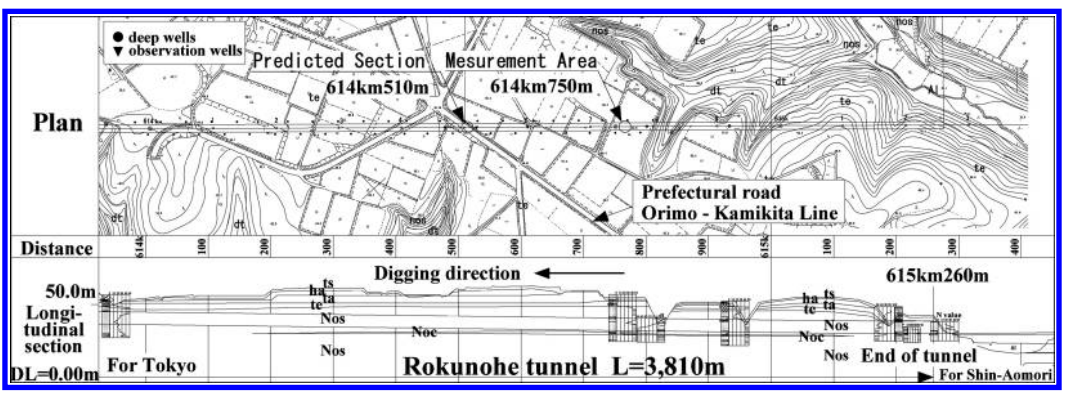


Figure 3. Geologic profile around the measurement area.

Copyright © 2005 Taylor & Francis Group plc, London, UK

were installed to take the distribution of settlement. Because the auto tracking level itself settles down, it was necessary to compensate the measured values. Therefore, reference points were set at the location outside the area uninfluenced by the tunnel excavation. Photograph 1 shows the equipment to measure the ground surface settlement.

In the main cross section, ground settlement and ground horizontal displacement were measured. Owing to thin overburden, pipe strainmeters were installed to measure the shear bands that would be generated by tunnel excavation (Figure 5).

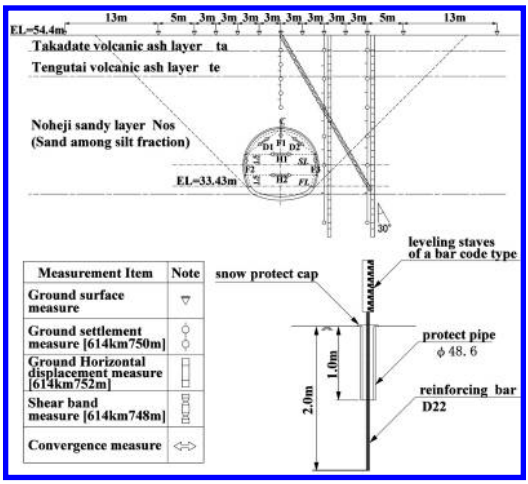
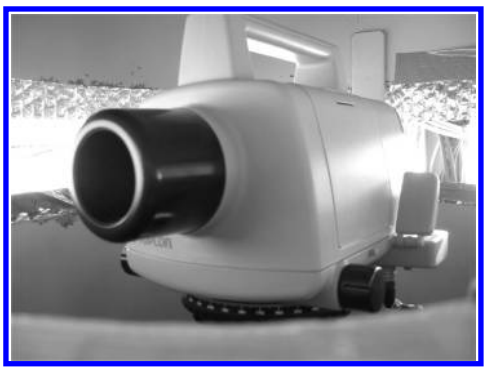


Figure 5. Main Cross Section of the Measurement Area.

4 MEASUREMENT RESULTS

Figure 6 shows the ratio of ground surface settlement to ultimate settlement right above the tunnel center with the distance from the face of the top heading. The maximum settlement was 13 mm. The settlement began when the face of the top heading reached the section 12 m (1.5D) – ahead of the measuring section. The fraction to the total settlement at each stage of excavation, were the 60% (upper half section), 30% (lower half section), and 10% (invert). Upper limit of the advanced settlement was 40% of the whole deformation.

Figure 7 shows the distribution of the ground settlement in monitored cross sections at the final excavation



(a) Auto tracking level



(b) View of the Measurement Area



(c) Leveling Staves of a Bar Code Type

Photograph 1. Equipments for Measurement

Copyright © 2005 Taylor & Francis Group plc, London, UK

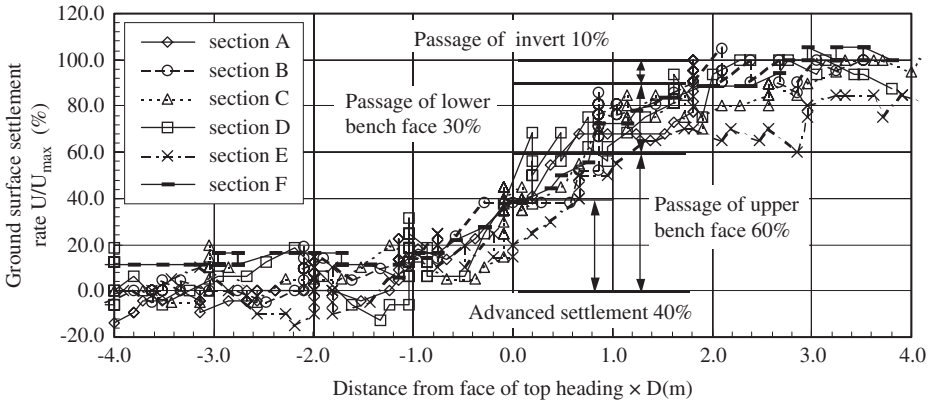


Figure 6. Characteristic of the Ground Settlement with the advance of the top heading.

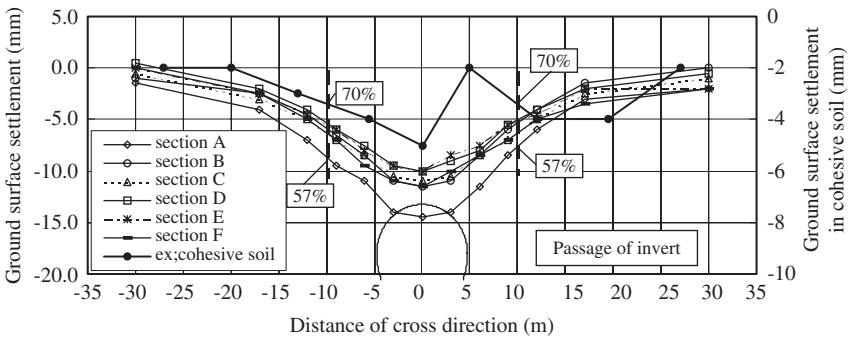


Figure 7. Distribution of Ground Surface Settlement in the final State.

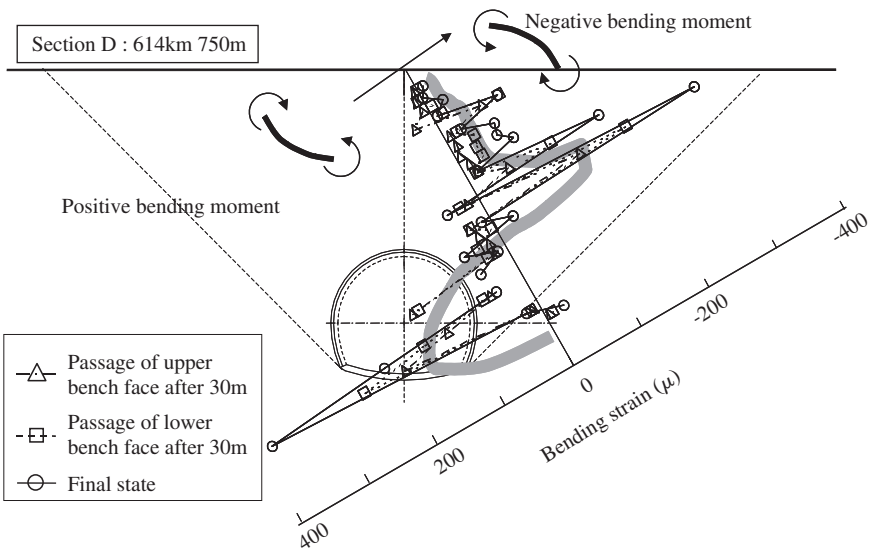


Figure 8. Deformation in the vicinity of the Tunnel.

Copyright © 2005 Taylor & Francis Group plc, London, UK

stage. The ground settlement at a position 15 m away from the center axis of the tunnel would reduce to 1/3. The measurement result that is in the cohesive soil ground is also shown in Figure 7, for example. Similar to a general tendency, the influence of settlement of this case is within the range to narrower than that of the case in the cohesive soil ground. At a position 10 m away from the center, it is obvious that the ratio of ground surface settlement to the maximum value in the cohesive soil ground (70%) is larger than the measurement results in the sandy ground (54–57%). While marginal settlement (1 to 2 mm) was observed at the point 30 m away from the center. This is considered to be the influence of the groundwater drainage from the deep wells.

Figure 8 shows the bending deformation that is estimated from the measurement data of the pipe strainmeters. In this figure, it appears that the mode of deformation with growing the shear bands forms at the side of the tunnel.

5 UTILIZATION OF MEASUREMENT RESULTS

Rokunohe tunnel passed through underneath a prefectural road at 45 degrees, and this point was about 250 m ahead from the measurement point.

Figure 9 shows the schematic cross section along to the tunnel. The stratum above the tunnel was 17 m thick volcanic ash layer accumulated about 10 m thick from the surface of ground over Nos layer. To predict the ground settlement resulting from tunnel excavation, elasto-plastic finite element analysis were carried out. Table 2 shows the soil properties based on available result of ground survey. The results of analysis are given in Table 3. The analysis results were well expressive of the measurement result. The maximum settlement of ground surface was 22 mm and deflection angle was 1.4×10^{-3} radian. Since it seemed to be of little influence for the traffic, it was anticipated that there were no need for applying any auxiliary methods.

Only this area consists of unconsolidated sandy ground. To avoid the expansion of loosened ground zone and the increase of deformation due to collapse at the crown, self-drilling type rockbolts were installed. Figure 10 shows the ground settlement distribution of cross section at each excavation steps.

While the predicted values well simulated the measured value until the top heading support was installed, the settlement exceeded the predicted values after the excavation of the bench.

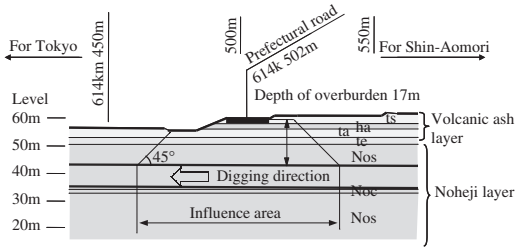


Figure 9. Longitudinal Section of the Prediction Area.

Table 2. Soil Properties for Predictive Analysis.

	Item	Bulk density γt (kN/m^3)	Modulus of deformation E_0 (kN/m^2)	Poisson's ratio ν	Cohesion c (kN/m^2)	Friction angle ϕ (degree)
Ground property	Towada volcanic ash layer [ts]	15.7	1.08×10^4	0.40	27.0	0
	Hachinohe volcanic ash layer [ha]	15.7	1.08×10^4	0.40	27.0	0
	Takadate volcanic ash layer [ta]	14.0	6.30×10^4	0.40	51.8	0
	Tengutai volcanic ash layer [te]	16.4	4.25×10^4	0.40	45.0	0
	Upper Noheji sandy layer [Nos 1]	18.5	6.00×10^4	0.35	30.0	35
	Noheji clayey soil layer [Noc]	15.5	1.39×10^4	0.40	70.0	15
	Lower Noheji sandy layer [Nos 2]	20.0	4.58×10^4	0.35	50.0	35
Support	Shotcrete and steel support	$E_{sc} = 7.416 \times 10^6$ kN/m^2 $I_{sc} = 7.644 \times 10^{-4}$m^4				Beam element
	Rockbolt	$E_s = 2.1 \times 10^8$ kN/m^2				Lod element

Copyright © 2005 Taylor & Francis Group plc, London, UK

Table 3. Result of the Predictive Analysis.

Evaluation item	At the upper bench support was installed	Passage of the upper bench	Passage of the lower bench
Maximum ground surface settlement right above the tunnel (mm)	9.0	21	22
Deflection angle (degree)	0.6/1000 (0.03)	1.4/1000 (0.08)	1.4/1000 (0.08)
Roofsubsidence (mm)	–	22	24
Footsubsidence (mm)	–	15	21

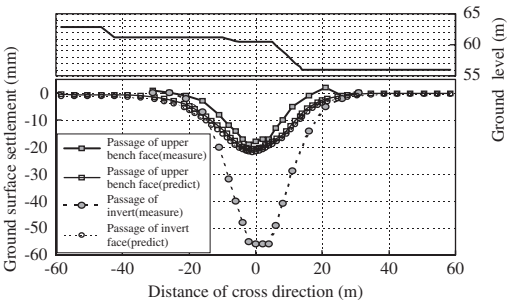


Figure 10. Distribution of Ground Settlement around the Prefectural Road.

This seemed to be resulted from the thin silt layer intervened in the floor ground and water inflow around the ground, where the bearing capacity at the footing of the steel sets became insufficient. There is a possibility that unexpected phenomena will occur in unconsolidated ground; therefore, in order to excavate the tunnel carefully, other auxiliary method should be prepared against trouble.

6 CONCLUSION

The optical measurement system by means of the auto tracking level worked in the cold district effectively.

Further predictive analysis by considering the measurement results enabled the reduction in use of the auxiliary methods in other sections.

It will be important to improve the analytical model and to interpret the tunnel behaviors by using inverse analysis. The knowledge will be made use of in investigating the influence by the planned tunnel excavation underneath crossing roads, railways and water channels.

Copyright © 2005 Taylor & Francis Group plc, London, UK

Construction method of shallow railway tunnel in loose sandy ground

T. Kitagawa, H. Iida & Y. Tadenuma
Japan Railway Constraction,Transport and Technology Agency, Japan

S. Konishi & T. Ono
Railway Technical Research Institute, Japan

K. Okutsu
Nihonkokudokaihatsu Joint Venture, Japan

ABSTRACT: Overburden, stiffness of the ground, underground water level and size of a tunnel are influential factor in tunnel stability. An extremely shallow tunnel (Ushikagi tunnel) is currently under construction with ground stabilizing method. The tunnel is constructed with the shotcrete tunneling method, so-call NATM (New Austrian Tunneling Method) in the Tohoku Shinkansen (between Hachinohe and Shin-aomori). The tunnel is a double-line tunnel with a length of 2,070 m. There are two remarkable points. Firstly, the tunnel is drilled in a loose sandy ground with high groundwater level. Secondly, the overburden of the tunnel is less than 10 m (between 2 m and 10 m) in whole section of the tunnel. In these conditions, the stability of the tunnel was a point to notice and the tunneling method with the ground stabilization was applied as a measure to keep the tunnel stability. This paper describes an outline of the construction, results of measurements and analysis, and evaluate on the effect of ground stabilization. We investigated the effect of the measurement on the face stability by use of measurement results. After that, the face stability with measure was evaluated by the elastic FEA and FEA based on plastic theory (so-call rigid-plastic FEA, RPFEA). Finally, the effect of the ground stabilization based on the results of the measurements and analysis was considered.

1 INTRODUCTION

In Japan, Cut and cover method has been widely used for shallow tunnel projects in unconsolidated ground. On the other hand, the recent development of various construction techniques has made it possible to construct shallow tunnels in unconsolidated ground by the shotcrete tunneling method (so-called NATM). In this case, it is necessary to construct measurements for the face stability and ease of the influence of tunneling on the ground surface including inventive division of heading, additional support, and ground stabilization.

In the Tohoku Shinkansen Line under construction between Hachinohe and Shin-aomori, there are some shallow tunnels which are constructed by NATM in unconsolidated sandy ground, of which. The Ushikagi tunnel is a 2,070 m-long tunnel. The tunnel is drilled in a loose sandy ground with high groundwater level. The overburden of the tunnel is less than 10 m (between 2 m and 10 m) through the whole section.

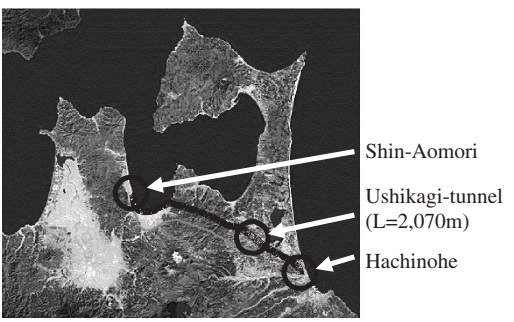


Figure 1. Position of the Ushikagi tunnel.

This paper firstly describes the outline of the tunneling method with ground stabilization which was adopted to the tunnel, and secondly, considers the mechanism of the stabilization with reference to the results of measurements and analyses.

Copyright © 2005 Taylor & Francis Group plc, London, UK

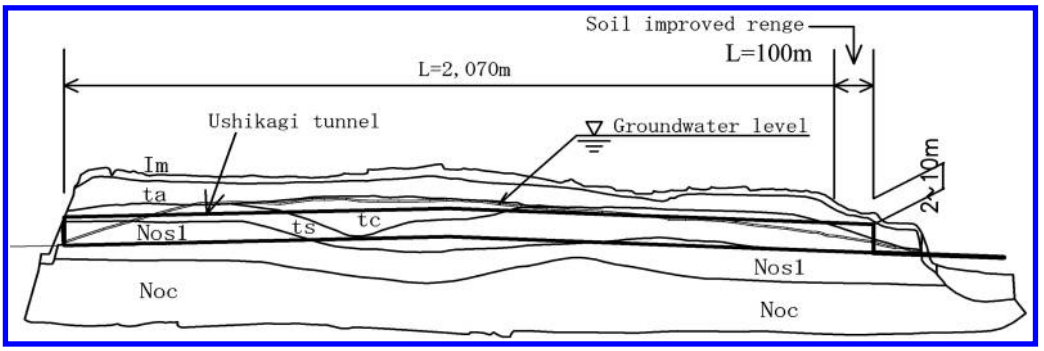


Figure 2. Geological profile of the Ushikagi tunnel.

2 GEOLOGICAL PROFILE

Figure 2 shows the geological profile of the Ushikagi tunnel, and Table 1 shows the soil parameters. The geology around this tunnel is mainly classified as the Noheji layer of Pleistocene epoch (sandy and cohesive soil), new term volcanic products (and soil and loam), alluvial fan sediments (sandy and cohesive soil). The candidate for excavation is the loose sandy ground (N value ≦ 10, Modulus of elasticity $E = 2.7 \times 10^{-4}$kN/m^2) at a high groundwater level, and the overburden of the tunnel is 2 to 10 m thick through the whole section. This sandy soil consists of gravel in mixture silt; the ratio of granule part content is 20% or less, and the coefficient of uniformity is 5 or less. Therefore, the flow of the sandy ground posed a problem.

3 OUTLINE OF TUNNEL CONSTRUCTION

3.1 *Selection of tunnel measurements*

Before the construction of the tunnel, three types of tunneling methods were compared with the viewpoint of economy, construction period, and safety: the first was the open-cut method, the second was the "NATM" with forpoling, and the third was the "NATM" with ground stabilizing method from the ground. Consequently, a tunneling method with a ground stabilizing was adopted, with the view point of both tunnel face stability and economy.

3.2 Outline of the ground stabilizing method

The soil near crown was improved by the soil mixing stabilizing method from the surface of the crown to the foot area before drilling. Figure 3 shows the process of the ground stabilization, and

1) Open cut between ground surface and tunnel crown.
2) Shallow mixing method by blending soil and cement at side zone.

Table 1. Soil parameters.

Stratum	γ(KN/m^3)	φ(deg)	c(KN/m^2)	Characteristic
Im	–	–	–	Surface soil
ta	14	0	35	Loam
ts	18	30	0	Sandy soil
tc	15	0	70	Cohesive soil
Nos1	18	30	0	Sandy soil
Noc	18	30	35	Cohesive soil

3) Pre-mixed method by blending soil and cement at top zone.
4) Replacing soil near ground surface.

Figure 4 shows the cutting face after the ground stabilization.

Next, Table 2 shows the outline of a ground stabilization. The strength of the improved soil was decided by the results of the elastic finite element method, and the blending mixing value of cement was decided after trials.

3.3 *Dewatering method*

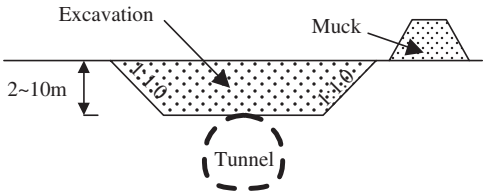
The groundwater that has strongly influences the face stability is lowered below to the tunnel S.L line through some weep holes and by the well point method from inside the tunnel.

4 MESUREMENT

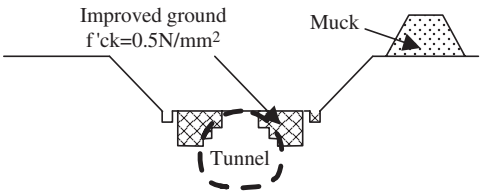
4.1 *Outline of measurement*

In the 100 m-section from the tunnel entrance, several items were measured to investigate the effect of ground improvement on stabilization during the construction of the tunnel. Measurement was performed at the 623 k 296 m point (30 m from the tunnel entrance). Figure 5 shows an outline of the measurement. Monitoring items are as follows.

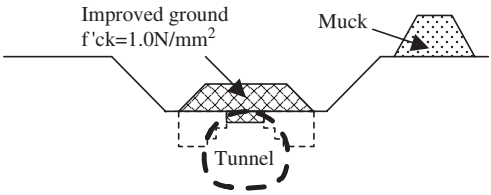
Copyright © 2005 Taylor & Francis Group plc, London, UK



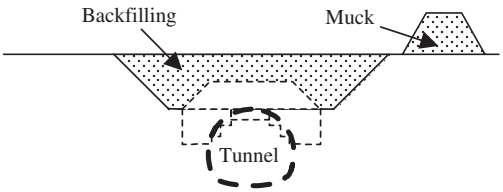
1) Open cut between ground surface and tunnel crown



2) Blending soil and cement at side zone



3) Blending soil and cement at top zone



4) Replacing soil near ground surface

Figure 3. The process of the ground stabilization.

1) Convergence displacement
2) Settling of crown and foot
3) Surface settlement
4) Earth pressure of the improved ground
5) Displacement of the ground
6) Stress of shotcrete and steel support

4.2 *Measurements results*

(1) Displacement of the ground

Figure 6 shows the displacements in the tunnel. Settling was about 30 mm at the crown and 20 to 30 mm at the foot, convergence was 5 mm expanding in the closing phase. The settling at the foot is about

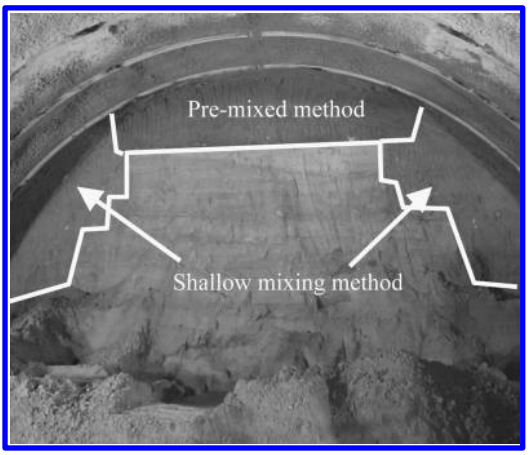


Figure 4. Cutting face after the ground stabilization.

Table 2. The outline of ground stabilization.

Method	Design strength of the improved soil (N/mm^2)	Blend mixing value of cement (kg/m3)
Shallow Mixing method	0.5	50 (clay soil) 90 (sandy soil)
Pre-mixed method	1.0	50

Legend	
○	Earth pressure
⧫	Displacement of the ground
●	Stress of shotcrete and steel support
×	Settlement of the ground
◎	Surface settlement
A	Convergence displacement, Settling of crown and foot
△ |	Inclinometer of the ground

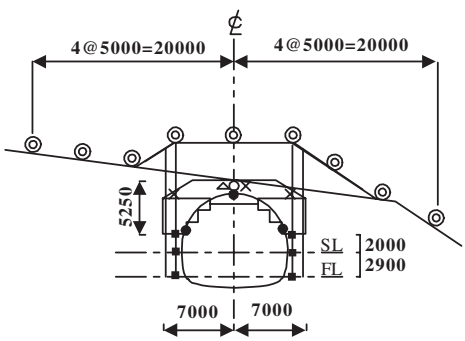


Figure 5. Outline of measurement.

Copyright © 2005 Taylor & Francis Group plc, London, UK

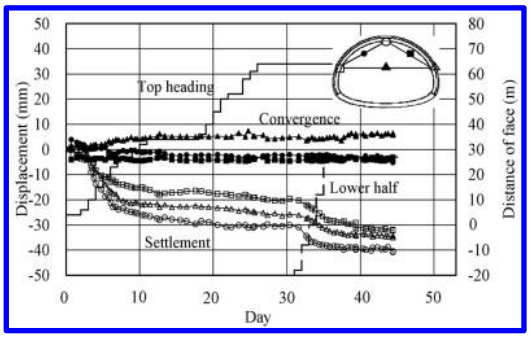


Figure 6. Displacement in the tunnel.

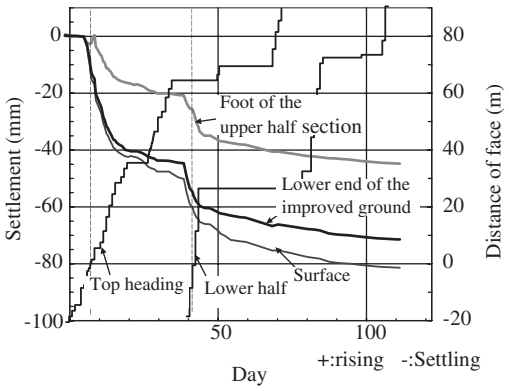


Figure 7. Vertical ground displacement around the tunnel.

75% of that at the crown. It was understood that the part of top heading settled down on the whole. During and after the excavation of the lower half, little change of the convergence was observed in the measurement results.

Figure 7 shows the vertical ground displacement around the tunnel. When the face approached a 10 m point, tunnel, improved ground and surface started to settle down. On the other hand, when the face of the lower half section approached a 20 m point, noticeable settle-down started. This mechanism is likely that the load around the face increased, and was transmitted to the ground ahead of the face. Next, settling at the surface was similar to that at lower end of the improved ground. It was understood that the improved ground and upper embankment settled on the whole.

The settling at the foot was smaller than that at the lower end of the improved ground. This is because the self-weight of the improved ground was supported at the foot of the upper half section.

(2) Earth pressure of the improved ground

Figure 8 shows the vertical earth pressure of the improved ground at the crown.

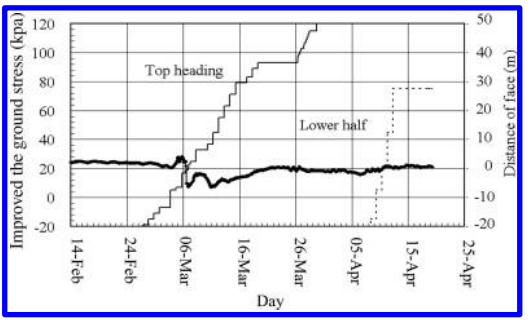


Figure 8. Improved ground stress at the crown.

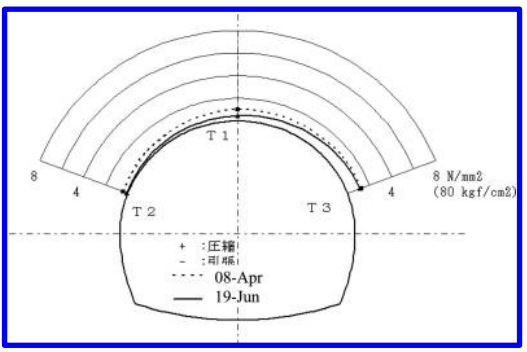


Figure 9. Distribution in the stress of the shotcrete.

When the face of the upper half section approached a 2 m point, the earth pressure of the improved ground decreased rapidly. After face passage, it increased again due to the construction of the primary lining. When the lower half has approached, it was almost fixed. It is thought that the stress relaxation of the improved ground was mitigated by digging.

(3) Stress of the primary lining

Figure 9 shows the stress of the shotcrete. The stress of the shotcrete is finally about 1.2 N/mm^2 in the top heading. It convergences 12 percent of a allowable stress.

Figure 10 shows the axial force of the steel support. Maximal value of axial force was measured at the right shoulder of tunnel. Because it was considered that the clay with the N value of equal about 2 is distinguished from other positions. The maximal value of generating stress which calculated from axial force was 107 N/mm^2, about 50 percent to the allowable stress.

Table 3 shows the stress of the primary lining. The stress of the primary lining was smaller than the allowable stress. It was understood that the safety of tunnel was ensured by the primary lining.

Copyright © 2005 Taylor & Francis Group plc, London, UK

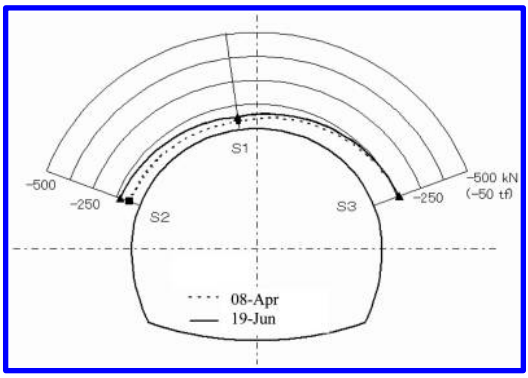


Figure 10. Distribution in the axial force of the steel support.

Table 3. Stresses of the primary lining.

Primary lining	Stress at crown (N/mm^2)	Stress at side area (N/mm^2)	Allowable stress (N/mm^2)
Shotcrete	0.8	1.2	9.3
Steel support	40	102	206

5 NUMERICAL ANALYSIS

5.1 *Outline of numerical analysis*

Stability of the cutting face with and without the measurement was evaluated by the elastic FEA and FEA based on plastic theory (so-called Rigid Plastic Finite Element Analysis, RPFEA).

RPFEA is the limit analysis based on the upper bound theorem and has following merits.

1) The elastic coefficients, which is useless under the critical state, is unnecessary in this analysis. They are γ (=unit weight), c (=cohesion), ϕ (=angle of internal friction).
2) The method can well express the elastic flow near the critical state, of which errors become large with an elastic-plastic model.
3) The initial stress is not required.
4) It does not greatly depend on the setup of analysis domain.

In this analysis, face stability was evaluated to calculate the load of collapse by RPFEA which was formulated by yield criteria of Drucker-Prager and associated flow rule.

Since RPFEA is ultimate analysis, displacement and stress of the ground in the digging process cannot be obtained by it, so some displacements and stresses in the tunnel and the ground in the digging process were evaluated by applying the elastic finite element method (Elastic FEA). Major material properties and the analysis model are shown in Figure 11 and Table 4.

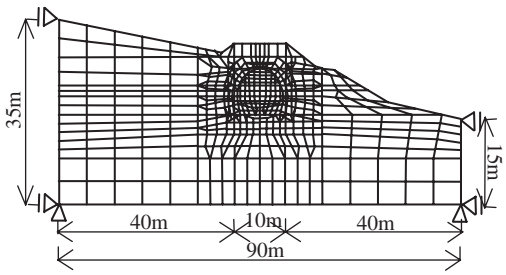


Figure 11. Analysis model of cross-section (Elastic FEA).

5.2 *Results of analysis*

(1) RPFEA

The stability of the face in the unimproved state and improved state were estimated by applying RPFEA through the following procedure.

1) Calculate acceleration μg when the ground collapses (g: gravity acceleration, μ: acceleration ratio, load coefficient).
2) If μ, which is the measure of the face stability, is $\mu > 1$, it judges that the face is stable, and if it is $\mu < 1$, it judged that collapse of the face.

Figure 12 shows velocity fields of a cross section with and without the ground stabilizing method. The scale bars on the right hand in the Figure 12 shows the unit calculated by dividing the maximum displacement velocity into 10 parts.

Since the analysis results without measurement was μ (=0.6)<1, we judged that the face collapsed in the states. On other hand, the result with measurement was μ (=1.1) >1. Therefore, we judged that the face is stable in this case.

(2) Elastic FEA

The displacement of the tunnel and the stress of the improved ground in the excavating process were evaluated by applying the Elastic FEA.

Figure 13 shows these results in the digging process.

1) Displacement of the tunnel
   - Crown: 17 mm~27 mm
   - Foot: 10 mm~21 mm
   - Convergence: 11 mm (max, expansion)
2) Stress of the improved ground
   - Crown: 42 kPa (max)

Figure 14 shows the distribution of the safety ratio obtained by elastic FEA based on Mohr-Coulomb's failure criterion. In the case without the ground stabilization method, the face became unstable because a

Copyright © 2005 Taylor & Francis Group plc, London, UK

Table 4. Input data of analysis.

Stratum parameter	ta (loam)	ts (sandy soil)	Nosl (sandy soil)	Noc (cohesive soil)	Improved ground of crown	Improved ground of shoulder
E (kN/m^2)	3.5×10^3	2.0×10^4	2.7×10^4	1.8×10^4	5.0×10^4	10×10^4
γ (kN/m^3)	14	18	18	16	19	19
ν	0.35	0.35	0.35	0.35	0.35	0.35
c (kN/m^2)	35	0	0	40	165	330
ϕ (Deg)	0	30	30	0	30	30

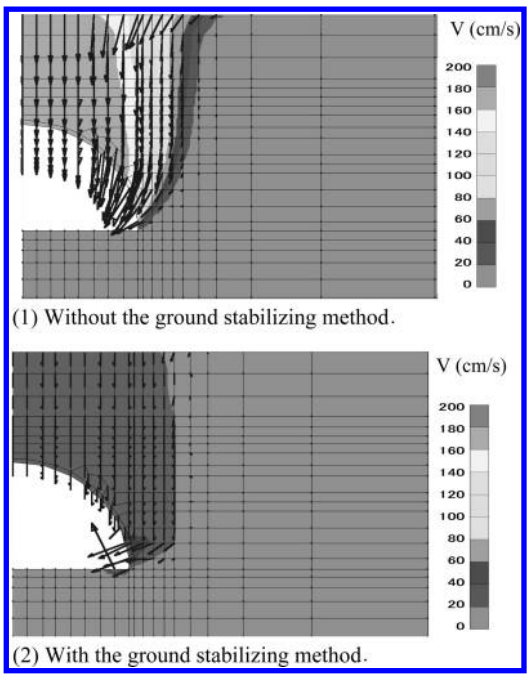


Figure 12. Velocity fields of a cross section.

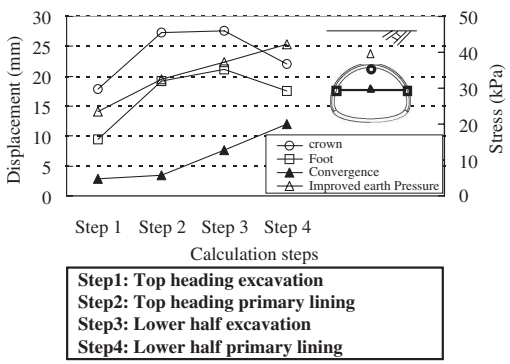


Figure 13. Displacement and stress (Elastic FEA).

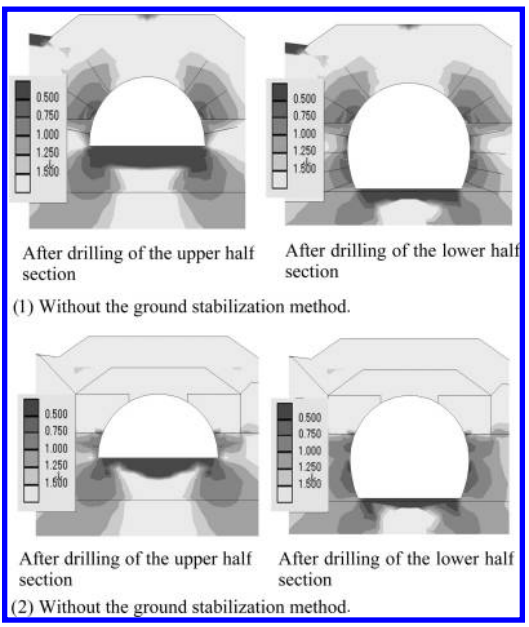


Figure 14. Distribution of safety ratio by elastic FEA.

zone with low safety ratio existed around the ground near the tunnel-arch.

In the case with the method, the face became stable because the ground around tunnel was an elastic condition. However, after drilling of the lower half section, a zone with a low safety ratio existed around the ground near the side wall of the tunnel. This meant that the load of the ground over the arch of the tunnel was supported at the foot of the upper half section.

6 CONCLUSION

In this paper, the effect of the tunneling method with the ground stabilization is evaluated by the results of measurements and analyses.

Results of the study from a cross section are as follows.

Copyright © 2005 Taylor & Francis Group plc, London, UK

1. When the shallow tunnel is excavated without the ground stabilizing method, it is highly possible that plastic strain enlarges at the ground near the tunnel-arch and collapse happens.
2. When the tunnel is excavated with the method, arch of the tunnel become stable. However, earth pressure at the feet of the upper half section increases due to supporting load of the ground over the arch of the tunnel. When the phenomenon is excessive, settlement of ground surface or collapse of the ground happen due to sinking of the tunnel. With careful attention to this point, it is necessary to plan the reinforcement of the feet or ground.

REFERENCES

Konishi, S., Asakura, T., Tamura, T. & Tsuji, T. 2002 Evaluation of tunnel face stability for sand strata with clay layers, Journal of geotechnical engineering, JSCE, No.659/III-52, pp. 51–62.

Konishi, S., Nishiyama, T. 2002 Study on evaluation of tunnel face stability by rigid plastic finite method, Railway Technical Research Institute Report, Vol.16, No.9, pp. 41–46.

Konishi, S., Tamura, T., & Nishiyama, T. 2002 Tunnel face stability of sandy ground with a clay layer on the crown, Proceedings of tunnel engineering, JSCE, Vol.12, pp. 25–32.

Murayama, S., & Matsuoka, H. 1971 Evaluation of tunnel face stability for sand strata with clay layers, Journal of geotechnical engineering, JSCE, No.187, pp. 95–108.

Tamura, T., Adachi, N., Konishi, S., & Tsuji, T. 1999 Rigid-plastic finite element method for frictional materials, Journal of geotechnical engineering, JSCE, No.638/III-49, pp. 301–310.

Tamura, T., Kobayashi, S. & Sumi, T. 1984 Limit analysis of soil structure by rigid plastic finite element method, Soils and Foundations, JSSMFE, Vol.24, No.1, pp. 34–42.

Tamura, T., Kobayashi, S. & Sumi, T. 1987 Rigid-plastic finite element method for frictional materials, Soils and Foundations, JSSMFE, Vol.27, No.3, pp. 1–12.

Copyright © 2005 Taylor & Francis Group plc, London, UK

Behavior of center diaphragm tunnel with large cross section in earth ground

Naoki Tomisawa
Civil Engineering Div. Konoike Construction Co., Ltd

Matsui Tamotsu
Dept. of Architecture and Civil Engineering, Fukui University of Technology

ABSTRACT: Cross-sections of road tunnels have been enlarged in Japan because of increasing traffics and spaces for sidewalks. Also locations and geological conditions of newly planned tunnels have become difficult. For large-scale tunnels in earth ground under such conditions, it is important to grasp deformation behavior of surrounding ground of tunnels especially in urban area to consider influence on environments such as ground settlement. Besides, increasing number of divided cutting faces is very effective to keep ground deformation within very small level, in addition to applying auxiliary methods. In this paper, the behavior of a center diaphragm tunnel with large cross section in earth ground was shown using results of monitoring, 2D-FEM and 3D-FEM analyses. Besides, the practical control measurement method was proposed for such tunnels based on above results, followed by demonstrating its applicability.

1 INTRODUCTION

NATM is generally applied to construct mountain tunnels. The method had made construction of tunnels easy and safe in case of rather bad geological condition and tunnels with large cross sectional area. In Japan, cross sections of road tunnels have been enlarged because of increasing traffics and spaces for sidewalks. Such large-scale tunnels are generally designed individually because their standard design techniques have not established yet. And locations and geological conditions of newly planned tunnels have become more difficult. Under such conditions, it is important to predict deformation behaviour of surrounding ground of large-scale tunnels especially in urban area to consider influences on environments such as ground settlements. Pre-support methods are usually applied to secure stability of cutting faces of tunnels in earth ground. Besides, especially in cases of tunnels with large cross section, it is needed to increase number of divided heading sections to keep ground deformation in very small level. In such cases, it is important to predict deformation behaviour of surrounding ground in each construction stages. Amanosan No.1 tunnel mentioned in this paper is a road tunnel with three lanes mainly in earth ground of sands and gravels. To ensure stability of the tunnel and control ground settlements, the center diaphragm method was applied and many kinds of measurements were carried out during the construction. In this paper, behaviour of the large-scale tunnel with center diaphragm in earth ground and deformation of the surrounding ground are described, based on the measured data and results of 2D-FEM and 3D-FEM analyses. Besides, the practical control measurement method for such tunnels will be proposed based on above results, followed by demonstrating its applicability.

2 OUTLINE OF TUNNEL

Amanosan No.1 tunnel is a 214 m long road tunnel with three lanes as shown in Figure 1 (Tomisawa & Matsui, 2000). The shape of its excavated cross section is 16 m wide and 11.5 m high, and its area is 145 m^2 as shown in Figure 2.

The geological condition of the ground mainly consists of unconsolidated sands and gravels of Pleistocene. Table 1 shows the mechanical properties of the ground. The maximum overburden is 18.7 m high. The center diaphragm method was applied to excavate the tunnel. Figure 3 shows the sequence of the center diaphragm method with 4 divided sections.

Copyright © 2005 Taylor & Francis Group plc, London, UK

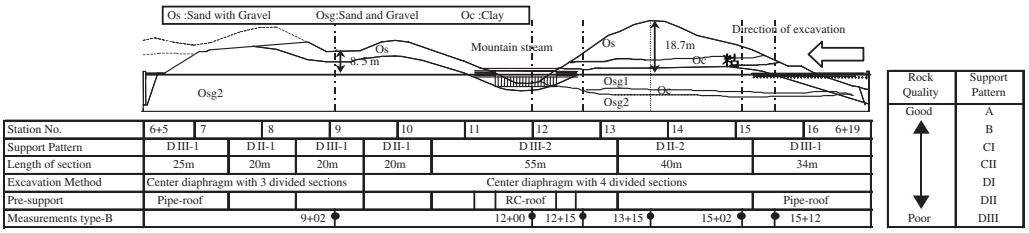


Figure 1. Longitudinal cross section of the Amanosan No. 1 Tunnel.

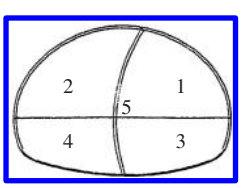


Figure 2. Center diaphragm method.

Table 1. Mechanical properties of ground.

Geology	Elastic Modulus N/mm^2	N value
Os1	60.7–74.3	33–60
	–	–
Osg1	65.3	54
	38.0–142.0	20–60
Os	–	–
	157.0–177.0	60<
Osg2	123.0–125.0	60<
	115.0–234.0	60<

Upper column: investigation data before tunnel construction
Lower column: investigation data during tunnel construction



1 Excavation of advanced upper section (the first face)
2 Excavation of backward upper section (the second face)
3 Excavation of advanced lower section (the third face)
4 Excavation of backward lower section (the fourth face)
5 Removal of center diaphragm

Figure 3. Sequence of the center diaphragm method with 4 divided sections.

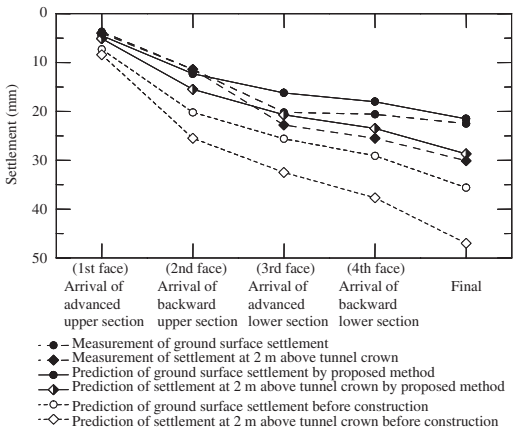


Figure 4. Settlement changes in the excavation sequence (No. 15 + 02).

3 DEFORMATION BEHAVIOUR OF GROUND BASED ON MEASURED DATA

Deformation behaviour of ground is shown below, based on the measured data (Tomisawa & Matsui, 2000). Many kinds of measurements, such as settlements and horizontal displacements in the ground, ground surface settlements, axial forces of rockbolts, stresses of shotcrete, stresses of steel arches, were carried out at 6 cross sections during the construction.

Figure 4 shows an example of measured settlement changes in the excavation sequence (broken lines), together with the predictions analyzed by using 2D elastic FEM before the construction (dotted lines). Solid lines show the predictions by proposed control method mentioned later on. Although predictions show increasing tendency from the third face to the fourth face, measurements hardly show such tendency. This might be because the actual interval between cutting faces may be different from the analytical conditions.

Figure 5 shows an example of measured and predicted distributions of ground settlements. Although

Copyright © 2005 Taylor & Francis Group plc, London, UK

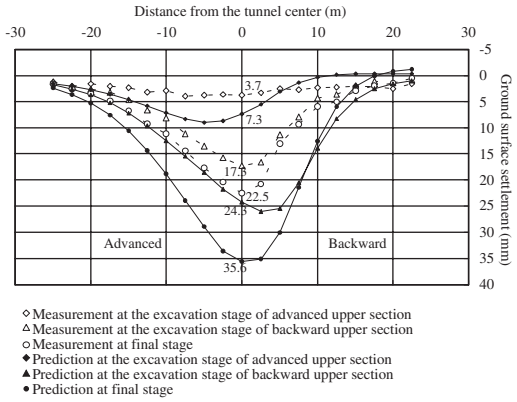


Figure 5. Distribution of ground surface settlement at each excavation stage (No. 15 + 02).

measured values are different from predictions quantitatively, the shapes of both distributions are similar. It seems that deformation behaviour of surround ground is almost like elastic.

4 DEFORMATION BEHAVIOUR OF GROUND BASED ON RESULTS OF 3D-FEM

4.1 *Outline of 3D-FEM analysis*

In Japan, 2D-FEM is generally used to analyze behaviour of tunnels. When the method is applied to Amanosan tunnel constructed using center diaphragm method with low overburden, excavation stress release ratio should be set according to the actual construction conditions. On the other hand, it is not necessary to consider the ratio when 3D-FEM is applied.

Figure 6 shows the 3D-FEM mesh. The input data for the mechanical properties of the ground and supports are the same as those for 2D-FEM.

4.2 *Results of 3D-FEM analysis*

Figure 7 shows the predicted settlement changes of ground along the tunnel center in the excavation sequence. Preceding settlements are very small as 1 mm. Increment of settlements caused by advanced sections excavation is larger than those by backward sections excavation. Before removal of center diaphragm, settlements never converge clearly except for the step of advanced lower section excavation. During upper section excavation, the closer the measured point locates to the tunnel crown, the smaller the ground settlements are. It is seen that there is a compressive zone between the tunnel crown and the ground surface. After removal of the diaphragm, the ground

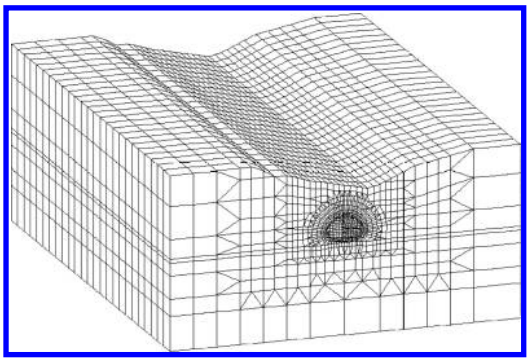


Figure 6. Meshes used in 3D-FEM analysis.

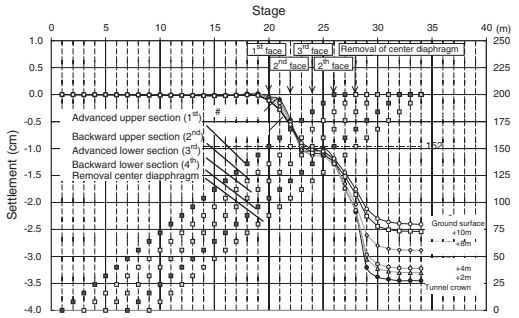


Figure 7. Settlement changes in the excavation sequence predicted by 3D-FEM analysis.

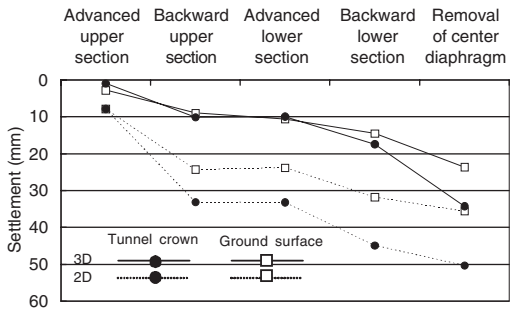


Figure 8. Comparison of settlement changes predicted by 2D-FEM and 3D-FEM analyses.

settlements become larger than the ground surface settlements.

Figure 8 shows the results of settlement changes of ground surface and tunnel crown predicted by 2D-FEM and 3D-FEM. The settlements by 3D-FEM are smaller than those by 2D-FEM. It is confirmed that the effect of center diaphragm is estimated higher by 3D-FEM than by 2D-FEM.

Copyright © 2005 Taylor & Francis Group plc, London, UK

5 OUTLINE OF PROPOSED CONTROL MEASUREMENT METHOD

5.1 *Problems on predicting deformation behaviour of centre diaphragm mountain tunnel*

In Japan, FEM is generally used to analyze behaviour of tunnels. And 2D elastic analyses are supposed to be enough to understand ground deformations during tunnel constructions by the following reasons.

(1) Three dimensional treatments

3D analyses are rarely applied because of problems on cost and time. Besides, quality and quantity of geological information obtained before tunnel constructions are not enough to apply 3D analyses.

(2) Nonlinear treatments

Geological materials are often treated as linear materials because enough geological information to express nonlinear behaviour is not obtained. Besides, nonlinear analyses are often unstable on their convergence.

(3) Time dependent treatments

Although properties of supports change with elapsed time, equivalent values are used because they are sufficient to predict deformation of ground but stress.

(4) Actual construction conditions

In most of tunnel analyses, predicted values are converged ones in each construction stage of subsequent cutting faces. Nevertheless, in actual construction controls, the predicted values have to be compared with measured data that do not always converge within each stage, because subsequent faces may influence them, especially in case of multi faces excavation like center diaphragm method.

5.2 *Outline of proposed control measurement method*

Amanosan No.1 tunnel was constructed by applying center diaphragm method with 3 or 4 divided sections with the minimum overburden of approximately 1D. The results of measurements did not converge in each construction stage, because intervals between faces were very close. In this study, therefore, the analysis sequence shown in Figure 9 is considered to fit predictions to measurements. There are two stages in the proposed method. The first is preparation stage in the upper part of the figure and the second is prediction stage in the lower part of the figure. In the preparation stage, preparation analyses and initial prediction are carried out. In the preparation analyses, three dimensional effects of both the interval between faces and the distance from tunnel wall are considered.

(1) Setting of excavation stress release ratio

There are four cutting faces in a cross section. The ratio for the first face is calculated by using axially symmetrical 2D analysis, considering actual overburden and cross section area.

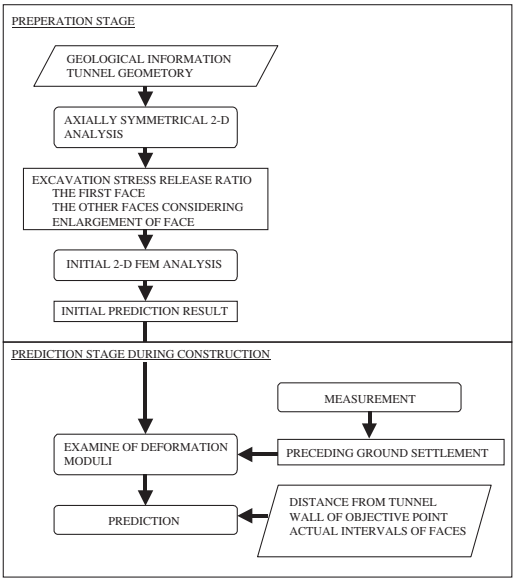


Figure 9. Sequence of proposed method.

(2) Setting of settlement characteristic curve caused by approach of subsequent faces

When applying center diaphragm method, deformation behaviour of surrounding ground is influenced by subsequent faces because the interval of faces are often less than 2D. Then, settlement curves are calculated by using axially symmetrical 2D analysis, for cases of several intervals between faces considering the actual overburden and cross section area.

(3) Setting of settlement characteristic curve on distance from tunnel wall in cross section direction

Settlement ratios to converged values vary with distance from tunnel wall. Then, relationships between settlement ratios and distance from tunnel wall are calculated considering the actual overburden and enlarged cross section area.

(4) Initial prediction analyses

Initial prediction analyses are carried out as the same as in general prediction using 2D-FEM considering the calculated stress release ratios.

(5) Setting of deformation moduli of geological materials

Geological materials are treated elastically. Conditions of initial stresses are hardly measured. And deformation moduli obtained from laboratory and insitu tests are often not suitable as the representative one of the ground as a whole. Then, in the prediction stage, it is assumed that deformation moduli can be decided based on a preceding ground settlement at the reference point close to the tunnel crown of the first face as shown by the solid circle in Figure 10.

Copyright © 2005 Taylor & Francis Group plc, London, UK

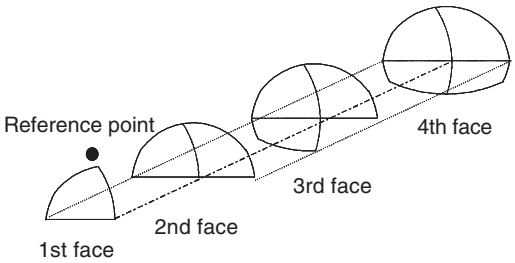


Figure 10. Position of preceding ground settlement.

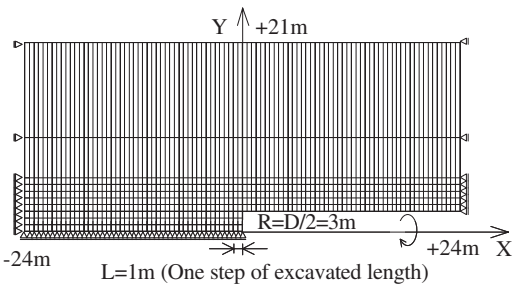


Figure 11. Example of meshes used in axially symmetrical analysis.

(6) Prediction of deformation behaviour of surrounding ground

Using parameters obtained in from (1) to (5) mentioned above, deformation behaviour of the surround ground are calculated by 2D-FEM, corresponding to the actual interval between faces and the distance from tunnel wall.

5.3 *Decision of parameters and characteristic curves used in proposed control measurement method*

Parameters and characteristic curves described in (1) to (3) in the previous section are decided by using axially symmetrical 2 dimensional analyses corresponding to actual overburden and cross section area. Figure 11 shows the FEM mesh for the analyses of the first face. Diameters on the mesh of each stage are calculated as the equivalent circle one to total area of each cutting face. The Y axial analytical area is decided as 21 m considering the fourth face diameter of 14 m (R = 7 m) and its minimum overburden of 1D.

(1) Excavation stress release ratio

Figure 12 shows settlement characteristic curves at the points of tunnel crown changing excavation diameter in cases of D = 6 m (A1 = 28 m^2), D = 10 m (A2 = 79 m^2), D = 12 m (A3 = 113 m^2) and D = 14 m (A4 = 154 m^2). The ratio at the distance of one

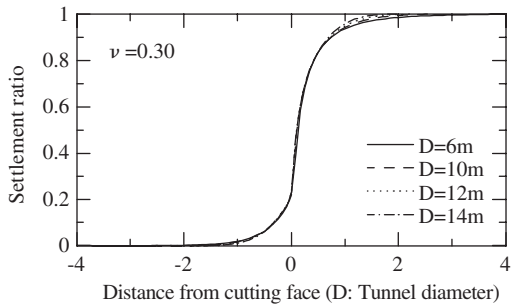


Figure 12. Effect of excavation diameter on settlement characteristic curve.

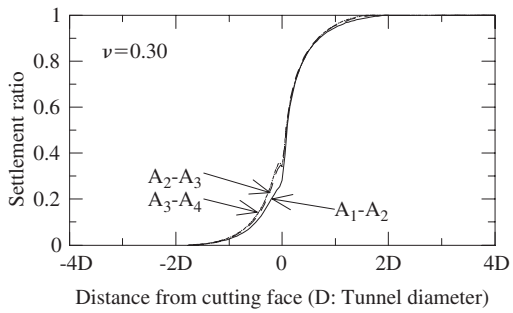


Figure 13. Effect of enlargement on settlement characteristic curve.

excavation length of 1 m for the first face of D = 6 m is 0.586.

Figure 13 shows settlement characteristic curves changing enlargement in three cases from A1 to A2 (enlargement ratio: 228%), from A2 to A3 (143%) and from A3 to A4 (136%). The ratios at the distance of one excavation length of 1 m are 0.527, 0.533 and 0.501 respectively. It is seen from this figure that deformation behaviour of surrounding ground are influenced by subsequent faces.

(2) Settlement characteristic curve caused by approach of subsequent faces

Figure 14 shows an example of settlement characteristic curves changing interval between neighboring faces in case of enlargement of D = 10 m. It is seen from this figure that the closer the distance from the subsequent face, the larger the settlement ratio to the converged value.

(3) Settlement characteristic curve on distance from tunnel crown in cross section direction

Figure 15 shows settlements characteristic curves changing distance from tunnel crown in case of D = 6 m. The smaller the distance from tunnel crown, the wider the range of settlements before arriving subsequent faces and the later the converged period.

Copyright © 2005 Taylor & Francis Group plc, London, UK

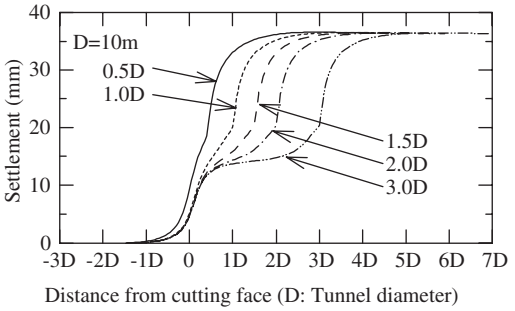


Figure 14. Effect of interval between neighboring faces on settlement characteristic curve.

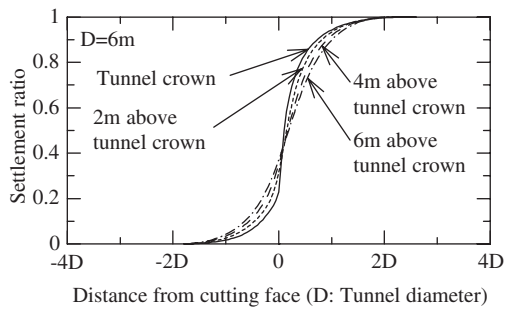


Figure 15. Effect of distance from tunnel crown on settlement characteristic curve.

6 APPLICABILITY OF PROPOSED CONTROL MEASUREMENT METHOD

Based on the sequence and results described in the previous chapter, the authors tried to predict deformation behaviour of the surrounding ground of the Amanosan No.1 tunnel, considering actual intervals of faces and distance from tunnel wall, followed by comparing with measured data. The deformation moduli were examined, based on the measured value at the reference point which is the nearest point to the tunnel crown at the first face arrival as shown in Figure 10, resulted in 2.33 times the value used in the initial analysis before construction.

The solid lines shown in Figure 4 are the predictions of ground settlements by the proposed method. The final prediction values agree with the measured ones, much better than predictions before construction which is shown by the dotted lines. Therefore, the applicability of the proposed method for practical use can be confirmed.

7 CONCLUSION

In this paper, the deformation behaviour of large-scale tunnel with center diaphragm in earth ground was described, followed by comparing both the results of 2D-FEM and 3D-FEM and by proposing its control measurement method for practical use. The proposed method is based on 2D-FEM, considering three dimensional effects such as multi face excavations and distance from tunnel crown, and also modifying deformation moduli based on measured data of preceding ground settlement. The main conclusions are summarized as follows;

(1) As for the interval between neighboring faces in this study, the settlements predicted by 3D-FEM never converge clearly as the construction steps proceed. It shows that 2D-FEM is not enough to predict settlement changes of tunnels using center diaphragm method.
(2) The results by 3D-FEM show that the closer the reference point locates to the tunnel crown, the smaller the settlement during excavation of upper sections is. It shows that there is a compressive zone between the tunnel crown and the ground surface.
(3) The settlements by 3D-FEM are smaller than those by 2D-FEM. It is confirmed that the effect of center diaphragm is higher by 3D-FEM than by 2D-FEM.
(4) The settlement changes of both tunnel crown and ground surface predicted by the proposed control measurement method agree well with the measured ones. Therefore, the applicability of the proposed method for practical use can be confirmed.

REFERENCES

Tomisawa N. & Matsui T. (2000). *Case history of a flat tunnel with large cross section in unconsolidated ground of gravel and sand*. Proc. AITESITA 2000 World Tunnel Congress, pp. 505–511.

Tomisawa N., Matsui T. & Hino M. (2001). *Behavior of mountain tunnel with large cross section in earth ground.* Modern Tunneling Science and Technology, Proc. ISKYOTO, pp. 403–406.

Tomisawa N. & Matsui T. (2002). *Prediction of deformation behaviour of large-scale mountain tunnel with multiple cutting faces in earth ground.* Proc. 28th ITA General Assembly and World Tunnel Congress, Sydney, pp. 795–799.

Copyright © 2005 Taylor & Francis Group plc, London, UK

Longitudinal arching characteristics around face of a soil-tunnel with crown and face-reinforcement – laboratory investigation

Yong-Ki Choi & Jong-Ho Park
Daewon Soil Co., Ltd, 29-11 Karakbon-dong, Songpa-gu, Seoul, Korea

Oh-Yeob Kwon
Dept. of Civil Engr. Konkuk University, 1 Hwayang-dong, Gwangjin-gu, Seoul, Korea

Sang-Baik Woo
GeoEng Co., Ltd, 1916 Jamsil-rezion, 22-5, Bangi-dong, Songpa-gu, Seoul, Korea

ABSTRACT: Pre-reinforcement ahead of a tunnel face using long steel or FRP (Fiberglass Reinforced Plastic) pipes in NATM (New Austrian Tunnelling Method), known as the UAM (Umbrella Arch Method), is the promising method to sustain the stability of a shallow tunnel face and reduce the ground settlements. In addition, horizontal reinforcing of the face is recently emphasized to improve the stability of the face. However, the characteristics on longitudinal arching around the face has not yet been established quantitatively with the RPUM (crown-reinforcing) and/or the face horizontal reinforcing. In this study therefore, the behavior of cohesionless soil around the face reinforced by the reinforcing member representing the RPUM and horizontal reinforcing is investigated through the two-dimensional laboratory model tests. A series of tests were carried out on various conditions by changing lengths and angles of the reinforcing members. Based on the vertical pressure around the face, the longitudinal extent of longitudinal arching have been found for the case of non-reinforced and reinforced.

1 INTRODUCTION

UAM (Umbrella arch method) is a pre-reinforcement technique, ahead of a tunnel face, which is obtained by installing steel or FRP (Fiberglass Reinforced Plastic) pipes at the tunnel boundary (Figure 1). The pipes are formed by an umbrella with a truncated cone shape and which allows the overlapping of two adjacent umbrellas (Oreste & Peila, 1998).

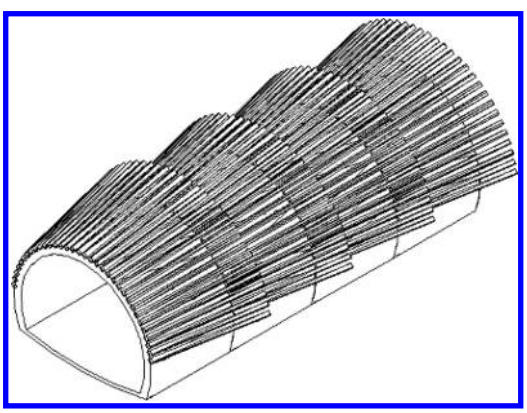


Figure 1. Schematic view of UAM (Umbrella arch method).

This technique allows safe excavation even in poor geotechnical grounds and at a low overburden. The evaluation and diffusion of the method were helped by an important technological development in act on the construction of bigger and efficient installation machine. Longitudinal ground arching develops generally parallel to the tunnel axis as tunnel is advanced. Principle of supports of NATM is based on this arching effect. It is therefore consistent to be analyzed the UAM in the Longitudinal arching. But most experimental studies on the UAM have been executed mainly on the face itself so far.

To find characteristics of the longitudinal arching laboratory model tests under two dimensional plane strain conditions carried therefore in this study. It was measured under various types of face-reinforcing that vertical pressure, settlements before and behind the face and horizontal pressure on the face to find characteristics of the longitudinal arching. The arching characteristics, reinforcing effects with the type and length of the reinforcing members are found from the test results.

Copyright © 2005 Taylor & Francis Group plc, London, UK

2 ARCHING EFFECT AROUND THE FACE

When a tunnel is excavated, initial stress in the ground before excavation is disturbed and changed into induced stress. With this simultaneously displacements around the face occur (Walter, 1990). Some of the initial stress is transferred to parallel (longitudinal) and perpendicular (transverse) to the tunnel axis so the remained stress is redistributed around the tunnel face. These are called "longitudenal arching" and "transverse arching" (Gnilsen, 1989) (Figure 2 and Figure 3).

The magnitude of the redistributed stress by the arching depends on the distance from the face, that is, two arching are developed simultaneously around the face. But along the ahead of the face, the longitudinal arching occurs mainly and along the rear of the face, transverse arching is developed. Therefore the longitudinal arching developing ahead of the face is closely connected with the face stability.

3 LABORATORY MODEL TEST

3.1 *Test configuration*

A series of laboratory model tests was conducted in a test box made of a steel frame, having inside dimensions of 1.13 m (width) × 0.87 m (height) × 0.3 m (thickness) (Figure 4). The condition of test is under two dimensional plane strain to investigate the longitudinal arching parallel to tunnel axis. The two side walls of the test box were constructed using the plate of transparent acrylic plate for ease of observing the failure mechanism during testing. To minimize side friction between model ground and acrylic plate two glass plates are inserted onto the inside acrylic wall.

The face of tunnel was represented by using six vertical plates (300 mm × 250 mm × 6 ea) connected to load cell that can measure horizontal pressure on the face (Figure 5). The vertical pressure along the ahead and rear of face was also measured using twenty-one horizontal plate connected to load cell. To reproduce the longitudinal behavior according to the advance of a tunnel, the face of the model is translated horizontally with speed of 1 mm/min backward to the excavated direction, monitoring the vertical pressure, horizontal pressure on the face, and ground settlement.

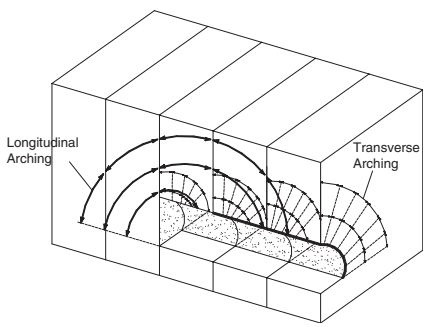


Figure 2. Arching effects at the tunnel face (Gnilsen, 1989).

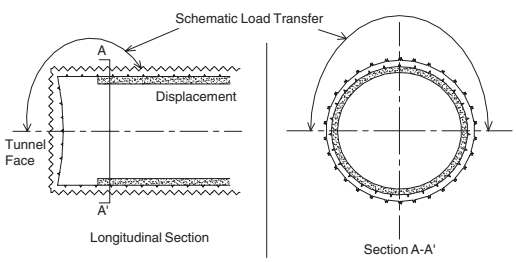


Figure 3. Load and displacement at the tunnel face (Gnilsen, 1989).

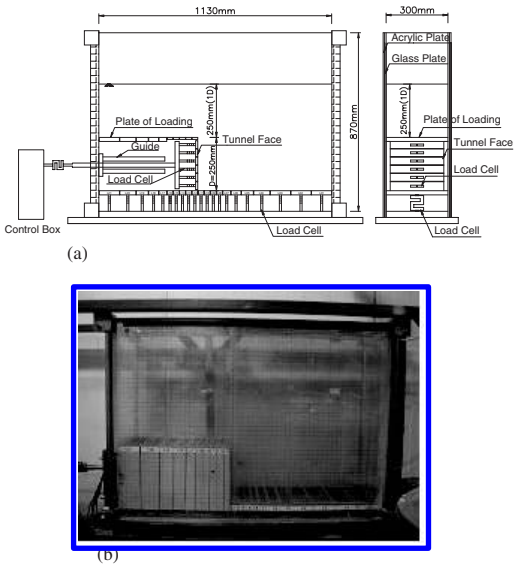


Figure 4. Tunnel model device, (a) Schematic diagram of tunnel model device, (b) Photograph of tunnel model device.



Figure 5. Load cells connected with tunnel face.

Copyright © 2005 Taylor & Francis Group plc, London, UK

3.2 *Model ground*

The model ground was constructed using fine sand by a raining technique with a specially designed hopper system as shown in Figure 6. The effective size (D_{10}), uniformity coefficient (C_u), and coefficient of curvature (C_c) for the sand were 0.14 mm, 1.43, and 1.03, respectively. The raining technique adopted in this study provided a uniform relative density of approximately 82% with a unit weight of 16 kN/m^3. To evaluate the shear strength parameters of the model ground, a series of direct shear tests were performed using specimens prepared by dry tamping in the same density. The estimated internal friction angle and cohesion were 41° and 0.

A number of evenly spaced markers were placed at the interface between the wall facing the tunnel and the model ground during model preparation for the purpose of facilitating visualization of the ground movements during testing. The vertical displacements of the ground during test were measured by the LVDT (Linear Variable Deformation Transformer) situated in the ground during ground preparation as shown Figure 6.

3.3 *Conditions and types of model test*

Conditions tested include both the non-reinforced (NR) and the reinforced cases for the tunnels with the cover depth ratio of H/D = 1.0. For reinforced cases, there are three types of test. Namely the first is crown-reinforced (C) that is obtained by installing reinforcements at the upper boundary of the face. The second is face-reinforced (F) reinforced horizontally in the face. Finally the third is crown and face-reinforced (CF) reinforced both crown and face. The type, number, length, and angle (with reference to the horizontal) of the reinforcement were varied in the reinforced cases. The lists of test are shown in Table 1 and Figure 7.

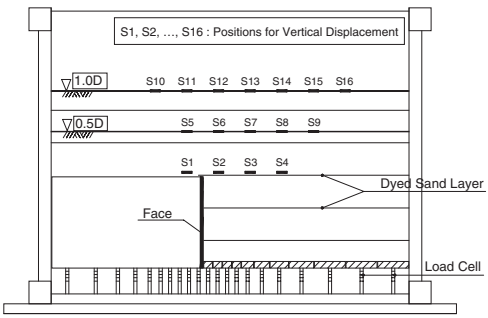


Figure 6. Schematic diagram of monitored positions for vertical displacement.

Table 1. Physical properties of testing material.

Unit Weight γ (kN/m^3)	Relative Density *Dr* (%)	Specific Gravity *Gs*	Friction Angle *ϕ* (degree)	Cohesion Intercept c (kN/m^2)	Soil Classification (USCS)
16.28	82	2.63	41	0	SP

Table 2. The list of model test.

		Reinforcement Member					
		Line (ea)		Angle (degree)		Length	
Reinforced type	Test notation	Crown	Face	Crown	Face	Crown	Face
Non	NR	–	–	–	–	–	–
Crown	C0.7	1	–	10	–	0.7D	–
	C1.0	1	–	10	–	1.0D	–
	C1.5	1	–	10	–	1.5D	–
Face	F0.7N1	–	1	–	0	–	0.7D
	F0.7N2	–	2	–	0	–	0.7D
	F0.7N3	–	3	–	0	–	0.7D
	F1.0N3	–	3	–	0	–	1.0D
	F1.5N3	–	3	–	0	–	1.5D
Crown + Face	C0.7A10F0.5	1	1	10	0	0.7D	0.5D
	C0.7A10F0.7	1	1	10	0	0.7D	0.7D
	C0.7A10F1.0	1	1	10	0	0.7D	1.0D
	C0.7A20F0.7	1	1	20	0	0.7D	0.7D
	C0.7A30F0.7	1	1	30	0	0.7D	0.7D
	C0.7F0.7N3	1	3	10	0	0.7D	0.7D
	C1.0F1.0N3	1	3	10	0	1.0D	1.0D
	C1.5F1.5N3	1	3	10	0	1.5D	1.5D

Copyright © 2005 Taylor & Francis Group plc, London, UK



Figure 7. Schematic diagram of the tests changing the type reinforcement, (a) NR (Non-Reinforced), (b) C0.7, (c) C1.0, (d) C1.5, (e) F0.7N1, (f) F0.7N2, (g) F0.7N3, (h) F1.0N3, (i) F1.5N3, (j) C0.7A10F0.5, (k) C0.7A10F0.7, (l) C0.7A10F1.0, (m) C0.7A20F0.7, (n) C0.7A30F0.7, (o) C0.7F0.7N3, (p) C1.0F1.0N3, (q) C1.5F1.5N3.

4 TEST RESULTS AND DISCUSSION

4.1 *Vertical pressure pattern*

Figure 8 shows the vertical pressure pattern according to horizontal displacement of the face backward for the non-reinforced case of H/D = 1.0 where D is tunnel height and H is distance from ground surface to tunnel crown. The vertical pressure was decreased at the ahead of the face whereas increased at the rear of the face. The reason of the decrease ahead of the face is assumed that the vertical pressure ahead of the face was transferred to the horizontal pressure on the face. On the other hand, the increase at the rear of the face may be owing to an arching action transferred from ahead to rear of the face.

Figure 9 is also shown that the vertical pressure pattern for the reinforced cases. The pattern of the vertical pressure resembled that of non-reinforced for the changing the length (Figure 9(a)) and angle (Figure 9(d)) of crown reinforcement, that is, decreased at the ahead of the face and increased at the rear of the face. Whereas for the changing the length (Figure 9(b))

Copyright © 2005 Taylor & Francis Group plc, London, UK

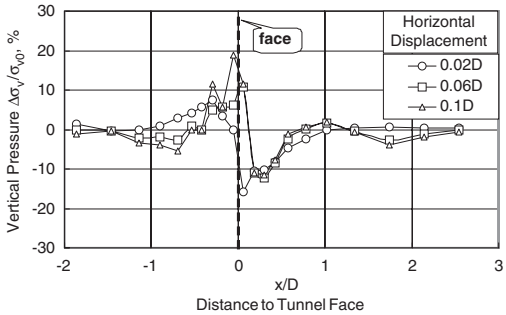


Figure 8. Vertical Pressure – Distance to the Face Relationships Changing the Horizontal Displacement of Tunnel Face **(Non-Reinforced)**.

and the line number (Figure 9(c)) of face reinforcement, the vertical pressures were shown opposite pattern. This reason that the pressure was increased at the ahead of the face would be due to the enhancement of supporting role in the face by face-reinforcing (Figure 9(b) (c) (e)).

In the mean time, the vertical pressure pattern for the crown and face-reinforced (Figure 9(e)) were changed mainly at the ahead of the face. It was also noted that the changes of the vertical pressure were increased significantly for the all reinforced cases, compared with that of non-reinforced.

It is found that the extent of longitudinal arching action at the ahead and rear of the face is about 2.5D, 1.5D respectively for the non-reinforced. For the crown-reinforced and face-reinforced the extent is about 2.0D, 1.5D and for crown and face-reinforced 2.0D, 1.0D respectively.

4.2 *Horizontal pressure on the face*

Figure 10 shows the horizontal pressure on the face for non-reinforced. As seen according to horizontal displacement of the face backward, the pressure in lower part of the face were decreased but increased in upper face.

Figure 9(a) is shown that the horizontal pressures were increased with the increase of crown reinforcement length in crown-reinforced. This reason would be due to the constraint of ground deformation ahead of the face, increasing the length of crown reinforcement.

Figure 9(b) shows also the pressure pattern for the angle of crown reinforcement. The pressure was decreased with decreasing of the reinforcement angle with reference to the horizontal.

4.3 *Ground settlement pattern*

Figure 12 illustrates the ground settlement pattern in the 0.0D, 0.5D, and 1.0D above the face at the horizontal

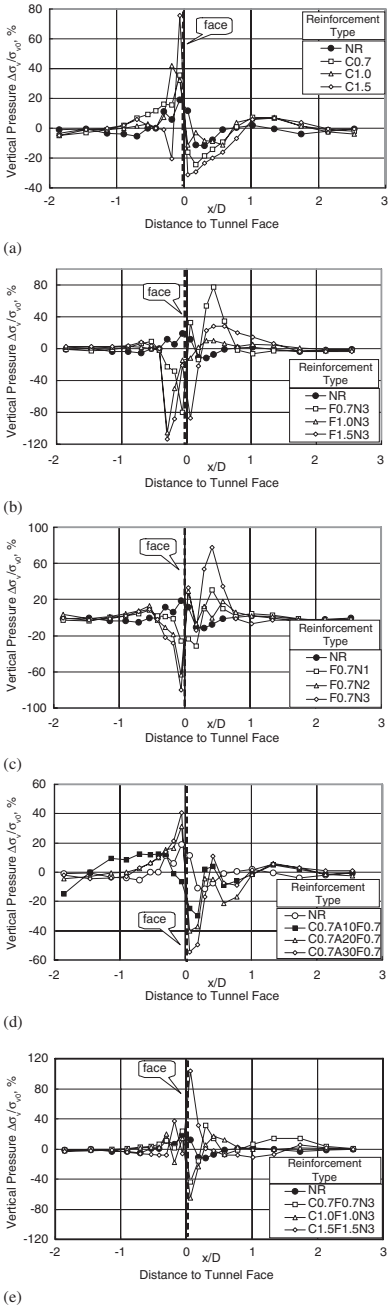


Figure 9. Vertical Pressure – Distance to the Face Relationships at the Horizontal Displacement (= 0.1D) **(Reinforced)**, (a) Crown-Reinforced changing the length, (b) Face-Reinforced changing the length, (c) Face-Reinforced changing the line, (d) Crown-Reinforced changing the angle, (e) Crown and Face-Reinforced changing the length.

Copyright © 2005 Taylor & Francis Group plc, London, UK

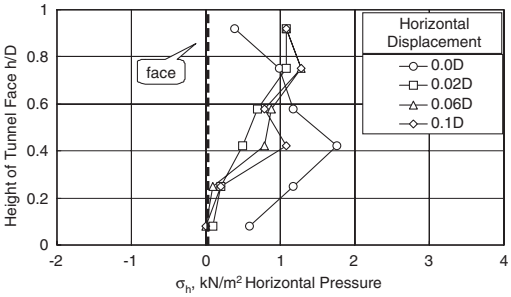
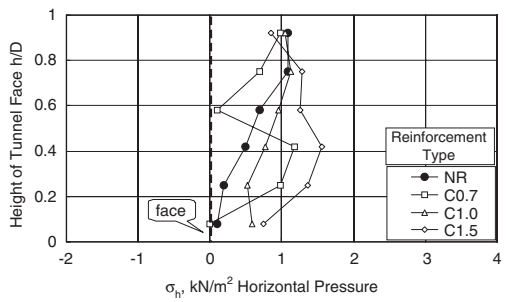
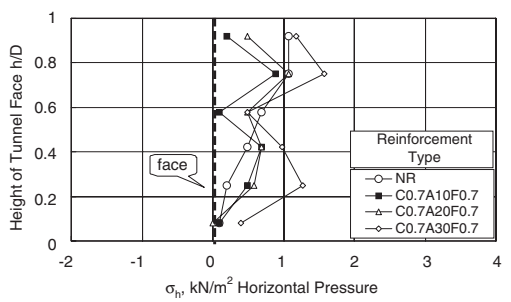


Figure 10. Horizontal Pressure Acted on the Tunnel Face with the Variation of Horizontal Displacement **(Non-Reinforced).**



(a)



(b)

Figure 11. Horizontal Pressure Acted on the Tunnel Face with the Variation of Horizontal Displacement (= 0.02D) **(Reinforced)**, (a) Crown-Reinforced changing the length, (b) Crown and Face-Reinforced changing the angle.

displacement of 0.1D for the non-reinforced. As seen the settlement in the ground was increased near the face.

In case of crown-reinforced the settlement in the ground was decreased significantly, compared with that of non-reinforced. Figure 13(a) shows the settlement ratio defined by the ratio of the settlement in reinforced case to that in non-reinforced. As seen the Figure 13(a) the ratio was shown less than 10% for

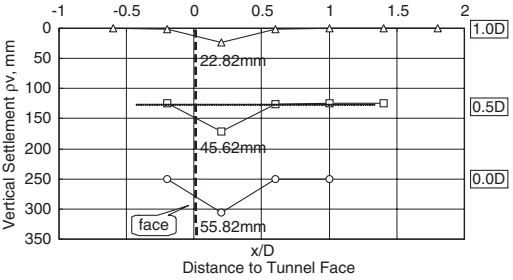


Figure 12. Vertical Settlement, ρ_v (mm) above the Tunnel – Distance to Tunnel Face Relationships at the Horizontal Displacement (= 0.1D) **(Non-Reinforced).**

the crown-reinforced. It is therefore thought that the crown reinforcement plays an important role in keeping the settlement in the ground.

The settlement ratios with the change of length and line number of face reinforcement for the face-reinforced are shown in Figure 13(b) and (c). Figure 13(d) shows the ratios with the angle change of crown reinforcement. Finally the ratios with the change of reinforcement length of both crown and face reinforcement in crown and face-reinforced cases. It was noted that the case of crown-reinforced was more effective than the face-reinforced in the point of settlement restraint.

5 CONCLUSIONS

A series of reduced-scale laboratory tests was conducted to investigate the longitudinal arching characteristics of tunnels reinforced with pipes by umbrella arch method. The two-dimensional model tunnel are constructed and tested under the various reinforcing conditions. Based on the results of the present investigation, the following conclusions can be drawn.

1. It was found that the extent of longitudinal arching action was decreased with the reinforcing on the based of the vertical pressure. That is, the extent at the head and rear of the face is about 2.5D and 1.5D (where D is tunnel height) respectively for the non-reinforced. For the crown-reinforced and face-reinforced the extent is about 2.0D, 1.5D and for crown and face-reinforced 2.0D, 1.0D respectively.
2. However the change of vertical pressure with the reinforcing was increased significantly. Thus, it was sure that the reinforcements on the crown and face have played an important role in safe tunneling.
3. The effectiveness of the crown and face reinforcement depends on the reinforcement layout such as the length, the number and the angle of the reinforcements.

Copyright © 2005 Taylor & Francis Group plc, London, UK

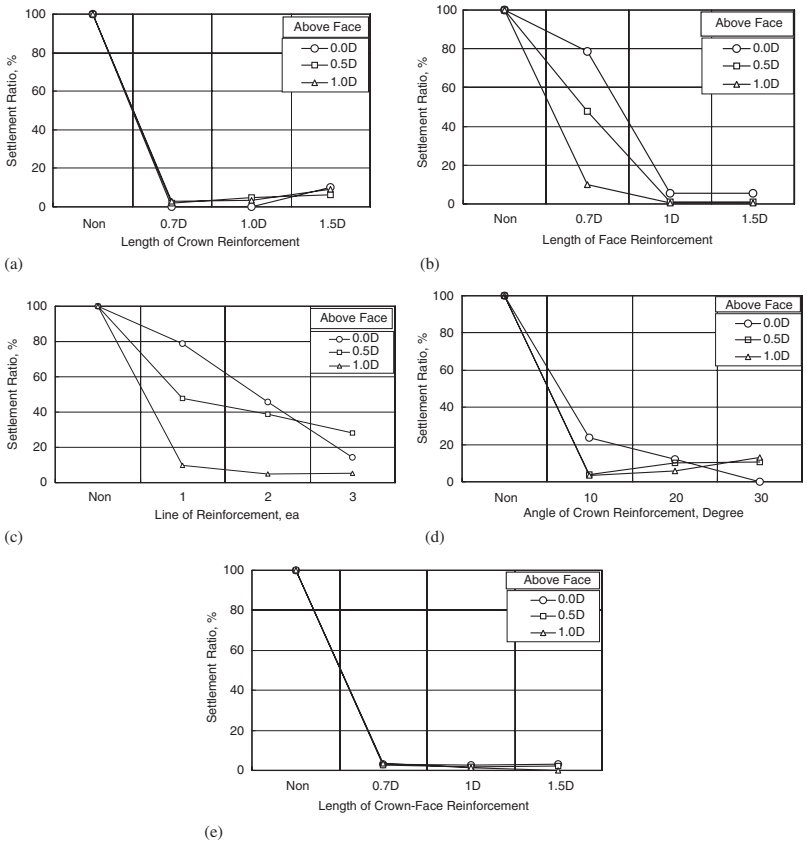


Figure 13. Settlement Ratio above the Face **(Reinforced)**, (a) Crown-Reinforced changing the length, (b) Face-Reinforced changing the length, (c) Face-Reinforced changing the line, (d) Crown-Reinforced changing the angle, (e) Crown and Face-Reinforced changing the length.

REFERENCES

Broms, B.B. 1967. Stability of Clay at Vertical Openings, *Journal of the Soil Mechanics and Foundations Division, ASCE,* 93(SM1): 71–95.

Gnilsen, R. 1989. Numerical Analysis: *Underground Structures Design and Instrumentation*: 84–128, Developments in Geotechnical Engineering, 59A: Elsevier.

Terzaghi, K. 1943. *Theoretical Soil Mechanics*: 66–77, York: JohnWiley & Sons.

Walter, W. 1990. Rock Mechanics: *Theory and Applications with Case Histories*: 444–471, Springer-Verlag.

Copyright © 2005 Taylor & Francis Group plc, London, UK

State-of-the-art microcement pre-injection for the Jong–Asker Rail Tunnel, Norway

H.O. Hognestad
Degussa UGC International, Switzerland

E. Frogner
AF Spesialprosjekt AS, Norway

ABSTRACT: The Jong–Asker, lot JA2, double track rail tunnel situated south of Oslo, has been constructed by AF Spesialprosjekt. The geology is hard rock, with a cross sectional area of about 104 m^2. There is a conservative water ingress specification split into three classes. The most stringent being a maximum allowed water ingress of 4 l/min/100 m, and with the use of microcement and rapid hardening cement pre-injection, the contractor has achieved less than 1 l/min/100 m tunnel in some sections. The paper highlights the need for correct choice of performance microcement and mix design to ensure full penetration of the fissured rock mass. An insight into the state of the art pre-injection equipment is reviewed, in addition to the use of alkali-free accelerators to effectively deal with high grout takes and grout in-leaks into the tunnel through the face and constructed tunnel, previously a considerable problem not sufficiently solved in pre-injection works underground.

1 INTRODUCTION

Jernbaneverket Utbygging (Railroad Department) is the Client for the total Sandvika–Asker project. (almost 4 billion NOK) The project is situated south of Oslo. The construction of the project permits a two fold increase of the rail capacity between Oslo and Drammen, currently the most dense traffic route in Norway.

The project Jong–Asker, lot JA2, a double track rail tunnel was constructed by AF Spesialprosjekt in near cooperation with their subsidiary company Scandinavian Rock Group (SRG). This tunnel is 2700 meter long, and was completed in 2004 after a building period of 18 months. Throughout its length of 2.7 km, the geology is hard rock (limestone), with a cross sectional profile of about 104 m^2. The overburden to the tunnel is between 2 and 50 m.

2 PRE-INJECTION OF ROCK: APPROACH, STRATEGY AND BASIC PRINCIPLE

2.1 *Basic concepts of pre-injection of rock*

There is international pressure for all companies to reduce risks and achieve even further economy in tunneling activities. Furthermore, the control of waste or contaminated water from the tunneling process has become increasingly relevant in minimizing environmental impacts on the ground surface. To achieve these goals, contractors can:

- Limit groundwater in excavations by pre-injecting cementitious grout ahead of the excavation advance face.
- Use modern drilling equipment in combination with state-of-the-art injection equipment and materials to improve and widen the application of pre-injection grouting.

Pre-injection of rock in underground construction involves pressure grouting into the rock mass through drill holes. The actual injection is part of a cycle that comprises exploratory drilling (probe drilling), injection drilling, injection, and control drilling. The holes are mostly drilled with modern, conventional drilling equipment e.g. a drill jumbo, with drill hole diameters of 45 to 64 mm, similar to those shown in Figure 1.

Cementitious grouts are recommended (and also required) for most injection work, but different types of chemical grouts are available for particular situations. The grout is pumped into the drill holes through hollow lances that are connected to the grout pump with hoses. With sufficient pressure, the grout will penetrate into the joints and discontinuities of the rock mass and replace the groundwater with grout and hence, block the seepage channels. The holes are

Copyright © 2005 Taylor & Francis Group plc, London, UK

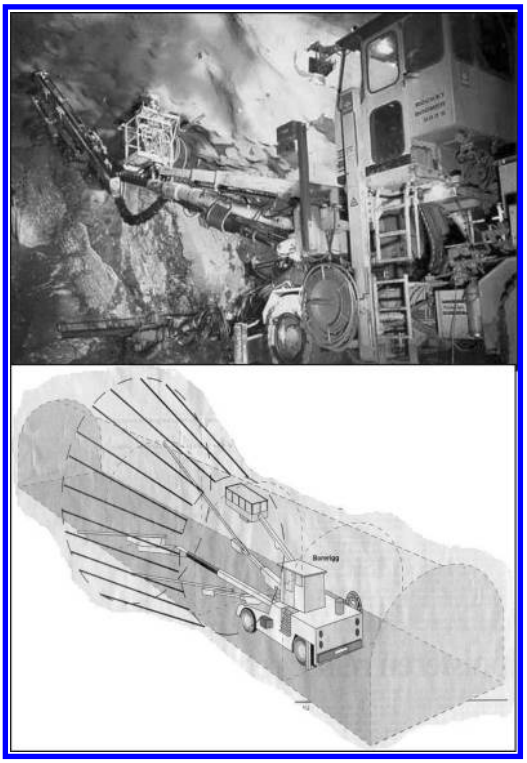


Figure 1 Typical drilling jumbo for tunnel applications preparing fan of pre-injection holes ahead of the excavation face.

drilled in a cylindrical fan around the tunnel, in order to encompass the tunnel with a zone of low conductivity. The general layout of a pre-injection fan is shown in Figure 1.

The basic strategy for pre-injection is to define a maximum accepted level of water seepage into the tunnel (a certain allowed volume of water per tunnel meter). A systematic pattern of exploratory drill holes repeatedly performed with overlap ahead of the tunnel face is then decided. Action criteria for grouting based on observed water inflow through the exploratory drill holes are then defined based on the maximum allowed seepage levels.

2.2 *Main motivations for pre-injection*

The problems that inflowing water can cause in an underground construction are numerous, and include:

- Consequences at the surface caused by a lowered groundwater table because of the drainage effect of the tunnel. It is very important to avoid ground water lowering in tunnels in urban areas. It can not be accepted to lower the groundwater because this will lead to settlement of roads, buildings etc.
- Consequences in the actual tunnel caused by an increased amount of inflowing water, including the possible deterioration of the temporary road in the tunnel and need for pumping, as well as the deterioration of the immediate stability of unsupported rock after excavation and the reduced feasibility of producing a high quality single shell support based on sprayed concrete and rock bolts.
- Unacceptably high costs to maintain excavation progress.

In many situations, one simply cannot allow a water inflow to occur with the intent of treating it behind the advancing tunnel face because of possible difficult or devastating consequences. In most cases today, the construction of any underground structure will be required to limit the inflow of water to a defined maximum. This amount will depend on the type and location of the underground structure.

The difficulty and cost implications of handling a significant water inflow in an already excavated tunnel can be extreme compared to the cost of the injection works carried out ahead of the tunnel face. A total cost difference of a factor of 10 or more is not unusual.

However, controlling water seepage by pre-injection is a complicated and time-consuming operation and is unavoidably time critical. Hence, detailed focus on overall cost-effectiveness including definition of action criteria, determination of drill hole patterns, selection of grouting materials, and definition of grouting procedures included efficient equipment will improve the total tunnelling performance significantly.

2.3 *Drilling of injection holes*

The fan or umbrella of injection holes should normally encompass the entire tunnel, including the bottom. The spacing between the holes is normally between 1.2 and 2 m. In certain cases, with clay-filled joints or seepage channels with a low degree of communication, it is necessary to have a smaller spacing to get a good grout distribution.

The length of the holes for injection depends on several factors, like safety, round length, and tightness requirements, but generally lies between 15 and 25 m. The drilling of longer holes is generally too time-consuming, and the risk of excessive drill hole deviation is too big. It is easier to get a good result with shorter holes, but this will also require much drill time. Careful optimization of the drilling injection cycles with proper hole lengths and overlaps is important in order to achieve the best possible total cost effectiveness.

Thorough washing of the holes after drilling is important for removal of drill cuttings and loose

Copyright © 2005 Taylor & Francis Group plc, London, UK

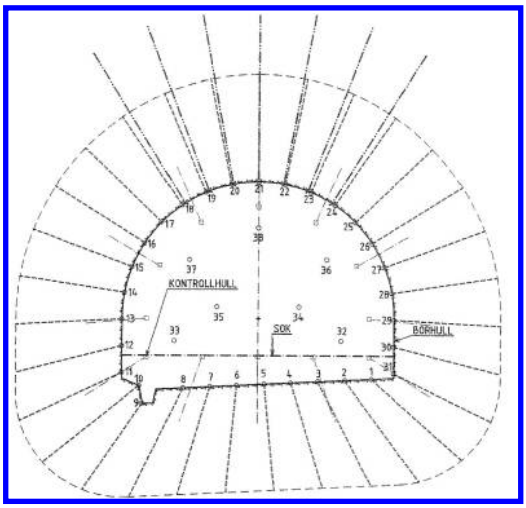


Figure 2. Typical injection fan for the most stringent Class 3 (4 litres/min/100 m tunnel).

ground material that could cover the joints in the drill hole. If left in the hole, this can block the penetration when the injection starts.

It is important to have an already injected bulkhead from the previous injection round in front of the tunnel face. Problems with backflow of grout into the tunnel and difficulties with fixing the packers could result if the overlap treated by injection is too short.

The diameter of the injection holes can be adjusted to the most practical. There is no need for large diameter holes. The main point is that the holes intersect the seepage channels. Diameters between 48 to 60 mm are most common. When encountering high water pressures, small diameter holes make the practical work far easier, e.g. the installation of packers. The use of small diameter packers also enables the packer itself to resist higher pressures, in comparison with a packer with a larger diameter.

2.4 *Injection fan layout*

Normally, injection holes are drilled in a fan as indicated in Figures 2 and 3, with an angle out from the tunnel contour. In most cases, it is not necessary to treat the rock mass directly in front of the tunnel. Typical drill angles are between 10 and 15° longitudinally out from the tunnel contour. The goal is to place the grout in a cylindrical body in the rock mass around the tunnel periphery. The intended thickness of this grout body depends on many factors. An important factor is the length of the rock anchors in use. If the grouted body is 3 m thick and the anchors have a length of 4 m, the anchor hole will create a seepage channel through the grouted body.



Figure 3. The Jong–Asker tunnel face being drilled ready for pre-injection.

2.5 *Injection*

When the entire fan is drilled, injection can commence. The injection should generally start at the bottom, and move upwards towards the ceiling in order to assure a well treated base for the upper part of the grout body. The importance of treating the bottom part thoroughly is emphasized, since a leakage through the floor will create problems with the road later on. These problems will be difficult to handle by post-injection at a later stage. Therefore, it is important to be particularly aware of the positioning of the injection holes in the bottom to ensure sufficient coverage of the injection fan. Often the drilling booms aren't directed sufficiently downwards.

Before injection of a hole can start, the packer needs to be installed. Normally the packer is placed at a depth between 1.5 and 2 meters at the end of a hollow lance. The packer has to be placed in sound and solid rock to be able to tight enough. The packer has to fill the entire drill hole.

3 THE JONG–ASKER, LOT JA2 PROJECT WATERTIGHTNESS REQUIREMENTS

The tunnel is designed as a single shell lining with sprayed concrete. As a result of this, the water had to be kept inside the rock.

The tunnel was driven through an environmentally sensitive area, and a conservative water ingress specification was in place. The tunnel is divided into three separate watertightness classes as follows:

Class 1: Allowable 16 litres/min/100 m tunnel
Class 2: Allowable 8 litres/min/100 m tunnel
Class 3: Allowable 4 litres/min/100 m tunnel

The most stringent class 3 allowed a maximum water ingress of 4 l/min/100 m, and was in force for more than 50% of the tunnel length.

Copyright © 2005 Taylor & Francis Group plc, London, UK



Figure 4. State-of-the-art specialist injection rig for pre-injection works.



Figure 5. Control panel at the injection rig.

4 THE PRE-INJECTION SOLUTION

In the normal expected geology, systematic pre-injection with the microccement RHEOCEM® 800 (D_{95} 12 micron) and standard rapid hardening cement was chosen, with the following consumption rates:

- RHEOCEM® 800 microcement: 900 kg/tunnel meter
- Rapid hardening cement: 860 kg/tunnel meter

As seen in Figures 4 and 5, AF Spesialprosjekt-SRG developed and built for the project, a state-of-the-art injection rig with computer controlled batching, mixing and injection systems. The set-up included 2 colloidal mixers, 4 agitator tanks, 4 pumps, and 4 separate lines that feed the injection lances at the face. The mixers were able to mix 4000 l/h, and the pumps delivered grout up to 100 bar pressure. The cements were delivered to the rig from 2 cement silos, 1600 liters each, which were fed with cements from 1000 kg big bags. All operations were done from the control board (see fig. 5) All necessary data like volume, pressure, time etc. were logged in a logging unit. This allowed the Clint to have full control over the injection work. This set up made it possible to rapid and efficient inject the 21 m long, up to 50 number pre-injection holes in the face for watertightness class 3, with up to 100 bar injection pressure. Overlap between injection rounds was 5 m, permitting three uninterrupted excavation rounds between grouting cycles.

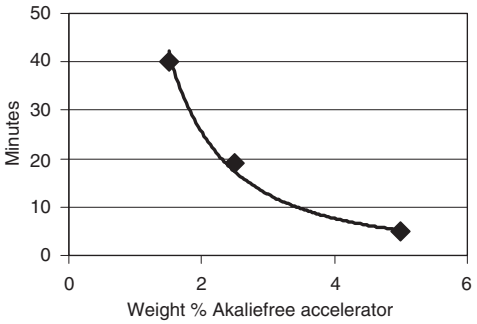


Figure 6. Setting time of cement grout with increasing alkali-free accelerator dose.

An injection round typically took between 20 to 30 hours, approximately 50% for long hole drilling, and 50% for pumping grout.

The total time used for injection, was about 50% of the total tunnel structure construction time.

Furthermore, with the assistance of Degussa UGC, AF – SRG developed an alkali-free accelerator dosing system with an in-line mixer positioned near the packer connection. The accelerator pump was electronically connected to the grout pumps.

For the first time this gave the contractor the possibility to control the grout take, and the setting time of the grout.

This approach allowed the contractor to significantly reduce the amount of grout used in zones of high water flow or large grout takes, thereby reducing the cycle times considerably! The accelerated grout was also used to stop out-leaks in the face and behind the face. This is normally difficult and time consuming tasks during injection. With this system it was possible to have a controlled open time of the grout between about 5 minutes and 20 minutes as shown in Figure 6.

The typical mix design for the RHEOCEM® grout was as follows:

- RHEOCEM® 800 – water ratio 0.8 to 1
- RHEOBUILD® 2000PF 1.5%
- MEYCO® SA162 AF Accelerator at injection point when required: 2 to 10% by weight of cement.

From the quality point of view, deliveries to the site were made on the "first in, first out" basis in large big-bag packaging (Figure 7), so that the RHEOCEM®

Copyright © 2005 Taylor & Francis Group plc, London, UK



Figure 7. Rheocem® 800 microcement being lifted to feed hoppers at back of injection rig at the tunnel face.

was always fresh and reactive. The Client, Jernbaneverket Utbygging, were given each month a Quality Control Certificate, so that each kilo of cement delivered to site was accounted for. This stringent requirement was a world first for the microcement pre-injection business.

5 RESULTS

In some zones, the contractor achieved tightness of less than 1 l/min/100 m tunnel, while the average for the hole tunnel is 5,15 l/min/100 m.The use of RHEOCEM® 800 microcement for pre-injection enabled the contractor to achieve the demanding total inleak requirements for the whole tunnel. In fact the total inleak is 40% lower than the already strict requirement! The overall goal to avoid settlements on the surface was also achieved.

Nearing the final tunnel breakthrough the ground conditions became worse as the rockmass had become weaker. As a result, the contractor needed to reduce the injection pressures to prevent face instability, but still required excellent grout penetration properties. To achieve this, AF Spesialprosjekt successfully switched their grout system to only RHEOCEM® 800 microcement, with a consumption of approximately 1500 kg per tunnel meter. Total project usage was 2,580 tonnes RHEOCEM® 800, and 115 tonnes of RHEOBUILD® 2000PF.

This high amount of injection also had a positive effect on the stability of the rock. This led to a reduced numbers of anchor bolts and less sprayed concrete. This reduction in cost should not be underestimated.

The capacity of long hole drilling will vary a lot depending on the rock quality, and the type of fissures.

The injection work was paid per kilo cement, and the drilling of injection holes and the pumping of the cement was paid after used hours for these operations. The used hours for the injection activities were then reimbursed as permitted construction time.

This method of payment was important for the achieved high quality and good results in waterproofing the tunnel. It is important to appreciate the Client had strict minimum requirements for the productivity capacities for the injection equipment, drilling jumbo and cement quality from the project outset to ensure rapid progress of the tunnel construction.

Finally, it must be stated that the intimate, close co-operation and teamwork between UGC, the Client and the Contractor on this project was one of the keys to success. All parties were focused on achieving the same goal, and stands as a model for future projects.

Copyright © 2005 Taylor & Francis Group plc, London, UK

Significance of grouting for controlling leakage in water tunnels – a case from Nepal

K.K. Panthi & B. Nilsen
Department of Geology and Mineral Resources Engineering, Norwegian University of Science and Technology (NTNU), Alfred Getz vei 2, N-7491 Trondheim, Norway

ABSTRACT: The rock itself is a significant barrier against groundwater movement if it has low porosity and is unweathered. The existence of discontinuities in the rock mass however increases the permeability and it may vary widely. In the Himalayas, active tectonic movement and shearing have made rock masses weathered and fractured and increased the permeability. Having such rock masses has direct impact on stability caused by water inflow and leakage in tunnelling. If the tunnel is excavated for conveying water, the leakage problem is not limited only to the tunnelling phase, since there is also high risk of water loss through unlined tunnels during operation. The paper discusses the role that preinjection and postinjection grouting played for controlling leakage through the unlined headrace tunnel of the 60 MW Khimti I hydropower project in Nepal Himalaya.

1 INTRODUCTION

The rock mass is typically a jointed aquifer where water moves through the most permeable discontinuities or through open channels along them. In general, the rock masses close to the surface are more jointed and the joints are more open than deeper in the rock mass. Visual observation carried out in many ungrouted tunnels indicates that most water leakage in general occurs in the part of the tunnel which is closest to the surface and is confined in fractures, faults and weathered zones (Nilsen and Thidemann, 1993 and Karlsrud, 2002).

Water leakage problems in unlined or shotcrete lined water tunnels are not new issues in tunnelling. In many occasions severe water inflow as well as leakage problems have been faced that not only reduced the stability of the rock mass surrounding the tunnel but also valuable water has been lost from the tunnel causing huge economic loss to the projects. According to Kassana and Nilsen (2003), some of the notable projects, which have suffered excessive water leakage problems are Chivor II (Columbia), Whatshan (Canada), Askora and Bjerka (Norway) and Kihansi (Tanzania). Consequently, water leakage control in the tunnels plays a vital role not only in improving the rock mass quality, but also in saving economic loss caused by leakages. The innovative solutions that exist at present in tunnelling makes it easier to control and reduce the amount of water leakage to a target level by pre and even post-grouting technique. However, the main concerns are the cost and time, which must be accounted and optimized. Thus, the proverb "prevention is better than cure" fits very well when it comes to water leakage control in tunnels.

In the Himalaya, due to active tectonics in this region, the rock masses are highly fractured, folded, sheared and deeply weathered. Tunneling through numerous zones of weakness, fractures and faults is thus a matter of reality. Moreover, the majority of these zones are in general highly conductive, representating potential sources of ground water aquifer as well as possible sources of water leakage from the completed unlined/shotcrete lined tunnels. Accordingly, treating the rock mass with injection grouting against water leakage might be very cost effective and environmentally friendly solutions for tunnels in this region. As an example on the effectiveness of grouting, Karlsrud (2002) indicates that the hydraulic conductivity of the rock mass closest to the tunnel periphery can be reduced to approximately one tenth the conductivity of ungrouted rock if systematic pregrouting is carried out during tunnel construction.

This paper is thus focused on the significant role that grouting may play in controlling the water leakage. For this the headrace tunnel of the Khimti I Hydropower Project in Nepal Himalaya has been taken as a case. In this Project, the grouting contributed significantly in reducing permeability and meeting the contractual requirements concerning water leakage. The main focus of the paper is the effective use of pre-injection and post-injection cement grouting.

Copyright © 2005 Taylor & Francis Group plc, London, UK

2 KHIMTI PROJECT

Khimti I Hydropower Project is located in the Himalayan region about 100 kilometers due east of Kathmandu, Nepal, see Figure 1.

The Project is owned by Himal Power Limited (HPL), Nepal and is among the first privately owned hydropower projects in the country. The Project started its commercial operation in June 2000. The Civil Construction Consortium (CCC) (a joint venture between Himal Hydro, Nepal and Statkraft AS, Norway) undertook the construction work on a turn key basis in 1996 and the construction work was completed in the summer 2001 after a one year defect liability period. The Project has an installed capacity of 60 MW and generates approximately 350 GWh electrical energy annually. To generate this energy the Project utilizes water from the very steep Khimti River, which has an average gradient of about 7 percent. Khimti I is a high head scheme, with a design discharge of 10.75 m^3/s and a gross head of 684 meters. The total waterway length of the Project is approximately 10 kilometers (HPL, 2000).

The headrace tunnel, which is the major focus of this paper, is a pressurized tunnel with maximum and minimum static water head of 4 bars and 1.1 bars at its downstream and upstream end respectively. The tunnel is approximately 7.9 kilometers long with inverted D-shape and 14 square meters cross-section. Except first downstream end of 418 meters with full reinforced concrete lining, the tunnel is built based on Norwegian tunnelling principles and is unlined or shotcrete supported. Modern support means such as pre and post-grouting, steel fiber shotcrete, spiling and rock-bolts have been used.

2.1 Project geology

Geologically, the project lies in the crystalline Tamakoshi gneiss complex representating Kunchha Group of the lesser Himalaya. Structurally the area is bounded or surrounded by a major fault system of the Himalaya called "the Main Central Thrust (MCT)", see Figure 2. The rocks in the project area are mainly augen gneiss with inter-bedded bands of chlorite and talcose schist. This intercalation has been observed frequently at an interval of 5–10 meters at the downstream section of the headrace tunnel.

In contrast, at the upstream stretch the interval is longer and the rocks are more fractured and open jointed.

The foliation planes are generally striking towards northeast – southwest direction and dipping towards northwest. Since the project area is bounded with the Main Central Thrust (MCT) the rocks along the headrace tunnel are highly jointed, sheared, deeply weathered and deformed. The area is also influenced by several minor faults and weakness zones represented by very weak sheared schist and crushed zones.



Figure 1. Location Map of Khimti I Hydropower Project.

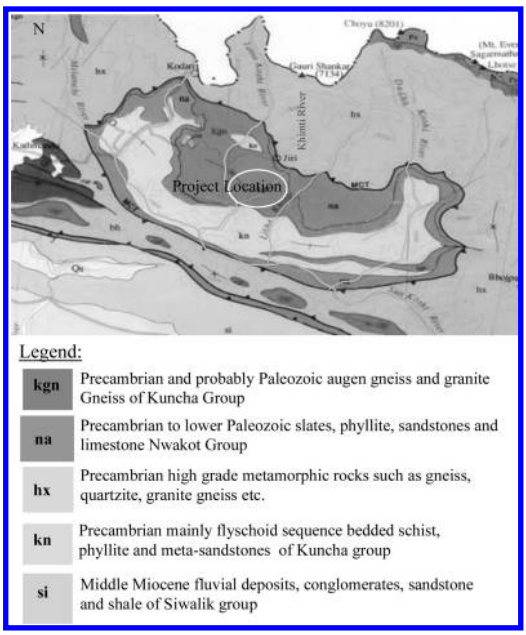


Figure 2. Geological map of the Project (source: Department of Mines and Geology, 1994).

2.2 *Actual rock mass conditions*

For a successful tunneling a method characterized by cost effectiveness and flexibility to adapt changing ground conditions is a must. In case of the Khimti headrace tunnel this concept is fully utilized with a maximum use of the self-supporting capacity of the rock mass. This is done by adopting a good system of water leakage control and by deciding the rock support at spot based on predefined rock mass classes and rock support procedures.

Copyright © 2005 Taylor & Francis Group plc, London, UK

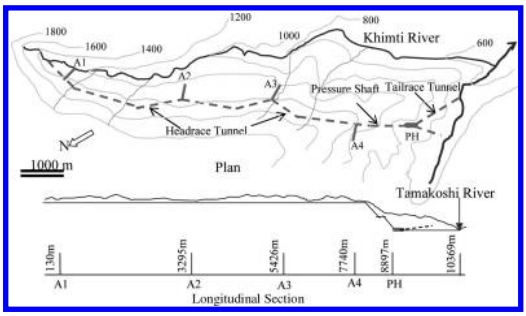


Figure 3. Plan and longitudinal profile of the Project.

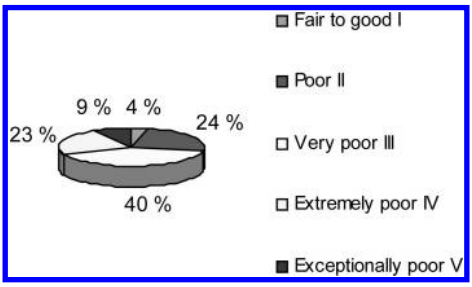


Figure 4. Headrace tunnel actual rock mass class distribution summarized after finish.

On the other hand, the planning phase investigation and predictions of the rock mass conditions along the tunnel in Khimti Project were rather poor and gave false impression to the contractor in planning the tunnelling work. The Design Basis Memorandum (HPL, 1995), which was the main guideline for the contractor in planning and detail design of the project, states that most of the tunnel length will be in sound rock. Exceptions were described to be the construction adits, the initial section close to intake and at the downstream end of the headrace tunnel, see Figure 3, where the tunnel was predicted to be in weathered rock where lining might be needed.

Accordingly, it was believed that the rock mass along the headrace tunnel would be of good quality and no measures such as water leakage control were considered at the initial phase of tunnelling. However, huge deviations have been found on the rock mass quality along the tunnel during construction. Less than 5 percent of the tunnel stretch was found to pass through sound rock, and the remaining 95 percents went through poor, very poor to extremely poor rock class (Bajracharya and Panthi, 2002), see Figure 4.

With respect to the discontinuity patterns, three sets of joints with occasional random joints have been observed along the tunnel alignment. The general

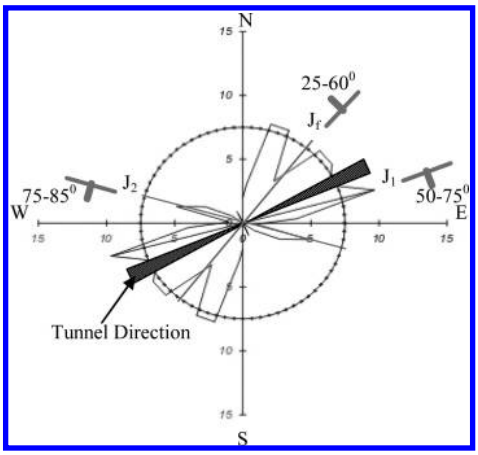


Figure 5. Joint rosette showing the orientation of the main joint sets and tunnel direction.

strikes of the main foliation joints (J_f) have been found varying from N15 to 60°E. This is not very favorable relatively to the headrace tunnel alignment, which also is oriented in northeast/southwest direction, see Figure 3 and 4. The foliation joints are mostly dipping towards northwest with a varying dip angle of 50 to 60 degrees at the southern part of the tunnel (adit 4 area) and this trend changes gradually making the dip angle more flat with almost 25 degrees at its northern part. The joint set number one (J_1) is oriented with almost the same strike direction as the foliation joints and is very close to parallel to the tunnel alignment, but is dipping opposite to the foliation joints (dip angle 50 to 75 degrees towards southeast). Joint set number two (J_2) is oriented in northwest southeast direction with very steep dip angle (70 to 85 degrees) towards southwest, see Figure 5.

Relating to joint filling and alteration, most of the discontinuities at the southern section (downstream from Adit 3) of the headrace tunnel are filled with clay and bands of chlorite and talcose schist, and have been characterized as impermeable with respect to water leakage. In contrast, the discontinuities present at the northern section of the headrace tunnel are either open or filled with coarse grained, permeable silt materials. In this northern section several open joints with aperture of up to 10 cm have been observed. Moreover, the degree of weathering along the tunnel alignment varies greatly and classifies as medium to highly weathered according to ISRM (1978). In some sections the degree of weathering was so deep that decomposed organic soil was found in the tunnel. Especially the tunnel section 500 meters downstream from Adit 2 was deeply weathered (CCC, 2002). The valley side slope in this stretch of the tunnel is flatter (about 25 degrees) and the rock cover is approximately 100 meters.

Copyright © 2005 Taylor & Francis Group plc, London, UK

Figure 5 indicates that the orientation and dip angle of two cross joints sets (J_1 and J_2) increase the possibility for large leakage from the headrace tunnel during operation as the valley side slope is oriented in northeast/southwest direction with a dip towards south, see also Figure 3. Moreover, most of the discontinuities upstream from Adit 3 are either open or filled with permeable materials that further increase the possibilities of large leakage during operation.

After tunnelling almost two and half kilometers of the headrace tunnel from different adits, the contractor realized this problem and had to change the tunnel construction methodology. He also incorporated a detail plan for preinjection grouting for the remaining tunnel stretch. However, there were only two alternatives left for water leakage control in the section of headrace tunnel where the excavation was already completed; full concrete lining or post-grouting. Even though it is well known that post-grouting is not as effective as pre-grouting in water leakage control, the contractor decided to go for post-grouting due to very tight construction schedule. Even if there were many uncertainties and risk connected to the postinjection grouting, success was achieved with tremendous amount of cost and time saving.

3 GROUTING CRITERIA AND PROCEDURE

The contractual limit for maximum water leakage from the 7,923 meters long headrace tunnel at the Khimti Project was defined as 150 liters per second, which gives specific leakage of 1.13 liters per minute per meter length of tunnel and is considered to be very strict with respect to water conveying tunnels. According to the Khimti civil works contract (KC2), failing to reach this criterion would have resulted in considerable economic penalties (CCC, 2002). In contrast, the traditional approach of full concrete lining in the tunnel would have been a very expensive and time consuming solution. In addition, concrete lining is not a fully watertight structure due to shrinkage cracks and there would be a need for contact grouting to make the tunnel water tight for full hydrostatic pressure.

Therefore, the decision was made to utilize the self supporting capability of the rock mass with modern means of support and to use mainly injection grouting in the headrace tunnel to reduce water leakage, see Figure 6.

As previously discussed, the best way to control the water leakage out of the tunnel would have been to carry out preinjection grouting ahead of the tunnel face during excavation. However, since almost 2.5 kilometres of the headrace tunnel was already excavated when the need of grouting was realized, both preinjection and post injection grouting was performed.

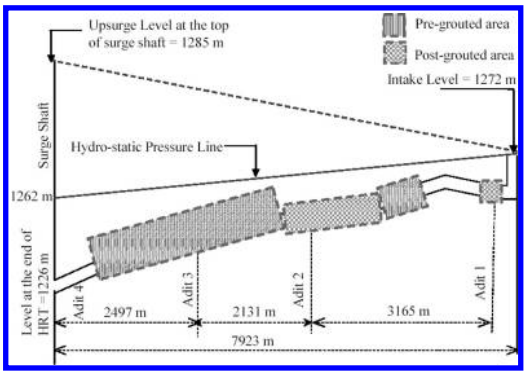


Figure 6. Headrace tunnel profile showing hydro-static line and areas with preinjection and postinjection grouting.

3.1 *Preinjection grouting*

Two criteria were mainly followed to decide whether there was a need for injection grouting or not. These were; (a) if the pressure of groundwater inflow to the tunnel is less than 1.5 times hydrostatic pressure during operation, (b) if the leakage through the rock mass exceeded a certain limit (water loss after pumping the water through exploratory drillhole with 1.5 times hydrostatic pressure). In general the criterion (b) is considered to be more reliable as criterion (a) is valid only in sections where groundwater inflow may occur during tunnel excavation and therefore (b) was used extensively for defining the preinjection grouting at the Khimti headrace tunnel.

First, one 21 meters long exploratory drillhole was drilled from the valley side wall of the tunnel face at an angle of 8 degrees relatively to the tunnel axis and slightly upwards with an angle of about 5 degrees. During the drilling regular observation was made to record possible water inflow as well as loss of flushing water, and the approximate depth of such incidents. Secondly, after drilling was finished, the water inflow (if any) into the tunnel was measured using packer and flow-meter. After that water leakage test was carried out by pumping water into the drillhole (through the packer) with 1,5 times the hydrostatic pressure. Finally, if the water leakage exceeded one litre per minute per meter length (lugeon value exceeding one) preinjection grouting was recommended. For preinjection grouting 12 drillholes with 21 meters length were drilled around the tunnel perimeter at an angle of 8 degrees relatively to the tunnel axis to establish a grouting cone, see Figure 7.

The preinjection grouting was performed using micro cement (Reocom) with some accelerator added to it. Three different mixes were used, starting with mix one having water/cement ratio 2. If mix one reached 1.5 times the operational hydrostatic pressure in the

Copyright © 2005 Taylor & Francis Group plc, London, UK

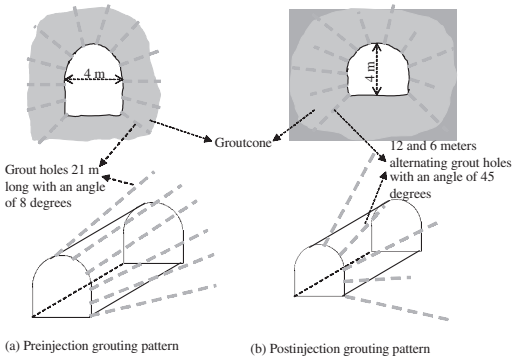


Figure 7. Used preinjection and postinjection grouting pattern.

tunnel, or the grout volume exceeded 200 litres in each hole, the grouting was stopped. However, if the grout pressure after 200 litres was still below 1.5 times the hydrostatic pressure, mix two with water cement ratio 1.5 was used with criteria as for mix one. In case of failing to reach the criteria, mix three with water cement ratio one was used. Finally, sawdust was added in case the desired pressure was not achieved.

3.2 *Postinjection grouting*

The orientation of joints shown in Figure 5 and the open character of the joints gave clear indication that there was a strong need for postinjection grouting at the section of tunnel where no preinjection grouting was performed during early stage of tunnel excavation, see Figure 6. Nevertheless, to be able to concentrate the postinjection grouting operation only to the required sections of the tunnel, it was very important to identify the areas from where maximum leakage could be expected. To verify that, early test water filling was performed in the headrace tunnel. A temporary plug was constructed at the downstream end of the headrace tunnel at chainage 7,505 meters, since the construction work at the pressure shaft and powerhouse were still not completed. The test water filling carried out in January 2000 indicated considerable leakage from the tunnel (approximately 700 liters per second), see Table 1.

As expected, the leakage was insignificant from Adit 3 and Adit 4, giving indication that the preinjection grouting was effective. On the other hand, the leakage from Adit 2 reached approximately 200 liters per second, giving indication that unacceptable leakage was occurring from the headrace tunnel near the Adit 2 area, where no preinjection grouting had been performed.

Based on the test water filling results and review of the geological tunnel log, a plan was made for the implementation of comprehensive postinjection

Table 1. Water leakage measured after test water filling.

Headrace tunnel locations	Leakage (Q) (liters/second)
Total leakage from headrace tunnel	700
From Adit 1 tunnel near concrete plug	2.6
From Adit 2 tunnel near concrete plug	200
From Adit 3 tunnel near concrete plug	0.4
From temporary plug at Adit 4	1.8
From remaining headrace tunnel	495.2

grouting. Main focus during grouting was on the ungrouted 910 meters upstream and 330 meters downstream stretch of the headrace tunnel from Adit 2 (chainage 2385 to 2965) where the joints were very open and the rock mass highly weathered. In addition, some length of the headrace tunnel near Adit 1 area where it was suspected that water was leaking, was also grouted, see Figure 6. Since the joints in these sections of the tunnel were more open, ordinary cement was used for the grouting. In addition, five percent bentonite clay was added in the grout mix to increase grouting effect. Four bars maximum pressure was used for postinjection grouting with a grouting pattern as shown in Figure 7-b. As indicated in the Figure, a 45 degrees angle relatively to the tunnel axis was used for drilling of the grout holes with alternating length of 12 and 6 meters.

4 GROUTING RESULTS

Both pre- and postinjection grouting were found to be very effective and economical solutions for controlling water leakage from the pressurized headrace tunnel. Compared to preinjection, the postinjection grouting was found somewhat difficult and challenging as there was a tendency of grout coming out in the tunnel wall, and due to very open joints it was often difficult to achieve the desired pressure. Consequently, the grout consumption was considerably higher than for preinjection grouting, and the grouting operations more costly. Nevertheless, the grouting costs were found much lower than those of concrete lining. The total consumption of grout material in the headrace tunnel is presented in Table 2.

The final water filling of the tunnel in March 2000, and leakage measured according to the performance guarantee in the civil works contract (KC2), gave a leakage of 120 liters per second in the 7,923 meters long headrace tunnel. This water leakage gives specific leakage (q) of 0.91 liters per minute per meter tunnel length, see Table 2, which is far below than the contractual leakage limit.

An analysis has been done to find out whether there exists correlation between the specific leakage

Copyright © 2005 Taylor & Francis Group plc, London, UK

Table 2. Grouting results and final water leakage measured.

Activity descriptions	Units	Quantity
A. Preinjection grouting		
Total grouted length	m	4612
Grout pressure used	bars	2.8–6
Total grout consumptions	kg	754,975
Specific grout consumption	kg/m tunnel	164
B. Postinjection grouting		
Total grouted length	m	1359
Grout pressure used	bars	4
Total grout consumptions	kg	941,260
Specific grout consumption	kg/m tunnel	693
C. Water leakage after final water filling		
Headrace tunnel length	m	7923
Total water leakage	liters/second	120
Specific water leakage	lt/min/m tunnel	0.91

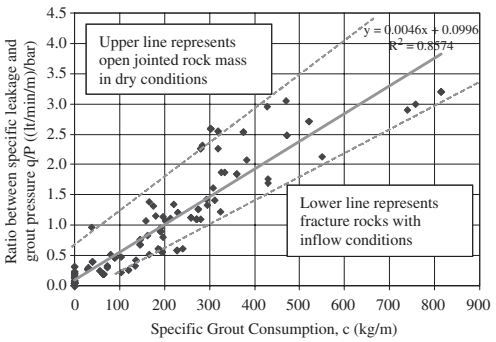


Figure 8. Correlation between specific leakage, grout pressure and specific grout consumption.

(q), the grouting pressure (P) (1.5 times static pressure during operation) and the specific grout consumption (c) for preinjection. As shown in Figure 8, a correlation has been found that might be used to estimate preinjection grout consumption for future tunnels in similar ground conditions.

Analysis has also been carried out of the specific grout consumption with respect to the rock mass quality of the tunnel section were both preinjection and postinjection grouting was performed. The results of this analysis are presented in Figure 9.

Figure 9 clearly indicates that the grout consumption for both preinjection and postinjection grouting is highest for rock class II and III. This is because the rock mass in these categories of rock class are typically open jointed. Poorer rock mass quality typically has clay filled joints, deformed rock mass and folding, which reduce the permeability. Figure 9 also indicates that the postinjection grouting has a considerably higher consumption than pregrouting.

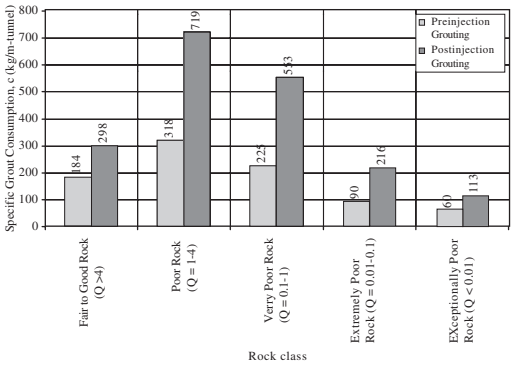


Figure 9. Relation between specific grout consumption and rock mass class.

5 CONCLUDING REMARKS

By applying systematic preinjection and postinjection grouting at the headrace tunnel of Khimti I Hydropower Project it was not only possible to control the water leakage to the contractual limit, but also to reduce the cost and time. The grouting carried out at this project clearly demonstrates that the use of systematic preinjection as well as postinjection grouting played a very significant role in the reduction of water leakage from the pressurized unlined / shotcrete lined water conveying headrace tunnel. Moreover, the grouting has played a major role in improving the rock mass quality by cementing the cracks and joints with grout material and reducing the need of excessive rock support.

The factual based analysis carried out has confirmed that there exists good correlation between the specific leakage (q), grout pressure (P) and specific grout consumption (c) that could be used for estimating grout consumption for future water conveying tunnels in similar rock conditions. The Khimti case also illustrates that the grouting operations are not easy tasks especially when it comes to postinjection grouting, which may reach a cost of many times that of preinjection grouting. Therefore, systematic preinjection grouting should be used as much as possible. Finally, to achieve a good grouting result at lowest possible cost, a good understanding of the ground conditions is of great importance.

REFERENCES

Bajracharya B. B. and Panthi K. K. 2002. Rock support optimization in Himalayan tunnels. *Proceedings. 28th ITA General Assembly & World Tunnel Congress:* 461–467. Sydney: Australia.

Civil Construction Consortium. 2002. Construction report. *Khimti I Hydropower Project. Volume 1-main text:* Nepal.

Copyright © 2005 Taylor & Francis Group plc, London, UK

Himal Power Limited. 1995. Project definition report. *Khimti I Hydropowe Project:* Nepal.

Himal Power Limited. 2000. Final design report. *Khimti I Hydropower Project. Volume 1 – main text:* Nepal

ISRM. 1978. Suggested methods for the quantitive description of discontinuities in rock mass. *International Journal of Rock Mechanics, Mining Sciences & Geomechanics Abstracts*. Volume 15: 319–368.

Karlsrud K. 2002. Control of water leakage when tunnelling under urban areas in the Oslo region. *Norwegian Tunnelling Society (NFF)*. Publication 12. 27–33.

Kassana L. B. and Nilsen B. 2003. Analysis of water leakage at Lower Kihansi Hydropower Plant System in Tanzania, East Africa. *Waterpower XII – HCI Publications*.

Nilsen B. and Thidemann A. 1993. Rock Engineering. *Hydropower Development Series*. Volume 9: 156. Norwegian Institute of Technology. Division of Hydraulic Engineering. Trondheim: Norway.

Copyright © 2005 Taylor & Francis Group plc, London, UK

Deformed ground massif state during tunnel construction

G.G. Balandyuk
Russian Tunnelling Association, Moscow, Russia

ABSTRACT: The results of monitoring of ground massif and tunnel lining deformations during construction of a deep multi-vaulted column transit station of Moscow subway are considered in this paper. The study results allow to foresee the zones of ground massif displacements during tunnels excavation that is important for the preliminary support including compensation grouting to minimize the influence of the excavation upon the structures located underground and on the ground surface.

Such a task positing is famous: during underground construction the structures (tunnel linings) and the surrounding ground massif are considered as a united (common) deformed system and all the necessary parameters are determined in the process of united calculations (Bulychev 1982, 2002).

It has also been established that the main feature of determination of the ground massif state after the strength limit point is the study of deformations; and stresses and strains are not connected by a one-valued relationship while stresses are decreasing. And the deformations (displacements) are determined taking into consideration the dilatance. The most essential is change of volume because of displacements. When the ground massif state is after the strength limit point it is necessary to take into consideration the connection of stresses with displacements on planes of sliding and not with the deformations (Shemyakin 2002).

The study of mechanism of the ground massif and tunnel structures (linings) deformation was performed in-situ when a deep multi-vaulted transit column station of Moscow subway was constructed. According to methods of experimental research special monitoring sections were set in tunnels (Balandyuk 1971, 1988).

The results of monitoring of displacements of tunnel structures and the ground massif in the vault of a side station tunnel as a consequence of the excavation of the neighbouring middle station tunnel are considered in the paper. The tunnels are located in solid Carbon clays with marl interlayers underlined by thick limestone strata. The clays are overlapped by thick limestone strata, then by carbon clays, sand loam and moraine deposits covered with cultural layers. Preliminary in the side station tunnel control cement grouting was performed beyond the tunnel lining for 3 days. It was made also with the aim to study the united work of the linings and ground massif in the monitoring section of the side station tunnel. In this situation the approaching face of the neighbouring middle station tunnel was located at 7 m distance from the monitoring section of the side station tunnel.

The relationships between the increase of the station structures displacements (Fig. 1, curve 1) and the overlapping limestone strata (Fig. 1, curve 2) have been got. Here along the axis OX there is a distance in meters from the plane of the moving face of the neighbouring side tunnel and along the axis OY there are displacements of the ground massif in mm.

During the period of the face approach of the middle station tunnel along the monitoring section in the neighbouring side tunnel the displacements of the linings and the ground massif are different. The lining

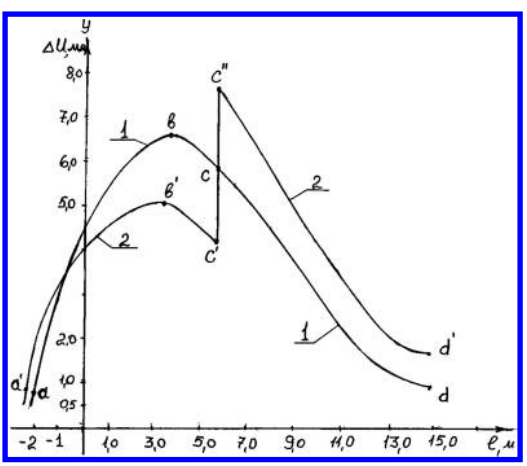


Figure 1. The velocities of the ground massif displacements and the lining displacement in the station side tunnel during the neighbouring middle station tunnel construction.

Copyright © 2005 Taylor & Francis Group plc, London, UK

begins to be displaced inside the tunnel when the face of the neighbouring parallel constructed tunnel is 2 m far from the considered plane. Then during permanent neighbouring tunnel construction vertical structural displacements in the studied tunnel reach maximum values when the neighbouring tunnel face has crossed the considered plane and has left it for a distance of 3/3.5 m (Fig. 1, curve 1, part a–b). Then the velocity of the lining displacements decreases intensively and stops at a distance 14 m from the tunnel face (Fig. 1, curve 1, part b–d).

The results of the ground massif displacements are of the most interest (Fig. 1, curve 2). In the part a′–b′–c′ (Fig. 1, curve 2) the ground massif working in an elastic state is displaced slower than the tunnel structure. When the face of the neighbouring tunnel No. 2 is as far as 6 m from the studied plane an immediate displacement (shear) happens, there is a stage of intensive ground massif displacement (Fig. 1, curve 2, part c′–c″). Here the velocity of the ground massif displacement is more than the velocity of the structure displacement. The ground massif being displaced leans on the structure passing from the elastic stage to the plastic one; the ground pressure develops, the structure and the ground massif work together till the neighboring tunnel face is as far as 14 m. Then the displacements practically fail. The overlapping limestone strata together with the ground massif have been displaced (Fig. 1, curve 2, part c′ – c″) up to the ground surface.

The results of the performed studies give the possibility to foresee the ground massif displacements while tunnel excavation takes place under similar engineering and geological conditions that is important for preliminary support works performing including compensation grouting.

REFERENCES

Bulychev, N. Mechanics of Underground Structures. Nedra Publishing House, 1982, 270 p. (in Russian).

Bulychev, N. Development of the Theory and the Calculation Methods for Underground Structures. *Proc. of the International Scientific and Practical Conference.* Moscow, 2002, 356–361 (in Russian).

Shemyakin, V. Deformations and Failure of Rocks. *Proc. of the International Scientific and Practical Conference.* Moscow, 2002, 334–342 (in Russian).

Balandyuk, G. Methodology of ground displacements during a deep subway station construction. *Proc. of TsNIIS*, Moscow, 1971, No. 40, 36–40 (in Russian).

Balandyuk, G. Patent of RF No. 1544974: Method of Control of Ground Massif Displacements. Priority of 27.04.1988. The Patent has been acting since 13.07.1993.

Copyright © 2005 Taylor & Francis Group plc, London, UK

Laboratory testing of grout properties and their influence on back fill grouting

A. Bezuijen & W.H. van der Zon
GeoDelft, Delft, Netherlands

A.M. Talmon
WL | Delft Hydraulics, Delft, Netherlands

ABSTRACT: Functions of tail void grout are described and necessary properties of the grout mortar to fulfil these functions are discussed. A simple model is derived to show the loading on the lining as a function of the mortar properties and the possible movement of the lining. When it takes a long time for the grout mortar to consolidate or to harden, this can lead to considerable forces in the lining of a tunnel as well as on the TBM as is shown with some example calculations in this paper.

1 INTRODUCTION

Back-fill grouting is a crucial process in TBM tunnelling. The grouting process determines the loading on the soil and with that an important part of the surface settlement. It also determines the loading on the lining. Field and laboratory measurements (Bezuijen et al. 2004, Bezuijen & Talmon, 2003) have revealed mechanisms that are of importance: the flow of the grout around the tunnel, the yield stress that determines the maximum resistance against the buoyancy forces and the influence of consolidation of the grout on the loading on the lining. The parameters necessary to describe these mechanisms are not given in the traditional grout tests and therefore a new test was developed.

The paper describes the functions of grout during and after injection in the tail void and the available and new developed laboratory experiments. A calculation method is presented that gives an indication about the loading along the lining. It presents some example calculations before ending with conclusions.

2 FUNCTIONS OF GROUT

2.1 *General*

Grout is injected in the tail void between the soil and the lining. In some cases it is injected through the lining, but most common is a grouting system that is constructed in the backside of the TBM and that can inject grout during drilling continuously, see Figure 1.

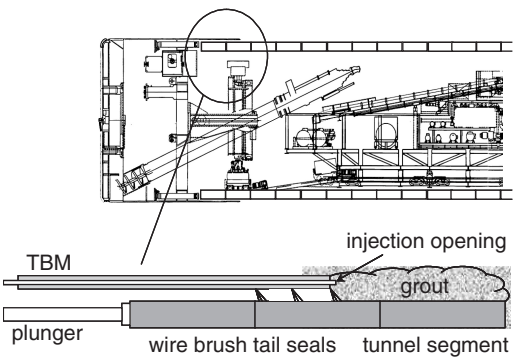


Figure 1. Sketch of TBM and detail of injections system.

The grout has different functions, as summarized by Shirlaw et al. (2004):

1. To ensure that there is uniform contact between the lining and the ground: The ground both loads the lining and provides resistance to distortion. Consistent filling of the tail void will avoid uneven loading.
2. To reduce the surface settlement over the tunnel: If the void is not filled with grout, the ground will move into the void, resulting in settlement. Typically, the volume of the tail void is in the range 3% to 16% of the internal volume of the tunnel. There can be high surface settlements if the grouting is ineffective, and the tail void closes as a result.
3. To hold the ring in place during shield advance: Soft ground and mixed face tunnel boring machines

Copyright © 2005 Taylor & Francis Group plc, London, UK

are typically advanced by thrusting off the installed lining. If the lining is surrounded by liquid grout, then it can float upwards, see Figure 2. This can lead to stepping on the circumferential joint, birds' mouths developing on the radial joints, loss of plane and damage to the lining.
4. To carry the load transmitted to the lining by the shield back-up trailers.
5. To reduce seepage and loss of fine particles where the gasket is ineffective due to damage or because of stepping of the lining.

In addition to this, grout also has to provide sufficient resistance to overcome the buoyancy forces that occur in the first rings after the TBM. These buoyancy forces occur because the average density of lining and air that forms the tunnel is less than the density of the grout. This is comparable with what is mentioned under 3, but it can be compensated by reduction of the grout density as well as by an increase of the yield stress.

Some of these functions can only be taken into account by the construction of the TBM (sufficient grout injection points) or craftsmanship (taking care for open injection points, consistent filling of the tail void). However, for some it is possible to 'design' the grout. In this paper we will discuss the influence of the density, the initial yield stress, the consolidation properties and the hardening of the grout on the loading on the lining. It is focused on forces and moments along the lining. Ring loading is not taken into account.

2.2 *Density of the grout and initial viscosity*

The density of grout mortars usually varies from 1000 to 2200 kg/m^3. The average density of the cross-section of tunnel lining and the air in the tunnel is in general around 400 kg/m^3. This means that there will be a buoyancy force on the tunnel. This can lead to upward directed movement of the tunnel lining when it is released from the TBM. Furthermore it induces stresses and moments in the TBM as will be explained later.

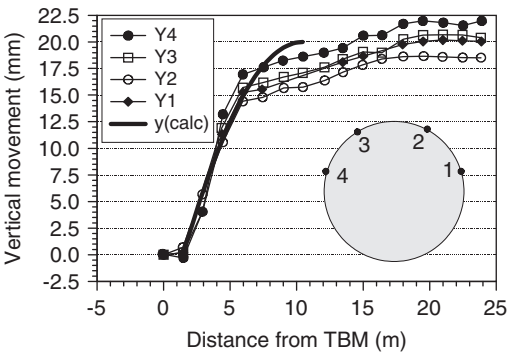


Figure 2. Rising of lining measured at 4 points on the lining after placement of lining segments (Sophia Rail Tunnel, The Netherlands) and calculated rising, see further text.

The grout mortar can be designed to minimize this buoyancy force by reducing the density and/or decrease the yield strength. The yield strength changes the pressure distribution over the lining. Assuming that the shear strength between the tunnel lining and the grout is small and the shear strength between the soil and the grout determines the pressure distribution, the relation between the yield strength and the maximum buoyancy force that can be compensated by the grout mortar can be written (Bezuijen et al. 2004):

$$F = \tau_y \frac{D^2}{s} \tag{1}$$

Where F is the maximum force per metre tunnel lining that can be compensated by the yield stress in the grout, τ_y the shear strength of the grout, D the diameter of the tunnel and s the width of the tail void. The buoyancy force K per metre lining exerted by the tunnel lining can be written as:

$$K = \frac{\pi}{4} D^2 (\rho_g - \rho_t) g \tag{2}$$

Where ρ_g is the density of the grout, ρ_t the average density of the tunnel (lining and air) and g the acceleration of gravity.

Equilibrium in a cross-section is reached when $F \geqslant K$. Such a situation can be reached when:

$$\tau_y \geq \frac{\pi}{4} s (\rho_g - \rho_t) g \tag{3}$$

This relation shows that a stable cross-section can be reached by using grout with high yield strength, or a low density or by increasing the average density of the tunnel (and/or dead weight or back-up train).

2.3 *Properties along the lining*

Although Eq. (3) looks rather simple, it is in a lot of cases not so easy to fulfil this equation directly behind the TBM due to other requirements on the grout mortar. The grout has to flow easily through the piping of the injection system and it has to fill the tail void completely and last but not least also costs play a role. These requirements quite often result in a grout mortar where Eq. (3) is not fulfilled directly after the TBM because the yield stress is too low. When this is the case, a part of lining directly after the TBM will have the tendency to move upward. However, this upward movement will be stopped by the friction forces between the lining elements still in the TBM on one side and the elements in the already hardened or consolidated grout on the other side. In such a situation

Copyright © 2005 Taylor & Francis Group plc, London, UK

it is necessary to know the hardening and consolidation properties of the grout as will be described later.

2.4 *Consolidation and hardening*

The yield strength of the grout mortar after injection will increase due to consolidation of the grout and hardening. It is of importance to have data to describe this strength increase because this determines for what length the tunnel lining has only limited support. Consolidation can lead to a strength increase for only a limited thickness of the grout layer (Bezuijen & Talmon 2003). This is the case when the tunnel is bored in stiff sand.

3 LOADING ON THE TUNNEL LINING

An example where Eq. (3) was not fulfilled is the Sophia Rail Tunnel (Bezuijen et al. 2004). The measured hydraulic gradient along a cross section of the tunnel lining is comparable to the average density of the tunnel at some distance from the TBM, there where the pressure gradient is more or less constant, see Figure 3, but increases close to the TBM. This leads to an upward directed loading on the tunnel lining close to the TBM until consolidation of the grout led to a yield strength that is high enough to overcome buoyancy forces further away from the TBM.

Using the pressure data during drilling it is possible to construct the load distribution on the tunnel for the part where the lining has the tendency to float. This loading can be used in a numerical program to calculate the shear forces and moments in the lining. The resulting shear forces and moments depend to a large extend on the moments and force exerted by the TBM. In this paper we focus on the influence of the grout and the influence of consolidation and hardening. We therefore assume a rather simple calculation model only to get an idea how the loading on the lining is influenced by the TBM induced moments and consolidation or hardening.

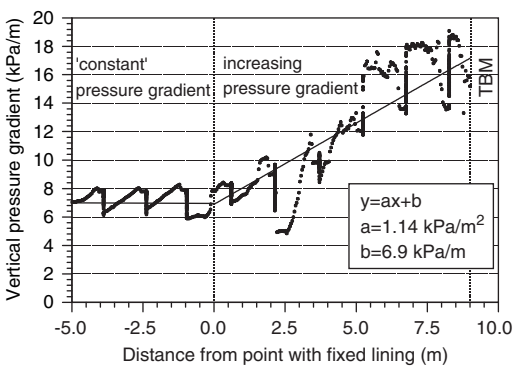


Figure 3. Example of gradient in the grout pressure as a function form the distance (0 on the X-axis represents the point where the lining is more or less fixed. The TBM is at 9 m). Results measured at Sophia Rail tunnel (Bezuijen et al. 2004).

The lining is approximated to a beam that is fixed at the end where the grout is consolidated or hardened. Usually it is assumed that the lining rests on an elastic foundation. However, the measurements, Figure 3, show that forces on the lining are more or less constant at some distance (more than 9 m in the figure) from the TBM. Movement of the lining in the grout would lead to pressure variations in the grout that are not measured. This justifies this approximation.

The other end of the lining bears at the TBM. The TBM can exert a certain moment M on the lining. A loading distribution on the lining is assumed that increases linearly with the distance from where the tunnel lining is fixed in the consolidated grout. This is again only an approximation of the real loading that occurred, see Figure 3.

As can be seen from Figure 2, there is a certain permanent movement in the lining. With the boundary conditions mentioned before it is possible to solve the beam equation:

$$EI\frac{d^4y}{dx^4} = -q.x \tag{4}$$

With the boundary conditions:

$$y(0)=0,\ \frac{dy(0)}{dx}=0,\ y(L)=A,\ \frac{d^2y(L)}{dx^2}=\frac{M}{EI} \tag{5}$$

Where E is Young's modulus, I the moment of inertia, $x = 0$ the position where the grout is hardened, $x = L$ the other end of the lining connected in the TBM, A the vertical displacement of the lining with respect to the TBM, q the increase of the loading with distance x and M the moment the TBM exerted on the lining. For these boundary conditions the movement of the lining can be written as:

$$y(x) = -\frac{x^2\,(2\,q\,x^3\,L^3 - 9\,x\,q\,L^5 + 120\,x\,A\,EI - 60\,x\,L^2\,M + 7\,q\,L^6 - 360\,L\,A\,EI + 60\,L^3 M)}{240\,L^3\,EI} \tag{6}$$

and the shear force (F_s) as:

$$F_s = 0.5qx^2 + \frac{3AEI}{L^3} - \frac{9}{40}qL^2 - 1.5\frac{M}{L} \tag{7}$$

Consequence of the assumptions is that F_s had to be 0 at x = 0 (a large F_s at x = 0 would be reflected in the measured pressure gradient, which is not measured).

Copyright © 2005 Taylor & Francis Group plc, London, UK

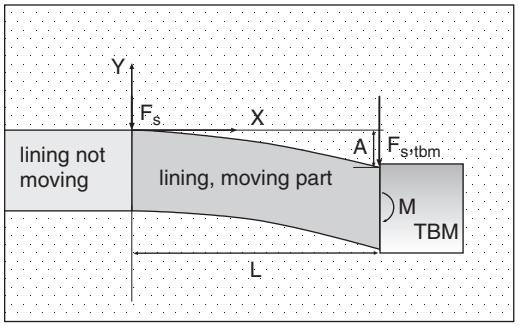


Figure 4. Definition sketch for calculating the loading on the lining.

With a length of the liquid zone of approximately 9 m and a tunnel with a diameter of 10 m, a beam equation cannot be more than an approximation, but as said before that is enough to get an idea of the importance of various parameters.

4 LABORATORY TESTS

Shirlaw et al. (2004) emphasize the importance of performance tests for grout, since it is likely that also in the future most grout mortars will be tailor made from locally available constituent materials. They mention possible tests to test grout mortar:

- grading curves on individual constituents and the combined mix.
- Cube tests (compressive strength).
- Segregation of mortar components under gravity.
- Relaxation, height variations in time.
- Washout. Dissolving of the sample in water.
- Bleeding under pressure (Bariod filter press).
- Sump cone or Prepakt cone for workability.
- Cohesion or yield stress by a vane apparatus.
- Internal friction.
- Density of the grout.

More information on these tests is given by Shirlaw et al. (2004).

Comparing these tests with a definition of a performance test: A performance test is a test in which the product is used under actual service conditions, it must be concluded the test mentioned are no performance tests but index tests. Index tests are useful to compare different materials, but present limited information of the performance in service conditions.

The following properties are of importance to describe the behaviour of the grout just after the TBM that is the focus of this paper:

- the yield stress or cohesion this describe the loading on the tunnel, see Eq. (1).
- the density of the grout to determine the buoyancy forces, Eq.(2).
- the time necessary for the grout to consolidate or before hardening starts. This time and the drilling velocity determines L in the beam equations.

The first 2 parameters can be measured with index tests mentioned before. This is not possible for the third parameter and therefore a new developed test is described in the next section.

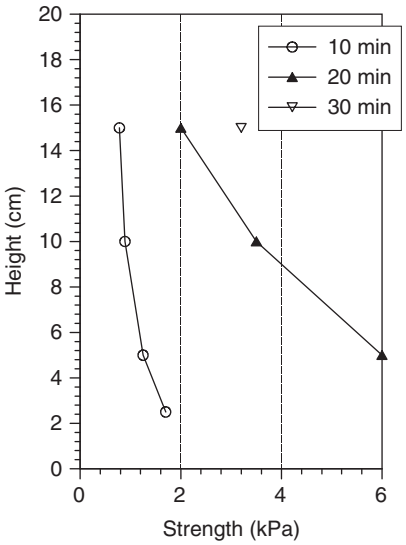


Figure 5. Strength development as measured with a vane during consolidation of grout.

5 'FULL SCALE' CONSOLIDATION TEST

It is difficult to measure the consolidation of grout in a traditional oedometer test or filter press test, because the consolidation is fast compared to the consolidation of clay or peat, as will be shown later in this section. Furthermore it is possible that there will be hardening of the grout during the consolidation process. Therefore consolidation experiments have been performed in a cylindrical cell with a diameter of 0.3 m in which a grout layer was made of 0.2 m height, comparable to the average thickness of a grout layer in the tail void for tunnels with diameters in the range of 6 to 11 m.

The test set-up is described by Bezuijen & Talmon (2003). A result is shown in Figure 5 for a grout sample that was loaded with 300 kPa pressure. It shows that due to consolidation the strength of the grout increases considerably within 30 minutes. This time is much shorter than the time necessary for strength increase due to hardening of the grout, which was approximately 5.5 hours (Bezuijen et al. 2004).

Copyright © 2005 Taylor & Francis Group plc, London, UK

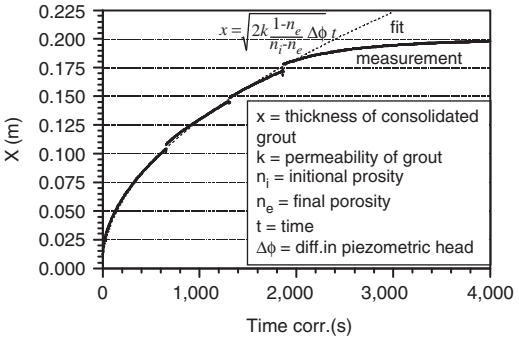


Figure 6. Experimental data on consolidation fitted with theory. x is the thickness of the consolidated layer.

Consolidation of grout, sometimes called bleeding, cannot be described by linear consolidation theory. It can be approximated quite well assuming it behaves as a grain-water mixture with little strength until the water is expelled from the grout and there is an effective stress between the grains. A description is presented in Bezuijen & Talmon (2003), see Figure 6. There it is also shown that the increase in yield stress of the grout corresponds with consolidation. This figure shows that the consolidation of a 0.2 m thick grout sample takes 2000s. A traditional oedometer test would last only 20s, which is rather short to perform good measurements of the deformation and amount of expelled water and will not take into account possible hardening.

6 EXAMPLE CALCULATION

6.1 *Sophia Rail tunnel*

As example the measurements for the Sophia Rail Tunnel are used. The measured pressure gradients are already shown in Figure 3. In this figure the pressure gradient during drilling is most prominent; because then the TBM is moving and x is changing (the pressures were measured in one ring of the lining). The vertical points in the plot show the change in gradient during stand still. The constant value of 6.9 kPa/m is higher than the value that corresponds to the weight of the tunnel (4 kPa/m) but will also be influenced by weight of equipment in the lining. The value of q can be determined from a in Figure 3:

$$q = a.O \tag{8}$$

With O the cross-sectional area of the tunnel lining. q is 80 kN/m^2 for a tunnel with a diameter of 9.45 m as the Sophia rail tunnel.

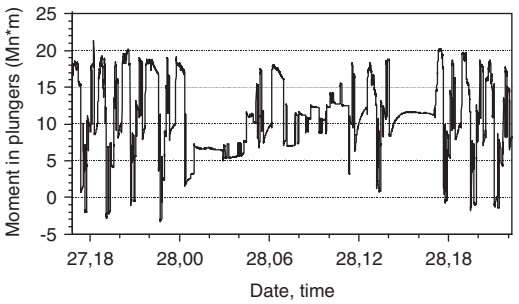


Figure 7. Momentum in vertical direction that is exerted on the lining by the plungers in the TBM. A positive momentum means that the forces on the lower part of the tunnel are higher than on the upper part.

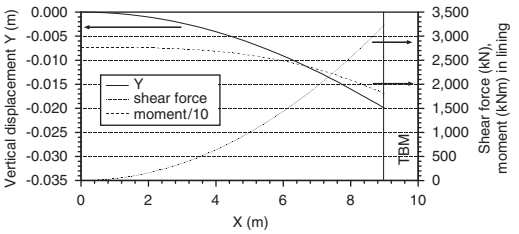


Figure 8. Results of calculation model. Calculated moments are divided by 10.

The momentum on the tunnel lining for the Sophia Rail tunnel as given in Bezuijen et al. (2004) is shown in Figure 7. Momentum is approximately 10 MNm during stand still and 18 MNm during drilling.

The stiffness of the lining is not well known. We used Eq. (7) to determine the stiffness. A very stiff lining will lead to a large downward directed shear force at $x = 0$ and a flexible lining to an upward directed shear force, which are both not measured according to the pressure gradients in the grout. By adjusting the stiffness of the lining to $EI = 5.4*10^7$ kNm^2 no shear force is present at $x = 0$. Results of this calculation are shown in Figure 8.

The calculated vertical displacement is also compared with the measured displacement in Figure 2 and showed reasonable agreement. This result means that the effective stiffness of the lining in liquid grout is less than normally assumed. It is possible that the segmented lining has more degrees of freedom than is assumed traditionally. It further implies that there is a considerable shear force present at the TBM that is counterbalanced by the weight of the TBM and the lining elements in the TBM. In this example a measured q was used, but this q is not the result from the grout properties only. For a situation with zero shear force F_s at $x = 0$, the values of the parameters in Eq. (5) also determine q so that $F_s = 0$ for $x = 0$, or to say

Copyright © 2005 Taylor & Francis Group plc, London, UK

it differently: not always all available shear stress in the grout is mobilized.

Consequence is that the influence of L (the length with linearly increasing grout pressure gradient) cannot be found by simply increasing L in Eq. (6) and (7). Assuming that the pressure gradient in the grout remains the same, it is also necessary to change q. Furthermore A has to be changed to fulfill the condition that $F_s = 0$ at $x = 0$. The value A can be found by changing the boundary condition $y(L) = A$ to $F_s(0) = 0$ in Eq. (5) and solving Eq. (4) for these conditions leading to:

$$y(x) = -\frac{x^2\,(q\,x^3 - 10\,q\,L^3 - 60\,M)}{120\,EI} \tag{9}$$

and to a simple expression for the shear force $F_s(x)$:

$$F_s(x) = 0.5\,q\,x^2 \tag{10}$$

Eq. (9) for $x = L$ presents A as a function of q, L, M and EI, see the example below.

A calculation was run where L was increased with a factor of 2, see Table 1. It is clear that 18 m unsupported length leads already to totally unacceptable movement of the tunnel.

An interesting result is further that it appears that only with a finite value of A it is possible to get a condition of $F_s = 0$ for $x = 0$. This condition is not always fulfilled in numerical calculations leading to shear forces in the lining that have no relation with reality.

A decreases quadratic with L therefore A can be minimized by using grout that acquire quickly a certain strength to develop the necessary shear strength. The 'full scale' consolidation tests described provide data on the consolidation properties. With the properties of the surrounding soil: shear modulus at unloading, permeability, it is then possible to calculate the time it takes before the necessary shear strength is available.

6.2 *Variations*

The calculation model presented in the section above, allows investigating the influence of various parameters. The loading on the lining close to the TBM exerted by the buoyancy force from the grout is q^*x and thus 720 kN/m. Using eq. (1) and (2) it can be derived that for such a situation $\tau_y = 0.5$ kPa (a bit lower than measured in the test shown in Figure 5 for fresh grout, but the maximum shear stress is a vector and therefore horizontal flow during injection decreases τ_y). It can be tested what will be the influence on the loading on the lining when this value is increased until 1 kPa. The loading on the lining reduces than to 432 kN/m close to the TBM and q to 48 kN/m^2 Another possible variation is to use the same shear stress (0.5 kPa) but to decrease the volumetric weight of the grout from 21 kN/m^3 as it was for Sophia Rail Tunnel to for example 12 kN/m^3. This will reduce the buoyancy force according to Eq. (2) to 78.3 kN/m close to the TBM, which, assuming again a linear increase in loading on the TBM, lead to a q of 8.7 kN/m^2. Table 2 shows results of calculation results obtained with the model described before.

Table 1. Parameters and results of beam calculations.

Parameter	Calc 1	Calc 2	dimension
Input			
L (length of 'unsupported' zone)	9	18	m
q (distributed loading near TBM)	80	40	kN/m^2
EI (stiffness of lining)	5.4×10^7	5.4×10^7	kNm^2
M (moment on TBM)	18	18	MNm
Result			
A (displacement of lining)	0.02	0.16	m
M (x = 0)	28	57	MNm
$F_{s,TBM}$ (shear force at $x = L$)	3.2	6.5	MN

Table 2. Influence of some variation in the parameters on the results of beam calculations.

Parameter	Calc 3	Calc 4	dimension
Input			
L (length of 'unsupported' zone)	9	9	m
q (distributed loading near TBM)	48	8.7	kN/m^2
EI (stiffness of lining)	5.4×10^7	5.4×10^7	kNm^2
M (moment on TBM)	18	18	MNm
Result			
A (displacement of lining)	0.017	0.015	m
M ($x = 0$)	24	19	MNm
$F_{s,TBM}$ (shear force at $x = L$)	1.9	0.35	MN

As expected, both a larger shear stress in the grout and a lower density leads to a lower displacement of the lining, a smaller moment and shear force. Especially the reduction in shear force at $x = L$ is considerable. In this way the model can be used to get quantitative information on the influence of using a different grout.

Further research will focus on deformation and grout pressure measurements for different tunnels to see how general applicable the proposed model is.

7 CONCLUSIONS

The work described in the paper has led to the following conclusions:

– The thickness of a grout layer in a consolidation test has to be comparable to the thickness of the

Copyright © 2005 Taylor & Francis Group plc, London, UK

grout layer in the field if hardening and consolidation both has an influence.

- The stability of the tunnel in longitudinal direction depends on various parameters. The tunnel more or less 'seeks' the equilibrium conditions.
- A minimum grout strength is necessary for an equilibrium condition of the lining.
- The length of the insufficient supported zone is of crucial influence on the movement of the tunnel, the shear force at the TBM and the moments in the lining. Movements and moments can be reduced by reducing the length of this zone by changing the hardening or consolidation properties of the grout. Yield strength and density of the grout also influences the longitudinal loading on the lining.
- The model presented show quantitatively what is the influence of changing the grout parameters on the loading on the lining.

REFERENCES

Bezuijen A., Talmon A.M., Kaalberg F.J. and Plugge R. Field measurements of grout pressures during tunneling of the Sophia Rail tunnel. *Soils and Foundations vol, 44, No 1, 41–50, Feb. 2004*

Bezuijen A., Talmon A.M, 2003, Grout the foundation of a bored tunnel, 2003, *Proc ICOF 2003 Dundee.*

Shirlaw J.N., Richards D.P., Ramon P., Longchamp P., 2004, Recent Experience in Automatic Tail Void Grouting with Soft Ground Tunnel Boring Machines. *Proc. ITA 2004, Singapore*

Copyright © 2005 Taylor & Francis Group plc, London, UK

Modified New Austrian Tunneling Method in clay soils

Y. Eyigun
Civil Engineer, Istanbul Greatercity Municipality, Technical Affairs Department, Istanbul, Turkey

K. Moroy
Geology Engineer, Yüksel Proje Uluslarasi AŞ. (Consultant Company for Istanbul Metro Project) Istanbul, Turkey

A. Saglamer
Prof. Istanbul Technical University, Head of Soil Mechanics & Geotechnical Engineering Department

ABSTRACT: In Yenikapi area where lies in Yenikapi-Taksim Section of Istanbul Subway Construction, the umbrella arch method and other supporting elements are used in clay soils. In order to minimize the deformations those occur during tunnel excavation in clay soils the excavation is made as upper and lower parts and the distance and duration between these two stages are kept short. As soon as the lower part excavation is finished the ring is must be completed and all the cross section must be transformed to a circular shape. Controlling deformations with geotechnical measurements during construction in NATM is very important. The success of the excavation and supporting method is related with the results of the deformation measurements before, during and after the excavation. When high deformations are measured the excavation is strengthened with further means such as temporary linings and increased number of support elements.

1 INTRODUCTION

Umbrella-Arch method and other extra reinforcement elements have been utilized for the tunnels that are bored in clay ground at Yenikapi Section at the construction of Yenikapi-Taksim route of Istanbul Metro administered by Istanbul Greater City Municipality.

In order to limit deformations below the boundary values and at minimum level when boring tunnels at clay grounds, the distance between excavation levels must be short at tunnel boring that is performed as upper half and lower half at two levels; the ring must be completed by excavating the lower half quickly and also the cross-section of the tunnel must be brought to circular shape.

During boring tunnels at rocky environment with the classical New Austrian Tunneling Method, advancing with leaving the middle section unexcavated for tunnel face stability provides benefit without any risks, whereas moving ahead by leaving the core at soft (clayey) grounds, the distance between excavation grades increases and the time to put the tunnel cross-section into circular shape gets longer and undesired deformations occur. In order to avoid this situation, excavation should not be done at clay grounds by leaving the middle section unexcavated for the tunnel face stability.

2 ISTANBUL METRO TAKSIM-YENIKAPI SECTION CONSTRUCTION

Metro construction between Taksim and Yenikapi constitutes an important section of Istanbul metro system. The route is 5200 meters from Taksim point of the commissioned Taksim – 4. Levent Metro to Yenikapi. This route with four stations is composed of the following sections:

- Around 3500 m. A-type tunnel (double track). These are the main-track tunnels with cross-sectional area of 36 square meters.
- 230 m long C-type single track tunnel. It has a cross-sectional area of 78 square meters and it has been designed to be at the junction of tracks.
- About 500 m P-type platform tunnels. Tunnel is 64 square meters and it is used at drilling station tunnels.
- 115 m excavation with retaining wall and backfill. (cut and cover).
- 850 m Golden Horn Transit Bridge.

3 GEOLOGY OF YENIKAPI-TAKSIM ROUTE

The parent rock at Yenikapi-Taksim route that is being constructed at present for Istanbul Metro is

Copyright © 2005 Taylor & Francis Group plc, London, UK

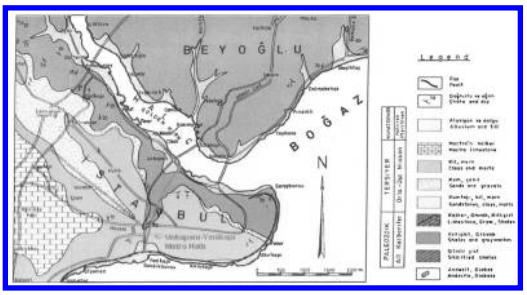


Figure 1. Geological plan of Istanbul Metro construction site.

Thrace (Trakya) Formation with carboniferous age (about 200 million years).

The construction between Unkapani-Taksim is completely bored inside Thrace Formation as shown Figure 1 upper region. In this section, there is a Backfill Ground (artificial filling) over Thrace Formation with a thickness between one to five meters. Also in this region, there are Diabase dikes here and there within Thrace Formation. Diabase dikes have also been found at tunnel excavation elevation.

At Yenikapi region of Yenikapi-Unkapani construction, extremely consolidated, very solid-hard Miocene aged (around 5 million years) Suleymaniye Clay (Gungoren Formation) with a thickness of five to fifteen meters is present above Thrace Formation. Over this layer, Loose-Medium tight Sandy and Graveled Alluvium containing water is present and its thickness is around five to fifteen meters. Over alluvium is Backfill Ground with thickness from four to seven meters.

4 GEOTECHNICAL MEASUREMENT STUDIES

The geotechnical measurement studies for Yenikapi-Taksim section of Istanbul Metro consists of two groups: Inside the tunnels and over the surface shown Figure 2.

4.1 *Geotechnical measurements at the tunnels*

- Convergence measurements inside the tunnel
- Opto-trigonometric measurements inside the tunnel
- Rock bolt load cells
- Hydraulic pressure cells
- Tension meters
- Drawing of the tunnel face geology

4.1.1 *Convergence and opto-trigonometric measurements in the tunnel*

The convergence measurements are done by an extensimeter with 0.01 mm sensitivity in order to observe

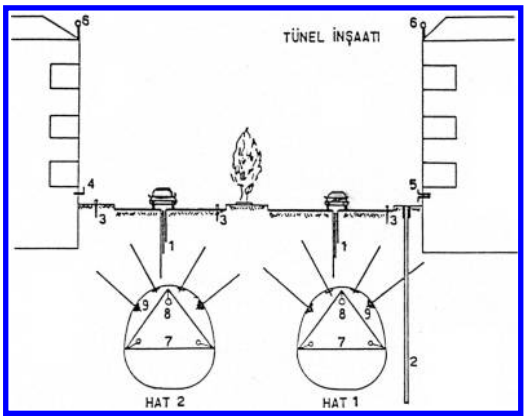


Figure 2. A general view of geotechnical instruments (1. Extensiometre, 2. Inclinometer, 3–5. Surface and building settlement rods, 6. Reflector, 7–8. Convergence 9. Rock bolt load cell.

relative movements of the tunnel ceiling and walls whereas opto-trigonometric measures are performed in order to measure the absolute horizontal and vertical movements of the walls.

Both of the measurement methods are carried out by using five measurement bolts located one on the ceiling and two at each of the walls.

The special measurement method designated for the convergence measurements of Istanbul Metro has provided reliable determination of the deformations. In classical measurement method, convergence bolts are driven into the finished structural wall concrete surfaces and relative time-dependant deformations are measured. In Istanbul Metro, these bolts are the rods that were welded to the shorings and the absolute deformations made by shorings were measured optically as soon as they were placed (x-y-z axes).

4.1.2 *Rock bolt load cells*

They are used to examine the tension changes at rock bolts. Main principle is just like the load cells in anchorages. However, dimensions of load cells are smaller due to the fact that pre-tension force applied to the rock bolts is lower.

The frequency of measurement is configured by checking the distance between measurement point and tunnel face, just like the convergence and opto-trigonometric measures.

4.1.3 *Hydraulic pressure cells*

They are placed in order to observe the radial and tangential tensions applied to shotcrete.

The measurements are obtained according to the distance between measurement point and tunnel face.

Copyright © 2005 Taylor & Francis Group plc, London, UK

4.1.4 *Tension meters*

Tension meters are used to evaluate the concrete deformations at foundations, bridges, dams, nuclear power plants and tunnel coatings.

4.2 *Geotechnical measurements on the surface*

These measurements are used not only for measuring the deformations that can occur during tunnel excavations, but also for measuring the deformations that may occur at open excavation constructions like station constructions.

- Rod Extensimeter
- Inclinometer
- Surface and building settlement measures
- Load cells with anchorage disks
- Reflector
- Crack measurer
- Optical measurements at station walls

4.2.1 *Rod extensimeter*

They are placed into a bore in order to observe vertical movement of the ground. In general, they consist of three levels. The lowest level is placed into the bore in a way to be one meter over the tunnel ceiling. The location of other levels is determined in accordance with the geological structure. The number of the levels can be increased or decreased when needed. The measures are taken from the extensimeter head placed on the surface.

4.2.2 *Inclinometers*

The inclinometers measure the horizontal displacements every 0.5 meters, in the special guiding pipe placed along the bore that is excavated from the surface to 1 meter below the excavation base. They are used to determine the horizontal ground movements around the tunnel and open excavation area.

4.2.3 *Surface and construction settlement measurements*

Settlements are measured by bolts driven to the surface and buildings. For this job, measurement cross-sections are placed on the surface every 25 meters in a way to be vertical to the axes of the tunnels.

The frequency of the measurement is determined according to the measurement cross-section of the tunnel face, similar to rod extensimeter measurement. However, the settlements at the station regions are obtained every day or once in every few days in accordance with the critical levels.

4.2.4 *Load cells with anchorage disk*

These are cylindrical devices connected to an oil-filled manometer that are placed at the anchorage heads in order to observe the tensile forces at the anchorages. Every cell is tested and calibrated in laboratory before placement. After the placement, measurements are obtained daily.

4.2.5 *Optical measurements at station walls*

Measurements are obtained to follow the displacements of the walls for which primary support processes have been completed. Measurements are performed by measuring the distance and angle from a fixed point.

Measurements are obtained daily or once in every few days in accordance with the dimensions of the displacements.

4.3 *Assessment of measurements*

During the excavation of the tunnels, tunnel face is examined at every phase of the excavation and engineering geology characteristics observed here are recorded in the "Underground Excavation Geotechnical Information" form.

All geotechnical measurements, measurement devices and their characteristics have been outlined in the project layout. However, additional measurements may be performed besides defined measurements in the layouts if required.

Displacements obtained with rod extensimeter, convergence, opto-trigonometric, surface and building settlement measurements with respect to tunnel progres are presented in graphical format through computer programs. Through these softwares, increases or decreases in tension at load cells may also be displayed in graphical format. Moreover, this software provides monitoring of graphics for tangential and radial tensions at shotcrete.

5 TUNNEL EXCAVATION SUPPORT TYPES IN NEW AUSTRIAN TUNNELING METHOD

The essential parameters in determining excavation support types are stability of the rock that is being excavated, thickness of the covering arch over the tunnel, quality of the buildings or structures along the route of the tunnel and the regions within the tunnel where stresses have been especially intensified during project phase.

The structural characteristics of the ground constituting the tunnel face and water content determine the stability. If the stability is low, related reinforcement support is increased. In the same manner, cover thickness is indirectly proportional to the excavation support amount. Intensification of the tension inside the tunnel and characterization of surface constructions as excessive are directly proportional with increasing the excavation support ratio.

Copyright © 2005 Taylor & Francis Group plc, London, UK

Table 1. Excavation support types for different soils.

Soil	A1 Solid rock	A2 Medium-solid rock	A3 Weak rock	A4 Soft Ground
Steel shoring	No	Yes	Yes	Yes
Wire mesh	Single layer	Single layer	Double layer	Double layer
Shotcrete	10–15 cm.	20 cm.	25 cm.	30 cm.
Rock Bolt	4–5	6–7	7–8	7–8
Slide Rod (quantity)	No	12 (max)	20 (max)	30 (max)
Each step	1,5 m (max)	1.0–1.2 m	0.8–1.0 m	0.6–0.8 m

In the Table 1, excavation support types are shown with characteristics and differences of reinforcement elements.

6 APPLICATION OF NEW AUSTRIAN TUNNELING METHOD ON CLAYEY GROUNDS (MODIFIED UMBRELLA-ARCH METHOD)

Undesired deformations exceeding project limit deformation values may occur while boring tunnels by using classical version of New Austrian tunnel boring method on clay and other soft ground environments.

Umbrella-Arch system has been used as the main element of Modified New Austrian Tunnel Boring method at soft ground environment and in this way, to reduce deformations inside the tunnel and on the surface have been aimed below the limit deformation values.

Umbrella Arch method comprises driving umbrella pipes with Φ144 mm. diameter and 9.00 meter length – through the tunnel ceiling section with an angle of 6–8° every 6 meters as driving the tubes and filling-in with injection as given in Figure 3. Due to the fact that holes of umbrella pipes are opened with a 130 mm auger, both inside of pipe and the region between outer surface of pipe and well wall is filled with injection solution during injection work.

Soil nails are driven to the tunnel face as additional reinforcement elements of this method. Holes of soil nails are bored again by a 130 mm auger with an angle of 8°–10°; deformed steel with Φ14 mm. diameter (16 to 24 pieces) and 12.00 meter in length; the region between steel and well wall is filled with injection.

The umbrella pipes compensate the pressure applied to the tunnel ceiling and moreover, it is possible to apply injection to the periphery of the pipe and cavities at

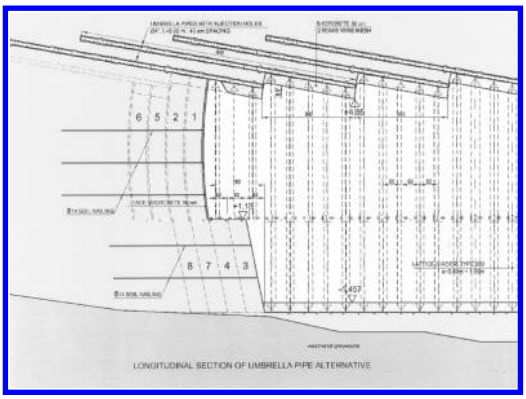


Figure 3. Excavation-support profile with Umbrella Arch pipe.

foundation as they are perforated. Soil nails function as anchorage for blocking the movement applied horizontally on the tunnel face. Tunnel face is covered with 5 cm. shotcrete in progressive steps.

In Umbrella Arch method, excavation is performed at three levels at main track tunnels and maximum distance between excavation levels is 2.40 meters. Furthermore, 6-meter long "Self Drilling Bolts" driven to shoring base have great importance for providing stability. Following primary and secondary level excavations, these bolts that are driven to shoring base with an angle of 45° function as punching. In this way, shoring is prevented from going downward within clayey ground.

Umbrella-Arch is an excavation method suite that should be considered along with other reinforcement elements. The procedure to be carried out is as follows:

1. Drawing the excavation tunnel face
2. Placing tunnel face soil nails and performing the injection
3. Boring a hole at the tunnel face for Umbrella-Arch pipes; installation and injection of U.A. pipes.
4. Performing Excavation + Reinforcement.

The purpose of three-level excavation is decreasing the cross-section of excavated surface and decreasing the area of application thereby.

All these processes performed to reach 6 meters progress take approximately 7 (seven) days.

7 MODIFIED TYPE OF NATM AT ISTANBUL METRO WITH FIELD APPLICATIONS

Excavation of Yenikapi tunnels at Istanbul Metro construction along Yenikapi-Unkapani route has started with the classical version of New Austrian Tunnel Boring Method. However, undesirable deformations

Copyright © 2005 Taylor & Francis Group plc, London, UK

have occurred in the clayey ground environment containing especially high-activity minerals.

7.1 *Main track (A-Type) tunnel excavations*

Excavation work has commenced in main track tunnels (A-Type) of Yenikapi Shaft by considering tunnel deformation limit values.

By placing special shorings (4 shorings placed as one within the other with 40 cm. intervals and repeating the same process in the lower half and by applying 50 cm. thick shotcrete) in the approach tunnel entrances of both tracks, excavation has commenced at Km: $4 + 564_{45}$ for H1 Unkapani tunnel and at Km: $4 + 628_{44}$ for H2 Unkapani tunnels. Progress has continued in both tunnels with progress steps of 0.80-0.60-0.80 meters after the 1.20 meter entrance structure. In order to distribute the loads of shorings, fender with 25 × 20 cm. dimensions has been placed behind the shoring panels in addition to 20 × 20 cm. shoring panels. The application was designated as 10 m. upper half excavation progress followed by 5 m. excavation of lower half. In this case, crack formation in shotcrete has occurred at the completion of excavation of lower half, similar to the case in approach tunnels. Shotcrete thickness here was 25 cm. Therefore, 5 m. lower half excavation process has started in H1 Unkapani tunnel following 8 m. upper half excavation at Km. $4 + 474_{60}$. In this way, the distance between upper half and lower half has shortened as shown Figure 5. Due to the obligation of advancing with leaving the middle section unexcavated in the tunnel face, it was not possible to keep upper and lower halves in alignment. After this application, it has been observed that crack formation in shotcrete for the regions in question is still evident. However, it has also been observed that rate of deformation increase has stopped after completion of lower half excavation and the increases have been recorded as 1 to 2 mm. For consequent operations, shorings have been applied at each step in the lower half as well in the 20-meter section between Km: $4 + 589_{40}$ and $4 + 609_{40}$ of H1 Unkapani tunnel to stop crack formation in shotcrete. Up to this section, shorings were placed as skipping one piece after the other (one full after one empty). Following this application, crack formation stopped in the boundary of lower half shotcrete endpoint. In the lower half, 25 cm. shotcrete was applied. The same application was also used in H2 Unkapani tunnel.

In the meantime, increases have been observed about level of deformation increase that had stopped at the 1 mm/week criterion after completion of lower half excavation. However, deformation values according to convergence measurements (90 mm. total contraction at sides) were very close to limit values whereas limit values measured by topography team were exceeded (122 mm. total contraction at sides). In this case, cross-section clearance check has been performed to reveal the actual condition of deformations and to check whether limit values have been exceeded or not. On June 15, 2000, cross-section clearance check was performed at 5 m. intervals in H1 Unkapani tunnel and it was observed that contraction has indeed exceeded the limit values. By placing convergence measurements to the closest points of the top of cross-section clearance measurements, it was observed that numerical values of deformations are different but geometrical appearance at both measurements look similar. Tunnel excavation has started with these increased deformation margins at Km: $4 + 630_{00}$ for H1U and at Km: $4 + 654_{40}$ for H2U. Furthermore, shorings have been interconnected with 100 mm. (U) profiles at shoring bases so as to make them work together.

Now that the desired values below limits have not been reached with all these actions, radical changes have been implemented, i.e. requesting U.A. preliminary reinforcement, avoiding unexcavated middle section (core) (see Figure 4 and 5) arranged at tunnel face and providing support with soil nail, driving 6 m. bolts to shoring base. The distance between upper and lower part excavation was limited maximum 2.4 m.

Modified Umbrella Arch method detailed in section 5 above was implemented in Yenikapi tunnels starting from Km: $4 + 650_{40}$ and Km: $4 + 675_{40}$ for YH1U and YH2U tunnels respectively.

Excavation works have been completed with Umbrella-Arch method in (A) Type tunnels with average deformation values at inside of the tunnel of 2.5 cm. and 1 cm. for YH1U and YH2U tunnels respectively. These values may be observed in deformation measurement graphics as shown Figure 6. The view inside tunnel after excavation-support and inner reinforced concrete lining is shown in Figure 7.



Figure 4. Excavation with leaving core.

Copyright © 2005 Taylor & Francis Group plc, London, UK



Figure 5. Excavation without leaving core.

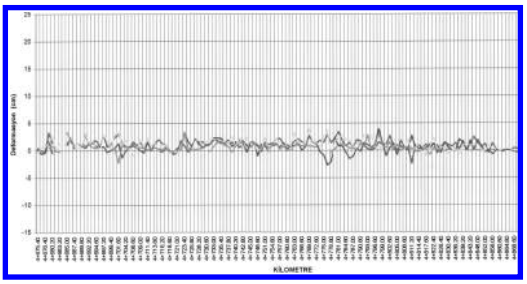


Figure 6. Deformation grafic after extra supports.

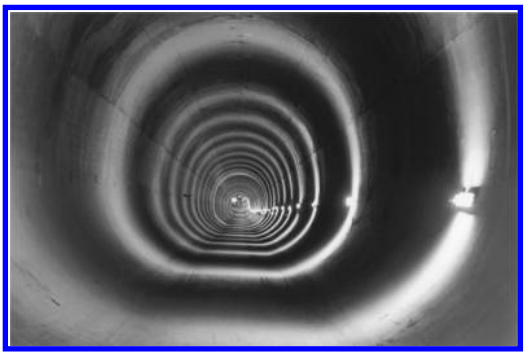


Figure 7. A view from same tunnel after inner lining.

8 CONCLUSIONS

Deformations in clayey ground which occurred during tunnel boring by New Austrian Tunnel Boring Method that could not be prevented were stopped within the same clayey environment by utilization of Modified New Austrian Tunnel Boring Method.

1. Tensions applied on tunnel ceiling have been transferred to sides and soil via umbrella pipes with injection in Umbrella Arch application.
2. By driving soil nails to tunnel face, obligation of leaving unexcavated middle section at tunnel face has been eliminated. In this way, ring has been completed by shortening the distance between upper and lower half excavations and circular formation of cross-section has been constituted. Furthermore, possible activity from tunnel face to excavation area has been prevented.
3. Excavation steps has been maintained as short as 0.60 m. and in this way, through fast completion of excavation for single shoring, it has been possible to cover clay surfaces with shotcrete in a short time and thereby, longer exposure to air has been prevented.
4. Exposure of clay surface to air has been prevented by application of 5 cm. shotcrete to excavation face at each shoring step and furthermore, this has provided stability for tunnel face.
5. Downward movement of shoring base into the clayey ground has been prevented by mutual driving of 6.00 m SDBs (Self Drilling Bolt) from shoring bases and anchoring them to the rock (Thrace Formation) 2 m. below the tunnel basement elevation and consequently, deformation occurrence has been considerably prevented. Occasionally, holes with 125 mm. diameter have been drilled with 45^0 angle from shoring base in application phase instead of SDB bolts and inside these holes, 26 mm. L = 5.00–6.00 m. tor steel is placed and filled with injection; these soil nails have been used functioning as punching bolts.
6. Various geotechnical measurement elements have been applied and collected-evaluated all data very sensitively.

Due to the features outlined above, Modified New Austrian Tunnel Boring Method has been utilized as a successful system for preventing excessive deformations in clayey grounds.

REFERENCES

1. Ketin, I. 1988. Structural Characteristics of Carboniferous Thrace Formation in Istanbul Region, Engineering Geology Journal, Issue 11, Istanbul
2. T.M.M.O.B. 1994. Chamber of Mining Engineers, 1994 First Symposium of Underground Excavations in Transportation, Chamber of Mining Engineers Publication, Macka – Istanbul
3. Yalcin, A. 1994. Istanbul Metro Construction Works 1992–1993 Period Technical Report, Istanbul

Copyright © 2005 Taylor & Francis Group plc, London, UK

Advanced grouting techniques for tunnel constructions under sensitive buildings

Ulvi Arslan
Technical University Darmstadt, Germany

Wolfgang Krajewski
CDM Consult AG/ University of Applied Sciences Darmstadt, Germany

Peter Ripper
CDM Consult AG, Darmstadt, Germany

ABSTRACT: In urban areas the overburden of tunnels sometimes have to be minimized to only few meters in an increasing number of projects. In consequence the limitation of deformations due to the tunnel construction is getting more important but also more difficult. In some cases an usual NATM- advance of the tunnel is not possible, even using strong supporting systems. However, it is possible to compensate unallowable large settlements by grouting techniques, as will be shown in the present paper.

The procedure demands a careful design and survey. Due to the three- dimensional geometry and the time-dependency of tunnel- driving and grouting work, numerical calculations are an important and even indispensable part of the engineering work. In the paper, two difficult projects are presented, where grouting techniques have been executed respectively designed to allow a safe tunnel construction.

1 TECHNIQUE OF COMPENSATION GROUTING

Compensation grouting belongs to the group of the so-called crack or fracture injection techniques. Contrary to fill injections where the voids of the subsoil are filled, during fracture injection artificially created joints are filled with a hardening cement based suspension. Fracture injection leads to a volume increase in the subsoil and causes a lifting of the ground surface.

The method of compensation grouting is based on repeated injections of small volumes of grout in regularly distributed boreholes. The total lifting of a building is the result of many partial heaves in the millimeter range (*Raabe & Stockhammer, 1995*).

The injection boreholes usually are fan-like distributed in the subsoil below the building that is going to be lifted. After the drilling of the boreholes is finished, steel or plastic pipes with packing rings made of rubber are installed into the boreholes. The annular space between the hole wall and the pipes is filled by a hardening suspension.

For the injection a double packer is placed at a chosen packing ring. The double packer is fastened by compressed air and suspension is injected into the internal space between the double packers.

After opening of the packing ring, and breaking of the hardened suspension in the annular space, fractures in the subsoil are created and filled with suspension. The injection volume is limited and the injection pressure result from the injection rate.

Electronic hydrostatic tube balances usually measure the heaves and the subsidence of settlement-sensitive buildings. The hydrostatic tube balances, which are known for a high standard of measuring accuracy, are connected on-line with the control desk. By that method the heaves and the subsidence of the building are continuously interpreted. The results are the basis for further injections (*Wittke, Wawrzyniak & Hardt, 2001*).

2 NUMERICAL SIMULATION OF COMPENSATION GROUTING

Usually compensation grouting is designed and carried out using empirical analysis methods and experience from former projects. However, the displacements and stress changes due to grouting cannot be evaluated, even not estimated using such methods. In practice, numerical calculations, which simulate the grouting process are indispensable (*Krajewski, Wawrzyniak, 2004*).

Copyright © 2005 Taylor & Francis Group plc, London, UK

The numerical model is developed to fulfil a variety of demands. On the one hand the design parameters, injection volumes and grouting pressure used in the model must agree with the construction. Also the subsidence of the building due to tunnel driving as well as the lifting of a building by compensation grouting should be simulated realistically. The stress changes in the tunnel lining and in the foundation of the building should be computed as well.

One of the fundamentals of the model is the question for the direction in which the fractures occur in the subsoil. For answering the question a single borehole is considered and the initial stress state is simulated. In most cases the horizontal principal stress σ_H is smaller than the vertical principle stress σ_V, which results from the load of the overlying ground. As a result of the grouting pressure inside the borehole, tensile stress occurs in tangential direction in the subsoil around the borehole. In the top and the bottom of the borehole, the tensile stress is higher than beside the borehole. Therefore, predominantly vertical fractures develop. Due to the vertical fractures the subsoil becomes compressed in a horizontal direction and the principle horizontal stress increases until a secondary stress state is reached, in which $\sigma_H > \sigma_V$. The injections that lead to the secondary stress state are the so-called contact-injections (fig. 1).

When the borehole is strained by injection pressure, the highest tensile stress occurs in the subsoil beside the borehole. Predominantly horizontal fractures develop. These injections are the essential heave injections.

Another fundamental question is the length of the fracture caused by the injections. For the determination of the length of the fractures used in the model, a separate FE-calculation has to be done. The FE-net copies the borehole as well as the vertical and the horizontal fractures. A surface load at the inside of the elements that replicate the fracture simulates the injection pressure. At the same time, a very low stiffness is assigned to the fracture elements. The injection volume results from the spreading of the fracture elements. In the computation, the fracture extends a certain amount at every calculation step. The computation is finished when the spreading of the fracture elements is the equivalent of the limited injection volume. Therefore the length of the fracture results from the last calculation step.

From the above-mentioned fundamentals an analysis model with horizontal and vertical fractures of determined length can be derived (*Wawrzyniak, 2001*).

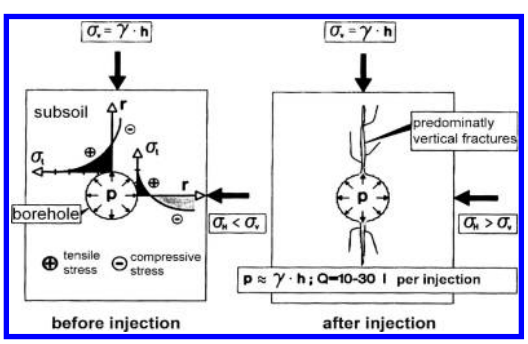


Figure 1. Fractures in the subsoil during contact injections.

3 EXAMPLES FOR APPLICATION

3.1 *Undercrossing a high stack warehouse by the Limburg tunnel*

The application of the method, will be explained by a compensation grouting carried out during the construction of the Limburg Tunnel, a part of the Cologne-Rhine/Main high-speed railway line in Germany (*Krajewski et al., 2000*). The tunnel is 2400 m long and has been constructed using the NATM-method. The subsoil consists of Devonian slates and quarzites respectively of tertiary clay and silt (fig. 2).

Near to the southern portal, the tunnel undercrosses an industrial area with several sensitive high stack warehouses. The overburden of the tunnel amounts only to 11.7 m, that means less than the width of the excavation (15.2 m, fig. 3). In the present area, the

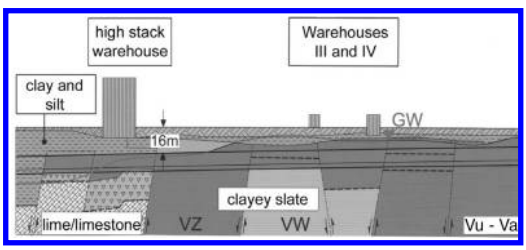


Figure 2. Limburg tunnel, longitudinal section.

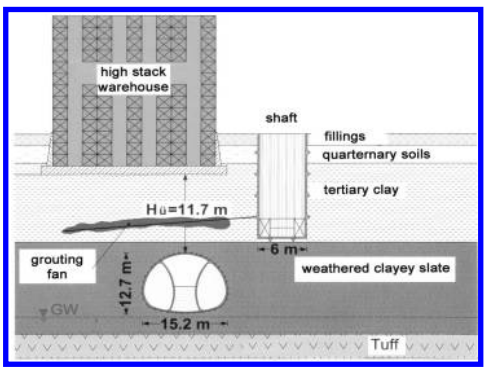


Figure 3. Undercrossing of a high stack ware house by the Limburg tunnel, cross-section.

Copyright © 2005 Taylor & Francis Group plc, London, UK

tunnel has been driven in weathered slates. However, the overburden consists mostly of stiff clay (fig. 3).

The procedure needs one ore more fans of tube-à-manchettes, which are bored horizontally from special shafts. At the Limburg tunnel two fans have been used, which have been installed from two separate shafts (figs. 3, 4). The shafts have a diameter of about 6 m and a depth of approx. 15 m. Cement suspensions are used as grouting material. In a first grouting- step, the soil is cracked in horizontal planes and prestressed vertically. During the following tunnel advance, the settlements are measured with high precision by a hydraulic and geodetic leveling systems (for example: hydrostatic tube balance), which reports the occurring deformations automatically. Subsequently, the deformations are compensated by selective grouting of different quantities of cement-suspension. The groutings effect heavings, which are also documented by the leveling system. Dependent on the measurements, the injection pressure and grouting volumes are managed. However, it is to consider, that the grouting works effect stress changes in the tunnel lining as well as in the foundation of the building. These demands cannot be not evaluated by general measuring systems. Hence, numerical calculations, which simulate the grouting process are necessary, to avoid cracks and damages in the constructions.

The steps of the numerical simulation copy the different phases of injection and tunnel heading (*Krajewski, Wawrzyniak, 2004*). The injection pressures and the resulting grout volumes of the numerical calculation are similar to the pressures and volumes that were carried out during the construction of the Limburg tunnel. Moreover the calculated heaves and subsidence agree with the heaves and subsidence measured during the heading of the tunnel. The numerical calculation shows, that stress changes caused by the injections occur in the shotcrete lining of the tunnel. At the crown of the lining the bending moments caused by the injections are twice as high as without injections. The normal stress increases, especially in the sidewalls of the tunnel lining, amount to about 25%.

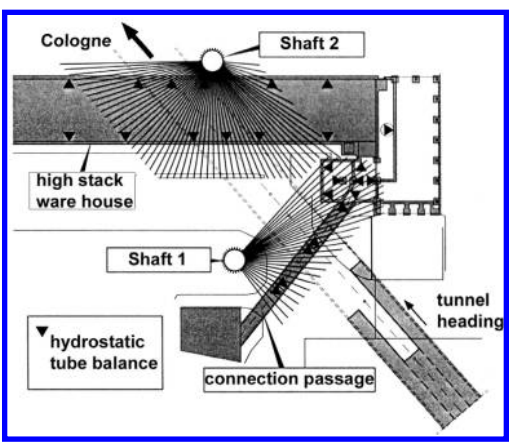


Figure 4. Undercrossing of a high stack ware house by the Limburg tunnel.

3.2 *Undercrossing of the Juridicum-Passage building by the "City-Tunnel" in Leipzig*

In the city of Leipzig, a hydro-shield full-face cutter will drive the new railway "City-Tunnel" (*Scheffler et al., Kleffner et al., 2004*). Numerous buildings have to be undercrossed by the tunnel, which consists of two parallel tubes. As the distance between tunnel lining and foundations is rather small at several estates, technical means have to be chosen to support the buildings and to avoid damage. At the Juridicum-Passage building near to the market place of Leipzig, an extraordinary difficult situation has to be solved. The building consists of several upper floors and four underground floors. The bearing construction is very complex due to several halls, which interrupt the concrete slabs. At the foundation level, the tunnel passes within a distance of only 1.4 m. The subsoil consists of river gravels and the so- called Bitterfeld sands.

It is agreed by contract that differential settlements of more than 2 cm respectively $>$1:800, due to the tunnel driving, have to be avoided or compensated by technical means. The probability of inadmissible deformations and the effect of technical countermeasures, especially the advantage of heave grouting, have been investigated by extensive three-dimensional Finite-Element calculations. As a characteristic result of the investigations fig. 5 shows the settlements due to tunnel driving as well as the corresponding principal stresses acting in the subsoil around tunnel and building foundation. It is obvious that the settlements of the building are rather small and amount only to $\leqslant$1.5 cm. However, the fact that the vertical stresses below the overhanging part of the building are reduced significantly, may be critical for the stability of the building, as the necessary bedding of this part of the foundation is reduced almost completely. The investigation of the concrete structure shows inadmissible loadings. In a further calculation step, the effect of heave grouting has been evaluated. The injections will be performed using a horizontal grouting curtain, which is already installed between the roof of the inner tunnel tube and the overhanging part of the building. The grouting causes a pre-stressed zone between tunnel and building. Hence the necessary bedding of the foundation can be generated (fig. 6). Moreover, it is obvious that no significant settlements of the building occur as the deformations due to tunnel driving are compensated by the injections. However, this positive result is accompanied by

Copyright © 2005 Taylor & Francis Group plc, London, UK

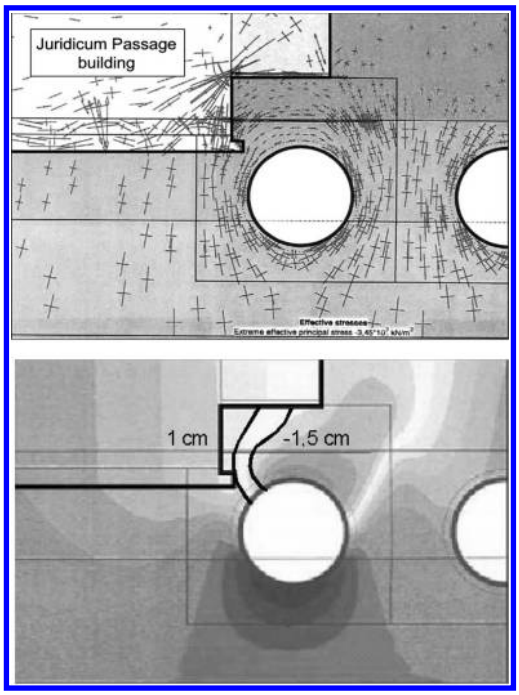


Figure 5. Undercrossing of the Juridicum-Passage building by the "City Tunnel" in Leipzig, principal stresses and settlements due to tunnel driving (FE- calculation).

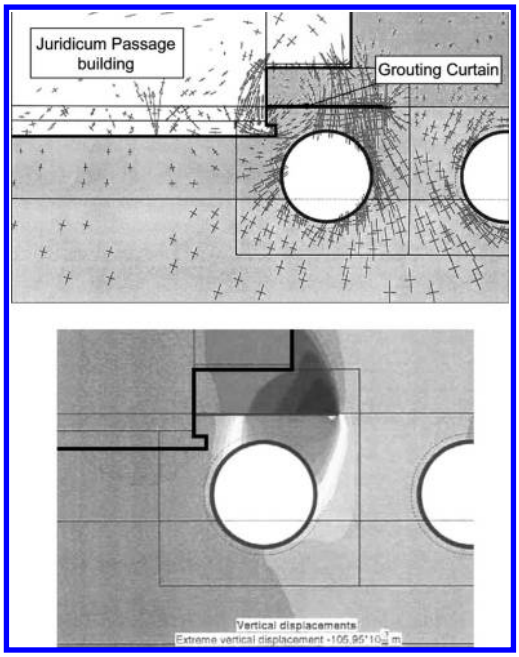


Figure 6. Calculated principal stresses and settlements due to tunnel driving and heave grouting.

a considerable additional loading of the tunnel lining. This fact is illustrated in fig. 6 by the red coloured area between tunnel and grouting curtain. This area is characterized by large settlements due to the injection pressures, which cause corresponding large bending moments in the tunnel lining.

REFERENCES

Arslan, U.; Krajewski, W.; Ripper, P. 2003. Risk and damage prevention in shallow tunneling, International Conference on Tunneling and Underground Space Use, Istanbul, Turkey.

Krajewski, W. 2004. Numerical calculations in tunnel engineering, Festschrift zum 60. Geburtstag von Herrn Prof. Dr.-Ing. P. Vermeer, Balkema-Verlag, Rotterdam, Netherlands.

Raabe, E.W. & Stockhammer, P. 1995. Einsatz von Soilcrete und Soilfrac im Tiefbau – Möglichkeiten und Grenzen beider Injektionstechniken. 10. Christian Veder Kolloquium, Graz.

Wawrzyniak, C. 2001. Berechnungsgrundlagen für den Entwurf und die Ausführung von Hebungs-injektionen. WBI Print 10, Hrsg. Prof. Dr.-Ing. W. Wittke Beratende Ingenieure für Grundbau und Felsbau GmbH, Aachen, Verlag Glückauf, Essen.

Krajewski, W.; Hardt, D.; Hosang, K.-H. 2000. Gerhardt, P.; Gebirgsbeschreibung für den Tunnelbau nach Funktionaler Ausschreibung – Erfahrungen aus der geotechnischen Bauüberwachung der ICE-Neubaustrecke Köln-Rhein/Main, 26. Baugrundtagung, Hannover.

Wittke, W.; Pierau, B.; Wawrzyniak, C.; Hardt, D. 2001. Hebungsinjektionen beim Auffahren des Limburger Tunnels der Neubaustrecke Köln-Rhein/Main unter dem Hochregallager der Firma TetraPak. Taschenbuch für den Tunnelbau 2002, Verlag Glückauf, Essen.

Krajewski, W.; Wawrzyniak, Chr. 2004. Compensation of settlements due to tunnel driving by grouting cement suspensions, EUROCK 2004 & 53rd Geomechanics Colloquium.

Scheffler, H.; Mißling, K.; von den Berg, M.; Spang, R. 2004. Geotechnische Verhältnisse im Zentrum von Leipzig und deren Bedeutung für Planung und Ausführung des Vorhabens City-Tunnel Leipzig, 28. Baugrundtagung, Leipzig.

Kleffner, H.-J.; Maidl, R. 2004. Baugrundtechnische Herausforderungen beim Bau des City-Tunnels Leipzig im Schildvortrieb, 28. Baugrundtagung, Leipzig.

Copyright © 2005 Taylor & Francis Group plc, London, UK

Improvement of wet-mix shotcrete performance by addition of High Reactivity Metakaolin

Gyu-Jin Bae, Soo-Ho Chang & Hyu-Soung Shin
Korea Institute of Construction Technology, Goyang, Gyeonggi-do, Korea

Hae-Geun Park, Myeong-Sub Lee & Jae-Kwon Kim
Samsung Engineering & Construction, Sungnam, Gyeonggi-do, Korea

Jong-Pil Won
Konkuk University, Seoul, Korea

ABSTRACT: High-performance shotcrete lining is necessary to improve the durability of a tunnel and to apply the single-shell tunneling method. Among a lot of shotcrete admixtures, pozzolan materials such as silica fume have positive effects on increasing the strength and the durability of shotcrete. In addition, a cement-based accelerator is much faster in setting time and more eco-friendly than conventional accelerators. This study aimed to improve wet-mix shotcrete properties by High-Reactivity Metakaolin (HRM) and the cement-based accelerator. To compare HRM with silica fume, dosages of each material were varied as 4% and 8% of cement weight. Moreover, HRM was blended with silica fume, and their binder was also set to 4% and 8% of cement weight. Setting time, compressive strength, flexural strength, permeability and freezing-thawing resistance were measured from each mixing condition. From the study, it was revealed HRM could be a substituting material for silica fume.

1 INTRODUCTION

High-performance shotcrete lining is highly in demand to improve the durability of a tunnel structure and to apply the single-shell tunneling method such as the NMT (Norwegian Method of Tunnelling) where shotcrete lining is a permanent support member.

Generally, accelerators and mineral admixtures are known to play a key part in improving shotcrete performance.

A lot of mineral admixtures such as fly ash, slag and silica fume with fine particle size improve concrete performance, and are becoming commonly used. Among them, the ultra-fine pozzolan material, silica fume, has been habitually used to make high-strength shotcrete since 1990s, especially in European countries (Dimmock, 1999). Addition of silica fume induces a pozzolanic reaction with cement's calcium hydroxide to produce additional calcium silicates that contribute to strength development, a reduction in permeability and durability improvement. As a result, silica fume increase fresh concrete cohesion and results in a lower rebound and improved pumpability (EFNARC, 1999).

However, silica fume with its large specific surface area makes shotcrete highly viscous and results in slump loss of unhardened concrete. Therefore, it is highly recommended to use silica fume with superplasticizer. In addition, its higher dosage decreases bleeding of unhardened concrete, and may induce plastic shrinkage cracks in early ages under a dry condition (Melbye, 2000). Especially, because the production of silica fume needs high electricity, it is totally imported from foreign countries in the countries such as Korea where electricity cost is very expensive. As a result, its unit cost is expensive, approximately 20 times higher than cement.

Recently, the use of High Reactivity Metakaolin (HRM) in concrete has shown effectiveness as close as to silica fume. Since HRM is its lighter color over silica fume, which makes it more suitable for applications related to repair and restoration. It has also been reported that in fiber reinforced concrete, mixes with HRM exhibit a greater post-peak energy dissipation capacity and a better fiber-matrix bond over silica fume (Bindiganavile & Banthia, 2001).

While silica fume is a by-product from an electric arc furnace used for manufacturing silicon metal or silicon alloy, HRM is derived from the calcinations of kaolin in the range of 600∼800°C. As a result, the variation of physical and chemical properties of HRM is smaller.

Copyright © 2005 Taylor & Francis Group plc, London, UK

In addition, Korea is abundant in kaolin, and the unit cost of HRM is much cheaper than that of silica fume.

Unfortunately, HRM has not been fully investigated in shotcrete. Bindiganavile & Banthia (2001) only verified the applicability of HRM to shotcrete. However, their study was restricted to dry-mix shotcrete that is not commonly used in tunnels and underground caverns.

It is generally reported that the conventional sodium silicate and aluminate type accelerators do harms to the human body and decrease long-term strength of shotcrete. Recently, alkali-free and cement mineral based accelerators were developed. It is known that they are eco-friendly, and do not decrease long-term strength of shotcrete.

The powder-type accelerator based on cement-like minerals such as calcium aluminate is actively used in Korea and Japan. The calcium aluminate based accelerator has a very quick-setting property and show no disadvantage in long-term strength development. Since the composition of the accelerator is close to cement, it does not do harm to the human body (Ishida et al., 1999).

This study aims to improve wet-mix shotcrete by HRM as well as calcium aluminate based accelerator. HRM was compared with silica fume to evaluate the applicability of HRM as a substitute for silica fume. In addition, the effects of HRM blended with silica fume on shotcrete properties were also investigated.

2 EXPERIMENTAL SETUP AND PROCEDURES

2.1 *Materials*

In this study, shotcrete materials were mixed in laboratory conditions. Although the characteristics of shotcrete materials mixed in laboratory might be different from those of sprayed concrete in field, it was judged that there might be no problems with simulating reactivity of shotcrete admixtures in laboratory.

The type of cement used in experiments was the ordinary Portland cement (OPC). Crushed rock with the maximum size of 13 mm was used as coarse aggregate. In addition, river sand with fineness modulus of 2.86, specific gravity of 2.6 and the percentage of water absorption of 0.67 was used as fine aggregate.

The basic properties of the calcium alumniate based ($C_{12}A_7$) accelerator used in this study are summarized in Table 1.

The pozzolan materials, namely, silica fume and metakaolin were used as an admixture to improve shotcrete performance. The content of SiO_2 in silica fume were over 85% (Table 2). Its average grain size and fineness were 0.2 μm and 240,000 cm^2/g respectively.

Fineness, specific gravity, 44 μm-passing grading and absorbed water content of HRM were 10,000 cm^2/g, 2.53, 90% and 0% respectively. The chemical composition of HRM is summarized in Table 3.

Table 1. Properties of the calcium alumniate based accelerator.

Main component	Type	True specific gravity	Bulk specific gravity	pH
Calcium aluminate	Light-gray powder	2.76	0.93	11.7

Table 2. Chemical composition of silica fume.

SiO_2	Al_2O_3	$K_2O + Na_2O$	$CaO + MgO$
Min. 90%	Max. 2%	Max. 2%	Max. 5%

Table 3. Chemical composition of HRM.

SiO_2	Al_2O_3	Fe_2O_3	TiO_2	K_2O	Na_2O	CaO	MgO
52%	40%	3%	0.4%	0.6%	0.4%	1.2%	0.5%

Table 4. Mixing conditions used in experiments.

Mixing condition	Unit weight (kg/m^3) W	C	Silica fume	HRM	S	a
P	205	420	–	–	1124	545
SF4	205	403.2	16.8	–	1124	545
SF8	205	386.4	33.6	–	1124	545
MK4	205	403.2	–	16.8	1124	545
MK8	205	386.4	–	33.6	1124	545
SM4	205	403.2	8.4	8.4	1124	545
SM8	205	386.4	16.8	16.8	1124	545

2.2 *Mixing design*

In the mixing design, slump, air content, water-cement ratio (W/C) and fine aggregate percentage (S/a) of unhardened concrete were set to 10 ± 2 cm, 4 ± 1%, 45% and 68% respectively. The dosage of accelerator was 5~6% of cement weight.

4% and 8% of cement weight were replaced by both of HRM and silica fume. In addition, binder dosages of HRM blended with silica fume were also set to 4% and 8% of cement weight, where dosages of HRM and silica fume were as same as each other (Table 4). The dosages of plasticizer for shotcrete material without and with pozzolan materials were 3,360 and 4,200 g/m^3 respectively.

Copyright © 2005 Taylor & Francis Group plc, London, UK

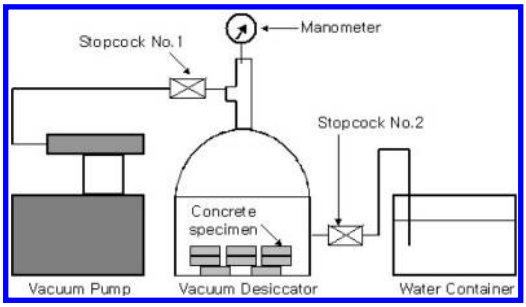


Figure 1. Pre-treatment of specimens before a chloride ion penetration test.

2.3 *Experimental procedures*

Setting time of unhardened concrete for the mixing conditions shown in Table 4 was measured by a penetration resistance needle (KS F 2436).

Uniaxial compression tests were carried out for 1, 3, 7 and 28-day aged specimens since they were first mixed in circular moulds with the diameter of 100 mm and the length of 200 mm (KS F 2405). For each day, compressive strength was measured six times. Specimens were water-cured in a curing room with constant temperature of 23 ± 2°C and relative humidity of 50%.

To measure flexural strength, specimens were cured in rectangular moulds with the size of 150 × 150 × 550 mm for 1, 3, 7 and 28 days (KS F 2408). For each day, flexural testing was carried out 3 times. As in uniaxial compression tests, specimens were water-cured in constant temperature of 23 ± 2°C.

Chloride ion penetration test (ASTM C 1202) was applied to investigate indirect permeability of shotcrete with different mixing conditions. Cylindrical specimens with the diameter of 100 mm and the length of 200 mm were prepared, and their middle part was cut into two parts (ϕ100 × 50 mm) by a diamond saw in 28 days. After cutting, entrained air in the specimens was eliminated in a desiccator by operating a vacuum pump during three hours. Then, the specimens were saturated again by supplying the desiccator with water and operating the vacuum pump during one hour, and then the specimens were submerged into water during 18 ± 1 hours (Fig. 1). After the pre-treatment procedure of the specimens was completed, they were fixed to the A.V. Cell (Applied Voltage Cell) where the positive (+) electrode was filled with a NaOH solution of 0.3 N and the negative (−) electrode was filled with a 3% NaCl solution (Fig. 2). Figure 3 shows the equipment to measure chloride ion permeability.

Then, electric charge was measured during six hours by supplying the specimens with a voltage of 60 V (direct current). Table 5 shows the indirect permeability of concrete depending upon different electric charges (ASTM C 1202).

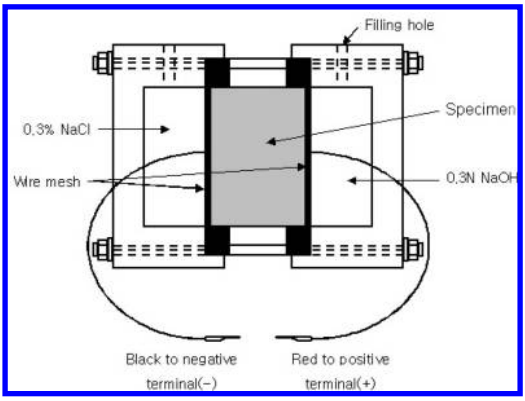


Figure 2. A.V. Cell to measure chloride ion permeability.

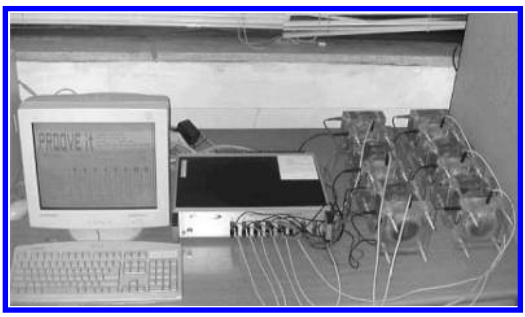


Figure 3. Equipment to measure chloride ion permeability.

Table 5. Criteria of chloride ion permeability.

Coulombs	Chloride ion permeability	Typical of
>4,000	High	High W/C ratio
4,000~2,000	Moderate	0.4~0.5 W/C ratio
2,000~1,000	Low	W/C ratio <0.4
1,000~100	Very low	Latex modif. con'c.
<100	Negligible	Polymer concrete

Freezing and thawing tests (KS F 2456) were carried out to investigate freezing-thawing resistance of shotcrete materials with different mixing conditions. The rectangular specimens with the size of 100 × 100 × 400 mm were prepared and cured in a curing tank with the constant temperature of 23°C during 14 days. Freezing stage to decrease the temperature in the middle of a specimen from 4°C to −18°C and thawing stage to increase the temperature to 4°C were repeated. Freezing-thawing resistance was estimated by measuring the relative dynamic elastic modulus of a specimen every 30 cycle (Fig. 4).

Copyright © 2005 Taylor & Francis Group plc, London, UK

3 EXPERIMENTAL RESULTS

3.1 *Setting time*

Independent of admixtures, the initial and the final setting time values from different mixing conditions were as close as to each other (Fig. 5). In other words, there was no retardation effect induced by dosing HRM and silica fume. The reason is why the setting mechanism is dominated not by admixtures but by the accelerator that accelerates the hydration of cement.

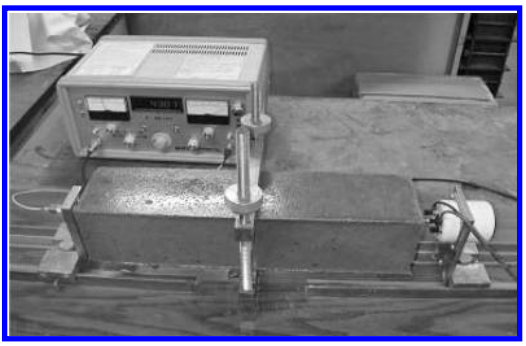


Figure 4. Equipment to measure the relative dynamic elastic modulus.

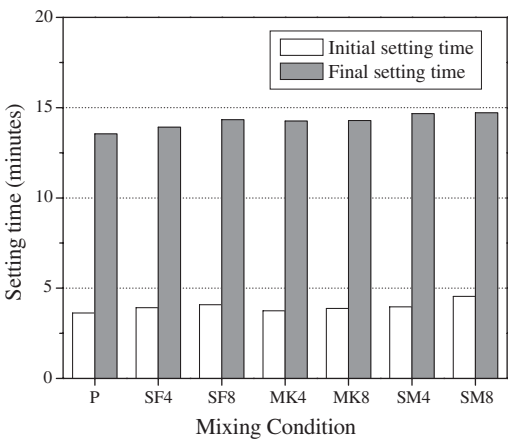


Figure 5. Initial and final setting time at different mixing conditions.

3.2 *Compressive strength*

In early ages when compressive strength of shotcrete is mainly dominated by the accelerator, compressive strength values were not so different from each other. However, in later ages, compressive strength obtained from the specimens mixed with HRM and silica fume is much higher than that from the specimens without admixtures (Fig. 6). The reason is why pozzolan materials such as HRM and silica fume react with calcium hydroxide formed during cement hydration and constitute C-S-H gel.

When the dosage of an admixture is 4% of cement weight, silica fume, HRM and HRM blended with silica fume increased compressive strength by 19.52%, 19.77% and 18.86% respectively. When the dosage of an admixture is 8% of cement weight, silica fume, HRM and HRM blended with silica fume increased compressive strength by 33.76%, 31.95% and 28.72% respectively. It shows that a higher dosage of an admixture makes shotcrete stronger and harder (Table 6).

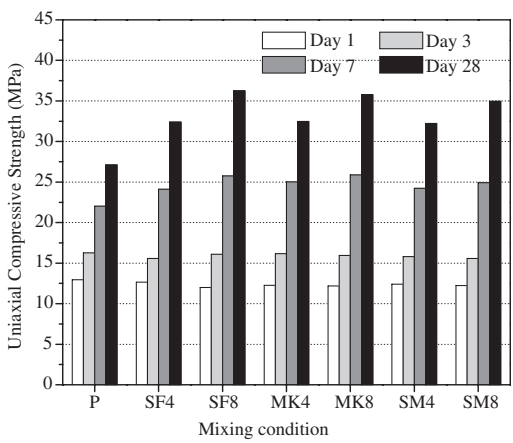


Figure 6. Compressive strength at different mixing conditions.

Table 6. Summary of compressive strength (unit: MPa).

Mixing condition	Day 1	Day 3	Day 7	Day 28
P	12.94 ± 0.23	16.27 ± 0.55	22.03 ± 0.79	27.10 ± 0.42
SF4	12.66 ± 0.32	15.57 ± 0.64	24.10 ± 0.30	32.93 ± 0.54
SF8	11.85 ± 0.51	16.10 ± 0.57	25.75 ± 0.60	36.25 ± 0.38
MK4	12.71 ± 1.43	16.16 ± 0.52	25.02 ± 0.39	32.46 ± 0.60
MK8	12.19 ± 0.51	15.94 ± 0.43	25.88 ± 0.43	35.76 ± 0.54
SM4	12.41 ± 0.82	15.66 ± 0.45	24.24 ± 0.99	32.21 ± 0.59
SM8	12.24 ± 0.30	15.57 ± 0.57	24.92 ± 0.54	34.94 ± 0.38

Copyright © 2005 Taylor & Francis Group plc, London, UK

However, it is recommended that the optimal dosage of an admixture should be determined by considering its economic efficiency and its effects on unhardened concrete.

Although the effect of silica fume on strength development was the best, strength differences between each mixing condition except the case without an admixture were not apparent.

3.3 *Flexural strength*

The effects of admixtures on flexural strength development are very close to those on compressive strength.

In later ages, flexural strength obtained from the specimens mixed with HRM and silica fume is much higher than that from the specimens without admixtures (Fig. 7).

When the dosage of an admixture is 4% of cement weight, silica fume, HRM and HRM blended with silica fume increased flexural strength by 12.29%, 11.11% and 8.75% respectively. When the dosage of an admixture is 8% of cement weight, silica fume, HRM and HRM blended with silica fume increased compressive strength by 20.80%, 17.97% and 16.08% respectively (Table 7).

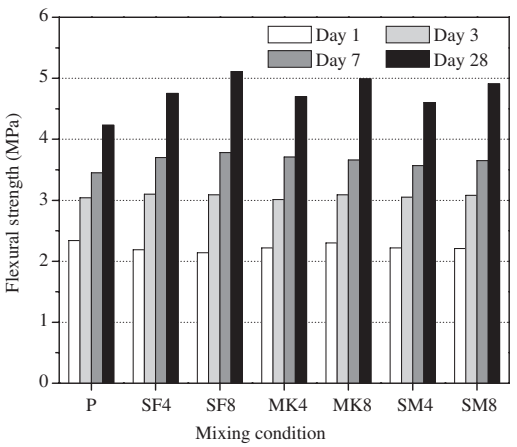


Figure 7. Flexural strength at different mixing conditions.

Table 7. Average flexural strength (unit: MPa).

Mixing condition	Day 1	Day 3	Day 7	Day 28
P	2.34	3.04	3.45	4.23
SF4	2.19	3.10	3.70	4.75
SF8	2.14	3.09	3.78	5.11
MK4	2.22	3.01	3.71	4.70
MK8	2.30	3.09	3.66	4.99
SM4	2.22	3.05	3.57	4.60
SM8	2.21	3.08	3.65	4.91

3.4 *Chloride ion permeability*

Except the shotcrete without admixtures, shotcrete from other mixing conditions has the permeability below moderate (Fig. 8).

The lowest permeability was obtained from the shotcrete with silica fume by 8% of cement weight and approximately 18.59% lower than shotcrete only with the accelerator (Table 8).

As the dosage of an admixture increased, the chloride ion permeability decreased proportionally. The reason is that the admixtures such HRM and silica fume have the micro-filter effect that they fill up pores between cement particles. In addition, they combine with calcium hydroxide from the early hydration stage, decrease micro-pores by pozzolan reaction and make the cement hydrate denser.

While shotcrete only with HRM shows the moderate permeability, shotcrete in which HRM and silica fume were mixed by equal percentage shows moderate or low permeability. In other words, the permeability of shotcrete where HRM was blended with silica fume by 8% of cement weight was very close to that of shotcrete with silica fume by 4% of cement weight. The average particle size of HRM is 1∼2 μm and much smaller than a cement particle with the size of 10 μm. However, it is 10 times bigger than a silica fume particle with the size of 0.1 μm. Such difference

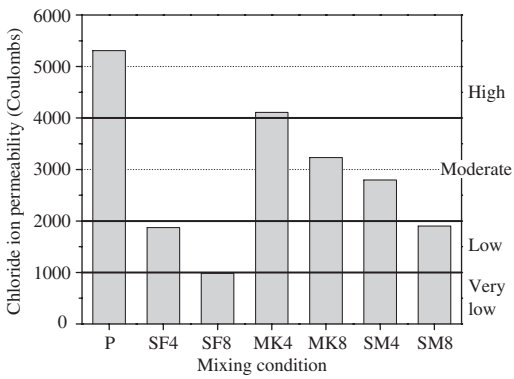


Figure 8. Chloride ion permeability of shotcrete.

Table 8. Summary of chloride ion permeability.

Mixing condition	Chloride ion permeability (Coulomb)
P	5,307 ± 241
SF4	1,870 ± 417
SF8	982 ± 405
MK4	4,109 ± 110
MK8	3,231 ± 316
SM4	2,794 ± 131
SM8	1,900 ± 123

Copyright © 2005 Taylor & Francis Group plc, London, UK

Table 9. Summary of the relative dynamic elastic moduli every 30 cycle.

Cycle	P	SF4	SF8	MK4	MK8	SM4	SM8
0	100	100	100	100	100	100	100
30	99.20	99.64	99.49	99.43	99.53	99.44	99.71
60	98.25	99.02	98.91	98.35	99.02	97.71	98.80
90	96.98	98.32	98.62	97.68	98.52	96.44	98.04
120	95.93	97.56	97.76	97.06	98.04	95.70	96.83
150	94.21	97.02	96.70	96.06	97.32	94.86	95.24
180	93.39	95.93	96.40	95.45	96.87	94.47	94.67
210	92.10	95.12	96.18	94.74	95.81	93.57	93.82
240	90.59	94.82	95.11	93.75	95.33	92.08	92.32
270	88.37	93.00	93.80	91.90	93.71	90.53	90.69
300	85.94	91.23	92.83	90.32	92.32	89.04	89.32

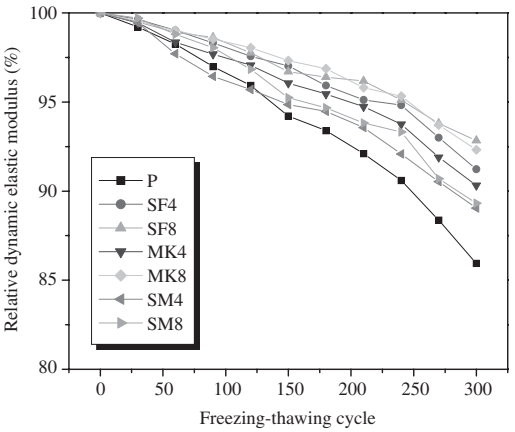


Figure 9. Relative dynamic elastic modulus every 30 cycle.

between fineness of HRM and silica fume induced different permeability of shotcrete.

Because the mechanical properties of shotcrete with admixtures are very close to each other, the choice and the dosage of an admixture should be determined by considering permeability required in shotcrete or permissible permeability of shotcrete liner. If both of economic efficiency and durability are considered, the use of shotcrete with HRM blended with silica fume is suggested.

3.5 *Freezing-thawing resistance*

Table 9 and Figure 9 show the dynamic elastic modulus measured every 30 cycle. Every specimen had the relative dynamic elastic moduli over 85% at 300 cycles and showed excellent freezing-thawing resistance.

Shotcrete with admixtures had slightly higher freezing-thawing resistance than that only with the accelerator. This arose from the fact that the admixtures such as HRM and silica fume fill up micro-pores between cement particles, decrease pore fraction in a specimen and make the cement hydrate denser by the pozzolan reaction. In other words, admixtures prevented water from permeating into shotcrete and increased freezing-thawing resistance. However, compared with the results of chloride ion penetration tests, the difference of freezing-thawing resistance between shotcrete with and without admixtures was not so high.

4 CONCLUSIONS

In unhardened shotcrete specimens, there was no retardation effect induced by dosing HRM and silica fume. The reason is why the setting mechanism of shotcrete is dominated not by admixtures but by the accelerator.

In early ages when mechanical properties of shotcrete are mainly dominated by the accelerator, compressive and flexural strength values were not so different from each other. Since the pozzolan materials such as HRM and silica fume react with calcium hydroxide formed during cement hydration and constitute C-S-H gel, higher long-term strength was obtained from the usage of admixtures. In other words, it was verified that the pozzolan materials are very effective in improving the long-term performance of shotcrete. However, the mechanical properties of shotcrete were not sensitive to the choice between HRM and silica fume.

Except the shotcrete without admixtures, shotcrete from other mixing conditions has the permeability below moderate. As the dosage of an admixture increased, the permeability of shotcrete decreased proportionally. The reason is why HRM and silica fume fill up pores between cement particles and make the cement hydrate denser. Considering that mechanical properties of shotcrete with admixtures are very close to each other, the kind and the dosage of an admixture should be determined by considering the permeability required in shotcrete. If both the economic efficiency and the durability of shotcrete are

Copyright © 2005 Taylor & Francis Group plc, London, UK

considered, the use of shotcrete with HRM blended with silica fume is highly recommended.

Every shotcrete specimen used in this study had the relative dynamic elastic modulus over 85% at 300 cycles and showed excellent freezing-thawing resistance. Shotcrete with admixtures had slightly higher freezing-thawing resistance than that only with the accelerator. However, the difference between them was not so high.

From the results, HRM was shown to be very effective in improving the long-term mechanical properties and the durability of shotcrete. Especially, considering the economic efficiency and the durability of shotcrete, the usage of HRM blended with silica fume in wet-mix shotcrete is highly recommended.

To increase the applicability of HRM to shotcrete, further studies on the determination of the optimal mixing condition and the verification of the effects of HRM on field sprayed concrete are in demand.

ACKNOWELDGEMENTS

This work is a part of results from the research project of "Development of high-performance shotcrete lining" funded by Samsung Engineering & Construction, Korea.

REFERENCES

ASTM C 1202. 1997. *Electrical indication of concrete's ability to resist chloride ion penetration*.

Bindiganavile, V. & Banthia, N. 2001. Fiber reinforced dry-mix shotcrete with metakaolin. *Cement & Concrete Composites* 23: 503–514.

Dimmock, R.H. 1999. Permanent Sprayed Concrete for UK Tunnels. In Nick Barton et al. (eds), *Proc. 3rd* Int. Symp. on Sprayed Concrete, Norway, 26–29 September 1999: 186–195. Norwegian Tunnelling Society.

EFNARC. 1999. *European Specification for Sprayed Concrete – Guidelines for Specifiers and Contractors*.

Ishida, A., Teramura, S., Hirano, K. & Nakagawa, K. 1999. Calcium sulfo-alumniate based accelerator for high-strength shotcrete in Japan. In T.B. Celestino & H.W. Parker (eds), *Shotcrete for Underground Support VIII*: 202–215. ASCE.

KS F 2405. 2002. *Method of test for compressive strength of concrete*.

KS F 2408. 2000. *Method of test for flexural strength of concrete*.

KS F 2436. 2002. *Method of test for time of setting of concrete mixture by penetration resistance*.

KS F 2456. 1993. *Method of test for resistance of concrete to rapid freezing and thawing*.

Melbye, T. 2000. *Sprayed Concrete for Rock Support*. MBT International Underground Construction Group.

Copyright © 2005 Taylor & Francis Group plc, London, UK

The use of horizontal inclinometers for the optimization of the rock mass – support interaction

G. Volkmann & W. Schubert
Graz University of Technology, Institute for Rock Mechanics and Tunneling, Austria

ABSTRACT: Nowadays a number of tunnels are constructed in urban areas in weak rocks with high or low overburden. In both cases geodetic methods are used to monitor displacements and control stability. In special cases additional other measurement systems are used to supplement the information gained by geodetic methods. This paper deals with the information gained by using a continuously recording horizontal chain inclinometer installed from the tunnel face. The increased information on the rock mass – support interaction can be used to better control the construction process and allows detecting unexpected changes in the rock mass earlier than with traditional measuring methods.

1 INTRODUCTION

The uncertainties inherent in each ground model with respect to geological setup and mechanical parameters require a continuation of the design into the construction phase. The behavior of the ground – support system is continuously monitored and excavation and support adjusted to the real rock mass conditions and requirements.

Urban tunneling is usually associated with limitation of settlements and/or differential settlements. By means of continuous monitoring and prediction of displacements critical developments can be detected in time and excavation and support methods adjusted in time.

This process of optimization the construction not only increases safety, but is also very economical, as an "overdesign" to account for uncertainties is not required.

All these facts call for an intensive observation program of the system behavior. Normally this observation is done using geodetic methods, as well on the surface as in the tunnel. As those methods only measure displacements on surfaces (ground surface and tunnel perimeter), deformations of the rock mass can only be estimated. Thus in some cases additional measuring methods have to be applied to obtain a full picture of the processes associated with tunnel excavation.

2 STATE OF THE ART MEASUREMENTS

Observations and measurements already have a long tradition in tunneling (Rabcewicz, 1944). The measurement data are used to control the excavation induced displacements (Rabcewicz 1963, Pacher 1964, Steindorfer et al. 1997). Nowadays geodetic three dimensional observations are state of the art for the collection of displacement data.

2.1 *Geodetical measurements*

Geodetic survey is performed both in the supported tunnel sections and on the surface. Due to the influence of temperature and air pollution the accuracy of the measurements is around +/− 1 mm.

The displacement observation is normally performed in cross sections with five to nine points in the total excavation area. The distances between those cross sections are rarely shorter than 10 m in the longitudinal direction.

The displacements induced by shallow tunnels are normally also measured on the surface. The layout of the measuring points on the surface frequently is determined by the surface structures, such as roads, and buildings, preventing a systematic and regular grid, which would be preferable for complete information on the subsidence.

The frequency of the measurements commonly is one per day, in some cases readings are taken twice a day.

2.2 *Evaluation*

Various methods of data evaluation and presentation exist and are used to support the control of the system

Copyright © 2005 Taylor & Francis Group plc, London, UK

behavior. By using different display methods like development of displacements as a function of time or tunnel advance, deflection curve diagrams, displacement vector diagrams, etc. it is possible to observe the spatial and timely influence of the construction process on the displacements. (Schubert et al. 2002). The information is used to better understand mechanisms and rock mechanical processes in the ground. (Steindorfer 1997, Golser et al. 2000, Schubert et al. 2003 Schubert 2004).

Special software has been developed to predict the development of displacements after a few readings only, considering the influence of time, advance and various support options. (Sellner 2000, Sellner et al. 2000, Sellner et al. 2002).

2.3 *Shortcomings*

With the geodetic measurement system it is not possible to measure the total settlement path at the tunnel level. Due to the fact that the measurement targets are installed only behind the face after support installation displacements ahead of the face and between face and monitoring section cannot be measured.

Considering the different distances and times in between the face and the zero reading it is possible to extrapolate the pre-settlements to the face with evaluation programs. That makes the collected data behind the face more comparable and results in a better quality of the geotechnical evaluation. (Sellner 2000)

Due to the commonly long interval between the geodetic measurements:

- it is not possible to evaluate single excavation steps or single excavation phases;
- it is not possible to evaluate the influence of the support installation on the displacements.

The measured cross sections are often not correlated to periodically installed support like face anchors or pipe roof systems. Due to the fact that the efficiency of such support systems changes with position to the installation the evaluation of the geodetical data becomes more difficult (Volkmann, 2003).

3 INCLINOMETER MEASUREMENT SYSTEM

The estimation of the system behavior using the geodetic survey is more difficult in weaker ground, where the stiffness contrast between the support and the rock mass is more significant and support ahead of the face is used.

For such conditions a measurement system was developed consisting of horizontal in-place chain inclinometers and a data acquisition system.

3.1 *Positioning*

The measurement system was installed in the crown of the tunnel parallel to the pipe roof (figure 1). One chain consists of ten 2 m long links connected to each other. The data acquisition system situated approximately 20 m behind the actual face collects the data. Thus the measurements did not disturb construction.

3.2 *Differences to the geodetical measurements*

The density of the observed points in the longitudinal direction is with 2 m much higher than that one from the geodetically monitored points.

The position of the chain inclinometer is primarily ahead of the face (figure 1). The length ahead of the face ranged between 8 m and 20 m (directly after the installation) depending on the position to the last installation in the applications till now.

Data can be acquired in predetermined intervals. For the applications described in this paper one minute reading intervals were chosen.

Even though the longitudinal and horizontal displacements cannot be measured this system supplements the information obtained from the geodetic measurement system.

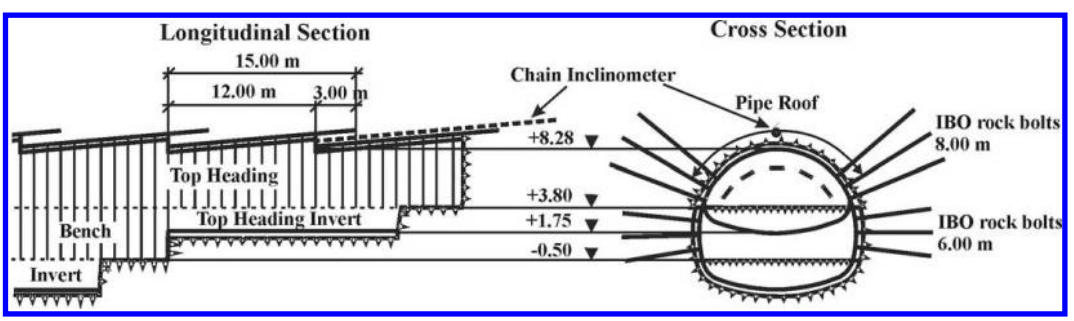


Figure 1. Position of the chain inclinometers (Volkmann et al. 2003).

Copyright © 2005 Taylor & Francis Group plc, London, UK

4 ADDITIONAL RESULTS

4.1 *Displacements during excavation*

In weak ground frequently sequential excavation is applied. A typical excavation procedure includes excavation of the top heading, followed by the bench and the invert. In case of an instable face the top heading excavation can also be divided into several phases.

Figure 2 shows the development of the settlements during the excavation of a round of 1 m length, which was done in two steps. After each step a shotcrete sealing was applied, with the completion of the support, including lattice girders, wire mesh and shotcrete following after step 2.

At the beginning of each excavation phase the displacement rate increases. After completion of the excavation the rate decreases significantly, indicating stabilization.

By using this system an excavation dependent evaluation is possible that can show the influence of each phase on the settlements in the excavation process. The combination of all simultaneously measured inclinometer links creates a deflection curve for an excavation step (figure 3).

Figure 3 shows the settlements induced by the excavation step from Station 254.21 to station 254.88.

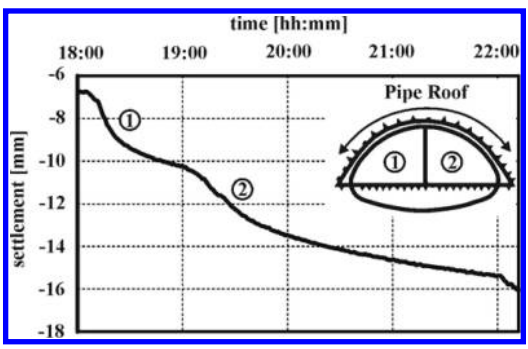


Figure 2. Time settlement line of one top heading excavation.

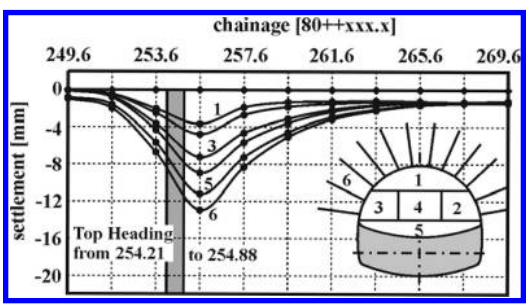


Figure 3. Deflection curve of one excavation step – normal settlement behavior (Volkmann & Button, 2003).

The top heading was excavated in 3 phases that were followed by the installation of the lining. After that the supporting rock wedge at the face and the top heading invert were excavated and supported. The work in this round was finalized with the installation of radial rock bolts.

A major proportion of the settlements occur in the area from 9 m ahead of the new face to 4 m behind the new face. The maximum settlement value is approximately 1 m ahead of the new face. Due to the pretty stiff lining used in this project, the settlements induced by this excavation phase behind the face are rather low.

This behavior showed to be characteristic on this particular site. With a geodetic monitoring alone, only a minor part of the total displacements could have been recorded (Volkmann et al. 2003), probably leading to wrong conclusions.

A detailed evaluation of the single excavation phases present different stress transfer areas defined by the occurring settlements. Depending on the relative position of the excavation phase the maximum values as well as the area where major displacements occur varies. When excavating the upper portion of the tunnel, the highest settlement values are recorded near to the unsupported area. When excavating the lower parts of the face, the maxima of the settlements are recorded further ahead of the face.

Using the settlement characteristic displayed in figure 3 the expected final settlement amount can be extrapolated. With the assumption of homogeneous ground conditions the area in between zero and the deflection curve defines the final settlement amount due to the excavation of the top heading.

With the detailed information on the spatial and timely deformation process, the excavation layout and timing of support installation can be optimized on site.

4.2 *Displacements during installation of support*

Due to the fact that conventional monitoring systems do not continuously record displacements, the influence of different activities in the tunnel cannot be evaluated in detail.

Figure 4 shows the development of the settlements during the excavation and support installation process. After the excavation of the first 3 phases a pronounced stabilization process can be observed, which continues through the installation of steel arch and shotcrete. The following installation of radial rock bolts and micro piles at the top heading footing cause additional settlements.

This additional settlement caused by the drilling of bolts and micro piles can be seen also in figure 3. The process causes additional settlements of maximum around 2 mm (difference between the last two lines). The influence can be observed as well ahead, as also behind the face on a couple of meters.

Copyright © 2005 Taylor & Francis Group plc, London, UK

In contrast to this face bolts, spiles or pipe roof installations increase the settlements primarily in sections ahead of the face (figure 5, face position = 0).

The comparison of two different methods of pipe roof installation showed that especially in weak ground a cased-drilling system is less susceptible to settlements than a pre-drilling system (Volkmann, 2004). The reasons for this are the immediate support of the drill hole and the flushing inside the pipe. This way of flushing does not erode the walls of the drill hole. The pre-drilling system should therefore only be chosen when the stability of the pre-drilled holes is guaranteed and the deformations of the unsupported hole are negligible. It has been observed that the installation of the pipes in uncased drill holes was rather difficult due to the convergence between drilling of the hole and installation of the pipe.

The result of the measurements made till now demonstrate that the installation of support like shotcrete with or without wire meshes and all types of arches do not increase the settlements. Supports like radial rock bolts, face bolts or pipe roof systems increase the settlements. The magnitude of this increase is a function of the strength and stiffness of the ground.

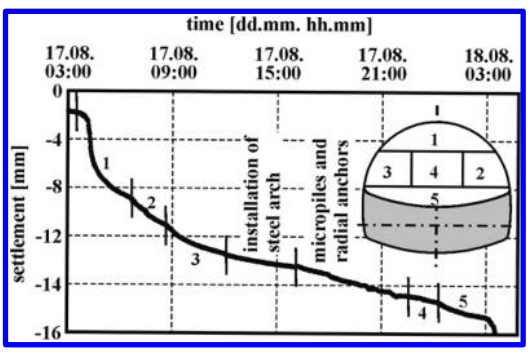


Figure 4. Time settlement line including the installation of radial rock bolts.

4.3 *Detection of changes in rock mass quality*

Methods have been developed to use the changes in the displacement vector orientation from geodetic monitoring data for the short term prediction of changes of the rock mass quality ahead of the face. In cases of a rather stiff lining however the value of this method of data evaluation is limited. The chain inclinometer on the other hand extends up to 20 m ahead of the face, allowing observing untypical deformations in this section directly.

The measurement of the total deformation path with the inclinometer clearly indicates changes in the rock mass ahead of the face.

The deflection curve shown in figure 6 is a good example how a weaker zone ahead of the face influences the displacements. While influence of the excavation cycle shown in figure 3 can be observed up to about 8 m ahead of the face, the cycle shown in figure 6 influenced a much longer section, which extended beyond the end of the inclinometer. This clearly indicates weaker material ahead of the face.

The total settlement path evaluated in a deflection curves diagram (figure 7) can also be used to determine the rock mass quality ahead of the face. When excavating from chainage 252.49 to 253, 36 an increase in the displacements between the face and approximately chainage 258 could be observed, with not

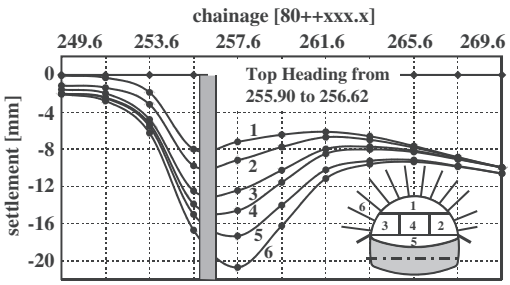


Figure 6. Deflection curve of one excavation step – non normal settlement behaviour.

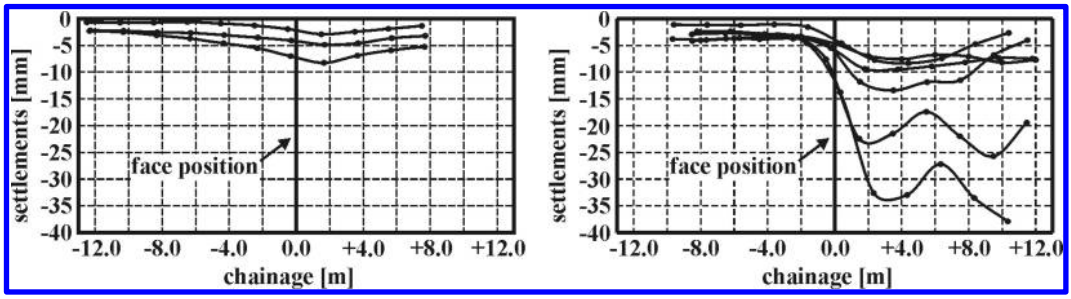


Figure 5. Settlements measured in the time of the installation of the cased-drilling (left) and the pre-drilling (right) pipe roof system (Volkmann, 2004).

Copyright © 2005 Taylor & Francis Group plc, London, UK

much influence on the section beyond this station. The next rounds did not cause a significant increase in the displacements, while a considerable increase can be observed again after the face passing chainage 256. The reason for this behavior was a stiffer block embedded in the weak matrix around chainage 258, which "blocked" the progression of the displacements beyond this station. Only when the bedding of the block due to excavation became weaker, the displacements progressed considerably ahead of the face again. At face position 2593 it was decided to install a new round of pipe roof support, which decreased the displacements during further advance. The weak zone could be passed without further problems (Likar et al. 2004).

4.4 *Further results*

In shallow tunnels the geodetically measured data on the surface generally display higher settlement amounts than in the tunnel. This fact in many cases is explained by consolidation processes of the material. Only when also underground total displacements are measured it can be determined if a consolidation process or relatively high displacements ahead of the face are the reason for high subsidence.

The continuous recording of displacements ahead of the face allows detecting failure mechanisms in the ground practically in real time. This enables to initiate appropriate mitigation measures in time to guarantee stability of the structure.

5 OPTIONS FOR THE OPTIMIZATION

The optimization of support or excavation methods can have different reasons. In some projects the use of support should be minimized to save time and money, while at the same time guarantee stability and safety. In other projects the most important factor is the control of surface settlements or differential settlements to prevent damage to surface structures.

The continuous recording of displacement data with high resolution can help to better understand the complex interaction between rock mass and construction measures. The analysis and interpretation of the geodetic data set can be used for this optimization in normal rock mass conditions.

In environmentally sensible areas with weak ground this system preferably is supplemented by a system as described in this paper to enhance the level of information and to allow for prompt reaction to unusual or unexpected processes.

By using the accurate evaluation results of a chain inclinometer measurement the excavation and support system can be changed depending on the aims of a project. The excavation can be adjusted to the ground conditions. The possibility to "look ahead" of the tunnel face also provides preparation time for any required changes.

The knowledge about the displacements ahead of the face allows optimizing the overlapping length of support systems reinforcing the area ahead the face, like face bolts or pipe roof supports.

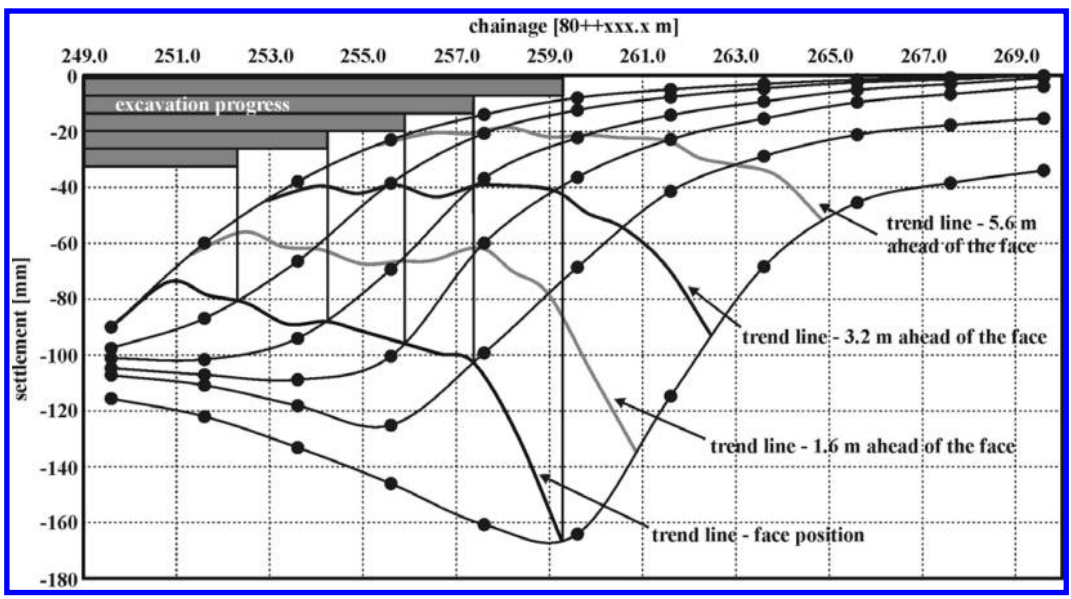


Figure 7. Settlements measured by the chain inclinometer system.

Copyright © 2005 Taylor & Francis Group plc, London, UK

By a continuous adaptation of the installed support the system behavior can be fitted to the actual demands. A precondition for a successful adaptation and optimization process is the availability of complete quality data, collected in intervals, which allow for a timely response to any changes in the ground conditions.

6 CONCLUSION

Tunnels in weak ground and environmentally sensible areas require special attention during design and construction. An extended monitoring program considerably can help in better understanding the complex processes of the interaction between ground and construction, and identify significant influences on the displacements. A continuous recording chain inclinometer system has been successfully applied for a tunnel in faulted rock in a built up area. The complete and in time information on the displacements in the ground allowed an optimization of the construction process, thus minimizing the damages to the surface structures.

REFERENCES

Golser, H. & Steindorfer, A., 2000.Displacement Vector Orientation in Tunneling – What Do They Tell? Felsbau 18, Nr. 2, 16–21.

Likar, J., Volkmann, G.M. & Button, E.A., 2004. New Evaluation Methods in Pipe Roof Supported Tunnels and ist Influence on Design during Construction. Proceedings of the 53rd Geomechanics Colloquy and EUROCK 2004, 277–282.

Pacher, F. 1964. Deformationsmessungen im Versuchsstollen als Mittel zur Erforschung des Gebirgsverhaltens und zur Bemessung des Ausbaues. In: Felsmechanik.

Rabcewicz, L. 1944. Gebirgsdruck und Tunnelbau. Vienna: Springer Verlag.

Rabcewicz, L. 1963. Bemessung von Hohlraumbauten. Die “Neue österreichische Bauweise” und ihr Einfluss auf Gebirgsdruckwirkungen und Dimensionierung. Felsmechanik und Ingenieurgeologie, Sonderabdruck aus Vol. I/3–4, 224–244. Vienna: Springer Verlag.

Schubert, W., 2004. Tunneling in Alpine Fault Zones – Excavation and Support Strategies. Proceedings of the 5th International Conference on Case Histories in Geotechnical Engineering, New York.

Schubert, W., Button, E. A., Sellner, P. & Solak, T., 2003. The Use of Monitoring Data and Geological Documentation as a Basis for Defining Rock Mass Behavior Types. Proceedings of the 6th International Geotechnical Conference, Bratislava, 89–98.

Schubert, W., Steindorfer, A., Button, E.A., 2002. Displacement Monitoring in Tunnels – an Overview. Felsbau 20, Nr. 2, 7–15.

Sellner, P.J., 2000. Prediction of Displacements in Tunneling. PhD Thesis, Graz University of Technology, Institute for Rock Mechanics and Tunneling.

Sellner, P.J., Grossauer, K. & Schubert, W., 2002. Advanced Analysis and Prediction of Displacements and System Behaviour in Tunneling. In Proceedings of ISRM international Symposium on Rock Engineering for Mountainous Regions, EUROCK 2002. Funchal, Madeira, Portugal. 539–546.

Steindorfer, A., 1997. Short Term Prediction of Rock Mass behaviour in Tunneling by Advanced Analysis of Displacement Monitoring. PhD Thesis, Graz University of Technology, Institute for Rock Mechanics and Tunneling.

Steindorfer, A. & Schubert, W. 1997. Application of new Methods of Monitoring Data Analysis for Short Term Prediction in Tunneling. Proceedings of the 23rd General Assembly of the International Tunneling Association, Vienna. Balkema, Rotterdam, 65–69.

Volkmann, G.M., Button, E.A. & Schubert, W. 2003. Influence of Zero Reading Time and Position on Geodetical Measurements. International Symposium on GeoTechnical Measurements and Modelling. Karlsruhe, 101–104.

Volkmann, G.M. 2003. Rock Mass – Pipe Roof Support Interaction Measured by Chain Inclinometers at the Birgltunnel. International Symposium on GeoTechnical Measurements and Modelling. Karlsruhe, 105–109.

Volkmann, G.M., 2004. A Contribution to the Effect and Behavior of Pipe Roof Supports. Proceedings of the 53rd Geomechanics Colloquy and EUROCK 2004, 161–166.

Copyright © 2005 Taylor & Francis Group plc, London, UK

Tunnel excavation works in Taksim–Kabataş funicular system project

E. Aykar & B. Arıoğlu
Yapı Merkezi Construction Industry Inc., Head Office, Çamlıca,İstanbul, Turkey

N. Erdirik, A.Yüksel & T. Özbayır
Yapı Merkezi Construction Industry Inc., Taksim–Kabataş Funicular System Project, Kabataş, İstanbul, Turkey

E. Arıoğlu & R. Yoldaş
Yapı Merkezi Construction Industry Inc., R&D Department Çamlıca, İstanbul, Turkey

ABSTRACT: Taksim–Kabataş Funicular System Project is planned to integrate the metro system and sea transportation routes by connecting the Taksim Station of the Metro System and the Kabataş Sea Bus Pier. The system is also connected to the tramway line in Meclis-i Mebusan Street. The funicular system consists of two cut and cover underground stations and a deep tunnel with 5 to 22% inclinations and 544 m length. In this paper, the unfavorable geological conditions at the tunnel entrance, the results of the subsequent soil improvement works and their effects on the tunnel deformations are presented in detail. Approximately 2500 m^3 artificial fill was treated with an average of 0.97 t/m^3 grout intake. Thanks to the soil improvement, the tunnel was bored safely and without any damages to buildings.

1 TAKSİM–KABATAŞ FUNICULAR SYSTEM

The funicular system is aligned at 55° NW direction, with total length of 643.5 m between Taksim and Kabataş. The system was designed as a funicular system due to the difference of altitude between Taksim (+81.5) and Kabataş (+2.0). Kabataş and Taksim stations are build underground using the cut-cover method. The stations are connected with a deep tunnel which is constructed with the New Austrian Tunnelling Method (NATM). The alignment starts in Kabataş at −11.29 m elevation and 5% inclination. The inclination increases up to 22.19% maximum at km 0+488 and then decreases to 5% at km 0+537. Finally the alignment ends at Taksim Station at +64.7 m elevation (Fig. 1).

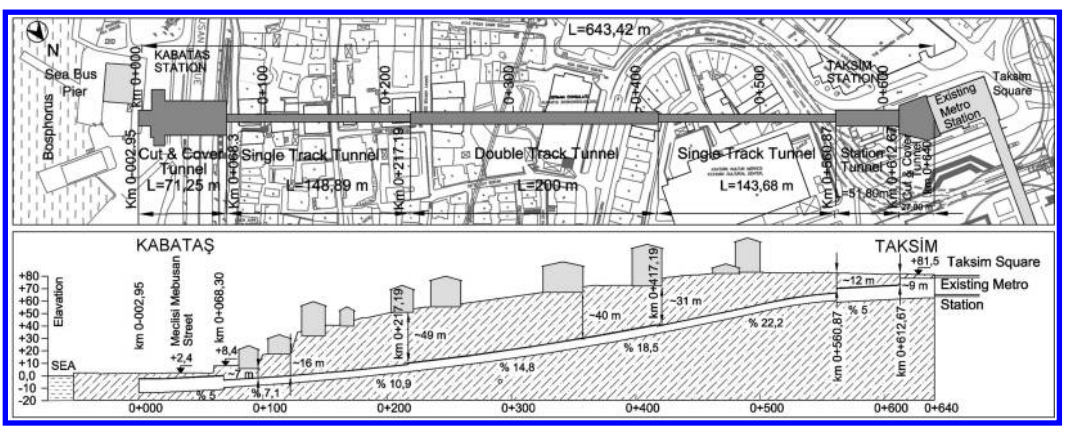


Figure 1. Kabataş–Taksim funicular system.

Copyright © 2005 Taylor & Francis Group plc, London, UK

2 GEOLOGY AND GEOMECHANICAL PROPERTIES OF THE FORMATION

A major part of the alignment passes through Greywacke formation. Carboniferous aged Greywacke referred to as Trakya Formation consists of sandstone, siltstone and claystone which occasionally display vertical and horizontal transitions with andesite and diabase dike or sills (Yoldaş, 2003). Rocks are very closely jointed and frequently faulted with E-W direction more or less and 60°–80° inclined both N and S. The geomechanical properties of the formation are summarized in Table 1.

Limited amount of investigation borings could be carried out due to the closely spaced buildings over the deep tunnel alignment. However, the geological conditions faced during the excavation are in a reasonable agreement with the predicted geological profile (Fig. 2). According to the bore-hole findings and the tunnel excavation records, the ground water level around the Kabataş Station is the same level with sea water level, then in the Taksim direction rises upwards with the topography and it stays in the cross section to be excavated before the Taksim station tunnel and in the station tunnel it approaches the invert of the tunnel (∼+60.0). Generally the water inflow encountered during the excavation had no negative influence on the excavation progress of the works because of low permeability.

Table 1. Summaries of geomechanical properties.

Geomechanical properties	Rock type		
	Sandstone	Claystone	Diabase
Unit weight, kN/m^3	26.1–27.5	27.4	27.8
Uniaxial compressive Strength, MPa	24.6–67.3	33.9–67.2	67
Modulus of elasticity, GPa	4.7–9.6	9.25	12
Poisson ratio	0.2	0.19	0.16
RQD, %	0–10	0–10	25
Geological strength Index, GSI	10–45	15–50	35–65
Rockmass compressive Strength, MPa (*)	0.7–7.8	1.2–9.5	5.2–17.1
Rockmass cohesion, MPa	0.4–2.9	0.7–3.0	2.5–4.2
Rockmass internal Friction angle,°	24–36	26–38	34–42
Rockmass modulus of elasticity, GPa	0.5–6.2	0.77–8.2	8.2

(*) Insitu values were predicted utilizing GSI concept (Hoek et al. 2002)

3 KABATAŞ STATION

3.1 *Station structure*

The Kabataş station lies directly under the Meclis-i Mebusan Street which is main artery of urban with high traffic volume. The width of the station is 26 m. and the length is 71.25 m. The depth of station varies from 13.50 m to 16.50 m because of inclined alignment. There is a layer with a more or less uniform thickness of 2.0–2.5 m, recently formed, consisting of artificial fill materials (construction debris, broken roof tiles etc.) just below the surface at the station area. Below the artificial fill lies the sand layer which contains sea mussels. The thickness of this layer increases up to 8.5 m towards the sea. Starting from 10 to 12 m depth, the sandstone and claystone layer begins. The upper parts of this layer are extremely weathered. A fault zone, cutting the station diagonally in E–W direction and 60° inclined to South, was encountered at the tunnel entrance of the station.

The excavation pit of the station is supported by Ø100 cm bored piles which are spaced 45 cm apart with 16.5–22 m variable lengths. Water impermeability is ensured by application of jetgrout columns between the piles down to the rock layer. The lateral loads are supported by the Ø80 cm steel pipe braces placed at 4 m spacing.

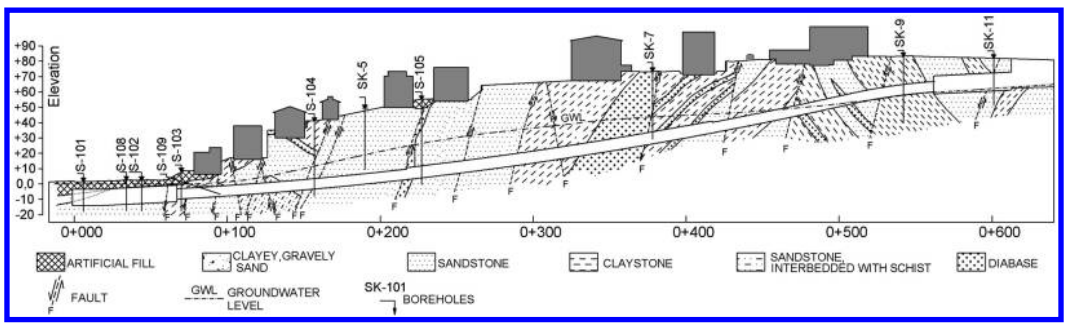


Figure 2. Geological section of the alignment.

Copyright © 2005 Taylor & Francis Group plc, London, UK

3.2 *Kabataş tunnel portal*

A 12 m length of Kabataş station is reserved for the portal of the deep tunnel. The lateral walls at this part of the station have been supported by post tensioned anchors except for a single row of steel pipe bracing at the top of the lateral walls. The soil profile at this location according to the borehole findings from S-103 and S-109 (this bore hole was inclined), shows 7.0 m artificial fill layer on the top and sandstone, schist and claystone under this layer which are significantly weathered at the interface with the artificial fill (Yoldaş, 2003). It is projected that the retaining wall in Inebolu Street which is placed at the side of tunnel entrance, parallel with the main street with a 6 m height must be supported by 9 m long mini piles + shotcrete and 12 m long soilnails, which are to be executed in 4 different levels. Due to existing infrastructural system the soilnails at the first level could not be executed and it is decided to make use of post-tensioned anchors with 20 ton of capacity and 18 m of length instead of the 2nd level of soilnails. It has been observed that during the drilling the holes for anchors are going trough artificial fill, due to this reason it has been decided to carry out a detailed soil investigation on the area behind the mini-piled wall and three additional bore holes with 15° of inclination and 30 m length have been executed. These investigations proved that the two buildings located on the tunnel axis had been constructed on artificial fill material which is formed of weathered and loose waste building materials. This layer reaches down to ~2 m near of the tunnel roof and has an approximate height of 5 m (Fig. 3).

4 SOIL IMPROVEMENT WORKS

4.1 *Procedure of grouting*

After evaluating the geological findings and environmental conditions around the portal, about it was decided that improvement of the artificial fill area above the tunnel by cement grouting is needed for safe and efficient execution of the works (Saglamer, 2003).

These factors have been effective on the decision:

- The existing mini piled retaining structure is stabilized by improving the geomechanical properties of the soil which is surrounding the nails.
- The distance between the tunnel crown and the foundation of the building is 7 m, out of which the artificial fill area comprises the upper ~5 m. This means that the forming of a natural arch around the tunnel crown was not likely without significant settlements which could result in damages to the buildings.

The soil improvement area, which is finally decided upon, is 20 m wide and 20 m long (max.) and ~6.0 m deep and it covers the effect area of the tunnel, where the foundations of Malatya and Kabataş Apartments are located.

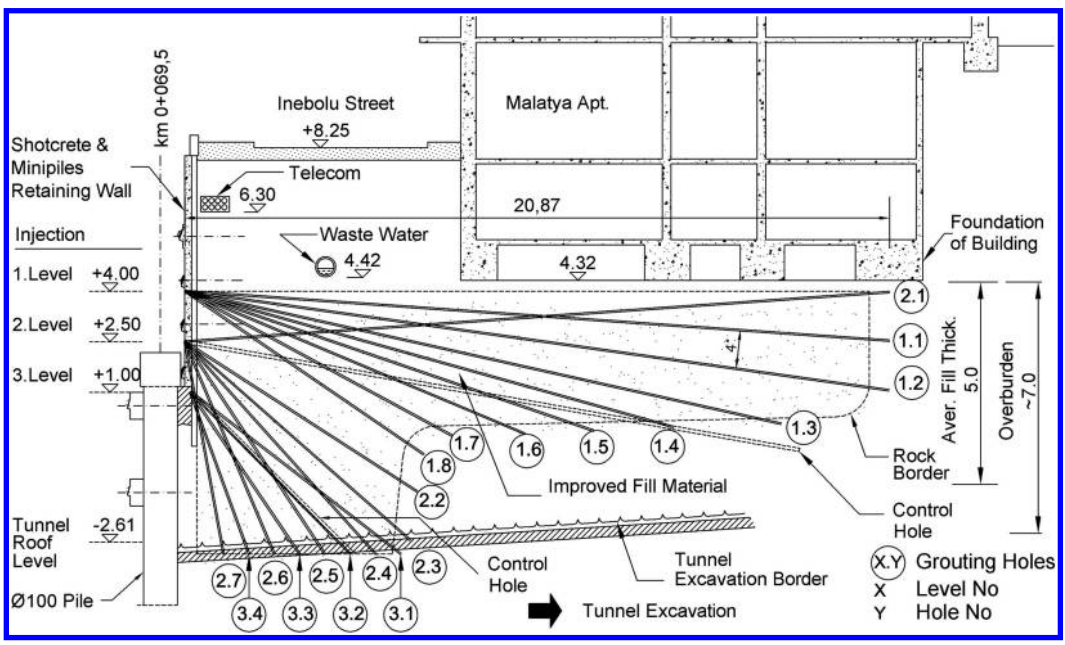


Figure 3. Vertical layout of the grouting pattern applied.

Copyright © 2005 Taylor & Francis Group plc, London, UK

The horizontal and vertical spacing of grouting pattern are 1.6 m and 1.5 m respectively. The numbers of the grouting location are 13 nos on the first level (A1, B1, … , M1), 12 nos on the second level (A2, B2, … , L2) and 11 nos on the third level (A3, B3, … , K3) The vertical arrangement of the drilling pattern is illustrated in Figure 3. The lengths of the drillings, which are entering at least 1 m into rock, are varying between 6 m and 21 m.

Drillings with 89 mm diameter have been executed by roto-percussion method, with Casagrande C6 drilling rig. The "water/cement" ratios of the grouting mixtures are chosen as 3/1, 2/1, 1/1. In addition, bentonite is added to mixture with an amount of % 3∼0.5 cement weight for stabilizing the grout. As a plasticizer agent, Sikament R4 is used 1∼0.8% amount of cement weight.

Low pressures (1.5 bars) for grouting are applied down to 5 m, due to concern for building foundations and infrastructures. On deeper holes the grouting pressures are applied up to 3 bars.

According to split spacing method, primary holes (skipping one hole vertically and horizontally) are grouted "up to down" in 3 m divisions. The holes of secondary are drilled completely then they are grouted "down to up" in 3 m divisions. The grouting procedure of each division is shown in Table 2.

4.2 *Grouting works*

The grouting works commenced in 25.09.2003 and finished 45 workdays after. Totally 3194 m holes (including redrilling) are bored, 244 ton cement, 5.4 ton bentonite and 1.9 ton plasticizer agent is used. Grouting intakes average is 186 kg/m in terms of dry cement for first level and 40 kg/m for the second level. The amounts of second level intakes are nearly % 20 of the first levels. This situation caused by the diffusing of grouting material that was executed in the first level.

After completion of grouting works, in order to control the grouting quality two control holes are drilled and pressure water tests are applied in these holes. According to the test results the average permeability of the grouted soil is 4.5 Lugeon (lt/m.min). This means that the cavities are properly filled and the soil is impermeable (Nonveiller, 1989). The degree of the grout intake is 7.14 kg/m in the first hole, 16.6 kg/m in the second hole. Taking the results of control tests into consideration, grouting work was found to be satisfactory and execution of a third level of grouting was determined unnecessarily.

Table 2. Grouting procedure.

	Mix	Refusal criterion		Refusal condition	
Item	w/c	Cement intake, kg/m	Press. bar	Yes	No
1	3/1	17	3	Stop	→ item 2
2	2/1	300	3	Stop	→ item 3
3	1/1	300	3	Stop	→ item 4
4	2/1	Σ1200	3	Stop	Wait 6 Hours then → Item 5 (*)
5	1/1	300	3	Stop	Information to Client

(*) w/c = 1/1 mix with 25% sand of cement amount-by weight.

5 TUNNEL WORKS

5.1 *Tunnel excavation*

Taksim–Kabataş tunnel has been bored from two sides. Excavation works have begun in October 2003 from Taksim side and in May 2004 from Kabataş side. The difficulties of the geological conditions and soil improvement above the Kabataş tunnel will be taken into consideration in this chapter.

Elevations of the tunnel roof and bottom are −2.61 and −9.86 at the tunnel entrance. Also the thickness of overburden is 11.5 m at the entrance. But, the distance between tunnel crown and foundation of buildings is

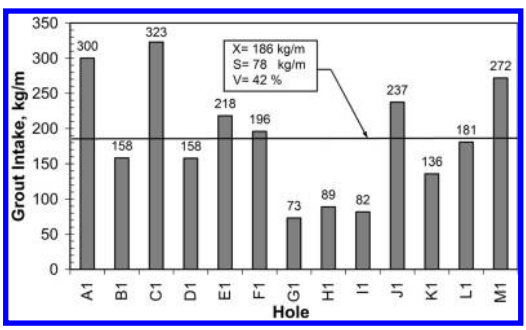


Figure 4. Distribution of grout intakes at 1st level (X = Average, S = Standard deviation, V = Coefficient of variation).

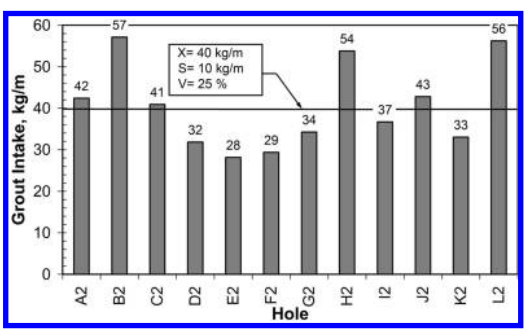


Figure 5. Distribution of grout intakes at 2nd level.

Copyright © 2005 Taylor & Francis Group plc, London, UK

approximately 7 m which is located between 8th and 26th meters of the tunnel. A sudden increase in the overburden thickness is observed on the consequent sections of the tunnel due to topographic elevations, such that it reaches 16 m below the second row of buildings which is located between 35th and 52nd meters of the tunnel (Fig. 1).

New Austrian Tunnelling Method (NATM) has been used as an excavation and supporting technique. Excavation height and width are 6.56 m and 6.40 m respectively and the tunnel was designed as a single track tunnel for the first 148.89 m. Excavation and supporting details are illustrated in Figure 6. The Umbrella Arch Method is applied on the first 37.8 m of the tunnel due to very poor rock conditions and insufficient overburden thickness for the formation of the natural arch (Arioğlu et al. 2003a). Umbrella arch pipes are acting as horizontal piles and forming an artificial arch over the crown of tunnel (Fig. 6). This supporting measure has been abandoned after km 0+107.8 where a 16 m of overburden thickness has been reached. Forepoling application has started at the tunnel roof instead of umbrella arch to prevent collapsing of rock pieces.

5.2 *Deformation measurements*

In accordance with the main principles of New Austrian Tunnelling Method, the tunnel geology and has been examined closely and deformation measurements have been taken in order to control and monitor the excavation and supporting systems (Arioglu et al. 2003b).

Face mapping and rock classification has been executed in every ~10 m of the tunnel as well as tunnel displacement and surface settlement measurements. The tunnel sidewall displacement measurements and surface settlements records of the first 100 m of Kabataş Project are displayed in Figures 7, 8 respectively (Yapi Merkezi, 2004).

If the tunnel displacement and surface settlement measurements are evaluated, the following observations can be made:

- As for relationship between face distance from the monitoring section and the recorded tunnel displacement, when the top heading face passes an approximate distance of 10 m, the rate of the tunnel

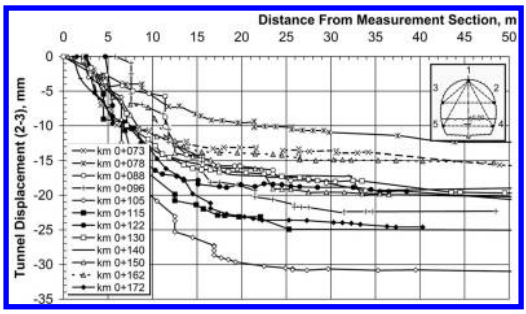


Figure 7. Relationship between the tunnel sidewall displacement and distance from measurement section.

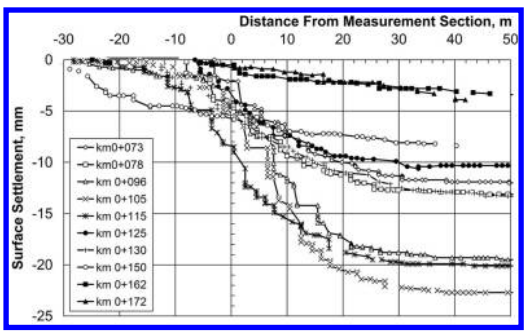


Figure 8. Relationship between the surface settlement and distance from measurement section.

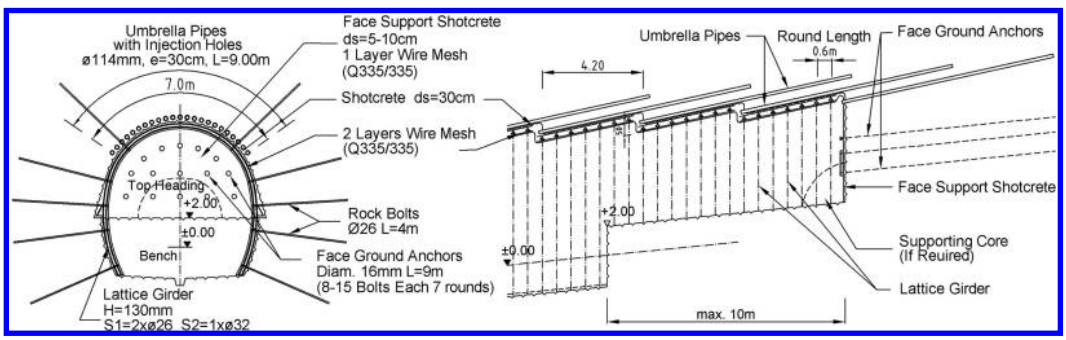


Figure 6. Type "A3" excavation and support detail of single track tunnel.

Copyright © 2005 Taylor & Francis Group plc, London, UK

displacement is noticeable. Regardless of the overburden depth the rate of the displacement behind of the tunnel face becomes insignificant at an approximate distance of 30 m. The ultimate displacement observed during the tunnel construction varies between 1.2 cm and 3.1 cm depending upon mainly rock mass mechanical properties and support density used.

- When taking the maximum tunnel displacement measured into account the normalized tunnel closure in percent may be calculated to be (u/R = 0.032 m/6.5 m = % 0.5), where: u = maximum tunnel sidewall displacement, R = tunnel diameter. This finding reveals that the tunnel is not subjected to "Stability Problems" (Barla, 1995, Arıoğlu et al. 2002).
- The grouting that have been executed into the artificial fill which is located between the beginning and the 20th meters of Kabataş Tunnel is likely to have a positive effect on the magnitude of the tunnel displacement and surface settlement measurements owing to the fact that the deformation modulus of the media under consideration is increased drastically for a given ratio of support pressure to in situ stress (Table 3). In other words, the plastic zone size is surrounding the tunnel decreases. The deflection ratio "Δ/L" can be utilized in conjunction with the measured surface settlements to predict the potential associated building damage. While the tunnel face was at km 0 + 091 the ratio in question was determined to be 1/2170. The estimated value is approximately 11 times smaller than the structural damage limit (Arıoğlu & Yüksel, 1999). (Δ is the relative settlement, L is length of a rectangular beam representing the building)
- When the face is ahead of measurement section at the distance of more or less 30 m the rate of the surface settlement diminishes. The final values recorded range from 0.3 cm to 2.3 cm.
- As expected the overburden depth effect on the surface settlement is observed i.e., the surfaces settlement reduces with increase in the depth.

Table 3. Effects of soil improvement.

	Section	
Parameters	km 0+078	km 0+115
Overburden thickness	~7 m	~16 m
Rock/soil type	Sandstone and Clay stone and Artificial Material above Tunnel	Sandstone
Rock classification, GSI, (Hoek et al. 2000, Ulusay et al. 2000)	Disintegrated/Very Poor (Fault Zone) 15	Blocky – Seamy/ Poor 30
Soil improvement	Improved Artificial Fill Material above tunnel	No Improvement
Supporting type (*)	A3 (with umbrella arch system)	A2
Round length	0.60 m	1.00 m
Tunnel fisplacement	12.4 mm	24.9 mm
Surface settlement	12.6 mm	19.9 mm

(*) A3: 30 cm shotcrete + lattice girder + 2 layer wire mesh + rock bolt + umbrella arch system.

A2: 25 cm shotcrete + lattice girder + 2 layer wire mesh + rock bolt + forepoling.

6 SUMMARY AND CONCLUSIONS

The crown of the Kabataş tunnel entrance has no enough room for natural arching, which transfer safely the external loadings resulting from the building foundations (Fig. 3). Furthermore, the formation in which the tunnel excavation was carried out, consists of fill materials and generally weathered, completely fractured sandstone, siltstone claystone alternations. In order to generate stable working media for the above-mentioned project conditions, the cement grouting was carried out. Details of the cement grouting procedure, such as the pattern of the borehole drilled and the distribution of the grout intake various levels are covered in Chapter 4. According to Lugeon test performed after cement grouting, permeation grouting into cavities/fissures of the soil/rock mass surrounding the tunnel was found to be efficient.

From the magnitudes of measured surface settlements and the overall tunnel displacements (Fig. 7), (Fig. 8) it is concluded that good stability control was realized under the unfavorable geotechnical conditions (Fig. 2 and Table 1) i.e. portal zone and poor, varying ground conditions of the site as well as foundation loads due to nearby buildings.

ACKNOWLEDGMENTS

The authors would like to express grateful acknowledgments to Dr. Eng. Ersin ARIOĞLU-Honorary Chairman of the Yapi Merkezi Inc.,-for his academic interests and supports. Special thanks are also due to the consulting team of the Municipality of Greater City of İstanbul. The authors would also like to recognize Dr. Eng. Nejat AYAYDIN-project engineer- and Prof. Dr. Ahmet SAĞLAMER-consulting engineer-for their valuable contributions to the Kabataş-Taksim Funicular System Project. The evaluations, comments and conclusions expressed herein are those

Copyright © 2005 Taylor & Francis Group plc, London, UK

of the authors and not necessarily the Yapı Merkezi–Doppelmayr Consortium.

REFERENCES

Arıoğlu, B, Yüksel, A., Arıoğlu, Ergin, 2002. Geotechnical works and it's evaluation in Nenehatun Tunnel of İzmir Metro Project, *ECAS 2002-International Symposium on Structure and Earthquake Engineering*, 14th October 2002, Middle East Technical University, Ankara, pp 358–368, (In Turkish).

Arıoğlu, Ergin, Yüksel, A., 1999. *Solved Shotcrete Problems in Tunnel and Underground Engineering Structures*, The Chamber of Mining Engineers-İstanbul Branch, İstanbul, 178 pp, (In Turkish).

Arıoğlu, Ergin, Girgin, C., 2003a. Investigation on the stability of the old building in 0 + 085 km of Kabataş–Taksim Funicular System Project, *Yapi Merkezi R&D Department, Report No: 2003/10*, İstanbul, 8 pp, (In Turkish).

Arıoğlu, Ergin, Girgin, C., Yoldaş R., 2003b. Practical notes with regard to construction works in Kabataş–Taksim Funicular System Project, *Yapı Merkezi R&D Department, Report No: 2003/11*, İstanbul, 13 pp, (In Turkish).

Barla, G., 1995, Squeezing in Tunnels, *News Journal International Society For Rock Mechanics,* Vol.2, Number 3&4, Lizboa, pp 14–44.

Hoek, E., Marinos, P., Benissi, M. 2002. Applicability of the Geological Strength Index (GSI) Classification for Every Weak and Sheared Rock Masses: the Case of the Athens Schist Formation *Bulletin of Engineering Geology and the Environment*, Volume 57, pp 151–160

Nonveiller, E., 1989. *Grouting Theory and Practice*, Elsevier, Amsterdam, 250 pp

Sağlamer, A. 2003. Kabataş–Taksim Funicular System Tunnel portal structure progressing report, FS-TR-J2003 *Yapi Merkezi*, İstanbul. 8 pp (In Turkish)

Ulusay, R. & Sönmez, H., 2000. Suggested modifications to the empirical Hoek-Brown failure criterion and their applicability: *Geological Engineering Journal*, Volume 23/24 Number 1. pp 77–99

Yapı Merkezi, 2003–2004. Kabataş–Taksim Funicular System, Deformation Measurement Records, *Yapi Merkezi*, İstanbul (In Turkish).

Yoldaş, R, 2003. Kabataş–Taksim Funicular System Geotechnical evaluation report for bored tunnel region, *Report No: FS-TR-J0115, Yapi Merkezi*, İstanbul, 39 pp, (In Turkish).

Copyright © 2005 Taylor & Francis Group plc, London, UK

Resin-injection soil stabilization techniques used in underground construction carried on in big cities in Russia

A.B. Kondratov
Specialized Research & Production Operations "Geoinjection", Perm, Russia

ABSTRACT: To solve the problems typical for municipal underground construction work such as tunneling a new loose water saturated rocks resin-injection stabilization technique has been developed and implemented in construction practice. Construction procedure is based on preliminary formation of in situ bearing elements in stabilized rocks and further project realization under their protection. The paper presents methods of design and simulation of stabilized ground physical and mechanical properties as well as the concepts of geomechanical variables design for in-situ load-bearing structures.

1 INTRODUCTION

Problems typical for municipal underground construction work arise as tunnels, operation mines and other jobs are driven within the area of big cities of Russia (Perm, Saratov, Kaliningrad, etc.). Very often the jobs are located in a city centre where underground utility systems, office and residential buildings are concentrated. Host rocks down to 20–30 m depth are presented by loose water-bearing deposits composed of loamy sands, loams, sand, gravel, pebble and boulders. Coefficient of permeability makes up 60–70 m per day and over.

Loose water saturated rocks resin-injection stabilization technique has been developed and implemented in construction practice. Construction procedure is based on preliminary formation of in situ bearing elements in stabilized rocks and further project realization under their protection.

2 ADOPTED APPROACHES

Typical complicated situation has occurred in the area of municipal underground construction work in Kaliningrad (former Konnigsberg). Main building of the institution AtlantNIRO is located in the vicinity to the line of route of the discharge header gallery that is under construction. The quoin is 7 m distant from the gallery center line. The gallery of 2.56 m dia. is driven at a depth of 14 m below surface. Accordingly significant part of the building equipped with unique hydraulic testing machines and a basin of 2000 m^3 capacity gets into area of gallery influence. Foundation is a bay of pilings with a thick concrete layer being placed over as a floor. Concrete plate – floor serves as a base for heavy hydraulic testing stand.

Geologic setting in the area of the building foundation and the gallery is rather complex. Downward section is presented by filled soil, loamy sand, loams, dust sand containing gravel and pebble as much as 10%, sandy-clayey floating earth, hard mix of loamy sand with gravel and pebble making up 10–15% and partings of water saturated sand. A bed of confined shifting sand consistent in area and thickness occurs at a depth of 17–18 m right under the building.

In terms of physical and mechanical properties the section presented theoretically may be divided into three basic elements – layers:

1. filled soil, loams (7–8 m thickness);
2. watered dust sand, sandy-clayey floating earth (6–7 m thickness);
3. hard loamy sands with watered confined sand (over 10 m thickness).

The second layer exhibits maximum threat of soil in-rush to the gallery. However, the first layer is also hazardous because of sewerage type pipes laid in it with respective leakages and soil getting soaked. Confined sands of the third layer occur below the gallery foundation base but being hydraulically connected to the overlying layers they exhibit a real threat of soil in-rush to the gallery.

Geomechanical analysis has shown that to prevent from a potential abnormal situation in this area preliminary resin injection stabilization of soil along the gallery route has to be supplemented by protective polymer soil "diaphragm wall" to be formed along

Copyright © 2005 Taylor & Francis Group plc, London, UK

perimeter under threat (face is 20 m long, building rear side is 20 m long).

The project sequence is presented in Fig. 1. Physical, mechanical properties and permeability of polymer soil "diaphragm wall" material are presented in Table 1.

3 VALIDATION OF STRUTURAL MODEL

The polymer soil "diaphragm wall" is aimed to protect the building at surface subsidence related to potential shifting sand in-rush to the gallery. In this connection the proposed structure has to provide for positive foundation waterproofing and in case of shifting sand in-rush to prevent from the building foundation hazardous lateral strains occurrence. According to the "Regulations on Facilities and Environmental Objects Protection from Hazardous Underground Mining Induced Effects" the ultimate lateral strain for buildings of the given type is estimated as $[\tau_g] = 0.44\%$. Strength of a "diaphragm wall" is calculated by Culona-Mohr's criterion:

$$[\tau_g] = C + tg\varphi \cdot \delta_n \quad (1)$$

where C, φ – a coefficient of cohesion and an angle of internal friction of stabilized ground respectively. Preliminary estimates have been made using average data corresponding to lithologic type of rocks and presented in Table 2.

While the problem statement it is assumed that the "diaphragm wall" is put deeper into hard loamy sands. At that its rigid bond to solid base is provided for and no lateral movement is allowed. Physical and mechanical properties of polymer rock compound estimated by means of laboratory tests are presented in Table 3.

Piling as per [5] is considered as a conditional in-deep foundation with the base area (at pile ends level) being estimated within the boundaries cut off by straight lines drawn at angle φ_{av} that is a mean value of internal friction angle for rocks where piles are driven.

Physical and mechanical properties of conditional foundation are estimated by procedure described in [1], that is as the properties of unilateral reinforced compound (with ground as basic material and piles as reinforcing elements). Write E_1 and υ_1 respectively for Young's modulus and Poisson's ratio for piles; write E_2 and υ_2 for ground properties, then elastic

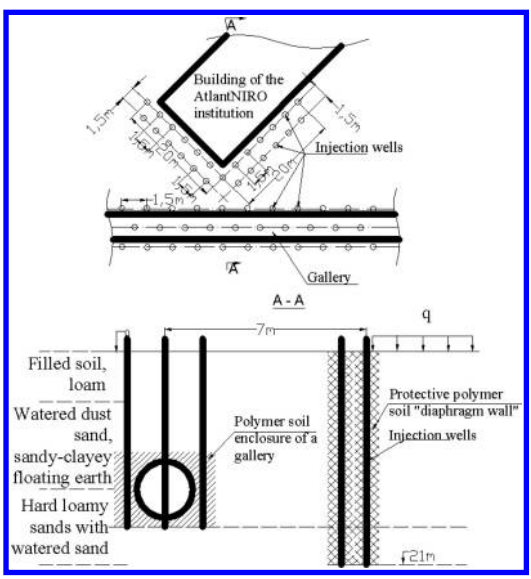


Figure 1. Protective polymer soil "diaphragm wall" formation pattern.

Table 2. Physical and mechanical propertied of rocks.

Rock type	$\gamma \cdot 10^4$, n/m^3	φ, deg	E, KPa	C, KPa	υ
Filled soil	2.1	22	21	21.0	0.33
Dust sand	1.7	42	10	2.5	0.48
Hard loamy sand	2.7	34	14000	1500.0	0.30

Table 3. Physical and mechanical properties of polymer rock compound.

$\gamma \cdot 10^4$, n/m^3	φ, deg	C, MPa	E, MPa	υ
2.0	25	0.45	22.8	0.3

Table 1. Physical and mechanical properties of stabilized loose watered rocks.

Type of rock concrete	Strength, MPa		Young's modulus, MPa		Poisson's ratio	Hydraulic conductivity, m/day
	σ_c	σ_t	E_s	E_d	μ	K_f
Gravel earth mass + urea resin	2.63	0.49	24.7	32.1	0.26	0.0014
Gravel-sand deposits + urea resin	2.97	0.51	23.2	31.5	0.25	0.0012
Loam + urea resin	3.14	0.53	22.8	31.2	0.24	0.0011

Copyright © 2005 Taylor & Francis Group plc, London, UK

properties of a conditional foundation can be calculated from the following formulae:

$$\upsilon_{xy} = K \cdot \upsilon_1 + (1 - K) \cdot \upsilon_2;$$

$$\upsilon_{xy} = \frac{K \cdot E_2 \cdot \upsilon_1 + (1 - K) \cdot E_1 \cdot \upsilon_2}{K \cdot E_2 + (1 - K) \cdot E_1};$$

$$G = \frac{G_1 \cdot G_2}{K \cdot G_2 + (1 - K) \cdot G_1} \qquad (2)$$

where K – relative piles material content by volume in a conditional foundation; Z-axis is directed along the building; X-axis is perpendicular to the building line; Y-axis goes vertically down. Calculated mechanical specifications for a conditional foundation are presented in Table 4. Note that in this case the foundation characteristics tend to exhibit particularly pronounced anisotropy.

As the structure geomechanical variables having been estimated the following options of potential shifting sand in-rush to the gallery have been considered. For the first structural model it is assumed that a fall-through has a natural slope shape (triangular form), where d_2 – depth of a gallery; $L_2 = d_2 \cdot ctg\alpha$ (α – angle of repose). The second option represents a limiting structural model when ground is carried away completely and the "diaphragm wall" is exposed.

Design has been made at fixed in value thickness of "diaphragm wall", $h = 4$ m, distance L between the "diaphragm wall" and the building foundation is variable.

The building dead weight (30 000 tonnes) is accounted for as a distributed load q applied to a conditional foundation.

3 DESIGN METHOD

The finite-element method [2, 7] is the most efficient method in estimation of stress–strain state of rock mass of complex basic geometry. This numerical method enables to account for difference of mechanical properties for rock mass and grounds and their anisotropy. By the finite-element method the domain of interest is approximated by first order triangular elements. Elastoplastic problem statement is based on Lagrange's variational method, the problem has been solved in movements. Elastoplastic model integrating plastic and hard-plastic media has combined two theories that the up-to-date soil mechanics is based on: the elastic theory and the theory of limit state. Regular set of mechanical characteristics obtained during the site investigation will be sufficient to describe the model.

Plastic strains have been accounted for by method of initial stresses with the iteration being used. Anisotropy of the foundation properties being of transversal-isotropic character was accounted for at rigidity matrix generation.

Numerically the method has been implemented on PC by means of double precision computation. Algebraic equations have been solved for unknown joint displacement by Gauss method with a number of degrees of freedom making 1168. Mean processor time per an option makes up 20 minutes.

Table 4. Physical and mechanical properties of a conditional foundation.

Basic material	$\gamma \cdot 10^4$, n/m^3	φ, deg	C, MPa	E, MPa	υ
Loamy sand, loam	2.1	23	0.12	21.8	0.33
				641	0.33
Shifting sand	1.7	42	0.12	2.6	0.48
				623	0.47

*The foundation characteristics in lateral direction are given as numerator; the ones in downward direction are given as denominator.

4 ANALYSIS OF COMPUTATION RESULTS

One of the basic factors contributing to the building stability as a whole is interference between the pile foundation and the base. Potential alternatives of interference are as follows:

– all piles are put deeper into hard ground;
– a part of piles is presented by friction piles;

all piles used are friction piles.

Results of design for a completely earth-sheltered foundation show that even in case of full shifting sand in-rush to the gallery the "diaphragm wall" retains its load-supporting ability and peak lateral strains do not exceed allowable level. In this case distance between "diaphragm wall" and the building has no significant effect on peak tangential stresses working in "diaphragm wall" (τ_{max}). Table 5 presents maximal values of strength criterion $n = \tau_{max}/\tau_g$ where τ_g – allowable tangential stress calculated from the formulae (1).

The "diaphragm wall" position relative to the building effects on value and pattern of the outer foundation boundary lateral strains distribution (Fig. 2), in view

Table 5. Maximum values of the "diaphragm wall" strength criterion (n).

Type of abnormal situation in the gallery	L = 1 m	L = 2 m	L = 5 m
Limited ground in-rush	0.36	0.35	0.36
Unlimited ground in-rush with the "diaphragm wall" being exposed	0.55	0.55	0.56

Copyright © 2005 Taylor & Francis Group plc, London, UK

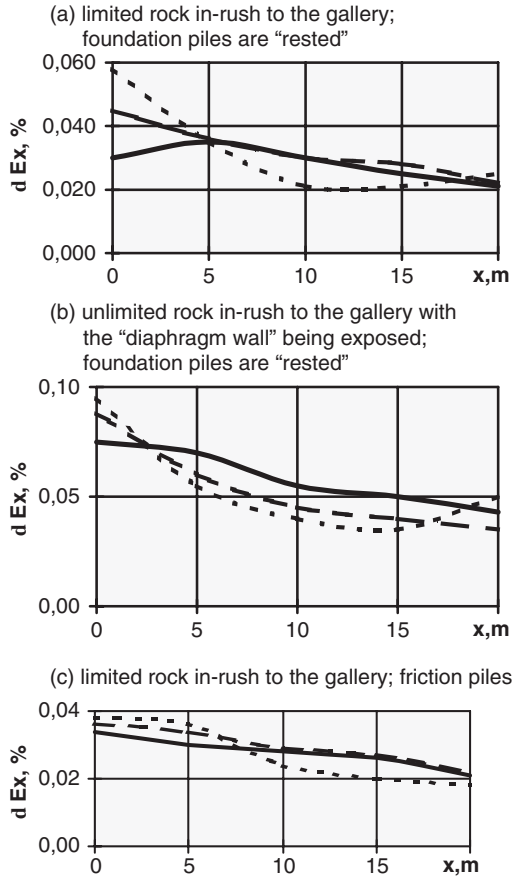


Figure 2. Distribution of lateral strains in AtlantNIRO building foundation under various abnormal situations.

of maximal strains the "diaphragm wall" location in the vicinity to the building is the most favorable.

In case of floating pile foundation being used limited shifting sand in-rush to the gallery will not result in the "diaphragm wall" failure. Maximal lateral strains of the foundation do not reach limiting values. In case of unlimited shifting sand in-rush and floating pile foundation being available realized lateral displacements of a building may reach 1.5 m and significantly exceed limiting values independent of the "diaphragm wall" location. Consequently with this rock mass plastic strains build-up a designed "diaphragm wall" may also fail.

Analysis of the "diaphragm wall" design results with stabilized ground plastic strains being accounted for enable to come to the following conclusions:

– at limited by angles of repose abnormal rock in-rush to the gallery selected specifications of the polymer soil "diaphragm wall" provide for the building protection from hazardous strains at any arrangement of its foundation piles – "rested" or "floating", at that 2–3- fold safety factor will be guaranteed;
– at unlimited rock in-rush to the gallery with polymer soil "diaphragm wall" of specified variables that is completely exposed and the foundation piles being of "rested" type lateral strains in the foundation will not exceed the limiting values; in case of completely "floating" piles the foundation ultimate strains may be exceeded therefore extra protective measures may be called for;
– the "diaphragm wall" position in the vicinity to the building is more favorable in view of strains localization.

Developed package of special measures provides for complete elimination of strains and the building failure risk both at tunnel drivage and during the header operation period. Similar works on the undermined 14-storey building protection have been successfully carried out earlier in Perm [3]. It has to be noted that geodetic survey and the project monitoring are to be considered as a prerequisite [3, 6].

REFERENCES

1 Bolotin, V.V. & Novichkov, Yu.N. 1980. *Mechanics of multiple-lift construction*. Moscow: Mashinostroyenie Publishers.
2 Fadeyev, A.B. 1987. *The finite-element method in geomechanics*. Moscow: Nedra Publishers.
3 Kondratov, A.B. 1996. Strains monitoring at special utility gallery drivage in Perm. In *Global underground space. Proc. world tunnel congress, Stuttgart, N. 3–4.*
4 Russian Building Code 2.02.03-85. 1986.*Pile foundations*. Gosstroy SSSR.
5 Tsytovich, N.A., Berezantsev,V.G. et al.1970. *Basements and foundations*. Moscow: Vysshaya Shkola Publishers.
6 Valet, J.-L. 2002. Compensating injection: real-time technique. Lefortovo tunnel in Moscow. *Metro and tunnels 4*.
7 Zenkevich, O. 1979. *The finite-element method in engineering*. Moscow: Mir Publishers.

Copyright © 2005 Taylor & Francis Group plc, London, UK

Calculation of the stress intensity index of a sprayed concrete lining

R.B. Rokahr, R. Zachow & D. Zander-Schiebenhöfer
University of Hanover, Hanover, Germany

ABSTRACT: The problem in interpreting measured data is to assess the daily changes of the displacements with respect to the stability of the combined system involving the lining and the ground. The displacement of the roof alone is not decisive: it is crucial to consider the roof in combination with the remaining displacements (i.e. convergence, divergence, settlement of the footing). A critical factor is the number of days and/or the period over which the changes in displacement are measured, e.g. the evaluation of the increase of the displacements within the first few days is completely different in comparison to the same increase that occurs after 10 or 20 days. Structural analysis carried out during the design stage merely takes time into consideration in a very simplified manner. However, the stability of the combined lining/ground system is strongly influenced by time. The validity of such a simplified stress analysis approach is inevitably very limited. Therefore, a method was developed for daily monitoring of the lining on the basis of the geotechnical measurements. This method permits the monitoring of the stress intensity of the sprayed concrete lining at any time and at any place within the tunnel, and has three main advantages. First, because of the ongoing calculation of the stress intensity, critical processes can be identified at an earlier stage in their development. Second, during the construction stage it is possible to optimise the supporting measures to meet the requirements of stability, security and economy. Third, calculations for the inner lining can be carried out based on the stress intensity of the sprayed concrete lining.

1 INTRODUCTION

The need to control the stability of tunnels using geotechnical measurements is undisputed. Most construction contracts stipulate that the validity of the preliminary structural investigations must be guaranteed by the interpretation of these measurements. Unfortunately, less and less time is available for this task within the framework of functional tenders. If no plans are included to have a geotechnican on site carrying out this task, it is down to the construction supervisor to interpret the measurement results. However, the construction supervisor is usually so busy with other things that he only carries out an interpretation if particularly difficult situations arise. In the end, the surveying technician has to decide which measuring cross-sections are given priority – unfortunately there are no general rules available to help him reach his decision. If the stability of a tunnel is to be assessed, the deformation behaviour of the combined ground/sprayed concrete lining – as the load-bearing system – must be taken into consideration.

The various possible displacements shown in figure 1 immediately show that settling of the roof is not only the crucial factor, but also the other measured displacements (convergence, divergence and settling of the footings) have to be considered. In Case A, a translation takes place which leaves the sprayed concrete lining unstressed. In Case B, the sprayed concrete lining is only subjected to pure normal forces. In Case C, the normal force is joined by a bending moment. Case D is dominated by bending stress. So we see here that the same degree of roof settlement can be associated with at least four different stress states.

The measurement results are difficult to interpret because the daily changes in deformation or rather increases in deformation, need to be assessed with regard to the stability of the load-bearing system. It is

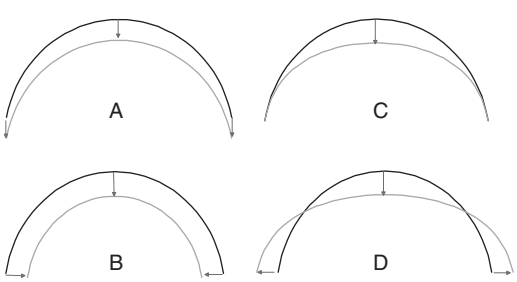


Figure 1. Deformation examples of a roof lining.

Copyright © 2005 Taylor & Francis Group plc, London, UK

particularly important to make allowance for the number of days after construction and the time periods over which the increases in displacement were measured. For instance, as a result of the construction method and the material behaviour increases in displacement occurring within the first few days should be assessed completely differently from displacement of the same order taking place after ten or twenty days. Because the time factor is usually not allowed for in structural calculations during the planning phase, the results of this preliminary investigation are inappropriate to be utilised during the construction phase to assess stability.

The method developed by ROKAHR/ZACHOW, which has now been implemented within the STRESS program system, includes as part of the daily interpretation of measuring results, a calculation of the stress intensity of the sprayed concrete lining by reverse calculation based on the measured deformation (this is in addition to the standard assessment of the time-displacement curves and the vectoral displacement diagrams). Calculation of the stress intensity in the sprayed concrete lining separately for each measuring section and each measurement takes into consideration the following boundary conditions:

- the actual contour of the sprayed concrete lining,
- the actual absolute position of the measuring points related to the tunnel axis,
- the deformation of the sprayed concrete lining at each point in time,
- the non-linear stress-strain relation for a change in load taking into consideration:
  - the dependence on cube compressive strength and calculated strength development,
  - the time-dependent fracture strength and calculated strength development,
  - the time-dependent development of ultimate elongation in the sprayed concrete,
  - the time-dependent stress-strain relation of the sprayed concrete (creep and relaxation).

The stress intensity calculated using this method is defined as relationship between the stresses calculated from the measured displacement and the time-dependent calculated strength of the sprayed concrete. With this method, the measuring results of all geotechnical surveys can be continuously analysed and updated after each measurement.

Updating takes place separately for

- each measuring section,
- each lining section,
- for the inner and outer lining margin.

Whilst the absolute displacements play a crucial role in assessing the usability, when it comes to stability, the most important aspect is the relative displacement between neighbouring points in the lining.

Generally, measuring inaccuracies can be smoothed out by subsequent interpolation. At least one additional subsequent measurement is usually required to assess whether a change in measured value is due to inaccuracy or is actually part of a displacement trend.

Another intention of this method is to extrapolate the interpreted strain curve to estimate the probable stress intensity of the sprayed concrete lining and the stability boundary.

Another requirement for the further interpretation of the measuring results, and in particular, for the stipulated confirmation of stability on the basis of geotechnical measurements demanded by almost all regulations, is the determination of the strain of individual lining sections so that conclusions can be drawn on the amount of stress involved.

The strain derived by the STRESS program system from the displacement of discrete points in the outer liner is checked with the calculation of a tunnel model using the FLAC3D FE program system from ITASCA. A sprayed concrete roof liner is subject here to a stepwise increase in vertical and horizontal stress.

The displacements of 5 boundary points of the opening determined by the FE calculation, whose positions correspond approximately with the convergence measurement points on an outer liner (one roof point, 2 abutment points at around 50 degrees, and two footings points, which lie approx. 1.5 metres above the roof base) are used to acquire the strain at the inner and outer margin of the liner with the help of the STRESS program, and compared with the integral strains of the roof zone derived from the FE calculations. This reveals that the strain calculated from the displacement of 5 discrete points describes the strain in the sprayed concrete liner with sufficient accuracy.

The irregularities in the calculated curves for the vertical and horizontal displacements, the subsequently calculated strains, and the ultimately calculated stress intensity are always caused by the measured values provided by the surveyor – independent of whether the reason is a reading error, damage to a measuring point or real displacement. It would therefore make sense to already correct any major errors at this phase by interpolation or regression calculations, and thus to smooth the curve.

However, in the case of a reference point correction, the resulting smoothed curves would falsify the situation and result in errors in the strain calculations.

On the other hand, smoothing which only takes place for the first time at the stress calculation phase would also be erroneous because this would be preceded by false strain increases at false points in time of the sprayed concrete liner which reacts in a time-dependent way.

For this reason, the following analysis calculates the strains from the raw measurement values in each case, and their change over time is then smoothed with the

Copyright © 2005 Taylor & Francis Group plc, London, UK

help of a regression calculation. The stress intensity is then calculated from the resulting values.

2 MATERIAL BEHAVIOUR OF SPRAYED CONCRETE

Just as in structural engineering, it is also necessary in tunnel engineering to check the material parameters of the construction materials on site from time to time for each structure on the basis of tests. This control is particularly important for fresh sprayed concrete because the tunnel lining already plays a load-bearing role at a very early stage.

2.1 *Compressive strength*

Several investigations are described in the literature for the development of the cube compressive strength of fresh sprayed concrete. Figure 2 shows the recommendations from CEB-FIP and WEBER for the temporal dependence of the strength of concrete class B25.

The reduction in calculated strength compared to the cube compressive strength of the sprayed concrete as designated in DIN 1045, are shown as blue squares in figure 3. This dependence can be determined to an adequate degree of accuracy by the red function

$$\beta_R = - 0{,}005 * \beta_{WN}^2 + 0{,}83 * \beta_{WN}$$

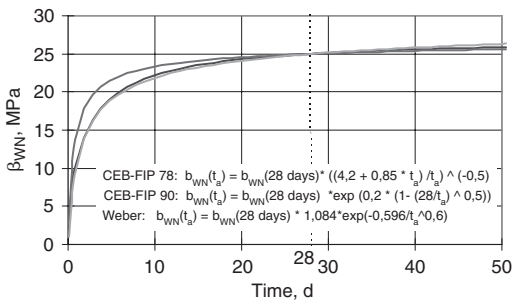


Figure 2. Cube compressive strength versus concrete age t_a.

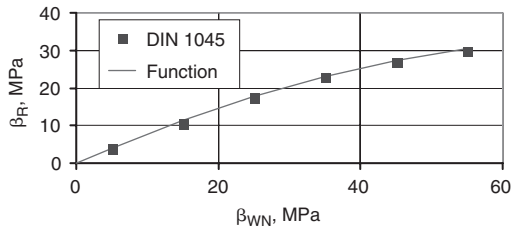


Figure 3. Calculated strength versus nominal cube compressive strength.

2.2 *Ultimate elongation*

The elongation of the fresh concrete is also dependent on the age of the concrete. It is often claimed in discussions that the elongation of fresh concrete is larger than that of hardened concrete. It is true that in the case of young concrete, the slow build-up of load only causes failure at a *measured* strain which far exceeds the elongation stipulated by DIN 1045. However, this measured strain includes a large proportion of creep strain which already occurs during the loading phase. When the load increases quickly, the elongation of fresh concrete is far below that of hardened concrete. WIERIG, KHAN et al. and XIANJU et al. are just a few examples in the literature referring to this situation, see figure 4. The blue and red functions were developed on the basis of measured values. The total of elastic and early creep strain during the testing phase is often also erroneously described as elongation.

In the following, elongation is described as strain after which no further increase in stress occurs and when the calculated strength has been reached.

2.3 *Stress–strain behaviour*

For the calculation of deformation, DIN 1045 stipulates Hook's law for the first approximation. Dimensioning can take place in a simplified way according to a bilinear stress–strain line which reaches a stress level corresponding to the calculated strength at strain of 1.35%.

A more accurate assessment is then carried out using a parabolic-rectangle diagram in which the stress curve follows a quadratic parabola until the calculated strength is reached at an elongation of 2%. If one incorporates into the stress–strain expression in DIN 1045 the fracture strength dependent on time and cube compressive strength determined in figures 2 and 3, and the calculated elongation which is also time-dependent (figure 4), then the curves shown in figure 5 can be derived for concrete of different age, and can be expressed by the following relationship:

$$for \quad \varepsilon < \varepsilon_R \quad \sigma = \beta_{R,(t)} * \left(-\frac{\varepsilon^2}{\varepsilon_R^2} + 2 * \frac{\varepsilon}{\varepsilon_R} \right)$$

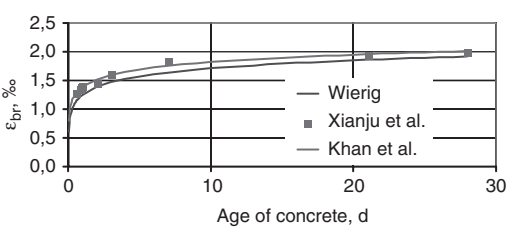


Figure 4. Ultimate elongation versus concrete age.

Copyright © 2005 Taylor & Francis Group plc, London, UK

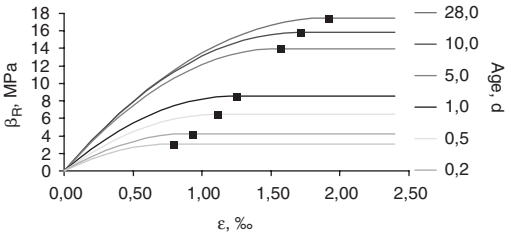


Figure 5. Example of stress-strain lines for sprayed concrete (B25) dependant on concrete age.

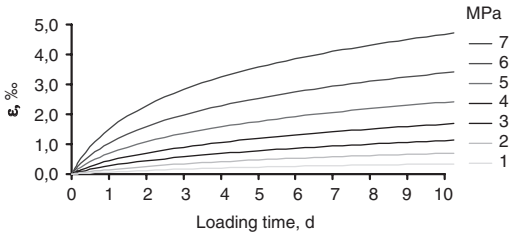


Figure 6. Creep strain ε_v versus time.

2.4 *Creep strain*

In addition to the elastic strain which is assumed to be reversible, there is also an irreversible proportion of viscose strain which is dependent on the stress as well as on the duration t of the stress and the age of the sprayed concrete ($t + t_a$).

The viscous strain is considered to be a better way of revealing the development of the concrete over time. This concept led to a further development of the previously used material law with a time-dependent diminution factor derived according to the development in fracture strength.

$$\psi = \left[\frac{4{,}2 + 0{,}85 * t}{t}\right]^{-0{,}5}$$

A formula was developed which asymptotically approaches a limiting value over time.

The expression for the creep rate is therefore as follows:

$$\dot{\varepsilon}_v(t) = (1-\psi) * \alpha * \exp\left(-\frac{s_1}{s_2} * t\right) * \frac{\left[\sigma + \left[n_1 * \exp\left(-\frac{t^{n_2}}{\sigma}\right) * \left(n_2 * t^{n_2} * \ln(t+t_a) - \sigma * \frac{t}{t+t_a}\right)\right]}{s_2}$$

where,

$$s_1 = s_1^* * \exp(k_1 * \sigma)$$

is the spring strength

$$s_2 = s_2^* * \exp(k_2 * \sigma) * (t + t_a)^{n_1 * \exp\left(-t^{n_2}/\sigma\right)}$$

is the viscosity and

$$\alpha = \frac{1}{1 - \psi_0}$$

is the correction factor.

The parameters referred to in the aforementioned formulae are factors determined from laboratory tests. For concrete with an age t_0 at the beginning of the test, this gives:

$$\psi_0 = \psi(t_0).$$

The development of the factor is associated with an error because it gives rise to a creep strain of 0 after a stress period of 28 days. A limiting value is therefore fixed beyond which any further decline in the creep curves is exclusively attributed to viscosity. Empirical data from laboratory tests reveal that this point is reached after approx. 8 to 12 days. The creep curves determined in the laboratory tests are aggregate-dependent and weathering dependent and therefore need to be determined specifically for each tunnel.

In figure 6, the calculation of the creep curves for an initial concrete age of e.g. $t_a = 1.25$ days and a stress period of $t < 10$ days uses the modified material law for sprayed concrete with the aforementioned functions.

3 RESULTS

Figure 7 shows the result of controls carried out in practice during the course of tunnel construction for a completed section of tunnel. The red line corresponds to the maximum stress level occurring in each measuring section since installation. With the help of the STRESS program system, it is possible to carry out controls of this type on a daily basis during the course of tunnel construction and to update the stress curve on a daily basis.

4 SUMMARY

The methods discussed in this paper take into consideration the time-dependent material behaviour of the sprayed concrete, and enable the stress on a sprayed concrete lining to be controlled at any time and at any place in the tunnel on the basis of geotechnical measurements. The daily updating of the stress intensity calculations enables critical situations to be identified early, as well as an optimisation of the necessary safety measures in an ongoing way parallel to the construction progress. The calculated stress intensity of the sprayed concrete external liner can then be taken into consideration for dimensioning the inner liner. Although structural calculations are essential for planning the

Copyright © 2005 Taylor & Francis Group plc, London, UK

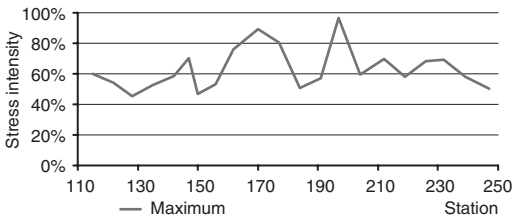


Figure 7. Example of the maximum stress intensity of the sprayed concrete lining in a tunnel section.

construction of a tunnel, they only produce a single deformation figure per stress approach, whereas the ROKAHR/ZACHOW method reflects the actual deformation occurring at the site.

In 1995 the first attempt was made to calculate the stress intensity during the building of the Römerberg tunnel by HL-AG (Vienna). Ever since, the resulting STRESS program system has continuously been advanced. It was used to construct the Melk underpass (Melk tunnel and Wachberg tunnel). Other references include the Egge tunnel completed in 2003, as well as the Geissberg tunnel on the new Nuremberg/Ingolstadt railway line. The method was also used in the Spital tunnel, the Lainzer tunnels in Vienna, the crossing of the Matzenpark in Brixlegg, the Steinhaus tunnel and the local traffic hub in Linz.

The ROKAHR/ZACHOW method was checked by stress measurements in the sprayed concrete external liner carried out by gbm, Limburg, using the compensation method. This method involves reversing the deformation arising from artificial release of the stress in the liner as a result of cutting stress-releasing slots in the external liner. The deformation is reversed by establishing a compensation pressure with suitable loading equipment. The compensation pressure built up in this way usually corresponds to the original stress. In addition, the strain calculated in the Geissberg tunnel using the ROKAHR/ZACHOW method was checked by measurements carried out with the help of ssm-1-concrete strain transmitters.

The usability of the method has so far been confirmed on site by over 1,500 cross-section measurements along 16,000 tunnel metres.

REFERENCES

Model Code 1990; International Federation for Structural Concrete (FIB); Comité Euro-Internacional du Béton (CEB) 1990.

DIN 1045; Fassung Juli 1988, Beuth-Verlag Berlin.

WEBER, J. W.; Empirische Formeln zur Beschreibung der Festigkeitsentwicklung und des E-Moduls von Beton. Beton- und Fertigteiltechnik, Heft 12, 1997.

WIERIG, H. J.; Eigenschaften von "grünen, jungen" Beton, beton (1968), Heft 3, 1968.

KHAN, A.; COOK, W.; MITCHEL, D.; Early Age Compressive Stress–Strain Properties of Low-, Medium- and High-Strength Concretes, ACI Journal, Vol. 92, 1995.

XIANJU Jin und ZONGJIN Li; Investigation of Mechanical Properties of Young Concrete, Materials and Structures, Vol. 33, 2000.

PÖTTLER, R.; Konsequenzen für die Tunnelstatik aufgrund des nichtlinearen Materialverhaltens von jungem Spritzbeton, Felsbau 8, (1990), Nr.3, Essen; 1990.

ROKAHR, R.; ZACHOW, R.; Ein neues Verfahren zur täglichen Kontrolle der Auslastung einer Spritzbetonschale. Felsbau 15 (1997) Nr.6; 1997.

ZACHOW, R.; VAVROVSKY, G. M.; Abschätzung der Auslastung des Spritzbetons mit Hilfe geotechnischer Messungen. Felsbau 13 (1995) Nr.6; 1995.

FRÖHLICH, B.; Spannungsmessungen nach der Kompensationsmethode in der Außen-schale des Eggetunnels, gbm – Gesellschaft für Baugeologie und – meßtechnik mbH, Dezember 1998.

Copyright © 2005 Taylor & Francis Group plc, London, UK

Prediction of ground deformation response for double tunnel Bangkok MRT subway

W. Teparaksa
Center of Soft Ground Engineering, Department of Civil Engineering, Chulalongkorn University, Bangkok, Thailand

ABSTRACT: The first MRT subway project of Bangkok city consists of dual tunnels about 20 km long with 18 subway stations. The tunnels are seated in the firm first stiff silty clay layer between 15–22 m. depth below ground surface having outside and inside diameter of 6.3 m., and 5.7 m., respectively. The behavior of ground deformation response based on instrumentation is presented. The back analysis based on plain strain FEM analysis was also presented and agreed with field performance. The shear strain of FEM analysis is in the range of 0.1–1% and agrees with the results of self boring pressuremeter tests.

1 INTRODUCTION

Construction of the first blue line subway 20 km long, the Metropolitan Rapid Transit Authority (MRTA) project has been started since 1996. The project consists of 18 underground stations running from the central main state railway station called the Hualamphong Station (S1) and goes through the business area, passes the bus terminal and ended at the Bangsue Station (S21) as shown in Figure 1. The project is a turnkey project divided into two parts as the South Contract awarded to BCKT JV, and North Contract awarded to ION JV. This first subway was completed and opened in August 2004. The next phase of the MRT subway will be extended from next year 2005. This paper briefly describes the MRT project, the principle of instrumentation to meet all design requirements, and safety control. The behavior of ground surface settlement during tunneling was presented based on instrumented record at various stages and time of construction. Back-analyses of ground surface response by means of FEM analysis are also presented.

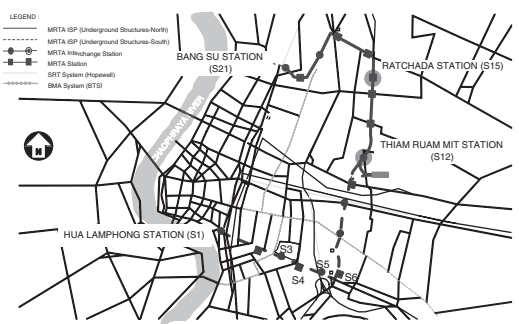


Figure 1. MRT Bangkok blue line subway.

2 GENERAL BANGKOK SUBSOIL CONDITIONS

Subsoil investigations were initially carried out during feasibility study and reported by Halcrow (1993). The post-tender site investigation were carried out during construction in order to confirm the subsoil conditions, to determine the existing piezometric levels, and to determine the design soil parameters. Over 200 boreholes as well as six numbers of self-boring pressuremeter tests were carried out. The general subsoil conditions are presented in Figure 2.

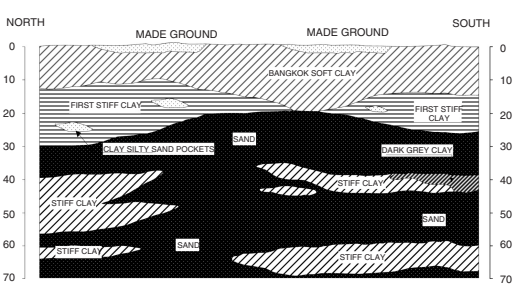


Figure 2. General Bangkok subsoil profile.

Copyright © 2005 Taylor & Francis Group plc, London, UK

The subsoil consists of 13–16 m. thick soft marine clay. This clay is sensitive, anisotropic and creep (time dependent stress-strain-strength behavior) susceptible. These characteristics have made the design and construction of deep basements, filled embankments and tunneling in soft clay difficult. The first stiff to very stiff silty clay layer is encountered below soft clay and medium clay varying from 21 to 28 m. depth. This first stiff silty clay having low sensitivity and high stiffness is appropriate to be the bearing layer for the subway tunnels. The first dense silty sand layer is located below stiff silty clay. The groundwater condition is hydrostatic starting from 1.0 m. below ground level. Deep well pumping from the deep aquifers has led to the under drainage of the soft clay and stiff clay as well as deeper soil layer. The piezometric level or the pheratic surface of the Bangkok aquifer is, therefore, reduced and quite constant at about 23 m, below ground surface (Teparaksa, 1999) as shown in Figure 3. This low piezometric level contributes to increase in effective stress, causing ground subsidence. However, the benefit of this lower piezometric level is easy to make a dry excavation of basement construction or subway station up to the silty clay level without any dewatering or pumping system. The subway tunneling was designed to be seated mainly in the first stiff silty clay layer between 15–22 m. depth below ground surface which is of very high stiffness and expecting very low or minor ground loss during TBM boring (Teparaksa, 1999, a, c and 2000).

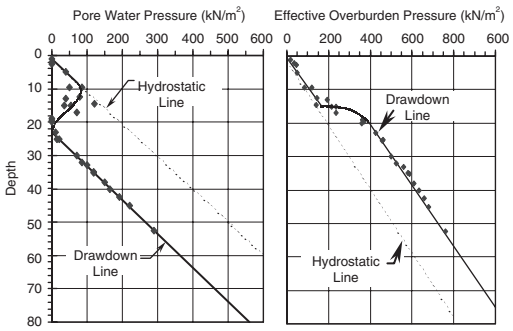


Figure 3. Piezometric level of Bangkok subsoils.

3 MRT SUBWAY CONSTRUCTION

The subway construction technique proposed by the JVs of the North and South contracts is different. Construction of the North route was firstly started with only a small launching shafts at one end of the station, then followed by tunneling works and concurrently subway station construction by top down construction technique. The South route construction, however, was started with firstly completion of the whole subway station structures and then followed by tunneling works. Therefore, the tunneling work of the North route was started earlier than the Southern route, although the South contract was awarded earlier than the North. The instrumentation related to monitoring the soil displacement during tunneling consists of the surface settlement

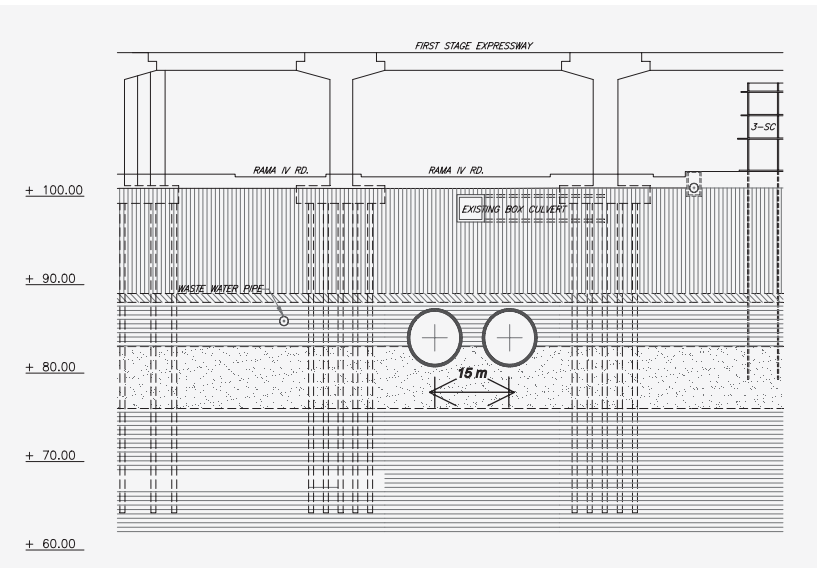


Figure 4. Parallel dual tunnel.

Copyright © 2005 Taylor & Francis Group plc, London, UK

points, extensometer, inclinometer and convergent bolts. Even though the convergent bolts mainly aims to monitoring the deformation of the segmental tunnel after installation, however, it is very useful for cross checking the ground settlement especially when some soil improvement techniques are applied near the completed tunnel. The tunnel was designed as a reinforce concrete segmental lining of about 0.3 m. thick with outside and inside diameter of 6.3 m., and 5.7 m., respectively. The Earth Pressure Balance (EPB) shield technique was used to bore the tunnel and the tunnells are seated in the firm first stiff silty clay layer between 15–22 m. depth below ground surface. Generally, dual tunnels in parallel arrangement with spacing between tunnel of about 15 m. is designed as shown in Figure 4. However, between station S1 (Hua Lumpong) to S6 (Sirikit) due to the obstruction of the existing main Bangkok water supply tunnel (MWA Tunnel) of about 3.5 m. in diameter, the dual tunnels were arranged in vertical stack direction as shown in Figure 5. Between station S6 to S5 (Bonkai) the tunnel was bored underneath and cross through this existing this main water supply tunnel in perpendicular direction as shown in Figure 6.

The clear space between the MRT tunnel and the existing main water supply tunnel is about 4.0 m.

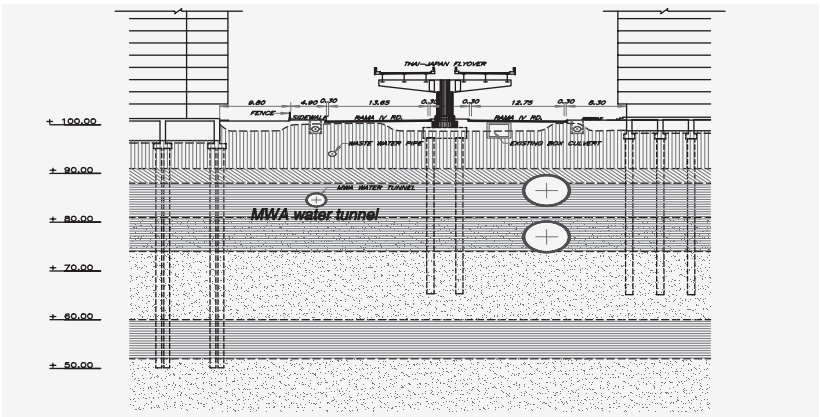


Figure 5. Vertical stack dual tunnel.

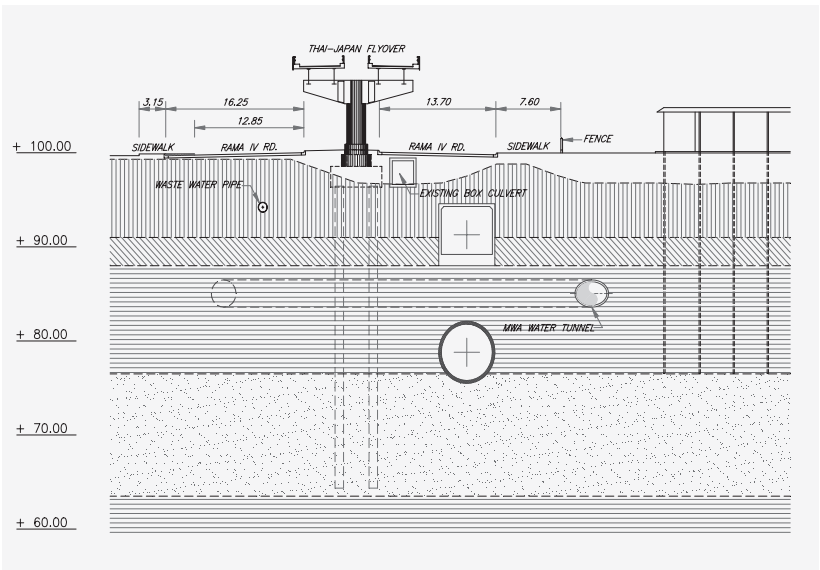


Figure 6. Tunnel bored underneath the existing MWA tunnel.

Copyright © 2005 Taylor & Francis Group plc, London, UK

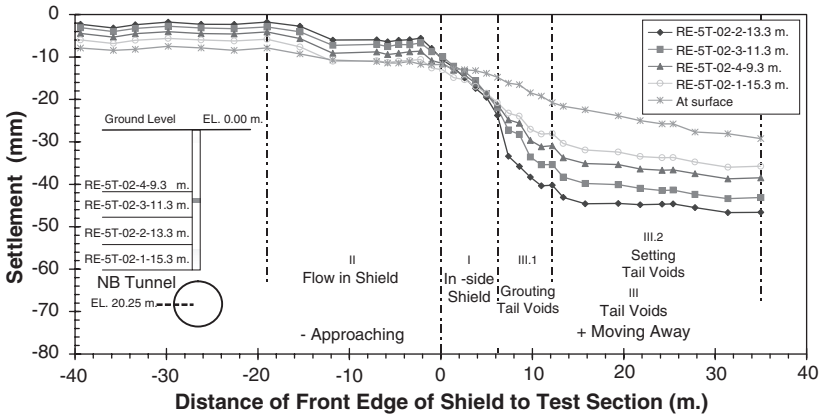


Figure 7. Behavior of ground displacement caused by EPB bored tunnel.

During MRT tunnel boring, the main water tunnel is under service discharge water pressure of 50–80 kN/m^2. The structure of the existing main water tunnel is the concrete segmental lining of 0.2 m. thick with secondary steel liner.

4 SOIL DISPLACEMENT RESPONSE DUE TO BORED TUNNELING

The ground surface response during bore tunneling was monitored by means of geotechnical instrumentation (Teparaksa, 2001). The ground surface and subsurface response due to shield tunneling can be classified according to position of TBM passing through the measured point into 3 stages as the deformation ahead the shield, deformation at the shield, and deformation behind the shield. This deformation behavior recorded between stations Bonkai (S5) to Sirikit (S6) is presented in Figure 7. The deformation ahead the shield is mainly due to soil flow into the shield, while deformation behind the shield is due to effect of tail void and setting time. It is clearly showed that the displacement behind the shield is the major displacement both surface and subsurface due to tail void phenomena.

5 PREDICTION OF GROUND DISPLACEMENT RESPONSE

The numerical approach to predict ground displacement response was performed based on FEM analysis. The two dimensional FEM namely PLAXIS (Teparaksa, 2002) is used for modeling of the interaction between soil and structure. With this approach, a complete modeling of the system including the stress-strain distribution and ground water condition, the deformation and section force in the lining was also possible.

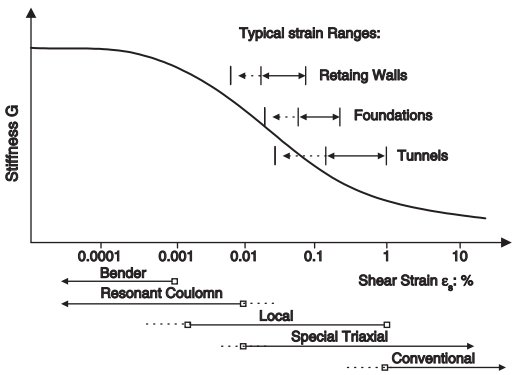


Figure 8. Typical shear modulus and shear strains for foundation works (after Mair 1993).

5.1 *Soil modeling*

The constitutive model was based on an elasto-plastic (Mohr-Coulomb) failure criteria. As the recorded ground displacement response, it was occurred in the short term conditions, therefore undrained soil parameters were assumed for the cohesive soil layers. The effect of ground water flow as well as consolidation was not considered in the model. The standard ground model used for the FEM analysis was based on the soil stiffness parameters. Generally the stiffness of the Bangkok subsoils has the non-linear behavior depended on the shear strain level (Teparaksa, 1999, c and 2000). For practical point of view, the plain strain concept with the Mohr-Coulomb soil model was used in the FEM analysis. Mair (1993) proposed the soil stiffness depending on the order of the shear strain as shown in Figure 8. The range of shear strain for bored tunnel was recommended in the range of 0.1–1.0%. Six number of self boring pressuremeter test were carried out along

Copyright © 2005 Taylor & Francis Group plc, London, UK

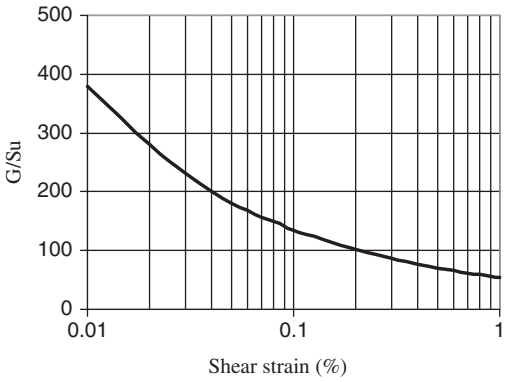


Figure 9(a). Shear modulus of soft Bangkok clay.

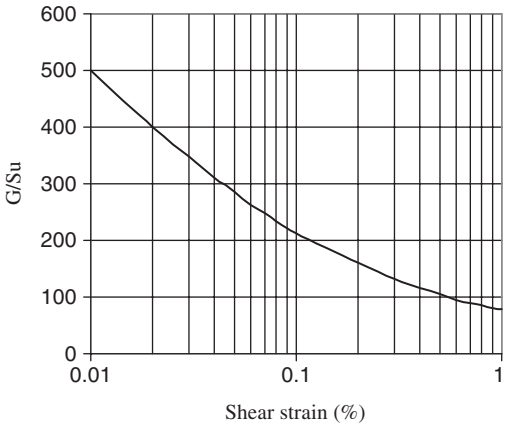


Figure 9(b). Shear modulus of stiff Bangkok clay.

the MRT route. Teparaksa (1999, a and b) reported the results of the self-boring pressuremeter tests in Bangkok subsoil that the soil stiffness was depended on the degree of shear strain. Figure 9 (a) and (b) show the variation of shear modulus with shear strains for soft clay and stiff clay respectively. According to the shear modulus from pressuremeter test and the order of shear strain for tunneling works recommended by Mair (1993) between 0.1–1%, the soil stiffness was assumed for FEM analysis as Eu/Su = 240 and 480 for soft clay and stiff clay, respectively. The strength and definition soil parameters were summarized in Table 1.

Table 1. Soil parameters for FEM analysis.

Soil layer	Su (kN/m^2)	Eu/Su	E′ (kN/m^2)
Made ground	35	300	–
Soft clay	17–22	240	–
Stiff clay	100–150	480	–
Silty sand	–	–	$2000N_{60}$

Su: Undrained shear strength
Eu: Undrained modulus
E′: Drained modulus

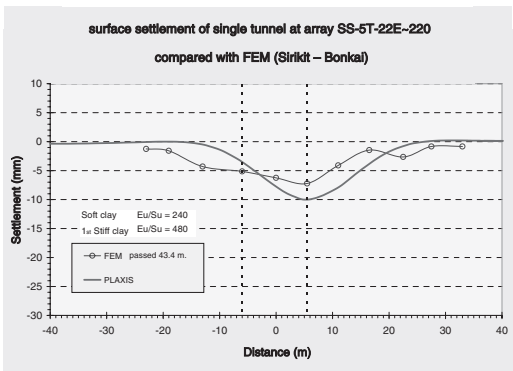


Figure 10(a). FEM prediction of ground surface displacement for single (parallel) tunnel.

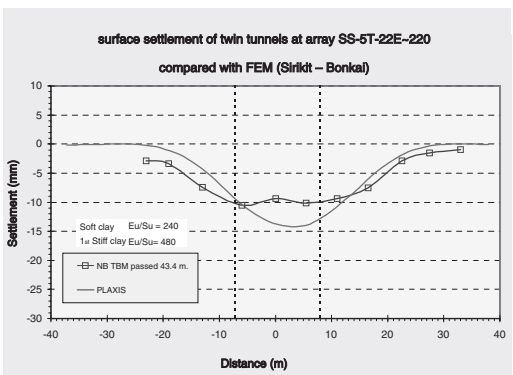


Figure 10(b). FEM prediction of ground surface displacement for twin parallel tunnels.

5.2 *FEM analysis*

Figure 10 shows the comparison between FEM predictions of ground surface deformation response with the field performance for case of parallel dual tunnel between stations Sirikit (S6) – Bonkai (S5). Figure 11 presents the comparison between FEM predictions of ground surface deformation response with the field measurement for case of vertical stack dual tunnel between Lumpini (S3) to Silom (S4) station.

It can be seen that the FEM prediction of ground surface deformation response agrees well with the

Copyright © 2005 Taylor & Francis Group plc, London, UK

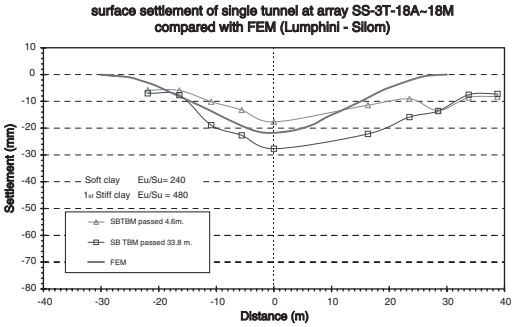


Figure 11(a). Predicted surface settlement from FEM for single tunnel.

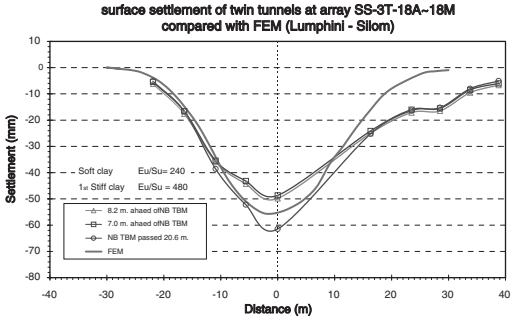


Figure 11(b). Predicted surface settlement from FEM for twin vertical stack tunnels.

field performance. The range of shear strain between 0.1–1% as recommended by Mair (1993) and Menzies (1997) as well as the soil stiffness in terms of modulus tested by means of self boring pressuremeter tests, therefore, can be used combination with Mohr-Coulomb constitutive soil modeling to predict ground response due to bored tunnel.

6 CONCLUSIONS

The ground surface settlement was monitored during and after completion of the MRT subway tunnelling in Bangkok city. The behavior of ground surface deformation response based on instrumentation was presented. The soil stiffness based on self boring pressuremeter test is proposed. The predicted ground surface settlement based on plain strain condition FEM analysis using Mohr-Coulomb soil modeling was also presented. The prediction of ground surface response due to shield tunneling by FEM analysis agreed with field performance.

ACKNOWLEGEMENT

The authors would like to express their gratitude to the Mass Rapid Transit Authority of Thailand (MRTA) for their permission of publishing this paper. Thanks also to all staff of the Strategia Engineering Consultants Co., Ltd. (SECC) for their supporting in the analysis as well as preparing the manuscript.

REFERENCES

Halcrow. 1993. Metropolitan Rapid Transits Authority Initial Project, *Geotechnical Report*.

Mair, R.J. 1993. Development in geotechnical engineering research, application to tunnels and deep excavations, *Proceedings of the Institution of Civil Engineers and Civil engineering*.

Menzies, B. 1997. Applying modern measures, *Ground Engineering*, pp. 22–23.

Teparaksa, W. 1999 a. Geotechnical aspects on the design and construction of the MRTA subway in Bangkok, *Journal of the Society of Professional Engineering Thailand*, Vol. 24, pp. 21–34.

Teparaksa, W. 1999 b. Performance of diaphragm wall and soil parameters for design and construction of sub structures in Bangkok subsoil, *Annual Conference on National Civil Engineering*, Engineering Institute of Thailand.

Teparaksa, W. 1999 c. Principle and application of instrumentation for the first MRTA subway project in Bangkok, 5th International Symposium on Field Measurements in Geomechanics, Singapore.

Teparaksa, W. 2000. Displacement behavior of soil for the first MRTA subway in Bangkok subsoil, *13th KKNN Symposium on Civil Engineering*, Taipei, Taiwan, pp. 349–354.

Teparaksa, W. 2001. Performance and behavior of soil and tunnel displacement due to bored tunnelling of MRT project, Guest speaker, 7th *National Conventional Conference*, Engineering Institute of Thailand, pp. INV 75–90.

Teparaksa, W. 2002. Training course on PLAXIS, *Two Plus Soft Co. Ltd.*, Bangkok, Thailand.

Copyright © 2005 Taylor & Francis Group plc, London, UK

Safety

Copyright © 2005 Taylor & Francis Group plc, London, UK

New guidance on safety standards for road and railway tunnels

A. Focaracci
Ministry of Infrastructures and Transports, Roma, Italy

ABSTRACT: European Directive 54/2004/EC may represent a turning point in the field of safety in the use of transport infrastructures and tunnels in particular: finally we are passed from a phase in which, in the aftermath of dramatic events all tunnel, safety measures seemed to be inadequate, to a phase in which safety is approached in engineering terms through a logical sequence of analyses and evaluation, mainly of a numerical and quantitative type.

In order to ensure that sentimental considerations do not lead to exaggerated reactions, with economic implications, it is necessary to plan the safety of infrastructures in the same way that the static safety of the work is planned. Italy's commitments to the subjects of road and railway tunnel safety undoubtedly represents a valid reference on which to base further developments on a international level and in the various scientific consensuses.

1 ITALIAN ACTION FOR SAFETY IN TUNNELS

1.1 *Safety engineering as a reference for new standards*

In recent years great attention has been dedicated to the theme of road and railway tunnel safety by all those parties that recognise the need to integrate transport infrastructure engineering with safety engineering.

Within the European Council and Parliament, the Italian Government has played a particularly active role in road safety in general and tunnel safety in particular.

In many cases transport infrastructures constructed a decade or more ago are unsuited to meeting the demands of the increase in passenger and freight transport, an index of the social and economic development of the continent as a whole and Italy in particular. This leads to infrastructure safety-related problems that are in some cases dramatic and call for studies and investigations at levels that have not always been reached in the past.

Safety engineering, intended as a subject for the in depth study of the phenomena that produce excessive accident rates, is able to provide the correct scientific elements and mental processes for evaluating the factors on which to act in the most objective way possible. Dealing with infrastructure safety now calls for the introduction of risk analysis, which by being based on the statistical analysis of the main factors behind the cause of accidents, makes it possible to identify the most suitable procedures to reduce the probability of accidental events.

The need to use "deterministic" type assessment criteria is obvious, given that the perception of danger, that is the mental perception of risk, is subjective and too closely linked to the individual's familiarity with the system (vehicle, system, structure, etc.) used. Recent risk perception studies have demonstrated great discrepancies between the danger of certain daily activities as perceived by the general public and subject experts. In certain other cases activities that in actual fact have a death rate ten time greater are considered to be less dangerous.

The scientific approach that allows the evaluation of all risk factors, their possible intensity and probability of an event occurring, must lead to the identification, monitoring and reduction of accidents. Infrastructure safety operations will focus primarily on preventing accidents and secondarily on protection in order to restrict the effects that an accident can have on users.

It is not possible to proceed with a hasty list of the measures to be adopted for the safety of an infrastructure unless the boundaries of the problem in terms of the most probable risks and the permissible safety levels have been established.

In the transport infrastructure field, accident cause factor analysis and a meticulous investigation into the parameters that reduce safety must guide the identification of the measures required to make the structure safer. Such measures, in the case of existing infrastructures can concern:

– the adaptation of the infrastructure from a structural and/or functional point of view;

Copyright © 2005 Taylor & Francis Group plc, London, UK

– the drafting of operative procedures aimed primarily at guaranteeing steady performance levels over time and throughout the year;
– the adoption of systems, appliances and/or instruments that reduce the risk of harmful events and incorrect behaviour or, at least the effects generated by them.

In the case of new infrastructures the safety criteria examined must become rules to be adopted in the definition of project input and performance standards.

Following the necessary technical investigations performed in universities in recent years, the concepts described have become standard reference points for railway and road tunnel safety.

In particular, these are, in the road tunnel field, Directive 2004/54/CE of the 29th April 2004 on "Minimum safety requirements for tunnels on the trans-European road network" and in the railway field the publication of the Technical Standards for Railway Tunnel safety, ordered by the Ministry of Infrastructures and Transport.

2 ROAD TUNNEL SAFETY

2.1 *Directive 54/2004/EU*

On 29th April 2004 the European Parliament and European Council adopted Directive 2004/54/EC, relating to the "Minimum Safety Requirements for tunnels on the Trans-European Road Network. As part of the Directive's dealings with tunnel safety, the Ministry of Infrastructures and Transport's contribution was decisive for the introduction of new scientific criteria for the choice of the minimum action to be adopted in order to harmonise the safety of TEN network users on a European level.

The European Directive on Safety in Tunnels is an important initiative for the improvement of road safety in tunnels. It aims to achieve a uniform outlook on safety and common safety levels within the European Union and consequentially a single interface for the users of tunnels across Europe.

The Directive originates from the requests by the European Council and European Parliament to improve road tunnel safety standards, in the light also of the tragic accidents in the Mont Blanc and Gottard tunnels.

The paper proposes:

– the establishment of minimum safety requirements for all tunnels belonging to the trans-European road network longer than 500 metres;
– the harmonisation of tunnel safety organisation in Member States, defining the roles and responsibilities of the various subjects involved;
– the harmonisation of road signs and markings.

Although the spirit of the initiative was appreciated immediately, there has been a certain difference of opinions concerning the approach followed by the Commission in the draft published in December 2002, establishing the criteria to be adopted in order to guarantee that the minimum requirements are adopted for all tunnels.

The new Directive is the result of the intensive work conducted by the Commission and subsequently by the European Council and European Parliament, which brought about substantial amendments to the draft proposal put to the Commission in December 2002, in order to achieve a text approved by all the delegations and that represents a modern, engineering-based approach to tunnel safety.

2.2 *The European Commission's proposal*

From the very first meetings of the European Council and subsequently during European Parliament debates, Italy and the other Alpine range countries (the Alpine countries' Group), which have the greatest number of tunnels (see figure) pointed out that the draft proposal presented in December 2002 seemed to exceed the European Commission's mandate, as the paper proposed by the Commission did not merely formulate the general guidelines for the harmonisation of minimum safety levels, but rather contained a detailed analysis, with precise operative provisions that were not within the European Commission's specific competence.

As a general rule, at least according to the Treaty, legal harmonisation enforced on a European level through a Community Directive must simply establish essential requirements (safety requirements, in this case), leaving each Member State the freedom to establish the way in which to achieve the harmonised levels, which may therefore take into consideration the differences in geographical, climatic, and living conditions, as well as the different levels of protection on national, regional or local levels.

This would have particularly serious consequences for Italy, given the extremely high number of tunnels present on the Italian portion of the TERN; in actual fact the draft Directive points out that according to the Commission, Italy owns approximately 50% of all European tunnels, far lower than the true figure, which has been given to the Commission, of 61% (Figure 1).

Considering that the estimates contained in the foreword to the draft Directive set the overall cost of tunnel adaptation work in order to satisfy the minimum safety requirements established by the Directive to be paid by Member States at between 2.6 and 6.3 billion Euros, it goes without say that more than half would be paid by Italy, thus heavily conditioning the criteria for the allocation of financial resources, and, above all, future national infrastructure policy choices.

Copyright © 2005 Taylor & Francis Group plc, London, UK

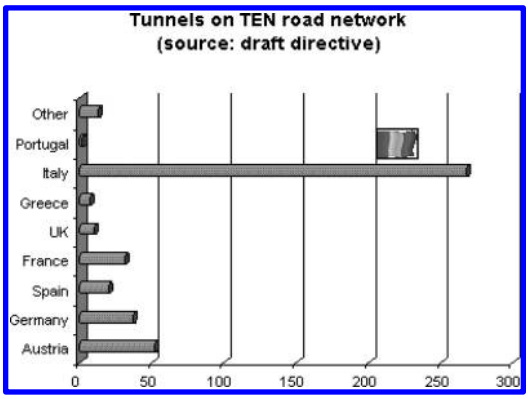


Figure 1. Tunnels on TEN road network (source: draft directive).

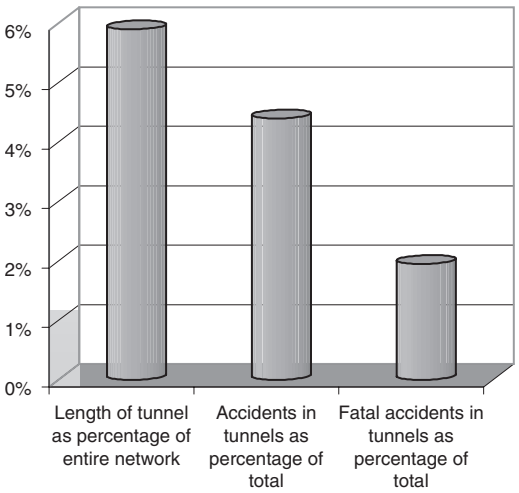


Figure 2. Effects of tunnels on safety. Percentage on pay motorway network.

In actual fact, according to the classification proposed in appendix one of the draft Directive, almost 54% of the tunnels situated on the Italian TEN network, belongs to Class I or II, and consequentially Italian tunnels would be obliged to adopt all the installation and structural measures envisaged. This circumstance would have caused:

– objective difficulties in performing work on certain stretches in which tunnels are close together;
– an extremely high impact on the surrounding area and traffic flows caused by the simultaneous opening of numerous work sites;
– obvious consequential repercussions on road safety for many years.

This would have caused a dangerous precedent in European legislation and cannot and must not commit Member States with regard to the detailed choices made but rather only with regard to the general objectives as part of the relative financial planning.

Apart from the economic considerations and the collateral effects mentioned above, doubts remain regarding the efficacy of this strategy: according to 2001 figures, the total length of tunnels on the Italian motorway network accounts for some 6% of the total TERN network, compared with a 4.6% of accidents in tunnels and an underground accident death rate of 2.1% of the network as a whole (Figure 2).

There is no reason to believe that the phenomenology would be any different wee national traffic flows any lower.

Furthermore, tunnel work is as a general rule more expensive than that above ground, especially in the case of work on existing structures. The same cost/benefit analysis produced by the European Commission showed the low efficacy of tunnel investments aimed at improving the overall safety levels of the network.

This would entail, especially in Italy, which is characterised by a considerable extent of the network underground, an inefficient use of the financial resources dedicated to road safety, as it is known that the result in terms of accident reduction, per unit of expenditure, is lower for tunnel work that above ground work.

The draft text also configured an atypical standard situation concerning the crucial question of choices for safety as although the draft Directive established obligations and identified operative solutions in detail, it left the relative respnsabilities to the various Member states.

In addition, the draft Directive provided no indication as to the strategies to be adopted for the following main objectives:

– risk minimisation through forecasting and prevention actions;
– the mitigation of effects through technical and operative instruments for managing emergencies.

No less fundamental is the observation by which the Directive based itself on the traffic-accident rate relations, which does not correspond in any way with any of the scientific analyses performed on the basis of data recorded on a European level. Consequentially, this unbalanced and incoherent approach undermined the credibility and scientific value of the draft Directive.

It is absolutely debatable – and was confirmed during recent meetings of the UN and AIPCR – that certain guidelines and most of the solutions identified do not coincide with recognised European or international consensus.

Lastly, the administrative procedures identified were complex, thus conditioning the choices of each Member State even with regard to technological

Copyright © 2005 Taylor & Francis Group plc, London, UK

innovation, which was bound to approved European procedures that had been uselessly complicated.

2.3 *The contribution of Alpine Countries*

Thanks to the contribution of the Alpine Countries, the European Directive now provides clear strategic lines and safety objectives and calls on Member States to implement appropriate procedures (defined in the Directive) in order to achieve those objectives. Each technical rule is based on technical-scientific criteria referring to safety engineering without going into detail, but rather leaving the precise definition and implementation of underground infrastructure safety measures to the Member States, with the aid of recommendations in the form of technical appendices, in the interest of the European Commission and other European and International organisations.

It is also envisaged that risk analysis, an analytic calculation instrument, will be used, when some of the structural requirements listed in appendix I can be satisfied through technical solutions that are substantially more expensive than those for similar new tunnels, but also in cases in which the requirements are not feasible, for example, due to justified and specific local conditions.

The tables at the end of the text exemplify and summarise the minimum operations envisaged, divided into:

- Work compulsory for all tunnels;
- Compulsory work with exceptions;
- Non-compulsory work;
- Recommended work.

Tunnel-by-tunnel studies of traffic conditions and road and surrounding environmental geometries will allow the identification of the set of operations that, with suitable risk analysis, may be sufficient to satisfy the safety objectives established by the Directive.

3 RAILWAY TUNNEL SAFETY

3.1 *Draft standard*

It was thought that the criteria that Italy had insisted on introducing into the European Directive on road tunnel safety could be included in the new technical standards on railway tunnel safety, in order to preventively provide the European Commission with a standard reference deemed suitable by the Member State with the largest number of tunnels in Europe.

The Decree of the Minister for Infrastructures and Transport n° 4462 of the 10.09.2003 established a technical work group composed of representatives of the Ministry of Infrastructures and Transport, the Home Office and the Italian National Railway Company, in order to standardise the subject of railway tunnel safety, in the same way as had already been performed by the European Commission for road tunnels.

The objectives assigned to the work group were:

- to create a clear reference standard for the objective and quantitative analysis of railway tunnel safety;
- to make the transition from a logic of rigidly preset standards to that of quantified system safety objectives;
- to identify an optimal balance between the safety objectives to be satisfied and the relative technical and economic consequences connected to the realisation of the work.

The structure of the paper is once again composed of a standard presented in articles and four technical appendices: appendix I Definitions, Appendix II Safety Requirements, appendix III Risk Analysis, Appendix IV Procedures. This streamlined structure makes for the easy future updating (dictated for example by technological evolution) of the technical appendices, without having to resort to complex legal instruments such as the issue of a new inter-ministerial decree.

The new standard therefore defines the safety provisions (minimum and integrative requirements) to be adopted for the safety of the more than 2000 railway tunnels in our country. These provisions refer to the infrastructure, transportable material and operating procedure subsystems. Within this framework, the Group adopted a clear choice: to minimise infrastructure work, which is always costly and affects operation, in order to favour prevention systems. In particular great importance is dedicated to fire extinguishing systems, which within the timeframes envisaged by the standard, will become compulsory for all passenger vehicles, including sleeper and restaurant cars.

The choice of the operations, both integrative ones and those exceptions to minimum requirements, is conditioned by the achievement of safety objectives, evaluated through quantitative risk analysis. For the first time in Italian or European legal history, details are provided on how risk analysis should be performed, for the attainment of the preset (individual or collective) safety objectives.

Lastly, the new standard deals with the technical – administrative procedures for the approval of tunnel projects, for their use with regard to the material permitted for rail transportation, the performance of simulation exercises and the documentation to be produced.

A risk analysis methodology, studied and devised through a number of simulations conducted by the La Sapienza University of Rome on the basis of the Italian railway database, was also presented.

3.2 *Risk analysis for railway tunnel safety*

The risk analysis proposed has the initial aim of evaluating the probability of the occurrence of previously

Copyright © 2005 Taylor & Francis Group plc, London, UK

identified accidental events together with the evaluation of an indicator of the gravity of the consequences connected to the evolution of the events.

Should suitable measures and devices for the reduction of risk be adopted, the analysis is repeated in order to analyse the residual risk.

In particular, the safety measures and devices that aim to reduce risk must distinguish (ref. *UIC* document – Codex 779-9 "Safety in Railway Tunnels") between:

- Prevention measures (prevention of incidents, *UIC*), aimed at reducing the probability of triggering characteristic accidental events (Initial Events, IE) relating to the train – tunnel system;
- Protection measures (individual and collective) and measures for the mitigation of consequences deriving from the occurrence of the aforesaid accidental events (mitigation of impact, *UIC*);
- Measures facilitating the escape from hazard sites (self-escape) (facilitation of escape, *UIC*);
- Measures facilitating rescue operations (facilitation of rescue, *UIC*).

Integrative measures may be adopted for very long tunnels.

The risk analysis procedure introduced into the standard is based on the critical application of consolidated probability methods for the evaluation of complex risk events using the usual Event Tree and Cause Tree techniques, combined with scenario studies for the evaluation of the consequences associated to each possible final outcome.

The information used to construct the procedure's input data came from the reference source of the Reports on the State of Safety in Railway Tunnels envisaged by the standard integrated as required with information contained in officially accredited databases on accident indices and malfunction or breakdown rates of system components.

A number of main reference scenarios were identified, relating to tunnel emergencies, consequentially to the onset of the following critical initiating events:

- *FIRE (S_1)*;
- *DERAILMENT (S_2)*;
- *COLLISION (S_3).*

The three reference accident scenarios may evolve towards different steady end of emergency configurations characterised by different levels of damage to humans, material and the infrastructure depending on the correct or incorrect functioning of the protection and mitigation measures relating to the:

- *INFRASTRUCTURE subsystem;*
- *TRANSPORTABLE MATERIAL subsystem;*
- *OPERATING PROCEDURE subsystem.*

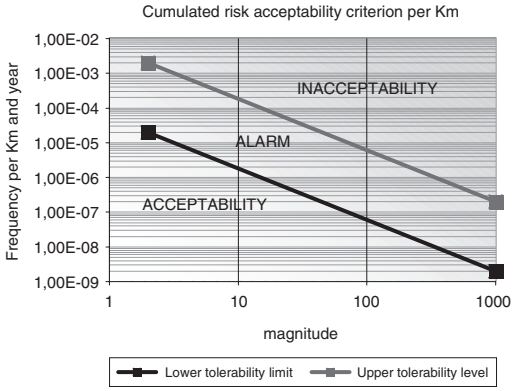


Figure 3. Cumulated risk acceptability criterion per Km.

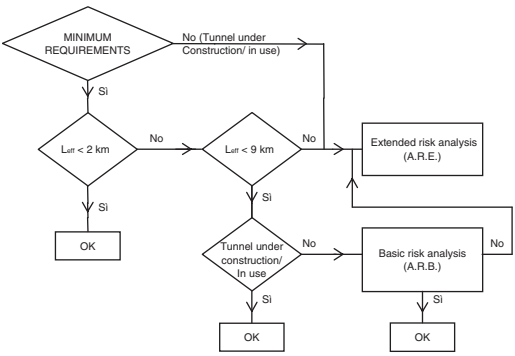


Figure 4. Criteria for exended or basic risk analysis choice.

The overall data obtained by Risk Analysis, performed on all the tunnels distributed along the railway network, compared on the one hand with accident rate figures and on the other with the public's safety expectations, allows the definition of risk objectives.

With regard to the call for the validation of minimum requirements as sufficient conditions for guaranteeing the safety of passengers for a given class of tunnel, it is necessary to be able to evaluate the risk level for a single tunnel.

The graph below (Figure 3) demonstrates the cumulated probability function acceptability criterion and indicates the probability that the number of victims per km/year is greater than preset reference thresholds.

The use of risk analysis and the various different methodologies envisaged (extended and basic) occurs according to the following criteria (Figure 4):

- Extended risk analysis is performed for all those tunnels where it is not possible to exclude the simultaneous presence of hazardous freight trains and passenger trains;

Copyright © 2005 Taylor & Francis Group plc, London, UK

– Tunnels with lengths between 1000 m and 2000 m, that comply with minimum requirements guarantee an adequate level of safety for passenger evacuation (self-rescue): this category of tunnel defines the Minimum Requirement Zone;
– For tunnels with lengths between 2000 m and 9000 m, the evaluation of the sufficiency of the applied safety measures is performed using Basic Risk Analysis. Should the Basic Risk Analysis demonstrate the insufficiency of the applied measures, extended risk analysis is required;
– Tunnels longer than 9000 m must be subject to extended risk analysis.

The Basic Risk Analysis procedure was defined on the basis of the tunnel fire accident scenario, with loss of mobility of the vehicle, assuming the probability of tunnel malfunction of the transportable material and operative procedures to be unitary. The "fire" initial event is therefore assumed to be connected to the stop in tunnel event: $S_1 = (stop_in_galleria) \cap 1$, with the consequential impossibility of the train to remove itself from critical conditions. It was also supposed that a rescue operation will be inefficient in saving the passengers and crew from the train involved.

The sufficiency of minimum requirements is therefore essentially conditioned by the successful evacuation of passengers (self-rescue) in the hypothesis of a central fire and advance of the smoke wall through the tunnel.

Safety conditions are determined according to the relationship between the trend of the concentrations of toxic products from combustion, concentration of oxygen and the visibility along the tunnel and passenger evacuation times.

4 CONCLUSIONS

European Directive 54/2004/EC, the national assimilation phase and draft directive compiled by the ad hoc inter-ministerial work group may represent a turning point in the field of safety in the use of transport infrastructures and tunnels in particular.

There has been an evolution from a phase in which in the aftermath of the dramatic events of the Mont Blanc and Gottard tunnel accidents all tunnel safety measures, including those with the most modern equipment seemed to be inadequate, to a phase in which safety is approached in engineering terms through a logical sequence of analyses and evaluation, mainly of a numerical and quantitative type.

In order to ensure that sentimental considerations do not lead to exaggerated reactions, with economic implications capable of jeopardising a country's investment abilities, it is necessary to plan the safety of the use of infrastructures in the same way that the static safety of the work is planned.

A correct approach that is coherent with the real necessity of a given infrastructure certainly allows an optimisation of investments, which are essential to recover the infrastructure gap that separates Italy from many other central European countries.

Italy's commitments to the subjects of road and railway tunnel safety undoubtedly represents a valid reference on which to base further developments on a international level and in the various scientific consensuses.

Copyright © 2005 Taylor & Francis Group plc, London, UK

Study on anti-fire panel for vehicle fire in immersed tunnel

Y. Matsuo
Krosaki Harima, Chiba, Japan

Arito Mizobe
Krosaki Harima, Chiba, Japan

O. Kiyomiya
Waseda University, Tokyo, Japan

ABSTRACT: Composite members made of steel and concrete are adopted for immersed tunnel. Since steel plates are exposed to the internal side of the road, vehicle fire countermeasures in tunnels are required. Investigation about the temperature rise at the composite member was made for test specimen with a ceramic anti-fire board. For the design temperature curve by the vehicle fires, the fire tests were carried out in a heating furnace. It is explained that the temperature rise in the composite members covered by the anti-fire board was within the allowable temperature, accompanied with a exfoliation phenomenon of the steel plates, spotty temperature rise on the joint portions, etc. On the other hand, the heat transfer analysis with which existence of the moisture in the concrete and separation of the steel plates from concrete can well explain the phenomenon in the fire test.

1 INTRODUCTION

The vehicle fire accidents that broke out in the Mont Blanc Tunnel (mountain tunnel) in 1999 and in the Towel Tunnel (mountain tunnel) in the same year brought about many victims. The recovery of the disasters required a voluminous amount of expenditure and month-long period. Thus the disasters have reminded us of importance of the tunnel fire countermeasures. With the fire accident countermeasures in Japan, investigations were promoted after the disasters including Nihon-zaka Tunnel. Various types of the countermeasures such as placement of fireplugs, security of evacuation routes, etc. are being taken. Danger of traffic accidents and fires induced by the accidents in tunnels is believed to be low in comparison with that of the general roads, inferring from the fact that the inside of a tunnel is usually liberated from bad weather and no crossing roads. However in a under sea tunnel, the damage in the structure materials caused by vehicle fires is, different from the mountain tunnels, is liable to bring about destroy of the whole of the facilities due to inflow of water or mud into the tunnel. Thus danger in human life loss is also very high. From such a point of view, anti-fire (fire-resisting) panel came to be settled inside of under sea tunnels such as Kobe Port Island Tunnel, the 2nd Channel-route Tunnel of Tokyo Bay, Marine Road Tunnel of Tokyo Bay, etc.

With the immersed tunnel, sandwich-composite members where steel plates and filled concrete are utilized (hereinafter called SC structure) are widely used in recent years. This type of the composite members is applied for several immersed tunnels. An example of the immersed tunnel having the SC structure is illustrated in Figure 1. The authors of this paper have long been engaged not only in the manufacture of the anti-fire boards and attachment of such boards but also in the extensive study on the evaluation of the performance of the anti-fire boards, thermal analysis, etc. this paper describes the fire test and heat transfer analysis for the composite member with anti-fire panel.

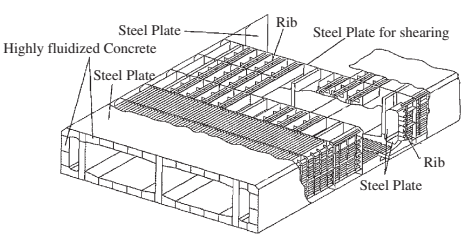


Figure 1. Outline of the immersed tunnel by sandwich member.

Copyright © 2005 Taylor & Francis Group plc, London, UK

2 MATERIALS AND STRUCTURE OF THE TEST SPECIMEN

2.1 *Outline of the test specimen*

The anti-fire test was carried out for the SC members of the immersed tunnel. As shown in Figure 2 as an outline, the test specimen has the length of 1416 and width of 1016 mm, respectively. The thickness of the ordinary type concrete was 200 mm, though the thickness of prototype composite members was about 1 m and self compacted concrete (high flowabilty concrete) is filled inside of steel chambers. The mixing ratio of the concrete used is listed in Table 1. The quality of the steel plate was SM490Y, and its thickness was 8 mm the same as that of the prototype. The reinforcement rib was aligned by an angle $150 \times 90 \times 9$ mm at 600 mm interval.

2.2 *Material characteristics of anti-fire boards*

The anti-fire boards are the materials composed of the alumina-silica ceramic substances whose major constituents are the inorganic materials such as alumina cement, burnt aggregates, etc. Burnt aggregates and light-weight aggregates are used as main aggregates, whereas main combined (bonding) agent is composed of alumina-cement and several types of fiber. Material characteristics are listed in Table 2, where bulk specific gravity is 1.0, heat conductivity is 0.17 W/mK, and bending strength is 4.1 N/mm^2. The material is excellent enough in heat stability, hydraulic resistance, acid resistance, freezing/melting resistive performance, and impact resistance. Almost none of shrinkage can be observed to the extent of 1250°C from the test result, and shrinkage as high as 6.5% is made at 1350°C. Also up until this temperature, none of phenomena such as dissolution, crack, etc. can be observed.

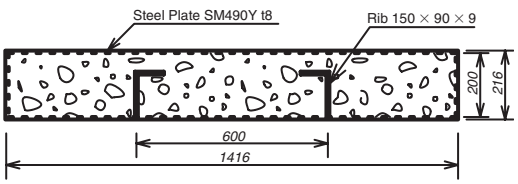


Figure 2. Outline of the immersed tunnel by sandwich member.

Table 1. Mixing of concrete.

Maximum size of ag. (mm)	Slump (cm)	W/C (%)	Nominal strength (N/mm^2)
20	15	43	30

Table 2. Physical properties of the anti-fire boards

	Anti-fire boards of ceramic type
Bulk specific gravity	1.03
Heat conductivity (W/mK)	0.17
Bending strength (N/mm^2)	4.1

2.3 *Shapes of the anti-fire boards and attaching method*

The anti-fire board has the dimension of 600 mm length, 500 mm width, and 20 mm thickness. The thickness was aligned according to previous finite element analysis which the equation of thermal transfer was solved so that the backside temperature of the anti-fire board will remain within 250°C complying with the surface temperature of 1000°C. Two plates in parallel were inserted into the studs that were welded on the steel plate, and were fixed by special hexagonal bolts. The quality of the hexagonal bolts was stainless steel of SUS316 in consideration of the test temperature. Into the gap between the anti-fire board and the hexagonal bolts, ceramic fiber was filled for prevention from heated air flow from the heating furnace.

3 METHODS FOR THE ANTI-FIRE TEST AND MEASUREMENT

For the anti-fire test, the multi-heating furnace shown in Figure 3 was used. With the assume fire in the anti-fire test, the time/temperature curve at 1000°C as shown in Figure 4 was adopted referring to the RABT curve. The locations for measurement of the in-furnace temperature were in accordance with JIS A1304, and

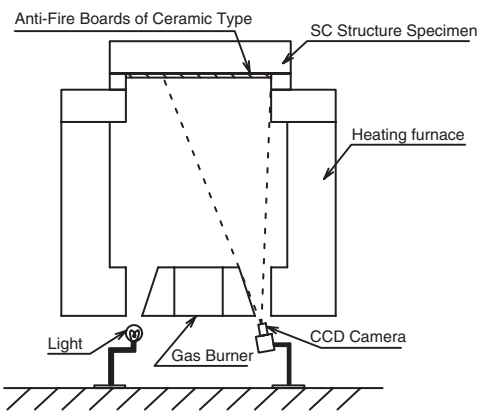


Figure 3. Outline of the multi-heating furnace.

Copyright © 2005 Taylor & Francis Group plc, London, UK

measurement of the 5 points 30 mm distant from the lower part of the anti-fire board were carried out by B-type thermocouples. In Figure 5, the temperature measurement points are shown.

4 TEMPERATURE CHARACTERISTICS OF STEEL MATERIAL AND CONCRETE

In general it is widely known that when high temperature of more than 200∼300°Cis reached, strength of both the materials is exceedingly lowered. With both the steel material and the concrete, the material strength is almost nullified at about 500°C temperature. With anti-fire tests, it is well known that when the temperature exceeds 200°C, exfoliation by concrete burst phenomena continuously related to water vaporization come out resulting in destruction of the concrete members. The utilization limitation temperature of the steel materials was determined to be 250∼350°C. Meanwhile the allowable temperature of the concrete was also determined to be 250∼380°C. This allowable temperature depends on the strength of the concrete, kinds of aggregate and so on.

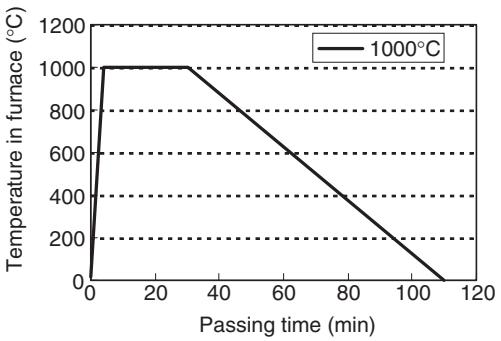


Figure 4. Heating time–temperature relationship.

5 ANTI-FIRE TEST RESULT

5.1 *Observation of test specimen*

During a heating test, no abnormalities such as blasting, fissure, removal, etc. were observed with anti-fire boards and attaching bolts. However with respect to the joint portions, a separation of the anti-fire board was instantaneously noticed in rise of the temperature where steel plate temperature (No.S0) exceeded 300°C. Meanwhile after approximately 30 minutes from the start of the test, slight joint opening

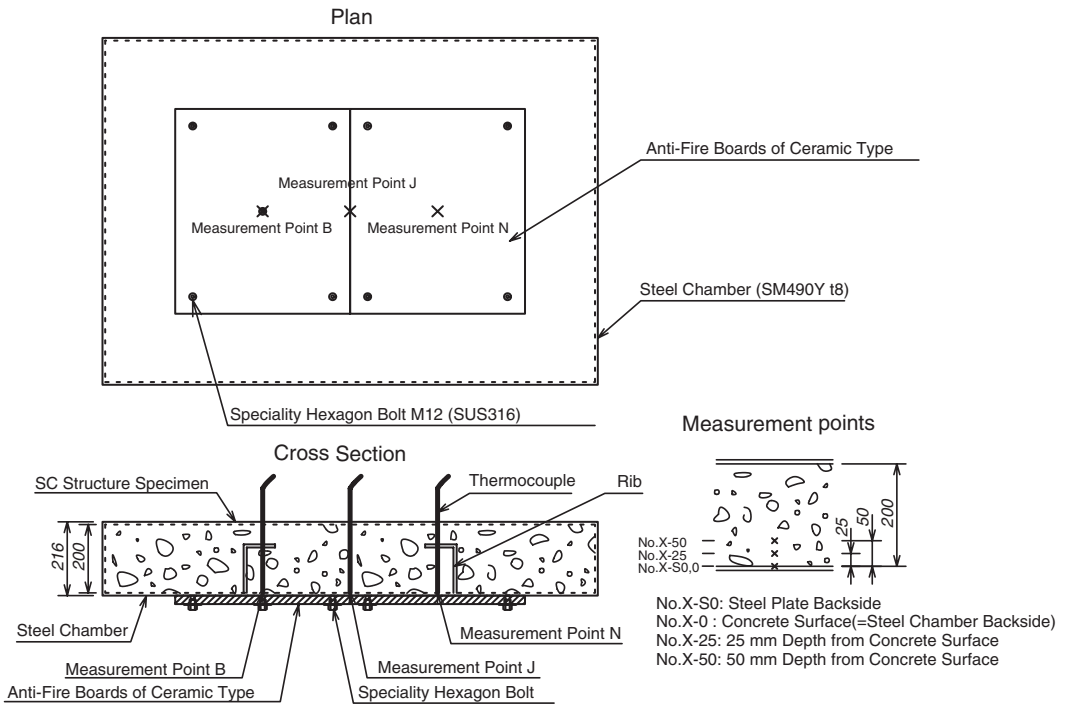


Figure 5. Anti-fire structure and measurement points.

Copyright © 2005 Taylor & Francis Group plc, London, UK

between the anti-fire boards was noticed. Judging from the comparison with the diameter of the thermocouple on the monitor, the joint opening was approximately 1～2 mm when visually observed.

5.2 *Temperature measurement result*

The in-furnace temperature during the anti-fire test stood 968°C after 4 minutes, whereas the average temperature since the lapse of 10 minutes ranged from 1002°C to 1007°C. Furthermore the deviation on the 5 points was ±16°C after 10 minutes. The processes of the general portion, joint portion, and bolt portion during the anti-fire test per temperature time are shown in Figures 6, 7 and 8. In any of the temperature measurement points, the highest temperature of the steel plate (No.S0) was less than 350°C. On the other hand, the highest temperature of the concrete surface (No.0) was less than 150°C. With respect to the bolt portion, temperature rise was high, different from the general portion or joint portion, noticed immediately after the heating. But the highest temperature remained 242°C (55 minutes after). Although a tendency the same as that of the general portion or joint portion was noticed with the concrete surface temperature (NO.B-0), the highest temperature remained 146°C (after 85 minutes).

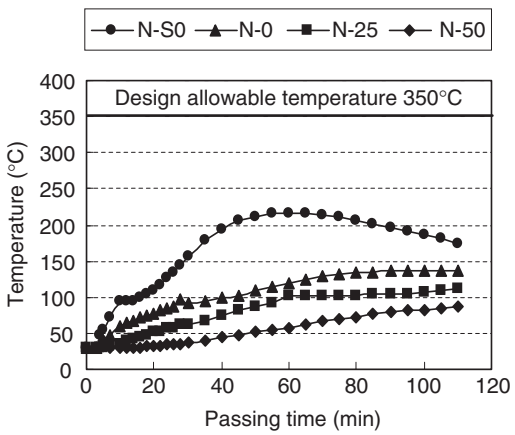


Figure 6. Result of the anti-fire test (General portion).

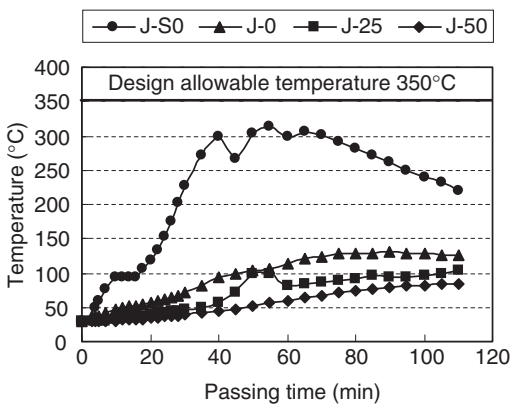


Figure 7. Result of the anti-fire test (Joint portion).

5.3 *Consideration of the experimental result*

The steel plate temperature and the concrete surface temperature showed different behaviors, although the temperature measurement positions in case that the thermocouple was settled at same points in depth. The concrete surface temperature was lower (that is to say: the steel plate temperature is higher) despite the fact that the concrete is intrinsically on the position the same as that of the steel plate, which might imply that an air layer that becomes an adiabatic layer, i.e. a gap has been created on the interface. The reason why a gap was created on this interface might be that owing to the pressure produced by the evaporation of the moisture in the concrete or thermal expansion of the steel plate, the steel plate swelled. However the steel plate temperature has often been separated from the concrete surface temperature from the initial stage of the heating, it is imagined that some amounts of air layer have already been generated before the anti-fire test. The temperature of the joint portion of the steel plate was higher than that of the general portion. This might be because of the fact that since the joint portion was located on the central point between the reinforcement ribs, the amount of the swell of the steel plate, i.e. the gap between the steel plate and the concrete interface is greater than that of the general portion. Thus heat is hard to be conducted to the concrete. This might have resulted in further heightening of the temperature. Meanwhile since the joint portion of the

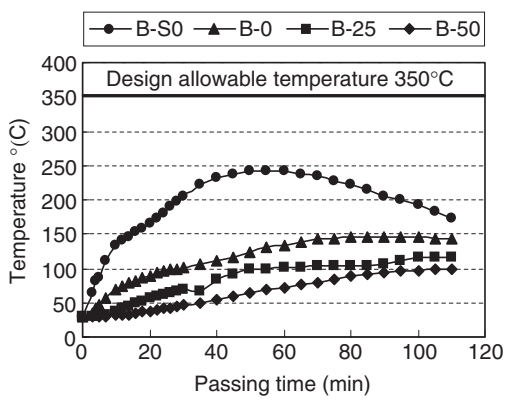


Figure 8. Result of the anti-fire test (Bolt portion).

Copyright © 2005 Taylor & Francis Group plc, London, UK

anti-fire board was slightly opened during the test, invasion of the heat flow from this gap might be one of the causes of the temperature rise. With the bolt portion, it can very easily be understood that the temperature made rise very rapidly starting from the initial stage of the heating because the bolt head is exposed to the inner side of the furnace. Meanwhile the highest temperature was lower than the temperature of the joint portion and showed a value rather closer to that of the general portion. With the joint portion, the joint opening was made wider accompanied with the rise of the temperature resulting in the enlargement of heat-acceptance area. However with the bolt portion, just spotted heat acceptance was observed.

6 THERMAL ANALYSIS

Fourier's heat transfer equation is generally known as Equation (1).

$$\frac{\partial T}{\partial t} = a\left(\frac{\partial^2 T}{\partial x^2} + \frac{\partial^2 T}{\partial y^2} + \frac{\partial^2 T}{\partial z^2}\right) \quad (1)$$

where a = λ/(ρ c), λ: thermal conductivity, ρ: bulk specific gravity, c: specific heat, T: temperature, t: time.

This time an analytical model for the sandwich members is illustrated in Figure 9. The thickness of the individual layers is modeled under the condition that ceramic anti-fire board is 20 mm, steel plate is 8 mm, and concrete is 200 mm in thickness. 2-dimensional simplex elements were adopted, and the node number was 142, element number was 140, and the atmosphere temperature on the boundary on the model periphery was 22°C. Physical properties of the materials used for thermal analysis are listed in Table 3 and Figure 10. As shown in the table, the heat conductivity was given with temperature dependency. Temperature dependency was not remarkable with the steel plate in a range of the calculation of this time, whereas the heat conductivity hardly changed to the extent of approximately 1000°C with the ceramic anti-fire board.

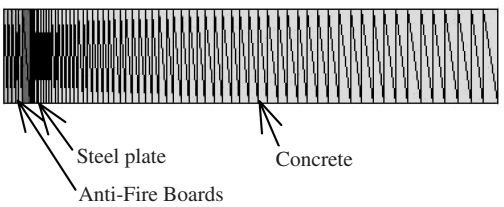


Figure 9. One dimensional thermal analysis.

Table 3. Physical properties of the materials.

	Steel	Concrete		Anti-fire boards of ceramic type
Density (kg/m^3)	7800	2300		1000
Specific heat (kJ/kgK)	0.461	<90°C 90~100°C >100°C	0.955 5.904 0.611	0.837
Heat conductivity	34.9	Fig. 10		0.163

7 THERMAL ANALYSIS RESULT AND OBSERVATION

7.1 *Influence of the moisture in the concrete*

As shown in Figure 11 is the calculation results, influence of the evaporation amount of the moisture

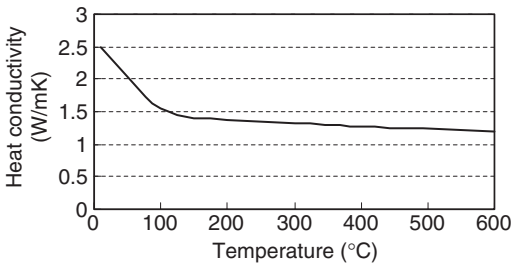


Figure 10. Heat conductivity of concrete.

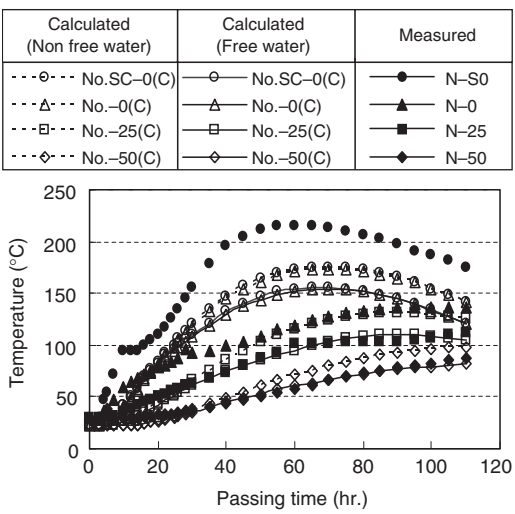


Figure 11. Influence of evaporation latent heat in concrete.

Copyright © 2005 Taylor & Francis Group plc, London, UK

was not so large. This effect is observed only at 100°C and presents the delay of temperature rise. The calculation value was rather separated from the measured value and especially the steel plate temperature (No.SC-0) was considerably deviated, it is necessary to take account of the other influence.

7.2 *Influence of the gap between the steel plate and the concrete*

The calculation results brought about by changing the gap between the steel plate and the concrete to 0.4, 0.8, 1.5, and 3.0 mm are shown in Figures 12～16. The highest temperature of the steel plate No.N-S0(C) is 187°C in case that the gap is 0.4 mm, 218°C in case that the gap is 0.8 mm, 263°C in case that the gap is 1.5 mm, and 323°C in case that the gap is 3.0 mm. That is to say, the wider the gap was, the higher the temperature was. On the other hand, the temperature on the concrete surface No.N-0(C) shows a tendency contrary to that of the steel plate. The temperature is 145°C in case that the gap is 0.4 mm, 135°C in case of

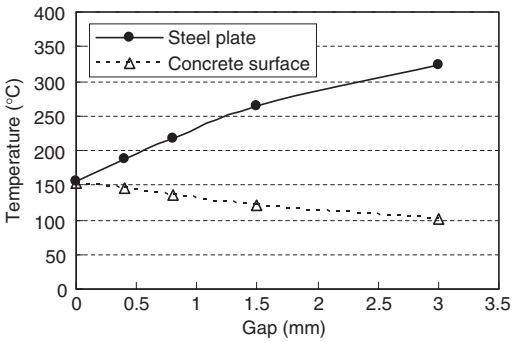


Figure 12. Relationship between the gap and steel chamber, concrete surface temperature.

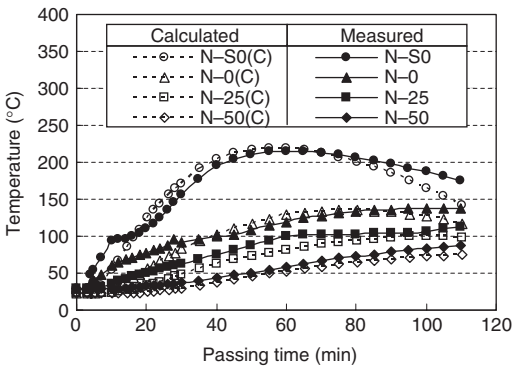


Figure 13. Comparison between calculation value and measurement value (General portion).

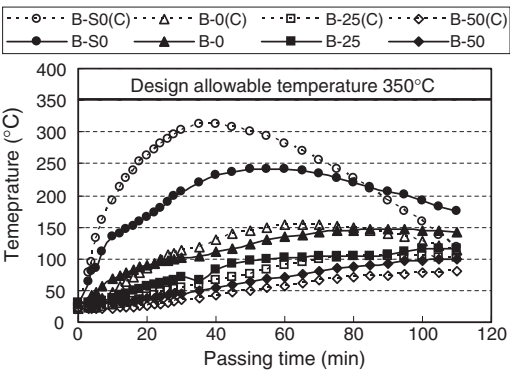


Figure 14. Comparison between calculation value and measurement value (Bolt portion).

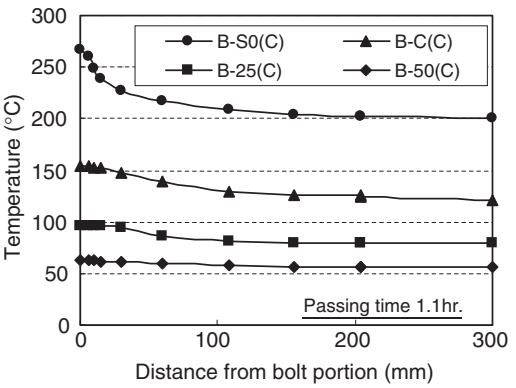


Figure 15. Relationship between the distance from bolt portion and temperature.

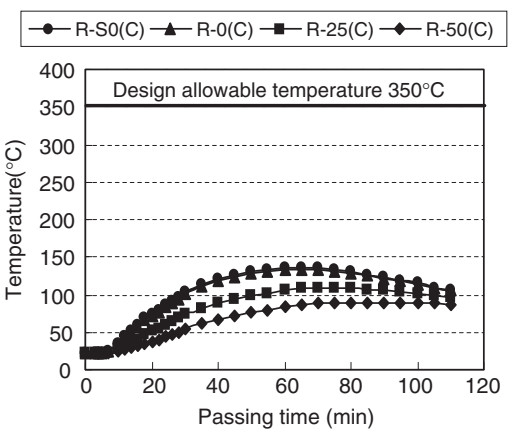


Figure 16. Transition of rib temperature on rib portion.

Copyright © 2005 Taylor & Francis Group plc, London, UK

0.8 mm, and 102°C in case that the gap is 3.0 mm. Meanwhile with the depth of the concrete of 25 mm and 50 mm as well, a tendency the same as in case of the concrete surface was shown. It can be said that the gap plays a role of an adiabatic layer helps raise the temperature of the steel plate, the temperature rise of the concrete was contrarily restrained.

8 CONCLUSIONS

(1) During the anti-fire test, no abnormality such as explosion was noticed with the test specimen. Although no abnormality such as fissure, removal, etc. was noticed with the anti-fire board, some joint opening (visually recognized as approximately 2 mm) possibly caused by the thermal expansion was noticed with the joint portion. Meanwhile with the specific hexagonal bolts, no abnormality such as falling was noticed.
(2) It is explained that coverage by ceramic anti-fire boards with a thickness of 20 mm makes it possible to protect the steel plate temperature to the extent of less than 350°C that is believed to be normal allowance temperature. At that time, the highest temperature on the concrete surface was less than 150°C.
(3) The highest temperature on the general portion was 215°C with the steel plate, whereas the temperature was 137°C with the concrete surface This is, it is explained, due to the fact that a gap was created on the boundary surface between the steel plate and the concrete.
(4) Higher temperature was reached on the joint portion than on the general portion. However this might not be due to the shrinkage of the anti-fire board, but might be due to the swell of the steel plate, the anti-fire board was pushed out from the backside.
(5) With the bolt portion whose bolt head part is exposed, the temperature at the initial stage of the heating is liable to be heightened. However since the heat acceptance areas are scattered, none of remarkable temperature rise was observed in concrete.
(6) When thermal transfer analysis by finite element method is made, behaviors of the full sandwich structure in case of heating can well be simulated provided that the influence of the moisture in the concrete or gap on the interface is taken into consideration.

REFERENCES

(1) A. Haack: 1992, Fire Protection in Traffic Tunnels Initial Findings from Large-scale Tests, *Tunneling and Ground Space Technology*, Vol.7,No.4, pp.363–375
(2) Studiengesellschaft Stahlanwendung e.V: Fires in Transport Tunnels, 1995 *Report on Full-Scale Test EUREKA-Project EU 499*
(3) Osamu Kiyomiya, et al: 2004, Design and countermeasure for vehicle fire in the immersed tunnel, *Tunneling und under ground space, Japan*, *April*, pp.63–70
(4) Hiromitsu Iida, et al: 1998, Fire model test and numerical calculation for joint part of immersed tunnel, *Symposium of Structural Engineering, Japan,* Vol.44A, pp.93–101

Copyright © 2005 Taylor & Francis Group plc, London, UK

Proposed safety facilities for highway tunnels in Turkey

İ. Ünal & A. Nitta
General Directorate of Turkish Highways, Ankara, Turkey
Motorway Structures Maintenance Chief

Honshu Shikoku Bridge Authority, Kobe, Japan
JICA Expert of General Directorate of Turkish Highways

ABSTRACT: Emergency Facilities in tunnels are applied to mitigate damage in the event of natural disaster, fire, sabotage or heavy accidents occur in a highway tunnel. Purpose of utilizing these emergency equipments are prevention of disaster and prevention of secondary damage after disaster. Tunnels are classified into five categories considering the tunnel length and traffic volume. Installation Standarts of Emergency Facilities are determined regarding these categories. Tunnel Emergency Facilities should be planned with full deliberation of the administrative system under which the facilities are to be operated, and the installation objectives and their utilization should be clearly defined. All types of emergency equipments are not necessary for each tunnel. Excessive equipment causes not only the increases in the construction of the facilities and maintenance costs but also causes a difficult equipment operation. Number of tunnels in Turkey is increasing every passing year. This presentation will compare the Specifications used in the construction of Turkish Tunnels emergency facilities with the Japan Tunnel Safety Specifications.

1 INTRODUCTION

For the recgnition the important role of tunnel emergency facilities in tunnel disaster prevention; the purpose of installation and operation method must be chosen and planned. In this paper the design of emergency facilities of two tubes two lanes tunnel for expressway and motorway is studied. In other tunnels having three or more lanes, it is possible to apply this design after making necessary modifications. Sufficient disaster prevention measures, are necessary against fire or other accidents since tunnel is a closed space. Statistically, fire accidents in tunnel are rare but if it happens, fire accidents cause big disasters. Fire spreads easily from one car to another and smoke fills inside of the tunnel. There are many examples of these kinds of accidents which happened in Mont-Blanc, Tauern, Gothard and Nihonsaka Tunnels and so on. A disaster in a tunnel, can never be managed only by the highway authorities. Help and the cooperation of road users and relevant organizations such as the Fire Brigade, the Police and Ambulance are indispensable.

2 CLASSIFICATION OF TUNNELS

Classification of tunnels is divided into five classes according to its length and traffic volume from AA to D as shown in Figure 1. Recently, disaster prevention inside tunnels became more important throughout the world especially in Europe. Therefore, emergency equipment in tunnel is planned not only for fire accident but also ordinary traffic accidents which may become the cause of fire accidents. In tunnels having long length and small traffic volume, traffic accidents are not so many. This kind of tunnels with traffic volume less than 4000 vehicles per day, is classified

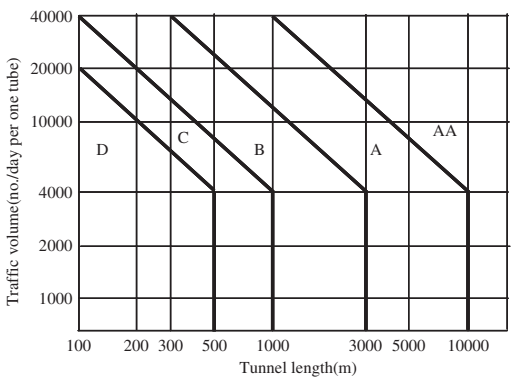


Figure 1. Tunnel classification (For two tubes two lanes tunnels).

Copyright © 2005 Taylor & Francis Group plc, London, UK

considering its length. Tunnel classification is decided basing on the accident occurence possibility. In figure, traffic volume (number of vehicles per day per one tube) is usually taken as the half of the estimated traffic volume after 10 years from opening date of the tunnel. This duration is decided considering the fact that economic life of emergency equipment is usually between 10 to 15 years. This study applies to the design of emergency facilities of 2 lanes double tube tunnels for expressways and motorways. Motorway tunnels in Turkey, are constructed usually as 3 lanes double tube that is why after 10 years traffic multiply with 1,5 can be made classification that kind of tunnels. Tunnel classification is to be reviewed in every 5 years after tunnel is taken into operation. In this case, traffic volume to be adopted, is the estimated traffic volume after 10 years from review date. And some facilities can be constructed using stage construction method. For example, water sprinkler must be constructed step by step considering the estimated traffic volume after every 5 years following the opening date of tunnel.

If the tunnels which have the radius of curvature below 500 m or longitudinal gradient over 3% or at the locations where there exist high possibility of accident. It is desirable to classify the tunnel as one class upper than the classification shown in Figure 1. In addition, if there are group tunnels i.e. two or more tunnels with short distance between facing of two tunnels should be taken as the total length including the distance between the two tunnels. Tunnel classification must be decided after considering these conditions.

3 INSTALLATION STANDARDS OF TUNNEL EMERGENCY FACILITIES

Tunnels shall be installed with emergency facilities for the prevention of disaster and fire and other emergency conditions according to the tunnel classification shown in table 1.

3.1 *Information and alarm equipment*

Information and alarm equipment are to be used to inform of the accident to road administrator, fire department and police and to alarm the road users of the accident occurrence. Information equipment consist of emergency telephone, push button type information equipment and emergency alarm equipment.

3.2 *Fire extinguisher equipment*

Extinguishing activities are consisted of first stage extinguishing by road users and large-scale extinguishing by fire department. Therefore, this equipment must have the function for road users to use easily and quickly and also have effective function to fire. This equipment consists of fire extinguisher and plug.

3.3 *Escape and guidance equipment*

Escape guidance equipment is used to let road user encountered accident or fire in tunnel, to escape to outside of tunnel safely. There are two types of this equipment. First type of equipment such as guidance board, supports escape activities indirectly by providing information. Second type of equipment, such as smoke discharge equipment and evacuation adit, supports escape directly.

3.4 *Other equipment*

Other equipment is used to supplement information and alarm equipment, escape and guidance equipment to make escape, rescue and extinguishing activities more effective. Other equipment consists of hydrant, radio communication equipment, radio re-broadcasting equipment, loudspeaker, water sprinkler, monitoring equipment, illumination equipment which can be used in power failure and emergency power supply equipment.

4 HIGHWAY TUNNELS IN TURKEY

As shown in Table 2, in Turkey now total 117 tunnels are in operation and 72 tunnels are under construction. 18 tunnels in operation have a length more than 500 meter and this number will reach 46 by the year of 2010. When motorway construction was started in Turkey at late of 1980's, new equipments and new technologies in tunnel constructions like New Austrian Tunnel Method (NATM) have encouraged Turkish Road Administration and Turkish Contractors. Tunnel construction having double tubes in motorways have been started very rapidly at the beginning of 1990's. Contrary to this, before 1980's all State Road tunnels were one tube and generally short and avalanche tunnels. The tunnels with high traffic volume and tunnels having a length more than 500 meter, should be given the priority in rehabilitation plans.

The experience and knowledge of construction techniques obtained from motorway tunnels were transferred also to the expressways. But these knowledge and experience could not be transferred to the long expressway tunnels in tunnel safety area. Therefore, first of all we need a tunnel administration with qualified personnel for motorways and expressways. After length and number of tunnels are increased very rapidly tunnel safety is in the agenda of the General Directorate of Highways. The importance of installation of emergency facilities of tunnels in Turkey,

Copyright © 2005 Taylor & Francis Group plc, London, UK

Table 1.

Emergency Facilities \ Classification of Tunnel			AA	A	B	C	D	Remark
Information and Alarm Equipment	Emergency telephone		○	○	○	○	○	Omitted in Class D tunnels less than 200m in length
	Pushbutton type information equipment		○	○	○	○		
	Fire detector		○	○				Omitted in tunnels without ventilation system
	Emergency alarm equipment	Tunnel entrance information board	○	○	○	○	○	Can be omitted in tunnels less than 200m in length
		In tunnel information board	○	△				To be installed in Class A tunnels 3,000m or more in length
Fire Extinguishing	Fire extinguisher		○	○	○	○	○	
	Fire plug		○	○	△			To be installed in Class B tunnels 1,000m or more in length
Escape and guidance equipment	Guide board	Emergency exit lump	To be installed in tunnels with evacuation adits					
		Guide board (A)	To be installed in tunnels with evacuation adits					
		Emergency exit direction board	To be installed in tunnels with evacuation adits					
		Guide board (B)	○	○	○			To be installed in tunnels with evacuation adits
	Smoke discharge equipment and Escape passage		Evacuation adits to be provided in tunnels of around 750 m or more in length. Smoke discharge equipment to be provided in tunnels of around 1,500 m or more in length. Evacuation tunnels provided for those Class AA tunnels and Class A tunnels of a length of 3,000 m or more which employ a two way traffic system and a longitudinal ventilation system in which the length of one ventilation section (length divided by vertical shaft) is more than 2,000 m.					
Other equipment	Hydrant		○	○	△			To be installed in Class B tunnels 1,000m or more in length Tunnels equipped with hydrants are to be provided with a water supply ports near the entrance
	Radio communication auxiliary equipment	Leakage coaxial cables	○	△				To be provided in Class A tunnels 3,000m or more in length
		Entrance/exit telephone	○	○				
	Radio re-broadcasting equipment	Interrupt function provided	○	△				To be provided in Class A tunnels 3,000m or more in length
	Loudspeaker equipment		To be provided in tunnels equipped with a radio re-broadcasting equipment (with interruption function)					
	Water sprinkler system		○					To be provided in Class A tunnels 3,000m or more in length, and serviced in two way traffic.
	Observation	Type A(200m intervals)	To be provided in tunnels with water sprinkler					
		Type B (Emergency parking area)		△				To be provided in Class A tunnels 3,000m or more in length
	Lighting equipment for power failure		To be provided in tunnels 200m or more in length					
	Emergency power supply equipment	Independent power plant	To be provided in tunnels 500m or more in length					
		Non-failure power supply equipment	To be provided in tunnels 200m or more in length					

○ Mandatory
□ Optional

Copyright © 2005 Taylor & Francis Group plc, London, UK

Table 2. Number and length of Turkish highway tunnels.

Type of road	Current status	L < 500 m	500 m < L L < 1000 M	1,000 m < L L < 3,000 M	L > 3,000 m	Double tube	Total number	Total length
MOT	OP	11	4	3	1	19	19	26.2 km
	UC	3	7	2		12	12	19.4 km
EXP	OP	88	5	5			98	23.7 km
	UC	41	10	8	1	20	60	32.3 km

MOT : Motorway OP : Operation
EXP : Expressway UC : Under Construction.

increased especially after Mont Blanc, Tauern and Gotthard tunnel disasters.

Turkish Motorway long tunnels have got the following equipment:

- Traffic management system
- Illumination
- Ventilation
- Safety equipment
- Communication equipment
- Fire extinction equipment
- Close-circuit TV
- Central operation system
- Energy supply
- Maintenance equipment
- Loudspeakers
- Radio broadcasting system.
- Monitoring
  (a) CO concentration
  (b) Turbidity/soot
  (c) Air speed and direction of air flow
  (d) Fire alarm
  (e) Traffic data

All Motorway tunnels in Turkey were constructed having double tubes and generally having triple lanes. And mostly these tunnels have got alternate roads. This provides advantage in case of emergency situation. Motorway tunnels in operation are young and contemporary tunnels and were generally constructed as long tunnels after 1998. When Turkish tunnels are compared with the World tunnels, the Turkish tunnels are not very long and their maximum lengths are about 3000 meters. Motorway tunnels are located outside of cities. There is not any directive or legal documents pertaining to tunnel safety in Turkey. Turkey can be more important for the Trans European network in future. One of the main policies of the EU is the transportation policy and Turkey should work in harmony with the European transportation policy and the criteria of tunnel safety.

Up to now, Installation Emergency Facilities in these tunnels were applied according to PIARC specifications or any other European country codes and criteria to the Turkish motorway tunnels and in some specific conditions the designers make Projects and Motorway Department approves and projects are realized. Engineers gained a great experience at this Emergency Facilities in Motorway Tunnels. As a result of all these experiences, in General Directorate of Highways, a Commission was set up on 6th September 2004 and this Commission is preparing a specification for "The Minimum Requirements of the Infrastructure" in double tube tunnels having a length more than 500 meters in Turkey. All these equipment should be designed according to this criteria. Installation of excess equipment increases not only the construction cost but also the maintenance cost. Therefore, the place of facilities must be chosen with right distances or numbers. In Turkey, we reviewed the Japan Specifications, PIARC documents and European tunnel safety studies. Turkey is eager to be included into the European Union. Therefore, the Commission decided to act in harmony with European Directives. But in some specific conditions Turkish Highway Authority will make use of the Turkish engineers' and contractors' experience in certain areas such as; group tunnels evaluation, emergency escape path doors which should be resistant to fire and smoke, tunnel inside pavement construction etc. The Commission made a meeting nearly every week and with all multidisciplinary engineers such as; civil engineers, electric and electronical engineers, mechanical engineers and discussed the topics of "Turkey tunnels safety and environmental preservation of tunnels". The final report will be presented to the approval of General Directorate of Highway. But till this date since no organization was established in General Directorate of Highways transporting dangerous goods via heavy vehicles were forbidden to enter the inside of tunnel. Advance technologic devices have got tunnels for maintenance and operation need qualified personnel.

5 CURRENT TURKEY MOTORWAY TUNNELS

(a) All motorway tunnels are twin tubes and generally triple lanes.
(b) They are not very long tunnels. Maximum length is Selatin Tunnel (3043 m).

Copyright © 2005 Taylor & Francis Group plc, London, UK

(c) They are young and contemporary tunnels. Most of them opened traffic after 1990.
(d) Turkey is a bridge with Europe and Caucasia and Middle East countries.
(e) Motorway Department was set up a tunnel safety commission and this commission decided adoptation of European Tunnel Safety Directives.

6 CONCLUSIONS

(a) The appropriate precautions should be taken to avoid the accidents happen.
(b) The teams of disaster caution should be located in convenient places.
(c) The personnel and the teams for the disaster caution should be capable for their effective operability in the emergency.
(d) When disaster finish immediately initiate recovery works.
(e) Establishing emergency system including manual system.
(f) Including tunnel control and maintenance personnel must be given necessary traning to police, fire brigadet and resque team.
(g) Daily inspection of emergency equipment and necessary maintenance immediately must be done
(h) For getting rid of consequences of fire catastrophe, it must be set up disaster precaution system and emergency facilities must be installed completely.
(i) Traffic control after accident inside and outside of tunnels.
(j) Extinction and rescue activities is done practically exercise once time annually.

REFERENCES

1. Japan Highway Public Corporation, November1997, Installation Standarts of Tunnel Emergency Facilities.
2. National Expressway Practices in Japan Tunnels.
3. Japan International Cooperation Agency Ministry of Land, Infrastructure and Transport, 29 Sept. 2003, Road Tunnel Technology in Japan.
4. General Directorate of Highways, June 2003, Motorway Maintenance and Operation Services.
5. United Nations Economic and Social Council, 10 December 2001, Recommendations of the Group of Experts on Safety in Road Tunnels.
6. European Commission Directorate General for Energy and Transport, 30 December 2002, Proposal for an European Parliament and Council directive-Safety in European Road Tunnels.
7. Directive of the European Parliament and of the Council on min. safety requirement for tunnels in the Trans-European Road Network, 29 April 2004.
8. www.kgm.gov.tr
9. Old Road Tunnels Inspection Reports from Division of General Directorate of Highways, 2001.
10. 1st European Road Congress Lisbon, 24–26 Nov. 2004, "Emergency Facilities for Tunnel Safety and Turkish Highway Tunnels, İrfan Ünal.
11. 2nd Traffic and Road Safety International Congress Ankara, 5–7 May 2004, "Tunnel Emergency Facilities", İrfan Ünal.

Copyright © 2005 Taylor & Francis Group plc, London, UK

Advanced studies on the propagation of fire in a motorway tunnel – case history by the test center

S.J. Seirer & V. Wetzig
Hagerbach Test Gallery Ltd. Sargans, Switzerland

ABSTRACT: Cofiroute is the largest private motorway operator in France, with responsibility for a motorway network of approximately 900 km in the west of the country. The centerpiece of the A86 in the west of Paris is a tunnel which carries traffic on two storeys. In the event of a fire, this gives rise to a variety of questions regarding the safety of tunnel users and intervention forces as well as the tunnel staff. Extensive tests on the basis of an experimental simulation of a serious accident resulting in a fire are to be used in order to study the propagation of fire between the vehicles in the tunnel, both above and below the seat of the fire.

1 INTRODUCTION

1.1 *The A86 project*

The centerpiece of A86 in the west is a single-tube road tunnel with a length of approx. 10 km and an inner diameter of 10.40 m which carries traffic on two storeys. This gives a clearance height of 2.55 m for each traffic level, so only vehicles with a maximum height of 2.00 m are permitted in this tunnel. Each level has two traffic lanes, one breakdown lane, its own ventilation system and its own emergency exits, and may be used irrespective of the other level.

1.2 *Terms of reference and objectives*

Early in 2003, Cofiroute commissioned Hagerbach Test Gallery Ltd. to realize the most realistic possible test environment in order to carry out studies on fire propagation. The aim is to study the propagation conditions for a fire and – with respect to the possibilities for people to escape –the environmental conditions in the area of the out flowing fire gases. Toxic smoke gases resulting from a fire, reduced oxygen content, diminished visibility and high temperatures together with thermal radiation can impose sustained restrictions on the actions that tunnel users can take to save themselves.

In detail, the terms of reference for Hagerbach Test Gallery Ltd comprised the following items:

– erect the test section;
– carry out the tests;
– design and operate extensive measurement and video technology.

2 THE TEST SECTION

2.1 *General*

Tests and experiments aimed at increasing safety in tunnels have been carried out continuously in the fire gallery at the Hagerbach Test Gallery since 2000. The fire gallery has a gradient of about 4% with a length of approx. 230 m, a width of approx. 9.5 m and a height of approx. 6.5 m, giving it the same cross-section as a two-lane motorway tunnel. Prior to these tests, the surfaces were largely of a rocky nature and only a short section of the floor was concreted. Extensive building work was required in order to be able to carry the tests out under near-real conditions and with the required quality.

2.2 *The intermediate ceiling*

The greatest challenge in connection with the adaptation of the fire gallery was posed by the installation of an intermediate ceiling throughout the entire test area (145 m). There was a clash of conflicting interests here: on the one hand, safety reasons called for a ceiling with the maximum possible stability while on the other hand, it had to be possible to dismantle the ceiling again at reasonable costs. It very quickly emerged

Copyright © 2005 Taylor & Francis Group plc, London, UK



Figure 1. Construction of the concrete ceiling.

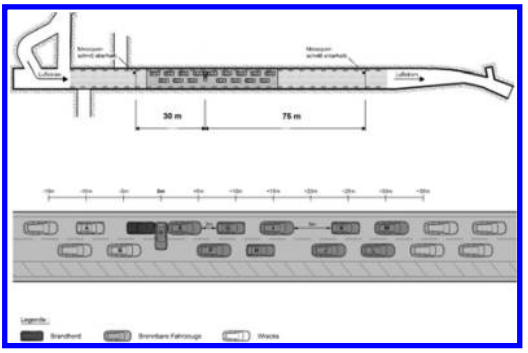


Figure 2. Test section (top) and fire section (below).

that a design based on lightweight construction would be out of question, mainly due to the high temperatures that were to be expected. After weighing the pros and cons a "mobile ceiling" (concrete and steel) was made. The basic framework was provided by steel girders in the tunnel walls, on which transverse girders were placed at intervals of approx. 2 m. Reinforced concrete slabs were placed between the transverse girders. The ceiling was protected with fireproof panels in the area of the seat of the fire.

2.3 *Floor, walls*

A concrete floor was made throughout the entire length of the test section, following the gradient of the gallery. The tunnel walls were spray-coated with a special fire protection mortar to prevent the high temperatures from causing any damage.

2.4 *Lighting*

The test area was lit with fluorescent lights of the sort used in the A86 road tunnel. 55-watt fluorescent lights (l = 1.5 m) were positioned at intervals of 5 m on both sides. In the area from −60 to −15 m, the lights were positioned below the tunnel ceiling. In the area from −10 m to +85 m, they were placed near the ground (30 cm from the ground) in order to protect the lamps against the high temperatures so that the lighting could be guaranteed for as long as possible even when smoke developed.

2.5 *Fire zone*

The centre of the fire is located at ±0 m (vehicle "D"). Starting from the centre of the fire, the distances in meters are prefixed with a positive sign in the direction of flow and with a negative sign against the direction of flow. The descriptive terms "downstream" (positive) and "upstream" (negative) are used analogously.

The fire zone is the part of the test area where the fire takes place. The fire zone starts at −25 m and ends at +30 m, giving it a total length of 55 m. In the area covered by the fire zone, the intermediate ceiling was protected against high temperatures by two layers of fireproof panels.

2.6 *Air speed*

Overpressure in the fire gallery was used to produce the required longitudinal flow in the test section. The air was accelerated and forced into the test section by two axial fans with a diameter of 1.8 m. The air speed in the test section was controlled by the sensor V1002 in the upstream measurement cross-section. In the access area of the test gallery, two gates were controlled on the basis of the effectively measured air speed, enabling the required air speed to be set.

The progression over time of the air flow in the test area was specified by the client.



Figure 3. Fans of the ventilation system.

Copyright © 2005 Taylor & Francis Group plc, London, UK

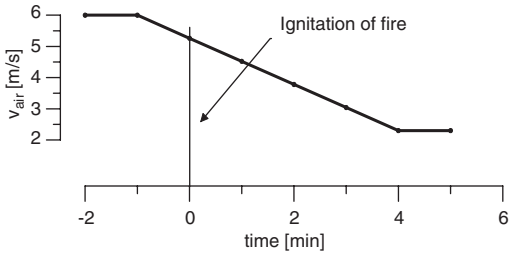


Figure 4. Run of the air-velocity at the beginning of the test.

3 SAFETY

The safety of the test team and the visitors were ensured by a fire engine with 12 men of a local Fire Brigade with operational equipment. To enable people to exit safely from the test area in the event of a power failure, the marked escape route was additionally safeguarded by lighting which was independent of the power mains.



Figure 5. Fire fighter operation.

4 MEASUREMENT TECHNOLOGY

4.1 *General*

All the technical measuring equipment had to be reliable and robust in order to operate without faults under the extreme test conditions such as humidity, high temperatures, smoke and aggressive gases.

4.2 *Central measurement technology unit*

The central measurement technology unit was located at the entrance to the fire gallery; it consisted of two rooms, one used as the command room and for data acquisition, and the other used to produce the video recordings. The central measurement technology unit was linked to the data network of the gallery installation and was also connected directly to the seminar room in the Hagerbach Test Gallery. During the tests, all the visitors were present in the seminar room and they were able to follow events on three screens. Two of these were used for video transmission and one was used for real-time data transmission.

4.3 *Data recording*

Central recording of the measured data was handled by the MDA-600 multi-channel measurement and monitoring system. One or more limit values can be assigned to each channel. These values are stored in a non-erasable, protected memory. All the measurement cards were tested by the manufacturer according to the DIN standard. The CSTB accepted the entire system after further testing prior to the start of experiments.

The MDA-600 was accommodated in the central measurement control room and was protected against power failures by an uninterruptible power supply.

4.4 *Sensors*

Measurement cross-sections were located on both sides of the fire scene, but all the data cables ran together in the central measurement technology unit; this meant that sections of the cable had to be routed past the seat of the fire. In order to circumvent this weak point, we decided to place all the measurement cables and part of the measurement electronics on the intermediate ceiling. The advantage of this choice was that the cables and electronics were not only protected against the high temperatures but also against the extinguishing water used by the fire brigade. The test area contained a total of 227 sensors and about 4800 m of measurement and data cable. Specifically, the sensors were for:

- temperature
- air speed
- air pressure
- air humidity
- heat flow density
- visibility
- gas (CO, CO_2, O_2, NO_x, HCl, HCN, SO_2).

4.5 *Measurement cross-section*

See figures 6 and 7.

4.6 *Cameras*

The tests were monitored by ten cameras mounted in fixed positions and one mobile camera. Given that restricted visibility was to be expected below the seat of the fire in particular, six normal image cameras and four thermal image cameras were used. All the video signals were converted into PAL signals via a central

Copyright © 2005 Taylor & Francis Group plc, London, UK

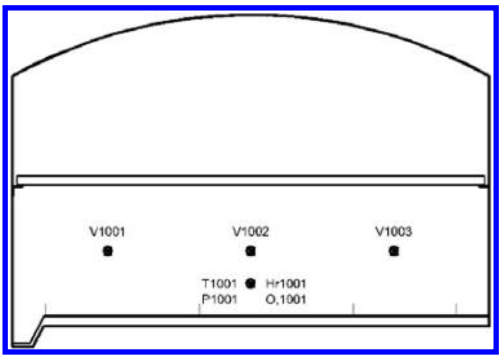


Figure 6. Measurement cross-section upstream.

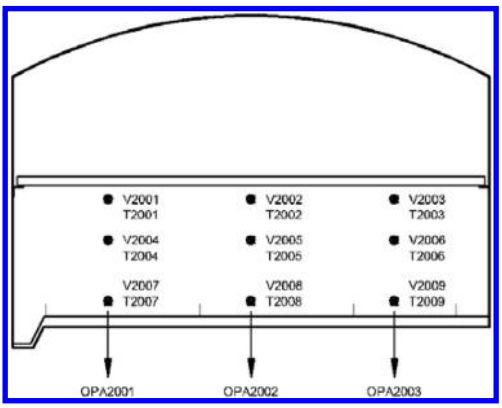


Figure 7. Measurement cross-section downstream.

production unit for recording on eleven analogue VHS recorders. The time code (min/sec) was added when the DVD was produced.

5 VEHICLES

To make the tests as meaningful as possible and in order to carry them out realistically, the choice of vehicles was to be based as closely as possible on the European average. The categories of vehicles were specified by the client and the selection of the individual vehicles within these categories was made by Hagerbach Test Gallery Ltd, depending on their availability on the used vehicle market. About 70 vehicles were burned in the course of the entire series of tests (with and without a water mist system).

5.1 *Ready-to-operate vehicles*

These vehicles were designated for those positions to which the fire can spread during the test period.

The combustible vehicles serve the purpose of making the test procedure realistic, and they had to meet the following conditions:

- engine in working order;
- undamaged bodywork;
- all window glass must be complete;
- it must be possible to drive the vehicles
- the tire must be complete;
- the fuel system (tank, pipes) must be tight (no leaks);
- the interior finish of the vehicles must be complete;

5.2 *Wrecked cars*

The non-combustible wrecks were designated for those positions where the possibility of the fire "skipping" could be ruled out. Their primary purpose was to create an air flow as realistic as possible in the test area.

The wrecked vehicles had to meet the following conditions:

- all the combustible materials (engine, tire, interior finish, fuel system, insulation material) had to be removed;
- the bodywork must not show any major damage;
- all window glass must be complete.



Figure 8. Ready-to-operate cars for the tests.

6 WATER MIST SYSTEM

A fixed-position water mist system from Aquasys, was used for this series of tests. Erection, dismantling and operation of the system were undertaken by Aquasys staff.

The system comprised five controllable pipe trains with a total length of 66 m (−33 to +33 m) per train. The system was operated at about 500 l/min and a pressure (sensor 2) of approx. 30 bar.

Copyright © 2005 Taylor & Francis Group plc, London, UK

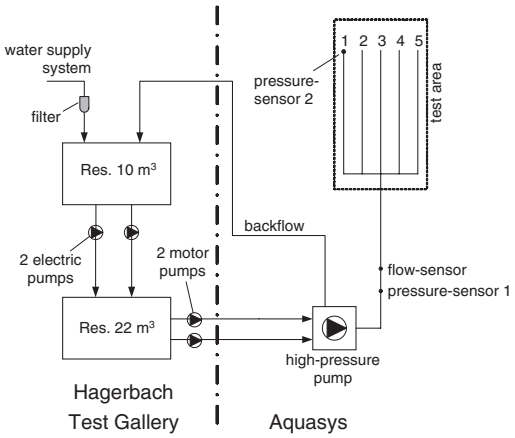


Figure 9. Scheme of the water mist system.

7 TESTS UNDER LIVE CONDITIONS

7.1 *Tests without the water mist system*

7.1.1 *Preliminary tests*

Preliminary tests were carried out to verify the entire measurement and camera system. Normal oil was used as the combustible for the preliminary tests. The seat of the fire consisted of four cylindrical steel pools with a combustion surface of 1.07 m^2 each and a height of 30 cm. Each container was filled with 40 l of heating oil and one liter of heptane. In order to create the most realistic flow conditions possible, four wrecked cars were placed behind the fire troughs and four were placed in front of them. The distance to the fire centre was selected so as to make it impossible for the fire to skip over.

Two preliminary tests were carried out.

7.1.2 *Main tests*

The vehicles were set up for the main tests as per Figure 2. The tanks of vehicles C, D and E were open and were each filled with 2 l of petrol + 5 l of diesel fuel; the tanks of the remaining vehicles were empty. On vehicle D, a leak was simulated by a drip point on the tank. On vehicle C, the front windscreen was damaged and on vehicle D, the rear window glass on the passenger's side was missing.

Using heptane (250 ml) as the fire accelerator, vehicle C was set on fire. A total of three main tests took place between September 25th and October 9th, 2003.

7.2 *Test with a water mist system*

7.2.1 *Preliminary tests*

The objective of the preliminary tests was to verify the entire measurement system and the camera system, and to verify the water mist system. Vehicles were used as per 5.1. depending on the position of the vehicles, they were filled with fuel: 2 l of petrol +15 l of diesel. In addition, a controllable drip point was installed in the tank system to simulate the escaping fuel.

7.2.2 *Main tests*

Vehicles as per 5.1 and 5.2 were used for the main tests; these were filled with fuel in the same way as for the preliminary tests. A computer program written by BG made it possible to monitor the measured values in real time on the computer and to assess the progression of the fire. The water mist system was activated manually on the basis of these assessments.

Between 4.11.2003 and 27.11.2003, a total of 6 preliminary tests and 4 main tests were carried out with a water mist system.

8 SUMMARY

Cofiroute's concept for the tunnel on the A86 only allows for vehicles with a maximum height of 2 m due to the clearance height – this systematically rules out hazards caused by larger quantities of goods. The special geometric parameters and the specific features of the organizational measures have nevertheless thrown up a large number of novel questions.

This series of tests, the nature and scope of which make them unique in the world, are intended to answer as many of the open questions as possible with the necessary care. In the future too, technical and organizational measures will be necessary in order to improve tunnel safety.

Tests of this sort can play a major part in enabling the residual risk in tunnel installations to be reduced to a negligible minimum, even though – sadly – the risk will always be present. For this reason, it will also be indispensable to carry out tests on a 1:1 scale in the future.

Copyright © 2005 Taylor & Francis Group plc, London, UK

Dynamic fire spreading and water mist tests for the A86 East tunnel – description of the test set up and overview of the water mist tests

X. Guigas & A. Weatherill
BG Consulting Engineers Ltd., Lausanne, Switzerland

C. Bouteloup
Cofiroute, France

V. Wetzig
Hagerbach Test Gallery Ltd., Hagerbach, Switzerland

ABSTRACT: This paper outlines the organisation and an overview of the results of the extensive fire test campaign organised in Switzerland for the A86 East tunnel (double deck) currently under construction in Paris. The objectives of the tests, the constraints imposed (realism, safety) and the general arrangement of the test gallery are described. Extracts from the results of the water mist tests are presented qualitatively and are commented.

1 INTRODUCTION, WHY THESE FIRE TESTS

In single direction tunnels, the most common ventilation strategy in case of fire is to create a sufficient longitudinal air velocity in order to push the smoke in the traffic direction and evacuate this smoke either at the tunnel portal or, for long tunnels, at an intermediate extraction point. Due to the ventilation flow, the tunnel part upstream of the fire is free of smoke, allowing a safe escape for the tunnel users. This straightforward ventilation procedure is based on the hypothesis that the vehicles located downstream the fire can leave freely the tunnel and, therefore, is well suited for non urban tunnels (low traffic jam occurrence) or for tunnels where the traffic can be efficiently controlled.

However, what would happen in case of an accident causing a fire at the end of a queue of cars formed by a traffic perturbation (or first accident)? Would the fire propagate to other vehicles? What would be the tenability and evacuation conditions downstream of the fire? What would be the conditions faced by the fire brigades? Would fixed fire fighting systems improve the egress conditions and diminish the risk of fire spreading?

These questions are generally ignored, mainly because they result from what is considered as a low probability event but also because they are difficult to answer. Nevertheless, the construction by COFIROUTE of the astonishing 11 km long single tube two decks

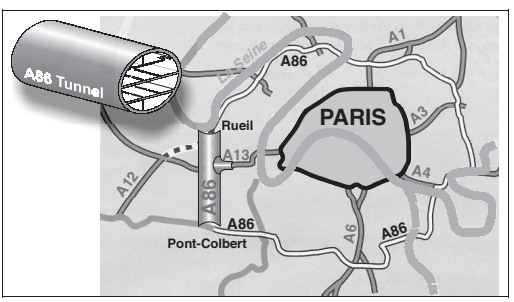


Figure 1. Localisation of the A86 tunnel.

A86 East Tunnel (Paris), with its reduced gauge (2.55 m from floor to ceiling, light vehicles only) revived the discussion on these safety questions.

2 OBJECTIVES OF THE TESTS

The objectives of these tests were, in a situation called "over-accident" (accident at the end of a forming queue of vehicles), and for real tunnel conditions (geometry, ventilation, vehicles, etc.):

(a) To observe and measure the fire propagation conditions between the stopped vehicles.
(b) To measure the ambient conditions downstream the fire place, zone where the vehicles of the tunnel users might be blocked.

Copyright © 2005 Taylor & Francis Group plc, London, UK

(c) To test and qualify the equipment of the COFIROUTE emergency services.
(d) To test different fire detection system and signaling equipment.
(e) To observe and measure the benefits and possible disadvantages of using fixed fire fighting systems.

3 PREPARATORY WORK

3.1 *Test organisation*

The A86 East tunnel being under construction, the fire tests took place in Switzerland (VSH Hagerbach). Several actors were involved in the test organisation (see table 1).

3.2 *Key aspects of the tests specifications*

As already mentioned, the tests conditions had to be as close as possible to the reality, this implied:

– A realistic ventilation flow: Numerical simulations of the transient tunnel ventilation flow during over-accident situation have been analysed leading to the following approached time-velocity curve (see figure 2). This curve has been used as a velocity target during all the tests.
– A realistic accident configuration: The over accident has been supposed to involve three vehicles (C–D–E) which were in contact. The distance between the other vehicles in the queue has been set to 2 m. The fire ignites in the engine compartment of vehicle C (small pot filled with heptane soaked rag, hood slightly open), a fuel leakage was created from the tank of vehicle D (roughly 1 l/min). Vehicle D had its lateral windows broken. The engines of vehicles C–D were running during 20 minutes before the ignition. The fuel content of all the vehicles was a mixture of 51 gasoline and 151 of diesel.
– A realistic selection of cars: This selection has been made from the result of a traffic analysis conducted by COFIROUTE in the A86 existing network. The 70 vehicles bought for the test campaign (almost 60 have been burned from them) were coming from the second-hand market.
– A realistic intervention scenario: Safety studies have shown that the longest intervention time needed by the COFIROUTE emergency services to reach the fire place was of 10 minutes after the alarm. Therefore, some of the fire tests included intervention trials aiming to see the capacity of these emergency services to approach and control the fire. Note: Parallel to the COFIROUTE emergency services, the Paris fire brigades will intervene on the fire scene. The maximum intervention time from the alarm) is assumed to be about 30 minutes.

Table 1. Main actors involved in the fire test campaign.

Actor	Role
COFIROUTE	Owner and future operator of the A86 tunnel
A86 Safety committee	Definition of the fire test objectives, validation of the test concept.
BG Consulting engineers Ltd.	Fire test definition and design; project management; post processing; treatment and presentation of the results, analysis
VSH Hagerbach test gallery Ltd.	Test realisation
CSTB	External quality control of the measurements
AQUASYS	Supply and operation of the water mist system

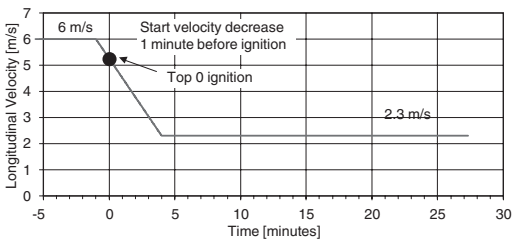


Figure 2. Ventilation flow rate used during the tests.

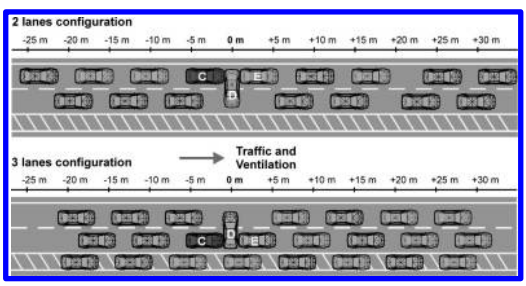


Figure 3. Test configuration for 2 lanes and for 3 lanes.

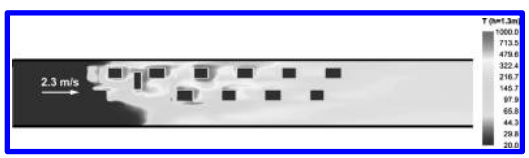


Figure 4. Calculated temperature field during fire propagation (slice at 1.3 m from the gallery floor) longitudinal velocity = 2.3 m/s.

Copyright © 2005 Taylor & Francis Group plc, London, UK

3.3 *CFD fire simulations*

CFD simulations (using FDS3 from NIST) have been performed prior to the fire tests in order to explore the patterns of the different fields (temperature, velocity, radiation, etc.), to adapt or control the sensor positions and to test the data processing method. The figure 4 shows an example of temperature slice calculated for a two lanes configuration.

The accuracy of the predicted results is of course strongly depending on the fire propagation criterions (thermal flux on the target object, temperature of this object). Moreover and according to test results, the fire propagation appears to be partly conducted by random processes, an efficient modelling of the fire spreading may require the use of statistical simulation (coupling of Monte Carlo/CFD methods for example).

4 ORGANISATION OF THE TEST GALLERY

4.1 *Geometry: recreating the A86 environment*

The gallery used during the test is part of the underground network (galleries, caverns) of the Hagerbach site. Its total length is approximately 220 m, 150 m have been dedicated for the recreation of the A86 geometry.

The recreation of the A86 geometry consisted in:

- Creating a false ceiling and a smooth concrete floor on the whole test length (150 m) in order to obtain the A86 tunnel gauge (2.55 m).
- Correcting the side walls (milling of the main irregularities) to get the A86 width (9.3 m).

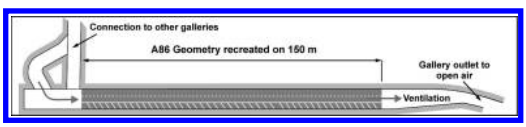


Figure 5. General layout of the test gallery.



Figure 6. Final test gallery arrangement.

4.2 *Instrumentation*

The instrumentation, gathering roughly 160 sensors, has been set up in three sections of the tests gallery:

- Upstream measurement section: Reference values, incoming airflow (sensors used for the air velocity regulation – input of the regulation loop).
- Fire zone: measurement of the "near field" ambient conditions (mainly air/smoke temperature and heat flux) together with fire propagation (temperature inside cars).
- Downstream measurement section: "Far field" ambient conditions (mainly gas concentrations, opacity).

The fire scene has been constantly filmed during the fire tests, the video system consisted in 6 normal cameras, 4 thermal (IR) cameras and a portable camera, all of them being connected to a video control room from where they were recorded and dispatched to the conference room (see chapter concerning test safety). The cameras submitted to hot smoke were protected by boxes ventilated from the upper part of the false ceiling.

4.3 *The water mist systems*

The general specifications of a water mist system compatible with the A86 East Tunnel were analysed in former studies (SOCATOP). The system installed and tested during this fire campaign was therefore adapted to this particular geometry (traffic area 9.3 m wide and 2.55 m high). It has to be noted that this water mist system was not designed to extinguish the fire but to keep its power to a value manageable by the emergency services (the waterflow needed for an extinction system would imply an outsized water network).

The layout of the tested water mist system is presented in the figure 7. The main characteristics of this system are: the droplet size (median diameter = 200 μm) – the water flow rate (roughly 0.5–1.5 L/min/m^2) – the pressure (medium pressure, in between 20 and 40 bars).

5 WATER MIST TESTS: OVERVIEW OF THE TEST RESULTS

The overall campaign consisted in a total of **19** fire tests for which all the data described above have been collected and stored. An important effort has been put on the preparatory runs, especially to be confident on the method used to estimate the heat release rate (HRR calculated from enthalpy flow, and from gas concentration: O_2–CO_2–CO) but also to set up the ignition method.

Copyright © 2005 Taylor & Francis Group plc, London, UK

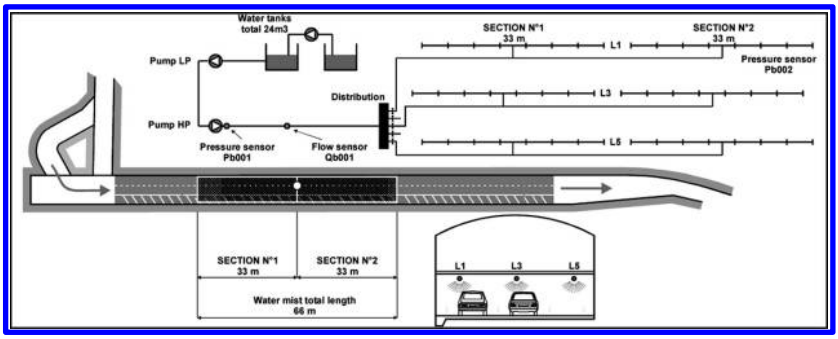


Figure 7. General layout of the water mist system.

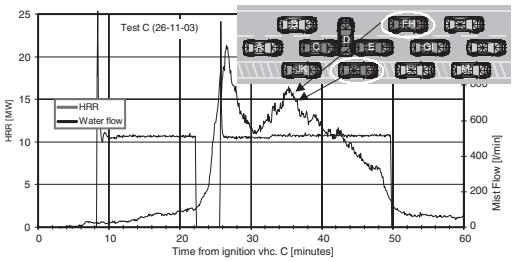


Figure 8. HRR and water flow measured during test C.

As pointed during the description of the installation, the tested water mist system was not designed to extinguish the fire but to keep the released power at a reasonable level. This was confirmed during the tests. However, the water mist (as tested) has shown its capacity to prevent the fire spreading to adjacent vehicles (2 m space).

Figure 8 (above) shows an example of fire behaviour experienced during the test campaign. During this test (called test C) the water mist system was operated in three phases:

– Phase 1: Water mist is operated approximately 8 min from the vhc. C ignition, at this time the engine compartment of vhc. C is gently burning (it is assumed that at this stage the fire can be detected from the CCTV network of the future tunnel). Under the water mist, the fire develops slowly, the flames lick vhc. D (left side and underside) and the underside of vhc. E. This situation evolves gradually during 14 minutes, the fire is under control.
– Phase 2: 22 minutes after ignition the fire mist is intentionally stopped during 4 minutes. The fire behaviour changes radically, the passenger compartments of D and E (heated up during phase 1) suddenly ignite, the HHR rapidly increases, the heat flux ignites vhc. K and vhc. F.
– Phase 3: About 26 minutes after first ignition the water mist is re-operated. The temperature of the gases surrounding the fire place together with the heat flux are sharply decreased, stopping the possible fire spreading. The ignition of the passenger compartments of vhc. K and F lead to a second maximum on the measured HRR curve. After this second maximum, the energetic contents of the cars are slowly consuming and the HRR decreases monotonically. The water mist is stopped 50 minutes after ignition.

During the tests the water mist was observed to diminish the total heat flux, the radiation heat flux being partially absorbed or scattered by the droplets, the convection flux being diminished as the global temperature level decreased. Qualitatively it was possible, during water mist activation, to approach (3–4 m) the actively burning fire place without felling heat sensation. figure 9 gives an example of comparison between heat flux with and without water mist.

As the droplet flow has a washing effect on the smoke (driving of part of the soot particles toward the floor), the visibility conditions downstream the fire place (but outside the mist section) were improved. This is illustrated by Figure 9 showing the visibility distance vs the heat released rate for test with and without water mist. However, in the mist section (downstream the fire place) it is likely (but not quantitatively measured) that the visibility conditions are deteriorated by the water mist.

No notable variation on the toxic gas concentration due to water mist operation has been noticed during the tests (at least for CO, CO_2, NO_x).

The visibility conditions upstream the fire place were undeniably deteriorated by the operation of the water mist system (see Figure 10), but the visibility level was still compatible with the principle of self evacuation. It is worthwhile to note that the water mist system, as tested, did not caused any respiratory problems and that the sound level generated by the nozzles was acceptable.

Copyright © 2005 Taylor & Francis Group plc, London, UK

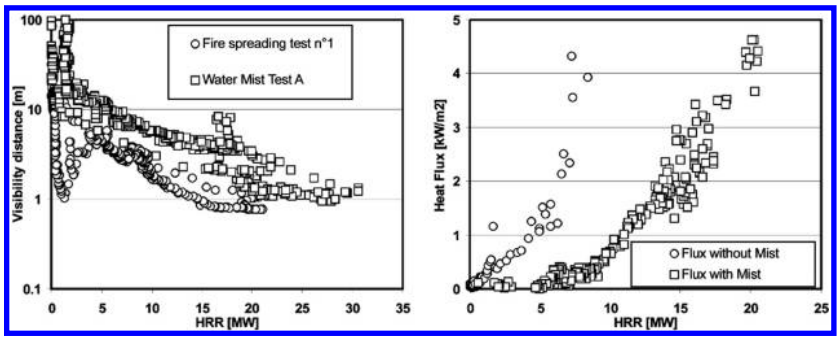


Figure 9. Visibility level and heat flux vs HRR with and without water mist (heat flux +10 m downstream the fire place, visibility measured at +75 m) – Examples.



Figure 10. Visibility of the fire place as the water mist is activated (left) and during operation (right).

6 CONCLUSION AND ACKNOWLEDGEMENTS

The test campaign highlighted the following points:

- The HRRs measured during the tests are in accordance with the values expected for a fire of grouped cars. During the growing phase of the fire, the time evolution of the HRR differs considerably from one test to another.
- For the test conditions the fire spreading toward adjacent vehicles has been observed. However the fire situation stays manageable for two well trained and equipped fire fighters, intervening within roughly 10–12 minutes after the ignition.
- The water mist system has been observed to stop the fire propagation by cooling considerably the combustion gases, reducing strongly the radiative heat flux together with a reduction of the HRR.
- It has been noted that the water mist system improves the visibility conditions downstream the fire place (smoke washing). On the other hand the visibility upstream the fire place was reduced. No significant effect on the toxic gas concentration downstream the fire place has been measured.

The present work was undertaken under contract of COFIROUTE, France. The Authors would like to thank here:

- COFIROUTE for permitting the publication of this paper.
- M. Bignand Colonel (er) from the Paris Fire Brigades for the management of the COFIROUTE emergency services during the intervention tests.
- The Flums and Flumserberg fire brigades for insuring the safety of the tests.

Copyright © 2005 Taylor & Francis Group plc, London, UK

Use of advanced fire fighting technologies of finely atomized water for fire protection of metro objects and tunnels

A.S. Chirko
Mosinzhproekt, Moscow, Russia

A.V. Karpyshev & M.D. Segal
The Research Institute of Low Temperatures of Moscow Aviation Institute (NIINT), Moscow, Russia

ABSTRACT: Consequences of major fires in Metro mean mass death of people and transportation collapse of a town Fires in Metro underground structures and tunnels are characterized by speedy temperature build-up, emission of considerable volumes of toxic combustion products, damage of tunnel structures, interruption of highway running. On the basis of advanced aerospace technology the specialists of NIINT have developed and patented fire fighting technologies by finely atomizated water, which surpass the well-known analogues, and several operating facilities have been created.

Nowadays the negative factors of technological, natural and terrorist character are the most hazardous threats for people's safety.

Safety system modification of the subway, transport tunnels, communication collectors and other underground city facilities as objects of a higher risk is directed to lowering the level of technological catastrophes and fires in the city tunnels that may lead to mass casualties and transport collapse.

It should be noted there is no distinct differentiation in spheres of responsibility for underground facility safety, and the control of extra-hazard area protection is, unfortunately, far from being perfect. The negative technological factor effects gain force.

There has been a stable tendency of terrorist act growth in the underground facilities over the past years, thus relating the underground facilities to a list of critically vital objects for Russian Federation.

Fires in the underground engineering arrangements and tunnels are characterized by a fast hazard area propagation effect on a considerable part of the facility, fast temperature growth in the tunnel space, escape way blocking out of the underground facilities and contaminating adjoining ground areas and buildings with toxic combustion products, tunnel structure damage, transport line service cut off. The consequence of a big underground fire may be mass casualties and transport collapse of the megalopolis.

A fire development in the underground train carriages, on the passenger platforms, escalators, railway and in the underground arrangements critical for security has the following features:

- limited space, a great number of people and, as a result, future difficulties for passenger evacuation;
- considerable total fire load, which is particular for different types of carriages amounting to more than 50 kg/m^2, it may include a good deal of materials releasing toxic components during combustion;
- a lot of, up to 10 kV, live power cables in the underground tunnels;
- a lot of live electric wiring in the carriages;
- a high rate of air exchange causing a high rate of temperature growth up to the values of a thousand and more degrees; actually in 3 … 5 minutes after the fire start the situation for the people in the tunnel becomes hazardous, herewith it is necessary to evacuate a few hundred people, when the fire develops;
- fast smoke spreading over the escape ways;
- considerable difficulties and, in a number of cases, practical inability to supply the required volume and flow rate of the extinguishing liquid delivery to the underground fires;
- possible panic rise among the passengers.

Smoke spreading presents a high risk and hazard for the passengers. The people die, as a rule, of asphyxia and poisoning by combustion products.

Copyright © 2005 Taylor & Francis Group plc, London, UK

A specific fire character of the underground facilities and in the tunnels demands strict and particular requirements for fire protection systems:

- fire extinguishants applied in the carriages, at the passenger platforms and escalators must be safe for the people;
- the system must be fast-acting including operation under motion blocking conditions in the tunnel;
- fire protection systems must provide safety for the people in the carriages, at the platforms and escalators;
- fire protection systems must provide fast temperature decrease and combustion product fallout;
- fire suppression and extinction must not result in the underground tunnel and engineering space flooding and cable bin submersion.

A higher degree of hazard and difficulties of subway and underground transport system passenger evacuation demand fire protection system availability characterized by fast response, high efficiency, and ecological friendliness, passenger and service personnel.

Atomized water fire protection technology allows fire suppression with maximum efficiency and minimum water consumption. These systems may be easily installed at the underground stations and in the carriages, in addition, they require minimum maintenance.

Russian atomized water fire fighting systems are highly competitive. The specialists of Low Temperature Research Institute (NIINT) of Moscow Aviation Institute (Technical University) have developed efficient atomized water fire fighting technologies on the basis of aerospace achievements surpassing prior state-of-the-art and designed a range of operating systems already proven by the service.

The NIINT has stored the atomized water fire protection system development and design experience in creating mobile and automatic fire extinguishing systems protected by tens of patents issued in the countries of Europe, the USA, Japan. The above systems have successfully functioned in different fields of national economy. The Institute possesses all necessary scientific and R&D abilities to solve particular problems of underground facility fire protection and it may come out as a leading organization in favor of this problem solution.

The best known development of this Institute product is RUPT-1-0,4 backpack fire fighting unit designed for fast suppression of solid combustible material, inflammable liquid and gas fires as well as live electrical system extinction.

The above unit is based on a gas-dynamic acceleration principle of an atomized two-phase (water-air) flow (mean water droplet size of about 100 microns), which allows fire suppression at the initial stage of the fire with a very high efficiency.

The unit features small dimensions and light gross weight of less than 20 kg, easiness and reliability in operation, constant readiness for work and safety. Just ordinary water or water and additives of about 9 L capacity serve as extinguishing liquid. The unit comprises a 2 L pressurized air bottle, 30 MPa operating pressure, which is similar to that used in a fireman's breathing apparatus, thereby allowing an atomized liquid jet generation with the lancing distance of 15–20 m.

During the approval tests of the unit in Russia and abroad it was confirmed suitable for the following purpose-oriented applications:

- Class 55A Fire extinction of solid combustible materials, which conforms to the burning surface area of about 60 m^2 including glowing combustion;
- inflammable liquid (petrol, kerosene, heptane, different oils and lubricants, etc.) fire extinction of up to 7.3 m^2 area and a greater area during fuel spillage, herewith in the course of the tests it was shown that 9 L unit capacity, water and foam agent components, is sufficient to extinguish approximately 200 L of burning petrol or heptane;
- up to 36000 V live electrical equipment fire extinction from the distance of more than 1 m (according to Dielectric Test Protocol).

These features of the unit demonstrate its promising application for the underground facility fire protection due to the following effect:

- a timely approach to fire suppression prior to major fire brigade arrival;
- exclusion of tunnel or facility water flooding and complete avoidance of a collateral damage;
- fire fighting, with the people not evacuated.

At firing tests in August, 2003 a burning car was extinguished by RUPT within 165s, only 3.5 L of extinguishing liquid spent.

On the basis of statistical data on a fire area by the moment of fire brigade arrival one may believe that almost 90% of all the fires can be successfully extinguished by a RUPT unit, which allows the least property damage.

This design was patented in many countries of the world, awarded Gold medals at the 48th World Exhibition "Brussels-Eurika 99" and the 28th International Exhibition (April 2000, Geneva), and the 2000-year Prize of Russian Federation Government A license for its production was purchased in Germany.

One of the Institute's latest developments is a fire extinguisher generating an atomized water jet for fast suppression of initial and considerably small fires.

The extinguisher water capacity (6 L) is sufficient to suppress A34 Class Fire (burn area of about 40 m^2) or IFL B183 Class Fire (approximately 180 L of any IFL on the tray 27 m in diameter). The total fire extinguisher

Copyright © 2005 Taylor & Francis Group plc, London, UK

weight is 9 kg. The atomized water jet range is 5–7 m, liquid flow rate is 0.3 L/s.

The extinguisher may also be used to suppress E Class Fires up to 10 kV.

The extinguisher is easy to operate, it requires no special maintenance and may be placed in the engine-driver's cab. A model range of these different-capacity fire extinguishers, 2 through 10 and more litres, is possible to manufacture.

These features of the said fire extinguisher allow to timely suppress such typical subway fires as, e.g., sleeper fire (including glowing combustion) or cable fire in the tunnels.

The NIINT specialists have developed and tested highly efficient atomized water deluge and sprinkler nozzles surpassing the best foreign analogs by their performance, the application of which is desirable to consider while designing automatic fire systems at the subway facilities including subway trains, since the above-mentioned systems feature a higher water consumption efficiency as against the well-known foreign analogs and lower operating pressures.

For automatic fire protection systems of the interior space in the subway train carriages the NIINT specialists also propose to design special modules containing a water tank, an air-expulsion system, and atomized water spray nozzles installed in the carriages. The model itself may be arranged in the space under the carriage.

Apart from other systems, the spray nozzles of which have operating water supply pressure of about 8.0 MPa, highly efficient NIINT atomized water spray nozzles operate by water supply pressure of about 0.6–1.2 MPa.

Application of gas, powder and aerosol fire systems is extremely dangerous for the people in a closed space. Atomized water application is not only efficient for fire suppression and safe for the people. Tiny water droplets intensively absorb heat radiation and adsorb active chemicals and asphyxiants, thereby completely protecting the people against fire hazard effects and creating local safe areas.

Pre-test studies carried out at NIINT have shown that another problem important for subway – creation of atomized water curtains preventing the smoke pread from the subway tunnel to a station in case of a fire.

In long tunnels with rare fire exits it is desirable to employ a Safe-Point installation – special fire protection equipment for a group of people in the tunnel. This is a new joint NIINT-and-Mosinzhproekt work especially efficient in deep tunnels as a compensating or extra measure developed to provide safety for those people who failed to escape. The tests show that the Safe-Point protects against a less than 65 kW/m^2 radiation flow and maintains not less tan 15% oxygen content. The installation is easily assembled, it has both remote and manual actuation. The Safe-Point is fitted with an advanced audible and light beacon system that allows to locate it with the visibility of less than 8 m from the distance of 50 m. The installation is of a high operation level, it may be integrated with automatic fire protection systems.

For long tunnels the first-due tunnel micro-engine has been developed. This micro-engine is able to deliver two firemen to the fire site at a speed of 55 km/hr. The equipment of the vehicle includes an atomized water fire protection system, 100 L capacity water/water and foam agent tank, which allows a timely extinction of solid combustible fires of up to 360 m^2 area or inflammable liquid fires of up to 40 m^2 area. In addition to a fire protection system of its own the micro-engine is fitted with two backpack fire fighting units and may also be equipped with a portable compressor of up to 33.0 MPa, a high-pressure pump to operate from an external water source, extra hoses and a breathing apparatus.

Hydraulic and firing tests of the design items have shown their high efficiency in suppressing a fire, their ability to lower the temperature in the vicinity of the fire and precipitate combustion products within a very short period of time (about a few seconds).

REFERENCES

Both, C. and A. Haack. *Present-Day Design Fire Scenarios and Comparison with Test Results and Real Fires: Structures and Equipment. Safe and Reliable Tunnels. Innovative European Achievements*. First International Symposium, Prague 2004, (73–87).

Copyright © 2005 Taylor & Francis Group plc, London, UK

Physical modeling of blasts and fires in tunnels

V.P. Efremov, V.E. Fortov, V.V. Golub, M.E. Povarnitsyn & S.B. Viktorov
Institute for High Energy Density Russian Academy of Sciences, Moscow, Russia

A.S. Chirko
Mosinzhproekt, Moscow, Russia

ABSTRACT: Prediction of terrorist attack consequences can be made by means of both experimental and numerical simulation.

1 INTRODUCTION

The specter of terrorist bombings is a haunting reality nowadays and needs urgent address in all of its aspects, including technical ones. Blast waves resulting from high explosive bursts in air cause death, injury and damage. The crucial parameters are high overpressure from the direct blast and from reflections that can cause excessive mechanical loading, and high temperatures that can cause a fire (Golub et al. 2004). These effects are most dangerous in tunnels where the critical energy of gas detonation ignition by factor 10 less than one in open air.

2 EXPERIMENTAL FACILITIES

Institute for High Energy Density Russian Academy of Sciences (IHED) is participating at such investigations and has the necessary equipment, including five shock tubes and two explosion chambers. The chamber 13YA3 has an internal diameter of 12 m and a mass of 450,000 kg, Figure 1. It was tested with a 600 kg charge of TNT.

Testing complex ST-5000 consist of uncial large-scale shock-tube and multifunctional complex for measurements, Figure 2 shows shock-tube of ST-5000. It has length about 100 m and consists of fourth sections with different lengths and diameters. Explosive charges of mass up to 20 kg TNT may be used for generation the blast wave. Assigning time – amplitude wave characteristic are reached by time – spatial explosion sources distribution into shock tube. Studied object is located into shock tube cannel or on its cross section at different angles with regard to blast wave front.



Figure 1. Chamber 13YA3.



Figure 2. Testing complex ST-5000.

Copyright © 2005 Taylor & Francis Group plc, London, UK

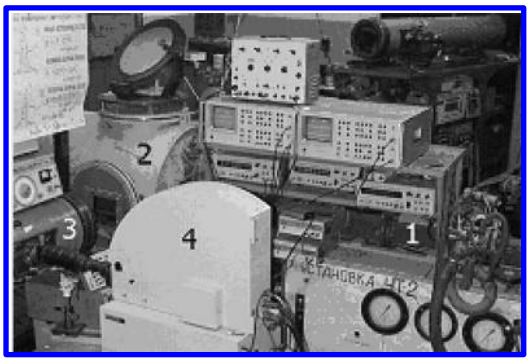


Figure 3. Shock tube with diagnostic apparatus: detonation/shock tube – 1, receiver/vacuum chamber – 2, IAB-451 schlieren device – 3, high-speed camera – 4.

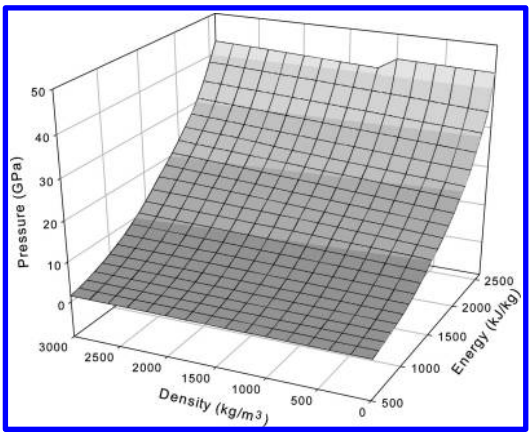


Figure 4. Pressure vs internal energy and density.

Systems are equipped by piezoelectric pressure transducers, which disposed on tube wall along the axis. Three dimensional visualization of shock wave processes can be obtained on unique UT-2M setup, Figure 3. High-speed camera VSK5 can operated up to 500,000 frames/sec and obtained 72 frames during the one experiment. Pressure gages have time resolution 1 mks.

Experimental base is used for detailed analysis of shock and combustion processes in collectors and tunnels.

3 THERMODYNAMIC EQUATION OF STATE

Accurate numerical modeling of shock and detonation processes requires realistic equation of state (EOS) for explosives and products of detonation. A thermodynamic EOS of the detonation products is often used in tabular form and can be obtained by means TDS code (Victorov et al. 2003), Figure 4.

The fluid products are described by a theoretical EOS, which is based on reliable statistical-mechanical theories and produces the excess thermodynamic properties of a fluid in excellent agreement with Monte Carlo and molecular dynamics simulations. The condensed graphite and diamond nanoparticles, which may be formed in the products, are treated with the model that takes into account the effect of the small size of carbon particles on their thermodynamics, Figure 5.

The current level of computer facilities does not allow yet for incorporating complete algorithms of an equilibrium thermodynamic solver directly into a hydrodynamic code. Millions of calls to such thermodynamic solver, which are required during hydrodynamic simulation, will lead to too significant expenses of computer time. For that reason, in this work we

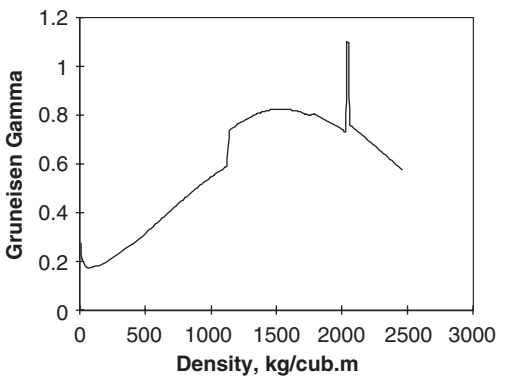


Figure 5. Gruneisen coefficient vs density along the CJ isentrope.

employ the TDS thermodynamic results in the form of a pre-calculated table with their subsequent accurate interpolation.

4 NUMERICAL SIMULATION

The numerical simulation is essential part of shock wave prediction and fire investigation. We present a numerical method for modeling strong shock waves in systems in which two or more substances are presented. The basis of our algorithm is a second-order Godunov method for the compressible Euler equations for a single material. This approach is second-order accurate in regions of smooth flow and captures shocks with a minimum of numerical overshoot and dissipation. By itself, this second-order Godunov methodology for a single gas phase has been used extensively to compute unsteady shock reflections in gases and has a demonstrated ability to resolve complex wave

Copyright © 2005 Taylor & Francis Group plc, London, UK

interactions in excellent agreement with experimental data (Colella & Glaz 1990).

Conservation laws for two-dimensional geometry in cylindrical coordinates can be written in divergent form as follows:

$$\frac{\partial \rho}{\partial t} + \frac{\partial (\rho U)}{\partial x} + \frac{1}{r}\frac{\partial (\rho V r)}{\partial r} = 0 \quad (1)$$

$$\frac{\partial (\rho U)}{\partial t} + \frac{\partial (\rho U^2 + P)}{\partial x} + \frac{\partial (\rho UV)}{\partial r} = -\frac{\rho UV}{r} \quad (2)$$

$$\frac{\partial (\rho V)}{\partial t} + \frac{\partial (\rho UV)}{\partial x} + \frac{\partial (\rho V^2 + P)}{\partial r} = -\frac{\rho V^2}{r} \quad (3)$$

$$\frac{\partial (\rho E)}{\partial t} + \frac{\partial (\rho EU + PU)}{\partial x} + \frac{1}{r}\frac{\partial (\rho EVr + PVr)}{\partial r} = 0 \quad (4)$$

$$E = e + (U^2 + V^2)/2 \quad (5)$$

$$P = P(\rho, e) \quad (6)$$

where P – pressure, ρ – density, U and V – axial and radial velocities, e – specific internal energy, E – specific total (kinetic plus internal) energy.

The latter equation describes dependences of pressure, density and specific internal energy. We use in our numerical experiments EOS in tabular form described earlier.

Our approach to modeling cells that contain more than one material species is based on an algorithm for modeling two or more gases. The interface between each substance is tracked with a volume-of-fluid interface reconstruction algorithm and the equations of motion for a single phase are supplemented with evolution equations for the volume fractions, total energy, and mass density of each phase in the multi-fluid cells (Miller & Puckett 1996). The resulting system of conservation laws is of hyperbolic type and thus can be solved using a straightforward extension of the second-order Godunov method for a single gas phase. Our formulation accounts for the thermodynamic properties of each phase separately, while modeling the pressure and velocity in all cells, including those that contain more than one phase, as single-valued quantities. In particular, given single uniform pressure acting on a multiphase cell, this algorithm will correctly account for the different compression or expansion that each phase undergoes as a result of that stress.

The Riemann problem solution is the backbone of any Godunov's approach. We computed the solution of the Riemann problem by using fifth-order Runge-Kutta method with varied step and accuracy control.

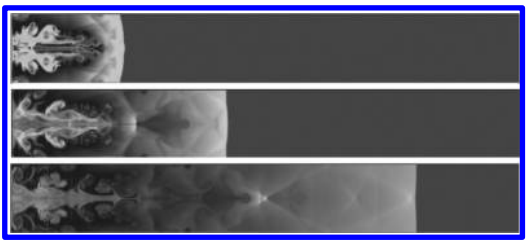


Figure 6. Three stages of shock wave traveling along the tube. Pressure distribution for different time moments, initial stages of shock wave formation – upper, stage of strong conical waves interference – middle, plane wave formation and propagation through tunnel – down.

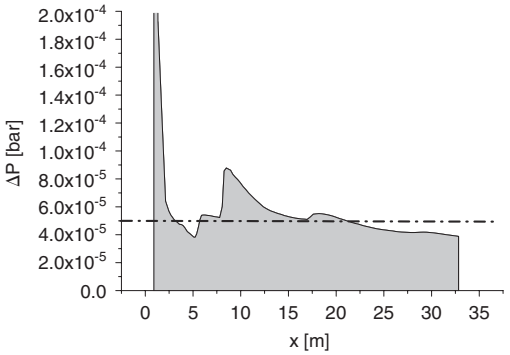


Figure 7. Mean pressure jump across the shock wave traveling along the tube towards the right. Initially energy release point was located at zero point. Dash-dot line is a critical pressure jump for human.

This set of numerical approaches allows us to model complex processes of shock wave physics with high accuracy.

On the Figure 6 represents the blast wave traveling along the tube for different time moments and mean intensity of the wave along the tube on Figure 7.

5 CONCLUSION

Reliable results of blasts and fires in tunnels investigation can be obtained only with integration of both experimental and numerical approaches.

Firstly, numerical simulation of high explosive in tunnel was made with taking into account chemical reactions in detonation products.

REFERENCES

Golub V.V., Lu F.K., Medin S.A., Mirova O.A., Parshikov A.N., Petukhov V.A. and Volodin V.V. 2004. Blast wave

Copyright © 2005 Taylor & Francis Group plc, London, UK

attenuation by lightly destructable granular materials. *In Proc. 24th International Symposium on Shock Waves*. Beijing, China. in press.

Victorov S.B., Gubin S.A., Maklashova I.V. and Revyakin I.I. 2001. Thermodynamic TDS code: Application to detonation properties of condensed explosives. *In Proc. Energetic Materials, Ignition, Combustion and Detonation. 32nd Int. Annual Conference of ICT*. Karlsruhe, Germany, pp. 69/1–69/15.

Colella P., Glaz H.M. 1990. Riemann problem for real gases. *J. Comput. Phys*. V.87. P.171.

Miller G.H., Puckett E.G. 1996. Second-order Godunov method for multiple condensed phases. *J. Comput. Phys.* V.128. P.134–164.

Copyright © 2005 Taylor & Francis Group plc, London, UK

Standardisation and research about fire safety in European traffic tunnels

A. Haack
STUVA, Cologne, Germany

ABSTRACT: A series of most tragic tunnel fire accidents has led to strong discussions among experts in Europe and around the world during the last couple of years. It also gave rise to intensified multinational efforts to improve the safety level for tunnel users and for the tunnel structure itself. In the result a comprehensive European research programme was launched, various related standards revised, and European directives set up.

1 INTRODUCTION

Fires in traffic tunnels can result in real catastrophes as we had to learn at least by the recent incidents in road tunnels as in the Mt. Blanc Tunnel (France/Italy, 24.3.1999), the Tauern Tunnel (Austria, 29.5.1999), the Gotthard Tunnel (Switzerland, 24.10.2001), or in the funicular tunnel of the Kitzsteinhorn (Austria, 11.11.2000), and most recently in the Metro of Daegu (South Korea, 18.2.2003). All these incidents cost too many lifes and they taught us some new aspects which were neither known nor expected before, if we do not consider the fire in the Nihonzaka road tunnel in Japan 1979, where about 189 vehicles were involved. One of the new lessons has been the extremely fast development of the fire combined with a tremendously fast increase of temperature up to about 1000°C (Fig. 1) and even more as well as the enormous emission of masses of smoke from the very beginning of the fire. The second was the fire jump from one car to another even over sections of more than 200 m as in the Mont Blanc Tunnel where no vehicle was stopped. The third and most shocking aspect was the behaviour of many road tunnel users. Too many of them did not realise the danger to which they were exposed. They felt safer in their cars which might be right for the very first minutes and they did not want to leave back their property unobserved. If ever and finally they realised that they are extremely endangered it was too late for a successful escape. They did not save their cars, but lost their not regainable lifes. This is by far the most tragic experience.

Against this background every proposal for any improvement in the direction of avoiding a vehicle fire especially in a tunnel, easing the escape conditions, rescuing tunnel users, and automatic fire combatting is welcome. There never is any stupid idea in this field. But immediately after a new or modified idea is born we have to evaluate systematically and seriously, if it is feasible, effective and reliable. In case the first theoretical judgement is positive we have to investigate carefully the details for realisation and finally we should do tests under conditions as realistic as possible. Those tests are a key issue to avoid investments in systems which at the end do not keep what they according to the theoretical thoughts promised. In this connection it is highly recommended – not to say essential – to come to an international agreement and co-operation for planning and conducting the various steps of those practical tests. The increasing shortage of public money asks for a concentration of financial sources. National going it alone must be



Figure 1. Fire test with an HGV (Fires in transport tunnels; Eureka research project EU499 Firetun; 1995).

Copyright © 2005 Taylor & Francis Group plc, London, UK

avoided last but not least against the necessity of harmonised safety concepts in multinational units such like the European Union (EU) or the North America Free Trade Agreement (NAFTA). Purely national efforts will lead to a situation where the first and simplest specific technical aspects are investigated several times again and again instead of combining various important questions in one multinational project supplemented by collecting the different national experience.

2 EUROPEAN DIRECTIVES AND RECOMMENDATIONS

2.1 *Road tunnels*

In April 2004 the European Commission released a directive concerning the minimum standard for safety in tunnels of the Trans-European Road Network. The purpose of this important regulation is a harmonized and high safety level for the users of tunnels along the Trans-European road network in all of Europe. The minimum standards are related to the organisational, structural, and operational safety aspects of road tunnels. The draft for this directive was discussed in the member states of the European Union and in all the related technical commissions as well as in the international associations since December 2002.

The directive is based on the results of thorough analyses of major accidents during the last years. By this it came out that the most frequent reasons for accidents were wrong behaviour of the road users, an insufficient safety equipment of the road infrastructure, technical defects of the vehicles, and problems regarding the transport of dangerous goods. Against this background the main objectives of the directive can be described as follows:

- Prevention in form of avoiding critical incidents endangering persons, environment, and the tunnel structure
- Mitigation of possible effects especially in case of car fire, providing the tunnel users with optimum preconditions or escape and rescue

The application of the new directive is obligatory for all tunnels along the Trans-European road network longer than 500 m independent of being in operation (Fig. 2), in construction or in the planning phase. The paper is divided into organisational as well as technical prescriptions. The organisational prescriptions are as follows:

- National administrative authorities
  The member states have to install an administrative authority which takes the responsibility for following the directive on a national level. The administrative authority can be set up at national, regional or local level. Tunnels crossing the border of two member states can be controlled by a national administrative authority in each of the two related member states or alternatively by one administrative authority designated jointly by these two member states. If the first solution is given, the decisions taken by one of the two national administrative authorities, have to be adopted with the prior agreement of the other national authority. The administrative authority responsible for a specific tunnel has the power to suspend or restrict the operation of a tunnel, if safety requirements are not met properly. In this case it has to specify the conditions under which normal traffic may be resumed. The administrative authority has also to ensure that the tunnels for which it is responsible are inspected on a regular basis with a focus on safety requirements.
- Tunnel manager
  For each road tunnel in the Trans-European Network the administrative authority has to identify a tunnel manager who is responsible for the management of the tunnel regardless whether it is in the design-, construction-, or operation-phase. For those tunnels crossing the border of two member states the two administrative authorities or the joint administrative authority shall recognize only one tunnel manager in charge of the operation of that tunnel.
- Safety officer
  The tunnel manager shall, with the prior approval of that administrative authority, nominate for each tunnel one safety officer. This safety officer has to coordinate all preventive and safeguarding measures to ensure the safety of the tunnel users as well as of the operational staff. He has to be independent in all tunnel safety issues and shall not be under instructions from an employer in respect to these issues.
- Inspection entity
  The member states have to take care that inspections, evaluations and tests of all the tunnels on their territory are carried out by experienced inspection



Figure 2. Longer road tunnel in operation (Austria).

Copyright © 2005 Taylor & Francis Group plc, London, UK

entities. The administrative authority may perform this function. The entities must be functionally independent from the tunnel manager.

In addition to these organisational prescriptions the technical regulations of the directive are related to the tunnel structure, the operation of the tunnel, the vehicles passing through the tunnel, and the means for communication to inform tunnel users in an emergency case. These prescriptions are very detailed and can be found on the following website: http://europa.eu.int/comm/transport/road/roadsafety/roadinfra/tunnels/index_en.htm.

Summarizing, it can be stated that with the publication of this directive a European compromise could be found in a difficult field which is influenced by many national interests. The directive deals with minimum requirements concerning the safety of road tunnels, but is certainly a very important first step with truly international approach. Against the background that the technical standards are permanently adapted to the state-of-the-art the directive offers sufficient space for the implementation of future and further developed technologies.

2.2 *Rail tunnels*

2.2.1 *Generalities*

Concerning heavy rail systems, similar European directives to those already published for the Trans-European road network are in preparation. They will follow the European directive on interoperability of conventional Trans-European railway network edited in March 2001. For the moment there are two recommendations dealing with safety concepts in railway tunnels available. One was prepared by the UIC (Union Internationale de Chemins de Fer) and published in August 2003, the other one was prepared by the United Nations – Economic Commission for Europe (UNECE) and published in December 2003.

Considering new tunnels the recommendations are structured in four categories of safety measures:

- Prevention of accidents
- Mitigation of the consequence of accidents
- Facilitation of escape
- Facilitation of rescue

They focus on a minimum requirement to any tunnel. Exceptions to these standards could be allowed, provided that the desired safety level in the tunnel could be reached by a combination of other measures. In specific cases where tunnels cross the border between two countries all of the minimum safety recommendations or standards concerning the infrastructure, rolling stock, and operational procedures should be consistantly applied in both countries and harmonised among the various network managers and train operators. Rescue and fire fighting measures should also be harmonised and coordinated between the responsible services of the two countries, although they may be governed by different national practices.

Where the desired safety level in the existing tunnels cannot be reached by improving the infrastructure, it may be achieved by a combination of measures concerning the rolling stock and the operations. In existing tunnels structural upgrading measures have to be planned carefully in terms of costs versus efficiency. Momentarily a large European funded research project is conducted investigating the most cost-efficient upgrading measures currently available (see under UPTUN in chapter 4).

In the following the measures recommended are described in details.

2.2.2 *Prevention of accidents*

The preventive measures recommended by these guidelines for new tunnels deal with the infrastructure, the rolling stock as well as the operational process. Regarding to the infrastructure it is stated that in the context of safety, both single-tube, double-track and double-tube, single-track tunnels have their advantages and disadvantages. Double-tube single-track tunnels might be safer as they avoid accidents caused by derailments obstructing the adjacent track and they provide the second tube as the possible safe haven. On the other hand, double-track tunnels have not only more space for possible rescue operations, but they also have more space for smoke retention. For high-speed lines (Fig. 3) single-tube double-track tunnels might be preferable taking aerodynamic factors into account. On the other hand, for mixed traffic (passengers and goods) two single-tube single-track tunnels might be more appropriate. The choice should finally be the result of a thorough evaluation of all parameters (length



Figure 3. High speed train leaving a tunnel (Germany).

Copyright © 2005 Taylor & Francis Group plc, London, UK

of the tunnel, type of traffic, speed, etc.) related to safety as well as cost considerations.

Fire protection measures for **rolling stock** should include the construction and design of vehicles to prevent the outbreak and spread of fire. The use of materials producing toxic substances and a large amount of smoke in the event of fire should be avoided. This is also valid for the renovation and refurbishing of older passenger train sets. In this context the proposal for the new European standards on fire resistance for railway passenger waggons prEN 45545 should be considered.

Various types of on-board detectors (heat, smoke, flame, etc.) may be installed on locomotives and rolling stock. They might be more effective than those installed in the tunnels.

Operational safety measures aim mainly at a separation of passenger trains and freight trains in double-track tunnels. The time-table of both train categories should be optimised in this direction to prevent passenger and freight trains especially containing dangerous goods from passing through a tunnel at the same time. So, very strong traffic through particular tunnels can be made safer by separation of operation for passenger and freight trains with dangerous goods into day and night. Lower speed can also reduce the potential consequences.

2.2.3 *Mitigation*

To mitigate the consequences of accidents some infrastructural measures are given. Concerning fire, smoke, and gas detectors in the tunnel it is stated that the nowadays available technology cannot give reliable detection of fire on trains driving through a tunnel at normal speed. However, fire detectors are highly recommended for technical rooms to give an alarm of any threat to the essential safety equipment or to staff. Cables and other equipment in the tunnel should be protected from the consequences of derailment or fire. Wherever possible, cable installations should be of low smoke and low fire type. Fire extinguishing systems for technical rooms should be determined depending on the potential courses of fire. An effective fire suppression system in the main tunnel is generally not practical and is not recommended. Smoke extraction systems and ventilation systems must be designed to keep emergency exits, cross-passages and safety tunnels free of smoke.

Concerning the rolling stock train radio is highly recommended as a particularly effective device to provide communication between the operation center and train crew. As normally all passenger trains are equipped with a passenger operated emergency brake it is highly recommended that the train driver should be able to override this emergency brake when passing through a tunnel and to drive the train into the open air.

For trains using long tunnels the installation of manually operated fire-extinguishing equipment is recommended on-board passenger waggons. The installation of automatic fire extinguishing systems in passengers cars might not be necessary but is recommended in sleeping cars. Automatic or manually operated extinguishing systems are particularly important and highly recommended on traction units. Unmanned power units (push-pulled trains, multiple traction units, etc.) should have automatic fire extinguishing equipment installed.

2.2.4 *Facilitation of escape*

For facilitation of escape properly designed and indicated escape walkways are essential for self-rescue. In case of double-track tunnels those walkways should be provided on both sides. Their width should be at least 700 mm, and preferably 1200 mm. Hand rails should be placed at an appropriate height above the walkway. In tunnels used by passenger trains emergency tunnel lighting shall be installed. This lighting shall be reliable and operating under autonomous conditions, visible under smoke and poor visibility conditions.

The distance between escape exits is varying from country to country. It is recommended that a maximum distance between two safe places (portal of the tunnel, cross passage, emergency exit) is defined to enable efficient self-rescue. The exact distance depends on the local situation, operating parameters and the safety concept. In double-tube single-track tunnels and parallel safety tunnels this distance should not exceed 500 m.

Vertical exits should be designed in such a way that smoke is prevented from spreading into the safe area by means of air locks or pressurisation. A stair flight should not be higher than 6 m between landings with a width of at least 1200 mm. Where the shaft is higher than 30 m, a fire fighting lift should be installed. Both, stairways and lifts should be pressurised and/or be equipped to ensure a smoke-free environment.

The maximum length for lateral exits should be about 150 m. In case of longer lateral exits an access for road vehicles should be provided. Cross passages should be lit, have means of communication, and be designed to prevent spreading of smoke into the safe area. They should be separated against the main tunnels by doors which should be able to resist fire for 30 minutes and the aerodynamic pressures caused by the trains.

The **operational measures** include emergency information for passengers and training of the railway staff.

2.2.5 *Facilitation of rescue*

For facilitation of rescue some **infrastructure measures** are given including a system for disconnection and earthing of traction current. Care must be taken not to disconnect power too fast in order to prevent the stopping of trains in the tunnel. At the tunnel entrances or exits rescue areas of about 500 m^2 with road access should be reserved for emergency services vehicles. A fire-fighting water supply should be made

Copyright © 2005 Taylor & Francis Group plc, London, UK

available in all tunnels covered by the recommendations. In addition, the electricity power distribution system in the tunnel should be suitable for emergency/rescue services' equipment. All the electrical equipment should be protected against damage caused by mechanical impact, heat or fire. The electrical supply should be reliable with safety related key elements having 90 minutes back-up, e.g. two independent supplies, stand-by generator, battery back-up. Suitable breathing apparatus shall be provided based on the intended role of the rescue services in an emergency. The breathing equipment could be stored either at the nearest fire station or in a secure place inside the tunnel. It has to be checked and tested regularly.

Concerning the **operational measures** especially exercises for the rescue services are recommended.

2.2.6 *Existing tunnels*

For existing tunnels a general demand to install all of the safety measures described for new tunnels may not be reasonable or appropriate. Therefore, existing tunnels should be equipped with as many standard measures as is reasonably possible during any maintenance and replacement actions. Priority should be given to rolling stock and operational measures as they do not require structural changes in the existing tunnels.

3 RESEARCH ON EVACUATION OF METRO STATIONS

On principle, the safety measures regarding mass-transit systems consist of a similar concept as it is described for heavy railway systems in chapter 2.2. They also focus on prevention, mitigation, facilitation of escape as well as facilitation of rescue.

A crucial task during the design phase of an underground metro station is the appropriate lay-out for escape and rescue in case of fire on the train. One of the first and vital demands in such a situation is to avoid a train stop in the running tunnel. If ever possible, the driver should by technical means be enabled to override the emergency brake and to drive the train into the next station. There the conditions for escape and rescue are significantly better as inside the running tunnel. This concept requires an appropriate design concerning the width of the platform, the stairways, the special emergency exits and in case of a fire also all the smoke control.

For harmonisation of the various design criteria for safety matters in underground mass-transit systems the German Ministry of Transport funded a comprehensive research programme, which was recently conducted by STUVA in cooperation with many other institutions and authorities. In the frame of this project several benchmarking definitions were agreed upon. So, it was postulated to keep the platform area during the phase of self-rescue at most free of smoke up to a height of 2.5 m for the first 15 minutes after the breakout of a fire. In the following rescue phase, which is assumed to last again 15 minutes, the smoke-free zone should reach a height of minimum 1.5 m to enable rescuers to find injured persons or those who are not able to escape within short time. The escape speed is assumed to be an average of 1 m/s on horizontal even ground. Beside the staircases also escalators (assumed to stand still) are included in the evacuation process, but not elevators. The basis for the calculation of the evacuation time is given by the American regulation NFPA 130.

The release of smoke and energy is defined depending on the type of rolling stock using the tunnel system. For the calculation of the smoke distribution along the station versus time either a zone model or a field model can be used. The mathematical model additionally gives an indication of the distribution of temperature and toxic gases as well as the visibility.

The final step of such an assessment is the comparison of the time needed for a sufficient evacuation with the time span until the smoke is reaching a level below 2.5 m above platform surface. The evacuation time must be significantly shorter (at least by 2 minutes) than the critical time in the smoke dispersion. If this requirement is not met, the capacity of the escape ways has to be extended or the smoke extraction system has to be improved.

To support the evacuation process on the structural side, all the staircases have to be protected against critical smoke ingress during the phase of self-rescue which means during the first 15 minutes after fire breakout. This can be ensured by using fire and smoke protective curtains as well as fire walls and fire doors. For architectural purposes, the sides of stairways can be sealed with specially certified glass instead of using massive concrete walls. For smoke extraction appropriate ventilation systems or shafts using the natural chimney effect have to be installed in various appropriate positions. In general, all platforms are to be provided with at least 2 separate exits. An escape from an underground station through the running tunnel should be avoided and not systematically be taken into account.

The principle concept developed by this important research work is increasingly used for designing new underground metro stations throughout all of Germany.

4 EUROPEAN RESEARCH PROGRAM

The European Commission has developed directives concerning the minimum safety equipment of road tunnels, which will soon be followed by directives for rail tunnels. This trend is supplemented by intensive domestic and international research activities. For example, researchers are working to create new or improved fireproof construction materials for tunnel

Copyright © 2005 Taylor & Francis Group plc, London, UK

construction. At the same time, work is underway to develop automatic systems for detecting, localizing, and fighting of fires as well as to determine fire ratings.

Another aspect pertains to general recommendations for suitable fire protection concepts. Knowledge and experience that already exist in Europe and around the world must be integrated into comprehensive, holistic safety concepts for planning new tunnels or retrofitting existing projects. This is the only way to overcome the public unease and anxiety about using tunnels.

Fires in transport tunnels can cause catastrophic disasters. The accidents in the Mont Blanc Tunnel, in the Tauern Tunnel, in the Gotthard Tunnel, in the subway system in Daegu/South Korea, and most recently in the Baregg Tunnel have made this more than clear. The detailed analysis of the cause and progression of these fires have yielded new insights that had not been expected or calculated to this extent (see chapter 1).

In the context of subway fires, the example of Daegu also showed how crucial the impact of railcar engineering and equipment, operational organisation and safety training of train conductors and station managers can be. Severe shortcomings in these criteria were a crucial factor in the tragic outcome with 196 fatalities.

One consequence of the devastating fire accidents has been that the European Commission issued directives regarding the minimum fire prevention equipment of road and rail tunnels. In addition, a number of important research projects were initiated. These are seven multinational projects that have already been awarded and funded in conjunction with the fifth Research Framework Program of the EU.

The following overview briefly discusses the objectives and general structure of these projects:

Fire in Tunnels (**FIT**) was established in March 2001 and is limited to four years. This "thematic network" includes 33 partners from twelve European countries and is coordinated by the Belgian Building Research Institute (BBRI). The Institute gathers information from all over Europe and around the world about existing research results and general experiences with fire prevention in transport tunnel facilities.

Six dedicated databases focus on research projects, tunnel test site facilities, numerical models for course of fires and smoke propagation, safety equipment, reports on fire accidents and case studies for upgrading tunnels. Three work packages within the FIT project are focused on a number of fundamental questions. This includes the determination of fire ratings, compilation of guidelines and recommendations for optimized principles of design that are suitable for fire prevention as well as advocating optimized measures for escape routes, assisted rescue and fire fighting. The corresponding partial reports have been completed in their draft versions. For further details visit: www.etnfit.net.

Durable and Reliable Tunnel Structures (**DARTS**) also started in March 2001 and ended in early 2004. The project had been coordinated by COWI Consulting Engineers & Planners AS, of Denmark. The initiative included eight European partners and was structured into six technical work packages. It was primarily dedicated to the problem of exceeded cost during the construction of underground transport facilities. In some cases, cost was exceeded by more than 100 percent of the originally calculated budget. In addition, project participants discussed how to limit or avoid construction delays. Furthermore, the quality and lifetime of tunnels as the most cost-intensive component of the entire traffic infrastructure was to be improved. More information is available at: www.dartsproject.net.

Innovative Systems and Frameworks for Enhancing of Traffic Safety in Road Tunnels (**Safe Tunnel**), begun in September 2001, and is designed for a project term of three years. The Centro Ricerche FIAT, Italy, is in charge of coordinating the nine members. This research project will primarily contribute to reducing the number of accidents in road tunnels with the help of preventive safety measures. The main focus is to reduce the extent and number of fire accidents.

The basic idea is to filter out and stop vehicles with irregularities such as overheated engines, blocked brakes or existing smoldering fires before entering the tunnel. This will be possible by using suitable measurement equipment. At the same time, devices need to be in place to monitor vehicle speed in order to reliably determine and prosecute speed violations. The web address of this project is: www.crfproject-eu.org.

Virtual Real Time Emergency Simulator (**Virtual Fires**) was started for a duration of three years with eight partners from five European countries. The Institute for Structural Analysis of TU Graz, Austria serves as the project coordinator. The objective is to develop a suitable and practical simulator to train firefighters in confining and fighting fires in tunnels. A computer model will be used to create virtual simulations of fires in tunnel situations.

Such a device would be more cost-efficient and environmentally friendly than the currently used method of training firefighters by setting real vehicles and liquids on fire in tunnels that are no longer in use. The simulator may also be used for studying and assessing tunnel facilities and their equipment with regard to their fire safety. Tunnel operators, planners and governmental safety agencies could be among the possible users of such a simulation device. For more information visit: www.virtualfires.org.

Cost-effective, sustainable and innovative Upgrading Methods for Fire Safety in existing Tunnels (**UPTUN**) is designed as a research and development project for four years and was started in September 2002. 41 partners from 13 EU member states as well as three newly joined member states are part of this cooperative effort, which is coordinated by TNO (Netherlands Organisation for Applied Scientific

Copyright © 2005 Taylor & Francis Group plc, London, UK

Research), Netherlands, and ENEA (Italian Agency for New Technology, Energy and Environment), Italy.

The principal goals of this large-scale project with a budget of approximately 12 million Euros can be described as follows:

1 To develop, assess and promote innovative, sustainable and cost-efficient measures in order to prevent, locate, record and fight fires. The essential goal is to reduce the probability of fires in existing tunnels and to limit the extent of the resulting damage.
2 To create and promote holistic and integrated assessment criteria and upgrading methods for tunnels that are already in operation, on the basis of previous insights (Fig. 4).

The results are intended to give planners and operators of tunnels, but also emergency and rescue services a better basis for measuring and increasing safety standards with regard to personal and material safety. Further details are available from the project website at: www.uptun.net.

Safety in Tunnels (**Safe-T**) represents another thematic network with a three-year term that was started in fall 2003 and is coordinated by TNO in the Netherlands. The primary objective is to harmonize the European requirements regarding tunnel safety. Experiences gathered at the national level are to be compiled and assessed in such regulations. Given the background of the negative experiences with the former operative concept of the Mont Blanc Tunnel, special emphasis will be on cross-border operative concepts. The experience of regional authorities, firefighters and emergency rescue services are of special importance for this project. Further details are available from the website at: www.safetunnel.net.

Safety Improvement in Road& Rail Tunnels using Advanced Information Technologies and Knowledge Intensive Decision Support Models (**SIRTAKI**) was initiated in September 2001 for a term of three years. The initiative is shared by twelve European partners under the project management of the Spanish ETRA Group. The main focus of the project is to reform operative concepts with regard to safety and emergency management. Once the concept has been developed, it will be tested in a variety of road and rail tunnels. The project outcome will include better prevention of critical situations, decision-making aids for tunnel operation, the introduction of a European operating network as well as the improvement of sensor-based vehicle and facility monitoring. Further details are available at: www.sirtakiproject.com.



Figure 4. Upgraded Klauser tunnel in Austria with central rumple strip.

5 OUTLOOK

The research efforts of the European Commission described here to improve the safety in transport tunnels are an essential prerequisite for an all-European harmonization in this field. Tunnels are an indispensable part of the Trans-European traffic network. Given this backdrop, the research activities are making a crucial contribution to guarantee the mobility of persons and goods, which represents a high political priority.

REFERENCES

Bendelius, A.G. 2002. Tunnel fire and life safety within the world road association (PIARC); *TUST* 17, pp. 159–162

Dahl, J. & Richter, D. 2001. Fire protection: new development to avoid concrete Splintering; *Tunnel* 20/6; pp. 10–22

European Commission. 2001. European Directive on interoperability of conventional Trans-European Railway Network

European Commission. 2004. European Directive on minimum safety requirements for tunnels located on the Trans-European Road Network

Haack, A. 2001. Commentary on the newly developed fire protection for single-shell tunnel linings; *Tunnel* 20/6; pp. 23–31

Haack, A. 2002. Current Safety issues in traffic tunnel; *TUST* 17; pp. 117–127

Haack, A. 2004a. Safety in transport tunnels; *FuE-Forum, Forschung und Entwicklung bei Hochtief*, Essen, 26/2004

Haack, A. 2004b. Latest achievement and perspectives in tunnel safety, Balkema/Singapore

Kirkland, C.J. 2002. The fire in the Channel Tunnel; *TUST* 17; pp. 129–132

NFPA. 2003. standard 130; editor: National Fire Protection Agency of USA

Studiengesellschaft Stahlanwendung e.V, Düsseldorf. 1995. Fires in transport tunnels; report on full-scale tests; EUREKA-project EU499 FIRETUN

UIC. 2003. Safety in Railway Tunnels, recommendations 779–9, August 2003

UNECE. 2003. Recommendations of the multidisciplinary Group of experts on safety in Tunnels (Rail), TRANS/AC. 9/9

Copyright © 2005 Taylor & Francis Group plc, London, UK

Safety management – Checking Engineer in Conventional Tunnelling

Andreas Beil
D2-Consult Dr. Wagner Dr. Schulter GmbH & Co-KG

Faïza Aïssaoui
D2-Consult Engineering GmbH

ABSTRACT: In recent years it has been shown that there is a valuable contribution to the management of safety of a tunnel project to use the checking engineer in project realisation. This relates to the phases of preliminary works and conceptual design, to the detailed design for the tender and to the final design for construction. The paper relates to experiences made during design and construction of the lower Inntal tunnels in Tyrol, Austria.

1 PREFACE

There is a successful practice since several years to use the so called Checking Engineer within Safety Management for Conventional Tunnelling. Its specific services have been standardized and defined within the relevant Honorary Regulation (HO-BK).

The interdisciplinary project team such has been extended by another valuable member, to gain synergy effects from long term experiences in Conventional Tunnelling.

2 CHECKING ENGINEERS POSITION

2.1 *Responsibility*

The Checking Engineer must participate already at the beginning of the project. Its cooperation must be considered already during conceptual design as well as during the phase of permit in order to optimise as early as possible working procedures between all project partners.

The Checking Engineer provides both technical, contractual and financial control for the client. He takes care of the clients interests especially in regard of actual standards and guidelines. With regard of its remuneration the Checking Engineer is evaluated according to HO-BK (Honorary Guidelines) to be a secondary control [3].

According to HO-BK (as of May 1, 2001, § 4 (1)) the specification of the Checking Engineer relates to all basic services of the following activities in each project phase.

- Organisation, Information, Coordination, Documentation
- Quality and Quantity
- Cost and Financing
- Schedule and Working Capacity

According to HO-BK (05/01/2001, § 4 (2)) related project phases are divided as follows:

- PPH 1 Project Preparation
- PPH 2 Design
- PPH 3 Construction Preparation
- PPH 4 Construction
- PPH 5 Project Completion

The Checking Engineer is influencing the project realisation. He must guarantee the projects quality assurance by early recognition of deviations from the clients requirements and by further respective indication such providing a double check principle.

The Checking may influence the project development such carrying responsibility to a very high degree. He requires a lot of competence in regard to know and experience in all aspects of the project.

3 CHECKING ENGINEER SERVICES

3.1 *Conceptual an tender phase*

During conceptual and tender phase there is a need for intense cooperation between designer, other authorities and client. On the other hand during construction face the client gives priority to new project members e.g. construction company and to construction supervision together with comprehensive control,

Copyright © 2005 Taylor & Francis Group plc, London, UK

thus corresponding to HO-BK and its primary project control.

Services to be provided by the Checking Engineer in Conventional Tunnelling depend on the individual planning phase. Such services are both technical, cost and contractual very different. They go hand by hand together with numerous project meetings.

Early recognition of planning deviations will lead both to more effective planning and more rational constructions.

Technical control relates to all documents used on site. As well as to the tender documents, bill of quantities, general and technical conditions of contract, construction description, construction schedule, geomechanical, geotechnical, geological, hydrogeological reports, conditions of survey and services of structural review of any kind.

Through technical control of all documents there is an indirect cost control, leading to a project designed and constructed according to the latest state of the art.

Together with the project there is a technical, contractual and cost related of the project with ends together with the project it self.

Detailed tender design, as required by the client should be primarily precise and of highest quality. It will lead as intended by the construction supervision and Checking Engineer to a project in construction, which is technically sound, costwise reasonable and friction free due to the efficient use of both control instruments.

3.2 *Construction phase*

Depending on the size of the project, this phase represents the most important and longest project phase. It requires most effective use and cooperation by all members of the project as well as minimised conflicts in communication.

During this phase there are new responsibilities for the Checking Engineer when compared the previous phases. The Checking Engineer is using additional control instruments, which are since quit some time state of the art in Conventional Tunnelling.

The most important instruments for controlling tunnel excavation are among others geologic and geotechnical survey as well as deformation monitoring.

Geologic survey represents since long time classical means to control tunnel excavation. Geotechnical deformation measurements are representing the more advanced instrument to control tunnelling. It contributes to the performance of tunnelling with out interference.

Last but not least this instrument became widely used due to extensive progress in research and development of measurement technology.

When using this instrument the following goals can be achieved [1]:

- Stability control by geologic and geotechnical survey as well as geotechnical deformation measurements known as “monitoring”.
- Interpretation of measurement results by structural calculation known as “Back Analysis”.

Tunnel survey requires close cooperation between geologist and geotechnical engineer. The geologist is responsible for correct interpretation of geologic conditions, while the geotechnical engineer has to take responsibility for geotechnical deformation measurements. In summary it defines further construction procedure and related support.

The Checking Engineer is using this interpretation of the results of the geotechnical deformation measurements in the contest of the geologic conditions in order to correspond with its responsibility.

3.3 *Geotechnical measurements*

In the mean time the interpretation of results of geotechnical deformation measurements for control of tunnel excavation became a fixed link in safety management of tunnelling.

The results of deformation measurements are recorded for vertical, horizontal and longitudinal displacement measurements. They are time related. There is an additional possibility to use the data by showing lines of influence, areas of influence, tendency lines, tendency areas and vectors [1].

Lines of influence are most widely used. They are connecting measurements values recorded at a certain time along the axes of the tunnel to become one measurement line. This type of presentation gives a good three dimensional and timely overview of the deformation development in order to recognise any change in rock behaviour by indicated changes of the line of influence.

The deformation behaviour of the rock is indicated by enlarged areas created by different lines of influence when the tunnel face is getting close to the measurement cross section. It allows to estimate the size of displacements. Production and interpretation of lines of influence is the responsibility of the experienced geotechnical engineer on site.

Control systems are only efficient if its planning and its use are carefully performed. Accuracy and power of interpretation depend on geotechnical deformation measurement they are defined by the requirements of the projects. Geomechanical planning has to be adopted accordingly.

However, the instrument of geotechnical deformation measurement remains an auxiliary instrument with uncertainties in spite of its improved used together

Copyright © 2005 Taylor & Francis Group plc, London, UK

with data controlled interpretation. It contributes to a better understanding of rock and system behaviour.

4 TUNNEL AND TECHNICAL CONSULTANCY

Within the instrument of Checking Engineer there is tunnel consultancy responsible for interpretation of deformation measurement results. Within the frame of services of Checking Engineer, Tunnel Technical Consultancy should provide long term experience in Conventional Tunnelling as working requirement together with best understanding for the mechanism of rock behaviour.

In order to be prepared for unforeseeable events during construction, regular control, analysis and evaluation of results of geotechnical deformation measurements, are representing a valuable instrument of construction.

The Tunnel Technical Consultant should be responsible to relate between submitted data and rock behaviour in connection with the used support system.

In consideration of technical and financial project conditions and in cooperation between individual project members it is possible to overcome problems during construction and to switch from “difficult” to “easy” construction.

During construction it is tough to overcome problems. It will be achieved by careful documentation, followed by interpretation of geologic, hydrogeologic and geotechnical data together with the results of deformation measurements.

An interdisciplinary interpretation of data is required during fact finding of an event during construction. It could be material ingress near to the tunnel face, it could be settlement of footing or even collapse progressing to the surface in the case of shallow overburden.

In spite of an adopted measurement system and in spite of its qualified interpretation demonstrated at the example of construction of Tunnel Vomp, Lower in Valley Railway, it can be shown that face instability during construction can occur.

Tunnel face location and related measurement cross sections are shown in Figure 1 at the time when the event happened.

On March 28, 2004, 9 pm at TM 373.7 a major material ingress of the face happened in the area of the left side wall covering a 2.5 m face support core. At the surface there was at the same time a 6 m wide and 6 m deep cone like funnel at TM 376.

In the area of the event the overburden amounts to approx. 22 m. Tunnel excavation was performed in sandy gravels which have been drained with pre running pipes. At the time of the event the face was fully supported with shotcrete and welded wire fabric.

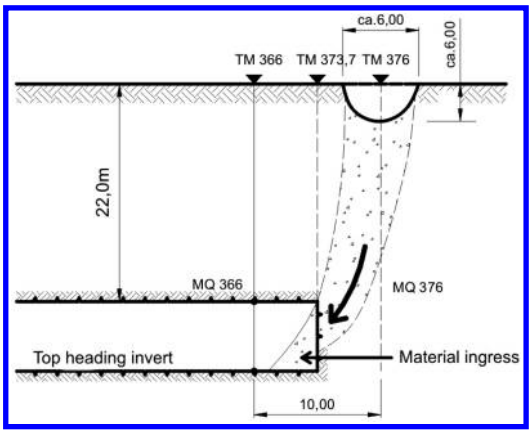


Figure 1. Location of face instability.

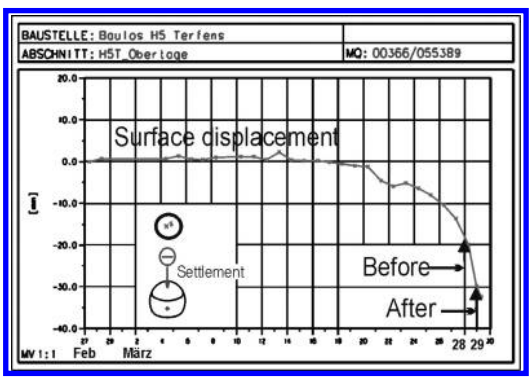


Figure 2. Surface displacement above roof TM 366.

Crown Invert was constructed up to 367.3. Bench and Invert have been constructed up to TM 79 and TM 78 respectively.

Respective measurements cross sections in the area of the event are located at TM 366 and TM 376, where as for TM measurement data have been delivered both for the surface and underground.

In order to analyze the event all available geotechnical deformation measurements (Figures 2 and 4) and geological conditions have been carefully analyzed an interpreted.

Surface settlement above the crown at TM 366 and TM 376 are recorded in Figures 2 and 4 [2]. Measurement values ahead of the event are stabile at TM 376 its values are small and far away from the alarm values. As measurement cross section at TM 376 is located directly in the area of the material ingress it became damaged. No further measurement values could be recorded prior to complete the rehabilitation of the area.

Copyright © 2005 Taylor & Francis Group plc, London, UK

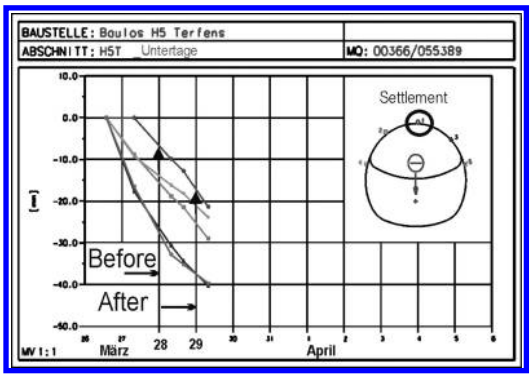


Figure 3. Tunnel crown displacement TM 366.

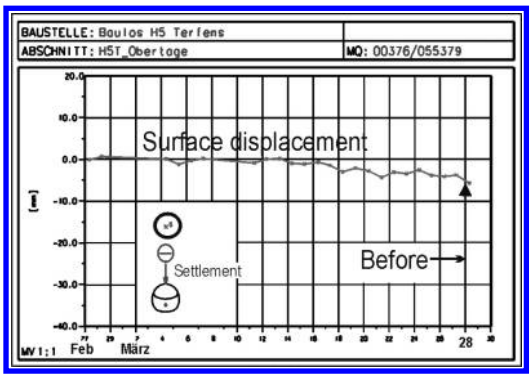


Figure 4. Surface displacement above roof TM 376.

Surface measurement values at TM 386 and TM 396 prior to the event have been stabile and smaller than the alarm values, such not allowing any indication for the event.

At TM 366 (Figures 2 and 3) [2] settlement deformations are more inclined with bigger values both underground and on surface but even so not indication event in 10 m distance. They have been smaller than the calculated alarm value. From measurement results it can be interpreted that support measures have not been sufficient in this area and rock load has been fully resting on the shotcrete lining. There was no reason for concern as the loading diagram of the shotcrete lining has been considered safe.

Efforts have been undertaken to find reasons at the time of the event resulting from the deformation measurements which should allow for recognition of warning ahead of time.

The history of deformation regarding face instability of the very cross section did not give any indication. There for interpretation of geologic conditions has been used for explanation. There has been an unfavourable coincidence of several faults as well as predominantly cohesionless sandy terrace gravels. Additionally it has been interpreted that the surrounding rock did cause the event due to missing three dimensional stress conditions.

The role of the Tunnel Technical Consultancy was as simple as useful. It did act as the experience mediator between construction supervision, geotechnical engineer and construction contactor. In order to find proper solutions numerous meetings took place leading to the successful rehabilitation of the area of instability and finally for restart of regular tunnelling.

In order to correspond with the tradition of tunnelling there is a need for implementation of long term experience. There are many possibilities for interpretation of the deformation behaviour between rock and the tunnel it self. It is the essence of many tunnel projects in comparable conditions of corresponding geologic and hydrogeologic criterias. As the underground is never perfectly comparable there will be always differences between forecast and actually measured data.

5 CONCLUSION

It is of utmost importance that interpretation of results of geotechnical deformation measurements contributes in the course of explaining unexpected events during tunnel construction aside of most accurate documentation of all geologic, hydrogeologic and geotechnical rock behaviour.

In Conventional Tunnelling the combination of interpretation and documentation is a reliable tool for control. The more experience and understanding is collected in this field, the more safe it will be for the Tunnel Engineer when using the instruments of interpretation.

REFERENCES

[1] Schubert, W. & Steindorfer, A. 1996. Selective Displacement Monitoring during Tunnel Excavation. Felsbau 14, Nr. 2.

[2] Arbeitsgemeinschaft AVD-Geodata 2004. Geotechnische Messergebnisse des Tunnelvortriebes Vomp.

[3] Bundeskammer der Architekten und Ingenieurkonsulenten 2001 Honorarordnung für Begleitenden Kontrolle HO-BK.

[4] TEAM Baugeologie Vomp: Berichte des Geologen. 2004. Bau- und Projektbesprechungsprotokolle des Tunnels Vomp der Unterinntaleisenbahnstrecke.

Copyright © 2005 Taylor & Francis Group plc, London, UK

Prevention of accidents during the tunnel construction phase

M. Bandmann & W. Chromy
Tiefbau-Berufsnossenschaft, Munich, Germany

A. Haack
STUVA e.V., Cologne, Germany

ABSTRACT: The importance of preventive measures for occupational safety during the construction phase of a tunnel has steadily increased over the recent years. During the planning phase it is one of the client's and his advisors' key responsibilities to ensure that the planned methods and sequences of construction will be safe. The contractor then draws up the safety concept for construction based on these premises and his excavation concept. Requirements posed on occupational and health safety increase both in conjunction with technical developments as well as the ever greater excavation lengths and the complexity of the construction measures. The conception presented here relates to fire, water, gas and cave-in incidents, i.e. events that occur suddenly and unexpectedly. A distinction is drawn between the shotcrete methods and mechanised tunnelling methods for the sake of clarity. The recommendations of DAUB (the German National Tunnelling Committee), which are presented here in excerpt form, are intended to assist clients and contractors with the preparation of the necessary safety concepts and of project-related safety risk assessments.

1 GENERAL REQUIREMENTS

1.1 *Duties of the client*

The responsibilities of the client for the planning of safety measures in tunnel construction are as follows:

- The client is responsible for the preparation of a design which guarantees construction methods and work processes that are safe to work in.
- He is responsible for the description of measures and requirements pertaining to safety concepts, specifying possible major incidents, geogenic hazards and hazards inherent in construction (gas, water, fire, caving in).
- The client specifies the maximum number of visitors (including personal safety equipment and self-rescue devices), i.e. the number of visitors allowed in the tunnel at the same time for the fire protection, escape and rescue concept during construction. This number should be kept as low as possible.
- The client is responsible for stipulating the applicable site procedures including access control.
- The client is responsible for obtaining required access permits for the emergency exits and shafts in due time prior to commencement of construction work.
- The client is responsible for commissioning an independent health and safety co-ordinator during the design and implementation phase. During the implementation phase, the client can also commission a health and safety co-ordinator, who is provided by the contractor executing the work.

1.2 *Duties of the contractor*

The responsibilities of the contractor during the realisation of the safety concept provided by the client with the planning documents are as follows:

- The major principles of the safety concept during the construction period must be plausibly specified in the tender. The same level of safety should also apply to special proposals and additional tenders.
- The contractor is responsible for preparing the safety concept for the construction period taking as a basis the specifications provided by the client and his heading concept and shall co-ordinate this concept with the local emergency and fire fighting services, with the participation of the health and safety co-ordinator.
- Every person working in the tunnel is to be informed about possible fire hazards and trained in initial fire-fighting measures. There must be at least 1 person trained in first-aid measures in each driving crew, who must be present on site.
- For the efficient operation of the emergency services (fire brigade, paramedics) the construction

Copyright © 2005 Taylor & Francis Group plc, London, UK

site is compelled to provide competent persons to guide them should this be required. These persons must accompany the rescue forces to the danger area.
– In the case of an incident, the alarm must be sounded immediately in compliance with the alarm plan and all available persons should undertake fire-fighting measures. Should there be an imminent threat of the fire getting out of control, the responsible supervisor must order immediate evacuation with self-rescue devices.
– The responsible project manager or his representative is responsible for alarming the emergency services and his superiors in the company, as specified in the alarm plan.
– The access of persons to the tunnel during the heading phase is to be defined (when, how many).

2 PROJECT-RELATED MEASURES FOR THE CONTRACTOR REGARDLESS OF THE TYPE OF EXCAVATION

A detailed fire protection, escape and rescue concept is to be drawn up within the framework of the safety concept for the construction period.

2.1 *Escape ways*

– All escape and rescue ways, above and below ground, must be clearly marked and kept free and properly illuminated at all times.
– Cross-passages should be produced immediately after the initial heading in order to minimise risks (in order to create an escape way).

2.2 *Oxygen self-rescue devices*

– An oxygen self-rescue device has to be available for each person present underground (client, contractor, visitor); the device must safely cover the maximum duration required for evacuation.
– The contractor must make sure that each person, who is provided with such a device, is capable of using it properly.
– Each person must carry his self-rescue device or alternatively it can be set down close to the workplace.

2.3 *Escape or fume-shelter container*

Escape or blasting fume-shelter containers (Fig. 1) serve to house persons to protect them from toxic explosion gases during drill and blast operations and from any toxic smoke gases that may develop in the event of fire. Escape or fume-shelter containers should be set up as close to the face as possible depending on the excavation method that is chosen.



Figure 1. Escape or blasting fume-shelter container.

The escape or fume-shelter container does *not* qualify as a safe area.

Various minimal requirements for escape or fume-shelter containers:

– The container serves to house persons and visitors should an incident occur. The size should be geared to the number of persons (min. 1.0 m^2 per person) requiring protection should an incident occur (size of crew + visitors).
– Static dimensioning corresponding to project-related loads (e.g. load imposed by drill + blast drive).
– The necessary external over-pressure sustention is to be ensured via the tunnel's compressed air supply with container over-pressure amounting to ≅ 0.001 bar or 100 Pa.
– Additional internal over-pressure sustention can be installed with automatic feed once the limit values are attained via bottles for at least 4 hours given the failure of the external over-pressure sustention, relating to 40 l/min and max. permissible number of persons in container.
– Lighting.
– Telephone supply.
– Power supply – external, emergency lighting via torches should failure occur.
– Oxygen self-rescue devices corresponding to the max. permissible number of persons and period to be worn, depending on the length of escape way (approx. 40 m/min).
– Stretcher for injured, first-aid kit, sanitary installations.

2.4 *Rescue container as safe area*

The rescue container serves to safety house staff and visitors in the event of a fire incident and/or gases for a minimum of 8 h/d.

The following requirements are valid for rescue containers in addition to those applicable under 2.3.

Copyright © 2005 Taylor & Francis Group plc, London, UK

– The container should be set up on the floor if possible, at an adequate distance away from fire loads.
– The rescue container is provided with a connection to an external compressed air and a power supply line (electricity, water) for air-conditioning, while at the same time, the components must be safeguarded, e.g. by means of lines and emergency power supply for the compressors laid in the floor (covered by concrete or soil filling).
– If it is not possible to lay lines in the floor, they (compressed air, power, and water) must be capable of safely enduring a fire incident (e.g. as a result of cased steel lines, correspondingly heat-resistant gaskets).
– The temperature effects of an incident on the interior of the rescue container should be restricted as far as possible (e.g. through sprinkler systems, insulation, cooling). Air-conditioning at $t_{eff} \leqslant 30°C$ is called for (at 60°C surrounding temperature over a period of at least 8 hours).

2.5 *Various other measures*

– The conception of the ventilation system must be orientated to the occurrence of possible fire incidents (switching possibilities at the face and along the route) in addition to taking the circumstances of the construction measure into consideration.
– The supply lines have to be laid outside of the area endangered by vehicle movements (mechanical hazards).
– An optical and acoustic warning device must be installed in the tunnel for cases of evacuation.
– Suitable means of communication have to be provided to ensure that the excavation crews are immediately informed about a case of alarm. Communication cables must be laid on the route in such a manner that they are protected against mechanical damage.
– A system must be installed, which provides details about the number of persons involved in the drive at any time.
– All vehicles and machines with diesel or electric drives have to be equipped with suitable fire extinguishers.

3 PROJECT-RELATED MEASURES FOR THE CONTRACTOR IN THE EVENT OF FIRE, DEPENDING ON THE TYPE OF EXCAVATION

3.1 *Definitions*

Drives are divided up into 3 hazard categories for the case of fire incident taking existing technical codes of practice [1, 2, 3] into account.

– Hazard category A (lowest hazard stage):
  During driving operations, there are escape way lengths to a "safe area" amounting to less than 500 m.
– Hazard category B:
  During driving operations, there are escape way lengths to a "safe area" amounting to more than 500 m but less than 1,000 m.
– Hazard category C (highest hazard stage):
  During driving operations, there are escape way lengths to a "safe area" amounting to more than 1,000 m.

The hazard categories govern further measures to be undertaken. Regardless of the escape way lengths, special regulations apply for conventional small drives and mechanised drives with nominal widths between 1.00 and 3.80 m.

3.2 *Conventional drives*

3.2.1 *Conventional drive category A*

The following measures apply in addition to those listed under Ch. 2.5:

– Deployment of suitable fire extinguishers, extinguishing installations etc. at major danger points (this applies in particular, to transformers in the tunnel).
– Installation of an extinguishing water supply (also industrial water line) with sufficient connections in the tunnel.
– A communication system has to be installed (e.g. telephone with stored short-dial numbers for cases of emergency).
– Deployment of suitable resources for escape and rescue where the tunnel telephones are located.
– Hardly inflammable plastics (at least fire class B 2) must be used for waterproofing (Fig. 2) as well as the sheeting for the curing machine in order to reduce the fire risk.

3.2.2 *Conventional drive category B*

The following measures apply in addition to those listed under Ch. 2.5 and for Category A:

– Appointment of a person to be responsible for initial rescue co-ordination until the arrival of the emergency services for the entire duration of the construction measure with the right to make decisions and institute initial assignment co-ordination in keeping with the emergency plans drawn up.
– Presence of an escape or blasting fume-shelter container.
– Installation of an automatic fire alarm system (smoke alarm, CO alarm, heat sensors) at main danger points (transformer, hazardous materials storage, tanks, explosives storage), with automatic

Copyright © 2005 Taylor & Francis Group plc, London, UK



Figure 2. Fixing the waterproofing in the tunnel crown area.

initiation of the fire alarm and additional alarm in the office of the person responsible.
– The length of the advance structural waterproofing, laid out prior to concreting but still exposed, can be stipulated up to a maximum of 150 m, given correspondingly defined additional fire protection measures.

3.2.3 *Conventional drive category C*
The following measures apply in addition to those listed under Ch. 2.5 and for Categories A and B:

– 2 independent communication systems (telephone/radio).
– Direction finding aids for persons located underground.
– Diesel operated working and transport machines, which are regularly used for underground operations, must be equipped with strapped down, manually activated or automatic extinguishing units.
– The necessity of establishing a tunnel fire brigade for the project by the contractor must be examined depending on the equipment, the training and the given local conditions of the fire brigades and emergency services in the vicinity.

3.2.4 *Conventional small drives*
In the case of tunnel drives in accordance with Categories B or C, where an escape or blasting fume-shelter container would essentially be necessary in terms of length, but cannot be accommodated on account of the cross-section ($<12\,m^2$), additional measures must be taken, which reduce the probability of a fire incident resulting at the face and along the route, which herald in immediate combating of the fire, prevent the escape way rapidly becoming filled with smoke and facilitate escape over a major distance e.g.:

– Water curtains every 250 m from the portal along the escape way, water supplied via cased pipes.
– No tasks likely to cause fire to be undertaken along the route without trained auxiliary firemen present.
– Diesel operated working and transport machines, which are regularly used for underground operations, must be equipped with strapped down, manually activated or automatic extinguishing units.

3.3 *Mechanised drives*

3.3.1 *Mechanised drive category A*
The following measures apply in addition to those listed under Ch. 2.5:

– A communication system must be installed (e.g. telephone with stored short-dial numbers for cases of emergency).
– Should only one person be in the machine, a hands-free connection to a source outside the tunnel must be set up?
– Transformers located within the tunnel must be provided with automatic/manual extinguishing units (e.g. fire extinguishers, foam, inert gas).
– Superfluous supplies of combustible consumables should not be stored on the driving installation.

3.3.2 *Mechanised drive category B*
The following measures apply in addition to those listed under Ch. 2.5 and for Category A:

– Installation of water curtains along the escape way in the proximity of the machine, at least at the end of the back-up.
– 2 independent communication systems (e.g. telephone/radio). These must be installed so that they are protected.
– A suitable fire alarm system, e.g. with CO as key component must be installed.
– An escape container must be carried on the back-up, whose size is geared to the number of persons present underground.

3.3.3 *Mechanised drive category C*
The following measures apply in addition to those listed under Ch. 2.5 and for Categories A and B:

– Appointment of someone to be responsible for initial rescue co-ordination until the arrival of the emergency services (temporary on-scene commander) on the construction site and his deputy, who takes charge of the initial on-scene co-ordination in keeping with the emergency plans drawn up. All working sectors operating underground have to be informed.
– Installation of an automatic fire alarm system (smoke alarm, heat sensors) at main danger points

Copyright © 2005 Taylor & Francis Group plc, London, UK



Figure 3. Example for a mechanised tunnel drive category C.

(transformer, hazardous material store, tank depot, explosive store), with automatic initiation of the fire alarm and additional alarm in the office of the person responsible.
– Diesel operated working and transport machines, which are regularly used for underground operations, must be equipped with strapped down, manually activated or automatic extinguishing units.
– The construction site makes available employees, who are both familiar with the local conditions and breathing equipment, if required to ensure efficient assignment of the emergency services.

Figure 3 shows exemplarily a mechanised drive of category C.

3.3.4 *Manned mechanised small drives*

Special measures have to be undertaken in the case of tunnel diameters less than 1.8 m together with the measures applying for mechanised driving category A and regardless of the escape way length:

– Every employee must be well-versed in first aid and extinguishing fires.
– Water curtains every 250 m along the escape way from the portal, water supply with cased pipes.
– Self-rescue devices must be stored every 500 m from the portal (appropriate for number of staff and visitors).

In the case of tunnel internal diameters less than 3.80 m (Fig. 4), where an escape or blasting fume-shelter container cannot be accommodated and where the speed of escape is substantially restricted, additional measures must be taken, which reduce the probability of a fire incident resulting at the face and along the route, which activate immediate combating of the fire, prevent the escape way rapidly becoming filled with smoke and facilitate escape over a major distance.



Figure 4. Example for a mechanised tunnel drive with a diameter less than 3.8 m.

– Automatic sprinkler system for the entire machine area.
– Water curtains every 250 m along the escape way, water supply with cased pipes.
– Self-rescue devices to be stored every 1,000 m.
– Separate fire-protected and emergency power supplied emergency lighting, or separate battery-operated emergency lighting, capable of functioning for longer than the possible escape duration.
– No tasks likely to cause fire to be undertaken along the route without trained auxiliary firemen present.

4 OTHER PROJECT-RELATED MEASURES FOR THE CONTRACTOR REGARDLESS OF THE TYPE OF DRIVE

The advance investigations carried out by the client can lead to different measures in keeping with the selected excavation method.

4.1 *Gas incident*

Should gases e.g. methane or radon be likely to escape from the ground, then the construction ventilation has to be designed correspondingly. A catalogue of measures, which contains the special installations and the processes to be introduced, has to be drawn up.

– An advance alarm has to be set off and the ventilation increased should the measured value of methane reach 10% of the lower explosion limit. At 20%, the endangered area must be cleared and all non-intrinsically safe electric equipment should be deactivated immediately.

Copyright © 2005 Taylor & Francis Group plc, London, UK

– In the event of a radon gas concentration in excess of 1,000 Bq/m^3, the workforce must be provided with dosimeters and the ventilation increased. Regular measurements have to be carried out. Further measures may become necessary depending on the measured radon concentrations, e.g. cutting down the amount of time worked.

4.2 *Water/muck run*

– The power supply should be set up in such a way that it is located in a safe area. It must conform to Level IP 54 (splash proof).
– A sufficient pump capacity reserve must be maintained in order to provide an adequate emergency power supply.
– It must be assured that any water present can be correspondingly removed.
– The pump lines have to be designed to cope with the incidence of muck and serviced at regular intervals.

4.3 *Cave-in/collapse incident*

In the event of conventional drives the threat is principally posed by the workforce being buried or trapped.

Ongoing investigation and observation methods have to be undertaken in order to plan a safe means of excavation, the selection of the correct excavation classes and the required supporting means.

In the case of mechanised drives the threat posed to the excavation crew for shielded drives (segments, pipe-jacking) with pre-cast lining is merely of secondary importance. A threat posed to the excavation crew by cave-in/collapse can exist given an open TBM and special shield machines with selective excavation. As a preventive measure, it is advisable to secure the roof in advance by means of suitable measures (e.g. reinforcement matting and anchors) in order to protect the head.

4.4 *Incidents in the working chamber of tunnel boring machines*

In the case of full-face cutting machines, any incidents occurring in the working chamber during the drive generally do not pose a threat to the driving crew. Normally the chamber is entered for inspection purposes, maintenance, repair or in order to salvage non-workable obstacles.

Potential dangers when inspecting the chamber are on the one hand, of a geological nature such as water, muck run, blow-outs and collapse (or face failure); all kinds of mechanical effects such as can result during the recovery of non-workable obstacles as well as fire hazards, toxic smokes and dusts.

Additional equipment for the machine to support (improve) face stability should be catered for prior to a chamber inspection such as e.g. possibilities of grouting to improve the soil from the machine, supporting the face by means of lagging plates or some similar measure or to create an enlarged working area.

5 FINAL REMARK

The incident conception presented in the form of excerpts was passed by the German Committee for Underground Construction (DAUB) as a recommendation. Currently, a harmonisation process is taking place with colleagues from Switzerland, Austria and the United Kingdom.

REFERENCES

[1] RABT – Richtlinien für die Ausstattung und den Betrieb von Straßentunneln. Ausgabe 2003; Köln, Forschungsgesellschaft für Straßen- und Verkehrswesen
[2] BOStrab – Verordnung über den Bau und Betrieb der Straßenbahnen (Straßenbahn-Bau- und Betriebsordnung) vom 11. Dezember 1987; Editor: Ministry of traffic
[3] Richtlinie “Anforderungen des Brand- und Katastrophenschutzes an den Bau und Betrieb von Eisenbahntunneln”; Bonn, Eisenbahnbundesamt, 1997
[4] Tunnelbau – sicher arbeiten. Leitfaden für Tunnelbauer; Editor: Tiefbau-Berufsgenossenschaft, München, 1987

Copyright © 2005 Taylor & Francis Group plc, London, UK

Analytical methods and numerical modelling

Copyright © 2005 Taylor & Francis Group plc, London, UK

From documentation to prediction – a computer-based method for discontinuity analysis and block stability assessment in tunnelling

M. Pötsch & W. Schubert
Institute for Rock Mechanics and Tunnelling, Graz University of Technology

A. Gaich
3G Software & Measurement GmbH

ABSTRACT: Tunnel face documentation done by a geologist is a well-established task during tunnel excavation. It mainly serves for the establishment of a geotechnical model and for the "conservation of evidence" for later contractual claims. This contribution describes a method for the documentation of the rock mass conditions, the establishment of a geotechnical model and the prediction of stability of keyblocks. This method is based on a hierarchical procedure which digitally processes discontinuity data from the acquisition to the analysis. The acquisition is performed using a remote sensing system, JointMetriX3D, a three-dimensional imaging system based on photogrammetry. It uses a pair of high-resolution digital panoramic images to establish a metric 3D image of the tunnel face. Geometrical properties are measured from these 3D images serving as the basis for the determination of the discontinuity system of the rock mass. Subsequently a geometrical model is determined which relates the thoroughly determined discontinuity system to the excavation. This geometrical model is analysed with respect to the identification of keyblocks which may result with proceeding excavation. Finally, the stability of keyblocks is calculated. The result serves for decision aids on site and for the final design of excavation and support as well.

1 INTRODUCTION

A rock mass containing a considerable number of discontinuities with low strength compared to the rock material is referred to as a blocky rock mass. The behaviour of a blocky rock mass is dominated by the properties of the discontinuity system. Despite its importance the determination of the discontinuity properties is subjected to several restrictions. In tunnelling the documentation of the faces is performed while construction work proceeds. Due to the pressure of time and the limited access only selected discontinuities are mapped in a manual sketch. Due to the lack of information detailed stability analyses of blocks are not possible to provide an objective basis for the final design of excavation and support. A new approach to overcome the described problems is currently under development. The approach includes the data acquisition process, the establishment of a geotechnical model, and the analysis of keyblocks. The stability analysis of keyblocks in a blocky rock mass is addressed and the important influencing factors such as the keyblock geometry are discussed. This method follows a hierarchical structure which allows for a consistent analysis and objective auditing. An additional benefit of this computer-based method is gained from the high visualisation capability.

2 DISCONTINUITY DATA PROCESSING

2.1 *Discontinuity data acquisition*

The JointMetriX3D documentation and measurement system (Gaich et al. 2004) provides 3D images of the tunnel faces representing the geometry of the surface and its geological assembly. The area of the 3D images captures the entire region of interest, i.e. a complete image of the rock mass structure is obtained.

A digital panoramic camera with a resolution up to 100 Megapixels acquires two images of the tunnel face from which a highly detailed 3D image is computed. The process includes digital image processing, photogrammetry, and computer graphics together with data management skills (Gaich et al. 2003). The camera locations can be individually selected. The typical distance from the tunnel face is around 6 m with a separation of the two locations of around 2 m. From these

Copyright © 2005 Taylor & Francis Group plc, London, UK

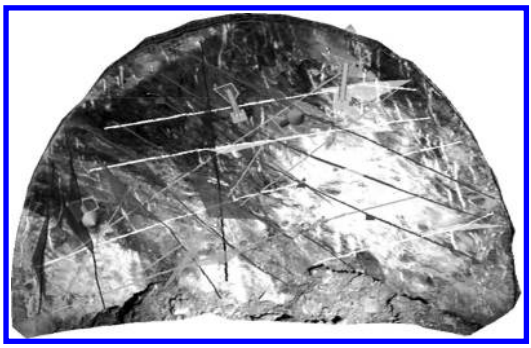


Figure 1. Evaluated 3D image showing discontinuity traces and areas with corresponding orientations.

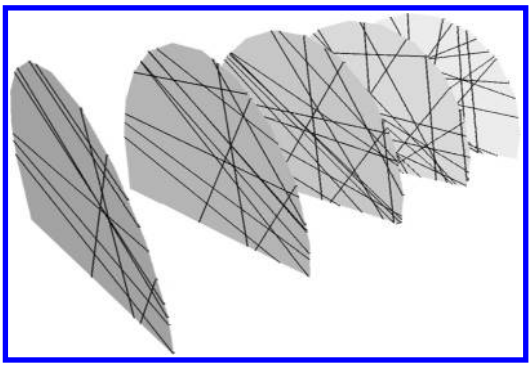


Figure 2. Sketch of tunnel faces at a regular separation of 2.5 m. The traces represent already the modelled discontinuity network.

two images a 3D model is reconstructed using the Shape from Stereo principle. In order to obtain a 3D image the 3D model and one image have to be aligned.

Applying the 3D assessment tool "JMX Analyst" measurements of geometrical properties can be taken directly from the 3D images. Discontinuity traces are identified as lineaments and areas. The length and area, respectively, and the spatial location of the marked elements are instantly available. For identified discontinuity planes the orientations can be determined both from area and linear outcrops. One area element usually covers a number of smaller surface elements from which the mean normal vector is calculated. This magnitude represents the discontinuity orientation which is instantly provided by dip and dip direction and a graphical marker. Having a discontinuity trace with a significant change in depth, i.e. the trace is not observed to be on a planar surface, its dip and dip direction is determined by fitting a plane to the resulting 3D polygonal line. Figure 1 shows an evaluated 3D image of a tunnel face. Discontinuities are represented by linear or area elements. The orientation of traces is represented by an equally oriented spatial triangle. The orientation of the areas is represented by the plane's normal vector.

2.2 *Establishment of a discontinuity network*

In order to establish a discontinuity network accompanying the tunnel excavation, consecutive tunnel faces have to be evaluated. This is done by recording several faces (best every round) using the JointMetriX3D system and generating 3D images. These 3D images are evaluated which allows defining the visible discontinuities. In order to avoid introducing the same discontinuity several times into the network it is necessary to inspect consecutive faces with respect to traces which belong to the same plane.

Face mapping as a data acquisition method (either conventional or by 3D imaging) implies that only discrete sampling locations are available. Depending on the sampling density it is possible that some discontinuities cannot be recorded as they do not appear in the face (especially steeply dipping discontinuities striking normal to the tunnel axis). Therefore, the discontinuity system has to be audited with geological judgement. In order to complete the system discontinuities can be manually introduced.

Figure 2 shows schematically the modelled discontinuity network which has been based on a frequent face documentation and evaluation.

2.3 *Establishment of a geometrical model*

For the following analysis a geometrical model has to be established which relates the discontinuity network with the excavation geometry. The geometrical model contains all relevant information of the geometry of the excavation and the identified discontinuities. The evaluated discontinuities are intersected with the excavation geometry and analysed from the trace network. Figure 3 shows the geometrical model obtained from acquired discontinuity data.

2.4 *Keyblock analysis*

Once the geometrical model is established, the trace network is searched for closed polygons (loops) of traces in order to identify the superficial block faces (Lu 2002). The traces are subdivided into stretches between their intersections. Reverse directions are assigned to each trace (directed traces). After randomly selecting the first directed trace, the subsequent traces have to comply with the following two constraints:

- The subsequent directed trace must point away from the endpoint of the current directed trace.
- The subsequent directed trace is the one which forms the maximum right-handed angle with the current directed trace whereby 360° are treated as 0°.

Copyright © 2005 Taylor & Francis Group plc, London, UK

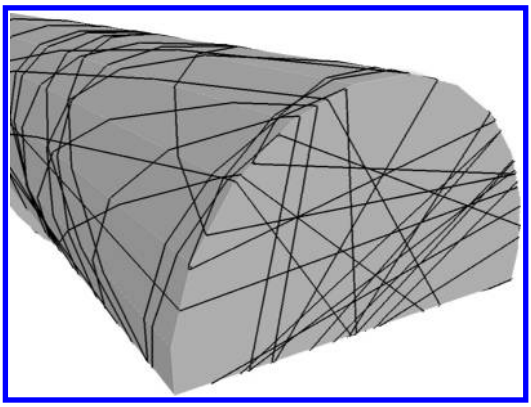


Figure 3. Geometrical model including discontinuity network and excavation.

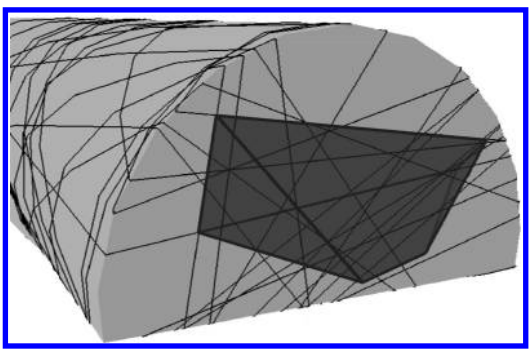


Figure 4. Visualisation of a removable block in the tunnel face.

This trace search criterion is applied to the entire trace map. This results in a subdivision of the tunnel wall into polygons. Each polygon forms part of the free surface of a block.

Since each polygon is formed by discontinuity traces, information about their orientations is assigned. For each polygon the joint and block pyramids are determined. This leads to the analysis of the removablility of the corresponding blocks (Goodman & Shi 1985). Figure 4 shows a removable block in the tunnel face. Compared to commercially available software (for instance Unwedge, PT Workshop) this analysis covers the identification of keyblocks at the tunnel wall, the tunnel face, and the edges of the intersections of wall and face. This is especially important in tunnelling where the rock mass is not supported at the face and the adjacent wall.

Basic keyblock analyses do not cover the entire block failure mechanisms. A number of blocks which are not necessarily individually removable can form a removable keyblock. These types of blocks are referred to as united keyblocks. Chan (1987) proposes a mathematical formulation for identifying united keyblocks. The drawback of this formulation is that it is applicable only for joint sets containing perfectly parallel discontinuities and one free surface. Its application is therefore restricted to slope analysis problems with a simple geometry of the surface and the discontinuity system. A generalisation for joints sets with non-parallel discontinuities is currently under development.

After determining the kinematically removable blocks they are analysed with respect to their mode of failure. The mode of failure of the block is dominated by the resulting force of the external force system of the block. Block theory provides the analysis of translational failure modes such as falling and lifting, single-face sliding, double face sliding. For instance, the mode of failure of a block whose joint pyramid contains the direction of the resulting force is identified as a falling or lifting block. Criteria for further failure mechanisms are provided by block theory (Goodman & Shi 1985).

Conventional block theory covers the translational failure modes. The force system acting on a block may also result in force couples which induce rotational displacements. Especially under conditions with high frictional resistance rotation is more likely than translation. This fact is relatively simple indicated by the problem of a block on an inclined plane discussed by Goodman & Bray (1976). They proposed criteria for sliding and toppling depending on the (cuboidal) block geometry, the inclination of the base plane, and the frictional resistance. The assumption of an increasing stability level with increasing friction led to a non-conservative design considering only translational failure modes. Mauldon (1992) and Tonon (1998) proposed expressions for the analysis of kinematics, modes and stability of rotations of tetrahedral blocks.

Once the failure modes of the blocks are determined, their stability can be calculated by means of a limit equilibrium analysis. Driving forces can be gravity or inertia forces as well as external water or gas pressure. On the other hand, resisting forces result from friction, clamping or support measures. Traditionally, limit equilibrium calculations provide fast design procedures but are usually conservative. It is inherently assumed that the shear resistance of the joints has fully developed while at the same instance the support provides its maximum bearing capacity.

Going further into detail, there is a complex interaction between a block, the surrounding rock mass, and the rock support. If an unstable block displaces along a rough discontinuity, it tends to dilate. If the block is free to dilate, its resistance is increased by the dilation angle of the discontinuity due to the asperities. This fact has been already discussed by Patton (1966). However, if the dilation of the block is restrained, e.g. by the surrounding rock mass, rock support, and as a result of rock mass stress, etc., additional normal

Copyright © 2005 Taylor & Francis Group plc, London, UK

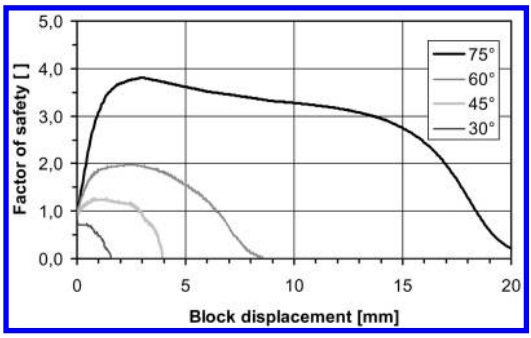


Figure 5. Example for the development of the factor of safety throughout the block displacement. Different lines refer to different dip angles of the planes of pyramidal keyblocks.

stresses can develop and significantly increase the resisting forces (Blümel et al. 2002). On the other hand, forces in rock bolts are mobilised only by displacement of the block. The displacement of the block causes a mobilisation of normal forces in the rock bolts due to dilation of the joints. As a consequence the interaction of driving and resisting forces causes a change of the factor of safety throughout the displacement. This phenomenon predominantly is influenced by the geometry of the discontinuity surface, the strength of the asperities, the geometry of the block, the stress condition and the stiffness of the restraining boundary (support, rock mass, etc.).

Non-linear constitutive models and iterative algorithms have to be applied in order to account for this interaction. Pötsch (2002) proposed an iterative shear model which considers a stiff boundary based on the expression of Barton & Choubey (1977) and Barton & Bandis (1990). Using this model he calculated the factor of safety of pyramidal keyblocks with four discontinuities in the tunnel crown. Figure 5 shows the development of the factor of safety for keyblock displacement under the same initial stress. The different lines refer to different block geometries. This highlights the importance of the accurate determination of the geometry of keyblocks for stability analysis.

3 SUMMARY

A method for discontinuity data analysis for tunnelling has been presented. The method includes the data acquisition process, the establishment of a geotechnical model and the analysis with respect to instabilities of discrete rock blocks. Using the described mapping method by 3D imaging data acquisition is decoupled from the evaluation task – the evaluation can be performed even when actual rock faces do no longer exist. Quantification from 3D images is an indirect measurement principle. Therefore only visually determinable features can be identified in contrast to other parameters, for example discontinuity filling or strength parameters. This results in the measurement of geometrical properties. A 3D image resulting from the JointMetriX3D system represents an objective record of a tunnel face due to its high resolution, true colour, visual information and its three-dimensional information. As presented in this paper information gained from 3D images support and improve rock mass analyses as the data give a realistic impression.

Taking 3D images of a tunnel face in a regular manner leads to a highly detailed and consistent rock mass model. It facilitates the establishment of a discontinuity network. The analysis of this network allows determining the development of the spatial properties along the tunnel alignment and identifying trends. Based on the obtained information the discontinuity system ahead of the face can be predicted. Simulating the excavation process allows determining removable blocks and their stability. This serves as a basis for the final design of the excavation geometry (e.g. round length) and the installed support.

ACKNOWLEDGMENT

This research work has been funded by 3G Software & Measurement GmbH and the FFG Austrian Industrial Research Promotion Agency Ltd.

REFERENCES

Barton, N. & Choubey, V. 1977. The shear strength of rock joints in theory and practice. *Rock Mechanics* 10: 1–54.

Barton, N. & Bandis, S. 1990. Review of predictive capabilities of JRC-JCS model in engineering practice. In Barton & Stephansson (eds), *Rock Joints:* 603–610. Rotterdam: Balkema.

Blümel, M., Button, E.A. & Pötsch, M. 2002. Steifigkeitsabhängiges Scherverhalten von Fels. *Felsbau* 20(3): 22–32.

Chan, L.-Y. 1987. *Application of block theory and simulation techniques to optimum design of rock excavations.* PhD Dissertation, University of California, Berkeley

Gaich, A., Fasching, A., & Schubert, W. 2003. Improved site investigation. Acquisition of geotechnical rock mass parameters based on 3D computer vision. In G. Beer (ed), *Numerical Simulation in Tunnelling*: 13–46. Springer: Wien.

Gaich, A., Pötsch, M., Fasching, A. & Schubert, W. 2004. Measurement of rock mass parameters using 3D imaging. In G. Barla & M. Barla (eds), *Caratterizzazione degli amassi rocciosi nella progettazione geotecnica: X Ciclo di Conferenze di Meccanica ed Ingegneria delle Rocce*, *Torino, 24–25 November 2004:* 21–45. Pàtron editore: Bologna.

Copyright © 2005 Taylor & Francis Group plc, London, UK

Goodman, R.E. & Bray, J.W. 1976. Toppling of Rock Slopes. *Proc. of the Specialty Conference on Rock Engineering for Foundations and Slopes, ASCE/Boulder, Colorado, 15–18 August 1976.*

Goodman, R.E. & Shi, G.-H. 1985. *Block Theory and its Application to Rock Engineering.* Prentice Hall: New Jersey.

Lu, J. 2002. Systematic identification of polyhedral rock blocks with arbitrary joints and faults. *Computers and Geotechnics* 29: 49–72.

Mauldon, M. 1992. *Rotational failure modes in jointed rock: A generalization of block theory.* PhD Dissertation. University of California, Berkeley.

Patton, F.D. 1966. Multiple modes of shear failure in rock, *Proc. of the 1st Cong. Int. Soc. Rock Mech., Lisbon:* 509–513.

Pötsch, M. 2002. *Influence of the three-dimensional stress condition at the tunnel face on the stability of removable blocks.* Diploma thesis, Graz University of Technology PT Workshop www.pantechnica.com

Tonon, F. (1998). Generalization of Mauldon's and Goodman's Vector Analysis of Keyblock Rotations. *Journal of Geotechnical and Geoenvironmental Engineering* 124(10): 913–922.

Unwedge www.rocscience.com

Copyright © 2005 Taylor & Francis Group plc, London, UK

Gallery connection between the annexed structure and the TBM tunnel in soft ground

Ashraf A. Abu-Krisha
National Authority for Tunnels (NAT), Cairo, Egypt

ABSTRACT: Construction of underground structures located on water bearing soil deposits is considered one of the challenging tasks facing civil engineers. In the subway lines of the Greater Cairo Metro, the annexed structures are normally located at the deepest location between any two-subway stations. The connections between these stations and the bored tunnel are at right angles in the form of galleries constructed by handmade excavation and supported by steel and shotcrete. The grouting technique was used to stabilize the soil at these tunnel links.

Modelling of deep excavations of subway structures is usually considered as one of the most complicated soil-structure interaction problems. The finite element calculation is achieved by a 2D model, which takes into account the different phases of tunneling, annexed structure and gallery building. The problem is actually a 3D model, so a 2D model is conservative for our objective. The purpose of this paper is to justify the overall stability of the soil mass around linked tunnels, taking into account local grouting and temporary supports. Furthermore, the results were discussed and compared with actual field measurements compiled during construction.

1 INTRODUCTION

Construction of the subway lines of Greater Cairo Metro had lots of challenges. Conventional underground connection methods required ground stabilization or mechanical protection to control ground collapse and groundwater inflow during galleries construction. The purpose of our calculation is to analyze the variation of the forces in the lining, close to the annex structure during the various construction stages of connection with the shafts. We have selected the section of the tunnel presenting the largest normal forces within the project adjacent to an annex structure.

Advanced diaphragm wall drilling machines, called hydro-phrase machines, had been used for the installation of the diaphragm walls of annexed structures. The sequence of excavation and construction within the annexed structures was done in a top-down sequence of work. The model of the annexed structure was based on a 2D finite element analysis by Abu-Krisha 2004. A pressurized face slurry shield tunnelboring machine with 9.4 m diameter executed the tunnels of Greater Cairo Metro line 2. The final internal diameter for design was 8.35 m with lining thickness 0.40 m. The lining design provided a ring width of 1.50 m. The model of the tunnel was based on a 2D finite element analysis by Abu-Krisha 2002.

The target of this paper is to demonstrate the analysis of the gallery by 2D modeling. The purpose of this investigation is to check carefully the distribution of deformations and forces and hence the safety of tunneling operations in the gallery zone, in addition, the reporting the fluctuations on stress that occurred at the opening of the existing segments in the process of the underground joining operation.

2 STRATIGRAPHY AND GEOTECHNICAL PROPERTIES

The region of Greater Cairo was built in the Nile valley on Quaternary deposits. These recent deposits consist mainly of silt and clay layers of several meters thick underlain by sand and gravelly sand layers. The medium sand, dense sand and gravel represent the main aquifer under the Greater Cairo and hence have main role on the change of groundwater levels under this area. A surface fill layer of heterogeneous mixture of silt, clay, sand, bricks, pottery and pieces of limestone is commonly encountered at these locations. According to the geotechnical reports by NAT, the properties of the four main soil deposits in Cairo are given in Table 1 (NAT soil report, 1980 to 2002).

The ground water table under the greater Cairo region tended to be higher than the relatively stable

Copyright © 2005 Taylor & Francis Group plc, London, UK

Table 1. Layers and geotechnical parameters.

Soil layer	Depth (m)	γ	E MPa	ν	ϕ	C	K_o	$K_{x,y}$ (m/s)
(1)	0–7	18.5	20	0.4	30	10	0.66	$4E^{-8}$
(2)	−7–12	19.0	70	0.3	33	0	0.46	$1E^{-6}$
(3)	−12–30	20.0	100	0.3	36	0	0.41	$3E^{-5}$
(4)	−30–80	20.0	160	0.3	37	0	0.4	$2E^{-4}$

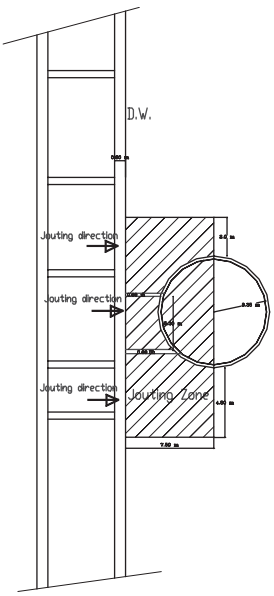


Figure 1. Layout of gallery with grouting zone.

water level in the Nile River. The ground water level was taken to be at −3.00 m from the ground level.

3 SOIL TREATMENTS

The treated soil gallery between the tunnel and annex structure is supposed to react as an elastic material with Young's modulus E = 500 MPa and Poisson's ratio ν = 0.30. The grouting materials are injected in two stages, bentonite-cement slurry followed by soft-silica gel through the annex structure until the center-line of the tunnel. The grouted soil is tested and the Young's modulus achieved E = 1500 MPa with a safety factor of 3. The grouted area of the gallery was performed as described in Figure 1. The thickness of the grouting and its elevation are calculated to satisfy a safe limit of the uplift pressure on the lower part of gallery, (NAT documents 1990–2002).

4 CONCRETE AND STEEL STRUCTURE

The concrete for tunnel lining, annexed structure and gallery beams are modeled as an elastic material: E = 28500 MPa, ν = 0.20, weight density = 2.5 t/m^3. The shotcrete is modeled as an elastic material with E = 10000 MPa and ν = 0.20, (NAT documents 1990–2002).

The temporary steel structure consists of two columns and two circular beams and is distributed every 1.5 m along the tunnel axis at the gallery location. Also, the steel is supposed to be an elastic material with E = 210000 MPa and ν = 0.30, (NAT documents 1990–2002).

5 CONSTRUCTION SEQUENCE

The annexed structures were constructed at first by utilizing the cut-and-cover technique similar to underground stations. This construction technology includes execution of supported deep excavations within a box of reinforced concrete diaphragm walls. The grouting materials are injected for gallery construction through the diaphragm walls as illustrated in Figure 1. The Tunneling Boring Machine (TBM) was advanced from the station shaft to excavate the tunnel. The tunnel advance was excavated through the grouted zone of gallery. After the tunneling processed and the temporary steel supports constructed, the gallery was excavated by using handmade techniques in the grouted zone and the shotcrete was performed. Finally, the gallery structure was constructed and the tunnel lining was demolished (NAT documents 1990–2002).

6 NUMERICAL ANALYSIS

For our problem, no analytical solution is available to simulate the construction process. The possible way is to use numerical methods. In this paper the Finite Element Method (FEM) is used to solve this problem. It is only possible to obtain rough information on the distribution of deformation and forces in the gallery zone by means of plane, two-dimensional (2D) models. It is thought that more realistic modelling of these problems can be achieved with three-dimensional (3D) models. However, considering 2D is conservative for our present objective. FINAL package (Swoboda 2001) with its new improvements has been used to model and solve this problem.

The soil is assumed to react according to an elasto-plastic Mohr-Coulomb law to describe its behavior in the non-linear stages. The discretization of the soil is made by using six node Linearly Strain Triangular elements (LST). The circular beams of the tunnel, the

Copyright © 2005 Taylor & Francis Group plc, London, UK

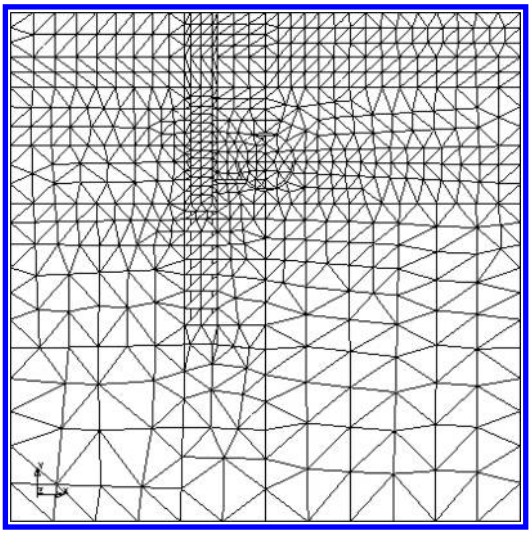


Figure 2. Finite element mesh for 2D analysis.

diaphragm walls of the annexed structure and the beams of gallery are modeled by six node beam elements (BEAM 6). This element can achieve the combined action with LST elements used for the surrounding soil. BEAM6 element nodes are arranged to form three couples, each couple with two nodes, Abu-Krisha 2002 & 2004. The columns and beams of the temporary steel supports inside the tunnel are modeled by 2D beam elements. The removal of precast segments and temporary steel are modeled through the application of forces within the segments and steel elements and decreasing the Young's modulus to zero. The 2D FE mesh for modeling is shown in Figure 2.

7 DESCRIPTIONS OF LOADING PHASES

The execution of the annex structure, the board tunnel and the gallery are modeled through seven loading phases:

1. Execution of the annex structure loads:
   - Initial geostatic state of stresses (for all the problem).
   - Full deconfinement load applied to the outer wall of the annexed structure.
   - Execution of the diaphragm walls, construction of the slabs and hydrostatic water pressure applied to the annex structure.
2. Treatment of soil between the diaphragm walls and the bored tunnel centerline is achieved by increasing the Young's Modulus E of the grouted zone.
3. Execution of the bored tunnel loads:
   - Tunnel excavation (Stress relief of the excavation soil by reducing its stiffness).
   - Installation of the concrete lining.
   - Application of the concrete lining weight and hydrostatic water pressure to the lining.
4. Setting the temporary steel structure in side the tunnel.
5. Execution of the gallery loads:
   - Excavation of the upper part of the gallery and shotcreting.
   - Applying the hydrostatic water pressure to the shotcrete.
   - Excavation of the lower part of the gallery and shotcreting.
   - Applying the hydrostatic water pressure to the bottom of shotcrete.
   - Casting of the concrete slabs of the gallery and applying its weight.
6. Demolition of the precast segments at junction with the gallery.
7. Removal of the temporary steel.

8 FIELD MEASUREMENTS

Field measurements were taken to secure safety of construction in the process of underground gallery. The monitoring of the groundwater levels was utilized by a number of piezometers stating at the first execution step. Where as the measuring instruments were installed after ground improvement. Measurements were taken continuously for the underground joining work, which were compared with prediction values of analysis to verify work safety.

9 NUMERICAL RESULTS

Figure 3 presents the predicted distribution of settlement in soil mass around the underground structures. The following table 2 shows the variation of vertical and horizontal deformation of lining, from loading 3 to loading 7. Figure 4 illustrates the deformation in the lining and gallery at different loadings. The vertical deformation at different section at loading 6 is shown in Figure 5.

The contour of the vertical effective stress at loading 6 and loading 7 are shown in Figures 6, 7. The maximum difference between extreme principal stresses $\sigma 1 - \sigma 2$ is 0.9 MPa while the allowable compressive strength of treated soil is 1.0 MPa. The large stresses were observed at the upper and the lower sides of the opening. Large stresses occurred at the temporary steel structures. No plastic zones around the tunnel or gallery were observed, so the soil failure will not occur and there is no expected risk for the surface structures.

The normal forces and the bending moments are developed in the lining and gallery according to the construction stages. The internal forces diagrams in

Copyright © 2005 Taylor & Francis Group plc, London, UK

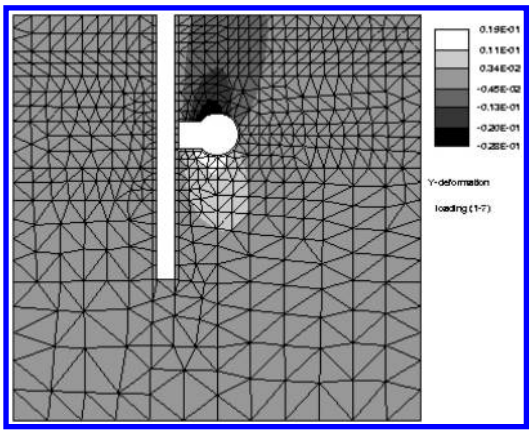


Figure 3. Contour of predicted settlement in soil mass.

Table 2. Variation of vertical and horizontal deformations.

Deformation (mm)	L(3)	L(4)	L(5)	L(6)	L(7)
Vc (Vll at center line)	3.7	4.6	6.2	6.6	9.8
Vo (Vll at opening)	1.2	2.5	4.8	5.7	5.9
Hc (Hzl at center line)	−2.1	−3.8	−6.9	−7.1	−7.3

* Vll = Vertical & Hzl = Horizontal & L = Loading

lining resulting from analysis are shown in Figures 8, 9. The computed normal forces and bending moment's values were complying with the interaction diagram of 40 cm thick reinforced segments and of the 24 cm thick joints between segments, Figure 10. Namely, the precast concrete lining can carry the additional internal forces.

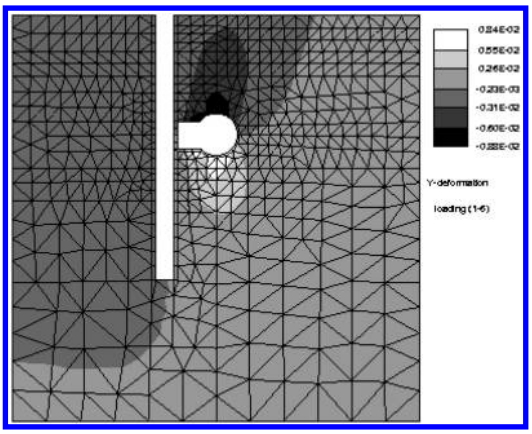


Figure 5. Contour of predicted settlement at loading 6.

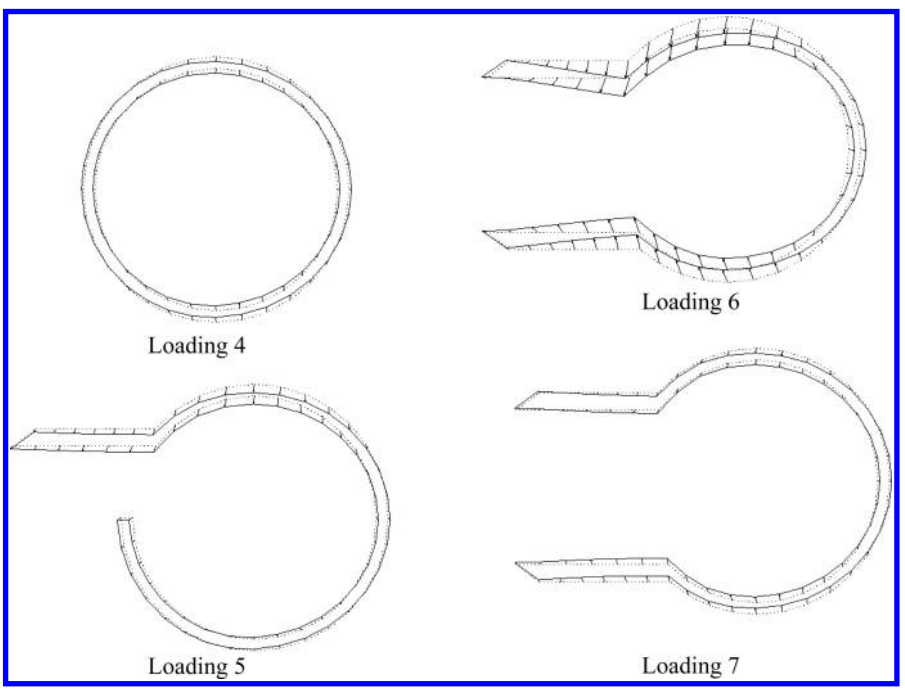


Figure 4. Deformations in lining and gallery.

Copyright © 2005 Taylor & Francis Group plc, London, UK

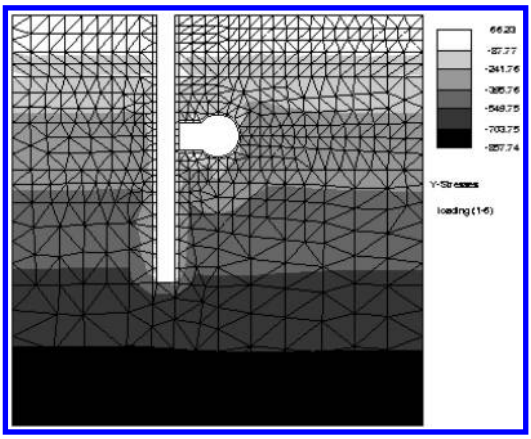


Figure 6. Contour of stresses at loading 6.

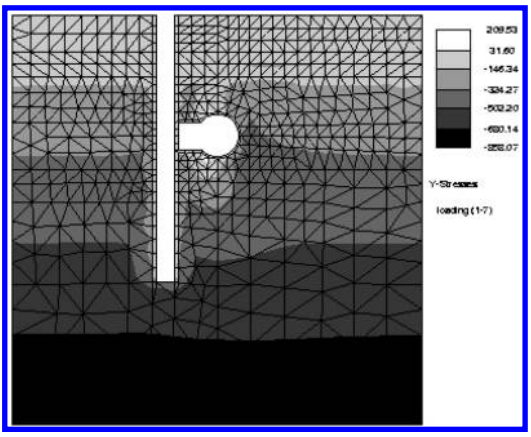


Figure 7. Contour of stresses at loading 7.

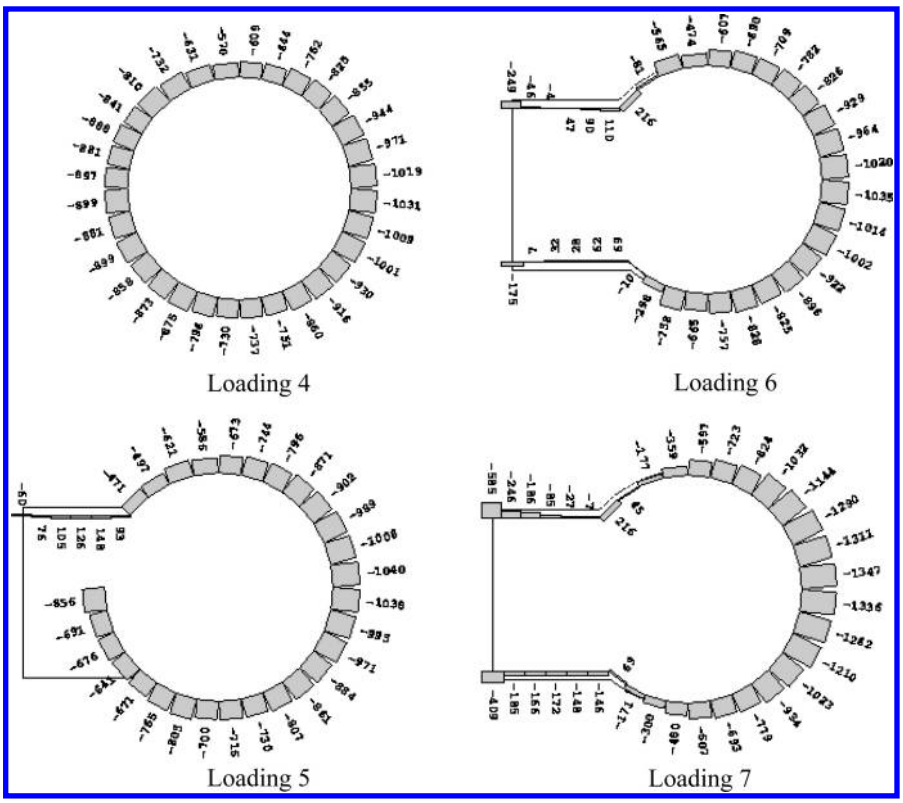


Figure 8. Normal forces in lining at different loadings.

10 CONCLUSIONS

The analysis of the gallery construction was successful to predict and control the deformations. The demolition of precast segments induced a vertical displacement of 3 mm close to the opening. The gallery construction succeeded and its deformation was within the allowable alignment tolerance.

Copyright © 2005 Taylor & Francis Group plc, London, UK

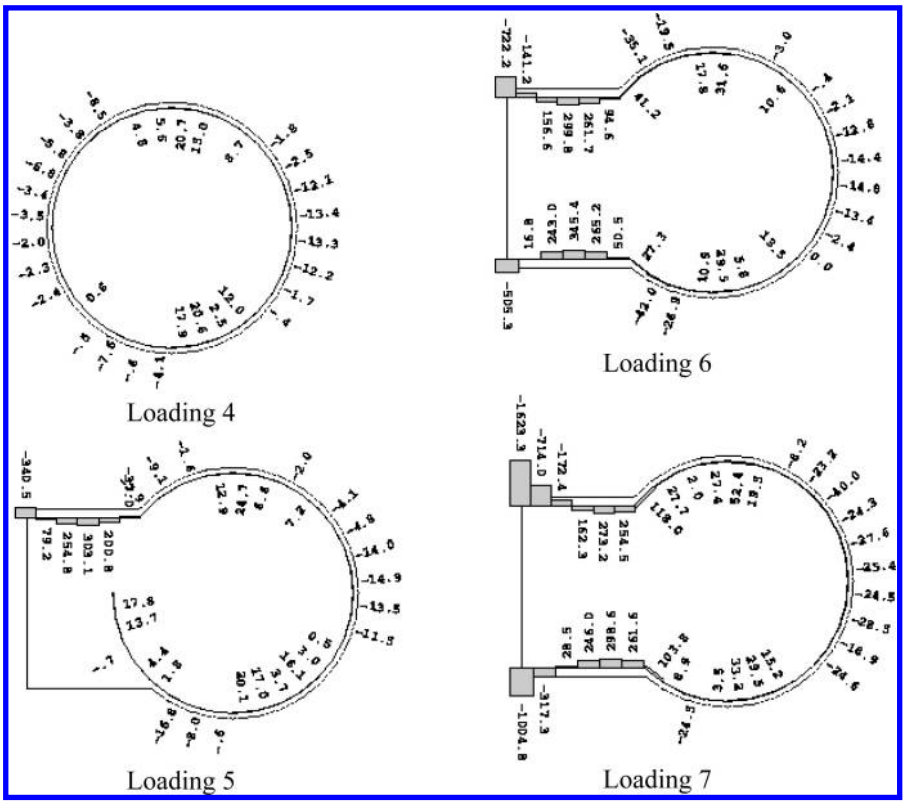


Figure 9. Bending moments in lining at different loadings.

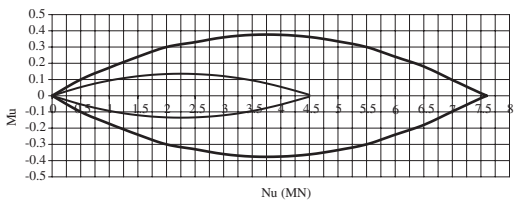


Figure 10. The interaction diagram of concrete lining.

The opening of the tunnel segments during the gallery construction works caused large stress on lining. The maximum difference between principal stresses was less than the allowable for the treated soil, so there will be no plastification at all. Moreover, the strengths obtained in-situ by tests are much higher than allowable.

The normal forces and the bending moments remain acceptable within the remaining lining according to the interaction diagram for a 0.24 m thickness concrete section. The steel temporary structure inside the ring was supporting the free edges of the ring and decreasing the deformations and internal stresses and increasing the safety factor.

Finally, the design and construction of the gallery was adequate to provide minimal disturbance and did not cause any harmful distress to the underground surrounding structures.

REFERENCES

Abu-Krisha A., 2002, "New 2d Simulation of TBM Tunneling and Application on El-Azhar Road Tunnels", Proc. of the AITES-ITA Downunder 2002, 28th ITA General Assembly and world tunnel Congress, Sydney, Australia.

Abu-Krisha A., 2004, "Design and construction of the deepest Diaphragm Walls in Cairo", Proc. of the 30th AITES-ITA world tunnel congress, Singapore.

El-Nahhas F., 2003, "Geotechnical aspects of controlling groundwater levels in urban areas", Proc. of the 10th International colloquium on structural and Geotechnical Engineering, Cairo, Egypt.

National Authority for tunnels (NAT). 1990 to 2002. Project Documents.

National Authority for tunnels (NAT). 1980 to 2002. Soil report. Project Documents.

Swoboda G., 2001. Program System FINAL, Finite Element Analysis Program for Linear and Nonlinear Structures, Version 7.1, University of Innsbruck, Austria.

Copyright © 2005 Taylor & Francis Group plc, London, UK

Development and application of a long face reinforcing method with GFRP tubes in mountain tunneling

Y. Mitarashi, T. Matsuo & H. Tezuka
Kumagai Gumi Co.Ltd., Tokyo, Japan

T. Tsuji, T .Haba & T. Okabe
KFC Ltd., Tokyo, Japan

ABSTRACT: The long face reinforcement with GFRP tube, forms an improved ground core ahead of the face. This method uses a double-tube drilling system. Glass fiber reinforced tubes are driven into the face, which serve as casings, and a polyurethane or a cement agent are injected through the tubes. It not only stabilizes the tunnel face, it also prevents loosening ahead of the face. This paper discusses the development of the FIT method and its application to tunneling projects. In addition, its effectiveness is verified on the basis of the measurements and identification analysis results by the finite difference method.

1 INTRODUCTION

Because of diversified social demands, urbanization and environment preservation concerns, strict conditions have been imposed on mountain tunneling projects, with restrictions on the alignments of tunnels. Recently, injection type long steel forepiling has been widely used, aimed at stabilizing the face and limiting displacement ahead of the face. However, under the requirement that impact of tunnel excavation should be minimized, this method fails to satisfactorily control loosening ahead of the face in some ground conditions, because this technique reinforces the portion around the crown ahead of the face but it does not strengthen the face.

To provide an effective solution for this problem, the FIT (FRP Injection Tube) method has been developed, which uses glass fiber reinforced plastic tubes.

This paper deals with the development of the FIT and cases where it has been applied. In addition, it discusses the effect of the FIT, using in-suit measurement results and analysis results by the three dimensional finite difference method and the distinct element method with a model of granular media.

2 OVERVIEW OF THE FIT METHOD

Long GFRP tubes are driven into ground ahead of the face, using the double-tube drilling technique. The reinforcement solidified with the injection agent strengthens the regions where stresses are redistributed under the influence of excavation. Figure 1 and 2 show the schematic diagram of this method and overview of placement.

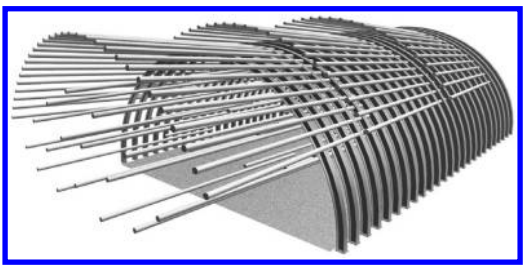


Figure 1. Schematic diagram of long face reinforcement.

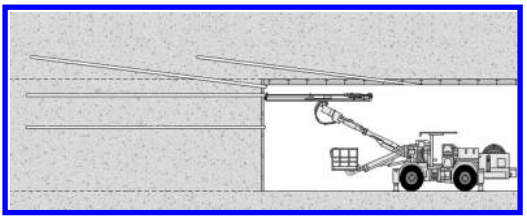


Figure 2. Overview of placement of long face reinforcement.

Copyright © 2005 Taylor & Francis Group plc, London, UK

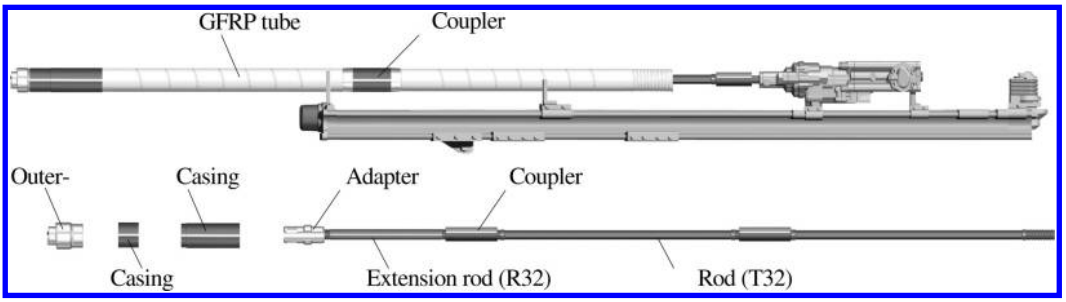


Figure 3. Drilling system.

The drilling system is composed of GFRP tubes that can be cut, ring bits, casing shoes, and rods with bit adapters. The drilling impact and rotational forces are transmitted from the rod mounted on the drifter, through the bit adapter, to the ring bit Figure 3. After a specified length is drilled by a drill jumbo, the ring bit and GFRP tube are left in the drilled hole, and the bit adapter and rod are retrieved. The standard length of a GFRP tube is 3 m. By connecting tubes, a desired length of reinforcement is made. A polyurethane or a cement injection agent is used. Two types of injection methods are available, to be selected on the basis of ground conditions and work cycles. These methods are valve injection by which the agent is poured through the mouth hole, and divided injection method using a packer.

3 FEATURES OF THE LONG FACE REINFORCEMENT

This method features the following.

1) The double-tube drilling is applicable under a ground where the wall of drilled hole is not self-supporting. Long reinforcing tubes are more easily driven than conventional face bolting techniques.
2) Since cuttable GFRP tubes are used, they can be driven in any direction. Depending on the extent to which pre-loosening must be prevented, tubes can be driven also into the circumference of the face, without extending the excavated section.
3) This method can be implemented by a drill jumbo that is generally used in tunneling sites, without requiring any special machines.
4) Although the GFRP tube diameter is small, its tensile strength is as large as 600 MPa, and the rigidity (modulus of elasticity) is as high as 20,000 to 30,000 MPa. The grooved surface of the tube provides a large force for anchoring to ground (Table 1).
5) The GFRP is light, weighing only about 3 kgs per meter. It is easy to handle and install, and safe.

Table 1. Properties of GFRP tube.

Contents glass fiber	⩾50% (Wt.)
Unit weight	3 kg/m
Young's modulus	20,000～30,000 MPa
Tensile strength	⩾600 MPa
Shear strength	⩾100 MPa

4 CASES OF APPLICATION OF THE LONG FACE REINFORCEMENT TO MOUNTAIN TUNNELING

4.1 *Application to a brittle fractured zone*

During excavation in a weathered sandstone/shale stratum, using forepiling (3.0 m long) and face shotcreting, a fractured zone was suddenly encountered, resulting in face collapse ahead of the edge of the forepiling (3.0 m long). Its impact reached the surface. Aimed at stabilization of the face, long GFRP forepiling (13.5 m long) and long face reinforcement (13.5 m long) were driven. Figure 4 shows the driving pattern. These face reinforcing measures stabilized the face, without gradually increasing the impact of collapse at the time of excavation restart. Then, breakthrough was safely achieved at the portal sector with a small earth overburden. Photo 1 shows the states of the face before and after the long face reinforcements were placed. Since application of these auxiliary methods stabilized the face, it was not necessary to make the face section smaller.

4.2 *A case of application to a ground with a large face extrusion*

The face and crown were unstable, with a large face extrusion, immediately after excavation (in soft block mudstone). The unstable state continued, and it was difficult to keep the face self-supporting, using only face shotcreting (10 cm thick). Even with forepoles driven into the face, the face and crown intermittently

Copyright © 2005 Taylor & Francis Group plc, London, UK

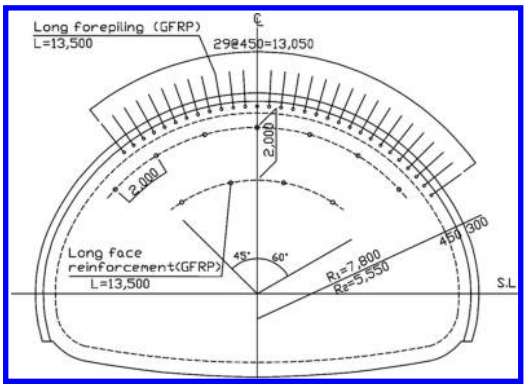


Figure 4. Long face reinforcement CASE 1.

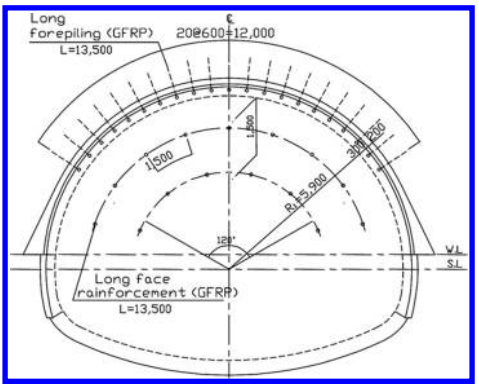


Figure 5. Long face reinforcement CASE 2.

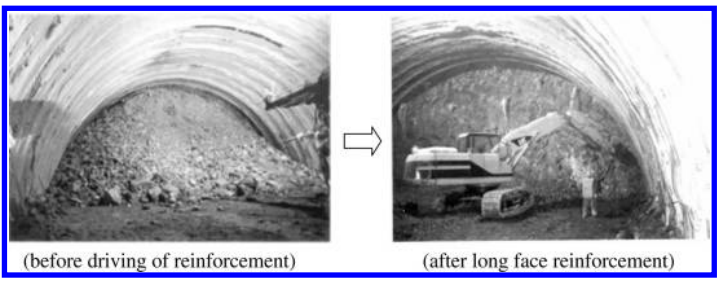


Photo 1. States of tunneling.

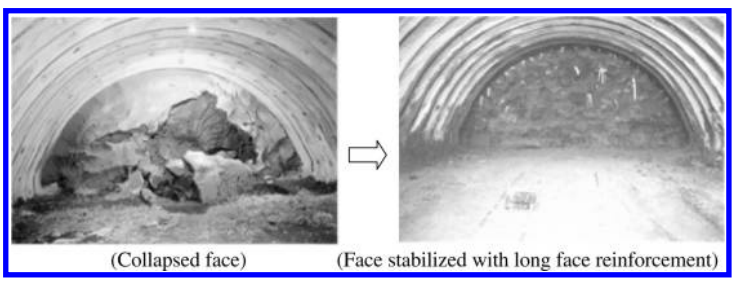


Photo 2. States of tunneling.

collapsed, inducing plastic deformation of the surrounding ground. Consequently, the gradual increase in displacement was noticeable.

For providing a solution, long GFRP forepiling (13.5 m long) and long face reinforcement (13.5 m long) were driven. Figure 5 shows the driving pattern. This measure effectively limited the face extrusion and plastic deformation of the surrounding ground. As a result, rock spalling from the crown was reduced, and as the face was more and more stabilized, the deformation converged earlier, and convergence and settlement at the foot of the upper half were remarkably reduced, as proved by the measurements. Photo 2 shows the states of tunneling.

5 MEASUREMENT RESULTS OF THE LONG FACE REINFORCEMENT AND DISCUSSION

5.1 *Measuring method of the forces in members of long face reinforcement*

A data logger was installed at the edge of GFRP tube. It was retrieved when ground at its location was excavated, to obtain data. With this casing-injection

Copyright © 2005 Taylor & Francis Group plc, London, UK

technique (GFRP tube casing), it is not appropriate to use a GFRP to which a strain gauge is attached in advance, because the gauge and lead wire would be damaged. Instead of this ordinary measurement method, a sensor tube (with a strain gauge attached inside) illustrated in Figure.6 is inserted into the GFRP tube, and the inside and outside of the tube is filled with silica resin.

5.2 *Measurement records*

The geology of the Minoh tunnel site is heavily fractured shale of the Tanba zone, with groundwater. Figure.7 illustrates the measuring points of the long face reinforcements.

The measurement was done with two GFRP tubes, i.e., F1 (axial force) and F2 (bending stress and axial force). Figure.8 shows the axial force distribution, Figure.9 the change in force increment against distance from the face, and Figure.10 the change in bending moment increment against distance from the face. The axial force increment and moment increment plotted against the ordinate axis represent the increment or decrease of axial force and moment per meter of face advance. The abscissa axis represents the distance between measuring point and face. The plus sign of axial force expresses the tensile force, and the plus sign of bending moment means a deformation convex

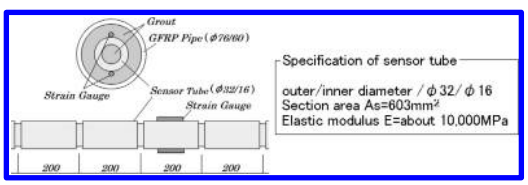


Figure 6. Measurement of strain of long face reinforcement.

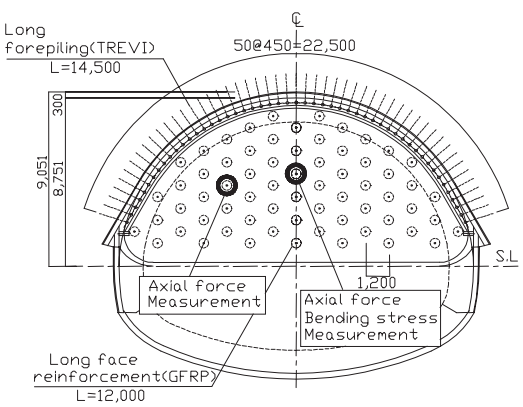


Figure 7. Layout of measuring points of auxiliary methods.

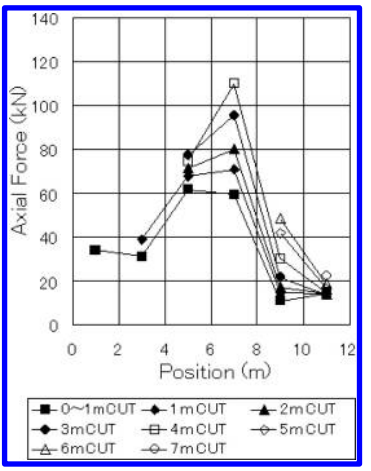


Figure 8. Axial force distribution.

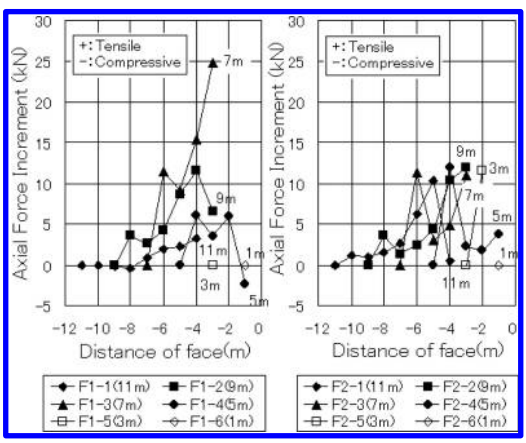
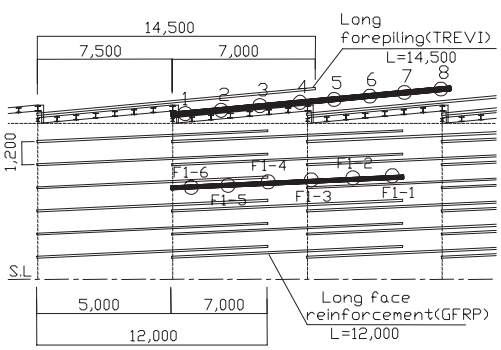


Figure 9. Axial force increment against distance from the face.



Copyright © 2005 Taylor & Francis Group plc, London, UK

upward. The distance of each measuring position given in the graphs is the distance from the tube mouth. The graphs show that, at 5 m or deeper from the tube mouth, the axial force suddenly increases when the face reaches 4 to 6 m from the face. The abrupt increase at F1-3 (7 m) in Figure 5-4 can be explained by the fact that, when the face reached about 3 m from the measuring point, the reading of the strain gauge became the maximum measurable value. These results demonstrate that when the face is at 4 to 6 m from each measuring point, the long face reinforcement develops the largest restraining force, thereby limiting the face extrusion. Since the absolute values of bending moments are relatively small, the limiting effect of the long face reinforcement is predominant. In the case reported here, where the long face reinforcement with GFRP tubes is applied to heavily fractured shale, the overlapping length of tubes (5 m) was determined on the basis of 3D finite difference analysis implemented in advance. The measurement results verify that the overlapping length of 5 m was appropriate.

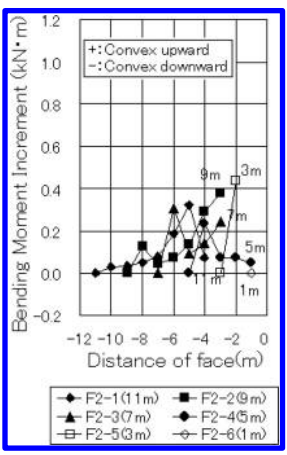


Figure 10. Moment increment against distance from the face.

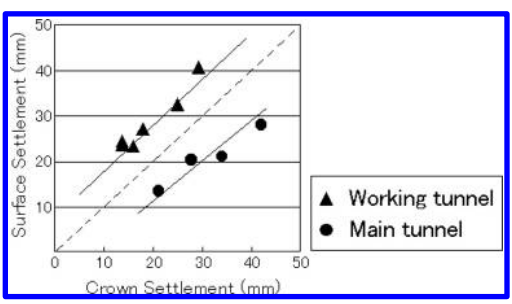


Figure 11. Settlements at main tunnel and working tunnel.

The excavation was done in the order of working tunnel, main tunnel and evacuation tunnel. From the measurements of surface settlement and displacement in ground near the welfare facility on the surface, the displacement ratio ahead of the face is 20 to 50%. It is smaller than 50% measured at the working tunnel executed without any auxiliary stabilizing methods.

Figure 11 shows the relationship between surface settlement and crown settlement of the working and main tunnels. The excavation section of main tunnel (100 to 190 m^2) is 2.5 to 5 times as large as that of the working tunnel (41 m^2). However, the surface settlement is smaller with the larger main tunnel. From the results addressed above, we verify that the long face reinforcement and long steel forepiling effectively worked to limit the impact of excavation of the larger main tunnel.

6 VALIDATION OF THE LONG FACE REINFORCEMENT BY NUMERICAL ANALYSIS

6.1 *Comparison between analytical results and measurements*

Figure 12 illustrates the axial force distributions in the long face reinforcement along with the face advance, analytically obtained and given by measurements, in the Minoh tunnel (CASE 1). The abscissa axis represents the position of each measuring point, and the ordinate axis the axial force distribution. Table 2 lists the properties inputted in the analysis. The input properties of the ground were determined as follows: Using measured convergences and surface settlements, parametrical analysis was implemented by the 2D finite element method (Central Research Institute of Electric Power Industry type non-linear elastic analysis); then, property values similar to the measured data were selected. The grout bond stiffness

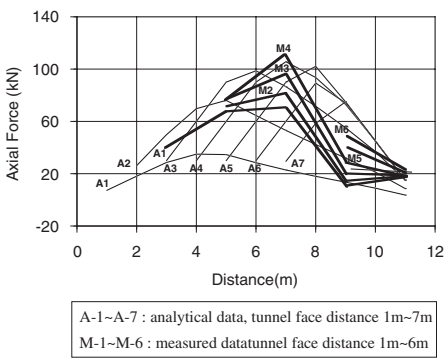


Figure 12. GFRP tube axial force distribution.

Copyright © 2005 Taylor & Francis Group plc, London, UK

Table 2. Input properties (Minoh tunnel).

Density (kN/m^3)	Young's modulus (MPa)	Poisson's ratio	Cohesion (MPa)	Friction angle (ϕ)
Input ground properties				
22	70	0.35	0.0098	30
Structure element	Density (kN/m^3)	Young's modulus (MPa)	Cross-section area (m^2)	Thickness (m)
Input properties of supports				
Shell	24.6	8650	0.3	0.3

	Density (kN/m^3)	Young's modulus (MPa)	Cross-section area (m^2)	Grout spring stiffness (N/m/m)	Grout spring cohesion (N/m/m)
Input properties of forepiles					
Steel Pipe	78	210000	4.0e−3	3.0e7	8.48e7
GFRP Tube	17.5	35000	1.7e−3	3.0e7	8.48e7

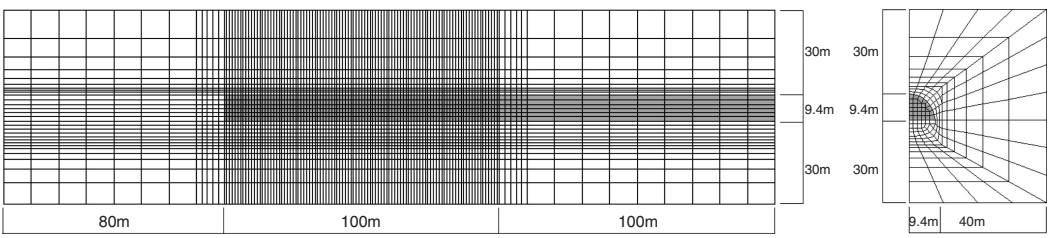


Figure 13. Mesh of analytical model.

of the long face reinforcement was determined from the results of the pull-out tests made during the phase of the development. The element mesh of the FDM analytical model is shown in Figure.13. The position where the peak axial force is produced in the long face reinforcement shifts toward deeper locations, as the face advances. Since the measuring point interval is relatively large, 2 m, it is impossible to clearly evaluate such shift from the measured data. However, both the analytical and measured values present the same tendency in the profile of axial force distribution and peak axial force.

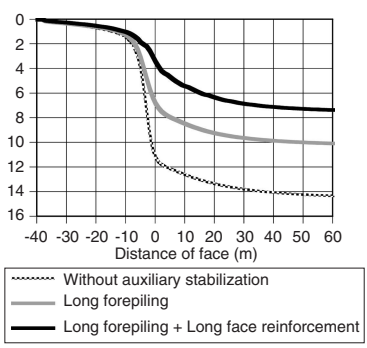


Figure 14. Crown settlement against distance from face.

6.2 *Validation by numerical analysis*

The analytical model is based on the Minoh tunnel (CASE 1). Three cases were analyzed, 1) case without auxiliary stabilization, 2) case with long steel forepiling only, and 3) case with both long steel forepiling and long face reinforcement. Figure.14 shows the crown settlement vs. distance from the face, Figure.15 the surface settlement vs. distance from the face, and Figure.16 the face extrusion. The graphs verify that both auxiliary methods reduce the crown and surface settlements. However, the face extrusion are remarkably reduced in case 3). This verifies that the long face reinforcement effectively works to reduce the deformation.

Copyright © 2005 Taylor & Francis Group plc, London, UK

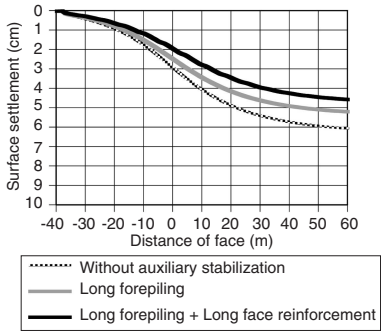


Figure 15. Surface settlement against distance from face.

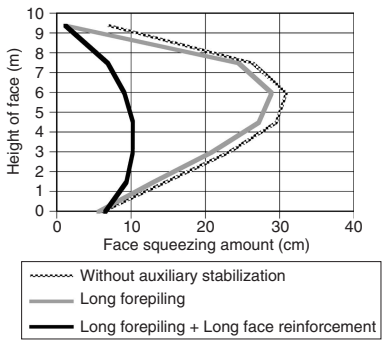


Figure 16. Face extrusion.

7 DISCUSSION ON THE EFFECT OF THE LONG FACE REINFORCEMENT BASED ON MEASURED DATA AND ANALYSIS

The behavior of a tunnel with GFRP tube long face reinforcement was investigated by measurements, and inputting the data thus obtained. The authors verified the effect of the reinforcement by the 3D numerical analysis. This study verifies that the long face reinforcement controls the extrusion of ground ahead of the face, thereby decreasing the loosening zone ahead of the face. From the measured data, we learned that the impact of tunnel excavation is noticeable up to the distance of 4 to 5 m ahead of the face. The axial force in the long face reinforcement takes on a peak value when the face reaches about 3 m from the measuring point. As the face advances, the peak-axial-force position moves toward the deeper side beyond the face. The GFRP tubes deeper than this peak position develop a tensile resistance to effectively restrain face extrusion.

Thus it is necessary to review the function of face bolts 3 to 4 m long. Such short face bolts are satisfactory, if the goal is only to restrain the ground near the face for improving the stability of the face. However, when it is imperative to minimize the impact upon structures existing on the surface and underground, long face reinforcement is essential to prevent loosening ahead of the face and increase in load on the tunnel.

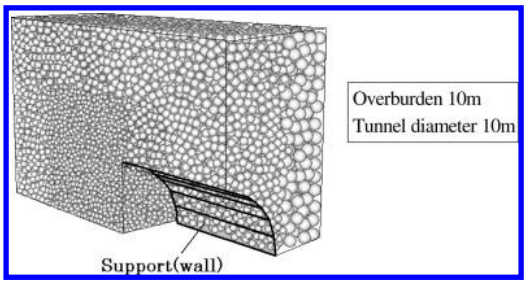


Figure 17. Analytical model.

Table 3. Input properties.

Contact stiffness (MN/m)	50
Bond strength (MN)	0.01
Friction	0.25

Table 4. Input values of mechanical characteristics.

	Long forepiling	Long face bolting
Contact stiffness (MN/m)	18,140	1,814
Parallel bond stiffness (MPa/m)	2,100,000	200,000

8 COMPARATIVE STUDIES ON FACE-STABILIZING METHODS

Available face stabilizing methods include long forepiles driven from the circumference of the tunnel and the long GFRP face bolting method with removable sections placed at the face. This paper compares cases using these two methods. Figure.17 shows an analysis model diagram assuming ground around the face. Table.3 and 4 shows input properties of the ground and of the respective cases of face-stabilization. In place of bolt members used in actual face-stabilizing work, parallel bond (elastic disk-shaped bond) is used to bond particles The bond strength of particles around the subject reinforcement work was assumed to be 1 MN considering the injection effect.

Figure.18 shows the results of analysis. With long forepiling, the tunnel face that is exposed during tunneling is prone to extrusion, leading to collapses. The face bolting restrains the face from extruding, and prevents the ground ahead of the face from collapsing.

Copyright © 2005 Taylor & Francis Group plc, London, UK

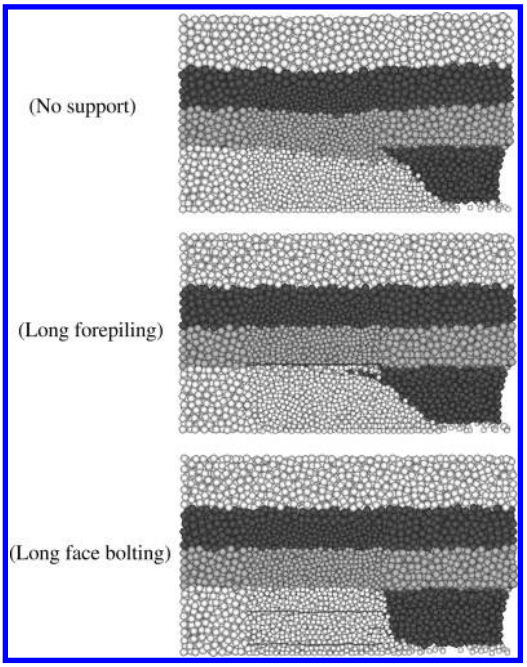


Figure 18. Condition of ground ahead of the tunnel face.

9 CONCLUSIONS

The long face reinforcement is applicable even to adverse ground conditions, easily and surely stabilizing the face. As a result, large section excavation has become possible even in a weak ground. The capability of efficient tunneling by this type of reinforcement has been demonstrated.

The face extrusion and behavior of the ground ahead of the face influenced by excavation have come to receive more attention, as various techniques for the NATM were developed. These behaviors have been quantitatively determined by measurements, offering very helpful data for studying effective measures to prevent impact due to excavation from being exerted around the tunneling site. Prevention of surface settlement is a typical example of such measures.

Utilization of underground space has been recently more actively promoted in urban areas. In this context, higher expectation has been given to the mountain tunneling technique from the viewpoint of its flexibility of application and economic efficiency. The long face reinforcement will satisfy such expectations, though there still remain many points to be improved.

The authors hope this paper would contribute to more rational tunnel design and construction.

REFERENCES

Kouji Isozaki etc, *Study on effect and evaluation of auxiliary methods for mountain tunneling in weak ground.* Proceedings of tunnel engineering. 2001, vol.11, 215–220

Toshirou Shimizu etc, *Behavior of the ground ahead of the face reinforced with long GFRP face forepiling.* Proceedings of tunnel engineering. 2003, vol.13, 225–230

Copyright © 2005 Taylor & Francis Group plc, London, UK

Probabilistic analysis of blasting-induced rock damages in tunneling

I. M. Lee
Department of Civil Engineering, Korea University, Seoul, Korea

B. K. Park
ESCO Consultant, Co., Seoul, Korea

K. H. Cho
Disaster Prevention Research Center, Korea University, Seoul, Korea

C. W. Park
DONG IL Engineering Consultants Co., Ltd, Seoul, Korea

ABSTRACT: Blast-induced rock damage and overbreak in tunneling construction may result in increasing construction costs and declining the stability of tunnel. In this paper, the rock mass behavior induced by tunnel blasting is analyzed by using numerical analysis based on continuum damage mechanics and fuzzy-random probability theory so that the degree of damage in remaining rock and overbreak can be estimated. An equation to estimate the blasting pressure is derived from the application of shock wave theory; statistical analysis is also performed to systematically assess the uncertainty of the proposed pressure equation. A numerical continuum damage model is proposed to assess the rock mass behavior induced by tunnel blasting. The proposed model is coded and linked to a commercial software ABAQUS/Explicit through user subroutine. The result of numerical analysis showed that the degree of overbreak can be reasonably evaluated by adopting the concept of fuzzy-failure probability.

1 INTRODUCTION

When a fully coupled explosive is initiated in the blast hole, the shock wave generated in the blast hole subsequently impacts the blasthole wall and propagates through surrounding rock. The propagation, reflection, and interaction of this shock wave result in crushing, spalling, and fragmentation of the surrounding rock. The energy conversion process of blasting pressure transformed to rock fragmentations, vibrations, and energy losses depends on explosive and rock properties. In order to realistically predict the effect of the blasting pressure on rock fragmentations and vibrations, the blasting pressure has to be modeled accurately and realistically.

One of the earliest efforts to solve the blast problem mathematically was made by Sharpe (1942). Using the theoretical solution proposed by Sharpe (1942), Duvall (1953) developed a general form of the blasting pressure equation which was a function of peak blasting pressure and an appropriate known definite function of time such as an exponential time decay function. Most researchers have used step or exponential functions to model the wave-shape of the blasting pressure. Starfield and Pugliese (1968) introduced a combination of exponential and sinusoidal functions as the pressure function. Farsangi, et al. (1999) analyzed the effect of detonation wave velocity on the blast-induced vibration using the blasting pressure which was a function of peak blasting pressure, detonation wave velocity, and exponential time decay function. Simha (1996) modeled the blasting pressure as a function of peak blasting pressure, rise time, and exponential time decay function to analyze the effect of rise time on the blast-induced vibration. In this study, the concept of rise time is introduced based on shape, velocity, and travel distance of these waves. Parametric analysis was performed to identify the most influential parameter that affects blasting pressure and rise time.

Numerical analysis was performed to figure out the effect of explosive and rock properties on the uncertainty of blast-induced vibration.

Copyright © 2005 Taylor & Francis Group plc, London, UK

2 RISE TIME AND RELATIONSHIP BETWEEN BLASTING PRESSURE AND TIME

2.1 *Relationship between blasting pressure and time*

The relationship between blasting pressure and time in a cylindrical fully coupled charge is generally specified by rise time t_R and corresponding peak magnitude of blasting pressure p_x. This relationship can be expressed by equation (1). The wave-shape, function $f(t)$, is an exponential time decay function. The relationship between blasting pressure and time can be modeled by equation (2). This relationship yields equation (3) by substituting $N = e/t^a{}_R$ into equation (2).

$$p(t) = p_x \cdot f(t) \tag{1}$$

$$p(t) = p_x (N \cdot t^a e^{-t/t_R}) \tag{2}$$

$$p(t) = p_x \cdot \left(\frac{t}{t_R}\right)^a \cdot e^{\frac{t_R - t}{t_R}} \tag{3}$$

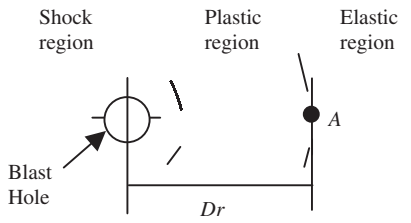
2.2 *Rise time*

The rise time of blasting pressure can be defined by the sum of elastic wave rise time (Δt_e) and plastic wave rise time (Δt_p) as shown in Figure 1 and expressed by equation (4). Since the plastic wave rise time is very short, it can be neglected. The rise time of the blasting pressure in the plastic region located at D_r from blasthole can be expressed by equation (5).

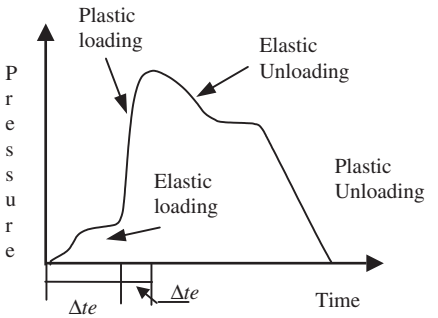
$$t_R = \Delta t_p + \Delta t_e \tag{4}$$

$$t_R = \Delta t_e = \frac{D_r}{C_p} - \frac{D_r}{C_e} = D_r \frac{C_e - C_p}{C_e C_p} \tag{5}$$

The peak magnitude of blasting pressure at the interface between plastic and elastic regions is equal based on continuity at the interface. The interface is located where the peak magnitude of blasting pressure is equal to dynamic yielding stress (σ_{DY}) of rock. Equation (6) shows a mathematical form of blasting pressure attenuation to find the interface location between plastic and elastic regions (Liu, etc, 1993). Distance, D_r (Figure 1 (b)), the location of the interface between plastic and elastic region from blasthole, is described in equation (7) derived from equation (6). The peak blasting pressure on blasthole wall can be obtained using equation (8) proposed by Park (2004). The rise time of blasting pressure is shown in equation



(a) Wave characteristics



(b) Rise time

Figure 1. Wave characteristics and rise time at point A.

(9) and can be obtained by substituting equation (7) and (8) into equation (5). The relationship between blasting pressure and the rise time is shown in equation (10) and can be obtained by substituting equation (9) into equation (3).

$$p_r = p_x \left(\frac{r}{r_0}\right)^n \tag{6}$$

where p_r = peak blasting pressure at radius r; p_x = peak blasting pressure on blasthole wall; r_0 = original blasthole radius; and n = exponential coefficient of peak pressure attenuation.

$$D_r = r_0 \left(\frac{\sigma_{DY}}{p_x}\right)^{\frac{1}{n}} \tag{7}$$

where, σ_{DY} = dynamic yielding stress

$$p_x^4 + f_1 p_x^3 + f_2 p_x^2 + f_3 p_x + f_4 = 0 \tag{8}$$

Copyright © 2005 Taylor & Francis Group plc, London, UK

Table 1. Fixed values of explosive and rock.

	Property	Value
Rock	Radius of charge r_0 (mm)	16.0
	n	1.559
	C_p (m/sec)	1850
	C_e (m/sec)	3700
	σ_{DY} (MPa)	155
	ρ_r (g/cm^3)	2.60
	S	1.63
Explosive	D (m/sec)	4600
	γ	2.61
	ρ_w (g/cm^3)	1.25

Table 2. Uncertainty characteristics of rock and explosive properties.

Probabilistic distribution	$m+\sigma$	m	$m-\sigma$
Elastic wave velocity (m/sec)	4424	3716	3008
Detonation velocity (m/sec)	4640	4602	4567
Rise time (μsec)	103	70	37

where $f_i = f(\rho_r, C, S, \gamma, \rho_w, D)$; $i = 1, 2, 3, 4$; and $p_x = f(\rho_r, C, S, \gamma, \rho_r, \rho_w, D)$.

$$t_R = r_0\left(\frac{\sigma_{DY}}{p_x}\right)^{\frac{1}{n}} \cdot \frac{C_e - C_p}{C_e C_p} = f(\sigma_{DY}, C_e, S, C_p, \rho_r, \rho_w, \gamma, D) \quad (9)$$

$$p(t) = p_x\left(\frac{t}{t_R}\right)^{a} \cdot e^{\frac{t_R - t}{t_R}} = f(t, \sigma_{DY}, C_e, C_p, \rho_r, \rho_w, \gamma, D) \quad (10)$$

2.3 *Parametric analysis for relationship of blasting pressure and time*

Parametric analyses were performed to identify the most influential parameter affecting rise time and the relationship between blasting pressure and time. During the parametric analysis for a chosen parameter, the other parameters were fixed as shown in Table 2. The results of parametric analysis for rise time are shown in Figure 2. Sensitive parameters in rise time were in order of exponential coefficient of peak pressure attenuation, plastic wave velocity, detonation wave velocity, radius of a charge, elastic wave velocity, dynamic yield stress, isentropic exponent, explosive density, rock density, and Hugoniot parameter S. Also, sensitive

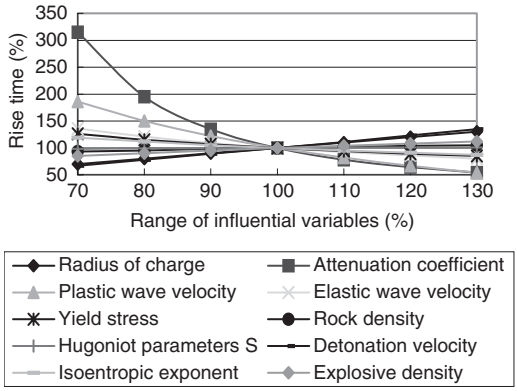


Figure 2. Parametric analysis results for rise time.

parameters on peak blasting pressure were in order of detonation velocity, isentropic exponent, explosive density, rock density, elastic wave velocity, and Hugoniot parameter S. According to the above analysis results, both rise time and peak blasting pressure were affected by detonation wave velocity, isentropic exponent, explosive density, rock density, elastic wave velocity, and Hugoniot parameter.

3 UNCERTAINTY ANALYSIS OF BLAST-INDUCED VIBRATION

3.1 *Uncertainty characteristics*

The most influential factors in the relationship between peak blasting pressure and time were elastic wave velocity and detonation velocity based on the results of explosion test and rock property test (Park, 2004). Therefore, elastic wave velocity and detonation velocity can be regarded as the representative values in rock property and explosive property, respectively. Uncertainty characteristics of blast-induced vibration were evaluated by substituting values in Table 2 into equations (8) and (9), and are summarized in Table 3.

3.2 *Numerical modeling*

Blast-induced vibration analysis was performed by using Finite Element Method (F.E.M) program ABAQUS/Explicit. A numerical modeling was performed using a two-dimensional solid explicit four-node module. The infinite elements were used for boundary conditions to avoid interferences from reflected wave. The numerical modeling is shown in Figure 3. The finite element model was assumed to be homogeneous, isotropic and continuous medium.

Copyright © 2005 Taylor & Francis Group plc, London, UK

Table 3. Uncertainty of peak blasting pressure and rise time.

Probabilistic distribution	$m + \sigma$		m		$m - \sigma$	
	Peak pressure (GPa)	Rise time (μsec)	Peak pressure (GPa)	Rise time (μsec)	Peak pressure (GPa)	Rise time (μsec)
Elastic wave vel.	10.858	64	10.382	70	9.943	76
Detonation vel.	10.566	71	10.382	70	10.286	69

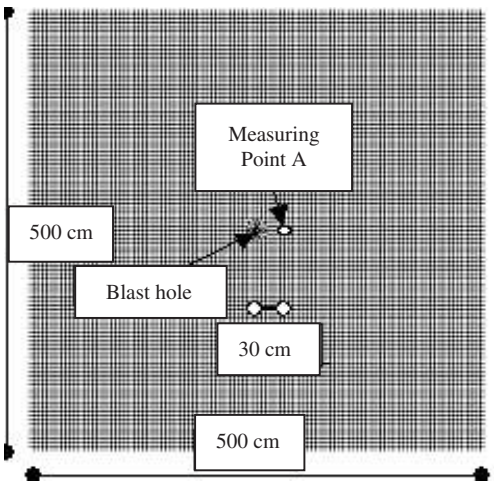


Figure 3. Numerical model.

3.3 *Uncertainty analysis of blast-induced vibration*

The uncertainty analysis results of blast-induced vibration are shown in Figure 4. The uncertainty of blast-induced vibration was influenced by rise time (approximately 20%), elastic wave velocity (approximately 10%), and detonation velocity (approximately 1%). The blast-induced vibration uncertainty was more influenced by rock property than explosive property.

Numerical analysis indicated that the loading rate, the ratio of peak blasting pressure to rise time, was the major influential factor on blast-induced vibrations. Uncertainties in peak blasting pressure, rise time, and loading rate were more influenced by rock property than explosive property.

4 ROCK DAMAGE EVALUATION INDUCED BY BLASTING

Over-breaks cannot be avoided in most of tunneling works, which are caused by misleading drilling hole direction, short distance between drilling holes, initial damage in rock mass. Minimized over-break by optimum blasting procedure can cause reduction of unnecessary rock waste and excessive casting of concrete lining, which saves construction costs in tunneling.

Remained rock around excavation line after blasting is usually damaged by transmitted blasting pressure. A numerical continuum damage model with initial damage and the fuzzy-random probabilistic theory (Wu, et al., 1999) was adopted to assess the rock mass behavior under blasting loads to overcome a fuzziness of the failure criterion. The adopted model was coded and linked a commercial program ABAQUS/Explicit through user's subroutine.

The numerical analysis was focused on rock damages around excavation line. Damages in the rock around excavation line are usually generated by blasting in the contour hole as well as the stopping hole as shown in Figure 5. Therefore, the numerical modeling was performed for the part of excavation area as shown in Figure 5. Infinite element was used for the boundaries in the model to eliminate interruptions from reflected wave from boundaries.

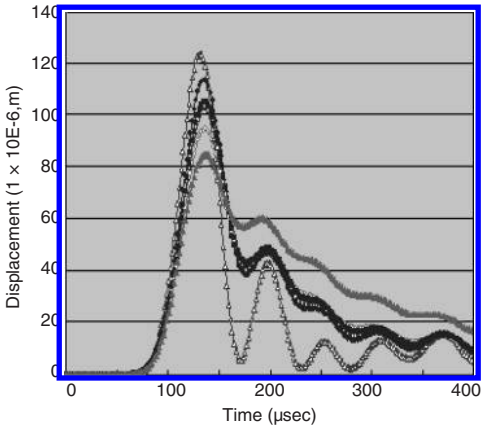
4.1 *Rock damage from stopping and contour hole blasting*

Rock damage analyses were performed for three cases of blasting patterns: blasting only in stopping holes; blasting only in contour holes; and blasting in both holes.

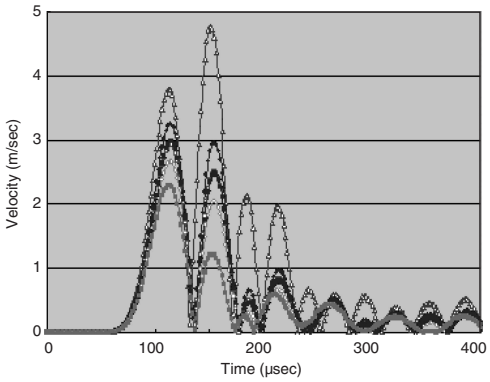
The analysis results from each case are shown in Figure 6. As shown in Figure 6, scarce rock damage was generated under blasting only in contour holes, which may be caused by low blasting pressure under decoupled charge condition. This analysis result can be verified by comparing with observed data in the field.

Rock damage zone from blasting pressure applied only stopping hole case and applied both of holes case are almost identical as shown in Figure 6, which indicates that rock damages can be minimized by matching damage zone occurred from each hole's blasting as shown in Figure 7.

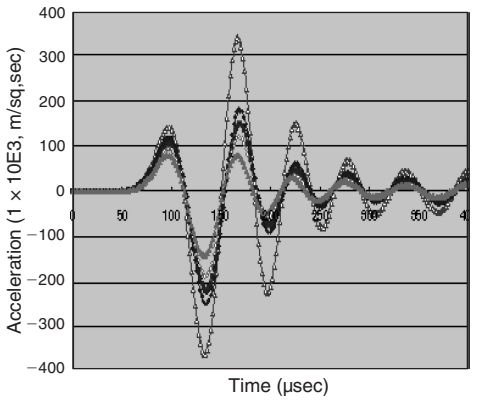
Copyright © 2005 Taylor & Francis Group plc, London, UK



(a) Particle displacement from numerical analysis

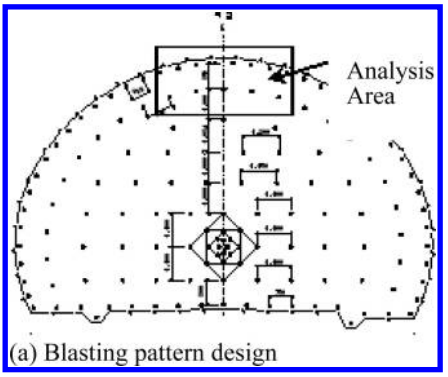


(b) Particle velocity from numerical analysis



(c) Particle acceleration from numerical analysis

Figure 4. Results of numerical analysis.



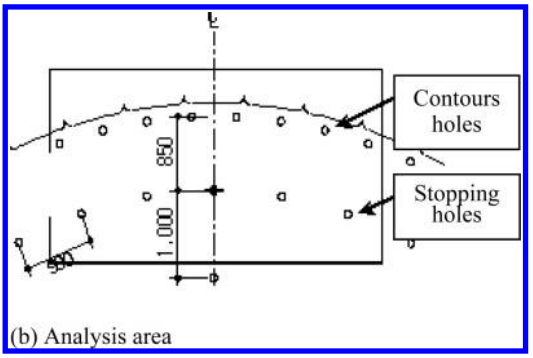


Figure 5. Analysis area for numerical analysis.

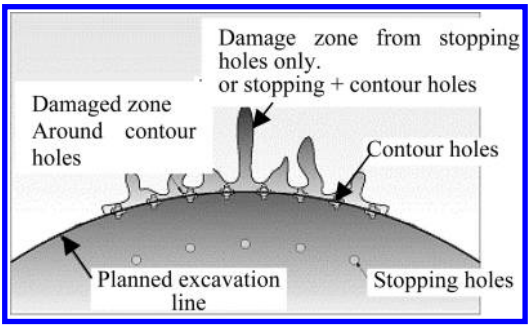


Figure 6. Rock damage zone under stopping and contour hole blasting.

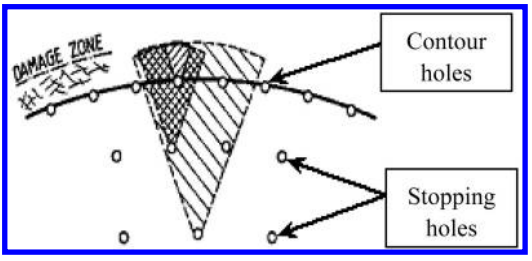


Figure 7. Optimized blasting design.

Copyright © 2005 Taylor & Francis Group plc, London, UK

5 CONCLUSIONS

Based on this study, conclusions are summarized as follows:

1. The concept of rise time is proposed by analyzing shape, velocity, and travel distance of these waves. Rise time is expressed as a function of explosive density, isentropic exponent, detonation wave velocity, exponential coefficient of the peak pressure attenuation, dynamic yield stress, plastic wave velocity, elastic wave velocity, rock density, and Hugoniot parameter. Parametric analysis was performed to identify the most influential parameter that affects rise time. It was found that the rock properties were the most sensitive parameters.
2. Uncertainty analysis of blast-induced vibration was performed to find the most sensitive parameter among rock and explosive properties. The blast-induced vibration uncertainty was more influenced by elastic wave velocity than detonation wave velocity. Vibration effects of elastic wave velocity and detonation velocity were approximately 10% and 1%, respectively.
3. Numerical analysis showed that the loading rate, the ratio of peak blasting pressure to rise time, was the major influential factor in blast-induced vibration. The uncertainties in the peak blasting pressure and the rise time were more influenced by rock property than explosive property. Therefore, the loading rate uncertainty was more influenced by rock property than explosive property.
4. Rock damage zone from blasting pressure applied only on stopping hole case and applied on both of holes case were almost identical. Therefore, rock damages can be minimized by matching damage zone occurred from each hole's blasting in design.

REFERENCES

Duvall, W. I. 1953. Strain-Wave Shapes in Rock near Explosions, *Geophysics*, vol. 18. 310–326.

Farsangi, M. A. E., Durucan, S. and Kunimatsu, S. 1999. The Effects of Velocity of Detonation of Explosives on Ground Vibration in Time and Frequency Domains. *Proceedings of The Sixth International Symposium on Rock Fragmentation by Blasting*, 203–206. Johannesburg. South Africa.

Liu, Q. and Katsabanis, P. D. 1993. A Theoretical Approach to the Stress Waves around a Borehole and Their Effect on Rock Crushing. *Proceedings of The Fourth International Symposium on Rock Fragmentation by Blasting*, 9–16. Vienna, Austria.

Park, B. K. 2004, *Probabilistic Assessment of Blast-induced Rock Pressure And Damage in Tunneling*. Ph.D. Dissertation. Korea University. Seoul. Korea.

Sharpe, J. A. 1942. The Production of Elastic Waves by Explosion Pressures I. Theory and Empirical Field Observations, *Geophysics* vol 7. 144–154.

Simha, K. R. Y. 1996. Effect of Open Joint on Stress Wave Propagation. *Proceedings of The Fifth International Symposium on Rock Fragmentation by Blasting.* 81–86. Montreal. Canada.

Starfield, A. M. and Pugliese, J. M. 1968. Compression Waves Generated in Rock by Cylindrical Explosive Charges, A Comparison between a Computer Model and Field Measurement. *International Journal of Rock Mechanics and Mining Science & Geomechanics Abstracts*, Vol. 5. 65–77.

Wu, C., Hao, H. and Zhau, Y. 1999. Fuzzy-Random Probability Analysis of Rock Mass Responses to Explosive Loads. *Computers and Geomechnics* 25. 205–225.

Copyright © 2005 Taylor & Francis Group plc, London, UK

Re-analysis of Şanlıurfa tunnels by finite element method

H. Tosun
Osmangazi University, Eskişehir, Turkey

ABSTRACT: Numerical solutions are widely utilized as a design tool to analyze stresses and deformations around an underground structure. One of them is finite element method (FEM) that can be used to provide analysis in which the rock is modeled with appropriate boundary conditions and support system. Beside design analysis of an underground structure, it can provide rational solutions to the problems which can develop in evaluating existing structures, post failure analysis, monitoring and control of construction, in location of instrumentation and in the analysis of laboratory test specimens. It also considers the influence of sequential excavation and construction procedure that can be best represented by three-dimensional models. This paper introduces the results of FEM analyses performed for Şanlıurfa Tunnels, which is the longest water conveyance tunnels of the world. All analyses were performed under external loading conditions.

1 INTRODUCTION

The Şanlıurfa tunnel is one of the most important aspects of the Southeastern Anatolian Project. The tunnel is located between Şanlıurfa city and the Atatürk dam. It is designed to convey water from the reservoir of the Atatürk dam to the Harran plain and also to generate electricity at its outlet. It is a pressurized tunnel with an internal water pressure of approximately 400 kPa. The system is consisted of two concrete-lined (double tube) tunnels each 26.4 km long and 7.62 m in diameter. Their excavated diameter is approximately 9.0 m. The tunnels will convey 328 cu.meter per second of water at an average flow rate of 3.5 m/s that will be utilized for the irrigation of 4.6×10^5 hectares of land in the Şanlıurfa and Mardin Plains, when fully used in operation stage. Their excavation and installation of support system were entirely completed in 2003, but their contact grouting is still under construction now. One of them is used with free flow.

The temporary support system is consisted of shotcrete and rock bolts. Shotcrete is applied in double layers (15 cm thick) with wire mesh combined with rock bolts of 3 m long and 2×2 m spacing. Cast-in-place concrete lining of varying thickness (minimum 40 cm) provides the permanent support of the tunnels (Fig. 1). Excavation was performed in three steps by tunnel boring machines (TBM) and locally by blasting. The rate of advance of the TBM was 6 m per day (Tosun, 2001 and 2002).

The permanent support system of tunnel includes concrete lining with various thickness. Tosun (1985) investigated the performance of concrete lining by four different 2-D models of finite element method. At the study, one-step construction sequence was assumed for all models and the gravity load was applied after excavation of the tunnel and installation of the supports, as external loading condition described by Einstein vd. (1980). The major difference between the models was only at the loading conditions.

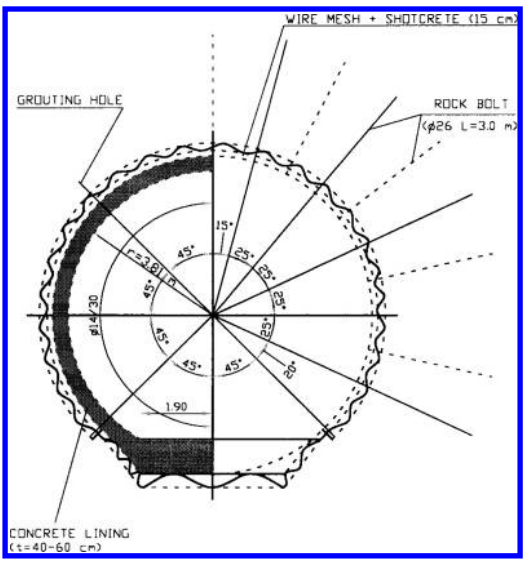


Figure 1. Support system used in the Şanlıurfa Tunnels.

Copyright © 2005 Taylor & Francis Group plc, London, UK

The weight of loosened zone was considered as an external load on the structure. Influence of minor geological features is eliminated to simulate a construction media. Finite element analysis was performed for the right-hand upper quarter section of tunnel with 762 cm internal diameter. The selection of the model geometry and the stress pattern was based on the in situ stress and deformation measurements (Tosun, 1991).

The tunnels were entirely completed now, but are not under operational stages because of being some deficiencies in the construction of irrigation facilities in downstream of the tunnels. At this study, the tunnels are reanalyzed by FEM models with considering actual data and results are compared with those obtained from observation and measurements during excavation of rock masses and installation of temporary support system.

2 GEOLOGY AND GEOTECHNICS

Detail geological surveys along the alignment of Şanlıurfa tunnel was performed by State Hydraulic Works (DSI, 1977). Approximately 85 percent of its total length excavated within the marl formation. Along the tunnel alignment, the bedrock possesses rather uniform and/or relatively homogeneous lithological characteristics. Thus, a special emphasis was given to the types and characteristics of the discontinuities encountered within the bedrock.

Numerous faults and shear zones intersect the tunnel alignment. The faults generally dip 40 to 90 degrees and their displacement range between 6 to 80 cm for the 1200 section considered in the study of Tosun (1992). The width of the fault or shear zones is rather narrow and infrequent intersect the tunnel at low angles. The joint surveys conducted between stations 11+200 and 15+000 indicate that the dominant set strikes Northeast and dips at angles greater than 40 degrees. Generally one or two major sets plus random are encountered within the bedrock. Spacing of the joints is highly variable. Their apertures are narrow to tight with smooth, planer, and rarely polished and/or slickensided surfaces. Infilling materials are generally calcite and clay. Iron oxide staining of joint surfaces is rather common.

Various laboratory and in-situ tests were conducted to determine the mechanical behavior of the bedrock. The plate loading tests conducted within the adits GT2 and YT1 have yielded the modulus of deformation values ranging between 570 MPa and 1825 MPa within the pressure range of 0 to 3.5 MPa, respectively. On the samples obtained from borehole 21, the average values of the poisson's ratio, the secant modulus of elasticity, and the uniaxial compressive strength were determined as 0.16, 1500 MPa, and 8.5 MPa, respectively.

In the tunnel, three stations were selected to determine the mechanical properties of rocks and two stations to monitor the convergence behavior of the tunnel. At station 25+500, the plate loading test has yielded an average deformation modulus of 6315 MPa within the pressure range of 0 to 3.5 MPa, whereas by Rocha dilatometer an average value of 1500 MPa was determined within the pressure range of 0 to 5.0 MPa. At station 24+500, three deformation moduli tests were conducted. The pressumeter, Goodman jack and plate loading tests have yielded average deformation values of 1312, 1186 and 3958 MPa, respectively.

At station 13+700 plate loading and laboratory rock mechanics tests were conducted. The modulus of deformation ranges between 2520 MPa and 11100 MPa, averaging 6255 MPa within the pressure range of 0 to 3.5 MPa. The compressive strength, dry density and Poisson's ratio averages 24.0 MPa, 2.01 Mg/m^3 and 0.20, respectively. The triaxial test results yielded cohesion values within the range of 0.4 to 1.0 MPa and the angle of internal friction value of 25 degrees.

The field measurements and instrumentation have been performed in the tunnel. The mechanical properties of the rock mass were determined in station 13+700. The rod and wire type extansometers were used to monitor the movement of the rock mass at station 25+550. Single point rod extansometers to measure the vertical movement of rock mass were installed at 2, 4 and 6 m away from the crown and to monitor the convergence of tunnel and deflection of the completed support system at three different direction. As a result of this measurements, the extreme deformation was obtained as 2.9 cm in the crown of tunnel, as a function of time and partial advance of the tunnel (Tosun, 1985).

3 FEM ANALYSES

Four different 2-D models were used to provide the Finite Element Analysis of Şanlıurfa Tunnel. The models assume different step of construction sequence. The gravity load is applied after excavation of the tunnel and placement of the supports, as external loading conditions (Desai, 1972; Kulhawy, 1974 and Schwartz, 1979). The weight of zone is considered as an external load on the structure (Kripakov, 1974 and Smith, 1982). Influence of minor geological features is eliminated to simulate a continuous media. In all models, upper boundary was free to displace vertically and horizontally. The left-hand and lower boundaries were rollered. The vertical boundary was restrained laterally, but was free to move vertically. Lower boundary was restrained from moving vertically, yet allowed to displace horizontally.

All models considered in this study have different loading and excavation sequences. Their limitations and loading conditions are summarized in Table 1.

Copyright © 2005 Taylor & Francis Group plc, London, UK

Table 1. The FEM models used for the analyses.

Model	Geometry	Number of stage	Stages
URFA1	One tunnel-semi section	2	Excavation + installation of shotcrete
URFA2	One tunnel-semi section	2	Excavation + installation of shotcrete and rock bolts
URFA3	One tunnel-semi section	3	Excavation + installation of shotcrete and rock bolts + excavation of invert section
URFA4	Two tunnel-full section	4	Excavation of Tunnel T1 + installation of temporaray support for tunnel T1 + excavation of Tunnel T2 + installation of temporary support for tunnel T2

Urfa1 considers two-steps construction. Urfa2 has similar geometrical and excavation conditions with exception of temporary supports and also describes two separate stages. Excavation of rock mass and installation of temporary supports are considered as first and second stages, respectively. For the first model only shotcrete is considered as temporary support, while shotcrete and systematic rock bolts are used for Urfa2. Urfa3 has same loading and excavation sequences with Urfa2, but it also includes the excavation of invert section as third stage. First three models have same geometric configuration and material properties.

URFA4 is modelled to investigate stress and deformation distribution when considered double tube tunnels described as actual case. Therefore, full section of tunnels is taken into account in the model. For each tunnel, two stages are defined to obtain exact solutions. First stage is excavation of rock masses excluding the invert section and second stage is installation of temporary support including only shotcrete.

All models represent the external rock stress consisting of vertical and horizontal components. In the models, external rock stress is entirely resisted by the temporary supports such as shotcrete and rock bolts. The models were restrained by the shotcrete lining (15 cm in thick) from inside of the tunnel. This lining was represented by members, which are lying through the center of structure. The rock bolts are represented by the node-to-node elements with 3 m of length and 2×2 m of spacing. Each rock bolt for a section is pre-stressed with a value of 100 kN/m.

As discussed in the pervious section, the excavated material has a wide range in elastic constants. For this

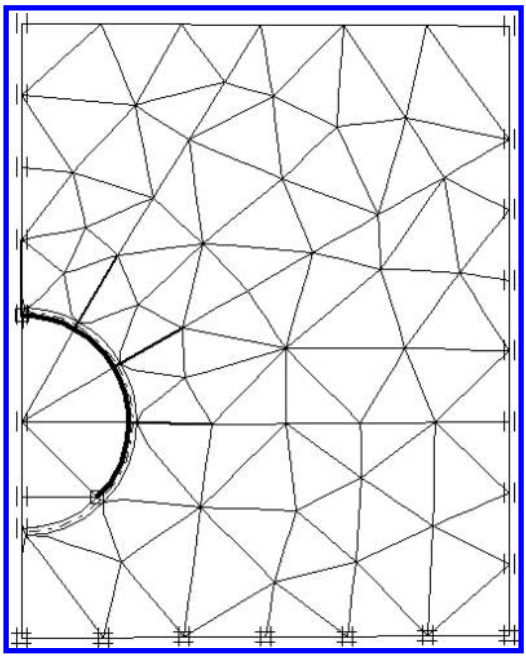


Figure 2. One of the finite element model for Şanlıurfa tunnels (Urfa3).

study worst ground condition was taken into account. Therefore, the minimum values of modulus of elasticity and poisson ratio were selected as 5×10^5 kN/m^2 and 0.2, respectively for all analyses. The shear strength parameters were considered as based on the Geomechanical Classification and laboratory tests ($c = 400$ kN/m^2 and $\Ø = 25°$). It is assumed that the excavated material is fully impermeable. All calculations are performed for drained conditions.

First three models were used to provide the finite element analysis which will be compared with other methods subjected to the arching theory and the principles belonging to the rock-support interaction. They represents the external rock stress consisting of vertical and horizontal components. Lateral rock stress is determined by the plane strain relationship. For the poisson's ratio of 0.20, the lateral stress coefficient is calculated as 0.25. The last model is used to analyse the influence of second tunnel to other one during excavation. Figure 2 gives the finite element model with three different materials for Urfa3.

All models were restrained by the shotcrete lining from inside of tunnel. This lining was represented by members which are lying through the center of structure. Urfa2 also includes systematic rock bolts, while Urfa1 has only the lining as temporary supports. The Urfa3 also has excavation of invert section as addition to the second model. Thrust and bending moment

Copyright © 2005 Taylor & Francis Group plc, London, UK

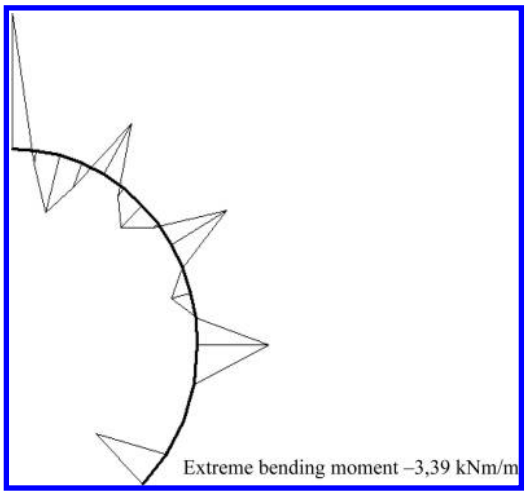


Figure 3. The distribition of bending moment for Urfa3.

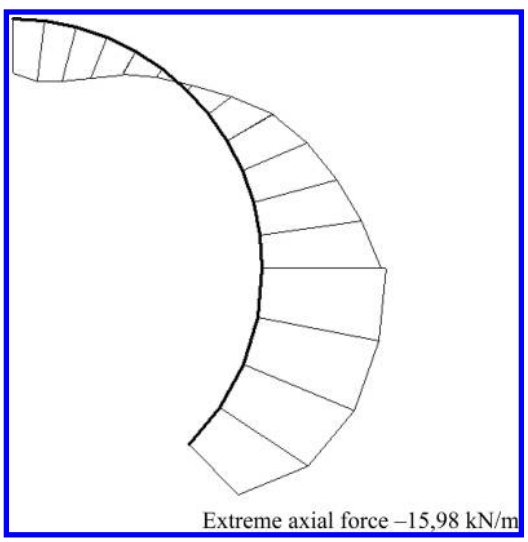


Figure 4. The distribition of thrust for Urfa3.

values acting on each member were illustrated in figures 3 and 4 for the model of Urfa3. The maximum values of bending moment were determined as 2.07 and −3.39 kNm/m for the models of Urfa1 and Urfa3. The distibution of bending moment is not simple for Urfa3, while Urfa1 reflects just the behaviour of a ring element. The maximum thrust values for each section and their distribution are significiantly different when compared two models. As a result of this study, Urfa3 provides more safe conditions for the tunnels.

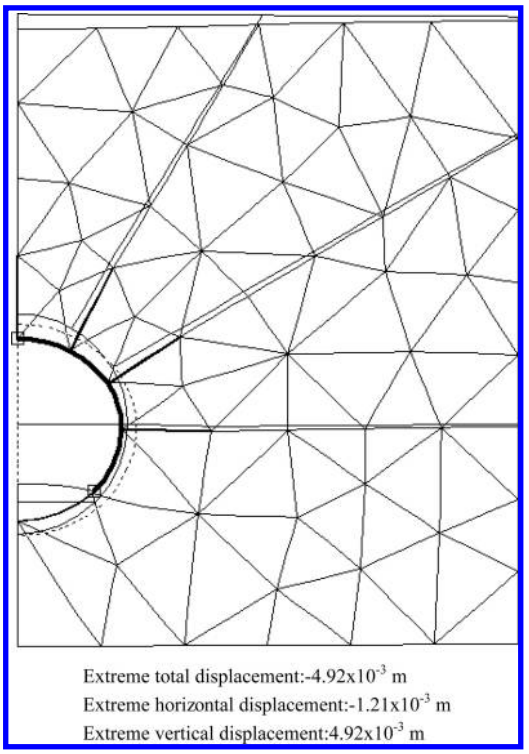


Figure 5. The deformed mesh and extreme displacement values for Urfa3.

As a result of the analyses, the deformed mesh was obtained and total displacement, horizontal displacemet and vertical displacemet were calculated for each elements. The maximum value for total displacemet was obtained in the model Urfa3. But the extreme values for horizontal and vertical displacements were very close to each other for the first three models. The deformed mesh and maximum values of displacements for Urfa3 are given in figure 5. The calculated values of displacement by FEM models are significiantly different than those of the measured ones.

Urfa4 is used to examine the influence of construction sequence on the original stress distrubiton, when two double tube is considered. As a result of analysis, it was obtained that there is no main difference on the stresses acting on the ortogonal directions for each tunnels (Fig. 6). In other words, the excavation of rock of tunnel2 has no influence on the stability of Tunnel1.

4 CONCLUSIONS

In this study, different models were considered to investigate the stability of Şanlıurfa Tunnels under

Copyright © 2005 Taylor & Francis Group plc, London, UK

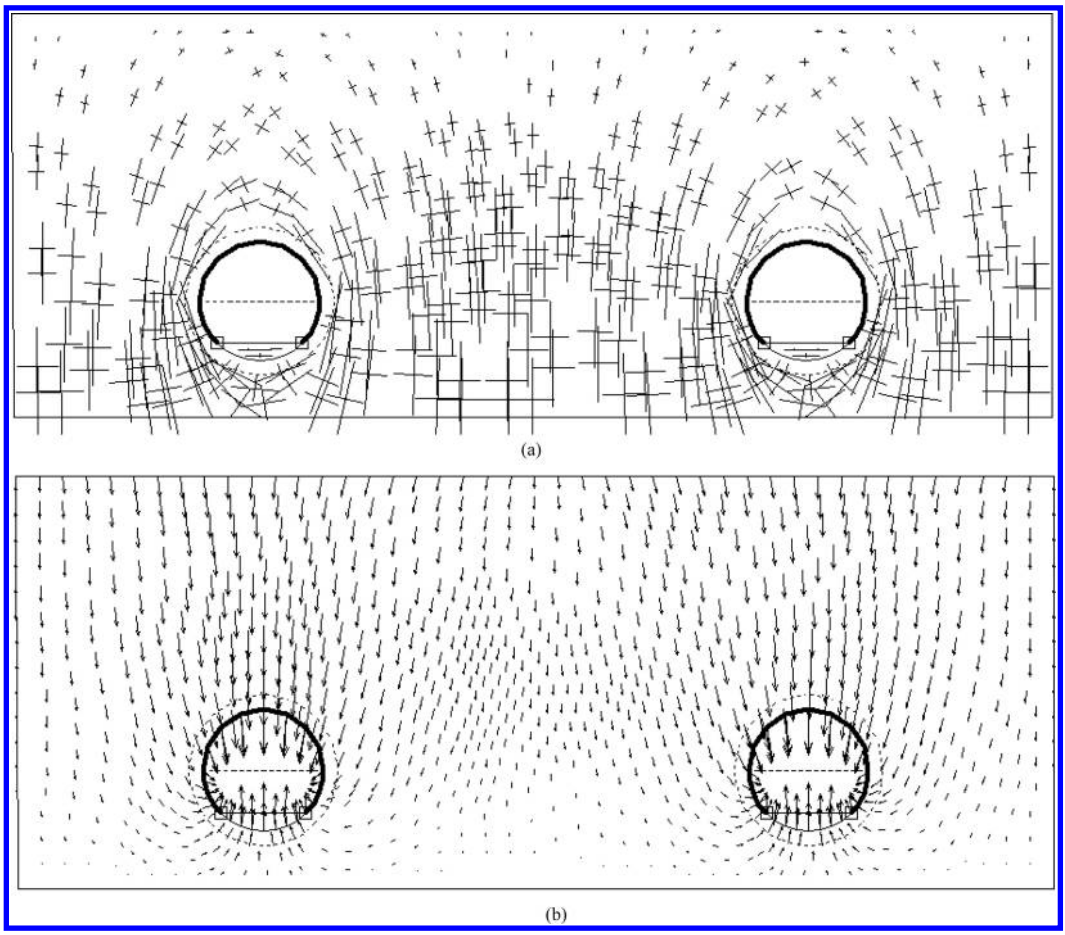


Figure 6. The finite element model for double tube system for Urfa4: (a) effective stresses, (b) vertical displacements.

external loading conditions. In other words, the behaviour of temporary supports consisting of shotcrete and rock bolts, as different combinations, was investigated under only rock loads. From this study, following conclusions have been derived:

i. The finite element analysis can effectively be used to determine the influence of construction procedure on the support loads.
ii. The calculated displacements obtained from the FEM models are less than those of the measured ones.
iii. For the weak ground conditions, the temporary support system composed of shotcrete and systematic rock bolts are safe to provide the stability of the tunnel.
iv. The stability of the first excavated tunnel is not influenced by other tunnel to be excavated later.
v. This study doesnot include the influence of internal water pressure for all models. Internal loading condition is most critical for the stability of tunnels. Therefore, new models should bu considered to investigate the stresses and displacements of permenant concrete lining under internal water pressure. The performance of grouting will influence the stability of tunnel for the cases under internal water pressure.

REFERENCES

Desai, C.S. 1972. Theory and application of the finite element method in geotechnical engineering. *Symposium on the application of the finite element method in geotechnical engineering:* 3–8. Vicksburg. Missisippi.

DSİ, 1977, Asağı Fırat projesi Urfa tüneli ilave jeoloji çaliş maları: DSİ Genel Müdürlüğü, 10 sayfa (kurum içi rapor.

Enstein, H.H., Schwartz, C.W., Stenier, W., Baligh, M.M and Levitt, R.E. 1980. *Improvement design for tunnel supports-Analysis method and ground structure behaviour:* U.S.

Copyright © 2005 Taylor & Francis Group plc, London, UK

Department of Transportation, Report no: DPB-50/79/10.
Kripakov, F.H. 1974. Finite element method of design. US Bureau of Mines, Denver, Colorado,17p.
Kulhawy, F.H. 1974. Finite element modeling criteria for underground opening in rocks. *Int. J. Rock Mech. and Geomech. Abs.* December, V.11, N.12, 445-472.
Schwartz, C.W. 1979. Numerical analysis of underground structures. *Computing in civil engineering*, 217–229.
Smith, I.M.1982. *Programing the finite element method with application to geomechanics*. John Wiley and Sons, Chichester, 345p.
Tosun, H. 1985. *Comparison of the tunnel design methods and their application to Urfa Aqueduct Tunnel.* M.S. Thesis in the Middle East Technical University, Ankara, 141p.
Tosun, H. 1991. Tünel tasariminda sonlu eleman metodunun kullanımı. *Su mühendisliginde bilgisayar uygulamalari semineri bildiriler kitabı,* Şanlıurfa, 7–11 Ekim, 1–28.
Tosun, H. 1992. Comparison on design methods of temporary supports using Şanlıurfa tunnels. *Proceeding of the 2nd Int. Conference on Hydropower*, Lillehammer, Norway, 201–208.
Tosun, H. 2001. Basınçlı tünel ve şaftların tasarım esasları dünyada ve ülkemizdeki bazı uygulamalar. *Yapı Dünyası,* Ekim, S.67, 23–28.
Tosun, H. 2002. Geotechnical experience obtained from the pressurized tunnel and shaft structures in Turkey. *Int. Conference on Tunnelling and Underground Space Use* Istanbul. Turkey 145–155.

Copyright © 2005 Taylor & Francis Group plc, London, UK

Tunnel convergence analyses in heterogeneous/anisotropic rock masses

C.Y. Kim, K.Y. Kim, S.H. Baek, S.W. Hong & G.J. Bae
Geotechnical Eng. Research Dept., Korea Institute of Construction Technology, Korea

S.H. Lee
Civil Eng. Dept., Sangji University, Korea

W. Schubert, K. Grossauer & Y.Z. Lee
Institute for Rock Mechanics and Tunneling, Graz University of Technology, Austria

ABSTRACT: It is very difficult task to excavate a tunnel in poor and heterogeneous ground. Although with a good geological investigation, uncertainties due to the local rock mass structures will still remain. Especially for such conditions, a reliable prediction of the conditions ahead and outside the tunnel profile are of paramount importance for the choice of appropriate excavation and support methods. In this paper, we present the effects of the heterogeneity/anisotropy of the weakness zone on tunnel convergence. Three dimensional Finite Element simulations of different weakness zone properties, thickness, and orientation relative to the tunnel axis were carried out and the function parameters evaluated from the results. The results are compared to monitoring results from Alpine tunnels in heterogeneous/anisotropic rock. The good qualitative correlation between trends observed on site and numerical results gives hope that by a routine determination of the function parameters during excavation the prediction of rock mass conditions ahead of the tunnel face can be improved.

1 INTRODUCTION

Displacements around tunnel are strongly influenced by small or large scale weakness zone such as heavily jointed and faulted zone, sometimes shear zones etc. Several case histories on large deformations and collapses due to these kinds of weakness zone show the importance of heterogeneity/anisotropy of the embedded weakness zones. If we can predict all these kinds of influencing factors during tunnel excavation, we can more be safe from the excavation induced hazards.

Henceforth, during the tunnel excavation a reliable monitoring and feed-back is very important for the determination of the proper support type and quantity, and for controlling the tunnel stability. Geodetic measurements of absolute displacement allow us to understand what happened ahead and outside of tunnel face in 3-dimensional monitoring space. These methods to a large extent have replaced relative displacement measurements in many countries, but still be used the conventional tape extensometers for measuring tunnel convergence in Korea. Comparing with the relative displacement measurement, the absolute monitoring results give us very useful information about the ahead or outside of tunnel face and several things etc. The evaluation of data gained from the excavation of tunnels constructed in Austria showed, that the ratio between radial and longitudinal displacement varied in a wide range. Matching the observed phenomena with the geological documentation, it was found that deviations of the ratio appeared when zones of different deformability were approached with the excavation (Schubert 1993). To verify the hypothesis, numerical 3-D simulations have been performed. The results showed that changing rock mass conditions ahead of the tunnel face clearly influence the displacement vector orientation (Schubert & Budil 1995, Steindorfer & Schubert 1997, Steindorfer 1998). To quantify the influence of weak zones on stresses and displacements, further research has been conducted (Grossauer 2001). Sellner (2000) developed software, which allows the short-term displacement prediction, namely GeoFit. Particularly, Kim (2003) suggest the relationship between convergence function parameter X, C and the rock mass quality of the ahead of tunnel face through several 3-D FE analyses, and verified by several Alpine tunnel case histories.

The function parameter X, C, T, m and the displacement vector orientations show some relationship between the modulus contrasts and the thickness of the weakness zones (Kim 2003). So, this paper suggests several qualitative clues for the effects of the

Copyright © 2005 Taylor & Francis Group plc, London, UK

heterogeneous/anisotropic nature of rock masses on the tunnel convergence results and the possibility of the prediction of the rock mass quality ahead of tunnel face during tunnel excavation using 3-D FE simulations.

2 INFLUENCE OF WEAKNESS ZONES

2.1 *Stresses*

A weakness zone has a significant influence on the stresses and displacements during tunnel excavation. In the case of normal, namely without weakness zone (Fig. 1(a)), at all measuring points, similar stress concentrations are detected, but, in the case of the excavation through the weakness zone, near and around weakness zone, severely high or low stress concentrations are shown. In the weakness zone (Ch. 50, 52.5), very low stress concentrations are observed, on the other hand, near the weakness zone such as Ch. 45, 55, more higher stress concentrations are detected in Figure 1.

When the excavation approaches a weakness zone, stresses increase in the stiffer material. On the other hand, due to an arching effect in the weakness zone, stresses close to the stiffer boundaries decrease within the weakness zone. Figure 2 shows the stress and displacement changes in the vicinity of a weakness zone for different modulus contrasts. Variations of the embedded weakness zone widths and lead to similar results (Grossauer 2001).

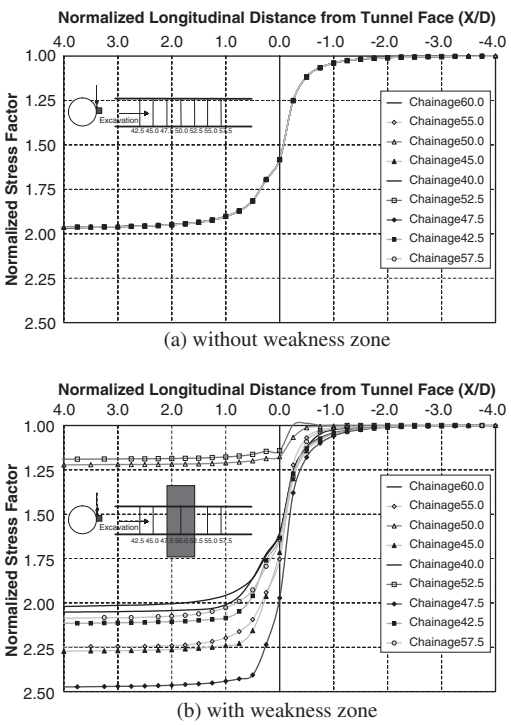


Figure 1. Stress concentrations of two cases; (a) without weakness zone, (b) with weakness zone (MC = 10, T_w = 0.5D). MC; modulus contrasts, T_w; thickness of weakness zone, D; tunnel diameter.

2.2 *Displacements*

The changed spatial stress situation around a tunnel in the vicinity of a fault zone strongly influences the

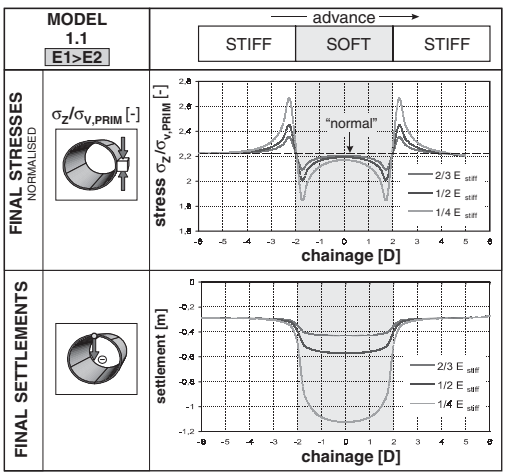


Figure 2. Stress distribution and final displacements when tunneling through a weakness zone (different modulus contrasts). Stresses are normalized to the primary stresses.

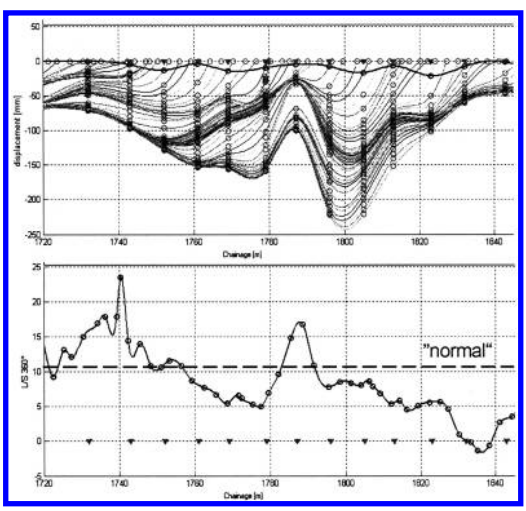


Figure 3. Settlement and displacement vector orientation trend for a side wall point at the tunnel Spital, Austria.

Copyright © 2005 Taylor & Francis Group plc, London, UK

deformations of the rock mass. It could be shown, that the displacement vector orientation shows significant changes much earlier than radial displacements.

Figure 3 shows settlements and the trend of the displacement vector orientation for a tunnel in a tectonic melange in Austria. Pronounced changes in the displacement vector orientation can be observed well before the excavation actually reaches the stronger or weaker rock masses.

3 NUMERICAL SIMULATIONS

3.1 *Finite element mesh*

In these numerical simulations, we mainly focus on the influence of the heterogeneity/anisotropy of the weakness zone due to tunnel excavation. Specially, the influences on the thickness, modulus contrasts and the orientations of the weakness zone are investigated. So, the support effects are neglected and purely excavation effects are analyzed in these parametric studies. The full face circular tunnel excavation is simulated by 2.5 m in each round length. The tunnel diameter is 10 m, and the maximum overburden is about 50 m. Total 30 excavation steps are considered. In order to simplify the numerical model, pure elastic and gravity controlled models are investigated with non-linear elasto-plastic 3 dimensional FE code UTAH III.

Figure 4 shows the 3-D FE model which consisted of 10260 elements and 10912 nodal points.

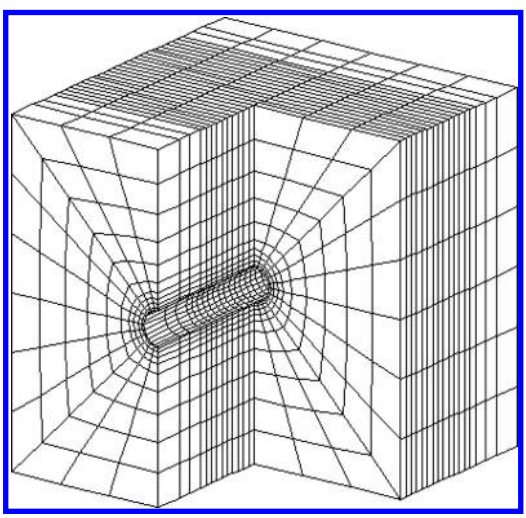


Figure 4. 3-D finite element model for the parametric study.

3.2 *Weakness zone embedded model*

The FE code UTAH III has several pre-processors such as VOL4, PM etc. VOL4 program is the one of these pre-processors. VOL4 program can detect the arbitrary oriented joints or fault planes which can pass through the 3 dimensional space elements as shown in Figure 5. PM program also can calculate the overall modulus of the matrix which is consisted of the weakness plane and the intact rock masses.

3.3 *Anisotropic model*

Simplified transversely isotropic models are investigated on the convergence function parameter X, C. Figure 6 shows 4 models. One isotropic model (Fig. 6(a)) and three transverse isotropic models (Fig. 6(b), (c), (d)) are considered. Rock masses properties are shown as Table 1. The Volume fraction means the ratio between total volume of weakness zone and intact rock. In this research, we assumed approximately 20% of the volume fraction. The modulus of the intact rock is ten times higher than the weakness zone.

Table 2 shows the function parameter X, C value on 4 models. In isotropic case, the X value is about 5.40 and the C value is approximately −6.70 mm, but, the case of the transverse isotropic plane perpendicular to x-axis shows the highest value of X among these models. On the other hand, the case of the transverse isotropic plane perpendicular to z-axis shows the lowest value of X. In the case of C value, the isotropic case shows the lowest value, but, the case of the transverse isotropic plane perpendicular to y-axis indicates the highest value. Figure 7 indicates the normalized displacement history. The displacements are normalized by maximum settlements. The displacement history

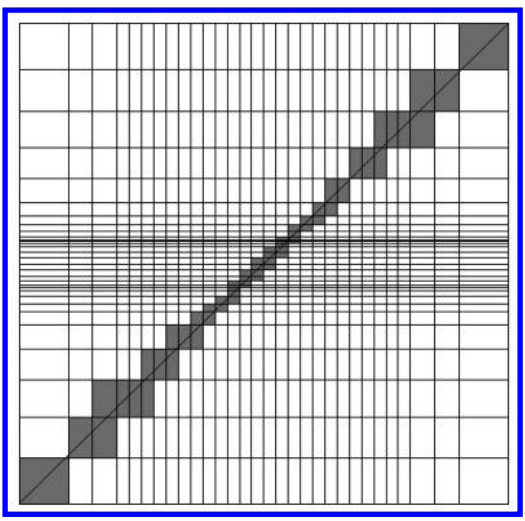


Figure 5. Weakness zone embedded model.

Copyright © 2005 Taylor & Francis Group plc, London, UK

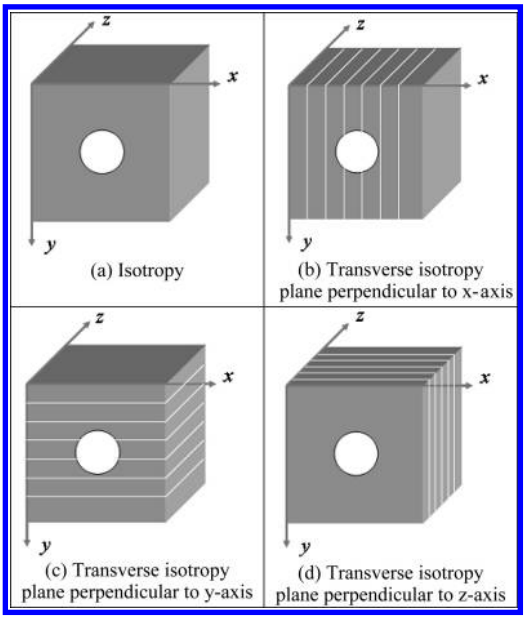


Figure 6. 3-D anisotropic model for RVE (Representative Volume Element).

Table 1. Rock masses properties for numerical analyses.

	Intact rock mass (MPa)	Weak/ fractured zone (MPa)	Volume fraction (V_{weak}/V_{intact})
Young's modulus	1000	100	0.2
Shear modulus	400	40	

Table 2. Function parameter X, C value.

	X		C	
	Crown	Side wall	Crown	Side wall
Isotropy	5.40	2.21	−6.70	−3.55
Transverse isotropy plane perpendicular to x-axis	7.24	2.42	−11.50	−7.57
Transverse isotropy plane perpendicular to y-axis	6.17	2.04	−16.19	−5.83
Transverse isotropy plane perpendicular to z-axis	4.35	1.27	−8.06	−4.09

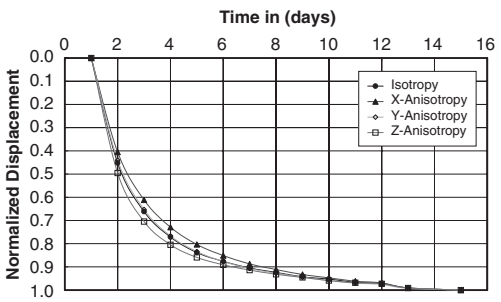


Figure 7. Normalized displacement history in each model.

of the case of Y-anisotropy indicates very similar with the isotropic case. Although the case of X-anisotropy is more smoothly converged, the case of Z-anisotropy is more quickly converged than the isotropic case. It means that the value of X is very important to evaluate the influence of face advancing.

3.4 *Heterogeneous model*

When excavating in uniform rock mass and primary stress conditions, it can be assumed that the single displacement vector components have a certain relationship. With different deformability of the ground, the absolute displacement values change but the ratios between the single components do not vary substantially. Evaluations of data from tunnels constructed in poor rock show that the average angle between longitudinal displacements and settlements have a certain value against the direction of excavation. This vector orientation can be considered as 'normal'. Different boundary conditions, like changes in the rock mass structure or in the primary stress situation, influence the stress distribution around the cross section of the tunnel as well as ahead of the face, which leads to deviations of the vector orientation from 'normal'. When the excavation approaches a 'stiffer' rock mass the vector orientation shows an increasing tendency to point in direction of excavation. On the other hand when excavation approaches 'weaker' rock mass the vector orientation shows an increasing tendency to point against the direction of excavation. Figure 8 indicates the concept of the differential vector orientation.

Figure 9 shows the displacement vector orientation tendency of the case, which the weakness zone thickness is 10 m, according to change the modulus contrasts. Similar pattern of vector orientation is observed in every modulus contrasts case (MC = 2, MC = 5, MC = 10).

Copyright © 2005 Taylor & Francis Group plc, London, UK

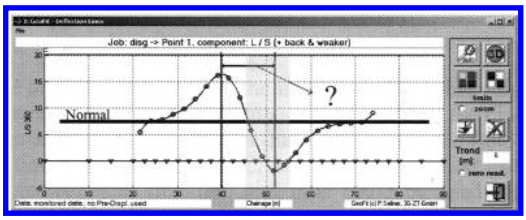


Figure 8. Normalized displacement history in each model.

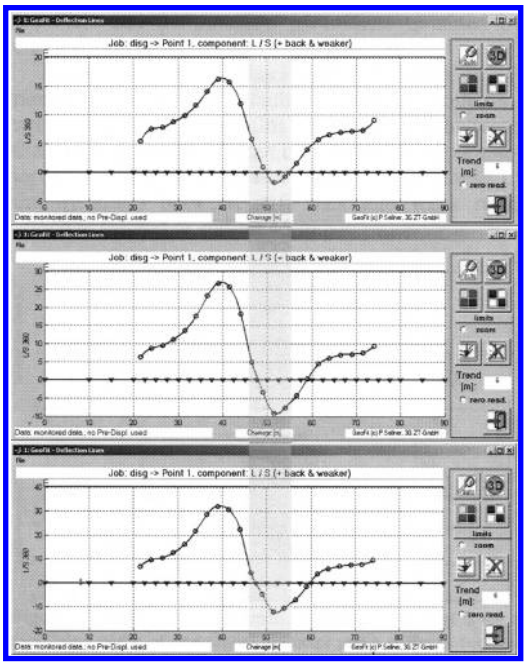


Figure 9. Displacement vector orientations with MC change.

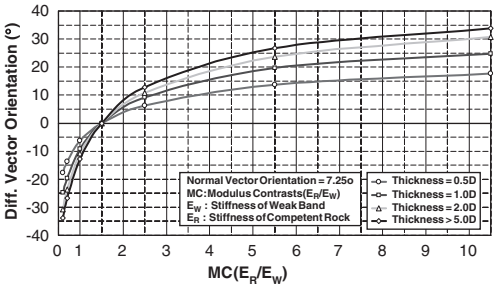


Figure 10. Differential vector orientation variations according to the change of the modulus contrasts and thickness of the weakness zone.

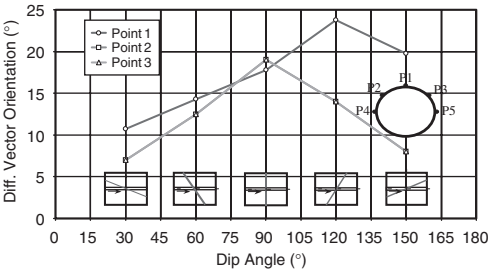


Figure 11. Differential vector orientation variations according to the change of dip angle of the weakness zone.

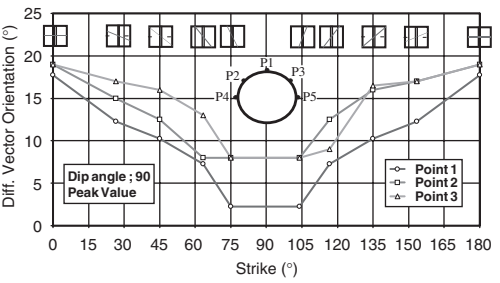


Figure 12. Differential vector orientation variations according to the change of strike of the weakness zone.

Before the weakness zone, the displacement vector orientation is increased to certain value, and then steeply decreased. The peak value indicates the influence of the weakness zone thickness and modulus contrasts etc. The concept of the differential vector orientation (D.V.O) means the difference value between the peak value and normal value which shows in the case of the intact rock mass. From Figure 10, we can see the tendency of the differential vector orientation variations according to the change of the modulus contrasts and thickness of the weakness zone. In brief, the weaker the modulus of the weakness zone, the higher the differential vector orientation, and the wider the thickness of the weakness zone, the higher the differential vector orientation.

Figure 11 shows the variations of the D.V.O according to the change of dip angle of the weakness zone. In this case, the plane of the weakness zone is perpendicular to the tunnel axis. The maximum D.V.O in tunnel crown measuring point is occurred in 60° dip angle against the direction of the tunnel. On the other hand, the maximum D.V.O in tunnel shoulder measuring point is occurred in vertical case as shown in Figure 11.

Figure 12 shows a change of the value of a D.V.O by the variation of strike of the weakness zone. When the strike is 0 degrees, a D.V.O value becomes the maximum, and the minimum works when parallel to tunnel excavation direction as shown in Figure 12. Also,

Copyright © 2005 Taylor & Francis Group plc, London, UK

the results of measurement point of shoulder show the same trend.

When try to summarize the results, the strike and dip angle of the weakness zone are important for the D.V.O value.

4 FUNTION PARAMETER CALCULATIONS

4.1 *Back calculation*

Following the ideas on the influence of the changing stress field in a heterogeneous rock mass on the displacements, it is obvious that the trends of the function parameters X, T, C, and m should reflect the geotechnical situation, and thus could be used for prediction. The results of numerical models with elastic rock mass behaviour were imported into GeoFit® and the function parameters obtained by curve fitting (Kim 2003).

Figure 13 shows the back-calculated function parameters X and C for a fault zone width of one tunnel diameter and a modulus contrast of 2.0 between the two rock masses. It can be seen, that the parameter X significantly increases already 15 m ahead of the transition between stiff rock and weak rock, which is located at station 45 m.

Figure 14 shows the distribution of the function parameters X and C for lengths of the weak zone of 0.5, 1.0 and 2.0 tunnel diameters. Besides the increase of the parameter X well ahead of the weak zone, the results clearly show the influence of the fault zone length on the final displacements within the weak zone, which are reflected through the parameter C. With some experience in this kind of monitoring data evaluation, the combination of displacement vector orientation trends and distributions of function parameter trends can be used to predict quality and extension of weak zones ahead of the tunnel face.

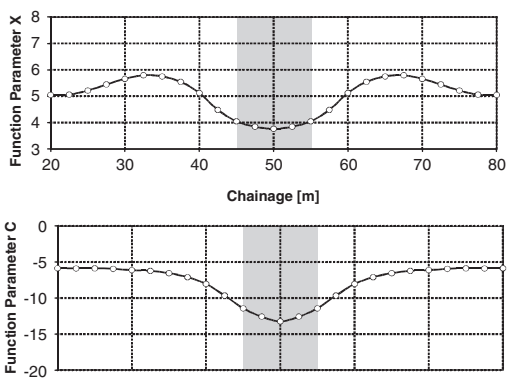


Figure 13. Back calculated function parameters X and C for a fault zone width of one tunnel diameter and a stiffness contrast of 2,0 between the two rock masses.

4.2 *Case histories*

On several projects the program GeoFit® was used to predict displacements. Figure 15 shows the vertical displacements of the tunnel crown and the parameter sets for a tunnel in phyllites at the transition to a major fault zone. As in the numerical simulations a

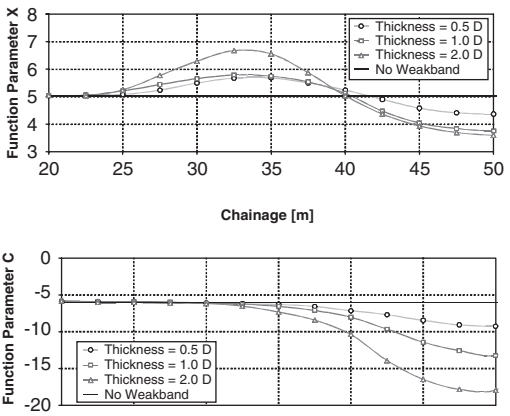


Figure 14. Distribution of the function parameters X and C for different fault zone widths.

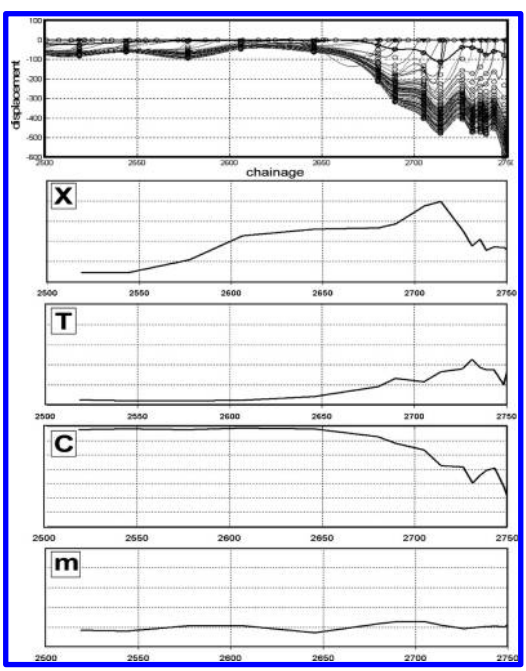


Figure 15. Vertical displacements of the crown point and the appropriate distribution of the function parameters X, T, C and m.

Copyright © 2005 Taylor & Francis Group plc, London, UK

significant increase of the parameter X can be observed well before the excavation reaches the fault zone.

5 CONCLUSIONS

The 3D absolute monitoring technologies in combination with newly developed methods of data evaluation have improved the possibilities for the prediction ahead and outside of tunnel face. In particularly, in heterogeneous/anisotropic rock masses, the prediction of the vector orientation and function parameters plays an important role with respect to safety and economical aspects of a tunnel project. Software for the evaluation of displacement monitoring data is continuously improved and functions added. With the evaluation of a number of projects in different geological environments under various boundary conditions a knowledge base will be developed, eventually leading to a 'smart' data evaluation tool.

REFERENCES

Grossauer, K. 2001: Tunnelling in Heterogeneous Ground – Numerical Investigation of Stresses and Displacements. Master thesis at the Institute for Rock Mechanics and Tunnelling, Graz University of Technology, Austria.

Grossauer, K, Schubert, W & Kim, C.Y. 2003: Tunnelling in Heterogeneous Ground – stresses and displacements. ISRM 2003, South African Institute of Mining and Metallugy.

Kim, C.Y. 2003: Investigation of fault zones on displacements. Project report at the Institute for Rock Mechanics and Tunnelling, Graz University of Technology, Austria. Unpublished.

Schubert, W. & Budil, A. 1995: Importance of longitudinal deformations in tunnel excavation. In T. Fujii (ed.), Int. Congress on Rock Mechanics, Proc. intern. Symp., Tokyo: 1411–1414. Rotterdam: Balkema.

Sellner, P.J. 2000: Prediction of Displacements in Tunnelling. Ph.D. thesis, Graz University of Technology, Austria. In G. Riedmüller, W. Schubert, S. Semprich (eds.). Schriftenreihe der Gruppe Geotechnik Graz, Heft 9. Graz.

Steindorfer, A. & Schubert, W. 1997: Application of new methods of monitoring data analysis for short term prediction in tunnelling. Tunnels for People. Golser, Hinkel, Schubert (eds.). Balkema. Vol. I: 65–69.

Sulem, J., PANET, M. & Guenot, A. 1987: Closure analysis in deep tunnels. In Int. Journal of Rock Mechanics and Mining Science 24: 145–154.

Copyright © 2005 Taylor & Francis Group plc, London, UK

Determination of the mechanical properties of discontinuous rock masses by using PFC2D

Eui-Seob Park & Chang-Ha Ryu
Korea Institute of Geoscience & Mineral Resources, Daejeon, Korea

Seong-Ho Bae
Geogeny Consultants, Seoul, Korea

ABSTRACT: Although the evaluation of the mechanical properties and behavior of discontinuous rock masses is very important for the design of underground openings, it has always been considered the most difficult problem. One of the difficulties in describing the rock mass behavior is assigning the appropriate constitutive model. This limitation may be overcome with the progress in discrete element software such as PFC, which does not need the user to prescribe a constitutive model for rock mass. Instead, the mirco-scale properties of the intact rock and joints are defined and the macro-scale response results from those properties and the geometry of the problem. In this paper, a 30 m × 30 m × 30 m jointed rock mass of road tunnel site was analyzed. A discrete fracture network was developed from the joint geometry obtained from core logging and surface survey. Using the discontinuities geometry from the DFN model, PFC simulations were carried out, starting with the intact rock and systematically adding the joints and the stress-strain response was recorded for each case. With the stress-strain response curves, the mechanical properties of discontinuous rock masses were determined and compared to the results of empirical methods such as RMR, Q and GSI. The values of Young's modulus, Poisson's ratio and peak strength are almost similar from PFC model and Empirical methods. As expected, the presence of joints had a pronounced effect on mechanical properties of the rock mass. More importantly, the mechanical response of the PFC model was not determined by a user specified constitutive model.

1 INTRODUCTION

Although the evaluation of the mechanical properties and behavior of discontinuous rock masses is very important for the design of underground openings, it has always been considered the most difficult problem. The reason is that it is often impossible to carry out large-scale in situ tests and, although widely used, the correlations between strength parameters and quality indexes (for instance GSI or Q index) are still affected by considerable uncertainties (Ribacchi 2000).

Experimental investigations have shown that the presence of joints reduces the strength of the rock mass relative to the intact rock material. The strength of this reduction is governed by such factors as joint geometry configuration, and intact and joint material properties.

At present, the rock mass strength and deformation characteristics are evaluated using empirical methods such as the rock mass classification systems of Bieniawski's RMR (1976) and Barton's Q-Values (1974). More recently Hoek at al. (1995) introduced the Geological Strength Index (GSI) to provide a system for estimating the rock mass strength for different conditions.

Deformation properties and rock mass strength are not only dependent on the intact rock, but also on the fracture network (number and orientation of fracture sets, intensity, mineralization, and so on) and the presence of deformation zones. Therefore, characterization of both the intact rock and of the fractures is required to define the mechanical behavior of the rock mass.

One of the difficulties in describing the rock mass behavior is assigning the appropriate constitutive model. This limitation may be overcome with the progress in discrete element software such as PFC, which does not need the user to prescribe a constitutive model for rock mass. Instead, the mirco-scale properties of the intact rock and joints are defined and the macro-scale response results from those properties and the geometry of the problem.

Recent developments in numerical modeling that allow study of the overall response of a synthetic material containing discrete heterogeneities and discontinuities both at the micro (particle) scale and at the

Copyright © 2005 Taylor & Francis Group plc, London, UK

larger scale of jointed rock masses can greatly aid the interpretation and application of laboratory test results on these materials (Potyondy & Fairhurst 1999).

2 BACKGROUND OF PFC MODELING

One of the limitations of numerical models, such as UDEC, that rely on a user specified constitutive model is that the results are prescribed by the constitutive model assigned to both the intact rock and the fractures. This limitation may be overcome with the progress in discrete element software such as PFC, which does not need the user to prescribe a constitutive model for rock mass.

Instead, the mirco-scale properties of the intact rock and joints are defined and the macro-scale response results from those properties and the geometry of the problem. By assigning a tensile bond strength and frictional bond strength, the micro strength properties can be expressed in terms familiar to geotechnical engineers. However, the challenge is finding the appropriate micro-scale parameters to represent the macro-scale response.

One of the earliest applications of the discrete element method to rock was the modeling of brittle failure observed around AECL's Mine-by test tunnel (Martin et al. 1996). That effort, using *PFC*, began in 1995 and resulted in many refinements to the *PFC* code that is commercially available today. In this modeling effort the basic "*PFC* Model for Rock" is used, which provides a numerical laboratory for simulating the full dynamic response of particle-based systems using the discrete-element method.

The particle flow code PFC2D, also available from Itasca Consulting Group Inc. was used to model the intact rock sample and the 30 × 30 m rock mass. The PFC2D model simulates the mechanical behavior of a collection of distinct, non-uniformly sized circular particles that displace independently and interact only at contacts. The movement and interaction of the particles is modeled using the discrete element method, as described by Cundall and Strack (1979). Also PFC models are categorized as direct, damage-type numerical models in which the deformation is not a function of prescribed relationships between stresses and strains, but of changing microstructure.

In the present PFC modeling the parallel bond model was considered. The required micro-properties are stiffness and strength parameters for the particles and the bonds. The difficulty with PFC is in determining the micromechanics contact parameters to represent the rock mass response. Fortunately, Potyondy and Cundall (2001) have investigated the relationship between micro and macro properties for Lac du Bonnet granite and their findings were used to establish the micro parameters for granite of this site.

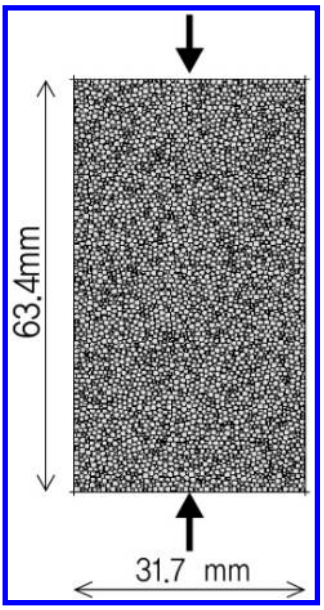


Figure 1. The PFC2D model for intact rock.

3 PFC2D MODEL FOR INTACT ROCK

Two and three dimensional "particle-flow codes," identified as PFC2D and PFC3D respectively, have recently been developed which can be applied directly to the interpretation of laboratory compression tests in terms of the particle-particle interactions and bond strengths (Itasca 1999a and 1999b).

A description of the PFC2D model of rock can be found in Potyondy *et al.* (1996a) and Potyondy and Fairhurst (1999).

All PFC2D specimens were created using the specimen-genesis procedure which produces a rectangular specimen containing a densely packed, bonded particle assembly with low locked-in stress.

Simulating a compression test involves two primary steps. First, a synthetic rock specimen is created that consists of a densely packed assembly of arbitrarily sized particles that are bonded to one another at their contact points. The specimen is constructed such that any locked-in stresses are low relative to the unconfined compressive strength of the specimen. Second, the specimen is loaded by surrounding walls. The top and bottom walls serve as loading platens, while the side walls serve to maintain a specified confining stress.

Numerical tests have been conducted to simulate the behavior of laboratory specimens of Lac du Bonnet granite. Figure 1 shows the particle assembly prior to loading.

The PFC2D model predicts the behaviors under both confined and unconfined conditions. The PFC2D

Copyright © 2005 Taylor & Francis Group plc, London, UK

Table 1. Comparison of results between lab test and PFC2D modeling for intact rock.

	Lab test	PFC model
Young's modulus (GPa)	41.3	41.1 ± 1.2
Poisson's ratio	0.24	0.237 ± 0.02
Uniaxial compressive strength (MPa)	150.0	151.8 ± 11.3

model produces a quantitative match of strength and deformation characteristics of the intact rock sample in terms of Young's modulus and unconfined compressive strength and so on.

To simulate the mechanical behavior of a particular rock of granite, some numerical calibration tests were necessary. Calibration involves finding the micromechanical parameters of the assembly from the macroscopic properties such as Young's modulus and the uniaxial compressive strength. In the calibration process, the responses of the model are compared to the responses of the rock samples in the laboratory and the micro-properties of the model are modified in an iterative way to achieve good agreement.

4 PFC2D MODELS FOR ROCK MASSES

To assess the rock mechanical considerations for a deep repository, the tunnel scale with resolution of 30 × 30 m in the numerical model is most likely sufficient to cover rock mechanical aspects in "the repository scale" (Staub et al. 2002). So the size of the fractured rock mass was set as 30 m × 30 m. This 900 m^2 contained a sufficient representative number of both large scale and small scale fractures.

The three-dimensional DFN generated by FracMan®, which is the software used to generate fractures in three dimensions within a given rock volume, must be transferred to two-dimensional fracture trace sections to provide the ground data for simulations of fractures in the PFC2D model. A discrete fracture network was developed from the joint geometry obtained from core logging and surface survey.

For the PFC2D model for rock masses, the minimum radius of particles is 100 mm, the ratio of maximum to minimum radius is 1.66, and it consists of approximately 13,000 particles.

The PFC model for discontinuous rock masses is built in the following steps. First, the intact rock is modeled as a single rock block of the model size. Then the fracture traces are integrated in the model. The fracture model in PFC2D was generated from 2D trace sections extracted from the 3D Discrete Fracture Network (DFN) model developed for this tunnel site.

Figure 2 shows the PFC2D models for discontinuous rock masses with regard to tunnel intersections at each 20° rotation angles in order to find out how the joint geometry affect the properties of rock masses.

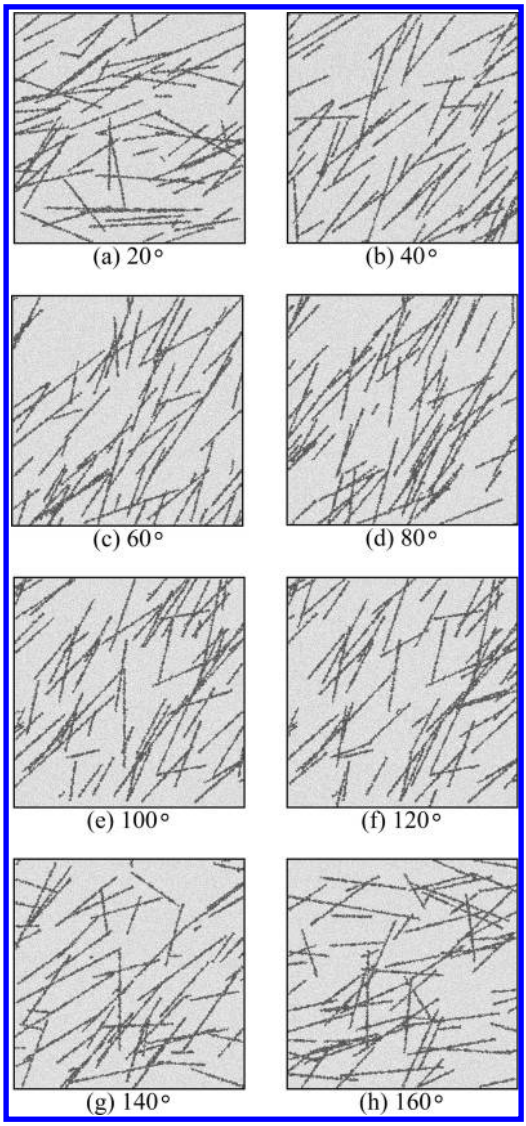


Figure 2. PFC models for discontinuous rock masses with regard to tunnel intersection at each 20° rotation angle (Class I).

After installation of joints in PFC model, the micro-properties of the joint set particles and bonds are modified. The given factors are applied to reduce the particle and bond stiffnesses and strengths, as it is assumed that the joint is softer and weaker than the matrix.

The mechanical testing is simulated by a vertical loading applied on the top of the model by means of a constant velocity displacement obtained by a constant

Copyright © 2005 Taylor & Francis Group plc, London, UK

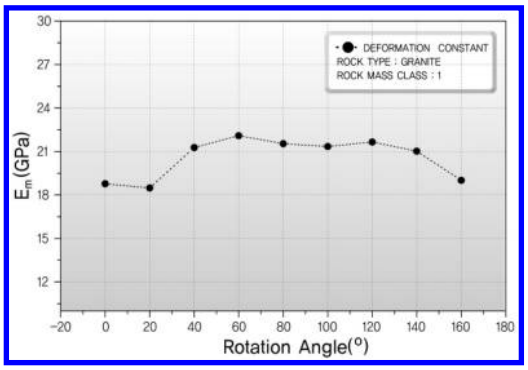


Figure 3. Estimated deformation modulus with regard to rotation angle (Class I).

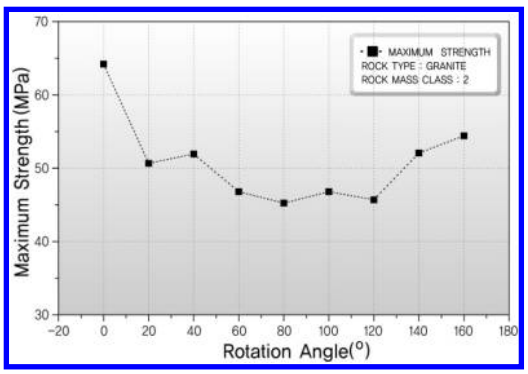


Figure 4. Estimated maximum strength with regard to rotation angle (Class I).

Table 2. Rock mass properties according to confining pressure (Class I).

Conf. pressure (MPa)	Peak strength (MPa)	Cohesion (MPa)	Friction angle (°)
S3 = 0.0	52.07	11.20	41.04
S3 = 2.5	60.66		
S3 = 5.0	70.18		
S3 = 10.0	87.14		

boundary velocity applied during a specified number of computational cycles. The vertical loading is applied to the model beyond the elastic behavior of the components of the model (rock material and fractures) so that the estimation of the rock mass strength can be assessed.

Figures 3–4 show the estimated deformation modulus and maximum strength with regard to rotation angle for rock mass Class I.

Table 3. Rock mass properties estimated by empirical method and PFC modeling (Class I).

	Empirical method	PFC modeling
Deformation modulus (GPa)	20.0	20.57
Peak strength (MPa)	–	50.9
Cohesion (MPa)	6.0	11.2
Friction angle (°)	46	41.4
Poisson's ratio	0.18	0.27

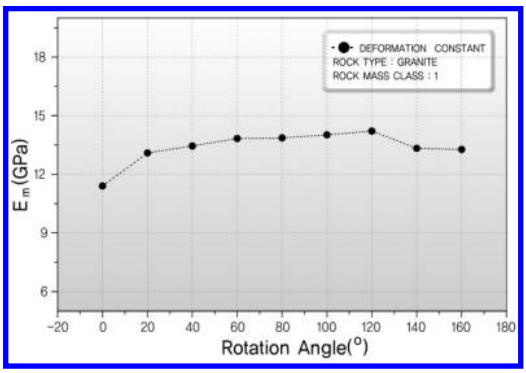


Figure 5. Estimated deformation modulus with regard to rotation angle (Class II).

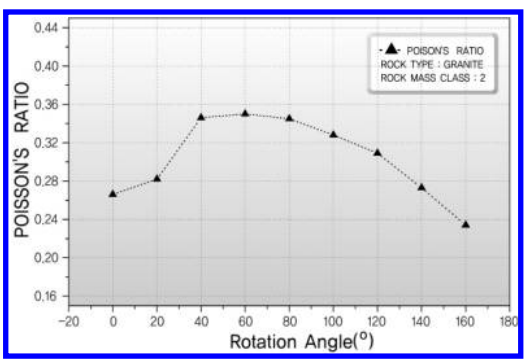


Figure 6. Estimated Poisson's ratio with regard to rotation angle (Class II).

The peak strength of rock masses was computed according to confining pressure, and the cohesion and friction angle are estimated for Mohr-Coulomb failure criteria which is used for conventional numerical modeling. Also the result by PFC modeling is compared with the result of empirical methods in Tables 2–3.

Figures 5–6 show the estimated deformation modulus and Poisson's ratio with regard to rotation angle for rock mass Class II.

Copyright © 2005 Taylor & Francis Group plc, London, UK

Table 4. Rock mass properties according to confining pressure (Class II).

Conf. pressure (MPa)	Peak strength (MPa)	Cohesion (MPa)	Friction angle (°)
S3 = 0.0	41.04	9.1	39.8
S3 = 2.5	50.23		
S3 = 5.0	57.88		
S3 = 10.0	74.33		

Table 5. Rock mass properties estimated by empirical method and PFC modeling (Class II).

	Empirical method	PFC modeling
Deformation modulus (GPa)	13.0	13.38
Peak strength (MPa)	–	41.4
Cohesion (MPa)	4.5	9.1
Friction angle (°)	43	39.8
Poisson's ratio	0.20	0.30

Like rock mass Class I, the peak strength, cohesion and friction angle are estimated for Mohr-Coulomb failure criteria, and the result by PFC modeling is compared with the result of empirical methods in Tables 4–5.

5 CONCLUSIONS

Using the discontinuities geometry from the DFN model, PFC simulations were carried out starting with the intact rock and systematically adding the joints and the stress–strain response was recorded for each case.

With the stress–strain response curves, the mechanical properties of discontinuous rock masses were determined and compared to the results of empirical methods such as RMR, Q and GSI. The values of Young's modulus, Poisson's ratio and peak strength are almost similar from PFC model and Empirical methods. And the cohesion and friction angle are estimated for Mohr-Coulomb failure criteria which is used for conventional numerical modeling. While the value of cohesion estimated by PFC modeling is much higher than that by empirical method, the value of friction angle by PFC modeling is a little lower than that by empirical method.

As expected, the presence of joints had a pronounced effect on mechanical properties of the rock mass. More importantly, the mechanical response of the PFC model was not determined by a user specified constitutive model.

Considering that increases in computing power have made it feasible to model entire boundary-value problems with direct approaches, thereby simulating the physical micromechanics directly and bypassing development of complex constitutive laws, the PFC model could be used further on to simulate the behavior of fractured rock masses that cannot yet be encompassed by existing continuum theories.

REFERENCES

Barton, N.R., Lien, R. & Lunde, J. 1974. Engineering classification of rock masses for the design of tunnel support. *Rock Mech*. 6(4): 189–239.

Bieniawski, Z.T. 1976. Rock mass classification in rock engineering. In *Exploration for rock engineering, Proceedings of the Symposium*, eds. Z.T. Bieniawski, 97–106. Cape Town: Balkema.

Cundall, P.A. & Strack, O.D.L. 1979. A discrete numerical model for granular assembles. *Geotechnique*. 29: 47–65.

Hoek, E., Kaiser, P.K. & Bawden, W.F. 1995. *Support of underground excavations in hard rock*. Rotterdam: Balkema.

Itasca Consulting Group Inc. 1999. *PFC2D* – Particle Flow Code in 2 Dimensions, Minneapolis: Itasca.

Martin, C.D. & Read, R.S. 1996. AECL's Mine-by Experiment: A test tunnel in brittle rock. *Proceedings of the 2nd N ARMS Symposium*, Montreal. Edited by M. Aubertin, F. Hassani & H. Mitri. Vol 1 pp. 13–24. A.A. Balkema, Rotterdam.

Potyondy, D.O. & Cundall, P.A. 2001. *The PFC Model for Rock: Predicting rock-mass damage at the underground research laboratory*, Itasca Consulting Group, Inc. Report to Atomic Energy of Canada Limited (AECL), Report No. 06819-REP-01200-10061-R00.

Potyondy, D. O. & Fairhurst, C.E. 1999. The Value of Numerical Modeling in Understanding the Complete Load/Deformation Behavior of Cohesive-Frictional Materials. *Nondestructive and Automated Testing for Soil and Rock Properties, ASTM STP 1350*, W.A. Marr and C.E. Fairhurst, Eds., American Society for Testing and Materials: 290–299.

Ribacchi, R. (2000). Mechanical Tests on Pervasively Jointed Rock Material: Insight into Rock Mass Behaviour. *Rock Mechanics and Rock Engineering* 33(4): 243–266.

Staub, I., Fredriksson, A. & Outters, N. 2002. *Strategy for a Rock Mechanics Site Descriptive Model: Development and testing of the theoretical approach*. SKB Report R-02-02, Stockholm, Sweden.

Copyright © 2005 Taylor & Francis Group plc, London, UK

Numerical simulations of SFRC precast tunnel segments

G.A. Plizzari & L. Cominoli
Department of Engineering Design and Technologies, University of Bergamo, Italy

ABSTRACT: The paper addresses precast tunnel segments for the new Line 9 of the Barcelona (Spain) Metro where the conventional reinforcement (rebars) may be partially substituted by steel fibers.

After the experimental determination of the material properties, NonLinear Fracture Mechanics analyses allowed to study the structural behavior of the tunnel segments with different types of reinforcement. Finally, an optimized reinforcement, based on a combination of rebars and steel fibers, is proposed.

1 INTRODUCTION

Fiber Reinforced Concretes (FRC) are composite materials with a cementitious matrix and a discontinuous reinforcement (the fibers) that may be made of metal, glass, synthetic or natural materials.

After almost four decades of research, mechanical properties of FRC have become well known, Standards for material characterization are widely available and design guidelines have been recently proposed (Naaman & Reinhardt, 2003; di Prisco et al., 2004; RILEM, 2002).

Among the structural applications of FRC, there is a growing interest in precast tunnel segments to be used with the Tunnel Boring Machine (TBM), where steel fibers may substitute, partially or totally, the conventional reinforcement (rebars).

In the present paper, the structural behavior of the tunnel segments for the new Metro line (Line 9) of Barcelona (Spain) are numerically simulated with FE analyses based on Non Linear Fracture Mechanics (NLFM; Hillerborg et al., 1976).

The new TBM-excavated tunnel of Barcelona has a diameter of about 12 m, a length of more than 40 km and is located from 30 to 70 m below the surface. The tunnel is made of 7 segments with a length of about 4.70 m and 1 key segment of half that length (Fig. 1). According to the original design project, the segments are made of conventional reinforcement with an addition of steel fibers whose contribution to the bearing capacity of the segment was not taken into account. In fact, the fibers were incorporated only to control cracking that may occur during handling and placing of the segments.

After the experimental characterization of the material properties of FRC with two types of steel fibers, NLFM analyses allowed to study the structural behavior of the segments with several combinations of reinforcement under different loading conditions.

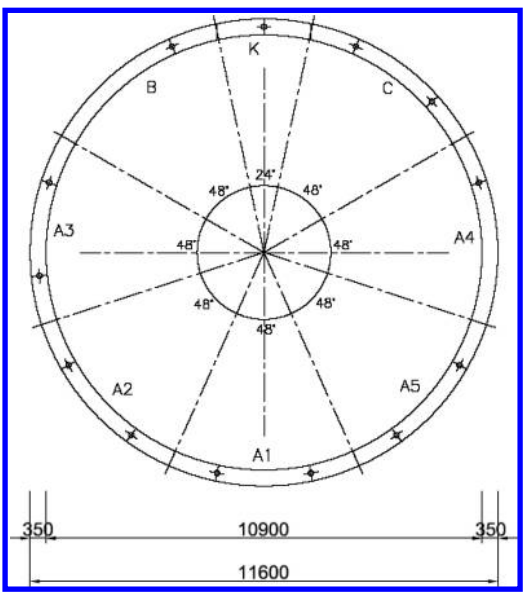


Figure 1. Transverse section of the tunnel for the new line (9) of the Barcelona Metro with evidenced the 8 tunnel segments (Gettu et al., 2004).

The numerical model was previously validated by using the experimental results on full-scale tests performed in Barcelona (Gettu et al., 2004).

Finally, an optimized reinforcement, based on a combination of rebars and steel fibers, is proposed.

Copyright © 2005 Taylor & Francis Group plc, London, UK

Table 1. Concrete composition (quantities refer to 1 m^3).

	Weight [Kg]	Volume [l]
Cement Portland 52,5R	425	134,92
Water	142	142
Superplasticiser	–	3,20
Aggregates	1885	699,88
Air assumed	–	20,00
Water/cement ratio	0,33	–

Table 2. Geometrical characteristic of the fibers.

Fiber code	L_f [mm]	ϕ_f [mm]	L_f/ϕ_f [-]	Fiber shape
Wirand FF1	50.0	1.00	50.0	
Wirand FF3	50.0	0.75	67.0	

2 MATERIALS

The concrete matrix was made with cement CEM I 52.5R (UNI-ENV 197) and a natural river gravel with a rounded shape and a maximum diameter of 15 mm; its composition is summarized in Table 1. The grain size distribution of aggregates was chosen very close to the Bolomey curve by using nine classes of aggregates. An acrylic based super-plasticizer was used.

The two different types of fibers that were considered in this research are reported in Table 2 where the fiber length (L_f), the fiber diameter (ϕ_f) and the aspect ratio (L_f/ϕ_f) are shown. All the fibers are cold drawn, have a hooked shape, a rounded shaft and a tensile strength higher than 1100 MPa.

Fibers with an aspect ratio equal to 50 (FF1) were used with two different volume fractions (V_f), equal to 0.45% (35 kg/m^3) and to 0.58% (45 kg/m^3). Fibers with a higher aspect ratio (FF3) were used with a lower dosage, equal to 25 kg/m^3 (V_f = 0.32%) and to 35 kg/m^3 (V_f = 0.45%).

Eight beam specimens were made for each type of SFRC; in addition, 8 beams of plain concrete were used as reference specimens.

The slump(s) of the fresh concrete was always greater than 150 mm.

Specimens were stored in a fog room (R.H. > 95%; T = 20 ± 2°C) until 24 hours before testing.

Table 3 reports the mechanical properties of concrete (average values), as determined after about 60 days of curing; in particular, tensile strength (f_{ct}) from cylinders (ϕ = 80 mm, L = 240 mm), compressive strength from cubes ($f_{c,cube}$) having 150 mm side and Young's modulus (E_c) from compression tests on cylinders (ϕ = 80 mm, L = 240 mm), are reported.

Table 3. Mechanical properties of concrete (average values).

	$f_{c,cube}$ [MPa]		f_{ct} [MPa]		E_c [GPa]	
FF1	64.7	64.1	4.11	4.07	38.8	38.1
FF3	63.5		4.04		37,4	

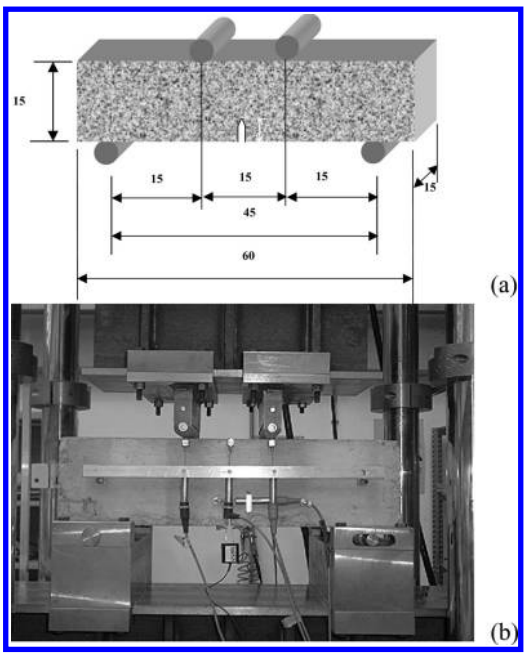


Figure 2. Geometry (a) and instrumentation (b) of the notched specimen for the beam tests.

Fracture properties were determined from notched beams (150 × 150 × 600 mm) tested under four point bending according to the Italian Standard (UNI, 2003; Fig. 2a). The tests were carried out with a closed-loop hydraulic testing machine by using the Crack Mouth Opening Displacement (CMOD) as a control parameter, which was measured by means of a clip gauge positioned astride a notch in the mid-span, having a depth of 45 mm (Fig. 2a). Additional Linear Variable Differential Transformers (LVDTs) were used to measure the Crack Tip Opening Displacement (CTOD) and the vertical displacement at the beam mid span and under the load points (Fig. 2b).

Figure 3 shows typical experimental results from bending tests on beams with fibers FF1.

Inverse analyses of the bending tests, based on NLFM, allowed to determine the best-fitting softening law for the SFRCs adopted in the present research (Roelfstra & Wittmann, 1986). The Young's modulus (E_c) was the one experimentally measured from the

Copyright © 2005 Taylor & Francis Group plc, London, UK

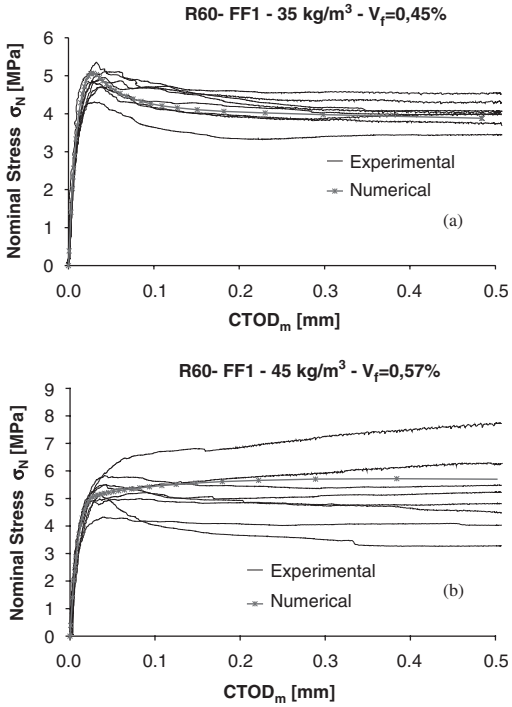


Figure 3. Experimental and numerical results obtained from beam tests on beams with fibers FF1.

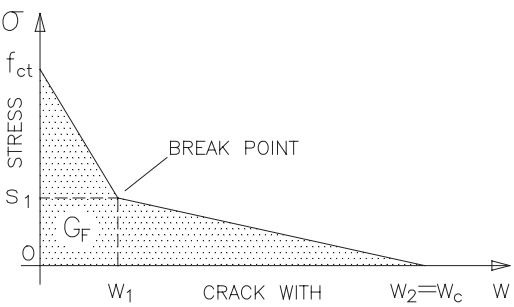


Figure 4. Bilinear law for the approximation of the post-cracking behavior of SFRC.

cylinders while the Poisson ratio (ν) was assumed equal to 0.15. The softening law was approximated as bilinear where the first steeper branch can be associated with (unconnected) micro-cracking ahead of the stress-free crack while the second branch represents the aggregate interlocking or the fiber bridging (Fig. 4). The numerical analyses were initially performed by assuming both a discrete crack approach with Merlin (1994) and a smeared crack approach with Abaqus (release 6.4.1; 2003); the latter was also used for the numerical simulations of the tunnel segments.

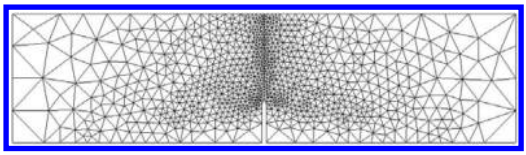


Figure 5. Mesh adopted for the numerical simulations of the beam tests based on a discrete crack approach.

Table 4. Parameters for the bilinear softening law for cracked concrete.

SFRC	V_f(%)	f_{ct} [MPa]	w_1 [mm]	σ_1 [MPa]	w_{cr} [mm]
FF1	0.45	4.1	0.031	1.450	3.50
	0.58	4.1	0.023	2.134	5.35
FF3	0.32	4.1	0.031	1.227	3.2
	0.45	4.1	0.028	1.505	3.9

Figure 5 shows the mesh used for Merlin with triangular plain stress elements and interface elements for the crack. The material parameters identified from the bending tests (f_{ct}, σ_1, w_1, w_{cr}) are summarized in Table 4. The best-fitting numerical curves obtained with Merlin are compared with the experimental ones in Figure 3.

2 VALIDATION OF THE FE MODEL

Experimental studies on the tunnel segments for the Barcelona Metro were carried out by Gettu and co-workers (2004) at the Universitat Politècnica de Catalunya. The studies aimed to study the possibility of using only fiber reinforcement in the tunnel segments (without any conventional reinforcement). The experimental program included the material characterization and structural scale tests under critical loading conditions: flexure, concentrated in-plane loads and possible stress concentrations in the joints between segments of the same ring.

The experimental results were used to validate the FE model used in the present research work. In particular, the simulation of the bending tests performed under three point loading is presented herein. These tests aimed to simulate the inadequate filling of the space between the lining and the excavated surface (Gettu et al., 2004; Fig. 6). Figure 7 shows the configuration of a bending test.

Figure 8a shows a comparison between the experimental and the numerical load-deflection curve for specimens reinforced with both conventional and fiber reinforcement as well as for specimens with steel fibers only. The good agreement between the numerical and the experimental results should be noticed. A further comparison, shown in Figure 8b,

Copyright © 2005 Taylor & Francis Group plc, London, UK

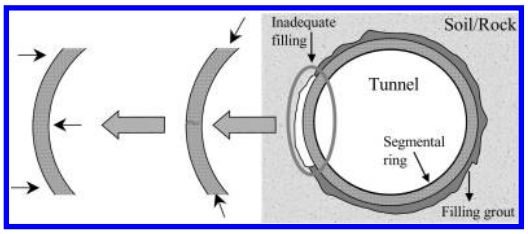


Figure 6. Motivation for the flexure tests performed at UPC (Gettu et al., 2004).



Figure 7. Configuration of the flexure test (Gettu et al., 2004).

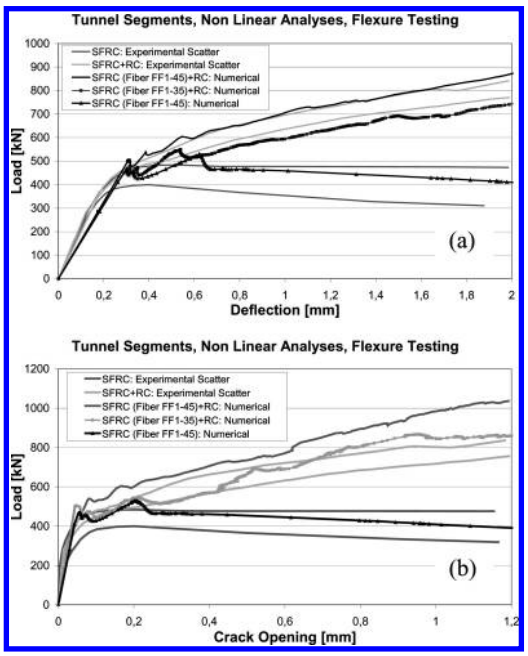


Figure 8. Comparison between the numerical curves and the experimental load displacement (a) and load-crack opening (b) curves obtained by Gettu et al., (2004) for two different materials.

concerns the crack opening displacement measured in the mid-section (Fig. 7); once again, the numerical curves fit the experimental ones quite well.

4 DESIGN ASPECTS

An open question for the construction companies and the precast industry concerns the reinforcement for these precast elements. In fact, a heavy conventional reinforcement is undesired in the construction process due to the placement of many curved rebars and for pouring the fresh concrete. Figure 9 shows the conventional reinforcement adopted for the segments of the Barcelona Metro that, as already mentioned, also included 30 kg/m^3 of steel fibers (FF1).

In order to verify the structural behavior of the tunnel segments towards an optimization of the reinforcement, several NLFM analyses were performed in the present research work. Based on the material properties described in §2, the damaged plasticity model provided in ABAQUS 6.4.1 (2003) was adopted for the FE simulations of the tunnel segments. The numerical analyses were carried out by adopting a 3D solid model with 4032 first order hexahedral elements (C3D8-eight node linear brick elements). The constitutive law for concrete under compression was assumed according to EC2 (2003).

The actions on the tunnel segments result from transportation, placing process and soil pressures in the final state. The numerical results concerning the high compression force exerted by the 30 TBM actuators on the ring during excavation are presented herein. The service load applied by a single actuator for the Barcelona Metro was 3 MN.

One single segment with four actuators was considered for the numerical analyses and its boundary conditions (i.e. presence of the adjacent segments) were simulated by elastic springs whose stiffness was calibrated with previous FE analyses of the full ring.

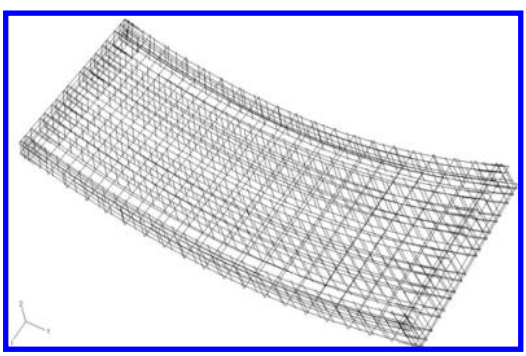


Figure 9. Caption of a typical figure. Photographs will be scanned by the printer. Always supply original photographs.

Copyright © 2005 Taylor & Francis Group plc, London, UK

Structural behavior of segments with different types of reinforcement was compared. Numerical results from segments with conventional reinforcement only (RC), with rebars and 35 kg/m^3 of fibers (RC35FF1, similar to the reinforcement adopted in Barcelona), or with 45 kg/m^3 of fiber reinforcement only (45FF1), are presented. To better evaluate the reinforcement effects, a reference specimen of plain concrete was also considered. Figure 11 shows the numerical results in terms of load (from four actuators) versus the longitudinal displacement of the middle section (average value under the four loading areas). One can notice the brittle failure of the plain concrete specimen and the minor contribution of fibers to the bearing capacity of the segment with conventional reinforcement. Specimens with fibers only have the same ultimate load but it is reached with larger displacements and, therefore, larger crack openings.

To better understand the structural behavior of segments with fiber-reinforcement only, Figure 12 shows the load-displacement curve of the specimen with 45 kg/m^3 of fibers FF1, without conventional reinforcement. It can be noticed that a splitting crack starts to open at the service load and that, because of the stress-redistribution along the longitudinal direction of the segment, this crack can propagate in a stable way up to the ultimate load which is almost twice the service load.

The distribution of radial stress σ_r (see Fig. 13) along the longitudinal section at the service load is represented in Figure 14; one can notice the tensile stresses under the actuator (on the left side) up to a distance from the segment surface of about 400 mm.

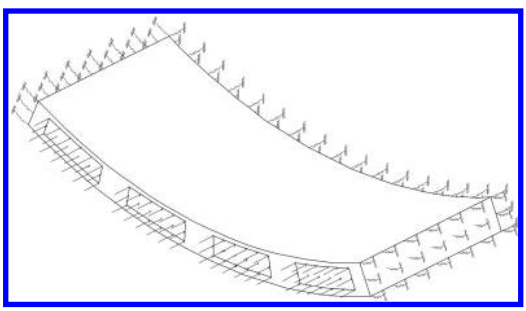


Figure 10. Scheme of a segment with the load from four actuator and the springs representing the neighbor segments.

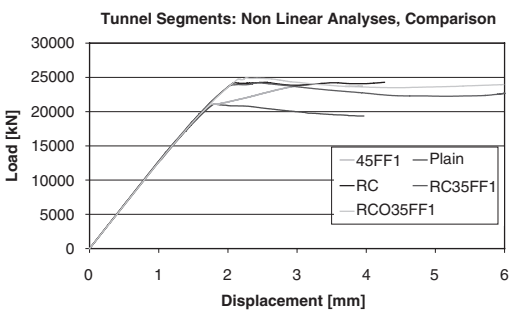


Figure 11. Comparison between the load-displacement curves as obtained from specimens with different types of reinforcement.

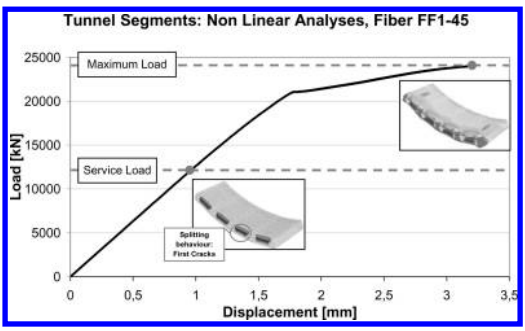


Figure 12. Caption of a typical figure. Photographs will be scanned by the printer. Always supply original photographs.

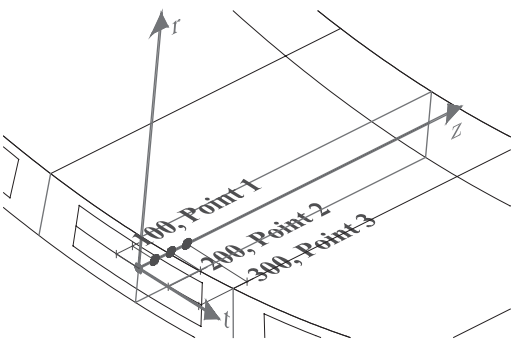


Figure 13. Reference system adopted for stresses and strains.

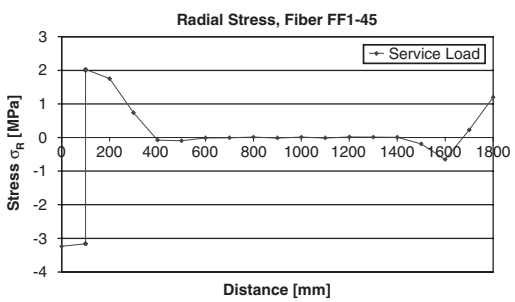


Figure 14. Distribution of radial strains ε_r along the longitudinal section of the element under service loads.

Copyright © 2005 Taylor & Francis Group plc, London, UK

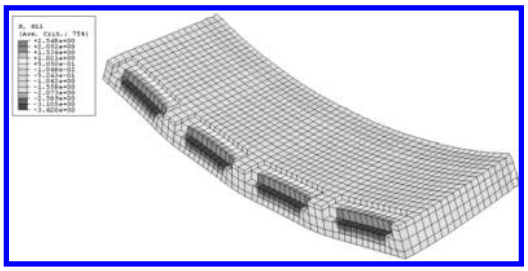


Figure 15. Distribution of radial strains ε_r under service loads.

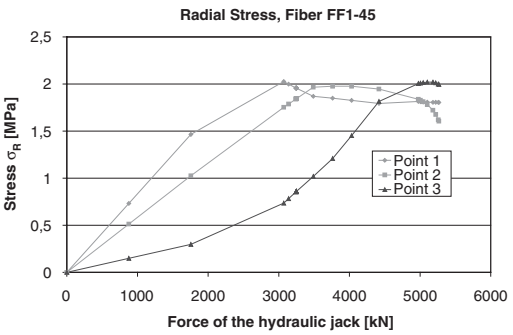


Figure 16. Distribution of the radial stresses (ε_r) at three different distances under the loading area of the actuator.

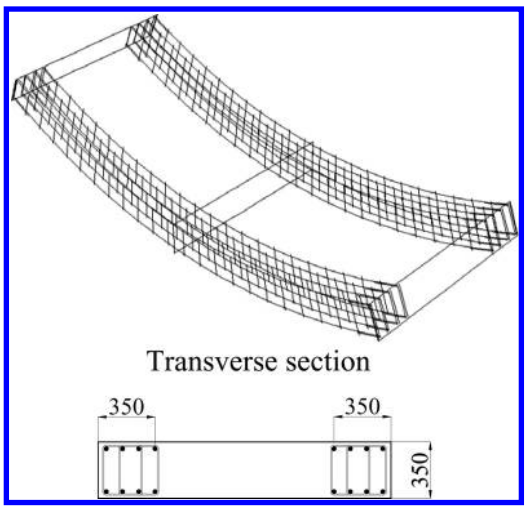


Figure 17. Optimized rebars proposed for the tunnel segment (the reinforcement in the middle of the specimen is provided by 35 kg/m^3 of fibers FF1.

Figure 15 shows the 3D distribution of the radial strains (in plane x-r of Figure 13) in the element under service load (3 MN in 4 actuators), and evidences the strain concentration under the actuators (some elements are removed to better show the strains inside the element).

Table 5. Reinforcement and maximum load obtained form the segments.

	Reinforcement [kg/m^3]			Max. Load [kN]
	Rebars	Fibers	Total	
Plain	–	–	–	21024
45FF1	–	45	45	24016
RC35FF1	97	35	132	24234
RC	97	–	97	24232
RCO35FF1	31	35	66	24943

The load increase in the SFRC elements is possible because of the stress distribution along the longitudinal section of the segment. This is clearly evidenced in Figure 16 that reports the radial stresses vs. the load at three different distances under the loading area (100, 200 and 300 mm; Fig. 13).

The previous numerical results showed that the use of fiber reinforcement with only 3 MN actuators may provoke larger crack openings and that tensile stresses are mainly concentrated in the first 30–40 cm under the actuators. In order to optimize the reinforcement of the tunnel segment, the rebars could be limited to the chords along the two longer sides (that are loaded by the actuators), as shown in Figure 17. The corresponding numerical results are shown in Figure 11 (RCO35FF1); note that the load displacement curve is very similar to the one related to the full conventional reinforcement with steel fibers. These results evidence that, although the considered loading condition is very severe, a lot of conventional reinforcement adopted in Barcelona may be substituted by steel fibers.

Table 5 reports the different amounts of steel reinforcement (fibers and rebars) considered for the tunnel segments and the corresponding ultimate load. It can be noticed that the proposed optimized reinforcement guaranties the same ultimate load and allows a savings of half of the reinforcement adopted in Barcelona.

5 CONCLUDING REMARKS

The present paper shows results of a numerical study of precast tunnel segments for the new Line 9 of the Barcelona Metro. Numerical analyses were performed under the assumptions of NLFM.

The numerical model allows a good approximation of the experimental results from full-scale tests obtained at the Universitat Politècnica de Catalunya.

The total reinforcement adopted in Barcelona may be reduced by using an optimized combination of conventional and fiber reinforcement.

Copyright © 2005 Taylor & Francis Group plc, London, UK

REFERENCES

ABAQUS *v. 6.4.1. 2003.* Theory manual. *Hibbitt, Karlsson & Sorensen, Pawtucket,* Rhode Island (USA).

di Prisco, R., Felicetti, R. & Plizzari, G.A. 2004. Proceedings of the 6th RILEM Symposium on Fibre Reinforced Concretes (FRC), Varenna (Italy), September 20–22, *RILEM PRO 39*, Bagneaux (France), 1514 p.

Gettu, R., Barragán, B., García, T., Ramos, G., Fernández, C. & Oliver, R. 2004. Steel Fiber Reinforced Concrete for the Barcelona Metro Line 9 Tunnel Lining. In BEFIB 2004, *Proceedings of the 6th RILEM Symposium on FRC, Varenna (Italy), Sept. 20–22*, RILEM PRO 39, 141–156.

Hillerborg, A., Modeer, M. & Petersson, P. E. 1976. Analysis of crack formation and crack growth in concrete by means of fracture mechanics and finite elements. *Cement and Concrete Research*, 6, 773–782.

Naaman, A.E. & Reinhardt, H.W. 2003. High performance fiber reinforced cement composites–HPFRCC4. *RILEM PRO 30*, Bagneaux (France), 546 p.

Reich, R., Cervenka, J. & Saouma, V.E. 1994. MERLIN, a three-dimensional finite element program based on a mixed-iterative solution strategy for problems in elasticity, plasticity, and linear and nonlinear fracture mechanics. E-PRI, Palo Alto, http://civil.colorado.edu/ ~saouma/Merlin.

RILEM TC 162 TDF. 2002. Test and Design Methods for Steel Fiber Reinforced Concrete. Design of Steel Fibre Reinforced Concrete using the σ-w method: Principles and Applications. *Materials and Structures*, 35, 262–278.

UNI EN 1992-1-1. 2003. Eurocode 2 – Design of concrete structures – Part 1-1: General rules and rules for buildings.

UNI 11039. 2003. Steel fibre reinforced concrete – Part I: Definitions, classification specification and conformity – Part II: Test method for measuring first crack strength and ductility indexes. *Italian Board for Standardization* (UNI).

Roelfstra, P.E. & Wittmann, F.H. 1986. Numerical method to link strain softening with failure of concrete. In *Fracture Toughness and Fracture Energy of Concrete,* Wittmann F.H. Ed., Elsevier, Amsterdam, 163–175.

ACNKNOWELEDGEMENTS

The research project was financed by Officine Maccaferri S.p.A. (Bologna, Italy) whose support is gratefully acknowledged. A special thanks goes to Prof. Paolo Riva for his useful suggestions for the numerical model and to Engineer Giuseppe Tiberti for his assistance in carrying out the beam tests and the numerical analyses.

Copyright © 2005 Taylor & Francis Group plc, London, UK

Observed behavior of three-arch tunnel constructed in weathered soil

Kang Ho Shin
Senior Engineer, Samsung Engineering and Construction, Sung-nam, South Korea

Jae Kwon Kim
Executive Director, Samsung Engineering and Construction, Sung-nam, South Korea

Seung Rae Lee
Professor, Korea Advanced Institute of Science and Technology, Daejeon, South Korea

Yun Ki Kim & Jeong Hyun Noh
Graduate students, Korea Advanced Institute of Science and Technology, Daejeon, South Korea

ABSTRACT: A three-arch NATM tunnel has been constructed for a metropolitan subway station in Daejeon, Korea. The tunnel has been supported by shotcrete and rock-bolt system and partially reinforced by pipe-roof grouting method. In this paper, the observed behavior of a large section three-arch tunnel constructed in weathered soil stratum was illustrated. As far as its excavation step is concerned, center tunnel was excavated from a previously-excavated pilot tunnel. The both side tunnels were then excavated along with the center tunnel maintaining the face-to-face distance to approximately 10 m. Each tunnel section was excavated in partitions by breaker and road-header. During the construction, large amount of ground settlement has occurred probably due to the outward movement of the portal, accompanied with lowering of ground water level. The maximum ground settlement up to 134 mm was observed at the center of tunnel section during the side tunnel excavation period. This settlement is approximately 3.2 times larger than the original design estimation. The maximum tunnel crown displacement was 29 mm during the side tunnel excavation period. Outward movement of the portal has increased with the ground settlement as well. The results of three dimensional FEM analysis using DIANA-3D and in-situ measurement data of ground settlement, ground water level, and member stresses were presented and explained.

1 INTRODUCTION

The tunneling method, the site condition and the reinforcement of the ground are important factors for tunneling in urban regions. Especially in the case of tunneling for the subway, the excavation or construction of the tunnel must be well executed in spite of the unsuitable soil condition such as the weathered soils or rocks.

The horizontal excavating sequences after the vertical excavation induce the surface subsidence of the ground and the outward movement of the portal of the tunnel. Therefore the prediction of the portal behavior and measurements of the stress and the displacement of the retaining wall structures or the rakers in construction stage are substantial. If the design of the support and reinforcement is not appropriate, the subsidence or the differential settlement of the surface ground excessively occurs and it causes the cracking of the adjacent buildings and even the collapse of the structures. For the prevention of the problems that occur in the portal of the subway tunnel, continuous measurements and numerical analyses should be conducted.

This paper illustrates an example of design and support systems for a three-arch tunnel constructed in Korea. The results of the ground surface subsidence measurements and the numerical analysis are discussed.

2 GEOMETRY AND CONSTRUCTION SEQUENCES

A three arch NATM tunnel has been constructed for a metropolitan subway station in Daejeon, Korea (Figure 1). The three-arch tunnel which has a total length of 53.5 m is a part of 104 station and the other part of station has been constructed using 78.8 m-long

Copyright © 2005 Taylor & Francis Group plc, London, UK

braced excavation method. The tunnel crown is located at 22 m below the ground level and it crosses the Daejeon KTX station underneath. The underpinning method by pipe-roofing was considered as an original design because of the wide section, but the tunneling method was selected due to the construction time schedule and the expected ground surface subsidence. Since the tunnel comprises a very wide section (10 × 28 m) to be used as a subway station, it reveals complicated mechanical behavior, especially near portal, due to its short length relative to its width.

2.1 *Geometry*

As shown in Figure 1, there are the KTX station and the railroad track over the subway station to be constructed. The allowable degree-displacement of the KTX station floor was set up 1/500∼1/600 mm/mm from the detailed stability report of the station. Besides, the allowable subsidence for the railroad track connecting Seoul to Busan was suggested below 7 mm, which is hard to be satisfied practically. It should be required to make the subsidence of the surface minimized and to repair the railroad track in time. Thus, the geometry and the tunnel construction method must be considered to prevent the subsidence of the ground surface and to fulfill the stability of the tunnel. A three-arch tunnel section (Figure 2) was designed since the depth from the crown of the tunnel to the ground surface was low (22 m) and the width of the subway station (28 m) was wide relative to the height (10 m). The ground is composed of fill soil, weathered soil, weathered rock and soft rock from the surface in order. The tunnel was located within the weathered rock layer. These features are shown in Figure 3. The underground-water table is maintained 1∼2 m above the recent excavated depth because of the open cut excavation.

2.2 *Excavation sequences and support system*

The mechanical excavation method (NATM) has been applied because the noise and the vibration induced

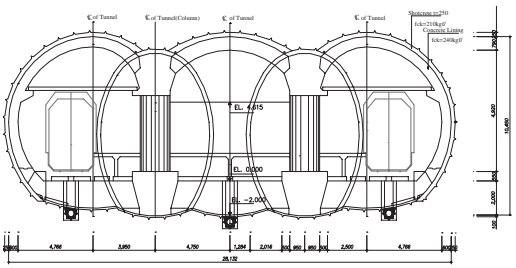


Figure 2. Cross-section of three-arch tunnel.

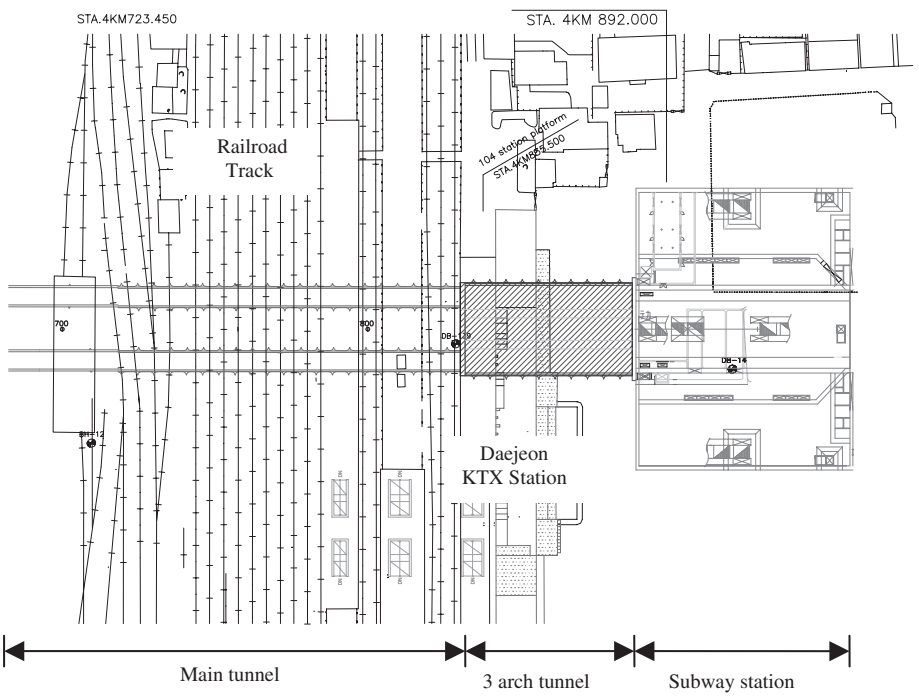


Figure 1. Geometry of Daejeon subway station.

Copyright © 2005 Taylor & Francis Group plc, London, UK

from an explosive method can cause the passenger's uncomfortable feeling and the cracking of the existing station structure. Ring-cut and temporal invert method was used for the pilot tunnel excavation to ensure the stability of the face and to prevent the subsidence. The excavation length for each excavation was 0.8 m and the short bench cut was applied. The support system was 25 cm-thick shotcrete.

The excavation sequences of the tunnel are schematically shown in Figure 4. At first, the left pilot tunnel was excavated and the columns were constructed. The center tunnel was excavated after the complete pilot tunnel excavation. Then the widened tunnels beside the pilot tunnel were excavated. The lining and invert of the center tunnel was early constructed to support the tunnel after the center tunnel excavation. The excavation sequences were designed for not only the small amount of ground subsidence but also the short construction duration.

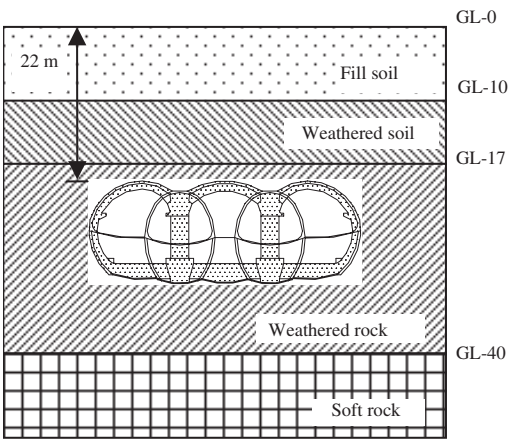


Figure 3. Ground profile.

2.3 *Reinforcement methods of the tunnel*

Several reinforcing methods had been applied to minimize the subsidence and to maintain the stability of the tunnel during the construction of the wide section of the three-arch tunnel in the poor soil condition. First of all, the crown and shoulder of the tunnel were reinforced by a 12 m-long steel pipe-reinforced multi-step grouting method (SPRG). Before the first excavation of the tunnel, three rows of SPRG were applied at the portal. After that, one row of SPRG was applied for each 4 m-long excavation sequence to keep supporting the three rows of SPRG in the tunnel.

2.4 *Temporary retaining structure of the portal*

The temporary retaining structure of the portal was constructed between the three-arch tunnel and the open-cut excavated area. This structure composed of the thumb-piles, earth retaining wall, earth anchors and soil nailings as shown in Figure 5. The 6 rows of earth anchors were constructed at the upper area of the portal to prevent the deformation of the earth retaining wall, while 7 rows of soil nailings were constructed below the earth anchors. The inclined reinforcing structures (rakers or struts) were also added to the retaining wall below the soil naillings. These structures were designed to maintain the stability of the retaining wall.

3 NUMERICAL ANALYSIS

The 3D FEM commercial program DIANA 8 (TNO, Netherlands) has been used to predict the behavior of the portal of the three-arch tunnel for each construction sequence. This program has the ability to carry out the phased analysis and to use appropriate elements for the reinforcing structures.

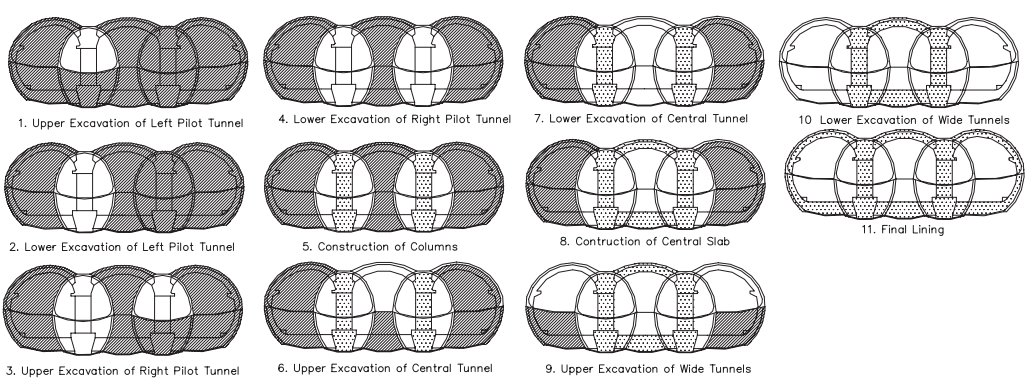


Figure 4. Sequences of three-arch tunnel excavations.

Copyright © 2005 Taylor & Francis Group plc, London, UK

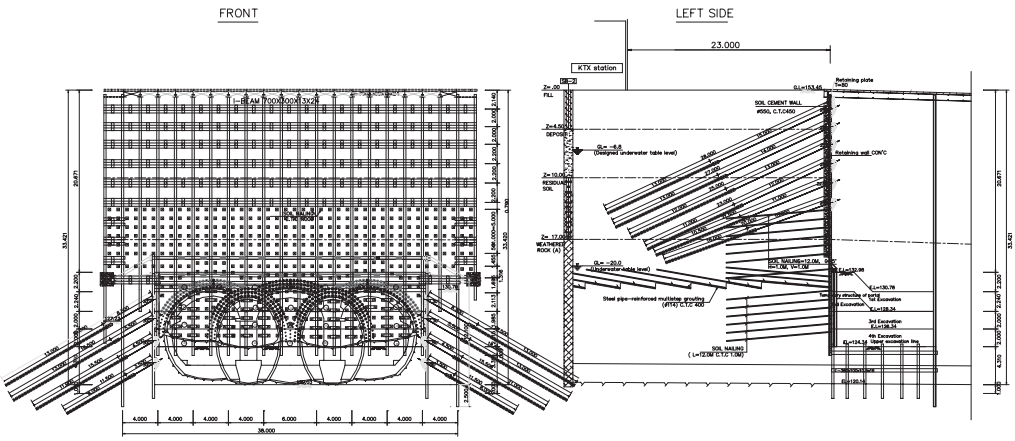


Figure 5. Features of the temporary structres supporting the portal.

Table 1. Element types for numerical model.

Element type	Applied structures
Solid	Soil, Rock, Grouting and Column
Shell	Shotcrete and Earth retaining wall
Embedded (Nobond)	Free cable
Embedded (Bond)	Fixed anchor and Soil nailing
Beam	Raker (strut)

3.1 *Element types and phase analysis*

The types of element used are summarized in Table 1. Especially DIANA supplies the EMBEDDED elements to describe the earth anchors and the soil nailings. These embedded elements add the corresponding stiffness to the finite element mother model. Bonded types are used for the fixed anchorage and the soil nailings, and nobonded types for the free cables of the anchor system. The SHELL elements are used for the shotcretes and the earth retaining wall because the thickness is thin relative to the other element scale.

The final mesh of the three-arch tunnel model is shown in Figure 6. This model has 72 phased sequences including 3 vertical front excavations. For each analysis, the material properties for the elements of the grouting and shotcretes are changed according to the construction sequences. The excavated elements (5 m for each sequence) are eliminated from the model and the reinforcing embedded elements are installed. The model has been analyzed by a Linear Static method. The pore water pressure under the tunnel has been excluded in the analysis.

The properties of materials used are displayed in Tables 2 and 3.

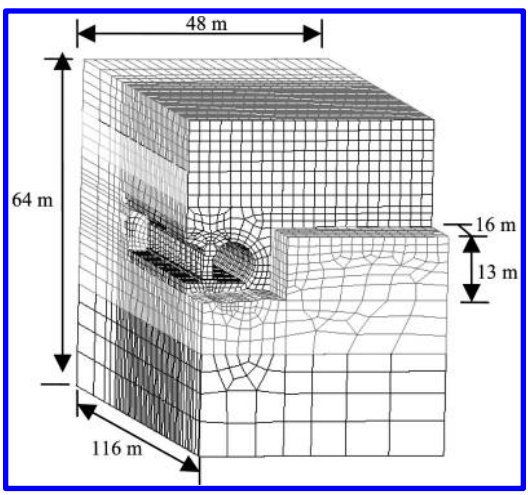


Figure 6. Final mesh of tunnel model.

Table 2. Properties of soils and rocks.

Type	γ (kN/m^3)	E (MPa)	ν	c (kPa)	φ (°)
Fill soil	17.6	12	0.35	20	28
Weathered soil	19.6	29	0.30	5	36
Weathered rock	22.5	130	0.23	50	36
Soft rock	24.5	3300	0.20	400	45
Grouting	22.5	850	0.20	250	36

3.2 *Analysis results*

The estimated maximum surface subsidence was 35 mm around 30 m apart from the portal along the

Copyright © 2005 Taylor & Francis Group plc, London, UK

Table 3. Material parameters.

Type	E (MPa)	Thickness (m)	Area (m^2)
Shotcrete	15000	0.25	–
Retaining wall	30500	0.164	–
Anchor (free)	210000	–	0.0003948
Anchor (fix)	20000	–	0.00785
Soil nailing	20000	–	0.00785
Concrete lining	26000	–	–
Raker	210000	I = 300 × 305 × 15 × 15	

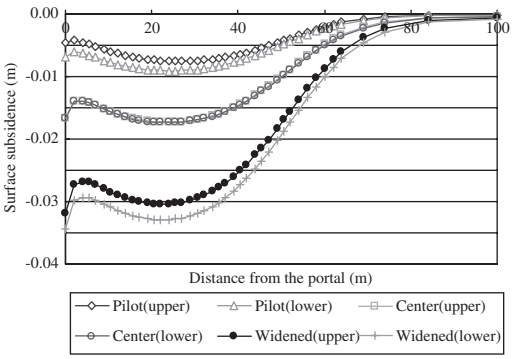


Figure 7. Estimated surface subsidence along the center line.

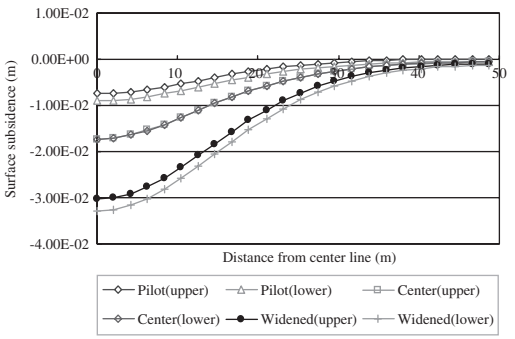


Figure 8. Estimated surface subsidence across the ground 20 m apart from the portal.

center line as shown in Figure 7. Each sequence of changing the tunnel type causes large subsidence relative to the partial excavation in a tunnel. This phenomenon happens during excavation along the tunnel. The subsidence develops the maximum at the center and decreases close to the boundary (Figure 8). At the

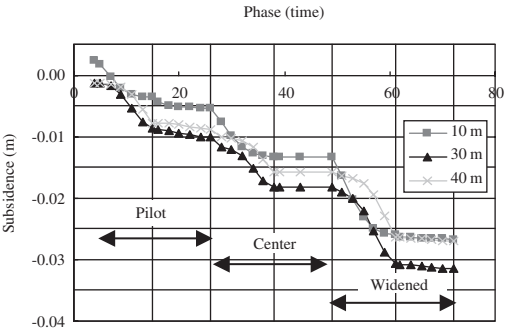


Figure 9. Estimated surface subsidence across the tunnel apart from the portal of the tunnnel to construcion.

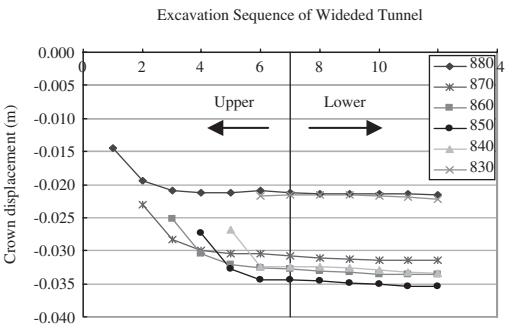


Figure 10. Estimated crown displacements according to the excavation in widened tunnel.

center tunnel, the lower section excavation has a very small effect on the subsidence.

The crown displacements of the widened tunnel have the convex shape in which the mid point has the largest displacement 40 mm. The large deformation occurs immediately after the excavation, and the displacements converge rapidly. However, in the phases of the lower section excavation of the tunnel, a little amount of displacement occurs (Figure 10).

The maximum column stress is about 19,700 kPa (197 kgf/m^2) at the closest column to the portal of the tunnel (#880). This value is much larger than the design stress 73 kgf/m^2. However, the other columns have values in the range of 50 to 80 kg/m^2.

The stresses in the rakers are around 50∼100 kN (5∼10 tonf) and the maximum value is 500 kN in the inner raker.

Except the raker, the other rakers have similar values. The second row of rakers reveals the larger stress than the first row. This means the lower part of the retaining wall structure moves out toward the open area.

Copyright © 2005 Taylor & Francis Group plc, London, UK

4 MEASUREMENTS

4.1 *Surface subsidence*

The maximum surface subsidence was observed around the center line above the three-arch tunnel 30 m apart from the portal (Figure 11). The value of the maximum subsidence was 134 mm at the stage of widened tunneling, that is 3.2 times much larger than the original design estimation (41.8 mm). The ground already settled 65 mm after the pilot tunneling, additionally 8 mm after the center tunneling and 61 mm during the final widened tunneling as shown in Figure 11. From these observed measurements, we could notice that the large subsidence occurred in the stages of the large excavated section such as the pilot and widened tunnels.

4.2 *Crown displacements*

The measured value of the crown displacement was 12 mm after the pilot tunneling, additionally 8 mm after the center tunneling and 29 mm during the widened tunneling.

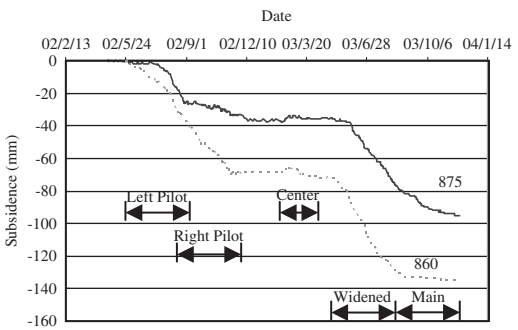


Figure 11. Measured surface subsidence according to the construction sequences of the tunnel.

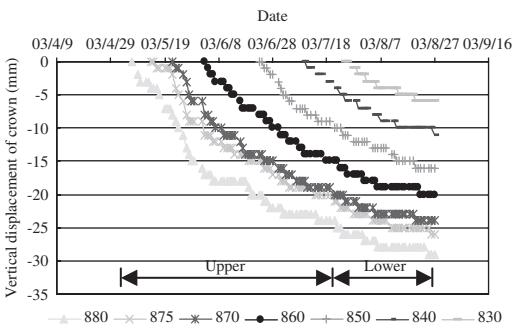


Figure 12. Measured crown displacements due to the widened tunneling.

4.3 *Axial forces developed in the rakers*

The reinforced struts had not been supported in the open-cut station until the complete excavation of the pilot tunnel. Therefore this might cause considerably large longitudinal displacement of the earth retaining wall. To prevent this deformation, each end of the wales was fixed to a concrete structure for the station at the stage of the center tunneling. As a result, the displacements of the rakers had been reduced but the axial forces of the rakers had been greatly increased. The maximum axial force of the raker was increased up to about 110 tonf at the final tunneling stage.

5 DISCUSSION

As compared, the predicted numerical behavior of the portal of the three-arch tunnel is different from the measured results. This might be caused by the earth anchors. The ground numerically reinforced by embedded element may have more stiffness than the in-situ situation and hence the stress release around the fixed anchor could not been modeled. On the other hand, the stress release around the anchor induces much larger deformation of the earth retaining wall and hence much larger settlement in the ground surface.

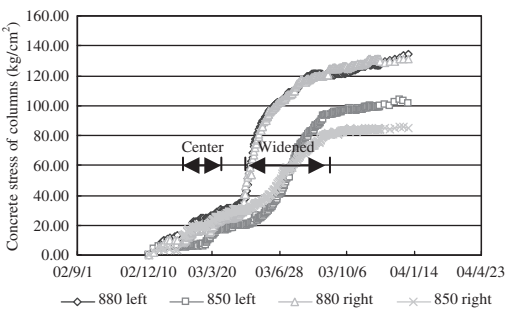


Figure 13. Measured stress in columns.

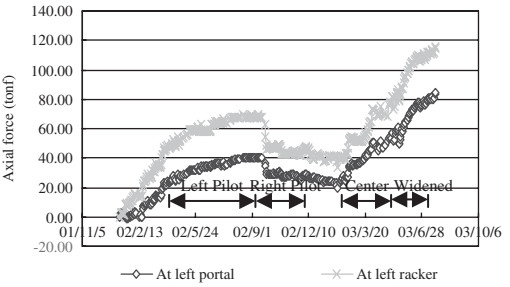


Figure 14. Measured axial forces in the second row of the raker.

Copyright © 2005 Taylor & Francis Group plc, London, UK

Furthermore, in the linear analysis, the plastic behavior of the ground and so on cannot be appropriately modeled. This gives more stiff deformation and some different estimated behavior of the portal. The nonlinear analysis might be required to model the measured large deformation characteristics of the tunnel structure.

6 CONCLUSIONS

It is very important to properly predict the behavior of the portal of the tunnel and to measure the surface subsidence and the displacement of the earth retaining wall, especially in the case of tunneling structures constructed in weathered soil or rock in urban area. In this paper, a three-arch tunnel constructed in Korea for the subway station was introduced. The phased analysis was carried out to describe the construction sequences of excavation, and the numerical results were shown and compared with the measured results. The measured surface subsidence 30 m apart from the portal was 134 mm which is much larger than the estimated value from a linear analysis. This large subsidence might be caused by the lateral deformation of the earth retaining wall. The longitudinally short tunnel relative to the width has been much influenced by the portal behavior. Therefore the design of the portal support system of such a tunnel must be carefully carried out.

REFERENCES

Chang, S.B., Moon, S.J., Kwon, S., Huh, D.H. & Bae, G.J. 2002. A design case study of the very wide 3-arch tunnel Daejeon railroad station building (I). *Tunnelling Technology* 4(3): 247–259.

Galli, G., Grimaldi, A. & Leonardi, A. 2004. Three-dimensional modeling of tunnel excavation and lining. Computers and Geotechnics 31: 171–183.

You, K.H. & Park, Y.J. 2002. Stability analysis of a 2 arch tunnel considering excavation sequence. *Tunneling Technology* 4(2): 167–173.

Daejeon subway construction center. 2001. *Analysis report of 3-arch tunnel in Daejeon Metropolitan Rapid Transit*.

Copyright © 2005 Taylor & Francis Group plc, London, UK

Evaluation of the stability and support design for the underground caverns in an abandoned gold mine

S.K. Chung, Y.S. Jeon, C. Sunwoo & Y.B. Jung
Korea Institute of Geoscience and Mineral Resources, Daejeon, Korea

ABSTRACT: A series of geotechnical surveys and in-situ tests were carried out to evaluate the stability of the natural caves and the man-made underground mine openings for an abandoned gold mine. After the closure of the mine, both the natural caves and the man-made underground openings are being served as tourist route. Therefore, it has become essential to analyze the stability of the entire subsurface caves for ensuring safety of visitors. Multistage convergent photography technique was applied in order to determine joint characteristics in one of the large natural caves. Detailed investigations are performed to evaluate RMR, GSI and Q values for stability analysis of caves and for designing required support systems of the unstable openings. Numerical analysis has been carried out to examine the risk of rock fall. Based upon the stability analysis, support patterns for the underground openings are recommended. A special structural design was also introduced in order to protect the visitors from unexpected collapse of the large natural caves and the mined caverns.

1 INTRODUCTION

Hazardous abandoned mine problems include catastrophic land subsidence or sinkhole due to collapse of subsurface cavities, environmental impacts associated with harmful minewater drainage and muckpile of tailings. For a decade, these problems have been occupying one of the global concerns and millions of dollars have been put into solving that. The abandoned underground mines have been utilized as food storage, waste repository, mining museum or tourist attraction.

This study has been carried out to evaluate the stability of underground caves in an abandoned gold mine. Mine caves had been excavated until the whole mine was closed. After the closure of the mine in 1940's, both the natural caves and the man-made underground openings have been served as a tourist route since 1990's.

Rock mass classification and numerical analysis were carried out to evaluate the stability of caves. Rock fall analysis has been carried on the rock masses of the largest cave where discontinuities were investigated by the multistage convergent photographing method. From the results of rock mass classification and numerical analysis, the support design was recommended. Also, several special structural design were introduced in order to protect the visitors from unexpected collapse of the large natural caves and the mined caverns.

2 GEOLOGY AND GENERAL FEATURES

Figure 1 shows the regional geological map of the studied area. The geology of this area consists of Joseon supergroup belonging to Paleozoic Era intruded by granitic rocks and dykes of Jurassic or

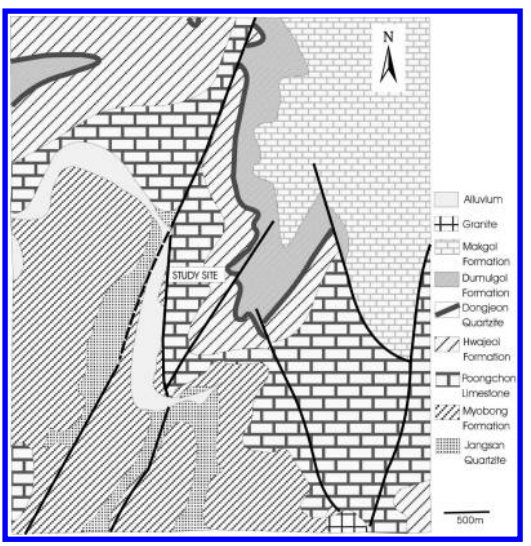


Figure 1. Geological strata.

Copyright © 2005 Taylor & Francis Group plc, London, UK

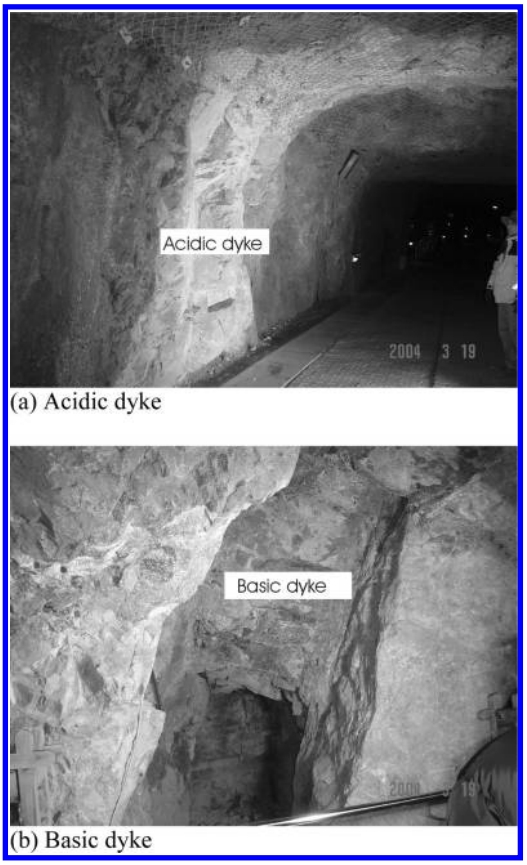


Figure 2. Dykes intruded in limestone.



Figure 3. Natural limestone cavity.

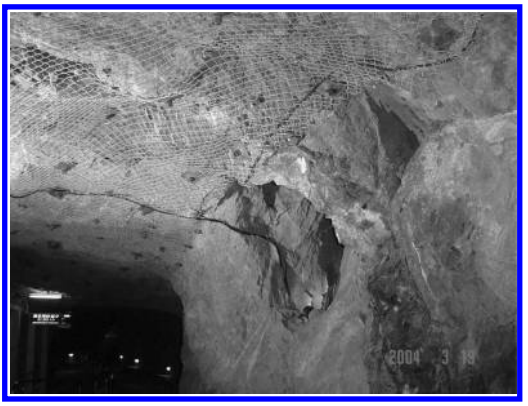


Figure 4. Rockbolts and wire net installed on the crown of the main visitors route.

Cretaceous Period. The predominant surrounding rock of the main roadway is Poongchon limestone intruded by acidic or basic dykes (Fig. 2). The formation of gold is expected to being created due to intrusion of these igneous rocks.

Mining had been carried out the gold vein which develops along the fault zone inside the limestone bedrock. Rock raises and in-vein drifts were used as the main mining structure. The dimension of main roadways of the mine is about 4–5 m wide and 2–3 m high and its total length is about 1.8 km. Many natural limestone caves can be found along the fault zone (Fig. 3). Figure 4 shows rockbolts and wire net installed on the crown of the main visitors route.

3 CHARACTERISTICS OF ROCK MASSES

3.1 *Rock mass classification*

Rock mass classification systems have been developed over the year to describe the rock mass or ground and to formalize an empirical approach to tunnel design. The different classification systems place different emphasis on various engineering geological parameters. In this study, detailed investigations were performed on the Rock Mass Rating (RMR), Geological Strength Index (GSI) and Q classification to evaluate the actual stability of the caves on the one hand and to design the reasonable support systems of the unstable openings on the other. The data required for the classification of the rock mass were collected from 33 underground locations.

Figure 5 shows the location of geological and geotechnical survey. As shown in this figure, investigations were carried out along the whole visitors routes. Multistage convergent photographing was applied to

Copyright © 2005 Taylor & Francis Group plc, London, UK

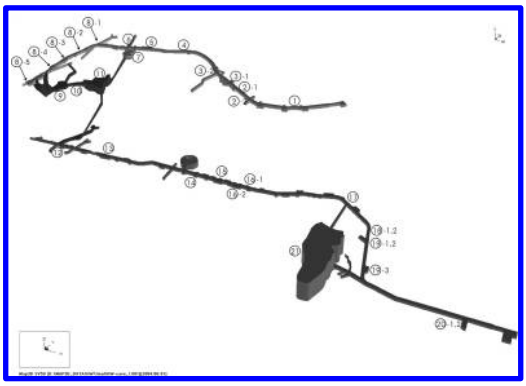


Figure 5. Three dimensional view and Location of geotechnical survey.

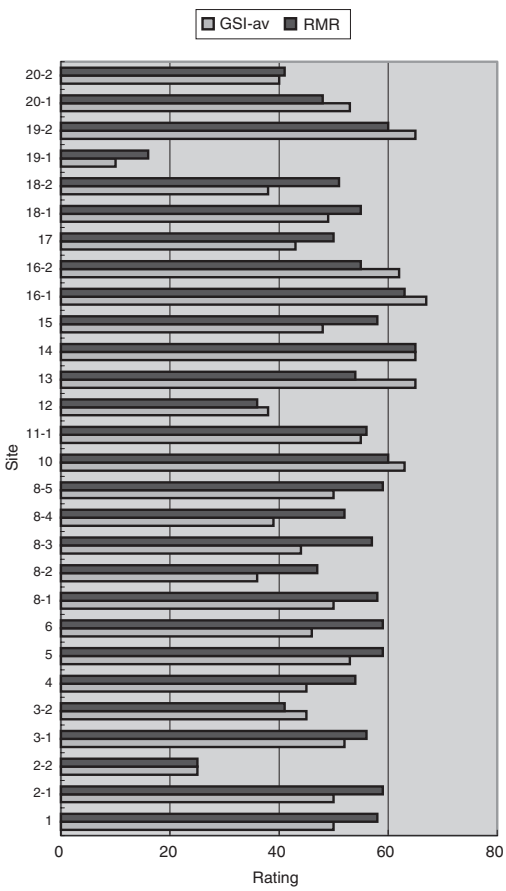


Figure 6. Summary of RMR and GSI classification.

Table 1. Summary of Q-system classification.

Site	RQD	Jn	Jr	Ja	Jw	SRF	Q-value
2-1	65	12	3	2	1	1	8.13
2-2	20	12	3	8	0.66	1	0.41
3-2	20	12	1.5	0.75	1	1	3.33
4	35	15	1.5	6	1	1	0.58
5	50	12	3	2	1	1	6.25
8-2	35	12	3	6	1	1	1.46
12	65	12	1	4	0.66	1	0.89
15	65	12	0.5	1	1	1	2.71
17	40	12	1	6	1	1	0.56
18-1	65	12	1	1	0.66	1	3.58

determine the joint characteristics in location 21 since direct investigation was impossible.

Figure 6 shows the results of rock mass classification both RMR and GSI. It is seen from the plot (Fig. 6), RMR values of the rock masses were classified in the range of fair to good except for the location 2-2 and 19-1 encountered with the fault zone. The Q values of the rock masses were classified as very poor to fair (Table 1). According to the support categories proposed by Grimstad & Barton (1993), these classes fall in the reinforcement category of the type 4 to type 1. A systematic bolting with a shotcrete of 4–10 cm thick can be designed for the type 4 and no support is necessary for the type 1.

There are a few fundamental differences between the rock mass rating RMR of Bieniawski (1973) and the rock mass quality Q system of Barton et al. (1974). RMR does not consider the stress condition of the rock masses, while Q system does not consider joint orientation and intact strength parameter. Regardless of these differences, inter-relations between RMR and Q system have been proposed by many researchers (Rutledge & Preston, 1978; Moreno, 1980; Abad et al., 1983; Bieniawski, 1976; Sunwoo & Hwang, 2001). These correlations have extensively been used in designing of rock tunnels or slopes.

For the comparison of results obtained in the present study, the correlations between Q and RMR or GSI are drawn (Figs 7–8). As shown in the figures, the correlation coefficient between GSI and Q is higher than that of RMR. The correlation equation between GSI and Q is $GSI = 5.98 \times \ln Q + 39.5$. Table 2 shows the Q values calculated from this equation and support categories.

3.2 *Digital photogrammetric technique*

In this study, digital photogrammetric technique, called as multistage convergent photographing system, was applied in order to determine joint characteristics in one of the large natural caves. This technique interprets joint information from a pair of image of the rock

Copyright © 2005 Taylor & Francis Group plc, London, UK

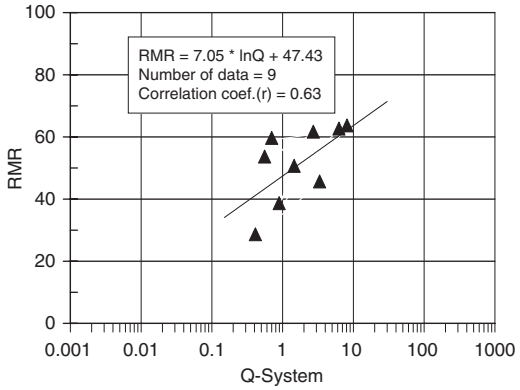


Figure 7. Relationship between Q system and RMR.

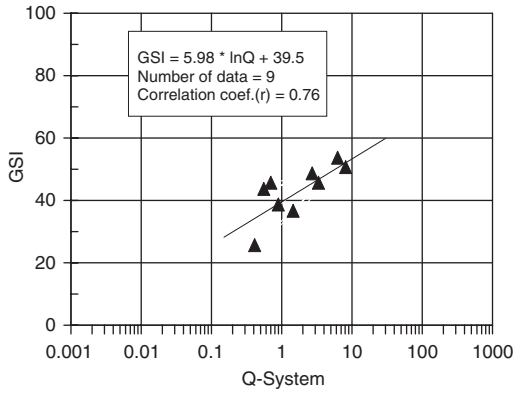


Figure 8. Relationship between Q system and GSI.

Table 2. Proposed support categories based on Q system.

Site	Q-value	Support category*
1	5.79	(1)
2-1	8.13	(1)
2-2	0.41	(5)
3-1	8.09	(1)
3-2	3.33	(4)
4	0.58	(5)
5	6.25	(1)
6	2.97	(4)
8-1	5.79	(1)
8-2	1.46	(4)
8-3	2.12	(4)
8-4	0.92	(4)
8-5	5.79	(1)
10	50.9	(1)
11-1	13.36	(1)
12	0.89	(5)
13	71.1	(1)
14	71.1	(1)
15	2.71	(4)
16-1	99.35	(1)
16-2	43.06	(1)
17	0.56	(5)
18-1	4.90	(1)
18-2	0.78	(5)
19-2	71.1	(1)
20-1	9.56	(1)
20-2	1.09	(4)

*(1): unsupported; (4): systematic bolting with 40–100 mm unreinforced shotcrete; (5): Fiber reinforced shotcrete, 50–90 mm, and bolting.

surface. The dimension of the natural cave is about 40 m wide and 20–30 m high and its length is about 80 m. Figure 9 shows the investigation location of photogrammetric technique. The results of multistage convergent photographing are shown in Table 3.

4 NUMERICAL ANALYSIS

Rock fall analysis has been carried out on the location 15 and 21. UNWEDGE program is originally designed for a quick and interactive use to analyze the geometry and the stability of underground wedges defined by intersecting structural discontinuities in the rock mass surrounding an underground excavation.

The dimension of the location 15 cave is 4 m wide and 3 m high. The dominant joint sets are 255/12 (dip direction/dip) in set 1, 202/80 in set 2, 312/88 in set 3 and 018/73 in set 4. In the case of unsupported, the safety factor of blocks was less than 1 except for combination of set 1, 2 and 4. Therefore, a support system using shotcrete and rockbolt was taken into consideration (Fig. 10). After installation of support member, the safety factor of all wedges became greater than 4.8 which is considered effective for this location (Table 4).

The UNWEDGE analysis has been carried on the rock masses of the largest cavern where discontinuities were investigated by the multistage convergent photographing method. Maximum width of the cavern is about 40 m and height is about 80 m. The locations of analysis and the characteristics of discontinuities are shown in Figure 9 and Table 3. Figure 11 shows the wedges formed in the case of site 2 for the three joint planes 1, 2 and 4 defined in Table 3. In the case of roof wedge, the wedge weighs about 880 tonnes and the safety factor is 0.25. However, since the dimension of wedge is too large to install the equipments in the cavern, it is impossible to support the cavern. Therefore, it is recommended to change the visitors routes which can avoid unexpected rock falls.

Copyright © 2005 Taylor & Francis Group plc, London, UK

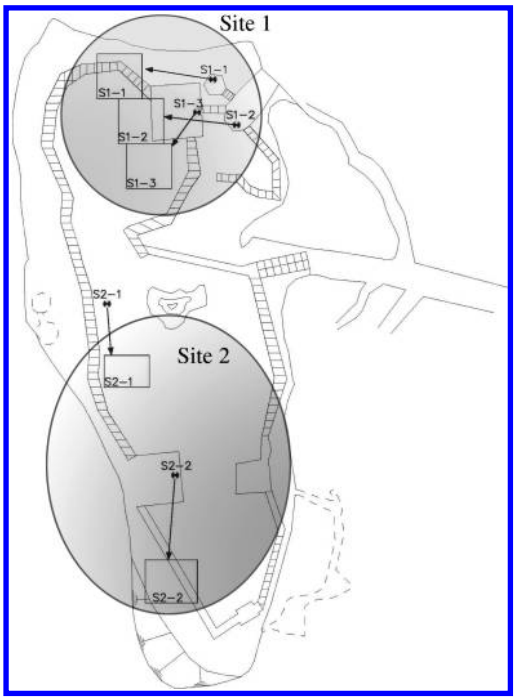


Figure 9. Investigation location of multistage convergent photographing.

Table 3. Results of multistage convergent photographing.

Site	Joint set	Dip direction/ dip (°)	Length (m)	Spacing (m)
S1-1	1	061/29	2.09	1.78
	2	003/35	0.71	10.0
	3	302/67	2.09	9.35
S1-2	1	061/29	N/A*	37.04
	2	003/35	0.36	16.39
	3	302/67	0.84	3.39
S1-3	1	061/29	16.08	1.56
	2	003/35	9.20	10.87
	3	302/67	N/A*	N/A*
S2-1	1	346/50	15.9	6.29
	2	019/70	N/A*	17.86
	3	336/80	9.95	5.03
	4	098/30	N/A*	19.23
S2-2	1	346/50	2.90	17.24
	2	019/70	2.70	9.26
	3	336/80	2.50	40.0
	4	098/30	3.34	5.99

* N/A: Not Available.

5 CONCLUSIONS

This paper presents a case study of utilization of abandoned mining. In this study, various investigations

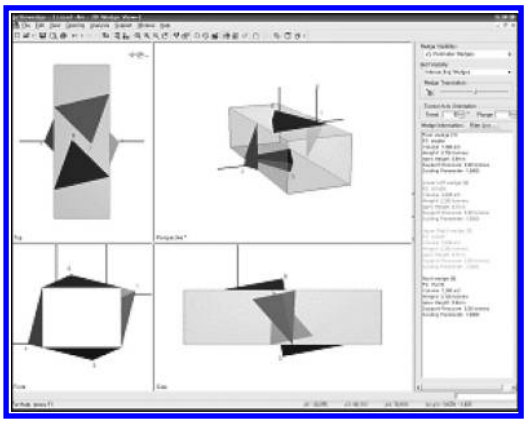


Figure 10. A result of rock fall analysis after reinforcement.

Table 4. Variation of safety factor on the blocks.

Combination no.	Joints	Safety factor		Weight of block (ton)
		Unsupport	Support	
1	1,2,3	0.26	15.76	0.489
2	1,3,4	0.04	13.53	2.283
3	1,2,4	4.79	4.85	526.856
4	2,3,4	0.03	19.09	4.514

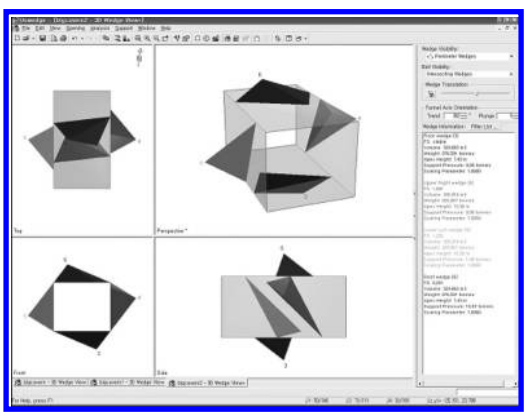


Figure 11. A result of rock fall analysis (Site 2).

and analyses were carried out to evaluate the stability of the natural caves and the man-made underground mine openings for an abandoned gold mine. The dimension of main roadways of the mine is about 4–5 m wide and 2–3 m high and its total length is about 1.8 km. Many natural limestone caves can be found along the fault zone. Rock raises and in-vein drifts were used as the main mining structure. It is

Copyright © 2005 Taylor & Francis Group plc, London, UK

essential to analyze the stability of the entire tourist route to ensure the safety of the visitors.

Detailed investigations were performed on the RMR, GSI and Q classification to evaluate the actual stability of the caves and to design the reasonable support systems of the unstable openings. The Q values of the rock masses were classified as very poor to fair. Based on the Q value, reinforcement category of the type 1, 4 and 5 is recommended. A systematic bolting with a shotcrete of 4–10 cm thick can be designed for the type 4 and no support is necessary for the type 1. The rock fall analysis has been carried on the typical roadway and in the largest cave where discontinuities were investigated by the multistage convergent photographing method. The risk of rock fall in the form of wedges by the principal joint sets from the roof or from the sidewall of the cave is also examined. It is inferred that the support system recommended by Q system will be effective to arrest any rock fall.

REFERENCES

Abad, J. Celada, B. Chacon, E. Gutierrez, V. & Hidalgo, E. 1983. Application of geomechanical classification to predict the convergence of coal mine galleries and to design their supports, *Proc. 5th Int. Congr. Rock Mech., ISRM*, 2: E15–E19. Melbourne.

Barton, N.R. Lien, R. & Lunde, J. 1974. Engineering classification of rock masses for the design of tunnel support. Rock Mech. 6(4): 189–239.

Bieniawski, Z.T. 1973. Engineering classification of jointed rock masses. *Trans. S. African Instn. Civil Engrs* 15: 335–342.

Bieniawski, J.T. 1976. Rock mass classifications in rock engineering. *Proc. of the Symp. On Exploration for Rock engineering, Johannesburg.* 11: 27–32. Rotterdam: Balkema.

Bieniawski, Z.T. 1989. *Engineering rock mass classification*. New York: John Wiley & Sons.

Grimstad, E. & Barton, N. 1993. Updating for the Q-system for NMT, In Kompen, Opsahl and Berg(eds), *Int. Symposium on Sprayed Concrete – Modern use of wet mix sprayed concrete for underground support*, Oslo: Norwegian Concrete Association.

Hoek, E. Kaiser, P.K. & Bawden, W.F. 1995. *Support of underground excavations in hard rock*. Rotterdam: Balkema.

Moreno Tallon, E. 1982. Comparison and application of the geomechanics classification schemes in tunnel construction, *Proc. Tunneling '*82: 241–246.

Reid, T.R. & Harrison, J.P. 2000. A semi-automated methodology for discontinuity trace detection in digital images of rock mass exposures, *Int. J. Rock Mech. & Min. Sci.* 37(7): 1073–1089.

Rutledge, J.C. & Preston R.L. 1978. Experience with engineering classification rock, *Proc. Int. Tunneling Symp*: A3.1–A3.7. Tokyo.

Sunwoo, Choon & Hwang Se-Ho. 2001. Correlation of rock mass classification methods in Korean rock mass, In S. Wang, B. Fu & Z. Li (eds.), *Proc. of the 2001 ISRM Symo.-2nd Asian Rock Mech. Symp. Beijing*: 11–14. Rotterdam: Balkema.

Zhang, L. & Einstein, H.H. 1998. Estimating the mean trace length of rock discontinuities, *Rock Mechanics and Rock Engineering* 31(4): 217–235.

Copyright © 2005 Taylor & Francis Group plc, London, UK

Stability analyses of the dump site culvert in Tınaz Surface Mine

Ö.C. Özcan & E. Ünal
Department of Mining Engineering, Middle East Technical University, Ankara, Turkey

ABSTRACT: In this paper stability analyses of the box-shaped dump-site culvert constructed in Tınaz Surface Mine of Turkish Coal Enterprises (TKİ) are presented. In addition, stability conditions of other culvert alternatives are evaluated. Existence of creeks in a surface mining area is a significant factor to be considered in selection of dump-site location. Since, the dumped overburden material on the valley acts as a barrier and behaves like a dam causing flood problem behind the dump-site. TKİ engineers prevented the flood potential that might have occurred behind the dump-site by constructing a 480-meter long reinforced-concrete culvert on the downstream of Gevenez Creek Valley. However, considerable amount of deformations occurred in the first 100 meters of the culvert as a result of overburden material being replaced on this structure. In order to determine the failure mechanism associated with the culvert, a series of numerical modeling analyses were carried out utilizing back analysis technique. The validity of the numerical model was justified by convergence measurements and observations carried out inside the culvert as overburden material being replaced on the stable part of the structure. Finally, based on the numerical model developed, the stability of other culvert alternatives that could be used in future projects were evaluated considering different embankment conditions (positive projecting and negative projecting), bedding conditions (impermissible, ordinary, first-class and concrete cradle), culvert shapes (box and circular) and dumping conditions.

1 INTRODUCTION

In a surface mine, considerable amount of overburden material has to be removed to produce coal or ore hence location of dumpsite has paramount importance in decreasing the cost of production. Existence of a creek valley on the selected dump site is a significant issue to be considered. Since, the dumped overburden material on the valley acts as a barrier and behaves like a dam; it disturbs the natural flow pattern of the surface waters and cause flood problem behind the dump site.

A similar problem was observed in Tınaz Surface Mine of Turkish Coal Enterprises (TKİ). TKİ tried to solve this problem by constructing a cast-in-place concrete box-shape-culvert on the existing valley and decided to convey water through this culvert without disturbing the natural flow pattern of the creek. After construction of the culvert, TKİ started to dump the overburden material on the valley including the culvert. However, when the height of the overburden material, dumped on the culvert, reached to 33 m, which is much lower than the designed height of 80 m, TKİ engineers observed a considerable deformation inside part of the culvert.

In this study, a numerical model of Tınaz Culvert is developed by making use of back analysis technique and validity of the numerical model is justified by convergence measurements and field observations carried out inside the culvert as overburden material is being replaced on this structure. Additionally other alternatives that could be used in future culvert projects of surface mines are analyzed.

2 METHODOLOGY

Predicting the mechanical behavior of the engineering structures like tunnels, large caverns and dams with sufficient accuracy is a difficult task. This is simply due to the fact that there are many uncertainties involved in the input data for the numerical analysis. Thus, the actual behavior of the structures offer differs from those predicted (Sakurai, 1997).

In order to overcome this inadequacy in design, inverse solution techniques are used in rock mechanics. The essence of the inverse solution approach is to derive the unknown material properties, system geometry, and boundary or initial conditions based on a limited number of laboratory or usually in-situ measured values of some key variables. In the case of rock engineering, the most widely applied inverse solution technique is back analysis (Jing and Hudson, 2002). It can bridge the gap between prediction and reality (Sakurai, 1997).

Copyright © 2005 Taylor & Francis Group plc, London, UK

In order to model dump site culvert of Tınaz Mine, back analyses method is used in combination with numerical modeling. Observed deformations during preliminary field studies are used to predict unknown data about the culvert and dump site.

3 PRELIMINARY FIELD STUDIES

Tınaz lignite mine is located near to Tınas town of Muğla, Turkey. In general, lignite was formed in a subsided basin in this area. Paleozoic schists and Mesozoic marbles, composing the upper layers of the subsided basin, border the lignite zone. Middle-upper Miocene aged Neogene deposit, including lignite horizon, fills the subsided basin.

The dump-site culvert in Tınaz Mine consists of two parts, namely "old culvert" and "new culvert", as shown in Figure 1. The total length of the old culvert, and the first 85 meters of the new culvert were constructed on Middle-Miocene aged Turgut Formation. This formation is intercalated with foliated clays and silts, well-cemented silt, clay and fine-grained gravel. During investigations it was observed that a discontinuity plane is passing through the 85th – 100th meters of the new culvert (Ünal et al., 2002). The new culvert, which is considered in this study, is 480 m in length from a joint connection to the old culvert. It has a cross-section of 3 × 3.7 m.

During initial stages of the overburden dumped on the new culvert deformations were observed between the 4th and 96th meters of the culvert when the overburden height reached to 33 meters. The maximum deformation estimated was about 30 cm. There were also considerable deformations taking place in the upper left and lower right corners, when looking from the entrance towards to the exit of the culvert, as seen in Figure 2.

Prior to this study the height of overburden material on different parts of the culvert was changing significantly (Figure 1). This non-homogenize dumping was one of the reasons why deformations occurred inside the culvert (Özcan, 2003).

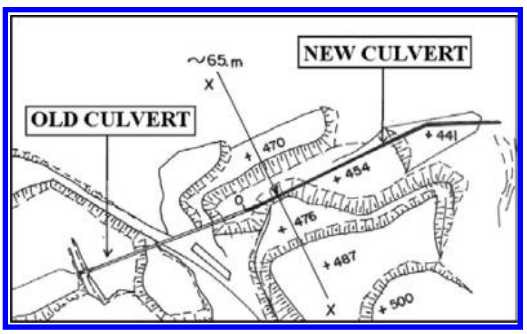


Figure 1. Existing culverts and heights of dump sites prior to study.



Figure 2. Deformations in "new" culvert.

4 NUMERICAL STUDIES ON EXISTING CULVERT

Significant deformations were observed in the first 100 meters of the new culvert due to the affect of overburden material dumped on this structure. During preliminary field investigations, on the other hand, it was observed that the maximum deformation has taken place in the 65th meter of the culvert. Consequently 65th meter of the culvert is taken into consideration in modeling. The culvert and dump site model, created by using Phase 2, is presented in Figure 3.

In order to characterize the applied construction method in the model, five different stages are identified namely: (i) the initial condition of the dump site before construction of the culvert; (ii) excavation of the foundation; (iii) replacement of boulders to the foundation excavation; (iv) construction of the cast-in-place reinforced concrete culvert; (v) dumping of overburden material on dump site including culvert.

During preliminary field studies, four different material types were identified, namely undisturbed

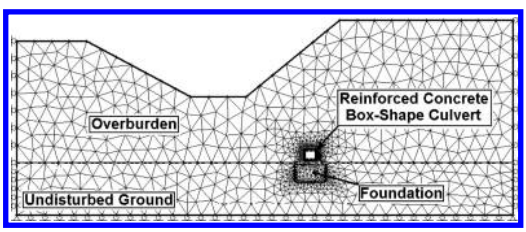


Figure 3. Culvert, dump site model and identified materials prior to study.

Copyright © 2005 Taylor & Francis Group plc, London, UK

ground, foundation, reinforced concrete and overburden as illustrated in Figure 3. The input parameters used for each material type are given in Table 1.

In order to reflect the physical observations made (failed locations) inside the culvert to the output obtained from the software (safety factors) and thus to be able to obtain comparable results, the "back analyses" technique was used. In order to obtain safety factor less then one at the locations where failure was observed the tensile strength and cohesion of the reinforced concrete was reduced. In that, the tensile strength and cohesion of the reinforced concrete was taken as 3.25 MPa and 5.2 MPa, respectively, reducing the original values about 35%, which could be considered as groundwater affect.

Safety factor distribution in the inner walls of the culvert in existing situation considering the groundwater is shown in Figure 4. In this figure, the safety factors in the upper-left and lower-right corners are below 1.00, meaning that compression failures occur in this two regions.

As a result of numerical studies carried out on the deformed part of the culvert in Tınaz Mine, an acceptable agreement between the behavior of actual deformations in the culvert (Figure 2) and in the model is evident. Consequently, it is concluded that numerical model, including model characteristics and input parameters for four identified materials, represents the existing failure mechanism in the dump site culvert of Tınaz Mine.

To determine the maximum height of the overburden material that could be dumped on the non-deformed part of the culvert (100–480 m), a new numerical model was considered.

In view of the fact that, the results obtained from numerical and back analyses of the deformed part of the culvert represent the behavior of the actual culvert of Tınaz Mine, the same input parameters, presented in Table 1, could be used for the non-deformed part with confidence. During these studies, homogeneously dumped overburden height of 80-meters, and existence of groundwater were considered.

As an outcome of these numerical analyses, a relationship between the minimum safety factor in the inner walls of the culvert and height of the overburden material that could be dumped on the culvert was determined, as shown in Figure 5. It is clearly seen from the figure that maximum height of the overburden material that could be dumped on the culvert is 30 m. considering the affect of groundwater and a safety factor of 1.10.

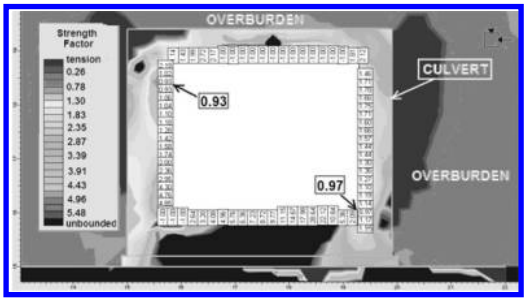


Figure 4. Safety factor distributions in the inner walls of the culvert in existing situation considering the groundwater effect.

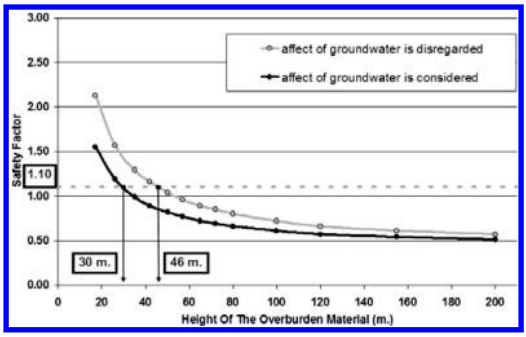


Figure 5. Relationship between minimum safety factor in the inner walls of the culvert and height of the overburden material on the culvert.

Table 1. Input parameter for each material type identified in existing situation (Özcan, 2003).

Input parameters	Undisturbed ground	Foundation	Reinforced concrete	Overburden
Loading condition	Field stress & Body force	Body force	Body force	Body force
Unit weight (MN/m^3), γ	0.027	0.027	0.027	0.0255
Young's modulus (MPa), E	5000	20000	30000	20
Poisson's ratio, ν	0.2	0.2	0.3	0.2
Material type	Elastic	Elastic	Elastic	Elastic
Failure criteria	Mohr-Coulomb	Mohr-Coulomb	Mohr-Coulomb	Mohr-Coulomb
Tensile strength (MPa), σ_t	0	0	5	0
Internal friction angle (°), φ	30	35	30	30
Cohesion (MPa), c	3	10.5	8	0

Copyright © 2005 Taylor & Francis Group plc, London, UK

5 FIELD MEASUREMENTS IN EXISTING CULVERT

In order to justify the validity of numerical modeling studies on the non-deformed part of the existing dump site culvert and to determine the maximum height of the overburden material a series of convergence measurements were carried out during overburden material being dumped on the non-deformed part of the culvert.

Dumping process has started following the installation of 14 convergence stations in the culvert. Convergence measurements were taken daily, as the overburden material being dumped. As a result of these measurements, the deformations occurring due to dumping of overburden material were identified.

Deformations occurring due to controlled and homogeneous dumping of the overburden material was evaluated based on (i) "Convergence" vs. "Time" and (ii) "Convergence" vs "Height of the Overburden Material" plots (Özcan and Ünal, 2002).

The maximum total convergence measured in the culvert was −55.78 mm in Station Y6 when the overburden replaced on the non-deformed part was 31.08 meters. The maximum convergence-rate was found as 6.15 mm/day, and the maximum convergence occurring as a result of unit dumping-height was found as 5.4 mm/m in that station. "Convergence" vs. "Time" and "Convergence" vs "Height of the Overburden Material" graphs are presented for Station Y6 in Figures 6 and 7 respectively.

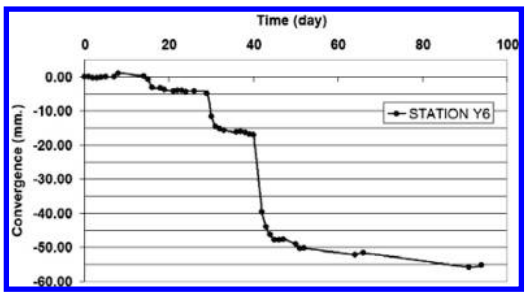


Figure 6. "Convergence" and "time" relation for Station Y6.

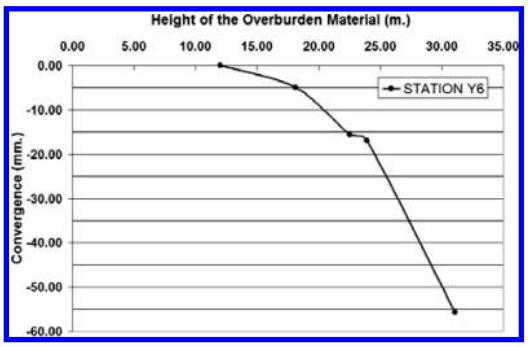


Figure 7. "Convergence" and "height of the overburden material" relation for Station Y6.

Considering the changes in convergence rate and total convergence, and observing the deformations in the culvert, the maximum height of the overburden material reached on the culvert was about 31 meters.

Based on the results obtained from the numerical modeling studies, carried out on the deformed part of the culvert, the maximum height of the overburden material that could be replaced on the culvert was determined as 30 meters (see Figure 5).

Consequently, by comparing the results obtained both from numerical analyses and field studies it is concluded that there is an acceptable agreement between the predicted and actual behavior of the culvert. Thus, the numerical model developed can be used to predict the actual behavior of dump site culvert in Tınaz Mine. In view of the fact that existing culvert model could not be able to stay stable under 80 meters of overburden height, alternative culvert models should be derived for future culvert projects based on the justified numerical model (Özcan, 2003).

6 NUMERICAL STUDIES ON ALTERNATIVE CULVERT MODELS

Embankment (overburden) culverts can be divided into two namely positive projecting and negative projecting culverts (Yang, 2000).

6.1 *Positive projecting embankment condition*

A positive projecting embankment culvert is one which is installed in shallow bedding with its top projecting above the surface of natural ground and which is covered with an embankment (Spangler and Handy, 1973).

The positive projecting culvert models for four different bedding conditions defined by U.S. Army Corps of Engineers (1997) namely, impermissible, ordinary, first class, and concrete cradle are taken into account to derive alternative circular culvert models.

As a result of numerical analyses carried out on alternative positive projecting culvert models, none of them stay stable under an overburden height of 80 meters under any groundwater condition (Özcan, 2003).

6.2 *Negative projecting embankment condition*

A negative projecting culvert is the one, installed in a relatively narrow and shallow trench with its top at an elevation below the natural ground surface and which

Copyright © 2005 Taylor & Francis Group plc, London, UK

is then covered with an embankment. This is a very favorable method of installing a culvert since the load produced by a given height of fill is generally less than it would be in the case of positive projecting culvert (Spangler and Handy, 1973).

Since the existing dump-site culvert of Tınaz Mine, analyzed previously, could not be included in this category, a box-shape culvert model was analyzed as an alternative in negative projecting embankment condition as well. Additionally negative projecting circular-shape culvert models for three different bedding conditions defined by U.S. Army Corps of Engineers (1997) namely, impermissible, ordinary and first class are taken into account to derive alternative circular culvert models. Numerical model for first class bedding condition is illustrated in Figure 8.

As a result of numerical analyses carried out on alternative negative projecting culvert models, all of the alternative culverts stay stable under an overburden height of 80 meters under any groundwater condition.

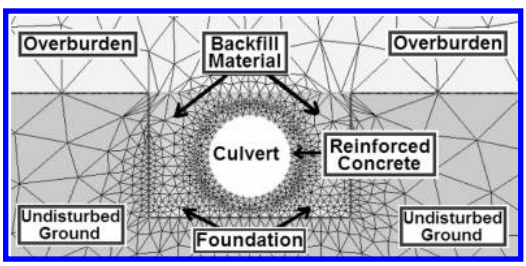


Figure 8. Negative projecting circular-shape culvert model having first-class bedding condition.

6.3 *Comparison of existing culvert and alternative culvert models*

In order to compare the existing dump-site culvert of Tınaz Mine with alternative culverts, the most stable culverts (culverts having higher safety factor under same overburden height and groundwater condition) are selected from each embankment type.

In positive projecting embankment condition, the culvert having first class bedding, which could stay stable under 26 m. of overburden load, is determined as the most stable alternative. The existing box-shape culvert on the other hand, stays stable under 30 meters of overburden load.

In negative projecting embankment condition, again the culvert having first-class bedding, which stays stable under 130 meters of overburden load, was determined as the most stable alternative among the other culvert models. The alternative box-shape culvert on the other hand, stays stable under 87 meters of overburden load.

The plots, showing the relation between the "lowest safety factor" in the inner walls of the existing and alternative culverts and the "height of the overburden material" on the culverts, is illustrated in Figure 9.

7 DISCUSSION

Information about the numerical studies on future dump site culverts has been presented in previous section. However, one part of the numerical analyses requires further discussion.

According to the numerical studies, it is found that the existing box-shape positive projecting culvert of

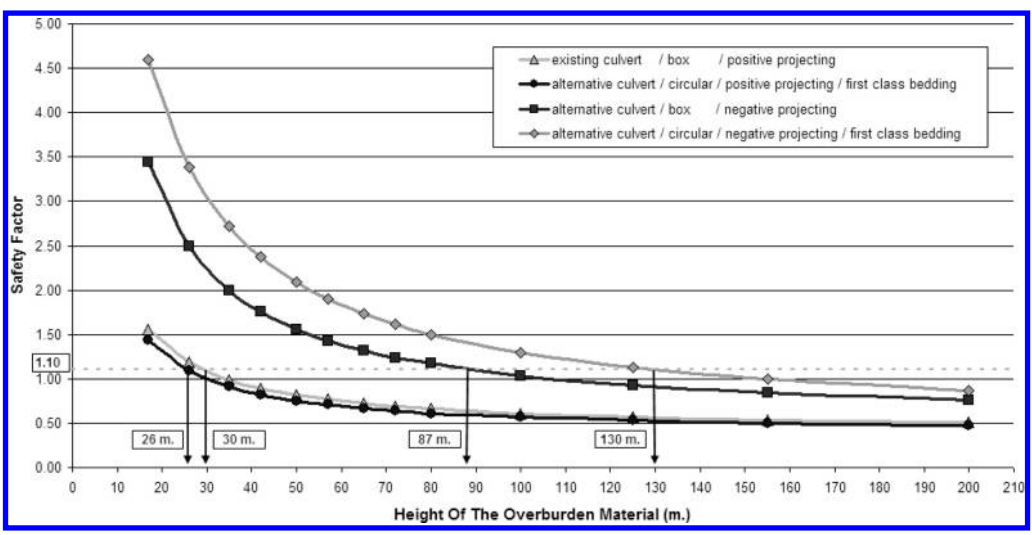


Figure 9. Relationship between "safety factor" and "height of the overburden" for existing and alternative culverts.

Copyright © 2005 Taylor & Francis Group plc, London, UK

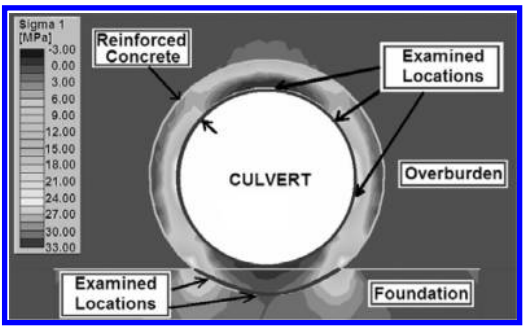


Figure 10. Examined locations of major principle stresses.

Table 2. Examination results of major principle stresses including lowest safety factors in the inner walls of the culverts.

Culvert shape	Bedding condition	Max. σ_1 (MPa) (inner walls)	Max. σ_1 (MPa) (basement)	Min. SF (inner walls)
Circular	Impermissible	45.70	57.15	0.62
Circular	Ordinary	29.12	22.00	0.78
Circular	Concrete cradle	19.66	18.34	0.88
Circular	First-class	17.18	14.05	0.96
Box	–	20.48	10.01	0.99

Tınaz Mine is more stable than any of the alternative circular-shape positive-projecting culvert models under same conditions. In order to examine the result of these analyses, which is interesting enough since lower safety factors are expected in the box-shape culvert as a result of higher stress concentrations in the edges distribution of principle stresses were examined in the inner walls and in the basement of the culverts. Examined locations of principle stresses are illustrated in Figure 10. Results are given in Table 2 including lowest safety factors in the inner walls of the culverts.

As can be seen from Table 2, the highest value of major principle stress occurred in circular-shape culvert having impermissible bedding. As the contact area between the culvert and foundation increases (from circular-shape culvert having impermissible bedding towards box-shape culvert), value of major principle stress decreases on basement, since the load on culvert is better transferred to the ground. Although principle stress in the inner walls of the box-shape culvert is higher than principle stress in the inner walls of the circular-shape culvert having first-class bedding as a result of stress concentration in the edges, box-shape culvert transfers that stress better because of having larger contact surface consequently it has the highest safety factor.

8 CONCLUSIONS

Based on the studies carried out in paper, the following conclusions can be drawn:

– Considering the results of convergence measurements, evaluating the plots of "Convergence vs. Time" and "Convergence vs. Height of the Overburden Material", and observing the deformations inside the culvert, the maximum height of the overburden material attained in the field, was about 31 meters justifying the validity of numerical modeling, computing 30 meters.
– After the completion of the dumping process it has been justified that the methods of dumping possess significant effect on the stability of a culvert. In that, when the overburden reaches to a height of 31.08 meters as a result of controlled and homogeneous replacement along the culvert axis, the maximum total convergence occurring inside the culvert reaches to a value of −55.78 mm. This value is considerably small when compared to the deformations occurred (about 30 cm) in failed part of the culvert as a result of non-homogeneous and uncontrolled replacement (about 33-meters in height), carried out perpendicular to the culvert axis, for approximately the same overburden heights.
– Bedding conditions of circular-shape culvert models, having positive or negative projecting embankment conditions, have significant affect on the stability of culvert. In the developed models first-class bedding provides better safety factors than concrete cradle, ordinary and impermissible beddings, under the same conditions.
– From stability point of view, any culvert in negative projecting embankment condition is significantly better than any culvert in positive projecting embankment condition.
– For optimum design, the ease of construction of the culvert should also be considered. Although the most stable alternative culvert is determined as circular-shape culvert with first-class bedding in negative-projecting embankment condition, the box-shape culvert in negative projecting embankment condition could also be chosen.

REFERENCES

Jing, L. & Hudson, J.A. 2002. Numerical methods in rock mechanics. *International Journal of Rock Mechanics & Mining Sciences* 39 (4): 409–427.

Özcan, Ö.C. 2003. Stability analyses of the dump site culvert in Tınaz Surface Mine. *M.Sc. Thesis. METU, Ankara, Turkey*: 155 pages.

Özcan, Ö.C. & Ünal, E. 2002. Tınaz Ocağı'nda inşa edilen kutu menfezin duraylilik koşullarinin belirlenmesi, *6th*

Copyright © 2005 Taylor & Francis Group plc, London, UK

Regional Rock Mechanics Symposium, Konya, Tukey: 317–324.
Sakurai, S. 1997. Lessons Learned From Field Measurements in Tunneling. *Tunneling and Underground Space Technology* 12 (4): 453–460.
Spangler, M.G. & Handy, R.L. 1973. Soil Engineering. *Intext Educational Publishers*: 748 pages.
US. Army Corps of Engineers, 1996. Engineering and Design: Conduits, Culverts and Pipes. *US. Army Corps of Engineers, Department of the Army, Washington DC., USA*: 87 pages.
Ünar, E., Öztürk, H. & Özcan, Ö.C., 2001. "GELİ Tınaz Açıkocağı'nda inşa edilen menfezin duraylılık koşullarının belirlenmesi". *Project No: 01-03-05-01-2-00-05, METU, Ankara, Turkey*: 117 pages.
Yang, M.Z. 2000. Evaluation of Factors Affecting Earth Pressures on Buried Box Culverts, *PhD Thesis, The University of Tennessee, Knoxville, USA*: 565 pages.

Copyright © 2005 Taylor & Francis Group plc, London, UK

Automated finite element model generation for tunnel forms

Ahmet Türer
Asst. Prof. Dr., Civil Engineering Dept., Middle East Technical University, Ankara, Turkey

Ökkeş Sultanoğlu & Ahmet Şuyun
MİM Mühendislik A.Ş., Kazan, Ankara, Turkey

ABSTRACT: The construction stages of tunnels are composed of geotechnical survey, excavation, stabilization with steel-mesh placement and shot grid concrete, post-tensioned soil anchorage, and immediately following up with reinforced concrete wall casting. Although some methods – such as in the case of Austrian – would use casting just for decoration, the thickness of the reinforced concrete walls is a function of excavated material characteristics and the tunnel geometrical dimensions. The concrete wall preparation needs to be fast to avoid any premature collapses. Reinforcement placement and concrete casting requires special forms which should be easily and quickly installed and removed. The forms are usually custom made for the specific needs and geometric properties of a tunnel. This paper explains the automated finite element (FE) model generation tool developed at Middle East Technical University. The mesh generation algorithm intelligently constructs complicated FE models within minutes and allows the flexibility to modify the original form dimensions (such as form depth, plate thickness, etc.) to optimize the design parameters. The loading on the tunnel form is also automatically generated for different levels of concrete hydrostatic pressure. The liquid concrete height assumptions can be based on the average pumping speed (m^3/hour), concrete wall thickness, form's longitudinal length, and concrete setting time. Conservative loading conditions, such as all concrete staying at its liquid state (for low temperatures or concrete retarders) or additional concrete pumping pressure, can be easily defined for any generated tunnel form FE models. Load combinations and envelope curve generations are also streamlined using a simplified "load combination matrix". All of the FE model and load condition generation is carried out using spreadsheets and developed macro codes.

1 INTRODUCTION

The forming and casting of concrete walls inside the tunnels is the last and probably one of the most critical stages of the tunnel construction in addition to the other stages of construction such as geotechnical survey, excavation, stabilization with steel-mesh placement and shot grid concrete, and post-tensioned soil anchorages. The stability of a tunnel most commonly relies on the shape and quality of walls, with the exception of Austrian method which uses concrete wall just for decoration.

The thickness of the reinforced concrete walls is a function of excavated material characteristics and the tunnel geometrical dimensions. The concrete wall reinforcement placement and concrete casting need to be fast to avoid any premature collapses. Special tunnel forms are required to cast the concrete. The general characteristics of the forms are categorized as:

(1) Have the proper shape of the inner line of the tunnel,
(2) Withstand concrete and pumping hydrostatic pressures,
(3) Easily and quickly mountable and dismountable,
(4) Repeatedly usable and durable,
(5) Have proper vibration tools to settle the concrete.

The first criterion is supplied by the client. The second one in the list is provided through detailed finite element (FE) modeling and repetitive modifications and analyses using commercially available analysis tools. An automated FE model generation module is prepared at Middle East Technical University, Civil Engineering Department to simplify and streamline the complicated geometry modeling and mesh generation work. Numerous loading conditions are also automatically generated to simulate the various loads on the forms and explained in further detail in the coming sections. The ease of use in the operation of the forms is provided by the smartly placed hinges along the perimeter of the forms. The forms can basically bend their arms inside to shrink their size in to a smaller

Copyright © 2005 Taylor & Francis Group plc, London, UK

shape which will easily move inside the tunnel to its subsequent location along its path and expand again to take its original shape. The durability and long life is achieved by using steel as the material of the forms. The surface vibrators located evenly at the inner surface of the forms to enable proper placement of low water content and low workable concrete between the tunnel rock/soil surface and the forms. This paper will mainly concentrate on the automated FE modeling and analysis of the tunnel forms.

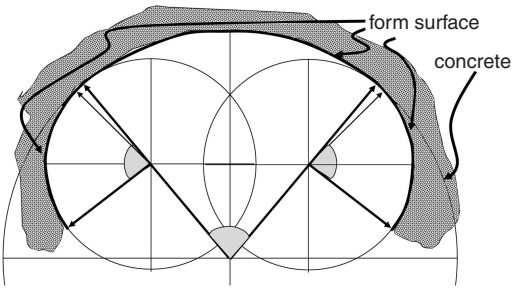


Figure 1. General cross section of a circular tunnel form.

2 FINITE ELEMENT MODEL GENERATION

The tunnel forms do not usually have regular shapes such as rectangle or circle. The shapes are usually more complicated, generated by combinations of two or more circles with different centers and radiuses (Figure 1). The inner sides of the forms are also irregular due to fabrication constraints and formed by linear pieces of steel members connected to each other by means of welded and hinged joints. The analysis and design of such complicated structures cannot be carried out in closed from neither by using generous assumptions and simplifications; however, a detailed three-dimensional (3D) finite element (FE) modeling and analysis is required. Generation of the 3D FE model manually inside the commercially available analysis software is inefficient and generally not possible due to the complexity of the model geometry. A generic FE model generation tool is necessary to streamline the modeling process and simplify the modeling efforts. FE model generator also minimizes the possibility of human error in definition of joint coordinates, element connection, loading values etc. The modeling algorithm written in MS Excel is briefly explained below.

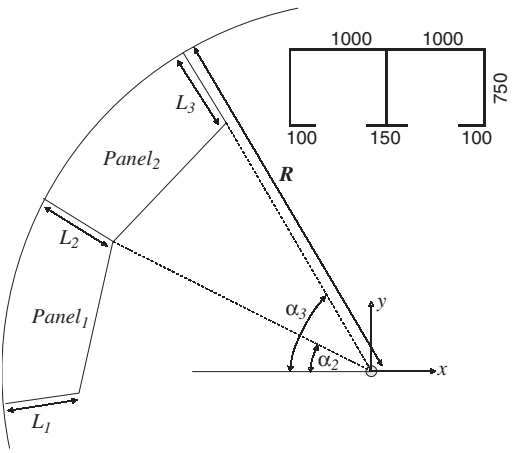


Figure 2. Detailing of the form sides and cross section.

2.1 *Mesh generation*

The round shaped tunnel forms have a tube-like shape in the longitudinal direction with rounded surfaces on the sides which are composed of a number of different centered circles having different radiuses.

The cross section of the forms are composed of "ribs" that are usually two meters long, which can be mounted next to each other to form a continuous form, giving the flexibility to maneuver pieces and modify total form length. The side view and the cross section of the ribs are somewhat complicated and usually look like the ones shown in Figure 2.

The first challenge to model the form automatically is to generate the sides (panels) as shown in Figure 2. The (two meter) surface and the rest of the form can easily be generated in analytical model by duplication as the circular shaped outer edge of the form is once generated. The meshing of the sides is intelligently generated using the centroid of the outer circle, panel numbers, edge thicknesses of the panels (L_1, L_2,...), and panel edge location angles (α_1, α_2,...). The outer edge of the form can be generated making use of sine and cosine functions, edge location angles (α_1, α_2,...), and radius of the section:

$$(xL4_i, yL4_i) = (x_{centroid} - R * \cos(\alpha_1 + \Delta\alpha * i), y_{centroid} + R * \sin(\alpha_1 + \Delta\alpha * i),) \quad (1)$$

$\Delta\alpha$ shown in the above equation is the angle increment step which is calculated by dividing the angle difference ($\alpha_3 - \alpha_2$) by the number of segments in each panel (Figure 2 and Figure 3). The number of segments is calculated by dividing the arch length by pre-defined FE member length and rounding it to the closest integer. The geometric definition of (xL4, yL4) is shown in Figure 3. (xL1, yL1) and (xL2, yL2) points shown on the same figure are also easily calculated using centroid of the circle but subtracting length of the panels l_{panel} and $l_{\text{panel}+1}$ from the circle radius as shown in Figure 3.

Copyright © 2005 Taylor & Francis Group plc, London, UK

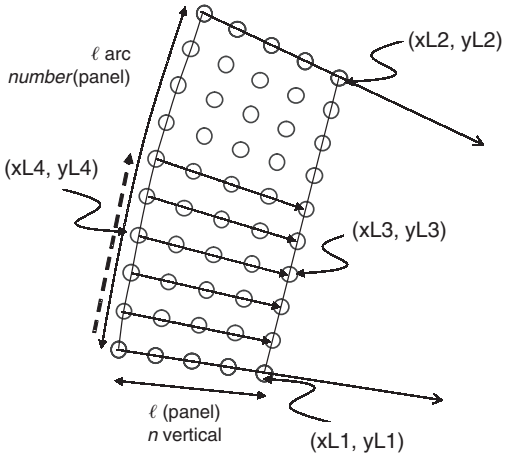


Figure 3. Meshing form's side.

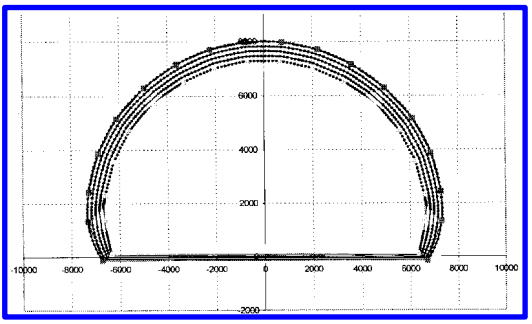


Figure 4. Overall meshing of the form sides.

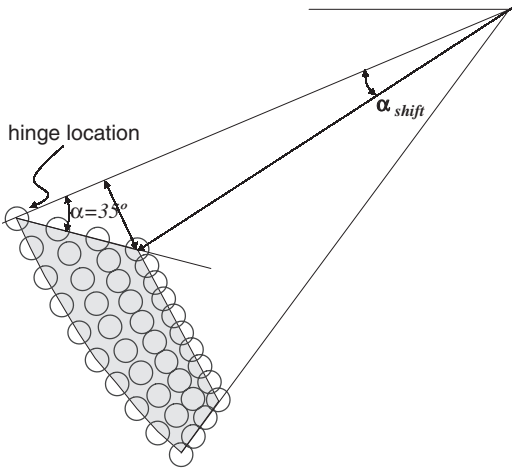


Figure 5. Correction of meshing for hinge locations.

After the coordinates (xL1, yL1) and (xL2, yL2) are calculated, (xL3, yL3) point can be found by linear interpolation between coordinates (xL1, yL1) and (xL2, yL2). All of these efforts to calculate coordinates (xL3, yL3) and (xL4, yL4) is to compute the intermediate nodes at the face of the panels which are located at the sides of the circular tunnel form and more difficult to generate. All of the other nodes are computed by linearly interpolating between coordinates (xL3, yL3) and (xL4, yL4) giving the nice transition of shapes between the rounded edge at the outer surface and straight edge at the inner surface. All of the nodes can now be automatically generated to form the general shape of the form as shown on an example in Figure 4.

The automated generation works nicely to form the sides of the form, however, problems arise if there are hinges at various locations of the form. Existence of hinges is a necessity to make the form bend inside, in a way the form shrinks to a smaller size to detach from the concrete surface and move inside the tunnel to the next casting position. When hinges are located, the sides of the forms are wedged to permit the form pieces to close. The FE model has to include these modifications so that the stress concentrations and strut forces at the hinge joints be calculated. The model generation program searches for the predefined hinge locations and defines a 35 degree wedge at the edges to compute modified (xL1, yL1) and/or (xL2, yL2) locations. Once these locations are corrected, the rest of the algorithm works fine to compute intermediate joint locations.

(xL1, yL1) and (xL2, yL2) coordinates are corrected by modifying the edge location angle(s) α_1 and/or α_2 to include the wedge angle. The change in the angle is computed by calculating the distance of shift along the (xL1, yL1) and (xL2, yL2) line. The distance shift is equal to l_{panel} distance times $\tan(\pi*35°/180°)$ which is also equal to $(R_{circle} - l_{panel})*\tan(\alpha_{shift}*35°/180°)$. Shift angle "$\alpha_{shift}$" can be calculated using the following equation.

$$l_{panel}*\tan(\pi*35°/180°) = (R_{circle}-l_{panel})*\tan(\alpha_{shift}*35°/180°) \quad (2)$$

Corrected position(s) of (xL1, yL1) and/or (xL2, yL2) coordinates are found using the original angle "α" and "α_{shift}" (Figure 5).

An MS Excel spread sheet is prepared for automated FE model generation. A tabular format in the Excel worksheet enables easy entry and alteration of tunnel form related parameters, and execution of a Visual Basic code embedded in Excel Macros generates nodal coordinates and shell member connection information between the generated nodes.

Copyright © 2005 Taylor & Francis Group plc, London, UK

2.2 *Load generation and analyses*

The FE generator algorithm also generates the hydrostatic concrete pressure around the form for predefined number of cases with worksheet entered heights of the concrete (Figure 6). The heights of the fresh concrete are defined based on the pumping speed.

Under normal conditions a pumping speed of 25 m^3/hour is expected. The spacing between the form and the tunnel soil times the perimeter of the form times the length of the form approximately gives the total volume of concrete that needs to be cast. Dividing the total volume by the pumping speed gives the average time to complete the casting job. Assumption of concrete settlement time as 1–2 hours is a good estimate to define different levels of hydrostatic concrete pressure. For the unlikely event of having

(a) low temperature,
(b) using admixtures to delay the concrete settling time (such as under hot weather or low water/cement content,
(c) or having casting concrete too fast (many concrete pumps working at the same time or small form size with small amounts of concrete volume,

the tunnel form can be totally filled with liquid concrete, therefore the form loading should also include the case of totally filled liquid concrete.



Figure 6. Numerous loading conditions on the tunnel form rib by concrete and pump.

	Comb01	Comb02	Comb03	Comb04	Comb05	Comb06	Comb07	Comb08	Comb09	Comb10	Comb11	Comb12	Comb13	Comb14	Comb15	Comb16	Comb17	Comb18	Comb19	Comb20	Comb21	Comb22	Comb23	Comb24
Load1	x																							
Load2		x																						
Load3			x																					
Load4				x																				
Load5					x																			
Load6						x																		
Load7							x																	
Load8								x																
Load9									x															
Load10										x	x													
Load11												x	x											
Load12														x	x									
Load13																x								
Load14																	x	x						
Load15																			x	x				
Load16																					x	x		
Load17																							x	x
Pompa											x		x		x			x		x		x		x
DL	x	x	x	x	x	x	x	x	x	x	x	x	x	x	x	x	x	x	x	x	x	x	x	x

Figure 7. Combination of loading cases to form an envelope of combinations.

A separate loading case of pump pressure should be included (e.g., minimum of 3 ton/m^2 = 30 kPa) acting on all surfaces of the form as the concrete fills up the empty volume and pump generates an overall pressure at the outer surface of the form. The loading cases generated in this way can be combined together with the dead load (DL) acting on the form and pressure load to generate the worst loading combination (Figure 7). The member forces and stresses calculated in each loading condition will then be combined using the load combination table (again by the modeler macro) and the maximum of the absolute stresses and forces are found using an "envelope case" which will combine the worst of all combination cases for all members.

All of the joint coordinate, member connection, and hydrostatic pressure calculations take place inside the macro and model data are generated on a separate excel work-sheet in text format (Figure 8) in SAP90 format. The results are manually copied from the

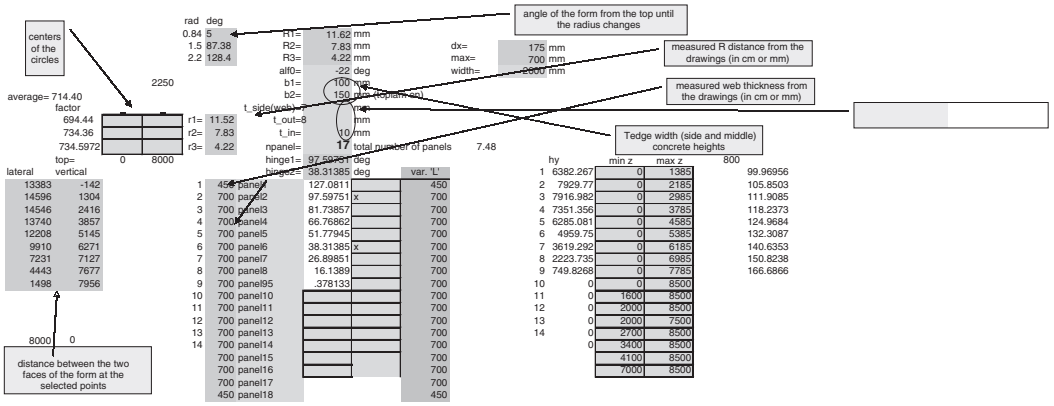


Figure 8. Excel interface to define important parameters of the form for automated generation.

Copyright © 2005 Taylor & Francis Group plc, London, UK

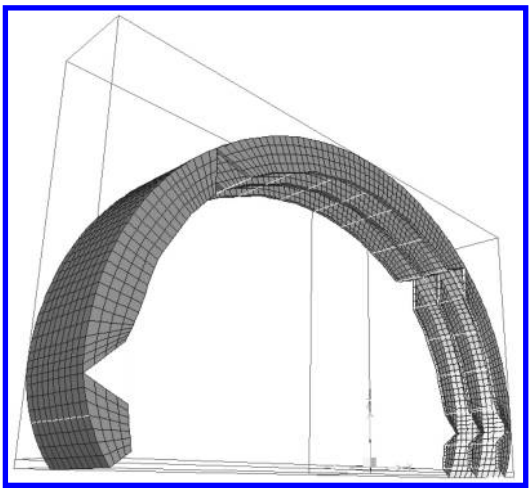


Figure 9. General view of a completed FE model.

excel worksheet and pasted into a text document using Notepad. The results are saved in a directory where the model will be analyzed. SAP90 formatted input file is imported to SAP2000 using import utility from program's file menu.

Minor manual corrections and additions (such as bars, supports, cart etc.) to the generated complicated geometry of the tunnel form are possible inside the analysis program. Shell thickness of the plates can also be manually modified without regenerating the model. Following the execution of the analysis program, the results are obtained in the form of stresses and forces, which are compared against stress and force capacities of the members. Local buckling of flanges and global buckling of axial load members are manually checked. If critical members are found, model is manually updated to include additional stiffeners and/or modification to plate thicknesses. If adequate capacity is not achieved in this way, a new model is generated using the FE model generator again for a larger geometry.

3 CONCLUSIONS

The FE model generator developed for multi radius circular tunnel forms proved to be an extremely useful tool for the modeling and design purposes. The complicated geometry of the forms makes it impossible to manually generate models in analysis programs. The model generator prepared in Excel not only simplifies and extremely speeds up the model generation phase but also enables repeated modeling by changing the geometry for an optimum design. Another advantage of automated model generation comes from the calculation of hydrostatic concrete pressure values acting on each and every shell element defined on the tunnel form. All of the pressure values are individually computed by the program and automatically applied on the corresponding shell members. Automated model generation also prevents possible human errors in nodal coordinates and node number connection to shell/frame member definitions, misplacement of loads, typo and similar errors. The final FE model generated using the developed program is exact, complete, and error-free to guide the design process which will achieve the best results and performance during its usage lifetime (Figure 9).

Copyright © 2005 Taylor & Francis Group plc, London, UK

Three-dimensional numerical simulation of tunnel advancement on adjacent pile foundation

C.H. Pang, K.Y. Yong & Y.K. Chow
National University of Singapore, Singapore

ABSTRACT: In this paper, the development of a three-dimensional finite element model to back-analyse a case history on the response of pile foundation subjected to shield tunnelling is described. The case history is from the construction of the MRT North-East Line Contract 704 in Singapore. The FE model was created to back-analyse the behaviour of one of the instrumented pile group at Pier 20 where the full shield tunnelling process, including the application of face pressure, shield tunnel advancement, over-cutting, tail void closure and installation of lining was simulated. The effect of single tunnel advancement was simulated and discussed. Good agreement between the results from analysis and measured data was obtained which validated the FE model.

1 INTRODUCTION

The increase demand for underground system in urban area particularly for transportation purpose as can be seen in Singapore, Hong Kong and London has inevitably resulted in tunnel being constructed in close proximity to superstructures due to space constraint. For superstructure supported on pile foundation, there is a need to carry out proper assessment of the pile response when subjected to the new tunnel construction. Tunnelling induced movement on nearby pile foundation is complex. Depending on the pile-tunnel relative position, additional loading from downdrag caused by soil settlement and bending moment caused by lateral soil movement can be undesirable.

The response of pile foundation when subjected to tunnel construction is principally a three-dimensional problem whether it is the tunnel advancement or the pile foundation. In current practice, the problem has been analysed using either the boundary element method (Poulos 2003) or two-dimensional finite element method (Vermeer & Bornier 1991, Lee et al. 1994). These approaches are idealised with plane strain tunnel and do not simulate the real construction process such as tunnel advancement. Furthermore, pile foundation is modelled as plane strain element (i.e. wall) in two-dimensional FE analysis with smeared properties. The accuracy of the analysis is jeopardised with the assumed properties especially for pile group where soil flow is not allowed in between piles. Three-dimensional analysis is essential for more accurate prediction and gives more flexibility in handling complex tunnelling process and soil condition. In this paper, the development of a three-dimensional finite element model to back-analyse a case history from the MRT North-East Line Contract 704 in Singapore is presented. Full tunnel construction process including the application of face pressure, shield advancement, over-cutting, tail void closure and installation of lining was simulated.

2 MRT NORTH-EAST LINE C704 SINGAPORE

The Mass Rapid Transit (MRT) North-East Line (NEL) is the third major MRT line in Singapore which comprised 22 km long underground track and 16 stations. Contract 704 involved the construction of two cut and cover stations i.e. Woodleigh Station and Serangoon Station, 992 m twin tunnels from Woodleigh Station to Serangoon Station and 1522 m twin tunnels from Serangoon Station to Kovan Station. In addition, the package included the construction of a 1.9 km long dual-lane viaduct bridge. The viaduct bridge which consists of 2 abutments and 39 piers was constructed in parallel alignment with the new twin tunnels configuration and located in between the tunnels. The typical relative position of the pile foundation and the tunnels is shown in Figure 1. The piers are supported mainly on bored piles of 1.2 m diameter in a group of four piles. Along the alignment, the tunnels were located as close as 1.6 m between the extrados and pile edge. The tunnels were bored with two Earth Pressure Balance (EPB) machines of 6.5 m diameter and mainly went through the weathered Granite. An instrumentation

Copyright © 2005 Taylor & Francis Group plc, London, UK

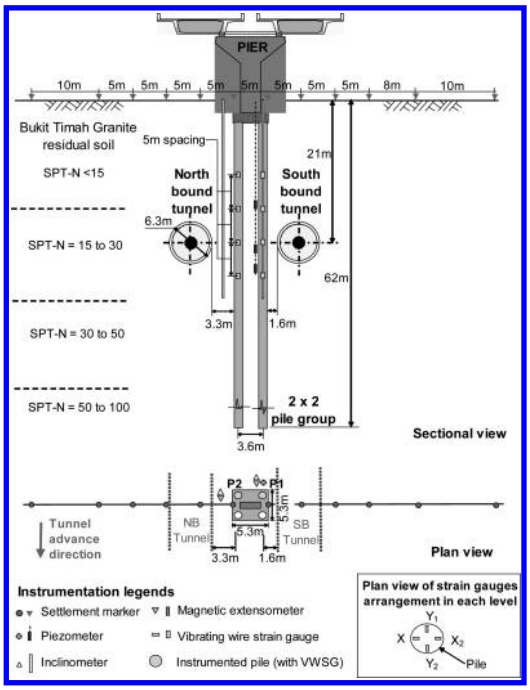


Figure 1. Typical section and instrumentation at Pier 20.

programme was implemented at six piers location. A total of twelve piles were installed with strain gauges at various levels to obtain the axial force and bending moment developed during tunnelling. In addition, in-situ instrumentation such as settlement marker, inclinometer, magnetic extensometer and piezometer were installed at the vicinity of the piles. For back-analysis work described in this paper, monitoring results of Pier 20 were used for comparison since it is the most critical section in term of tunnel-pile distance (i.e. 1.6 m) and volume loss (i.e. 1.38% for SB tunnel and 1.67% for NB tunnel).

3 THREE-DIMENSIONAL FE MODELLING

3.1 *Finite element mesh*

The analysis described in this paper were performed using finite element program ABAQUS (Hibbitt, Karlsson & Sorensen Inc., 2001). Figure 2 shows the typical finite element mesh adopted for the simulation. Only the effect of single tunnel advancement was studied here. All the soils, tunnel lining, pile foundation were modelled using 20-noded continuum solid element. Approximately 5080 elements with total up to 19107 nodes were present in the mesh. Assuming the pile foundation existed on both sides of the tunnel, only half the mesh was created taking the plane of symmetry

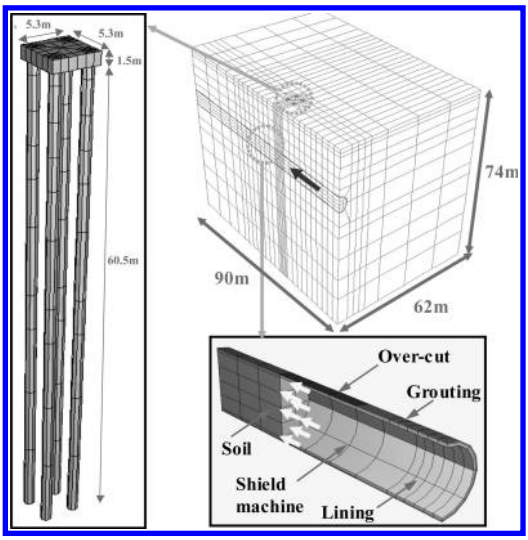


Figure 2. Typical finite element mesh adopted.

at the tunnel axis. Although this was not the case in reality, it was demonstrated through full mesh analysis that there was no significant effect on the results of analysis.

After preliminary study on the boundary effects, the mesh was determined to be 74 m on the vertical length, 62 m on the transverse width and 90 m on the longitudinal length. Out of the 90 m length, the excavation was simulated up to 60 m, which left 30 m of soil in front of the tunnel face. In the model, lateral boundary fixity was assigned perpendicular to the vertical plane, and both the lateral and vertical fixities were assigned to the bottom of the mesh. The pile group was located far enough such that the effect of tunnel approaching and leaving on the pile response could be studied. Therefore, the centre of pile group was modelled 33 m away from the mesh front boundary. The piles were assumed wished-in-place. Pile group of four piles with pile diameter of 1.2 m and length of 60.5 m were modelled. A clear distance of 1.6 m between the pile edge and the SB tunnel extrados was examined. The actual pilecap size of 5.3 m $\times$ 5.3 m with a thickness of 1.5 m was simulated. No interface element was prescribed between the pile and the soil. In the actual condition at Pier 20, the piles at that time were only loaded up to pilecap level prior to tunnel advancement. Therefore, no loading was prescribed on the pile head in the analysis.

3.2 *Geology and ground conditions*

The soil profile was modelled according to the boreholes nearest to Pier 20. At this section, only the Bukit Timah Granite residual soil was encountered. The residual soil is classified as Grade VI material according to

Copyright © 2005 Taylor & Francis Group plc, London, UK

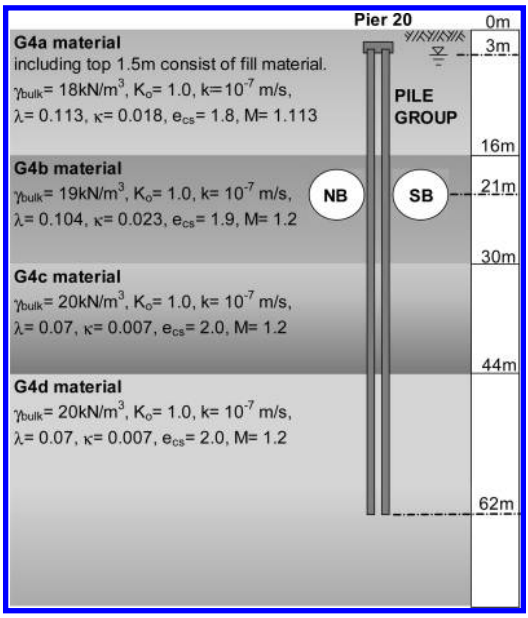


Figure 3. Typical soil profile simulated in FE analysis.

the British Code of Practice (BS5930 1981) or better known as the G4 material according to classification system by Dames & Moore (1983). The G4 material is predominantly reddish brown, sandy silty clay.

Figure 3 shows the idealised soil profile for analysis. Within the G4 material, further layering is classified according to the SPT-N value (Wang 2003). G4a, G4b, G4c, G4d and G4e represent respectively the residual soil with SPT-N $<$ 15, 15 to 30, 30 to 50, 50 to 100 and $>$100. The twin tunnels were located at a depth of 21 m below ground surface. The water table was assumed at 3 m.b.g.l. All the analyses were carried out with coupled consolidation model to simulate the rate of tunnel advancement.

3.3 *Tunnel advancement simulation procedures*

The magnitude of ground movement during the EPB shield tunnelling is highly related to the operational and human factor rather than the ground condition (Shirlaw 2000).

To simulate the effect of shield tunnelling on ground movement as accurate as possible, four main phases of the construction process have to be considered in the model. This includes the face pressure, shield machine advancement (i.e. over-cutting), tail void closure and lining installation. In this paper, the tunnel was modelled using solid elements to represent the shield machine, over-cut, grout and lining. The tunnel face was supported by application of horizontal pressure during the shield advancement. A pressure of 100 kPa as measured (Knight-Hassell & Tan 2000) was assigned in the analysis.

In the FE analysis, advancement was simulated by step-by-step removal of soil element and activation of shield, lining and grout elements. The excavation was simulated with 3 m per step. The advancement rate of 9 m/day was simulated in the analysis. During each excavation step, soil elements were removed with simultaneous application of pressure on the tunnel face and activation of shield and over-cut elements. At the same step, the shield and over-cut elements at the back are removed to simulate the shield length of 9 m. In addition, the initial grout and lining elements were activated there. In C704, the grout mix setting time was in the range of 5 to 12 hours (Shirlaw et al. 2004). With the tunnel advancement rate of 9 m/day, the length of grout to be in fluid state would be between 1.875 m and 4.5 m. Therefore, the length of initial grout was modelled as 3 m length. In the subsequent tunnel advancement, the initial grout element was replaced with grout of hardened property.

3.4 *Material models and parameters*

To consider the pre-failure non-linear stress-strain behaviour, the Strain Dependent Modified Cam Clay (SDMCC) model developed by Dasari (1996) was used. Within the elastic part, the model incorporated the variation of shear and bulk modulus with strain which follow the power laws. On the wet side of the critical state, the classical MCC yield surface was assumed. However, on the dry side of critical state, the Hvorslev surface and a no-tension cut off line were further incorporated into the SDMCC model. More details of the formulations and parameters selected are presented in Appendix A. The general soil properties and standard MCC parameters adopted for different soil layers are shown in Figure 3.

The structural properties such as lining and shield machine were modelled as linear elastic material. The shield machine was modelled with solid elements with Young's modulus of 200 GPa and poisson ratio of 0.25. The concrete lining was modelled with Young's modulus of 28 GPa, density of 24 kN/m^3 and poisson ratio of 0.2. In this study, the over-cutting was modelled using solid elements to induce deformation. Therefore, calibration with measured surface settlement during shield passage was necessary. After sensitivity studies, these elements were assigned Young's modulus of 1000 kPa and a poisson ratio of 0.2. Similarly, an initial Young's modulus of 1000 kPa, poisson ratio of 0.2 and density of 24 kN/m^3 were assigned to the grout of liquid state. The hardened grout element which replaced the liquid grout was assigned stiffness of 50 MPa. The pile was assumed to be linear elastic. From the back-analysis carried out on the instrumented pile load test at the C704 site, Young's modulus of

Copyright © 2005 Taylor & Francis Group plc, London, UK

28 MPa was selected for the strain gauge interpretation and also for the finite element analysis. Poisson ratio of 0.2 was assigned.

4 RESULTS OF ANALYSIS

4.1 *Surface settlement*

Figure 4 shows the comparison between the computed and measured transverse surface settlement trough after the tunnel face had passed the monitoring section by 27 m (i.e. plane strain condition). A fairly good agreement of trough shape and magnitude is achieved although the trough is slightly wider numerically at the far-field. The effect of piles on the surface settlement was also noted with the reduction in settlement extending as far as 25 m away from the tunnel axis.

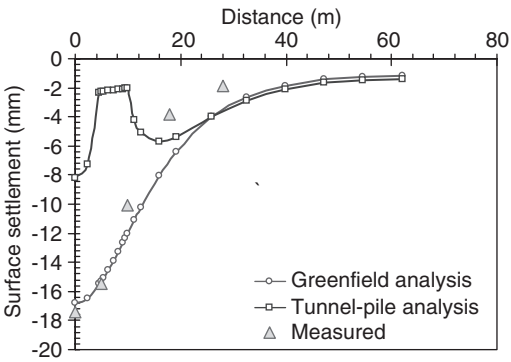


Figure 4. Transverse surface settlement profile.

4.2 *Axial response of piles*

Figure 5 shows the predicted axial and bending responses of the piles when the tunnel face was 27 m away from the centre of the pile group (where plane strain condition had been achieved). The measured data for axial force, transverse BM and longitudinal BM are also included for comparison. As can be seen in Figure 5a, the axial force of piles in the same row i.e. P1 & P4 (front row) or P2 & P3 (rear row) behaved in the same manner and magnitude. The axial force is increasing with depth down to the tunnel springline which indicated the piles are subjected to downdrag from the soil settlement. Below the tunnel springline, the axial force reduced owing to the positive skin friction developed to support the dragload. The predicted axial force is slightly higher than the measured for both the front and rear piles. Piles settlements predicted were very small with maximum magnitude at the pile head up to 2.5 mm only.

4.3 *Bending response of piles*

Figure 5b shows the bending moment of piles in the transverse direction. The maximum magnitudes occurred at the tunnel springline. The maximum computed lateral deflection of piles was only up to 13 mm. The rear piles were subjected to a lower magnitude compared to the front piles. Looking in another direction parallel to the tunnel advancement i.e. longitudinal, the bending moment reduced by more than half the magnitudes observed in the transverse direction (Fig. 5c).

For clearer visualisation of the development of piles responses, the computed deformation of the three-dimensional analysis were extracted for different stages of the tunnel advancement as shown in Figure 6

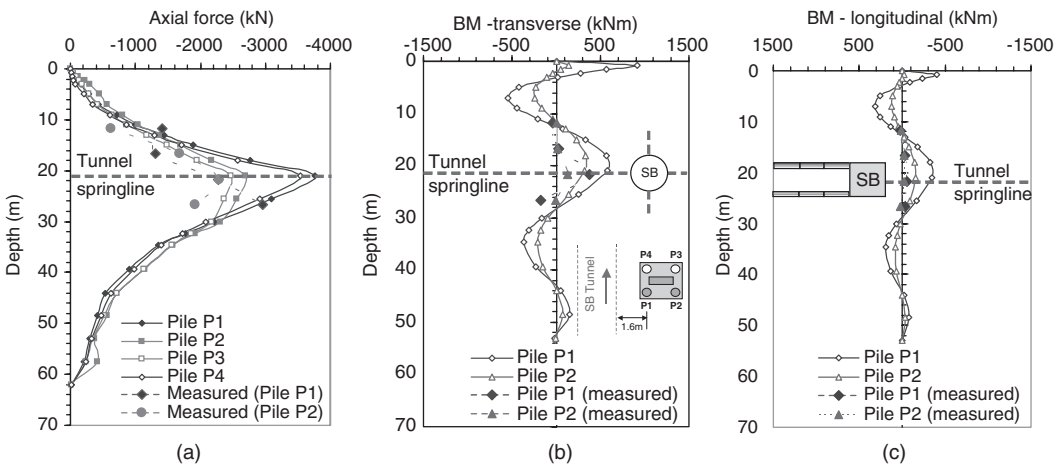


Figure 5. Response of pile foundation (a) axial force (b) transverse bending moment (c) longitudinal bending moment.

Copyright © 2005 Taylor & Francis Group plc, London, UK

for both the transverse and longitudinal planes. On the transverse plane, as the tunnel progressively approached the pile group, the deformation became noticeable particularly when the tunnel face passed by the pile group. As the tunnel face gradually left the pile group, the piles in the same row, i.e. front piles and rear piles behaved similarly which indicated that plane strain condition had been reached. The response of piles were rather different in the longitudinal plane. Prior to the tunnel arriving at the pile group, the piles deflected towards the tunnel with maximum movement at the pile head level and not at the tunnel springline. Subsequently, as the tunnel advanced pass the pile group, the piles were gradually pushed forward in the same direction of the tunnel advancement. The response was caused by the lateral soil movement which moved in the same trend. Similar observations were also noted in measured data reported by Phienwej (1997) and Abu-Farsakh & Voyiadjis (1999) for shield tunnelling work. It was also noted that the piles in the same row were subjected to different magnitude of deflection even after plane strain condition has been achieved unlike in the transverse deflection.

Figure 7 plots the ratio of the maximum responses of the front pile to the rear pile in both the pile group analysis and single pile analysis. Apparently, the front pile was subjected to higher magnitude compared to the rear pile in both the axial and bending responses up to 2.5 times. However, the ratio of axial response was rather insignificant. The measured ratio also showed good agreement with the finite element analysis. As a fact, the soil movement caused by tunnelling reduces as the distance is further away from the tunnel. The positive ratio was attributed to the fact that the front

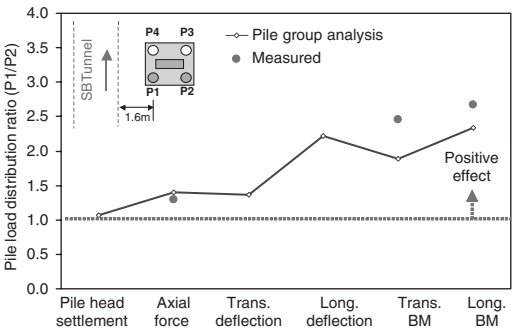


Figure 7. Distribution ratio of front pile to rear pile response.

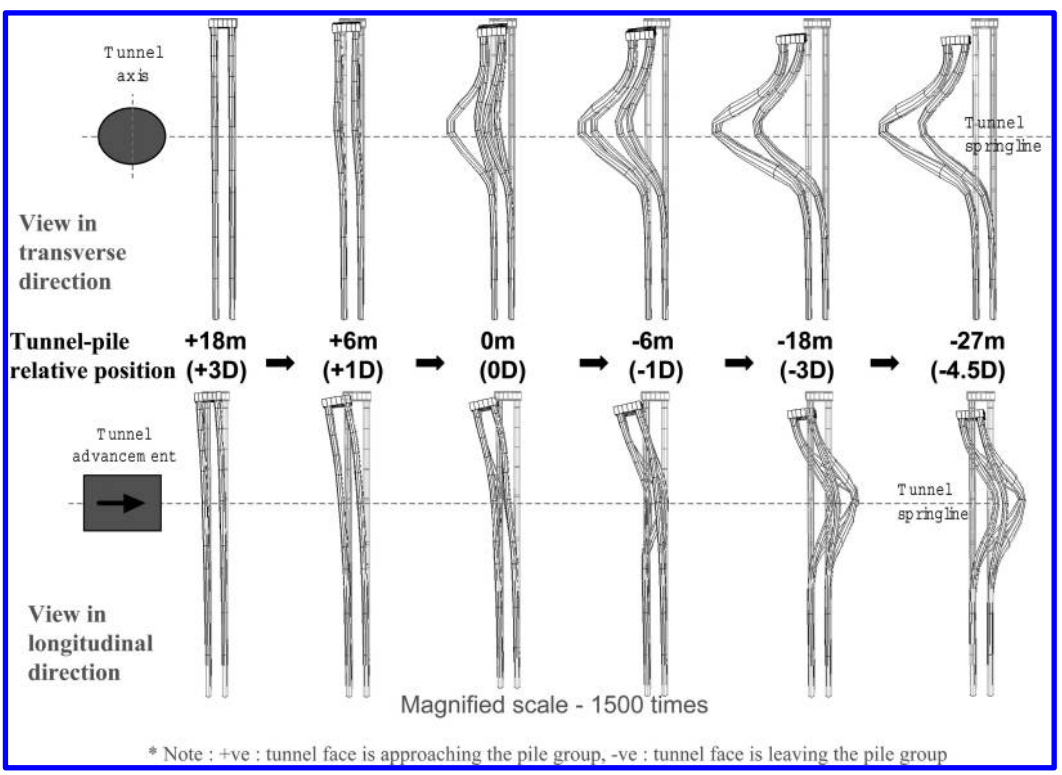


Figure 6. Visualised pile group response at different stages of tunnel advancement computed from finite element analysis.

Copyright © 2005 Taylor & Francis Group plc, London, UK

pile was subjected to more soil movement compared to the rear pile which was located three times pile diameter away (i.e. 3.6 m). Besides, pile group interaction effect also played a part.

5 CONCLUSIONS

A three-dimensional finite element model was created with phase tunnel construction simulated. A case history from the MRT North-East Line C704 in Singapore was back-analysed and good agreement between measured data and prediction was achieved. The trend of pile group deformation was shown to deflect towards the tunnel transverse direction. In the longitudinal direction, prior to the tunnel arriving at the pile group, the piles deflected towards the tunnel with maximum movement at the pile head level and not at the tunnel springline. Subsequently, as the tunnel advanced pass the pile group, the piles were gradually pushed forward in the same direction of the tunnel advancement. In addition, the front pile was found to be subjected to higher response of up to 2.5 times compared to the rear pile.

ACKNOWLEDGEMENT

The first author would like to thank National University of Singapore for a research scholarship to pursue his doctoral studies. The authors would like to thank the Land Transport Authority of Singapore and Dr. J. Wang for providing access to the C704 data for back-analysis work. Special thanks also to Dr. G.R. Dasari for his guidance on the use of ABAQUS and the SDMCC soil model.

REFERENCES

Abu-Farsakh, M.Y. & Voyiadjis, G.Z. 1999. Computational model for the simulation of the shield tunneling process in cohesive soils. International Journal for Numerical and Analytical Methods in Geomechanics, 23, pp.23–44.

BS5930 1981. Code of Practice for Site Investigations. BSI, London, 1999.

Dames & Moore 1983. Mass rapid transit system, Singapore: Detailed geotechnical study. Interpretative Report, Provisional Mass Rapid Transit Authority, Singapore.

Dasari, G.R. 1996. Modelling the variation of soil stiffness during sequential construction. PhD thesis. Cambridge University.

Hibbitt, Karlsson & Sorensen, Inc 2001. ABAQUS User's manual, Version 6.31.

Knight-Hassell, C.K. & Tan, K.B. 2000. Tunnelling through challenging ground conditions in Singapore. Proceeding of the International Conference on Tunnels and Underground Structures, Singapore, 26–29 November 2000, pp.633–638.

Lee, R.G., Turner, A.J. & Whitworth, L.J. 1994. Deformations caused by tunneling beneath a piled structure, XIII ICSMFE, New Delhi, India.

Phienwej, N. 1997. Ground movements in shield tunnelling in Bangkok soils. 14th International Conference on Soil Mechanics and Foundation Engineering, Hamburg.

Poulos, H.G. 2003. Effects of urban construction on existing pile foundations. State of the Art Report. European Conference on Soil Mechanics and Geotechnical Engineering.

Shirlaw, J.N. 2000. Discussion: Can settlement be accurately predicted using advanced numerical method. Geotechnical Aspect of Underground Construction in Soft Ground. Fujita & Miyazaki (eds).

Shirlaw, J.N., Richards, D.P., Ramond, P. & Longchamp, P. 2004. Recent experience in automatic tail void grouting with soft ground tunnel boring machines. ITA-AITES World Tunnel Congress, 22–27 May 2004, Singapore.

Vermeer, P.A. & Bonnier, P.G. 1991. Pile settlements due to tunneling, 10th European Conference on Soil Mechanics and Foundation Engineering, Florence, Italy, pp: 869–872.

Wang, J. 2003. Field monitoring and back-analysis of soldiers piles retaining wall for deep excavation. PhD thesis. National University of Singapore.

APPENDIX A

In SDMCC model, within a very small shear strain ($\varepsilon_q < \varepsilon_q^e$), the shear modulus is independent of strain but varies with mean effective pressure, p' and over-consolidation ratio, OCR as follow:

$$G_{max} = A\, P'^{n1}\, OCR^{m1} \tag{1}$$

In the small strain ($e_q^e < e_q < \varepsilon_q^p$), the shear modulus decreases with shear strain and is given by

$$G = B\, P'^{n2}\, OCR^{m2} \varepsilon_q^{\,b2} \tag{2}$$

where A, n1, m1, B, n2, m2 and b2 are another set of experimental parameters from curve fitting. In the large strain ($\varepsilon_q > \varepsilon_q^p$), the shear modulus varies according to equation (2) but with a constant $\varepsilon_q = \varepsilon_q^p$.

Similarly, the bulk modulus, K is assumed to follow the same degradation curve as shear modulus but varying with volumetric strain. For very small strain ($\varepsilon_v < \varepsilon_v^e$), K is defined as

$$K_{max} = C\, P'^{n3}\, OCR^{m3} \tag{3}$$

Again within the small strain ($e_v^e < e_v < \varepsilon_{qv}^p$), K varies with strain according to

$$K = D\, P'^{n4}\, OCR^{m4} \varepsilon_v^{\,b4} \tag{4}$$

Copyright © 2005 Taylor & Francis Group plc, London, UK

Table 1. Parameters for shear modulus in SDMCC model.

A	n1	m1	B	n2	m2	b2
4500	0.7	0.2	0.71	1.0	0.2	−0.62

Table 2. Parameters for bulk modulus in SDMCC model.

C	n3	m3	D	n4	m4	b4
800	1.0	0.2	1.2	1.0	0.2	−0.61

where C, n3, m3, D, n4, m4 and b4 are another set of experimental parameters from curve fitting. For $\varepsilon_v > \varepsilon_v^p$, constant $\varepsilon_v = \varepsilon_v^p$ is assumed, i.e. independent of strain. Bulk modulus on yield surface is according to the MCC formulation.

Copyright © 2005 Taylor & Francis Group plc, London, UK

Some considerations in finite element analysis of tunnelling

C.H. Pang & K.Y. Yong
National University of Singapore, Singapore

G.R. Dasari
Upstream Research Company, ExxonMobil, USA

ABSTRACT: As ground is practically an unbounded medium, selection of only a small area around a tunnel for analysis purpose is sure to introduce some errors. Also the boundary conditions imposed on these boundaries will influence the shape and magnitude of displacement profiles. This paper investigates effect of boundaries on predicted ground movements due to tunnelling in plane strain analysis. A review of published finite element analyses was carried out and general observations on the magnitudes and trends of movement are summarised. Subsequently, a detailed parametric study was carried out to identify the factors which influence mesh size. It is shown that the size of mesh required is highly dependent on the C/D ratio, soil model, K_o condition and the boundary fixity. A mesh configuration scheme is proposed to obtain sizes of mesh to produce near mesh-independent results.

1 INTRODUCTION

The discretisation of ground into finite element would impose an assumption of confined area. Generally, the appropriate boundary would be infinite. The simulation of the infinite condition has been explored by Kumar (1986) and Beer et al. (1987) with the use of infinite elements and boundary elements in two and three-dimensional analyses respectively. Since infinite elements are not available in most commercial finite element software, a substantial number of finite elements are required to solve the problem.

In the study by Burd et al. (1994), it has been shown that the mesh configuration has great effect on the predicted settlement profile. The surface heaving is observed instead of settlement, as the mesh got larger. Another critical factor is the fixity of the bottom boundary of the mesh whether it may be on roller (fixed vertically only) or pinned (fixed both vertical and horizontal). The objective of the paper is to explore sizes of meshes required for tunnelling analysis in various geometries and stress-states of soil.

2 REVIEW OF FINITE ELEMENT MESH

The geometry and symbols used to describe various dimensions are shown in Figure 1. The dimension Y_1 is used in some circumstances represented by the dimension C (which is the depth from ground surface to tunnel crown).

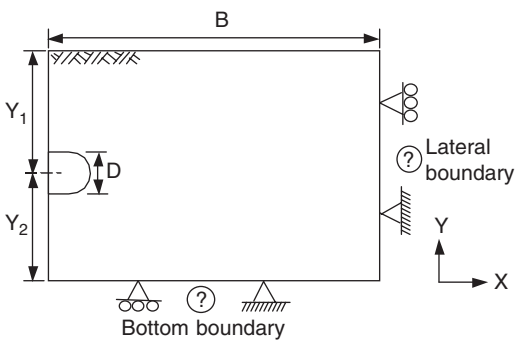


Figure 1. Geometry of the problem analysed in this study.

A review on 49 available publications has found that tunnelling analyses were carried out with different mesh configuration particularly on the above-mentioned factors, which ranges from very narrow to wide meshes or very shallow to deep meshes and to no debate which mesh configuration is appropriate and the effect on the result as given in Table 1. The review also shows that analyses were carried out both with and without the lateral fixity at the bottom boundary of the mesh (60% with pinned fixity where as 36% on

Copyright © 2005 Taylor & Francis Group plc, London, UK

roller and 4% on infinite elements). It will be shown in the present study that in tunnelling, the effect is substantial especially when the tunnel is near the bottom boundary.

Oteo & Sagaseta (1982) proposed that in plane strain analysis in linear elastic model, the lateral boundary has no effect and is negligible if the B/D ratio is greater than 9 and the maximum influence is less than 10% if B/D is between 5 and 9. It will be shown latter in this paper that the boundary distance depends on various factors.

3 GENERAL OBSERVATIONS

3.1 *Effect of mesh width (B)*

Four tunnelling analyses were carried out by changing mesh width (B) from 5D to 40D. Soil model was linear elastic which stiffness increases with depth (Gibson soil) and analyses were undrained. The analyses are for C/D ratio of 2.5 and diameter of tunnel (D) was 8.0 m. The analyses were carried out using the commercial finite element program ABAQUS (HKS 2002). Figure 2a shows the surface settlement profiles for mesh of different widths. The results show that the mesh width has large effect on both the trough shape and also the magnitude. As the width gets larger, there is a reduction in settlement. It can also be seen that the settlement at far-field is decreased with increasing mesh width but with identical material parameters. However, beyond a critical value of mesh width, further increase in mesh width did not cause appreciable change in results (compare results of 20D and 40D). This means that the soil movements converged as the boundary has represented near infinite condition. A similar trend is also observed in the surface horizontal movement as shown in Figure 2b but with an increase of magnitude as the mesh got larger. It is to be noted that the volume loss for the 4 meshes are close. There is only a slight increase in volume loss as the mesh width increases, generally less then 0.05% (as shown in Figure 3a). For comparison, the results from analyses with linear elastic model with constant stiffness were plotted in Figure 3b. The near constant volume loss results in larger settlement for meshes with smaller width.

Table 1. Mesh size adopted for tunnelling.

Y_1/D	Y_2/D	B/D
<3.0	0.5 to 10.0	2.0 to 12.0
>3.0	1.8 to 8.8	3.5 to 19.6

3.2 *Effect of mesh extension below tunnel springline (Y_2)*

The distance below tunnel springline (Y_2) is usually chosen based on presence of a rigid stratum. However, if no such rigid stratum is present within reasonable distance justification of the mesh depth (Y_2) is uncertain. The mesh depth and boundary condition on the boundary will influence surface settlement profile. Results from analyses with various Y_2/D ratios are shown in Figure 4. Three analyses are with pinned boundary condition and three analyses are with roller boundary condition.

Modelling the large Y_2 would create substantial upward soil movement at the invert. This behaviour therefore, leads to a higher far-field displacement

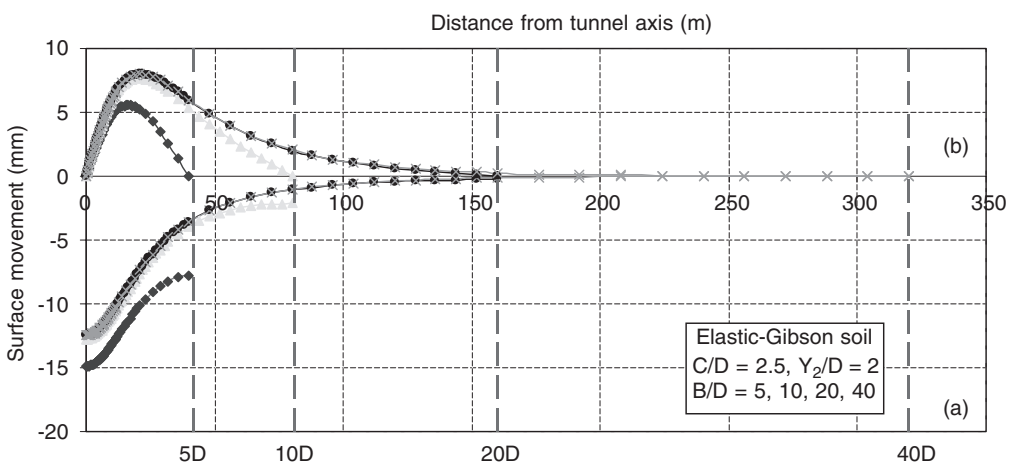


Figure 2. Variation of surface movement in 2-D plane strain analysis (a) settlement (b) horizontal movement.

Copyright © 2005 Taylor & Francis Group plc, London, UK

due to the volumetric constraint in an undrained analysis. This also means higher Y_2/D ratio, lower surface settlement.

There is a convergence of the settlement after certain value of Y_2/D ratio similar to mesh width as shown in previous section. Obviously, convergence will be reached as opposed to the observations by Burd et al. (1994) and Oteo & Sagaseta (1982). Surprisingly, an 'apparently' better surface profile (deeper surface settlement and lesser far field settlement) will result when Y_2/D ratio is less than 2.

An observation shows that volume loss decreases slightly as Y_2 increases (see Fig. 3). The difference of volume loss between Y_2/D of 2 and 10 is about 0.025% where as for Y_2/D of 10 and 20, it reduces to 0.02%. Upward strain at the invert is same for both meshes as the amount of stress reduction is same (i.e. strain = decrement of stress/Young's modulus). An additional strain in deeper mesh would leads to higher upward displacement at the invert. However, after a certain depth, no more strain or displacement will be observed and further extension will not change the volume loss very much.

3.3 *Effect of boundary fixity*

The study carried out here shows the presence of huge horizontal soil movement along the bottom boundary and the tunnel vicinity when the boundary is on roller particularly when the bottom boundary is

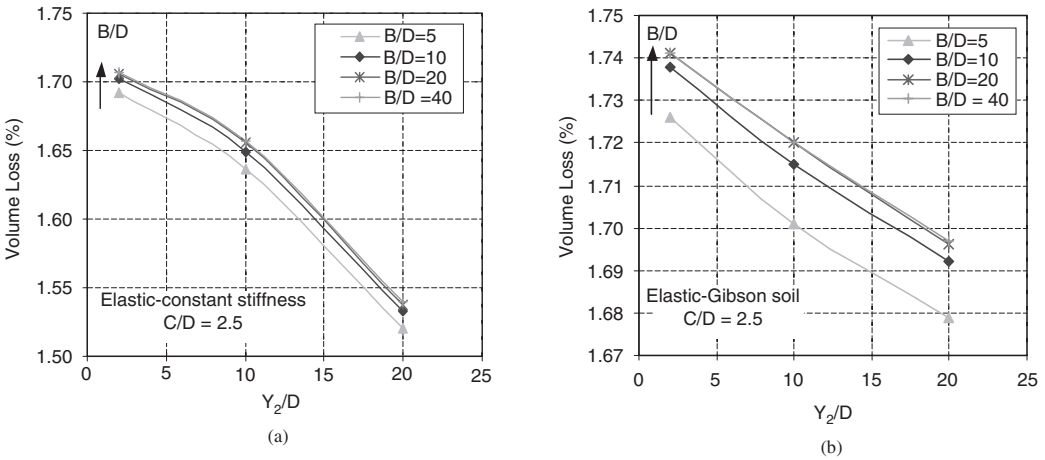


Figure 3. Variation of volume loss with Y_2 and B in (a) Elastic-Gibson soil (b) Linear Elastic with constant stiffness.

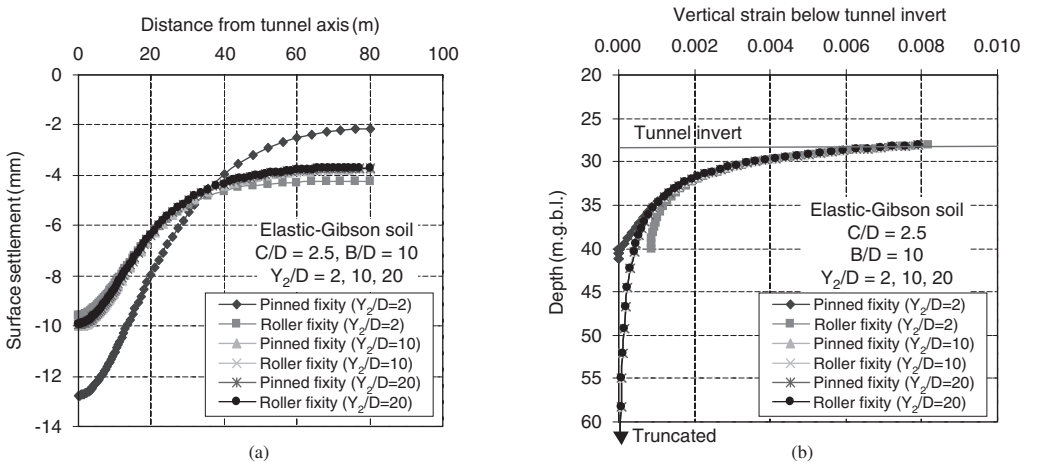


Figure 4. (a) Variation of surface settlement profile with Y_2 (b) Vertical strain below tunnel invert in Elastic-Gibson soil.

Copyright © 2005 Taylor & Francis Group plc, London, UK

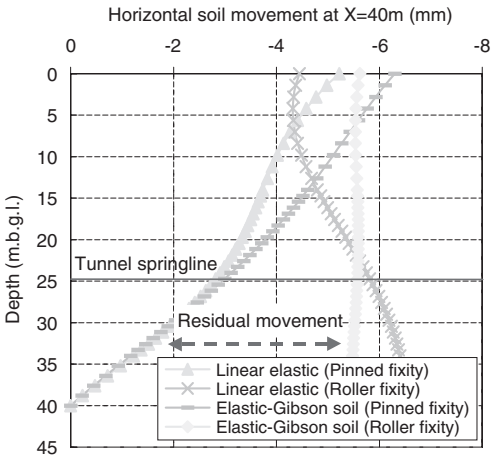


Figure 5. Horizontal soil movement along the depth at 40 m from tunnel axis.

very close to the tunnel. Figure 5 shows the trend of horizontal soil movement along the vertical section 40 m from tunnel axis where the boundary is pinned or on roller. In linear elastic soil (with constant stiffness), the horizontal subsurface soil movement is increasing with depth where as a constant movement in Gibson soil. In reality, the movement is expected to taper off with depth. The problem can be arrested by prescribing pinned fixity. The pinned boundary leads to an improved surface settlement curve as to a lesser far-field settlement and higher maximum settlement at the tunnel axis Figure 4a. However, it should be noticed that when the mesh is very deep, the fixity would have no influence on the result.

Constraint in the lateral boundary is always subjected to lateral movement only. Vertical constraint is not common or perhaps not at all being applied in any geotechnical modelling, therefore allowing settlement. However, some analyses were carried out here to identify the possibility of improving the result with this type of boundary fixity. The vertical fixity at the far end lateral boundary does not help to improve the result but only restrain the movement near the boundary locally.

4 PARAMETRIC STUDIES

4.1 *Numerical model*

In the previous section, it was reported that beyond certain width, further extension of mesh width will not affect the results. It is recognised that vertical soil movement would be over-estimated where as the horizontal soil movement would be under-estimated as the mesh gets smaller. In this section, a more refined parametric

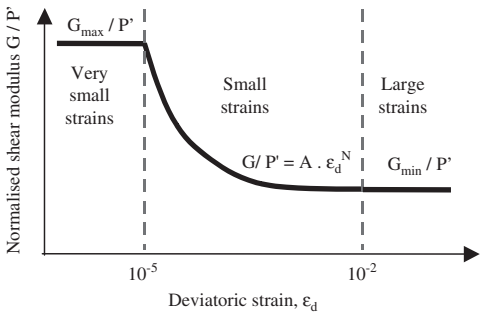


Figure 6. Variation of shear modulus with deviatoric strain.

study is carried out to assess the degree of error quantitatively. A very large mesh (i.e. B = 40D) is used to represent the infinite condition. The error is defined as

$$Error(\%) = \frac{(Result\ of\ B_{40D} - B_{vary})}{(Result\ of\ B_{40D})} \times 100 \quad (1)$$

Three soil models, Gibson, Modified Cam Clay (MCC) and simple non-linear elastic model are used with parameters typically representing stiff clay. The simple non-linear elastic model, which is incorporated into ABAQUS, in general, is stress and strain dependent where the soil shear modulus is formulated in the form of power function and is given by :

$$G / P' = A.\varepsilon_d^{\ n} \quad (2)$$

where G is the shear modulus, P′ is the mean effective stress, ε_d = deviatoric strain and A and n defined as the G multiplier and strain exponent respectively. The degradation is categorised into 3 main parts; very small strain, small strain and large strain (see Figure 6). For very small strain and large strain, the elastic behaviour is considered to be linear with a specific maximum (G_{max}) and minimum shear modulus (G_{min}) respectively. The tunnel is allowed to deform to its full stress relief by removing the tunnel elements. Short analysis time is adopted to model the problem as an undrained case.

4.2 *Results of analyses*

4.2.1 *Effects of soil models*

The results from parametric studies on plane strain analyses are shown in Figure 7 in terms of percentage error and B/D ratio. The variables in the analyses include C/D ratio and K_o. The figures 7a, b and c correspond to Gibson, MCC and non-linear elastic soil models. Generally, the error in surface settlement is large for meshes with B/D less than 10, which are indicated by the sharp slopes change. Beyond B/D of

Copyright © 2005 Taylor & Francis Group plc, London, UK

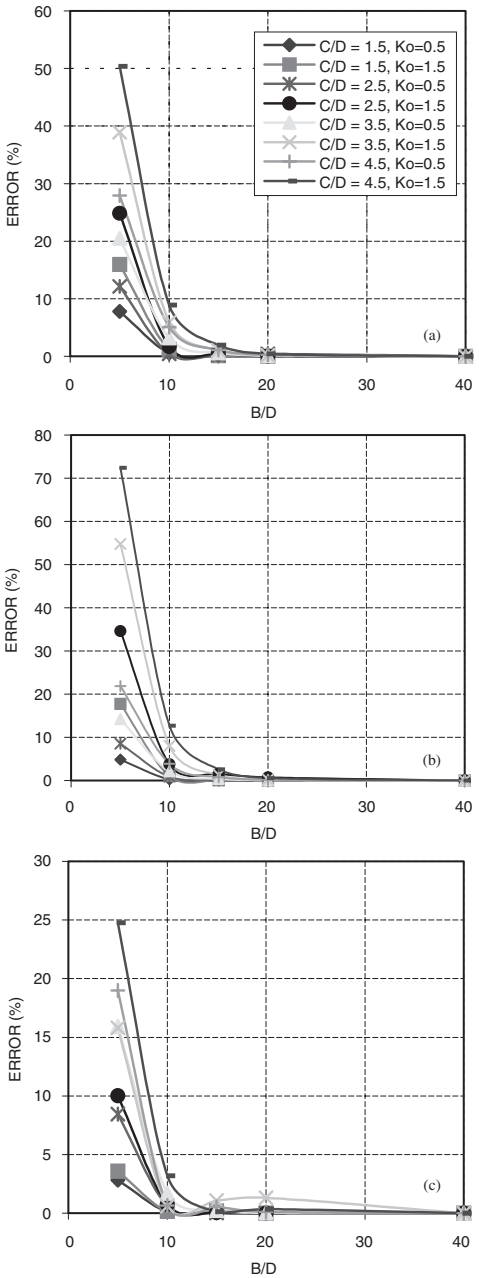


Figure 7. Percentage error with respect to maximum surface settlement (a) Gibson soil (b) MCC (c) Non-linear elastic model.

10, the error reduces and at about B/D = 20, the error is virtually zero.

The error observed is maximum in MCC and followed by Gibson and non-linear elastic model. The highest errors observed in the three models respectively are 72%, 50% and 25%. In non-linear elastic model, the error induced is significantly reduced even with a small mesh. The error ranges from 2.5 to 25% for B/D = 5 and within 3% for B/D = 10 or greater. This is due to the progressive degradation of soil stiffness with strain, which leads to a localised deformation around the tunnel and therefore reducing the mesh size.

4.2.2 *Effect of soil earth pressure at rest (K_o)*

The coefficient of earth pressure at rest, K_o is one of the important soil parameters, which has considerable influence on the soil movement in excavation due to the horizontal stress relief. Therefore, K_o parameter is another factor contributing to the error. Apparent from Figure 7, consistently for $K_o = 0.5$, the error induced is smaller compared to $K_o = 1.5$ for all C/D ratios and soil models investigated. As horizontal stress gets larger, the extent of lateral boundary has to be increased. The error difference between a K_o of 0.5 and 1.5 could range from 10 to 22% for Gibson soil where as 12 to 50% for MCC and 1 to 5% for non-linear elastic model.

4.2.3 *Effect of tunnel depth/diameter ratio (C/D)*

The error induced is highly influenced by the depth of tunnel below ground surface. Generally, the error gets larger as the tunnel gets deeper. It is noticed that the curves are shallower as C/D decreases Figure 7. The depth effect is possibly well explained empirically. The zone of influence of the soil movement above ground due tunnelling is typically spread within 45° from tunnel axis for clay. The zone of influence would be larger as the tunnel gets deeper and indirectly, the mesh adopted would be wider.

4.2.4 *The influence of the extent of Y_2 on the result*

The results in Figure 7 are based on a fixed mesh below tunnel invert Y_2/D of 2. The results actually present a lower bound case. As Y_2 increases, the error increases dramatically especially at small B/D ratio. A precaution should always be exercised when the mesh adopted gets larger. However, in non-linear elastic soil, due to its localised deformation, the increase of Y_2/D from 2 to 20 yields an increase of error up to the most 5% only.

Another significant observation is the crown/invert displacement ratio. The smaller the Y_2, the higher the ratio. A good assessment of displacement around tunnel is vital for prediction of surface movement. As observed in practice, this ratio could be as large as 20. This could be achieved by varying Y_2 although it is not a practical boundary. Far-field settlement could be reduced to zero within a practical distance. Vermeer & Bonnier (1991) has shown in their analysis with the mesh terminated at tunnel invert (i.e. Y_2/D = 0.5), presumably prescribing a zero invert heave and good settlement trough is obtained.

Copyright © 2005 Taylor & Francis Group plc, London, UK

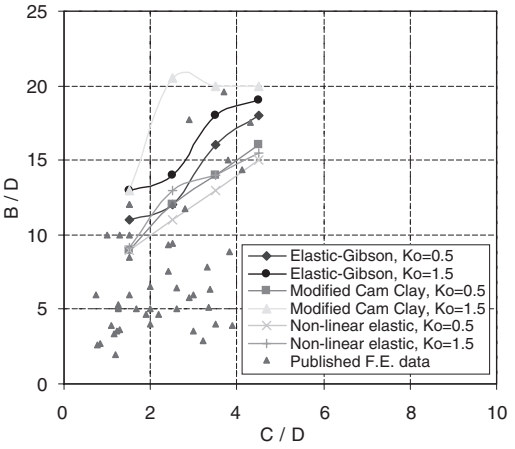


Figure 8. Relationship of B/D and C/D for maximum surface settlement.

5 PROPOSED MESH CONFIGURATION

To obtain an optimised mesh width, a relationship between C/D and B/D ratio is extracted from error charts as shown in Figure 7 above either by interpolation or extrapolation Figure 8. The first observation is the increasing requirement of B/D for increasing C/D to fulfill the convergence of settlement. Although it is apparently increasing with C/D, there is actually no clear and linear trend. Secondly, soil with higher K_o would require a higher B/D especially in MCC where the influence is tremendous for intermediate C/D between 1.5 and 4.5. A difference of B equal to 5D is obvious between K_o of 0.5 and 1.5. In non-linear elastic model, there is a huge increase of mesh width for C/D of 3.5 to 4.5. Nevertheless, due to the variation of the soil models used and K_o parameter, an upper bound of B/D = 24 formed the maximum mesh width for C/D ranging from 1.5 to 4.5. If an error of 5% can be allowed, a much smaller mesh could be used (i.e. B/D can range from 4 to 14 for all the models and C/D under consideration).

For comparison, the review of mesh sizes adopted in the industry as shown in Section 2 is plotted together in Figure 8. It can be noticed that the meshes are much scattered over a large range of C/D ratio. Most of the analyses does not meet the 100% converged soil movement. It should be noted that the result in Figure 8 is presented for Y_2/D of 2.0. This represent a lower bound and the size requirement increases with Y_2/D.

6 CONCLUSIONS

The analyses carried out in this study have shown that the soil movement predicted by finite element model can be highly subjected to the mesh size. The prediction of surface settlement trough can be improved for adequate mesh size adopted. For preliminary understanding, Figure 8 can be referred as a guide on the estimation of mesh sizes. The accuracy of the above results is indicative only and there are other factors that could jeopardise the convergence such as the boundary fixity, soil stiffness and particularly the effect of Y_2 as described in Section 4.2.4.

It is not inconvenient but time consuming to carry out a mesh study prior the use of finite element in analysis of tunnelling. If a small relaxation on the accuracy is allowed, i.e. 5 to 10%, a significant saving on computational time could be achieved by lesser elements. Strictly speaking, the convergence of meshes highly depends on the point which is of concern. Care should be exercised for each different case under consideration and it is worth carrying out a mesh study before using the results.

Besides, the boundary fixity at the mesh bottom has shown to produce great effect on the overall soil movement. The above study has shown that a pinned fixity would produce a better result in term of settlement trough shape and magnitude and therefore, is strongly recommended.

REFERENCES

Hibbitt, Karlsson and Sorensen, Inc 2002. ABAQUS User's manual, Version 6.3.

Beer, G., Watson, J.O. & Swoboda, G. 1987. Three dimensional analysis of tunnels using infinite boundary elements. Computer and Geotechnics Vol.3: 37–58.

Burd, H.J., Houlsby, G.T., Chow, L., Augarde, C.E. & Liu, G. 1994. Analysis of settlement damage to masonry structures. Proceeding of the 3rd European Conference on Numerical Methods in Geotechnical Engineering, I M Smith (eds), Manchester, 203–208.

Kumar, P. 1986. A contribution to an accurate analysis of shallow underground openings. Computers and Geotechnics Vol.2: 141–151.

Oteo, C.S. & Sagaseta, C. 1982. Prediction of settlements due to underground openings. International Symposium on Numerical Models in Geomechanics, Zurich, 13–17 September 1982, 653–659.

Vermeer, P.A. & Bonnier, P.G. 1991. Pile settlements due to tunnelling. Proceeding of the 10th European Conference on Soil Mechanics and Foundation Engineering, Florence, 869–872.

Copyright © 2005 Taylor & Francis Group plc, London, UK

3-D FEM analysis of closely spaced vertical twin tunnel

Yuchao Zheng & Wenge Qiu
School of Civil Engineering, Southwest Jiaotong University, Chengdu, Sichuan, PRC

ABSTRACT: The closely spaced twin tunnel or multi-bored tunnel is frequently encountered in Metro projects. To study this problem, a 3D FEM is adopted to simulate the excavation of vertical twin tunnel by Drill and Blast method in ShenZhen Metro Phase I. Alternative sequences of up-down or down-up construction is considered in this paper. Therefore, the coverage of internal forces and ground settlement of first-driven tunnel are obtained during the other tunnel is driven. In addition, the tunneling-dependent history and peak values of various indexes are derived. Based on the analysis of relation between each index and surrounding rock class, net spacing and relative location of closely-spaced twin tunnel, conclusion to this project is drawn.

1 BACKGROUND

With the constraint of surrounding buildings and structures, vertical twin tube is adopted in ShenZhen Metro Phase I Project for the first time in national Metro history. It is designed for the running tunnels of three sections: Luohu-Guomao, Guomao-Laojie and Laojie-Dajuyuan. Typical section is seen as Figure 1.

Luohu-Guomao inter-station tunnel passes through soft ground, hence it is planed to be driven with shield method. While the ground Guomao-Laojie and Laojie-Dajuyuan inter-station tunnel passes through is relatively good, plus much underpinning works within planned tunnel envelope, hence drill and blasting method is adopted. In such case the common practice worldwide is with shield method which is technically sophisticated but risk is mitigated. Therefore the key and focal point is put upon the running tunnel by drill and blasting method, particularly on the Laojie-Dajuyuan interstation tunnel where the vertical twin-bored tunnel with intersection is adopted. Dual-layer single-bored tunnel is designed for Guomao-Laojie inter-station.

The ground formation running tunnel passes through mainly is Silty clay (1.2～4.1 m), (silty, medium, gravelly) sand (0～6 m) and gravelly clay (0～19.2 m). The overburden is man-made accumulative formation marine alluvium of Quaternary Holocene series and the eluvium of Quaternary mid Pleistocene series, and the bed rock is of Yanshan Era granite. The Ground water is 1.7～4.2 m below the surface, mainly composed of porosity water and bedrock fracture water. With its source of precipitation, water level ranges from 0.5 to 1.0 m.

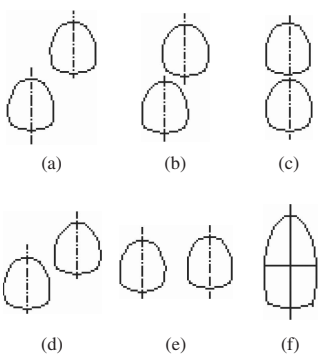


Figure 1. Typical section.

2 FEM NUMERIC MODEL

Dynamic simulation of tunneling for Laojie-Guomao vertical twin tunnel with varying spacing is carried out by 3D FEM based on elastic-plastic theory.

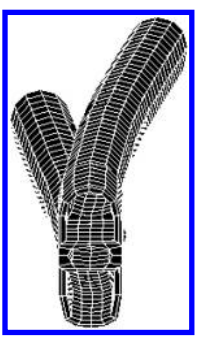


Figure 2. FEM model of tunnel structure.

Copyright © 2005 Taylor & Francis Group plc, London, UK

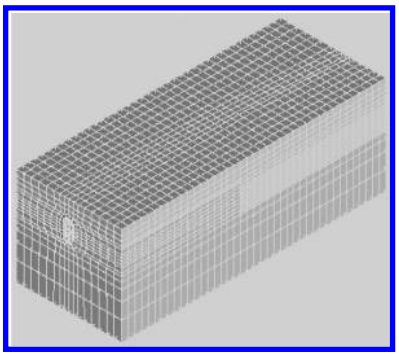


Figure 3. Global FEM model (calculation scope).
* The longitudinal direction of tunnel is axis Z; The vertical direction of tunnel is axis Y; The direction of tunnel is axis X.

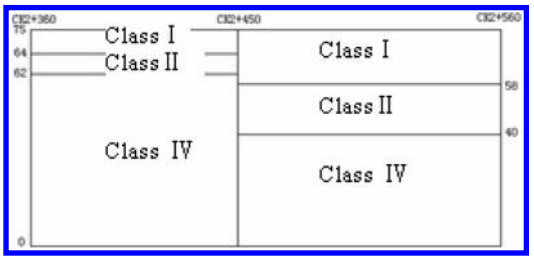


Figure 4. Rock mass classification log.

2.1 *Calculation scope*

CK2+390 is the boundary chainage between the dual-layer single-bored tunnel and the vertical twin tunnel. We focus on the latter in this paper, however, taken account the boundary effect, 30 m double-floor tunnel is added in FEM model, so the start section is CK2+360. According to the result of the plane calculation, clear space of 6 m is critical distance, so the end chainage is CK2+560, therefore, the total length of the model is 200 m. Considered of twin tunnel, cross section area is 80 m (width) × 75 m (height) in the model. The global FEM model is seen as Figure 3.

2.2 *Stratum formation and mechanical parameters*

Based on the geological log of several typical sections and geological profile, ground is sorted as Figure 4, and material parameter is seen as Table 1. Rock mass classification and material parameters are referred to «Code for design of railway tunnel with NATM method» (1985).

2.3 *Geometric relation of vertical twin tunnel*

The geometric relation of Laojie-Dajuyuan running-tunnel is seen as Figure 5 and Table 2.

Table 1. Material parameters.

Rock mass classification	E (GPa)	P (kg/m^3)	μ	C (MPa)	ϕ(°)
I	0.2	1800	0.44	0.0125	22.5
II	0.6	2000	0.38	0.0500	27.5
IV	5.5	2400	0.26	0.8000	37.5
Pre-injection ground	2.0	2200	0.32	2.0000	32.5
C25 concrete	29	2500	0.20	2.74	55

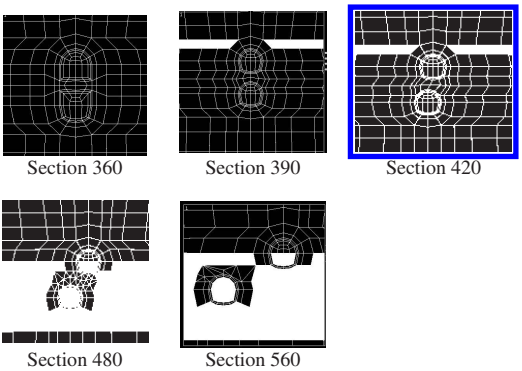


Figure 5. Varying typical section of FEM model.

Table 2. Spacing between two tunnels.

Chainage	CK2 +360	+390	+450	+480	+510	+560
Horizontal spacing (m)	0	0(0.4)	2.40	5.4	7.4	12.4
Vertical spacing (M)	7.867	8.415	9.373	9.08	8.82	7.535
Clear spacing (M)	1.4	1.9	3.0	3.4	4.6	8.0

Note: the section at chainage CK2+*** is hereinafter referred as Section ***.

2.4 *Tunneling simulation*

Tunneling is composed of multi-step excavation and lining applying. The equation of mechanical behavior of different procedures simulation is:

$$\{[K_{i-1}]+[\Delta K_i]\}\{\Delta\delta_i\}=\{\Delta F_{ir}\}+\{\Delta F_{ia}\}, \quad (i=1\sim M)$$

Where: M – total step number of tunneling;
$[K_{i-1}]$ – rigidity matrix of model after step i-1;
$[\Delta K_i]$ – increment/decrement of rigidity of surrounding-rock and structure at step i;

Copyright © 2005 Taylor & Francis Group plc, London, UK

$\{\Delta F_{ir}\}$ – array of nodal force increment/ decrement at the boundary nodes due to release of stress.
$\{\Delta F_{ia}\}$ – array of nodal force increment/ decrement due to tunneling.

2.5 *Work case*

Tunneling procedures can be combined in many ways, such as straight up-down or down-up and staggering tunneling with certain distance of cutting face. Whereas the key point lies in the close-in construction influence, the former two cases are simulated respectively so as to investigate the influence imposed on the firstly-driven tunnel accompanying the driving of lag tunnel in terms of internal force and ground settlement.

2.6 *Boundary condition and yield criterion*

The displacement boundary condition adopted in FEM model is as follows, the top is free ground surface, the rest sides are constrained in normal direction. In accordance with Drucker-Prager yield criterion, Elastic-plastic FEM models is adopted. Nonlinear deformation character of the structure is activated in tunneling simulation.

2.7 *The element adopted*

Lining and ground are simulated by hexahedral or tetrahedral solid isotropic element.

2.8 *Analytical index and analytical section*

Typical Section Analyzing Method (TSAM) is adopted to investigate the varying index of typical cross section pertinent to the driving of the lag tunnel, i.e., to analyze the history of each index such as internal forces, ground settlement as well as its peak value. As above-stated, the focal point of this study is to investigate the vertically stacked twin tunnel, hence the analytical sections are twin tunnel section after the chainage of CK2 + 390. Section 390 and 480 are taken as the analytical sections, among which section 390 twin tunnel are basically in class IV rock mass, while section 480 twin tunnel are buried in class II surrounding rock.

3 RESULT ANALYSIS

3.1 *The internal force variation and envelop diagram*

3.1.1 *The variation of internal force*

As is seen from Figure 6, the moment M_z of the upper tunnel lining at section 390 obviously reduce (absolute value), particularly at crown and invert, the value at invert reduce from 38.9 to 4.1 by about 85%, and reduce less at the spring line. Furthermore, the internal

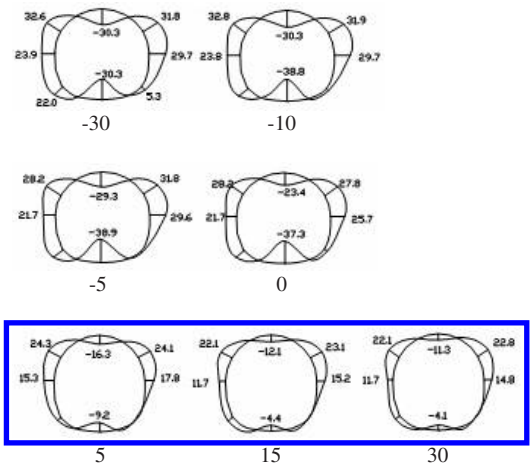


Figure 6. Case1, the moment Mz (KN · m) of upper tunnel lining of section 390 accompanying with driving of lower tunnel.

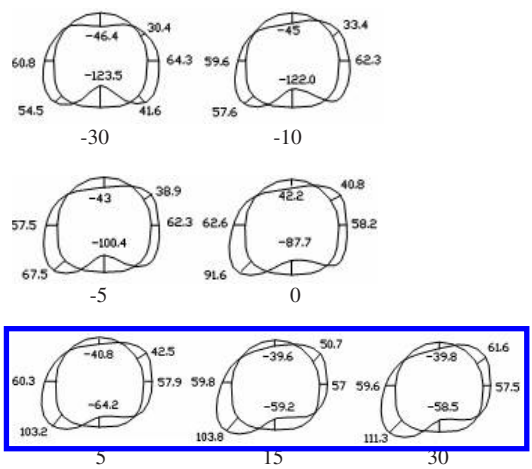


Figure 7. Case1, the moment Mz (KN · m) of upper tunnel lining of section 480 accompanying with driving of lower tunnel.

force diagram is basically symmetrical because the twin tunnel in the area close to section 390 is vertically centered.

The variation of moment (M_z) of tunnel lining at section 480 accompanying with the driving of lower tunnel indicates that: the moment diagram is basically symmetrical before the effect by excavation of the lower tunnel takes place. With the approaching of lower tunnel, the moment obviously deflect, the moment at crown and invert reduces dramatically, and the moment of left spring and right shoulder obviously increase. The amplitude reaches 50 KN · m. at left spring and invert.

Copyright © 2005 Taylor & Francis Group plc, London, UK

3.1.2 *Maximal internal force, variation value and the moment envelop diagram*

As Table 3 shows, because of different cover depth, generally the internal force of lower tunnel is greater than the upper tunnel. However, the maximal variation of internal force of upper tunnel in case 1 is greater than that of lower tunnel in case 2, i.e., case 1 is relatively disadvantageous in terms of influence degree of internal force. Besides, according with the result of plane calculation, with the rise of horizontal distance, the asymmetry of internal force is increasingly evident. Generally, the maximal variation value is in the center-center direction of twin tunnel. As following, it shows the Mz envelope diagram of the upper tunnel in Case 1 affected by the excavation of lower tunnel. The changing of two tunnels' spatial location, that is from the basically overlap to slant interleave, the moment Mz vary from the basically symmetry distribution to asymmetrical distribution. The moment at each position fluctuates with some amplitude, some position even appear opposite sign. See Figure 8.

3.2 *History and envelope diagram of longitudinal moment*

As for the upper tunnel structure of cross-section 390, no longitudinal moment occurred initially. When the lower tunnel is driven to about 20 m behind the reference section, Mx is minus moment. With the driving of the lower tunnel, it turns into plus moment when the lower tunnel face is about 5 m ahead. It appears minus moment to My when the lower tunnel is 5 m behind, and it reaches to maximum 3 m ahead, but the value is small, Seen as Figure 9.

As above-mentioned, inflection point exists round the zero distance in longitudinal moment curve to obvious lagging effect. The Max value generally appear in the 15 m scope front or behind the face, the lagging effect of My is much less than the Mx. Besides, at basic overlapping zone, the Mx value is major, and the My can ignore, this is in accordance with the two tunnels' spatial location relationship.

Figure10 indicates the driving-dependent history of longitudinal moment in the upper tunnel at cross-section 480 in class II ground. As same as in Figure 9, after completing of the upper tunnel itself, on the whole it has no longitudinal moment. By comparing with Figure 9 of section 390 in ground IV, influence scope in Figure 10 is bigger than in Figure 9. Although the distance between two tunnels is increasing, the maximal longitudinal moment is greater than it at the cross-section 390, it shows the rock mass is the greater influence. The contribution of My to resultant moment is obviously increasing, it is consistent with the change of spatial location.

It has no longitudinal internal force before excavation of the late-constructed tunnel, so the longitudinal internal force value reflects the influence degree of early-constructed tunnel is affected by late- constructed tunnel. Table 4 shows the value of case 1 is greater than case 2, the maximal value increment of case 1 is 58% greater than case 2 in class rock mass, and in class

Table 3. The Max. & Min. internal force and Max increment/decrement in different cases.

Case:	Case 1		Case 2	
Rock mass class	IV	II	IV	II
Section	390	480	390	480
Clear distance (m)	1.9	3.5	1.9	3.5
Max Mz (KN · m)	32.8	111.3	35.6	122.2
Min Mz (KN · m)	−38.9	−123	−53.3	−188.2
Min Normal force (KN)	−2231	−2384	−2901	−3350
Max Mz (KN · m) variation N (KN)	94.8 808	23.4 718	63.9 417	63.9 417

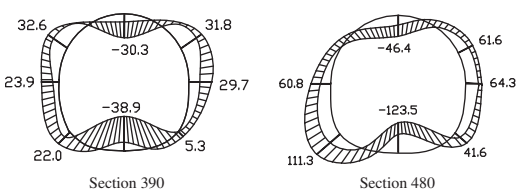


Figure 8. Moment Mz envelope diagrame in Case 1.

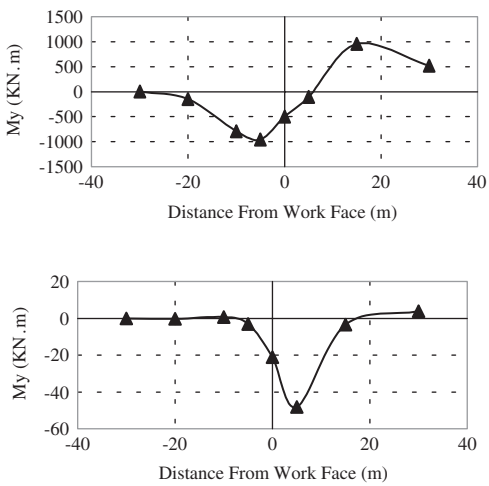


Figure 9. The longitudinal moment Mx, My of the upper tunnel at Section 390 with driving of the lower tunnel in Case 1.

Copyright © 2005 Taylor & Francis Group plc, London, UK

rock mass, that is 120%. So from the comparison of longitudinal internal force, case 2 is advantageous.

We can see from Figures 9 to 12 just as follows: both Mx and My have wave character and limitedly influenced by excavation. Their occurrence, development and extinction or remained distributions are in accordance with stress-released regularity caused by excavation. The essence is that stress redistribution caused by excavation of the later construction tunnel.

3.3 *Ground settlement*

As a matter of fact, tunneling simulation is not really carried on the early-constructed tunnel which was excavated and supported once for all. Hence settlement caused by early tunneling is not too big, the calculation settlement is mainly caused by excavation of the lag tunnel. Curve diagram of typical section in cross direction is shown as follows. The zero point is projection at ground surface of the middle point of the two tunnel centre at same cross section.

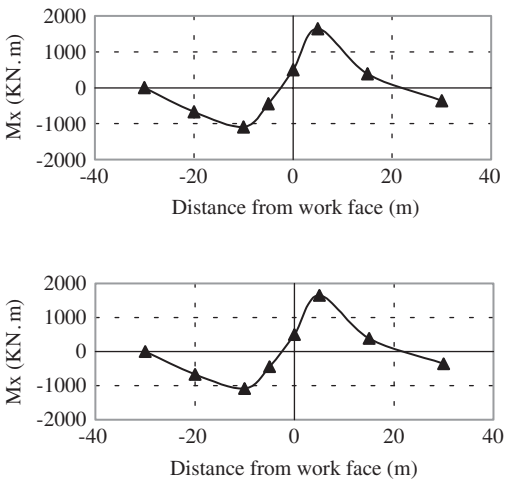
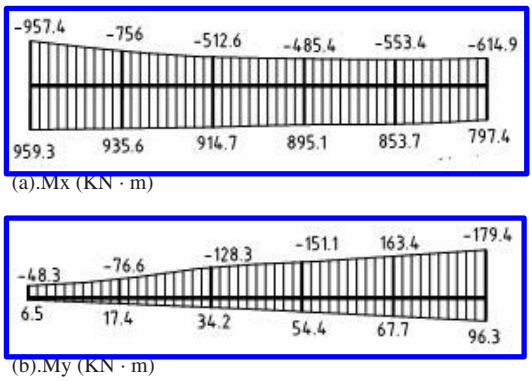


Figure 10. The longitudinal moment Mx, My of the upper tunnel at Section 480 with driving of the lower tunnel in Case 1.

Table 4. The Max longitudinal direction internal force and Max changing value among differents cases in class rock mass sections.

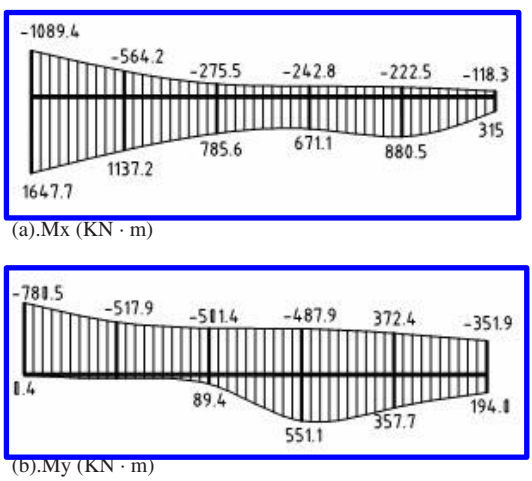
Case:	Case 1		Case 2	
Rock mass class	IV	II	IV	II
Section	390	480	390	480
Clear distance (m)	1.9	3.5	1.9	3.5
Max Mx (KN · m)	959.3	1647.7	62.3	180.4
Min Mx (KN · m)	−957.4	−1089.4	−719.9	−513.2
Max variation (KN)	1916.8	2737.2	786.2	759.6
Max My (KN · m)	6.5	0.4	21.3	183.7
Min My (KN · m)	−48.3	−780.5	−44.3	−10.7
Max variation (KN)	54.8	780.9	65.6	194.4



(a).Mx (KN · m)

(b).My (KN · m)

Figure 11. Case 1 IV class rock mass tunnel moment envelope diagram.



(a).Mx (KN · m)

(b).My (KN · m)

Figure 12. Case 1 II class rock mass tunnel longitudinal moment envelope diagram.
** The tunnel in class IV rock mass is from section 360 to section 450; the tunnel in class II rock mass is from section 450 to section 540.

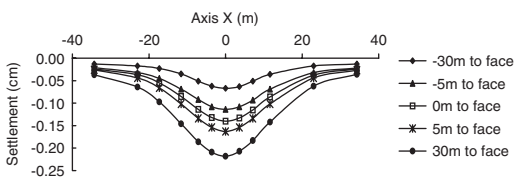


Figure 13. The curve of ground surface settlement at section 390 with difference work face of the lower tunnel in Case 1.

Copyright © 2005 Taylor & Francis Group plc, London, UK

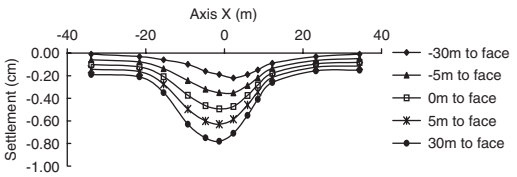


Figure 14. The curve of ground settlement at section 480 with different work face of the lower tunnel in Case 1.

Table 5. The initial and final value of ground settlement.

Case:	Case 1		Case 2	
Rock class	IV	II	IV	II
Section	390	480	390	480
Net spacing (m)	1.9	3.5	1.9	3.5
Initial value (cm)	0.07	0.20	0.04	0.09
Final value (cm)	0.22	0.76	0.41	1.24
Increment	0.15	0.56	0.37	1.15

The maximal settlement of case 1 is obviously less than that of case 2. Of them, the maximal increment/decrement in case 2 is 140 per cent bigger than that of case1 in rock mass, and 92 per cent bigger in class rock mass. It indicates that settlement can be better controlled in the case1 for the reinforcement action on the lower tunnel by the firstly-constructed upper tunnel.

4 CONCLUSIONS

(1) As above-discussed, influence degree and value increment/decrement of internal force in case 1 is greater than in case 2,while ground settlement in case 1 is less than in case 2. Therefore, in terms of influence degree, the tunneling sequence of case 2 is better than that of e case 1. On the contrary, in terms of ground settlement, the construction method of case 1 is preferable than that of case 2.

(2) The longitudinal forces vary with the face of late-constructed tunnel, obviously decreasing or disappearing when the face ahead the review section with a given distance. i.e., the longitudinal influence is closely associated with tunneling process. Suppose parallel twin tunnel is in homogeneous ground, the influence in longitudinal direction will not remain after completion; comparatively twin tunnel with varying spacing is in non-homogeneous ground, inhomogeneous deformation will occur in the firstly-constructed tunnel and certain internal force in longitudinal direction will remain. Correspondingly temporary measures should be adopted at certain time and distance interval from the cutting face during construction in case of slightly remained longitudinal influence. Therefore, permanent reinforcement measures are not necessarily needed.

(3) The cross direction and longitudinal direction of structure should be designed according to envelope diagram of excavation influence. In order to decrease the longitudinal influence, deformation joint can be considered at certain interval, but it is unfavorable to waterproof.

REFERENCES

Qiu Wenge. The Study on Mechanics Principle and Countermeasure of Approaching excavation in Underground Works. Southwest Jiaotong University Doctor Degree Thesis. 2003.

Qiu Wenge etc. Research Report about Vertically Stacked Tunnel Technique in the First Phase of Shenzhen Metro South-West Jiaotong University 2001.

Guan Baoshu. An Introduction to Tunnel Mechanics South-West Jiaotong University 1993.

Copyright © 2005 Taylor & Francis Group plc, London, UK

3D FEM analysis on mechanics behaviour of a new style railway tunnel portal

Junru Zhang, Wenge Qiu & Fei Wang
School of Civil Engineering, Southwest Jiaotong University, Chengdu,Sichuan, China

ABSTRACT: Aim at down bamboo-truncating tunnel portal, a 3D Numerical Simulation Analysis by FEM is carried out. Meantime,in this thesis,the result is compared with the result of model experiment which the geometric similarity ratio is 1:30. So we can get the basic mechanics character of the type of down bamboo-truncating portal, whose tunnel opening is under stress of three dimension and can not be simplified as plane strain model. Only if it has been come into the cave for some distance (such as 18 m , the result in our calculation) can it be simplified as plane strain model; On the common boundary between the salience place of lining and the face of terrane, the vertical axis-force of the vault reach the Max and that with the state of tension. We should pay more attention to this point in structure design.

1 FOREWORD

With the quick development of high-grade railway and highway, the design of tunnel portal which from domestic and oversea has upper breakthrough and innovation, such as the appearance of bamboo-truncating, sunglasses tunnel portal and so on. The mainly form of this portal is extrude style, the extend of lining to the outboard of slope of altitude to form ring-frame, that makes portal. So it can reduce the slope-brushing around the portal, even no slope-brushing, protecting the circumjacent environment, meantime,it also according with the "early in late out" principle which bring out by our country's railway tunnel design, it bring people more and more attention. Such as the Xianniangmiao-one tunnel portal from Ganzhou-Longyan railway and many highway tunnels portal in JAPAN (Figure 1), the design collect many theoretics, principles and viewpoints from architectonics, gardening and environment aesthetics, and bring them to the design of tunnel portal, it receiving the beauty effect, giving people beauty enjoy and it deserving use for reference[2]. The study of railway new style tunnel portal and it's characteristic is well mean, it not only in pursuit of the aesthetics effect, environment protection but also it should ensure the using require, and the last is very important. So many years, the mechanics characteristic of tunnel portal is considered at complex 3D state qualitative, the design of tunnel portal is adopting the mode of standard-drawing empirically. Though the literature [3] bring out a kind of no-headwall (bamboo-truncating) portal, for the part

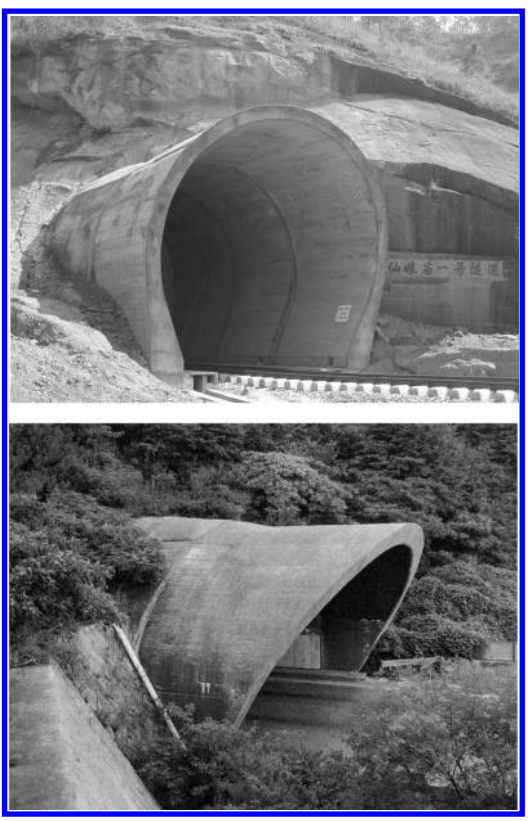


Figure 1. Down bamboo-truncating portal.

Copyright © 2005 Taylor & Francis Group plc, London, UK

lining structure internal force extend from the portal: one hand, carrying out check computations based on the traditional earth-retaining wall principle, the other hand, carrying out design according to the lining structure directly, this viewpoint has great sense datum, so carrying out further research to the mechanics principle of protuberant portal has great engineering and learning meaning.

The down bamboo-truncating tunnel portal is applied on the hilly terrain condition of the portal and the zones of good wall-rock condition, the author according to the Xianniangmiao-one tunnel outlet belong to the new constructing Gan(zhou)-Long(yan) railway, carrying out 3D numerical simulation analysis using the method of FEM, and checking up via model experimentation.

2 COMPUTATIONAL MODEL AND STRATUM LAYER PHYSICS MECHANICS PARAMETER

For the sake of the authenticity of calculation, using 3D model in this compution, the range of the computational model is: in order to simulate the 3D-space effect adequately, the horizontal width along the tunnel transverse is 7 times as long as the true tunnel span, the horizontal width along the tunnel lognitudinal is 10 times as long as the true tunnel span, the overburden of tunnel's vault is shallow so choosing rock stratum thickness according to the actual overburden thickness, the rock stratum thickness below the tunnel motherboard is 3.5 times as long as the tunnel span. Simulative calculation using the ANSYS FEM universal program[4]. Constraint condition: horizontal constraint at front and back, left and right, the underside enduring vertical constraint, the top face is free face in vertical direction. In the whole simulation process, 24536 units are divided totally of the FEM model, the tunnel lining is simulated by the elastic shell unit in calculation, the stratum layer is simulated by the elasto-plastic entity unit. The calculation model of down bamboo-truncating tunnel portal as Figure 2.

The physics mechanics index of wall-rock and concrete in calculation is selected by the combination of <The detailed report about project geology of new constructing Gan(Zhou)Long(Yan) railway> and <The wall-rock classification standard of spray-anchor constructing method>. The details such as Table 1.

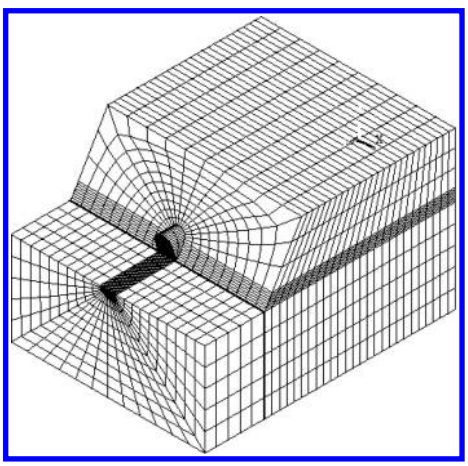


Figure 2. The calculation model of the down bamboo-truncating portal.

3 CALCULATION LOAD AND THE REALIZATION OF EXCAVATION SUPPORT EFFECT

In the place of tunnel portal which belong to the shallow overburden area, mainly consider the dead load stress field of stratum layer and the gravity force of concrete lining. The simulation of excavation effect is achieved by the using of null-unit method, the specific method is realized by the unit "dead" function which offer through ANSYS software, in other words, in the case of the equation has no morbidity, a very small proportion factor is multiplied on the rigidity matrix to the unit which is going to excavate, make it rigidity contribution change little so it can be ignored, at the same time, setting the quality, load effect value to 0, in this way it can adopt a same kind of FEM to carve up graticule in the whole process of excavation

Table 1. Physical mechanic parameters.

Stratum and material	Elastic ratio E (GPa)	Poisson ratio (μ)	Bulk volume γ (kN/m^3)	Cohesion force c (MPa)	Internal friction angle φ (°)
II Degree wall rock	30	0.22	27.0	1.8	50
C25 Reinforced concrete	26	0.18	25.0	–	–

Copyright © 2005 Taylor & Francis Group plc, London, UK

calculation. The construction of secondary lining is completed by the unit "live" function which providing by the program, in other words, in appropriate load process, make the previous "dead" condition unit's rigidity, quality, load recover it original numbers in current model, so the simulation analysis can reflect the dynamic process of construction absolutely. In the 3D FEM calculation, the constitutive equations of surrounding rock adopting the nonlinear constitutive model of Drucker-Prager elasto-plasticity.

4 CALCULATION RESULT AND THE ANALYSIS

In order to convenience the analysis of the result, drawing the each cross-section's inner force relation chart along the tunnel longitudinal direction(Z direction of the model), choosing four sites which are vault, side wall and invert arch to analyse separate. From the inner force distributing chart that show obviously, in stated scope of tunnel portal, the inner force has changed obviously, in the sector of tunnel body, the inner force has keeping stabilize basically[5].

4.1 *The inner force analysis of tunnel vault*

The circumferential axis-force P_x, longitudinal axis-force P_y and the circumferential bend moment M_x, longitudinal bend moment M_y of tunnel vault is as change as the distance of tunnel longitudinal direction, the changing chart such as Figure 3, it tell us:

In the range of the lining emergent parts and the rock face, longitudinal direction axis-force and bend moment reach the Max at the same time, for the design of tunnel portal structure, it should treat as control cross-section.

On the adjacent face, the longitudinal direction axis-force value at vault is 2 times as great as the circumferential direction axis-force value, it reach 37 KN, and it in the condition of stretching force.

When entering into 12 m from the tunnel entrance to the interior, the circumferential, longitudinal direction bend moment has kept stabilization basicly; and entreing into 18 m from the entrance to the interior, the circumferential, longitudinal direction axis-force has astringed gradually.

4.2 *The inner force analysis of tunnel's arch-loin*

The circumferential axis-force P_x, longitudinal axis-force P_y and the circumferential bend moment M_x, longitudinal bend moment M_y of tunnel's loin is as change as the distance of tunnel longitudinal direction, the changing chart such as Figure 4, it tell us:

The circumferential axis-force of tunnel portal is –24 KN, along with entering into the tunnel, the circumferential axis-force value has increased gradually, when entering 18 m into the tunnel, the circumferential axis-force has became stabilized basically; the longitudinal axis-force of tunnel portal is –8.8 KN, when entering into 18 m from the portal, the longitudinal axis-force also has became stabilized basically; the circumferential axis-force is 5–10 times as great as the longitudinal axis-force in the 5 m scope of the portal, it become 20 times in the tunnel body area.

In the position of tunnel portal, circumferential bend moment and longitudinal bend moment reach the Max at the same time, when entering 12 m into the tunnel, both two value has became stabilized, the circumferential bend moment is 10 times as great as the longitudinal bend moment in the area of tunnel body.

4.3 *The inner force analysis of tunnel side wall*

The circumferential axis-force P_x, longitudinal axis-force P_y and the circumferential bend moment M_x, longitudinal bend moment M_y of tunnel side wall is as

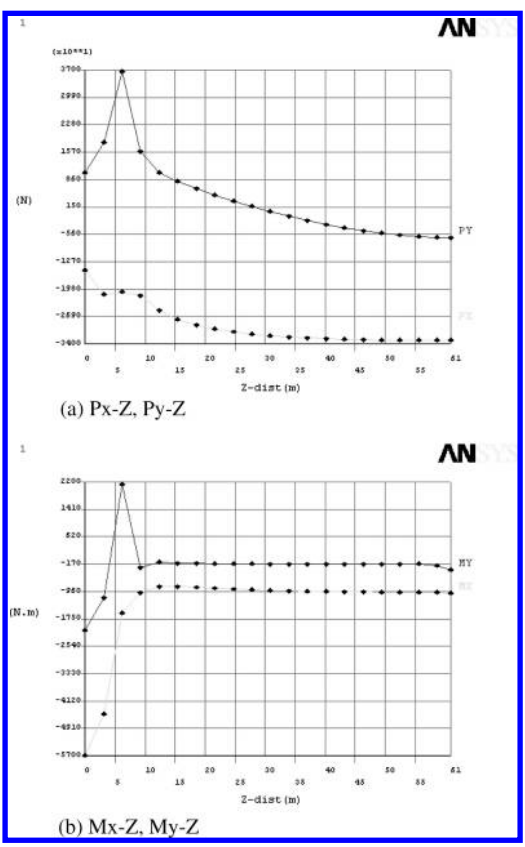


Figure 3. Relation between the internal force of vault and longitudinal distance in the tunnel.

Copyright © 2005 Taylor & Francis Group plc, London, UK

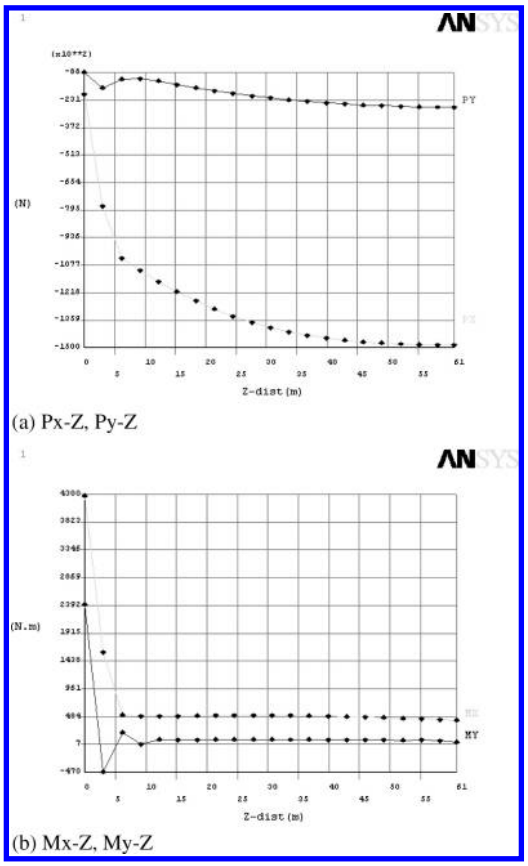


Figure 4. Relation between the internal force of the hance and longitudinal distance in the tunnel.

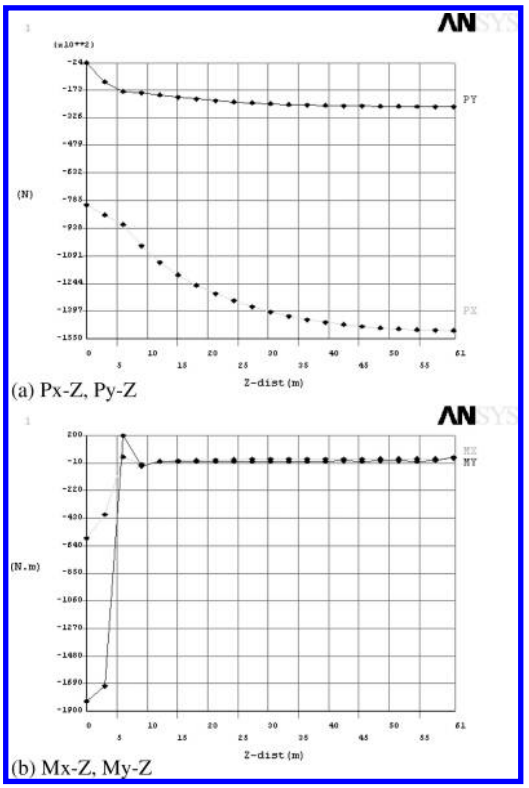


Figure 5. Relation between the internal force of the abutment wall and longitudinal distance in the tunnel.

change as the distance of tunnel longitudinal direction, the changing chart such as Figure 5, it tell us:

The circumferential axis-force of tunnel portal is –80 KN, along with entering into the tunnel, the circumferential axis-force value has increased gradually, when entering 18 m into the tunnel, the circumferential axis-force has became stabilized basically; the longitudinal axis-force of tunnel portal is –2.4 KN, when entering into 18 m from the portal, the longitudinal axis-force also has became stabilized basically.

In the position of tunnel portal, circumferential bend moment and longitudinal bend moment reach the Max at the same time, the longitudinal bend moment is 4 times as great as the circumferential bend moment, when entering into the tunnel site at the interface of the emergent of lining and the rock face, both value become negative from positive at the same time, but the Max value is 0.2 KN·m, when entering 10 m into the tunnel, both value has became stabilized, and the value drive to zero.

4.4 *Analysis on inner force in the invert arch of tunnel*

In the invert arch of tunnel, the circumferential axis-force P_x, the circumferential bend moment M_x, the axial force in longitudinal direction P_y, and the longitudinal bend moment M_y changing with the longitudinal length are showed in the Figure 6, What we can see from the Figure 6 just as follows:

The axial forces in circumferential direction are all pressure force, but the axial forces in longitudinal direction are stretching forces only at the export of tunnel and the others are all pressure forces . The stretching forces are very small, for they are only about 0.09 KN. Both the axial forces tend to stabilize after entering 18 m from the export of tunnel, and the axial forces in circumferential direction are fifth to eighth times of the axial force in longitudinal direction.

Both the bend moment tend to stabilize after entering 15 m from the export of tunnel, and the bend moment in circumferential direction are fifth to eighth times of the bend moment in longitudinal direction. The bend moments are all small, and the biggest one is only 1.9 KN·m.

Copyright © 2005 Taylor & Francis Group plc, London, UK

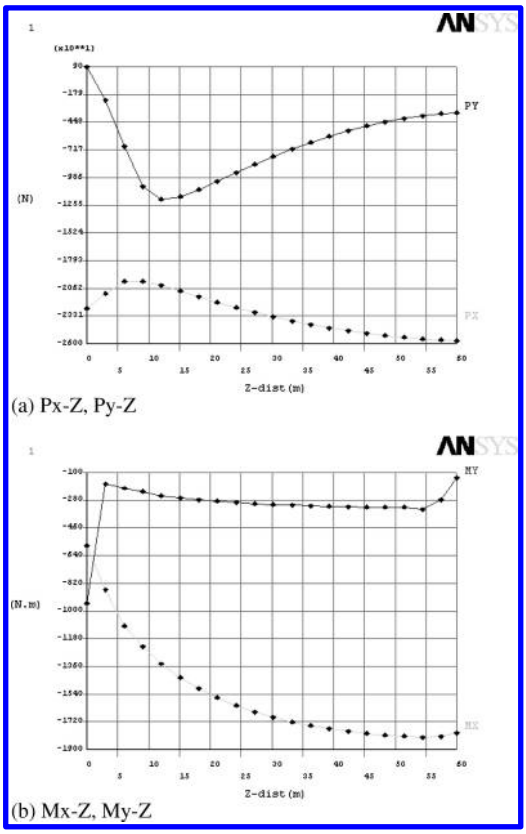


Figure 6. Relation between the internal force of the invert arch and longitudinal distance in the tunnel.

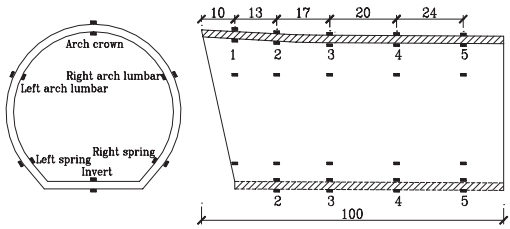


Figure 7. Layout of observation points(unit:cm).

5 THE SIMILARITY MODEL EXPERIMENT AND ANALYSIS

5.1 *General situation of the experiment*

Similarity model experiment was carried on at the same time for substantiating and supplying the result of numerical calculation. Self-weight stress was only considered among the original ground stresses for the sector of the export of tunnel was buryed shallowly. Considering the three-dimensional effect of the export of tunnel, similarity model experiment was tridimensional. Similarity ratio based on geometric similarity ratio $C_L = 30$ and volume weight similarity ratio $C_\gamma = 1$. According to the π theorem of Buckingham[6], The similarity ratio of Poisson's ratio, deformation and angle of friction were all equal to 1, $C_\gamma = C = C_\varphi = 1$, The similarity ratio of stress, cohesive force and elastic ratio were all equal to 30, $C_\sigma = C_C = C_E = 30$.

In theory in the cross direction of tunnel, the influence to the surrounding rock during excavation will tend to disappear with the increasing of the distance from the excavated sector (according to the Saint Venant theorem).The experience has proved that the influence to the surrounding rock during excavation only is limited in the range of the sector third to fifth times of distance far from the center of rough tunnel. The scope of similarity model experiment just as follows: the distance in the cross direction of tunnel is 3.5 m, the distance in longitudinal direction of tunnel is 1 m, the distance under the invert arch is 0.25 m. The structure is considered as a member in bending and compression and required to be analysised at the load component method. The strain gauge transducers in cross direction are installed both in and out of the structure. Considering the longitudinal effect of structure, the strain gauge transducers in longitudinal direction are also installed both in and out of the structure. Figure 7 shows the spot where the strain gauge transducers are.

5.2 *Analysis the result of experiment*

In order to be easy to analysis and compare the result of experiment, the test date and the result of numerical calculation are displayed in Table 2. Because of limitation, it only displays the result of vault and invert arch of the lining.

It indicates in Table 2 that the test dates are all greater than the results of numerical calculation at the same numbering of cross-section of vault and invert arch. But the inner force distribution and changing tendency of lining have the same style.

6 CONCLUSIONS

Tridimensional numerical simulation analysis conjunct with model experiment have been done to down bamboo-truncating tunnel portal. We can draw a few conclusions as follows after analysis and compare the result of experiment, the test date and the result of numerical calculation.

1. To the down bamboo-truncating tunnel portal, the stress characters of lining structure among a given scope of the opening have significant difference

Copyright © 2005 Taylor & Francis Group plc, London, UK

Table 2. The comparison of model experiment data and the result of numerical calculation.

Position	Numbering of cross-section	Axial force of across direction (kN)		Flexural torque of cross direction (kN · m)		Axial force of longitudinal direction (kN)		Flexural torque of longitudinal direction (kN · m)	
		Test date	Result of numerical calculation	Test date	Result of numerical calculation	Test date	Result of numerical calculation	Test date	Result of numerical calculation
Arch crown	1	−570.3	−21.2	−61.1	−4.5	430.7	18.5	−28.4	−1.1
	2	−489.5	−20.8	−36.8	−1.6	703.4	37.0	50.6	2.2
	3	−604.1	−25.5	−22.7	−0.8	263.1	11.4	−6.3	−0.2
	4	−645.3	−29.7	−23.8	−0.8	138.0	5.8	−6.8	−0.2
	5	−648.2	−30.4	−24.2	−0.8	70.8	3.1	−5.9	−0.2
Invert	2	−462.7	−20.1	−27.3	−1.0	−134.9	−5.6	−6.7	−0.2
	3	−473.8	−20.3	−29.9	−1.3	−258.7	−6.9	−6.9	−0.2
	4	−570.3	−21.2	−34.3	−1.5	−247.4	−7.2	−7.2	−0.3
	5	−600.4	−22.0	−36.8	−1.6	−240.5	−6.8	−6.8	−0.3

from that of the main body of tunnel. It spears space distribution, so special designing is necessary to lining structure among a given scope of the opening.

2. The inner forces of lining structure tend to stabilize after entering 18 m from the export of tunnel. That is to say, when designing lining structure of the opening, we can regard 18 m of the opening as integrality. Three-dimensional effect should be considered among such scope of the opening. Both stress of cross-section and lengthwise section must be considered. Moving forward deeper to tunnel, it can be treated as traditional plane strain case. So the safety of structure can be guaranteed and the economical efficiency of engineering also can be increased.
3. At the interface of the lining ledge and rock stratum, the axial forces in longitudinal direction of vault reach the Maximum and they are all in tension. So distributed steel designing should be done to structure in longitudinal direction when designing lining structure of the opening.
4. At the main body of tunnel, the axial forces in longitudinal direction are much less than the axial forces in circumferential direction, and the bend moment in circumferential direction are sixth to tenth times of them in longitudinal direction. So structure can be treated as plane strain case and endogen force can be ignored when designed.
5. What we can find from the result of numerical simulation analysis just as follows : The opening structure of tunnel is in tridimensional stress case, so it can not be simplified as plane strain case. It must be paid attention to that it can be simplified as plane strain case only after entering a give distance from the export of tunnel (e.g. 18 m in this paper) when designed.

This article was completed with Professor Qiu Wenge' meticulous guidance. In the selection of academic thesis subject, theoretical calculation, experimental investigation and final version is embodied tutor's painstaking work. I hereby express my thanks to Doctor Gao Xinqiang, senior fellow apprentice and Master Wang Fei, Master Li Shufeng, junior fellow apprentice. They give me strong support and help during writing this article.

Finally, I express heartfelt thanks to every Expert and Professor for reading and appraising the article during busy work.. Please oblige me with your valuable comments and a critical opinion.

REFERENCES

[1] Yu Rufa. Discussing About Conception And Expression Format [J]. Tunnel And Underground Engineering, 1985, 6 (4):39–45
[2] Qiu Wenge. Research About The New Style Railway Tunnel Portal [R]. Chengdu. South-West Jiaotong University, 2003.3
[3] Gao Shufeng. Portal Without Headwall's Application In Jing-Hu High-speed Railway [J]. Railway Engineering Transaction, 2000, No. 2, 62–64
[4] Liu Tao. Be Proficient in ANSYS[M]. Beijing: Tsinghua University Publishing Company, 2002
[5] Pan Changshi. Mechanical Numerical Method Of Tunnel [M]. Beijing: Railway Publishing Company, China, 1995
[6] Xia Caichu,Li Yongsheng. Theory and Technique about Test and Measurement in Underground Engineering[M]. Shanghai. Tongji University Publishing Company, 1999

Copyright © 2005 Taylor & Francis Group plc, London, UK

Study on calculation method of frost force of tunnel in frozen earth

Wenge Qiu & Jian Wu
School of Civil Engineering, Southwest Jiaotong University, Chengdu, Sichuan, China

ABSTRACT: In studying on tunnel in frozen earth, studying mutual action among not-freezing surrounding rock, freezing surrounding rock, lining and making frost force of tunnel clear in frozen earth are the key problem. Half-theory and half-experience calculation method of frost force of tunnel in frozen earth is put forward in this paper according to elasticity-plasticity mechanics and FEM. This calculation method is practiced by FEM and proved by model experiment.

1 PREFACE

The essential factors of frost damage of tunnel in frozen earth are as follows: the temperature situation, the hydrological condition, the condition of surrounding rock and the measure of tunneling. Through researches to lots of tunnels' frost damage phenomena and its mechanical principle, we discover that the mechanical character of frozen soil differs greatly from other types of soil. The main reasons for frost damage taking place include: the volume expansion and the change of physical mechanical character of soil when the unfrozen soil transforms to frozen one, and frost force to tunnel lining. Therefore, the key point of study to tunnel in frozen earth is the mutual effect of unfrozen surrounding-rock, frozen-area and tunnel lining, and we should make frost force of tunnel in frozen earth clear.

At present, we adopt a method that couples stress field, temperature field and seepage field together to study the frost force in frozen earth in theory, however, due to the complexity of practical engineering and the limit of mathematical mechanics, there is a long way for us to apply this method to practice. So that, in the paper, we choose a calculation method of theoretical-experiential style, that's we firstly give the frozen area of tunnel's surrounding-rock according to temperature test of earth and the physical mechanical parameters of both frozen and unfrozen surrounding-rock according to original mechanics test, then do numerical simulation analysis for the coupling of gravity field and temperature field.

2 THEORY CALCULATION METHOD OF FROST FORCE OF TUNNEL IN FROZEN EARTH

2.1 *Summarize of calculation method of frost force*

The calculation method of frost force is as follows: first of all, through test to get the distribution of stress field of tunnel's surrounding-rock in frozen earth, the physical mechanical parameters (such as: γ, E, μ, c, φ, η and so on.) of surrounding-rock when it is either frozen or unfrozen, the frozen area of surrounding-rock, the physical mechanical parameters of tunnel's lining support structure; then we choose a FEM program (e.g. ANSYS) to create a calculation model of mutual effect among tunnel's lining, the frozen and unfrozen surrounding-rock; basing on displacement-response and rigidity-distribution principle, considering the interaction effect of the active pressure (the pressure of surrounding-rock in frozen area for frost force reason) and the passive pressure (the reaction of the unfrozen surrounding-rock and tunnel's lining structure), we can do the calculation of the frost force of tunnel in frozen earth.

Some researches indicate that: in fissured rock, the volume expansion of fissured water when which is being frozen is the main reason that leads to frost force, during the transfer of frost force from surrounding-rock to tunnel's lining, the surrounding-rock partakes a major part, a minor part do effect on tunnel's lining. For the uncertainty of crack's distribution in fissured rock, we can calculate the frost force of tunnel's lining after we make sure the distribution of crack through geological investigation. However,

Copyright © 2005 Taylor & Francis Group plc, London, UK

in homogeneous fracture rock, the main reason leads to frost force is the expansion of the surrounding-rock that includes water, the effect of frost force is obvious because it acts on tunnel's lining directly. Therefore, the calculation method of frost force in frozen earth introduced in this paper mainly aims at homogeneous rock, that is the surrounding-rock class of IV, V, VI referred in «Code for design of railway tunnel».

2.2 *The FEM elastic-plastic calculation method of frost force*

Using the elastic-plastic FEM numerical calculation method, it is easy to simulate these transformation and their process. We choose the FEM program – ANSYS to create the calculation model of interaction of tunnel's lining support structure, the frozen and unfrozen surrounding-rock; basing on displacement-response and rigidity-distribution principle, considering the interaction effect of the active pressure and the passive pressure, then we can do the calculation of frost force. Tunnel's excavating, lining's constructing and frozen-area forming are simulated by a method that is through killing and activating FEM elements and changing material's parameters.

In the calculation, we adopt elastic-plastic FEM models and Drucker-Prager yield-principle to calculate structure's nonlinear deformation character of structure during excavation.

The equal stress of DP FEM model is:

$$\sigma = 3\beta\sigma_m + \left[\frac{1}{2}\{S\}^T[M]\{S\}\right]^{\frac{1}{2}}$$

In the formula:

$$\{S\} = \{\sigma\} - \sigma_m[1 \quad 1 \quad 1 \quad 0 \quad 0 \quad 0]^T;\ \sigma_m = \frac{1}{3}(\sigma_x + \sigma_y + \sigma_z);$$

$$\beta = \frac{2\sin\varphi}{\sqrt{3}(3-\sin\varphi)};\quad \sigma_y = \frac{6c\cos\varphi}{\sqrt{3}(3-\sin\varphi)};$$

Where c – cohesion of material; φ – inner-friction degree of material.

The yield-principle is:

$$F = 3\beta\sigma_m + \left[\frac{1}{2}\{S\}^T[M]\{S\}\right]^{\frac{1}{2}} - \sigma_y = 0$$

After the creation of calculation model, we do the FEM solution by 3 steps:

2.2.1 *The initial ground-stress calculation of tunnel's surrounding-rock*

In shallow tunnels, initial ground-stress is mainly formed by the gravity field of surrounding-rock, we can get its value through solution on the original FEM model. In deep tunnels, initial ground-stress is formed by the gravity field and geological structure stress field of surrounding-rock, we can get its value through spot test, we put the stress on FEM model as boundary condition, in some simplified cases, we may consider the gravity field only and calculate its value through solution on the original FEM model.

2.2.2 *The calculation for simulating tunneling process*

Tunneling process includes the excavation of surrounding-rock and constructing of tunnel's lining, both step by step. The equation of mechanical behavior of different process simulation is:

$$\{[K_{i-1}] + [\Delta K_i]\}\{\Delta\delta_i\} = \{\Delta F_{ir}\} + \{\Delta F_{ia}\},\quad (i = 1 \sim M)$$

In the formula: M – the total steps of tunneling;

$[K_{i-1}]$ – the rigidity matrix of model after the tunneling of step i − 1;

$[\Delta K_i]$ – the amount increasing and decreasing of rigidity of surrounding-rock and structure during tunneling of step i;

$\{\Delta F_{ir}\}$ – the boundary increasing amount nodal stress array for excavation reason;

$\{\Delta F_{ia}\}$ – the new nodal stress array in tunneling process.

2.2.3 *The calculation of frost force that is after the frozen-circle forms*

When tunneling completed, new frozen-circle will form and surround tunnel. In the calculation, we will get the frozen area according to theory calculation or spot test, the temperature changing will lead to volume expansion of the surrounding-rock in frozen-circle and the change of physical mechanical parameters of the surrounding-rock, we calculate the frost force of tunnel in frozen earth basing on displacement-response and rigidity-distribution principle.

3 MODEL EXPERIMENTATION STUDY ON FROST FORCE OF TUNNEL IN FROZEN EARTH

3.1 *General situation of model experimentation*

3.1.1 *The purpose and content of model experimentation*

The purpose of model experimentation is to simulate the mutual effect of surrounding-rock and tunnel's lining in frozen-circle when the volume of surrounding-rock is expanding, analysis the principle and value of tunnel's frost force from the result of model experimentation, and check the result of numerical simulation.

Copyright © 2005 Taylor & Francis Group plc, London, UK

3.1.2 *The project of model experimentation*

3.1.2.1 Summarize of model experimentation

Model experimentation demands to simulate the geometry size of surrounding rock and tunnel, in addition, the physical mechanical character on model, the model's material, size and loads must follow a rule, that's similar law. The physical mechanical parameters we need in model experimentation include: γ, μ, E, c, φ, F (loads) and displacement etc. For the limit of experimentation condition, we adopt plane-strain models with a similar ratio of 50.

Basing on similar law, we can get the similar ratio of parameters in model experimentation and listed them in Table 1.

3.1.2.2 The component and physical mechanical parameters of similar material in model experimentation

The similar materials of surrounding-rock in model experimentation mainly include: barite power, fine sand and machine oil, the similar material of tunnel's lining is made of plaster and water.

Materials' physical mechanical parameters in model experimentation are listed in Table 2

3.1.2.3 Area of model experimentation

According to past research experience, frost force will effect on lining along a whole tunnel, in a perfect instance of model experimentation, we shall consider the longitudinal effect of frost force to simulate the mechanical condition of a whole tunnel. But because of the limit of experimentation condition, it is difficult to simulate the longitudinal effect, in this experimentation, we simplify the model to a plane problem model without the considering of space effect. The disposals of transect and profile are listed in figure 1.

3.1.2.4 Data test of model experimentation

We set a testing section in model, consider the lining as pressed-bending structure, adopt some low-temperature strain-slices which is made in Shanghai and put them on lining model's inner and outer side at positions of vault, spring, wall and invert; we use pressure-boxes to test the contact pressure between surrounding-rock and tunnel's lining, put them at the strain-slices' position, and the pressure-boxes are made in Qiu-Long sensor company of DanDong. The transects and profiles of model data test are listed in figure 2. We lay the model of lining structure and similar material of surrounding-rock in a iron-box, do some waterproof measure to plaster model, connect the thrum of strain-slice and pressure-box with outer lines, and then put the whole model in an icebox to do a freezing experiment. We collect the strain data of structure and the pressure data of surrounding-rock by special instrument.

Table 1. Similar ratio of parameters in model experimentation.

Parameter name	Similar ratio	Parameter name	Similar ratio
Geometrical ratio C_l	50	Density ratio C_γ	1
Stress ratio C_σ	50	Ratio of E C_E	50
Strain ratio C_ε	1	Ratio of c C_c	50
Displacement ratio C_u	50	Ratio of φ C_v	1

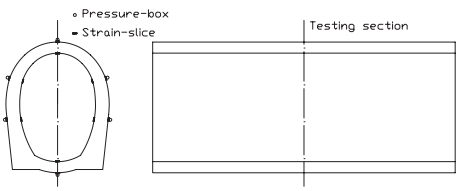


Figure 1. Transect & Profile of model experimentation.

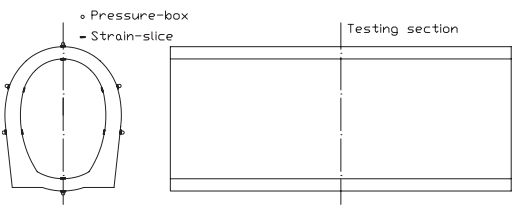


Figure 2. Transect & Profile for data test.

Table 2. Physical mechanical parameters of original model and similar materials.

System	Case	γ (kN/m^3)	E (MPa)	μ	C (KPa)	φ (°)	Frost expansion ratio η
Surrounding rock	Unfrozen model	18	2000	0.40	150	25	0.5%
	Unfrozen model	18	40	0.40	3	25	
	Frozen model	18	3600	0.32	450	33	
	Frozen model	18	72	0.32	9	33	
Lining	Original model	23	30000	–	–	–	–
	Similar model	23	600	–	–	–	

Copyright © 2005 Taylor & Francis Group plc, London, UK

Table 3. Frost force between surrounding-rock and tunnel's lining.

Position	Vault	Left-spring	Right-spring	Left-sidewall	Right-sidewall	Invert
Frost force (MPa)	0.032	0.081	0.084	0.030	0.032	0.054

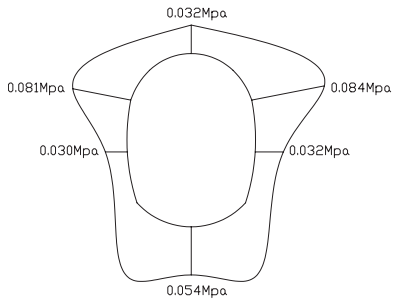


Figure 3. Frost force between lining and surrounding-rock.

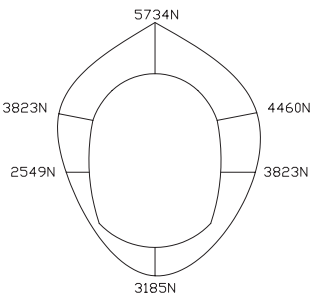


Figure 4. Force of tunnel's lining structure.

Table 4. Inner-force of tunnel's lining structure.

Position	Vault	Left-spring	Right-spring	Left-sidewall	Right-sidewall	Invert
Moment (N · m)	40	12	15	20	17	10
Force (N)	5734	3823	4460	2549	3823	3185

* for force value – positive sign represents pull; minus represents pressure.
Force's maximum is 5734N and at the position of Vault.
Moment's maximum is 40N · m and at the position of Vault.

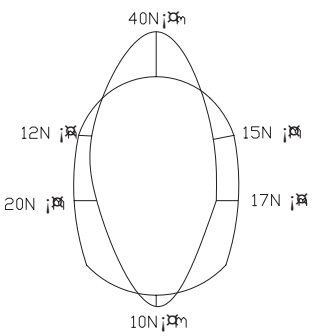


Figure 5. Moment of tunnel's lining structure.

3.2 *The result of model experimentation and analysis for it*

3.2.1 *Frost force between surrounding-rock and tunnel's lining*

According to demarcate information of pressure-box, we can deal with the original data of model experimentation and analyze it, and then get the value of frost force between surrounding-rock and tunnel's lining, and list them in table 3 and figure 3.

The result show that the distribution of frost force is anisomerous, the maximum value of frost force is 0.84 Mpa at the position of right spring.

3.2.2 *The inner-force of tunnel's lining caused by frost force*

According to related theories, we can deal with the original data of model experimentation and analyze it, and then get the inner-force of tunnel's lining, and list them in table 4, figure 4 and figure 5.

4 NUMERICAL CALCULATION OF FROST FORCE OF TUNNEL IN FROZEN EARTH

4.1 *The numerical calculation model*

4.1.1 *The calculation area and model*

According to the situation of model experimentation, we don't consider the space-effect in experimentation, just simplify the model to a plane problem one. So, we simplify the FEM model to be a plane-strain one when we create it in ANSYS. The calculation area of numerical simulation refers to model experimentation size, see figure 6, longitudinal direction is Z axis, vertical direction is Y axis, transverse direction is X axis.

Copyright © 2005 Taylor & Francis Group plc, London, UK

After we decide the calculation area, we can create the calculation model. The model is divided to be 3 parts: the iron box (to simulate the boundary condition), surrounding-rock and tunnel's lining structure, when temperature down, all the surrounding-rock of tunnel will be frozen. The calculation model is listed in figure 7.

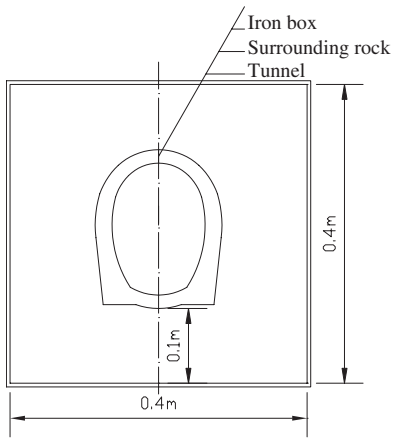


Figure 6. Calculation area.

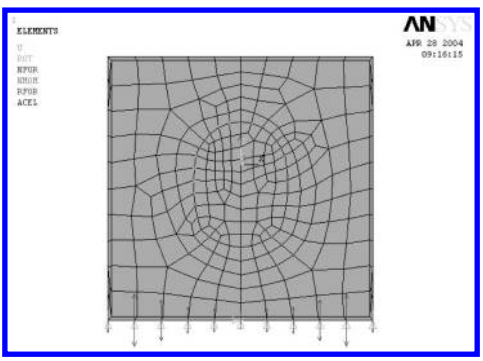


Figure 7. Calculation model.

4.1.2 *Simulation of surrounding-rock and tunnel's lining structure*

In the calculation model, we adopt four-side body isoparametric elements to simulate iron model(to simulate boundary condition) and surrounding-rock, beam elements to simulate tunnel's lining structure.

Table 6. Frost force between surrounding-rock and tunnel's lining.

Position	Vault	Left-spring	Right-spring	Left-wall	Right-wall	Invert
Frost force (MP)	0.037	0.064	0.064	0.030	0.030	0.057

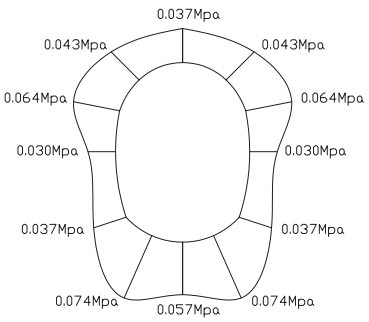


Figure 8. Frost force between surrounding-rock and tunnel's lining.

Table 7. The inner force of tunnel's lining structure.

Position	Vault	Left-spring	Right-spring	Left-sidewall	Right-sidewall	Invert
Moment (N · m)	23	8	8	23	23	8
Normal axis-Force (N)	4167	3241	3241	3704	3704	4167

* for force value – positive sign represents pull; minus represents pressure.

Table 5. The physical mechanical parameters which will be used in calculation.

Type	Material	γ (kN/m^3)	E (MPa)	μ	C (KPa)	φ (°)	Frozen-expanded ratio η
Unfrozen-surrounding-rock	Class V surrounding-rock	18	40	0.40	3	25	–
Unfrozen-surrounding-rock	Class V surrounding-rock	18	72	0.32	9	33	0.5%
Iron box	Iron board	23	600	–	–	–	–
Tunnel's lining	plaster	78	210000	–	–	–	–

Copyright © 2005 Taylor & Francis Group plc, London, UK

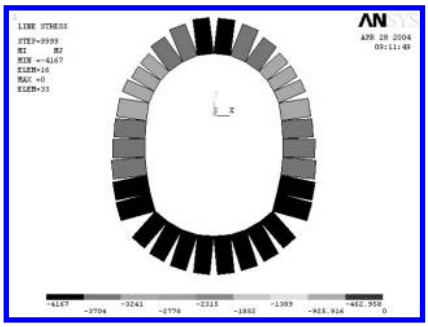


Figure 9. Force of tunnel's lining structure.

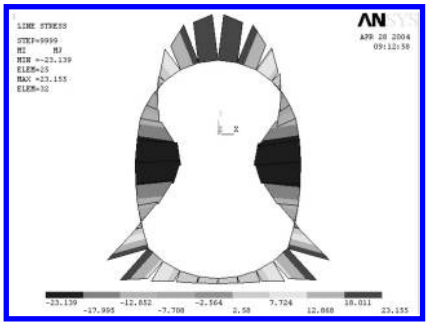


Figure 10. Moment of tunnel's lining structure.

The physical mechanical parameters which will be used in calculation are listed in table 5.

4.1.3 *The simulation for the forming process of the frozen-circle of tunnel's surrounding-rock*

In model experimentation, the main purpose is to observe tunnel's frost force, so the excavation and support of tunnel are not simulated. We don't consider the effect of tunneling, but consider tunnel to have existed in surrounding-rock, the simulation for the forming process of the frozen-area of surrounding-rock is divided into 2 steps: ① The calculation for tunnel's initial condition in surrounding-rock ② The calculation for the forming process of the frozen-circle of surrounding-rock.

4.1.4 *The plastic principle and boundary adopted in calculation*

In calculation, we adopt elastic-plastic model and Drucker-Prager yield principle to calculate the elastic-plastic nonlinear transformative character of tunnel's lining during the forming process of surrounding-rock's frozen-area.

We adopt displacement boundary conditions, use an iron box to simulate the top face, side face and bottom face, put a normal boundary conditions on bottom face.

4.2 *Numerical calculation result and analysis for it*

4.2.1 *Frost force between surrounding-rock and tunnel's lining*

According to numerical calculation result we can get the frost force values between surrounding-rock and tunnel's lining, and list them in table 6, figure 8.

4.2.2 *The inner force of tunnel's lining structure caused by frost force*

According to numerical calculation result we can get the inner force of tunnel's lining structure caused by frost force and list them in table 7, figures 9, 10.

Force's maximum is 4167N and at the position of invert.

Moment's maximum is 23N · m and at the position of vault and wall.

5 CONCLUSION AND PROPOSAL

Comparing with the result of model experimentation and numerical calculation, we know that there are some differences for the frost force value between surrounding-rock and tunnel's lining and the inner force of tunnel's lining. The main reason for the differences is the discreteness of material's physical mechanical parameters in model experimentation, but the rules that two methods reflect are inosculated on the whole. Therefore, the model experimentation indicate that, the method we firstly find out the area of surrounding-rock's frozen circle through test of earth temperature, get the physical mechanical parameters of surrounding-rock both frozen and unfrozen through original mechanical test, and then do the coupling for gravity field and temperature field is feasible, we call it an experiential-theoretical method for the calculation of frost force in frozen earth.

REFERENCES

The third railway survey & design institute. Permafrost Engineering [M]. China railway press. 1994.

Yuanfang Hu etc. Calculation of Frost Force of Kunlun Mountain Tunnel in Qing-Zang Railway [J]. Modern tunnel technology 2002, 39 (2).

Copyright © 2005 Taylor & Francis Group plc, London, UK

Design, construction and supervision of tunnels in swelling rock

W. Wittke & M. Wittke
WBI – Prof. Dr.-Ing. W. Wittke Consulting Engineers for Tunneling and Geotechnical Engineering Ltd., Aachen/Stuttgart, Germany

ABSTRACT: Long sections of the tunnels planned for the project Stuttgart 21 are located in anhydrite bearing, swelling Gypsum Keuper, which also contains swelling clay minerals. The fundamentals of swelling behavior of Gypsum Keuper and its analytical description are illustrated. In chapter 3, the support principles for tunnels in swelling rock are illustrated. With the aid of exemplary analyses, which were carried out with a FE-program developed and calibrated by WBI, it is shown that the more economic principle of resisting support can be realized with small deformations, if a layer of competent rock with sufficient thickness is available above the tunnel's roof as abutment against swelling pressure. For such conditions the principle of resisting support is to be recommended. In addition, there is a chance for a self-sealing effect of the rock mass in the area of the tunnel due to swelling, which would enable more economic solutions.

FE-analyses and observations for the tunnels Heslach II and Wagenburg showed that heaving of the tunnel tubes, which may extend up to the ground surface, results, if the principle of resisting support is applied to cases where leached Gypsum Keuper is located directly above the tunnel's roof or in the upper area of the cross-section. In such cases the principle of yielding support is to be recommended, if the installation of a slabtrack does not allow for such heavings.

As executed example for the principle of yielding support, the Freudensteintunnel is illustrated. Further, rules are set up which should be considered during construction of tunnels in swelling rock.

1 INTRODUCTION

Single-track tunnels with a total length of almost 50 km are planned for the project Stuttgart 21 in Germany (Marquart 2004). The longest of these tunnels is the Fildertunnel with a total length of approx. 2 × 9.5 km (no. 28, Figure 1). 4.3 km of both tubes of this tunnel are located in the swelling unleached Gypsum Keuper.

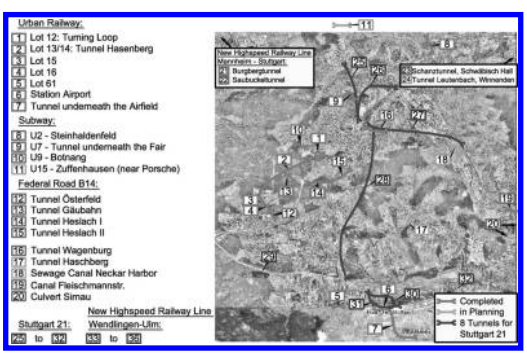


Figure 1. Tunneling in Stuttgart, experience of more than 30 years.

Also three other tunnels of this project are partly located in this rock formation (no. 25–27, Figure 1).

Tunneling in the unleached Gypsum Keuper is very challenging and often lead to damages to the structure and thus to an increase of construction time and costs in the past. Experience in tunneling gained by WBI in the area of Stuttgart during the past 30 years will surely help to build the tunnels of the project Stuttgart 21 economically and according to schedule (Wittke 2004).

2 FUNDAMENTALS

In case water gains access to the anydritic rock of the unleached Gypsum Keuper, the anhydrite is transformed into gypsum. This chemical process leads to a volume increase of the anhydrite of $\Delta V = 61\%$ (Figure 2, Kiehl 1990, Wittke-Gattermann 1998). Tremendous swelling pressures develop, if this volume increase is prevented.

The relation between the swelling pressures and swelling strains can be described by the law given in Figure 3 (Grob 1972, Wittke & Wittke & Wahlen 2004). This one-dimensional swelling law was extended to

Copyright © 2005 Taylor & Francis Group plc, London, UK

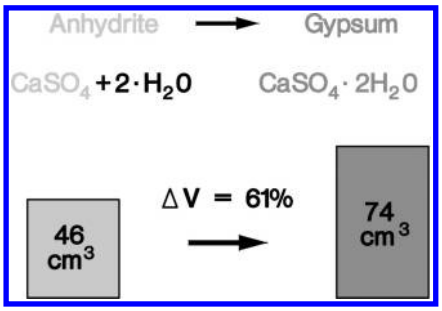


Figure 2. Swelling of Gypsum Keuper.

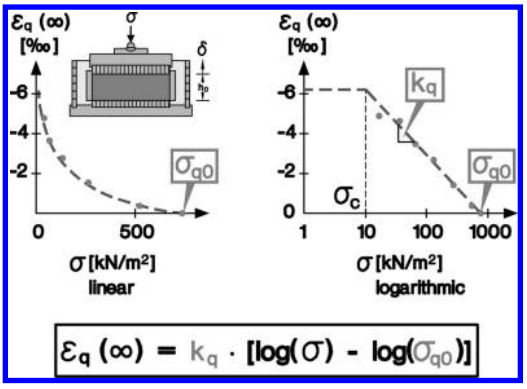


Figure 3. One-dimensional swelling law for full saturation.

three dimensions in a way that also anisotropic behavior of the rock can be accounted for (Kiehl 1990, Wittke-Gattermann 1998). Furthermore, the time-dependency of swelling is accounted for in the model so that stability analyses to design tunnels in swelling rock can be carried out (Kiehl 1990, Wittke-Gattermann 1998, Wittke 2003).

3 STABILITY ANALYSES AND SUPPORT PRINCIPLES

Two different support principles are foreseen for those sections of the tunnels of Stuttgart 21, which are located in the unleached Gypsum Keuper (Figure 4). In case the principle of resisting support is used, the internal lining will be designed to withstand the swelling pressure. For the yielding principle, a highly deformable yielding zone is placed underneath the invert of the tunnel. The planned shoulders of concrete make the construction of the yielding zone easier and prevent a loading of this zone by the dead-weight of the concrete lining. On the other hand, this shoulder will be highly loaded due to its great stiffness. Investigations carried

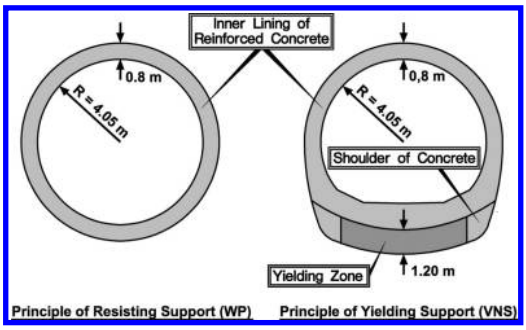


Figure 4. Support principles.

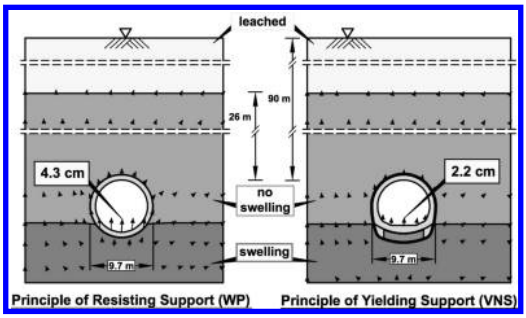


Figure 5. FE-Analyses, intact rock above the tunnel, displacements.

out by WBI lead to the result, that the shape of the yielding zone given in figure 4 is the optimum with regards to static aspects and construction works.

Both support principles have a different static mode of functioning. The results of FE-analyses for tunnels and the two support principles are illustrated in Figures 5 to 8. The given parameters result from comparative analyses for an investigation gallery in Germany, carried out with the FE-program FEST03 (Wittke-Gattermann 1998). In case the tunnel is well covered with competent unleached Gypsum Keuper and water is only available underneath the invert of the tunnel, the invert is subjected to higher bending in case of a resisting support than in case of a yielding support (Figure 5). Heaving of the tunnel cannot be observed in both cases. The high loading of the shoulders of concrete for the yielding principle is remarkable (Figure 6). It leads to high shear forces in the corresponding area of the inner lining. Nevertheless, the bending moments and normal thrust in the internal lining are lower for the yielding principle than for the resisting principle.

In case leached Gypsum Keuper is located above the roof, tunnels constructed according to the resisting principle are subjected to heaving (Figure 7). Due to the low shear strength and Young's modulus, the

Copyright © 2005 Taylor & Francis Group plc, London, UK

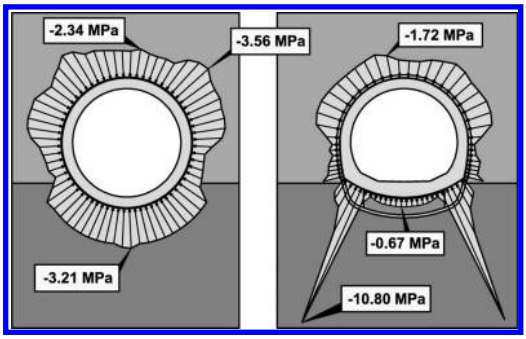


Figure 6. FE-Analyses, intact rock above the tunnel, radial loading.

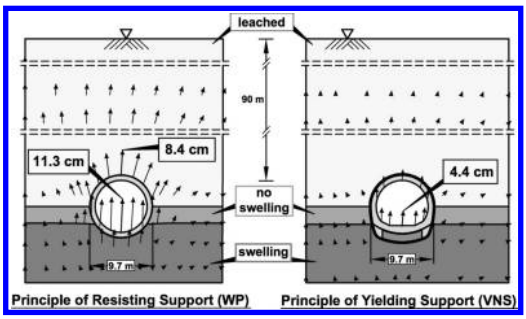


Figure 7. FE-Analyses, leached rock above the tunnel, displacements.

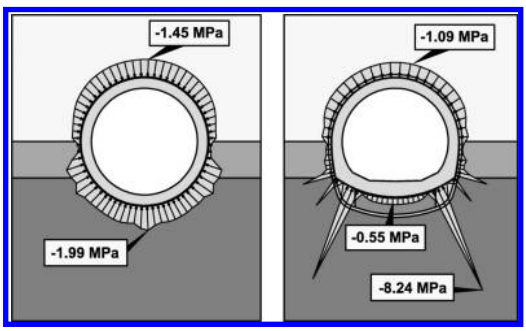


Figure 8. FE-Analyses, leached rock above the tunnel, radial loading.

leached Gypsum Keuper provides only small resistance against swelling pressures. Thus, in this case the load of the internal lining due to swelling is comparatively small (Figure 8). Also the difference between the radial loading on both linings is comparatively small. However, the heaving of the tunnel and the ground above are much smaller in case the yielding principle is used (cp. Figure 7).

	Intact Rock above Tunnel		Leached Rock above Tunnel	
	WP	VNS	WP	VNS
Heavings	+	+	−	+
M, N	−	+	−	+
Q	+	−	+	−
Costs	+	−	+	−
Chance of Self-sealing	+	−	−	−

Figure 9. Comparison of the two support principles.

Dry Tunneling

- careful excavation ⇒ avoid loosening of rock
- dry drilling of blastholes
- don't condense dust by water
- sealing of rock with shotcrete
- no use of anchors if possible

Water Inflow in the Area of the Leaching Front

- collect and discharge
- in case of swelling ⇒ temporary anchoring of invert (if needed, additional excavation)

Figure 10. Demands on construction.

The first three lines in Figure 9 illustrate again the described result. However, if the two support principles are compared, one has to account for the higher costs for construction of tunnels according to the yielding principle. Moreover, the yielding zone is very permeable and due to the large swelling strains loosening occurs in the rock underneath. Thus, the chance for self-sealing of the swelling rock and for the corresponding limitation of swelling pressures is only very low in case the principle of yielding support is used (Wittke 2003).

4 CONSTRUCTION

A basic rule for tunneling works in swelling rock is to avoid water inflow by all means until the internal lining is completed. Therefore, it is essential to observe the rules given in Figure 10. If the tunnel is located in the unleached Gypsum Keuper (Anhydrite, Figure 10) with a sufficient distance from the leaching front, it is possible to keep the rock completely dry during construction, if these rules are considered.

However, if the tunnel is located in the area of the water-bearing leaching front, it will be extremely difficult to keep the anhydritic rock completely dry. In

Copyright © 2005 Taylor & Francis Group plc, London, UK

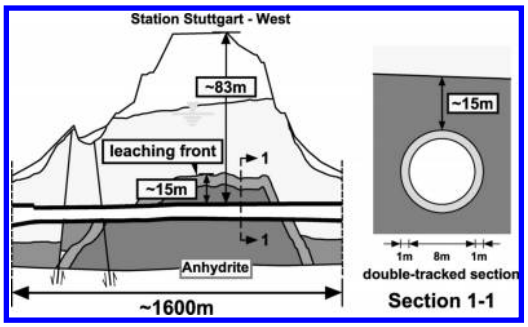


Figure 11. Urban railway Stuttgart, Lot 12.

such cases, the water must be collected and discharged carefully. If this fails, temporary anchoring of the invert and shotcrete support can be installed to keep the heaving due to swelling within acceptable limits until the final lining is installed (Klonsdorf & Schaser 1991).

5 EXAMPLES

5.1 *Suburban railway line Stuttgart, Lot 12*

The turning loop of the suburban railway system in Stuttgart, Germany (Lot 12) was constructed in the 1960s (Grüter & Liening 1976, Wittke & Rißler 1976). A long section of this tunnel is located in the anhydritic unleached Gypsum Keuper (Figure 11). The leaching front is located approximately 15 m above the roof. The ground water table is located in the leached Gypsum Keuper (Figure 11). Construction works of the tunnel were carried out strictly according to the rules given in figure 10. The rock was covered with a 5 to 10 cm thick sealing of shotcrete immediately after excavation. Anchors and steel arches were not used. The tunnel thus was stable with very little support, and the rock was found to be completely dry. The internal lining was designed according to the principle of resisting support with a thickness of 1 m. Up to now, no damages were observed in this tunnel.

5.2 *Road tunnel Heslach II and tunnel Wagenburg, Stuttgart*

The tunnel Heslach II is approximately 1000 m long and is located in the area of the city of Stuttgart in Germany. The maximum overburden results to approx. 91 m (Figure 12). In the middle section of the alignment, the invert of the tunnel is located in the swelling Gypsum Keuper, whereas the upper part of the cross section is located in the leached Gypsum Keuper. A through-going ground water table was not observed, however, in the area of the leaching front seepage water from rainfall was found. The tunnel was

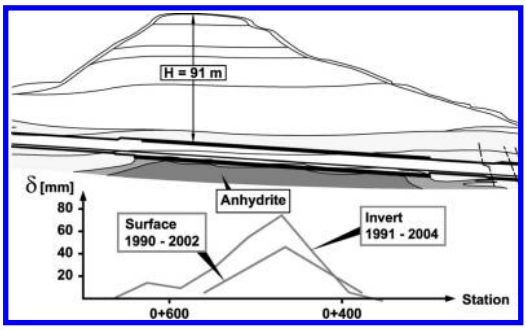


Figure 12. Tunnel Heslach II, longitudinal section and vertical displacements.

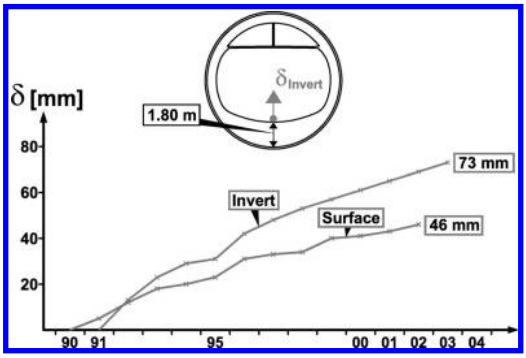


Figure 13. Tunnel Heslach II, cross section and vertical displacements.

built according to the principle of resisting support with an excavated diameter of 12.4 m. The design of the internal lining lead to a 1.8 m thick invert (Figure 13, Beiche 1991). In the course of construction works, heaving due to swelling did not occur. However, in the following 12 to 14 years after construction heaving of the invert was observed as shown in figure 12. Also leveling at the surface showed heaving. The increase of the displacements over the time is illustrated in figure 13. It can be clearly seen that the observations made for the tunnel Heslach II in principle correspond very well with the analysis results described above.

Similar observations were made for the Tunnel Wagenburg, which is located near to the central station of the city of Stuttgart (Wittke 2004).

5.3 *Tunnel Freudenstein*

The Tunnel Freudenstein of the new highspeed railway line from Mannheim to Stuttgart is approximately 6,8 km long (Klonsdorf & Schaser 1991, Kirschke et al. 1991). Over a length of 5 km, the tunnel is located in the unleached Gypsum Keuper (Figure 14). For the major part of this section the leaching front is located

Copyright © 2005 Taylor & Francis Group plc, London, UK

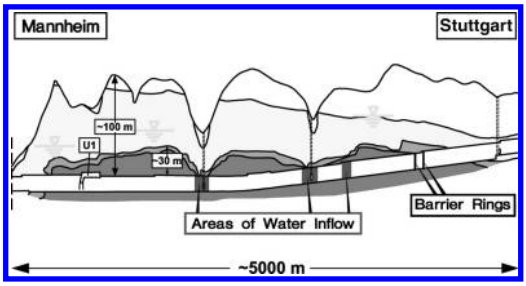


Figure 14. Tunnel Freudenstein, longitudinal section.

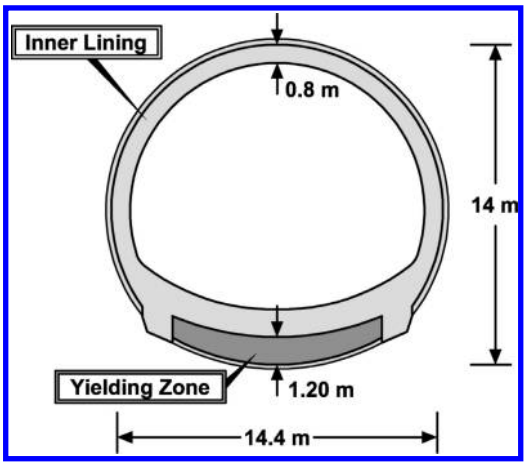


Figure 15. Tunnel Freudenstein, cross section.

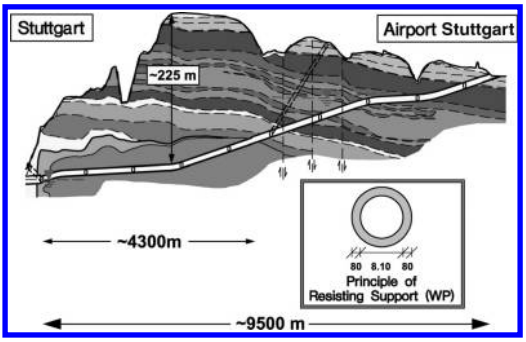


Figure 16. Filder tunnel.

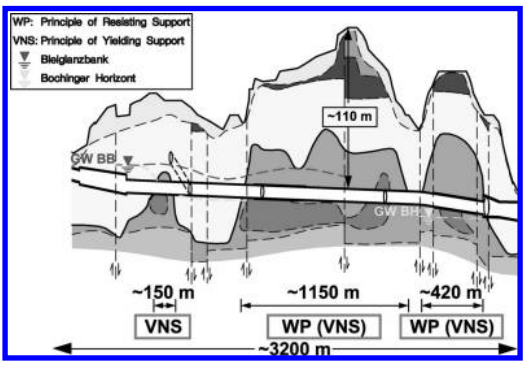


Figure 17. Tunnel to Feuerbach.

well above the tunnel, however, in the areas of two valleys the leaching front is located in the area of the tunnel's roof. Mainly along these sections water inflow was observed during construction. This is not surprising, because the ground water table is located in the leached Gypsum Keuper, well above the tunnel (Figure 14). The tunnel Freudenstein was constructed according to the principle of yielding support (Figure 15, Kirschke et al. 1991).

6 SUMMARY

Based on the theoretical investigations and the experience gained from tunnels constructed in the past, the following conclusions were drawn for the design and construction of those tunnels of the project Stuttgart 21, which are located in swelling Gypsum Keuper: The gradient of the Fildertunnel in the unleached Gypsum Keuper was determined in a way that the water-bearing leaching front is located well above the tunnel. It is expected that this tunnel can be constructed under completely dry conditions and thus it is designed according to the principle of resisting support (Figure 16). Analyses have shown that a thickness of the internal lining of 80 cm is sufficient to withstand the occurring swelling pressure. Moreover, the chance of self-sealing of the rock is apparent and thus, construction of an even thinner lining might be possible (Wittke 2003).

For the tunnel to Feuerbach, the principle of yielding support is foreseen to be used over short distances, because the rock cover above the tunnel is not sufficient (Figure 17). In other sections, it is planned to use the cheaper principle of resisting support. However, explorations will be carried out during construction. In case the rock cover is not sufficient to withstand the swelling pressure, it is planned to use the yielding principle also in these sections. Special measures, such as temporary anchoring or yielding support, are also foreseen in case swelling occurs during construction, although it is not expected.

REFERENCES

Beiche, H. 1991: Bemessung und Bau eines Tunnels in anhydrithaltigem Gebirge. Proc. 9. Nat. Felsmechanik

Copyright © 2005 Taylor & Francis Group plc, London, UK

Symposium, Aachen 1990, Sonderheft der Geotechnik, 208–215.
Grob, H. 1972: Schwelldruck am Beipiel des Belchentunnels. Sitzungsberichte Int. Symp. Für Untertagbau, Luzern, 99–119.
Grüter, R.; Liening, B. 1976: S-Bahn Stuttgart, Planung und Bau der Haltestelle Schwabstraße (Baulos 11) und der unterirdischen Wendeanlage (Baulos 12), Teil I. Deutsche Gesellschaft für Erd- und Grundbau e.V., Vorträge der Baugrundtagung in Nürnberg.
Kiehl, J. R. 1990: Ein dreidimensionales Quellgesetz und seine Anwendung auf den Felshohlraum. Proc. 9. Nat. Felsmechanik Symposium, Aachen 1990, 185–207.
Kirschke, D.; Kuhnhenn, K.; Prommersberger, G. 1991: Der Freudensteintunnel: Eine Herausforderung für den planenden Ingenieur. Ibw 7, 5–39.
Klonsdorf, G.; Schaser, F. 1991: Baudurchführung des Freudensteintunnels, Bergmännische und offene Bauweisen. Ibw 7, 118–172.
Marquart, P. 2004: Die Geologie weist den Weg – Tunnelbau in den Gebirgsformationen rund um Stuttgart und auf der Schwäbischen Alb. Geotechnik 27, Nr. 2.
Wittke, M. 2003: Begrenzung der Quelldrücke durch Selbstabdichtung beim Tunnelbau im anhydritführenden Gebirge. Geotechnik in Forschung und Praxis, WBI-Print 13, Verlag Glückauf GmbH, Essen.
Wittke, W.; Rißler, P. 1976: S-Bahn Stuttgart, Planung und Bau der Haltestelle Schwabstraße (Baulos 11) und der unterirdischen Wendeanlage (Baulos 12), Teil II. Deutsche Gesellschaft für Erd- und Grundbau e.V., Vorträge der Baugrundtagung in Nürnberg.
Wittke, W. 2004: Planung, Bau und Überwachung von Tunneln in quellfähigem Gipskeuper. Geotechnik 27, Nr. 2.
Wittke, W.; Wittke, M.; Wahlen, R. 2004: Zum Quellgesetz für den anhydritführenden, unausgelaugten Gipskeuper. Geotechnik 27, Nr. 2.
Wittke-gattermann, P. 1998: Verfahren zur Berechnung von Tunnels in quellfähigem Gebirge und Kalibrierung an einem Versuchsbauwerk. Geotechnik in Forschung und Praxis, WBI-PRINT 1, Verlag Glückauf, Essen.

Copyright © 2005 Taylor & Francis Group plc, London, UK

Building response to tunnelling in Brazil Salvador Metro

S.B. Foá, I. Chissolucombe & A.P. Assis
University of Brasilia, Brasilia, Brazil

ABSTRACT: The socio-economic development usually generates an increasing demand for mass transit systems. In Brazil, the urban population has been increasing enormously since the 50s, from less than 40% to more than 80%. In Salvador (Bahia), the number of inhabitants increased more than 10% from 1996 to 2000, and required an implementation of a mass transit system, which is called Salvador Metro. This subway includes a tunnel, with 1200 m of length and 12 m of width. This work presents a building response to tunnelling, where the tunnel axis crosses its garage ramp. Building foundations are footings, placed in a clayed-silt soil layer. An extensive instrument programme for monitoring ground and building movements was installed. The building behaviour due to tunnelling was numerically simulated with the programme called PLAXIS 3D-Tunnel (Brinkgreve & Vermeer, 2001), specifically intended to three-dimension analysis of deformation and stability. The forecasted results are compared to monitoring data.

1 INTRODUCTION

The importance of tunnels continues to expand progressively in every modern urban environment, as tunnels provide a viable, environmentally acceptable solution to ever-growing traffic congestion, and to the need to optimise the integral use of the underground space. When designing and constructing a tunnel, engineers should worry about the excavation impact on adjacent buildings. Many researchers have focused on the assessment of the ground surface settlement trough above the tunnel and its effects on the settlement, in special the differential settlement, of adjacent buildings.

In Brazil, the unplanned population increase in many urban centres has generated serious problems. In the 1950s, the industrialization process played an important role in generating employment in the cities and triggering a migration process from rural to urban areas. Salvador city, the capital of Bahia State (Figure 1), suffered the same process. Its population increased more than 10% from 1996 to 2000 and now exceeds 2.5 millions inhabitants.

The construction of the first metro line, from *Lapa* to *Pirajá* (Figure 2), began on April 2000. This line will be 11.9 km long, of which 1.2 km will be in tunnel, 4.8 km elevated, and the rest on the surface level. There will be eight stations; four of them will be bus/metro interchanges. The first line is expected to cost US$ 307 million, of which US$ l50 million comes from the World Bank, US$ 40 million from Brazil's federal government, US$ 67 million from Bahia state and Salvador city, and US$ 50 million from private enterprise. The Salvador metro will be operated initially by a fleet of 11 four-car trains, with full capacity for 1250 passengers. Traffic forecast is of 200,000 passengers a day.

In a second phase, Line 1 will be extended by 2.9 km to *Pau da Lima* (Figure 2). For the future, it is



Figure 1. Location of Salvador, Bahia, Brazil.

Copyright © 2005 Taylor & Francis Group plc, London, UK



Figure 2. Salvador Metro and Suburban Lines.

proposed to extend Line 1 to *Cajazeiras*, and to build a second line, 9.4 km long, from *Calçada* (the suburban railway terminal) to *Rodoviária* (the intercity bus terminal). At this phase, the suburban line will be reconstructed to conform to a metro line.

2 STATEMENT OF THE PROBLEM

This paper will focus on a section of the tunnel that was excavated under a building constructed in the 1970s. The building has 35 m of height. It is a reinforced concrete structure with 9 floors and basement. The elevator machine house and a water tank are located below the building. The tunnel axis crosses the garage ramp, 23 m below the street level. The building foundations are footings installed at 6 m of depth. A complete instrumentation programme was implemented to measure building displacements, tunnel movements and water levels.

A soft ground tunnel was designed to be constructed with sequential excavation and flexible shotcrete lining, following the NATM philosophy commonly used in Brazil since 1970. Sequential excavation methods have become quite preferable in Brazil because of their flexibility to adapt to different soil conditions, contractual aspects and required tunnelling equipment.

Different excavation methods were used in Salvador metro. Due to poor soil conditions and the existence of sensitive structures nearby, a construction method with partial face excavation was chosen for the section under consideration. It is divided in three stages (Figure 3). Each stage was totally completed, stabilised and passed a safe distance thought the building, before the next stage was started. After the excavation of each

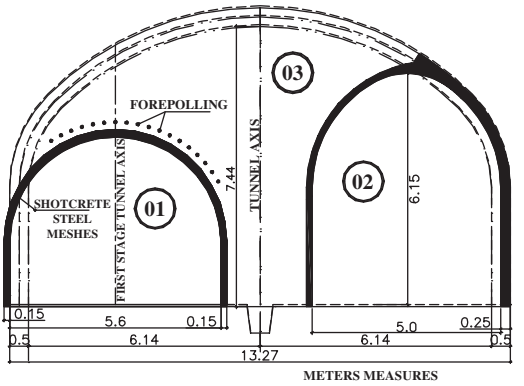


Figure 3. The excavation sequence method used in the tunnel.

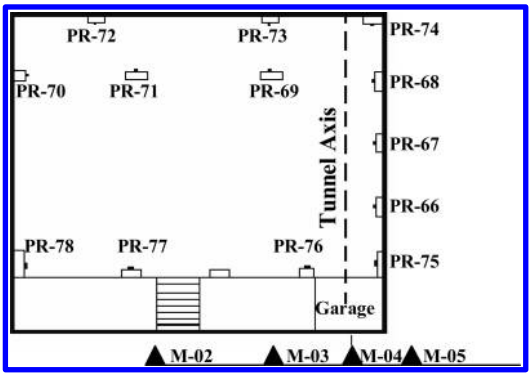


Figure 4. Displacement pins (PR-66 to PR-78) in the building.

stage, the lining was constructed using steel girders (spaced from 0.6 to 1.0 m, depending on the excavation and deformation conditions), shotcrete for the primary lining layer (10 cm thick) and finally, placement of the secondary lining layer (5 cm thick and one layer of steel meshes).

3 INSTRUMENTATION

A complete instrumentation programme was implemented to measure building settlements, tunnel movements and water levels. Thirteen displacement pins, PR-66 to PR-78 were installed in the building (Figure 4). A fully instrumented section, SI-15 (Figure 5), was installed in front of the building and also where either tunnel geometry or geologic conditions changed. It comprises the following instruments: six surface marks (M02 to M07), two vertical single point extensometers (T1 and T2), a piezometer (PZ3) and three convergence pins (P1 to P3) embedded in the shotcrete.

Copyright © 2005 Taylor & Francis Group plc, London, UK

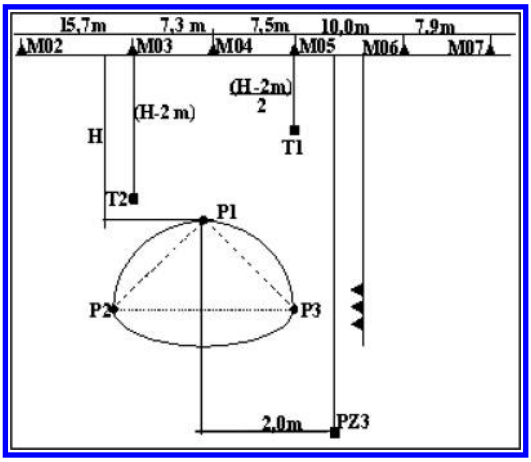


Figure 5. A fully instrumented section, SI-15.

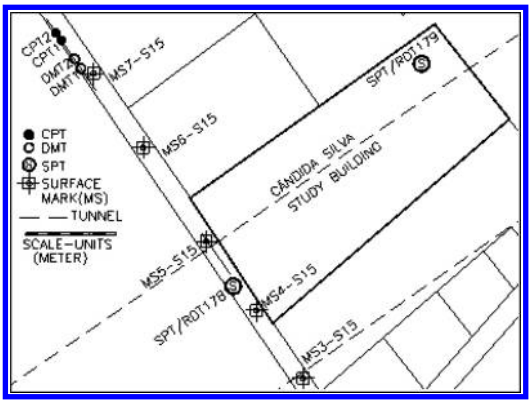


Figure 6. Location of SPT, CPT and DMT tests.

4 GEOTECHNICAL CHARACTERISATION

For this research, the Federal University of Bahia executed a laboratory test programme on undisturbed samples obtained near the building at a depth of 6 m (the same layer where building foundations were installed). A summary of some laboratory test results is presented. The Atterberg limits are: liquid limit $w_L = 64\%$ and plastic limit $w_P = 35\%$. The clay fraction (percentage of particles smaller than 2 μm) lies between 43 and 50% and the percentage of fines (grain sizes smaller than 60 μm) varies from 67 to 70%. The average unit weight of the soil is $\gamma = 17.5\ kN/m^3$. The strength parameters of this material were obtained from triaxial tests carried out on undisturbed saturated specimens, yielding the following Mohr-Coulomb drained parameters: cohesion $c' = 30\ kPa$ and friction angle $\phi' = 29°$.

Figure 6 shows the location of in situ tests performed such as Standard Penetration Test (SPT), Cone

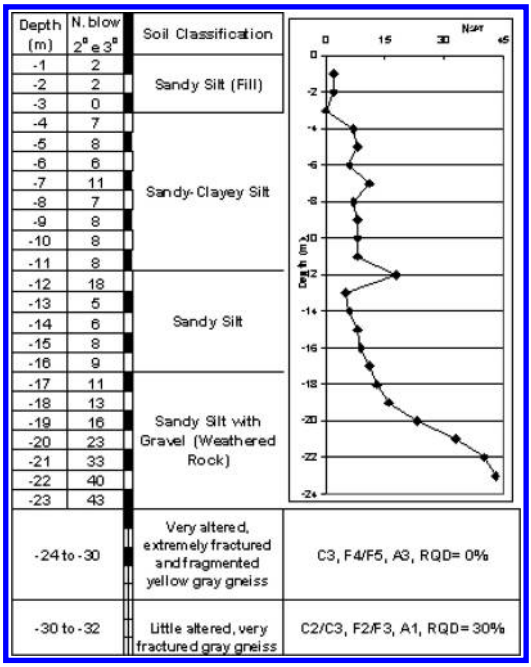


Figure 7. Soil profile obtained from SPT/RDT tests.

Penetration Test (CPT) and Flat Dilatometer Test (DMT). Figure 7 depicts the soil profile (from SPT/RDT) in front of the building. The first 3 m comprise a layer of sandy silt (fill). Then, it follows a layer of sandy-clayey silt, with number of SPT blow counts (NSPT) of 8 blows. A transition zone to sandy silt, with gravel, is found at 11 m of depth, without any major change in the NSPT (around 8 blows). The number of SPT blow counts increases steadily from NSPT = 11 to 43 for depths between 17 and 23 m, which is the domain of weathered rock (saprolitic soil). Below this zone, it is found a layer of very weathered, fractured and fragmented yellow and grey gneiss up to a depth of 30 m. Less weathered, but rather fractured, gneiss layer in then found until the drill limit of 32 m.

5 NUMERICAL ANALYSES

Ground control criteria, settlement trough and interference with existing public utilities and buildings are the main concerns of underground works in urban areas. In Salvador, three-dimensional finite element analyses are carried out in large scale to investigate the real ground behaviour due to tunnelling. Numerical analyses were done using the program PLAXIS 3D-Tunnel (Brinkgreve & Vermeer, 2001). This is a geotechnical finite element package specifically intended

Copyright © 2005 Taylor & Francis Group plc, London, UK

to three-dimension analysis of deformation and stability in tunnel projects.

The PLAXIS 3D has an automatic mesh generation of unstructured 2D finite element mesh with options of global and local refinement. In the study case, the 2D mesh used a triangular 6-node element to model the deformations in the soil and rock. In contrast to displacements stress and strain were calculated at individual Gaussian integration points rather than at the nodes. A 6-node element contains 3 stress points. The plate 8-node elements were used to model the building structure behaviour and it is defined using a flexural rigidity, a normal stiffness and an ultimate bending moment. The plate element behaviour follows Mindlin's Theory.

The 3D model is created simply by a linear extension of the mesh in z-direction. The previously generated 2D mesh is repeated at each z-plane. The 3D mesh is created by connecting the corners of the 2D triangular elements to the corresponding points of the corresponding elements in the next z-plane. In this paper, only the first stage excavation was simulated and analysed. The 2D mesh analysed had 254 elements, in a total of 546 nodes and 762 stress points. The Z-coordinates was 2 or 2.5 m, and the total longitudinal dimension mesh was 35.5 m, 10 m before the building and 10 m after it. After that, the 3D mesh had 10829 3D-elements (each one with 15-nodes and 6 stress points), 30210-nodes and 64974 stress points. Figure 8 shows the 3D mesh from The PLAXIS 3D Tunnel program.

Geotechnical applications require advanced constitutive models for simulating the behaviour of soil and rock. In this study, the elastic-plastic Hardening-Soil model was assumed. In the special case of a drained triaxial test, the observed relationship between the axial strain and the deviatoric stress can be well approximated by a hyperbola. Such a relationship was first formulated by Kondner (1963) and later used in the well-known hyperbolic model (Duncan & Chang, 1970). The Hardening-Soil model uses the theory of plasticity rather than the theory of elasticity and includes soil dilatancy and a yield cap, more details can be found in Schanz et al. (1999).

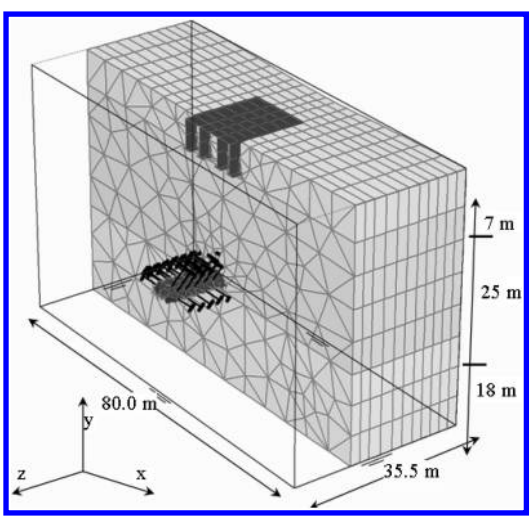


Figure 8. The 3D mesh used at the PLAXIS 3D Tunnel.

This model involves six input soil parameters. The parameters are effective cohesion (c), effective internal friction angle (ϕ) and a dilatancy angle (ψ). Besides that, basic parameters for soil stiffness are secant stiffness in standard drained triaxial test (E_{50}^{ref}), tangent stiffness for primarily oedometer loading (E_{oed}^{ref}) and power for stress-level dependency of stiffness (m). The initial soil conditions and initial horizontal soil stress (generated by k_o – coefficient earth pressure) play an important role in soil settlement problems.

The rock behaviour was modelled by the Hooke's law as a linear, isotropic and elastic medium. This model involves two input rock parameters: E and ν. Table 1 displays the soil and rock parameters assumed.

The building structure has twelve columns, which are not longitudinally aligned. However, for numerical simulation it was necessary to simplify and assume four sections with four columns in each longitude alignment. Table 2 shows the ER – equivalent structure rigidity (structure rigidity for one structure per square meter); the distance (d) between columns, lining thickness and thick floor and the Poisson's ratio ν assumed for the analyses.

The length of the tunnel was crossed by 19 plans and it was divided into 17 tunnel slices with 2 or 2.5 m of width for excavating slice by slice. Each section is divided into almost equally two parts (the top and bottom parts). Top part was indicated by index T and the arch invert or the bottom part was indicated by index

Table 1. The soil and rock parameters assumed.

Material	γ_{dry} (kN/m^3)	E_{50}^{ref} (MPa)	E_{oed}^{ref} (MPa)	E_{ur}^{ref} (MPa)	c (kPA)	ϕ°	K_o
Soil 1	13,6	33	44	99	30	30	0,6
Soil 2	13.6	31	41.6	93	25	30	0,6
Rock	22	40000	–	–	–	–	0,5

Table 2. The ER – structure rigidity equivalent.

	Column	Footing	Lining	Thick floor
ER (GPA)	21	30	4.5	150
d (m)	0,25	–	0,15	3
ν	0,15	0,15	0,15	0,15

Copyright © 2005 Taylor & Francis Group plc, London, UK

B. The whole excavation process had 36 stages and it can be described as follows:

1. Generating initial soil conditions and initial horizontal soil stress (generated by ko – coefficient earth pressure);
2. Loading structure and soil with dead loads;
3. Excavation of the upper part of the tunnel (T) for the first section (1st T);
4. Lining activation around excavated 1st T part, the forepooling installation at 2nd section and the excavation of the 1st bottom part (1st B);
5. Total lining activation at the first section and excavation of the upper part of the tunnel (T) for the second section (2nd T);
6. Lining activation of the 2nd T part, the forepooling installation at 3rd section, excavation of bottom part at 2nd section (2nd B);
7. Total lining activation at 2nd section, excavation of the 3rd T part;
8. Lining activation of 3rd T part, the forepooling installation at 4th section, excavation of 3rd B part;
9. Total lining activation at 3rd section, excavation of the 4th T part,
10. Repeat steps (8) and (9) until the tunnel end.

Tunnel excavations inevitably cause ground deformation and it may affect existent structures near to the tunnel. The induced displacements can influence the structure behaviour, as well as the structure is able to influence the path deformation. The effects of the tunnel construction on overlying and adjacent structures should be evaluated in urban areas. For this reason, the results presented herein show the soil and structure settlement due to tunnelling.

Figures 9 and 10 displayed the settlement pattern at two cross-sections when the tunnel finished: the 1st excavation slice (S1 – 0 to 2 m) and the 9th slice (S9 – 16 to 18.50 m), only for the 1st excavation stage. At the roof tunnel, the S1 presented 8.5 mm displacement and S9 showed 7.1 mm. Probably, this effect was observed because of the forepooling action. This element decreased the roof displacement and by the consequence the ground deformations.

The behaviour of soils during tunnelling is significantly affected by the soil overburden or the ratio D/R, where D is the depth from the ground surface to the tunnel top and R is the radius of the tunnel. At this study, the tunnel was classified as deep tunnel, because the ratio D/R was 11.8. In this case, there is less influence on surface settlements as represented on Figures 9 and 10 (around 3.7 mm). Figure 11 pointed out the 3D surface settlements at the end of tunnelling, where the maximum value was 4.5 mm.

Potts & Addenbrooke (1997) concluded that the ground displacement magnitude decreases and its form is more distorted as the axial relative rigidity and the soil-structure flexibility increases. Chissolucombe (2001) analysed the interferences at the Brasilia Metro (Brazil). Several soil models were used and concluded that the pattern and the magnitude of the displacements suffered few changes regarding the elastic-plastic soil models (Cam-Clay and Hardening Soil) compared to the linear-elastic and Mohr-Coulomb constitutive models, although the behaviour trend was the same.

Figure 12 demonstrated the vertical settlements of the first structure column section versus transverse

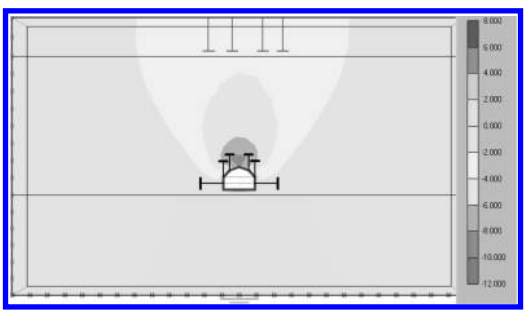


Figure 9. The settlement occurred at the S1 slice.

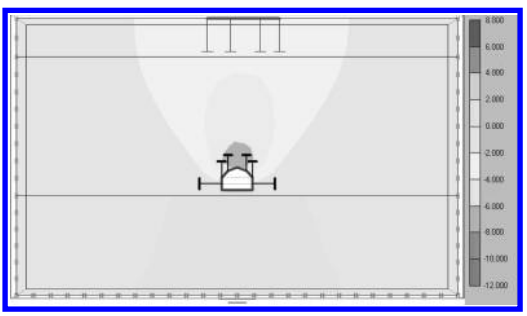


Figure 10. The settlement occurred at the S9 slice.

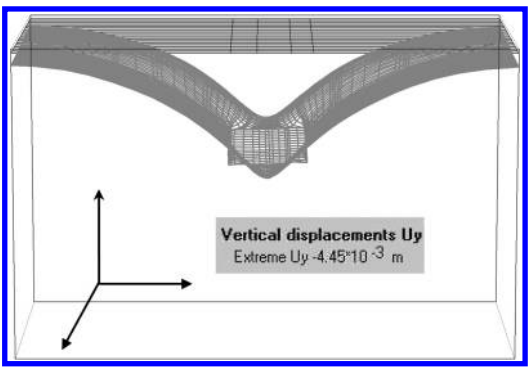


Figure 11. The 3D surface settlements at the end of tunnelling.

Copyright © 2005 Taylor & Francis Group plc, London, UK

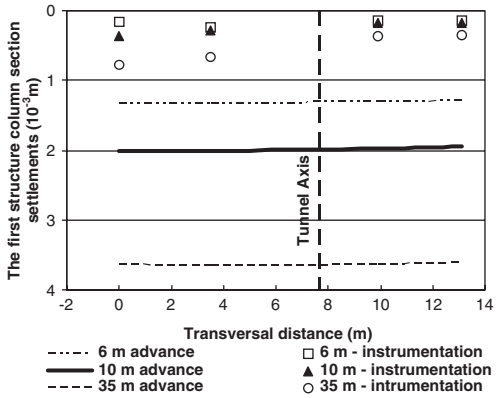


Figure 12. The vertical settlements of the first structure column section versus transverse distance and tunnelling advance.

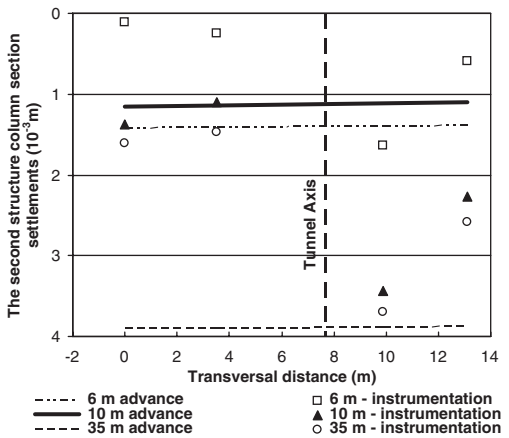


Figure 13. The vertical settlements of the second structure column section versus transverse distance and tunnelling advance.

distance and tunnelling advance. Numerical simulation results showed that the structure suffered settlement increases with the excavation front progression, but the angular distortion values did not present great variability. About the instrumentation, the measured values were smaller than the simulation values. The maximum simulation settlement was around 3.7 mm and the maximum measured settlement was around 0.8 mm. According to Mair et al. (1996) damage criterion, when the settlements structure are inferior to 10 mm, it will not suffer significant damages due tunnelling.

Figure 13 verified the vertical settlements of the second structure column section versus transverse distance and tunnelling advance. This showed that structure suffered again settlement increases with the excavation front progression. The simulation angular distortion values did not present great variability. However, the angular distortion measured values presented variability and the third column presents the biggest settlements. The maximum simulation settlement was around 3.9 mm and the maximum measured settlement was around 3.8 mm. At this time, the simulation and measured values had an excellent agreement.

6 CONCLUSIONS

This paper presents back-analyses for predicting settlement during tunnelling by using the actual collected data from the Salvador Metro in Brazil. An extensive instrument programme for monitoring ground and building movements was installed in the building and surrounding ground. Numerical simulations were performed using the programme PLAXIS 3D-Tunnel intended to three-dimension analysis of deformation and stability in tunnel projects.

It was investigated the pattern of displacements at the tunnel roof. Besides, the structure behaviour was also analysed. At the structure, the forecasted results were compared to monitoring data. For the first columns section, the predictions were bigger than the measured data. For the second columns section, the settlements obtained from numerical simulation were quite well matched with monitoring data; however the angular distortions were not good. In conclusion, the PLAXIS 3D-Tunnel was able to satisfactorily model the maximum building response to tunnelling in Salvador.

ACKNOWLEDGEMENTS

The authors would like to express their gratitude to the Salvador Metro Company, Federal University of Bahia, University of Brasilia, National Research Council of Brazil (CNPq) for the financial support, and the Brazilian companies Camargo Correa and Andrade Gutierrez (joint-venture contractors).

REFERENCES

Brinkgreve, R.B.J. & Vermeer, P.A. 2001. Finite Element Code for Soil and Rock Analyses. Plaxis Manual. Balkema, Rotterdam, Netherlands.

Chissolucombe, I. 2001. Numerical Simulation for evaluate the structure damages nearby a tunnelling. M.Sc. Thesis, G.DM – 088A/01, Civil and Environmental Engineering Department. University of Brasilia. Brasília, DF, 194 p. (In Portuguese).

Duncan, J.M. & Chang, C.Y. 1970. Nonlinear analysis of stress and strain in soil, Journal of Soil Mechanics Foundation Division. ASCE 96, 1629–1653.

Copyright © 2005 Taylor & Francis Group plc, London, UK

Kondner, R.L. & Zelasko, J.S. 1963. A hyperbolic stress strain formulation for sands. Proc. 2nd Pan American. ICOSFE Brazil, 289–394.

Mair, R.J., Taylor, R.N. & Burland, J.B. 1996. Prediction of ground movements and assessment of risk of building damage due to bored tunneling. Geotechnical Aspects of Underground Construction in Soft Ground, Mair & Taylor (eds), London, pp. 713–718.

Potts, D.M. & Addenbrooke, T.I. 1997. A structure's influence on tunnelling-induced ground movements. Proc. Instn. Civ. Engrs. Geotech. Engng, 125(1).109–125.

Schanz, T., Vermeer, P.A. & Bonnier, P.G. 1999. The hardening soil model: formulation and verification, Beyond 2000 in Computation Geotechnics – 10 years of Plaxis, Balkema, Rotterdam, ISBN 90 5809040 X.

Copyright © 2005 Taylor & Francis Group plc, London, UK

Prediction of ground-condition ahead of tunnel face using electric resistivity – analytical study

G.C. Cho & J.S. Choi
Korea Advanced Institute of Science and Technology, Daejeon, Korea

G.H. Lee
Posco E&C., Seoul, Korea

J.K. Lee
Dodam E&C., Gyeonggi, Korea

ABSTRACT: During tunnel construction, ground failures often occur due to existence of weak zones, such as faults, joints, and cavities around tunnel face. It is hard to detect effectively weak zones, which can lead underground structure to failure after excavation and before supporting, by using conventional characterization methods. In this study, an enhanced analytical method of predicting weak zones ahead of tunnel face is developed to overcome some problems in the conventional electrical resistivity-based characterization methods. The analytical method is based on Coulomb's and Gauss's laws with considering the characteristics of electric fields subjected to rock mass. A series of case studies are performed using the developed analysis. The presence of weak zones and their sizes, location, and states can be accurately predicted by combining a proper inversion process with electrical resistivity measured from several electrodes on the tunnel face.

1 INTRODUCTION

When a long tunnel or a large underground structure is made, the precise assessment of ground condition controls its safety and success. Therefore in-situ site characterization (or investigation) is often performed to assess the ground condition of construction site before a design stage. However, it may be impossible to detect detailed ground information in the whole area along the axes of tunnel with high resolution. When there is weak zone or fault zone around tunnel face, the failure of tunnel face or crown has been often reported after excavation and before installation of primary support (Hasegawa et al., 1993; Cho et al., 1999; Kim et al., 2000). This makes time delay in construction schedule and causes a lot of casualties. For this reason, it is necessary to develop an enhanced geophysical characterization method which allows predicting ground-condition ahead of tunnel face during construction.

The Tunnel Seismic Profiling (TSP) method has been generally used for that purpose. This is suitable for detection of faults and weak zones for hard rock mass in 100 m–200 m ahead of tunnel face. However, the TSP is not applicable to detection in a near range such as 10 m–20 m ahead of tunnel face (Sattel et al., 1992; Lee, 2001; Lee et al., 2002; KGE, 2002). Therefore this study will present an enhanced detection method for a near field inner twice of a tunnel diameter from tunnel face which affects tunnel safety most likely. This method overcomes shortcoming of elastic wave and analyzes more precise than the conventional resistivity-based geophysical characterization method. This method uses the characteristics of current that is charged through water inner pores and joints of rock mass.

2 ELECTRIC FIELD ANALYSIS BETWEEN TWO-ELECTRODES IN AN IDEAL INFINITE MEDIUM

Let us consider that two spherical electrodes (+q, −q) are placed at a certain distance (L) in an ideal infinite medium. The electrode +q is anode where current goes out, and the electrode −q is cathode where current comes in. An electric field (E) at the center of two electrodes can be expressed using Coulomb's law and Gauss' law (Fig. 1):

$$E_{+q} = \frac{1}{4\pi\varepsilon_m} \cdot \frac{q}{x^2 + r^2} \tag{1-1}$$

Copyright © 2005 Taylor & Francis Group plc, London, UK

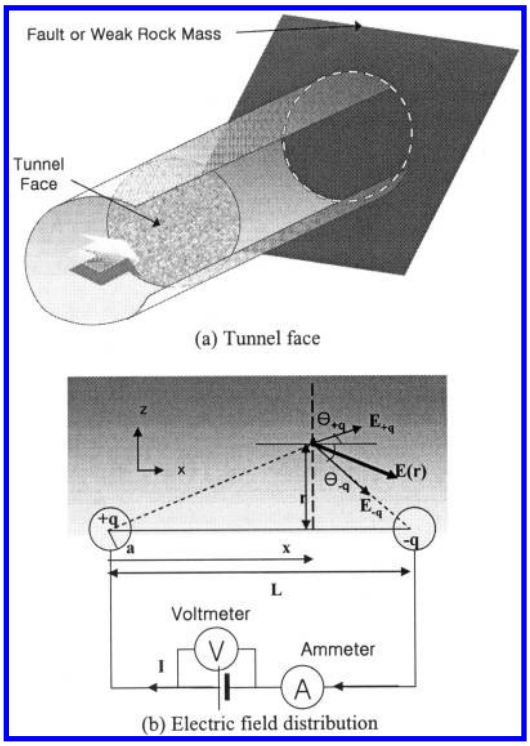


Figure 1. Electric field between two electrodes equipped on a tunnel face in a semi-infinite medium.

$$E_{-q} = \frac{1}{4\pi\varepsilon_m} \cdot \frac{q}{(L-x)^2 + r^2} \tag{1-2}$$

where E_{+q} = the electric field formed by the electrode +q, E_{-q} = the electric field formed by the electrode −q, ε_m = the permittivity of the medium, q = the electric charge of +q and −q, L = the distance between two electrodes, x = the distance from the electrode +q on the line of two electrodes, r = the normal distance from the line of two electrodes. The current density can be expressed as multiplying conductivity and electric field as follows:

$$\overline{E(r)} = \overline{E}_{+q}\cos\theta_{+q} + \overline{E}_{-q}\cos\theta_{-q} \tag{2}$$

where

$$\cos\theta_{+q} = \frac{x}{x^2 + r^2} \tag{2-1}$$

$$\cos\theta_{-q} = \frac{L-x}{(L-x)^2 + r^2} \tag{2-2}$$

The current (I) can be obtained by integrating current density (J) on the surface:

$$I = \int J \cdot ds = \int \sigma\overline{E} \cdot \overline{ds} = \int_0^\infty \sigma \cdot \overline{E(r)} \cdot \pi r dr \tag{3}$$

The voltage at the surface of electrode (V′) is equal to half of the voltage between two electrodes (V):

$$V' = \frac{1}{4\pi\varepsilon} \cdot \frac{q}{a} = \frac{V}{2} \tag{4}$$

where a = the diameter of an electrode. If combining Eq. (1), Eq. (3), and Eq. (4) together, the current between two electrodes becomes:

$$I = \frac{\sigma \cdot q}{\varepsilon} = \frac{\sigma}{\varepsilon} \cdot \pi\varepsilon \cdot a \cdot V = \frac{\pi a \cdot V}{\rho} \tag{5}$$

Finally, resistance (R) is a function of electrode's radius (a) and electric resistivity (ρ) as follows:

$$R = \rho\frac{1}{\pi a} \tag{6}$$

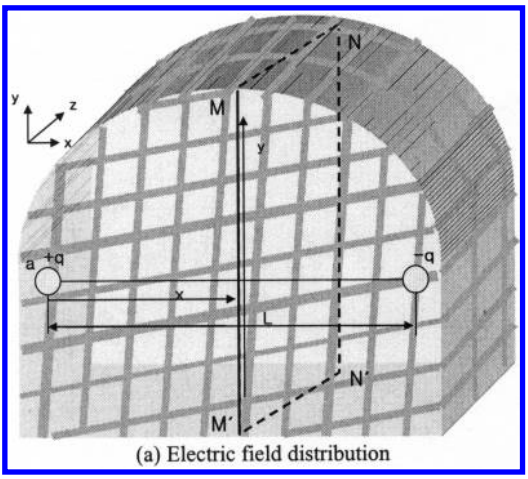
The electric resistivity of a medium can be assessed by measuring resistance with voltmeter and ammeter. An interesting observation is that the distance between two electrodes has no effect on resistance.

3 ELECTRIC FIELD ANALYSIS IN SEMI-INFINITE ROCK MASS

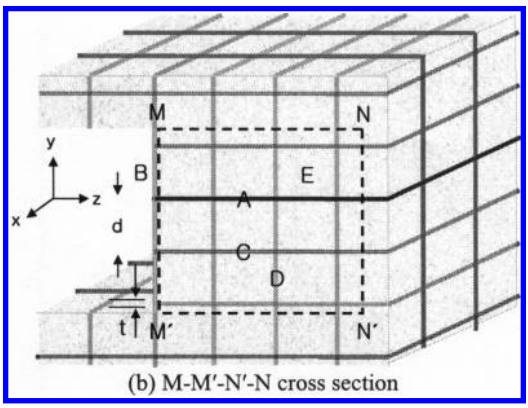
The resistance of an ideal semi-infinite medium subjected to electric current can be calculated from the previous section, rendering twice of the resistance of an ideal infinite medium. In general case, joints in rock mass around tunnel are saturated with water because most tunnels are below the groundwater table. Especially, if weathering process is developed, the width of joint surface will become larger and the electric resistivity will become lower. Figure 2(a) shows configuration of two electrodes on tunnel face in rock mass having 3 joint sets. Suppose that the orientations of three joint sets are identical to three axes, the direction of tunnel excavation is on z-axis and the tunnel face is on x–y plane, and the center of tunnel face is the origin of rectangular coordinate. If the width of joints is t and the distance between joints is d, the current (I) and resistance (ρ) of y–z plane including section M–M′–N′–N can be expressed as follows:

$$I = 2\sum_{k=0}^{\infty}[A + B + C + D] \cdot V \tag{7-1}$$

Copyright © 2005 Taylor & Francis Group plc, London, UK



(a) Electric field distribution



(b) M-M′-N′-N cross section

Figure 2. Electric field of joint surface in semi-infinite medium.

$$R = \frac{1}{2\sum_{k=0}^{\infty}[A+B+C+D]} \tag{7-2}$$

Also, in case that base material is shale or sandstone which has good connection of water in pore (Archie, 1942; Sen et al., 1981; David and Kennedy, 1994; Olivar, 1995; Chinh, 2004), the current and resistance of rock mass can be expressed as follows:

$$I = 2\sum_{k=0}^{\infty}[A+B+C+D+E]\cdot V \tag{8-1}$$

$$R = \frac{1}{2\sum_{k=0}^{\infty}[A+B+C+D+E]} \tag{8-2}$$

where the section A, B, C, D and E are summarized in Table 1.

Table 1. Double integral analysis of jointed rock mass.

Equation	Plane-Integral	
	z-axis	y-axis
	Description	
$A=\int_0^{t/2}\int_0^{\infty}\sigma_J E_J dzdy$	∞	t/2
	At y=o, x-z plane, Joint surface	
$B=\int_{(d+t)+t/2}^{(d+t)+t/2+d}\int_0^{t/2}\sigma_J E_J dzdy$	t/2	d
	At z=0, x-y plane, Joint surface	
$C=\int_{(d+t)+t/2+d}^{(k+1)(d+t)+t/2}\int_0^{\infty}\sigma_J E_J dzdy$	∞	t
	At y=const., x-z plane, Joint surface	
$D=\int_{(d+t)+t/2}^{(d+t)+t/2+d}\int_{(k+1)(d+t)+t/2+d}^{(k+1)(d+t)+t/2}\sigma_J E_J dzdy$	t	d
	At z=const., x-y plane, Joint surface	
$E=\int_{(d+t)+t/2}^{(d+t)+t/2+d}\int_{(d+t)+t/2}^{(d+t)+t/2+d}\sigma_{IR}E_{IR}dzdy$	d	d
	Rock zone	

Note: $\sigma_J E_J = \frac{2\sigma_J q}{4\pi\varepsilon_J}\frac{L/2}{\left[(L/2)^2+y^2+z^2\right]^{3/2}}$

$\sigma_{IR}E_{IR} = \frac{2\sigma_{IR}q}{4\pi\varepsilon_{IR}}\frac{L/2}{\left[L/2^2+y^2+z^2\right]^{3/2}}$

Notation: σ_J = the conductivity of joint, E_J = the electric field in joint, ε_J = the permittivity of joint, σ_R = the conductivity of a porous medium, E_R = the electric field in a porous medium, ε_{IR} = the permittivity of a porous medium.

4 ELECTRIC FIELD ANALYSIS IN SEMI-INFINITE ROCK MASS WITH A SPHERICAL WEAK ZONE

Consider that a weak zone is ahead of tunnel face. The shape of the weak zone is assumed to be a spherical shape. If its shape is not spherical, its equivalent diameter to sphere can be calculated. As shown in Fig. 3, the point O is the center of a spherical weak zone and E_w is the electric field of a weak zone. Laplace's equation for sphere coordinate can be expressed as follows (Fig. 4):

$$\nabla^2\varphi \equiv \frac{1}{r^2}\frac{\partial}{\partial r}\left(r^2\frac{\partial\varphi}{\partial r}\right)+\frac{1}{r^2\sin\theta}\frac{\partial}{\partial\theta}\left(\sin\theta\frac{\partial\varphi}{\partial\theta}\right)+\frac{1}{r^3\sin^2\theta}\frac{\partial^2\varphi}{\partial\phi^2} \tag{9}$$

$$\lim_{r\to\infty}\varphi(r,\theta)=\lim_{r\to\infty}\left(\frac{\partial}{\partial r}\left(r^2\frac{\partial\varphi}{\partial r}\right)+\frac{1}{\sin\theta}\frac{\partial}{\partial\theta}\left(\sin\theta\frac{\partial\varphi}{\partial\theta}\right)\right)=0 \tag{10}$$

Eq. (10) shows the condition that electric potential of the point at infinity is zero in Eq. (9). Using Legredre's equation, the electric potential can be deduced as

Copyright © 2005 Taylor & Francis Group plc, London, UK

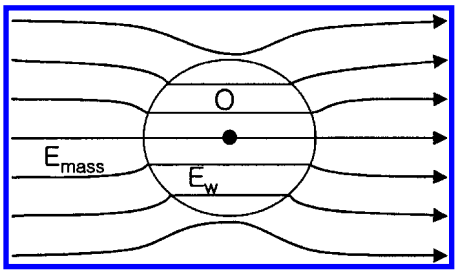


Figure 3. Electric field variation in spherical.

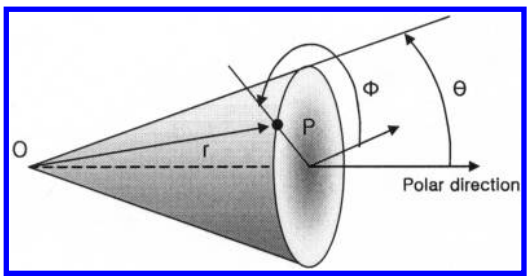


Figure 4. Location of the point P in terms of the spherical coordinates r, θ,Φ.

sphere's inner potential (φ_1) and outer potential (φ_1) as follows:

$$\varphi_1(r,\theta) = A_1 r\cos\theta + C_1 r^{-2}\cos\theta \tag{11-1}$$

$$\varphi_2(r,\theta) = A_2 r\cos\theta + C_2 r^{-2}\cos\theta \tag{11-2}$$

where A_1, A_2, C_1, and C_2 are the unknown constants and can be determined from boundary condition. The area of existing electric field is supposed to have homogeneous properties, and A_1 ($=-E_0$) A_2 ($=-3\ E_{mass}/(K+2)$), C_1 ($=((K-1)a^3E_{mass}/(K+2))$, and C_2 ($=0$) are estimated from boundary condition (Reitz et al., 1993). The electric field of weak zone can be expressed in terms of relation permittivity (K) and the electric field of rock mass (E_{mass}):

$$E_w = \frac{3}{K+2}E_{mass} \tag{12}$$

where K = the ratio of the permittivity of rock mass to the permittivity of weak rock mass ($=\varepsilon_w/\varepsilon_{mass}$). The current (I) shown in Fig. 5(a) is following:

$$I = \int_0^{r-b}\sigma_{mass}E_{mass}\cdot\pi r dr + \int_{r-b}^{r+b}\sigma_w E_w\cdot\alpha r dr + \int_{r-b}^{r+b}\sigma_{mass}E_{mass}(\pi-\alpha)r dr + \int_{r+b}^{\infty}\sigma_{mass}E_{mass}\cdot\pi r dr \tag{13}$$

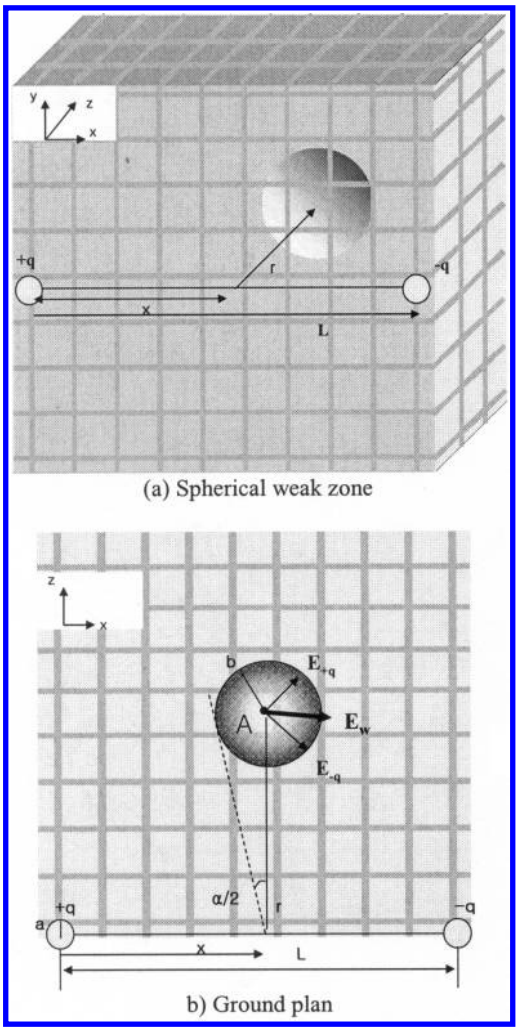


Figure 5. Electric field analysis of weak zone in semi-infinite medium.

where $\alpha = \sin^{-1}(b/r)$, b = the radius of weak zone, r = the distance between the center of electrode and that of weak zone, σ_w = the conductivity of weak zone, σ_{mass} = the conductivity of rock mass. After substituting Eq. (12) for Eq. (13) and considering Eg. (4), the resistance of total rock mass with weak zone is

$$R = \frac{1}{\left[\pi\sigma_{mass}A + \left[\frac{3\sin^{-1}\frac{b}{r}\cdot\sigma_w}{K+2} + \left(\pi - \sin^{-1}\frac{b}{r}\right)\sigma_{mass}\right]\cdot B\right]\cdot\frac{a}{2}} \tag{14}$$

Copyright © 2005 Taylor & Francis Group plc, London, UK

$$A = 2 + \cos\left(\tan^{-1}\frac{r+b}{x}\right) + \cos\left(\tan^{-1}\frac{r+b}{L-x}\right) - \cos\left(\tan^{-1}\frac{r-b}{x}\right) - \cos\left(\tan^{-1}\frac{r-b}{L-x}\right) \quad (14\text{-}1)$$

$$B = \cos\left(\tan^{-1}\frac{r-b}{x}\right) + \cos\left(\tan^{-1}\frac{r-b}{L-x}\right) - \cos\left(\tan^{-1}\frac{r+b}{x}\right) - \cos\left(\tan^{-1}\frac{r+b}{L-x}\right) \quad (14\text{-}2)$$

where x = the distance from electrode +q to the point, meeting perpendicularly the line passing the center of spherical weak rock mass with the line passing the center of two electrodes simultaneously, and L = the distance between two electrodes.

5 ELECTRIC FIELD ANALYSIS OF SEMI-INFINITE ROCK MASS WITH A FAULT ZONE

The configuration of semi-infinite rock mass with a fault zone is shown in Fig. 6. It is assumed in analysis that the base medium is homogeneous and the width of the fault zone is fixed to be a constant. As electric current flows through, the direction of electric field is altered because the fault zone has different properties from the base medium. This case can be analyzed in view of mutated electric field, by using electrostatic image effect which is considered as virtual charge, actually not existing charge (Reitz et al., 1993). The boundary of two different properties is considered as x = 0 on x–y plane as shown in Fig. 7. The point charge q is located in right medium with the distance d from x = 0. Thus, if an imaginary point charge exists in an opposite direction (−x), the coordination r and coordination r′ are

$$r = \sqrt{(x+d)^2 + y^2 + z^2} \quad (15\text{-}1)$$

$$r' = \sqrt{(x-d)^2 + y^2 + z^2} \quad (15\text{-}2)$$

Therefore, the potential of the right medium can be expressed as:

$$\varphi = \frac{1}{4\pi\varepsilon_{mass}} \cdot \left(\frac{q}{r} + \frac{q'}{r'}\right) \quad (16)$$

The imaginary charge q′ exists in the location (−d, 0, 0) in the left medium. Hence, the effect of electric field in any point of the right medium is received by the point charge q and q′. The left medium is affected by

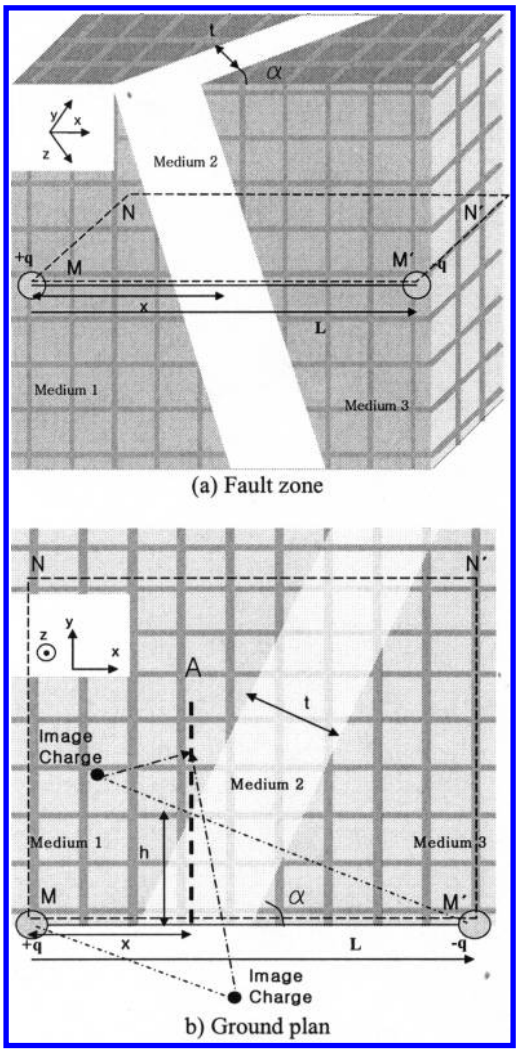


Figure 6. Electric field analysis of fault zone in semi-infinite medium.

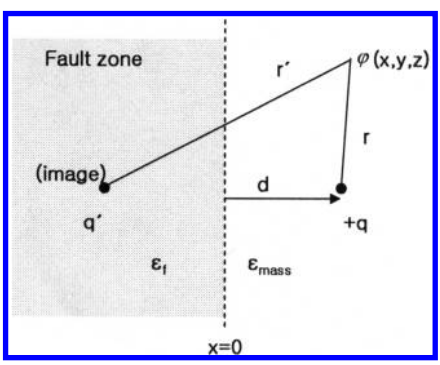


Figure 7. Electric field analysis using image effect: φ(*x*, *y*, *z*).

Copyright © 2005 Taylor & Francis Group plc, London, UK

the effect of the right point charge q, and the electric field is altered by a different material. Thus, the potential in the left medium is

$$\varphi'' = \frac{q''}{4\pi\varepsilon_f r''} \tag{17}$$

where ε_f = the permittivity of fault zone. The charges q' and q'' can be determined by using the same conditions of electric field and electric displacement in boundary condition.

$$q' = \frac{\varepsilon_{mass} - \varepsilon_f}{\varepsilon_{mass} + \varepsilon_f} q \tag{18-1}$$

$$q'' = \frac{2\varepsilon_{mass}}{\varepsilon_{mass} + \varepsilon_f} q \tag{18-2}$$

This satisfies the boundary condition and Laplace's equation in bi-medium.

$$\varphi_1 = \frac{+q}{4\pi\varepsilon_{mass}}\left[\frac{1}{r_1} + \left(\frac{\varepsilon_{mass} - \varepsilon_f}{\varepsilon_{mass} + \varepsilon_f}\right)\cdot\frac{1}{r_1'}\right] + \frac{-q}{4\pi\varepsilon_{mass}}\left[\left(\frac{4\varepsilon_{mass}\varepsilon_f}{(\varepsilon_{mass} + \varepsilon_f)^2}\right)\right]\frac{1}{r_1''} \tag{19-1}$$

$$\varphi_2 = \frac{+q}{4\pi\varepsilon_f}\left[\left(\frac{2\varepsilon_f}{\varepsilon_{mass} + \varepsilon_f}\right)\cdot\frac{1}{r_L}\right] + \frac{-q}{4\pi\varepsilon_w}\left[\left(\frac{2\varepsilon_f}{\varepsilon_{mass} + \varepsilon_f}\right)\cdot\frac{1}{r_R}\right] \tag{19-2}$$

where r_1 = the distance in medium 1 from +q to integral plane, r_1' = the distance in medium 1 from image effect of +q to integral plane, r_1'' = the distance in medium 1 from −q to integral plane, r_L = the distance in medium 2 from +q to integral plane, r_R = the distance in medium 2 from −q to integral plane. The effect for +q existed in medium 1 is about q in Eq. (16), the image effect for +q in medium 1 substitutes Eq. (18-1) for Eq. (16), and the effect for −q existed in medium 3 including the effect for medium 2 substitutes Eq. (18-2) for Eq. (17). Eq. (19-1) is arranged for the previous sections. And Eq. (19-2) is considered as the effect of medium 2 for +q and −q in mediums 1 and 3 by substituting Eq. (18-2) for Eq. (17). The current calculated after electric field using Eq. (19-1) and Eq. (19-2) can be expressed as follows:

$$\therefore I_{total} = I_1 + I_2 \tag{20}$$

$$I_1 = \int_h^{\infty}\int_{-\infty}^{\infty}\sigma_{mass}\left[\frac{+q}{4\pi\varepsilon_{mass}}\left[\frac{1}{r_1} + \left(\frac{\varepsilon_{mass} - \varepsilon_f}{\varepsilon_{mass} + \varepsilon_f}\right)\cdot\frac{1}{r_1'}\right] + \frac{-q}{4\pi\varepsilon_{mass}}\left[\left(\frac{4\varepsilon_{mass}\varepsilon_f}{\varepsilon_{mass} + \varepsilon_f}\right)\right]\frac{1}{r_1''}\right]dzdy \tag{20-1}$$

$$I_2 = \int_0^{t}\int_{-\infty}^{\infty}\sigma_w\left[\frac{+q}{4\pi\varepsilon_w}\left[\left(\frac{2\varepsilon_f}{\varepsilon_{mass} + \varepsilon_f}\right)\cdot\frac{1}{r_L}\right] + \frac{-q}{4\pi\varepsilon_f}\left[\left(\frac{2\varepsilon_f}{\varepsilon_{mass} + \varepsilon_f}\right)\cdot\frac{1}{r_R}\right]\right]dzdy \tag{20-2}$$

Substituting q in Eq. (4) for Eq. (20) renders.

$$R = \frac{1}{\pi\sigma_{mass}\left[\left(\frac{\pi}{2} - \tan^{-1}\frac{h}{x}\right) + \frac{1-K}{1+K}A + \left(\frac{\pi}{2} - \tan^{-1}\frac{h}{L-x}\right)\frac{4K}{(1+K)^2}\right]\cdot a + \frac{2\pi\sigma_f}{1+K}\left[\tan^{-1}\frac{h}{x} + \tan^{-1}\frac{h}{L-x}\right]\cdot a} \tag{21}$$

where

$$A = \left[\frac{\pi}{2} - \tan^{-1}\left[\frac{h + \left(x - \frac{h}{\tan\alpha}\right)\sin 2\alpha}{2\left(x - \frac{h}{\tan\alpha}\right)\sin^2\alpha - x}\right]\right] \tag{21-1}$$

where a = the radius of electrode, α = the fault discretion against x–y plane, K = relative permittivity ($=\varepsilon_w/\varepsilon_{mass}$), h = the shortness thickness of fault (t)/ 2cosθ, x = the distance from +q to the center of fault, L = the distance between two electrodes, σ_{mass} = the conductivity of fault zone, σ_w = the conductivity of rock mass.

6 FINAL REMARKS

This study developed an enhanced prediction method of ground condition ahead of tunnel face using resistivity to overcome some problems in the conventional electrical resistivity-based characterization methods. The analytical method is based on Coulomb's and Gauss's laws with considering the characteristics of electric fields subjected to rock mass. The presence of weak zones and their sizes, location, and states can be accurately predicted by using the developed analysis method and combining a proper inversion process with electrical resistivity measured from several electrodes on the tunnel face.

ACKNOWLEDGEMENTS

This work was supported by the POSCO E&C and the Underground Space Construction Technology Center under the Ministry of Construction and Transportation in Korea (grant C04-01).

Copyright © 2005 Taylor & Francis Group plc, London, UK

REFERENCES

Archie, G. E. 1942, The electrical resistivity log as an aid in determining some reservoir characteristic: *Trans, AIME* 146: 54–62.

Bittar, M. S., Rodney, P. F., Mack, S. G. and Bartel, R. P. 1993, A Multiple-Depth-of-Investigation Electromagnetic Wave Resisivity Sensor: *Theory, Experiment, and Field Test Results, SPE Formation Evaluation*: 171–176.

Blaricom, R. V. 1992, Practical Geophysics 2 – for the Exploration Geologist-, *Northwest Mining Association, Spokane*: 39–139.

Chinh, P. D. 2000, Electrical Properties of Sedimentary Rocks having interconnected Water-Saturated Pore Spaces, *Geophysics* 65(4): 1093–1097.

Cho, Y., Lim, J. S., Jeong, Y. Y. and Choi, S. Y. 1999, A Case Study on the Ground Reinforcement Method and Effect of the Failed Tunnel (in Korea), *KTS Spring Conference*: 293–300.

Herrick, C. D. and Kenndy, W. D. 1994, Electrical Efficiency − A Pore Geometric Theory for Interpreting the Electrical Properties of Reservoir Rocks, *Geophysics* 59(6): 918–927.

Hasegawa, M., Usui, M., and Gotoh, K. 1993, Geological prognosis ahead of a tunnel face, *Engineeing Geology* 35: 229–235.

Jackson, J. D. 1999, *Classical Electrodynamics*, John Wiley & Son, U.S.A: 24–134.

Karwatowski, J. and Habberjam, G. M. 1981, A Tunnel Resolution Investigation using Automated Resistivtiy Tank Analog, *Geophysics Prospecting* 29: 891–905.

Kim, N. Y., Kim, S. H. and Joeng, H. S. 2000, Analysis of Collapse Shape and Cause in the Highway Tunnel (in Korea), *Korea Tunnel Assocation*, 2(3): 13–23.

Korea Geophysics Exploration Association 1998, Electric resistivity Exploration 1 (in Korea), *Proceedings of Korea Geophysics Exploration Association* 1(2): 140–143.

Korea Geophysics Exploration Association 1998, Electric resistivity Exploration 2 (in Korea), *Proceedings of Korea Geophysics Exploration Association Proceeding* 1(3): 188–194.

Korea Geophysics Exploration Association 2002, TSP (Tunnel Seismic Profiling) Exploration (in Korea), *Geophysics* Exploration Practical Guide: 253–261.

Lee, I. M., Choi, S. S., Kim, S. T., Kim, C. K. and Jun, J. S. 2002 3D analysis of fracture zones ahead of tunnel face using seismic reflection (in Korea), *Tunneling Technology* 4(4): 301–317.

Lee, S. W. 2001, Investigation Skill of TBM Tunnel ahead of Tunnel Face (in Korea), *Construction Skill Information*: 25–27.

Militzer, H., Rösler, R. and Lösch, W. 1977, Theoretical and Experimental Investigations for Cavity Research with Geoelectrical Resistivity Methods. *Geophysics Prospecting* 25: 640–652.

Olivar, A. L. de Lima, 1995, Water Saturation and Permeability from Resistivity, Dielectric, and Porosity Log, *Geophysics* 60(6): 1756–1764.

Reitz, J. R., Milfore, F. J. and Christy, R. W. 1993, *Foundations to Electromagnetic Theory*, Addison Wesley, U.S.A: 26–126.

Sattel, G, Frey, P. and Amberg R. 1992, Prediction ahead of the tunnel face by seismic methods, *pilot project in Centovalli Tunnel, Locarno, Switzerland. First Break* 10: 19–25.

Sen, P. N., Scala, C. and Cohen, M. H. 1981, A self-similar model for sedimentation rocks with application to the dielectric constant of fused glass beads, *Geophysics* 46: 718–795.

Suzuki, K., Nakata. E., Minami. M., Hibino. E., Tani, T., Sakakibara, J. and Yamada, N. 2004, Estimation of the Zone of Excavation Distribution around Tunnels, using Resistivity and Acoustic Tomography, *Geophysics Prospecting* 33: 62–69.

Copyright © 2005 Taylor & Francis Group plc, London, UK

3D numerical simulation of the future Pinheiros Station – Line 4-Yellow of the São Paulo Subway

Flávio Massayuki Kuwajima
ITA – Instituto Tecnológico de Aeronáutica and SGP Engenharia S/C Ltda- Sao Paulo, Brazil

Hugo Cássio Rocha
Companhia do Metropolitano de Sao Paulo- Metrô, Sao Paulo, Brazil

ABSTRACT: The paper describes some aspects of a sequential evolutive three-dimensional numerical modeling using the Finite Elements Method for the excavation of the future Pinheiros Station, Line 4 – Yellow, of the São Paulo Subway. It includes the excavation of the central access shaft, the tunnels of station body and lateral tunnels of access of the CPTM (Regional Track line) line. The excavation presents large geological and geotechnical variability, including earthfill, Quaternary and Tertiary sediments, residual soil, saprolite and gnaiss at different degrees of weathering.

1 THE METROPOLIS

São Paulo is the Latin America biggest city and there are more than 17 million inhabitants. São Paulo represents 18% of the Brazilian GDP and it is the most important the financial center not only in Brazil but also in Latin America. The metropolis is served by a well managed and efficient subway system which needs immediate expansion. Currently the São Paulo Subway carries approximately 486 million passengers/year with a total extension lines of 49,2 kilometers long with 46 stations. Under the *PITU*'s guidelines (Integrated Program of the Urban Transport), of the São Paulo State Government, the subway system is being expanded and the construction of the new line 4 (yellow) is an important stage in this program, improving the life quality of passengers that use of the public transport in São Paulo.

2 THE PROJECT

The line 4 (yellow) will connect the Luz quarter, downtown, with the Vila Sônia one, at west side, crossing the regions of the Consolação, Paulista Avenue and Pinheiros. There will be 11 stations and an extension of 12,8 kilometers, which allows connections with the lines of the CPTM – São Paulo Metropolitan Railway Company, as well as the other lines of the Subway. The project will be developed in two phases. The phase 1, to be concluded in 48 months, consisting of 12,8 km of extension including total construction of track tunnels, complete construction of 5 stations, partial construction of 4 stations and the Vila Sônia maintenance yard. The phase 2 consists of the conclusion of 4 stations of phase 1 and construction of two new stations and complementation of the yard. The line will be entirely underground except for the Vila Sônia yard.

As occurs in similar projects, design modifications always are allowed, even after the conclusion of the basic project. In the case of line 4 it was not different, and soon after the conclusion of the project for the implantation of the Station Pinheiros, it was necessary to review the project. 3D analyses with the FEM took place during the project review.

3 GEOLOGY

The regional geology of São Paulo Metropolitan area, can be summarized in three great geologic units: Precambrian basement, tertiary sediments of the São Paulo Sedimentary Basin, and quaternary sedimentary deposits. The local Precambrian rock mass can be divided in three different groups, based in its mineralogical, textural and structural characteristics such as: the granite-gneiss, biotitic gneiss and striped gneiss, with different degrees of weathering and fractures. The values of Q (Barton) vary locally between 0.1 and 15.

The São Paulo Sedimentary Basin is a depression with coluvial, alluvial and lacustrine sediments Tertiary

Copyright © 2005 Taylor & Francis Group plc, London, UK

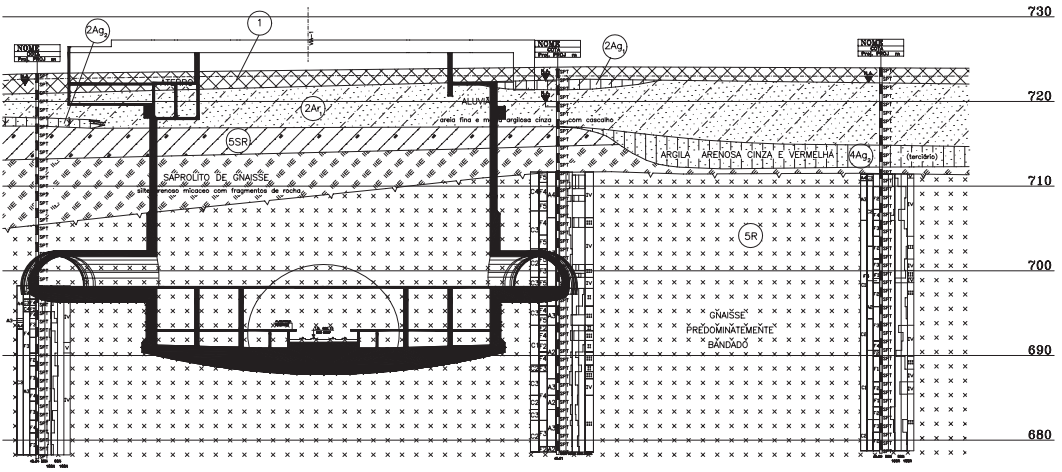


Figure 1. Pinheiros station geological cross section.

located above the basin, which can be gathered in the following formations:

- Resende Formation – consisting of intercalations of gray silty clay (Taguá) and gray and yellow silty sands, usually little clayed. It occurs predominantly below of elevation 750;
- São Paulo Formation – it occurs predominantly above of elevation 760 in downtown. It is formed by sandy clay, silty clay and clayey sand, sometimes conglomeratic.
- The modern quaternary sediments are at the most part alluvial deposits and occur along the Tietê River valley and its tributaries. They are composed by clays, gravels and sands deposits along the current fluvial system.

At the future Pinheiros Station site, there are quaternary sediments related to alluviums of the river Pinheiros. Also, the Resende's Formation tertiary sediments, represented by gray clays, and the Precambrian basin formed by residual soils and saprolites of granite-gneiss and biotitic, besides the rock in different degrees of weathering. (Figure 1 geologic Section: 1- earthfill, 2Ag alluvial clays, 2Ar alluvial sands, 4Ag1- gray tertiary clay, 5S- gneiss saprolite, 5SR gneiss residual soil, 5R granite gneiss striped).

4 CONSTRUTIVE METHODOLOGY

Along the São Paulo Subway Pinheiros Station there is a mixed construction method: cut & cover for the central body and adjacent tunnels, and NATM, for the platforms. There are also two tunnels (in slope) which make the connection between the Metro Station and the CPTM-Pinheiros railway station located in the east side of the Pinheiros river. The construction method comprises the following stages: central body (shaft), platforms tunnels in half section (heading), tunnels of interconnection between the Stations Pinheiros (Metro and CPTM), bench of platform tunnels and construction of the internal structures of the tunnels and shafts and other constructions of the station.

The central body of the Pinheiros Station consists of the opening of a great elliptical shaft with approximately 720 m^2 excavation area, which, as function of its shape and constructive methodology creates great clean spaces without internal struts and slender structures of containment. The executive conditionings of the shaft are the same of NATM tunnels. The executive attention should be addressed to the horizontal e vertical steps compatible to the stand-up-time of local material and the first phase stabilization as fast as possible.

5 CALCULATIONS METHODS

TOCHNOG, a FEM code, was used for the calculation of soil and tunnel lining interaction. TOCHNOG was originally developed by Dennis Roddeman at the University of Twente, with GNU type public license. It is a program that possesses extensive library of elements and constitutive models. The results from this program is being tested by many users in many different countries, and as result, many improvements have been implemented. During the analyses, one can model the different phases of tunnel construction.

A three-dimensional mesh was used to model the station. It was possible to model the each excavation phase and then the lining application. Due to practical reason restriction, it was necessary to introduce some

Copyright © 2005 Taylor & Francis Group plc, London, UK

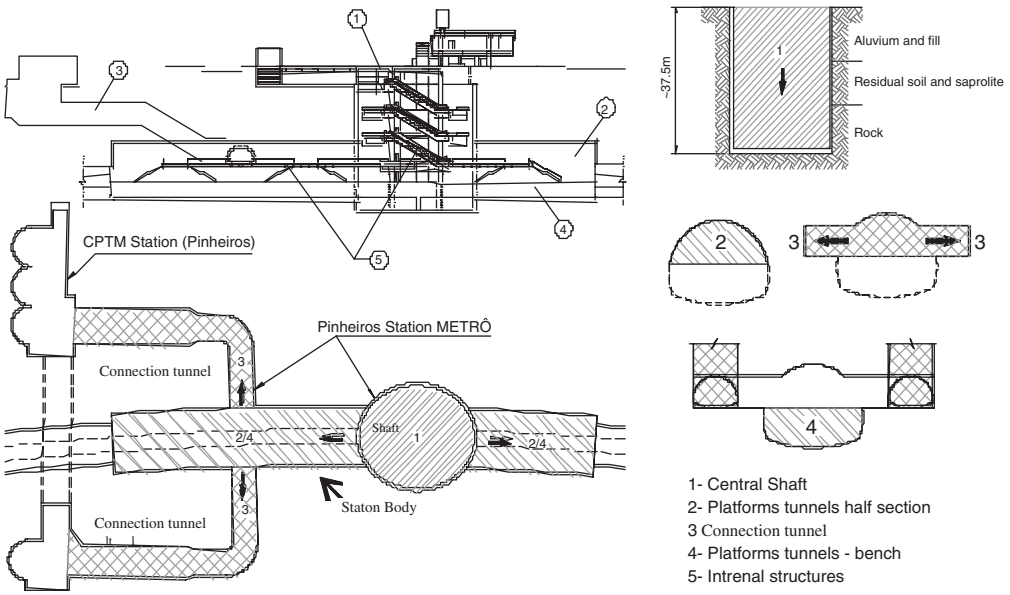


Figure 2. Schematic implantation drawing.

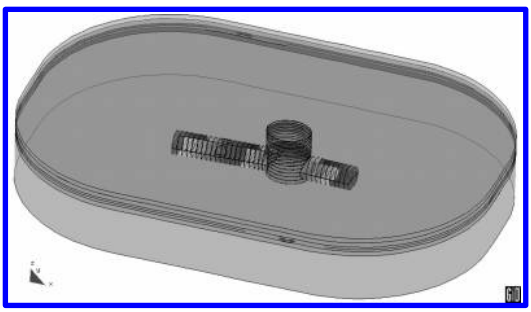


Figure 3. Geometric configuration of the problem.

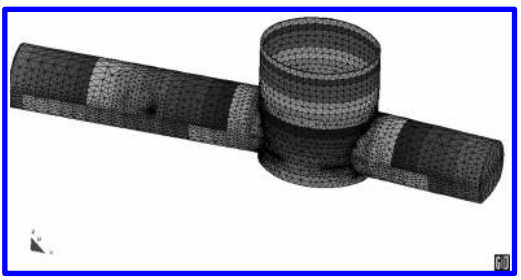


Figure 4. General view of the lining elements.

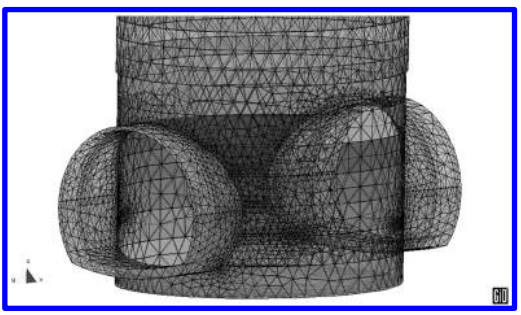


Figure 5. Lining element detail with the transparency resource.

simplifications such as the use of tetrahedron volumetric elements with 4 nodes. For the lining, an elastic linear model was used. For the rock mass, a Mohr-Coulomb model elasto-plastic with no associated plastic flow was used (null plastic flow and therefore soil at the critical state).

The simulation sequence started with the in-situ stresses, then a stage of excavation followed by lining, then the advances shown in Figures 3 the 5, in a total of 59 simulation phases. Figure 3 shows the geometry of the region of simulation. One can notice that if was used a cylindrical contour around de ground mass. It was necessary to avoid volumetric angularity, which in turn would increase the number of elements during the mesh generation process.

The Figures 4 and 5 present details of the lining mesh. It can be observed that the mesh generator used tends to increase the density of the mesh in the corners of changing materials (of each phase of simulation). The bigger the density of these intersections, the greater the density of mesh in these places and

Copyright © 2005 Taylor & Francis Group plc, London, UK

this causes big impact in the mesh size. Consequently, the number of material intersections is the biggest restriction to a detailed analysis. In Figure 5, one can see the change in lining thickness from 0,35 m in soil to 0,15 in rock.

6 RESULTS

Just some results are presented because the analyses produce a large amount of information. Figures 6 and 7 present resulted for phase 15 of the simulation, when the excavation reached the final depth of the shaft and the last ring of the lining was still not installed. Analyzing these figures it is possible to define plastic plans and the probable failure conditions. McCreath (1980) already had shown the necessity of the verifications of the potential plastic plans in order to improve the application of stabilization devices. In this case, it was verified that the biggest plastic zones and its space extension are in the plan xy, therefore trends of local failure mechanism are larger in the horizontal plan. At the field, if local failures is exaggerated, the best form to achieve stabilization is to diminish the size of the lateral excavation step. If larger plastic blocks occurred in the vertical plane, there would be necessary to reduce the excavation step.

These figures show that the largest plastic zones are concentrated in the upper region of alluvial and earth fill. No significant plastic zone is noted in tertiary or residual soil, saprolites or rock masses.

(a) plan xz (b) plan yz

Figure 8 presents the settlements next to the contour to the shaft in false ellipse. Larger values are observed in the region of bigger ray and smaller values in region of small ray. Thus the contour trend of the lining in the region of bigger ray is to converge while that in the region of lesser ray is to diverge. The figure also shows the distribution of settlements inside of the mass and can be verified that the vertical displacements are concentrated in the superior layers. The displacements in the rock are insignificant.

The Figure 9 presents the results of the vertical displacement fields in the final phases of the analysis, after the execution of the tunnels. The Figure 9a shows surface settlements around the shaft. Comparing with Figure 8, the phase 15 has the same deformed shape. The Figure 9b shows settlements of subsurface for the top of the rock, in phase 58 of the simulation (final phase). As the magnitude of the displacements in the Figure 9a is bigger than that in Figure 9b, it is clear that the surface settlements that depend on the construction method of the shaft and of the surface soft layers. On the other hand, excavation of tunnels in rock mass has little influence on surface settlements.

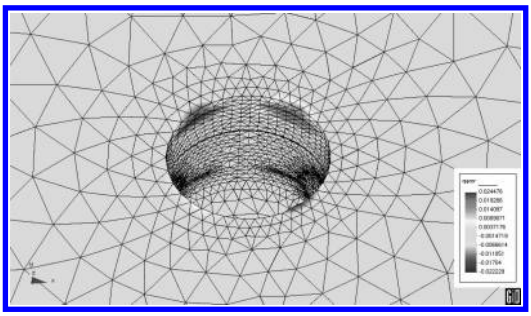
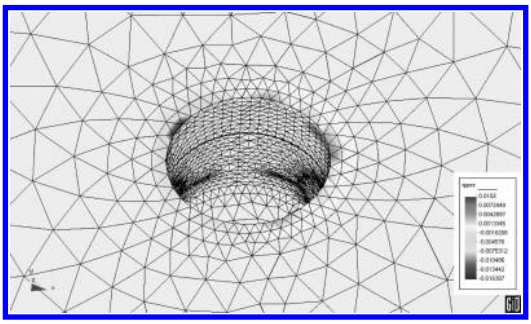


Figure 6. Shear plastic deformation in the soil, horizontal plan xy, phase 15.



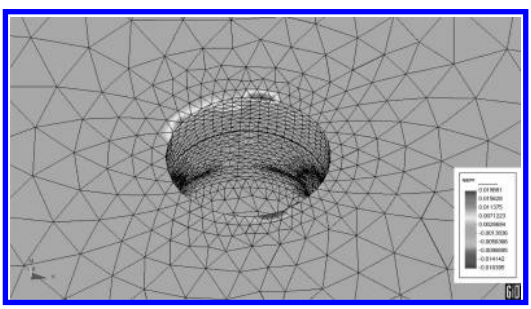


Figure 7. Plastic shear deformation in the soil, vertical plans, phase 15.

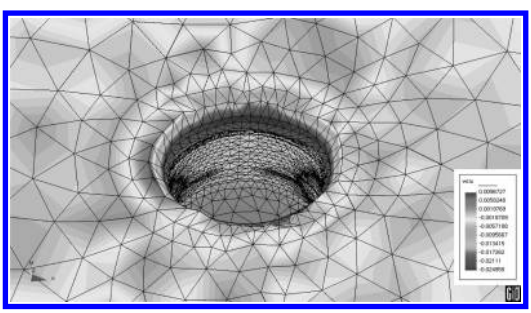


Figure 8. Iso-settlements over deformed surface (increase by 200 times), phase 15.

Copyright © 2005 Taylor & Francis Group plc, London, UK

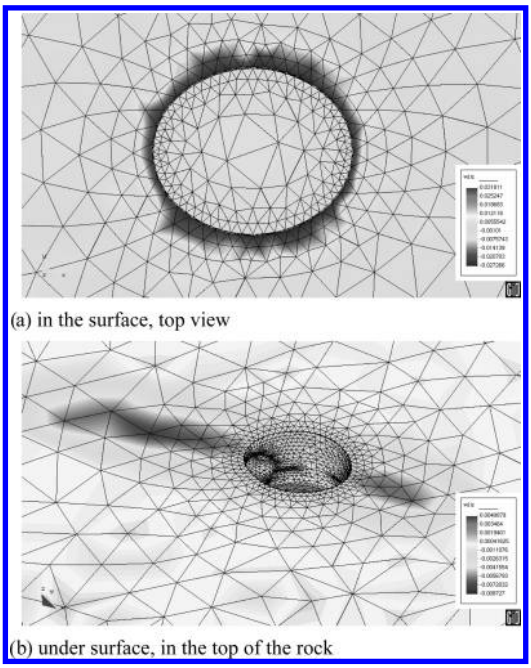


Figure 9. Equal- settlements.

7 CONCLUSIONS AND COMMENTARIES

An economic feasibility study showed that for a conventional microcomputer of last generation, with good configuration of hardware and an operational system Linux 7,2 Redhat default, the limit size of three-dimensional finite elements mesh, with 60 phases of simulation reaches from 150000 to 200000 elements. The mesh used for the Pinheiros station, was created by GiD program version 6.1.2a, and totals approximately 187000 elements. This mesh size was close to the minimum limit to the GiD program. The program can only generate meshes with larger number of elements. Analysis in the field of plastic shear deformations allowed the verification of potential plans of failure in the shaft, of similar form to the ones considered in McCreath (1980). The same type of analysis can be made for the tunnels. This type of analysis can anticipate mechanisms of local failures, and also identify the yielding plans and thus making possible one better use of the stabilization measures. The largest plastic zones are located in the alluvium layer which influences the shaft design. The simultaneous excavation of portals and tunnels would be potentially critical for design, but they were immersed in very competent material (rock) and did not presented critical loads neither to the lining nor the ground.

The vertical settlements were influenced by the Alluvium layer. It was observed that around the shaft opening, the larger the ray the bigger the displacement, and vice-versa. The Mohr-Coulomb model of no associated flow lead to lower values of settlement because this model takes null volumetric plastic deformation. As the tunnels are immersed in rock, the displacements associates to its execution have worthless effect in surface settlements. Bahac et al (2002) had carried out numerical studies for designs of tunnels in Prague, where some tectonic faults existed and various constitutive models had been used in the program TOCHNOG. Laboratory tests of great scale had been carried out and had identified the necessity of the use of better constitutive models to preview of the displacements. For shafts, settlements are due to horizontal tension release and the constitutive model will cause greater impact in the analysis. Thus, for a better evaluation of settlements more realistic constitutive models are necessary.

ACKNOWLEDGMENTS

The authors thank the São Paulo Subway Company – Metrô for allowing accomplishment of this work, and Figueiredo Ferraz for the supplied support.

BIBLIOGRAPHY

BOHAC, J., HERLE, I. AND MASIN, D., 2002, Stress and strain dependent stiffness in the numerical model of tunnel, Proc. 2nd Int. Conference on Soil Structure Interaction in Civil Urban Engineering, Zurich, p. 357–364.

MCCREATH, D.R., 1980, Analysis of formation pressure on tunnels and shaft lining, MSc Thesis, Department of Civil Engineering, University of Alberta.

Copyright © 2005 Taylor & Francis Group plc, London, UK

Field measurements and monitoring

Copyright © 2005 Taylor & Francis Group plc, London, UK

Deformation monitoring of large tunnel wall under construction by digital photogrammetry measurement at Ritto Tunnel

T. Nakai & M. Ryu
Earthtech Toyo Corporation, Japan

H. Miyauchi
Japan Highway Public Corporation, Japan

S. Miura
KAJIMA Corporation, Japan

Y. Ohnishi & S. Nishiyama
School of Civil Eng., Kyoto University, Japan

ABSTRACT: The second Meishin (Tokyo-Kobe) highway that will be the most important to Japanese economy in the 21st century, is under construction. In this highway tunnels are the major structures which go through many mountainous areas. The standard cross-section of the tunnel in this highways is very large (250 m^2) compared to ordinary tunnels and the tunnel width is very wide (18 m). The tunnel is first bored by 5 m diameter TBM and it is enlarged later. Photogrammetry measurement with a CCD camera is applied to deformation monitoring of large tunnel. Tunnels on construction sites like highways must be carefully and continuously observed for deformation during construction. Although geology is granite, it has many fractures under Tectonic process in Japan. In the tunnel, the fractured zone was detected widely by investigation by TBM pilot tunnel, we needed to check the stability of tunnel wall after enlarge section process. Conventionally proposed monitoring methods include total station. However, none of these are widely employed because of poor workability, insufficient precision and/or high running cost under tunnel work. For this reason, it decided to apply precision photogrammetry and the technique of investigating the tunnel deformation of the whole visually by three dimensions was developed. The reflective target of 121 or more sheets was stuck on tunnel wall, by taking a photograph, the 3-dimensional coordinates of a target were acquired and deformation of tunnel wall was visualized. In this paper, we show an example of the result.

1 INTRODUCTION

1.1 *Ritto Tunnel*

Ritto Tunnel construction site located in Kinki District include KIX (Kansai Airport) shown in Figure 1. A mountainous region around the tunnel is 300 to 600 meters above the sea level and a comparatively gentle slope is seen at the summit of the mountain. In addition, steep V shape valley develops along swamp and river around the tunnel. The geology of the tunnel mainly consists of biotite granite of the latter period of Cretaceous period called Tanakami granite, which is fresh and hard. Maximum unconfined compressive strength is 100 MPa and seismic velocity is more than 4.7 kilometers per second. However, a lot of small scale faults and fractures are distributed in this area. Longitudinal geological section is shown in Figure 2.

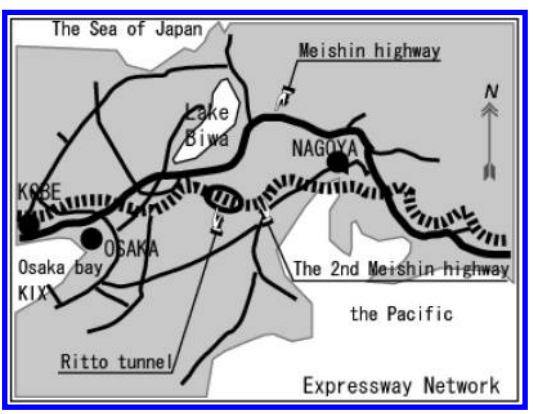


Figure 1. Location of Ritto Tunnel.

Copyright © 2005 Taylor & Francis Group plc, London, UK

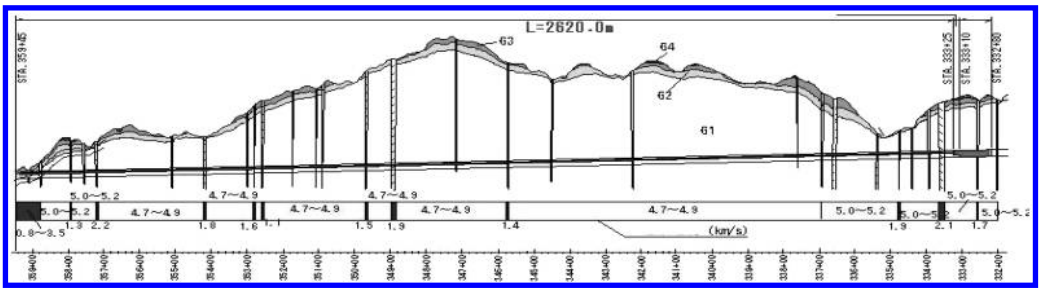


Figure 2. Geological section. Geology is granite. Solid lines are faults.

1.2 *Approach using photogrammetry*

Photogrammetry with a CCD camera is applied to deformation monitoring of tunnels. Tunnels on construction sites like highways must be carefully and continuously observed for deformation at least during construction and, depending on the circumstances, for several months after completion. Conventionally proposed monitoring methods include total station, GPS and an optical fiver strain sensor. However, none of these are widely employed because of poor workability, insufficient precision and/or high running cost.

This paper discusses monitoring of tunnel deformations by photogrammetry with a CCD camera. Reflective targets are placed over a tunnel wall, and their object coordinates are measured by a photogrammetric technique. Their displacements are then statistically detected every two epochs of time. Since it is usually hard to deploy long scales at construction sites, an observation equation has been developed to detect target displacements without the need for scales. At every time epoch, object coordinates of targets are independently adjusted by a free-network. Parameters for detecting displacements are tested, in which the inconformities of coordinate systems are incorporated in test equations.

The strengths of the observation networks are compared by simulation and validated by experiments using a model space on a reduced scale of 1/20. In a typical case, 3 mm target displacement over a 20 m × 30 m tunnel wall are proved to be detectable.

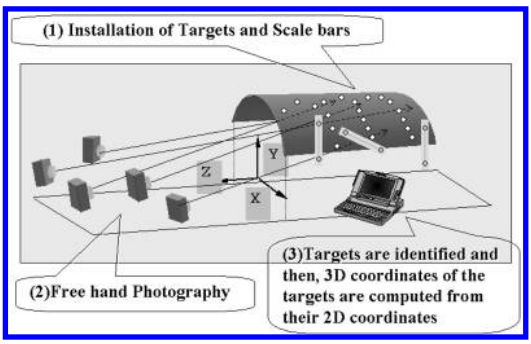


Figure 3. Procedure of measurement.

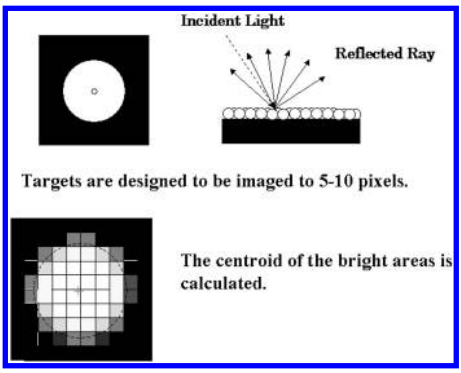


Figure 4. Target that we install on the object.

2 MEASUREMENT BY PHOTOGRAMMETRY

The procedure for digital photogrammetry is generally illustrated in Figure 3.

In order to measure the displacements, we need to install the targets that can reflect the flashlight of camera as shown in Figure 4. The fundamental mathematical model of digital photogrammetry is an optical triangulation that describes the perspective transformation from two dimensional image coordinates into three dimensional object space coordinates. The ultimate extension of the principles is to adjust many photogrammetric measurements to ground control values in a single solution known as a bundle adjustment. The analytical process is so named because of the many lights rays that pass through each lens position constituting a bundle of rays. Any object point can be determined as the intersection of the corresponding rays from each of many images.

All parameters describing the perspective transformation process can be also determined without prior knowledge of camera positions and calibration parameters.

Copyright © 2005 Taylor & Francis Group plc, London, UK

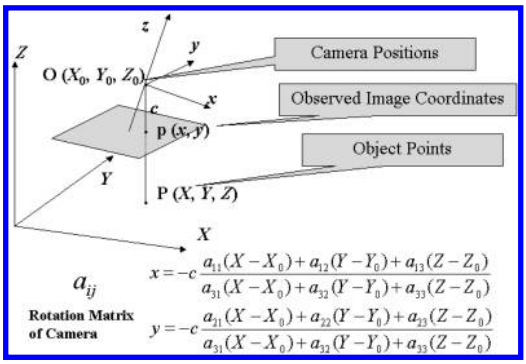


Figure 5. The concept of collinearity equations.

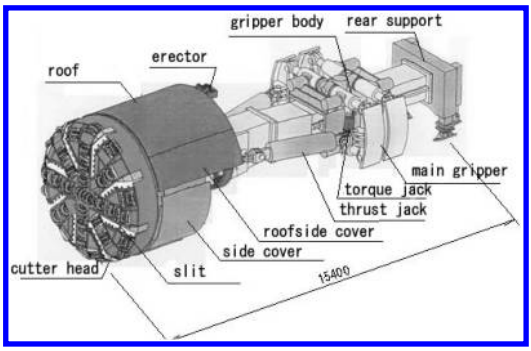


Figure 6. Tunnel boring machine.

The computational model of the bundle adjustment is based on the well-known collinearity equations as shown in Figure 5:

$$x = \square x - c\frac{a_{11}(X-X_0)+a_{12}(Y-Y_0)+a_{13}(Z-Z_0)}{a_{31}(X-X_0)+a_{32}(Y-Y_0)+a_{33}(Z-Z_0)}$$
$$y = \square y - c\frac{a_{21}(X-X_0)+a_{22}(Y-Y_0)+a_{23}(Z-Z_0)}{a_{31}(X-X_0)+a_{32}(Y-Y_0)+a_{33}(Z-Z_0)} \quad (1)$$

where x and y are the observed image coordinates; X_0, Y_0, Z_0 and X, Y, Z are the object space coordinates of the camera positions and object points, respectively; the a's are functions of three rotation angles of each image; Δx, Δy and c are the interior orientation elements; Δx and Δy are perturbation parameters which describe departures from collinearity due to lens distortion and in-plane and out-of-plane image distortion, c being the focal length. This model including the interior orientation elements is known as a self-calibrating bundle adjustment. This method has the advantage of obtaining high photogrammetric accuracies with cameras having unknown calibration parameters.

The collinearity equations can be recast into the following observation equations by linearization:

$$v = A_1X_1 + A_2X_2 + \Delta \quad (2)$$

where A_1,A_2 are the design matrices of the unknown exterior orientation elements, vector X_1, and object point coordinates, X_2; is the discrepancy vector, is the vector of image coordinate residuals. Solution for X_1 and X_2 is according to the method of least-squares.

3 TUNNEL EXCAVATION SYSTEM

The first excavation procedure at Ritto tunnel was bored by TBM shown in Figure 6. First, after TBM pilot tunnel was excavated, main tunnel is enlarged with NATM method. Before excavating a main tunnel, support pattern for the big section is designed based on the actual TBM excavation results. When we discover unstable blocks or zones of the main tunnel, additional reinforcement was applied. The procedure of this excavation system is shown in Figure 7.

4 FIELD EXPERIMENT AT RITTO TUNNEL

4.1 *The observational zone of the tunnel*

As shown in Figure 8, several discontinuous zone alternated with hard part of granite. Weak discontinuous zone classified D class shown as orange parts and especially claylike zone is colored by sky blue area located center part of tunnel along with the tunnel line. We observed these STA349 + 15 ~STA349 + 35 (20 m long).

The rock masses have bedding joint planes and also faults that are developed along with tunnel line. The geological property thus indicates that a sheared rock mass model should be applied for this site.

4.2 *Photogrammetry-based observed tunneling*

We applied enough rockbolts to the weak zone which observed large deformation for the excavation of upper part of the tunnel. However, since cutting face is very large, observational method was indispensable. In case of space of discontinuity is narrower than observational points as shown in Figure 9 and 10, we could not recognize failure. For this reason, it decided to install many targets to observe deformation of the tunnel wall in the process of excavation of remaining bottom section. It determined to apply digital precision photogrammetry so that the monitor of the deformation of the whole surface of the tunnel wall can be carried out in detail. With regard to the unstable

Copyright © 2005 Taylor & Francis Group plc, London, UK

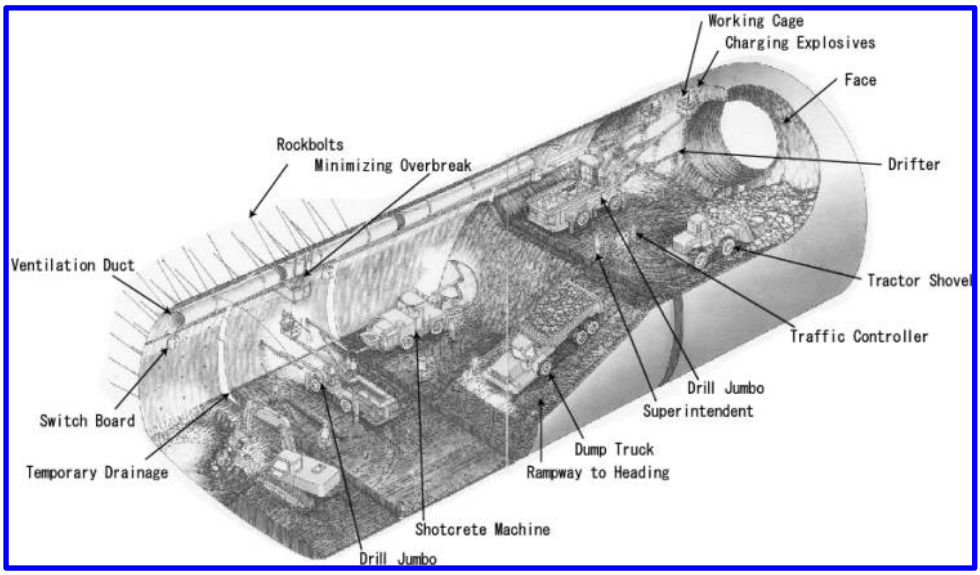


Figure 7. Procedure of TBM and enlargement system of large tunnel.

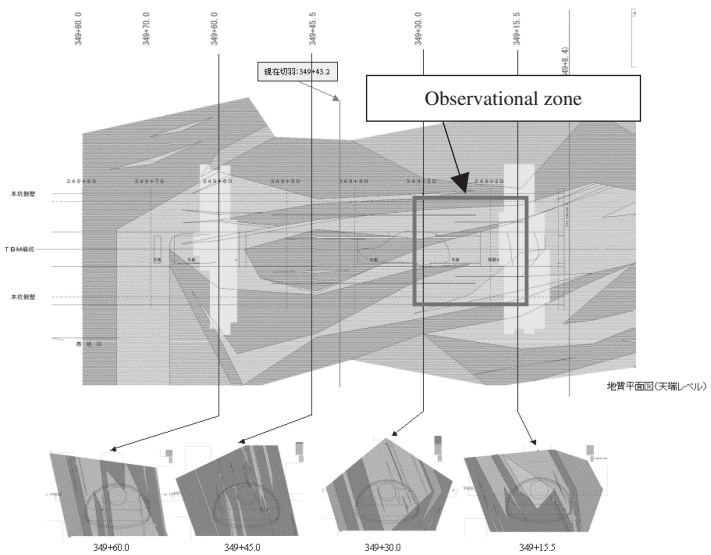


Figure 8. Geological plan and sections nearby target zone. purple: B class, blue: C class, orange: D class, sky blue: weathered (clay)

blocks identified in the block analysis and the block borders, i.e. faults, displacements of rock masses were monitored by photogrammetry right below the observational zone as shown in Figure 10.

During the observation procedure, 121 targets placed tunnel wall were photographed by the digital photogrammetry technology, each time when the cutting face progressed by excavation of bottom section.

(1) Photographing equipment

Nikon D1 camera and a 18 mm lens of the same manufacturer were selected. Nikon SB-28DX Speedlight Flash was used inside the TBM pilot tunnel.

(2) Targets

After selecting the camera and lens, the diameter of targets was determined according to the measured

Copyright © 2005 Taylor & Francis Group plc, London, UK

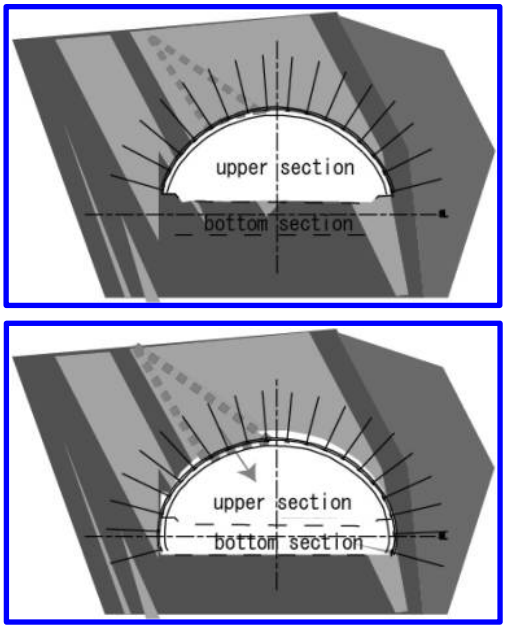


Figure 9. Excavation procedure and increasing risk for block failure.

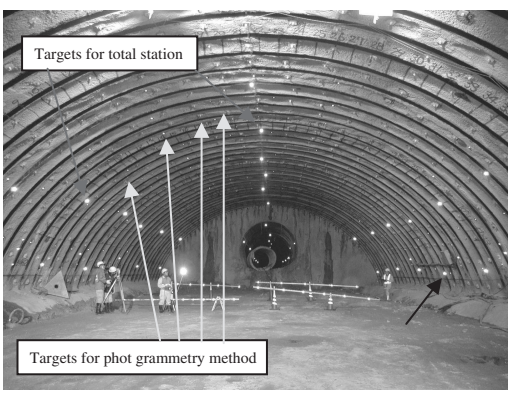


Figure 10. Setting of photogrammetry targets.

distance to ensure the images of the targets could come out in 5 pixel or larger in diameter. The diameter was set at 30 mm here, and the targets were placed every 2 m (11 targets in the transversal circumference direction) or 2 m (11 targets in the longitudinal direction). As a result, 40 targets were photographed per image on average, which was sufficient for use in the analysis. An example of target layout is shown in Figure 11.

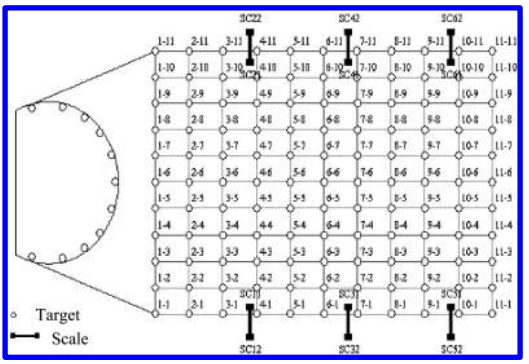


Figure.11 Target layout.

(3) Installation of scales

At the Ritto Tunnel, it was difficult to install scales for external measurement due to such restrictions as the photographing cycle and the access from cutting face during the excavation work. It would be often the case in a tunneling work that there are no external fiducial points. Therefore, six to ten 1 m-long fiducial scales were prepared and installed.

(4) Photographing conditions

The lens stop was set at F22 at maximum. The infinite focus was selected. The shutter speed and ISO sensitivity were set at 1/250 and 200, respectively.

Photographs were taken for every 6 m at 3 points each at both upper and lower locations for each transversal direction.

4.3 *Result of observed tunneling*

The estimated accuracy was about 0.5 mm shown as Table 1, This must be considered of good quality, given the unfavorable condition of on-site photographing during the tunneling work.

First, to make use of the 3-D coordinates consisting of 121 targets obtained by bundle adjustment, the displacement represented this way can compare the distance between corresponding to the convergence and roof settlement were defined, not only those on a same transversal section but also any given targets.

Once the 3-D coordinates have been obtained, various displacement diagrams can be shown by moving the view point three dimensionally on a computer screen.

As shown in Figure 12, bird views only are shown here due to space limitation. The dots in vertical and horizontal directions indicate the initial positions of photo targets. The lines extending from the initial positions represent displacement vectors. The displacements are multiplied for emphasizing purposes here.

Copyright © 2005 Taylor & Francis Group plc, London, UK

Table.1 Precision of image coordinate measurements.

	Estimated accuracy (mm)					
Date	X	Y	Z	Max X	Max Y	Max Z
2002/01/06	0.307	0.185	0.362	0.881	0.422	1.514
2002/01/20	0.317	0.179	0.252	0.983	0.358	0.731
2002/02/17	0.516	0.314	0.470	1.568	0.685	1.884
2002/03/16	0.523	0.348	0.487	1.996	0.691	2.698

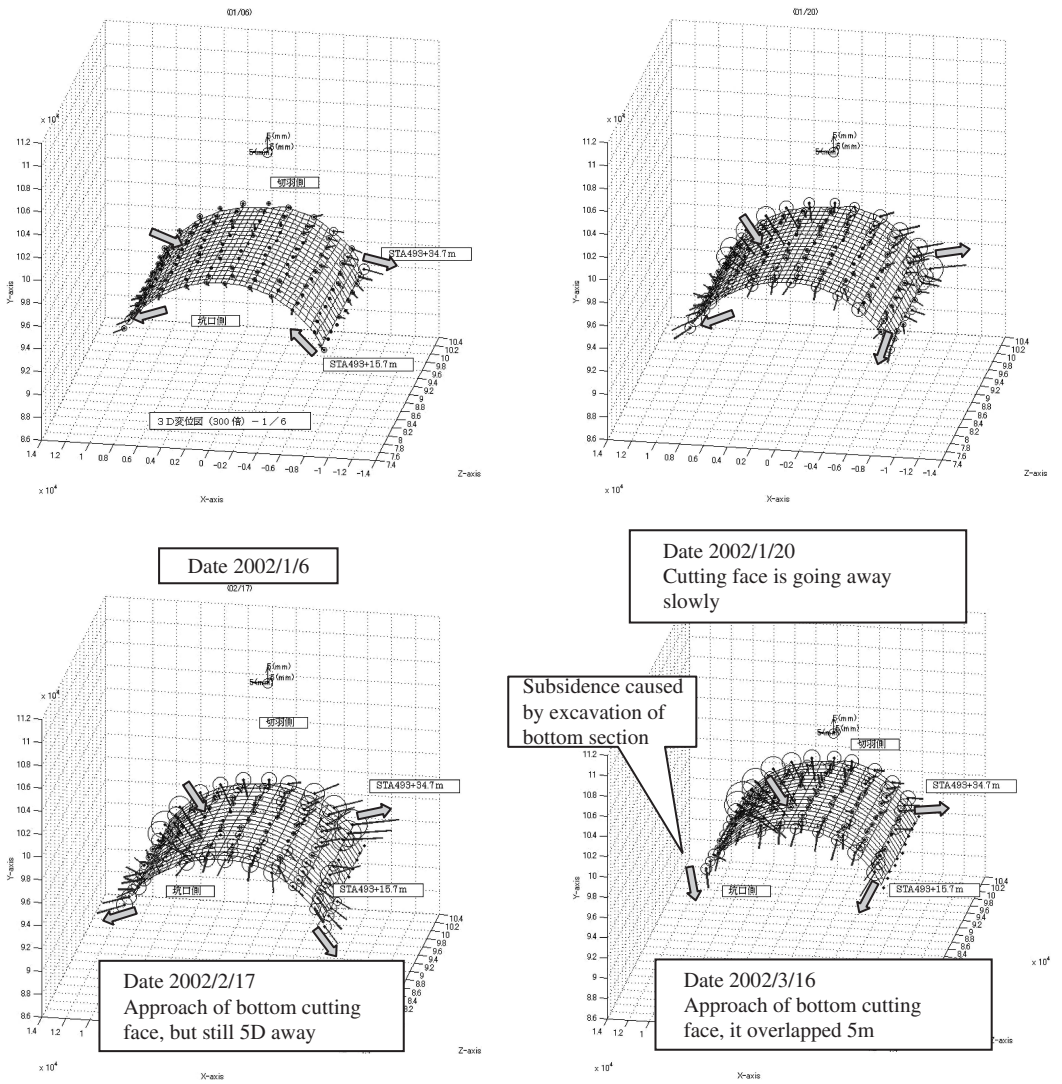


Figure 12. Results of observation at each excavation.

Copyright © 2005 Taylor & Francis Group plc, London, UK

They remained within the threshold in practice, i.e. less than a few millimeters and 5 mm in the horizontal and vertical directions, respectively.

The displacement, size and orientation of the rock masses were three dimensionally monitored with these diagrams. We can not detect an extraordinary rock behavior during excavation of bottom section carried out.

Figure 12 shows a region defined by as showed Figure 8, which is around the STA349 + 15 ~STA349 + 35 section. Here, the rock mass is not showing a discontinuous behavior, with the vectors having continuous movements. There are some movements on the both-hand side of the borders due to enlargement toward bottom section, which are nonetheless considered as homogeneous movement of the rock mass as a whole.

5 CONCLUSIONS

A new control system for discontinuous rock masses has been proposed, which combines computer power and photogrammetry technologies. The effectiveness or stability of the countermeasure was proved through digital photogrammetry-based monitoring.

During enlargement sequence, many photo targets were placed in the pre-existing part of tunnel wall. The digital photogrammetry system to observe movement of pre-existing tunnel wall could tell us safety of enlargement excavation of bottom section and effectiveness of countermeasures for potential unstable rock blocks. Also this digital photogrammetry system could forecast the existence of weak zone and the information was utilized to take warning.

It was proved at this tunnel that the digital photogrammetry observation can verify the results. And according to this system a suitable construction and counter-measure method was properly decided.

This research proposes a new technology for controlling the complicated discontinuity-dependent rock mass behavior, which treats the behavior as 3-D data throughout the process from investigation to construction work using the digital photogrammetry and computer aided imaging technique. The authors believe that this research will greatly contribute to the further advancement of rock engineering.

REFERENCES

Okamoto, A.: General Free Net Theory in Photogrammetry, Intl. Archives of Photogrammetry and Remote Sensing, XXVII-B3, pp. 599–608, 1988

Ohnishi, Y., Niida, H., Ryu, M. & Nakai, T.:An Application of Key Block Analysis to Large Section Tunnel Excavation, Fourth International Conference on Analysis of Discontinuous Deformation, pp. 357–365, 2001

Ohnishi, Y., Ohtsu, H., Nishiyama, S., Okai, N., Seya, T., Yoshida, Y., Nakai, T.& Ryu, M.: The International Symposium on Modern Tunneling Science and Technology (IS-Kyoto 2001), pp. 281–284, 2001

Nakai, T., Ohnishi, Y., Ohtsu, H., Nishiyama, S. & Ryu, M.: Monitoring and Analysis of Tunnel in Discontinuous rock Masses by using Digital Photogrammetry and Key Block Theory at Houou Tunnel, EIT-Kyoto University-AIT Joint Workshop on Development of Rock Mechanics and Engineering, pp. 57–63, 2002

Copyright © 2005 Taylor & Francis Group plc, London, UK

Channel Tunnel – monitoring strategy for the tunnel lining

C. Choquet, A. Schwenzfeier & D.R. Lamont
Channel Tunnel Safety Authority, France and UK

ABSTRACT: Safety in the Channel Tunnel is overseen by a Safety Authority responsible to an Intergovernmental Commission representing the French and UK Governments. The remit of the Authority includes ensuring the structural integrity of the tunnel infrastructure. The paper describes how this is being done through the development and adoption of a tunnel lining monitoring strategy. The strategy allows for both routine monitoring and the identification of problem areas should they arise.

1 ORIGINS OF THE FIXED LINK

The construction and operation of the Fixed Link, as the Channel Tunnel is formally know as, was agreed between the French and UK Governments under the Treaty of Canterbury in 1986. By this Treaty, the French and UK Governments allowed the construction and the operation, by private concessionaires, of a fixed twin bore tunnel rail link, with associated service tunnel, under the Channel between Cheriton in Kent and Fréthun in the Pas-de-Calais Region.

A Concession Agreement in March 1986 completed the legal and financial framework of the Treaty and awarded the Concession to Eurotunnel. It indicated the general characteristics of the Fixed Link and the rules to be applied during its construction and subsequent operation. Originally planned to last 55 years, the Concession has been extended to 99 years and is now due to expire in 2086.

Commercial operations began in May 1994 with goods trains and shuttle services carrying lorries. Eurostar services commenced in October 1994 and shuttle services for tourist vehicles were introduced between December 1994 and June 1995.

2 THE SAFETY AUTHORITY'S DUTIES

Through the Treaty and the Concession Agreement, the Governments acquired the power to monitor the construction and operating conditions of the Tunnel. An Intergovernmental Commission was established to supervise safety on behalf of the two Governments. In turn, a Safety Authority was established to advise the Intergovernmental Commission on all matters relating to safety in the construction and operation of the Tunnel. The main duties of the Safety Authority are to ensure that national and international safety law is enforced in the Tunnel; to examine reports concerning any incident affecting safety in the Tunnel, and to carry out any necessary investigations and report to the Intergovernmental Commission.

The Safety Authority is a bi-national body. Each of the delegations is made up of five members who may be replaced by an alternate member if they are unable to attend. It is chaired alternately, and for a period of one year, by the Head of each Delegation. For the purpose of its duties, the Safety Authority may call on the assistance of the authorities in each Government and any body or expert whom it may choose. Five permanent and specialist working groups, led jointly by a member of each delegation, have been set up by the Authority covering civil engineering and fixed equipment, rescue and public safety, railway safety, transport of dangerous goods and occupational health and safety. The working groups provide the detailed technical analysis on which the Authority's advice to the Intergovernmental Commission is based:

The Civil Engineering Working Group (CEWG) is responsible for the infrastructure of the tunnels and terminals. A major aspect of its work is to ensure the structural integrity of the tunnels and that there is a proper asset management system in place for this to be achieved. In all its activities, CEWG has worked towards ensuring the asset management system treats the infrastructure as single tunnel complex. This has involved the integration of inspection and reporting procedures through the development, by Eurotunnel, of a comprehensive tunnel lining monitoring strategy. The strategy was accepted by CEWG in 2004 and in future will inform the production of CEWG's annual inspection plan.

Copyright © 2005 Taylor & Francis Group plc, London, UK

3 DESCRIPTION OF THE EUROTUNNEL SYSTEM

3.1 *General*

The Eurotunnel system comprises two Running Tunnels on either side of a service tunnel. The tunnels are approximately 50 km long, of which approximately 37 km are under the English Channel. They connect the Channel Tunnel terminals at Coquelles, Pas de Calais region in France, and at Cheriton, Kent, in the United Kingdom.

The Running Tunnels contain the track for the movement of trains. There is a closed circuit of track from one terminal to the other used for Eurotunnel's shuttle trains, with connections at the French terminal to the SNCF system and in the United Kingdom terminal to that of Network Rail. Running Tunnel North normally handles traffic from the United Kingdom to France, and Running Tunnel South from France to the United Kingdom.

The Service Tunnel has three main safety functions:

- To provide normal ventilation for the running tunnels.
- To provide a safe haven for passengers and crew members in the event of the need for evacuation.
- To facilitate the speedy arrival of emergency teams.

Four main categories of trains use the Running tunnels:

- Single and Double Deck tourist shuttles carrying coaches and cars respectively.
- Heavy Goods Vehicle shuttles carrying lorries and trucks.
- Passenger trains, currently the Eurostar trains which operate between London and Paris and London and Brussels.
- National freight trains operating between the Fréthun sidings in France and the Dolland's Moor sidings in the United Kingdom.

3.2 *Civil engineering*

The two Running Tunnels and the Service Tunnel are lined with precast reinforced concrete segments or, in some places, cast iron segments. The nominal diameter of the Running Tunnels is 7.6 m, and of the Service Tunnel 4.8 m. Each Running Tunnel contains a walkway on the Service Tunnel side for the evacuation of passengers and crew in the event of an incident. On the opposite side, there is a walkway for maintenance purposes or for the inspection of trains, which have broken down.

The tunnels were driven by TBM from each side of the English Channel between 1987 and 1991.

The Running Tunnels are connected to the Service Tunnel by cross-passages at intervals of about 375 m. At each cross-passage and recessed into the side of the Running Tunnels, are cross passage doors which separate the Running Tunnels from the safe haven of the Service Tunnel. These doors are fire resistant and are normally closed.

Piston Relief Ducts, some 2 m in diameter are found at intervals of about 250 m, and connect the two running tunnels in order to relieve the build up of air pressure caused by the passage of trains and thus to reduce aerodynamic resistance.

The Piston Relief Ducts have dampers, which are kept open during normal operations.

There are two under-sea crossovers, and two land crossovers to enable trains to pass from one running tunnel to the other, when part of either tunnel is closed for maintenance. The undersea crossovers are equipped with massive sliding fire-resistant doors, which when closed, maintain the separation between the two Running Tunnels. These doors are controlled from the Rail Control Centre. The crossovers separate each tunnel into three intervals, each approximately 17 km long.

4 PRINCIPLES BEHIND THE STRATEGY

This was developed by Eurotunnel within a framework, agreed with CEWG, which required that it should:

- cover the periodic routine monitoring of all tunnel lining and deliver results of the monitoring in a report to CEWG every two years. The report should be interpretative as well as providing factual data, should give opinion as to the likely future safety of the structures and should be in the same format for all the tunnel complex.
- identify parts of the tunnel complex with special monitoring requirements.
- permit the identification of locations within the tunnels where additional monitoring would be required as a result of unexpected corrosion, significant leakage or movement.
- cover the provision and maintenance of instrumentation as necessary to give continuity of monitoring data.
- define both relative and absolute alarm thresholds.
- require appropriate testing of materials where necessary for the monitoring programme.

5 DEVELOPMENT OF THE STRUCTURAL MONITORING STRATEGY

5.1 *General points: two approaches to be harmonised*

Monitoring and maintenance of the underground structures of the Channel Tunnel is carried out in accordance with a document entitled: "Civil engineering maintenance strategy for the tunnels".

Copyright © 2005 Taylor & Francis Group plc, London, UK

This document is the result of prolonged development work, in which members of CEWG played a major role.

The objectives of the operator and the regulator clearly cannot coincide completely:

- For the operator, the requirement is to maintain the structure in a functionally operational state, to ensure that the tunnel can be used with the minimum of disruption to traffic. So the operating and monitoring system is specifically developed to deal with all structural faults, which could disrupt traffic, as quickly as possible. For example, everything possible is done to deal expeditiously with minor leakage through joints in the lining. Even slight amounts of water dripping on to sensitive equipment such as signalling equipment or the catenary, can cause corrosion or short-circuiting, both of which are very disruptive to traffic operations. Dust is also a major problem.
- For the regulator, the objective is to check that the operator's monitoring policy actually guarantees safety in terms of the integrity of the lining and any changes to it. This supposes that information about any part of the structure must be easily accessible, and that it enables any change in the condition of the structure to be identified, through successive reports on its condition.

5.2 *Background to the development of the monitoring strategy*

From 1994, when the tunnel opened, until 1997, the regulator mainly depended on annual reports of measurements of the 22 sections of lining fitted with instrumentation, to check the adequacy of condition monitoring of the linings.

From 1997, the CEWG requested its inspectors and civil engineering experts to analyse these reports and to make comments, which would enable the monitoring policy to be improved. This was done through meetings between Eurotunnel, its consultants (Mott McDonald, SETEC), and CEWG experts.

At the same time, Eurotunnel started to formalise its monitoring strategy in a single document. This document was submitted to the CEWG experts, and its content was discussed through correspondence and meetings. The outcome of this work was the document "Civil engineering maintenance strategy for the tunnels".

5.3 *The two principal components of monitoring*

5.3.1 *Instrumentation of the structures*

The instrumentation in the tunnels was originally installed to verify the validity of the assumptions made during the design and construction phase, and to check whether behavior of the structures was as predicted.

Location of these sections were proposed by the designer and constructor of the Tunnel, TransManche Link, taking in account the geological properties of the ground and the strata profile, and approved by Eurotunnel. Factors considered when locating instrumented sections included depth of overburden, chalk interface profile, proximity of the Gault clay, proximity of the Service Tunnel at the cross-overs etc.

Having verified the validity of the design assumptions, the in-situ instrumentation now provides information, which is proving to be extremely valuable for long-term structural monitoring purposes.

Because the design assumptions for the tunnel lining differed between the UK and French sides, the instrumentation is also slightly different. On the UK side, the lining is assumed to be drained, whereas on the French side, the lining is fully gasketed.

5.3.1.1 Brief decription of the instrumentation

Normal sections of the tunnels

A normal section generally covers the 3 tunnels. During construction, 8 sections on the French side, and 6 sections on the UK side were fitted with instrumentation. Instrumentation is divided between the two running tunnels and the service tunnel. Each instrumented section has:

- 24 to 30 vibrating wire strain gauges, to measure strain
- 1 piezometer
- 6 to 8 monitoring points for measuring convergence by invar wire and optical techniques

Cross-overs

These are fitted with:

- extensometers of 1m, 4.5 m, 9 m in length.
- piezometers
- monitoring points for measuring horizontal convergence
- levelling markers
- rock pressure cells
- monitoring points across the joints between the central wall and the vault
- monitoring points on the headwalls

Fire damaged section of running Tunnel South

- monitoring points for measuring convergence by invar wire and optical techniques
- vibrating wire strain gauge to measure strain
- extensometers

Frequency of monitoring

The frequency of monitoring varies from 6 months (for the piezometers and extensometers) to 2 years for optical convergence, to 6 years for the highly accurate but time-consuming invar wire convergence monitoring.

Castle hill

The final section of tunnel before the UK portal passes for some 500 metres through an ancient landslip on

Copyright © 2005 Taylor & Francis Group plc, London, UK

the seaward slope of Castle Hill. Instrumentation consists of boreholes fitted with inclinometers and piezometers. Regular monitoring of instrumentation is carried out from the hillside, as well as checks being made of the flow of water from drainage galleries within the body of the slip.

5.3.1.2 Harmonisation of monitoring practices

Until 1998, the data from the instrumentation were interpreted by two firms of consultants, Mott McDonald on the UK side and SETEC on the French side. Differences in approach to reporting the information arose between the two consultants, and to resolve this, the CEWG experts requested that the monitoring and reporting policy should be harmonised for both sides of the tunnel.

Consequently a compromise was arrived at whereby tunnel measurements are now interpreted by the French consultants and geotechnical measurements on the ancient landslip at Castle Hill are now interpreted by the UK consultants.

Monitoring reports for the tunnels and Castle Hill are prepared annually to an agreed schedule. The reporting period ends in the spring and thus should cover the wettest half of the year (autumn–spring) within a single reporting period. The reporting schedule is as follows: reports on the results for a year are submitted to the Safety Authority no more than 6 months, after the last measurement, and presented orally to the experts 3 months later. Clarification or additional measurements may be requested by CEWG experts to address any concerns they may have. The experts report to the CEWG, who may then propose inspections, or additional investigations, to verify the behavior of sections where the measurements appear to be abnormal. Finally, the CEWG co-chairmen report the results to the Safety Authority.

5.3.2 *Visual inspections*

Visual inspections form the second part of the structural monitoring regime. They are based on French regulations for the monitoring of civil engineering structures forming part of the national road network, but they are implemented in markedly different ways, to take account of the specific features of the Tunnel, as it is of a totally different magnitude than conventional civil engineering structures.

There are two types of visual inspections:

- primary inspections, made every 6 years, consist of a visual examination of all surfaces accessible from the walkways. They are supplemented by an inspection of the vault using an access platform where there is a need to monitor changes to specific defects, or to deal with these (for example, by the injection of grout to stop seepage dripping on to the catenary).
- general inspections of the lining are carried out annually, chiefly to identify the need for operational cleaning, surveying of obvious major defects, the development of fresh defects and the functioning of the drainage networks.

In areas known to be problematical, particularly due to the influx of water, more frequent monitoring may be required.

Finally, if routine monitoring has indicated the presence a serious defect, a detailed expert appraisal is organized immediately. That appraisal may lead to repairs, or to other actions such as increased frequency of monitoring or the installation of instrumentation and an inspection by the CEWG experts.

6 CONCLUSIONS

The monitoring and maintenance strategy for the tunnel lining has been established by Eurotunnel through a development programme, taking into account the requirements of the Regulator. The strategy is based in part on the monitoring defined at the time of the design and construction of the Tunnel, but equally it takes into account changes in the structure over time, as evidenced by the monitoring results. For sections of the tunnels where lining defects are identified, the response must take into account the history of their development along with anticipated future changes and all in sufficient time to limit the adverse effects on Tunnel operation.

The strategy is set down in a living document, subject to change in the light of the information thrown up by the monitoring and maintenance operations.

ACKNOWLEDGEMENTS

The Authors wish to make it clear that the experiences and opinions reported herein are their own and are do not necessarily reperesent the views of the CTSA or Eurotunnel.

The Authors wish to acknowledge and thank Christian Huchon of Eurotunnel for the major contribution made by him in drafting this paper, and to thank Marc Houlé, formerly of Eurotunnel, for his assistance.

Copyright © 2005 Taylor & Francis Group plc, London, UK

Measurements of lining loads on a 3-arch tunnel in Daejeon subway, Korea

H.J. Kim
Department of Geological Engineering, Daejeon University, Daejeon, Korea

S.H. Kim
Sambo Engineering, Seoul, Korea

G.J. Bae
Korea Institute of Construction Technology, Goyang-Si, Gyeonggi-Do, Korea

J.K. Kim & D.S. Park
Samsung Corporation, Seoul, Korea

ABSTRACT: The 3-arch tunnel in Daejeon subway has an excavated cross-sectional area of 284.7 m^2. Since the tunnel passes at depth of 23 m below the railroad station, the stability of the tunnel is very crucial. In order to measure lining loads in the tunnel, vibrating wire strain gauges and pressure cells are installed in steel ribs and shotcrete linings respectively. The measured load ratio between the rib and shotcrete in the 3-arch tunnel ranged from 0.05 to 0.25 with an average of 0.14, which were close to the theoretical value of 0.1. The liner pressure carried by the primary lining ranged from 33% to 143% of the overburden pressure with an average of 83%.

1 INTRODUCTION

Prediction of lining loads due to tunnelling is one of the major issues to be addressed in the design of a tunnel. However, the problem is not easily solved due to uncertainties of the ground conditions and the differences in construction procedures. Therefore, field measurements are often necessary to obtain the lining load. Lots of measured data on the lining were accumulated in Korea due to the active construction of subway and road tunnels. However, the prediction of the lining load using the previous results may cause errors because most of the load measurements were obtained in the shotcrete lining. The interpretation of shotcrete lining instrumentation is very difficult due to stress independent strains. On the other hands, the strain measurements in the steel rib can give more reliable results for the estimation of the lining loads.

The stability of the 3-arch tunnel is very crucial because the tunnel passes at depth of 23 m below the railroad station. In order to measure lining loads in the tunnel, vibrating wire strain gauges and pressure cells are installed in steel ribs and shotcrete linings respectively. Lining instrument program for the 3-arch tunnel is presented in detail in this paper.

2 SCOPE AND METHODS

It is a common tunnelling practice in Korea to take strain measurements in the shotcrete. However, the interpretation of shotcrete lining instrumentation is very difficult due to stress independent strains such as shrinkage and temperature changes and time-dependent creep deformations. For a NATM tunnel, these problems are obvious because the shotcrete is loaded at an early age. During this period, the curing shotcrete exhibits a complex mechanical behaviour that changes with the age. Cording et al. (1975) described methods for estimating these strains, which are not related to ground loads. The variation of the modulus of elasticity of the shotcrete lining with age can be estimated by means of an extensive series of laboratory tests as Kuwajima (1991) did. However, the suggested method can be very inconvenient. Therefore, the strain measurement in the shotcrete is usually used only for the estimation of the relative amount of the displacement of the shotcrete lining to ensure the stability of the tunnel.

For geotechnical engineering research purposes, the loads due to earth pressure are a major concern. The axial strain in the steel rib can be converted to an axial load without the uncertainty of the elastic modulus of

Copyright © 2005 Taylor & Francis Group plc, London, UK

the rib. Furthermore, strain gauges can be easily attached to the surface of steel ribs. Vibrating wire strain gauges and pressure cells are installed in steel ribs and shotcrete linings respectively to measure the lining loads in the 3-arch tunnel.

3 3-ARCH TUNNEL

The 3-arch tunnel in Daejeon subway is approximately 55 m long has an excavated cross-sectional area of 284.7 m^2, which are 10 m high and 28 m wide. The cross section of the tunnel is shown in Figure 1. The sequence of excavation was as follows:

Step 1: Top heading and bottom heading excavation of Tunnels A and B
Step 2: Installation of pillars in Tunnels A and B
Step 3: Excavation of center heading
Step 4: Excavation of left and right headings

The tunnel is located within weathered Jurassic granites. The tunnel was constructed using a breaker road-header to prevent any noise and vibration damages. The primary lining is composed of segmented steel ribs at 0.8 m centers and 0.5 m thick shotcrete in order to reduce ground settlements.

4 MEASUREMENTS ON THE PRIMARY LINING

The loads in a combined lining system of the rib and shotcrete are shared by the rib and shotcrete separately. Therefore, vibrating wire strain gauges and pressure cells are installed in steel ribs and shotcrete linings respectively to measure lining loads. It has been suggested that the load share between shotcrete and steel ribs in terms of thrust, T, can be expressed as the ratio between the product of Young's modulus versus the area (EA) of each of these structural elements:

$$\frac{T_{rib}}{T_{shotcrete}} = \frac{(EA)_{rib}}{(EA)_{shotcrete.}} \quad (1)$$

The ratio can be used as a simplified way to predict the load share between the shotcrete and rib in NATM tunnels. In other words, if lining loads are measured only in either shotcrete or steel ribs, an average lining load can be obtained by adding the loads in the rib and shotcrete using the equation 1 and dividing the total loads by the combined length of the rib and shotcrete.

A more rigorous solution can be obtained for estimating the load share between the shotcrete and rib using a procedure recommended by Hoek & Brown (1980). However, Eisenstein et al. (1991) showed that the relative differences between these two evaluations were smaller than 5% and suggested the use of ratio $(EA)_{rib}$ /$(EA)_{shotcrete}$ due to its simplicity. The ratio of $(EA)_{rib}$ and $(EA)_{shotcrete}$ in the 3-arch tunnel is 0.10.

Two sections were selected for the load measurements. The location of the instruments in the tunnel is shown in Figures 1–2 and Table 1. Six steel ribs were instrumented to allow for variation in the load as shown in Table 1. Three vibrating wire strain gauges, one at the crown and two at the springlines, were installed for each steel rib. Forty-eight strain gauges were installed for the steel ribs.

The axial load in the steel ribs is obtained from axial strain measurements. Two strain gauges are located on opposite sides of the rib web at the neutral axis to minimize the influence of bending strains. The axial strain, which is obtained by averaging the two strain measurements, is converted to an axial load by multiplying the strain by the cross-sectional area and elastic modulus of the rib. Axial loads and bending moments were found, assuming a linear distribution of strain across the lining thickness.

The lining load on the shotcrete was measured using embedded pressure cells. Nine pressure cells were installed for the shotcretes. The deflection of the cell is sensed by a vibrating-wire transducer. The pressure

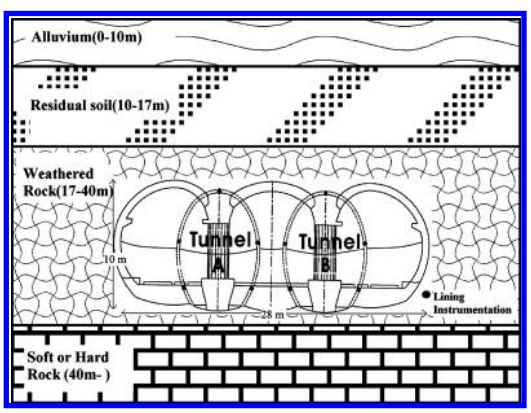


Figure 1. Cross section of the 3-arch tunnel.

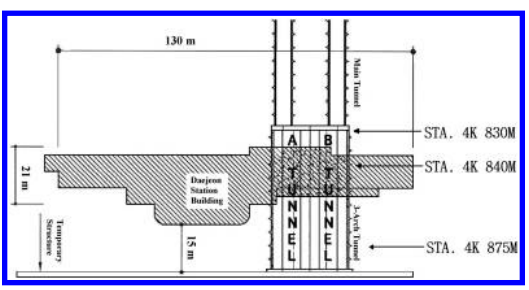


Figure 2. Plane view of the 3-arch tunnel.

Copyright © 2005 Taylor & Francis Group plc, London, UK

cell was designed to measure the radial stress and tangential stress at the same time as shown in Figure 3.

The axial strains measured in the shotcrete and the steel rib were converted to axial loads. The axial loads were divided by the radius of the lining and the spacing of the steel rib to estimate stress distribution around a tunnel.

Table 1. Summary of the lining instrumentation.

Location	Instruments
Tunnel A 830M, Bottom Heading (Crown, Springlines left, right) Tunnel B 875M, Top Heading (Crown, Springlines left, right) Tunnel B 840M, Top Heading (Crown, Springlines left, right)	Shotcretes 9 Pressure Cells
Tunnel A, 830 Rib A, Bottom Heading (Springlines left, right) Tunnel A, 830 Rib B, Bottom Heading (Springlines left, right(malfun.)) Tunnel B, 875 Rib C, Top Heading (Crown, Springlines left, right) Tunnel B, 875 Rib D, Top Heading (Crown, Springlines left, right) Tunnel B, 840 Rib D, Top Heading (Crown, Springlines left, right) Tunnel B, 840 Rib E, Top Heading (Crown, Springlines left, right)	Steel Ribs 48 Strain Gauges (16 × 3)

5 DISCUSSION OF RESULTS

Table 2 shows the measured stresses on the steel rib and shotcretes, the load ratio between shotcrete and steel ribs, and the percentage of overburden pressure acting

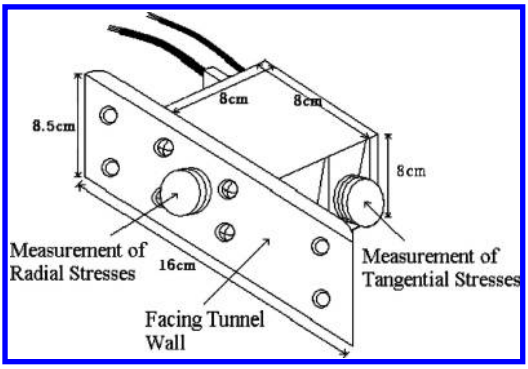


Figure 3. Pressure cell used for shotcretes.

Table 2. Summary of primary liner loads for the 3-arch tunnel.

Location			Stresses (KN/m^2)	Ratio of the rib & shotcrete loads	% of Overburden Pressure
Tunnel A 830M	Crown	Shotcrete	4987		
		Rib A			
		Rib B			
Bottom Heading	Right	Shotcrete	3313		
		Rib A	24721	0.07	96
		Rib B	(Broken)		
	Left	Shotcrete	2428		
		Rib A	30695	0.13	74
		Rib B	28635	0.12	
Tunnel B 875M	Crown	Shotcrete	4184		
		Rib C	93323	0.22	97
		Rib D	55623	0.13	
Top Heading	Right	Shotcrete	4836		
		Rib C	46970	0.10	143
		Rib D	40790	0.08	
	Left	Shotcrete	2360		
		Rib C	34404	0.15	76
		Rib D	54387	0.23	
Tunnel B 840M	Crown	Shotcrete	3663		
		Rib D	27811	0.08	79
		Rib E	43262	0.12	
Top Heading	Right	Shotcrete	2261		
		Rib D	10713	0.05	68
		Rib E	42850	0.19	
	Left	Shotcrete	998		
		Rib D	24515	0.25	33
		Rib E	17511	0.18	

Copyright © 2005 Taylor & Francis Group plc, London, UK

on the lining. The measured lining loads considered in this study were obtained before the installation of pillars in Tunnels A and B. The liner pressure carried by the primary lining ranged from 33% to 143% of the overburden pressure with an average of 83%. The measurements indicate that the most of ground section located above the tunnel crown exerted pressure on the tunnel lining in several locations. In other words, arching was not developed due to shallow ground cover. The plastic zone may be extended to the ground surface, which was indicated by the surface settlement of 65 mm in STA. 4K 880M during the excavation of Tunnels A and B. However, the stability of the tunnel could be maintained because the stress acting on the shotcrete was lower than the strength of the shotcrete ($8{,}240\ KN/m^2$).

The load share between shotcrete and steel ribs in terms of thrust ranged from 0.05 to 0.25 with an average of 0.14. Since the ratio of $(EA)_{rib}$ and $(EA)_{shotcrete}$ in the 3-arch tunnel is 0.10, the results encourage the use of this ratio as a simplified way to predict the load share between the shotcrete and rib in NATM tunnels. In other words, if lining loads are measured only in steel ribs, an average lining load can be obtained by adding the loads in the rib and shotcrete using the above equation and dividing the total loads by the combined length of the rib and shotcrete.

6 CONCLUSIONS

It is a common tunnelling practice in Korea to take strain measurements in the shotcrete. However, the interpretation of shotcrete lining instrumentation is very difficult due to stress independent strains. Vibrating wire strain gauges and pressure cells were installed in steel ribs and shotcrete linings respectively to measure the lining loads in the 3-arch tunnel. The load share between shotcrete and steel ribs in terms of thrust ranged from 0.05 to 0.25 with an average of 0.14. Since the ratio of $(EA)_{rib}$ and $(EA)_{shotcrete}$ in the 3-arch tunnel is 0.10, the results encourage the use of this ratio as a simplified way to predict the load share between the shotcrete and rib in NATM tunnels. In other words, lining loads can be measured using the steel rib.

The liner pressure carried by the primary lining ranged from 33% to 143% of the overburden pressure with an average of 83%. The measurements indicate that the most of ground section located above the tunnel crown exerted pressure on the tunnel lining in several locations. However, the stability of the tunnel could be maintained because the stress acting on the shotcrete was lower than the strength of the shotcrete.

The measured lining loads considered in this study were obtained before the installation of pillars in Tunnels A and B. The lining loads after construction of pillars and the excavation of the whole tunnel section will be presented in the future study.

REFERENCES

Cording, E.J., Hendron, A.J., MacPherson, H.H., Hansmire, W.H., Jones, R.A., Mahar, J.W., and O'Rourke, T.D. 1975. Methods for geotechnical observations and instrumentation in tunneling. Report prepared for U.S. national science foundation, Washington, D.C., 1(2).

Eisenstein, Z., Kuwajima, F.M. and Heinz, H.K. 1991. Behaviour of shotcrete tunnel linings. Proc. rapid excavation and tunnelling conf., Seattle: 47–57.

Hoek, E. and Brown, E.T. 1980. Underground excavations in rock. The institution of mining and metallurgy, London.

Kuwajima, F.M. 1991. Behavior of shotcrete in shallow tunnels. Ph.D. Thesis, Depart. of civil eng., Uni. of Alberta, Edmonton.

Copyright © 2005 Taylor & Francis Group plc, London, UK

Impact on the environment of a shallow gallery excavated in Toulouse's molasses by a conventional method

E. Vanoudheusden*, G. Petit* & J. Robert
Arcadis ESG, Paris and Toulouse (*), France

F. Emeriault & R. Kastner
URGC Géotechnique, INSA, Lyon, France

J.Y. de Lamballerie
Maîtrise d'œuvre du Métro de l'Agglomération Toulousaine, Toulouse, France

B. Reynaud
Société du Métro de l'Agglomération Toulousaine (SMAT), Toulouse, France

ABSTRACT: A fifty-meter-long part of the Toulouse's underground line B has been excavated in molasses by a conventional method. This paper presents the results of the measurement devices installed in this part of the project to evaluate vertical and horizontal movements of the surrounding soil and the deformations of the buildings. The monitoring devices include two inclinometric boreholes, a multipoint extensometer borehole, high precision levelling on several profiles, and measures of horizontal distances and rotations for a two floors house. Results show settlements of the surface and house, quickly stable after the excavation works ending.

1 INTRODUCTION

The excavation of a shallow tunnel induces deformations of the soil volume in the vicinity and above the tunnel and consequently on the buildings. The range of these deformations depends among other on the geological conditions, the geometry of the tunnel, the excavation method.

The 12.6 km long underground line B of Toulouse has been realized with three different tunnel boring machine (TBM) techniques: earth-pressure balanced TBM, slurry shield TBM and compressed-air TBM. Moreover, a small part has been excavated by a conventional method. This fifty-meter-long part of the tunnel (10 m wide and 8 m in height) has been excavated sequentially, by two-half-sections, with an excavator. The upper half section has been excavated at a rate of 1.5 m per day, in 3 shifts; the lower half section has been excavated after the completion of the upper half section of the gallery, at a rate of 2.5 m per day. The temporary support consisted of HEB 200 steel arches and 20 cm of fiber reinforced shotcrete.

Monitoring devices have been installed in order to evaluate vertical and horizontal movements of the surrounding soil and the deformations of the buildings.



Figure 1. Gallery during lower half section excavation.

The instrumentation included two inclinometric boreholes, one multipoint extensometer, a precise levelling of borehole extensometer head and levelling points on the pavement and houses, and finally tiltmeters and horizontal extension measurements on one house.

Copyright © 2005 Taylor & Francis Group plc, London, UK

This paper presents the results of these measurements and analysis of the soil movements occurring due to the excavation of a large diameter gallery by a conventional method in Toulouse's molasses.

2 GEOLOGICAL CONDITIONS

Several boreholes were made within the gallery area. The corresponding borehole logs indicate relatively uniform ground conditions:

- 1.5 m of made ground and alluvium
- 1.5 m of alluvial sandy clay
- over 20 m of overconsolidated molasses consisting in hard clay and lenses of very dense sand, with some calcareous layers.

The water table is found 2.5 m below the ground level. The overburden thickness is around 14 m.

Results of laboratory tests give the main geotechnical parameters of molasses (see Table 1).

3 INSTRUMENTATION

The location of all the measuring points and instruments are presented in Figure 2 and Figure 3.

The monitoring devices included two inclinometric boreholes, one at the axis of the tunnel (I1), and the other 1.5 meter away from the tunnel sidewall

Table 1. Overconsolidated molasses mean geotechnical parameters.

kN/m^3		kPa		kPa	MPa	
γ	ϕ_u	C_u	ϕ'	C'	E	K_0
22	0	300	32	30	100–400	1–1.5

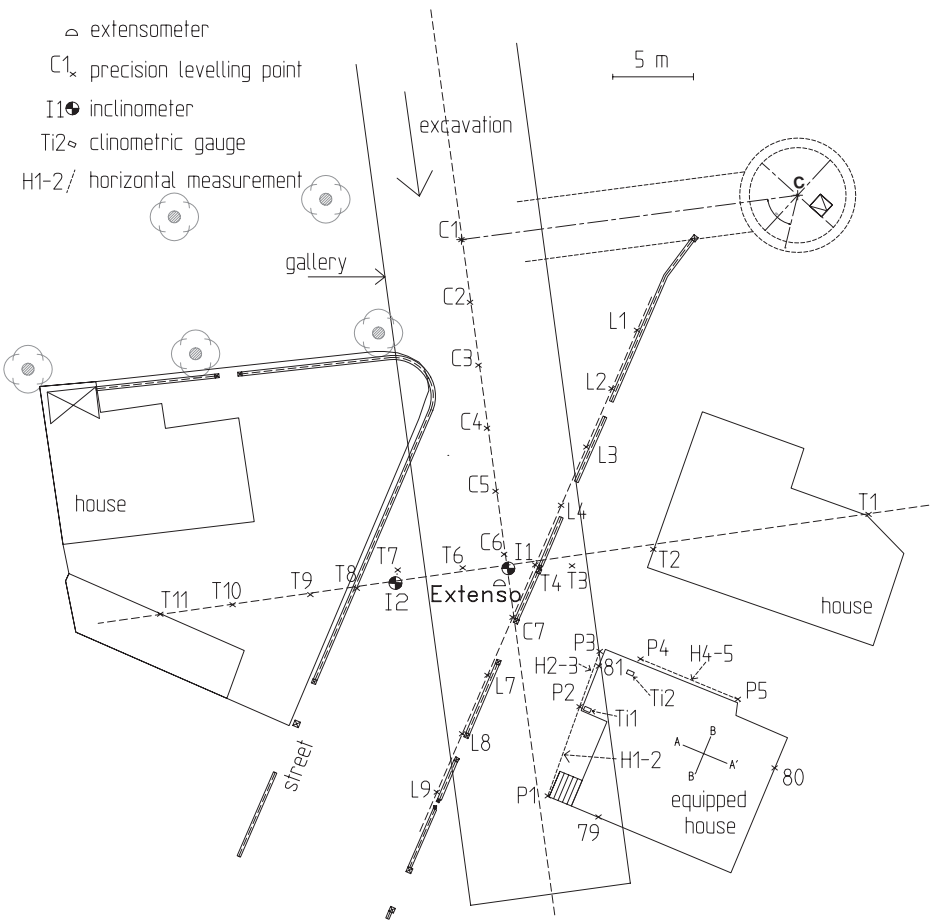


Figure 2. Location of instrumentation devices.

Copyright © 2005 Taylor & Francis Group plc, London, UK

(I2), and one multipoint extensometer borehole with automatic data acquisition. High precision levelling of borehole extensometer head was regularly performed, as well as that of levelling points on the pavement and houses close to the tunnel axis. Besides, a two storey building has been equipped in order to evaluate the variations of horizontal distances (measures with invar thread) and rotations (automatic clinometric gauges). An initial precision levelling was done on the 4th of February, when excavation works were at 14 m ahead of I1. All others initial measurements dated of the 11th of February, when excavation works were at 4 m ahead of I1. A complete set of data has been obtained regularly during the whole excavation works and after completion of the gallery, in order to appraise surrounding soil's movements and building deformations.

4 OBSERVED BEHAVIOUR

4.1 *Ground surface vertical movements*

Precision levelling consisted of 3 profiles of levelling points on the pavement (see Figure 2): the axis profile with points along the axis of the gallery (from C1 to C7), the lateral profile with points along a lateral line of the gallery axis (from L1 to L9) and the transversal profile with points along a transversal line (from T1 to T11).

4.1.1 *Excavation of the upper half section*

Figure 4 and Figure 5 show the settlements observed during the upper half section excavation. Different settlement curves have been established, corresponding to different position of the excavation front regarding to the position of I1 (−4 m, −0.5 m, +1 m, +2.5 m, +5.5 m, +12.5 m, +13.5 m, +21 m). Because of the date of the initial measurement (the 11th of February when excavation works are at 14 m of I1), we did not record the complete displacement of the first points of the central profile C1 and C2.

Figure 4 shows settlement plotted against distance to the excavated face for points C3 to C7. Settlements of points C1 and C2 are not represented. We can distinguish two phases of displacements: first, until the +5.5 measure, longitudinal points located between 7 m ahead of excavation works and 20 m behind settled progressively; behind the tunnel face, settlements logically increase with the distance to the excavation. From the +12.5 measure the settlement behavior is different: the maximum settlement is recorded for the last four points of the profile (from C5 to C7 and the extensometer head). This may be explained by a difference of geology: a sand layer was found in the area of point C7, and some crown instabilities took place.

In the transversal direction (Figure 5), until the +1 m measurement, surface settlements were within 1 mm; afterwards, there is a more important increase in the vertical settlement. This increase stopped after the +13.5 m measure. We can see that this transversal settlement curve is slightly asymmetric; this could be mainly due to the rigidity of the house.

Figure 6 presents contour plot of settlements at the end of the upper half section excavation. We can observe that the maximum settlement is above to the axis of the gallery around the levelling point C7.

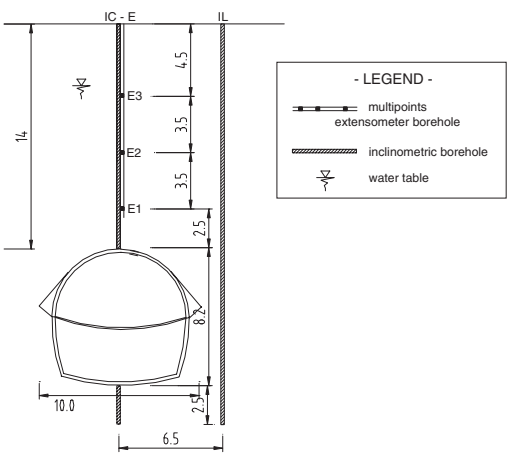


Figure 3. Description of the section.

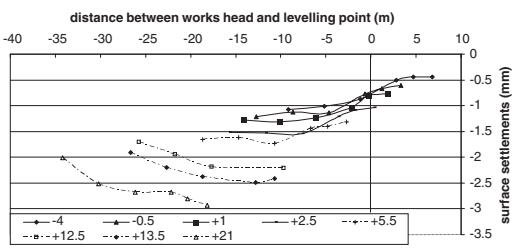


Figure 4. Longitudinal profile settlements – upper half section.

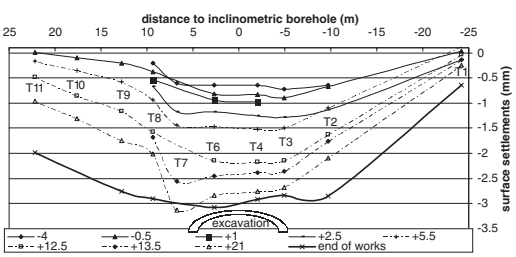


Figure 5. Transversal profile settlements – upper half section and end of excavation works.

Copyright © 2005 Taylor & Francis Group plc, London, UK

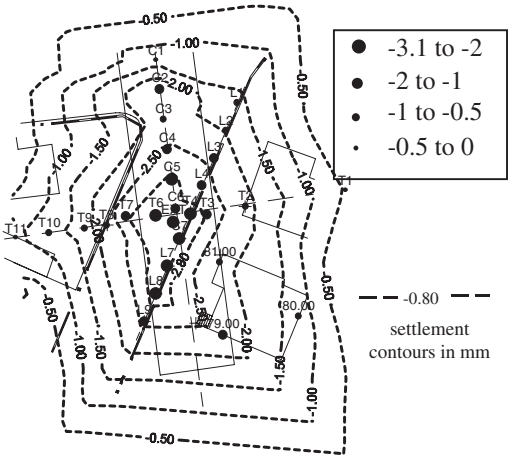


Figure 6. Contour plot of settlements at the end of the upper half section excavation.

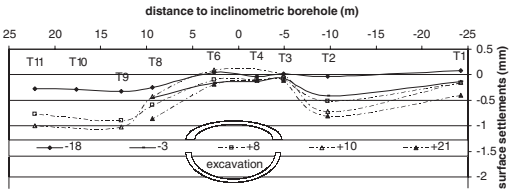


Figure 7. Transversal profile settlements – lower half section.

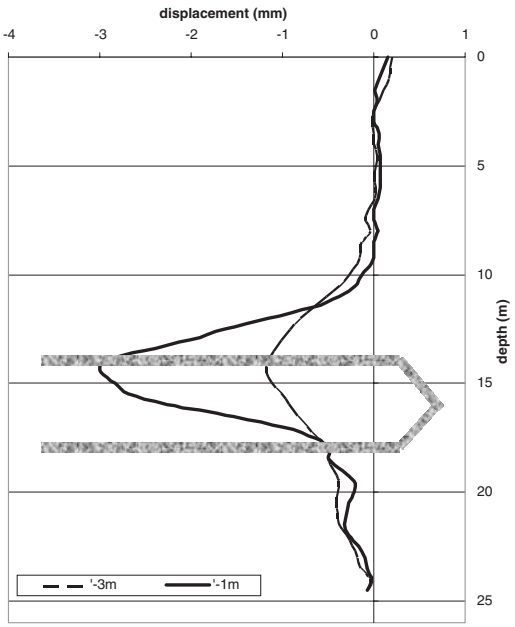


Figure 8. Horizontal displacements of I1.

4.1.2 *Excavation of the lower half section*

Levelling measurements done during this phase show that all points on central and lateral profiles have no particular vertical movements. In fact, the surface displacement is quite obvious when we observe the results on the transversal profile (Figure 7): the 3 points close to the axis of the gallery (from −5 m to +3 m) did not move, the others settled after the −3 m measure. The maximum settlement was recorded for points T2, T8 and T9, set at around 10 m away from the gallery axis. This settlement was slow and stopped after the +21 m measure.

4.2 *Soil deformation*

4.2.1 *Horizontal movements*

Figure 8 presents the central inclinometric boreholes results. The two measures, that were taken before the tube was destroyed by the excavation, show that the soil at the gallery depth moved towards the excavation; the maximum displacement recorded was worth 3 mm at 14 m depth (i.e. at crown).

Evolution of horizontal displacement of the lateral inclinometric borehole is presented in Figure 9 for the upper half section. It should be noted that a real displacement was obvious with the third measure; the bulb increased slowly (4th and 5th measures), and seems to be stable at the last measure. The maximum displacement reached 3 mm at 14 m depth.

Figure 10 presents horizontal displacements recorded during the lower half section excavation. The initial reference measure was taken after the end of the upper half excavation. We observed again the formation of a bulb, increasing with the progress of excavation works. This displacement seems to be stable when the excavation works were 14 m after the inclinometric borehole position. The maximum displacement reached 4.6 mm at 17.5 m depth.

4.2.2 *Vertical movements*

The vertical movements of the soil have been monitored with one multipoint extensometer borehole with automatic data acquisition. This device has been bored on the axis of the gallery and the three anchors were fixed at 4.5, 8 and 11.5 m depth (see Figure 3).

Figure 11 presents results of the extensometer monitoring during the excavation of the upper half section; these results are presented in terms of absolute movements (sum of relative movements of one anchor relative to the surface and movements of extensometer head); moreover the figure shows excavation works progress during this phase.

Copyright © 2005 Taylor & Francis Group plc, London, UK

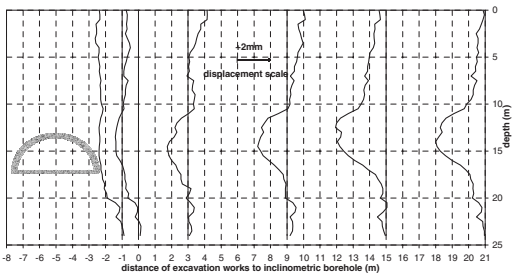


Figure 9. Horizontal displacements of I2 during the upper half section excavation.

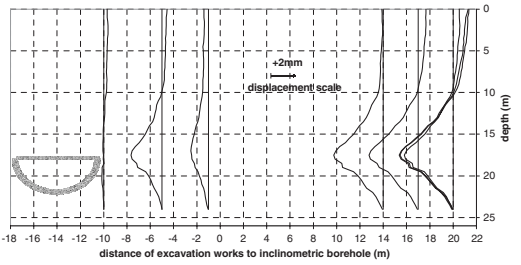


Figure 10. Horizontal displacements of I2 during the lower half section excavation.

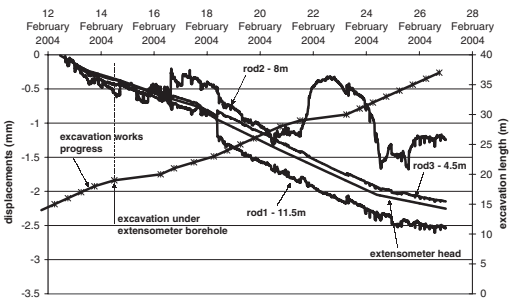


Figure 11. Extensometer results – absolute movements.

First we can see that rod3 had almost the same vertical movements than the surface point. At the beginning of excavation works, movements of rod1 were close to surface movements; suddenly the 18th of February, this anchor settled of 0.6 mm relatively to the extensometer head; after this date, movements of rod1 were similar to surface movements. At the same date of 18th of February, we observe a little movement upwards for rod3 (0.15 mm). Results of the rod2 are not reliable.

In conclusion, during the upper half section excavation, the anchor at −4.5 m had the same settlement than the surface, and the soil just above the gallery settled a little bit more.

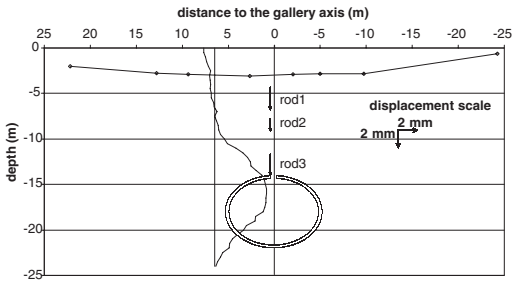


Figure 12. Total displacements of ground surface and within the soil.

Displacements of the anchors during the lower half section excavation were not significant.

4.3 *Global results of soil and surface deformations*

Figure 12 presents results of vertical (levelling surface points and extensometer borehole anchors) and horizontal movements of the soil. We can see that final horizontal displacements are twice the final vertical displacements. This could be explained by a value of the K_0 coefficient greater than 1.

Figure 12 presents the shape of the surface settlement at the end of all excavation works. The left part of this curve (not influenced by the building) may be approximated by a Gaussian distribution, as proposed by Peck (1969), where the maximum settlement S_{max} equals 3 mm and the parameter i (distance to the inflection point of the curve) equals 25. This value of i is high compared to values obtained with Peck's abacus, completed by Attewell (1977) and Clough & Schmidt (1977).

The "volume loss" caused by excavation depends on the maximum settlement S_{max} and parameter i:

$$V_S = 2.5 * i * S_{\max} \quad (1)$$

thus, in this case, $V_S = 0.19\ m^3/ml$.

We can express the "volume loss" as a percentage of the theoretical excavated volume of the gallery V_{exc}:

$$\frac{V_S}{V_{exc}} = \frac{0.19}{63} = 0.3\%$$

We can conclude that if the width of the settlement trough is particularly high, the volume loss at the end of the excavation works is low, compared to usual values.

Copyright © 2005 Taylor & Francis Group plc, London, UK

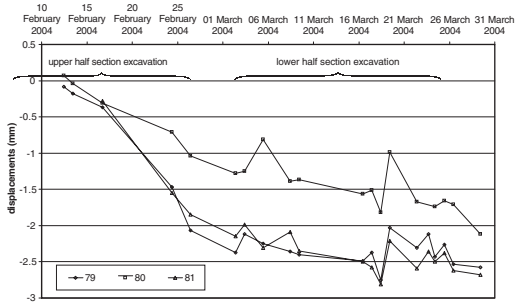


Figure 13. House precision levelling results.

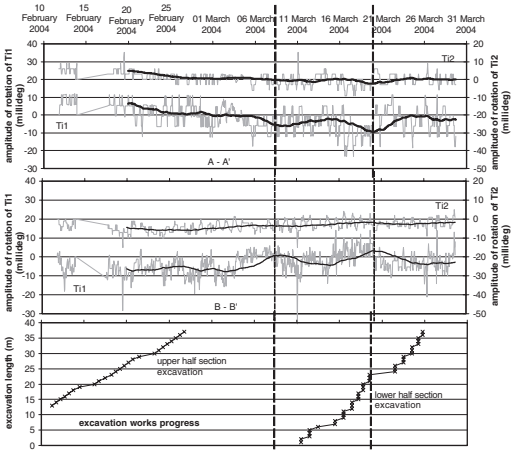


Figure 14. Results of clinometric gauges.

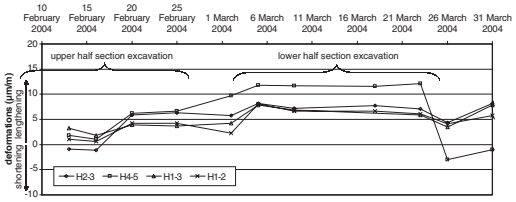


Figure 15. Results of measures with invar thread.

4.4 *Building deformations*

A two storey house close to the axis of the gallery has been equipped in order to evaluate its deformations. House settlements have been controlled with precision levelling measures, rotations with automatic clinometric gauges and variations of horizontal distances with an invar thread (see Figure 2).

Three levelling points have been controlled during the excavation works (points 79, 80 and 81 Figure 2). Settlements of these points versus time are presented in Figure 13. Points 79 and 81 have nearly the same behavior. During the upper half section excavation, settlements of point 80 were half those of points 79 and 81. Stabilization seemed to be just reached in June. Finally complete displacement of those three points was quite the same (−3 mm).

Two clinometric gauges controlled rotations of the house. These devices have been installed at the second storey of the house (Ti1 and Ti2, see Figure 2). They were composed of two captors, for longitudinal A-A′ and transversal B-B′ movements. Sensibility of longitudinal captors was 3 millideg, sensibility of transversal captors was 1 millideg. Figure 14 presents results of the two clinometric gauges in the two directions. In the A-A′ direction, negative value means a rotation towards excavation works; in the B-B′ direction, positive value is a rotation towards point 79. Ti1 and Ti2 had the same behavior, but amplitudes of movements of Ti2 were less important.

In the A-A′ direction, we had a slow rotation of the house towards excavation works until the 20th of March. At this date, excavation works of lower half section were situated at 5 meters behind the position of central inclinometer I1 (see Figure 2). After this date, captor rotated rapidly in the opposite direction, and became relatively stable.

In the B-B′ direction, during the upper half section and the start of the lower half section excavation, tilt values increased slowly; between the 7th and the 20th of March, values decreased and then increased. After this transition date, values decreased and became stable.

Qualitatively, these results are coherent with precision levelling on house points. But, quantitatively, amplitudes of rotations are so different between the two gauges that it seems impossible to compare with the levelling results.

The house was equipped for a control of variations of horizontal distances: this equipment consisted of 5 points fixed on the house and one invar thread for measure distances between these points. Three distances have been measured (see Figure 2): H1-2 and H2-3 in the front of the house and H4-5 in the side, H1-3 is an additional measure for control of H1-2 and H2-3.

Figure 15 presents deformations of the four measures at several dates. The deformation is the measured increment ΔH divided by the distance between the two points H. A positive value means a horizontal distance increase.

During the excavation works (until the 23rd of March), the three horizontal distances increased slowly. This can be related to the position of the house on the hogging part of the settlement trough. Between the 23rd and the 26th of March, just at the end of excavation works, we could observe a sudden decrease of horizontal extension, especially on H4-5 (on the house side). This can be explained by the flattening of the

Copyright © 2005 Taylor & Francis Group plc, London, UK

settlement trough near the tunnel observed during the lower part excavation.

The maximum extension remains small (12 μm/m) compared to the limits usually used to avoid damage on the building.

5 CONCLUSION

The construction by a conventional method of a 50 m long tunnel in Toulouse molasses lead to very small volume losses and surface settlements, without any risk of damage to existing buildings.

The monitoring of horizontal and vertical movements around the tunnel showed unusual deformation scheme, the maximum horizontal movements being twice the maximum vertical movements.

This can be explained by the highly overconsolidated character of the Toulouse molasses, which resulted also in a very flat settlement trough in the vicinity of the tunnel axis, the width of the trough being much larger than that given by empirical estimations.

ACKNOWLEDGEMENTS

The authors would like to thank for their financial support the French Ministry of Research and the Réseau Génie Civil & Urbain (RGC&U). They also would like to acknowledge the help of the different contractors in collecting data.

REFERENCES

Peck, R.B. 1969. Deep excavations and tunneling in soft ground. Proceedings of the 7th International Congress of Soil Mechanics and Foundation Engineering, Mexico: p 225–285.

Attewell, P.B. 1977. Ground movements caused by tunneling in soil. Proceedings of the First Conference on Large Ground Movements and Structures, Cardiff: p 812–948.

Clough, G.W. & Schmidt, B. 1977. Design and performance of excavation and tunnels in soft clay: state-of-the-art report. International symposium on soft clay, Bangkok: p 980–1032.

Copyright © 2005 Taylor & Francis Group plc, London, UK

Geotechnical online support for tunnels in difficult ground

W. Schubert & K. Grossauer
Graz University of Technology & 3G Gruppe Geotechnik Graz ZT GmbH, Austria

B.A. Moritz
Geoconsult ZT GmbH, Salzburg, Austria

ABSTRACT: Tunnel construction in difficult geological conditions requires special attention in order to satisfy safety demands and economical requirements. In particular in heterogeneous ground the prediction of the behavior of the rock mass is essential to be able to adjust excavation and support in time. Very rarely is the required know-how to cope with geotechnical problems available on site. The Internet allows a nearly real time site assistance by experts located somewhere in the world. Relevant data are transferred via Internet, and the data analyzed with special tools by experts. The behavior of the tunnel is analyzed on its "normality", predictions of the future development of displacements and the geotechnical situation ahead of the face (short term prediction) are made. The result of the analyses and recommendations are communicated by Internet or via phone in urgent cases within a few minutes to a few hours. The intervals of data transmission and duration of involvement of the expert(s) is adjusted to the needs of the site. The paper demonstrates the possibilities of this type of online expertise with the help of selected case histories.

1 INTRODUCTION

Even with a good geological and geotechnical investigation and an up to date design, the adjustment of excavation and support to the local conditions has to be done on site in order to achieve an economical and safe tunnel construction. The uncertainties in the ground model increase with increased overburden and complex geological conditions. Thus considerable effort and expertise is required to continuously update the ground model, predict ground conditions ahead of the face, identify possible failure modes, determine excavation and support, and predict and verify the system behavior.

In most cases it is impossible to maintain appropriately experienced staff on site to cope with all expected and unexpected scenarios. For an optimal construction the involvement of experts is required. This involvement may be necessary only for short periods or over the whole construction time, depending on the complexity of the ground conditions, and the expertise available on site. The traditional way of acquiring external expertise is to call in an expert to the site, brief him on the situation, and expect a sound advice within hours. This procedure is not only time consuming and expensive, but also inefficient, as even nowadays nobody carries all the supporting hard- and software around the world. In addition the appropriate expert might be unable to allocate the time to go to a site being far away from his office.

The solution to this problem is to dispatch an experienced geotechnical engineer to the respective site and allocate appropriate experts for the problems expected, which support him from their offices in case needed. Data exchange and information is done via Internet.

2 REQUIREMENTS

2.1 *Acquisition of experts*

It is recommendable that already in the preconstruction phase the respective expert(s) are contacted and made familiar with the project. This will generate some costs, but is a good investment, as a familiarization during the construction inevitably leads to delays and/or lower quality advice.

2.2 *Identification of required data and organization of data transfer*

Depending on the problems expected during construction, the type of data, their quality and quantity need to be determined. In general this will be geological

Copyright © 2005 Taylor & Francis Group plc, London, UK

data from face mapping and on-site modeling, data on excavation and support, and in particular displacement monitoring results. Photos can supplement the information.

As the experts working off site lack a bit a "feeling" for the ground conditions, and cannot acquire a personal impression, the data collected and transmitted must be objective, complete, and of high quality.

The format of the data has to be agreed upon to allow a processing in the office of the expert(s). Preferably the data are uploaded to a server, to which the expert(s) have access at any time.

2.3 *Co-ordination with geologist and geotechnical engineer on site*

For a successful co-operation between the expert(s) and the on-site geological – geotechnical staff a start up meeting is very useful. In this meeting the site conditions should be discussed, as well as other boundary conditions clarified, like site organization, reporting scheme, etc. As in many cases the external expert(s) will not be involved on a daily basis, but more intensive in times of more critical geotechnical conditions, rules have to be established for the alert of the expert(s). This may be done by fixing warning criteria as appropriate.

3 HARD AND SOFTWARE

3.1 *Geological on-site mapping*

Traditionally this is done by sketches of the tunnel face, accompanied by the measurement of the orientation of some features, like joints or foliation, and occasionally some photographs. Experience shows that due to the unfavorable working conditions such data often are biased, inaccurate, and incomplete. Another disadvantage of this method of data collection is the requirement to digitize the sketches and measurement data prior to transmission, a process which usually does not improve the quality of the data.

To obtain complete, accurate and unbiased structural data, stereo photographic systems have recently been developed (Gaich et al. 2003). With the evaluation software it is possible to measure the orientations of discontinuities, areas, distances, etc. directly in the 3D image. The software also includes statistical routines for clustering of joint sets.

The processing of the images and the 3D reconstruction can be either done on site or in off-site offices. The latter option in the moment is preferable, as still considerable computer power is required for the processing. Within a few hours after the images were taken, the evaluation can be back on the site.

The advantage of such a system is that the evaluation can go into as many details as needed, as all features are recorded. In contrast to that a conventional face map contains only what the geologist did see or recognize. Any feature overlooked during the mapping hence is lost.

The off-site service not necessarily is limited to the 3D reconstruction, but can include also updating of the geological model and prediction of the geological conditions in the volume of interest ahead and around the tunnel. Also the preparation of reports (daily, weekly, monthly, or final) can be outsourced to off site facilities. This allows the on-site staff to concentrate on the daily duties, not being distracted from routine drawing work, which can be done much more efficiently in well equipped offices with experienced staff.

3.2 *Software for the evaluation of displacement monitoring data*

Over the last decade a number of programs have been developed for the evaluation and display of displacement monitoring data. On site an easy to use and flexible tool should be used to be able to quickly view results. The software should allow plotting displacement histories, deflection lines, and displacement vector plots in the cross section as a minimum. It should be also possible to calculate the predisplacements to compensate different zero reading times in different measuring sections.

It is important that the data format of the software on site is compatible with that of the users off site. The most advanced product presently is the evaluation software Tunnel:Monitor (Tunnelmonitor, 2004) because of its flexibility, open data format (XML), and the various display options.

For more advanced analyses and prediction of displacements we use the software GeoFit (Sellner, 2000, 3G). This tool allows predicting the development of displacements under consideration of nonsteady advance, sequential excavation and various support options. The actual displacements can be continuously

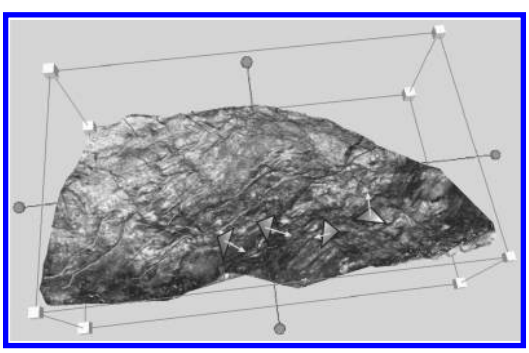


Figure 1. Evaluation of joint traces and measurement of discontinuity orientations from a 3D image.

Copyright © 2005 Taylor & Francis Group plc, London, UK

compared to the predicted ones, and thus any deviations from the "normal" behavior identified immediately. In addition the tool allows predicting also the ground quality outside of the visible area, e.g. ahead of the face. This allows a timely adjustment of excavation and support. For an optimal result expert knowledge is required for interpretation and reliable conclusions.

4 APPLICATION

4.1 *Shallow tunnel in a tectonic mélange, Case 1*

Extremely heterogeneous ground conditions characterized this tunnel site. Frequently changing deformation characteristics made the adjustment of excavation and support and the prediction of the system behavior very difficult. The owner sought for expert assistance after considerable difficulties were encountered during excavation. The geotechnical engineer on site had standard evaluation software, while in the expert's office GeoFit was used. To save costs, data were transferred only when the geotechnical engineer thought he needed some assistance. Unfortunately the Internet connection of the site was rather poor, making the data transfer unreliable. In addition the discontinuous delivery reduced the efficiency of the expert advice, as time consuming familiarization with the conditions was required each time data arrived. Even with this less than perfect procedure valuable advice could be given in several critical situations, without the necessity to go to the site frequently.

An example shall show the advantage of using advanced software for the evaluation of displacement monitoring data (Sellner et al. 2002). The tunnel was excavated in a top heading – bench – invert sequence, with a temporary top heading invert, where required.

The development of the displacements was predicted with GeoFit. Figure 2 shows a crown settlements of a measuring section which was installed immediately before the Christmas break. It can be seen that the observed displacements were pretty close to the predicted ones for a long period of time.

When the excavation met exceptionally weak material displacements even 30 m back from the face increased considerable, deviating from the predicted "normal" behavior (figure 2).

Two scenarios were considered. One option was that the temporary invert failed the other one that there was also a failure in the rock mass itself. In the first case, the displacements after the sudden increase should stabilize again and follow the predicted displacements for a support without temporary invert (dashed line in figure 2). In the second case, displacements would exceed the values predicted for the support without temporary invert.

As can be seen from figure 3 the assumption of the failure of the top heading invert was correct, as the further displacements followed those predicted for the case without temporary top heading invert. The pause during the Christmas break allowed the shotcrete to cure, increasing its stiffness, and thus make it more sensible to additional displacement caused by the further advance of the face than would be the case with a continuous advance.

As the trend of the displacements was not indicating any stability problem, but only a slight increase in total displacements it was decided to accept the additional displacements. No strengthening of the support or other mitigation measure was required. The fact that shotcrete linings suffer damage after the restart of the excavation after a longer break is well known. In this special case this effect was superimposed by additional displacements due to the weak material at the face.

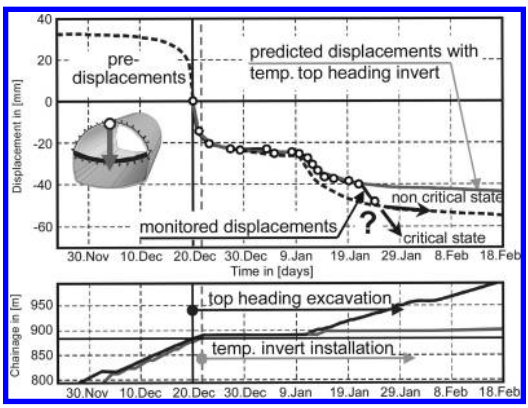


Figure 2. Predicted displacements without temporary invert (dashed line) and with temporary invert (solid line). Deviation of the observed displacements from the predicted ones.

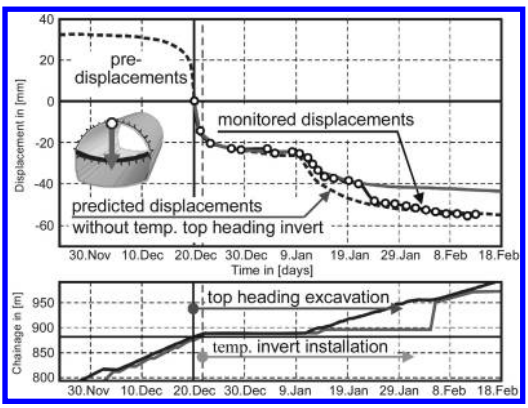


Figure 3. Displacements stabilizing at the level of those predicted without top heading invert after its failure.

Copyright © 2005 Taylor & Francis Group plc, London, UK

4.2 *Shallow tunnel in a tectonic mélange, Case 2*

This tunnel is located basically in the same formation as that described above. The excavation of this tunnel started later than that described above. The assistance of the on-site geotechnical engineer was planned right from the beginning. The transfer of the displacement monitoring data was done on a nearly daily basis, allowing a continuous follow up of the project from the off-site offices. On demand also face maps and data sheets were transferred. Besides a continuous evaluation of the stability, the focus of the assistance in this project was put on the short term prediction of the conditions ahead of the face to allow for a timely adjustment of excavation and support to the frequently changing ground conditions.

For the evaluation of the displacement monitoring data on site standard software was available (ARGUS), while in the experts' offices GeoFit was used. In the course of the project the geotechnical engineer on site was trained in the use of GeoFit, and the software installed on site as well. This showed to be very efficient, as the same graphs could be displayed in both offices, easing the communication.

The trend of displacement vector orientation proved to be a good parameter to predict changes in the rock mass quality ahead of the face in the past in tunnels with high overburden (Steindorfer, 1998). At this project it could be shown that this is also applicable for tunnels with shallow overburden provided the quality of the measurement data is excellent.

Figure 4 shows the transition from a larger block to a block-in-matrix structure. It shows that the displacement vector orientation changes already when the face is well ahead of the transition, while the radial displacements still remain at a pretty low level (Moritz et al. 2004).

Although such findings have been published since quite some time (Schubert & Budil 1995, Steindorfer 1998, Golser & Steindorfer 2000, Schubert et al. 2002) not many engineers on site are familiar in using these techniques.

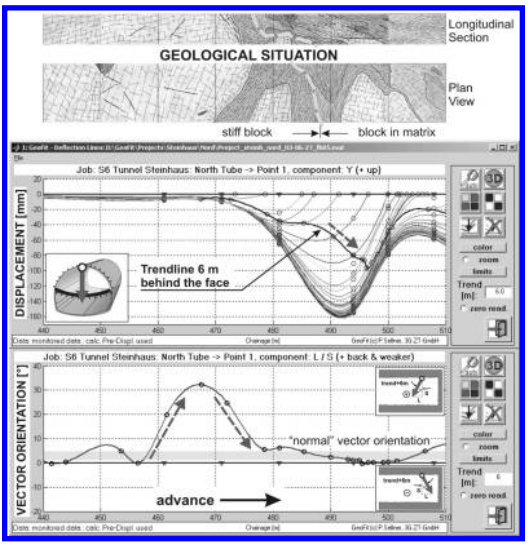


Figure 4. Geological map of a transition from a block to a block-in-matrix structure (top); deflection curves of the crown settlement (center), and trend line of the displacement vector orientation (bottom).

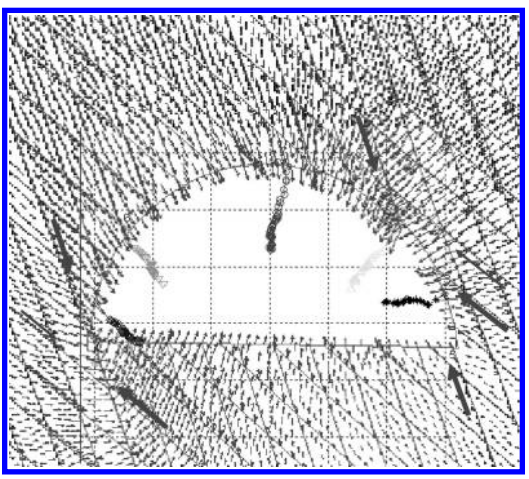


Figure 5. Analysis of displacements and mechanisms; comparison with monitored displacements.

4.3 *Tunnel in foliated rock with high overburden*

This case deals with an Alpine tunnel in foliated rocks with an overburden of up to 600 m. The orientation of the tunnel axis is nearly parallel to the foliation, which is dipping steeply. Here the off-site advice was done for the contractor, who wanted to optimize excavation and support to achieve good advance rates.

An analysis of the displacement patterns observed was followed by an identification of basic behaviors for different rock mass structures. Figure 5 shows a typical displacement vector plot in the cross section within this material. It can be seen that the displacements are rather unsymmetrical. The numerical simulation clearly shows that shearing along foliation and discontinuities is responsible for this behavior.

Evaluation of monitoring data and numerical analyses showed that the largest displacements usually are at the shoulder situated below the foliation, obviously due to a pronounced dilation more or less perpendicular to the foliation. Displacements on this side in average were 1.5 to 1.7 times the displacements of the

Copyright © 2005 Taylor & Francis Group plc, London, UK

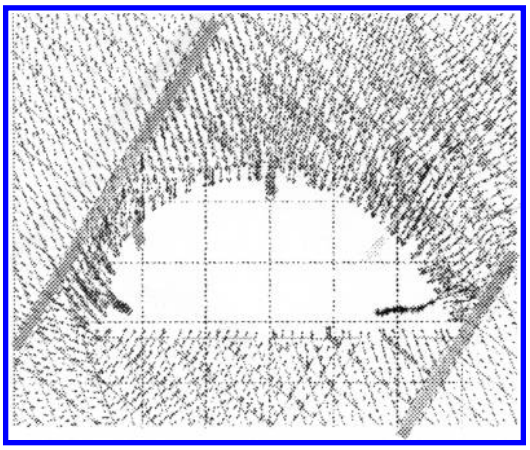


Figure 6. Analysis of mechanisms by a numerical analysis and comparison to the measured displacements.

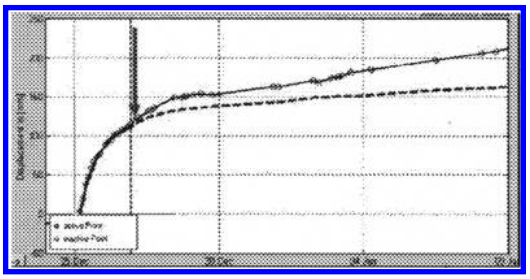


Figure 7. Predicted horizontal displacements for the left sidewall (dashed line), and observed displacements (solid line), showing a deviation approximately 20 days after excavation.

opposite side, where the tunnel is above the foliation (Button 2004). With the numerical simulations typical behavior patterns could be recognized, which again allow understanding the rock mass response and thus enable to appropriately adapt the support.

By adding typical smaller shear zones to the basic model, good agreement could be achieved with the measured displacement patterns (Figure 6). Analyses like the ones shown here are not at all common on site due to lack of time and resources, but can provide valuable input for the selection of excavation and support.

Although the models used were rather simple, the basic phenomena could be shown and the understanding of the rock mass response enhanced. This put the on-site team in a position to quicker react to changes in the system behavior. This is especially important in squeezing ground, where the amount of overexcavation to allow for expected displacements has to be continuously adjusted.

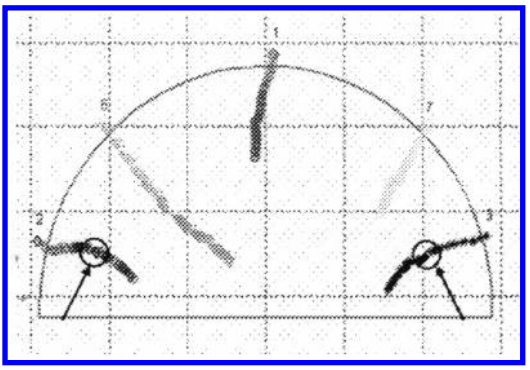


Figure 8. The onset of the invert heaving can be seen from the change in displacement vector orientation (marked with circles).

In a section with an overburden of more than 600 m a pronounced deviation of the measured displacements from the predicted ones was observed (Figure 7).

One might be tempted to interpret the long lasting displacements as a creeping process, which is higher than originally expected. Using the displacement vector plot in the cross section, one can see that at a certain time the mechanism must have changed (marked with circles at the sidewall vectors in figure 8). It was found that a wedge in the top heading invert had been squeezed upwards, leading to a relaxation in the bench area, which again caused the increased displacement in the top heading.

5 CONCLUSION AND OUTLOOK

Off-site expert support can considerably help in onsite decisions at relatively low costs. The quick and easy transmission of even large data volumes via Internet allows the off-site expert to keep track of the ground conditions and system behavior. The accumulated experience of many cases can thus be utilized for the benefit of a site. Up to now, fixed rules for the evaluation and interpretation of monitoring data are rare. Thus an individual judgment of specific situations is required by an experienced expert. As the experience of on-site engineers not always is adequate to cope with non-standard situations, unbiased external support can be helpful in preparing and making the required decisions. The involvement of the expert depends on the complexity of the ground conditions, on the available experience on site, as well as the boundary conditions of the project. The support can be asked for, when there is a real demand on site and reduced in sections with less difficulty. Thus a very economical use of the resources is possible, avoiding maintaining high-level expertise all the time on site, which is difficult to acquire anyway.

Copyright © 2005 Taylor & Francis Group plc, London, UK

To solve difficult questions, sometimes the use of special software for data evaluation and simulations is required. It would be rather uneconomical to provide all the tools for an on-site application, especially as the on-site staff would require extensive training to be able to use them appropriately.

The easy access to the data from anywhere in the world also does not require the expert being at his office, increasing his availability.

As the services of the off-site expert can be ordered as required and reduced to a minimum involvement in sections with less difficulty, this model is very cost efficient.

An efficient support however is only possible when the data made available by the site are of excellent quality. With incomplete and poor quality data even a most experienced expert will have difficulties to draw correct conclusions.

The quick and easy data transfer via Internet also allows outsourcing other services from the site, like evaluation of stereo photographic face maps, geological short term prediction, or preparation of geological and geotechnical final reports. In most cases the external offices will be better equipped with software and trained personnel than the site itself. This allows the on-site staff to concentrate on their key tasks. An additional advantage is that the offsite personnel in general are less biased and less strained by contractual boundary conditions, allowing concentrating on the technical matters. The value of an independent second opinion should not be underestimated.

In Austria for sites with difficult geotechnical conditions it is common to appoint an independent expert right from the beginning of construction, supporting the site in all geotechnical and stability issues, as well as serving as an arbitrator in case of technical disagreement between contractor and client.

With the further development of telecommunication online communication with the engineers on site directly at the face will be possible. With the help of a video camera carried by the on-site engineer it is possible that the off-site expert sees the same as the on site engineer and gets a better "feeling" for the conditions on site.

REFERENCES

Button, E. A., 2004. A Contribution to the Characterization of Phyllitic and Schistose Rock Masses for Tunnelling. Doctoral thesis, Graz University of Technology

Gaich, A., Fasching, A., Schubert, W., 2003. Determining Structural Rock Mass Parameters Using a Computer Vision System. Felsbau 21, Vol. 2, 46–50. VGE Essen

Golser, H., Steindorfer, A. 2000. Displacement Vector Orientations in Tunnelling – What do they tell? Felsbau 18, Vol. 2, 16–21. VGE Essen

Moritz, B., Grossauer, K., Schubert, W., 2004. Short Term Prediction of System Behaviour of Shallow Tunnels in Heterogeneous Ground. Felsbau 22, Vol. 5, 44–52. VGE Essen

Schubert, W., Steindorfer, A., Button, E.A., 2002. Displacement Monitoring in Tunnels – an Overview. Felsbau 20, Nr. 2, 7–15. VGE Essen

Schubert, W., Budil, A., 1995. The Importance of Longitudinal Deformation in Tunnel Excavation. Proceedings of the 8th International Congress on Rock Mechanics (ISRM), Vol. 3, 1411–141. Balkema, Rotterdam

Sellner, P.J., 2000. Prediction of Displacements in Tunnelling. Ph.D. Thesis, Graz University of Technology, Austria. In Schubert, Riedmüller & Semprich (eds.) Schriftenreihe der Gruppe Geotechnik Graz, Heft 9

Sellner, P., Grossauer, K., Schubert, W., 2002. Advanced Analysis and Prediction of Displacements and System Behaviour in Tunnelling. In Dinis da Gama, C., Ribeiro e Sousa, L. (eds), Proceedings ISRM International Symposium on Rock Engineering for Montainous Regions, 539–546. Sociedade Portuguesa de Geotecnia, Lisboa

Steindorfer, A., 1998. Short term Prediction of Rock Mass Behaviour in Tunnelling by Advanced Analysis of Displacement Monitoring Data. Ph.D. Thesis, Graz University of Technology, Austria. In Schubert, Riedmüller & Semprich (eds.), Schriftenreihe der Gruppe Geotechnik Graz, Heft 1

Tunnel:Monitor, 2004. http://tunnelmonitor.com 3G- Gruppe Geotechnik Graz, 2004. GeoFit Homepage. http://www.geofit.3-g.at

Copyright © 2005 Taylor & Francis Group plc, London, UK

Evaluation of the influence of the rock mass structure on the deformation behavior of tunnels

T. Solak
General Directorate of Turkish Highways, Turkey

W. Schubert
Graz University of Technology, Austria

ABSTRACT: During the construction of tunnels, the system behaviors derived from the design are verified and updated by absolute displacement monitoring. Advanced evaluation methods of the monitoring data enable detecting the influence of geological features on the rock mass behavior around the tunnel. Displacement data from Alpine tunnels were analyzed in correlation with the geological structure. The influences of the geological features (orientation of the joint sets and their strength properties) and fault zones on the deformation behavior of the tunnel were investigated. The monitoring data were compared to the results of the numerical simulations of the tunnel excavation in rock masses with two joint sets with UDEC.

1 INTRODUCTION

The Austrian Society of Geomechanics (ÖGG 2001) recommended a procedure for the geomechanical design both at design and construction stage. At the design stage for the evaluation of the potential rock mass behavior, rock mass types and local influencing factors including the relative orientation of relevant discontinuities to the excavation are considered. Relative orientation of the underground structure and discontinuities are used as a basis for kinematical analyses and the influence of the rock mass structure on the stress redistribution are evaluated.

Failure mechanisms are determined by numerical analyses which allow the modeling of discrete failure planes. At the construction stage observations during excavation such as signs of excessive stress, deformation pattern and observed failure mechanisms and results from probing ahead are used to continuously update the geological model. The reaction of the ground to the excavation has to be observed, using appropriate geotechnical monitoring methods.

With the displacement vector plots the influence of the rock mass structure can easily be observed as well as failure mechanisms detected. Using vector plot in a cross section, structures like faults outside the tunnel profile can be detected before they can be seen at the face and influence of dilatation and shearing on displacement vector orientations can be seen (Schubert 2002).

Considering the value of evaluation methods for specific questions, vectors in the cross section give good results for detection of weak zones outside profiles (Schubert et al. 2002).

Sellner developed software (GeoFit) for the prediction of displacements. This software has been applied on several Austrian tunnel projects to predict normal behavior and detect deviations from the normal behavior (Sellner et al. 2002, 3G).

Case histories from the tunnels in phyllites, where 3 D absolute displacement monitoring was carried out, have been used to identify the influence of the rock mass structures. For phyllites basic key parameters are stated as anisotropic strength and deformability associated with the foliation. The main influencing parameters are relative orientation of foliation to the excavation, fault orientations and spatial characteristics. For the identification of failure modes for the tunnels in phyllites the documented geological conditions and monitored displacements were evaluated (Button 2004 & Button et al. 2004).

2 EVALUATION OF MONITORING DATA

The absolute displacement measurements from the Strenger tunnel are analyzed to evaluate the influence of the rock mass structure on the deformation behavior of the tunnel. The Strenger Tunnel on the S16 four lane express way between Landeck and Bludenz has

Copyright © 2005 Taylor & Francis Group plc, London, UK

two tubes with a diameter of approximately 10 m. Maximum overburden reaches more than 600 m. The rock mass primarily is quartz phyllite consisting mainly of quartz phyllonites and phyllonitic mica schists. The uniaxial compressive strength of the phyllites is between 15–25 MPa. The foliation strikes nearly parallel to the tunnel axis, and its dip angle is between 50° to 80° to the South. Additional joint sets striking nearly parallel to the tunnel axis show dip angles between 40°–70°.

Due to this condition monitored displacements in the cross section can be compared to the results of 2 dimensional numerical simulations carried out considering the characteristics of the Strenger tunnel (Solak & Schubert 2004). The comparison is done based on the general behavior considering the influence of block size, shape and joint residual strength. For the sake of simplicity sequential excavation and supports are not considered in the numerical analyses.

In Figure 1 the displacement vector orientations from a section of the tunnel with lower overburden are shown. In this case the foliations dip is to the left. The displacements are more or less uniform and directed radially. It is interesting to note that the biggest displacements in general are at the shoulder/sidewall located under the foliation, with an orientation approximately perpendicular to the foliation (points 2 and 6 in Figure 1).

With increasing overburden stresses and displacements increase. In Figure 2 the measured displacements at the station 1935 m are compared to the calculated values shown with arrows. The measured displacement orientations agree well with those calculated with the numerical model (block size = 2.9 m, apex angle = 20°, joint residual friction angle = 20°) at the early stages of measurements.

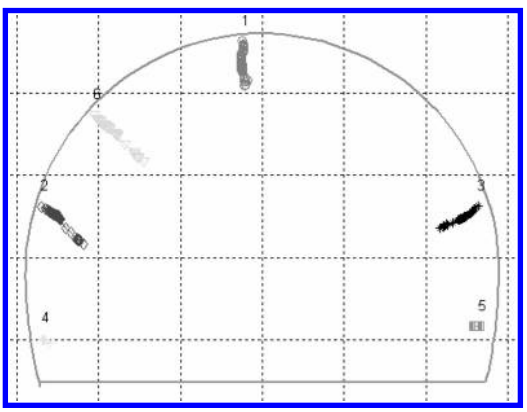


Figure 1. The displacement vector orientation in cross section.

As shear failures occur along joints the displacement vectors change their directions at the side walls and displacements increase. This process was not captured in the numerical model. A variation of parameters or an addition of additional singularities would definitely yield a better agreement. Another cause for this increase can be the heaving at the left invert measured as 20–50 cm.

The deformation history graph shows the significant increase at the side wall due to the change in mechanism. The deformation curve deviates from the normal behavior which is predicted by GeoFit considering the first measurements (Figure 3).

In Figure 4 the measured displacements at station 2188 m are compared to the calculated values from

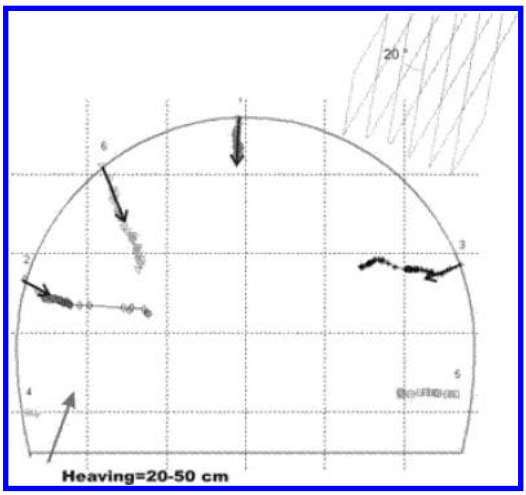


Figure 2. Measured and calculated displacement vectors at the cross section (1935 m).

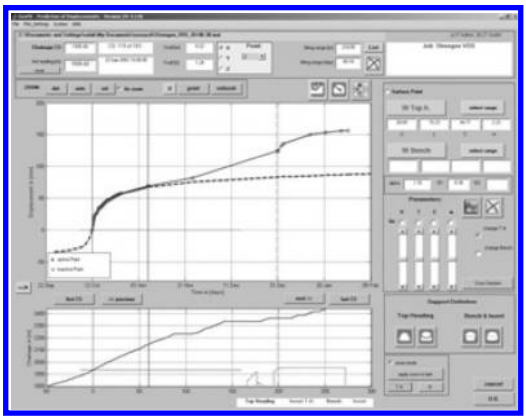


Figure 3. Development of horizontal displacement of the left sidewall and deviation from the predicted one.

Copyright © 2005 Taylor & Francis Group plc, London, UK

the numerical simulation. The measured displacement amounts and orientations at the crown right shoulder and sidewall agree well with those calculated (block size = 1.4 m, apex angle = 20°, joint residual friction angle = 16°, no additional features). The difference in orientation and magnitude between the measured and calculated displacements at the left side of the tunnel cross is caused by a fault zone located outside the profile (Figure 5).

Similar to the last example the deformation curve deviates from the predicted normal behavior (Figure 6).

In the numerical analysis a subvertical fault zone located in a distance of 5 m from the left side wall, with a thickness of 10 m was introduced. It shows that the orientations of the computed displacement vectors now are very similar to those observed, while the magnitude of displacements at the crown and right shoulder are a bit overestimated.

In Figure 8 the measured displacements at the station 2230 m are compared to the calculated values. The measured displacement amounts are similar to those from the numerical model (block size = 1 m, apex angle = 20°, joint residual friction angle = 18°, no additional features).

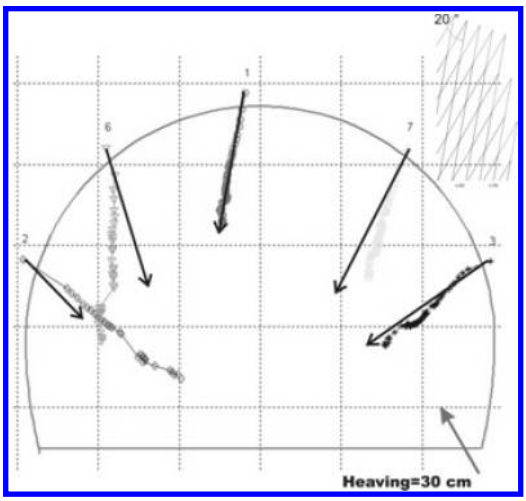


Figure 4. Measured and calculated displacements and their vectors at the cross section (2188 m).

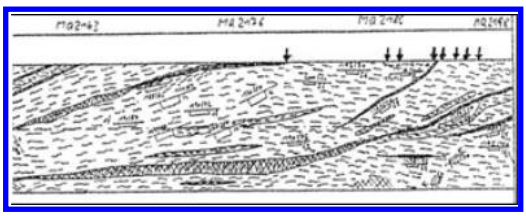


Figure 5. Geological plan view.

The difference between measured and calculated displacement orientations are attributed to a fault zone located at the left side of the cross section and the heaving at the right invert (Figure 9). A numerical analysis including a steeply dipping fault zone with a width of 5 m yields a better agreement between measured and calculated displacement vector orientations, as well as an increase in magnitude.

In Figure 11 the measured displacements at station 2306 m are compared to the calculated values. The measured displacement orientations are similar to those calculated from the numerical model (block size = 1.6 m, apex angle = 40°, joint residual friction angle = 16°). The calculated displacement at the right shoulder significantly exceeds the measured one. The reason is that in the simulation no support was used,



Figure 6. Y displacement curve of Point 6 and deviation from the predicted one (2188 m).

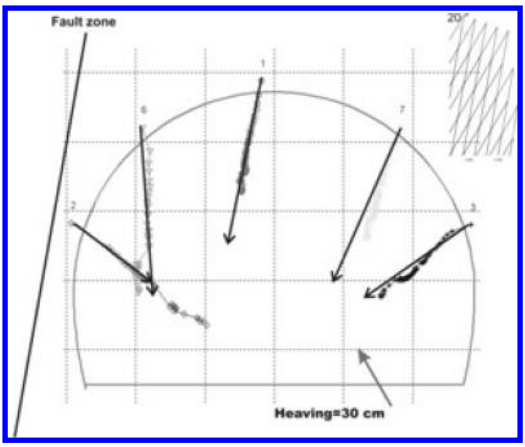


Figure 7. Measured and calculated displacements and their vectors at the cross section (2188 m) considering a fault zone outside the tunnel cross section.

Copyright © 2005 Taylor & Francis Group plc, London, UK

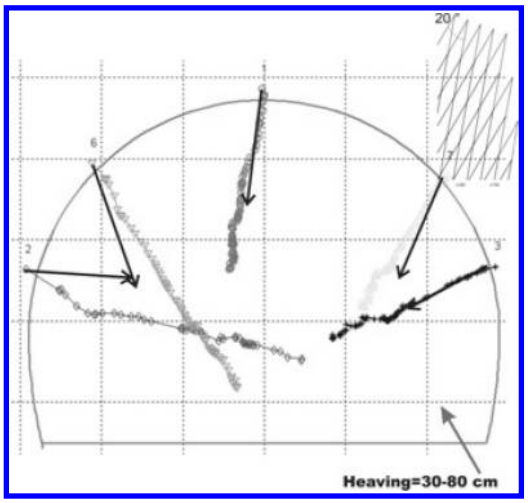


Figure 8. Measured and calculated displacements and their vectors at the cross section (2230 m).

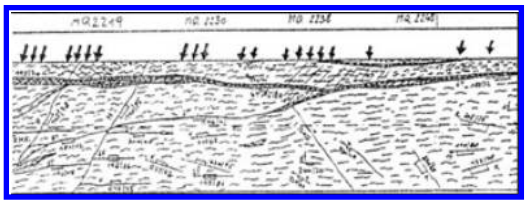


Figure 9. Geological plan view.

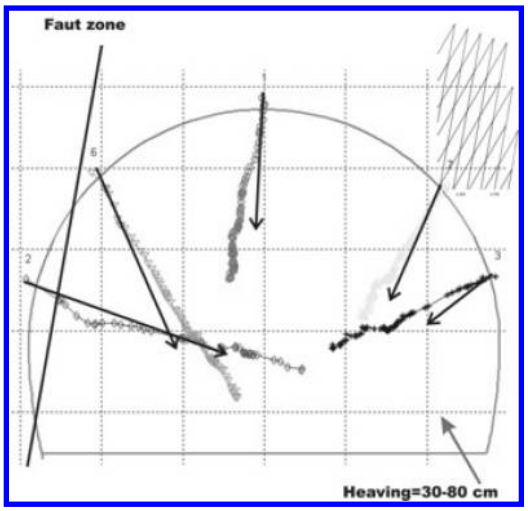


Figure 10. Measured and calculated displacements at cross section 2230 m, considering a fault zone at the left side of the tunnel cross section.

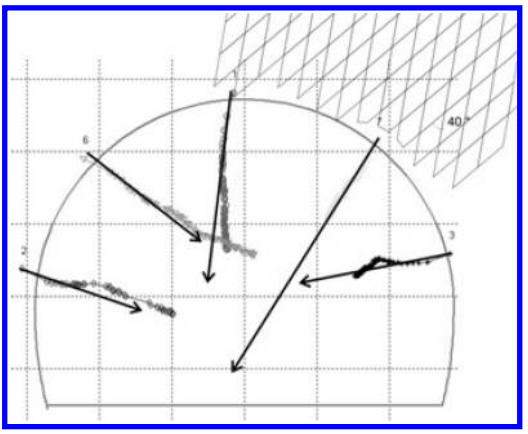


Figure 11. Measured and calculated displacements and their vectors at the cross section (2306 m).

allowing a wedge to slide into the excavation, which on site was held back by the dense bolting.

3 CONCLUSION

Absolute displacement monitoring enables to evaluate the influence of the rock mass structure and fault zones located outside the tunnel profile. In blocky rock mass the relative orientation of the joints, joint spacing and strength properties determine the failure modes, displacement amounts and directions. Discrete numerical analyses are valuable tools to evaluate failure modes and deformation behavior of tunnels in jointed rock masses. The study shall contribute to a better understanding of rock mechanical processes during tunneling. It is hoped that the results will contribute to safer and more economical tunneling.

REFERENCES

Button, E. A. 2004. Characterization of Phyllites for Tunnelling, *International Journal of Rock Mechanics and Mining Sciences*. Vol 41. 396.

Button, E. A., Schubert, W., Riedmueller, G. 2004. The Use of Monitoring Data and Geologic Documentation as a Basis for Defining Rock mass Behavior Types for Tunnelling, In: Prakash (ed), *Proc. of the Fifth Conference on Case Histories in Geotechnical Engineering*, USA.

ÖGG 2001. *Richtlinie für Geomechnische Planung von Untertagebauarbeiten mit zyklischem Vortrieb*. Österreichische Gesellschaft für Geomechnik, Salzburg.

Schubert, W. & Vavrovsky, G.M. 2003. Innovations in Geotechnical on-site Engineering for Tunnels. In O. Natau, E. Fecker, E. Pimentel (ed.), *Geotechnical*

Copyright © 2005 Taylor & Francis Group plc, London, UK

Measurements and Modelling; Proc. intern. symp., Karlsruhe, 35–44. Rotterdam: Balkema.

Schubert, W., Steindorfer, A., Button, E. A. 2002. Displacement Monitoring in Tunnels – an Overview. *Felsbau 20*, *No 2*, p 7–15. VGE.

Sellner et al. 2002. Advanced Analysis and prediction of Displacements and System Behavior in Tunnelling. In Dinis da Gama, C., Riberio e Sousa, L. (ed.), *Proc. of the ISRM International Symposium on Rock Engineering in Mountainous Regions*, Portugal, 539–546. Rotterdam: Balkema.

Solak, T. & Schubert, W. 2004. Influence of the Block Size and Shape on the Deformation Behavior and the Stress Development around the Tunnels. In Schubert (ed), *Rock Engineering-Theory and Practice*, Proceedings EUROCK 2004. 695–700, VGE.

3G- Gruppe Geotechnik Graz ZT GmbH, 2004. GeoFit homepage http://www.geofit.3-g.at/

Copyright © 2005 Taylor & Francis Group plc, London, UK

The importance of displacement prediction

K. Grossauer
Graz University of Technology, Graz, Austria

W. Schubert & P. Sellner
3G Gruppe Geotechnik Graz ZT GmbH, Graz, Austria

ABSTRACT: Tunnel construction in faulted and/or heterogeneous rock mass is in general associated with stability problems, high deformations and frequently changing stress conditions. Depending on the encountered conditions, different strategies for excavation and support of the tunnel must be applied.

The decisions on site thereby are widely influenced by the magnitude and development of the tunnel displacements. To allow for a reliable and relatively accurate prediction of displacements, the program GeoFit® was developed. GeoFit® is based on analytical functions which simulate the face advance effect and the time-dependent behaviour of the rock mass and support. Several parameters are used to describe the complex system behaviour. The program allows considering several options, including the installation of supports, sequential excavation, and non-steady tunnel advance. It provides several options of displaying measured and predicted data, thus allowing a continuous control of the "normality" of the displacements, and reacting in time in case the measured values deviate from the predicted ones. In addition the follow-up of trends of function parameters and displacements enables for short term prediction of the geological condition ahead of the face. This again increases the quality of decisions on site, increases safety and economic efficiency, and reduces the uncertainties.

The paper will show some basic principles of the displacement prediction and methods of data evaluation. Selected case histories will be used to illustrate the evaluation techniques and the benefit gained from these methods.

1 INTRODUCTION

The prediction of the magnitude and development of the expected displacements has a considerable impact on a large number of issues during tunnel construction.

On the one hand, excavation and support methods are influenced by the magnitude of displacements. On the other hand, the over-excavation has to be adjusted to the expected displacements to guarantee the clearance after stabilisation. In case of a misjudgement of displacements serious consequences have to be expected.

When underestimating the displacements, the danger of destruction of the lining exists by exceeding the deformability. Figure 1 illustrates such a case where shearing of the shotcrete occurred at the right side wall. In addition displacements in excess of the anticipated ones may lead to the necessity of reshaping, a process which in general costs as much as the original excavation and support.

In case of overestimation of displacements the remaining volume between primary lining and planned inner lining has to be filled with concrete. This also causes additional costs.

To allow for a safe and economic construction, the accurate prediction of displacements and conditions ahead of the face is essential.



Figure 1. Damaged lining after excessive displacements and exceeded deformability of the shotcrete.

Copyright © 2005 Taylor & Francis Group plc, London, UK

2 ADVANCED EVALUATION OF DISPLACEMENT MONITORING DATA

Prediction of rock mass behaviour, in particular when tunnelling under high overburden is a most challenging task, during design as well as during construction. Heterogeneous rock mass conditions significantly increase the difficulties in prediction of the tunnel performance.

Although the general geological situation may be known, changes of rock mass stiffness or structure ahead of the face, to a great extent influencing stresses in the vicinity of the tunnel and thus deformations, generally cannot be determined with sufficient accuracy. Exploration by drilling ahead or questionable results from geophysical methods are time consuming and costly.

The introduction of absolute displacement monitoring during tunnel excavation by geodetic methods to a large extent has replaced relative displacement measurements (Rabensteiner 1996). The resulting increase in the amount of available information has led to additional possibilities in data visualisation. Plots of deflection curves, trend lines along the tunnel axis and displacement histories have become common practice in many countries. The improved tools have led to a better understanding of geomechanical processes during tunnel excavation, and valuably assist the geotechnical engineer on site in his daily work.

2.1 *Qualitative evaluation of the displacement vector orientation*

During the excavation of the Inntaltunnel Schubert (1993) observed that the ratio between longitudinal and radial displacements (L/S) considerably changes when the face approaches a zone of different stiffness. Using data from absolute displacement monitoring from different sites, Budil (Budil 1996, Schubert & Budil 1995) studied the phenomenon of longitudinal displacements. He found a relation between displacement vector orientation and rock mass heterogeneity. This work was continued by Stein-dorfer (Steindorfer 1998, Steindorfer & Schubert 1997), who in detail analysed the development of stresses and displacements in heterogeneous ground during tunnel excavation.

When tunnelling in homogeneous rock mass and primary stress conditions, the vector orientation (ratio between longitudinal displacements and settlements – L/S) shows a certain value which can be considered as "normal". With different deformability of the ground, the absolute displacement values change but the ratios of the single components do not vary substantially. Different boundary conditions, like changes in the rock mass structure or in the primary stress situation,

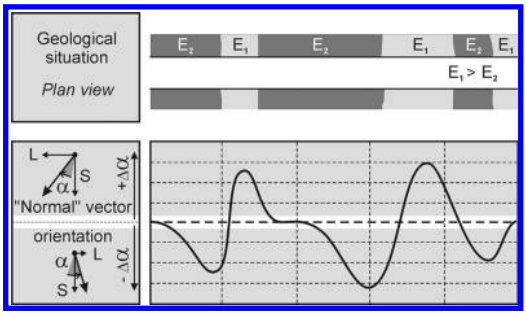


Figure 2. Variation in the vector orientation when tunnelling through rock mass with frequently changing stiffness.

influence the stress distribution around the cross section of the tunnel as well as ahead of the face, which leads to deviations of the vector orientation from "normal". When the excavation approaches a section consisting of "stiff" rock mass the vector orientation drops below "normal", which means an increasing trend of the vector orientation in the direction of excavation.

The opposite tendency can be observed when the face approaches a section consisting of "soft" rock. The vector orientation shows an increasing trend against the direction of excavation. A certain prediction of the extension of a fault zone is possible with the help of vector orientation trends.

Figure 2 illustrates the results from numerical simulations for tunnelling through rock mass with frequently changing stiffness. When the excavation approaches "stiff" rock (section 2) the vectors tends to point in the direction of excavation. Shortly after the excavation enters the "stiff" rock, the vector orientation shows an opposite tendency, which means an increasing trend against the direction of excavation. With further advance of the face into the relatively "stiff" section, the vector orientation does not normalise, but rather continues its increasing trend against the direction of the excavation. This deformation pattern indicates that rock mass conditions ahead of the face will change within one or two diameters and "soft" rock will be encountered.

After the face enters section 3 which consists of "soft" rock mass, the vector orientation tends back to "normal". When excavating in section 3 the vector orientation remains "normal", which is an indication that "soft" rock mass is ahead of the face for at least two or three diameters.

The practical value of this information is obvious. When tunnelling through a rock mass with frequently changing stiffness at short distances, stresses will concentrate in the "stiff" sections. When these sections of "stiff" rock are comparatively narrow, they may become overloaded and already fail in the vicinity of

Copyright © 2005 Taylor & Francis Group plc, London, UK

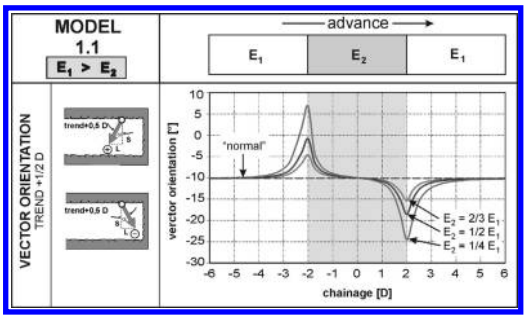


Figure 3. Deviation of the displacement vector orientation from "normal" for different stiffness contrasts.

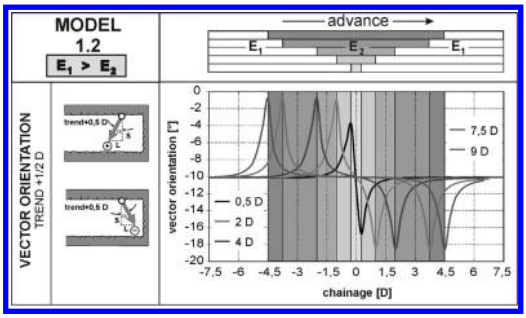


Figure 4. Deviation of the displacement vector orientation from "normal" for a certain stiffness contrasts and different fault zone widths.

the face or at some distance from the face. This again leads to a redistribution of loads to the previously "weaker" rock. This process may continue for a while, and in many cases is interpreted as creeping.

2.2 *Quantitative evaluation of the displacement vector orientation*

To quantify the influence of weak zones on stresses and displacements, further investigations with numerical simulations have been conducted by Gros-sauer (2001).

Figure 3 shows the deviation of the displacement vector orientation from "normal", obtained from numerical 3D model for different stiffness contrasts between the fault zone and the adjacent rock mass. The amount of the deviation does not only depend on the stiffness contrast between the rock masses, but also on the width of the embedded zone. Figure 4 illustrates the increasing deviation with increasing fault zone length up to a certain critical length, beyond this no further increase of the vector orientation can be observed. This critical zone length was determined to be in between 2.5 and 4 tunnel diameters.

3 PREDICTION OF DISPLACEMENTS

Guenot et al. (1985) and Sulem et al. (1987) proposed a method based on analytical functions that describe displacements in a plane perpendicular to the tunnel axis as a function of time and the advancing face. Barlow (1986) and Sellner (2000) modified this approach. The displacement behaviour of the rock mass and support basically is represented by four function parameters. Two parameters (T, m) are used to simulate time dependency and another two parameters (X, C) the face advance effect. These parameters can be back-calculated from case histories using curve fitting techniques. Artificial intelligence (neuronal networks) is planned to be involved to identify dependencies between the function parameters and the geological and geotechnical conditions encountered.

The system of these analytical functions was implemented in the program package called GeoFit® (Sellner 2000). It provides easy-to-use tools for back-calculating displacement monitoring data (curve fitting technique), for prediction of displacements and for handling the expert system. The application is acting interactively. Each change in the calculation assumptions is displayed on the screen immediately. Both monitored and predicted results are shown. This procedure allows to predict displacements for any time and point of the tunnel wall as well as the ground surface considering different construction stages and supports. Trend lines, deflection lines, displacement plots and spatial displacement vector orientations can be evaluated and displayed on the basis of monitored, calculated and predicted data, allowing a continuous comparison of the actually measured and predicted data.

3.1 *Prediction methods*

Basically, there are two possibilities for predicting displacements. The first, a very simple but accurate method is to predict final displacements after a few displacement readings at a given cross section. The rock mass behaviour is determined form previously excavated sections in combination with the short-term prediction gained from the evaluation of the monitoring data (Steindorfer 1998). By fitting the analytical displacement function to the measured displacements, a prediction for the future displacement development is possible. Figure 5 shows a displacement history plot for the crown settlement at the Inntaltunnel (cross section 3009). The readings of the first two days after the zero reading are used to back calculate the function parameters (X, T, C, m). The obtained function parameters represent the displacement behaviour of the observed section and the displacements can be calculated for any desired excavation advance. The dashed line shows the displacement prediction for this cross section. This method is called

Copyright © 2005 Taylor & Francis Group plc, London, UK

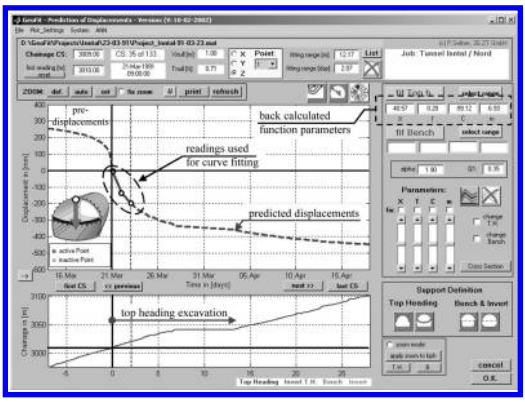


Figure 5. Back calculation of the function parameters using the readings of the first 2 days and prediction of displacements.

the "Extrapolating Prediction Method" (EPM). The accuracy of the prediction increases with the number of available displacement readings at the observed cross section.

The second method is used for sections ahead of the face, when no readings are available yet. The information required for the determination of the rock mass behaviour and support influence is gained from a database, which stores knowledge from back-calculated case histories. Information describing the geological and geotechnical conditions for the specific section is gained by modelling ahead, using the predicted geological conditions, as well as extrapolations of the observed behaviour on previous sections. Easy-to-obtain parameters such as overburden, joint parameters, RMR and weathering conditions are used as input parameters for the artificial neural network, which calculates the function's parameters and thus displacements. This method is called the "Pure Prediction Method" (PPM).

3.2 *EPM versus PPM*

While the latter method, the PPM, requires a database of back-calculated values to predict the function parameters, the first method, the EPM, only needs some a few displacement readings and information of the previously excavated tunnel sections. The EPM has been tested on several sites and shows a high accuracy and reliability. The prediction procedure is simple and quick and supports the site engineer in his daily work.

3.3 *Function parameters for prediction*

Following the ideas of the influence of the changing stress field in a heterogeneous rock mass on the displacements, it is obvious that the trends of the function parameters X, T, C, and m should reflect the geotechnical situation, and thus could be used for prediction. The results of numerical models with elastic rock mass behaviour were imported into GeoFit® and the function parameters obtained by curve fitting (Kim 2003). The back calculated function parameters X and C for a fault zone width of one tunnel diameter and a stiffness contrast of 2.0 between the two rock masses showed that the parameter X significantly increases already 15 m ahead of the transition between stiff and weak rock. The investigation of different fault zone widths showed larger increase of the parameter X for with increasing widths. Besides this increase of X well ahead of the weak zone, the results clearly show the influence of the fault zone length on the final displacements within the weak zone, which are reflected through the parameter C. With some experience in this kind of monitoring data evaluation, the combination of displacement vector orientation trends and distributions of function parameter trends can be used to predict quality and extension of weak zones ahead of the tunnel face, as well as the magnitude and development of the displacements.

4 CASE HISTORIES

During the last few years advanced methods were used on many tunnel sites to support the geotechnical engineer in the ongoing evaluation of the displacement monitoring data and to assist him in the interpretation of geotechnical situations and consequently in the decision making process.

To illustrate the evaluation techniques and the benefit gained from the methods explained in this paper, examples of two selected case histories will be shown.

4.1 *Inntaltunnel, Austria*

The 12.7 km long, double track railway tunnel bypasses the city of Innsbruck. During the excavation of the north heading with an overburden of approx. 300 to 350 m, a major fault zone was encountered.

The following figures (Figure 6 & Figure 7) will show the advantages of advanced monitoring data evaluation for chainage 3060 m up to 3200 m and the left sidewall point.

From chainage 3100 to 3135 the settlements dropped to about 5 to 10 mm. In contrast the trend of the vector orientation 20 m behind the face showed a significant increase against direction of excavation, indicating a zone of weakness outside the excavation area.

Shortly before the excavation entered the major fault zone, the settlements showed a slight increase, which did not provide a clear indication of changing rock mass conditions ahead of the face as the variation was within the usual range (Figure 7).

Copyright © 2005 Taylor & Francis Group plc, London, UK

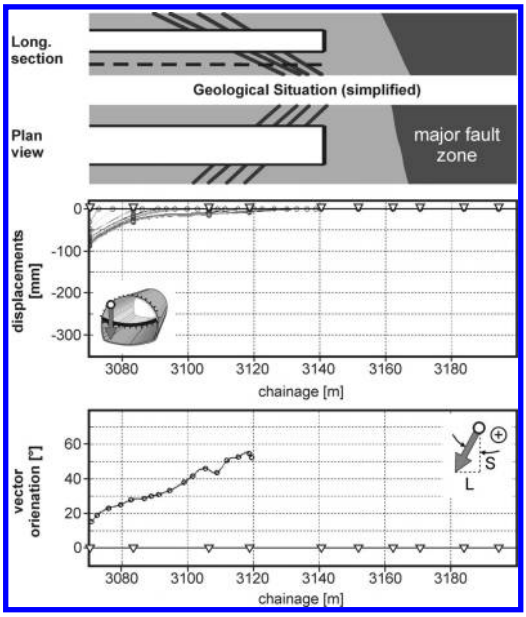


Figure 6. Development of settlement and displacement vector orientation trend (L/S), face position at chainage 3140 m.

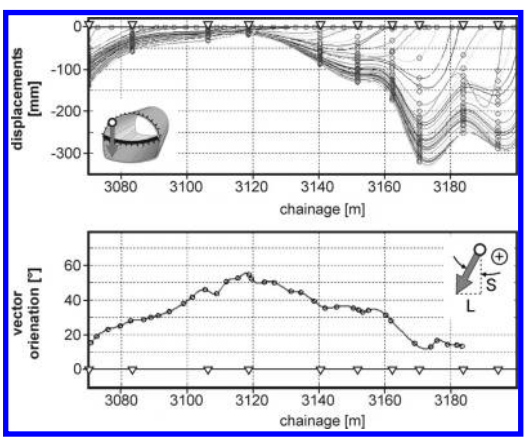


Figure 7. Settlement and displacement vector orientation (L/S) after entering the major fault zone.

After the face entered the fault zone at chainage 3170, the vector orientation dropped to about 10° against direction of excavation which could be considered to be "normal" behaviour while settlements increased considerably due to the "soft" fault material.

4.2 *Strenger tunnel, Austria*

The Strenger tunnel, a twin tube, two lane road tunnel is located between Innsbruck and Bregenz in the western

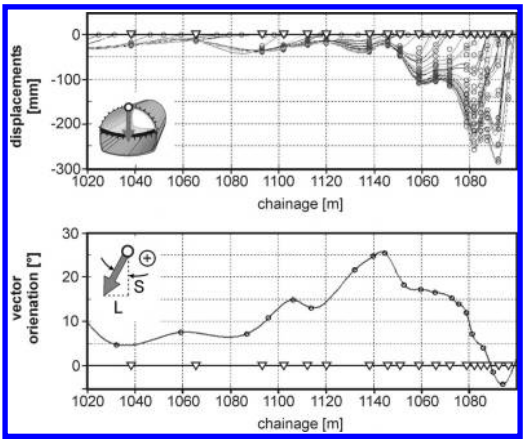


Figure 8. Settlements and displacement vector orientation trend after encountering a fault zone.

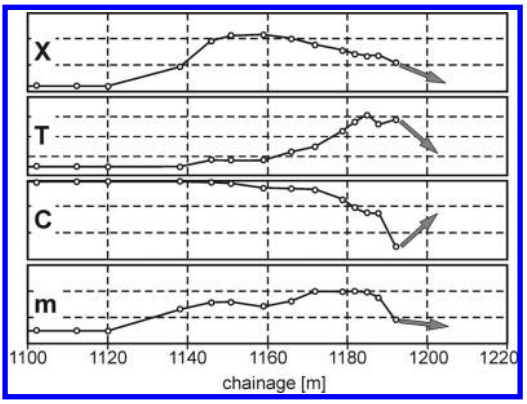


Figure 9. Distribution of the function parameter trends; extrapolation of the parameters for the next monitoring section.

part of Austria. The geological situation is dominated by Quartzphyllite with an overburden up to 600 m. The foliation typically dips steeply to the south, which results in a strike oblique to parallel to the tunnel axis.

Figure 8 shows the development of the settlements and the trend of the vector orientation for the crown point of the south heading from the west portal, after entering a fault zone.

Similar to the case displayed above, a significant increase of the displacement vector orientation trend against direction of excavation could be observed well before the excavation entered the fault zone. In contrast, the development of the displacements don't show a significant increase until the fault zone was entered.

Figure 9 demonstrates the distribution of the four function parameters X, T, C and m back-calculated from the vertical displacements of nearly the same section described before.

Copyright © 2005 Taylor & Francis Group plc, London, UK

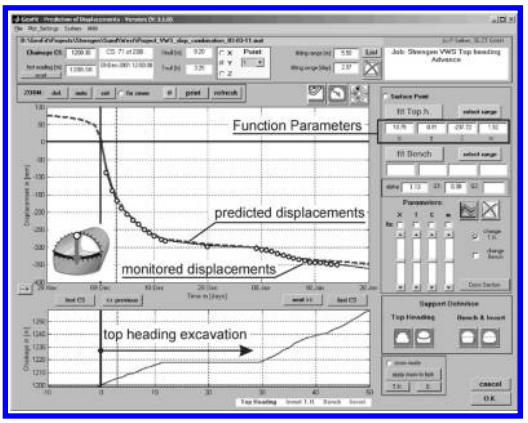


Figure 10. Displacement history plot; comparison of the predicted and finally observed displacements for the crown point of cross section 1200.

Similar to the distribution of the displacement vector orientation, a significant increase in the trend of the parameter X can be observed well before the excavation encounters the fault zone at approx. chainage 1175.

Some experience in the field of the advanced evaluation of displacement monitoring data in combination with the distribution of the parameter trends allows for an extrapolation of these parameters for the next monitoring section. Figure 10 demonstrates the displacement history plot of the monitored settlements (circles) and the predicted ones (dashed line) for the crown point of cross section 1200. For the prediction of the displacements the function parameters, extrapolated from the section before, were used. After the third reading a fine adjustment of the predicted curve was made. Finally, the predicted displacements fit well to the displacements monitored on site.

5 CONCLUSION

The prediction of the geotechnical conditions ahead of the face and, especially the prediction of the expected displacements is a crucial issue for safe and economical tunnelling in faulted or heterogeneous rock mass.

Advanced methods of data evaluation have significantly improved the value of information gained from monitoring data. Experience with tunnels in Austria during the last decades has shown that the ratio between longitudinal and radial displacements can be used to identify zones of different stiffness ahead of the face. Based on analytical functions it is possible to back-calculate displacement monitoring data with curve fitting techniques and to predict displacements. The combination of displacement vector orientation trends and distributions of function parameter trends can be used to predict weak zones ahead of the tunnel face, as well as the magnitude and development of the expected displacements.

With the increasing number of projects evaluated with these methods in different geological environment and boundary conditions a knowledge base can be developed leading to a “smart” data evaluation tool.

REFERENCE

Barlow, J.P. 1986. Interpretation of Tunnel Convergence Measurements. MSc Thesis, Dep. of Civil Engineering, University of Alberta, Canada.

Budil, A. 1996. Längsverschiebungen beim Tunnelvortrieb. Ph.D. thesis at the Institute for Rock Mechanics and Tunnelling, Graz University of Technology, Austria. 100pp.

Grossauer, K. 2001. Tunnelling in Heterogeneous Ground – Numerical Investigation of Stresses and Displacements. Diploma Thesis at the Institute for Rock Mechanics and Tunnelling, Graz University of Technology, Austria.

Guenot, A., Panet, M. & Sulem, J. 1985. A New Aspect in Tunnel Closure Interpretation. In Ashwoth, E. (ed). *Research and Engineering Applications in Rock Masses. Proc. 26th US Symposium on Rock Mechanics, Rapid City, South Dakota, 26–28 June, 1985*: 445–460. Rotterdam: Balkema.

Kim, C.Y. 2003. Investigation of fault zones on displacements. Project report at the Institute for Rock Mechanics and Tunnelling, Graz University of Technology, Austria. (unpublished).

Rabensteiner, K. 1996. Advanced Tunnel Surveying and Monitoring. In Felsbau 14, Vol. 2: 98–102. Essen: VGE.

Schubert, W. 1993. Erfahrungen bei der Durchörterung einer Großstörung im Inntaltunnel. In Felsbau 11, Vol. 6: 443–447. Essen: VGE.

Schubert, W., Budil, A. 1995. The Importance of Longitudinal Deformation in Tunnel Excavation. In Fujii, T. (ed.). *Proceedings of the 8th International Congress on Rock Mechanics (ISRM), Vol. 3, Tokyo, 25–30 September 1995:* 1411–141. Rotterdam: Balkema.

Sellner, P.J. 2000. Prediction of Displacements in Tunnelling. Ph.D. Thesis, Graz University of Technology, Austria. In Schubert, Riedmüller & Semprich (eds.). Schriftenreihe der Gruppe Geotechnik Graz, Heft 9.

Steindorfer, A. 1998. Short term Prediction of Rock Mass Behaviour in Tunnelling by Advanced Analysis of Displacement Monitoring Data. Ph.D. Thesis, Graz University of Technology, Austria. In Schubert, Riedmüller & Semprich (eds.), Schriftenreihe der Gruppe Geotechnik Graz, Heft 1.

Steindorfer, A. & Schubert, W. 1997. Application of new methods of monitoring data analysis for short term prediction in tunnelling. In Golser, Hinkel & Schubert (eds.). *Tunnels for People. Proc. 23rd General Assembly of the Int. Tunnelling Association, Vienna, 12–17 April 1997:* 65–69. Rotterdam: Balkema.

Sulem, J. Panet, M. & Guenot, A. 1987. Closure analysis in deep tunnels. In Int. Journal of Rock Mechanics and Mining Science 24: 145–154. Amsterdam: Elsevier.

Copyright © 2005 Taylor & Francis Group plc, London, UK

The development of an in-situ AE monitoring system and its application to rock engineering with particular emphasis on tunneling

H. Tano
Dept. of Civil Engineering, College of Engineering, Koriyama, Japan

T. Abe
Kokusai Kogyo, Sendai, Japan

Ö. Aydan
Dept. of Marine Civil Engineering, Tokai University, Shizuoka, Japan

ABSTRACT: This paper discusses the response of tunnel lining using an AE monitoring system and a portable laser distance meter in a landslide area and the AE response of rockmass nearby the tunnel face during excavation to assess its stability. This AE system has been developed for in-situ measurements with the use of dry batteries. Therefore the set up of this device can be done in all in-situ environments and measure the AE responses induced by sliding of ground and micro fracturing of rock mass. A portable laser distance meter was used to measure the convergence of tunnels.

1 INTRODUCTION

There are many measurement equipments using advanced technologies. However, their cost is generally high and their operations are not simple for field measurements. We have tried to develop a more simple method with low cost equipments. In this article, two portable systems are explained and the results obtained from field applications are presented. The first system is a portable laser distance measuring equipment and the second one is an AE counting system.

2 MONITORING SYSTEMS

2.1 *Portable laser distance measurement system*

A commercially available laser distance-meter used in the portable system and its measurement accuracy is about 1.5 mm for a maximum distance of 40 m. Generally a total accuracy of measurement of distance depends on the equipment accuracy, which can not be improved by ourselves, and a setting error in field. However there may be some room for us to minimize the setting error in measurements. We developed an end attachment device to reduce the setting error of a laser distance-meter as shown in Figures 1 and 2. A device together with a small pin having a diameter of 1.5 mm is attached at the end part of the laser distance-meter. A small base having a spherical concave seating with the same diameter as that of the pin is used. With the use of this attachment, the setting error associated with measurements can be less than 1 mm even we change the direction of measurements. Furthermore, the operation is quite simple and a convergence measurement of one section of a tunnel can be performed within a few minutes. The target is a non-mirror type and a small aluminum plate is used as a target.

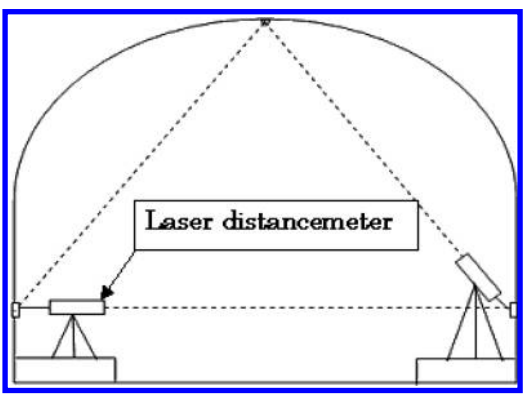


Figure 1. Schematic diagram of convergence measurement using by portable laser distance-meter.

Copyright © 2005 Taylor & Francis Group plc, London, UK

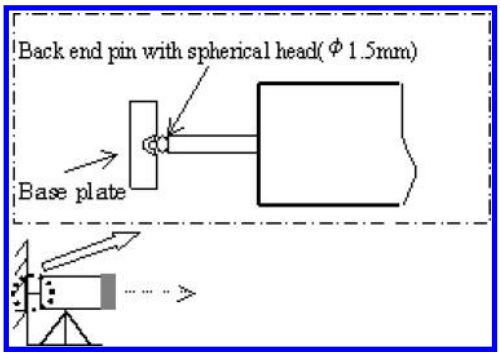


Figure 2. The attachment at the end part of the distance-meter for reducing setting error.

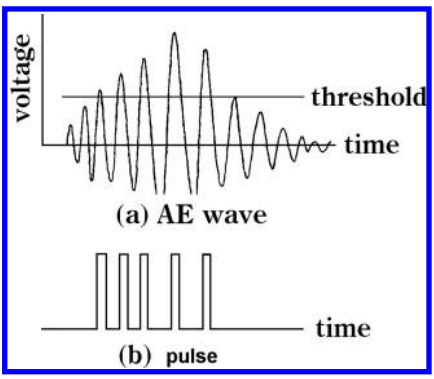


Figure 3. The principle of AE counting.

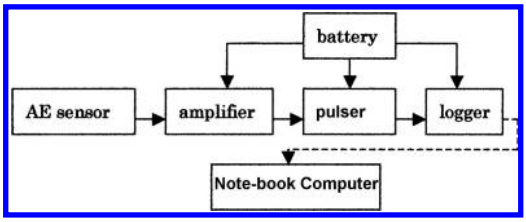


Figure 4. A block diagram of AE counting system.

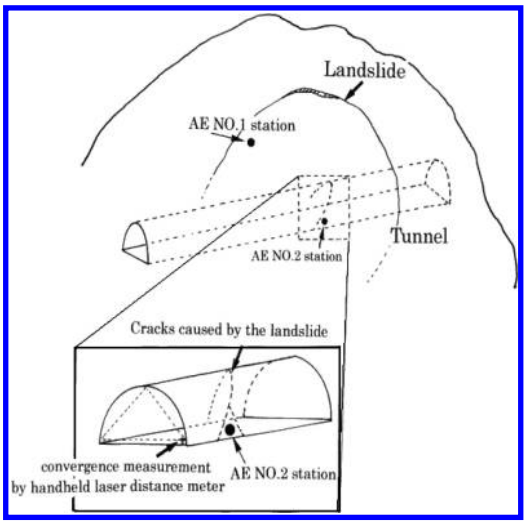


Figure 5. Schematic diagram of tunnel S damaged by the landslide and AE set-up locations.

2.2 *AE counting system*

It is well known that AE activities of rock mass occur in association with micro fracturing and it is one of useful parameters for monitoring the behaviour of a rock structure. If an AE system used with a wave memory, it is possible to measure many parameters related to fracturing and deformation of surrounding medium. However, such a full utilization of AE system has several problems, especially in field use as follows:

(1) AE system cost is generally high,
(2) A noise condition of AE in field is not clear,
(3) AC power is required for a long term monitoring.

With the consideration points mentioned above, we developed a simple AE system which was limited only to counting AE events as illustrated in Figures 3 and 4. Pulse signals, which correspond to AE waves exceeding a threshold are discriminated through a pulsar and recorded onto a pulse counter (logger) as AE rate counts. Such limited specification of the rate counting reduces the system cost so that we are always capable of using two AE systems as one set. One of the AE systems is called an active unit while the other one is called a dummy unit. The active unit is directly attached onto the object while the dummy AE sensor is not in contact with the object. If any noise, for example, due to electrical switching occurs, such a noise may be simultaneously counted both active and dummy systems as AE events. If signals are counted on both systems, the count of active unit is neglected from the measured data. This active-dummy counting system can improve the reliability of the AE monitoring and check the noise condition in field.

3 APPLICATIONS

3.1 *Behaviour of tunnel affected by landslide*

Figure 5 shows a schematic diagram of tunnel S passing through a landslide area in Fukushima, Japan and the tunnel has been experiencing very large deformation and fracturing for about 8 years. The tunnel is 400 m long, 6 m high and 7 m wide. We have been measuring the convergence of this tunnel through the laser distance-meter with some improvements. In addition, we have installed the AE counting systems in the tunnel and on the rock slope as shown in Figure 5.

Copyright © 2005 Taylor & Francis Group plc, London, UK

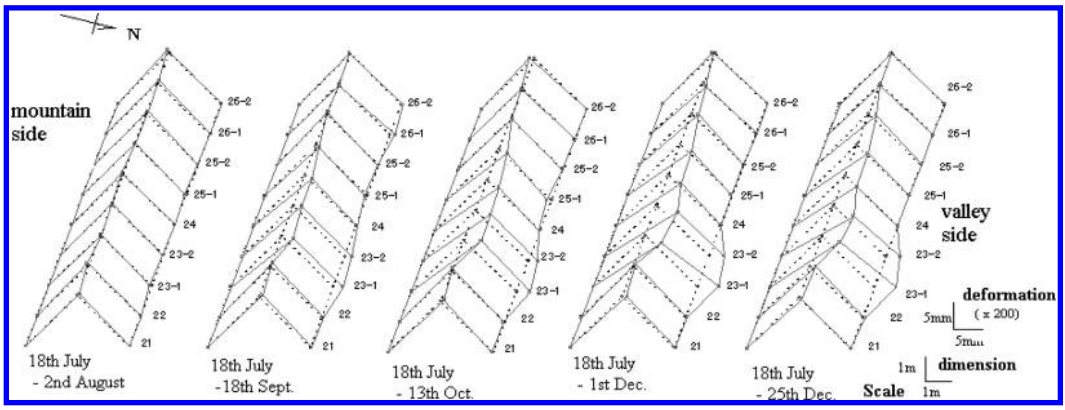


Figure 6. The deformation of tunnel S under landslide.

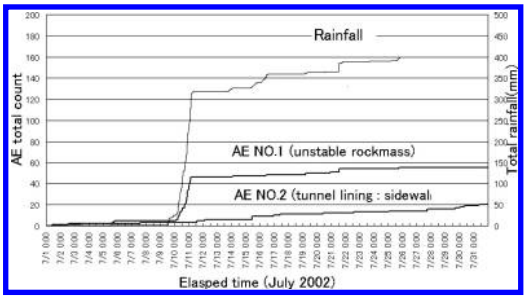


Figure 7. An example of AE measured results and relations among rainfall, and AE activities on landslide (AE NO.1) and damaged tunnel-lining wall (AE NO.2).

The NO.1 AE station was set up nearby the sliding plane and the NO.2 AE system was set on the tunnel lining, which was damaged by the landslide plane.

Figure 6 shows the convergence of tunnel S for about six months from July 2001 to December 2001. As noted from this figure, the sidewall on the mountainside is stable while the lining on the valley-side is deforming. The measurement was performed for about 30 meters long section of the tunnel where cracks were observed in the lining. The maximum deformation of the sections was about 5 millimeters.

Figure 7 shows the AE events at measurement stations on the landslide zone (NO.1) and on tunnel lining (NO.2) in relation to rainfall. It seems that there are some correlations between the amount of rainfall and AE responses. This aspect is further discussed in Subsection 4.1.

3.2 *AE activities near tunnel face just after blasting*

Figures 8 and 9 show views of the AE system fixed directly onto a rock bolt, which acts as an AE waveguide. The set up time is about one or two minutes.

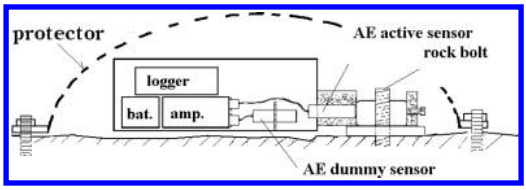


Figure 8. Schematic diagram AE system for rock bolt.

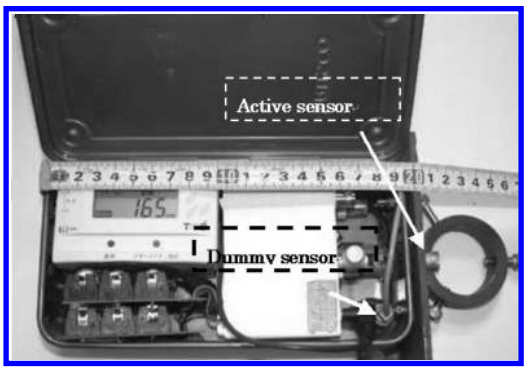


Figure 9. AE system with active and dummy sensors.

Figure 10 shows the setup nearby a tunnel face just before blasting. The systems were guarded by a protector against impacts of fragments of rocks resulting from blasting (Figures 8 and 10). Figure 11 shows the locations of three AE systems setup as a schematic diagram. The left sidewall set up was NO.1 AE system, which was faced the direction of excavation face. The NO.2 system was located at the crown as seen in Figure 12. The purpose of this measurement was to assess the stability of rockmass surrounding a tunnel. Two tunnels are under construction at the time of installation of this AE counting system and their characteristics are given in Table 1. The rock mass was granodiorite.

Copyright © 2005 Taylor & Francis Group plc, London, UK



Figure 10. Set up AE system covered by protector at tunnel crown.

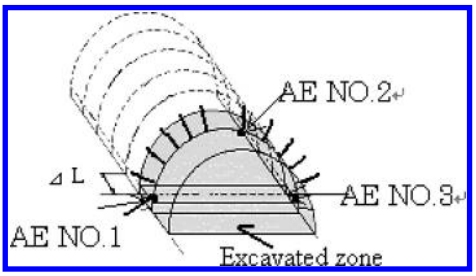


Figure 11. The locations of three AE stations near the face.

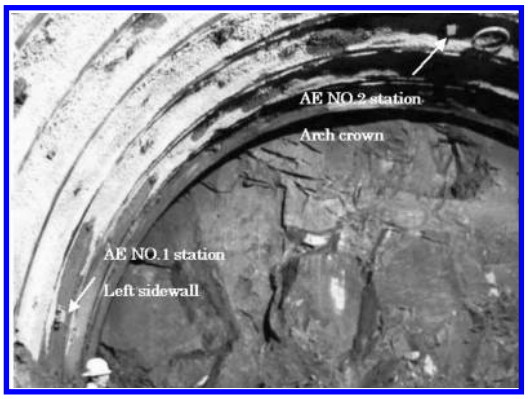


Figure 12. AE-NO.1 station and AE-NO.2 stations nearby tunnel face.

Figure 13 shows a standard cross section in tunnel G. An example of records obtained at tunnel G listed in Table 2. As it is noted from the table, AE activities occurred during the measuring interval of 10 seconds, which correspond to the blasting operation period. Therefore, it is contemplated that the conditions of the rockmass was very good and the tunnel face was stable. The rock quality at the section where instruments were installed was good and the number of joint was a few. Therefore, it is expected that the AE activities should be terminated within a short period of time. In this particular case the locations of AE systems were fixed while the tunnel face advanced after each blasting. Figure 14 shows the relation between the AE activity and the distance from the tunnel face. It seems that when the face was near the AE systems, AE activities are less than when the tunnel face is far from the instrumentation location at tunnel G. It is also interested to notice that the AE activities in the crown are much higher than those at two sidewalls. Figure 15 shows the results obtained in tunnel K. In this case the AE activities also terminated within 10 seconds and it was to the case of tunnel G shown in Figure 14.

4 DISCUSSIONS

4.1 *Delay time among rainfall, landslide behavior and tunnel deformation*

According to the variations of deformations shown in Figure 6, the location of the landslide plane crossing

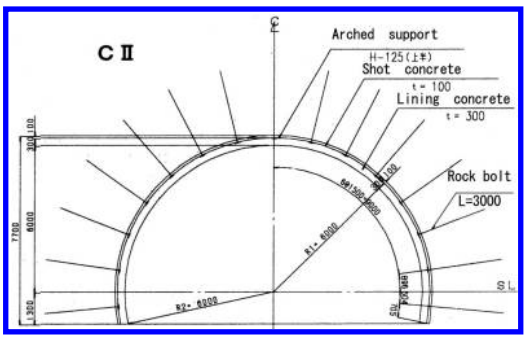


Figure 13. Standard cross section and support system at C II rock class in tunnels G and K.

Table 1. Characteristics of tunnels and AE counting intervals.

Tunnel	Dimension (m) Length × width × height	Station (m)	Overburden at station	(Max.) m	Rock bolt pattern*	Geology	AE counting interval (sec.)
G	1385 × 12 × 6	1045	90	(160)	C II	granodio rite	10
G	1385 × 12 × 6	1252	18	(160)	C II	granodio rite	2
K	4345 × 9.3 × 6.45	776	240	(480)	C II	tuff breccia	2

* Rock bolt length = 3 m

Copyright © 2005 Taylor & Francis Group plc, London, UK

Table 2. An example of AE activities nearby the face for 10 seconds after blasting in tunnel G (10 seconds interval).

	Left side wall		Arch crown		Right side wall		
Time	Active	Dummy	Active	Dummy	Active	Dummy	Estimation of operations using by AE records
06:50′50″	0	0	0	0	0	0	
06:51′00″	2	0	4	0	0	2	←Start of operations
06:51′10″	0	0	0	0	0	0	
06:51′20″	1	0	3	0	0	0	
06:51′30″	3	0	1	0	0	3	
06:55′00″	0	0	86	2	51	90	←Working
06:55′10″	178	21	193	41	124	202	
06:55′20″	236	126	220	120	138	215	
06:55′30″	235	127	216	116	133	207	
06:55′40″	229	124	218	114	134	206	
06:55′50″	233	124	227	126	141	215	
07:37′40″	181	62	191	39	88	170	
07:37′50″	125	25	107	6	39	95	
07:38′00″	112	32	99	14	42	93	
07:38′10″	14	0	0	0	0	1	←Talking in the shelter
07:38′20″	0	0	1	0	0	2	
08:10′10″	6	0	0	0	0	0	
08:10′20″	0	0	0	0	0	0	
08:10′30″	0	0	0	0	0	0	
08:10′40″	0	0	0	0	0	0	
08:10′50″	0	0	0	0	0	0	
08:11′00″	0	0	0	0	0	0	
08:11′10″	0	0	0	0	0	0	
08:11′20″	0	0	0	0	0	0	
08:11′30″	0	0	0	0	0	0	
08:11′40″	0	0	0	0	0	0	
08:13′40″	0	0	0	0	0	0	
08:13′50″	0	0	0	0	0	0	
08:14′00″	0	0	0	0	0	0	
08:14′10″	0	0	0	0	0	0	
08:14′20″	0	0	0	0	0	0	
08:14′30″	0	0	0	0	0	0	
08:14′40″	0	0	0	0	0	0	
08:14′50″	**47**	**45**	**62**	**73**	**14**	**40**	**←Blasting**
08:15′00″	0	0	0	0	0	0	
08:15′10″	0	0	0	0	0	0	
08:15′20″	0	0	0	0	0	0	
08:15′30″	0	0	0	0	0	0	←Waiting
08:15′40″	0	0	0	0	0	0	
08:15′50″	0	0	0	0	0	0	
08:16′00″	0	0	0	0	0	0	
08:16′10″	0	0	0	0	0	0	
08:16′20″	0	0	0	0	0	0	
08:16′30″	0	0	0	0	0	0	
08:19′20″	0	0	0	0	0	0	
08:19′30″	6	0	0	0	0	2	←Continuation of operations
08:19′40″	1	0	0	0	0	0	
08:19′50″	4	0	0	0	0	2	
08:20’00”	1	0	0	0	0	0	

tunnel S can be easily inferred. After a heavy rainfall in August, the deformation of lining increased. It is easily noted that there is a delay time between the rainfall and AE activities. The AE counts starts about 12 hours nearby the landslide zone while the same AE activity on the tunnel lining was observed after about 36 hours. In other words, the total delay time for AE activities in the tunnel is two days. This may be

Copyright © 2005 Taylor & Francis Group plc, London, UK

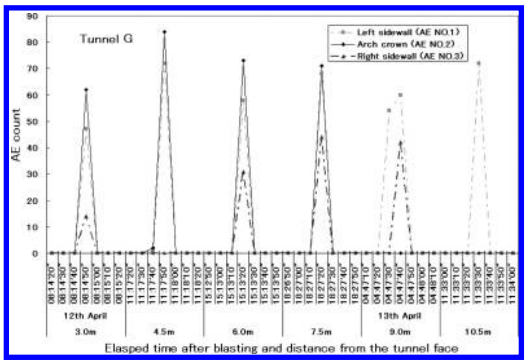


Figure 14. AE activities nearby the face for 10 seconds after blasting in tunnel G (10 seconds measurement interval).

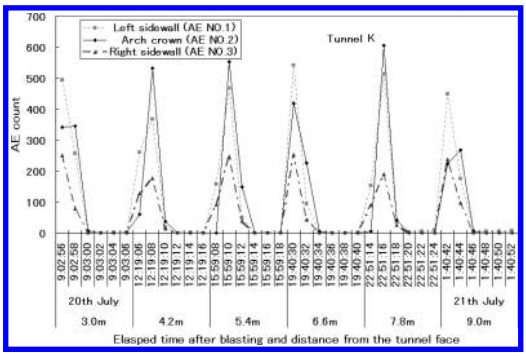


Figure 15. Relation between AE activities and face distance after blasting in tunnel K (2 seconds measurement interval).

Table 3. An example of AE activities nearby the tunnel face after blasting in tunnel K (2 seconds measurement interval).

	Left side wall		Arch crown		Right side wall		
Time	Active	Dummy	Active	Dummy	Active	Dummy	Estimation of operations using by AE records
06:50′50″	0	0	0	0	0	0	
06:51′00″	2	0	4	0	0	2	←Start of operations
06:51′10″	0	0	0	0	0	0	
06:51′20″	1	0	3	0	0	0	
06:51′30″	3	0	1	0	0	3	
06:55′00″	80	0	86	2	51	90	←Working
06:55′10″	178	21	193	41	124	202	
06:55′20″	236	126	220	120	138	215	
06:55′30″	235	127	216	116	133	207	
06:55′40″	229	124	218	114	134	206	
06:55′50″	233	124	227	126	141	215	
07:37′40″	181	62	191	39	88	170	
07:37′50″	125	25	107	6	39	95	
07:38′00″	112	32	99	14	42	93	
07:38′10″	14	0	0	0	0	1	←Talking in the shelter
07:38′20″	0	0	1	0	0	2	
08:10′10″	6	0	0	0	0	0	
08:10′20″	0	0	0	0	0	0	
08:10′30″	0	0	0	0	0	0	
08:10′40″	0	0	0	0	0	0	
08:10′50″	0	0	0	0	0	0	
08:11′00″	0	0	0	0	0	0	
08:11′10″	0	0	0	0	0	0	
08:11′20″	0	0	0	0	0	0	
08:11′30″	0	0	0	0	0	0	
08:11′40″	0	0	0	0	0	0	
08:13′40″	0	0	0	0	0	0	
08:13′50″	0	0	0	0	0	0	
08:14′00″	0	0	0	0	0	0	
08:14′10″	0	0	0	0	0	0	
08:14′20″	0	0	0	0	0	0	
08:14′30″	0	0	0	0	0	0	
08:14′40″	0	0	0	0	0	0	
08:14′50″	**47**	**45**	**62**	**73**	**14**	**40**	**←Blasting**
08:15′00″	0	0	0	0	0	0	
08:15′10″	0	0	0	0	0	0	

Copyright © 2005 Taylor & Francis Group plc, London, UK

Table 3. *Continued*

Time	Left side wall		Arch crown		Right side wall		Estimation of operations using by AE records
	Active	Dummy	Active	Dummy	Active	Dummy	
08:15′20″	0	0	0	0	0	0	
08:15′30″	0	0	0	0	0	0	←Waiting
08:15′40″	0	0	0	0	0	0	
08:15′50″	0	0	0	0	0	0	
08:16′00″	0	0	0	0	0	0	
08:16′10″	0	0	0	0	0	0	
08:16′20″	0	0	0	0	0	0	
08:16′30″	0	0	0	0	0	0	
08:19′20″	0	0	0	0	0	0	
08:19′30″	6	0	0	0	0	2	←Continuation of operations
08:19′40″	1	0	0	0	0	0	
08:19′50″	14	0	0	0	0	2	
08:20′00″	1	0	0	0	0	0	

related to seepage of ground water. The tunnel convergence was measured every three or four weeks intervals while AE activity was measured at ten minutes intervals. Therefore, the deformation measurements can not be directly compared with AE activities.

4.2 *AE activities nearby tunnel face just before and after blasting*

As mentioned Subsection 3.2, it seems that the behavior of rock mass nearby the tunnel face in tunnel G is elastic and AE activity ceases during the measurement interval of ten seconds (Table 2). Therefore, another attempt was done to measure the AE activities of tunnel K at an interval of two seconds and the results are shown in Figure 15 and they are listed in Table 3. As seen in Table 3, the AE activities decreased quickly during the first two intervals (four seconds) after the blasting. In other words, the AE activities in the first half of about ten seconds was directly affected by shock waves resulting from blasting. It is recognized that the influence of impact was stronger at the location of about 0.5D (D: diameter of the tunnel) from the tunnel face. Taking the experiences gained during the measurements in tunnel K and tunnel G into account, the measurements were carried out at two seconds interval thereafter and they are shown in Figure 16. The AE activities in the seconds half of the ten seconds are shown in Figures 17 and 18.

These observations on the AE activities may be caused by the redistribution of the in-situ stresses around the tunnel as a result of blasting. It is interesting to notice that the tendency of AE activities at the second half of ten seconds after blasting were similar to those in the first half when Figures 14 to 18 are compared with each other. It seems that AE counts in

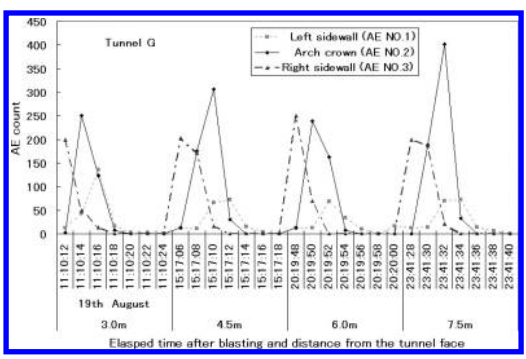


Figure 16. AE activities for about 5 seconds after the first 4 seconds following blasting in tunnel G.

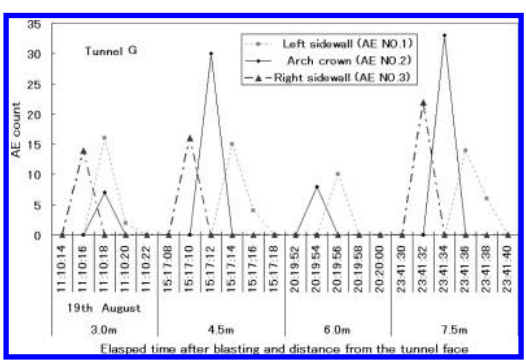


Figure 17. Relation between AE activities and the locations of the face after blasting in tunnel G (2 seconds interval).

Copyright © 2005 Taylor & Francis Group plc, London, UK

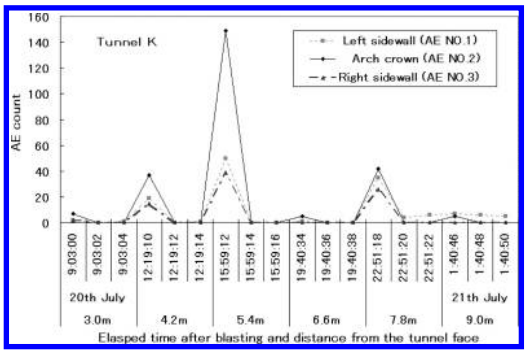


Figure 18. AE activities for about 5 seconds after 4 seconds following blasting in tunnel K.

the second half has a maximum value when the tunnel face distance is about 0.5D. Furthermore, the AE activities in the crown (AE-NO.2 station) are higher than those in the sidewall stations (AE-NO.1 and 2).

5 CONCLUSIONS

From this study, the following conclusions may be drawn as follows:

(1) A portable laser distance-meter could measure the convergence of tunnel S caused by the landslide.
(2) By installing AE counting systems near the landslide plane and on tunnel lining, the delay time between rainfall and AE responses of landslide and tunnel lining can be measured and there is a time delay of about 48 hours in this particular case.
(3) The real-time stability of the tunnel face may be assessed using AE counting system during the excavation.
(4) When the tunnel face is stable, AE activities nearby the tunnel face ceases within about ten seconds.
(5) The AE activities in the second half of ten seconds period may be indicators that the rock mass surrounding the tunnels is stable.
(6) The AE activities have a maximum value when the tunnel face distance is 0.5D.
(7) This AE system is useful for monitoring not only the stability of tunnels but also of other rock engineering structures. One of such systems has been already set up to monitor the landslide in Turkey since 2002 (Tano et al. 2003a) and in Egypt (Tano et al. 2003b). A wireless type AE system may be also useful for real time monitoring for assessing rock burst phenomenon in tunnelling.

REFERENCES

Tano, H., Kumsar, H., Aydan, Ö., Ulusay, R. (2003a). Assesment on Babadağ landslide using by simple field measuring systems. Int. Colloquium on Instrumentation and Monitoring of Landslides and earthquakes in Japan and Turkey, Koriyama, (Edited by H. Tano and Ö. Aydan), 1–10.

Tano, H., Aydan, Ö., Ulusay, R., Tokashiki, N., Ito, T., Akagi, T., Yoshimura, S. (2003b). The assessment of the performance of historical rock structures for preservation and restoration. *International Symposium on Industrial Minerals and Building Stones*, Istanbul, 371–379.

Copyright © 2005 Taylor & Francis Group plc, London, UK

A real-time multi-parameter monitoring system for assessing the stability of tunnels during excavation

Ö. Aydan & M. Daido
Tokai University, Shimizu-Orido, Shizuoka, Japan

H. Tano
Nihon University, Koriyama, Japan

T. Tokashiki
Ryukyu University, Okinawa, Japan

K. Ohkubo
Japan Roadway Authority, Tokyo, Japan

ABSTRACT: The real time monitoring of the stability of tunnels are of great importance when tunnels are prone to failure during excavation such as rockbursting or squeezing. It is also known that when rock starts to fail, the stored mechanical energy in rock tends to transform itself into different forms of energy. Experimental studies by the authors showed that rock indicates distinct variations of multi-parameters during deformation and fracturing processes. These may be used for the real-time assessment of the stability of rock structures. An application of this approach was done to the third Shizuoka tunnel of the second Tomei Expressway in Japan. The parameters measured involve electric potential variations, acoustic emissions, rock temperature, temperature and humidity of the tunnel in addition to the measurements of convergence and loads on support members during the face advance. The in-situ stress state was inferred from the AE method and from striations on the faults. In addition, the model tunnels in large rock samples gathered from the tunnel were tested in laboratory to see the multi-parameter responses beforehand. A series of analytical and numerical studies were performed to understand the likely locations of the high stress concentrations by taking into account the in-situ stress state. This article describes the results obtained from the application of the multi-parameter real-time monitoring system for the assessment of the stability tunnels during excavation and their implications in tunneling.

1 INTRODUCTION

Squeezing and rock bursting problems in underground excavations are often encountered and they are major modes of failure in both short-term and long-term (Aydan et al. 1993, 1996, 2001). While squeezing problem is often observed in weak rocks, rock-bursting problem is commonly seen in underground excavations in hard rocks. Rockburst could be particularly a very severe problem during the excavation as it involves detachment of rock fragments with high velocity. Mont Blanc tunnel in France, Gotthard tunnel in Switzerland, Dai-Shimizu tunnel and Kanetsu tunnel in Japan are some of the well-known examples of rock bursting in tunneling. Rockburst problems are also one of the common instability modes in deep mining in hard rocks and numerous examples are reported from South Africa and Canada.

It is known that when rock starts to fail, the stored mechanical energy in rock tends to transform itself into different forms of energy according to the energy conservation law. Some of these transformations involve the electrical potential, magnetic field, heat release, kinetic energy. Recent experimental studies by the authors (Aydan et al. 2001, 2002, 2003) showed that rock indicates distinct variations of multi-parameters during deformation and fracturing processes. This implies that they may be used in the assessment of the stability of rock structures.

A real time multi-parameter monitoring system for assessing the stability of underground structures has been developed and it has been applied to the third Shizuoka tunnel, which is a part of the second Tomei Expressway under construction (Figure 1). The multi-parameter measurement system involve electric potential (EP) variations, acoustic emissions (AE),

Copyright © 2005 Taylor & Francis Group plc, London, UK



Figure 1. Location of Shizuoka third tunnel along Tomei Expressway alignment.

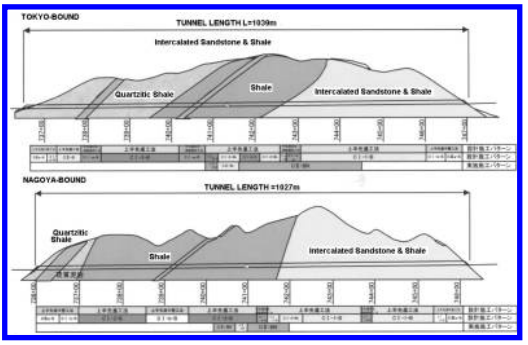


Figure 2. Geology and overburden along the tunnel alignments.

rock temperature (RT), temperature and humidity of the tunnel in addition to the measurements of convergence and loads on support members. The initial in-situ stress state in the vicinity of the tunnel was determined by using the AE method and stresses inference technique from fault striations on the faults. Besides these, the model tunnels drilled into large rock samples gathered from the tunnel used to measure the multi-parameters under laboratory conditions and a series of analytical and numerical studies were performed to understand the likely locations of the high stress concentrations by taking into account the in-situ stress state. This article describes the outcomes of the application of the multi-parameter real-time monitoring system for assessing the stability of tunnels during excavation in addition to various laboratory tests and in-situ explorations. The possibility of the developed multi-parameter system to actual underground excavations is also discussed.

2 GEOLOGY

The geological cross-sections of the Tokyo-bound and Nagoya-bound tunnels are shown in Figure 2. The Rock formations are mainly intercalated sandstone and shale, shale (wrongly named as mudstone on the basis its age) and quartzitic shale. The tunnels pass through the Sasayama tectonic line. The rock formations are folded and folding axis is aligned NW-SE. The layers steeply inclined (300/60–80) and dips NW. The angle between the strike of layers and the alignement of tunnels ranges between 20–30°. The layer thickness generally varies between 30–100 cm.

3 INITIAL STRESS STATE

The tunnels are linear structures and the stress measurements are very rare unless some rockburst problems occur. The stress state of the tunnel, however, must be known for design purposes. It is a common practice that the tunnels are almost designed and constructed without knowing the initial stress state, although very complex stability analyses are performed under some certain assumptions. One of the problems associated with initial stress measurements is the cost of performing such measurements. Since the current methods are generally expensive, some methods with low cost must be developed. The AE method is one of the promising methods for a such purpose and the authors group have initiated such a program in a very large scale in Turkey and Japan (Aydan et al. 2002, Ulusay et al. 2003, Watanabe et al. 2004). In addition to the AE method as a direct method, the first author developed a method to infer the stress state from geological features such as fault striations, folding, kinking, focal plane solutions of earthquakes (Aydan 2000a, 2000b, Aydan et al. 2002, Aydan and Kim 2002, Aydan and Tokashiki 2003). Oriented rock samples parallel, perpendicular to layering were gathered from the tunnel and tested under laboratory conditions at rock Mechanics Laboratory of Ryukyu University. The overburden was 75 m and the estimated vertical stress was 1.88 MPa and the inferred stresses are given in Table 1.

Table 1. Inferred stresses from AE method.

Minimum horizontal (MPa)	Vertical (MPa)	Maximum horizontal (MPa)
0.70–0.80	1.84–2.25	2.07–2.71

Table 2. Inferred stresses from fault striation.

Normalised minimum horizontal stress σ_h/σ_v	Normalised maximum horizontal stress σ_H/σ_v
0.442	1.236

A fault in the tunnel was observed and its striation was measured as 330/78/155. From this measurement, the inferred stresses are given in Table 2. Comparing

Copyright © 2005 Taylor & Francis Group plc, London, UK

Table 2 and Table 1, the estimated stresses are almost the same. Furthermore, the estimations for the regional stress state reported by Aydan and Kim (2002) are consistent with those given in Tables 1 & 2. The estimated horizontal and vertical stresses on the tunnel cross-section from these results should be close to the hydrostatic stress state.

4 PROPERTIES OF INTACT ROCK AND ROCK MASS

The rock units are sandstone and shale. Some laboratory tests were performed on the samples. The results are given Table 3.

Rock masses along the tunnel alignment are classified as CI and DI on Japan Roadway Authority on the basis of elastic wave velocity and type of rocks. The RMR and Q-system classifications are given in Table 4. These classification results are based on in-situ observations by the first author.

5 STABILITY ANALYSIS

5.1 *Ground reaction response analyses*

The rock mass according to Japan Roadway Authority was classified as CI and DI. The rock mass properties were estimated from elastic wave velocity of rock mass with the use of the Aydan's approach (Aydan et al. 1993, 1996, 2001) for the deepest section of the tunnel for two rock classes (Figure 3). The estimated ground reaction curves are shown in Figure 4. The surrounding rock for CI-Class rock mass should behave elastically and there should not be any stress induced plastic zones around the tunnel. As for DI-Class rock mass the behaviour of rock mass becomes elasto-plastic. However, the displacement of ground terminates after a certain amount. In other words, these estimations indicate that there should be no severe stability problem during the excavation of tunnel.

Table 3. Physical and mechanical properties of intact rock.

Rock	Unit weight (kN/m^3)	Elastic wave velocity (km/s)	Uniaxial compressive strength (MPa)	elastic modulus GPa
Sandstone	25.0–26.6	4.8–5.7	40–46	19.6–24.3
Shale	24.2–25.5	4.6–5.5	24–40	12.9–13.4

Table 4. Classification of rock masses.

Wave velocity (km/s)	JRA class	RMR	Q-value
4.2–4.8	CI	71–74	8.33–10.0
2.0–3.4	DI	57–60	5.2–6.6

5.2 *2D stress analysis*

Next, 2D elastic analyses were carried to see the likely locations due to in-situ stress-induced yielding of rock mass as well as yielding due to existing discontinuities. The original analyses were carried out on three stages of the bench excavation and the results for final stage are only given herein. Figure 5 shows the yield zones for yielding zones for rock mass and discontinuities. As expected from the previous analyses, if there should be any yielding of rock mass, it should be quite limited. The yielding occur only at both side-walls of the tunnel for a depth of about 1 m. As for the yielding zones due to sliding of discontinuity sets with a frictional resistance (Friction angle was taken as 30°) around the tunnel, the yielding zone is much larger and the yielding zone is about 2–3 m. Since the tunnel is supported with 6 m long rockbolts and shotcrete of 150–200 mm thick, these zones should not cause any major problem during the excavation. Nevertheless, the blocks bounded by discontinuities at the crown and shoulders of the tunnel are prone to fall into the tunnel under gravity.



Figure 3. Overburden and analyses section.

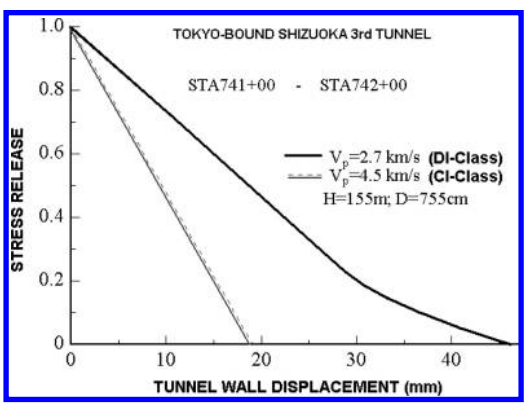


Figure 4. Computed ground reaction curves for DI 6CI Classes.

Copyright © 2005 Taylor & Francis Group plc, London, UK

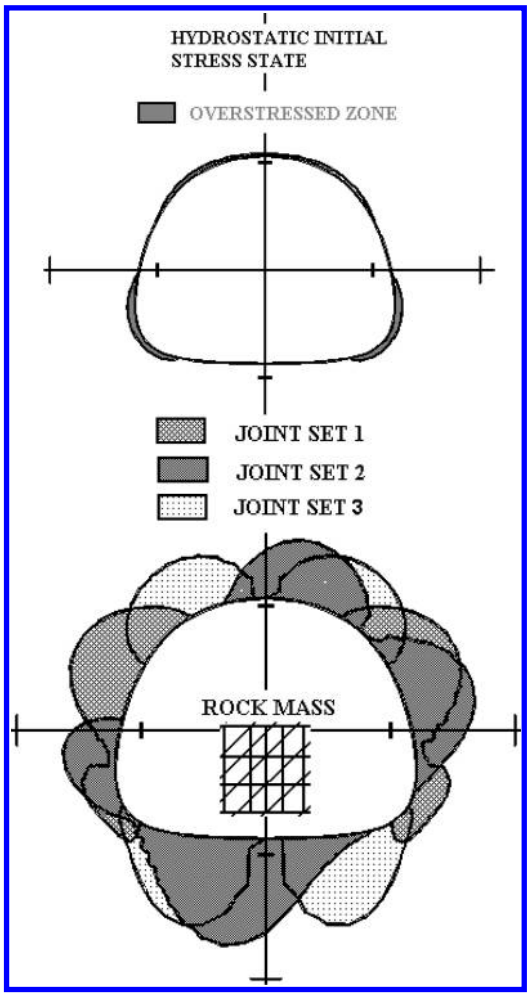


Figure 5. Computed yielding zones around the tunnel.

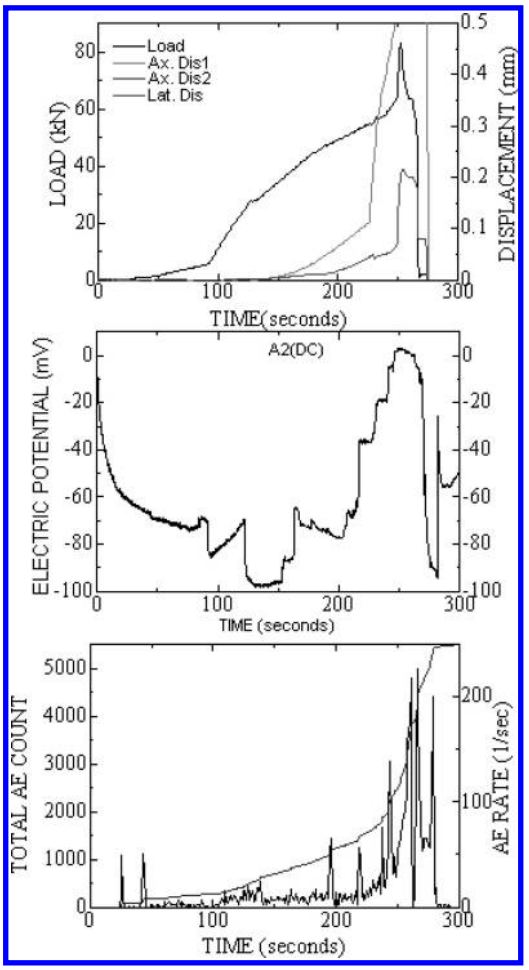


Figure 6. Multi-parameter responses of sandstone sample A2 during deformation and fracturing process.

6 MULTI-PARAMETER RESPONSES

6.1 *Laboratory tests*

Laboratory tests were performed on the multi-parameter responses of sandstone and shale from the tunnel during the deformation and fracturing processes. The multi-parameters were electric potential (EP) variations, acoustic emissions (AE), rock temperature (RT), the load and displacement. Figure 6 shows an example of multi-parameter responses for sandstone sample numbered A2. As noted from the figure, there are distinct variations of acoustic emissions, electric potential during both deformation and fracturing processes. During deformation and fracturing process, it is noted that temperature variations do occur. However, they are not so distinct. It is of great interest that the failure of rock sample occurs after some distinct variations of both acoustic emission and electrical potential. The variation of electric potential takes place earlier than the acoustic emissions. Therefore, they may be considered as some good indicators of the approaching failure event.

6.2 *Model tests*

The model tunnels drilled into intercalated sandstone and shale samples with dimensions of 300 mm high, 200 mm wide and 140–160 mm thick. The model tunnels were 58 mm in diameter. Figure 7 shows an illustration of the instrumentation of a model tunnel sample. Besides the multi-parameter measurements,

Copyright © 2005 Taylor & Francis Group plc, London, UK

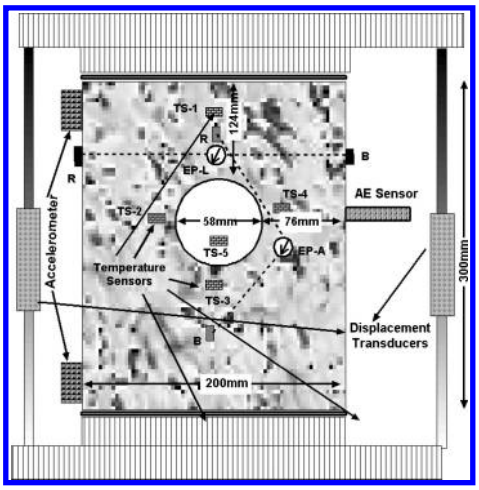


Figure 7. Instrumentation of model tunnel samples.

the samples were instrumented with accelerometers in order to see the induced accelerations, which may be of some value for the estimation of ejection velocity of rock fragments. Two experiments were carried out and the electric potential was measured as either AC or DC due to the limitations of the measuring device. Figure 8 shows the measured multi-parameter responses. Basically, the measured responses show similarity to those observed in uniaxial compression tests and the same conclusions are valid.

7 A MULTI-PARAMETER MEASUREMENT SYSTEM FOR REAL TIME MONITORING

The multi-parameters such as acoustic emission, electric potential and rock temperature in addition to conventional convergence measurements in tunnels are selected for the real time monitoring of the tunnel advance and it was the first application to the real-time stability assessment of tunnels. The tunnel excavation of the tunnel was done through drilling-blasting technique. Each blasting operation causes both dynamic and static stress variations around the tunnel and its close vicinity. Measurements were carried out at two phases. In the first phase, the effect of the face advance of Nagoya-bound tunnel on Tokyo-bound tunnel was investigated. Figure 9 shows the layout of instrumentation. Figure 10 shows the measured AE and electric potential responses as a function of time. Vertical bars in the same figure indicate the blasting operations. After each blasting operation, distinct AE and EP variations were observed. These variations cease after a certain period of time. The electric potential increase simultaneously and tends to decrease as time goes by. AE response also showed the same type

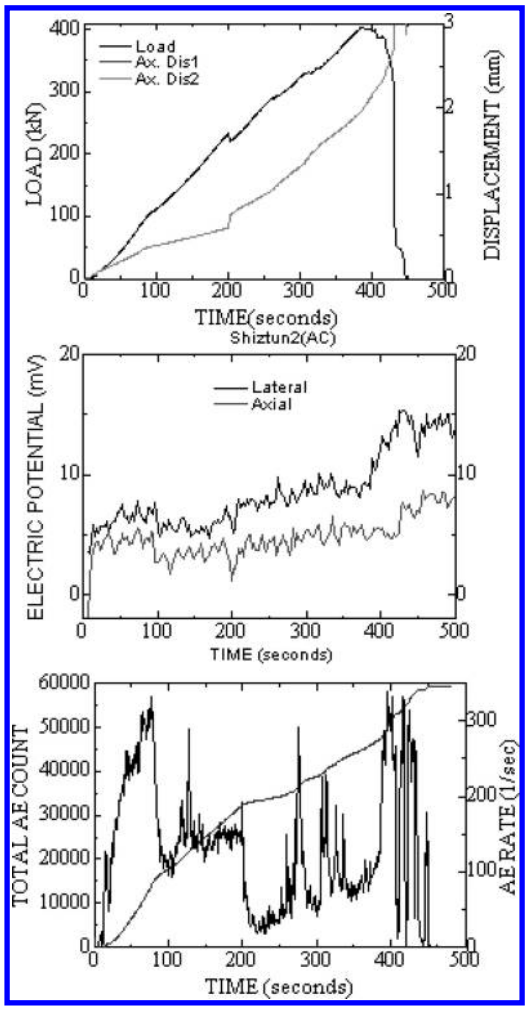


Figure 8. Multi-parameter responses of model tunnel sample Shiztun-2 during deformation and fracturing process.

of response. When the tunnel is stable, it is expected that these variations should disappear on the bases of experimental observations and theoretical considerations by the first author (Aydan et al. 2000, 2001, 2003, Aydan and Daido, 2002).

The second phase measurements were planned to see both the effect of face advance on AE and EP responses in the same tunnel as well as that of adjacent tunnel. Furthermore, two new electric potential measurement devices with higher impedance were used in addition to low impedance electric potential measurement devices. Figure 11 shows the layout of instrumentation and face advance schedule.

The responses of AE and EP are shown in Figure 12 and they were basically similar to those of the first

Copyright © 2005 Taylor & Francis Group plc, London, UK

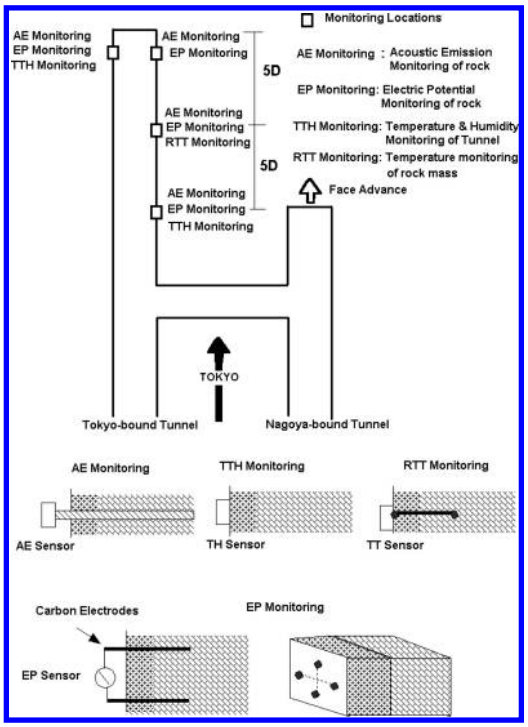


Figure 9. The layout of instrumentation and face advance.

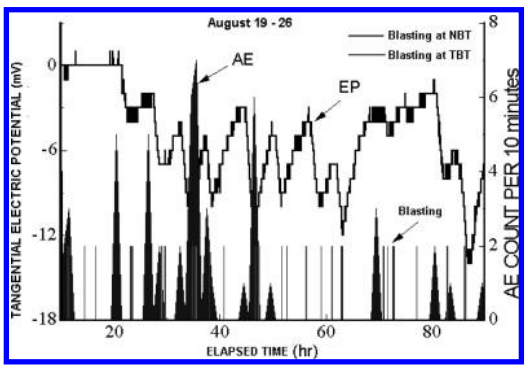


Figure 10. AE and EP responses measured resulting from face advance during the period from August 19 to August 26.

phase. Nevertheless, the amplitude of variations was much larger than those of the previous phase. This was thought to be the closeness of the instruments to the tunnel face where blasting operations were carried out. The electric potential measurements with low impedance and high impedance electric potential devices were almost the same. However, the high impedance electric potential measurement devices are desirable.

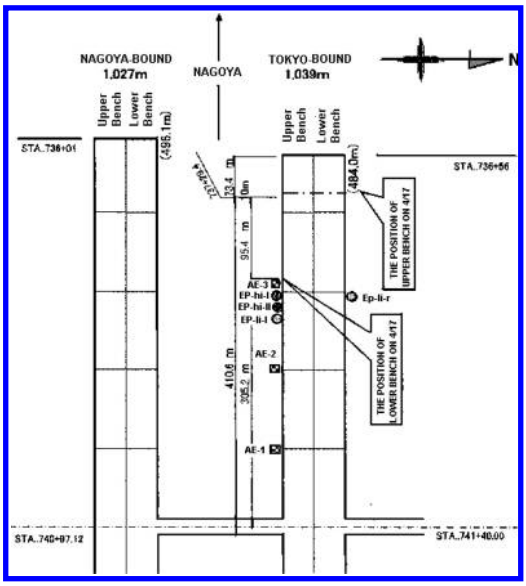


Figure 11. The layout of instrumentation and face advance schedule.

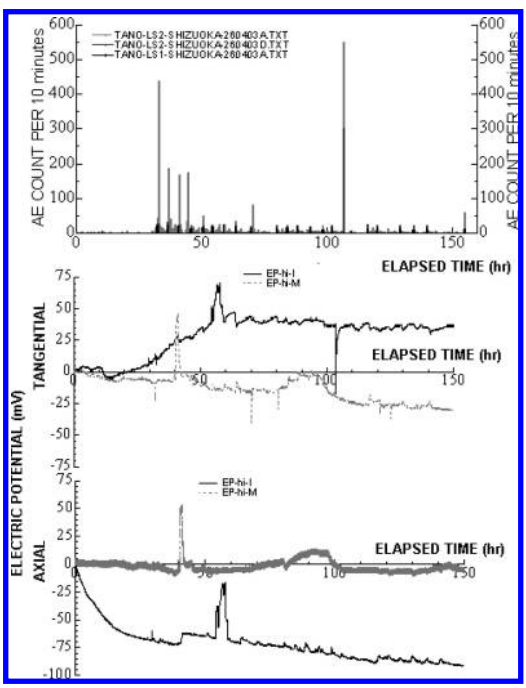


Figure 12. The measured AE and EP responses during face advance.

Copyright © 2005 Taylor & Francis Group plc, London, UK

In addition to that, some problems were noted with the fixation of electrodes into the rock mass and the damage by flying rock fragments during the blasting operation. However, the electric potential variations may sometimes include the far field effects from the deformation of the earth's crust associated with earthquakes. During the measurement of electric potentials an additional device would be necessary outside of the tunnel. In this particular case, such a device was installed at a place about 2 km west of the tunnel.

8 CONCLUSIONS

A multi-parameter real time monitoring system in which acoustic emission, electric potential and rock temperature are measured, is applied to assess the stability of advancing tunnels during excavation. Although the tunnel was statically stable, the blasting operations induced stress and deformation variations in surrounding rock mass, which, in turn, induced both acoustic emission and electric potential variations. Since the tunnels were stable after each face advance, both electric potential and acoustic emission variations ceased after a short period of time. If the tunnels should had been unstable, it was expected to have very large variations of the multi-parameters as observed during the deformation and fracturing of model tunnels in the same rock tested in the laboratory.

ACKNOWLEDGEMENTS

The authors thank Japan Roadway Authority for giving a chance to apply this system to the real tunneling project and the Join Venture consisting of Shimizu and Aoki Construction Companies for their excellent collaborations. Mr. M. Katayose from Japan Roadway Authority and Mr. I. Shimizu are sincerely acknowledged for their help in the installation and maintenance of the system and gathering real-time data.

REFERENCES

Aydan, Ö. (2000a): A stress inference method based on structural geological features for the full-stress components in the earth' crust, *Yerbilimleri*, 22, 223–236.

Aydan, Ö. (2000b): A New Stress Inference Method for The Stress State of Earth's Crust and Its Applications. Western Japan Rock Engineering Symposium, Kumamoto.

Aydan, Ö., and Kim, Y.U. (2002): The inference of crustal stresses and possible earthquake faulting mechanisms in Shizuoka Prefecture from the striations of faults. J. of the School of Marine Science and Technology, No. 54, 21–35.

Aydan, Ö. and Daido, M. (2002). An experimental study on the seepage induced geo-electric potential in porous media. Journal of School of Marine Science and Technology, Tokai University, No. 55.

Aydan, Ö. and Tokashiki, N. (2003). The Inference of crustal stresses in Ryukyu Islands. *Int. Symp Rock stress, Sugawara, Obara & Saito (eds), 349–354.*

Aydan, Akagi, T. and Kawamoto, T. (1993). Squeezing potential of rocks around tunnels; theory and prediction. *Rock Mechanics and Rock Engin*eering, **26**(2), 137–163.

Aydan, Ö., Akagi, T. Kawamoto, T. (1996). The squeezing potential of rock around tunnels: theory and prediction with examples taken from Japan. *Rock Mechanics and Rock Engineering*, **29**(3), 125–143.

Aydan, Ö., Kumsar, H. and Ulusay, R. (2001). How to infer the possible mechanism and characteristics of earthquakes from the strations and ground surface traces of existing faults. *Workshop on Seismic Fault Induced Failures*, Japan, 153–162.

Aydan, Ö., Minato, T. & Fukue, M. (2001). An experimental study on the electrical potential of geomaterials during deformation and its implications in Geomechanics. 38th US Rock Mech. Symp., Washington, Vol. 2, 1199–1206, 2001.

Aydan, Ö., Geniş, M., Akagi, T. and Kawamoto, T. (2001). Assessment of susceptibility of rockbursting in tunnelling in hard rocks. Int. Symp. on Modern Tunnelling Science and Technology, IS-KYOTO, Vol. 1, 391–396.

Aydan, Ö., Ito, T., Akagi, T., Watanabe, and H. Tano, H. (2002). An experimental study on the electrical potential of geomaterials during fracturing and sliding. Korea-Japan Joint Symposium on Rock Engineering, Seoul, Korea, July, 211–218.

Aydan, Ö., Tokashiki, N., Ito, T., Akagi, T., Ulusay, R. and Bilgin, H.A. (2003). An experimental study on the electrical potential of non-piezoelectric geomaterials during fracturing and sliding, 9th ISRM Congress, South Africa, 73–78.

Watanabe, H., Tano, H., Aydan, Ö., Ulusay, R., Tuncay, E. and Bilgin,A. (2003). The measurement of the in-situ stress state by acoustic emission method in weak rocks. *Int. Symp* on *Rock stress, Sugawara, Obara & Saito (eds,), 389–402.*

Ulusay, R., Tuncay, E., Watanabe, H., Tano, H. and Aydan, Ö. (2003). The measurement of the stress state of Turkey by Acoustic Emission (AE) method. *Int. Symp* on *Rock stress, Sugawara, Obara & Saito (eds,), 255–260.*

Copyright © 2005 Taylor & Francis Group plc, London, UK

Immersed tunnels

Copyright © 2005 Taylor & Francis Group plc, London, UK

Hydrodynamic forces on immersed tunnel elements during transportation and foundation

B.P. Rigter
Ministry of Public Works and Water Management, Civil Engineering Division, Utrecht, The Netherlands

D. Schwanenberg
WL|Delft Hydraulics, River Engineering and Morphology, Delft, The Netherlands

ABSTRACT: The elements of immersed tunnels generally are constructed in a separate building pit, where they are prepared for the FTIF-process (Flotation, Transport, Immersion, Foundation). This paper deals with hydraulic forces on a tunnel element during transportation phase and temporary foundation phase caused by passing ships.

If tunnel elements have to be transported through waterways of limited cross-section the drag force on the elements may become very high.

After the element is placed on its temporary foundations but is not yet backfilled, passing ships will exert hydraulic forces on the tunnel element. These forces can sometimes become very high and could move the element from its foundation.

From new experiments it appears that these forces are higher during the passage of the bow of the ship than during the passage of its stern.

In this paper a theory is presented which explains both phenomena.

1 INTRODUCTION

In the seventies of the past century the elements of an immersed tunnel, which were constructed in a separate building pit, had to be towed through a small river with tidal movement to the trench where they were immersed. As the dimensions of the elements were impressive (50 m wide, 7.5 m high and 110 m long) compared to the dimensions of the river (100 m wide at the bottom, variable depth due to the tidal wave between 8.5 m and 10.0 m) and as the water in the river flows with considerable velocities, which also change direction due to the tidal movement, it was decided to perform laboratory investigations in order to estimate the forces necessary to control the elements during the transportation phase.

It resulted that the drag coefficient was very sensitive not only to the blockage ratio (which was expected) but also to the Froude Number of the river (De Reus 1973; Glerum et al., 1976).

Some years after these experiments the first author developed a one-dimensional theory, which explains this behavior (Rigter 1989). In the second section the outlines of the theory will be presented.

When tunnel elements are immersed on their temporary foundations they are for some time unprotected by the future backfill and thus could be exposed to dangerous forces due to passing ships. Eysink (1978) has developed a gracious mathematical model to estimate the forces on the tunnel element and its temporary foundations, which was verified by measurements. The third section describes the main elements of this mathematical model.

This model was developed further to account for various parameters (Eysink & de Jong 1993). During the construction of a recent tunnel in the harbour of Rotterdam doubts arose concerning the validity of this further developed model. Therefore the Civil Engineering Division of the Ministry of Public Works and Water Management decided to have a closer look at the problem. A CFD-consultant was commissioned to simulate the flow pattern, pressures and forces around and on a tunnel element on temporary foundations in a trench during the passage of a ship with a blunt bow. Furthermore Delft Hydraulics was commissioned to verify the simulations with experiments in a hydraulic model.

It appeared that the measured forces differed much both from the CFD calculations and from the further developed Eysink model. However the theory developed by the first author to estimate the drag coefficient of towed tunnel elements appeared to be applicable to

Copyright © 2005 Taylor & Francis Group plc, London, UK

this case as well. The fourth section describes the experiments and the application of the "drag" theory.

2 THE "DRAG" THEORY FOR TUNNEL ELEMENTS IN RESTRICTED WATER

The towing force F on a floating element in water is generally expressed as:

$$F = \frac{1}{2}\rho A_T C_D u^2 \tag{1}$$

where ρ = specific mass; A_T = area of "wet" tunnel cross section; C_D = drag coefficient and u = velocity of element relative to the water.

For wide and deep water the drag coefficient is a constant indeed (provided the Reynolds Number is high enough), but for elements in restricted water this appears not to be the case. In order to derive an expression for the drag coefficient in this case we consider the water-element system in Figure 1.

If the friction force between the water and the profile of the waterway is neglected the towing force F equals the hydrostatic forces in the cross sections 1 and 5 plus the transport of momentum:

$$F = \rho g (h_1 - h_5) A_w + \rho A_w u^2 - \rho A_{w5} u_5^2 \tag{2}$$

where g = gravitational constant; h_1, h_5 = water levels or hydrostatic heads in cross sections 1 and 5; A_w = cross section area of the waterway in cross section 1; A_{w5} = cross section area of the waterway in cross section 5; u_5 = water velocity in cross section 5.

In order to determine the difference in water level $h_1 - h_5$ various sections of the water-element system are discerned and on each section either the theorem of Bernoulli (conservation of energy) or the theorem of Newton (conservation of momentum) is applied.

In the section between the cross sections 1 and 2 it is supposed that the streamlines detach from the "bow" of the tunnel element. Figure 2 shows a detailed scheme of the contraction of the streamlines That is why the water particles will be accelerated even more than when the streamlines would remain attached. In this section the loss of energy is supposed negligible, thus "Bernoulli" can be applied. Due to the acceleration there will be a considerable drop of the hydraulic head in cross section 2.

Of course the pattern of this contraction under the "bow" of the element will be different from that in the horizontal plane. Therefore the contraction coefficient μ, used in this paper must be considered as "averaged". A contraction coefficient μ means that the water in cross section 2 only is transported through the confined area $\mu(A_{wT} - A_T)$, where A_{wT} is the area of the cross section of the waterway in sections perpendicular to the axis of the tunnel element. Applying "Bernoulli" on the section between cross sections 1 and 2 yields an expression for the drop of hydrostatic head:

$$h_1 - h_2 = \left[\left(\frac{\beta}{\mu(1-\beta)\beta_0}\right)^2 - 1\right]\frac{u^2}{2g} \tag{3}$$

where $\beta = A_T/A_{wT}$; and $\beta_0 = A_T/A_w$.

Note that due to the squat of the tunnel element, which in this one-dimensional consideration is equal to the lowering of the water level at the sides of the tunnel element, the blockage ratio β in flowing water is higher than in stagnant water where it is β_0.

In the section between cross sections 2 and 3 water is retarded and energy is dissipated. "Newton" can be applied, supposing that the hydraulic pressures in the planes 2 and 3 are hydrostatic. The result is:

$$h_2 - h_3 = -2(\mu - \mu^2)\left(\frac{\beta}{\mu(1-\beta)\beta_0}\right)^2 \frac{u^2}{2g} \tag{4}$$

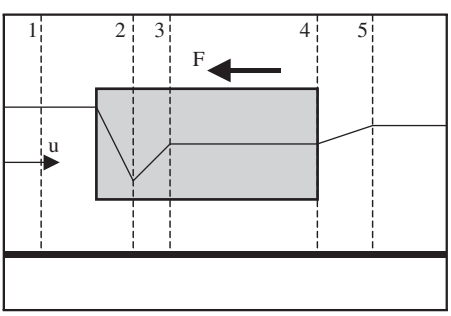


Figure 1. Schematization of the system of water and tunnel element, with sections.

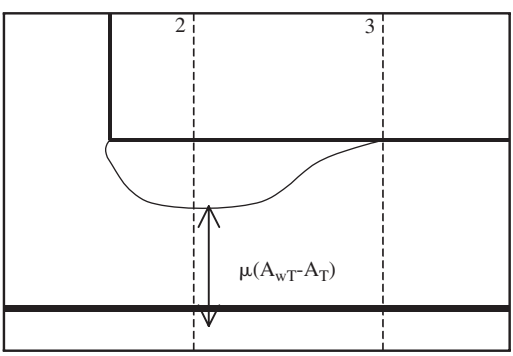


Figure 2. Detail of contraction of streamlines and reattachment.

Copyright © 2005 Taylor & Francis Group plc, London, UK

In the section between cross sections 3 and 4 friction forces act between the hull of the element and the water and also between water and the profile of the waterway. For very long elements and a high blockage ratio these friction forces might become important, but normally they are negligible. In this paper they are neglected as well.

Finally in the section between cross sections 4 and 5 retardation losses occur and only the momentum equation can be applied, assuming hydrostatic pressure in the cross sections 4 and 5. The result is:

$$h_4 - h_5 = -2\left(\frac{\beta}{(1-\beta)\beta_0}\right)\frac{u^2}{2g} + \frac{u_5^2}{g} \tag{5}$$

Summation of Equations 3, 4 and 5 yields an expression for $(h_1 - h_5)$ which can be substituted in Equation 2. This yields:

$$\frac{F}{\rho g A_w} = \left(\frac{\beta}{(1-\beta)\beta_0}\right)^2\left[\left(\frac{1-\mu}{\mu}\right)^2 + \left(1 - \frac{(1-\beta)\beta_0}{\beta}\right)^2\right]\frac{u^2}{2g} \tag{6}$$

Finally eliminating F from Equations 6 and 1 yields this expression for the drag coefficient C_D:

$$C_D = \left(\frac{\beta}{(1-\beta)\beta_0}\right)^2 \frac{1}{\beta_0}\left[\left(\frac{1-\mu}{\mu}\right)^2 + \left(1 - \frac{(1-\beta)\beta_0}{\beta}\right)^2\right] \tag{7}$$

At moderate velocities and moderate blockage ratio the blockage ratio β will not differ much from the blockage ratio at zero velocity β_0, then Equation 7 reduces to:

$$C_D = \frac{1}{\beta_0(1-\beta_0)^2}\left[\left(\frac{1-\mu}{\mu}\right)^2 + \beta_0^2\right] \tag{8}$$

Equations 7 and 8 show both the influence of the blockage ratio β and the influence of the contraction coefficient μ on the value of the drag coefficient.

It is also possible to derive an equation for the vertical balance. When the effect of the contraction on the squat of the tunnel element is neglected, assuming that the length of the contraction is small compared to the length of the tunnel element, it can be shown that the relation between the squat of the element (which is the same as the depression of the water level) and the blockage ratio is:

$$\frac{h_1 - h_3}{\bar{h}} = \frac{\beta - \beta_0}{\beta} \tag{9}$$

in which $h = A_w/B$ with B: the width of the waterway at water level. Summation of Equations 3 and 4 yield an expression for $h_1 - h_3$ and this inserted in Equation 1 finally yields:

$$Fr = \sqrt{\frac{2\left(\frac{\beta-\beta_0}{\beta}\right)\left[\frac{(1-\beta)\beta_0}{\beta}\right]^2}{\left(\frac{1-\mu}{\mu}\right)^2 + 1 - \left(\frac{(1-\beta)\beta_0}{\beta}\right)^2}} \tag{10}$$

where Fr $(=u/\sqrt{gh})$ is called the Froude Number.

Equation (10) gives a relation for the actual blockage ratio β and the Froude Number. The tunnel element will have a greater squat (or greater blockage ratio β) when the contraction is greater (smaller μ). Also β increases with increasing Fr.

Together with Equation 7 it is then possible to make graphs for the drag coefficient as function of the Froude Number and the blockage ratio in stagnant water (β_0). By choosing a certain value for the contraction coefficient it is possible to explain all the values measured in the experiments.

3 FORCES ON A TUNNEL ELEMENT ON TEMPORARY FOUNDATIONS DURING PASSAGE OF SHIPS

When an element of the immersed tunnel has been immersed it is placed on temporary foundations in the trench. In this situation the stability of the element is quite poor and therefore can be sensitive to hydrodynamic forces due to the passage of ships. As port authorities only allow the closure of the waterway for navigation for a very short period, it is necessary to consider these dynamic forces. The theory presented by Eysink and De Jong (1993) is schematized is Figure 3.

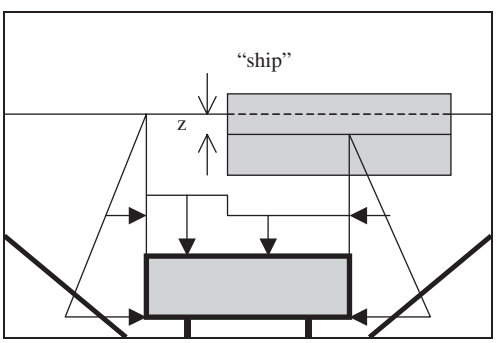


Figure 3. Hydrodynamic pressures on tunnel element during passage of a ship.

Copyright © 2005 Taylor & Francis Group plc, London, UK

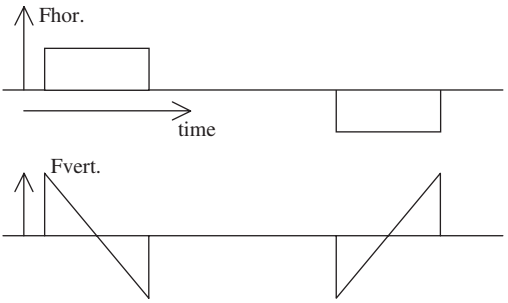


Figure 4. Theoretical time history of horizontal and vertical force fluctuations during ship passage.

The passing ship causes a depression "z" of the water level. This causes a drop in the hydrostatic pressure at the top of the tunnel element equal to ρgz. Also there is a difference in water pressure between the sidewalls of the tunnel element. Finally water pressure under the tunnel element is supposed to vary linearly according to the laws of movement of water through slits. These pressures cause horizontal and vertical forces as well as moments. The time histories of the resulting horizontal and vertical forces are as shown in Figure 4.

The value z of the depression of the water level is found using one of the methods developed to calculate return flow and water level depressions caused by ships in restricted water (e.g. Bouwmeester (1977)). None of these methods takes into account the loss of energy at the front of ships as described in section 2 of this paper. Moreover it is assumed that the water level at the stern is equal to that before the bow, which is only possible for self-propelling ships. Therefore the time histories of the forces on the tunnel element are essentially asymmetric as shown in Figure 4.

In the course of time, at the occasion of several more investigations the theory has been adapted to take into account effects due to asymmetrical sailing ships and variation of the water level across the width of the waterway, introduction of a "mass coefficient", and a more detailed schematization of lowering of the water level along the length of the ship. The resulting calculating tool is called FORTUN. However the effect of possible losses of energy at the bow of the ship on the depression of the hydraulic head was not taken into account.

4 CFD AND HYDRAULIC MODEL STUDY WITH SHIP WITH BLUNT BOW

4.1 *Set up of the study*

Due to the questions raised during the construction of a recent tunnel in the harbour of Rotterdam, it was decided to set up a fundamental study. As the theoretical model described in the previous section is based on more or less simple one-dimensional considerations it was concluded to simultaneously apply a three dimensional Computer Fluid Dynamic models (CFD) to make use of the rapid developments in this field. One of the problems however is that not only the water flows relative to the waterway and the tunnel element in the trench but also the ship moves relative to both the water and the waterway. Nevertheless a CFD-consultant offered to try and calculate the pressures and forces exerted by a passing ship on a tunnel element in a trench. In order to verify the CFD-simulations it was decided as well to perform experiments on a physical hydraulic model using the same boundary conditions as applied in the CFD-simulations.

As it already was clear that the forces on the tunnel element would be especially important when a ship with a blunt bow was used it was decided to use a completely rectangular (shoe box model) ship. The other relevant dimensions of the "prototype"situation were:

Channel width:	225 m
Channel depth:	10 m
Ship width:	22 m
Ship draught:	7 m
Ship length:	150 m
Tunnel element width:	33 m
Tunnel element height:	8.40 m
Trench depth:	11.75 m
Blockage ratio β_0:	0.055
Velocity water:	1.0 m/s

Various runs were performed with different values for the speed of the ship, varying between 2.90 m/s downstream and 2.90 upstream.

The model scale for the hydraulic model was 1:50 resulting in a velocity scale of 1:7.

The tunnel element was provided with several pressure sensors as well as horizontal and vertical force sensors.

The CFD model was as well set up to calculate the pressures using the same dimensions as the physical hydraulic model.

4.2 *Results of model measurements*

4.2.1 *Water level depressions*

A full report of the model investigation is described in Verheij, Schwanenberg & Sprengers (2002). From the pressure sensors on the roof of the tunnel element it appeared that they all could be characterized by an extreme drop in pressure just after the passage of the bow. During the passage of the ship the pressure remains relatively constant. After the stern of the ship has passed the element the pressure increases but not to the original level. Figure 5 shows a typical time history of the pressure measured on the roof.

Copyright © 2005 Taylor & Francis Group plc, London, UK

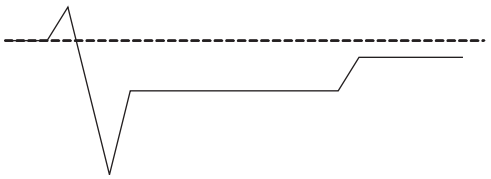


Figure 5. Typical time history of pressure measured on the roof.

This is in accordance with the schematization of the hydraulic level as schematized in Figure 1 of this paper. The first author (Rigter 2002) has shown that Equations 3, 4 and 5 predict the time history very well using a contraction coefficient of 0.75. The only feature not mentioned in section 2 of this paper is that just before the bow passes the pressure sensor the pressure increases somewhat.

This increase is related to the stream pattern in front of the bow where water is urged to change direction from the middle of the bow to the side of the ship. This causes a stagnation of the water just in front of the bow and this, according to Bernoulli gives rise to an over pressure of the order of $^1/_2\rho u^2$. Also this formula appears to be correct.

4.2.2 *Horizontal forces*

The time history of the measured horizontal force can be characterized as shown in Figure 6.

Comparison with Figure 4 shows that during the passage of the bow the horizontal force is much higher than during the passage of the stern. Moreover there is at first a sharp peak, followed by a lower value. The occurrence of the peak is in full accordance with the sharp drop in hydrostatic head under the bow due to the contraction of the streamlines. This is illustrated in Figure 7. Furthermore during the passage of the stern of the ship at first there is a negative force, which is lower than the average (positive) force during passage of the bow. This can be explained by the fact that the difference in water levels at the bow is higher than at the stern. Finally after the passage of the stern there remains a horizontal force, witch is logical as the external force, which moved the ship causes a difference in water level before and behind the ship in accordance with Equation 2. Calculations by the first author (Rigter 2002) show good agreement between theory and measurements.

Thus it appears that the theory of the high drag coefficients is also applicable to the case of dynamic forces on tunnel elements on temporary foundations during the passage of ships. It should be noticed that in the case the ship has its own propulsion the time history of the horizontal force would be more in accordance with the Eysink theory.

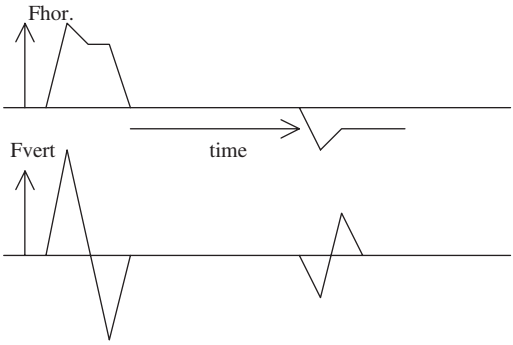


Figure 6. Typical time history of horizontal and vertical forces on tunnel element as measured in experiments.

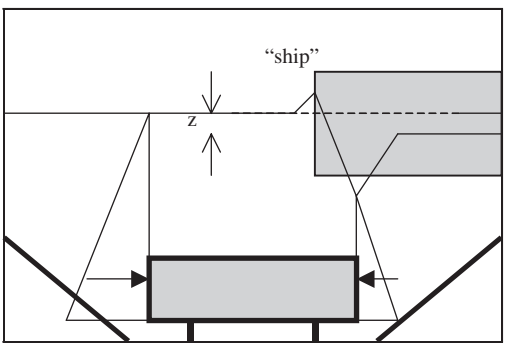


Figure 7. Explaining the peak value of the horizontal force.

4.2.3 *Vertical forces*

As regards the vertical force it is seen that during passage of the bow this force is much higher than during the passage of the stern. This can be attributed as well to the sharp drop in hydraulic head under the bow.

4.3 *Comparison of measurements with results of CFD and FORTUN calculations*

As regards the CFD calculations it was concluded that the results were very unclear. This applies to both the pressures and the forces. When the forces are compared to the results of the hydraulic model differences up to 100% are found. For cases with low relative velocities the differences are even greater.

Calculations also were performed with the FORTUN programme. Also this program resulted in important differences. As explained in section 4.2 this mainly must be attributed to the facts that FORTUN does not take into account the contraction effect at the bow, neither is fit for ships that are towed!

Copyright © 2005 Taylor & Francis Group plc, London, UK

5 CONCLUSIONS

1. The detachment of streamlines from blunt bows of ships and towed tunnel elements causes a drop in hydraulic head and a loss of hydraulic energy which increases the squat of the ship and the depression of the water level. Together with the loss of energy at the stern of the ship (or tunnel element) it causes a high value of the drag coefficient, which is dependent on the Froude Number and the blockage ratio.
2. The theory of detachment of streamlines also can be applied to determine the hydrodynamic forces on tunnel elements on temporary foundation during the passage of (big) ships.
3. We do not know of a CFD-program that effectively can reflect the time history of pressures and forces on tunnel elements during the passage of ships.
4. FORTUN is not fit for reproducing the time history of pressures and forces on tunnel elements during the passage of ships due to ships with blunt bows and external propulsion. Nevertheless it will do for common ships with streamlined bows, which have their own propulsion.
5. In order to gain better insight in the reality of the hypothesis of detachment of streamlines detailed research is necessary.

REFERENCES

Bouwmeester, J.1977. Calculation of return flow and water level depression, New method. In *Proc. XXIV PIANC Congress Leningrad*: 148–151. PIANC.

Glerum, A., Rigter, B.P., Eysink, W.D. & Heins, W.F. 1976. *Motorway tunnels built by the immersed tube method.* The Hague: Government Publishing Office.

Eysink, W.D. 1978. *Immersion of the Botlek tunnel, forces on and displacements of tunnel elements due to flow forces. Report M 1458.* Delft: WL | Delft Hydraulics.

Eysink, W.D. & Jong, R.J. de. 1993. Forces due to ship maneuvering during immersion of tunnels. In H. Burger (ed), *Options for Tunnelling*: 291–302. Elsevier Science Publishers.

Reus, J.H. de 1973. *Road tunnel at Dordrecht, hydrodynamic behaviour of the tunnel elements, Report M 1169*. Delft: WL | Delft Hydraulics.

Rigter, B.P. 1989. *Forces on floating objects in restricted water.* Not published.

Rigter, B.P. 2002. *Analysis model measurements pressures and forces on immersed tunnel element during passage of a ship*. Not published.

Verheij, H.J., Schwanenberg, D. & Sprengers, C.J. 2002. *Validation tests forces on immersed tunnels by passing ships, Report Q2550*. Delft: WL|Delft Hydraulics.

Copyright © 2005 Taylor & Francis Group plc, London, UK

Marmaray project: requirements for the design and construction of the Bosphorus tunnel

L.C.F. Ingerslev
Parsons Brinckerhoff Quade & Douglas, Inc., New York, USA

H. Sakaeda
Pacific Consultants International, Japan

M. Takahashi
Oriental Consultants, Japan

Raymond Castelli
Parsons Brinckerhoff Quade & Douglas, Inc.

ABSTRACT: This paper addresses requirements that must be met during the design and construction of the immersed tunnel. The Bosphorus and the historic city of Istanbul are located in a highly seismic zone. Important elements of the Employer's Requirements that form part of the design-build contract are discussed. Some of the requirements for the Bosphorus tunnel are highly project specific, yet give the Contractor latitude for choice. The paper also outlines the geotechnical requirements, the seismic conditions and how they are to be applied, and how these and other loads are to be applied to the immersed tunnel structure. Other requirements particular to this immersed tunnel are also discussed.

1 INTRODUCTION

The 50 m deep Bosphorus is an international waterway that connects the Black Sea to the Sea of Marmara, with the European side of Istanbul on one side, and the Asian side on the other (Figures 1 & 2). The existing rail systems on each side of the Bosphorus are to be upgraded to a commuter rail system connected by a tunnel. While that tunnel descends through soft ground into rock each side of the Bosphorus, an immersed tunnel is used to traverse the very soft deposits beneath the Bosphorus and thereby to connect the two rock tunnels.

Two single-track tunnels are each to be capable of operating in either direction. The immersed tunnel will accommodate the two tunnels within one structure.



Figure 1. Bosphorus tunnel location.



Figure 2. Bosphorus tunnel alignment (end to end).

Copyright © 2005 Taylor & Francis Group plc, London, UK

Besides the tunnels, there will be three underground stations. Floodgates are to be provided each side of the Bosphorus to prevent any unexpected flooding from affecting the land tunnels and below-ground stations.

Since this is a design-build project, most of the Employer's Requirements have been written to give the contractor considerable flexibility in achieving the required fitness for purpose. This is the overriding requirement of the tunnel, fitness for purpose.

Considerable emphasis is placed on safety and the ability to escape in case of emergency, complying with NFPA 130. Furthermore, no point in the immersed tunnel is to be more than 62.5 m from a point of access to a place of refuge or egress. Escape into the adjacent train tunnel using the emergency walkways and cross-passage doors or cross passages into the other train tunnel will comply.

2 UNUSUAL FEATURES

This immersed tunnel is special in a number of ways. It will be the deepest immersed tunnel. Its nearest rival, BART in San Francisco, has 40.5 m water depth to underside of structure, whereas this tunnel will have almost 60 m. Structures have to be watertight ignoring the mandatory waterproofing membrane, an additional protection. If the membrane does not adhere to the concrete (e.g. a steel membrane), ribs anchored in the concrete must compartmentalize the surface to facilitate the repair of potential leaks.

The 3 to 6 knot constant current through the Bosphorus is driven by the head difference between the Black Sea to the north and the Sea of Marmaray to the south that leads ultimately to the Mediterranean; consequently, there are almost no tidal effects. Differences in salinity between the two seas cause a 1 to 2 knot contra-flowing current at depth and a turbulent layer between them.

The North Anatolian Fault (N.A.F.), which is not only active but also expecting a 7.5 Richter seismic event within 40 years in the Istanbul area, lies only about 16 km to the south of the immersed tunnel. The soft soil conditions appear to be such that some potential for liquefaction exists at the immersed tunnel location even though the ends will be in rock.

The tunnel will be used for freight as well as passengers and is to have a two hour 100 MW fire rating for the Rijkswaterstaat hydrocarbon curve, and a four hour rating for the harmonized curve. Where the partial loss of the tunnel structure can compromise the safety of passengers within it, such as beneath the Bosphorus, the train tunnels must have fire insulation over the ceiling and walls. There must be no spalling of concrete beneath the insulation, and concrete and reinforcement temperatures are limited.

The concept design of 1985, like other historical designs before it, envisaged the bored tunnels meeting a connecting structure (ventilation building and access shaft) at the western shore with an immersed tunnel beyond. At the shoreline, the open trench would be about 53 m deep, half in rock. Such an excavation would have been unprecedented and is viewed today with skepticism taking into account nearby utilities, the adjacent current and that the existing slope is probably at its maximum angle of repose. The bidding documents therefore left it to the Contractor to determine the optimum location and method to transition between tunnel types. The suggested location for each end of the immersed tunnel in the bidding documents was therefore shown only just sufficiently into rock to allow safe rock tunneling. The successful bidder elected to terminate the immersed tunnel at the transition between soft ground and rock, resulting in a limited quantity of rock excavation. The transitions between the immersed tunnel and adjoining bored tunnels are therefore offshore at both the European and Asian sides of the crossing.

The ends of the immersed tunnel are in deep water where the sides of the Bosphorus rise rapidly. Bored tunnels will connect directly to the immersed tunnel without any interface structure. The ends of the immersed tunnel will be designed such that tunnel boring machines can bore directly into them. This has been done before in Hong Kong for the 1977 transit (MTRC) tunnel across Victoria Harbour between Admiralty and Tsimshatsui, and is also being proposed for a new rail tunnel across the Hudson River in New York. Two immersed tunnels under the Tama River in Tokyo, Japan (Ref. 1) also connect to bored tunnels, but do so through pneumatic caissons as connecting structures.

Once protection is placed over the top of the immersed tunnel, it is customary to allow natural siltation to fill any remaining trench. However, environmental issues related to maintaining the delicate saltier-fresher water ecosystem within the Bosphorus requires the original bed profile to be reestablished on this project. Similar ecosystem issues were faced on the Øresund project at the entrance to the Baltic.

Another challenge will be excavation and backfill. Due to the great depth (up to nearly 60 m) and high currents, southwards in the upper layers and northwards in the lower layers, it will be difficult to determine exactly where operations are taking place at bed level, and therefore how complete such operations are. A rigid connection such as provided by a trailing cutter-suction dredger will identify bed location, but operating and control in such currents would then be the challenge. Similar challenges would occur if placing backfill using tremie pipes.

Construction of the immersed tunnel must also contend with the extremely heavy navigation traffic at

Copyright © 2005 Taylor & Francis Group plc, London, UK

the location of the crossing. This traffic includes frequent ferry services connecting the European side of Istanbul to various points on the Asian side, as well as heavy cargo ship traffic transiting the Bosphorus, a designated international waterway between the Black Sea and the Sea of Marmara.

3 SOIL CONDITIONS

An initial soil exploration between the two shores took place in 1985–1987, using conventional drilling methods with Standard Penetration Tests and undisturbed Shelby tube samples. These conventional techniques for the testing and recovery of soft materials at depth were problematic and yielded unreliable results. Undue reliance cannot be placed therefore on the results of those early tests. To assist bidding contractors in interpreting earlier results and to provide additional data, a drill ship was commissioned in 2003 to carry out additional borings, the results of which were available before the contractors' tenders were due. The selected contractor is required to commission more soil exploration at design-specific locations, such as at the transitions between the immersed and bored tunnels.

The findings of the initial and pre-tender phase geotechnical investigations are described by Simsek, et al (2005). In general, the principal soil strata anticipated along the tunnel horizon include very soft to soft silty clay for a distance of about 500 m from the European end of the immersed tunnel; then loose to dense sand with interlayering of firm to stiff sandy clay layers and shell deposits for a distance of about 800 m; then variable deposits of sand, gravel, cobbles and boulders for a distance of about 100 m to the Asian end of the immersed tunnel. Rock at both ends of the immersed tunnel consists of moderately to highly fractured, interbedded sandstone, siltstone and mudstone (shale), locally designated as the Trakya formation. Generally, the rock is moderately strong, but contains faulted and sheared zones with low to very low strength, as well as local zones of more competent, higher strength dyke intrusions.

4 GEOTECHNICAL ISSUES

The Contractor faces challenges in maintaining stability of underwater slopes, particularly in the soft silty clay on the European side of the crossing. In addition, the excavation in this area is adjacent to underwater utility lines that must be protected from movement during construction. Where utility lines, shore protection and marine and historic structures are located within the influence of tunnel construction, underwater slopes are to be designed using limit state for a minimum factor of safety of 1.3 for temporary conditions and 1.4 for permanent. In addition, cut slopes at all areas are to be no steeper than 1 vertical:2 horizontal in soil, nor 4:1 in rock. For underwater areas that do not impact existing structures or utilities, the Contractor is required to design the permanent slopes with a minimum factor of safety of 1.3.

Of particular concern so that the final alignment is fit for rail traffic are the expected movements of tunnel elements from the time they are placed. Estimates of the foundation rebound due to excavation of the overburden soils, and of the recompression of the foundation soils including the foundation course (as a result of the installation of the tunnel and backfill materials) are required so that the placement level at which to set the tunnel can be calculated. In addition, the contractor is required to estimate both short term and long term settlement and potential longitudinal and transverse differential settlements within each tunnel element, between adjoining tunnel elements, and at the transitions to the bored tunnels at the ends of the immersed tunnel. If the tunnel element cannot be designed to accommodate the resulting stresses, mitigating measures must be employed. Measures could for example include changing joint locations or joint type. The magnitude of the potential movements may also require additional tolerances to the internal dimensions to ensure that a viable track profile can be obtained.

Tunnel design must also consider post-earthquake seismic settlement in the foundation soils. Seismic design issues are discussed in further detail by Wang, et al (2005), and summarized in the following section of this paper.

Preliminary analyses of the subsurface investigation data indicated that deposits of loose to medium dense sand on the eastern portion of the crossing may be susceptible to liquefaction to a depth of 10 m, or more, below the tunnel base level. The contractor is required to further evaluate the liquefaction potential of these soils, and to design mitigation measures, if necessary, to prevent liquefaction. Such measures may include stone columns, sand compaction columns, or compaction grouting. The implementation of mitigation measures and the corresponding quality control procedures are greatly complicated by the water depth (approximately 40 m), the strong current, and the reversed direction of flow at depth.

The contractor must provide trench backfill material that is free-draining and not susceptible to liquefaction, even when loosely placed under water. This requirement is necessary to avoid the risk of floatation of the tunnels during a high level earthquake event.

Strict measures are required to minimize dispersion of fines during excavation and backfill. Fish migration occurs during spring and autumn and at different water levels; operations will need to be modified or curtailed to minimize effects on migrating fish.

Copyright © 2005 Taylor & Francis Group plc, London, UK

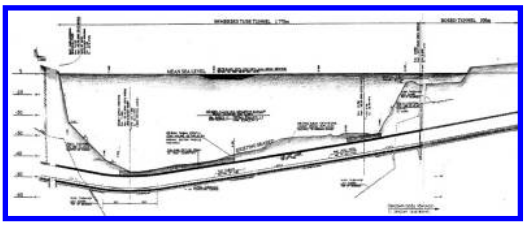


Figure 3. Bosphorus tunnel profile.

Surficial soils to a depth of about 3 m along a length of approximately 600 m of the immersed tunnel alignment on the European side of the crossing have been found to be contaminated. These contaminated soils will be dredged and disposed of in a confined disposal facility. All other dredged material will be disposed of in a designated deep water site in the Sea of Marmaray.

5 SEISMIC CONDITIONS

The seismic hazards at the project site are dominated by the "Characteristic Earthquake" associated with segments of the North Anatolian Fault (N.A.F.) located within the Sea of Marmara rather than by various other line or zone sources; because of the quiescent period on these segments of the fault since the mid 1700s, there exists a substantial probability of occurrence of a major earthquake in the Sea of Marmara area during the service life of the project. As a result, the intensity of the high-probability event (functional evaluation earthquake, FEE) is approaching that of the low-probability event (safety evaluation earthquake, SEE), resulting in a single design basis earthquake (DBE) for this project. The DBE is defined as an Mw = 7.5 (moment magnitude) earthquake occurring within the Sea of Marmara at a location that is 16 km from the immersed tunnel site.

Seismic loads to be applied include any dynamic earth pressures and/or hydrodynamic pressures during an earthquake, earthquake loads in the form of ground deformations during shaking, and post-earthquake loads due to permanent ground movements such as post-liquefaction settlements and lateral spread, if applicable. Furthermore, the facility is to remain operational following an earthquake, allowing not more than a few days for inspection. Hence, structural elements have to be designed in such a way that, in the post-elastic range, damage and deformations are controlled and the structural elements are ductile. Tunnel elements and joints must remain watertight during and after the earthquake.

Sets of site-specific design ground-motion time-histories for bedrock outcrops were derived for appropriate shortest distances to the N.A.F. (ranging from 13 to 21 km) and provided as design data. Each set comprises three components, two horizontal and one vertical bedrock ground-motion time histories for acceleration, velocity, and displacement. All three components have to be applied simultaneously. Furthermore, the effect of spatial variations of ground motions on long structure such as the immersed tunnel that results from the effects of wave passage and local soil overburden also needs to be considered.

The site at the immersed tunnel location is underlain by deep soil deposits with highly variable characteristics. The presence of the deep soil overburden can modify the bedrock motions considerably as they travel both horizontally and vertically to the soils surrounding the tunnel, necessitating site-specific site response analysis for this project. There are several analysis methods available for evaluating the effect of local soil conditions on ground response during earthquakes, including the equivalent-linear one-dimensional total stress method (e.g. SHAKE), the non-linear one-dimensional total and effective stress method, the two- and three-dimensional equivalent-linear total stress methods (e.g. 3-D FLUSH), and the two- and three-dimensional non-linear total and effective stress methods.

The soils surrounding the immersed tunnel have to be investigated to determine their vulnerability to liquefaction and liquefaction-induced settlements, lateral spread and slope stability problems. Liquefaction can cause uplift and flotation of the immersed tunnel. The tunnel backfill materials will have to be designed to be resistant to liquefaction. Empirical procedures by Seed and Idriss (or Japan's Design Specifications for Highway Bridges) can be used for liquefaction potential evaluations. These procedures are based on standard penetration test blow counts or cone penetrometer testing data. Even if tunnel flotation/uplift is not an issue, post-liquefaction settlements and lateral spread of foundation soils after the shaking ends can be a major concern and must be considered in the design. Sufficient extra space may therefore be needed in the internal cross-section for a new serviceable rail alignment to be established, depending not only upon total settlements but also upon differential settlements and horizontal displacement.

Where liquefaction may occur and/or movements are too large, ground improvement will be necessary. One way of achieving this is to change the soil properties and thereby minimize the liquefaction potential, perhaps most easily achieved by installing sand compaction piles or other similar ground improvement methods. Sand compaction piles have been installed before in deep water in Japan. Additional measures may include providing free draining aggregates to allow excess pore water pressure to escape. The aggregates need to be placed beneath the immersed tunnel and up the sides to the bed surface. This method

Copyright © 2005 Taylor & Francis Group plc, London, UK

was used for the 1984 Kaohsiung Harbor Tunnel in Taiwan and for tunnels in Japan. Measurement of the actual improvement achieved to validate the methods used is a requirement for this project.

Steep underwater soil slopes, such as that at the western shoreline, may be susceptible to seismically-induced landslides. Were that to happen, a very large surcharge could suddenly arrive on top of the immersed tunnel. It is vital that any potential for such slope instability be identified and either designed for or mitigated. Out in the Sea of Marmara, there are steeply shelving slopes extending down to a depth of 1000 m at the N.A.F. that are also potentially unstable. Landslides there can trigger tsunamis and there is historical evidence that Tsunamis have affected Istanbul. With a period of about 5 minutes and an estimated height of 4 m at the tunnel location, a tsunami is not expected to have a significant effect on the immersed tunnel, though effects at the surface and on the tunnel scour protection may be significant. At the low-lying Üsküdar Station at entrances susceptible to tsunami effects, flood doors are required that close if such a flood were to occur and emergency exits are to be provided above predicted flood level.

The overall sliding stability of the immersed tunnel transversely during and after the design basis earthquake must also be checked. Factors influencing this may include dynamic earth pressures and hydrodynamic pressures against tunnel walls, inertial force of the dead load, the potential for lateral movement of the tunnel in gently sloping ground in either liquefied or soft soils, and strength degradation potential in soils below, adjacent to and over the tunnel structure (such as strength reduction in cohesive soils and excess pore pressure or liquefaction in granular soils).

6 IMMERSED TUNNEL FOUNDATIONS

Some immersed tunnels are placed on a prepared foundation while others are placed on temporary supports and the foundation completed below the tunnel. In poor ground the tunnel may even be founded on piles. If the immersed tunnel foundation is not continuous bedding, e.g. piles or temporary supports, then the individual supports have to be adjustable during the construction phase to ensure even support. Continuous foundations must be at least 500 mm thick. Foundations after placement of the immersed tunnel have been completed using sand flow, sand jetting, or grouting (usually within bags).

On this project, the foundation and backfill up to the seabed are to be free-draining to assist in preventing the development of excess pore-water pressure (and hence liquefaction) within the soils adjacent to and below the immersed tunnel during and following an earthquake.

Armour protection to the tunnel backfill is to be provided to prevent erosion at the sides and on top of the tunnel. For environmental reasons, the final bed level is to restore the original seabed profile. Anchor release bands either side of the tunnel are to form part of this to force a dragging anchor over the top of the tunnel.

7 TUNNEL STRUCTURES

The general procedure for seismic design of tunnel structures is based on the ground deformation approach. During earthquakes, tunnel structures will move together with the surrounding geologic media and must therefore be designed to accommodate the deformations imposed by the ground. The effects of soil structure interaction should be taken into account, especially in soft soils.

Three primary modes of deformation occur during seismic shaking: racking, axial and curvature deformations. The racking deformation is caused primarily by seismic waves propagating normal to the tunnel longitudinal axis for which vertically propagating shear waves are often considered the most critical. The axial and curvature deformations are induced by components of seismic waves that propagate along the longitudinal axis and/or by spatially varying ground motions resulting from local soil/site effects.

When modeling the length of the structure for overall behavior, particular attention must be paid to discontinuities such as at flexible joints between immersed tunnel elements, between immersed tunnel elements supported on different foundation conditions (e.g. piled, grouted, rock and soil), at changes in section where there is a significant change in the type of construction. Relative motion across such discontinuities may differ significantly. It is essential to consider in detail the effects of these discontinuities on the earthquake resistance of the structure, as well as to the abilities of these discontinuities to remain watertight during and after earthquakes. A three-dimensional finite element/difference structural model can be developed along the tunnel axis to do this, with the soil represented by discrete springs onto which the seismic ground motions can be imposed. Any non-linear behavior of the soil needs to be reflected in the springs. The ultimate frictional (drag) resistance between the tunnel and the surrounding soil must be accounted for in deriving the longitudinal spring parameters to permit slippage, should it occur.

Both temporary structures and permanent structures under construction must be designed to resist at least 50% of the DBE design load.

Safety is especially important for a tunnel that is as deep as this one is. The external pressure of 5 to 6 bar results in higher general level of stress than is

Copyright © 2005 Taylor & Francis Group plc, London, UK

usually encountered in immersed tunnels. It was therefore considered important to try and keep concrete stresses low by having as much structural concrete as possible. Hence a decision was made not to permit the usually octagonal "double-shell" type of tunnel where some of the concrete is placed by tremie and is non-structural.

For single-shell and sandwich-type immersed tunnels where the outer structural steel shell also serves as a membrane for waterproofing, an additional condition is that a minimum shell thickness of 10 mm must exist throughout the design life of the tunnel. Furthermore, critical design stresses in that membrane are permitted only for temporary loadings during construction, such as during outfitting, towing and placing.

In considering the effects of applied loads during normal operating conditions, the tunnel is naturally to remain fully serviceable without damage (full performance level). Under extreme loads such as sunken or stranding ships, anchor impact, ship collision, flooded tunnel, train derailed with collision, explosion and fire, it is anticipated that the tunnel may be closed. However, full performance level is also required with no more than light damage needing minor repairs, and only brief interruptions to public traffic, perhaps minor leaks, and above all effectively no significant loss of service under the most adverse combination of events. Under the design-basis earthquake (DBE) predicted for the location and the resulting movement of soils, the result is to be no worse than a limited performance level with intermediate damage, repairable over not more than 12 months, limited emergency and public traffic within hours, limited leakage, full lighting and ventilation, and essentially normal public traffic restored within a few days despite ongoing repairs. This is a tough requirement, but necessary because of the high likelihood that the DBE will occur within 40 years and the tunnel is to function for at least another 60 years. Above all, primary structural members have to be designed to be ductile in the overload range with no shear failures.

For the purposes of long term monitoring, each immersed tunnel element is to have permanent embeddable reference electrodes as well as a corrosion monitoring system for the structural steel and/or reinforcement at or near the external surface. In concrete immersed tunnels, embeddable corrosion monitoring probes are also required at about 500 m intervals to monitor the ingress of aggressive chloride ions through the cover concrete. The design of the tunnel elements is also to provide for possible future impressed-current cathodic protection of the structural steel and/or reinforcement at or near the external surface of the tunnel. For that to be effective, the various layers of reinforcement and exposed steel on the exterior have to be electrically isolated from each other. Electrical continuity is required within each layer of reinforcement, although each immersed tunnel element is to be electrically isolated from adjacent elements (unless rigid joints are used with the steel plate continuous on the outside).

The internal size of the tunnel has to incorporate tolerances for construction, installation and settlements as well as potential displacements due to a seismic event. Furthermore, differential settlements may result in an angular change at a joint and extra space may be needed to ensure that a satisfactory rail alignment can be achieved. Direct track fixation is required in all tunnels, but it must also be capable of adjustment following a seismic event. At joints where an angular rotation or a displacement is possible, such as at seismic joints, track may need to be "floating" so that the change occurs across a manageable distance.

8 CONCLUSIONS

The Bosphorus crossing will be the deepest immersed tunnel ever constructed. It also requires offshore transitions to bored tunnels on both sides of the crossing. The project will be constructed as a design-build contract in which the tender documents establish design and performance requirements for the tunnel structure.

Considering the unprecedented depth of the tunnel, provisions were included in the tender documents to assure a waterproof tunnel. Other engineering challenges to be addressed in the design of the tunnel include seismic loading of the structure and liquefaction potential of the foundation soils; liquefaction mitigation of the foundation soils on the Asian side of the crossing; settlement and stability of soft cohesive soils along the European side of the crossing; and differential settlement due to variable foundation conditions and at the transitions to the bored rock tunnels on both sides of the crossing; design of tunnel joints to accommodate anticipated tunnel displacements; and designing the trench backfill material to resist liquefaction.

Construction issues include excavation control in the deep waters of the Bosphorus; tube segment placement with difficult currents and ship navigation conditions; rock excavation at the end transitions; dredging and disposal of contaminated soils at the European side of the crossing; trench excavation and foundation preparation in deep water; placing, positioning and linking the tube elements; and placement of the trench backfill materials in the adverse underwater conditions while protecting the marine environment.

The design-build contract was awarded to the Joint Venture team of Taisei, Kumagai, Gama and Nurol (TKGN) in September, 2004. The project is scheduled for completion in 2008.

Copyright © 2005 Taylor & Francis Group plc, London, UK

REFERENCES

Simsek, O., Castelli, R. J., and Mitani, S. (2005), "Bosphorus Crossing: Geological and Geotechnical Investigations," International Tunneling Association (ITA) World Tunnel Congress, Istanbul.

Wang, J., Erdik, M., Otake, S., Tanal, V., Ozerkan, Z., and Pehlivan, S. F., (2005), "Seismic Hazards Assessment and Earthquake Resistant Design Considerations for the Bosphorus Tunnel Project," International Tunneling Association (ITA) World Tunnel Congress, Istanbul.

State-of-the-Art Report, 1997 International Tunnelling Association Immersed and Floating Tunnels Working Group, second edition, Pergamon Press, Oxford, 1997.

Copyright © 2005 Taylor & Francis Group plc, London, UK

Marmaray project: designing an immersed tunnel for the Bosphorus

L.C.F. Ingerslev
Parsons Brinckerhoff Quade & Douglas, Inc., New York, USA

H. Sakaeda
Pacific Consultants International, Tokyo, Japan

M. Takahashi
Oriental Consultants, Tokyo, Japan

ABSTRACT: The rail tunnel under the Bosphorus will be the deepest immersed tunnel yet constructed. Unlike most other similar tunnels, the strong currents in the Bosphorus are relatively unaffected by tides. This paper discusses how the local conditions and the design requirements affect the actual design and construction of the immersed tunnel. Options are evaluated as to permissible types of tunnel and its method of construction, i.e. steel composite construction or reinforced concrete, and why shape could be important. Details of particular significance include water tightness and waterproofing, main principles regarding joints, and installation issues. Handling of structural issues such how the structure can accommodate seismic effects, external pressure, and resistance to fire are described.

1 INTRODUCTION

A companion paper *Requirements for the design of the Bosphorus Tunnel* addresses requirements particular to the Bosphorus that must be met during the design and construction of the immersed rail tunnel now under construction. This paper looks at the immersed tunnel and considers how it might be designed to meet these stringent requirements.

2 TUNNEL TYPE

Two main types of immersed tunnel have emerged, known as steel and concrete. The two types contain about equal quantities of concrete but differ in construction methodology. Steel tunnels use structural steel, usually in the form of stiffened plate, working compositely with the interior concrete, whereas concrete tunnels do not, relying on steel reinforcing bars or prestressing cables. The number of concrete tunnels constructed is almost twice that of steel tunnels. Steel tunnels can have an initial draft of as little as about 2.5 m before concrete is placed afloat, whereas most concrete tunnels have almost no freeboard because they are usually complete before being floated out. Tunnel cross-sections may have flat faces or be curved. Straight tunnel elements with flat faces will result in the cheapest formwork. However, under high external hydrostatic pressures, transverse moments and shears are reduced as the exterior cross section becomes more nearly circular such as is shown in Figure 1.

Historically, concrete tunnels have been circular, or curved with a flat bottom, but the predominant shape has been rectangular, which is particularly attractive for wide highways and combined road/rail tunnels. In Europe, Southeast Asia and Australia, virtually all immersed tunnels are concrete. In Japan, steel and concrete tunnels are in approximately equal numbers. Most tunnels in North America are steel tunnels.

Steel tunnels have been circular, curved with a flat bottom, and rectangular (particularly in Japan), but

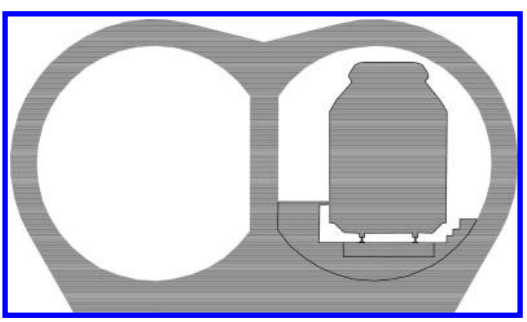


Figure 1. Illustrative design.

Copyright © 2005 Taylor & Francis Group plc, London, UK



Figure 2. Construction of the BART tunnel shells.



Figure 3. Ted Williams tunnel shells arrive at Boston.

the predominant shape in the past in the US has been a circular shell within an octagonal shape, with ventilation ducts above and below the roadway, either in single tube or binocular versions. This arrangement of ventilation ducts may change, since current techniques permit the use of longitudinal ventilation in much longer tunnels, often obviating the need for separate ventilation ducts. Most or all of the concrete in steel tunnels is placed while the steel shell is afloat, in direct contrast to concrete tunnels that are virtually complete before being floated out. The order in which concrete is placed afloat for a steel tunnel must be tightly controlled to minimize deformations and the resulting moments. Construction joints in the concrete are areas of weakness in all tunnels and can be vulnerable to leakage, particularly if the external membrane is punctured. Steel tunnels can be categorized into three sub-types.

Single shell tunnels have the external structural shell plate working compositely with the interior reinforced concrete and the shell plate requires corrosion protection. The BART tunnel is typical of this type.

The so-called steel double-shell tunnel has an interior circular structural shell plate that works compositely

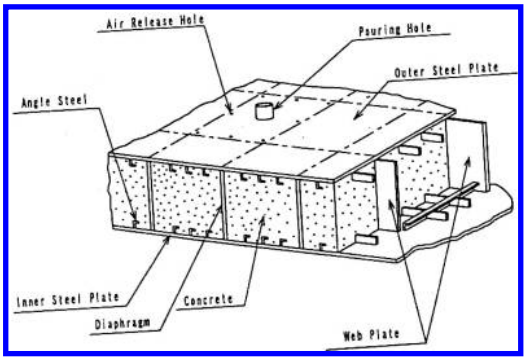


Figure 4. Japanese “sandwich” construction.

with reinforced concrete within it and is protected by external concrete placed within non-structural steel form plates. This shape has also been used in pairs for several tunnels, the most recent being Ted Williams in Boston, Massachusetts. Double shell tunnels are only found in the USA.

The newest form of tunnel, a recent development in Japan, is the “sandwich”, wherein internal steel diaphragms form the connection between structural steel face plates, both internal and external, and the space between them is subsequently filled with unreinforced non-shrink self-compacting concrete. Naha Port and Kobe Port tunnels are constructed by this method, the latter being the first steel tunnel to carry three lanes per duct.

The type of immersed tunnel selected is often dictated by a number of factors that could include local custom, familiarity to the designer, availability of fabrication facilities, contractor experience, suitability of the final product, safety, and cost. Whilst a concrete tunnel and all three types of steel tunnel are considered viable for the challenging conditions of the Bosphorus, the relative advantages and disadvantages of each type were compared, together with the fact that this tunnel will be placed deeper than previous immersed tunnels and in fast flowing water. The steel double-shell tunnel was considered less desirable than the other types for two reasons and therefore eliminated as a permissible type. Firstly, because the overall height might be higher than other types so that a lowering of the rail profile might be required. Secondly, because the structural concrete ring must be thinner than for concrete in a single shell or sandwich-type tunnel due to the weight of external tremie concrete provided; stresses will therefore be higher in the structural concrete ring than for other types of steel tunnel.

For the Bosphorus, it was decided to allow contractors to have freedom of choice in selecting the tunnel shape. However, the illustrative conceptual design that was included with the bidding documents was circular and is shown in Figure 1. There was no obligation

Copyright © 2005 Taylor & Francis Group plc, London, UK

to mimic this example and at the time of writing this paper, the successful contractor has elected to design a rectangular concrete tunnel with an overall width of about 15.3 m (Fig. 6).

In order to maximize the use of available facilities at Tuzla belonging to the Employer, the Contractor's proposed construction method is more akin to that of a steel tunnel in that the end bulkheads and the steel waterproofing membrane on the soffit and sides, suitably stiffened, are to be constructed in pairs in a small graving basin, sufficiently deep so that the elements can be floated out after the lower half of the concrete is placed. The tunnel elements are then to be floated out and towed to the adjacent harbour, made available by the Employer, and the remaining concrete placed there while the elements are afloat. The proposed tunnel element is designed as reinforced concrete with the steel waterproofing membrane not acting compositely with the concrete.

3 SIZING THE TUNNEL

A comprehensive transportation study by the Turkish Ministry of Transport and Communications concluded that, in the long term, Istanbul required a tunnel across the Bosphorus connecting the European and Asian rail networks. Rail operations dictated that it be a two-track tunnel primarily for commuter rail but which will also carry inter-city trains and freight. The dynamic gauge is sized to accommodate both the UIC 506 GC structural gauge and Turkish rolling stock, and assumes overhead catenary traction power. Besides rolling stock, items required within the internal tunnel space for the Bosphorus tunnel include:

- Line-side cables 320 × 555 mm each side
- Radiating cables 840 × 200 mm
- Traction power feeders 200 × 100 mm
- Overhead line equipment fixings 400 × 300 mm
- Return current cables 150 × 150 mm
- Earth wires 150 × 150
- Tunnel drainage
- Drainage sump discharge pipe
- Water supply pipes for firefighting
- Surveillance cameras
- Signals (0.5 × 1 m above walkway)
- Wayside telephones 150 × 400 mm
- Other miscellaneous wayside equipment
- Tunnel lighting
- Emergency egress illuminated signs at low level (so that they are not in smoke)
- Escape walkway 0.9 m above track 1.4 m wide and 55 mm clear of the kinematic gauge
- "Squeezeway" opposite the escape walkway, as a safe refuge for staff as trains pass, 0.5 m wide clear of the structure gauge
- Fireproofing of the walls and ceiling.

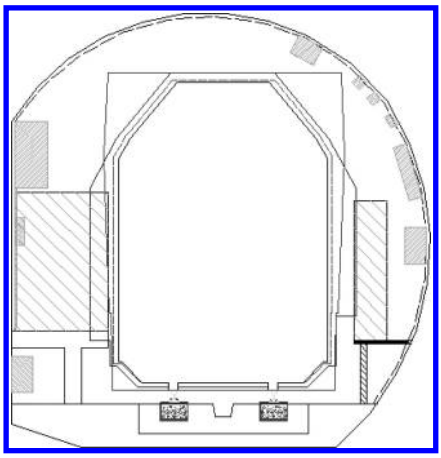


Figure 5. Space Requirements.

Additional space is also required for construction tolerances, installation tolerances and to ensure that the alignment still fits after backfill, differential settlements, and during and after seismic events. While difficulties can be expected with installation due to the great depth and strong currents in the Bosphorus, these very issues may result in greater attention being paid to methodology and therefore greater control; perhaps placing may end up being more accurate? Items that can fit within the walls and floor include emergency doors and cross passages, fire fighting panels, emergency equipment, sumps and pumps.

Having thus defined the minimum internal space, calculations have to be made to determine whether ventilation and safety requirements to meet NFPA 130 are adequate. Conceptual design for the illustrative section indicated that the internal space even around a stalled vehicle may be adequate. Preliminary estimates of structural thicknesses can then be made, taking into account the needs to be able to make the tunnel both float and stay submerged, as appropriate to the construction stage. It is important at this stage to have real data relating to the density not of only the concrete to be used but also of the water at the surface and at depth. This work will require the design of the immersion, seismic and other joints, as well as the weight of typical bulkheads and other fittings needed during floating and immersion.

The cross-section design then needs to be evaluated to determine what changes can be made to simplify construction, to reduce reinforcing steel requirements, to optimize for economy the reinforcing steel layout, and to minimize cost. This is a vital step that can save the contractor a considerable amount of money. Of particular concern are sharp transitions from soil to rock foundations, and hard spots within the length of a tunnel. Full soil-structure interaction analysis may

Copyright © 2005 Taylor & Francis Group plc, London, UK

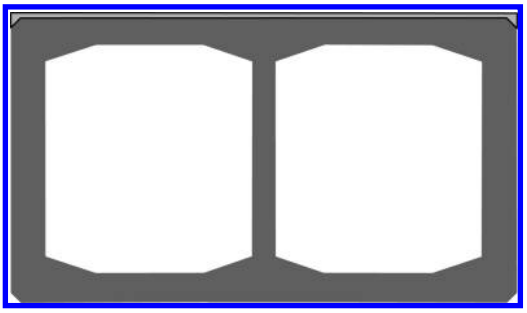


Figure 6. Typical section, Contractor's design.

be needed to identify resulting stresses such that the tunnel structure is reinforced in both directions to accommodate the stresses arising, although removal, mitigating or avoiding the offending problem may be more economical. These issues can also arise from temporary supports to the tunnel if they are not fully released.

Terminal and final joints may then be designed and any further changes to the cross-sections incorporated. In this case, both the engineer and all the bidders proposed that the adjacent tunnels be bored after the immersed tunnel is laid. By making the ends circular and sized slightly larger than the TBM shield, the TBM can be driven right into the ends of the immersed tunnel, as was done for the Wanchai to Tsimshatsui transit tunnel in Hong Kong. Soil in the vicinity of the end of the tunnel may need to be treated to ensure compatibility with the type of TBM and to reduce the risk of leaks.

Immersion joints will need to be designed to carry any shear resulting from differential settlements and to ensure that relative displacements do not affect rail operations. Horizontal and vertical shear keys may be required across the joints if they remain flexible, depending on .movements expected. If the immersion joints are made rigid, then the effects of differential settlements due to variations in thicknesses of the underlying soil layers as well as their stiffness must be thoroughly investigated to ensure that allowable design stresses are not exceeded.

4 SEISMIC DESIGN

The requirements and methodology for seismic analysis of the immersed tunnel is discussed in the companion paper *Requirements for the design of the Bosphorus Tunnel* and will not be repeated here. Needless to say, tunnel structures will be constrained to move together with the surrounding geologic media. Taking soil-structure interaction into account may reduce such movements and hence the induced stresses. Designing a tunnel to meet seismic loads is significantly different from resisting other loads. If a section is overstressed by seismic loads, stiffness may have to be reduced so that the structure may more easily deform to follow the movements of adjacent geologic media. It is also essential that ductility is ensured even in the overload range.

It may be necessary to reduce or eliminate corner haunches if racking deformations cause overstress. For imposed curvature due to longitudinal waves, a reduction in the overall length of a tunnel element between flexible joints can reduce transverse shear stresses. Significant transverse shear at joints may similarly also be reduced, but another option might be to consider eliminating flexible joints if the overall section is able to resist the moments and shears. For a wide section, this may not be possible. After immersion and joint dewatering, the joint can be designed to be as rigid as elsewhere, as was done for the BART tunnel in San Francisco. Longitudinal seismic waves could result in flexible joints opening up. Any such tendency must be resisted, often achieved through the use of short prestressing bars across the joints. Under normal loads such bars may have little or no stress. A number of immersed tunnels have been longitudinally prestressed to about 2 MPa in the belief that this helps to keep incipient cracks closed.

5 EARLY AGE CRACK CONTROL

Due to the depth of the installed tunnel, nearly 60 m to the underside at the deepest point, potential leakage is of great concern. A design requirement is that the concrete must be watertight in its own right ignoring the mandatory waterproofing membrane.

Historically, some of the most vulnerable areas for leakage are the construction joints. Any reduction in the number of construction joints must therefore reduce the risk of leakage. For the Øresund tunnel between Denmark and Sweden, each 22 m tunnel segment was cast in a single operation including floor, walls and roof, which resulted in each tunnel element only having seven circumferential joints. Whilst the Contractor is not proposing to cast the elements in a single operation, the Bosphorus tunnel elements are probably small enough to do so, which would reduce joint locations to the immersion joints only.

Immersed tunnel sections are often about a metre thick and are therefore classified as thick concrete. Early-age thermal cracking is not permitted. For the control of it, there are two important temperature differences:

- the peak temperature rise above that of the adjoining concrete, affecting the external restraint;
- the maximum temperature gradient within the section, affecting the internal restraint.

Copyright © 2005 Taylor & Francis Group plc, London, UK

External restraint causes through-cracking of the concrete with the associated risk of direct leaks. Internal restraint causes surface cracking which will place reinforcement at a high risk of corrosion. Also contributing to early-age cracking are early shrinkage and creep, and settlements. As part of the design process, the Contractor is to document that the planned risk of early-age cracking is acceptable for the ambient climatic conditions that may occur. Temperature and stress analyses by finite-elements are required for this.

For the base slab, potential cracking would be due mainly to external restraint from an adjacent previously placed slab and to temperature gradient between the cold top surface and the hot interior. The foundation can effectively provide a high degree of insulation to the underside. The effects of the steel formwork on the external sides will therefore be of minor importance. The walls will have external restraints along the bottom and along one or both vertical ends when cast against adjacent sections, and internal restraints due to the cooling effects of steel on both faces, assuming steel forms are used internally. Similarly, the roof, if cast separately, will have external restraints on three or four edges and internal restraints due to the cooling effects of the underside steel form and the cold top surface.

In evaluating ways to limit the design temperature rise and hence cracking, at least the following parameters have to be taken into account:

- Section thickness.
- Formwork and insulation. Results of tests to determine conductivity will be needed.
- Ambient conditions (wind, temperature and humidity vary with the season).
- Types and sources of cementitious materials.
- Concrete mix proportions.
- Concrete placing temperature.
- Results of tests to determine adiabatic heat development of the actual concrete.
- Active forms for temperature control such as internal cooling pipes, if used.

Inner walls are often thinner than outer walls and slabs. The thicker sections will have a greater temperature rise and may require more effort to limit cracking. Formwork affects both the temperature rise and the temperature gradient across the section thickness. Although the steel waterproofing membrane, which also acts as a steel form, has high conductivity, the concrete sections are sufficiently thick that the peak temperature will effectively not be reduced.

Clearly, for all surfaces, external insulation can reduce the transverse temperature gradient and hence surface cracking. One of the causes of through-cracking is casting concrete (which gets hot for several days) against cold concrete, i.e. adjacent to construction joints. When the new concrete cools and shrinks, it is restrained by the old cold concrete and can crack. In the past, the joint areas have often been cooled through tubes in the fresh concrete near the joints so that the temperature change at joints is more gradual. This can also be achieved by casting the concrete on successive days while the adjacent concrete is still hot.

Design shade temperatures in Istanbul range between $+31°C$ and $-4°C$ although under extreme conditions the range could be $+41°C$ to $-20°C$. Chemical reactions are at their most virulent during the hottest part of the year, and this is when the temperature differential between the heart of the concrete and the exterior will reach the maximum that can be expected. Use of a low-heat cement and partial cementitious content replacement (for example by PFA) can further reduce the maximum temperature reached. Winds can affect the rate of cooling at the surfaces of the forms, and both wind and humidity affect evaporation and cooling at the exposed concrete surface, though proper curing can compensate for this. For the greatest success in achieving watertight crack-free concrete, protection from wind and sun, limiting the maximum temperature of the concrete while it is being placed and after placement, insulated forms and adequate curing will all be required.

During construction, unless the ground is very hard, relative settlements will occur each time concrete is placed, inducing strain in the freshly set concrete while it is still weak. The construction sequence and timing may become critical if cracking and distortion are to be avoided. Computations are required to demonstrate that resulting stresses are within limits. The Contractor is proposing to place some of the concrete in the tunnel elements while afloat, and this is really the same situation where the ground has become particularly weak (in fact water).

6 INSTALLATION

Life safety is not only to be considered for operation, it is relevant also for construction. Especial care will be required for the design of the temporary bulkheads to ensure sufficient strength and adequate support, as well as a watertight fit. Depths are such that repair from the exterior will be difficult if not impossible. For the same reason, should the immersion joints between the elements for some reason not obtain their initial seal so that the joints can be dewatered, a backup method of obtaining a seal must be designed into the elements.

Although guides can be provided to align the elements as they are brought together, the usual survey tower to locate the element from above the surface will not be possible. The strong currents acting on the tall tower will tend to force the underlying tunnel

Copyright © 2005 Taylor & Francis Group plc, London, UK

element to rotate. The design will therefore have to incorporate alternate methods of determining and correcting position. Furthermore, access into the tunnel elements is required after immersion. This is most easily achieved at the eastern end of the immersed tunnel section, which is located in the immediate vicinity of Kiz Kulesi (Leander's Tower), using a temporary access shaft installed immediately after laying the first tunnel element. This access shaft will have to be stabilized externally to ensure that the tunnel element below remains in the correct position. Design of the temporary access to the first laid element of the Bosphorus tunnel is therefore crucial to the success of the project and is therefore as important as the design of the elements themselves. Naturally, sealing up of the temporary access when no longer needed will have to be done in a manner that will ensure that it remains watertight for the entire design life.

7 CONCLUSION

From the options available, the Contractor has elected to design a rectangular concrete immersed tunnel with a steel waterproofing membrane on the sides and underside. A relatively shallow drydock will be used to construct the steel waterproofing membrane and to place the concrete in the lower half. After flooding the drydock, the incomplete tunnel element will be moved to the adjacent DLH harbour in Tuzla for completion afloat.

The size of the tunnel internally is governed by space requirements for rolling stock, cables, traction power, utilities and safety requirements as detailed by the Employer. Additional space is required to allow for construction tolerances and expected movements due to settlements and seismic effects. If necessary to ensure that tunnel elements can float, additional space may be required. The train ducts in the terminal elements splay outwards to form circular holes into which tunnel boring machines can be driven directly to complete the tunnels. The immersion joints and their rubber gaskets are temporary and will be made rigid after installation.

Due to the great depth at which the tunnel elements are to be installed, early age crack control to produce a watertight tunnel will be particularly important. High surface currents and a contra-flowing bed current will create challenges for the contractor to overcome for his excavation and backfilling operations, as well as immersion and placing the tunnel elements. As part of the temporary installations, the crucial ability to install and support temporary access shafts in the vicinity of the fourth century Leander's Tower will succeed only if it is an integral part of the tunnel's design.

REFERENCES

Tanal, V. and Grantz, W.C., 1989, Bosporus railroad tunnel crossing design alternatives, *Immersed Tunnel Techniques*, London, Thomas Telford.

State-of-the-Art Report, second edition, 1997, International Tunnelling Association Immersed and Floating Tunnels Working Group, Pergamon.

Ingerslev, L.C.F., Concrete Immersed Tunnels: The Design Process, 1989, *Immersed Tunnel Techniques*, The Institution of Civil Engineers, London, Telford.

Copyright © 2005 Taylor & Francis Group plc, London, UK

Dredged material management in immersed tube tunnel construction

Vahan Tanal
Senior Vice President, Parsons Brinckerhoff, New York, USA

F. Simin Pehlivan
Former Deputy Director General, Ministry of Transport & Communication, General Directorate of Railways, Harbours and Airports Construction, Ankara, Turkey

Jaw-Nan Wang
Senior Engineering Manager, Parsons Brinckerhoff, New York, USA

Zafer Ozerkan
Railway Advisor, Yuksel Proje, Ankara, Turkey

Isikhan Guler
Marine Works Division Manager, Yuksel Proje, Ankara, Turkey

ABSTRACT: Four case histories are described approximately 10 years apart, where unique solutions were implemented in the disposal of dredged materials for immersed tube tunnel construction. The earliest project in the 1970s used the dredged materials to construct a manmade island for the Second Hampton Roads Crossing in Virginia. The second project, the Fort McHenry Tunnel in Baltimore, built in the 1980s, separated clean and contaminated sediments and used the materials to reclaim the nearshore confined disposal facility (CDF) as a modern container terminal. The third, the Ted Williams Tunnel built in the 1990s in Boston Harbor, used large scale solidification/stabilization for contaminated sediments in an upland CDF. The most recent project, the Marmaray Rail Tunnel Crossing under the Bosphorus, will utilize a CDF for contaminated sediments – the first facility of its type in Turkey. The four projects illustrate a dramatic increase in dredging and disposal costs in the past three decades due primarily to continually tightening environmental restrictions. Furthermore, the escalating disposal costs threaten the economic feasibility of an otherwise attractive method of subaqueous tunnel construction.

1 INTRODUCTION

Up until the 1970s dredged sediments were commonly disposed of in specially designated open water disposal sites. In immersed tube tunnel construction, the material dredged to form the tunnel trench would be temporarily stored underwater near the trench. Once the tubes were sunk, the material would be used as ordinary backfill to cover the immersed tubes. In 1980, during the planning and design of the Fort McHenry Tunnel in Baltimore that practice was deemed environmentally unacceptable. It has since become common practice to plan and engineer confined disposal facilities to mitigate negative environmental impacts.

2 SECOND HAMPTON ROADS CROSSING

In 1954, the Virginia Department of Highways and Transportation retained Parsons Brinckerhoff (PB) to design a crossing of the Hampton Roads ship channel. In 1957, the first Hampton Roads Bridge-Tunnel opened, connecting Hampton and Norfolk, Virginia across the James River, a major shipping channel. Twelve years later, in 1969, the firm was once again retained to provide design and construction inspection services for a parallel second crossing to meet increasing traffic demands. The Second Hampton Roads Crossing was opened to traffic in 1976.

The second crossing was composed of a 1,930-meter southern approach trestle; a 965-meter northern approach trestle; 600 meters of open approaches on the two enlarged portal islands; and a 1,920-meter immersed tube tunnel under the channel. During this project, dredged material was beneficially re-used to enlarge a man-made island used for the south tunnel portal (Figure 1), and the process was completed without polluting the water and with no damage to extensive clam and oyster beds and other nearby marine

Copyright © 2005 Taylor & Francis Group plc, London, UK



Figure 1. Enlarged man-made tunnel portal island.

habitats. Although a federal environmental impact statement (EIS) was not required – as it would be today – all work was closely coordinated among various state and federal agencies and the construction industry to reduce the risk of disturbing or damaging the environment.

3 FORT MCHENRY/SEAGIRT NEARSHORE CDF

As part of the design and construction work for the Fort McHenry Tunnel in Baltimore, PB was part of a joint venture that designed a nearshore CDF 3.2 kilometers from the tunnel site.

After a detailed study of alternative upland, nearshore and open water disposal site options, the 59-hectare Seagirt site in Baltimore Harbor was selected as the optimum location which provided sufficient capacity and met the design criteria and environmental requirements in regards to dredging, disposal, and construction. The $60 million disposal facility, which included a 1,700-meter cellular cofferdam offshore containment structure and 6-meter-high clay-lined upland perimeter dikes, was constructed so that it could be converted into a marine terminal by the Maryland Port Administration.

During the site search, PB evaluated various upland and harbor locations. Our findings were reported and reviewed in frequent meetings with the Interstate Division for Baltimore City (IDBC); the Federal Highway Administration (FHWA), which funded 90 percent of the cost of the tunnel, and an environmental task force composed of representatives of nine different federal, state, and local regulatory and permitting agencies. Because these agencies were regularly informed of our technical findings during the study of alternative sites, the required dredging and disposal permit for the selected site was obtained shortly after completion of the study. The proactive participation of the regulatory bodies in the site search was instrumental in streamlining and expediting the permitting process.

The principal environmental requirement governing the design of the CDF stated that any discharge from the disposal site could contain no more than 400 mg/L of suspended solids. Since the size of the site was too small for adequate settling basins, it was necessary to accelerate the settling of the solids from the dredge slurry by flocculation before the effluent could be discharged back into Baltimore Harbor.

The facility was designed to receive 2.7 million cubic meters of dredged material, including 460,000 cubic meters of highly contaminated sediments, excavated from the 55-meter trench for the construction of a twin-tube, eight-lane vehicular immersed tube tunnel. Subsurface profiles developed from borings drilled at the tunnel site indicated that the materials to be dredged would consist of very soft harbor bottom deposits (460,000 cubic meters), organic clayey and sandy silt deposits (500,000 cubic meters), gravelly sands (920,000 cubic meters), and stiff-to-hard clays and clayey silts (730,000 cubic meters).

The requirement to reclaim the CDF for the development of a marine terminal shortly after filling, was a major factor in the design of the Seagirt site. If all the dredged materials were placed in one area in an uncontrolled manner, the resulting non-homogenous fill would take many years to consolidate at great cost. To provide a design to accelerate site reclamation, the softest (and hardest to consolidate) materials which were also the contaminated shallow sediments were isolated and placed in a separate partitioned area. This area would require special ground improvement techniques and its development into usable land would take approximately 10 to 20 years. The better materials, e.g. sands and hard clays, were placed in the "spoil area" where a stabilization effort would commence soon after the completion of disposal operations.

The CDF capacity was engineered to accommodate the increased volume (bulking) of the materials after being dredged and redeposited. With allowance for bulking, which varies both with the type of material being dredged as well as the dredging method, the required disposal site design capacity was estimated at 3.8 million cubic meters.

The materials dredged by a cutter suction dredge were pumped the 3.2-kilometer distance from the tunnel trench by a 0.7-meter underwater pipeline to the disposal site where the contaminated materials were separated using shut-off valves on the pipeline (Figure 2). The effluent was diverted through shaft-type weirs into the treatment and the settling basins before discharge. Rapid mixers installed inside the weirs and slow mixers in the treatment basin accelerated the agglomeration of the flocculants.

Copyright © 2005 Taylor & Francis Group plc, London, UK



Figure 2. Y-valves on the pipeline separated the clean and contaminated sediments during disposal operations.



Figure 3. Seagirt nearshore CDF during construction.

The Seagirt nearshore CDF project (Figure 3) was the first major dredging project to be designed for effluent treatment by large-scale flocculation and sedimentation – a state-of-the-art system in dredged material disposal which has worked remarkably well in settling the finer solids in the effluent and containing them at the disposal site. During disposal operations, the solids that settled inside the settling basin were continuously removed by a small hydraulic dredge operating inside the basin to maintain the required ponding depth.

To maximize capacity, the dredged material received in the disposal area was piled and compacted by bulldozers to build a 3.4-meter-high dike 30 meters behind the cells at the elevation of the land dikes at +6.4 meters. The land dikes were constructed of compacted granular fill and lined on the inside face with a clay blanket to prevent seepage. Dredging and disposal operations were completed on schedule (Figure 4). The site was later consolidated through ground improvement and converted into a container port by the Maryland Port Administration (Figure 5).



Figure 4. CDF at completion of disposal operations.



Figure 5. Seagirt CDF after conversion into marine terminal.

4 TED WILLIAMS TUNNEL/GOVERNORS ISLAND UPLAND CDF

In 1990, PB in joint venture, designed and managed the construction of a solidification/stabilization and upland CDF for the contaminated sediments dredged for the construction of the Ted Williams Tunnel in Boston. Earlier, in the late 1980s, the solidification/stabilization of contaminated marine sediments for reclamation projects was a state-of-the-art technology that had been tested in bench scale and applied in demonstration projects (mainly in Japan). The primary thrust of Japanese research was improving the handling and enhancement of bearing capacities for fill to improve or reclaim land, with minor emphasis on contaminant stabilization (Kita and Kubo 1983). In the U.S., such techniques had been used almost exclusively in oil and gas drilling operations and on wastes from power plants, sewage treatment, chemical manufacturing, and the nuclear industry. More than a decade later, the lime stabilization of dredged contaminated sediments in Boston represents the first

Copyright © 2005 Taylor & Francis Group plc, London, UK

known case history of a large-scale application of immobilization technology for contaminated harbor sediments in the U.S.

The construction of the tunnel required the excavation of a subaqueous trench to accommodate 11 immersed tubes to be sunk across the harbor. Approximately 840,000 cubic meters of material were dredged/excavated from the tunnel alignment that is across the main channel of Boston's Inner Harbor. Approximately 68,000 cubic meters of shallow marine sediments, from within 1.5 meters of the harbor bottom, were highly contaminated and did not meet Massachusetts requirements for open water disposal. It was therefore necessary to identify a suitable upland disposal site to meet Massachusetts Department of Environmental Protection (MDEP) regulations and permit requirements for disposal.

The contaminated fraction of the marine sediments were dredged by clamshell, chemically stabilized by adding quicklime, and contained in a lined and capped site on Governors Island adjacent to Logan International Airport. The site, owned by Massport, was made available on the condition that the materials be stabilized, solidified, and placed in a completely sealed environment. A design requirement called for the solidification of sediments in the shortest possible period after disposal, as additional land-excavated material from the East Boston portion of the tunnel construction would be filled over the stabilized sediments. To provide for adequate bearing capacity, the desired shear strength of the compacted solidified sediments was established as 207 kPa in order to accommodate a 4.6-meter-high embankment. Additionally, the convenient site adjacent to Logan Airport would later be reclaimed and developed into a parking area or used for storage facilities. To meet the environmental and engineering requirements, the dredged sediments were chemically stabilized and solidified by adding ten percent quicklime by volume.

The containment site was enclosed by a 4.6-meter-high dike and entirely lined with a double geomembrane sandwiching a geonet to intercept leachate in the event of a rupture in the primary geomembrane. A gravel and perforated pipe underdrain system was installed below the double liner to intercept high groundwater and drain it into a sump for long term monitoring. A leachate collection pump was also provided to collect any leachate intercepted by the geonet.

The lime admixture and mixing ratio were selected on the basis of a sampling and laboratory testing program on the marine sediments which included stabilization, solidification, and leaching tests with varying admixture proportions of lime, fly ash, kiln dust and cement. The primary goals were to design a method to stabilize the contaminants, as well as to rapidly solidify the soft sediments so that the CDF could be reclaimed for future use. Tests were conducted on raw samples and on mixed samples at various curing conditions to assess both the geotechnical properties and the leachability of contaminants. Test results indicated that the lime would react with the sediments to produce a pozzolanic reaction that would significantly improve the unconfined compressive strength of the sediments. Both Toxicity Characteristics Leaching Procedure (TCLP) tests and Sequential Batch Leach Tests (SBLT) indicated undetectable levels of contaminants in leachates from sediments mixed with powdered quicklime. Based on the test results, it was determined that the primary controlling parameters for a successful field mix would be uniform mixing, effective compaction, and a temperature greater than 4.4°C during curing of the mix. Since the initial water content of raw dredged sediments is very high, it is necessary to either add sorbents or air-dry the amended sediments prior to compaction.



Figure 6. Governors Island CDF solidification/stabilization.

During construction, the sediments were dredged by clamshell, transported by scows to a silt curtain-enclosed unloading wharf, transferred into sealed trucks through a hopper, and hauled to the pre-constructed CDF. A fully satisfactory means for homogenous lime mixing was impossible to achieve in spite of the contractor's trials with several mixing locations and methods. Mixing in the open caused unacceptable lime dust propagation to the nearby airport. However, mixing in a pugmill was slow because of frequent mechanical breakdowns caused by debris in the dredged materials. Ultimately, the contractor was permitted to add and mix the lime within the CDF during periods of low air traffic – and when wind direction was away from the runways (Figure 6). As a result, most mixing work was performed at night, and airborne lime dust concentrations and winds were monitored to ensure compliance with the established criteria.

Massport and DEP also required odor control measures to prevent seagulls from being attracted to the sediments and straying into the path of aircraft. A special odor neutralizing foam was sprayed on the sediment stockpiles, forming a protective membrane after

Copyright © 2005 Taylor & Francis Group plc, London, UK



Figure 7. Odor neutralizing foam sprayed on sediment stockpiles.



Figure 8. Cinarcik Basin disposal site in the Marmara Sea.

every hauling and mixing shift (Figure 7). During and after construction, a field sampling and laboratory testing program was carried out in the CDF to test the effectiveness of chemical stabilization and solidification. It was found that the amended sediments were completely stabilized as no detectable levels of contaminants were observed in periodic leachability testing on representative field samples. Required unconfined compressive strengths were also generally achieved. The stabilized sediments were leveled in the CDF, mechanically compacted in layers, and set aside for future land use. The total cost of the Governors Island CDF solidification and stabilization facility was approximately $5 million.

5 MARMARAY RAIL TUNNEL CROSSING

This immersed tube tunnel crossing currently under construction beneath the Bosphorus involves a multiple of technical issues, both on land and beneath the waves. Excavation work is being undertaken in a historic district of Istanbul – a city designated as a World Heritage Site. As has been the case during past projects in this ancient city, encountering underground artifacts is a likely event during this major project.

Increasing the complexity of this construction are the challenges presented by the strait itself – one of the world's busiest international waterways. This narrow channel provides the only shipping access from the Mediterranean to Black Sea ports, in addition to handling a large volume of local marine traffic. The Bosphorus is also noteworthy for its two-layer water flow, consisting of an upper layer of freshwater runoff from the Black Sea as well as a salty lower layer of water migrating north from the Mediterranean to the Black Sea. It is within these swift currents that the immersed tube tunnel will be laid.

Although it is feasible to perform immersed tube placement operations in the Bosphorus using conventional methods, the heavy ship traffic and two-layer water flow will present significant construction challenges that will necessitate a great amount of care and careful planning. In part, this is because dredging, screeding and tube laying equipment and barges will not be permitted to block ship traffic and extensive safeguards will be necessary to guard against accidental collisions. Additionally, the two-layer water flow will become a factor as tube elements pass through the turbulent transition zone between the upper and lower water flows, setting up significant opposing hydrodynamic forces.

Subsurface investigations, including bathymetric and geophysical surveys, soil borings and laboratory tests performed in 1985 and 2003 identified and characterized the subaqueous soil and rock profile along the tunnel alignment. Soil characterization tests indicated that on the European side of the alignment, near the Golden Horn, the upper 1- to 3-meter layers of underwater sediments along a length of approximately 600 meters were contaminated, and therefore unsuitable for open water disposal. The limits of the contaminated sediments were delineated and the quantity of contaminated sediments to be dredged was established on the basis of dredged trench slopes of one vertical on three horizontal within those depths. The contaminated sediments will be dredged by closed environmental buckets and transported to a permitted CDF designed by the contractor. The CDF will be permanently capped upon the completion of disposal operations. The clean dredged material will be disposed of in open water at the designated historic disposal site at Cinarcik Basin in the Sea of Marmara (Figure 8).

Dredging and disposal operations will be sensitive to fish migrations, and curtailed during restrictive periods. Precautions will be taken to prevent any adverse

Copyright © 2005 Taylor & Francis Group plc, London, UK

impacts to the natural water flow, to keep the water clean, to minimize turbidity, and to meet the requirements of the Clean Water Act and related regulations. The Marmaray Project will be the first application of a CDF for contaminated dredged sediments in Turkey.

6 CONCLUSION

The four case histories presented in this paper illustrate the evolution of CDF design and permitting processes in the last 30 years: relatively simple handling of dredged materials in the 1970s during the construction of the Second Hampton Roads Crossing; to the $60 million CDF in Baltimore in the 1980s; to the $42 per cubic meter solidification/stabilization process in the 1990s in Boston; to the first CDF in Turkey today. All four projects have dealt with the dredging and disposal of contaminated sediments in a similar fashion in seeking a close review of the planning and design parameters and criteria by regulatory and permitting agencies, involving them very early in the planning stages. Environmental permitting rules require costly state of the art testing and analyses for sediment characterization and for containment mobility effects on the adjacent environment both during construction and in the long term.

Innovative engineering and construction techniques such as the temporary wastewater treatment facilities at the Seagirt CDF and the solidification/stabilization process application at the Governors Island CDF are no longer isolated exceptional case histories. On the contrary, such progressive practices are becoming commonplace to meet more and more severe environmental and regulatory criteria. All these projects demonstrate that the scarcity and high real estate value of nearshore and upland sites in proximity to dredging projects make it necessary to design confined disposal facilities that can be converted into usable land at the completion of disposal operations. Finally, the beneficial use of dredged materials, whether amended or naturally pristine clean, is mandatory as the only alternative to costly CDFs, as open water disposal is no longer an option. Experience shows that we must be prepared to stand up to ever-growing engineering challenges to deal with contaminated dredged sediments lest the dramatic increase in disposal costs threaten the economic feasibility of immersed tube tunnel construction.

REFERENCES

DiGiano, F.A., C.T. Miller, and J. Yoon, 1995. "Dredging Elutriate Test (DRET) Development," *Contract Report D-95-1*, U.S. Army Engineer Waterways Experiment Station, Vicksburg, MS.

Kita, D. and H. Kubo, 1983. "Several Solidified Sediment Examples," *Proc. 7th Annual U.S.-Japan Experts' Meeting*, U.S. Army Corps of Engineers, Fort Belvoir, VA.

Myers, T.E., J.M. Brannon, B.A. Tardy, and D.M. Townsend, 1996. "Leachate Testing and Evaluation for Estuarine Sediments," *Technical Report D-96-1*, U.S. Army Engineer Waterways Experiment Station, Vicksburg, MS.

Samtani, N.C., Tanal, V., Wang, J-N, and T. Lancellotti, 1994. "Effect of Lime Admixtures on Contaminated Dredged Sediments," *Proceedings, First International Congress on Environmental Geotechnics*, Edmonton, Alberta, Canada, 10–15 July, pp. 57–63.

Copyright © 2005 Taylor & Francis Group plc, London, UK

Sustainable design and construction aspects of immersed tube tunnels

Vahan Tanal, P.E.
Senior Vice President, Parsons Brinckerhoff, New York, USA

F. Simin Pehlivan
Former Deputy Director General, Ministry of Transport & Communication,
General Directorate of Railways, Harbours and Airports Construction, Ankara, Turkey

ABSTRACT: *Over the past decade, sustainability has had an increasing impact on the engineering profession. As defined by the chair of the 1987 UN World Commission on Environment and Development, Dr. Gro Harlem Brundtland, sustainable development "meets the needs of the present without compromising the ability of future generations to meet their own needs." This paper answers the question as to what are the sustainable elements in the design and construction of immersed tube tunnels. It presents sustainable aspects of immersed tube tunnels, such as the use of prefabricated elements under controlled conditions; protection of aquatic habitats during construction; environmental controls during dredging; special controls and precautions in dredging contaminated sediments; confined disposal of dredged materials; beneficial reuse of both clean and processed contaminated sediments; mitigation measures and compliance monitoring; sensitivity to current and salinity impacts; and others. The sustainable design aspects of the current Marmaray Bosphorus Immersed Tube Tunnel Project are presented as a local case study.*

1 INTRODUCTION

Recent years have brought extraordinary developments in engineering. Innovative engineering techniques are emerging in a host of practice areas, from traditional civil engineering to high-tech telecommunications, renewable energy development, "intelligent" building design, and high-tech instrumentation. High-performance materials are being researched or utilized in virtually every type of major construction project. Even the way projects are planned and financed, before engineers and contractors go to work, is changing – there are more methods presently available to deliver a project than at any time in engineering history. At the same time, the needs of the modern world are becoming ever more complex and challenging. And when these needs and our new capabilities intersect, tremendous engineering movements are created.

This paper will focus on one of these movements – sustainable design – as well as immersed tube tunnels as a special case study that is directly relevant to life in Istanbul, now that a railway tunnel under the Bosphorus is becoming a reality.

2 WHAT IS SUSTAINABILITY?

Sustainability represents the best engineering approach of all—the recognition that no project exists in a vacuum, but in a social and natural context that affects the project and is, in turn, affected by it. If we take this holistic view of engineering, which involves respecting the natural and human environment in the design, construction and operation of projects, we find distinct benefits in terms of quality, technical innovations, and long-term social, economic and environmental returns.

As engineers, we need to go one step further in defining sustainability. What does it mean for our profession? How is it related to the practice of civil engineering, whether we're designing ports and waterways, bridges, highways, buildings, dams, or power plants? What, in short, does sustainable design involve?

Full answers are still taking shape as engineers explore additional ways to design sustainable projects – but the outlines have come together. Some of the ways in which sustainability is relevant to specific engineering practice are listed below. They demonstrate that a sustainable approach is an integral part of that practice, and not just something imposed upon it.

3 PORTS AND WATERWAYS

Green ports and sustainability in the design of waterways often involve air and water quality, dredged material disposal, processing and beneficial re-use of contaminated sediments, protection of endangered

Copyright © 2005 Taylor & Francis Group plc, London, UK

and threatened species, habitat restoration, health and environmental impacts. It aims to control land-based water pollution, oil pollution and ship and port generated solid waste. Ports promote sustainability through community relation and environmental stewardship.

4 BUILDINGS

Green building design involves energy and water efficiency through daylighting, thermal efficiency, use of solar panels and water-saving fixtures, and landscaping that captures rainwater and reduces maintenance needs. It also involves conserving resources through the use of recycled and locally available materials and the re-use of existing structures where it is safe to do so. Green construction methods such as waste reduction and noise and pollution control, help to minimize environmental impacts (reducing materials sent to landfills) and community impacts (preserving the quality of life during construction). Indoor safety and air quality are also features linked to sustainability. Around the world, standards have been or are being developed to guide owners, designers and builders in achieving green designs.

5 ENERGY

In power generation, sustainability involves the exploitation of renewable sources of energy – solar, wind, hydroelectric, geothermal, tidal, and biomass – as clean, cost-effective alternatives to fossil-fuel combustion. Clearly, systems based on these sources will have to meet the supply standard that has been set by fossil fuels, but committed efforts to tap green power sources, including wind, hydroelectric and geothermal, are already yielding significant results on various parts of the globe.

6 WATER AND WASTEWATER MANAGEMENT

Sustainability may involve water conservation and reclamation, the application of technologies such as desalination to secure long-term supplies of potable water while reducing groundwater stress, and environmental protection and wastewater treatment measures to clean up polluted waterways or prevent environmental damage.

7 HIGHWAYS

Sustainability is related to highway development through the consideration of aesthetic and community impacts, the preservation of important cultural and historic resources, and wildlife protection.

8 MASS TRANSIT

Sustainable design can be achieved with energy efficiency in train operations, green design and construction of transit facilities, and resource conservation (for example, through the use of rainwater and gray water for washing operations). In fact, the very existence of mass transit promotes sustainability because it reduces fuel consumption, traffic congestion and vehicle pollution, while improving air quality—major quality-of-life issues in cities around the world.

9 WHEN IS AN IMMERSED TUBE TUNNEL PROJECT SUSTAINABLE?

Let us briefly review what an immersed tube tunnel project involves. Under certain conditions, tube tunnels are less expensive and more quickly implemented than bored tunnels, which involve deeper alignments due to tunneling requirements and often encounter unforeseen subsurface conditions. In immersed tube tunnel construction, a trench is dredged in the bed of the channel, then sanded and screeded. Meanwhile, tunnel elements are constructed in the dry, such as a fabrication yard or casting basin, and the ends are temporarily sealed with bulkheads. Each element is unique and has a specific place in the tunnel construction. Work can proceed simultaneously on entrance portals at both ends of the tunnel.

The elements are then floated to the site and lowered into position. The elements must be precisely aligned with each other and with the portals to create a watertight seal. Water is then pumped from between the bulkheads; the resulting hydraulic pressure compresses a rubber seal and the joint is tightly closed. The last major step involves placing backfill around and over the tunnel to protect it. The process is illustrated in Figure 1.

Several aspects of this process involve activities that incorporate sustainability. First and foremost, the use of tunnel elements that are prefabricated under controlled conditions helps reduce the potential for pollution and other environmental impacts from construction activities. Additionally, the dredging of the tunnel trench can be controlled to protect animal and plant life as much as possible during construction. Because contaminated sediments from dredging operations pose a significant risk to the environment if not properly disposed of, the confined disposal and treatment of these sediments is essentially a sustainable technique. Moreover, the processing and re-use of dredged material can create reclaimed land for safe future development. Careful

Copyright © 2005 Taylor & Francis Group plc, London, UK

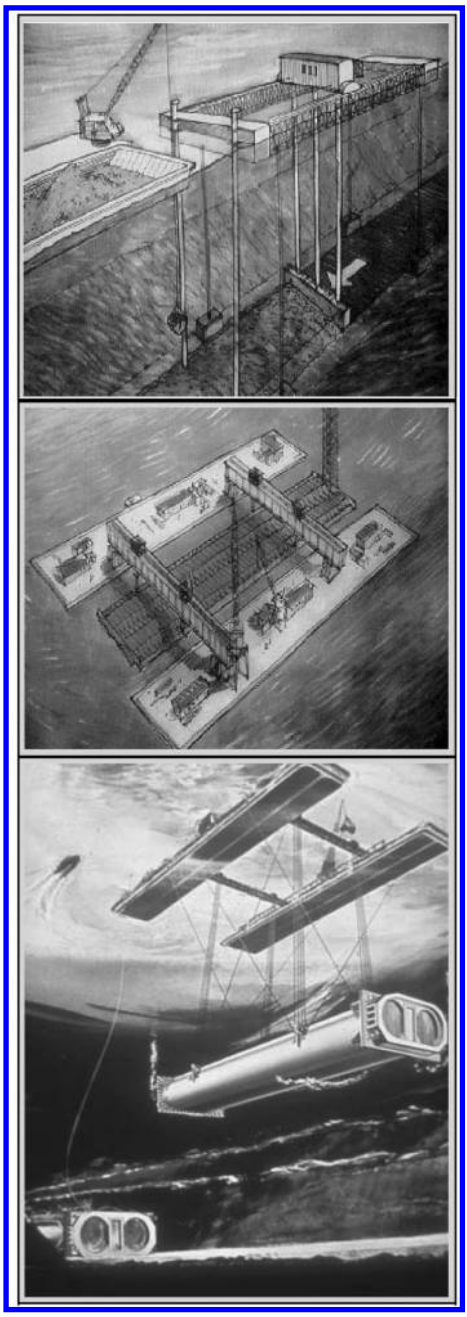


Figure 1. Steps in immersed tube tunnel placement.

monitoring of the project's impact on wetlands and on plant and animal species, along with appropriate prevention and mitigation measures, can also help ensure that water quality and marine life are affected as little as possible, if at all.



Figure 2. Hampton Roads Tunnels in Virginia. Project featured the re-use of dredged material to enlarge a man-made island and resulted in no water pollution or damage to marine habitat.

Three immersed tube tunnel projects constructed in the past 30 years in which Parsons Brinckerhoff (PB) has been involved are briefly described below from a sustainable engineering perspective. In each case, close coordination between authorities, planners, design engineers and the building contractors were instrumental in the successful completion of the projects. The fourth project presented is the Istanbul Bosphorus tunnel crossing, currently under construction.

10 SECOND HAMPTON ROADS CROSSING, HAMPTON TO NORFOLK, VIRGINIA

The first Hampton Roads Bridge-Tunnel crossing, which connects the cities of Hampton and Norfolk in the state of Virginia, was designed by PB in 1954 and opened to traffic in 1957. Twelve years later, in 1969, PB designed a parallel second crossing to meet projected traffic demands. The second bridge/immersed tube tunnel was opened to traffic in 1976 (Figure 2). This second crossing involved a number of sustainable techniques that were quite visionary for their time.

A major design issue involved enlarging the south portal island, underlain by soft silt to a depth of 30 meters, without seriously disturbing the existing tunnel and island. The soft foundation soils were consolidated by using the sand drain and surcharge method prior to construction of the new tunnel to minimize post-construction settlements and prevent any subsurface deformations toward the existing tunnel (Figure 3). Special design and construction measures were implemented for dredging and dredge material placement to minimize turbidity and protect nearby clam and oyster beds. The dredged material was re-used to enlarge the south portal island within protective containment dikes to prevent the spillage of silt into the harbor.

Copyright © 2005 Taylor & Francis Group plc, London, UK



Figure 3. Sand drain installation at the south portal island.



Figure 4. Fort McHenry Tunnel in Maryland. Project featured extensive dredged material processing in a confined disposal facility, which was subsequently used for a new container terminal.

Although a federal environmental impact statement (EIS) was not required – as it would be today – the design engineers cooperated with state and federal agencies and the construction industry to develop methods to minimize the environment consequences of the construction work.

11 FORT MCHENRY TUNNEL, BALTIMORE, MARYLAND

The design and construction of Fort McHenry Tunnel under Baltimore Harbor, which opened to traffic in November 1985, also involved sustainable techniques that were ahead of their time. At 2,680 meters in length, with 32 tube sections, each containing two bores and carrying four lanes of traffic, it is the largest subaqueous tunnel in the world. It is located near Fort McHenry, a historic site from the War of 1812. To preserve the view from Fort McHenry, a tunnel was selected instead of a bridge crossing. To avoid construction work beneath the fort, the design involved a unique horizontally and vertically curved alignment to keep the tunnel at a safe distance away from the fort—thus the world's first tunnel sections with both horizontal and vertical curvature were built.

The 2.7 million cubic meters of material dredged from the tunnel trench were transported to a nearshore confined disposal facility (CDF) where the contaminated sediments were separated from the clean soils. The materials were processed at the 59-hectare disposal site which was consolidated and converted into a modern container terminal, the Seagirt Marine Terminal in Baltimore Harbor (Figure 4). Wetlands lost to the construction of the disposal site were mitigated by the development of a number of tidal marshes in the harbor to restore benthic animal and plant communities (Figure 5).



Figure 5. A mitigation tidal marsh was created over the west approach to restore benthic animal and plant communities.

12 TED WILLIAMS TUNNEL, BOSTON, MASSACHUSETTS

The Ted Williams Tunnel, Boston's new harbor crossing to Logan International Airport, opened to traffic in 1995, as part of the Central Artery/Tunnel (CA/T) Project, a massive program to upgrade the area's transportation infrastructure. The project represents a spectacular case history of sustainable development implementation. The scope of the environmental protection and mitigation program reflects the monumental size of the CA/T Project itself. The project included ocean disposal, enclosed marine containment and upland disposal of nearly 9.5 million cubic meters of dredged and excavated material.

The construction broke ground in many areas of state-of-the-art engineering applications, including the solidification/stabilization of contaminated dredged sediments. For the first time anywhere, this project involved processing 53,000 cubic meters of contaminated dredged material in an upland CDF, chemically

Copyright © 2005 Taylor & Francis Group plc, London, UK



Figure 6. Ted Williams Tunnel in Massachusetts. Project involved processing 53,000 cubic meters of contaminated dredged material in an upland confined disposal facility, as well as large-scale lime solidification and stabilization.

solidifying the material, and reclaiming the CDF for future use (Figure 6).

Within the U.S., stabilization had been applied in areas other than dredging, such as oil and gas drilling operations and treatment of waste from power plants, sewage treatment plants, and chemical and nuclear facilities, but this was the first case of extensive stabilization applied to contaminated harbor sediments. The process was also conducted in a way that significantly reduced impacts on nearby Logan International Airport. The contractor added and mixed lime within the confined disposal facility only when air traffic was diminished and the wind was blowing away from the runways. Airborne lime dust concentrations were measured by a computerized instrumentation system for compliance monitoring. Odor control measures were also successfully used on dredged sediment stockpiles to avoid attracting seagulls that might interfere with aircraft operations.

An extensive public outreach program ranged from one-on-one contacts with residents and businesses, to mitigation-related negotiations with the city and community groups affected by construction. The project has been recognized through dozens of awards for engineering excellence and aesthetics.

13 MARMARAY BOSPHORUS CROSSING

Split in two by the Bosphorus Strait, the city of Istanbul has always sought ways to move people and goods



Figure 7. The Bosphorus Strait separates Europe and Asia in Istanbul.

across this narrow and busy waterway separating two continents (Figure 7). In 1985, PB led a consortium to conduct feasibility studies, plan and perform the preliminary design of a railroad tunnel beneath the strait to connect the European and Asian sides of the Bosphorus. In March 2002 the Ministry of Transport & Communication, General Directorate of Railways, Harbours and Airports Construction, commissioned Avrasya, a joint venture led by Pacific Consultants International of Japan to assist the Ministry in implementing the project as its general engineering consultant. In 2004, the design/build contract was awarded to a joint venture of Taisei, Kumagai, Gama and Nurol.

The project, involving the world's deepest immersed tube tunnel as well as the related upgrade of 63 kilometers of at-grade rail lines, will be one of the most ambitious and complex undertakings of its kind. It will feature a 1.8-kilometer tunnel in 50 meters of water below one of the busiest waterways in the region, where international shipping traffic is constant (Figure 8). The Bosphorus, the only access from the Mediterranean to the Black Sea, with two opposing currents, provides a pathway for seasonal migrations of fish between the two bodies of water. Additionally, the shallow current carries freshwater southward whereas the deeper flow provides the only saltwater supply to the Black Sea.

This mass transportation project will significantly alleviate road congestion and vehicle pollution. Mass transport is vital to sustainable development, particularly in highly developed urban areas. Other sustainable features of the Marmaray Project mirror those of the immersed tube tunnel projects previously discussed, such as the confined disposal of contaminated dredged material and the fact that this project will have no permanent effect on the aquatic habitats of the very rich marine life of the Bosphorus. This is due to the fact that the tunnel will be buried entirely beneath the channel,

Copyright © 2005 Taylor & Francis Group plc, London, UK



Figure 8. Marmaray Immersed Tube Tunnel Project in Istanbul. This project will feature the confined disposal of dredged material and will not impact aquatic habitats, currents, salinity, or its visual surroundings.

and as such will not affect currents or salinity. Similar to the Fort McHenry Tunnel, it will not create a negative visual impact and will preserve the spectacular view of the Bosphorus and the historic Istanbul skyline.

14 CONCLUSION

The case histories presented in this paper demonstrate that the design and construction of immersed tube tunnels can be performed totally within sustainable engineering principles. A common denominator key to the success of such major construction projects is to develop a harmony between the engineers, the authorities, and the communities affected by the construction.

As civil engineers, we have chosen a profession that can both serve the public good and enhance the quality of life. Sustainable design provides a means to accomplish that mission. Major engineering firms such as Parsons Brinckerhoff are embracing sustainability in both their technical and business practices. Although we are still in the opening stretch – as Sir Mark Moody-Stuart observed in 2002 in Johannesburg, "Even those companies at the forefront of sustainable development are close to the start of the journey. We are very much on the first rung of the ladder." In time, it will become clear that sustainability – and sustainable design – are genuinely worthwhile goals.

REFERENCES

1. Rachel Carson (1907–1964) was a biologist, ecologist and writer. *Silent Spring*, which appeared in 1962, exposed the dangers of the powerful pesticide DDT and the threat it posed to a wide range of species and to the world food supply. More generally, it revealed the devastating effect human activity could have on the natural environment. Other relevant studies from the period are Paul Ehrlich's exploration of the dangers of overpopulation and its relation to sustainability, and E.F. Schumacher's 1973 book *Small Is Beautiful*, which proposed the use of earth-friendly technology that is proportionate to the scale of the community using it.
2. The report of the *World Commission on Environment and Development*, chaired by Dr. Brundtland, was entitled *Our Common Future* and was published in April 1987.
3. The U.S. Green Building Council (USGBC) describes the *Leadership in Energy and Environmental Design* (LEED) Green Building Rating System™ as a "voluntary, consensus-based national standard for developing high-performance, sustainable buildings." Information on the USGBC and the LEED program may be found on the organization's web site. The Building Research Establishment's *Environmental Assessment Method* (BREEAM) in the U.K. assesses building performance in overall management, energy use, health and well-being, pollution, transport, land use, ecology, use of materials, and water use and efficiency.

Copyright © 2005 Taylor & Francis Group plc, London, UK

Seismic hazard assessment and earthquake resistant design considerations for the Bosphorus tunnel project

Jaw-Nan (Joe) Wang
Senior Engineering Manager, Parsons Brinckerhoff Quade & Douglas, Inc., New York, U.S.A.

Mustafa Erdik
Professor, Chairman, Department of Earthquake Engineering, Bogazici University, Turkey

Shogo Otake
Manager, Oriental Consultants Co., Ltd, Japan

ABSTRACT: In this paper the fundamental considerations and methodology used in deriving the project Design Basis Earthquake (DBE) are discussed. Both probabilistic and deterministic approaches were used for assessing the seismic hazards. In the probabilistic approach the homogeneous Poisson model was used to assess the hazard on the regional basis while time-dependent conditional probability model was used to characterize the segmentation behavior of Main Marmara Fault which is an extension of the North Anatolian Fault (NAF). Due to the exceptionally high exceedance probabilities of large events based on results from the probabilistic hazard analysis, it was determined that results from the deterministic approach are more appropriate for the seismic design of the Bosphorus tunnel project. Also included in this paper are discussions of tunnel performance criteria, general design and analysis methodology for tunnel structures using the deformation-based approach, effects of liquefaction and liquefaction-induced ground deformations on the tunnel structures, and other geotechnical design requirements under the Design Basis Earthquake.

1 INTRODUCTION

The proximity of the proposed Bosphorus tunnel site to the fault system in the Sea of Marmara (see Figure 1) as well as the critical site soil conditions makes the safe seismic design of the tunnel one of the most critical elements of the project. Current seismic design methodology for mass transit rail facilities has in general adopted a performance-based two-level design earthquake approach – a low level, high probability Functional Evaluation Earthquake (FEE) and a high level, low probability Safety Evaluation Earthquake (SEE). However, because of the unique seismological settings in the project region, the generally adopted two-level design earthquake approach is modified for this project.

The seismic hazards at the project site are dominated by the "Characteristic Earthquakes" associated with segments of the North Anatolian Fault in the Marmara Sea area rather than by various other line or zone sources. Because of the quiescent period on these segments of the fault (since the mid 1700s), there exists a substantial probability of occurrence of a major earthquake in the Marmara Sea area during the service life of the tunnel. As a result, the magnitude of the high probability event (FEE) is approaching that of the low probability event (SEE), making the use of the two-level design earthquake approach not appropriate.

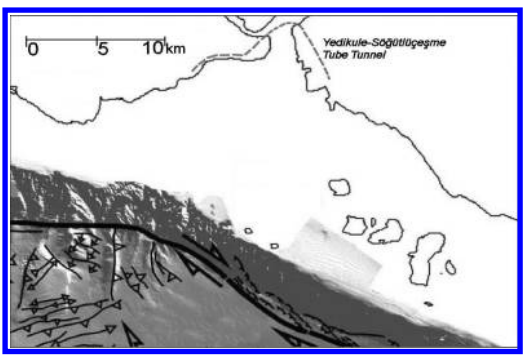


Figure 1. Project alignment relative to main Marmara fault.

Copyright © 2005 Taylor & Francis Group plc, London, UK

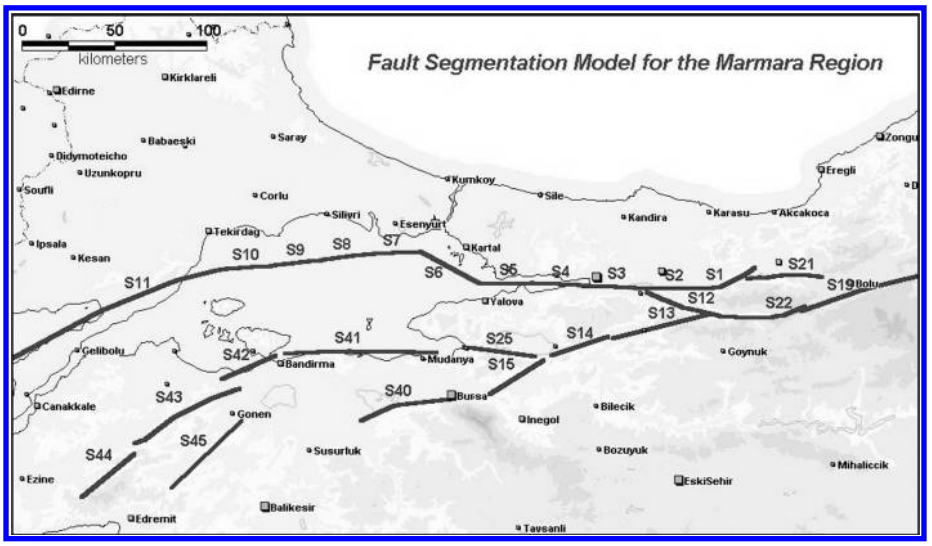


Figure 2. Fault segmentation model.

For this project, the minimum seismic design requirements for this project are based on a single level design earthquake, defined as the Design Basis Earthquake (DBE), corresponding to a $M_W = 7.5$ (moment magnitude) earthquake. When subjected to the DBE, the minimum performance requirements of the tunnel structures are: (1) damage shall be easily repairable and shall not result in a loss of functionality or lives, (2) the tunnel shall remain watertight, and (3) facility shall remain operational following the earthquake, allowing not more than a few days for inspection and re-adjustment of the rail alignment as necessary, and (4) repair work can be performed with minimum disruption to the operation of the facility. Additional requirements for the design of the Bosphorus tunnel are presented and discussed by Ingerslev et al. (2005).

2 REGIONAL TECTONICS AND SEISMICITY

The primary tectonic feature affecting the project site is the Marmara Fault System in the Marmara Sea to the south of the project site. The Marmara Fault System is an extension of the North Anatolian Fault Zone (NAFZ), splaying westward toward the Marmara Sea region into a complex system. The Main Marmara Fault is the northern strand of the complex system and exhibits features typically associated with a strike-slip fault (i.e., Segments S1 through S11 shown in Figure 2). The other active faults in the area are located in the southern part of the Marmara Sea. These southern-strand faults are generally of extensional type. Based on the long-term seismicity and GPS measurements the northern strand of the fault zone (i.e., the Main Marmara Fault) is more active than the southern strand and governs the seismic design of the proposed tunnel structures.

Figure 3 shows the historical seismicity of the Marmara region for earthquake events with magnitude greater than 5.0. In the time period from 1500 to present there have been a number of $M > 7.0$ earthquakes in the Marmara region. After detailed assessment of the distribution of reported earthquake damages, these major historical earthquakes have been correlated to the fault segmentation model presented in Figure 2. Fault ruptures associated with the fault segmentation are summarized in Table 1 below.

3 PROBABILISTIC HAZARD ANALYSIS

Two probabilistic models were used. The homogeneous Poisson model was used to assess the hazard on the regional basis while time-dependent conditional probability model was used to characterize the segmentation behavior of Main Marmara Fault. The "no-memory" feature of the homogeneous Poisson model however is not applicable for this project because of the unique time-dependent behavior of fault system in the Marmara Sea area.

In the time-dependent conditional probability model, consideration was given to the time elapsed since the last event (when the segment ruptured) in estimating the probability of future events. The fault segmentation model (Figure 2) was derived based on the assumption that the segment boundaries exist where faults change direction or where the fault displacement varied substantially in the past earthquakes.

Copyright © 2005 Taylor & Francis Group plc, London, UK

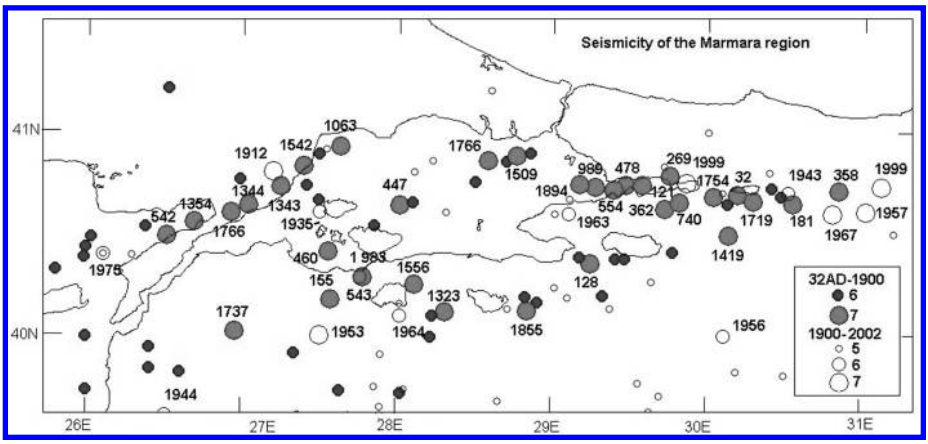


Figure 3. Historical seismicity of marmara region (M > 5.0).

Table 1. Correlation between historical major earthquakes and fault segmentation model (See figure 2 for fault segment).

Earthquake	Fault segment
10/9/1509 (Ms = 7.2)	S7, S8
10/5/1556 (Ms = 7.2)	S9
25/5/1719 (Ms = 7.4)	S2, S3, S4, S5
2/9/1754 (Ms = 6.8)	S6
22/5/1766 (Ms = 7.1)	S7, S8
5/8/1766 (Ms = 7.4)	S11
10/7/1894 (Ms = 7.3)	S3, S4, S5
9/8/1912 (Ms = 7.3)	S11
17/8/1999 (Ms = 7.8)	S1, S2, S3, S4

The associated median recurrence time for each segment assumed in the analysis is presented in Table 2 below. These median recurrence times were determined from the ratio of the displacement (D) of the previous segment rupturing earthquakes to the best estimated median value of the regional slip rate (V). For the Marmara Sea the median slip rate was assumed to be in the range of 2∼3 cm/year.

The results of the time-dependent conditional probability model indicated that the probability for an Mw > 7.0 earthquake to occur in the Marmara Sea area for the next 50-year is about 50%. If the interaction effect of "Stress Transfer" is considered (i.e., the occurrence of earthquake on one fault segment has an impact on the probability of occurrence on another segment), then the probability of the occurrence for an Mw > 7.0 earthquake will be further increased. This findings is consistent with that reported by Parsons et al. (2000), who based on recent studies after the 1999 Kocaeli (Mw = 7.4) and Duzce (Mw = 7.2) earthquakes suggested about 65% probability for the occurrence of an Mw ⩾ 7.0 earthquake affecting Istanbul in the near future.

Table 2. Median recurrence times of fault segments.

Fault seg.	Last earthquake	Median recurrence time
S1	12/11/1999(Ms = 7.3)	
S2	17/8/1999 (Ms = 7.8)	140 ± 35 years
S3	17/8/1999 (Ms = 7.8)	140 ± 35 years
S4	17/8/1999 (Ms = 7.8)	140 ± 35 years
S5	10/7/1894 (Ms = 7.3)	175 years
S6	2/9/1754 (Ms = 6.8)	210 ± 40 years
S7	22/5/1766 (Ms = 7.1)	250 years
S8	22/5/1766 (Ms = 7.1)	250 years
S9	10/5/1556 (Ms = 7.2)	200 ± 50 years
S10	–	200 ± 50 years
S11	9/8/1912 (Ms = 7.3)	150 years

The exceptionally high probability for a major earthquake occurring in the project area suggests that it is prudent to use the deterministic approach for the assessment of the project DBE ground motions. The results based on the deterministic approach are discussed in the following section.

4 DETERMINISTIC HAZARD ANALYSIS

The deterministic hazard analysis involves two primary elements: (1) determination of the scenario earthquake, and (2) identification of the proper attenuation relationships. There are various procedures in determining the maximum credible earthquake scenario. For the Istanbul area, almost all of these procedures converge to a large earthquake associated with the un-ruptured sections of the Main Marmara Fault. On these bases and other technical considerations, an Mw = 7.5 earthquake (similar to the 1999 Kocaeli earthquake in Magnitude and in total rupture length)

Copyright © 2005 Taylor & Francis Group plc, London, UK

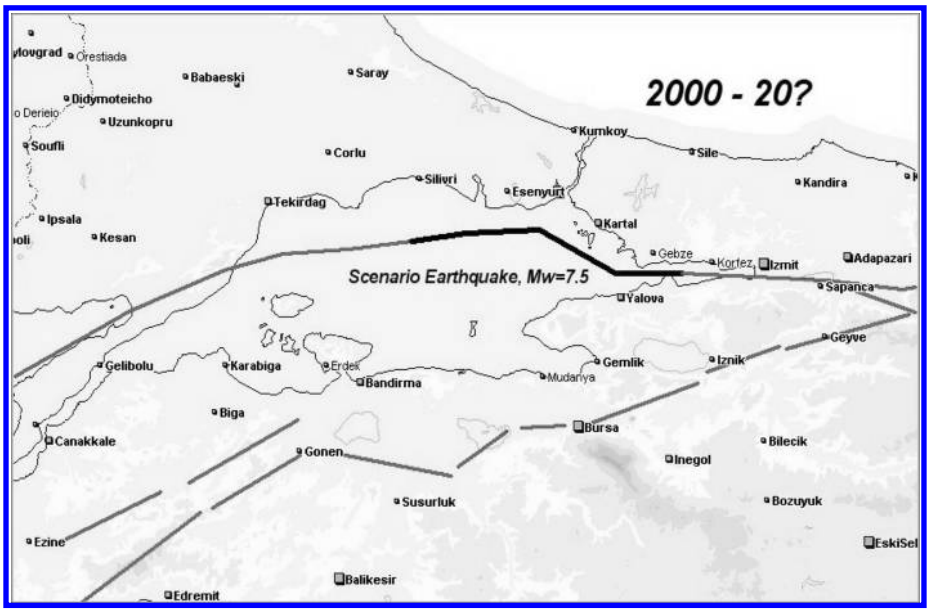


Figure 4. The maximum credible earthquake scenario.

was selected as the maximum credible earthquake scenario. This scenario event was assumed to take place on Segments S5 through S8 along the Main Marmara Fault, as shown in Figure 4. This fault section lies only about 16 km (the closest distance) to the proposed immersed tunnel (refer to Figure 1 for the relative location of the tunnel alignment to the fault rupture).

Due to the importance of the project and the relatively higher uncertainties associated with large magnitude earthquakes in the near field conditions, the attenuation relationships used in deriving ground motion parameters were based on the median-plus-one-standard deviation values (i.e., the 84th percentile values). The ground motion parameters (on free-field rock outcrop) derived by the deterministic approach includes the short-period spectral acceleration S_s (i.e., the spectral acceleration at T = 0.2 sec), the long-period spectral acceleration S_1 (i.e., the spectral acceleration at T = 1.0 sec), the peak ground acceleration (PGA), the peak ground velocity (PGV), and the peak ground displacement (PGD). For assessment of S_s, S_1 and PGA the attenuation relationships proposed by Boore et al. (1997) were used. For the PGV and PGD the relationships developed by Campbell (1997) and Gregor (1995) were adopted. The results of the hazard analysis and the DBE ground motion parameters are summarized in Table 3 below for three different distances – 13, 16, and 20 km to represent the shortest distance to fault from the various structure components along the project alignment.

Table 3. DBE Ground motion parameters – on rock outcrop.

Distance to fault	13 km	16 km	20 km
S_s (g)	0.90	0.74	0.65
S_1 (g)	0.50	0.40	0.37
PGA (g)	0.42	0.38	0.32
PGV (cm/sec^2)	30	24	22
PGD (cm)	29	25	21

The design rock spectra were derived by using the S_s and S_1 values following the 1997 NEHRP procedure. The rock quality at the project site is characterized as soft rock and meets the "B/C Boundary" site classification in accordance with the NEHRP procedure (i.e., with an average shear wave propagation velocity of 750 m/sec in the upper 30 meters of the rock). Figure 5 shows the resulting DBE rock response spectra (5% damping) from the scenario earthquake of Mw = 7.5 at the fault distance of 16 km (representing the closest distance from the immersed tunnel to the fault). The vertical component spectral values are assumed to be two-thirds of the horizontal component values for design purposes.

The spectrum-compatible DBE ground motion time histories were also developed. Two sets of three-components (i.e., the longitudinal, transverse and vertical components) were developed for each distance to fault.

Copyright © 2005 Taylor & Francis Group plc, London, UK

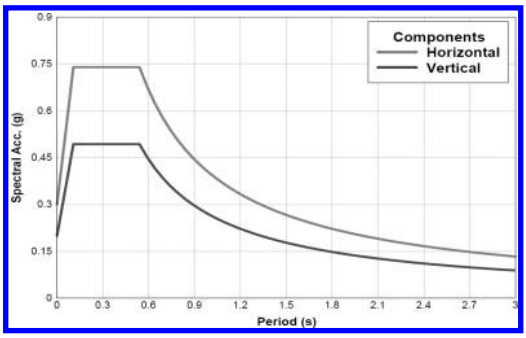


Figure 5. Design bedrock response spectra – for R = 16 km.

The design criteria specify that both sets of the time histories shall be used in the response analysis and the maximum response values of all time history analyses shall be used for design purposes.

Detailed descriptions, assumptions, and results of the site-specific hazard analysis are contained in a report by Erdik, Ozbey and Sesetyan (2002).

5 SEISMIC EFFECTS ON TUNNELS

The general seismic effects on tunnels can be divided roughly into two categories: (1) ground shaking, and (2) ground failure. Ground failure as a result of seismic shaking can include liquefaction, post-liquefaction movements (settlements and lateral spread), and slope instability (landslide). This section focuses on the ground shaking effects on tunnel response.

The response of a tunnel to seismic shaking motions can be described in terms of three principal types of deformations: (1) axial deformation, (2) curvature deformation, and (3) ovaling (for circular tunnels) or racking (for rectangular tunnels). The first two types, axial and curvature deformations, are induced by components of seismic waves that propagate along the tunnel axis (i.e., longitudinal response of the tunnel). When the component waves produce particle motions parallel to the longitudinal axis of the tunnel, they cause alternating axial compression and tension strains (Figure 6a). Curvature deformations result from component waves that produce particle motions in the direction perpendicular to the tunnel axis. The curvature deformation results in bending and shear demands on the tunnel structures (Figure 6b). The ovaling/racking deformation (i.e., the transverse response of the tunnel) is caused primarily by seismic waves propagating perpendicular to the tunnel longitudinal axis. Vertically propagating shear waves are generally considered the most critical type of waves for this mode of deformation, as shown in Figure 7 (Wang, 1993).

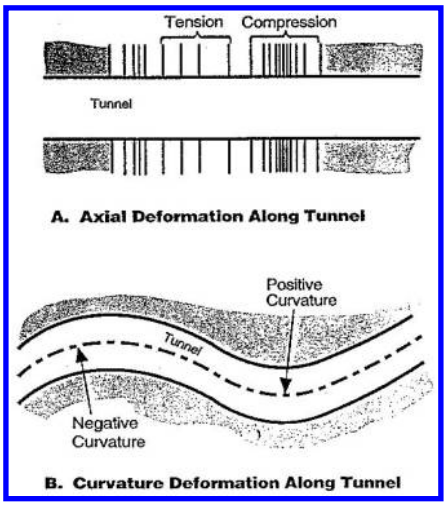


Figure 6. Longitudinal deformation of tunnels.

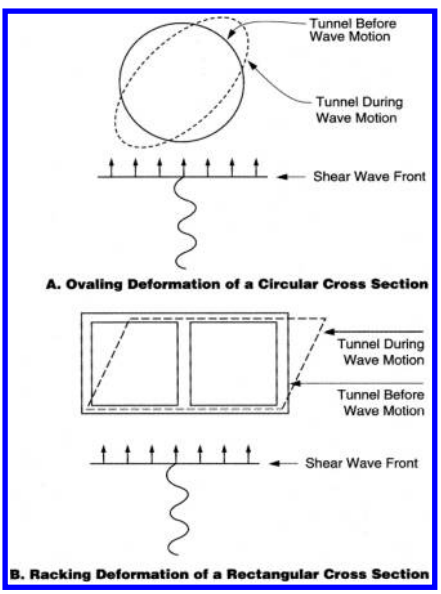


Figure 7. Transverse ovaling/racking of tunnels.

6 FREE-FIELD SITE RESPONSE ANALYSIS REQUIREMENTS

The subsurface conditions at the site are highly variable. The top of the rock varies from EL − 25 m to EL − 115 m along the proposed tunnel alignment, creating a basin filled by deep deposit of soft clayey and sandy deposits. At its deepest location the soil overburden thickness is about 85 m, while rock was encountered at the tunnel invert elevations at the two

Copyright © 2005 Taylor & Francis Group plc, London, UK

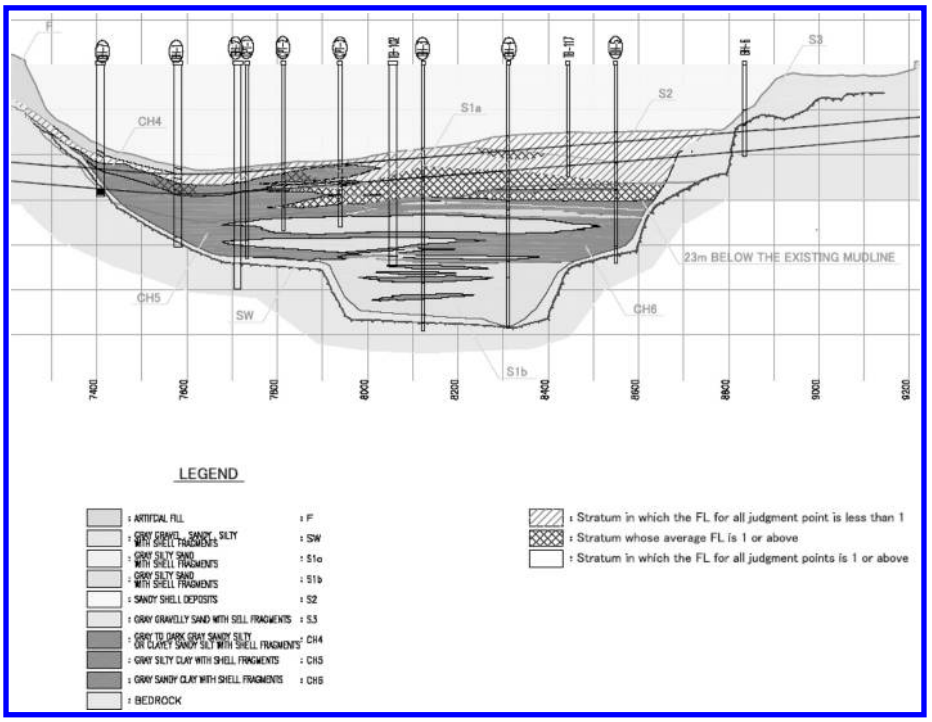


Figure 8. Subsurface conditions along the immersed tunnel.

ends where the immersed tunnel connects with the land tunnels (Figure 8).

Detailed descriptions and discussions of the subsurface conditions are presented by Simsek, et al. (2005). In general, a very soft to soft silty clay stratum was encountered for a distance of about 500 m from the European end of the immersed tunnel. Based on in-situ seismic shear wave velocity measurements, the soft clayey stratum has a shear wave velocity varying from about 100 m/sec at the mudline gradually increasing to about 250 m/sec at 40 m below the mudline. Further eastward, the soil stratum consists primarily of loose to dense sand with interlayering of firm to stiff sandy clay layers. Within about 100 m of the Asian end of the immersed tunnel, variable deposits of sand, gravel, cobbles and boulders were encountered.

Site response analysis was performed to (1) account for the site amplification effect due to the presence of the deep soil deposits, (2) derive free-field displacement time histories as input for the tunnel longitudinal response analysis, (3) derive free-field ground deformation profiles for the tunnel transverse racking response analysis, and (4) derive earthquake-induced shear stresses for liquefaction potential evaluations.

Due to the highly non-linear soil properties during earthquake, the free-field response analysis was performed using non-linear dynamic time history analysis in time domain. The modified Ramberg-Osgood model was used to account for the non-linear characteristics of the soils. In addition, the two-dimensional finite element method (FEM) was used for the longitudinal and vertical excitations and the three dimensional FEM was used in the transverse direction (due to the presence of non-horizontally layered soil/rock strata and to account for the deep basin effect under the Bosphorus).

Figure 9 presents a schematic diagram (provided by TKGN, JV) showing the three-dimensional free-field site response analysis using the FEM. It should be noted that only one unit width of the domain in the direction normal to plane is needed in the analysis.

7 LONGITUDINAL TUNNEL RESPONSE ANALYSIS

Using the free-field displacement time histories (at the tunnel position) discussed in Section 6 above, the longitudinal tunnel response analysis was carried out using the seismic deformation method. The important factors considered in the analysis include the following:

A. The tunnel is modeled as beam elements, taking into account the non-linear characteristics of the tunnel member rigidity.

Copyright © 2005 Taylor & Francis Group plc, London, UK

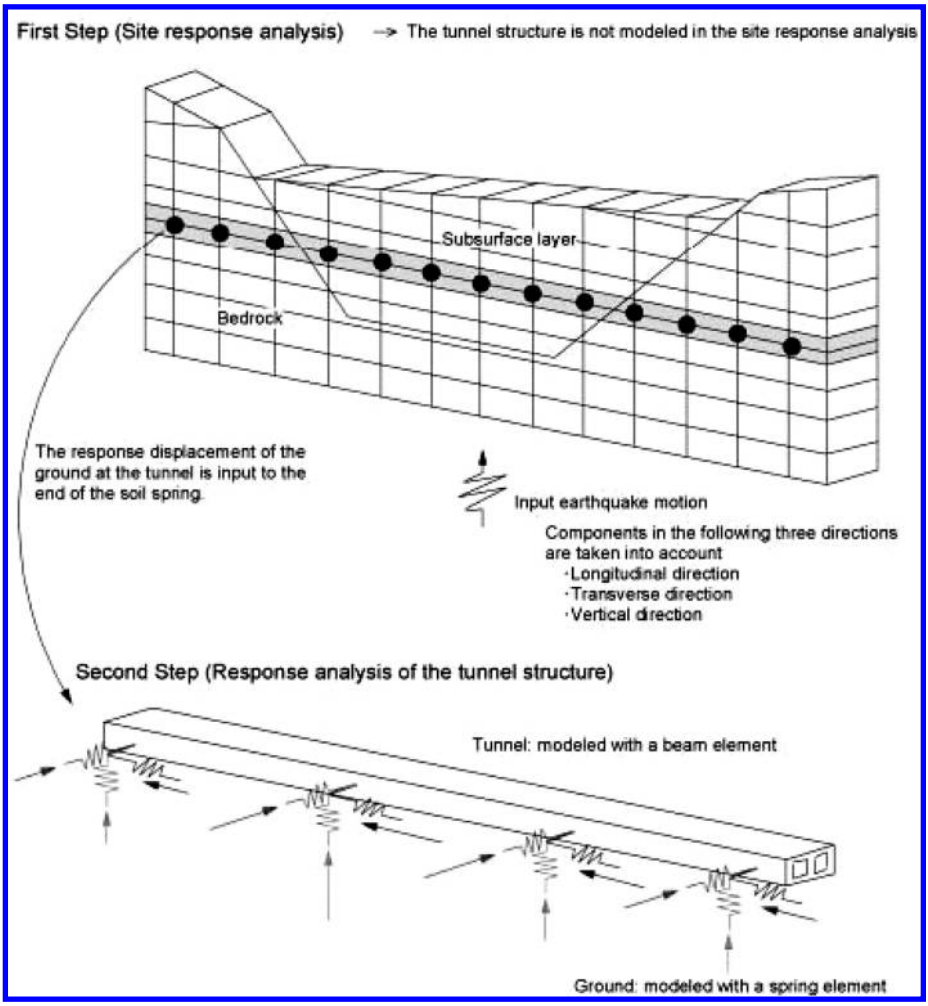


Figure 9. Free-Field site response analysis and tunnel response analysis using seismic deformation method.

B. The interaction between the surrounding ground and the structure is modeled as non-linear spring elements with limiting resistance.
C. The structural characteristic of the joints (e.g., the immersed joints) and discontinuity (e.g., the flexible and seismic joints) must be considered. The project criteria require that joint properties used in the model be derived based on validated experimental data.

8 TRANSVERSE TUNNEL RACKING ANALYSIS

The seismic racking response of the immersed tunnel structure was analyzed using the Pseudo-static seismic deformation method, whose general concept is illustrated in Figure 10 (Wang, 1993).

The analysis consists of the following steps:

A. Determine the free-field deformation profile from site response analysis (Refer to Section 6).
B. Develop a two-dimensional free-field finite element plane-strain model.
C. Apply boundary displacements or loads on the model boundaries (or a pseudo-static seismic coefficient) to achieve the free-field soil deformation profile discussed in Step A above.
D. Add tunnel structural elements in the model and remove the soil elements to be excavated.
E. Apply to the model the same boundary displacements or loads (or the pseudo-static seismic

Copyright © 2005 Taylor & Francis Group plc, London, UK

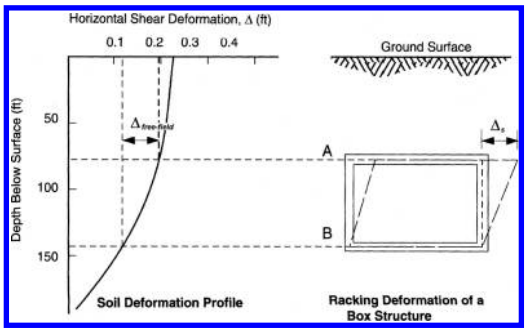


Figure 10. Tunnel racking response analysis.

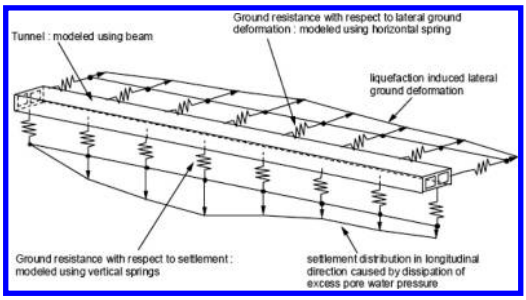


Figure 11. Effect of residual ground movements on tunnel.

coefficient) as used in Step C. The resulting sectional forces and displacements in the structural elements are the seismic demands under the transverse racking deformation effect.

9 LIQUEFACTION AND LIQUEFACTION-INDUCED GROUND DEFORMATIONS

The effects of liquefaction to be considered for the tunnel design included the following: (1) uplift, buoyancy, and flotation, (2) post-liquefaction settlements and lateral deformations (total as well as differential), and (3) lateral sliding stability. The empirical procedure based on CPT (cone penetrometer testing) data was used for preliminary liquefaction potential evaluations (NCEER, 1997).

Based on the preliminary investigation of the subsurface data, deposits of liquefiable soils (loose to medium dense sands) are present at the elevations above the proposed tunnel invert along almost the entire alignment. During the construction these problem soils surrounding the tunnel elements will be excavated and replaced by properly designed backfill materials that are not vulnerable to liquefaction. Below the invert, the soils on the western portion of the crossing are composed primarily of silty clay and therefore liquefaction is not of main concern along this section of the tunnel.

On the eastern portion of the crossing, however, loose to medium sandy soils are present to a depth of about 10 m, or more, below the tunnel invert. Preliminary analysis indicated that the sandy deposits on this portion of the crossing are liquefiable and post-liquefaction settlements as high as 35 cm can be expected. In addition to the post-liquefaction settlements, the design must also consider the liquefaction-induced lateral spread due to the sloping channel bottom in the transverse direction of the tunnel.

Figure 11 presents the schematic diagram (provided by TKGN, JV) showing the methodology used in evaluating the effects of post-liquefaction settlements and liquefaction-induced lateral ground deformations on tunnels.

For the final design, further evaluations of the liquefaction potential of the soils are required. If necessary, design mitigation measures are to be provided to minimize the post-liquefaction deformations. Such measures may include sand compaction piles (SCP), and/or compaction grouting.

10 SEISMIC SLOPE STABILITY AND LANDSLIDE

The potential for seismically induced landslides and slope instability are to be identified along the proposed alignment, particularly for steep underwater soil slopes such as that near the western shoreline. Pseudo-static seismic stability analysis and time history deformation analysis are proposed for analyzing such slope using appropriate seismic coefficient and ground motion time histories derived from the DBE parameters. If any potential for such slope instability is identified, design mitigation measures will be developed and implemented.

REFERENCES

Boore, D. M., Joyner, W. B., and Fumal, T. E., (1997), "Equations for Estimating Horizontal Response Spectra and Peak Acceleration from Western North American Earthquakes: A Summary of Recent Work", Seismological Research Letters, Vol. 68, No. 1, pp. 128–153.

Campbell, K. W., (1997), "Empirical Near-Source Attenuation Relationships for Horizontal and Vertical Components of Peak Ground Acceleration, Peak Ground Velocity, and Pseudo-Absolute Acceleration Response Spectra", Seismological Research Letters, Vol. 68, No. 1, pp. 154–179.

Erdik, M., Ozbey, C., and Sesetyan, K., (2002), "Earthquake Hazard Assessment, Earthquake Resistant Design Considerations and Design Basis Ground Motion for the Marmaray Project," Interim Report Submitted to the Avrasya Joint Venture, Department of Earthquake Engineering, Bogazici University, Istanbul, Turkey.

Copyright © 2005 Taylor & Francis Group plc, London, UK

Gregor, N. J., (1995), "The Attenuation of Strong Ground Motion Displacements," Report No: UBC/EERC-95/02, University of California, Berkeley, CA.
Ingerslev, L. C. F., Sakaeda, H., and Takahashi, M., (2005), "Requirements for the Design of the Bosphorus Tunnel," International Tunneling Association (ITA) World Tunnel Congress, Istanbul.
Parsons, T., Toda, S., Stein, R. S., Barka, A., and Dieterich, J. H., (2000), "Heightened Odds of Large Earthquake Near Istanbul: An Interaction-based Probability Calculation," Science, 288, pp. 661–665.
Simsek, O., Castelli, R. J., and Mitani, S. (2005), "Bosphorus Crossing: Geological and Geotechnical Investigations," International Tunneling Association (ITA) World Tunnel Congress, Istanbul.
Youd, T. L., and Idriss, I. M., (1997), "Proceedings of the NCEER Workshop on Evaluation of Liquefaction Resistance of Soils," National Center of Earthquake Engineering Research, Technical Report NCEER-97-0022.
Wang, J., (1993), "Seismic Design of Tunnels – A Simple State-of-the-Art Design Approach," 1991 William Barclay Parsons Fellowship, Parsons Brinckerhoff Monograph No. 7.

Copyright © 2005 Taylor & Francis Group plc, London, UK

Marmaray project: safety and ventilation strategy, Bosphorus crossing tunnels

Steen Lykke
Project Manager, Marmaray Project, Pacific Consultants International, Japan

William D. Kennedy
Vice President, Parsons Brinckerhoff International Inc., USA

M.M. Babur
Mechanical Engineer, Bosphorus Crossing, Yuksel Proje, Turkey

F. Aşci
Mechanical Engineer, Project Implementation Unit, DLH

ABSTRACT: The total closed length of the tunnels, portals and deep stations under the Bosphorus and under Istanbul is more than 13 km. The tunnels consist of two tubes, one tube for mixed train traffic in each direction. The Bosphorus is a very deep Strait, and therefore the deepest point of the Immersed Tunnel will be some 55 m below the water surface level. This paper describes the safety philosophy used, the safety systems installed and the functionality of these systems seen in the light of potential abnormal situations in the tunnels and stations. The paper also focuses on the fire scenarios to be considered and the related requirements to functionality and reliability of the Ventilation Systems to be installed. The paper also discusses the requirements to and functionality of relevant systems important for escape routes and rescuing operations.

1 INTRODUCTION

In the relatively recent past a number of serious accidents in tunnels have been experienced. Examples are the Mont Blanc Tunnel, the … tunnel and the Channel Tunnel. These accidents have caused relatively large numbers of fatalities and casualties.

The examples mentioned above all included motor vehicles either as direct road traffic or indirect (trucks loaded on trains). The track record when it comes to serious accidents for tunnels not including road traffic or vehicles loaded on to trains is much better than the track record for road tunnels for obvious reasons.

However, this fact is not commonly recognized by people not involved in the planning, design and construction of tunnels. Therefore, it has been imperative for the planning and design of the Marmaray Project to ensure that the safety of people passing through the tunnels and the deep stations can be compared to the safety of people being passengers onboard modern mass transport train systems in service on surface and or on elevated structures and people using on-surface stations. Furthermore, there is an obligation on all involved in the Project to do what can be done to inform about all the efforts that have and will be done to ensure a high degree of safety for people using the commuter rail system.

2 SAFETY, MAIN PRINCIPLES

During the preparation of the Employer's Requirements related to safety the following main incidents and principles of major importance for the overall safety of people in the tunnels have been considered.

2.1 *Safety, main philosophy*

The Marmaray Project is an international project and therefore the philosophy has been that the level of safety for the Bosphorus crossing, which includes the tunnels, underground stations and associated facilities, shall be comparable to similar modern facilities in Japan, Europe and the United States.

The purpose of the design related to safety is to ensure that

- passengers that are capable of rescuing themselves can escape to a place of refuge;

Copyright © 2005 Taylor & Francis Group plc, London, UK

- rescue of those passengers not capable of rescuing themselves is possible and can be initiated immediately;
- passengers and staff can be evacuated;
- access is available to emergency services;
- normal operation can quickly be resumed.

In tunnels, the place of safe refuge will always be the adjacent tunnel and in stations, the place of safe refuge will always be at surface outside the station building. All design has to be prepared in accordance with the requirements of NFPA130.

2.2 *Fire scenarios*

The tunnels will be used by mixed types of train traffic including commuter trains, inter city passenger trains and freight trains. Therefore one of the "worst case scenarios" will be a freight train on fire in one of the bores. In this scenario a 100 MW fire has been considered, and the gas temperature curve has been taken as the well known Rijkswaterstaat curve which has duration of 2 hours and a max gas temperature as high as 1,350°C. Furthermore, the structures shall be able to withstand the effects from the standard hydrocarbon fire curve with a maximum temperature of 1,100°C but duration of 4 hours whichever creates the most severe effects.

Another possible "worst case scenario" is a fully loaded passenger train on fire; either in one of the bores or at a station. In this scenario a 20 MW fire must be considered.

2.2.1 *Escape routes*

In case of a serious accident including fire in one of the bores the escape routes are the first facility that will enable people that can rescue themselves to flee from the affected area. Modern philosophies and studies of serious accidents and people's behavior indicate that the distance between escape doors is a crucial factor.

In immersed tunnel construction it is not very costly and it does not involve any risk for people during construction to establish such escape doors. Therefore, it has on the Marmaray Project been required that the Contractor establish escape doors with a distance of not more than 125 m. This is a considerably shorter distance than what a standard calculation in accordance with NFPA130 and a maximum evacuation time to a place of refuge of 4 minutes would be implied, but it has been considered a very cheap way of improving safety conditions in the tunnel in general.

In the bored tunnels the situation is different. To establish escape tunnels between the two bores is normally costly and time-consuming. And even more important, such connections are often established by conventional mining tunnel techniques done "by hand" by human beings. Therefore, the establishment of these tunnels represents a considerable risk for casualties during construction. On this basis it has been considered reasonable to set the minimum requirement to the distance as 200 m.

To allow people to reach the escape door an emergency escape walkway alongside the centre wall of the tunnels will be needed. The width of such an escape route must be calculated in accordance with the NFPA130 regulations. The detailed calculation will depend on the detailed design in general but will generally in case of the Marmaray Project come out in the order of 1,200 mm. However, recently there has been a general acceptance worldwide of the importance of sufficient space in the escape routes in order to ensure that panic will not cause people to be killed because other people try to escape over people who have fallen in the escape route and in order to enable wheel chairs to escape as well. For this reason and to avoid the bidders competing at the expense of safety by minimizing the width of the escape walkway to an absolute minimum, it was decided to include a minimum width of 1.40 m for this walkway.

2.2.2 *Smoke control*

In case of a heavy fire breaking out in tunnels, all experience show that it is not the fire as such that causes the death of most of the casualties, it is the smoke and the poisonous gasses that develop during the fire. Therefore, it is imperative that the smoke is controlled to the extent possible and that visibility in the tunnels can be maintained in the critical phases just after the fire has broken out in order to enable people and rescuing personnel to find the escape and access routes.

How to arrange ventilation systems and the main principles behind the smoke control have been heavily discussed during the past decade and especially in connection with the severe accidents we have seen recently.

On the Marmaray Project simple but effective requirements have been introduced. The airflow in a tunnel with normal operation will generally be in the direction of the train operation. This happens due to the "piston effect" of the trains. There will, of course, be secondary effects from outside pressure differences, from wind on the portal structures, chimney effects due to hot air, local pressure differences in areas at cross-over and the like but normally these effects are of very minor importance compared to the piston effect. It is also a well known fact that it takes quite a long time and requires quite high fan capacity to change this direction of the airflow because of the inertia in the moving amount of air inside the tunnels. It has therefore on the Marmaray Project been decided that in case a fire breaks out inside the tunnels, the fan-systems shall immediately start operation in push-pull mode and drive the smoke out in direction of the train

Copyright © 2005 Taylor & Francis Group plc, London, UK

movement. The fans in the other bore shall start up in "push-push" mode to ensure that there will be an over-pressure in the adjacent bore and thereby a limited flow of smoke from the effected bore to the safe refuge bore through the doors that may be open between the bores because people are fleeing through those doors.

Arguments against this philosophy are often that if the fire has broken out for example in the last car of the train, the smoke is blown in the direction of the fleeing passengers where it would be safer to blow the smoke in the other direction. This is in our opinion not a good argument. First of all; there is only a 50% possibility that the fire will brake out behind the midpoint of the train. Secondly, it will take some time to realize where exactly the fire has broken out, and in this period an awful lot of smoke has already been blown in the direction of the train. If the fans then try to revert the flow direction, all this smoke will be blown back in the direction of the train already on fire, and even worse, the smoke has now cooled down and will not stay up under the ceiling as hot smoke will do, but smoke will fill the tube from floor to ceiling and visibility will be zero. And loss of visibility in the first critical minutes is a critical factor in whether the evacuation will be swift and successful or slow and fatal.

At the time this paper was written, the basic design of the ventilation systems was in progress, but the main principles will be that in both ends of the deep stations there will be a group of main fans combined with saccardo nozzles. All fans will be of the reversible type, and therefore the push-pull and push-push functions as described above will be possible for all bores between two stations.

In the Stations, conventional over platform and under platform exhaust systems will be installed.

2.2.3 *Fire fighting systems*

The main philosophy related to fire fighting is that the fire fighting operation will be done by systems operated and managed by human beings if the fire fighting has to take place in the tunnels.

Consequently, sprinkler systems will not be allowed in tunnels, because if such systems are activated – automatically or manually – the sprinkler systems will, of course, have a fire distinction and cooling effect, but all experience and laboratory tests indicates that the positive effects in no way can compensate for the extreme negative effect such sprinkler systems have because the smoke will be cooled down and immediately mixed up with the fresh air that will exist under the smoke layer; and this will happen within seconds and create a disastrous situation. Sprinkler systems will be installed in areas such as equipment rooms, fan and fire pump rooms, escalators, moving walkways, elevators, refuse stores, stores and other similar areas.

In the stations and tunnels automatic wet standpipe systems will be installed. In the stations at both ends of the platforms and in the tunnels the maximum distance between any fire hose cabinet will be not more than 45 m.

The main principle in fighting a fire in the tunnels will be that the fire fighters will enter the fire either downstream in the effected bore or from the non effected bore via the escape doors. Special vehicles for the purpose of rescuing will be part of the Rolling Stock contract.

2.2.4 *Detection systems*

A number of automatic detection systems will be installed. Fire detection systems will be in all station buildings and tunnel sections including cross passages, adits, stairwells and ventilation shafts, cable chambers and galleries, equipment and plant rooms, station operation rooms and in all other covered or concealed spaces.

Detection systems for control of air quality will be installed. These detection systems will as a minimum provide control of temperature, CO and NOx, and alarm systems if such gases or extreme temperatures are detected will warn the operators and the customers.

2.2.5 *Fire protection systems*

The structures in the tunnels and relevant parts of the stations will be protected against the excessive heat that will be the consequence of a serious fire in such areas. The requirements to the protection material are that the temperature on the backside of the material will not exceed 380°C and the temperature at the backside of the concrete cover of reinforcement does not exceed 250°C. These temperatures have been selected in order to prevent permanent adverse chemical reactions of the concrete and in order to prevent the reinforcement to loose too much strength.

The Contractor has in the very early stages of the construction period carried out very extensive tests of a sprayed on insulation mortar based material, thickness approximately 40 mm, and this material is furthermore physically fixed to the concrete with a fine stainless steel mesh.

The results have been very promising but further tests are still ongoing. The spray will be applied to all walls and slabs that may be affected by high temperatures.

2.3 *Flooding*

Because of the extreme depth of the Bosphorus, a potential flooding of the tunnels under the Bosphorus and the nearby connection tunnels has to avoided to the extent possible. However, no matter how well you plan the works, no matter how careful all the stakeholders are in the construction of the tunnels and

Copyright © 2005 Taylor & Francis Group plc, London, UK

no matter how many precautions you include to avoid a flooding after the commercial operation has started, there will always be a risk – albeit an extremely remote risk, that such flooding may occur. The type of flooding we talk about here is flooding where there will be a connection from the tunnel to the seawater of the Bosphorus Strait through a major opening; not potential flooding the source of which is surface water that may enter through the portal buildings or stations.

Because this risk can not fully be mitigated, it was decided to include flood gates at the ends of Sirkeci and Uskudar Stations on the seaward side; the two stations on both sides of the Bosphorus. These flood gates will be installed as early as possible during construction in order to be able to utilize them if flooding occurs during construction.

However, to close the flood gates on both sides may be an effective tool to limit serious consequences for people and equipment in the adjacent tunnels and the deep station, but closing the flood gates may increase the risk for people that for one reason or the other may still be in the immersed tunnel part of the system. Therefore, there is also another requirement that there must be proper escape routes on the potential "wet side of the flood gates" for people to flee from the Immersed Tunnel even if the gates have been closed.

Closing of such gates should not be triggered automatically, and therefore, the gates can only be closed after a manual triggering has taken place. The gates are furthermore counter-balanced in such a way that they can be manually opened as well. For inspection and maintenance purposes the gates can furthermore be manually operated via hydraulic systems.

2.4 *Hazardous goods*

The rail traffic that will use the tunnel under the Bosphorus will comprise freight trains as well as mixed passenger train traffic. Of late the issue of the transportation of people and hazardous materials through a confined corridor has generated much heated discussion. As is often the case much of this discussion is driven by emotion rather than analysis and reason. Sensibly, if hazardous materials are to be transported then decisions on how they are allowed to be transported should be based on a systematic analysis of the risk involved with the transportation of such goods through the tunnels compared to the risk of other modes of transportation of such goods. There are many examples around the world, where no dangerous goods or only very limited amounts are allowed to be transported through such tunnels despite the fact that it can be demonstrated by well proven statistical methods that the risk related to tunnel transportation is order of magnitudes less than the risk related to the existing mode of transportation of such goods.

Unfortunately, the design team of the Bosphorus Tunnels is not in a position today to conduct such risk analysis because the analysis will depend on many decisions that will be taken by the Operating Company later on as well as decisions that will be made by other Operating Companies responsible for the alternative modes of transportation. And at the end of the day, sometime in the future, such decisions will have to be made by politicians based on global risk assessments because they will be the ones that will have to explain to the public in the future why the transportation of hazardous goods was arranged as it was in case of major accidents.

However, there is an obligation on the design team of the Bosphorus Tunnels to offer a "balanced solution for the Bosphorus Tunnels" that will ensure, that should the decision in the future be to take certain types of dangerous goods through the tunnels, then reasonable precautions have been made to enable that to be realised – may be taking into account some reasonable restrictions on the operation plans when hazardous goods are present in the tunnels. It is for example often seen that certain types of dangerous goods are allowed through such tunnels, but only during nighttime, the train has to be the only train in the tube, and no passengers are allowed in the tubes or onboard the train.

Therefore, and based on the above described philosophy regarding the final decision making in the future, some requirements have been included regarding potential risks related to hazardous goods.

The drainage sumps and the equipment in such sumps shall be capable of handling up to $50\,m^3$ of hydrocarbon spillage and shall be explosion proof.

Should fire break out anyway, all the precautions described above will improve the chances for the few people present in the tunnels and the rescuing crew to evacuate safely or to fight the fire.

All structures shall be able to withstand an explosion load of not less than a permanent overpressure of $100\,kN/m^2$.

All trains will – before entering the tunnels – be checked for gauge requirements, hot axles, flat wheels and the like, and if anything is non-complying, the trains will not be allowed access.

Copyright © 2005 Taylor & Francis Group plc, London, UK

Marmaray project: geological and geotechnical investigations

Orhan Şimşek
Engineering Geologist (Bosphorus Crossing); (Sial Yerbilimleri, Turkey)

Satoshi Mitani
Design Supervisor (Bosphorus Crossing); (Pacific Consultants International, Japan)

Osman Altun
Geophysichts (Bölge Müdürlüğü, Turkey)

ABSTRACT: Preliminary site investigations for the Bosphorus rail tube tunnel project were carried out in 1985–1987. Additional site investigations for offshore and on-shore sections using modern techniques were conducted in 2002 and 2003. The objective of the off-shore investigations was to define the soil types of the marine deposits, soil/rock boundaries and geotechnical parameters of the soil layers to enable contractors to evaluate potential risk for liquefaction under seismic conditions, slope stability of the dredged trench, heave and settlement of clay layers at the bottom of the trench along the immersed tunnel alignment and the dynamic properties of soil and rock to be used in seismic hazard assessment. The objective of the investigations along the bored tunnels and cut & cover sections was to determine the soft ground and rock boundaries, geotechnical and structural properties of rock and soil, groundwater conditions and permeability.

1 INTRODUCTION

The Bosphorus railway tube crossing project extends from Söğütlüçeşme to Kazlicesme with a total length of 13,558 km (Figure 1). The project includes;

- 1600 m immersed tube, (at base elevation of −55 to −60 m, deepest immersed tube in the world),
- 10133 m bored tunnel (double tube),
- 1910 m cut & cover tunnel (stations included),
- 1300 m retaining fill and cut and at grade structures



Figure 1. Plan view of gunnel alignment.

Initial geological and geotechnical investigations were carried out in 1985–1987 during a preliminary design stage. Detailed site investigations were conducted in 2002 and 2003 during the final design stage and construction tender period.

2 INVESTIGATION PERFORMED

2.1 *Investigation in 1985–1987*

The 1985 to 1987 investigations were performed between Yenikapi and Söğütlüçeşme stations and included core drilling in rock and soil with systematic Standard Penetration Testing (SPT) and sampling. A total length of 772 m boreholes at 20 locations on water and 1394 m at 37 locations on land were carried out. Geophysical and bathymetric surveys were conducted across the Bosphorus. Physical properties of the rock and soil were determined by laboratory tests.

The off-shore investigation was carried out on a barge using conventional drilling equipment. In this method, the casing sunk into soft soil from mud line to some depth by its own weight and many of the SPT N values were counted as 0. This situation caused misleading measurements of water depth at the borehole locations and unreliable estimate of the shear strength of the soil.

Copyright © 2005 Taylor & Francis Group plc, London, UK

2.2 *Investigation in 2002–2003*

An additional investigation program was carried out for the section from Yedikule to Söğütlüçeşme in 2002 and 2003. This program included:

- A total length of 1070 m core drilling in 26 location,
- Undisturbed and SPT sampling in soil layers,
- Geophysical survey (up/down hole and cross hole) at deep stations,
- Laboratory testing to define the physical and geomechanical properties of the rock and soil.

Off shore

- A total number of seven boreholes with total length of 350 m and maximum 85 m depth from seabed level with continuous Cone Penetration Testing (CPT) and undisturbed sampling every 3 m in soil and continuous coring in rock,
- Continuous CPT tests down to maximum depth of 40 m below seabed at 3 locations,
- P-S logging in 2 holes, from seabed level to 10 m into bedrock,
- Environmental sampling and testing from seabed down to approximately 9 m,
- Geotechnical laboratory testing.

Off-shore drilling was performed by Fugro Engineers, from the Netherlands, using the marine vessel Bavenit, which maintains its location on water by a dynamic positioning system.

CPT testing was conducted using the Wison type equipment (Figure 2), which consist of a down hole jacking unit with a 3 m stroke and a thrust capacity of 90 kN. The Wison type CPT equipment is used in conjunction with a flush rotary drilling system and open bit. After the borehole has reached the required depth, the Wison unit is lowered by its electro-hydraulic umbilical to the bit, where it seats and latches under its own weight. The cone penetrometer is then hydraulically pushed into the soil at a constant rate of 20 mm/s. The measurements of cone tip resistance, sleeve friction and pore pressure are displayed graphically in the control cabin and electronically recorded.

The geophysical and bathymetric surveys extended to a width of 500 m on both sides of the immersed tube tunnel alignment. The geophysical survey included single channel boomer and sparker methods. The single channel boomer was carried out with parallel (parallel to the route corridor) profiles spacing of 100 m and cross profiles (at right angle to the route corridor) at a spacing of 25 m. The sparker method was measured along 3 parallel profiles (along the proposed alignment centerline and one profile along each side of the alignment) and cross profiles at spacing of 100 m.

The first 50 m of depth below the channel have a vertical resolution of less then 25 cm for boomer operation. The sparker system was used down to approximately 100 m from seabed, with a vertical resolution of less than 2 m.

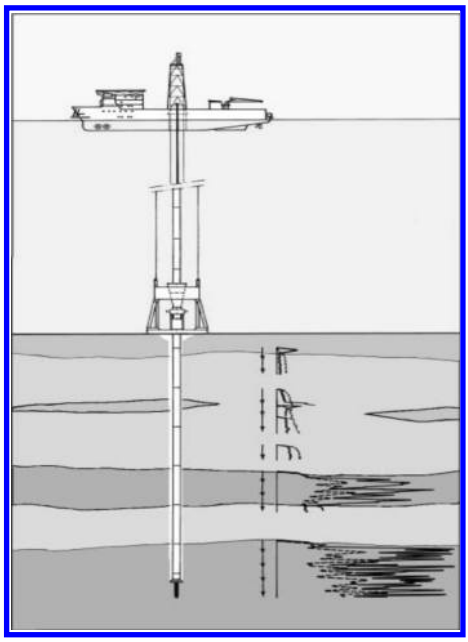


Figure 2. Wison type CPT equipment.

3 RESULTS OF INVESTIGATION

3.1 *Bored tunnel*

Based on the findings of the site investigation described above, the predicted ground conditions along the bored tunnel alignment can be summarized as indicated in Table 1 and in geological profiles (Figures 3 and 4):

As seen in Table 1, three major formations will be encountered along the bored tunnel alignment:

Bakirköy Formation will likely be encountered from km 0 + 960 to km 2 + 400 and consist of silty sandy clay with calcareous lenses. The clayey layers are highly over-consolidated and are in stiff to very stiff consistency. The calcareous lenses bear groundwater. SPT N blows are usually higher than 30 at tunnel level and generally increase with the depth (Figure 5). According to Unified Soil Classification System (Casagrande 1948), the cohesive layer of the Bakirköy Formation is classified as CH and the cohesionless layers are classified as SC, SP-SC and SW-SC (see Figure 6).

Süleymaniye Formation will likely be encountered along the bored tunnel section from km 2 + 400 to 4 + 560 consisting of silty clay with sandy lenses. The clayey layers are highly over-consolidated and are in stiff to very stiff consistency. The sandy lenses bears

Copyright © 2005 Taylor & Francis Group plc, London, UK

Table 1. Summary of ground conditions along Bored tunnel.

Chainage (km)	Structure	Formation
Till km 0 + 960	At Grade	Artificial Fill
0 + 960–1 + 500	Cut & Cover	Artificial Fill Bakirköy Formation
1 + 500–2 + 420	Bored Tunnel	Bakirköy Formation
2 + 420–3 + 310	Bored Tunnel	Süleymaniye Formation
3 + 310–4 + 090		Artificial Fill Marine Deposits
	Cut & Cover (Yenikapi Station)	Süleymaniye Formation Trakya Formation
4 + 090–4 + 140	Bored Tunnel	Süleymaniye Formation
4 + 140–4 + 420	Bored Tunnel	Trakya Formation
4 + 420–4 + 560	Bored Tunnel	Süleymaniye Formation Trakya Formation
4 + 560–6 + 240	Bored Tunnel	Trakya Formation
6 + 240–6 + 420	Sirkeci Station	Trakya Formation
6 + 420–7 + 320	Bored Tunnel	Trakya Formation
8 + 890–9 + 550	Bored Tunnel	Trakya Formation
9 + 550–9 + 880	Üsküdar Station	Artificial Fill Marine Deposits Trakya Formation
9 + 880–12 + 795	Bored Tunnel	Trakya Formation
12 + 795–12 + 920	Bored Tunnel	Alluvium Trakya Formation
12 + 920–13 + 415	Bored Tunnel	Trakya Formation
13 + 415–13 + 860	Cut & Cover, At Grade Structures	Artificial Fill Alluvium Trakya Formation

usually confined perched groundwater. According to the Unified Soil Classification System, the cohesive layer of the Süleymaniye Formation is usually classified as CH and MH-OH (Figure 7). The sandy lenses are classified as SC, SP-SC and SW-SC. SPT N blows versus depth relation is shown in Figure 8.

The Trakya Formation is made up of yellowish brown to dark gray colored sandstone, siltstone and mudstone (shale) sequences. The rock mass is usually medium weathered to fresh and exhibits closely to moderate closely spaced discontinuities. The strength properties of the intact rock are in the range of weak to very strong. Dyke intrusions will likely be encountered frequently during tunneling.

From a geotechnical point of view the Trakya Formation can be divided into three groups;

Faulted/sheared rock mass: This zone will usually be encountered at fault zone areas with thickness of from several decimeters to few meters, at sheared mudstone (shale) layers and at dyke contact. Intact rock Uniaxial Compressive Strength values (UCS) vary from 2 MPa to 20 MPa.

Average rock mass: This rock mass is composed of sandstone, siltstone and mudstone (shale) sequences. The rock mass is medium strong to very strong and shows 70 MPa UCS in average. Abrasiveness of the rock mass is expected in the range of from not abrasive-to-abrasive.

Competent rock: This rock mass represents fresh and very strong sandstone (intact UCS is higher than 180 MPa) and fresh diabase type dyke intrusion.

3.1 *Immersed tube section*

Based on the investigation results, the geological conditions and lithological stratification are interpreted as shown in the geological profile (Figure 10). Taking into consideration the grain size distribution, density and consistency of the soils along the immersed tube tunnel alignment, the marine deposits can be distinguished into eight geotechnical units (excluding rock), as summarized in Table 2.

Geotechnical unit A refers to contaminated soil. These layers will be dredged and disposed in a confined disposal facilities.

Geotechnical unit B refers to gray colored, fine to coarse – grained sand with silt and little clay content. This unit is encountered at the upper level of the tube tunnel profile and is not present below the foundation level of the tube between km 7 + 390 and 7 + 900. The cone resistance in this unit is generally rather low, in the range of 0.5 MPa to 4 Mpa, which corresponds to very loose to loose soil. Locally, the cone resistance is as high as 12 MPa. This unit will be encountered below the invert of the tube alignment between km 7 + 900 and km 8 + 680. The CPT cone resistance is relatively high and increases with depth. It ranges from 4 MPa to 12 MPa in first 8 m to 12 m. Below this depth, unit B has higher cone resistance (more than 12 MPa) due to interlayering with unit E.

Geotechnical Unit C represents the gray colored sandy clay/clayey sand layer, which is situated above the immersed tube foundation level. This unit is located from km 7 + 390 to 7 + 900. CPT tests indicate rather low cone resistance (0.2 MPa to 2 MPa), which corresponds to very soft to soft/very loose to loose consistency and density.

Geotechnical unit D consists of gray colored silty clay (Golden Horn Clay) with medium plasticity and very soft-to-soft consistency. This unit is present below the foundation of the immersed tube tunnel between km 7 + 390 and km 7 + 900 and therefore is considered one of the main geotechnical units influencing the construction works. The cone resistance of this clay is rather low, averaging about 0.5 MPa, which corresponds to very soft consistency (see Figure 9).

Geotechnical Unit E is composed of gray sandy clay with low to medium plasticity, and firm to stiff consistency. H2S gasses were measured from the

Copyright © 2005 Taylor & Francis Group plc, London, UK

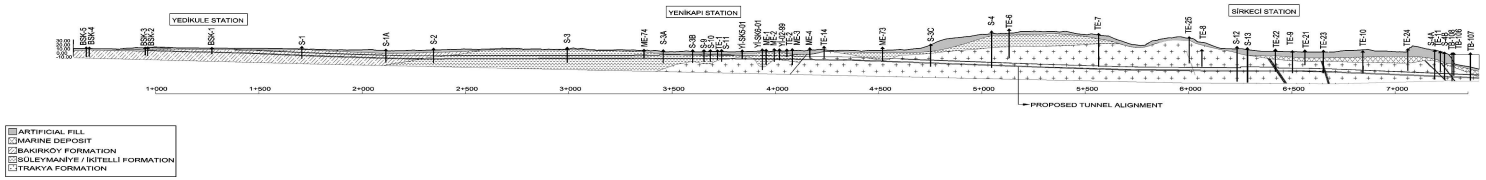


Figure 3. Geological profile of European side.

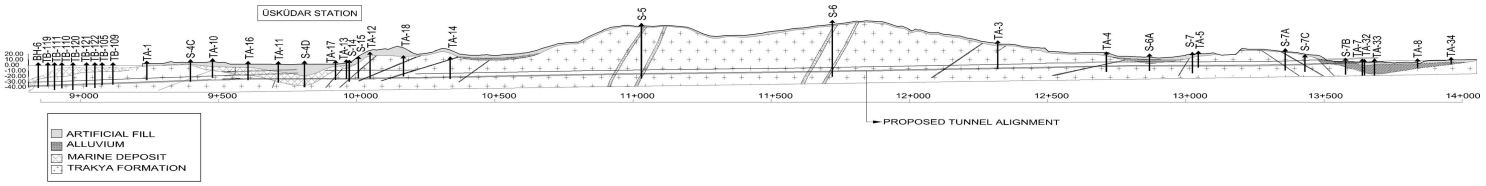


Figure 4. Geological profile of Asian side.

Copyright © 2005 Taylor & Francis Group plc, London, UK

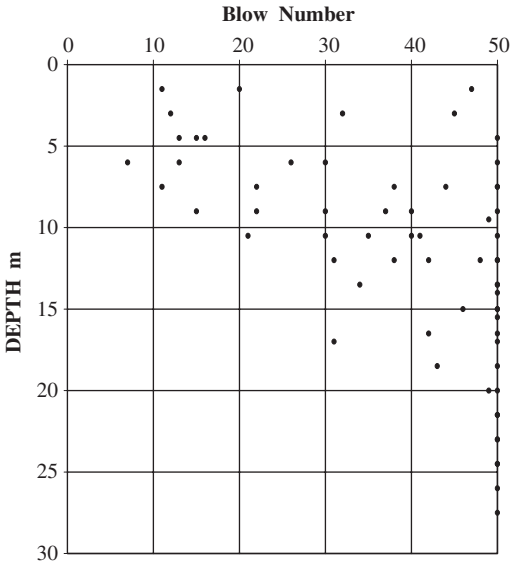


Figure 5. SPT N values versus depth.

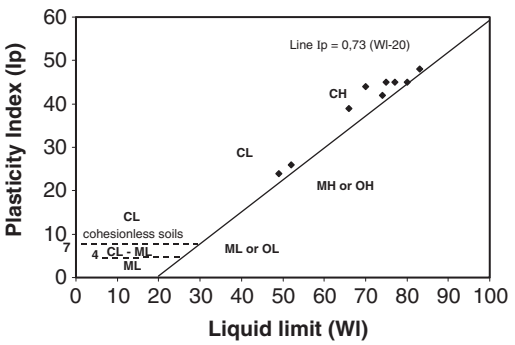


Figure 6. Plasticity chart, Bakirköy formation.

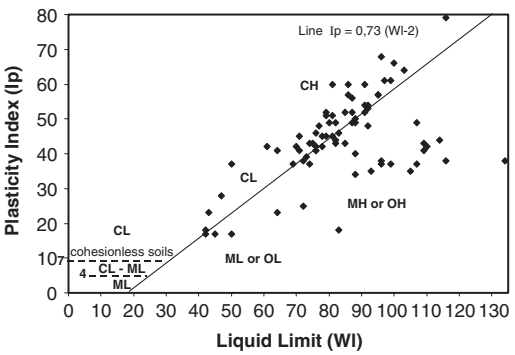


Figure 7. Plasticity chart, Süleymaniye formation.

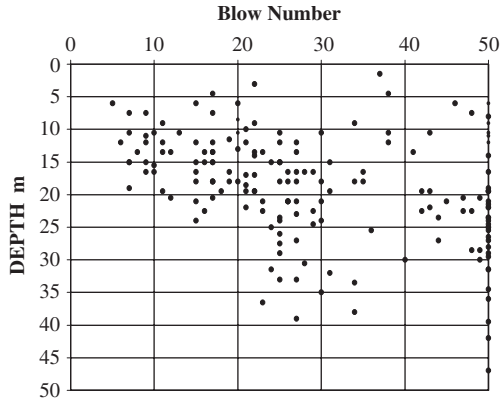


Figure 8. SPT N values versus depth.

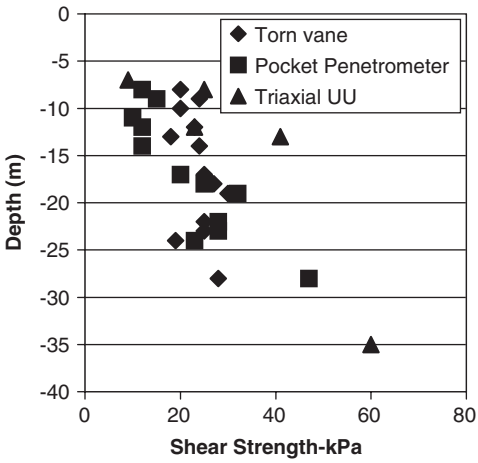


Figure 9. Depth un-drained shear strength of unit D.

sample obtained from this unit. This unit is encountered in the central and eastern part of the tube tunnel alignment. Since it is found below elevation −55.0 m, it is assumed that this unit will not appear within the limits of proposed tunnel trench. The cone resistance of this unit generally ranges from 1.0 to 2 MPa, which corresponds to firm to stiff consistency.

Geotechnical Unit F contains light gray-to-gray sandy shell deposits, which is present between km 8 + 180 and 8 + 780. This unit appears from seabed level to −43.0 m.

Geotechnical Unit G is made up of gray silty sandy gravel with shell fragments. This coarse grained soil is present at the eastern side of the tube tunnel alignment between approximately km 8 + 680 and 8 + 790.

Geotechnical Unit H contains coarser gain size marine deposits composed of sand, gravel, cobble and boulders. Maximum boulder size is expected to be approximately 1 m diameter.

Copyright © 2005 Taylor & Francis Group plc, London, UK

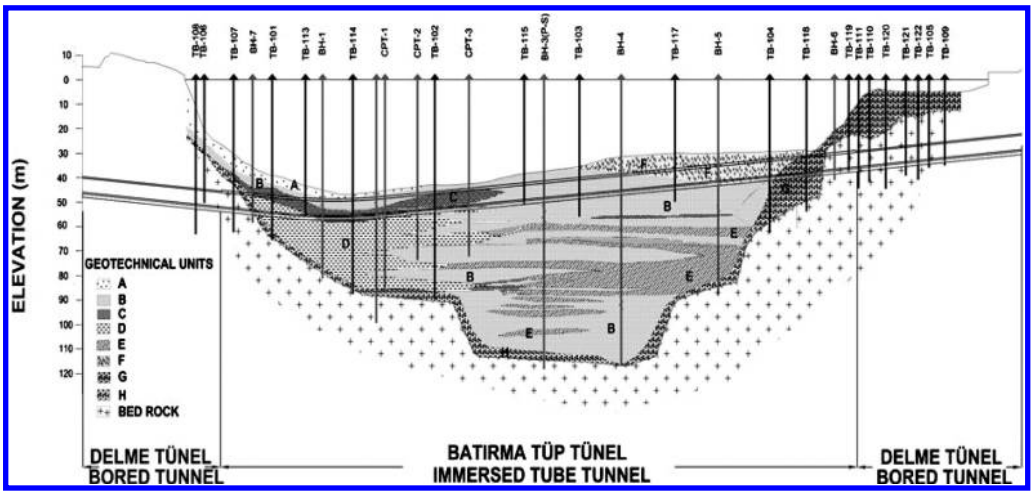


Figure 10. Geological profile, immersed tube section.

Table 2. Summary of ground conditions.

Units	Lithological descriptions
A	Artificial fill, contaminated soil
B	Light gray to dark gray sand
C	Gray Sandy Clay/clayey sand
D	Gray Silty clay, very soft with sandy lenses
E	Gray sandy clay
F	Light gray to gray sandy shell deposits
G	Gray Silty sandy gravel
H	Gray sandy gravel

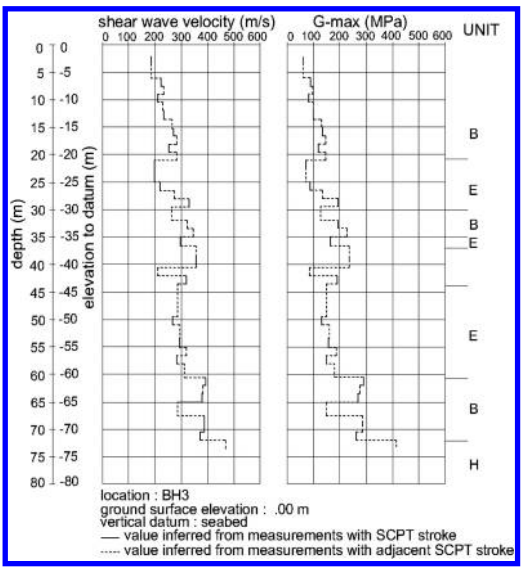


Figure 11. Shear wave velocity (m/s) and small-strain shear modulus at borehole BH-3.

P-waves, S-waves and shear modulus of the various geotechnical units were measured in two boreholes by Seismic CPT tools. Shear wave velocity and small-strain shear modulus profiles measured in one of these borings is presented in Figure 11.

4 CONCLUDING REMARKS

Geological and geotechnical investigations for the proposed Bosphorus rail tube tunnel crossing were carried out during a preliminary design phase in 1985–1987 and a final design and construction tender phase in 2002–2003.

The off-shore preliminary geotechnical investigation in 1985–1987 was performed using conventional drilling methods with SPT tests and undisturbed samples, whereas modern investigation techniques were used during final design and construction tender stage by means of a vessel which is capable of maintaining its location by a dynamic positioning system. In this system, continuous CPT testing was performed and undisturbed soil samples were obtained at 3 m intervals. The data obtained from the recent investigation were found more reliable for defining the soil stratification, index properties and strength properties of the various soil layers.

REFERENCES

Büchi E., Mathier J. –F., Wyss Ch., 1995, Rock abrasivity – a significant cost factor for mechanical tunnelling in loose and hard rock, Tunnel 5/95, Cologne: 38–44.

Casagrande A. (1948), Classification and identification of soil, Transaction ASCE, vol. 113, pp. 901–991.

Copyright © 2005 Taylor & Francis Group plc, London, UK

Marmaray project: tunnels and stations in BC contract

Satoshi Mitani
Design and Construction Supervisor (Bosphorus Crossing); Pacific Consultants International, Japan

Hideki Sakaeda
Assistant Project Manager (Bosphorus Crossing); Pacific Consultants International, Japan

Halil Şahin
Bored Tunnel Engineer (Bosphorus Crossing) ; Yüksel ProjeUluslararası A.Ş., Turkey

Ümit Çelik
M.Sc., CE (Bölge Müdürlüğü, Turkey)

ABSTRACT: The areas on each side of the Bophorus, in what is now Istanbul, have been continuously inhabited for millennia. The city's historical and cultural heritage is an amalgam of influences from the early Roman Empire, the Byzantium Empire, Selçuk Turkey, the Ottoman Empire and the modern state of Turkey. The bored double tunnels and the cut & cover tunnels of the project will run under the heart of the historic peninsula, under the Bosphorus and under historic Uskadar. The tunnels will run under many historical and cultural structures of world and local importance, and will no doubt run through important archeological strata. Great cities need to adjust to the needs of their inhabitants while maintaining cultural and historical continuity; and railway transport links in tunnels meets those objectives. It has been the general practice in Istanbul to excavate tunnels using the New Austrian Tunneling Method (NATM). Although the method has many advantages, there are many difficulties when it is applied in these particular circumstances. For instance the rate of progress is relatively slow, there is a risk of subsidence due to contraction of the excavated space and it is difficult to control leakage and subsequent drawdown of groundwater, which may lead to uncontrolled settlement on the ground surface. Preferably, tunnel excavation by Tunnel Boring Machine (TBM) was recommended for the excavation of main lines of tunnels to minimize the possible impact of the construction on structures at or below ground level.

1 INTRODUCTION

The Marmaray Project is the upgrading of approximately 76 km of commuter rail from Halkali, European end, to Gebze, Asian end. The black alignment in Figure 1 shows the parts of the railway that are above ground (CR Project) and the white alignment shows the new railway system that will be constructed in tunnels under the Bosphorus (BC Project).

The paper deals with the BC project which is currently in the early stage of design and construction.



Figure 1. Alignment of Marmaray project.

2 BACKGROUND OF THE BC PROJECT

The idea of connecting Europe and Asia with a traffic connection under the Bosphorus Strait was first suggested in 1860. The desire to construct a railway mass transit connection from west to east in Istanbul became stronger in the early 1980s, and consequently the first comprehensive feasibility study was carried out in 1985. This study concluded that such a connection would be feasible and cost-effective, and the alignment

Copyright © 2005 Taylor & Francis Group plc, London, UK

we see in the project today was selected as the best of a range of alignments.

The project, as outlined in 1985, was discussed during the following years, and around 1995 it was decided to make more detailed studies and update the feasibility studies. These new studies were concluded in 1998, and the conclusions underlined the earlier conclusions that the project would offer many advantages to the people working and living in Istanbul, and would ease the rapidly growing problems of traffic congestion in the city.

In 1999, a funding agreement between the Republic of Turkey and the Japanese Bank for International Cooperation (JBIC) was signed, and the pre-qualification of groups for the contract – the Bosphorus Crossing – was finalized in December 2002, and in May 2004 a design and build contract was signed between the Employer and the TKGN Joint Venture.

3 OUTLINE OF THE BC PROJECT

The Bosphorus Crossing project, the total length of which is approximately 13 km, consists of immersed tube tunnel, bored tunnels and cut & cover tunnels, 3 underground stations and one at grade station as shown in Figure 2.

3.1 *Immersed tube tunnel*

The immersed tunnel under the Bosphorus will be approximately 1,500 m long, including the connections between the immersed and bored tunnels. The tunnel will provide a vital link in the two-track rail crossing beneath the Bosphorus, and is located between the districts of Eminönü on the European side and Üsküdar on the Asian side of Istanbul. The maximum depth of sea floor is about 60 m, which means that this tunnel will be the deepest of its type to date.

3.2 *Bored tunnels and underground stations*

Connecting to the immersed tunnel are tunnels bored through rock using tunnel boring machines (TBMs). One tunnel in each direction is provided with one track in each. The tunnels are spaced far enough apart to avoid affecting each other significantly during construction. Short connecting tunnels are provided at frequent intervals so that escape to the parallel tunnel is possible in an emergency.

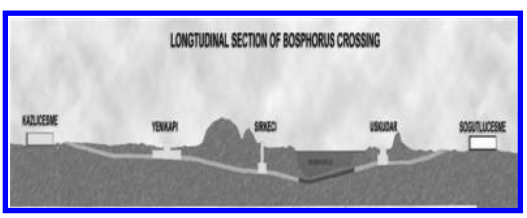


Figure 2. Longitudinal section of Bosphorus Crossing project.

When the tunnels become very shallow, or the rock becomes very soft, the tunnels are constructed either using a soft-ground TBM or by cut-and-cover construction. In places where the tunnel shape changes, such as where trains can cross from one tunnel to the other, other methods using a number of specialized procedures may be used (such as NATM, drill-and-blast and pipe-jacking). Similar procedures may be used to excavate Sirkeci Station which will be formed in a cavern deep underground. Two other stations, Yenikapi and Üsküdar, will be constructed below ground using cut-and-cover techniques. Where cut-and-cover tunnels are used, they will most probably be constructed as a single box with a central dividing wall between the two tracks.

Altogether, there will be approximately 12 km of tunnels constructed by these methods. These works extend from west of the existing Yedikule Station to the end of the immersed tunnel somewhere east of Sarayburnu Park on the European side, and from end of the immersed tunnel north of Kiz Kulesi near the Üsküdar Ferry Terminal to the Commercial Complex Center near Söğütlüçeşme Station on the Asian side. TBM tunnels will all be lined with pre-cast segmental linings. All tunnels and stations will be waterproofed to prevent leaks and ventilation will be provided.

4 SITE CONDITION

4.1 *Works in historic peninsula*

The Project is situated in Istanbul, where many buildings and structures exist that are of national and international historical importance. These important aspect of national and world heritage have to be preserved as they are. Many of these buildings and structures on the surface ground are vulnerable to tilting movement, differential settlement of the ground or vibration, which may possibly be induced by tunnelling works, partly by the loss of the ground and partly by dewatering and blasting. In addition, it has been anticipated that subsurface antiquities will be encountered, preservation of some of which may also be necessary.

Thus, tunnelling work as well as cut and cover work will be executed under very careful control to keep the ground condition as close as possible to that which existed before tunneling commenced and coordination with Historical Heritage Preservation Committee is scheduled during the whole construction period.

Due to the limited land available for Works Area and PTFA (Permanent Track Facilities Area), the places where work areas for temporary shafts or adits are

Copyright © 2005 Taylor & Francis Group plc, London, UK

limited. The method of construction therefore has to be selected in accordance with these limitations, and the sensitive conditions. The construction program and schedule under these difficult site conditions will be complex and very tight.

4.2 *Geology and geotechnical condition*

4.2.1 *Geological setting*

Details on geology and geotechnical conditions are introduced briefly here.

Palaeozoic sedimentary rock formations, from Ordovician to Carboniferous, develop widely along the alignment of the Project, forming the main rock unit for tunnelling works. This basement rock consists of a sequence of alternating layers of sandstones (greywacke) and siltstones. Thrusting and folding highly develop throughout the basement rocks.

Tertiary sedimentary rocks of middle to upper Miocene consist of bone-bearing sands and gravels of Çukurçesme Formation, clays and marls of Güngören Formation and Mactra (molluscs) bearing limestone of Bakirkoy Formation develops at old Istanbul area. These sediments unconformably overlie the Palaeozoic formation and are gently deformed.

Quaternary sediments and artificial fill overlie the Palaeozoic and Tertiary sediments. Quaternary marine sediments distribute in a thick series in sea bed as unconsolidated sandy and silty material and thin out to the lowland. In places onshore colluviums deposit. Artificial fill consists of clayey silty gravel with rock fragments and bricks.

4.2.2 *Geotechnical condition*

1. Stations and Cut & Cover Tunnel Works in European side:- Artificial fill, with varying thickness from few meters to 15 m, develops as a superficial layer. Beneath the layer Tertiary sediments are distributed widely around the Yedikule and Yenikapi area. These consist of gravelly sandy hard clays with occasional intercalations of calcareous layers and hard clays; they seem to be of sufficient bearing capacity and no heaving is expected. In Yedikule and Sirkeci area Quaternary marine deposits underlie the artificial fill and up 7 m thick. This layer consists of sandy-silty clay to clayey-sandy silt with shell fragments. At Sirkeci station beneath the marine deposits there is basement rock in which the deep station structure is to be constructed. Groundwater level is few meters above sea level.
2. Stations and Cut & Cover Tunnel Works in Asian side:- Uskudar Station is located in a buried old valley. The lowest point of the top of the basement rock, which forms the floor of the buried valley, is about 38 m below sea level. Quaternary marine deposits of sand and basal gravel abut the basement rock with thickness of 10 to 20 m. Artificial fill covers these deposits to a thickness of 6 to 20 m. Groundwater level is slightly higher than sea level.
3. Bored tunnel in European side:- From western end portal to Yenikapi Station there are Tertiary sediments consisting of silty to clayey layers associated with calcareous lenses and sandy and gravelly lenses. Overburden is very thin in the section between Yedikule station and 2 + 080, where TCDD trains operate on the surface. From Yenikapi Station to Immersed tunnel the bored tunnel is to be constructed mainly in basement rocks, however, near Yenikapi Station, the rock cover is very thin and around 4 + 500 the Tertiary weak rock mass may appear at the tunnel face for about 150 m where the thickness of this Tertiary formation above the tunnel crown may be sufficient to create arch action. After passing through Sirkeci Station, the possibility of sea-water ingress becomes higher. At the connection between bored tunnel and immersed tunnel the rock cover will be less than 1tunnel diameter (1D).
4. Bored tunnel in Asian side:- From the immersed tunnel to Üskudar Station the conditions are similar to those mentioned previously where the tunnel is to be constructed in basement rock. Minimum rock cover is less than 1D near the connection with immersed tunnel and then it becomes greater than 1D. Where the tunnel connects to Üskudar Station the rock cover reduces to few meters. From Üskudar Station to eastern end portal the tunnel excavation may start in a mixed ground condition which consists of marine sediments and basement rock, and in few tens of meters of excavation rock cover increases to more than 2D. At about 12 + 800, where cut & cover tunnel was originally designed the tunnel may drive in a mixed ground which consists of basement rock and colluviums for about 150 m. From here to the eastern end of the tunnel the tunnel is under thin overburden with rock cover less than 1D.

4.3 *Seismic condition*

Istanbul is located some 20 km from the extension of the North Anatolian Fault Zone, which runs from east to west to the south of the Princess Islands in the Marmaray Sea. The project area is therefore in a location where the risk of a severe earthquake must be taken into account.

5 TUNNELS AND UNDERGROUND STATIONS

5.1 *Preliminary design concept*

In the preparation of the Employer's Requirement for design and construction care was taken to introduce preliminary design constraints that dealt not only with

Copyright © 2005 Taylor & Francis Group plc, London, UK

the quantitative aspect of design and the physical constraints of limited and cramped working conditions but also the qualitative aspects of design that need to relate to the unique historical environment in which the project is to be placed. The broad points considered are given below;

- Selection of alignment and station locations to preserve historical heritage;
- Archaeological investigation; in cooperation with Historical Heritage Preservation Committee;
- Architectural expression to be in keeping with location;

Consideration on site, geotechnical, hydrological and seismic condition

- Setting of work areas and PTFA with respect to site condition
- Choice of type of tunnels and method of construction
- Safety of the structure.

Passenger flow forecast

5.2 *Why TBM?*

There are two choices as for the method of tunnel excavation, one is the excavation by TBM and the other is the excavation by non-TBM methods. The Employer's Requirement specifies that the main running tunnels are to be excavated by closed-face shield TBM or Semi-mechanical shield and that where tunnels are to be excavated in any area where there is a risk of flooding from the sea, excavation shall be by means of a TBM which can seal off the tunnel against flooding. Other tunnels and shafts are to be excavated by non-TBM method.

Due to the time constraints of the project and difficulty to allocate adequate numbers of shafts or adits for tunnel excavation, the main running tunnels are specified to be excavated by TBMs with shield. Only Sarayburnu work area and shafts at station areas are possible to be fixed as starting portals of tunnelling. Thus, the main running tunnels of significant length must be excavated within a limited duration. The expectations are that the TBMs will achieve the progress needed to meet the time constraints and the adoption of segmental lining tunnel will be result in a high quality, permanently lined structure with a resulting long life. To minimize the collapse of the ground, or if it happens to minimize the result and thereby prevent the ground surface from subsidence the TBM is required to be equipped with shield shell which eases the erection of segmental lining as well.

Tunneling by NATM in poor ground, as is the case of this project, requires considerably heavy support pattern associated with various auxiliary supporting methods to prevent the working face from excess deformation and collapse. This means that varieties of activities are required to complete the one round of excavation, which results in slow advance rate of progress, which doesn't meet the targeted schedule of the completion of the Project. Besides, there may be indeed a serious risk when the connection part with Immersed tunnel is to be excavated by NATM under high water pressure under the sea.

In general the best way to excavate tunnels is to commence excavation from a portal at the lower point of the tunnel alignment and to proceed in an uphill direction to ease the excavation, which in this project means to fix portals at both ends of the immersed tunnel. However, the reality of the Site does not allow the "best" approach to be adopted and it is inevitable that sections of the tunnels will have to be excavated in a downhill direction. This will involve difficulty to some extent if groundwater ingress is significant and the TBM is without face control mechanism. The probability of groundwater ingress is largest in tunnels under the sea or at such sections being affected by the sea and a closed face TBM is required to be used.

5.3 *Application of NATM*

5.3.1 *Sirkeci underground station*

Two platform tunnels of about 9 m high and 11 m wide are planned either to be constructed by enlargement of tunnels excavated by TBM or independently through the shafts at both ends of the station. Non-TBM mechanical excavation may be used. Occasional grouting may be necessary to cope with difficult ground, and fore-piling with chemical injection may be required to prevent the fractured rock mass in arch portion from collapse. The central platform tunnel of about 8 m in diameter and 175 m long will be excavated from the bottom of the shaft by non-TBM mechanical excavation. The sequence of excavation may be similar to that of platform tunnel; however, this tunnel shall be supported rigidly enough to cope with the anticipated large stress which will be induced by the excavation of platform tunnels at both sides. Four connection tunnels of about 20 m long each and two inclined, tunnels for escalators are to be excavated in the same manner. Excavation of two shafts, about 48 m deep and about 55 m deep respectively, will be done from the surface ground.

5.3.2 *Connection tunnels and crossover tunnels*

Connection tunnels are to be constructed every 200 m in the onshore running tunnels with cross section of about 10 m^2. Depending on the geological conditions these will be excavated by NATM or pipe-jacking. Crossover tunnels, one at both sides of the Bosphorus Strait, connect the running tunnels which are about 15 m to 40 m apart. Excavation will be done using the short-bench-cut method. Both ends of the tunnel are

Copyright © 2005 Taylor & Francis Group plc, London, UK

close to and in contact with running tunnels, which may require a large cross section and may need adequate auxiliary supporting methods as well, including grouting and reinforcement of the running tunnels. Secondary in-situ lining will be placed after the completion of excavation.

6 DIFFICULTIES AND NECESSARY CARES FOR TUNNEL EXCAVATION

6.1 *TBM*

The connection between the bored tunnels and the immersed tunnels under on under high water pressure requires specific measures to be considered so as not to flood the tunnel. The clearance between the two bored tunnels is very narrow and the stability of the leading tunnel may be affected by the excavation of the following tunnel. Therefore the segments and backfill of the preceding tunnel have to be strong enough to resist these affects and it may be necessary to reinforce the surrounding ground. If the Contractor were to use double track TBM, connection with the immersed tunnel could be very difficult, due to the big difference in tunnel shapes and the possible need for futile excess excavation as well. If the Contractor were to use multi-face TBM capable to install partition, MF shield may be physically not capable to drive through hard rock ground and cost of TBM will become enormously high.

When driving through poor quality rock mass it is highly possible that the TBM will get jammed at the face due to collapse of friable rock mass in both open-face and closed-face excavation, which will obstruct the progress of the work significantly. Depending on the situations encountered necessary counter measures may be adopted but occasional grouting will be necessary to rescue TBM.

When driving under railway operation precise monitoring on settlement and the application of necessary counter measures to prevent the surface track base from settling beneath the TCDD train operation where the overburden is thin is required.

Generally in shield tunnelling most of the accidents occur when the shield starts from the shaft or arrives at the shaft. The main causes of such accidents are ingress of groundwater accompanied by soil around the shaft, where ground has been disturbed during the construction of shafts. Auxiliary method such as grouting is generally necessary.

6.2 *NATM*

To prevent the settlement of the surface ground which will be caused by the lowering of groundwater table, injection grouting against surrounding rock mass is often necessary to seal off fissures in the rock mass. Grouting may also be necessary to prevent the friable, sheared rock mass at the working face from collapsing under the ingress of groundwater. Rock mass in the Project, as a general, is of rather poor quality, where fore-piling along the periphery of the tunnel arch as well as to the tunnel face will be necessary in tunnelling by NATM. Tunnelling by NATM under thin overburden needs to proceed with specific care not to generate excess subsidence of surface ground. Auxiliary supporting measures are generally required in such circumstance. Tunnelling by NATM in poor ground requires considerable heavy support pattern associated with various auxiliary supporting methods to prevent the working face from excess deformation and collapse. This means that varieties of activities are required to complete the one round of excavation, which results in slow advance rate of progress.

7 CONSTRUCTION TIME SCHEDULE

Design and Construction commenced on 27th August 2004 and is scheduled to be completed by April 2009.

Copyright © 2005 Taylor & Francis Group plc, London, UK

Marmaray project: marine operations, the Bosphorus crossing

Steen Lykke
Project Manager, Marmaray Project, Pacific Consultants International, Japan

Hideki Sakaeda
Assistant Project Manager, Bosphorus Crossing, Pacific Consultants International, Japan

Vahan Tanal
Dredging Specialist, Marmaray Project, Parsons Brinckerhoff Quade & Douglas, Inc., USA

F. Koyama
Project Manager, Immersed Tunnel, Taisei Corporation

Isikhan Guler
Marine Works Engineer, Marmaray Project, Yuksel Proje, Turkey

ABSTRACT: This paper describes the most important factors influencing the marine regime of the Bosphorus, and present and explain the measurements done up till now in the Bosphorus. It also describes the other constraining factors influencing the immersion processes in the area, and discusses the background for the final requirements to the Contractor related to how to control and predict the marine conditions. It also describes in broad terms the results of the initial investigations performed by the Contractor regarding the immersion process as of the time of writing this paper.

1 INTRODUCTION

The Bosphorus Strait is one of the busiest sea lanes in the world. All commercial traffic to and from the Black Sea have to pass the Bosphorus, and therefore a large number of commercial ships traverse the length of the Bosphorus every year. On top of that a vast number of smaller commercial ferries carrying passengers and cars across the Bosphorus find their way in between the bigger ships in the area near Uskudar and where the immersed tunnel will be constructed.

The current in the strait varies dramatically and the current regime is of a complex nature. The current is stratified. Non saline water from the rivers leading to the Black Sea and general surface water is normally flowing in the upper layers of the Bosphorus from the Black Sea towards the Marmaray Sea, and saline water is normally flowing in the lower layers in the opposite direction from the Marmaray Sea towards the Black Sea.

However, major variations due to many different factors in this regime occur during the seasons, and a further complicating factor is that water from the Golden Horn – a side stream to the Bosphorus – is flowing into the Bosphorus exactly in the area where the deepest immersed tube tunnel of the world will be constructed – the Bosphorus Crossing Immersed Tunnel.

2 FORECASTING OF THE CURRENT AND RELATED RISKS

At the time of planning the requirements that would be incorporated in the Contract and defining the risk sharing between the Contractor and the Employer regarding the control of the immersion process, not much factual information about the actual current in the Bosphorus could be found. Sporadic measurements had been done by different organizations and companies, but no measurement campaign over longer periods where the "quality" of the measurements had been documented could be made available to the engineers.

To ensure safety and to minimize risks have been very important guidelines for the management in everything that has been done on the project up till now, and it is generally accepted that accidents and uncontrolled processes related to the immersion process of the elements constitutes high risks. Therefore more comprehensive studies had to be established.

Copyright © 2005 Taylor & Francis Group plc, London, UK

The sporadic measurements available indicated that the current in the Bosphorus can vary quite dramatically and the surface current velocity can be as high as 3–4 m/s in extreme situations. The bottom current is generally low and does normally not exceed 1 m/s. It was therefore decided that a simple measuring campaign would be performed by the Employer in the period before the bid was initiated and as long into the bid period as was reasonably possible in order for the bidders to be able to utilize the results. Such a campaign could not and was not designed to give a solid basis for the bidders planning in details but served only the purpose of giving the bidders a better basis for limiting the costs for the risk they had to allocate in their bids related to the immersion process.

It was also decided that a requirement for the Contractor to establish a comprehensive data base of the current regime in the entire immersion area would be included in the bid documents. The purpose of this campaign would be two fold. Firstly, to enable the Contractor to develop a reliable forecasting model that would be sufficient to avoid major surprises and unnecessary risks during the last critical phases of the immersion processes, and secondly to ensure the establishment of a database that could be used to define a risk sharing mechanism between the Employer and the Contractor of "unforeseen current conditions".

The mechanism to establish "reference conditions for the current regime in the Bosphorus for the purpose of risk sharing related to immersion processes" becomes complicated because the current will vary substantially from place to place of each elements position on the alignment. Therefore, it would be almost impossible to establish continuous monitoring (baseline conditions) of the current in each immersion position, and later on during construction it would be impossible to monitor the actual current in the same positions due to dredging and construction activities taking place in the alignment. It was therefore decided that the "reference condition in each immersion position" would not be direct monitoring of the current in that position, but the reference condition would be defined as the output of a calibrated computer model (a micro environment model) using input from three monitoring stations placed strategically in the water column near the alignment. Continuous monitoring at these three points can be done during the whole period, and therefore the risk sharing mechanism will also be effective over the whole period. The monitoring in these three positions is continuing and the monitoring is done from seabed to water surface. Important information will not only be the current profile itself, but also other factors such as salinity, the transition layer between the upper and lower current and the temperatures.

The mechanism and the requirements to establish reliable forecasts of the current in the immersion position for the needed critical window was based on experience from similar situations, for example the Oeresund Immersed Tunnel established between Denmark and Sweden where quite similar physical conditions like stratified current exist. The forecast mechanism was furthermore combined with the monitoring we would have to do anyway in three positions as described above for the purpose of establishing the reference conditions for current. The input to a current forecasting model is known to be all relevant meteorological and hydrologic data, and the forecast of such weather data, as they change in the regions surrounding the Bosphorus Strait. The area we talk about here can be quite large, but how large it is and which input data are required can only be decided later, after the calibration and optimization of this "macro model" has been done. However, most likely the regions have to cover the Black Sea and the surrounding land areas, the Marmaray Sea and the surrounding land areas and major land areas east and west of Istanbul in general. The most important weather systems and hydrological systems are expected to be low and high atmospheric pressure in the region, wind systems, temperatures in the air as well as in the water, salinity profiles, precipitation and fresh water inflow to the Black Sea. The output of this forecasting model should then be the current in the three fixed points, and because the current will be monitored continuously in these points these data can be used to calibrate the "macro model". The development, calibration and verification of the reliability criteria is progressing.

The minimum requirement for the accuracy of this forecasting model is that the confidence level of the maximum velocity of the current not exceeding the threshold level of 1.5 m/s in the critical period shall be not less than 90%.

3 OTHER CONSTRAINTS FOR IMMERSION

As described, the Bosphorus Strait is one of the world's busiest straits when it comes to commercial ship. The statistics tell us that approximately 50,000 major commercial ships pass through the navigation channel of the strait every year. This channel changes direction several times along the length of the strait and especially in the alignment area of the tunnel heavy navigation is required by the ships. The channel is also narrow, of the order of 800 m. The set-up of the immersion equipment will require a working area free of ship traffic of approximately 600 m in the cross direction of the channel, and therefore it will most likely be necessary to close the channel down completely for traffic when the 3–4 center placed tunnel elements will have to be immersed. Such a close down can, in such situations, be arranged, but international notices will be needed.

Copyright © 2005 Taylor & Francis Group plc, London, UK

The specific requirements of such notices do not go well in hand with the uncertainty of natural events, and this only emphasizes the importance of the need for reliable forecasting systems.

4 THE IMMERSION PROCESS, MODEL TESTS

The Contractor on the Bosphorus Crossing contract (the TKGN Joint Venture) performed tests of the immersion process in detail as early as in the bid period. These tests have been repeated and improved on a running basis as more information has become available during the process. The following information is based on the status of these tests as of October 2004.

The Basic Design of the IMT indicates that there will be 11 elements differing in length between 98 m and 140 m with a typical length of 130 m. The model tests were performed in Taisei Corporation's advanced testing facilities available in the Technology Center in Japan. The model scale used was 1:120. The flow condition simulated was one directional uniform flow of 2, 3 and 4 knots similar to 1.0 m/s, 1.5 m/s and 2.0 m/s.

The complete immersion procedure consists of three different and sequential processes; the towing process, the mooring process and the lowering process. The purpose of the model tests is:

- to determine the maximum forces during all phases to enable the Contractor to design the mooring equipment;
- to check the behavior and the handling of the immersion barge and the element during lowering, and
- to confirm the preliminary procedures regarding the handling of winches.

The elements will be produced and fitted out in the construction yard in Tuzla Harbor. When the forecasting system indicates that the weather window needed will be there, the towing of the elements will be initiated. It is expected that the traditional set-up of towing boats with one boat connected to each of the four corners of the immersion pontoon will be used. The route will be to the south of the Princess Islands. An alternative route north of the Princess Islands between these islands and the main land of Turkey has been discussed but two arguments do not favour this route. One is an area of relative shallow water that has to be passed, and another is the more frequent traffic of passenger boats and other boats that exists in this area. The southern route will have a last check-point where an update of the weather forecast and the model output will be performed. If the forecast has changed in such a way that the required window is no longer available, this point will be the area where the element is temporarily moored and secured in waiting for the next window to emerge. If the forecast has not changed for the worse, the towing will continue to the last "go/no-go point" which will be the immersion position in the Bosphorus Strait before the first mooring line is established.

Since the early days of the planning of this procedure was considered, it has been in the mind of engineers experienced in immersion techniques that the extreme forces on the element that would occur if the element was turned from a streamlined position where the element is parallel to the current to a position perpendicular to the current in the upper layer strong currents should be avoided. This idea has been further developed and adopted by the Contractor, so the first step of the mooring process is to moor the immersion pontoon carrying the element in a streamlined position parallel to the current. Only one mooring line (number 5) is used for this purpose together with some of the tug-boats to maintain full control. From this position, the element will be lowered until it is in the relative calm zone between the upper and the lower current and further up-stream mooring lines will be activated to control the immersion pontoon (number 3, 6, 7 and 8). Tug boats are not required anymore, but will be on stand by. In this position the immersion pontoon and the element will be turned in the horizontal plan into the correct position in order to be lowered further down into the trench. Before the final lowering is initiated, the remaining four down-stream mooring lines (number 1, 2, 3 and 9) connected to the pontoon are activated to ensure full control of the immersion pontoon.

The element will in this position only be kept in place by the down force on the 4 "sling lines" (number 10, 11, 12 and 13) carrying the element. This total down force is temporarily being designed for approximately 800 tons. However, before the final positioning of the element in the trench takes place the four adjusting wires (number 14, 15, 16 and 17) connected directly to the four corners of the element are activated for detailed control of the element.

Many different tests with this set-up have now been carried out, and the preliminary design of the mooring equipment has been done. The designed winch capacity (brake force) of the mooring wires (1–9), the sling wires (10–13) carrying the element down force and the adjusting wires (14 – 17) are as follows:

Wire no	Brake force, tons	Wire no	Brake force, tons
1	60	10	250
2	60	11	250
3	60	12	250
4	80	13	250
5	140	14	50
6	100	15	50
7	100	16	50
8	80	17	50
9	60		

Copyright © 2005 Taylor & Francis Group plc, London, UK

Marmaray Project: Project Management, the Marmaray Project

Steen Lykke
Project Manager, Pacific Consultants International, Japan

Hüseyin Belkaya
Deputy Project Manager, Yuksel Proje, Turkey

Hideki Sakaeda
Assistant Project Manager, Pacific Consultants International, Japan

Haluk Özmen
Ph.D. and Coordinator of the Project Implementation Unit (PIU), DLH, Turkey

ABSTRACT: The Bosphorus Crossing and the Commuter Rail upgrading project is one of the most complex major infrastructure projects being implemented in the world. The complexity does not only include major challenges of a technical nature but also challenges of more indefinable character like the funding set-up of a 3 billion US$ project originating from different sources, the complex nature of the necessary permissions and approvals from the relevant authorities, the cultural differences in a region where Europe meets Asia and the complexity of the organizations of the stakeholders.

This paper will describe the processes and the main philosophies used for managing the Project seen from the perspective of the Employer's representative, Avrasyaconsult. The paper will furthermore describe the challenges that have to be addressed establishing new organizations and effective procedures when senior staff with many different nationalities and backgrounds have to be brought together in a very limited time period and with limited resources for the purpose of producing top quality Enquiry Documents for the Project.

The paper will address the managerial challenges we have been facing because the contract concept is based on the Conditions of Contract for the FIDIC EPC/Turnkey Projects or better known as the "Silver Book". The paper will describe the inherent problems all organizations of this nature will face during the coming 5 to 10 years if they use the "Silver Book concept" simply because it takes decades to change the mindset of managers and engineers from an Employer's-design type of concept to a design-build concept.

The paper will as conclusions outline the lessons learned so far and what can be done better next time a similar challenge lies ahead of us.

1 INTRODUCTION

The management of modern mega-projects is usually based on the ideas and principles of the ISO9001 and related standards. The problem with this set of standards is that the principles may be clear but they are very general, and the principles, terms and definitions are – in the opinion of the author – focusing on and adopted to organizations of a "going concern" where cultures, business principles and attitudes are developed during generations. Furthermore, the ISO standards are written by Quality Managers for Quality Managers and not by Project Managers for Project Managers. Therefore, it takes effort and time to develop management systems suitable for a project and on these types of project time, in the early days of the project, is a very limited resource.

A project organization is established and based on senior managers and engineers being brought together in a very short time period and as these engineers and managers invariably have different backgrounds, experience, cultures and nationalities they cannot by their nature form a homogeneous project team in the early days of a project.

The engineering and management services that must be provided by Avrasyaconsult the Employer's Representative on the Marmaray Project – were procured through a competitive bidding process that started in 1999, however, the contract was not awarded until February 2002 with work starting a month later.

Copyright © 2005 Taylor & Francis Group plc, London, UK

A consequence of this delay and developments in the arrangements for funding was that the project definition today is not what it was at the time when the planning and staffing of the organization was done. In other words; a project of this nature is constantly evolving and therefore the management of the project by its very nature has to adapt to change.

Many different organizations have to work closely together. The Employers project organization – the Project Implementation Unit (PIU), the Employer's running organization, the Contractors project organization, the authorities, the independent committees like the Historical Committees of Istanbul and the involved stakeholder groups and NGOs are examples of such organizations that have to develop good working relationships, but all these organizations do not as basis have the same objectives. To the contrary, often the objectives are directly contradictory.

The above given descriptions set the scene and outline the challenges which have to be met by the management of the Project.

2 PROJECT MANAGEMENT

The problems related to the ISO9001 standards as described above were to a certain extent decreased by the introduction in 2003 of the ISO10006 international standard which deals with *"Quality management systems – guidelines for quality management in Projects"*. In this guideline Project Management is defined as the "planning, organizing, monitoring, controlling and reporting of all aspects of a Project and the motivation of all those involved in it to achieve the project objectives". So in order to set up Project Management Systems it is necessary to define "the project objectives". And here it must be realized that there are more than one "project" involved. The overall "Project" is, of course, the Marmaray Project; but the "project" for Avrasyaconsult is not only the Marmaray Project, but also the "Avrasyaconsult project" which is the engineering and consulting services we have to deliver to the Employer; and for the Contractors the "project" is not only the Marmaray Project but also the design and construction works they have to deliver to the Employer.

3 PURPOSE AND OBJECTIVES

The intended purpose of the Marmaray Project is to provide bi-directional, safe, robust, reliable, comfortable, durable, cost-effective and uninterrupted train transportation of passengers and freight throughout the Istanbul area of Turkey, on both sides of as well as under the Bosphorus Strait for design life of 100 years.

The Objectives of the Marmaray Project are:

- to open for commercial operation of the Commuter trains on track 1 and 2 and for other train operations on track 3 (and track 1 and 2 through the tunnels) from Halkali to Gebze on or before 15th March 2010.
- to stay on or below the cost estimates and to stay on or above the income estimates established July 2004 during implementation as well as during the operation and maintenance period up to the point in time where the Project "has been paid for by the users".
- to establish the Project in the required quality which is a quality that can be compared to other modern projects of a similar nature established during the last three decades in Japan, Europe or the USA, with a design lifetime of the structures of minimum 100 years.
- to meet all fitness for purpose, performance and minimum criteria as described in the contract documents for all Contracts.

It should be observed that inherent in these objectives are internal conflicts that have to be dealt with during the processes of the Project. There are three quality aspects built into these objectives; time, cost and technical quality. At a given point in time only two of them can have first priority and the third must take second priority. In the planning and description of performance criteria phase it is common to give first priority to time and technical quality, and therefore these two facets will automatically take priority over cost. Later in the Project when the minimum requirements for technically quality have been defined the first priority can be given to time and cost by constantly following up on ensuring the technical quality.

The Objectives and the priority of the Avrasyaconsult Joint Venture are:

- the overall Objectives of the Marmaray Project.
- to ensure customer (DLHs) and funding agency satisfaction with the performance of Avrasyaconsult, to the extent possible the performance of the Contractors and the progress of the Project.
- to create a positive and international atmosphere on the Project and in the organization within which it will be attractive for highly skilled and committed staff to perform their duties.
- to ensure and make visible the success of the Project as well as success for the individuals working in the organization in order to strengthen the opportunities for their carees ahead.
- to meet the profitability requirements of the Avrasyaconsult's engagement on the Project to the benefit of the Partners and the associated companies of the Joint Venture.
- to ensure technical and managerial success for the JV-Partners.

Copyright © 2005 Taylor & Francis Group plc, London, UK

4 MANAGEMENT PRINCIPLES

The policies established for managing the Project and the Avrasya organization are:

- to manage by objectives, delegation and follow up.
- to manage by controlled processes and pro-activity.
- to limit the need for reactive processes by taking due care in time.
- to manage by obeying and observing "the 7 C's":
  - Clarity
  - Commitment
  - Communication
  - Coordination
  - Cooperation
  - Consistency and
  - Continuity.
- To respect the integrity of each staff member of the Avrasyaconsult team and request the same from each staff member.
- The management systems must be build up on the basis of the philosophy of ISO9000/2000; however, the systems must at all times be adjusted where needed to meet the objectives and requirements of the Project, the Employer and the Avrasyaconsult organization and to limit bureaucracy and internal friction.
- In providing transportation as described in the intended purpose of the Project, the implementation and the operation of the railway must be done with respect to the Environment and the people that will be directly or indirectly affected by the Project.

5 STRATEGIES

The Strategies have to be formulated with respect to the Objectives and it has furthermore to be realized that this Project belongs to a small group of maybe not more than 5 "Mega – Infrastructure Projects" of the same complexity going on in the world right now, and this Project can therefore hardly be compared to any other project ever constructed in Turkey; be it national as well as international projects.

The most important strategies are:

- The "Employer" (DLH, the PIU and Avrasyaconsult) must be and must be seen as an experienced, international, open, honest, unified, trustworthy and professional Employer with respect for professionalism, roles and responsibilities and the environment in which we perform our duties.
- The Employer and his Representative must have the necessary but sufficient staffing in the organization at all times of the process and matching at all times the workload and the Scope of Works.
- Bureaucracy must be limited to an absolute minimum in all processes in order to increase efficiency and avoid unnecessary internal friction.
- A Partnership relationship with respect of the different roles and responsibilities should be developed between the Employer, the Employer's Representative and the Contractors if all parties "deserve" such a partnership relation to be established ("It takes two to tango").
- Efficient and intelligent use of modern IT systems is a cornerstone in modern Project Management, and such systems must therefore be developed and maintained on all levels of the Project Organization.
- Observe early in all phases the importance of identifying internal as well as external interfaces; inside and between organizations as well as inside and between all involved organizations and develop clear procedures of how to ensure consistency in all matters on both sides of the interfaces.

6 CHALLENGES RELATED TO "DESIGN & BUILD" CONCEPT

Due to the very nature of the Project and the Terms of Reference governing the engineering and Services Contract between the Avrasyaconsult Joint Venture and the Employer, the majority of staff employed in the Joint Venture are very senior managers and engineers. Such staff has for historical reasons gained most of their experience from contracts performed in accordance with conventional Employer's-design where the Employer has already prepared the detailed design and all the specifications and construction methods have also been fixed.

Very few people have extensive experience of the "Silver Book" type of design and build contract. The main difference in describing the contract requirements are that under the Silver Book type of contract, the Employer (through his consultant) must describe the criteria that the end product has to fulfill; i.e. the purpose of the component or the system and the related performance and documentation criteria related to that component or system. In a "conventional" or Employer's-design type of contract the Employer normally does not bother to describe the purpose or performance criteria of the components and systems, because that is input already used by himself for the purpose of actually performing the detailed design of the Project. Actually it is often seen that these overall fitness for purpose and performance criteria are never written down in clear language even on Mega-projects like the Marmaray Project.

The challenge on this project and similar projects is to organize the change of mindset that has to take place on all levels of the organization in order to ensure a high and consistent quality of the Employer's Requirements. These requirements have been described

Copyright © 2005 Taylor & Francis Group plc, London, UK

on different levels and within four different categories as follows:

- Fitness for purpose descriptions. Typically these descriptions have been given on three different levels; the overall Marmaray Project level, on "Contract level" and on system or component level.
- Performance criteria. Such criteria are requirements that can be tested and documented via approved test methods or by other means.
- Minimum Requirements. In order to ensure a minimum quality within certain important issues and thereby also to ensure a common basis for all the competing Contractors and/or to limit risks for the Employer and the Contractors a number of minimum requirements have been stated in the contract documents.
- Exclusion of design solutions or construction methods that will not be accepted to be introduced or used on the Project.

This way of building up the Contract Documents is not familiar to most managers and engineers, and therefore it has been necessary to conduct many and repeated internal education sessions in the organization.

The next phase of performing supervision and inspections will also constitute big challenges for the organizations. In the traditional Employer's-Design type of contract the Engineer has most often produced the design and the related specifications, and therefore the supervision and inspection is more or less straight forward. All engineers are therefore familiar with this type of supervision. However, on a "Silver Book" type of contract this is not the case, and the supervision and inspection of the works has a different nature. All such activities start with a requirement that the Contractor must supply a Basic Design, a Detailed Design, all specifications and method statements and all this information has to be organized in proper Quality and Inspection and Test Plans. The Engineers job is then to perform inspection and check of this documentation and to ensure that all requirements related to the intended purpose and the performance criteria are likely to be fulfilled, and later on to conduct audits and supervision works including random inspections of the Contractors quality and management systems on site. In short, the nature of performing supervision and inspections on a "Silver Book" type of Contract is quite different from that with which most engineers are familiar.

7 ORGANISATION AVRASYACONSULT

Some main principles have been used in establishing the Project Organization for Avrasyaconsult:

- There is a Top Management Team (M-team) of five persons consisting of the Project Manager, the Deputy Project Manager, two Assistant Project Managers for the "line management" of the Bosphorus Crossing and the Commuter Rail respectively and the Assistant Project Manager for General Project Support (Contracts, Programming & Planning and Quality Management). The Project Manager is the ultimate responsible person for the M-team and reports to the Policy Committee of the Joint Venture.
- The Deputy Project Manager has his own team being responsible for the general administration – all aspects of the Joint Venture.
- Each Assistant Project Manager (APM) has his own team of managers and engineers and the maximum number of persons reporting to a member of the Top Management Team must not exceed 7. Each APM is the ultimate responsible person for his own Division and reports to the PM and DPM.
- Clear demarcations are described between the line divisions and the General Project Support division and the General Administration Department. Only line divisions are responsible for the management of the Contractors.
- The line divisions request the General Project Support Division for assistance as necessary in the areas of contract administration, claims, variations, cost, programming and quality control. However, the General Project Support Division monitors, audits and instructs the line divisions on internal procedural matters.
- All internal interfaces between divisions and or departments have only two parties; the fulfilling party and the receiving party. The receiving party has the obligation to "drive the interface".
- Internal "matrix organization" conflicts must be eliminated via clarity in job descriptions and procedures and via a high daily level of internal communication, coordination and pro-activity.

8 LESSONS LEARNED SO FAR

The conclusions under this heading will be formulated as a number of questions and related answers. Of course this is not a scientific approach because others should judge whether the outcome of the management efforts done by the Employer and the Employer's Representative live up to what could be expected, but we will do it this way anyway.

8.1 *Was the "lead in" time to set up the organization and get organized on management systems and procedures sufficient?*

No, as is normal on this type of Project, all involved parties are too optimistic when it comes to evaluation of

Copyright © 2005 Taylor & Francis Group plc, London, UK

the capability for all involved parties to "get organized". However, it is our opinion that this "optimism" helps in driving the process in the early phases of the Project, and it is also our opinion that the main output of the pre-award phase up until now – the BC1 Contract Documents and the management philosophy in general – despite this over-optimism, has a very high quality.

8.2 *After the lead-in period, did the outcome of the planning and programming of the Project constitute a robust product and did we up until now act pro-actively?*

Yes, the Illustrative Design and the related planning and programming has not revealed any "surprises" up till now and all known potential future problems have been dealt with in the planning and programming of the Works. However, decisions not fully under the control of the Employer and his Representative like for example obtaining permits from authorities and decisions from Historical committees and the funding of the remaining portions of the Project may influence the future planning and programming.

8.3 *Do the Organization Structure and the underlying management principles work out in practice?*

Yes, it is our opinion that the Organization and the described management principles work out very satisfactory and leads to a high degree of satisfaction for the involved persons and a high quality of the output from the organization. However, the organisation is a fresh product and will require constant adjustments and alertness to ensure that the ultimate objectives for the Project, the Employer, the Contractors and for Avrasyaconsult will be met.

8.4 *Has the Organisation been able to observe the "7 Cs" to the extent required?*

Yes and No. In general, it is our opinion that we have been able to observe and follow up to a satisfactory extent on 5 out of the 7 Cs; that is on Clarity, Commitment, Coordination, Cooperation and Consistency. However, on Communication and Continuity room still exists for improvements. Every time an internal dispute or problem has been analyses to find the root of the problem, lack of communication has played a role in the process. This is not surprisingly. The working language is English. The Team consists of people with many different nationalities and cultural background and therefore it is inevitable that communication problems will occur from time to time.

An analysis of the roots of potential problems often also shows links to lack of continuity. This problem arises out of the fact that many people for different reasons can not work consistently and permanently on the Marmaray Project. Therefore discontinuities in processes will occur and discontinuity is a common root of potential problems. It was expected that short input, specialist staff would be less productive than assumed at the original planning stage and that management time would be consumed to coordinate their contributions. However, the problems associated with continuity were not fully appreciated. When the team realized the full extent of this problem the solution was to decrease the number of people working short time or part time on the Project and then convert the related resources into full time staffing fully dedicated to the Project.

8.5 *Has the introduction of ISO9001/2000 management principles been a success?*

Yes and No. It has up until now been demonstrated that the main philosophy of the ISO standards creates a good basis for the management principles of such major projects. However, it has taken too long for the management to realize that the ISO9000/2000 structure, vocabulary and terminology is not very suitable for use on projects like the Marmaray Project, which has a nature of producing one and only one "prototype" not followed by "mass production" of the prototype.

Copyright © 2005 Taylor & Francis Group plc, London, UK

Marmaray Project: contract strategy and minor tactics

R. Harrison
Assistant Project Manager, (Contracts, Cost and Planning)Pacific Consultants International, Tokyo, Japan

S. Lykke
Project Manager, Pacific Consultants International, Tokyo, Japan

H. Sakaeda
Assistant Project Manager, (Bosphorus Crossing) Pacific Consultants International, Tokyo, Japan

M. Çilingir
Former Deputy Project Manager, Yüksel Proje, Turkey

ABSTRACT: This paper focuses on the way the principal decisions on contract strategy were made on the Marmaray Project, and the influence of the type of contract on those decisions. It also touches upon risk allocation, the use of the FIDIC Silver Book and the structure and drafting of design-build contracts.

1 INTRODUCTION

This paper looks very briefly at the strategic decisions that were made with respect to the contractual aspects of implementing the Marmaray Project. The terms "Employer" and "Contractor" are as used in FIDIC contracts; however, the term "Consultant" is used to refer to the firm employed to assist the Employer.

2 STRATEGIC DECISIONS

The overall contractual strategy was decided in February 1999 and it originated from the first International Funding Institution (IFI1) involved, not the Employer. The Employer proposed a single contract covering the whole project because:

1. "if a juridical problem occurs in one part of the Project the other parts could not be operated although they are completed properly.
2. In case of a problem occurring in the whole system it would be difficult to find the responsible authority.
3. if synchronization could not be managed for any reason, the parts completed would not be taken into the commissioning tests without the completion of the other parts (and) this might cause juridical problems."

The IFI1 proposed financing one contract and indicated that the remainder of the project be split into two contracts because:

1. "the amount in the case of one lot is too huge.
2. division of procurement is technically possible, because the nature of each procurement is different from (the) others.
3. (the) consultant will ensure the synchronization of several procurement lots.
4. by dividing procurement (into) lots, more opportunity for competition among competent bidders can be provided."

The Employer accepted packaging and financing of one contract (the Bosphorus Crossing or BC1), with packaging of the balance of the project (the upgrading of the commuter rail and the procurement of the rolling stock) to be decided.

Both the Employer and the IFI1 agreed that the form of the contracts would be "design and build". This decision was partially reflected in the terms of reference upon which the Consultant was hired to assist the Employer in implementing the project.

The next strategic decision again related to financing. The Employer proposed that the commuter rail and the rolling stock be procured as a single contract because the Employer, and the Consultant in this instance, sought not to dilute the liability for fitness

Copyright © 2005 Taylor & Francis Group plc, London, UK

for purpose inherent in a design-and-build contract. However, the IFI involved in financing (IFI2) proposed that there be a number of contracts, selected by discipline (i.e. civil works and various electrical and mechanical-type works). Their reasoning was essentially identical to that offered by IFI1. IFI2 finally accepted a more general grouping: a contract for the Commuter Rail (CR1) and a contract for the rolling stock (CR2). This split was also influenced by the Government's planning process which would not allow the rolling stock component of cost to be committed before 2005. The final split of contracts is thus Contract BC1 for the tunnel crossing of the Bosphorus and underground stations, CR1 for the rest of the commuter rail system and CR2 for the supply of rolling stock.

There are compelling reasons for splitting a project up into multiple packages. One is if finance cannot be arranged to cover the entire project, and another is if the project is simply so large that no individual contractor, or even group of contractors, would take it on. However, these were not the arguments presented by the IFI and this may partly be explained by the fact that breaking projects into parts is not restricted to mega-projects. Many projects well within the capacity of the construction industry and for which finance is available in full are broken into parts, and this is the case whether the projects are large and single-disciplinary (such as roads) or large and multi-disciplinary (such as railways and airports). What, then, are the underlying arguments for this "subdivision" approach?

One argument may be that large projects are frequently beyond the financial capacity of "local" companies and are seen to deny those companies the opportunity to participate in the economic development of their area by reason of their lack of size. This is a strong emotional argument for fragmentation of projects. However, if this reason is accepted, it must be either that it brings economic, if not financial, benefits or that it is acceptable for the taxpayer to pay a higher price, providing the higher price is subsidizing local companies.

Another factor is the view, sometimes promoted as being self-evident, that splitting works to be done into a large number of smaller contracts results in substantially lower costs. There is not much evidence to support this view. Civil engineering projects are rarely, if ever, identical and Employers do not run control sample projects for the purpose of comparison. In short, we don't know – our views are based on a bit of experience, a smidgen of data, some thought and a lot of habit. But we do know that Employers frequently give contractors the opportunity to provide discounts if they are awarded packages of contracts rather than single contracts. These discounts, which usually run at about 2%, have a rational basis encapsulated in the "economies of scale". We also know that multiple small contracts must, inevitably, duplicate effort and costs in matters as simple as unit costs of office space, administration and personnel management. They also must, in theory, lose out on the cost savings arising from bulk purchasing.

It is also unlikely that cost saving could arise from multiple small contracts being run more efficiently than a single large contract. Indeed, the reverse is the more likely. A large project is more likely to be given a high priority in the allocation of resources. The key decision-makers in each of the multiple small contracts are unlikely to have the same degree of experience as those in the equivalent positions in the single large contract. Cost savings might be available in the area of reduced regulatory and social costs but size of firm at which these cost savings become significant is likely to be well below the size of firm involved in construction.

That leaves increased competition as the sole supporting argument for a subdivision approach being less "expensive". The smaller the contract, the more contractors have the resources needed to do the job, so the more contractors available to bid. Ten contractors vying for each of twenty contracts certainly has an intuitive feel of increased competition over, say, four or five contractors vying for a single contract. However, there are not that many small jobs where a firm's organization or method of doing the work can lead to a substantial cost savings. So the cost reductions that come about through increased competition result from a reduction of the margin allowed for profit and risk. Increasing the number of bidders to twenty from five increases the opportunity for the incompetent or desperate to win a job. This increased risk is of little interest if what is being contracted for is a series of independent items of work, but the increased risk should be of considerable interest if what is being built is a complex system. So the cost saving that comes at the expense of increased competition is not a true reduction in cost, it is rather a transfer of risk. Perhaps it is the theoretical financial consequences of this risk transfer that form the basis for the "less expensive" school of thought. However, the effort (and costs) needed to ensure that the sum of the parts actually works properly and the cost of risk associated with the fact that it might not, do not disappear. They are simply transferred to the Employer. So the argument that a large number of smaller contracts can result in substantially lower costs and that, conversely, a single large contract is often more expensive (than a lot of smaller contracts) is, even if there was evidence to support it, comparing apples with turnips.

In addition to the cost argument, there is also the view that, if the whole job is given to a single company or JV, then the success of the project is dependent on that one company and that this gives the company "too much power" and places the project at risk of

Copyright © 2005 Taylor & Francis Group plc, London, UK

that one company or JV failing – for example, going bankrupt. The "too much power" argument appears to be an emotional or ideological belief or "feeling" and is not amenable to analysis. The "project at risk" argument is also suspect. One of the purposes of pre-qualification is to establish whether a bidder has the financial capability to do the job, i.e. whether it is sound. The questions are then whether it is more or less likely for a financial risk to be missed in evaluation if the Employer is researching and analyzing five firms, or fifty firms; whether large firms or medium or small firms are more susceptible to bankruptcy; whether the failure of a medium-sized firm doing a key part of a project has any less of a consequence than the failure of a large firm doing all of the project, and whether the questions have any meaning in the case of joint ventures and joint and several liability.

In a conventional "Employer's design" contract, the type that probably reflects the bulk of any engineer's experience, it really does not make much difference with respect to liability if the project is split into multiple small contracts. The cost differences are submerged in the difference between bids. However, there is a fundamental difference between Employer-design contracts and design-and-build contracts:

1. In a design-and-build contract, the builder is responsible for the design.
2. In an Employer-design contract, the Employer is responsible for the design.

Clearly, if the Employer divides the project into a number of parts, and arranges the design of those parts, and gives that design to the builder to construct, then it makes eminent sense for the Employer to arrange the coordination of the design and interfaces between the designs. This can be done by the Employer forming a team to manage the integration of the designs or by paying one of the contractors to do this work. As the Employer is responsible for the individual designs, the Employer is responsible for the whole design.

Where the Employer has chosen the design-and-build route, the builder is responsible for the design. Indeed, the law and, increasingly, the contracts themselves impose a "fitness for purpose" liability on the Contractor. If a project is split into two or more contracts, the responsibility for design and build must inevitably be split between the contractors involved. Who, then, is responsible for ensuring that the overall design actually works? Who is responsible for the "fitness for purpose" of the project?

It is not the contractors who, sensibly, can be responsible only for the fitness for purpose of what they have designed. In an effort to resolve this problem, which arises solely because of splitting the project into parts, an Employer may take on that responsibility himself. If the Employer should do so, he immediately removes, or at least dilutes, the "fitness for purpose" obligation. In addition, the Employer is faced with the problem of how, practically and contractually, he can get the changes needed to ensure compatibility between designs incorporated in the design. What mechanism exists for changing a design? That mechanism is the contractual authority to vary the Work. However, if the Employer varies the Work, he may well destroy what is left of the "fitness for purpose" obligation, and varied works lead to increased costs.

The Employer may seek to incorporate an interface obligation within each of the design-and-build contracts. This is much easier to say than it is to do, or at least to do well – that is, in a way that works effectively and maintains the fitness for purpose obligation. A contract may be written that appears to have direct contractual obligations on both parties to address interface problems but it is quite likely that problems will not be addressed effectively, primarily because, despite what appear to be clear reciprocal obligations, the multiple contractors have distinct and divorced organizations and it is extraordinarily difficult to create a contractually robust mechanism for actually implementing the changes that coordination of interface design actually demands. In such a situation, changes in design have to be made by one or both of the contractors. Who decides which one makes the changes and what happens to the cost of those changes? And there are more complications. When an Employer is having a project designed and built, it sometimes makes sense to include a maintenance obligation. This is not a difficult matter to arrange if either the design is the responsibility of the Employer and is thus known to the builder when the Employer tendered, or if the builder is responsible for the design. It is extremely difficult (i.e. expensive) to have such an obligation incorporated in a design-and-build contract where the design of a critical part is being done by another design-and-build builder and the design is not even known at the time the first design-and-build builder has to bid.

The question is then not why do Employers actually split design-and-build contracts; they do so in order to facilitate financing or because they think no-one will bid for the complete project. The question is why it is thought necessary to seek to justify the decision to split by presenting arguments that do not stand up well to scrutiny.

Before we leave matters of strategy, let us take a fleeting look at that other strategic decision: design-and-build rather than Employer-design. Was this the correct decision, particularly given that one of the key selling points for design-and-build – sole-source responsibility – had effectively been negated?

The answer is probably "yes", primarily because of the (technically) strategic decision to have the main part of the tunnel under the Bosphorus as an immersed tunnel where the method of construction, which truly

Copyright © 2005 Taylor & Francis Group plc, London, UK

falls within the expertise of the contractor, is of overwhelming importance. In addition, from the perspective of financing, a fixed-price design-and-build contract is more certain as to final price than a floating-price, remeasured Employer-design contract.

3 CHOICE OF CONTRACT

The basic choice as to the form of the contracts to be used was between a contract drafted, from the beginning, to meet the needs of the Employer and a standard contract modified to meet the needs of the Employer. A custom contract was rejected because it would take a considerable time and cost a considerable amount to create a new contract for this specific project, there was little or no evidence to indicate that custom contracts are any "better" than modified standard contracts, and a custom contract would, of itself, inject a degree of uncertainty into a bidder's perception of risk and this would either be reflected in a reluctance to bid or an increased price associated with that uncertainty.

The standard contracts evaluated were:

1. FIDIC Design-Build and Turnkey 1st Edition (Orange Book).
2. FIDIC Plant and Design-Build Contract 1st Edition (New Yellow Book).
3. FIDIC EPC/Turnkey Projects (Silver Book).
4. ICE Design and Construct Conditions of Contract 1st Edition.
5. EJCDC Standard General Conditions of Contract between Owner and Design/Builder.

The Orange Book was rejected on the assumption that the more recent FIDIC contracts would incorporate experience gained from its use. ICE was rejected on the grounds that, in an international environment, it would be viewed as country and legal-system specific. EJCDC was rejected for the same reasons and as being unnecessarily complicated. That left the New Yellow Book or the Silver Book. The Silver Book was chosen primarily because it provided a better base on which to build the modifications that best suited the needs of the Employer than did the New Yellow Book, and this was because of Sub-Clause 4.12 and the question of what can be reasonably foreseen by an experienced contractor.

The Silver Book has been quite heavily criticised since its introduction. This criticism appears generally to be at the instigation of contractors. While the Silver Book may deserve criticism for scrapping the "Turnkey" part of the title, it does not deserve criticism in that area which has attracted the most attention, and that is Sub-Clause 4.12; indeed, it deserves praise in that particular area.

Sub-Clause 4.12 attracts criticism because it does away with the idea of the Employer carrying the risks of the Contractor encountering adverse physical conditions that were not reasonably foreseeable by an experienced contractor. This is seen by contractors as being a major and unfair shift in the allocation of risk. It does nothing of the sort, as should be clear if the sub-clause is actually read. What it says is "Except as otherwise stated in the contract" and this actually allows the Employer to override the allocation of risk contained in the standard Sub-Clause 4.12 and to allocate risks in the manner that best suits his approach to risk, the nature of the contract, the degree of certainty needed for financing, and how much he is prepared to pay for the Contractor to carry various risks.

It even allows the Employer to include, verbatim, the risk allocation described in Sub-Clause 4.12 of the FIDIC Design and Build Contract if he should be so ill advised to do so. Why ill advised? Simply because "Clause 12" in its varied forms in FIDIC contracts has been a fertile source for disputes (perhaps the most fertile) as long as there have been FIDIC contracts but also, as was pointed out years ago, its effect is not what it was thought to be: it actually encourages the rash and inexperienced contractor to the detriment of the prudent and experienced one. A rash contractor may foresee what may happen and ignore it, pinning his hopes on a successful claim under Clause 12. An inexperienced contractor will not foresee what may happen, and that will be reflected in a low price and a successful tender. A prudent and experienced contractor will foresee what may to happen, allow for it and then lose the job because his tender is high.

The reality is that, with respect to Clause 12, a contractor is not identifying those physical obstructions that are "… in his opinion not foreseeable by an experienced contractor …" but rather those physical obstructions that are commercially impracticable for him to allow for in his tender and which he has a reasonable expectation of convincing the Employer were not reasonably foreseeable.

It was therefore concluded that the Employer's interests would best be served by not leaving this to the vagaries of judgment of individual contractors and the consequent uncertainty but to insert a "changed conditions clause" and a set of "reference conditions". The principle is exactly the same as that introduced in North America with the idea of a Geological Baseline Report, although in the implementation the "baseline", or reference, conditions were expanded to cover more than just geological conditions.

The manner in which the risk of the "unforeseeable" was finally treated in the contract documents is more elaborate than originally intended because it was, in essence, a radical departure from that with which the IFI were familiar, and was the subject

Copyright © 2005 Taylor & Francis Group plc, London, UK

of considerable debate before its final form was accepted.

4 CONTRACT STRUCTURE

The broad structure of the contracts is relatively conventional. One point of interest is that interpretive reports were not included in the Contract Documents, nor in the Enquiry Documents. This omission is against the advice of various tunnelling associations, including ITA. This is because interpretation is the contractual obligation of the contractor. However, if both factual and interpretive data are provided, then either the interpretation provided will confirm the Contractor's own interpretation – in which case the Contractor will be reassured but no other purpose will have been served – or the interpretative report will contradict or at least differ from the Contractor's own interpretation. In such a case, the Contractor has to depend on his own interpretation. If the Contractor's interpretation of what is foreseeable is more favourable than that given in the interpretative reports, then what does he do? If he depends on his own interpretation and it proves to be wrong, he is unlikely to be able to demonstrate that what was actually encountered was not reasonably foreseeable, even though the interpretation used to counter his demonstration is unlikely to have been made by an experienced contractor. Sensibly, therefore, the interpretations provided to him form the lower bound of what is foreseeable.

Put simply, interpretive reports do not contain facts; they contain interpretations derived from facts, and these are opinions. Sensibly, interpretive reports should be included as contract documents only where their contents have contractual meaning, as, for example, in geological baseline reports.

With respect to the detailed structure of the contract documents, the Employer's Requirements posed the usual and still unsolved problem of taxonomic consistency – specifically, how to present the Employer's Requirements (or indeed any specifications) in a systematic manner where the underlying system is reachable by logic. Unfortunately, there is no correct solution to this problem and, given the time constraints, the solution was to adopt a structure that had been used on a previous similar project. This approach, to replicate what has been used in the past, is a sensible approach in a situation where a considerable amount of work has to be done in a very limited time. Unfortunately, there is no guarantee that what you are using has been carefully considered; indeed, it is highly probable that it is simply the repetition of something that was used before and that in turn is the repetition … etc.

The net result was that, during the drafting, it became apparent that there was a danger that inconsistencies in the logic of the structure would threaten the overall contractual stability of the document, primarily through that bane of all contracts – mutated repetitions. This forced a restructuring and, even so, the structure of the Employer's Requirements in BC1 has obvious taxonomic peculiarities.

Contract BC1 Employer's Requirements

Chapter 1: General
Chapter 2: Scope of Work
Chapter 3: Management Systems
Chapter 4: Design
Chapter 5: Construction
Chapter 6: Definition Drawings
Chapter 7: Design, Construction and Materials (EM Works)
Chapter 8: Standards
Chapter 9: Reference Conditions

However, the more egregious flaws were addressed in CR1.

Contract BC1 Employer's Requirements

Chapter 1: General
Chapter 2: Scope of Work
Chapter 3: Project Management
Chapter 4: General Requirements for Design
Chapter 5: General Requirements for Materials Plant and Workmanship
Chapter 6: Definition Drawings
Chapter 7: Trackwork
Chapter 8: Traction Power System
Chapter 9: Overhead Catenary System
Chapter 10: SCADA System
Chapter 11: Telecommunications System
Chapter 12: Signaling System
Chapter 13: Rolling Stock: Not used
Chapter 14: Automatic Fare Collection System
Chapter 15: Depots and Stabling yards
Chapter 16: Stations
Chapter 17: Operations Control Centre & Administration Building
Chapter 18: Building Services & E&M
Chapter 19: Bridges and Other Structures
Chapter 20: Interfaces – CR2 and BC1 Contracts

Payment was addressed through the use of a priced activity schedule. Payment for any activity is made when it is complete and when it is demonstrated, through the documents of the quality system, that it complies with the Contract. An alternative proposal, namely payment via a payment schedule fixed at the time of bid and controlled by a series of milestones related to progress and quality, was rejected. It remains to be seen how efficient the selected approach will prove to be. Consideration was given to a hybrid approach in CR1. If adopted, this would combine the advantages of the priced activity approach of linking payment directly to quality with the incentive advantages offered by a Milestone Contract.

Copyright © 2005 Taylor & Francis Group plc, London, UK

5 DRAFTING OF THE CONTRACT

Perhaps this should have been called "Drafting the Employer's Requirements" because that is where serious difficulties were encountered. The award of the consultancy contract was made very much later than originally planned, which meant that the provisional planning for mobilization of staff was meaningless as they had been assigned to other projects. Specialists from the international joint venture, many of whom had never worked together, mobilized in the order they became available, to temporary and overcrowded quarters. With the computer system yet to be delivered and installed, they worked on their own laptops using their own software and languages while the management structure was created around them. Many of the technical writers of the Employer's Requirements were writing in English as a second language and all of them brought with them the mindset of their own organization and their own experience; in short, a typical project startup.

As these specialists became available, there was an equally typical imperative to have them produce something – firstly, because of a tight timetable for the production of the Enquiry Documents and, secondly, because they were short-term specialists with limited time allocated to this project. The result was that many of them, with the best of intentions, started turning out what they thought was required in the fashion with which they were familiar. Unfortunately, because of their consultancy background, what they were familiar with was how to design and how to write "specifications" for Employer-design contracts. This was expected and they were informed of what was required of them, namely that this was a design-and-build project and what was wanted was carefully considered definitions of intended purpose and associated performance requirements, not mechanistic specifications. Simple guidelines on how to draft documents were given, as were guidelines on how to use standard document templates and even how to punctuate. Naturally, most of this was simply ignored. This in itself was expected; the difficulties involved in taking a disparate set of people of different nationalities, cultures and languages, placing them in a time-critical environment and requiring them to adopt a new way of thinking and a new way of writing were obvious. What was not expected was just how tenaciously people would adhere to a mechanistic specification approach and how reluctant they would be to recognize the fundamental differences between Employer-design and design-and-build contracts and how those differences had to be reflected in the documents.

The approach required of the writers was to identify and describe the intended purpose of what it was they were dealing with. A "fitness for purpose" obligation is generally one imposed by law in common-law systems. However, in addition in the Silver Book Sub-Clause 4.1, it is an expressed obligation that the Works be fit for their intended purpose as defined in the Contract. This means the Contract has to contain a definition of the intended purpose. If there were a single contract covering the whole project, then this "top level" definition would be relatively straightforward to develop. Dealing with three separate contracts, none of which serves much purpose without the contribution of the others, makes such a definition more thought provoking.

After they had that clear in their minds, they were required to identify what measurable "performance requirements" should be stipulated to assist in judging whether the component parts of the Works would, individually and collectively, be fit for their respective intended purposes.

The next stage involved the identification of "minimum requirements". The principle of minimum requirement was difficult to communicate to the writers of the technical parts of the documents. The intention was not to specify minimum requirements for every last part of the Works. If this were done, the Works would be defined by the minimum requirements. The intention was for the writers to identify within particular aspects of their specialty subjects key requirements that they would not under any circumstances forego. In other areas, the Employer included minimum requirements in order buy freedom from specific risks. Rather than forming the outer shell defining the entirety of the Works, the minimum requirements were intended to be nodes defining the framework of the Works. Similar in principle was the exclusion of specific solutions. While the Employer allows the Contractor the freedom to design and build much as he should so wish, there are certain design and construction solutions that carry a risk to the project that the Employer is not prepared to carry notwithstanding that intermediary carriers of that risk may be the Contractor and the insurers. In these situations, the Employer specifically excluded certain solutions.

6 CONCLUSIONS

The compelling reason for splitting a design-and-build project into separate contractual packages is if that is what is necessary to be done in order to obtain funding or to get firms interested in bidding. However, the arguments actually deployed in favour of splitting are along the lines that it actually makes sense to have such a split. These arguments are flawed in general and fail properly to distinguish between Employer-design and design-and-build contracts. Splitting a design-and-build project into parts removes many, if not all, of the benefits of the design-and-build approach.

A multi-disciplinary, multi-lingual, international consulting joint venture takes time to establish and to meld into an effective team. This is obvious and will

Copyright © 2005 Taylor & Francis Group plc, London, UK

inevitably result in a degree of inefficiency in the utilization of resources in the early stages of a project. This inefficiency is increased if the time schedule for the startup phase of the project is unrealistic – and it is always unrealistic.

Drafting the technical aspects of design-and-build contract documents needs a particular approach, a common "mindset" in the writers. This mindset takes considerable time to achieve and, if not repeatedly reinforced, rapidly reverts to the specification approach of Employer's-design contracts. Merely explaining what is required is insufficient. It is essential that the writers of design–build contracts not only understand what is required but why it is required, and that is best achieved by regular meetings to discuss and criticize what has been written. A lengthy re-education and indoctrination programme is required that hammers the principles home.

Copyright © 2005 Taylor & Francis Group plc, London, UK